TRANSACTIONS

OF THE

AMERICAN SOCIETY

OF

CIVIL ENGINEERS

(INSTITUTED 1852)

VOLUME 122

1957

Edited by the Executive Secretary, under the direction of the Committee on Publications.

Reprints from this publication, which is copyrighted, may be made on condition that the full title of paper, name of author, and page reference (or paper number) are given.

NEW YORK
PUBLISHED BY THE SOCIETY

1957

Transportation
Library

TA
1
A526
V.122

Copyright 1957 by the AMERICAN SOCIETY OF CIVIL ENGINEERS

NOTE.—The Society is not responsible for any statement made or opinion expressed in its publications.

CONTENTS

No. PAGE

2845 HIGH-STRENGTH STEEL BOLTS IN STRUCTURAL PRACTICE
BY MACE H. BELL.......... 1

DISCUSSION:
By WILLIAM HANSEN.......... 20
MACE H. BELL.......... 20

2846 THE DESIGN OF PIERS, JETTIES, AND DOLPHINS
BY DAVID A. HOPKINS.......... 22

DISCUSSION:
By ZUSSE LEVINTON.......... 37
DAVID A. HOPKINS.......... 37

2847 IMPACT ON PIN-JOINTED TRUSSES
BY BRUNO A. BOLEY AND CHI-CHANG CHAO.......... 39

2848 SIGHT DISTANCE AT UNDERCROSSINGS
BY PAUL HARTMAN.......... 64

DISCUSSION:
By THOMAS F. HICKERSON.......... 72

2849 PHOTOSYNTHESIS IN SEWAGE TREATMENT
BY WILLIAM J. OSWALD AND HAROLD B. GOTAAS.......... 73

DISCUSSION:
By ISADORE NUSBAUM.......... 98
WILLIAM J. OSWALD AND HAROLD B. GOTAAS.......... 101

2850 STIFFENING LOCK GATES BY PRESTRESSING DIAGONALS
BY CARL L. SHERMER.......... 106

2851 DRAINAGE IN THE HUMID AREAS OF THE UNITED STATES
BY JOHN G. SUTTON.......... 115

2852 MOMENT-ROTATION CHARACTERISTICS OF COLUMN ANCHORAGES
BY CHARLES G. SALMON, LEO SCHENKER, AND BRUCE G. JOHNSTON.. 132

2853 BEACH REHABILITATION BY FILL AND NOURISHMENT
BY JAY V. HALL, JR. AND GEORGE M. WATTS.......... 155

2854 INTEGRATION OF STREETS WITH AN EXPRESSWAY SYSTEM
BY KARL A. BEVINS.......... 178

2855 DISCHARGE COEFFICIENTS FOR SPILLWAYS AT TVA DAMS
BY KENNETH W. KIRKPATRICK.......... 190

2856 WATER CONTROL IN CENTRAL AND SOUTHERN FLORIDA
BY HAROLD A. SCOTT.......... 211

No. PAGE

2857 PUMPING GROUND WATER FOR IRRIGATION AND DRAINAGE
BY CLEVE H. MILLIGAN.................... 228

2858 MOMENTS IN DOMES BUILT INTO CYLINDERS
BY JOHN V. HUDDLESTON AND MARIO G. SALVADORI.................... 235

2859 NATURAL FREQUENCIES OF CONTINUOUS FLEXURAL MEMBERS
BY ANESTIS S. VELETSOS AND NATHAN M. NEWMARK.................... 249

DISCUSSION:
BY JACOB KAROL.................... 279
ANESTIS S. VELETSOS AND NATHAN M. NEWMARK.................... 281

2860 OBSERVATIONS ON THE URBAN TRANSPORTATION PROBLEM
BY HARMER E. DAVIS.................... 286

2861 IMPULSIVE MOTION OF ELASTO-PLASTIC SHEAR BUILDINGS
BY EDWARD COHEN, LEON S. LEVY, AND LEONARD E. SMOLLEN... 293

2862 AN EXPERIMENTAL STUDY OF BOUNDARY-LAYER TRANSITION
BY HENRY W. BENNETT AND CHARLES A. LEE.................... 307

2863 URBAN RENEWAL OF AMERICAN CITIES
BY JAMES W. FOLLIN.................... 330

2864 SOIL MECHANICS AND WORK-HARDENING THEORIES OF PLASTICITY
BY DANIEL C. DRUCKER, ROBERT E. GIBSON, AND DAVID J. HENKEL.. 338

2865 MEASUREMENT OF CANAL SEEPAGE
BY AUGUST R. ROBINSON, JR. AND CARL ROHWER.................... 347

DISCUSSION:
BY RAYMOND A. HILL.................... 364
DEAN C. MUCKEL.................... 364
CALVIN C. WARNICK.................... 366
N. SZALAY.................... 368
CYRIL W. LAURITZEN.................... 369
AUGUST R. ROBINSON, JR. AND CARL ROHWER.................... 371

2866 LATERAL BUCKLING OF ELASTICALLY END-RESTRAINED I-BEAMS
BY WALTER J. AUSTIN, SHAHEN YEGIAN, AND TIE P. TUNG.................... 374

R 2867 THE HIGHWAY SPIRAL FOR COMBINING CURVES OF DIFFERENT RADII
BY PAUL HARTMAN.................... 389

DISCUSSION:
BY THOMAS F. HICKERSON.................... 400
C. C. WILEY.................... 402
ALLEN H. BROWNFIELD.................... 404
PAUL HARTMAN.................... 408

2868 RIGID CULVERTS UNDER HIGH OVERFILLS
BY R. ROBINSON ROWE.................... 410

2869 GROUND-WATER DEVELOPMENT: A SYMPOSIUM
PLANNED UTILIZATION
BY ROBERT O. THOMAS.................... 422

DISCUSSION:
BY HAROLD E. THOMAS.................... 434
FRANK B. CLENDENEN.................... 437
ROBERT O. THOMAS.................... 439

No. Page

IRRIGATION ASPECTS
BY HARRIS R. MCDONALD....... 443

BASIN RECHARGE
BY PAUL BAUMANN.... 458

Discussion:
By **Robert T. Knapp**.. 474
Frederick L. Hotes.. 475
Norman H. Brooks.. 483
James A. Harder.. 486
Charles H. Lee.. 488
Paul Baumann.. 491

HYDRAULICS OF WELLS
BY DEAN F. PETERSON, JR.. 502

2870 VIRTUAL MASS AND ACCELERATION IN FLUIDS
BY THOMAS E. STELSON AND FREDERIC T. MAVIS........................ 518

Discussion:
By **Joseph M. Caldwell**.. 526
Edward Silberman.. 527
Thomas E. Stelson and Frederic T. Mavis........................ 529

2871 FLOOD-EROSION PROTECTION FOR HIGHWAY FILLS
BY CHESLEY J. POSEY.. 531

Discussion:
By **Gerard H. Matthes**.. 543
Emory W. Lane.. 544
Carl F. Izzard and Joseph N. Bradley........................ 544
Carl E. Kindsvater.. 548
Parley R. Neeley.. 552
Chesley J. Posey.. 554

2872 RECOVERY OF USABLE WATER FROM SALINE WATER
BY DAVID B. SMITH AND CHARLES E. RICHHEIMER........................ 556

2873 OSCILLATORY GRAVITY WAVES IN FLOWING WATER
BY TURGUT SARPKAYA.. 564

2874 PERMEABILITY, PORE PRESSURE, AND UPLIFT IN GRAVITY DAMS
BY ROY W. CARLSON.. 587

Discussion:
By **Bryant Mather**.. 603
J. Laginha Serafim.. 603
Serge Leliavsky.. 608
Roy W. Carlson.. 612

2875 EFFECT OF AIRPORT DISTANCE ON TRAFFIC GENERATION
BY JAMES C. BUCKLEY.. 614

2876 STRESSES IN ELASTIC PLATES OVER FLEXIBLE SUBGRADES
BY ERIC REISSNER.. 627

2877 MISSOURI RIVER BASIN PLAN IN OPERATION
BY WENDELL E. JOHNSON.. 654

2878 SHEAR DEFLECTION OF WIDE-FLANGE STEEL BEAMS IN THE PLASTIC RANGE
BY WILLIAM J. HALL AND NATHAN M. NEWMARK........................ 666

No. PAGE

2879 RIVER-BED DEGRADATION BELOW LARGE-CAPACITY RESERVOIRS
BY M. GAMAL MOSTAFA 688

DISCUSSION:
BY WHITNEY M. BORLAND AND CARL R. MILLER 696
MAURICE L ALBERTSON AND HSIN-KUAN LIU 699
SERGE LELIAVSKY 701
M. GAMAL MOSTAFA 702

2880 STRUCTURAL VIBRATIONS PRODUCED BY GROUND MOTION
BY DONALD E. HUDSON AND GEORGE W. HOUSNER 705

2881 INELASTIC BUCKLING OF NON-UNIFORM COLUMNS
BY JOHN E. GOLDBERG, JOHN L. BOGDANOFF, AND HSU LO 722

2882 THE ACTION OF SOFT CLAY ALONG FRICTION PILES
BY H. BOLTON SEED AND LYMON C. REESE 731

DISCUSSION:
BY LAWRENCE A. DUBOSE 755
YOSHICHIKA NISHIDA 757
JAMES D. PARSONS AND RALPH B. PECK 758
H. BOLTON SEED AND LYMON C. REESE 760

2883 EDUCATION OF CIVIL ENGINEERS: A SYMPOSIUM
FOREWORD
BY EDWIN H. GAYLORD, JR. 766

NEED FOR RECONSIDERATION
BY L. E. GRINTER 767

DISCUSSION:
BY DANIEL C. DRUCKER 776
L. E. GRINTER 778

TRAINING FOR CIVIL ENGINEERING
BY BENJAMIN A. WHISLER 779

DISCUSSION:
BY ALFRED R. GOLZÉ 783
BENJAMIN A. WHISLER 784

2884 A CONCEPT OF THE REGIME THEORY
BY NING CHIEN 785

DISCUSSION:
BY GERALD LACEY 794
EMORY W. LANE 797
THOMAS BLENCH 799
NING CHIEN 803
HANS A. EINSTEIN 804

2885 METHODS OF DETERMINING CONSUMPTIVE USE OF WATER IN IRRIGATION
BY RALPH D. GOODRICH 806

DISCUSSION:
BY DON M. FORESTER 818
RALPH D. GOODRICH 820

2886 LATERAL BUCKLING OF ROLLED STEEL BEAMS
BY ROBERT A. HECHTMAN, JOHN S. HATTRUP, EUGENE F. STYER, AND JOHN L. TIEDEMANN 823

No. Page

2887 FIELD VANE SHEAR TESTS OF SENSITIVE COHESIVE SOILS
BY HAMILTON GRAY 844

DISCUSSION:
BY EBENEZER VEY 858
CARL W. FENSKE 860
DALE T. HARROUN 861
HAMILTON GRAY 862

2888 A PATTERN OF INTERSTATION AIR TRAVEL
BY DANIEL M. BELMONT 864

2889 THE ANALYSIS OF WATER SAMPLES FOR CYCLICAL VARIATIONS
BY ALEX N. DIACHISHIN 872

2890 TRAFFIC DIVERSION TO TOLL ROADS
BY JOHN T. LYNCH 883

2891 MODEL TESTS, ANALYSIS, AND OBSERVATION OF AN ARCH DAM
BY MANUEL ROCHA, J. LAGINHA SERAFIM, ANTÓNIO F. DA SILVEIRA, AND JOSÉ M. RESSURREIÇÃO NETO 903

DISCUSSION:
BY MERLIN D. COPEN 935
A. WARREN SIMONDS 938
JOE T. RICHARDSON 942
A. CARVALHO XEREZ 945
MANUEL ROCHA, J. LAGINHA SERAFIM, ANTÓNIO F. DA SILVEIRA, AND JOSÉ M. RESSURREIÇÃO NETO 946

2892 A GENERAL METHOD OF ANALYSIS OF RIGID FRAMES
BY PANAGIOTIS D. MOLIOTIS 950

2893 TRANSPORT HELICOPTER COST AND HELIPORT CONSIDERATIONS
BY F. DAVID SCHNEBLY 973

2894 UNDERSEEPAGE, MISSISSIPPI RIVER LEVEES, ST. LOUIS DISTRICT
BY CHARLES I. MANSUR AND ROBERT I. KAUFMAN 985

2895 A PRELIMINARY STUDY OF HIGH-RATE COMPOSTING
BY JOHN S. WILEY AND GEORGE W. PEARCE 1009

DISCUSSION:
BY PIETER R. KRIGE 1031
JOHN S. WILEY AND GEORGE W. PEARCE 1032

2896 THE EFFECT OF TRAFFIC ON THE CROSS SECTION OF A RUNWAY PAVEMENT
BY ROBERT HORONJEFF AND JOHN HUGH JONES 1035

DISCUSSION:
BY ROGER H. WILLIAMS 1046
JOHN F. REDUS 1046
ROBERT HORONJEFF AND JOHN HUGH JONES 1047

2897 FAILURE OF PLAIN CONCRETE UNDER COMBINED STRESSES
BY BORIS BRESLER AND KARL S. PISTER 1049

DISCUSSION:
BY FRANK A. BLAKEY AND F. DONALD BERESFORD 1060
PAUL RICE 1061
HENRY J. COWAN 1063
BORIS BRESLER AND KARL S. PISTER 1066

No. PAGE

2898 THICK RECTANGULAR PLATES ON AN ELASTIC FOUNDATION
BY DANIEL FREDERICK 1069

DISCUSSION:
By HAROLD G. LORSCH 1086
DANIEL FREDERICK 1086

2899 FLOW INTO A WELL BY ELECTRIC AND MEMBRANE ANALOGY
BY CHONG-HUNG ZEE, DEAN F. PETERSON, AND ROBERT O. BOCK .. 1088

DISCUSSION:
By ROBERT E. GLOVER 1106
VAUGHN E. HANSEN 1107
JAMES N. LUTHIN 1109
CHIA-SHUN YIH 1110
CHONG-HUNG ZEE, DEAN F. PETERSON, AND ROBERT O. BOCK 1111

2900 ANALYSIS FOR SHEET-PILE RETAINING WALLS
BY F. E. RICHART, JR. 1113

DISCUSSION:
By PETER W. ROWE 1133
F. E. RICHART, JR. 1135

2901 PLASTIC STRENGTH OF STEEL FRAMES
BY LYNN S. BEEDLE 1139

DISCUSSION:
By JACK R. BENJAMIN 1161
ZDENĚK SOBOTKA 1162
LYNN S. BEEDLE 1165

2902 WATER SUPPLY IN ARCTIC AREAS: DESIGN FEATURES
BY LLOYD K. CLARK AND AMOS J. ALTER 1169

2903 INTERMITTENT DISCHARGE OF SPENT SULFITE LIQUOR
BY HERMAN R. AMBERG AND ROBERT ELDER 1179

2904 THE USE OF STATISTICS IN RESERVOIR OPERATIONS
BY VICTOR A. KOELZER 1187

2905 AN APPROACH TO THE DESIGN OF TRICKLING FILTERS
BY WILLIAM T. INGRAM 1202

2906 TIME TO THINK: ADDRESS AT THE SUMMER CONVENTION, BUFFALO, N. Y., JUNE 5, 1957
BY MASON G. LOCKWOOD, PRESIDENT 1221

MEMOIRS OF DECEASED MEMBERS: ABSTRACTS 1229

SUBJECT INDEX 1264

AUTHOR INDEX 1301

ERRATA

Transactions, Vol. 121, 1956

Page 49, Eq. 2, the coefficient "6" in the denominator should be omitted.

Page 56, in the line immediately following Eq. 7*a*, the fraction bar between "k" and "x_s" should be omitted.

AMERICAN SOCIETY OF CIVIL ENGINEERS
Founded November 5, 1852

TRANSACTIONS

Paper No. 2845

HIGH-STRENGTH STEEL BOLTS IN STRUCTURAL PRACTICE

By Mace H. Bell,[1] A. M. ASCE

With Discussion by Messrs. William Hansen, and Mace H. Bell

Synopsis

A brief history of the development of the high-strength bolt is presented, together with a resume of the development of specifications for field assembly using high-strength bolts. The use of the pneumatic wrench and procedures for determining bolt tension are described. Numerous examples of use of high-strength bolts are cited and illustrated.

Bolts have been used in structural steel connections since the very early days of steel fabrication, and in various specifications governing the design, fabrication, and erection of steel their use under certain conditions has been recognized. Until the early 1950's the types of bolted joints permitted could be broadly classified as:

1. The "unfinished," "common," or "machine-bolt" joint, with $\frac{1}{16}$-in. clearance in holes;
2. The "turned-bolt" joint with a "close" fit, usually with $\frac{1}{50}$-in. clearance in reamed or drilled holes; and
3. The "ribbed" or "rivet-bolt" joint, in which the fluted shank of the bolt is slightly larger than the holes in the connected material and bearing between the bolt shank, and the plies of connected material are obtained by means of a "driving fit" at the time of installation.

In 1947 an entirely new concept of bolted connections for structural joints came into being as a result of the research work and investigations sponsored by the Research Council on Riveted and Bolted Structural Joints of the Engineering Foundation (referred to herein as the Research Council). The principle of this connection places it in a different category from that of the other types of bolted connections previously mentioned. This joint

---

Note.—Published, essentially as printed here, in March, 1955, as *Proceedings-Separate No. 651*. Positions and titles given are those in effect when the paper or discussion was approved for publication in *Transactions*.

[1] Chief of Dist. Engrs., A.I.S.C., New York, N. Y.

depends on friction between the faying surfaces of the connected members for stress transfer. The list of broad classifications of bolted connections can thus be completed with:

4. The pretensioned "high-strength steel bolt" joint, having hardened washers and $\frac{1}{16}$-in. clearance in holes.

Since January 15, 1947, when the Research Council was organized, this new type of joint has had an increase in acceptance and usage that has seldom been matched by any other newly introduced method in structural steel assembly. It has been accepted by both structural engineers and bridge engineers as a connection that is suitable not only for static loads but also for all ranges of dynamic loads.

William H. Munse, A. M. ASCE, has written[2] of the laboratory research and field research that led to the development of the "Specifications for Assembly of Structural Joints Using High Strength Steel Bolts."[3] The material that follows is confined to the practical aspects of use of this new "high-strength steel bolt" in structural connections.

Within a short time after the Research Council's specifications were first issued in 1951, the American Institute of Steel Construction (AISC) endorsed them. This action constitutes full acceptance by the AISC of this method of connecting structural members. Therefore, when the AISC "Specification for the Design, Fabrication, and Erection of Structural Steel for Buildings" is next revised, these provisions controlling the use of high-strength bolts will be incorporated into the body of that document. Meanwhile, the two specifications are referred to jointly in any job specification in which it is intended that high-strength bolting be used.

Similarly, the American Railway Engineering Association (AREA) and the American Association of State Highway Officials (AASHO) have accepted the Research Council's specifications with only minor editorial changes, thus permitting the use of high-strength bolted connections in railway bridges and in highway bridges.

From the practical viewpoint, there are six principal features of the Research Council's brief specifications that should be emphasized in detail.

The first important feature is that the connections are designed and fabricated to conform to the requirements of applicable existing codes or specifications for riveted structures. In the case of rivet quality, American Society for Testing Materials (ASTM) specifications provide criteria. A high-strength bolt of the same diameter may be substituted for each rivet of ASTM-A 141 quality[4] in any joint so designed.

The cut-away view in Fig. 1 is a high-strength bolt in a three-ply structural connection. The joint is fastened with a bolt, a heavy nut, and two hardened washers, assembled into standard $\frac{1}{16}$-in.-clearance holes as used for rivets. There are certain differences in physical appearance that distinguish it from the ordinary bolted joint used in structural practice. These are indicated in the sketch of Fig. 1. They are: (1) The use of heavy, hardened washers under both the bolt head and the nut; (2) the use of heavy, semifinished hexagon nuts; (3) a distinctive bolt-head marking of three radial lines, as required by ASTM specification[5] A 325; and (4) the bolt is black in color as a result of heat treatment.

---

[2] "Research on Bolted Connections," by William H. Munse, *Transactions*, ASCE, Vol. 121, 1956, p. 1255.

[3] "Specifications for Assembly of Structural Joints Using High Strength Steel Bolts," approved by Research Council on Riveted and Bolted Structural Joints, The Engineering Foundation, February, 1954. (With Appendix B, approved December, 1955.)

[4] "Standard Specification for Structural Rivet Steel (A 141-55T)," Book of Standards, A.S.T.M. Pt. 1, 1955, p. 632.

A point of interest to engineers is that no special provision for locking the nut is required. When the bolts are properly installed and the nut is tightened to induce the high tension specified, both field tests and laboratory tests have proved that there is no tendency for the bolt to lose tension even after millions of cycles of loading. The friction of the threads and of the bearing surface of the nut keeps the connection permanently tight.

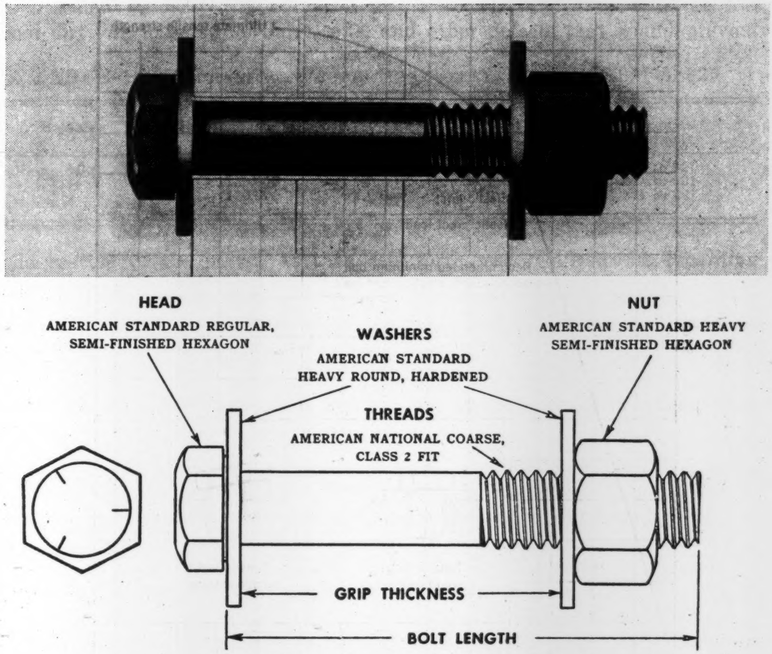
HEAD
AMERICAN STANDARD REGULAR, SEMI-FINISHED HEXAGON
WASHERS
AMERICAN STANDARD HEAVY ROUND, HARDENED
NUT
AMERICAN STANDARD HEAVY SEMI-FINISHED HEXAGON
THREADS
AMERICAN NATIONAL COARSE, CLASS 2 FIT
GRIP THICKNESS
BOLT LENGTH

Fig. 1.—A High-Strength Bolt

The second important feature of the Research Council's specification concerns the bolts, nuts, and washers. These are all required to conform to ASTM specification A 325 and to the dimensions established by the American Standards Association (ASA).[6] The bolt is made from a medium carbon steel and is heat-treated, quenched, and tempered. The nut is made from a similar steel but no heat treatment is required. The hardened washers are either quenched and tempered, or carburized, quenched, and tempered.

---

[5] "Tentative Specifications for Quenched and Tempered Steel Bolts and Studs with Suitable Nuts and Plain Hardened Washers (A 325-55T)," Book of Standards, A.S.T.M., Pt. 1, 1955, p. 705.

[6] "Square and Hexagon Bolts and Nuts," A.S.A. B 18.2-1952.

Fig. 2 illustrates the typical stress-strain curve obtained in tests of A 325 bolts. The line is straight below the elastic limit, beyond which it curves gradually without any clearly defined yield point to an ultimate strength that is 70% above the recommended preload to which the bolts are tightened. The strain beyond the yield point is 1.75 times the total elastic strain. The mechanical properties required for three commonly used bolt sizes are shown in Table 1, and the relative position of the elastic proof load, the elastic limit, and the ultimate tensile strength, in addition to the recommended minimum bolt preload, are all indicated in Fig. 2. The tension test, from zero to the elastic proof load, is determined by axial loading, as indicated in the sketch of a bolt head labeled "axial loading." The ultimate load is determined with a 10° wedge under the bolt head, as shown in the second sketch in Fig. 2.

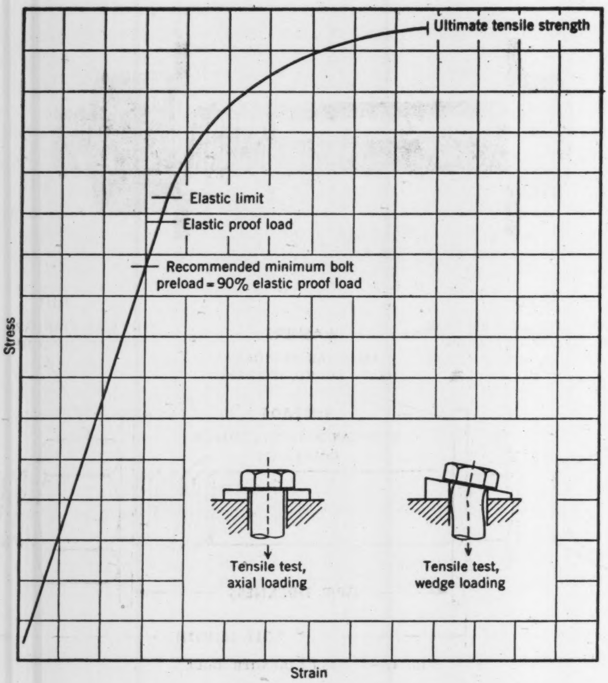

Fig. 2.—Stress-Strain Curve, ASTM-A 325 Bolts

Two conclusions can be drawn from Fig. 2. First, it is evident that there is no danger in tightening the bolts to tensions considerably exceeding the minimum values required by the Research Council's specification because there is a considerable reserve strength in the bolt beyond those values. The strain in the bolt at its ultimate strength is approximately 3.25 times the strain at the recommended minimum bolt preload point on the curve. Second, the bolt strength, at its proof load and upper limits, is not materially affected when the bolt head and nut bear on nonparallel surfaces having slopes as great as 1 on 6, or 10°.

The third important provision of the Research Council's specification requires that the contact surfaces, including those adjacent to the washers, be descaled or carry the normal tight mill scale, and they must be free from dirt, oil, loose scale, burrs, pits, and other defects that would prevent solid seating of the parts. It then sets forth two requirements regarding shop painting.

TABLE 1.—MECHANICAL PROPERTIES, STEEL BOLTS, ASTM-A 325

Bolt size (in.)	Ultimate tensile strength (lb per sq in.)	Elastic proof load (lb per sq in.)	Hardness (Brinell)
¾	120,000	85,000	241 to 321
⅞	120,000	78,000	241 to 321
1	120,000	78,000	241 to 321

> "Contact surfaces of joints where slippage into bearing is acceptable may carry a shop coat of protective paint or lacquer.
>
> "Contact surfaces of joints subjected to stress reversal, impact, or vibration, or where stress redistribution due to joint slippage would be undesirable, shall be free of paint or lacquer."

Most bridge specifications and the AISC specification ordinarily permit shop paint in the connections. Therefore, when high-strength bolts are to be used, the engineer must give consideration to the requirements of the various joints in a specific job before arriving at a decision as to which of the two provisions is applicable. Since this paper first appeared in *Proceedings* of ASCE, the Research Council has issued Appendix B to the specification[3] to give authoritative guidance on the application of these and other provisions.

Taking into consideration the strength of a connection subject to static or pulsating loads, the Research Council has made shear tests of joints in which the bolts have slipped into bearing and found the shearing strength of such joints considerably greater than that of riveted joints. The omission of paint, including the additional work of indicating unpainted areas in the drafting room and masking or marking them in the shop before painting, is an expensive operation reflected in bid prices.

From the standpoint of accepting some slippage, which could probably not exceed $\frac{1}{16}$ in. even with perfectly matched holes, the engineer should consider (1) the direction in which the slip can occur and the consequence of maximum slip and (2) the rate of slip under service conditions. The laboratory investigations that have been performed thus far on painted surfaces have indicated long-term slip, and if the joint is loaded to its full design capacity with static loads one can expect slip. On the other hand, with normal loads which are apt to be less than maximum, it may require hours or days before the bolts slip into bearing. For the usual condition a joint load is composed of a combination of dead load and live load, and when there are live loads of a transient nature, such as wind loads and certain classes of dynamic loads, the joints are stressed to full capacity only for short periods of time.

If these two considerations are applied to the connections of a tier building, for example, one can reason as follows: The milled column splices cannot slip as they are already in bearing. The web or seat connections could move downward only and, should this occur, the effect would be negligible. The wind connections are subject to fluctuating short-term loads which normally would not cause slip. It is doubtful whether painted joints would experience any greater slip under such conditions than that which has occurred in riveted joints.

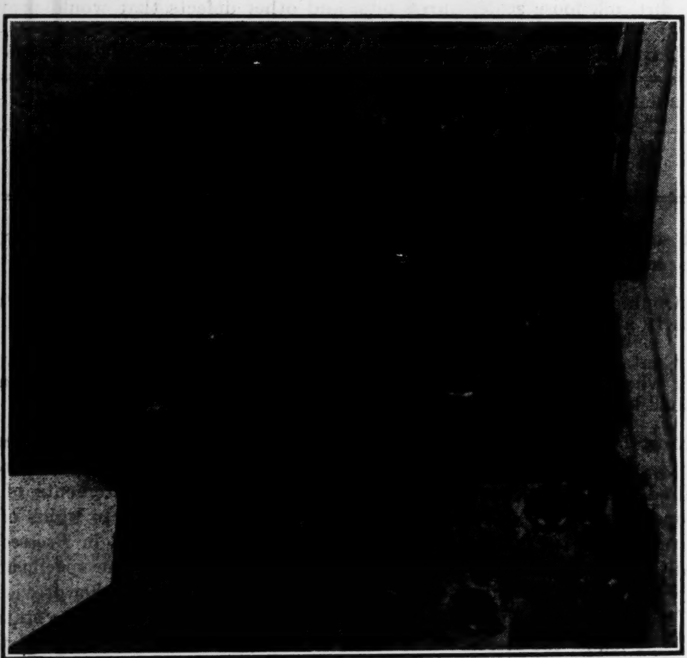

FIG. 3.—USE OF SQUARE, BEVELED WASHERS

The fourth important feature of the Research Council's specification provides that flat washers may be used if the abutment surfaces adjacent to the bolt head and nut do not have a slope of more than 1 on 20 with respect to a plane normal to the bolt axis, and provided that the nut is tightened against a nonsloping surface. There are two slopes on structural shapes rolled in the United States. These are given in the AISC manual of steel construction,[7] and can be summarized as follows:

Shape	Slope	Percentage	Angle
Certain WF beams	1 on 20	5	2° 52′
American Standard beams and channels	1 on 6	16.67	9° 28′

This clause of the specification thus permits the use of flat washers under bolt heads when bolts pass through the flanges of WF shapes but requires the use of beveled washers for flange connections for American Standard beams and channels.

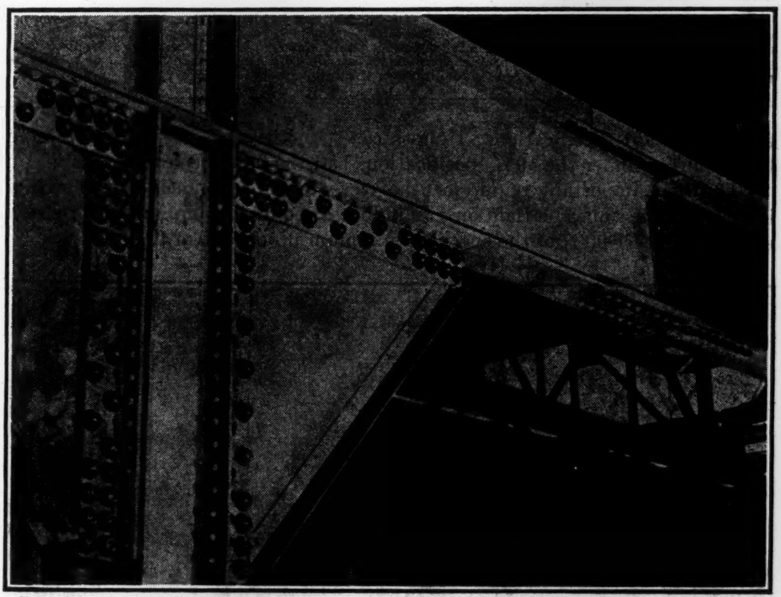

FIG. 4.—HIGH-STRENGTH BOLTS IN A FIELD CONNECTION

Fig. 3 shows a part of the connection of a 36-in. WF floor beam to a plate girder in a single-track, trough-type railway bridge. The lateral bracing gusset plate at the bottom of this floor beam, one with a 5% flange slope, is bolted with square beveled washers under the nuts as required by the 1954 specification. Fig. 4 pictures the connection of a crane runway girder to a column and shows a splice in the girder to the right. Flat circular washers are used in the angle-to-web, knee-brace connections, in the girder web splice, and on the outside face of the girder flange splice. The square beveled washers seen on the inside face of the girder's upper flange splice were installed under

---

[7] "Steel Construction," A.I.S.C., 5th Ed., 1956.

TABLE 2.—REQUIRED MINIMUM TENSION IN HIGH-STRENGTH BOLTS, RESEARCH COUNCIL SPECIFICATION

Bolt size (in.)	Recommended[a] bolt tension for calibrating wrenches (lb)	Required minimum[b] bolt tension (lb)	Approximate[c] equivalent torque for required minimum bolt tension (lb-ft)
½	12,500	10,850	90
⅝	20,000	17,250	180
¾	29,000	25,600	320
⅞	37,000	32,400	470
1	49,000	42,500	710
1⅛	58,000	50,800	960
1¼	74,000	64,500	1350

[a] Approximately 15% in excess of the required minimum bolt tension. [b] Equal to 90% of the minimum proof load of the bolt (ASTM-A 325). There is no recommended maximum bolt tension. [c] Equal to 0.0167 lb-ft per in. of bolt diameter per lb tension for nonlubricated bolts and nuts. Values listed are experimental approximations. If torque rather than tension is to be measured, the ratio of torque to tension shall be determined by the actual conditions of the application.

the earlier 1951 specification. In both cases, the beveled washers could have been omitted under the 1954 specifications had the bolts been reversed.

The fifth important requirement of the Research Council's specification is that all bolts must be tightened to induce a required minimum bolt tension equal to at least 90% of the specified minimum proof load of the bolt.

FIG. 5.—TIGHTENING BOLTS WITH (a) A TORQUE WRENCH AND (b) AN IMPACT WRENCH

Table 2 shows values taken from the specification to show these requirements. It should be noted that the tension values shown represent total tension per bolt, and not pounds per square inch. The second column of Table 2 gives a recommended bolt tension for calibrating wrenches. This is not a requirement but is recommended as a "target" value that will insure that all bolts will be tightened to the required minimum tensions shown in the third column. If wrenches are calibrated to produce a particular average tension, the actual tensions in a group of bolts making up a connection will vary from that average by perhaps 5% to 10%. For this reason the target value is set at 15% above the required minimum tension. The fourth column lists the approximate equivalent torques needed to produce the specified minimum tensions. These, too, are not a requirement of the specification. They are experimental approximations obtained from studies of torque applied to nonlubricated bolts and nuts. Such variables as the amount of lubricant on threads and the condition of the thread, nut, and washer surfaces all affect these values considerably. They are included as a guide which is useful in the first steps of calibration to determine the requirements of a particular job application.

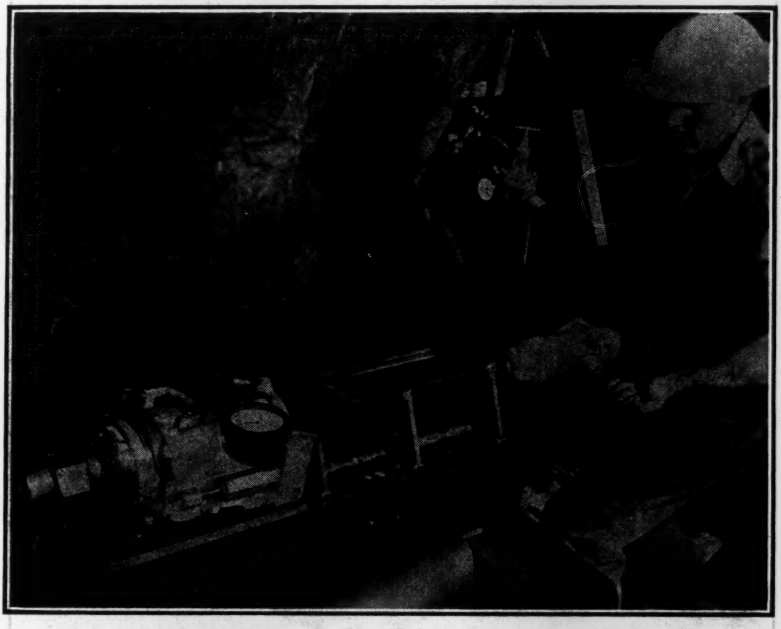

FIG. 6.—CALIBRATION OF A PNEUMATIC IMPACT WRENCH

Although manual wrenching of the bolts has been used where only a few connections are required, it is slow, cumbersome, and relatively expensive for general application. The size of wrench required for tightening the nuts on

⅞-in.-diameter bolts can be judged from Fig. 5(*a*). The workman is using a hand torque wrench. For these particular bolts he must exert a pull of approximately 100 lb. As contrasted to this, the use of an electric impact wrench or pneumatic impact wrench is fast and requires a minimum of effort (Fig. 5(*b*)).

The usual method of assembling joints is to use the pneumatic impact wrench. In addition to having the advantages of speed and ease with which high torques can be applied, the pneumatic impact wrench is particularly suited to a remarkably dependable method of reproducing uniform tension in the bolts. Field experience on many different jobs has proved that, by controlling the air pressure to the wrenches, they can be calibrated to deliver the required tension without any reference to torque.

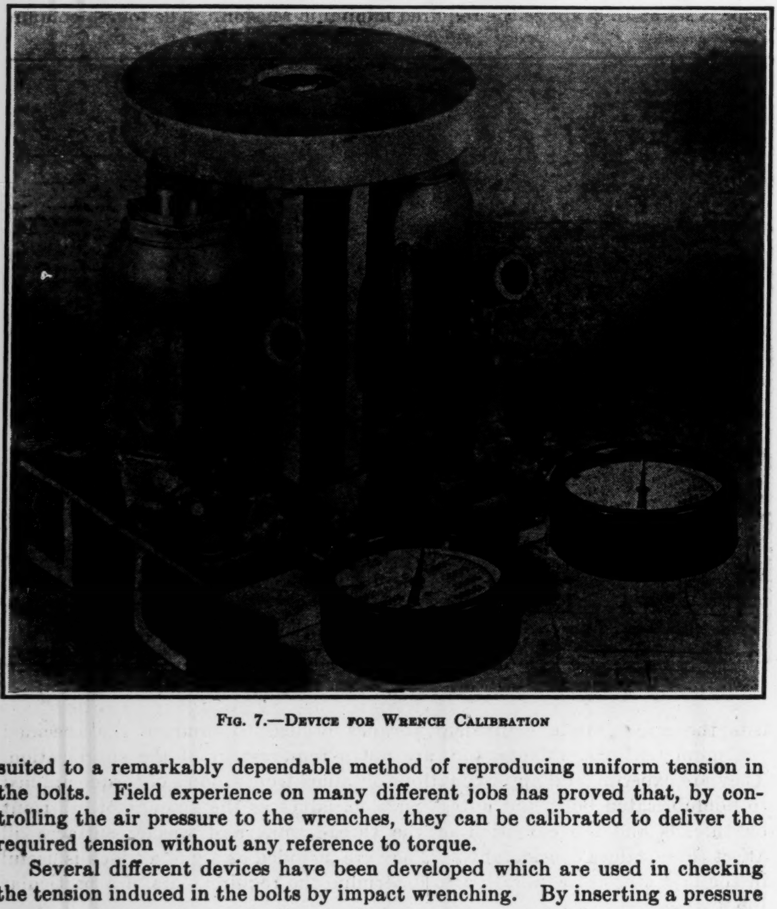

FIG. 7.—DEVICE FOR WRENCH CALIBRATION

Several different devices have been developed which are used in checking the tension induced in the bolts by impact wrenching. By inserting a pressure regulator in the air supply line leading to each wrench, the wrench can be calibrated or adjusted to "stall" when the desired tension is reached. In practice, several bolts of the size being used are tested in the device, and the air pressure and approximate time of operation required to stall the wrench are determined. At the point of stalling, the wrench continues to exert impact but there is no visible turning of the nut. This point can be determined by watching a series of crayon marks on the wrench chuck.

One such device is shown in Fig. 6. It consists of a 60-ton-capacity hydraulic puller mounted on a steel base. By means of a yoke arrangement at the base of the puller, the tension induced in the bolt by the impact wrench is read directly on the gage mounted on the jack. In the photograph, the bolt being tested is hidden by the supporting frame. The nut bears against the frame and the bolt head bears against the yoke which is, in turn, connected to the heavy threaded rod extending through the jack.

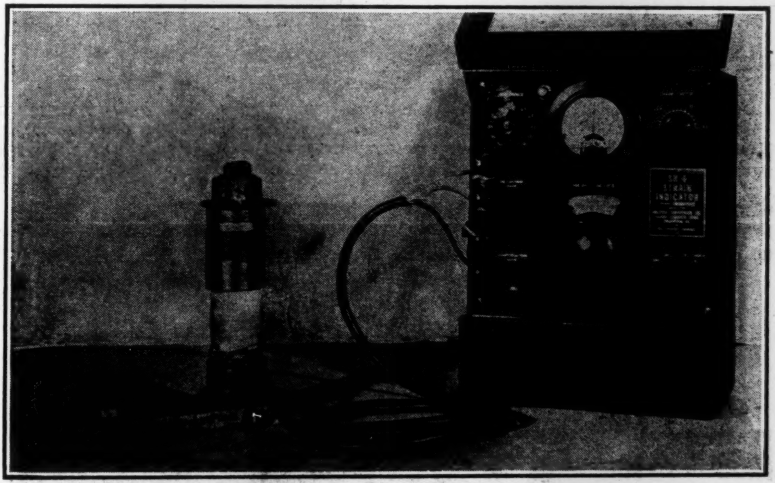

FIG. 8.—STRAIN-GAGE TYPE CALIBRATION METER

A similar device in which a pair of hydraulic jacks and gages are used to read the induced tension directly is shown in Fig. 7.

All these devices are rugged, simple to operate, and easy to move. They can be used to calibrate a wrench in only a few minutes. They can also be used to train wrench operators and to recheck wrench adjustments and operator performance at any time.

Other devices have been used for calibration. One of these consists of a heavy steel testing yoke made of two plates separated by two spacer bars at opposite edges. The deflection of these yokes under increments of load is first measured in a hydraulic press, and a calibration table is prepared. When a bolt is placed in the yoke and tightened, its tension can be determined by measuring the yoke deflection with micrometer calipers. Another device consists of a steel tube with electrical strain gages and a meter calibrated to read the bolt tension directly in pounds (Fig. 8).

Another method of reproducing uniform tension in bolts, which is an even simpler operation than those previously described, is based on the fact that after the connected plies have become seated there is a definite relationship between turns of the nut and the tension that is induced in the bolt. The method has been reported by F. P. Drew,[8] A. M. ASCE. The Research Council has approved tension control by rotation of the nut in Section 9 of Appendix B of its specification.[3] The method is rapidly gaining favor in the United States because of its simplicity.

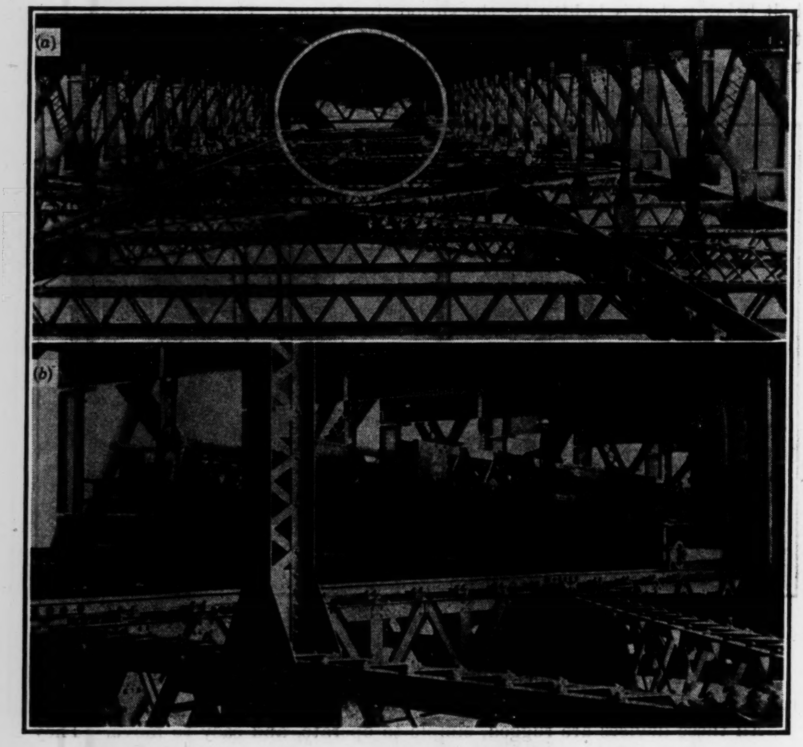

FIG. 9.—BOTTOM LATERAL STIFFENING SYSTEM ADDED TO GOLDEN GATE BRIDGE

The sixth and last feature of the Research Council's specification covers inspection of the bolting. The specification, when first issued in 1951, recommended that between 5% and 10% of all bolts installed be checked by a procedure of loosening and retightening, and suggested that the torque required to retighten be equal to the approximate equivalent torque previously shown in Table 2. This procedure was time-consuming and not altogether satisfactory because, at best, the torque-tension relationship is apt to be somewhat erratic. The development of the calibrating devices that have been described has made possible automatic accounting for all the variables that affect bolt tightness—wrench capacity, bolt size and length, and lubrication and condition of the threads.

---

[8] "Tightening High-Strength Bolts," by F. P. Drew, *Proceedings Paper 786*, ASCE, August, 1955.

FIG. 10.—FLOOR-BEAM CONNECTION THROUGH PLATE-GIRDER RAILWAY BRIDGE

Four years of field experience made it increasingly evident that inspection by means of approval of the procedures for calibration of wrenches and installation of bolts, followed by observations to assure that the procedures were being followed, insured even closer control of bolt tensions. With the issuance of the current 1954 specification, the Research Council approved this method of inspection and eliminated the requirements that torque be used as a measure of tension.

In practice every wrench is calibrated at least once each day, using the same length of hose that will be required on the job between the wrench and the regulating valve. The inspectors check closely to make sure that the impact wrenches are correctly calibrated for use on the bolts that are to be installed.

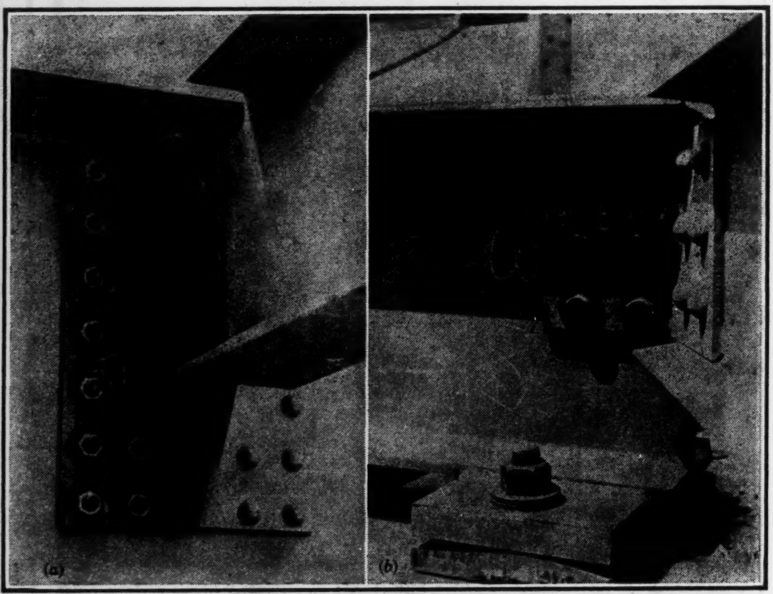

FIG. 11.—BOTH ENDS OF A BRIDGE STRINGER, SHOWING (a) FLOOR-BEAM CONNECTION AND (b) END-DIAPHRAGM CONNECTION

After the joints are made up, the bolts are tightened, usually beginning at the center and working toward the ends of a connection, as each bolt is tightened.

Since the first commercial installation of high-strength bolts in 1950, the use of this new connection has increased at a phenomenal rate. It has been impossible to keep account of all of the structures in which they have been used. Partial lists that were compiled indicate that they have been used in all types of buildings—hospitals, office buildings, schools, Atomic Energy Commission plants, and steel mills—and in both new construction and maintenance work on railway bridges and highway bridges. Special applications have also been reported, as in radio transmission towers, refinery structures, and boiler-supporting frameworks.

The new bottom lateral stiffening system on the great Golden Gate Bridge in San Francisco, Calif., designed to give the bridge additional resistance to vibrations induced by wind, was installed with high-strength bolts. Fig. 9(*a*) shows a part of the system as installed between the main stiffening trusses. The 4,700 tons of steel used required 190 tons of high-strength bolts for connections. Fig. 9(*b*) provides a closer view of some of the joints. Because of the varying nature of wind loads these joints will be subject to stress reversals, fatigue, and vibrations.

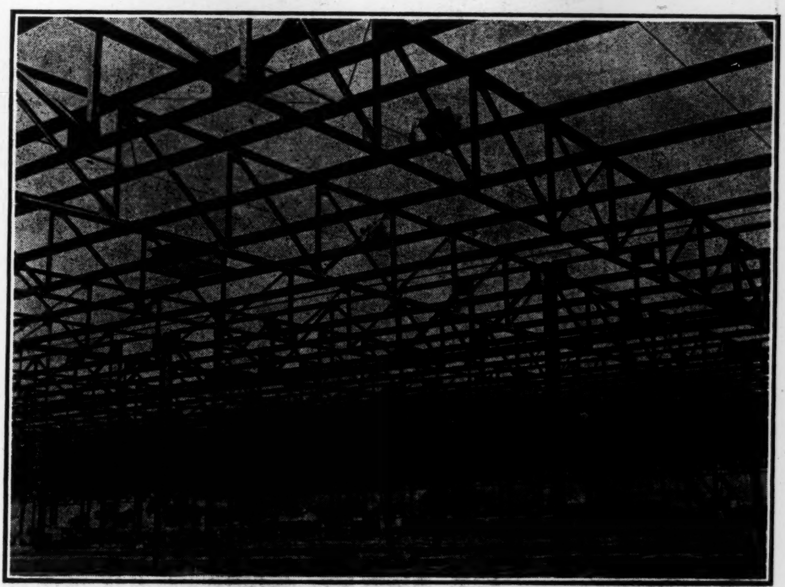

FIG. 12.—AN AUTOMOBILE ASSEMBLY PLANT UNDER CONSTRUCTION

There have been many bridges constructed recently in which all floor-beam, stringer, and lateral-bracing connections are made with high-strength bolts in order to avoid having to move riveting equipment to a job site for a comparatively small number of connections.

The details of the floor-beam-to-girder connection of a typical through plate-girder railway bridge are shown in Fig. 10. Connection details of the lateral-bracing gusset plate and trough-support beam can be seen.

Fig. 11(*a*) illustrates a stringer-to-floor-beam connection of the same bridge. The unpainted areas for the field-bolted parts of the connection show

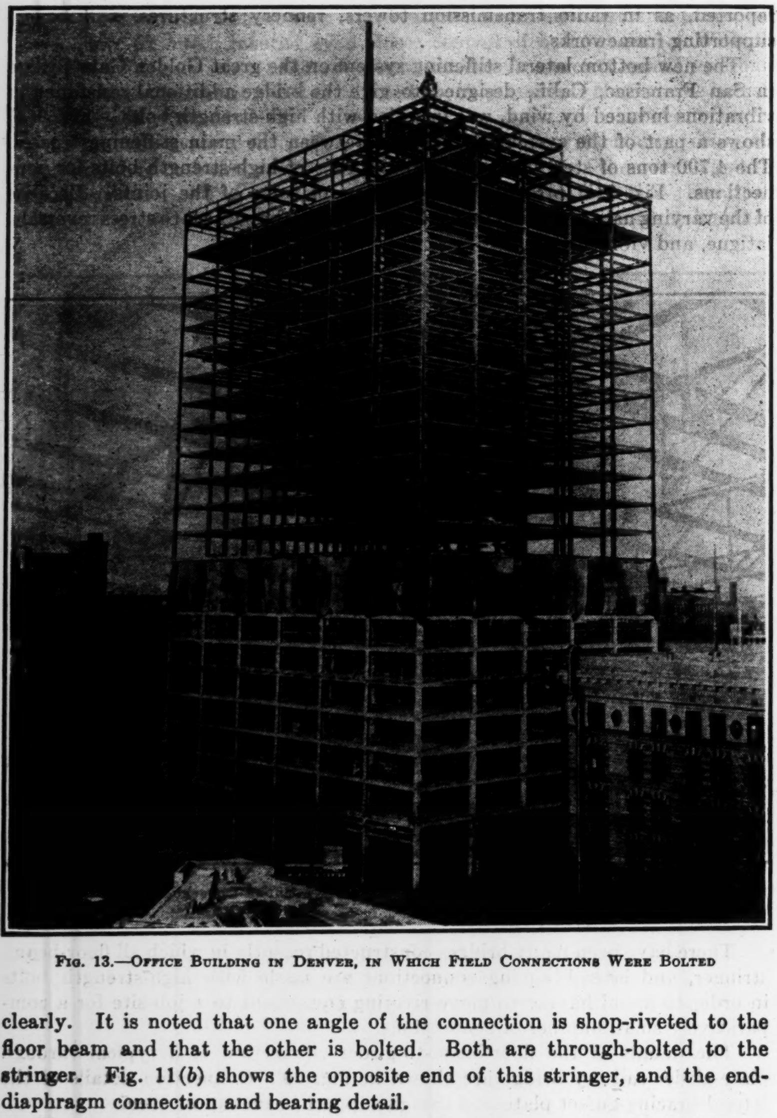

FIG. 13.—OFFICE BUILDING IN DENVER, IN WHICH FIELD CONNECTIONS WERE BOLTED

clearly. It is noted that one angle of the connection is shop-riveted to the floor beam and that the other is bolted. Both are through-bolted to the stringer. Fig. 11(*b*) shows the opposite end of this stringer, and the end-diaphragm connection and bearing detail.

The framing of an automobile assembly plant in the western United States (Fig. 12) was erected at the rate of a half acre per day, using high-strength bolts for field connections of all the 2,600 trusses. The building has a total of 38 bays at 45 ft in its long dimension of 1,710 ft, and 14 bays at 50 ft and 1 bay 90 ft long in its short dimension of 790 ft. The area covered is 1,351,000 sq ft or 31 acres.

The Mile-High Center in Denver, Colo., has attracted much attention in the construction press. The 23-story framework (Fig. 13), an office building, will be the dominant feature of the Mile-High Center. The 4,500-ton framework was erected in only 82 days. All column splices, beam-to-column connections, and bracing connections were fastened with high-strength bolts. Fig. 14 pictures the bolting of a wind-bracing member in this structure.

One of the most unusual frameworks ever used in a tier building (shown in Fig. 15) has been completed in San Francisco. This 25-story office building, designed to resist earthquake forces under the rigid San Francisco code, has tapered exterior columns and spandrel beams in the lower floors. Riveting, welding, and bolting were all used in this framework. High-strength bolts were used to splice the columns and to make all beam-to-column connections (Fig. 16(*a*)) with the exception of the spandrels below the 16th floor, which are welded. Both shop-riveting and welding were used in fabricating the various members. Fig. 16(*b*) is a view of a splice in one of the exterior tapered columns, illustrating the combination of shop-welding and riveting with the use of high-strength bolts for field connections.

FIG. 14.—BOLTING OF A WIND-BRACING MEMBER

Since the first commercial installation at Keene, N. H., in 1950, many millions of high-strength bolts have been used to erect hundreds of thousands

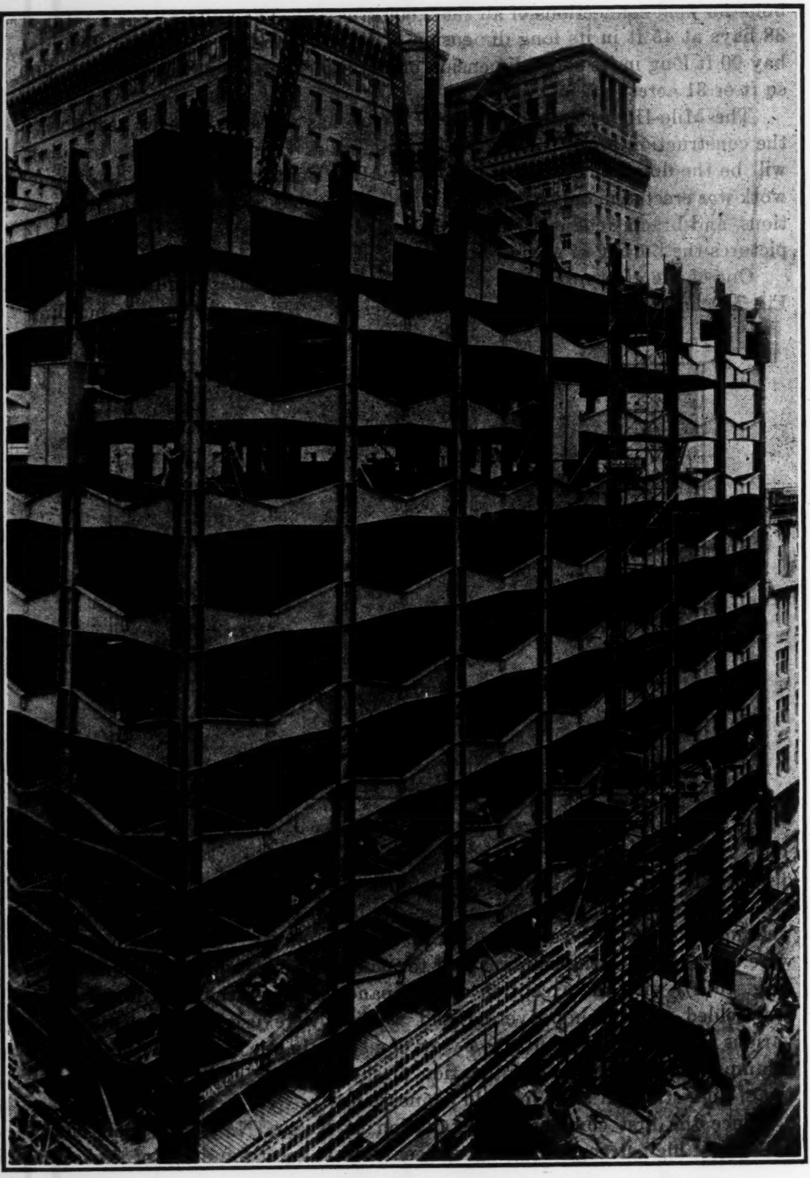

FIG. 15.—TIER BUILDING HAVING TAPERED EXTERIOR COLUMNS AND SPANDRELS

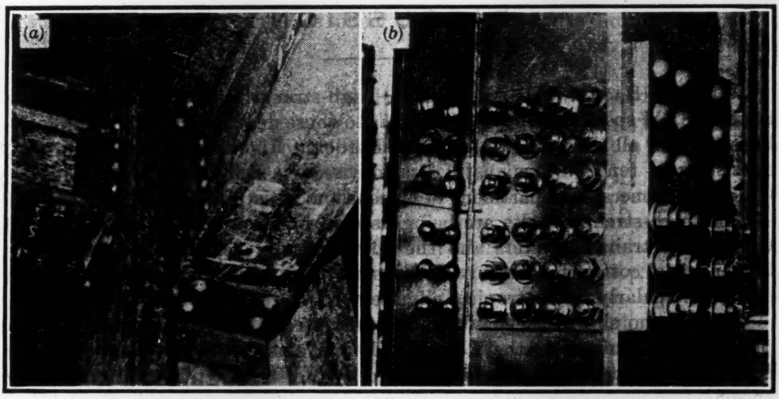

FIG. 16.—DETAILS OF THE BUILDING OF FIG. 15

of tons of structural steel. The Research Council is continuing its program of research, and it is easily conceivable that the results of these investigations can lead to the development of specification provisions and installation techniques that will make the use of high-strength bolted connections even more attractive to bridge and structural engineers.

DISCUSSION

William Hansen,[9] A. M. ASCE.—High-strength steel bolts conforming to the ASTM specification A 325, similar to those described by Mr. Bell, have been used in all the field joints of the Burdekin River Bridge. This bridge, consisting of ten 250-ft spans of Pratt trusses, is being erected by the Co-Ordinator General's Department of Queensland, Australia.

The high-strength bolts are being used in preference to rivets because of the lack of trained riveters and the advantages of easier scaffolding. The higher initial cost of the bolts has been more than offset by lower installation costs, particularly in the tropical climate.

Because no slip in the joints can be accepted, all faying surfaces are unpainted and conform to the Research Council's assembly specification. The bolts are tightened to the torque required by the Research Council's assembly specification using pneumatic impact wrenches with the air supply throttled to produce stalling of the wrench at the required torque.

Experiments on the bolts used, with threads of a medium fit made[10] to British Standard Specification 84, agree with the torque-tension relationship used in the Research Council's assembly specification.

In addition to checking the calibration of the wrenches at the stalling point, it has been found necessary to check the torque on the bolts in position. About 1% of the bolts used are checked in this manner with a torque wrench. The fit of the socket on the nut and the rigidity of the member being bolted have been found to affect considerably the tension developed in the bolt.

Multiple thickness of plates giving some spring in the joint also produces a reduced tension in the bolt below that obtained on a rigid testing device.

Losses in sockets due to cracking and splitting have been great. The writer would like to know whether special sockets are in use in the United States and what is the anticipated life of a socket.

Mace H. Bell,[11] A. M. ASCE.—The writer thanks Mr. Hansen for his discussion comparing the paper with experiences on the erection of the Burdekin River Bridge in Queensland, Australia. It is interesting to note that the cost experience in the two countries is similar. The favorable cost of high-strength bolted connections is one of the factors that has contributed to the fast increase in their use in the United States.

Some erectors in the United States check a small percentage of the bolts after tightening by means of a manual torque wrench, even though it is not required by the specifications. Where this "check procedure" is used, the "equivalent torque" required is first determined by calibrating the manual torque wrench on the calibrating device. It is the writer's understanding that where such "spot checks" are used, the objective is to insure that consistently good workmanship is being obtained from the bolting crews. In addition, such a "double check" serves to insure accuracy of the impact-wrench calibration.

---

[9] Engr. in charge, Burdekin Bridge Erection, Co-Ordinator General's Dept., Queensland, Australia.

[10] "Limits of Screw Thread of Whitworth Form," *British Standards Specification 84*, British Standards Inst., London, 1940.

[11] Chief of Dist. Engrs., A.I.S.C., New York, N. Y.

Since the paper was written, the Research Council has issued an Appendix B[12] which contains answers and authoritative guidance to certain questions that have been raised on the application of the "Specifications for Assembly of Structural Joints Using High Strength Steel Bolts."[3]

In Section 9 of this Appendix, the Research Council has approved a so-called "one-turn-of-the-nut method" as a satisfactory means of insuring sufficient pretension in the bolts. This method, mentioned briefly in the writer's paper, is gaining in favor in the United States because of its simplicity.

The writer agrees with Mr. Hansen that connections made up of multiple plies must be drawn tightly together during erection to insure that the specified bolt tensions are obtained when all bolts in the connection are tightened. The current practice in the United States is to install and tighten enough bolts during erection to insure a tight "drawdown" of the assembled parts. The remainder of the bolts are then installed and properly tensioned. On completion of this step, those bolts used during fitting-up and erection are retightened, or if the erector has elected to use special erection bolts during the fitting-up stage these are removed and new bolts are installed and tightened.

No complaints concerning cracking or splitting of the wrench sockets have come to the writer's attention. There is no doubt that the chance of wear in the socket and the chance of possible failure of the socket are increased if there is a loose fit between the socket and the nut. Erectors in the United States report that a loose fit of the socket on the nut or on the wrench drive shaft results in loss of power and requires increased air pressure in the wrench.

It may be that the sockets referred to by Mr. Hansen were not properly heat treated. There is also the possibility that the sockets used were originally designed for use with manual wrenches.

The anticipated socket life is undoubtedly subject to many variations. One large fabricating firm reports that the sockets they use, purchased as a standard accessory from one of the leading impact-wrench manufacturers, tighten 40,000 high-strength bolts before showing undue signs of wear.

---

[12] "Specifications for Assembly of Structural Joints Using High Strength Steel Bolts, with Appendix B," Research Council on Riveted and Bolted Structural Joints, A.I.S.C., December 15, 1955.

AMERICAN SOCIETY OF CIVIL ENGINEERS
Founded November 5, 1852
TRANSACTIONS

Paper No. 2846

THE DESIGN OF PIERS, JETTIES, AND DOLPHINS

BY DAVID A. HOPKINS,[1] A. M. ASCE

WITH DISCUSSION BY MESSRS. ZUSSE LEVINTON, AND DAVID A. HOPKINS

SYNOPSIS

This paper deals with the design of piers, jetties, and dolphins with particular reference to the lateral loads from berthing ships which these structures must withstand. Design principles are examined, and two examples of pier design are reviewed: (*a*) Guayacan Bay Pier, Chile (built for Bethlehem Chile Iron Mines) and (*b*) Hoboken Pier "C", Hoboken, N. J. (built for the Port of New York Authority).

The paper shows how the impact energy of a berthing ship may be absorbed by the elastic deformation of the structure, without the need for any special system for spring fendering.

INTRODUCTION

The design of piers and other maritime structures for lateral loads is a subject that is dealt with in many textbooks. Port and harbor engineers, however, continue to hold widely divergent opinions on the provisions that should be made for lateral loading, and this paper is presented with the object of examining some of the basic assumptions that are made in the practical design of port structures.

Lateral loads due to sea action, wind, or impacts from ships must all be considered, but the heaviest load is usually the last of these three—the impact of ships when berthing.

To illustrate contrasting types of marine structures and the trend of modern pier construction, Figs. 1 and 2 show sections of an old-fashioned concrete jetty and a representative New York (N. Y.) timber pier—designs

---

NOTE.—Published, essentially as printed here, in June, 1955, as *Proceedings-Separate No. 727.* Positions and titles given are those in effect when the paper or discussion was approved for publication in *Transactions.*

[1] Project Engr., Tippetts-Abbett-McCarthy-Stratton, New York, N. Y.

that were typical of pier construction fifty years ago. Those examples represent the two extremes—the rigid mass-concrete jetty which is not susceptible to damage but may cause damage to ships and the flexible timber pier which minimizes impact forces by its deflection under load.

Figs. 3 and 4 show sections of H-piled piers that are described in this paper. It is found that these structures possess some of the flexibility and resilience that give timber piers their well-known resistance to repeated berthing impacts.

The Estimation of Lateral Impact Loads.—The critical factor in estimating berthing impact loads is the assumed speed of approach of the ships. The question of what speed of approach a designer should assume as a worst case in order to compute the lateral force on the pier is inherently unanswerable by reference to statistical evidence or experimental data. Damage to piers and fenders is not the kind of subject on which reliable statistics can be easily accumulated. It is unfortunate that, on the rare occasions when a ship's master or pilot makes an error of judgment resulting in damage to the pier or fenders, it is unusual to find a competent and impartial observer present on the pier.

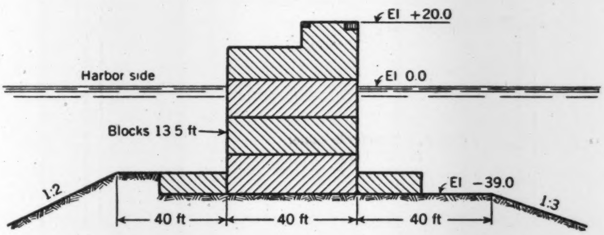

FIG. 1.—A MASS-CONCRETE PIER AND BREAKWATER AT VALENCIA, SPAIN

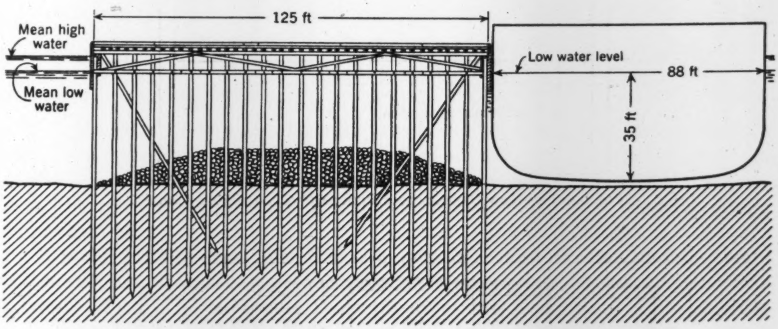

FIG. 2.—A TYPICAL TIMBER PIER BUILT IN THE NORTH RIVER IN 1905

Some of the factors that will influence the probable berthing speeds are:

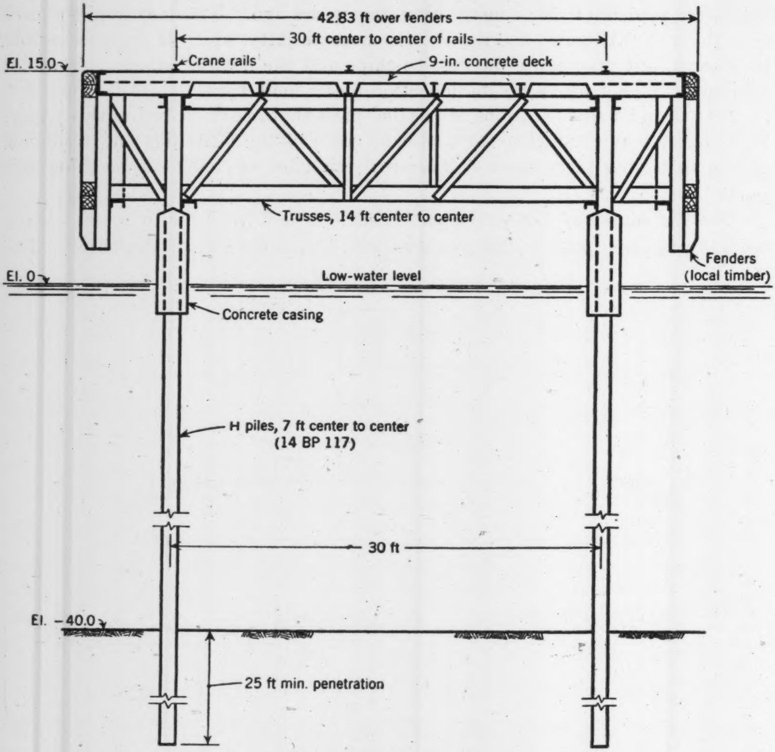
42.83 ft over fenders
30 ft center to center of rails
El. 15.0
Crane rails
9-in. concrete deck
Trusses, 14 ft center to center
Fenders (local timber)
El. 0
Low-water level
Concrete casing
H piles, 7 ft center to center (14 BP 117)
30 ft
El. −40.0
25 ft min. penetration

FIG. 3.—THE NEW ORE-LOADING PIER AT GUAYACAN BAY, CHILE

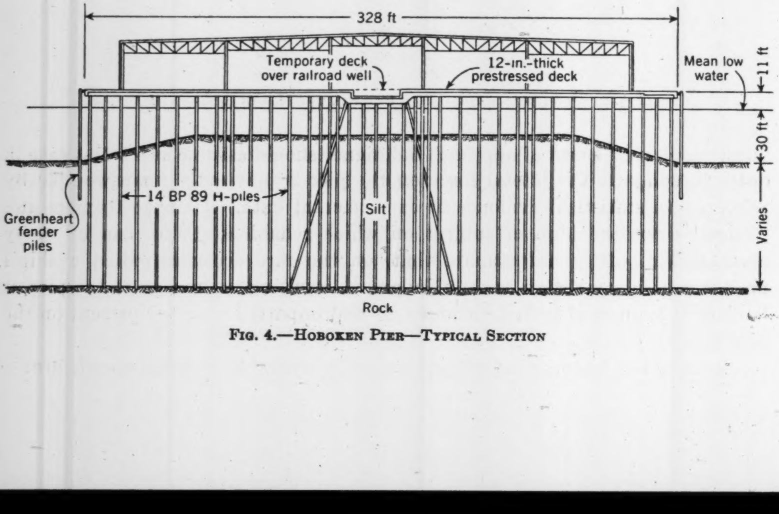
328 ft
Temporary deck over railroad well
12-in.-thick prestressed deck
Mean low water
11 ft
30 ft
Varies
14 BP 89 H-piles
Silt
Greenheart fender piles
Rock

FIG. 4.—HOBOKEN PIER—TYPICAL SECTION

1. The Location of the Pier or Dolphin.—A ship in a confined waterway, enclosed harbor, or dock is less likely to be moving fast than when it is in an open channel. Enclosed harbors also minimize the risk of high winds blowing a vessel against a pier. Conversely, piers or dolphins in open channels or exposed situations are more liable to receive impacts at higher speeds of approach.

2. Currents.—The presence of river currents or tidal currents will obviously increase the risk of serious impact due to an error of judgment on the part of the pilot, whereas a ship coming alongside in still water has a better chance of making a smooth approach.

3. Size and Type of Vessel.—As a general rule, the larger the ship, the greater the care with which it is handled and warped alongside. Ships of the large passenger lines, for example, are handled with extreme caution when in port, whereas ferries, tugs, and harbor craft are apt to exhibit much less respect for the structures alongside which they are berthing. These smaller harbor craft are often built with heavy rubbing strakes and thicker plating, and as the ship itself is less liable to sustain damage, even when handled carelessly, it is understandable that the master or pilot will not exercise the same degree of caution when berthing.

4. The Type of Traffic.—Regular dockings by pilots who are familiar with local conditions are likely to be smoother than those of ships docked by masters who are unfamiliar with the port. A further point to be considered, however, is that if the ship is sailing on a tight time schedule there will be less time available for cautious berthing.

The estimation of approach speeds at berthing is thus a matter of judgment for the designing engineer in consultation with ship owners, pilots, and others with knowledge of local conditions. It should be noted that the "approach speed" referred to in this paper is the speed in a direction normal to the face of the pier. In the case of an oblique approach, which is of course the general rule, the resolved component in a normal direction must be used for design computations.

It is the writer's experience that ship owners and pilots often underestimate the maximum probable approach speed and quote low figures. One of the manuals of the United States Department of the Navy until quite recently specified a design figure of 1/6 knot (equal to 0.3 ft per sec), which is certainly too low. At the other extreme, some bridge engineers assume approach speeds of 3 ft per sec or 4 ft per sec when designing bridge piers against accidental lateral loading—figures that are too high for general use in the design of port and harbor structures.

In practice a design speed of 1 ft per sec is commonly used for piers in enclosed harbors but in other cases speeds as low as 0.5 ft per sec or, in exposed situations, as high as 1.5 ft per sec or 2 ft per sec, are sometimes adopted.

The Computation of Impact Forces.—If the assumption is made that 40% of the ship's kinetic energy is the amount of energy that is absorbed by the deformation of the structure, then

$$\frac{P\,\delta}{2} = \frac{0.4\,m\,v^2}{2\,g}$$

from which P can be computed for various values of δ. In this expression, m equals the weight of the ship; v, the speed of approach; P, the maximum force of the ship on the structure; and δ, the maximum deflection of the structure at the point of impact. The two principal assumptions are that (*a*) the pier structure acts as an elastic spring and (*b*) the 40% of the ship's energy that is assumed to be absorbed by the deformation of the structure is the residue after allowing for impact and other losses such as the loss due to the elastic deformation of the ship's hull and to the oblique angle of approach. The value 40% is essentially empirical. Some research on the subject was undertaken by H. T. Horsfield in 1948,[2] but no conclusive results were reached.

A further energy equation is required when the mass of the pier is large compared with the mass of the ship:

$$m v = (M + m)V.$$

The effective kinetic energy to be absorbed is

$$\frac{0.4(M + m)V^2}{2g}$$

in which v equals the speed of the ship before impact; V, the speed of the ship and pier structure immediately after impact; m, the weight of the ship; and M the weight of the pier structure.

The foregoing momentum equations are not required in the design of piers or structures that do not have a heavy deck structure. If the structure has a heavy concrete deck, the use of these equations yields a slightly lower value for the kinetic energy.

Working Stresses.—In considering the allowable working stress, it should be borne in mind that the estimated speed of approach that has been discussed is the assumed maximum probable speed of a ship that is not under proper control. This condition is in some respects analogous to designing for earthquake shocks or hurricanes, in the sense that severe impact loading is a contingency that will not be a regular occurrence, and higher working stresses are therefore permissible.

The advantage of adopting a high working stress lies in the greatly increased energy absorption which results—the elastic energy of deformation in bending being proportional to the square of the working stress. If, for example, the working stress is doubled, the energy absorption is multiplied by four. In this paper, stresses 50% greater than normal working stresses are used as allowable stresses.

In timber structures the flexural stress at failure may be as high as 6,000 lb per sq in. and this is the reason for the well-known reserve of strength which timber piers and dolphins show when subjected to impact loads. The subject of stresses in timber and steel dolphins has been fully discussed in a paper by D. H. Little to the British Institution of Civil Engineers in 1949.[3]

---

[2] "The Impact of a Vessel with a Pier," by H. T. Horsfield, *The Dock and Harbour Authority*, London, June, 1948, p. 45.

[3] "Some Dolphin Designs," by D. H. Little, *Journal*, Inst. of C. E., London, November, 1946, p. 48.

The adoption of high working stresses is, of course, contingent upon the assumption of a maximum probable value for the berthing speed. If the assumed berthing speed is a normal speed occurring frequently, then ordinary working stresses should be used.

Fenders.—The design of fendering, which has in the past been considered of minor importance as compared with the design of the pier structure itself, has lately attracted increasing attention from engineers. Spring fenders of the coil-spring and rubber-buffer types have been fitted to several piers and jetties that have been constructed in recent years.[4] The suspended gravity fender, developed during World War II, has also been installed in several ports.[5]

Fender design will not be examined herein in any detail. The subject has been treated comprehensively by D. H. Little in a recent paper[6] and also by A. M. Robertson.[7] It should be noted, however, that special attention to fendering design is essential if the structure itself is rigid. In the past the need has been met with brushwood fenders, camels, or catamarans floating alongside the face of the pier and absorbing the energy of impact by crushing the timber. Spring fenders or gravity fenders are refinements of these traditional expedients, and on rigid structures their value in minimizing impact loads on the structure or damage to the ship's hull is indisputable.

For a structure as flexible as the type of pier illustrated in Fig. 3, a rubbing face only is required, and the fenders are not required to absorb energy. Although in practice the fenders will be crushed to a limited extent, the amount of energy absorbed will be small compared with that of the energy absorbed by the structure itself and may be neglected.

It is to be expected, therefore, that the fenders on this type of pier will be subjected to less wear and damage and will have a longer life than others. A general conclusion may be drawn that a flexible structure will demonstrate an economy in the cost of fender maintenance in addition to the economy of low initial construction cost due to the reduction of the lateral loading.

The Guayacan Bay Pier

Design Principles.—Guayacan Bay is the loading point for iron ore from the ore-handling plant of the Bethlehem Chile Iron Mines. The type of pier construction adopted—a deck structure supported on two rows of H-piles, without batter piles or underwater bracing (Fig. 3)—is designed to facilitate easy erection from the land, without the use of floating equipment. All the trusses are prefabricated and are used as templates to guide the piles during driving. On completion of the steelwork erection the reinforced concrete deck slab is poured, the forms being supported on the structural steel members.

The pier deck is designed to carry H-20 truck loading and also a traveling ore loader. When lateral impact loads are considered—an important consideration for this type of pier which has no batter piles—the deck slab and steel trusses are assumed to act as a composite beam, continuous for the 700-ft length of the pier, and supported by the H-piles acting as embedded cantilevers when resisting horizontal loads. The entire length of deck is therefore, in effect, a beam on elastic supports, and the design analysis, which includes consideration of the relative deflection of the pier deck and the H-piles, shows how the load is distributed.

---

[4] "Oil-Loading Docks in Venezuela Built of Welded Steel," by Theodore T. Knappen, *Civil Engineering*, March, 1949, p. 33.

[5] "Huge Oil Pier Built in Open Water," by D. C. Wolfe, *Engineering News-Record*, May 25, 1950, p. 34.

[6] "Some Design for Flexible Fenders," by D. H. Little, *Proceedings*, Inst. of C. E., London, February, 1953, p. 42.

[7] "Fendering, Lead-in Jetties and Dolphins," by A. M. Robertson, *The Dock and Harbour Authority*, London, May, 1953. p. 15.

Berthing Impact Loads.—Because of the sheltered situation of the pier, and because berthing is effected by first making fast a line to a mooring buoy and then warping the ship alongside, the assumed approach speed of 1 ft per sec is not likely to be exceeded. The effective kinetic energy of a ship with a displacement tonnage of 14,000 long tons will be

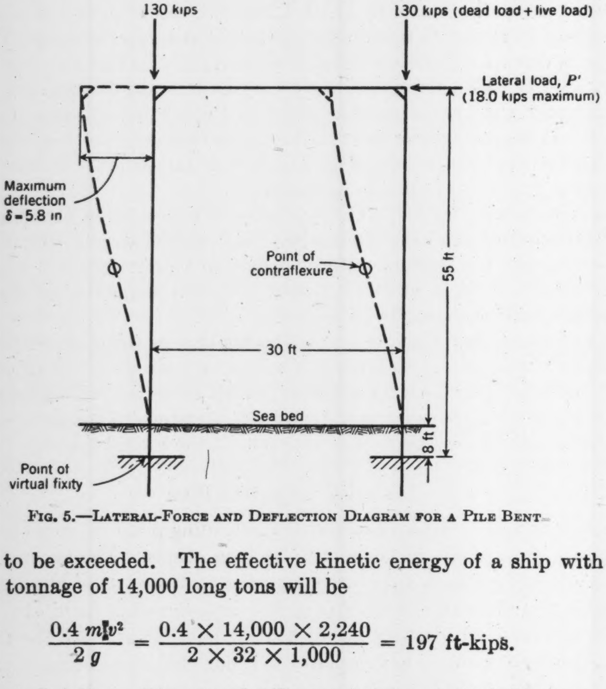

FIG. 5.—LATERAL-FORCE AND DEFLECTION DIAGRAM FOR A PILE BENT

$$\frac{0.4\, mv^2}{2\,g} = \frac{0.4 \times 14{,}000 \times 2{,}240}{2 \times 32 \times 1{,}000} = 197 \text{ ft-kips.}$$

H-Piles in Bending.—Figs. 5 and 6 illustrate the mode of deflection assumed for an individual pile bent and also for the deck of the pier when lateral loads are applied.

In Appendix I and Table 1 are summarized the results of the design computations for a lateral impact load applied to the pier deck at the center, the quarter-points, and the end of the pier. The design criterion for the maximum permissible lateral load is that the combined bending and direct stress in the piles shall not exceed the stresses permitted by the column formula of the American Institute of Steel Construction. It is found in this case that the maximum lateral load (allowing 50% overstress) produces a deflection of the deck of 5.8 in.

In computing the pile bending stresses, no attempt has been made to evaluate the passive earth pressures on the embedded portion of the pile because the necessary soil data were not available. A point of virtual fixity has been assumed 8 ft below the sea bed and, because the soil was a dense gravel, the assumption is considered to have been conservative. In any event, a small variation in the assumed depth of the point of fixity would not have any significant effect on the result.

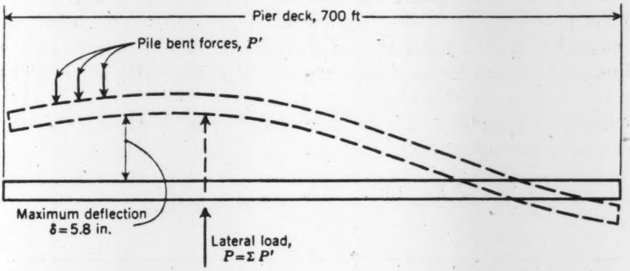
Pier deck, 700 ft
Pile bent forces, P'
Maximum deflection $\delta = 5.8$ in.
Lateral load, $P = \Sigma P'$

FIG. 6.—LATERAL-FORCE AND DEFLECTION DIAGRAM FOR THE PIER DECK

TABLE 1.—MAXIMUM PERMISSIBLE LATERAL LOADS ON THE GUAYACAN BAY PIER

Point of application	Maximum Lateral Load, P, in Kips		Pier-deck deflection diagram, $\delta_{max} = 5.8$ in.
	Case A[a]	Case B[b]	
Center	980	995	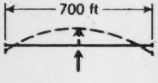
Quarter-Point	880	975	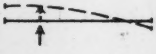
End	270	390	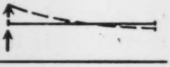

[a] In case A, 14 BP 117 H-piles were used, 7 ft center to center throughout. [b] Case B same as case A except that 14WF 158 H-piles were used for the 14 bents in the 100-ft section at each end of the pier.

When the first analysis of deflections and loads shown in Table 1 (case A) had been completed and the comparative weakness of the ends of the pier was appreciated, it was decided that some stiffening of the ends was necessary. The 14 BP 117 piles originally proposed for the full length of the pier were replaced by 14 WF 158 piles in the fourteen bents at each end, resulting in a 50% increase in the stiffness of the ends. The revised values of the lateral load, P, are shown in Table 1 (case B).

In arriving at a decision as to the necessary stiffening of the ends, application of the load at the quarter-point was used as the governing factor. The ends of the pier are protected by 40-ft-diameter sheet-pile caisson dolphins, which are located at each end of the pier so that their fendering is 3 ft in front of the pier fender line, and impact loads of any magnitude on the extreme ends of the pier are therefore highly improbable.

Pier Energy Absorption.—In the case of an impact load on the center of the pier, the energy absorption is

$$\frac{P\,\delta}{2} = \frac{995 \times 5.8}{2 \times 12} = 240 \text{ ft-kips.}$$

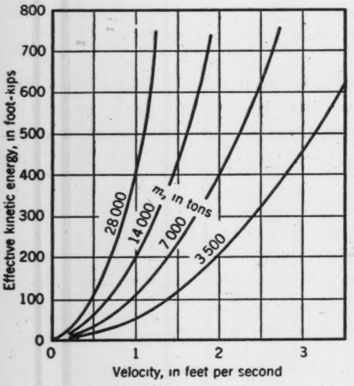

Fig. 7.—Guayacan Bay Pier—Kinetic Energy ($0.4\, m v^2/2 g$) Related to Velocity

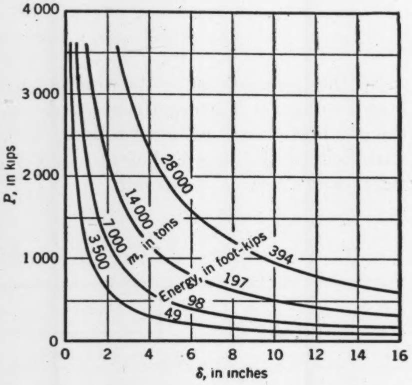

Fig. 8.—Guayacan Bay Pier—Elastic Energy Values Equal a Ship's Kinetic Energy at 1 Ft per Sec

This value provides a reasonable margin over the design requirement of 197 ft-kips and has been accepted as satisfactory.

Further Investigations.—The value of energy methods of analysis of a structure under impact loads lies in the general picture of its behavior that can thus be presented, rather than in the attempt to compute design stresses with great accuracy. In this respect, graphs similar to Figs. 7, 8, and 9 are of great assistance.

Fig. 7 shows the increase in effective kinetic energy with the square of the speed. Large ships moving at any appreciable speed have enormous kinetic energies and produce correspondingly heavy loads on the structures unless the energy is adequately absorbed.

Fig. 8 shows the maximum lateral load on the pier and the substantial decrease in load that results from providing for adequate deflection.

Fig. 9 shows the structure's resistance to impact loads for varying lengths of pile, the effective length of the pile being the distance from the lower chord of the lateral truss to the point of virtual fixity in the sea bed. Although the allowable load is less for a long pile than for a short one, the energy absorption is greater because of the increased deflection. A long unbraced length of pile is therefore advantageous in absorbing the energy of impact loads, and, conversely, any system of rigid bracing that reduces the deflection of the pile would reduce the resistance to impact loads.

HOBOKEN PIER C

Design Principles.—The Port of New York Authority's Hoboken Pier C, a general description of which has been previously published,[8] is a general cargo terminal pier designed to accommodate C.2 class, Liberty class, or Mariner class merchant ships. The pier has an over-all length of 700 ft and a width of 328 ft and is of prestressed concrete construction supported on steel H-piles. It is not structurally connected to the shore; there is a 1.5-in. expansion gap at the inshore end. The gap is provided with keys, which restrain this end of the pier from lateral movement, but do not provide fixity. The offshore end of the pier is free to deflect under lateral loads.

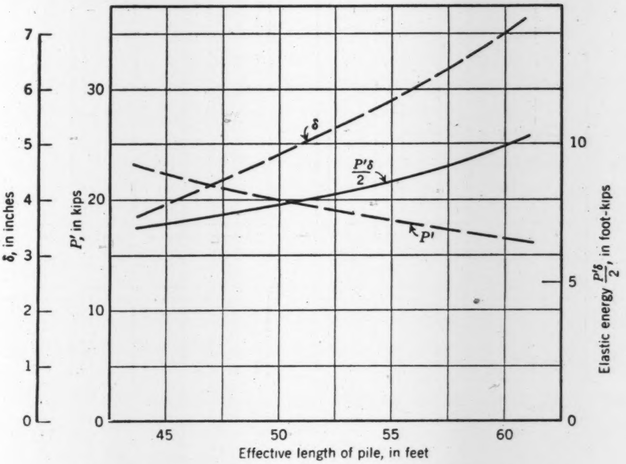

FIG. 9.—GUAYACAN BAY PIER—ELASTIC ENERGY, 2-PILE BENT (EACH PILE STRESSED TO 18 KIPS PER SQ IN. + 50%)

Fig. 4 shows a typical cross section, and Fig. 10 shows details of the deck stringers. The sequence of construction was as follows:

---

[8] "Prestressed Deck Proves Cheapest for New Hoboken Pier," by Theodore O. Blaschke and David A. Hopkins, *Civil Engineering*, February, 1954, p. 50.

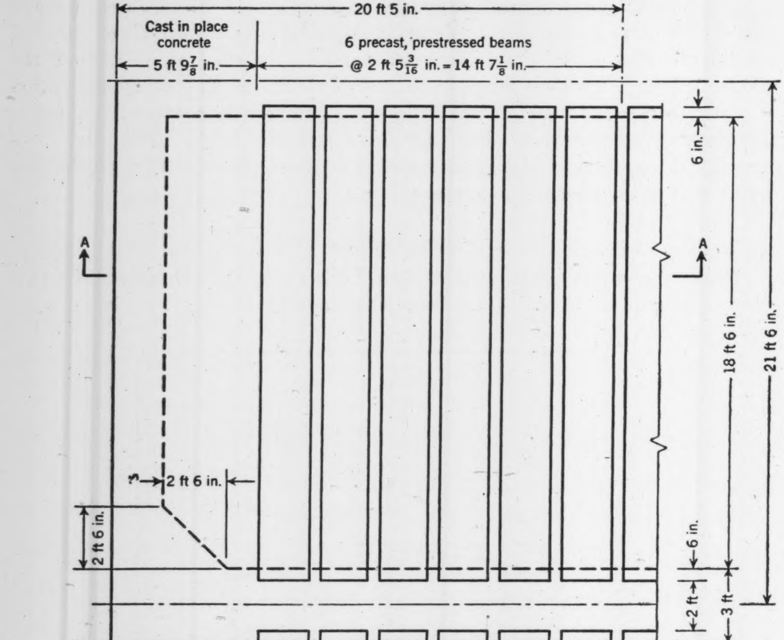
20 ft 5 in.
Cast in place concrete
5 ft 9⅞ in.
6 precast, prestressed beams
@ 2 ft 5 3/16 in. = 14 ft 7⅛ in.
A
A
6 in.
18 ft 6 in.
21 ft 6 in.
2 ft 6 in.
2 ft 6 in.
6 in.
2 ft
3 ft
2 ft 6 in.
6 in.
2 ft
2 ft 6 in.
PLAN
20 ft 5 in.
Cast in place concrete
5 ft 9⅞ in.
6 precast, prestressed beams
@ 2 ft 5 3/16 in. = 14 ft 7⅛ in.
Wall
4th pour
1 ft
1 ft
1st pour
3 ft 9 in.
2 ft 9 in.
2 ft 9 in.
3 ft 9 in.
2 ft
2 ft 6 in.
SECTION A-A

FIG. 10.—HOBOKEN PIER—PLAN AND SECTION, SHOWING PRETENSIONED STRINGERS ON CAST-IN-PLACE PILE

1. The pile caps, 21.5 ft center to center, were poured with ducts embedded for use in post-tensioning cables extending the length of each pile cap.

2. The precast, prestressed concrete stringers were laid in place, spanning between pile caps.

3. The concrete in the upper section of the pile-cap beam and in the keys between the stringers was poured so that the poured concrete was flush with the upper surface of the stringers.

4. The pile-cap beams were post-tensioned. The purpose of the post-tensioning is to provide a lateral compression in the pier deck, and thus insure that the concrete deck will be monolithic. The compressive stress induced in the deck in this manner is low—less than 100 lb per sq in.—but it is sufficient to eliminate the risk of shear failure between stringers in a longitudinal direction. Without the post-tensioning there would be no positive provision against distortion of the deck and failure in shear when subjected to lateral loads from berthing ships.

Impact Loads.—The design provisions for lateral loading on the pier are either the impact energy of a ship of 25,000-short-tons displacement moving at 1 ft per sec, or a concentrated load of 1,500 kips.

If the weight of the offshore half of the concrete pier is assumed to be 30,000 kips, then, using the momentum and energy equations: $50{,}000 \times 1 = (50{,}000 + 30{,}000) \times V$ and $V = 0.625$ ft per sec. The effective kinetic energy equals $\frac{0.4 \times 80{,}000 \times (0.625)^2}{2 \times 32} = 195$ ft-kips.

Loading for H-Piles.—Because the 14 BP 89 H-piles were between 90 ft and 150 ft long, driven to a point bearing on rock through soft silt, a design investigation was undertaken based on the analyses by A. E. Cummings[9] and G. W. Glick[10] in order to determine the permissible loads—both in bearing and in a lateral direction—which the piles would carry. The results were of course dependent on the value assigned to the lateral soil modulus, although for this modulus there is no generally acceptable method of computation or standard soils laboratory procedure. There was also some doubt as to the extent to which the theoretical considerations forming the basis of the analyses would be realized in practice.

The conclusions reached were as follows:

a. The safe bearing load would be considered to be 90 tons per pile. However, it was stipulated by the design engineers that this value should be confirmed by the proof loading of a test pile to 150 tons before construction was begun.

b. When subjected to lateral loads, the piles would act as embedded cantilevers, with a length of approximately 60 ft from the lower point of virtual fixity in the silt to the upper point of fixity in the pile cap.

---

[9] "The Stability of Foundation Piles Against Buckling Under Axial Load," by A. E. Cummings, *Proceedings*, Highway Research Board, National Research Council, Washington, D. C., Vol. 18, Pt. II, December, 1938, p. 112.

[10] "Influence of Soft Ground on the Design of Long Piles," by G. W. Glick, *Proceedings*, 2d International Conference on Soil Mechanics, Vol. IV, Rotterdam, 1948, p. 84.

c. It would be unwise to rely solely on the cantilever strength of the H-piles to provide the pier's resistance to lateral loads because of the uncertainties involved in the design analyses. Batter piles were therefore required to provide lateral resistance.

d. The maximum lateral deflection of the pier would be governed by the permissible deflection of the batter-pile bents, computed to be 0.24 ft.

Other assumptions relating to the design for lateral loading were that:

e. As a "worst case" the impact load would be applied to one of the knuckles at the offshore end of the pier.

f. The deflection of the pier would be a maximum at the offshore end and zero at the inshore end, which is laterally restrained.

g. Only 550 of the bearing piles and 40 of the batter piles, which are located in the offshore half of the pier, would be effective in resisting lateral impact.

Energy Absorption.—In Appendix II is summarized the design computations for the absorption of energy resulting from lateral impacts. The total energy absorption, 462 ft-kips is more than double the design requirement of 195 ft-kips. The pier thus possesses a large reserve of resistance to lateral loads. Furthermore, it may be noted that the fendering, consisting of greenheart fender piles backed by southern pine wales, provides an additional reserve of energy absorption, consideration of which has not been included in this paper. The margin available for collision risks is therefore even greater than indicated by the foregoing values. This margin is considered a wise form of insurance in a structure designed to have a life of one hundred years.

CONCLUSIONS

The values quoted in this paper are not intended as exact loads and deflections because the velocity of a berthing ship can never be estimated with precision or certainty. However, the formulation of energy equations will often give the port and harbor engineer a sense of perspective when dealing with lateral loads.

It is hoped that this paper will lead to discussion and the wider application of energy-absorption criteria. Investigation into cases of piers damaged by berthing ships would provide guidance for design engineers in the future.

APPENDIX I. GUAYACAN PIER

DESIGN ASSUMPTIONS FOR A TWO-PILE BENT (FIG. 5)

1. The horizontal cross-member is assumed completely rigid.

2. The piles are assumed to have a theoretical point of fixity 8 ft below the sea bed.

3. The piles are considered as columns with combined bending and direct stresses for which $(f_a/F_a) + (f_b/F_b)$ must not exceed 1.

4. The allowable compressive stress, F_a, is taken as an allowable column load + 50% for a 52-ft-high column, equal to 17,600 lb per sq in. (This short column length provides allowance for soil support at the foot of the pile.)

5. The allowable bending stress, F_b, is taken as 18,000 + 50% = 27,000 lb per sq in.

The maximum load (direct compression) on the pile equals 130 + (55/30) P' kips. The maximum bending moment in the pile equals (55/4) $P' + 130 \times (\delta/2)$. Obtaining corresponding equations for direct and bending stresses, and solving graphically the expression, $(f_a/F_a) + (f_b/F_b) = 1$, it is found that $P'_{max} = 18.0$ kips and $\delta_{max} = 5.8$ in.

Design Assumptions for the Pier Deck (Fig. 6)

1. The resisting force of the pile bents, P', varies with the deflections, δ, and has a maximum value of 18.0 kips when $\delta = 5.8$ in.

2. The deflection equation is $E\,I\,\frac{d^4y}{dx^4} = -\,k\,y$, in which E is the modulus of elasticity; y, the deflection; x, the distance along the member; and I and k are as defined subsequently.

3. The moment of inertia of the deck, I, is considered as that of a cracked section of reinforced concrete beam plus 50% of the longitudinal steel in the trusses equal to 120×10^6 in.^{4}

4. The resistance modulus, k, equals 37 lb per in. of deflection per in. of length.

The general solution for a beam of infinite length is $y = \frac{P\,\beta}{2\,k}\,e^{-\beta x}(\cos\beta\,x + \sin\beta\,x)$, in which $\beta = \sqrt[4]{K/(4E\,I)} = 0.00042$. For beam of length, l, with a center load, $y_{max} = \frac{P\,\beta}{2\,k}\left(\frac{\cosh\beta\,l + \cos\beta\,l + 2}{\sinh\beta\,l + \sin\beta\,l}\right)$. Values of P in Table 1 are all computed for $\delta_{max} = y_{max} = 5.8$ in.

APPENDIX II. HOBOKEN PIER

Lateral Load.—All piles of this pier are 14 BP 89, for which $I = 909.1$ in.^{4} The maximum pile loading equals 90 tons plus 50%, or 135 tons. The maximum pile length is 150 ft. The maximum permissible lateral design load for batter-pile bents (2 batter piles in each bent) was 55.5 tons. The batter-pile loading was computed by means of simple statics, and uplift was found to govern in the case of the left-hand batter pile. The maximum permissible lateral load on 20 batter-pile bents was thus computed to be 1,110 tons.

Energy Absorption by Batter Piles.—If the maximum axial compression or extension of batter piles under design load is computed for the full 150-ft pile length, the maximum permissible deflection of the pile bent equals 0.24 ft (Fig. 11). Therefore, the energy absorption will be $0.24 \times 1{,}110 \times 2/2 = 264$ ft-kips.

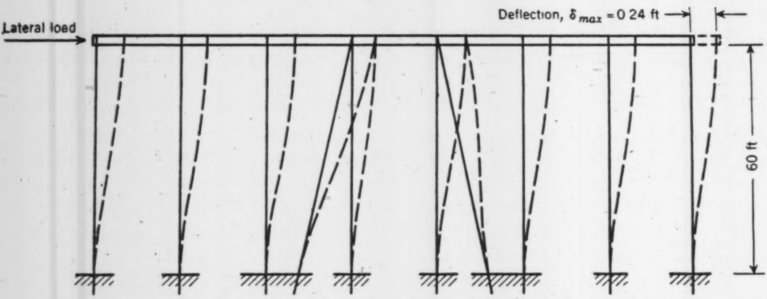

FIG. 11.—CAPS WHICH WERE POST-TENSIONED; DIAGRAM SHOWING LATERAL DEFLECTION

Energy Absorption by Bearing Piles.—If the maximum permissible lateral deflection of the pier equals 0.24 ft and the bearing piles are considered to act as embedded cantilevers 60 ft long, fixed top and bottom, the maximum permissible lateral load equals 3 kips per pile. On 550 piles the maximum permissible lateral load equals 550 × 3 = 1,650 kips. Therefore, the energy absorption will be 1,650 × 0.24/2 = 198 ft-kips.

Total Energy Absorption.—The total energy absorption for this pier is thus 264 + 198 = 462 ft-kips.

DISCUSSION

Zusse Levinton,[11] M. ASCE.—The author is to be congratulated on having made a simple and concise statement of design methods relating to ship impact on piers. The two examples of piers on flexible piling show how the impact energy may be absorbed by the deflection of the structure. However, it would be erroneous to conclude that, in general, flexibility of the structure itself is preferable to flexibility provided by resilient fendering. High flexibility in the structure is usually accompanied by weakness of the structure. This point is illustrated in the author's statement (under the heading, "The Guayacan Bay Pier: H-Piles in Bending") that when "* * * the comparative weakness of the ends of the pier was appreciated, it was decided that some stiffening of the ends was necessary." In the same example, "the ends of the pier are protected by 40-ft-diameter sheet-pile caisson dolphins, which are located at each end of the pier * * *." Having thus protected the ends by stiff structures, the middle could be made flexible to allow a computed deflection of 5.8 in. which was possibly expedient in this case.

In general, it is not desirable to have a pier bounce as much as 6 in. from ship impact, a condition similar to earthquake shock. For such large deflections, special flexible connections may be required for pipelines and utilities on the pier, and special provisions in the design of superstructures, such as cranes, conveyer towers, or hoppers. These deflections also involve inconvenience and even danger to the personnel.

The advantage of lesser wear and tear of the rubbing face when the structure is flexible is correctly pointed out by the author. The same advantage will, of course, ensue when the rubbing face is backed by flexible springs attached to a stiffer pier structure.

In the second case cited by the author, the pier is wide, with a large number of piles in each bent. The computed 3-in. deflection is rather small and would be even smaller if the soil were stiffer and the point of virtual fixity of the piles much higher. Under such conditions the structure would require resilient fendering.

In the writer's practice, there were numerous cases in which fewer and heavier piles were preferred to larger numbers of lighter piles. This preference resulted in stronger and stiffer structures where the necessary flexibility was provided by spring fendering. The saving in the cost of the structure more than equaled the cost of the springs.

Higher velocities of approach and larger ships require greater deflections for absorption of the energy. Deflections of from 12 in. to 18 in. are quite easily obtainable by means of various types of steel springs. To incorporate such flexibility in the structure itself is impracticable.

David A. Hopkins,[12] A.M. ASCE.—Mr. Levinton's discussion of the general considerations which affect spring fender design indicates an intelligent appreciation of fundamental principles and raises a number of controversial points. It was certainly never intended that the paper should disparage the use of spring fenders. On rigid structures their value in minimizing impact loads on the structure or damage to the ship's hull is indisputable. A study of fender design cannot properly be included in this closure. For further study the reader is referred to the footnote references listed in the original paper dealing with the subject.

---

[11] Chf. Structural Engr., Tippetts-Abbett-McCarthy-Stratton, New York, N. Y.

[12] Project Engr., Tippetts-Abbett-McCarthy-Stratton, New York, N. Y.

The following points, however, are selected for further comment:

1. The strength and flexibility of any particular structure are separate characteristics, not interrelated in any way. Considering the analogy of an elastic spring—a spring may be designed for light or heavy loads and also for small or large deflections. In the same way the rigidity or flexibility of a structure may vary, quite independently of its strength. Piers subjected to lateral impact loads commonly deflect from 2 in. to 6 in.

2. A sentence from the paper (under the heading, "The Guayacan Bay Pier: H-Piles in Bending") stated that "when * * * the comparative weakness of the ends of the pier was appreciated, it was decided that some stiffening of the ends was necessary." The use of the word "stiffening" in this case was possibly misleading because it was used in the sense of spring stiffness and not structure stiffness. The stiffening referred to involved the substitution of heavier section H-piles at the ends of the pier as finally designed. The lateral load-carrying capacity of the ends of the pier was thus increased without any loss in flexibility.

The problem of protecting the end of a pier is, of course, common to both flexible and rigid structures because in practice the ends of piers are usually most vulnerable to accidental damage.

3. Deflections of pier structures as great as 6 in. are common for piers under lateral impact loads. In the case of the Guayacan Bay pier, no difficulty was experienced in providing for 6 in. of movement when designing pipe work and mechanical equipment because the movement is gradual and the curvature of the structure extremely small. Modern design techniques require a more careful evaluation of the effects of deflection than was customary in the past.

In conclusion, the necessity for the absorption of lateral impact energy—either by deflection of the structure or by spring fenders, or by a combination of the two—should be emphasized.

The examples described in the paper illustrate how structural deflection can be utilized advantageously to absorb this impact energy. The relative economy, however, of utilizing structural deflection as compared with spring fenders for the absorption of energy can only be evaluated by a study of particular cases. The two methods are available to design engineers, and no design study would be complete without an evaluation of the extent to which either method is likely to be of value.

AMERICAN SOCIETY OF CIVIL ENGINEERS
Founded November 5, 1852
TRANSACTIONS

Paper No. 2847

IMPACT ON PIN-JOINTED TRUSSES

By Bruno A. Boley[1] and Chi-Chang Chao[2]

Synopsis

A method is presented for the analysis of pin-jointed trusses subjected to impact. Expressions are derived describing the behavior of the various types of joints which may exist; with the aid of these, a numerical computation procedure is developed. This procedure makes use of "distribution factors," dependent only on the joint geometry, to describe the relationship between the waves arising in the bars meeting at an unloaded joint. The analogous relationships at a loaded joint are determined with the aid of a finite-differences technique. The method suggested can be used whether impact is caused by a known pressure pulse or by collision with a solid object. The criterion for establishing the time at which impact ends is cited in detail for the latter of these cases. An illustrative example is presented for which stresses, deflections, and reactions are computed. The basic equations governing the behavior of the various joints are derived for three-dimensional trusses as well as plane trusses; the proposed method of analysis is equally applicable to both.

Notation

The letter symbols adopted for use in this paper are defined where they first appear and are arranged alphabetically, for convenience of reference, in the Appendix.

Introduction

The behavior of pin-jointed trusses under time-dependent loadings is examined herein by use of a dynamic analysis which considers, in detail, the elastic waves set up in the various bars of the truss. Such an analysis is necessary if the loads are rapidly applied, either by a sudden pressure wave or through collision with a fast-moving solid object. Of course, if the loads are gradually applied, the customary static analysis (or an analysis taking into

---

Note.—Published, essentially as printed here, in January, 1955, as *Proceedings-Separate No. 605*. Positions and titles given are those in effect when the paper was approved for publication in *Transactions*.

[1] Associate Prof. of Civ. Eng., Inst. of Flight Structures, Columbia Univ., New York, N. Y.

[2] Research Assistant, Dept. of Civ. Eng. and Eng. Mechanics, Columbia Univ., New York, N. Y.

account the excitation of the first few normal modes of vibration) may be adequate. The types of loadings cited, however, are becoming increasingly important in a number of engineering applications and therefore make necessary a more accurate method of computation. The purpose of this investigation is, therefore, the development of a procedure suitable for practical use which is general enough to include structures of arbitrary configuration.

General Description

The method of solution presented herein consists essentially of a procedure for following the waves that arise in the various bars of the truss and of determining how these waves are distributed among the bars meeting at any one joint. For a truss with arbitrary configuration or with a large number of joints and bars, this procedure can become cumbersome unless it is performed in a systematic manner. It is therefore desirable to consider separately the various sources of difficulties and to determine how each may best be treated.

The first requirement of the computation procedure is that it account for all the waves at any one time at whatever joint is considered. This is best accomplished by first solving for all the waves affecting the loaded joint and subsequently extending the solution to the other parts of the truss. The computation of the waves at the loaded joint is, in turn, divided into the consideration of the following three distinct items: (*a*) The condition in which only waves emanating from the loaded joint are present and the waves have not yet reached the neighboring joints, (*b*) the distribution of these waves among the bars at the neighboring joints, and (*c*) the arrival and distribution of these new waves at the loaded joint. The actual steps of a procedure in which these items are followed is described subsequently.

It is now necessary to determine how the waves are distributed at any one joint. The distribution process obeys two rules:

1. The vector sum of the bar forces must vanish (for an unloaded joint) or balance the inertia force of the striking mass (at a loaded joint).
2. The velocity of each bar must be compatible with the condition that all bars remain attached at the joint.

These two conditions, one concerning stresses and one velocities, could be simplified if a simple relationship existed between the stress and the velocity of any one bar. In the foregoing item *a* the stress and velocity of the end points of each bar are found to be proportional whereas in items *b* and *c* this is true only for a part of the distributed waves; the remaining part is proportional to the incoming wave and is therefore known. Subsequently, these statements are expressed mathematically in Eq. 4 for item *a*, in Eqs. 11*a* and 11*b* for item *b*, and in Eqs. 12*a* and 12*b* for item *c*.

It is also shown herein that the distribution of waves at an unloaded joint (item *b*) is readily performed by means of Eq. 13 whereas that at a loaded joint (item *c*) requires the use of a finite-differences technique. For this reason these items are kept separate in the final procedure.

The general ideas indicated in the foregoing form the basis of the proposed solution which the writers will present in detail. Particular reference will be made to the truss of Fig. 1, but it should be clear that this in no way restricts the generality of the method because it is, in fact, valid for either two-dimensional or three-dimensional trusses.

It is convenient in the following development to consider separately the behavior of the various types of joints which may be encountered in a truss of general configuration; therefore, five types of joints, defined as follows, are studied in detail:

Type a—A loaded joint, in which all waves are traveling away from the joint;
Type b—An interior unloaded joint, after the arrival of a wave in one of the bars;
Type c—A loaded joint, after the arrival of a wave in one of the bars;
Type d—A joint with roller support; and
Type e—A joint with a fixed hinge support.

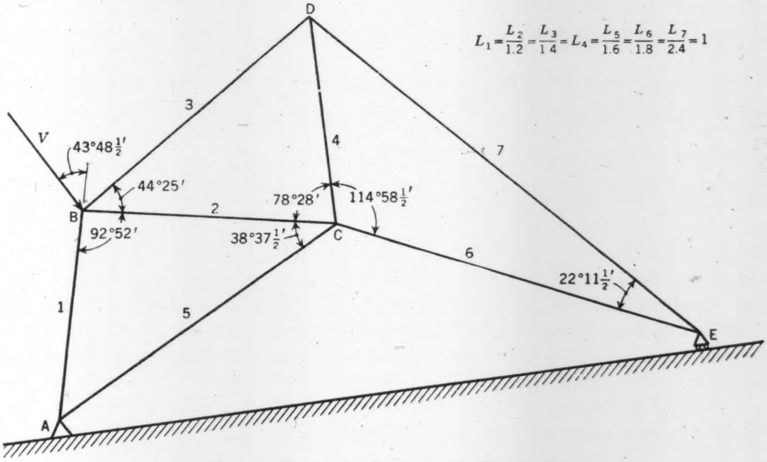
D
$L_1 = \frac{L_2}{1.2} = \frac{L_3}{1.4} = L_4 = \frac{L_5}{1.6} = \frac{L_6}{1.8} = \frac{L_7}{2.4} = 1$
3
V
43°48½′
4
7
44°25′
78°28′
114°58½′
2
B
92°52′
38°37½′
C
6
22°11½′
1
5
E
A

FIG. 1.—TRUSS FOR ILLUSTRATIVE EXAMPLE

If the truss in Fig. 1 is struck at joint B by a mass, *M*, with a velocity, *V*, in the direction shown, waves immediately arise in all the bars meeting at that joint; the corresponding axial displacement, u_i, in the *i*th bar satisfies the wave equation[3]:

$$\frac{\partial^2 u_i}{\partial t^2} = a^2 \frac{\partial^2 u_i}{\partial x^2_i} \qquad (1)$$

in which t is time, a denotes the speed of wave propagation, and x_i is the axial distance along bar i, positive when measured from the joint in question. Bending deflections are neglected herein as this type of deflection is probably of little importance in most applications. It would, of course, become significant if the applied loads were such as to excite the lower normal modes of vibration which involve considerable transverse deflections; in such problems a more thorough analysis would be required. At first only waves traveling away from the joint are present; hence,

---

[3] "The Mathematical Theory of Elasticity," by A. E. H. Love, Dover Publications, New York, N. Y., 4th Ed., 1944.

$$u_i = f_i\,(a\,t - x_i) \qquad (2)$$

for any bar, in which f_i is an arbitrary function. The stress,

$$\sigma_i = \frac{\partial u_i}{\partial x_i} E \qquad (3)$$

(in which E is the modulus of elasticity) and the velocity $(\partial u_i/\partial t)$ in bar i at $x_i = 0$ (struck end, joint B) are related by

$$\frac{\partial u_i}{\partial x_i} = -\frac{1}{a}\frac{\partial u_i}{\partial t} = -f'_i\,(a\,t) \qquad (4)$$

in which primes indicate differentiation with respect to the argument of the function, f_i.

The mass, M, is acted upon by the stress of Eq. 3 and behaves in accordance with Newton's law of motion which, written in the direction of each of the bars, is

$$M\frac{\partial^2 u_i}{\partial t^2} = \sum_{j=1}^{n} A_j\,\sigma_j \cos\theta_{ij}, \qquad i = 1,2,3,\cdots n \qquad (5)$$

in which n is the number of bars meeting at the joint; A_j denotes the area of bar, j; θ_{ij} represents the angle between bars i and j positive when counterclockwise; and all quantities are evaluated at $x_j = 0$. A joint of the truss which obeys Eqs. 2 and 5 is a loaded joint with all waves traveling away from it and is termed "type a." With the subsequent arrival of reflected waves this will no longer be true, and the joint will then be one of "type c."

In Eq. 5 it is assumed that the mass and the struck joint remain in contact; if contact were to cease, this equation would reduce to

$$\sum_{j=1}^{n} A_j\,\sigma_j \cos\theta_{ij} = 0, \qquad i = 1,2,3,\cdots n \qquad (6)$$

A joint which obeys Eq. 6 is termed "type b."

The solution of Eqs. 2 and 5 completely determines the wave in any bar (for example, the ith) until a time $t = L_i/a$ (in which L_i is the length of bar i)—that is, when the wave has reached the far end of the bar in question. For example, the wave in bar 2 in the truss of Fig. 1 will first affect joint C at $t = L_2/a$ by striking it with wave f_2 of Eq. 2. If the origin is now shifted to joint C, the magnitude of f_2 becomes

$$u_p = -f_p\,(a\,t - L_p + x_p) \qquad (7)$$

in which $p = 2$. In general, the subscript, p, will denote the bar along which a wave arrives. The wave, f_p, causes disturbances in all bars emanating from joint C and traveling away from it (item *b*); hence, they all satisfy Eq. 2. The governing equations for this joint are obviously Eqs. 6. Therefore, this joint is of type b, and these new waves can be determined from those equations. If the new wave in bar 4 is denoted by f_{24} (or, in general, the wave in bar i by f_{pi}), then

$$u_4 = f_{24}\,(a\,t - L_2 - x_4) \tag{8}$$

or, in general,

$$u_i = f_{pi}\,(a\,t - L_p - x_i), \qquad i \neq p \tag{9}$$

in which $f_{pi}(0) = 0$. The corresponding equation for bar p must, in addition, take into account the incoming wave of Eq. 7 and is

$$u_p = -\,f_p\,(a\,t - L_p + x_p) + f_{pp}\,(a\,t - L_p - x_p) \tag{10}$$

It follows from the foregoing that, at $x_i = 0$,

$$\frac{\partial u_i}{\partial t} = a\,f'_{pi}, \qquad p \neq i \tag{11a}$$

$$\frac{\partial u_i}{\partial t} = a\,(f'_{pp} - f'_p), \qquad p = i \tag{11b}$$

and

$$\frac{\sigma_i}{E} = \frac{\partial u_i}{\partial x_i} = -\,\frac{1}{a}\,\frac{\partial u_i}{\partial t} = -\,f'_{pi}, \qquad p \neq i \tag{12a}$$

$$\frac{\sigma_i}{E} = \frac{\partial u_i}{\partial x_i} = -\,f'_p - f'_{pp} = \frac{1}{a}\,\frac{\partial u_i}{\partial t} + 2\,f'_p, \qquad p = i \tag{12b}$$

It should be noticed that in all but the p-bar, Eq. 4 still holds; for the bar p, only a part of the stress is proportional to the velocity whereas the remainder is proportional to the known incoming wave, f'_p.

Solution of Eq. 6 will show that the simple relationship,

$$f'_{pi} = D_{pi}\,f'_p \tag{13}$$

holds for all bars, in which D_{pi} is a "distribution factor" dependent only on the geometry of the joint in question and its bars. In general, the relationship,

$$D_{ip} = D_{pi} \tag{14}$$

holds; D_{pp} is, in general, different when computed at different ends of the same bar. Thus, for example, in Fig. 1, D_{44C} does not equal D_{44D}.

Of the new waves just started at joint C, f_{22} will reach joint B at $t = 2\,L_2/a$; f_{24} will reach joint D at $t = (L_2 + L_4)/a$, and so forth. The wave, f_{24}, will distribute at joint D (which is of type b) according to the distribution factor appropriate to that joint; it will thus give rise to the following new waves (traveling away from joint D):

$$f'_{243}\,(a\,t - x_3) = D_{24}\,D_{43}\,f'_2\,(a\,t - L_2 - L_4 - x_3) \tag{15a}$$

$$f'_{244}\,(a\,t - x_4) = D_{24}\,D_{44D}\,f'_2\,(a\,t - L_2 - L_4 - x_4) \tag{15b}$$

and

$$f'_{247}\,(a\,t - x_7) = D_{24}\,D_{47}\,f'_2\,(a\,t - L_2 - L_4 - x_7)\,\ldots\ldots\ldots(15c)$$

in which x_3, x_4, and x_7 are measured from joint D. Thus, when

$$a\,t = (L_2 + L_4 + L_3)\,\ldots\ldots\ldots\ldots\ldots\ldots\ldots(16)$$

wave f_{243} reaches the loaded joint B.

Wave f_{342} will, of course, reach joint B at the same time as f_{243} (note $f_{342} \neq f_{243}$), but before that happens it has been seen that f_{22}, in addition to f_{11} and f_{33}, has already arrived there. With the exception of f_{11}, all these waves encounter only joints of type b and therefore behave as described previously. Joint A is a fixed hinged support and therefore cannot be displaced; such a joint is termed type e and can be treated in a manner analogous to that of type b. The distribution factors for joints of type b are found in the next section to be

$$D_{pi} = -\,4\,\frac{\sum\limits_{k=1}^{n} A_p\,A_k \sin\theta_{ik} \sin\theta_{pk}}{\sum\limits_{k=1}^{n}\sum\limits_{q=1}^{n} A_k\,A_q \sin^2\theta_{kq}}, \qquad i \neq p\,\ldots\ldots\ldots(17a)$$

and

$$D_{pp} = 1 - 4\,\frac{\sum\limits_{k=1}^{n} A_p\,A_k \sin^2\theta_{pk}}{\sum\limits_{k=1}^{n}\sum\limits_{q=1}^{n} A_k\,A_q \sin^2\theta_{kq}}\,\ldots\ldots\ldots\ldots\ldots(17b)$$

For type d joints the distribution factors are found to be

$$D_{pi} = -\,2\,\frac{A_p \sin\theta_{pR} \sin\theta_{iR}}{\sum\limits_{j=1}^{n} A_j \sin^2\theta_{jR}}, \qquad i \neq p\,\ldots\ldots\ldots\ldots(18a)$$

and

$$D_{pp} = 1 - 2\,\frac{A_p \sin^2\theta_{pR}}{\sum\limits_{j=1}^{n} A_j \sin^2\theta_{jR}}\,\ldots\ldots\ldots\ldots\ldots\ldots(18b)$$

For type e joints the distribution factors are found to be

$$D_{pi} = 0, \qquad i \neq p$$

and

$$D_{pp} = 1.$$

One must also consider item c, namely, the behavior of the loaded joint (B in this case) after the arrival of waves along its component bars (type c). This joint is a combination of types a and b in that it follows Eqs. 5, 9, 10, 11, and 12. The solution of these equations cannot be put in terms of distribution factors similar to those introduced previously; the governing relationships are derived subsequently by use of a finite-differences technique.

EQUATIONS FOR VARIOUS TYPES OF JOINTS

Type a.—Type a joints have two degrees of freedom; hence, there can be only two independent equations in Eq. 5. For example, if the ith and jth equations ($i \neq j$) are taken to be the independent ones, any other (say, the kth) may be obtained from them by multiplying the ith equation by $\sin \theta_{jk}/\sin \theta_{ij}$ and the jth equation by $\sin \theta_{ki}/\sin \theta_{ij}$, adding the results, and simplifying the expression thus obtained with the aid of the equations:

$$\theta_{ii} = 0 \qquad (19a)$$

$$\theta_{ij} + \theta_{ji} = 2\pi \qquad (19b)$$

and

$$\theta_{ij} + \theta_{jk} = \theta_{ik} \qquad (19c)$$

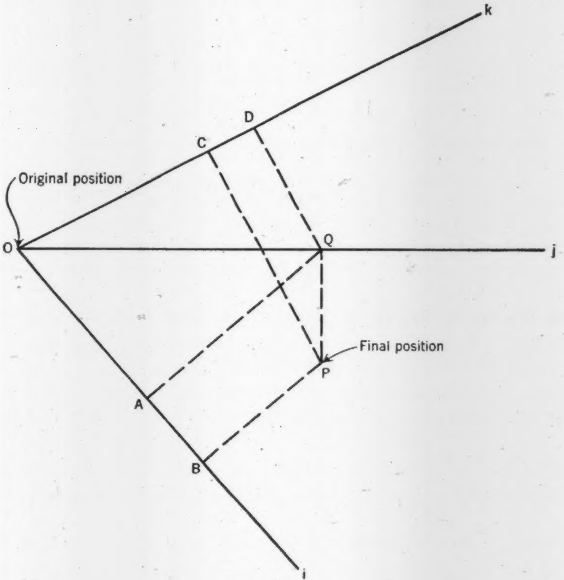

FIG. 2.—DISPLACEMENT OF A JOINT IN A PLANE TRUSS

and the compatibility relationships,

$$u_i \sin \theta_{jk} + u_j \sin \theta_{ki} + u_k \sin \theta_{ij} = 0, \qquad x_i = x_j = x_k = 0 \ldots (20)$$

In two special cases ($k = i$ and $k = j$) Eq. 20 is trivial; in the remaining ($n - 2$) cases it may be derived by equating the following two expressions for the distance PQ of Fig. 2:

$$\text{PQ} \sin \theta_{ij} = \text{AB} = \text{OB} - \text{OA} = u_i - u_j \cos \theta_{ij} \qquad (21a)$$

and

$$\text{PQ} \sin \theta_{jk} = \text{CD} = \text{OD} - \text{OC} = u_j \cos \theta_{jk} - u_k \qquad (21b)$$

Eq. 20 holds also if u_i is replaced by $\partial u_i/\partial t$; then use of Eq. 4 shows that one may also write

$$f'_i \sin\theta_{jk} + f'_j \sin\theta_{ki} + f'_k \sin\theta_{ij} = 0 \qquad (22)$$

With Eqs. 22 and 4, all displacements but two may be eliminated from the two independent equations of Eq. 5. Taking again the *i*th and *j*th equations as the independent ones, one obtains

$$f''_i + \frac{f'_i}{\sin\theta_{ji}} \sum_{k=1}^{n} \frac{\sin\theta_{jk}\cos\theta_{ik}}{m_k L_k} + \frac{f'_i}{\sin\theta_{ji}} \sum_{k=1}^{n} \frac{\sin\theta_{ki}\cos\theta_{ik}}{m_k L_k} = 0 \qquad (23a)$$

and

$$f''_j + \frac{f'_j}{\sin\theta_{ji}} \sum_{k=1}^{n} \frac{\sin\theta_{jk}\cos\theta_{kj}}{m_k L_k} + \frac{f'_j}{\sin\theta_{ji}} \sum_{k=1}^{n} \frac{\sin\theta_{ki}\cos\theta_{jk}}{m_k L_k} = 0 \qquad (23b)$$

in which

$$m_k = \frac{M}{\rho A_k L_k} \qquad (24)$$

and ρ is the mass density. Eq. 23*a* gives

$$f'_j = -\frac{f''_i + \dfrac{f'_i}{\sin\theta_{ji}} \displaystyle\sum_{k=1}^{n} \frac{\sin\theta_{jk}\cos\theta_{ik}}{m_k L_k}}{\dfrac{1}{\sin\theta_{ji}} \displaystyle\sum_{k=1}^{n} \frac{\sin\theta_{ki}\cos\theta_{ki}}{m_k L_k}} \qquad (25)$$

Substitution into Eq. 23*b* yields, after some algebraic manipulation and with the aid of Eqs. 19,

$$f'''_i + P_1 f''_i + P_2 f'_i = 0 \qquad (26)$$

in which the constants, P_1 and P_2, independent of the choice of reference bars, are

$$P_1 = \sum_{k=1}^{n} \frac{1}{m_k L_k} \qquad (27a)$$

and

$$P_2 = \tfrac{1}{2} \sum_{k=1}^{n} \sum_{p=1}^{n} \frac{\sin^2\theta_{kp}}{m_k L_k m_p L_p} \qquad (27b)$$

The initial conditions for Eq. 26 are provided by the known initial velocity and displacement of the joint; they are

$$f'_i(0) = \frac{V}{a}\cos\theta_{Vi} \qquad (27c)$$

$$f'_j(0) = \frac{V}{a}\cos\theta_{Vj} \qquad (27d)$$

and

$$f(0) = 0 \qquad (27e)$$

The final result is

$$f_i = \frac{C_1}{r_1}\left[e^{r_1(a t - x_i)} - 1\right] + \frac{C_2}{r_2}\left[e^{r_2(a t - x_i)} - 1\right] \dots\dots\dots\dots (28)$$

in which C_1 and C_2 are to be determined from Eqs. 27*c* and 27*d*, and

$$r_{1,2} = \tfrac{1}{2}\left(-P_1 \pm \sqrt{P^2_1 - 4P_2}\right) \dots\dots\dots\dots (29)$$

Type b.—For bars other than the pth one, Eqs. 9, 10, 11, and 12 show that the compatibility condition (Eq. 20) may be simplified as in Eq. 22; that is,

$$f'_{pi}\sin\theta_{jk} + f'_{pj}\sin\theta_{ki} + f'_{pk}\sin\theta_{ij} = 0, \qquad p \neq i, j, k \dots (30a)$$

If $p = i$, then use of Eqs. 11 gives

$$(f'_{pp} - f'_p)\sin\theta_{jk} + f'_{pj}\sin\theta_{kp} + f'_{pk}\sin\theta_{pj} = 0 \dots\dots\dots (30b)$$

By use of Eqs. 30 and 12, Eq. 6 can be reduced to

$$\frac{f'_{pi}}{\sin\theta_{ji}}\sum_{k=1}^{n}\frac{\sin\theta_{jk}\cos\theta_{ik}}{m_k L_k} + \frac{f'_{pi}}{\sin\theta_{ji}}\sum_{k=1}^{n}\frac{\sin\theta_{ki}\cos\theta_{ik}}{m_k L_k} = -\frac{2f'_p}{m_p L_p}\cos\theta_{pi} \dots (31a)$$

$$\frac{f'_{pi}}{\sin\theta_{ji}}\sum_{k=1}^{n}\frac{\sin\theta_{jk}\cos\theta_{jk}}{m_k L_k} + \frac{f'_{pi}}{\sin\theta_{ji}}\sum_{k=1}^{n}\frac{\sin\theta_{ki}\cos\theta_{jk}}{m_k L_k} = -\frac{2f'_p}{m_p L_p}\cos\theta_{pj} \dots (31b)$$

with $i, j \neq p$. For the case in which $i = p$, the quantity f'_{pi} appearing in Eqs. 31 must, of course, be replaced by $f'_{pp} - f'_p$. The relationship between f'_{pi} and f'_p is the desired distribution factor; it can be obtained by algebraic solution of Eqs. 31*a* and 31*b* and is given as Eqs. 17.

Type c.—The basic equations for joints of type c are Eqs. 5, in which the velocities and stresses are given by Eqs. 11 and 12, respectively. The solution could be obtained by a treatment similar to that for joints of types a and b; such an analytical solution, however, would become complicated except in the simplest examples, and it was therefore considered more practical in the work which follows to use a finite-difference technique for this type of joint. Both methods are, however, presented herein.

The analytical solution gives, similarly to Eq. 26,

$$f'''_{pi} + P_1 f''_{pi} + P_2 f'_{pi} = F_{pi}, \qquad i \neq p \dots\dots\dots\dots (32)$$

in which

$$F_{pi} = -\frac{2}{m_p L_p}\left(f''_p\cos\theta_{ip} + \sum_{k=1}^{n}\frac{\sin\theta_{kp}\sin\theta_{ki}}{m_k L_k}f'_p\right) \dots\dots\dots (33)$$

If $i = p$, f'_{pi} is replaced by $f'_{pp} - f'_p$.

If t_0 is the time at which the incoming wave arrives at this joint, the solution of Eq. 32 satisfying the conditions that the velocity of the striking mass is continuous at $t = t_0$, is

$$f' = a^2 e^{-r_1 a t}\int_{t_0}^{t}\left[e^{(r_1 - r_2)at}\int_{t_0}^{t} e^{r_2 a t}F_{pi}\,dt\right]dt \dots\dots\dots\dots (34)$$

The basic equations for the finite-difference solution (Eqs. 23 and 31*b*) are

$$\begin{aligned} f''_{pi} + \frac{f'_{pi}}{\sin\theta_{ji}} \sum_{k=1}^{n} \frac{\sin\theta_{jk}\cos\theta_{ik}}{m_k L_k} \\ + \frac{f'_{pi}}{\sin\theta_{ji}} \sum_{k=1}^{n} \frac{\sin\theta_{ki}\cos\theta_{ik}}{m_k L_k} = -\frac{2 f'_p}{m_p L_p} \cos\theta_{pi} \quad \text{..(35}a) \end{aligned}$$

and

$$\begin{aligned} f''_{pi} + \frac{f'_{pi}}{\sin\theta_{ji}} \sum_{k=1}^{n} \frac{\sin\theta_{jk}\cos\theta_{jk}}{m_k L_k} \\ + \frac{f'_{pi}}{\sin\theta_{ji}} \sum_{k=1}^{n} \frac{\sin\theta_{ki}\cos\theta_{jk}}{m_k L_k} = -\frac{2 f'_p}{m_p L_p} \cos\theta_{pj} \quad \text{..(35}b) \end{aligned}$$

for $i, j \neq p$. Letting

$$f''_{pi} = \frac{f'_{pi}(\tau + \Delta\tau) - f'_{pi}(\tau)}{\Delta\tau} \quad \text{..................(36)}$$

developing a similar expression for f''_{pj}, and using the average values of the functions, f'_{pi} and f'_{pj}, within each interval, $\Delta\tau$, one obtains the final finite-difference equations:

$$\begin{aligned} & f'_{pi}\,(\tau + \Delta\tau) \left\{ 1 + \frac{\Delta\tau}{2\sin\theta_{ji}} \sum_{k=1}^{n} \frac{\sin\theta_{jk}\cos\theta_{ik}}{m_k L_k} \right\} + f'_{pj}\,(\tau + \Delta\tau) \left\{ \frac{\Delta\tau}{2\sin\theta_{ji}} \right. \\ & \left. \times \sum_{k=1}^{n} \frac{\sin\theta_{ki}\cos\theta_{ki}}{m_k L_k} \right\} = -\,\Delta\tau \left\{ \frac{f'_p\,(\tau + \Delta\tau) + f'_p\,(\tau)}{m_p L_p} \cos\theta_{ip} - \left[\frac{1}{\Delta\tau} \right. \right. \\ & \left. \left. - \frac{1}{2\sin\theta_{ji}} \sum_{k=1}^{n} \frac{\sin\theta_{jk}\cos\theta_{ik}}{m_k L_k} \right] f'_{pi}\,(\tau) + \frac{f'_{pj}\,(\tau)}{2\sin\theta_{ji}} \sum_{k=1}^{n} \frac{\sin\theta_{ki}\cos\theta_{ki}}{m_k L_k} \right\} \quad \text{..(37}a) \end{aligned}$$

$$\begin{aligned} & f'_{pi}\,(\tau + \Delta\tau) \left\{ \frac{\Delta\tau}{2\sin\theta_{ji}} \sum_{k=1}^{n} \frac{\sin\theta_{jk}\cos\theta_{jk}}{m_k L_k} \right\} + f'_{pj}\,(\tau + \Delta\tau) \left\{ 1 + \frac{\Delta\tau}{2\sin\theta_{ji}} \right. \\ & \left. \times \sum_{k=1}^{n} \frac{\sin\theta_{ki}\cos\theta_{ki}}{m_k L_k} \right\} = -\,\Delta\tau \left\{ \frac{f'_p\,(\tau + \Delta\tau) + f'_p\,(\tau)}{m_p L_p} \cos\theta_{jp} + \frac{f'_{pi}\,(\tau)}{2\sin\theta_{ji}} \right. \\ & \left. \times \sum_{k=1}^{n} \frac{\sin\theta_{jk}\cos\theta_{jk}}{m_k L_k} - \left[\frac{1}{\Delta\tau} - \frac{1}{2\sin\theta_{ji}} \sum_{k=1}^{n} \frac{\sin\theta_{ki}\cos\theta_{jk}}{m_k L_k} \right] f'_{pj}\,(\tau) \right\} \quad \text{..(37}b) \end{aligned}$$

It should be noted that, as in Eqs. 31, the quantity, f'_{pi}, appearing in Eqs. 35 must be replaced by $f'_{pp} - f'_p$ when $i = p$. From this point, the solution is purely numerical.

Type d.—A joint on a roller support has only one degree of freedom; this type of constraint is obtained by letting the direction, k, in Eq. 20 be that of the reaction; then $u_k = 0$ and

$$\frac{u_i}{\sin\theta_{iR}} = \frac{u_j}{\sin\theta_{jR}} = \ldots = \frac{u_n}{\sin\theta_{nR}} \quad \text{................(38)}$$

As in the case of Eq. 22,

$$\frac{f'_{pi}}{\sin \theta_{iR}} = \frac{f'_{pj}}{\sin \theta_{jR}} = \frac{f'_{pp} - f'_p}{\sin \theta_{pR}} = \ldots = \frac{f'_{pn}}{\sin \theta_{nR}} \tag{39}$$

Selecting again two independent equations from the governing set,

$$\sum_{j=1}^{n} \sigma_j A_j \cos \theta_{ij} + R \cos \theta_{iR} = 0 \tag{40}$$

one may solve for the unknown reaction, R, and the stress in the independent bar by purely algebraic manipulation. The result for the latter is given in Eqs. 18 and for the former is

$$R = \frac{-2 E f'_p \sum_{i=1}^{n} \sin \theta_{iR} \sin \theta_{pi} A_i A_p}{\sum_{i=1}^{n} (\sin^2 \theta_{iR}) A_i} \tag{41}$$

The angle between the ith bar and the reaction is denoted by θ_{iR}.

Type e.—Type e joints do not displace; therefore, all values of u_i and σ_i vanish with the exception of σ_p which can be obtained from Eqs. 11 as

$$f'_{pp} = f'_p \tag{42}$$

The distribution factors for joints of type e are $D_{pi} = 0$ for $i \neq p$ and $D_{pp} = 1$. The reaction is equal and opposite to $\sigma_p A_p$.

Criterion for the End of Impact

If a rigid mass, M, moves in space with a certain velocity and its uniform motion is then disturbed by a collision with an elastic object—in this case, the joint of a truss—its velocity will change both in magnitude and direction and will be, in fact, identical with that of the joint. Eventually, however, the mass will leave the joint either by rebounding or by slipping off. The time at which this happens is the time of end of impact.

Immediately after the start of impact, the mass and joint move together in some curvilinear path—that is, at any one time the mass is restrained from escaping along the tangent to that path with its instantaneous velocity (as it tends to do because of its inertia) by the interference provided by the truss. Should that interference suddenly end, the mass will of course leave and impact will cease. The meaning of the term "interference," as used herein, must now be made precise.

The striking mass is assumed to hit the loaded joint, which is either of type a or of type c, within the angle defined by the ith and the $(i + 1)$th bars, so that $0 \leq \theta_{iV} \leq \theta_{i,i+1}$. The velocity with which the joint and the mass are moving at a certain instant $t = t_0$ may be denoted by V; the subsequent motion of the joint and of the mass must now be investigated on the hypothesis that impact ends at that instant. The mass will then travel in a straight line a distance $(V\,dt)$ during a short interval dt. The joint will be one of type b

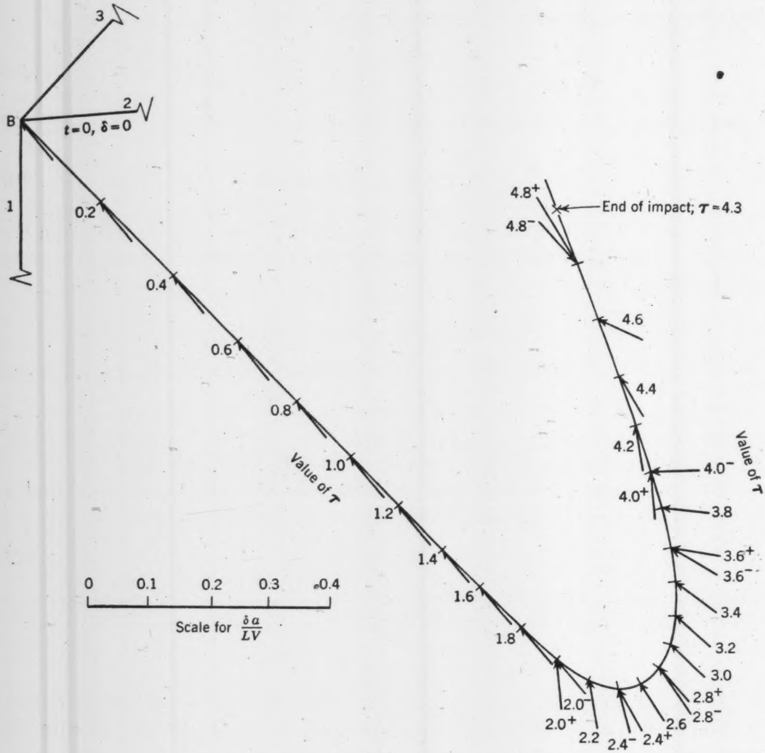

FIG. 3.—DISPLACEMENTS OF JOINT B OF FIG. 1

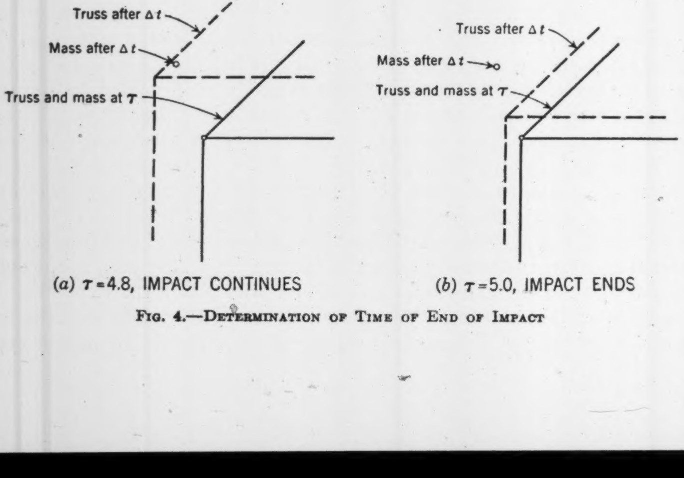
Truss after Δt
Mass after Δt
Truss and mass at τ
Truss after Δt
Mass after Δt
Truss and mass at τ

(*a*) $\tau=4.8$, IMPACT CONTINUES (*b*) $\tau=5.0$, IMPACT ENDS

FIG. 4.—DETERMINATION OF TIME OF END OF IMPACT

during that interval and will therefore travel along a cuve so that, in general, the final positions of joint and mass will not coincide. The positions of bars i and $(i + 1)$ will have changed slightly during the interval dt; in certain cases the mass will be found to be (after the foregoing straight-line displacement) outside the angle defined by these bars. As the mass was originally taken to be within this angle, the situation just described is physically impossible and it may be concluded that interference exists. In such a case, therefore, impact will continue. On the other hand, should no interference arise between the position of the mass and that of the truss, the calculations mentioned previously would yield the actual motion of the system, and impact would have ended. These conditions are illustrated in Figs. 3 and 4 for the example of the truss of Fig. 1.

The following criterion for the time of end of impact may now be written; a necessary and sufficient condition for impact to continue is the persistence of interference as previously defined or, in other words, impact will end the first time that interference is not present. Practical use of this criterion may be quite laborious for some cases. The computations may be shortened by observing that interference will always exist when the component of the force, F (on the mass), between mass and joint parallel to the direction of the mass velocity, V, has the same sense as V, namely, when

$$F \cdot V \leq 0 \qquad (43a)$$

in which the dot indicates the scalar product. It is thus sufficient to restrict the investigation of interference to the times at which Eq. 43*a* fails—that is, only the limiting case

$$F \cdot V = 0 \qquad (43b)$$

need be considered. It is of interest to note some special problems in which the limiting case of Eq. 43*b* holds. The most important of these is the example of longitudinal impact on the free end of a single bar. In this case $F \cdot V < 0$ until the time of maximum deflection, when $V = 0$ and therefore $F \cdot V = 0$. However, inspection shows that interference is always present and hence impact persists. As the mass rebounds, Eq. 43*a* holds until $F = 0$; at this time again $F \cdot V = 0$, and impact will end. A similar situation will arise in all cases in which the direction of the mass velocity (and force) is unchanged during impact, as in the case whenever a symmetrical truss is subjected to impact in its plane of symmetry.

Numerical Solution and Illustrative Example

The truss of Fig. 1 which is used in this example allows no simplifications such as might be caused by conditions of symmetry or by a too-restricted number of bars and of joints. Furthermore, it contains joints of all five types. The loading is applied by collision with a solid object; a solution corresponding to a prescribed force would be considerably simpler and is briefly cited subsequently.

The steps in the proposed numerical solution are as follows:

1. A scale drawing is made of the truss in question and all the mechanical and geometrical parameters that are required in the solution are listed. For Fig. 1 they are:

$$A_1 = A_2 = A_3 = A_4 = A_5 = A_6 = A_7 = 1$$

$$L_1 = \frac{L_2}{1.2} = \frac{L_3}{1.4} = L_4 = \frac{L_5}{1.6} = \frac{L_6}{1.8} = \frac{L_7}{2.4} = 1$$

$$m_1 = 2,\ m_2 = \tfrac{5}{3},\ m_3 = \tfrac{10}{7},\ m_4 = 2,\ m_5 = \tfrac{5}{8},\ m_6 = \tfrac{10}{9},\ m_7 = \tfrac{5}{6}$$

$$m_1 L_1 = m_2 L_2 = m_3 L_3 = m_4 L_4 = m_5 L_5 = m_6 L_6 = m_7 L_7 = 2$$

TABLE 1.—DISTRIBUTION FACTORS D_{pi} FOR FIG. 1

Joint	Value of p	VALUE OF i						
		1	2	3	4	5	6	7
A	1	1	...	...	...	0	...	...
	5	0	...	...	...	1	...	...
B	1	−0.49699	−0.48756	0.71783	...	...	...	...
	2	−0.48756	−0.52741	−0.69579	...	...	...	...
	3	0.71783	−0.69579	0.02440	...	...	...	...
C	2	...	0.22876	...	−0.18956	−0.58000	0.75850	...
	4	...	−0.18956	...	−0.41442	0.72887	0.51094	...
	5	...	−0.58000	...	0.72887	0.00864	0.36368	...
	6	...	0.75850	...	0.51094	0.36368	0.17703	...
D	3	...	...	−0.56753	−0.62654	...	...	0.53419
	4	...	...	−0.62654	−0.09230	...	...	−0.77390
	7	...	...	0.53419	−0.77390	...	...	−0.34017
E	6	...	...	...	...	...	−0.27420	−0.96167
	7	...	...	...	...	...	−0.96167	0.27420

2. The distribution factors D_{ip} are listed for all bars at all joints, as in Table 1. The distribution factors listed in Table 1 for joint B (loaded joint) will be needed for the computation of the time of end of impact and if the calculations are to be continued beyond that time.

3. A total of 2 n tables are prepared, in which n is the number of bars meeting at the struck joint; in this case, $n = 3$. Of these tables one-half will be used for incoming (traveling toward the loaded joint) waves and the other half will be used for outgoing (traveling away from the loaded joint) waves. The tables required in the present problem are included herein as Tables 2 and 3, respectively, for the first and second halves of the 2 n tables. The first column of each part of Tables 2 and 3 gives the time, τ, in nondimensional form ($\tau = a\,t/L$). The characteristic length, L, was chosen in this case as the length of the shortest bar—that is, $L = L_1 = 1$. It is convenient to list the quantity, τ, in equal intervals of magnitude, $\Delta\tau$, chosen in such a way that the quantity, L_i/L, is, for all bars, an integral multiple of $\Delta\tau$. In the present example, $\Delta\tau = 0.2$.

4. As soon as impact starts, the loaded joint B is of type a (item *a*). From Eq. 28 the functions f' for any two (for example, the ith and jth) bars meeting at

TABLE 2.—INCOMING WAVES AT JOINT B

(a) Bar 1

τ	f_{I1}
2.0 −	0
2.0 +	0.72166
2.2	0.65213
2.4	0.58967
2.6	0.53350
2.8	0.48291
3.0	0.43733
3.2	0.39622
3.4	0.35911
3.6	0.32558
3.8	0.29527
4.0 −	0.26786
4.0 +	0.98952
4.2	0.76756
4.4	0.58523
4.6	0.43641
4.8	0.31338
5.0	0.21619

(b) Bar 2

τ	f_{22}	f_{242}	f_{2442}	f_{24442}	f_{2552}	f_{2662}	f_{744442}	f_{2762}	f_{I2}
2.4	0.14989	. . .	. . .	. . .	. . .	. . .	. . .	. . .	0.14989
2.6	0.13723	. . .	. . .	. . .	. . .	. . .	. . .	. . .	0.13723
2.8	0.12554	. . .	. . .	. . .	. . .	. . .	. . .	. . .	0.12554
3.0	0.11477	. . .	. . .	. . .	. . .	. . .	. . .	. . .	0.11477
3.2	0.10487	. . .	. . .	. . .	. . .	. . .	. . .	. . .	0.10487
3.4	0.09577	. . .	. . .	. . .	. . .	. . .	. . .	. . .	0.09577
3.6 −	0.08742	. . .	. . .	. . .	. . .	. . .	. . .	. . .	0.08742
3.6 +	0.08742	−0.00721	. . .	. . .	. . .	. . .	. . .	. . .	0.08021
3.8	0.07977	−0.00589	. . .	. . .	. . .	. . .	. . .	. . .	0.07388
4.0	0.07276	−0.00481	. . .	. . .	. . .	. . .	. . .	. . .	0.06795
4.2	0.06634	−0.00393	. . .	. . .	. . .	. . .	. . .	. . .	0.06241
4.4 −	0.06047	−0.00321	. . .	. . .	. . .	. . .	. . .	. . .	0.05726
4.4 +	0.06047	−0.00321	−0.00217	. . .	. . .	. . .	. . .	. . .	0.05509
4.6	0.05583	−0.00263	−0.00199	. . .	. . .	. . .	. . .	. . .	0.05121
4.8 −	0.05008	−0.00215	−0.00182	. . .	. . .	. . .	. . .	. . .	0.04611
4.8 +	0.08437	−0.00215	−0.00182	. . .	. . .	. . .	. . .	. . .	0.08040
5.0	0.06904	−0.00176	−0.00166	. . .	. . .	. . .	. . .	. . .	0.06562
5.2	0.05509	−0.00144	−0.00152	. . .	. . .	. . .	. . .	. . .	0.05213
5.4	0.04161	−0.00118	−0.00139	. . .	. . .	. . .	. . .	. . .	0.03904
5.6 −	0.02983	−0.00097	−0.00127	. . .	. . .	. . .	. . .	. . .	0.02759
5.6 +	0.02983	−0.00097	−0.00127	−0.00028	0.22043	. . .	. . .	. . .	0.24774
5.8	0.01960	0.01008	−0.00116	−0.00023	0.20181	. . .	. . .	. . .	0.23010
6.0 −	0.01110	0.01803	−0.00106	−0.00018	0.18462	. . .	. . .	. . .	0.21251
6.0 +	0.00945	0.01803	−0.00106	−0.00018	0.18462	−0.10339	. . .	. . .	0.10747
6.2	0.00025	0.02135	−0.00096	−0.00015	0.16879	−0.09465	. . .	. . .	0.09463
6.4 −	−0.00734	0.02340	−0.00088	−0.00012	0.15422	−0.08659	. . .	. . .	0.08269
6.4 +	−0.00734	0.02749	−0.00088	−0.00012	0.15422	−0.08659	−0.00009	. . .	0.08669
6.6	−0.01296	0.02715	−0.00081	−0.00010	0.14084	−0.07916	−0.00008	. . .	0.07494
6.8 −	−0.01879	0.02647	−0.00073	−0.00008	0.12856	−0.07233	−0.00007	. . .	0.06303
6.8 +	−0.01929	0.02647	−0.00122	−0.00008	0.12856	−0.07233	−0.00007	0.02365	0.08567
7.0	−0.02463	0.02554	−0.00100	−0.00007	0.11730	−0.06606	−0.00007	0.01931	0.07033

(c) Bar 3

τ	f_{33}	f_{243}	f_{2443}	f_{I3}
2.8	0.03444	. . .	. . .	0.03444
3.0	0.02813	. . .	. . .	0.02813
3.2	0.02298	. . .	. . .	0.02298
3.4	0.01878	. . .	. . .	0.01878
3.6 −	0.01535	. . .	. . .	0.01535
3.6 +	0.01535	0.07785	. . .	0.09320
3.8	0.01255	0.07127	. . .	0.08382
4.0	0.01027	0.06520	. . .	0.07547
4.2	0.00841	0.05961	. . .	0.06802
4.4	0.00689	0.05447	. . .	0.06136
4.6	0.00565	0.04974	. . .	0.05539
4.8 −	0.00463	0.04541	. . .	0.05004
4.8 +	0.00463	0.04541	0.00987	0.05991
5.0	−0.04816	0.04143	0.00806	0.00133

TABLE 3.—OUTGOING

(a) Bar 1							(b) Bar 2			
τ	f_1	f_{I1}	$f_{1B1}-f_{I1}$	f_{2B1}	f_{3B1}	fO_1	τ	f_2	f_{1B2}	f_{I2}
0	0.72166	...	...	...	...	0.72166	0	0.65529	...	...
0.2	0.65213	...	...	...	...	0.65213	0.2	0.59992	...	...
0.4	0.58967	...	...	...	...	0.58967	0.4	0.54883	...	...
0.6	0.53350	...	...	...	...	0.53350	0.6	0.50177	...	...
0.8	0.48291	...	...	...	...	0.48291	0.8	0.45846	...	...
1.0	0.43733	...	...	...	...	0.43733	1.0	0.41869	...	...
1.2	0.39622	...	...	...	...	0.39622	1.2	0.38219	...	...
1.4	0.35911	...	...	...	...	0.35911	1.4	0.34873	...	...
1.6	0.32558	...	...	...	...	0.32558	1.6	0.31808	...	...
1.8	0.29527	...	...	...	...	0.29527	1.8	0.29004	...	...
2.0 −	0.26786	...	...	...	...	0.26786	2.0	0.26438	0	...
2.0 +	0.26786	0.72166	0	...	...	0.98952	2.2	0.24095	0.00312	...
2.2	0.24306	0.65213	−0.12763	...	...	0.76756	2.4 −	0.21952	−0.00057	...
2.4	0.22059	0.58967	−0.22503	0	...	0.58523	2.4 +	0.21952	−0.00057	0.14989
2.6	0.20025	0.53350	−0.29799	0.00065	...	0.43641	2.6	0.19998	−0.00866	0.13723
2.8	0.18181	0.48291	−0.35123	−0.00011	0	0.31338	2.8	0.18213	−0.01937	0.12554
3.0	0.16510	0.43733	−0.38861	−0.00181	0.00418	0.21619	3.0	0.16585	−0.03136	0.11477
3.2	0.14995	0.39622	−0.41329	−0.00407	0.00681	0.13562	3.2	0.15101	−0.04369	0.10487
3.4	0.13620	0.35911	−0.42784	−0.00668	0.00833	0.06912	3.4	0.13747	−0.05569	0.09577
3.6	0.12374	0.32558	−0.43437	−0.00936	0.00905	0.01464	3.6 −	0.12514	−0.06690	0.08742
3.8	0.11242	0.29527	−0.43459	−0.01190	0.01917	−0.01963	3.6 +	0.12514	−0.06690	0.08021
4.0 −	0.10215	0.26786	−0.42990	−0.01424	0.02623	−0.04790	3.8	0.11390	−0.07703	0.07388
4.0 +	0.10215	0.98952	−0.42990	−0.01424	0.02623	0.67376	4.0	0.10366	−0.08591	0.06795
4.2	0.09282	0.76756	−0.53720	−0.01636	0.03093	0.33775	4.2	0.09433	−0.09063	0.06241
4.4	0.08435	0.58523	−0.59219	−0.01819	0.03380	0.09300	4.4 −	0.08584	−0.10074	0.05726
4.6	0.07666	0.43641	−0.60922	−0.01977	0.03531	−0.08061	4.4 +	0.08584	−0.10074	0.05509
4.8	0.06968	0.31338	−0.59919	−0.02106	0.03577	−0.20142	4.6	0.07810	−0.11284	0.05121
5.0	0.06334	0.21619	−0.57067	−0.02196	0.03315	−0.27995	4.8 −	0.07106	−0.12471	0.04617
							4.8 +	0.07106	−0.12471	0.08040
							5.0	0.06465	−0.13498	0.06562

that joint are determined; the values of f'_k for the kth bar are then computed from Eq. 22. The final numerical results are

$$\left(\frac{a}{V}\right) f'_1(\tau) = 0.04356\, e^{-r_1 \tau} + 0.67810\, e^{-r_2 \tau} \qquad (44a)$$

$$\left(\frac{a}{V}\right) f'_2(\tau) = -\,0.04246\, e^{-r_1 \tau} + 0.69775\, e^{-r_2 \tau} \qquad (44b)$$

and

$$\left(\frac{a}{V}\right) f'_3(\tau) = -\,0.05936\, e^{-r_1 \tau} + 0.00133\, e^{-r_2 \tau} \qquad (44c)$$

in which $r_1 = -\,1.02501$ and $r_2 = -\,0.47499$. The values of these f'-functions are entered (for the appropriate values of τ) in the second column of Tables 3(*a*), 3(*b*), and 3(*c*). These quantities represent all the waves present at the loaded joint until the first reflected wave arrives. The stresses σ_i and velocities $\partial u_i/\partial t$ during this period can then be easily found from Eqs. 3 and 4.

5. Item *b* is next considered. Tables 2(*a*), 2(*b*), and 2(*c*) are filled in according to Eqs. 13 and 15 for all times, τ, for which this can be done without consideration of any joints of type c. For example, wave f'_{342} in Table 2(*b*) arrives at joint B at $\tau = (L_3 + L_4 + L_2)/L = 3.6$; hence, all entries for this wave are

WAVES AT JOINT B

(*b*) Bar 2			(*c*) Bar 3						
$f_{2B2}-f_{I2}$	f_{3B2}	$f0_2$	τ	f_3	f_{1B3}	f_{2B3}	f_{I3}	$f_{3B3}-f_{I3}$	$f0_3$
...	...	0.65529	0	−0.06069	...	...	...	...	−0.06069
...	...	0.59992	0.2	−0.04957	...	...	...	...	−0.04957
...	...	0.54883	0.4	−0.04049	...	...	...	...	−0.04049
...	...	0.50177	0.6	−0.03309	...	...	...	...	−0.03309
...	...	0.45846	0.8	−0.02705	...	...	...	...	−0.02705
...	...	0.41869	1.0	−0.02212	...	...	...	...	−0.02212
...	...	0.38219	1.2	−0.01810	...	...	...	...	−0.01810
...	...	0.34873	1.4	−0.01482	...	...	...	...	−0.01482
...	...	0.31808	1.6	−0.01214	...	...	...	...	−0.01214
...	...	0.29004	1.8	−0.00995	...	...	...	...	−0.00995
...	...	0.26438	2.0	−0.00816	0	...	...	...	−0.00816
...	...	0.24407	2.2	−0.00669	0.09155	...	...	...	0.08486
...	...	0.21895	2.4	−0.00550	0.15730	0	...	...	0.15180
0	...	0.36884	2.6	−0.00452	0.20293	−0.01860	...	...	0.17981
−0.02671	...	0.30184	2.8−	−0.00372	0.23296	−0.03216	...	...	0.19708
−0.04746	0	0.24084	2.8+	−0.00372	0.23296	−0.03216	0.03444	0	0.23152
−0.06332	−0.00405	0.18189	3.0	−0.00306	0.25101	−0.04174	0.02813	−0.00568	0.22866
−0.07516	−0.00661	0.13042	3.2	−0.00252	0.25993	−0.04820	0.02298	−0.00926	0.22293
−0.08379	−0.00809	0.08567	3.4	−0.00208	0.26198	−0.05223	0.01878	−0.01133	0.21512
−0.08833	−0.00880	0.04853	3.6−	−0.00172	0.25894	−0.05344	0.01535	−0.01232	0.20681
−0.08833	−0.00880	0.04132	3.6+	−0.00172	0.25894	−0.05344	0.09320	−0.01232	0.28466
−0.09101	−0.01863	0.00111	3.8	−0.00143	0.25221	−0.05348	0.08382	−0.02609	0.25503
−0.09230	−0.02548	−0.03208	4.0	−0.00118	0.24289	−0.05271	0.07547	−0.03569	0.22878
−0.09246	−0.03003	−0.05638	4.2	−0.00098	0.31488	−0.05134	0.06802	−0.04207	0.28851
−0.09170	−0.03282	−0.08216	4.4	−0.00082	0.34654	−0.04954	0.06136	−0.04598	0.31156
−0.09170	−0.03282	−0.08433	4.6	−0.00068	0.35026	−0.04720	0.05539	−0.04802	0.30975
−0.08989	−0.03427	−0.10769	4.8−	−0.00057	0.33517	−0.04472	0.05004	−0.04865	0.29127
−0.08757	−0.03472	−0.12977	4.8+	−0.00057	0.33517	−0.04472	0.50991	−0.04865	0.30114
−0.08757	−0.03472	−0.09554	5.0	−0.00050	0.30821	−0.04583	0.00133	−0.04507	0.21814
−0.09016	−0.03216	−0.12703							

zero for $0 < \tau < 3.6$. The first reflected wave to reach joint B is that traveling along the shortest bar and is, in this example, f'_{11}; this wave arrives at B when $\tau = 2\,L_1/L = 2$; at that time it is divided (joint of type c) among bars 1, 2, and 3. In particular, this last fraction of f'_{11} will be felt as part of f'_{342} as an incoming wave at joint B when $\tau = 3.6 + 2\,L_1/L = 5.6$. Hence, entries for f'_{342} in Table 2(*b*) can be made during this step for the range $3.6 < \tau < 5.6$. It should be noted that all entries are zero for $0 < \tau < 2\,L_i/L$ in the table corresponding to the *i*th bar. The sum of all incoming waves is written in the last column on the right in Tables 2 and is denoted by f_{Ii} for the *i*th bar.

6. At this time the loaded joint is considered as one of type c and the distribution of an incoming wave there is examined (item *c*). Such a distribution can no longer be effected, as in step 5 for joints of type b, simply by multiplication by a distribution factor; use of Eqs. 37 is therefore suggested. In the present case these equations reduce (with $i = 2$, $j = 3$, and $\Delta\tau = 0.2$) to

$$10.47577\,f'_{pB2}\,(\tau + 0.2) + 0.39282\,f'_{pB3}\,(\tau + 0.2) = -\,[f'_p\,(\tau + 0.2) + f'_p\,(\tau)]\cos\theta_{2p} - 9.52423\,f'_{pB2}\,(\tau) + 0.39282\,f'_{pB3}\,(\tau) \quad \text{..(45}a\text{)}$$

and

$$0.00106\,f'_{pB2}\,(\tau + 0.2) + 11.02425\,f'_{pB3}\,(\tau + 0.2) = -\,[f'_p\,(\tau + 0.2) + f'_p\,(\tau)]\cos\theta + 0.00106\,f'_{pB2}\,(\tau) - 8.97575\,f'_3\,(\tau) \quad \text{..(45}b\text{)}$$

in which $p = 1, 2$, or 3 depending on the bar traveled by the incoming wave. For this joint, Eq. 22 becomes

$$0.69986\,f'_{pB1} - 0.67837\,f'_{pB2} + 0.99875\,f'_{pB3} = 0 \ldots\ldots\ldots (46)$$

The term f'_{pBi} denotes the influence on bar i of the total wave entering joint B through bar p. It should be noted that, according to Eqs. 30, f'_{pBp} must be replaced by $f'_{pBp} - f'_{Ip}$. In the details of the numerical solution, the quantity, $-f'_{Ip}$, is entered first in the pth of Tables 3; it represents the wave arriving along the pth bar. Then the quantities f'_{pBi} are calculated by simultaneous solution of Eqs. 45 and subsequent use of Eq. 46. The initial conditions for Eqs. 45 are obtained from the fact that there cannot be, at a loaded joint, any sudden change in velocity; therefore, all functions, f'_{pBi}, for $i \neq p$ (and $f'_{pBp} - f'_{Ip}$ if $i = p$) must vanish at the time of arrival of the incoming wave.

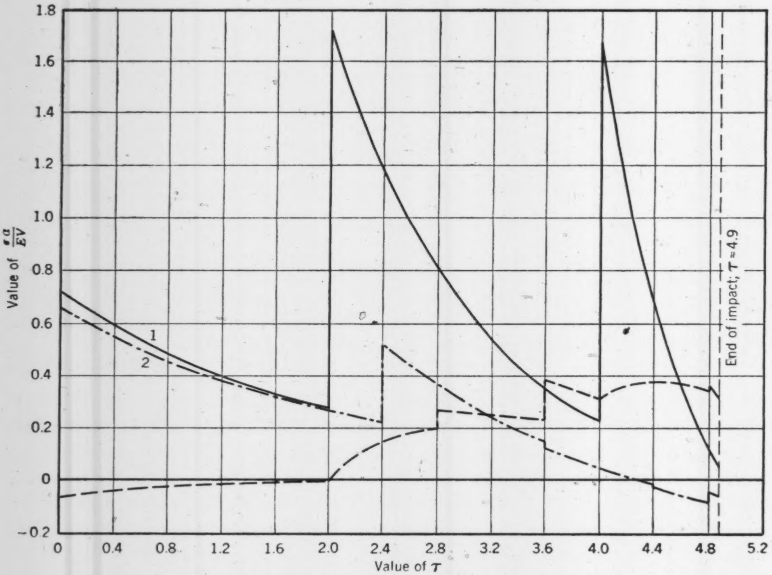

FIG. 5.—STRESSES AT JOINT B IN BARS 1, 2, AND 3 OF FIG. 1

7. The sum of all the columns of each of Tables 3, for the rows which have been completed, is listed in the last column on the right in each table. This column is denoted as f'_{0i} for the ith table of Tables 3 and represents the total outgoing wave in bar i at the loaded joint. The stress σ_i and the velocity $\partial u_i/\partial t$ in bar i at that joint are then

$$\sigma_i \frac{a}{E\,V} = -f'_{Ii} - f'_{0i} \ldots\ldots\ldots\ldots\ldots\ldots (47a)$$

and

$$\frac{1}{a}\frac{\partial u_i}{\partial t} = f'_{Ii} - f'_{0i} \quad \text{(47b)}$$

which may be calculated for all times by means of the previously described steps. Their values in the present problem are listed in Table 4, and the stresses in bars 1, 2, and 3 are plotted in Fig. 5.

The resultant velocity, V, of the loaded joint, the resultant force, F, acting on the striking mass, and the angles, θ_{Vi} and θ_{Fi}, between bar i and these quantities are also given in Table 4. These terms were computed from

$$V^2 \sin^2 \theta_{ij} = \left(\frac{\partial u_i}{\partial t} - \frac{\partial u_j}{\partial t}\cos\theta_{ij}\right)^2 + \left(\frac{\partial u_j}{\partial t}\sin\theta_{ij}\right)^2 \quad \text{(48a)}$$

$$\cos\theta_{Vi} = \frac{1}{V}\frac{\partial u_i}{\partial t} \quad \text{(48b)}$$

$$F^2 = \left(\sum_{j=1}^{n} \sigma_j A_j \cos\theta_{ij}\right)^2 + \left(\sum_{j=1}^{n} \sigma_j A_j \sin\theta_{ij}\right)^2 \quad \text{(48c)}$$

and

$$\tan\theta_{Fi} = \frac{\sum_{j=1}^{n} \sigma_j A_j \sin\theta_{ij}}{\sum_{j=1}^{n} \sigma_j A_j \cos\theta_{ij}} \quad \text{(48d)}$$

The displacement, δ, of the loaded joint at any time is

$$\vec{\delta} = \Sigma\, \vec{V}\, \Delta t \quad \text{(49)}$$

where the terms under the summation must be added vectorially, a process which is here most conveniently performed graphically. In the present numerical examples the average value of the velocity within each interval, Δt, was used. A plot of the displacement of the loaded joint is shown in Fig. 3.

Duration of Impact.—It has been shown that impact can end only when Eq. 43b holds; in the present example this is true for $0 < \tau < 2.7$ and $4.7 < \tau$. These limiting values are approximate; they correspond to the time at which

$$\tan\theta_{Vi}\tan\theta_{Fi} + 1 = 0 \quad \text{(50)}$$

and can be obtained by inspection of Table 4. The final determination of the time of end of impact requires use of the definition of interference and is illustrated in Figs. 4(*a*) and 4(*b*), respectively, for presence and absence of interference. The velocities of the mass and joint are required for drawing these figures; the quantity, $\partial u_i/\partial t$, is given by Eq. 47b in the case of the mass and by the relationship,

$$\frac{1}{a}\left(\frac{\partial u_i}{\partial t}\right)_{joint} = -f'_{Ii} + \sum_{j=1}^{n} D_{ij} f'_{Ij} \quad \text{(51)}$$

in the case of the joint (considered temporarily as one of type b). The approximate time of end of impact for the illustrative example is $\tau = 4.9$.

TABLE 4.—MAGNITUDES AND DIRECTIONS OF STRESSES, VELOCITIES, AND FORCE AT JOINT B IN BARS 1, 2, AND 3 OF FIG. 1

τ	$\frac{\sigma_1 a}{E V}$	$\frac{\sigma_2 a}{E V}$	$\frac{\sigma_3 a}{E V}$	$F_{\parallel 1} \frac{a}{E V}$	$F_{\perp 1} \frac{a}{E V}$	$\tan \theta_{F1}$	θ_{F1}	$\frac{1}{V} \frac{\partial u_1}{\partial t}$	$\frac{1}{V} \frac{\partial u_2}{\partial t}$	$\frac{1}{V} \frac{\partial u_3}{\partial t}$	$\frac{1}{V} \frac{\partial u_{\perp 1}}{\partial t}$	$\frac{1}{V} \frac{\partial u}{\partial t}$	$\tan \theta_{V1}$	θ_{V1}	$\tan \theta_{F1} \times \tan \theta_{V1}$
0	0.72166	0.65529	−0.06069	0.73348	0.61330	0.83615	219°54′	0.72166	0.65529	−0.06069	0.69225	1.00000	0.95925	43°48′	0.80208
0.2	0.65213	0.59992	−0.04957	0.65855	0.56554	0.85877	220°39′	0.65213	0.59992	−0.04957	0.63332	0.90905	0.97116	44°10′	0.83400
0.4	0.58967	0.54883	−0.04049	0.59197	0.52068	0.87957	221°20′	0.58967	0.54883	−0.04049	0.57904	0.82644	0.98197	44°29′	0.86371
0.6	0.53350	0.50177	−0.03309	0.53272	0.47870	0.89859	221°57′	0.53350	0.50177	−0.03309	0.52911	0.75139	0.99177	44°46′	0.89119
0.8	0.48291	0.45846	−0.02705	0.47986	0.43954	0.91597	222°29′	0.48291	0.45846	−0.02705	0.48321	0.68315	1.00062	45° 1′	0.91653
1.0	0.43733	0.41869	−0.02212	0.43264	0.40316	0.93186	222°59′	0.43733	0.41869	−0.02212	0.44111	0.62116	1.00864	45°15′	0.93991
1.2	0.39622	0.38219	−0.01810	0.39041	0.36943	0.94627	223°25′	0.39622	0.38219	−0.01810	0.40251	0.56481	1.01588	45°27′	0.96130
1.4	0.35911	0.34873	−0.01482	0.35256	0.33824	0.95938	223°49′	0.35911	0.34873	−0.01482	0.36715	0.51357	1.02239	45°38′	0.98086
1.6	0.32558	0.31808	−0.01214	0.31859	0.30945	0.97130	224°10′	0.32558	0.31808	−0.01214	0.33478	0.46699	1.02826	45°48′	0.99875
1.8	0.29527	0.29004	−0.00995	0.28808	0.28293	0.98211	224°29′	0.29527	0.29004	−0.00995	0.30519	0.42465	1.03360	45°57′	1.01511
2.0 −	0.26786	0.26438	−0.00816	0.26063	0.25851	0.99188	224°46′	0.26786	0.26438	−0.00816	0.27812	0.38613	1.03830	46° 5′	1.02987
2.0 +	1.71118	0.26438	−0.00816	1.70395	0.25851	0.15171	188°38′	0.26786	0.26438	−0.00816	0.27812	0.38613	1.03830	46° 5′	0.15752
2.2	1.41969	0.24407	0.08486	1.34514	0.30133	0.22401	192°38′	0.11543	0.24407	0.08486	0.25016	0.27551	2.16720	65°14′	0.48547
2.4 −	1.17490	0.21895	0.15180	1.05242	0.32165	0.30563	197° 0′	−0.00444	0.21895	0.15180	0.21900	0.21905	−49.32432	91°10′	−15.07499
2.4 +	1.17490	0.51873	0.15180	1.03743	0.62106	0.59865	210°54′	−0.00444	0.21895	0.15180	0.21900	0.21905	−49.32432	91°10′	−29.52800
2.6	0.96991	0.43907	0.17981	0.81584	0.56050	0.68702	214°30′	−0.09709	0.16461	0.17981	0.15995	0.18711	−1.64744	121°15′	−1.13182
2.8 −	0.79629	0.36638	0.19708	0.63317	0.49962	0.78907	218°17′	−0.16953	0.11530	0.19708	0.10696	0.20045	−0.63092	147°45′	−0.49784
2.8 +	0.79629	0.36638	0.26956	0.57992	0.54878	0.94631	223°25′	−0.16953	0.11530	0.19708	0.10696	0.20045	−0.63092	147°45′	−0.59705
3.0	0.65352	0.29666	0.25679	0.45002	0.47049	1.04548	226°16′	−0.22114	0.06712	0.20053	0.05613	0.22815	−0.25382	165°46′	−0.26536
3.2	0.53184	0.23529	0.24591	0.33940	0.40181	1.18388	229°49′	−0.26060	0.02555	0.19995	0.01253	0.26090	−0.04808	177°15′	−0.05692
3.4	0.42823	0.18144	0.23390	0.24731	0.33988	1.37432	233°58′	−0.28999	−0.01010	0.19634	−0.02463	0.29104	0.08493	184°51′	0.11675
3.6 −	0.34022	0.13595	0.22216	0.17020	0.28649	1.68324	239°17′	−0.31094	−0.03889	0.19146	−0.05451	0.31568	0.17531	189°57′	0.29509
3.6 +	0.34022	0.12153	0.37786	0.05652	0.37771	6.68271	261°30′	−0.31094	−0.03889	0.19146	−0.05451	0.31568	0.17531	189°57′	1.17155
3.8	0.27564	0.07499	0.33885	0.02293	0.30476	13.29097	265°42′	−0.31490	−0.07277	0.17121	−0.08863	0.32713	0.28145	195°43′	3.74074
4.0 −	0.21996	0.03587	0.30425	−0.00537	0.24222	−45.10600	271°16′	−0.31576	−0.10003	0.15331	−0.11597	0.33638	0.36727	200°10′	−16.56608
4.0 +	1.66328	0.03587	0.30425	1.43745	0.24222	0.16851	189°34′	−0.31576	−0.10003	0.15331	−0.11597	0.33638	0.36727	200°10′	0.06189
4.2	1.10531	0.00603	0.35653	0.84306	0.24788	0.29403	196°23′	−0.42981	−0.11879	0.22049	−0.14046	0.45218	0.32680	198° 6′	0.09609
4.4 −	0.67823	−0.02490	0.37292	0.40548	0.22811	0.56257	209°22′	−0.49223	−0.13942	0.25020	−0.16424	0.50891	0.33367	198°27′	0.18771
4.4 +	0.67823	−0.02924	0.39292	0.40570	0.22377	0.55158	208°53′	−0.49223	−0.13942	0.25020	−0.16424	0.50891	0.33367	198°27′	0.18404
4.6	0.35580	−0.05648	0.36514	0.09035	0.19129	2.11722	244°43′	−0.51702	−0.15890	0.25436	−0.18499	0.54912	0.35780	199°41′	0.75754
4.8 −	0.11196	−0.08360	0.34131	−0.13463	0.14804	−1.09961	312°17′	−0.51480	−0.17594	0.24123	−0.20194	0.55300	0.39277	201°25′	−0.43189
4.8 +	0.11196	−0.01514	0.36105	−0.15255	0.22980	−1.50639	303°35′	−0.51480	−0.17594	0.24123	−0.20194	0.55300	0.39277	201°25′	−0.59166
5.0	−0.06376	−0.06141	0.21947	−0.22194	0.08755	−0.39448	338°28′	−0.49614	−0.19265	0.21681	−0.21773	0.43885	0.43885	203°42′	−0.17312

Interior Joints and Bars.—The computation of the stresses, velocities, and displacements in the interior of the truss can now be completed. This part contains no loaded joints and therefore the use of the finite-difference solution is no longer necessary; in fact, repetition of step 5 for the joint currently considered is all that is required.

Consider, for example, the bars meeting at joint C. The wave, $f'_{02}(\tau_0)$, appearing in Table 3(*b*) is also the total wave entering joint C from bar 2 at $\tau = \tau_0 + 1.2$, and is therefore known. Similarly, the total outgoing wave in that bar at joint C at $\tau = \tau_0 - 1.2$ appears in Table 2(*b*) as $f'_{I2}(\tau_0)$. These two waves are entered in Table 5. As in Eqs. 47 and 48 the stress and the velocity can be evaluated at this end of bar 2; they are also listed in Table 5.

For the other bars at joint C, the incoming and outgoing waves must be found from the procedure described in step 5. This step makes use of the distribution factors; as these have already been listed in Table 1, no difficulties arise because of supported joints such as A and E. The deflections of an interior joint and the stresses and velocities arising in all bars are computed in the same manner as for the loaded joint; some of these are listed in Table 6. Plots of these and additional quantities (deflections of joint C and reactions, for example) have been presented elsewhere.[4,5] The solution may thus be considered complete.

TABLE 5.—STRESSES AND VELOCITIES IN BAR 2 AT JOINT C IN FIG. 1

τ	f_{in}	f_{out}	$\frac{a}{E\,V}\sigma_2$	$\frac{1}{V}\frac{\partial u_2}{\partial t}$
1.2	0.65529	0.14989	0.80518	0.50540
1.4	0.59992	0.13723	0.73715	0.46269
1.6	0.54883	0.12554	0.67437	0.42329
1.8	0.50177	0.11477	0.61654	0.38700
2.0	0.45846	0.10487	0.56333	0.35359
2.2	0.41869	0.09577	0.51446	0.32292
2.4 −	0.38219	0.08742	0.46961	0.29477
2.4 +	0.38219	0.08021	0.46240	0.30198
2.6	0.34873	0.07388	0.42261	0.27485
2.8	0.31808	0.06795	0.38603	0.25013
3.0	0.29004	0.06241	0.35245	0.22763
3.2 −	0.26438	0.05726	0.32164	0.20712
3.2 +	0.26438	0.05509	0.31947	0.20929
3.4	0.24407	0.05121	0.29528	0.19286
3.6 −	0.21895	0.04617	0.26512	0.17278
3.6 +	0.36884	0.08040	0.44924	0.28844
3.8	0.30184	0.06562	0.36746	0.23622
4.0	0.24084	0.05213	0.29297	0.18871
4.2	0.18189	0.03904	0.22093	0.14285
4.4 −	0.13042	0.02759	0.15801	0.10283
4.4 +	0.13042	0.24774	0.37816	−0.11732
4.6	0.08567	0.23010	0.31577	−0.14443
4.8 −	0.04853	0.21251	0.26104	−0.16398
4.8 +	0.04132	0.10747	0.14879	−0.06615
5.0	0.00111	0.09463	0.09574	−0.09352

ADDITIONAL INFORMATION

Some additional information is presented herewith concerning checks on the numerical computations, possible simplifications, and the adaptation to other loading conditions.

---

[4] "The Analysis of Plane Trusses Under Impact," by Bruno A. Boley and Chi-Chang Chao, *Technical Report No. 1*, NOnr 266 (20), Columbia Univ., New York, N. Y., 1953.

[5] "Equations for Three-Dimensional Trusses Under Impact," by Chi-Chang Chao and Bruno A. Boley, *Technical Report No. 3*, NOnr 266 (20), Columbia Univ., New York, N. Y., 1954.

TABLE 6.—MAGNITUDES AND DIRECTIONS OF STRESSES, VELOCITIES, AND FORCE AT JOINT C IN BARS 2, 4, 5, AND 6 IN FIG. 1

τ	$\frac{\sigma_2 a}{E\,V}$	$\frac{\sigma_5 a}{E\,V}$	$\frac{\sigma_6 a}{E\,V}$	$\frac{\sigma_4 a}{E\,V}$	$\frac{1}{V}\frac{\partial u_2}{\partial t}$	$\frac{1}{V}\frac{\partial u_5}{\partial t}$	$\frac{1}{V}\frac{\partial u_6}{\partial t}$	$\frac{1}{V}\frac{\partial u_4}{\partial t}$	$\frac{1}{V}\frac{\partial u_{\perp 2}}{\partial t}$	$\frac{1}{V}\frac{\partial u}{\partial t}$	$\tan \theta_{2u}$	θ_{2u}
1.2	0.80518	−0.38006	0.49704	−0.12422	0.50540	−0.38006	0.49704	−0.12422	−0.02368	0.50597	−0.04685	− 2°41′
1.4	0.73715	−0.34795	0.45504	−0.11372	0.46269	−0.34795	0.45504	−0.11372	−0.02167	0.46320	−0.04683	− 2°41′
1.6	0.67437	−0.31832	0.41629	−0.10404	0.42329	−0.31832	0.41629	−0.10404	−0.01983	0.42375	−0.04685	− 2°41′
1.8	0.61654	−0.29102	0.38059	−0.09512	0.38700	−0.29102	0.38059	−0.09512	−0.01814	0.38743	−0.04687	− 2°41′
2.0	0.56333	−0.26590	0.34774	−0.08691	0.35359	−0.26590	0.34774	−0.08691	−0.01657	0.35398	−0.04686	− 2°41′
2.2	0.51446	−0.24284	0.31758	−0.07937	0.32292	−0.24284	0.31758	−0.07937	−0.01512	0.32327	−0.04682	− 2°41′
2.4 −	0.46961	−0.22167	0.28989	−0.07245	0.29477	−0.22167	0.28989	−0.07245	−0.01381	0.29509	−0.04685	− 2°41′
2.4 +	0.46240	−0.19395	0.30932	−0.05019	0.30198	−0.19395	0.30932	−0.12623	−0.06724	0.30938	−0.22266	−12°33′
2.6	0.42261	−0.17962	0.28038	−0.04792	0.27485	−0.17962	0.28038	−0.11004	−0.05624	0.28054	−0.20466	− 11°34′
2.8	0.38603	−0.16600	0.25422	−0.04544	0.25013	−0.16600	0.25422	−0.09618	−0.04712	0.25453	−0.18838	−10°40′
3.0	0.35245	−0.15311	0.23059	−0.04284	0.22763	−0.15311	0.23059	−0.08430	−0.03961	0.23105	−0.17401	− 9°52′
3.2 −	0.32164	−0.14099	0.20919	−0.04019	0.20712	−0.14099	0.20919	−0.07409	−0.03336	0.20979	−0.16107	− 9°9′
3.2 +	0.31947	−0.13263	0.21505	−0.03347	0.20929	−0.13263	0.21505	−0.09031	−0.04947	0.21506	−0.23637	−13°18′
3.4	0.29528	−0.12381	0.19759	−0.03200	0.19286	−0.12381	0.19759	−0.08072	−0.04303	0.19760	−0.22312	−12°35′
3.6 −	0.26512	−0.11172	0.17677	−0.02924	0.17278	−0.11172	0.17677	−0.07112	−0.03727	0.17676	−0.21571	−12°10′
3.6 +	0.44924	−0.19866	0.29047	−0.05766	0.28844	−0.19866	0.29047	−0.09954	−0.04275	0.29159	−0.14821	− 8°26′
3.8	0.36746	−0.16190	0.23818	−0.04664	0.23622	−0.16190	0.23818	−0.08278	−0.03628	0.23899	−0.15359	− 8°44′
4.0	0.29297	−0.12830	0.19067	−0.03649	0.18871	−0.12830	0.19067	−0.06775	−0.03065	0.19118	−0.16242	− 9°14′
4.2	0.22093	−0.09562	0.14489	−0.02654	0.14285	−0.09562	0.14489	−0.05366	−0.02560	0.14513	−0.17921	−10°10′
4.4 −	0.15801	−0.06704	0.10495	−0.01781	0.10283	−0.06704	0.10495	−0.04141	−0.02130	0.10501	−0.20714	−11°42′
4.4 +	0.37816	−0.44932	−0.03253	−0.29397	−0.11732	0.31080	−0.03253	−0.32047	−0.35107	0.37015	2.99241	251°31′
4.6	0.31577	−0.43408	−0.08499	−0.29672	−0.14443	0.26182	−0.08499	−0.20496	−0.23867	0.27897	1.65250	238°49′
4.8 −	0.26104	−0.41377	−0.12421	−0.29307	−0.16398	0.22287	−0.12421	−0.11593	−0.15181	0.22346	0.92578	222°48′
4.8 +	0.14879	−0.45916	−0.29010	−0.36133	−0.06615	0.17748	−0.01752	−0.18419	−0.20153	0.21211	3.04656	251°50′
5.0	0.09574	−0.41738	−0.30642	−0.33862	−0.09352	0.16466	−0.05688	−0.12502	−0.14674	0.17401	1.56908	237°29′
5.2 −	0.05061	−0.37726	−0.31579	−0.31527	−0.11477	0.15454	−0.08749	−0.07887	−0.10393	0.15483	0.90555	222°10′
5.2 +	0.05461	−0.39268	−0.32660	−0.32764	−0.11877	0.13912	−0.09830	−0.04896	−0.07422	0.14005	0.62491	211°58′
5.4	0.01856	−0.35082	−0.32446	−0.30048	−0.13132	0.13486	−0.11574	−0.02436	−0.05169	0.14113	0.39362	201°29′
5.6 −	−0.01913	−0.30880	−0.32417	−0.27381	−0.14519	0.13454	−0.13347	−0.00373	−0.03382	0.14908	0.23294	193° 7′
5.6 +	0.00134	−0.26657	−0.27770	−0.23572	−0.17000	0.12133	−0.14934	0.02912	0.01839	0.17099	−0.10818	175°50′
5.8	−0.03736	−0.23500	−0.28535	−0.21741	−0.17802	0.12424	−0.16211	0.04019	0.02377	0.17960	−0.13352	172°24′

1. In the computations at any one joint it is necessary to choose two bars to be considered as independent and then to determine the waves in the remaining bars from Eq. 22. The choice of independent bars is arbitrary; therefore, a check may be obtained by deriving the same results with different independent coordinates. Another check is provided by the fact that the vector sum of the forces in all the bars meeting at an interior joint must be zero.

2. A certain number of joints must be traveled to reach any one bar from the loaded joint. As this number increases, the stresses decrease because each wave is distributed at each joint according to distribution factors which are smaller than unity; that is, the truss configuration at large distances from the loaded joint has little influence on the stresses near the load. In Fig. 1, for example, impact has already ended when waves which passed through joint E return to the loaded joint.

3. It follows that the maximum stresses will usually occur in one of the bars meeting at the loaded joint. An upper limit for these stresses can be obtained by considering all joints adjacent to the loaded one as fixed hinges. Because joint A is of such a type in Fig. 1, in this particular case this procedure gives the actual maximum stress.

4. If the loading consists of a prescribed force varying with time, joints of types a and c are eliminated and therefore no finite-difference solution is necessary. The modifications necessary to reduce the loaded joint to one of type b have been cited in the discussion of that type of joint.

6. If impact occurs at more than one joint, either simultaneously or not, the stresses and velocities can be obtained by superposing the values obtained by considering each impact separately. Care must be exercised, however, because it is necessary to consider together the effects of all loadings when the time of end of impact for any one of the striking masses is determined.

7. In the computations previously described only the stresses and velocities at the ends of each bar were determined. It is easy to find the values of these quantities at a distance, x_i, from one of the ends (M) of bar i with the aid of the expressions:

$$\sigma(\tau, x_i) = \sigma_{out}\left(\tau - \frac{x_i}{L}\right) + \sigma_{in}\left(\tau + \frac{x_i}{L}\right) \qquad \text{(52a)}$$

and

$$\frac{\partial}{\partial t}[u_i(\tau, x_i)] = \frac{\partial}{\partial t}\left[u_i\left(\tau - \frac{x_i}{L}\right)\right]_{out} - \frac{\partial}{\partial t}\left[u_i\left(\tau + \frac{x_i}{L}\right)\right]_{in} \qquad \text{(52b)}$$

in which the subscripts indicate the total outgoing or incoming wave at $x_i = 0$—that is, at joint M.

8. The striking mass was assumed perfectly rigid in the present example so as not to introduce any complications extraneous to the truss proper. Should the mass be elastic, some modifications in the computations pertaining to joints of types a and c would be required, perhaps using the Hertz theory of impact[6] for the determination of the impulsive force.

---

[6] "Theory of Elasticity," by S. P. Timoshenko and J. N. Goodier, McGraw-Hill Book Co., Inc., New York, N. Y., 2d Ed., 1951.

EQUATIONS FOR SPACE TRUSSES

The procedure described in the foregoing for the analysis of trusses under impact is quite general and can therefore be applied directly to three-dimensional trusses; some of the basic equations, however, must be modified to take into account the additional degree of freedom. The principal equations are listed herewith and are derived with the aid of some well-known formulas of vector analysis.[7] It should be noted that all equations, under the heading, "General Description," are still valid, with the exception of the specific expressions for distribution factors. Eq. 20 becomes, for the three-dimensional case,

$$u_k = C^1{}_k\, u_1 + C^2{}_k\, u_2 + C^3{}_k\, u_3 \qquad (53)$$

in which bars 1, 2, and 3 are not coplanar, and in which

$$C^i{}_k = g^{i1} \cos \theta_{1k} + g^{i2} \cos \theta_{2k} + g^{i3} \cos \theta_{3k} \qquad (54a)$$

$$g^{11} = \frac{1}{g} \sin^2 \theta_{23} \qquad (54b)$$

$$g^{22} = \frac{1}{g} \sin^2 \theta_{13} \qquad (54c)$$

$$g^{33} = \frac{1}{g} \sin^2 \theta_{12} \qquad (54d)$$

$$g^{12} = g^{21} = \frac{1}{g} (\cos \theta_{23} \cos \theta_{13} - \cos \theta_{12}) \qquad (54e)$$

$$g^{13} = g^{31} = \frac{1}{g} (\cos \theta_{12} \cos \theta_{23} - \cos \theta_{13}) \qquad (54f)$$

$$g^{23} = g^{32} = \frac{1}{g} (\cos \theta_{13} \cos \theta_{12} - \cos \theta_{23}) \qquad (54g)$$

and

$$g = 1 - \cos^2 \theta_{23} - \cos^2 \theta_{12} - \cos^2 \theta_{13} + 2 \cos \theta_{12} \cos \theta_{13} \cos \theta_{23} \qquad (54h)$$

Eqs. 23, in the three-dimensional case, are replaced by

$$f''_i + f'_i \sum \frac{C^i{}_p}{m_p\, L_p} \cos \theta_{ip} + f'_j \sum \frac{C^j{}_p}{m_p\, L_p} \cos \theta_{ip} + f'_k \sum \frac{C^k{}_p}{m_p\, L_p} \cos \theta_{ip} = 0 \qquad (55)$$

and two other similar equations for bars j and k, where, in the summations, $p = 1, 2, 3 \ldots n$. Eq. 26 becomes in this case,

$$f''''_i + P_1 f'''_i + P_2 f''_i + P_3 f'_i = 0 \qquad (56)$$

in which the quantities P_1 and P_2 are identical with those given by Eqs. 27*a* and 27*b*, respectively, and

$$P_3 = \frac{1}{3!} \sum_{s=1}^{n} \sum_{q=1}^{n} \sum_{r=1}^{n} \frac{g_{sqr}}{m_s\, L_s\, m_q\, L_q\, m_r\, L_r} \qquad (57a)$$

---

[7] "Vector Analysis, with an Introduction to Tensor Analysis," by A. P. Wills, Prentice-Hall, Inc., New York, N. Y., 1931, Sections 94–95.

in which

$$g_{sqr} = 1 - \cos^2\theta_{sq} - \cos^2\theta_{qr} - \cos^2\theta_{rs} + 2\cos\theta_{sq}\cos\theta_{qr}\cos\theta_{rs} \,..\, (57b)$$

It should be noted that $g = g_{123}$ and that $g_{sqr} = g_{srq} = g_{rqs}$ and so forth.

With the foregoing equations, joints of type a can be treated. For joints of type b the necessary distribution factor D_{ip} of Eq. 13 becomes

$$D_{ip} = -\frac{1}{P_3}\sum_{q=1}^{n}\sum_{r=1}^{n}\frac{(g_{iqr}\,g_{pqr})^{1/2}}{m_i\,L_i\,m_q\,L_q\,m_r\,L_r}, \qquad i \neq p \,......\, (58a)$$

and

$$D_{ii} = 1 - \frac{1}{P_3}\sum_{q=1}^{n}\sum_{r=1}^{n}\frac{q_{iqr}}{m_i\,L_i\,m_q\,L_q\,m_r\,L_r} \,..............\, (58b)$$

For joints of types c, the finite-differences technique should again be used; the pertinent equations (corresponding to Eqs. 37) are cumbersome but otherwise easily derived.

APPENDIX

The following symbols, adopted for use in the paper and for the guidance of discussers, conform essentially with "American Standard Letter Symbols for Structural Analysis" (ASA Z10.8—1949), prepared by a committee of the American Standards Association with Society representation, and approved by the Association in 1949:

A = cross-sectional area of a bar;
a = speed of wave propagation;
C = constants;
D = distribution factor;
E = modulus of elasticity;
f_i = wave in bar i;
F = force;
L = length of a bar;
M = mass;
m = term defined in Eq. 24;
n = number of bars meeting at a joint;
P = term defined by Eqs. 26;
R = reaction;
r = term defined in Eqs. 28;
t = time;
u = axial displacement;
V = velocity;
x = distance along a bar;
δ = displacement;
θ = angle;
ρ = mass density;
σ = normal axial stress; and
τ = nondimensional time.

AMERICAN SOCIETY OF CIVIL ENGINEERS

Founded November 5, 1852

TRANSACTIONS

Paper No. 2848

SIGHT DISTANCE AT UNDERCROSSINGS

By Paul Hartman,[1] M. ASCE

With Discussion by Mr. Thomas F. Hickerson

Synopsis

Daylight sight distances on highway vertical curves in sag may be limited by a structure crossing the right of way. Conventional formulas for the determination of this sight distance are based on the special case in which the critical edge of the structure is directly above the vertex of the vertical curve. Despite this limitation, these equations are considered to be applicable regardless of the position of the critical edge with respect to the vertex of the vertical curve.

Specific formulas are derived which are correct for any position of the structure; the results obtained by use of the conventional equations are compared with those using the specific formulas.

Introduction

In Fig. 1, A is the critical edge of the underpass structure; $\overline{MN}$ is the line of sight with M the driver's eye at a height, h, above the pavement; and N is a point on the object the driver must see at a height, h_1, above the pavement. The horizontal projection of $\overline{MN}$ is the sight distance, S. The grades of the entering and leaving tangents are g_1 and g_2, respectively, with direction of travel always assumed to be from left to right unless otherwise noted. The length of the vertical curve is L, and a is a constant of the parabola given by

$$a = \frac{g_2 - g_1}{2\,L} \qquad (1)$$

All horizontal distances are expressed in stations and vertical distances are expressed in feet; grades are expressed in percentages.

Note.—Published, essentially as printed here, in January, 1955, as *Proceedings-Separate No. 597.* Positions and titles given are those in effect when the paper or discussion was approved for publication in *Transactions.*

[1] Associate Prof. of Civ. Eng., The City College of New York, New York, N. Y.

Case I. Sight Distance Less Than Length of Vertical Curve.—In Fig. 1 (*a*), A is any point such that the line of sight remains entirely within the vertical curve. The vertical clearance is $\overline{AC}$ and the horizontal distance from A to the object end of the line of sight is $k\,S$ in which k is an unknown ratio. The line $\overline{FJ}$ is a tangent of the parabola drawn parallel to chord $\overline{HK}$. The point of tangency, E, will be at the midpoint of $\overline{FJ}$. The clearance,

$$\overline{AC} = \overline{AB} + \overline{BD} - \overline{CD} \qquad (2)$$

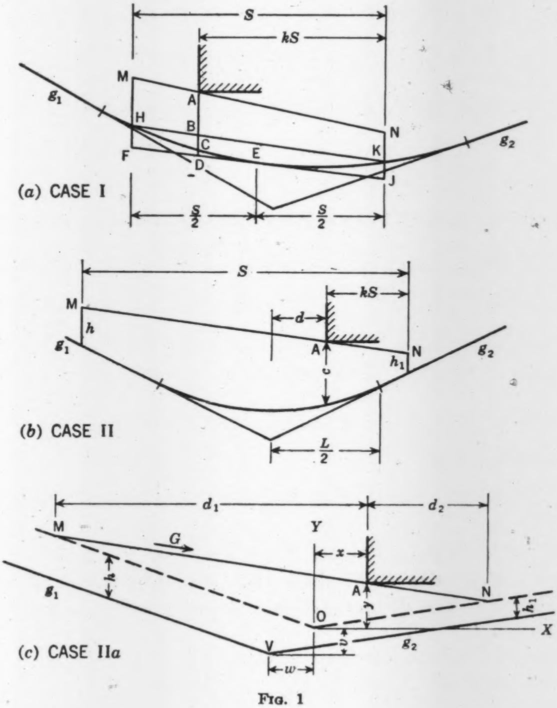
S
kS
M
g_1
A
H
B
N
C
E
K
g_2
F
D
J
(*a*) CASE I
$\frac{S}{2}$
$\frac{S}{2}$
S
kS
M
d
h
g_1
A
N
g_2
c
h_1
(*b*) CASE II
$\frac{L}{2}$
d_1
d_2
M
Y
G
x
h
A
N
g_1
O
y
h_1
X
v
V
g_2
w
(*c*) CASE II*a*

FIG. 1

By proportion,

$$\overline{AB} = h_1 + (h - h_1)\,k \qquad (3)$$

From the rule of offsets from a tangent to a parabola,

$$\overline{BD} = \overline{HF} = \frac{1}{4}\,a\,S^2 \qquad (4)$$

and

$$\overline{CD} = a\left(k\,S - \frac{S}{2}\right)^2 \qquad (5)$$

Letting the clearance $\overline{AC}$ equal c and substituting Eqs. 3, 4, and 5 into Eq. 2 results in

$$c = h_1 + (h - h_1)\,k + \frac{1}{4}\,a\,S^2 - a\left(k\,S - \frac{S}{2}\right)^2 \qquad (6)$$

which, upon simplification, is

$$a\,k^2\,S^2 - a\,k\,S^2 - (h - h_1)\,k = h_1 - c \qquad (7)$$

Differentiating with respect to k and equating dS/dk to zero yields the value of k for which S is a minimum—

$$k = \frac{1}{2} + \frac{h - h_1}{2\,a\,S^2} \qquad (8)$$

Substituting this value of k into Eq. 7 and simplifying results in

$$S^2 = \frac{2\,c - (h + h_1)}{a} \pm \frac{2}{a}\sqrt{(c - h)(c - h_1)} \qquad (9)$$

The values recommended[2] by the American Association of State Highway Officials (AASHO) are $h = 6$ ft, $h_1 = 1.5$ ft, and $c = 14$ ft. Substituting these values into Eq. 9 leads to

$$S^2 = \frac{40.5}{a} \qquad (10)$$

Substituting Eq. 1 into Eq. 10 and solving for L results in

$$L = \frac{g_2 - g_1}{81}\,S^2 \qquad (11)$$

The AASHO formula is

$$L = \frac{g_2 - g_1}{82}\,S^2 \qquad (12)$$

Case II. Sight Distance Greater Than Length of Vertical Curve.—In Fig. 1 (*b*), A is the critical edge of the obstruction, distant d from the vertex of the the vertical curve. The distance, d, is assumed positive to the right and it must be less than $L/2$. The distance from A to the object end of the line of sight is $k\,S$, in which k is an unknown ratio.

The elevations of M, A, and N, above the vertex, are

$$\mathrm{El}_M = -\,g_1\,(S - k\,S - d) + h \qquad (13a)$$

$$\mathrm{El}_A = g_2\,d + a\left(\frac{L}{2} - d\right)^2 + c \qquad (13b)$$

and

$$\mathrm{El}_N = g_2\,(k\,S + d) + h_1 \qquad (13c)$$

By proportion,

$$\frac{\mathrm{El}_M - \mathrm{El}_N}{S} = \frac{\mathrm{El}_A - \mathrm{El}_N}{k\,S} \qquad (14)$$

---

[2] "A Policy on Grade Separations for Intersecting Highways," A.A.S.H.O., 1944, p. 28.

or

$$k[-g_1(S-kS-d)+h-g_2(kS+d)-h_1]$$
$$=g_2d+a\left(\frac{L}{2}-d\right)^2+c-g_2(kS+d)-h_1 \quad (15)$$

Simplifying and using Eq. 1 leads to

$$kS-k^2S-kd+\frac{h-h_1}{g_2-g_1}k=\frac{L}{8}-\frac{d}{2}+\frac{d^2}{2L}+\frac{c-h_1}{g_2-g_1} \quad (16)$$

Differentiating S with respect to k and setting dS/dk equal to zero results in

$$S-2kS-d+\frac{h-h_1}{g_2-g_1}=0 \quad (17)$$

For a minimum value of S,

$$k=\frac{1}{2}-\frac{d}{2S}+\frac{1}{2S}\frac{h-h_1}{g_2-g_1} \quad (18)$$

Solving Eq. 16 for L leads to

$$L^2-8L\left[kS(1-k)-d\left(k-\frac{1}{2}\right)+k\frac{h-h_1}{g_2-g_1}-\frac{c-h_1}{g_2-g_1}\right]+4d^2=0 \quad (19)$$

Denoting the multiplier of 8 L by F causes Eq. 19 to be changed to

$$L=4F+2\sqrt{4F^2-d^2} \quad (20)$$

Substituting the value of k from Eq. 18 into the expression for F and simplifying results in

$$F=\frac{S}{4}+\frac{1}{4S}\left(\frac{h-h_1}{g_2-g_1}-d\right)^2-\frac{2c-h-h_1}{2(g_2-g_1)} \quad (21)$$

With $h = 6$ ft, $h_1 = 1.5$ ft, and $c = 14$ ft, Eq. 21 becomes

$$F=\frac{S}{4}+\frac{1}{S}\left(\frac{2.25}{g_2-g_1}-\frac{d}{2}\right)^2-\frac{10.25}{g_2-g_1} \quad (22)$$

It should be noted that Eq. 22 assumes that the clearance at the critical edge is 14 ft. This is not necessarily so, as the critical edge may be the one with a clearance of more than 14 ft. To determine the critical edge, it is necessary to know whether the line of sight has a positive or negative slope in the direction of travel of the vehicle. To avoid confusion, the vehicle will always be assumed to be traveling from left to right unless otherwise noted.

If the elevation of N minus the elevation of M is termed E, the sign of E will be the same as that of the slope of the line of sight. Then,

$$E=g_2(kS+d)+h_1+g_1(S-kS-d)-h \quad (23)$$

Simplifying and substituting for k its value in Eq. 18, with $h = 6$ ft and $h_1 = 1.5$ ft, as before, results in

$$E = g_1 S - 2.25 + \frac{S + d}{2} (g_2 - g_1) \quad \text{(24)}$$

Should Eq. 24 indicate that the slope of the line of sight is such that the critical edge is the one with a clearance of more than 14 ft, it is necessary to modify Eq. 22 by adding the additional clearance to the constant of the last term.

To illustrate the use of Eqs. 20, 22, and 24, the following problem will be solved:

A -2% slope meets a $+3\%$ slope at Station 10 + 00 at El. 100. An overcrossing structure 100 ft wide which crosses the right of way at right angles extends from Station 7 + 00 to Station 8 + 00. The required sight distance is 1,320 ft. What length of vertical curve is required?

Because it is not at once apparent which is the critical edge, it is assumed that the critical edge is at Station 7 + 00—that is, $d = -3$. Then, solving Eq. 24, E is found to be -3.15. The magnitude is not important; the sign is important because it confirms the assumption as to the critical edge. Solving Eq. 22, F is found to be 1.538 and from Eq. 20, L is 7.51 stations.

This is not a complete solution as the sight distance in the opposite direction must also be considered. Solving Eq. 24 with $d = +3$, $g_1 = -3\%$, and $g_2 = +2\%$, E is negative and the critical edge is that at Station 8 + 00. The clearance at Station 8 + 00 must be greater than 14 ft which is the clearance at Station 7 + 00. To determine this additional clearance, it is necessary to assume a value of L. Assuming $L = 7.50$ stations, the clearance at Station 8 + 00 corresponding to a 14-ft clearance at Station 7 + 00 is 15.17 ft. This changes Eq. 22 to

$$F = \frac{S}{4} + \frac{1}{S}\left(\frac{2.25}{g_2 - g_1} - \frac{d}{2}\right)^2 - \frac{11.42}{g_2 - g_1} \quad \text{(25)}$$

and F is 1.081 and L is 5.97 stations.

Hence, for a sight distance in both directions of 1,320 ft, the vertical curve must be 750 ft long. The AASHO formula for L when $S > L$ is

$$L = 2\,S - \frac{82}{g_2 - g_1} \quad \text{(26)}$$

Eq. 26 requires a vertical curve for the foregoing conditions to be 1,000 ft long as compared with the correct value of 750 ft. Shortening the curve to 750 ft reduces the required elevation of the critical edge by 0.81 ft.

A comparison of the value of L obtained from Eq. 20 and Eq. 26 for various values of S, g_1, g_2, and d is made in Table 1. In each case the obstruction has been so located with respect to the vertex that the critical edge is the one with the minimum (14 ft) clearance. The length of curve required by Eq. 20 has been computed for travel in both directions, as indicated by the arrows. Where the tabular value of d is, for example, $+ 1$, the obstruction is one station to the right of the vertex. In computing the value of L for travel from right to left the value of d used is $- 1$. The grade to the left of the vertex is always numerically equal to g_1 but, of course, its sign is changed when travel from right to left is considered.

Referring again to the foregoing problem, if the overcrossing structure were shifted 50 ft farther away from the vertex, the value of L determined by Eq. 20 would be imaginary. A study of Table 1 shows that, for any given set of conditions, there is a critical value of d beyond which Eq. 20 is not applicable —that is, L becomes imaginary. This critical value of d is $2\,F$.

TABLE 1.—A COMPARISON OF LENGTHS OF VERTICAL CURVES AS DETERMINED BY THE CONVENTIONAL METHOD (EQ. 26) AND THE PROPOSED METHOD (EQ. 20)

S, in stations	g_1, in %	g_2, in %	d, in stations	L, in stations, from Eq. 20		Minimum L, in stations	
				→	←	Eq. 20	Eq. 26
13.2	−2	+3	0	10.12	10.12	10.12	10
			+1	9.58	10.15	10.15	
			+2	8.23	9.62	9.62	
			+3	...	7.51	7.51	
16.25	−3	+1	0	12.15	12.15	12.15	12
			−1	12.24	11.66	12.24	
			−2	11.84	10.59	11.84	
			−3	10.73	7.87	10.73	
			−3.5	9.41	...	9.41	
18	−1.5	+2	0	12.75	12.75	12.75	12.60
			+1	12.24	12.83	12.83	
			+2	11.17	12.48	12.48	
			+3	8.79	11.46	11.46	
			+3.5	...	10.38	10.38	
21	−1	+2	0	14.88	14.88	14.88	14.67
			+1	14.41	15.01	15.01	
			+2	13.50	14.76	14.76	
			+3	11.84	14.03	14.03	
			+4	...	12.40	12.40	

When d exceeds $2\,F$ another relationship is required. This relationship is considered as Case II*a*. It is also applicable for values of d less than the critical but it is not as convenient to use as Eq. 20.

Case IIa. Sight Distance Greater Than Length of Vertical Curve.—In Fig. 1(*c*), A is any point within the sag. The line of sight, $\overline{MN}$, has an unknown slope, G. The lines $\overline{MO}$ and $\overline{ON}$ are parallel to the grade tangents and vertically above them by distances h and h_1, respectively. The coordinates of A with respect to coordinate axes through point 0 are x and y. The coordinates of the vertex, V, with respect to the same axes are w and v. Point A divides the sight distance, S, into segments, d_1 and d_2. Therefore,

$$y = - g_1 (d_1 - x) + G\,d_1 \quad\text{.................. (27)}$$

and

$$y = g_2 (d_2 + x) - G\,d_2 \quad\text{.................. (28)}$$

Solving Eqs. 27 and 28 for d_1 and d_2 and adding leads to

$$S = \frac{y - g_1 x}{G - g_1} + \frac{y - g_2 x}{g_2 - G} \qquad (29)$$

Differentiating Eq. 29 with respect to G and equating dS/dG to zero results in

$$\frac{y - g_1 x}{(G - g_1)^2} = \frac{y - g_2 x}{(g_2 - G)^2} \qquad (30)$$

which becomes

$$G = \frac{y}{x} \pm \sqrt{\left(\frac{y}{x}\right)^2 - \frac{y}{x}(g_1 + g_2) + g_1 g_2} \qquad (31)$$

The value of G obtained by substituting the known values of x, y, g_1, and g_2 in Eq. 31 is then used in Eq. 29 which may be rearranged into

$$S = \frac{(y - xG)(g_2 - g_1)}{(G - g_1)(g_2 - G)} \qquad (32)$$

With proper regard to sign, the coordinates of the vertex are

$$w = \frac{h - h_1}{g_1 - g_2} \qquad (33)$$

and

$$v = \frac{g_1(h - h_1)}{g_1 - g_2} - h \qquad (34)$$

To illustrate the use of Eqs. 31, 32, 33, and 34, the data given in the foregoing problem are assumed except that the overcrossing extends from Station 6 + 50 to Station 7 + 50. From the previous solution it is logical to assume that the curve will be shorter than 700 ft. The elevation of the critical edge is then 121.00, and the distance from the vertex is − 3.50 stations. From Eqs. 33 and 34, w and v are − 0.90 stations and − 4.20 ft, respectively. Then x and y are − 4.40 stations and 16.80 ft, respectively. From Eq. 31, G is − 0.30% and from Eq. 32, S is 13.80 stations.

Thus, the actual sight distance is greater than the required sight distance without a vertical curve. If S had been less than 1,320 ft, it would have been necessary to increase y by introducing a vertical curve longer than 700 ft or by increasing the clearance. A check of the sight distance in the opposite direction shows that the critical edge is the one at Station 7 + 50 and S is 14.63 stations. In so far as daylight sight distance is concerned, it is not necessary to have a vertical curve in this sag. The length of the vertical curve would be determined by some other design criterion.

CONCLUSIONS

For Case I, sight distance less than length of vertical curve, the conventional formula is, for all practical purposes, identical with the proposed correct formula. This will be true for any reasonable values of c, h, and h_1.

For Case II, the conventional formula (Eq. 26) is remarkably accurate if the critical edge is within approximately 200 ft of the vertex of the vertical curve, and if sight distance is considered in each direction as it must be because passing sight distances are involved in most practical problems involving Case II. However, when the critical edge is more than 200 ft from the vertex, the conventional formula will usually yield results which are considerably in error.

As the critical edge moves farther away from the vertex, Eq. 20 becomes invalid, and it is necessary to resort to Eq. 32 to determine the sight distance. Both of these equations, when used in conjunction with the equations from which they were developed, permit exact location of the line of sight. This permits rigorous solutions for complicated sight-distance problems such as a sag with more than one structure crossing the right of way.

DISCUSSION

Thomas F. Hickerson,[3] M. ASCE.—As a partial check on Mr. Hartman's formulas for Case II, if $d = 0$, then $k = \frac{1}{2}$; hence,

$$F = \frac{S}{4} - \frac{C - \frac{1}{2}(h + h_1)}{g_2 - g_1} \qquad (35)$$

With $C = 14$ ft, $h = 6$ ft, and $h_1 = 1.5$ ft,

$$F = \frac{S}{4} - \frac{10.25}{g_2 - g_1} \qquad (36)$$

Substituting Eq. 36 into Eq. 20,

$$L = 8\,F = \frac{S}{2} - \frac{82}{g_2 - g_1} \qquad (37)$$

which agrees with Eq. 26, the AASHO formula.

In view of Mr. Hartman's conclusions, the writer is firmly convinced that the conventional formulas are satisfactory if attention is called to the range of errors (on the side of safety) for the rather extreme situations (in Case II or Case II*a*) in which the critical edge is more than 200 ft from the vertex of the vertical curve. The conventional formulas possess the great advantage of simplicity in derivation and application. Because the hazards of passing sight distances are involved in most practical problems involving Case II, the erroneous results are rendered less important.

In conclusion, it must be stated that Mr. Hartman's paper is a valuable contribution to the technical information of the profession.

---

[3] Formerly Prof. of Civ. Eng., Univ. of North Carolina, Chapel Hill, N. C.

AMERICAN SOCIETY OF CIVIL ENGINEERS
Founded November 5, 1852
TRANSACTIONS

Paper No. 2849

PHOTOSYNTHESIS IN SEWAGE TREATMENT

BY WILLIAM J. OSWALD,[1] A. M. ASCE, AND HAROLD B. GOTAAS,[2] M. ASCE

WITH DISCUSSION BY MESSRS. ISADORE NUSBAUM, AND WILLIAM J. OSWALD AND HAROLD B. GOTAAS

SYNOPSIS

The stabilization of organic matter in sewage wastes requires oxygen, which in secondary treatment plants is normally obtained from the atmosphere. The primary source of atmospheric oxygen is photosynthesis, for which the sun supplies the energy and water supplies the oxygen. Sewage contains the necessary nutrients for photosynthetic organisms to produce oxygen and at the same time to fix these valuable nutrients as well as solar energy in reclaimable material. Laboratory and pilot-plant investigations of sewage treatment in open ponds by photosynthetically produced oxygen have been conducted during the years 1951–1955. These studies have provided some basic principles which can be utilized for the engineering design of the process as well as for the prediction of the operational performance of new or existing oxidation ponds. In this paper the authors have formulated design criteria based on these principles. The chemical, biological, operational, and economic factors that affect the use of engineered photosynthesis as a method for producing oxygen and reclaimable wastes are outlined.

INTRODUCTION

The impounding of domestic sewage and industrial wastes in natural and artificial ponds has been practiced under various circumstances for a long time. In recent years, however, descriptions of pond designs and structures have appeared in engineering literature with increasing frequency, indicating that impounding is emerging as a distinct treatment process. Such facilities have been most commonly called "sewage lagoons" and "industrial waste lagoons."

NOTE.—Published, essentially as printed here, in May, 1955, as *Proceedings-Separate No. 686*. Positions and titles given are those in effect when the paper or discussion was approved for publication in *Transactions*.

[1] Asst. Research Engr., Inst. of Eng. Research, Univ. of California, Berkeley, Calif.

[2] Prof., San. Eng. Chem., Civ. Eng. Div., Univ. of California, Berkeley, Calif.

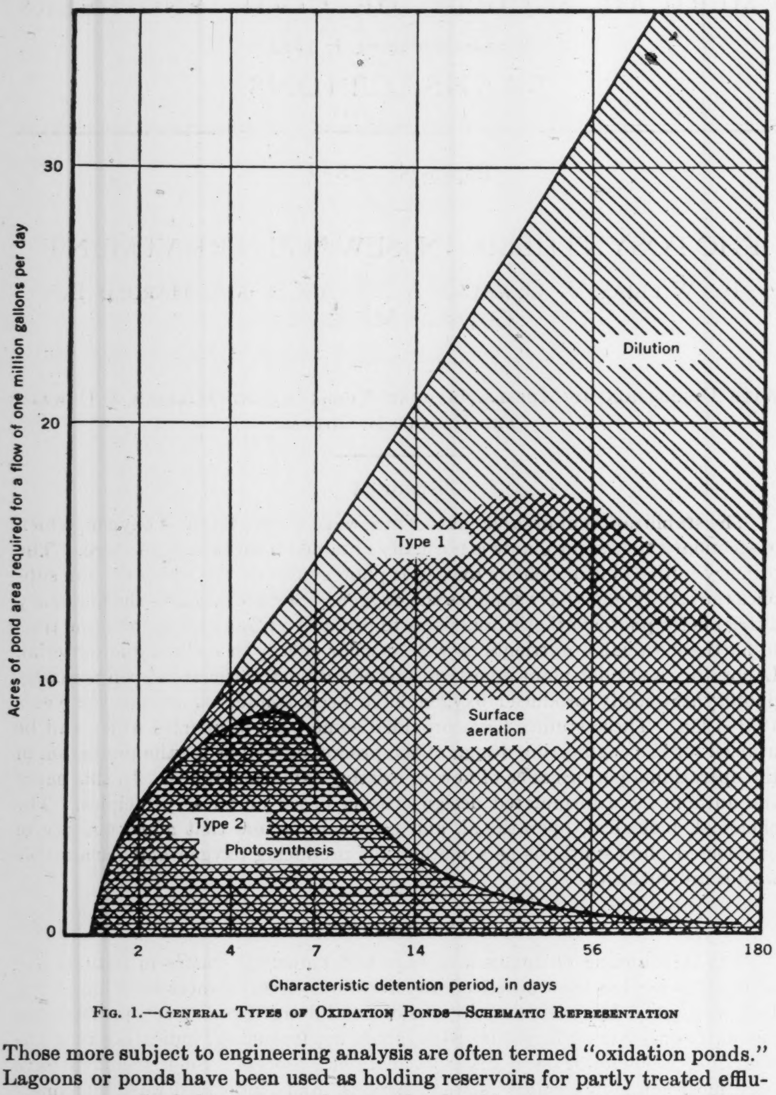

Fig. 1.—General Types of Oxidation Ponds—Schematic Representation

Those more subject to engineering analysis are often termed "oxidation ponds." Lagoons or ponds have been used as holding reservoirs for partly treated effluents from overloaded treatment plants and as leaching reservoirs for percolating liquid wastes into the soil; they have also been used in either primary or secondary sewage treatment, or in both. Ponds of this kind have certain characteristics in common: They accomplish a degree of treatment by biological oxidation, and they may produce growths of photosynthetic organisms, principally green algae.

Oxidation-Pond Types.—Studies indicate that oxidation ponds which differ greatly in detention time or physical size may also differ greatly in the principal mechanism by which oxygen is supplied to newly introduced wastes. For a fixed rate of inflow to ponds of various relative sizes and detention periods, the two principal mechanisms and corresponding pond types may be shown schematically as in Fig. 1.

In oxidation ponds of Type 1, having detention periods ranging from three weeks to six months or more, surface aeration is the most important source of oxygen. The larger units of this type which furnish oxygen by dilution are comparable to natural lakes because their physical size is so great that they may receive wastes with little depletion of their oxygen reserves. The design of such units has been described recently by W. Van Heuvelen and Jerome H. Svore.[3]

The smaller Type 1 oxidation ponds are commonly designed for detention periods of from three weeks to six weeks. They depend principally on surface reaeration with atmospheric oxygen which is accelerated by partial depletion of their oxygen reserve as oxidation of organic matter progresses. The design of this type of pond has been described by D. H. Caldwell,[4] A.M. ASCE.

Type 2 ponds utilize detention periods of less than one week. Their small size makes them highly dependent on the biological process of photosynthesis to yield the oxygen needed for oxidizing the entering wastes. This type of pond has not previously been described in the literature and thus far has been built only on a pilot scale.

As indicated in Fig. 1, no sharp distinctions are made between the pond types because there is overlapping in their oxygenation mechanisms. Photosynthesis, the major source of oxygen in ponds of Type 2, may also contribute to the oxygen resources of ponds of Type 1 whenever conditions are favorable for vigorous algal growth and also where recirculation is used. Surface aeration is a source of oxygen for ponds of Type 2, especially at night when photosynthetic oxygen production is nonexistent.

The principles of waste treatment by dilution and, to some degree, by surface aeration have been described in the engineering literature.[5,6] Few practical data on the principles of waste treatment by engineered photosynthesis are available however. It is the purpose of this paper to present such information, which has been developed in laboratory studies and pilot-plant studies during the past five years.

Photosynthesis.—Photosynthesis is the most basic process of biology. Through it green plants are able to make use of solar energy in appropriating carbon dioxide for incorporation into their own organic structure. Photosynthesis represents the ultimate origin of almost all organic matter and, thus, is the only important mechanism by which solar energy is stored in a form available for living organisms. It is also the basic mechanism by which oxygen is released from water; oxygen in turn is the only substance that makes it possible for living organisms to gain sustained access to the energy stored in organic matter. More simply stated, the production of organic matter by photosynthesis is accompanied by the absorption of energy and the release of oxygen whereas the destruction of organic matter involves the utilization of an equivalent amount of oxygen and the release of energy. In general, the value of this equivalence of oxygen and any amount of a specific organic matter may be determined from the elementary composition of the organic matter when newly formed.

---

[3] "Sewage Lagoons in North Dakota," by W. Van Heuvelen and Jerome H. Svore, *Sewage and Industrial Wastes*, Vol. 26, 1954, p. 771.

[4] "Sewage Oxidation Ponds—Performance Operation and Design," by D. H. Caldwell, *Sewage Works Journal*, Vol. 18, 1946, p. 433.

[5] "Stream Sanitation," by Earle B. Phelps, John Wiley & Sons, Inc., New York, N. Y., 1944.

[6] "Sewage Treatment," by Karl Imhoff and G. M. Fair, John Wiley & Sons, Inc., New York, N.Y., 1940.

Photosynthesis in Sewage Treatment

It is generally recognized that organic matter is most rapidly oxidized biologically by bacteria, and there is much evidence that it is most rapidly synthesized on a sustained basis by green algae. It is also well known that the principal products of aerobic bacterial oxidation of organic matter are CO_2, NH_3, and H_2O which, except for the additional requirement of light energy, are identical to the principal requirements for algal photosynthesis. Thus, in theory, the decomposition of organic matter by bacteria may occur at the same time that new organic matter is being synthesized by algae, provided that light is available as the energy source. Under such circumstances the efficiency of oxygen utilization is greatest because oxygen is used as soon as it is formed. This cycle of photosynthetic oxygen production is shown in Fig. 2. Organic matter entering the system as sewage is oxidized by sewage bacteria utilizing

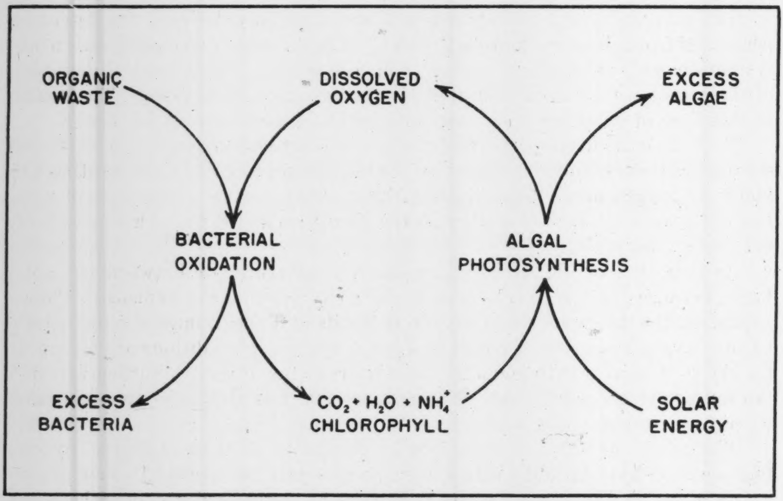

Fig. 2.—The Cycle of Oxygen and Algal Production in Sewage Treatment by Photosynthesis

oxygen released by algae. The algae, utilizing solar energy, are simultaneously synthesizing organic matter from hydrogen liberated in their chlorophyll pigments and from the carbon dioxide and ammonia produced by bacteria. Although this entire reaction may occur in a closed system, some carbon dioxide is normally drawn into the cycle from the atmosphere and excess oxygen may be lost.

The cycle shown in Fig. 2 is the basic principle on which the Type 2 oxidation pond of Fig. 1 is operated. In order to develop practical equations for the design of such a unit, it is desirable to assume that it will be operated so that all the oxygen required by bacteria will result from the development of new photosynthate. It is desired also to evaluate some of the previously cited basic factors of photosynthesis and to express them in simple mathematical symbols. These factors are: (1) The relationship between oxygen and organic photosynthate; (2) the relationship between stored energy and organic photosynthate; and (3) the relationship between energy stored in organic photosynthate and the solar energy required to produce it.

The ratio of the weight of oxygen released, W_o, to the weight of organic matter synthesized, W_{om}, may be expressed as a factor, p:

$$p = \frac{W_o}{W_{om}} \qquad (1)$$

The available stored energy content, H, of the organic photosynthate is equal to its unit heat of combustion, h, times its weight, W_{om}, or

$$h = \frac{H}{W_{om}} \qquad (2)$$

The fraction of solar energy, E_s, fixed in the form of organic matter is equal to the total available heat energy, H, of the organic matter divided by a factor, F, which is the efficiency of energy conversion.

$$E_s = \frac{H}{F}, \quad \text{or} \quad F = \frac{H}{E_s} \qquad (3)$$

The ratios from Eqs. 1, 2, and 3 may be combined so as to show the basic relationships between algal cell concentration, depth, detention period, solar-energy input, and photosynthetic efficiency in photosynthetic oxygen production. These relationships may then be utilized with certain modifications to determine rational values for the physical dimensions of a pond of Type 2.

As shown by Eq. 3, the heat of combustion of algal cell material is proportional to the amount of the total light energy which has been fixed ($H = F\,E_s$). Because efficiency, F, is dimensionless, both H and E_s should be expressed in the same units. The energy, E_s, is related to insolation as follows:

$$E_s = S\,A\,D \qquad (4)$$

in which S is the insolation in langleys (gram-calories per square centimeter) per day; A is the surface area exposed to light, in square centimeters; and D is the time, in days.

Substituting in Eq. 3 the value of H from Eq. 2 and the value of E_e from Eq. 4,

$$S\,A\,D\,F = h\,W_{om}, \quad \text{or} \quad F = \frac{h\,W_{om}}{S\,A\,D} \qquad (5a)$$

in which W_{om} equals the weight of organic matter produced in area A and F is the efficiency of light utilization.

From the considerations shown in the development of Eq. 4, Eq. 3 may be written as

$$H = S\,A\,D\,F \qquad (5b)$$

The energy fixed in algal cells, H, may also be evaluated by multiplying the heat of combustion of the algae, h, by the concentration of algae, C_e, expressed in milligrams per liter rather than as W_{om}. Thus, $H = S\,A\,D\,F = h\,C_e$. Because the surface area, A, for one liter of liquid of depth, d, in centimeters is 1,000/d sq cm,

$$h\,C_e = \frac{S\,1{,}000\,D\,F}{d}, \quad \text{or} \quad D = \frac{h\,C_e\,d}{S\,1{,}000\,F} \qquad (6)$$

Since in deriving Eq. 6 the oxygen demand of a waste is assumed to be met through photosynthetic oxygen production, the biochemical oxygen demand, L_t, in any time, t, may be substituted for oxygen produced, W_o, and C_e may be substituted for W_{om}. That is,

$$p = \frac{W_o}{W_{om}} = \frac{L_t}{C_e} \quad \text{or} \quad C_e = \frac{L_t}{p} \qquad (7)$$

Combining Eqs. 5*a* and 7,

$$D = \frac{h\,L_t\,d}{1{,}000\,F\,S\,p} \qquad (8)$$

The efficiency, F, in Eqs. 6 and 8 is modified by many environmental factors.

The quantitative effects of each of the several environmental factors are not usually known. Experimental coefficients representing them can be determined, however, and then be applied to the factor, F. For example, temperature strongly affects both bacterial and algal growth. Hence, a temperature coefficient, T_e, is required in Eqs. 6 and 8.

$$d = \frac{h\,C_e\,d}{F\,T_e\,1{,}000\,S} = \frac{h\,L_t\,d}{F\,p\,T_e\,1{,}000\,S} \qquad (9)$$

EVALUATION OF THE DESIGN EQUATION

The actual application of Eq. 9 to the design of oxidation ponds depends on a knowledge of the interrelationships between the several factors in the equation in addition to the influence of environmental factors on the efficiency of algal and bacterial growth.

Depth.—The depth, d, necessary for a pond to produce by photosynthesis the oxygen required by a waste can be developed in terms of algal cell concentration, C_c. Experimental data have shown conclusively that a suspension of algal cells absorbs light, within close limits, in accordance with the Beer-Lambert law:

$$\frac{I}{I_i} = e^{-C}\, c^{\alpha d} \qquad (10)$$

in which I is the measured light intensity at depth d, I_i is the incident light intensity, and α is the specific absorption coefficient. Taking the natural log of both sides of Eq. 10,

$$\log_e I - \log_e I_i - C_c \alpha d \qquad (11)$$

For a practical design it should be assumed that all the available light is absorbed; therefore, at the pond bottom the transmitted light, I, should be approximately zero. Equating I to 1.0 and solving Eq. 11 for d,

$$d = \frac{\log_e I_i}{C_c \alpha} \qquad (12)$$

If one neglects the possibility of unusual turbidity other than algal cells, Eq. 12 expresses the depth, d, to which light penetrates through a culture. Thus, Eq. 12 defines the effective depth for photosynthetic oxygen production inasmuch as there is no visible light and, hence, no algal growth below depth, d.

Because daylight intensities vary from a few hundred foot-candles to more than 10,000 ft-c and α and C_c vary between 1×10^{-3} and 2×10^{-3} and between 1×10^2 and 3×10^2, respectively, it might seem that light intensity would have the greatest effect on the depth of light penetration. Actually light intensity may increase tenfold with but a 33% increase in the depth of penetration. On the other hand, reducing cell concentration by a factor of 2 will double the depth of penetration. The value of the coefficient α depends on the algal species and their pigmentation and is not normally subject to close control. In practice, however, it may remain approximately 1.5×10^{-3}. Hence, it may be concluded that algal cell concentration is the most important of three factors which determine the depth to which light will penetrate into a pond. The value of d determined from Eq. 12 is the depth which normally should be substituted in Eq. 6, Eq. 8, or Eq. 9.

Values of the Factor, h.—The heat content of algal cell material is a variable factor. It may be measured by calorimetric methods or computed from the chemical content of the algae. In general, it has been shown to be proportional to a factor termed the "R-value," which represents degree of reduction of the organic matter synthesized. If the percentage by weight of carbon, hydrogen, and oxygen in the organic matter is known, R may be determined. H. A. Spoehr and H. W. Milner[7] have shown that $R = \left(\frac{\%\,C \times 2.66 + \%\,H \times 7.94 - \%\,0}{398.9}\right) 100$. It may also be shown that there is a relationship between R and h which closely follows the empirical expression, $h = R/7.89 + 0.4$. Thus, a hypothetical material having an R-value of 60 should have a heat of combustion of about 8 kg-calories per gram. These relationships have been confirmed in the laboratory by calorimetric methods for algal cell material grown on sewage. Normally for sewage-grown algae, h is near 6 kg-calories per gram on an ash-free basis.

---

[7] "The Chemical Composition of Chlorella; Effect of Environmental Conditions," by H. A. Spoehr and H. W. Milner, *Plant Physiology*, Vol. 24, 1949, p. 120.

Values of the Factor, p.—The relationship between the weights of oxygen released and organic matter synthesized varies within relatively narrow limits. As in the case of h, one fundamental method for its evaluation is to measure carbon, hydrogen, oxygen, and nitrogen in the algal cell material. For example, an analysis of a certain culture of algal cells shows carbon to be 59.3%; hydrogen, 5.24%; oxygen, 26.3%; and nitrogen, 9.1%, on an ash-free, dry-weight basis. By dividing each of these percentages by the atomic weight of the corresponding element and by correcting the resulting numbers proportionately to make the value of the nitrogen coefficient equal to one, the following formula for algal cell material is developed: $C_{7.62}\,H_{8.08}\,O_{2.53}\,N_{1.0}$. Inasmuch as all evidence indicates that ammonia is the source of the nitrogen, carbon dioxide is the principal source of the carbon and water is the source of the oxygen, it may be assumed that the synthesis of this material is expressed by the equation,

$$1.0\,NH^+_4 + 7.62\,CO_2 + 2.53\,H_2O \rightarrow C_{7.62}\,H_{8.08}\,O_{2.53}\,N_{1.0} + 7.62\,O_2 + 1.0\,H^+.$$

Considering only cell material and oxygen on the right-hand side of the equation, $(12 \times 7.62) + (1 \times 8.08) + (16 \times 2.53) + (14 \times 1) = 153.56$ g cell material, and $(7.62 \times 32) = 243.84$ g oxygen, from which 1 g of cell materials is found to be equivalent to 1.587 g of oxygen. Because algal cell material may contain approximately 85% organic matter, the oxygen yield per gram of ash-included organic matter is 1.587×0.85 or approximately 1.35 g. Experimental work has shown that, under environmental conditions which are practical for photosynthetic oxygen production, the value of factor, p, is normally between 1.25 and 1.75. Thus, it may be concluded that synthesis of a unit weight of freshly produced algal cells has been accompanied by the production of a greater weight of oxygen in a form available for bacterial oxidation of organic matter.

Limitations on Efficiency.—It is to be expected that every factor affecting living cells will influence the efficiency with which green algae utilize solar energy. No firm value has been established for the maximum efficiency of photosynthesis although it may be more than 50% under certain conditions.[8] However, for purposes of application to sewage treatment, the question of maximum photosynthetic efficiency is largely academic because a practical barrier to high efficiency occurs long before the maximum reported values are reached.

This practical barrier is evolved from the fact that there is a maximum intensity of light which individual algal cells can utilize during a sustained period. All light energy supplied at a higher rate is therefore partly wasted. The critical light intensity above which no additional light is utilized has been termed the "saturation intensity," I_s. The importance of this factor in pond design is due to its effect in placing a practical upper limit on the efficiency, F, that can be used in Eqs. 6 and 8.

---

[8] "Quantum Mechanism and Energy Cycle Process in Photosynthesis," by Dean Burk and Otto Warburg, *Naturwissenschaften*, Vol. 37, 1950, p. 560.

According to Vannevar Bush, as quoted by John S. Burlew,[9] the maximum fraction of available light that may be utilized by an individual alga is

$$f = \frac{I_s}{I_i}\left(\log_e \frac{I_i}{I_s} + 1\right) \dots\dots\dots\dots\dots\dots (13)$$

in which I_i is the incident light intensity, I_s is the saturation light intensity, and f is the fraction of the available light utilized.

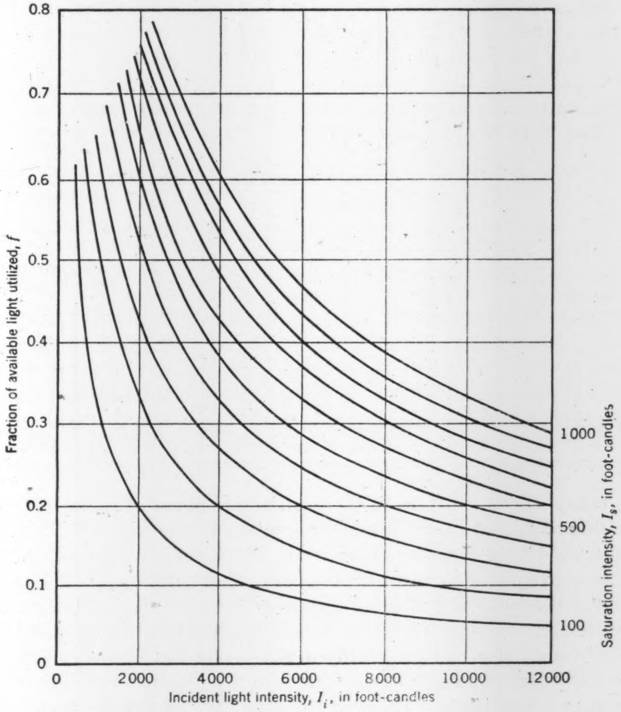

FIG. 3.—INFLUENCE OF SATURATION INTENSITY ON LIGHT UTILIZATION BY ALGAE

Fig. 3 shows graphically how f is influenced by changes in the incident and saturation light intensities. It is evident that, as the saturation intensity increases, the percentage of incident light which is utilized also increases. Thus, for example, for an I_i-value of 8,000 ft-c and an I_s-value of 400 ft-c, only 20% of the available light energy is utilized whereas, for an I_s-value of

---

[9] "Algal Culture from Laboratory to Pilot Plant," by John S. Burlew, *Publication 600*, Carnegie Institution of Washington, D.C., 1953.

700 ft-c, 30% of the energy is used. As I_i increases, f decreases regardless of the value of I_s. Investigations[9] have shown as one result of the foregoing that, if algal cells can be brought intermittently into contact with high-intensity light through turbulence created by vertical mixing, the percentage of available light that may be utilized is increased. This increase in the availability of light theoretically increases the depth which can be used in Eq. 6, Eq. 8, or Eq. 9 above that which might be determined from Eq. 12. Hence, the economically effective depth could be greater than the depth determined from Eq. 12. Further data are required, however, before any permissible increase in depth can be predicted under conditions of vertical mixing.

The value of I_s is not the same for all cultures of sewage-grown algae but rather it is a function of the physiological makeup of the particular cells in the culture. Their mechanisms for light absorption, hydrogen transfer, organic synthesis, and cell multiplication, when functioning at peak efficiency provide the highest saturation intensity. It has been previously demonstrated by the writers[10] that these functions are performed most effectively by young, rapidly growing cells. Thus, cultures in the logarithmic phase of cell growth attain a higher value of I_s and utilize a greater fraction of the available light than do older cultures. To support a population of young cells in the logarithmic phase of growth, a substrate rich in nitrogen and other vital elements is necessary. This condition is met only at short detention periods—that is, low values of D.

TABLE 1.—TEMPERATURE COEFFICIENTS FOR PILOT–PLANT CHLORELLA

Mean Temperature, in Degrees		Photosynthetic temperature coefficient, T_c
Centigrade	Fahrenheit	
0	32	...
5	41	0.26
10	50	0.49
15	59	0.87
20	68	1.00
25	77	0.91
30	86	0.82
35	95	0.69
40	104	...

Only moderate values of efficiency are practical in sewage treatment because high values of F can occur only in substrates that are very rich in nutrients and hence are not stabilized. Values of F exceeding 10% are believed to indicate such a condition. Because the objective of sewage treatment is to produce a substrate depleted in organic matter, a relatively low average efficiency during the process is implied.

Temperature data are used to typify the manner in which photosynthetic efficiency is modified by environmental factors. In Table 1 are presented typical values for the temperature coefficient, T_c. This table is based on data for cultures of chlorella isolated in pilot-plant studies and grown in the laboratory at a light intensity of 1,200 ft-c, illuminated an average of 14.4 hr daily, and at a detention period of 4 days. As previously indicated different values of T_c might be obtained under different experimental conditions and with different species of algae. This fact is illustrated by the observation that the dominant species of algae in an oxidation pond tends to change with the seasons.[11] Sustained low temperatures require consideration. Data obtained in the laboratory indicate that low-temperature adaptation is a characteristic of the chlorella encountered in pilot-plant studies.[11] This strain, or comparable strains of algae, may be expected to occur in low-temperature ponds and will sustain photosynthetic oxygen production at temperatures nearly as low as freezing. However, as shown in Table 1, temperature coefficients which modify efficiencies are greatly reduced at the lower temperatures. The rate of bacterial oxidation of sewage is also reduced at low temperatures, and it may become reduced to a point where little oxidation is accomplished regardless of the oxygen supply. In regard to high temperatures, a strain of chlorella that has a high temperature tolerance has been reported by Jack Myers.[12] This and other strains will undoubtedly develop under favorable conditions particularly if afforded an adaptation period.

---

[10] "Algae Symbiosis in Oxidation Ponds. II. Growth Characteristics of *C. pyrinoidosa* Cultured in Sewage," by W. J. Oswald, H. B. Gotaas, H. F. Ludwig, and V. Lynch, *Sewage and Industrial Wastes*, Vol. 25, 1953, p. 26.

Values of the Factor, S.—The daily amount of solar energy, S, that reaches the earth's surface is a function of astronomical, geographical, and meteorological phenomena. As might be expected it is subject to wide daily and seasonal variation, but on a monthly basis it may be closely predicted at any particular location if certain geographical and meteorological data are available. Table 2 represents predicted maximum and minimum plausible values of S for the indicated segment of the earth, as computed by the writers from relationships published by H. H. Kimball[13] together with other data collected and published by the Weather Bureau (United States Department of Commerce).[14,15] Use of Table 2 to determine the value of S is illustrated by the following example:

The numbers in the columns under each month represent the visible and total insolation (solar radiation), both direct and diffuse, incident on a horizontal surface at sea level, expressed in langleys (gram-calories per square centimeter) per day. Values in the right-hand column for any month are total insolation (ultraviolet, visible, and infrared) whereas those in the left-hand column are the portion of this total radiation which lies in the visible range—that is, the amount of radiation of wave lengths from 4,000 A° to 7,000 A° that will penetrate a smooth water surface. The maximum (max) values represent in each case the average daily amount of radiant energy which may be received during clear weather. These maximum values have been computed taking into consideration all the important factors influencing insolation. Hence,

---

[11] "Photosynthetic Reclamation of Organic Wastes," by H. B. Gotaas, W. J. Oswald, and H. F. Ludwig, *Scientific Monthly*, Vol. 79, 1954, p. 368.

[12] "Growth Characteristics of Algae in Relation to the Problems of Mass Culture," by Jack Myers, *Publication 600*, Carnegie Institution of Washington, 1953.

[13] "Intensity of Solar Radiation at the Surface of the Earth and its Variations with Latitude, Altitude, Season, and Time of Day," by H. H. Kimball, *Monthly Weather Review*, Vol. 63, 1935, p. 1.

[14] "Solar Radiation Data by Stations," *Monthly Weather Review*, U. S. Dept. of Agriculture, Nos. 71–77, U. S. Govt. Printing Office, Washington, D. C.

[15] "Solar Radiation Data Annual Summary," *Climatological Data: National Summary*, U. S. Dept. of Commerce, Nos. 1–3, U. S. Govt. Printing Office, Washington, D. C., 1943–1953.

TABLE 2.—SOLAR RADIATION[a]; PROBABLE AVERAGE VALUES SURFACE AT SEA LEVEL,

NORTH LATITUDE		MONTH											
Degree	Range	January		February		March		April		May		June	
		vis[c]	tot[d]	vis	tot	vis	tot	vis	tot	vis	tot	vis	tot
0	max[e]	255	685	266	700	271	708	266	690	249	645	236	626
	min[f]	210	580	219	583	206	536	188	462	182	480	103	274
2	max	250	670	263	693	271	706	267	697	253	655	241	642
	min	206	560	213	560	204	534	188	464	184	484	108	288
4	max	244	650	259	688	270	704	268	701	258	665	247	656
	min	200	540	206	543	202	532	187	466	187	492	113	300
6	max	238	630	254	675	268	702	270	705	262	675	252	668
	min	193	520	199	530	200	530	186	467	189	500	118	310
8	max	230	610	249	665	267	700	270	709	266	685	258	678
	min	187	495	192	510	196	523	185	467	191	506	124	320
10	max	223	595	244	655	264	694	271	711	270	694	262	688
	min	179	475	184	490	193	513	183	464	192	512	129	330
12	max	216	572	239	645	262	690	271	710	273	702	267	700
	min	172	455	176	470	189	500	181	462	193	518	133	343
14	max	208	555	233	630	258	680	271	709	276	710	272	710
	min	163	430	167	450	184	487	179	460	194	524	137	354
16	max	200	530	226	610	255	670	272	707	279	718	276	720
	min	154	400	159	430	180	473	177	456	194	528	141	363
18	max	192	515	220	590	250	664	272	705	282	723	280	728
	min	144	380	150	410	174	459	174	452	194	530	145	375
20	max	183	500	213	575	246	652	271	703	284	730	284	738
	min	134	360	140	390	168	440	170	447	194	532	148	383
22	max	174	480	206	560	241	644	270	701	286	734	286	747
	min	123	335	132	370	162	426	167	440	193	530	152	392
24	max	166	460	200	545	236	625	268	697	288	738	290	753
	min	111	310	123	340	156	410	164	433	191	525	155	403
26	max	156	440	192	530	230	615	266	690	288	741	292	760
	min	99	280	114	310	149	390	160	425	189	518	158	409
28	max	146	420	184	510	224	603	264	683	289	743	294	764
	min	87	250	106	290	142	373	156	415	187	506	161	418
30	max	136	400	176	490	218	587	261	675	290	744	296	768
	min	76	220	96	260	134	362	151	405	184	490	163	425
32	max	126	380	169	470	212	570	258	663	290	744	296	772
	min	63	180	87	240	126	340	146	395	181	475	166	431
34	max	114	360	160	450	204	553	254	657	290	743	297	775
	min	53	155	78	215	118	320	141	385	176	462	168	439
36	max	103	335	150	430	196	538	250	650	288	741	298	776
	min	44	133	70	200	111	300	136	375	172	444	170	443
38	max	90	310	140	415	189	520	246	640	287	738	298	778
	min	36	120	62	180	103	280	131	365	166	428	171	448
40	max	80	280	130	390	181	500	241	630	286	732	298	778
	min	30	105	53	160	95	270	125	355	162	415	173	450
42	max	68	255	119	370	172	485	236	618	283	728	298	777
	min	24	90	45	140	88	250	120	344	157	405	174	451
44	max	55	228	106	340	165	470	230	607	280	722	298	777
	min	20	80	37	130	80	230	114	325	153	395	175	453
46	max	45	200	94	315	156	450	224	598	278	716	298	776
	min	16	74	30	110	72	210	108	315	150	385	175	455
48	max	35	180	82	290	149	430	218	582	274	710	297	776
	min	12	64	25	99	64	190	102	307	146	378	176	458
50	max	28	164	70	265	141	410	210	568	271	703	297	776
	min	10	54	19	80	58	173	97	300	144	371	176	458
52	max	22	140	60	240	134	390	202	555	267	695	296	776
	min	8	45	14	62	51	158	92	295	141	366	176	460
54	max	16	120	50	215	126	370	194	542	263	687	296	776
	min	6	40	11	45	46	145	88	289	139	360	176	460
56	max	12	102	43	200	120	350	188	528	258	680	295	775
	min	4	35	8	35	41	132	85	283	136	352	175	460
58	max	9	80	37	170	113	330	182	516	254	670	294	774
	min	3	28	6	28	37	118	82	277	134	346	175	460
60	max	7	64	32	150	107	310	176	500	249	660	294	773
	min	2	20	4	20	33	105	79	270	132	340	174	460

---

[a] Calculated from data published by the Weather Bureau. Approximate corrections for elevation up to 10,000 ft: (1) Total radiation = (total at sea level) (1 + 0.0185 × El.), and (2) Visible radiation = ("visible" at sea level) (1 + 0.00925 × El.). Correction for cloudiness (approximate): Min + [(max − min) cl.] in which cl. is the fraction of time the weather is clear. [b] Gram calories per square centimeter. [c] "Visible" = radiation

OF INSOLATION—DIRECT AND DIFFUSE—ON A HORIZONTAL IN LANGLEYS[b] PER DAY

Month												North Latitude	
July		August		September		October		November		December		Range	Degree
vis	tot	vis	tot	vis	tot	vis	tot	vis	tot	vis	tot		
238	630	252	666	269	690	265	694	256	683	253	667	max	0
137	368	167	432	207	533	203	530	202	543	195	527	min	
244	646	255	673	269	693	262	688	251	666	249	646	max	2
141	375	169	442	206	531	200	523	198	526	189	505	min	
250	657	258	678	269	695	260	680	246	650	244	628	max	4
146	385	171	448	204	529	196	513	194	510	183	480	min	
255	669	261	683	269	697	256	670	240	634	238	610	max	6
150	395	172	452	202	524	191	500	188	494	176	460	min	
260	680	263	688	267	695	252	660	234	616	231	590	max	8
154	405	174	456	200	518	186	486	182	478	169	440	min	
265	690	266	693	266	693	248	650	228	600	225	570	max	10
158	414	176	460	196	510	181	474	176	462	162	420	min	
269	700	267	697	264	691	244	640	221	585	217	550	max	12
161	421	176	464	193	502	176	462	169	446	154	400	min	
273	708	269	700	262	688	240	627	214	567	209	536	max	14
164	429	177	467	189	496	170	449	162	430	146	380	min	
277	715	270	703	259	684	234	615	206	554	200	520	max	16
167	435	177	469	185	489	164	434	154	410	138	360	min	
280	723	272	705	256	680	229	605	198	538	192	500	max	18
170	442	177	471	180	479	157	418	146	390	129	340	min	
282	729	272	706	252	674	224	596	190	520	182	480	max	20
172	450	177	472	176	467	150	400	138	370	120	320	min	
285	736	273	707	248	668	218	582	183	500	172	460	max	22
173	454	176	472	170	455	143	380	128	350	110	300	min	
287	742	273	708	244	659	212	568	175	480	161	440	max	24
176	459	174	471	165	443	136	360	119	326	101	280	min	
288	749	273	706	240	652	205	552	166	460	149	420	max	26
177	463	172	469	160	429	128	332	109	300	90	260	min	
288	755	272	704	236	635	199	537	157	440	138	400	max	28
178	467	169	466	154	415	120	310	99	278	80	236	min	
289	759	271	702	231	625	192	524	148	420	126	380	max	30
178	469	166	462	147	399	113	290	90	256	70	210	min	
289	761	269	700	226	615	185	510	138	400	114	360	max	32
178	472	163	458	140	385	104	270	80	224	60	184	min	
289	763	267	696	221	602	178	490	128	380	101	338	max	34
178	472	159	448	134	368	96	250	70	202	47	158	min	
289	765	264	690	215	590	170	470	118	360	88	314	max	36
177	470	155	438	127	350	88	230	60	180	39	134	min	
288	766	262	684	210	576	162	450	106	336	77	290	max	38
175	464	152	429	120	330	80	216	50	158	30	111	min	
288	765	258	680	203	562	152	430	95	313	66	270	max	40
172	455	147	416	112	310	72	202	42	134	24	94	min	
287	761	254	670	196	547	144	410	84	289	56	244	max	42
167	442	143	403	105	290	65	187	34	112	19	78	min	
285	755	250	660	189	530	132	390	72	263	47	218	max	44
164	430	139	389	98	270	58	173	28	98	15	62	min	
284	749	245	650	181	512	122	370	61	238	39	194	max	46
161	420	134	374	90	250	52	158	23	86	11	48	min	
282	740	241	640	174	496	111	350	50	210	32	170	max	48
158	410	129	358	81	230	45	144	18	70	9	37	min	
280	733	236	625	166	480	100	329	40	183	26	144	max	50
155	403	125	342	73	210	40	130	15	60	7	30	min	
278	725	232	615	158	460	87	307	32	160	21	121	max	52
153	398	120	326	65	190	34	120	12	53	4	27	min	
276	720	224	602	150	440	76	285	25	140	16	99	max	54
150	394	116	312	58	170	29	106	9	43	3	23	min	
273	714	218	587	141	420	64	261	20	120	12	78	max	56
148	390	110	297	51	150	24	95	7	36	2	18	min	
270	710	212	575	134	402							max	58
146	385	106	285	44	132							min	
268	708	205	556	126	386							max	60
144	380	100	270	38	116							min	

---

of wave lengths of 4,000 A° to 7,000 A° penetrating a smooth water surface. [d] "Total" = radiation of all wave lengths in the solar spectrum. [e] Value which will not normally be exceeded. [f] Value based on, or extrapolate from, lowest values observed for indicated month and latitude during ten years of record.

there is little chance that any particular value will be exceeded during the month for which it is listed. Minimum (min) values represent average daily amounts that may be received during weather with heavy incidence of clouds. These minimum values reflect graphic interpolations or extrapolations of minimum observations reported in Weather Bureau records during the ten-year period, 1943 to 1952, inclusive. Thus, although these minimum values do not reflect the most cloudy days of record, there is little chance that any of the stations will experience monthly averages appreciably lower.

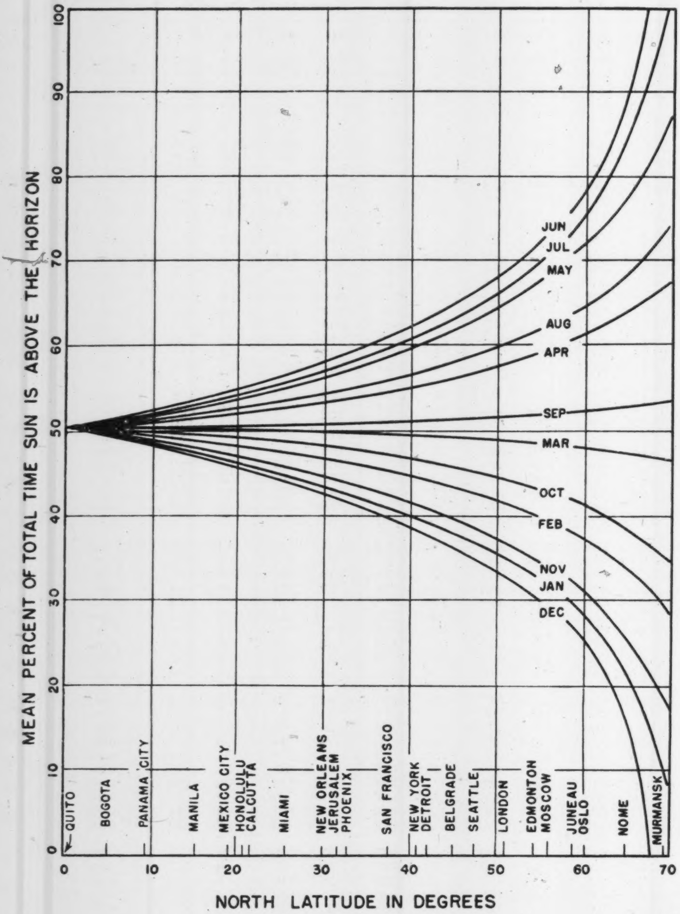

Fig. 4

When corrections are made for elevation and cloudiness in the manner noted at the bottom of Table 2, values of visible radiation obtained from the table may be used as a quantitative measure of the energy available for photosynthesis—that is, as values of S to be used in Eq. 6, Eq. 8, or Eq. 9.

Table 2 may also be used in connection with Fig. 4 in order to estimate a value of I_i to be substituted in Eq. 12 to determine an approximate value of d for use in Eq. 6, Eq. 8, and Eq. 9. Studies by the writers have shown that the mean light intensity at a point for the entire twenty-four hour period of a day is about ten times the total insolation expressed in langleys per day, multiplied by the fraction of the time the sun is visible. A value so estimated is altered by many variable factors and is not subject to precise evaluation. However, this method is relatively accurate for determining the average light intensity during a period of time and may be used for the estimation of I_i by the following steps:

1. The total solar radiation is determined from Table 2.
2. The necessary corrections are made for elevation and cloudiness.
3. The resulting value is multiplied by 10.
4. One evaluates I_i for use in Eq. 12 by multiplying the result of step 3 by the fraction of time the sun is visible for the appropriate latitude and month as determined from Fig. 4.

For example, following the foregoing steps a station at latitude 37°, El. 2000, with clear weather 50% of the time may have a mean light intensity in December of approximately 870 ft-c on a horizontal surface.

INFLUENCE OF CHEMICAL FACTORS

Nitrogen.—The writers[16] have collected considerable evidence indicating that the species of algae which are effective in photosynthetic oxygen production utilize ammonia as the principal source of nitrogen with which to build their proteinaceous cell material. At moderately long detention periods of 3 days or 4 days when temperature and light are optimum, almost all the available ammonia nitrogen appears in the form of algal cell material. In this way nitrogen is conserved and at the same time the ultimate oxygen demand of a waste material is greatly diminished because little ammonia remains to be oxidized to nitrate.

Under some conditions, supernatant analyses show the presence of reduced nitrogenous compounds. Although there can occur a small carry-over of sewage unoxidized during the short detention periods normally effective in the process, the quantity of these compounds increases with increasing detention periods; this fact indicates that a small amount of inseparable organic matter is produced in the process. A portion of the nitrogenous material is fixed in living bacterial cells, which are dispersed as colloids and are discharged in the supernatant liquid. Whatever the nature of this supernatant nitrogen, under proper operating conditions it normally amounts to less than one-third the total nitrogen in the waste while the remainder appears in the algal cells.

---

[16] "Algae Symbiosis in Oxidation Ponds. III. Photosynthetic Oxygenation," by W. J. Oswald, H. B. Gotaas, H. Ludwig, and V. Lynch, *Sewage and Industrial Wastes*, Vol. 25, 1953, p. 692.

The nitrogen content of a waste material places a practical upper limit on the concentration of cell material which can be developed from it. A useful rule-of-thumb relationship between sewage nitrogen and growing algae is that $C_c = 10 \times N$, in which C_c (the maximum algal cell concentration) and N (nitrogen) are expressed in the same units. The constant 10 stems from the assumption that 80% of the nitrogen in the waste is recovered and that algal cells are 8% nitrogen. For example, it has been observed that a waste material containing 30 ppm of total nitrogen will support $0.8 \times 30/0.08 = 300$ ppm of algal cells before nitrogen becomes a limiting factor to cell growth.

Phosphorus.—Phosphorus rarely becomes a limiting factor to algal growth in sewage. The best information now available indicates that phosphorus does not normally exceed 1.5% of the dry weight of algae. In this case a typical sewage containing 6 ppm or more of phosphorus would sustain an algal concentration of 400 ppm or more if all the phosphorus were available. Increased use of detergents in the home and in industries makes it unlikely that either phosphorus or nitrogen (both components of detergents) will be limiting factors in the nutritional makeup of domestic sewage.

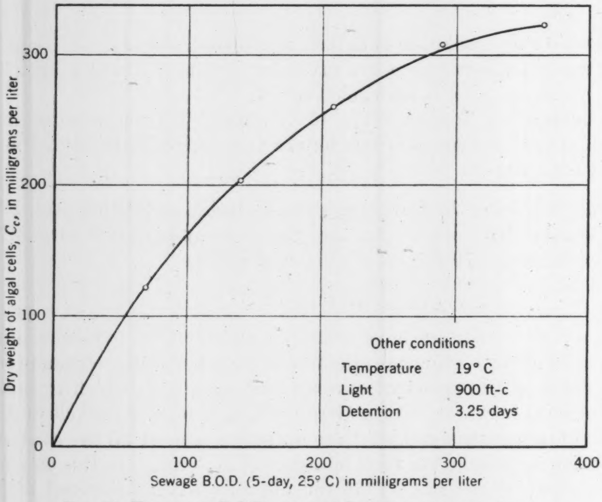

FIG. 5.—EFFECT OF B.O.D. ON THE CONCENTRATION OF ALGAL CELLS IN CONTINUOUS CULTURES

Magnesium and Potassium.—Both magnesium and potassium are essential to algal growth. Magnesium is essential because it is an integral part of the chlorophyll molecule, and potassium because salts of this metal are prime constituents of algal cell sap. Normally domestic sewage contains more than 5 ppm of both these elements. Since algal cells may contain 0.5% potassium and 1% magnesium, it can be concluded that if these elements are fully available domestic sewage contains them in sufficient amounts to support algal concentrations in excess of 500 ppm.

Carbon.—Carbon is usually the limiting element when algae are cultured in sewage. However, the use of artificially introduced carbon is neither essential nor desirable when algae are cultured in sewage for purposes of photosynthetic production of oxygen. Although the amount of carbon contained in sewage may be inadequate to produce growths large enough to meet the oxygen demand of the waste, the culture may also obtain carbon dioxide from the air. Active photosynthesis causes the pH to increase to 10 or more, accelerating the absorption of atmospheric CO_2 by the culture. Under such conditions this CO_2 appears in the solution as a bicarbonate ion and becomes available to the algae at once. From this fact it is seen that algae may compensate for a shortage of CO_2 by increasing the CO_2 absorbing properties of the solution in which they grow.

Biochemical Oxygen Demand.—The B.O.D. test is unique in its significance as a measure of the response of microbial growth to the nutritional character of wastes. Fig. 5 shows the effect of the B.O.D. of a sewage on the algal growth it will support. It is noteworthy that in continuous cultures such as those reported in Fig. 5 the dry weight of algal cell material appears to be a logarithmic function of B.O.D. up to approximately 400 ppm. Evidence indicates that for B.O.D.-values greater than 300 ppm light rather than nutrition is normally limiting to outdoor algal growth. The effect of increasing light intensity above that shown for the tests in Fig. 5 would be to increase culture density slightly. However, the shape of the curve would remain similar.

Actual laboratory tests are needed to determine whether a given domestic sewage will support enough algal growth to produce its oxygen requirements by photosynthesis.

DESIGN CONSIDERATIONS

Detention Period.—Inasmuch as the detention period, D, as shown in Eq. 9 is a function of light and temperature, theoretically it should be capable of much greater variation than is possible in practical pond design. For example, to apply Eq. 9 to a sewage having a B.O.D. of 150 ppm under December conditions at latitude 37°, it may be assumed that $p = 1.5$, $h = 6.0$, $d = 30$ cm, $F = 0.1$, and $T_e = 0.87$. From Table 2, S (min) may be taken as 34 langleys per day. Using these values it is computed that a detention period of nearly 6 days might be required for complete sewage treatment. In the summertime the efficiency of a pond designed for such a detention period would become very low. Without proper variations in operating procedures the result could be overproduction of algae, a part of which might die and be decomposed, thus producing a pond effluent having a high supernatant B.O.D. On the other hand, if a pond were designed for the same location on the basis of June light and temperature conditions using S (average) $= 234$, $T_e = 1.0$, and other factors remaining the same, from Eq. 9 a detention period of only 0.77 day is determined. Pilot-plant units have been successfully operated at detention periods as low as 0.75 day for sustained periods with otherwise optimum environmental conditions, and chlorella as well as other algae easily maintain a rate of growth sufficient to prevent being diluted out of the pond under these conditions. However, it has been found from pilot-plant experience that cultures cannot withstand either low temperatures or a long succession of cloudy days at this low detention period without some nuisances occurring. Hence, if a pond were to be designed for the June conditions previously stated, it would be better to increase the detention period and the pond depth. For the stated June conditions of light and temperature the depth, *d*, determined from Eq. 12 is increased to 48 cm, in which case the detention period determined from Eq. 9 would become 1.25 days, a value more in keeping with the growth capabilities of organisms under varying outdoor conditions. In order to provide a detention period suitable for effective photosynthetic oxygen production in both winter and summer and with "buffer capacity" against changes in light and temperature and against shock loading, certain compromises are necessary. In some cases it might be feasible to design with the expectation that only about 50% of the B.O.D. would be removed by the process in winter when, because of low temperatures and higher stream flow, complete treatment should not be necessary. It would be unnecessary to produce oxygen photosynthetically when the temperature was too low for a high rate of bacterial oxidation.

In general, it may be concluded that for most conditions detention periods should not be less than 1 day for summer conditions nor more than 6 days for winter conditions. A pond having a detention period of about 3 days and a depth of 12 in. should, for example, satisfactorily produce adequate oxygen by photosynthesis more than 80% of the time in latitudes up to 40° north, providing that continuous freezing conditions do not prevail. Under summer conditions it may be computed that Type 2 ponds should operate successfully as far north as the arctic circle or beyond.

Depth.—As previously shown by Eq. 12, the depth of a pond depends on light intensity for effective photosynthetic oxygen production as well as on light absorption and algal cell concentration. From Eq. 9 it may be observed that computed depth varies greatly with both the cell concentration, C_c, and the sewage strength, L_t. Strong wastes requiring dense algal growths must therefore be treated in relatively shallow ponds whereas weak domestic sewage may be processed at larger depths. The appropriate depth required for treating a particular sewage may be computed as illustrated in the following example. Assuming that the sewage has a B.O.D. of 125 ppm, p is 1.25, I_i has a mean value of 1,500 ft-c, and α is 1.2×10^{-3}, then from Eq. 12,

$$d = \frac{\log_e I_i}{\alpha\, C_c} = \frac{\log_e 1{,}500}{1.2 \times 10^{-3}\, C_c} \approx \frac{6{,}000}{C_c}.$$

From Eq. 7,

$$C_c = \frac{L_t}{P} = \frac{125}{1.25} = 100.$$

Hence,

$$d = 6{,}000/100 = 60 \text{ cm, or approximately 2 ft.}$$

Organic matter at depths below this value would presumably be in darkness and not subject to photosynthetic oxygenation. If a waste material with a B.O.D. of 1,250 ppm had been utilized in the computations, a depth of light penetration of less than 3 in. would have been determined. Economic utilization of land, pond-construction costs, mixing methods, and similar factors place a practical lower limit on the depth of the pond and a practical upper limit on the concentration of wastes. For instance, wastes of B.O.D. greater than 300 ppm result in computed depths so shallow that pond areas become very large. In such cases vertical mixing or primary dilution should be considered as alternatives to shallow depths.

Deposition of Sludge.—Rapid oxidation of organic matter in a pond accelerates the deposition of sludge, which may become so dense near the pond inlet as to include more than 50% of the influent organic matter. Such sludging has been observed in oxidation ponds of all types, especially in those having only a few inlets. Small ponds and long narrow ones are more subject to this difficulty than are large ponds or broad ponds, indicating that wind mixing is beneficial in the open structures. These anaerobic sludge deposits tend to exclude light, retain nutrients needed by the algae in the liquid, and, hence, decrease permissible pond depth. Suggestions for combating sludging by proper design considerations include reduction of depth, increasing dilution factor, distributing the load by multiple inlets, orientation of the pond to obtain wind mixing, and producing turbulence by vertical mixing.

If a Type 2 pond is to be maintained aerobic by photosynthetic oxygen production despite sludge deposition, it must be kept shallow so that light penetrates a relatively large portion of the volume, or some form of vertical mixing must be used. Present evidence indicates that vertical mixing is particularly desirable if algal cell recovery is to be practiced. In this case maximum algal growth is encouraged because the products of bacterial oxidation are made uniformly available to the algae in the light. It is probable that some artificial vertical mixing must be considered an essential feature for Type 2 oxidation ponds. Mixing, however, must not be prolonged because the resultant increase in turbidity decreases light penetration, hindering photosynthesis.

Recirculation.—Pilot-plant studies have indicated that recirculation is important to photosynthetic oxygen production because it permits seeding of influent sewage with algal cells and brings abundant oxygen into it. In other words, recirculation produces good overlapping of bacterial oxidation and of photosynthetic reduction, thereby preventing loss of CO_2 and ammonia from the bacterial phase and providing an efficient outlet for the oxygen liberated by algal growth.[10] This overlapping produces more abundant growths of bacteria and would produce more abundant growths of algae were it not for the problem of sludge deposition. Algae tend to remain dispersed in the solution whereas bacteria tend to form a floc which, together with coagulated sewage colloids containing a large part of the carbon and nitrogen, settles quite rapidly to the bottom of the pond. Some recirculation accelerates sludge deposition with the accompanying possibility of anaerobic conditions in the sludge layer as well as the withholding of nutrients from the algae in the liquid. Because the principal benefits of recirculation are seeding and aeration of the influent, it is possible that these benefits may be duplicated by increasing the uniformity of load distribution together with a low rate of recirculation to accomplish seeding.

Retention of Sludge.—If continuous vertical mixing is used some aerobic sludge may be carried into the pond effluent. This material may be readily removed from the algal suspension by sedimentation and returned to the pond.

If intermittent vertical mixing is used, carry-over of sludge may be prevented by interrupting the discharge of effluent during and shortly after the mixing period. In either case, retention of sludge is advantageous because it allows more complete oxidation of the organic matter, resulting in increased algal growth and improved removal of suspended solids other than algae.

The Need for Paving.—Several factors suggest the possibility that there may be important advantages gained by lining oxidation ponds of Type 2. Any form of vertical mixing considered essential for raising precipitated sludge and increasing light utilization might cause undue turbidity in unpaved ponds. The result would be reduction if not termination of photosynthesis. Furthermore, unpaved ponds designed to make full use of winter sunlight might have excess light at the bottom in the summer, a factor which would probably encourage growth of water weeds such as tule.

Asphaltic or rubber membranes sprayed over shaped and compacted earth appear to be an economic type of pond lining. Sealed asphaltic concrete or thin reinforced concrete would have the advantage of durability and low maintenance. The possibility of application of commercially manufactured preformed channels of plastic or aluminum should not be overlooked. The design and fabrication of economical pond linings does not appear to be a difficult technical problem because the indicated pond size of nearly one-half acre per thousand population is not prohibitively large. The decision on linings depends primarily on the value of photosynthate in the sewage treatment process.

Disposal of Algae.—In the process of producing controlled quantities of oxygen for bacterial stabilization of waste, the concentration of algae produced in moderately strong domestic sewage (200 ppm B.O.D.) may attain levels in excess of 300 ppm, dry weight. Two questions immediately arise: (1) If algae are discharged with the pond effluent, what is the effect on a receiving body of water; and (2) can these algae be economically separated from the effluent?

In answer to the first question, it should be noted that there is a limit to the concentration of algae that can survive in any body of water for a sustained period of time. Algal cells are living organic matter which may grow, vegetate, or die. If the cells grow they will produce oxygen. If they vegetate they will have a small but finite continuous oxygen demand. (For sewage-grown algae by Warburg measurement, this usually is about one-tenth the ash-free dry weight of cells per day at 25° C.) If they die they will be decomposed like any other organic matter. Which of these three possible avenues the cells will first take depends on the environment in the receiving water. As discussed by the writers in an earlier paper,[17] if the receiving water contains nutrients (indicating pollution) and light, the cells will grow and divide, thus producing oxygen. If there is light but few nutrients, the cells will vegetate for long periods of time producing little objectionable pollution in a stream. Cultures of algae having concentrations of 200 ppm or 300 ppm have been held for three months without putrefaction as long as light and access to atmospheric CO_2 are afforded. Ultimately, however, the cells will settle to the bottom. In the dark, algae remain alive for a length of time, which is principally a function of temperature. Algal cells will keep in the dark for 2 weeks at temperatures near freezing but will die and be decomposed in a few days in the dark at temperatures above 25° C. It may be concluded that living algal cells will do little pollutional damage to receiving waters unless their concentration is so large that their endogenous respiration depletes the oxygen reserve of the water. However, should the algal cells for some reason be killed in the receiving waters, they will exert an oxygen demand approximately equivalent to their dry weight.

---

[17] "Algae Symbiosis in Oxidation Ponds. I. Growth Characteristics of *E. gracilis* Cultured in Sewage," by H. F. Ludwig, W. J. Oswald. H. B. Gotaas, and V. Lynch, *Sewage and Industrial Wastes*, Vol. 23, 1951, p. 1337.

Economical separation of algal cells is a highly important aspect of the general use of photosynthesis in sewage treatment. At least two systematic investigations have been conducted recently on algal separation, and three processes have been demonstrated to be technically effective. Two of these processes, centrifugal separation and alum coagulation, have been partly investigated by the writers and other methods are scheduled for investigation. E. W. Steele, M. ASCE, and E. F. Gloyna, A.M. ASCE,[18] performed a series of investigations on screening and filtering devices for separating algae. These showed rather conclusively that separation of algae is a difficult and costly procedure which may require extensive research and development before the most economical procedures are established.

Because of the relatively low concentration at which algae grow, the cost of separation is almost completely proportional to the volume of liquid processed and relatively independent of the concentration of algae in the liquid. Therefore, some level of algal concentration may be attained which will pay for the cost of harvesting, and some higher concentration might support the entire photosynthetic process.

Pond Performance

Algal Yields.—Pilot-plant observations summarized in Fig. 6 show that the rate of algal yield may vary from 1 ton per acre per month in the winter to 5 tons per acre per month in the summer. The total annual rate of yield was 30 tons per acre. In order to visualize such yields, it is useful to compare yields of algae to field crop yields. During 1953 the average field crop yield in California was less than 1.5 tons dry weight per acre per year. Thus, the rate of yield attained in the pilot plant was twenty times the agricultural average. The actual annual yield of algae may be expected to vary strongly with light and temperature and, hence, with geographical location.

B.O.D. Removal.—The operation of an oxidation pond to produce maximum algal yields can at the same time accomplish a high degree of sewage treatment in terms of B.O.D. removal. Data from pilot-plant experiments shown in Table 3 demonstrate that effluents of the quality desired in sewage treatment may be produced. It is believed that samples 2, 3, and 4 would have exerted much less B.O.D. in a stream than is indicated from the data because the residual algae would have continued to produce some oxygen following discharge.

Coliform Removals.—In laboratory and pilot-plant tests no reduction in coliform organisms other than normal die-away has been noted, except in certain light-saturated cultures. In these cultures it is probable that the germicidal effect of natural sunlight was responsible. In other words, no specific anticoliform activity can be credited to the algae produced in the cultures tested. These findings were supported by inoculating with human intestinal coliform a solid medium made up with 25% porcelain-filtered pond supernatant. The fact that the coliform organisms were found to grow abundantly in this medium indicates that no specific anticoliform substance was present in the samples tested. It should be noted that, if an adequate separation procedure is used to remove algae, extensive removal of coliform as well as other bacteria should be attained.

---

[18] "Oxidation Ponds-Radioactivity Uptake and Algae Concentration," by E. W. Steele and E. F. Gloyna, *Technical Report No. 1*, AECU-2837, U. S. Atomic Energy Commission, Technical Information Service, Oak Ridge, Tenn., 1954.

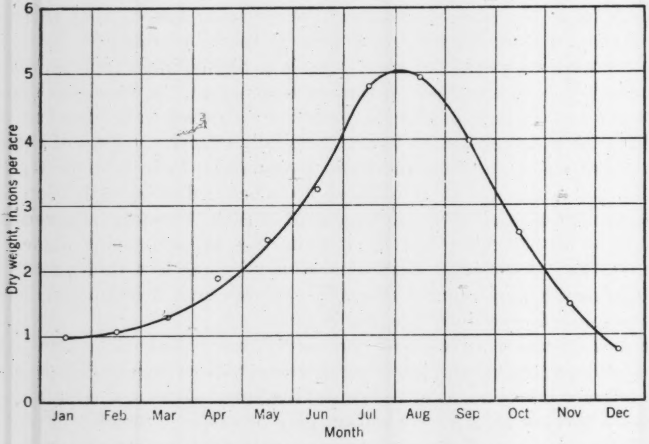

Fig. 6.—Estimated Monthly Yields of Algae from Domestic Sewage at Richmond, Calif.

TABLE 3.—Typical Values for B.O.D. as a Function of Separation Procedure Following Photosynthetic Oxygenation

No.	Sample	Separating procedure	B.O.D., in parts per million	Percentage removal
1	Influent	None	210	0
2	Pond	No separation	195	7
3	Tailing	Settling 1 hr	105	50
4	Tailing	Laboratory centrifuging 10 min at 500 times gravity	25	88
5	Supernatant	Coagulation (followed by 30 min settling)	9	96

Odors.—During the two years of operation of the pilot plants under proper conditions no odors have been observed, with the exception of a faint grassy odor which is a characteristic of the process. These observations include the all-night periods during which the pond was undergoing high loadings. When the ponds were overloaded in a deliberate attempt to break down the photosynthetic process foul odors were noticeable. These resulted principally from anaerobic bottom sludges brought to the surface during stirring. Under proper operating conditions, photosynthetic oxygenation is a process without objectionable odors.

Contaminants.—Any biological or chemical agent that interferes with the process of green algal growth may be considered a "contaminant." Chemical contaminants are those materials which may occur in sewage and are specifically toxic to algae. Although this factor has not been studied directly, indirect evidence indicates that such chemicals normally do not attain high enough concentrations in sewage to destroy the algal population.

Blue-green algae, some of which are toxic to animals, could conceivably ruin the algal cell material as a useful food product. There is little evidence of any tendency for blue-green algae to grow in fresh domestic sewage. In two years of open-air pilot-plant operation, blue-green algae have appeared only in negligible concentration.

The principal contaminants found in pilot-plant studies were green algae of the genus chlamydomonas. These organisms grow swiftly, covering the pond surface with a foamy scum in 1 or 2 days. This scum prevents light from reaching underlying strata and, hence, interrupts oxygen production. Fortunately, chlamydomonas blooms are of short duration and the organisms are easily skimmed from the pond surface by means of wind or jet skimming.

ECONOMIC FACTORS

Reclamation of Nutrients.—Green algae, growing in wastes, are capable of accumulating needed elements from solutions that contain these elements only in minute concentrations. Thus, green algae have great potential as agents of reclamation. For example, in growth-unit experiments algae growing in sewage were supplied a small excess of carbon dioxide. As a result, all but a trace of ammonia nitrogen was incorporated in algal cell material. If a culture is supplied air containing 0.03% CO_2, from 60% to 80% of the sewage nitrogen is fixed in algal cell material within a few days. Similar reclamation of other critical elements occurs. These facts indicate that photosynthesis for waste reclamation may have intrinsic values to the national economy over and above its usefulness as a sewage treatment process. This may be further understood when it is considered that sewage is not truly a waste. Derived from the most nutritive photosynthate harvested from the land, sewage contains the low energy forms of every element critical to life. Nitrogen might be cited as a typical example. Nitrogen is essential in the human body and yet if a daily nitrogen balance were made on a normal human subject, it would be difficult to demonstrate any significant utilization of nitrogen because the amount excreted would be found to be almost identical to the amount consumed. Only the form and energy level of the nitrogenous compounds would be changed. Living animals are thus in dynamic equilibrium with their environment, and the amounts of critical elements permanently affixed in their bodies are negligible when compared with the total amounts which are consumed and excreted during their lifetime. Thus excreted, organic matter has undergone little more than a reduction in its chemical energy content, and it would be surprising if it were not an ideal medium for algal growth.

Mention should be made also of some of the possibilities of this process for water reclamation. For example, the quantity of water required to produce a pound of protein by this process can be computed to be less than 1/100th of that required to produce a pound of protein by conventional agricultural methods. This difference is mainly due to the relatively high photosynthetic efficiency of the process. When coagulation is used for algae removal, effluents are of high quality and there does not appear to be any technical reason why they could not directly supplement a water supply if first processed by sand filtration and chlorination.

Algae as Food and Raw Material.—Results of investigations[9] have indicated the value of algae as a food and as a source of industrial raw materials. Sewage-grown algae have been fed satisfactorily to a number of animals with no evidence of toxic effects. One group of chicks received dried sewage-grown algae as their sole source of protein. Gain in live weight of these chicks average 4.2% per day. This may be compared with a maximum gain for chicks of approximately 8% per day obtained with a protein mixture considered ideal. From this, as compared with vegetable protein, the value of sewage-grown algae as a chicken feed supplement should be approximately $100 per ton.

In tropical areas of the world, which receive much solar energy but which often lack fixed nitrogen and other essential elements for food production, it is possible that the photosynthetic process could be applied to recycle these elements, thereby greatly increasing the food supply.

The fuel characteristics of dry algae are similar to those of medium-grade bituminous coal although their heat content is somewhat less, ranging up to 10,000 BTU per pound. For a few more years, however, the food value of dry algae will probably be its greatest economic value.

The high protein content—more than 50%—is not the only important quality of algae. Algae may become an important source of vitamins, or of starting products for organic synthesis, or as organic collectors of elements such as germanium, which algae concentrate. Exploration of these possibilities has been seriously restricted by a lack of algae with which to experiment. It is possible that one or more of these uses could at once make sewage treatment by photosynthesis an economically feasible process.

Plant Costs.—No attempt will be made to present detailed estimates of the cost to build and operate a plant to treat sewage by photosynthetic oxygenation. The cost of each plant where the process might be used must be evaluated specifically in accordance with the design principles set forth. It does appear that the total cost for a plant to grow algae would be less than that for conventional secondary treatment when the cost of land is not excessively high. The development of economical methods of harvesting the yield of from 1 ton to 1.5 tons of algae that can be grown per million gallons of sewage might bring the actual cost much below that of conventional treatment because of the value of the harvested algae.

SUMMARY AND CONCLUSIONS

Oxidation ponds are classified in accordance with the principal source of oxygen. Type 2 ponds in which oxygen is produced essentially by photosynthesis can be much smaller than ponds of Type 1 in which the necessary oxygen is supplied primarily by surface aeration.

Basic rational formulations for pond detention periods and pond depths are derived by utilizing the law of conservation of energy together with solar energy data and data on the light-transmitting characteristics of algal cultures. The application of these formulations to design of Type 2 ponds is illustrated and discussed. When design criteria are correctly applied, photosynthetic oxygenation will result in sewage treatment equivalent to complete treatment achieved by other methods.

Successful technical design of a plant for the photosynthetic oxygenation process requires consideration of the influences of such variables of light, temperature, and sewage quality on symbiotic bacterial and algal growth. Although the interrelationship between these variables is complex, when applied to algal growth their effects can be conveniently incorporated into design equations as coefficients. No firm value can be assigned to the over-all photosynthetic efficiency because of the modifying effects of environmental factors which are largely unknown. For the present, a value approaching 0.1 can be attained in experimental work whereas values exceeding 0.20 do not appear likely because of the limited ability of algae to utilize light of high intensity.

Before photosynthetic oxygen production in Type 2 ponds can attain its maximum potential as a practical form of sewage treatment, economical methods for algal separation must be further evaluated, developed, and demonstrated.

The technical feasibility of photosynthetic oxygenation in sewage treatment may be considered an accomplished fact. The reclamation of animal food from sewage in the form of algae appears highly promising, but practical attainment will be deterred pending further investigation of separation procedures. More studies of photosynthetic efficiency, separation of algae from cultures, and of other factors are necessary—particularly of the value of the algal cell materials produced in the process.

ACKNOWLEDGMENTS

Appreciation is extended to P. H. McGauhey, W. F. Langelier, Edwin W. Lee, Jerome Thomas, Richard J. Hee, Norma O. Goldstein, William R. Kellen, Allan Beattie, Gerhard Klein, and Yvonne Barker of the University of California, and to Harvey F. Ludwig of the United States Public Health Service for their cooperation and assistance.

This research is supported in part by a grant from the National Institutes of Health, United States Public Health Service.

DISCUSSION

ISADORE NUSBAUM,[19] A.M. ASCE.—In the past decade much interest has developed in the use of oxidation ponds for the treatment of liquid wastes from small and moderate-sized communities, institutions, military establishments, and industry. As a result of increased construction and operating costs for conventionally designed sewage treatment works, the use of oxidation ponds has been presented as a means of attaining a high degree of treatment at low cost. The use of oxidation ponds for the treatment of sewage has now become extensive, particularly throughout the southwest and far west regions of the United States; yet only few empirical data are available for their design. The authors have presented basic data on the role of photosynthesis in sewage treatment. Much remains to be clarified before the fundamental data available through the study of phytoplankton can be used for the realistic design of a sewage treatment plant.

Until this work is complete, frequently used deviations from the present empirical data, such as organic loadings of 50 lb of B.O.D. per acre of surface area per day, minimum depths of from 3 ft to 4 ft, and minimum detention periods of 30 days, must be viewed with caution. This attitude should not discourage any community from including in the pond arrangement such flexibility that these characteristics might be varied in the interest of obtaining pertinent data, for the area and waste involved, upon which to base extensions and operating practice.

The authors have divided oxidation ponds into two rather artificial classifications: Type 1 ponds are those which, by the authors' definition, obtain the oxygen necessary for waste stabilization through surface reaeration and have detention periods of from at least three weeks to six weeks. Type 2 ponds are those which have detention periods of less than one week and which are highly dependent on photosynthesis for oxygen. The qualification is then introduced that Type 1 ponds may obtain large amounts of oxygen through photosynthesis when conditions are favorable. A brief analysis of the situation demonstrates that photosynthesis, or causes other than surface reaeration, must be responsible for the stabilization which takes place in the many hundreds of oxidation ponds now in use in the southwest and which are characterized by the authors as Type 1 ponds. The rate at which oxygen is transferred from the atmosphere to a water media through the air-water interface depends on several factors, but primarily on the extent of the dissolved-oxygen deficit in the water. If the water is saturated or supersaturated with oxygen, there is no net transfer of oxygen from the atmosphere and indeed there may be a loss of oxygen from the water to air. The upper 12 in. or more of conventionally designed ponds are frequently supersaturated with oxygen only for short periods, principally during hours of darkness, and have oxygen concentrations appreciably below saturation. A typical example of such variation is pictured by D. F. Smallhorst, B. N. Walton, and Jack Myers.[20]

---

[19] Senior Water Pollution Control Engr., San Diego Regional Water Pollution Control Board, San Diego, Calif.

[20] "The Use of Oxidation Ponds in Sewage Treatment," by D. F. Smallhorst, B. N. Walton, and Jack Myers, *Manual for Sewage Plant Operators*, Texas Water & Sewage Works Assn., 1955, Chapter XIII.

The amount of oxygen which may be transferred through the air-water interface is limited by the characteristics of the pond itself. For example, Karl Imhoff and G. M. Fair[6] state that for ponds approximately 3 ft in depth the rate of reaeration from the atmosphere at 100% oxygen deficit is 13 lb of oxygen per acre of surface area per day. This condition rarely exists, and for the more realistic mean limiting condition of a 20% oxygen deficit in ponds designed for loadings of 50 lb of B.O.D. per acre of surface area per day, the atmosphere would supply 3 lb of oxygen per acre per day. It is quite evident that a deficit of 47 lb of oxygen per acre per day would exist, together with an extremely offensive anaerobic condition, unless oxygen for aerobic microbial action were supplied by other means. Experiences in southern California and Texas have shown that at the 50-lb B.O.D. loading oxygen concentrations in the ponds are extremely favorable throughout the year.

Although pond loadings are conveniently computed in terms of available surface area, depth plays an important part in the satisfactory operation of an oxidation pond. It is necessary to maintain at least 3 ft of water in the pond in order to avoid the growth of nuisance vegetation. Messrs. Smallhorst, Walton, and Myers[20] have pointed out that temperatures in very shallow ponds may become too high during the summer to permit the growth of algae such as chlorella. Depth through the larger-volume plant also permits the retention of greater quantities of oxygen during periods of supersaturation. Although the bottom layers may be anaerobic in deeper ponds, this factor may contribute to the over-all reduction of B.O.D. which occurs. Otherwise all the carbon dioxide produced by aerobic bacteria from the organic matter in the waste might be used by the algae in the resynthesis of organic matter. Increased depths also permit the rapid dispersion of the incoming waste, thus avoiding shock loading effects and minimizing the resuspension of solids from the bottom of the pond.

Recirculation has been found to have a distinctly salutary effect on the operation of both ponds and the entire sewage treatment plant. Offensive odors surrounding some treatment works have been entirely controlled by the recirculation of pond effluent. Where the sewage is given some secondary treatment before it is discharged to the pond, the secondary units have been found to function with fewer problems when recirculation is practiced. The most important effect of recirculation is to reduce the shock loading of high-B.O.D. wastes on the pond.

The writer has observed the operation of many oxidation ponds in southern California and doubts that the shallow, short-detention-period ponds proposed by the authors will withstand the intermittent high loadings that occur unless some form of recirculation is practiced or the ponds are merely used as a final treatment following secondary treatment.

The amount of recirculation to be used has never been determined except by trial-and-error methods. Messrs. Smallhorst, Walton, and Myers[20] have recommended that provisions for recirculation of the effluent be included in plants utilizing oxidation ponds and that recirculation ratios of from 15% to 50% should prove satisfactory. The writer believes, based on his experience, that recirculation ratios of at least one part pond effluent to two parts of sewage flow should be provided and should be necessary for recirculation, particularly where primary effluent is discharged to the ponds. It appears likely that the amount of or necessity for recirculation depends on the initial oxygen requirement of the waste.

Aerobic bacteria are necessary inhabitants of oxidation ponds because it is by their action that organic matter in the wastes is destroyed or converted to carbon dioxide to be used by the phytoplankton. Algae have been cultivated in synthetic media without the presence of bacteria and extraneous organic substances. Because coliform organisms, and presumably pathogens, have shown marked reductions in numbers in passage through oxidation ponds, it has been postulated that some antibiotic or toxic substance may be generated by the algae. However, as indicated by the authors, no such change other than the normal die-off expected on storage has been observed in their experiments. The writer has found significant coliform densities in ponds with detention periods of from 10 to 15 days. Effluents from ponds with 30 days or more of detention are found to have bacterial reductions comparable to or greater than effluents from the chlorinated sewage treatment plant. Because the use of chlorination in small sewage treatment works is usually quite ineffective due to insufficient operation and maintenance, oxidation ponds have been used to produce bacterially safe effluents. For ponds having short detention periods, it will be necessary to provide some means of chemical disinfection until more information is available on any bacterial hazards. However, virtually nothing is known about the disinfection of pond effluents.

Several preliminary tests have been conducted by the writer on the chlorine requirements of oxidation-pond effluents. The effluents have had low chlorine requirements of from 2 ppm to 3 ppm. The coliform population was rapidly reduced to extremely low values on chlorination in this range. The effect on the algae was undetermined, but they also may have been destroyed. If so, chlorination may decrease some of the pond effectiveness.

The authors have stated that there is little tendency for blue-green algae to grow in oxidation ponds. The presence of large numbers of blue-green algae has been reported from Texas. Also, in the San Diego (Calif.) area two separate ponds, thirty miles apart, have been afflicted with an almost pure culture of blue-green algae of the genus arthrospira. The vegetative cells of these organisms are found in free-floating filaments which are helical in shape. Apparently, organisms rising to the surface collect in small clumps which then are driven by the wind into pockets where large mats of the arthrospira accumulate. As the surface of the mats putrefies, an extremely foul, offensive odor is produced.

Nevertheless, the effluent from these ponds was well treated. Some investigational work has indicated that the growth of these specific algae is connected with the salinity of the ponds involved. The arthrospira have previously been found in ponds of brackish water. Both the infested ponds have sodium chloride concentrations of approximately 3,500 ppm; in one case, this was because of saline ground-water infiltration and in the other because a slough with no outlet was being used as the pond.

As reported in an earlier paper[11] the total inorganic solids content of the sewage used for these experiments, conducted at the Sanitary Engineering Research Laboratory of the University of California, is quite low. Data are lacking on the use of ponds in areas where the normal solids content of the water is high. It is true that synthetic media for the culture of algae are high in mineral solids; however, such media have been carefully prepared to produce optimum growth.

There is some evidence[21] to indicate that relatively small changes in chloride concentrations may have definite effects on the cultivation of certain phytoplankton. The City of Oceanside (Calif.) has experienced difficulties with an experimental oxidation pond having a surface area of 5 acres. The oxidation pond contains between 800 ppm and 1,000 ppm of sodium chloride because of the high salinity of the community water supply. Many other factors may be involved and some have been investigated with no positive results. Attempts to seed chlorella into one of the brackish ponds mentioned earlier were completely unsuccessful.

R. W. Krauss[22] has pointed out that much work remains to be done on the total nutrient requirements of algae grown in mass culture and that, even in complex organic media with large numbers of compounds in solution, it is possible that growth may be limited by the absence or unavailability of some element. Iron, zinc, copper, molybdenum, manganese, cobalt, and other elements are believed to be essential micronutrients for the cultivation of algae. It is quite conceivable that, despite the heterogeneous makeup of sewage in some regions, the sewage may be deficient in some element necessary for a vigorous, healthy growth of algae.

Few data have been found on the effects of insecticide formulations on the operation of oxidation ponds. Ponds do, under some circumstances, harbor mosquito and gnat larvae, and health departments justifiably demand that insect control be exercised. In at least two cases with which the writer is familiar, the spraying of ponds with diesel-oil solutions of DDT were followed by almost complete algal inactivity. Much less impairment was suffered when a water-type emulsion of lindane was used.

Despite the lack of knowledge about many aspects of the use of oxidation ponds for sewage treatment, they do serve a useful purpose in sanitary engineering. The limited information has undoubtedly resulted in lower efficiencies than might otherwise be possible.

The use of oxidation ponds for sewage treatment must be justified principally on their effectiveness and their cost for that specific purpose. The recovery of valuable by-products other than water for agricultural or industrial purposes is in an elementary stage of development and does not yet merit consideration in the design of oxidation ponds for sewage treatment.

WILLIAM J. OSWALD,[23] A. M. ASCE, AND HAROLD B. GOTAAS,[24] M. ASCE.—Mr. Nusbaum's remarks concerning conventional oxidation ponds commonly used for sewage treatment in the western and southwestern United States indicate concern regarding any deviation from the present empirical design criteria: Organic loadings of 50 lb of B.O.D. per acre of surface area per day, minimum depths of from 3 ft to 4 ft, and minimum detention periods of 30 days. Actually there has been very little scientific analysis or investigation on which to base these criteria. They were proposed and used before photosynthesis was given particular consideration as a source of oxygen for bacterial decomposition. The early oxidation ponds were designed on the basis that oxygen would be supplied by surface aeration from the atmosphere and detention periods were determined on the basis of what experience had indicated would provide satisfactory removal of B.O.D. without the creation of nuisances. The ponds were designed sufficiently deep to prevent penetration of light to the bottom, thus inhibiting the growth of nuisance vegetation. Oxidation ponds can be operated over a wide range of conditions and still provide a reasonably satisfactory effluent.

---

[21] "Relative and Limiting Concentrations of Major Mineral Constituents for the Growth of Algal Flagellates," by Luigi Pravasoli, V. V. A. McLaughlin, and I. J. Pinter, *Transactions*, New York Academy of Sciences, Series II, Vol. 16, 1954, p. 412.

[22] "Nutrient Supply for Large-Scale Algal Cultures," by R. W. Krauss, *Scientific Monthly*, Vol. 80, 1955, p. 21.

[23] Assistant Research Engr., Inst. of Eng. Research, Univ. of California, Berkeley, Calif.

[24] Prof. of San. Eng. Chem., Civ. Eng. Div., Univ. of California, Berkeley, Calif.

The writers indicated two types of oxidation ponds: Type 1, depending primarily on surface aeration as the oxygen source with oxygen from photosynthesis coincidental but not essential in the maintenance of aerobic conditions, and Type 2, depending primarily on photosynthetic oxygen sources. Naturally there is no fine line of demarcation because these types are the two extremes. As indicated in the paper, long-detention-period oxidation ponds may receive considerable oxygen produced by algae growing near the pond surface. Mr. Nusbaum's value of 47 lb of oxygen per acre per day could easily have been produced by photosynthesis; in fact, oxygen is produced at many times this rate in Type 2 ponds. Although some oxygen may be produced photosynthetically in the conventional pond, it should be emphasized that the two types of ponds are very different. The conventional Type 1 ponds treat the waste at a low rate, requiring a relatively small quantity of oxygen per acre and often have sludge deposits on the bottom which decompose anaerobically. The high-rate Type 2 ponds, however, may treat wastes at ten times the conventional rate, developing dense algal cultures which supply nearly all the oxygen requirements for the maintenance of aerobic conditions throughout. The purpose of photosynthetic oxygenation is to treat the waste more rapidly on a smaller area while developing sufficiently dense cultures of algae to permit harvesting and reclamation of many of the valuable nutrients in the waste.

Conventional oxidation ponds designed for a B.O.D. loading of 50 lb per acre per day and a 30-day detention period often contain a sludge deposit on the bottom which undergoes anaerobic decomposition. Much of the dissolved and colloidal organic matter of the sewage is flocculated and settles to the bottom. If aerobic conditions are maintained in the upper part of the pond water, only the B.O.D. of the nonsettling material and the residual B.O.D. of the anaerobically decomposed sludge are satisfied aerobically. Thus, less oxygen is required than if all the organic matter were decomposed aerobically. If the anaerobic sludge deposits are not too large, odor and nuisance conditions are not developed because adsorbed atmospheric oxygen and photosynthetic oxygen in the supernatant may be sufficient to prevent odor nuisances. It may be seen that the average B.O.D. loading per acre per day is an inaccurate parameter because the amount of deposition and anaerobic decomposition of

B.O.D. may be greater than the aerobic oxidation and the algal oxygen production may vary widely depending on sunlight and other factors.

Oxidation ponds may be operated with detention periods and loadings between those of conventional Type 1 practice and values shown for the Type 2, high-rate ponds. The Type 2 pond requires some vertical mixing to keep the sludge, the bacteria, and the algae in close proximity so that the sludge will be aerobic and the algae can obtain the carbon dioxide and ammonia released by the bacteria. The writers have been able neither to develop dense algal cultures in deep, long detention period ponds nor to find any conventionally designed ponds which produce high algal concentrations. There is a valid physical reason for this which was presented as Eq. 12. This equation shows that algal concentrations exceeding 40 ppm cannot be sustained in ponds 3 ft deep. Algal densities greater than 25 ppm are rare in the conventional pond, compared to densities of from 200 ppm to 350 ppm in the Type 2 pond when ample sunlight and nutrients are available.

Studies indicate that the Type 2 high-rate ponds will have the greatest economic possibilities when high-quality secondary treatment is desired. Pilot-plant experience indicates that an effluent is produced from which 95% to 97% of the B.O.D. has been removed.

Mr. Nusbaum refers to the desirability of recirculation for overcoming shock loads on the pond. The operation of the high-rate pond requires recirculation for seeding the influent waste with algae and adding oxygen initially to provide aerobic conditions. However, recirculation is desirable in the operation of any oxidation pond. In the Type 2 pond, the amount of recirculation should be controlled because extensive recirculation hastens bioflocculation and settling of organic matter. Separation of the bacteria and nutrients from the algae which do not settle retards algal growth.

Reference was made to the die-away or removal of coliform bacteria in high-rate oxidation ponds. If the algae are chemically coagulated and precipitated, practically all the coliform organisms are removed to the sludge, and the effluent may be satisfactorily filtered through a rapid sand filter. Many observations of the change in coliform densities in the high-rate oxidation ponds have shown that the most probable number decreases from 10^7 or 10^8 in the sewage to between 10^2 and 10^4 in the pond effluent. The variation between 10^2 and 10^4 is affected by the detention period and the depth. Ponds of shallow depths and longer detention periods in intense sunlight show lower coliform counts in the effluent.

Mr. Nusbaum indicated that oxidation ponds have low chlorine requirements of 2 ppm to 3 ppm. The writers have found that the effluents from Type 2 ponds have a high chlorine demand due to their high algal concentration. They have also found that the effluent from Type 2 ponds, after harvesting the algae, has a very low demand. This indicates, therefore, that the pond effluents referred to by Mr. Nusbaum contained very few algae, and hence probably obtained little oxygen from photosynthesis.

The writers are unable to answer completely the question of blue-green algal development in long-detention-period ponds and the lack of such development in high-rate ponds. There are several factors which may influence the development of the blue-green algae. First, blue-green algae seem to grow better in partly nitrified sewage than do green algae, but appear unable to compete with green algae when ammonia nitrogen, rather than nitrate nitrogen, is the nitrogen source. Only ammonia nitrogen is available in the short-detention-period ponds. Secondly, blue-green algae will grow when sewage nitrogen is low or absent because they have the capacity to fix nitrogen from the air. There is usually an excess of nitrogen in high-rate ponds. Inasmuch as blue-green algae often grow around mats of organic sludge, which may rise from the bottom of the pond where a sludge blanket has developed, they may require longer detention periods than green algae. It is therefore believed possible that the detention periods of the Type 2 pond may be too short for growth of blue-green algae, permitting only fast growing green algae to develop on the available nutrients.

Mr. Nusbaum has raised the question of growing chlorella and other algae in ponds high in sodium chloride or total solids. There is little information indicating that brackish waters influence algal growth when total salt concentrations are less than 3,000 ppm and no toxic minerals are present. It is possible that the noted unsuccessful results of attempts to seed chlorella into brackish ponds were due to insufficient seed or excessively long detention periods. Because chlorella are small, rapidly growing algae, they dominate when detention periods are short, and other larger, more slowly growing organisms do not have the opportunity to overgrow them. Chlorella, scenedesmus, and other small, rapidly growing cells seldom predominate when the detention period is long.

Much additional study of photosynthetic oxygenation of sewage and of separation of the algae from the liquid has been accomplished since the paper was written. Pilot-plant investigations have shown that the algae and other suspended and colloidal matter can be continuously precipitated, and an effluent can be produced that contains a very low B.O.D. and bacteria count. The investigations indicate that during summer weather considerably more than one ton, dry weight, of algae can be produced per million gallons of average domestic sewage. Based on pilot-plant studies, the cost of growing, separating, and drying the algae while also providing a high-quality effluent is believed to be less than $100 per million gallons for average conditions. The algae contain from 45% to 55% protein as well as carbohydrates, fats, and minerals, and have an indicated value of more than $100 per ton as an animal food. Hence, even though this process is now only in the developmental stage and accurate cost and operational data for a full-scale plant are not available, it seems probable that Type 2 short-detention-period ponds and algae harvesting may provide high-quality sewage treatment for a very low net cost. The most economical use of the process may be for cities requiring complete, year-round sewage treatment in areas where the climate and sunlight are satisfactory. This would generally be in areas between the equator and 35° latitude. The process may also be economical for use during the summer in places farther from the equator where only partial treatment is necessary during the cold winter period.

A rational formulation was presented of the major fundamental biological, physical, and chemical factors that govern the production of oxygen and algae in sewage ponds together with engineering applications of these fundamentals. These principles are applicable under a wide variety of conditions and can be utilized in the design of either conventional or high-rate type ponds whenever photosynthesis is considered as a source of oxygen. Naturally, caution should be exercised in designing high-rate ponds of large magnitude until the process has been operated at plant-scale installations. Present information indicates, however, that conventional detention periods and loadings can be changed for greater efficiency and economy. Future designs of conventional oxidation ponds should include provision for conversion to high-rate operation, a step which is essential for the development of sufficient algae to permit economical harvesting and reclamation.

Pilot-plant experience with this process indicates the possibilities for much more extensive reclamation of the valuable nutrients now being wasted in costly treatment processes. The high-rate process, which utilizes sunlight as a source of energy for growing algae to treat wastes and to reclaim nutrients, has one less degree of freedom for general application than the more conventional processes because of light requirements. However, in many localities sunlight is an unusually abundant item and it is unwise to waste either nutrient materials or sunlight if a process can be developed for their economical utilization. Engineered control of photosynthesis offers a means to this end. Certainly civilization might have been retarded if engineers had chosen to allow natural processes to proceed only at their primordial rate.

AMERICAN SOCIETY OF CIVIL ENGINEERS
Founded November 5, 1852
TRANSACTIONS

Paper No. 2850

STIFFENING LOCK GATES BY PRESTRESSING DIAGONALS

By Carl L. Shermer,[1] M. ASCE

Synopsis

A method is presented for the control of the warping or twisting of mitering-type navigation lock gates when the gates are swung through the water. The gate leaf is analyzed, and the function of the diagonal members in resisting torsional forces is explained. Expressions for torsional deflection and corresponding stresses in the diagonal members are developed; it is found that the prestressing of the diagonal members increases their effectiveness. The steps in applying the theory and the field technique for prestressing are presented.

Introduction

The warping or twisting of mitering-type navigation lock gates when the gates are swung through the water has often posed serious problems. In the Mississippi River navigation system there are a number of locks in which the gates are all of similar design; all the gates twisted excessively at first when they were being opened or closed. To remedy this situation, the machinery was redesigned so that the speed of operation was cut in half, thus causing less of a twisting force. This correction involved considerable expense, but no simple method of stiffening the gate leaves was known at that time (prior to 1942).

It was observed that gates which are thick twist less than thin gates and diagonal members on the gates prevent much of the twisting; however, there was (prior to 1942) no rational method of designing or of determining, in advance, how much a given gate would twist in operation. Diagonal members were assumed to carry all or a part of the dead-load shear in the leaf, and although this design assumption led to diagonals which looked reasonable, the method has no rational basis and the results of applying it were sometimes disastrous.

Actually, the skin plate on most lock gates is so rigid in its own plane that it carries practically all the dead-load shear, and the shear carried by the

---

Note.—Published, essentially as printed here, in September, 1955, as *Proceedings Paper 804*. Positions and titles given are those in effect when the paper was approved for publication in *Transactions*.

[1] Prof. of Civ. Eng., Michigan State Univ., East Lansing, Mich.

diagonals is negligible. The actual function of the diagonal members is to make the gates torsionally rigid; the method of design is explained subsequently. This design method has been used successfully on several lock designs in the United States (for example, the MacArthur Lock at Sault Sainte Marie, Mich., and the Chain of Rocks Lock at St. Louis, Mo.) and has even been applied to the stiffening of gates on some older locks in the Mississippi River system. In the latter case the gate leaves were analyzed and the existing diagonals prestressed without structurally altering the leaves in any way.

The first design using this method of torsional analysis (1942) involved gates for the 80-ft-wide MacArthur Lock. Each leaf of the gate at the downstream end of the lock is 56 ft high and 45 ft wide but only 3 ft thick. Such a thin gate had never been tried before, but the gate operates under all conditions with no noticeable twist. Indeed, it is so rigid that the lock operators swing the leaves back and forth to clear floating masses of ice out of the channel in the winter.

ANALYSIS

In Fig. 1 there is shown the surface of a lock-gate-leaf panel with skin plate and vertical end girders or diaphragms; in plan, the surface may be of any shape whatsoever. The vertical lines, gj and fk, are drawn a small, but finite, distance apart on the surface. Now let the element, fgjk, of the surface be warped in such a way that side gj rotates about the lower edge, jk, into the new position, g′j. The other portions of the surface remain rigid so that the whole segment, gjbc, also rotates about axis jk but undergoes no twisting. If the angle, g′fg, in the plan view is denoted by α, the angle through which g′j rotates is $\alpha\,\Delta u/h$ and, because α is small, point c is displaced vertically by

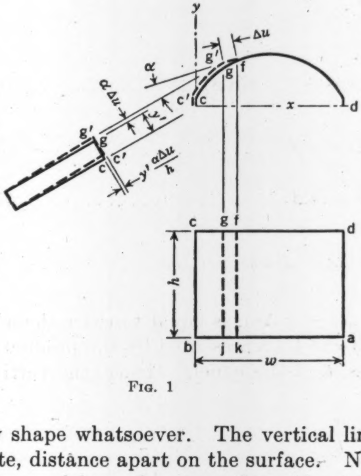

FIG. 1

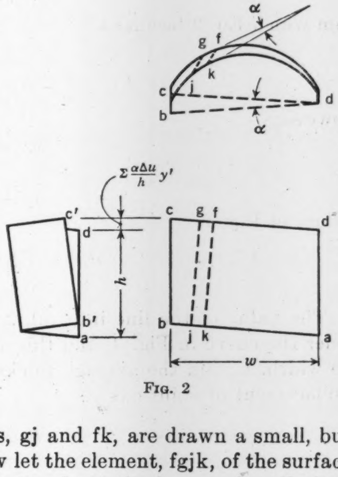

FIG. 2

$$d_{cv} = y' \frac{\alpha}{h} \Delta u. \qquad (1)$$

If a lock-gate leaf is twisted, the horizontal girders prevent any change in the shape of any horizontal cross section as seen in the plan view, the warping of the sections producing only second-order changes as seen in this same view. Each element of the surface, therefore, is warped by the same amount, α (Fig. 2), and the total vertical displacement of point c is

$$d_{ctv} = \frac{\alpha}{h} \Sigma \, \Delta u \, y' \quad \text{(2)}$$

However, from Fig. 3,

$$y' = y \cos \beta - x \sin \beta \quad \text{(3)}$$

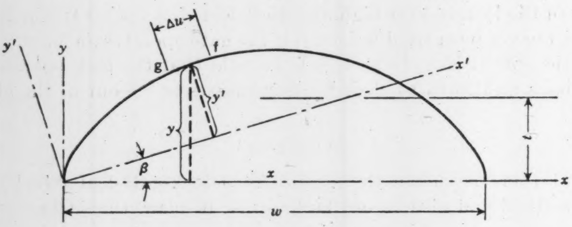

FIG. 3

from which Eq. 2 becomes

$$d_{ctv} = \frac{\alpha}{h} \Sigma \, \Delta u \, (y \cos \beta - x \sin \beta) \quad \text{(4)}$$

However,

$$\Delta x = \Delta u \cos \beta \quad \text{(5a)}$$

and

$$\Delta y = \Delta u \sin \beta \quad \text{(5b)}$$

By use of Eqs. 5,

$$d_{ctv} = \frac{\alpha}{h} \Sigma \, (y \, \Delta x - x \, \Delta y) \quad \text{(6)}$$

The value of the line integral, $\Sigma(y \, \Delta x - x \, \Delta y)$, is equal to twice the area under the curve in Fig. 3, and this area can be represented by the product of the width, w, and the average thickness, t, of the panel. Hence, the vertical displacement of point c is

$$d_{cv} = 2 \frac{\alpha}{h} w \, t \quad \text{(7)}$$

Taking the component of this vertical displacement of point c along the diagonal chord, ac, the change in length of the diagonal distance, ac, produced by the twisting of the surface is

$$\delta_0 = 2 \frac{\alpha \, w \, t}{h} \frac{h}{m} = 2 \frac{\alpha \, w \, t}{m} \quad \text{(8)}$$

in which m is the length of the diagonal chord, ac.

Lock-gate leaves may be subdivided, either horizontally or vertically, into any number of panels (Fig. 4). If D represents the total amount by which the miter end of the leaf is out of plumb, the angle, α, for any panel is (D/v) (h/H). Substituting this in Eq. 8 leads to

$$\delta_0 = \pm\, 2\, \frac{D\, h\, w\, t}{H\, v\, m} \qquad (9)$$

Eq. 9 is a general equation referring to either diagonal ac or diagonal bd because it is evident that, for small angles of twist, diagonal bd decreases in length by the same amount that ac increases in length. If the twist is in the opposite direction, diagonal ac will decrease in length whereas bd will increase.

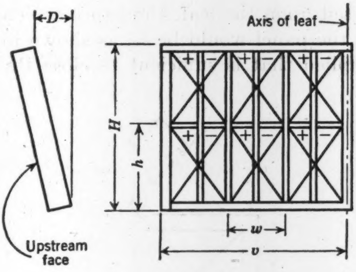

FIG. 4

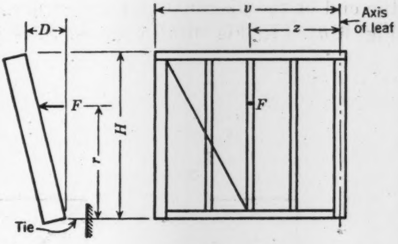

FIG. 5

On the right-hand side of Eq. 9 all factors except D are dimensions of the leaf and may be combined into a single constant, R_0. Therefore,

$$\delta_0 = R_0\, D \qquad (10)$$

in which

$$R_0 = \pm\, \frac{2\, w\, h\, t}{H\, v\, m} \qquad (11)$$

The values of R_0 are not necessarily the same for all panels but will vary with the dimensions of the panel. The sign of R_0 is positive for positive diagonals—that is, those which increase in length with a positive deflection, D, of the leaf; R_0 is negative for negative diagonals which are those which decrease in length with a positive deflection of the leaf. The term D is considered positive when the top of the leaf is twisted upstream regardless of which of the leaves of the gate is being considered. A positive deflection is shown in Fig. 4, and the positive and negative diagonals are marked.

A leaf with one diagonal member is shown in Fig. 5. The leaf is initially vertical, and there is no stress in the diagonal member. A force, F, applied as shown, will twist the leaf and in doing so will do work that is given by

$$W_F = \frac{F}{2}\, \frac{r}{H}\, \frac{z}{v}\, D \qquad (12)$$

Assuming that the leaf itself, without a diagonal member, has a negligible resistance to twisting (this will be true if the leaf does not have skin plates on both faces over any large part of its area), all of the work done by F can be equated to the work done by the stress, S, in the diagonal member. The work done by this stress is

$$W_S = \frac{S}{2}\delta_0 = \frac{S}{2} R_0 D \quad (13)$$

Equating this to the work done by F and rearranging,

$$S R_0 H v = F r z \quad (14)$$

If the diagonal member of Fig. 5 had not been connected at the upper end and if a deflection, D, had been imposed upon the leaf, the gap between the end of the diagonal and the corner of the panel would be δ_0, as shown in Fig. 6(*a*). In Fig. 6(*b*) a stress, S, is applied that is sufficient to close the gap while the deflection, D, is maintained. The diagonal member will elongate an amount,

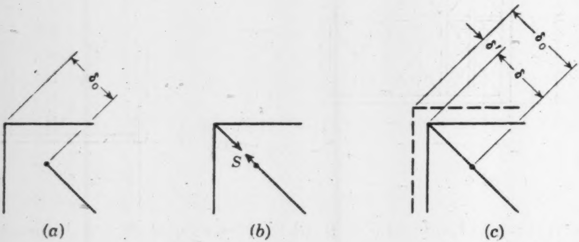

(*a*) (*b*) (*c*)

FIG. 6

$$\delta = \frac{S L}{A E} \quad (15)$$

and the corners of the panel will be pulled together an amount,

$$\delta' = \frac{S L'}{A' E} \quad (16)$$

in which L'/A' is a measure of the flexibility of the panel in the direction of the diagonal. The term L'/A' cannot be evaluated analytically because so many factors enter into it. However, it has been experimentally determined for a number of different gates by computing, for a given value of D, the strain, δ, and the stress, S, in the diagonal from strain-gage measurements. The term δ' is then the difference between the computed value of δ_0 and the measured value of δ, and from this L'/A' can be found.

Even when a gate leaf has many panels, the value of S, as determined from the torsional loads, is affected very little or not at all by the value of L'/A'.

The computed deflection of the leaf is influenced by the value of L'/A', but even here the influence is not great because L'/A' is usually small compared with L/A, and hence δ' is correspondingly small compared with δ.

If L' is taken arbitrarily to be equal to L, then experiments show that, without serious error, A' may be taken equal to one-half of the average cross-sectional area of the girders which bound the panel.

If $K = L/A$ and $K' = L'/A'$,

$$\frac{\delta}{\delta'} = \frac{K}{K'} \qquad (17)$$

Substituting $\delta_0 - \delta$ for δ' (Fig. 6(*c*)) and solving for δ,

$$\delta = \frac{K}{K + K'} \delta_0 = \frac{K}{K + K'} R_0 D \qquad (18)$$

The coefficient of D in Eq. 18 is a constant for any particular diagonal member.

If

$$\frac{K}{K + K'} R_0 = R \qquad (19)$$

then

$$\delta = R\,D \qquad (20)$$

The total stress, S, in any diagonal member is therefore

$$S = \frac{\delta}{L} E\,A = \frac{R\,E\,A}{L} D \qquad (21)$$

In the foregoing it was assumed that when $D = 0$ (leaf vertical) there is no stress in the diagonal. However, if the point of zero stress for a diagonal occurs at some other position, D_0, of the leaf, the elongation of the diagonal member is $R\,(D - D_0)$, and the total stress in the diagonal member is

$$S = \frac{R\,E\,A}{L} (D - D_0) \qquad (22)$$

Substituting this value into Eq. 14 leads to

$$\frac{R_0\,H\,v\,R\,E\,A}{L} (D - D_0) = F\,r\,z \qquad (23)$$

For any given diagonal member the coefficient of $(D - D_0)$ is a constant. Furthermore, the constant is always positive for both positive and negative diagonals as R_0 and R always have the same sign. If Q represents this constant,

$$\frac{R_0\,H\,v\,R\,E\,A}{L} = Q \qquad (24)$$

and

$$Q\,(D - D_0) = F\,r\,z \qquad (25)$$

in which Q is an elastic constant of the diagonal member which measures the resistance which that member offers to the torsional deflection of the leaf.

For more than one diagonal and for any number of loads,

$$\Sigma Q\ (D - D_0) = \Sigma F\ r\ z \qquad (26)$$

and, solving for D,

$$D = \frac{\Sigma F\ r\ z + \Sigma Q\ D_0}{\Sigma Q} \qquad (27)$$

For the leaf to hang vertically ($D = 0$) under its own weight, the numerator on the right-hand side of Eq. 27 must equal zero for dead load; that is,

$$(F\ r\ z)_{DL} + \Sigma Q\ D_0 = 0 \qquad (28)$$

The value of F in Eq. 28 is the total dead-load weight of the leaf, r is the distance from the center of gravity of the leaf to the shear center of the leaf cross section, and z is the distance from the center line of the pintle to the center of gravity of the leaf, all of which are shown in Fig. 7. Separating live load and dead load in Eq. 27,

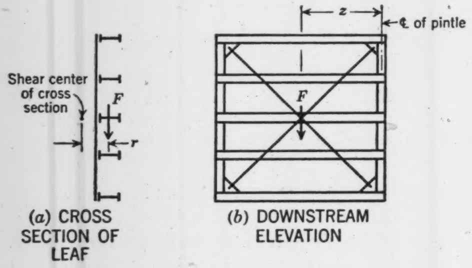

Shear center of cross section
F
r
z
℄ of pintle
F

(a) CROSS SECTION OF LEAF

(b) DOWNSTREAM ELEVATION

FIG. 7

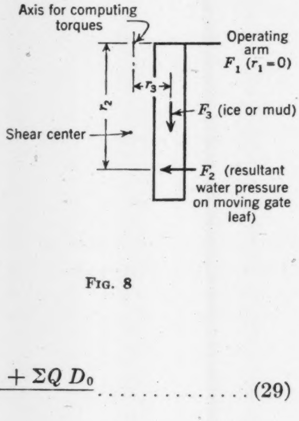

Axis for computing torques
Operating arm
F_1 (r_1 = 0)
r_3
r_2
F_3 (ice or mud)
Shear center
F_2 (resultant water pressure on moving gate leaf)

FIG. 8

$$D = \frac{(\Sigma F\ r\ z)_{LL} + (F\ r\ z)_{DL} + \Sigma Q\ D_0}{\Sigma Q} \qquad (29)$$

However,

$$(F\ r\ z)_{DL} + \Sigma Q\ D_0 = 0 \qquad (30)$$

Hence, when the leaf is being operated, the torsional deflection will be

$$D = \frac{(\Sigma F\ r\ z)_{LL}}{\Sigma Q} \qquad (31)$$

If the diagonal members have sufficient initial prestress so that the stress in none of them is ever reduced to zero regardless of the torsional deflection, then in Eq. 31 ΣQ includes all diagonal members whether positive or negative. If the summation of the torsional live loads is positive, D will be positive; the stress in the positive diagonals will increase, and the stress in the negative diagonals will decrease. The negative diagonals, in giving up some of their tensile stress, behave exactly as if they were able to withstand compression and they add just as much to the torsional stiffness of the leaf. For negative values of $\Sigma F\, r\, z$, the function of the positive and negative diagonals is reversed. It has been assumed herein that diagonal members are so slender that they cannot sustain compression; if this were not so, the foregoing analysis would still be valid, but prestressing would not be necessary.

Any horizontal axis parallel to the leaf and lying in the same vertical plane as the shear center may be used in computing the values of r, the torque radius. One such choice of axes is shown in Fig. 8. For any given condition of loading the value of $\Sigma F\, r\, z$ is independent of the axis chosen.

DESIGN

The following steps should be taken in applying the theory to a design problem:

1. Design the leaf completely except for the diagonal members. Make provision for placing the diagonal members as far from the skin plate as practicable. Do not increase the thickness of the leaf, however, beyond that which is required by other considerations.

2. Compute the value of R_0 from Eq. 11 for each diagonal; for greatest efficiency all values should be approximately the same. Any diagonal with a very low value of R_0 might just as well be omitted as it will be ineffective. It is not necessary to have diagonal members in every panel.

3. Compute the maximum positive and negative dead-load plus live-load values of $\Sigma F\, r\, z$. Using an average value of R_0 and the maximum positive value of $\Sigma F\, r\, z$, determine the total of the stresses in all positive diagonals from

$$\Sigma S = \frac{\Sigma F\, r\, z}{R_0\, H\, v} \qquad (32)$$

By dividing the total of the stresses, ΣS, by the number of positive diagonals, the stress in each is obtained and the required size can be determined. All positive diagonal members should be made the same size regardless of their position on the leaf. Similarly, the required sizes of the negative diagonal members are determined using the maximum negative value of $\Sigma F\, r\, z$.

4. Compute the value of Q for each diagonal from Eq. 24.

5. Using the maximum positive and maximum negative values of $\Sigma F\, r\, z$ for live load only, compute the maximum positive and maximum negative values, respectively, of the torsional deflection, D, of the leaf from Eq. 31. In each computation ΣQ contains all diagonals, both positive and negative.

6. Select a negative value of the prestress deflection, D_0, for the positive diagonals which is slightly greater numerically than the maximum negative deflection computed from Eq. 31. With this value of D_0 the diagonals will never become slack during operation of the gates. Then select a positive value of D_0 for the negative diagonals that is slightly greater than the expected positive deflection of the leaf. The values of D_0 may have to be adjusted somewhat to satisfy Eq. 28 in order for the leaf to hang plumb under its own weight.

7. Inasmuch as the stresses computed in step 3 may not be exact, they should be checked for each diagonal by using Eq. 22. If it is found necessary to revise the size of any member, all the design steps will have to be repeated, but such repetition will not usually be necessary.

8. Details of the diagonal members may now be determined and the design is then complete.

Diagonal members which are adjustable by a turnbuckle or sleeve nut are the best type. The initial adjustment is easy, and if the gate should become damaged in subsequent service it is a simple matter to readjust it. However, adjustable diagonals are not necessary.

Field Work

The diagonals with the largest numerical prestress deflection, D_0, should be adjusted first. For the case in which the negative diagonals have the greatest amount of prestress, the leaf should be swung against the lock wall and the top tied to the wall. The bottom is then jacked away from the wall until the leaf has a positive twist equal to the prestress deflection desired for the negative diagonals. At this point the turnbuckles in the negative diagonals should be tightened just enough to remove all slack but not so much that there is any significant stress in the members. During this operation the positive diagonals should be kept loose.

The bottom of the leaf is then held and the top is jacked away from the wall until the leaf has a negative twist equal to the prestress deflection required for the positive diagonals. At this point all the slack is removed from the positive diagonals. When the leaf is released it will hang plumb and it will be rigid in operation.

If a diagonal member is not adjustable but is of a fixed length, it may be attached (by welding) when the leaf is in the proper position for that diagonal. It should have no slack in it when it is attached or else D_0 may be increased slightly to compensate for any slack which might exist.

Conclusions

Diagonal members of lock-gate leaves can be designed to resist forces which cause twisting or wracking of the leaves as they are swung through the water. Prestressing these diagonal members adds much to their effectiveness. Maximum stresses in diagonals are not increased by prestressing so that many existing gates which are not prestressed can be prestressed without any structural alteration. The method has proved successful on both old and new installations.

AMERICAN SOCIETY OF CIVIL ENGINEERS
Founded November 5, 1852
TRANSACTIONS

Paper No. 2851

DRAINAGE IN THE HUMID AREAS OF THE UNITED STATES

By JOHN G. SUTTON,[1] M. ASCE

SYNOPSIS

The object of this paper is to acquaint the engineer briefly with the extent, needs, and current problems of drainage in the humid areas. In addition to the extent of drainage, improvements and accomplishments of the principal assistance programs are discussed. Examination of the changes brought about by drainage and some brief historical notes are included. Drainage is an activity in which federal, state, and local agencies, such as drainage enterprises and the individual farmer, cooperate in the planning and construction of drainage improvements. The functions of the various agencies responsible for drainage are described. Further described are the kinds of assistance furnished by technicians of the Soil Conservation Service, United States Department of Agriculture (SCS), working through soil conservation districts on drainage problems. Construction of adequate farm drainage systems for cultivated lands is the most extensive need, but there are some 20,000,000 acres of wet lands that could be drained and cultivated if required. The programs adopted by the states of Louisiana and North Dakota to meet special drainage needs are described. In many cases agricultural drainage has been impaired by inadequate culverts under roads or railroads. The paper cites the need for attending to this problem and refers to the Ohio Turnpike drainage standards as an example of how this problem may be met. Other technical problems, including those met with in the use of tile drainage, and some of the principal research needs are outlined.

INTRODUCTION

A third of the cultivated land in the humid areas of the United States requires drainage. Shallow surface drains, the bedding system of cultivation, and land clearing or smoothing are farm-drainage practices for collecting and removing surface water from cultivated fields. Tile drains are used to lower

---

NOTE.—Published, essentially as printed here, in July, 1954, as *Proceedings-Separate No. 460*. Positions and titles given are those in effect when the paper was approved for publication in *Transactions*.

[1] Head, Drainage Section, Eng. Div., Soil Conservation Service, U. S. Dept. of Agriculture, Washington, D. C.

the ground-water table and to provide the aeration of soil that is needed for optimum plant growth. Open drains are also used for ground-water control in some places. Outlet drains are constructed to transport flow from surface drains and subsurface drains to streams or other outlets. Levees, dikes, and diversion ditches are used to protect drained lands from overflow. Drainage pumping plants are used where it is not feasible to remove drainage water by gravity flow. Drainage is controlled through the regulation of water levels by means of structures installed in open or closed drains. Various types of structures are required in connection with all drainage practices.

In many places the farms lack adequate outlets for drainage under natural conditions, and two or more landowners must act jointly to construct the necessary outlets and other drainage works. Such construction is done through community or group drainage enterprises, such as drainage districts, county and township drains, state enterprises, and informal groups. The construction of group drainage works in the humid areas has been in progress since the United States was settled. It has permitted development of large areas of the country's most fertile lands.

TABLE 1.—SUMMARY OF DRAINAGE WORK OF ORGANIZED DRAINAGE ENTERPRISES FOR FOURTEEN STATES WITH UNITED STATES TOTALS[a]

State	Land in enterprises, 1950 (acres)	Increase since 1940 (acres)	Length of ditches, 1950[b] (miles)	Length of tile drains, 1950[b] (miles)	Length of levees and dikes, 1950[b] (miles)	Area served by pumps (acres)
Ohio	8,923,362	1,194,095	18,770	10,171	5	
Indiana	11,017,709	895,757	22,206	10,803	159	5,412[c]
Michigan	10,194,439	1,216,053	20,163	3,375	14	800[c]
Minnesota	11,269,962	279,553	16,214	9,973		1,315[c]
Iowa	6,734,863	570,519	5,393	13,038	492	81,754[c]
North Dakota	1,572,220	196,179	1,034	10		
Illinois	5,370,825	279,461	7,135	4,314	1,177	315,363
Missouri	3,147,484	60,421	5,222	170	704	67,217
Florida	6,083,676	384,654	7,285	16	1,132	293,124
Mississippi	3,023,744	133,126	4,716	34	191	8,040[d]
Arkansas	4,701,095	108,357	6,153	11	347	3,900[c]
Louisiana	12,161,665	7,942,041	9,222	6	790	179,266
Texas	5,794,786	1,575,936	5,854	18	69	17,990[c]
North Carolina	1,128,509	302,933	2,250		5	
All other states	11,563,992	582,207	23,836	4,376	2,728	
Total U. S.	102,688,331	15,721,292	155,453	56,315	7,813	

[a] Data from the 1950 Census of Drainage, except as noted. [b] Data obtained by adding totals reported in the 1940 census and new works constructed during the period from 1940 to 1950. [c] Data from the 1940 census. [d] Data from the 1930 census.

EXTENT OF DRAINAGE

Fig. 1 shows the location of drainage enterprises according to the "1950 Census of Agriculture,"[2] hereinafter referred to as "the 1950 census." The principal drainage works constructed through these drainage enterprises include open ditches, tile drains, and levees or dikes. Interest in the practice of draining by pumping is increasing. Table 1 shows the extent of land drained,

---

[2] "1950 Census of Agriculture," Vol. IV, "Drainage of Agricultural Lands," U. S. Govt. Printing Office, Washington, D. C., 1952.

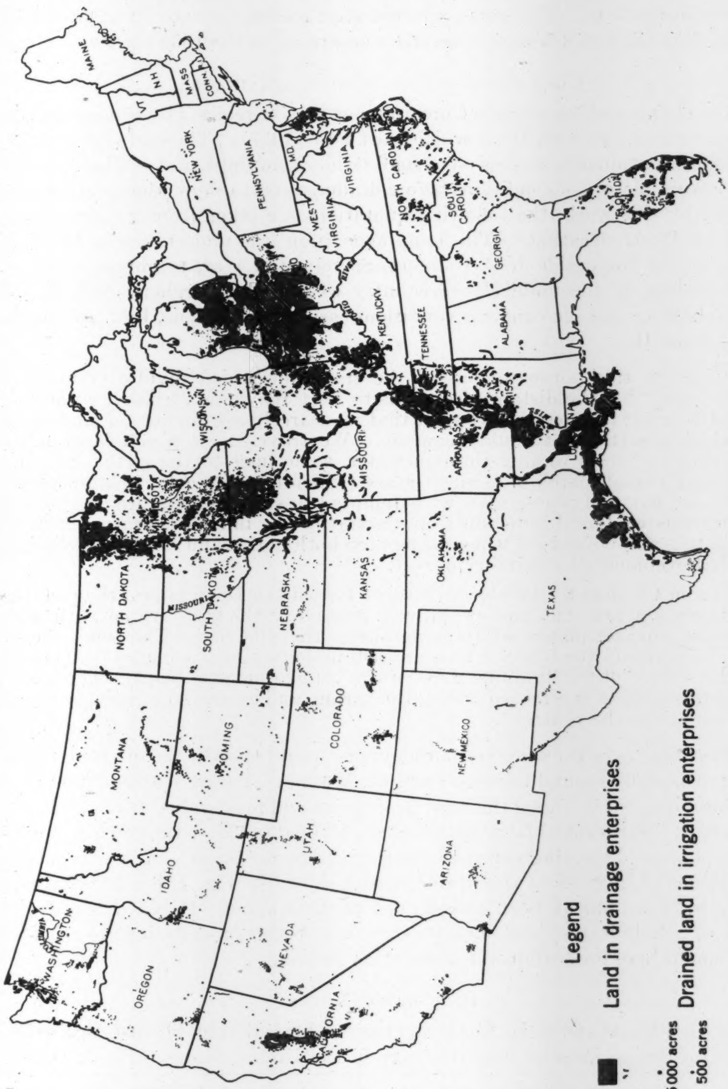
MAINE
VT
N H
MASS
CONN
R I
N J
NEW YORK
PENNSYLVANIA
MD
WEST VIRGINIA
VIRGINIA
NORTH CAROLINA
SOUTH CAROLINA
GEORGIA
FLORIDA
OHIO
OHIO RIVER
KENTUCKY
TENNESSEE
ALABAMA
MISS
LA
ARKANSAS
MISSOURI
WISCONSIN
MINNESOTA
IOWA
NORTH DAKOTA
SOUTH DAKOTA
MISSOURI
NEBRASKA
KANSAS
OKLAHOMA
TEXAS
MONTANA
WYOMING
COLORADO
NEW MEXICO
IDAHO
UTAH
ARIZONA
WASHINGTON
OREGON
NEVADA
CALIFORNIA
Legend
Land in drainage enterprises
Drained land in irrigation enterprises
5000 acres
500 acres

FIG. 1

the principal items of drainage works in fourteen states in the humid areas, and the national totals. The states selected are those which showed an excess of one million acres in drainage enterprises according to the 1950 census.

CHANGES AND BENEFITS OF DRAINAGE

The changes which resulted from drainage may be realized by comparing the original conditions with those which exist now (1957). The midwest prairies originally contained a succession of shallow lakes, swamps, and wet lands. To give a word picture of conditions before drainage and to show what was accomplished by this work, the following quotations are taken from a passage in a book by W. H. Keating.[3] The Long expedition was undertaken in 1823 by order of the Honorable J. C. Calhoun, Secretary of War, to obtain information relating to the undeveloped country west of the Allegheny Mountains. The following passage concerns conditions east of Fort Wayne, Ind., and south of Chicago, Ill.

> "Near to this house we passed the state line which divides Ohio from Indiana * * * The distance from this to Fort Wayne is 24 miles, without a settlement; the country is so wet that we scarcely saw an acre of land upon which a settlement could be made. We traveled for a couple of miles with our horses wading through water, sometimes to the girth. Having found a small patch of esculent-grass (which from its color is known here by the name of blue-grass), we attempted to stop and pasture our horses, but this we found impossible on account of the immense swarms of mosquitoes and horse flies, which tormented both horses and riders in a manner that excluded all possibility of rest.
>
> "From Chicago to the place where we forded the Des Plaines, the country presents a low, flat and swampy prairie, very thickly covered with high grass, aquatic plants, and among others the wild rice. The latter occurs principally in the places which are still under water; its blades floating on the surface of the fluid like those of the young domestic plant. The whole of this tract is overflowed during the spring, and canoes pass in every direction across the prairie."

Traveling over the same route today, one would observe the urban development, especially around Chicago and Fort Wayne. The agricultural land that has been drained is among the most productive and most valuable of any in the corn belt. Substantial farm buildings are located in places that formerly were swampland and thriving villages serve the prosperous farms. A similar change has occurred in most of the drained areas shown in Fig. 1, but the drainage problems have not all been solved even in these areas. Public drains are in need of rehabilitation and maintenance, and better farm drains are required as a sound base for sustained conservation farming.

HISTORICAL NOTES

C. G. Elliott[4] and S. H. McCrory[5] have published valuable historical references on the progress of land drainage in the United States. H. C. Darby[6] covered the historical development of drainage of the English Fens from about 1500 to the date of publication. Experience with drainage in England served as a basis for the drainage of rice lands in South Carolina in colonial times and for early state laws for community drainage projects.

---

[3] "Long's Expedition to the Source of St. Peter's River in 1823," by W. H. Keating, Carey and Lea, Philadelphia, Pa., 1824.

[4] "Engineering for Land Drainage," by C. G. Elliott, John Wiley & Sons, Inc., New York, N. Y., 1919, pp. 1-20.

[5] "Historical Notes on Land Drainage in the United States," by S. H. McCrory, *Transactions*, ASCE, Vol. 92, 1928, p. 1250.

[6] "The Draining of the Fens," by H. C. Darby, Cambridge Univ. Press, London, 1940.

In 1754, the colony of South Carolina passed a drainage act providing for drainage of the Cacaw Swamp. The colony of New Jersey enacted a drainage law in 1772. Several states passed drainage laws soon after the Revolutionary War. Progress in the formation of drainage enterprises was slow until about 1870, when several states enacted drainage laws similar to those now (1957) in force. They provided for drainage districts and county drains.

In Table 2 is shown the rate of development of organized enterprises according to the 1950 United States Census.

Underdrainage with manufactured tile was instituted in the United States in 1835 by John Johnston of Seneca County, New York. Mr. Johnston's tiles were manufactured by hand from patterns brought over from Scotland.[5] A total of 1,140 tile factories were in operation by 1880, chiefly in Indiana, Illinois, Ohio, Michigan, and Iowa.

TABLE 2.—RATE OF DEVELOPMENT OF DRAINAGE ENTERPRISES IN THE UNITED STATES

Date of organization	Land, in acres	Capital invested prior to January 1, 1950, in dollars
Before 1870	919,117	1,263,389
1870–1879	2,516,942	11,317,896
1880–1889	6,052,807	28,035,384
1890–1899	5,957,503	32,838,911
1900–1904	7,665,823	34,139,656
1905–1909	18,328,017	111,612,254
1910–1914	16,448,377	125,953,183
1915–1919	15,802,902	190,583,008
1920–1924	7,428,179	102,976,838
1925–1929	3,288,426	42,012,361
1930–1939	2,558,946	10,991,639
1940–1949	15,721,292	23,872,422[a]
All enterprises	102,688,331	715,596,941

[a] In addition, a total of $179,033,770 was spent by drainage enterprises during the period between 1940 and 1949, classified as "Construction, operation and maintenance."

In 1883, a large drainage district in Illinois, Mason and Taswell Counties, began construction of a main drain 14.5 miles long.[5] This was the longest drainage ditch in the country at that time and its construction was the first instance in which steam-driven dipper dredges were used successfully in drainage work. This was said to have worked a revolution in drainage. In 1903, the first drag-scraper excavator was built. The dragline excavator has gradually supplanted the floating dipper dredges.

DRAINAGE ENTERPRISES

In most states, community-type drainage enterprises are organized under general or special state laws. Drainage districts usually have their own board of managers whereas the development and maintenance of county drains is usually under the direction of the governing body of the county. Organization of both forms of enterprises is based on a petition in which from a majority to two-thirds of the landowners and acreage are usually represented. For the establishment of a drainage enterprise, it is usually required that the project be conducive to the health and welfare of the community, that a feasible plan of drainage be prepared by a competent engineer, that the benefits to be derived be shown to exceed the costs, and that objectors be given a fair opportunity to be heard in court if grievances cannot be settled by other means.

The present extent of drainage enterprises may be reviewed by a study of the 1950 census. Thirty states reported 14,066 drainage enterprises comprising 50,655,190 acres, nearly all of which were classed as drainage districts. In ten states, drainage enterprises consist principally of county drains and for census purposes the drainage in each county was considered as a single enterprise. In these ten states, 52,033,141 acres were reported to be included in drainage enterprises.

The large number and small size of drainage enterprises was emphasized in the 1940 drainage census,[7] in which were recorded 41,691 drainage enterprises of less than 500 acres each, comprising a net land area of 4,378,743 acres, and 37,529 enterprises in excess of 500 acres, comprising 82,588,296 acres. Although the land area quoted was net area, the totals of enterprises included subdistricts and informal groups which often overlapped other drainage enterprises. Because of their small size, many drainage enterprises have been unable to employ adequate managers and competent engineers.

LAND IN NEED OF DRAINAGE

The most extensive problem at present is the development of adequate farm drainage systems. These are the works needed on each farm after outlets have been provided. There is a vast difference in the productive capacity of well-drained land, used with proper conservation practices, and the partly drained land so frequently found on farms. Adequate drainage is so important for efficient crop production that it is often the first practice to be instituted in a farm conservation program. Many cultivated fields which appear to have satisfactory drainage are actually in need of a well-planned drainage system. On the basis of present information, there seems little doubt that the construction and maintenance of farm-drainage systems is needed for approximately one-third of all cultivated land.

Land that is now wet but on which drainage is possible constitutes a valuable asset for future development of agricultural land. The current crop surpluses discourage the immediate drainage of wet noncrop lands on a large scale, and technical and other assistance is not provided on projects the primary purpose of which is to bring new land under cultivation. H. H. Bennett, in his testimony before a subcommittee on agriculture and forestry in the United States Senate on June 5, 1944,[8] made estimates of land which can be drained, by states, as shown in Table 3. Since then, estimates of conservation needs have indicated that the total is somewhat larger, or about 20,000,000 acres.

---

[7] "1940 Census of Agriculture," Volume entitled "Drainage of Agricultural Lands," U. S. Govt. Printing Office, Washington, D. C., 1942.

[8] "Construction of Drainage Works in the United States," Hearings Before a Subcommittee of the Committee on Agriculture and Forestry, United States Senate, 78th Cong., 2d Session on S.1289, U. S. Govt. Printing Office, Washington, D. C., 1944.

This figure is now generally accepted as the estimate of land which can be drained and cultivated. These lands include mostly timbered areas and marsh areas. However, on some of the included lands, crops are grown occasionally, but the land is too wet to be utilized efficiently. Not included are 70,000,000 acres of wet lands now considered most adaptable to wildlife, recreation, and limited use for grazing and timber growing.

It also has been estimated that the outlet works in existing drainage enterprises, including 30,000,000 acres, are in need of rehabilitation or improvement. There is a considerable volume of reconstruction, improvement, and maintenance to be done each year to improve land drainage, and advancements in designs have made much of the earlier drainage work obsolete.

One of the principal problems in this field is to secure regular maintenance of drainage works, which will insure good drainage and stable agricultural production. Many drains overflow until the damage due to inadequate outlets becomes excessive and the drains must be reconstructed. Rehabilitation of the more successful outlet drains has occurred at intervals of from 10 years to 20 years. However, labor and equipment shortages and economic conditions have caused much needed drainage work to be delayed.

TABLE 3.—Areas of Fertile Undeveloped Wet Land in the Humid Section of the United States That Can Be Provided with Drainage at Reasonable Cost[a]

State	Area, in acres	State	Area, in acres
Alabama	683,000	New Jersey	60,000
Arkansas	1,870,000	New York	100,000
Connecticut	22,000	North Carolina	1,157,000
Delaware	34,000	North Dakota	29,000
Florida	1,970,000	Ohio	95,000
Georgia	1,721,000	Oklahoma	64,000
Illinois	69,000	Oregon	61,000
Indiana	135,000	Pennsylvania	90,000
Iowa	56,000	Rhode Island	4,000
Kansas	30,000	South Carolina	966,000
Kentucky	170,000	South Dakota	88,000
Louisiana	2,197,000	Tennessee	242,000
Maine	64,000	Texas	1,690,000
Maryland	63,000	Vermont	18,000
Massachusetts	19,000	Virginia	514,000
Michigan	690,000	Washington	137,000
Minnesota	874,000	West Virginia	15,000
Mississippi	1,272,000	Wisconsin	316,000
Missouri	323,000		
Nebraska	22,000		
New Hampshire	18,000		17,948,000

[a] Does not include 78,000,000 acres of wet land suited for wildlife, recreational uses, the growth of timber, and similar purposes.

The chief type of work involved in the construction and rehabilitation of drainage outlets is clearing and excavation with draglines. Much structural work is also included, in addition to work on such drainage facilities as levees and tile drains.

SOIL CONSERVATION DISTRICTS PROGRAM

In furthering the program of soil conservation districts, the Soil Conservation Service, United States Department of Agriculture (SCS), has provided a broad program of technical assistance to drainage enterprises and individual farmers. Drainage has become an integral part of the soil and water conservation program. All states have made it possible for farmers to organize soil conservation districts, and more than 80% of all farmers are now located in such districts. On request, the SCS and the Office of the Solicitor of the Department of Agriculture have cooperated with states and local agencies on problems in respect to state drainage laws.

The governing body of these districts receives requests from farmers or group enterprises for assistance on specific drainage problems and authorizes technicians to provide such assistance where possible. Frequently, a preliminary study and survey are required in order to determine drainage needs and the feasibility of drainage, and to supply the information needed for planning a drainage system for a large area. Local people interested in drainage then consider the proposals and determine whether or not they can finance the necessary expenditures. Most of the group projects are small, financed by an existing drainage organization or an informal group. After construction is assured, detailed surveys, plans, and designs are prepared. Drainage groups or enterprises usually let contracts for construction and they arrange for financing the work.

TABLE 4.—GROUP ENTERPRISE PLANS (INVOLVING TWO OR MORE FARMS) IN SOIL CONSERVATION DISTRICTS: UNITED STATES TOTALS FOR THE CALENDAR YEAR 1952 AND CUMULATIVE TO DECEMBER 31, 1952

Item	GROUP DRAINAGE	
	1952	Cumulative
(a) PLANS		
Number of group job plans	1,344	9,538
Areas to be benefited, in acres	683,034	6,744,090
Estimated total cost, in dollars	3,950,677	33,733,145
Number of group jobs completed	1,130	7,475
Number of farms benefited	6,925	44,922
Area benefited, in acres	522,189	4,256,413
(b) SOME PRINCIPAL INSTALLATIONS		
Ditch and canal excavation, in miles	1,177	9,477
Ditch and canal excavation, in cubic yards	10,155,966	85,332,638
Spoil bank leveling, in cubic yards	6,957,330	41,968,132
Levees and dikes, in miles	31	240.1
Levees and dikes, in cubic yards	333,301	3,121,460
Channel stabilization, in miles	12	202
Closed drains and pipe, in feet	545,597	2,490,328
Number of structures	908	6,325

[a] Group enterprise plans are defined as any job involving two or more landowners or operators who agree to work together to accomplish the construction, operations, and maintenance specified in the plans.

The SCS encourages those in charge of drainage enterprises and soil conservation districts to employ private engineers. Frequently, the SCS prepares a preliminary plan evaluating the capability of soils for agricultural use and the feasibility of drainage, and giving the approximate locations and designs of drainage works. On many projects, after the preliminary report has been accepted, private engineers make the detailed surveys and designs in accordance with recognized standards, supervise construction, and represent the drainage enterprises in legal and court work.

TABLE 5.—FARM DRAINAGE MEASURES APPLIED BY SOIL CONSERVATION DISTRICT COOPERATORS, WITH TECHNICAL ASSISTANCE FROM THE SOIL CONSERVATION SERVICE, DURING THE CALENDAR YEAR 1952 AND CUMULATIVE TO DECEMBER 31, 1952

State, territory, or insular possession	FARM DRAINAGE (ACRES)		OPEN DRAINS (MILES)		TILE DRAINS (MILES)	
	Applied, 1952	Cumulative to December 31, 1952	Applied, 1952	Cumulative to December 31, 1952	Applied, 1952	Cumulative to December 31, 1952
Alabama	46,126	230,451	387	2,010	1	8
Arizona	14	411	1	5		2
Arkansas	106,832	405,888	942	3,434		9
California	32,623	87,653	215	576	339	903
Colorado	7,028	34,171	52	261	43	147
Connecticut	454	3,382	10	78	2	12
Delaware	3,497	16,710	86	408		1
Florida	95,671	702,647	2,473	10,841	16	286
Georgia	27,849	224,555	223	1,735	6	30
Idaho	13,473	33,744	132	289	22	39
Illinois	39,169	233,927	295	1,280	659	3,526
Indiana	26,032	131,708	170	712	702	2,330
Iowa	40,783	191,020	258	980	1,950	5,131
Kansas	65,022	249,767	490	2,308	2	3
Kentucky	37,579	195,532	489	2,473	219	1,137
Louisiana	116,451	763,324	2,400	11,480		
Maine	390	5,155	19	174	6	32
Maryland	11,082	90,500	273	2,269	10	63
Massachusetts	578	5,019	13	114	5	21
Michigan	20,269	89,991	230	758	672	1,952
Minnesota	49,766	186,991	602	1,527	568	1,774
Mississippi	191,814	1,311,597	2,427	9,714		1
Missouri	43,250	103,632	301	920	21	24
Montana	13,051	87,574	151	793	3	10
Nebraska	37,224	155,002	324	1,520	34	48
Nevada	1,596	14,986	25	110		1
New Hampshire	736	1,877	11	47	7	14
New Jersey	2,452	12,820	58	316	42	143
New Mexico	1,231	3,987	3	27		2
New York	12,516	92,415	137	1,210	233	1,384
North Carolina	59,374	335,968	967	6,097	197	1,355
North Dakota	167,122	678,758	1,309	4,925		2
Ohio	19,524	90,411	142	528	1,184	3,806
Oklahoma	17,166	144,526	115	1,166		
Oregon	13,250	62,909	142	693	86	245
Pennsylvania	4,015	14,645	51	199	138	390
Rhode Island	49	772	1	15		2
South Carolina	63,186	427,662	530	3,437	20	188
South Dakota	33,489	217,170	685	3,243	7	28
Tennessee	21,408	233,948	219	1,258	1	6
Texas	40,732	234,649	400	2,478	20	30
Utah	3,308	12,159	29	178	14	41
Vermont	1,698	19,209	31	444	4	32
Virginia	18,451	105,915	469	2,698	74	496
Washington	20,078	117,264	318	1,539	95	334
West Virginia	2,787	19,438	64	445	96	513
Wisconsin	23,984	83,735	649	1,797	196	758
Wyoming	9,526	46,907	59	332	12	35
United States Total	1,563,705	8,512,481	19,377	89,841	7,706	27,294
Alaska	5	19	1	1		
Hawaii	103	204	6	20		
Caribbean Area	4,620	17,901	654	3,419		
Grand Total	1,568,433	8,530,605	20,038	93,281	7,706	27,294

Some of the principal accomplishments in providing technical assistance in the matter of group drains are shown in Table 4.

Technical assistance on farm drainage work is provided the individual farmer in connection with farm conservation planning. These plans provide for technical assistance on other conservation practices as needed, including a soil map and a determination of land capability and the proper use for each field. Soil amendments, including lime and fertilizers, are generally required to secure optimum crop production. A proper crop rotation is usually essential in order to maintain and improve soil fertility and to maintain the soil structure and soil permeability. Erosion control measures are often required in the watershed, including streambank control to protect drainage systems. Soil conservation districts do not furnish any funds to farmers but conservation payments are made under the Agricultural Conservation Program Service, Department of Agriculture, described subsequently.

TABLE 6.—OPEN DITCHES AND CLOSED DRAINS INSTALLED UNDER THE 1952 AGRICULTURAL CONSERVATION PROGRAM AND THE CUMULATIVE TOTAL EXTENT FOR 1942–1952, INCLUSIVE

Areas of the United States	OPEN DITCHES			CLOSED DRAINS		
	1952 Program		Cumulative	1952 Program		Cumulative
	Area[a] drained, in acres	Length of all ditches,[b] in rods	Area drained, in acres	Area[c] drained, in acres	Length of all drains installed, in rods[d]	Area drained, in acres
North Atlantic States	26,962	195,519	329,393	22,444	199,749	170,110
North Central States	607,033	2,462,450	12,792,415	339,579	5,393,738	3,088,599
South Atlantic States	167,081	414,598	2,080,776	6,174	54,733	149,241
South Central States	389,494	1,071,109	9,207,662	6,601	64,111	36,512
Western States	224,700	383,055	2,291,281	59,377	439,597	447,787
Islands, Territories	7,058	33,275	11,678			
Total	1,422,328	4,560,006	26,713,205	434,175	6,151,928	3,892,249

[a] Acreage drained by open ditches installed during the 1952 crop year was located on 35,683 farms.

[b] The estimated gross assistance to farmers for 1952 for open ditches amounted to $3,888,849.

[c] The acreage drained by means of closed drains installed during the 1952 crop year was located on 35,275 farms.

[d] The estimated gross assistance to farmers during 1952 for closed drains amounted to $4,450,279.

The accomplishments in drainage in humid-area states under the soil-conservation-district program are summarized in Table 5. Accomplishments in drainage for the western states are listed, but drainage work in those states was principally on irrigated lands. However, a considerable volume of drainage work has been accomplished on the humid western slopes of Washington and Oregon. Many farm drainage systems include dikes, drainage structures, pumping plants, and other practices in addition to the open and closed drains indicated in Table 5.

AGRICULTURAL CONSERVATION PAYMENTS

The Congress of the United States has enacted legislation providing financial assistance to farmers who complete needed conservation practices in accordance with provisions of a program that was operated for several years under the Production and Marketing Administration, Department of Agriculture, and more recently has become the Agricultural Conservation Program Service. Payments are made for a large list of practices, including measures for erosion control, irrigation, and drainage. The County Agricultural Stabilization and Conservation Committees, composed of elected farmers acting with local representatives of state and federal agricultural agencies, have considerable discretion in determining the practices for which assistance is made available in the county. Payments for drainage work are not available in some places.

Since 1951, the SCS has been responsible for furnishing technical assistance for this program. This includes assistance in the preparation of practice standards and specifications. After the farmer makes application for assistance, the SCS technician determines the feasibility of the measure, approves the site selection, makes necessary designs and layout, and checks compliance to determine that the installation complies with specifications. In Table 6 are outlined some of the major accomplishments in the drainage phase of this program for the 1952 program year.

Special State Programs

Difficulties encountered in the financing, organization, management, and operation of drainage enterprises have led to many special programs for handling drainage work. Those in Louisiana and North Dakota are examples of particular significance.

The state-wide drainage plan of Louisiana, begun in 1941 by the Louisiana Department of Public Works, has resulted in outstanding long-range accomplishments. This program has been primarily responsible for the increase of 7,942,041 acres in drainage enterprises in Louisiana in the decade ended in 1950. This program benefited greatly from the levees and main outlet channels constructed by the Corps of Engineers, United States Department of the Army. Many of these works of improvements were directly responsible for making land drainage possible in the lower Mississippi delta.

Previously, the drainage works in the state were constructed by small drainage districts. In the 1950–1951 Biennial Report of the Louisiana Department of Public Works it is stated that the works of these drainage districts were constructed without regard to capacity, to outlet streams, or to the effect on small local improvements, without provisions for adequate maintenance, and with high interest rates on bonds.

Under the Louisiana program, the governing board of parishes (counties) has constructed main ditches and laterals. The engineering assistance has been provided under supervision of the state department of public works, which has employed an experienced staff of drainage engineers. The parishes have assumed responsibility for bonds and assets of the previous drainage districts. An election is held for the issuance of bonds. If the election is favorable, the parish issues the bonds for construction of a system and the retirement of old bonds.

State general funds frequently have provided about 40% of construction costs and parish funds have provided about 60%. The state-wide program was financed through a special state appropriation of $5,000,000 to the department of public works in 1945 and in 1948. The 1951 report showed progress in twenty-seven parishes which undertook major drainage construction, with the initial program complete or nearly complete in nineteen parishes.

Soil conservation districts have an extensive program after parish outlets are constructed. They assist small groups of farmers in providing cooperative drains to reach the outlet. Farm drainage is one of the most important practices in the soil-conservation-district program.

North Dakota has provided substantial state assistance to organized drainage enterprises in the past decade. The state has approximately 1,500,000 acres in drainage enterprises, of which a large proportion are in the Red River Valley. During the prolonged drought of the 1930's, there was little need for drains. In fact, many miles of ditches were almost closed by wind-blown soil. Many of the section-line roads were constructed so that they greatly retarded drainage because road fills were raised and small culverts placed too high. When rainfall became normal again the lack of effective drainage resulted in extensive crop failures. Emergency measures were undertaken to improve the drainage.

The state legislature made some state funds available through the State Water Conservation Commission. State funds were used to pay approximately 40% of the reconstruction costs of the public drains that qualified for assistance. The farmers organized soil conservation districts throughout the area, and these districts secured technical help for the program from the SCS. The Agricultural Conservation Program Service made an important contribution toward the success of the program by making conservation payments to farmers for farm drains. This program, utilizing resources from several agencies, has been highly successful and has re-established the Red River Valley as a highly productive area.

Engineers of the SCS made most of the surveys, prepared the plans, made the designs, and supervised construction in connection with this work. Assistance of this type was furnished on 670 group jobs—benefiting 3,922 farms and 947,850 acres—which were completed in the state prior to December 31, 1952. This work included 1,007 miles of open ditches, requiring 10,212,443 cu yd of excavation. The group job included work on county drains and on projects for informal groups of farmers. In addition, technical assistance under the district program was provided for the completion of 4,925 miles of farm drains which served 678,758 acres.

A few counties in Texas have undertaken construction of county-wide drainage systems, financed by county funds but otherwise under a plan similar in principle to the coordinated county drainage systems described for Louisiana. Another interesting venture has been undertaken in Washington County, Mississippi, where several drainage districts combined resources for rehabilitation and maintenance of their drainage works while they maintained their separate legal identities. The drainage districts jointly employed an engineer, erected a machine shop, and purchased equipment to carry on drainage work as a regular activity.

Some of the larger drainage districts have employed highly competent technical staffs. In most states, however, the drainage work is still being done by small drainage districts, with great variations in operating results. Most districts conduct maintenance and rehabilitation work by letting construction contracts, a plan which is found to be economical.

Several states have recognized problems in connection with state drainage laws and have undertaken revisions of these statutes. In recent years the State of Delaware has enacted legislation and commenced operation of a simplified drainage program. Technical control is invested in a state drainage engineer, and the assistance of soil conservation districts is fully utilized. The program is working smoothly as a result of the improved legal procedures. Maryland put into effect a new and simplified drainage code in 1941 which has also been quite successful.

DRAINAGE AND FLOOD CONTROL

Congress has enacted legislation which for many years has authorized large flood-control projects and programs. The watershed protection, conservation, and upstream flood-control aspects of these programs have been administered by the Corps of Engineers, and more recently by the Department of Agriculture. Programs of both agencies often have an important or decisive influence on the feasibility of draining land. The levees and major channel improvement work of the Corps of Engineers have made it possible for drainage enterprises and landowners to drain large areas of fertile bottom lands along the Mississippi River, Missouri River, Red River, Arkansas River, Illinois River, and other major rivers.

The Department of Agriculture is working on watershed protection projects, flood prevention, and erosion control in many locations.

The Watershed Protection and Flood Prevention Act (Public Law 566), authorized by the 83d United States Congress, which includes drainage systems or channels with other necessary works will provide works of protection for many bottom-land and other areas. The program under which large numbers of small projects are being planned is reaching the initial construction stage. It offers great promise for future development of many of the bottom lands and improvement of other flat lands which can be developed in cooperation with soil conservation districts, drainage enterprises, or landowners. Such development will provide for control of flash floods in the upstream reaches by means of small flood-control dams.

ASSISTANCE BY OTHER AGENCIES

Other types of assistance have been provided to drainage enterprises and farmers undertaking drainage work. The Department of Agriculture provided technical assistance through the Office of Drainage Investigations from 1904 to about 1920. This latter organization employed several drainage engineers who made plans for drainage and reclamation of large areas throughout the country. Costs of surveys were borne partly by local interests. Many of these plans are still available and, where available, form a valuable reference for rehabilitation of drainage works.

In about 1920, the main emphasis in drainage investigations was shifted to research. Research work continued as a major Department of Agriculture activity in drainage, and numerous technical bulletins were published by the department as a result of such research.

Forty-six Civilian Conservation Corps (CCC) camps for drainage work were assigned in 1935 to the Bureau of Agricultural Engineering, which then had the responsibility for drainage work. These camps were located in ten states Their work, which benefited about 12,000,000 acres, consisted chiefly of clearing and excavating open drains. A total of 6,444 miles of ditches was excavated, involving 64,000,000 cu yd of earth. This program was limited to rehabilitation and improvement of existing drainage enterprises organized under state drainage laws.

The public works programs and the work relief programs also contributed extensively to the work on drainage systems in the late 1930's. The CCC and these public works programs enabled many drainage enterprises to rehabilitate drainage works that had become ineffective during depression years.

In legislation enacted by the United States Congress in 1933, the Reconstruction Finance Corporation (RFC) was authorized to lend money to drainage and irrigation enterprises in financial distress. This agency provided the assistance that permitted many districts to continue operations during the depression years. Where bonds were in default, a settlement could usually be negotiated by the bondholders, the RFC, and the drainage enterprise. Bondholders generally accepted as a cash settlement sums ranging from 30% to 75% of the face value of their bonds. The RFC secured new bonds from the drainage enterprise to retire the old ones and provided additional funds, if necessary, for rehabilitating the works of the district. Thus, a sound financial plan enabled the drainage enterprise to keep operating and to improve drainage works. Under the program, the RFC loaned $40,000,000 for approximately 300 drainare enterprises in about twenty-six states. Many of these enterprises were among the larger drainage districts. With minor exceptions, the funds advanced by the federal government have been paid as due under this program.

The Federal Land Bank System maintains a staff of engineers to advise the banks on factors to be considered in making long-term farm mortgage loans in areas affected by drainage, flood control, and irrigation problems. This system consists of twelve farmer-owned banks, which are privately financed but operate under federal supervision of the Farm Credit Administration. The engineering staff periodically investigates and prepares reports on physical and economic conditions in areas involving some 60,000,000 acres of land affected by drainage and overflow problems in the humid sections of the country. This work is privately financed, and the engineering reports are not published for distribution to the public. Nevertheless, the Federal Land Banks have been cooperative in giving agencies interested in improving conditions access to the information contained in these reports. These banks have been helpful also in making loans to farmers for the purpose of financing drainage improvements that will increase crop production.

Current Problems in Technical Phases

There is a need for improved methods of maintenance and more detailed information relating to the effectiveness and costs of the different methods.

Considerable interest has developed in spraying ditch banks with chemicals to control undesirable vegetation. In some cases, damages to adjoining crops and unsuccessful trials have curtailed further use. Some ditches have been maintained by mowing weeds with a tractor and mower or by pasturing. Comparisons of these methods with other methods should be made in order to determine relative costs and effectiveness.

DRAINAGE REQUIREMENTS OF CULVERTS AND BRIDGES

Inadequate culverts under highways, roads, or railroads have caused many delays and additional costs in providing proper drainage for farm land. This has been one of the major problems in rehabilitating drains to adequate standards. It is desirable for civil engineers who are responsible for the design of culverts and bridges to observe carefully the drainage needs of agricultural lands. Probably the greatest difficulty arises from placing culverts too high for agricultural drainage needs. This problem has not been solved in many states. The writer recently observed twin culverts that had been installed under a new four-lane divided highway of the most modern design. All the details had been planned carefully except the elevations of the culverts which were at least 2.5 ft too high to serve the agricultural drainage needs.

On the Ohio Turnpike, excellent drainage requirements have been incorporated in the design standards. This highway traverses the "Old Black Swamp" section for more than 100 miles, over which the right of way crosses many networks of tiles and open drains. The Ohio Turnpike Commission recognized that it was essential to provide for future agricultural drainage along its right of way.

The Ohio Turnpike drainage standards have been described by H. Luebcke[9] in detail. Standards for capacity and other drainage criteria were developed in consultation with landowners, county engineers, Ohio State University (Columbus), and the SCS. In numerous cases, provision for future drainage across the turnpike was made by installing culverts of adequate size and depth and sealing both ends. This procedure safeguards the right of landowners to drain their lands in accordance with the provisions of state laws.

Provisions for adequate drainage have been of great help in securing rights of way from farmers who understand that drainage needs of their lands will be provided for. The structures installed by this turnpike in accordance with these standards will not be a limiting factor in either existing or future drainage improvements.

TILE DRAINAGE

There have been many complex technical problems associated with the design and maintenance of tile drains. Many tile drains have failed through frost action on the clay tile and the action of sulfates and acids on concrete tile. In many cases, tile having inadequate strength or tile that is highly absorptive has been manufactured and sold. This fact caused early failures in areas exposed to overloading or freezing and thawing conditions.

---

[9] "Special Drainage Along Ohio Turnpike to Protect Tiling," by Henry Luebcke, *Roads and Streets*, July, 1953, pp. 73–76, 79–81.

The American Society for Testing Materials (ASTM) prepared specifications for various grades of drain tile. The SCS is working on methods of improving the quality of drain tile, including recommendations for the adoption of ASTM specifications where applicable. Many drain tiles manufactured from surface clays cannot meet recent ASTM specifications (C4-55) but may furnish satisfactory service in farm drain installations, especially in the southern United States where freezing and thawing are not of much consequence. Investigations to establish the quality requirements of drain tile for various conditions of exposure should be undertaken.

Effective research work has been done on the resistance of concrete tile to acids and sulfates. The publications by Dalton G. Miller and Philip W. Manson[10,11] contain much information relating to durability of concrete and mortar under exposure to acid and alkaline conditions.

In many states, the engineers, soil scientists, and technicians of the SCS and of the state agricultural college cooperate to produce recommendations for the depth and spacing of tile drains. Such recommendations have been based on experience with soil groups and dominant soil types. In some states specific recommendations are available for from 50 to 100 soil types.

A committee of the American Society of Agricultural Engineers has published tentative standards for design and construction of tile drains in humid areas.[12] This report is to be amended after comments are received.

Research Needs

There are many investigations of a general nature that should be made in order to encourage further improvement in drainage. Research studies are needed to determine criteria for the effective design of outlet ditches and farm drainage systems, including types, capacity, spacing, and depth. Much interest has been evident in developing formulas and procedures to determine the depth and spacing of tile drains based on the permeability of soil. Research should be conducted on criteria for and methods of laying tile, including protection and spacing of joints in sandy and erosive soils and on steep slopes. This research should cover the use of interceptor systems and other tile systems on sloping lands.

Grading land to improve drainage is a comparatively new practice in the humid area. Specific guides need to be developed in order to establish desirable grades, maximum depths of cut, and soils and crops for which this practice is recommended.

Mole drainage has been used extensively in Great Britain and other European countries. In the United States, the practice has been emphasized infrequently outside of Florida where it has been used commonly in organic soils. A hydraulic-lift mole drainage machine has been developed by the SCS.

---

[10] "Durability of Concretes and Mortars in Acid Soils with Particular Reference to Drain Tile," by Dalton G. Miller and Philip W. Manson, *Technical Bulletin No. 180*, Univ. of Minnesota Agri. Experiment Station, Minneapolis, Minn., 1948.

[11] "Long-time Tests of Concretes and Mortars Exposed to Sulfate Waters," by Dalton G. Miller and Philip W. Manson, *Technical Bulletin No. 194*, Univ. of Minnesota Agri. Experiment Station, Minneapolis, Minn., 1951.

[12] "Design and Construction of Tile Drains in Humid Areas," by Committee on Design and Construction of Tile Drains, *Agricultural Engineers Yearbook*, 1955, Am. Soc. of Agri. Engrs., St. Joseph, Mich., 1955, p. 117.

Further trials to determine feasibility, depth, and spacing of this type of drainage are needed.

The widespread availability of electric power and tractors on farms is responsible for considerable interest in the construction of small pumping plants. Small drainage pumping plants have been used to drain lake-plains soil, such as in northwest Ohio, and to drain depressional areas in which it was not feasible to deepen outlet ditches. Studies should be made to establish criteria for the design and installation of such plants.

Additional investigations are needed to determine proper locations, procedures, and feasibility of drainage facilities required for the development of wet lands in theUnited States.

AMERICAN SOCIETY OF CIVIL ENGINEERS
Founded November 5, 1852
TRANSACTIONS

Paper No. 2852

MOMENT-ROTATION CHARACTERISTICS OF COLUMN ANCHORAGES

By Charles G. Salmon,[1] J. M. ASCE, Leo Schenker,[2] A. M. ASCE, and Bruce G. Johnston,[3] M. ASCE

Synopsis

In this paper are presented methods of determining the moment-rotation characteristics for common types of column anchorages found in light industrial buildings. These characteristics are useful in methods of analysis or design, particularly for cases in which resistance to rotation may be critical to the survival of the structure under heavy lateral loads such as earthquakes or blast loads. Upper and lower bounds for maximum resisting moment and maximum rotation, respectively, are developed. Shear is found to have little effect on the ultimate resisting moment but has somewhat more effect on the maximum rotation.

Formulation of the complete moment-rotation curve is developed in five stages. Appendixes illustrate the use of the formulas. The variables involved are examined, and the effect of each on the ultimate moment and rotation is shown graphically. The procedure developed may provide at least a first approximation until experimental data become available which will allow corroboration or correction of the assumptions that have been made.

Introduction

To permit the analysis of a complete structure, knowledge of the ultimate strength of the column anchorages must be supplemented by an estimate of their moment-rotation characteristics, particularly in the case of structures subjected to lateral blast loads.

Because analytical and test information on the ultimate strength-rotation behavior of column anchorages is largely lacking, a theoretical analysis of the problem applicable to simple types of anchorages is developed herein.

Note.—Published, essentially as printed here, in April, 1955, as *Proceedings-Separate No. 660*. Positions and titles given are those in effect when the paper was approved for publication in *Transactions*.

[1] Instructor, Civ. Eng. Dept., Univ. of Wisconsin, Madison, Wis.

[2] Member of Technical Staff, Bell Telephone Labs., Inc., Murray Hill, N. J.

[3] Prof. of Structural Eng., Univ. of Michigan, Ann Arbor, Mich.

The degree to which anchorages affect the capacity of structures to resist lateral loads, such as could occur as a result of a bomb blast, varies with the type of structure. This fact follows from consideration of the three ways in which a column anchorage can fail: (a) Failure in shear resistance, (*b*) failure in moment resistance, and (*c*) failure in tensile resistance.

Shear failure of an anchorage might occur in a low, wide building. This failure could take the form of cracking of the concrete pier to which the anchorage is secured or shearing of the anchor bolts. The latter type of failure might result from shear alone or might occur in combination with the applied moment, causing combined tension and shear failure of individual bolts. Anchorages of multistory buildings are unlikely to fail in shear because they are so rigid and because friction due to the vertical loads is so great. Although each design should be examined individually, in general, the anchorages of tall buildings, being heavily embedded in concrete, can be considered fully fixed; hence, deformation and failure would be governed by the properties of the columns. A related problem outside the scope of this paper is the possibility of over-all footing failure.

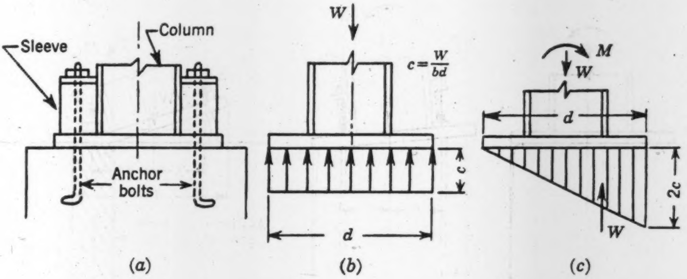

FIG. 1

Between the two extreme cases of fixed and flexible anchorages are the anchorages encountered in most light industrial buildings. These consist of plates attached to the bottom of columns and held down by anchor bolts embedded in a concrete pier (Fig. 1(*a*)). The moment-rotation relationship of this type of anchorage will be investigated, omitting consideration of any relative movement between the concrete foundation and the surrounding soil.

Several technical articles have appeared on the subject of the design of simple anchorages,[4] but a review of the literature has not revealed any experimental or analytical investigation of such anchorages. Empirical procedures have been used for design purposes with the knowledge that a large factor of safety is available to absorb discrepancies between the assumptions and the actual behavior of anchorages. The assumptions made herein are more realistic and are readily adjustable to results of tests as they become available.

---

[4] "Analysis of Anchor Bolts and Concrete Piers for Large Stills and Kettles," by A. A. Brown, *Civil Engineering*, Vol. 22, 1952, p. 491.

UPPER BOUND OF MOMENT

The "upper bound" of moment is an approximate evaluation of a resisting moment below which the actual resisting moment must lie.

Rectangular Base Plate.—The most important variables that enter into the moment-rotation relationship for a column anchorage are: (*a*) The dimensions of the base plate; (*b*) the dimensions, location, and stress-strain characteristics of the anchor bolts; (*c*) the dimensions and stress-strain characteristics of the concrete pier; and (*d*) the vertical loading. As a first step in determining the manner in which changes in these variables affect the moment-rotation relationship of the anchorage, the upper bound of the moment and the corresponding minimum rotation will be estimated.

It is convenient to express many variables in terms of the dimensions of the base plate; thus, all primed symbols in this paper signify such a manner of expression. For example, e is defined as the distance of an anchor bolt from the center line of the base plate and $e' = e/(d/2) = 2\,e/d$. The only exception to this use of primed symbols is f'_c which has the conventional meaning of ultimate concrete (cylinder) compressive strength.

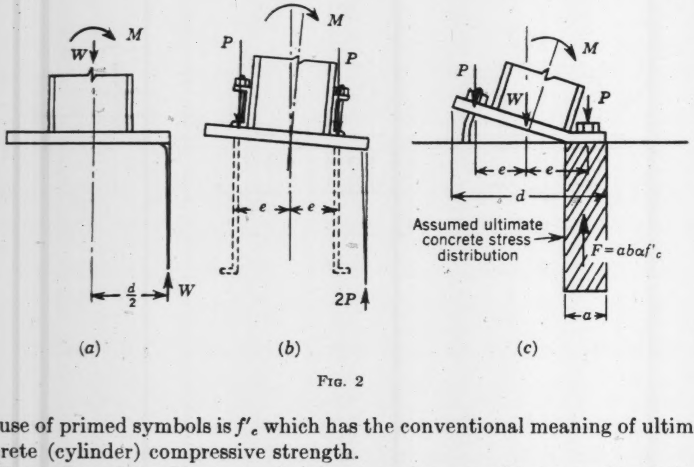

(*a*) (*b*) (*c*)

FIG. 2

Upper Bound for Moment.—A column anchorage without anchor bolts is shown in Fig 1 (*b*), in which b is the width of the base plate. The unit bearing pressure, c, due to a concentric vertical load, W, is assumed to be uniform. On a concrete foundation, the maximum value for c permitted by most codes is 600 lb per sq in. or 800 lb per sq in. If a moment applied by the column is added, the stress distribution at some stage is assumed to be approximately as shown in Fig. 1 (*c*). Evidently, the resisting moment is $W\,d/6$, in which d is the length of the base plate. If, hypothetically, the concrete had infinite strength and the bearing plate were infinitely rigid, equilibrium considerations alone would determine the maximum moment that could be resisted. Just before the column toppled over, as shown in Fig. 2 (*a*), the resultant base pressure would be at the edge of the plate and the "upper-bound" moment would be

$$M_u = \tfrac{1}{2}\,W\,d \ldots\ldots\ldots\ldots\ldots\ldots\ldots\ldots (1)$$

Fig. 2(*b*) shows the same column-and-base-plate arrangement supporting no weight at all but held down by anchor bolts. The plate and the concrete are again assumed as infinitely rigid. The tension to which the bolts have been tightened is immaterial. The ultimate strength of the bolt or bolts on one side of the center line of the base plate is designated P_u. The distance from the anchor bolts to the center line is e. In this case the upper bound for the resisting moment is

$$M_u = P_u \left(\frac{d}{2} + e\right) + P_u \left(\frac{d}{2} - e\right) = 2\,P_u \frac{d}{2} \ldots\ldots\ldots\ldots (2)$$

Adding the upper-bound moments for the two cases (Eqs. 1 and 2), the upper-bound moment for an anchorage supporting a weight, W, and held down by anchor bolts of ultimate strength, $2\,P_u$, is

$$M_u = (W + 2\,P_u)\frac{d}{2} \ldots\ldots\ldots\ldots (3a)$$

If one is interested only in the moment which would doubtless cause complete structural failure of the type of anchorage under consideration, Eq. 3(*a*) would provide sufficient information.

The symbol p is now introduced as equaling $A_t/\,(b\,d)$, in which A_t is the cross-sectional area of one-half the anchor bolts and b is the width of the base plate. Thus, p has a meaning similar to that in reinforced concrete theory, in which d is the distance from the extreme compression fibers to the reinforcing steel. Eq. 3(*a*) can thus be rewritten

$$M_u = (c\,b\,d + 2\,p\,\sigma_u\,b\,d)\frac{d}{2} \ldots\ldots\ldots\ldots (3b)$$

in which σ_u is the ultimate steel strength. Thus, $M_u = (c + 2\,p\,\sigma_u)(b\,d^2)/2$.

Setting

$$\left.\begin{aligned} \frac{M_u}{b\,d^2} &= M'_u \\ \text{one may write} \qquad M'_u &= \tfrac{1}{2}\,(c + 2\,p\,\sigma_u) \end{aligned}\right\} \ldots\ldots\ldots\ldots (3c)$$

Hence, the upper-bound moment divided by $b\,d^2$ is the same for similar anchorages of different size, provided that the original uniform bearing stress and the ratio of anchor-bolt area to base-plate area remain the same.

Next, a more realistic assumption than that of infinite strength is made with regard to the concrete. The actual ultimate concrete strength depends somewhat on the relative size of the base plate and the concrete footing. It is known that the compressive strength of concrete confined in one or more directions is greater than the value of f'_c determined from standard cylinder tests. It will be assumed, therefore, that the concrete strength is $\alpha\,f'_c$, in which $\alpha \geqq 1$ and must be either estimated or determined by suitable tests.

Theoretical considerations based on elastic theory[5] suggest that α might be between 1 and 1.5. Tests conducted by the Hydro-Electric Power Commission of Ontario (report unpublished) on concrete cubes loaded over a small central square indicate that α may be proportional to the cube root of the ratio of total area to loaded area. Values for α as high as 10 have been obtained in tests at the Hydro-Electric Power Commission's laboratories.

---

[5] "Theory of Elasticity," by S. Timoshenko and J. N. Goodier, McGraw-Hill Book Co., Inc., New York, N. Y., 1951.

From the viewpoint of determining the moment resistance of anchorages, the effect of loading a rectangular strip is of more importance than that of loading a small square. O. Graf[6] reports on tests performed on concrete cubes in which ultimate strength under a loading on a strip covering only a third of the top surface was 1.6 times as high as the ultimate strength of a cube loaded uniformly over all its cross section. Loading on a strip one-seventh the width of the cube resulted in values for α varying from 2.5 to 2.8. Moving the loaded strip toward the edge of the cube resulted in reducing α to from 1.2 to 1.5. Fortunately, as will be shown subsequently, the values M_u are relatively insensitive to changes in α.

The concrete stress distribution just before failure is likely to be nearly trapezoidal but it is considered that, in view of the large strains involved, no great error is introduced by assuming the stress distribution to be uniform, as shown in Fig. 2(*c*). The width of the strip of concrete in touch with the base plate is designated by a. Then

$$\alpha f'_c a b = W + P_u, \qquad \left(\frac{d}{2} - e\right) < a \ldots\ldots\ldots\ldots\ldots (4a)$$

or

$$\alpha f'_c a b = W + 2 P_u, \qquad \left(\frac{d}{2} - e\right) > a \ldots\ldots\ldots\ldots\ldots (4b)$$

Analyzing first the case in which $(d/2 - e) < a$—that is, in which the bolts near the compression zone are not effective—and defining a_1 as the width of concrete bearing area in this particular case,

$$\left.\begin{aligned} a_1 &= \frac{W + P_u}{\alpha f'_c b} = \frac{(c + p\,\sigma_u)\,d}{\alpha f'_c} \\ \text{and} \qquad & \\ M_{u1} &= W\left(\frac{d}{2} - \frac{a_1}{2}\right) + P_u\left(\frac{d}{2} + e - \frac{a_1}{2}\right) \end{aligned}\right\} \ldots\ldots\ldots\ldots (5a)$$

Setting

$$\left.\begin{aligned} e' &= \frac{e}{(1/2)\,d} = \frac{2\,e}{d} \\ &\text{one may write} \\ M_{u1} &= \frac{c\,b\,d^2}{2}\left(1 - \frac{c + p\,\sigma_u}{\alpha f'_c}\right) + \frac{p\,\sigma_u\,b\,d^2}{2}\left(1 + e' - \frac{c + p\,\sigma_u}{\alpha f'_c}\right) \end{aligned}\right\} \ldots (5b)$$

and

$$M'_{u1} = \frac{M_{u1}}{b\,d^2} = \tfrac{1}{2}\,(c + p\,\sigma_u)\left(1 - \frac{c + p\,\sigma_u}{\alpha f'_c}\right) + \tfrac{1}{2}\,p\,\sigma_u\,e' \ldots\ldots (5c)$$

---

[6] "Die Eigenschaften des Betons," by O. Graf, Springer, Berlin, 1950.

For the second case, in which $\left(\frac{d}{2} - e\right) > a$,

$$\left.\begin{aligned} a_2 &= \frac{W + 2\,P_u}{\alpha\,f'_c\,b} = \frac{(c + 2\,p\,\sigma_u)\,d}{\alpha\,f'_c} \\ \text{then}& \\ M_{u2} &= W\left(\frac{d}{2} - \frac{a_2}{2}\right) + P_u\left(\frac{d}{2} + e - \frac{a_2}{2}\right) + P_u\left(\frac{d}{2} - e - \frac{a_2}{2}\right) \\ &= W\left(\frac{d}{2} - \frac{a_2}{2}\right) + 2\,P_u\left(\frac{d}{2} - \frac{a_2}{2}\right) \end{aligned}\right\} \quad \ldots (5d)$$

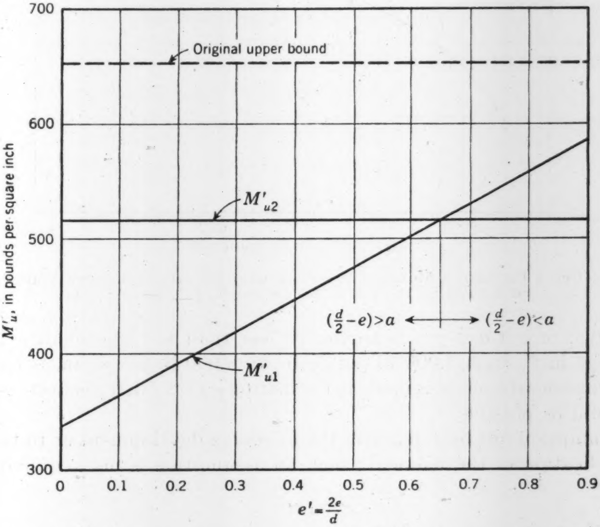

FIG. 3.—UPPER BOUND FOR MOMENT; VARIATION WITH ECCENTRICITY USING TYPICAL VALUES; $\alpha f'_c = 6{,}000$ LB PER SQ IN., $c = W/(b\,d) = 300$ LB PER SQ IN., AND $p\,\sigma_u = P/(b\,d) = 500$ LB PER SQ IN.

and

$$M'_{u2} = \tfrac{1}{2}\,(c + 2\,p\,\sigma_u)\left(1 - \frac{c + 2\,p\,\sigma_u}{\alpha\,f'_c}\right) \quad \ldots\ldots\ldots\ldots (5e)$$

from which M'_{u2} is seen to be independent of e.

The moment resistance coefficients, M'_{u1} and M'_{u2}, are shown in Fig. 3, plotted relative to e' for specific values of c, p, $\alpha\,f'_c$, and σ_u. The larger of the two coefficients represents the upper-bound moment.

In most cases the value e' does not differ greatly from 0.8, and the effective value of the upper bound will be in the range in which M'_{u1} is greater than M'_{u2}. In the following, the expression for M'_{u1} will be used for M'_u with rectangular base plates.

A study of Eqs. 5c and 5e reveals that, in any practical case, all variables except $\alpha f'_c$ are known. To illustrate the effect on M'_{u1} of any error in estimating $\alpha f'_c$, Fig. 4 was prepared, again using specific typical values of c, p, e', and σ_u. The value of M'_{u1} is greater than that of M'_{u2} up to values of $\alpha f'_c$ of approximately 11,000 lb per sq in., which is near the limit of practicality. Hence, M'_{u1} represents the effective upper bound for moment on most anchorages, whether or not $d/2 - e$ is greater or less than a. The change in M'_{u1} for a change in f'_c from 4,000 lb per sq in. to 8,000 lb per sq in. is only 7%. Even if a considerable error is made in estimating $\alpha f'_c$, a fairly accurate estimate of M_u should be possible.

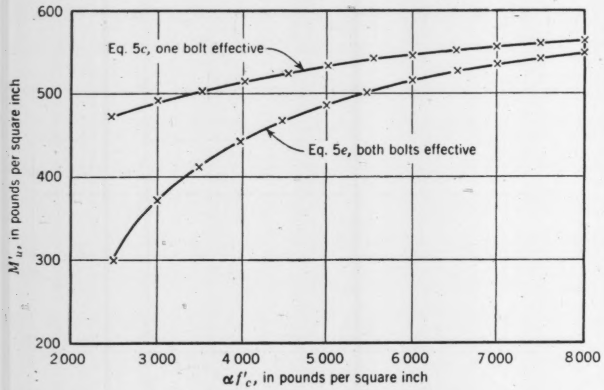

Fig. 4.—Upper Bound for Moment; Variation with Ultimate Concrete Strength; $c = 300$ Lb per Sq In., $p\,\sigma_u = 500$ Lb per Sq In., and $e' = 0.81$

No assumption has been made in the foregoing development as to the manner of application of the moment; such an assumption is not required. The moment that is considered herein is the total external moment and, in the case of large lateral displacements of the structure, vertical loads may be responsible for a considerable fraction of the total moment.

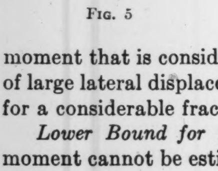

Fig. 5

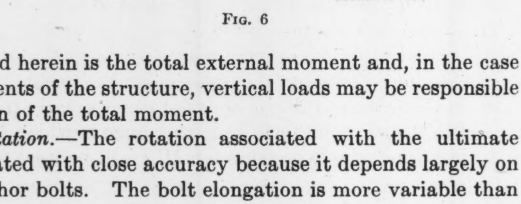

Fig. 6

Lower Bound for Rotation.—The rotation associated with the ultimate moment cannot be estimated with close accuracy because it depends largely on the elongation of the anchor bolts. The bolt elongation is more variable than that of plain rods and, although the elongation of a tensile specimen made of the same material may be from 20% to 30%, the bolt may be elongated no more than 5% at failure. However, it is possible to estimate a minimum value for the rotation based on the extension of the bolt at the maximum stress.

From Fig. 5, the lower bound for the rotation is

$$\theta_L = \frac{\epsilon_u \, (L_1 + L_2)}{\frac{d}{2} + e - a}$$

in which ϵ_u denotes strain, corresponding to the maximum stress for the material of the anchor bolts (from the stress-strain diagram); L_1 is the length of bolt above the surface of the concrete; and L_2 is the equivalent free length of the embedded part of the bolt (Appendix I). The length, L_2, can be assumed to be at least eight times the diameter of the plain portion of the bolt (Appendix I).

Circular Base Plate.—Pipe columns, such as those used to support water towers, rest on circular base plates and these can be treated similarly to rectangular plates. The case of two diametrically opposed anchor bolts is considered here, but other types of anchorages can be analyzed in a similar manner to find the upper bound moment.

As in the case of rectangular plates, it is assumed that at the ultimate moment only part of the base plate is in contact with the concrete (Fig. 6) and that the bearing pressure on this contact area is uniform and equal to $\alpha f'_c$. The distance to the center of gravity of the compression area from the center of the base plate is

$$z = \frac{d \sin^3 \gamma}{3 \, (\gamma - \sin \gamma \cos \gamma)}.$$

With one bolt ineffective because it is in the compression zone,

$$M_{u1} = W \, z + P_u \, (z + e) = W \, z + A_s \, \sigma_u \, (z + e).$$

Letting $M'_{u1} = \frac{M_{u1}}{(\pi/4)d^3}$, $c = \frac{W}{(\pi/4)d^2}$, $p = \frac{A_t}{(\pi/4)d^2}$, and $e' = \frac{e}{d/2}$,

$$M'_{u1} = \frac{(c + p \, \sigma_u) \sin^3 \gamma}{3 \, (\gamma - \sin \gamma \cos \gamma)} + \frac{p \, \sigma_u \, e'}{2} \qquad \text{(6a)}$$

which can also be written

$$M'_{u1} = \frac{\alpha f'_c \sin^3 \gamma}{3} + \frac{P \, \sigma_u \, e'}{2} \qquad \text{(6b)}$$

Furthermore, because at the stage considered the compression force in the concrete must equal the ultimate strength of one bolt plus the load, W,

$$\left.\begin{aligned} \left(\frac{d^2}{4}\gamma - \frac{d^2}{4}\sin \gamma \cos \gamma\right) \alpha f'_c &= p \, \pi \frac{d^2}{4} \sigma_u + c \, \pi \frac{d^2}{4} \\ \text{and} \qquad \alpha f'_c &= \frac{\pi \, (p \, \sigma_u + c)}{\gamma - \sin \gamma \cos \gamma} \end{aligned}\right\} \qquad \text{(7)}$$

It is difficult to eliminate γ from Eqs. 6 and 7 but they can be used together with γ as a parameter in the same way that Eq. 5 is used alone. For example, a curve relating M'_{u1} to $\alpha f'_c$ can be plotted (Fig. 7). Comparing Fig. 7 with Fig. 4, it is seen that, for the same values of $\alpha f'_c$, M'_{u1} is slightly smaller for a circular base plate. It should be recalled, however, that the factor by which

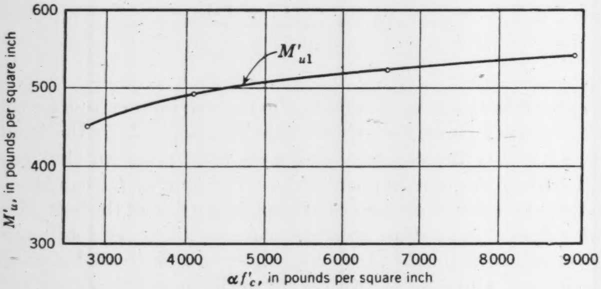

FIG. 7.—VARIATION OF THE UPPER-BOUND MOMENT WITH VARIATION IN ULTIMATE CONCRETE STRENGTH FOR A CIRCULAR BASE PLATE

M'_{u1} is multiplied in the two cases to determine the upper-bound moment is not the same.

EFFECT OF SHEAR

Horizontal shear on a simple anchorage is resisted by the anchor bolts and by friction. The resistance of the anchor bolts is, of course, the shear strength multiplied by the cross-sectional area.

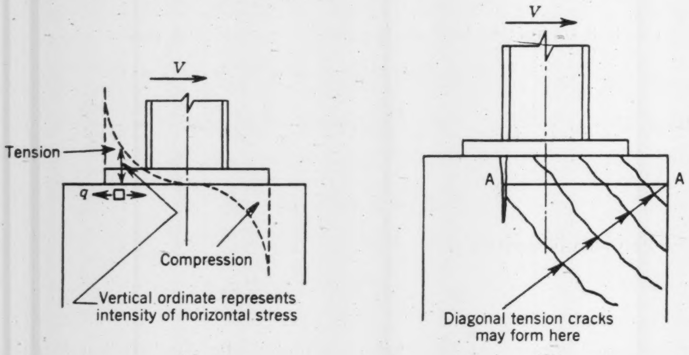
V
Tension
q
Compression
Vertical ordinate represents intensity of horizontal stress
(a)
V
A
A
Diagonal tension cracks may form here
(b)

FIG. 8

The horizontal resistance due to friction is νW. When the base plate has been rotated so as to cause its toe to dig into the concrete, a larger horizontal force than νW will be transmitted.

In analyzing the effect of the friction forces alone (assuming uniform bearing pressure), it is found that they produce compression in a horizontal direction under one-half of the base plate and tension under the other half. The variation of these stresses is shown in Fig. 8(*a*) and, theoretically, infinite stresses exist near the edges. Actually, plastic deformation reduces the peaks and, furthermore, when cracks on the tension side reduce the rigidity of the concrete on that side, all, or almost all, of the resistance is provided on the compression side. When the toe of the base plate digs into the concrete, all the resistance is concentrated along one line. Tracing further the path of the horizontal forces it is found that, unless the footing is completely embedded in fairly rigid material, the forces have to be transmitted to lower parts of the footing through shear along sections such as A–A in Fig. 8(*b*). When the horizontal load is concentrated at the toe of the base plate, the distance A–A is quite short and the high diagonal tension may result in the corner of the footing spalling off. Failure due to excessive compression could, however, be evidenced by similar symptoms and the two should not be confused. One may conclude that not all the horizontal resistance which appears to be available as a result of friction between base plate and concrete may be effective because of the possibility of premature failure in another mode.

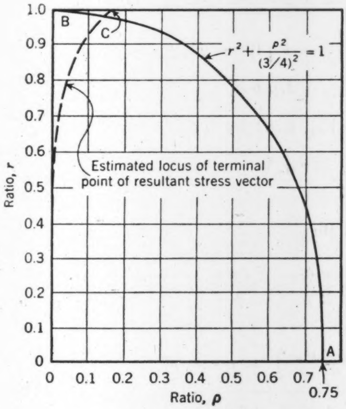

FIG. 9.—THE EFFECT OF COMBINED SHEAR AND TENSION ON THE ULTIMATE STRENGTH OF A ROUND STEEL BAR

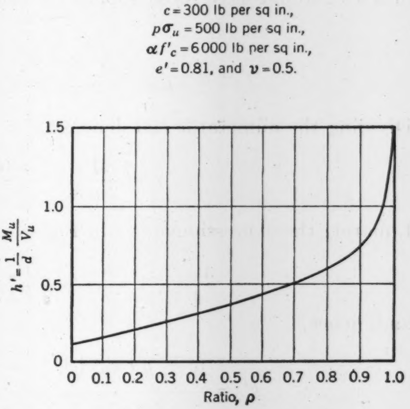

FIG. 10.—THE EFFECT OF THE MOMENT–SHEAR RATIO ON THE ULTIMATE ANCHOR-BOLT STRENGTH

The Effect of Shear on the Ultimate Moment.—The effect of combined tension and shear on the strength of a rivet was studied by H. L. Cox,[7] with correlation to test results. He pointed out that the relationship between the tensile and shear components and their resultant at failure can be represented by a quarter ellipse, as shown in Fig. 9, in which r is the ratio of the tensile component at failure to the ultimate tensile strength and ρ is the ratio of the shear component at failure to the ultimate tensile strength. It is proposed to assume that a similar relationship exists for the unthreaded portion of an anchor bolt.

---

[7] "Static Strength of Rivets Subjected to Combined Tension and Shear," by H. L. Cox, thesis presented to the University of Illinois at Urbana, in 1952, in partial fulfilment of the requirements for the degree of Master of Science.

The question arises as to what fraction of the ultimate tensile strength of the anchor bolts is available to resist moment if shear forces are also acting on the bolts. If $r\,\sigma_u$ is this remaining strength when the shear stress on the anchor bolts is τ, then from Fig. 9 the relationship between τ, r, and σ_u is

$$\tau = 0.75\,\sigma_u \sqrt{1 - r^2} \quad \text{(8)}$$

The shear force causing this shear stress may be represented by V_s. Because this force is resisted by all the anchor bolts, $V_s = 2\,A_t\,\tau = 2\,p\,b\,d\,\tau$. The additional shear force due to friction between the base and the concrete is $V_F = \nu\,F = \nu\,(W + P)$. (The full frictional force is used here for illustration, but its complete omission does not greatly affect the numerical results.) Hence, the total applied shear, V, is equal to $V_s + V_F$. The ratio, M_u/V, is set equal to h, which equals $h'\,d$—that is, the distance from the base plate at which the shear, V, would have to be applied to result in a moment, M_u. Hence,

$$\tau = \frac{V_s}{2\,p\,b\,d} = \frac{V - V_F}{2\,p\,b\,d} = \frac{\dfrac{M_u}{h'\,d} - \nu\,(W + P_u)}{2\,p\,b\,d} \quad \text{(9a)}$$

Dividing the numerator and denominator of Eq. 9(*a*) by $b\,d$,

$$\tau = \frac{M'_u}{2\,p\,h'} - \frac{\nu\,(c + p\,r\,\sigma_u)}{2\,p} \quad \text{(9b)}$$

Equating the expressions for τ in Eqs. 8 and 9*a*,

$$\frac{3\,\sigma_u}{4}\sqrt{1 - r^2} = \frac{M'_u}{2\,p\,h'} - \frac{\nu\,c}{2\,p} - \frac{\nu\,r\,\sigma_u}{2},$$

and, hence,

$$h' = \frac{(c + p\,r\,\sigma_u)\left(1 - \dfrac{c + p\,r\,\sigma_u}{\alpha\,f'_c}\right) + p\,r\,\sigma_u\,e'}{3\,p\,\sigma_u\sqrt{1 - r^2} + 2\,\nu\,(c + p\,r\,\sigma_u)} \quad \text{(10)}$$

Eq. 10 establishes a relationship between h' and that fraction r of the ultimate tensile strength that is available at failure. The relationship is shown in graph form in Fig. 10 for some typical values of c, p, σ_u, $\alpha\,f'_c$, e', and ν. This illustration shows that, for values of $h' > 1.38$, $r = 1$—that is, no shear stress exists in the anchor bolts, implying that all the shear is resisted by friction.

Although the shape of the graph would change with changes in the values of the various parameters, it is evident that only for very small values of h' would the ultimate tensile strength be seriously reduced by the action of shear. As the anchorage yields and rotates, the value of h' is decreased and will approach zero as the plastic hinge is formed. This could change the relative magnitude of the shear and tensile components in a manner illustrated by the dashed line in Fig. 9. Point C determines the stress components at failure. Although free rotation may eventually occur, it is unlikely that C will be less than $r = 0.9$. In general, it is suggested that, in regard to the degree of accuracy to which the ultimate strength is known, the effect of shear on the ultimate strength can be neglected.

THE GENERAL MOMENT–ROTATION RELATIONSHIP

The method described earlier of computing the upper bound for the resisting moment of an anchorage, in addition to being of interest in itself, helps one to visualize the relationship between the variables at all stages.

It will be assumed that during the first stage of application of moment the concrete stress distribution is as shown for "stage 1" in Fig. 11. If the highest stress is f_c, then the least stress must be $2\,c - f_c$ because the average stress is $W/b\,d = c$. At the end of stage 1, $2\,c - f_c = 0$—that is, $f_c = 2\,c$.

During the second stage the point of zero stress is moved across from the edge of the plate toward the first anchor bolt. Stage 2 ends as the point of zero concrete stress passes the anchor bolt and tensile stress is induced in the bolt.

Stage 3 is considered to end when yield-point stress is first reached in the anchor bolts. The forces on the anchorage during stage 3 are also shown in Fig. 11. Equilibrium considerations yield only one equation—namely,

$$P + W = F.$$

This is not sufficient, however, to permit the calculation of the concrete stress-distribution diagram. Specifically, the distance, w, shown in Fig. 11 is required in order to compute values of M at any stage:

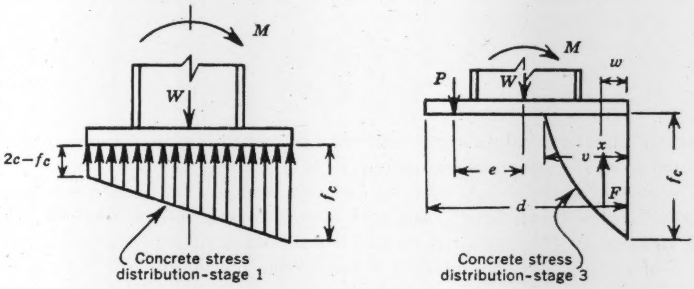
M
W
2c−fc
fc
Concrete stress distribution-stage 1
M
w
P
W
x
v
e
d
F
fc
Concrete stress distribution-stage 3

FIG. 11

$$M = W\left(\frac{d}{2} - w\right) + P\left(\frac{d}{2} + e - w\right) \ldots\ldots\ldots\ldots (11a)$$

or, if

$$w' = \frac{w}{d/2} = \frac{2\,w}{d} \ldots\ldots\ldots\ldots\ldots\ldots\ldots\ldots (11b)$$

then

$$M' = \tfrac{1}{2}\,(c + p\,\sigma)(1 - w') + \tfrac{1}{2}\,p\,\sigma\,e' \ldots\ldots\ldots\ldots (11c)$$

Stage 4 is considered to terminate when the anchor-bolt strain reaches the strain-hardening range. Eq. 11c for M' is still applicable in stage 4 but the value of w' is changed from that in stage 3. The remaining stage, up to failure, will be called stage 5.

In a previous section, the ultimate value of M' was estimated by assuming that the concrete stress just before failure would be uniformly distributed and equal to the ultimate concrete strength as modified by the prevailing conditions of restraint.

To estimate the value of θ, which is the angle of rotation of the column base corresponding to a moment, M, and a steel stress, σ, the strains at the end of stage 1 are considered—when the concrete stress is zero under one edge of the base plate and $2\,c$ under the other edge. The difference in the displacement at the two edges can be computed approximately in two ways. Assuming that the depth to which the stresses are transmitted is equal to width, d, and ignoring the effect of the concrete all around the base plate, the differential movement is $2\,c\,d/E_c$ and $\theta = 2\,c/E_c$. Alternatively, S. Timoshenko[5] has presented an approximate expression for the average deflection under a rectangular plate subject to a load, F,

$$F\,\frac{1-\mu^2}{E_c\sqrt{b\,d}} = \frac{(c + p\,\sigma)\,\sqrt{b\,d}\,(1-\mu^2)}{E_c}$$

in which μ denotes the Poisson ratio. Assuming that the maximum deflection is twice the average deflection,

$$\theta = \frac{2\,\sqrt{b\,d}\,(1-\mu^2)}{E_c\,d},$$

and when numerical values are substituted, the result is almost the same as that obtained from the previous expression for θ.

The second stage is only of brief duration and can be treated similarly to stage 1. In the third, fourth, and fifth stages, rotation is due to three causes: (*a*) Extension of the anchor bolts, (*b*) compression of the concrete, and (*c*) flexure of part of the base plate. A knowledge of the anchor-bolt extension and the distance, v (Fig. 11), would permit the calculation of θ for any value of σ and for any value of M', if w were also known. In this stage,

$$\theta = \frac{\sigma\,L_e}{E_s\left(\frac{d}{2} + e - v\right)} \quad\ldots\ldots\ldots\ldots\ldots\ldots\ldots (12)$$

in which $E_s = \sigma/\epsilon$ = stress/strain, for any point on the stress-strain diagram of the anchor-bolt material in the elastic or plastic ranges, and L_e is the equivalent total length of the anchor bolts. By L_e is meant the length of a similar bolt, not embedded but fixed at the end only, that would have the same extension under a stress, σ.

For use in similar anchorages in which all linear dimensions are proportional to d, Eq. 12 can be so written as to eliminate the dimension, d. Because in similar anchorages L_1 is proportional to d and because in Appendix I it is shown that L_2 is also likely to be proportional to d, one may set L_e, which is the sum of L_1 and L_2, equal to $L'_e\,d$. From the previous definition, $e' = 2\,e/d$ and

$v' = 2\,v/d$. Therefore,

$$\theta = \frac{2\,\sigma\,L'_e}{E_s\,(1 + e' - v')} \qquad (13)$$

The foregoing considerations of the relationship between M and θ can be summarized as follows: If M' were plotted against θ, the first part of the graph would be a straight line of approximate slope—$(c/6) \div (2\,c/E_c) = E_c/12$. Beyond that region, Eqs. 11*c* and 12, with σ as a parameter, define the shape of the curve.

It was explained previously that the values, v' and w', the equivalent anchor-bolt length, L_e, and the stress-strain relationship of the anchor bolts must be known before the moment-rotation curve can be drawn. Sufficient basic test information exists to make possible a fairly accurate estimate of the stress-strain relationship of the anchor bolts. An idealized curve is shown in Fig. 12, drawn as far as the maximum stress value. Alternatively, it would be relatively easy to test anchor bolts of a type proposed in any new design.

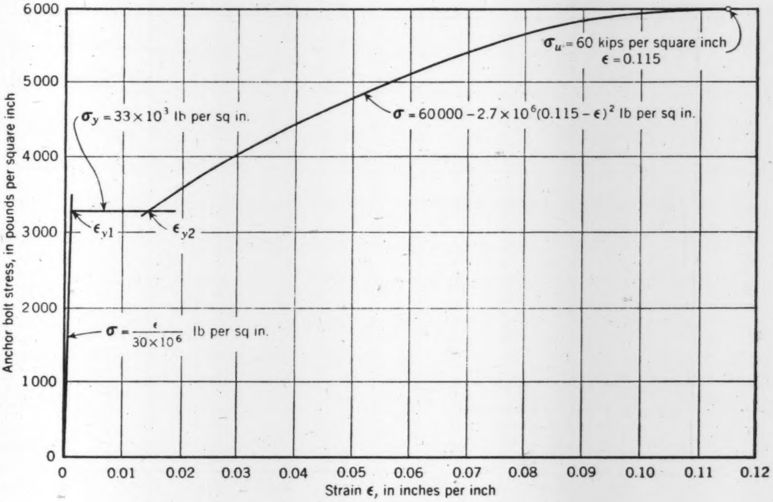

FIG. 12.—IDEALIZED STRESS-STRAIN CURVE FOR ANCHOR BOLTS

The estimate of L_e—the sum of L_1 and L_2—is somewhat more difficult. However, H. J. Gilkey, M. ASCE, S. J. Chamberlin, A.M. ASCE, and R. W. Beal[8] suggest that, for a long embedded steel bar being pulled out of concrete, bond is not effective over the entire length of the bar; it is only effective over a length of approximately 24 diameters. Assuming that this is so, the tensile stress in the bar varies from σ at the point where it emerges from the concrete to zero at 24 D (D being the bar diameter). It is shown in Appendix I that the length of bar, L_2—which under a stress, σ, would be strained by a distance equal to the slip, s, of the embedded bar—is equal to the distance of the center of gravity of the bond-stress diagram from the concrete edge at the loaded end. Hence, in order to estimate L_2, the bond-stress distribution must be assumed. Assuming a linear decrease of bond stress from a value u_o at the loaded end to zero at 24 D, $L_2 = \frac{1}{3} \times 24\ D = 8\ D$, and

---

[8] "Bond Between Concrete and Steel," by H. J. Gilkey, S. J. Chamberlin, and R. W. Beal, *Bulletin No. 147*, Iowa Eng. Experiment Station, Ames, Iowa, 1940.

$$L_e = L_1 + 8\ D.$$

The length, L_1, of the anchor bolt above the concrete surface as well as D are known.

If v and w (Fig. 11) are known at the various stages, the diagram relating M' and θ can be drawn. When this is done, a moment-rotation curve such as the one in Fig. 13 would result for a particular combination of values of p, c, $\alpha f'_c$, e, L, and a given anchor-bolt stress-strain diagram. The initial slope of the curve has been estimated to be $E_c/12$. The ultimate values of M' and θ estimated previously (Eq. 5) were based on the assumption of rectangular bearing-stress distribution. Hence, the coordinates of the terminal point of the curve can be estimated and the slope of the curve at that point would be zero. To fill in the rest of the curve, the bearing-stress distribution must be estimated at intermediate stages—that is, the values of v and w must be estimated. For this purpose it is considered justifiable to use the reinforced concrete theory for the stresses at the end of stage 3 (yield point reached) and a modified theory for the stresses at the end of stage 4 (strain-hardening range reached). (The modifica-

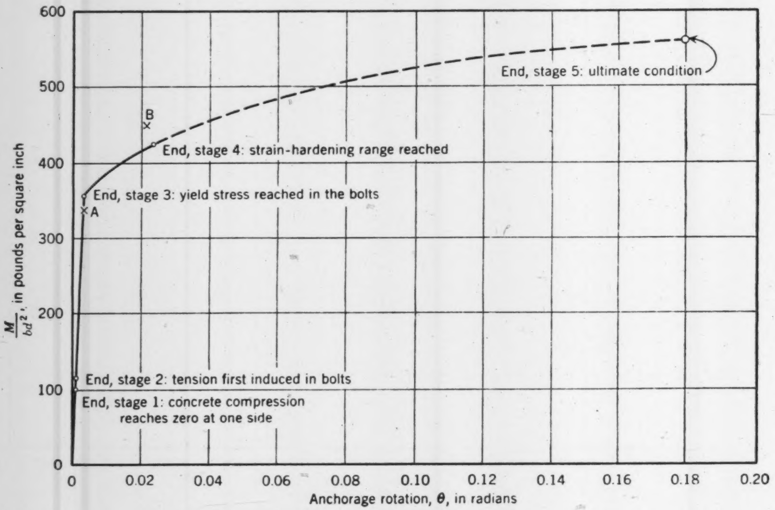

FIG. 13.—TYPICAL THEORETICAL MOMENT–ROTATION CURVE FOR A SIMPLE COLUMN ANCHORAGE; $p = 0.6\%$, $c = 600$ LB PER SQ IN., $\sigma_y = 33{,}000$ LB PER SQ IN., $\sigma_u = 60{,}000$ LB PER SQ IN., $\alpha f'_c = 6{,}000$ LB PER SQ IN., $e = 0.4\ d$, AND $L_1 = 2\ d/3$

tion consists of assuming trapezoidal stress distribution at the end of stage 4, with the maximum bearing stress limited to $\alpha f'_c$.)

Details of typical computations for the moment-rotation curve in the manner here outlined are shown in Appendix II, and the results are plotted in Fig. 13. In Fig. 13 there are two points marked A and B which approximate the sensitivity of the method to variations in assumptions. Point A corresponds to the end of stage 3, but a modular ratio of 10 was used for the end of stage 3 whereas 15 was used for A. Point B corresponds to the end of stage 4, but rectangular stress distribution was assumed for B (similar to the distribution at failure) whereas trapezoidal distribution was assumed for the end of stage 4.

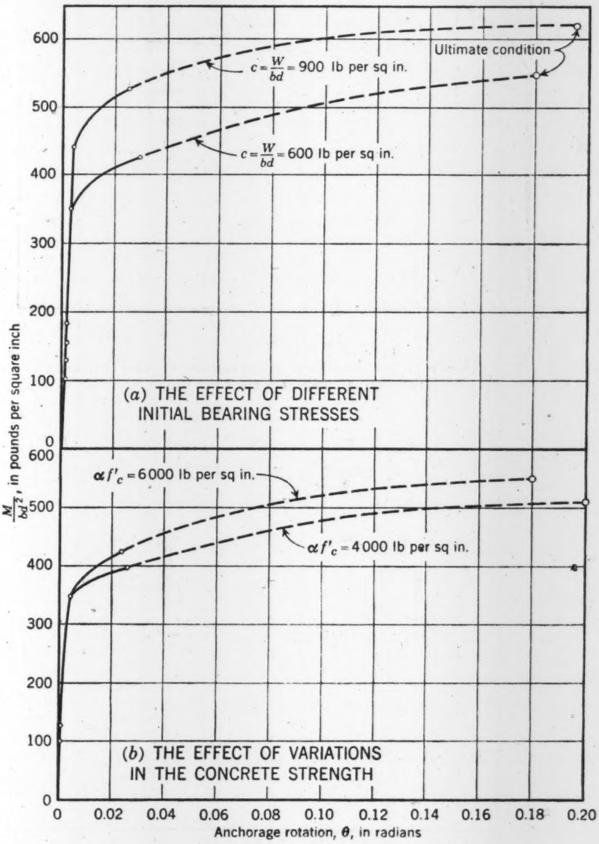

FIG. 14.—THE EFFECT OF VARIATION IN INITIAL BEARING STRESSES AND IN CONCRETE STRENGTH FOR THE CONDITIONS OF FIG. 13

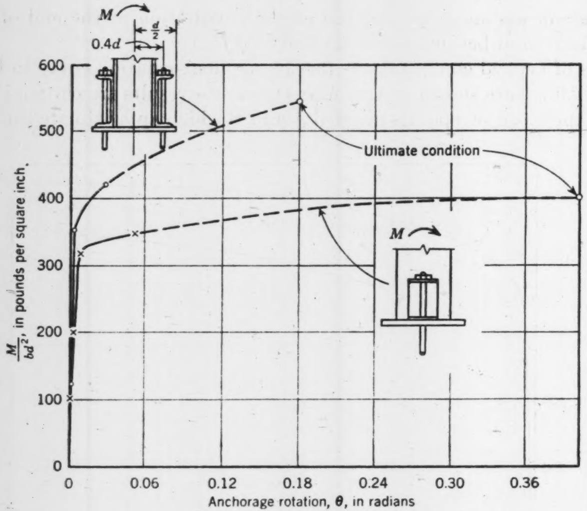

FIG. 15.—THE EFFECT OF VARYING THE ECCENTRICITY OF THE ANCHOR BOLTS FOR THE CONDITIONS OF FIG. 13

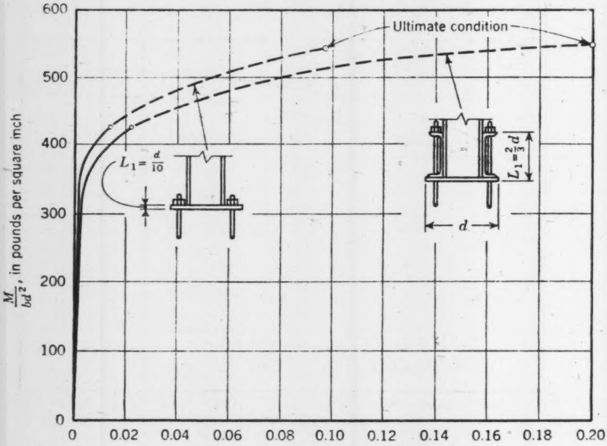

FIG. 16.—THE EFFECT OF VARYING THE FREE ANCHOR-BOLT LENGTH, L_1, FOR THE CONDITIONS OF FIG. 13

Figs. 14, 15, and 16 further illustrate the effect on the moment-rotation curve of the variation of c, $\alpha f'_c$, e, and L_1. The effect of increasing p would be similar to that produced by increasing c—it would result in more rigidity and a high ultimate resistance moment. The effect of changes in the concrete

strength is not very great. The result of reducing e to zero is interesting because such a procedure could be followed for estimating the $(M\text{–}\theta)$-curve for anchorages with only two bolts about an axis joining the bolts (axis of least resistance).

CONCLUSIONS

The foregoing procedure for estimating the moment-rotation characteristics of a simple column anchorage should be satisfactory as a first approximation. Experimental verification and subsequent correction of the assumptions should be made. Such a correction of the assumptions, after an initial series of tests on anchorages, may result in a refinement of the method permitting the estimate of the moment-rotation curve for any similar anchorage without further tests, or it may be necessary, at times, to conduct small supplementary tests in the nature of combined pull-out and tension tests on anchor bolts.

ACKNOWLEDGMENTS

This investigation has been supported by the Bureau of Yards and Docks, United States Department of the Navy, under Contract NOy-74521, in connection with a broad study of the subject of structural steel connections. The work has been a regular research project of the Civil Engineering Department of the University of Michigan (at Ann Arbor), through the administrative facilities of the Engineering Research Institute of that university.

APPENDIX I. EQUIVALENT FREE LENGTH OF AN EMBEDDED BAR

It is necessary to investigate whether the equilvaent free length of embedded bars of various sizes is proportional to d, the length of the base plate, provided that p and σ do not vary.

If p is the same for all anchorages,

$$\frac{A_t}{b\,d} = \frac{\pi D^2}{4\,b\,d} = \text{a constant}$$

in which D is the diameter of the bar. Also, if the ratio of b to d is kept the same, $b = k\,d$, and

$$\frac{D^2}{t^2} = \text{a constant}$$

and it remains to be proved that the equivalent length is proportional to D.

The equivalent length, L_2, is defined as follows: If the slip is s, then $s = P\,L_2/(E_s\,A_t) = \sigma\,L_2/E_s$ or $L_2 = s\,E_s/\sigma$. Since this is a comparison among various cases at a stage when θ, and therefore σ, are the same, σ can be considered a constant. Furthermore, for L_2 to be proportional to D, s must be proportional to D.

From Fig. 17,

$$P_x = P - \int_0^x u_x \pi D \, dx$$

and

$$\sigma_x = \sigma - \int_0^x \frac{4\,u_x}{D}\, dx.$$

Hence, σ_x decreases as x increases and is zero at $x = L_t$. The part of the bolt at a distance greater than L_t is of no importance.

$$0 = \sigma - \int_0^{L_t} \frac{4\,u_x}{D}\, dx, \quad \text{or} \quad \sigma = \int_0^{L_t} \frac{4\,u_x}{D}\, dx.$$

The strain $\epsilon_x = \frac{1}{E_s}\sigma_x$. Therefore,

$$E_s\,\epsilon_x = \int_0^{L_t} \frac{4\,u_x}{D}\, dx - \int_0^x \frac{4\,u_x}{D}\, dx = \int_x^{L_t} \frac{4\,u_x}{D}\, dx$$

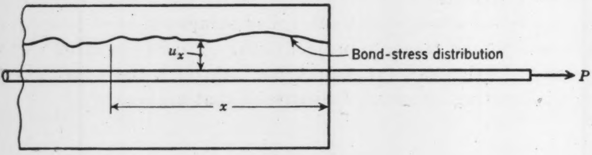

FIG. 17.—EMBEDDED BAR

and

$$s = \int_0^{L_t} \epsilon_x \, dx = \frac{4}{D\,E_s}\int_0^{L_t}\int_x^{L_t} u_x \, dx^2.$$

Case 1.—If u_x is constant and independent of x,

$$s = \frac{2\,u\,L^2_t}{D\,E_s}.$$

It has been shown[8] that the effective length, L_t, is approximately 24 D. In any case, L_t can be assumed to be proportional to D. Hence,

$$u = \frac{\sigma D}{4\,L_t} = \frac{\sigma}{4\,K}$$

in which K is a constant and

$$s = \frac{2\,u\,L^2_t}{D\,E_s} = \frac{2\,\sigma\,K^2\,D^2}{4\,K\,D\,E_s} = \frac{\sigma\,K\,D}{2\,E_s}.$$

That is, for any particular σ-value, the slip is proportional to the diameter. Furthermore, the equivalent length, L_2, is found to be

$$\frac{E_s}{\sigma} = \frac{K\,D}{2} = \frac{L_t}{2}.$$

This means that the equivalent free length, L_2, is one-half the effective length, L_t. In other words, the distance of slip at the loaded end is the same as the extension of a nonembedded bar fixed at a point equivalent to the center of gravity of the bond-stress distribution diagram for the embedded bar.

Case 2.—If the bond stress varies linearly, as shown in Fig. 18,

$$s = \frac{2\,u_o\,L^2_t}{3\,D\,E_s}$$

and

$$\sigma = \frac{2\,u_o\,L_t}{D} = 2\,u_o\,K = \frac{\sigma\,K\,D}{3\,E_s},$$

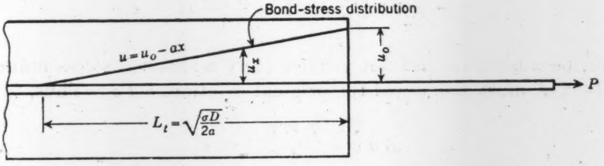

FIG. 18.—EMBEDDED BAR—LINEARLY VARYING BOND STRESS

or s is proportional to D, and

$$L_2 = \tfrac{1}{3}\,L_t.$$

It would appear to be generally true that $s \propto D \propto d$ for a constant p-value and σ-value.

APPENDIX II. TYPICAL COMPUTATIONS FOR THE MOMENT-ROTATION CURVE

The following data are assumed: $c = 600$ lb per sq in., $p = 0.6\%$, $\alpha f'_c =$ 6,000 lb per sq in., $e = 0.4\,d$, $L_1 = 2\,d/3$, the stress-strain curve for anchor-bolt material is as shown in Fig. 12, and the n-value for concrete is 10. By definition, $e' = 2\,e/d = 0.8$ and $L'_1 = L_1/d = 2/3$. Also $p = A_t/(b\,d) = 0.006$; therefore, $\pi\,D^2/4 = 0.006\;\,b\,d$. Assuming that $b \approx d$, $D = d\,\sqrt{0.012/\pi} =$ $0.062\,d$.

Furthermore, assuming a bond-stress distribution as in Fig. 18 (Appendix I) and a total effective length of embedment of 24 D, the equivalent length, L_2, of the embedded portion of the bolt is 8 D. Thus, $L_2 = 8\,D = 0.496\,d$. The total equivalent length of the anchor bolt $L_e = L_1 + L_2 = (0.667 + 0.496)\,d =$ $1.163\,d$. By definition, $L'_e = L_e/d = 1.163$.

Stage 1.—At the end of stage 1 (as defined under the heading, "The General Moment-Rotation Relationship") the stress distribution under the plate is as shown in Fig. 19(*a*). The moment of resistance is

$$M = \frac{1}{6}\,dF = \frac{b\,d^2\,c}{6}\ .$$

By definition,

$$M' = \frac{M}{b\,d^2} = \frac{c}{6}\ .$$

Therefore, $M'_1 = 100$ lb per sq in. Similarly, the rotation at the end of stage 1 is

$$\theta_1 = \frac{2\,c}{E_c}$$

and $\theta_1 = 4 \times 10^{-4}$ radian.

Stage 2.—At the end of the second stage, tensile stress is just beginning to be induced in the anchor bolt on one side. The stress distribution under the plate is as shown in Fig. 19(*b*). The reaction is

$$F = \frac{1}{2} f_c\, b \left(\frac{d}{2} + e \right) = \frac{f_c\, b\, d}{4}\,(1 + e').$$

However, because there has not yet been any additional stress induced in the anchor bolt, F must also equal the original reaction, $b\,d\,c$. Thus,

$$b\,d\,c = \frac{f_c\, b\, d}{4}\,(1 + e')$$

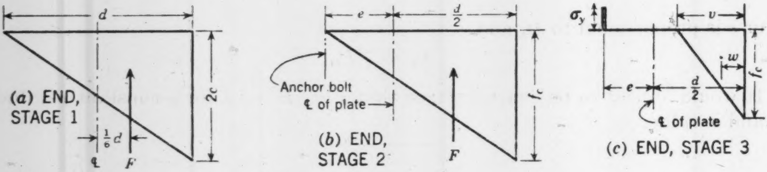

(*a*) END, STAGE 1

(*b*) END, STAGE 2

(*c*) END, STAGE 3

FIG. 19

and

$$f_c = \frac{4\,c}{1 + e'}\ .$$

The moment of resistance is

$$M_2 = b\,d\,c \left[\frac{d}{2} - \frac{1}{3} \left(\frac{d}{2} + e \right) \right] = \frac{b\,d^2\,c}{2} \left[1 - \frac{1}{3}\,(1 + e') \right]$$

and

$$M'_2 = \frac{c}{6}\,(2 - e') = 100\,(2 - 0.8).$$

Therefore, $M'_2 = 120$ lb per sq in. The strain in the concrete due to a stress, f_c, is given by

$$\frac{f_c}{E_c} = \frac{4\,c}{(1 + e')\,E_c}\ .$$

Assuming, as indicated in the text, that this concrete strain is over an effective depth, d,

$$\theta_2 = \frac{4\,c\,d}{(1 + e')\,E_c} \left[\frac{1}{e + \frac{d}{2}} \right] = \frac{8\,c}{(1 + e')^2\,E_c}$$

from which $\theta_2 = 5 \times 10^{-4}$ radian.

Stage 3.—During stage 3, the anchor plate is tilted sufficiently so that it is in contact with the concrete over a strip of width, v. At the end of the stage (by definition) the stress in the anchor bolt has reached the yield point (Fig. 19(c)).

In order to determine v and w, the following two equations can be written and solved. By geometry,

$$\frac{\sigma_y}{f_c} = \frac{n\,(d/2 + e - v)}{v} = \frac{n\,(1 + e' - v')}{v'}.$$

Because of equilibrium requirements, $p\,b\,d\,\sigma_y + b\,d\,c = \dfrac{v\,b\,f_c}{2}$. Thus,

$$\frac{\sigma_y\,(v')^2}{4\,n\,(p\,\sigma_y + c)} + v' + (1 + e') = 0$$

from which v' equals 0.92, and $w' = v'/3 = 0.307$. From Eq. 11*c*, $M' = 0.5 \times 798\,(1 - 0.307) = 0.5 \times 198 \times 0.8$; therefore, $M'_3 = 354$ lb per sq in.

Using Eq. 13,

$$\theta_3 = \theta_2 + \frac{2 \times 33 \times 1.163}{30 \times 10^3\,(1.8 - 0.92)} = 34 \times 10^{-4} \text{ radian.}$$

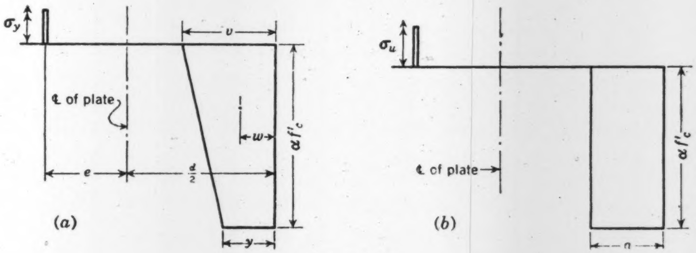

(*a*) (*b*)

FIG. 20

Stage 4.—This stage ends when the strain in the anchor bolts reaches the value ϵ_{y2} (Fig. 12). At this time the concrete stress distribution is nonlinear and may be approximated by a trapezoid (Fig. 20(*a*)). In order to determine v and y, two equations can be written and solved. By geometry

$$\frac{\epsilon_{y2}}{\alpha\,f'_c/E_c} = \frac{d/2 + e - v}{v - y}.$$

From equilibrium, $p\,b\,d\,\sigma_y + b\,d\,c = 0.5\,\alpha\,f'_c\,(v + y)\,b$, from which $v' = 2\,v/d = 0.353$, and $y' = 2\,y/d = 0.178$. Also,

$$w' = \frac{(v')^2 + v'\,y' + (y')^2}{3\,(v' + y')} = 0.137.$$

As in stage 3, $M' = 0.5 \times 798\,(1 - 0.137) + 0.5 \times 0.198 \times 0.8$, or $M'_4 = 423$ lb per sq in. Using Eq. 13, but replacing σ_y/E_s by ϵ_{y2},

$$\theta_4 = \theta_2 + \frac{2\,\epsilon_{y2}\,L'_s}{1 + e' - v'}$$

from which $\theta_4 = 246 \times 10^{-4}$ radian.

Stage 5.—This stage represents the condition of ultimate moment. From Eqs. 5*a* and 5*c*, $a = [(c + p\,\sigma_u)d]/(\alpha f'_c) = 0.16\ d$. Hence, $M'_u = 0.5 \times 960\ (1 - 0.16) + 0.5 \times 360 \times 0.8 = 547$ lb per sq in. Also,

$$\theta_5 = \theta_2 + \frac{\epsilon_u L_e}{\frac{d}{2} + e - a} = \theta_2 + \frac{2\,\epsilon_u L'_e}{1 + e' - a'}$$

or $\theta_5 = 0.18$ radian. The foregoing values of M' and θ are shown in graphical form in Fig. 13.

AMERICAN SOCIETY OF CIVIL ENGINEERS
Founded November 5, 1852
TRANSACTIONS

Paper No. 2853

BEACH REHABILITATION BY FILL AND NOURISHMENT

By Jay V. Hall, Jr.,[1] M. ASCE, and George M. Watts,[2] A. M. ASCE

Synopsis

Shore stability and alinement have been greatly influenced by the progressive development of seaside resorts and the construction of navigable inlets. During the past several years various methods of artificial nourishment by means of beach fill have been used with varying success. The basic methods of utilizing beach fill to maintain artificial nourishment are: (*a*) Stockpiling, in which fill is placed at one point and allowed to function as a feeder beach; (*b*) direct placement, in which the material is placed along the beach and an adequate beach width for immediate protection is created, which in turn provides the downdrift area with a littoral supply and continuous nourishment; and (*c*) a fixed or semifixed plant is positioned on the updrift side of a jettied inlet where it intercepts and bypasses the littoral drift to the downdrift side of the inlet. This paper will review several cases in which these methods of artificial nourishment have been used and will show the experience record.

Introduction

The mechanics of transporting sediment by water is not completely understood; however, it is known that, for a movable bed to be in a state of equilibrium, there must be a balance of energy distribution in terms of bed aggradation and degradation. For this reason, coastal beaches can reach stability or equilibrium and maintain this condition only when there is a sufficient supply of littoral-drift material for the natural forces involved. Insufficient littoral supply will tend to create beach erosion; an overabundant supply will cause accretion. In terms of geological time, no coast line is in a completely stable state. However, in terms of decades, there are stable reaches of shore line.

Note.—Published, essentially as printed here, in February, 1955, as *Proceedings-Separate No. 616*. Positions and titles given are those in effect when the paper was approved for publication in *Transactions*.

[1] Chief, Eng. Div., U. S. Beach Erosion Board, Washington, D. C.

[2] Asst. Chief, Eng. Div., U. S. Beach Erosion Board, Washington, D. C.

It is only natural that the economic development of a coastal region will be greatest in these stable zones.

Prior to the extensive economic development of the United States, natural forces built and molded the beaches, drawing from an abundant supply of material which was derived from stream sediments carried to the shore during periods of flood and from eroding headlands. The discovery and ensuing development of the beaches as a playground have brought about a gradual change in the beach stability of these areas. Also, shore stability and alinement have been influenced by navigable inlets and by inlets constructed to alleviate stagnant conditions in bays and lagoons.

The first seaside resorts were supported mainly by local inhabitants but, with improved transportation and increased leisure time, beach development grew. These centers of recreation, however, did not line the shores but were scattered, usually near the large centers of population where economic justification permitted the construction of public-transportation systems. The primary purpose in building a resort area is for the convenience of those who prefer to live on the beach when they visit it. The ensuing growth of hotels and other facilities soon established a line beyond which the shore could not be allowed to erode. In view of this condition coastal engineers used structures such as sea walls to prevent the erosion of the fast land and groins to impound the littoral materials. Such structures were reasonably successful for holding and building a beach when the updrift shore line was undeveloped and supplied material to the littoral stream. As the intervening beach area was developed and protected from erosion, as harbor entrances were constructed and improved with jetties, and as flood-control dams were built on the rivers, the quantity of material supplied to the littoral zone gradually decreased. This condition of inadequate sand supply has developed at many beaches.

The problem that confronts the coastal engineer is: What is the best and most economical method of protecting and rehabilitating a beach receiving an inadequate supply of littoral material? The problem appears to be simple because all that is required is to re-establish the supply of material. However, the method of placing the beach fill, in order that it will supply material at the natural replenishment rate, is an extremely important factor.

The intended functions of beach fills have not been fully understood by the public, or, to some extent, by the engineering profession. There are several purposes for which such fills are designed, one of which is to supply nourishment to shores downdrift of the filled area. This type of fill often includes a part of its width that is intended to be permanent, the remaining seaward part of the fill being used as a stockpile. The stockpile is designed to erode at the natural rate of littoral drift and, by eroding, to provide nourishment for the downdrift shore. The establishment and periodic replenishment of such a stockpile beach are called artificial nourishment.

When artificial nourishment is applied as a remedy for a long reach of starved and eroded shore, it is often necessary to rehabilitate the shore by filling in order to provide the desired protective beach without delay. This type of fill is termed direct placement and normally has those dimensions which it will preferably maintain. When such a fill is made it will remain effective only if it is artificially nourished. The two methods of artificial nourishment are the stockpile method previously described and the almost continuous feeding, which results from a fixed or semifixed, bypassing installation. Artificial nourishment is, therefore, a sand-moving operation and the method depends on the required rate and the source of material. Because it is suitable for maintaining long reaches of shore by a single operation, artificial nourishment is often more economical than defensive works, such as sea walls or groins. It also prevents rather than causes the spreading of an erosion problem.

During the past several years these methods of artificial nourishment have been applied with varying success. It is the writers' purpose to review several cases in which these methods of nourishment have been used and to show the experience record. Some of the protective measures applied to the cases presented herein have not been in effect long enough to provide conclusive results; however, the problem of the choice of protection is believed to be of great significance. The references cited in each beach problem present a comprehensive description of the area and only the most pertinent information is included.

Direct Placement at West Haven, Conn.

The West Haven shore line, shown in Fig. 1, comprises the shores of Long Island Sound near the entrance to New Haven Harbor, which is approximately 50 miles east of New York (N. Y.). In general, all the shore line of Long Island Sound is interesting because of the reduced wave action, as compared to the open-ocean shore lines; however, there exist serious problems of beach restoration and stabilization. The West Haven area has been selected to show a typical problem along these shores and the measures taken to improve the shore-line condition.

The headlands and lowlands of the West Haven area are composed of unconsolidated glacial-drift materials which are easily eroded by wave action. This source of supply of beach-building material has gradually been reduced by the intensive development of the shore for residential and resort purposes. Protective structures have been erected in developed areas to limit the recession of the shore line, thereby transferring the erosion to undeveloped areas. As indicated in a Beach Erosion Control study[3] of this area,

> "The problem is to stabilize and improve the shore line so that existing and future development on the shore front may benefit from restored beach conditions and also to prevent future damages and losses which will otherwise inevitably result from the present deterioration."

The present quantity of littoral drift in the West Haven area and, in general, along the coast of Connecticut, is small. There appear to be many nodal points created by rocky headlands, where the direction of littoral drift divides. In the West Haven area between Bradley Point and Sandy Point, the predominant direction of drift is to the east. Long Island acts as a natural breakwater, which shields nearly all the shore of Connecticut; therefore, the wave action in this area is greatly reduced as compared to the shores that are completely exposed to the open ocean. The moderately flat nearshore and offshore slopes, combined with maximum fetches of from 20 miles to 30 miles, do not permit severe wave action to reach the actual backshore and only relatively small waves contribute to the gradual erosion and deterioration of the shore line.

---

[3] "Area 3—New Haven Harbor to Housatonic River," *House Document No. 203*, 83rd Cong., 1st Session, Beach Erosion Control Study, Corps of Engrs., U. S. Dept. of the Army, Washington, D. C., March, 1952, pp. 19–20.

This condition of hydrography and a short fetch tends to produce a wave climate of short-period waves that, in general, create offshore deposition along with the small quantity of material movement in the littoral stream. In this area the offshore deposits are within a practicable distance for hydraulic dredging and pumping to the foreshore. The Beach Erosion Control study, previously mentioned, included the shore line from New Haven Harbor to the Housatonic River; this study indicated that the most economical and practical approach to restoration and stabilization of this area is by the direct

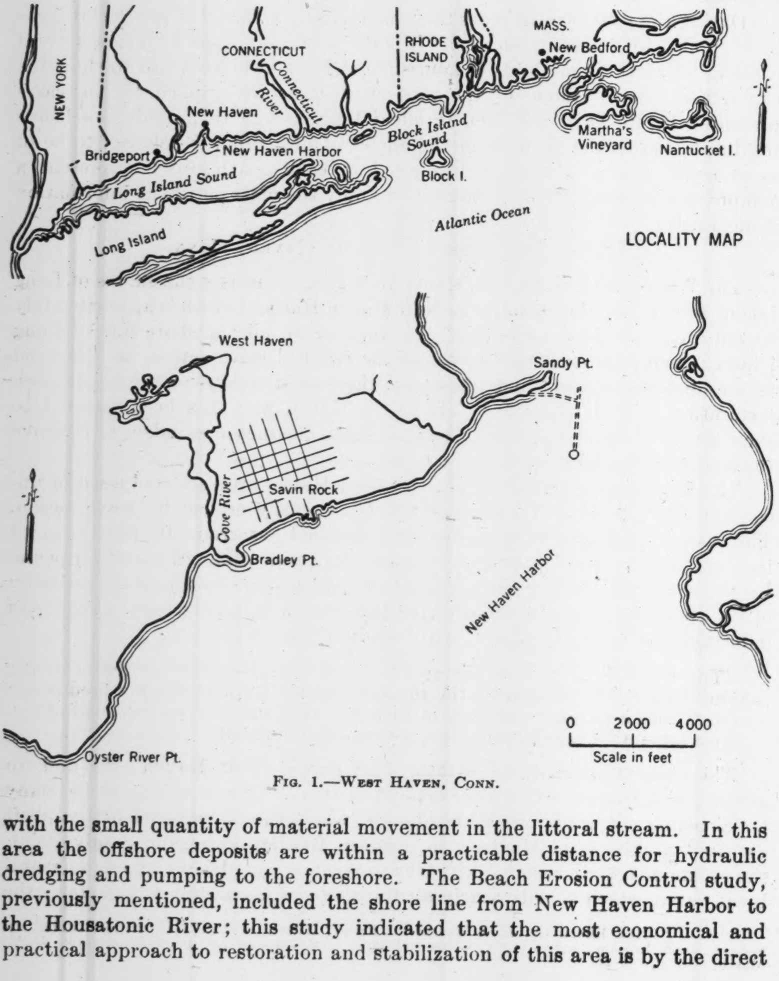
NEW YORK
CONNECTICUT
Connecticut River
RHODE ISLAND
MASS.
New Bedford
New Haven
Bridgeport
New Haven Harbor
Block Island Sound
Martha's Vineyard
Nantucket I.
Block I.
Long Island Sound
Long Island
Atlantic Ocean
N
LOCALITY MAP
West Haven
Sandy Pt.
Savin Rock
Cove River
Bradley Pt.
New Haven Harbor
Oyster River Pt.
N
0 2000 4000
Scale in feet

FIG. 1.—WEST HAVEN, CONN.

placement of sand on the beaches and by groin construction to prevent alongshore erosion of restored beaches.

From July, 1948, to January, 1949, more than 1,000,000 cu yd of sand were pumped from the New Haven Harbor in order to maintain the navigation channel and deposited on the shore south of Sandy Point. Prior to the placement of this spoil sand, this reach of shore was in a critical condition regarding possible danger to works located on the immediate backshores. The direct placement of sand on the beach in this area provided protection to the backshore in addition to providing an extensive recreational area. A comparison of surveys made in October, 1949, and April, 1950, covering the area from Sandy Point to Bradley Point, indicates that the mean-high-water line has not changed appreciably. A comparison of plan areas between the lines at mean high water and mean low water for these two surveys indicates a reduction of approximately 25%; this rather rapid reduction of the foreshore zone indicates that a readjustment of the foreshore slope is occurring, and until this readjustment is completed, over-all evaluation of the sand placement in this area would be difficult to establish.

The significant feature of this problem is that the construction of shore structures, such as groins, to retain the littoral drift must be coupled with the placing of artificial fill. In general, groins alone in the area are ineffective because of small rates of drift; they also deprive the downdrift zones of the limited littoral supply, which results in excessive erosion of the downdrift shore line. It becomes increasingly evident why the most economical and practical approach to the restoration and stabilization of this area is by direct placement of sand and groin construction where necessary.

OFFSHORE DEPOSITION AND DIRECT PLACEMENT AT ATLANTIC CITY, N. J.

Atlantic City lies on the coast of New Jersey, approximately 45 miles northeast of Cape May, which is the southern tip of the state at the entrance to Delaware Bay. Atlantic City comprises nearly one-half of the barrier beach known as Absecon Island; Absecon Inlet is the northeastern boundary of the city and island.

Atlantic City has been developed rapidly since 1900 because of its location near extensively developed and densely populated urban areas. Philadelphia, (Pa.) and New York City lie approximately 60 miles and 125 miles, respectively, from this resort area.

The broad sand beach for which Atlantic City is famous was originally supplied with material transported southward along Absecon Island. Dredging volumes removed from Absecon channel between 1935 and 1946 indicate that approximately 400,000 cu yd of material reach the southern end of the island annually. It is not known whether the serious erosion of the ocean beach at Atlantic City is the result of a diminished rate of supply of sand to the beach or of a greater rate of loss of sand from the beach because of an increase in power of the eroding forces. It is believed that both factors contribute to the erosion, but the prominence of one factor over the other would be extremely difficult to determine in this case.

Although prior to 1940 the beach remained relatively stable, it was decided that augmented nourishment to the beach would be beneficial; this nourishment was derived from hopper-dredging operations in Absecon Inlet. From April, 1935, to September, 1943, approximately 3,554,000 cu yd of sand were deposited off the beach in from 15 ft to 20 ft of water (Fig. 2). This operation was observed closely to determine whether any perceptible quantity of the dumped material was moved to the beach. The findings were negative and reports indicate that in 1940 serious erosion of the beach for a distance of 6,000 ft south of the inlet became evident.

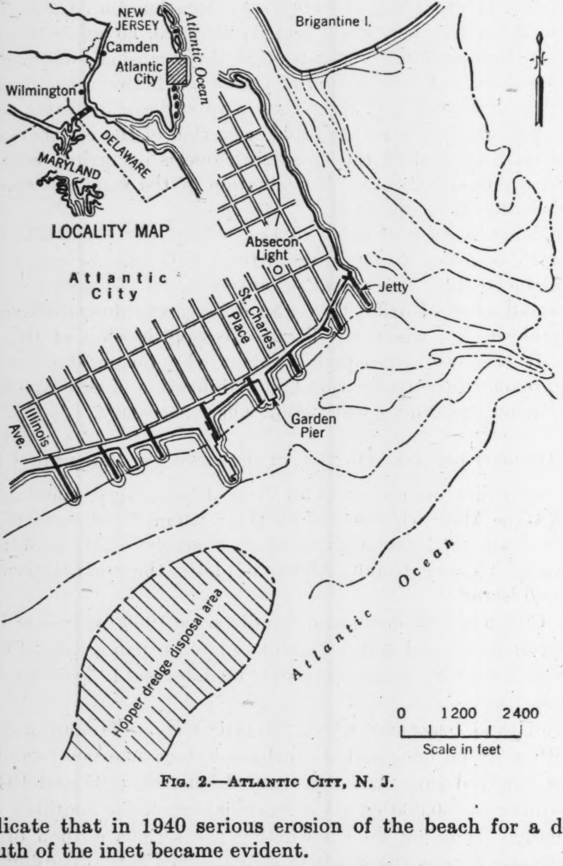
NEW JERSEY
Camden
Atlantic City
Atlantic Ocean
Wilmington
DELAWARE
MARYLAND
LOCALITY MAP
Brigantine I.
Absecon Light
Jetty
Atlantic City
St. Charles Place
Illinois Ave.
Garden Pier
Atlantic Ocean
Hopper dredge disposal area
0
1200
2400
Scale in feet

FIG. 2.—ATLANTIC CITY, N. J.

Realizing that a positive method of construction and rehabilitation of the beach would be required if the expensive real estate lining the shore was to be preserved, Atlantic City entered into an agreement with the Corps of Engineers (United States Department of the Army), to make a study concerning erosion control of this beach.

As a result of this study[4] the following plan of improvement was recommended for the ocean-beach section:

a. The channel of Absecon Inlet should be maintained on an east-west alinement away from the ocean beach.

b. Five timber groins should be constructed and one stone groin should be extended, starting with the one farthest west and working eastward as the beach filled in.

c. The beach should be replenished and maintained with artificial nourishment as required.

The State of New Jersey and Atlantic City began rehabilitation in 1948. They constructed a stone jetty at Oriental Avenue to divert the inlet channel eastward away from the beach and placed approximately 700,000 cu yd of sand on the beach from the jetty to a point approximately 6,000 ft southward. The sand used for nourishment was pumped from the southern tip of Absecon Island.

Immediately upon the completion of the fill, the beach began to erode at a greater rate than is normally encountered during the adjustment of the beach profile. In fact, the erosion progressed at such a rapid rate that the city constructed the five-timber groins that were recommended in the plan of improvement. The groins immediately began to function and reduced the rate of loss of material to the downdrift beaches; the eroding beach started to rebuild itself.

In 1954 the beach, as far south as St. Charles Place, accreted to a width equal to or greater than the width it had immediately after the direct placement of sand. City officials indicate that the rebuilding process is gradually moving southward and evidences of improvement are apparent at the North Carolina Avenue groin.

This information indicates that the beach would have been built up by means of groins without artificial nourishment; this fact was never questioned. The nourishment was provided to restore the beach to its former dimensions as rapidly as possible in order to protect the beach-front property from unusual storms.

This type of rehabilitation will often be needed, and the delay in constructing groins in order to observe the behavior of the new fill is economically sound because in some instances groins will not be required.

Direct Placement at Virginia Beach, Va.

The City of Virginia Beach, shown in Fig. 3, is 3.5 miles south of Cape Henry, which is the southern point of the entrance to Chesapeake Bay. The shore frontage of the city is approximately 3.3 miles in length. The shore line of this area has been developed chiefly for resort and recreational purposes.

Use of this beach area as a resort was begun around 1890. It has steadily gained in popularity, and, at the present time (1956), a conservative estimate of the gross annual business is $12,000,000. Prior to the shore-frontage development, sand dunes of considerable size existed and the erosion of these dunes supplied material to create and maintain the beach. With the erection of buildings and protective structures, these fore-dunes were removed, a procedure which severely reduced the supply of sand that normally fed the beach or foreshore zone. In 1927 the Town of Virginia Beach constructed 1.93 miles of concrete sea wall and promenade to protect the most extensively developed shore frontage. The initial cost was $250,000; as of April 1, 1949, the maintenance and repair expenditures were $326,534. In 1950 the high-water line was, in general, at the toe of the sea wall and endangered many of the shore-line resort facilities.

---

[4] "Atlantic City, N. J.," *House Document 538*, 81st Cong., 2d Session, Beach Erosion Control Study, Corps of Engrs., U. S. Dept. of the Army, Washington, D. C., January 30, 1950, p. 36.

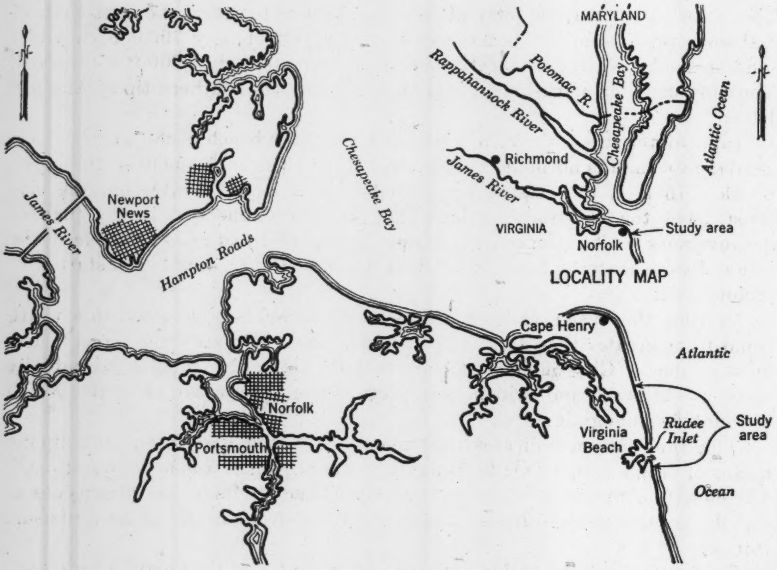
MARYLAND
Potomac R.
Rappahannock River
Chesapeake Bay
Atlantic Ocean
Richmond
James River
VIRGINIA
Norfolk
Study area
LOCALITY MAP
James River
Newport News
Chesapeake Bay
Hampton Roads
Cape Henry
Atlantic
Norfolk
Portsmouth
Virginia Beach
Rudee Inlet
Study area
Ocean

FIG. 3.—VIRGINIA BEACH, VA.

A Beach Erosion Control report[5] on the cooperative study of Virginia Beach was submitted in 1951. The purpose of this investigation was to determine the most suitable method of restoring and preserving an adequate beach for the protection of the sea wall and the upland area and for recreational use.

Statistical data on wind and ocean swell that could be applied to Virginia Beach indicated a predominant direction from the northeast and east; however, offshore-bottom hydrography and tidal currents from the entrance to Chesapeake Bay influence the wave pattern to an extent that littoral characteristics cannot be defined. Seasonal reversals in the direction of drift are apparent with an appreciable volume being transported in either direction. Based on forty-six years of record, the high-water line has shown continual recession, representing a net loss of 36,000 cu yd per yr in the problem area.

---

[5] "Virginia Beach, Va.," *House Document 186*, 83rd Cong., 1st Session, Beach Erosion Control Study, Corps of Engrs., U. S. Dept. of the Army, Washington, D. C., August 22, 1952, p. 6.

After all the evidence involved in the problem area had been considered, the recommended plan, as presented in the report cited herein, was to widen the existing beach by means of artificial placement of fill to provide sufficient protection of the sea wall and the upland area, and to maintain it by means of replenishing losses at suitable intervals in order to insure continuous protection. The plan included deferred groin construction for protection works with the provision that their construction be undertaken at such times as the estimated annual charges therewith, including material replenishment, would be less than the annual cost of beach replenishment without groins.

By the summer of 1953, 1,400,000 cu yd of sand had been hydraulically placed on the beach along the town's shore frontage. The material was obtained by dredging Rudee Inlet and Lake, which are located at the southern limit of the study area. To date, the placed fill has protected the property along the shore line, and the annual loss of material from the beach has been of the order of magnitude of the expected maintenance program. There has been insufficient time, in terms of the initial placement and the subsequent maintenance, to evaluate the deferred groin-construction plan.

STOCKPILING AT PALM BEACH, FLA., AND CONTINUOUS NOURISHMENT AT SOUTH LAKE WORTH INLET, FLA.

Prior to the start of the rehabilitation measures, the shore frontage of the Town of Palm Beach and the shores south of South Lake Worth Inlet were experiencing recession which was mainly due to the reduction of a natural supply of littoral-drift material after inlets with entrance jetties had been constructed.

As indicated in Fig. 4, Palm Beach is on the east coast of Florida, approximately 70 miles north of Miami. The town has been built on a barrier beach that separates Lake Worth from the Atlantic Ocean. The barrier varies in width from 250 ft to approximately 3,600 ft and extends about 16 miles between Lake Worth Inlet and South Lake Worth Inlet, these inlets being the only waterways between Lake Worth and the ocean. The major development of the Palm Beach shore line is situated in the reaches south of Lake Worth Inlet. This inlet was dredged through the barrier and two entrance jetties were constructed between 1918 and 1925. The north jetty is approximately 2,000 ft long and the south jetty is approximately 1,900 ft long, as measured by the shore line in 1920. The direction of littoral drift in this area is predominantly from north to south, and estimates of the annual impounding rate of the north jetty, after construction of this jetty, ranged from 150,000 cu yd to 225,000 cu yd. After the inlet and jetties had been constructed, the normal supply of material to the southern reaches of the inlet was greatly reduced. In the interval between 1926 and 1946 approximately $1,548,000 was extended for the construction and maintenance of bulkheads and groins designed for shore protection. Groins were virtually ineffective in retaining material because the supply was limited. In 1944 hydraulically dredged material, obtained from the turning basin in Lake Worth, was deposited on the beach 1,500 ft south of the south jetty of Lake Worth Inlet. It was estimated that 282,000 cu yd of sand were deposited on the beach in the form of a stockpile. It was reported that this material was transported up and down the coast and that it became impounded between the groin fields. This 282,000 cu-yd stockpile of sand was beneficial for 0.25 mile north and 1.5 miles south of the stockpile.

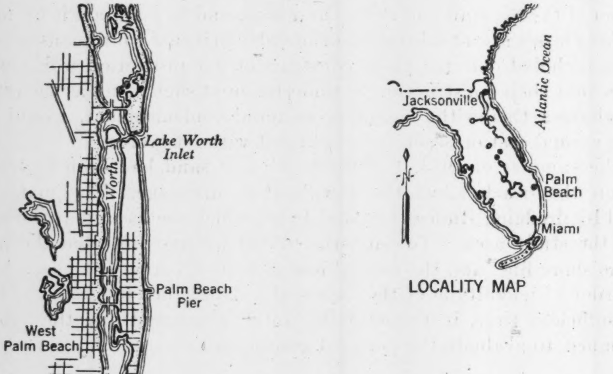
Lake Worth Inlet
Worth
Palm Beach Pier
West Palm Beach
Lake
Atlantic Ocean
South Lake Worth Inlet
0 1 2 3
Scale in miles
Jacksonville
Atlantic Ocean
Palm Beach
Miami
LOCALITY MAP
Atlantic
Bridge
Pipe line
Pumping plant
South Lake Worth Inlet
Middle ground (shoal)
Detention drain
Ocean
SOUTH LAKE WORTH INLET

FIG. 4.—PALM BEACH AND SOUTH LAKE WORTH INLET IN FLORIDA

This relatively small quantity of sand for artificial nourishment was a temporary measure until a more comprehensive beach-rehabilitation program could be undertaken. Accordingly, a Beach Erosion Control study[6] was completed in 1947. In this report it was considered that the most suitable minimum plan of improvement for the rehabilitation and protection of Palm Beach would be the placement of 1,000,000 cu yd of suitable material, dredged from Lake Worth, in five stockpiles on the beach; thereafter, periodic replenishment of sand, maintenance of existing sea walls and bulkheads, and groin maintenance would be undertaken. The stockpiles were to be placed at critical portions of the beach; it was estimated that the initial volume of placement would be depleted in about five years. The rehabilitation plan was undertaken and the stockpiling was completed in 1948. Approximately 2,000,000 cu yd of material was stockpiled instead of the recommended 1,000,000 cu yd; the total cost of this operation was $400,000. This artificial nourishment has provided adequate protection for the 13 miles of ocean-front property in Palm Beach since 1948.

---

[6] "Palm Beach, Fla.," *House Document 722*, 80th Cong., 2d Session, Beach Erosion Control Study, Corps. of Engrs., U. S. Dept. of the Army, Washington, D. C., February 13, 1947, p. 22.

During 1953 town officials followed the recommended plan of shore-line maintenance. The officials have also been considering the most feasible plan to transport mechanically the sand impounded by the north jetty of Lake Worth Inlet to the shores south of the jetty.

South Lake Worth Inlet, which is approximately 16 miles south of Lake Worth Inlet, was dredged through the barrier beach in 1927 in order to create a circulation of water through Lake Worth. The north and south entrance jetties protecting this channel are, respectively, 310 ft long and 320 ft long. After the construction of the inlet and jetties there was an immediate reduction in the supply of littoral material to the shores south of the south jetty. The predominant direction of littoral drift in this area is from north to south. In the period from 1932 to 1937, property owners in these reaches constructed protective works, such as sea walls and groins, to check the erosion; however, the supply of drift was so small that the groins were ineffective in providing a beach and the sea walls were in danger of being undermined. The concern of the South Lake Worth Inlet District Commission with this erosion problem and the growth of the shoaling problem in Lake Worth resulted in a decision to install a sand bypassing plant on the north jetty of the inlet.

The plant was installed in 1937 and consisted basically of (*a*) a swinging boom to which was attached an 8-in. suction line; (*b*) a 6-in., 65-hp, diesel-driven centrifugal pump; and (*c*) 1,200 ft of 6-in.-diameter discharge line. It was estimated that 60,200 cu yd of sand were transported to the shores south of the south jetty in the first year of operation. Pronounced accretion to the area south of the inlet was immediately noticed. By 1941 beneficial nourishment was apparent for a distance of approximately 1 mile south of the inlet. During this period an average of 50,000 cu yd of sand per yr were pumped. The plant was not operated from 1942 to 1945 because of fuel shortages and, during this three-year period, there was considerable erosion south of the inlet. Since 1945 the pumping plant has been modified to handle a greater volume of material, and recent studies[7] indicate the yearly pumping rate to be between 70,000 cu yd and 80,000 cu yd.

The shoaling rate in Lake Worth has been greatly reduced by this bypassing installation; however, the present magnitude of shoaling is still considered a maintenance problem. The downcoast area from the inlet is in excellent condi-

---

[7] "A Study of Sand Movement at South Lake Worth Inlet, Florida," *Technical Memorandum No. 42*, U. S. Beach Erosion Board, Washington, D. C., October, 1953.

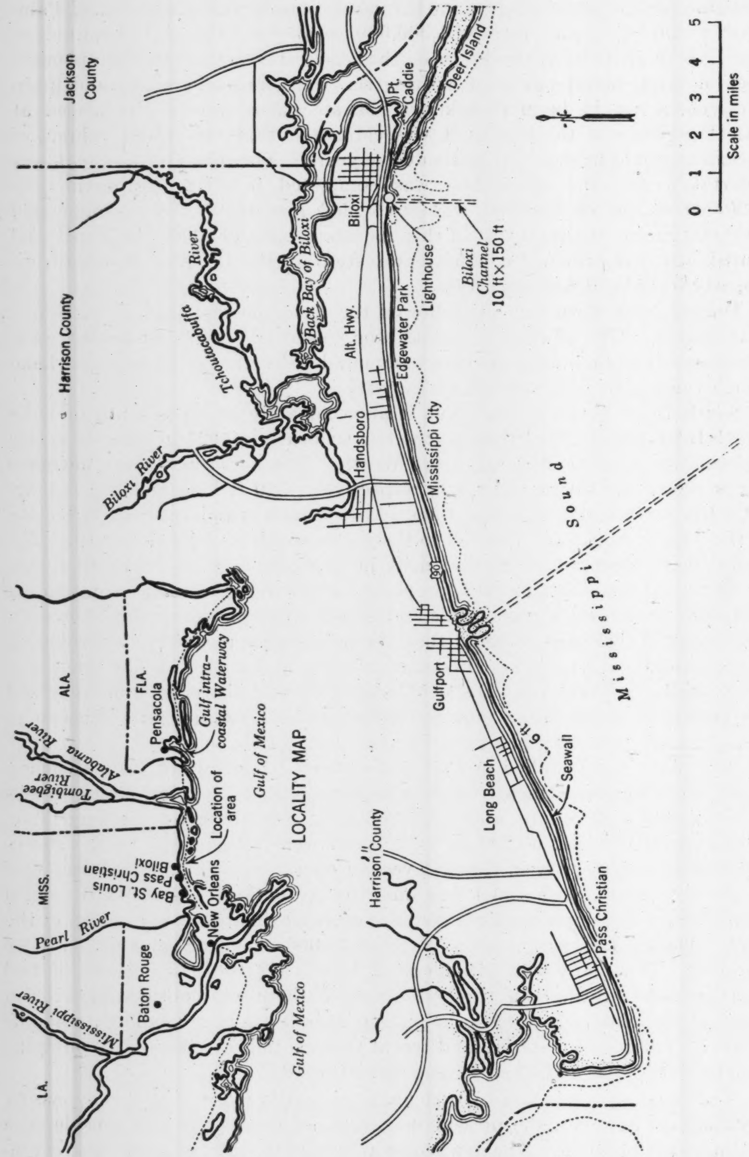
LA.
MISS.
ALA.
FLA.
Baton Rouge
Mississippi River
Pearl River
New Orleans
Bay St. Louis
Pass Christian
Biloxi
Tombigbee River
Alabama River
Pensacola
Location of area
Gulf intra-coastal Waterway
Gulf of Mexico
Gulf of Mexico
LOCALITY MAP
Jackson County
Harrison County
Biloxi River
Tchoutacabouffa River
Back Bay of Biloxi
Biloxi
Pt. Caddie
Deer Island
Alt. Hwy.
Handsboro
Edgewater Park
Lighthouse
Biloxi Channel 10 ft×150 ft
Mississippi City
90
Gulfport
Long Beach
6 ft
Seawall
Harrison County
Pass Christian
Mississippi Sound
0 1 2 3 4 5
Scale in miles

FIG. 5.—HARRISON COUNTY, MISSISSIPPI

tion and there is ample shore protection resulting from the bypassing operation. The estimated annual maintenance of the bypassing plant is $10,000—including the salaries of two operators.

This stationary sand-pumping plant, as it is operated at South Lake Worth Inlet, is one of the first installations of its type in the United States. The design and the shore-control processes of the plant have caused considerable interest. It is significant that the estimated rate of littoral drift 16 miles north of the bypassing plant ranges from 150,000 cu yd per yr to 225,000 cu yd per yr, or perhaps an average of 200,000 cu yd per yr. This indicates that the bypassing operation stabilizes the downcoast beaches by pumping only one-third of the total volume of littoral-drift material. Earlier observations indicate that the bypassed material is the main source of supply to the shore immediately south of the inlet. One of the reasons for the successful operation of this installation is that the sand reservoir at the pump's intake is a natural trap for the coarser-sized fraction of the littoral supply and, consequently, when this material is placed on the reaches south of the inlet, it quickly and adequately stabilizes the foreshore.

Direct Placement at Harrison County, Mississippi

As shown in Fig. 5, Harrison County is situated on the Gulf of Mexico, midway between New Orleans (La.) and Mobile (Ala.). The general coast line alinement of the county is east and west. The beach-rehabilitation problem covers the entire gulf-exposed shore line of the county, which is about 25 miles in length.

Transcontinental highway U. S. 90 borders the county shore line. In 1915 a severe hurricane created high tides and wave action which inflicted heavy damage to this heavily traveled roadway. Damage to the highway and extensive damage to beach-front property necessitated the construction of a 25-mile-long, reinforced concrete sea wall. This stepped-type structure is probably the longest continuous sea wall in the world.[8]

The sea-wall construction was completed in 1928 at the cost of $3,400,000. The bottom step was at the original ground level, and a low, narrow beach existed at the time the sea wall was constructed. Through the years wave action eroded this beach and exposed the curtain wall which supported the toe of the sea wall. Difficulties in making the curtain wall sandtight were encountered in the initial construction and, when it became exposed to direct wave action on the seaward face, extensive leaching of sand from the backfill behind the wall resulted. This action endangered the highway foundation in back of the sea wall; therefore, the sea wall was not completely effective in its primary purpose.

A Beach Erosion Control study[9] of the Harrison County shore line was completed in 1947. The recommended plan of improvement was to provide structural repair of the sea wall with particular emphasis on a sandtight curtain wall, revision of the existing drainage system, replacement of backfill, and construction of an artificial beach. The plan included periodic maintenance of the sea wall and the replenishment of sand to the beach.

---

[8] "Shore Protection in Harrison County, Mississippi," by F. F. Escoffier and W. L. Dolive, *Bulletin*, U. S. Beach Erosion Board, Washington, D. C., Vol. 8, No. 3, July 1, 1954, p. 1.

[9] "Harrison County, Miss.," *House Document 682*, 80th Cong., 2d Session, Beach Erosion Control Study, Corps of Engrs., U. S. Dept. of the Army, Washington, D. C., March 8, 1948, p. 18.

This plan was undertaken in 1951. After the sea wall had been repaired, approximately 6,000,000 cu yd of sand were placed hydraulically, directly in front of the sea wall, to create a beach 300 ft wide (mean sea level) and about 24 miles long. Adjacent to the wall, the beach elevation is 5 ft above mean sea level for a distance of 50 ft from the wall, and the beach is sloped at 1 on 100 to the naturally adjusted foreshore slope, which is 1 on 10. The material for this beach was obtained 1,500 ft directly offshore in Mississippi Sound.

Recent surveys indicate that this beach is in excellent condition, offering protection to the sea wall and providing recreational facilities. The loss of beach material because of erosion and natural adjustment of the beach has been estimated to be 32,500 cu yd annually. At present (1956), no replenishment by means of dredging has been undertaken.

The reasons for using the direct-placement method in this beach restoration problem are apparent. The sheltering effect of the islands between 12 miles and 15 miles offshore results in a small westerly rate of littoral drift; this sheltering effect also provides excellent conditions for floating plant operations which are reflected in the project costs. The sand deposits that are 1,500 ft offshore are apparently suitable to the wave climate in the area because a minimum natural foreshore adjustment has occurred.

Direct Placement at Surfside Beach, Calif., and Sunset Beach, Calif.

As shown in Fig. 6, Surfside and Sunset Beaches are located on the coast of southern California in Orange County, approximately 4 miles southeast of the mouth of the Los Angeles River at Long Beach. Anaheim Bay Harbor lies at the western limit of the area, and the two communities are situated on a barrier beach fronting tidal marshland beyond which the topography rises gradually inland. The beaches were formed in a prehistoric era along the face of the marsh by abundant easterly moving littoral-drift material supplied by eroding headlands and by debris carried to the shore by the Los Angeles River and the San Gabriel River.

Recent erosion of these shores, which are adjacent to the Anaheim Bay Harbor, has resulted because of a lack of nourishment. This lack of nourishment is due to a change in the local shore regimen resulting from the effects of flood control and water conservation in the tributary drainage areas, from the effects of the offshore detached breakwater extending eastward from San Pedro to a point opposite the mouth of the San Gabriel River, and from the effects of the converging breakwaters protecting Anaheim Bay Harbor. The rate of the littoral drift that built the beaches is not known, but recent studies show that material is carried eastward from Surfside at a rate of 155,000 cu yd per yr.

Before 1933 private interests built a series of short groins to combat the erosion; these failed to accomplish their purpose. In 1942 a series of longer groins was built to retain the 452,000 cu yd of sandfill placed between them during the period from 1942 to 1945. These groins were partly effective in holding the fill, but by 1947 erosion had progressed so far that eight large beach homes were threatened. At this time the United States Congress appropriated $250,000 as an emergency measure[10] to provide 1,220,000 cu yd of sandfill to the beach. It was estimated that this nourishment would last approximately five years. During the succeeding years erosion occurred, and by the summer of 1951 the shore line had receded to the 1947 predredging position at the western end of the beach. Since that time the erosion has moved progressively southward and has caused the loss of several beach homes.

A recent report[11] of a comprehensive study of the area recommends that artificial beach nourishment derived from Anaheim Harbor and the marshes be placed behind the barrier at a rate of 1,000,000 cu yd every five years. It is estimated that this quantity of material will provide protection for approximately six to seven years. It is proposed to nourish the beach after five years by allowing a remaining protecting fillet of beach in the area adjacent to the east-harbor jetty. The initial dredging will be from the harbor area, which is mainly sand; subsequent dredging will be from the marsh areas, which contain foreign material and, consequently, 1,000,000 yd cannot be depended on to last more than five years.

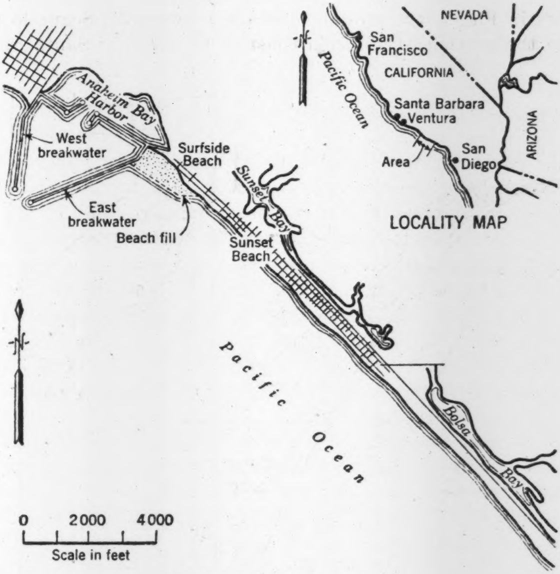
Anaheim Bay Harbor
West breakwater
East breakwater
Beach fill
Surfside Beach
Sunset Bay
Sunset Beach
Pacific Ocean
Bolsa Bay
N
0 2000 4000
Scale in feet
NEVADA
San Francisco
CALIFORNIA
Pacific Ocean
Santa Barbara
Ventura
Area
San Diego
ARIZONA
LOCALITY MAP

FIG. 6.—SUNSET BEACH, CALIF.

This problem shows the need for considering an entire littoral compartment, which, if considered, will show the economic value of artificial nourishment for constructing and rehabilitating beaches. The study of this problem indicates that beach stabilization can be attained more economically by means of artificial nourishment, because a supply of sand is close at hand, than by means of a sea wall. Artificial nourishment provides the added advantage of supplying material to the littoral zone for nourishing the beaches downdrift whereas a sea wall would merely transfer the erosion problem downdrift. Once sea-wall protection is started, it may be necessary to extend the sea wall progressively downdrift until the entire shore of the littoral compartment is protected.

---

[10] *Public Law 122*, 80th Cong., approved June 27, 1947.

[11] "Anaheim Bay Harbor, Calif.," *House Document 349*, 83rd Cong., 2d Session, Beach Erosion Control Study, Corps of Engrs., U. S. Dept. of the Army, Washington, D. C., November 30, 1953, p. 42.

Direct Placement at El Segundo, Calif., and Ocean Park, Calif.

As shown in Fig. 7, the stretch of beach between El Segundo and Ocean Park lies on the southern California coast at the head of Santa Monica Bay.

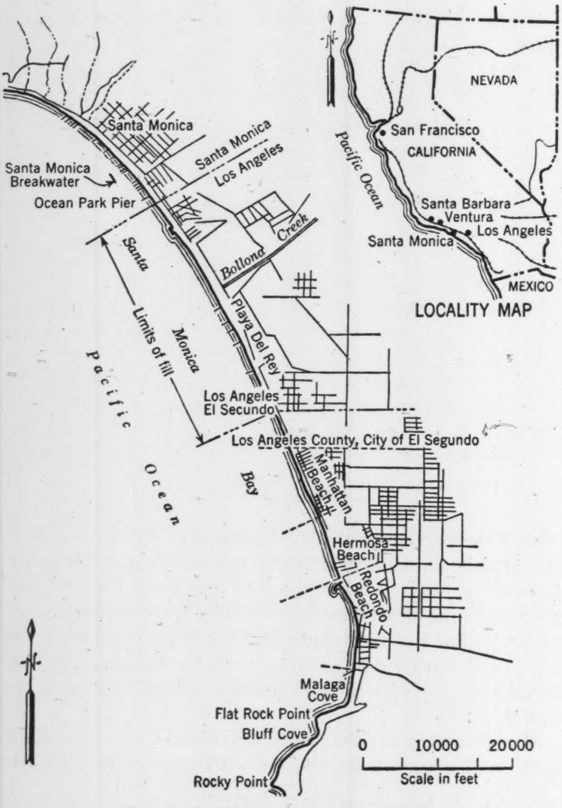
N
Santa Monica
Santa Monica
Los Angeles
Santa Monica Breakwater
Ocean Park Pier
Bollona Creek
Santa Monica Bay
Limits of fill
Pacific Ocean
Playa Del Rey
Los Angeles
El Secundo
Los Angeles County, City of El Segundo
Manhattan Beach
Hermosa Beach
Redondo Beach
Malaga Cove
Flat Rock Point
Bluff Cove
Rocky Point
0 10000 20000
Scale in feet
N
NEVADA
San Francisco
CALIFORNIA
Pacific Ocean
Santa Barbara
Ventura
Los Angeles
Santa Monica
MEXICO
LOCALITY MAP

Fig. 7.—Santa Monica Bay, California

Immediately behind the beach the coastal area is covered with wind-blown sand dunes extending several thousand feet inland and rising to an elevation of 175 ft.

The problem in this area was not entirely one of erosion but one of pollution. The outfall sewer of the City of Los Angeles in the Hyperion District discharged solid sewage into Santa Monica Bay and contaminated the beaches in the area. Public use of the beaches was prohibited in 1943. In order to alleviate this condition, a sewage-disposal plant was planned to be constructed in the sand-dune area at El Segundo. The construction of this plant required the removal of 14,000,000 cu yd of sand to reduce the elevation of the dunes from 175 ft to a general elevation of 40 ft. The problem of disposing of this spoil was simple because Los Angeles County had a master plan of shoreline development,[12,13] which provided for the widening of the beach with fill. The fill is to be developed into a park area by means of roads, vehicle parking areas, bathhouses, playgrounds, and similar installations.

In conformity with the master plan, the 14,000,000 cu yd of material were dumped on the beach over the 6-mile stretch from El Segundo to Ocean Park in 1948. The beach was widened from 600 ft to 800 ft. Because of the nature of the littoral-drift material in this area which moves downcoast at a rate of about 160,000 cu yd per yr, the master plan indicates that some stabilization of the shore line by artificial nourishment should be used to replace that carried downcoast. Because man-made structures will undoubtedly appear upcoast in the future, a stockpile of sand will be needed at the updrift end of each littoral segment. A stockpile of approximately 800,000 cu yd is estimated to be sufficient for about five years. Sand for this fill can be procured from the foothills and dunes at a cost of from 30¢ per cu yd to 50¢ per cu yd.

From the time the fill was first placed (1948) until the present (1956) no additional material has been placed. Surveys made to a depth of − 20 ft in the area during the period from 1949 to 1953 indicate that there has been considerable movement of the material with losses approximately as expected. From the southern limit of the fill to Ballona Creek, a distance of about 4⅓ miles, the loss has been approximately 1,000,000 cu yd, or an average of 250,000 cu yd per yr. This is in agreement with the 160,000-cu-yd estimated annual loss, if readjustment of the artificial fill is considered, together with the supply demand in the littoral stream. Reaches farther north (the remaining 2 miles of the study area) indicate stability and considerable accretion at certain points, the most apparent being behind the Santa Monica breakwater. This accretion is due to the material movement from upcoast as the littoral-drift material moves from north to south in this area.

CONTINUOUS NOURISHMENT AT DURBAN (PORT NATAL), SOUTH AFRICA

Durban (Port Natal) lies on the southeast coast of Africa (Fig. 8) approximately 800 miles northeast of the Cape of Good Hope and adjacent to Cape Natal. This city, which had a population of 367,000 in 1949, is one of

---

[12] "Appendix II—Coast of California, Point Mugu to San Pedro Breakwater," *House Document 277*, 83rd Cong., 2d Session, Corps of Engrs., U. S. Dept. of the Army, Washington, D. C., June 5, 1952, p. 23.

[13] "Los Angeles $41,000,000 Hyperion Project Ends Beach Contamination," by Lloyd Aldrich and H. G. Smith, *Civil Engineering*, Vol. 18, July, 1948, p. 419.

the leading year-round holiday resorts in South Africa. Like most coastal resort cities, Durban depends on its beach to attract visitors. However, erosion has gradually reduced the proportions of the beach to such a size that the city officials feel there is a danger of losing the lucrative tourist trade.

The erosion problem in this case is concerned with the harbor breakwaters, whose construction was started in the 1880's and, in particular, with the intensive dredging that has been necessary in the vicinity of the harbor entrance channel. This navigation channel has prevented an abundant littoral drift from reaching the Durban beaches. As a consequence, more than 40 acres of foreshore have been lost in about forty years. During a period of many years, 60,000,000 cu yd of material have been removed from the vicinity of the harbor entrance to maintain a low-water, ordinary-spring-tide (LWOST) channel elevation of − 42 ft.

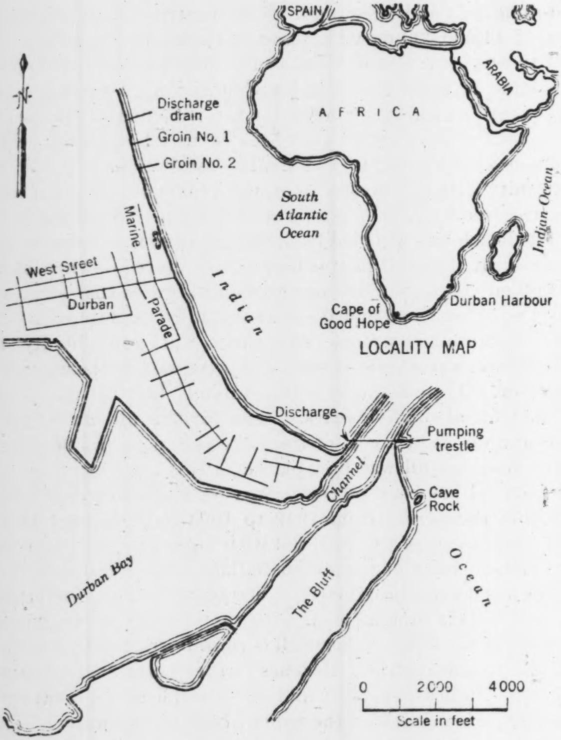
N
Discharge drain
Groin No. 1
Groin No. 2
Marine
Parade
West Street
Durban
Indian
Ocean
Discharge
Pumping trestle
Channel
Cave Rock
Durban Bay
The Bluff
0
2000
4000
Scale in feet
SPAIN
ARABIA
AFRICA
South Atlantic Ocean
Indian Ocean
Cape of Good Hope
Durban Harbour
LOCALITY MAP

FIG. 8.—DURBAN HARBOR, SOUTH AFRICA

In 1938 sand, derived from channel maintenance, was pumped onto the beach from a hydraulic dredge operating along the inside face of the north jetty. The dredge had a 42-in.-diameter discharge line. In nine years more than 5,000,000 cu yd of sand were placed on the beach. This pumping operation restored the foreshore and reclaimed approximately 75 acres, except in the area north of West Street along lower Marine Parade where a rubble wall had been built to combat the inroads of erosion; in this area relief was only temporary.

In 1950, in order to reduce harbor-maintenance dredging and also to supply sand to the beach, a 16-in. dredge pump was installed on a steel trestle in Cave Rock Bight. The unit, which consists of a crane and pump, moves along the trestle to provide storage at the inner end in stormy weather. During operational weather the unit works at the outer end of the trestle, dredging over a semicircular area (radius 36 ft) to a depth of − 20-ft LWOST. The discharge line of the pump, when it is in dredging position, is connected to a steel line with a rubber sleeve. The line crosses the harbor at − 42-ft LWOST and discharges on the beach near the base of the north jetty. Previously, the discharge point was 5,000 ft farther north, effected by two booster pumps spaced approximately 2,000 ft apart. The pump has been operated almost continuously since it was constructed in 1954. The estimated output of the plant operating 7 hr per day, 5 days per week, is 268,000 cu yd of sand per yr. Prior to the pumping in Cave Rock Bight, the LWOST line was 65 ft beyond the end of the trestle; in 1954 it was 135 ft shoreward therefrom. Occasionally the plant is unable to operate continuously because of a lack of littoral material.

Engineers feel certain that channel-maintenance dredging has been reduced by the amount bypassed. The sand supply to the Durban shore has maintained the position of the beach except in the lower Marine Parade area where damage has occurred during the heaviest storms.

A discharge drain acting as a groin is located approximately 3,600 ft north of the parade area. In April, 1953, two groins were constructed—one 700 ft and the other 1,400 ft south of the discharge drain. Since that time the low-water line has been forced seaward immediately south of Groin No. 1 for a maximum of 135 ft, but subsequent storms have reduced the gain to approximately 85 ft. Although the stormy period each year has reduced the volume of material that was impounded during the fine weather, there has been a substantial gain in the width of the beach.

The engineers responsible for the construction and rehabilitation of this beach consider that the annual nourishment, aided by the groins to reduce the rate of loss from the beach, will rehabilitate this beach area. The entire downdrift stretch of shore will be stabilized after the groins are full and material passes around the ends of the groins.

CONTINUOUS NOURISHMENT AT SALINA CRUZ, MEXICO

The Port of Salina Cruz[14] is located on the Pacific Ocean side of southern Mexico, approximately 1,800 miles southeast of Los Angeles. The entire harbor has been artificially constructed. The shore line in the Salina Cruz area is oriented in an essentially east-west direction, and the littoral drift is in an easterly direction. The rate of littoral drift is 500,000 cu yd annually.

---

[14] "Draga Fija," Junta Directiva de Puertos Libres Mexicanos (1950), Translation in *Bulletin*, U. S. Beach Erosion Board, Washington, D. C., Vol. 5, No. 3, July, 1951, p. 1.

The initial breakwater for the protection of the harbor docks was approximately parallel with the general shore alinement, which allowed navigation into the harbor from the southeast. It was quickly realized that there were extensive shoals in the eastern end of the breakwater; therefore, the direction of the breakwater was changed to nearly due south and it was extended toward the open ocean. Another breakwater was constructed on the eastern side of the harbor, thus forming the inner and outer harbors as shown in Fig. 9. The impounding area west of the harbor entrance was soon filled and, for the

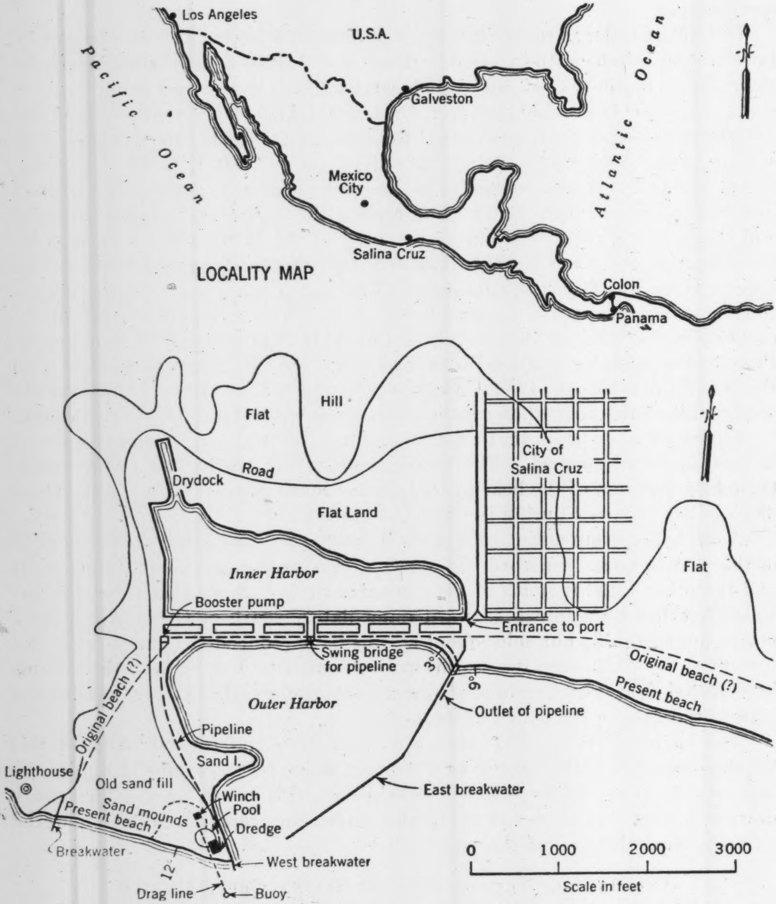
Los Angeles
U.S.A.
Pacific Ocean
Galveston
Atlantic Ocean
N
Mexico City
Salina Cruz
LOCALITY MAP
Colon
Panama
Flat
Hill
City of Salina Cruz
Drydock
Road
Flat Land
Inner Harbor
Flat
N
Booster pump
Entrance to port
Swing bridge for pipeline
3°
9°
Original beach (?)
Present beach
Outer Harbor
Outlet of pipeline
Original beach (?)
Pipeline
Sand I.
Lighthouse
Old sand fill
Winch
Pool
Sand mounds
Present beach
Dredge
East breakwater
Breakwater
West breakwater
12°
Drag line
Buoy
0
1000
2000
3000
Scale in feet

Fig. 9.—Salina Cruz, Mexico

past forty years, extensive maintenance dredging has been required to keep the entrance channel and harbor open to navigation.

As a solution of this maintenance problem, the Board of Mexican Free Ports constructed what is considered the largest stationary dredge in the world. The fixed dredge consists of two 450-hp motors to operate two dredge pumps equipped with 18-in.-diameter intake and discharge lines. The location of the pumping station, discharge line, and general features are shown in Fig. 9. Six swivel-type intake lines feed into the dredge pumps, and the pond or reservoir created by these intakes can be approximately 200 ft long, 100 ft wide, and 32 ft deep.

After the initial plant construction, the seaward limit of this pond was approximately 150 ft from the mean-low-water line on the beach. The plan was to breach this barrier and allow the sand to flow naturally into the pool or reservoir. Attempts to open the barrier between the pond and beach were not successful with a conventional dragline and land equipment. Each time an opening was made, large quantities of sand were deposited in the reservoir area and the pumps lacked sufficient capacity to maintain the opening. Eventually a reinforced concrete sheet-piling passageway was constructed and a drag scraper, operated by a winch and guided by steel cables passing over a pulley installed on a float anchored at sea, pulled the material into the reservoir. A spur dike (groin) was constructed approximately 1,800 ft west of the bypassing plant in order to reduce the rate of littoral drift at the plant. The development of this sand bypassing plant has afforded some revealing information. Because of the difficulties of attaining the desired readjusted shore line, the success of the operation has yet to be evaluated. In July, 1952, the beach line in front of the reservoir pools had not appreciably receded. It appeared at that time that the sand must be artificially pulled within reach of the suction lines at considerably greater rates in order that the beach might recede sufficiently to allow the sand to flow naturally into the pool. A final appraisal of this operation should lead to a better understanding of large-scale sand bypassing plants, their effect on updrift shore lines, the effect of shoaling in the navigation channel, and the effects to the downdrift areas, and should indicate the comparative maintenance costs for navigation inlets.

CONCLUSIONS

It can be noted, from the cases presented herein, that there are two basic methods of artificial nourishment to beaches; these methods are stockpiling and continuous nourishment. To state that one method is superior to the other method would not be true because it is common for coastal engineers to find that a method applicable in a particular locality would be most unsound in another locality. For example, the distribution of material into the littoral zone from a stockpile of material depends on the hydrography and predominant wave characteristics. It would be unwise to stockpile material on a foreshore zone when the hydrography is of steep slopes and the predominant waves have high steepness values (ratio of wave height to wave length).

Because the technique of artificial nourishment was not extensively used until after World War II, this method of rehabilitating beaches is relatively new. In the beach restoration at Atlantic City, the method of offshore deposition did not appear encouraging. However, conclusive criticism of this technique cannot be made until more is known about the actual mechanics of material transport by waves. After the offshore deposition was completed, the foreshore area indicated continued erosion, but there could possibly be a reduced rate of erosion because of this offshore deposition. In some coastal waters it is known that, during a period of years, a tremendous volume of material is moved in the offshore zone; however, the actual mechanics of this material movement are yet to be understood fully.

When immediate protection is needed and the fill is placed directly on the beach, there can be no actual failure of beach rehabilitation. The success of the operation can be measured by the length of time the protective beach has existed. The sand is placed directly on the foreshore, protection is provided for the onshore area, and success of the operation is measured by the length of time this protective beach exists. Perhaps one of the most important considerations in using direct-placement fill is the characteristic of the material placed on the beach. A material with a fine gradation, relative to the material environment where it is being placed, will probably be quickly transported to the offshore zones and the net residual of this placed material will be insufficient to provide the required beach width for protective measures. In cases of direct placement, a material with a coarser gradation than that of the native beach material will be best for foreshore adjustment and will provide the desired protective beach width over the longest span of time. Obviously an optimum exists for the coarseness of material in considering a beach for recreational purposes.

Current experiences indicate that there is always a gradation toward finer materials as progression is made from the foreshore area toward the offshore area. In general, too, the coarsest fraction is found at the plunge point of the waves. These residuals of sand movement, which are due to the hydraulic characteristic of the waves, all favor the operation of a continuous-nourishment type of beach rehabilitation. In such a case, the plant is positioned to intercept this coarse fraction and to transport it to the downdrift areas where it will function as a feeder to the littoral stream. When the outfall of the bypassing plant is not systematically extended, the operation becomes a form of stockpiling, which requires additional time for the natural forces to transport the material downcoast. Observations made at the sand bypassing plant at South Lake Worth Inlet tend to indicate that this type of artificial nourishment is the solution to all inlet problems. However, observations made of the sand bypassing operations at Salina Cruz show that the over-all planning is not so simple. Here again, this method of providing nourishment to the downdrift area from an inlet, with the additional purpose of the operation being to reduce maintenance dredging for navigation in the inlet, is new. It is reasonable to assume that this type of operation would always provide the downdrift area with material having desirable characteristics; however, this operation must be studied from the standpoints of reducing the maintenance costs of dredging in the inlet and of determining the possibilities of the plant becoming "landlocked." This type of operation is receiving much attention and can be evaluated better as more is known about the basic movement of sands by wave action.

The cost of beach restoration has the greatest bearing on the selection of artificial nourishment. In one case the cost of protecting a reach of shore line by means of artificial nourishment may be only a few cents per linear foot because of the accessibility of the source material; in another case the cost would be extremely high because of the scarcity of materials. In the latter case it is often more economical to consider permanent protection, such as massive sea walls or bulkheads for protecting valuable onshore property, and, in some cases, the value of the onshore property does not justify the total cost of adequate protection from ocean waves.

AMERICAN SOCIETY OF CIVIL ENGINEERS
Founded November 5, 1852
TRANSACTIONS

Paper No. 2854

INTEGRATION OF STREETS WITH AN EXPRESSWAY SYSTEM

By Karl A. Bevins,[1]

Synopsis

The problem of providing for traffic expansion in Atlanta, Ga., involves revising a primarily radial street pattern to provide streets bypassing the downtown area. In addition, a "screen line" of railroads surrounds the downtown area. The major street plan includes an expressway, belt routes, improvement of radial streets, and a one-way traffic pattern. Government and business people are being effectively organized to plan and administer the program.

Coordination of Government and Business

Governmental Agencies.—In Atlanta, Ga., the governmental agencies most active in the field of traffic improvement include the City of Atlanta, through its Municipal Planning Board and consultants, its Construction Department, and its Traffic Commission and Traffic Engineering Department; Fulton County, through its Department of Public Works; DeKalb County, through its Commissioner of Roads and Revenues; the Metropolitan Planning Commission, which is financed jointly by the City of Atlanta, Fulton County, and DeKalb County; the Joint Bond Commission, a citizens' commission which administers the bond funds voted by the citizens of the City of Atlanta and Fulton County for traffic improvement; the Georgia State Highway Department; and the Bureau of Public Roads (United States Department of Commerce).

The Role of Businessmen.—In order to minimize duplications and avoid omissions, the Atlanta Traffic and Safety Council organized the Transportation Planning Council composed of one administrative official and one technical man from each of the agencies working on traffic plans. This council is an unofficial advisory group. Its work is done by special committees appointed for specific jobs. One standing committee, called the Technical Coordinating Committee, holds regular meetings and carries the bulk of the work load.

Note.—Published, essentially as printed here, in January, 1955, as *Proceedings-Separate No. 603*. Positions and titles given are those in effect when the paper was approved for publication in *Transactions*.

[1] Traffic Engr., Atlanta, Ga.

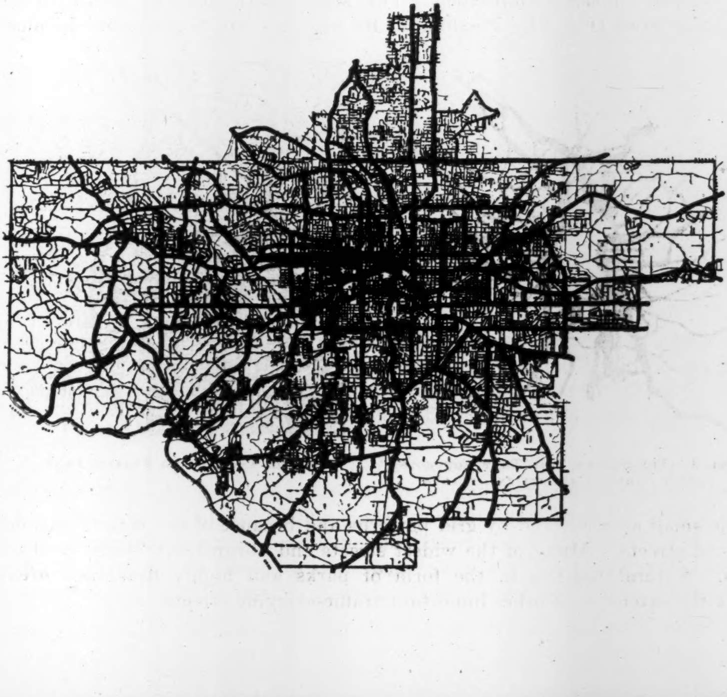

FIG. 1.—RADIAL PATTERN FORMED BY EXISTING STREETS

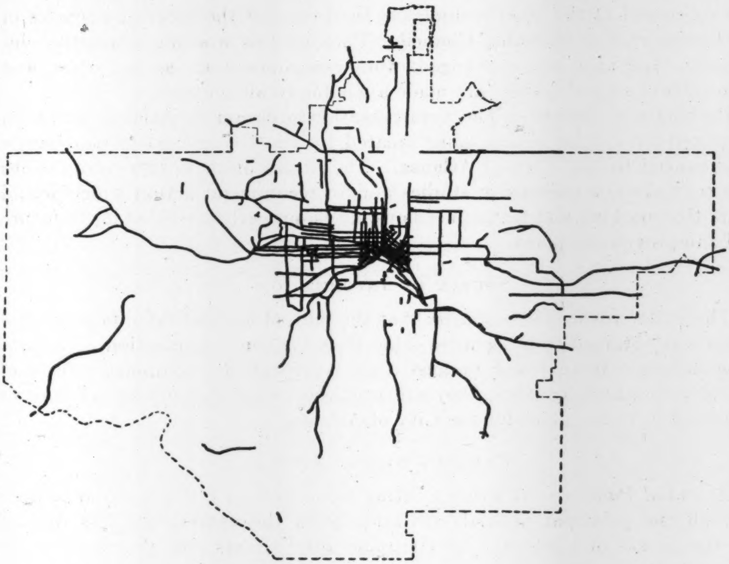

FIG. 2.—WIDE STREETS ARE SCARCE AND DISCONNECTED

It is composed of the chief technicians from each of the member agencies of the Transportation Planning Council. Through this working committee, information and ideas are exchanged, work assignments are agreed upon, and the results of special studies are made available to all agencies.

Parking and Transit.—The transportation program in Atlanta has been completed by special commissions created by the Georgia State Legislature and financed by the City of Atlanta. The duties of these two commissions were to make comprehensive studies and to recommend action which would insure that parking and transit needs would be properly provided for in future traffic improvement plans.

SOURCE OF INFORMATION

The writer wishes to emphasize that the bulk of the factual data presented herein was obtained from agencies other than his own organization. Because these data are factual and because they represent the combined efforts of several responsible agencies, they are worthy of careful study by all persons interested in traffic plans for the City of Atlanta.

EXISTING STREET SYSTEM

A Radial Pattern.—Atlanta's existing street system forms a radial pattern with all the principal arterials radiating from the central business district like the spokes of a wheel. No circumferential streets and almost no crosstown streets exist (Fig. 1).

Vehicular Capacity Limitations.—Few streets with roadway widths of 40 ft or more exist (Fig. 2). Possibilities for one-way streets are scarce because of the small area covered by grid patterns and because of the lack of parallel pairs of streets. Many of the widest streets end abruptly at "jogs" or dead ends. Natural barriers in the form of parks and highly developed areas block the extension of other important traffic-carrying streets.

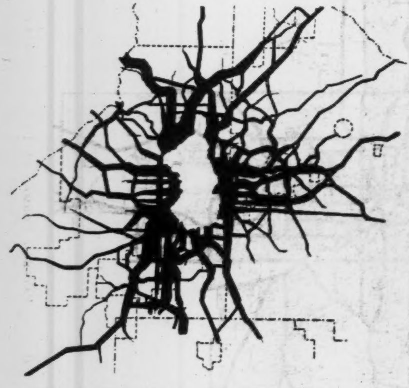

FIG. 3.—THE SCREEN LINE THAT CONTROLS USEFUL STREET CAPACITY IN ATLANTA

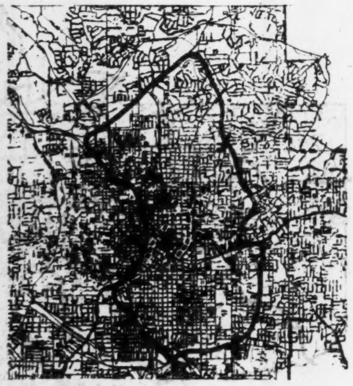

FIG. 4.—EXISTING TRAFFIC FLOW

The "Screen Line".—The central business district, from which radiate most of the main streets, is completely surrounded by railroads. These railroads form a circular belt line which may be termed the "screen line" (Fig. 3). The streets radiating from the central business district and crossing this screen line will be referred to as "gateways." There are 29 of these gateways piercing the screen line. At present, these 29 gateways provide a total of 74 traffic lanes, 37 being inbound and 37 outbound. The practical operating capacity of these 29 gateways in one direction is 16,650 vehicles per hour (vph). The maximum capacity, which is an unsatisfactory operating figure, is 18,500 vph. For all practical purposes this capacity of 16,650 vph is the useful capacity of the existing radial street pattern.

TRAFFIC LOAD RELATED TO USEFUL STREET CAPACITY

Radial Streets.—Existing traffic flow data show that few streets, other than the radial system, now carry large amounts of traffic (Fig. 4). The lack of routes bypassing the central district accounts for this. As the city grows and new secondary focal points develop, the need for bypass facilities will increase. However, the radial system, with the screen line controlling its capacity, must continue to carry the bulk of the traffic load to and from the important central business district.

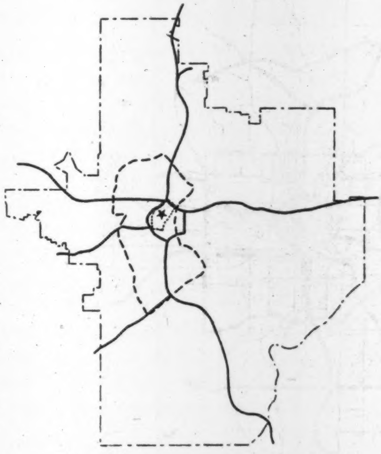

FIG. 5.—BYPASSING OF THE SCREEN LINE WITH BELT ROUTES

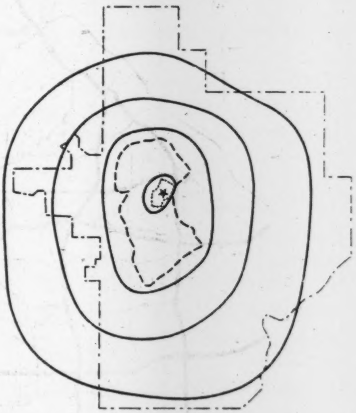

FIG. 6.—USE OF EXPRESSWAYS AS A SKELETON SYSTEM

Screen-Line Traffic Load Related to Its Capacity.—The maximum inbound movement through the screen line occurs during the morning peak period with a load of 14,250 vph. The maximum outbound load of 17,000 vph occurs during the afternoon peak period. Comparing the 17,000 vph now carried through the 29 gateways at the screen line with the practical operating capacity of only 16,650 vph emphasizes a critical problem. The congestion experienced at the capacity-controlling screen line confirms the fact that many of the gateways are badly overloaded during peak hours.

IMPORTANCE OF A STREET IMPROVEMENT PROGRAM

Possible Means of Improvement.—If the gateways through the screen line are overloaded at present, how can the city provide for its future growth?

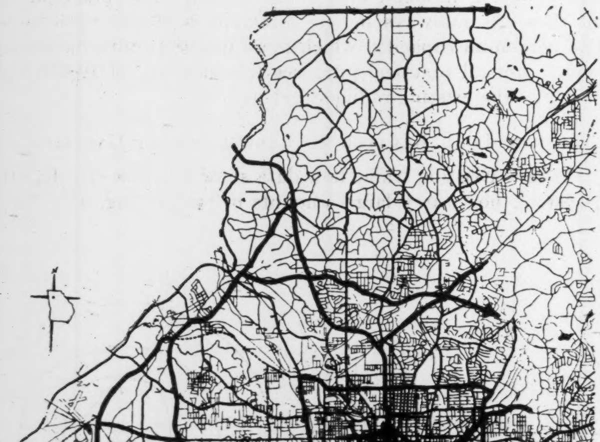

FIG. 7.—PROPOSED MAJOR STREET PLAN (HEAVY LINE INDICATES EXPRESSWAY OR LIMITED-ACCESS BOULEVARD)

The following possible means of relief have been proposed: (1) Construction of bypass, cross-town, and circumferential streets to carry around the area bounded by the screen line all traffic that does not have destinations within that area (Fig. 5); (2) construction of expressways piercing the screen line, thus creating additional high-capacity gateways (Fig. 6); (3) construction of new surface gateways; and (4) improvement of existing gateways by (*a*) eliminating parking, (*b*) installing staggered lanes, (*c*) widening existing streets, and (*d*) using various combinations of measures (*a*), (*b*), and (*c*).

The Proposed Major Street Plan.—The proposed plan makes use of all these devices. Five expressways form the "backbone" of the proposed plan. The heart of the central business district is to be surrounded by an expressway "ring." From this connector ring one expressway is to run north and split into a northwest leg and a northeast leg; another is to run east; the third is to run east and southeast; the fourth is to run south; and the fifth is to run west. A series of strategically located circumferential routes and cross-town routes are to be spaced at intervals outward from the central business district to tie together the expressways and to relieve the radial feeder system. Major improvements for the radial system and the downtown streets are to be included to permit and encourage the dispersion of traffic (Fig. 7).

ANTICIPATED PERIOD OF ADEQUACY

Increasing the Screen-Line Capacity.—All justifiable methods have been used to increase the screen-line capacity. These measures include bypass routes, expressways, new surface gateways, widenings by means of construction and no-parking, one-way streets, staggered lanes, and special traffic-signal timing. These changes have all been assumed to increase the traffic-carrying capacity of the screen-line gateways, which in turn control the useful capacity of the Atlanta street system.

Screen-Line Demand Related to Practical Capacity.—Lane capacities of surface streets were computed using an average of 450 vph as the operating lane capacity and 500 vph as the maximum possible lane capacity. On expressways, 1,200 vph was used as the operating lane capacity and 1,500 vph was used as the maximum possible lane capacity. The proposed plan utilizes some of the streets to their maximum capacity. This heavy loading of some streets became necessary when it was judged impracticable to add more traffic lanes through certain sectors of the screen line. The traffic demand at the screen line in 1980 has been estimated at 53,600 vph, but the practical operating capacity of the streets available under the major street plan is only 51,600 vph. The difference between these two values can be made up by loading some of the streets at or near their maximum possible capacities rather than adhering to operating capacities.

Overloading of Streets.—In order to anticipate better 1980 traffic needs at the various gateways, the screen line has been divided into four sectors (Fig. 8).

North Sector.—The estimated demand for the north sector is 10,900 vph whereas the operating capacity is only 6,450 vph and the maximum capacity, only 7,500 vph. By loading all the northbound gateways to maximum capacity, the deficiency can be reduced to 3,400 vph. Assigning 750 vph to leave the screen line westbound on Tenth Street and then turn north, and assigning another 2,650 vph to leave the screen line eastbound on the Expressway (N.E.), Piedmont Avenue, and Boulevard before turning north to their ultimate destinations, makes possible a balance between demand and capacity for the north sector.

East Sector.—The estimated 1980 demand is 19,900 vph whereas the operating capacity is 21,900 vph. However, the east sector has been required to absorb 2,650 vph from the north sector, leaving an operating capacity of only 19,250 vph available for east-sector traffic. This will undoubtedly result in some congestion on gateways in the east sector.

South Sector.—In comparison to the capacity of 11,700 vph the estimated demand in 1980 is 12,600 vph. The difference can be eliminated by requiring some of the gateways to carry nearly their maximum possible capacities.

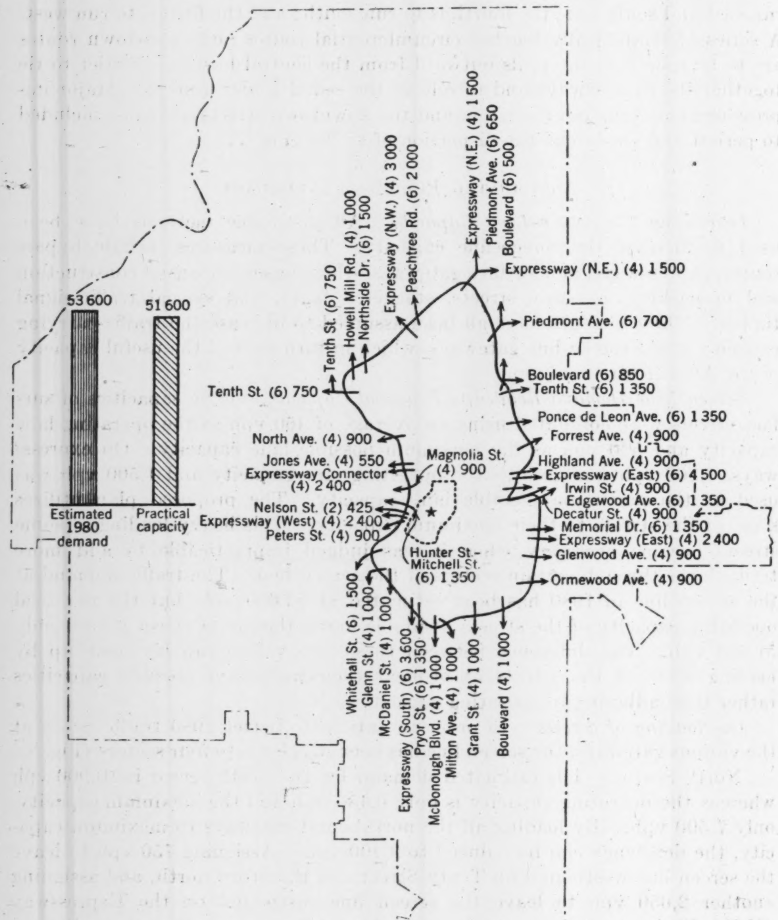
53 600
51 600
Estimated 1980 demand
Practical capacity
Tenth St. (6) 750
Howell Mill Rd. (4) 1 000
Northside Dr. (6) 1 500
Expressway (N.W.) (4) 3 000
Peachtree Rd. (6) 2 000
Expressway (N.E.) (4) 1 500
Piedmont Ave. (6) 650
Boulevard (6) 500
Expressway (N.E.) (4) 1 500
Piedmont Ave. (6) 700
Boulevard (6) 850
Tenth St. (6) 1 350
Tenth St. (6) 750
Ponce de Leon Ave. (6) 1 350
Forrest Ave. (4) 900
North Ave. (4) 900
Magnolia St. (4) 900
Jones Ave. (4) 550
Highland Ave. (4) 900
Expressway Connector (4) 2 400
Expressway (East) (6) 4 500
Irwin St. (4) 900
Edgewood Ave. (6) 1 350
Nelson St. (2) 425
Expressway (West) (4) 2 400
Decatur St. (4) 900
Memorial Dr. (6) 1 350
Peters St. (4) 900
Expressway (East) (4) 2 400
Hunter St.-Mitchell St. (6) 1 350
Glenwood Ave. (4) 900
Ormewood Ave. (4) 900
Whitehall St. (6) 1 500
Glenn St. (4) 1 000
McDaniel St. (4) 1 000
Expressway (South) (6) 3 600
Pryor St. (6) 1 350
McDonough Blvd. (4) 1 000
Milton Ave. (4) 1 000
Grant St. (4) 1 000
Boulevard (4) 1 000

FIG. 8.—ESTIMATED 1980 DEMAND EXCEEDS PRACTICAL CAPACITY

West Sector.—The west sector is the least crowded of the four, having an estimated demand of 10,200 vph and an operating capacity of 11,550 vph. The 750 vph, which the west sector has been required to absorb from the north sector, leaves available a comfortable 10,800 vph in operating capacity.

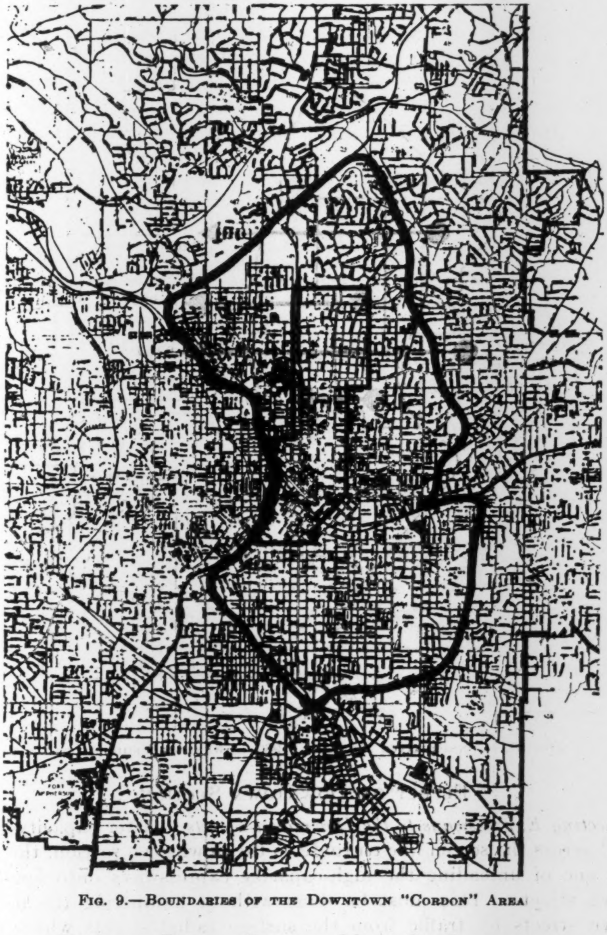

Fig. 9.—Boundaries of the Downtown "Cordon" Area

Existing Radial Streets Must Be Improved

The proposed major street plan includes five expressways through the screen line in addition to major widenings on nearly every existing gateway and the construction of several new surface gateways. However, even with these costly improvements, the gateway capacity at the screen line can only be increased enough to equal the demand that is expected by the year 1980. The expressways alone cannot solve the problem. If future traffic is to have access through the screen line to the important central business district, all existing surface radial streets must not only be kept open across the expressway lines but also greatly improved.

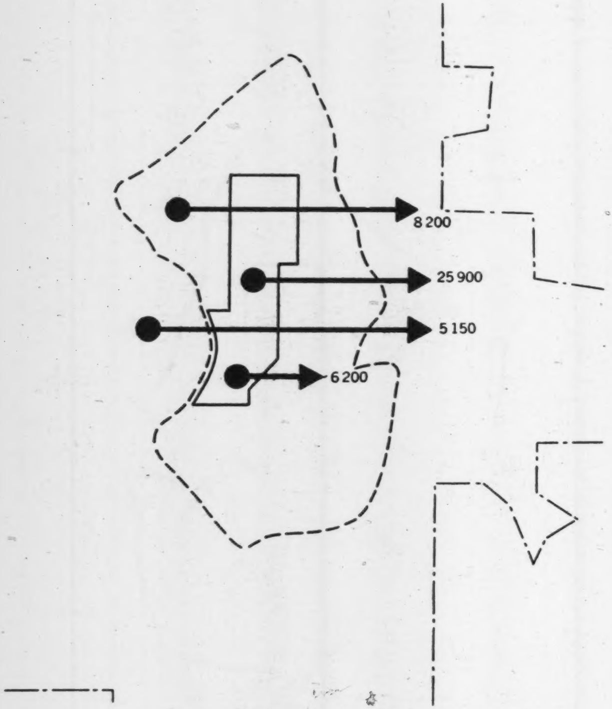

Fig. 10.—Conservative Estimate, 1980 Downtown Vehicle Load

Effect on Downtown Section

Connecting Expressways to the Downtown Streets.—After capacity has been increased across the screen line en route to the downtown section, the problem becomes one of unloading the high-capacity expressways onto low-capacity downtown streets. This must be done without hampering the use of the downtown streets by traffic from the surface radial streets which feed the downtown section. There are three distinct phases to this problem: (1) To determine the future traffic load downtown; (2) to arrange the downtown streets to provide the most efficient traffic flow pattern, and to determine the capacity of this arrangement; and (3) to design a system of ramps to provide the best possible ingress and egress for the expressways, meanwhile preserving the highest possible capacity on the downtown street system for feeding the radial streets leading from the downtown section through the critical screen-line barrier.

ESTIMATED 1980 DOWNTOWN TRAFFIC VOLUME

Boundaries.—Based on planning studies, the downtown section of 1980 is expected to cover a larger area than that which is now considered the downtown section. A cordon was thrown around this 1980 downtown section; the streets forming this cordon line are shown in Fig. 9.

The Estimated 1980 Demand.—In estimating the downtown traffic volume for the year 1980, consideration was given to the ability of the downtown section to grow and to provide parking space; an increased use of transit facilities, especially by all-day workers, was assumed; all reasonable assumptions regarding the bypassing of traffic not bound for the central district were used; and no adjustment was made for a change in driver habits due to the improved street system. These conditions tend to make the estimated demand of 45,450 vph conservative. The distribution of this estimated load is shown in Fig. 10.

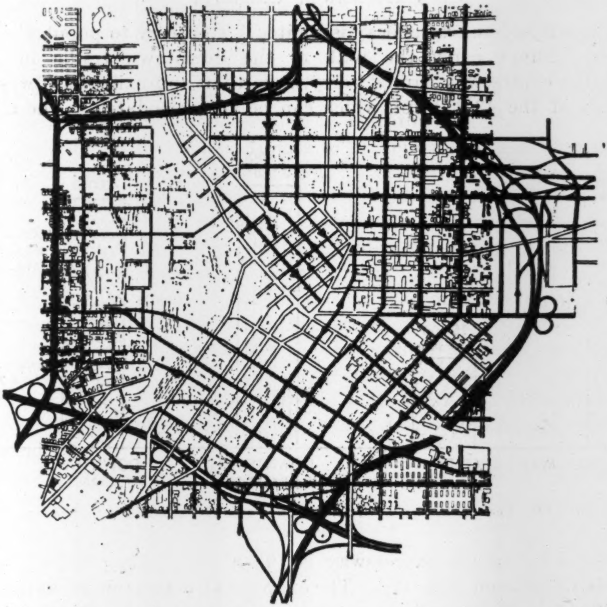

FIG. 11.—PROPOSED DOWNTOWN TRAFFIC PATTERN AND EXPRESSWAY RAMP SYSTEM

The Greatest Operating Capacity Downtown Is 43,050 Vph.—In an effort to obtain the greatest possible capacity from the downtown street system, one-way streets were planned with due consideration for transit needs; absence of parking regulations was assumed; major widenings were assumed on Memorial Drive, Edgewood Avenue, Bartow Street, and Magnolia Street; the Hunter Street viaduct was planned as a four-lane structure; and the connections of Mitchell Street to Hunter Street, Capitol Avenue to Piedmont Avenue, Peters Street to Garnett Street, Cain Street to Magnolia Street, and Baker Street to Luckie Street were assumed (Fig. 11). The highest practical capacity obtainable on the streets and expressways crossing the cordon line into the downtown section, even with all these improvements, is 43,050 vph. The expressways were assumed to be carrying 18,300 vph, and the surface streets the remaining 24,750 vph.

EXPRESSWAY CAPACITY

The capacity of an expressway is limited. Contrary to popular belief, the expressway cannot carry the bulk of the downtown traffic in Atlanta. Actually, the expressway cannot carry more than approximately two-fifths or 18,300 vph of the 43,050 vph which can be accommodated. The maximum possible capacity of the expressway is 19,500 vph. Its practical operating capacity is 15,600 vph (Fig. 12). The expressway load assumed in the analysis was 18,300 vph, which will be in excess of its practical operating capacity. Of these 18,300 vph, 15,000 vph were assumed to come from within the cordon area and 2,800 vph were assumed to be "through" traffic. It was estimated that this assumed load of 18,300 vph would result in an overload on the expressway northbound from the proposed downtown Piedmont Avenue ramp to Peachtree Road and on the Expressway (East) just east of Harris Street. It is believed that a maximum of 24,750 vph will be able to cross the cordon line on surface streets to bring the total capacity of streets crossing the cordon line to 43,050 vph (Fig. 12). It is also believed that the traffic representing the difference between the demand of 45,450 vph and the capacity of 43,050 vph can filter around the cordon area on minor streets. Some of the 45,450 vph is through traffic which will use streets in the cordon area as long as they

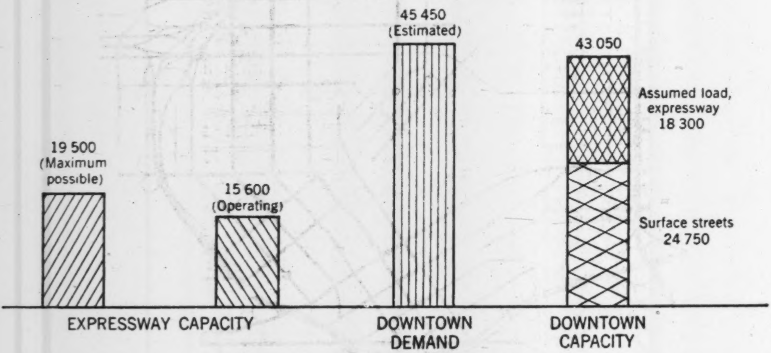

FIG. 12.—PROPORTIONING OF TRAFFIC BETWEEN EXPRESSWAY AND STREETS

are available but which could use bypass streets. Although all the major streets will be loaded to capacity with radial traffic from the cordon area, some minor streets will be available for bypass traffic.

RAMP-SYSTEM DESIGN

A ramp system designed to permit maximum use of surface streets will control downtown traffic. A consideration of ramp construction costs as against the service factor will prove that adequate ramps can be provided without seriously impairing the capacity of the surface feeder-street system (Fig. 11). The ramp design should (1) provide the best possible service for the expressways and (2) preserve sufficient capacity in the local streets to permit the growth of the downtown section. The following should be included as basic principles in the design of the downtown expressway ramps in Atlanta:

a. The ramp capacity should be balanced against the expressway capacity.

b. The ramps should be so located with reference to origin-and-destination information as to minimize travel on local downtown streets.

c. Ramps should be placed in pairs to prevent unnecessary circulation on downtown streets. If an unloading ramp is justified, a corresponding loading ramp of equal capacity is needed to return the movement to the expressway in the direction from which it came. Ramps are less expensive than street widenings in the downtown section. Too wide a separation of complementary ramps causes unnecessary use of surface streets.

d. Ramps should not be connected to streets feeding the important surface radial system. Ramps tend to fill the street to capacity with expressway traffic and to make it useless as a feeder for surface traffic beyond the ramp.

e. In the future it may be advantageous to make Whitehall Street and Forsyth Street a pair of one-way streets with Whitehall Street northbound and Forsyth Street southbound. The ramp design should not prevent this arrangement.

f. Capitol Avenue and Washington Street also may be possible future one-way streets, with Capitol Avenue northbound and Washington Street southbound. The ramp design should provide for this arrangement.

CONCLUSIONS

A "team" of public and private agencies is working on the "Atlanta Plan." Immediate action is indicated in order to relieve existing critical congestion, and an aggressive, large-scale, street-improvement program appears essential to the growth of Atlanta. Expressways are urgently needed as the "backbone" for an improved radial and added circumferential surface street system. However, the existing feeder streets for the downtown section must not be cut off by the expressway roadway or by expressway traffic at ramp connections. Ramps should be so located as to provide maximum service with a minimum of circulation on downtown streets. The most efficient possible traffic flow pattern should be adopted for the streets of the downtown section including provision for efficient transit routing.

AMERICAN SOCIETY OF CIVIL ENGINEERS
Founded November 5, 1852
TRANSACTIONS

Paper No. 2855

DISCHARGE COEFFICIENTS FOR SPILLWAYS AT TVA DAMS

By Kenneth W. Kirkpatrick,[1] A. M. ASCE

Synopsis

Spillway ratings derived from model studies have been used in the preparation of spillway rating tables for the Tennessee Valley Authority dams. As a result of these studies, discharge coefficients for eleven of the Tennessee Valley Authority dams are given in this paper. Coefficients for both submerged and free discharge conditions are presented for discharges over standard spillway crests, irregular spillway crests, and a vertical-lift spillway gate. Discharge coefficients for Tainter gates placed on curved spillway crests are also given for various gate openings under free discharge conditions. In addition, data on the effect of model scale on the discharge coefficient and the effect of closing adjacent spillway bays and gates are presented. The coefficient relationships are shown in a form that may be used by designers as a guide in making determinations of the discharges for future spillways.

Notation

The letter symbols adopted for use in this paper are defined where they first appear, in the illustrations or in the text, and are arranged alphabetically, for convenience of reference, in the Appendix.

Introduction

The Tennessee Valley Authority (TVA) operates a system of nine dams on the Tennessee River and twenty-three on the tributary rivers. The successful operation of such a system requires accurate discharge ratings for each structure. Although enough water is seldom available to make complete ratings for most spillways from measurements conducted on the prototype structure, ratings can be determined from scale model tests. Therefore, the necessary ratings for the TVA spillways have been determined by this means. Model studies have been made at the TVA Hydraulic Laboratory at Norris, Tenn.,

---

Note.—Published, essentially as printed here, in February, 1955, as *Proceedings-Separate No. 626*. Positions and titles given are those in effect when the paper was approved for publication in *Transactions*.

[1] Hydr. Engr., Hydr. Lab., Tennessee Valley Authority, Norris, Tenn.

on nine different spillway crest shapes equipped with three types of control gates.

Seven of the nine crests were curved sections which approximated the shape of the lower nappe of a sharp-crested weir. The other two crests were flat. The two flat-crested weirs and one of the curved crests were equipped with double-leaf vertical lift gates. Five of the curved crests were equipped with Tainter gates and the other with vertical lift gates.

Data Presented.—Data are presented for the following conditions: (1) Free, ungated flow through a series of spillway bays; (2) submerged, ungated flow through a series of spillway bays; (3) free, ungated flow through a series of spillway bays, with adjacent bays fully open or closed; (4) free flow over a vertical lift gate; (5) submerged flow over a vertical lift gate; (6) flow under a series of Tainter gates set with equal openings; and (7) flow under a series of Tainter gates with adjacent gates closed.

Data are also presented to show the effect of model scale for the condition of free, ungated flow through a series of spillway bays.

General Model Arrangement.—The models were tested in flumes either 3.5 ft wide or 8 ft wide. Models installed in the smaller flume usually consisted of a reproduction of three of the prototype spillway bays. In the larger flume five or six spillway bays were reproduced. Each of these flumes was provided with glass panels for observation purposes. The models placed in the larger flume were constructed at scale ratios of from 1:28.72 to 1:50 with a ratio of approximately 1:35 generally used. Those tested in the smaller flume were built at scale ratios of 1:50, 1:100, and 1:200.

The models were usually provided with concrete crests and concrete piers to insure dimensional stability. Half piers were constructed on the ends of each model. If the model did not completely fill the flume one side was placed against the glass side of the flume and the other against a false wall. The river bed upstream and downstream from the model was reproduced at the elevation of the prototype river bed. Suitable baffling was provided to obtain a uniform distribution of flow in the spillway approach channel. The tailwater level was controlled at the end of the flumes by means of slat gates. Model discharges were determined from readings of a carefully calibrated diaphragm orifice located in the water supply line.

Headwater heights were measured at two piezometers at distances equal to approximately 5 and 8 times the design head upstream from the spillway crest. Tailwater heights were obtained at 2 piezometers at distances equal to approximately 9 and 12 times the design head downstream from the spillway crest—in all cases, sufficiently far enough downstream to eliminate the effect of the spillway apron.

In most studies the headwater and tailwater levels were determined by means of hook gages reading to 0.001 ft. For the 1/200-scale model the heads were measured with a micrometer point gage reading to 0.0001 ft.

Discharge Equations.—The model data have been reduced by the use of two commonly accepted discharge equations. For both free and submerged flow over a spillway crest the equation,

$$Q = C\,L\,H^{3/2} \qquad (1)$$

was used, in which Q is the discharge in cubic feet per second, C is the coefficient of discharge determined from the model tests, L is the length of the crest, and H is the total head as shown in Fig. 1(*a*). Use was made of the same equation in the reduction of the data for free and submerged flows over a vertical gate with D, H, d, and P (Fig. 1(*a*)) being measured from the top of the gate.

For flow under a gate the equation for a rectangular orifice under low head,

$$Q = C\,L\,[H^{3/2} - (D_1 + h)^{3/2}] \ldots\ldots\ldots\ldots\ldots\ldots\ldots (2)$$

was used, in which D_1 is the depth of water to the bottom of the gate as defined in Fig. 1(*b*) and h is the approach velocity head.

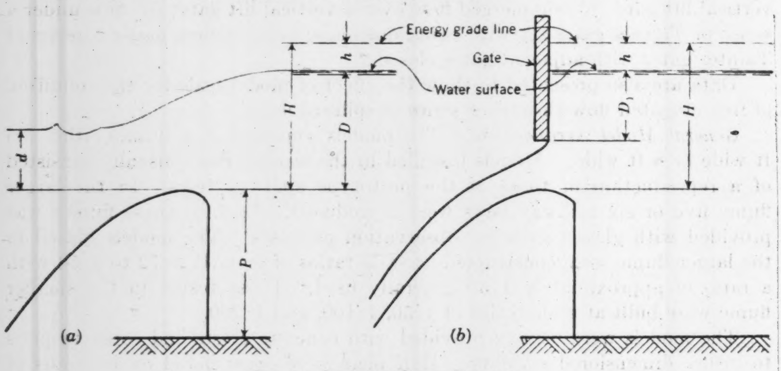

FIG. 1.—SPILLWAY-CREST DIAGRAM

FREE-DISCHARGE COEFFICIENTS, FLOW OVER SPILLWAY CRESTS

It is common practice for engineers to design spillway crests to approximate closely the shape of the lower portion of a jet issuing from a sharp-crested weir, and this type of crest is designated a standard crest.[2] Because the shape of the jet changes with the head on the weir, some particular head must be used for each design. This head for which a particular crest is designed is termed the design head. At this head, pressures approximating atmospheric pressure are developed at the spillway surface. At smaller heads, pressures are greater than atmospheric. Seven of the nine TVA crests for which data are available approximate standard crests in shape whereas the other two crests, which are flat, do not. Fig. 2 shows the basic details and dimensions of each of these crests. Fig. 3 presents the coefficient data obtained on the crests of Fig. 2. Pertinent design data concerning each crest, together with the scale to which each was modeled, appear in Table 1. Eleven spillways are also listed in Table 1. Two pairs of these, the Ocoee No. 3-Apalachia set, and the Douglas-Watts Bar set, both in Tennessee, have crest shapes that are identical within the pair but which were tested for different values of the approach depth, P.

---

[2] "Hydroelectric Handbook," by W. P. Creager and J. D. Justin, John Wiley & Sons, Inc., New York, N. Y., 2d Ed., 1950.

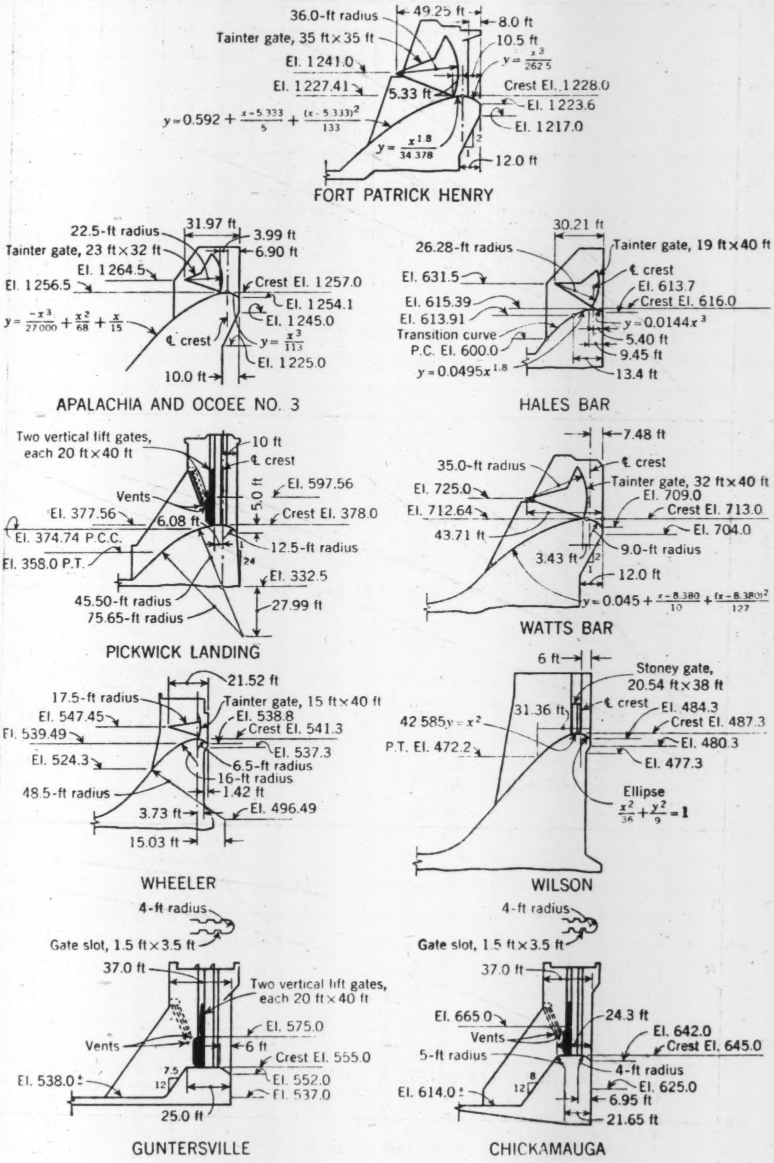
36.0-ft radius
49.25 ft
8.0 ft
Tainter gate, 35 ft × 35 ft
10.5 ft
El. 1241.0
$y = \frac{x^3}{262.5}$
El. 1227.41
5.33 ft
Crest El. 1228.0
El. 1223.6
$y = 0.592 + \frac{x - 5.333}{5} + \frac{(x - 5.333)^2}{133}$
El. 1217.0
$y = \frac{x^{1.8}}{34.378}$
2
1
12.0 ft
FORT PATRICK HENRY
22.5-ft radius
31.97 ft
3.99 ft
Tainter gate, 23 ft × 32 ft
6.90 ft
El. 1264.5
El. 1256.5
Crest El. 1257.0
El. 1254.1
$y = \frac{-x^3}{27{,}000} + \frac{x^2}{68} + \frac{x}{15}$
El. 1245.0
℄ crest
$y = \frac{x^3}{113}$
El. 1225.0
10.0 ft
APALACHIA AND OCOEE NO. 3
30.21 ft
26.28-ft radius
Tainter gate, 19 ft × 40 ft
El. 631.5
℄ crest
El. 613.7
El. 615.39
Crest El. 616.0
El. 613.91
$y = 0.0144x^3$
Transition curve
5.40 ft
P.C. El. 600.0
9.45 ft
$y = 0.0495x^{1.8}$
13.4 ft
HALES BAR
Two vertical lift gates, each 20 ft × 40 ft
10 ft
℄ crest
Vents
5.0 ft
El. 597.56
El. 377.56
Crest El. 378.0
6.08 ft
El. 374.74 P.C.C.
12.5-ft radius
El. 358.0 P.T.
1
24
El. 332.5
45.50-ft radius
27.99 ft
75.65-ft radius
PICKWICK LANDING
7.48 ft
35.0-ft radius
℄ crest
El. 725.0
Tainter gate, 32 ft × 40 ft
El. 709.0
El. 712.64
Crest El. 713.0
El. 704.0
43.71 ft
9.0-ft radius
3.43 ft
2
1
12.0 ft
$y = 0.045 + \frac{x - 8.380}{10} + \frac{(x - 8.380)^2}{127}$
WATTS BAR
21.52 ft
17.5-ft radius
Tainter gate, 15 ft × 40 ft
El. 547.45
El. 538.8
El. 539.49
Crest El. 541.3
El. 537.3
El. 524.3
6.5-ft radius
16-ft radius
48.5-ft radius
1.42 ft
3.73 ft
El. 496.49
15.03 ft
WHEELER
6 ft
Stoney gate, 20.54 ft × 38 ft
31.36 ft
℄ crest
El. 484.3
$42.585y = x^2$
Crest El. 487.3
El. 480.3
P.T. El. 472.2
El. 477.3
Ellipse
$\frac{x^2}{36} + \frac{y^2}{9} = 1$
WILSON
4-ft radius
Gate slot, 1.5 ft × 3.5 ft
37.0 ft
Two vertical lift gates, each 20 ft × 40 ft
El. 575.0
Vents
6 ft
Crest El. 555.0
7.5
12
El. 538.0±
El. 552.0
El. 537.0
25.0 ft
GUNTERSVILLE
4-ft radius
Gate slot, 1.5 ft × 3.5 ft
37.0 ft
El. 665.0
24.3 ft
Vents
El. 642.0
Crest El. 645.0
5-ft radius
4-ft radius
8
12
El. 625.0
El. 614.0±
6.95 ft
21.65 ft
CHICKAMAUGA

FIG. 2.—TVA SPILLWAY CRESTS (DATA IN FIG. 3)

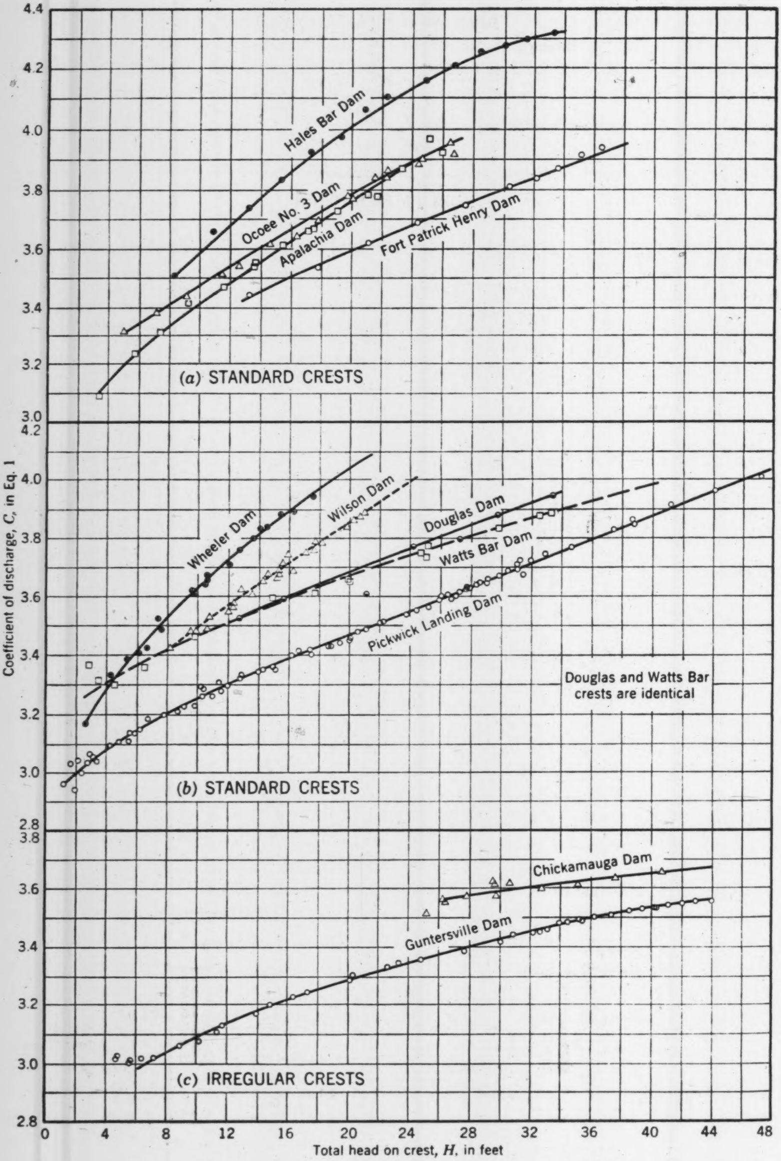

FIG. 3.—DISCHARGE COEFFICIENTS FOR FREE FLOW OVER THE SPILLWAY CRESTS OF FIG. 2

The accuracy of the data is evidenced by the plotting of the data points in Fig. 3. Except in some cases at low heads, the deviation of any plotted point from the coefficient curve does not exceed 0.5%.

Standard Crests.—It has been shown by various authors that the discharge coefficients for all standard crests can be related to each other and that, conversely, the coefficients to be used for a new design can be taken from previous test data.[2,3,4,5] Unfortunately, in most crest designs, due to other design considerations, it is necessary that the shape be varied from the standard form. Nevertheless, satisfactory coefficients can be obtained as sufficient data are now available on a range of crest shapes. By comparison of crest shapes designers may select a coefficient for any particular crest.

Dimensionless plotting provides a means for comparison of crest shapes. This method is used in Fig. 4 on which seven TVA crests which closely approximate standard crests are shown by the solid lines, with the dashed line representing a standard crest shape.[3] The horizontal coordinate, x, and the vertical coordinate, y, of the crest curve have been divided by the design head, H_o.

TABLE 1.—DESIGN DATA FOR ELEVEN MODELS OF TVA SPILLWAYS

Project	Model scale	Design head, H_o, in feet	Upstream depth, P, in feet	$\frac{H_o}{P}$	Pier nose radius, in feet
Hales Bar	1:34.76	18	32	0.56	3.00
Ocoee No. 3	1:28.72	23	67	0.35	3.00
Apalachia	1:28.72	23	97	0.24	3.00
Fort Patrick Henry	1:50	35	43	0.81	3.25
Wheeler	1:34.35	16.5	43	0.38	2.50
Wilson	1:39.4	19	75	0.25	4.00
Douglas	1:35	23.5	133	0.18	3.25
Watts Bar	1:35	23.5	52	0.45	3.25
Pickwick Landing	1:50	31.5	32	0.98	3.75
Chickamauga	1:50		20		4.00
Guntersville	1:50		18		4.00

The design head was determined by fitting the real and standard curves at the crest point ($x = 0$) and at the intersection of the curve with the upstream vertical face. These design-head values are presented in Table 1. The design-head discharge coefficients (C_o) determined from Fig. 3 are shown in Fig. 4.

The TVA crests all fairly closely approximate the standard curve from the upstream spillway face to a point somewhere downstream from the crest which was determined by the position of the gate seal. Below this latter point, the crest shape was modified to fit the trajectory of a jet issuing from under the gate when set at a small opening. The upstream face for a standard crest is vertical. The upstream face of the TVA crests, as shown in Fig. 4, deviates from the vertical. Other experimenters have established the fact that the shape of the upstream face generally has little influence on the discharge coefficient.[3]

---

[3] "Final Reports of Boulder Canyon Project," *Bulletin No. 3*, Part VI, Hydraulic Investigations, Bureau of Reclamation, U. S. Dept. of the Interior, Washington, D. C., 1947.

[4] "Engineering Hydraulics," edited by Hunter Rouse, John Wiley & Sons, Inc., New York, N. Y., 1950.

[5] "Discharge Coefficients for Irregular Overfall Spillways," by J. N. Bradley, *Engineering Monograph No. 9*, Bureau of Reclamation, U. S. Dept. of the Interior, Washington, D. C., 1952.

Fig. 4 indicates that the shape of the curve from the crest to a point somewhere in the neighborhood of $x/H_o = 0.5$ materially affects the coefficient. As the curve is raised above the standard curve, the coefficient is decreased. This can be seen by comparing the (y/H_o)-values at $x/H_o = 0.5$ with C_o. The comparative crests in Fig. 4 have been placed in the order of decreasing (Y/H_o)-values. No reasonable correlation of C_o with either upstream shape of H_o/P can be determined.

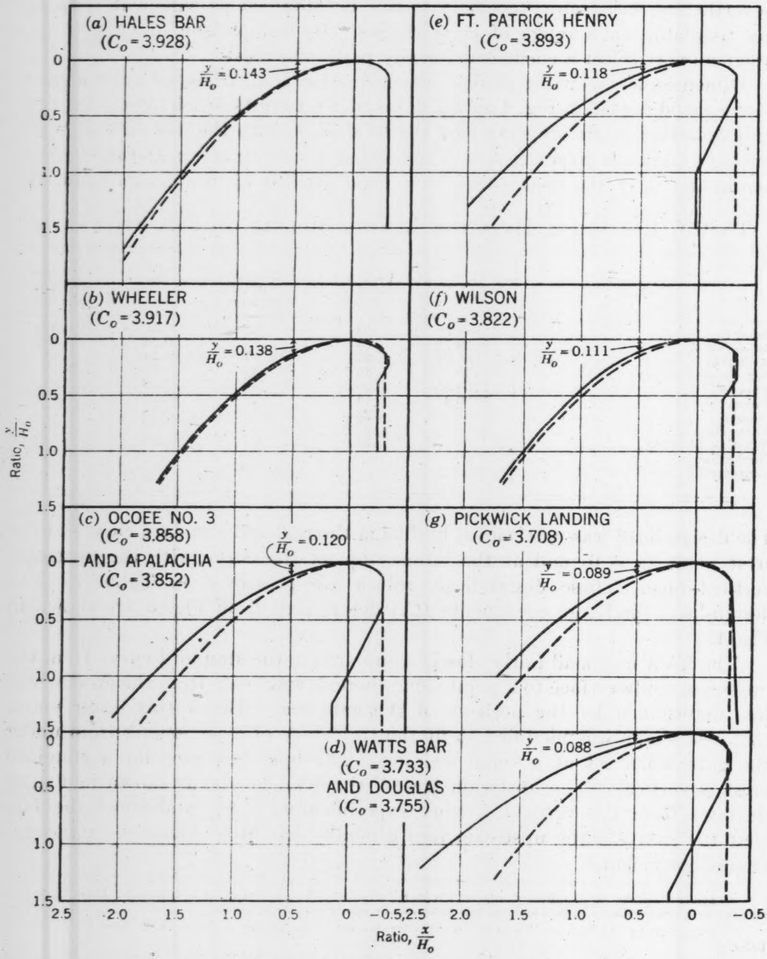

FIG. 4.—COMPARATIVE CRESTS (H_o/P SHOWN IN TABLE 1)

The relationships between the discharge coefficient and the ratio of any head to the design head, H/H_o, are shown in Fig. 5. In Fig. 5(*a*) the value of C is plotted against H/H_o for the four crests—Apalachia, Ocoee No. 3, Hales Bar (Tennessee), and Fort Patrick Henry (Tennesse)—that most closely follow the standard crest shape. The maximum variation of the individual points from the average curve for TVA crests is 0.5%. The standard-crest curve shown by the dashed line in Fig. 5 is that of W. P. Creager and J. D. Justin.[2] This curve is approximately 2% higher than the TVA curve. Fig. 5(*b*) is a dimensionless plot of the data from Figs. 3(*a*) and 3(*b*). The deviation of the points from the average curve is greater than in Fig. 5(*a*) because all crests are included, but for design purposes the curve should be useful. Actually, the

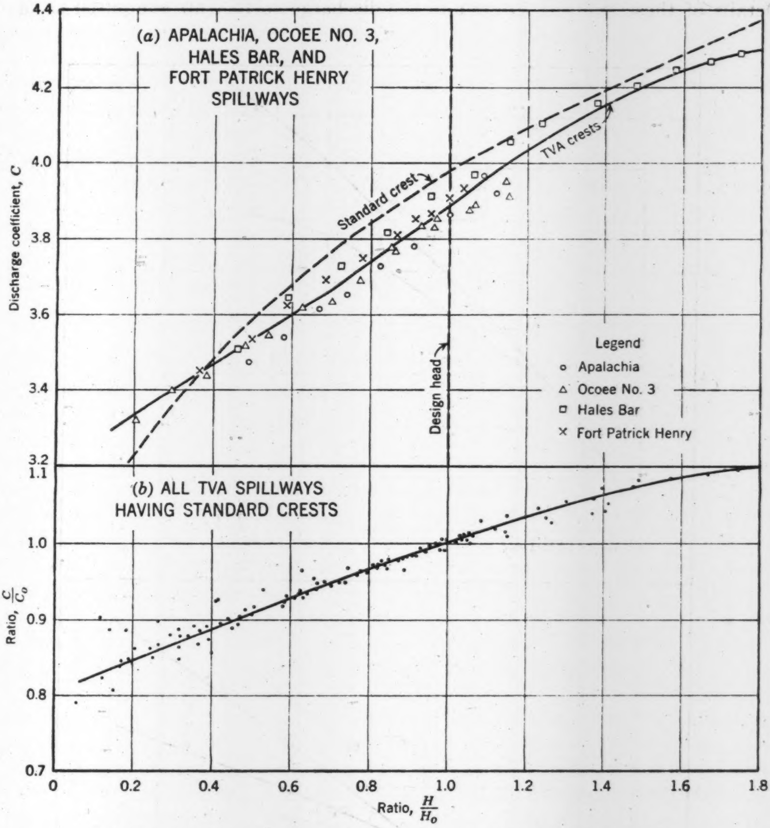

FIG. 5.—DISCHARGE COEFFICIENTS FOR SPILLWAYS HAVING STANDARD CRESTS

curve is more firmly established than it may appear because the curve itself obliterates several test points.

Irregular Spillway Crests.—The designation "irregular spillway crests" is used to distinguish between standard spillway crests and other crest forms. Only two of the TVA spillways, those at Chickamauga, Tenn., and Guntersville, Ala., have irregular spillway crests. Both are trapezoidal in cross section. Details of these spillway crests and the discharge coefficients computed using

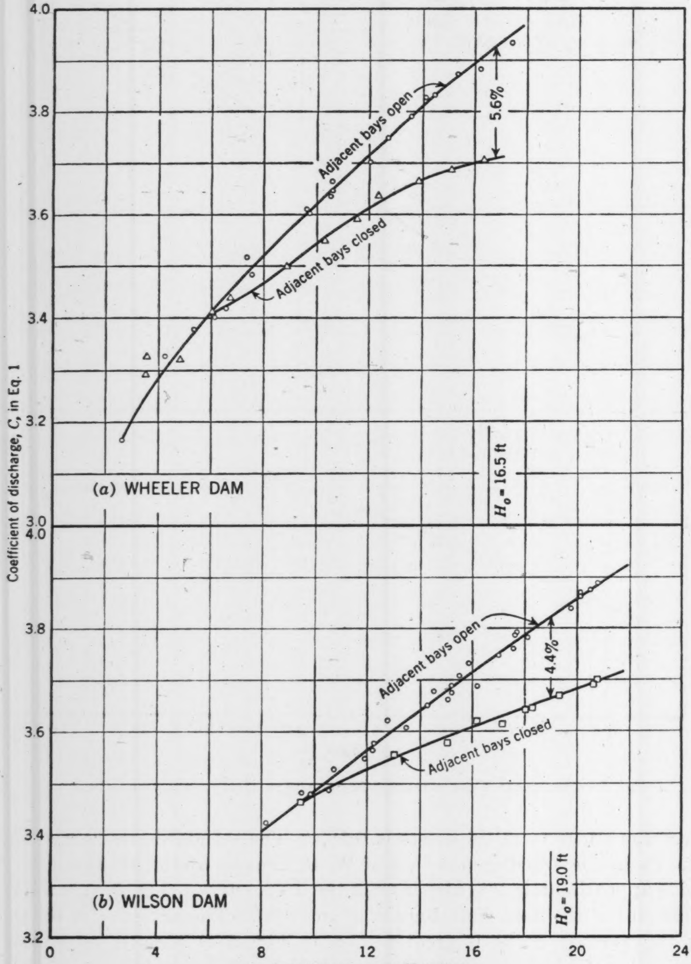

FIG. 6.—EFFECT OF OPERATION OF ADJACENT SPILLWAY BAYS

Eq. 1 from the model-study data are shown in Fig. 3(*c*). The two crests differ chiefly in the shape of the upstream and downstream edges of the crest and the height above the apron. Over the range of the tests of the Chickamauga spillway the coefficients are consistently from 3% to 5% greater than those for the Guntersville spillway. The additional height of the crest above the apron and the rounding of the near upstream edge of the Chickamauga crest would operate to increase the discharge coefficients.

The Effect of Operating Adjacent Spillway Bays.—In the TVA water-control operations, it is necessary to operate single spillway bays and groups of consecutive spillway bays. Because a greater contraction forms at a pier situated next to a closed bay, models of the Wilson and Wheeler spillways in Tennessee were tested with adjacent spillway bays open and closed to determine the difference in contraction effects at the piers.

Fig. 6 shows the head-coefficient relationships for the two conditions tested. The discharge coefficient at the design head was 5.6% higher at Wheeler Dam with adjacent bays opened and 4.4% higher at Wilson Dam than with these bays closed. These relationships show the importance of spillway pier contraction effects in spillway discharge determinations.

SUBMERGENCE DISCHARGE COEFFICIENTS FOR FLOW OVER SPILLWAY CRESTS

Chickamauga Dam, Guntersville Dam, Pickwick Landing Dam (Tennessee), and Watts Bar Dam are subject to submergence of the crest at periods of high discharge. To determine the effect of this submergence model tests were conducted by establishing a constant rate of discharge and varying the tailwater elevation to determine the relationship between the headwater and tailwater elevations. This procedure was repeated for several discharge rates covering the operating range at the dam.

Two flow conditions were observed in the model tests which are characterized as "plunging nappe" and "flowing nappe." In the condition of plunging nappe the discharge issuing from the spillway plunges down into the tailwater and appears to follow the boundary surface of the spillway.

In the condition of flowing nappe the flow is nearly horizontal, producing an undulating surface flow in the tailrace channel. The plunging nappe usually occurs with low submergence whereas the flowing nappe occurs with high submergence. When the headwater and tailwater head relationship at a constant rate of discharge was plotted for each series of tests, it was found that the change from plunging nappe to flowing nappe had no apparent effect on the discharge coefficient.

The results from these tests on the four spillways have been plotted in Fig. 7 in the dimensionless form, d/H, against C_s/C, in which d is the depth of submergence and H is the total head above the crest. The coefficient, C_s, was computed from Eq. 1 using the H-value for the submerged conditions; C was determined using the H-value for the free-flow condition.

No systematic variation of C_s/C could be determined for any variable except the (d/H)-ratio for any of the conditions tested. However, no relatively low discharges were tested because in practice the TVA installations can never be submerged at low discharges.

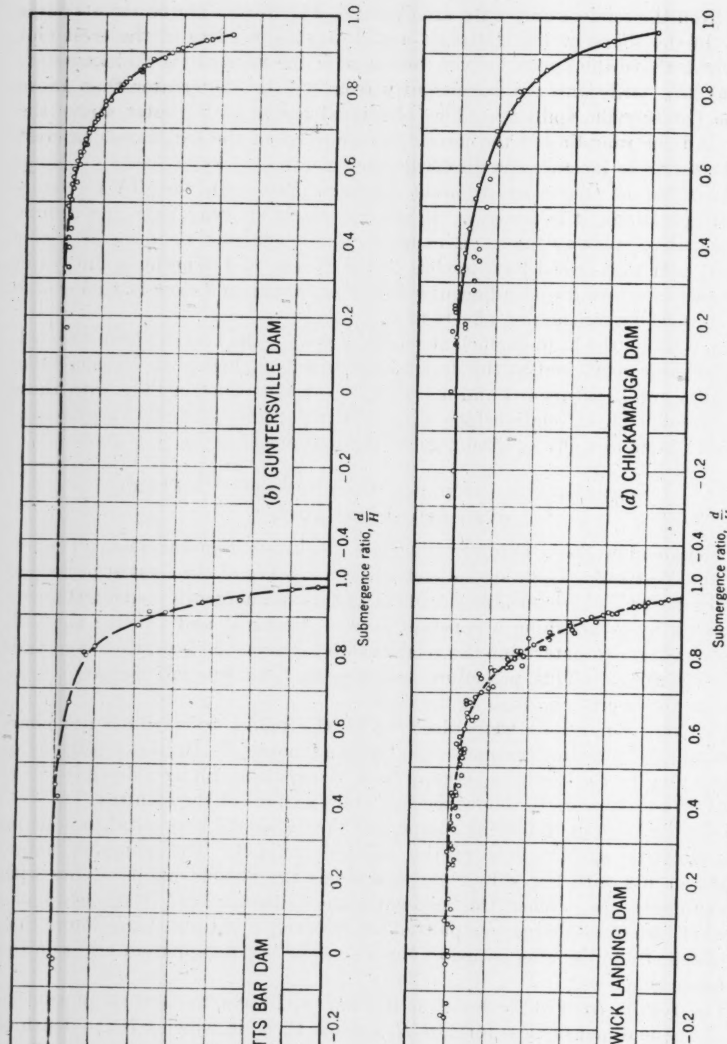

FIG. 7.—EFFECT OF SUBMERGENCE ON DISCHARGE COEFFICIENTS (*C*-VALUES FROM FIG. 3)

In Fig. 8 the four curves of Fig. 7 are shown on a single plot. Although the maximum spread between curves is about 10%, this is to be expected considering the wide range of crest shapes used in the tests.

FREE-DISCHARGE COEFFICIENTS FOR FLOW OVER VERTICAL LIFT GATES

The Pickwick Landing vertical lift gates are representative of this type of gate, which has been used on several TVA projects. In Fig. 9(*a*) are shown details of the lower spillway gate leaf. For heads greater than 2 ft, this gate is essentially a sharp-crested weir 40 ft long and 20 ft high with piers 7.5 ft thick at each end of the gate. Air intakes were installed in the sides of the piers just below the top of the gate to ventilate the underside of the nappe.[6] Model tests were conducted with the 1/50-scale, 3-bay spillway model.

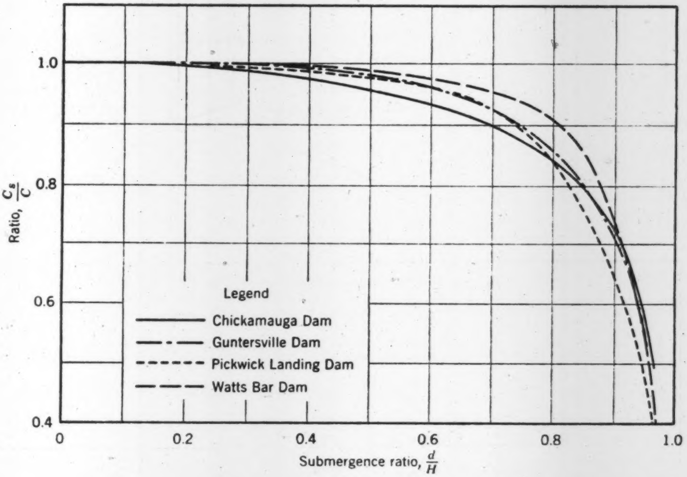

FIG. 8.—COMPARISON OF SUBMERGENCE EFFECTS FOR VARIOUS SPILLWAY CREST SHAPES

In Fig. 9(*b*) is shown the head-coefficient relationship for flow over the crest of the spillway gate. The coefficient, C, was computed from Eq. 1 using the top of the gate as crest elevation. The points define the head-coefficient relationship for heads between 3 ft and 28 ft. Each point was determined from the average of from 3 to 5 separate tests. A constant value of C equal to 3.428 is shown for heads in excess of 12 ft. For heads of from 12 ft to about 4 ft the model test curve shows a gradual rise in the coefficient, with an abrupt drop-off when the heads are approximately 4 ft and less. This curve takes the characteristic form for the coefficients of a sharp-crested weir, the rise and fall in the coefficient curve being due to the nappe clinging to the surface of the weir. This phenomenon is a function of the absolute head. Therefore, similarity between the model and prototype did not exist for prototype heads of less than 12 ft. Because the gate has a 10-in.-wide flat top, at low heads the prototype can be expected to exhibit discharge characteristics similar to those of the model. However, for a head in excess of about 2 ft the prototype can be expected to act similarly to a sharp-crested weir and to have a flat coefficient curve.

---

[6] "Aeration of Spillways," by G. H. Hickox, *Transactions*, ASCE, Vol. 109, p. 537.

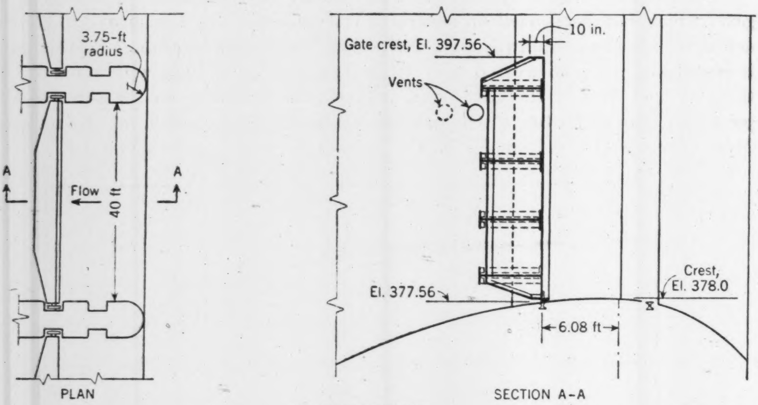

(*a*) GATE DESIGN

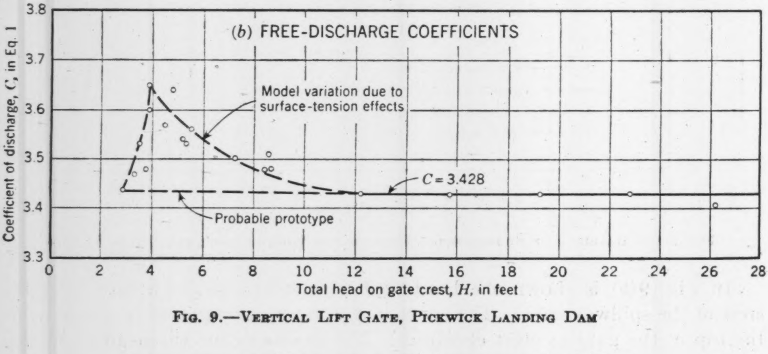

FIG. 9.—VERTICAL LIFT GATE, PICKWICK LANDING DAM

SUBMERGENCE DISCHARGE COEFFICIENTS FOR FLOW OVER A VERTICAL LIFT GATE

To obtain data on the effect of the submergence of flow over vertical-lift gates, model tests were conducted in a manner similar to that used in determining submergence effects on spillway crests. The coefficient, C_s, was computed from Eq. 1 in a manner similar to that used for the spillway crest data but using the top of gate as the crest elevation. Fig. 10 shows a plot of the headwater-tailwater relationships that have been determined. The data presented in Fig. 10 represent the rating of a three-bay, 1/50-scale model of the Pickwick Landing Dam. The total equivalent prototype crest width was

117.8 ft. The discharge was for three spillway bays. These curves illustrate the characteristic flow phenomena associated with this type of gate. Each constant-discharge curve begins with a horizontal line where the head-discharge relationship is not affected by the tailwater level. Just before the tailwater elevation reaches the gate crest level there is a drop in the headwater level for an increase in the tailwater level. Observations of the model operation showed that at this point the air vents, located in the sides of the piers just below the crest of the spillway gate, became submerged by the tailwater, reducing the contraction of the lower nappe issuing from the gate crest. The

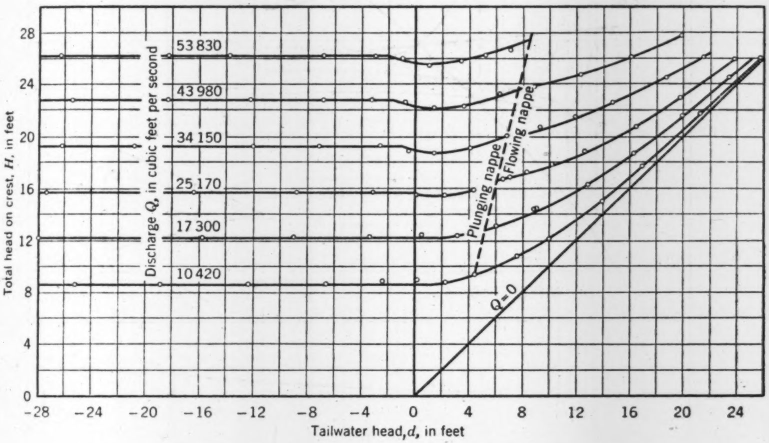

FIG. 10.—HEADWATER-TAILWATER RELATIONS FOR FLOW OVER A VERTICAL LIFT GATE (PROFILE SKETCH IN FIG. 11)

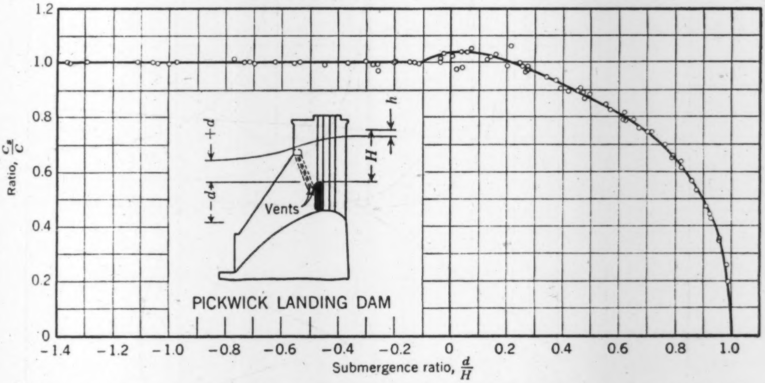

FIG. 11.—SUBMERGENCE EFFECT FOR FLOW OVER A VERTICAL LIFT SPILLWAY GATE ($C = 2.428$)

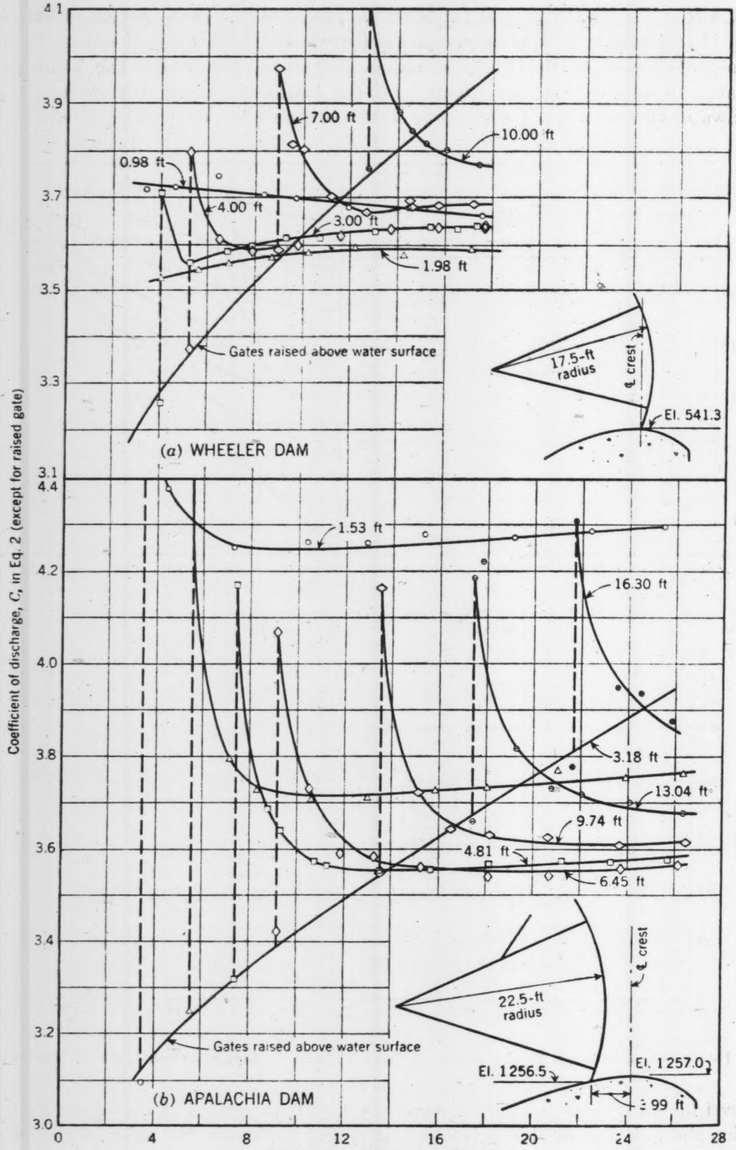

FIG. 12.—TAINTER-GATE SPILLWAY DISCHARGE COEFFICIENTS (DIMENSIONS ON CURVES ARE GATE OPENINGS)

discharge over the gate was thus increased with a consequent lowering of the headwater level.

The flow conditions of plunging nappe and flowing nappe, previously described, also occurred in this type of flow. In this case the change from one to the other is apparent in the data. The dashed line in Fig. 10 indicates the approximate location of the change. At these points the curves show a definite discontinuity in shape. The data of Fig. 10 can be reduced in coefficient form to the single-curve representation shown in Fig. 11. In this illustration, a constant value of C, equal to 3.428, was used in computing the ratio of C_s/C.

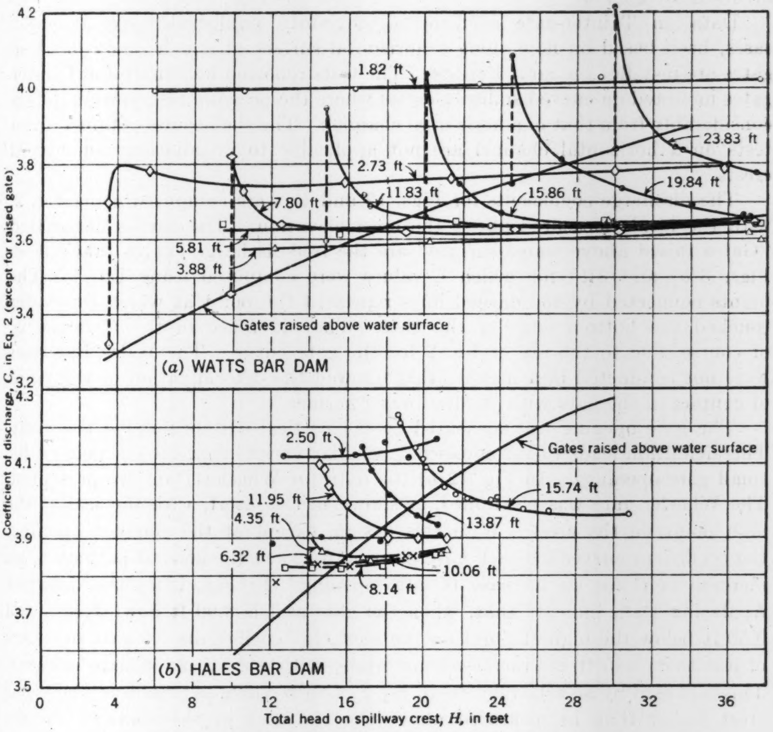

FIG. 13.—TAINTER-GATE SPILLWAY DISCHARGE COEFFICIENTS (DIMENSIONS ON CURVES ARE GATE OPENINGS)

DISCHARGE COEFFICIENTS FOR FLOW UNDER TAINTER GATES

The flow under Tainter gates mounted on curved crests is controlled by the geometry of three interrelated variables—the crest shape, the gate, and the gate setting. The major factors which influence the discharge relationships are the position of the gate seal point with respect to the highest point of the spillway crest and the curvature of the upstream face of the gate. In obtaining the model data on the various TVA Tainter-gate installations no attempt has been made to determine the quantitative effect of these factors taken individually. The data presented in Figs. 12 and 13 for the gate settings at Wheeler Dam, Apalachia Dam, Watts Bar Dam, and Hales Bar Dam are not, therefore, applicable to other installations unless the several variables involved are similar.

Data on Tainter-gate coefficients previously published have, in most cases, been based on flow along a horizontal surface although many of these gates are installed on curved crests. The tests reported herein are for Tainter gates mounted on curved spillway crests where the pressure distribution differs considerably from that in a horizontal channel. The coefficients obtained from tests on a horizontal channel are not applicable to installations on curved crests.

The discharge coefficients for Figs. 12 and 13 were computed using Eq. 2, with the heads measured above the crest elevation. The curves designated "Gates raised above water surface" are the free-discharge curves taken from Figs. 3(*a*) and 3(*b*) for which C-values were computed using Eq. 1. The points connected by the dashed lines represent the point at which the water touched the bottom edge of the gate. The difference in the C-values is, of course, due to the use of Eq. 2 for the gate curve. The Hales Bar tests were not conducted in a manner that allowed the determination of the point of contact of the gate with the free water surface.

The gate opening was measured as the vertical distance above the crest. This definition leads to the somewhat peculiar variation in the coefficients for small gate openings. In Fig. 12(*a*) the data for Wheeler Dam are presented. The Wheeler gate was positioned, as shown in the insert, with the seal at the high point on the crest. With this design, except at the smallest opening, the coefficient curves for each gate position followed the general pattern of an increase in C for an increase in gate opening. In Fig. 12(*b*) the data for Apalachia Dam indicate that, when the gate seal is 3.99 ft downstream and 0.50 ft below the highest point on the crest, the coefficients for gate openings of less than 6.45 ft are increased materially with a decrease in gate opening. This is caused by an arbitrary use in Eq. 2 of an H-value as measured above the crest rather than as measured above the elevation of the spillway surface below the gate. Thus, although the H-value is consistently too small at the smaller gate openings, the effect becomes more appreciable and results in the increase in C.

TAINTER-GATE DISCHARGE COEFFICIENTS WITH ADJACENT GATES OPENED OR CLOSED

The results of tests on the six-spillway-bay model of Wheeler Dam with one gate in operation and with six gates in operation are shown in Fig. 14. In operating with all six gates the contraction effect of the end piers was the same as that for the intermediate piers because the model was constructed with half piers against the sidewalls of the flume. This operation thus represented the case in which all adjacent bays are open.

EFFECT OF MODEL SCALE ON FREE-DISCHARGE COEFFICIENTS

In developing discharge ratings for prototype structures from model data, it is important that the scale at which the model is built be such that the coefficients determined are applicable to the prototype structure. One author has presented data to indicate that with an increase in the model size the discharge coefficients increase.[7] To study this relationship, a series of precise tests was made at the TVA Hydraulic Laboratory under the joint sponsorship of the American Society for Engineering Education, the University of Tennessee (Knoxville) and the TVA.[8] In this study three models of Pickwick Landing spillway were constructed to scales of 1:50, 1:100, and 1:200. Each model consisted of a reproduction of three spillway bays. The shape of the spillway crest and the piers of Pickwick Landing Dam are shown in Figs. 2 and 9(*a*). Similar techniques were used in all tests with one exception. Hook gages reading to 0.0001 ft were used for the 1/200-scale

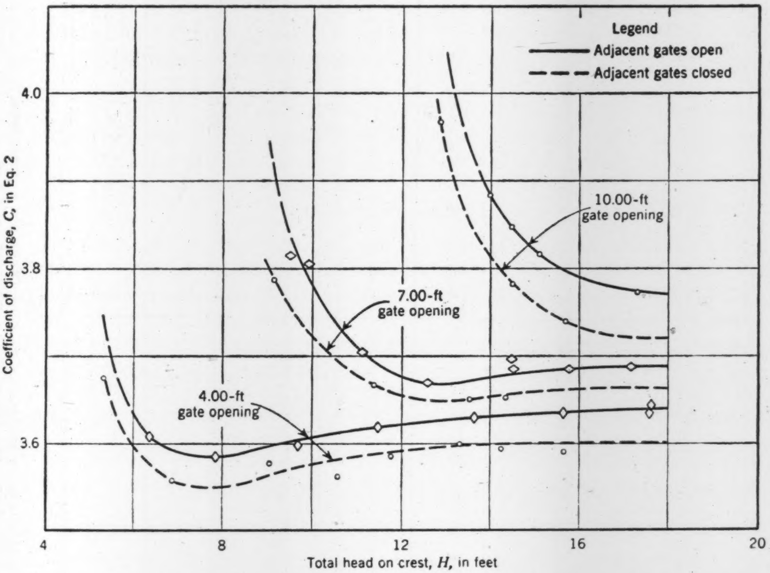

FIG. 14.—TAINTER-GATE DISCHARGE COEFFICIENTS, *C*, WHEELER DAM

---

[7] "Überfallversuche in Berschiedener Modellgrosse," by F. Eisner, The Prussian Experiment Station for Hydraulic Structures and Shipbuilding, Berlin, 1933.

[8] "A Study of the Effect of Model Size on Spillway Coefficients," by C. R. Ownbey, thesis presented in 1949 to the University of Tennessee at Knoxville, in partial fulfilment of the requirements for the degree of Master of Science.

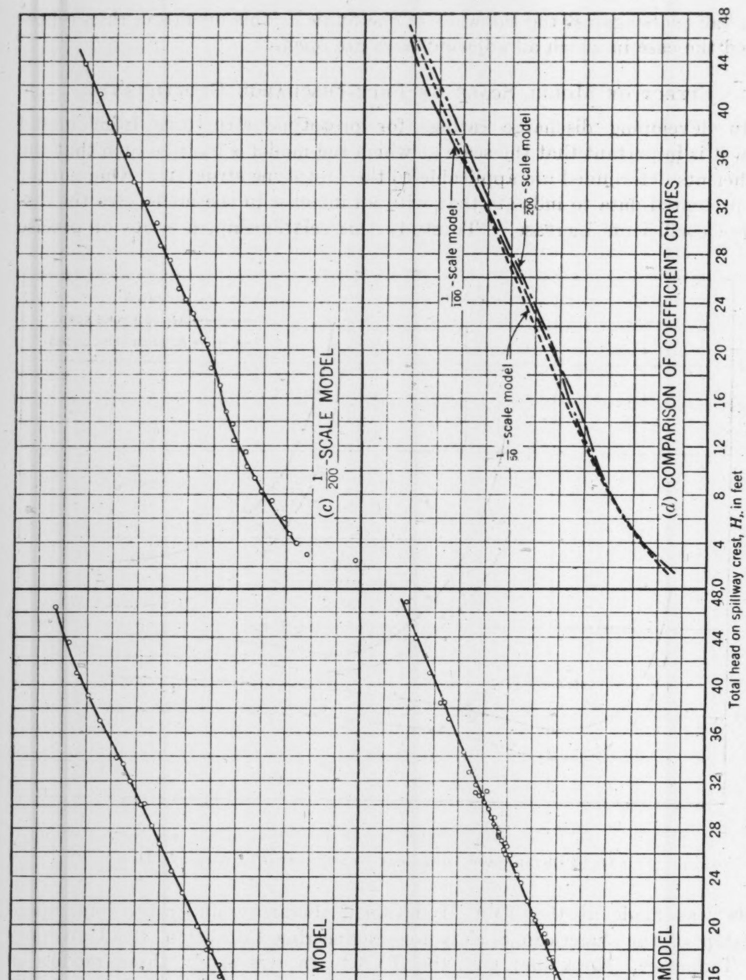

FIG. 115.—EFFECT OF MODEL SCALE ON DISCHARGE COEFFICIENTS, FLOW OVER PICKWICK LANDING SPILLWAY CREST

tests, and gages reading to 0.001 ft were used in the 1/50-scale tests and 1/100-scale tests.

Discharge coefficients for free flow over the crest of each model are shown in Figs. 15(*a*), 15(*b*), and 15(*c*). The coefficients of discharge were computed using Eq. 1. Each curve was drawn through the average of the plotted points.

A comparison of the three coefficient curves is shown in Fig. 15(*d*). The maximum spread of the curves does not exceed 2%. For prototype heads between 2 ft and 8 ft, the three coefficient curves are almost identical. At 13 ft the coefficient curve for the 1/100-scale model is approximately 1% lower than those for the 1/50-scale model and the 1/200-scale model. At 43 ft the curve for the 1/100-scale model is 1% higher than the data for the 1/50-scale model, and that of the 1/200-scale model is 1% lower than that of the 1/50-scale model. Because there is no consistent relationship between the coefficient curves, it is logical to conclude that these variations are merely the result of experimental error and that the model scale did not affect the stage-coefficient relationship. The close agreement of the coefficient curves at the three scales supports the validity of the preparation of prototype ratings based on model tests.

ACKNOWLEDGMENTS

The model studies were made under the general direction of Albert S. Fry, M. ASCE, chief of the Hydraulic Data Branch of the TVA, and under the immediate supervision of G. H. Hickox, M. ASCE, former head of the TVA Hydraulic Laboratory, and Rex A. Elder, M. ASCE, head of the TVA Hydraulic Laboratory. The assistance of Jack C. Jones, J. M. ASCE, is acknowledged in making the computations and preparing the illustrations in this paper. The writer also acknowledges the many helpful suggestions made by Mr. Hickox and Mr. Elder.

APPENDIX. NOTATION

The following letter symbols, adopted for use in the paper and for the guidance of discussers, conform essentially with American Standard Letter Symbols for Hydraulics (ASA-Z10.2-1942), prepared by a committee of the American Standards Association with Society representation, and approved by the Association in 1942:

C = coefficient of discharge for any head:
  C_o = coefficient of discharge for the design head;
  C_s = coefficient of discharge for submerged flow;
D = depth of flow above the crest, in feet (Fig. 1(*a*));
D_1 = depth, bottom of gate to water surface, in feet (Fig. 1(*b*));
d = submergence tailwater, measured above the crest, in feet (Fig. 1(*a*));
g = acceleration due to gravity, in feet per second per second;

H = total head above the crest, including the velocity head of approach, in feet (Fig. 1);
H_o = design head for a standard crest, including the velocity head of approach, in feet;
h = velocity head of approach, $v^2/2g$, in feet (Fig. 1);
L = spillway crest length, in feet;
P = depth of the approach channel, crest to river bed, in feet (Fig. 1(*a*));
Q = total discharge, in cubic feet per second;
v = average velocity of approach, in feet per second; and
X, Y = crest coordinates, in feet.

AMERICAN SOCIETY OF CIVIL ENGINEERS
Founded November 5, 1852
TRANSACTIONS

Paper No. 2856

WATER CONTROL IN CENTRAL AND SOUTHERN FLORIDA

By Harold A. Scott,[1] M. ASCE

Synopsis

This paper describes the historical efforts made to provide drainage and water control for central and southern Florida. Distribution and utilization of water in the comprehensive plan for flood control and multiple purposes are described. The need for a secondary water-control plan is emphasized.

Introduction

The area described in this paper (Fig. 1) lies south of an east-west line through Lake Harney (about 35 miles north of Cocoa) in Florida in the St. Johns River basin and east of the ridge that extends through Haines City and Sebring. The ridge divides the waters which flow into the Atlantic Ocean and those which flow into the Gulf of Mexico. Water-control problems are quite common throughout the area, although there are a few variations in topography and soil. The area consists of approximately 15,000 sq miles of groveland, pastures, rich agricultural lands, lakes, and marshlands. Elevations range from approximately 7 ft in the vicinity of Miami and 15 ft around Lake Okeechobee to 80 ft in the area of the headwaters of the Kissimmee River basin. (All stages and elevations throughout this paper refer to mean sea level data.) However, the lands of a large part of the area are extremely flat, and natural water courses are not common. Except for the St. Johns River, the Kissimmee River, Fisheating Creek, and a few minor streams, most of the water control is accomplished by man-made canals and drainage districts. Soils in the area vary from sand to peat with a small amount of marl. The areas with higher elevations in the St. Johns and Kissimmee River basins consist of sand mixed with a small amount of organic material in the upper 6 in. to 12 in. In the low areas and marshes, deposits of peat of thicknesses ranging to several feet are found. The Everglades is covered with a layer of peat of thickness ranging to approximately 15 ft at Lake Okeechobee and gradually diminishing to zero at

---

Note.—Published, essentially as printed here, in October, 1954, as *Proceedings-Separate No. 521*. Positions and titles given are those in effect when the paper was approved for publication in *Transactions*.

[1] Cons. Engr., Reynolds, Smith, and Hills, Jacksonville, Fla.

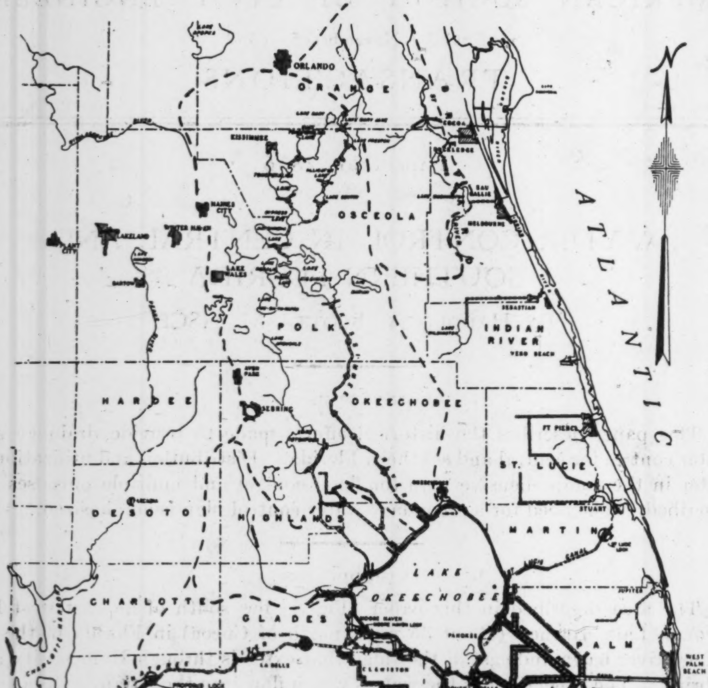
ATLANTIC
OCEAN
ORLANDO
ORANGE
KISSIMMEE
COCOA
OSCEOLA
HAINES CITY
WINTER HAVEN
LAKELAND
PLANT CITY
LAKE WALES
POLK
INDIAN RIVER
VERO BEACH
SEBASTIAN
MELBOURNE
EAU GALLIE
AVON PARK
SEBRING
HARDEE
OKEECHOBEE
FT PIERCE
ST. LUCIE
ARCADIA
DE SOTO
HIGHLANDS
MARTIN
STUART
LAKE OKEECHOBEE
JUPITER
CHARLOTTE
GLADES
MOORE HAVEN
PAHOKEE
PALM BEACH
WEST PALM BEACH
LAKE WORTH
BOYNTON BEACH
CLEWISTON
LA BELLE
FT MYERS
PROPOSED LOCK AND SPILLWAY
HENDRY
LEE
BOCA RATON
BROWARD
FORT LAUDERDALE
HOLLYWOOD
SOUTH NEW RIVER CANAL
ST. LUCIE CANAL
COLLIER
EVERGLADES
MIAMI
MONROE
DADE
HOMESTEAD
STRUCTURE 5A
LEGEND
PROPOSED SPILLWAY
PROPOSED PUMPING STATION
PROPOSED CULVERT
EXISTING LEVEE
EXISTING LEVEE TO BE ENLARGED
PROPOSED LEVEE
PROPOSED LEVEE WITH HIGHWAY ON CROWN
PROPOSED CANAL
EXISTING CANAL TO BE IMPROVED
EXISTING CANAL NOT TO BE IMPROVED
EXISTING LOCK AND DAM, SPILLWAY TO BE ENLARGED
EXISTING LOCK
EXISTING HURRICANE GATE
SCALE IN MILES

FIG. 1.—THE CENTRAL AND SOUTHERN FLORIDA COMPREHENSIVE PLAN

the edges. From the St. Lucie Canal south to the tip of Florida, a low ridge of sand, limestone, and marl forms a divide between the Everglades and drainage to the ocean. In the vicinity of Miami the area is underlain by porous limerock which makes the problem of water control quite difficult.

The mean annual rainfall is approximately 58 in. in Miami, 70 in. in West Palm Beach, and 51 in. in Kissimmee. The mean values are rather deceptive when studied for water-control purposes. For instance, 10 in. of rainfall during any summer month is quite common. Furthermore, 70% of the rainfall occurs from May to October, inclusive, which is considered the wet season. During the wet season, rainfall averages approximately 7 in. a month whereas the average is only from 2 in. to 3 in. for the remaining six dry months.

The mean annual temperatures vary from 75° F in Miami to 72° F in Kissimmee. The water areas provided by the lakes and marshes and the proximity of the Atlantic Ocean and the Gulf of Mexico temper the climate. Therefore, the extreme variations are not great or frequent. The highest summer temperatures seldom exceed 100° F; winter temperatures as low as 20° F have been experienced. The relative humidity is generally high throughout the area.

Evaporation and transpiration rates are very high throughout the area, particularly where large water surfaces are exposed. Estimates indicate an excess of the average annual rainfall over evaporation of about 9 in. in the vicinity of Lake Okeechobee and about 12 in. in the Everglades. Therefore, the effect of evaporation is a primary factor in water control.

Numerous floods have covered the central and southern Florida area. However, the 1947 flood was the most serious of record. The entire area was under water except for a few drainage districts, which were protected by dikes, and a few high areas in 15,000 sq miles. The water was not able to drain to the ocean because it was hindered by the low ridge parallel to, and 5 to 10 miles inland from, the coast. The storage areas are shallow and have a limited capacity. In 1948 a similar flood of lesser proportions covered the area, and again only those areas protected by dikes or having a higher elevation were saved from flood damage.

The area has suffered many severe droughts. The most notable droughts occurred in 1942–1943, and 1945. Those droughts did not occur through a lack of water because there were many lakes with an abundant supply, but because there was no distribution system to conduct the water to the areas of greatest need.

In view of the severe floods and droughts, the uneven distribution of rainfall, and the generally flat topography, the need for a sound water-control program becomes a paramount problem.

HISTORY

In order to understand better the value and need for a plan, it appears desirable to review briefly the history of drainage and water control in central and southern Florida. The first report on the Everglades was made in 1847–1848 by Buckingham Smith, an agent appointed by the Secretary of the Treasury of the United States. In 1881 the Board of Trustees of the Internal Improvement Fund contracted with Hamilton Disston and associates for the sale of 4,000,000 acres of land. Mr. Disston concentrated his efforts in the Caloosahatchee and Kissimmee River basins. The Everglades, approximately 2,862,080 acres of land, was conveyed to the State of Florida in 1903 under the Swamp and Overflow Land Grant Act of September 28, 1850. That area has presented one of the most difficult engineering problems.

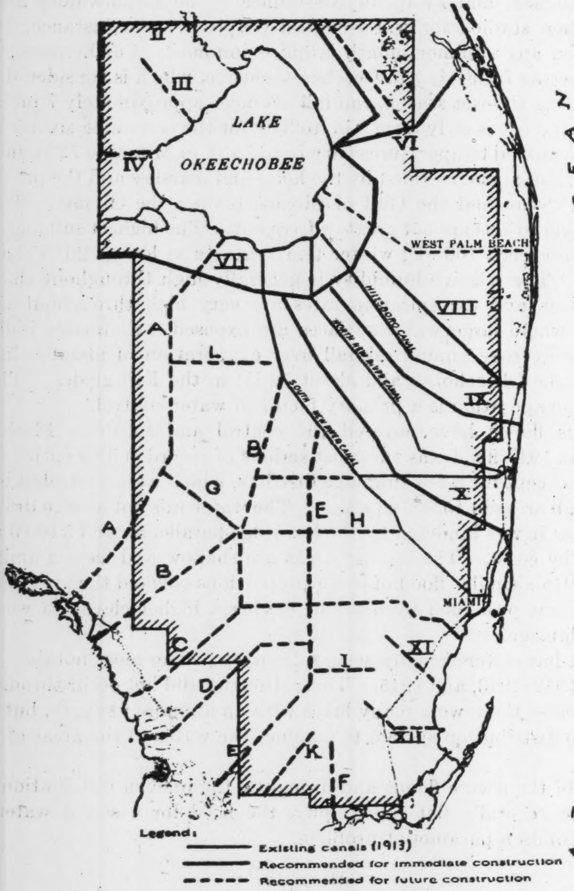
II
III
LAKE
OKEECHOBEE
IV
V
VI
WEST PALM BEACH
VII
VIII
HILLSBORO CANAL
NORTH NEW RIVER CANAL
SOUTH NEW RIVER CANAL
A
L
IX
B
G
X
E
H
A
B
MIAMI
C
XI
I
D
XII
E
K
F
OCEAN
ATLANTIC
Legend:
Existing canals (1913)
Recommended for immediate construction
Recommended for future construction

FIG. 2.—RECOMMENDATIONS OF THE FLORIDA EVERGLADES ENGINEERING COMMISSION

The state's drainage plan for the Everglades was started in 1905 when the Legislature adopted a drainage law providing for the establishment of boundaries of an Everglades Drainage District. Actual construction was started in 1906; by 1912, eight dredges were at work on canal excavation in the Everglades. In 1913 the Everglades Drainage District was created. The Board of Commis-

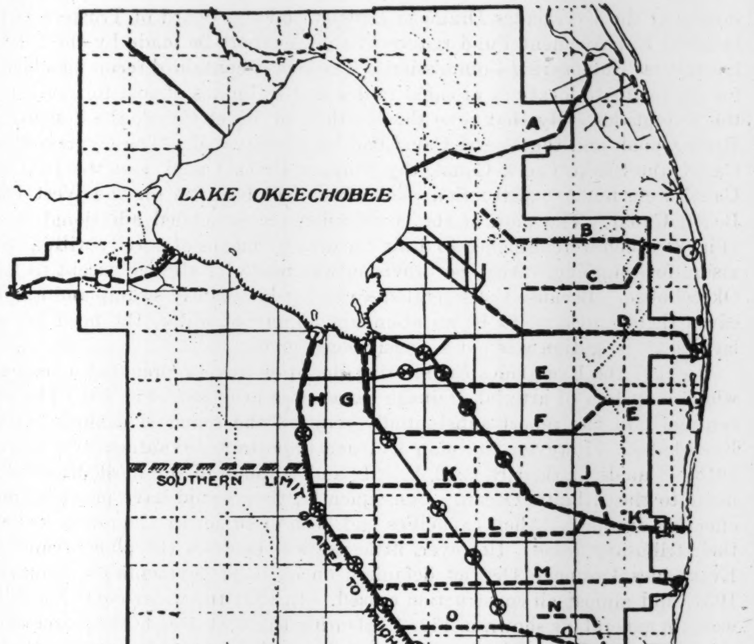
LAKE OKEECHOBEE
A
B
C
D
E
E
F
G
H
I
J
K
K
L
M
N
O
O
P
Q
R
S
T
U
SOUTHERN LIMIT OF AREA TO WHICH OUTLETS INDICATED WILL BE AVAILABLE
ATLANTIC OCEAN
CANAL
IMPROVEMENT OF EXISTING LOCK & DAM
CONTROL DAM
EARTH DAM
LEVEE
Scale Miles
5 0 5 10 15

FIG. 3.—PROPOSED WORKS OF THE EVERGLADES ENGINEERING BOARD OF REVIEW

sioners of the Everglades Drainage District and the Board of Trustees of the Internal Improvement Fund requested that a report be made by the Florida Everglades Engineering Commission. The report contained recommendations for approximate locations of canal routes and estimates of cost for reclaiming the Everglades. By that time the North New River Canal, the South New River Canal, and the Miami Canal had been excavated. The Cypress Creek Canal, the Snake Creek Canal, the Snapper Creek Canal, and the Hillsboro Canal were under construction; a contract had been let for the West Palm Beach Canal. The plan of the commission recommended additional canals (Fig. 2) which were designed to drain the area by means of gravity with no provision for pumping. Also, no provision was made for storage except in Lake Okeechobee. Because the Everglades was predominantly swampland and because there appeared to be an abundant supply of water, the need for any large-scale irrigation was not seriously considered.

In 1927 the Everglades Engineering Board of Review prepared a report in which a system of arterial drainage canals was proposed (Fig. 3). The plan contained in the report substantially reduced the scope of drainage of the Everglades. However, the plan had one important advantage over that of 1913. Canals marked B, C, E, F, J, L, and Q followed the most direct alinement to the Atlantic Ocean. Consequently, they would have provided more effective drainage if their capacities had been of sufficient magnitude to serve their tributary areas. However, little use was made of the plan because the Everglades Drainage District defaulted on its bond payments on January 1, 1931, and almost all construction ceased. In 1931 the water-control facilities were, in general, as shown in Fig. 4. During the next decade the works of the Everglades Drainage District deteriorated; canals became filled with hyacinths, the locks fell into disuse, damage was sustained from either too much water or no water, and the entire project become ineffective.

After the 1926 and 1928 hurricanes the local residents made numerous requests of the federal government for assistance. As a result of those requests, the Caloosahatchee-Lake Okeechobee Drainage Area Project was authorized. This project consisted of 75 miles of levees around the lake, hurricane-gate structures, locks on the St. Lucie and Caloosahatchee canals, and the enlargement of those two canals. Although that construction helped the water-control problem of Lake Okeechobee, the Everglades still lacked adequate facilities. Troubles with water control continued, and new requests for assistance were made of the federal government during the 1940's.

At the time that efforts were directed toward reclaiming the Everglades, other efforts were being made to dig canals, build dikes, and create drainage districts in the basins of the Kissimmee River and the upper St. Johns River. Most notable are the numerous drainage districts astride the eastern divide between the upper St. Johns and Indian river basins from the vicinity of Stuart to Rockledge (Fig. 1). An active program to join the lakes by canalization in the headwaters of the Kissimmee River basin was also initiated.

By 1947 the Corps of Engineers (United States Department of the Army) had received thirteen authorizations for reports in the central and southern Florida area covering flood control, navigation, and allied purposes. After

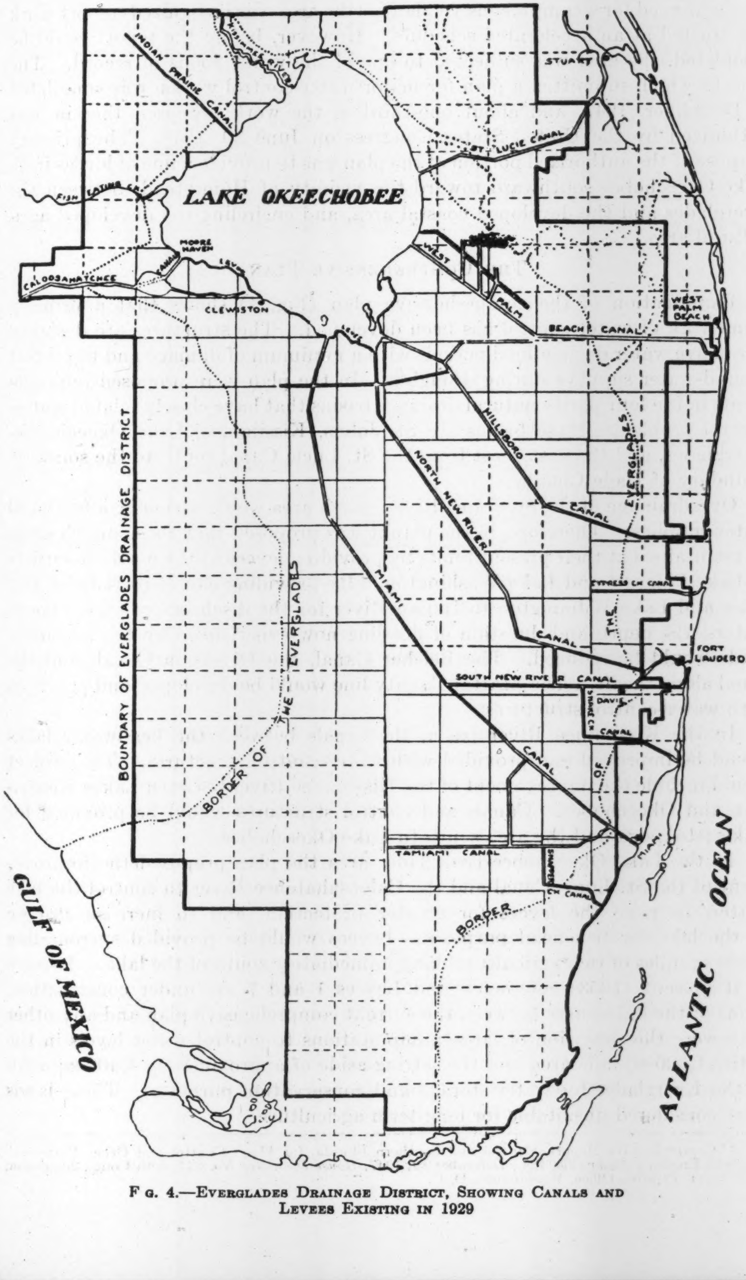
INDIAN PRAIRIE CANAL
KISSIMMEE RIVER
STUART
ST. LUCIE CANAL
FISH EATING CR.
LAKE OKEECHOBEE
MOORE HAVEN
CALOOSAHATCHEE
CANAL
LEVEE
CLEWISTON
WEST PALM BEACH CANAL
WEST PALM BEACH
LEVEE
HILLSBORO
NORTH NEW RIVER CANAL
MIAMI CANAL
BORDER OF THE EVERGLADES
BOUNDARY OF EVERGLADES DRAINAGE DISTRICT
CYPRESS CR CANAL
FORT LAUDERDALE
SOUTH NEW RIVER CANAL
DAVIE
SNAKE CR CANAL
TAMIAMI CANAL
MIAMI
SNAPPER CR CANAL
BORDER
GULF OF MEXICO
ATLANTIC OCEAN

FIG. 4.—EVERGLADES DRAINAGE DISTRICT, SHOWING CANALS AND LEVEES EXISTING IN 1929

the great need for a comprehensive plan for the area was recognized, report work was started at an accelerated schedule. However, before the report could be completed, the area was subjected to one of the worst floods of record. The report,[2] which submitted a plan for major water-control works, was completed in December, 1947, and about one-third of the work proposed therein was authorized by the United States Congress on June 30, 1948. The primary purpose of the authorized portion of the plan was to provide a line of levees from Lake Okeechobee southward toward the vicinity of Homestead, between the Everglades and the developed coastal area, and encircling the developed agricultural area.

THE COMPREHENSIVE PLAN

Examination of the comprehensive plan (Fig. 1) shows that a primary framework of water control has been developed. The structures are designed to remove water during flood periods with a minimum of damage and to protect ground-water supplies during droughts. In the plan were proposed improvements in the four partly natural drainage basins that have closely related water-control problems; these basins are St. Johns, Kissimmee, Lake Okeechobee-Everglades, and the east coast from the St. Lucie Canal south to the southern boundary of Dade County.

Overdrainage of the St. Johns River marsh area would seriously affect local water supplies. Therefore, in the plan it was proposed that those marsh areas be maintained at their present limits by providing levees at the northern outlets of Lake Poinsett and Lake Washington. By providing canals from those two lakes and Lake Wilmington to Indian River for the discharge of excess floodwaters, the depth and duration of flooding now experienced by the adjoining lands would be reduced. The Belcher Canal, the Diversion Canal, and the canal along the St. Lucie-Martin County line would be developed and provided with water-control structures.

In the Kissimmee River basin, the canals between the headwater lakes would be improved and provided with water-control structures. The project would include the improvement of the Kissimmee River between Lakes Kissimmee and Okeechobee. Canals and control structures would be provided for Lake Istokpoga and the area south to Lake Okeechobee.

In the Lake Okeechobee-Everglades area the plan proposed the improvement of the St. Lucie Canal and the Caloosahatchee River to control the lake better, to raise the levees for greater protection, and to increase storage in the lake for beneficial purposes. Levees would be provided surrounding 1,000 sq miles of rich agricultural land immediately south of the lake. Levee 8 is at present (1953) completed and Levees 1 and 7 are under construction. Some of the differences between the current comprehensive plan and any other plan were the provision of large pump stations to control water levels in the entire 1,000-sq-mile area and the setting aside of approximately 1,400 sq miles of the Everglades for water storage and conservation purposes. These lands were considered unsuitable for long-term agriculture.

---

[2] "Comprehensive Report, Central and Southern Florida, for Flood Control and Other Purposes," Corps of Engrs., Jacksonville, Fla., December 19, 1947, *House Document No. 643*, 80th Cong., 2d session, U. S. Govt. Printing Office, Washington, D. C.

The east-coast area would secure water control through improvement of existing canals capable of carrying storm runoff rapidly to the ocean. Water-control structures would be provided near the lower ends of the canals to control ground water and to retard the salt-water flow upstream.

Because the authorized part of the comprehensive project is situated in the Everglades and east-coast areas, the problems of water control in those areas have received more study.

In order to meet the needs of the region and to achieve optimum use of the available water, it is necessary to store large quantities when excess water is available and to restrict wasteful discharge to a minimum. Maintenance of a water supply in Lake Okeechobee and in the conservation areas would provide the following benefits:

a. Water supply for agricultural areas;
b. Improved ground-water control;
c. Improvement and replenishment of east-coast well fields and streams for municipal water supply;
d. Salinity control for east-coast areas;
e. Recreational facilities on Lake Okeechobee and related waterways;
f. Increased navigation depths in Lake Okeechobee and related waterways;
g. Conservation of peat and muck lands of the agricultural area; and
h. Conditions favorable for the propagation of fish and wildlife in Lake Okeechobee, the conservation areas, and Everglades National Park.

A study of the use and distribution of available water requires a knowledge of the optimum and normal requirements of the areas for the benefits cited herein, the present and ultimate demands of the affected areas, the total water supply available, and the amount of available water that can be distributed to satisfy the entire or partial needs of those areas.

The principal areas that would benefit from, or be affected by, the sources and quantity of water that would be made available by the construction of project impoundment facilities are the Everglades area and the adjacent east coast. This region averages 40 miles in width, extends part of the way around the eastern and western shores of Lake Okeechobee, and extends southward approximately 100 miles from the lake to the southern tip of Florida. It includes the entire lower east coast of Florida—the narrow coastal ridge where West Palm Beach, Fort Lauderdale, Miami, and many smaller communities are located. The major water-demand areas are: (*a*) The Lake Okeechobee agricultural area, (*b*) the Lake Worth agricultural area and adjacent east-coast areas, (*c*) the Davie and Plantation agricultural areas and adjacent east-coast areas, (*d*) the Davie and Miami agricultural areas and adjacent east-coast areas, and (*e*) the Everglades National Park. The sources of water supply for those areas, the resulting benefits, and other pertinent data are listed in Table 1.

The available water storage in Lake Okeechobee for the agricultural area would be the volume between the maximum conservation-pool level and the lowest lake stage acceptable to local agricultural and navigational interests. Local agricultural interests prefer that the minimum lake stage be not lower than approximately 13 ft; however, under natural conditions, the lake has fallen below 13 ft sixteen times in the thirty-eight years of record. The maximum acceptable conservation-pool elevation depends on the stage at which seepage damage to highly developed lands on the lake margins would be great enough to require appreciable remedial measures. Attempts to maintain conservation-pool stages in excess of that level would necessitate establishing a buffer strip adjacent to the landward toe of the lake levees from the vicinity of Port Mayaca to Moore Haven and constructing a ditch to collect seepage water to be conveyed to the main canals of the agricultural area. Because the required strip would include highly developed agricultural lands and would require relocation of highways, bridges, and other structures, the cost would be considerable. The results of several routing studies made to determine the volume of storage that could be economically provided for agricultural use, assuming maximum conservation pool elevation at 13 ft, 14 ft, 15 ft, and 16.4 ft, are shown in Table 2. If the upper limit of the conservation pool had been at 16.4 ft, the volume of agricultural-use storage, approximately 2,440,000 acre-ft, would have been adequate to meet all requirements arising from the ultimate development of the area in the thirty-eight years of record except in 1922 when the lake would have been below El. 10.5 for four months. Under the same conditions of storage, nearly all the capacity would have been needed to satisfy requirements of the two next driest years. Approximately 400,000 acre-ft of additional storage would have been needed to satisfy fully the agricultural re-

TABLE 1.—SOURCE OF WATER SUPPLY AND AREA OF DEMAND

Area of demand	Area, in square miles	Area of supply	Area, in square miles	Benefits
Lake Okeechobee	730	Kissimmee River Basin[a]	4,812	Navigation, recreation, fish and wildlife.
Agricultural area	1,130[b]	Lake Okeechobee	730	Water for agricultural use; conservation of peat and muck lands.
Conservation areas				
No. 1	216	Lake Okeechobee and agricultural area	1,748	Fish and wildlife.
No. 2	204			
No. 3	924			
Total	1,344			
Lake Worth agricultural area	340	Conservation area No. 1	216	Water for agricultural and urban use.
Davie and Plantation agricultural areas	85	Conservation area No. 2	204	Water for agricultural and urban use.
Davie and Miami agricultural areas	220	Conservation area No. 3	924	Water for agricultural and urban use.
East-coast area	...	Conservation areas Nos. 1, 2, and 3	1,344	Water supply and salinity control.
Everglades National Park	1,240	Conservation area No. 3, and adjacent area runoff	...	Fish and wildlife, birdlife, and vegetation.

[a] Includes drainage areas of numerous streams in the northeast and also of lake shores. [b] Of this area, 112 sq miles drain to the Caloosahatchee River.

quirements in 1922 assuming that the ultimate development would not drop below El. 10.5, but this amount of water could not have been stored without raising the lake to above El. 17. However, by assuming that water was stored to an elevation above 17 ft, the lower limit would have been higher than 10.5 ft in 1922. Increased benefits resulting from the provision for additional storage at this time would be relatively insignificant.

Water control in the agricultural area south of Lake Okeechobee depends on pumping. The capacities chosen for the pump stations and agricultural canals are those required for the removal of 0.75 in. of rainfall per day from the drainage area. Those capacities were selected after investigations of rainfall, flood duration, and crop losses. Based on long-range considerations, as much water as possible should be stored and the remainder should be discharged through the Everglades National Park in order to obtain the maximum benefits for conservation purposes.

Routings, which were computed for the three conservation areas, established pool elevations of 17 ft and 15.9 ft to provide the maximum water-control benefits for conservation areas No. 1 and No. 2. In conservation area No. 3 the surface storage was found to be limited not by the capacity but by the available supply. The conservation pools would be used primarily to replenish ground water.

TABLE 2.—Routing Studies for Agricultural–Use Storage: Ultimate Development of the Area

Upper limit, conservation pool elevation, in feet	Minimum lake stage reached, in feet	Times lake below El. 10.56	Months lake below El. 10.56	Storage capacity available for agricultural use, in acre-feet	Agricultural Demands Not Satisfied	
					(Acre-feet)	(Months)
16.4	10.0	1	4	2,440,000	178,000	2
15.0	9.9	5	21	1,800,000	1,038,000	14
14.0	9.4	7	41	1,350,000	2,325,000	18
13.0	9.2	17	79	925,000	4,553,000	39

The water requirements of the various urban areas of the region were determined. The major requirement of the region is supplemental water to permit orderly development of agricultural lands lying south and east of Lake Okeechobee and also those lying east of the conservation areas, although municipal water demands during the course of the project may require supplementing of existing supplies. The provision of an adequate water supply to meet these two fundamental requirements for the development of the area would constitute making the best use of available water. Such a provision would also provide supplemental benefits in the maintenance of sufficiently high ground-water levels to conserve peat and muck soils and would assist materially in restricting the intrusion of salt water into coastal lands. It is also apparent that the creation of additional water supplies would provide attendant benefits to fish and wildlife resources; the recreational facilities of the region would also be increased. Table 3 summarizes the present water consumption and the estimated consumption for the year 2000 for agricultural and municipal water supply in the major subdivisions of the region of demand.

Municipal water supply for the coastal urban centers would depend somewhat on releases of water from the conservation areas; however, the major part of the supply would be obtained from ground-water sources that would be maintained by rainfall, by seepage of water from nearby farm areas, and by seepage from the conservation pools and from several lakes. Because the existing water supply for the area would be adequate for ultimate development under normal conditions, any additional water that might be required during severe droughts would be available from increased seepage from the conservation and agricultural areas.

Routings were computed to determine the flow distribution of a design flood, an average water year, and a drought year (Figs. 5, 6, and 7). The distribution of the design flood (Fig. 5) is similar to that which would occur during any large flood; the larger the flood, the more the water which will have to be discharged through the St. Lucie Canal and the Caloosahatchee Canal, and into Everglades National Park. The distribution of the average year (Fig. 6) is representative of long-term utilization and was developed from twelve years of record. During the average year, evaporation claims the greatest quantity of water; only a small amount is discharged for nonproductive uses, indicating that only a small increase in land area can be supplied with water during normal times. Data for the drought year (Fig. 7) shows how critical the water supply will be; no water will be discharged for nonproductive uses and only a small amount is available.

TABLE 3.—PRESENT AND PROSPECTIVE WATER CONSUMPTION FOR PRINCIPAL AREAS OF DEMAND

Region of demand	Area, in square miles	Water usage	DEVELOPMENT—YEAR 1950			DEVELOPMENT—YEAR 2000		
			Acreage under water control	Population	Water consumption, in acre-feet	Acreage	Population	Maximum water demand, in acre-feet
Lake Okeechobee agricultural area	1,130	Agriculture	127,000	...	155,000	723,200	...	883,000
Lake Worth area	340	Agriculture	36,000	...	20,000	150,000	...	147,000
		Municipal	...	139,000	22,000	...	417,000	71,000
Davie and Plantation areas	85	Agriculture	17,000	...	7,400	54,000	...	56,300
		Municipal[a]	...			...		
Davie and Miami areas	220	Agriculture	46,000	...	23,700	123,000	...	134,000
		Municipal	...	535,000	60,000	...	1,605,000	269,000

[a] Population and water consumption included in the values for the Lake Worth area.

In Fig. 8 the utilization of water is shown in percentage of the total available water supply. During the average year the water that is discharged through the West Palm Beach Canal and the Hillsboro Canal is available in conservation areas No. 1 and No. 2.

The significant purpose in these distribution routings is to indicate the volume of water available to the area. However, in addition to the area pre-

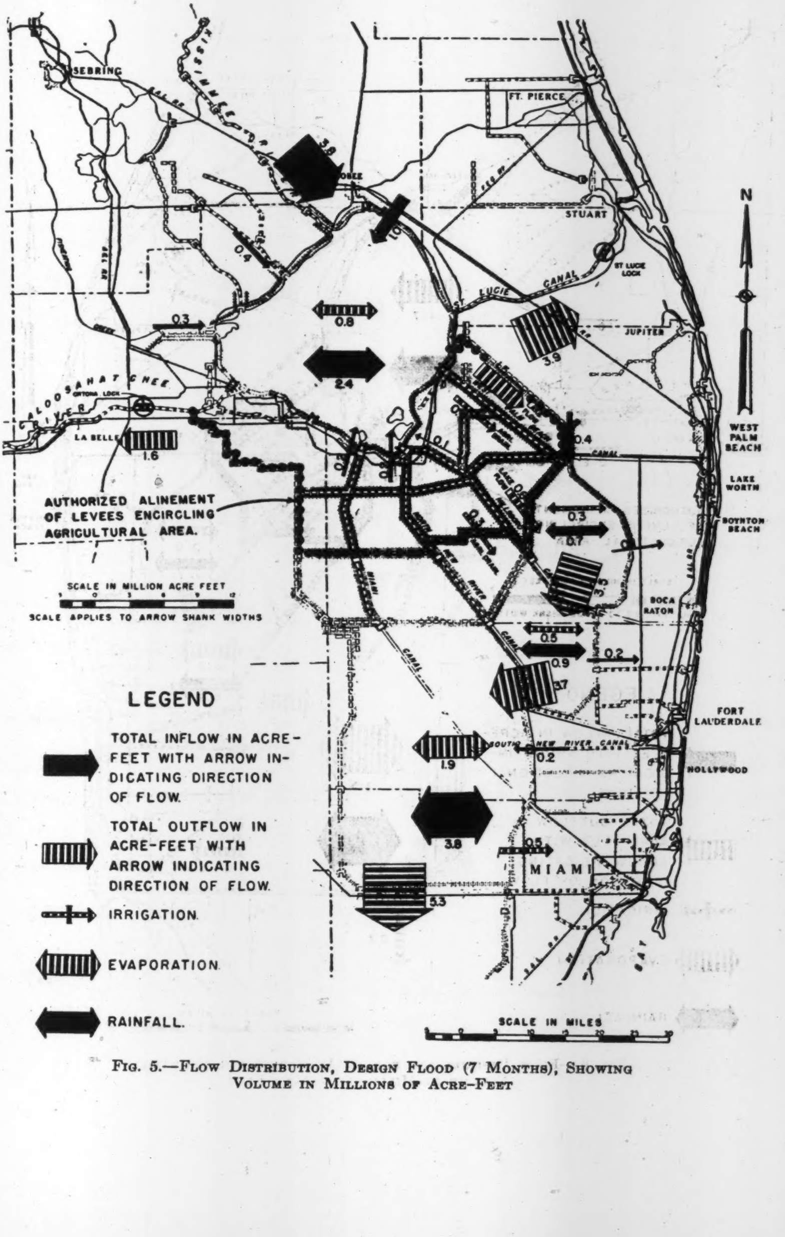
SEBRING
KISSIMMEE RIVER
3.8
OKEECHOBEE
1.0
FT. PIERCE
STUART
N
ST LUCIE LOCK
ST. LUCIE CANAL
0.4
0.8
2.4
0.3
3.9
JUPITER
CALOOSAHATCHEE RIVER
ORTONA LOCK
LA BELLE
1.6
0.1
0.4
WEST PALM BEACH
LAKE WORTH
BOYNTON BEACH
AUTHORIZED ALINEMENT OF LEVEES ENCIRCLING AGRICULTURAL AREA.
0.3
0.7
3.1
MIAMI CANAL
NEW RIVER CANAL
SCALE IN MILLION ACRE FEET
3 0 3 6 9 12
SCALE APPLIES TO ARROW SHANK WIDTHS
BOCA RATON
0.5
0.9
0.2
3.7
FORT LAUDERDALE
LEGEND
TOTAL INFLOW IN ACRE-FEET WITH ARROW INDICATING DIRECTION OF FLOW.
TOTAL OUTFLOW IN ACRE-FEET WITH ARROW INDICATING DIRECTION OF FLOW.
IRRIGATION.
EVAPORATION.
RAINFALL.
1.9
SOUTH NEW RIVER CANAL
0.2
HOLLYWOOD
3.8
0.5
MIAMI
5.3
BAY
SCALE IN MILES
5 0 5 10 15 20 25 30

FIG. 5.—FLOW DISTRIBUTION, DESIGN FLOOD (7 MONTHS), SHOWING VOLUME IN MILLIONS OF ACRE-FEET

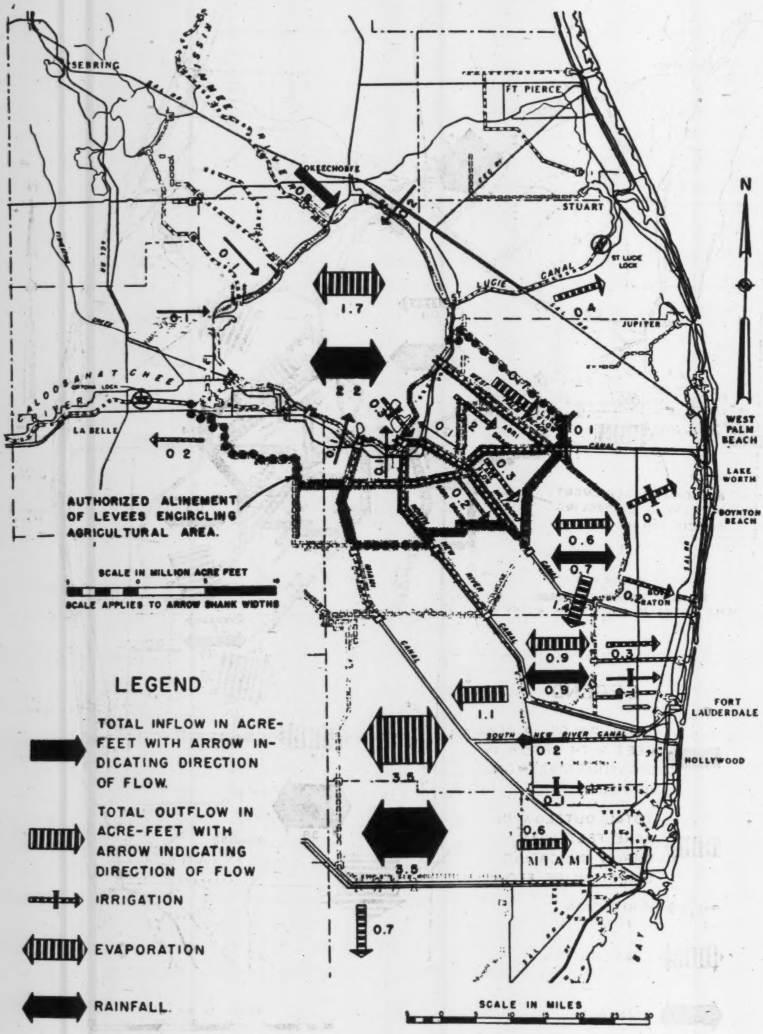
SEBRING
KISSIMMEE RIVER
OKEECHOBEE
FT PIERCE
STUART
ST LUCIE LOCK
ST LUCIE CANAL
N
JUPITER
WEST PALM BEACH
LAKE WORTH
BOYNTON BEACH
CALOOSAHATCHEE RIVER
ORTONA LOCK
LA BELLE
1.7
2.2
0.1
0.2
0.4
0.3
0.6
0.7
1.4
0.9
0.9
1.1
3.5
3.5
0.7
BOCA RATON
FORT LAUDERDALE
HOLLYWOOD
SOUTH NEW RIVER CANAL
MIAMI
BAY
AUTHORIZED ALINEMENT OF LEVEES ENCIRCLING AGRICULTURAL AREA.
SCALE IN MILLION ACRE FEET
SCALE APPLIES TO ARROW SHANK WIDTHS
LEGEND
TOTAL INFLOW IN ACRE-FEET WITH ARROW INDICATING DIRECTION OF FLOW.
TOTAL OUTFLOW IN ACRE-FEET WITH ARROW INDICATING DIRECTION OF FLOW
IRRIGATION
EVAPORATION
RAINFALL.
SCALE IN MILES
0 5 10 15 20 25 30

FIG. 6.—FLOW DISTRIBUTION FOR AN AVERAGE YEAR, SHOWING VOLUME IN MILLIONS OF ACRE-FEET

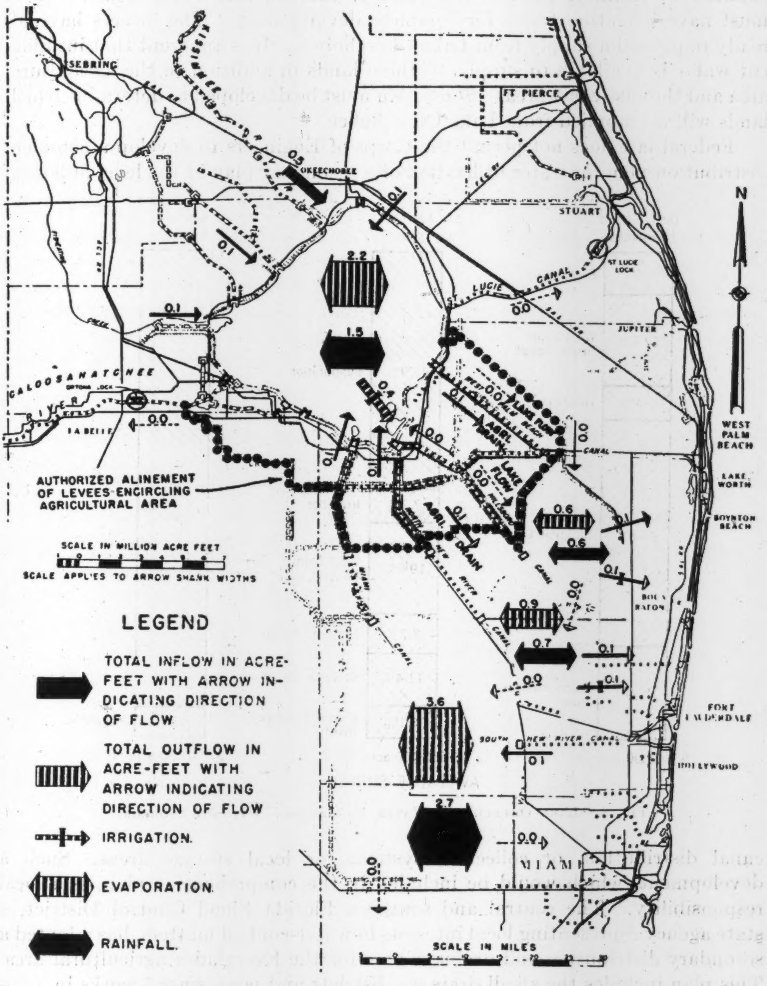
SEBRING
KISSIMMEE
OKEECHOBEE
FT PIERCE
STUART
ST LUCIE LOCK
LUCIE CANAL
JUPITER
N
WEST PALM BEACH
LAKE WORTH
BOYNTON BEACH
BOCA RATON
FORT LAUDERDALE
HOLLYWOOD
MIAMI
CALOOSAHATCHEE RIVER
ORTONA LOCK
LA BELLE
NEW RIVER CANAL
WEST PALM BEACH CANAL
HILLSBORO CANAL
MIAMI CANAL
LAKE FLOW
AGRI. DRAIN
0.5
0.1
1.0
0.1
2.2
1.5
0.0
0.4
0.1
0.0
0.6
0.6
0.9
0.7
0.1
0.1
0.0
3.6
2.7
0.1
0.0
0.0
AUTHORIZED ALINEMENT OF LEVEES ENCIRCLING AGRICULTURAL AREA
SCALE IN MILLION ACRE FEET
SCALE APPLIES TO ARROW SHANK WIDTHS
LEGEND
TOTAL INFLOW IN ACRE-FEET WITH ARROW INDICATING DIRECTION OF FLOW
TOTAL OUTFLOW IN ACRE-FEET WITH ARROW INDICATING DIRECTION OF FLOW
IRRIGATION.
EVAPORATION.
RAINFALL.
SCALE IN MILES
0
5
10
15
20
25
30

FIG. 7.—FLOW DISTRIBUTION FOR A DROUGHT YEAR, SHOWING VOLUME IN MILLIONS OF ACRE-FEET

viously mentioned for which water would be available during an average year, there are thousands of acres of lands in the adjacent area—that is, in the counties of Hendry, Glades, Okeechobee, Martin, and Palm Beach—which must have irrigation water for complete development. The owners have already requested a supply from Lake Okeechobee. It is apparent that insufficient water is available to supply all these lands in addition to the agricultural area and the east-coast area. Some plan must be developed to determine which lands will be supplied from Lake Okeechobee.

Federal law does not permit the Corps of Engineers to develop a complete distribution plan for water utilization or a secondary plan at the level of lateral canal distribution, or collection systems, or local storage areas. Such a development, which would be included in the comprehensive plan, is a local responsibility. The central and southern Florida Flood Control District, a state agency representing local interests in water-control matters, has adopted a secondary distribution-and-drainage plan for the Everglades agricultural area. This plan includes the small drainage districts and landowners' works in addition to the canals and controls that would permit the maximum benefits to be realized from the primary comprehensive plan.

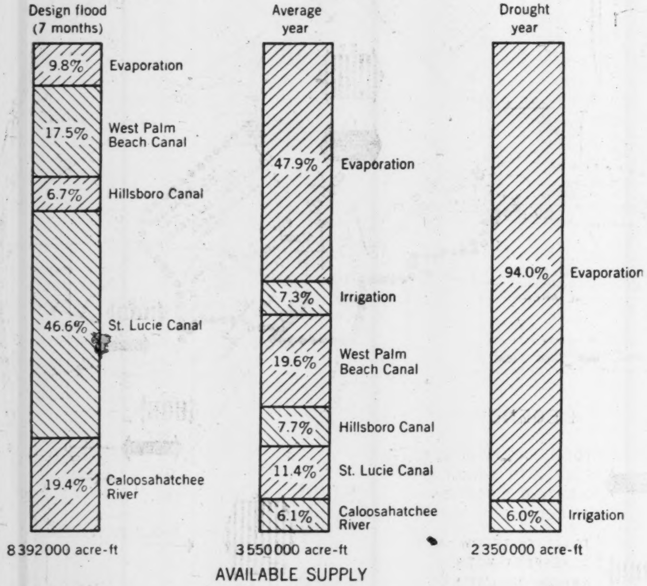

FIG. 8.—LAKE OKEECHOBEE WATER UTILIZATION (WITHOUT STORAGE)

In order to realize the maximum development throughout the central and southern Florida area, it is imperative that a secondary water-control plan be prepared for the entire 15,000 sq miles. This plan would develop an understanding by local residents of the inadequacy of the water supply in the area and would produce a cataloging of possibilities for water supply, land use, and storage. The plan would result in classification of lands that are susceptible to complete water control and of those that would have only limited facilities. The flood control district, in cooperation with individual counties in the area, is developing a secondary plan. The problems of water control are being understood by the people of Florida.

SUMMARY

Water control in central and southern Florida has been under intensive consideration ever since the first white settlers arrived. Primary efforts in this field have been made by the state and federal governments. The existing comprehensive plan for flood control and other purposes forms a basic framework for satisfactory water control in the area. Studies indicate a greater demand for water than can be supplied throughout the entire region. Planning is necessary to develop those lands which would yield the greatest benefits by being provided with water control.

ACKNOWLEDGMENTS

The studies described in this paper are those of the Planning and Reports Branch of the Jacksonville District, Corps of Engineers, under the supervision of the writer. He wishes to thank the Corps of Engineers for permission to use the material presented herein and to express appreciation to his associates in the preparation of this paper.

AMERICAN SOCIETY OF CIVIL ENGINEERS
Founded November 5, 1852
TRANSACTIONS

Paper No. 2857

PUMPING GROUND WATER FOR IRRIGATION AND DRAINAGE

By Cleve H. Milligan,[1] A. M. ASCE

Synopsis

Ground water is an important but neglected national resource. Existing developments illustrate the need for planned utilization of ground water which produces both irrigation and drainage benefits. Physical data, legal concepts, and administrative principles and practices must be improved and developed to stimulate and guide sound ground-water development.

Introduction

Pumping ground water provides both irrigation and drainage; this fact is demonstrated in California, Arizona, Colorado, New Mexico, Utah, and other parts of the western United States. However, there is little mention of ground water in the plans for basin-wide development of the Tennessee Valley, the Missouri Valley, and the Columbia Basin and other basins. Perhaps integration in the plans of both surface water and ground water would delay development. Data needed for planning ground-water utilization are meager, and there are many legal and administrative problems; these factors have delayed the utilization of ground water. Nevertheless, any future ground-water development in the basins cited will probably be initiated as a result of individual effort; this has characterized many past underground-water developments.

The costs of future irrigation projects will be enormous. Before this expense is undertaken consideration should be given to the utilization of ground water and ground-water-storage reservoirs, in addition to surface-water development. This utilization should be an integral part of the development of the water economy of the basin. Ground-water reservoirs may have advantages over surface reservoirs in that they may provide economical hold-over storage for many years with minimum evaporation losses. Also, utilization of ground water produces two benefits—additional water is provided and drainage is accomplished.

Note.—Published, essentially as printed here in February, 1955, as *Proceedings-Separate No. 618.* Positions and titles given are those in effect when the paper was approved for publication in *Transactions.*

[1] Head, Dept. of Civ. and Irrig. Eng., Utah State Agri. College, Logan, Utah.

In the past fifty years the population of the United States has doubled, and both agriculture and industry have expanded at tremendous rates. In order to meet increasing future demands many states are seeking to develop their "last water holes."

The President's Materials Policy Commission, in its report, "Resources for Freedom," estimates that water use will nearly double in the period, 1950–1975. This increased use will result from such developments as nuclear fission, hydrogenation of coal and oil shales, supplemental irrigation in the eastern United States, air conditioning, waste disposal, new irrigation projects in the west, expansion of industry, increase of population, and many other developments. To meet these needs, the utilization of ground water should not be overlooked. Ground-water reservoirs often have tremendous hold-over capacities and other advantages not possessed by surface reservoirs. Moreover, pumping from underground reservoirs may relieve or alleviate drainage problems which always accompany irrigation to some degree. The Soil Conservation Service (United States Department of Agriculture) estimates that 8,000,000 acres of land in seventeen western states need improved drainage.

Unrestricted, or unplanned, pumping has created problems in some areas; these problems include excessive land settlement, salt intrusion, and high pumping costs. However, probably not more than 5% of the ground-water resources have been overdeveloped. There are more than 100 ground-water basins in the Great Basin, those parts of Utah, Idaho, Wyoming, and Nevada which do not drain into the oceans, but only three may be classified as overdeveloped. Additional means of recharging the underground reservoirs may solve the problems created by high pumping rates in those areas where pumpage is excessive if the annual recharge can be made to equal the annual draft.

Some authorities[2] claim that ground water is one of the most neglected national resources. Although there are too few statistics to permit an accurate appraisal of such a claim, there is some justification for it. Water-loving plants in the wet areas of the west probably transpire about 25,000,000 acre-ft of water per yr. This is approximately twice the annual flow into Lake Mead (upstream from Hoover Dam on the Colorado River in Nevada and Arizona) but it does not include evaporation from natural evaporation pans, such as Great Salt Lake (Utah), which receive part of their supply from underground sources. This great waste may indicate that the "last water holes" are in the underground reservoirs.

GROUND-WATER UTILIZATION IN HISTORY

Primitive man in arid climates dug for water. Thomas Ewbank[3] states that

> "Man's ingenuity was, perhaps, first exercised in procuring water; and it is not improbable, that the art of constructing wells was more rapidly carried to perfection than any other."

The Bible contains many references to wells—early Biblical romances were enacted at wells—and Joseph's well in Cairo, Egypt, is still in operation.

---

[2] "The Conservation of Groundwater," by H. E. Thomas, McGraw-Hill Book Co., New York, N. Y., 1951.

[3] "Hydraulics and Mechanics," by Thomas Ewbank, Charles Scribner and Co., New York, N. Y., 1870, p. 25.

The well was and still is, in many areas, the center of religious and social activity. These areas include southern Europe, the Middle East, the Far East, Latin America, and many islands of the sea. The pagans worshipped their wells; the Greeks consecrated them to their gods; the Moslems constructed mosques over them; and the Hindus constructed temples near important wells.

In many countries the development of ground waters far surpassed the development of surface waters. The ghanats of Persia are of great interest because they serve not only as a source of water for municipal and agricultural purposes but also as deep drains which have prevented waterlogging and alkalinity for centuries. The ancient Chinese drilled wells as deep as 3,600 ft with primitive churn-drill methods; some of these wells were cased with bamboo.

The French developed modern drilling methods which were introduced into the United States in 1850. The first wells for culinary purposes were drilled in Charleston, S. C., Louisville, Ky., and St. Louis, Mo. The oil-drilling industry gave well drilling its greatest impetus.

Historical ground-water developments illustrate the importance of ground water in the development of civilizations. The ground-water development projects have usually survived the ravages of time and many are still in use, whereas many great historic projects to conserve surface waters are no longer in use.

PRESENT UTILIZATION

In the United States approximately 20% of the water utilized for industrial, municipal, and agricultural purposes comes from ground-water sources. This ground-water use is approximately 30,000,000,000 gal per day, which is equivalent to a continuous flow of 46,500 cu ft per sec. This stream would produce 33,500,000 acre-ft per yr, or more than enough to fill Lake Mead in one year.

Approximately 14,000,000 acre-ft of ground water were utilized in seventeen western states in 1945; of this volume 11,000,000 acre-ft were used for irrigation. In 1950 California pumped approximately 10,000,000 acre-ft of water from underground sources. There are more than 54,000 wells in Arizona, California, Colorado, Idaho, and Utah. If these wells were all pumped simultaneously into a common stream, the resulting flow rate would be approximately 75,000 cu ft per sec, which would fill Lake Mead in a little more than one-half year. Pumping from ground-water reservoirs involves a considerable investment in well-drilling machinery, wells, pumps, and water distribution facilities.

Some of the development to date (1954) has been haphazard and not according to a systematic plan based on good physical and hydrologic data. This has resulted in annual pumpage in excess of annual recharge, salt-water intrusion, and, in a few areas, growing pumping costs. However, the problems which have resulted from haphazard development merely emphasize the need for planned utilization and should not deter the maximum safe development of ground-water resources.

Present utilization of ground water has demonstrated the feasibility of pumping for both irrigation and drainage and has illustrated the problems which must be considered in the future planned utilization of ground water.

Examples of Ground-Water Utilization

Texas.—The daily use of ground water for industry, agriculture, and municipalities is considerably more than 5,000 acre-ft. Nearly 75% of the urban water supply in Texas comes from underground sources. The use of ground water doubled in nine years; in the same time, the use of water for irrigation multiplied four times. The rate of ground-water utilization in many parts of Texas far exceeds the rate of replenishment of the ground-water reservoirs. This is especially true in the high plains of Texas where the annual pumpage is estimated to be twenty times the annual recharge. In 1934 in the high plains area there were 300 pumped wells which irrigated 16,000 acres. In 1948 there were 10,000 wells irrigating 1,000,000 acres. At the present time pumped wells irrigate approximately 2,500,000 acres in the high-plains region. Developments in this region illustrate the need for planned utilization of ground water so that the average annual draft can more nearly approximate the average annual replenishment.

California, Modesto Irrigation District.—From 1907 to 1922 the Modesto Irrigation District spent $356,000 for the construction and maintenance of regular gravity drains for 45,000 acres; in 1922 the district drilled its first drainage well; by 1939 there were 77 pumped wells which pumped 207 cu ft per sec. The total construction cost of the wells, pumps, and pipelines was $159,000. The comparable cost for gravity drains and facilities was $308,000. The operation and maintenance costs for the pump system was $60,050 compared to $148,700 for the gravity drains. Power costs for pumps amounted to $393,100. However, the value of the pumped water utilized for irrigation at $1.36 per acre-ft was $612,050. The cost of drainage with the open drains was prohibitive. Thus, pumping from ground-water sources produced both irrigation and drainage benefits with considerable financial advantage for the Modesto District.

California, Central Valley.—Ground-water development has been rapid since 1910. By 1919 the total capacity of wells in the San Joaquin Valley was 7,300 cu ft per sec, and by 1929, 20,600 cu ft per sec. The usable underground-reservoir capacity is approximately 20,000,000 acre-ft. In 1948 there were approximately 35,000 pumped wells in the San Joaquin Valley with a gross pumpage of 7,000,000 acre-ft. The annual recharge is about 2,000,000 acre-ft. Plans are being made to increase the recharge, and pumping ground water in the Central Valley has practically eliminated drainage problems. Because of the utilization of underground-storage reservoirs, deep percolation and seepage from canals and ditches are relatively unimportant so far as utilization of water in the basin as a whole is concerned.

Utilization of ground water and of the reservoirs which store it is of great economic importance in the Central Valley. Surface-storage reservoirs cannot compete with the great underground reservoirs. Although the annual use from the reservoir exceeds the annual recharge rate, one cannot state that development has been excessive until all possibilities of increasing the annual recharge have been fully developed. When a surface reservoir fails to fill, means of getting additional water into the basin are explored. The same should be done for ground-water reservoirs.

Arizona, Salt River Valley.—Irrigation was greatly expanded in the Salt River Valley by completion of the Roosevelt Dam. Drainage became a problem in 1918 because such a problem usually follows irrigation developments. In 1920 and 1921 the Salt River Valley Water Users' Association pumped 50,000 acre-ft of ground water in order to alleviate the drainage problem and at the same time to provide additional irrigation water. In 1922 the volume of pumped water was increased to 100,000 acre-ft, and in 1948 the total was 400,000 acre-ft, which is one-third the irrigation water supply. The water table is now at an average depth of about 50 ft, and pumping ground water has solved the drainage problem. This is an example of the two benefits of utilizing ground water.

A Private Ranch in Idaho.—The benefits of pumping ground water for both irrigation and drainage are illustrated by a development on a ranch near Arco, Idaho. This example, cited because of its simplicity and because it was within the economic reach of an individual farmer and his sons, illustrates on a small scale some of the possibilities on a much larger scale of many ground-water reservoirs in the west. Twenty years ago this ranch was a marginal enterprise mainly because of an inadequate supply of late-season water for the higher lands and because of the waterlogging of lower lands. This paradox exists in many areas in the west—low productivity of the higher lands because of an inadequate water supply and reduced productivity of the lower lands because of too much water.

Part of the ranch was situated on a bench with shallow, highly permeable soils that could not be irrigated without excessive seepage from irrigation ditches and deep percolation losses from the irrigated soils. Also, the land was steep so that excessive surface runoff accompanied irrigation. Part of the ranch was situated on low-lying river-bottom land which produced poor pasture grasses and other water-loving plants with high consumptive-use rates. The water losses from the higher lands produced waterlogging of the lower lands.

A ravine, which was rather deep in the upper lands and shallow in the lower lands, extended through the ranch. It served as a natural drain for irrigation-waste water from upper lands and for floodwaters from precipitation and snowmelt. Flow in the ravine was erratic but it contributed to the drainage problem in the lower lands. The rancher's best water right, from the point of view of the volume of water, priority, and seasonal distribution, was on the ditch serving the lower lands. Even though the soil was already filled with water, the rancher always used the water on these lower lands because of the possibility of losing his right through disuse. Thus, he further contributed to the drainage problem.

The rancher and some neighbors hoped that the dam on the river, from which they received their water, would be raised so that additional late-season water could be provided for the high benchlands; this proved uneconomical. Here is the solution produced by the rancher and his son with some technical assistance.

The water in the lower canal was transferred to the higher land, providing adequate water for that area. Two pumped wells were installed on the low-lying land. The rancher's sons purchased an old well-drilling rig and repaired it. They then drilled their own wells. During the slack season on the ranch a small dam was built across the ravine with their equipment. This provided a small reservoir of approximately 50 acre-ft of storage capacity. The reservoir fills from two to three times during a season with waste water from the higher lands and with floodwaters. Water from the surface reservoir and from the two pumped wells provides an ample water supply for the lower lands. Excessive seepage from ditches and reservoirs does not cause the rancher much worry because these waters are almost all reclaimed by the two pumped wells. In addition, the water table on the low lands has been lowered sufficiently to make the pastures highly productive. The difference in consumptive use between the water-loving plants and the high-grade pastures has resulted in a net savings in water. Even if the consumptive use had been the same, the exchange of a poor pasture for a good one was a sensible business venture because the ranch has been transformed from a marginal operation to a profitable enterprise.

Individual farmers could profit by the foregoing example. Its principles should be considered in the planned utilization of water resources on a basinwide scale.

PROBLEMS OF DEVELOPMENT

There is a need for adequate consideration of ground water in planning future water-development projects, but ground-water development problems are extensive and varied. Most of these problems are physical, legal, and administrative.

Physical Problems.—Physical problems arise from a lack of basic hydrologic and geologic data. If water resources are to be fully and efficiently utilized, an inventory of almost every aspect of the hydrologic cycle should be made. The measurement of precipitation and surface runoff has been adequate to date, but no phase of the hydrologic cycle has been completely inventoried. Data on the ground-water aspects of the hydrologic cycle are lacking. Good basic data are indispensable to planned utilization and the lack of these data has contributed to the inadequate consideration given ground water in water-development projects. The recommendations[4] of the Hydrologic Subcommittee of the Federal Interagency River Basin Committee on basic data needs are inadequate with respect to ground-water development. This illustrates one of the difficult problems which must be solved if ground water is to receive ample consideration in future water plans.

There is a lack, too, of adequate geologic data on the size, configuration, and water-yielding capacities of underground water reservoirs. Obtaining good data is expensive, but if millions, and sometimes billions, of dollars can be expended to construct some of the projects proposed for the future, the costs of obtaining good basic data upon which to base such tremendous expenditures can also be expended.

Legal Problems.—Legal definitions, classifications, and concepts have tended to limit development and full utilization of ground water in some areas.

---

[4] "The Conservation of Groundwater," by H. E. Thomas, McGraw-Hill Book Co., New York, N. Y., 1951.

The classification and separation of surface water from ground water and, in many instances, the application of different rules to them, has limited ground-water development. Uniform policies and rules are necessary for the administration of all water whether above or below ground. Actually, underground and surface waters are so closely related in the hydrology of a basin that it is academic and impractical to separate them.

Some court decisions have tended to limit future ground-water development. This is partly due to the lack of basic data and partly to the failure of the courts to make due allowance for changing conditions and demands. In Utah, for example, courts have rendered decisions which make junior appropriators of ground water liable for damages resulting from lowering artesian pressures in flowing wells. This has discouraged full development of underground water. Prior appropriators could still have obtained water by pumping. In other words, in the case of development of underground water, the courts have guaranteed the means of diversion of the water from underground-storage. In the case of development of surface waters, however, the courts have not guaranteed the original means of diversion of water. This is typical of some of the inconsistencies in court decisions. In some states there is no legislative control or constitutional control of ground-water development. Control is based largely on court decisions, but often court decisions are delayed until after irreparable damage has occurred.

These legal problems must be resolved even though to do so will be difficult. However, it may be no more difficult than the consummation of a river compact or the working-out of the large number of water-right exchanges that will be required in many future water-development projects.

Administrative Problems.—The coordinated development and utilization of ground and surface waters on a basin-wide, and frequently, an interbasin basis will require the solution of many administrative problems. A closer coordination of the efforts of separate agencies which deal with surface and underground waters will be necessary. Perhaps these agencies can be merged into an over-all agency to plan, develop, and administer all waters. Another problem will be that of making appropriate water transfers so that surface water may be utilized on higher lands and pumped water on lower lands. Lowering the water table on low lands in order to reduce consumptive waste and to improve drainage will alter the regimen of stream flow on the lower sectors of streams.

CONCLUSIONS

Ground water is a neglected natural resource. Basin-wide plans for developing many of the great river systems seldom mention the utilization of ground water. Existing developments demonstrate the economic importance of ground water and the need for planned utilization. They also show that utilization of ground water produces two benefits—drainage and additional irrigation water. Physical data, legal concepts, and administrative principles and practices must be improved and developed to stimulate sound development of this important resource.

AMERICAN SOCIETY OF CIVIL ENGINEERS
Founded November 5, 1852
TRANSACTIONS

Paper No. 2858

MOMENTS IN DOMES BUILT INTO CYLINDERS

By John V. Huddleston,[1] J. M. ASCE, and
Mario G. Salvadori,[2] M. ASCE

Synopsis

In thin shells of revolution that are symmetrically loaded and built into vertical cylinders, significant moments occur in the neighborhood of the junction between dome and cylinder.

These moments and the accompanying shears (under dead load and live load) are evaluated approximately herein for domes having vertical boundaries. Membrane displacements and rotations at the dome edge are first determined, and moments and shears are found that satisfy the requirements of continuity between shell and cylinder.

The results are plotted as nondimensional curves allowing the immediate evaluation of moments and shears in the range of parameters usually encountered in practice.

Introduction

In the investigation of thin shells it is commonly found that, in large parts of a shell, only membrane stresses are developed. However, bending moments and transverse shears are required in some parts of the shell (for example, near boundaries) in order to eliminate the discontinuities predicted by membrane theory.

The purpose of this investigation is to facilitate the approximate determination of bending stresses at the edge of certain types of shells of revolution (usually termed "domes"). The type of shell considered has a vertical axis of rotation, is loaded symmetrically with respect to that axis, and is built into a circular cylinder with the same axis and radius as that of the shell at the point of juncture. This investigation is concerned with the effect of dead load and live load, and particularly with the evaluation of bending moments and transverse shears caused near the junction of shell and cylinder by such loads. The standard procedure for such an investigation consists in determining first

---

Note.—Published, essentially as printed here, in August, 1955, as *Proceedings Paper 772*. Positions and titles given are those in effect when the paper was approved for publication in *Transactions*.

[1] **Instructor in Civ. Eng., Columbia Univ., New York, N. Y.**

[2] **Prof. of Civ. Eng., Columbia Univ., New York, N. Y.**

the displacements and rotations at the edge of the shell due to membrane stresses. To restore continuity, the edge moments and shears must produce equal and opposite displacements and rotations, which can be computed with close approximation by substituting for the part of the shell near the edge a part of the cylinder tangent to the shell, provided the thickness of shell and cylinder are small in comparison with their common radius (the Geckeler assumption).[3]

EDGE DISPLACEMENTS

Membranes of Revolution Under Dead Load.—A shell of revolution is considered to be formed by the rotation of a meridian curve, $y(x)$, about the y-axis (Fig. 1). The principal radii of curvature at any point (x, y) of the shell are r_1 and r_2; r_1 is the radius of curvature of the surface in the meridian plane (that is, the radius of curvature of the meridian itself) and r_2 the radius of curvature of the surface in a plane perpendicular to the meridian. The angle between the normal to the shell and the shell axis is ϕ. The following assumptions are made in this investigation:

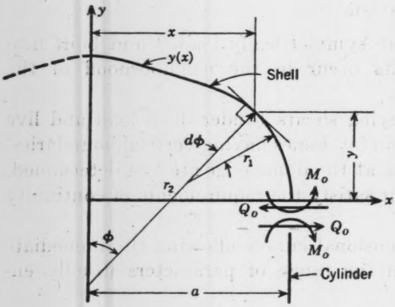

FIG. 1

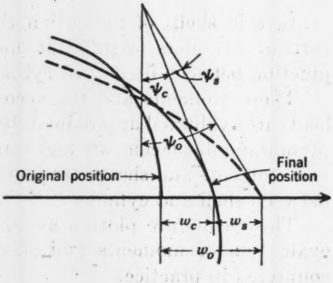

FIG. 2

1. The shell has a vertical tangent at the lower edge—that is,

$$\left.\frac{dx}{dy}\right|_{y=0} = 0 \qquad (1)$$

from which it follows that

$$\left.\frac{dr_2}{d\phi}\right|_{\phi=\pi/2} = 0 \qquad (2)$$

2. The derivative of r_1 with respect to ϕ is zero at the lower edge—that is,

$$\left.\frac{dr_1}{d\phi}\right|_{\phi=\pi/2} = 0 \qquad (3)$$

---

[3] "Theory of Plates and Shells," by S. Timoshenko, McGraw-Hill Book Co., Inc., New York, N. Y., 1940, pp. 407–408, and p. 467.

This condition is satisfied by all meridional sections symmetrical about the equator (x-axis).

3. The thickness of the shell is essentially constant in the neighborhood of the edge.

4. Poisson's ratio is equal to zero.

The symmetrical dead load acting on the shell at any height y is p per unit area of shell, and p is expressed as a function of ϕ, as follows:

$$p = p_o\, g(\phi) \qquad (4)$$

in which p_o is the value of p at $\phi = \pi/2$. The value of p is determined at any point by multiplying the thickness of the shell at that point by the unit weight of the material.

It has been shown[4] that, under the foregoing specified conditions, the radial displacement, w_o, at the edge, $\phi = \pi/2$ (positive outward), and the rotation, ψ_o, at the same edge (positive outward—that is, positive if counterclockwise at $\phi = \pi/2$) are

$$w_o = \frac{p_o\, a^2}{E\, h_s}\left(\frac{a}{r_o}\right) S \qquad (5)$$

and

$$\psi_o = 2\, \frac{p_o\, a}{E\, h_s}\left(\frac{a}{r_o}\right) \qquad (6)$$

in which a is the radius of the equator (that is, r_2 at $\phi = \pi/2$, or x at $y = 0$), E is the modulus of elasticity of the material, h_s is the thickness of the shell in the neighborhood of the equator, and r_o is the radius of curvature of the meridian at the equator (that is, r_1 at $\phi = \pi/2$).

The quantity, S (the nondimensional static moment of the load with respect to the shell axis), is defined as

$$S = \frac{1}{a^2}\int_0^{\pi/2} g(\phi)\, r_2 \sin\phi\, r_1\, d\phi \qquad (7)$$

and its evaluation for various meridional curves and thickness variations is studied subsequently.

Bending Displacements in the Shell.—If a uniformly distributed bending moment, M_o, per unit of circumference and a uniformly distributed shear, Q_o, per unit of circumference are applied to the edge of the shell as shown in Fig. 1, the edge will undergo a radial displacement, w_s (positive inward), and a rotation, ψ_s (positive inward). To evaluate w_s and ψ_s for shells having a small value (less than 1/30) of the ratio, h_s/a, it can be assumed (without appreciable error) that the displacements caused by M_o and Q_o will be felt only in the vicinity of the boundary and that this part of the shell can be analyzed[3] as a part of a long cylindrical shell of radius, a. On the basis of these assumptions, w_s and ψ_s are given by[5]

---

[4] "Boundary Displacements in Membranes of Revolution under Vertical Loads," by Mario G. Salvadori, *Annali di Matematica Pura e Applicata*, Series IV, Vol. XXXIX, Bologna, 1955.

$$w_s = -\frac{1}{2\,\beta^3_s\,D_s}\,(\beta_s\,M_o - Q_o) \qquad (8)$$

and

$$\psi_s = -\frac{1}{2\,\beta^2_s\,D_s}\,(2\,\beta_s\,M_o - Q_o) \qquad (9)$$

in which

$$\beta_s = \frac{\sqrt[4]{3}}{\sqrt{a\,h_s}} = \frac{1.32}{\sqrt{a\,h_s}} \qquad (10)$$

and

$$D_s = \frac{E\,h^3_s}{12} \qquad (11)$$

Bending Displacements in the Cylinder.—If equal and opposite edge moments and shears are applied to the cylinder as shown in Fig. 1, its edge will undergo a radial displacement, w_c (positive outward), and a rotation, ψ_c (positive inward), which can be determined from

$$w_c = \frac{1}{2\,\beta^3_c\,D_c}\,(\beta_c\,M_o + Q_o) \qquad (12)$$

and

$$\psi_c = -\frac{1}{2\,\beta^2_c\,D_c}\,(2\,\beta_c\,M_o + Q_o) \qquad (13)$$

Terming h_c the thickness of the cylinder in the neighborhood of the edge, β_c and D_c are defined by changing the subscript from s to c in Eqs. 10 and 11, respectively.

CONTINUITY BETWEEN THE SHELL AND CYLINDER

Two conditions of continuity arise from the fact that there can be no relative displacement or rotation between the shell and the cylinder at the edge. Using the nomenclature of Fig. 2 they are

$$w_s + w_c = w_o \qquad (14)$$

and

$$\psi_s + \psi_c = \psi_o \qquad (15)$$

Substitution of Eqs. 5, 6, 8, 9, 12, and 13 into Eqs. 14 and 15 leads to two equations and the two unknowns, M_o and Q_o. Solution of these equations permits writing M_o and Q_o as

$$M_o = m_o\,p_o\,a\,h_s\left(\frac{a}{r_o}\right)S \qquad (16)$$

---

[5] "Theory of Plates and Shells," by S. Timoshenko, McGraw-Hill Book Co., Inc., New York, N. Y., 1940, p. 393.

and

$$Q_o = q_o\,p_o\,a\left(\frac{h_s}{a}\right)^{1/2}\left(\frac{a}{r_o}\right)S \quad\text{.................}(17)$$

in which

$$m_o = f_1(r) - \frac{1}{S}\sqrt{\frac{h_s}{a}}\,g_1(r) \quad\text{..................}(18)$$

$$q_0 = f_2(r) - \frac{1}{S}\sqrt{\frac{h_s}{a}}\,g_2(r) \quad\text{..................}(19)$$

$$f_1(r) = \frac{\dfrac{1}{2\sqrt{3}}(1 - r^2)}{(1 + r^2)^2 + 2\,r^{3/2}\,(1 + r)} \quad\text{...............}(20)$$

$$g_1(r) = \frac{\dfrac{1}{\sqrt[4]{27}}(1 + r^{3/2})}{(1 + r^2)^2 + 2\,r^{3/2}\,(1 + r)} \quad\text{...............}(21)$$

$$f_2(r) = \frac{\dfrac{1}{\sqrt[4]{3}}(1 + r^{5/2})}{(1 + r^2)^2 + 2\,r^{3/2}\,(1 + r)} \quad\text{...............}(22)$$

$$g_2(r) = \frac{\dfrac{1}{\sqrt{3}}(1 - r^2)}{(1 + r^2)^2 + 2\,r^{3/2}\,(1 + r)} = 2\,f_1(r) \quad\text{...........}(23)$$

and

$$r = \frac{h_s}{h_c} \quad\text{.........................}(24)$$

Values of m_o and q_o as functions of r for various values of the parameter $(1/S)\sqrt{h_s/a}$ are presented in Figs. 3 and 4, respectively. For intermediate values of $(1/S)\sqrt{h_s/a}$, a linear interpolation gives the correct result because m_o and q_o are linear functions of this parameter.

MAXIMUM MOMENT IN THE SHELL OR CYLINDER

Assuming again that the part of the shell affected by the edge moments and shears behaves as a long cylinder, the bending moment, M_s, per unit of circumference of the shell at a distance, s_s, from the edge along the meridian may be approximated by[5]

$$M_s(s_s) = M_o\,\phi(\beta_s\,s_s) - \frac{Q_o}{\beta_s}\zeta(\beta_s\,s_s) \quad\text{...............}(25)$$

in which the functions, ϕ and ζ, are given by

$$\phi(\beta_s\,s_s) = e^{-\beta_s s_s}(\cos\beta_s\,s_s + \sin\beta_s\,s_s)$$

and

$$\zeta(\beta_s\,s_s) = e^{-\beta_s s_s}\sin\beta_s\,s_s$$

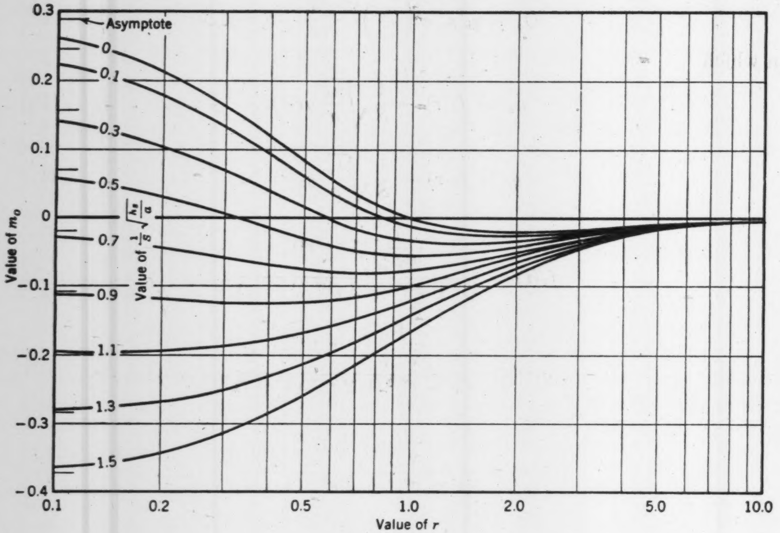
Asymptote
0
0.1
0.3
0.5
0.7
0.9
1.1
1.3
1.5
Value of $\frac{1}{s}\sqrt{\frac{h_s}{a}}$
Value of m_0
0.3
0.2
0.1
0
−0.1
−0.2
−0.3
−0.4
0.1
0.2
0.5
1.0
2.0
5.0
10.0
Value of r

Fig. 3

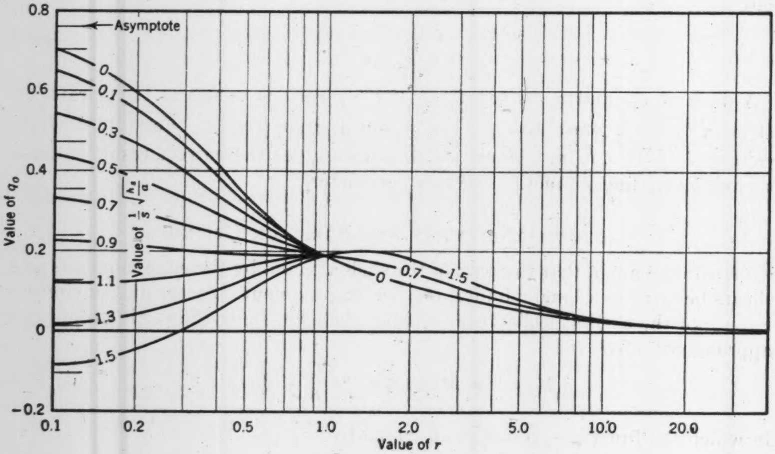
Asymptote
0
0.1
0.3
0.5
0.7
0.9
1.1
1.3
1.5
0
0.7
1.5
Value of $\frac{1}{s}\sqrt{\frac{h_s}{a}}$
Value of q_0
0.8
0.6
0.4
0.2
0
−0.2
0.1
0.2
0.5
1.0
2.0
5.0
10.0
20.0
Value of r

Fig. 4

and are tabulated by S. Timoshenko.[5,6] The moment, M_s, has a first maximum at a distance, $\bar{s}_s$, defined by

$$\tan (\beta_s \bar{s}_s) = \frac{q_o}{q_o - 2 \sqrt[4]{3}\, m_o} \tag{26}$$

The maximum value of $M_s(s_s)$ is given by

$$\bar{M}_s = M_s(\bar{s}_s) = m_s\, p_o\, a\, h_s \left(\frac{a}{r_o}\right) S \tag{27}$$

in which

$$m_s = m_o\, \phi(\beta_s \bar{s}_s) - \frac{q_o}{\sqrt[4]{3}} \zeta(\beta_s \bar{s}_s) \tag{28}$$

Similarly, the bending moment, M_c, per unit of circumference of the cylinder at a distance, s_c, from the edge is

$$M_c(s_c) = M_o\, \phi(\beta_c s_c) + \frac{Q_o}{\beta_c} \zeta(\beta_c s_c) \tag{29}$$

which has a first maximum at a distance, $\bar{s}_c$, defined by

$$\tan (\beta_c \bar{s}_c) = \frac{q_o}{q_o + 2 \sqrt[4]{3} \sqrt{r}\, m_o} \tag{30}$$

The maximum value of $M_c(s_c)$ is given by

$$\bar{M}_c = M_c(\bar{s}_c) = m_c\, p_o\, a\, h_s \left(\frac{a}{r_o}\right) S \tag{31}$$

in which

$$m_c = m_o\, \phi(\beta_c \bar{s}_c) + \frac{q_o}{\sqrt[4]{3} \sqrt{r}} \zeta(\beta_c \bar{s}_c) \tag{32}$$

To make possible the determination of the point of greatest internal moment and the value of the moment coefficient (m_s or m_c) for both shell and cylinder from a single graph, the quantities β, $\bar{s}$, and m without subscripts are understood to be applicable to either the shell or the cylinder. The point of maximum internal moment is then given by

$$\tan (\beta \bar{s}) = \frac{\lambda}{\lambda - 2} \tag{33}$$

in which, for the shell,

$$\lambda = \frac{q_o}{\sqrt[4]{3}\, m_o} = 0.760 \frac{q_o}{m_o} \tag{34}$$

and, for the cylinder,

$$\lambda = -\frac{q_o}{\sqrt[4]{3} \sqrt{r}\, m_o} = -0.760 \frac{q_o}{\sqrt{r}\, m_o} \tag{35}$$

---

[6] "Theory of Plates and Shells," by S. Timoshenko, McGraw-Hill Book Co., Inc., New York, N. Y., 1940, p. 394.

The value of the coefficient, m, for maximum moment is thus given by

$$m = m_o\,[\phi(\beta\,\bar{s}) - \lambda\,\zeta(\beta\,\bar{s})] \quad \text{(36)}$$

The ratio, $\mu = m/m_o$, therefore becomes

$$\mu = \frac{m}{m_o} = \phi(\beta\,\bar{s}) - \lambda\,\zeta(\beta\,\bar{s}) \quad \text{(37)}$$

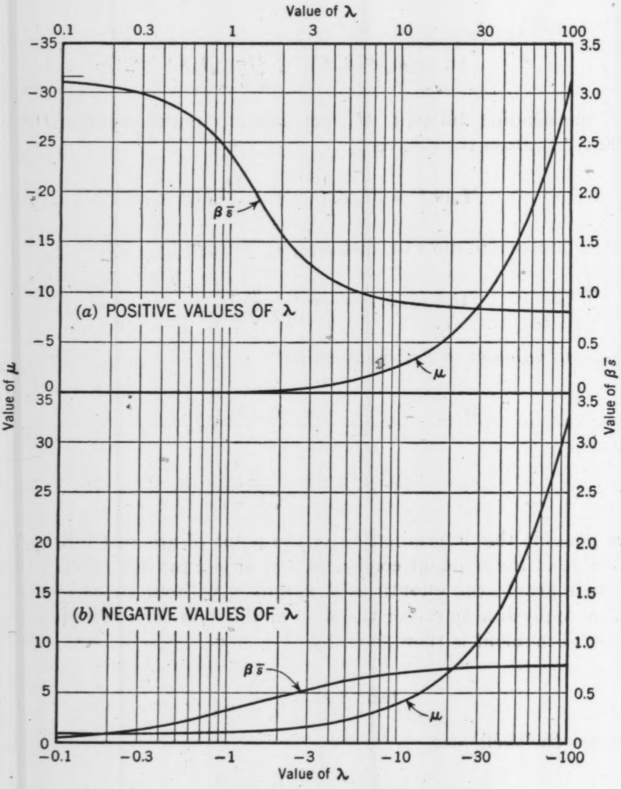

FIG. 5

Fig. 5 contains graphs relating $\beta\,\bar{s}$ and λ (Eq. 33), and also μ and λ (Eq. 37). Fig. 5(*a*) represents positive values of λ from 0.1 to 100 (in which range μ is always negative), and Fig. 5(*b*) represents negative values of λ from 0.1 to 100 (for which μ is always positive). After values of m_o and q_o have been determined from Figs. 3 and 4, two values of λ (one for the shell and one for the cylinder) can be found from Eqs. 34 and 35. Fig. 5 can then be used for either the shell or the cylinder to determine the location and magnitude of maximum internal moment. In the range in which μ is positive, μ is always greater than unity, and the design moment is of the same sign as M_o but greater than M_o. In the range in which μ is negative, it may be greater or less than unity and yields a design moment of opposite sign to that of M_o. The second peak moment (which may be greater than M_o but is always small as compared with the first peak moment) is located in any case by increasing $\beta\,\bar{s}$ by an amount, π, and is evaluated by multiplying the first peak moment by $-e^{-\pi}$, which is -0.0432.

The approximate values of $\bar{M}_s$ determined by means of Eq. 27 will be acceptable for practical purposes provided the shell does not deviate greatly from the tangent cylinder. This deviation may be easily checked by noticing that

$$\bar{s}_s = \frac{\beta_s\,\bar{s}_s}{\beta_s} = (\beta_s\,\bar{s}_s)\,\frac{\sqrt{a\,h_s}}{1.32} \ldots\ldots\ldots\ldots\ldots\ldots (38a)$$

and that the angle, $\bar{\phi}$, subtended in the shell by $\bar{s}_s$ is expressed approximately by

$$\bar{\phi} \le \frac{\bar{s}_s}{r_o} = 0.76\,(\beta_s\,\bar{s}_s)\left(\frac{a}{r_o}\right)\sqrt{\frac{h_s}{a}} \ldots\ldots\ldots\ldots\ldots (38b)$$

It is seen that the angular deviation, $\bar{\phi}$, depends not only on $\sqrt{h_s/a}$ but also on a/r_o. Because $\beta_s\,\bar{s}_s \le \pi/4$ for negative values of λ and, in most practical cases, λ is negative for the shell, the angular deviation may be taken to be

$$\bar{\phi} \le 0.60\left(\frac{a}{r_o}\right)\sqrt{\frac{h_s}{a}} \ldots\ldots\ldots\ldots\ldots\ldots\ldots\ldots (39)$$

For the case of spherical shells, angular deviations of the order of 0.10 have been shown to introduce errors of less than 1% in the moments.[3] Angular deviations of the order of 0.20 are acceptable for practical purposes.[7]

THE CASE OF SMALL EDGE MOMENTS

If the value of m_o obtained from Fig. 3 is small, the resulting value of λ may be large enough to be out of the range given in Fig. 5. It can be shown, however, that, for λ-values greater than $+100$ or less than -100, the contribution of the first term of the right-hand member of Eq. 28 or of Eq. 32 will always be less than 2.1% of the second term and that the first term can therefore be neglected in comparison with the second, giving the following approximate equations for $|\lambda| > 100$:

$$m_s = -\frac{q_o}{\sqrt[4]{3}}\,\zeta\,(\beta_s\,s_s), \qquad |\lambda| > 100 \ldots\ldots\ldots\ldots (40)$$

---

[7] "Scienza delle Costruzioni," by O. Belluzzi, Vol. III, Nicola Zanichelli Editore, Bologna, 1953, pp. 393–394.

and

$$m_c = \frac{q_o}{\sqrt[4]{3}\,\sqrt{r}}\,\zeta(\beta_c\, s_c), \qquad |\lambda| > 100 \tag{41}$$

Eqs. 40 and 41 can be further simplified by noticing that, for absolute values of λ larger than 100, $\beta\, s$ is nearly equal to $\pi/4$. Using this value in Eqs. 40 and 41, the following equations are obtained for m_s and m_c:

$$m_s = -\,0.245\, q_o \tag{42}$$

and

$$m_c = 0.245\, \frac{q_o}{\sqrt{r}} \tag{43}$$

LIVE-LOAD MOMENTS

When the load on the shell is a live load defined by

$$p = p_o\, f(x) \tag{44}$$

in which p is the load per unit area of horizontal projection of the shell and p_o is the load intensity at the lower edge or at the shell top, the edge displacement and rotations are given by[4]

$$w_o = \frac{p_o\, a^2}{E\, h_s}\left(\frac{a}{r_o}\right) S_L \tag{45}$$

and

$$\psi_o = 0 \tag{46}$$

In Eq. 45, S_L is the nondimensional static moment of the live load with respect to the shell axis, defined as follows:

$$S_L = \frac{1}{a^2}\int_o^a f(x)\, x\, dx \tag{47}$$

Because in Eqs. 18 and 19 the terms involving $(1/S)\ \sqrt{h_s/a}$ are derived from the rotation, ψ_o, due to the load, and ψ_o is zero for the live load of Eq. 44, the graphs of Figs. 3 and 4 corresponding to $(1/S)\ \sqrt{h_s/a} = 0$ may be used directly to obtain values of m_o and q_o for the case of the live load. The maximum moments are then evaluated as was done for the case of the dead load. (The bending stresses due to live load depend on the single parameter, r, and have also been evaluated directly elsewhere.[8])

EVALUATION OF S AND S_L

The evaluation of S as defined by Eq. 7 can be accomplished by numerical integration in most cases and by analytical integration in some instances. Results will be presented herein for ellipsoidal shells generated by half ellipses of various ratios of the minor semiaxis, b, to the major semiaxis, a, (Fig. 6), including spherical shells, for the cases of constant thickness and of thickness varying linearly with ϕ.

---

[8] "Live Load and Temperature Moments in Shells of Rotation Built into Cylinders," by Mario G. Salvadori, *Journal*, A. C. I., Vol. 27, No. 2, 1955.

For constant thickness, $g(\phi) = 1$ and Eq. 7 becomes, upon proper substitution[9] for r_1 and r_2,

$$S = \left(\frac{b}{a}\right)^2 \int_0^{\pi/2} \frac{\sin\phi \, d\phi}{[\sin^2\phi + \left(\frac{b}{a}\right)^2 \cos^2\phi]^2} \quad \text{(48)}$$

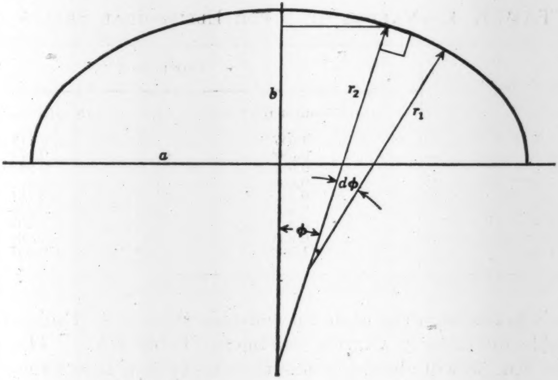

FIG. 6

Eq. 48 can be integrated exactly and yields

$$S = \frac{1}{2} + \frac{1 - k^2}{4\,k} \log\frac{1 + k}{1 - k} \quad \text{(49)}$$

in which

$$k = \sqrt{1 - \left(\frac{b}{a}\right)^2} \quad \text{(50)}$$

Values of S for various values of b/a are given in Table 1(a).

For the case of linearly varying thickness, $g(\phi) = (2/\pi)\,\phi$, and Eq. 7 becomes

$$S = \frac{2}{\pi}\left(\frac{b}{a}\right)^2 \int_0^{\pi/2} \frac{\phi \sin\phi \, d\phi}{\left[\sin^2\phi + \left(\frac{b}{a}\right)^2 \cos^2\phi\right]^2} \quad \text{(51)}$$

Eq. 51 can be integrated by numerical methods, and values obtained by means of Simpson's one-third rule and h^4-extrapolation[10] are given in Table 1(b).

---

[9] "Theory of Plates and Shells," by S. Timoshenko, McGraw-Hill Book Co., Inc., New York, N. Y., 1940, p. 365.

[10] "Numerical Methods in Engineering," by Mario G. Salvadori and Melvin L. Baron, Prentice-Hall, Inc., New York, N. Y., 1952, pp. 72 and 75.

For the case of a thickness varying linearly from some value, h_1, at the crown to another (greater) value, h_o, at the edge—that is, for

$$g(\phi) = \frac{h_1}{h_o} + \frac{2}{\pi}\left(1 - \frac{h_1}{h_o}\right)\phi \quad \text{.................. (52)}$$

the quantity, S, can be computed from

$$S = \frac{h_1}{h_o} S_1 + \left(1 - \frac{h_1}{h_o}\right) S_2 \quad \text{.................. (53)}$$

TABLE 1.—VALUES OF S FOR ELLIPSOIDAL SHELLS

Value of b/a	VALUE OF S	
	(a) Constant thickness	(b) $g(\phi) = 2\,\phi/\pi$
0.2	0.547	0.114
0.3	0.588	0.171
0.4	0.637	0.228
0.5	0.690	0.295
0.6	0.747	0.361
0.7	0.807	0.428
0.8	0.870	0.497
0.9	0.934	0.566
1.0	1.000	0.637

in which S_1 is taken from the table for constant thickness (Table 1(a)) and S_2 from the table for linearly varying thickness (Table 1(b)). The value of S computed by Eq. 53 will always be less than unity if h_1 is less than h_o.

In most practical cases, S will be greater than 0.1, and the graphs of Figs. 3 and 4 have been extended to include all values of h_s/a from zero to 1/50, assuming that S will not be smaller than 0.1.

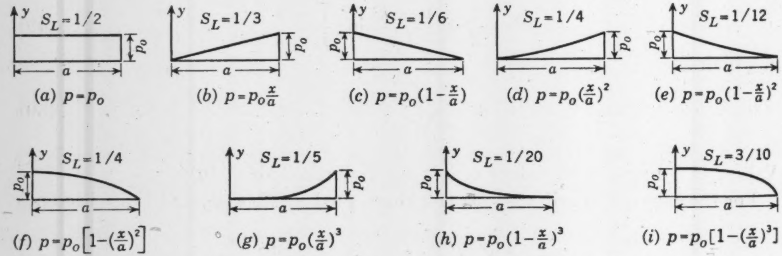

(a) $p = p_o$ (b) $p = p_o\frac{x}{a}$ (c) $p = p_o(1-\frac{x}{a})$ (d) $p = p_o(\frac{x}{a})^2$ (e) $p = p_o(1-\frac{x}{a})^2$

(f) $p = p_o\left[1-(\frac{x}{a})^2\right]$ (g) $p = p_o(\frac{x}{a})^3$ (h) $p = p_o(1-\frac{x}{a})^3$ (i) $p = p_o[1-(\frac{x}{a})^3]$

FIG. 7

For any other function, $g(\phi)$, when the meridian is elliptical, Eq. 7 can be integrated by expressing it in the form:

$$S = \left(\frac{b}{a}\right)^2 \int_0^{\pi/2} g(\phi)\, \frac{\sin\phi\, d\phi}{\left[\sin^2\phi + \left(\frac{b}{a}\right)^2 \cos^2\phi\right]^2} \quad \text{.......... (54)}$$

If $g(\phi)$ can be evaluated pointwise, Eq. 54 can be integrated numerically.

For more complicated meridian shapes and thickness variations, including those specified only by an architect's drawing, values of S can be determined by numerical or graphical methods using Eq. 7 as a definition and, if necessary, expressing the quantities under the integral sign in terms of other angles and distances.

Fig. 7 gives the values of S_L as defined by Eq. 47 for some of the most commonly encountered live-load distributions.

EXAMPLE

As an example of the use of the equations and graphs contained herein, an elliptical shell is considered, with $a = 40$ ft and $b = 20$ ft and with a thickness varying linearly from 2 in. at the crown to 4 in. at the edge, the shell being built into a cylinder having a thickness of 4 in. Because for elliptical shells $r_o = b^2/a$, in this example $r_o = 10$ ft and the ratio, h/r_o, takes the value 1/30, and hence the present theory will give close approximations of the dead-load moments. With $b/a = 0.5$, Table 1 yields $S_1 = 0.690$ and $S_2 = 0.295$, and by Eq. 53,

$$S = \frac{2}{4}\,(0.690) + \left(1 - \frac{2}{4}\right)(0.295) = 0.492.$$

With $h_s = h_o = \frac{1}{3}$ ft, the parameter $(1/S)\sqrt{h_s/a}$ is equal to 0.185. From Figs. 3 and 4, with $r = h_s/h_c = 1$, there is obtained $m_o = -0.023$ and $q_0 = 0.190$, and from Eqs. 34 and 35, for the shell,

$$\lambda = 0.760\,\frac{0.190}{-0.023} = -6.3$$

and, for the cylinder,

$$\lambda = -0.760\,\frac{0.190}{\sqrt{1}\,(-0.023)} = +6.3.$$

Figs. 5(*b*) and 5(*a*) give, therefore, respectively:

$$\beta_s\,\bar{s}_s = 0.60; \qquad \mu = 2.9; \qquad \text{and} \qquad m_s = 2.9\,(-0.023) = -0.067$$

and

$$\beta_c\,\bar{s}_o = 0.96; \qquad \mu = -1.4; \qquad \text{and} \qquad m_c\,(-1.4)\,(-0.023) = +0.032.$$

The angular deviation in the shell, by Eq. 39, is

$$\bar{\phi} \leq 0.60 \times \frac{40}{10}\sqrt{\frac{1/3}{40}} = 0.219 \text{ radian} = 12.5°$$

and is small enough to guarantee an acceptable error in the shell moments.

Assuming the shell material to be concrete weighing 150 lb per cu ft, the dead-load intensity at the edge becomes

$$p_o = 150 \times 0.333 = 50 \text{ lb per sq ft}$$

and, with $r_o = \dfrac{20^2}{40} = 10$ ft,

$$p_o\, a\, h_s \left(\frac{a}{r_o}\right) S = 50 \times 40 \times \frac{1}{3} \times \frac{40}{10} \times 0.492 = 1{,}310 \text{ lb-ft per ft.}$$

Hence, by Eqs. 16, 27, and 31,

$$M_o = -\,0.023 \times 1{,}310 = -\,30.2 \text{ lb-ft per ft}$$
$$\bar{M}_s = -\,0.067 \times 1{,}310 = -\,88.0 \text{ lb-ft per ft}$$

and

$$\bar{M}_c = 0.032 \times 1{,}310 = 42.0 \text{ lb-ft per ft.}$$

With

$$\beta_s = \beta_c = \frac{1.32}{\sqrt{40 \times 1/3}} = 0.362 \text{ per ft}$$

one finally obtains

$$s_s = \frac{0.60}{0.362} = 1.65 \text{ ft}$$

and

$$s_c = \frac{0.96}{0.362} = 2.65 \text{ ft.}$$

Thus, the shell must be reinforced with outside steel at the edge to resist a moment of 30.2 lb-ft per ft and outside steel 1.65 ft from the edge to resist a moment of 88.0 lb-ft per ft; the cylinder must have the same outside steel as the shell at the edge and inside steel 2.65 ft from the edge to resist a moment of 42.0 lb-ft per ft.

CONCLUSIONS

The results obtained show that the analysis of a statically indeterminate structure consisting of a shell of rotation and a cylinder can be greatly simplified without essential loss of accuracy. The use of the graphs for the solution of moments and shears, valid for both shell and cylinder under either live load or dead load, makes this analysis simpler than the analysis of a framed structure. It is therefore to be hoped that the practicing engineer will not avoid the economical use of such structures because of nonexistent analytical difficulties.

AMERICAN SOCIETY OF CIVIL ENGINEERS
Founded November 5, 1852

TRANSACTIONS

Paper No. 2859

NATURAL FREQUENCIES OF CONTINUOUS FLEXURAL MEMBERS

By Anestis S. Veletsos,[1] J. M. ASCE, and Nathan M. Newmark,[2] M. ASCE

With Discussion by Messrs. Jacob Karol, and Anestis S. Veletsos and Nathan M. Newmark

Synopsis

A numerical method is presented for determining the natural frequencies of undamped flexural vibration of continuous beams on rigid supports and of rigid-jointed plane frameworks without sidesway. The method is based on concepts which are familiar to structural engineers, and it is reduced to a routine system of numerical computations which, when repeated a sufficient number of times, will give the natural frequencies of the system considered to any desired degree of accuracy. Numerical values for the various physical constants which are necessary in the analysis by this method are tabulated. The application of the method is illustrated by three numerical examples.

Introduction

The problem of computing natural frequencies of vibration of structures is of great practical importance in the analysis and design of structures subjected to time-dependent forces or dynamic forces. This problem is particularly significant in the study of the behavior of structures under stationary periodic forces, such as those which arise from rotating or reciprocating machinery. If the frequency of the disturbing force is sufficiently close to one of the natural frequencies of the structure, the structure will undergo vibrations which, in the absence of appreciable damping effects, may become prohibitively large.

The purpose of this work is to describe a method of computing the natural frequencies of flexural vibration of elastic beams continuous over rigid supports, and of rigid-jointed, plane, elastic frameworks without sidesway. The mass of

---

Note.—Published, essentially as printed here, in July, 1955 as *Proceedings Paper 735*. Positions and titles given are those in effect when the paper or discussion was approved for publication in *Transactions*.

[1] Research Asst. Prof. of Civ. Eng., Univ. of Illinois, Urbana, Ill.

[2] Research Prof. of Structural Eng., Univ. of Illinois, Urbana, Ill.

the members composing the structure is assumed to be uniformly distributed along each member. A system with distributed mass and elasticity has an infinite number of natural frequencies; using the method presented herein one is able to determine as many of the natural frequencies as desired.

The application of classical analytical methods for determining natural frequencies of continuous beams and frames has been described by, among others, E. R. Darnley,[3] S. Timoshenko,[4] S. Bennon,[5] and K. Hohenemser and W. Prager,[6] M. ASCE. Additional methods, having a fairly general applicability, have been presented by W. Mudrak,[7,8] E. Saibel,[9] and C. T. G. Looney,[10] M. ASCE. A numerical method applicable primarily to fundamental frequencies has been developed by E. F. Masur,[11] A.M. ASCE.

The method presented herein is an extension of the method for determining the natural frequencies of torsional vibration of shafts developed by H. Holzer.[12,13,14,15] It is based on principles which are familiar to structural engineers and is reduced to a straightforward system of numerical computations which, when repeated a sufficient number of times, will give any of the natural frequencies of the system considered to any desired degree of accuracy. This procedure is simple, of wide applicability, and appears to be less subject to computational errors than any of the other methods known to the writers.

GENERAL DESCRIPTION OF METHOD

Basic Principles.—The method is based on the fact that, in the absence of damping, the exciting couple which is necessary to maintain a dynamical system in a steady state of forced vibration with finite amplitudes becomes equal to zero when the frequency of the couple is equal to one of the natural frequencies of the system. It is assumed that the exciting couple is applied at a joint for which the amplitude of rotation is different from zero for all the natural frequencies that are to be determined.

For example, one may consider a continuous beam or frame that is in a steady state of forced vibration under the action of a harmonically varying exciting couple applied at a suitable joint, designated as joint z. The amplitude of this couple is assumed to be such that the amplitude of the rotation (or of the internal bending moment) at a joint of the structure different from z—say, at joint 1—has a prescribed finite value. The vibration of the structure ist hen harmonic and its frequency is equal to that of the exciting couple. Furthermore, because the effect of damping is neglected the amplitude of vibration is constant and the response is either in phase with, or 180° out of phase with, the exciting couple.

---

[3] "The Transverse Vibrations of Beams and the Whirling of Shafts Supported at Intermediate Points,' by E. R. Darnley, *Philosophical Magazine*, Vol. 41, 1921, p. 81.

[4] "Vibration Problems in Engineering," by S. Timoshenko, D. Van Nostrand Co., Inc., New York, N. Y., 3d Ed., 1955, pp. 342–345.

[5] "Natural Modes of Vibration of Simple Frames," by S. Bennon, *Journal*, Franklin Inst., Vol. 243, 1947, pp. 13–19.

[6] "Dynamik der Stabwerke," by K. Hohenemser and W. Prager, J. Springer, Berlin, 1933.

[7] "Zur Ermittlung der Grundschwingungszahlen von durchlaufenden Trägern," by W. Mudrak, *Ingenieur-Archiv*, Vol. 7, 1936, pp. 51–55.

[8] "Bestimmung der Eigenschwingungszahlen von durchlaufenden Trägern und Rahmen," by W. Mudrak, *Zeitschrift für Angewandte Mathematik und Mechanik*, Vol. 28, 1948, pp. 258–263.

[9] "Vibration Frequencies of Continuous Beams," by E. Saibel, *Journal of the Aeronautical Sciences*, Vol. 11, 1940, p. 88.

[10] "Behavior of Structures Subjected to a Forced Vibration," by C. T. G. Looney, *Proceedings-Separate No. 451*, ASCE, June, 1954.

[11] "On the Fundamental Frequencies of Vibration of Rigid Frames," by E. F. Masur, *Proceedings*, First Midwestern Conference on Solid Mechanics, Urbana, Ill., 1953, pp. 89–94.

[12] "Die Berechnung der Drechschwingungen," by H. Holzer, J. Springer, Berlin, 1921.

[13] "Mechanical Vibrations," by J. P. Den Hartog, McGraw-Hill Book Co. Inc., New York, N. Y., 3d Ed., 1947, p. 239.

[14] *Ibid.*, p. 290.

[15] "Vibration Analysis," by N. O. Myklestad, McGraw-Hill Book Co., Inc., New York, N. Y., 1944, pp. 165–168.

For a given system, the magnitude of the exciting couple necessary to maintain the prescribed amplitude of vibration at joint 1 depends on the frequency of the couple. For the limiting case of zero frequency the magnitude of the couple is obviously finite; if desired, its value may be computed by any of the available methods of indeterminate stress analysis. As the frequency of the exciting couple increases above zero the structure is acted on by distributed inertia forces of increasingly greater magnitudes. These forces are at first in phase with the exciting couple and produce displacements in excess of those produced by the couple acting statically. With a further increase in the frequency of the exciting couple the inertia effects predominate, and for a frequency equal to the fundamental or lowest natural frequency of the structure, the magnitude of the couple becomes equal to zero. This condition of the vanishing exciting couple is characteristic of all the natural frequencies of an undamped elastic system.

Therefore, to determine the natural frequencies of a structure the following approach may be used:

1. Consider that the structure oscillates in a steady state at an assumed frequency of vibration and with a fixed amplitude of rotation (or internal bending moment) at joint 1.
2. Determine the magnitude of the exciting couple at joint z necessary to maintain the vibration.
3. Repeat these steps for a number of assumed frequencies.
4. Plot the magnitude of the exciting couple as a function of the frequency of vibration. The frequencies for which the exciting couple vanishes represent the desired natural frequencies of the structure.

It should be noted that the amplitude of rotation (or internal bending moment) at joint 1 is assumed to be different from zero in this method. Accordingly, if there exists a natural frequency for which this assumption is not satisfied the method will fail to detect it. Such a condition may occur in the case of continuous frames. A supplementary technique for determining the natural frequencies which the main procedure may fail to detect is described subsequently.

The primary computational task in the method outlined is the evaluation of the exciting couple; this may be accomplished by a number of different procedures. The conditions to be satisfied are simply those of equilibrium and continuity for each joint of the structure. These may be expressed by a set of linear equations in a number of different ways, and the equations may be solved by a variety of procedures. In the procedure presented herein, these conditions are expressed in the form of a dynamic three-slope equation and the distortions of the joints are computed by the repeated application of this equation, working progressively from one end of the structure to the other.

Elastic Constants for a Vibrating Bar.—The following terms refer to a bar which is simply supported at one end and fixed at the other, and is in a steady state of oscillation under the action of a harmonically varying bending moment applied at the simply supported end:

The amplitude of the bending moment necessary to produce, at the end at which the exciting moment is applied, a steady-state rotation of unit amplitude is termed as the "dynamic flexural stiffness" and will be denoted by the symbol, K.

The ratio of the bending moment developed at the far fixed end to the exciting moment at the near end is defined as the "dynamic flexural carry-over factor" and will be denoted by k.

The foregoing terms are generalizations of those introduced by Hardy Cross,[16] Hon. M. ASCE, for the analysis of frames under static loads. These terms were first used by R. E. Gaskell[17] in applying the method of moment distribution to the analysis of the steady-state forced vibration of frames.

For certain conditions of symmetry, antisymmetry, and for those cases for which the degree of restraint at the far end of a member is known, it may be convenient to use effective stiffnesses. The effective stiffness for a symmetrically deformed bar is

$$K^s = K\,(1 - k) \qquad \text{(1)}$$

For an antisymmetrically deformed bar, the corresponding stiffness is

$$K^a = K\,(1 + k) \qquad \text{(2)}$$

For a bar, the far end of which is subjected to a rotational elastic restraint of stiffness, R, the effective stiffness is

$$K' = K - \frac{(k\,K)^2}{K + R} \qquad \text{(3)}$$

Eqs. 1, 2, and 3 are identical to those for the static case.[18,19]

The present investigation is restricted to members having both uniform cross section and uniform mass per unit of length. The stiffness and the carry-over factor for both ends of such a member are equal.

Numerical Values of Constants.—The pertinent analytical expressions for the quantities previously defined are available.[17] The dynamic stiffness may be expressed as

$$K = C_K \frac{E\,I}{L} \qquad \text{(4)}$$

in which C_K is a dimensionless factor depending on the dimensionless parameter,

$$\lambda = \sqrt[4]{\frac{m\,\omega^2}{E\,I}}\,L \qquad \text{(5)}$$

---

[16] "Analysis of Continuous Frames by Distributing Fixed-End Moments," by Hardy Cross, *Transactions*, ASCE, Vol. 96, 1932, p. 1.

[17] "On Moment Balancing in Structural Dynamics," by R. E. Gaskell, *Quarterly of Applied Mathematics*, Vol. 1, 1943, pp. 237–249.

[18] "Continuous Frames of Reinforced Concrete," by Hardy Cross and N. D. Morgan, John Wiley & Sons, Inc., New York, N. Y., 1932, p. 119.

[19] "A Direct Method of Moment Distribution," by T. Y. Lin, *Transactions*, ASCE, Vol. 102, 1937, pp. 561.

In Eqs. 4 and 5, m is the mass per unit of length of the bar; ω is the circular frequency of vibration; E is the modulus of elasticity of the material in the bar; I is the moment of inertia of the cross section of the bar about its centroidal axis; and L is the span length of the bar. The carry-over factor, k, is dimensionless and depends also on the parameter, λ.

A graphical representation of the variation of the stiffness and the carry-over factor as a function of λ is given in Fig. 1. For $\lambda = 0$ these quantities have the well-known static values of $K = 4\,E\,I/L$ and $k = 0.5$. Values of λ equal to 3.927, 7.069, and 10.210 correspond, respectively, to the first, the second, and the third natural frequencies of a bar fixed at one end and simply supported at the other. For these frequencies, the value of the dynamic stiffness is equal to zero because no exciting moment is required to maintain the vibration. Furthermore, because the amplitude of the moment at the fixed end of the bar is different from zero for these frequencies, the value of the carry-over factor is infinite. Values of λ equal to 4.730 and 7.853 correspond to the first and the second natural frequencies of a bar fixed at both ends. For these frequencies, the stiffness of the bar becomes infinite because the end rotations are zero.

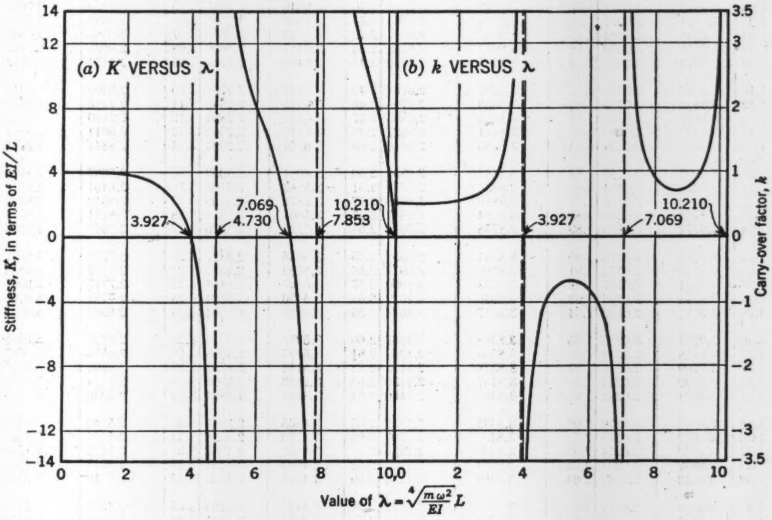

FIG. 1.—RELATIONSHIP BETWEEN K, k, AND λ

In the procedure presented herein, only the stiffness and the product of the stiffness and the carry-over factor are needed. Numerical values of these quantities have been computed to seven significant figures[20] for values of λ between zero and 10.20 at increments of 0.01. A part of these results is tabu-

---

[20] "A Method for Calculating the Natural Frequencies of Continuous Beams, Frames and Certain Types of Plates," by A. S. Veletsos, thesis presented, in 1953, to the University of Illinois at Urbana, in partial fulfilment of the requirements for the degree of Doctor of Philosophy.

TABLE 1.—DIMENSIONLESS COEFFICIENTS (AS A FUNCTION OF THE DIMENSIONLESS PARAMETER, λ) OF K AND $k\,K$ FOR A UNIFORM BAR FIXED AT THE FAR END

λ	$K\frac{L}{EI}$	$kK\frac{L}{EI}$	λ	$K\frac{L}{EI}$	$kK\frac{L}{EI}$	λ	$K\frac{L}{EI}$	$kK\frac{L}{EI}$	λ	$K\frac{L}{EI}$	$kK\frac{L}{EI}$
0	4.0000	2.0000	1.65	3.9285	2.0538	2.30	3.7200	2.2129	2.95	3.1691	2.6473
0.20	4.0000	2.0000	1.66	3.9267	2.0552	2.31	3.7149	2.2169	2.96	3.1560	2.6579
0.40	3.9998	2.0002	1.67	3.9249	2.0565	2.32	3.7096	2.2209	2.97	3.1427	2.6686
0.60	3.9988	2.0009	1.68	3.9231	2.0579	2.33	3.7043	2.2250	2.98	3.1292	2.6795
0.70	3.9977	2.0017	1.69	3.9212	2.0593	2.34	3.6989	2.2292	2.99	3.1155	2.6906
0.75	3.9970	2.0023	1.70	3.9193	2.0608	2.35	3.6935	2.2334	3.00	3.1016	2.7018]
0.80	3.9961	2.0029	1.71	3.9174	2.0622	2.36	3.6879	2.2377	3.01	3.0875	2.7132
0.85	3.9950	2.0037	1.72	3.9154	2.0637	2.37	3.6823	2.2421	3.02	3.0732	2.7248
0.90	3.9937	2.0047	1.73	3.9134	2.0653	2.38	3.6766	2.2465	3.03	3.0587	2.7366
0.95	3.9922	2.0058	1.74	3.9113	2.0668	2.39	3.6708	2.2510	3.04	3.0440	2.7485
1.00	3.9905	2.0072	1.75	3.9092	2.0684	2.40	3.6649	2.2555	3.05	3.0290	2.7607
1.02	3.9897	2.0077	1.76	3.9071	2.0700	2.41	3.6589	2.2601	3.06	3.0139	2.7730
1.04	3.9888	2.0084	1.77	3.9049	2.0717	2.42	3.6528	2.2648	3.07	2.9985	2.7855
1.06	3.9879	2.0090	1.78	3.9027	2.0733	2.43	3.6467	2.2696	3.08	2.9828	2.7983
1.08	3.9870	2.0097	1.79	3.9005	2.0750	2.44	3.6405	2.2744	3.09	2.9670	2.8112
1.10	3.9860	2.0105	1.80	3.8982	2.0768	2.45	3.6341	2.2793	3.10	2.9509	2.8243
1.12	3.9850	2.0113	1.81	3.8959	2.0785	2.46	3.6277	2.2843	3.11	2.9346	2.8377
1.14	3.9839	2.0121	1.82	3.8935	2.0803	2.47	3.6212	2.2894	3.12	2.9180	2.8513
1.16	3.9827	2.0130	1.83	3.8911	2.0821	2.48	3.6146	2.2945	3.13	2.9011	2.8651
1.18	3.9815	2.0139	1.84	3.8886	2.0840	2.49	3.6079	2.2997	3.14	2.8841	2.8791
1.20	3.9802	2.0149	1.85	3.8862	2.0859	2.50	3.6011	2.3050	3.15	2.8667	2.8933
1.21	3.9795	2.0154	1.86	3.8836	2.0878	2.51	3.5942	2.3104	3.16	2.8491	2.9078
1.22	3.9788	2.0159	1.87	3.8810	2.0898	2.52	3.5872	2.3159	3.17	2.8312	2.9225
1.23	3.9781	2.0164	1.88	3.8784	2.0917	2.53	3.5801	2.3214	3.18	2.8131	2.9374
1.24	3.9774	2.0170	1.89	3.8758	2.0938	2.54	3.5729	2.3270	3.19	2.7947	2.9526
1.25	3.9767	2.0175	1.90	3.8731	2.0958	2.55	3.5656	2.3327	3.20	2.7759	2.9681
1.26	3.9759	2.0181	1.91	3.8703	2.0979	2.56	3.5582	2.3385	3.21	2.7569	2.9838
1.27	3.9751	2.0187	1.92	3.8675	2.1000	2.57	3.5507	2.3444	3.22	2.7377	2.9997
1.28	3.9743	2.0193	1.93	3.8646	2.1022	2.58	3.5430	2.3504	3.23	2.7181	3.0160
1.29	3.9735	2.0199	1.94	3.8617	2.1044	2.59	3.5353	2.3564	3.24	2.6982	3.0325
1.30	3.9727	2.0205	1.95	3.8588	2.1067	2.60	3.5275	2.3625	3.25	2.6779	3.0493
1.31	3.9718	2.0212	1.96	3.8558	2.1089	2.61	3.5195	2.3688	3.26	2.6574	3.0663
1.32	3.9709	2.0218	1.97	3.8528	2.1113	2.62	3.5114	2.3751	3.27	2.6366	3.0837
1.33	3.9700	2.0225	1.98	3.8497	2.1136	2.63	3.5033	2.3815	3.28	2.6154	3.1013
1.34	3.9691	2.0232	1.99	3.8465	2.1160	2.64	3.4949	2.3881	3.29	2.5939	3.1193
1.35	3.9682	2.0239	2.00	3.8433	2.1184	2.65	3.4865	2.3947	3.30	2.5720	3.1375
1.36	3.9672	2.0246	2.01	3.8401	2.1209	2.66	3.4780	2.4014	3.31	2.5498	3.1561
1.37	3.9662	2.0254	2.02	3.8368	2.1234	2.67	3.4693	2.4082	3.32	2.5272	3.1750
1.38	3.9652	2.0261	2.03	3.8334	2.1260	2.68	2.4605	2.4151	3.33	2.5043	3.1942
1.39	3.9642	2.0269	2.04	3.8300	2.1286	2.69	3.4516	2.4222	3.34	2.4810	3.2138
1.40	3.9632	2.0277	2.05	3.8265	2.1312	2.70	3.4426	2.4293	3.35	2.4573	3.2337
1.41	3.9621	2.0285	2.06	3.8230	2.1339	2.71	3.4334	2.4365	3.36	2.4332	3.2539
1.42	3.9610	2.0293	2.07	3.8195	2.1366	2.72	3.4241	2.4439	3.37	2.4087	3.2746
1.43	3.9599	2.0301	2.08	3.8158	2.1394	2.73	3.4147	2.4513	3.38	2.3839	3.2955
1.44	3.9587	2.0310	2.09	3.8121	2.1422	2.74	3.4051	2.4589	3.39	2.3586	3.3169
1.45	3.9576	2.0319	2.10	3.8084	2.1451	2.75	3.3954	2.4666	3.40	2.3329	3.3386
1.46	3.9564	2.0328	2.11	3.8046	2.1480	2.76	3.3855	2.4744	3.41	2.3067	3.3607
1.47	3.9552	2.0337	2.12	3.8007	2.1510	2.77	3.3755	2.4823	3.42	2.2802	3.3833
1.48	3.9539	2.0346	2.13	3.7968	2.1540	2.78	3.3654	2.4904	3.43	2.2531	3.4062
1.49	3.9527	2.0356	2.14	3.7928	2.1570	2.79	3.3551	2.4985	3.44	2.2256	3.4296
1.50	3.9514	2.0366	2.15	3.7887	2.1601	2.80	3.3447	2.5068	3.45	2.1977	3.4534
1.51	3.9500	2.0376	2.16	3.7846	2.1633	2.81	3.3341	2.5152	3.46	2.1692	3.4776
1.52	3.9487	2.0386	2.17	3.7805	2.1665	2.82	3.3234	2.5237	3.47	2.1403	3.5023
1.53	3.9473	2.0396	2.18	3.7762	2.1697	2.83	3.3125	2.5324	3.48	2.1109	3.5274
1.54	3.9459	2.0407	2.19	3.7719	2.1730	2.84	3.3015	2.5412	3.49	2.0809	3.5531
1.55	3.9445	2.0418	2.20	3.7675	2.1764	2.85	3.2903	2.5501	3.50	2.0505	3.5792
1.56	3.9430	2.0429	2.21	3.7631	3.1798	2.86	3.2790	2.5592	3.51	2.0194	3.6058
1.57	3.9415	2.0440	2.22	3.7586	2.1832	2.87	3.2674	2.5684	3.52	1.9879	3.6329
1.58	3.9400	2.0451	2.23	3.7540	2.1868	2.88	3.2558	2.5778	3.53	1.9557	3.6605
1.59	3.9385	2.0463	2.24	3.7494	2.1903	2.89	3.2439	2.5872	3.54	1.9230	3.6887
1.60	3.9369	2.0475	2.25	3.7447	2.1939	2.90	3.2319	2.5969	3.55	1.8897	3.7174
1.61	3.9353	2.0487	2.26	3.7399	2.1976	2.91	3.2197	2.6067	3.56	1.8558	3.7467
1.62	3.9336	2.0500	2.27	3.7350	2.2014	2.92	3.2073	2.6166	3.57	1.8213	3.7766
1.63	3.9319	2.0512	2.28	3.7301	2.2052	2.93	3.1948	2.6267	3.58	1.7861	3.8071
1.64	3.9302	2.0525	2.29	3.7251	2.2090	2.94	3.1820	2.6369	3.59	1.7503	3.8381

TABLE 1.—(*Continued*)

λ	$K\frac{L}{EI}$	$kK\frac{L}{EI}$	λ	$K\frac{L}{EI}$	$kK\frac{L}{EI}$	λ	$K\frac{L}{EI}$	$kK\frac{L}{EI}$	λ	$K\frac{L}{EI}$	$kK\frac{L}{EI}$
3.60	1.7138	3.8698	4.25	−4.0214	9.1797	4.90	33.375	−28.966	5.55	10.660	−7.5873
3.61	1.6766	3.9022	4.26	−4.2335	9.3832	4.91	31.822	−27.428	5.56	10.576	−7.5312
3.62	1.6387	3.9352	4.27	−4.4548	9.5958	4.92	30.431	−26.053	5.57	10.494	−7.4768
3.63	1.6001	3.9689	4.28	−4.6859	9.8180	4.93	29.179	−24.816	5.58	10.413	−7.4242
3.64	1.5607	4.0033	4.29	−4.9274	10.051	4.94	28.045	−23.698	5.59	10.334	−7.3732
3.65	1.5206	4.0384	4.30	−5.1801	10.294	4.95	27.014	−22.682	5.60	10.256	−7.3239
3.66	1.4797	4.0742	4.31	−5.4447	10.550	4.96	26.072	−21.756	5.61	10.179	−7.2761
3.67	1.4380	4.1108	4.32	−5.7221	10.818	4.97	25.207	−20.907	5.62	10.103	−7.2298
3.68	1.3954	4.1482	4.33	−6.0133	11.100	4.98	24.411	−20.127	5.63	10.029	−7.1850
3.69	1.3520	4.1864	4.34	−6.3194	11.397	4.99	23.676	−19.408	5.64	9.9555	−7.1416
3.70	1.3078	4.2254	4.35	−6.6415	11.710	5.00	22.994	−18.743	5.65	9.8832	−7.0996
3.71	1.2626	4.2653	4.36	−6.9809	12.040	5.01	22.361	−18.126	5.66	9.8120	−7.0590
3.72	1.2165	4.3060	4.37	−7.3390	12.389	5.02	21.771	−17.553	5.67	9.7418	−7.0196
3.73	1.1694	4.3477	4.38	−7.7174	12.757	5.03	21.219	−17.018	5.68	9.6726	−6.9815
2.74	1.1214	4.3902	4.39	−8.1180	13.148	5.04	20.702	−16.518	5.69	9.6042	−6.9447
3.75	1.0724	4.4338	4.40	−8.5427	13.563	5.05	20.217	−16.050	5.70	9.5368	−6.9091
3.76	1.0223	4.4783	4.41	−8.9938	14.005	5.06	19.761	−15.611	5.71	9.4702	−6.8747
3.77	0.97110	4.5239	4.42	−9.4739	14.475	5.07	19.331	−15.199	5.72	9.4044	−6.8414
3.78	0.91884	4.5705	4.43	−9.9858	14.977	5.08	18.925	−14.811	5.73	9.3394	−6.8092
3.79	0.86543	4.6182	4.44	−10.533	15.514	5.09	18.542	−14.445	5.74	9.2752	−6.7781
3.80	0.81084	4.6670	4.45	−11.119	16.089	5.10	18.178	−14.099	5.75	9.2116	−6.7481
3.81	0.75504	4.7170	4.46	−11.748	16.708	5.11	17.833	−13.772	5.76	9.1488	−6.7192
3.82	0.69799	4.7682	4.47	−12.425	17.375	5.12	17.505	−13.462	5.77	9.0866	−6.6912
3.83	0.63965	4.8206	4.48	−13.156	18.096	5.13	17.193	−13.169	5.78	9.0251	−6.6643
3.84	0.57997	4.8744	4.49	−13.948	18.877	5.14	16.895	−12.890	5.79	8.9642	−6.6384
3.85	0.51891	4.9294	4.50	−14.808	19.727	5.15	16.612	−12.625	5.80	8.9038	−6.6134
3.86	0.45642	4.9858	4.51	−15.747	20.655	5.16	16.341	−12.373	5.81	8.8441	−6.5893
3.87	0.39246	5.0436	4.52	−16.774	21.671	5.17	16.081	−12.133	5.82	8.7848	−6.5662
3.88	0.32697	5.1029	4.53	−17.904	22.790	5.18	15.833	−11.904	5.83	8.7261	−6.5439
3.89	0.25990	5.1638	4.54	−19.152	24.027	5.19	15.595	−11.685	5.84	8.6678	−6.5226
3.90	0.19119	5.2262	4.55	−20.539	25.403	5.20	15.367	−11.477	5.85	8.6101	−6.5021
3.91	0.12079	5.2902	4.56	−22.088	26.941	5.21	15.148	−11.277	5.86	8.5527	−6.4824
3.92	0.048634	5.3560	4.57	−23.831	28.672	5.22	14.937	−11.086	5.87	8.4958	−6.4636
3.93	−0.025344	5.4235	4.58	−25.805	30.635	5.23	14.734	−10.903	5.88	8.4393	−6.4457
3.94	−0.10121	5.4928	4.59	−28.060	32.879	5.24	14.538	−10.728	5.89	8.3832	−6.4285
3.95	−0.17904	5.5641	4.60	−30.662	35.469	5.25	14.350	−10.560	5.90	8.3275	−6.4121
3.96	−0.25890	5.6373	4.61	−33.697	38.492	5.26	14.168	−10.399	5.91	8.2721	−6.3966
3.97	−0.34087	5.7126	4.62	−37.282	42.066	5.27	13.992	−10.245	5.92	8.2170	−6.3818
3.98	−0.42504	5.7900	4.63	−41.583	46.355	5.28	13.823	−10.096	5.93	8.1622	−6.3677
3.99	−0.51150	5.8696	4.64	−46.839	51.599	5.29	13.658	− 9.9534	5.94	8.1077	−6.3544
4.00	−0.60034	5.9516	4.65	−53.407	58.155	5.30	13.500	− 9.8160	5.95	8.0536	−6.3419
4.01	−0.69164	6.0360	4.66	−61.849	66.585	5.31	13.346	− 9.6839	5.96	7.9996	−6.3301
4.02	−0.78553	6.1229	4.67	−73.102	77.826	5.32	13.197	− 9.5567	5.97	7.9459	−6.3190
4.03	−0.88210	6.2124	4.68	−88.850	93.561	5.33	13.052	− 9.4342	5.98	7.8925	−6.3086
4.04	−0.98148	6.3046	4.69	−112.46	117.16	5.34	12.911	− 9.3162	5.99	7.8392	−6.2989
4.05	−1.0838	6.3997	4.70	−151.79	156.48	5.35	12.775	− 9.2024	6.00	7.7862	−6.2899
4.06	−1.1891	6.4978	4.71	−230.36	235.04	5.36	12.643	− 9.0926	6.01	7.7333	−6.2817
4.07	−1.2977	6.5991	4.72	−465.43	470.09	5.37	12.514	− 8.9868	6.02	7.6806	−6.2741
4.08	−1.4096	6.7036	4.73+	∓∞	±∞	5.38	12.388	− 8.8846	6.03	7.6280	−6.2671
4.09	−1.5249	6.8115	4.74	480.58	−475.95	5.39	12.266	− 8.7860	6.04	7.5756	−6.2609
4.10	−1.6439	6.9230	4.75	242.62	−238.00	5.40	12.147	− 8.6908	6.05	7.5233	−6.2553
4.11	−1.7668	7.0383	4.76	163.51	−158.91	5.41	12.031	− 8.5988	6.06	7.4711	−6.2504
4.12	−1.8937	7.1575	4.77	124.00	−119.40	5.42	11.918	− 8.5099	6.07	7.4190	−6.2461
4.13	−2.0247	7.2809	4.78	100.30	−95.717	5.43	11.808	− 8.4240	6.08	7.3670	−6.2425
4.14	−2.1603	7.4086	4.79	84.501	−79.934	5.44	11.701	− 8.3409	6.09	7.3151	−6.2396
4.15	−2.3004	7.5410	4.80	73.219	−68.666	5.45	11.595	− 8.2606	6.10	7.2632	−6.2373
4.16	−2.4455	7.6781	4.81	64.757	−60.218	5.46	11.493	− 8.1829	6.11	7.2113	−6.2356
4.17	−2.5957	7.8203	4.82	58.176	−53.650	5.47	11.392	− 8.1078	6.12	7.1595	−6.2346
4.18	−2.7513	7.9679	4.83	52.909	−48.398	5.48	11.294	− 8.0351	6.13	7.1077	−6.2342
4.19	−2.9127	8.1212	4.84	48.600	−44.103	5.49	11.198	− 7.9647	6.14	7.0559	−6.2344
4.20	−3.0802	8.2805	4.85	45.008	−40.525	5.50	11.104	− 7.8966	6.15	7.0041	−6.2353
4.21	−3.2540	8.4461	4.86	41.967	−37.499	5.51	11.011	− 7.8307	6.16	6.9522	−6.2368
4.22	−3.4347	8.6183	4.87	39.360	−34.907	5.52	10.921	− 7.7668	6.17	6.9003	−6.2389
4.23	−3.6225	8.7977	4.88	37.100	−32.661	5.53	10.832	− 7.7051	6.18	6.8484	−6.2416
4.24	−3.8179	8.9847	4.89	35.122	−30.698	5.54	10.745	− 7.6452	6.19	6.7964	−6.2450

TABLE 1.—(*Continued*)

λ	$K\frac{L}{EI}$	$kK\frac{L}{EI}$	λ	$K\frac{L}{EI}$	$kK\frac{L}{EI}$	λ	$K\frac{L}{EI}$	$kK\frac{L}{EI}$	λ	$K\frac{L}{EI}$	$kK\frac{L}{EI}$
6.20	6.7444	−6.2490	6.65	4.1064	−7.1371	7.10	−0.46186	−10.384	7.55	−16.576	−25.287
6.21	6.6922	−6.2536	6.66	4.0356	−7.1755	7.11	−0.61625	−10.511	7.56	−17.474	−26.158
6.22	6.6400	−6.2589	6.67	3.9639	−7.2150	7.12	−0.77445	−10.642	7.57	−18.434	−27.091
6.23	6.5876	−6.2648	6.68	3.8914	−7.2555	7.13	−0.93663	−10.777	7.58	−19.464	−28.094
6.24	6.5351	−6.2713	6.69	3.8179	−7.2971	7.14	−1.1030	−10.917	7.59	−20.571	−29.173
6.25	6.4825	−6.2785	6.70	3.7436	−7.3398	7.15	−1.2736	−11.060	7.60	−21.764	−30.339
6.26	6.4297	−6.2862	6.71	3.6683	−7.3836	7.16	−1.4488	−11.208	7.61	−23.054	−31.602
9.27	6.3768	−6.2946	6.72	3.5920	−7.4286	7.17	−1.6286	−11.361	7.62	−24.454	−32.974
6.28	6.3237	−6.3037	6.73	3.5147	−7.4747	7.18	−1.8134	−11.519	7.63	−25.977	−34.470
6.29	6.2704	−6.3134	6.74	3.4364	−7.5220	7.19	−2.0034	−11.682	7.64	−27.643	−36.108
6.30	6.2169	−6.3237	6.75	3.3570	−7.5706	7.20	−2.1987	−11.850	7.65	−29.470	−37.908
6.31	6.1631	−6.3347	6.76	3.2765	−7.6204	7.21	−2.3996	−12.024	7.66	−31.486	−39.895
6.32	6.1092	−6.3463	6.77	3.1949	−7.6715	7.22	−2.6065	−12.204	7.67	−33.720	−42.101
6.33	6.0550	−6.3585	6.78	3.1121	−7.7240	7.23	−2.8195	−12.391	7.68	−36.210	−44.564
6.34	6.0006	−6.3715	6.79	3.0281	−7.7778	7.24	−3.0391	−12.583	7.69	−39.003	−47.329
6.35	5.9459	−6.3850	6.80	2.9428	−7.8330	7.25	−3.2655	−12.783	7.70	−42.159	−50.457
6.36	5.8909	−6.3993	6.81	2.8563	−7.8896	7.26	−3.4990	−12.990	7.71	−45.754	−54.024
6.37	5.8356	−6.4142	6.82	2.7684	−7.9476	7.27	−3.7400	−13.204	7.72	−49.886	−58.128
6.38	5.7800	−6.4298	6.83	2.6791	−8.0072	7.28	−3.9890	−13.426	7.73	−54.687	−62.900
6.39	5.7241	−6.4461	6.84	2.5885	−8.0683	7.29	−4.2464	−13.657	7.74	−60.333	−68.518
6.40	5.6679	−6.4630	6.85	2.4963	−8.1310	7.30	−4.5125	−13.896	7.75	−67.070	−75.227
6.41	5.6113	−6.4807	6.86	2.4027	−8.1953	7.31	−4.7879	−14.145	7.76	−75.250	−83.379
6.42	5.5544	−6.4990	6.87	2.3075	−8.2613	7.32	−5.0732	−14.403	7.77	−85.392	−93.492
6.43	5.4970	−6.5181	6.88	2.2107	−8.3290	7.33	−5.3688	−14.672	7.78	−98.301	−106.37
6.44	5.4393	−6.5379	6.89	2.1123	−8.3985	7.34	−5.6754	−14.952	7.79	−115.29	−123.33
6.45	5.3812	−6.5584	6.90	2.0121	−8.4698	7.35	−5.9936	−15.243	7.80	−138.66	−146.67
6.46	5.3226	−6.5796	6.91	1.9101	−8.5430	7.36	−6.3242	−15.547	7.81	−172.84	−180.82
6.47	5.2636	−6.6016	6.92	1.8064	−8.6181	7.37	−6.6679	−15.864	7.82	−227.60	−235.55
6.48	5.2042	−6.6243	6.93	1.7007	−8.6952	7.38	−7.0256	−16.195	7.83	−329.54	−337.46
6.49	5.1442	−6.6478	6.94	1.5930	−8.7744	7.39	−7.3981	−16.541	7.84	−585.85	−593.75
6.50	5.0838	−6.6720	6.95	1.4834	−8.8556	7.40	−7.7864	−16.902	7.85	−2441.7	−2449.6
6.51	5.0229	−6.6971	6.96	1.3716	−8.9391	7.41	−8.1916	−17.281	7.86	1164.5	1156.7
6.52	4.9615	−6.7229	6.97	1.2577	−9.0249	6.42	−8.6149	−17.677			
6.53	4.8995	−6.7496	6.98	1.1415	−9.1129	7.43	−9.0576	−18.093			
6.54	4.8369	−6.7770	6.99	1.0230	−9.2034	7.44	−9.5210	−18.530			
6.55	4.7738	−6.8053	7.00	0.90203	−9.2964	7.45	−10.007	−18.989			
6.56	4.7101	−6.8344	7.01	0.77860	−9.3919	7.46	−10.516	−19.471			
6.57	4.6458	−6.8644	7.02	0.65256	−9.4901	7.47	−11.052	−19.980			
6.58	4.5808	−6.8953	7.03	0.52383	−9.5911	7.48	−11.616	−20.517			
6.59	4.5152	−6.9270	7.04	0.39231	−9.6950	7.49	−12.209	−21.084			
6.60	4.4489	−6.9597	7.05	0.25789	−9.8018	7.50	−12.836	−21.683			
6.61	4.3818	−6.9933	7.06	0.12045	−9.9117	7.51	−13.498	−22.319			
6.62	4.3141	−7.0278	7.07	−0.020117	−10.025	7.52	−14.200	−22.993			
6.63	4.2457	−7.0632	7.08	−0.16394	−10.141	7.53	−14.944	−23.710			
6.64	4.1764	−7.0997	7.09	−0.31114	−10.261	7.54	−15.734	−24.473			

lated to five significant figures in Table 1. It should be noted that some of these values could have been obtained from functions tabulated by Messrs. Hohenemser and Prager.[6]

CONTINUOUS BEAMS

Characteristics of Beams Considered.—The beams considered herein are assumed to be initially straight and continuous over nondeflecting supports. The cross section and the mass per unit of length of each beam may vary from one span to the next, but in any one span these quantities are considered constant. It is assumed that the vibration is restricted to one of the principal planes of flexure of the beam and that the cross-sectional dimensions of each span are small in comparison to its length, so that the effects of shearing deformation and rotatory inertia are negligible.

Sign Convention and Nomenclature.—Downward deflections and clockwise rotations are taken as positive herein. Internal bending moments in a member at its connection with other members, and external couples, are taken as positive when acting in a clockwise direction.

The supports are numbered consecutively starting with 1 at the extreme left end and terminating with z at the extreme right end. The quantities, L_j, $E_j I_j$, m_j, λ_j, K_j, and $(k K)_j$, refer to the span between supports j and j + 1. The symbol, θ_j, denotes the amplitude of the rotation at the jth support and M_j denotes the corresponding amplitude of internal bending moment. The subscripts, L and R, designate, respectively, sections just to the left and just to the right of the support. The amplitude of the exciting couple at support z is denoted by $\bar{M}_z$.

Fundamental Equations.—Fig. 2 shows, to an exaggerated scale, the extreme deflected position of spans j − 1 and j of a continuous beam undergoing steady-state forced vibration. The vibration is assumed to be maintained by a single exciting couple applied at support z. The rotations and bending moments at the ends of each span are indicated in their positive directions. Their value at a time, t, for support j are

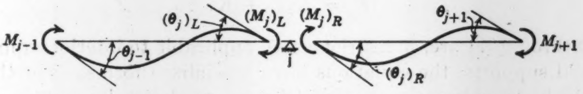

FIG. 2.—SPANS j-1 AND j OF A CONTINUOUS BEAM

$$\theta_j(t) = \theta_j \cos \omega t \qquad (6a)$$

and

$$M_j(t) = M_j \cos \omega t \qquad (6b)$$

In the equations to be used, the term, $\cos \omega t$, appears as a common factor; for convenience this will be omitted, and in the remainder of this investigation the terms "amplitude of rotation" and "rotation" and the terms "amplitude of moment" and "moment" will be used interchangeably.

From the conditions of continuity and equilibrium it follows that, at the interior support, j,

$$(\theta_j)_L = (\theta_j)_R = \theta_j \qquad (7)$$

and

$$(M_j)_L + (M_j)_R = 0 \qquad (8)$$

The moments, $(M_j)_L$ and $(M_j)_R$, can be expressed in terms of the end rotations of spans j − 1 and j, respectively. For span j, one can assume, first, that the right end of the span is held fixed while the left end is rotated through an angle, θ_j; then, the moment at the end being rotated is equal to the product of the rotation, θ_j, and the flexural stiffness of the member, K_j. Next, the left end of the span can be kept fixed while the right end is rotated through θ_{j+1}; the moment induced at the fixed left end is equal to the rotation, θ_{j+1}, multiplied by the product of the flexural stiffness and flexural carry-over factor of the member,

$(k\,K)_j$. Because the governing differential equation is linear and the principle of superposition is valid,

$$(M_j)_R = K_j\,\theta_j + (k\,K)_j\,\theta_{j+1} \tag{9a}$$

By considering span j − 1, one obtains, in a similar manner,

$$(M_j)_L = K_{j-1}\,\theta_j + (k\,K)_{j-1}\,\theta_{j-1} \tag{9b}$$

Substitution of Eqs. 9*a* and 9*b* into Eq. 8 yields

$$(k\,K)_{j-1}\,\theta_{j-1} + (K_{j-1} + K_j)\,\theta_j + (k\,K)_j\,\theta_{j+1} = 0 \tag{10a}$$

It is convenient to rewrite Eq. 10*a* into the form,

$$\theta_{j+1} = -\,\frac{(k\,K)_{j-1}\,\theta_{j-1} + \bar{K}_j\,\theta_j}{(k\,K)_j} \tag{10b}$$

in which $\bar{K}_j$, the total flexural stiffness at support j, is

$$\bar{K}_j = K_{j-1} + K_j \tag{11}$$

Eqs. 9 through 11 are, in a strict sense, applicable to interior supports only. For the end supports, the equations have specialized forms. For the general case in which the extreme ends of the beam are elastically restrained against rotation, the restraining end moments are related to the corresponding rotations by the equations:

$$M_1 = -\,R_1\,\theta_1 \tag{12a}$$

and

$$M_s = -\,R_s\,\theta_s \tag{12b}$$

in which R_1 and R_s are known stiffnesses of the rotational restraints at the left end and the right end, respectively. For a hinged end, $R = 0$, and for a fixed end, $R = \infty$. The negative signs in Eqs. 12 denote that, for a positive restraint (positive value of R), the restraining moment acts in a direction opposite to the direction of rotation of the span.

For a hinged or partly fixed condition at the extreme left end of the beam, Eq. 10*a* reduces to

$$\bar{K}_1\,\theta_1 + (k\,K)_1\,\theta_2 = 0 \tag{13a}$$

in which

$$\bar{K}_1 = R_1 + K_1 \tag{13b}$$

For a fixed condition, $\theta_1 = 0$, and the relationship between the internal moment at the fixed end and the rotation at the second support is

$$M_1 = (k\,K)_1\,\theta_2 \tag{14}$$

For a hinged or a partly fixed end at the right end of the beam, the magnitude of the exciting couple is obtained from a specialized form of Eq. 10*a* as

$$\bar{M}_s = (k\,K)_{s-1}\,\theta_{s-1} + \bar{K}_s\,\theta_s \tag{15a}$$

in which

$$\bar{K}_z = K_{z-1} + R_z \quad \text{(15}b\text{)}$$

At a natural frequency, $\bar{M}_z$ must be identically equal to zero. For a fixed end, $\theta_z = 0$, and the criterion for a natural frequency is that this equation must be satisfied. The magnitude of the internal bending moment at the fixed end is of no practical interest but, should it be desired, it can be computed from Eq. 15 by taking $\theta_z = 0$.

Outline of the Procedure.—As previously noted, the principal computational task of the procedure is the determination of the exciting force at the right end of the beam necessary to maintain a given amplitude of rotation (or internal bending moment) at the left end. Because the natural frequencies of a system depend on the relative rather than on the absolute values of the displacements, any arbitrary amplitude consistent with the actual boundary conditions may be chosen for the amplitude of vibration at support 1. For a hinged or a partly fixed end, θ_1 is taken, for convenience, to equal unity; for a fixed end, θ_1 is equal to zero, and M_1 or M_1 times L/EI of some reference span r is taken to equal unity.

The procedure is outlined as follows:

1. Assume a value of λ for some reference span, r; this step is equivalent to assuming a frequency of vibration,

$$\omega = \frac{\lambda^2_r}{L^2_r}\sqrt{\frac{E_r I_r}{m_r}} \quad \text{(16)}$$

Compute then the values of λ for the remaining spans from the expression,

$$\lambda_j = \sqrt[4]{\frac{m_j}{m_r}\frac{E_r}{E_j}\frac{I_r}{I_j}}\,\frac{L_j}{L_r}\lambda_r \quad \text{(17)}$$

The pertinent computations are conveniently carried out in a tabular form, as shown in the subsequent illustrative example. Eq. 17 is obtained readily by equating the expression for ω of the rth span to that of the jth span.

2. From Table 1, obtain the values of K and $k\,K$ for the various spans.

3. From Eq. 13 or Eq. 14 compute the rotation of the beam over the second support and, by successive applications of Eq. 10*b*, evaluate the rotations, θ_3 to θ_z. A convenient scheme for arranging the computations is described in the illustrative example. If support z is fixed, the determination of the rotation, θ_z, completes one cycle of the procedure. However, if this support is hinged or only partly fixed, it is necessary to proceed further and evaluate Eq. 15*a*.

4. Repeat steps 1 through 3 for different values of λ_r, and plot the values computed for θ_z or $\bar{M}_z$ as a function of λ_r. The zero intercepts of the resulting curve which, in general, has the shape shown in Fig. 4 (to be presented subsequently), correspond to the natural frequencies of the system considered.

Illustrative Example.—The continuous beam in Fig. 3(*a*) is elastically restrained against rotation at the left end and simply supported at the right end. The stiffness of the end restraint and the properties of the various spans are shown in Fig. 3(*a*).

For convenience in performing the computations, the natural frequencies of this beam will be expressed in terms of the pertinent properties of a reference span, r; in this case, r is assumed to equal 1. In terms of the $E\,I/L$ of the rth span, the values of K and $k\,K$ for a span, j, are equal to those obtained from Table 1 multiplied by the dimensionless factor,

$$\alpha_j = \frac{E_j\,I_j}{E_r\,I_r}\,\frac{L_r}{L_j} \qquad (18)$$

The quantities, λ_j/λ_r and α_j, are evaluated in Table 2. It should be noted that these computations are independent of the frequency of vibration. A complete cycle of the procedure will be presented herewith for a trial

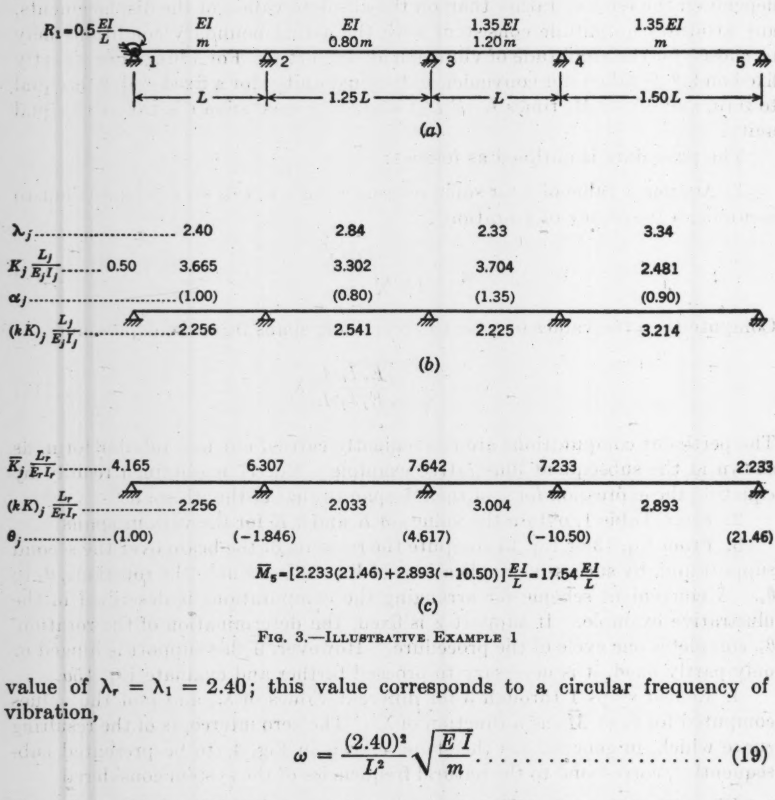
$R_1 = 0.5\frac{EI}{L}$
EI
m
EI
$0.80m$
$1.35EI$
$1.20m$
$1.35EI$
m
1
2
3
4
5
L
$1.25L$
L
$1.50L$
(a)
λ_j 2.40 2.84 2.33 3.34
$K_j\,\frac{L_j}{E_jI_j}$ 0.50 3.665 3.302 3.704 2.481
α_j .... (1.00) (0.80) (1.35) (0.90)
$(kK)_j\,\frac{L_j}{E_jI_j}$ 2.256 2.541 2.225 3.214
(b)
$\overline{K}_j\,\frac{L_r}{E_rI_r}$ 4.165 6.307 7.642 7.233 2.233
$(kK)_j\,\frac{L_r}{E_rI_r}$ 2.256 2.033 3.004 2.893
θ_j .... (1.00) (−1.846) (4.617) (−10.50) (21.46)
$\overline{M}_5 = [2.233(21.46) + 2.893(-10.50)]\frac{EI}{L} = 17.54\frac{EI}{L}$
(c)

FIG. 3.—ILLUSTRATIVE EXAMPLE 1

value of $\lambda_r = \lambda_1 = 2.40$; this value corresponds to a circular frequency of vibration,

$$\omega = \frac{(2.40)^2}{L^2}\sqrt{\frac{E\,I}{m}} \qquad (19)$$

The values of λ for the various spans are recorded at the top of the diagram in Fig. 3(*b*). These values are obtained as the product of the assumed λ_r-value and each of the values in Col. 5 of Table 2. The values of α for the various members are recorded in parentheses on the same diagram. The numbers above the values of α give the stiffnesses of the various spans whereas those below the values of α give the corresponding products of the stiffnesses and the carry-over factors. These quantities are expressed in terms of the $E\,I/L$ of the span to which they refer, and they are obtained directly from Table 1.

Before using them in the fundamental equations, it is convenient to express the quantities, K and $k\,K$, in terms of a common factor. In Fig. 3(*c*), these quantities are given in terms of the $E\,I/L$ of the reference span. In this diagram, the number above each support represents the value of $\bar{K}$ for that support, and the number at the middle of each span represents the value of $k\,K$ for that span. The value of $\bar{K}$ for the jth support is determined by taking the sum of the products of the α-values and the K-values in Fig. 3(*b*) for spans j-1 and j. Thus, the total stiffness at support 3 is

$$\bar{K}_3 = [3.302(0.80) + 3.704(1.35)]\frac{E\,I}{L} = 7.642\,\frac{E\,I}{L} \quad\ldots\ldots\ldots (20)$$

Similarly, the values of $k\,K$ are obtained by multiplying the values of $k\,K$ given in Fig. 3(*b*) by the corresponding values of α.

TABLE 2

Span	$\dfrac{m_j}{m_r}$ (1)	$\dfrac{E_j\,I_j}{E_r\,I_r}$ (2)	$\sqrt[4]{\dfrac{\text{Col. 1}}{\text{Col. 2}}}$ (3)	$\dfrac{L_j}{L_r}$ (4)	$\dfrac{\lambda_j}{\lambda_r} = \text{Col. 3} \times \text{Col. 4}$ (5)	$\alpha_j = \dfrac{\text{Col. 2}}{\text{Col. 4}}$ (6)
1 = r	1.00	1.00	1.00	1.00	1.00	1.00
2	0.80	1.00	0.9457	1.25	1.182	0.80
3	1.20	1.35	0.9710	1.00	0.9710	1.35
4	1.00	1.35	0.9277	1.50	1.392	0.90

With the foregoing information established, one can compute readily the rotations of the beam. In Fig. 3(*c*), the number in parentheses below each support represents the value of the rotation at that support; the rotation, θ_1, is taken equal to unity. The rotation, θ_2, is evaluated from Eq. 13(*a*) which, it should be recalled, is a specialized form of Eq. 10*b*. Thus,

$$\theta_2 = -\frac{4.165(1.00)}{2.256} = -1.846.$$

The rotations, θ_3, θ_4, and θ_5, are determined by the application of Eq. 10*b* to joints 2, 3, and 4, respectively. Thus,

$$\theta_3 = -\frac{2.256(1.00) + 6.307(-1.846)}{2.033} = 4.617$$

$$\theta_4 = -\frac{2.033(-1.846) + 7.642(4.617)}{3.004} = -10.50$$

and

$$\theta_5 = -\frac{3.004(4.617) + 7.233(-10.50)}{2.893} = 21.46.$$

These results are recorded in Fig. 3(*c*) as they are computed.

The exciting couple is found to be

$$\bar{M}_5 = [2.233(21.46) + 2.893\,(-\,10.50)]\,\frac{E\,I}{L} = 17.54\,\frac{E\,I}{L} \quad\ldots\ldots (21)$$

Because $\bar{M}_5$ is different from zero the assumed value of $\lambda_1 = 2.40$ does not correspond to a natural frequency of the system. The negative of the value of $\bar{M}_5$ divided by the rotation, θ_5, is

$$-\,\frac{17.54}{21.46}\,\frac{E\,I}{L} = -\,0.8173\,\frac{E\,I}{L} \quad\ldots\ldots\ldots\ldots\ldots\ldots (22)$$

and represents the stiffness of a rotational constraint which, if applied at the right end of the beam, would make the assumed frequency correspond to a natural frequency of the system.

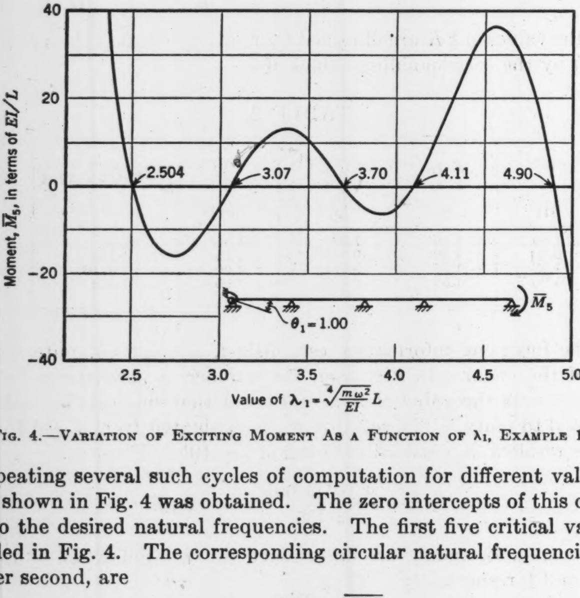

FIG. 4.—VARIATION OF EXCITING MOMENT AS A FUNCTION OF λ_1, EXAMPLE 1

By repeating several such cycles of computation for different values of λ_1, the curve shown in Fig. 4 was obtained. The zero intercepts of this curve correspond to the desired natural frequencies. The first five critical values of λ are recorded in Fig. 4. The corresponding circular natural frequencies, ω_N, in radians per second, are

$$(\omega_N)_1 = \frac{6.27}{L^2}\sqrt{\frac{E\,I}{m}} \quad\ldots\ldots\ldots\ldots\ldots\ldots (23a)$$

$$(\omega_N)_2 = \frac{9.42}{L^2}\sqrt{\frac{E\,I}{m}} \quad\ldots\ldots\ldots\ldots\ldots\ldots (23b)$$

$$(\omega_N)_3 = \frac{13.7}{L^2}\sqrt{\frac{E\,I}{m}} \quad\ldots\ldots\ldots\ldots\ldots\ldots (23c)$$

$$(\omega_N)_4 = \frac{16.9}{L^2}\sqrt{\frac{E\,I}{m}} \quad\ldots\ldots\ldots\ldots\ldots\ldots (23d)$$

and

$$(\omega_N)_5 = \frac{24.0}{L^2}\sqrt{\frac{E\,I}{m}} \qquad (23e)$$

The natural frequencies, in cycles per second, may be computed from the relationship,

$$f_N = \frac{\omega_N}{2\,\pi} \qquad (24)$$

In this example and in the subsequent ones the computations have been carried out to four significant figures. In the particular cycle described, this accuracy was greater than actually required. In general, for the determination of the lower natural frequencies of continuous beams, slide-rule accuracy will prove satisfactory. However, for the higher natural frequencies, particularly in the case of frames involving closed panels, the computations may involve small differences between large quantities and it may be necessary to retain a minimum of four significant figures.

CONTINUOUS FRAMES WITHOUT SIDESWAY

The following material applies to rigid-jointed, plane, elastic frameworks for which the joints do not translate. The individual members of each frame are considered to be of both uniform cross section and uniform mass per unit of length. The vibrations are assumed to take place in the plane of the framework. The change in length of the members due to axial deformation and the effect of the axial forces on the bending moment in the members are neglected. In addition, no account is taken of the influence of axial vibrations. As before, the cross-sectional dimensions of the members are considered to be small in comparison to their length, so that the effects of shearing deformation and rotatory inertia are negligible.

For the purpose of this investigation, structural frames will be divided into (*a*) open frames, including those which do not involve any closed panels and have known conditions of restraint at all terminals; and (*b*) closed frames, including those which do involve closed panels. Each group will be examined separately. It is first necessary, however, to develop the appropriate slope equations applicable to frames.

Fundamental Equations.—Fig. 5 shows s members of a structure rigidly connected at their common intersection, O. The ends of the members are assumed to be fixed against translation but free to rotate subject to the restraint imposed by the adjoining members. It is assumed that the structure is in a steady state of forced vibration under the action of an exciting moment applied at a joint different from joint O.

The term, θ_{O-j}, denotes the amplitude of rotation at end O of member $O - j$, and θ_{j-O} denotes the amplitude of rotation at end j of the same member. Similarly, M_{O-j} and M_{j-O} are the corresponding moment amplitudes at the same ends and, K_{O-j} and $(k\,K)_{O-j}$ are, respectively, the values of K and $k\,K$ for member $O - j$.

Because all members are rigidly connected at their joints,

$$\theta_{O-1} = \theta_{O-2} = \ldots = \theta_{O-j} = \ldots = \theta_{O-s} = \theta_O \ldots\ldots\ldots\ldots (25a)$$

and

$$\theta_{j-O} = \theta_j \ldots\ldots\ldots\ldots\ldots\ldots\ldots\ldots\ldots\ldots (25b)$$

Furthermore, because no external moment acts at joint O,

$$M_{O-1} + M_{O-2} + \ldots + M_{O-j} + \ldots + M_{O-s} = \sum_{j=1}^{s} M_{O-j} = 0 \ldots\ldots (26)$$

The moment, M_{O-j}, may be expressed in terms of the end rotations of member $O - j$ as follows:

$$M_{O-j} = K_{O-j}\,\theta_O + (k\,K)_{O-j}\,\theta_j \ldots\ldots\ldots\ldots\ldots\ldots (27)$$

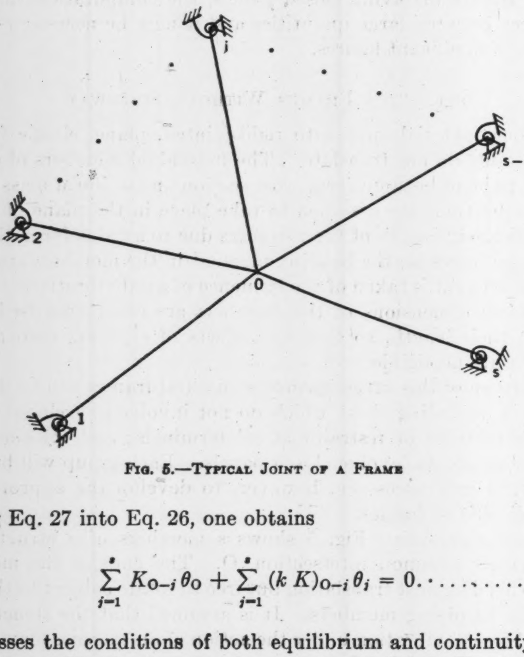

FIG. 5.—TYPICAL JOINT OF A FRAME

Substituting Eq. 27 into Eq. 26, one obtains

$$\sum_{j=1}^{s} K_{O-j}\,\theta_O + \sum_{j=1}^{s} (k\,K)_{O-j}\,\theta_j = 0 \ldots\ldots\ldots\ldots\ldots (28a)$$

which expresses the conditions of both equilibrium and continuity for joint O of the structure. If only two members meet at joint O, Eq. 28*a* reduces to Eq. 10*a* for continuous beams.

If the restraints at the far ends of the members meeting at a joint are known, it is convenient to use effective stiffnesses. If it is assumed that the restraints at ends 1 and 2 of the part of the structure shown in Fig. 5 are known, and if K'_{O-1} and K'_{O-2} are the effective stiffnesses of members $O - 1$ and $O - 2$, respectively (determined from Eq. 3), then Eq. 28*a* may be written as

$$(K'_{O-1} + K'_{O-2})\,\theta_O + \sum_{j=3}^{s} K_{O-j}\,\theta_O + \sum_{j=3}^{s} (k\,K)_{O-j}\,\theta_j = 0 \ldots\ldots (28b)$$

Open Frames.—Simple L-frames and portal frames, such as those shown in Figs. 6(*a*) and 6(*b*), behave as continuous beams on rigid supports. Therefore, their natural frequencies can be computed by the procedure presented previously under the heading, "Continuous Beams."

The natural frequencies of open frames, such as those shown in Figs. 6(*c*) through 6(*e*), can be evaluated by a variation of the procedure applicable to beams. In any of the frames in Figs. 6(*c*) through 6(*e*), 1 denotes the joint of the frame at the extreme left terminal and z denotes the joint at the extreme right terminal. Without loss of generality, it may be assumed that joint z is either hinged or elastically restrained. A fixed end may be treated in the same manner as a fixed end of a continuous beam. It can be assumed that the structure is in a steady state of forced vibration under the action of an exciting couple, $\bar{M}_z$, applied at joint z. The amplitude of the slope or of the bending moment at joint 1 is assumed to have a fixed value. If the joint is hinged or is elastically restrained, the amplitude of the slope is taken equal to unity. If the joint is fixed, the amplitude of the internal bending moment is taken equal to unity instead. For an assumed frequency of vibration, it is generally possible to compute the magnitude of the exciting moment, $\bar{M}_z$, in a manner entirely analogous to that used for continuous beams—that is, by working progressively from one end of the frame to the other, the only difference being that one must use the more general Eqs. 28 rather than Eqs. 10. By repeating this procedure for several frequencies of vibration, the magnitude of $\bar{M}_z$ may be plotted as a function of the frequency of vibration. The frequencies for which the amplitude of the exciting couple vanishes are the natural frequencies of the frame.

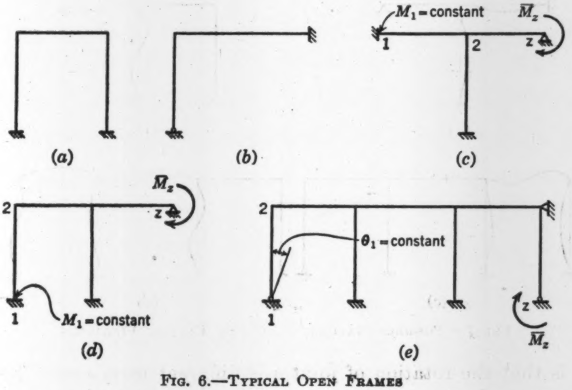

FIG. 6.—TYPICAL OPEN FRAMES

Natural Modes of Partial Vibration.—When a continuous beam is in a natural mode of vibration each span oscillates with finite amplitudes. In the case of frames, however, it is possible for only a part of the frame to oscillate while the rest remains stationary (vibrates with zero amplitude). Fig. 7 presents several such modes for the structures shown in Figs. 6(*c*) through 6(*e*). Such modes can, of course, exist only if the dimensions of the various members satisfy certain definite relationships. Natural modes for which only a part of a structure vibrates while the rest remains still are referred to as "natural modes of partial vibration."

Because of the assumptions on which it is based, the procedure described thus far may fail to detect natural frequencies corresponding to natural modes of partial vibration. It may be recalled that the amplitude of the slope or bending moment at joint 1 of the structure is assumed to be fixed in the procedure. Accordingly, the procedure will fail to reveal those natural frequencies for which bar 1–2 remains stationary. A second assumption implicit in the procedure is that the rotation of joint z is different from zero. Because this condition is not always satisfied, the procedure will fail also to reveal the natural frequencies for which the bars meeting at joint z are stationary.

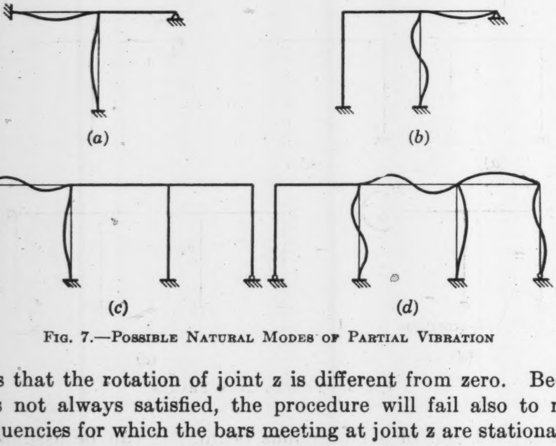

FIG. 7.—POSSIBLE NATURAL MODES OF PARTIAL VIBRATION

The natural frequencies which the main procedure fails to detect may be determined by (*a*) computing the frequencies for which bar 1–2 and the bars meeting at joint z can remain still, and (*b*) ascertaining whether or not these frequencies are natural frequencies of the system. The details of this supplementary procedure are described subsequently by a numerical example.

It is worth noting that natural modes of partial vibration occur rather infrequently; they are most likely to occur in the case of frames involving panels of uniform members. It is worth noting also that, for most practical applications, it may be entirely unnecessary to determine natural frequencies corresponding to such modes. In practice, one is usually interested in determining natural frequencies comprised within specified ranges of frequencies. Therefore, if the values computed in the first step of the supplementary procedure are found to lie outside the ranges of interest, it will be superfluous to perform the second step. The first step of this procedure, as will be shown subsequently, can usually be performed almost by inspection. It should finally be noted that natural modes of partial vibration always correspond to higher natural frequencies. Therefore, no consideration need be given to these modes if only the fundamental natural frequency of a frame is to be determined.

Illustrative Example.—As an illustration, the first few natural frequencies of the simple frame shown in Fig. 8 (*a*) will be determined. The bars identified by 1 are assumed to be identical, whereas the bar designated as 2 is considered to have such dimensions that

$$\frac{E_2\,I_2}{L_2} = \frac{E_1\,I_1}{L_1} \quad \text{(29a)}$$

$$L_2 = 0.80\,L_1 \quad \text{(29b)}$$

and

$$\lambda_2 = \frac{3.927}{4.730}\,\lambda_1 = 0.8302\,\lambda_1 \quad \text{(29c)}$$

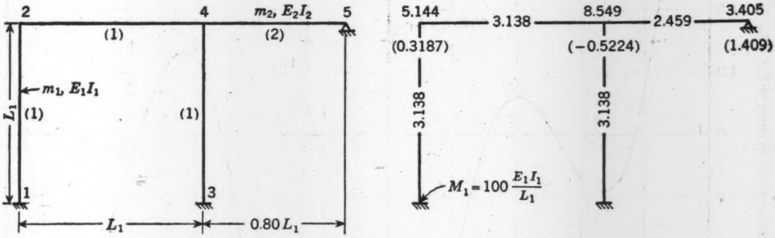

(*a*) (*b*) $\lambda_1 = 3.30$

FIG. 8.—ILLUSTRATIVE EXAMPLE 2

The subscripts 1 and 2 refer to bars 1 and 2, respectively. These proportions have been chosen so that the frame can vibrate in a natural mode of partial vibration.

For the sake of brevity, only one cycle of the procedure is presented herein. The computations are given for a value of $\lambda_1 = 3.30$, which corresponds to a value of $\lambda_2 = 2.74$.

The appropriate values of K and $k\,K$, obtained from Table 1 are, for bars 1,

$$K_1 = 2.572\,\frac{E_1\,I_1}{L_1} \quad \text{(30a)}$$

and

$$(k\,K)_1 = 3.138\,\frac{E_1\,I_1}{L_1} \quad \text{(30b)}$$

and, for bar 2,

$$K_2 = 3.405\,\frac{E_1\,I_1}{L_1} \quad \text{(31a)}$$

and

$$(k\,K)_2 = 2.459\,\frac{E_1\,I_1}{L_1} \quad \text{(31b)}$$

The data necessary in the analysis are compiled in Fig. 8(*b*). The number without parentheses opposite each joint is the sum of the stiffnesses of the members meeting at that joint. The number at the middle of each member is the product of the stiffness and the carry-over factor for the member. Both quantities are expressed in terms of $E_1 I_1/L_1$. The numbers in parentheses denote the rotations of the joints. These quantities are evaluated in the manner described subsequently and are recorded on the diagram as they are computed.

The procedure is begun by taking $M_1 = 1.00\ E_1 I_1/L_1$. Then, θ_2 is computed by application to joint 1 of Eq. 27,

$$\theta_2 = \frac{1.00}{3.138} = 0.3187.$$

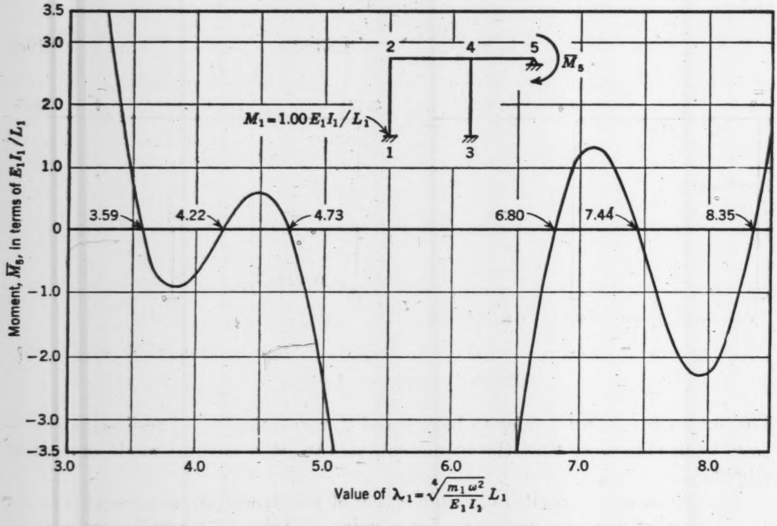

FIG. 9.—VARIATION OF EXCITING MOMENT AS A FUNCTION OF λ_1, EXAMPLE 2

The rotations, θ_4 and θ_5, are then determined successively by application of Eq. 28*a* to joints 2 and 4:

$$\theta_4 = -\frac{3.138\ (0) + 5.144\ (0.3187)}{3.138} = -\ 0.5224$$

and

$$\theta_5 = -\frac{3.138\ (0.3187) + 3.138(0)\ + 8.549\ (-\ 0.5224)}{2.459} = 1.409.$$

The magnitude of the exciting moment is determined from Eq. 27 as

$$\bar{M}_5 = [3.405\ (1.409) + 2.459\ (-\ 0.5224)]\ \frac{E_1 I_1}{L_1} = 3.513\ \frac{E_1 I_1}{L_1} \ldots . (32)$$

Because $\bar{M}_5$ is different from zero the asumed frequency does not correspond to a natural frequency. By repeating this procedure for several values of λ_1, the curve shown in Fig. 9 was obtained. The values of λ_1 corresponding to natural frequencies are recorded in Fig. 9.

It is next necessary to investigate whether there are any natural frequencies for which $M_1 = 0$. To this end, the following reasoning is used: In order for M_1 to be equal to zero, bar 1–2 must be stationary; then, the rotation and the internal bending moment at joint 2 must be also equal to zero. This condition requires that bar 2–4 be stationary and that

$$\theta_4 = M_{4-2} = 0 \qquad (33)$$

But with joint 4 remaining fixed against rotation, bar 3–4 can oscillate freely only at frequencies represented by values of

$$\lambda_1 = 4.730, 7.853 \qquad (34)$$

During a natural frequency, every member of a structure vibrates with the same frequency. Therefore, in order for these frequencies to be natural frequencies of the frame, they must also be natural frequencies of the remaining part of the frame (bar 4–5 in this particular case). The natural frequencies of bar 4–5, considering that its left end is fixed, correspond to values of

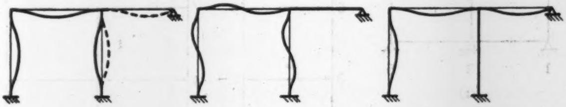
(a) $\lambda_1 = 4.73$ (b) $\lambda_1 = 7.85$ (c) $\lambda_1 = 4.73$

FIG. 10.—NATURAL MODES OF PARTIAL VIBRATION FOR EXAMPLE 2

$$\lambda_2 = 3.927, 7.069 \qquad (35a)$$

which, in turn, correspond to values of

$$\lambda_1 = 4.730, 8.514 \qquad (35b)$$

Comparing the values given in Eq. 35*b* with those given in Eq. 34 one concludes that, within the range of frequencies considered in Fig. 9, the values, $\lambda_1 = 7.853$ and $\lambda_1 = 8.514$, do not correspond to natural frequencies whereas the value $\lambda_1 = 4.730$ does. The natural mode of partial vibration for $\lambda_1 = 4.730$ is shown by the dotted curve in Fig. 10(*a*).

Finally, it is necessary to investigate whether there are any natural frequencies for which $\theta_5 = 0$. One reasons that θ_5 can be equal to zero only if bar 4–5 is stationary. Under this condition,

$$\theta_4 = M_{4-5} = 0 \qquad (36)$$

Then, bar 3–4 can vibrate freely only at frequencies represented by the values of λ_1 given in Eq. 34. Because members 1–2 and 2–4 of the remaining part of the frame are identical to member 3-4, each of the members composing the panel, 1-2-3-4, can vibrate in a fixed-ended condition for the same frequencies; therefore, the λ_1-values given in Eq. 34 correspond to natural frequencies of the frame. The natural mode of partial vibration corresponding to $\lambda_1 = 4.730$ is shown by the solid curve in Fig. 10(*a*) and the mode corresponding to $\lambda_1 = 7.853$ is shown in Fig. 10(*b*).

It should be noted that a total of three natural modes have been determined for a frequency corresponding to a value of $\lambda_1 = 4.730$. It can be shown, however, that of these three modes only two are independent; the mode shown in Fig. 10(*c*) is a linear combination of the other two.

From the foregoing, one concludes that, within the range of frequencies considered in Fig. 9, the complete set of λ_1-values corresponding to natural frequencies is 3.59, 4.22, 4.73 (double), 6.80, 7.44, 7.85, and 8.35.

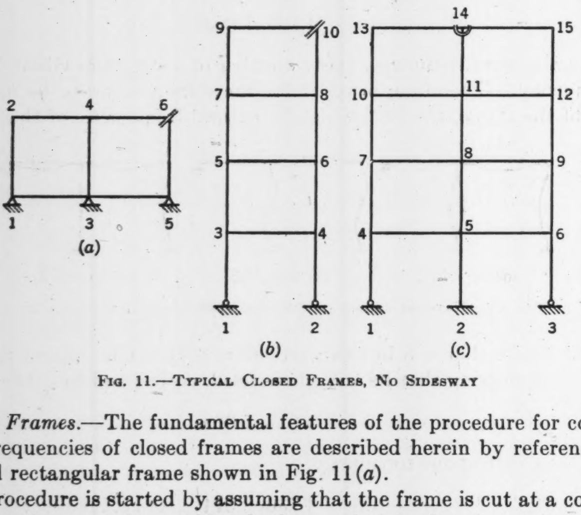

FIG. 11.—TYPICAL CLOSED FRAMES, NO SIDESWAY

Closed Frames.—The fundamental features of the procedure for computing natural frequencies of closed frames are described herein by reference to the two-celled rectangular frame shown in Fig. 11(*a*).

The procedure is started by assuming that the frame is cut at a convenient joint. For the example considered, the cut is introduced at joint $z = 6$, as shown in Fig. 11(*a*). It is next assumed that the frame undergoes a steady state of forced vibration with finite amplitudes and known frequency under the action of an exciting couple applied at the cut joint. In general, there will be a discontinuity in slope in the cut joint. However, for a natural frequency of vibration, both the amplitude of the exciting moment and the discontinuity in slope will vanish. Therefore, the criterion for a natural frequency is that equations,

$$\theta_{6-4} - \theta_{6-5} = 0 \;\ldots\ldots\ldots\ldots\ldots\ldots \quad (37a)$$

and

$$\bar{M}_6 = 0 \;\ldots\ldots\ldots\ldots\ldots\ldots\ldots\ldots \quad (37b)$$

be satisfied simultaneously. It is, of course, assumed that the frame does not oscillate in a natural mode of partial vibration.

Determination of the Discontinuity in Slope and of the Exciting Moment.—The discontinuity in slope and the magnitude of the exciting moment may be determined by working progressively from joint to joint across the structure in the same general way as for open frames, except for one major difference. Whereas for the cases considered thus far the equation for the first joint involved only two unknowns, in the present case the corresponding equation involves a minimum of three unknowns.

To illustrate this point, reference is again made to the frame shown in Fig. 11 (*a*). One begins by applying Eq. 28*a* to joint 1. The resulting expression will then involve the three unknowns, θ_1, θ_2, and θ_3, only one of which can be taken equal to a constant. Thus, it becomes necessary to express θ_3 in terms of both θ_1 and θ_2. One next selects consecutive joints in such an order that each new equation involves only one additional unknown, which is also expressed in terms of both θ_1 and θ_2. The rotation, θ_4, is determined by applying Eq. 28*a* to joint 2. The rotations, θ_5, θ_{6-4}, and θ_{6-5}, are determined by the successive application of the same equation to joints 3, 4, and 5, respectively. Finally, the exciting moment, $\bar{M}_z$, is obtained from equations similar to Eq. 27. Having expressed all these quantities in terms of θ_1 and θ_2, one may write Eqs. 37 in the form:

$$c_{11}\theta_1 + c_{12}\theta_2 = 0 \ldots\ldots\ldots\ldots\ldots\ldots\ldots (38a)$$

$$c_{21}\theta_1 + c_{22}\theta_2 = 0 \ldots\ldots\ldots\ldots\ldots\ldots\ldots (38b)$$

In Eqs. 38, the coefficients, *c*, are numerical constants, the magnitudes of which depend on the assumed frequency of vibration and on the properties of all the members of the structure. Eqs. 38 are a set of linear, homogeneous equations for the unknowns, θ_1 and θ_2, and have a solution different from zero when the determinant of the coefficients of θ_1 and θ_2 is zero—that is,

$$\Delta_6(\theta_1, \theta_2) = \begin{vmatrix} c_{11} & c_{12} \\ c_{21} & c_{22} \end{vmatrix} = 0 \ldots\ldots\ldots\ldots\ldots\ldots (39)$$

It should be noted that, in this procedure, the cut is always introduced at the joint, the rotation of which is evaluated last by the procedure described. Furthermore, the number of members meeting at the cut is always equal to the number of unknowns necessary to express the rotations of the joints.

The foregoing criterion of the vanishing determinant will fail to reveal the natural frequencies from which θ_1 and θ_2 are simultaneously equal to zero. It will also fail to reveal the natural frequencies for which the bars meeting at the cut are stationary. If necessary, the natural frequencies corresponding to these conditions of partial vibration may be determined by the supplementary procedure described previously.

The natural frequencies of vertical vibration of the single bay, multistory building frame shown in Fig. 11 (*b*) may be found in identically the same manner as for the frame in Fig. 11 (*a*). The rotations may be expressed in terms of θ_1 and θ_2 and the cut may be introduced at joint 9 or 10. For the two bay, multistory frame shown in Fig. 11 (*c*), one needs to express the rotations of the joints in terms of three quantities, such as θ_1, M_2 and θ_3, so that succeeding equations involve only one additional unknown. In this case, the cut is introduced at joint 14. The conditions of continuity and equilibrium at the cut may then be expressed as

$$\theta_{14-13} - \theta_{14-11} = c_{11}\theta_1 + c_{12}M_2 + c_{13}\theta_3 = 0 \qquad (40a)$$

$$\theta_{14-11} - \theta_{14-15} = c_{21}\theta_1 + c_{22}M_2 + c_{23}\theta_3 = 0 \qquad (40b)$$

and

$$\bar{M}_{14} = c_{31}\theta_1 + c_{32}M_2 + c_{33}\theta_3 = 0 \qquad (40c)$$

Therefore, the criterion for a natural frequency is

$$\Delta_{14}(\theta_1, M_2, \theta_3) = \begin{vmatrix} c_{11} & c_{12} & c_{13} \\ c_{21} & c_{22} & c_{23} \\ c_{31} & c_{32} & c_{33} \end{vmatrix} = 0 \qquad (41)$$

It is seen that, for this problem, it becomes necessary to evaluate a third order determinant. In general, the order of the determinant to be evaluated is equal to the number of unknowns used to determine the rotations of the joints.

Simplified Approach.—Even if only two unknowns are needed to express the rotations of the joints, the numerical work required to compute the exciting moment and the discontinuity of slope at the cut may be fairly involved. One may simplify this work by determining the desired quantities as a linear combination of partial solutions. For illustration, for the frame in Fig. 11 (*a*), one first assumes that $\theta_1 = 1.00$ and that $\theta_2 = 0$. If Eq. 28*a* is applied to joint 1, it will be found that the rotation of joint 3 will be the only unknown in the resulting expression. One then determines this unknown and, proceeding from joint to joint across the frame in the order described previously, one evaluates the rotations of the remaining joints and designates them by θ'. One also computes the magnitude of the exciting moment corresponding to the rotations θ' and designates it by $\bar{M}'_s$. Next, one assumes that $\theta_1 = 0$ and that $\theta_2 = 1.00$ and, in the same manner, one computes the rotations of the joints and the corresponding exciting moment. Denoting these quantities by θ'' and M''_s, respectively, the actual rotation at a joint, j, is

$$\theta_j = \theta'_j\theta_1 + \theta''_j\theta_2 \qquad (42)$$

For the frame shown in Fig. 11 (*a*), the total discontinuity of slope at the cut is

$$\theta_{6-4} - \theta_{6-5} = (\theta'_{6-4} - \theta'_{6-5})\theta_1 + (\theta''_{6-4} - \theta''_{6-5})\theta_2 = 0 \qquad (43)$$

and the total exciting moment is

$$\bar{M}_6 = \bar{M}'_6\theta_1 + M''_6\theta_2 \qquad (44)$$

The coefficients of θ_1 and θ_2 in Eqs. 43 and 44 correspond to the coefficients, *c*, in Eqs. 38. The direct combination of the foregoing partial effects is justified by the fact that the differential equation for steady-state forced vibration is linear.

Outline of Procedure.—The details of the main procedure can now be summarized. Some of the steps described herewith are repeated for the sake of completeness.

1. Assume that the frame is cut at a suitable joint. For some member of the frame, say member r, assume a value of λ_r (Eq. 5). This is equivalent to assuming a frequency of vibration, ω.

2. From Eq. 17 compute the values of λ for the remaining members of the frame, and from Table 1 obtain the appropriate values of K and $k\,K$ for each member.

3. The values of K and $k\,K$, as given in Table 1, are expressed in terms of $E_j\,I_j/L_j$, in which the subscript, j, refers to the particular member considered.

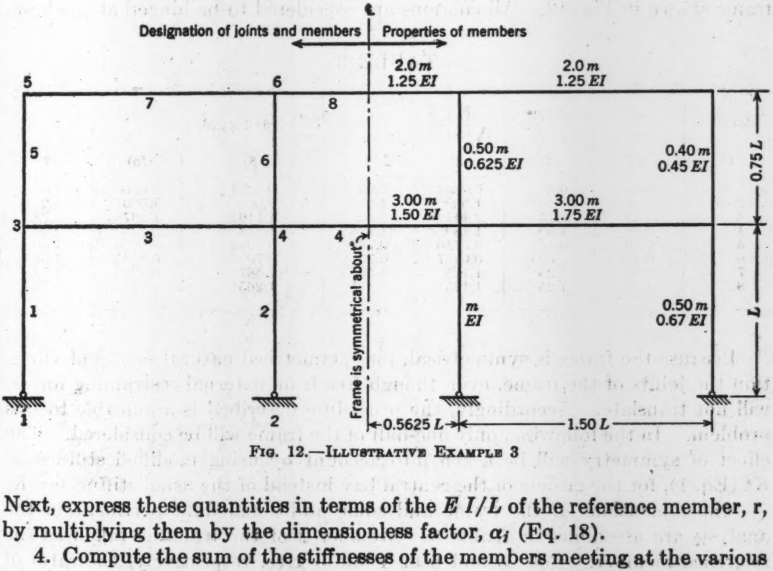
℄
Designation of joints and members
Properties of members
5
6
7
8
5
6
3
3
4
4
1
2
1
2
2.0 m
1.25 EI
2.0 m
1.25 EI
0.50 m
0.625 EI
0.40 m
0.45 EI
3.00 m
1.50 EI
3.00 m
1.75 EI
m
EI
0.50 m
0.67 EI
0.75 L
L
Frame is symmetrical about ℄
0.5625 L
1.50 L

FIG. 12.—ILLUSTRATIVE EXAMPLE 3

Next, express these quantities in terms of the $E\,I/L$ of the reference member, r, by multiplying them by the dimensionless factor, α_j (Eq. 18).

4. Compute the sum of the stiffnesses of the members meeting at the various joints and record them on a diagram of the frame. On the same diagram also record the product of the stiffness and the carry-over factor for each member. These quantities must be expressed in terms of the $E\,I/L$ of the same reference member, r. A convenient scheme for arranging the computations is shown in the illustrative examples.

5. Choose the unknowns in terms of which the distortions of the frame will be expressed. In general, the number of unknowns that must be selected is equal to the number of the main longitudinal members in the frame. Consider the first of these unknowns equal to unity and the other equal to zero. By working across the structure, in the manner described previously, compute the

rotations of the joints. Denote these by θ'. Compute also the exciting moment at the cut and denote it by $\bar{M}'_z$.

6. Repeat step 5, taking the second unknown equal to unity and the others equal to zero. Denote the resulting rotations by θ'' and the corresponding exciting moment by $\bar{M}''_z$. In general, steps 5 and 6 must be repeated as many times as there are unknowns in the expressions for the distortions of the system.

7. Determine the total discontinuity of slope and the total exciting moment at the cut, and evaluate the determinant of the coefficients of the unknowns.

8. Repeat steps 1 through 7 for a number of values of λ_r and plot the variation of the determinant evaluated in step 7 as a function of λ_r. The values of λ_r for which the determinant becomes equal to zero correspond to the desired natural frequencies of the frame.

Illustrative Example.—As an illustration there will be computed herein, the first eight natural frequencies of symmetrical vibration of the symmetrical frame shown in Fig. 12. All columns are considered to be hinged at the base.

TABLE 3

Member	$\frac{m_j}{m_r}$ (1)	$\frac{E_j I_j}{E_r I_r}$ (2)	$\sqrt{\frac{\text{Col. 1}}{\text{Col. 2}}}$ (3)	$\frac{L_j}{L_r}$ (4)	$\frac{\lambda_j}{\lambda_r} = \text{Col. 3} \times \text{Col. 4}$ (5)	$\alpha_j = \frac{\text{Col. 2}}{\text{Col. 4}}$ (6)	λ_j (7)
1	0.50	0.67	0.9294	1.00	0.9294	0.6700	2.04
2 = r	1.00	1.00	1.000	1.00	1.000	1.000	2.20
3	3.00	1.75	1.144	1.50	1.716	1.167	3.78
4	3.00	1.50	1.189	1.125	1.338	1.333	2.94
5	0.40	0.45	0.9710	0.75	0.7282	0.6000	1.60
6	0.50	0.625	0.9457	0.75	0.7093	0.8333	1.56
7	2.00	1.25	1.125	1.50	1.687	0.8333	3.71
8	2.00	1.25	1.125	1.125	1.265	1.111	2.78

Because the frame is symmetrical, for symmetrical natural modes of vibration the joints of the frame, even though free from external restraining forces, will not translate. Accordingly, the procedure described is applicable to this problem. In the following, only one-half of the frame will be considered. The effect of symmetry will be taken into account by using modified stiffnesses, K^s (Eq. 1), for the girders of the central bay instead of the usual stiffnesses, K.

The dimensions of the frame and some additional data pertinent in the analysis are assembled in Table 3. Member 2 of the frame is taken as the reference member. Cols. 5 and 6 of Table 3 give, respectively, the ratio of λ_j/λ_2 (Eq. 17) and the values of α_j (Eq. 18) for each member. For the sake of brevity, only one cycle of the procedure is presented. Detailed computations are given for a value of $\lambda_2 = 2.20$, which corresponds to a circular frequency of vibration,

$$\omega = \frac{(2.20)^2}{L^2} \sqrt{\frac{EI}{m}} \quad \ldots\ldots\ldots\ldots\ldots\ldots (45)$$

The values of α for the various members are recorded in parentheses in Fig. 13(a). The numbers above these values give the stiffnesses of the various members whereas those below the values of α give the products of the stiffnesses and the carry-over factors. These quantities are expressed in terms of the $E\,I/L$ of the member to which they refer, and they are obtained directly from Table 1.

In Fig. 13(*b*), the number without parentheses opposite each joint represents the total stiffness of the members framing into that joint. These stiffnesses are expressed in terms of the $E\,I/L$ of reference member 2. Thus, the total stiffness of the members connecting at joint 4 is

$$\bar{K}_4 = [3.768(1.00) + 0.9188(1.167) + 3.943(0.8333) + 0.5451(1.333)] \times \frac{E\,I}{L} = 8.853\,\frac{E\,I}{L} \quad (46)$$

The number at the middle of each member represents the product of the stiffness and the carry-over factor for that member; these values are also expressed in terms of the $E\,I/L$ of reference member 2.

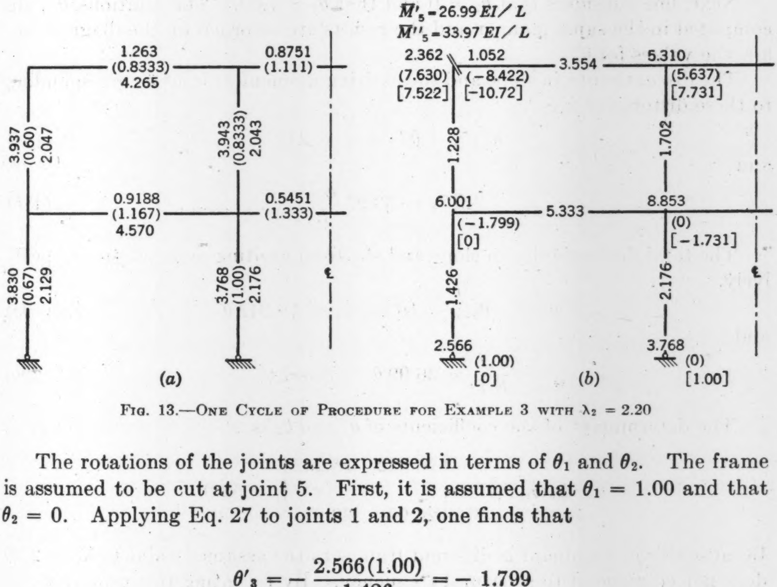
$\bar{M}'_5 = 26.99\,EI/L$
$\bar{M}''_5 = 33.97\,EI/L$
1.263
(0.8333)
4.265
0.8751
(1.111)
3.937
(0.60)
2.047
3.943
(0.8333)
2.043
0.9188
(1.167)
4.570
0.5451
(1.333)
3.830
(0.67)
2.129
3.768
(1.00)
2.176
℄
(a)
2.362
(7.630)
[7.522]
1.052
(−8.422)
[−10.72]
3.554
5.310
(5.637)
[7.731]
1.228
1.702
6.001
(−1.799)
[0]
5.333
8.853
(0)
[−1.731]
1.426
2.176
2.566
(1.00)
[0]
3.768
(0)
[1.00]
(b)
℄

FIG. 13.—ONE CYCLE OF PROCEDURE FOR EXAMPLE 3 WITH $\lambda_2 = 2.20$

The rotations of the joints are expressed in terms of θ_1 and θ_2. The frame is assumed to be cut at joint 5. First, it is assumed that $\theta_1 = 1.00$ and that $\theta_2 = 0$. Applying Eq. 27 to joints 1 and 2, one finds that

$$\theta'_3 = -\frac{2.566(1.00)}{1.426} = -1.799$$

and

$$\theta'_4 = -\frac{3.768(0)}{2.176} = 0.$$

These values are shown in parentheses in Fig. 13(*b*), and they are recorded on the diagram as they are computed. Applying Eq. 28*a* successively to joints

3, 4, and 6, one obtains

$$\theta'_{5-3} = -\frac{6.001(-1.799) + 1.426(1.00) + 5.333(0)}{1.228} = 7.630$$

$$\theta'_{6} = -\frac{0 + 5.333(-1.799) + 0}{1.702} = 5.637$$

$$\theta'_{5-6} = -\frac{0 + 5.310(5.637)}{3.554} = -8.422.$$

The discontinuity in slope at joint 5 corresponding to these distortions is

$$\theta'_{5-3} - \theta'_{5-6} = 16.052$$

and the corresponding exciting moment is

$$\bar{M}'_5 = [2.362(7.630) + 1.228(-1.799) + 1.052(-8.422) + 3.554(5.637)] \times \frac{EI}{L} = 26.99\,\frac{EI}{L} \;..\; (47)$$

Next, one considers that $\theta_1 = 0$ and that $\theta_2 = 1.00$. The rotations, θ'', are computed in the same manner and the results are recorded on the diagram below the values for θ'.

The discontinuity in slope and the exciting moment at joint 5 corresponding to these distortions are

$$\theta''_{5-3} - \theta''_{5-6} = 18.242 \;\ldots\ldots\; (48a)$$

and

$$\bar{M}''_5 = 33.97\,\frac{EI}{L} \;\ldots\ldots\; (48b)$$

The total discontinuity in slope and the total exciting moment are, respectively,

$$\theta_{5-3} - \theta_{5-6} = 16.502\,\theta_1 + 18.242\,\theta_2 \;\ldots\ldots\; (49a)$$

and

$$\frac{\bar{M}_5 L}{EI} = 26.99\,\theta_1 + 33.97\,\theta_2 \;\ldots\ldots\; (49b)$$

The determinant of the coefficients of θ_1 and θ_2 is

$$\Delta_5(\theta_1, \theta_2) = \begin{vmatrix} 16.052 & 18.242 \\ 26.99 & 33.97 \end{vmatrix} = 52.9.$$

Because this determinant is different from zero the assumed value of $\lambda_2 = 2.20$ does not correspond to a natural frequency. By repeating this procedure for several values of λ_2 and by evaluating, in each case, the resulting determinant, the curve given in Fig. 14 was obtained. The values of λ_2 corresponding to the natural frequencies of the frame are recorded in Fig. 14. The fundamental natural frequency, in radians per second, is

$$(\omega_N)_1 = \frac{(2.163)^2}{L^2}\sqrt{\frac{EI}{m}} \;\ldots\ldots\; (50)$$

It can be shown that, for the range of frequencies considered, there are no natural frequencies corresponding to modes of partial vibration.

CONCLUSIONS

A numerical method has been presented for determining the undamped natural frequencies of flexural vibration of continuous beams on rigid supports and of rigid-jointed, plane frameworks for which the joints do not displace. The members composing the structures have been considered to be of uniform cross section and mass per unit of length.

In this presentation, the effect of permanent axial forces has been neglected. This effect, which may be important when the magnitude of the external load on the structure is a sizable fraction of the critical buckling load, may be taken into account by using modified stiffness and carry-over factors which include the influence of the axial forces. These quantities may be expressed conveniently in terms of the dimensionless parameter, λ, and the ratio, P/P_o, in which P is the axial compressive or tensile force and P_o is the fundamental buckling load of the member considered, computed on the assumption that the ends of the member are simply supported. For the limiting case of $\lambda = 0$, the foregoing values of stiffness and carry-over factor reduce to those for an axially loaded bar which does not vibrate. Thus, the problem of investigating the elastic instability of continuous beams and frames becomes a special case of the more general problem of determining the natural frequencies of flexural vibration of structures in which the component members are subjected to axial forces.[20]

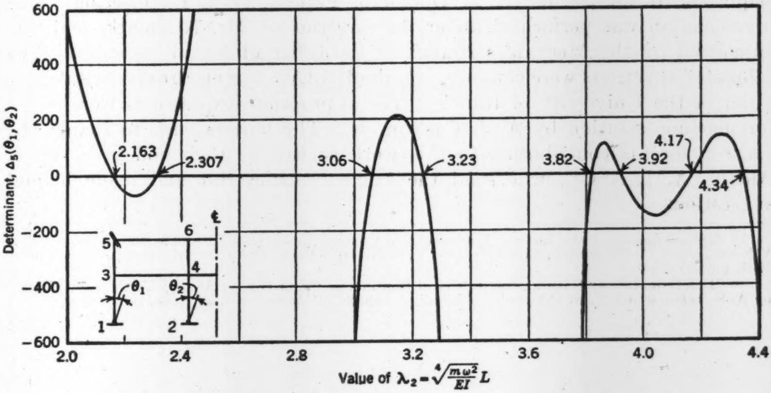

FIG. 14.—VARIATION OF DETERMINANT AS A FUNCTION OF λ_2, EXAMPLE 3

The procedure may be used also to compute natural frequencies of beams having variable cross section or variable mass per unit of length. A further extension of the method can be made to the case of continuous beams on an elastic foundation of the Winkler type.[20] To accomplish this, it is only necessary to tabulate the pertinent quantities of stiffness and of the product of the stiffness and the carry-over factor.

An obvious extension of the method is in the analysis of the steady-state forced vibration of continuous beams and frames subjected to harmonically varying forces.[20]

The extension of the method to the case of continuous beams on flexible supports and of simple frames with sidesway has been described elsewhere.[21] The method has been applied also to the case of rectangular plates which are simply supported along two opposite edges and, in one direction, are continuous over rigid supports transverse to the simply supported edges.[22]

ACKNOWLEDGMENTS

This paper is based on a thesis by Mr. Veletsos submitted to the Graduate College of the University of Illinois at Urbana in partial fulfilment of the requirements for the degree of Doctor of Philosophy in Engineering. The investigation was performed under the direction of Mr. Newmark, and was supported by the Mechanics Branch of the Office of Naval Research. The tabulated constants were computed on the ILLIAC, the electronic digital computer of the University of Illinois. The appropriate expressions were coded for machine solution by A. J. Carlson, Jr. The writers wish to thank Mr. Carlson for his contribution to this work as well as their colleague, W. J. Austin, A.M. ASCE, who read the original manuscript and made helpful suggestions.

---

[21] "Determination of the Natural Frequencies of Continuous Beams on Flexible Supports," by A. S. Veletsos and N. M. Newmark, *Proceedings*, 2d U. S. National Cong. of Applied Mechanics, ASME, June, 1954, pp. 147-155.

[22] "Determination of Natural Frequencies of Continuous Plates Hinged Along Two Opposite Edges," by A. S. Veletsos and N. M. Newmark, *Journal of Applied Mechanics*, Vol. 23, 1956, pp. 97-102.

DISCUSSION

Jacob Karol,[23] M. ASCE.—The paper is a notable contribution to the field of vibration analysis of beams and plane frameworks. The comprehensive tables of the physical constants required for analysis are of great value in the solution of a particular problem. The method of analysis should be readily understood by structural designers because it is based on the familiar concepts of moment distribution.

The determination of the natural frequencies using the authors' procedure still involves considerable computation. Alternate solutions for the three numerical examples will be presented which, it is felt, are simpler and more expeditious. The sign convention and nomenclature established by Messrs. Veletsos and Newmark will be retained.

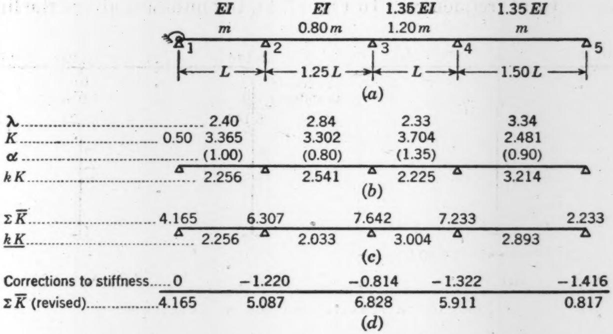
EI
m
EI
0.80m
1.35EI
1.20m
1.35EI
m
1
2
3
4
5
L
1.25L
L
1.50L
(a)
λ 2.40 2.84 2.33 3.34
K 0.50 3.365 3.302 3.704 2.481
α (1.00) (0.80) (1.35) (0.90)
kK 2.256 2.541 2.225 3.214
(b)
ΣK̄ 4.165 6.307 7.642 7.233 2.233
kK 2.256 2.033 3.004 2.893
(c)
Corrections to stiffness 0 −1.220 −0.814 −1.322 −1.416
ΣK̄ (revised) 4.165 5.087 6.828 5.911 0.817
(d)

Fig. 15.—Alternate Solution to Example 1

Illustrative Example 1.—This example involves the determination of the natural frequencies of a four-span continuous beam. The authors' procedure requires the application of a unit rotation at the left support if the end is hinged or partly fixed, or a unit moment if the end is fixed. Rotations are computed at the successive supports by Eq. 10*b*; for a hinged or partly fixed end at support *z*, the moment must be determined from Eq. 15.

The alternate procedure involves the computation of the effective stiffness at the successive supports using Eq. 3. The second term on the right side of Eq. 3 represents the change in stiffness. The detailed calculations for Example 1 are shown in Fig. 15. The bottom line in Fig. 15(*d*) shows the effective stiffness at the supports. It should be noted that the value of $K_5 = 0.817\ E I/L$ represents the moment required to produce a unit rotation and agrees with the value determined by the authors.

If the end support had been fixed, the computation of the effective stiffnesses would be carried only to the penultimate support, and the natural frequency would be that for which the effective stiffness at that support was zero.

---

[23] Prin. Design Engr., Howard, Needles, Tammen & Bergendoff, Kansas City, Mo.

Illustrative Example 2.—This example considers an open frame without sidesway which can be solved by the procedure used for continuous beams. The alternate solution is shown in Fig. 16. Because joint 1 is fixed there is no change in stiffness at joint 2. Because joint 3 is fixed the only change in stiffness at joint 4 is that involving member 2–4. The effective stiffness at $K_5 = 2.492\ E_1\ I_1/L_1$. Dividing the moment by the rotation computed by Messrs. Veletsos and Newmark for joint 5, $K_5 = 2.493\ E_1\ I_1/L_1$.

Illustrative Example 3.—This example involves a closed frame without sidesway. For this type of frame the authors present a general procedure requiring the solution of a second-order determinant. The particular frame chosen for analysis is not as complicated as it may appear at first glance. Because it is only two stories high and symmetrical about the center line, the frame is basically a single quadrangular loop with branching members. Such a frame can be analyzed directly without the use of determinants.

The solution is shown in Fig. 17 for $\lambda_2 = 2.163$, which the authors indicate is the lowest natural frequency. In Fig. 17 (*b*), the numbers above the line represent the stiffnesses and the numbers below the line the product of the stiffnesses and carry-over factors. The numbers at joints 3, 4, and 6 represent the total joint stiffness, except that the stiffnesses of members 1–3 and 2–4 have been modified to account for the hinged ends at 1 and 2.

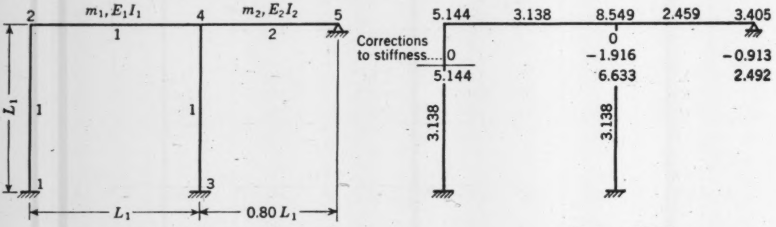

(*a*) (*b*) $\lambda_1 = 3.30$

FIG. 16.—ALTERNATE SOLUTION TO EXAMPLE 2

For convenience, the loop, 5–3–4–6, has been straightened out to simulate a continuous beam. It is first necessary to compute the effective stiffness at joint 4 using Eq. 3. Next, a unit rotation is applied at the cut ends of joint 5. The rotations induced at joints 3 and 6 are computed using Eq. 13*a*. These rotations in turn produce rotations at joint 4. The rotation of joint 4 induces rotations at joints 3 and 6. The final rotations are shown in Fig. 17 (*c*). An independent analysis for these rotations using simultaneous slope-deflection equations checked the results shown. Knowing the rotations at the joints, the moment at 5 is computed using Eq. 9.

$$M_5 = (2.365 - 1.227 \times 0.767 + 1.268 - 3.365 \times 0.787) \times \frac{E\,I}{L} = 0.042\,\frac{E\,I}{L} \quad \text{. . (51)}$$

Because the moment is almost zero, the assumed frequency is very close to the natural frequency. The natural frequency determined by the writer corresponds to $\lambda_2 = 2.164$.

An analysis for the lowest natural frequency assuming the columns fixed at joints 1 and 2 showed that it occurs at a value of $\lambda_2 = 2.182$. This indicates that it may be possible to isolate and analyze the two top stories of a multistory building and obtain reliable results. Comment regarding the limitations of such a procedure is invited from Messrs. Veletsos and Newmark.

It is worth noting that the solutions presented herein permit the recording of all the computations directly on the structural diagram and make use of only three simple equations from the basic theory. All computations were made with a slide rule. The suggested procedure also saves considerable computation. Designers may therefore find it preferable to the authors' procedure for problems where it is applicable.

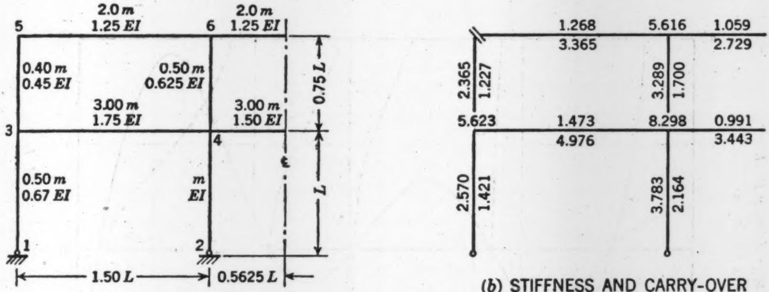
5
2.0 m
1.25 EI
6
2.0 m
1.25 EI
0.40 m
0.45 EI
0.50 m
0.625 EI
0.75 L
3.00 m
1.75 EI
3.00 m
1.50 EI
3
4
0.50 m
0.67 EI
m
EI
L
1
2
1.50 L
0.5625 L
1.268
5.616
1.059
3.365
2.729
2.365
1.227
3.289
1.700
5.623
1.473
8.298
0.991
4.976
3.443
2.570
1.421
3.783
2.164

(a) PROPERTIES OF MEMBERS

(b) STIFFNESS AND CARRY-OVER FACTORS, $\lambda_2 = 2.163$

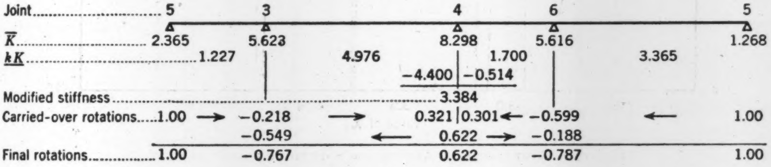
Joint
5
3
4
6
5
K̄
2.365
5.623
8.298
5.616
1.268
kK
1.227
4.976
1.700
3.365
−4.400
−0.514
Modified stiffness
3.384
Carried-over rotations
1.00
−0.218
0.321
0.301
−0.599
1.00
−0.549
0.622
−0.188
Final rotations
1.00
−0.767
0.622
−0.787
1.00

(c) JOINT ROTATIONS FOR CLOSED LOOP 5-3-4-6

FIG. 17.—ALTERNATE SOLUTION TO EXAMPLE 3

ANESTIS S. VELETSOS,[24] J.M. ASCE, AND NATHAN M. NEWMARK,[25] M. ASCE.—The procedure presented by the writers for the computation of the natural frequencies of continuous flexural members is indeed only one of a number of possible procedures for applying the general method described in the paper. Mr. Karol discusses an alternate procedure based on the "effective-stiffness criterion." This procedure consists of (*a*) computing, for a number of frequencies, the effective stiffness of some joint of the structure; and (*b*) determining the frequencies for which this stiffness becomes identically equal to zero. The information presented by Mr. Karol is of considerable value and his discussion is greatly appreciated.

---

[24] Research Asst. Prof. of Civ. Eng., Univ. of Illinois, Urbana, Ill.

[25] Research Prof. of Structural Eng., Univ. of Illinois, Urbana, Ill.

It may be of interest to note that, in the course of the investigation which resulted in the present paper, the writers studied several alternate procedures, including the procedure described by Mr. Karol. An account of these alternate procedures together with a brief discussion of their relative merits is available.[26] For particular problems some of these alternate procedures—especially the procedure described by Mr. Karol—may be somewhat simpler to apply than the procedure presented. However, for the fairly broad class of problems considered, the procedure described is found to be generally superior to all the other procedures investigated.

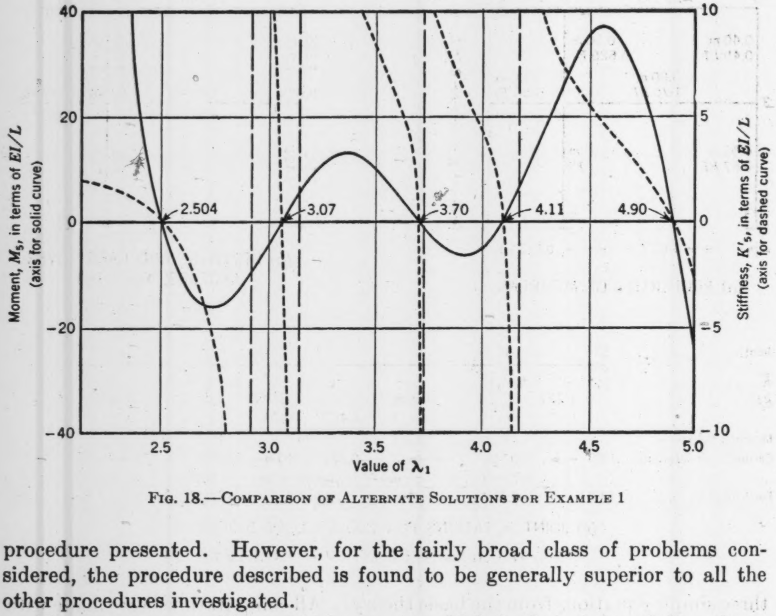

FIG. 18.—COMPARISON OF ALTERNATE SOLUTIONS FOR EXAMPLE 1

There are presented herewith the reasons which, in the opinion of the writers, make the procedure described in the paper generally superior to the procedure involving the computation of the effective stiffness.

1. In so far as the computation of only the fundamental frequencies of continuous beams is concerned, there is no advantage in using one procedure over the other. However, for the determination of the higher natural frequencies, the procedure described requires fewer trials than the procedure involving the computation of the effective stiffness.

---

[26] "A Method for Calculating the Natural Frequencies of Continuous Beams, Frames and Certain Types of Plates," by A. S. Veletsos, thesis presented to the University of Illinois at Urbana, in 1953, in partial fulfilment of the requirements for the degree of Doctor of Philosophy, pp. 31-37.

As an illustration, consider the curves in Fig. 18. These curves pertain to the beam analyzed in Example 1. The solid-line curve is the same as that given in Fig. 4. The dashed-line curve[27] shows the variation of the effective stiffness at support 5, K_5', as a function of the frequency parameter, λ_1. For both curves the λ_1-intercepts correspond to the unknown natural frequencies. One observes that, for the range of frequencies corresponding to the fundamental frequency of the beam, the variations in shape of the two curves with variations in the frequency parameter, λ_1, are of the same type and order of magnitude. Accordingly, either curve can be defined with the same number of points. Because the computation of each individual point involves essentially the same amount of work by either procedure, it makes little difference which of the two procedures is used in this case. However, for the range of frequencies corresponding to the higher natural frequencies, the situation is quite different. In this range of frequencies, the curve represented by the dashed line is discontinuous (the discontinuities correspond to the natural frequencies of the beam when fixed at the right end), and in certain regions it varies from positive values to infinite negative values and then returns to positive values over a small range of frequency. One can easily miss one of the natural frequencies by investigating the problem with too coarse a variation in forcing frequency. The dotted-line curve can be said to be "sensitive" to minor variations of the frequency. On the other hand, the curve represented by the solid line is both continuous and much less sensitive to variations in frequency. It becomes apparent that the number of points necessary to approximate the dashed-line curve is considerably larger than that required to establish the solid-line curve. That is, the higher natural frequencies can be determined with fewer trials by the procedure described than by the procedure involving the computation of the effective stiffness.

2. The procedure presented by the writers has a wider field of application than the procedure involving the computation of effective stiffnesses. Whereas the first procedure has been generalized to apply to continouus frames involving any number of closed loops, the second procedure does not appear to be capable of extension to frames involving more than a single closed loop.

Mr. Karol's procedure for determining the effective stiffness of the frame analyzed in Example 3 is both interesting and efficient. However, as appropriately pointed out, this frame is basically a single quadrangular loop with rotational restraints at the joints. Extension of the same procedure to multiple-loop frames does not appear to be possible.

In some cases the effective stiffness of a multiple-loop frame may be determined by moment distribution or slope distribution. It should be noted, however, that these procedures do not always converge to an answer. Convergence of the moment-distribution procedure can be assured only for frequencies of vibration which are smaller than the lowest natural frequency of the system considered.[17] A similar condition appears to exist for the slope-distribution procedure. In general, these procedures can be used to determine only the fundamental frequency of a structure. However, even for the range of frequencies corresponding to the fundamental frequency, the procedures of moment distribution and slope distribution may converge so slowly that they become of questionable practical value.

---

[27] "A Method for Calculating the Natural Frequencies of Continuous Beams, Frames and Certain Types of Plates," by A. S. Veletsos, thesis presented to the University of Illinois at Urbana, in 1953, in partial fulfilment of the requirements for the degree of Doctor of Philosophy, p. 190, Fig. 20.

3. An important feature of the procedure described in the paper is that it also provides information on the distortions of the structure during vibration. Because the rotations of the joints are evaluated in this procedure, the natural modes can be sketched readily. From the shape of a natural mode, it may be possible to determine also the order of the corresponding natural frequency.

With reference to the solution of Example 1 by the effective-stiffness criterion, Mr. Karol states:

> "If the end support had been fixed, the computation of the effective stiffnesses would be carried only to the penultimate support, and the natural frequency would be that for which the effective stiffness at that support was zero."

For the computation of the fundamental frequency, which is actually the problem considered by Mr. Karol, this procedure is quite satisfactory. However, it is worth noting that the same procedure when applied to the computation of the higher natural frequencies will, in general, fail to detect those natural frequencies for which the joint at the penultimate support remains stationary. To avoid this difficulty one should compute the effective stiffness at the fixed support. The natural frequencies are then those frequencies for which the effective stiffness at that support becomes infinite. If these frequencies were to be evaluated graphically, it would be more convenient to plot the reciprocal of the effective stiffness, which is proportional to the rotation of the joint, and then to determine the frequencies for which the reciprocal of the stiffness becomes equal to zero.

Some explanation appears necessary regarding the use of determinants in the procedure described in the paper. The reason for using determinants was to make it possible to compute also the natural frequencies corresponding to modes of partial vibration.

Mr. Karol refers to the possibility of determining the natural frequencies of a multistory building by considering only the two top stories rather than the complete structure. In commenting on the limitations of such a simplification it is necessary to distinguish between fundamental frequencies and higher natural frequencies.

In so far as the computation of the fundamental frequencies is concerned, it is believed that the proposed simplification will be sufficiently accurate for most practical purposes. Obviously, if the stiffness of the restraints at the base of the simplified structure could be determined accurately, the natural frequencies of both structures would be the same. The fact that these restraints cannot be evaluated in advance is not very serious. The natural frequencies of a system, such as a two-story frame which involves several members, are not very sensitive to the conditions of restraint at the ends. Therefore, any reasonable approximation for the dynamic stiffness of these restraints should lead to an accurate prediction of the desired natural frequency. The fact should not be overlooked, however, that these stiffnesses may actually be negative rather than positive. As a possible aid in estimating the magnitude of the dynamic restraints at the base of the equivalent two-story frame, one may use an approximate equation presented elsewhere.[28]

With reference to the computation of the higher natural frequencies, an analysis which considers only a part of the structure rather than the complete structure does not appear to be promising. For multistory frames, the spectra of natural frequencies are functions of the number of stories. It appears, therefore, unlikely that all significant higher natural frequencies of a multistory frame can be determined by considering only the top two stories. Additional studies are necessary before the degree of accuracy and the range of applicability of this simplification can be established adequately.

In the solution of the illustrative examples, the use of short cuts which may confuse the casual reader was purposely avoided. As may readily be inferred from Mr. Karol's discussion, the solution of Example 3 could be simplified by replacing columns 1 and 2 by rotational springs and by expressing the distortions of the structure in terms of θ_3 and θ_4 rather than in terms of θ_1 and θ_2. An additional simplification could be achieved by using available tabular data[20] for the dynamic stiffness of bars simply supported at the far ends.

Mr. Karol is to be thanked for his pertinent comments. His discussion of the effective-stiffness procedure and of some of the practical aspects of the problem are very valuable, indeed.

---

[28] "A Simple Approximation for the Fundamental Frequencies of Two-Span and Three-Span Continuous Beams," by A. S. Veletsos and N. M. Newmark, *Proceedings*, ASME, 2d U. S. National Cong. of Applied Mechanics, 1954, p. 144, Eq. 6.

AMERICAN SOCIETY OF CIVIL ENGINEERS
Founded November 5, 1852
TRANSACTIONS

Paper No. 2860

OBSERVATIONS ON THE URBAN TRANSPORTATION PROBLEM

By Harmer E. Davis,[1] A. M. ASCE

Synopsis

To provide a setting for an examination of the problem of urban transportation, the interrelationship of urban development and transportation is presented, and a series of observations pertaining to the urban transportation problem is made.

In the case of a widespread problem, it must be attacked by parts; but chances for a successful solution are enhanced by having an over-all strategy. In attempting to solve the transportation problem in large cities today (1957), it seems to be the policy to solve separate problems by short-term expedients. Policies based on an over-all view are lacking.

It is obvious that the various elements of the urban transportation problem are interrelated and that alterations in one phase of transportation facilities and services can markedly affect some of the other phases—and sometimes adversely. Although many measures for facilitating the movement of people and goods in congested urban areas are earnestly and sincerely advocated as a means of improving transportation services, when taken collectively the various proposals for relief often appear as aggregations of contradictions.

Whether it is possible to develop a unified transportation policy for an urban area is uncertain. However, with a better understanding of the effects of various transportation factors on the functioning of a community, it would be more feasible to appraise the numerous proposals which are being urged.

Interrelationship of Transportation and Urban Development

As a first step in attempting to provide some perspective on the urban transportation problem, it is helpful to review in retrospect a typical development of an urban pattern as related to the availability of transport service. For this purpose, an imaginary city is pictured as passing through many stages of development to become a metropolitan center in a period of approximately 125 years (1830 to 1957).

Note.—Published, essentially as printed here, in August, 1955, as *Proceedings Paper 769*. Positions and titles given are those in effect when the paper was approved for publication in *Transactions*.

[1] Prof. of Civ. Eng. and Director, Inst. of Transportation and Traffic Eng., Univ. of California, Berkeley, Calif.

In the 1830's it must be remembered that in daily activities, most of the people walked to their destinations—to work, to the store, to market, to church, or to school—with the exception of a few more opulent citizens. Industries were relatively small and the workers lived close by. Many small businesses were conducted on the same premises where the owner lived with his family. The size of such businesses were generally dependent on their accessibility by walking.

As time passed, a mass transportation system in the form of horse-drawn cars was established. For a moderate cost, many more workers and their families could travel faster and with less effort than walking. The business section developed and became more specialized because owners, clerks, and shoppers could live some distance away. Some factories became larger because they could draw workers from a greater radius, and the city gradually expanded as improvements in speed, comfort, and scope of the public system of conveyance followed in succession. Schedules, tandem cars, and steam dummies on the major routes gradually made public transportation on fixed routes a part of the urban way of life.

After approximately 50 years (circa 1880) the electric streetcar made its appearance. These electric cars could transport people twice as fast as the horse car and three times as fast as they could walk. People now had an even broader choice of where to live and work. Expansion accelerated, and specialization of economic function in parts of the city was more greatly emphasized. Trolley lines extended outward from the central area of the city, encouraging the development of new residential areas. Some businesses and factories developed along the main trolley routes, and more homes were built within walking distance of feeder routes to the main arteries.

In 1910, after a period of 80 years, nearly 90% of the people rode to work and to most other places on streetcars. Streetcar operation on extended routes made the central business district easily accessible to large numbers of people. As a result, the central business district became compact; downtown land values soared; and skyscrapers were built. There was appreciable congestion on the downtown streets because of the horse-drawn drays, hacks, and streetcars. The building of an elevated railroad system or a subway similar to those in Chicago, Ill., and New York, N. Y., was planned, but such facilities were costly and it was difficult to decide in which direction the first line should be built. In addition, the interurban railway which operated partly on private right of way was fairly satisfactory.

About this time, a new vehicle, the automobile, was appearing on the streets, and its price was gradually lowered by an industry that was using mass-production techniques. Increasing numbers of people bought them because they were pleased to have an increasingly dependable, private means of transportation. Whereas in 1900 people could live three miles from the heart of the city and reach the downtown section in from 30 min to 45 min, by 1920 the traveling time by automobile was from 10 min to 15 min. With a few more minutes of travel time, they could live still farther away, or they could build homes in the rather sparsely settled tracts between the now (1920) extended trolley routes. A star-like pattern of growth was beginning to fill in; an over-all pattern of development was emerging although it was spotty because clusters were forming around former villages, or new satellite communities were being developed around rudimentary small business communities.

The foregoing sketch of the pattern and rate of growth of this imaginary city illustrates the observation that the real city limits (that is, limits of the urban complex, not political boundaries) are set by time rather than by distance. A basic feature in the functioning of a city is the interchange of goods and services on a daily basis. For interchange within this time scale, the speed of transport appreciably conditions the functional size of the community.

Because of the increasing use of the automobile, the public transportation system ceased to be a monopoly. Competition between the streetcar and the automobile became more marked and more complex. Because it provided flexible, convenient, and rapid personal transportation, the automobile attracted many users who could have or otherwise might have used the streetcar. In addition, the automobile competed for space on the city streets. Congestion mounted but was partly allayed by street-widening programs, the building of boulevards and arterials, and other traffic facilitation devices. Nevertheless, a long-term decline in the use of mass transit became discernible by the 1930's.

New situations were created by the accelerated use of the automobile. Lines of cars parked at the curbs cut down the space for movement. Curb space became so limited that a new business developed—the parking lot and the parking garage.

Today (1957) perhaps the most significant problem that has resulted from the crowded streets is the fact that elapsed travel time from one point to another is increasing. For many people in the suburbs, the time to make the trip downtown by either automobile or public transit (which includes a variety of buses) is almost intolerable, at least as a daily occurrence. As a result, many of them are shopping and using the services in satellite business areas which are becoming a prominent characteristic in the city pattern; even many large factories and warehouses are moving out of the so-called industrial district to open land areas at or beyond the edges of the city. All such moves are requiring more and more transportation service.

As a result of the business nuclei which are developing, there seems to be a new kind of competition, an economic competition between the satellite community and the central business district. This complicates efforts to establish new rapid transit routes.

Factors in the Urban Transportation Problem

As a second step in attempting to contribute some perspective on the general problem, a condensed series of observations concerning transportation in urbanized areas is presented. Not all the concepts can be considered as exact or unchanging; the intent here is to provide a general summary of factors which may be useful in appraising current developments.

1. When daily travel times rise above some tolerable value, people tend to alter their commuting patterns. There appears to be a maximum travel time

which the average person is willing to spend on daily trips for various purposes. As a corollary to this, the general limits of daily movement in an urban community appear to be set by time rather than distance. Technologic advances in transport, which made possible higher speeds, were accompanied by expansions in size of, and shifts in, the urban pattern.

2. Delays, inconvenience, and rising costs resulting from congestion cause shifts in travel habits. Some congestion is a natural result of the aggregation of human beings in urban communities. Up to some point, the behavior of the majority of people will not be markedly or adversely affected by congestion. However, beyond that point, congestion may become intolerable to appreciable numbers of people, and they will react so as to avoid the congested area as much as possible. Deciding factors, however, in influencing individuals to shift their transportation habits will not be congestion, per se, but increased travel time, delays that are judged to be intolerable, inconvenience, and increased costs. However, little appears to be known factually concerning tolerable journey times or the range in tolerable journey times although there has been considerable opinion and speculation. (Tolerable travel times are probably affected by habit and differ as between small towns and metropolitan areas.)

3. The pattern of urban growth and functioning is conditioned by the kind of transportation available. Urban growth when transit was the dominant mode of transportation occurred along and close to the transit routes; central business districts tended to be compact with high land values. Communities that have grown and developed predominantly with the automobile as the mode of transportation show a more diffuse pattern. The development of vast suburban residential areas has been made possible by a supply of this flexible, individualized transportation within reach of large numbers of people. The average density of population in cities that have undergone great growth and expansion during the automobile age is in striking contrast to cities which saw their major expansion during the streetcar age. It appears now that mass transportation cannot be supplied to the great outlying areas at a fare and service level that will induce a sufficient number of people to become transit riders so that general street transit operations are a profitable enterprise, at least at fare structures that are acceptable.

4. With respect to technical efficiency, mass transit is superior to the privately owned automobile in moving large numbers of people from one location to another within a relatively congested urban area. In large cities, transit is still depended on for moving much of the population during peak hours. Furthermore, it is difficult to see how central cities could accommodate the number of automobiles which would be used if all the peak-hour transit riders used them.

5. Higher transit operating costs have resulted from the trend toward the high ratio of peak-hour to off-peak-hour patronage. The present pattern of transit usage—namely, high peak-hour loads with very low off-peak-hour patronage has resulted in disproportionately high operating costs in comparison with income under present fare structures. Attempts to adjust income to

expenditures by raising fares and cutting off-peak-hour service have been accompanied by a further decrease in patronage during off-peak hours.

6. Slower trainsit schedules resulting from congestion contribute to decreased patronage and increased costs. Congested streets have resulted in slowing the movement not only of automobile traffic but also of the transit schedules, especially during rush hours. The result is that transit riding is less and less attractive, and there is a tendency toward decreased transit riding during peak hours as well as during off-peak hours. In addition, operating costs are further increased, and the efficiency of transit as a mass carrier is reduced under these conditions.

7. Parking supply is an important factor in placing a ceiling on the number of cars which can be accommodated in business districts. It appears that the supply of parking and the price of parking are important factors in determining how many cars will come into a central business district. (A pricing policy with respect to short-time parking as against long-time parking would influence the total number of cars which could provide transport service per day in a business district; this would also affect peak-hour against off-peak-hour traffic loads on the streets and the problem of transit usage.)

8. The uses of the public streets both as arteries for traffic flow and for vehicle storage are in direct conflict. Community decisions to provide large off-street parking programs are, in effect, the development of a policy to resolve this conflict, but often the community policy is not widespread nor consistent. Frequently much curb parking is retained, and the efforts are not commonly coordinated with the capacity for ingress by expressways or improved arterial street systems.

9. Extended travel time also places a general ceiling on the number of cars that would provide transportation service into the downtown areas; this condition appears to be contributing to the establishment and success of suburban shopping and business centers. (These centers, however, may become equally congested due to the same factors which in turn tend to contribute to a proliferation of such centers and a diffuse pattern of urban economic activity.)

10. The decline of the central business district is not inevitable, but strong remedial measures are needed to prevent further deterioration of transport services which can affect the central business district. It appears that the central business districts of some cities have reached a plateau of economic activity, but marked deterioration in the quantity and quality of present transport service can conceivably lead to an appreciable decline. The situation does not appear to be stable. However, at the present time (1957) there is no appreciable backlog of statistics on which to estimate trends, nor is there an over-all urban transportation policy which can be relied on to promote stability.

11. Mass transit, either rapid or local, is no longer a monopoly. However, tax and regulatory policies which evolved when transit was the only form of public transportation are still applied, in some degree, to transit operations. Policies which would permit carriers to adapt operations to current conditions would appear to be worthy of formulation and serious consideration.

12. Rapid transit cannot be expected to operate successfully unless conditions favorable to inducing large-volume patronage are created. Successful rapid transit operations which have so far been instituted appear to be associated with two population characteristics: (1) A large total population and (2) a high density of population. These characteristics have assured mass origins and destinations of large-volume patronage on selected routes. Large passenger volumes are necessary to provide revenue to underwrite investment in very costly facilities. A problem facing communities with a diffuse pattern of residential development is that of obtaining mass origins. Some students of the rapid transit problem claim that for a new system to be successful, riders must be collected at stations to which they can drive and park with ease, and patronage must be induced by superior service.

The current pattern of over-all urban transportation management—if indeed it is management—is chaotic; coordination would appear to be essential for satisfactory operation. The responsibility of designing and constructing the street, road, and expressway systems lies in the departments of the state, city, and county governments and in special districts in some locations. The routing and operation of transit systems is centered in a separate department of city government or in a private company. The maintenance and servicing of streets and lights and the utilities which lie along the streets are in still other departments. The control of traffic movement usually is the responsibility of another department. The regulation of public carriers is by one or more separate agencies of state and local government. The general urban planning functions are directed in yet another department. The lack of adequate coordination between these disperse managment functions is well known. More serious, however, is the fact that this kind of management pattern has also severely lessened the possibility of an over-all transport policy being evolved by those directly concerned. This condition in turn has prevented the presentation of any coordinated policy to the citizens of the community on whom the final endorsement rests.

CONCLUSIONS

If the urban transportation problem is to be solved with maximum efficiency in transportation and at minimum costs, a comprehensive and coordinated treatment and a consideration of complementary and alternate forms of transportation are required. Especially to be considered in the large metropolitan areas are the interrelationships between the provision and use of facilities for automobiles and the offering and use of mass transportation service. A coordinated and comprehensive approach would necessitate the coordinated planning of facilities and their operations. Realistic, coordinated planning, in turn, would require a backlog of factual information and a factual appraisal. Furthermore, an effective scheme of management of all the complementary forms of transportation, a scheme which would result in efficiency but retain the essence of native democratic processes, would have to be found. Finally, new problems in financing, both with respect to source of funds and to allocation, would have to be solved.

A coordinated attack offers the best promise of success in alleviating urban traffic congestion and improving transportation service. The questions still remain: How can such an attack be made? Why has it been delayed? A part of the answer to the latter question lies in a lack of sufficient basic data. Appraisal of the urban transportation problem is no simple task; the planning and design of adequate and publicly acceptable transportation systems will require the technical knowledge and skills of many engineers and specialists and the use of a great variety of factual data concerning the functioning of urban areas.

In the middle 1930's, most of the state highway departments began the more-or-less systematic collection of data pertinent to the financing, construction, and use of rural state highways—data which have since been found to be indispensable to sound highway planning. The urban areas have not been so fortunate with respect to accumulating the statistical tools with which to plan. The necessity for the routine collection of basic information was not always apparent in most areas, and until recently no apparent urgency existed. There is no single agency which is responsible for the collection of data. The resulting situation is one in which existing factual data are insufficient to permit a comprehensive appraisal of the problem. However, the recent establishment of the National Committee on Urban Transportation may provide a means of overcoming this deficiency.

It should not be impossible to devise coordinated transportation systems which meet the social and economic needs of the entire population of an area. The devising of such a scheme will require a great deal of patience, wise use of existing laws and the enactment of new ones, fullest cooperation among existing and potential governmental agencies, and great expense. It is obvious that finding the right solution to the transportation problem will require not only the full use of technical knowledge and skills but also the wide citizen participation. It is the public which will determine, through their support or lack of it, whether or not the right solution has been found.

AMERICAN SOCIETY OF CIVIL ENGINEERS
Founded November 5, 1852
TRANSACTIONS

Paper No. 2861

IMPULSIVE MOTION OF ELASTO-PLASTIC SHEAR BUILDINGS

BY EDWARD COHEN,[1] J. M. ASCE, LEON S. LEVY,[2] AND LEONARD E. SMOLLEN,[3] J. M. ASCE

SYNOPSIS

The method of normal modes is applied to the analysis of elasto-plastic shear buildings subjected to impulsive loads, foundation uplift, and nonuniform viscous damping. Interaction of foundation rotation and plasticity in the superstructure is described. A short table of approximate modes and frequencies is included.

INTRODUCTION

The use of the normal modes of vibration for the solution of dynamic problems involving shear buildings is extended in this paper to include the displacement of structures subjected to (*a*) impulsive torsional loads, (*b*) the development of plastic action in the frame and the foundation, (*c*) "temporary instability" or uplift of the foundation, and (*d*) nonuniform viscous damping. The interaction of foundation rotation and plasticity in the superstructure is described herein, and a general approach to the solution of the problem is outlined.

Shear buildings are defined as idealized multistory structures with the following properties:

1. The mass of the building and the applied forces are concentrated at the various floor levels.
2. The motion of the building is due to shear only. The displacements due to flexure of the building as a whole are negligible.
3. The elastic shear in any story is a function only of the elastic deflection between adjacent floors.

For the purpose of dynamic analysis such idealized buildings are analogous to rigid frame structures with stiff floor systems and flexible columns and to

---

NOTE.—Published, essentially as printed here, in April, 1955, as *Proceedings-Separate No. 676.* Positions and titles given are those in effect when the paper was approved for publication in *Transactions.*

[1] Associate, Ammann and Whitney, Cons. Engrs., New York, N. Y.

[2] RCA David Sarnoff Fellow, Harvard Univ., Cambridge, Mass.

[3] Senior Vibrations Engr., Sikorsky Aircraft, Bridgeport, Conn.

many other structures of such height-to-width ratios that over-all flexural deformation can be neglected. A typical five-story shear building is shown in Fig. 1. The equations of motion for a multistory shear building with impulsive lateral loads will be developed in terms of the normal modes of vibration. The use of normal modes is advantageous because the problem is thereby reduced from the solution of the N simultaneous equations that would be required by the direct application of the Newton equation of motion to the solution of N independent equations for a building with N degrees of freedom.

Numerical methods, such as finite differences, trial and error, and similar procedures, may be used effectively in the solution of the dynamic problems treated herein. However, the methods described are also applicable where it is possible to obtain analytic solutions. They have been used by the writers for the numerical analysis of a three-story building subjected to a long-duration blast loading. The computations followed the finite-difference theory and were done with the aid of only ordinary automatic desk-type calculators. However, it is recognized that as the number of stories increases the volume of computations also increases rapidly, and when the number of stories exceeds approximately five the use of high-speed digital computers or analog computers becomes necessary.

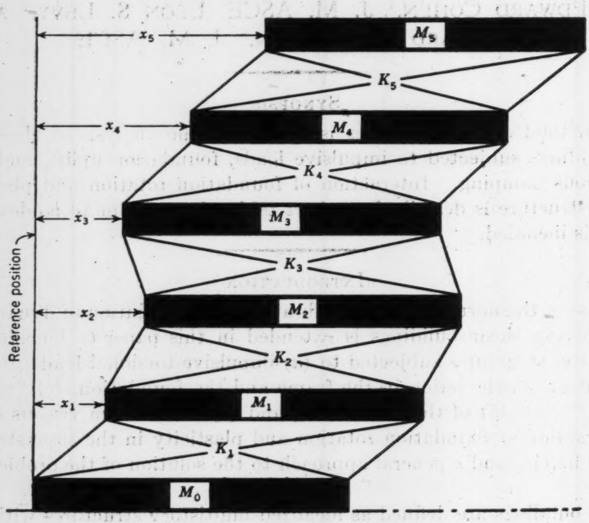

FIG. 1.—DISTORTED POSITION OF AN IDEALIZED FIVE-STORY BUILDING ON A RIGID FOUNDATION

GENERAL RELATIONSHIPS

The equation of free vibration for the ith floor of a shear building (Fig. 2) on a rigid foundation, in which the vertical load divided by the story height is negligible compared to the story stiffness, K_i, is

$$M_i \ddot{x}_i = K_{i+1}(x_{i+1} - x_i) - K_i(x_i - x_{i-1}), \qquad i = 1,2,\cdots n \ldots\ldots (1)$$

in which M_i is the mass concentrated at the ith floor, K_i is the spring constant for that portion of the building under the ith floor, and $x_i(t)$ equals the absolute horizontal displacement of the ith floor at the time, t.

The displacement at any time, t, may be expressed in terms of normalized modes, ϕ_j, and the generalized coordinates, $q_j(t)$, as

$$x_i(t) = \sum_{j=1}^{N} \phi_j(i)\, q_j(t) \ldots\ldots (2)$$

By application of the Lagrangian equations,

$$\frac{d}{dt}\frac{\partial T}{\partial q_k} + \frac{\partial U}{\partial q_k} = Q_k \ldots\ldots (3)$$

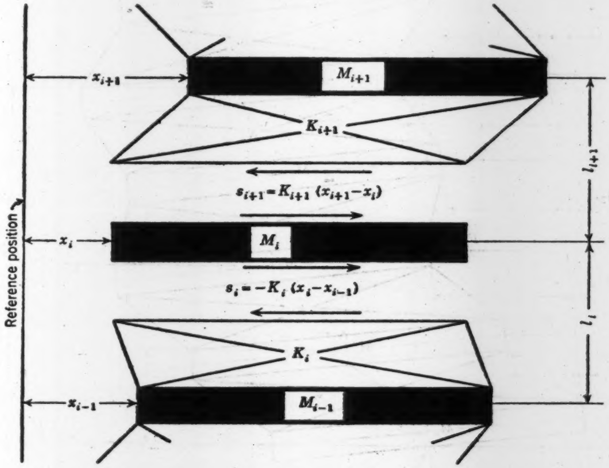

FIG. 2.—TYPICAL FORCE SYSTEM FOR THE iTH FLOOR

in which Q_k is the generalized force,

$$Q_k = \sum_{i=1}^{N} P_i \frac{\partial x_i}{\partial q_k} \ldots\ldots (4)$$

P_i is the real force applied to the ith floor; T is the kinetic energy,

$$T = \tfrac{1}{2} \sum_{j=1}^{N} \dot{q}^2{}_j \ldots\ldots (5)$$

U is the potential energy,

$$U = \tfrac{1}{2} \sum_{j=1}^{N} \omega^2{}_j\, q_j \ldots\ldots (6)$$

N is the number of stories; and ω_j is the frequency of the jth mode.

The equations of forced vibration in terms of the generalized coordinates become

$$\ddot{q}_j + \omega^2{}_j\, q_j = \sum_{i=1}^{N} P_i\, \phi_j(i), \qquad j = 1, 2, \cdots N \ldots\ldots\ldots\ldots (7)$$

Thus far it has been assumed that the story masses undergo horizontal motion only. This assumption is valid if the foundation material is infinitely rigid. If the foundation is elastic, the building will also rotate about an axis through the centroid of the base and perpendicular to the direction of motion, as shown in Fig. 3.

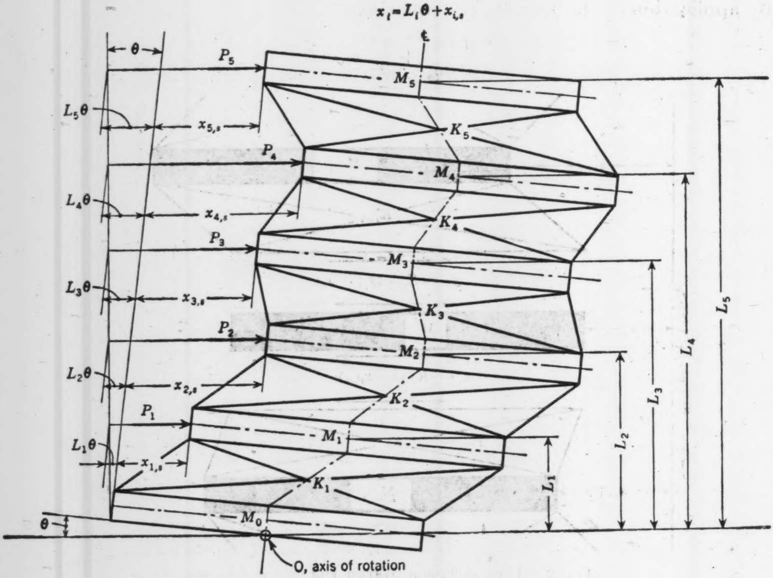
$x_i = L_i\theta + x_{i,s}$
℄
θ
P_5
M_5
$L_5\theta$
$x_{5,s}$
K_5
P_4
M_4
$L_4\theta$
$x_{4,s}$
K_4
P_3
M_3
$L_3\theta$
$x_{3,s}$
K_3
P_2
M_2
$L_2\theta$
$x_{2,s}$
K_2
P_1
M_1
$L_1\theta$
$x_{1,s}$
K_1
M_0
θ
O, axis of rotation
L_1
L_2
L_3
L_4
L_5

FIG. 3.—DISTORTED POSITION OF AN IDEALIZED BUILDING ON A NONRIGID FOUNDATION

For this case, the following equation of motion may be obtained:

$$\ddot{q}_k + \Omega^2{}_k\, q_k = \sum_{i=1}^{N} P_i\, \psi_k(i), \qquad k = 1, 2, \cdots N + 1 \ldots\ldots\ldots (8)$$

in which q_k, Ω_k, and $\psi_k(i)$ are the modified generalized coordinates, frequencies, and modes, respectively, of a building rotating elastically about the centroid of its base.[4]

---

[4] "Earthquake Stresses in Shear Buildings," by M. G. Salvadori, *Transactions*, ASCE, Vol. 119, 1954, p. 171.

The mode, $\psi_k(i)$, may be expressed as

$$\psi_k(i) = C_k \phi_A(i) + \sum_{j=1}^{N} C_{kj}\, \phi_j(i), \qquad k = 1, 2, \cdots N + 1 \ldots\ldots (9)$$

in which the coefficients, C_k and C_{kj}, are given by

$$\frac{\omega^2{}_A}{\Omega^2{}_k} C_k = \sum_{i=1}^{N} \phi_A(i)\, \psi_k(i)\, M_i \ldots\ldots\ldots\ldots\ldots\ldots (10)$$

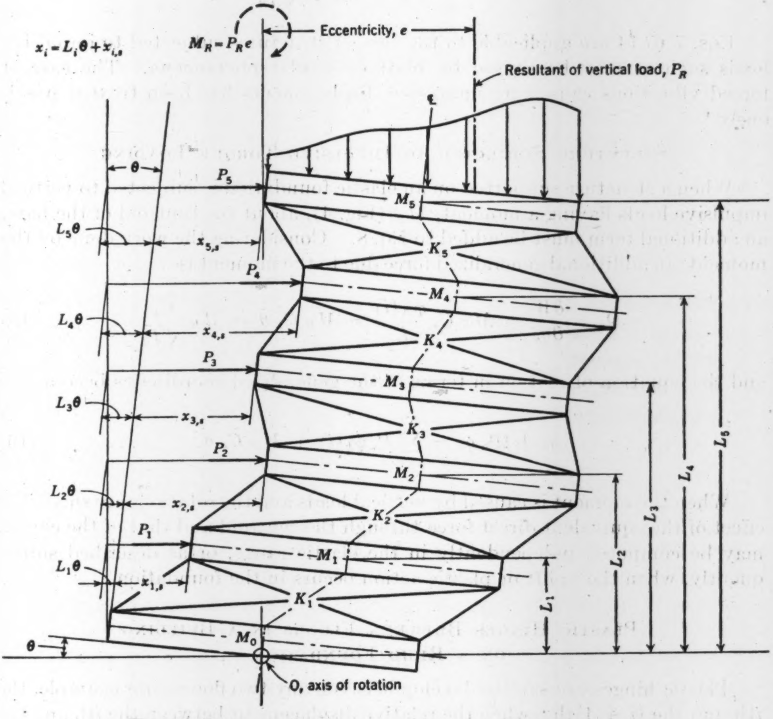
$x_i = L_i\theta + x_{i,s}$
$M_R = P_R e$
Eccentricity, e
Resultant of vertical load, P_R
℄
θ
P_5
M_5
$L_5\theta$
$x_{5,s}$
K_5
P_4
M_4
$L_4\theta$
$x_{4,s}$
K_4
P_3
M_3
$L_3\theta$
$x_{3,s}$
K_3
P_2
M_2
$L_2\theta$
$x_{2,s}$
K_2
P_1
M_1
$L_1\theta$
$x_{1,s}$
K_1
M_0
θ
O, axis of rotation
L_1
L_2
L_3
L_4
L_5

FIG. 4.—DISTORTED POSITION OF AN IDEALIZED BUILDING ON AN ELASTIC FOUNDATION

and

$$\frac{\omega^2{}_A}{\Omega^2{}_k} C_{kj} = \sum_{i=1}^{N} \phi_j(i)\, \psi_k(i)\, M_i \ldots\ldots\ldots\ldots\ldots\ldots (11)$$

In Eq. 10, $\phi_A(i)$ denotes the "rocking mode" of the building:

$$\phi_A(i) = \frac{L_i}{\sqrt{I_0}} \ldots\ldots\ldots\ldots\ldots\ldots\ldots\ldots (12)$$

The symbol, I_0, represents the total moment of inertia about the axis of rotation.

The rotation may be expressed as

$$\theta = \sum_{k=1}^{N+1} \bar{\theta}_k \, q_k \ldots\ldots\ldots\ldots\ldots\ldots\ldots\ldots (13)$$

in which

$$\bar{\theta}_k = C_k \, \bar{\theta} = C_k \frac{\phi_A}{L_i} = \frac{C_k}{\sqrt{I_0}} \ldots\ldots\ldots\ldots\ldots\ldots (14)$$

Eqs. 7 to 14 are applicable to the case of structures subjected to impulsive loads such as may be caused by blast or similar phenomena. The case of forced vibrations caused by impressed displacements has been treated previously.[4]

Structure Subjected to Impulsive Torque Loading

When a structure supported on an elastic foundation is subjected to vertical impulsive loads having a moment, M_R (Fig. 4), about the centroid of the base, an additional term must be added to Eq. 8. Considering the work done by the moment, an additional generalized force due to the moment is

$$Q_k = \frac{\partial W}{\partial q_k} = M_R \, C_k \frac{\phi_A(i)}{L_i} = M_R \, C_k \, \bar{\theta} = M_R \frac{C_k}{\sqrt{I_0}} \ldots\ldots\ldots (15)$$

and the equation of motion in terms of the generalized coordinates becomes

$$\ddot{q}_k + \Omega^2{}_k \, q_k = \sum_{i=1}^{N} P_i \, \psi_k(i) + M_R \, C_k \, \bar{\theta} \ldots\ldots\ldots\ldots\ldots (16)$$

When the moment is caused by vertical loads and the rotations are small, the effect of the equivalent direct force through the centroid and that of the couple may be computed independently in the elastic range, or as described subsequently, when the uplift or plastic action occurs in the foundation.

Plastic Hinges Between Floors in a Building on a Rigid Foundation

Plastic hinges are said to develop between any two floors—for example, the *i*th and the $(i + 1)$th—when the relative displacement between the *i*th and the $(i + 1)$th floor masses is such that the shear, $K_{i+1} \, (x_{i+1} - x_i)$ exceeds the yield-point resistance. Fig. 5 shows an idealized plot of shear resistance related to displacement if the horizontal components of the axial forces in the columns can be neglected. For a more accurate solution the horizontal components should be subtracted from the plastic shear values. From the time a plastic hinge is first developed until such time as the relative velocities of the two adjacent floors are reversed and the story shear returns to the elastic range, the method of analysis must take into account the first, and all subsequent, plastic hinges as they are developed.

If the problem is solved analytically, it is necessary to revise the equations of motion whenever any story exceeds its yield-point displacement. This requirement also holds for a numerical solution. Because the duration of the time intervals must be kept to a small fraction of the period of the mode being computed, the possibility that a new hinge may develop within any one step is usually unimportant, the change in equations being made either at the beginning or the end of that time interval.

Considering a shear building in which plastic hinges have developed between certain stories, it is clear that the plastic hinges divide the building into a number of smaller "independent" constituent structures (as shown in Fig. 6) each with its own modes and frequencies of vibration. Therefore, the shear-building analysis can be applied to each of the constituent structures after certain modifications due to the plastic resistance, $S_p(i)$, have been applied and the initial conditions established. Relative motion between the foundation and the soil may be treated in exactly the same way.

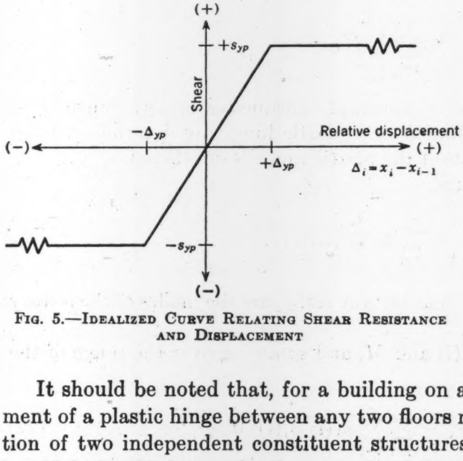

FIG. 5.—IDEALIZED CURVE RELATING SHEAR RESISTANCE AND DISPLACEMENT

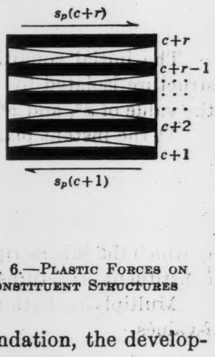

FIG. 6.—PLASTIC FORCES ON CONSTITUENT STRUCTURES

It should be noted that, for a building on a rigid foundation, the development of a plastic hinge between any two floors reduces the problem to the solution of two independent constituent structures. Thus, a four-story building in which the third story has become plastic is reduced to two independent two-story buildings with a consequent simplification of the problem and, in the case of numerical solutions, a great reduction in the required labor.

If *r* stories are isolated by plastic hinges they may be considered to form an *r*-story structure. The equations of motion of the new *r*-story structure are also expressed by the Lagrange equations,

$$\frac{d}{dt}\frac{\partial T}{\partial q_k} - \frac{\partial T}{\partial q_k} = -\frac{\partial \bar{U}}{\partial q_k} + Q_k, \qquad k = 1, 2, \cdots r \ldots\ldots\ldots\ldots (17)$$

in which the kinetic energy, *T*, and the potential energy, *U*, are for the new system under consideration.

The kinetic energy is defined as before:

$$T = \tfrac{1}{2} \sum_{i=1}^{r} M_i \, \dot{x}^2{}_1 = \tfrac{1}{2} \sum_{j=1}^{r} \dot{q}^2{}_j \quad \ldots\ldots\ldots\ldots \quad (18)$$

The potential energy is defined as the effect of both the internal and external work. This energy will also include the work done in overcoming the plastic resistances, $S_p(i)$, so that after plastic hinges have been developed, the potential energy, $\bar{U}$, is equal to U as previously defined, plus the work done by the plastic resistances:

$$\bar{U} = U + S_{p(c+r)} \, x_{(c+r)} - S_{p(c+1)} \, x_{(c+1)} \quad \ldots\ldots\ldots\ldots \quad (19)$$

or

$$\bar{U} = U + S_{p(c+r)} \sum_{j=1}^{r} \phi_j(r) \, q_j - S_{p(c+1)} \sum_{j=1}^{r} \phi_j(1) \, q_j \quad \ldots\ldots\ldots \quad (20)$$

The displacements, x_i, can be computed from

$$x_i = \sum_{j=1}^{r} \phi_j(i) \, q_j.$$

The initial conditions for the generalized coordinates of any constituent structure isolated by the development of a plastic hinge are determined from the value of $x^p{}_i$ and $\dot{x}^p{}_i$ at the instant the plastic hinge is developed.

At the instant plasticity occurs,

$$x^p{}_i = \sum_{j=1}^{r} \phi_j(i) \, q_j(t) \quad \ldots\ldots\ldots\ldots \quad (21)$$

in which the superscript p defines that instant and ϕ_j are the modes of the r-story constituent structures.

Multiplying both sides by $\phi_j(i)$ and M_i and summing over the range of the i-values,

$$\sum_{i=1}^{r} \phi_j(i) \, M_i \, x^p{}_i = \sum_{j=1}^{r} \sum_{i=1}^{r} \phi_k(i) \, \phi_j(i) \, M_i \, q^p{}_j \quad \ldots\ldots\ldots\ldots \quad (22)$$

However,

$$\sum_{j=1}^{r} \sum_{i=1}^{r} \phi_j(i) \, \phi_k(i) \, M_i = 1 \quad \ldots\ldots\ldots\ldots \quad (23)$$

and

$$q^p{}_j = \sum_{i=1}^{r} \phi_j(i) \, M_i \, x^p{}_i \quad \ldots\ldots\ldots\ldots \quad (24)$$

Similarly,

$$\dot{q}^p{}_j = \sum_{i=1}^{r} \phi_j(i) \, M_i \, \dot{x}^p{}_i \quad \ldots\ldots\ldots\ldots \quad (25)$$

TEMPORARY INSTABILITY AND PLASTICITY IN THE FOUNDATION SOIL

The analysis presented for a rocking building is valid only if the building can be considered to be rotating about the centroid of the foundation. This is approximately true only if the building exerts a compressive force along the entire base. However, if the analysis indicates tension on part of the foundation, the building will actually pull away from the ground and the center of rotation will shift.

From the soil-pressure analysis, a force diagram such as that shown in Fig. 7 may be found.

The fictitious tensile forces that must be eliminated are equivalent to a vertical downward force, F_T, through the centroid of the base, and a counterclockwise moment, $F_T\,e$, in which e is the lever arm of the centroid. An upward vertical force, F'_T, and a clockwise moment, $F'_T\,e$, equal in magnitude to the quantities to be subtracted are therefore applied to the structure.

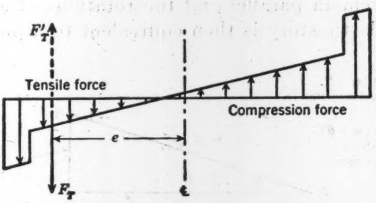

FIG. 7.—FORCE DIAGRAM ON A FOUNDATION FOOTING

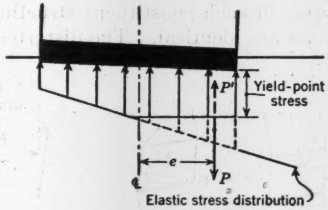

FIG. 8.—PLASTIC ACTION IN SOIL

Using a step-by-step, finite-difference method, a solution by successive trials may be attained as follows:

1. A value is assumed for the vertical force, F_T, and the moment, $F_T\,e$;
2. The displacements, x_i, are computed from Eqs. 15 and 16 by adjusting Eq. 16 so that

$$\ddot{q}_k + \Omega^2_k\, q_k = \sum_{i=1}^{N} P_i\, \psi_k(i) + M_R\, c_k\, \frac{\phi_A(i)}{L_i} + \lambda_k \qquad (26)$$

in which

$$\lambda_k = \frac{F'_T\, e\, c_k\, \phi_A(i)}{L_i} \qquad (27)$$

3. The soil-pressure diagram is determined on the basis of the values assumed, and F_T and $F_T\,e$ are computed.
4. If a check is obtained, one may proceed to the next time interval. If not, Steps 1 to 3 are repeated.

It may be noted that the proposed method of solution results in a uniformly asymptotic approach to the final condition of equilibrium, the computed resisting moment of the foundation always being greater and the rotation always smaller than the actual values.

Plastic action in the soil may be accounted for in a similar manner by equilibrating the difference between the plastic and elastic soil resistance, as shown in Fig. 8.

ROTATION OF BUILDING WITH LARGE PLASTIC DISTORTIONS IN SUPERSTRUCTURE

Plastic hinges in a building rotating about the center of its base divide it into a number of independent constituent structures, any one of which may be treated separately if the effects of the plastic hinges above and below are included in the analysis. Each plastic hinge is assumed to transmit only a horizontal plastic resistance, S_{pi}, and axial force, F_{Ti}, and a moment, M_i. Throughout this section it will be assumed that the plastic resistance, S_{pi}, is known at any specified time, t, that it acts in a horizontal direction, and that it may be treated as an additional applied force.

If it is also assumed that the plastic story is axially stiff—that is, that the column lengths do not change—both the columns in each story and the floor masses in each constituent structure remain parallel and the rotations of all stories are identical. The distorted plastic story is then equivalent to a pin-connected parallelogram or a series of parallelograms when the number of columns exceeds two. The adjacent masses are moved both horizontally and vertically relative to each other as the structure is rotated. The new unknowns are the horizontal and vertical components of the column reactions and the story-to-story distortion, α, as modified by rotation.

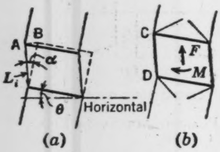

FIG. 9.—REACTIONS AT A PLASTIC HINGE

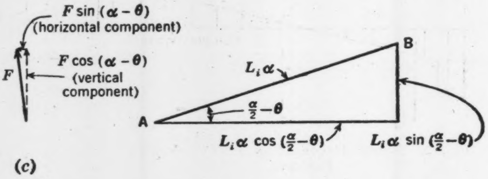
$F \sin(\alpha-\theta)$ (horizontal component)
$F \cos(\alpha-\theta)$ (vertical component)
F
(c)
B
$L_i\alpha$
$\frac{\alpha}{2}-\theta$
A
$L_i\alpha \cos(\frac{\alpha}{2}-\theta)$
$L_i\alpha \sin(\frac{\alpha}{2}-\theta)$

FIG. 10.—VERTICAL AND HORIZONTAL COMPONENTS OF PLASTIC DISPLACEMENT

Fig. 9(a) shows the plastic hinge at time, t, in which AB is the relative displacement of the upper constituent structure at the plastic hinge and α is the angle of distortion of the plastic story. Fig. 9(b) shows the resultant, F, of the final axial column forces, and their couple, M, resulting from the rotation. This moment is a measure of the contribution of the upper constituent structure to the total rotational inertia of the structure. The contribution diminishes as the distortion, α, increases. The resultant force, F, which is superimposed on the pure couple, is caused by applied vertical loads and the vertical inertia forces. The vertical and horizontal components of the plastic displacements, AB, are shown in Fig. 10.

The following parameters are then obtained for an N-story building having n plastic hinges: N shear displacements, x_i; $n + 1$ rotations, θ_i; n plastic axial forces, F_{Ti}; and n plastic displacement angles, α_i. The following independent equations also prevail: N equations for shear displacement; $n + 1$ equations for rotation; n equations of rotational compatibility—that is, $\theta_i = \theta_{i+n}$; and n equations of displacement compatibility.

The initial conditions (at rest) are:

$$\begin{aligned} x^o{}_i &= 0, & \dot{x}^o{}_i &= 0 \\ \theta^o{}_i &= 0, & \dot{\theta}^o{}_i &= 0 \\ \alpha^o{}_i &= 0, & \dot{\alpha}^o{}_i &= 0 \\ F^o{}_i &= 0, & \dot{F}^o{}_i &= 0 \end{aligned}$$

For plastic-hinge development at any later time, t, suitable initial conditions may be derived by means of the procedure outlined in Eqs. 21 through 25.

For a step-by-step solution in which the number of plastic hinges is small (less than 3 or 4), x_i and θ_i at the end of any time interval may be found by trial and error by assuming values of α_i and F_i for computing θ_i and x_i. The equations of shear displacement and displacement compatibility serve as a check on the accuracy of the assumed values of α_i and F_i. This method is restricted to a structure with a limited number of hinges because the solution itself has no inherent properties of convergence and depends entirely on the computer's judgment and ability to visualize the action of the structure.

UNEQUAL VISCOUS DAMPING IN A COMPLEMENTARY SYSTEM

Because of the large difference in magnitude that may exist between the damping due to the soil foundation and that due to the shear displacements of the structure, it is desirable to account for both these factors—that is, to evaluate the actual damping coefficients, μ_k, of the kth mode of the rotating structure in terms of the damping coefficients, μ_A, of the foundation and μ_j of the shear modes of the structure on a rigid foundation. Both μ_j and μ_A may be determined experimentally.

It may be noted that in Eq. 1, the equation of motion of the floor mass of the ith floor, viscous damping may be introduced by the addition of linear velocity terms, so that Eq. 1 becomes

$$M_i\,\ddot{x}_i = K_{i+1}\,(x_{i+1} - x_i) - K_i\,(x_i - x_{i+1}) + \sum_{I=1}^{N} \mu_{iI}\,(\dot{x}_I) \ldots\ldots (28)$$

in which μ_{iI} is the coefficient of the damping between the Ith and ith floor masses and in which, in general, only the $I = (i + 1)$, i, and $(i - 1)$ velocities affect the motion of the ith floor. Therefore,

$$\begin{aligned} M_i\,\ddot{x}_i = K_{i+1}\,(x_{i+1} - x_i) - K_i\,(x_i - x_{i-1}) + \mu_{i(i+1)} \\ \times (\dot{x}_{i+1} - \dot{x}_i) - \mu_{i(i-1)}\,(\dot{x}_i - \dot{x}_{i-1}) \ldots (29) \end{aligned}$$

The damping coefficients which account for the effect of one story mass upon another are difficult to evaluate directly even in the case in which rotation is not allowed.

However, if it is assumed that the damping of single-degree-of-freedom systems is a linear function of the velocity, a damping term may be added to the equation for the generalized coordinates, which then becomes

$$\ddot{q}_k + \mu_k \dot{q}_k + \Omega^2{}_k \, q_k = \sum_{i=1}^{N} p_i \, \psi_k(i) + M_R \, c_k \, \ddot{\bar{\theta}} \ldots\ldots\ldots\ldots (30)$$

The damping coefficient, μ_k, may be evaluated in terms of μ_j and μ_A by considering the dissipative function of the damping.

A dissipative function,[5] D, is such that the damping force is the negative of the derivative of the dissipative function with respect to the velocity. The dissipative function may also be defined by

$$D = -\tfrac{1}{2} W \ldots\ldots\ldots\ldots (31)$$

in which W is the instantaneous work, so that $-W$ is the time rate of energy dissipation. The dissipative function may be introduced into the Lagrange equations so that

$$\frac{d}{dt}\frac{\partial T}{\partial \dot{q}_k} - \frac{\partial T}{\partial q_k} + \frac{\partial V}{\partial q_k} + \frac{\partial D}{\partial \dot{q}_k} = 0 \ldots\ldots\ldots\ldots (32)$$

Because of the second definition of the dissipative function, the total dissipative function may be equated to the sum of the soil and shear dissipative functions.

$$D_V = D_{Vs} + D_{V\theta} \ldots\ldots\ldots\ldots (33)$$

in which D_V, the total dissipative function, is

$$D_V = \tfrac{1}{2} \sum_{k=1}^{N+1} \mu_k \, \dot{q}^2{}_k \ldots\ldots\ldots\ldots (34)$$

D_{Vs}, the shear dissipative function, is

$$D_{Vs} = \tfrac{1}{2} \sum_{i=1}^{N} \sum_{I=1}^{N} \mu_{iI} \, \dot{x}_{is} \, \dot{x}_{Is} = \tfrac{1}{2} \sum_{i=1}^{N} \sum_{I=1}^{N} \mu_{iI} \sum_{k=1}^{N} \psi_{ks}(i) \, \dot{q}_k \sum_{k=1}^{N+1} \psi_{ks}(I) \, \dot{q}_k \ldots\ldots (35)$$

and $D_{V\theta}$, the soil dissipative function, is

$$\left.\begin{aligned} D_{V\theta} &= \tfrac{1}{2} \mu_A \sum_{k=1}^{N+1} \bar{\theta}^2{}_k \, \dot{q}^2{}_k \\ \text{in which} \qquad \bar{\theta}_k &= \frac{C_k}{\sqrt{I}} = C_k \frac{\phi_A(i)}{L_i} \end{aligned}\right\} \ldots\ldots\ldots\ldots (36)$$

Substituting in the foregoing equations the values of the dissipative function and differentiating with respect to the kth generalized velocity, one obtains

$$\mu_k = \mu_A \, \bar{\theta}^2 + \sum_{i=1}^{N} \sum_{I=1}^{N} \mu_{iI} \, \psi_{ks}(i) \, \psi_{ks}(I) \ldots\ldots\ldots\ldots (37)$$

---

[5] "Mathematical Methods in Engineering," by Th. von Kármán and M. A. Biot, McGraw-Hill Book Co., Inc., New York, N. Y., 1940, p. 219.

Proceeding to the limit at which $\bar{\theta}_k = 0$,

$$\mu_j = \sum_{i=1}^{N} \sum_{I=1}^{N} \mu_{iI}\, \phi_j(i)\, \phi_j(I) \qquad (38)$$

Because $\mu_{iI} = \mu_{Ii}$, $\mu_{ii} = -[\mu_{i(i+1)} + \mu_{i(i-1)}]$ and because $\mu_{iI} = 0$ if I represents any story other than the $(i+1)$th, ith, or $(i-1)$th, Eq. 38 may be solved for the pertinent value of μ_{iI} in terms of μ_j. If μ_j is known, these may then be substituted in Eq. 37 to obtain the required value of μ_k.

If the effect of damping in the shear modes is small enough to be neglected relative to the soil damping, Eq. 37 becomes

$$\mu_k = \mu_A\, \bar{\theta}_k^2 \qquad (39)$$

TABLE 1.—APPROXIMATE MODES AND FREQUENCIES

Ratio, λ	Story, i	$\frac{M_i}{M_1}$	$\phi_1\sqrt{M_1}$	$\phi_2\sqrt{M_1}$	$\phi_3\sqrt{M_1}$	$\phi_4\sqrt{M_1}$	$\phi_5\sqrt{M_1}$	Mode	$\frac{\omega_j}{\sqrt{\beta}}$
FIVE-STORY BUILDING									
1	5	0.75	0.615	−0.599	0.555	−0.456	0.278	5	1.93
1	4	1.00	0.575	−0.265	−0.205	0.559	−0.500	4	1.72
1	3	1.00	0.483	0.268	−0.590	−0.067	0.587	3	1.35
1	2	1.00	0.348	0.599	0.140	−0.496	−0.512	2	0.867
1	1	1.00	0.182	0.480	0.608	0.531	0.297	1	0.298
FIVE-STORY BUILDING									
0.2	5	0.40	0.837	−1.03	0.835	−0.212	0.028	5	1.61
0.4	4	0.80	0.696	−0.116	−0.710	0.485	−0.115	4	1.29
0.6	3	0.80	0.506	0.443	−0.170	−0.776	0.407	3	0.962
0.8	2	1.00	0.322	0.552	0.399	0.098	−0.650	2	0.668
1.0	1	1.00	0.150	0.326	0.365	0.551	0.660	1	0.290
FIVE-STORY BUILDING									
1	5	1.00	0.599	−0.546	0.462	−0.322	0.165	5	1.92
1	4	1.00	0.550	−0.170	−0.333	−0.595	−0.456	4	1.68
1	3	1.00	0.456	0.326	−0.550	−0.165	0.604	3	1.30
1	2	1.00	0.326	0.599	0.174	−0.452	−0.555	2	0.831
1	1	1.00	0.170	0.456	0.596	0.546	0.331	1	0.287
FOUR-STORY BUILDING									
1	4	1.00	0.658	−0.582	0.434	−0.233		4	1.88
1	3	1.00	0.577	0.00	−0.582	0.582		3	1.53
1	2	1.00	0.429	0.582	−0.224	−0.658		2	1.00
1	1	1.00	0.228	0.582	0.658	0.429		1	0.346
THREE-STORY BUILDING									
1	3	1.00	0.736	−0.586	0.328			3	1.80
1	2	1.00	0.591	0.327	−0.736			2	1.24
1	1	1.00	0.327	0.743	0.591			1	0.445
TWO-STORY BUILDING									
1	2	1.00	0.854	−0.528				2	1.62
1	1	1.00	0.528	0.854				1	0.616

Eq. 35 has been used because it is a general mathematical expression for a dissipative function in a building of N stories. In physical terms it represents the damping action between any two (not necessarily adjacent) stories, i and I. The damping for any floor mass as given by the equation for D substituted in the Lagrange equation is equal to $\partial D/\partial \dot{q}_k$ so that the damping force for the fifth floor mass, for example, will be

$$-\frac{\partial D}{\partial \dot{x}_5} = \frac{-\partial}{\partial \dot{x}_5}\left(\sum_{i=1}^{N}\sum_{I=1}^{N} \mu_{iI}\, \dot{x}_{i5}\, \dot{x}_{I5}\right) = -\left(\sum_{i=1}^{N}\sum_{I=1}^{N} \mu_{iI}\, \frac{\partial \dot{x}_{i5}}{\partial \dot{x}_5} \dot{x}_{i5} + \sum_{i=1}^{N}\sum_{I=1}^{N} \mu_{iI}\, \dot{x}_{i5}\, \frac{\partial \dot{x}_{I5}}{\partial \dot{x}_5}\right)$$

TABLES OF MODES AND FREQUENCIES

Approximate modes and frequencies of some typical shear buildings having from two stories to five stories are presented in Table 1. In this tabulation, M_i is the mass of the ith story, K_i is the stiffness of the ith story, β equals K_1/M_1, and λ equals K_i/K_1.

AMERICAN SOCIETY OF CIVIL ENGINEERS
Founded November 5, 1852

TRANSACTIONS

Paper No. 2862

AN EXPERIMENTAL STUDY OF BOUNDARY-LAYER TRANSITION

By Henry W. Bennett[1] and Charles A. Lee,[2] M. ASCE

Synopsis

Transition on a smooth flat plate in a zero pressure gradient was studied in a wind tunnel using conventional surface-tube and hot-wire techniques.

In the range of free-stream turbulence used (0.1% to 0.5%) it is shown that the laminar oscillations predicted by the Tollmien-Schlichting theory of laminar-layer stability play an important role in transition. The process of transition in this case is shown to be similar to the development of a turbulent wake from a vortex street, the amplified frequency feeding the rest of the spectrum. The effect of free-stream turbulence on the process was studied in terms of the energy concentrated at the amplified frequency. As anticipated, free-stream turbulence hastens the feeding of energy from the amplified frequency to the rest of the spectrum. It is indicated that, at a much higher level of free-stream turbulence than used in these tests, laminar oscillations will play no part in transition and, possibly, the phenomenon is controlled by the laminar-separation theory proposed by G. I. Taylor.

Notation

The letter symbols adopted for use in this paper are defined where they first appear and are arranged alphabetically, for convenience of reference, in the Appendix.

Introduction

Since L. Prandtl introduced[3] the concept of the boundary layer—a region near the surface of a body or the wall of a pipe where the velocity changes from that of the body right at the surface to the velocity of the free stream some distance away—much research has been accomplished to discover the char-

---

Note.—Published, essentially as printed here, in September, 1955, as *Proceedings Paper 796*. Positions and titles given are those in effect when the paper was approved for publication in *Transactions*.

[1] Hydr. Engr., Kimberly-Clark Corp., Neenah, Wis.

[2] Supt. of Fluid Mechanics Lab., Kimberly-Clark Corp., Neenah, Wis.

[3] "Über Flüssigkeiten bei sehr kleiner Reibung," by L. Prandtl, *Verhandlung*, 3d International Mathematics Cong., Heidelberg, 1904.

acteristics of the layer because of its importance in many problems in fluid mechanics.

For some distance down a flat plate that is immersed lengthwise in a flowing stream (if the leading edge is well sharpened, the plate is smooth, and the free stream is fairly nonturbulent), the boundary layer is laminar. The laminar boundary layer is thin and has the gradual velocity profile characteristic of laminar flow. After some distance, depending on the roughness of the plate, the free-stream turbulence, and other factors, the boundary layer becomes turbulent and assumes the usual turbulent-layer profile. Although it is usually tacitly assumed that this transition occurs instantaneously, it is well known that this is not the case. Transition occurs over a considerable length of the plate and has its beginnings considerably upstream of the modification of the laminar-layer velocity profile. It is toward a fuller understanding of this region, the conditions that determine where it will occur, and the conditions within the region that the research reported on herein is aimed. This research was prompted by the need of fundamental information along this line by those engaged in ship-model testing. In model testing the frictional resistance cannot be "scaled up" directly because of the presence of a considerable relative length of laminar boundary layer on the model and a much shorter one on the prototype. The correction for this condition has always been somewhat in doubt, in no small part because of a lack of knowledge concerning the position of transition on the model and how this position is affected by the other variables in the water channel.

Because previous work on this problem has been reviewed extensively in some well-known reports[4] the literature review presented herein will be brief and will be concerned primarily with work dealing with the effect of turbulence on transition on a smooth plate with zero pressure gradient.

Causes of Transition.—The major items affecting transition on a flat plate are (*a*) roughness of the plate, (*b*) free-stream turbulence, (*c*) pressure gradients along the plate, (*d*) plate curvature, (*e*) temperature variations, and (*f*) vibration or noise. In order to limit this study, only the effect of turbulence was considered; the effects of the other items have been studied elsewhere.[4,5,6]

Effect of Turbulence.—One of the earlier, more notable investigations of the effect of turbulence on transition was that of G. I. Taylor.[7] Mr. Taylor theorized that transition was caused by separation, either momentary or permanent, in the laminar layer; thus, transition should be governed by the von Kármán-Pohlhausen parameter for laminar separation. For isotropic turbulence such as occurs in the wake of a grid, Mr. Taylor was able to relate the von Kármán-Pohlhausen parameter to the measurable free-stream quantities, scale, and intensity, and was thus able to relate the pressure forces causing intermittent separation to free-stream quantities. Mr. Taylor evolved the expression $(u'/U_0)(x/L)^{1/5}$ as the parameter which determines at what R_x-value the boundary layer will become turbulent. In these expressions u' is the root-mean velocity fluctuation in the direction of flow; U_0 denotes the mean velocity in the free stream; x is the distance from the leading edge of the flat plate along the plate; L represents the scale of the u'-fluctuations; and R_x is the Reynolds number based on x and U_0. Mr. Taylor confirmed that this parameter does control transition with fairly large values of free-stream turbulence on flat plates, spheres, and elliptic cylinders. This theory has met with some objections, not the least of which is that separation has not been proved to be a necessity for transition.

---

[4] "Some Recent Contributions to the Study of Transition and Turbulent Boundary Layers," by Hugh L. Dryden, *Technical Note No. 1168*, National Advisory Committee for Aeronautics, Washington, D. C., April, 1947.

[5] "Investigation of Effects of Surface Temperature and Single Roughness Elements on Boundary Layer Transition," by H. W. Liepmann and Gertrude H. Fila, *Report No. 890*, National Advisory Committee for Aeronautics, Washington, D. C., 1947.

[6] "Review of Published Data on the Effect of Roughness on Transition from Laminar to Turbulent Flow," by Hugh L. Dryden, *Journal of the Aeronautical Sciences*, Vol. 20, 1953, p. 477.

[7] "Statistical Theory of Turbulence V—Effect of Turbulence on Boundary Layer," by G. I. Taylor, *Proceedings*, Royal Soc. of London, Series A, Vol. 156, August, 1936, p. 307.

Theory of Laminar Oscillations.—From a purely theoretical standpoint it has been found that the laminar layer, by virtue of its thickness, the kinematic viscosity of the fluid involved, and the free-stream velocity, is able to amplify certain frequencies of disturbance. This is in decided contrast to the theory wherein the magnitude of the disturbance was felt to be the essential factor. In this theory the type of disturbance, particularly with regard to what frequencies are present, was considered to be the essential thing.[8] The essential result of this theory is the "curve of neutral stability" shown in Fig. 1. In Fig. 1, $\beta_r \nu/U_0$ is plotted as a function of R_δ, in which β_r is $2\pi f$ (f is frequency), ν represents the kinematic viscosity, and R_δ is the Reynolds number based on δ and U_0 (δ is the boundary-layer-displacement thickness). This curve is a loop, the two branches meeting at infinity. This curve was first plotted by H. Schlichting[9] and subsequent corrections have been made to the theory by C. C. Lin[10] which changed somewhat the position of the right side of the loop (usually referred to as Branch II). Essentially, this loop defines which

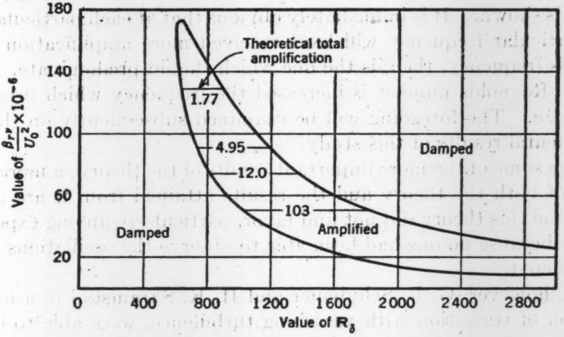

FIG. 1.—CURVE OF NEUTRAL STABILITY

---

[8] "General Instability Criterion of Laminar Velocity Distributions," by W. Tollmien, *Technical Memorandum No. 792*, National Advisory Committee for Aeronautics, Washington, D. C., 1936.

[9] "Amplitudenverteilung und Energiebilanz der kleinen Storungen bei der Plattenstromung," by H. Schlichting, *Nachrichten*, Gesellschaft der Wissenschaften zu Gottingen, Mathematische-Physikalische Klasse, Vol. 1, 1935, pp. 47–78.

[10] "On the Stability of Two-Dimensional Parallel Flows," by C. C. Lin, *Quarterly of Applied Mathematics*, July, 1945, pp. 117–142; October, 1945, pp. 218–234; and January, 1946, pp. 277–301.

disturbances present in the boundary layer will be amplified and which disturbances will be damped. Any combination of disturbance, free-stream velocity, and boundary-layer Reynolds number which puts the situation inside the loop should theoretically cause the disturbance to be amplified. If the point falls outside the loop, the disturbance will be damped, and a point falling right on the curve should neither be damped nor amplified. Assuming a disturbance of constant frequency is impressed on the laminar layer at a small value of boundary-layer Reynolds number, the disturbance will be damped until the boundary-layer Reynolds number reaches the value where the frequency parameter intersects Branch I of the stability curve. From here on, as the point of observation is moved down the plate, the disturbance will be amplified until the boundary-layer Reynolds number reaches the value of the intersection with Branch II. At this point the wave is again damped. The question remains, if a single frequency is to be present in the boundary layer at a particular value of boundary-layer Reynolds number, what should this frequency be? In Fig. 1, the theoretical total amplification for several frequencies is shown. It is immediately obvious that at each particular value of R_δ, one particular frequency will have received more amplification than any other. This frequency, then, is the one which should predominate. If this is true, as the Reynolds number is increased the frequency which predominates should change. The foregoing will be examined subsequently on the basis of the experimental results of this study.

These are some of the more important results of the theory; a more complete discussion of both the theory and the results attained from it are available.[8] For some time this theory did not find favor, particularly among experimentalists, mainly because no one had been able to observe the oscillations which the theory predicted.

In 1938, however, G. B. Schubauer and H. K. Skramstad in a near-classic investigation of transition with vanishing turbulence, were able to detect the astonishingly pure laminar oscillations.[11] Evidently, previous investigators had been unable to detect the oscillations because transition had occurred simultaneously or nearly simultaneously with the appearance of the waves.

Even more important than merely discovering the existence of the waves, Messrs. Schubauer and Skramstad introduced oscillations of known frequency and amplitude into the boundary layer by vibrating a very thin metal ribbon at different frequencies and amplitudes in the boundary layer. By using a very narrow band-pass filter on the amplified output of a hot wire moved progressively down the plate, they were able to follow the growth and decay of the frequency being considered. They proved conclusively not only the existence of the waves but also that the waves would grow and decay according to Fig. 1. From this information, Messrs. Schubauer and Skramstad formulated a new proposal of how transition occurs, particularly when the free-stream turbulence is low.

The analogy of the formation of turbulence from a free vortex sheet was used by Messrs. Schubauer and Skramstad. The boundary layer becomes wavelike and, eventually, discrete eddies appear. These eddies, in themselves, are unstable and eventually decay into turbulence. The decay into turbulence is gradual, the random turbulent motion only occurring a part of the time. This explanation seems to fit the quantitative data presented by Messrs. Schubauer and Skramstad better than the explanation of intermittent separation cited previously.

---

[11] "Laminar Boundary Layer Oscillations and Transition on a Flat Plate," by G. B. Schubauer and H. K. Skramstad, *Report No. 909*, National Advisory Committee for Aeronautics, Washington, D. C., 1948.

Some support is lent to the theory of Messrs. Schubauer and Skramstad by F. R. Hama and I. Tani.[12] In connection with a study of the effect of a single roughness element on transition, Messrs. Hama and Tani towed a flat plate horizontally in water and attached a small-diameter pipe transversely to the plate as a roughness element. Dye was injected through a small hole in the top of the pipe in the center of the plate into the surrounding water. The motion of the dye was photographed as it progressed down the plate. At first, vortices were emitted from the top of the pipe at a constant rate and would move down the plate with this orientation. Soon, however, neighboring vortices would join with one another to form a larger vortex. At some point further down the plate these vortices would "explode" and the motion become random. Messrs. Hama and Tani postulate that this may be transition.

Of course, conditions behind a single roughness element are not the same as conditions on a smooth plate, but photographs[12] do show that oriented vortices in the laminar boundary layer are not stable and seem to explode suddenly some distance down the plate. In the case of a smooth plate, the vortices are a product of the amplified boundary-layer oscillations and in the wake of a roughness element the vortices are, of course, caused by the element. Nevertheless, the "exploding" of the waves is probably the same in both cases.

Probability Transition Theory.—One further approach to the problem is that taken by H. W. Emmons.[13] In an observation on a water-table analogy to supersonic flow, Mr Emmons observed boundary-layer transition. The transition could be viewed clearly because the thin layer of water, when it became turbulent, was considerably changed in appearance with either transmitted or reflected light. It was noted that transition is not a clearly defined phenomenon, but is rather an intermittent process. Mr. Emmons noted that by virtue of disturbances carried into the layer by outside turbulence, plate roughness, vibration, or other factors, the laminar layer is disturbed. When these disturbances reach a certain value a turbulent "burst" occurs. This turbulent "spot," as Mr. Emmons terms it, moves along with the fluid and gradually fans out, making turbulent everything before it. Mr. Emmons notes that the "bursts" which are noted by the hot wire are these turbulent spots passing over the wire. The farther down the plate one observes the flow, the larger the number of turbulent spots which have been born upstream and hence the larger percentage of time the particular point under observation is turbulent. Mr. Emmons states that one cannot describe transition in terms of a single point, but rather one should be able to define what percentage of the time any point on the plate would be turbulent. Mr. Emmons then develops

---

[12] "Some Experiments on the Effect of a Single Roughness Element on Boundary Layer Transition," by F. R. Hama and I. Tani, *Journal of the Aeronautical Sciences*, Vol. 20, 1953, p. 289.

[13] "The Laminar-Turbulent Transition in a Boundary Layer: Part 1," by H. W. Emmons, *ibid.*, Vol. 18, 1951, p. 490.

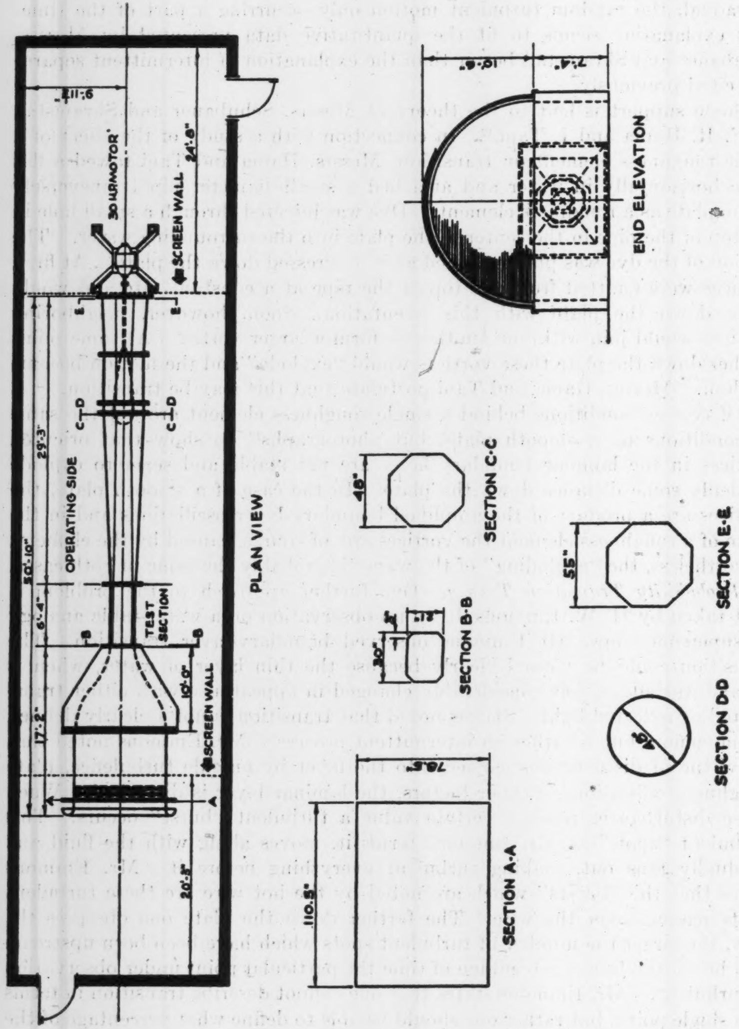
SECTION A-A
110.5"
78.5"
20'-5"
17'-2"
10'-0"
SCREEN WALL
A
B
TEST SECTION
6'-4"
50'-10"
OPERATING SIDE
PLAN VIEW
29'-3"
C-D
E
SCREEN WALL
24'-8"
30 H.P. MOTOR
11'-6"
SECTION B-B
30"
SECTION C-C
48"
SECTION D-D
SECTION E-E
55"
END ELEVATION
10'-6"
7'-4"

Fig. 2.—Tunnel Installation

a theory for predicting what percentage of the time each position on the plate will be turbulent by considering not only the effect of spots formed at the point in question but also those that form upstream. Some rather complicated expressions result for the probability that a certain spot on the plate will be turbulent. Much additional experimental evidence is necessary to complete this theory, however—primarily data on the rate of spot production, the initial size of a turbulent spot, the rate at which a spot grows as it moves downstream, and how these parameters are affected by free-stream turbulence.

Although this theory will undoubtedly aid in better defining the conditions in the boundary layer through transition, the lack of definitive data does not make it too useful. This information, however, was included merely to indicate yet another method of defining transition and the conditions immediately surrounding it.

APPARATUS AND METHODS

The Tunnel.—The experimental work was performed in the single-pass wind tunnel which is shown in Fig. 2. The tunnel is placed in a long building composed of two quonset huts in tandem, each hut being raised 7 ft from the floor level to give a maximum ceiling height of 17 ft. The tunnel has a 14-to-1 contraction ratio and test-section dimensions of 20 in. by 30 in. and 6 ft long. To eliminate a longitudinal static pressure gradient in the test section, the sidewalls are adjustable in fixed increments as indicated in Fig. 3. The velocity distribution, as measured in several transverse planes across the test section, was found to be uniform to within 0.5% over the working range of the jet.

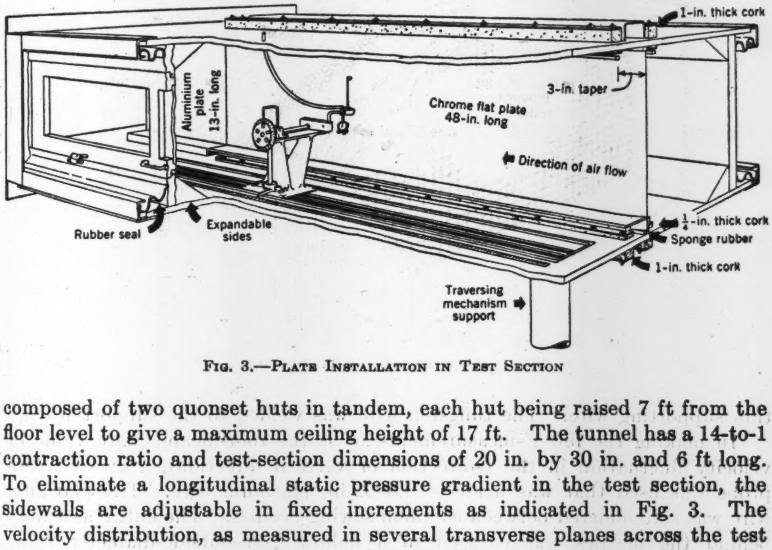
1-in. thick cork
3-in. taper
Aluminium plate 13-in. long
Chrome flat plate 48-in. long
Direction of air flow
$\frac{1}{4}$-in. thick cork
Sponge rubber
1-in. thick cork
Rubber seal
Expandable sides
Traversing mechanism support

FIG. 3.—PLATE INSTALLATION IN TEST SECTION

To distribute the return flow of air over the cross section of the room, two walls of 60-by-60 mesh wire were introduced across the hut as indicated in Fig. 2. To eliminate any remaining large-scale irregularities in the incoming flow, a 30-by-30 mesh screen with 0.013-in.-diameter wire was placed immediately following the bell mouth. This screen was directly followed by a honeycomb of paper tubes with an inside diameter of 0.5 in., an outside diameter of

0.625 in., and a length of 12 in. Following the honeycomb was a short settling length as indicated in Fig. 4 and two more 30-by-30 mesh screens. To change the turbulence level in the tunnel, rope grids with various diameter ropes were introduced immediately downstream of the last screen.

Hot-Wire Equipment.—The hot-wire equipment was of the constant-current type, the changes in voltage across the wire being an indication of the velocity changes. Included with the hot-wire heating equipment and the amplifier was the usual assortment of galvanometers, potentiometers, switching circuits, bridge circuits, and similar devices. The amplifier is of the capacitance-compensated type with a flat response from 0 cycle to 10,000 cycles.

The wires used for u'-measurements were of 0.00031-in.-diameter tungsten wire supported as shown in Fig. 5. The probes consisted of two brass strips separated by an insulating material. To each of the strips was fastened a thin supporting wire. The tungsten wire was welded to the support wires.[14]

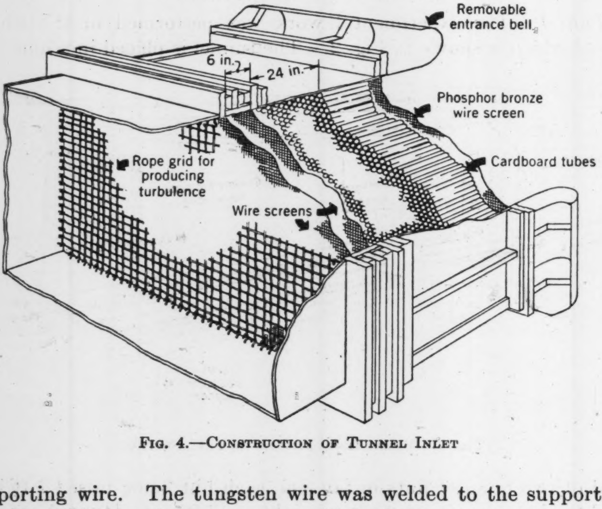
Removable entrance bell
6 in.
24 in.
Phosphor bronze wire screen
Cardboard tubes
Rope grid for producing turbulence
Wire screens

Fig. 4.—Construction of Tunnel Inlet

In making the few v'-measurements (v' is the root-mean-square value of velocity fluctuation in the y-direction or vertical direction), a crossed wire probe was used that was made of 0.0002-in. platinum wire. The platinum wire was soft-soldered between common sewing needles. The entire assembly behind the needles was encased in a hollow $\frac{3}{8}$-in.-outside-diameter tube, approximately 6 in. long, as shown in Fig. 5.

To traverse the wire, the carriage assembly shown in Fig. 3 was used. A part of the tunnel floor was removed and the metal bed, on which the carriage traveled, was inserted. A long lead screw, operated externally, gave the entire carriage longitudinal motion; the short precision-lead screw shown in Fig. 3, also operated from an external handwheel through a shaft and gear system, gave crosswise motion to the mount. Although the probe wire is rather close to the carriage as shown in Fig. 3, no observable pressure-field effects were encountered. To position the probe wire relative to the plate, feeler gages were used, and the reading on the dial indicator attached to the probe holder was noted.

---

[14] "On the Construction of Hot-Wire Aneomometers for the Investigation of Turbulence," by B. G. van der Hegge Zijnen, *Applied Scientific Research*, Vol. A2, The Hague, 1951.

To measure the distribution of fluctuation energy with frequency, a panoramic sonic analyzer was used. This instrument, which is similar to an oscilliscope, samples (once a second) the frequency spectrum from 20 cycles to 20,000 cycles and automatically plots the output as a function of frequency.

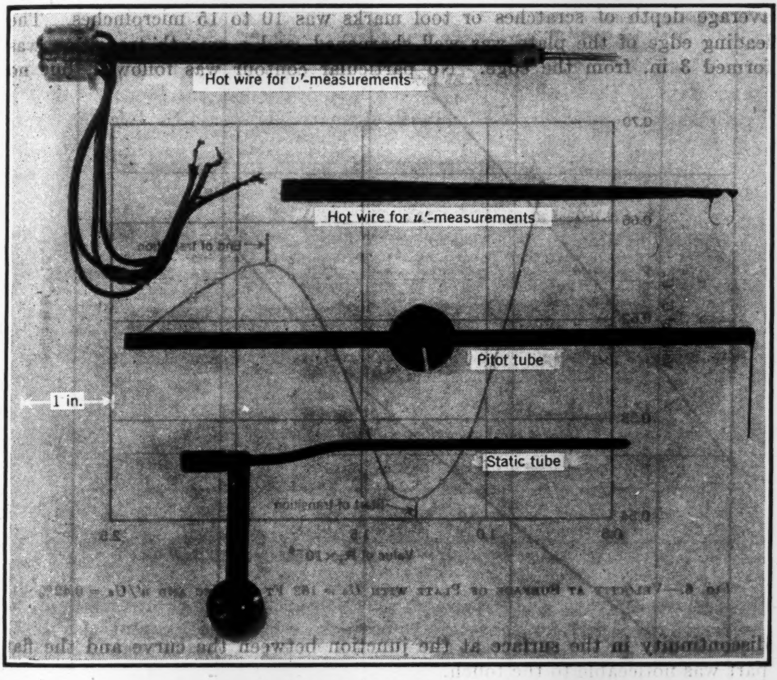
Hot wire for v'-measurements
Hot wire for u'-measurements
Pitot tube
1 in.
Static tube

FIG. 5.—INSTRUMENTS

To obtain an average picture of the spectrum, a long-time photograph of the face of the instrument was taken and the image "burned in" the photographic paper. Interpretation of these photographs was somewhat difficult, but by connecting points of equal optical intensity it is felt that a fair picture of the frequency spectrum was obtained.

Velocity Measurements.—To measure the velocity at the surface of the plate, the dynamic pressure was measured using the impact tube shown in Fig. 5. This tube consists of a hypodermic needle of 0.0010-in. inside diameter and 0.0020-in. outside diameter. The needle was fastened into the end and perpendicular to the axis of a $\frac{3}{16}$-in. hollow brass tube. A simple mounting arrangement permitted the probe to be mounted in the traversing carriage. The static pressure was measured using the static probe also shown in Fig. 5. This probe consisted of a long cylinder with an ogive-shaped nose and pressure ports around the cylinder eight diameters back from the tip of the nose. This probe was used for measuring the test-section static-pressure gradient and also as a reference for the impact tube when measurements were being made with the latter near the surface of the plate.

Flat Plate.—The flat plate was of $\frac{1}{4}$-in. sheet steel, prepared on a surface grinder, hand-polished, and then chromeplated. The root-mean-square average depth of scratches or tool marks was 10 to 15 microinches. The leading edge of the plate was well sharpened, and a smooth transition was formed 3 in. from the edge. No particular contour was followed, but no discontinuity in the surface at the junction between the curve and the flat part was noticeable to the touch.

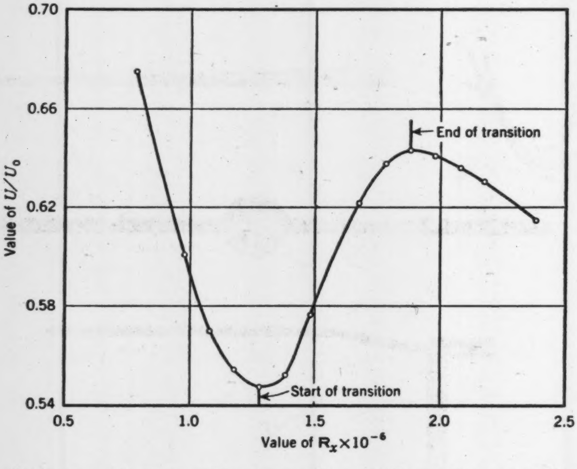

FIG. 6.—VELOCITY AT SURFACE OF PLATE WITH $U_0 = 162$ FT PER SEC AND $u'/U_0 = 0.42\%$

The plate was supported both top and bottom by a row of bolts passing through the plate. To isolate the plate from the tunnel vibration, strips of cork and rubber were used as indicated in Fig. 3.

The plate did not, at first, extend back to the end of the test section, but it was soon observed that the balance between the flow on either side of the plate was upset when the carriage of the traversing mechanism was moved back behind the trailing edge of the plate. To correct this, an extension of $\frac{1}{4}$-in. aluminum was added to the plate. No measurements were made, of course, on the aluminum extension, but no further difficulty with the balance of air on the two sides of the plate was encountered.

RESULTS

Fig. 6 shows a typical series of velocity measurements a fixed distance away from the plate (approximately one-half the diameter of the hypodermic needle shown in Fig. 5) as a function of distance down the plate. The velocity

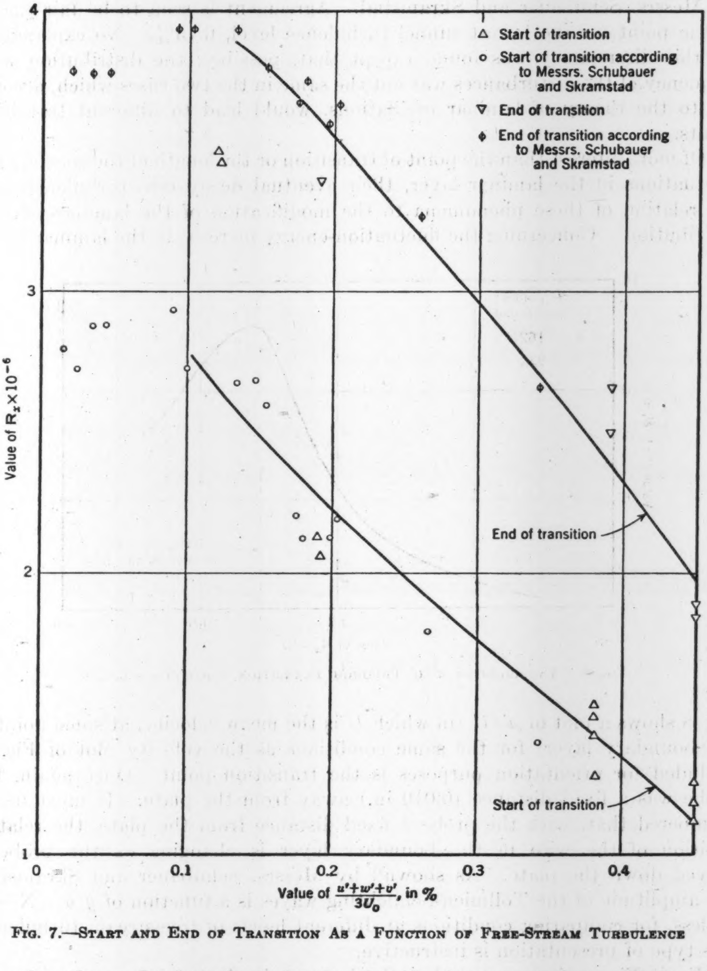

FIG. 7.—START AND END OF TRANSITION AS A FUNCTION OF FREE-STREAM TURBULENCE

was referred to a fixed static probe elsewhere in the test section. The sudden rise in pressure, caused by the "washing away" of the laminar profile by the steeper turbulent profile is usually defined as the "transition point." Immediately following the peak of this curve is the decrease in velocity a fixed distance from the surface, caused by the natural growth of the turbulent layer. The peak of this curve is termed the end of transition.

Fig. 7 shows the start and end of the transition region for several levels of free-stream turbulence; in Fig. 7, w' is the root-mean-square value of velocity fluctuation in the z (or longitudinal)-direction. Also shown are data taken[11] by Messrs. Schubauer and Skramstad. Agreement is seen to be fair except at the point for the lowest tunnel turbulence level, 0.13%. No explanation for this discrepancy was found except that, possibly, the distribution with frequency of the disturbances was not the same in the two cases which, according to the theory of laminar oscillations, would lead to different transition points.

Of more interest than the point of transition or the length of the zone are the fluctuations in the laminar layer, their eventual decay into turbulence, and the relation of these phenomena to the modification of the laminar-velocity distribution. Concerning the fluctuation-energy increase in the laminar layer, Fig. 8 shows a plot of u'/U (in which U is the mean velocity, at some point in the boundary layer) for the same conditions as the velocity plot of Fig. 6. Included for orientation purposes is the transition point. Once again, the probe was a fixed distance (0.010 in.) away from the plate. It must be remembered that, with the probe a fixed distance from the plate, the relative position of the wire in the boundary layer is changing as the probe is moved down the plate. As shown[11] by Messrs. Schubauer and Skramstad, the amplitude of the Tollmien-Schlichting waves is a function of y/δ. Nevertheless, for comparing conditions at different levels of free-stream turbulence, this type of presentation is instructive.

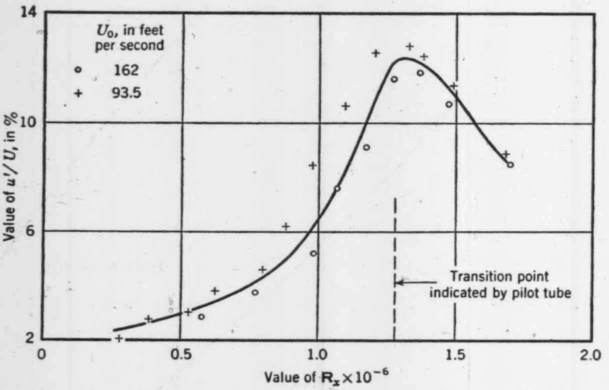

FIG. 8.—VARIATION OF u'/U THROUGH TRANSITION FOR $u'/U_0 = 0.42\%$

From Fig. 8, it is noted that the increase in fluctuation energy is not a sudden phenomenon, concurrent with the modification of the velocity profile, but is rather a more gradual process. To understand fully what occurs as the fluctuation energy increases, it is necessary to examine the frequency spectrum of the fluctuations.

Measurement of Spectrum.—Fig. 9 shows copies of a series of photographs of the panoramic analyzer which, in effect, are plots of output versus frequency of the compensated amplifier; in Fig. 9, the term M denotes the relative magnification. Initially the hot wire detects low-amplitude waves, some of which appear to be stray electrical or mechanical pickup. As the $\mathbf{R}_x$-value is increased, it is seen that a particular frequency is picked up by the boundary layer and amplified. The amplified frequency eventually becomes more and more distorted as the band of frequencies which are amplified becomes wider, and it appears that the rest of the spectrum "feeds" on the amplified frequency. This pattern of development was observed in all the tests made with the range of free-stream turbulence used (0.13% to 0.50%); however, important differences showed up as the free-stream turbulence and the free-stream velocity were changed. These differences, cited subsequently, offer much insight into the mechanism of transition.

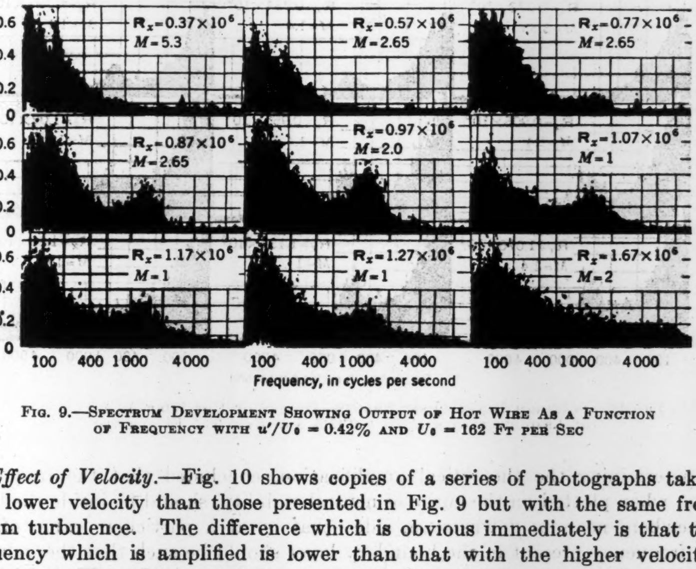

Fig. 9.—Spectrum Development Showing Output of Hot Wire As a Function of Frequency with $u'/U_0 = 0.42\%$ and $U_0 = 162$ Ft per Sec

Effect of Velocity.—Fig. 10 shows copies of a series of photographs taken at a lower velocity than those presented in Fig. 9 but with the same free-stream turbulence. The difference which is obvious immediately is that the frequency which is amplified is lower than that with the higher velocity. Referring to Fig. 1, however, it is seen that $\beta_r\, \nu/U^2_0$ is the important parameter in determining which frequency will be amplified. Computation of this frequency parameter showed it to be nearly constant for the same conditions of turbulence but for different velocities.

Effect of Free-Stream Turbulence on Oscillations and Eventual Transition.—Fig. 11 shows the development of oscillations for the lowest tunnel turbulence used (0.13%), and Fig. 9 gives the same information for the highest turbulence, $u'/U_0 = 0.42\%$. The speed was the same in both cases. It is immediately obvious that, with lower turbulence, the frequency which the boundary layer picks up is much lower than with the higher turbulence and, even more important, the oscillation is extremely pure. With the higher turbulence there is almost immediately, on the appearance of the oscillations, a feeding of energy from the central frequency to the surrounding frequencies. This process, with the higher level of free-stream turbulence, leads to transition almost immediately after the appearance of the waves. With lower turbulence, however, the oscillations are pure, and there is little transfer of energy to surrounding frequencies.

Concerning the frequency which the laminar layer amplifies, it was noted previously that the frequency present at the point of observation is a function of conditions at that point—that is, the frequency present will be that frequency which, at that particular value of boundary-layer Reynolds number, has received the most amplification up to that point. This implies that the frequency should be constantly changing as the hot-wire probe is moved down the plate. Messrs. Schubauer and Skramstad, using Mr. Schlichting's method of determining the theoretical amplification, concluded that the frequency data, when plotted on the curve of neutral stability, should be inside the loop, somewhere near its downstream side—that is, at a particular value of $\mathbf{R}_\delta$, the frequency present in the boundary layer should be such that the value of $\beta_r\,\nu/U^2_0$ places the point near the downstream (Branch II) side of the loop. Fig. 12 shows the values of $\beta_r\,\nu/U^2_0$ as a function of $\mathbf{R}_\delta$ as found in a few of the tests. Most of the data are near Branch II of the loop, although a few points fall outside the loop. Some of the error undoubtedly occurred in interpreting the photographs.

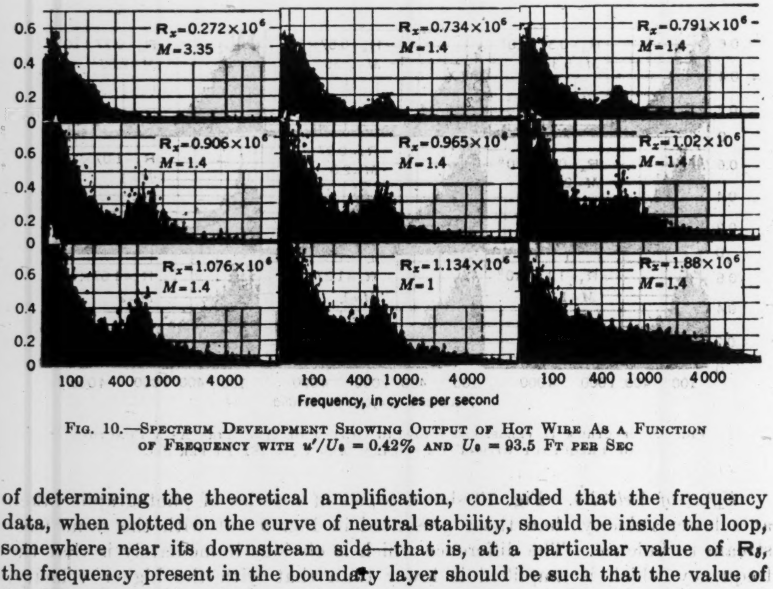

Fig. 10.—Spectrum Development Showing Output of Hot Wire As a Function of Frequency with $u'/U_0 = 0.42\%$ and $U_0 = 93.5$ Ft per Sec

It is interesting to note that, in some of the tests, the frequency amplified does not change as rapidly as would be predicted. In Fig. 11, for example, it is obvious that the amplified frequency remains nearly 1,000 cycles for some distance down the plate. In this respect, the experimental results did not agree too well with those predicted by the theory.

Also of interest in this regard is the frequency which first makes its appearance in the boundary layer as the free-stream turbulence is changed. From Figs. 9 and 11, it is seen that under conditions of higher turbulence the frequency which first appears with an amplitude of any importance is considerably higher than the frequency which first appears under conditions of low free-stream turbulence. This is shown in Fig. 13, in which the value of $\mathbf{R}_\delta$ at which oscillations first appear is shown as a function of u'/U_0 in the free stream. Fig. 13 shows clearly that at lower levels of free-stream turbulence the waves do not make their appearance until the observation is made at a higher value of $\mathbf{R}_\delta$. This can mean either that there is some minimum value of free-stream disturbance necessary to excite a particular frequency or that the product of disturbance and amplification at the lower turbulence does not give a measurable boundary layer wave—that is, one that would appear above the noise level of the sonic analyzer. This latter conjecture is rather difficult to believe because, as noted in Fig. 1, the amplification given a disturbance increases manyfold with only a slight decrease in $\beta_r \nu/U^2_0$. Assuming that the product of amplification and disturbance must reach some value before the wave becomes discernible, it is obvious from Fig. 1 that the amplification increases considerably more than the free-stream turbulence and that their product is nowhere near constant, even allowing for some difference in the initial energy distribution with frequency. It almost appears that there is some minimum level of free-stream disturbance necessary to excite a particular frequency. At any rate, it is important to note that the waves appear at a lower value of $\mathbf{R}_\delta$ the higher the level of free-stream turbulence.

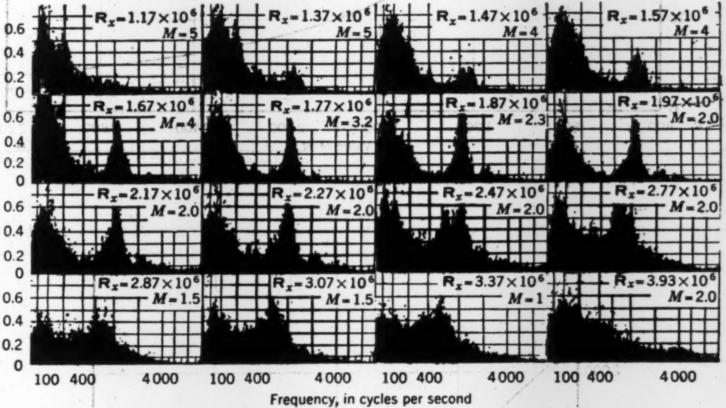

FIG. 11.—SPECTRUM DEVELOPMENT SHOWING OUTPUT OF HOT WIRE AS A FUNCTION OF FREQUENCY WITH $u'/U_0 = 0.13\%$ AND $U_0 = 162$ FT PER SEC

As noted previously, the photographs from the panoramic analyzer were analyzed by connecting points of equal optical intensity. If the values are then squared and suitably made nondimensional, curves of energy versus

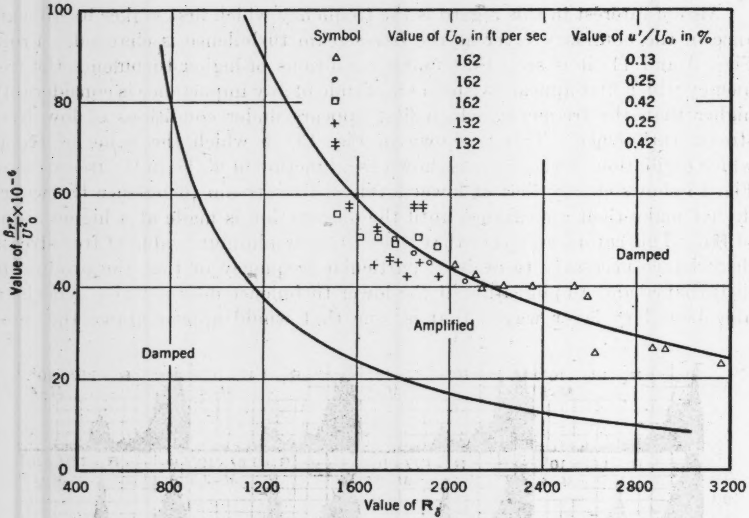

FIG. 12.—CURVE OF NEUTRAL STABILITY SHOWING EXPERIMENTAL DATA

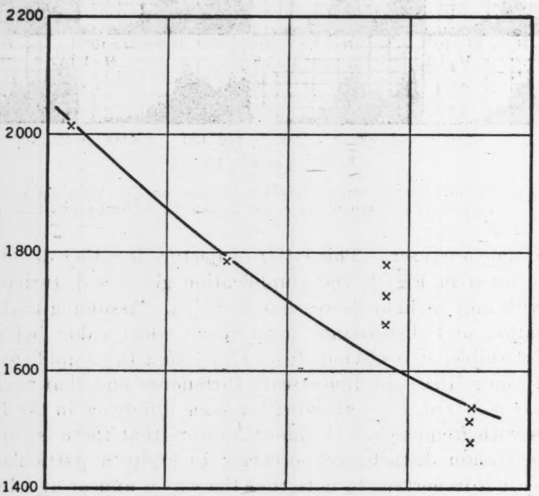

FIG. 13.—VALUE OF R_δ WHEN LAMINAR OSCILLATIONS FIRST APPEAR AS A FUNCTION OF FREE-STREAM TURBULENCE

frequency result. To make these curves nondimensional the maximum value of the squared output at zero frequency was used. Fig. 14 shows the photographs of Fig. 11 analyzed in this manner. A certain amount of judgment was necessary in interpreting the photographs, particularly at the lower frequencies where the trace from the panoramic analyzer never seemed to burn into the film with the same intensity as at the higher frequencies, making interpretation somewhat difficult. Also present, particularly at low values of $\mathbf{R}_x$, was a certain amount of unexplained low-frequency signal, probably due in part to mechanical vibration of the probe. Nevertheless, at higher values of $\mathbf{R}_x$ and particularly in the middle range of frequencies (from 600 cycles to 1,500 cycles), the curves of Fig. 14 present a true picture of the growth and decay of the laminar oscillations. In connection with Fig. 14 it should be noted that the change in velocity distribution started at $\mathbf{R}_x = 3.48 \times 10^6$.

It appears that the low-frequency end of the spectrum increased rather quickly after the appearance of the waves. This is undoubtedly due to the distortion of the regular frequency which can be observed on an oscilliscope. As the amplified frequency continues to grow, the low-frequency end of the spectrum tends to become constant, and the higher frequencies start to feed off the laminar oscillations. It appears that the regular wave in the laminar layer cannot undergo further distortion without bursting into random turbulent motion. The curve showing the final spectrum is somewhat misleading with regard to the general level. It must be realized that all measurements were taken a fixed distance from the surface, and in order to get a spectrum measurement without any traces of laminar oscillations it was found necessary to measure a distance following the modification of the laminar-layer velocity distribution. This, of course, meant that the value of y/δ was considerably less than in previous measurements and caused the decrease in total energy.

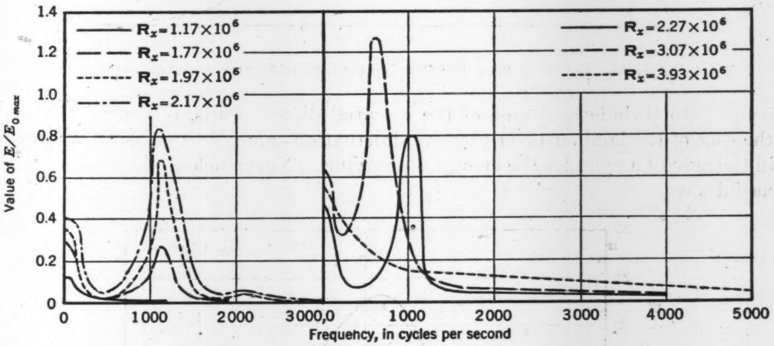

FIG. 14.—CHANGES IN SPECTRUM THROUGH TRANSITION WITH $u'/U_0 = 0.13\%$ AND $U_0 = 162$ FT PER SEC

An instructive method of showing these data is to separate from the continuous spectra the energy caused by the laminar oscillations. The method used is similar to that used[15] by A. Roshko for presenting data on the development of turbulent motion from a vortex street in the wake of a cylinder. The situation during transition is remarkably similar to conditions in the immediate wake of a cylinder. In both cases, a large percentage of the total energy is, for some distance, concentrated in discrete eddies which eventually decay into turbulence. One of the essential differences is, of course, that in the case of the laminar layer the total fluctuation energy is increasing, whereas in the case of a cylinder the energy is decaying. Nevertheless, the analogy is a useful one.

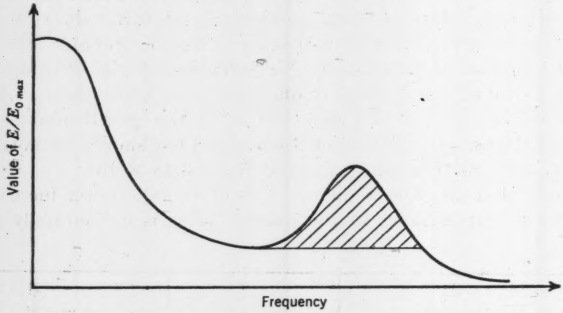

Fig. 15.—Separation of Discrete Energy from Continuous Spectra

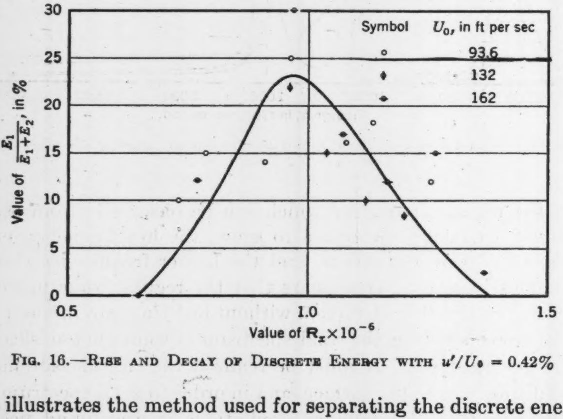

Fig. 16.—Rise and Decay of Discrete Energy with $u'/U_0 = 0.42\%$

Fig. 15 illustrates the method used for separating the discrete energy caused by the laminar oscillations. It was rather difficult to decide on a suitable method because of the large differences in the curves at the higher frequencies. Admittedly, the method used does not show exactly how much of the total energy is represented by the laminar oscillations, but no other method was found that would adequately portray the changes that occur. In this method the shaded area is the energy resulting from the laminar oscillations and is termed discrete and is designated as E_1; the remaining area is E_2 and the total area is E. Thus, $[E_1/(E_1 + E_2)]\,100$ is the percentage of the total represented by the discrete area.

---

[15] "On the Development of Turbulent Wakes from Vortex Streets," by A. Roshko, *Technical Note No. 2913*, National Advisory Committee for Aeronautics, Washington, D. C., March, 1953.

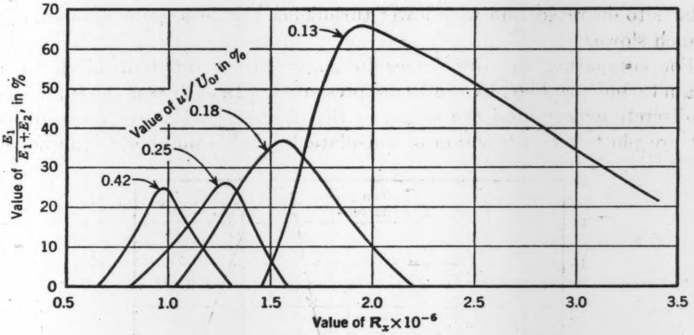

Fig. 17.—Rise and Decay of Discrete Energy for Different Levels of Free-Stream Turbulence

It was found that the rise and decay of discrete energy were independent of velocity. This is shown in Fig. 16, in which discrete energy is plotted as a function of R_x for three different speeds. Although there is a scattering of results there seems to be no systematic variation with velocity. This certainly

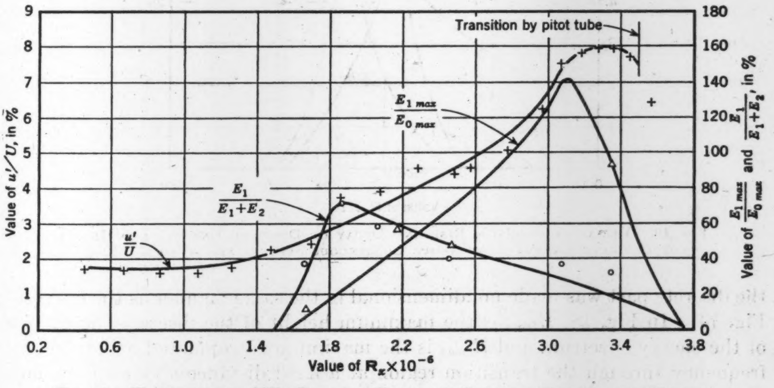

Fig. 18.—Variation of u'/U_0, Rise and Decay of Discrete Energy, and Height of Discrete Energy Part Above Continuous Spectra Through Transition for $u'/U_0 = 0.13\%$

shows the dependence of the entire phenomenon of transition on the free-stream turbulence and the Reynolds number. Fig. 13 showed that the Reynolds number at which the waves appear is a unique function of the free-stream turbulence. Fig. 16 indicates that the growth and decay of the discrete energy in the spectrum is a function of the Reynolds number, independent of velocity, despite the fact that the frequency found is a function of the reciprocal of the velocity squared.

With the different levels of turbulence used, the rise and decay of discrete energy are shown in Fig. 17. As anticipated, with decreasing turbulence the discrete energy reaches a much greater percentage of the total energy before it starts to decrease, and with lower turbulence the decrease in discrete energy is much slower.

For comparing the differences in transition at different levels of free-stream turbulence Figs. 18 and 19 are presented. In each case the total energy, the discrete energy, and the height of the discrete part above the continuous part are plotted as a function of flat-plate Reynolds number. The height of the discrete part was made nondimensional in the same manner as the curves of Fig. 14. In Fig. 18, E_{1max} is the maximum height of the discrete-energy part of the energy spectrum and E_{0max} is the maximum extrapolated energy at zero frequency through the transition region at a fixed distance above the surface. As indicated by Fig. 18, the total energy starts to increase at the same time that the discrete energy starts to increase. This corresponds to the initial introduction of the oscillations into the boundary layer. The discrete energy quickly reaches a peak and starts to decrease despite the fact that the amplified waves are still present, as indicated by the continuing increase in height of the discrete part. This indicates that the discrete part is feeding energy to the rest of the spectrum, initially the lower frequencies and finally the higher frequencies, as cited previously. Eventually the height of the amplified-

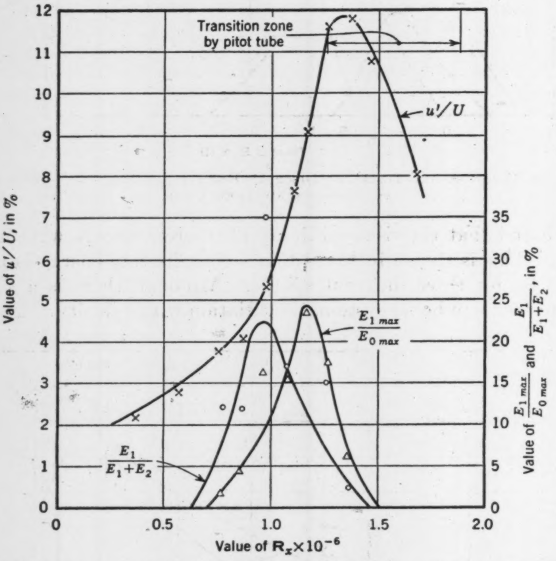

Fig. 19.—Variation of u'/U_0, Rise and Decay of Discrete Energy, and Height of Discrete Energy Part Above Continuous Spectra for $u'/U_0 = 0.42\%$

frequency part of the spectrum starts to decrease, indicating that the oscillations are bursting into high-frequency turbulence more rapidly than the oscillations can grow. Following this, modification of the velocity distribution occurs quickly as the pitot-tube pressure rise, shown for convenience, indicates. In Fig. 19, the same curves are shown but for a higher level of turbulence.

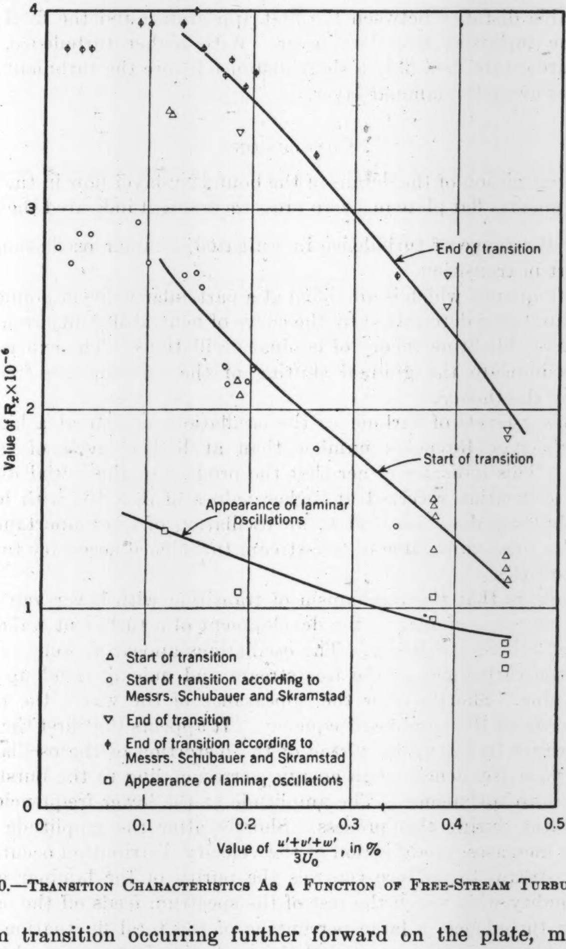

FIG. 20.—TRANSITION CHARACTERISTICS AS A FUNCTION OF FREE-STREAM TURBULENCE

Aside from transition occurring further forward on the plate, many other differences are discernible. The ratio of discrete energy to total energy never becomes very high which can only mean that, as quickly as the oscillations build up, they are distorted and quickly feed the rest of the spectrum. It is seen that the magnitude of the amplified frequency builds up in much the same manner as with lower turbulence, but the maximum is reached much faster and the magnitude of the amplified-frequency band relative to the rest of the spectrum decays much more rapidly than with lower turbulence.

As indicated in the foregoing and borne out by the data, it is incorrect to speak of transition as occurring at any one point—its beginnings occur far upstream on the plate. Fig. 20 shows the plot of Fig. 7 with more of the "landmarks" of transition included. It is seen that with low turbulence there is considerable distance between the first appearance and the final establishment of the turbulent boundary layer. With higher turbulence, however, the waves are established only a short distance before the turbulent boundary layer washes away the laminar layer.

CONCLUSIONS

This investigation of the details of the boundary-layer flow in the transition region on a smooth flat plate in a zero pressure gradient indicated the following:

1. Over the range of turbulence investigated, laminar oscillations play an integral part in transition.
2. The frequency which is amplified at a particular value of boundary-layer Reynolds number is determined by the curve of neutral stability resulting from the Tollmien-Schlichting theory of laminar oscillations. The experiments did not always indicate the gradual shifting of the predominate frequency as indicated by the theory.
3. At lower levels of turbulence the oscillations appear at a higher value of boundary-layer Reynolds number than at higher levels of free-stream turbulence. This indicates either that the product of the initial disturbance and the amplification received at higher values of $\beta_r \nu / U^2_0$ with lower free-stream turbulence does not lead to an oscillation of any importance or that there is some minimum value of free-stream turbulence necessary to excite the higher frequencies.
4. It appears that the mechanism of transition with lower values of free-stream turbulence is similar to the development of a turbulent wake from the vortex sheet behind a cylinder. The oscillations appear at some point determined by the turbulence in the free stream and quickly build up to an appreciable value. Shortly after the appearance of the waves the rest of the spectrum feeds off the amplified frequency. It appears that first the lower end of the spectrum builds up by virtue of the distortion of the oscillations, and then the higher frequencies gain energy, corresponding to the bursting of the oscillations into turbulence. The amplitude at the lower frequencies remains fairly constant during this process. Shortly after the amplitude at higher frequencies increases, modification of the velocity distribution occurs.
5. Free-stream turbulence controls the purity of the laminar oscillations and the rapidity with which the rest of the spectrum feeds off the oscillations. With lower turbulence, a large percentage of the total fluctuation energy in the boundary layer is concentrated at the oscillation frequency and the process covers a considerable distance on the plate. With higher turbulence in the free stream, the rest of the spectrum feeds quickly off the amplified frequency and only a small part of the total energy is concentrated at this frequency.

6. Extrapolating this information to even higher levels of free-stream turbulence than used for these tests, it is obvious that at some point the laminar oscillations will play no part in transition. This level of turbulence, however, is much higher than had been previously anticipated. Quite possibly at this level of turbulence and beyond, transition is controlled by the laminar-separation theory proposed by Mr. Taylor.[7]

APPENDIX

The following symbols, adopted for use in the paper and for the guidance of discussers, conform essentially with "American Standard Letter Symbols for Hydraulics" (ASA Z10.2-1942), prepared by a committee of the American Standards Association with Society representation, and approved by the Association in 1942:

E = **total energy in the boundary layer:**

  E_{0max} = **maximum extrapolated energy at zero frequency through the transition region at a fixed distance above the surface;**

  E_1 = **energy due to laminar oscillations;**

  E_{1max} = **maximum height of the discrete-energy part of the energy spectrum;**

  E_2 = **difference between total energy and energy due to laminar oscillations;**

f = **frequency;**

L = **scale of the u'-fluctuations;**

M = **relative magnification;**

$\mathbf{R}$ = **Reynolds number:**

  $\mathbf{R}_x$ = Reynolds number based on x and U_0;

  $\mathbf{R}_\delta$ = Reynolds number based on δ and U_0;

U = **mean velocity at some point in the boundary layer;**

U_0 = **mean velocity in the free stream;**

u' = **root-mean-square value of velocity fluctuation in the direction of flow;**

v' = **root-mean-square value of velocity fluctuation in the y-direction;**

w' = **root-mean-square value of velocity fluctuation in the z-direction;**

x = **distance from leading edge of the flat plate along the plate;**

y = **vertical direction;**

z = **longitudinal direction;**

$\beta_r = 2\pi f$;

δ = **boundary-layer-displacement thickness; and**

ν = **kinematic viscosity.**

AMERICAN SOCIETY OF CIVIL ENGINEERS
Founded November 5, 1852
TRANSACTIONS

Paper No. 2863

URBAN RENEWAL OF AMERICAN CITIES

By James W. Follin,[1] M. ASCE

Synopsis

The urban renewal program, authorized by the Federal Housing Act of 1954 provides for (*a*) prevention of the spread of blight, (*b*) rehabilitation of salvable areas, and (*c*) clearance and redevelopment of nonsalvable slums. Federal aids available under the Federal Housing Act of 1954 and community activity in undertaking an urban renewal program are outlined herein.

Introduction

The engineers who are responsible for planning or providing physical facilities or services in urban communities are aware of the serious problems facing American municipalities. After forty years' experience in this general field, in 1953 the writer was given responsibility to administer federal aid for slum clearance and urban redevelopment. Since that time he has participated in expanding the program authorized by the Federal Housing Act of 1949 into the urban renewal program provided by the Federal Housing Act of 1954. The potentialities of this new law deserve careful consideration.

Run-Down Urban Plant and Equipment

No city has been able to make the capital improvements required to keep plant and equipment up to date. For example, no city has solved the traffic problem. Every metropolitan area in the United States is struggling with this problem. Despite the money which has already been spent, additional millions of dollars will have to be expended; this is also true in the case of other physical facilities in the cities.

In viewing the past few decades, it is easy to see why this is so. Data for 21 large cities indicate that capital outlays averaged approximately $10.15 per capita per yr in 1910 and only $11.85 in 1940 despite price levels that were two or three times those in 1910. Current operating expenses meanwhile had increased from approximately $19.50 per capita to $65.40, or almost 235%. Thus, the ratio of capital outlays to operating expenses, which was about 52% at the beginning of the period (1910–1940), had dropped to approximately 18% at the end. This was a period in which the motor vehicle (among

---

Note.—Published, essentially as printed here, in August, 1955, as *Proceedings Paper 785*. Positions and titles given are those in effect when the paper was approved for publication in *Transactions*.

[1] Urban Renewal Consultant, De Leuw, Cather & Co., Chicago, Ill.

other things) contributed to the need for change in the physical pattern of the typical city.

For the most part, it has been impossible to raise the money to pay for such changes. Cities have found it difficult to increase revenues in proportion to the increased cost of the goods and services that were necessary from year to year. The result has been a relative decrease in expenditures for capital outlays. This means, in fact, an inability to replace worn-out and obsolete public facilities, of which an example is the replacement of school buildings. Difficulties in the older sections of cities have been complicated by the extraordinary demand for community facilities in the newer sections developed for the postwar population increment.

Therefore, it is obvious that where capital investment has been withheld and where plant has been allowed to run down, operating costs are correspondingly higher. Some cities have documented some of these costs and traced the source to which they are attributable. Baltimore, Md., for example, has discovered that it needs to spend on slum areas of the city $14,000,000 per yr more than it receives in taxes from those areas. This same type of subsidy exists in almost every community and is a luxury which municipal government cannot afford.

It is only a matter of time before cities will have to face obsolescence and high operating costs as industrial concerns have been facing them for years. Old installations must be redesigned and replaced and new installations must be made wherever necessary, either to meet new conditions or to increase the efficiency with which the locality meets its continuing obligations.

Slum Conditions

When a city allows its plant to deteriorate and rock-bottom slums to develop, it not only loses its efficiency but also some of the quality of its citizenship. Slums breed disease and crime; they destroy the incentive of inhabitants to improve themselves and their surroundings.

Necessary repairs to slum properties are seldom adequate or satisfactory. In making repairs or in adding a bath or bedroom, slum dwellers must use the services of any contractor and money lender they can interest in the job. All too often, this results in jobs poorly done at excessive cost and in second mortgages which keep the slum dwellers in debt for years.

People cannot be subjected to such conditions and treatment without becoming callous and indifferent; this destroys the ideals on which good citizenship is founded. The struggle of the slum dweller seems hopeless. Therefore, he ceases to fight, and it becomes easy to take advantage of him. Hence, he is a threat to the institutions which most people struggle to maintain.

This paper is directed to engineers who are also responsible citizens of their communities. Therefore, it is not necessary to overemphasize the fact that this problem will become increasingly important to society and that it must be solved to protect the future welfare of the United States.

Tools for the All-Out Attack

The tools to deal with this problem are just beginning to be developed. The federally-aided program of slum clearance and urban redevelopment, which has been in operation for approximately five years under the Federal Housing Act of 1949, has accomplished a great deal. Operations are being conducted in more than 200 cities and towns, large or small, and scattered over the United States. By the end of August, 1954, actual clearance or redevelopment or both was under way in 77 separate operations in 37 communities. In 83 communities final project planning for 103 separate operations was also being undertaken and in 94 communities, preliminary surveys for 112 separate operations were being conducted.

However, in spite of this progress and in spite of the substantial prospective benefits, it became evident that the program did not have a broad enough basis. Therefore, the President of the United States, in 1953, appointed an Advisory Committee on Government Housing Policies and Programs (Washington, D. C.) to study the problem of slums and blight; its contribution has been significant.

The committee's report,[2] completed in December, 1953, states the following:

> "A piecemeal attack on slums simply will not work—occasional thrusts at slum pockets in one section of a city will only push slums to other sections unless an effective program exists for attacking the entire problem of urban decay. Programs for slum prevention, for rehabilitation of existing houses and neighborhoods, and for demolition of wornout structures and areas must advance along a broad united front to accomplish the renewal of our towns and cities. This approach must be vigorously carried out in the localities themselves, and will require local solutions which vary widely from city to city."

In his message transmitting to Congress the recommendations now embodied in the Federal Housing Act of 1954,[3] the President stated:

> "In order to clear out slums and blighted areas and to improve our communities, we must eliminate the causes of slums and blight. This is essentially a problem for our cities. However, Federal assistance is justified for communities which face up to the problem of neighborhood decay and undertake long-range programs directed to its prevention. The main elements of such programs should include—
>
> "First. Prevention of the spread of blight into good areas of the community through strict enforcement of housing and neighborhood standards and strict occupancy controls:
>
> "Second. Rehabilitation of salvable areas, turning them into sound, healthy neighborhoods by replanning, removing congestion, providing parks and playgrounds, reorganizing streets and traffic, and by facilitating physical rehabilitation of deteriorated structures:
>
> "Third. Clearance and redevelopment of nonsalvable slums."

This new legislation differs from the old legislation in two important ways. First, it expands the scope of federal aid to include not only clearance and redevelopment but conservation and rehabilitation, and it provides other valuable benefits to the local communities. Secondly, it emphasizes local responsibility by making the bulk of federal financial aid conditional on the local initiation of a satisfactory "workable program" to deal with the entire problem of slums and blighted areas.

---

[2] "Recommendations on Government Housing Policies and Programs, A Report of the President's Advisory Committee on Government Housing Policies and Programs," U. S. Govt. Printing Office, Washington, D. C., 1953.

[3] *Public Law 560*, 2d Session, 83d Cong., approved August 2, 1954.

AVAILABLE FEDERAL ASSISTANCE FOR URBAN RENEWAL

The tools, which are available for this three-pronged attack on the problem of urban decay, have been created by the Federal Housing Act of 1954. Of course, these tools must be used by the inhabitants of various localities. However, when the tools are incorporated into local programs they can become powerful indeed; this will be discussed later in more detail. A list of the kinds of federal assistance that are available is as follows:

1. The urban renewal service, the chief purpose of which is to provide technical and professional assistance in preparing a workable program for the community and in planning and developing an urban renewal program, will consist of (*a*) a generalized series of pamphlets and information bulletins, and (*b*) specialized technical services developed through visits to the local communities. This service will be available without charge, on request.
2. Advances for surveys and plans and other preliminary work for urban renewal projects are available prior to approval of the workable program.
3. Temporary loans for urban renewal projects will be sufficient, if necessary, for all working-capital requirements.
4. Definitive (long-term) loans for urban renewal projects will be used when project land is leased rather than sold for redevelopment.
5. Capital grants for urban renewal projects will provide upward of two-thirds of net project cost.
6. Special grants for demonstration projects in urban renewal will also provide for upward of two-thirds of net project cost.
7. Special grants for urban planning assistance are authorized in a separate title of the Housing Act of 1954 and have no direct connection with urban renewal programs, although they may be of great importance to smaller cities and towns, and to metropolitan areas in community planning which is an indispensable element of the required workable program.
8. Special provisions for Federal Housing Administration mortgage insurance, under the new Section 220 of the National Housing Act,[4] will provide easier financing for building or rehabilitating residential property in an urban renewal area.
9. Special mortgage insurance provisions in the new Section 221 will facilitate construction or rehabilitation of low-priced residential accommodations to rehouse displaced families. This will be done either by urban renewal projects or by other governmental action.
10. Provision for low-rent public housing will be used to accommodate displaced families that cannot pay for adequate private housing.

Except for the urban renewal service, the advances for surveys and plans, and the special grants for urban planning assistance, the several types of federal aid mentioned previously are predicated on adoption by the locality of a workable program for dealing with slums and blight that is acceptable to the Housing and Home Finance Administrator. Specifications for such a workable program have recently been issued by the Housing and Home Finance Agency.

---

[4] *Public Law 479*, 2d Session, 73d Cong., as amended, approved June 27, 1934.

URBAN RENEWAL PROGRAMS AND PROJECTS

What happens when a local community starts an urban renewal program and wants to undertake urban renewal projects? One can assume at the outset that the workable program has evolved and has been approved. It will include establishment or designation of a local public agency, which is empowered by state and local law and which is technically and otherwise competent to carry out urban renewal projects. Under federal law that agency may consist of

> "***any State, county, municipality, or other governmental entity or public body, or two or more such entities or bodies, authorized to undertake the project for which assistance is sought." [5]

All the various governmental units in the community may constitute such an agency, assuming joint responsibility and setting up a technical and administrative staff to act for the community as a whole. It may be a special housing, redevelopment, or urban renewal organization established under enabling legislation or home-rule charter. Its initial task is the delineation of a suitable urban renewal area or areas, followed by a series of successive steps for organizing and carrying out a project or projects. A list of six principal steps follows with the first step described in detail:

1. Organization and planning, which will consist of:

a. Analytical surveys of the project area to determine the parts of that area that can be adequately handled through rehabilitation and conservation, and the parts that must be cleared for redevelopment;

b. Plans for a program of voluntary rehabilitation, involving organizing participation of area residents and owners, fixing standards for rehabilitated properties, and encouraging industry support and participation;

c. Plans for code enforcement to compel either rehabilitation, closing up, or demolition of substandard structures;

d. Plans for satisfactory relocation of families displaced from the urban renewal area;

e. Appraisals, title searches, and other preliminary work for the acquisition of any land for clearance and redevelopment; and

f. A complete plan for the urban renewal area showing what is to be done in each part. This plan must conform to the general plan for the locality as a whole and must indicate all the physical changes to be made. It includes not only re-use specifications for each part of the area to be cleared but also shows the improved street arrangements, public utilities, recreational and community facilities, and other supporting facilities, such as schools, required within the whole urban renewal area.

2. Any parts of the urban renewal area to be cleared for redevelopment will be acquired.

3. The project will also involve demolition and removal of buildings that are not to be retained in the areas acquired, and preparation of the land for redevelopment. Of course, the plan for relocating displaced families will be implemented prior to this.

---

[5] *Housing Act of 1949*, as amended, approved July 15, 1949. *Public Law 171*, 1st Session, 81st Cong., Section 110(h).

4. Installation, construction, or reconstruction of streets, utilities, parks, playgrounds, and other improvements necessary for the entire urban renewal area.

5. The land available for redevelopment will be disposed at its fair value for uses in accordance with the redevelopment plan.

6. Rehabilitation of the structures that are not demolished and do not meet the project standards will be completed by property owners with industry assistance.

The cost of the organization and planning may be covered by the federal-fund advances mentioned earlier. The outlays for the first five steps, including administrative expenses and carrying charges until completion of the project, may be included in gross project cost. The amount of any local grants-in-aid which are furnished in forms other than cash is added to such outlays to make up the total of gross project cost. The proceeds from disposal of land acquired are subtracted from this total, and the remainder is net project cost.

The federal capital grant for a project may amount to as much as two-thirds the net project cost. In addition, the gross and net project cost of all projects in the community may be pooled so that the federal contribution may amount to two-thirds the aggregate net cost. The remaining third must be provided for by local grants-in-aid. These may consist of cash, donations of land, work done in the project area, and supporting facilities, such as school buildings and other public facilities necessary to achieve urban renewal objectives.

Based on experience to date, one can expect that in many instances the local government will recover its contribution in a short time. In 1953, after making a study of the clearance and redevelopment operations of 10 cities chosen at random, the Advisory Committee on Housing Policies and Programs reported[2] that tax receipts in the affected areas could be expected to increase from approximately 2½ times to as much as 10 times. Using only 75% of the estimated tax-revenue increases, 15-yr bonds could be serviced in amounts sufficient to meet or substantially exceed the local grants-in-aid required in 7 of the 10 projects studied.

With reference to the net federal outlays, which amount to twice the local outlays, the recovery will, of course, be indirect rather than direct. However, in view of the large volume of construction and the better, stabler incomes of the residents and business concerns to be expected in the areas cleared and redeveloped or upgraded by rehabilitation and conservation, the federal government will undoubtedly realize a substantial recovery on its outlays. When the intangible benefits of sound, healthy communities, good neighborhoods, and accompanying higher levels of citizenship are added, these capital grants are apt to be a profitable investment for the federal government.

OTHER PROVISIONS OF THE HOUSING ACT OF 1954

There are three special programs connected with the urban renewal program which are of importance:

Title VII, Urban Planning and the Reserve of Planned Public Works. Section 701.—This section makes federal grants available through official state planning agencies, on a matching basis for assistance to cities with populations of under

25,000. It also provides official metropolitan and regional planning agencies with matching grants. It is directed toward filling two serious gaps in local planning: The spread of slums and blight in small towns and cities and in the periphery expansion areas of our big cities as well as in certain rural nonfarm counties and regions. These are problems for which no adequate plans and solutions have been provided. However, it is hoped that the additional source of funds will be of assistance in this respect.

Section 702.—The Division of Slum Clearance and Redevelopment does not have management jurisdiction over the reserve of Planned Public Works (Community Facilities Administration) whereas the Housing and Home Finance Agency does. This extension of previous legislation, which is familiar to civil engineers, is directed toward encouraging localities to maintain a planned public-works reserve. The federal government is not committed to aiding the construction developed under this program, but these loans would be repaid when the projects mature. All such construction plans must conform to approved over-all state, local, or regional plans.

Title III, Section 314.—Funds have also been provided for grants of two-thirds of the net cost for developing, testing, and reporting on methods and techniques, and demonstrations for preventing and eliminating slums and blight; the purpose of this program is to develop new ideas and attacks on complex urban problems. The ingenuity of the technical expert must be employed because much of the work will involve the science of city building and rebuilding.

POTENTIAL PUBLIC EXPENDITURES IN REDEVELOPMENT AND REHABILITATION

Clearance and redevelopment under the provisions of the Housing Act of 1949, and rehabilitation provided for in the Housing Act of 1954, comprise the potentialities of the urban renewal program. Only rough estimates of the cost and time involved are available, but these figures indicate the significance of urban renewal to the national economy.

Although urban decay usually concerns all types of property, it affects living accommodations most seriously. According to the 1950 census, approximately 10,000,000 nonfarm dwelling units in the United States are deficient according to modern standards and should be rehabilitated or displaced. About 5,000,000 will have to be demolished within a reasonable time. On the basis of figures quoted by the President's Advisory Committee on Housing Policies and Programs, the public cost of clearance and redevelopment per dwelling unit will be approximately $3,000. This means a total public cost for the 5,000,000 units of nearly $15,000,000,000.

Rehabilitation figures are not so exact because there has been little actual experience with mass rehabilitation. However, on the basis of the Advisory Committee's report,[2] one can assume that at least 15,000,000 dwelling units will need to be rehabilitated either extensively or slightly over a period of years. This figure includes the other 5,000,000 units cited as deficient in the 1950 census but which are in good enough condition to justify rehabilitation. It also includes another 10,000,000 units assumed to require repairs and modernization in neighborhoods needing upgrading or conservation protection, although they may not have deteriorated to the extent to which they are subject to rehabilitation under local police powers.

Public expenditures required to rehabilitate neighborhoods will amount to at least $9,000,000,000 before the 15,000,000 dwelling units have been rehabilitated and conserved against future deterioration. Thus, public expenditures of as much as $24,000,000,000 may be required to support and facilitate the displacement or rehabilitation of the 20,000,000 deteriorated and deteriorating dwelling units, which is half the present housing supply. This large expense can be spared from the overstressed public treasuries only over a period of years. The $500,000,000 authorized for slum clearance and redevelopment by the United States Congress in the Housing Act of 1949 is a significant start on federal participation. Congress will be asked for greater authorizations as soon as they are needed, and many believe Congress will meet the sum total of city requests. The rate of expenditure is the responsibility of all engineers, planners, and public officials throughout the United States who are interested in attempting projects that will benefit American communities.

Redevelopment Cost in the National Economy

At present (1954) experience indicates that new construction on cleared sites in redevelopment projects will amount to four times the public expenditure on redevelopment. In connection with the $15,000,000,000 of public cost for clearing 5,000,000 slum and substandard dwelling units, new construction might total as much as $60,000,000,000. This new construction will consist principally of residential, commercial or industrial buildings, and other improvements, and will be privately financed and constructed for the most part. Thus, the total private and public-redevelopment costs may amount to $75,000,000,000 which would give strong support to construction volume and, hence, to the national economy, even though it might be spread over a number of years. If this money were concentrated in a period of declining business it could be extraordinarily useful. The high ratio—four construction dollars to one public dollar—far exceeds that experienced on any previous federal-aid program.

AMERICAN SOCIETY OF CIVIL ENGINEERS
Founded November 5, 1852
TRANSACTIONS

Paper No. 2864

SOIL MECHANICS AND WORK-HARDENING THEORIES OF PLASTICITY

BY DANIEL C. DRUCKER,[1] M. ASCE, ROBERT E. GIBSON,[2] AND DAVID J. HENKEL[3]

SYNOPSIS

Soils having cohesion and internal friction are often considered to be perfectly plastic solids. A consistent approach has been proposed on the basis of the mathematical theory of perfect plasticity, and several interesting results were obtained. However, such an idealized treatment will often result in a marked difference between prediction and experimental fact. In particular, the strong dependence of the volume change under shearing action on the prior history of the soil cannot be properly taken into account. It is suggested herein that soil be treated as a work-hardening material which may reach the perfectly plastic state. A remarkable qualitative agreement is then obtained with the known behavior of soils in triaxial tests; additional study along similar lines appears most promising.

INTRODUCTION

There are many problems of soil mechanics in which the soil is considered (Fig. 1) to behave as a perfectly plastic material following a Coulomb criterion, $r = c \cos\phi + \frac{1}{2}(\sigma_x + \sigma_y) \sin\phi$ in which r is the radius of Mohr's circle at yield or failure; c, cohesion; ϕ, angle of friction; and $\frac{1}{2}(\sigma_x + \sigma_y)$, the mean normal stress in the plane, positive denoting compression. Some typical examples are the stability of slopes, the bearing capacity of footings, and the pressures on retaining walls. The familiar Rankine stress fields for active and passive pressure and the work of Karl Terzaghi,[4] Hon. M. ASCE, George G. Meyerhof,[5] A.M. ASCE, J. Brinch Hansen,[6] and R. T. Shield[7] are based essentially on the assumption

---

NOTE.—Published, essentially as printed here, in September, 1955, as *Proceedings Paper 798*. Positions and titles given are those in effect when the paper was approved for publication in *Transactions*.

[1] Chairman, Div. of Eng., Brown Univ., Providence, R. I.

[2] Scientific Officer, Building Research Station, Dept. of Scientific and Industrial Research, Watford, England.

[3] Lecturer, Dept. of Civ. Eng., Imperial College, London, England.

[4] "Theoretical Soil Mechanics," by Karl Terzaghi, John Wiley & Sons, New York, N. Y., 1943.

[5] "The Ultimate Bearing Capacity of Foundations," by George G. Meyerhof, *Géotechnique*, Vol. 2, 1951, pp. 301-332.

[6] "Earth Pressure Calculation," by J. Brinch Hansen, Danish Technical Press, Copenhagen, 1953.

[7] "Mixed Boundary Value Problems in Soil Mechanics," by R. T. Shield, *Quarterly of Applied Mathematics*, Vol. 11, 1953, p. 61.

of perfect plasticity. The implications of this basic assumption are far reaching and often unexpected, as shown by the writer and by William Prager,[8] M. ASCE. It was shown[8,9] that any generalization of the Coulomb criterion which lies within the framework of perfect-plasticity theory, such as the one shown in Fig. 2, requires a volume expansion to accompany shearing action in soil with a friction angle, ϕ. In Fig. 2, β is the half angle of the cone and σ_1, σ_2, and σ_3 are the three principal stresses.

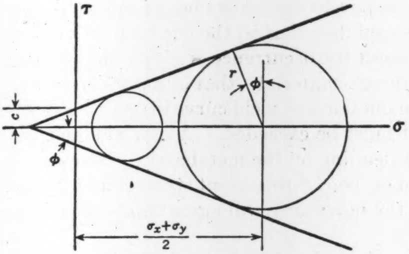
τ
c
φ
r
φ
σ
$\frac{\sigma_x+\sigma_y}{2}$

FIG. 1.—COULOMB CRITERION

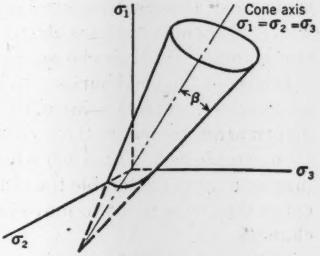
σ_1
Cone axis
$\sigma_1=\sigma_2=\sigma_3$
β
σ_3
σ_2

FIG. 2.—MISES TYPE OF EXTENSION OF COULOMB CRITERION

Whenever plasticity theory is applied to computations of the stress field, its consequences with respect to the displacement pattern cannot be ignored. If there is lack of agreement between physical reality and the prediction of a self-consistent theory, the underlying hypotheses of the theory need reexamination; inconsistent use of the theory is improper.

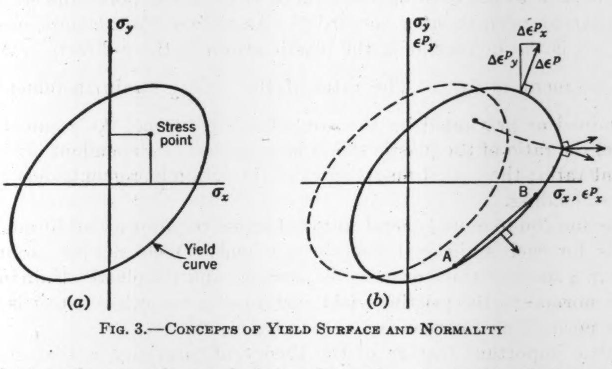
σ_y
Stress point
σ_x
Yield curve
(a)
σ_y
ϵ^P_y
$\Delta\epsilon^P_x$
$\Delta\epsilon^P_y$
$\Delta\epsilon^P$
B
σ_x, ϵ^P_x
A
(b)

FIG. 3.—CONCEPTS OF YIELD SURFACE AND NORMALITY

Although the general concept of plasticity is accepted in the field of soil mechanics, the relation between stress and strain in the plastic range involves terminology and special concepts that are not in common use. A brief description, therefore, will be given of the salient features of the theory of stress-strain relations in plasticity; a familiar two-dimensional state of stress in a metal sheet or thin-walled tube will be used to illustrate this theory.

---

[8] "Soil Mechanics and Plastic Analysis or Limit Design," by D. C. Drucker and William Prager, *Quarterly of Applied Mathematics*, Vol. 10, 1952, pp. 157–165.

[9] "Limit Analysis of Two and Three Dimensional Soil Mechanics Problems," by D. C. Drucker, *Journal of the Mechanics and Physics of Solids*, Vol. 1, 1953, pp. 217–226.

Assuming that the normal stresses, σ_x and σ_y, are principal stresses and that the third principal stress is zero, the state of stress then may be represented by a point (stress point) on a plot of σ_x versus σ_y (Fig. 3(*a*)). As the state of stress is changed, the resulting strains may be purely elastic or may be elastic-plastic. The curve which encloses elastic stress points—that is, the curve containing the stress points which can be reached without the occurrence of plastic deformation—is termed the yield curve. In an ordinary material—that is, a work-hardening material—the stress point must move outside the yield curve in order for plastic deformation to occur; the yield point must be exceeded. A new yield curve is then established (Fig. 3(*b*)) which, depending on the metal and the stress path, may or may not resemble the old yield curve. Subsequent stress changes which cause the stress point to move inside the new curve will again cause only elastic changes.

Strain coordinates can be superposed on the stress-coordinate axes in order to permit plotting strain and stress on the same diagram. The total strain consists of an elastic component and a plastic component; strain increments may also be decomposed into their elastic and plastic parts; and elastic strain increments can be computed from the stress increments by using the elastic stress-strain relation.

Fig. 3(*b*) shows only plastic strain increments. The theory of plasticity requires that each infinitesimal plastic strain increment, $\Delta\epsilon^p$, plot as a vector which is normal to the existing yield curve at a smooth point and which is between adjacent normals at a corner.[10,11] As shown, the x-component of the vector, $\Delta\epsilon^p$, is the increment in the plastic strain in the x-direction, $\Delta\epsilon^p{}_x$, and the y-component is $\Delta\epsilon^p{}_y$. The ratio of the plastic strain increments, $\frac{\Delta\epsilon^p{}_y}{\Delta\epsilon^p{}_x}$, is determined or bracketed by the normality condition. At a smooth point, therefore, the ratio of the plastic strain increments is independent of the stress-increment ratio; the actual magnitudes of the strain increments depend on the amount of loading.

The extension to more general states of stress requires an additional coordinate axis for each additional stress component. Yield curves become yield surfaces in a space of three or more dimensions, and the plastic strain increment vector is normal to the existing yield surface at a smooth point or is between adjacent normals at a corner or at a pointed vertex.

Another important feature of the theory of plasticity is that the fundamental definitions of work-hardening and perfect plasticity require that all yield surfaces must be convex.[11] Convexity means that a line between two points on the surface does not pass outside the region which is bounded by the surface. If the state of stress is changed in the most direct manner from one point inside the yield surface to another point (all the stress-difference compo-

---

[10] "Some Implications of Work Hardening and Ideal Plasticity," by D. C. Drucker, *Quarterly of Applied Mathematics*, Vol. 7, 1950, pp. 411–418.

[11] "A More Fundamental Approach to Stress-Strain Relations," by D. C. Drucker, *Proceedings*, 1st U. S. National Cong. for Applied Mechanics, ASME, 1951, pp. 487–491.

nents being kept in ratio), no plastic deformation will occur, as indicated in Fig. 3(*b*) by the straight line AB which lies within the yield curve.

Perfect plasticity is a limiting case of work-hardening in which the subsequent yield surfaces approach the original yield surface; in the limit there is one yield surface and the stress point cannot go outside it. Plastic deformations can occur when the state of stress is at yield—that is, when the stress point is on the yield surface.

Assuming that the Coulomb criterion represents a yield surface for a perfectly plastic solid, simple shear along a plane requires a motion away from the plane, as shown in Fig. 4(*a*) because the concept of perfect plasticity leads directly to the normality of $\Delta\epsilon^p$ (Fig. 4(*b*)). The vertical component of $\Delta\epsilon^p$ represents the increment of plastic shearing strain, $\Delta\gamma^p$. The horizontal component, which is always associated with the vertical component, points in the direction of the tensile stress and, therefore, represents a plastic extension increment, $\Delta\epsilon^p_e = \Delta\gamma^p \tan\phi$.

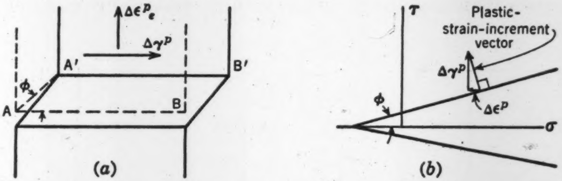

FIG. 4.—"SIMPLE" SHEAR PRODUCING VOLUME EXPANSION—PLASTIC MATERIAL WITH COULOMB YIELD

Although several important and interesting results are obtained by applying the theory of perfectly plastic bodies to soils, the theory obviously has severe limitations. Experiments indicate that the predicted dilation is usually larger than that found in practice. In fact, some materials decrease, rather than increase, in volume when shearing proceeds. The discrepancy between the prediction of simple theory and physical reality is not surprising because perfect plasticity is an extreme idealization for metals and is also so for soils. Furthermore, there are fundamental differences between plastic and frictional systems[10,11,12] and all soils are frictional systems to a certain extent.

It is possible that soil behavior can be described by a theory of plasticity. Metals are complicated, inhomogeneous, and anisotropic materials, as are soils. Nevertheless, the behavior of metal can be described by work-hardening, stress-strain relations for homogeneous material with initial isotropy.

SOME PHYSICAL FACTS AND THEIR SIGNIFICANCE

In any complete theory of plasticity for soil, a number of phenomena must be considered, one of the most important of which is the plastic component of volume change, $(v_o - v)^p$, which occurs when the hydrostatic or equal all around effective pressure is increased. The effective stress which controls the de-

---

[12] "Coulomb Friction, Plasticity, and Limit Loads," by D. C. Drucker, *Journal of Applied Mechanics*, Vol. 21, 1954, pp. 71–74.

formation of the soil[4] is the difference between the applied stress and the pore-water pressure.

One may consider, for example, a specimen of fully saturated clay which is subjected to gradually increasing pressure, p. (The test is conducted under fully drained conditions.) In drained tests the pore-water pressure is zero at equilibrium; the effective and applied stresses are then equal. A typical relation between the volume decrease and the pressure, p, is shown schematically in Fig. 5, in which the effective stress is plotted as in all the figures. If the pressure is reduced at a stage, A, of loading, the specimen volume increases to R. If the pressure is increased again to A, the subsequent relation for volume decrease under increasing pressure is similar to that which would have been obtained had no unloading-reloading cycle been conducted. The unloading and reloading loop (Fig. 5) may be replaced to a first approximation by an elastic line as shown at CDEB. If the hysteresis loop is averaged, the equivalent of a work-hardening, stress-strain relation is obtained in which the non-linearity of the elastic recovery may be quite pronounced. A similar type of curve is obtained for loose sand,[13] but the volume changes are much smaller than those for clay.

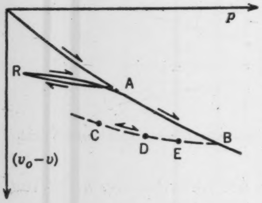

FIG. 5.—HYDROSTATIC PRESSURE PRODUCING PLASTIC VOLUME CHANGE—A WORK-HARDENING CURVE

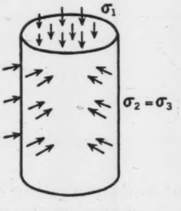

FIG. 6.—TRIAXIAL TEST

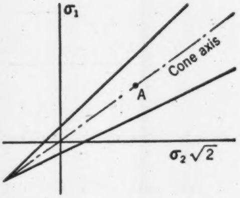

FIG. 7.—SECTION OF CONE OF FIG. 2 BY THE PLANE $\sigma_2 = \sigma_3$

If this type of behavior is to be considered, perfect plasticity, with an extended Coulomb criterion for a yield surface, cannot be assumed. The yield surface must cut the axis of the cone because yielding does occur for a state of stress which is represented by a point on the cone axis (Fig. 2). Also, the behavior involves work-hardening, not perfect, plasticity because continuing plastic volume decrease requires increasing pressure.

Consider the triaxial test shown in Fig. 6, in which $\sigma_2 = \sigma_3$, and in which σ_1 and σ_2 may be varied independently. It should be noted that the soil-mechanics convention is followed with compressive stress called positive and tensile stress called negative; a decrease in volume is also plotted as positive. The opposite convention has been used elsewhere.[8,9] With $\sigma_2 = \sigma_3$, the Coulomb criterion may be interpreted as the section of the cone shown in Fig. 2 by the plane, $\sigma_2 = \sigma_3$, as shown in Fig. 7. The points on the axis of the cone represent the hydrostatic pressure, $\sigma_1 = \sigma_2 = \sigma_3$. The abscissa is labelled

---

[13] "Fundamental Factors Controlling Shear Properties of Sands," by A. K. Gamal Eldin, thesis presented to the University of London in 1951 in partial fulfilment of the requirements for the degree of Doctor of Philosophy.

$\sigma_2\sqrt{2}$ because $\sigma_2 = \sigma_3$ and $\sigma_2\sqrt{2}$ is the magnitude of the vector sum or the distance along the line at 45° to the σ_2-axis and σ_3-axis in the plane, $\sigma_1 = 0$.

If the soil has been consolidated to point A (Fig. 5), the yield curve, which has been established for the material, must pass through the corresponding hydrostatic pressure point, A, shown in Fig. 7. Additional research and study is needed to determine the precise shape of the yield curve. As has been stated,[11] the yield curve or, in general, the yield surface, must be convex so that its rough outline is known even though only a few points and features are established. The yield curve can perhaps be approximated most simply by means of two straight lines and a circular arc closure as shown on curve 1 in Fig. 8(*a*), which corresponds to placing a spherical cap on the open end of the cone shown in Fig. 2. As the hydrostatic pressure increases to B, the yield surface may change to a similar curve 2 of Fig. 8(*a*), and the cone, which is established as part of the new yield surface, is apt to be larger than the previously existing cone.

As the writers have indicated, the concepts of work-hardening and perfect plasticity result in the normality of the plastic strain increment vector. The ratio of the components of the plastic strain increment is given by the direction of the normal to the yield surface. The components of the normal to the yield curves of Fig. 8 represent $\Delta\epsilon^{p}{}_2\sqrt{2}$ and $\Delta\epsilon^{p}{}_1$. The factor, $\sqrt{2}$, appears in the horizontal coordinate because $\Delta\epsilon^{p}{}_2 = \Delta\epsilon^{p}{}_3$ and $\Delta\epsilon^{p}{}_2\sqrt{2}$ is their vector sum.

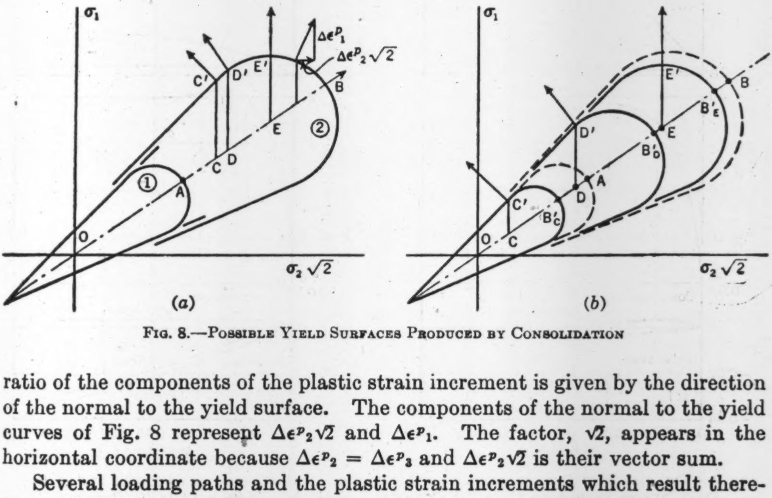

(*a*) (*b*)

FIG. 8.—POSSIBLE YIELD SURFACES PRODUCED BY CONSOLIDATION

Several loading paths and the plastic strain increments which result therefrom are illustrated in Fig. 8. Fig. 8(*a*) is a simpler illustration which, in analogy to metal plasticity, ignores the changes in the yield surface that may accompany elastic unloading and reloading. In a soil the elastic changes have much more significance. Release of pressure results in an elastic volume increase which, in the drained test, means an increase in water content. Yield strength is affected by water content so that the yield surface will change as the stress point moves inside it and only elastic strains occur. Fig. 8(*b*) is a schematic illustration of the effect of the increase in water content on unloading from B.

Unloading hydrostatically from B to C and increasing σ_1 to C′ and more causes a plastic volume increase somewhat as in Fig. 4. Another path, BDD′, in which the tangent at D′ is parallel to the axis, OB, of the cone, leads to zero plastic volume change almost as for a frictionless material. It can be seen that the ratio, OD/OB, is much smaller in Fig. 8(*b*) than in Fig. 8(*a*). All paths of the type described which are to the left of D′ give a plastic volume increase, all to the right give a plastic volume decrease. Path BEE′ is a special case of a plastic decrease in volume with $\Delta\epsilon^{p}_2 = 0$. Therefore, there will be a plastic increase in diameter of the triaxial specimen for paths to the left of E′ and a plastic decrease for paths to the right.

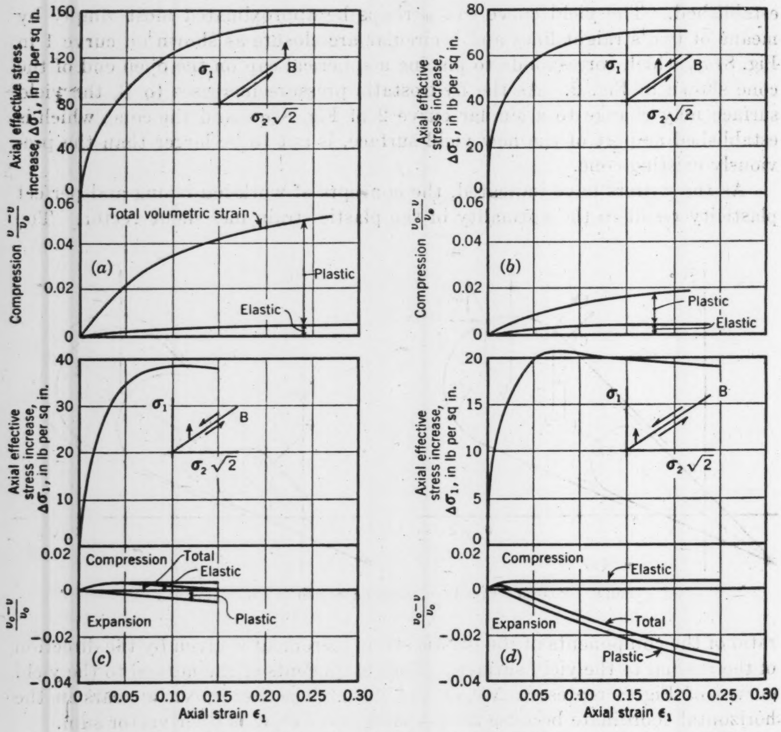

Fig. 9.—Triaxial Test Data on Silty Clay Consolidated at a Pressure of 120 Lb per Sq In., Axial Stress Increased from: (*a*) Consolidation Pressure (0 → 120); (*b*) Reduced Pressure of 60 Lb per Sq In. (0 → 120 → 60); (*c*) Reduced Pressure of 30 Lb per Sq In. (0 → 120 → 30); (*d*) Reduced Pressure of 15 Lb per Sq In. (0 → 120 → 15)

The paths described are easily produced in the triaxial test. Some typical data are given in Fig. 9, which were obtained from drained compression tests conducted on a remolded silty clay found in Haslemere, England. The clay was consolidated or overconsolidated as shown in Fig. 9, and the vertical stress,

σ_1, was increased from a point on axis OB (Fig. 8). The results shown in Figs. 9(*a*), 9(*b*), 9(*c*), and 9(*d*) can be summarized as follows: (1) From the consolidation point, B, the plastic volume decrease is quite large compared with the axial compression; (2) from a point situated halfway back to zero pressure from B, there is a moderate plastic volume decrease; (3) from a point at a distance three-quarters of the way back from B, the plastic volume increase is small; and (4) from a point which is seven-eighths of the distance back of B, there is a large plastic volume increase. One must remember that only plastic volume changes are indicated in Fig. 8. Elastic changes will accompany the plastic changes and they must be computed and subtracted from the total volume change in order to give the plastic change (Fig. 9). The qualitative agreement with the prediction of the simple theory is remarkable. As plastic deformation begins, plastic volume expansion, contraction, and an approximation of the transition case of no change are illustrated.

As plastic deformation proceeds, the rate of the change of volume does not usually remain constant. This means that as the stress, σ_1, is increased in the tests and as the point representing the state of stress moves outside the previously established yield surface, subsequent yield surfaces will be altered significantly. Even though more data must be accumulated and analyzed, one can speculate that the subsequent yield surfaces tend to rotate the normal to a perpendicular position with respect to the cone axis (Fig. 10); the rate of plastic volume increase or decrease would then become zero. A perfectly plastic state may be approached in which the yield surface is locally parallel to the axis of the cone and also in which no further hardening takes place. The shear stress required for continued plastic deformation will vary with the pressure, but no volume expansion is necessary.

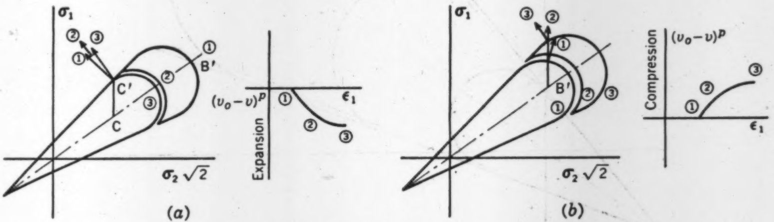

FIG. 10.—POSSIBLE SUCCESSIVE YIELD SURFACES IN TRIAXIAL TEST SHOWING TENDENCY TO APPROACH ZERO PLASTIC RATE OF CHANGE OF VOLUME: (*a*) EXPANSION; (*b*) COMPRESSION

With respect to the curves obtained for high overconsolidation, Figs. 9(c) and 9(*d*) indicate that there is a reduction in strength as deformation proceeds. This may be a result of frictional action and for that reason not be included in the existing theory of plasticity.[12] Therefore, the normality condition may be an approximation for curves 2 and 3 in Fig. 10(*a*).

THE COULOMB CRITERION

The Coulomb criterion may still be considered applicable as a limiting condition for soil but in a different sense. Although at times it might be convenient to consider that the straight lines of Figs. 1, 7, and 8 are yield curves for a perfectly plastic material, together with a reasonable closing circular arc, this is not necessarily true. Instead it is necessary that a succession of yield surfaces be considered (Fig. 11). At the failure condition the stress point may be on the end cap and the plastic deformation may involve volume decrease or increase, depending on the prior loading history. If the failure point is on the end cap, the Coulomb criterion is shown by the dotted line of Fig. 11 rather than by the outer line. The difference is not great except for the implied volume change, and it is necessary to obtain additional experimental information in order to achieve a better understanding of the behavior of soil. Because the limit line is indefinite and because perfect plasticity which follows work hardening is an oversimplification, there can be no detailed agreement.

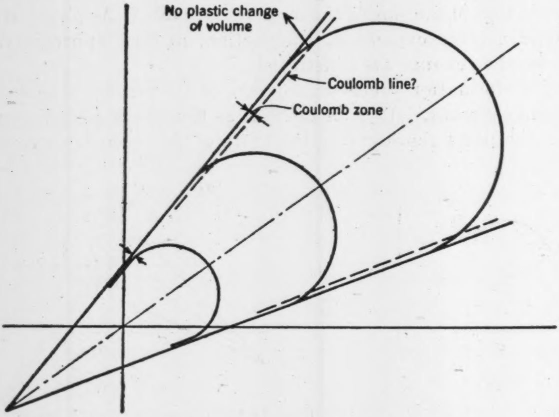

FIG. 11.—POSSIBLE MEANING OF COULOMB CRITERION

CONCLUSIONS

Much research has yet to be undertaken before one can say that practical soil-mechanics problems can be solved with a work-hardening theory of plasticity. However, an understanding of soil behavior can be obtained which will be helpful in design despite the difficulty in obtaining exact solutions. The new approach appears to offer many possibilities in this direction because it provides qualitative agreement with known data and with previously unexplained experimental data derived from triaxial tests.

No simple yield surfaces, as shown in Figs. 8 and 11, can explain all observable phenomena. The spherical end caps are probably not the correct shape, and other convex yield surfaces should be tried. The theory of stress-strain relations for work-hardening materials is so general that it certainly will be helpful when more experimental information is available.

AMERICAN SOCIETY OF CIVIL ENGINEERS
Founded November 5, 1852
TRANSACTIONS

Paper No. 2865

MEASUREMENT OF CANAL SEEPAGE

By August R. Robinson, Jr.,[1] J. M. ASCE,
and Carl Rohwer,[2] M. ASCE

With Discussion by Messrs. Raymond A. Hill; Dean C. Muckel; Calvin C. Warnick; N. Szalay; Cyril W. Lauritzen; and August R. Robinson, Jr., and Carl Rohwer

Synopsis

Existing methods of measuring seepage have been investigated by the authors in an effort to develop new methods and to study the factors affecting seepage. Special studies include the effect of depth of water on seepage, the effect of the depth to ground water, and the effect of temperature on the seepage rate. Seepage meters were found to indicate the order of magnitude of loss, although they do not provide accurate measurement. A method of analysis was developed for using the well-permeameter test results in forecasting seepage.

Introduction

Of the water diverted for irrigation in the seventeen western states of the United States, nearly 35,000,000 acre-ft, or approximately 40%, is lost before it reaches the farms. On forty-six operating projects constructed by the Bureau of Reclamation, United States Department of the Interior, it was determined that approximately 25% of the water was lost in transit. This loss consists of seepage, evaporation, transpiration, and leakage. The greatest amount of water is lost by seepage. This seepage water is not only lost to the canal to which it is appropriated but may also cause considerable damage to lands as a result of high water-table conditions and excess salts in the soil. Although the water is lost to the canal, it is not totally lost, as a considerable amount may go to replenish ground-water supplies or to increase the return flow to streams.

Note.—Published, essentially as printed here, in June, 1955, as *Proceedings-Separate No. 728.* Positions and titles given are those in effect when the paper or discussion was approved for publication in *Transactions.*

[1] Agri. Engr., Agri. Research Service, U. S. Dept. of Agriculture, Colorado Agri. and Mech. College, Fort Collins, Colo.

[2] Irrig. Engr. (Retired), Agri. Research Service, U. S. Dept. of Agriculture, Colorado Agri. and Mech. College, Fort Collins, Colo.

Methods of measuring seepage are necessary in order to determine the magnitude of the losses and also to isolate reaches of canals where high losses are occurring. Water is becoming increasingly valuable and it is necessary to determine whether the economic value of the water saved and the land reclaimed, plus the savings in cost of operation and maintenance, will exceed the cost of lining. It is also desirable to determine whether a new canal should be lined before construction is started.

Many factors have a definite effect on the seepage rate, but the permeability of the material forming the bed of the canal is the most important one. Other factors that influence the seepage rate are: (1) The depth of water in the canal, (2) the length of time the canal has been in operation, (3) the depth to ground water, (4) the temperature of the water and the soil, (5) the percentage of entrained air in the soil, (6) the soil-moisture tension, (7) the salt content of the soil or water, and (8) the volume of silt carried by the canal. Biological factors and the barometric pressure may affect the seepage rate, to a degree dependent on conditions. Because all these factors may act simultaneously and may, in some cases, counteract each other, it is difficult to segregate the effect of any one of them.

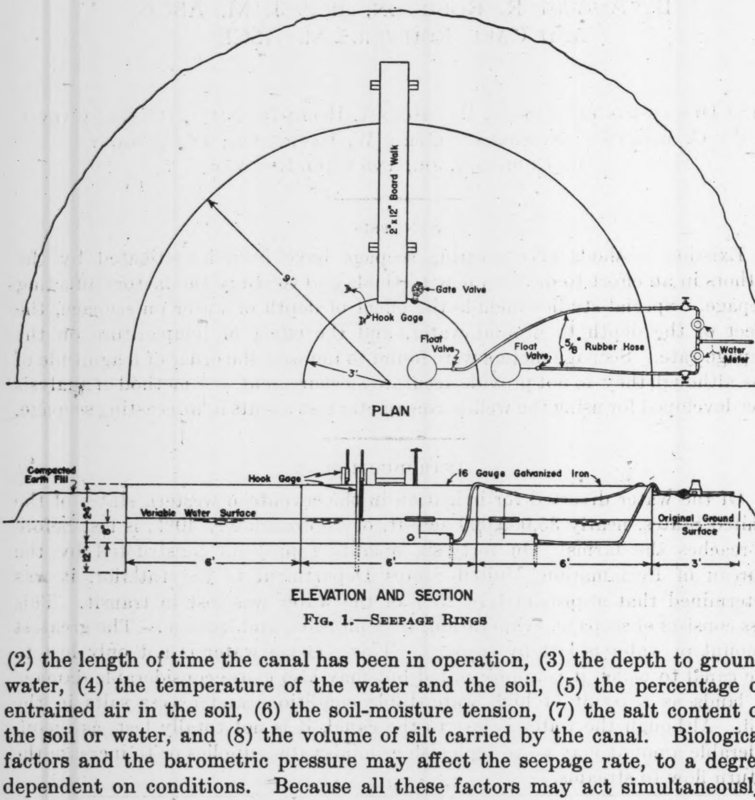
2"x 12" Board Walk
Gate Valve
Hook Gage
9'
3'
Float Valve
Float Valve
5/8" Rubber Hose
Water Meter
PLAN
Compacted Earth Fill
Hook Gage
16 Gauge Galvanized Iron
Variable Water Surface
Original Ground Surface
2'
8"
12"
6'
6'
6'
3'
ELEVATION AND SECTION

FIG. 1.—SEEPAGE RINGS

Various methods of measuring seepage have been devised which are adaptable for use in the field or in the laboratory. Some of these methods yield results which are the average seepage for a section of a canal, whereas others give the seepage rate for a small area or merely furnish information as to the permeability of a sample of the canal bed material, either in its undisturbed state or in a crushed, screened, and compacted condition. If methods are used that yield only the permeability, additional observation must be made to determine the hydraulic gradient.

The principal methods of measuring seepage now in use are: (1) Ponding, (2) inflow-outflow, (3) use of the seepage meter, (4) use of the well permeameter, (5) laboratory permeability measurements, and (6) special methods such as measuring electrical resistance in the areas where seepage is occurring or tracing radioactive material in the seepage water. Seepage rates based on the ponding tests are the most reliable but the cost of these tests frequently precludes the use of this method. For this reason, other methods must usually be adopted.

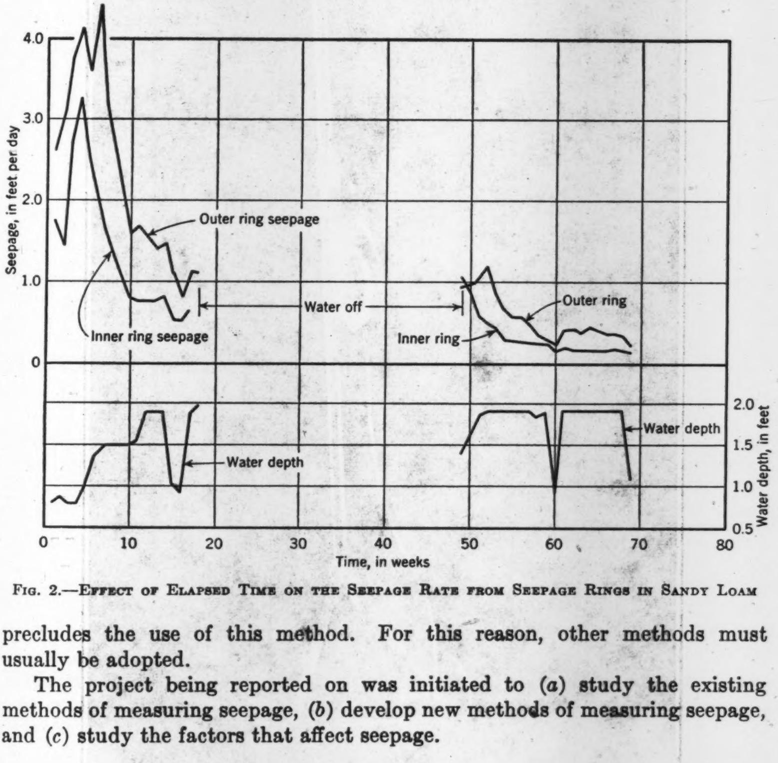

FIG. 2.—EFFECT OF ELAPSED TIME ON THE SEEPAGE RATE FROM SEEPAGE RINGS IN SANDY LOAM

The project being reported on was initiated to (*a*) study the existing methods of measuring seepage, (*b*) develop new methods of measuring seepage, and (*c*) study the factors that affect seepage.

MEASUREMENT OF SEEPAGE LOSSES

Seepage Rings.—Because of the limitations of the customary methods of measuring seepage, such as inflow-outflow and ponding methods, it was decided in the present study that some of the experiments would be conducted in artificial pools where the measurements and factors involved could be accurately determined. These pools were formed by concentric metal rings as shown in Fig. 1. The rings could accommodate a 2-ft depth of water, and the inflow necessary to maintain a constant depth of water could be accurately measured. The seepage meter was calibrated by using these rings with the meters installed in the outer ring and then by comparing the rate from the seepage meter with the seepage-ring rate. The rings were installed in several

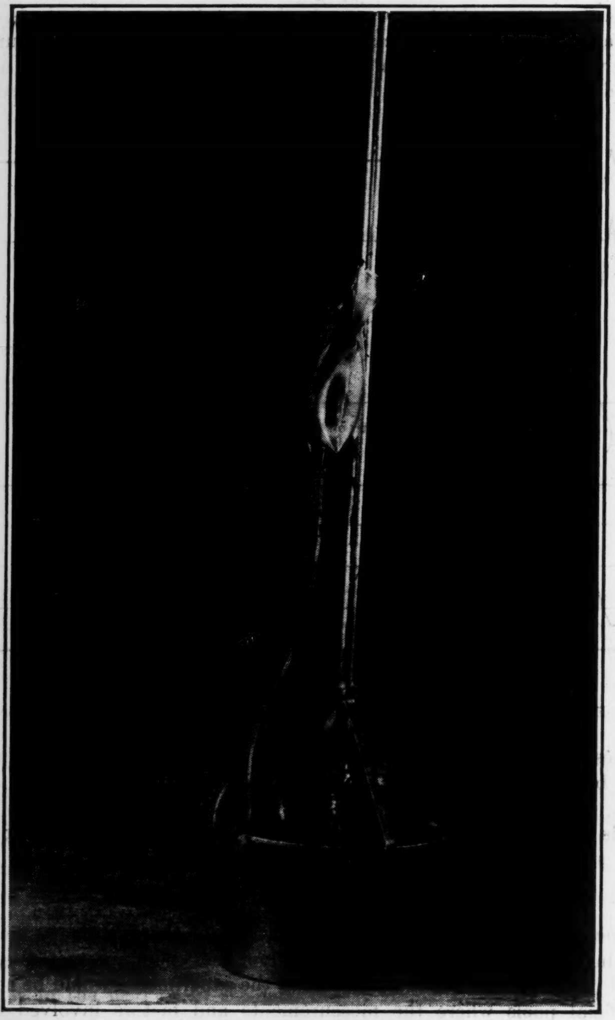

FIG. 3.—A SEEPAGE METER, WITH PLASTIC BAG

locations in soils ranging from clay to sand. These rings were operated continuously in each location for periods of approximately six months. The rings also provided facilities for studying the effect of depth of water, time, temperature, and other related factors on the rate of seepage through soils of different types.

In long-term seepage tests, it is significant to note the effect of time and its related factors on the seepage rates. Generally, the seepage rate decreases with time after the water is first introduced. Fig. 2 shows the seepage rate determined from use of rings installed in sandy loam during a period of two years. The seepage rates continued to decrease throughout the entire period although no silting occurred. This decrease was probably due to microbiological action, the decomposition of soil aggregates, and possibly the clogging of pores.

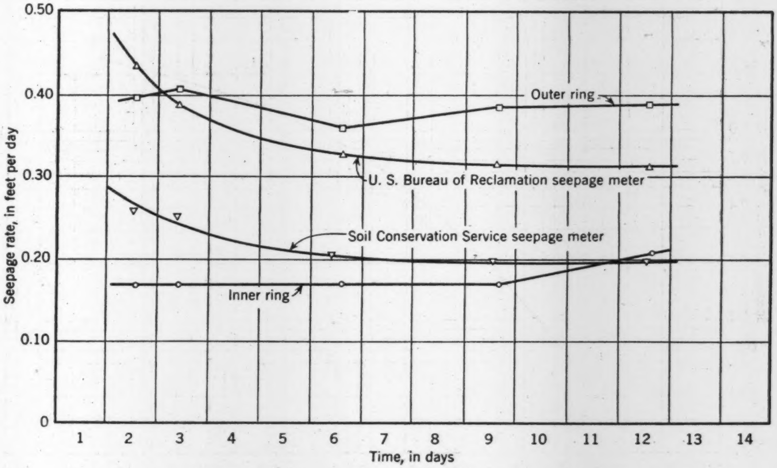

FIG. 4.—A TYPICAL EXAMPLE OF RESULTS OF SEEPAGE-METER AND SEEPAGE-RING TESTS IN SANDY LOAM

Seepage Meters.—Seepage meters have been widely used as a means of locating areas of canals where high seepage losses are occurring. Theoretically, they should measure the seepage through the area in which they are installed. However, such meters had never been calibrated to see if they actually did measure the true rate of seepage. Therefore, the main emphasis of the present study is on the calibration of the meters and on recommendations as to the best method of installation.

Fig. 3 shows one type of seepage meter which was adapted by the Bureau of Reclamation from the meter developed by the Regional Salinity Laboratory, Soil Conservation Service, United States Department of Agriculture (Riverside, Calif.), and used in this study. The bell of the meter is pressed into the canal bottom or side in order to isolate a small area. The meter is installed under water but the area under the bell is isolated so that water is fed into the bell from the plastic bag, which is submerged in the canal. A seepage rate can then be determined from the volume of water drawn from the bag during a certain period of time.

Several hundred tests were made with the seepage meter in the seepage rings. In some types of soil the initial rates measured by the meters were much higher than those indicated by the seepage rings. An example of this is shown in Fig. 4. In other cases the seepage-meter rates were lower than the seepage-ring rate. The method of installation seemed to affect the results. Hammering or jarring the meters during installation tended to influence the results in that the measured rates were much lower than the seepage-ring rates.

A calibration curve for the seepage meter is shown in Fig. 5. The rates measured by the seepage meter and those determined in the rings agree fairly well up to a rate of 1.0 ft per day (cubic feet per square foot per day). However, beyond this point the seepage-meter rates are greater than the seepage-ring rates.

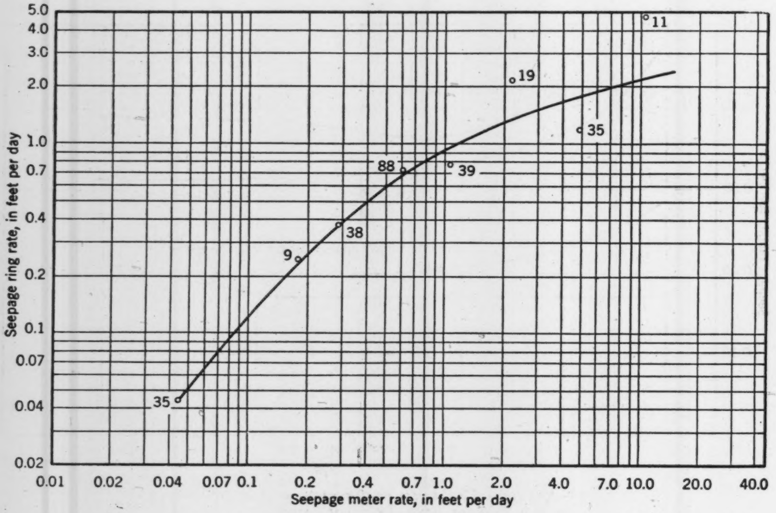

FIG. 5.—THE RELATIONSHIP BETWEEN SEEPAGE RATES FROM SEEPAGE RINGS AND SEEPAGE METERS (NUMBERS ON POINTS ARE NUMBER OF SINGLE DETERMINATIONS AVERAGED TO DETERMINE POINT)

Seepage-meter tests in canals which were checked by ponding tests yielded discouraging results. The seepage-meter tests were made only in the canal bottoms and at great distances apart. It is believed that the discrepancy in the results was due to the possibility that the seepage was greater through the sides than through the bottom of canals. In order for satisfactory results to be obtained with seepage meters in canals, the meters should be installed on the sides as well as on the bottom of canals. The measurements should be made at points as close together as possible.

Well Permeameters.—Whenever the feasibility of a new irrigation project is being investigated, there is need for information on the probable seepage loss from proposed canals. The well permeameter was developed by the Bureau of Reclamation for this purpose. This device measures the rate at which water seeps from a small well drilled in the soil on the center line of the proposed canal. After observations have been made on seepage from wells at intervals along the canal, an estimate of probable seepage loss can be made.

The well permeameter is shown in Fig. 6. This permeameter consists of a calibrated supply tank equipped with an indicator glass and an outlet pipe equipped with a float mechanism. The float maintains a constant water level in an uncased hole. This hole varies in depth but is usually drilled to the same elevation as the proposed canal invert.

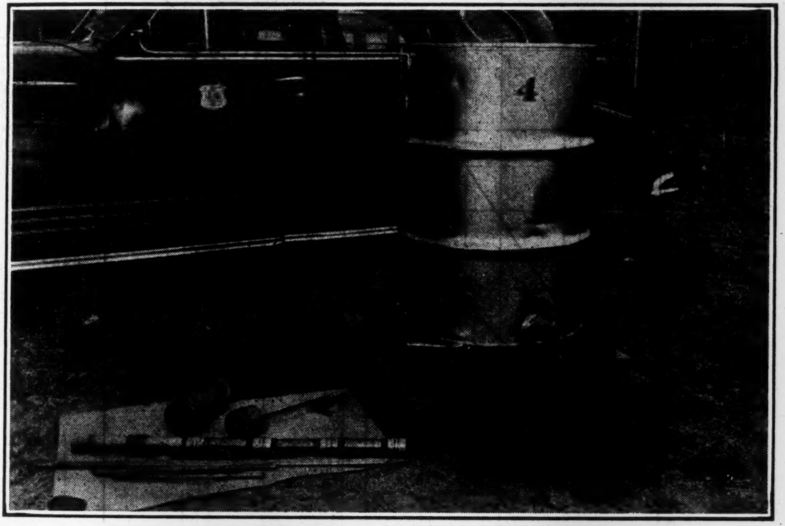

Fig. 6.—Equipment for the Well-Permeameter Test

A calibration curve for the well permeameter is shown in Fig. 7. The results of the well-permeameter tests have been compared to those from ponding tests on the canal after completion. The permeameter test results were computed on the basis of the outflow from the well converted to a unit seepage rate over the wetted area of the well. From Fig. 7 it can be seen that the correlation is not definite for line A. For this relationship the seepage from the ponding test was considered to be through the sides and bottom of the canal. From previous tests it had been determined that most of the seepage occurs through the sides of a canal in many instances. For this reason the data from the ponding tests were recomputed so that all the seepage was considered as passing through the canal sides. This relationship is shown as Line B in Fig. 7.

SPECIAL STUDIES

Effect of Depth of Water on Seepage.—Seepage measurements made by the ponding method during previous investigations of seepage have shown that the seepage rate increases as the depth of water in the canal increases. In some instances the sides of the canal are more permeable than the bottom, which results in an increased seepage rate as the depth of water is increased. In order to study the effect of water depth on seepage through the canal bottom, seepage rings were used in which all the seepage would occur through the bottom under a wide range in depths.

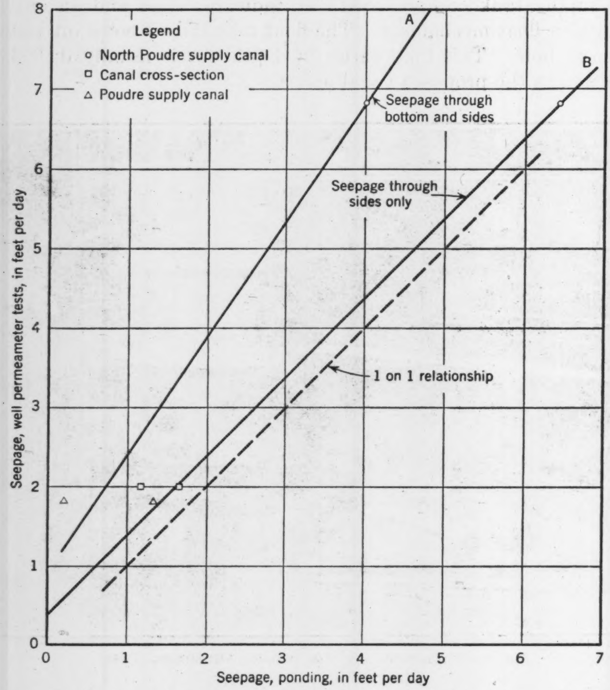

FIG. 7.—THE RELATIONSHIP BETWEEN SEEPAGE DATA FROM PONDING TESTS AND THOSE FROM WELL-PERMEAMETER TESTS (ALL RATES CORRECTED TO 60° F)

In order to determine the effect of depth on the seepage rate the water levels were allowed to drop in the seepage rings and every two hours readings were taken of the water depth, seepage rate, and water temperature. Fig. 8 shows the effect of depth on the seepage rate for sandy loam. The seepage rate always decreased as the depth decreased but seepage was indicated even as the depth approached zero. This shows that the seepage rate is not directly proportional to the depth of water but is proportional to this depth plus some distance below the surface. In all cases it should be noted that the seepage

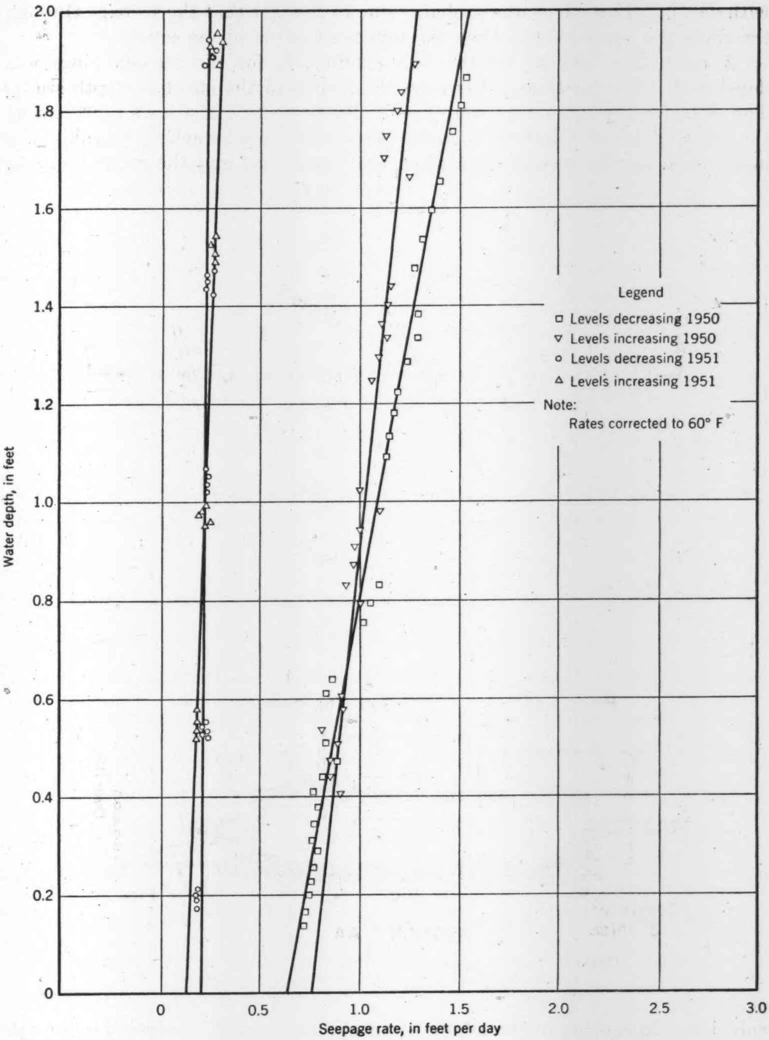

FIG. 8.—THE EFFECT OF WATER-DEPTH VARIATION ON THE SEEPAGE RATE IN SANDY LOAM, MEASURED IN THE OUTER SEEPAGE RING

rate did vary in a straight-line relationship and the rate increased with depth. Fig. 8 shows that the effect of depth on the seepage is greater as the permeability of the soil increases.

The results of several ponding tests on canals revealed, however, that the depth-seepage relationship was not linear, but that the slope usually increased with depth. This effect was probably due to the fact that the seepage through the sides was much greater than through the bottom of the canal.

A method of solving for the permeability, *k*, for the seepage rings was developed. This method is based on the results of the effect of depth study. The data for the inner ring were used. By projecting the lines representing the depth-seepage relationship until zero depth was reached, a value was determined for the seepage rate when the water level and the ground surface coincide. According to the Darcy equation, $q = k(h/l)$, in which q is the rate of flow per unit area, k is the permeability, h is the hydraulic head, and l is the length of the soil column. At zero depth of water, h and l are equal so that h/l equals unity, and q equals k at this point. It should be pointed out that this is true only if a negative head caused by soil-moisture tension does not exist or is negligible. This development may prove useful in other studies for determining the permeability of soils.

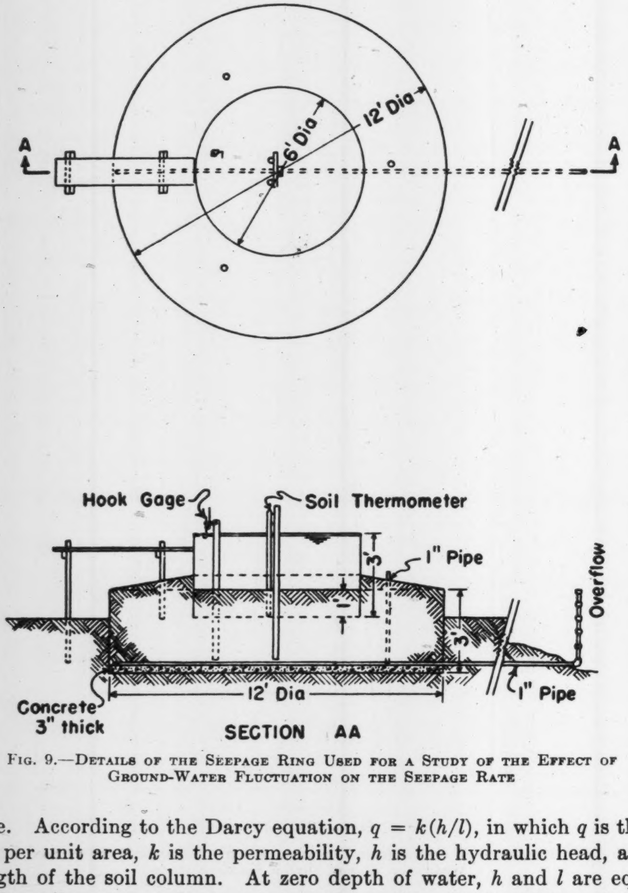

Fig. 9.—Details of the Seepage Ring Used for a Study of the Effect of Ground-Water Fluctuation on the Seepage Rate

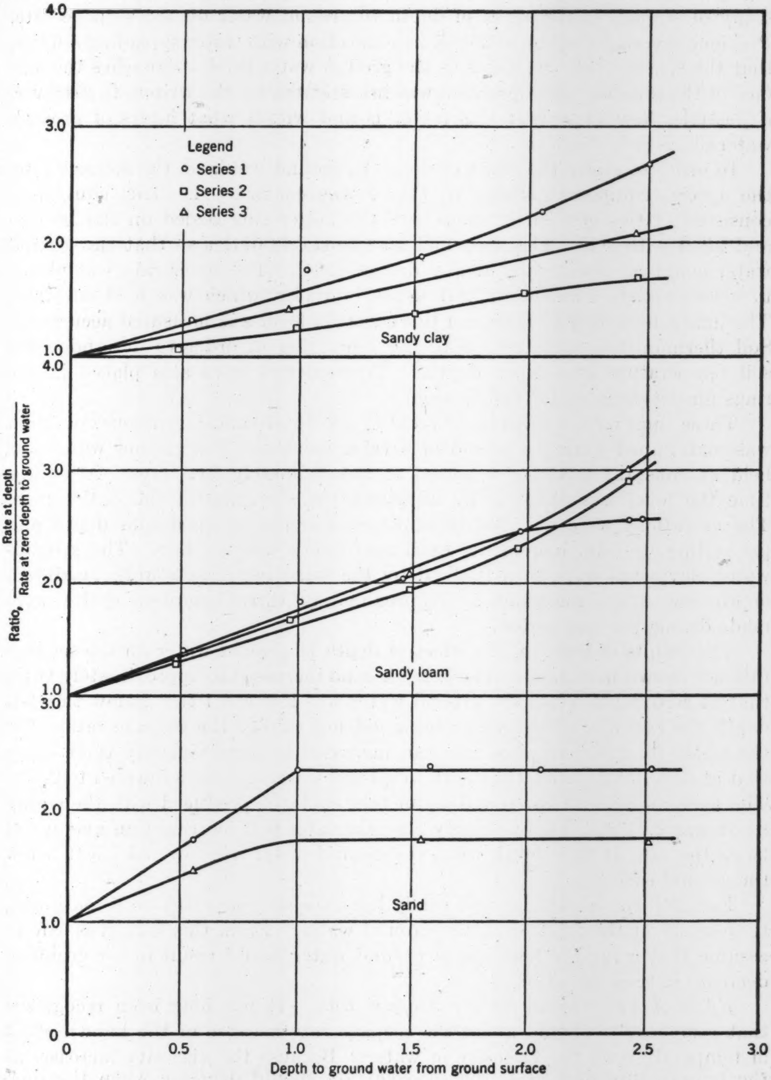

FIG. 10.—EFFECT OF VARIATION OF WATER-TABLE ELEVATION ON THE SEEPAGE RATE

Effect of Depth to Ground Water.—One of the problems encountered in the study of seepage is the effect of depth to ground water on the seepage rate. Previous investigators[3] have noted, in connection with water spreading studies, that the seepage rate decreases as the ground-water level approaches the surface of the ground. The problem was investigated by the writers to discover, if possible, how important this factor is and within what limits of ground-water levels it is effective.

In order to study the effect of depth to ground water on the seepage rate, the special equipment shown in Fig. 9 was constructed. This equipment consisted of two concentric rings with the larger ring sealed on the bottom and filled with soil. This ring had an adjustable outlet so that the ground water could be maintained at any desired level. The inner ring was placed to accommodate a maximum 2-ft depth of water, which was held constant. The inflow necessary to maintain this constant level was measured accurately. Soil thermometers were placed in the inner ring in order to determine the soil temperature at various depths. Tensiometers were also placed in the rings for determining the soil tension.

These rings were located in different types of soils, and continuous operation was maintained during a period of several months. The ground water was held at constant level for a period of approximately five days. After this time the level was changed by adjusting the elevation of the outlet pipe. The elevations were changed in sequence starting at maximum depth and proceeding by 6-in. increments until zero depth was reached. The ground-water elevations were then lowered by the same increments until maximum depth was again maintained. Approximately three complete cycles were made during the test period.

The results of tests on the effect of depth to ground water on the seepage rate are shown in Fig. 10. The rate for sand increased to approximately twice that at zero depth when the ground water was lowered 1 ft. Below this 1-ft depth the lowering of the water table did not change the seepage rate. For the sandy loam the seepage rate had increased to approximately three times that at zero depth, when the depth to ground water had been lowered to 2.5 ft. The maximum depth to ground water that could be produced with the equipment was 2.75 ft. For the sandy clay the rates had increased an average of twice the rate at zero depth when the ground water was lowered 2.5 ft below the ground surface.

For both the sandy clay and sandy loam the seepage rates were continuing to decrease at the 2.5-ft depth to ground water. From this fact, it is safe to assume that a further lowering of ground water would result in a continuing decrease in seepage rates.

Effect of Temperature on the Seepage Rate.—It has long been recognized that temperature should affect the seepage rate because of the known effect of temperature on the viscosity of water. Because the viscosity increases as the temperature decreases, the seepage rate should decrease when the temperature drops. However, continuous tests with well permeameters on the line of the proposed North Poudre Supply Canal (Colorado-Big Thompson

---

[3] "Spreading Water for Underground Storage," by A. T. Mitchelson and D. C. Muckel, *Technical Bulletin 578*, U. S. Dept. of Agriculture, Washington, D. C., 1937.

Project in Colorado) showed that the loss from the permeameters increased as the temperature decreased (Fig. 11) and that the maximum losses occurred when the temperature was a minimum. Readings twice daily of the seepage loss from the seepage rings in various types of soil had failed to disclose this tendency. For this reason several series of continuous observations for periods of three days were made on the seepage rings to determine whether temperature affected the seepage readings in the same way. The readings were taken at 2-hr intervals.

These tests were made on several different types of soil. The rings were refilled between readings to minimize the effect of the drop in the water level. These observations on the seepage rate also showed that it decreased as the temperature of the water increased.

There was considerable variation in the amount of the decrease in different types of soil, but the trend was unmistakable. The maximum variation in the seepage rates due to temperature occurred in the sandy soil. When the seepage rates were corrected for viscosity to the standard temperature of 60°F, the trend was made more noticeable. The results of typical series of observations in 1952 and 1953 are shown in Fig. 12.

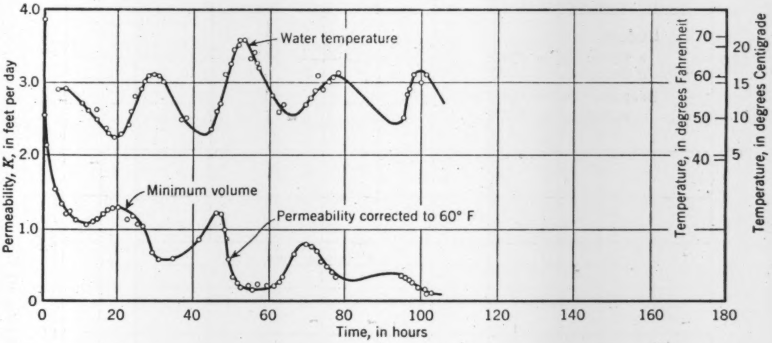

Fig. 11.—Effect of Temperature Variation on Permeability—Well-Permeameter Test

Attempts were made to explain this phenomenon on the basis of the expansion and contraction of the bubbles of air trapped in the soil as the temperature changed, but the change in volume of the air was too small to account for the difference in the seepage rate. The effect of the variation in solubility of air in water with variation in temperature was also investigated. Although this is a logical approach to the problem, the temperature gradient between the water and the soil was usually too small to account for the observed differences.

Apparently some other factor, dependent on temperature, was causing the variation in the seepage rate. Because the air that remains in the soil even after long periods of saturation would change in volume with changes in the vapor pressure of the saturated air in the bubbles, the effect of these changes was also investigated. Vapor pressure changes rapidly with an increase in

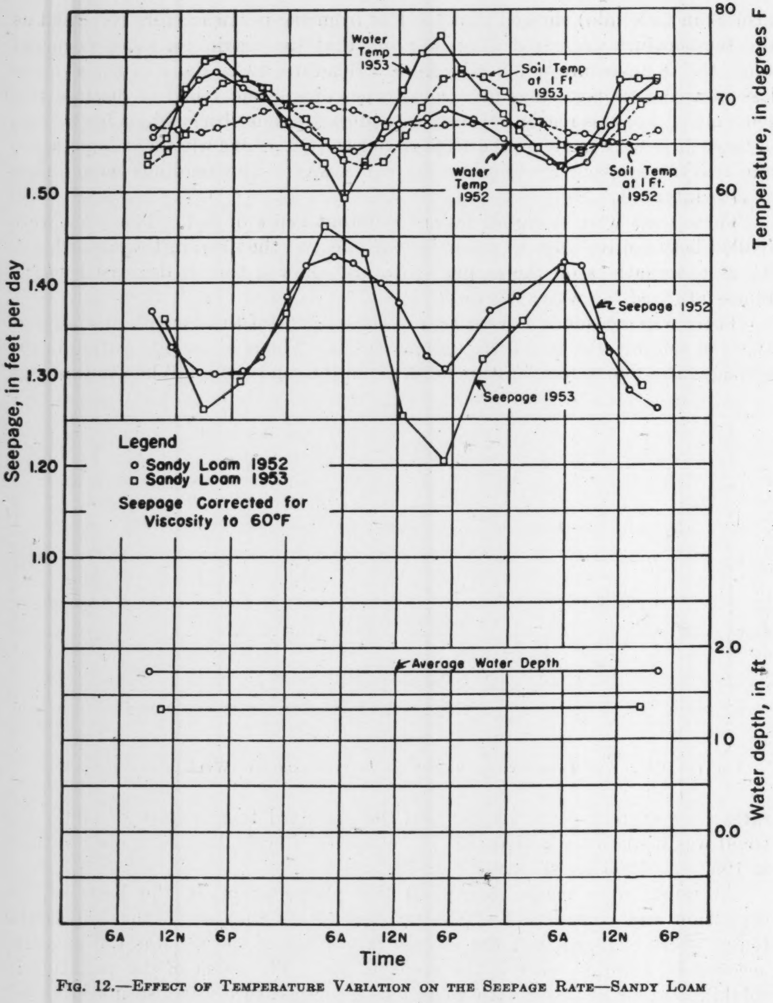

FIG. 12.—EFFECT OF TEMPERATURE VARIATION ON THE SEEPAGE RATE—SANDY LOAM

temperature and, for this reason, the expansion of the bubbles which reduces the permeability of the soil should decrease the seepage rate as was found by the tests.

The effect of change in porosity on the permeability of granular material has been shown by G. M. Fair, M. ASCE, and L. P. Hatch[4] to be proportional to $n^3/(1-n)^2$, in which n is the porosity of the material. Small changes in porosity produce large changes in the permeability, and consequently in the seepage rate, because seepage is directly proportional to permeability. Unfortunately, the percentage of air bubbles in the soil was unknown but by assuming various percentages of air the effect of changes in vapor pressure could be determined.

---

[4] "Porosity Factor for Case of Laminar Flow Through Granular Media," by J. B. Franzine, *Transactions*, Am. Geophysical Union, Vol. 32, 1951, pp. 443–446.

Seepage rates corrected in this manner for assumed values of 10% air and 15% air are shown in Fig. 13. The corrected seepage rates for 15% air and standard viscosity have a considerable variation, whereas if the assumption were correct the seepage rate should be constant. When the corrections are made on the assumption that the soil contains 10% air, the seepage rate approaches the observed rate. For this condition the correction for change in viscosity appears to balance approximately the correction for change in permeability due to the variation in vapor pressure with temperature. Although the vapor pressure of the entrapped air seems to have a definite effect on the seepage rate, the precise relationship of the factors to the seepage rate could not be determined from the available data.

In the study of the effect of temperature on the seepage rate it was observed that the seepage rate was small when the difference between the temperature of the water and that of the soil was large, and that the reverse was true when the temperature difference was small. This relationship was particularly noticeable when the temperature of the water was at the maximum during the day. This phenomenon can be explained by the fact that the temperature of the soil is soon raised to that of the water when the seepage rate is high, whereas the soil temperature is not greatly affected by the seepage if the rate is small. Preliminary studies indicate that the temperature difference might be used as the basis for determining the relative seepage rates from different parts of a canal.

Summary

The seepage rings provide an accurate method of measuring seepage rates in small, isolated areas. For this study the seepage rings were used as a standard for the calibration of seepage meters. Additional factors which affect seepage, such as time, temperature, and depth of water, were also studied using the seepage rings. The study demonstrated the fact that there are many other factors besides the soil type which determine the seepage rate.

The calibration of seepage meters showed that, although the meters do not provide an accurate method of measuring seepage, they do indicate the order of magnitude of the loss. For losses less than 1.0 ft per day the meters provide a fairly accurate measurement, but for greater rates the meters definitely overregister. Care must be exercised in installing the meters because hammering or jarring the meter was likely to affect the results. It was found that a period of from two days to a week should elapse after the meters are installed before reliable readings could be obtained. The plastic-bag seepage meter was the simplest type to operate and the results seemed to be reliable. It was concluded that seepage-meter measurements must be made both in the sides and in the bottom of canals in order to obtain reliable estimates of seepage.

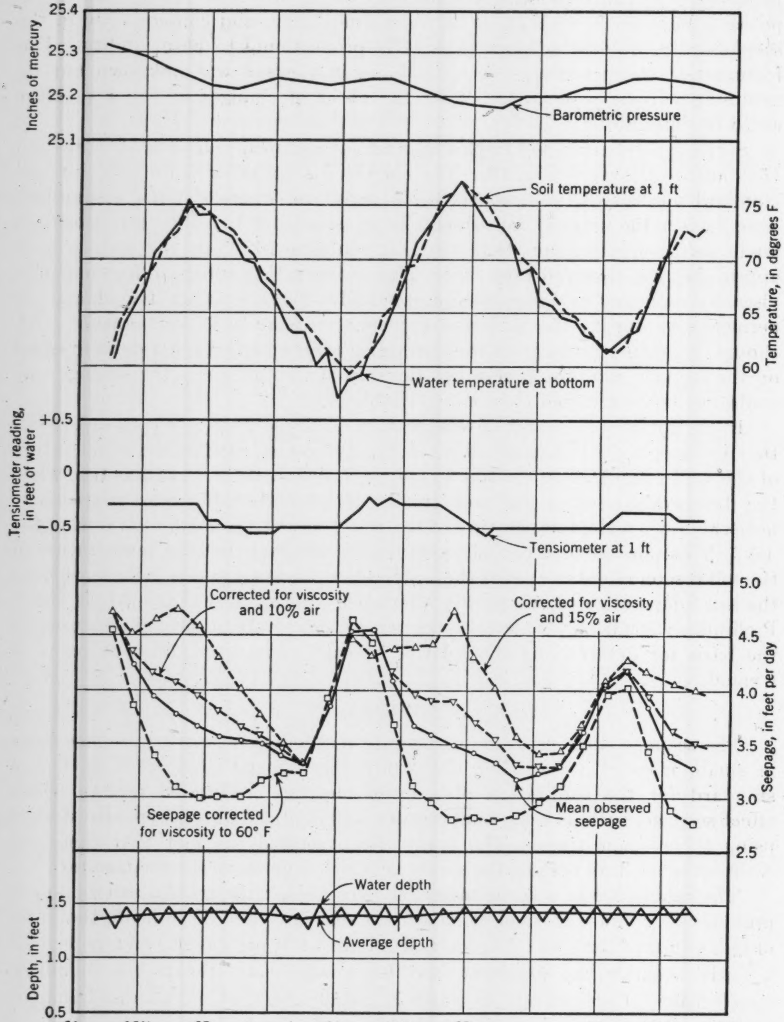

Fig. 13.—Effect of Temperature on the Seepage Rate in Sand; The Seepage Rate Is Shown Corrected for Viscosity and Porosity

A method of analysis was developed for using the well-permeameter test results in forecasting the seepage from proposed canals. A further study of this method is needed before its use can be recommended.

Studies of the effect of depth of water on seepage show that the rate increases as the depth increases but not in direct proportion to the increase in depth. For a high seepage rate, an increase in depth produced a proportionally greater increase in rate than it did for a low rate.

Variation of the depth to ground water had a definite effect on the seepage rate. The tests showed that the seepage rate increased as the depth to ground water increased within the range of depths tested, except in a sandy material. The tests on sand showed that increasing the depth beyond 1 ft did not further increase the seepage rate. At maximum depth to ground water (2.75 ft) the seepage rate in other types of soil was several times that when the groundwater level was at the ground surface.

In several tests it was found that the seepage rate is not a constant but may vary over wide ranges for periods of a few hours. In some cases, the highest seepage rates occurred at the lowest water temperatures and the lower rates at the higher temperatures. Because this phenomenon was contrary to present concepts of the influence of the factors involved, a detailed study was made to determine the cause of the fluctuations. These studies, however, have not been successful in explaining the variations.

Although much has been learned about seepage as a result of this study, many questions still remain unanswered and, because of the economic importance of seepage losses, the study of the problem should be continued.

Acknowledgment

This study was conducted by the Agricultural Research Service, United States Department of Agriculture, in cooperation with the Experiment Station of the Colorado Agricultural and Mechanical College and the Irrigation Operations Division, Region VII, Bureau of Reclamation.

DISCUSSION

Raymond A. Hill,[5] **M. ASCE.**—In the "Introduction," the following statement appears, to which exception must be taken:

> "Of the water diverted for irrigation in the seventeen western states of the United States, nearly 35,000,000 acre-ft, or approximately 40%, is lost before it reaches the farms. On forty-six operating projects constructed by the Bureau of Reclamation, United States Department of the Interior, it was determined that approximately 25% of the water was lost in transit."

The writer questions the validity of these figures, believing that the indicated losses are much greater than the actual losses on these projects. The quantities reported as lost in transit are merely differences between water that is diverted and that presumed to have been delivered to farms.

The quantity of water diverted from a river into a canal system is usually known within reasonable limits. The quantities of water delivered to individual farms, however, are not known accurately, even on extremely well-managed projects; they are only approximated on most irrigation projects. Overdeliveries to farms are the rule rather than the exception. Furthermore, the quantities of water reported as having been returned to the river through wasteways are too frequently no more than guesses by gate tenders.

In brief, the quantities of water reported by the Bureau of Reclamation and others as lost in transit represent only water not accounted for by measurements. Such measurements are generally inadequate and tend to exaggerate the apparent loss of water due to seepage.

Dean C. Muckel[6].—The measurement of canal seepage presents problems similar to those encountered in measuring infiltration on water-spreading areas for ground-water replenishment. The data presented by the authors are helpful in understanding some of the factors affecting this rate—whether it is called seepage or infiltration. In the case of canal seepage the desired end result will be to reduce the rate; in water spreading the aim is to increase it. In either case a thorough understanding of the factors involved will be necessary in order to reach a final solution.

The writer has made numerous measurements of infiltration on water-spreading areas in California, and it is noteworthy that the results obtained agree in general with those given in the paper. The shape of the curve in Fig. 2 is typical of an infiltration curve over the period of time shown. A suggested explanation of the variation in rate was presented in an earlier work by the writer[7] and agrees with the conclusions reached by the authors.

The use of seepage rings (commonly called infiltrometers in irrigation and water-spreading studies) is widespread. However, rarely does one find different workers using the same sizes of rings, depth of setting, or techniques of operation. Also, there is no general agreement as to the use of a buffer. Consequently, the results are not comparable and even results obtained by the same operator are often erratic. Standardization is needed for most effective use of the data being obtained throughout the irrigated western United States. The seepage ring used by the authors has a disadvantage because of its large size and the amount of water required to operate it, particularly if many isolated sites are to be investigated. In water-spreading investigations the writer was asked to determine infiltration rates at locations remote from any water supply so that water had to be transported by truck. A much smaller unit under these conditions would have a distinct advantage over that used by the authors.

---

[5] Cons. Engr., Leeds, Hill & Jewett, Los Angeles, Calif.

[6] Irrig. Engr., Soil and Water Conservation Branch, Agri. Research Service, U. S. Dept. of Agriculture, Washington, D. C.

[7] "Research in Water Spreading," by Dean C. Muckel, *Transactions*, ASCE, Vol. 118, 1953, p. 209.

The depth of setting of a seepage ring or infiltrometer is important, and the 1-ft depth used by the authors may not be sufficient in all cases to obtain the desired result. The fact that the curves for seepage through sand in Fig. 10 break at a depth to ground water of approximately 1.0 ft raises the question as to whether the same results would have been obtained if a different depth of setting has been used for the rings. In connection with water-spreading studies,[8] it was found that a saturated soil column extends below the soil surface during prolonged submergence. The length of this saturated soil column will vary with permeability and depth of water on the surface. For soils with low permeability the head loss in the soil is high and the column will be short. In soils with high permeabilities the column will be longer because the head losses per unit of length are less. If the depth of setting of a seepage ring is less than the length of the saturated soil column, lateral percolation will occur whereas if the depth of setting is greater than the length of the soil column, no lateral percolation should occur (except for a small capillary movement) and buffering should have no effect. It would be interesting to know whether the authors performed tests with the equipment shown in Fig. 1 while the buffering rings were not in operation and, if so, what the results were.

The effect of depth to ground water on the seepage rate also involves the saturated column. It is difficult to understand how ground water can affect the seepage rate unless the ground water rises and comes in actual contact with the saturated soil immediately below the surface. Possibly over the range tested the soil between the surface and the water table was saturated, or nearly so. A five-day period seems rather short for the time interval between changing of the depths to ground water. Stabilization may not have occurred in the heavier soils.

As to the effect of head on seepage rate, the authors correlated seepage rate with depth of water on the soil surface. Actually the total effective head is the depth of water on the surface plus the length of the saturated soil column immediately below the surface. In terms of the Darcy equation,

$$q = k\,\frac{d + l}{l}$$

in which d is the depth of water on the surface and l is the length of the saturated column. For the ranges in water depth used, the value of l is probably small in comparison to d.

---

[8] "The Effect of Surface Head on Infiltration Rates Based on the Performance of Ring Infiltrometers and Ponds," by Leonard Schiff, *Transactions*, Am. Geophysical Union, Vol. 34, 1953, pp. 257-266.

In connection with the authors' attempt to explain the effect of temperature on the basis of air entrapment, it might be mentioned that in water-spreading studies it was found that gases other than air were generated within a soil during a prolonged run. This was noticed particularly in laboratory experiments with soils containing quantities of organic matter and after anaerobic conditions developed. This information is not offered here as an explanation of temperature effects but merely to add another perplexity to the problem of measuring seepage over a prolonged period and to emphasize the difficulties involved in measuring an item affected by so many changing factors.

The authors cite the discouraging results in checking seepage-meter tests with actual canal losses determined by ponding. Similar discouraging results have been obtained in experiments with small ponds, 0.005 acre in size, located within a few feet of each other on soils supposedly uniform. Seepage rates ranging from the equivalent of that in adjacent ponds to several times that rate were obtained without apparent reason. The question is raised as to whether the authors reproduced their tests at a particular site with two or more seepage rings or accepted the results from an individual seepage ring.

The authors are to be congratulated on their work in dealing with a difficult problem, and the continuance of the study should be encouraged. The results will have widespread use not necessarily confined to canal seepage.

CALVIN C. WARNICK,[9] J. M. ASCE.—The authors have presented their investigation of the measurement of canal seepage in a very concise and interesting manner. The enumeration of eight principal factors that influence seepage rates and the presentation of data covering these factors shows a genuine thoroughness of the study.

The writer concurs in the opinion that the ponding method is the most reliable test for determining the average seepage loss from a given section. In the study of seepage meters it has been the writer's experience that the seepage meter shown in Fig. 3 is difficult to operate because the seepage bag is not always capable of transmitting the same pressure to the meter supply source as that outside the bag in the water surrounding the meter. Likewise, the operator cannot watch what is happening to be sure the meter is functioning properly. A meter adapted by Lloyd E. Meyers from the laboratory seepage meter and used on the Weber Basin Project of Utah has merit for canal seepage studies. The sketch of this meter is shown in Fig. 14. In order to maintain a constant head of water on the confined area of canal perimeter within the seepage meter cup, the principle of the Mariotte siphon is used. Water is supplied to the cup from the 500-milliliter burette as a reservoir. Atmospheric pressure exists at the lower end of the air inlet tube and the water in the burette above the end of the tube is actually under a pressure less than atmospheric. By setting the air inlet tube at the water surface in the canal, the water flowing into the soil from the seepage cup is actually under the same hydrostatic head as the water entering the canal perimeter outside the seepage meter. Actually, for operation, the end of the air inlet tube is set $\frac{1}{3}$ in. above the water surface in order to allow the bubbles of air to escape and rise to the vacuum zone of the burette. This type of meter has been used extensively in canal seepage studies conducted by the Engineering Experiment Station of the University of Idaho at Moscow. A number of these meters have been operated in test sections of irrigation laterals at the same time ponding tests were in progress. In an uncompacted silt section a rather consistent relationship has been developed by averaging the readings of numerous seepage-meter tests with the data from ponding tests. For three years of record the loss measured by seepage meter was 57%, 67%, and 69% of the loss measured by ponding. The writer agrees that this percentage will vary with the shape of section, degree of silting, and ground-water condition. However, if these can be standardized, a relationship can be established that should permit evaluation of an approximate rate of loss from a canal.

---

[9] Associate Research Prof., Eng. Experiment Station, Univ. of Idaho, Moscow, Idaho.

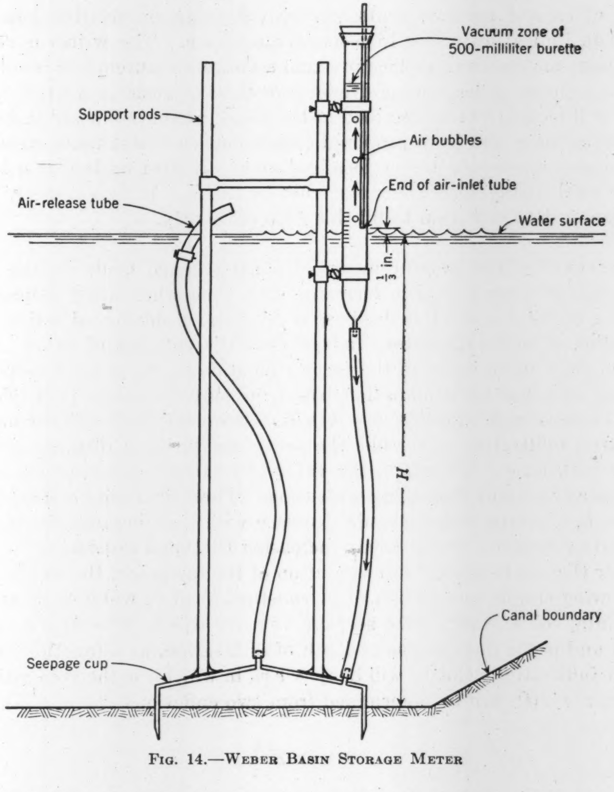
Vacuum zone of
500-milliliter burette
Support rods
Air bubbles
End of air-inlet tube
Air-release tube
Water surface
$\frac{1}{3}$ in.
H
Canal boundary
Seepage cup

FIG. 14.—WEBER BASIN STORAGE METER

The writer questions whether the comparison of seepage-meter rates with the rates from the seepage rings represents the measurement of an identical flow rate. From Fig. 4 it appears that the seepage rate from the inner ring approaches that rate measured by the seepage meter after a few days, yet the meter represented a localized area whereas the inner ring data represented a composite of a considerably greater area. Inserting the meter more than two or three times, it appears, would naturally change that composite figure by disturbing the soil. The fact that a seepage meter measures a localized area definitely limits the meter's value and, because of silting in the bottom, lack of homogeneity of soil strata through which a canal perimeter cuts makes the data of a single seepage-meter measurement of little real value. However, a series of careful measurements can provide data on relative loss that is valuable in indicating where high-loss sections are. The writer is confident that seepage meters have a place in canal seepage measurements because they represent a cheap, quick, and convenient method of measurement.

The well permeameter described in the paper presents a possible device for predicting seepage loss from proposed canals, but each test takes considerable time and also represents a very localized area. If data on loss at a localized area are used, many measurements must be taken. In this respect, the well permeameter does not seem to fill this need efficiently.

N. SZALAY[10].—The measurements of canal seepage made by the authors show a rate of seepage which decreases with time when using seepage rings. According to the authors this decrease is due to microbiological action, the decomposition of soil aggregates, and possibly the clogging of pores. It must be added that, in addition to the factors mentioned, decrease of seepage rate with time also has an explanation based on pure hydraulic principles. According to the Darcy equation, $q = k(h/l)$. However, if a canal becomes filled with water, infiltrating water fills the soil pores within a distance always increasing with time. Therefore, the value of l cannot be considered constant but is instead a value increasing with time. Thus, assuming a constant head of water, h, the rate of flow should decrease with time because the same head is used to overcome a continuously increasing frictional resistance.

As for the mathematical interpretation of the foregoing, the writer presents the following simple application.[11] A constant head of water, h, is applied to a horizontal soil surface. The seepage velocity will be $v_s = k(h/z)$, in which $z = z(t)$ and is the instantaneous depth of infiltration, as a function of time, t. The true infiltration velocity will be $v_i = e\, v_s$, in which e is the void ratio. The function, $z = z(t)$, can be determined from two equations,

$$v_i = n\,K\,\frac{h}{z}$$

and

$$v_i = \frac{dz}{dt}.$$

By setting equal the two expressions for v_i and separating the variables, one determines the basic differential equation for nonpermanent seepage flow—

---

[10] Associate Prof. of Hydr. Eng., Technical Univ. of Budapest, Budapest, Hungary.

[11] "Determination of the Permeability of Soil Layers Lying Above Groundwater Table," by N. Szalay, *Hidrologiai Közlöny*, November-December, 1954.

$z\,dz = n\,K\,h\,dt$. After integration,

$$z = \sqrt{2}\,n\,K\,h\,t - C.$$

In order to determine the rate of flow, the Darcy equation is used again:

$$q = K\frac{h}{z} = \sqrt{\frac{K\,h}{2\,n\,t}} = \frac{c}{\sqrt{t}}.$$

That is, the rate of flow is inversely proportional to the square root of the time.

The accuracy of rate-of-flow measurements depends on the infiltration area as lateral infiltration has greater influence on the pure vertical infiltration in small areas than in large areas. This fact was proved by the experiments of L. Szabo[12] who found that, under the foregoing conditions, the measured rate of infiltration depends on the infiltration area as follows:

Infiltration area, in square meters	Rate of seepage, q, in meters per second
0.01	$c_1 \quad t^{-0.45}$
0.02	$c_2 \quad t^{-0.45}$
0.25	$c_3 \quad t^{-0.46}$
16.00	$c_4 \quad t^{-0.48}$
100.00	$c_5 \quad t^{-0.48}$
Theoretically	$c \quad t^{-0.50}$

The values of c_1 through c_5, experimentally determined, show a tendency to decrease with increasing infiltration area.

Finally, it may be mentioned that the basic principles of the foregoing theory of nonsteady seepage were also applied to pure horizontal seepage flow, approximately as it occurs when using well permeameters[11] and when infiltration develops through flood-control levees. In both cases the results computed theoretically were in satisfactory agreement with experimental data.[13]

Cyril W. Lauritzen[14].—The ever-increasing demand for water in arid countries has focused attention on losses sustained in the conveyance of irrigation water. One of the most perplexing problems encountered has been the accurate determination of these losses. A few methods have been used for measuring seepage losses, but all have had their limitations and none has been entirely satisfactory. As pointed out by the authors, the results obtained from ponding measurements are probably the most reliable. However, ponding measurements can lead to erroneous conclusions unless one considers antecedent conditions as well as conditions at the time of measurement.

The extreme variability in seepage-meter measurements made in operating canals coincides with the results obtained by the writer and his associates.[15]

---

[12] "Influence of Lateral Seepage Upon Rate-of-Flow Standards of Surface Irrigations," by L. Szabo, *Hidrologiai Közlöny*, July–August, 1954.

[13] "Design of Flood-Control Levees with Special Regard to Seepage," by N. Szalay, *ibid.*, March–April, 1953.

[14] Project Supervisor, Agri. Research Service, U. S. Dept. of Agriculture, Logan, Utah.

[15] "Measuring Seepage from Irrigation Canals," by W. W. Rasmussen and C. W. Lauritzen, *Journal*, Am. Soc. of Agri. Engrs., Vol. 34, 1951, p. 326.

It has been their experience that, frequently, the difference between measurements made with meters set side by side is as great or greater than measurements made by the ponding method in canals of widely different subgrade material. The closer agreement between measurements with seepage rings in uniform material would seem to indicate that part of the variability is actual. Possibly this should be anticipated even though the material appears to be uniform. It is known, for example, that stratification of the material in a soil sample can greatly alter the permeability of the material as a whole. The fact that some variability persists in the measurements made in seepage rings may indicate that there is an inherent error in the results due to installation and operation of the meters. The consistent overregistration of the seepage rate, as indicated by the seepage rings, suggests the possibility of applying a correction factor to seepage-meter measurements. Correction factors, based on the relationship between seepage-meter measurements and ponding measurements, have been developed and used by Mr. Warnick[16] in an attempt to determine a better index of seepage losses. In developing a correction factor based on a comparison with ponding tests one must, of course, take into account the difference in seepage loss between the bottom and the sides of the canal.

At first, such a procedure might appear to be a solution to the problem and under certain circumstances might provide a reasonably accurate index of seepage losses. However, when one considers the fact that the relationship between the seepage from the bottom and sides of the canal may differ widely among canals and from one season to the next, the value of such an approach must be re-examined. Possibly a permeability measurement on disturbed samples of bed material would provide an equally accurate index of losses.

The authors have pointed out that there are other factors in addition to soil type which influence seepage losses; among those mentioned is temperature. Permeability measurements are commonly corrected for temperature in order to take into account the change in viscosity of water with temperature. It has been the writer's experience that corrections applied to permeability measurements as mentioned by the authors give contradictory results. Apparently, some factor other than the change in viscosity of water is operating. The authors seemed to have ruled out the possibility that the reduction in porosity is due to an increase in the size of air bubbles. The fact that a correction for viscosity seems to compensate more for temperature changes with coarse-textured material than with fine-textured material indicates that the discrepancy may be associated with the fine fraction. Possibly the reduction in permeability which sometimes accompanies an increase in the temperature during a measurement can be explained as resulting from a reduction in porosity due to greater hydration of the clay minerals at higher temperatures. This theory, at least, might well be explored. If this should be the situation, the greater transmission of water, which would be expected to accompany an increase in temperature and the corresponding decrease in viscosity of the water would tend to be compensated for by the reduced porosity of the profile due to swelling of the constituent material.

---

[16] "A Study of Canal Linings for Controlling Seepage Losses," by C. C. Warnick, *Progress Report No. 3*, Eng. Experiment Station, Univ. of Idaho, Moscow, Idaho.

The depth of water in the canal and the distance to the ground-water table have long been known to be important factors contributing to seepage losses. Engineers have generally attributed the increased seepage rate which accompanies an increased depth of water in the canal to the difference in permeability of the material constituting the upper side slopes, as compared to the lower side slopes and bottom of the canal. If only the bottom of a canal is being considered, corresponding to measurements in seepage rings, seepage should be proportional to the hydraulic gradient as the authors have shown. The problem has been to establish the value of the hydraulic gradient. It is of interest to note that as the seepage rate increases the effect of water depth on seepage increases. This might be explained by the steeper hydraulic gradient associated with coarse-textured material, which in effect, disproportionately increases water transmission as the water depth is increased. Additional information on this point would be valuable. The fact that the influence of water-table depth was restricted to 1 ft for sand as compared to a greater distance for fine-textured material supports this reasoning.

It is evident from the paper that all the questions related to seepage measurement have not been answered. The investigation has, however, done much to clarify certain aspects of the problem and the authors are to be commended for their careful work and the contribution they have made.

August R. Robinson, Jr.,[17] J. M. ASCE, and Carl Rohwer,[18] M. ASCE.—Seepage measurements, even when made under carefully controlled conditions, yield rates that are correct only at a specific place at the time of the tests. It does not necessarily follow that the same results should be obtained in the same area at a different time under different conditions. For this reason, widely divergent results are frequently obtained when seepage measurements are extended over a considerable period of time. This fact makes the solution of the seepage problem especially difficult.

Mr. Hill has taken exception to the total seepage losses reported by the writers for the seventeen western states because more water is delivered to farmers than is ordinarily shown by the records. This is probably true, but it should be pointed out that more water is frequently available for delivery than is shown by the diversions from streams and reservoirs at the canal intake, because many canals receive waste water from higher irrigated land and intercept runoff from rainfall. This inflow cannot be accurately measured and, although it is probably less than the excess deliveries to farmers, it is a compensating factor. Also, water records of the Turlock Irrigation District in California indicate a loss of water from diversion to irrigator of 27.2%. This record is for an irrigated area of 168,000 acres and is an average loss for the five-year period from 1950 to 1954. Whether the seepage losses for the seventeen western states quoted in the paper are correct or not is probably not important to the paper because they were cited merely to show the magnitude of the seepage problem.

---

[17] Agri. Engr., Agri. Research Service, U. S. Dept. of Agriculture, Colorado Agri. and Mech. College, Fort Collins, Colo.

[18] Senior Irrig. Engr. (Retired) Agri. Research Service, U. S. Dept. of Agriculture, Fort Collins, Colo.

The comments by Mr. Muckel, based on his extensive experience with ground-water recharge by water spreading, show that the difficulties encountered by the writers in the study of seepage are not unique. With reference to Mr. Muckel's question as to the effect of operating the inner ring when no water was in the buffer ring, this condition was not investigated by the writers. Mr. Muckel found that gases other than air were released in the soil under certain conditions. When this occurs, the seepage rate is reduced.

The fact that the depth of water in the rings is not the true head was recognized in the study of effect of depth of water on the seepage rate. By projecting the curves downward until they intersect the vertical axis, a head is determined which makes the seepage rate directly proportional to the depth, as should be the case according to the Darcy law. Since the seepage rings were used primarily for checking seepage meters, a single installation was used in each type of soil. However, many seepage-meter measurements were made in each seepage ring. Observations of seepage were made at intervals during a period of approximately two weeks for each setting of the seepage meter. At the end of the period, the seepage meter was installed at a new location inside the ring and the procedure repeated. As a result of this procedure, many replications of seepage-meter measurements in different soils were obtained where the seepage rate was accurately known.

An ingenious method of keeping the pressure inside the seepage meter equal to the head on the canal bed is described by Mr. Warnick. By using the Mariotte siphon principle, the reservoir of water for the seepage meter can be placed above the water surface in the canal. This equipment permits the observer to see whether the seepage meter is functioning properly and to note the rate at which water is seeping away through the cup of the meter. Mariotte controls were tried by the writers on well permeameters but the equipment did not prove satisfactory because it was affected by temperature. Furthermore, the surface tension at the bottom end of the air inlet tube affected the sensitivity of the device because the water level had to drop appreciably before the air bubble could break loose from the tube. A simple float control was found to be more sensitive and it was not affected by temperature.

It is difficult to understand why the plastic seepage bag is not capable of transmitting pressure at the same magnitude as that due to the water surrounding the bag, as indicated by Mr. Warnick. The writers had occasion to try different measuring devices on the meters at the same installations without finding any difference in the measured rate. The burette on the Weber Basin seepage meter is considered by many technicians to be too fragile for field use.

The tests reported by Mr. Warnick, which extended over a period of three years, showed that the losses measured by the seepage meter were 57%, 67%, and 69% of the losses measured by ponding. The writers found, however, that seepage meters installed in the seepage rings usually indicated a higher rather than a lower rate. This difference is probably due to the fact that all the seepage from the seepage rings had to pass through the bottom, whereas in the experiments reported by Mr. Warnick a large portion of the seepage probably occurred through the side slopes of the canals where it is difficult to install the seepage meters.

The development by Mr. Szalay is interesting but several inconsistencies should be pointed out. The true infiltration velocity is $v_i = v_s/n$, in which n is the porosity and v_s is the bulk velocity. The interpretation by Mr. Szalay is applicable only to the case of flow through a horizontal section on which the gravitational forces would be constant. For the case of a constant depth of water on a horizontal soil surface the hydraulic head would be $h + z$, so that the Darcy equation would be $v_s = K\,(h + z)/z$. In terms of infiltration velocity through the pores:

$$v_i = \frac{K}{n}\frac{h+z}{z}$$

and

$$v_i = \frac{dz}{dt}.$$

By eliminating v_i from these equations, the basic differential equation results:

$$\frac{z\,dz}{h+z} = \frac{K}{n}\,dt.$$

Integration of this equation results in

$$z = \frac{K\,t}{n} + h \log \frac{h+z}{h}.$$

In view of the foregoing analysis, it is difficult to understand how Mr. Szalay determined the relationship which he has tabulated from data on infiltration.

The possibility of utilizing permeability measurements on disturbed samples of bed material in determining seepage losses is mentioned by Mr. Lauritzen. It is believed that this method would not be an indication of a true seepage rate from a canal, owing to the difference in seepage rates on the sides and bottom. In many cases the sides have a higher seepage rate due to stratification and secondary structure—that is, cracks, root channels, and holes dug by rodents. The effect of these factors would be eliminated in disturbed soil samples.

In order for the greater hydration of clay minerals at a higher temperature to be a factor in a reduction of permeability at these temperatures, the process would have to be reversible. Referring to Fig. 12, it is noted that there is a cyclic variation so that when the water temperature decreases the seepage rate increases.

The comments of the discussers of the paper have emphasized the complexities of the seepage problem. Many uncertainties still exist and because of the importance of seepage the study of the problem should be continued.

AMERICAN SOCIETY OF CIVIL ENGINEERS
Founded November 5, 1852
TRANSACTIONS

Paper No. 2866

LATERAL BUCKLING OF ELASTICALLY END-RESTRAINED I-BEAMS

By Walter J. Austin,[1] A. M. ASCE, Shahen Yegian,[2] and Tie P. Tung[3]

SYNOPSIS

The purpose of this paper is to present the critical lateral loads and the corresponding critical bending stresses at midspan for prismatic I-beams having equal, linear, rotational restraints at both ends. In actual structures such end restraint is commonly provided by the connections. It is of importance to determine the increase of the lateral buckling load which results from this restraint. The critical loads for end-restrained bars of rectangular cross section have been considered by G. Winter,[4] M. ASCE, and A. R. Flint.[5]

THEORY

Considering an I-beam, the horizontal principal axis is denoted as x, the vertical principal axis as y, the longitudinal axis as z, the depth of the beam as d_2, and the distance between shear centers of the flanges as d_1, as shown in Fig. 1. Each flange at each end is assumed to be individually restrained against rotation about the vertical axis. The rotation of each end as a whole about the x-axis is elastically restrained and no rotation at the ends is allowed about the z-axis. The beam is loaded by vertical forces acting in the plane of the web. Two loadings are considered—uniform load and concentrated load at midspan—each load acting at three positions: (*a*) On the top flange, (*b*) at the centroid, and (*c*) at the bottom flange. The maximum stresses are assumed to be less than the proportional limit of the material. It is also assumed that the external loads remain parallel to their original direction when the points of application of these loads are displaced.

Note.—Published, essentially as printed here, in April, 1955, as *Proceedings-Separate No. 673.* Positions and titles given are those in effect when the paper was approved for publication in *Transactions.*

[1] Research Associate Prof., Dept. of Civ. Eng., Univ. of Illinois, Urbana, Ill.

[2] Research Assistant, Dept. of Civ. Eng., Univ. of Illinois, Urbana, Ill.

[3] Research Asst. Prof., Dept. of Civ. Eng., Univ. of Illinois, Urbana, Ill.

[4] "Strength of Slender Beams," by George Winter, *Transactions*, ASCE, Vol. 109, 1944, p. 1321.

[5] "The Influence of Restraints on the Stability of Beams," by A. R. Flint, *Structural Engineer*, September, 1951, p. 235.

The differential equations governing the lateral buckling of a symmetrical I-beam supported as described are as follows:[6]

$$E I_y u'''' = -(\beta M_x)'' \quad \ldots\ldots (1)$$

$$-D\beta'''' + C\beta'' + q s \beta = M_x u'' \quad \ldots\ldots (2)$$

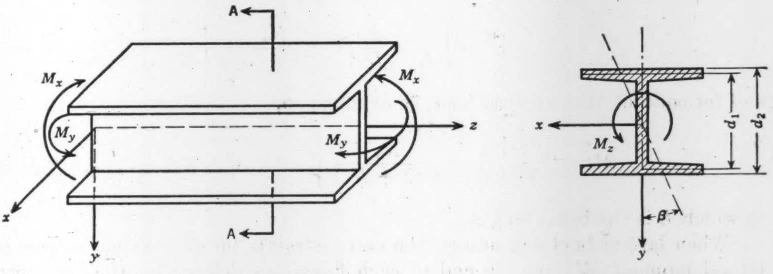

(a) COORDINATE SYSTEM (b) SECTION A-A

FIG. 1.—SIGN CONVENTION

in which each prime symbol denotes one differentiation with respect to z. The other symbols are defined as follows:

β = the angle of rotation of the cross section about its centroid (Fig. 1);
u = the displacement of the centroid in the x-direction;
M_x = the bending moment about the x-axis;
E = Young's modulus;
I_x, I_y = the moment of inertia of the cross section about the x-axis and y-axis, respectively;
C = the uniform torsion constant or torsional rigidity;
$D = E I_y d^2_1/4$ = the torsional bending constant;
q = the distributed vertical load; and
s = the distance from the centroid to the point of load application, assumed equal to $+d_1/2$, 0, or $-d_1/2$ for load at the top flange, centroid, or bottom flange, respectively.

The origin is considered to be at the left end of the beam. Due to symmetry, only the left half of the beam will be considered. The stiffness against rotation about the x-axis of the end restraint is characterized by the equation for the left end,

$$M_{xe} = -K_x (y')_{z=0} \quad \ldots\ldots (3)$$

in which K_x is the stiffness of the end restraint against rotation about the x-axis and M_{xe} is the moment exerted on the left end of the beam by the restraint. It is convenient to use a dimensionless quantity, N_x, related to the stiffness, K_z, in the following way:

---

[6] "Buckling Strength of Metal Structures," by F. Bleich, McGraw-Hill Book Co., Inc., New York, N. Y., 1952, p. 158.

$$N_z = \frac{K_z\,L}{E\,I_z} \qquad (4)$$

The flexural moments in the beam are given by the following equations: For uniform load, q, on the entire span,

$$M_z = \frac{q\,L^2}{2}\left[\frac{z}{L} - \frac{z^2}{L^2} - \frac{N_z}{6\,(2 + N_z)}\right] \qquad (5a)$$

and for concentrated vertical load, Q, at midspan,

$$M_z = \frac{Q\,L}{2}\left[\frac{z}{L} - \frac{N_z}{4\,(2 + N_z)}\right], \qquad 0 \leq z \leq \frac{L}{2} \qquad (5b)$$

in which L is the beam length.

When lateral buckling occurs, the end restraints on each flange impose a lateral moment, M_y, on the end of each flange, as defined by the following equations:

$$M_{y1} = \frac{K_y}{2}\,u'_1 \quad \text{and} \quad M_{y2} = \frac{K_y}{2}\,u'_2 \qquad (6)$$

in which the subscripts 1 and 2 denote the top and bottom flange, respectively, and $K_y/2$ is, for each flange, the stiffness of the restraint against rotation about the y-axis. The total stiffness for the beam, therefore, is equal to K_y. It is convenient to use a dimensionless quantity, N_y, related to the stiffness, K_y, in the following way:

$$N_y = \frac{K_y\,L}{E\,I_y} \qquad (7)$$

The curvature of each flange in the horizontal plane may be found from the ordinary beam equations, assuming that the flexural stiffness of each flange is one-half of the total beam stiffness, $E\,I_y$.

$$u''_1 = \frac{2\,M_{y1}}{E\,I_y} \quad \text{and} \quad u''_2 = \frac{2\,M_{y2}}{E\,I_y} \qquad (8)$$

The moments, M_y, may be eliminated from Eqs. 8 by the use of Eqs. 6:

$$u''_1 = \frac{K_y}{E\,I_y}\,u'_1 \quad \text{and} \quad u''_2 = \frac{K_y}{E\,I_y}\,u'_2 \qquad (9)$$

The lateral displacements of the top and bottom flanges may be expressed in terms of the lateral displacement, u, of the centroidal axis and the rotation, β, of the cross section about the centroidal axis. Thus,

$$\left.\begin{matrix} u_1 \\ u_2 \end{matrix}\right\rangle = u \pm \frac{d_1}{2}\,\beta \qquad (10a)$$

Differentiating Eqs. 10*a*, one obtains the following:

$$\left.\begin{matrix} u'_1 \\ u'_2 \end{matrix}\right\rangle = u' \pm \frac{d_1}{2}\beta' \qquad (10b)$$

and

$$\left.\begin{matrix} u''_1 \\ u''_2 \end{matrix}\right\rangle = u'' \pm \frac{d_1}{2}\beta'' \qquad (10c)$$

Eqs. 9 may now be expressed in terms of u and β by the use of Eqs. 10*b* and 10*c*. Thus,

$$u'' \pm \frac{d_1}{2}\beta'' = \frac{K_v}{E\,I_y}\left(u' \pm \frac{d_1}{2}\beta'\right) \qquad (11)$$

A sufficient condition for Eq. 11 to be satisfied is the following:

$$u'' = \frac{K_v}{E\,I_y}u' \qquad (12)$$

and

$$\beta'' = \frac{K_v}{E\,I_y}\beta' \qquad (13)$$

Eqs. 12 and 13 express two boundary conditions at the end of the beam. Two more are obtained from the requirement that lateral displacements and rotations at the end be prohibited. Hence,

$$u = 0 \qquad (14)$$

and

$$\beta = 0 \qquad (15)$$

At midspan, three boundary conditions result from symmetry, as follows:

$$u' = 0 \qquad (16)$$

$$u''' = 0 \qquad (17)$$

and

$$\beta' = 0 \qquad (18)$$

The final boundary condition at midspan depends on the loading. For distributed load,

$$\beta''' = 0 \qquad (19)$$

However, for a concentrated load, a couple equal to $Q\,s\,\beta$ acts at midspan. Therefore, just to the left of midspan,

$$D\,\beta''' = -\frac{Q}{2}s\,\beta \qquad (20)$$

Eqs. 1 and 2 were solved numerically using a successive-approximations procedure and an integration technique with twenty-four equal divisions in the length of the beam. All numerical computations were performed by the

TABLE 1.—CRITICAL VALUES OF $q L^4/(E I_y d_1)$ FOR THE CASE OF UNIFORM LOAD

N_y	N_z	Values of L/a									
		0	1	2	3	4	5	6	7	8	10
		(*a*) LOAD OF TOP FLANGE									
0	0	28.7	30.7	36.3	44.6	54.7	66.0	78.0	90.5	103.4	129.9
	2	36.1	38.9	47.0	59.1	74.2	91.2	109.5	128.8	148.7	189.8
	6	40.5	44.0	53.9	69.2	88.5	110.7	134.9	160.7	187.5	243.4
	18	43.1	47.0	58.2	75.8	98.5	125.0	154.4	186.0	219.2	288.9
	∞	44.6	48.8	60.9	80.1	105.2	135.1	168.6	205.1	243.7	325.8
$\frac{2}{3}$	0	35.5	37.5	43.1	51.5	62.0	73.8	86.5	99.9	113.8	142.3
	2	44.5	47.3	55.3	67.5	82.8	100.4	119.6	139.8	160.9	204.6
	6	50.0	53.4	63.2	78.4	97.8	120.4	145.3	172.0	200.0	258.3
	18	53.3	57.1	68.1	85.5	108.1	134.8	164.6	196.8	230.8	302.7
	∞	55.2	59.3	71.2	90.1	115.0	144.8	178.4	215.1	254.2	337.7
2	0	46.4	48.3	53.9	62.5	73.2	85.6	99.2	113.6	128.5	159.7
	2	58.1	60.8	68.7	80.8	96.4	114.4	134.4	155.7	178.0	224.8
	6	65.3	68.6	78.1	93.1	112.5	135.4	160.9	188.4	217.4	278.7
	18	69.7	73.4	84.1	101.2	123.5	150.2	180.2	212.9	247.6	321.6
	∞	72.5	76.4	88.0	106.5	131.0	160.4	194.0	230.8	270.2	354.8
6	0	66.6	68.5	74.0	82.5	93.5	106.5	120.9	136.4	152.7	187.1
	2	83.5	86.1	93.7	105.6	121.2	139.6	160.3	182.6	206.3	256.5
	6	94.2	97.3	106.5	121.0	140.2	163.1	189.0	217.2	247.2	311.3
	18	101.0	104.5	114.8	131.4	153.3	179.6	209.6	242.6	277.9	353.7
	∞	105.5	109.3	120.4	138.4	162.3	191.3	224.5	261.2	300.7	386.1
∞	0	113.8	115.6	121.0	129.6	141.0	154.7	170.3	187.3	205.5	244.5
	2	146.0	148.6	156.1	168.2	184.2	203.5	225.5	249.6	275.5	331.1
	6	168.3	171.4	180.7	195.5	215.3	239.2	266.6	296.8	329.2	399.0
	18	183.9	187.5	198.1	215.1	237.9	265.6	297.4	332.5	370.3	452.1
	∞	195.0	199.0	210.6	229.4	254.6	285.3	320.6	359.8	402.0	493.8
		(*b*) LOAD AT CENTROID									
0	0	44.7	46.9	53.0	61.8	72.3	84.0	96.3	109.0	122.1	148.8
	2	70.7	74.2	83.8	97.7	114.3	132.7	152.1	172.2	192.8	234.9
	6	98.4	103.3	116.6	136.0	159.1	184.6	211.6	239.5	268.1	326.5
	18	126.9	133.1	150.3	175.3	205.1	237.9	272.6	308.5	345.3	420.5
	∞	154.5	162.2	183.2	213.6	249.9	290.0	332.3	376.2	421.1	512.9
$\frac{2}{3}$	0	54.7	56.9	63.0	72.0	82.9	95.1	108.2	121.9	135.9	164.8
	2	85.4	88.8	98.2	112.2	129.3	148.3	168.7	189.9	211.8	256.7
	6	117.1	121.7	134.7	153.9	177.2	203.3	231.2	260.3	290.2	351.8
	18	148.6	154.5	171.0	195.3	225.0	258.1	293.5	330.5	368.5	446.5
	∞	178.6	185.7	205.5	234.7	270.4	310.3	352.8	397.3	443.0	536.9
2	0	70.4	72.5	78.5	87.6	98.9	111.8	125.8	140.5	155.7	187.3
	2	107.8	111.0	120.2	134.1	151.4	171.1	192.4	214.9	238.2	286.5
	6	145.0	149.4	161.7	180.4	203.7	230.2	258.9	289.1	320.4	385.3
	18	180.9	186.3	201.7	225.0	254.0	287.0	322.8	360.5	399.6	480.5
	∞	214.0	220.4	238.6	266.2	300.6	339.7	382.0	426.6	472.8	568.4
		(*b*) LOAD AT CENTROID (*cont'd.*)									
6	0	97.8	99.9	105.7	114.7	126.3	139.8	154.6	170.6	187.2	222.2
	2	146.0	149.0	157.7	171.2	188.4	208.5	230.7	254.5	279.3	331.5
	6	192.1	196.0	207.5	225.2	247.9	274.3	303.4	334.6	367.2	435.6
	18	235.0	239.9	253.8	275.5	303.2	335.4	370.9	408.9	448.7	532.0
	∞	274.1	279.7	295.9	321.1	353.3	390.7	431.9	475.9	522.0	618.4
∞	0	153.3	155.2	160.8	169.9	181.7	195.9	212.0	229.5	248.1	287.9
	2	225.1	227.9	236.2	249.4	266.7	287.5	310.9	336.4	363.6	421.5
	6	292.8	296.4	307.2	324.2	346.7	373.4	403.7	436.6	471.5	545.9
	18	355.9	360.3	373.3	393.9	420.9	453.2	489.5	529.0	571.0	660.0
	∞	414.2	419.3	434.2	458.0	489.2	526.3	568.1	613.4	661.5	763.2
		(*c*) LOAD AT BOTTOM FLANGE									
0	0	69.6	71.6	77.2	85.5	95.5	106.7	118.7	131.2	144.1	170.5
	2	138.0	140.8	148.8	160.8	175.6	192.4	210.6	229.6	249.4	290.1
	6	236.5	239.9	249.7	264.6	283.5	305.2	329.0	354.3	380.7	435.8
	18	366.0	369.8	380.7	397.8	419.9	445.8	474.5	505.4	538.0	606.6
	∞	522.2	526.3	538.1	556.9	581.4	610.6	643.5	679.3	717.3	798.1
$\frac{2}{3}$	0	84.3	86.3	91.9	100.3	110.7	122.5	135.2	148.5	162.3	190.7
	2	162.8	165.6	173.5	185.5	200.7	218.1	237.0	257.0	277.9	321.3
	6	270.9	274.2	283.8	298.7	317.8	340.0	364.6	390.8	418.4	476.1
	18	407.0	410.8	421.6	438.7	460.9	487.1	516.4	548.2	581.7	652.8
	∞	565.6	569.6	581.4	600.0	624.6	654.0	687.2	723.5	762.1	844.6
2	0	106.6	108.5	114.1	122.6	133.3	145.6	159.1	173.4	188.3	219.4
	2	198.2	200.9	208.7	220.7	236.1	254.0	273.8	295.0	317.1	363.6
	6	317.5	320.7	330.2	345.0	364.2	386.9	412.2	439.4	468.2	529.1
	18	460.8	464.5	475.1	492.1	514.3	540.8	570.7	603.1	637.7	711.2
	∞	621.0	625.0	636.5	654.9	679.3	708.7	742.0	778.5	817.7	901.6
6	0	142.8	144.7	150.1	158.6	169.6	182.6	196.9	212.4	228.7	263.1
	2	252.3	254.9	262.5	274.4	290.0	308.5	329.2	351.6	375.3	425.6
	6	385.6	388.8	398.0	412.7	432.0	455.1	481.1	509.5	539.7	604.1
	18	537.8	541.4	551.8	568.5	590.7	617.3	647.6	680.7	716.2	792.2
	∞	701.1	704.9	716.1	734.1	758.0	787.0	820.2	856.7	896.0	980.7
∞	0	204.7	206.6	212.1	220.8	232.4	246.2	262.0	279.3	297.7	337.2
	2	342.4	345.0	352.8	365.2	381.6	401.4	423.9	448.7	475.2	532.0
	6	501.4	504.6	514.2	529.6	550.1	574.8	603.1	634.1	667.5	739.2
	18	677.7	681.4	692.4	710.0	733.5	762.1	794.8	830.9	869.6	953.1
	∞	865.5	869.5	881.4	900.5	926.1	957.2	992.9	1032	1075	1167

TABLE 2.—CRITICAL VALUES OF $Q L^3/(E I_y d_1)$ FOR THE CASE OF A CONCENTRATED LOAD

N_y	N_x	Values of L/a									
		0	1	2	3	4	5	6	7	8	10
		(a) LOAD AT TOP FLANGE									
0	0	15.8	16.9	20.2	25.0	30.8	37.4	44.4	51.8	59.4	75.0
	4/3	18.0	19.5	23.5	29.6	37.1	45.5	54.7	64.3	74.2	94.7
	4	19.7	21.3	26.0	33.2	42.2	52.5	63.7	75.6	87.9	113.5
	12	20.8	22.6	27.9	36.0	46.3	58.2	71.4	85.3	100.0	130.6
	∞	21.6	23.5	29.2	38.0	49.3	62.6	77.4	93.3	110.0	145.3
$\frac{2}{3}$	0	19.2	20.4	23.6	28.4	34.4	41.2	48.5	56.3	64.3	80.9
	4/3	21.9	23.3	27.3	33.3	40.8	49.5	58.9	68.9	79.2	100.8
	4	23.9	25.5	30.0	37.1	46.1	56.4	67.8	80.0	92.7	119.2
	12	25.2	27.0	32.1	40.0	50.1	62.0	75.2	89.3	104.2	135.6
	∞	26.2	28.0	33.5	42.0	53.1	66.3	81.0	96.8	113.7	149.4
2	0	24.6	25.7	28.8	33.6	39.7	46.7	54.4	62.5	71.0	88.8
	4/3	28.0	29.3	33.1	39.0	46.5	55.2	64.9	75.3	86.1	108.8
	4	30.4	31.9	36.3	43.1	51.9	62.3	73.8	86.1	99.2	126.7
	12	32.1	33.8	38.6	46.2	56.1	67.8	80.9	95.1	110.2	142.2
	∞	33.3	35.1	40.2	48.4	59.2	72.0	86.5	102.3	119.1	155.0
6	0	34.2	35.2	38.1	42.8	48.8	56.0	63.9	72.5	81.5	100.7
	4/3	38.6	39.8	43.4	49.0	56.4	65.1	74.9	85.6	96.8	120.8
	4	41.9	43.3	47.4	53.8	62.3	72.5	84.0	96.5	109.8	138.2
	12	44.3	45.8	50.3	57.5	66.9	78.3	91.2	105.3	120.4	152.9
	∞	46.0	47.7	52.5	60.1	70.4	82.7	96.8	112.4	129.1	165.0
∞	0	55.0	55.9	58.8	63.3	69.4	76.6	84.9	94.0	103.8	124.7
	4/3	62.4	63.6	67.0	72.5	79.8	88.6	98.7	109.8	121.7	147.4
	4	68.2	69.5	73.4	79.7	88.1	98.2	109.9	122.8	136.7	166.7
	12	72.6	74.0	78.3	85.3	94.6	106.0	119.0	133.5	149.2	183.0
	∞	76.0	77.5	82.2	89.7	99.8	112.2	126.4	142.3	159.4	196.7
		(b) LOAD AT CENTROID									
0	0	26.9	28.2	31.8	37.1	43.4	50.4	57.8	65.4	73.2	89.1
	4/3	36.2	37.9	42.8	49.9	58.4	67.7	77.6	87.8	98.3	119.6
	4	46.4	48.7	54.9	64.0	74.8	86.8	99.4	112.4	125.7	152.9
	12	57.1	59.9	67.7	78.8	92.2	106.8	122.3	138.3	154.7	188.2
	∞	67.7	71.1	80.2	93.5	109.3	126.8	145.2	164.2	183.7	223.4
$\frac{2}{3}$	0	32.5	33.8	37.4	42.7	49.2	56.4	64.2	72.2	80.5	97.6
	4/3	43.2	44.9	49.6	56.7	65.3	74.8	85.1	95.7	106.7	129.2
	4	54.5	56.7	62.7	71.6	82.4	94.5	107.4	120.8	134.6	163.0
	12	66.1	68.7	76.0	86.8	100.0	114.6	130.2	146.5	163.3	197.6
	∞	77.3	80.4	88.9	101.6	116.9	134.1	152.4	171.5	191.1	231.3
2	0	41.1	42.3	45.8	51.1	57.7	65.2	73.3	81.8	90.7	109.0
	4/3	53.6	55.2	59.7	66.6	75.2	84.9	95.5	106.6	118.1	142.0
	4	66.5	68.5	74.1	82.6	93.3	105.3	118.4	132.2	146.5	176.0
	12	79.2	81.6	88.3	98.5	111.2	125.6	141.2	157.6	174.6	209.7
	∞	91.3	94.0	101.7	113.5	128.1	144.7	162.7	181.6	201.2	241.7
		(b) LOAD AT CENTROID (*cont'd.*)									
6	0	55.5	56.7	60.0	65.1	71.7	79.3	87.7	96.7	106.2	125.9
	4/3	70.9	72.3	76.5	83.0	91.4	101.1	111.9	123.3	135.4	160.6
	4	86.1	87.8	92.9	100.9	111.0	122.8	135.8	149.8	164.3	194.9
	12	100.7	102.8	108.8	118.0	129.9	143.7	158.9	175.2	192.2	227.8
	∞	114.4	116.8	123.5	134.0	147.5	163.1	180.4	198.8	218.1	258.4
∞	0	84.0	85.0	88.1	93.1	99.6	107.3	116.1	125.6	135.8	157.5
	4/3	105.4	106.7	110.6	116.8	124.9	134.6	145.6	157.5	170.2	197.2
	4	126.4	128.0	132.6	140.0	149.7	161.2	174.3	188.5	203.6	235.7
	12	146.6	148.4	153.7	162.3	173.4	186.8	201.8	218.1	235.5	272.4
	∞	165.7	167.7	173.8	183.3	195.9	210.8	227.7	246.0	265.4	306.6
		(c) LOAD AT BOTTOM FLANGE									
0	0	45.5	46.7	50.0	54.9	60.8	67.5	74.7	82.2	89.8	105.6
	4/3	71.9	73.3	77.5	83.7	91.4	100.1	109.4	119.3	129.4	150.3
	4	108.2	109.9	114.7	122.2	131.5	142.1	153.7	165.9	178.6	204.8
	12	154.8	156.7	162.2	170.7	181.5	194.0	207.7	222.2	237.4	269.0
	∞	208.3	210.4	216.5	226.0	238.2	252.4	268.1	285.0	302.6	339.6
$\frac{2}{3}$	0	54.6	55.8	59.0	63.9	70.0	76.9	84.4	92.3	100.4	117.2
	4/3	84.3	85.7	89.7	95.9	103.6	112.5	122.1	132.3	142.9	164.9
	4	123.2	124.9	129.6	136.9	146.2	156.9	168.6	181.2	194.2	221.4
	12	170.9	172.7	178.0	186.3	196.9	209.4	223.1	237.9	253.3	285.7
	∞	223.0	225.0	230.8	240.0	251.9	266.0	281.6	298.5	316.2	353.6
2	0	68.1	69.2	72.4	77.2	83.4	90.5	98.3	106.6	115.2	133.2
	4/3	101.9	103.3	107.1	113.1	120.8	129.8	139.7	150.2	161.2	184.3
	4	143.9	145.5	150.0	157.0	166.1	176.7	188.6	201.3	214.7	242.8
	12	192.5	194.2	199.2	207.2	217.5	229.7	243.3	258.1	273.6	306.6
	∞	243.0	244.9	250.4	259.1	270.5	284.1	299.4	316.0	333.6	371.0
6	0	89.9	90.9	93.9	98.6	104.7	111.9	120.0	128.6	137.8	157.1
	4/3	129.2	130.5	134.1	139.8	147.3	156.2	166.1	176.9	188.3	212.5
	4	175.2	176.6	180.7	187.3	196.0	206.4	218.0	230.8	244.3	273.1
	12	225.3	226.9	231.5	238.8	248.5	260.1	273.3	287.7	303.2	336.2
	∞	275.5	277.2	282.1	290.1	300.6	313.2	327.7	343.6	360.6	397.3
∞	0	127.9	128.9	131.7	136.3	142.4	149.8	158.2	167.4	177.2	198.4
	4/3	177.3	178.5	181.9	187.4	194.8	203.7	213.9	225.1	237.1	263.1
	4	232.9	234.2	238.1	244.4	252.8	263.0	274.8	287.7	301.6	331.7
	12	292.6	294.0	298.3	305.2	314.4	325.6	338.5	352.9	368.3	401.9
	∞	353.2	354.7	359.2	366.5	376.3	388.2	402.0	417.4	434.0	470.3

Illiac digital computing machine in ten hours. The details of the numerical procedure and the coding of the digital computing machine are not given here.

CHARTS AND TABLES

In Tables 1 and 2 are given the critical values of a dimensionless load parameter for ranges of the factors, L/a, N_x, and N_y, in which $a = \sqrt{D/C}$; Table 1 is for a uniform load over the entire length of the beam and Table 2 is for a concentrated load at midspan. To determine the critical load, one should multiply the coefficients in the tables by the appropriate value of $E\,I_y\,d_1/L^4$ for a uniform load, or $E\,I_y\,d_1/L^3$ for a concentrated load at midspan. The critical loads are tabulated for three common positions of the loading, which are: (*a*) At the top flange, (*b*) at the centroid, and (*c*) at the bottom flange.

The ratio L/a is the significant geometrical property of the beam for the problem of lateral buckling, somewhat like the slenderness ratio, L/r, for columns. Critical values of the load parameter are tabulated for values of the ratio L/a of 0, 1, 2, 3, 4, 5, 6, 7, 8, and 10; these values cover the range of practical interest.

TABLE 3.—RATIOS OF END TO MIDSPAN MOMENTS FOR TABULATED VALUES OF N_x

CASE OF UNIFORM LOAD		CASE OF CONCENTRATED LOAD AT MIDSPAN	
Restraint, N_x	$\frac{\text{End moment}}{\text{Midspan moment}}$	Restraint, N_x	$\frac{\text{End moment}}{\text{Midspan moment}}$
0	0	0	0
2	−0.5	4/3	−0.25
6	−1.0	4	−0.5
18	−1.5	12	−0.75
∞	−2.0	∞	−1.0

Five values of end restraint about each axis, N_x and N_y, were chosen to cover the complete range from no end restraint, $N = 0$, to a fixed condition, $N = \infty$, with intermediate values spaced approximately equal in effectiveness. For example, the values of N_x were so chosen as to yield equal increments in the ratio of end moment to midspan moment, as shown in Table 3. In using the tables and curves, it is often more convenient to use the concept of the ratio of end moment to center moment rather than the stiffness, N_x. The values of N_y were chosen in a similar manner.

Critical stress is usually the quantity that is most useful in design. Figs. 2 through 6 show the variation of a dimensionless critical-stress parameter with variation in L/a for all combinations of the values of N_x and N_y previously considered and for the three positions of loading. The symbol σ in the critical-stress parameter, $\sigma\,L^2\,I_x/E\,I_y\,d_1\,d_2$, denotes the extreme fiber stress at midspan corresponding to the critical load. This stress is always the maximum stress for the case of a concentrated load at midspan, but, as shown in Table 3, it is not the maximum stress in the beam for the case of uniform loading when $N_x > 6$.

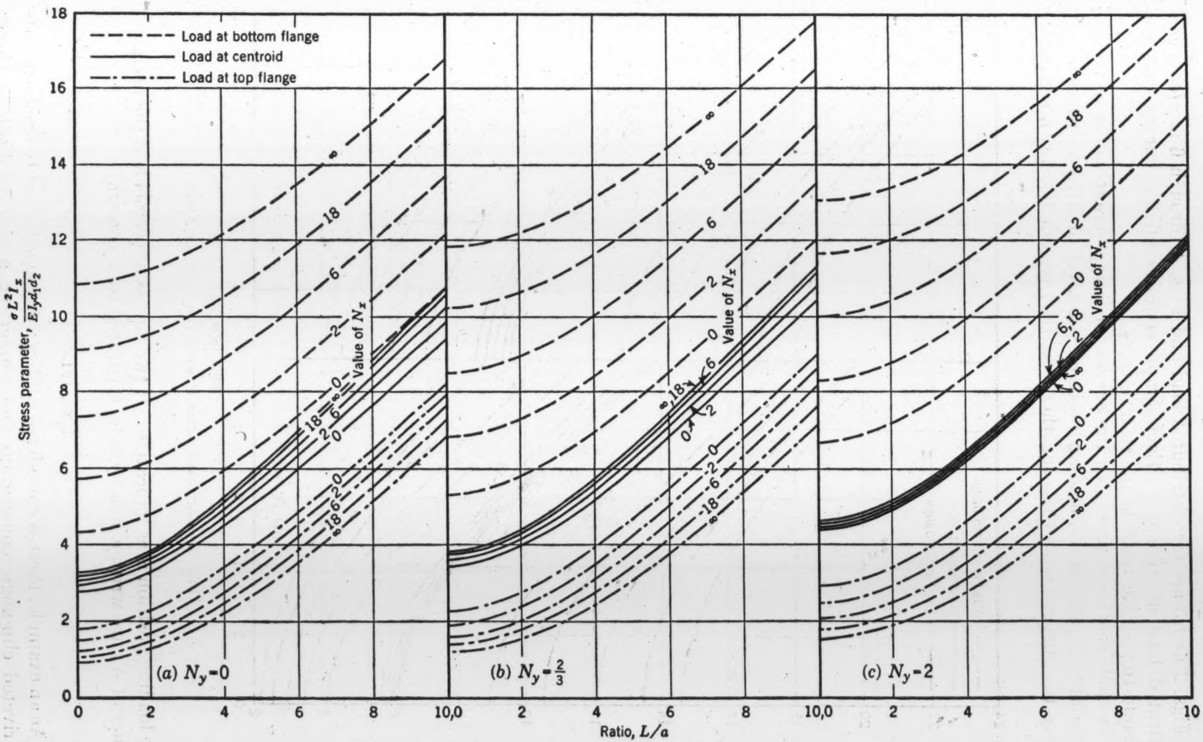

FIG. 2.—CRITICAL-STRESS CURVES FOR UNIFORM LOAD

Figs. 2 and 3 are for distributed load and Figs. 4 through 6 are for a concentrated load at midspan. Each graph contains all the curves that correspond to a single value of the restraint, N_y.

In each graph are presented the curves for five different values of the end restraint, N_x, and three loading positions—a total of fifteen curves except where the curves are so close together that they cannot be drawn separately.

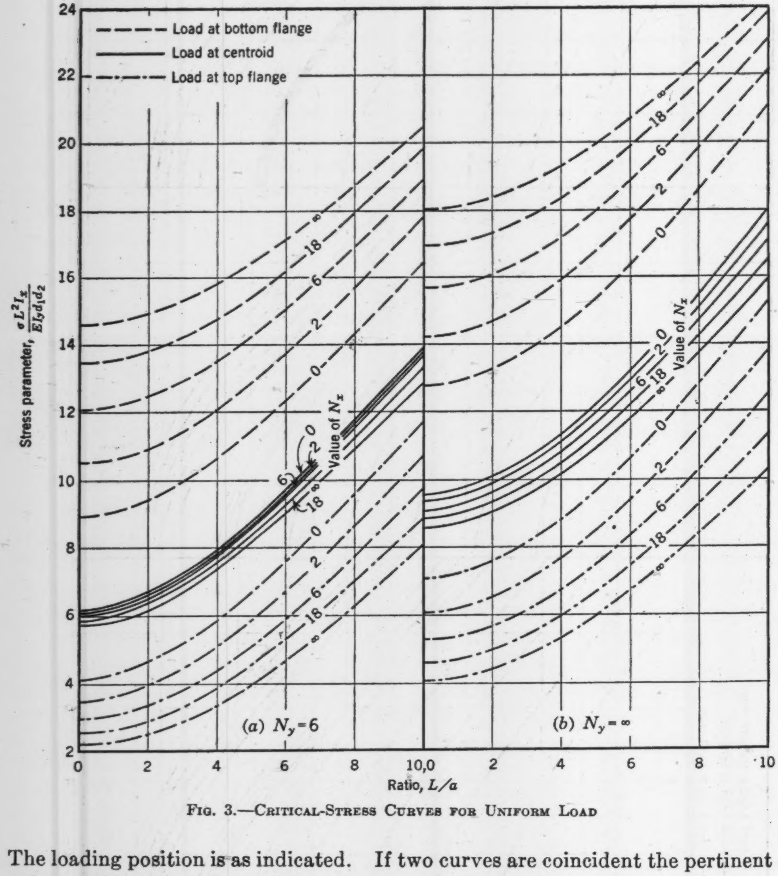

FIG. 3.—CRITICAL-STRESS CURVES FOR UNIFORM LOAD

The loading position is as indicated. If two curves are coincident the pertinent values of N_x are written side by side, separated by a comma.

EXAMPLE

As an example, there is considered a 12-in. I-beam attached to fixed supports by riveted clip-angle connections and supporting a uniform load, as shown

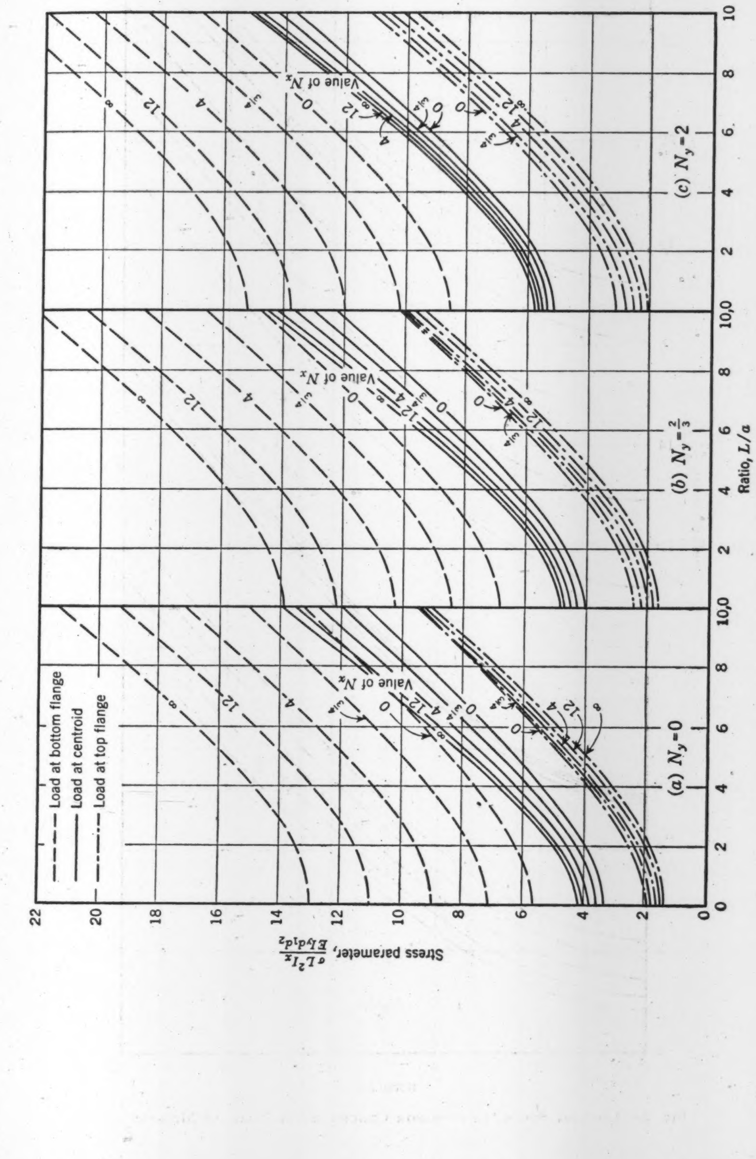

FIG. 4.—CRITICAL-STRESS CURVES FOR CONCENTRATED LOAD AT MIDSPAN

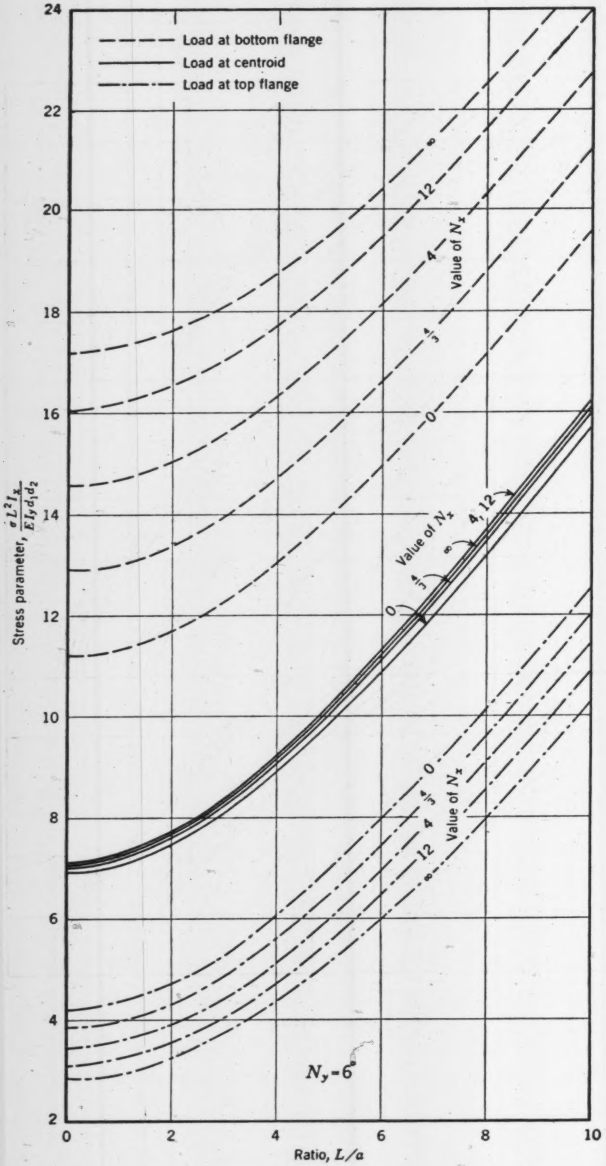

FIG. 5.—CRITICAL-STRESS CURVES FOR CONCENTRATED LOAD AT MIDSPAN

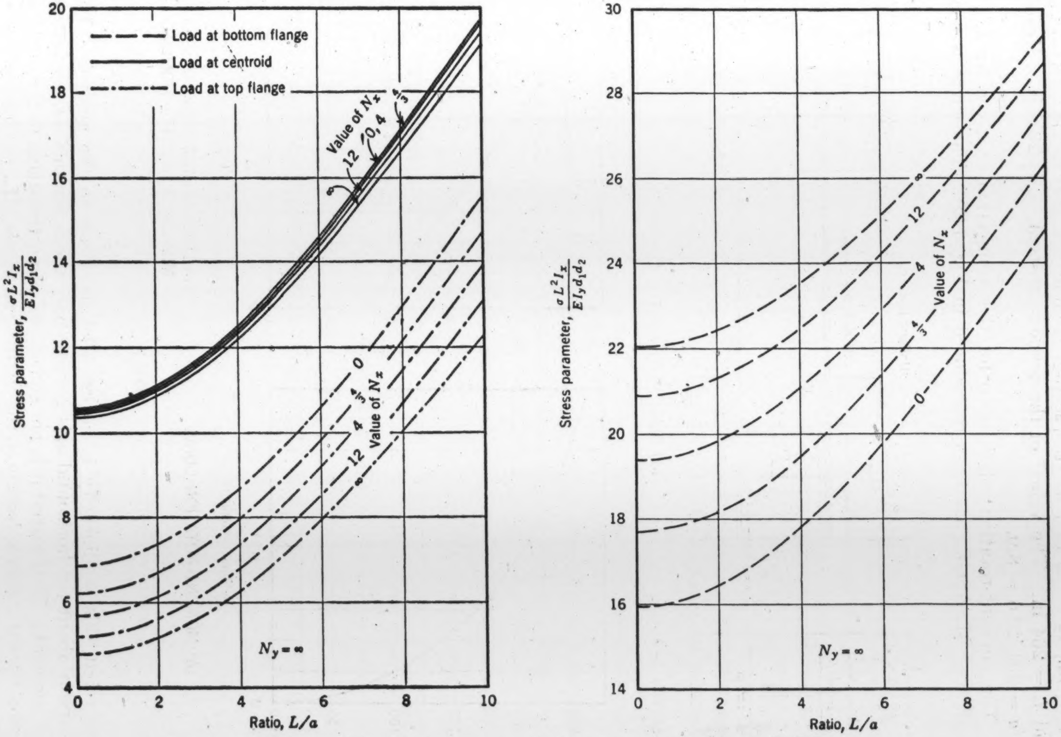

FIG. 6.—CRITICAL-STRESS CURVES FOR CONCENTRATED LOAD AT MIDSPAN

in Fig. 7(*a*). The properties of the beam are as follows: $E = 30 \times 10^6$ lb per sq in., $I_y = 9.5$ in.^{4}, Z_x (the section modulus) = 36.0 in.^{3}, $d_1 = 11.5$ in., and $L = 264$ in. The value[7] of the torsion constant, a, is 29.6 in. Hence, $L/a = 264/29.6 = 8.9$.

The moment-rotation relationship for this connection as given by J. C. Rathbun,[8] M. ASCE, has been reproduced in Fig. 7(*b*). The curve is nonlinear but this nonlinearity is no essential handicap to the analysis. The restraint about the horizontal axis governs only the magnitude of the vertical end moment. This restraint is not considered as participating in the buckling action because, during buckling, the vertical moments, M_x, are assumed to be independent of the lateral displacement and rotation.

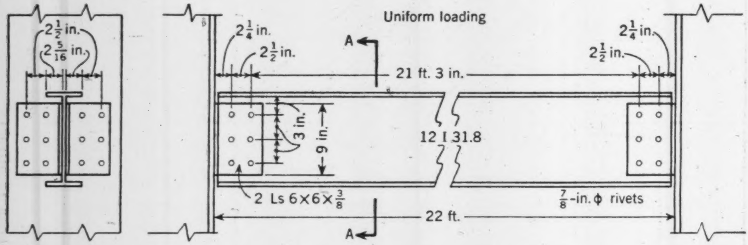
$2\frac{1}{2}$ in.
$2\frac{5}{16}$ in.
$2\frac{1}{4}$ in.
$2\frac{1}{2}$ in.
Uniform loading
A
21 ft. 3 in.
$2\frac{1}{4}$ in.
$2\frac{1}{2}$ in.
3 in.
9 in.
12 I 31.8
2 Ls $6 \times 6 \times \frac{3}{8}$
$\frac{7}{8}$-in. ϕ rivets
22 ft.
A

SECTION A-A

(*a*) BEAM WITH RIVETED CONNECTIONS

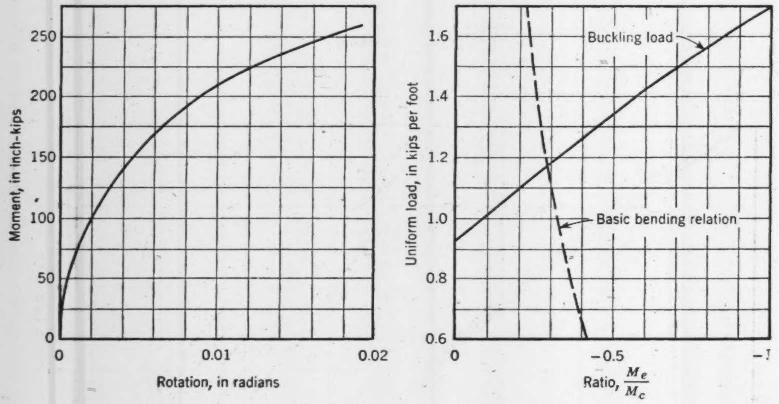

(*b*) MOMENT-ROTATION CURVE

(*c*) LOAD AGAINST RATIO OF END MOMENT TO CENTER MOMENT

Fig. 7

---

[7] "Torsional Stresses in Structural Beams," *Booklet S-57*, Bethlehem Steel Co., Bethlehem, Pa., 1950.

[8] "Elastic Properties of Riveted Connections," by J. C. Rathbun, *Transactions*, ASCE, Vol. 101, 1936, p. 524.

Because the moment-rotation relationship for the end connections is nonlinear the moments in the beam are not proportional to the magnitude of the uniform load. The flexural moments that result from any specified load may be found as explained by Mr. Rathbun. By making this computation for several assumed values of the load, one may obtain the curve relating the load to the moment ratio, M_e/M_c, which is shown as a dashed line in Fig. 7(*c*). This line is inclined downward to the right and is slightly curved; if the riveted connection were linearly elastic, this curve would be a straight vertical line. Of course, if the end connections were linearly elastic, Fig. 7(*c*) would be unnecessary because the critical stress could be read directly from Fig. 2. The dashed curve in Fig. 7(*c*) defines the flexural action of the beam on the assumption that the beam is in neutral or stable equilibrium.

The clip-angle connection affords no restraint against rotation of the flanges about a vertical axis. Therefore, $N_y = 0$. It is also assumed that the clip angles prevent rotation of the beam about the centroidal axis at both ends. The curve relating buckling load to the moment ratio, M_e/M_c, may now be established for this beam by interpolating between the pertinent values in Table 1. The buckling curve is shown as a solid line in Fig. 7(*c*). The moment ratio, M_e/M_c, is used instead of the parameter, N_x; the relationship between the two is given in Table 3 for the tabulated values of N_x.

The intersection of the buckling-load curve and the basic bending-relation curve defines the magnitude of the critical uniform load and also the moment ratio. In Fig. 7(*c*), this intersection occurs at the following values: Critical load = w = 1,180 lb per ft, and $M_e/M_c = -0.29$.

Because $M_c - M_e = w\,L^2/8 = 857$ in.-kips, it is true that $M_e = -193$ in.-kips, and $M_c = 664$ in.-kips. The maximum critical stress, in pounds per square inch, is thus

$$\sigma_{cr} = \frac{M_c}{Z_x} = \frac{664{,}000}{36} = 18{,}400.$$

If the beam were assumed to be simply supported at the ends, the critical load and critical stress would be as follows: Critical load equals 930 lb per ft, and critical stress equals 18,800 lb per sq in.

Thus, the restraint afforded by the clip angles raises the critical load by 28% for this particular case. On the other hand, the critical stress is slightly decreased.

In general, the critical maximum stress varies much less than the critical load as the restraint about the horizontal axis, N_x, changes. The critical load always increases as N_x increases, but the critical stress may either increase or decrease. The latter trend is illustrated in the curves for critical stress at midspan due to a concentrated load acting on the top flange, shown in Figs. 4 through 6.

In applying these solutions to actual problems there is seldom any difficulty in determining the proper value of N_x, or its equivalent, M_e/M_c. However, often the value of N_y can only be determined by making simplifying assumptions.

ACKNOWLEDGMENTS

The work described herein has been performed as part of the cooperative research contract between the Engineering Experiment Station of the University of Illinois at Urbana and the Office of Naval Research, under Contract N6ori-071(06), Project NR-064-183. The writers wish to express their appreciation to the members of Committee E of the Column Research Council of the Engineering Foundation for the encouragement and constructive advice offered. The writers also wish to thank the Digital Computer Laboratory of the University of Illinois for the use of the Illiac computing machine.

AMERICAN SOCIETY OF CIVIL ENGINEERS
Founded November 5, 1852
TRANSACTIONS

Paper No. 2867

THE HIGHWAY SPIRAL FOR COMBINING CURVES OF DIFFERENT RADII

By Paul Hartman,[1] M. ASCE

With Discussion by Messrs. Thomas F. Hickerson, C. C. Wiley, Allen H. Brownfield, and Paul Hartman

Synopsis

The highway spiral connecting a tangent and a circular arc is rigorously defined mathematically. When two adjacent circular arcs must be connected by a spiral, mathematical exactness is replaced by the approximations of the theory of the osculating circle. The theory is satisfactory for flat spirals but has distinct failings for sharper spirals.

In this paper rigorous equations for the highway spiral connecting circular arcs of different radii are derived, and the extent of the approximations involved in the theory of the osculating circle are shown. Three graphs based on these equations permit rapid and accurate determination of the corrections to be applied to values obtained from the theory. The engineer with a working knowlege of the theory should find that the determination and application of these corrections are straightforward and simple.

The derivations themselves are cumbersome and extensive. They are given in outline form but in sufficient detail to permit checking.

Introduction

The spiral connecting two circular arcs is a part of the spiral which would be used to connect the sharper arc to a tangent. Thus, a 200-ft spiral connecting a 4° circular arc and a 6° circular arc is the last third of a 600-ft spiral running from a tangent to a 6° arc. In order to distinguish between the 200-ft spiral and the 600-ft spiral of which it is a part, the former is termed a compound spiral and the latter a simple spiral.

A simple spiral (Fig. 1) is arc APB connecting tangent HE with circular arc BG. The symbol P is any point on the spiral, and the circular arc is extended

---

Note.—Published, essentially as printed here, in June, 1955, as *Proceedings-Separate No. 703*. Positions and titles given are those in effect when the paper or discussion was approved for publication in *Transactions*.

[1] Associate Prof. of Civ. Eng., The City College of New York, New York, N. Y.

backward to C where it is parallel to HE. Notations conform with the designations of Joseph Barnett,[2] M. ASCE, which will be used, for the most part, herein.

In Fig. 2(*a*) a compound spiral is shown, which is arc APB connecting circular arcs GA and BH, and P is, again, any point on the spiral. The sharper arc, GA, with radius, OA, is extended forward to C on the common radial line O′D. The flatter arc, BH, with radius, O′B, is extended backward to D. The shift, CD, is designated as p_a. The central angles, designated β and α, do not conform with Mr. Barnett's notation for reasons explained subsequently. The deflection angle, EAP, to any point, P, on the spiral is ϕ_a. The angle between the tangent to the spiral at P and the main tangent, AE, is θ (Fig. 2(*b*)).

Also, D_1 is the degree of flatter circular arc, in degrees; D_2, the degree of sharper circular arc, in degrees; $D = D_2 - D_1$, or the degree of curve for an equivalent simple spiral; L_s, the length of a simple spiral, in feet; L_a, the length of a compound spiral, in feet; $\Delta_1 = D_1 L_a/200$; $\Delta_2 = D_2 L_a/200$; $\theta_s = D L_s/200$; and $\theta_a = (D_2 - D_1) L_a/200 = \Delta_2 - \Delta_1$, the nominal spiral angle.

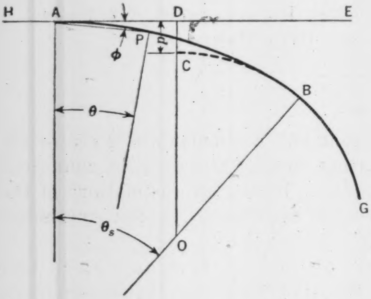

FIG. 1

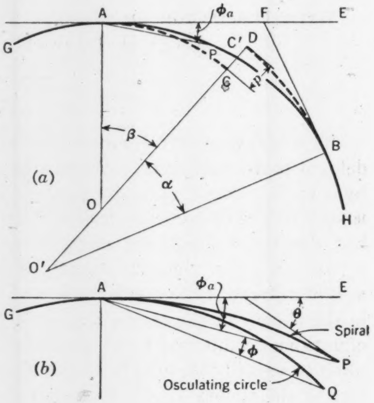

FIG. 2

The theory of the osculating circle assumes that a spiral departs from an osculating circle in the same manner that an equivalent simple spiral departs from the tangent. For the simple spiral to be equivalent to the compound spiral, the spiral angle, θ_s, of the simple spiral must be equal to the nominal spiral angle, θ_a, of the compound spiral and L_s must be equal to L_a.

Thus, in Fig. 2(*b*), which is an enlargement of a part of Fig. 2(*a*), the deflection angle, ϕ_a, to any point P, distant l (measured along the arc) from A, is the difference between two angles, the deflection angle to the osculating circle, EAQ, and the angle, PAQ. The latter is equal to ϕ, the deflection angle of an equivalent simple spiral to a point distant the same length l from point A in

---

[2] "Transition Curves for Highways," by Joseph Barnett, Public Roads Administration, U. S. Govt. Printing Office, Washington, D. C., 1940.

Fig. 1. Expressed mathematically,

$$\phi_a = \frac{D_2 l}{200} - \phi.$$

For a setup at B this equation would become

$$\phi_a = \frac{D_1 l}{200} + \phi.$$

The length, l, in each case is the distance along the spiral from the setup point to the sighted point.

The theory of the osculating circle further assumes that p_a (Fig. 2(a)) is equal to p (Fig. 1) and that β and α are equal to Δ_2 and Δ_1, respectively.

CORRECTIONS

The derivations show that all the assumptions of the theory of the osculating circle are in error, the magnitude of the errors varying with Δ_1 and Δ_2. For flat spirals the errors are negligible, but with increasing sharpness, the errors become so large that the theory cannot be used without applying the corrections cited herein.

The derivation of β shows that it is always larger than Δ_2 by a quantity which will be designated C_b:

$$C_b = 0.03655\, \Delta_2\, \theta_a\, (\Delta_2 - \theta_a) \{1 + 121\, [24\, \Delta_2\, (\Delta_2 - \theta_a) - 7\, \theta_a^2]\, 10^{-8}\} \ldots (1)$$

in which θ_a and Δ_2 are expressed in degrees and C_b, in seconds. The expression is set up in terms, θ_a and Δ_2, rather than in terms, Δ_1 and Δ_2, because the use of these terms simplifies a subsequent equation and it seems logical to use the same terms in all equations.

The correction, C_b, may be determined by using the graph of Fig. 3, which consists of curves of C_b versus θ_a for various values of Δ_2. In order to illustrate the use of the graph the value of β will be determined for a 400-ft compound spiral connecting a 10° arc with a 20° arc. The arguments are

$$\Delta_2 = \frac{20 \times 400}{200} = 40°$$

and

$$\theta_a = \frac{(20 - 10)\, 400}{200} = 20°.$$

The value of C_b, or the ordinate of the curve, $\Delta_2 = 40°$, at the point where θ_a is 20°, is 596″ or 9′56″. Then β is 40° 09′56″ and, because the complete central angle is $\Delta_1 + \Delta_2$, $\alpha = \Delta_1 - C_b = 19°50'04''$.

The value of the shift, p_a, is always less than p by a quantity which will be designated C_p:

$$C_p = 0.222\, L_a\, \Delta_2\, \theta_a\, (\Delta_2 - \theta_a)\, 10^{-7} \ldots\ldots (2)$$

in which C_p and L_a are expressed in feet and Δ_2 and θ_a, in degrees. In Fig. 4, the curves of C_p for a value of L_a of 1,000 ft versus θ_a are plotted for various

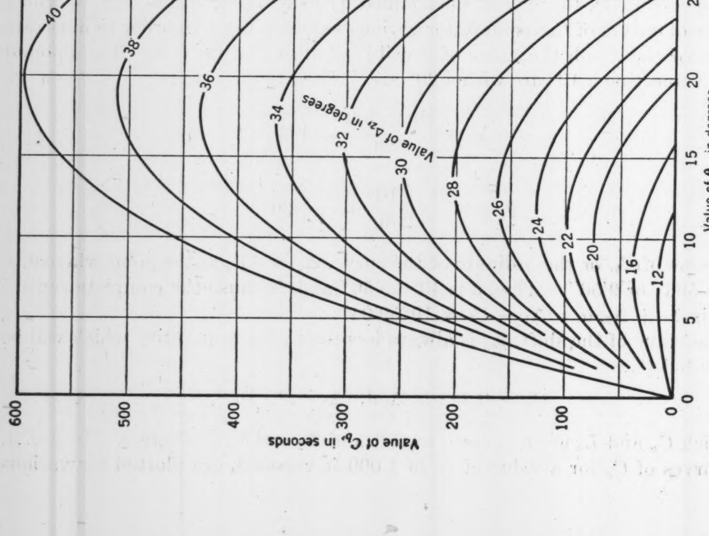
Value of C_p, in seconds
600
500
400
300
200
100
0
0
5
10
15
20
25
30
Value of θ_a, in degrees
Value of Δ_z, in degrees
40
38
36
34
32
30
28
26
24
22
20
16
12

Fig. 3

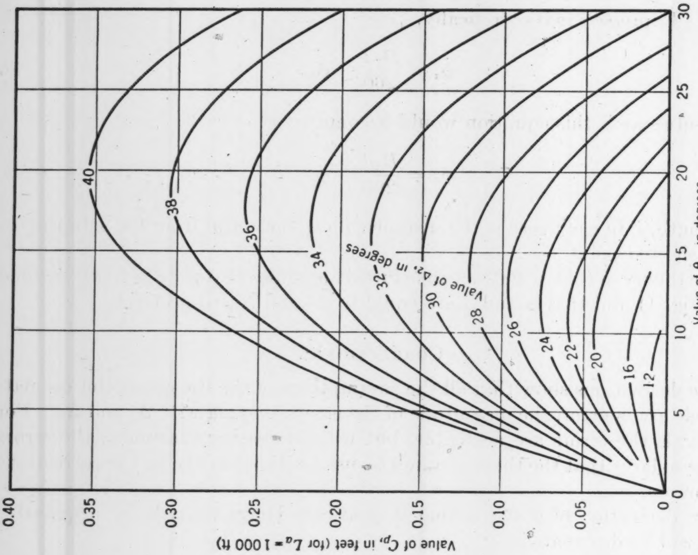
Value of C_p, in feet (for L_a = 1 000 ft)
0.40
0.35
0.30
0.25
0.20
0.15
0.10
0.05
0
0
5
10
15
20
25
30
Value of θ_a, in degrees
Value of Δ_z, in degrees
40
38
36
34
32
30
28
26
24
22
20
16
12

Fig. 4

values of Δ_2. Using the spiral of the preceding example, the value of C_p plots as 0.354, or, for 400 ft, $C_p = 400/1{,}000 \times 0.354 = 0.142$. From standard spiral tables the value of p for a value of θ_s of 20° is 11.584. Therefore, $p_a =$ 11.442.

The expression for the correction to be applied to intermediate deflection angles is cumbersome in its general form (Eq. 16 to be presented subsequently).

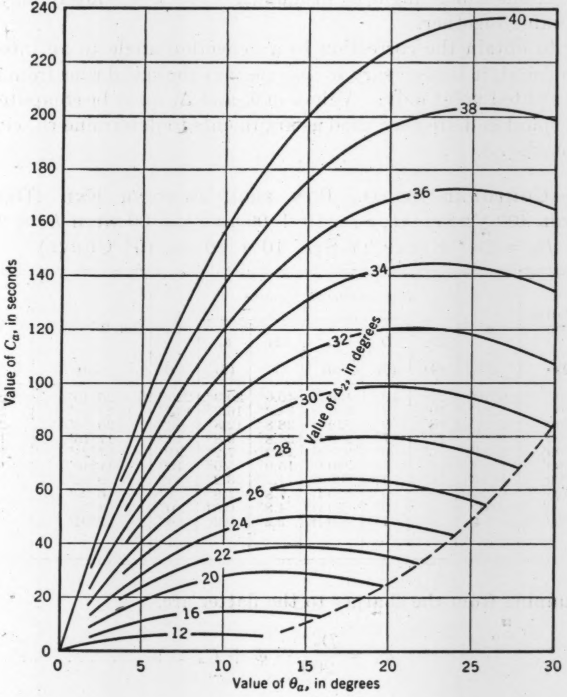

FIG. 5

The expression for the correction to the deflection angle to the end point of the spiral is simpler. It is

$$C_a = 0.01218\,\Delta_2\,\theta_a\,(\Delta_2 - \theta_a) + 0.0031\,\theta_a^3 + 0.23\,\theta_a^5\,10^{-7} + 0.353\,\Delta_2^3\,\theta_a \times (\Delta_2 - 2\,\theta_a)\,10^{-6} + 0.295\,\Delta_2\,\theta_a^3\,(181\,\Delta_2 - 61\,\theta_a)\,10^{-8} \quad (3)$$

in which C_a is in seconds and Δ_2 and θ_a are in degrees. Values of C_a may be obtained from Fig. 5 with more precision than is ordinarily required for any practical layout.

It should be noted that the deflection angle to the simple spiral is here assumed to be directly proportional to l^2—that is, $\phi = (\theta_s/3)\,(l/L_s)^2$. Standard spiral deflection angle tables list angles computed from the formula,

$$\phi = \frac{\theta_s}{3}\left(\frac{l}{L_s}\right)^2 - 0.31\,\theta_s^3\,10^{-2} - 0.23\,\theta_s^5\,10^{-7}$$

in which ϕ and θ_s are expressed in degrees and the two negative terms, in seconds. The negative terms are usually small and so is C_a. By including these terms in C_a, two corrections which might be insignificant taken separately may have an appreciable value together.

In order to obtain the correction to a deflection angle to an intermediate point on the spiral, it is necessary to assume that the spiral runs from the setup point to the sighted point only. Values of θ_a and Δ_2 must be computed for this abbreviated spiral and are then used as arguments to determine C_a, either from Fig. 5 or from Eq. 3.

TABLE 1.—COMPOUND SPIRAL, RUN FROM FLATTER END (DEFLECTION ANGLES FOR 400-FT SPIRAL, STA. 10 + 00 TO 14 + 00 WITH $D_1 = 10$ AND $D_2 = 20$. SETUP AT STA. 10 + 00 ON 10° CURVE)

Sta.	Osculating circle	ϕ	INTERMEDIATE VALUES					C_a	Col. 2 + Col. 3	ϕ_a, Col. 10 − Col. 9
			D_2	D	L_a	Δ_2	θ_a			
(1)	(2)	(3)	(4)	(5)	(6)	(7)	(8)	(9)	(10)	(11)
14 + 00	20°00′	6°40′	20°	10°	400 ft	40.0°	20.0°	225″	26°40′	26°36′15″
+ 60	18°00′	5°24′	19°	9°	360 ft	34.2°	16.2°	137″	23°24′	23°21′43″
13 + 20	16°00′	4°16′	18°	8°	320 ft	28.8°	12.8°	80″	20°16′	20°14′40″
+ 80	14°00′	3°16′	17°	7°	280 ft	23.8°	9.8°	42″	17°16′	17°15′18″
+ 40	12°00′	2°24′	16°	6°	240 ft	19.2°	7.2°	21″	14°24′	14°23′39″
12 + 00	10°00′	1°40′	15°	5°	200 ft	15.0°	5.0°	10″	11°40′	11°39′50″
+ 60	8°00′	1°04′	14°	4°	160 ft	11.2°	3.2°	4″	9°04′	9°03′56″
11 + 20	6°00′	0°36′	13°	3°	120 ft	7.8°	1.8°	1″	6°36′	6°35′59″
+ 80	4°00′	0°16′	12°	2°	80 ft	4.8°	0.8°	0″	4°16′	4°16′00″
+ 40	2°00′	0°04′	11°	1°	40 ft	2.2°	0.2°	0″	2°04′	2°04′00″
10 + 00										

When running from the sharper to the flatter arc,

$$\phi_a = \frac{D_2\, l}{200} - \phi + C_a \qquad (4)$$

and when running in the opposite direction,

$$\phi_a = \frac{D_1\, l}{200} + \phi - C_a \qquad (5)$$

Computation of deflection angles for the spiral used in the preceding illustrative examples is shown in Table 1. Instrument setup is assumed at the flatter end of the spiral, Sta. 10 + 00, and the deflection angles are computed to the tenth points.

The deflection angles to the osculating circle are listed in Col. 2 and equal $D_1\, l/200$. For the deflection angles of an equivalent simple spiral (Col. 3), $\phi = (\theta_a/3)\,(l/L)^2$ so that the value of ϕ (for Sta. 10 + 40) is $20/3\,(0.1)^2 = 0.067°$ or 4′. Cols. 4 to 8 contain values for the "abbreviated" spirals—that is, running from the setup point to the sighted point only. Thus, for the deflection angle to the midpoint of the spiral (Sta. 12 + 00), the abbreviated spiral runs from the 10° arc to a 15° arc and is 200 ft long; then $D_2 = 15°$, $D = 5°$, and $L_a = 200$ ft. From these values, Δ_2 and θ_a are determined as 15° and 5°, respectively. Using these values as arguments, Fig. 5 gives $C_a = 21''$. Values of C_a are listed in Col. 9, and the correct deflection angle is listed in Col. 11.

TABLE 2.—COMPOUND SPIRAL, RUN FROM SHARP END (DEFLECTION ANGLES FOR 400-FT SPIRAL, STA. 14 + 00 TO 10 + 00, WITH $D_1 = 10°$ AND $D_2 = 20°$. SETUP AT STA. 14 + 00 ON 20° CURVE)

Sta.	Osculating circle	ϕ	INTERMEDIATE VALUES					C_a	Col. 2 − Col. 3	ϕ_a, Col. 9 + Col. 10
			D_2	D	L_a	Δ_2	θ_a			
(1)	(2)	(3)	(4)	(5)	(6)	(7)	(8)	(9)	(10)	(11)
10 + 00	40°00′	6°40′	20°	10°	400 ft	40°	20.0°	225″	33°20′	33°23′45″
+ 40	36°00′	5°24′	20°	9°	360 ft	36°	16.2°	157″	30°36′	30°38′37″
+ 80	32°00′	4°16′	20°	8°	320 ft	32°	12.8°	104″	27°44′	27°45′44″
11 + 20	28°00′	3°16′	20°	7°	280 ft	28°	9.8°	65″	24°44′	24°45′05″
+ 60	24°00′	2°24′	20°	6°	240 ft	24°	7.2°	36″	21°36′	21°36′36″
12 + 00	20°00′	1°40′	20°	5°	200 ft	20°	5.0°	19″	18°20′	18°20′19″
+ 40	16°00′	1°04′	20°	4°	160 ft	16°	3.2°	8″	14°56′	14°56′08″
+ 80	12°00′	0°36′	20°	3°	120 ft	12°	1.8°	3″	11°24′	11°24′03″
13 + 20	8°00′	0°16′	20°	2°	80 ft	8°	0.8°	1″	7°44′	7°44′01″
+ 60	4°00′	0°04′	20°	1°	40 ft	4°	0.2°	0″	3°56′	3°56′00″
14 + 00										

Deflection angles for the same spiral run in from the sharp end (Sta. 14 + 000) are computed in Table 2. It should be noted that Cols. 3, 5, 6, and 8 are identical.

The corrections (Col. 9) applied to the deflection angles of the first half of the spiral (the half nearer the point of setup) are negligible. They are listed herein to illustrate the fact that the best method of laying out a spiral may be to work from both ends toward the middle. Such a procedure would eliminate the need for computing C_a-values and would also eliminate the long sights which are taken last in the field layout and are, therefore, most liable to error.

TABLE 3.—SIMPLE SPIRAL (DEFLECTION ANGLES FOR A 200-FT SPIRAL, STA. 31 + 00 TO 33 + 00 JOINING A TANGENT AND A 30° CURVE. SETUP AT STA. 31 + 00 ON THE 30° CURVE)

Sta.	Osculating circle	ϕ	INTERMEDIATE VALUES						Col. 2 − Col. 3	ϕ_a, Col. 9 + Col. 10
			D_2	D	L_a	Δ_2	θ_a	C_a		
(1)	(2)	(3)	(4)	(5)	(6)	(7)	(8)	(9)	(10)	(11)
33 + 00	30°00′	10°00′	30°	30°	200 ft	30°	30.0°	84″	20°00′	20°01′24″
+ 60	24°00′	6°24′	30°	24°	160 ft	24°	19.2°	49″	17°36′	17°36′49″
32 + 20	18°00′	3°36′	30°	18°	120 ft	18°	10.8°	21″	14°24′	14°24′21″
+ 80	12°00′	1°36′	30°	12°	80 ft	12°	4.8°	6″	10°24′	10°24′06″
+ 40	6°00′	0°24′	30°	6°	40 ft	6°	1.2°	0″	5°36′	5°36′00″
31 + 00										

As a check on the precision of the corrections, the coordinates of the end point of a 200-ft spiral running from a 40° curve to a 20° curve were computed by the following methods: (*a*) Theoretical equations for X and Y; (*b*) traverse along the radii, using the values of β and p_a obtained from Eqs. 1 and 2; and (*c*) traverse along the chords of a 10-point spiral. The theoretical coordinates are $X = 159.398$ and $Y = 105.088$. The coordinates computed by the other methods did not differ more than 0.001 from these values.

The one correction that applies to a simple spiral is C_a, and it applies only when the setup is at some point on the spiral other than the TS, the point of "tangent to spiral." For a setup at the SC, the point of "spiral to curve," D_2 is equal to the degree of the circular curve, D_1 is equal to the degree of the osculating circle at the sighted point, and L_a is equal to the difference in stationing of the ends of the line of sight. Similarly, for a setup between TS and SC, the spiral between setup and sighted point is treated as a compound spiral.

Computations of the deflection angles to the fifth points of a simple spiral are shown in Table 3. The spiral is 200 ft long to a 30° curve; the transit setup is assumed at Sta. 31 + 00, the SC; and the columns are identical with those in Tables 1 and 2.

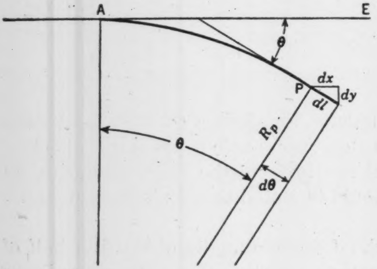

FIG. 6

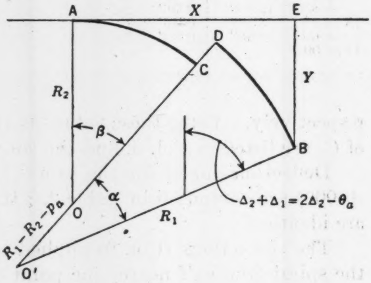

FIG. 7

DERIVATION

The degree of curvature of the highway spiral varies uniformly with length of curve. In Fig. 2(*a*) the degree of the spiral varies from D_2 at point A to D_1 at point B. The degree of curvature at any point, P, distant l from point A is

$$D_p = D_2 - (D_2 - D_1)\frac{l}{L_a} \quad \ldots\ldots\ldots\ldots\ldots\ldots (6)$$

Referring to Fig. 6, which shows an enlarged part of Fig. 2(*a*), the radius at any point, P, is R_p which is equal to $1/D_p$ if lengths are expressed in stations and angles are expressed in radians as they will be throughout the derivation. Then

$$dl = R_p\, d\theta = \frac{d\theta}{D_p} \quad \ldots\ldots\ldots\ldots\ldots\ldots (7)$$

Substituting for D_p its value from Eq. 6 and integrating,

$$\theta = D_2\, l = (D_2 - D_1)\frac{l^2}{2\,L_a} \ldots\ldots (8)$$

Letting l/L_a equal K and substituting θ_a for $(D_2 - D_1)L_a/2$ and Δ_2 for $D_2\, L_a/2$,

$$\theta = 2\,\Delta_2\, K - \theta_a\, K^2 \ldots\ldots (9)$$

Also,

$$dy = dl \sin\theta \ldots\ldots (10)$$

and

$$dx = dl \cos\theta \ldots\ldots (11)$$

Substituting for sine and cosine the respective series expansions in θ and integrating,

$$y = l\,(\Delta_2\, K - \tfrac{1}{3}\,\theta_a\, K^2 - \tfrac{1}{3}\,\Delta^3{}_2\, K^3 + \cdots) \ldots\ldots (12)$$

and

$$x = l\,(1 - \tfrac{2}{3}\,\Delta^2{}_2\, K^2 + \tfrac{1}{2}\,\Delta_2\,\theta_a\, K^3 - \tfrac{1}{10}\,\theta^2{}_a\, K^4 + \cdots) \ldots\ldots (13)$$

Dividing y by x

$$\tan\phi_a = \Delta_2\, K - \tfrac{1}{3}\,\theta_a\, K^2 + \tfrac{1}{3}\,\Delta^3{}_2\, K^3 - \cdots \ldots\ldots (14)$$

from which

$$\phi_a = \Delta_2\, K - \tfrac{1}{3}\,\theta_a\, K^2 + \frac{1}{90}\,\Delta^2{}_2\,\theta_a\, K^4 - \frac{1}{90}\,\Delta_2\,\theta^2{}_a\, K^5 + \cdots \ldots\ldots (15)$$

It should be noted that the first term on the right is the deflection angle to the osculating circle and that the second term is ϕ. Thus, these two terms are the deflection angle by the osculating-circle theory, and the remaining terms comprise a correction, C_a, or

$$C_a = \frac{1}{90}\,\Delta_2\,\theta_a\, K^4\,(\Delta_2 - \theta_a\, K) + \frac{8}{2{,}835}\,\theta^3{}_a\, K^6 + \frac{32}{467{,}775}\,\theta^5{}_a\, K^{10} + \frac{1}{945}$$
$$\times\,\Delta^3{}_2\,\theta_a\, K^6\,(\Delta_2 - 2\,\theta_a\, K) + \frac{1}{113{,}400}\,\Delta_2\,\theta^3{}_a\,(181\,\Delta_2 - 61\,\theta_a\, K)\, K^8 \ldots (16)$$

Eq. 5 is the same as Eq. 16 except for units and the fact that K has been taken equal to unity in Eq. 5.

To obtain equations for β and p_a the closed polygon, AEBO′O, in Fig. 7 is solved "by traverse." The direction of OA is assumed to be north, and the sums of the latitudes and departures of the polygon sides are equated to zero.

$$\Sigma\ \text{Lat.} = \text{O} = R_2 - Y - R_1 \cos\,(2\,\Delta_2 - \theta_a) + (R_1 - R_2 - p_a)\cos\beta \ldots (17)$$

$$\Sigma\ \text{Dep.} = X - R_1 \sin\,(2\,\Delta_2 - \theta_a) + (R_1 - R_2 - p_a)\sin\beta \ldots\ldots (18)$$

Solving Eqs. 17 and 18 for β,

$$\cos\beta = \frac{Y + R_1 \cos\,(2\,\Delta_2 - \theta_a) - R_2}{R_1 - R_2 - p_a} \ldots\ldots (19)$$

and

$$\sin\beta = \frac{R_1 \sin(2\,\Delta_2 - \theta_a) - X}{R_1 - R_2 - p_a} \qquad (20)$$

Dividing Eq. 20 by Eq. 19 to eliminate p_a,

$$\tan\beta = \frac{R_1 \sin(2\,\Delta_2 - \theta_a) - X}{Y + R_1 \cos(2\,\Delta_2 - \theta_a) - R_2} \qquad (21)$$

All terms of this fraction may be expressed in terms of Δ_2 and θ_a. Then,

$$\tan\beta = \Delta_2 + \tfrac{1}{3}\,\Delta_2^3 + \frac{1}{30}\,\Delta_2^2\,\theta_a - \frac{1}{30}\,\Delta_2\,\theta_a^2 + \cdots \qquad (22)$$

from which

$$\beta = \Delta_2 + \frac{1}{30}\,\Delta_2^2\,\theta_a - \frac{1}{30}\,\Delta_2\,\theta_a^2 + \frac{1}{315}\,\Delta_2^4\,\theta_a - \frac{2}{315}\,\Delta_2^3\,\theta_a^2 + \frac{17}{7{,}560}\,\Delta_2^2\,\theta_a^3 + \frac{1}{1{,}080}\,\Delta_2\,\theta_a^4 \ldots \qquad (23)$$

In Eq. 23, Δ_2 is the nominal central angle and the remaining terms comprise a correction, C_b, which is added to Δ_2 to obtain β and subtracted from Δ_1 to obtain α.

With β known either Eq. 19 or Eq. 20 may be used to solve for p_a. Using Eq. 20,

$$p_a = \frac{(R_1 - R_2)\sin\beta - R_1 \sin(2\,\Delta_2 - \theta_a) + X}{\sin\beta} \qquad (24)$$

Again, expressing all terms of the fraction in terms of Δ_2 and θ_a, and dividing, yields

$$p_a = L_a\left(\frac{1}{12}\,\theta_a - \frac{1}{240}\,\Delta_2^2\,\theta_a + \frac{1}{240}\,\Delta_2\,\theta_a^2 - \frac{1}{336}\,\theta_a^3 + \frac{1}{10{,}080}\,\Delta_2^4\,\theta_a - \frac{1}{5{,}040} \times \Delta_2^3\,\theta_a^2 + \frac{1}{18{,}900}\,\Delta_2^2\,\theta_a^3 + \frac{1}{21{,}600}\,\Delta_2\,\theta_a^4 + \frac{1}{15{,}840}\,\theta_a^5 \cdots\right) \qquad (25)$$

However,

$$p = L_s\left(\frac{1}{12}\,\theta_a - \frac{1}{336}\,\theta_a^3 + \frac{1}{15{,}840}\,\theta_a^5 - \cdots\right) \qquad (26)$$

Therefore,

$$p_a = p - L_a\left(\frac{1}{240}\,\Delta_2\,\theta_a\,(\Delta_2 - \theta_a) - \frac{1}{10{,}080}\,\Delta_2^4\,\theta_a + \frac{1}{5{,}040} \times \Delta_2^3\,\theta_a^2 - \frac{1}{18{,}900}\,\Delta_2^2\,\theta_a^3 - \frac{1}{21{,}600}\,\Delta_2\,\theta_a^4 \cdots\right) \qquad (27)$$

Calling the bracketed term C_p and ignoring all terms within the bracket after the first term because they are negligible for any practical highway spiral,

$$C_p = \frac{1}{240} \Delta_2 \theta_a (\Delta_2 - \theta_a) L_a \qquad (28)$$

in which C_p is the correction to be subtracted from p.

CONCLUSIONS

The derivations replace the theory of the osculating circle with mathematical exactness which permits the precise layout of a highway spiral between the branches of a compound curve regardless of sharpness. The procedure is, in effect, an extension of the osculating-circle theory. Figs. 3, 4, and 5 allow rapid and accurate determination of the corrections for any practical spiral, although, in cases where precise ties are desired, it would be preferable to compute C_b by use of Eq. 1.

Computations may be simplified and the precision of field layout increased if the spiral is laid out from both ends. Such a procedure eliminates the need for computing the corrections to deflection angles to the intermediate points of the spiral. It also eliminates the long sights to the far end of the spiral, which are a source of error in ordinary spiral layout.

DISCUSSION

Thomas F. Hickerson,[3] M. ASCE.—The paper is, in effect, a continuation of a paper by the writer.[4] Reference is made in the paper to the designations[2] of Mr. Barnett. Actually, Mr. Barnett's book was preceded by an earlier work[5] which he has acknowledged.[6]

So far as is known, Mr. Barnett first presented general formulas for the long and short tangent distances to the spiraled compound curve, based on a solution of oblique triangles. With his permission these were reproduced by the writer[5] but were accompanied by an alternate (and preferable) new set of tangent formulas based on the traverse method. There was also given a formula for β (like the author's Eq. 8 for θ) based on simple calculus, which was nevertheless a new concept.

Mr. Hartman offers no new procedure except the introduction of the angle, β, instead of a fixed angle, Δ_2, for the sharper curve. This method is a real contribution to the solution of the problem of combining very sharp curves of different radii.

Even with great precision in the deflection angles, slight errors in the curve layout may arise from the usual way of chaining and setting stakes. Actually an error of 100″ in angle causes a deviation transversely of not more than 0.1 ft at a distance of 200 ft. The long and short tangents of the spiral being known, frequently point B in Fig. 2(*a*) is set precisely on the forward tangent in advance of the curve layout by measurements from the point of intersection. In cases in which the point of intersection is inaccessible, point B might be established by well-known procedures. As a rule it would be desirable to hold to an independent location of B, although the end of the last chord misses it slightly. The eye could not detect small deviations in sharp curvature, but a displacement of the point of (forward) tangency is significant.

Applying the author's formula to a 200-ft spiral running from a 40° curve to a 20° curve gives theoretical coordinates which, it is stated, do not differ from those by other methods by more than 0.001. A careful check shows this to be precisely true. Curves of such extreme sharpness, even though not encountered in actual practice, serve as limiting values in Figs. 3, 4, and 5.

Letting $r = \Delta_2/\theta_a$, noting that $K = 1$ when $l = L_a$, and converting radians into degrees ($\pi = 3.1415927$), Eqs. 12 and 13, when extended, become

$$Y = L_a\left[\theta_a\left(\frac{\pi}{180}\right)\left(r-\frac{1}{3}\right) - \theta^3{}_a\left(\frac{\pi}{180}\right)^3\left(\frac{1}{3}r^3-\frac{2}{5}r^2+\frac{1}{6}r-\frac{1}{42}\right)\right.$$
$$\left.+\,\theta^5{}_a\left(\frac{\pi}{180}\right)^5\left(\frac{2}{45}r^5-\frac{2}{21}r^4+\frac{1}{12}r^3-\frac{1}{27}r^2+\frac{1}{120}r-\frac{1}{1{,}320}\right)\right] \quad \text{..(29)}$$

---

[3] Formerly Prof. of Civ. Eng., Univ. of North Carolina, Chapel Hill, N. C.

[4] "A Mathematical Examination of Spiraled Compound Curves," by T. F. Hickerson, *Proceedings-Separate No. 357*, ASCE, November, 1953.

[5] "Route Location and Surveying," by T. F. Hickerson, McGraw-Hill Book Co., Inc., New York, N. Y., 1953.

[6] "Transition Curves for Highways," by Joseph Barnett, Public Roads Administration, U. S. Govt. Printing Office, Washington, D. C., 1940, p. 12.

$$X = L_a\left[1 - \theta^2{}_a\left(\frac{\pi}{180}\right)^2\left(\frac{2}{3}r^2 - \frac{1}{2}r + \frac{1}{10}\right) + \theta^4{}_a\left(\frac{\pi}{180}\right)^4\right.$$
$$\times\left(\frac{2}{15}r^4 - \frac{2}{9}r^3 + \frac{1}{7}r^2 - \frac{1}{24}r + \frac{1}{216}\right) - \theta^6{}_a\left(\frac{\pi}{180}\right)^6\left(\frac{4}{315}r^6\right.$$
$$\left.\left. - \frac{13}{240}r^5 + \frac{1}{27}r^4 - \frac{1}{45}r^3 + \frac{1}{132}r^2 - \frac{1}{720}r + \frac{1}{9{,}360}\right)\right] \;..\; (30)$$

The subtractive term involving $\theta^7{}_a$ is omitted from Eq. 29 because it amounts to only 0.009 even when $L_a = 200$, $D_2 = 40°$, and $D_1 = 20°$. For all other cases this item is rarely (if ever) appreciable.

Three computations illustrate numerical applications that check the author's formulas.

a. Let $\Delta = \Delta_1 + \Delta_2$; T_1 = long tangent = BF (Fig. 2(*a*)); and T_2 = short tangent = AF. Then for the 200-ft spiral connecting the 40° and 20° curves:

$$T_1 = \frac{Y}{\sin\Delta} = \frac{105.088}{0.8660254} = 121.345 \ldots\ldots\ldots\ldots\ldots (31)$$

$$T_2 = X - Y\cot\Delta = 98.725 \ldots\ldots\ldots\ldots\ldots\ldots\ldots (32)$$

Also, $\theta_a = 40° - \frac{20°}{3} + C_a = 40° - \frac{20°}{3} + 226'' = 33°\,43'\,46''$.

b. For another method independent of Eqs. 29 and 30,

$$Y = R_2 + (R_1 - R_2 - p_a)\cos\beta - R_1\cos\Delta \ldots\ldots\ldots\ldots (33)$$

$$X = R_1\sin\Delta - (R_1 - R_2 - p_a)\sin\beta \ldots\ldots\ldots\ldots\ldots\ldots (34)$$

Now $R_1 = 286.479$, $R = 143.239$, $\beta = \Delta_2 + C_b = 40° + 9'\,54'' = 40°\,09'\,54''$, and $p_a = p = C_p = 5.792 - 0.071 = 5.721$. Substituting in Eqs. 33 and 34, $Y = 105.091$, $X = 159.399$. Then $T_1 = \frac{105.091}{\sin\Delta} = 121.349$ and

$$T_2 = X - Y\cot\Delta = 98.725.$$

These values of T_1 and T_2 are checks on computation *a*.

c. Replacing β with Δ_2 and p_a with p by the conventional method and noting also that $\phi_a = D_2 - \frac{1}{3}(20°) + C = 33°\,40'\,25''$ (in which $C = 25''$), Eqs. 33 and 34 give $Y = 105.291$ and $X = 159.748$, from which $T_1 = 121.58$ and $T_2 = 98.96$.

The error in T_1 and T_2 is approximately 0.2. A satisfactory adjustment might be to establish point B (Fig. 2(*a*)) at the end of the 200-ft spiral as determined by the last deflection angle, ϕ_a (slightly erroneous), of 33° 40′ 25″ causing a deviation of not more than 0.2 ft. Then with a transit set at this location of B, turn off the angle, BAF = $\Delta - \phi_a$, thus fixing the corresponding forward tangent.

C. C. WILEY,[7] M. ASCE.—The writer feels that the paper has several failings. It appears that the contentions have not been proved, that the derivations are not entirely correct, and that the ponderous formulas are likely to discourage rather than promote the adequate use of spirals.

The principle of the osculating circle is basic to the spiral and is derived directly from its definition. It is not a "theory" based on any assumption but is a geometrical principle universally applicable. Small discrepancies that may appear in the computations are the result of minute approximations in the derivations of certain formulas whereas larger differences are probably the result of incorrect assumptions in applying the principle.

At any point on the spiral, the degree of curve of the osculating circle is a constant whereas the degree of curve of the spiral changes at a rate that is the same throughout the length of the spiral. Therefore, the geometric relationship between the spiral and each osculating circle is exactly the same. Obviously, general formulas expressing this relationship would involve factors from both the osculating circle and the spiral.

The limit of the osculating circle is the initial point (TS) at which the degree of curve becomes zero. There, the radius is infinite and the osculating circle becomes a straight line which is the initial tangent. With $D = 0$ the circular factors disappear, hence formulas expressing the relationship of the spiral to the initial tangent become simple and easy to derive. At any point other than the TS, the same formulas express the relationship between the spiral and the osculating circle at that point. Therefore, all that is required to transpose the formulas from the initial tangent to any location is to add the proper factors from the given osculating circle. Such adjustment is evident in the formulas for the deflection angles.

It is a fact that a deflection angle for a simple spiral is not exactly one-third the change of direction and may be expressed by

$$\phi = \frac{1}{3}\theta - C_a.$$

Investigations of C_a show that this correction is normally so small it can be omitted and that even if it should be of some apparent magnitude, the ultimate effect on the actual location of the spiral is insignificant. Consequently, in common practice it is omitted. Mathematicians have habitually overemphasized C_a and have not attempted to reduce it to a practical form. However, the expression can be reduced to a simple form which can be computed in one setting on a slide rule, with an accuracy beyond any practical requirement.

The deflection angles for a compound spiral are merely the deflection angles for a setup at a point on the spiral. Consequently, the formulas should be applicable at any point and to any distance without being hampered by the limits of a specific problem. The principle of the osculating circle shows that the deflection angle at any point to any other is equal to the deflection angle of the osculating circle for the required distance plus (or minus, according to direction) the deflection angle of the simple spiral for the same distance. Because the circular deflection is mathematically exact the only theoretical correction is C_a as previously given.

---

[7] Prof. of Highway Eng. Emeritus, Univ. of Illinois, Urbana, Ill.

Early in the twentieth century a study was made of the foregoing by two independent methods—one analogous to that in the paper and the other entirely different. The combined effect was to show that

$$\phi_a = \phi_c \pm (\tfrac{1}{3}\theta - C_a).$$

The computation was subject to small discrepancies traceable to minute approximations in the formulas for some of the component factors. These solutions verified the correctness of C_a and the principle of the osculating circle.

Tables 1 and 2 conflict with the foregoing in two ways. First, the final value of C_a in both directions is 10 times (for example, 3.75′ rather than 0.38′) the value given by the formulas verified as indicated above and which have long been applied satisfactorily. Second, the intermediate corrections are not the same in both directions as they should be. The first difference possibly is the result of a misplaced decimal point. The second is more difficult to explain, but perhaps somewhere a mistake was made in combining terms.

It is hardly appropriate herein to discuss the mode of operation, and only a few comments will be included. The rate of change of the degree of curve of the spiral is the sole parameter that fixes the spiral and it is constant for a given spiral. If it had been used throughout in conjunction with the distances, if the complicating term, K, had been omitted, and if the extra work of reducing other factors to angles had been discarded, the derivations would have been simpler and the final formulas would have been both simpler and fully applicable to any point and to any distance. For a particular problem, L_a would then have been merely a specific case of l, and "abbreviated spirals" would not exist.

The derivation of C_b apparently is in error because of a basic misapplication of the geometry of the problem with consequent incorrect procedures. The specific item that causes the difficulty is the false assumption that $\alpha + \beta = \Delta_1 + \Delta_2$. This equality is the conventional approximation commonly used in practice and is not a geometric fact. The assumption that $\beta = \Delta_2$ and $\alpha = \Delta_1$ does not come from the "theory of the osculating circle" as stated by Mr. Hartman. It is merely the use of the common assumption in practice that the spiral is bisected by its offset, which is not mathematically exact.

The problem is to determine the effect of a spiral on a proposed layout, not the effect of an assumed layout on a spiral. The spiral is a fixed item. The proper position of the spiral (Fig. 2(*a*)) is with its offset, CD, on the line of compounding as designated by the general curve plan. The position of CD within the spiral is fixed by arc C′B = $\tfrac{1}{2} L_a$, which establishes the position of B with respect to the line of compounding. Therefore, $\beta = \Delta_2$ is a condition precedent to the correct solution of the problem, when only Δ_1 is subject to change.

At the other end of the spiral, AC′ is the length of the compound spiral from the line of compounding and is equal to $\tfrac{1}{2} L_s - C_t$, in which C_t is the "tangent correction" of the simple spiral which now, under the principle of the osculating circle, is to be measured on the D_1-circle. Reducing C_t to a central angle of D_1 gives an angular correction, C_a, to be added to the central angle of D_1 and subtracted from Δ_1. This is the only correction involved. Therefore, this and the preceding paragraph give the complete and correct solution of the whole problem.

Inasmuch as C_p is merely a by-product of the incorrect derivation of C_b it does not exist. The offset p is purely a function of the spiral. It is used in computing the tangent distances of the entire spiraled curve between the primary tangents; hence, any distortion would affect the accuracy of the entire layout.

In the paper, the example of a 400-ft spiral connecting a 10° circle with a 20° circle gives a value of C_b as approximately 10′. Reducing this to arcs of D_1 and D_2, the distances are 1.66 ft and 0.83 ft. The effects are that A is moved forward 1.66 ft to 198.34 ft from C′, whereas B is moved forward only 0.83 ft to maintain the correct length of spiral. The result is that the spiral as a whole is moved forward, and the offset is located 0.83 ft from the established line of compounding. The direct solution of C_t from its own formula gives 0.82 ft. Thus, the correct position of A is 199.18 from C' which puts the offset on the line of compounding and leaves B at the proper distance of 200.00 from C′. The tangent correction, C_t, reduced to terms of D_1 is 4.7′, or somewhat less than half of C_b as given. The correction found from Fig. 4, $C_p = -0.14$, simply does not exist because the geometry of the spiral requires p to be 11.58.

The suggestions concerning running half of a compound spiral from each end are not good. Point A is located from D_1 and B, from D_2. Therefore, each is subject to the field errors of the surveys leading up to it. If half the spiral is run from each, the combined field errors, or the total field error for the whole layout, would be concentrated at the middle of the spiral where it is difficult and undesirable to adjust the errors because of the changing curvature. The spiral should be run entirely from one end which will concentrate the errors at a junction with a circle, and the errors can easily be run out on the circle and at a uniform rate.

As a whole, this situation is largely "a tempest in a teapot." In the vast majority of cases the "errors" are so small as to be negligible. Even when they are of some apparent magnitude, the over-all effects are peculiarly insignificant. Small longitudinal changes have no effect on the lateral placement and appear only in the field errors of closure. Small errors in deflection angle are corrected for direction in the orientation at the new setup, hence their greatest possible fault is to cause a very small lateral displacement of the circular curve which would be lost in the normal field errors of the whole survey.

To a would-be user, the obviously cumbersome and complicated formulas of the paper are discouraging. An engineer with experience in laying out spirals would doubtless discard them because they are not in workable form. They have been carried to more terms than are reasonable and left without clarification as to practical use.

Allen H. Brownfield,[8] A.M. ASCE.—The writer found the paper very interesting. The purpose of this discussion is to offer additional data for the computer who wishes to lay out a true spiral and not to examine the present-day use of spirals or their desirable properties.

---

[8] Superv. Structural Engr., State Div. of Architecture, Sacramento, Calif.

This problem of connecting circular curves has been examined by C. L. Crandall,[9] and D. E. Hughes.[10] The writer[11] also gave a reasonably exact traverse of the Euler spiral that can be used for checking the author's method when R_2 becomes unusually short (for $D_2 = 20°$ and based on a 100-ft arc, $R_2 = 286.479$ ft).

Mr. Crandall has developed[9] a general expression for $\tan \phi_a$ using the rectangular system of coordinates, and he presented several tables for obtaining correct deflection angles at specific points along the spiral. Mr. Hughes derived a rigorous solution for the particular case in which one is given R_1, R_2, and p_a in which $p_a > 0$ and $R_1 > R_2$. Mr. Hughes derived θ_2 from a series based on the ratio of R_1 to R_2. Because the use of this series is tedious, he developed a correction table based on $R_1 L_1 = R_2 L_2 = k$ (a constant) for each particular spiral and the trial arc length (omitting the fractional terms of θ_3 after the first as given in Eq. 36). It should be noted that the intrinsic equation of the Euler spiral is $L_s = 2 R_s \theta_s$ and this then applies to any part of a simple spiral which includes the origin.

While working on the alinement for rails on the San Francisco-Oakland Bay Bridge in 1937 (San Francisco, Calif.), the writer found only one type of spiral problem that did not lend itself to a reasonably exact solution—the one indicated by Mr. Hughes. For this case a fairly accurate solution was developed, based on

$$R_3 = \frac{R_1 R_2}{R_1 - R_2} \quad \text{......................} (35)$$

in which R_3 is defined in Eq. 37 and is the terminal radius of a simple spiral having an arc length of L_a. Letting $n = 6\, p_a/R_3$, then

$$\theta_3 = \sqrt{n + \frac{n^2}{28} + \frac{29\, n^3}{16{,}170} + \frac{1{,}391\, n^4}{13{,}582{,}800} + \cdots} \quad \text{..........} (36)$$

This material was not submitted for publication in the previously cited discussion[11] because (*a*) it is not exact, (*b*) it is needed only for the solution of the problem noted by Mr. Hartman, and (*c*) the table developed by Mr. Hughes was available. This type of solution is pertinent to the author's paper because it is not clear how he would solve this particular problem, the problem in which one is given R_1, R_2, and p_a only.

If an arc length L_a is taken as 400 ft (Table 1), the curve can be rigorously computed by the method suggested by the writer[12] in conjunction with any one of several published tables of spiral functions. The deflection angles can then be computed using the author's methods or by traversing the spiral. It should be noted that there is a change in subscript for the radii of Mr. Hartman's paper from that used in the discussion by the writer.[11]

---

[9] "The Transition Curve by Offsets and by Deflections Angles," by C. L. Crandall, John Wiley & Sons, Inc., New York, N. Y., 1899, p. 7.

[10] "The Sickle; or, The Ideal Railway and Highway Transition Curve," by D. E. Hughes, a paper filed in the Engineering Societies' Library, 29 W. 39th St., New York, N. Y., 1941.

[11] Discussion by Allen H. Brownfield of "Mathematical Examination of the Highway Transition Spiral," by John Oran Eichler and Howard W. Eves, *Transactions*, ASCE, Vol. 111, 1946, p. 986.

[12] *Ibid.*, p. 988, Eqs. 56*a*, 56*b*, 56*c*, 58, 59*a*, 59*b*, and 60.

To illustrate the problem, one is given $p_a = 11.444$ ft, $R_1 = 572.958$ ft, and $R_2 = 286.479$ ft and one is asked to find the length of a Euler spiral arc required to join curves. Incidentally, the given value of p_a is the minimum for the particular curve and radii. Also, this example does not fit the usual spiral tables because it involves short radii and large angles.

Using Eq. 35, $R_3 = 572.958$ and by Eq. 36, $\theta_3 = 0.3469255$ (radian)—

$$L_a = L_2 - L_1 = 2\,R_3\,\theta_3 \ldots\ldots\ldots\ldots\ldots\ldots (37)$$

TABLE 4.—SPIRAL TRAVERSE (PROBLEM FROM TABLE 1)

Sta.	θ_s	θ_c	Chord correction	Chord	α_c	X (657.496 ft)	Y (323.597 ft)
14+00	80.0°					657.495 ft	323.598 ft
		7.8°	0.031 ft	39.969 ft	76.067°		
13+60	72.2°					647.871 ft	284.805 ft
		7.4°	0.028 ft	39.972 ft	68.467°		
13+20	64.8°					633.199 ft	247.623 ft
		7.0°	0.025 ft	39.975 ft	61.267°		
12+80	57.8°					613.982 ft	212.570 ft
		6.6°	0.022 ft	39.978 ft	54.467°		
12+40	51.2°					590.748 ft	180.037 ft
		6.2°	0.020 ft	39.980 ft	48.067°		
12+00	45.0°					564.031 ft	150.294 ft
		5.8°	0.017 ft	39.983 ft	42.067°		
11+60	39.2°					534.349 ft	123.506 ft
		5.4°	0.015 ft	39.985 ft	36.467°		
11+20	33.8°					502.193 ft	99.740 ft
		5.0°	0.013 ft	39.987 ft	31.267°		
10+80	28.8°					468.014 ft	78.986 ft
		4.6°	0.010 ft	39.990 ft	26.467°		
10+40	24.2°					432.215 ft	61.163 ft
		4.2°	0.009 ft	39.991 ft	22.067°		
10+00	20.0°					395.154 ft	46.139 ft

in which $L_2 - L_1 = 397.547$ ft. This is an approximate length and is always short because Eq. 36 was derived for a spiral starting at the origin. For the more usual problem this first computed value of L_a will be sufficiently accurate:

$$L_2 = \frac{R_1\,L_a}{R_1 - R_2} = 795.094 \text{ ft} \ldots\ldots\ldots\ldots\ldots (38)$$

$$L_1 = \frac{R_2\,L_a}{R_1 - R_2} = 397.547 \text{ ft} \ldots\ldots\ldots\ldots\ldots (39)$$

$$L_2 - L_1 = 2\,R_3\,\theta_3 = 2\,R_c\,\theta_c \ldots\ldots\ldots\ldots\ldots\ldots (40)$$

$$R_c = \frac{R_1\,R_2}{R_1 + R_2} \ldots\ldots\ldots\ldots\ldots\ldots\ldots\ldots (41)$$

From this $R_c = 190.986$ ft, $\theta_3 = 19.877°$,

$$\theta_c = \frac{R_3}{R_c}\,\theta_3 = 59.632° \ldots\ldots\ldots\ldots\ldots\ldots (42)$$

The total spiral angle is $\theta_3 + \theta_c = 79.509°$. Now this can be corrected by trial and error, by Mr. Hughes' table or by the author's Fig. 4, using $\theta_a = 19.9°$ and $\Delta_2 = 39.75°$. Then $C_p = 0.355 \times 0.397547 = 0.141$ ft. Thus, the correct value of $p_a = 11.444 + 0.141 = 11.585$ ft. If this value is substituted in Eq. 36, $L_a = 400$ ft and $\theta_3 = 20°$.

The traversing of the spiral in Table 4 is quite simple and accurate by the writer's method, as will be demonstrated. The computer should be equipped with a calculating machine, a slide rule, the tables of squares of Peter Barlow[13] and the 7-place trigonometrical functions (to 0.001°) as compiled by J. Peters.[14] He should also be aware that, for a column of numbers such as $k\,\theta^2$, the second differences are constant for equal intervals of θ, enabling him to set up the traverse (values of θ and α_c) by addition.

From an equation by the writer,[15]

$$C_e \approx 4\,R_e \sin\frac{\theta_e}{2} \ldots\ldots\ldots\ldots\ldots\ldots\ldots\ldots \text{(43)}$$

in which C_e is the chord length for a short piece of arc.

$$C_e \approx L_a - L_a\frac{\theta^2{}_e}{24} \ldots\ldots\ldots\ldots\ldots\ldots\ldots\ldots \text{(44)}$$

In Table 4, $L_a = 40$ ft and the correction to L_a is $-\,L_a\,(\theta^2{}_c/24) = -\,40/24\,(\theta_c)^2\,(\pi/180)^2 = -\,0.0005077\,(\theta_c)^2$

$$\alpha_c = \frac{\theta_1 + \sqrt{\theta_1\,\theta_2} + \theta_2}{3} = \frac{\theta_1 + 4\,\theta_m + \theta_2}{6} = \text{chord slope} \ldots\ldots \text{(45)}$$

in which θ_m is the total spiral angle at the mid-arc point.

$$L_m = \frac{L_1 + L_2}{2} = 4\,R_c\,\theta_m \ldots\ldots\ldots\ldots\ldots\ldots \text{(46)}$$

The sines and cosines were used directly from the tables and will not be included in the traverse.

Now for the particular spiral,

$D_1 = 10°$ $\qquad D_2 = 20°$
$R_1 = 572.958$ ft $\qquad R_2 = 286.479$ ft
$\theta_1 = 20°$ $\qquad \theta_2 = 80°$
$X_1 = 395.154$ ft $\qquad X_2 = 657.496$ ft
$Y_1 = 46.139$ ft $\qquad Y_2 = 323.597$ ft
$S_1 = 400$ ft $\qquad S_2 = 800$ ft

From the traverse,

$$\tan\alpha_c = \frac{Y_2 - Y_1}{X_2 - X_1} = \frac{277.459}{262.341} = 1.0576273$$

$$\begin{aligned} \alpha_c &= 46°\,36'\,15'' \\ \theta_1 &= 20° \\ \phi_a &= 26°\,36'\,15'' \end{aligned}$$

---

[13] "Tables of Squares, Cubes, Square Roots, Cube Roots and Reciprocals of all Integer Numbers up to 10,000," by Peter Barlow, L. J. Comrie, London, 1930.

[14] "Seven-place Values of Trigonometric Functions for Every Thousandth of a Degree," compiled by J. Peters, D. Van Nostrand Co., Inc., New York, N. Y., 1942.

[15] Discussion by Allen H. Brownfield of "Mathematical Examination of the Highway Transition Spiral," by John Oran Eichler and Howard W. Eves, *Transactions*, ASCE, Vol. 111, 1946, p. 989, Eq. 61*a*.

This value checks Table 4. Eq. 45 will give nearly correct values for α_c up to $L_a = 200$ ft for this particular spiral.

In Table 4 the starting values, X_1 and Y_1, at Sta. 10 + 00 could have been any values. The closure, Sta. 14 + 00, is very good in this case, being 0.001′ for both X_2 and Y_2. If a few engineers find the writer's data useful, he will feel justified in assembling them.

PAUL HARTMAN,[16] M. ASCE.—The able discussion of Mr. Brownfield is a valuable addition to the paper. The writer is particularly indebted to him for the completely independent traverse check of the spiral of Table 1; the work involved is extensive.

It is apparent that the complicated derivations of the paper have tended to obscure the simplicity of the proposed method of spiral layout. This method differs from that of the theory of the osculating circle only in the application of three corrections to elements of the compound spiral as computed according to the theory. The corrections are: (1) C_b, obtained from Fig. 3, which is added to Δ_2 and subtracted from Δ_1; (2) C_p, obtained from Fig. 4, which is subtracted from the offset, p, of the equivalent spiral to obtain p_a; and (3) C_a, obtained from Fig. 5, and added to the nominal deflection angle to the far end of the spiral when the setup is on the sharper circular arc and subtracted when the setup is on the flatter circular arc. Each correction is obtained by entering its graph with the values of Δ_2 and θ_a.

No corrections need be applied to deflection angles to intermediate points on the spiral provided not more than half the length of the spiral is set from one end. To lay the spiral out from each end it is necessary to establish one end of the spiral from the other by tangent distance and offset or by deflection angle and long chord. Either set of values may be obtained by traversing along the radii of the compound spiral.

Mr. Brownfield discusses the solution of the particular case when R_1, R_2, and p_a are fixed. With R_1 and R_2 fixed, p_a is a function of L_a. The most practical solution would be to assume various values of L_a and compute the corresponding values of p_a. A simple plot of L_a versus p_a would serve to determine L_a with any desired precision. However, it would seem more practical to fix L_a rather than p_a and thus avoid using an odd value of L_a which would complicate computation and layout work.

Messrs. Hickerson and Wiley contend that the error in locating the end point of a compound spiral laid out by conventional methods will be small and may be lumped with the field closure. They apparently overlooked the fact that the spiral so laid out deviates from the correct spiral at a rate which varies approximately as the fifth power of the distance (measured along the arc) from the transit setup.

The effect of this deviation on curvature may be significant as shown by comparing the correct spiral of Table 1 with a similar spiral laid out in accordance with the theory of the osculating circle. The deviations at the fifth, sixth, seventh, eighth, ninth, and tenth points are (in feet) 0.01, 0.02, 0.06,

---

[16] Associate Prof. of Civ. Eng., The City College of New York, New York, N. Y.

0.11, 0.22, and 0.40, respectively. The difference in successive deviations is a direct measure of the difference in curvature of the two spirals.

The curvature of the nominal spiral in this case is approximately 21.3° at the point where it joins the 20° circular curve. This error would have been still larger if the twentieth points had been set. Such a layout defeats the purpose of the spiral by introducing a sudden change of curvature in what is intended to be an easement curve.

Mr. Wiley criticizes the idea of laying out the spiral from both ends because the field error would appear at the midpoint. However, because one end of the spiral is located with respect to the other end, as already indicated, the field error should be small. The resulting curve would be a far better easement curve than that run in from one end only, using deflection angles obtained from the theory of the osculating circle.

The paper presents a practical method for the precise layout of a compound spiral, which is essentially that of the theory of the osculating circle. The difference lies in the computation and application of corrections, a procedure which will not increase the time required for computation by more than ten minutes. The extra time is well spent because it gives meaning to field closures and results in a proper easement curve.

AMERICAN SOCIETY OF CIVIL ENGINEERS
Founded November 5, 1852

TRANSACTIONS

Paper No. 2868

RIGID CULVERTS UNDER HIGH OVERFILLS

By R. Robinson Rowe,[1] M. ASCE

Synopsis

Progressively higher standards for highway width, alinement, gradient, and durability have been a challenge to designers of cross-drainage facilities. Relatively cheaper earthwork favors heavy earth fills with long culverts rather than bridges. Extrapolation of practice used for low-fill culverts to high-fill requirements would have indicated long barrels of great unit cost. Adaptation of the overlying earth arch to relieve culverts of part of the load promised a substantial reduction in cost. Experimental at first, this practice has been justified by more than ten years of satisfactory performance. Review of experience disclosed occasional distress, which can be obviated by more careful attention to detail. In the paper there are summarized the progressive developments in design and the findings of a field review of performance, including suggestion for further development of the practice.

Introduction

Early in the twentieth century, few culverts were more than timber boxes just below an earth or gravel road, the exceptions being masonry arches of stone or brick. Rarely did spans exceed 12 ft or overfills, 5 ft; for a wider stream or deeper gulch, bridges were cheaper. For such overfills, standard construction practices prevailed, here designated as "Method A" for distinction with an improved "Method B" developed particularly for use with high fills.

Highways have progressed sensationally with the passing of time. Modern (1956) standards of alinement and gradient aided by heavier and more efficient earth-moving equipment have led to high embankments, many of them more than 100 ft and some approaching 200 ft. Culvert lengths have increased even more, relatively, because of precautionary terracing of the higher embankments, greater skew angles of highways with respect to lines of cross-drainage, and greater roadway widths.

Then, too, culverts became more desirable than bridges for such locations because the alternating of fills in gulches with cuts through adjacent spurs

---

Note.—Published, essentially as printed here, in October, 1955, as *Proceedings Paper 823*. Positions and titles given are those in effect when the paper was approved for publication in *Transactions*.

[1] Prin. Bridge Engr., California Div. of Highways, Sacramento, Calif.

balanced earthwork on a lower and more economical profile and facilitated construction operations. However, the culvert had to equal in permanence the alternative use of the bridge and exceed it, if possible, because of the impracticability of replacing a deficient culvert in a deep fill.

At first, it was expedient to design by adaptation of low-fill types to higher and higher limits simply by specifying greater strength for conduit walls (Fig. 1(*a*)). This practice limited pipe culverts to 40-ft fills, but cast-in-place boxes or arches could be designed for greater depths. Multiple-cell culverts (Fig. 1(*b*)) could be used if debris were light or controllable.

When simple modification became expensive, other expedients were often cheaper. On a steep mountain stream, the culvert could be run on a mild gradient in a side-hill location to a chute on the face of the downstream embankment, thereby greatly reducing maximum overfill and length of culvert. For crooked channels, a tunnel might be cut on a direct line through solid material.

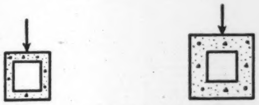

(*a*) HEAVIER SECTION

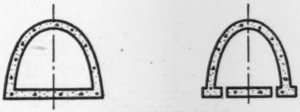

(*d*) FLOATING SLAB

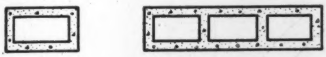

(*b*) MULTIPLE CELL

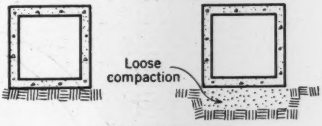

(*e*) YIELDING BASE

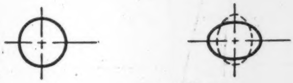

(*c*) STRUTTING

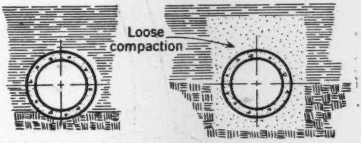

(*f*) LOOSE OVERFILL METHOD B

FIG. 1.—CULVERT SECTION UNDER FILL (SECTIONS FOR LOW FILL ON LEFT, FOR HIGH FILL ON RIGHT)

Because a tunnel lining is designed to meet the character of the soils surrounding it rather than the weight of soil above it, the principle was adaptable to culverts. For example, the fill could be built first and then tunneled for the culvert, or the fill could be built over arched falsework, leaving space for a future culvert. In either case, the embankment would become an earth arch on a large scale.

To avoid the expense of tunneling or falsework, an intermediate adaptation was developed to carry part of the load on an earth arch and part on the culvert structure. This could be done by building the culvert to yield as the fill was built over it, just as flexible culverts (Fig. 1 (*c*)) were cambered by struts during construction and yielded when the struts were removed. Rigid culverts (Figs. 1 (*d*), 1 (*e*), and 1 (*f*)) were built on yielding foundation or roofed with yielding overfill. To some degree, the tunnel analogy is applicable to such a method.

This paper is limited to rigid culverts, reporting (*a*) the standard designs adopted by the California Division of Highways for reinforced concrete arches, pipes, and boxes with the overfill limits applicable to each; (*b*) the observations of performance of typical installations; and (*c*) some conclusions on reliability of design, mistakes responsible for local overstress, and modifications of design and construction to avoid such mistakes.

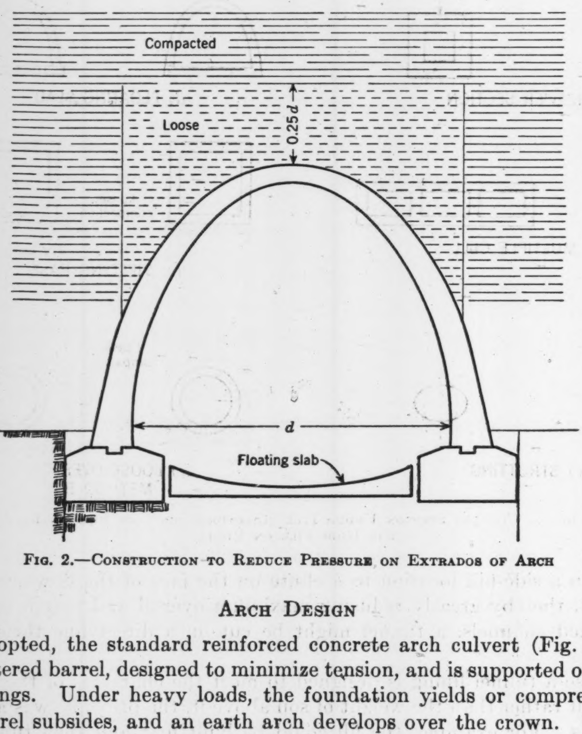

Fig. 2.—Construction to Reduce Pressure on Extrados of Arch

Arch Design

As adopted, the standard reinforced concrete arch culvert (Fig. 2) has a three-centered barrel, designed to minimize tension, and is supported on narrow wall footings. Under heavy loads, the foundation yields or compresses, the entire barrel subsides, and an earth arch develops over the crown. The wall footings are held apart by a floating invert slab. If subsidence of the arch transmits pressure under the invert slab, it moves upward to relieve the pressure.

Articulation is provided by building slab and footings continuous and the arch barrel in 30-ft segments. Struts are left to support the barrel until the overfill equals the span. The first overfill, up to 25% of the span (Fig. 2), is loosely compacted to provide an additional zone of yielding material.

The same geometric shape is used for spans, *d*, of from 6 ft to 22 ft (areas from 27 sq ft to 363 sq ft). Minimum overfill nominally equals the span, *d*, and maximum overfill is nominally 60 ft, but these limits can be exceeded by adding a relatively small percentage of reinforcement. A twin-arched culvert under a deep fill is shown in two stages in Fig. 3.

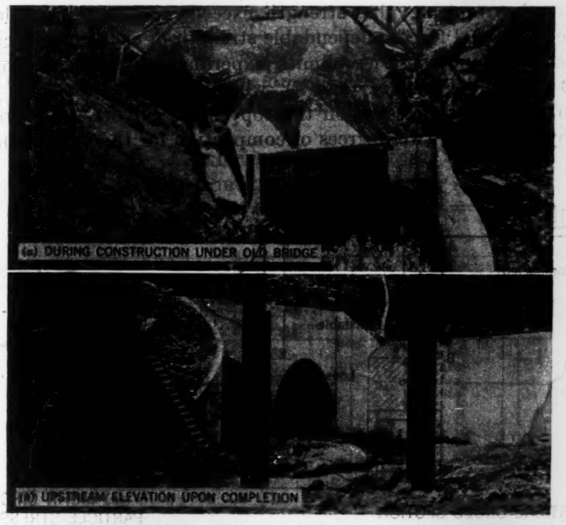
(a) DURING CONSTRUCTION UNDER OLD BRIDGE
(b) UPSTREAM ELEVATION UPON COMPLETION

Fig. 3.—Double 18-Ft Arch Culvert Under 70-Ft Fill

Pipe Practice

Rigid pipe for highway culverts is practically limited to reinforced concrete pipe. During the period of rapid increase in height of overfill and length of culvert, commercial prefabricated pipe was improving in quality and uniformity. Decentralization of centrifugal casting yards made it economical to use larger sizes because of reduced cost of haul to the site. Furthermore, the rapid increase in cost of field labor generally favored prefabrication.

Bedding practice received early attention. Four distinct combinations of bedding and backfill are influential in determining allowable overfill:

With unyielding foundation—no crown deflection, no bottom settlement—

Case I—Rigid culvert in trench
Case II—Rigid culvert under embankment

With yielding foundation—crown settlement equal to bottom settlement—

Case III—Rigid culvert in trench
Case IV—Rigid culvert under embankment

Of these, case III is most favorable and case II least favorable whereas cases I and IV are intermediate. Details are beyond the scope of this paper, except to report the objective of a uniformly yielding bed, often obtained by subexcavation and imported borrow. This practice is easier to inspect and control than a meticulous shaping of the bed to cradle the pipe fully.

Reappraisal of pipe strength was the second step in designing for higher overfills. Specifications for standard and extra-strength pipe govern the wall thickness, test strength of concrete, and percentage of reinforcement in such a way that the resulting pipe strength exceeds the test strength. Overfill limits were computed for the dependable strength of each commercial pipe.

For design beyond these new limits, experiments were begun in 1943 with Method B backfill (Figs. 2(*f*) and 4), which is an application of the tunnel analogy to reduce the pressure on the top of the culvert. This reduction is obtained by specifying two degrees of compaction for the embankment—loose compaction above the culvert for a height equal to the culvert span (or diameter), *d*, and dense compaction for the remainder of the section.

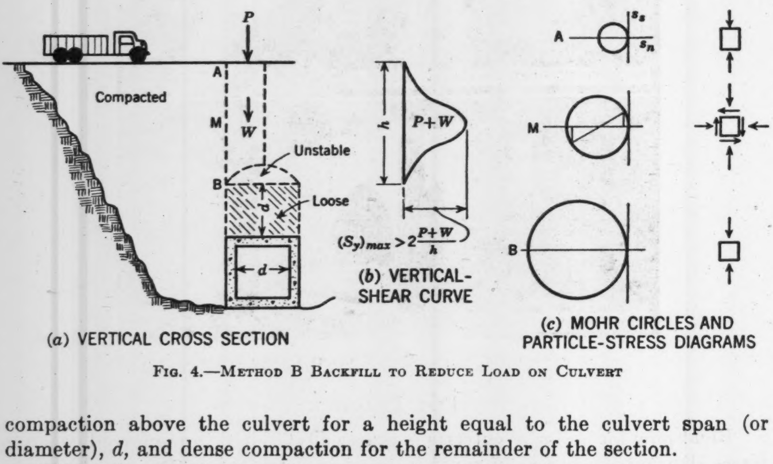

(*a*) VERTICAL CROSS SECTION

(*b*) VERTICAL-SHEAR CURVE

(*c*) MOHR CIRCLES AND PARTICLE-STRESS DIAGRAMS

FIG. 4.—METHOD B BACKFILL TO REDUCE LOAD ON CULVERT

The mechanics of reduced pressure can be visualized in several ways. From the tunnel analogy, the loose backfill and a small (unstable) segment of earth (Fig. 4(*a*)) become a part of a "tunnel," and the compacted zone above its intrados subsides just as the rock crown of a tunnel deflects when the supporting rock is removed. When the depth, *h*, is small, the earth structure is analogous to an arch, for which the zone of loose earth is the falsework which has been struck but not removed.

In Fig. 4, consistent units for measuring depths, weights, areas, length of section, and value of shear are understood. The subsidence of the compacted overfill, being greater than that of the compacted sidefill, develops vertical shear along the boundary. Along the haunch plane, AB, shear resistance should be adequate to support *W*, the weight of half the overfill, plus a live load, *P*. Hence, there must be a minimum depth, *h*, or the earth arch will fail in shear. The generalized shear-distribution curve (Fig. 4(*b*)) shows that maximum vertical shear, S_v, will exceed twice the average. This curve is based qualitatively on the Mohr circles for points A, M, and B (Fig. 4(*c*)) which show that shear must be zero at A and B where there is no horizontal compression.

After successful experience with this method, it became a standard alternative. Table 1, which has been abstracted from design tables, shows the limitation of the conventional Method A in comparison with Method B, and Fig. 5(*a*) is a guide to economy in its use. It should be understood that Method B is not a cheap expedient as it interferes with continuous operations in constructing large embankments with heavy machinery; Method A with extra-strength pipe is usually selected up to the limit for commercial pipe. Method B is used for overfills exceeding 60 ft for small pipe and 33 ft for large pipe up to the limits shown. Monolithic pipe has been designed for higher fills.

TABLE 1.—MAXIMUM OVERFILL FOR COMMERCIAL REINFORCED CONCRETE PIPE[a]

Diameter, in inches	Overfill, in Feet			
	Method A		Method B	
	Standard pipe	Special pipe	Standard pipe	Special pipe
12	36	62	Infinite	
24	27	51	Infinite	
36	25	52	Infinite	
48	23	53	Infinite	
60	23	48	32[b]	Infinite
72	23	45	28[b]	Infinite
84	23	37	27[b]	90
96	20	33		59
108	20	33		48

[a] "Special" commercial pipe is "standard" or "thick wall" with extra steel for specified D-load strength. The D-load is the three-edge test load per lineal foot of pipe divided by the inside diameter, *D*, at the appearance of a 0.01-in. crack. [b] Stronger pipe preferred under ordinary backfill.

BOX DESIGN

The reinforced concrete box has always been a popular design for culverts but its use lagged behind arches and pipe in adaptation to high overfills. Up to a practical limit, walls and slabs were made heavier. Next, working stresses were raised on the theory that dead loads do not need as large a safety factor as live loads. Finally, from the tunnel analogy, particular attention was given to bedding, and Method B backfill was specified as an alternative.

Box culverts ranging in size from 4 ft by 2 ft to 12 ft by 12 ft have been standardized with several strengths designed for each size, providing for each structural section an overfill limit for each of 4 combinations of bedding and backfill, one of which is equivalent to Method B backfill for rigid pipes. The upper limits of design with and without Method B are shown in Fig. 5(*b*). Using the 8-ft by 8-ft box with an area of 64 sq ft as an example, the strongest standard section would only support 22 ft of overfill (E), but the limit is extended to 32 ft by using Method B backfill or by building the box in a trench

(F). Further extension to 58 ft is possible by combining these two devices (G), but arch culverts would be used (H) for fills exceeding 58 ft. If natural ground is not satisfactory for ordinary entrenchment, an imperfect trench can be dug in a partly completed and well-compacted embankment.

In all extension of practice to high overfills, with either flexible or rigid culverts, it is important that there be uniform foundation under the bedding to avoid large differential settlement when the foundation is compressed by the heavy earth load. High fills require the use of long culverts, usually too long for the culvert to follow a sinuous channel. If the direct line and grade from channel intercepts on each side of the embankment resembled those shown in Fig. 6, uniform foundation can usually be obtained by (*a*) deflection of line to one side of the channel or (*b*) depression of grade below the natural bed of the stream.

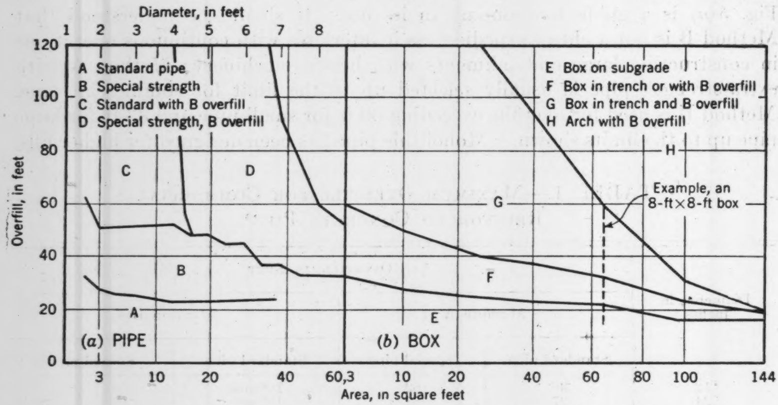

FIG. 5.—UPPER OVERFILL LIMITS, DESIGN OF REINFORCED CONCRETE CULVERTS

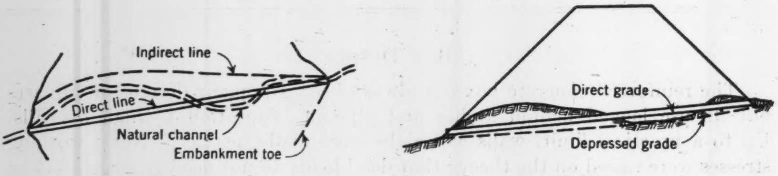

(*a*) PLAN (*b*) PROFILE.

FIG. 6.—INDIRECT LINE OR GRADE TO DEVELOP UNIFORM FOUNDATION

PERFORMANCE INSPECTION

In their early lives all the installations made on an experimental basis were periodically inspected. With few exceptions, the observations were favorable, the method was adopted for standard installations, and thereafter inspections were essentially limited to those required for maintenance. Large culverts classified as bridges were an exception; these were inspected regularly for structural deficiencies or distress.

In August, 1954, prompted by collateral interest of others, a joint review was made of rigid culverts under high overfills in the northern part of California. The results were so informative that the review was extended into southern California in November, 1954. Dozens of culverts were included. Most of the localities involved were in the coastal counties, extending from Mendocino in the north to San Diego in the south, in which the very first experiment was made with Method B in 1943.

Culverts selected for the review (Fig. 7) ranged from a 36-in. pipe under a 111-ft overfill to a 120-in. pipe under an 83-ft overfill. The largest section was a double 18-ft arch under a 70-ft fill. The longest was 1,400 ft of 60-in. reinforced concrete pipe under a 65-ft fill, of which the central 1,045 ft had been installed by Method B. In Fig. 7, below Curve I and above Curve II the limitations in the method of constructing overfill are obvious. Between the curves there may be a choice between Method B and Method A with stronger pipe.

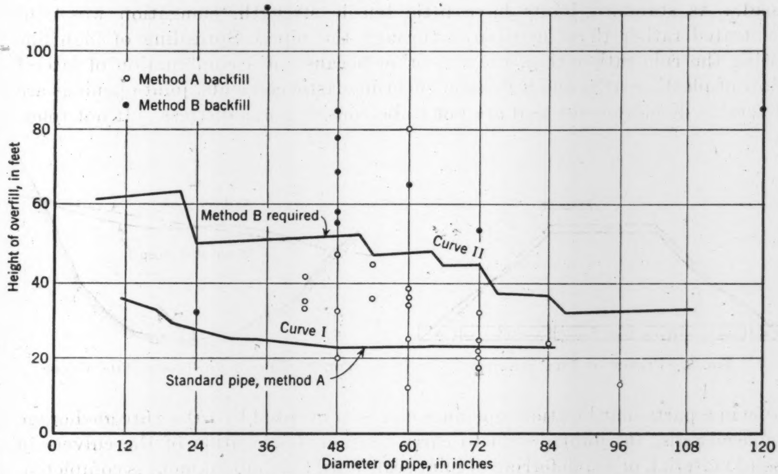

FIG. 7.—CULVERTS INVESTIGATED AND METHODS OF OVERFILLING

The review procedure was varied with the findings of a preliminary superficial examination. If there were signs of distress, measurements were made of visible evidence, such as cracking and joint separation. Where found, the position of the T marking the top of elliptically reinforced pipe was recorded. Photographs were taken of a few typical and of all extreme conditions. On the other hand, if there were no obvious signs of distress, the record was a qualitative appraisal of the average condition.

On the whole, the performance of all types of rigid culverts justified the adopted practice. Least distress was found in arches and one large monolithic pipe; the most was found in a box section. Installations using Method B were generally in excellent condition, independent of depth of overfill, but pipes installed under ordinary backfills were distressed somewhat in proportion to depth. In a few cases a long culvert would be found in excellent condition except for one or two signs of local distress; these were difficult to explain except as mistakes in construction and supervisory inspection. Where distress was uniform or consistent, the cause could be found. The principal causes will be examined in a concluding analysis.

By far the most common departure was the opened joint between pipe sections. Openings were largest near ends of culverts; this was ascribed to elongation of the culvert by spreading of the fill (Fig. 8) as it subsided under load. As standard joints have little tensile strength, elongation was concentrated rather than distributed through the pipe. Spreading of high fills being the rule rather than the exception because of a combination of lateral flow of plastic earths and a Poisson effect in elastic elements, joint openings are tolerable displacements and are not to be considered as distress. If not tolerable in a particular location, openings can be prevented by (*a*) secure anchorage of headwalls, (*b*) joint design to carry tension, (*c*) location of the culvert in solid material, or (*d*) deferring of joint seals until the embankment is completed. The latter remedy is preferred and it is believed that it should be standard practice for all large pipes.

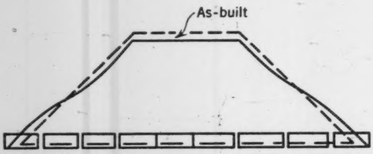

Fig. 8.—Effect of Fill Stretch

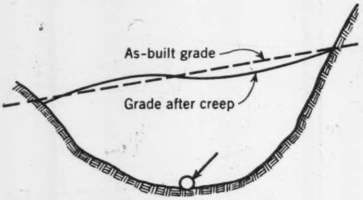

Fig. 9.—Effect of Plastic Fill Creep

Related to the spread of an embankment is the lengthwise creep of an embankment on a steep gradient (Fig. 9). Such an explanation seemed most logical for a longitudinal crack which appeared in the uphill side of two segments of an otherwise flawless culvert. Obviously, if the principal stress is deflected from the vertical by creep of the fill, maximum tension will not occur at the crown of the pipe but on the uphill side where tensile resistance is less in elliptically reinforced pipe. Although the single occurrence may not justify anxiety, this trouble could be remedied if inner and outer cages of circular reinforcement were specified for such pipes.

The most common departure after that of open joints was the longitudinal cracking of the crown of pipe, occasionally accompanied by corresponding cracks along the invert. Cracking to some degree in these locations is a normal expectancy because there tension is a maximum and the elongation of tensile reinforcement stretches the surrounding concrete beyond its low value in tension.

In the best pipes, the cracking should be distributed in fine hair lines, but any departure from homogeneity in concrete or bond concentrates the elongation in a single wide crack. This may not indicate greater distress than a manifold of hair cracks, but it can lead to real distress and ultimate failure if it admits corrosive air or water to the embedded steel. Hence, one remedy is to seal the cracks, particularly those on the invert, with a flexible adhesive crack filler or invert pavement. Prestressed pipe, of course, would probably not crack in this manner; if commercially available, it should be considered for difficult locations.

Causes and Relief of Distress

Perhaps all locations under high overfill should be considered difficult with the hazard generally proportional to the height, but there are other factors which increase the probability of distress for even moderate heights. Two, in particular, are plasticity of fill material and presence of ground water—the latter probably contributing to the former.

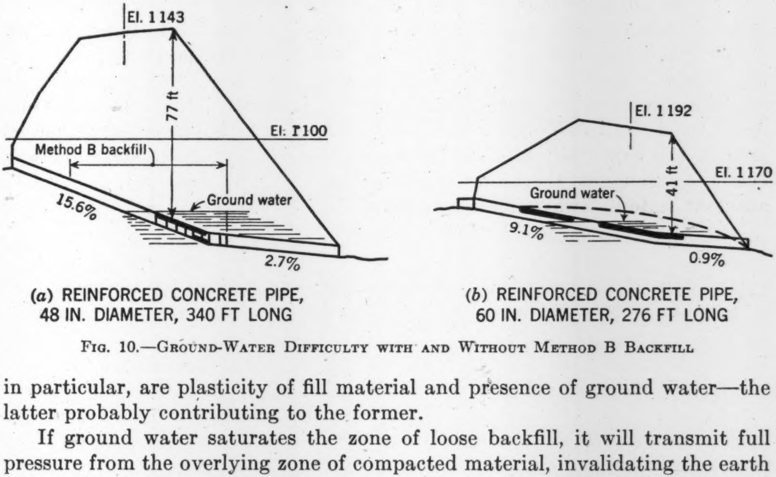

(*a*) REINFORCED CONCRETE PIPE, 48 IN. DIAMETER, 340 FT LONG

(*b*) REINFORCED CONCRETE PIPE, 60 IN. DIAMETER, 276 FT LONG

Fig. 10.—Ground-Water Difficulty with and Without Method B Backfill

If ground water saturates the zone of loose backfill, it will transmit full pressure from the overlying zone of compacted material, invalidating the earth arch and tunnel analogy. Two cases were observed where ground water was entering the pipe (Fig. 10) about 100 ft from the upper end; there was no unusual distress in the dry section, but cracks up to 0.09 in. appeared in the crown of the wet pipe. Distress was much greater in Fig. 10(*b*) with 41 ft of overfill placed by Method A than in Fig. 10(*a*) with 77 ft of overfill placed by Method B. Probably the saturated fill had become plastic, increasing the load on the pipe by unusual subsidence and a higher unit weight. Actually this possibility had been foreseen and underdrains were provided, but those had become clogged with sediment. The remedy may lie in perforation of the upper half of the culvert as a "safety valve" in case of failure of underdrains.

The severest trouble found in the investigations occurred in a 6-ft by 6-ft box culvert under a 63-ft overfill; this culvert had to be repaired. Measured deformation indicated further distress near the outfall where the fill was only from 18 ft to 35 ft. One 30-ft section between joints was deformed on both walls, and both slabs were deformed with shear offsets up to 5 in. The trouble was diagnosed as "hard foundation." This section had subsided much less than the adjoining sections. Method B backfill had been specified, but it is not a substitute for uniform bedding. The good condition of the box under the higher part of the overfill justified the basic design.

It was concluded from observation of performance that Method B backfill is correct in principle and practical in application to rigid culverts under high overfills but that inspection must be unusually alert because of the tremendous loads which may be shifted back to the structure by careless construction. In design it is important to foresee possible conflict between the principle of Method B backfill and the construction of large earth embankments and to consider the relative economy of a heavier structure installed by classical methods.

ACKNOWLEDGMENTS

The foregoing account of design and performance of rigid culverts under high overfills refers to practice of the California Division of Highways, but opinions and conclusions are those of the writer and not necessarily those of the division.

Aiding in the review were M. G. Spangler, M. ASCE, John G. Hendrickson, A.M. ASCE, and C. W. W. Abbott, A.M. ASCE. As bridge engineer, special studies, the writer serves under George T. McCoy, M. ASCE, state highway engineer and under the immediate direction of F. W. Panhorst, M. ASCE, assistant state highway engineer, bridges.

AMERICAN SOCIETY OF CIVIL ENGINEERS
Founded November 5, 1852
TRANSACTIONS

Paper No. 2869

GROUND-WATER DEVELOPMENT
A SYMPOSIUM

PAGE

Planned Utilization
By Robert O. Thomas, A.M. ASCE 422
With Discussion by Messrs. Harold E. Thomas, Frank B. Clendenen, and Robert O. Thomas 434

Irrigation Aspects
By Harris R. McDonald, A.M. ASCE 443

Basin Recharge
By Paul Baumann, M. ASCE 458
With Discussion by Messrs. Robert T. Knapp, Frederick L. Hotes, Norman H. Brooks, James A. Harder, Charles H. Lee, and Paul Baumann 474

Hydraulics of Wells
By Dean F. Peterson, Jr., M. ASCE 502

PLANNED UTILIZATION

BY ROBERT O. THOMAS,[1] A. M. ASCE

WITH DISCUSSION BY HAROLD E. THOMAS, FRANK B. CLENDENEN, AND ROBERT O. THOMAS

SYNOPSIS

There is reviewed herein the legal status of ground waters in California and the present (1955) development of ground-water supplies with particular reference to problems caused by haphazard development. An organization is recommended for the full beneficial control and use of available water supplies through the coordinated use of surface-water and ground-water storage capacity. The problems of such coordinated operation are examined, and an illustrative operational example of the benefits attributable to the planned utilization of underground storage is presented.

HISTORICAL SUMMARY

Legal principles applicable to rights in, control, and use of California ground waters are based almost entirely on the foundations established by court decisions. There was no mention of water rights in the 1849 constitution nor in legislation directly relating thereto prior to the codes adopted in 1872. At the first legislative session held in 1850, however, it was enacted that the common law of England, as developed by the courts of that country, would constitute the rule by which the California courts would be guided in their decisions in situations not otherwise provided for. Pursuant to that directive, the California courts, in the earliest cases, applied the English doctrine of absolute ownership of underlying ground water on the part of the owner of the overlying land. This was later overruled and another doctrine substituted in which various modifications of the "absolute ownership" theory were announced, many of the modified decisions being based on strained interpretations and definitions of physical facts and occurrences.

Historically, the courts have always attempted to differentiate between waters flowing in subterranean streams through "known and definite channels" and percolating waters. Those waters flowing in definite underground streams have been made subject to the same laws regarding rights of use as streams flowing on the surface. In making this distinction the courts have been at variance with the hydrologic principle which recognizes that all ground water (with minor exceptions such as unrecoverable soil moisture or waters in closed basins which are dissipated by excessive evapo-transpiration) constitutes a part of the general water supply and has a common ultimate disposal with surface streams by outflow to the ocean or other large body of water, becoming

---

NOTE.—Published, essentially as printed here, in June, 1955, as *Proceedings-Separate No. 706*. Positions and titles given are those in effect when the paper or discussion was approved for publication in *Transactions*.

[1] Senior Hydr. Engr., Div. of Water Resources, State of California, Sacramento, Calif.

indistinguishable from surface flows in the process. That is, all ground water eventually contributes to the maintenance of the surface supply.

In 1903 the California Supreme Court first definitely abrogated the English rule of absolute ownership in a leading case.[2] The principles enunciated therein and further developed in subsequent decisions have come to be known as the "doctrine of correlative rights" and are comparable in many respects to the riparian doctrine as applied to surface waters. The principle that all owners of overlying lands are entitled to the reasonable use of the waters occurring under the lands was established, with the further corollary that no owner was entitled, solely by virtue of the right of ownership, to injure other owners by unreasonable diversions for the purpose of "sale or carriage to distant lands." Many subsequent decisions amplified and extended this theory. In one[3] it was declared that, where the common supply was insufficient to provide for the needs of all users, those who had acquired prescriptive rights by use for a 5-yr period would, under the theory of "mutual prescription," be required to share equitably the burden of reducing the demand to the hydrologically determined safe yield. This decision was influenced by a stipulation, by all but one of the parties involved, which included a physical solution providing the necessary water supply to meet the needs of the water users.

Although the use of ground water in California has been one of the major factors contributing to the development of the state and the gross pumpage is estimated to be in excess of 10,000,000 acre-ft per yr (roughly 40% of the gross pumpage in the United States), there has been neither constitutional nor legislative control of the development of this basic resource except in minor instances such as control of unreasonable manner of use or wastage from wells tapping artesian supplies. Consequently, all disputes or differences of opinion regarding right and equities, based on the use of ground water, have been referred to the courts for decision—an expensive and time-consuming process definitely not contributing to the development of firm policies governing ground-water development. The principal beneficial result of such legal action is that it is possible to effect through the courts a determination of rights among all users of a common basin. However, such a procedure is usually initiated long after it is needed. It must be begun by one or more of the users and results in a decision which may be delayed until long after severe damage has been suffered by the basin. Such decisions relate only to the respective rights of each user and provide no method for instituting hydrologically feasible plans concerned with possible alteration of the regime of use within the basin. Also, they do not necessarily provide for the most economic and beneficial use of imported supplies.

There have been, however, two developments in California water law which appear to presage an awakening of the public consciousness to the desirability of establishing a program of maximum utilization for beneficial use of all the waters of the state—both surface and underground. The first was the passage, in 1928, of a constitutional amendment recognizing riparian rights but limiting them to reasonable use under reasonable methods of use. The amendment has been used by the courts to apply the reasonable-use doctrine to overlying users of a ground-water basin.

---

[2] Katz vs Walkinshaw, 141 Cal. 116.

[3] City of Pasadena vs City of Alhambra et al, 33 Cal. 2d 908.

The second development was the recognition by the courts that the storage of water underground for later withdrawal by the entity storing such waters was a beneficial operational use of such storage capacity. This principle was brought forth in a case[4] in which the points decided included the determination of the status of water imported by Los Angeles (Calif.) from a distant watershed, Owens Valley, and spread in the San Fernando Valley, either through sale of water for irrigation or other purposes, so that the water eventually found its way into an underground lake forming a part of the Los Angeles River. In due course it reached the diversion works by which the city takes water into its distribution system. The court declared that the city, in spreading water in the San Fernando Valley with the expectation that the water would in due time be recaptured, did not abandon the water nor was the water free to be taken by others, and that the city retained title to and could recapture the water.

Historically, progress in science has occurred far in advance of the acceptance and application of the physical theories involved in the determination of legal rights. The law, by its very nature, is conservative and rests to a large extent on precedents which were established, in many instances, long before the developments of scientific progress. Recently, the courts have shown an increasing awareness of the implication of physical and economic situations on the former implacable harshness of the legal nature of property rights. In a previously cited[3] case, it was stated:

> "Although the law at one time was otherwise, it is now clear that an overlying owner or any other person having a legal right to surface or ground water may take only such amount as he reasonably needs for beneficial purposes."

and

> "Public interest requires that there be the greatest number of beneficial uses which the supply can yield."

With reference to the 1928 constitutional amendment, the court[5] stated:

> "That the constitutional amendment now under consideration is a legitimate exercise of the police power of the state cannot be questioned. It is the highest and most solemn expression of the people of the state in behalf of the general welfare. The present and future well-being and prosperity of the state depend upon the conservation of its life-giving water."

It is evident that, with the legal basis for the acceptance of new and forward looking concepts for the conservation of the water resources of semiarid areas, legislation—which can be shown to be necessary for the greatest possible development of the available resources in order that the "greatest good for the greatest number" may be accomplished—can be adopted as a valid exercise of the police power and should be upheld by the courts. The surface storage and conservation of water is definitely limited in its application to the availability of suitable topographic sites, and the time is rapidly approaching when full control and use of the vast underground storage capacity will be required in order to provide the necessary water supplies for full development.

---

[4] City of Los Angeles vs City of Glendale, 23 Cal. 2d 68.

[5] Gin S. Chow vs City of Santa Barbara, 217 Cal. 673.

PRESENT STATUS OF DEVELOPMENT

At present (1955), utilization of underground storage capacity is principally confined to haphazard local development and individual or community use of the water thus made available. In a few instances, deliberate attempts to replenish the supply by other than natural cyclic means have been attempted with varying degrees of success.[6] In the usual case, the development is begun by the earliest pumpers, whose use of this resource is interfered with (in the course of time) by those who later tap the supply. Because the annual accretion to storage is limited to that which naturally percolates to the water table, supplemented by underflow into the basin from adjacent areas, it is evident that there is—considering the underground basin as a storage reservoir receiving variable annual accretions—a definite supply which can be withdrawn in uniform annual quantities without permanently exceeding the safe yield of the basin. Withdrawals in excess of that amount, occasioned by the growing demand for water, will result in overdevelopment of the basin, evidenced by progressive lowering of water levels over a long period of time and concurrent inability of the basin to return to a full reservoir status during the periods of above-normal surface supplies. When this occurs, legal action is necessary in order to establish the rights, expressed as annual withdrawals, for all users then pumping water from the basin. In a comprehensive adjudication it is evident that this procedure tends to inhibit all future use of the basin except by the parties to the original contest and those who derive their rights from such parties by sale or otherwise.

In general, such a procedure does not necessarily include a plan for the development and utilization of an imported supply. Under present (1955) law, it is difficult to make full use of the potential cyclic storage capacity and to increase the average annual quantity of water made available for future development. In California, the "court reference procedure," whereby such cases may be referred to the Division of Water Resources for determination of the physical facts and recommendation for solution, is utilized by the courts in many cases. The availability of supplemental or imported water supplies is considered in the investigation conducted by the division, and appropriate recommendations are made in the report rendered to the court. It is evident, however, that a feasible solution to the problem requires not only the determination of rights to water after an overdraft occurs but also legislation wherein provision is made for complete administrative and technical control of the basin for all purposes. Current (1955) proposals for administrative determination of rights to underground water, similar to the procedures which have been applied for many years to surface waters, would merely substitute an administrative agency for the courts, without change in the basic philosophy. Although time and expense to the water users might be saved by such procedures, no final solution to the over-all problem would be accomplished.

---

[6] "Ground Water Recharge," by Finley B. Laverty, *Journal*, A.W.W.A., Vol. 4, 1952, pp. 677–681.

The maximum development of the available water resources and the consequent economic development of the state can be realized only if the available ground-water storage capacity can be fully utilized for long-time holdover storage of surplus surface waters. Such planned utilization will enable full use of the possibilities inherent in the operation of the available reservoir space in the same manner and following the same general principles as in the operation of large surface reservoirs filling cyclic supply functions. The available capacity in underground reservoirs in California has been estimated to be in the order of 175,000,000 acre-ft, of which an estimated 133,000,000 acre-ft exist in the Central Valley. An intensive investigation of the storage capacity in the Sacramento Valley, a part of the Central Valley, has been made by the Geological Survey, United States Department of the Interior (USGS), and it has been determined that this valley contains approximately 34,000,000 acre-ft of storage capacity in the range of from 20 ft to 200 ft below ground surface. This capacity is, for all practicable purposes, largely unused at the present time (1955). The possibilities of large-scale conservation works, making use of the subsurface storage capacity in an area of surplus water supply, are almost unlimited. In addition to the conservation of surplus surface waters, the use of underground storage for the possible salvage of otherwise unusable waste waters from municipal and industrial developments is readily apparent. Such waters, of course, would have to be rendered suitable for admixture prior to being placed in storage in order that the quality of the underground waters would not be adversely affected.

Because planned utilization of the available underground storage capacity is inherent in a program of maximum conservation and use, it is evident that the retention of much of that part of the water supply which is presently wasted in outflow to the ocean and in excessive evaporation by phreatophytes will require the lowering of the water table during periods of less-than-average supply to a much greater extent than would otherwise occur in order to provide the storage capacity necessary for the maximum retention in the ensuing above-normal period. In such a program, the ground-water reservoir would be used for cyclic storage and would be operated in conjunction with surface reservoirs to provide a firm supply for both the overlying lands within the natural service area of the basin and for the exporting of surplus waters to areas of deficiency. Such an operation will undoubtedly require maximum artificial replenishment of ground water and the coordinate operation of surface reservoirs so as to make such recharge feasible. This will require over-all administrative control by an agency empowered to exercise jurisdiction between, as well as within, the geographical limits of the individual basins. With reference to water available for export, for example, it is actually unimportant whether the water is used to replenish a local basin and is later recovered and delivered to an area of deficiency or whether it is first exported to such an area and there stored underground for later use. The net result, or the net cost of the end product, should be approximately the same in both cases. Any plan for operation of underground storage which is approached from the purely local viewpoint will provide only temporary relief from periodic shortages and will eventually result in the waste of otherwise recoverable water to the detriment of areas in short supply.

A definite problem in the utilization of underground storage is the existence of present rights to water from such basins. If an attempt is made to coordinate the use of the storage capacity with the present pattern of withdrawals in a ground-water basin, there will be inevitable conflict between the holder of rights to pumpage and the operators of the basin for reservoir purposes. It is probable that no user will ever complain during periods when the water table is held at high levels and he consequently receives the benefit of lowered costs of pumping; however, when the basin is deliberately lowered in order to firm supplies during dry periods, the administrative agency responsible for such operation would be the target of innumerable lawsuits and injunctions by the local water users. It is therefore apparent that legislation which provides for the utilization of underground storage capacity must, of necessity, provide for appropriate adjustment with the owners of existing rights. Necessary water supplies will then be provided to the overlying service area by the agency operating the basin. A feasible method of evaluating the water right in such instances would be to establish the historical annual cost to the pumper and to subtract that cost from the proposed price at which a supply will be furnished for his lands; the difference can then be capitalized for an appropriate period—say, 50 yr—and the resulting amount can be termed the value of his right, for which he would receive compensation. Administrative difficulty, inherent in other proposed methods of control, would result if the operating agency computed the natural fluctuation occurring in the absence of planned utilization and compensated individual users for excess costs of pumping during periods of lowered water table. Such a system would equitably require that the user be charged an amount over and above his cost of pumping during periods of high water table.

Water-Control Agencies

It is evident from the foregoing that the enabling legislation permitting full utilization of ground-water storage capacity should provide for an organization with state-wide powers to control such usage. The usual type of public district organization, which in this case would deal only with individual ground-water basins or, at most, with entire stream basins, would not have the inherent authority to provide for the large-scale transfer of water supplies from areas of surplus to areas of deficiency. The limited organization, therefore, would not be able to accomplish the purposes for which the program was conceived and operated.

Enabling legislation designed to accomplish state-wide control of the ground-water storage capacity should provide for (*a*) the appointment or election of a governing board; (*b*) the purchase of, or other adjustment of conflicts with, existing water rights; (*c*) the conservation of the available supply through maximum use of underground storage; (*d*) the transportation of water supplies between stream basins; (*e*) the development and distribution of water to operating agencies for irrigation, municipal, and other uses; (*f*) the imposition of general taxation in order to share the burden of costly supplies, contributing to the general prosperity of the state, among those who ordinarily secure their water supplies by other means; (*g*) the artificial recharge of underground basins; (*h*) the treatment and conservation of waste waters; (*i*) the coordinated operation of surface reservoirs which are an integral part of the combined system; and (*j*) the issuance of either or both revenue and general taxation bonds to defray the capital investment of the operation.

Although the powers enumerated are far-reaching, anything less will inevitably fail to develop the available supplies to the maximum extent by means of planned operation of cyclic storage and redistribution of supplies on a state-wide basis from areas of surplus to those of deficiency. Above all, the water supply contributing to the development of the modern community must not be subject to intersectional jealousies or political expediency.

OPERATION OF UNDERGROUND STORAGE

The possibility of underground storage exists in any geological formation in which interstices are present; however, the particular storage capacity cited herein is that which exists in the broad alluvial valleys and coastal plains across which flow the major streams of California. Underground storage reservoirs are usually much larger in areal extent and have greater total storage capacity than available surface reservoir sites. Natural annual recharge, however, is usually much less in proportion to storage capacity than is the annual supply to surface reservoirs. Ground-water reservoirs may, in years of deficient surface supplies, be drawn down to the greatest practicable extent whereas surface storage, because of lesser capacity, has a definite limited annual ability to yield a water supply for beneficial use. Ground-water reservoirs serve frequently as regulators of stream flow, maintaining such flow over periods of deficient precipitation. In the operation of underground storage the average annual discharge may exceed the annual recharge for much longer periods than is possible with surface reservoirs, if the long-time average annual recharge and discharge are maintained in hydrologic equality.

The two principal types of ground-water reservoirs commonly found in alluvial formations are free ground-water reservoirs and artesian ground-water reservoirs. In a free ground-water reservoir the water table represents the upper surface of the reservoir; a change of storage is represented by a rise or fall of the water table and is equal to the product of the cubical contents of the material between the water table at the beginning and end of the period and the average specific yield of the material in which the change in storage occurs. Artesian ground-water reservoirs are reservoirs in which the water is confined under pressure and upon release will rise above the physical limits of the upper surface of the water in storage, and in which change in storage can occur only in the forebay area—a free ground-water reservoir at the head of the artesian area. In many artesian reservoirs, occasional changes will take place in the cubical capacity because of compression of the overlying impermeable strata. This change in capacity is relatively minor and is in reality a change in the transmission capacity of the reservoir rather than in the storage capacity. Storage in such an aquifer becomes important only after the forebay has been dewatered to the extent that the upper physical surface of the underground water becomes a free water table by receding from contact with the overlying confining strata. Change in storage capacity may occur in a free ground-water reservoir due to consolidation of the fill material, but available data on this aspect of loss of storage capacity do not provide a basis for its evaluation.

In order to perform a regulating function in the hydrologic cycle, a ground-water reservoir must maintain a constant cycle of recharge and discharge. In the natural state, and over a period of time during which the aggregate supply approaches the long-time mean, recharge and discharge are equal and no net change in storage occurs. In this process, a regular regimen is developed which is followed throughout a period of wet and dry years. During and following a period of above-normal supply, the water table rises, natural discharge is increased, and high water tables contribute to the disposal of surplus water by evaporation from moist areas and transpiration by phreatophytes. With a succession of below-normal seasons, the water table falls, the moist areas are dewatered, subsurface outflow is decreased, and phreatophytes wither as a result of the lack of adequate supply. This cycle of an alternately rising and falling water table is repeated interminably as time continues. Under active development, this regimen is affected by artificial extractions. In the early period of such development, water is actually mined from storage. That is, an excessive quantity is removed from storage in order to lower rapidly the water table to such an extent that the average annual recharge will not again raise the water table to an elevation where undue waste occurs. This excess removal of water in the early development period cannot be continued over a long-time period unless methods are found to increase the natural recharge to the extent necessary to maintain such withdrawals.

The planned utilization of underground storage must envision the lowering of the water table in the reservoir during a period of dry years and the subsequent recharge and storage of surplus flows during the ensuing wet period. Unless sufficient storage capacity is made available, a part of the surface supply during this period will be wasted; on the other hand, too great a lowering will result in the inability to recharge fully the basin because of the inadequacy of the available supply. Such loss of storage would occur in the zone closest to the ground surface where recovery costs are least. A concurrent problem, on which extensive research activities have been conducted, is the practicability of artificial recharge by the use of the surplus surface water available.[6,7] It is clear that the capacity of the underground reservoir to provide cyclic storage for the long-time average annual supply is solely dependent on the rate at which such surface supplies may be placed in storage in the underground basin. Present (1955) experimental projects concerned with inducing such artificial recharge are being conducted in many localities. These projects include experiments in the use of chemical additives and mechanical aids to maintain percolation rates[8] and in the use of recharge or injection wells. Significant contributions to ground water are also made by percolation from surface conduits, rivers, and streams, and deep percolation of water applied to lands for the irrigation of crops. Much interest has been aroused in the possibilities of recovering large quantities of otherwise waste water through reclamation or spreading of sewage.

---

[7] "Spreading Water for Storage Underground," by A. T. Mitchelson and Dean C. Muckel, *Technical Bulletin No. 578*, U.S. Dept. of Agriculture, Washington, D.C., 1937.

[8] "Some Factors Involved in Ground Water Replenishment," by R. S. Bliss and C. E. Johnson, *Transactions*, Am. Geophysical Union, Vol. 33, 1952, pp. 547–558.

A further operating problem arises in maintaining the water table at an elevation below the root zone of overlying vegetation and below the limits of capillary action in order to reduce the loss of storage due to excessive evapotranspiration. Other losses, principally those caused by water-loving vegetation and subsurface outflow from the basin, will occur, but these are also subject to a measure of control. Subsurface outflow is usually dependent on the elevation of the water table at a point some distance upstream or up-basin from the point of outflow, and such water may, in large measure, be salvaged for use as a part of the annual supply by a program of pumping from that part of the reservoir closest to the subsurface outlet. Much can be done in programming the extractive operations so that the maximum beneficial effect can be gained from the operation of the underground reservoir. The pattern of pumping should be planned to take the greatest advantage of the usable storage capacity and should be definitely related to the geologic structure of the basin, the areas of natural and artificial recharge, the transmissibility of the basin materials, the areas of use, the necessity and amount of drainage necessary for salt balance, and the desirability of controlling the subsurface outflow and effluent seepage from the basin.

The average annual firm supply which can be made available by operation of the underground reservoir will, to a large extent, be limited by (*a*) the rate of recharge, (*b*) the maximum economic cost of pumping, (*c*) the effect of the operation on the quality of the water supply, and (*d*) the sum of unavoidable losses. The effect of the cost of pumping would be greatest in irrigation developments, and the maximum permissible cost would be limited to the residual between income derived from irrigated crops and the total of all costs of production other than those attributable to water supply. In the case of municipal and industrial supplies, the cost of pumping would have less importance than other general economic factors—the desirability of continued full employment, the necessity of water for the purpose of maintaining life, and similar considerations—all having a decided bearing on the practicability of pumping water from great depths. The extent of works constructed to facilitate recharge will be determined by factors other than the cost of pumping because recharge at a rate in excess of that necessary to assure a full supply reservoir at the end of a wet period will result only in excessive loss through waterlogging of lower parts of the basin and uneconomic outflow.

Special operating problems will be evidenced in some basins due to local geographic and geologic factors as, for example, the problem of saline waters in many basins of California.[9] The prevention of sea-water intrusion is a continuing problem in coastal ground-water basins,[10] many of which have been drawn down to such an extent that sea water has penetrated into the aquifers with deleterious effect on the supply. Experiments in the prevention of such intrusion by operation of a line of coastal injection wells have been made by the Division of Water Resources and the Los Angeles County Flood Control

---

[9] "Water Quality Problems in California," by Harvey O. Banks and Jack H. Lawrence, *Transactions*, Am. Geophysical Union, Vol. 34, 1952, pp. 58–66.

[10] "Sea Water Intrusion into Ground Water Basins Bordering the California Coast and Inland Bays," by Harvey O. Banks, George B. Gleason, and Raymond C. Richter, *Report No. 1*, Water Pollution Investigations, Div. of Water Resources, State of California, Sacramento, Calif., 1950.

District,[11] and a research project covering the same general problem has been completed by the University of California,[12] at Berkeley.

Large parts of the Central Valley of California were formerly overlain by an arm of the ocean, and saline waters underlie the usable fresh waters. Excessive drawdown of the water table and heavy pumping rates have a tendency to cause these saline waters to rise in local areas and mix with the high quality waters in the upper zones. Other problems arise through intrusion of ground waters of inferior quality by lateral underflow when the free water table is lowered sufficiently to permit a differential head to occur. In pressure aquifers, problems arise as a result of downward infiltration of poor quality perched waters through defective wells when the underlying head is reduced through heavy pumping. It would appear that in large-scale operations many of these problems would not be confined to individual basins, and hence a multiplicity of ground-water basin districts concerned with the long-time cyclic management of the underground reservoirs would be unable to coordinate their operations to effect the best use of the available storage capacity.

ILLUSTRATIVE EXAMPLE

In order to emphasize the beneficial results of coordinated operation of surface and underground storage, an example of the utilization of a hypothetical underground basin is presented. The basin was operated in conjunction with surface storage over a 30-yr period, 1914–1915 to 1943–1944, using the full natural flow of the Tuolumne River, tributary to the Central Valley of California, as the assumed supply. Three studies, utilizing differing criteria, were made in order to derive comparative results. Basic assumptions used in all studies were:

Annual Demands

Irrigation	960,000	acre-ft, over a period of 7 months
Municipal	200,000	acre-ft, of which 42% occurred during the winter and 58% during the summer
Evaporation	50,000	acre-ft from the surface reservoir
Export	300,000	acre-ft constant flow
Total	1,510,000	acre-ft

Average annual supply	1,751,000 acre-ft
Dry period annual supply	1,550,000 acre-ft
Maximum surface reservoir	1,200,000 acre-ft
Maximum usable underground capacity	1,800,000 acre-ft
Surface minimum storage	50,000 acre-ft
Recharge capacity	45,000 acre-ft per month

---

[11] "Report on Tests for the Creation of Fresh Water Barriers to Prevent Salinity Intrusion Performed in West Coastal Basin, Los Angeles County," by Finley B. Laverty, L. W. Jordan, and H. A. van der Goot, Los Angeles County Flood Control Dist., Los Angeles, Calif., 1951.

[12] "Report on Sea Water Intrusion," by Thomas R. Simpson, James A. Harder, and Leung-ku Lau, San. Eng. Research Lab., Univ. of California, Berkeley, Calif., April, 1954.

It was assumed that subsurface outflow from the ground-water unit would occur at a maximum rate of 48,000 acre-ft per yr when the basin was at maximum capacity and would vary in a linear relationship with the storage.

In the first study (*a*) the surface reservoir was operated to supply the annual demand to the maximum extent possible and to furnish the water required for recharge to the underground basin; (*b*) deficiencies in surface supplies were augmented by withdrawals from underground storage; (*c*) the surface storage was depleted to the maximum extent annually; and (*d*) the ground-water storage was retained at maximum capacity for the greatest possible portion of the total time. The second study comprised the simultaneous recharge to and withdrawal from the ground-water basin in practically all years of the period in conjunction with partial supply of the annual demand from surface storage. It was found that the method of operation had little effect on the long-time results as long as the annual withdrawal from both surface and underground storage was held within reasonable limits. It was found that utilizing annual withdrawals from underground storage effected a slight reduction in the total loss due to subsurface outflow because of a somewhat lower average elevation of the water table. The third study, operating only the available surface storage, was made in order to determine the percentage of conservation of the total available supply which was obtained through the use of the underground storage capacity. It was found that the surface reservoir could supply only the local service area demand, amounting to 1,210,000 acre-ft per annum. Although some water could have been made available for export from surface storage alone during practically all years, it would have varied greatly in quantity and time of occurrence and excessively large transmission capacity would have been necessary in order to make the water available to the area of import. Also, operation of a ground-water reservoir in the area of import would have been necessary in order to reregulate the varying annual supply. When considering export supplies in the operation of coordinated ground and surface storage, it is unimportant from an engineering standpoint whether the supply is first used to charge a basin in the local area and later pumped and forwarded to the area of use or whether the supply is first exported and there regulated by underground storage. The economics of transmission will probably define the most feasible solution. The results of the three studies are set forth in Table 1. Demands were met in all years, except 1934, in operational studies 1 and 2, and

TABLE 1.—OPERATIONAL STUDIES

Item	OPERATIONAL STUDY		
	1	2	3
Storage			
Beginning of period, in 10^3 acre-ft	50	50	50
End of period, in 10^3 acre-ft	2,375	2,387	848
Annual yield, in 10^3 acre-ft	1,510	1,510	1,210
Total spill, in 10^3 acre-ft	4,325	4,335	15,512
Subsurface outflow, in 10^3 acre-ft	1,068	988	
Deficiency in one year, in 10^3 acre-ft	485	426	79
In percentage of demand	32.1	28.2	6.5
Conservation, in percentage of total water available	89.8	89.9	70.5

in 1931 in study 3. It will be noted that the deficiency in study 3 refers only to the reduced annual demand of 1,210,000 acre-ft.

The important fact illustrated by Table 1 is the tremendous increase in conservation of the available supply which is creditable to the operation of the ground-water storage capacity. It will also be noted that, in operational study 2, it was possible to meet total demands with a lesser deficiency even during the year of exhaustion of supply during the dry period from 1923–1924 to 1934–1935.

CONCLUSIONS

Control and conservation of available water supplies through development of surface storage are limited by the availability of suitable reservoir sites. Future large-scale development of necessary water supplies for beneficial uses will, in many cases, require complete control and utilization of the vast underground storage capacity.

Governmental agencies created to implement such water-supply developments should exercise adequate geographic control, including both areas of surplus and areas of deficiency. The inherent powers of such agencies should provide for large-scale transfers of required water supplies.

Planned utilization of underground storage, involving the lowering of the water table by increased draft during dry periods and the subsequent recharge and storage of surplus flows during wet periods, will create an array of new operational, hydrologic, economic, and financial problems.

It is indicated that a considerable increase in the conservation of water supplies may be obtained through conjunctive operation of surface and underground storage. This will permit an expansion of the general economic development, particularly in the semiarid areas subject to extreme fluctuations in the occurrence of available water supplies.

ACKNOWLEDGMENT

Much of the subject matter contained herein has been expressed in similar ways by many others to whom the writer is indebted for basic concepts. It is particularly desired to state that the opinions and conclusions expressed herein are solely those of the writer and do not represent the policies of the Division of Water Resources of California.

DISCUSSION

Harold E. Thomas.[13]—Although the paper is based largely on experiences in California, it has broad applicability to ground-water problems in many other states. As an example, the section entitled "Operation of Underground Storage" is an inclusive and yet concise statement of the complexities involved in operating California's ground-water reservoirs for maximum benefit to the greatest number of people. However, it is equally applicable to the broad, alluvium-filled, intermontane valleys of other western states. With only slight modifications it is also applicable to the gravel-and-sand aquifers of the great plains, the Atlantic and Gulf coastal plains, and the glaciated parts of the United States. Much of the information is basic to the operation of all ground-water reservoirs, large or small, in consolidated or unconsolidated rocks.

Under the heading, "Present Status of Development," Mr. Thomas presents a picture of haphazard local development—from the drilling of the first wells to interference by later users, and ultimately to overdevelopment—that also applies to many ground-water reservoirs in other states. However, California has gone further than have most states in the creation of ground-water problems and in the solution of some of them. This is to be expected in a state where the annual pumpage from wells is estimated to be 40% of the nation's total. Because California has only 5% of the area of the United States and 8% of its population, it is obvious that the state is far beyond the national average in development and use of ground water. In assuming leadership in this field, California has inevitably pioneered many aspects of ground-water development as well as regulation of that development. Thus, in many respects it can serve as an experimental laboratory for other states.

California has also served as an experimental laboratory for the development and application of legal doctrines pertaining to ground water. Mr. Thomas mentions the state's early adherence to the English doctrine of unlimited use, its development of the doctrine of correlative rights, the adherence of its state water code to the doctrine of reasonable use, and the recently developed doctrine of mutual prescription. The doctrine of appropriation is also recognized in California, as it is to a greater or lesser extent in all western states. It originated in the customs of California miners of 1849 and was accepted by the California Supreme Court as early as 1855. Finally, despite all these doctrines, or perhaps because of their diversity, there have been opportunities for unbridled competition for ground water, with the result that several basins have been overdeveloped. Specific instances of this have been acclaimed as good economic measures by experts on the basis that because of them California's largest cities were able to grow large enough and wealthy enough to finance the importing of water from remote sources.

The current (1955) haphazard patterns of ground-water development in all parts of the United States are similar in many respects to the early stages of development of many mineral resources. In 1849, in California, uncoordinated individual efforts, conflicting claims, and general confusion were the rule, but as gold mining became more difficult and expensive these difficulties gave way to consolidation of interests and technically supervised operations. The early development of oil fields by intense competition among individual landowners has similarly been generally replaced by unitization and scientific extraction from petroleum reservoirs.

---

[13] Staff Geologist, Ground Water Branch, Geological Survey, U. S. Dept. of the Interior, Salt Lake City, Utah.

Water is in significant contrast to these mineral resources in at least one respect, however. Gold, petroleum, and uranium are so rare that most persons have long since given up hope of ever owning property that contains such resources in profitable amounts. Fresh water, however, is common on the land masses of the earth. The populous regions, in particular, are sufficiently well watered by precipitation to make men feel that they have a right to it—at least enough for their reasonable needs. Unfortunately, the arid and semiarid regions—which embrace most of the western states—do not receive enough precipitation for the reasonable needs of agriculture or of other activities that the broad expanse of land might otherwise support. Water rights, therefore, involving the adaptation of the limited water supplies to the far more abundant land resources, have always been of major concern in western states. As Mr. Thomas notes, they will become a real problem in any effort to achieve maximum utilization of underground storage.

Part of the water-rights problem is the lack of clear definition as to what a right involves, or definitions that are inadequate or unworkable in the light of the knowledge of hydrology. For example, many well owners consider that their water right includes a right to a certain pressure head in flowing wells or to a specific static level in pumped wells, and this contention is supported by court decisions in some states. However, by such interpretation it would be impossible to achieve full development of a ground-water reservoir for beneficial use, or a firm sustained yield in the case of varying inflow to a ground-water reservoir. On the other hand, a significant lowering of water level is likely to put a well owner to considerable expense in deepening his well or enlarging it, or in purchasing new pumping equipment. Thus, society, by its increasing development of water supplies, may increase the cost of water to existing users and be put in conflict with the interests of those individuals.

Many water-rights difficulties arise because water rights are considered as personal property, and people commonly form a strong attachment for personal property. It might be possible for most people to drop this emotional attitude if they could delegate the responsibility for providing an assured satisfactory supply of water at reasonable cost. This has already occurred in most metropolitan areas for industrial, commercial, and residential users alike. Water is one of the utilities, like electricity or gas, and is furnished by a unit that specializes in water supply.

Assuming that water-rights problems can be resolved to permit scientific operation of a ground-water reservoir, an important question then will be: How much water can be withdrawn perennially from the reservoir? By analogy with a surface reservoir, the administrator of a ground-water reservoir would need basic data as to the capacity of the reservoir (which could perhaps be broken down into the "usable" storage of fresh water within economic pumping lifts and the "dead" storage at greater depth), the long-term average recharge to the reservoir, the annual and cyclic deviations from that average, the unavoidable losses by evapo-transpiration or surface or subsurface outflow, and the effects of use upon quality of the supply. Such information is not (1955) available to users of the great majority of the nation's ground-water reservoirs. Thus, in most areas, a considerably enlarged basic-data program would be an essential preliminary to planned ground-water utilization.

Not all difficulties in determining the "safe" yield of individual ground-water basins can be blamed on failure to make adequate studies. In some areas the necessary data have been collected for several years, and climatic fluctuations are such that one cannot be certain what the "average" conditions are. As a case in point, Utah has detailed information for Cedar City Valley since 1935 but cannot be sure how much of the recorded decline in water levels is due to natural drought conditions and how much to pumping from wells.[14]

One may ask what is likely to happen if development does go beyond the "safe" yield of a ground-water reservoir. Obviously, if pumping continues to exceed the average rate of recharge, the inevitable result is progressive depletion of storage until the ground-water reservoir is drained; at that time, of course, pumping will be cut back by natural conditions to a rate not exceeding the recharge. There are few, if any, instances where man (either in statutes or administrative edicts or court decisions) has succeeded in cutting back the pumpage in an overdeveloped area, unless there is an alternate source of water supply available to those who are cut off.[15] One hesitates to cut off the water supply after it has actually been developed and used.

An important element in Mr. Thomas' paper is the augmentation of the natural supplies, where necessary, to meet the demand. Thus, the natural inflow to ground-water reservoirs would be increased by artificial recharge, and the total water resources of deficiency areas would be increased by importation from areas of surplus. Many other states may not see any immediate need for such measures because their ground-water reservoirs have not been developed beyond the capabilities of natural recharge, or they may not have the opportunity because they have no areas of water surplus from which water can be transported economically to the areas of water deficiency.

Mr. Thomas points out that the usual type of public-district organization covering individual ground-water basins, or perhaps entire stream basins at the most, would not have the inherent authority necessary for long-distance transfer of water. However, organization of water users on this local pattern might be a significant first step. Certainly if such units were large enough to employ specialists in water development and supply, some of the handicaps of haphazard development by individuals might be overcome. After such units develop the capability of rational and comprehensive development in accordance with the resource potential, it might be possible for them to pool their resources and transfer water in accordance with demand in the same way that electric utilities care for local surpluses and deficiencies. Presumably, the development of such water utilities would require enabling legislation and then increasing pressure toward greater responsibility and authority on their part, particularly in regions of greatest controversy over the water resources.

---

[14] "Effect of Current Drought upon Water Supplies in Cedar City Valley, Utah," by H. A. Waite and H. E. Thomas, *Transactions*, Am. Geophysical Union, Vol. 36, 1955, pp. 805–812.

[15] "Water Rights in Areas of Ground-Water Mining," by H. E. Thomas, *Circular No. 347*, Geological Survey, U. S. Dept. of the Interior, Washington, D. C., 1955.

Frank B. Clendenen,[16] J. M. ASCE.—A valuable service to the civil engineering profession has been performed by Mr. Thomas in stating clearly the value and necessity of utilization of vast subsurface reservoirs. Although the author's remarks appear to pertain to the situation and conditions in California, they are just as relevant to many other areas of the United States and to other nations where underground storage potentialities exist. There has been (as of 1955) too great a reluctance on the part of project planners to give ground-water-storage utilization its proper place in their schemes. The result of this neglect has been the formulation of schemes where either surface storage has been overdeveloped or the allocation of surface storage for non-conservation purposes has been unnecessarily reduced. It is believed that the lack of use of ground-water storage in conjunction with surface storage is caused by the misconception that subsurface storage is not "tried and true," that it is still too new, and that it is not reliable. This misconception should be dispelled by considering a few pertinent facts. First, without any planned operation of the ground-water storage, more than half the irrigation water applied in California is obtained from ground-water storage. Second, ground-water basins such as the San Fernando Valley, the San Gabriel Valley, the Owens Valley and the Santa Clara Valley, all in California, have been successfully operated in conjunction with surface storage. Third, planners for the future can certainly see that one must either use the subsurface reservoirs to a large extent or many areas will be left to stagnate because of an insufficient water supply.

Mr. Thomas makes a plea (under the heading, "Water-Control Agencies") for enabling legislation designed to accomplish state-wide (California) control of the ground-water-storage capacity. One of the purposes of this regulated legislation is to provide for

> "* * * the imposition of general taxation in order to share the burden of costly supplies, contributing to the general prosperity of the state, among those who ordinarily secure their water supplies by other means."

There is no developed water supply being used that does not contribute to the general prosperity of the state. It is sounder economics to have the principal beneficiaries of a project pay the principal cost. The danger of using "general prosperity" as justification for state-tax support for regional projects is obvious.

It is further stated (under the heading, "Water-Control Agencies") that

> "* * * the water supply contributing to the development of the modern community must not be subject to intersectional jealousies or political expediency."

Because both of these feared deterrents of sound water-supply planning already exist (1955) it appears wiser to acknowledge their existence and plan to control them rather than to act on the basis that they do not exist. It is easy to comprehend the inherent appreciation that sectional groups have for their natural resources. The reluctance of lesser developed areas to help pay for the development of their resources for the benefit of already highly developed regions is just as understandable. The legislator must recognize that any issue as important to his constituents as their water supply, present and future, demands his attention. Such important issues have historically been settled by the interested parties getting together to discuss the problem and to find a mutually agreeable solution. It is true that the water problem becomes highly complex when the conduits are hundreds of miles in length and the ground-water basins underlie vast areas. It would seem that, when there is need for utilization of a ground-water basin, the overlying owners could be formed into a legal body and be dealt with as the owners by those desiring to exploit the storage capacity. Mr. Thomas has suggested a reasonable method of compensating existing basin-water users for the damage that would be done them by ground-water-storage-capacity utilization.

---

[16] Asst. Prof. of Civ. Eng. and Irrig., Univ. of California, Berkeley, Calif.

The basic fact that the author has expounded—that enabling legislation to allow the utilization of subsurface storage is required—is certainly recognized; such legislation is vital. It is hoped that this legislation will indeed avoid "dog in the manger" attitudes on the part of the inhabitants of areas of surplus water which would prevent sound water-supply development. It is also hoped that such legislation will not so quiet the critical individual that he will no longer feel his responsibility for local water-resources development.

It is generally concluded that ground-water recharge is the key to economic conjuctive utilization of surface and subsurface reservoirs. Under the heading, "Operation of Underground Storage," it is stated that

> "It is clear that the capacity of the underground reservoir to provide cyclic storage for the long-time average annual supply is solely dependent on the rate at which such surface supplies may be placed in storage in the underground basin."

This important factor in water conservation—ground-water recharge—has been receiving much attention of late (1955). Using the author's lucid illustrative example of the Tuolumne River basin, it is seen that an artificial recharge capacity of 45,000 acre-ft per month enables conjunctive use of surface and subsurface reservoirs to develop 30% more water than can be developed by the surface component of the storage singly. If one uses a very conservative infiltration rate of ½ ft per day, the 45,000 acre-ft can be placed in subsurface storage in one month by use of only 3,000 acres. This is a small price to pay for the 300,000 acre-ft average annual increase in conservation, yet it is doubtful if any spreading ponds would be required for this hypothetical operation because of the large quantity of secondary or indirect artificial recharge capacity existing in the area. More attention should be directed to the tremendous quantity of artificial recharge that is usually a by-product of other functions in an irrigated area.

Indirect artificial recharge of significant magnitude in the Tuolumne River area is composed of irrigation, deep percolation, canal seepage, and stream seepage. For this area the applied irrigation water that percolates below the plant-root zone is at least 1 ft per yr. Assuming that the 960,000 acre-ft of irrigation water is for consumptive use and that the entire service area is capable of being served surface water in a "wet" year, the seasonal deep percolation from irrigation is about 400,000 acre-ft. As for canal seepage, the water that has historically been "lost" to canal seepage in this region is about 30% of the gross diversion. If the total annual diversion for a wet year were obtained from surface supplies and if the average irrigation efficiency were 60%, the indirect recharge for a wet year would be approximately 630,000 acre-ft. This annual canal seepage could be increased by operation to keep the system wet for a longer period than that required for irrigation. The monthly seepage rate of the Tuolumne River would be about 11,000 acre-ft if a percolation rate of ½ ft per day and an effective wetted stream bed area of 30 miles by 200 ft can be assumed to exist.

These three sources of indirect artificial recharge yield an average monthly rate of 100,000 acre-ft. The variation of monthly irrigation requirement would cause the peak-requirement months of the summer to have a larger recharge rate than the winter months. This rather rough estimate serves as satisfactory proof that, for areas such as the Tuolumne River basin, ample recharge capacity is available to obtain the high degree of conservation indicated by the illustrative example. The writer has made similar operation studies on the American and Merced Rivers, which along with the Tuolumne River are located in the Central Valley, and has obtained results similar to those presented in the illustrative example.

Whereas Mr. Thomas has clearly depicted the important increase in conservation of the available supply which is creditable to the inclusion of ground-water-storage capacity in the scheme, attention should be drawn to the added emphasis this point requires in the light of the ever-increasing cost of surface storage and the rapid increase in water demand that is being experienced now and which will be aggravated with time.

Robert O. Thomas,[17] A. M. ASCE.—The important contributions made by Messrs. Thomas and Clendenen are appreciated. It is regretted that more extensive discussion of the problems involved, with particular reference to areas other than California, was not forthcoming.

The problem of determination of safe yield from an underground reservoir was discussed by Mr. Thomas. Evaluation of this aspect of ground-water storage has heretofore been expressed (in California) as the maximum rate of extraction of water from a ground-water basin which, if continued over an indefinitely long period of years, would result in the maintenance of certain desirable fixed conditions. This rate of extraction is determined by one or more of the following criteria:

1. Mean seasonal extraction of water from the ground-water basin does not exceed mean seasonal replenishment to the basin.
2. Water levels are not lowered sufficiently to cause harmful impairment of the quality of the ground water by intrusion of other water of undesirable quality or by accumulation and concentration of degradents or pollutants.
3. Water levels are not lowered sufficiently to imperil the economy of ground-water users by excessive costs of pumping from the ground-water basin or by the exclusion of users from the supply.

---

[17] Senior Hydr. Engr., Div. of Water Resources, State of California, Sacramento, Calif.

These criteria have usually been applied to the natural hydrologic balance of inflow and outflow in individual ground-water basins. Occasionally, they have been extended to include imported water supplies as an item of replenishment for basins where the annual draft is greatly in excess of the natural, or native, replenishment. The next step will, of course, be the deliberate utilization of the ground-water storage capacity as an addition to the volume of surface storage available in order to achieve maximum conservation of water supplies. Such a concept will result in the accomplishment of conjunctive use of surface and ground-water storage.

The yield derived from a conjunctive operation is the total yield resulting from the operation of both surface and underground storage capacity; the proportionate part derived from each source will vary annually and cyclically. The quantity of water pumped from the underground basin must, in order to utilize the basin conjunctively, conform to criterion 1. Criterion 2 must also be observed so that the water thus made available will be usable for beneficial purposes. The implication of single-agency inherent in conjunctive use, however, relegates criterion 3 to a position of subsidiary concern.

It would be desirable to denote the yield from conjunctive operation by the use of a new term such as "average operating yield." The annual extraction will vary from zero in a year of ample surface supply to a maximum in a year of grossly deficient surface supply. The quantity of average operating yield can be determined from an operational study covering a complete cycle of water supply, as in the case of a surface reservoir. The basin investigation required as a preliminary to such study, however, is far more complex than that necessary to determine the yield of a surface development.

The investigation of physical situations which are useful in conjunctive operation will generally be conducted along three broad phases of inquiry. The first phase of investigation may be termed the geological phase, in which the conditions to be encountered on and under the surface are determined. The primary requisite is the location of underground storage space, which may be found in those geological formations containing a sufficient number of voids to hold, transmit, and release water in the necessary quantities. After determining that usable storage space for practicable operation exists, the porosity, transmissibility, chemical composition, location of intake areas, and other basic physical characteristics of hydrologic and hydraulic operations are ascertained.

The second field of investigation of possible subsurface storage areas is the hydrologic phase. This is concerned with the determination of the water supply available for the project; the regimen of its occurrence; the quality of the native, imported, and subsurface waters available; the operation of surface facilities for storing, transporting, and percolating surplus in subsurface storage; and innumerable additional factors bearing on the problems of routing the water supplies between the place of origin and the place of final disposal.

The economic phase is the third field of inquiry. This phase is concerned with the determination of places and quantities of use. It involves the classification of land areas as to suitability for irrigated agriculture, domestic, industrial, or other uses; determination of water requirements for the various uses; production, distribution, salvage, and disposal of available water supplies; and other necessary studies. It may be noted that the grouping of phases of an operating study is made solely for convenience of illustration and bears no relationship to the order of work or usual concept of fields of endeavor. The engineer and geologist will function in close coordination throughout the investigation and will be assisted, as required, by other concerned specialists.

From the basic data collected, the limits of variability of factors entering into the determination of yield can be established and the operating studies completed. Such studies must begin with the disposal of the yield from the surface reservoir; this may be distributed in many ways. Part of the yield will be dissipated in surface evaporation; other quantities will be released to stream channels, irrigation, and domestic or municipal services; part will go to direct percolation to underground basins; and some may be exported permanently from the area. Items of accretion to ground-water storage are the deep percolation of water applied for irrigation—whether from surface or underground sources; the deep percolation of precipitation on overlying lands and of a portion of the water delivered for urban uses; the direct ground-water recharge from surface-water supplies; seepage from natural and artificial water channels; and subsurface inflow from adjacent areas. Depletion of ground-water supplies is caused by extractions for required water supplies to areas of use, rising water, uneconomic consumptive use in high water-table areas, extractions for purposes of salt balance, and subsurface outflow from the basin. From such studies, made with varying operating criteria, the average operating yield and the volume of underground storage capacity utilized may be determined.

The portion of the total underground storage capacity that is capable of being dewatered during periods of deficient surface supply and resaturated during periods of above-normal supply may be considered as the usable storage capacity. Obviously, the volume of the usable capacity is limited by the capacity of the basin to yield or absorb water at predetermined rates sufficient for cyclic operation. Criterion 2, pertaining to water quality, is applicable to this situation. Water-quality factors may reduce the volume of gross-storage capacity that could otherwise be classed as usable.

Maintenance of suitable quality of water supplies, particularly those intended to be used consumptively by irrigated agriculture, requires the consideration of the salt balance involved in the use and reuse of such supplies. The solution involves induced drainage of water from the ground-water basin in quantities sufficient to maintain satisfactory mineral quality. The water so drained will constitute a future demand on the developed water supply. Under natural conditions, most ground-water basins tend to fill with water and to overflow in the lower portions, thereby flushing out soluble salts contained in water originating in the tributary watershed and overlying lands. When aquifers in the basin are tapped by wells, the pumping draft lowers ground-water levels to such an extent that, in many cases, the natural flushing of the basins ceases. Because the pumped water is largely used on overlying lands, soluble salts accumulate within the basin and tend to degrade the quality of the ground water in storage. If the situation is such that no discharge of water from the area, either surface or subsurface, occurs, in the course of time the concentration of salt compounds in the remaining water will become so great as to inhibit it as a source of water supply. For this reason, the planned extraction and export of the quantity of water necessary for maintenance of adequate quality are required.

From the procedures outlined herein, the total firm yield of the conjunctive operation and the average operating yield of the underground reservoir can be determined. The average operating yield will vary, of course, in accordance with the method of operation selected for the surface component—that is, "carry-over" or "fill-and-draw" operation. The disposal of such average operating yield will determine the quantity of firm water supplies from the conjunctive operation which can be made available for beneficial uses.

Mr. Clendenen has noted that conjunctive operation of surface-water and ground-water storage capacity is presently (1955) being practiced in several areas of deficient water supplies in California. In other areas, an involuntary, or unplanned, operation has been in progress for many years. This is particularly true in extensive irrigated areas where a considerable portion of the applied water, from whatever source, finds its way to the main body of underground water in storage.

The writer cannot agree with Mr. Clendenen as to the basis of financing future water-supply developments. Supplies which have been developed in the past were generally those which were well within the ability of water users to repay. The history of irrigation development in the western states, however, is replete with instances of developments at excessive cost, followed by the dishonoring of bonds and other securities and the dismemberment or reorganization and refinancing of districts and other water agencies. In view of the fact that much of the "cream of the crop" of possible water-supply projects has already been developed, it is apparent that projects which are uneconomic in a repayment sense will necessarily have to be constructed in order to meet increasing demands for water. Whereas much of the cost of such projects should properly be paid by the principal beneficiaries, the water users, it is felt that support from governmental revenues is both required and proper in order to continue the maintenance of a modern, dynamic economy.

In the administration and operation of ground-water-storage capacity for conservation and use of available water supplies, a new field of operational problems will require solution. These problems may be divided into broad areas, tentatively designated as legal, hydrologic, managerial, and operational. The problems in each area will, of necessity, contain elements common to one or more of the other areas because the interrelationship is such that precise area boundaries cannot be drawn.

The present paper has, it is hoped, served to initiate effort in this direction. Engineers, particularly those engaged in water-resource activities, should take a position of leadership in the development of a sound foundation of theory and practice for the maximum ultimate utilization of all available resources for the conservation of the national water supplies.

IRRIGATION ASPECTS

By Harris R. McDonald,[1] A. M. ASCE

Synopsis

The advantages of coordinated use of surface and ground water for irrigation have not been fully realized in the planning and operation of irrigation projects. Because of transit losses, farm waste, and deep percolation, only about 50% of the water diverted from streams is used by crops. Significant quantities are commonly used nonbeneficially in poorly drained areas or along natural stream channels. There are cited herein the advantages of ground-water pumping to reduce losses, to prevent or reduce drainage problems, and to irrigate additional lands where the water is of suitable quality and aquifer characteristics are favorable for the development of large-capacity wells.

Introduction

Early irrigation development in the United States was based almost exclusively on the use of surface water—first, by direct river diversion and later with regulation by upstream storage reservoirs. From 1900 to the present (1955), many of the most economical reservoir sites were developed for power, irrigation, flood control, or other purposes. Millions of dollars were justly expended, and yet nature has provided reservoirs of far greater total capacity than all the reservoirs man has built; they are awaiting man's use or abuse.

Ground water and surface water are closely related. In fact, from the instant a particle of water falls on the ground, it may change form many times before it reaches the ocean. Practically all the fair-weather flow of streams represents ground-water discharge, the overflow of the ground-water reservoir temporarily held in storage.

Historical Development of Irrigation

Modern ground-water irrigation development as it now exists (1955) had its beginnings in the United States in about 1900. Artesian basins in which water supplies could be developed by natural flow represented the first significant use; to the layman who did not know its source, the supply was considered inexhaustible. However, with the drilling of more and more wells, the flows began to diminish and man became concerned. This concern led to the study of artesian basins by various state and federal authorities; it was then that modern ground-water hydrology was born. Attention was first given to the arid regions of the western states because in this area water supplies are extremely vital. Surface supplies were meager and unreliable, and the value of a perennial supply, even though limited, was recognized.

Note.—Published, essentially as printed here, in June, 1955, as *Proceedings-Separate No. 707*. Positions and titles given are those in effect when the paper was approved for publication in *Transactions*.

[1] Hydr. Engr., Hydrology Div., Bureau of Reclamation, U. S. Dept. of the Interior, Denver, Colo.

In the early stages of development, little was known about the construction and development of wells. The importance of ground water and the frequency of well failures led to the investigation of the causative factors and theoretical inquiry of the movements of underground waters. One of the earliest of these comprehensive investigations was the work of C. S. Slichter.[2]

Impetus was given to ground-water development by the perfection of the internal combustion engine and the improvement of the centrifugal pump. Better methods of drilling and finishing wells enabled the production of more water from a single well and at less cost. Thus, the stage was set for modern methods of ground-water irrigation.

The development of ground water for municipal and industrial use was no doubt largely responsible for technological improvements in the design and construction of wells, pumps, and motors. The high unit value of ground water and its advantages for municipal and industrial use provided not only the incentive but also the funds necessary to realize these improvements.

The development of the vertical turbine pump, the well screen, dependable electric motors, and low-cost electrical energy have all given added impetus to the growing use of ground water.

USE OF GROUND WATER

In 1950 the Geological Survey,[3] United States Department of the Interior (USGS), estimated the total water use in the United States as follows:

	Millions of acre-feet per year	Percentage of total
Irrigation	84.0	44.2
Industrial	86.2	45.4
Municipal	15.7	8.3
Rural, other than irrigation	4.0	2.1
Total	189.9	100.0

The total industrial use includes water for cooling and other purposes where the water is essentially unchanged in quantity or quality.

The total use of ground water for irrigation is difficult to estimate. In only a few areas are reliable data available, and even in these areas the quantity pumped changes significantly from year to year with the increase or decrease in acreage irrigated and with the increase or decrease in annual precipitation. In many areas, ground water is used as a supplement to surface supplies, and the amount used depends to a large extent on the quantity of surface water available.

In 1945 the USGS[4] estimated the total use of ground water in the United States as follows:

---

[2] "Theoretical Investigation of the Motion of Ground Waters," Nineteenth Annual Report of the U. S. Geological Survey, Geological Survey, U. S. Dept. of the Interior, Washington, D. C., 1899.

[3] "The Physical and Economic Foundation of Natural Resources: Part II, The Physical Basis of Water Supply and Its Principal Uses," Interior and Insular Affairs Committee, House of Representatives, United States Congress, 1952.

[4] "The Water Situation in the United States with Special Reference to Ground Water," by C. L. McGuinness, *Geological Survey Circular 114*, U. S. Dept. of the Interior, Washington, D. C., June, 1951.

	Millions of acre-feet per year	Percentage of total
Irrigation	11.2	50.2
Industrial	5.6	25.0
Municipal	3.4	15.2
Rural, other than irrigation	2.2	9.8
Total	22.4	100.0

In 1950 the USGS revised its estimate of the use for irrigation to 16,800,000 acre-ft per yr. Based on reported data from various sources, it is estimated that the present (1955) use of ground water for irrigation is in excess of 25,000,000 acre-ft per yr in the seventeen western states. Data on pumpage for irrigation in the more humid parts of the United States are almost totally lacking. However, the limited data available indicate that even in humid areas the use of ground water for irrigation is profitable for growing high-quality specialty crops and will be more extensively used as experience is gained.

The use of ground water for irrigation is vital to the agricultural economy of many of the western states, especially Arizona, Arkansas, California, Colorado, New Mexico, and Texas. With the possible exception of Arkansas, the total pumpage in each of these states exceeds 1,000,000 acre-ft per yr.

California.—California leads all other states in the use and development of ground water. It is estimated by T. Russel Simpson[5] that the total gross pumpage of ground water in California in 1950 was more than 10,000,000 acre-ft, including municipal and industrial use. It is assumed that for practical purposes, the small quantities used for municipal and industrial purposes would not significantly affect the estimated total use. This usage is broken down into seven major hydrographic areas as follows:

Area	Estimated average pumpage in acre-feet
South coastal area	1,500,000
Colorado desert	100,000 (for drainage only)
Lahontan basin	150,000
Central coastal area	600,000
San Francisco Bay area	300,000
North coastal area	50,000
Central Valley	8,000,000
Total	10,700,000

Ground-water pumpage has been concentrated in areas of deficient surface supplies, particularly in the south coastal area and in the San Joaquin Valley. Continued overdraft has been practical only because of the large storage capacity of the ground-water basins. Even with the large storage available, serious problems are arising. Along the coastal areas, the intrusion of sea water is becoming increasingly serious. In some parts of the San Joaquin Valley, pumping lifts are increasing, and economic conditions may largely determine the length of time the rate of overdraft can be continued.

---

[5] "Utilization of Ground Water in California," by T. Russel Simpson, *Transactions*, ASCE, Vol. 117, 1952, p. 923.

The coordinated use of surface and ground-water supplies for irrigation probably has been given more consideration in the Central Valley of California than elsewhere. In the upper San Joaquin Valley area, surface supplies for many years have been insufficient to meet the requirements, and ground-water pumping has been relied on. In some areas, crop requirements were met wholly by ground-water pumping. Such pumping has been largely from ground-water storage, and the tremendous quantities of water pumped without completely dewatering the most permeable aquifers is evidence of the vast storage capacity of the ground-water basins. Early reports recognized that without development of new water supplies, much of the productive area would necessarily be abandoned. Thus, in about 1930, the state water plan envisioned the diversion of surplus Sacramento River flows to the lower areas of the San Joaquin Valley, and by exchanging San Joaquin flows with the imported water, additional surface supplies could be made available to the higher lands in the San Joaquin Valley. With the execution of the exchange contract and the construction of Shasta Dam and the Delta-Mendota Canal by the Bureau of Reclamation, United States Department of the Interior (USBR), additional water supplies were potentially available for use on upper San Joaquin Valley lands. However, not until the construction of Friant Dam and the Friant-Kern and the Madera Canals were significant water deliveries made. Under the proposed plan of operation, ground-water pumping will be utilized to the maximum practical extent, and additional supplies of surface water will be available. So far as possible, a balanced surface-water and ground-water supply will be used to meet irrigation and municipal demands. The availability of an average of 1,500,000 acre-ft of additional surface water to the east side of the South San Joaquin Valley through the facilities of Friant Dam and appurtenant distribution system should prove effective in satisfying the deficiencies in water supply to areas now in production. The additional ground-water recharge and reuse of return flows resulting from the application of the 1,500,000 acre-ft of new water will probably increase the total available from the importation to an average of more than 2,000,000 acre-ft.

Similar plans are underway (as of 1955) for augmenting the water supply of the west side of the South San Joaquin Valley. In the San Luis area, approximately 500,000 acres are irrigated wholly by ground-water pumping. Pumping lifts are steadily increasing, and it has long been recognized that importation of surface supplies would be required if the economy of the area is to be stabilized or expanded. Irrigable lands in this area total nearly 1,000,000 acres. The USBR is supplying (1955) about 300,000 acre-ft of surface water annually to the west side of this valley from the Delta-Mendota Canal in addition to approximately 1,000,000 acre-ft to the lands below Mendota Pool under the terms of the exchange contract. Plans now (1955) being studied include the construction of San Luis Dam and distribution system which will obtain water from the Sacramento River, utilizing the off-peak capacity available in the Delta-Mendota Canal and Tracy Pumping Plant; storage would be in San Luis Reservoir. Here, also, the use of surface-water and ground-water storage would be coordinated to obtain the maximum practical quantity of water.

Arizona.—Although the use of ground water for irrigation in Arizona is only about one-half that of California, it is no less important to the economy of the area. In recent years, the 600,000 acres irrigated in the Salt River Valley area (including Pinal County) have received the greater portion of their water supplies by ground-water pumping. In 1951,[6] the ground-water pumpage in this area exceeded by almost four times the surface water diverted at Granite Reef Dam. The total area irrigated has increased from 436,000 acres in 1946 to 590,000 acres in 1951 and represents about one-half the total irrigated area in Arizona. During the same period, the number of wells increased from 850 to about 1,500. From this, it is apparent that the increase in number of wells (75%) is proportionately greater than the increase in the irrigated acreage (35%). It may be concluded that yields of older wells have diminished as the water table has declined, and the more productive aquifers have become unwatered. Consequently, new and deeper wells have had to be drilled, not only to irrigate new lands but also to compensate for the decreased production of the older wells.

TABLE 1.—Estimated Pumpage in Arizona

County	Area	Pumpage, in 1,000 Acre-Feet	
		1951	1953
Cochise	San Simon, Willcox, and Douglas	76	145
Graham	Safford Valley	125	120
Greenlee	Duncan Valley	33	30
Maricopa	Queen Creek, Salt River Valley	2,020	2,498
Pima	Part of Santa Cruz basin	240	380
Pinal	Santa Cruz and Gila basins	1,030	1,400
Santa Cruz	Part of Santa Cruz basin	30	27
Yuma	Gila basin	127	151
	Total	3,681	4,751

Smaller quantities of ground water are pumped for irrigation in other basins delineated by the USGS. Table 1 indicates the basin and the estimated pumpage in Arizona during 1951 and 1953.

When the amount of water pumped greatly exceeds the quantity of recharge to any basin, it is commonly referred to as "mining," the connotation being that in large measure the water pumped will never be replaced. Studies made by the USGS in cooperation with the State of Arizona have shown conclusively that most of the water pumped in recent years has been "mined." High agricultural prices, highly efficient pumps and motors, low-cost power, and decreases in surface supplies resulting from drought conditions are, no doubt, responsible for the large increase in ground-water pumping. This has occurred despite the fact that pumping lifts have steadily increased.

There is little doubt that the future of the highly developed agricultural economy in the Salt River Valley basin, including Pinal and Maricopa Counties, is dependent on the importation of additional supplies of surface water. Continued overdraft of the present (1955) magnitude cannot long be maintained even from a ground-water basin of such large capacity. The USBR has made a comprehensive study of the methods by which the importation of additional water could be made into the area. This study proposes the diversion of water from the Colorado River and, by a pump lift of several hundred feet, its delivery to a point near the existing Granite Reef Dam. Thus, by exchange with water now originating upstream, large areas would be furnished a supplemental water supply. The dispute over water rights and the interpretation of the Colorado River Compact is before (1955) the United States Supreme Court.

---

[6] "Pumpage and Ground-Water Levels in Arizona in 1953," by L. C. Halpenny et al, Geological Survey, U. S. Dept. of the Interior, Tucson, Ariz., June, 1954.

Shortly after the construction of Roosevelt Dam in about 1910 (on the Salt River), water levels within the project which is served by river diversions began to rise, and by 1920 about 31% of the Salt River Project area had a water-table depth of less than 10 ft, and in about 65% of the area the depth to the water table was from 10 ft to 50 ft. Because of ground-water pumping—first for drainage and later for water supply—the depth to ground water in 1945 was less than 10 ft in only 0.2% of the area and was between 10 ft and 50 ft in about 55%. Water levels in areas served wholly by ground-water pumping have declined at a much more rapid rate, and pumping lifts in excess of 300 ft are not uncommon.

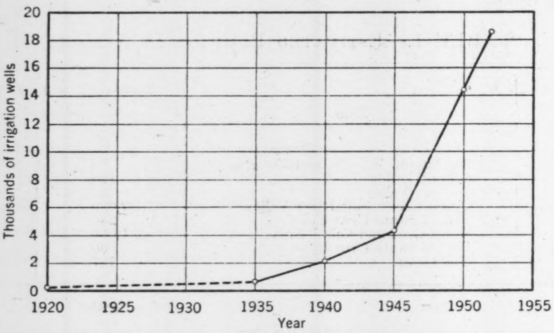

FIG. 1.—NUMBER OF WELLS IN THE SOUTHERN HIGH PLAINS OF TEXAS

Texas.—Irrigated acreage in Texas expanded from slightly more than 1,000,000 acres in 1940 to more than 3,150,000 acres in 1950,[7] the increased acreage being served principally by ground-water pumping. Nearly two-thirds of the total irrigated area is located in the high plains. About 600,000 acres are irrigated in the lower Rio Grande Valley and almost an equal amount in the coastal prairie rice-growing region, although these areas utilize surface-water supplies to a large extent. Total ground-water pumpage for irrigation in the southern high plains during 1951 was about 2,000,000 acre-ft, but because of drought conditions prevailing in 1952, pumpage was about 3,700,000 acre-ft. As shown in Fig. 1, the number of irrigation wells in this area has increased from about 2,000 in 1940 to more than 18,000 in 1952.

---

[7] "Irrigated Agriculture in Texas," *Miscellaneous Publication No. 59*, Texas Agri. Experiment Station, College Station, Tex., September, 1950.

In the high plains area where irrigation is practiced almost exclusively by ground-water pumping, average pumping lifts in 1949 were approximately 110 ft, the maximum being somewhat more than 250 ft. The principal aquifer in this area is the Ogallala formation, a heterogeneous mixture of gravel, sand, silt, clay, and caliche, varying from place to place as to sorting and cementation, as well as permeability. The average thickness of the Ogallala formation in the Amarillo, Lubbock, and adjacent areas is approximately 210 ft and has been estimated to contain 150,000,000 acre-ft of ground water in storage, of which about 100,000,000 acre-ft are within 200 ft of the land surface.

Colorado.—Considerable ground-water development for irrigation has occurred in Colorado, principally in the Arkansas, Rio Grande, and South Platte basins. In these areas, ground water is pumped primarily to furnish supplemental water, although considerable acreages in some of the tributary valleys rely entirely on ground-water pumping for their supply.

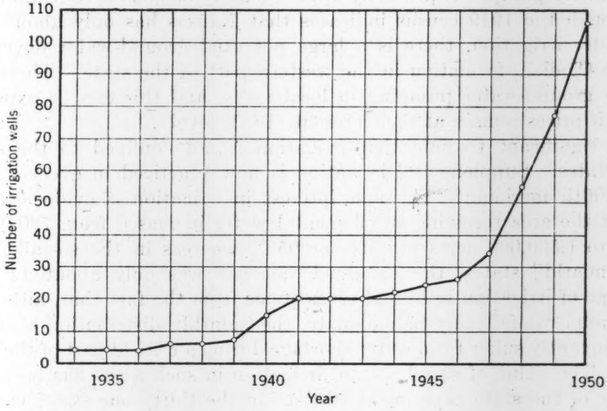

FIG. 2.—NUMBER OF WELLS IN THE PLAINS AREA OF EASTERN COLORADO

Recently somewhat localized but intensive development of ground water has occurred in the plains areas of eastern Colorado. In 1952 more than 100 wells had been drilled, which provided a full supply to approximately 6,000 acres. Development of ground water in this area is moving forward at a rapid pace (Fig. 2). Although a relatively small area is now irrigated in this manner (as of 1955), large areas are capable of being developed because they are underlain by the Ogallala formation and have sufficient saturated thickness to permit the construction of large-capacity wells. Recharge to the ground-water reservoir is limited, and pumping is almost wholly from storage.

Development of the San Luis Valley artesian basin in southern Colorado began in about 1890, and it has been estimated that more than 7,500 wells have been drilled to date (1955). Most of these wells are of small diameter and are cased only a few feet below the surface. Consequently, frequent cleaning is required to keep them open, and undoubtedly many of the casings have collapsed and the wells no longer flow at the surface. Recently several large irrigation wells have been drilled and pumping equipment has been installed. Total ground-water discharge by pumping or artesian flow during 1952 was estimated by the USGS to be approximately 480,000 acre-ft.[8]

The total area irrigated in Colorado, according to the 1949 agricultural census, was about 3,200,000 acres. It is probable that during 1952 total ground-water pumpage for irrigation was between 1,500,000 acre-ft and 2,000,000 acre-ft.

Other Areas.—Nebraska has approximately 900,000 acres irrigated (as of 1955), about one-fourth of which is supplied almost entirely by ground-water pumping. The most intensively pumped area lies in the Platte River Valley between Kearney and Grand Island. In 1952, George H. Taylor,[9] A. M. ASCE, estimated that close to 400,000 acres in Nebraska are irrigated wholly or in part by ground-water pumping from a total of about 8,000 wells. The total quantity pumped is probably approximately 600,000 acre-ft annually.

Although the 1949 census indicates that Kansas has only about 140,000 acres under irrigation, there is a large potential ground-water development from the Ogallala formation in the western part of the state. There is considerable ground-water pumping in local areas, and this can be expected to increase if prices remain at their present (1955) level.

It is significant to note that irrigation is not confined to the so-called "arid" states. Supplemental irrigation is now practiced in every state east of the 100th meridian. The new interest in irrigation is evidenced by the fact that the area receiving supplemental water increased from 780,000 acres in 1940 to 1,500,000 acres in 1950, or 95%, whereas in the so-called "arid" and "semiarid" states, the increased[10] acreage was only about 22%. The advantage of irrigation in humid areas stems from the fact that, although the total annual rainfall may be adequate, the monthly distribution is such that crops frequently suffer from water shortage during a critical part of the growing season. The value of supplemental irrigation in such areas has been studied by many of the state experiment stations in the thirty-one states east of the 100th meridian. The advantages of the development of ground-water supplies in favorable areas are evident. Ground-water supplies usually are not vulnerable to evaporation losses and, hence, are available when streams and farm ponds reach their low stages during dry periods.

GROUND-WATER STORAGE, RECHARGE, AND DISCHARGE

Because ground-water resources are a significant portion of the total water supply for irrigation and other uses, why has the United States, as a nation, not given more thought to their development and utilization? In the first place, the concepts of storage, recharge, and discharge are not well understood by the average engineer. Ground water is largely hidden from view, is difficult to measure, and in some respects behaves unlike surface water. Studies of ground-water reservoirs depend, in a large measure, on indirect evidence obtained from geological and engineering studies; yet, ground water forms a significant part of the total water resources, and as one reaches the limit of development of surface water, ground-water sources must be developed for additional supplies. Fortunately, the science of ground-water hydrology has provided techniques which were not available in 1900. It is now possible to estimate the capacity of underground reservoirs and to determine the inflow, outflow, and perennial yield. It is known that ground-water storage, if properly used, will provide water that is essentially free from silt and bacteria and is of relatively uniform temperature and chemical composition.

---

[8] "Geology and Ground-water Resources of a Part of the San Luis Valley, Colorado," Geological Survey, U. S. Dept. of the Interior, Washington, D. C., 1954 (unpublished report).

[9] "The Ground-Water Resources of Nebraska," by George H. Taylor, Geological Survey, U. S. Dept. of the Interior, Washington, D. C., January 24, 1952 (information release).

[10] "Economic Effect of Irrigation in a Subhumid Area," by Willis C. Boegli, *Proceedings-Separate No. 398*, ASCE, February, 1954.

Likewise, advances in the design and construction of wells, pumps, and power plants have provided the means by which the water stored in these natural reservoirs can often be utilized economically. Low-cost electric power or diesel power has made possible the use of great quantities of water that otherwise would not have been available.

In some respects, ground-water reservoirs are similar to surface-water reservoirs. They have a given capacity and must have a recharge and a discharge. The reservoirs are often irregular in shape and intricate in their construction, but their location can be mapped and their structure determined. The hydraulic characteristics of the aquifers comprising the reservoirs can be determined accurately with respect to recharge, discharge, storage, and movement. These processes involve laws of fluid mechanics which depend on the principles of physics but which have little significance in the hydraulics of surface water. The most efficient operation and use of these reservoirs can be accomplished by the practical application of the knowledge developed by these scientific methods of investigation.

One of the most difficult problems in regard to any ground-water development is how much of the water pumped is taken from storage and how much is supplied from surface sources. The latter quantity is dependent on the size and location of the intake area, the permeability of the surficial material, and the quantity and distribution of the water available for recharge. The "stage" of the reservoir must be determined by measuring the elevation of the water tables in wells. Because the water surface is not a plane, as in a surface reservoir, many wells must be used. If the reservoir is full, the water available for recharge will be rejected, and thus the potentialities of the reservoir are not being realized.

All ground-water reservoirs have some natural discharge. Withdrawals from the reservoir will either reduce the natural discharge, increase the natural recharge, or reduce the storage. The quantity of water that may be withdrawn perennially from the reservoir is dependent only on (*a*) the reduction of the pre-existing discharge or (*b*) the increase in recharge over what has occurred. This does not imply that water may not be withdrawn from storage for one year or even for several years, provided that accretions to storage are made in such a way that the average discharge is equal to the average recharge. The development of artesian basins is often limited in an attempt to maintain artesian pressures at a level which will maintain flowing wells. This means that only a small fraction of the total storage capacity of the reservoir is being utilized.

In some instances, the perennial yield of the reservoir is limited by the capacity of the aquifer to transmit water rather than by the quantity of water available for recharge. The aquifer thus serves as a conduit from the recharge area to the discharge area, although it may have some of the characteristics of both a reservoir and a conduit. For this reason, the manner in which a ground-water reservoir will operate is determined to a considerable extent by the characteristics of the aquifer of which it is comprised.

In studying the effects of pumpage or withdrawals from a ground-water reservoir, it has often been found useful to operate the reservoir through a critical period as is commonly done when determining the hypothetical function of a surface reservoir. In such instances, the capacity and the recharge must be known with a reasonable degree of accuracy.

Salvage of Water Supplies by Coordinated Use

When surface water is diverted for irrigation, a significant portion percolates below the root zone of plants, and with suitable drainage conditions, in due course of time, finds its way back to natural or artificial drainage channels. This water, together with farm waste, is usually termed return flow. Where the physical conditions are suitable, such water may be rediverted to additional lands and used for irrigation purposes. In instances where this water must be carried in natural drainage channels for long distances before rediversion, quite often the channels become choked with tules, cattails, and other water-loving vegetation termed "phreatophytes" which sometimes use a large part of the water available. In the southwestern states, a plant known as salt cedar or tamarisk (*Tamarix gallica*) is often found. This plant, introduced from the Middle East in about 1900, often infests deltaic deposits at the head of reservoirs, along streambanks, and drainage channels. The USGS, in an investigation of the Safford Valley (Arizona) in 1943–1944 found that these plants used from two to three times as much water as that required by most crops.

The water used by these plants varies as the depth to water, temperature, and the density of growth. Poorly drained areas such as those found near or in almost any irrigation project provide a suitable environment for these plants. In the aggregate, their total use is no doubt several million acre-feet per year. Although their total use is great, a difficult problem is presented when an attempt is made to recover this water economically. It is believed that, by proper coordination of surface-water and ground-water reservoirs, a significant quantity of the water thus lost could be salvaged in some areas.

Inasmuch as phreatophytes are commonly found in poorly drained areas, it is possible that large quantities of water could be salvaged by lowering the water table by ground-water pumping, if suitable aquifers occur. Peak demands for irrigation occur simultaneously with maximum use by phreatophytes, and continuous pumping during the growing season would be effective in reducing the water available to the phreatophytes.

In cases where natural streams flow through phreatophyte-infested areas, channelization has made possible significant salvage by lowering the water table within the area and by reducing the travel time of upstream reservoir releases or flood flows. For example, significant water salvage has been demonstrated by this method in the Middle Rio Grande Valley of New Mexico, even though construction has not been completed.

A situation similar to that in the Middle Rio Grande Valley also exists in the Pecos River basin (New Mexico). Because of more limited runoff in the Pecos River basin, the nonbeneficial depletion presents a more pressing problem.

McMillan Reservoir on the Pecos River was constructed in about 1900 to provide storage for the Pecos Irrigation Company, the predecessor of the Carlsbad Irrigation District. McMillan Reservoir had an original capacity of about 80,000 acre-ft but has been depleted by sedimentation so that its present (1955) capacity is only about 37,000 acre-ft. In addition, leaks have developed in the reservoir area and its effectiveness has been reduced further. After various studies of the possibilities for the enlargement and rehabilitation of McMillan Dam, it was recommended that a new dam be constructed farther upstream at Alamogordo. This was authorized in 1935, and construction was completed in 1937 by the USBR. At about the same time, the Red Bluff Reservoir was constructed farther downstream for the benefit of Texas interests. Meanwhile, phreatophytes consisting almost entirely of salt cedar gained a foothold in the Lake McMillan delta deposits. The phreatophytes spread rapidly upstream and provided an effective means of keeping the sediment out of the reservoir; apparently at that time no one realized how much water they were consuming.

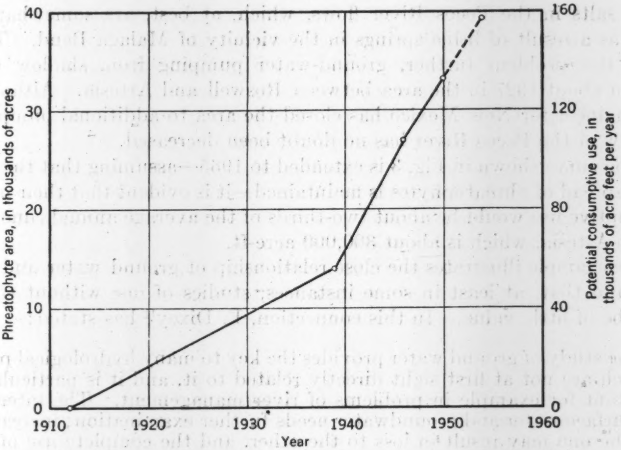

FIG. 3.—PHREATOPHYTE AREA AND COMSUMPTIVE USE IN THE PECOS RIVER BASIN OF NEW MEXICO

Because of the interstate problems involved, a compact commission was first appointed in about 1925, but it was not until 1948 that the Pecos River Compact became effective. The compact provided, among other things, that the depletion of stream flow in New Mexico by man's activities would be limited to that existing as of 1947 but would not be responsible for additional depletions resulting from natural causes. The Pecos River Commission was established to administer the compact.

Studies by the engineering advisers to the Pecos River Commission and others have revealed some startling facts. The phreatophytes have spread rapidly and their water consumption has been estimated (Fig. 3). Since being introduced into the area in about 1912, they covered an area of approximately 14,000 acres in 1939, about 27,000 acres in 1946, and by 1953 (assuming the same rate of increase) about 36,000 acres. These phreatophytes have a potential ability to consume between 140,000 acre-ft and 170,000 acre-ft of water annually. In effect, these plants are robbing the water supply of the river. Although it is obtained almost entirely from the ground-water reservoir, ground-water depletions are restored by river flows before they continue downstream. This use has also had the effect of further concentrating the soluble salts in the Pecos River flows, which, at best, are somewhat saline, largely as a result of brine springs in the vicinity of Malaga Bend. To complicate the problem further, ground-water pumping from shallow aquifers began in about 1927 in the area between Roswell and Artesia. Although the state engineer for New Mexico has closed the area to additional pumping, the base flow of the Pecos River has no doubt been decreased.

If the curve shown in Fig. 3 is extended to 1965—assuming that the present rate of spread of phreatophytes is maintained—it is evident that their potential consumptive use would be about two-thirds of the average annual runoff of the river at Artesia, which is about 300,000 acre-ft.

This example illustrates the close relationship of ground water and surface water and that, at least in some instances, studies of one without the other would be of little value. In this connection, F. Dixey[11] has stated:

> "The study of ground water provides the key to many hydrological problems which are not at first sight directly related to it, and it is particularly important for example in problems of river management. The interrelation of surface water and groundwater needs further examination; increasing use of the one may result in loss to the other, and the complete use of surface water for irrigation may stop accretion to ground water."

THE PROBLEM OF ECONOMIC YIELD

In the absence of legal restrictions and physical limitations, the economics of pumping is usually the determining factor not only for the location but also for the quantity of ground water pumped for irrigation in arid areas. Water has a higher value for domestic and municipal supplies than for irrigation, and, therefore, for these uses more elaborate installations and higher operational costs can be sustained.

Almost without exception, the history of ground-water irrigation development of arid areas demonstrates that where the land resources exceed the water resources, the ground-water reservoirs have been overdeveloped if it were profitable to do so. In some areas, the problems of overdraft have been recognized and appropriate measures taken before development reached the stage where legal control alone would not offer a practical solution. A prime example is the Roswell artesian basin in New Mexico. In other areas, such as parts of Texas and New Mexico, legal attempts to control unlimited ground-water pumping have been made, but have been partly successful because aquifer overdevelopment occurred prior to legal control.

---

[11] "Some Recent Studies in Ground-water Problems," by F. Dixey, Ankara Symposium on Arid Zone Hydrology, UNESCO, New York, N. Y., 1953, p. 47.

A unique problem is presented in such areas as the high plains region, which covers parts of New Mexico, Texas, Oklahoma, Colorado, Kansas, and Nebraska. Annual average recharge from precipitation is limited to perhaps $\frac{1}{4}$ in. to $\frac{1}{2}$ in. annually, depending on the average precipitation of the locality. Assuming an average recharge of $\frac{1}{4}$ in. and an average unit irrigation consumptive-use requirement of 1.0 ft, an average of only 1 acre in each 48 acres could be irrigated if the irrigation depletion were limited to the recharge. The question then arises as to the desirability of limiting irrigation by legal restrictions to such a degree, particularly in an area where the quantity of ground water in storage is very large in relation to the recharge. Obviously, if the ground water remains forever in storage, it will be of little economic benefit to the overlying landowners or to the public, but, if utilized by "mining," an irrigation economy may be developed and sustained for a given length of time depending on the quantity of water in storage, the extent of development, and the pumping lifts. Such development and utilization of the ground-water storage during that period would be of great value not only to the individuals involved but also to the state. However, many social and economic problems may result from such developments. Permanent improvements—such as buildings, roads, and utilities—in all probability must ultimately be abandoned, and persons dependent on irrigation agriculture must seek another means of livelihood, unless, of course, a new source of water can be made available.

In a speech on August 6, 1952, George Harris, attorney for the New Mexico state engineer, stated that the state engineer testified to the effect that he considered that the waters of such a basin were fully appropriated when there was enough water remaining in storage to supply the prior appropriators a reasonable quantity of water for a reasonable length of time. His testimony was to the effect that there are no means of utilizing water in storage in such a way that appropriators will have a right to the use of that water in perpetuity. Mr. Harris expressed the opinion that an irrigation economy should last for at least 40 yr and that appropriations for the use of ground water should be based on studies using this criteria.

Legal Aspects of Ground-Water Pumping for Irrigation

Laws relating to the use of ground water are generally based on and are similar to laws governing the use of surface water. Basically, two major doctrines have been followed in the United States—the common law doctrine of riparian rights and the doctrine of prior appropriation. As applied to ground water, the riparian right is based on the ownership of land overlying a water-bearing formation; the right is sustained even though it is not used. The doctrine of appropriation recognizes that "the first in time is the first in right," and generally is limited to the quantity of water that is used beneficially.

Also, the appropriative right is usually forfeited if not used for a specified period of time.

Attempts have been made by the court in some instances to distinguish between "percolating ground water" and "ground water flowing in definite underground channels," "artesian waters" and "diffused surface waters," and to apply different regulations based on those distinctions. Because this distinction is not based on scientifically defensible facts, it has caused much confusion. Regarding this, A. G. Fiedler, M. ASCE, and D. G. Thompson[12] state:

> "We believe, as a matter of fact, that from a scientific point of view, such an elaborate classification of ground water is neither justified nor necessary. All water in the part of the earth known as the zone of saturation is purely and simply ground water, moving according to certain well recognized laws of physics."

Because of the competition for limited water supplies under the riparian doctrine, the New Hampshire State Supreme Court in a decision rendered[13] in 1862, ruled that a man's right to use water percolating under his own land is limited by the corresponding right of his neighbor. This has since become known as the American Rule of Reasonable Use. The California Supreme Court further modified the American Rule and held that not only must the use be reasonable, but it must also be correlated with the uses of others and in times of shortage each should receive a fair and just share.

At present (1955), at least fifteen states have some form of ground-water law based on the appropriation doctrine, and about six states apply the American Rule of Reasonable Use to the riparian doctrine. In all the other states the common-law doctrine is followed.

Just as disputes have arisen between water users in the same state, disputes have also arisen between states. The earliest disputes pertained to territorial boundaries, and agreements were reached by compact—the first in about 1780. Since 1789 the compact method has been used extensively, dealing with problems of flood control, navigation, fishing, stream-pollution abatement, vehicular tunnels, municipal waterworks, and port facilities. Since 1900 many compacts dealing with surface-water allocation have been negotiated between two or more of the western states. So far as is known, none of these pertains specifically to the use of ground water, although the concept of stream depletion upon which some compacts are based would include stream depletions as a result of ground-water pumping.

In recent years, more emphasis has been placed on the coordinated operation of river systems. Experiences in the Tennessee Valley, the Missouri River and the Columbia River basins, and elsewhere have demonstrated the advantages of coordinated river operations. However, lacking some over-all governing body composed of representatives of the interested parties, such coordination would be difficult or impossible to obtain. The compact-commission method of approach would appear to meet these needs quite closely. In the past, it has generally been considered that, once a compact has been negotiated, nothing more need be done. In view of the ever-changing physical, economic, and social conditions, there may be advantages if compacts merely established operating principles with enough flexibility to permit operating rules to be modified by the commission when studies showed it would be beneficial to all parties concerned. Such a concept would require the compact commission to study continuously the changing physical and economic conditions within the basin as a whole, but it would provide a flexible mechanism capable of meeting the changing conditions. The increasing use of ground water for irrigation in some western river valleys, the sedimentation of reservoirs, and the constantly changing water quality emphasize that, if full benefit is to be realized from the available water resources, the rules must be flexible.

---

[12] "Some Problems Relating to Legal Control of Use of Ground Waters," by D. G. Thompson and A. G. Fiedler, *Journal*, A.W.W.A., Vol. 30, 1938, pp. 1049–1091.

[13] *Ibid*, p. 1062.

Potentialities of Ground-Water Development in Relation to Agriculture

The expansion of agriculture in the arid and semiarid western states is largely dependent on (*a*) the importation of water to shortage areas from regions having a surplus and (*b*) the judicious development and use of ground water.

It would be difficult indeed to predict the effect of changing economic and social conditions on the feasibility of transbasin diversion projects. In the final analysis, each must be evaluated in the light of prevailing conditions at the time they are studied.

In some shortage areas, transbasin diversions may not be practical or economical, and increased agricultural development may depend on the reduction of nonbeneficial consumptive uses. In areas having a shallow water table and high nonbeneficial uses, water may be salvaged by ground-water pumping. Because of the deterioration of water quality resulting from irrigation use, allowance should be made for adequate outflow from the basin to maintain the salt balance.

Irrigation in humid areas and especially the use of ground water for irrigation are certain to receive more attention in future years. For example, the increasing demand for high-value specialty crops by the frozen-food industries will stimulate the search for a reliable source of supplemental water as drought insurance. Ground water, if available in suitable areas, will admirably fulfill this need.

Conclusions

The rapidly expanding development of ground water for irrigation indicates that it is becoming increasingly important in the utilization of the total water resources. Coordinated development of surface water and ground water offers possibilities that should be considered in the planning of irrigation projects if maximum development is to be attained.

If properly planned, ground-water developments will often permit the serving of more land than if surface sources alone were used, and at the same time may prevent or greatly reduce drainage problems inherent in most irrigation projects.

Recent advances in the design and construction of wells, the availability of cheap electrical power, and the increasing demands for specialty crops have given impetus to the development and use of ground water for irrigation.

BASIN RECHARGE

By Paul Baumann,[1] M. ASCE

With Discussion by Messrs. Robert T. Knapp, Frederick L. Hotes, Norman H. Brooks, James A. Harder, Charles H. Lee, and Paul Baumann

Synopsis

In semiarid parts of the United States, water conservation is of great importance. The artificial recharge of ground-water basins, which in Los Angeles County (California) has been practiced for approximately 60 yr, has proved to be a beneficial conservation measure. Since June, 1915, the Los Angeles County Flood Control District has had the dual function of flood control and water conservation. From June, 1915, to January 1, 1955, the district, in cooperation with local agencies, has added approximately 1,200,000 acre-ft of potable water to the ground-water supply through both percolation from basins in off-channel spreading grounds and injection through wells. Percolation from basins is normally associated with shallow spreading basins overlying open aquifers and injection through wells with confined aquifers.

Introduction

In the study of ground-water phenomena related to basin recharge, one must examine separately the conditions caused by open and confined aquifers. Common to both types of conditions are the fundamental premises that (*a*) the flow of water through porous media, such as sand, is laminar; (*b*) its velocity is in accordance with the Darcy law; and (*c*) the rate of flow is based on vertical sections in accordance with the Dupuit theorem, except in special cases.

In applying these laws and theorems to undisturbed ground-water streams it is found that, in general, the velocities are low and that there is a lack of spectacular features compared to those of surface-water hydraulics. The concept changes, however, when the ground-water stream is disturbed as a result of influences such as recharge from the surface and the formation of a mound, which is superposed on the original, undisturbed ground-water table. In an open aquifer the mound will necessarily have a free-water surface whereas in a confined aquifer a pressure mound will form. The mathematical background of these phenomena has been developed by the writer,[2] and the material herein is confined to those features which are of practical interest.

Note.—Published, essentially as printed here, in September, 1955, as *Proceedings Paper 806.* Positions and titles given are those in effect when the paper or discussion was approved for publication in *Transactions.*

[1] Asst. Chf. Engr., Los Angeles County Flood Control Dist., Los Angeles, Calif.

[2] "Ground-Water Movement Controlled Through Spreading," by Paul Baumann, *Transactions*, ASCE, Vol. 117, 1952, p. 1024.

RECHARGE FROM SPREADING BASINS

Depending on the shape of the spreading basins, the mound will be cited as being two dimensional or three dimensional. Hence, two cases will be considered: (*a*) The recharge from a strip basin—for example, a canal or a stream channel whose width is smaller than its length— and (*b*) the recharge from a basin whose shape is approximately circular.

If clear water seeps into the ground from a shallow basin, it will trickle through the pores solely under the influence of gravity and free from hydrostatic pressure. The rate of infiltration is controlled by the properties of the soil and the viscosity of the water. Because viscosity varies with the temperature, the rate of infiltration must vary accordingly. However, in the study of ground-water phenomena related to basin recharge, one can use average values of temperature and consider them constant. In addition, idealization of soil properties is necessary by using average values of permeability and porosity and of the slope and magnitude of the aquifer.

STRIP BASIN

The Growing Mound.—When the seepage reaches the undisturbed ground-water table, a mound begins to form, which may be considered a two-dimensional ridge. The initial width of this mound will equal the width of the spreading strip, but the mound will subsequently grow in height and width. In the case of an initially horizontal ground-water table, the spreading will be symmetrical relative to the center of the strip basin and unsymmetrical if the ground-water table is initially inclined.

The mound spreads in the form of a wave, termed a "mound wave," both upstream and downstream from the spreading strip. The celerity of the wave may exceed more than ten times the initial velocity of a particle of ground water. The propagation of this mound wave resembles the propagation of a tidal wave in an estuary. The rate of propagation decreases with the increase of the wave length—that is, the distance from the spreading strip and the initial ground-water depth—and increases with the rate of infiltration.

The rate of growth in the height of the mound depends primarily on the rate of infiltration and on the distance from the spreading strip to a control. No ground-water movement can continue indefinitely without such a control, which may be the bank or bed of a stream, a trench or pit, a pumping trough, or the escarpment along a lake or the seashore. A control is principally an area of discharge by which the ground-water levels may be kept constant. The idealized control is a vertical seepage surface extending from the top to the bottom of the aquifer, and terminating along the respective vertical plane. The greater the distance from the spreading strip to the seepage surface the higher the mound may rise before control by the seepage surface becomes effective. The term "control," therefore, pertains primarily to the maximum depth the ground-water stream may sustain.

The ultimate height to which a recharge mound may rise above the initial surface of a ground-water stream in a given aquifer is governed by the rate and duration of infiltration and the vertical distance between the initial ground-water surface and the surface of the ground, or the distance between the spreading strip and the control. If the control is governing and the mound reaches its ultimate height without reaching the ground surface, steady flow will result. The native ground-water stream will flow through the stable-mound system and will be increased by the recharge flow on reaching its zone of influence.

When the recharge water reaches the undisturbed ground-water table and causes the mound to rise and thereby create an adverse gradient, the native stream is checked and must go into storage in the pore space above its initial surface. In addition, part of the recharge water will also flow into storage in an upstream direction; the balance will flow downstream toward the control and at a rate sufficient to (*a*) replace the native ground-water stream and (*b*) maintain the growth of the mound. Hence, the rate of growth of the mound will depend on the excess of the rate of infiltration per unit width of spreading strip over the rate of native ground-water flow. The ratio of infiltration rate to the rate of native ground-water flow per unit length of strip is, therefore, an important parameter of spreading operations. Normally this ratio is large because native ground-water movements are limited by gradients of generally less than 0.01 whereas the rate of infiltration is primarily governed by a gradient which approaches unity.

Therefore, it can be concluded that, in the absence of compensating extractions of ground water through pumping or other means, the growth of a mound will tend to be rapid and that, in the course of time and duration of recharge, the mound will reach both the surface of the ground and the free water in the spreading basin. A continuous pressure system will then have been created between the spreading basin and the ground-water body. Because this condition is dependent on the mound not attaining stability before reaching the ground surface, the rate of infiltration must diminish because of the progresive flattening of the slopes of the mound. If native ground-water flow existed, the rise of the mound to the surface might have serious consequences as a result of waterlogging of the ground—unless prevented by pumping extractions. Hence, it is advisable to combine spreading and pumping operations to achieve complete control of the mound phenomenon. Ground water extracted through pumping should, of course, be put to beneficial use. In Los Angeles County (California) approximately two-thirds of the total use of water is supplied from ground water; hence, pumping is performed in all areas where recharge is practiced. However, pumping, in general, lacks proper coordination with recharge. Consequently, proper control for the systematic accomplishment of maximum water conservation is not exercised.

The time requirement for a growing mound for an initial gradient of 0.01, a distance of 4 ft between the simulated spreading strip and the control, and a rate of infiltration of 0.82 cu ft per hr per unit length has been shown.[3] The width of the spreading basin was neglected[3] because the mound dimensions were carried far beyond the model dimensions. The spreading strip may be represented by a line and the infiltration by a line source. The rapid initial growth of the mound, which is associated with the correspondingly rapid movement of the mound wave in both the upstream and the downstream directions, is of special interest. It is obvious that the flow of recharge water in the upstream direction diminishes with time and approaches zero at the instant the adverse gradient disappears. The native ground-water flow then gradually passes through the mound and, together with the entire recharge flow, moves toward the control. Hence, at the time the mound has reached its ultimate height the entire native and recharge flows are discharged through the control. Theoretically, this time is infinite; however, it may be noted[3] that the time required for the mound to become quasi-stable is well within finite limits. For a smaller gradient and a greater distance to the control, the time requirement would be correspondingly increased. For example, for a gradient of 0.0025 and a distance of 30 ft to the control, approximately 2,400 hr, as compared with 10 hr, would be required for the establishment of quasi-stability.

---

[3] "Ground-Water Movement Controlled Through Spreading," by Paul Baumann, *Transactions*, ASCE, Vol. 117, 1952, p. 1031, Fig. 2.

The initial slope and depth of the native stream and the distance to the control combined with the rate of infiltration, the permeability, and the effective porosity determine the ultimate height of the mound and effective upstream distance of the backwater. Theoretically, this distance is likewise infinite. Practically, however, the rise of the backwater above the initial ground-water surface is of no importance after it is no longer measurable.

In model tests for maximum potential flow,[4] the "basic parabola" was observed. It is apparent that the Dupuit theorem is applicable with fair approximation except near the spreading basin and near the control. That is, the use of the tangent of the slope angle rather than the sine of the angle is permissible, as long as a ground-water problem can be treated without a flow net.

The model quantities could readily be applied to a prototype of comparable soil properties, initial slope, and linear dimensions N times those of the model. The rate of infiltration and the time required for the various stages of the mound would then be N times those of the model. Hence, if the linear dimensions of the prototype are, for example, 200 times those of the model ($N = 200$), the initial slope is 0.0025, and the distance to the control is 800 ft, then the time required for the mound to reach practical stability would be approximately 20,000 hr or 835 days, the ultimate height 50 ft, and the distance of measurable backwater 60,000 ft. If the distance between initial ground-water surface and land surface is less than the ultimate height of the mound—for example, one-half or 25 ft and is therefore governing—the time required for the mound to rise to the surface would be approximately 20 hr or less than a day. At this time, a measurable rise of the backwater would extend upstream from the spreading strip for a distance of 2,000 ft. This clearly illustrates the rapid spread of the mound wave even in the upstream direction. In the downstream direction the mound wave would require less than 4 hr to reach the control which is 800 ft from the spreading strip. Based on these soil properties, the time required for a water particle of the native stream to travel a distance of 800 ft would be 5,760 hr or 240 days. Hence, in this case, the average celerity of the mound wave is more than 1,400 times that of the velocity of native ground-water flow through the pores of the soil. This explains the sudden rise of water in observation wells that are several thousand feet from spreading grounds in much less time than that corresponding to the rate of native ground-water movement.

---

[4] "Ground-Water Movement Controlled Through Spreading," by Paul Baumann, *Transactions*, ASCE, Vol. 117, 1952, pp. 1055–1060.

The Disappearing Mound.—When a mound rises during spreading operations and recharge then is discontinued, the mound will drain itself in the course of time. Theoretically, this time is infinite; practically, effective drainage takes place within a time period comparable to that of the growing mound.

Using the same scale factor ($N = 200$) and a prototype specific yield equal to that for the rising mound, the time required effectively to drain the mound, which is 50 ft in height and with an initial gradient of 0.0025, would be 30,000 hr or 1,250 days. It would therefore take approximately one and one-half times as long for the mound to drain as for it to form. This time requirement, of course, increases with the increase of the distance to the control.

If the mound has not reached the control and is still in the state of growth at the time spreading is discontinued, the mound will not only fade away but will "float" downstream because of lack of hydraulic support from the control. Hence, the passage of the itinerant, fading mound will be demonstrated by progressive diminishing of the water level in wells along its route.

The foregoing example clearly indicates the controlling influence of the spreading itself; the position of the mound crest will remain fixed as long as infiltration from the surface is maintained.

CIRCULAR BASIN

The foregoing also applies, in general, to the circular spreading grounds except that in this case the mound will be three dimensional. Furthermore, the difference in the shape of the mound between a horizontal and an initially inclined ground-water table and the phenomenon as a whole is much more pronounced.

In the case of a horizontal ground-water table, the mound wave radiates uniformly in all directions from the center of the circle. Hence, the directrices are the traces of radial, vertical planes which diverge in the direction of flow. Therefore, for a recharge flow per unit length of circumference of the circular basin which is equal to that per unit length of the strip basin, the rate of growth of the three-dimensional mound is less than that of the two-dimensional mound. Thus, it may be postulated that sustained recharge from circular basins is more efficient than from strip basins because the three-dimensional mound in the same ground-water basin tends to spread more uniformly and over a wider area before it rises to the surface. Furthermore, after it rises to the surface, the rate of infiltration (acceptance rate) for the three-dimensional mound diminishes less rapidly than for the two-dimensional mound. In addition, the danger of waterlogging the area adjacent to the circular spreading basin is lessened despite the fact that the initial rate of infiltration per unit area of a strip basin is greater than that of a circular spreading basin because the rise to the surface, not the initial acceptance rate, is the criterion for sustained recharge.

If the seepage of a circular spreading basin is falling on an inclined ground-water table, the mound phenomenon is far more difficult to analyze. At present (1956), no exact solution has been given for the unsteady flow and wave motion. Mathematical expressions based on the streamline theory have been developed[5] only for the ultimate condition, which is the stable mound. It is necessary to assume even for this condition that the infiltration is concentrated in the center of the circle. Recharge through a well, which will subsequently be cited, closely satisfies this premise.

For the steady-flow condition the streamlines and equipotential contours may be computed. The formation of a recharge stream, which is entirely separate from the native ground-water stream and confined within vertical interfaces, means that, except for some diffusion along the interfaces, the two liquids, despite chemical and physical similarity, do not mix. This condition exists because of the difference in potentials, that of the recharge flow being the greater. Therefore, one may conclude that the spreading stream must asymptotically approach a width which is equal to the total rate of infiltration divided by the rate per unit width of native ground-water flow; the time required therefor is infinite.

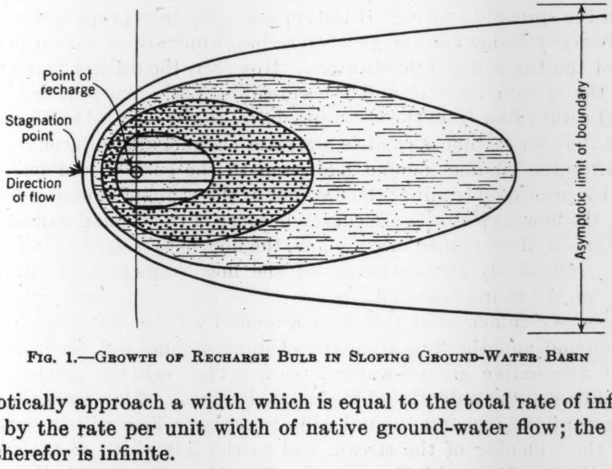

FIG. 1.—GROWTH OF RECHARGE BULB IN SLOPING GROUND-WATER BASIN

Attention must be directed with some speculation to those features which occur within finite times. It is safe to reason that in its early state this mound would not differ much from the circular mound if the initial slope of the ground-water table were quite small, which it usually is. The mound would be slightly egg-shaped rather than circular, the point of the "egg" facing downstream. With continued spreading the mound would be growing in all directions, but it would grow most rapidly in a downstream direction and least rapidly in an upstream direction. Because the streamline theory predicts a point of stagnation at the ultimate upstream boundary of the recharge flow, the mound therefore must approach this point by decelerating its upstream growth. On the other hand, the ultimate condition in the downstream direction is the aforementioned width of the spreading stream, which calls for the progressive elongation of the mound in the downstream direction. Although an exact analysis is difficult, intermediate stages of the mound may be practically evaluated by graphical methods. One condition must always exist for any particular time—the water content of the mound must be equal to the volume of water infiltrated. Fig. 1 shows the approximate shape of the mound for three early stages in relation to the ultimate shape of the mound.

---

[5] "Ground-Water Movement Controlled Through Spreading," by Paul Baumann, *Transactions*, ASCE, Vol. 117, 1952, pp. 1049–1050.

EFFECT OF SPREADING MOUNDS ON CHANNEL MOUNDS

A problem that often arises when spreading grounds are located on the bench land next to stream channels is as follows: Under what condition can the recharge water move across the stream channel if a mound, previously formed under the channel, has risen to its surface—that is, under what condition can the channel mound block the flow from the spreading mound?

It can be concluded that to stop the flow from the spreading basin the water surface of the channel mound would have to rise to the same elevation as that in the spreading basin. If the spreading basin is properly located this could only occur during flood stage when recharge operations are not performed because of the turbidity of floodwaters. However, the difference in elevation between the stream channel and the spreading basin must be such that a significant return flow from the spreading basin to the channel can be avoided.

Fig. 2 shows a section normal to a stream channel and adjacent spreading ground after the channel mound had risen to the surface and had become quasi-stable prior to spreading; the flow net of the channel mound is indicated. Actually, the flow trajectories are curved because of the sloping stream channel and aquifer but, if developed into a plane, the flow net resembles that shown in Fig. 2(*a*). Obviously the curvature of the flow trajectories facilitates the outflow from the channel mound.

If recharge commences at this time, a mound will form on the slope of the channel mound and the flow from the channel mound will act in a manner similar to the native ground-water stream. The recharge mound will rise rapidly and reach the potential of the channel mound. Flow from the channel mound toward the recharge mound will also cease, which will have the same effect as the widening of the stream bed to the full width of the spreading ground. Hence, the total infiltrated flow from the channel and the spreading ground will be divided relative to the center line of the combined width. Part of the recharge flow will therefore begin to move across the stream channel, together with all the channel percolation.

As the spreading mound continues to rise, an increasing part of its flow will move across the channel. This condition (Fig. 2(*b*)) may be accompanied by a return flow to the stream channel if the spreading basin is only separated from it by a levee. The flow net shown in Fig. 2(*b*) is likewise developed from a curved surface, and the curved trajectories will again facilitate the flow from both mounds. Only by taking the three dimensions of the net into consideration is it possible fully to understand this flow condition. The actual part of the recharge water crossing the stream channel for any given condition is obtained from a balanced-flow net.

In assuming the impervious stratum to be horizontal and the flow trajectories linear and at right angles to the stream channel, a relation between the average acceptance rate, q, per unit of wetted area and the parameter, D/W, is

$$q = K(1 - e^{-D/2W}) \ldots\ldots\ldots\ldots\ldots\ldots (1)$$

(a) CHANNEL MOUND

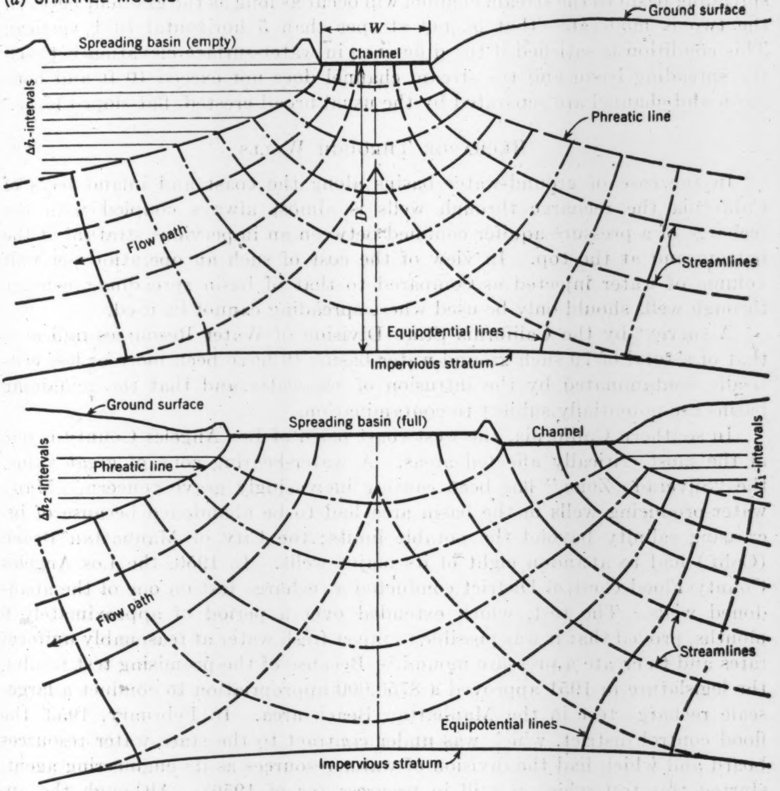
Ground surface
W
Spreading basin (empty)
Channel
Δh-intervals
Phreatic line
D
Flow path
Streamlines
Equipotential lines
Impervious stratum
Ground surface
Spreading basin (full)
Channel
Δh₂-intervals
Δh₁-intervals
Phreatic line
Flow path
Streamlines
Equipotential lines
Impervious stratum

(b) CHANNEL AND SPREADING MOUND

FIG. 2.—FLOW NETS

in which K is the permeability coefficient and e, the base of natural logarithms.

Eq. 1 was determined by computing the flow per unit length of channel for flow nets of constant depth, D, and variable width, W (Fig. 2(a)). The average acceptance rate per unit of wetted area decreases with the increase in width of the channel relative to a constant depth of the aquifer. However, the total acceptance rate, Q, increases with W although at a decreasing rate.

For example, the total acceptance rate for $D/W = 1$ and the stream channel only is $Q_1 = 0.387\ K\ W$, whereas for a combined width equal to 4 W of stream channel and spreading ground, $Q_2 = 0.468\ K\ W$. This relation between a given depth of aquifer and the width of the spreading area is of economic importance.

From Fig. 2(*b*) it is apparent that no significant return flow from the spreading basin to the stream channel will occur as long as the gradient between the two is moderate—that is, not steeper than 5 horizontal to 1 vertical. This condition is satisfied if the difference in water-surface elevation between the spreading basin and the stream channel does not exceed 10 ft and both basin and channel are separated by the usual broad-crested, flat-sloped levee.

Recharge Through Wells

In the case of ground-water basins along the coast and inland bays of California the recharge through wells is almost always coupled with the recharge of a pressure aquifer confined between an impervious stratum at the bottom and at the top. In view of the cost of such an operation per unit volume of water injected as compared to that of basin spreading, recharge through wells should only be used where spreading cannot be used.

A survey[6] by the California State Division of Water Resources indicated that of a total of 79 such ground-water basins 19 have been more or less critically contaminated by the intrusion of sea water and that the remaining basins are potentially subject to contamination.

In southern California, the west coast basin of Los Angeles County is one of the most critically affected areas. A water-bearing zone of great value, the "Silverado Zone," has been causing increasingly grave concern. Many water-producing wells in the basin area had to be abandoned because of increasing salinity beyond the potable limits; the City of Manhattan Beach (Calif.) had to abandon eight of its major wells. In 1950, the Los Angeles County Flood Control District conducted a recharge test on one of the abandoned wells. The test, which extended over a period of approximately 6 months, proved that it was possible to inject fresh water at reasonably uniform rates and to create a pressure mound.[7] Because of the promising test results, the legislature in 1951 approved a $750,000 appropriation to conduct a large-scale recharge test in the Manhattan Beach area. In February, 1953, the flood control district, which was under contract to the state water resources board and which had the division of water resources as its engineering agent, started this test which is still in progress (as of 1956). Although the appropriated state funds became exhausted in November, 1953, the flood control district, together with the west basin water association, managed to continue the test on a somewhat reduced basis after that date.

In facing the problem of stemming sea-water intrusion into a ground-water basin by a fresh-water barrier, a principle not previously cited herein pertaining to the difference in specific gravity between fresh water and sea water must be considered; it is termed the Ghyben-Herzberg principle.[8] In brief, the principle establishes the fact that in order to balance the pressure of sea water by fresh water at any depth below sea level, a differential head of fresh water between 2½% and 3% of the depth in question must be provided. The exact percentage depends, of course, on the actual relative density of sea water and fresh water at a particular location. At Manhattan Beach a differential head of 2½% of the maximum depth must be present. However, this differential head can only exist as long as the fresh-water gradient is seaward which, unfortunately, has not been the case under natural conditions in this and other ground-water basins along the ocean front of California. Hence, it is necessary to raise the water table artificially by a pressure mound created through the injection of fresh water into the aquifer through wells. Replenishment of the basin will be an important incidental achievement.

---

[6] "Seawater Intrusion into Ground Water Basins Bordering the California Coast and Inland Bays," *Water Quality Investigation, Report No. 1,* California State Water Resources Board, Sacramento, Calif., December, 1950.

[7] "Experiment with Fresh Water Barrier to Stem Sea Water Intrusion," by Paul Baumann, *Journal,* A.W.W.A., May, 1953, p. 521.

In connection with circular spreading basins and an inclined ground-water table it was noted that the native ground water and the infiltrated fresh water do not mix so long as the latter has a higher potential. This is also true if one of the liquids, such as the sea water, has a higher specific gravity than the other and thereby possesses the potentialities of a density current.

Therefore, sea water will intrude a ground-water basin lying below mean sea level in the form of a wedge which will creep along the bottom of the aquifer at an ever-increasing rate and will eventually displace the fresh water throughout its section unless it is repelled by recharge operations. Such pressure produced by fresh-water injection through wells must satisfy the foregoing minimum requirement at all points. Thus, the spacing of the recharge wells is an important hydraulic parameter in addition to being of economic significance. The mechanics of the pressure mound thus formed and of the free mound below a circular spreading ground are basically the same, except no significant change in storage is involved with the pressure mound. Hence, a simplified analysis can be made of the recharge of a confined aquifer. The maximum spacing of the recharge wells is determined by the ratio of injection rate and rate of native ground-water flow per unit length of barrier.

Fig. 3 is a map of the west coast basin and the ground-water contours of the confined aquifer prior to the recharge test. The location of the test front in relation to the possible, ultimate recharge line is indicated, together with the sites of tests conducted simultaneously on the Manhattan Beach well and on spreading plots. Areas A and B represent quasi-unconfined aquifer conditions. The depletion of the basin is evidenced through the deep depressions and the landward gradient. In general, the basin is confined between the ocean front and the Newport-Inglewood (Calif.) fault.

Sand dunes in the test reach, approximately 90 ft thick, are underlain at or near sea level by approximately 20 ft to 30 ft of relatively impervious Upper Pleistocene sediments which cap the affected major regional aquifer known as the "Merged Silverado." This confined nonhomogenous aquifer, consisting of approximately 100 ft of continental and shallow marine Upper and Lower

---

[8] Discussion by David K. Todd of "Ground-Water Movement Controlled Through Spreading," by Paul Baumann, *Transactions*, ASCE, Vol. 117, 1952, p. 1061.

Pleistocene deposits, bifurcates and appreciably thickens inland; it is also in hydraulic continuity with several important prolific west coast basin, water-bearing members, among which are the quasi-open aquifers in the areas marked A and B in Fig. 3.

At the test site, the effective bottom of the aquifer is approximately 110 ft below mean sea level. It follows, therefore, that, according to the Ghyben-Herzberg principle, the minimum differential fresh-water head required to balance sea-water pressure at that depth is 2.75 ft. The test front, 4,000 ft long, approximately 2,000 ft landward from the sea shore and parallel to it, is formed by nine 12-in.-diameter recharge wells, 500 ft apart. Thirty-six 8-in., four 4-in., and eighteen 2-in. wells were provided for observation of pressure levels and for sampling. Fresh water is supplied through a pipeline which connects to the west-coast-basin supply line of the Metropolitan Water District of Southern California; the arrangement is shown in Fig. 4, which

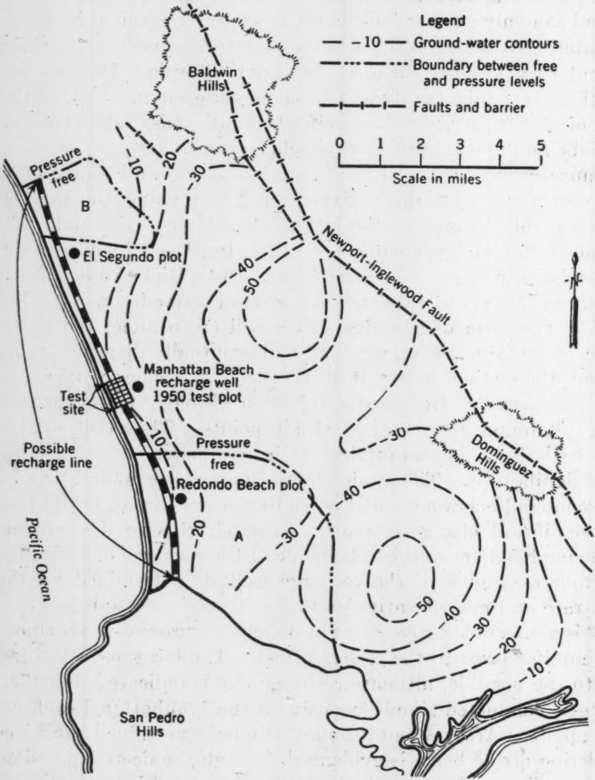
Legend
-10 Ground-water contours
Boundary between free and pressure levels
Faults and barrier
0 1 2 3 4 5
Scale in miles
Baldwin Hills
Pressure
free
B
El Segundo plot
-10
20
30
40
50
Newport-Inglewood Fault
Manhattan Beach recharge well 1950 test plot
Test site
Possible recharge line
Pressure
free
10
Redondo Beach plot
20
A
30
40
50
30
20
10
Dominguez Hills
Pacific Ocean
San Pedro Hills

FIG. 3.—WEST COAST BASIN TEST SITES, BARRIER LOCATION, AND GROUND-WATER CONTOURS

also shows the adjacent, abandoned, and producing wells and the isochlors prior to recharge (solid contours).

The possible detrimental effect of the "saline wave" has caused some apprehension. This wave was thought to be the result of displacing part of the saline water with injected fresh water which had extended landward beyond the well front. The test proved that this apprehension was unfounded. The sea-water intrusion itself is the damaging feature and not the saline wave caused by injection. Once the intrusion is stopped the effect of the saline wave is not important. These statements are, of course, made on the assumption that the saline intrusion had displaced the native ground water for a relatively small distance landward from the well front and that, therefore, the volume of saline water landward from the injection wells would be small compared to that of the native ground water. In general, it was found that the saline wave flattens as it moves landward. The contaminating effect diminishes approximately with the square of the distance from the recharge wells

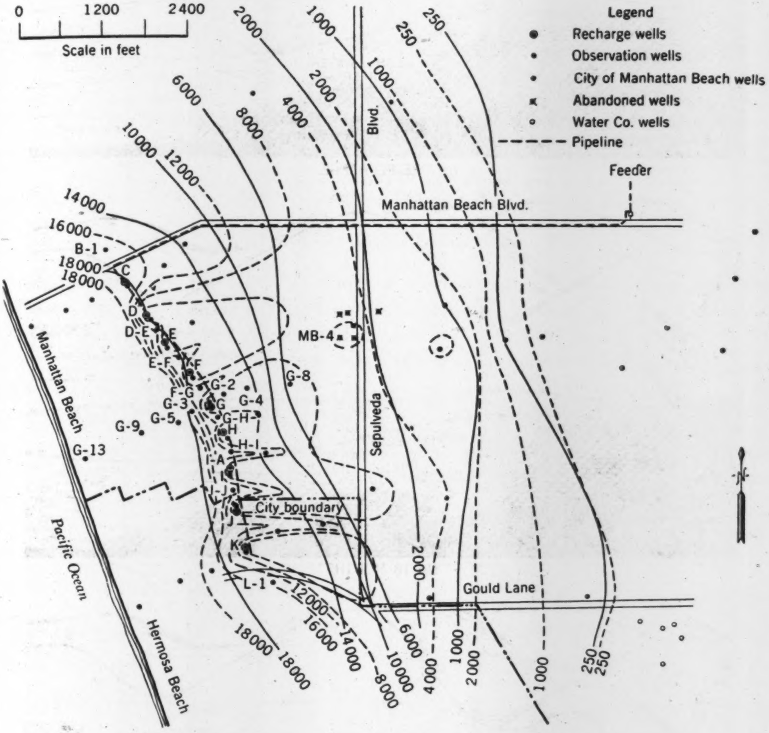
0
1200
2400
Scale in feet
Legend
Recharge wells
Observation wells
City of Manhattan Beach wells
Abandoned wells
Water Co. wells
Pipeline
Feeder
Manhattan Beach Blvd.
Sepulveda Blvd.
Gould Lane
City boundary
Manhattan Beach
Hermosa Beach
Pacific Ocean
MB-4
B-1
C
D
D-E
E
E-F
F
F-G
G-2
G-3
G
G-4
G-5
G-H
H
G-9
G-13
H-I
A
I
I-J
J
K
L-1
250
1000
2000
4000
6000
8000
10000
12000
14000
16000
18000

Fig. 4.—Barrier Test Arrangement with Isochlor Lines

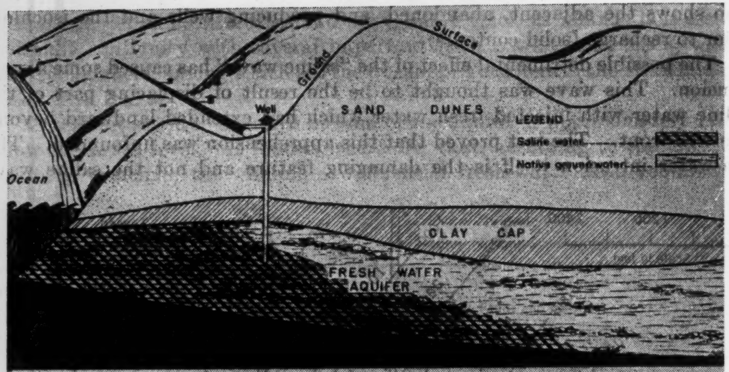
Ground Surface
Well
SAND DUNES
LEGEND
Saline water
Native ground water
Ocean
CLAY CAP
FRESH WATER AQUIFER

(a) PRE-RECHARGE

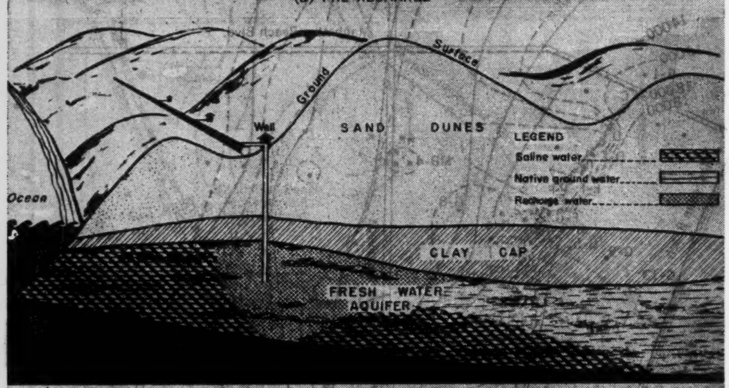
Ground Surface
Well
SAND DUNES
LEGEND
Saline water
Native ground water
Recharge water
Ocean
CLAY CAP
FRESH WATER AQUIFER

(b) 18 MONTHS

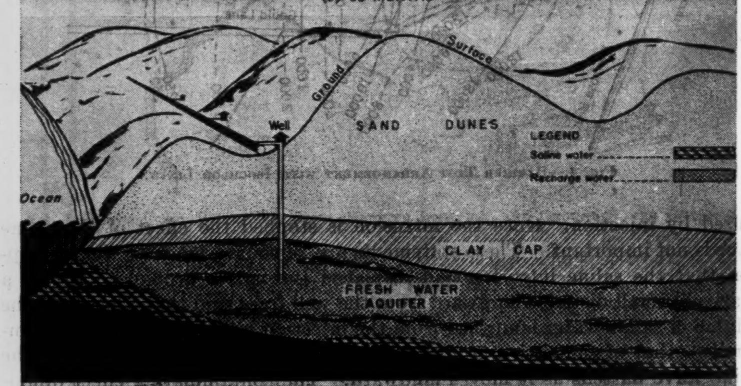
Ground Surface
Well
SAND DUNES
LEGEND
Saline water
Recharge water
Ocean
CLAY CAP
FRESH WATER AQUIFER

(c) ULTIMATELY

FIG. 5.—THE EFFECT OF RECHARGE ON SEA-WATER INTRUSION

if the rate of fresh-water injection is such that the minimum differential head of 2.75 ft at the internodal point between the wells can be maintained.

In a section through the center of the test front, in Fig. 5(*a*), is shown the extent of the sea-water intrusion prior to commencement of injection. Horizontal and vertical distances may be estimated from the distance between the recharge well and the seashore which is approximately 2,000 ft and from the depth below sea level of the aquifer which is approximately 110 ft. The saline water indicated by the cross-hatched area had displaced nearly all the native water between the ocean and the test front and had crept 3,500 ft landward in the form of a wedge. Wherever possible, the position of the interface between saline water and fresh water was determined by conductivity measurements.

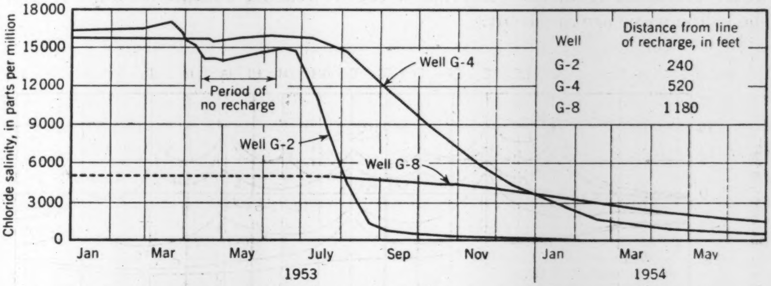

Fig. 6.—Passage of Saline Wells at Test Wells

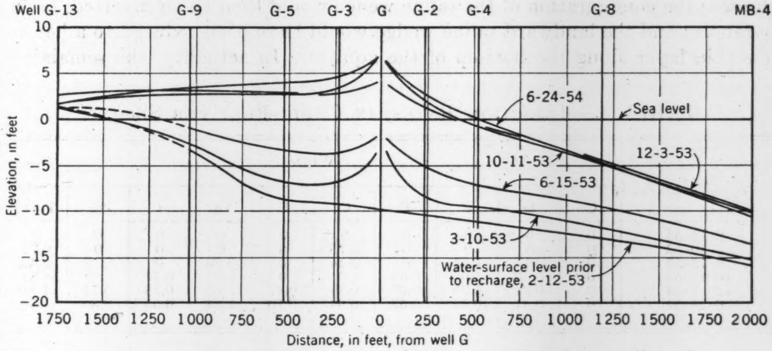

Fig. 7.—Cross Section of Barrier at Various Stages

Fig. 5(*b*) shows the aquifer conditions after fresh water had been injected for 18 months. The injected fresh water was contained in the dot-covered bulb. The recharge water had displaced the saline water in the form of a crater and had caused it to "slough" off landward and to retreat seaward. The rate of displacement of the saline water naturally depends on the rate of injection which, in turn, depends on the injection head, relative to mean sea level. The injected water, therefore, has a higher potential than both the sea water and the native fresh water and, unless agitated, does not mix with either except through diffusion along the interfaces as previously cited. Hence, the water volume of the recharge bulb must at all times be equal to the volume of water injected. The landward sloughing, the flattening-off of the saline water displaced from the crater, and the decreasing contaminating effect of the saline wave are apparent.

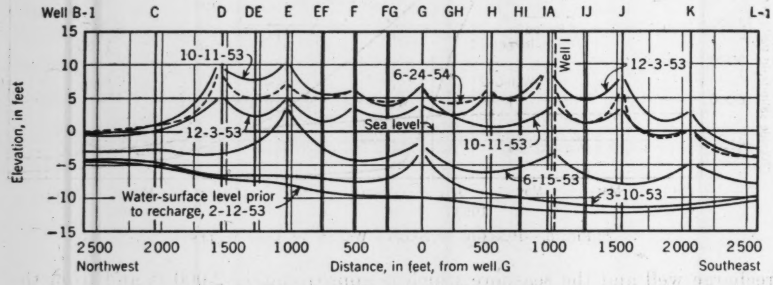

FIG. 8.—PROFILE OF BARRIER AT VARIOUS STAGES

Finally, Fig. 5(*c*) shows, on a speculative basis, the ultimate result of recharge—that is, the condition at a time when the recharge operations would have accomplished their objectives. At this time, the saline wedge would have been forced seaward far enough to enable recharge water to escape to the sea; the configuration of the saline wedge would then be an inverted, basic parabola; and the landward saline wedge would have been reduced to a harmless thin layer along the bottom of the aquifer. In actuality, the remaining sea water would have been trapped in depressions along the bottom of the aquifer or would have been depleted without harmful effect through pump extractions. The condition as shown in Fig. 5(*c*) would probably establish itself after approximately 10 yr of continuous fresh-water injection. Recharge would have to be resumed when the saline wedge had again advanced a critical distance landward or might be maintained at a rate sufficient to prevent re-invasion.

TABLE 1.—INJECTION RATES, IN CUBIC FEET PER SECOND

Date	Well									
	C	D	E	F	G	H	IA	J	K	Total
2-12-53	0	0	0	0	0	0	0	0	0	0
3-10-53	0	0	0	0	0.75	0	0	0	0	0.75
6-15-53	0	0	1.05	0	0.54	0	0.36	0	0.48	2.43
10-11-53	0	0.50	1.04	0.63	1.05	0	0.37	0.51	0.74	4.84
12- 3-53	0	0.24	0.39	0.37	0.39	0.47	1.03	0.78	0.74	4.41
6-24-54	0	0.41	0.45	0.59	0.64	0.70	1.13	0.55	0.30	4.77

Fig. 6 shows a typical manifestation of the saline wave in terms of chloride-ion concentration as it passed observation wells 240 ft, 520 ft, and 1,180 ft, respectively, landward from the injection wells.

Fig. 4 shows the isochlors (dashed contours) after 16 months of recharge in relation to the well front. It is interesting to note the articulation of the mounds at the recharge wells and the merging of these mounds landward from the recharge wells.

Fig. 7 shows the pressure-mound configuration at various times along the cross section normal to the test front; Fig. 8 shows the mound in profile; and the injection rates are shown in Table 1. It is evident that the pressure mound extends well beyond the terminal recharge wells. Unfortunately, the well at the north end had to be shut down and injection was discontinued after only a few days of operation because of failure of the clay cap at this location. Hence, the barrier shown in Fig. 8 was created by only 8 recharge wells.

CONCLUSIONS

The barrier test has clearly demonstrated the superiority of gravel-jacketed wells in relation to simple casing wells. Two of the 9 recharge wells were gravel-jacketed and performed satisfactorily throughout the test. Of the remaining 7 simple casing wells, one failed immediately after it was put in operation, and the others developed weaknesses at various times necessitating shut down and costly repairs. The main advantages of the gravel-jacketed well are the uniform distribution of perforations and the resulting freedom in the movement of recharge water through the gravel jacket into the aquifer, which requires considerably less head than a simple casing well for one and the same rate of recharge. Hence, the danger of "blowout" along the contact between well casing and clay cap is correspondingly lessened.

By sterilizing the injected water with approximately 8 ppm of chlorine it was possible to sustain a minimum total injection rate of 4.50 cu ft per sec at moderate head. Chlorination, or a similar method of sterilization, is believed essential in well recharge to prevent clogging of the pores by otherwise harmless microorganisms, which are somewhat prevalent in all sources of water and which are stimulated to great activity by unavoidable aeration of the recharge water. Sterilization of clear water diverted from streams attending large-scale recharge operations in spreading grounds has not been found essential.

ACKNOWLEDGMENTS

The writer is indebted to H. E. Hedger, M. ASCE, for his review of the paper; to Finley B. Laverty, M. ASCE, and his staff for assisting in the computations and the preparation of the original exhibits; and to Hazel M. Robertson for typing and assembling the original manuscript.

DISCUSSION

Robert T. Knapp,[9] **M. ASCE.**—Although the paper was undoubtedly stimulated by the author's interest in the water problems of southern California, the concepts and methods it presents are applicable to all semiarid and arid regions where water supply is a limiting factor in determining the population that can be supported by an area.

The writer was particularly interested in the Manhattan Beach experiments on the development of a fresn-water barrier to prevent salt-water intrusion in depleted ground-water basins. While observing the action of the fresh-water barrier as shown in Fig. 5, the writer noted a minor discrepancy—the free surface of the salt water appears to slope in the wrong direction.

One can assume that in a density-current flow in a porous medium there is no friction at the interface between the two liquids because the velocity difference is extremely small. The flow velocity of the overlying layer is determined by the shear between the liquid of the overlying layer and the fixed porous medium. Hence, within a salt-water intrusion which is in equilibrium with a ground-water flow, pressures will always be constant along any horizontal plane and will be equal to the weight of a unit column of sea water whose height is the distance from the horizontal plane to sea level. The slope of the interface will therefore be determined solely by the pressure from the overlying layer.

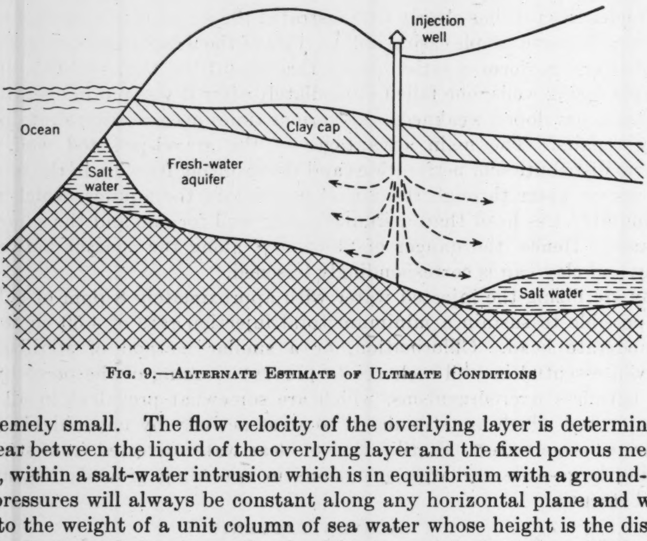

Fig. 9.—Alternate Estimate of Ultimate Conditions

In the case of the landward saline wedge cut off from the ocean by the recharge flow, pressures within the saline water must also be constant along horizontal planes. The pressure level will not be determined by the depth below the surface of the ocean but by the pressure in the overlying fresh water. When it finally reaches equilibrium, the configuration of the interface between this isolated body of salt water will depend on its geographical location at equilibrium. It will, of course, run downhill to the lowest available spot and form a lake. In Fig. 5 it appears as if this lake were formed within the recharge zone—that is, where the fresh-water mound is still sloping landward. If this is the case, the interface would slope seaward as shown in Fig. 9. If this salt-water lake rested under a region in which there were pumping wells, the interface would include salt-water mounds with peaks lying under these wells, as shown in Fig. 10.

---

[9] Prof. and Hydr. Engr., California Inst. of Technology, Pasadena, Calif.

This principle of zero shear at the interface makes it easy to compute the possible distance of salt-water intrusion from the known ground-water elevations because the hydrostatic pressure at the interface must exactly equal the depth below sea level of the interface. The slope of the interface is always in the opposite direction to that of the ground-water surface. The interfacial slope is always steeper because the ratio of the two slopes is equal to the ratio of the density of the fresh water to the difference in density between the salt water and fresh water. If the relative density of the salt water is assumed to have the nominal value of 1.025 with respect to the fresh water, the downward slope of the interface will be forty times the ground-water slope. However, these considerations apply only to equilibrium conditions and therefore represent only the maximum salt-water intrusion occurring for a given set of continuing ground-water elevations.

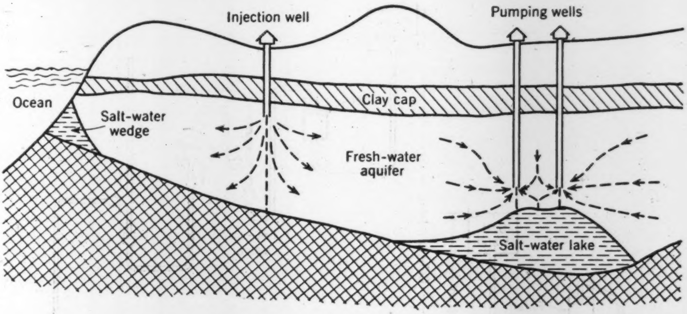

FIG. 10.—EFFECT OF PUMPING ON INTERFACE OF SALT-WATER LAKE

FREDERICK L. HOTES,[10] A.M. ASCE.—Ground-water problems are increasing throughout the United States and, although there are many complex phenomena that engineers and hydrologists would like to know more about, none is as important as basin recharge. Recharge, both natural and artificial, places definite limits on the safe, sustained yield of ground-water basins. The author has indicated some of the phenomena connected with recharge problems for both free and confined aquifers and has also indicated some of the practical limitations learned from his personal experience.

This discussion will be limited primarily to the problem of sea-water intrusion into pressure aquifers. Several research projects conducted at the University of California at Berkeley have contributed information of considerable assistance in interpreting ground-water behavior in coastal regions and on the effectiveness of injection wells in repelling sea-water intrusion.

---

[10] Associate Prof. of Irrig. Eng., Univ. of California, Berkeley, Calif.

Model Studies.—In addition to contracting with the Los Angeles Flood Control District, the California State Water Resources Board also contracted with the University of California to conduct laboratory and model studies of sea-water intrusion, which would supplement and aid in the prototype experiments being performed by the flood control district.

Model Aquifer.—After a thorough study of the literature had been made,[11] a sand and lucite model was constructed. A detailed description of the model and the experiments, together with the results of research on impermeable cut-off-wall materials, has been published.[12,13] Therefore, only a summary will be presented.

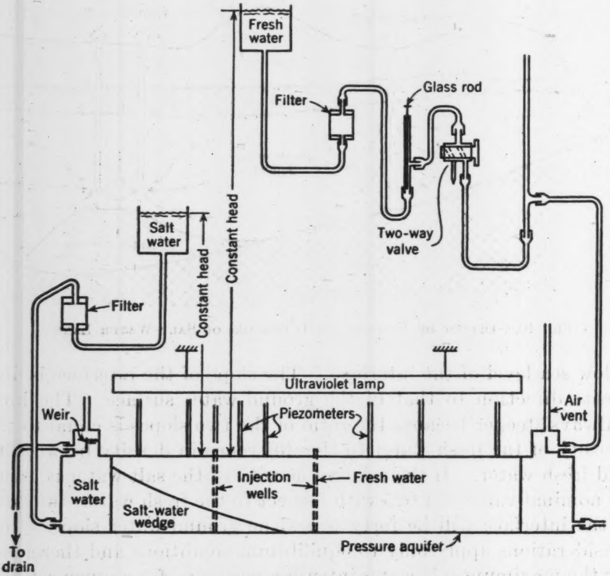
Fresh water
Filter
Glass rod
Two-way valve
Constant head
Salt water
Constant head
Filter
Ultraviolet lamp
Weir
Piezometers
Air vent
Salt water
Injection wells
Fresh water
Salt-water wedge
Pressure aquifer
To drain

FIG. 11.—SCHEMATIC SKETCH OF APPARATUS

Fig. 11 is a schematic sketch of the apparatus. The main chamber, representing an idealized pressure aquifer, was 4 ft long, 6 in. high, and 3 in. wide. It was packed with a commercially available washed-quartz sand; this sand has an effective size (10%) of 0.22 mm, a 50% size of 0.28 mm, and a uniformity coefficient of 1.3. When packed in the model its coefficient of permeability averaged 0.032 cm per sec (680 gal per sq ft per day). The salt water was introduced through the chamber on the left and the fresh water through the chamber on the right. Both fluids were supplied through constant-head-flow regulators.

---

[11] "An Abstract of Literature Pertaining to Sea Water Intrusion and Its Control," by D. K. Todd, *Technical Bulletin No. 10*, San. Eng. Research Lab., Univ. of California, Berkeley, Calif., July, 1953.

[12] "Report on Laboratory and Model Studies of Sea Water Intrusion," by J. A. Harder and F. L. Hotes, *Technical Bulletin No. 11*, San. Eng. Research Lab., Univ. of California, Berkeley, Calif., May, 1955, p. 11.

[13] *Ibid.*, p. 39.

The piezometric tubes were used to establish the piezometric surface under any desired condition of flow. The model injection wells were located only along the near side of the aquifer. They were made of split-glass tubing, $\frac{1}{4}$ in. in diameter. The near face represents a plane of symmetry, which is normal to the coast line and through the center line of one of a series of injection wells that are equally spaced along a line parallel to the coast. The far face represents the plane of symmetry, which is normal to the coast and midway between two injection wells. No flow crosses these planes of symmetry in a uniform injection process; therefore, they are represented by solid lucite walls in the model.

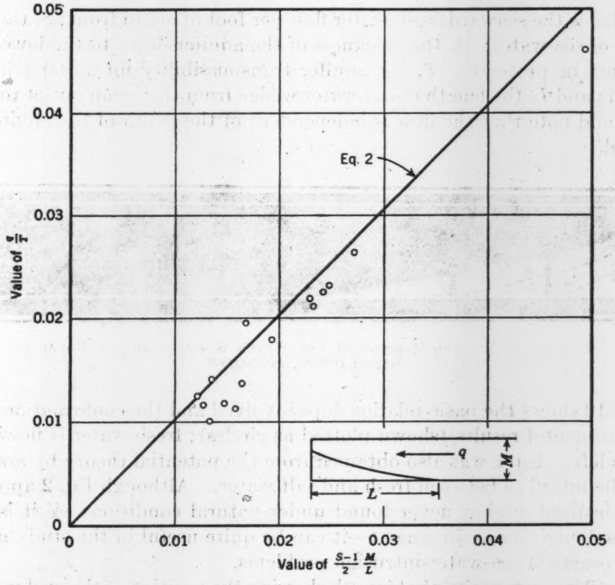

FIG. 12.—LENGTH OF INTRUDED WEDGE VERSUS SEAWARD FRESH-WATER FLOW

Model Fluids.—The salt water used in the model was adjusted to a specific gravity of 1.100, and solutions of both calcium chloride and sodium chloride were successfully used. The procedure increased the model flow rate and generally speeded up an otherwise slow action. The viscosity of these solutions was about 30% greater than that of sea water. This discrepancy did not affect measurements when the sea-water edge was stationary, but it did have some effect on rates of wedge movement.

An innovation that produced startling and successful results was the use of fluorescent dyes to aid in distinguishing the fresh water from the salt water. A convenient concentration of ordinary dyes does not show up well in the model because of the thin layer of solution visible between the transparent sides and the first layer of sand grains. An ultraviolet light source was also used to produce a strong, positive response from the thin-solution layer next to the wall. Rhodamine B in the salt water and fluorosol in the fresh water gave good contrasting colors of red and blue.

Results.—J. A. Harder,[12,13] using an adaptation of M. Muskat's[14] approach to the solution of seepage through an earth dam on an impervious foundation, derived the following expression for the fresh-water flow and length of intruded saline wedge under equilibrium conditions:

$$q = \tfrac{1}{2}(S - 1)\frac{M}{L}T \qquad (2)$$

in which q is the seaward fresh-water flow per foot of ocean front; S, the specific gravity of sea water; M, the thickness of the aquifer down to the lowest depth that must be protected; T, the aquifer transmissibility for a 100%-hydraulic gradient; and L, the length of sea-water wedge from the ocean outlet to the toe. One should note that the flow is independent of the depth of the aquifer below sea level.

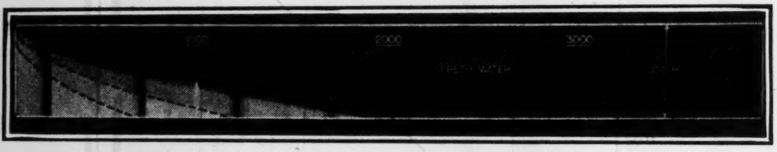

FIG. 13.—SHAPE AND POSITION OF SEA-WATER WEDGE WITH q/T EQUAL TO 0.0020, 0.0009, AND 0.0006

Fig. 12 shows the basic relationships involved and the confirmation of Eq. 2 by experimental results (shown plotted as circles); fresh water is flowing from right to left. Eq. 2 was also obtained from the potential theory by assuming a parabolic interface between fresh and salt water. Although Eq. 2 applies only to an idealized aquifer never found under natural conditions—if it is applied with good engineering judgment—it can be quite useful in the study and solution of practical sea-water-intrusion problems.

Fig. 13 is a composite photograph showing the position of the wedge for three different values of fresh-water flow. The dark vertical lines are caused by the metal bracing of the model. The shapes of the interface are typical. The distances shown are for a hypothetical prototype aquifer 100 ft thick but are not limited to this one case. One of the great advantages of such a model is that the results can be extended by model laws to any prototype aquifer. A new model does not have to be constructed for each aquifer—the single study serves all. Of course, models of aquifers with known variations in permeability might justify individual models for the study of peculiar conditions.

Fig. 14 shows the behavior of the sea-water wedge when water is injected through a line of wells 1,000 ft inland and spaced at 500-ft intervals. In this series there is no flow to or from the inland area. Hence, all the injected water

---

[14] "Flow of Homogeneous Fluids Through Porous Media," by M. Muskat, McGraw-Hill Book Co., Inc., New York, N. Y., 1937, pp. 377–380.

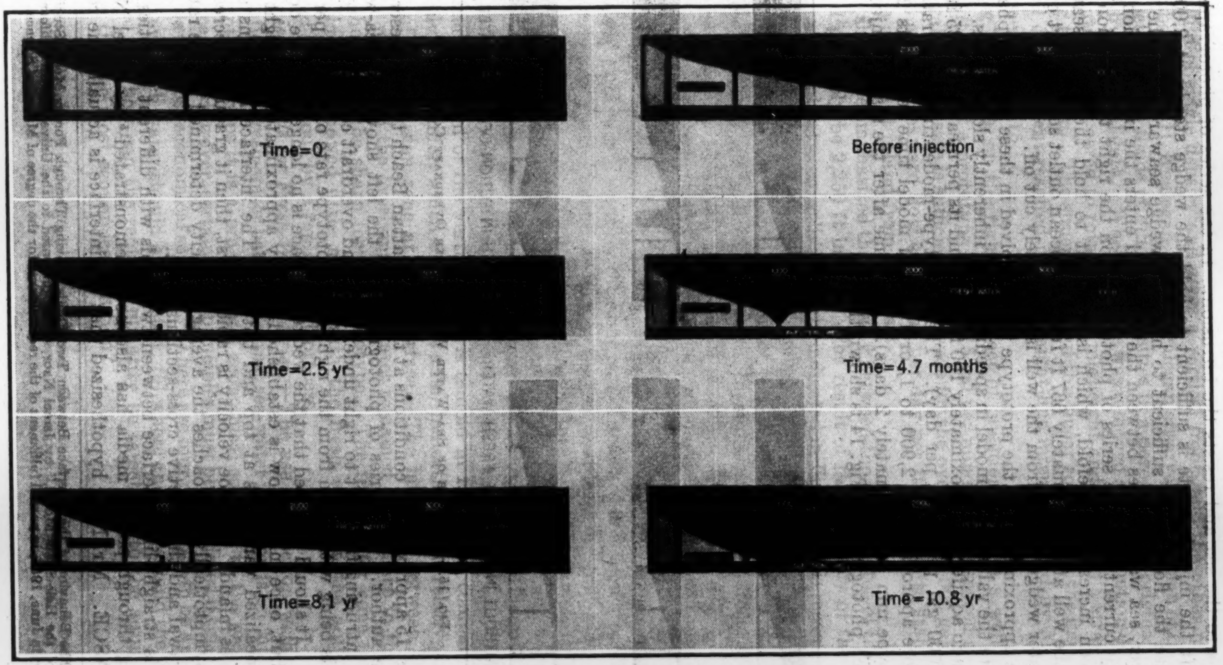
Time=0
Before injection
Time=2.5 yr
Time=4.7 months
Time=8.1 yr
Time=10.8 yr

FIG. 14.—BEHAVIOR OF SEA-WATER WEDGE AT VARIOUS INJECTION RATES

escapes to the sea and resists the intrusion. In the series of photographs on the left the injection rate is sufficient to hold the wedge steady at 2,000 ft. Because the flow is not sufficient to hold the wedge seaward from the well, however, sea water moves between the wells and enters the inland region as a density current. In the series of photographs on the right the injection rate has been increased threefold, which is sufficient to hold the wedge seaward from the well at approximately 667 ft from the ocean outlet so that part of the sea-water wedge inland from the well is completely cut off.

An approximation of the prototype time involved in these photographs will indicate the value of the model in speeding up an inherently slow process. The Silverado aquifer is approximately 100 ft thick and its permeability is 25 ft per hr (4,500 gal per sq ft per day). The prototype-model-time-scale ratio is therefore approximately 2,900 to 1, or 1 min of model time represents 2,900 prototype min (approximately 2 days). The time after the start of injection for each photograph in Fig. 14 is shown therein.

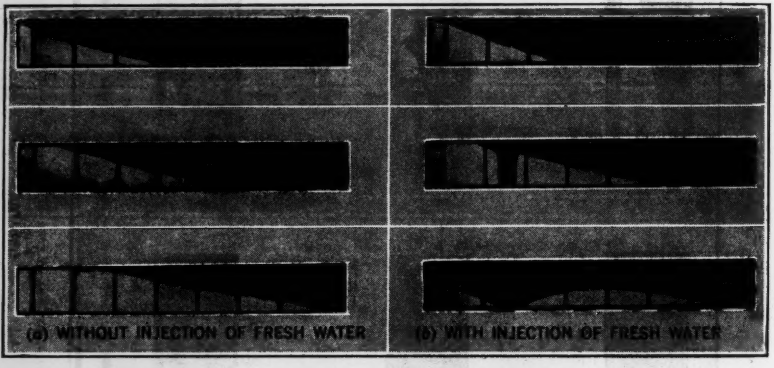
(a) WITHOUT INJECTION OF FRESH WATER
(b) WITH INJECTION OF FRESH WATER

FIG. 15.—BEHAVIOR OF SEA-WATER WEDGE UNDER OVERDRAFT CONDITIONS

Fig. 15 approximates conditions at the Manhattan Beach test site described by the author. The series of photographs on the left shows the sea-water wedge intruding from left to right under an inland overdraft condition. Fresh water is being withdrawn from the right at a prototype rate of 900 gal per day per ft. It should be noted that the wedge interface is no longer concave downward but, once inland flow is established, closely approximates a straight line with localized variations at top and bottom. The interface lengthens as it advances inland. The toe velocity is rapid at first, then it gradually decreases, and asymptotically approaches the average velocity determined by the rate of withdrawal and the effective cross-sectional area.

This straight-line interface between two fluids with different densities and moving through porous media has also been demonstrated[15] by Israel Naor, J.M. ASCE. Mr. Naor hypothesized that the interface is actually the result of two superimposed linear motions. One motion is the horizontal movement of a fluid of single density and gives a vertical front, and the other motion is described[16] by G. H. Keulegan. Mr. Keulegan observed the motion of the interface between two fluids of different densities in a porous media originally separated by a vertical gate. When the gate was removed a tilting motion occurred. The interface appeared to rotate about midheight and remained a straight line during the motion. The superposition of this linear rotation on the linear horizontal displacement resulted in the straight-line interface noted by Mr. Naor and seen in Fig. 15.

---

[15] "The Behavior of the Interface Between Two Fluids Moving Through Porous Media Studied by Means of the Hele-Shaw Model," by Israel Naor, thesis presented to the University of California, at Berkeley, in June, 1955, in partial fulfilment of the requirements for the degree of Master of Science.

Fig. 15 shows, on the right, the effect of injection through a well located 2,000 ft inland at a prototype rate of 415 gal per min for wells spaced at 500-ft intervals. This rate is sufficient to provide for the overdraft of 900 gal per day per ft and the seaward flow of 293 gal per day per ft required to stabilize the wedge at 2,000 ft inland from the coast.

It should be emphasized that midway between the wells the toe of the wedge would probably be 2,250 ft inland. The result of the tendency of the wedge to move inland between wells is clearly indicated in Fig. 4. It is recommended that the line of injection wells be located at least one half-well spacing inland from the allowed maximum intrusion of the wedge. The flows from the injection wells tend to equalize at this distance, and a relatively uniform flow rate per foot of coast is obtained. If the wells remain at 2,000 ft, a greater injection rate is necessary to keep the wedge at the midpoint between wells from passing beyond the line of wells, which would mean a greater loss of injected water.

One important result of the test was to show that the wedge would be stabilized at the same point for the same rate of seaward flow no matter how far the wells were spaced inland, as long as they were at least one half-well spacing beyond the maximum allowable intrusion distance. Tests were also made on wells penetrating only the upper or the lower half of the aquifer and on wells in distant inland areas. All results confirmed the theory that the location of the source of the seaward flow was immaterial within the limits cited.

The distortion of the vertical scale is tenfold in Fig. 15 as compared with the Silverado aquifer, which should give a fair indication of the relative importance of the diffusion zone at the interface. The interface between the sea-water wedge and the overlying fresh water remained quite sharp in the model and should also be sharp for the prototype. The fresh-water cone from the injection well showed little mixing with the fresh water in the aquifer but tended to move out by a replacement process.

Injection Wells for Fresh-Water Barrier.—The use of injection wells for the formation of a "fresh-water barrier" against sea-water intrusion is an interesting concept. Perhaps it is a practical and economical solution to the problem in some cases. However, certain basic principles must be considered if this method is to be the most economical solution. There are four questions to be answered: (*a*) How much water should be injected; (*b*) where and how should the wells be located; (*c*) how can the required quantity be injected into the aquifer; and (*d*) is this the most economical solution?

---

[16] "Ninth Progress Report on Model Laws for Density Currents," by G. H. Keulegan, *Report No. 3411*, National Bureau of Standards, U. S. Dept. of Commerce, Washington, D. C., June, 1954.

Amount of Water.—The solution to this problem lies in the principles of the conservation of matter and of continuity. Sea-water intrusion is caused by an inland-overdraft condition. The laws of nature require that a small quantity of fresh water continually flow out to sea to repel the sea water. This quantity can be estimated from Eq. 2 for any specified allowable location of the toe of the wedge. Whenever this seaward flow is reduced, the wedge will move inland. If the flow is reduced or eliminated, or is perhaps even made a negative quantity by inland pumping, sea water will flow inland. Wedge stability can be achieved only by furnishing a seaward flow of fresh water. Water in sufficient quantity will not flow seaward unless the overdraft causing the invasion is eliminated. That is, the total quantity of water required is equal to the sum of the seaward stability flow plus the existing overdraft. This quantity of fresh water can be supplied by several methods or combinations that will be cited subsequently.

Location of Wells.—The status of the sea water trapped inland from the line of injection wells, as shown in Fig. 5(*b*), presents a problem. It is believed that this salt water will continue to move inland and will begin to appear in wells that have previously been in a fresh-water zone only. Fig. 4 (dashed contours) indicates that this is what occurs at Manhattan Beach. The solid isochlors in Fig. 4 (solid contours) that are inland from the injection wells are even further inland in Fig. 4 (dashed contours). Any wells pumping near the wedge will induce some salt water to flow to them, which will mix with fresh water in the well and cannot be removed except by pumping as long as the injection wells remain in their present location.

It is recommended that injection wells to be used for sea-water repulsion be located inland from the most advanced intrusion of the wedge toe. The same quantity of injected water is required, but this location has the advantage of immediately causing the entire wedge to retreat toward the sea. The excess sea water will be flushed out into the ocean and the aquifer will again be fresh. All pumping wells should improve in quality whereas, under the plan shown in Fig. 4, some of the inland wells apparently have suffered further quality deteriorations.

Problems of Injection.—It is recognized that it is more difficult to pump water into the ground than to pump it out. The large-scale tests reported by the author are some of the most significant yet undertaken. Experiments conducted on a well field at the University of California have yielded interesting results on injection rates for both clear water and water containing 20% of primary settled sewage.[17,18] Clear-water injection rates of 8.4 gal per ft of aquifer having a permeability of 1,900 gal per sq ft per day were successfully obtained. The sewage-injection trials were also successful but a redevelopment technique is vital.[17,19] Of particular importance was the discovery that no coliform organisms appeared in the observation well 190 ft away whereas a few organisms did appear 100 ft away. Increasing the injection rate beyond a certain limit did not increase the travel distance of coliform organisms. These

---

[17] "Report on the Investigation of Travel of Pollution," *Publication No. 11*, California State Water Pollution Control Board, Sacramento, Calif., 1954.

[18] "Studies in Water Reclamation," *Technical Bulletin No. 13*, San. Eng. Research Lab., Univ. of California, Berkeley, Calif., July, 1955, pp. 24–34.

[19] "Report on the Investigation of Travel of Pollution," *Publication No. 11*, California State Water Pollution Control Board, Sacramento, Calif., 1954, pp. 136–139.

studies reconfirmed the inherent natural filtering action of an aquifer. If sewage rather than domestic water can be used for recharge by injection, considerable savings in cost are possible.

Economical Solutions.—The quantity of water required to repel sea-water intrusion can be estimated. The total water use in a critical area cannot be expected to decrease, but, on the contrary, present (1956) estimates predict greater water use in such areas. Solutions are additional importation of water, or reclamation of waste water, or both. Once this supplemental supply is brought into an overdraft region, it should become subject to economic analysis. The sea-water intrusion can be eliminated by injecting the water into the aquifer or by supplying the water directly to the users through a surface distribution system. The latter method reduces the draft on the aquifer and allows the required seaward flow to take place. The total quantity of water required is the same in both methods. However, the injection method requires that the water be pumped into the aquifer and then pumped out again. This method is expensive and probably should not be used unless it is less expensive than the construction of a surface distribution system. Thus, a pressure aquifer acts as a conduit. It provides no storage but provides a "spigot" (well) for each overlying landowner.

In the case of an unconfined aquifer there are additional benefits obtained from the injection method. It keeps sea water out of the reservoir during dry years when water users may lower the ground-water level below sea level. The value of the aquifer as a purifying filter for injected sewage must also be considered in cases where waste water is available in sufficient quantities.

Ground-water problems are inherently more difficult to understand than surface-water problems because in most instances they cannot be seen and must be dealt with in abstract terms, by mathematics and drawings. It is only through such studies and tests as the author has described that practical solutions can be found.

NORMAN H. BROOKS,[20] J.M. ASCE.—An excellent explanation of various physical phenomena encountered in ground-water recharge has been presented by the author.

The material under the heading, "Effect of Spreading Mounds on Channel Mounds," is particularly interesting. The writer agrees with the basic conclusion that the recharge from a stream channel does not prevent the recharge from an adjacent spreading ground from crossing under the stream. In fact, the recharge from the combination of stream channel and spreading ground is essentially the same as it would be from a stream of the same width as the combination.

However, it should be noted that there are some limitations in the analysis resulting in this conclusion and in Eq. 1. Each of the flow nets in Fig. 2 shows a zone of no flow which is roughly triangular in shape in the lower central part of the pervious stratum. Assuming that the ground-water flow follows Darcy's law, there is no theoretical justification for departing from conventional flow-net analysis. Hence, the center streamline should go to the bottom of the pervious stratum before dividing at the stagnation point, and the entire region should be included in the flow net.

---

[20] Asst. Prof. of Civ. Eng., California Inst. of Technology, Pasadena, Calif.

It might also be noted that the flow nets would be correct if the wedge-shaped sections, which have been excluded from the flow net, were impervious. Because they are not impervious there will be flow in them and the limiting streamlines cannot curve downward away from the center line to the impervious base, as the author has indicated.

The over-all effect of this approximation may not have a significant effect on the results inasmuch as the flow velocities in the excluded region are undoubtedly low. However, the approximation makes the drawing of the flow net considerably easier.

The writer has another misgiving about the flow nets shown in Fig. 2. The author states, under the same heading:

> "Actually, the flow trajectories are curved because of the sloping stream channel and aquifer but, if developed into a plane, the flow net resembles that shown in Fig. 2 (*a*)."

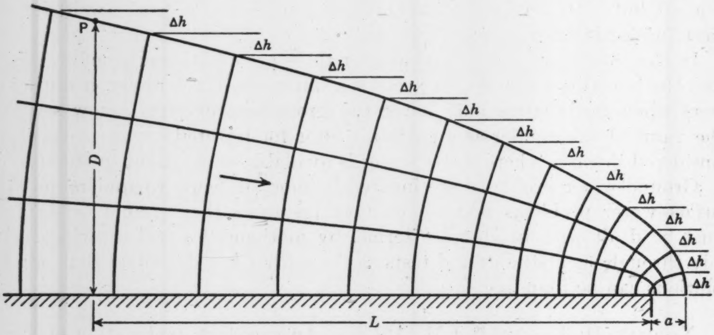

FIG. 16.—BASIC-PARABOLA SOLUTION FOR HORIZONTAL DISCHARGE FACE

Theoretically, flow nets apply only for two-dimensional flow although it is also possible to draw a special type of flow net for axially symmetric flow in three dimensions, but there is no axial symmetry in this case. Therefore, the development of a curved-flow pattern into a plane flow net is without theoretical basis. Although this development is helpful in visualizing the flow, it is nevertheless a faulty procedure for quantitative solutions of problems.

Furthermore, the way in which the streamlines curve in a plan view depends on the length of the reach of the stream from which water flows into the ground. If the recharging reach is very short, the streamlines can turn parallel to the stream quite close to it. If, however, the recharging reach is infinitely long, the streamlines for the ground-water flow cannot become parallel to the stream.

In making the analysis leading to Eq. 1, the author has avoided this difficulty by assuming the underlying impervious stratum to be horizontal and the flow, two dimensional. However, in drawing the various flow nets which resulted in Eq. 1 he must have assumed some type of downstream control.

Without a control point at a finite distance it is impossible to establish steady flow.

In order to make an approximate analysis of the effect of the distance to the control it will be assumed that the control consists of a horizontal discharge face. The flow net in the vicinity of this control, shown in Fig. 16, is the familiar solution[21] consisting of confocal parabolas. The line of seepage in this case is often termed the "basic parabola." This theoretical solution is fairly good except in the immediate vicinity of the spreading ground. At this point the curvature will be reversed because the water must initially flow downward from the spreading basin and then turn either to the right or to the left.

In Fig. 16, P is the point at which the actual flow net between the spreading ground and control starts to deviate substantially from the basic parabola. To obtain a maximum estimate of the discharge for comparison with Mr. Baumann's analysis, one can assume point P to be at the water surface at the edge of the spreading ground. Because point P cannot, in reality, be so high, the discharge computed subsequently will necessarily be somewhat larger than the actual discharge. In any event, the actual flow cannot exceed this maximum estimate because the line of seepage certainly cannot, at any point, be higher than the water level in the spreading ground.

From the properties of a parabola the length of the discharge face, a, is given by

$$a = \tfrac{1}{2} \left(\sqrt{L^2 + D^2} - L \right) \ldots\ldots\ldots\ldots\ldots\ldots (3)$$

in which D is the height of point P above the impervious base and L, the horizontal distance from P to the discharge face. Because the discharge, q', is simply $2\,K\,a$ (K is the permeability) the rate of flow can be expressed in terms of L and D as

$$q' = K \left(\sqrt{L^2 + D^2} - L \right) \ldots\ldots\ldots\ldots\ldots\ldots (4)$$

According to the author the acceptance rate, q, is equivalent to $2\,q'/W$, wherein the factor of 2 accounts for flow to either side of the spreading ground. Consequently, the maximum estimate of the acceptance rate may be given dimensionlessly as

$$\frac{q'}{K} = 2\,\frac{D}{W}\left(\sqrt{\left(\frac{L}{D}\right)^2 + 1} - \frac{L}{D}\right) \ldots\ldots\ldots\ldots\ldots (5)$$

Because this is a maximum estimate, the actual acceptance rate,

$$\frac{q}{K} < \frac{q'}{K}.$$

In Fig. 17 a comparison is made between Eq. 1 and Eq. 5. It is apparent that for many values of L/D Eq. 1 gives a value of the acceptance rate which exceeds the capacity of the pervious stratum for transmitting the flow horizontally to the control. For example, if L/D equals 10 and D/W equals 2, then the upper limit from Eq. 5 is q'/K equals 0.20 whereas Eq. 1 gives q/K equals 0.63, a value which is at least three times too large for this case. In fact, the distance to the control, L, must not be more than twice the depth, D, if the value of q found by Eq. 1 is to be consistently less than the maximum possible as indicated by Eq. 5. Therefore, the distance from the spreading ground to the control is an important variable to be taken into account.

---

[21] "Seepage Through Dams," by A. Casagrande, in "Contributions to Soil Mechanics, (1925–1940)," Boston Soc. of Civ. Engrs., p. 310.

It will be noted from Eq. 5 that, for some combinations of variables, the computed value of q'/K will exceed unity. This is physically impossible because the acceptance rate, q', can never exceed K which is the rate corresponding to downward percolation without hydrostatic pressure. The apparent inconsistency arises when the recharge mound cannot rise to the spreading ground level but reaches its ultimate height some distance below the spreading ground, with the recharge water percolating by gravity down to the top of the mound.

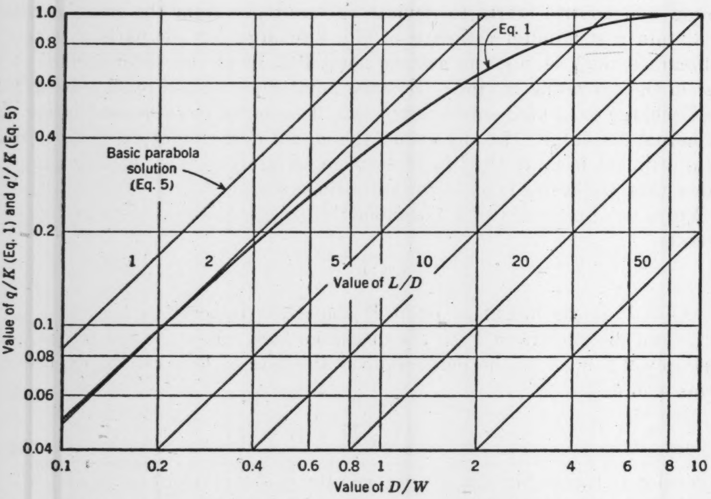

FIG. 17.—COMPARISON OF EQ. 1 FOR ACCEPTANCE RATE WITH MAXIMUM ESTIMATE BY EQ. 5

JAMES A. HARDER.[22]—The description of the ground-water recharge operations being conducted by the Los Angeles County Flood Control District is a welcome contribution to the study of water conservation. Water conservation is a subject not only of vital importance to such semiarid regions as southern California but also of increasing importance to other parts of the United States. The writer does not agree, however, that the importance of the "saline wave" should be minimized.

As shown by the isochlors in Fig. 4, at the time the injection was started the injection site was underlain by water having a chloride-ion concentration approximately 90% that of sea water. Therefore, it was feared that, if this particular site were used, the trapped sea water would cause trouble as it moved inland. Accordingly, the district was required either to use a site inland from the intrusion or to obtain waivers from major water users exempting the State of California from responsibility for damage. The waivers were obtained.

---

[22] Asst. Research Engr., Univ. of California, Berkeley, Calif.

From the isochlors in Fig. 4 an estimate may be made of the total chloride content of the water which lay behind the injection-well site before injection by making a profile of the concentration versus the distance inland from the injection-well site and applying graphical integration. Based on profiles through the end points and the center of the site and assuming an aquifer thickness of 100 ft and a porosity of 30%, the average quantity of chloride ion existing behind the 4,000-ft-long site is computed to be approximately 20 tons of Cl^- per ft of front or a total of 80,000 tons. This amount of Cl^-, by simple arithmetic, can contaminate 240,000 acre-ft of water to a concentration of 250 ppm, which is a generally accepted maximum for domestic use.

Of course, there is a large quantity of fresh water still remaining in the inland part of the aquifer which might be available for dilution of the saline wave. From Fig. 3, the distance from the injection-well site to the Inglewood fault, the inland boundary of the basin, is approximately 6 miles. Assuming that the aquifer thickens to 150 ft and continues to the fault, there are 150,000 acre-ft of fresh water in the 4,000-ft-wide strip between the injection-well site and the fault. The previously computed weight of chloride could contaminate this water to a concentration of approximately 400 ppm if it were uniformly distributed. All this fresh water will not be available for dilution, however, because inland-water users may be expected to pump out as much as possible before the saline wave arrives.

Furthermore, it does not appear that the natural recharge will contribute sufficient fresh water to be significant in the diluting process. On the basis of its area relative to the basin, the strip behind the injection site should probably receive no more than 2,000 acre-ft per yr of new water from natural recharge. Artificial recharge from the injection-well site is contributing a similar quantity according to the data presented in the paper.

It may still be hoped that the fresh water which overlies the saline water in the wave or is trapped in depressions along the bottom of the aquifer could be recovered free of salt from partly penetrating wells. This is possible only under severe restrictions on the average pumping rate. For example, a computation based on experimental data presented by Mr. Muskat[23] will show the maximum drawdown at which a well penetrating the top 50% of the fresh-water zone of an aquifer can operate without "coning." Assuming that there is a layer of sea water lying at the bottom of a 100-ft aquifer, a drawdown of only 3.5 ft will induce the salt water to rise in a "cone" and enter the bottom of the well. Obviously this is a much smaller drawdown than is normally feasible.

The past, present, and future status of sea-water intrusion in Manhattan Beach may be determined from Fig. 15. This series of photographs was taken of sea-water intrusion into a model aquifer constructed at the University of California.[12] Overdraft and injection rates were set up to approximate conditions at Manhattan Beach; with scale factors adjusted so that the 4-ft-long model represents a section of the aquifer 8,000 ft long perpendicular to the coast, the total time elapsed between the first and last frames represents 10 yr. The present situation (1956) would be similar to a frame following the second frame on the right. The saline wave is shown moving inland with the fresh water from the injection wells at a rate corresponding to approximately 500 ft per yr in the prototype. The shift in the isochlors in Fig. 4 seems to indicate the same approximate rate; the wave tends to flatten and spread with the passage of time. Little diffusion will occur across the salt water-fresh water interface; however, the interface slope is so sensitive to changes in the slope of the piezometric surface that there is little chance that salt water can be held in depressions along the bottom of the aquifer. For example, a piezometric surface slope of 1 ft per mile corresponds, at equilibrium, to a interface slope of 40 ft per mile in the opposite direction if the salt-water layer is pure sea water.

---

[23] "Flow of Homogeneous Fluids Through Porous Media," by M. Muskat, McGraw-Hill Book Co., Inc., New York, N. Y., 1937, pp. 480–496.

Charles H. Lee,[24] M. ASCE.—A very interesting equation (Eq. 1) is presented by the author to express the relationship between the average acceptance (infiltration) rate per unit of wetted area and the parameter, D/W. The writer agrees that the parameter is of economic importance but believes it is also of physical significance. In order to illustrate this graphically, in Fig. 18 the full range of D/W for $K = 1{,}000$ gal per sq ft per 24 hr for a gradient of unity has been plotted. The value of K is equivalent to a flow of 67.5 cu ft per sec per acre for a gradient of unity. The resultant curve closely approaches its asymptote, $q = 67.5$, for values of D/W exceeding 8. The depth of unconfined water-bearing alluvial deposits as found in nature seldom exceeds 500 ft and is usually much less. Spreading basins of from 500 ft to 1,500 ft in width and more are in common use. For a basin only 500 ft wide, the maximum value of D/W in actual practice would, therefore, seldom exceed unity and is usually much smaller. For $D/W = 0.1$, the value of q is 3.6 cu ft per sec for a gradient of unity, as indicated in Fig. 18.

In the model tests which the author has conducted to supplement his mathematical analysis, it is shown that the value of the parameter, D/W, in the model[2] was 12.8 in./1.2 in. = 10.7. This extreme divergence in value of the parameter, D/W, between model and prototype raises the question of the feasibility of relating model and prototype. In the second phase of mound growth, in which the surface of the mound contacts water in the spreading basin and acquires the potential control of its surface, there is a greater probability of waterlogging the surrounding ground for $D/W < 1$ than for $D/W = 10$. Wherever the spreading basin is adjacent to the stream channel, there is also a greater probability of substantial return flow from the spreading basin to the stream channel.

The author states, under the heading, "Effect of Spreading Mounds on Channel Mounds," that "* * * no significant return flow from the spreading basin to the stream channel will occur as long as the gradient between the two is moderate * * *." This statement suggests that a slope of 5 horizontal to 1 vertical is critical, but does not support this suggestion by theory or test. The only positive statement the author has made in connection with the foregoing is that "* * * to stop the flow from the spreading basin the water surface of the channel mound would have to rise to the same elevation as that in the spreading basin." Fig. 2(*b*) is used to illustrate this statement. In Fig. 19 a flow-net sketch is shown in the region of an assumed river levee. Fig. 19 is more detailed than Fig. 2 and is more in accord with actual field experience as well as with results of model tests for percolating flow under levees and dams. The percolating flow through the vertical section, A-A′, immediately behind the near river bank in a slice 1 ft wide perpendicular to the bank, can be computed from

---

[24] Cons. Engr., San Francisco, Calif.

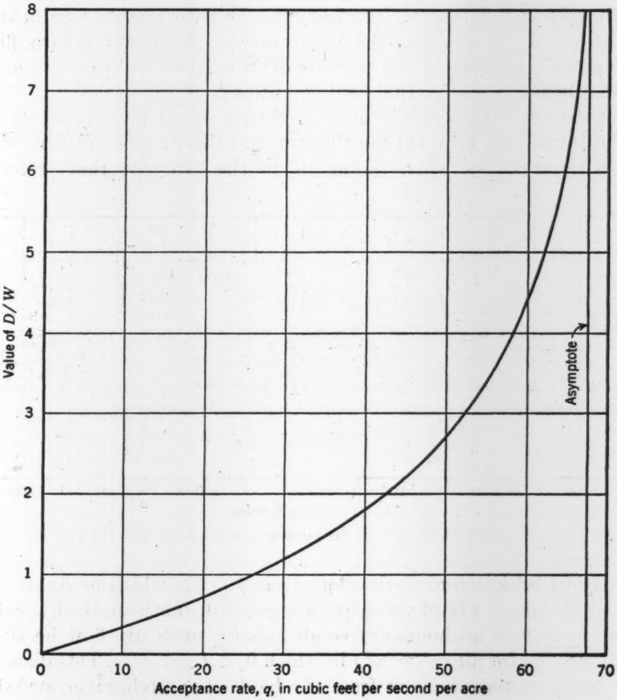

FIG. 18.—RELATIONSHIP BETWEEN D/W AND q IN EQ. 1 FOR K = 1,000 GAL PER SQ FT PER 24 HR FOR A GRADIENT OF UNITY

$$Q = K\,A\,i \qquad (6)$$

assuming K equal to 1,000 gal per sq ft per 24 hr, A as 92 sq ft, and i as 6 ft/37 ft to be

$$Q_A = \frac{1{,}000 \times 92}{7.5 \times 24 \times 60 \times 60} \times \frac{6}{37} = 0.32 \text{ cu ft per sec.}$$

A similar computation at the far bank of the river in vertical section, B-B′, is

$$Q_B = \frac{1{,}000 \times 92}{7.5 \times 24 \times 60 \times 60} \times \frac{6}{230} = 0.023 \text{ cu ft per sec.}$$

The indicated loss must be assumed to be seepage into the river channel—that is, $Q_A - Q_B = 0.286$ cu ft per sec. This value is 87% of the percolating flow at the near bank of the river and would be greater for sections taken at a lesser angle to the river. This computation illustrates that, even for a gradient flatter than of from 5 to 1, the seepage into the river may be significant. The author's optimism regarding the avoidance of significant return flow from spreading basin to channel at gradients of from less than 5 to 1 would appear unfounded in the case of actual field conditions.

The reason for the wide discrepancy between model and prototype (actual field conditions) may be sought in the fact that there is no law of physics which is true without limits. Mr. Baumann, in the "Introduction" refers to the mathematical background he developed[25] in 1952 in which he did not indicate within what ranges his physical phenomena are mathematically valid. For example, in setting up boundary conditions for unsteady flow he stated that $y = 0$ at $x = L_d$ for all values of t in which $0 < L_d < \infty$. This disregards the case in which seepage escapes from the bank of a ditch, river, or lake above the free water surface, or the existence of escape gradient. It also assumes that the advancing margin of the mound has a feather edge rather than a blunt nose. The rapid initial rise of water, as often observed in test holes following initial stream flow, would indicate a blunt nose.

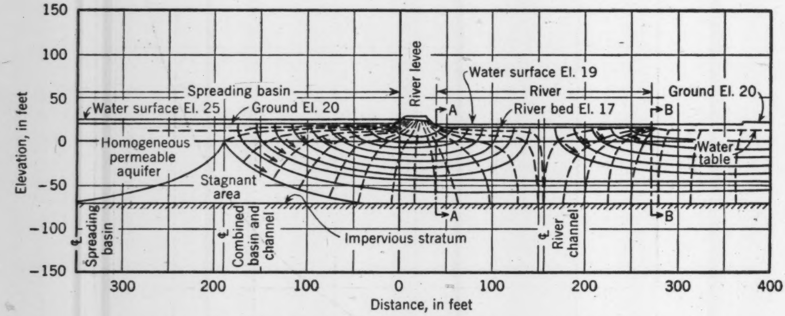
150
100
50
0
-50
-100
-150
Elevation, in feet
River levee
Water surface El. 19
Spreading basin
River
Ground El. 20
Water surface El. 25
Ground El. 20
A
River bed El. 17
B
Homogeneous permeable aquifer
Water table
Stagnant area
A
B
℄ Spreading basin
℄ Combined basin and channel
Impervious stratum
℄ River channel
300
200
100
0
100
200
300
400
Distance, in feet

FIG. 19.—FLOW NET OF SPREADING BASIN ADJACENT TO RIVER

Mr. Baumann also stated in 1952 that $y = f(x)$ at $t = \infty$, apparently assuming that the profile of the water table is a continuous linear function of the distance from the spreading ground throughout its length at any and all times. This assumption is predicated on the transmitting material being homogeneous for any value of x; this is a condition never met with in nature. It also omits consideration of discontinuity as a result of an intervening horizontal water surface in an open ditch or a river. Such condition is of common occurrence.

---

[25] "Ground-Water Movement Controlled Through Spreading," by Paul Baumann, *Transactions*, ASCE, Vol. 117, 1952, pp. 1027, Eq. 4.

The 'fitting" of the "basic parabola" observed in model tests with the parabolic type of equation developed mathematically for the mound profile for steady flow does not justify the extension of such equations beyond the specific limits of the model test. Obviously the results of such tests apply only to the conditions established by the model. In the absence of a great variety of conditions, which only a great number of tests made on many different models would provide, there exists no foundation for generalization or correlation with mathematical equations.

Mr. Baumann notes that his basic equation for unsteady flow has its analog in the flow of heat through a prismatic nonradiating bar. It is to be noted that for this condition to be attained for percolating flow through granular soil, the soil stratum must be enclosed in sealed surfaces which, in a flow net, would be represented by flow lines rather than by equipotential lines. In practice, this condition is fulfilled for a percolating stream in homogeneous unconfined granular material by the free water table and the impervious stratum at the bottom. When such a flow is intercepted by an open ditch, river, or lake, however, the upper limiting surface changes from the water table to the stream bank and bed. The stream bank and bed then become an equipotential line, thus changing the analog to heat transference through a radiating prismatic bar. Hence, at this point a discontinuity occurs in the mathematical equations relating to the percolating stream. Recognition of this condition is an aid in understanding why a substantial part of the percolating water seeps into the stream channel instead of moving across the channel.

PAUL BAUMANN,[26] M. ASCE.—Eq. 1 was correctly evaluated by Mr. Lee, although it would have been preferable to express the acceptance rate in cubic feet per second per square foot instead of per wetted acre because in the study of two-dimensional ground-water movements a strip 1 ft wide is normally considered. Hence, the spreading grounds and the stream channels, the widths of which are rarely constant, may be divided up into as many strips are as required reasonably to reflect the effect of the variable widths on the total acceptance rate.

In constructing the flow net (Fig. 19) Mr. Lee was apparently influenced by the textbook example of percolation from a reservoir for a unit length of a floating dam of infinite length on a saturated, porous foundation with the less-featured case of flow from a spreading ground under a river levee. However, the two cases are fundamentally different. The percolation flow from a saturated stream channel is approximately at right angles to the channel—that is, in the direction of both residual pore storage and a control as shown in Fig. 2(*a*). In the longitudinal direction of the saturated stream channel there is no residual pore storage, no control, and therefore no escape for additional subsurface flow. Therefore, in the absence of lateral escape, all percolation under a floating dam from a reservoir must rise to the surface whereas percolation under a levee from an adjacent spreading ground must not rise as long as there is an escape by means of residual pore storage and a control. However, return flow to the river from the spreading ground may occur depending on the gradient between the water surfaces of the spreading basin and the stream channel.

---

[26] Asst. Chf. Engr., Los Angeles Flood Control Dist., Los Angeles, Calif.

The flow net shown in Fig. 19 does not consistently satisfy the basic requirements, which are (*a*) the vertical drop, Δh, between the equipotentials along any phreatic line must be constant; (*b*) the flow, Δq, through each of the flow paths must be constant; (*c*) the flow, Δq, must be equal for all the flow paths; and (*d*) the streamlines and equipotential lines must form approximate squares between themselves except near the boundaries where distortion is unavoidable.

Fig. 20 shows a balanced-flow net for an extreme condition similar to that chosen by Mr. Lee. The gradient between basin and stream-channel water surfaces used in Fig. 20 is 2 horizontal to 1 vertical, as compared to the 5 horizontal to 1 vertical gradient referred to by the writer as the limiting value for insignificant return flow to the stream channel. By assuming a number of phreatic lines through the levee it was possible to find the one for which the return flow is a maximum. The return flow was found to be 7.5% of the total flow of percolation from the spreading basin toward the stream channel. Hence, for a gradient of 5 to 1, the return flow would indeed be insignificant. In deriving the return flow to the stream channel, Mr. Lee has computed the flow through the two vertical sections on the premise that the respective gradients are equal to the difference in water-surface elevation divided by the horizontal distance to the section. This method assumes horizontal flow throughout the entire reach in accordance with the Dupuit theorem. In the "Introduction," it was stated that "* * * the rate of flow is based on vertical sections in accordance with the Dupuit theorem, except in special cases" Subsequently, under the heading, "Strip Basin: The Growing Mound" it was stated that "it is apparent that the Dupuit theorem is applicable with fair approximation except near the spreading basin and near the control." At these points the flow conditions cannot be ascertained without a flow net. The total flow computed from the flow net checks that determined from Eq. 1 within 15%, which is a close check considering the extremity of the example.

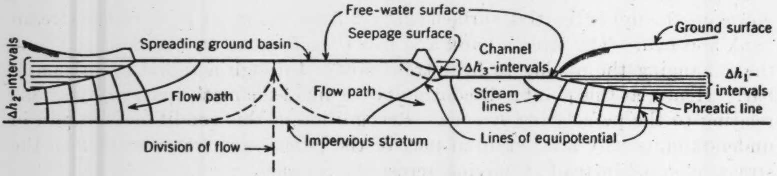

FIG. 20.—FLOW NET OF COMBINED SPREADING GROUND AND CHANNEL MOUND

For the water year, 1940–1941 (October 1 to September 30), the rainfall for Los Angeles County exceeded 200% of normal. Sustained runoff from the San Gabriel Mountains occurred throughout the winter, and, by the spring of 1941, recharge of ground-water basins by means of percolation from stream channels and spreading grounds caused mounds to rise to the surface in the "forebay" of the central coastal basin. Fig. 21 shows the ground-water contours and ground-surface contours in the vicinity of the San Gabriel and the Rio Hondo spreading grounds of the Los Angeles County Flood Control District as of May 6, 1941. These spreading grounds are located in the forebay, and, at stream channels, the ground-surface contours show average elevations between banks. Low-water channel beds would be from 2 ft to 3 ft lower. The merging of the mound beneath the San Gabriel spreading grounds with the channel mound is of special interest because of the fact that the percolation flow east of the San Gabriel stream channel was more restricted than the flow west of the Rio Hondo channel. Throughout this period there was no evidence of rising water in the saturated San Gabriel stream channel adjacent to the levee separating it from the spreading grounds, although the gradient from the spreading mound toward the stream channel is conspicuous in Fig. 21.

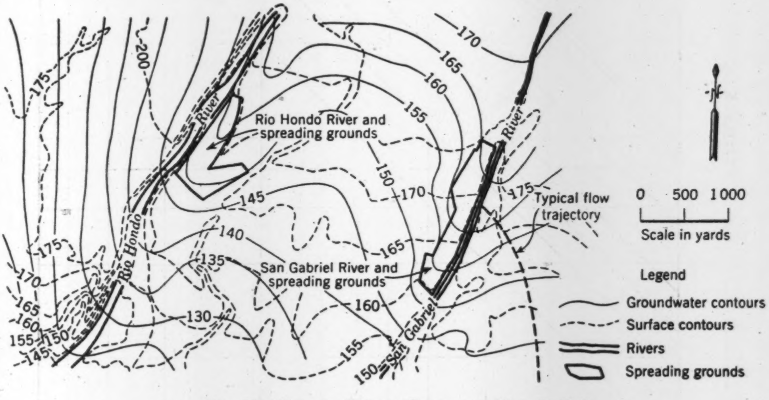
Rio Hondo River and spreading grounds
San Gabriel River and spreading grounds
Rio Hondo
River
San Gabriel
River
Typical flow trajectory
0 500 1000
Scale in yards
Legend
Groundwater contours
Surface contours
Rivers
Spreading grounds
N
200
175
170
165
160
155
150
145
140
135
130

FIG. 21.—GROUND-WATER CONTOURS, MAY 6, 1941

There is no evidence of blocking by the channel mound of percolation from the spreading grounds. Another interesting feature is the curvature of the streamline trajectories normal to the ground-water contours in connection with the channel-flow net. A typical trajectory is indicated by a dashed line in Fig. 21.

Mr. Lee questions the similarity between the model-test results and those of a prototype as expressed by Eq. 1. The model test, which was relatively free from capillary flow,[27] showed a maximum discharge parameter, $q/K = 0.097$, whereas Eq. 1 for $W = 2.4$ in. (not 1.2 in. as used by Mr. Lee) and $D = 12$ in. gives $q/K = 0.092$, a difference of $5\frac{1}{2}\%$.

Mr. Brooks undertakes to correlate the evaluation of Eq. 1 and Eq. 5 for the basic parabola. However, in developing Eq. 5 to appear in terms of

---

[27] "Ground-Water Movement Controlled Through Spreading," by Paul Baumann, *Transactions*, ASCE, Vol. 117, 1952, p. 1059.

D/W, Mr. Brooks apparently overlooked the fact that the depth, D, in his ingeniously conceived Fig. 17 can never be equal to D in Fig. 2(*a*). As previously shown[28] the phreatic line between the spreading ground and the control can be approximated by a double parabola. The depth, D, in Fig. 17 can therefore be considered as the depth below the point, P, of contraflexure. Therefore, D and L in Fig. 17 should be changed to d and l. Mr. Brooks' example for arbitrary values of $D/W = 2$, $L/D = 10$, and the apparent discrepancy between the results based on Eq. 1 and on the basic parabola are

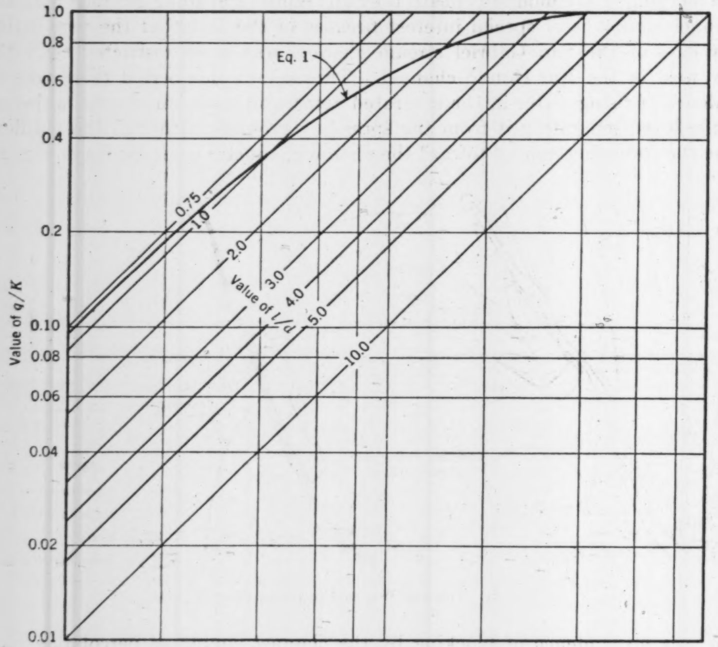

FIG. 22.—RELATIONSHIP AMONG d/W, q/K, AND l/d

therefore incompatible with the condition for potential flow between the spreading ground and the control because the ratio, q/K, must be common to both the spreading ground and the lower basic parabola. Eq. 1 was developed from flow nets which necessarily terminated in basic parabolas and attendant controls. Hence, all corresponding values are found as the intersection of the (l/d)-lines with the $(l - e^{-d/W})$-curve in Fig. 22. It is interesting to note that the line for $l/d = 3/4$ becomes tangent to the $(l - e^{-d/W})$-curve as q/K approaches zero. In developing $e^{-d/W}$ into a series it also follows that, as d/W

---

[28] "Ground-Water Movement Controlled Through Spreading," by Paul Baumann, *Transactions*, ASCE, Vol. 117, 1952, pp. 1042–1045.

approaches 0, q/K approaches d/W. Actually, as is indicated by Fig. 22, the (q/K)-ratio closely checks the (d/W)-ratio if the latter is less than 0.1.

In designing a spreading ground it is necessary to ascertain the economic limitations. Ordinarily, the depth $D = 2\,d$ to the impervious stratum is known. Therefore, by Eq. 1 and Eq. 5, corresponding values of q/K and W may be determined as shown in Fig. 23.

For the case mentioned by Mr. Lee—that is, $D \sim 100$ ft—it follows from Fig. 23 that, for $D/W = 0.10$ and, therefore, $W \sim 1{,}000$ ft, the infiltration parameter per sq ft, q/K, is 0.05 or $q = 3.35$ cu ft per sec per wetted acre for $K = 1{,}000$ gal per sq ft per 24 hr.

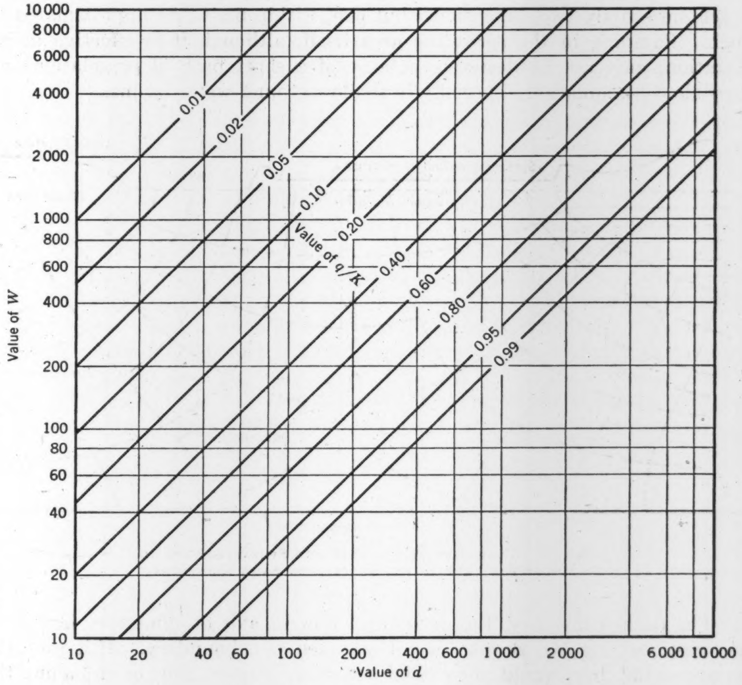

FIG. 23.—RELATIONSHIP AMONG d, W, AND q/K

Because Fig. 22 and Fig. 23 are correlated, the absolute value of l (half the distance between the edge of the spreading ground or stream channel and the control) may be ascertained from Fig. 22. As Mr. Brooks points out, the distance, $2\,l$, from the spreading ground to the control is an important variable for strictly two-dimensional flow. In arriving at the discrepancy mentioned herein, he considered the distance, $2\,l$, fixed and, correctly, the rate of flow q' thereby governed.

As previously stated, extraction of ground water through pumping must be expected where recharge through spreading is performed. Coordination of the two operations should include the locating of water wells as closely as possible to the theoretical control. However, as previously cited and indicated in Fig. 21, the curvature in the plan of the flow paths—that is, the approach to three-dimensional flow—makes unnecessary the precise location of the control based on strictly two-dimensional flow and thereby provides considerable flexibility for the distance, $2l$, in that, theoretically, this distance may be ∞ (Fig. 1). Prototype ground-water movement, contrary to that in models, is seldom strictly two dimensional but can, within limits, be approximated as such. Pumping in the spreading area itself, although it is effective in infiltration, may not be desirable because of a short path of percolation and possible contamination, especially in shallow ground-water basins.

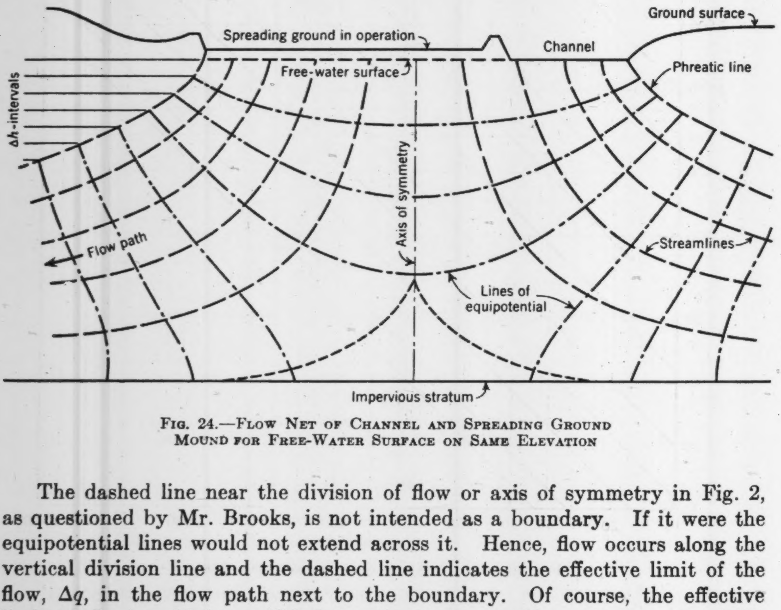

FIG. 24.—FLOW NET OF CHANNEL AND SPREADING GROUND MOUND FOR FREE-WATER SURFACE ON SAME ELEVATION

The dashed line near the division of flow or axis of symmetry in Fig. 2, as questioned by Mr. Brooks, is not intended as a boundary. If it were the equipotential lines would not extend across it. Hence, flow occurs along the vertical division line and the dashed line indicates the effective limit of the flow, Δq, in the flow path next to the boundary. Of course, the effective limit of flow could be modified to advantage, as shown in Fig. 24. This figure shows the symmetrical flow net for the free-water surface of stream channel and spreading ground at the same potential.

Mr. Knapp has found a flaw in the deliberations in connection with Fig. 5 in that they indicated ultimate conditions when, in fact, they were just "prior to ultimate." Mr. Knapp's reference to interface slopes under the influence of pumping is of particular significance. As indicated by Fig. 3, the drawdown gradients adjacent to the test site are one-half of 1%. Hence, in using the 40-to-1 ratio, as suggested by Mr. Knapp, the slope of the interface would be

20%. This phenomenon is somewhat startling at first glance. However, sea water spread along the bottom of an aquifer is normally sucked into wells at more moderate rates than fresh water because the lowest well perforations are at a distance above the bottom of the aquifer requiring the interface to assume its maximum slope in rising to the well.

This clearly shows the difference between the saline wave and sea-water intrusion questioned by Messrs. Hotes and Harder. During the passing of the saline wave the lowest perforations of affected wells may be temporarily blocked whereas no measure of protection will save a well from abandonment if sea-water intrusion is permitted to continue unchecked. Also, those wells adversely affected by the saline wave might be temporarily used to extract sea water cut off from the ocean by the barrier.

The writer had occasion to observe the ingeniously conceived model, shown in Fig. 11, at the University of California. This model simulated all probable prototype conditions and evaluated results quantitatively within reasonable limits of accuracy. As in all cases of ground-water studies, the time scale would have to be used on the assumption of the homogeneity of the aquifer as well as the uniformity in magnitude.

Eq. 2, which was developed by Mr. Harder and which is an adaptation of an example of flow through an earth prism analyzed by Mr. Muskat, is based on the assumption of a constant potential or equipotential along a vertical line through the injection well, a constant potential of equal magnitude along the horizontal sole, and a variable potential along the vertical line through the seaward control. Hence, the fresh-water flow passes through the control between the bottom of the clay cap and the sole of the aquifer with no flow along the latter. The same result obtained by Mr. Harder can be obtained by applying the Dupuit theorem to flow between the clay cap and the interface. The shape of the interface is such that balanced pressure between fresh water and sea water exists at all points. Its shape is expressed by

$$z = M \pm \sqrt{M^2 - \frac{2\,q\,x}{K\,(s-1)}} \qquad (7)$$

in which, as shown in Fig. 25, z is the ordinate of interface above the x-axis; M, the magnitude of the aquifer; x, the abscissa relative to the center of the recharge well; s, the specific gravity of sea water; and 1, the specific gravity of fresh water. For any stable condition of the interface, the rate of flow, q, must be constant and a maximum. Hence, because the radical in Eq. 7 must be real, the two terms under the radical for q_{max} must be equal. Thus, for $x = L$,

$$M^2 = \frac{2\,q\,L}{K\,(s-1)} \qquad (8)$$

and

$$q = \frac{1}{2}\,(s-1)\,\frac{K\,M^2}{L} = \frac{1}{2}\,(s-1)\,\frac{M}{L}\,T \qquad (9)$$

which agrees with Eq. 2.

For this condition to result, the product, $q\,L$, of the two variables must remain constant. Hence, as q increases, L decreases proportionately and vice versa, as shown in Fig. 13. From Eq. 7 it follows that for any stable condition of the interface and, therefore, any corresponding product, $q\,L$, the height, z, of the interface at the control is equal to M. Because this would leave no aperture for the discharge of fresh water, it is evident that Eq. 7 based on the Dupuit theorem is an approximation of the true solution. To satisfy $z = 0$ for $x = 0$ the sign before the radical must be negative.

From Eq. 7 it follows that the slope of the interface,

$$\frac{dz}{dx} = \frac{q}{K\,(s-1)\sqrt{M^2 - \dfrac{2\,q\,x}{K\,(s-1)}}} \ldots\ldots\ldots\ldots\ldots (10)$$

and that for $x = L$, the slope for any corresponding q-values and L-values is 90°. This answer again reflects the aforementioned approximation, and it appears reasonable if one remembers Mr. Knapp's 40-to-1 ratio between the fresh-water gradient and the slope of the interface. In accordance with this ratio, any fresh-water gradient in excess of $2\frac{1}{4}$° would need a slope of the interface at the control of 90° which, of course, cannot be exceeded.

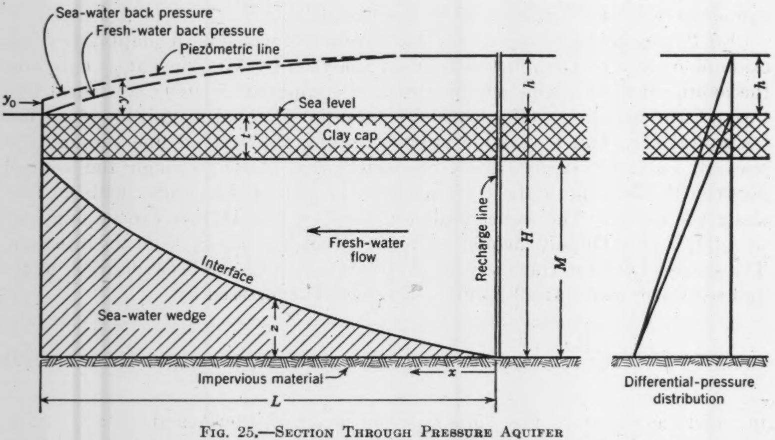
Sea-water back pressure
Fresh-water back pressure
Piezometric line
y_0
y
Sea level
t
Clay cap
h
Recharge line
H
M
Fresh-water flow
Interface
Sea-water wedge
z
Impervious material
x
L
h
Differential-pressure distribution

FIG. 25.—SECTION THROUGH PRESSURE AQUIFER

If the interface were treated as an inverted, basic parabola and if the boundary condition, $z = M - q/K$ at $x = L$, were imposed to bring the Dupuit solution in accord with the Kozeny solution,[29] then Eq. 7 would lead to

$$\frac{q}{K} = -\frac{L}{s-1} + \sqrt{\frac{L^2}{(s-1)^2} + M^2} \ldots\ldots\ldots\ldots\ldots (11)$$

---

[29] "Ground-Water Movement Controlled Through Spreading," by Paul Baumann, *Transactions*, ASCE, Vol. 117, 1952, p. 1040.

and

$$q = -\frac{K L}{s - 1} + \sqrt{\frac{K^2 L^2}{(s - 1)^2} + T^2} \quad \text{.............. (12)}$$

Although no authenticity is claimed for Eqs. 11 and 12, it is encouraging to find that the boundary conditions, $L = 0$ therefore $q = T$, and $L \rightarrow \infty$ therefore $q \rightarrow 0$, are satisfied. Also, q is of the same order as that quantity obtained from Eq. 9.

Putting Eq. 11 in the form,

$$\frac{q}{K} = \frac{L}{s - 1}\left[\sqrt{1 + \frac{M^2}{L^2}(s - 1)^2} - 1\right] \quad \text{.............. (13)}$$

and expanding the radical into a binomial results in

$$\frac{q}{K} = \frac{M^2 (s - 1)}{2 L} - \frac{1}{8}\frac{M^4 (s - 1)^3}{L^3} \quad \text{.............. (14)}$$

from which it follows that for any finite discharge face the rate of flow, q, must be smaller than in accordance with Eq. 2. Hence, the latter equation should be corrected to read

$$q = \frac{K (s - 1) M^2}{2 n L} \quad \text{.......................... (15)}$$

in which $n > 1$ and increases as the ratio, M/L, increases.

Obviously, if fresh water from the recharge well were discharged from a pressure level, h feet above mean sea level at the recharge well, into a fresh-water lake with the water surface at mean sea level and if the interface were fixed, y_0 at the control would be close to zero and the pressure gradient or piezometric line would be as indicated in Fig. 25. If it were possible suddenly to convert the back pressure due to fresh water to that due to sea water, the discharge would also stop suddenly. However, the pressure head, h, would now exert itself and would cause fresh-water pressure to exceed sea-water pressure except at the interface where the two pressures would be balanced. Hence, for a liquid interface, the blocking of flow at the base of the control is offset, at least in part, by the pressure head, y_0, on top of the control.

The foregoing focuses the danger of "blow out" at the control, which grows with q and diminishes with the increase in the distance, L, between the toe of the salt-water wedge and the control. Furthermore, this danger is greatest during the periods of extreme low tide, a feature which is particularly significant at locations subject to large tidal ranges. Fortunately, the extreme tidal range along the coast of Calfornia is moderate.

It is possible that offset in the model, shown in Fig. 11, between the back of the sea-water weir box and the control face caused the trapping of air split out of the fresh water and that the q-measurements were thereby affected to some extent. The determination of the equipotential lines and the flow distribution between the interface and the clay cap of the model would be interesting and would merit additional research.

The discharge of fresh water through the control[28] to the ocean could be more readily understood if the interface, as a basic parabola, were extended so as to terminate at the horizontal discharge face, $q/2\,K$, in width and flush with the bottom of the clay cap. The discharge of fresh water would then be vertically upward and would satisfy the physical premise of the buoyancy of fresh water relative to sea water.

The stages shown in Fig. 14, especially those pertaining to high injection rates, are interesting. It must be assumed that the condition, as shown at the bottom of the photographs on the right, would closely represent the ultimate condition of the sea-water wedge cut off by the barrier.

Mr. Harder computes the contamination of 240,000 acre-ft of water to a concentration of 250 ppm of chloride ions (Cl^-) because of dilution of that part of the sea-water wedge which had intruded landward from the injection wells. If sea water intruding a fresh-water aquifer mixed with fresh water as readily as Mr. Harder assumes, the correction of sea-water intrusion would indeed be nearly hopeless unless it were always possible to locate the injection wells landward from the extreme tip of a saline wedge, as suggested by Messrs. Hotes and Harder. At Manhattan Beach this procedure was carefully considered but had to be abandoned because of three principal features: (1) The landward pressure gradient of the aquifer would have made it necessary to create a barrier above mean sea level of approximately twice the height of that at the final location of the barrier; (2) the right of way necessary for the barrier, including pipelines, pressure regulators, and chlorinators, would have been far too expensive to be justified for experimental operation; and (3) facilities for the disposal of water that was produced during the development of the recharge wells were completely lacking. However, the writer maintains that the effect of the saline wave, under conditions similar to those at Manhattan Beach, is negligible compared to that of the sea-water intrusion. It is only necessary to visualize the irregularities that normally exist in the form of mounds and depressions along the bottom of an aquifer to realize the facilities needed for the ready absorption of the sea water cut off from the original wedge by the injection and forced landward. The average depth of absorbed sea water may require a relatively short landward distance of spread.

In referring to Fig. 4, Mr. Hotes concludes that the saline wave is worse than is herein indicated. Apparently, Mr. Hotes overlooked the significance of Fig. 6 which shows more graphically than Fig. 4 what happened when the cut-off sea-water wedge was forced landward by the barrier wells. For example, it shows that the salinity in well G8, 1,180 ft from the line of recharge wells, dropped from about 5,000 ppm of Cl^- concentration to approximately 1,000 ppm in 16 months of barrier operation. Since October, 1955, this particular well has been immersed in fresh water of less than 250 ppm of Cl^-. Prior to the recharge test, sea water displaced fresh water throughout the entire depth of the aquifer at a rate of approximately 500 ft per yr. Since the test was started (38 months as of 1956) unadulterated sea water would have intruded well G8 and would have advanced some 400 ft beyond it.

Messrs. Harder and Hotes are, however, justified in pointing out that sea water, which had intruded into a shallow aquifer for a considerable distance landward and which had completely displaced the fresh water, could not be checked by means of injection wells without seriously affecting adjacent inland wells by displacing the landward part of the saline wedge. On the other hand, under conditions similar to those at Manhattan Beach, wells close to the barrier would also be close to the ocean and, therefore, would be subject to permanent and irreparable damage instead of temporary damage.

The writer deeply appreciates the discussions which have added great value to the paper. It is regretted that he cannot agree with all the thoughts presented.

HYDRAULICS OF WELLS

BY DEAN F. PETERSON, JR.,[1] M. ASCE

SYNOPSIS

The development of theoretical well hydraulics and certain aspects of the application of these developments to practical problems are reviewed. Considerable information is available regarding the hydraulics of well components and hydrodynamic details existing near the well. Much research is needed, however, for a better understanding of the hydrodynamic conditions near and through the well and for relating such information to natural geologic conditions and practical well engineering.

INTRODUCTION

Ground water is used extensively not only for irrigation in the western United States and in other arid and semiarid regions, but throughout the world for domestic and industrial purposes. The basis for the development of this resource is a long history of practical experience and relatively recent developments of theory.

The study of well hydraulics is a fascinating subject and has occupied the attention of many capable investigators. Like many engineering sciences, however, it is not an exact science, and the mathematical assumptions which often have to be made represent only limiting cases of real conditions. For example, one interested in theoretical well hydraulics usually finds he must postulate at least some of the following conditions, which are not usually fully correct:

1. The natural ground-water regime affecting an aquifer remains constant with time.
2. The permeability is uniform and isotropic throughout the formation.
3. The porosity and thickness of the formation is uniform.
4. The well penetrates fully, and the hydraulic head is the same at all points on the well boundary.
5. The initial piezometric surface is level.
6. Only laminar flow exists in the region affected by the well.
7. The region from which the well draws is infinite in extent.

Despite the necessity for introducing some of these unrealities, excellent progress has been achieved by students of theoretical well hydraulics. Useful tools for taking into account specific deviations of natural conditions from the assumed idealized conditions have also been devised in many cases. Well hydraulics has contributed much toward a better and more economic development of ground water.

NOTE.—Published, essentially as printed here, in June, 1955, as *Proceedings-Separate No. 708.* Positions and titles given are those in effect when the paper was approved for publication in *Transactions.*

[1] Prof. and Head, Civ. Eng. Dept., Colorado Agri. and Mech. College, Fort Collins, Colo.

FLOW FORMULAS

Equilibrium Case.—J. Dupuit[2] is credited with first combining Darcy's law of laminar flow through sands and gravels with the statement of continuity in order to derive an equation for well discharge. For this equation there were assumed complete axial symmetry and steady flow through an infinitely extending aquifer; the effects of curvilinear motion were ignored. The equation deduced was

$$Q = \pi K \frac{h^2_2 - h^2_1}{\ln (r_2/r_1)} \quad \text{(1)}$$

in which Q is the discharge; K denotes the permeability or, more properly, the hydraulic conductivity; and h_1 and h_2 are the elevations of the water surface above a level, impermeable bed bounding the lower side of the aquifer at radial distances, r_1 and r_2 (Fig. 1). All quantities in Eq. 1 must be expressed in compatible units or the necessary conversion constants must be introduced.

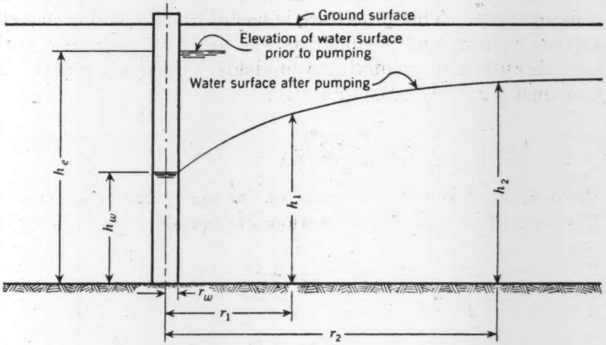
Ground surface
Elevation of water surface prior to pumping
Water surface after pumping
h_e
h_w
h_1
h_2
r_w
r_1
r_2

FIG. 1.—DEFINITION SKETCH FOR EQ. 1

Eq. 1 implies a well discharging from a water-table condition. However, all the common steady-flow formulas for fully penetrating wells stem from the Dupuit concept and may readily be deduced by algebraic manipulation of Eq. 1. It can be shown that

$$h^2_2 - h^2_1 = (h_2 - h_1)(h_2 + h_1) = (s_1 - s_2)(2\,m) \quad \text{(2)}$$

in which s_1 and s_2 are the drawdowns from the original water table or piezometric surface and m is the average thickness of the water-transmitting formation. Direct substitution of Eq. 2 into Eq. 1 yields

$$Q = \frac{2\,\pi\,K\,m\,(s_1 - s_2)}{\ln (r_2/r_1)} \quad \text{(3)}$$

---

[2] "Études théoriques et practiques sur le mouvement des eaux," by J. Dupuit, Dunod, Paris, 2d Ed., 1863.

Eq. 3 may also be used to describe a well discharging from an artesian aquifer of thickness, m.

Common practice of the Geological Survey, United States Department of the Interior (USGS), is to introduce the transmissibility term, T, into Eqs. 1 and 3. Transmissibility is the product of K and m and is widely used in characterizing an aquifer. Making this substitution into Eq. 3 yields

$$T = \frac{Q \ln (r_2/r_1)}{2 \pi (s_1 - s_2)} \qquad (4)$$

In USGS practice, T is ordinarily expressed in gallons per day per foot and Q in gallons per minute; length units are in feet. Introducing the necessary unit conversion constants into Eq. 4 yields

$$T = \frac{527.7\, Q \log_{10} (r_2/r_1)}{s_1 - s_2} \qquad (5)$$

Eqs. 1 through 5 are useful for determining K or T of water-bearing formations from pump tests. This procedure is useful in engineering investigations of dam foundations and land drainage as well as in water-supply work; these equations are also useful in predicting well yields. Ordinary practice is to plot drawdown against log r; then the quantity,

$$\frac{s_1 - s_2}{\log_{10} (r_2/r_1)} = \Delta s \qquad (6)$$

is simply the drop in piezometric surface for one log cycle of radii from the well center. The term, T, is directly proportional to Q and inversely proportional to Δs—that is,

$$T = 527.7 \frac{Q}{\Delta s} \qquad (7)$$

If

$$s_1 - s_2 = D \qquad (8)$$

is considered to be the drawdown of the well, r_1 corresponds to the well radius, r_w, and r_2 becomes the radius to a point where the functioning of the well does not disturb the existing piezometric surface, originally assumed as level. This latter distance is ordinarily termed the radius of influence. Obviously a well in equilibrium cannot exist in a finite, level, piezometric field. The concept of a radius of influence accordingly implies equilibrium between the flow discharged by the well and the flow replenished by nature to the region influenced by the well. The radius of influence is simply a length parameter describing the size of the influence region in a naturally replenishing field.

Orson W. Israelsen, M. ASCE, Vaughn E. Hansen, J.M. ASCE, and the writer, in 1950, postulated[3] a general functional relationship for steady-state wells expressed in the dimensionless form,

$$\frac{Q}{K\, r^2_w} = f\left(\frac{D}{r_w}, \frac{m}{r_w}, I\right) \qquad (9)$$

---

[3] "Hydraulics of Wells," by Dean F. Peterson, Orson W. Israelsen, and Vaughn E. Hansen, *Bulletin 351*, (Technical) Utah Agri. Experiment Station, Logan, Utah, 1950, pp. 21-29.

in which I represents the unit natural replenishment. In this work[3] there were presented expressions for natural seepage flow intercepted by the influence region of a well. Eliminating the radius of influence by substituting these expressions into the well-discharge equations (Eqs. 1 and 3), approximate functional relationships were obtained for fully penetrating wells in both artesian and unconfined aquifers having natural piezometric slopes, i_n, and for a well in an unconfined aquifer replenished vertically at a uniform rate.[3] For the unconfined case, this procedure results in

$$\frac{Q}{K h^2_e} = \frac{\pi \left[1 - \left(\frac{h_w}{h_e}\right)^2\right]}{2.303 \log \left[\frac{1}{2}\left(\frac{Q}{K h^2_e}\right)\left(\frac{h_e/r_w}{i_n}\right)\right]} \qquad (10)$$

in which h_e is the original height of the water surface above the impermeable stratum and i_n is the natural slope of the water table. For the confined case,

$$\frac{Q}{K D m} = \frac{2\pi}{2.303 \log \left[\frac{1}{2}\left(\frac{Q}{K D m}\right)\left(\frac{D/r_w}{i_n}\right)\right]} \qquad (11)$$

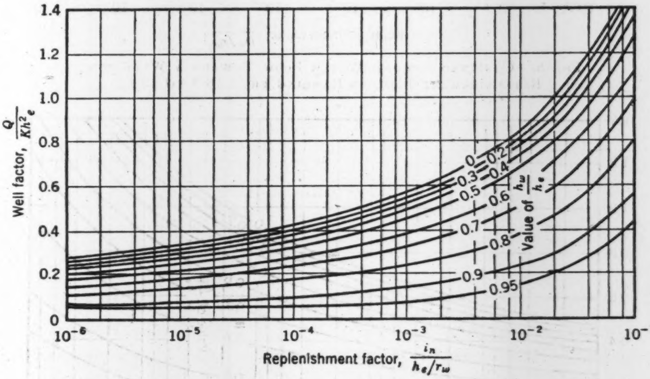

FIG. 2.—HORIZONTALLY REPLENISHED WELL IN UNCONFINED SYSTEM

For the case of a well in an unconfined aquifer, replenished both by vertical seepage at the uniform rate, q_v (volume per unit area per unit of time), and by horizontal seepage into the influence zone, a procedure embracing similar assumptions to those used in deriving Eq. 1 results in

$$Q = \frac{\pi K (h^2 - h^2_w)}{\ln \frac{r}{r_w} - \frac{n}{2}\left(\frac{r}{r_e}\right)^2} \qquad (12)$$

In Eq. 12, n is the proportion of total discharge, Q, originating by vertical replenishment and r_e is the radius of influence. If $n = 1$,

$$\frac{Q}{K\,h^2_e} = \frac{\pi\left[1 - \left(\frac{h_w}{h_e}\right)^2\right]}{1.151 \log\left[\frac{1}{\pi}\left(\frac{Q}{K\,h^2_e}\right)\left(\frac{h^2_e/r^2_w}{q_v/K}\right)\right] - \frac{1}{2}} \quad \ldots\ldots\ldots (13)$$

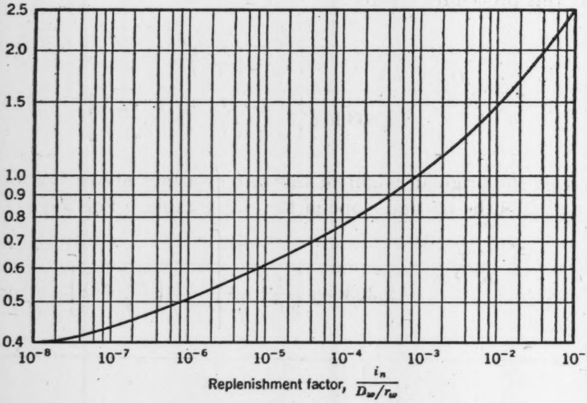

FIG. 3.—CONFINED GROUND-WATER FLOW TOWARD A WELL FOR REPLENISHMENT FACTORS RANGING FROM 10^{-8} TO 10^{-1}

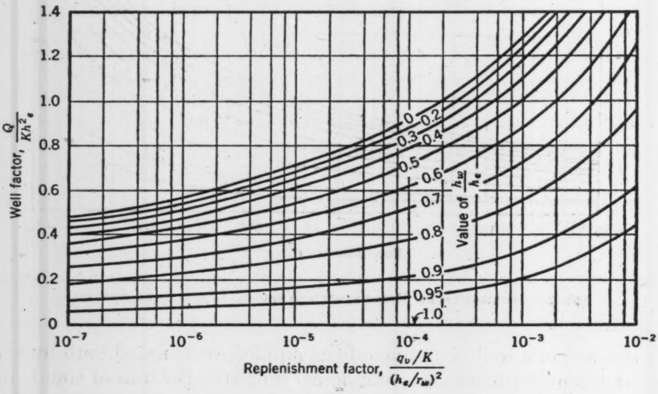

FIG. 4.—VERTICALLY REPLENISHED AND UNCONFINED GROUND WATER FOR REPLENISHMENT FACTORS RANGING FROM 10^{-7} TO 10^{-2}

Eqs. 10, 11, and 13 are not in the identical symbolic form of Eq. 9. However, m and D may be defined in terms of h_e and h_w for Eqs. 10 and 13; I is represented by i_n in Eqs. 10 and 11 and by q_v/K in Eq. 9.

The relationships expressed by Eqs. 10, 11, and 13 are shown graphically in Figs. 2, 3, 4, and 5. These figures should be useful in predicting the performance of wells for the limiting case when the discharge is in equilibrium with recharge by nature.

Letting $h = h_e$ and $r = r_e$, Eq. 13 may be rewritten in the form,

$$Q = \frac{\pi K \, (h^2_e - h^2_w)}{\ln \left[e^{-n/2} \left(\frac{r_e}{r_w} \right) \right]} \qquad (14)$$

in which e is the Naperian base. Eq. 14 is interesting because it implies that, if a transformation,

$$r_w = r'_w \; e^{-n/2} \qquad (15)$$

is introduced, the resulting flow system of a vertically replenished aquifer drained by a well of radius, r_w, will be geometrically similar to that of a Dupuit system drained by a well of radius, r'_w. Eq. 14 is subjected to the same theoretical approximations as Eq. 1 and, in addition, to the difficulty that the phreatic surface is not actually a streamline as for the Dupuit case. In spite of these approximations, Eqs. 13 and 14 are believed to be useful in the design of relief drainage systems using pumped wells. For such systems the average vertical replenishment is apt to be uniformly distributed over the influence area.

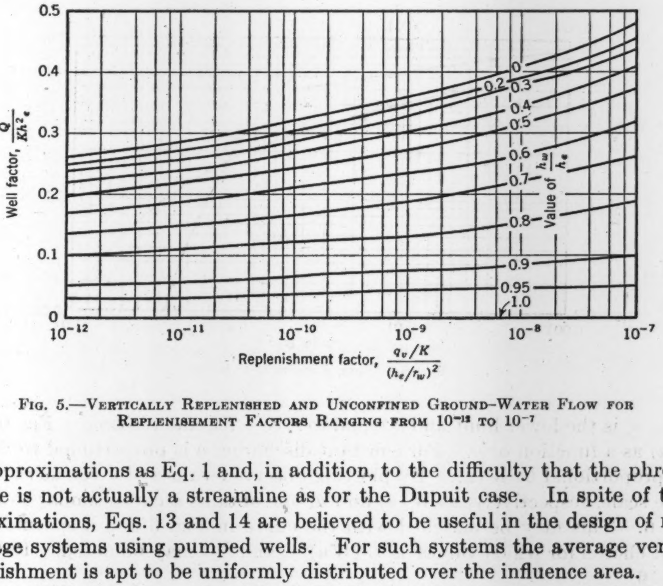

FIG. 5.—VERTICALLY REPLENISHED AND UNCONFINED GROUND-WATER FLOW FOR REPLENISHMENT FACTORS RANGING FROM 10^{-12} TO 10^{-7}

Nonequilibrium Case.—In 1935, C. V. Theis, utilizing mathematical methods developed in the study of heat flow, proposed[4] a method for analyzing the nonsteady flow of water into a well. Because the steady-flow condition or equilibrium condition is a limiting case rather than the rule in well hydraulics, this advance has led to a much greater understanding of well performance and to improved well engineering. This case takes into account the water drawn from storage in the aquifer as the result of unwatering in the water-table case, or volume changes associated with changes in pressure under pumping in the artesian case. An additional aquifer characteristic, the storage coefficient, S, was introduced by Mr. Theis. This coefficient, in common units, equals the volume of water released in 1 sq ft of area tributary to the well because of a unit decrease in piezometric head. For the water-table case this becomes the specific yield.

---

[4] "The Relation Between the Lowering of the Piezometric Surface and the Rate and Duration of Discharge of a Well Using Ground-Water Storage," by C. V. Theis, *Transactions*, Am. Geophysical Union, Vol. 16, 1935, pp. 519–524.

For the case of an infinitely extending aquifer and constant discharge,

$$s = \frac{Q}{4\,\pi\,T}\int_{r^2S/4\,T\,t}^{\infty} \frac{e^{-u}}{u}\,du \qquad (16)$$

This integral is termed the exponential integral, and tables of its values have been published.[5] It has also been termed the well function, $W(u)$, in which the

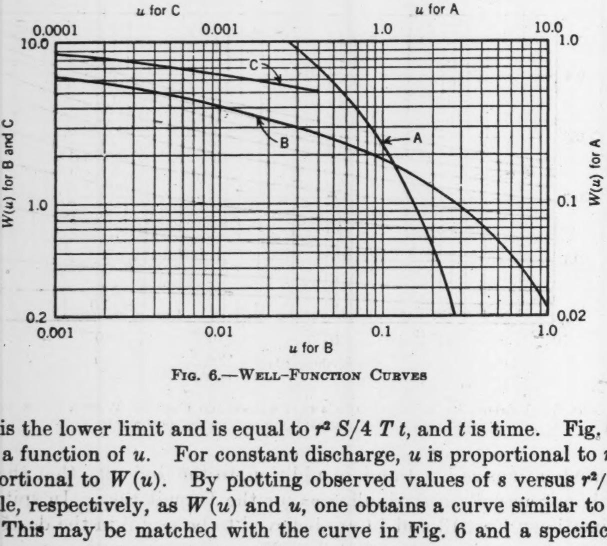

Fig. 6.—Well-Function Curves

term, u, is the lower limit and is equal to $r^2\,S/4\,T\,t$, and t is time. Fig. 6 shows $W(u)$ as a function of u. For constant discharge, u is proportional to r^2/t and s is proportional to $W(u)$. By plotting observed values of s versus r^2/t to the same scale, respectively, as $W(u)$ and u, one obtains a curve similar to that in Fig. 6. This may be matched with the curve in Fig. 6 and a specific match point chosen for which values of u, (Wu), s, and r^2/t may be noted. Rewriting Eq. 16,

$$s = \frac{Q}{4\,\pi\,T}\,W(u) \qquad (17)$$

and recalling,

$$\frac{r^2}{t} = \frac{4\,T\,u}{S} \qquad (18)$$

one may substitute these specific values to solve for T and S for the formation.

The exponential integral may be expressed by an infinite series. For small values of u only the first two terms are significant and

---

[5] "Smithsonian Physical Tables," Smithsonian Institution, Washington, D. C., 8th Ed., 1933, Table 32.

$$W(u) \cong -0.5772 - \ln u \ldots\ldots\ldots\ldots (19)$$

Substituting Eq. 19 into Eq. 17 yields

$$s = \frac{Q}{4\,\pi\,T}\left(\ln\frac{1}{u} - 0.5772\right) \ldots\ldots\ldots\ldots (20)$$

Taking into account the value of u from Eq. 18 for a well at a particular radial distance, one can demonstrate from Eq. 20 that

$$s_2 - s_1 = \frac{Q}{4\,\pi\,T}\ln\frac{t_2}{t_1} \ldots\ldots\ldots\ldots (21)$$

in which s_1 and s_2 are the values of drawdown at times t_1 and t_2, respectively. In USGS units,

$$s_2 - s_1 = \frac{264\,Q}{T}\log_{10}\frac{t_2}{t_1} \ldots\ldots\ldots\ldots (22)$$

In using Eqs. 21 and 22, s may be plotted against log t until the points fall on a straight line. Data from the straight-line portion of the curve are used to solve Eq. 22 for T (Fig. 7). By extending the straight line to a value of t_o when drawdown is zero, one may combine Eqs. 18 and 19 to give

$$s = 2.25\,\frac{T\,t_o}{r^2} \ldots\ldots\ldots\ldots (23)$$

The work of Mr. Theis is based on a boundary condition of constant discharge. In 1952, C. E. Jacob and Stanley W. Lohman published[6] a solution for the case of unsteady flow to a well at constant drawdown which resulted in

$$s = \frac{Q}{2\,\pi\,T\,G(\alpha)} \ldots\ldots\ldots\ldots (24)$$

In Eq. 24,

$$\alpha = \frac{T\,t}{S\,r^2_w} \ldots\ldots\ldots\ldots (25)$$

and $G(\alpha)$ is an irregular integral which has been evaluated by numerical methods.[6] For large values of α, $G(\alpha)$ was found to approach $2/W\,(\frac{1}{4}\,\alpha)$. The solution of Messrs. Jacob and Lohman is particularly applicable in analyzing flowing artesian wells.

The nonequilibrium formula may be applied to wells drawing from water-table conditions if proper correction is made to allow for the decrease in effective thickness owing to lowering of the water table. Mr. Jacob has shown[7] that a correction of $s^2/2\,m$ should be subtracted from the numerical values of observed drawdown, *s*. Failure to apply this correction results in rather considerable errors in the computed values of T and S.

---

[6] "Nonsteady Flow to a Well of Constant Drawdown in an Extensive Aquifer," by C. E. Jacob and Stanley W. Kohman, *Transactions*, Am. Geophysical Union, Vol. 33, 1952, p. 559.

[7] "Notes on Determining Permeability by Pumping Tests Under Water Table Conditions," by C. E. Jacob, Jamaica, N. Y., June, 1944 (mimeographed).

Since 1930, the nonequilibrium formula has been widely used with excellent results. Even where an equilibrium state may be possible, at the beginning of pumping the condition is always one of nonequilibrium. As time increases and the cone of influence becomes larger, the condition of the region near the well more closely resembles an equilibrium state because proportionately less of the flow through that part of the region comes from storage. Whether approximate equilibrium may occur eventually depends on the natural hydrology of the aquifer.

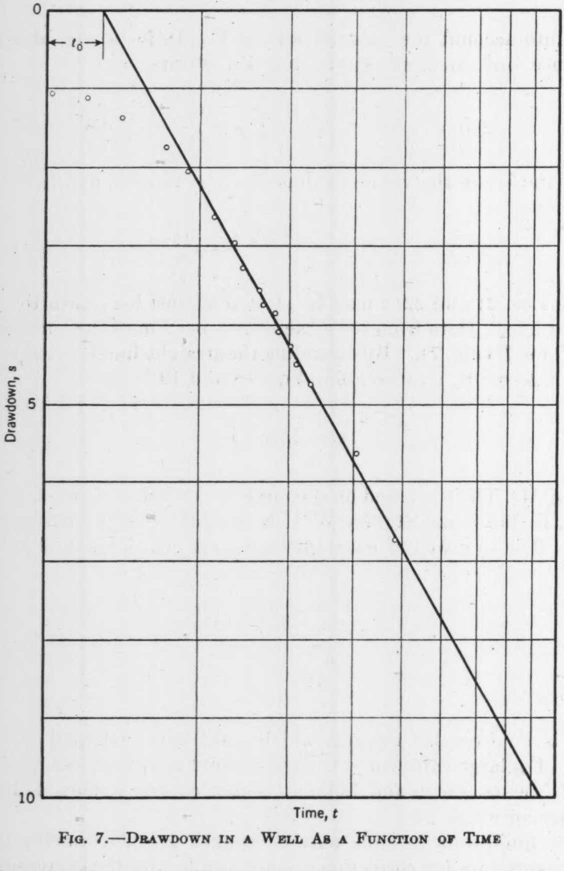

FIG. 7.—DRAWDOWN IN A WELL AS A FUNCTION OF TIME

Operation of a well depletes underground storage. Actually this increases the capacity of the underground reservoir to utilize available recharge. Ideally, for long-time continuous production, the management of a system of wells should be such as to deplete underground storage over the period of a recharge cycle in a quantity equal to the available recharge. Continual pumping in excess of this amount will lead to eventual complete depletion; pumping less than this quantity means some of the available recharge waters will be lost owing to lack of storage capacity.

METHOD OF IMAGES

By using the common mathematical device of assuming a set of images of the real condition, well hydraulics may take into account the effect of finite geologic boundaries deviating from the ideal assumed in deriving the various formulas. This may be illustrated by an example of an aquifer bounded by an impermeable boundary or aquiclude as shown in Fig. 8. If it is assumed that the aquiclude is approximately represented by the vertical plane, AB, no flow occurs through this plane. A set of images which makes this a plane of symmetry will provide a zero hydraulic gradient at the required boundary. The real drawdown will be the sum of the drawdowns for the real and the image wells in an infinite aquifer. In the event of two parallel boundaries, two planes of symmetry are necessary and may be achieved only by postulating an infinite set of images. The actual correction need be made only for the nearest few of the images, the number depending on the degree of accuracy desired.

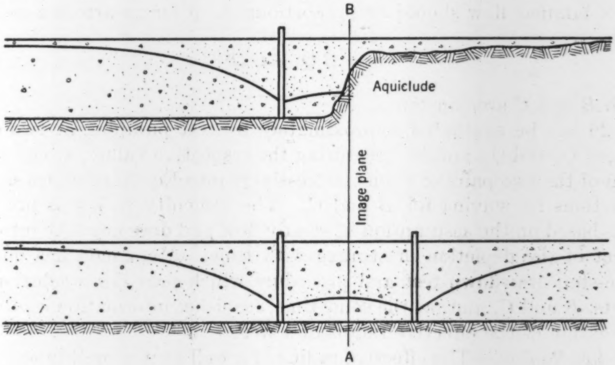

FIG. 8.—METHOD OF IMAGES

In the case involving a source of recharge at constant head, a symmetrical, but negative, set of images will provide the necessary boundary condition.

HYDRAULIC EFFECTS OF THE WELL

The flow of water through an aquifer under an energy gradient created by a well has been treated in this paper. The water must also be transferred through the screen and casing or pump column to the point of discharge. Under some circumstances the energy expended in moving the water through the well structure may exceed that used in moving it through the aquifer. A better understanding of hydraulic principles involved in this latter mechanism should lead to improved well engineering.

Specific Capacity.—Engineers have designated the ratio of discharge to drawdown as specific capacity. If the hydraulic head losses through the screen and casing were zero and the time effect of storage depletion were ignored, the discharge of an ideal artesian well could be expected to be directly proportional to the drawdown. This would lead to a constant value of specific capacity corresponding to all values of discharge of an artesian well—a condition usually assumed. For wells in unconfined aquifers, an increase in drawdown at the same time decreases the effective thickness of the aquifer. Thus, even discounting energy losses at the well, the specific capacity would decrease with discharge for the water-table case.

The hydraulic losses through the well cause further nonlinearity of the relationship of discharge to drawdown. As mentioned[8] by Mr. Jacob, flow through the screen and casing usually occurs in the turbulent regime, and the resulting head losses are thus proportional to Q^2. Furthermore, aquifer losses under conditions of laminar flow should be proportional to Q for an artesian well—thus,

$$s = B\,Q + C\,Q^2 \qquad (26)$$

in which B and C are constants.

Eq. 26 can be evaluated approximately by test pumping at two different discharges, Q_1 and Q_2, and by measuring the respective values, s_1 and s_2. Substitution of the two pairs of values successively into Eq. 26 provides simultaneous equations for solving for B and C. The difficulty with this procedure is that it is based on the assumption of steady flow and does not take into account the effect of the depletion of storage with time. Mr. Jacob has outlined[8] a multiple-step drawdown test and procedure which provides a solution for the constants, B and C, and, at the same time, furnishes information leading to the determination of the effective radius of a well.

Effective Radius.—The effective radius of a well as it is used in the formulas for flow may not be the same as the radius of the screen or hole, especially for wells in uncemented sediments. Development of the well or use of gravel envelopes increases the permeability of the formation immediately surrounding the casing. This effect is the same as increasing the radius. The effective radius is defined[9] by Mr. Jacob as

> "* * * that distance, measured radially from the axis of the well, at which the theoretical drawdown based on the logarithmic head distribution * * * equals the actual drawdown just outside the screen * * *."

Mr. Jacob also gives[8] a procedure for determining this quantity using the results of field tests.

Seepage Face.—For wells in unconfined aquifers, the Dupuit formula implies that the water surface outside the well intersects the water level in the well at the casing (Fig. 1). Even for a hydrodynamically perfect well this cannot be the case—a finite seepage face always exists between the water level in the well and the water surface outside. Mr. Hansen in 1949 proposed[10] the relationship,

---

[8] "Drawdown Test to Determine Effective Radius of Artesian Well," by C. E. Jacob, *Transactions* ASCE, Vol. 112, 1947, p. 1047.

[9] *Ibid.*, p. 1049.

$$\frac{Q}{K\,r^2_w} = F\left(\frac{h_w}{r_w},\ \frac{h_s}{r_w}\right) \qquad (27)$$

for a well in an unconfined aquifer bounded by a level impermeable stratum at the bottom. In Eq. 27, h_w is the elevation of the water level in the well and h_s is the corresponding elevation outside, both measured from the impermeable stratum. Using the experimental data available at that time, Mr. Hansen was able to propose curves graphing the functional relationship of Eq. 27. Additional information has since been made available by relaxation investigations[11] of Shih Te Yang and analogy investigations[12] which make possible presentation of Fig. 9. Fig. 9 also shows values of h_{115}/r_w corresponding to the values of the other parameters in which h_{115} is the height of the water level at a distance of 115 r_w. A field test of a well at Mosca (Colo.) by W. E. Code and the writer in 1954 correlated very well with the curves of Fig. 9. Results of this test gave $Q/K\,r^2_w = 30.5$, $h_s/r_w = 17.8$, $h_w/r_w = 13.9$, and $h_{115}/r_w = 27.1$. The results of this test appear as point A in Fig. 9.

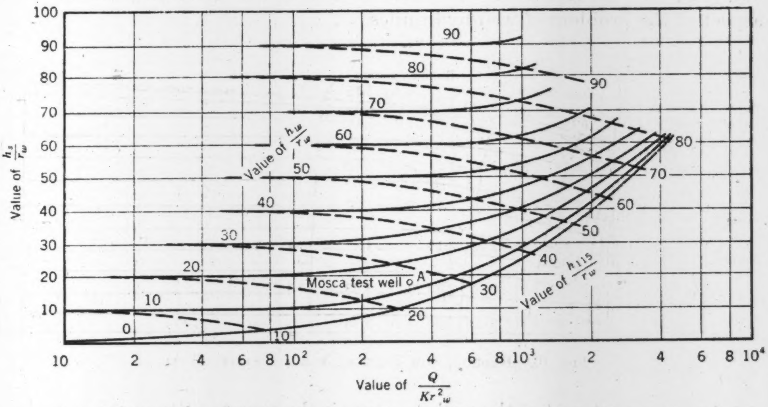

FIG. 9.—FUNCTIONAL RELATIONSHIP OF DISCHARGE AND GEOMETRIC PARAMETERS

The approach velocity in the neighborhood of an equipotential well is not constant as shown in Fig. 10, which is a flow pattern observed by C. H. Zee.[12] At the top of the seepage surface the approach velocity is K. Theoretically this increases with decreasing elevation and is proportional to the cosecant of the angle of inclination of the streamlines intersecting the seepage face. At the singular point, at the elevation of the water level in the well, this velocity theoretically becomes infinite but, practically, turbulent flow probably occurs. Below the singular point the velocity rapidly decreases to an almost constant value. Fig. 10 also shows the relationship between Dupuit's curve and the true water surface.

---

[10] "Evaluation of Unconfined Flow to Multiple Wells by the Membrane Analogy," by Vaughn E. Hansen, thesis presented to the State University of Iowa, at Iowa City, in 1949, in partial fulfilment of the requirements for the degree of Doctor of Philosophy.

[11] "Seepage Toward a Well Analyzed by the Relaxation Method," by Shih Te Yang, thesis presented to Harvard University, at Cambridge, Mass., in 1949, in partial fulfilment of the requirements for the degree of Doctor of Philosophy.

[12] "Flow into a Well by Electric and Membrane Analogy," by Chong-Hung Zee, Dean F. Peterson, and Robert O. Bock, *Transactions*, ASCE, Vol. 122, 1957.

Well Screens.—Frequently a large part of the energy imparted through a well is expended in transferring the water through the screen and pump. For this reason, attention should be given to the hydraulic performance of the well structure. Whereas considerable progress has been made, collection of data, especially in the field, is difficult because of rapidly changing flow conditions near the well. Laboratory experiments which simulate field conditions are expensive and arduous. Nevertheless, more attention should be given to this important aspect of the problem of well hydraulics.

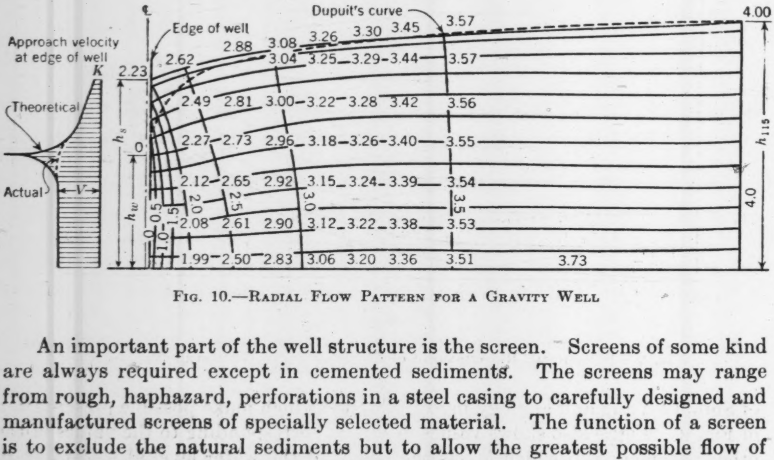

FIG. 10.—RADIAL FLOW PATTERN FOR A GRAVITY WELL

An important part of the well structure is the screen. Screens of some kind are always required except in cemented sediments. The screens may range from rough, haphazard, perforations in a steel casing to carefully designed and manufactured screens of specially selected material. The function of a screen is to exclude the natural sediments but to allow the greatest possible flow of water into the well. The factor of longevity influences the choice of screen.

The hydraulic performance of well screens has been ably treated.[13] Water enters the interior of a screen in the form of radial jets at relatively high velocities. The energy of these jets is dissipated, and the flow is accelerated in the axial direction. From a theoretical consideration of the mechanics involved, it was deduced that

$$\frac{\Delta h}{V^2/2\,g} = 2\,\frac{\cosh\,(C\,L/D + 1)}{\cosh\,(C\,L/D - 1)} \ldots\ldots\ldots\ldots\ldots (28)$$

in which Δh is the hydraulic head loss involved in the screen, V is the final average velocity along the screen axis, L is the axial length of the screen, and D is the screen diameter. The term, C, was defined as the screen coefficient—

---

[13] "Effect of Well Screens on Flow into Wells," by Jack S. Petersen, Carl Rohwer, and Maurice L. Albertson, *Transactions*, ASCE, Vol. 120, 1955, p. 563.

$$C = 11.31\, C_c A_p \ldots\ldots\ldots\ldots\ldots\ldots\ldots (29)$$

In Eq. 29, C_c is the orifice coefficient of discharge applying to the screen opening and A_p is the fractional ratio of screen opening to total screen surface. Eq. 28 was confirmed by large-scale laboratory experiments using specially made screens with machined openings and not surrounded by gravel (Fig. 11). Some coefficients were also determined for certain commercial-type screens.

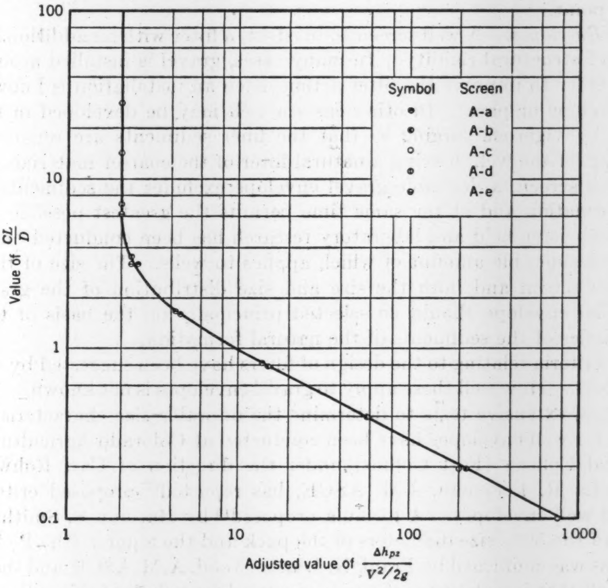

FIG. 11.—ADJUSTED VALUES OF $\Delta h_{pz}/(V^2/2\,g)$ AS A FUNCTION OF $C\,L/D$ FOR TYPE A SCREENS

The loss coefficient, $\dfrac{\Delta h}{V^2/2\,g}$, in Eq. 28, approaches 2 for values of $C\,L/D$ exceeding approximately 6. Apparently, for a particular screen of a certain diameter, increasing L beyond this value would not result in an appreciable decrease in screen losses for a particular discharge. The effect of gravel surrounding the screen was to reduce the screen coefficient but not appreciably for larger sizes of gravel. Where the gravel size was sufficiently small that it effectively reduced the percentage of open area of screen, the screen coefficient was also appreciably reduced. This important consideration needs to be taken into account in transferring the implications of Eq. 28 to the field. One should note that Eq. 28 does not imply that increasing the length of screen beyond a value corresponding to $C\,L/D = 6$ would fail to result in increased discharge but only that the ratio of screen losses to velocity head, whatever the effect on discharge, will not be improved by lengthening the screen.

The action of a well screen is such that the greatest flow through the openings occurs near the discharge point of the screen and decreases with distance from this point. In an actual installation, the discharge point would correspond to the intake for the pump bowls. In solving the conventional equations for flow through aquifers, the well boundary is assumed as a surface of constant head equal to the water level in the well. The effect of screens is to upset this; the head will be least opposite the pump inlet and will increase in both directions from this point.

Gravel Envelopes.—A well screen is, in effect, a filter with an additional characteristic of structural rigidity. In many cases, gravel is installed around the screen in order to improve the filter action; such an installation is known as a gravel envelope or pack. In other cases a well may be developed in natural materials by vigorous surging so that the finer sediments are removed and pumped out of the well, leaving a natural filter of the coarser materials.

As for a screen, a desirable gravel envelope excludes the sediments of the natural formation and at the same time permits the greatest possible flow of water. Extensive field and laboratory research has been conducted on gravel filters, a considerable amount of which applies to wells. The size of the slots in the well screen and both the size and size distribution of the gravel for the artificial envelope should be selected principally on the basis of the size characteristics of the sediments of the natural formation.

Many criteria relating to the design of filters have been suggested by various investigators. How well these apply to gravel envelopes is not known. During recent years, extensive tests to determine the desirable size characteristics for materials for well envelopes have been conducted at Colorado Agricultural and Mechanical College (Fort Collins) under the direction of Carl Rohwer, M. ASCE. John R. Lockman, J.M. ASCE, has reported[14] proposed criteria for filters and well envelopes. A formula proposed[15] by Harmon F. Smith is that the ratio of the 50% size diameters of the pack and the aquifer (the P–A ratio) be 5. This was confirmed by Frank N. Leatherwood, A.M. ASCE, and the writer who found[16] that instability of the sand occurred for values of this ratio exceeding 5.3. These investigators used gravels essentially uniform in size. Mr. Lockman, also using uniform-sized gravels sieved between adjacent size sieves, found, nevertheless, that the uniformity of the sand greatly affected the ability of the pack to resist plugging. Mr. Lockman proposed a criterion involving the uniformity coefficient (ratio of D_{60} to D_{10}) of the aquifer such that the product of the P–A ratio and the uniformity coefficient be in the range of 5 to 8; a uniform-sized pack gravel seemed to give best results.

---

[14] "Selection of Gravel Pack for Wells in Fine, Uniform, Unconsolidated Aquifers," by John R. Lockman, thesis presented to Colorado Agricultural and Mechanical College, at Fort Collins, in 1954, in partial fulfilment of the requirement for the degree of Master of Science.

[15] "Gravel Packing Water Wells," by Harmon F. Smith, *Water Well Journal*, January–February, 1954, pp. 15–17.

[16] "Hydraulic Head Loss at the Interface Between Uniform Sands of Different Sizes," by Frank N. Leatherwood and Dean F. Peterson, *Transactions*, Am. Geophysical Union, Vol. 35, 1954, p. 588.

CONCLUSIONS

The work of Dupuit and the formulas involved from the same general concept, based on assumed steady-flow conditions, have provided a valuable basis for well engineering and for field testing to determine the permeability of underground sediments. Nevertheless, a steady-state flow condition is not the usual case, and most well flow occurs by storage depletion. The formula proposed by Mr. Theis for a nonequilibrium well with subsequent adaptations to special conditions has yielded excellent results and has contributed greatly to the success of well engineering. Well-field developments, if they are to be permanent, should be designed to deplete storage only to the extent that subsequent periodical recharge may be expected. A development in which production continuously exceeds available recharge is doomed to eventual depletion, although in some instances the volume of storage is so large that this may not be imminent.

A well is, among other things, a mechanism for the transfer of energy to an underground body of water. The energy thus transferred causes flow toward the well. In inefficient wells, energy losses in and near the well may be excessive. Considerable information is available regarding the hydraulics of well components, such as screens and gravel envelopes, and of hydrodynamic details existing near the well. This has contributed greatly to the art of well construction. Much additional research is needed, however, principally in an effort to understand better hydrodynamic conditions near the well and through the well components and to be able to relate such information to natural geologic conditions and practical well engineering.

AMERICAN SOCIETY OF CIVIL ENGINEERS

Founded November 5, 1852

TRANSACTIONS

Paper No. 2870

VIRTUAL MASS AND ACCELERATION IN FLUIDS

By Thomas E. Stelson,[1] J. M. ASCE, and Frederic T. Mavis,[2] M. ASCE

With Discussion by Messrs. Joseph M. Caldwell; Edward Silberman; and Thomas E. Stelson and Frederic T. Mavis

Synopsis

The "effective inertia" of a body is greater in air than in a vacuum and is much greater in a liquid. This effective inertia, which is greater than the "quantity of matter" or mass (ratio of weight to the acceleration due to gravity) of a body, is termed "virtual mass." The excess of virtual mass over the quantity of matter is the added mass caused by the surrounding fluid.

Measurements were made on objects as they were immersed in water and accelerated in oscillatory motion. The added masses, which depend on the size and shape of the body, the direction of acceleration, and the density of the fluid, were determined from a mass-frequency relationship for the supporting beam. The experimental results are reasonable, consistent, and agree with previous analytical studies of potential flow.

Introduction

In 1779 Pierre Louis Gabriel DuBuat[3] published the results of his observations on spherical pendulum bobs of lead, glass, and wood vibrating in air and in water. He noticed that a simple buoyancy correction for the submerged sphere was not sufficient. In addition, the fluid had the same effect as increasing the mass of the sphere by approximately one-half the mass of the fluid that was displaced.

Since the time of DuBuat the added mass due to submergence in a fluid has been the subject of many analytical and experimental investigations.[4] Deter-

---

Note.—Published, essentially as printed here, in April, 1955, as *Proceedings-Separate No. 670.* Positions and titles given are those in effect when the paper or discussion was approved for publication in *Transactions.*

[1] Asst. Prof. of Civ. Eng., Carnegie Inst. of Technology, Pittsburgh, Pa.

[2] Prof. and Head, Dept. of Civ. Eng., Carnegie Inst. of Technology, Pittsburgh, Pa.

[3] "Principes d'hydraulique," by Pierre Louis Gabriel DuBuat, Paris, 2d Ed., 1786, Vol. 2, pp. 226–259.

[4] "Acceleration of Bodies in Fluids—A Study of Virtual Mass," by T. E. Stelson, thesis submitted to the Carnegie Institute of Technology at Pittsburgh, Pa., in 1952, in partial fulfilment of the requirements for the degree of Doctor of Science, pp. 5–16.

mination of added mass by experiment often has been inconsistent and unreasonable. Measured values for added mass have usually been larger than can be explained by theory and analysis. J. Luneau[5] reported on tests of circular disks where he found added masses from three to nine times the theoretical values. In 1951 H. W. Iverson and R. Balent[6] concluded that added mass is a variable which depends on the state of motion and is not a constant as had been shown by studies of potential flow.

In the present study a new method for determining the added mass of submerged bodies was developed. It is simple yet accurate and permits the easy measurement of added mass for bodies of any shape. The measured values are in substantial agreement with analytical values obtained from studies of potential flow. Thus, the practical value of added masses obtained from analytical studies is confirmed. In addition, for odd-shaped bodies a reliable experimental method is now available to determine the added masses which cannot be obtained by analysis alone.

THEORY

If a body of a mass, m, moves in rectilinear motion at a velocity, v, its kinetic energy is

$$T_B = \tfrac{1}{2}\, m\, v^2 \ldots\ldots\ldots\ldots (1)$$

If a body moves at a velocity, v, in an ideal, incompressible fluid of infinite extent, at rest of infinity, and in irrotational motion, the total kinetic energy of the fluid is

$$T_F = \tfrac{1}{2}\, c\, v^2 \ldots\ldots\ldots\ldots (2)$$

in which c is a constant that depends only on the density of the fluid, the size and shape of the body, and the direction of motion.[7] The total kinetic energy, T, of the system (body and fluid) is

$$T = T_F + T_B = \tfrac{1}{2}\,(m + c)\, v^2 \ldots\ldots\ldots\ldots (3)$$

When the body is accelerated, the rate of change in the total kinetic energy with respect to time, t, is

$$\frac{dT}{dt} = (m + c)\, v\, \frac{dv}{dt} \ldots\ldots\ldots\ldots (4)$$

Inasmuch as

$$\frac{dT}{dt} = F\, v \ldots\ldots\ldots\ldots (5)$$

in which F is the resultant of the external forces that act on the body to cause the acceleration, dv/dt. Therefore,

$$F = (m + c)\, \frac{dv}{dt} \ldots\ldots\ldots\ldots (6)$$

---

[5] "Sur l'effet d'inertie des sillages des disques circulaires se deplaçant dans l'eau d'un mouvement uniformement acceleré," by J. Luneau, *Comptes rendus de l'Academie des Sciences*, Vol. 229, 1949, pp. 927–928.

[6] "A Correlating Modulus for Fluid Resistance in Accelerated Motion," by H. W. Iverson and R. Balent, *Journal of Applied Physics*, Vol. 22, 1951, pp. 324–328.

[7] "Hydrodynamics, a Study in Logic, Fact and Similitude," by G. Birkhoff, Princeton University Press, Princeton, N. J., 1950, pp. 151–154.

Thus, the fluid has the effect of increasing the inertia or mass of the body from m to $(m + c)$. The term, c, is called the "added mass" and $(m + c)$ the "virtual mass." A more rigorous explanation of this phenomenon can be found in textbooks on hydrodynamics.[8,9] Energy rather than momentum expressions have been used in the foregoing explanation because in the analysis of potential flow the energy integrals usually converge and momentum integrals do not.

The virtual mass is the inertia coefficient or ratio of applied force to acceleration in fluid media. The actual mass of a body is the inertia coefficient that applies to movement in a vacuum. Thus, the quantity that is of practical importance in most dynamic problems is the virtual mass; the difference between actual and virtual mass is frequently overlooked or assumed to be of only academic interest. For movement in low-density fluids such as air, the difference may not be significant, but in fluids such as water the virtual mass may be many times the actual mass. Consequently, the difference between the two may really be important.

PRACTICAL IMPORTANCE

Investigating the effect of virtual mass on dams during earthquakes, H. M. Westergaard[10] found the inertia pressures to be neither excessively large nor negligible. Charles P. Dunn,[11] and Adolph J. Ackerman,[12] Members, ASCE, described a unique method of placing the Chute-à-Caron cofferdam in the Saguenay River (Quebec, Canada). The concrete dam, 92 ft long, 45 ft thick, and 42 ft high at the center, was built on one end on a pier and was toppled into place in the river which was 28 ft deep and flowed at a velocity of 20 ft per sec. Although the 11,000 tons of concrete in the dam fell an average distance of 86 ft and came to rest on bed rock, only a few hairline cracks developed. The water "cushioned" the fall so that the final impact was the equivalent of only a 4-in. drop through air. The potential energy of the falling dam was largely changed into kinetic energy of the water. Velocities of water were estimated to be as great as 600 ft per sec.

The added-mass effect has been considered in such diverse problems as roll, pitch, and vibration of ships; accelerations of submarines, ships, and dirigibles; entrance of projectiles and seaplane floats into water; sediment movement and wave action; tone of bells and strings; and the vibration of plates and structures. Whenever solids in contact with fluids accelerate, virtual mass is a factor that should not be overlooked.

EXPERIMENTAL METHOD

The apparatus used is shown in Fig. 1. The test bodies were immersed in a cylindrical tank of water. Supporting rods were rigidly attached to a

---

[8] "Theoretical Hydrodynamics," by L. M. Milne-Thompson, The Macmillan Co., New York, N. Y., 2d Ed., 1938, pp. 228–229.

[9] "Hydrodynamics," by H. Lamb, Cambridge University Press, London, 6th Ed., 1932, pp. 160–174.

[10] "Water Pressures on Dams During Earthquakes," by H. M. Westergaard, *Transactions*, ASCE, Vol. 98, 1933, pp. 418–434.

[11] "Blasting a Precast Dam into Place," by Charles P. Dunn, *Civil Engineering*, Vol. 1, 1930, pp. 159–164.

[12] "Models Predict Behavior of Falling Dam," by Adolph J. Ackerman, *ibid.*, Vol. 2, 1932, pp. 415–420.

beam, $\frac{3}{8}$ in. deep, $\frac{1}{8}$ in. wide, and 24 in. long, whose ends were simply supported on pivot bearings just above the surface of the water.

Before testing the bodies, the relationship between the natural fundamental frequency for vertical vibration of the beam and the mass in air attached to the center was determined by experiment. The frequency was measured by attaching a small magnet to the beam. When vibrated, the moving magnet produced a potential in a surrounding coil that was independently supported. An oscillograph recorded the varying potential. Frequency was obtained by averaging the time for 30 cycles to 50 cycles on the oscillograph record.

A test body was then submerged in water, attached to the center of the beam by a rod, and the beam was vibrated at its new natural fundamental frequency. The frequency of the body submerged in water was equal to the frequency of a body of larger mass attached to the beam and vibrating freely in air. The difference between the mass of the submerged body and the attached mass in air that gives the same frequency is the added mass effect of the fluid.

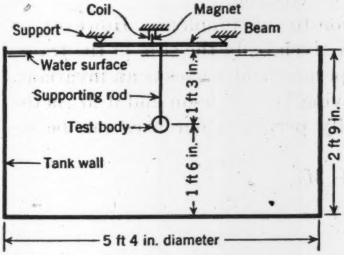

FIG. 1.—APPARATUS FOR MEASURING ADDED MASS

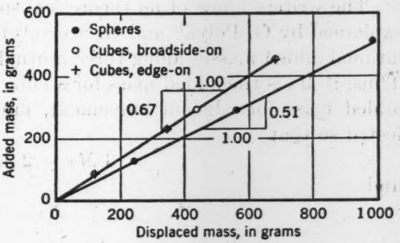

FIG. 2.—TESTS ON SPHERES AND CUBES

The foregoing statement is true only under the following assumptions:

1. The weight of air displaced by the weights attached to the beam is negligible compared to the weight of water displaced by the submerged bodies. Because the ratio of the densities of air and water is approximately 1 to 800 and the attached masses are relatively compact in shape and size, the error due to the added mass in air could not be more than 1 part in 2,000.

2. The effect of the viscosity of the water is assumed to be negligible. The validity of this assumption is supported by two experimental observations: (*a*) The oscillograph trace which represents the vertical velocity of the beam is as nearly sinusoidal as can be measured. (*b*) The damping is so slight that the amplitude of the vibration is reduced by only one-half in 20 cycles to 50 cycles—a logarithmic damping decrement of about 2% per cycle.

Analyzing the effect of viscosity on the inertia resistance of a sphere oscillating in simple harmonic motion, H. Lamb[13] found that, instead of $\frac{1}{2}$, the viscosity changes the inertia coefficient to

---

[13] "Hydrodynamics," by H. Lamb, Cambridge University Press, London, 6th Ed., 1932, p. 644.

$$\frac{1}{2} + \frac{9}{4\,a}\left(\frac{\nu}{\pi\,f}\right)^{\frac{1}{2}}$$

in which a is the radius of the sphere, f denotes the frequency of the vibration, and ν is the kinematic viscosity of the fluid. For typical test conditions of a sphere having a radius of 0.17 ft vibrating in water ($\nu = 0.00001$ sq ft per sec) at 20 cycles per sec, the change in inertia resistance due to viscosity is 0.0054, or approximately 1%. Thus, the viscosity would not seriously affect the experimental values for added mass.

RESULTS AND ANALYSIS

Spheres.—The measured added mass due to the fluid (Fig. 2) is 0.51 times the mass of fluid displaced. This agrees well with theoretical analyses[9] that show the added mass to be one-half the displaced mass.

Cubes.—The measured added mass (Fig. 2) is 0.67 times the displaced mass for cubes accelerated either "broadside-on" or "edge-on."

The writers know of no theoretical solution to this problem. However, as explained by G. Polya[14] and G. Szego,[15] for a given body the sum of the translational added masses along three mutually perpendicular axes is an invariant. Thus, if M_b is the added mass for a cube moving broadside-on and if M_e is the added mass for edge-on movement, mutually perpendicular axes can be selected so that

$$3\,M_b = 2\,M_e + M_b$$

and

$$M_b = M_e.$$

Thus, theory indicates that the added masses of a cube for edge-on motion and broadside-on motion should be identical as was shown by experiment.

The ratio of added mass to displaced mass for a cube was 0.67, which was one-third greater than the corresponding ratio, 0.51, for a sphere. Mr. Szego[15] has shown that a sphere has less added mass than any other nearly spherical solid of equal volume. Hence, theory would indicate that the ratio for cubes should be larger than the ratio for spheres as was shown by the writers' experiments.

Circular Cylinders.—The relationships (Fig. 3) between the ratio of length to diameter and the ratio of added mass to the displaced mass for square-ended circular cylinders of wood about 2 in. in diameter are plotted on "semi-hyperbolic" paper for which Y-distances from the origin vary directly as the variable, y, and X-distances from the origin vary inversely as the variable, x. Experimental data for circular cylinders (solid circles) define a line which intersects the axis of ordinates at 1.00. This means that, experimentally, for rigid circular cylinders whose ratio of length to diameter is "very large," the added mass is 1.00 times the displaced-cylinder mass—exactly the quantity indicated by mathematical analysis.

---

[14] "A Minimum Problem about the Motion of a Solid Through a Fluid," by G. Polya, *Proceedings*, National Academy of Sciences, Vol. 33, 1947, pp. 218–221.

[15] "On the Virtual Mass of Nearly Spherical Solids," by G. Szego, *Journal of Mathematics*, Duke Univ., Durham, N. C., Vol. 16, 1949, pp. 209–223.

Rectangular Plates.—Rectangular plates from 2 in. to 3 in. wide and from 2 in. to 8 in. long of 16-gage sheet steel were accelerated broadside-on (Fig. 3). As the length-to-width ratio for the plates becomes large, the ratio of added mass to displaced-cylinder mass approaches 1.05. The displaced-cylinder mass is by definition the mass of fluid displaced by a right circular cylinder, having a diameter equal to the width of the plate. The plate and cylinder lengths are the same.

In analyzing potential flow about a rod of infinite length having a rectangular cross section and moving broadside-on, D. Riabouchinsky[16] found the added mass, c, per unit length in a fluid of unit density to be

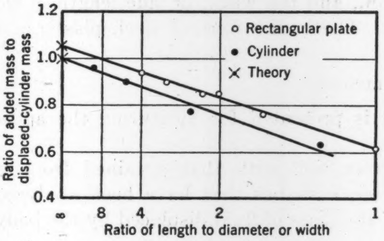

FIG. 3.—CIRCULAR CYLINDERS AND RECTANGULAR PLATES

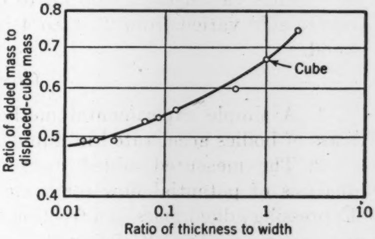

FIG. 4.—RECTANGULAR PARALLELEPIPEDS—SQUARE SIDE MOVING BROADSIDE-ON

$$c = \frac{\pi}{4} w^2 \left\{ \frac{\sin^2 \alpha}{[E - (\cos^2 \alpha)\, K]^2} - \frac{4}{\pi} \frac{d}{w} \right\} \qquad (7a)$$

in which α is a parameter so that

$$\frac{d}{w} = \frac{[E' - (\sin^2 \alpha)\, K']}{[E - (\cos^2 \alpha)\, K]} \qquad (7b)$$

The broadside width is w, and the thickness in the direction of motion is d. Terms K and E are complete elliptic integrals of the first and second kind and $\cos \alpha$ and $\sin \alpha$ are their respective moduli; E' and K' are the corresponding functions of the complementary angle $(90° - \alpha)$.

Mr. Riabouchinsky found that, when $\alpha = 80°$,

$$\frac{d}{w} = 0.025 \qquad \text{and} \qquad \frac{c}{\pi w^2/4} = 1.05.$$

The quantity, $\pi w^2/4$, is the displaced-cylinder mass in a fluid of unit density.

In the experiments described herein, $d = 0.0625$ in. and the mean width $w = 2.50$ in. Thus,

$$\frac{d}{w} = \frac{0.0625}{2.50} = 0.025,$$

---

[16] "Sur la résistance des fluides," by D. Riabouchinsky, *Comptes Rendus*, Congrès International des Mathematiciens, Strasbourg, 1920, pp. 568–585.

and by analysis the ratio of added mass to displaced-cylinder mass for such plates of infinite length should be 1.05, checking the experimental results (Fig. 3).

Rectangular Parallelepipeds.—In Fig. 4 is shown the relationship between (1) the ratio of added mass to displaced-cube mass and (2) the ratio of thickness in the direction of motion to the edge width perpendicular to motion—for rectangular parallelepipeds having a square side moving broadside-on. The displaced-cube mass is defined as the mass of fluid displaced by a cube having sides the same as the square sides of the parallelepiped. The thickness of the test bodies varied from 0.06 in. to 6 in., and the width or side length of the square side varied from 2 in. to 4 in. The bodies were of steel, plastic, and wood.

CONCLUSIONS

1. A simple experimental method is presented for measuring the added mass of bodies accelerated in liquids.

2. The measured added mass agrees well with that obtained from an analysis of potential flow for some simple shapes that have been analyzed. Expressing added mass as a fraction of the mass of fluid displaced by the body, a comparison of results follows:

Body	Added Mass	
	Analysis	Experiment
Sphere	0.50	0.51
Long circular cylinder, accelerated transversely	1.00	1.00 (asymptote)
Long, thin rectangular rod, accelerated broadside-on	1.05	1.05 (asymptote)

(The final quantities, 1.05, are in terms of the displaced mass of a circular cylinder inscribed in the broadside width.)

3. For those shapes that have not been analyzed the added mass has been measured as follows:

Body	Range	Added Mass
Cube accelerated, parallel to a side	...	0.67 displaced mass
Circular cylinder, accelerated transversely	$1.2 \le \dfrac{\text{length}}{\text{diameter}} \le \infty$	as shown in Fig. 3
Thin rectangular cylinder, accelerated broadside-on	$\le \dfrac{\text{length}}{\text{diameter}} \le \infty$	as shown in Fig. 3
Rectangular parallelepipeds with with square side, accelerated broadside-on	$0.016 \le \dfrac{\text{length}}{\text{diameter}} \le 2$	as shown in Fig. 4

ACKNOWLEDGMENTS

The study from which this paper is drawn was supported financially from a Gerard Swope Fellowship awarded by the General Electric Educational Fund.

The experiments were performed in the civil engineering laboratories at the Carnegie Institute of Technology at Pittsburgh, Pa.

C. F. Peck, Jr., A. M. ASCE, and T. E. Doyle, Jr., contributed significantly to the development of experimental methods of producing and recording vibrations.

DISCUSSION

Joseph M. Caldwell,[17] M. ASCE.—The authors are to be commended for presenting in a readily understandable manner the basic concept of virtual mass and for demonstrating its potential importance in engineering practice. Possibly the value of the experimental data in the paper could be further increased by a replot of Fig. 4. Unless accompanied by a careful reading of the text, Fig. 4 might give the impression that the relative importance of the virtual-mass effect increases as the thickness (or length) of the object increases whereas, actually, it decreases.

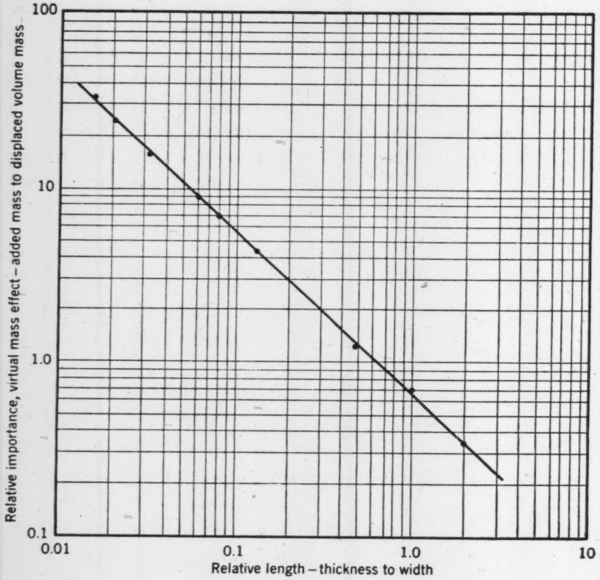

Fig. 5.—Relative Effect of Virtual Mass in Parallelepipeds—Square Side Moving Broadside-On

The decrease can be demonstrated by replotting the data with the ratio of added mass to displaced-volume mass as the parameter for the ordinates. In Fig. 5 is shown the result; the decreasing relative importance of the virtual-mass effect as the object becomes increasingly elongated in the direction of motion is apparent.

A possible worthwhile extension of the work of Messrs. Stelson and Mavis would be into the problem of the fixed object held in an accelerating fluid flow. This latter problem is being faced with increasing frequency in the design of offshore structures subjected to wave action around the continental shelf of the United States, and the concepts of virtual mass are not yet clarified in many such design problems.

---

[17] Chief of Research Div., Beach Erosion Board, Corps of Engrs., U. S. Dept. of the Army, Washington, D. C.

EDWARD SILBERMAN,[18] A.M. ASCE.—The method for measuring virtual mass introduced in the paper should prove extremely useful. The carefulness with which the work was done and the agreement with theory, where applicable, indicates that the results presented are of a high order of accuracy. However, the statement in the "Introduction"—"determination of added mass by experiment often has been inconsistent and unreasonable"—and the associated implication that results not in agreement with those of the authors are in error require further proof.

It should be observed that, in the cited references [5,6] involving added masses several times the theoretical values, the bodies were in unidirectional motion rather than in vibratory motion. A body in unidirectional motion sooner or later develops a boundary layer and wake. The question then arises as to what part of the resistance to motion is due to viscous and form drag and what part is due to added mass. The question can be best studied, perhaps, by reducing all resistance or drag values to the form of a drag coefficient, C_D, defined by

$$\text{Resistance} = C_D \, \rho \, S \frac{v^2}{2} \qquad (8)$$

in which ρ is the fluid density and S is the area of maximum cross section taken normal to the direction of motion. For a sphere of diameter, D, for example, the resistance attributable to added mass is

$$c \frac{dv}{dt} \approx \tfrac{1}{2} \rho \, \pi \frac{D^3}{6} \frac{dv}{dt} \qquad (9)$$

$$S = \frac{\pi D^2}{4}$$

with

$$C_D = \tfrac{2}{3} \frac{D}{v^2} \frac{dv}{dt} \qquad (10)$$

In Fig. 6 are plotted some experimental data for spheres in unidirectional acceleration.[19] Curve 1 follows the preceding equation for the drag coefficient attributable to added mass, and curve 2 is the drag coefficient for unaccelerated motion, for which C_D (steady motion at Reynolds number $\approx 10^5$) $= 0.5$. The abscissa is the dimensionless parameter $(D/v^2)\, dv/dt$ used by Messrs. Iverson and Balent.[6] Fig. 6 is typical of unidirectional acceleration data; the data of Messrs. Iverson and Balent for circular disks are plotted in a similar manner, for example.

It is apparent that the precision in unidirectional-acceleration measurements is not nearly so great as that in the authors' experiments. Nevertheless, the results are sufficiently consistent when plotted in this manner to indicate a definite trend. A first attempt toward predicting the fluid resistance in unidirectional acceleration would be to add the resistance attributable to the added mass of the body to the resistance attributable to viscous motion at the instantaneous Reynolds number of the motion. This has been tried, and the result is shown by the dotted line (1 + 2) in Fig. 6. It is apparent that this simple approach fails; a similar result occurs for all other unidirectional acceleration data known to the writer.

---

[18] Associate Prof., St. Anthony Falls Hydr. Lab., Univ. of Minnesota, Minneapolis, Minn.

[19] "The Resistance to Accelerated Motion of Spheres in Water," by G. Bugliarello, thesis submitted to the University of Minnesota, at Minneapolis, in July, 1954, in partial fulfilment of the requirements for the degree of Master of Science in Civil Engineering.

There are other possibilities for predicting the resistance in unidirectional acceleration: (1) The viscous drag corresponding to a Reynolds number much smaller than its instantaneous value should be used; (2) the added mass for a body longer than the actual body, to allow for the presence of the wake, should be introduced; and (3) a combination of smaller Reynolds number and larger added mass should be used.

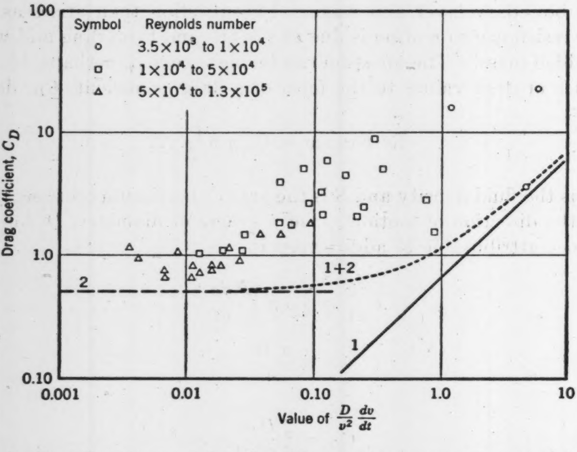

FIG. 6.—DRAG COEFFICENT FOR 3-IN. STEEL SPHERES ACCELERATED UNIDIRECTIONALLY

In support of choice (2), it is shown in Fig. 4 that as the length of a parallelepiped increases its added mass with respect to the displaced mass of a cube increases. If the wake behind a cube could be considered as adding to its length, the cube-wake combination would have a larger added mass and larger resistance than the cube alone. The writer believes that either choice (2) or choice (3) is the proper explanation for the trend of the data and that the added mass is actually a function of the state of the motion. Only at very large values of the parameter, $(D/v^2)\, dv/dt$ (that is, in the absence of a wake), do the authors' results apply to unidirectional motion.

Regarding the importance of added mass in low-density fluids, it should be noted that Fig. 6 is largely independent of the fluid used. Hence, even in air, at high values of the parameter, $(D/v^2)\, dv/dt$, the resistance attributable to added mass may be much more important than the viscous and form drag associated with the instantaneous Reynolds number of motion.

It is interesting to observe that in Fig. 3 the data for the rectangular plates can be used to extend the plotting to the right of the length-width ratio of unity. That is, the added mass for a plate of length-wide ratio of 4, say, must be the same as for a plate of the same area of length-width ratio of ¼, assuming no scale effect. The displaced-cylinder masses in the example cited are in the ratio of 1:16. Thus, the ordinate occurring at the length-width ratio of 4 may be divided by 16 and plotted at the length-width ratio of ¼. Proceeding similarly with all the data, the straight line drawn through the rectangular plate data in Fig. 3 is seen to be a curve asymptotic to the ordinate zero. (Actually, the curve and straight line are nearly identical in the region of Fig. 3.) By inference, the cylinder data may be assumed to follow a similar trend.

Thomas E. Stelson,[20] **J. M. ASCE, and Frederic T. Mavis,**[21] **M. ASCE.**—The writers' data on added mass of rectangular parallelepipeds with square side moving broadside-on (Fig. 4) have added meaning as they have been replotted by Mr. Caldwell. Using the ratio of added mass to displaced-volume mass as the ordinate, he shows quantitatively (Fig. 5) what every canoeist has experienced—namely, that for the same acceleration it takes much more force to push a paddle through water broadside-on (small relative length) than to feather it (large relative length). The same experimental data for rectangular parallelepipeds are shown in Figs. 4 and 5, but Mr. Caldwell's Fig. 5 shows them more clearly. The data can be formulated as follows:

$$\frac{c}{\rho V} = 0.67 \left(\frac{d}{w}\right)^{-0.94} \qquad \text{(11)}$$

in which c is the added mass, ρ denotes mass density of the fluid, V is the volume of fluid displaced, d signifies thickness in the direction of motion, and w designates the broadside width of square face.

Mr. Silberman questions these statements in the "Introduction":

> "Determination of added mass by experiment often has been inconsistent and unreasonable. Measured values for added mass have usually been larger than can be explained by theory and analysis."

Each sentence is intended merely to state a fact, and the second is not a conclusion drawn from the first, as Mr. Silberman may have inferred. In fact, the data shown in Mr. Silberman's Fig. 6 eloquently support both statements.

First, what was measured and plotted in Fig. 6 is expressed as a drag coefficient—a variable which combines velocity-dependent forces and acceleration-dependent forces inseparably. What the writers measured and reported in Figs. 2, 3, and 4 was an "added-force" term that was only dependent on acceleration because in their experiments accelerations were high and velocities were low. In fact, the writers consider this separation and control of variables (variables that have commonly been masked in earlier experiments) to be one of their more important contributions to experimental studies of virtual mass. Second, every point except one as plotted in Mr. Silberman's Fig. 6 shows the drag coefficient to be substantially higher than the solid line. Thus, Fig. 6 says, in the language of graphs, the same thing as the writers' two sentences.

---

[20] Asst. Prof. of Civ. Eng., Carnegie Inst. of Technology, Pittsburgh, Pa.

[21] Prof. and Head, Dept. of Civ. Eng., Carnegie Inst. of Technology, Pittsburgh, Pa.

There seems to be abundant evidence in the literature since 1779 to support the statement, "Determination of added mass by experiment often has been inconsistent and unreasonable." Many early investigators of virtual mass deserve great credit for their keen observation and analysis of fundamentals that are so elusively hidden by the simultaneous influence of uncontrolled variables. One of these was F. W. Bessel[22] who, in 1828, reported that because of added mass the period of pendulums was increased from 1 part in 3,000 to 1 part in 35,000. It is a tribute to Bessel and his experimental technique that he was able to detect such slight changes. However, it is not surprising that from such relatively small quantitative measurements he should have arrived at deduced added masses that were as much as 90% larger than can consistently and reasonably be expected today (1956).

Incidentally, all but two points shown in Fig. 6 are from 100% to 1000% higher than the dotted curve designated "1 + 2" which, presumably by his hypothesis, should represent the drag coefficient for steel spheres accelerated unidirectionally.

The closing suggestion by Mr. Caldwell—to study "* * * the problem of the fixed object held in an accelerating fluid flow" (particularly in a closed conduit)—may resolve whatever differences of interpretation there may be between Mr. Silberman and the writers. It is because of differences in analytical and experimental studies that engineers can acquire a better understanding of accelerated motion of structures and machines in fluids and of the associated forces they must anticipate in design.

---

[22] "Untersuchungen über die Länge des einfachen Secundenpendels," by F. W. Bessel, Abhandlung der Akademie Wissenschaft, Berlin, 1828, pp. 1-256.

AMERICAN SOCIETY OF CIVIL ENGINEERS
Founded November 5, 1852
TRANSACTIONS

Paper No. 2871

FLOOD-EROSION PROTECTION FOR HIGHWAY FILLS

BY CHESLEY J. POSEY,[1] M. ASCE

WITH DISCUSSION BY MESSRS. GERARD H. MATTHES; EMORY W. LANE; CARL F. IZZARD AND JOSEPH N. BRADLEY; CARL E. KINDSVATER; PARLEY R. NEELEY; AND CHESLEY J. POSEY

SYNOPSIS

As a result of a series of investigations sponsored by the Highway Research Board of the Iowa State Highway Commission, a method was developed for constructing highway fills that would not be appreciably damaged by inundation even when subjected to high velocities of flow over the grade or along the side slopes. Preliminary investigations gave considerable insight into the mechanism of failure of erosion protection and provided a rational basis for a design capable of being used for any required degree of resistance to scour. The recommended design embodies properly graded layers with the topmost layer bound in "rock sausages." The size of the sausages required for various exposures was not determined, but full-scale tests showed that a minimum practicable size would be ample to protect highway fills under the most severe conditions likely to be encountered.

INTRODUCTION

Before the introduction of the high-speed motor vehicle and earth-moving machinery of great capacity, the highway was usually built across a flood plain almost at grade, rising to cross a bridge set just above the estimated high-water elevation. With flooding, the approaches were soon inundated and the bridge which was probably still dry was rendered useless.

The demand for a highway that would be open at all times, which developed as the economy became more and more dependent on motor transport, has

---

NOTE.—Published, essentially as printed here, in August, 1955, as *Proceedings Paper 783.* Positions and titles given are those in effect when the paper or discussion was approved for publication in *Transactions.*

[1] Prof. and Head, Dept. of Civ. Eng., State Univ. of Iowa, Iowa City, Iowa.

resulted in a different type of valley crossing. High fills extend out from the hills on each side to meet the bridge without any intervening sag in grade, even where the flood plain is comparatively broad. Sight distances are better, with fewer and broader vertical curves, and the hills at the sides of the valley are less high and less steep.

When such a highway is subjected to floods somewhat above ordinary high water, however, serious defects are encountered. The waters that formerly flowed over the approaches are forced through the bridge opening. If the bridge opening is not adequate the water backs up to result in higher elevations upstream than would previously have existed for the same discharge. This backing up results in greatly increased velocities through the bridge—with attendant danger from underscour. Velocities approaching the bridge opening along the side of the fill often become high enough to wash out the shoulders and undermine the pavement slab. If the flow is sufficiently constricted for flood waters to overtop the pavement, heavy damages can occur within comparatively short periods, even when the depth of overflow is less than 1 ft. For example, on June 26, 1944, Sugar Creek, a tributary of the Cedar River, near Moscow, Iowa, had a flash flood that washed out several modern bridge crossings and a considerable length of pavement but did little damage to the older crossings, which were passable as soon as the flood waters had subsided. Washouts in high approach fills are extremely dangerous to traffic and expensive to repair.

Methods of Improving Valley Crossings

In many locations the bridge openings can be increased to accommodate the largest floods considered possible without any delay to traffic. For an important highway a comparatively large expenditure on the crossing will be justified, and the design flood chosen might be one which could be expected to occur only once in every 25 yr or more. However, bridges for a less important highway might be constructed with the expectation that they would be rendered temporarily impassable every 5 yr or less. A reasonable economic balance could be obtained between the losses to traffic and the cost of eliminating flooding, provided that washouts, with their uncertain cost, can be eliminated.

One solution to the problem is to lower the grade line to permit overflooding or to use less erosion-resistant construction at certain carefully chosen sections, with the expectation that severe flooding will wash them out. These "fuse-plug" sections, which must be of ample hydraulic capacity, should be located at points where the high-velocity jet that will flow through them will not endanger the bridge, either directly or through induced eddies, and where damage to adjacent properties will be the least. At the same time, consideration should be given to the speed and ease with which the washed-out fill and surfacing can be repaired. The disadvantages of this method, as well as its economies, are evident.

Another method that has frequently been tried is to surface the fill with a masonry slab. This protection is expensive and not dependable; builders of earth dams never attempt to build a masonry spillway on fill because full hydrostatic pressure may develop on the lower side of a slab which has little or no pressure above it. Unless the slab is heavy enough to balance the excess pressure a blowup will result. For example, a concrete thickness of 20 in. would be required to balance a head of only 4 ft of water.

MECHANISM OF RIPRAP PROTECTION

To prevent erosion, earth has always been protected by piling on stones or other loose objects. The stones may be simply thrown together or they may be carefully placed for a neat appearance. The cost varies greatly, depending on the availability of stone and the labor expended in its placement. The effectiveness varies greatly, also, but does not necessarily bear any relationship to the cost or to the appearance. The layer of stones is intended to prevent erosion by reducing the velocities that come into contact with the earth to a noneroding value. The stones exposed to the current must be of such size and weight as to resist removal.

In order to study how a layer of stone reduces the velocities at the surface of the material being protected, a glass-walled flume 27 in. wide was constructed in which the erosion from water flowing over layers of crushed stone or gravel of different thicknesses protecting a bed of fine sand could be observed throughout a length of 48 in. A bed of fine white sand was leveled and carefully covered over with the thinnest possible covering of red sand of the same size classification. A rock layer was then placed by hand in such a way as not to disturb the red sand but not in any special systematic fashion to secure good fit or minimize voids. After a sufficient thickness of rock had been placed by hand, the remainder was dumped in up to the required level.

Upstream and downstream from the 48-in. section the flume had a bottom which formed a straight line, on a slight downgrade, with the top of the protective layer of crushed stone or gravel. With an increase in discharge the velocity and erosive power of the current over the test section was increased.

The method of operation was to increase the discharge slowly, noting the point at which the sand grains in the thin red layer began to be displaced. The apparatus also permitted observation of the manner in which erosive velocities reached the bed. Grains of potassium permanganate distributed through the rock layer gave off streamers of colored water which could be traced for several inches and which indicated, to some extent, the intensity of the local velocity. Before the tests started, it was thought that induced eddies would be the principal medium by which the erosive velocities would reach the bottom; rotation in the topmost cavity would induce opposite rotation in the next, and so on down with decreasing intensity. Observations showed very little of this action. The streamers over wide regions tended to be roughly parallel and to fluctuate together in direction and intensity, indicating that the principal currents in the underflow were driven by the pressure differences originating from the main flow of the stream.

As the discharge increased, the intensity of these currents through the rock layer increased until finally violent bursts began to move the red sand at several points which could be observed through the glass wall. If the test was stopped at this point and the stones carefully removed by hand, the points of beginning movement were found to be uniformly scattered, in random fashion, over the whole area of the sand bed. If the test was not stopped but the discharge increased further, movement began at more points and rock and sand began to be mixed instead of having a sharp plane of demarcation.

UNIFORM RIPRAP

The first investigation with this apparatus was conducted with stone of uniform grading.[2] In Fig. 1 the "nominal size" (abscissa) is the mesh on which the rock was retained—the smaller of the limiting sizes. The ordinate is the ratio, in each instance, of the overflow velocity causing sand movement to the velocity which would move the unprotected bed (in this case, 1.5 ft per sec). The results show that it would be uneconomical to use material of uniform granular size to protect finer material because a great increase in thickness of protective layer is required for only a slight increase in velocity. This result is consistent with the observation that the pulses driven by turbulence in the stream were more likely to cause erosion than were the void eddies.

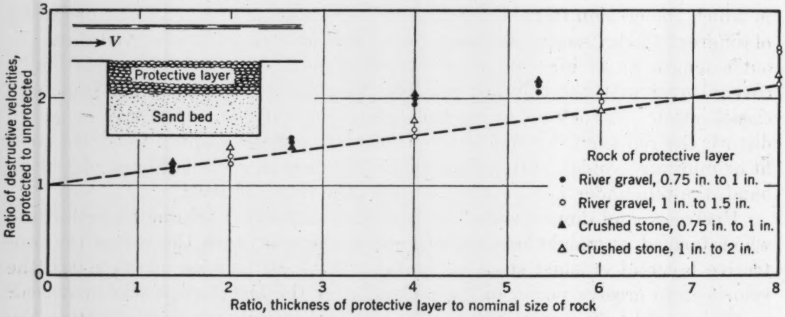

FIG. 1.—TESTS OF EFFECTIVENESS OF PROTECTIVE LAYER OF ROCK OF NEARLY UNIFORM SIZE

SPECIFICATIONS FOR GRADED RIPRAP

Nonuniform grading of the protective layer was attempted next—particularly a type proposed by Karl Terzaghi,[3] Hon. M. ASCE, and thoroughly tested[4, 5] by the United States Waterways Experiment Station at Vicksburg, Miss. This grading is intended to prevent the escape of the bed material into an overlying coarser layer when the flow is directly upward. In the Vicksburg tests the layers subjected to upward flow could, at the same time, be vibrated and subjected to surging without causing the fine material to migrate upward into the coarse material; to achieve this the original specifications suggested by Mr. Terzaghi had to be revised.[4,5] The resulting specifications relate the grading of the protective layer ("filter") to that of the bed material ("base") by the following three inequalities:

---

[2] "Protection of Earth Embankments by Rip-Rap of Uniform Size," by J. O. de Abreu-Lima and W. B. Morgan, thesis presented to the University of Iowa at Iowa City, in August, 1951, in partial fulfilment of the requirements for the degree of Master of Science.

[3] "Soil Mechanics in Engineering Practice," by K. Terzaghi and R. Peck, John Wiley & Sons, Inc., New York, N. Y., 1948, p. 50.

[4] "Investigation of Filter Requirements for Underdrains," *Technical Memorandum 183-1*, U. S. Waterways Experiment Station, Vicksburg, Miss., December, 1941.

[5] "Laboratory Investigation of Filters for Enid and Grenada Dams," *Technical Memorandum 3-245*, U. S. Waterways Experiment Station, Vicksburg, Miss., January, 1948.

$$\frac{D_{15}\text{ Filter}}{D_{85}\text{ Base}} < 5 \qquad (1)$$

$$4 < \frac{D_{15}\text{ Filter}}{D_{15}\text{ Base}} < 20 \qquad (2)$$

and

$$\frac{D_{50}\text{ Filter}}{D_{50}\text{ Base}} < 25 \qquad (3)$$

Fifteen percent, by weight, of the filter material is finer than the size indicated by D_{15} filter; 85%, by weight, of the base material is finer than the size denoted by D_{85} base.

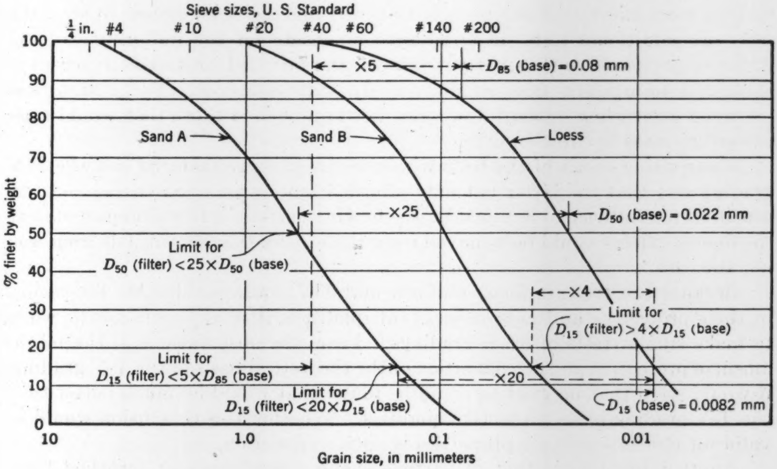

FIG. 2.—GRAIN-SIZE CURVES FOR T-V GRADINGS

In Fig. 2 are shown grain-size curves for materials meeting the specifications[3, 4, 5] to be referred to as the "T-V gradings." The base layer (loess) is to be protected by the filter layer (sand). From the grain sizes of the 15, 50, and 85 percentiles of the loess, the limits on the grading of coarser material that will protect it are determined. By the Terzaghi-Vicksburg specifications, sand A is about as coarse a sand as could be used for the loess shown. Sand B would be acceptable, but, being finer than necessary, would set lower limits on the crushed-rock layer next above, which has to have the same relationship to the sand that the sand has to the loess.

Because the abscissa scale is logarithmic each of the values (5, 4, 20, and 25) in Eqs. 1 through 3 corresponds to a fixed horizontal distance on the graph; hence, readings and computations are not necessary in plotting the permissible limits. When two materials must be blended to meet the specifications, computations are not necessary because the grading curve of a blend divides the vertical distances between the curves of its components inversely according to their proportions. Thus, the curve for a blend composed two-thirds of sand A and one-third of sand B (Fig. 2) would contain 80% finer than the 1.0-mm size.

PROTECTIVE QUALITY OF GRADED RIPRAP

Tests of the T-V grading in the same apparatus as was used previously showed that a 2-in. layer of T-V grading provided better protection over most of its area than an 8-in. layer of uniform particles of the same size as the largest component of the T-V mix.[6] Because the largest particles of the T-V mix barely passed a ¾-in. mesh sieve, it is not surprising that the 2-in. layer showed several imperfect spots. A 3-in. layer of T-V grading gave complete protection over the entire range of velocities up to that at which rock began to be torn from the top of the protective layer, making it necessary to stop the test. In additional tests, in order to compensate for the uniformity of the flume as compared with a natural stream, the bed and protective layer were subjected to upward flow simultaneously with overflow. No motion was observed even when upward-flow velocities approached those that would raise the entire mass by friction drag.

A surprising result of the tests with the uniform-size material and the T-V grading was that the latter not only afforded more protection to the bed but was itself less subject to removal by the flowing current. It was expected that the finer particles would be removed from the mix by the current, but such was not the case.

Because the two gradings, uniform and T-V, had considerable differences in their protective and erosion-resistant qualities, it might seem worth while to make similar tests of other gradings. From the observations of the mechanism of protection and consideration of the theoretical basis of the T-V grading, it would seem that no grading could be found that would be much better than the T-V grading in its protective qualities. Whether this conclusion would be valid for erosion-resistant properties is open to question.

Another problem is that of particle shape. Both angular (crushed limestone) and rounded (river gravel) particles were tested without finding significant differences, but the results from particles of very unusual shape (elongated or flat) might be significantly different.

Karl Jetter[7] has corroborated the conclusion that erosion of fine material from under the protective stones must be prevented. He made an extensive investigation of methods of protecting sand dikes which had been proposed for maintaining navigation depths on the upper Mississippi River. Mr. Jetter reasoned that the downward currents between the stones might be prevented from scouring the sand if a watertight covering were provided; he apparently overlooked the concomitant upward currents and pressures which would disrupt such a covering. Mr. Jetter rejected the idea of a concrete mat because it "would be expensive and any rupture in its surface would permit scouring of the sand." He also reasoned that for the upstream slope and berm satisfactory results "might be obtained by grading the covering from coarse sand next to the sand of the dike to large stones, heavy enough to withstand the current at the top."

---

[6] "Tests of Graded Rip-Rap for Protection of Erosible Material," by Henry de S. Manamperi, thesis presented to the University of Iowa at Iowa City, in June, 1952, in partial fulfilment of the requirements for the degree of Master of Science.

[7] "Tests on Sand Dikes Protected Against Erosion by Overflowing Water," by Karl Jetter, thesis presented to the University of Iowa at Iowa City, in August, 1931, in partial fulfilment of the requirements for the degree of Master of Science.

Erosion Resistance of Graded Riprap

At this stage of the investigation it was assumed that the problem of protecting the earth fill at its zone of contact with the protective layer was solved and that what remained was to learn how to prevent the protective layer itself from being washed away. Just as the T-V layer protects the earth, another layer of coarser material bearing a T-V relationship to the first one can protect it, and so on, until finally a layer is reached with particles large enough to resist movement by the stream velocities likely to be encountered. The problem is to find just how large the grading of this protective layer must be.

Erosion conditions are severe on a steep slope with water flowing directly down because gravity and the dynamic force of the water both have components down the slope, and the only resisting forces are compression in the top layer and friction along the bottom of the top layer. Previous analyses and attempts to develop a formula that would give the necessary size of rock, as recorded in the literature, were not made for T-V gradings and lacked verification on slopes steep enough for highway fills. Hence, another flume was built at the Iowa Institute of Hydraulic Research, at Iowa City, in which a T-V layer representing the top layer on the downstream face of a full-scale highway fill could be tested with varying depths of overflow over various sizes of aggregate placed to different side slopes. Limitations of space available and water available, at the time, fixed the width of the flume at only 15 in. It was decided that the largest aggregate particles should not have a maximum dimension of more than 6 in. in order to avoid wedging between the sides.

Despite the care taken in the use of this flume it was difficult to obtain consistent quantitative results. At the same time that it was being operated, a full-scale, highway-fill section was built in the river flume of the institute. The 10-ft width permitted the use of larger rock—the largest size that could be obtained from the local quarry. The fill section was not a full standard highway section because it lacked a slab, and the upstream section was replaced by a bulkhead and flow guide. Also, the shoulders were narrower than usual.

These changes from the standard section were not considered disadvantageous as far as possible results were concerned because their effect would be to increase slightly the severity of the exposure. The loess fill was protected by T-V layers which might be described as sand, fine gravel, coarse gravel, and riprap to a 14-in. maximum size. A total weight of 250 lb of hot asphalt was poured on top of the rock in a grid pattern of lines at 1-ft centers to increase the erosion resistance. By extrapolation from the results of the tests in the smaller flume, it was thought that this fill should stand an overflow head of about 1 ft. However, some movement of the riprap occurred within 5 min after the head had reached 1 ft, and the eroded patch enlarged rapidly during the next run of 10 min at a head of 0.7 ft.

Before the results of this test in the river flume were available, another series of tests with larger rock sizes was begun in the 80-in. flume of the Rocky Mountain Hydraulic Laboratory at Allenspark, Colo. Finally, all three series of tests were completed. The results are shown in Fig. 3. At greater heads than those presented in Fig. 3, the rock becomes unstable and is washed down the slope. All the tests were made with the tailwater at the lowest possible elevation, a series of preliminary tests in the 15-in. flume having shown that the condition of low tailwater was most likely to cause failure of the rock slope. It had been thought that the hydraulic jump that would form with moderate tailwater depths would aggravate the tendency to scour on the steep slope, but this was found not to be true.

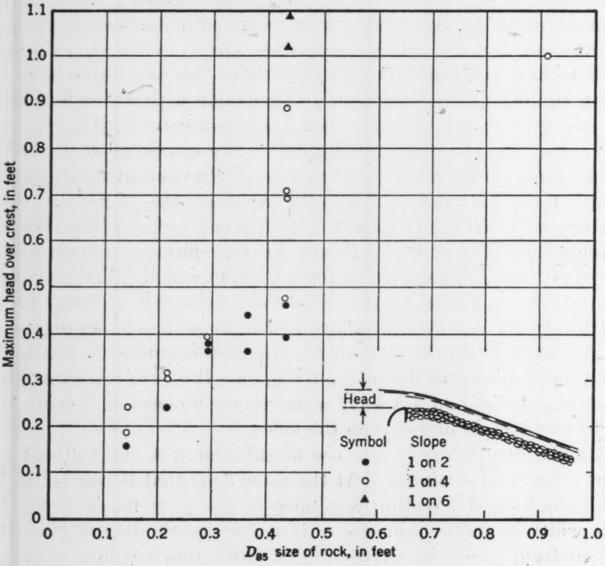

FIG. 3.—MAXIMUM HEADS FOR FLOW DOWN TYPICAL RIPRAP SLOPES

The riprap tests in the three flumes were inconclusive in determining the size of the rock in the topmost layer needed to resist various depths of overflow when covering reasonable highway-fill side slopes. However, it was evident that the rock sizes required for even moderate depths of overflow would be so large as to be impractical for the purpose and prohibitively expensive in many localities. Despite the care used in the laboratory tests there was great variation in the results. Under field conditions the variation would undoubtedly be even greater.

ROCK SAUSAGES

Another method used was to stuff the top T-V layer into wire-mesh sausages laid over the fill. By pulling the wired sausages up tight the rock was put into compression so that the layer gained compressive strength in the direction of the slope. The cross-sectional area of the wire envelope, if carried over the top of the fill, would also provide a tension to help carry the large downward force on the steep slope.

This method was first tested in the Rocky Mountain Hydraulic Laboratory erosion flume using strips of 2-ft-wide chicken wire which, when stuffed with rock of 3-in. maximum size, made sausages about 9 in. in diameter. Laid on a 3-to-1 slope, starting at the upper edge of a narrow "shoulder" and, hence, without the benefit of tension to hold them in place, these sausages withstood a greater depth of overflow than any loose layer tested. They were the only installation which remained in place up to the capacity of the flume.

The final test was of a loess fill built in 1953 in the river flume of the Iowa Institute of Hydraulic Research. The fill was protected by layers approximating the proper T-V gradings, consisting of sand and of fine crushed stone layers below 12-in.-diameter to 15-in.-diameter sausages made of No. 9 wire spiral woven to a 2-in. mesh. The stone available to fill the sausages was crusher-run, passing a 6-in. screen and being retained on a $\frac{3}{4}$-in. screen. The grading did not quite conform to the T-V requirements of the layer next underneath and was somewhat too small for the wire-mesh openings. The first row of sausages was filled in position and laced up tightly, but because the smaller rock particles tended to spill out, the remainder of the crushed stone was sifted to eliminate the sizes passing the 2-in. mesh. This operation was done by hand because the necessary equipment was not available; because of the magnitude of the job, it was not completely effective.

The rest of the sausages were filled from the end, in 10-ft lengths, and laid in place with a crane. The longitudinal spaces between the sausages, underneath the line of contact, were not completely filled with rock. Therefore, channels were formed down the slope through which the underlying fine rock could be washed away, as was shown by a preliminary test made on December 8, 1953, with the highest head available up to that time. After this test the sausages were wired together end to end and some small gaps on the downstream face were closed with chicken wire. Despite its imperfections the test section withstood depths of overflow up to 0.75 ft for more than 30 min in this preliminary test without appreciable signs of damage.[8]

PREVIOUS USES OF WIRE-BOUND ROCK SAUSAGES

During the preparation of a progress report[8] it was learned that rock sausages, or "gabions" as they were called, had been in use for more than 50 yr in the Himalayas. It was also found that an Italian firm specialized in gabions for erosion protection. Its brochure seems to indicate that the importance of T-V grading to protect the bed material had not been recognized. With the method of hand-filling bags and rectangular box cages, it would also seem that the benefits of putting the loose rock in compression would not be obtained. That the firm has been successful for so many years despite these omissions speaks well for this type of construction.

---

[8] "Rock 'Sausages' Provide Economical Protection Against Erosion," by C. J. Posey, *Engineering News-Record*, May 13, 1954, p. 45.

H. G. Strom[9] has described wire sausages used for river-control work in Australia.

In the previous uses of rock sausages the purpose was riverbank protection. There is no specific record of their use to protect relatively steep embankments from overflow; it was probably seldom feasible to install the sausages "in the dry" with opportunity to control the underlying layers, as would be possible in the construction of most highway fills.

Andrew Weiss[10] reported on a similar method used to pass flood waters over the partly completed San Ildefonso Dam in Mexico. Though imperfect as a reverse filter, his design, which embodied a network of steel bars with anchors, was adequate in preventing too much scour.

COMPLETION OF FULL-SIZE OVERFLOW TESTS

In May and June, 1954, occasional higher flows in the Iowa River permitted testing the sausage-protected overflow section under more severe conditions. The results are presented in Table 1. All the runs were made with no tailwater, and velocities at the foot of the 5½-ft-high embankment were estimated to be approximately 20 ft per sec. No damage could be found after Run 2, but after Run 3 it was found that some rock had been removed from inside one of the sausages. No further damage was noted until after Run 5, when there was found to have been some enlargement of the cavities where undersized rock had been torn out through the mesh. After Run 6 the general level of the sausages seemed to have sunk slightly at one location; the amount was no more than could have been accounted for by the fact that some fine rock had been washed out through the gaps between the sausages which had not all been effectively stopped up after the first run.

TABLE 1

Run	Date	Head, in feet	Duration
1	December 8	0.75	20 min
2	May 4	0.9	20 min
3	May 4	1.3 to 2.3	45 min
4	May 4	2.2	2 hr
5	June 3	2.5	3¼ hr
6	June 7	2.7	1 hr
7	June 8–9	1.1	28 hr

Finally, two of the sausages were slit longitudinally and the embankment subjected to a head of 1.5 ft for 10 min. The sausages on the downstream slope were approximately half emptied whereas those on the upstream slope were not affected. Further overflow failed to remove the installation sufficiently fast, and the sausages were finally lifted out with a crane.

It should be noted that the two tests in the 10-ft flume of the Iowa Institute of Hydraulic Research tested not only the resistance of the protective cover against removal but also the ability of the T-V graded sequence to protect the underlying loess from being leached out. In neither case was there any sign that the loess was being removed while the layers above were intact. The first was not as severe a test of the protection because, with riprap bound together only by bitumen, the rock covering was rapidly washed out and the loess exposed. In the second test the flow was maintained at higher depth for many hours but at no time was there any sign that the water was being muddied by loess, nor any sign that the sausages had been undermined except at the location where some of the rock layer next below the sausages seemed to have been removed.

---

[9] "River Control Structures," by H. G. Strom, *Technical Bulletin No. 6*, State Rivers and Water Supply Commission, Victoria, 1954.

[10] "Construction Technique of Passing Floods over Earth Dams," by Andrew Weiss, *Transactions*, ASCE, Vol. 116, 1951, p. 1158.

Field Installation Needed

Under field conditions in Iowa (*a*) tailwater would stand on the downstream face; (*b*) the total head would seldom, if ever, exceed 3 ft or 4 ft; and (*c*) the flood flow would, in most cases, last for hours rather than for days. Hence, the use of rock sausages may be recommended for a full-scale field test. Installation problems encountered in building the fill in cramped laboratory quarters are not representative of field conditions, but the information gained may be helpful and some suggestions may be offered.

TABLE 2

Material	Cost of mesh per square foot of surface protected, in dollars	Ultimate tensile stress, in pounds per square inch	Relative strength of wire
Galvanized steel No. 6	0.68	85,000	1.66
Galvanized steel No. 9	0.43	90,000	1.00
Stainless steel No. 11	1.25	130,000	0.95
Stainless steel No. 12	1.05	130,000	0.70
Aluminum No. 6	0.90	41,000	0.81
Aluminum No. 9	0.53	41,000	0.45

1. It is possible that only part, rather than the full length of a long fill, should be protected after the fashion of the fuse plugs mentioned previously. However, the flanks of adjacent nonoverflow sections should be protected wherever high-velocity currents may occur.

2. The T-V gradings may seem complicated and therefore expensive. However, natural deposits may be found to fit the specifications with little or no screening. In general, T-V gradings may be cheaper (in large quantities) than commercial gradings made for concrete.

3. With regard to the cost and durability of the wire sausages, the investigation can offer little more than tentative information. Prices quoted (1955) by a manufacturer of steel-wire mesh indicate the approximate costs per square foot for a single layer of sausages made of 2-in.-mesh, chain-link fabric (Table 2).

Experience with steel wire coated by hot-dip zinc galvanizing for river-protection work shows that its life is from 15 yr to 20 yr. When used on highway fills above water and not in direct contact with earth or sand, the probable life of the galvanized wire would exceed 20 yr. One cost-saving possibility would be to use stainless-steel wire for those parts subject to frequent inundation, but special precautions would have to be taken to avoid electrolytic corrosion where contact is made with galvanized wire.

The committee for the Regularisation of the Rhine River (Germany) reported[11] favorably on rock sausages, but it stated that efforts to improve the useful life by using aluminum wire were unsuccessful because the wire was "not sufficiently resistant to withstand the stresses to which it is subjected during manufacture and the putting in place of the rollers." Properly designed mechanized equipment might make the use of aluminum wire possible.

Most of the sausages used in the river-flume test were end-filled, but the writer believes that, if suitable equipment were constructed, the method used in the Allenspark test and for the first row of sausages placed in the river flume would be cheaper and more efficient with less strain on the wire. The end-filling method has certain advantages, however, and could also be improved. For example, filled sausages could be transported by truck and used for protecting piers or abutments of bridges threatened by underscour.

CONCLUSIONS

Important theoretical questions remain unanswered—namely, the sizes of the sausages, the rock fill, and the wire of which the sausages are woven. These sizes must be capable of resisting the action of the current at a given depth and velocity. To protect highway fills in Iowa these questions need not be answered until such time as the rock-sausage method has come into wide use and will bear further investigation to achieve maximum economy. If it is to be generally used for spillways, diversion channels, or bridge-pier protection or abutment protection, more information will have to be obtained.

ACKNOWLEDGMENTS

The Highway Research Board of the Iowa State Highway Commission provided the principal financial support for this project. J. de Abreu-Lima, W. B. Morgan, Henry de S. Manamperi rendered valuable contributions by their thesis projects as graduate students at the University of Iowa. The tests made at Allenspark were under the supervision of the staff of the Rocky Mountain Hydraulic Laboratory, assisted by I. M. Mostafa and R. E. Nava, Junior Members, ASCE. Various aspects of the project were conducted by J. W. Dinzole, Jr., M. T. Lwin, and F. A. Haag, Junior Members, ASCE. Many other staff members of the Iowa Institute of Hydraulic Research cooperated on the project.

---

[11] "Tests and Study of a Rational Method of Constructing Groynes on the Upper Rhine," *Bulletin*, Works Committee for Regularisation of the Rhine Between Strasbourg/Kehl and Istein, Permanent International Assn. of Navigation Congs., No. 38, July, 1953, p. 115.

DISCUSSION

Gerard H. Matthes,[12] **Hon. M. ASCE.**—The experiments described by Mr. Posey demonstrate the practicability of protecting earth embankments against erosion from flowing water by use of rock sausages. They recall the effective use that has been made of this method elsewhere for the protection of riverbanks against erosion by high-velocity flow. The author is to be commended for conducting full-scale experiments on an unregulated river. His findings should be of timely interest in view of the extraordinary toll taken by flooding (in 1955) of streams too small to warrant the construction of flood-control reservoirs by the Corps of Engineers (United States Department of the Army) under existing flood-control laws. Much can be accomplished, however, through state and local effort, by using the rock-sausage method of protecting highway fills and the riverbanks of the smaller streams, as shown by European practice.

Wire-bound rock sausages or gabions originally were introduced and patented by the Italian engineer, Giulio Serrazanetti,[13] in 1903 and have been extensively used along headwater streams in Italy, Austria, and Bavaria since 1908. European methods of applying rock sausages along earth fills or stream banks have included: (*a*) Horizontal tiers backed by boulders; (*b*) vertical walls built by standing sausages on end, with cross sections square instead of round; (*c*) the formation of dikes supported on layers of large boulders or on fascine mattresses; or (*d*) sinking the sausages in sandy river beds to serve as foundations for rock fills or sandbag cofferdams. In the United States, rock sausages have been used by the National Park Service (United States Department of the Interior) to counteract bed erosion[14] and by the California State Highway Commission to protect the banks of streams near Los Angeles, Calif.[15] An exhaustive investigation of the uses of rock sausages in Germany and Austria was made by Chr. Keutner in 1934.[16]

The limitations of the protection provided by rock sausages are the maintenance cost, covering inspection and repairs needed after each major flood, and the eventual breakdown of the galvanized wire netting by rusting at points of abrasion from boulders or careless handling. Repairs are usually made by patching with strips of new netting. In the Bavarian system the distribution[16] of the first cost was: (1) Wire netting and hexagonal mesh, 32.5%; (2) providing broken stone including the cost of transportation, filling, sewing, and placing, 56.5%; and (3) wear and tear of equipment and miscellaneous expenses, 11.0%.

Comparative costs of wires equal in strength and having a diameter of 2.8 mm or 3.0 mm showed steel wire to cost 2.4 times as much as ordinary galvanized-iron wire. The diameter of hexagonal mesh was 60 mm (2⅜ in.). Steel wire lost only one-fifth as much weight because of abrasion as did galvanized-iron wire.

---

[12] Cons. Hydr. Engr., New York, N. Y.

[13] "Wasserschutzbauten," by Giulio Serrazanetti, Bologna, Italy, 1903.

[14] "Rock-and-Wire Deflectors Protect Banks Against Floods," *Engineering-News Record*, November 9, 1922.

[15] "Wire-Bound Rock Training Walls Solve Zion Park Flood Problem," by Thomas C. Parker and Frank A. Kittredge, *ibid.*, November 14, 1935.

[16] "Die Verwendung von Drahtnetzkorpern im Wasserbau," by Chr. Keutner, Research Inst. for River Control, Munich, 1935.

EMORY W. LANE,[17] M. ASCE.—The paper presents, so far as the writer knows, the first report on scientific tests of the value of rock sausages. It should bring this effective device for bank protection into wider use. Mr. Posey's work is, therefore, a valuable addition to the hydraulic and highway engineering literature.

Although these sausages have come into use in the United States comparatively recently, they have long been used in China for stream-bank and bed protection and more recently for the closure of levee breaches along the Yellow River. Their use in the operation of the great Min River irrigation system was described elsewhere by the writer.[18] This great project, which irrigates 950,000 acres of land, has been in continuous use since about 200 B.C., and the sausages have no doubt been used for centuries. They are used to protect the stream bed at a structure for dividing the flow of the Min River and as pavement on a spillway. Thin strips of bamboo are woven to form the casing of the sausage. Similar construction was used on the Yellow River, with large, long sausages rolled into the gap in the levee from the banks. The gap was gradually closed by filling it with sausages placed in this manner.

CARL F. IZZARD,[19] A. M. ASCE, AND JOSEPH N. BRADLEY,[20] M. ASCE.—The author is to be commended for his valuable and timely study of erosion protection for highway fills. Such a study is especially appropriate just prior to an expansion of the national highway program.

Highway fills designed to be overtopped during floods have not been unusual in the past, especially on secondary roads. However, as a result of the steady increase in traffic volume, current (1956) trends tend to discourage designs that provide for overtopping of highway embankments on primary roads. Before taking a definite stand on the question it may be well to weigh the merits of the old concept of flow over highway fills against the apparent advantages to be gained by keeping embankments above high water at all times.

With the introduction of the modern turnpike and multilane divided highway, with long sweeping curves and adequate sight distance, bridges now assume a permanent role and can no longer be considered as short-term investments. Therefore, bridges on modern highways should be designed to accommodate extreme floods without failure or serious damage to the bridge. The higher the roadway embankment, the longer the bridge must be to be reasonably sure that a bridge will be safe during a superflood. Long, expensive bridges, of course, can be subject to severe criticism from those who bear the cost. On the other hand, delays to traffic by the inundation of bridge approaches can also lead to criticism. Cases are on record where old bridges have withstood record floods whereas newer and more modern bridges, both upstream and downstream, have failed. The old bridges built to accommodate flooding at intervals of once in 10 yr or 20 yr have remained intact because approach embankments were low, allowing floodwaters to spill over the road for discharges greater than the capacity of the bridge. Some bridges of this type have been inundated many times, and great quantities of debris have lodged against the superstructure without serious damage. There are other instances on record where the approach embankments to bridges of this category were later elevated and the old bridges replaced by modern ones of approximately the same length. It was reasoned that raising the superstructure provided additional effective waterway area under the bridge. The fallacy of this assumption is borne out by the fact that a fair share of bridges constructed on this premise have failed during the first sizeable flood. With embankments raised it was necessary for all flow to pass under the new bridge, increasing the backwater and velocity. Failure usually resulted from undermined footings of abutments and piers.

---

[17] Hydr. Engr., Fort Collins, Colo.

[18] "Great Min River Irrigation Project," by E. W. Lane, *Civil Engineering*, Vol. 1, 1931, pp. 397–400.

[19] Chief, Hydr. Research Branch, Bureau of Public Roads, U. S. Dept. of Commerce, Washington, D.C.

[20] Hydr. Engr., Bureau of Public Roads, U. S. Dept. of Commerce, Washington, D. C.

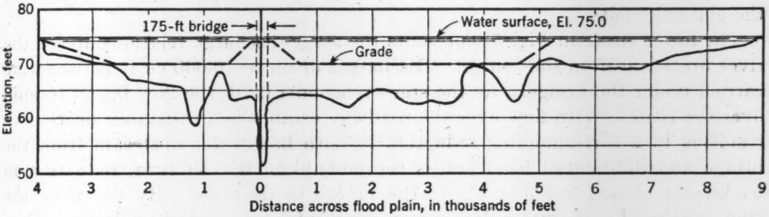

FIG. 4.—PROFILE OF FLOOD PLAIN, BRIDGE, AND ROAD GRADE FOR FLOOD OF 26,000 CU FT PER SEC IN 1940

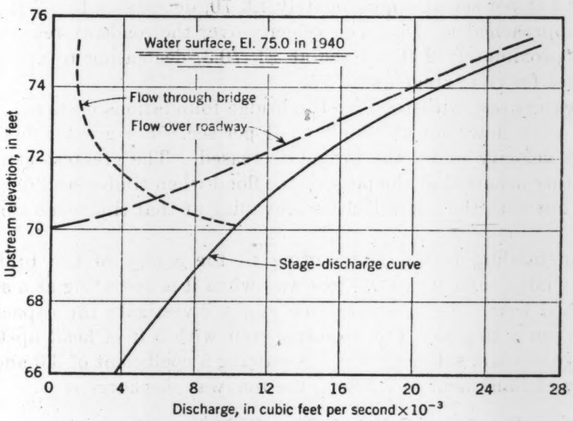

FIG. 5.—STAGE-DISCHARGE RELATIONSHIP

An explanation of the hydraulic principles involved is best illustrated by an actual case on which reliable observations and measurements were available. The 175-ft bridge shown in Fig. 4 has withstood several severe floods, one with a recurrence interval exceeding 100 yr. The capacity of the bridge itself is approximately 10,000 cu ft per sec. However, a flood of 26,000 cu ft per sec, or approximately $2\frac{1}{2}$ times that quantity, was accommodated with no damage to the bridge. Minor repairs were required on the downstream shoulders of the embankments.

The lower curve in Fig. 5 represents the stage-discharge relationship for the river upstream from the bridge. Discharges of up to 10,000 cu ft per sec were carried under the bridge. As the stage reached El. 70, the flow began to spill over the road. With flow over the roadway established, resistance decreased, resulting in a corresponding reduction in both backwater upstream from the bridge and differential head across the embankment. In turn, reduction in backwater caused the flow under the bridge to decrease. By the time the stage reached El. 75, water flowed to a depth of 5 ft over the roadway. Flow over the embankment at this point reached 24,000 cu ft per sec whereas flow under the bridge fell to less than 2,000 cu ft per sec.

The backwater upstream from the bridge reached a maximum of 0.37 ft for the stage at El. 70. The differential head across the embankment was approximately double this amount for the same stage but fell to 0.015 ft as the stage reached El. 75.

Measurements indicated that the highest mean velocity attained under the bridge was 4 ft per sec at approximately El. 70, decreasing to 0.7 ft per sec as the stage approached El. 75. The velocity over the roadway reached a maximum of approximately 2 ft per sec at El. 70.3, decreasing to approximately 0.7 ft per sec for river stage at El. 75.

The greatest test withstood by the bridge foundations occurred, therefore, not at the peak flow, but at 10,000 cu ft per sec. For greater flows the discharge and velocity under the bridge decreased. The greatest threat to the superstructure occurred at the peak of the flood when timber and debris lodged against it, but with the low velocities prevailing at that time even this was not serious.

The outstanding factor contributing to the safety of the bridge is the surprisingly large capacity of the roadway when it is operating as a submerged broad-crested weir. To illustrate, one might investigate the capacity of the roadway when acting as a broad-crested weir with 5 ft of head upstream and without downstream submergence. Assuming a coefficient of 3.0 and a length of roadway embankment of 7,500 ft, the roadway discharge is

$$Q = 3.0 \times 7,500 \times 5^{3/2} = 252,000 \text{ cu ft per sec.}$$

If essentially the same upstream conditions prevail but the downstream water level is 4.75 ft above the road grade, making the submergence 95%, the coefficient of discharge for this condition, as shown elsewhere,[21,22] would be

---

[21] "Discharge Characteristics of an Embankment-Shaped Weir," by Gunnar Sigurdsson, thesis presented to the Georgia Institute of Technology, at Atlanta, in 1955, in partial fulfilment of the requirements for the degree of Master of Science in Civil Engineering.

[22] "Flow of Water over Railway and Highway Embankments," by D. L. Yarnell and F. A. Nagler, *Public Roads*, April, 1930, p. 30.

$3.0 \times 0.73 = 2.20$. The discharge would then be

$$Q_s = 2.2 \times 7{,}500 \times 5^{3/2} = 185{,}000 \text{ cu ft per sec.}$$

Thus, with 95% submergence, flow over the roadway will still constitute about 75% of that for the free-flow condition. Thus, this favorable characteristic of the submerged broad-crested weir should not be discarded from bridge design without serious thought.

Enumerating the advantages of the sagged roadway used in bridge design:

1. The bridge waterway and foundations can, in many cases, be designed for a moderate flood rather than for an extreme one with considerable saving in initial cost.
2. Backwater will be reduced materially once flow over the road is established. This is important when parts of towns or improved property exist on the flood plain upstream from the bridge.
3. With the reduction in velocity the peak-flow loads placed on the bridge superstructure by floating debris will be lessened.
4. A saving can be effected in the cost of the sagged roadway embankments.
5. If hydrologic computations should prove inadequate, loads placed on the bridge by floods of unforeseen magnitude will not alter conditions materially.
6. Safety of the motorist is all important. Water on the roadway forms its own barricade, but an unbarricaded, washed-out bridge is much more dangerous.

The principal disadvantage to be weighed against these considerations is the occasional interruption of traffic and the resulting inconvenience and expense to the motorist caused by detours. For roads carrying a heavy volume of traffic this can well constitute the decisive factor.

The sagged-roadway design need not be limited to secondary roads but can be used to advantage on any highway where flood-plain conditions are favorable. The difference in concept between the secondary road and the modern highway lies only in the period of time to be allowed between inundations of the sagged part of the roadway. Where a bridge on a secondary road may be designed for a 20-yr flood, the bridge on the modern highway may be designed for a 50-yr flood. In the first case, flow over the road would be expected to occur on an average of 5 times every 100 yr whereas, in the second case, it would be expected only twice. However, both bridges could be subjected to an unexpected 500-yr flood without loss of the bridge proper.

The foregoing indicates that neither the low nor high approach embankment is entirely satisfactory for bridge design on primary roads. As stated previously, the principal objections are the interruption of traffic with low embankments and the initial bridge cost with high embankments. A compromise may retain some of the advantages of the low embankment design whereas a reduction in the height of the high embankment type will be favorable from a cost standpoint. A comparison of average annual cost for alternate designs is suggested. In such a study the cost of traffic delays and repairs due to flood damage to upstream property, reduced to average annual cost, should be added to the annual cost of amortizing the investment.

The information presented by Mr. Posey on flood-erosion protection agrees with current (1956) thinking in regard to bridge design on wide and reasonably wide flood plains. Information on low-cost embankment protection will undoubtedly be in demand. Therefore, further research on the subject, accompanied by prototype verification whenever possible, should stress simplicity of placement, permanence, and low cost.

Another phase of research in connection with embankment protection might be the fuse-plug design mentioned by the author, which sacrifices a section of roadway embankment to save the bridge during extreme floods. Heavy protection would be provided adjacent to, but omitted at, the plug. With up-to-date earth-moving equipment the time required for replacing a section of roadway embankment is measured in days as compared to the months necessary to rebuild or repair damage to a bridge. Thus, if one must be sacrificed the decision should not be difficult.

Carl E. Kindsvater,[23] M. ASCE.—Highway embankments in valley regions are inundated when flood discharges exceed the combined normal capacities of bridge and culvert waterways. Such an occurrence may be an unexpected disaster or it may have been anticipated in the design of the highway.

In those sections where highways are required to cross many miles of flood plain or swamp, planned periodic inundation of the embankments may be an economic necessity. This is especially true for roads which are of less than primary importance in the transportation system. The savings which make such a plan economically feasible usually result from lower embankments, shorter bridges, and smaller or fewer culverts. Tending to offset the savings, however, is the cost of preventing or repairing the damage due to submergence and overflow.

Mr. Posey has described a method of preventing damage to highway embankments which are subject to inundation by floodwaters. His conclusions, based on original research and analysis, show the advantages of a blanket of rock sausages as a protective device. His report, therefore, is a contribution to highway design as well as to highway-maintenance practices.

In his research the author was specifically concerned with the comparison of different methods of preventing flood damage to a typical highway embankment under representative conditions of submergence and overflow. It was logically beyond the scope of his investigation to study the hydraulics of overflow. Nevertheless, a complete understanding of the requirements for adequate protection will ultimately involve the discharge characteristics of the embankment. It appears appropriate, therefore, to add to the author's excellent report some comments regarding the flow of water over highway embankments, based on work at the Georgia Institute of Technology at Atlanta.

Intermittently since 1947 the writer has been engaged in a study of embankment hydraulics, beginning with his direction of a hydraulic model study sponsored by the Georgia State Highway Department at the Hydraulics Laboratory of the Georgia Institute of Technology. The study was subsequently continued as a thesis[21] sponsored by the Society's J. Waldo Smith Hydraulic Fellowship. It is the subject of a second thesis which is partly supported by the Geological Survey, United States Department of the Interior (USGS).

---

[23] Regents' Prof., School of Civ. Eng., Georgia Inst. of Technology, Atlanta, Ga.

The experimental phase of this research has been concerned with the overflow characteristics of a single form of embankment. Tests covering a full range of normal flow conditions have been conducted on several two-dimensional models, all having the shape shown in Fig. 6. The information collected includes surface profiles, velocity-distribution measurements, and discharge calibrations. The current (1956) investigation is concerned primarily with the internal characteristics of the flow pattern, including the character and influence of the boundary layer. The subsequent comments, however, emphasize the external characteristics of the flow pattern. It is believed that it is this knowledge which is most essential to a better understanding of the requirements for embankment protection.

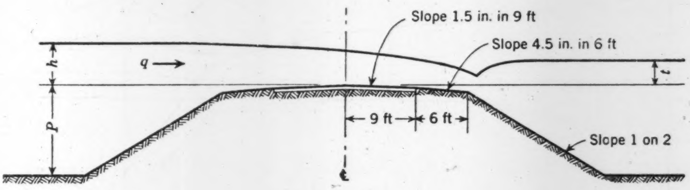

FIG. 6.—EMBANKMENT SECTION (SYMMETRICAL ABOUT CENTER LINE)

As an overflow structure, the highway embankment is a form of broad-crested weir. Depending on the boundary configuration, the rate of flow, the roughness of the surface, and the relative height of the tailwater, the discharge over an embankment may be described as either "free" or "submerged" flow. Free flow occurs when the embankment acts as a control section; that is, the discharge is controlled by the upstream water level. Therefore, it is associated with low tailwater levels. Submerged flow occurs when the discharge is controlled by the tailwater level as well as the headwater level. This condition, obviously, is associated with high tailwater levels. The transition regime between free and submerged flow is described as "incipient submergence."

Free flow is further subclassified as "plunging" flow and "surface" flow. Plunging flow occurs when the discharge over the downstream shoulder continues to follow the surface of the embankment, thus plunging under the tailwater. When the flow is plunging, maximum erosive velocities occur over the downstream face of the embankment. Surface flow occurs when the discharge separates from the embankment surface at the downstream shoulder and "rides" over the surface of the tailwater. Thus, when surface flows occur erosive tendencies are a minimum. In general, plunging flows occur when the tailwater level is low; surface flows occur at higher tailwater levels. Submerged flows are always surface flows.

It was first demonstrated during the exploratory tests at Georgia Tech in 1947 that the transition from plunging flow to surface flow, and vice-versa, occurs within a well-defined range of tailwater levels. It was also demonstrated that the tailwater level at which the transition occurs is critically related to the history of the overflow. That is, if the flow is initially plunging and the tailwater is low, the plunging flow will persist as the tailwater level rises to an upper limit before changing suddenly to surface flow. This sequence of events would normally occur during a rising flood stage. However, if the tailwater is initially high and the discharge is a surface flow, this condition will persist as the tailwater level drops to a lower limit before changing to plunging flow. This sequence of events would normally occur during a falling flood stage. The transition range is the difference in tailwater levels corresponding to the upper and lower limits.

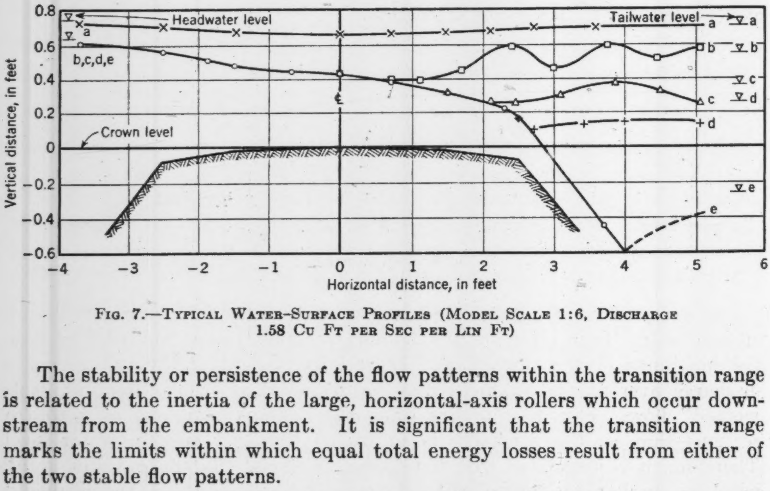

FIG. 7.—TYPICAL WATER-SURFACE PROFILES (MODEL SCALE 1:6, DISCHARGE 1.58 CU FT PER SEC PER LIN FT)

The stability or persistence of the flow patterns within the transition range is related to the inertia of the large, horizontal-axis rollers which occur downstream from the embankment. It is significant that the transition range marks the limits within which equal total energy losses result from either of the two stable flow patterns.

Fig. 7 shows measured water-surface profiles for typical 1:6-scale model tests illustrating the various flow regimes described. The transition range within which free discharge can be either plunging flow or surface flow is identified by the profiles marked c, which is the upper limit, and d, which is the lower limit. The remaining profiles are a, submerged flow; b, incipient submergence; and e, free, plunging flow.

From the same series of tests, Fig. 8 shows the transition range in terms of the tailwater ratio, t/h. On the basis of these tests, which were among the first completed, it was concluded that the limits of the transition range could be predicted accurately. It was recognized, of course, that the limits of the range might be influenced by the shape of the embankment. It was also reasoned that the flow separation which occurs at the downstream edge of the downstream shoulder during surface flows could be stimulated by artificial means. The result would be to lower the upper limit of the transition range and thereby extend the range of tailwater levels in which the occurrence of surface flow would be assured. The practical significance of this reasoning was related to the assumption that surface flows are less erosive than plunging flows. From the results of his research, Mr. Posey has doubtless formed an opinion regarding the correctness of this assumption.

The extent to which very slight variations in boundary characteristics would influence the tailwater limits of the transition range was revealed by subsequent experiments on other models. Three embankment models have been involved, each built to a different scale (1:6, 1:9, and 1:12) but all built to simulate the cross section shown in Fig. 6. In addition, several degrees of boundary roughness have been involved. It was soon apparent that each model and every modification of each model could be characterized by distinctive variations of the curves shown in Fig. 7. The curves obtained from each test series were well defined, but there was no reasonable correlation between the results of the tests and the differences in the models.

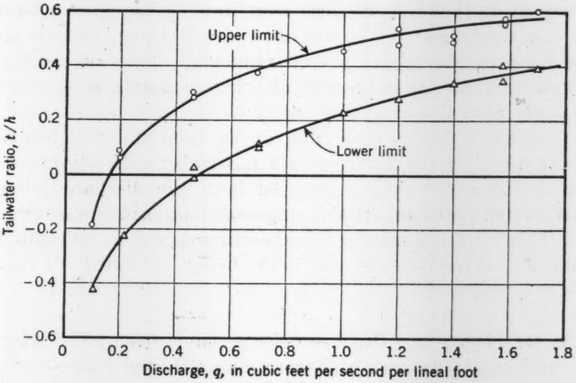

FIG. 8.—TAILWATER LIMITS OF TRANSITION RANGE (MODEL SCALE 1:6)

The extreme sensitivity of this relationship to the shape of the downstream shoulder was demonstrated by a special series of tests on the 1:9-scale model. In these tests a wire of $<.09$-in. diameter was fastened to the downstream edge of the shoulder. As a result, values of t/h corresponding to the upper and lower tailwater limits were changed an average of 15%. It is understandable, therefore, that the different models failed to define a single characteristic relationship of the kind shown in Fig. 7. It is also apparent that the flow pattern downstream from inundated highways will be critically dependent on the configuration of the downstream shoulder. It should be emphasized, however, that the flow pattern upstream from this shoulder is unaffected by the causes of the transition phenomena. It follows that, because the control section is at or near the crown for all free-flow conditions, the head-discharge relationship is unaffected by minor variations in the shape of the downstream surfaces of the embankment.

The studies have included an investigation of the discharge characteristics of submerged flow. It is significant that the results of the submergence tests on the different models were remarkably similar. It was revealed, for example, that the relative depth of tailwater required to produce incipient submergence is only slightly influenced by discharge, embankment height, and roughness. Thus, incipient submergence for practically all the conditions investigated occurred when the height of the tailwater measured above the crown was approximately 0.85 times the head. That is, the head-discharge relationship is unaffected by the tailwater until the ratio t/h exceeds approximately 0.85; unlike the transition from plunging to surface flow, the transition from free to submerged flow occurs at the same value of t/h for both the rising and falling sequences of tailwater variation.

Under the heading, "Methods of Improving the Modern Valley Crossing," the author suggests that in some locations bridge openings can be made large enough to pass the largest floods without causing the upstream water level to exceed the level of the adjacent embankments. This, of course, presumes adequate knowledge of the hydraulics of bridge waterways—knowledge which has been largely nonexistent until recently.

A comprehensive research program on the hydraulics of bridge openings was begun in 1951 by the USGS under the writer's direction. As a result, several publications[24,25,26] which describe both the discharge characteristics and the backwater characteristics of single-opening bridge waterways are now available. This work has involved field studies as well as laboratory research. The laboratory investigations are now being extended to multiopening waterways.

PARLEY R. NEELEY.[27]—Rock sausages have been effectively used for erosion control on the Bureau of Reclamation (United States Department of the Interior) Moon Lake project in the Uintah Basin of eastern Utah along banks of the Duchesne River that threatened to undercut the important Duchesne feeder canal.[28] This canal parallels the river for a distance of 1,500 ft near the diversion point, approximately 6 miles east of Duchesne City, Utah. The peak flood flow of the river has reached 9,000 cu ft per sec and normally ranges from 200 cu ft per sec to 1,000 cu ft per sec during the summer. Sausages also were provided for the Yellowstone Canal in Cottonwood, Wash., 20 miles northeast of Duchesne City.

The Uintah Basin has a complex geologic history. The high Uintah Mountains are composed of limestone, sandstone, shale, and quartzite. Erosion by the glacial-fed streams removed great quantities of these materials

---

[24] "Tranquil Flow Through Open-Channel Constrictions," by Carl E. Kindsvater and Rolland W. Carter, *Transactions*, ASCE, Vol. 120, 1955, p. 955.

[25] "Computation of Peak Discharge at Contractions," by C. E. Kindsvater, R. W. Carter, and H. J. Tracy, *Circular 284*, Geological Survey, U. S. Dept. of the Interior, Washington, D. C., 1953.

[26] "Backwater Effects of Open-Channel Constrictions," by Hubert J. Tracy and Rolland W. Carter, *Transactions*, ASCE, Vol. 120, 1955, p. 993.

[27] Area Engr., Bureau of Reclamation, U. S. Dept. of the Interior, Spanish Fork, Utah.

[28] " 'Sausages' for Erosion Control," by Parley R. Neeley, *Reclamation Era*, November, 1955, p. 87.

to the lower valleys, depositing sediments and quartzite boulders along the streams and forming large, sloping benchlands. Subsequently, the streams cut deep canyons through to the underlying rocks. The exposed shale, soft sandstone, and shale-formed sediments do not readily lend themselves to the growth of deep-rooted protective plants, shrubs, and trees. Such growths as are made are frequently destroyed by the shifting of the stream channels undercutting the banks, deepening the channel, or depositing silts over the flood plain. In an area such as the Uintah Basin, erosion control is a difficult and expensive undertaking. The nearest quarry rock may have to be hauled a distance as great as 50 miles.

In processing road-surfacing materials near the points where erosion control was undertaken, the Utah State Highway Department has left large waste piles of quartzite boulders. It was decided to use these boulders for the rock sausages. The use of rock sausages had been effectively demonstrated by the Denver and Rio Grande Western Railroad Company during the 1952 early spring runoff of mountain streams which approached the 50-yr flood frequency.

Each rock sausage was constructed by taking a 10-ft-long piece of 32-in., hog-wire fencing and then folding and lacing the two edges together with wire. The result was a cage approximately 3½ ft long and 20 in. in diameter which, when standing up, had a closed bottom and open top. The wire cage was filled with cobbles, the top was laced together, and the sausage was then ready for placing. Treated native timber piling was driven, and timbers were spiked horizontally between the piling. The sausages were stood on end, two tiers high, in back of the timber piling, and then were continued on the sloped bank.

The cost of preparing and placing the unit would have been less than two-thirds the estimate for quarried-rock riprap, had such a quarry been in close proximity to the work, and about one-third the estimated cost of riprap with quarried rock from the minimum distance available—approximately 50 miles.

When the cobbles were confined in the wire mesh, the sausage provided many advantages. The combination of confined cobbles made a heavy unit acting as one large compact piece. The eddies set up by the irregular surface tend to encourage deposition of silt. The unit was flexible, settling snugly into the soft foundation, and it was easily handled by hooking a dragline into the wire mesh for lifting and placing in position. The uniform size of the sausages made a closely knit, compact surface resistant to erosion or shifting.

At the time the Yellowstone feeder canal was constructed the natural channel was used to convey water for approximately 2 miles from one constructed part to another. It was not considered necessary to protect the banks of the natural channel because the channel was in a remote area. However, erosion was causing an expensive operation and maintenance problem in the canal below the natural channel. Rock sausages placed in the natural channel did a remarkable job of erosion control. Native cedar (juniper) posts were placed at 8-ft intervals, hog wire 3 ft high was stapled and wired to the posts, and the sausages were placed back of this wire screen. The vertical banks ranging in height from 15 ft to 40 ft were trimmed to approximately a 1:1½ slope. Not only was the erosion practically stopped but grass and willows took root in the silt retained by the rock sausage. The channel normally carries about 80 cu ft per sec and has at times exceeded 100 cu ft per sec.

Rock sausages have a place in erosion control and are adaptable to many conditions. The sausages are easy and economical to make, can be readily handled, and permit the utilization of rock fragments usually found adjacent to the point where erosion control is needed, without undertaking an expensive borrow-and-hauling operation. The fine materials retained between the rocks allow the growth of protective grasses and willows.

CHESLEY J. POSEY,[29] M. ASCE.—The contributions of the discussers provide much information concerning flood erosion protection not included in the paper. Mr. Matthes' report on the European use of rock sausages and Mr. Lane's reference to the ancient Chinese usage are especially welcome because they show the origins of this device and testify to its long history of successful application. The writer's approach ignored the literature, at least in the first stages of the investigation. However, if the customary historical review had been undertaken before the experiments were started, the observations of the mechanism of riprap protection would not have been made and the necessity for T-V grading of protective layers not discovered. These observations point the way to developing a completely dependable technique of rock-sausage protection.

The data comparing the cost and abrasive resistance of steel wire with the ordinary galvanized-iron wire mentioned by Mr. Matthes raise the question of whether the wires were comparable to those used in the United States or whether stainless-steel wire was used. For the protection of the flanks of embankments against water flowing down the slope, spiral-woven mesh is preferable to hexagonal mesh because greater springiness of the spiral weave insures that the sausage unit will maintain good compressive strength.

The sound argument presented by Messrs. Izzard and Bradley for the re-examination of the basis for constructing elevated road embankments deserves careful study by designers of highway-bridge crossings.

Mr. Kindsvater rightly emphasizes the importance of the hydraulic-flow characteristics; he notes that, if surface flows can be maintained over a wider range, less erosion resistance may be necessary. Although experience has taught the writer to be cautious in predicting when and where erosion will be severe, he agrees that surface flows are likely to be less erosive than plunging flows. The tests described in the paper were all made with minimum tailwater because it was desired to subject the embankments to the most severe tests. Preliminary experiments showed the condition of minimum tailwater to be even more severe than the case with a hydraulic jump forming on the slope.

The hydraulic data described by Mr. Kindsvater are of importance if the economic balance envisaged by Messrs. Izzard and Bradley is to be evaluated.

---

[29] Prof. and Head, Dept. of Civ. Eng., State Univ. of Iowa, Iowa City, Iowa.

The total costs involved are evidently enormous for the United States as a whole, making the hydraulic experimentation especially urgent.

Hubert E. Snyder, M. ASCE, has cited by letter the case of a highway fill built across a water-supply reservoir, realizing that it would occasionally be overtopped by flood waters. The fill successfully withstood one flood, only to be washed out under a later flood of approximately the same magnitude. In the interval a plate-type guard rail had been installed, and it was thought that the presence of the guard rail and posts caused the failure. That considerable differences in the flow pattern might be expected is shown in the data presented by Mr. Kindsvater. The effect of handrails on hydraulic and erosion characteristics needs further investigation. It is the writer's opinion that cable guard rails carried by slender posts, preferably of steel and carefully installed between sausages, would not appreciably affect the erosion resistance of a properly built fill.

Mr. Neeley describes an application of rock-sausage protection which has provided an economical solution to a difficult erosion problem. Again, the writer would suggest spiral-woven fencing which—although not as widely available as fencing marketed for agricultural purposes—is better for this special purpose and should be cheaper in quantity because it is easier to manufacture and much easier to "sew" in the field.

AMERICAN SOCIETY OF CIVIL ENGINEERS
Founded November 5, 1852

TRANSACTIONS

Paper No. 2872

RECOVERY OF USABLE WATER FROM SALINE WATER

By David B. Smith,[1] A. M. ASCE, and Charles E. Richheimer[2]

Synopsis

Future water demands require that all sources of water be used, and one potential source is in the vast quantities of saline water. The various methods for recovery of usable water from saline waters are cited herein, and the economics of each process are developed.

Within recent years much interest has been centered on the research and development program adopted to recover usable water from saline water. This interest has been promoted for the most part by the Saline Water Conversion Program of the United States Department of the Interior. This program was started in 1952. At the outset it was realized that the success of any technique or apparatus for recovering usable water from saline water must be judged entirely by the cost. A report[3] clearly illustrates this point:

> "At the beginning of the Saline Water Conversion Program, the cost of converting sea water was estimated at about $400 to $500 an acre-foot. Accordingly, two arbitrary criteria were set for the initial 5-year phase of the program, one for water for municipal and similar purposes and one for irrigation water. For these criteria no distinction is made as to whether the water to be converted is sea or brackish water. These goals were $125 and $40 per acre-foot (38 and 12 cents per 1,000 gallons) respectively and they were believed, on the basis of data then available, to represent about the maximum that could be borne by these types of use."

There are several publications[3, 4, 5, 6] which present descriptions of the various possible methods for reclaiming fresh water from saline water in

---

Note.—Published, essentially as printed here, in February, 1956, as *Proceedings Paper 890.* Positions and titles given are those in effect when the paper was approved for publication in *Transactions.*

[1] Prof. of Civ. Eng., Univ. of Florida, Gainesville, Fla.

[2] Partner, Reynolds, Smith & Hills, Archts. and Engrs., Jacksonville, Fla.

[3] "Third Annual Report of the Secretary of the Interior on Saline Water Conversion," U. S. Dept. of of the Interior, Washington, D. C., January, 1955.

[4] "Demineralization of Saline Water with Solar Energy," by G. O. G. Lof, *Research and Development Progress Report No. 4*, Saline Water Conversion Program, U. S. Dept. of the Interior, Washington, D. C., August, 1954.

[5] "Review of Research on Problems of Utilization of Saline Water," United Nations Educational, Scientific and Cultural Organization, New York, N. Y., April, 1954.

[6] "Fresh Water from the Ocean," by C. B. Ellis, and members of the staff of Nuclear Development Associates, Inc., Ronald Press, New York, N. Y., 1954.

addition to the theories involved. Each method can be classified as either (1) a proven method, for which standard equipment is available; (2) an unproven method, for which standard equipment is available; or (3) an unproven method, for which standard equipment is unavailable. (The term, "proven," designates those methods for which long-time operating data exist on a successful plant-scale installation.) The first group of methods includes various types of distillation processes. The second group includes the direct ion-exchange method and the electrodialytic method. The third group consists of demineralizing techniques, such as solar evaporation, freezing, reverse osmosis, and high temperature and pressure distillation. None of the techniques in the third group, however, is sufficiently developed to permit a cost comparison with the methods listed in the first two groups.

TABLE 1.—CHARACTERISTICS OF A RAW WATER WHICH MAY BE OBTAINED FROM CERTAIN DEEP-WELL SOURCES

Constituent	Average concentration
Total dissolved solids, in ppm	1,617
Silica as SiO_2, in ppm	14.3
Iron as Fe, in ppm	0.14
Manganese as Mn, in ppm	0
Calcium as Ca, in ppm	128
Magnesium as Mg, in ppm	64
Sodium and potassium as Na, in ppm	287[a]
Bicarbonate as HCO_3, in ppm	150
Carbonate as CO_3, in ppm	0
Sulfate as SO_4, in ppm	169
Chloride as Cl, in ppm	643
Fluoride as F, in ppm	0.32
Nitrate as NO_3, in ppm	0.52
Carbonate hardness as $CaCO_3$, in ppm	123
Noncarbonate hardness as $CaCO_3$, in ppm	458
Total hardness as $CaCO_3$, in ppm	581
Carbon dioxide as CO_2, in ppm	25
pH	7.4
Color (cobalt scale)	13
Total alkalinity as $CaCO_3$, in ppm	123
Hydrogen sulfide	appreciable
Temperature	23° C

[a] Adjusted.

Attempts that have been made to recover usable water from saline water can best be presented by comparing the unit-treatment costs of each method when it is applied to a saline water of given characteristics.

RAW AND TREATED WATER CHARACTERISTICS

To illustrate the problem it is assumed that 2.00 mgd of treated water is furnished from a deep-well supply producing raw water of the quality indicated in Table 1. In general, the objectionable qualities of this water are (1) a high dissolved-solids content, (2) a high chloride content, and (3) a high total-hardness content. Additionally, aeration and stabilization are needed to produce a nonaggressive, stable effluent water free from objectionable tastes and odors. If the quality criteria of the treated water are to conform to the Public Health Service (United States Department of Health, Education and Welfare) Drinking Water Standards (1946), a reduction is needed of the chloride concentrations and of the total dissolved-solids concentrations as shown in Table 2. Also, the 581-ppm total hardness should be reduced to the upper limit of 100 ppm which is normally accepted for municipal water supplies. Successful treatment of the raw well water to meet these standards would produce effluent water that would be generally satisfactory for municipal consumption.

TABLE 2.—COMPARISON OF RAW WATER CONSTITUENTS WITH THE 1946 UNITED STATES PUBLIC HEALTH SERVICE DRINKING WATER STANDARDS

Constituent	Raw water	Upper limits, 1946 Standards
Chloride	643 ppm	250 ppm
Total solids	1,617 ppm	500 ppm[a]
Taste and odor	objectionable	not objectionable

[a] 1,000 ppm may be permitted.

COST DETERMINANTS

In evaluating the various processes of the methods used to meet these water-quality criteria, it is necessary to estimate the capital outlay, the operational costs, and the total over-all costs of each method, based on a unit quantity of the finished water produced. The estimates given herein represent costs per 1,000 gal of finished water. Table 3 lists the unit prices of chemicals, labor, and power which were used in the various estimates. The equipment costs used were price quotations by manufacturers and an estimate of delivery, erection, and housing costs. The operational costs include an estimate for renewals and repairs needed to maintain the initial equipment in operating condition for an indefinite period of time. The total capital costs are based on an interest charge of 3% and on a 25-yr amortization period, which results in a gross annual charge of 5.74% of the capital outlay.

TABLE 3.—ESTIMATING UNIT COSTS

Item	Cost
Labor	$2.25 per man-hr
Fuel oil	0.075 per gal
Electricity	0.015 per kw-hr
Chemicals:	
Caustic soda—50% NaOH (liquid)	0.0357 per lb
Sulfuric acid—66° Be	0.0167 per lb
Soda ash	0.0215 per lb
Alum (Filter alum, American Water Works Association Specification)	0.0283 per lb
Sodium silicate	0.0205 per lb
Lime, slaked, bagged	0.0150 per lb
Rock salt	0.0085 per lb

Although the necessary costs for effluent stabilization and for taste and odor control are included in the cost estimates, it has been assumed that standard aeration and chlorination procedures will reduce the hydrogen-sulfide

TABLE 4.—COST ESTIMATES FOR VARIOUS TREATMENT PROCESSES

Item	(*a*) Multiple-effect evaporation treatment process	(*b*) Vapor-compression distillation treatment process	(*c*) Flash-type distillation treatment process	(*d*) Ion-exchange treatment process	(*e*) Electrodialytic process preceded by sodium-zeolite softening	(*f*) Electrodialytic process with acid pretreatment alone	(*g*) Goal of Saline Water Conversion Program for municipal consumption
COSTS OF FACILITIES, IN DOLLARS							
Pumphouse and laboratory	40,000	40,000	40,000	40,000	40,000	40,000	
Reservoir and piping	20,000	20,000	20,000	20,000	20,000	20,000	
Degasifier	15,000	15,000	15,000	15,000	15,000	15,000	
Evaporators and boiler plant (1.24 mgd)	2,500,000	...	...	...	...	...	
Vapor-compression distillation units (1.24 mgd)	...	3,000,000	...	...	...	...	
Flash-type boiler units (1.24 mgd)	...	...	2,120,000	...	...	...	
Cation and anion demineralization units	...	...	...	330,000	...	...	
Acid and caustic storage and transfer piping	...	...	...	70,000	...	...	
Electrodialytic units	...	...	...	...	720,000	720,000	
Pumps, piping, chlorinators	70,000	70,000	70,000	80,000	...	...	
Salt storage, transfer pumps, and housing	40,000	40,000	40,000	40,000	90,000	...	
Acid storage and handling	...	...	...	...	...	20,000	
Pumps, piping, chlorinators, housing, drain line and controls	...	...	...	...	119,000	119,000	
Zeolite softeners	80,000	80,000	80,000	80,000	398,000	...	
Brine disposal	10,000	10,000	10,000	10,000	20,000	20,000	
Soft-water storage	10,000	10,000	10,000	10,000	50,000	50,000	
Estimated capital outlay	2,785,000	3,285,000	2,405,000	695,000	1,472,000	1,004,000	
OVER-ALL COSTS FOR FINISHED WATER, IN DOLLARS PER THOUSAND GALLONS							
Fuel	2.00	0.21	0.83	...	...	...	
Labor	0.09	0.09	0.09	0.02	0.06	0.06	
Maintenance of equipment	0.09	0.21	0.09	0.02	0.05	0.04	
Power	...	0.02	0.12	...	0.12	0.12	
Salt	0.03	0.03	0.03	0.02	0.15	...	
Sulfuric acid	...	...	...	0.44	...	0.02	
Caustic soda	...	...	...	0.30	...	...	
Membrane replacement	...	...	...	...	0.14	0.14	
Stabilization of effluent	0.02	0.02	0.02	0.02	0.01	0.02	
Capital charges	0.22	0.26	0.19	0.05	0.12	0.08	
Estimated over-all costs	2.45	0.84	1.37	0.87	0.65	0.48	0.38

concentration to a nonobjectionable level. It has also been assumed that effluent stabilization is accomplished by the addition of silicate, lime, soda ash, or flue gas, as required. Primary considerations are thus resolved to methods of reducing the chlorides, total solids, and total-hardness concentrations.

MULTIPLE-EFFECT EVAPORATION

The process of vaporization applied to demineralization methods consists of evaporating a part of the saline water, after which the vapor is condensed to produce fresh water. In multiple-effect evaporation the vapor from one stage is condensed in heat-exchange units of the next stage, in which steam is being produced from brine at a temperature and a pressure less than those of the previous stage. Several stages may be used but three stages seem to be the normal limit. This method has been developed commercially, and, at present (1956), almost all fresh water is recovered from saline water by one of the evaporation methods.

In order to produce a finished water (with a chloride content of not more than 250 ppm) from the raw water (Table 1), it would be necessary to produce a distillate at a rate of 1.24 mgd. When the effluent water is mixed with 0.76 mgd of water which has bypassed the evaporators, it would satisfy the criteria for chlorides and total-solids concentrations, but it would contain 221 ppm of total hardness. The bypassed water would therefore require partial softening to reduce the hardness constituents of the final product to 100 ppm. For this purpose, sodium-zeolite softeners are satisfactory and have been used to determine the costs involved. Table 4(*a*) presents an estimate of the over-all costs for producing 1,000 gal of final effluent by means of a multiple-effect evaporation plant designed and operated at a rate of 2 mgd; the estimated over-all cost is $2.45 per 1,000 gal.

VAPOR-COMPRESSION DISTILLATION

The evaporation principle may be utilized with greater efficiency when the vapor-compression distillation process is used. This process operates on the heat-pump principle in which the latent heat of vaporization is continuously reused. The unit first vaporizes water from saline water at atmospheric pressure. The vapor is then compressed to raise its pressure and temperature and is returned to the heating side of the evaporator tubes where it condenses. In this process substantially all the latent heat of vaporization is transferred back to the boiling brine; the fresh-water condensate is then withdrawn.

In estimating the costs of treating the raw water by vapor-compression distillation units, the distillate production, as well as the water bypassed and softened, would be the same as that achieved in the multiple-effect evaporation process. Table 4(*b*) gives the estimated cost data for treating the raw water so as to meet the indicated standards of dissolved solids, chlorides, and hardness content. If diesel-driven compressors are used to compress the water vapor and if sodium-zeolite units are used to soften the bypassed water, the estimated over-all cost of producing 1,000 gal of finished water is $0.84, as shown in Table 4(*b*).

FLASH-TYPE DISTILLATION

A third process which uses the vaporization principle is flash-type distillation. In flash evaporation, saline water at a given temperature and pressure is released into a chamber of lower pressure where the water vaporizes. The vapor is then condensed in cooling chambers by the incoming raw saline water to produce fresh water.

Finished water containing 250 ppm of chlorides and 100 ppm of total hardness could be produced from the raw water by flash-evaporation equipment capable of furnishing 1.24 mgd of distilled water; this total hardness could also be produced by partial softening with sodium zeolite of 0.76 mgd of the bypassed raw water. Table 4(*c*) gives an itemized list of the estimated over-all costs, which amount to $1.37 per 1,000 gal of finished water.

ION EXCHANGE

Although the cation-exchange principle has long been used in conventional water-softening plants, recent developments of hydrogen-cation exchangers and anion exchangers have made practicable the complete removal of dissolved salts by ion exchange. The requirements for rinse and regeneration limit the ion exchange to waters of less than approximately 2,500 ppm of dissolved salts.[7] However, because the water selected for the present analysis contains only 1,617 ppm, ion exchange may be considered to be a feasible treatment method.

A finished water, containing 250 ppm of chlorides and approximately 630 ppm of dissolved solids, may be obtained from the raw water described in Table 1 by demineralizing 1.24 mgd in ion-exchange units and by mixing the treated water with 0.76 mgd of bypassed raw water. The total hardness of the finished water could be reduced to 100 ppm by the softening with sodium zeolite of 56% of the bypassed water. This would thus produce a finished water complying with the desirable water-quality criteria. Table 4(*d*) lists the estimated over-all costs which amount to $0.87 per 1,000 gal of finished water.

ELECTRODIALYSIS

The most recent development (as of 1956) in methods used to recover usable water from saline water is the electrodialysis process which utilizes the properties of semipermeable, selective ion membranes.[8] This process removes equivalent amounts of anions and cations from water almost without regard to the ionic constituents present. It is known, however, that ferrous, calcium, and magnesium cations tend to precipitate on the membranes. This shortens the life of the membranes and increases operational and maintenance costs. The water of the present example contains 192 ppm of calcium and magnesium, which is a concentration greater than is considered safe to apply to the membranes. Pretreatment methods are, therefore, desirable to reduce the calcium and magnesium ions to minimum feasible concentrations. The over-all production costs will be increased accordingly, but the membrane operating life, a major factor in determining the over-all costs, may then be estimated to be three years.

---

[7] "The Desalting of Saline Waters: A Review of the Present Status," by E. W. Moore, *Journal*, New England Water Works Assn., Vol. 65, 1951, p. 319.

[8] "Reclamation of Saline Waters by Electrodialysis Shows Promise," by Rolf Eliassen, *Civil Engineering*, Vol. 24, 1954, p. 366.

It has also been determined that the optimum demineralization rate in the electrodialytic units is 40% of the feed-water ionic concentration per treatment stage. The optimum wastage rate is 20% of the product water regardless of the number of stages used. For the present example, a two-stage treatment plant would be required to remove 64% of the original chlorides (40% of the original concentration plus 40% of 60% of the remaining concentration), or to produce a finished water containing 232 ppm of chlorides. In producing 2.00 mgd of finished water, the wastage rate would be 0.50 mgd requiring a feed-water rate of 2.50 mgd.

There are at least two processes to reduce the calcium and magnesium content of the feed water—sodium-zeolite and lime-soda ash softening. Lime-soda ash pretreatment would reduce the hardness content to approximately 40 ppm and would not alter significantly the total dissolved-solids content. Sodium-zeolite pretreatment would reduce the hardness constituents to almost zero and would increase the total dissolved solids approximately 5%. Cost estimates show that the over-all costs per unit of finished water are approximately equal for each method. Therefore, the sodium-zeolite process has been selected for the example cited herein because it accomplishes greater hardness removal.

Finished water containing 232 ppm of chlorides and 507 ppm of dissolved salts (as sodium chloride) may be obtained from the raw water described in Table 1 by producing 2.50 mgd of water softened by sodium zeolite and by passing the entire flow through two stages of the electrodialytic units. The finished water would be quite soft but would meet the quality criteria cited previously. Total over-all costs are estimated to be $0.65 per 1,000 gal of finished water, as shown in Table 4(*e*). The costs are based on salt-regenerated zeolite beds, but further economies can be realized if a source of sea water or brine is available for regenerating the zeolite units.[9]

There are some experimental data on the use of acid pretreatment of the feed water to render presoftening unnecessary.[10] The initial results are promising and, if this technique is successful on a long-time basis, the estimated over-all costs per 1,000 gal of finished water may be reduced materially by eliminating the construction, maintenance, and operational costs of the sodium-zeolite-softening units. It would be necessary, however, to include cost estimates for the acid pretreatment and for the subsequent additional pH-factor adjustment of the effluent water, as shown in Table 4(*f*). The estimated total over-all costs are $0.48 per 1,000 gal of finished water.

The last line in Table 4 summarizes the estimated over-all unit costs of the various methods considered herein, in addition to the cost estimated by the Saline Water Conversion Program, to be approximately the maximum cost that may be borne by municipalities.

---

[9] "Sea Water Regeneration of Zeolite Water Treatment Plants," by Charles E. Richheimer, *Southern Power and Industry*, July, 1948.

[10] "Third Annual Report of the Secretary of the Interior on Saline Water Conversion," U. S. Dept. of the Interior, Washington, D. C., January, 1955, p. 49.

CONCLUSIONS

From the cost analyses cited, it is seen that the electrodialytic process for demineralizing water is (as of 1956) the most economical means of recovering usable water from water of low salinity levels. Although the over-all unit costs of production are high, continuing research and development should improve existing methods or produce newer methods that will permit significant cost reductions. It is not yet possible, however, to recover usable water from moderately saline waters at costs that compete with conventional treatment and supply methods.

AMERICAN SOCIETY OF CIVIL ENGINEERS
Founded November 5, 1852
TRANSACTIONS

Paper No. 2873

OSCILLATORY GRAVITY WAVES IN FLOWING WATER

By Turgut Sarpkaya,[1] J. M. ASCE

Synopsis

The main objectives of this paper are (*a*) to determine the conditions of stability of progressive, oscillatory gravity waves in water flowing over smooth and artificially roughened surfaces and (*b*) to evaluate the combined effect on the wave propagation by various interrelated characteristics of flowing water, such as viscous shear, turbulent mixing shear, and nonuniform velocity distribution. Because neither experimental nor conclusive theoretical results are available for solving the problems discussed herein, it is necessary to evaluate the effect of various characteristics of flowing water on the velocity of stable-wave propagation by comparing results with those obtained from available theories, particularly those of G. G. Stokes[2] and D. J. Struik.[3]

For stable, ascendant, oscillatory gravity waves in smooth and artificially roughened rectangular channels, the period and various geometrical characteristics were measured for range of depth, velocity of flow, and settings of the wave generator. The following results were obtained:

1. For a given flow there is only one neutrally stable wave. All other waves show either an exponential damping or an amplification during their propagation along the channel. It is easy to separate the two regions by means of the surface of neutral stability, which was determined experimentally and is presented graphically.
2. The celerity of a stable ascendant wave is smaller than that obtained from the theories of Messrs. Stokes and Struik. The deviation in wave velocity from that obtained from potential theory increases with increasing Froude numbers and decreases with increasing Reynolds numbers.
3. For a channel with an artificially roughened bottom, the deviation is greater than that for a channel with a smooth bottom.
4. As described by Mr. Struik, the experimentally determined profiles of stable oscillatory gravity waves vary about the theoretical profiles.

Note.—Published, essentially as printed here, in October, 1955, as *Proceedings Paper 815*. Positions and titles given are those in effect when the paper was approved for publication in *Transactions*.

[1] Research Engr., Massachusetts Inst. of Technology, Cambridge, Mass.

[2] "On the Theory of Oscillatory Waves," by G. G. Stokes, *Transactions*, Cambridge Phil. Soc., Vol. VIII, 1847, p. 441.

[3] "Détermination rigoureuse des ondes irrotationelles périodiques dans un canal à profondeur finie," by D. J. Struik, *Mathematische Annalen*, Vol. XCV, 1926, pp. 595–634.

INTRODUCTION

Exact knowledge of the characteristics of waves in flowing water is important from both scientific and practical standpoints. This knowledge is necessary in the case of the penetration of waves into an estuary and in the determination of scour in the river bed caused by either ascendant waves or descendant waves generated by wind. The analysis of all these problems requires, first of all, a knowledge of the laws governing wave movement in a nonerodible channel.

Until the 1930's, knowledge of the motion of oscillatory gravity waves in water was based for the most part on theoretical studies. Several rigorous solutions were obtained, differing from each other chiefly in their results for the motion of the water particles involved.[2,3,4,5]

Experimental confirmation of these theoretical solutions has been the main purpose of a number of studies. For waves in still water these investigations[6,7,8] have shown that, except for mass transport, the difference in value of the wave characteristics defined by the theories of rotational and irrotational wave motion is smaller than the experimental error. If waves are generated in water that is already in motion, there is a difference between observations and classical theories that results from the effect of viscous shear, turbulent mixing shear, and nonuniform velocity distribution.

On the one hand, viscous action in the boundary layer produces vorticity which diffuses through the fluid and modifies the whole velocity distribution. The subsequent wave motion thereby inherits a rotational motion, and the usual assumption of a velocity potential becomes inadequate. On the other hand, turbulence becomes an important factor which takes precedence over gravity. Furthermore, both the velocity distribution and the turbulence structure of the primary flow are completely altered by the wave motion. In addition, perhaps the situation is most highly complicated by the factor that waves generated in flowing water are not always neutrally stable; some of these waves are damped and some are amplified, according to the existing flow conditions. Therefore, the effect of the various factors on the propagation of waves in flowing water can be evaluated but only after the conditions of neutral stability have been determined.

An attempt is made herein to establish the conditions of stability of ascendant waves and also to evaluate the effect of the various characteristics of flow on their propagation.

PREVIOUS INVESTIGATIONS

Certain phases of the general problem—that is, the effect of various characteristics of the primary flow on the velocity of propagation of the disturb-

---

[4] "Détermination rigoureuse des ondes d'ampleur finie," by T. Levi-Civita, *Mathematische Annalen*, Vol. XCII, 1925, pp. 264–314.

[5] "Mouvements ondulatoires de la mer en profondeur constante ou décroissante," by M. Miche, *Annales des Ponts et Chaussées*, Vol. 114, 1944, pp. 25–406.

[6] "A Study of Progressive Oscillatory Waves in Water," by M. A. Mason, *Technical Report No. 1*, Beach Erosion Board, Corps of Engrs., U. S. Dept. of the Army, Washington, D. C., 1942.

[7] "Remarques sur la célérité de la houle irrotationelle exacte au troisième ordre," by F. Biésel, *La Houille Blanche*, Vol. XXXIV, 1951, p. 414.

[8] "Basic Experimental Wave Research," by F. Suquet and A. Wallet, *Proceedings*, Minnesota International Hydr. Convention, Univ. of Minnesota, Minneapolis, Minn., 1953, pp. 173–191.

ances—have been studied previously. The problem is, however, so complex that none of these phases has been completely solved.

The experiments of H. Bazin[9] on the propagation of a solitary wave were the first demonstrations of the incongruity between observations and the theory despite agreement in still water. The effect of the nonuniform velocity distribution on translation waves has been studied in great detail by J. Boussinesq.[10] H. Favre[11] has employed the Boussinesq integrals to describe the motion of waves occurring during the operation of navigation locks. More than half a century after Mr. Boussinesq's analysis was completed, G. H. Keulegan and G. W. Patterson analyzed[12] the combined effects of turbulent resistance and inertia on the motion of flood waves and other waves of translation in open channels. All these investigations were conducted for the case of translatory gravity waves in flowing water.

S. S. Hough[13] presented a solution of certain problems that illustrated the effects of viscosity on the motion of the sea. Mr. Hough concluded that the velocity of wave propagation is slightly decreased by the resistance of the ocean bed, by the dissipation of energy through internal viscosity, and by turbulence. A. J. Abdullah[14] attempted to solve the problem of wave motion superposed on a current caused by winds; this current is assumed to follow the Ekman spiral law in speed but to remain constant in direction. In comparing his results with gravitational waves, Mr. Abdullah found that the total effect of turbulence and gravity gives a velocity smaller than that provided by gravity alone. F. Biésel[15] has presented a theoretical analysis of the effect of nonuniform velocity distribution on the velocity of propagation of small-amplitude oscillatory gravity waves in open channels; this analysis will be further discussed in detail because it partly confirms the present (1956) experimental results.

For very long waves—that is, for large values of $a\,L^2/d^3$—in the linearized theory, J. C. Burns[16] obtained a general equation, which connects the wave velocity with the velocity in the undisturbed stream; the equation was solved in several special cases. He showed that the velocity of a long wave, which is relative to the mean flow, is always greater than the value given by the classical theory. In the appendix of Mr. Burns' paper,[16] Williams Lighthill examined the critical Froude number above which no ascendant-wave propagation is possible. On the basis of assumptions which will be examined herein, Mr. Lighthill found that the nonuniformity in the velocity distribution has the opposite effect for large and small wave lengths. For waves that are represented in the Stokes theory, in which the motion is predominantly at the surface, the relatively high fluid velocity in this region causes the lowering of the critical Froude number which is based on the mean velocity. For longer waves, in which the motion is almost purely longitudinal, the decreased velocities near the bottom make a greater difference in wave velocity than do the increased velocities near the surface.

---

[9] "Recherches experimentales sur la propagation des ondes," by H. Bazin, *Mémoires Divers Savants à l'Académie des Sciences*, Vol. 19, 1865, p. 495.

[10] "Essai sur la théorie des eaux courantes," by J. Boussinesq, *ibid.*, Vol. 23, 1877, p. 1.

[11] "Étude théorique et experimentale des ondes de translation dans les canaux découverts," by H. Favre, Dunod, Paris, 1955.

[12] "Effect of Turbulence and Channel Slope on Translation Waves," by G. H. Keulegan and G. W. Patterson, *Journal of Research*, National Bureau of Standards, U. S. Dept. of Commerce, Washington, D. C., Vol. 30–31, 1943, pp. 461–512.

[13] "On the Influence of Viscosity on Waves and Currents," by S. S. Hough, *Proceedings*, London Math. Soc., Vol. XXVIII, 1896, pp. 264–288.

[14] "Wave Motion at the Surface of a Current Which Has an Exponential Distribution of Vorticity," by A. J. Abdullah, *Annals*, N. Y. Academy of Sciences, Vol. 51, 1942, p. 3.

[15] "Étude théorique de la houle en eau courante," by F. Biésel, *La Houille Blanche*, 1950, pp. 279–285.

[16] "Long Waves in Running Water," by J. C. Burns, *Proceedings*, Cambridge Phil Soc., Vol. 97, 1953, p. 243.

In considering the second part of the present investigation, one finds there has been no previous theoretical and experimental study in order to determine the stability conditions of an oscillatory gravity wave. However, because of the challenging nature of the stability problem, there have been many investigations of the stability of interfacial gravity waves, the stability of parallel flows, and the stability of dunes in the stream beds. D. J. Korteweg and G. de Vries[17] have shown that relatively long waves have a tendency to become steep ahead of their peaks at a rate proportional to a/d and that this tendency is resisted by an opposing tendency, which is independent of amplitude and results from the departures from uniformity in the distribution of velocity with depth. Messrs. Korteweg and de Vries have also shown that there is an infinite sequence of wave forms. Each sequence is such that, for a particular ratio of a/d to d^2/L^2, the tendencies to change in form are eliminated, which thereby leads to a wave of permanent type. These wave forms are conoidal—that is, they are graphs of the square of the Jacobian elliptic function, $\operatorname{cn} x$, for different moduli, k_1; one extreme, $k_1 = 0$, is the sinusoidal wave, which occurs when the ratio $a\, L^2/d^3$ is very small. At the other extreme, $k_1 = 1$, the wave length becomes large, and the character of the waves becomes increasingly like that of a sequence of solitary waves.

For the stability of an elementary wave starting from a uniform regime, the evolution with time of a sinusoidal undulation of small amplitude was studied by H. Jeffreys[18] and, depending on the case involved, an exponential damping or amplification was found. Recently, the stability of two-dimensional small disturbances in laminar flow on a plane boundary was studied by Chia-Shun Yih.[19] Mr. Yih found that, for each slope of the channel bottom, a hyperbolic type of curve with arms extending in the directions of the wave number, $2\pi\, d/L$, and of the Reynolds number separates the stable region from the unstable one.

There has been no previous theoretical and experimental investigation of the conditions of stability for an oscillatory gravity wave of finite amplitude in flowing water.

THEORETICAL CONSIDERATIONS

Because of the present status of turbulence theory and mathematical techniques, there is little hope that either the effect of turbulence and viscosity or the conditions of stability can be directly determined. In general, an oscillatory gravity wave is unsteady and involves both molar and molecular resistance. In addition to this complexity, turbulence characteristics, such as velocity and pressure fluctuations, cannot be determined deductively. However, neglecting the effect of turbulence and considering only the effect of viscosity with a nonuniform velocity distribution over the cross section and by using the Sommerfeld-Orr equation, as shown in the paper of A. Sommerfeld,[20] the problem of stability can be conveniently formulated. In spite of this simple formulation, it would be extremely difficult to evaluate a rigorous solution of the equations obtained for even a simple velocity distribution; such an evaluation has not been attempted.

---

[17] "On the Change of Form of Long Waves Advancing in a Rectangular Canal, and a New Type of Long Stationary Waves," by D. J. Korteweg and G. de Vries, *London, Edinburgh, and Dublin Magazine and Journal of Science*, Vol. 39, 1895, p. 139.

[18] "The Evolution with Time of a Sinusoidal Undulation of Small Amplitude," by H. Jeffreys, *Proceedings*, Cambridge Phil. Soc., Vol. 98, 1954, p. 139.

[19] "Stability of Parallel Laminar Flow with a Free Surface," by Chia-Shun Yih, *Proceedings*, 2d National Cong. of Applied Mechanics, Brown Univ., Providence, R. I., 1954, p. 239.

For very large Reynolds numbers, the theoretical and the practical values of this solution seem questionable. As the Reynolds number increases beyond the critical range, the eddy viscosity becomes increasingly important. In other words, if the Reynolds number is high, the viscous stresses in terms of the mean-velocity gradients are negligible compared with the apparent stresses that are due to momentum transport.

Despite these difficulties, the effect of nonuniform velocity distribution on the propagation of small stable gravity waves can be obtained analytically. Mr. Biésel[15] neglected the viscous terms in the Sommerfeld-Orr equation and made the wave motion steady by fixing the axes on the wave profile. He additionally assumed a linear-velocity distribution,

$$C = C_0(1 + k\,y) \qquad \text{(1)}$$

and obtained the velocity of an ascendant wave,

$$V_{as} = \sqrt{\left(\frac{U_0 - U_1}{2}\,\frac{\tanh m\,d}{m\,d}\right)^2 + \left(g\,\frac{\tanh m\,d}{m}\right)} - \left(U_0 - \frac{U_0 - U_1}{2}\,\frac{\tanh m\,d}{m\,d}\right) \qquad \text{(2)}$$

If the velocity of the ascendant wave were obtained from the superposition of a small-amplitude wave velocity on the mean velocity of flow, the result would be

$$V'_{as} = \sqrt{g\,\frac{\tanh m\,d}{m}} - \frac{U_0 + U_1}{2} \qquad \text{(3)}$$

The deviation, ζ, can be defined by the relationship,

$$\zeta = \frac{V_t - V_m}{V_m} \qquad \text{(4)}$$

If Eq. 2 is used for measured velocities and Eq. 3 is used for theoretical velocities, the deviation, ζ, can be obtained as

---

[20] "Ein Beitrag zur Hydrodynamischen Erklaerung der turbulenten Fluessigkeitsbewegungen," by A. Sommerfeld, *Proceedings*, 4th International Cong. of Math., Rome, 1908, pp. 116–124.

$$\zeta = \frac{\sqrt{g\,\frac{\tanh m\,d}{m}} - \frac{U_0 + U_1}{2}}{\sqrt{\left(\frac{U_0 - U_1}{2}\,\frac{\tanh m\,d}{m\,d}\right)^2 + g\,\frac{\tanh m\,d}{m}} - U_0 - \frac{U_0 - U_1}{2}\,\frac{\tanh m\,d}{m\,d}} - 1 \ldots\ldots (5)$$

The results obtained from this equation and their comparison with the experimental results will be examined herein in more detail because the experimental results are partly confirmed.

In the case of the breaking of waves in flowing water, one of the most important characteristics of oscillatory gravity waves is the continuous deformation of shape and the subsequent breaking under different factors from those in still water. The limiting condition beyond which no wave propagation exists is determined primarily from the consideration that the wave becomes unstable and breaks when the forward velocity of the water particles at the crest exceeds the velocity of the wave. In general, in still water this may be caused by the shoaling of the depth, accompanied by the complicated effects of backwash from previously broken waves, or by the action of an opposing wind as yet little understood. It has been known theoretically that the asymptotic limit for waves in deep water is $a/L = 0.14$. In fairly shallow waters, a good approximation is given by the solitary-wave theory despite the fact that it is not confirmed by the experiments in sloping channels conducted at the Massachusetts Institute of Technology at Cambridge. For intermediate conditions in medium depth, the limiting wave steepness is given by M. Miche[5] as

$$\frac{a}{L} = 0.14 \tanh \frac{2\,\pi\,d}{L} \ldots\ldots\ldots\ldots\ldots\ldots\ldots (6)$$

P. Danel[21] has reported experimental results which approximate this theoretical limiting curve.

However, in flowing water, in addition to the effect of the slope of the channel bottom which does not cause any shoaling, the retardation of the forward face of the wave by the opposing current and its being consequently overtaken by the remainder of the wave become predominant factors. Evidently the mean velocity of flow, as well as the particular velocity distribution, is important in determining the limiting condition. Therefore, the limiting wave steepness is additionally related to the Froude and Reynolds numbers of the primary flow as well as being related to the ratio, d/L.

However, in the theoretical determination of the limiting condition, all these parameters are as difficult to consider as the evaluation of the stability conditions. It is essential to simplify assumptions in order to achieve some insight into the phenomenon. Mr. Lighthill[16] made the assumption that a solution exists with $V = 0$, which corresponds to a stationary wave above which no upstream propagation is possible. The consideration of the equation of motion for a stationary wave of sufficiently small amplitude, with the particular velocity distribution,

---

[21] "On the Limiting Clapotis," by P. Danel, from "Symposium on Gravity Waves," *Circular 521*, National Bureau of Standards, U. S. Dept. of Commerce, Washington, D. C., 1952, p. 12.

$$U = U_1\left(\frac{y}{d}\right)^{\epsilon} \qquad (7)$$

and with the necessary boundary conditions, leads to the solution for the critical Froude number as follows:

$$\mathsf{F}_C = \frac{\bar{U}}{\sqrt{g\,d}} = \sqrt{\frac{L}{2\,\pi\,d}\,\frac{1}{(1+\epsilon)^2}\,\frac{I_{\frac{1}{3}-\epsilon}\left(\frac{2\,\pi\,d}{L}\right)}{I_{\frac{1}{3}-\epsilon}\left(\frac{2\,\pi\,d}{L}\right)}} \qquad (8)$$

To show the effect of nonuniformity in velocity distribution, if the ratio is taken of this expression to the classical expression (limit $\epsilon \rightarrow 0$) for uniform flow,

$$\frac{\mathsf{F}_C}{\mathsf{F}} = \sqrt{\frac{1}{\tanh\frac{2\,\pi\,d}{L}}\,\frac{1}{(1+\epsilon)^2}\,\frac{I_{\frac{1}{3}-\epsilon}\left(\frac{2\,\pi\,d}{L}\right)}{I_{\frac{1}{3}-\epsilon}\left(\frac{2\,\pi\,d}{L}\right)}} \qquad (9)$$

Mr. Lighthill's fundamental assumption in the derivation of the foregoing equations is not, however, fully acceptable. Propagation becomes impossible with the complete breaking of the wave. The velocity of flow becomes equal to the celerity of energy transmission, which is, in general, smaller than the wave velocity except in the case of anomalous dispersion. For waves of small amplitude the energy is transmitted by the group velocity, C_g,

$$\frac{C_g}{\sqrt{g\,d}} = \frac{1}{2}\left(1 + \frac{\frac{4\,\pi\,d}{L}}{\sinh\frac{4\,\pi\,d}{L}}\right)\sqrt{\frac{L}{2\,\pi\,d}\tanh\frac{2\,\pi\,d}{L}} \qquad (10)$$

The validity of the foregoing is limited to waves of sufficiently small amplitude. The assumption is made that the nature of the energy transmission for the waves under consideration is the same as the nature of the small-amplitude theory. Although the effect of the Froude and Reynolds numbers, **F** and **R**, can be included with the help of the deviation, ζ, it will be omitted.

If the assumption is made that no wave propagation is possible when the celerity of energy transmission is equal to the mean velocity of flow, the critical Froude number becomes

$$\mathsf{F} = \frac{1}{2}\left(1 + \frac{\frac{4\,\pi\,d}{L}}{\sinh\frac{4\,\pi\,d}{L}}\right)\sqrt{\frac{L}{2\,\pi\,d}\tanh\frac{2\,\pi\,d}{L}} \qquad (11)$$

It can easily be shown that the condition of the equality of the mean velocity of flow to the celerity of energy transmission corresponds precisely to the equality of the wave lengths of the two ascendant waves of the same period propagating in the same flow. In this case it should be noted that, in general, there are two different waves of the same period propagating in the same flow.

DIMENSIONAL ANALYSIS

The basic variables pertinent to this phenomenon are: (*a*) Amplitude, length, and velocity of a stable wave; (*b*) dynamic viscosity and density of the fluid; (*c*) depth and mean velocity of flow; (*d*) shape factor of the flume; (*e*) spacing and the dimensions of roughness elements; and (*f*) the acceleration of gravity. These variables yield the following functional relationships:

$$\begin{bmatrix} \dfrac{a}{d} \\[2mm] \dfrac{d}{L} \\[2mm] \dfrac{V_m}{\bar{U}} \end{bmatrix} = f_{1-3}\left(\frac{\bar{U}}{\sqrt{g\,d}}, \frac{\bar{U}\,d}{\nu}, \frac{k}{d}, \frac{\lambda}{d}, \beta \right) \quad \text{(12)}$$

in which ν is the kinematic viscosity of the fluid. In order to compare the wave velocities obtained experimentally with those obtained from the theory of irrotational motion, it is necessary to introduce the theoretical wave velocity, V_t. For an ascendant wave, V_t is given by the relationship,

$$V_t = C - \bar{U} \quad \text{(13)}$$

If both sides of this equation are divided by V_m and the numerator and the denominator of the right side are divided by $\sqrt{g\,d}$,

$$\frac{V_t}{V_m} = \frac{\dfrac{C}{\sqrt{g\,d}} - \dfrac{\bar{U}}{\sqrt{g\,d}}}{\dfrac{V_m}{\bar{U}}\,\dfrac{\bar{U}}{\sqrt{g\,d}}} \quad \text{(14)}$$

Because $C/\sqrt{g\,d}$ is a function of only a/d and L/d and is a function of only the independent dimensionless parameters, then $V_m/\bar{U}$ in Eq. 12 can be replaced by V_t/V_m or by the deviation, ζ. Replacing a/d by a/L, L/d by d/L, and d/k by k/d, the relationships take the form:

$$\begin{bmatrix} \dfrac{a}{L} \\[2mm] \dfrac{d}{L} \\[2mm] \zeta \end{bmatrix} = g_{1-3}\left(\frac{\bar{U}}{\sqrt{g\,d}}, \frac{\bar{U}\,d}{\nu}, \frac{k}{d}, \frac{\lambda}{d}, \beta \right) \quad \text{(15)}$$

The dependent dimensionless parameters to the left of the equations represent the wave steepness, the ratio, d/L, and the deviation, respectively. The parameters to the right of the equations represent, in order of appearance, the Froude number, **F**; the Reynolds number, **R**; the relative roughness; the relative spacing of the roughness elements; and a channel-shape factor.

It is almost impossible to consider all these variables in determining the stability conditions and in evaluating the deviation, ζ. A useful result can be obtained only in isolated instances and only if all but the most essential parameters are ignored. The existing experimental data and the theoretical knowledge are not sufficient to determine the characteristics of the shape factor, β. Furthermore, if the sides and bottom of the channel are smooth, d/k and λ/k need not be considered. Thus, for smooth channels of rectangular cross section, the relationships take the forms:

$$\begin{bmatrix} \dfrac{a}{L} \\ \dfrac{d}{L} \\ \zeta \end{bmatrix} = f_{1-3}(\mathsf{F}, \mathsf{R}) \qquad (16)$$

For the case in which the channel bottom is artificially roughened,

$$\begin{bmatrix} \dfrac{a}{L} \\ \dfrac{d}{L} \\ \zeta \end{bmatrix} = f_{1-3}\left(\mathsf{F}, \mathsf{R}, \frac{d}{k}, \frac{\lambda}{k}\right) \qquad (17)$$

In the present investigation only one type of strip roughness is used—that is λ/k is constant. Therefore,

$$\begin{bmatrix} \dfrac{a}{L} \\ \dfrac{d}{L} \\ \zeta \end{bmatrix} = f_{1-3}\left(\mathsf{F}, \mathsf{R}, \frac{d}{k}\right) \qquad (18)$$

The experimental results will be evaluated according to Eqs. 16 and 18.

APPARATUS

Wave Flume.—The glass-walled flume used in these experiments has a rectangular working section 85 ft long, 2 ft wide, and 1.5 ft deep. Depth and velocity measuring devices and probes for the wave recorder with necessary electrical circuits were mounted on two aluminum carriages which ran along the top of the walls.

Artificial roughness consisted of $\frac{1}{4}$-in. by $\frac{1}{4}$-in. continuous brass strips, placed at 1-in. intervals on the steel bottom of the flume and perpendicular to its longitudinal axis. The relative spacing, λ/k, was 4, and the depth of the flow was measured to the middle of the strips—that is, 0.011 ft was subtracted from the depth to the smooth bottom. Actually, the true depth would be between this depth and the depth to the top of the strips.

Water was supplied from the laboratory circulation system, and the discharge was measured by a calibrated venturi meter. In addition, a triangular weir conveniently placed at the end of the flume measured small discharges.

Wave Generator.—It was necessary to design a new wave generator that was simply constructed and easily operated. This generally had several concurrent functions; they were (*a*) to allow the passage of flow; (*b*) to approximate the water-particle motion in accordance with the theory under consideration; and (*c*) to cause minimum additional turbulence.

The wave generator, developed in the Iowa Institute of Hydraulic Research at Iowa City and used throughout the experiments (Fig. 1), is primarily a combination of the Ransford classical three-bar linkage (ballistic pendulum) with a system resembling a venetian blind with metal slats that can be set at any angle to regulate the passage of water only in one direction. The use of the metal slats originated at the St. Anthony Falls Hydraulic Laboratory in Minneapolis, Minn. This type of generator is very simple to operate and adequately produces the waves under investigation in varying depths of flow throughout the complete range of study.

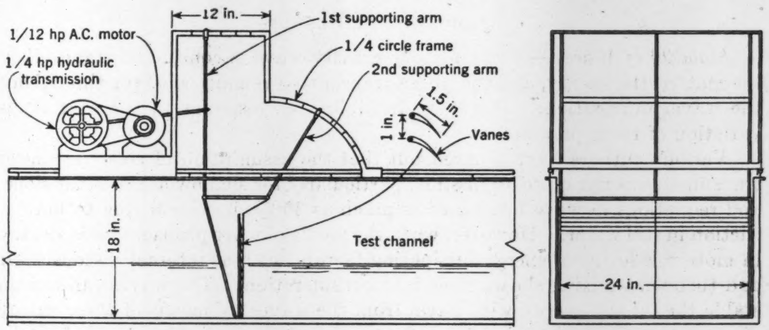

Fig. 1.—Venetian-Blind Type of Wave Generator

In order to eliminate wave reflections from the end of the flume opposite the generator, it was necessary to install wave dampers across the section. A basket made of No. 32 wire screen was filled with ¼-in. and ½-in. gravel and was hung on two parallel steel rails at a slope of approximately 30° in the direction of flow. It was adjusted so that its bottom was a half-wave height below the mean elevation of the water surface. This procedure, together with one or two wire screens stretched below the section, provided excellent wave absorption.

Experimental Procedure

The amplitude, length, and shape of waves were determined from photographs. Readings to thousandths of a foot were made under the microscope with no difficulty.

Wave periods were obtained from recordings made with a Sanborn Twin-Viso recorder. Wave velocities were also obtained by placing two parallel wire gages 10 ft apart and by registering the wave profile from these gages on the recorder. A timing device made 4 marks per sec on the recorded permapaper. Thus, having established the distance between the gages and the time required for the wave to travel from one gage to the next, it was possible to determine the wave velocity.

Velocity profiles on the flume axis were obtained by means of a $\frac{1}{8}$-in.-diameter pitot tube connected to two manometers. These manometers were set at a slope 45° from the vertical in order to magnify the differences by $\sqrt{2}$.

The general experimental procedure was as follows: The discharge was held constant for varying depths of flow. For each depth the setting of the wave generator was varied several times, and wave heights were recorded at different sections of the flume with the same wave recorder and compared with each other. Necessary adjustments of the generator, such as the period and the positions of the connecting rods, were made until a stable wave was obtained. After stability had been established, the characteristics of the resulting waves were photographed and recorded.

DISCUSSION OF RESULTS

Stability of Waves.—An oscillatory gravity wave is considered stable when the matter, the energy, and the phase transported remain constant throughout the wave propagation. Therefore, instability corresponds to the continuous variation of these parameters.

Various authors have pointed out that the assumption of constant power transmission is not quite admissible, particularly for shallow areas of flat slope, and reductions in wave heights of as much as 30% may occur due to bottom friction in still water. However, when the media of wave propagation is already in motion, additional energy dissipating factors, such as internal viscous shear and turbulent mixing shear, come into consideration. The waves can remain stable then if the energy withdrawn from the waves by means of these energy dissipating agencies is exactly in balance with the energy that is added by the flow.

Evidently the propagation of waves alters completely both the velocity distribution and the turbulence structure of the primary flow. The supplied and the dissipated energies, which are equal originally, become unbalanced because of the complete alteration of the characteristics of the primary flow. A certain amount of energy remains, which is the difference between the supplied energy and the dissipated energy; this unbalanced energy is used either to amplify or to damp the waves. Therefore, from the point of view of energy transfer, instability corresponds to an excess or a deficiency of the supplied energy with respect to that dissipated by various resistances.

The parameters which change the characteristics of the primary flow are essentially: (*a*) The oscillations of the laminar-boundary layer due to periodic variations of the pressure; (*b*) the orbital motion of the water particles due to wave movement; (*c*) the mass transport; and (*d*) a momentum transport in the direction of wave motion as a consequence of the mass transport. The momentum transported per wave length is equal to the wave velocity times the mass transported during one wave period. Recent studies have shown that the disturbances on water surface of small amplitude considerably change the mixing length of turbulence. It is an empirical fact that the turbulence creates a resistive force which is roughly dependent on a certain power of the velocity and is indirectly dependent on a certain power of the hydraulic radius with a proportionality constant depending on the stream bed. Perhaps this empirical formula could be better rationalized after the variation of the intensity and scale of turbulence as a function of Froude and Reynolds numbers has been determined in order that the wave energy scattered by turbulence can be formulated. Subsequently, the wave attenuation, which is of the same order of magnitude as the energy scattered, can be evaluated.

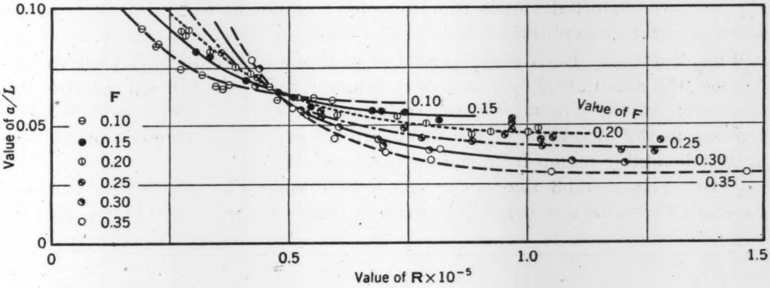

FIG. 2.—VALUES OF **R**, IN HUNDRED THOUSANDTHS

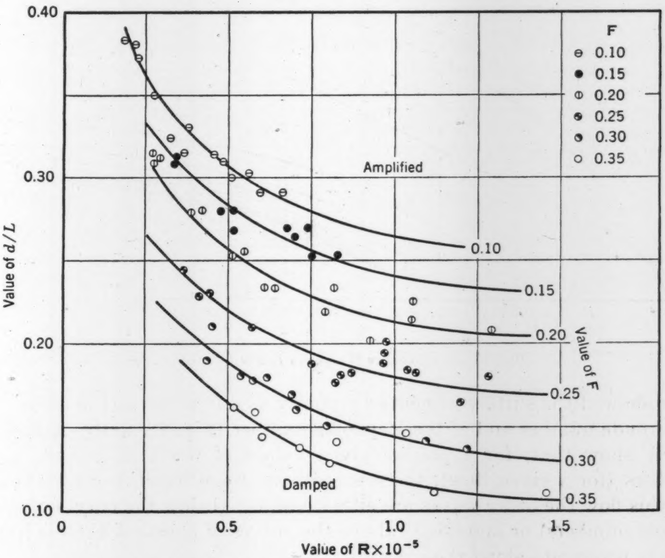

FIG. 3.—RELATIONSHIP OF d/L VERSUS **R** FOR CONSTANT **F**

Because there is no sound theoretical solution for the determination of the stability conditions, an experimental, direct approach appears to be a unique method and may yield satisfactory results. In order to obtain the stability conditions for oscillatory gravity waves in water flowing in a smooth channel, the steepness and the ratio, d/L, of stable waves were determined experimentally and were plotted versus the Reynolds number of the primary flow. A series of curves was obtained for constant values of Froude numbers, as shown in Figs. 2 and 3. Each curve is similar in shape to the one obtained by Mr. Yih for the small-amplitude waves in laminar flow. In the Yih solution for each slope of the channel bottom, a hyperbolic type of curve, with arms extending in the directions of the wave number and the Reynolds number, separates the stable region from the unstable region.

From Figs. 2 and 3, two new graphs were obtained; one showed the curves of constant Reynolds numbers for L/d versus the Froude number (Fig. 4), and the other showed the surface of neutral stability as a function of the ratio, L/d, of the Froude number and of the Reynolds number (Fig. 5). Figs. 2, 3, 4, and 5 clearly show that, for a pair of given values of the Froude and Reynolds numbers (for a given flow), there is only one wave which is neutrally stable. For this flow the other waves are either damped (below the curves of constant Froude numbers) or amplified (above the curves of constant Froude numbers) as they propagate along the channel.

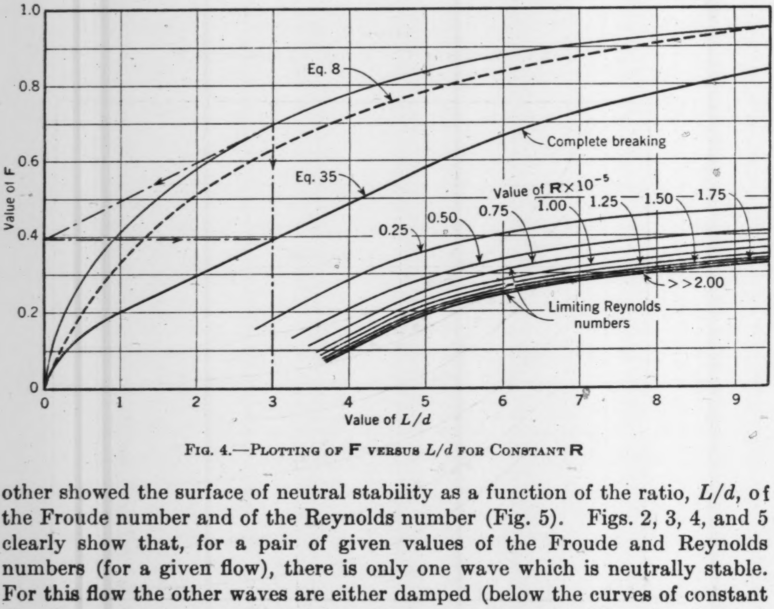

FIG. 4.—PLOTTING OF **F** VERSUS L/d FOR CONSTANT **R**

Obviously, a wave amplified along its course cannot grow indefinitely. After a certain distance during which the wave continuously grows in amplitude, breaking occurs near the crest and is accompanied by foam extending down the front slope of the wave. The foam appears to be detached from the mass of the water and to roll over the advancing face. The subsequent development of the wave was not examined; thus, the possibility of stabilization of a wave by breaking is excluded from consideration herein.

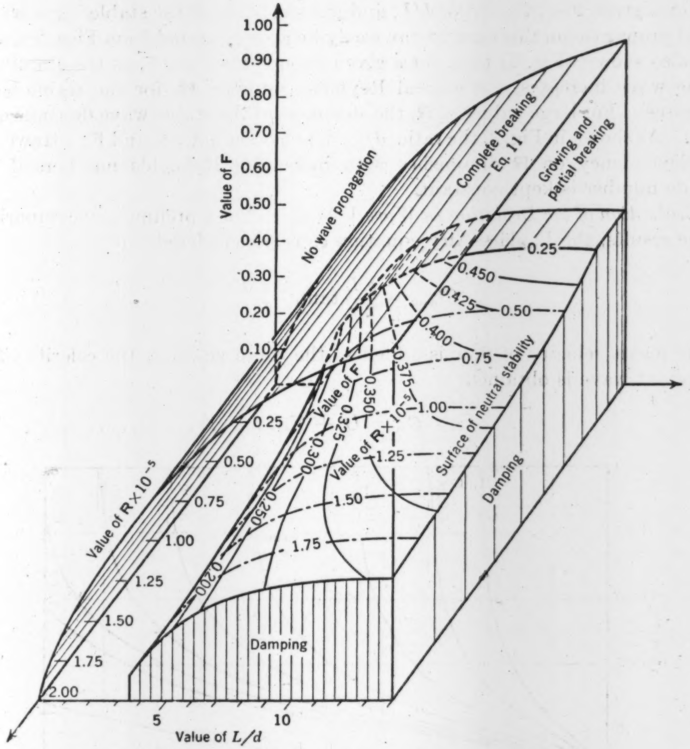

Fig. 5.—Surface of Neutral Stability—Triaxial Graph

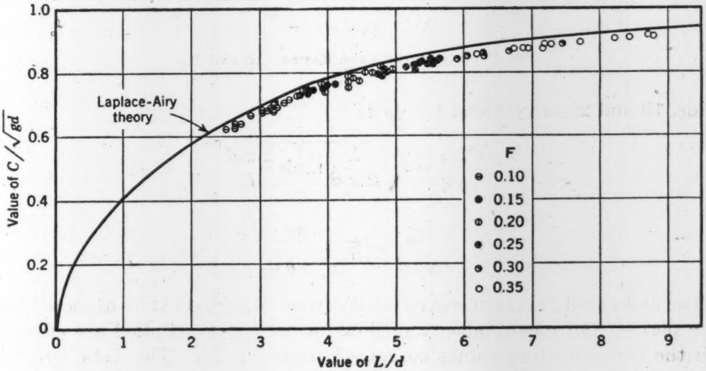

Fig. 6.—Comparison with Laplace-Airy Theory

For a given flow, the ratio, d/L, and the steepness of the stable wave which would propagate on this current can easily be approximated from Figs. 2 and 3. It is also shown (Fig. 2) that, for a given Froude number, **F**, as the amplitude of the wave increases, the critical Reynolds number, **R**, for the stable wave decreases. For large values of **R**, the steepness of the stable wave depends only on **F**. As shown in Fig. 3, the ratio, d/L, depends on both **R** and **F**. However, the dependency on **R** diminishes with increasing Reynolds numbers if the Froude number is kept constant.

Evaluation of the Deviation in Wave Velocity.—For a preliminary comparison of the results, the Laplace-Airy equation can be considered:

$$C^2_{\alpha=0} = \frac{g\,L}{2\,\pi}\tanh\frac{2\,\pi\,d}{L} \qquad (19)$$

If the mean velocity of flow is added to the wave velocity, the celerity of an ascendant wave is obtained:

$$C_m = \bar{U} + V_m \qquad (20)$$

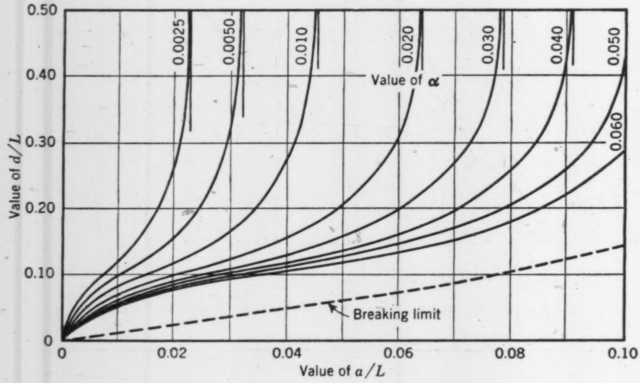

FIG. 7.—PARAMETER α FOR RATIOS, a/L AND d/L

If Eqs. 19 and 20 are divided by $\sqrt{g\,d}$,

$$\frac{C_{\alpha=0}}{\sqrt{g\,d}} = \sqrt{\frac{L}{2\,\pi\,d}\tanh\frac{2\,\pi\,d}{L}} \qquad (21)$$

and

$$\frac{C_m}{\sqrt{g\,d}} = \mathsf{F} + \frac{V_m}{\sqrt{g\,d}} \qquad (22)$$

The computed values of wave celerity from measured values of wave length, wave period, and mean velocity of flow for each wave studied are compared with the corresponding values computed from Eq. 21. The data, presented graphically in Fig. 6, show that ascendant waves consistently propagate more slowly in flowing water than the Laplace-Airy theory indicates. However, in this theory the significance of the comparison is limited by the fact that the effect of wave steepness on the celerity of the wave is not considered.

According to Mr. Struik,[3] the celerity of a wave, C_t, in the third approximation, is given by

$$C^2_t = \left(\frac{g\,L}{2\,\pi}\tanh\frac{2\,\pi\,d}{L}\right)\left[\,1-\left(\frac{\pi\,a}{L}\right)^2 A\,\right] \ldots\ldots\ldots\ldots (23)$$

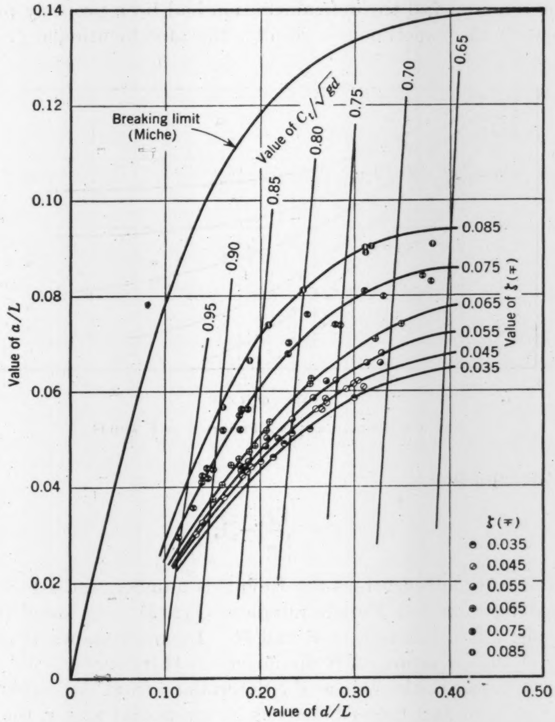

FIG. 8.—DEVIATION ζ AS A FUNCTION OF a/L AND d/L

in which

$$A = \frac{1}{8}\left(\,9\coth^4\frac{2\,\pi\,d}{L} - 6\coth^2\frac{2\,\pi\,d}{L} + 5\,\right)\ldots\ldots\ldots\ldots (24)$$

Thus, the velocity is a function of the wave steepness as well as of the ratio, d/L. The factor, A, becomes increasingly important as the ratio, d/L, becomes smaller. In order to show this importance and to facilitate the computation of C_t, a parameter, α, which is defined by the expression,

$$\frac{C_t}{C_{\alpha=0}} = 1 + \alpha \text{.........................} \quad (25)$$

is introduced into the analysis. The values of α are taken from Fig. 7 for corresponding values of wave steepness and the ratio, d/L, and the values of $C_{\alpha=0}$ are computed from Eq. 19. For the same parameters, Fig. 8 gives the values of C_t directly although less reliably because of the large variation of the celerity with wave steepness.

After the fundamental theoretical solution had been properly prepared for comparison with the experimental results, the aforementioned ζ, which was

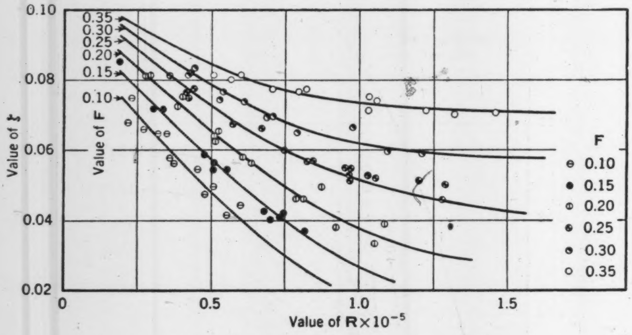

FIG. 9.—DEVIATION ζ AS A FUNCTION OF **F** AND **R**

defined by the equation,

$$\zeta = \frac{V_t}{V_m} - 1,$$

was computed and plotted versus the Reynolds number, and a series of curves was obtained for constant Froude numbers (Fig. 9). As found from dimensional analysis, ζ is a function of **F** and **R**. Figure 9 shows that for **F** the dependency of the deviation on **R** diminishes as **R** increases.

In order to compare the values of ζ determined from the experiments with those obtained from Mr. Biésel's analysis for sinusoidal waves, the ratio, d/L, was plotted versus **F** for neutrally stable waves; a series of curves of constant, ζ, was obtained in Fig. 10(a). Eq. 5 is presented in the same manner as in Fig. 10(b) for $U_0/U_1 = K = 1.34$, which was determined from the velocity profiles that were obtained experimentally. The similarity in trends of the experimental and theoretical results is obvious. Their agreement is not remarkable which, however, is to be expected because in the analysis turbulence was not taken into consideration, and the waves were of infinitesimal amplitude. As a result of the latter limitation, the mass transport in the direction of wave motion was impossible.

In Fig. 8, the deviation, ζ, is presented as a function of the ratio, d/L, and of the wave steepness. For the values of d/L less than approximately 0.40, ζ increases rapidly with increasing wave steepness. As the ratio, d/L, becomes larger, the wave steepness becomes the dominant factor. It should be remembered that the foregoing comparison and conclusions have until now been made only for experiments in which the channel walls and bottom were smooth. For a channel with an artificially roughened bottom and smooth sides, similar plots are presented in Figs. 11, 12, and 13, in which it is shown that the deviation for the roughened channel is greater than the corresponding deviation for the smooth channel.

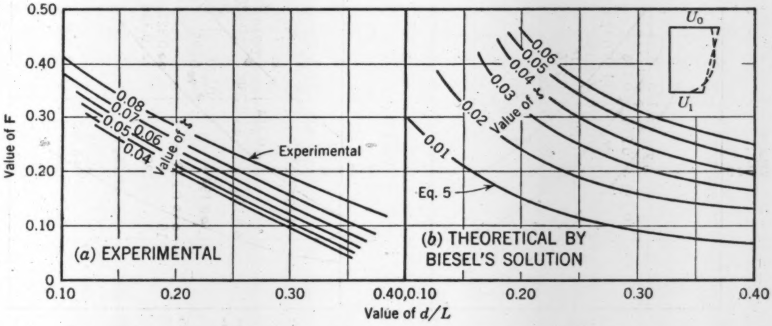

FIG. 10.—DEVIATION ζ AS A FUNCTION OF F AND d/L

Unfortunately, it is not possible to arrive at a definite conclusion about the dependency of the deviation on the Reynolds number, R. Moreover, a careful examination of Figs. 13 and 14 reveals that, for a given Froude number, F, the deviation does not vary greatly with the degree of roughness. Therefore, the dependency of the deviation on R is slight. However, there is some question whether, in the case of an artificially roughened channel, the deviation is a function of F alone or depends also on R. This point could be clarified by

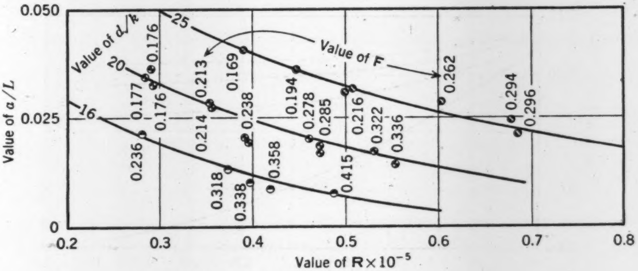

FIG. 11.—VARIATION OF a/L VERSUS R, d/k CONSTANT

means of experiments with new roughness elements geometrically similar to the one previously used but of different size. Such experiments would provide a family of plots with a constant **F** for each plot. Each one would contain a series of curves for constant relative roughnesses as a function of the deviation

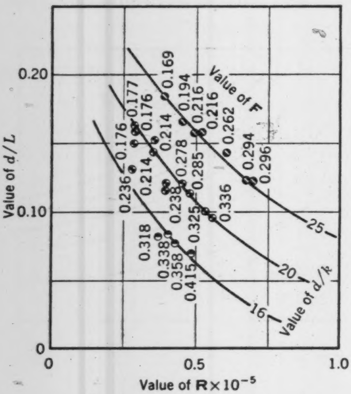

Fig. 12.—Variation d/L versus **R**, d/k Constant

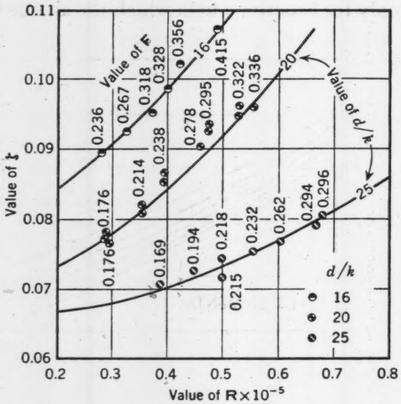

Fig. 13.—Variation ζ versus **R**, d/k Constant

and **R**. Such a family of curves (Fig. 14), although it is incomplete, is based on a Froude number of 0.30.

Relationship Between Ascendant and Descendant Waves.—If waves are generated in a fluid which is already in motion by means of placing the wave generator near the middle of the flume, it is observed that descendant waves are much longer than ascendant waves although their period is equal.

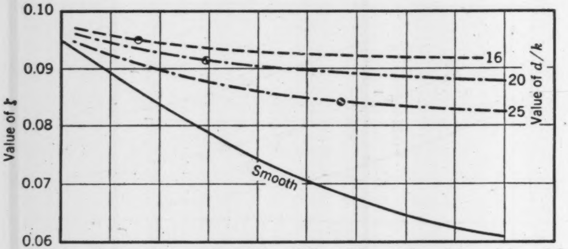

Fig. 14.—Plots of ζ versus **R**, **F** = 0.30 and d/k Constant

According to the Laplace-Airy solution, the ratio of the lengths, L_a and L_d, of an ascendant wave and a descendant wave of the same period can be written as follows:

$$\frac{\dfrac{L_d}{d}}{\dfrac{L_a}{d}} = \frac{\sqrt{\dfrac{L_d}{2\pi d}\tanh\dfrac{2\pi d}{L_d}} + \mathsf{F}}{\sqrt{\dfrac{L_a}{2\pi d}\tanh\dfrac{2\pi d}{L_a}} - \mathsf{F}} \qquad (26)$$

Constant Froude numbers are plotted versus L_d/d and L_a/d in Fig. 15 in which the periods, T_a and T_d, for ascending and descending waves are equal. Fig. 15 shows that a descendant wave propagates faster than an ascendant wave if both waves have the same period and travel in the same flow. This fact becomes more apparent as the Froude number is increased; the difficulty of testing descendant waves in a short test channel is thereby demonstrated. The limiting barrier beyond which no ascendant wave propagation is possible (Eq. 11) is also shown.

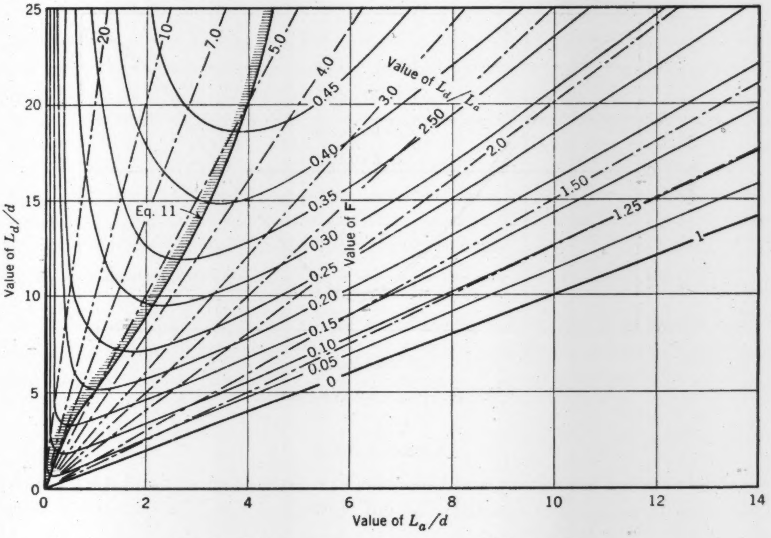

FIG. 15.—RELATIONSHIP OF L_d/d VERSUS L_a/d, $T_a = T_d$

Comparison of Theoretical and Experimental Wave Profiles.—Typical experimental profiles selected from the numerous runs are compared with the theoretical profiles given by Eq. 3:

$$\begin{aligned}\eta = {} & \tfrac{1}{2}\, m\, \delta^2 \coth m\, d + [1 + \tfrac{3}{8}\, m^2 \delta^2 \tanh^2 m\, d(1 + 2\coth^2 m\, d)]\, \delta \cos m\, x \\ & + \tfrac{1}{4}\, m\, \delta \coth m\, d(3\coth^2 m\, d - 1)\, \delta \cos 2\, m\, x + \tfrac{3}{64}\, m^2 \delta^2 (3\coth^2 m\, d - 1) \\ & \times (3\coth^4 m\, d + 1)\, \delta \cos 3\, m\, x \qquad (27)\end{aligned}$$

in which δ is determined from the equation,

$$a = 2\,\delta[1 + \tfrac{3}{64}\, m^2 \delta^2 (9\coth^6 m\, d + 13\coth^4 m\, d + 11\coth^2 m\, d - 1)] \qquad (28)$$

Although no theoretical function represents the wave profile exactly for all possible combinations of the ratio, *d*/*L*, and wave steepness, it was found that Eq. 27 gives the most consistent agreement between observations and theory within the range tested. The deviation was as follows: For large amplitudes the experimental profiles have a sharper crest with more gentle side slopes and a flatter trough than is given by the theory whereas the lower amplitudes exhibit opposite characteristics.

Thus, for the amplitudes and depths examined in this investigation, the experimental profiles vary about the theoretical profile, as described by Mr. Struik.[3] The wave profile in Fig. 16 is representative of the numerous profiles tested.

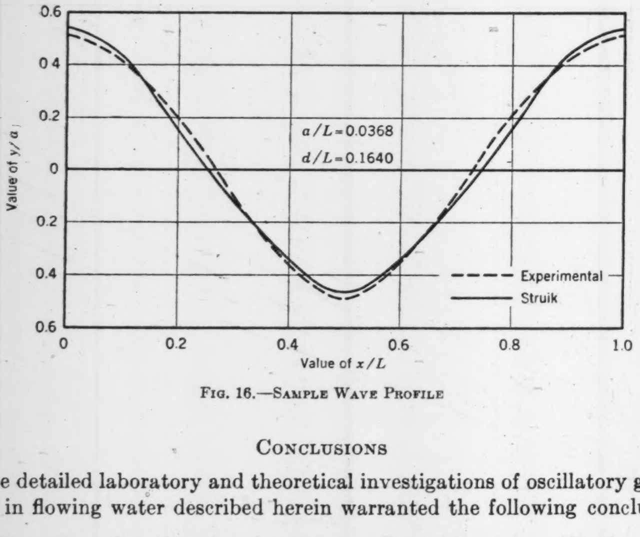

FIG. 16.—SAMPLE WAVE PROFILE

CONCLUSIONS

The detailed laboratory and theoretical investigations of oscillatory gravity waves in flowing water described herein warranted the following conclusions:

1. For a given flow there is only one neutrally stable wave. All other waves show either exponential damping or amplification during their propagation along the channel. It is easy to separate the two regions by the surface of neutral stability, determined experimentally and presented graphically. In view of the complexity of stability phenomena, it is difficult to find a reasonable solution for the stability of oscillatory gravity waves in flowing water. No basic solution is presented herein, and the theoretical determination of this problem will have to be investigated further.

2. The celerity of a stable ascendant wave in flowing water may be as much as 10% smaller than that obtained from the theories of Messrs. Stokes and Struik.[2,3] This finding is contrary to the commonly held assumption that the characteristics of waves propagated in flowing water are identical with those propagated in still water. Thus, the rule of superimposition is not permissible; two presently existing theories are found inadequate for waves in flowing water.

The deviation of the measured wave velocity from that obtained from potential theory increases with increasing Froude numbers and decreases with increasing Reynolds numbers. The larger the Reynolds number the smaller the dependency of the deviation on it.

3. For a channel with an artificially roughened bottom, the deviation is greater than the corresponding deviation in a channel with a smooth bottom. For example, for a Froude number, 0.30, and a Reynolds number, 10^{-5}, deviation is approximately 6% for a smooth channel and approximately 9% for a rough channel. For rough channels, however, there can be no conclusion as to the dependency of the deviation on the Reynolds number because of experimental limitations; indications are that the Reynolds number has little or no effect on the deviation.

4. The experimentally determined profiles of stable, ascendant, oscillatory gravity waves vary about the theoretical profiles described by Mr. Struik.[3] It was found that Mr. Struik's profile equation gives the most consistent agreement between observations and theory within the range tested.

5. Hydraulic engineers concerned with the problems of oscillatory gravity waves in flowing water should consider this paper a basic introduction to the body of knowledge and small amount of literature available. There remain many unsolved theoretical and practical problems. In order to solve them, one should have an understanding of the mechanics involved and an appreciation of the importance of sound theoretical concepts.

ACKNOWLEDGMENTS

The experiments reported herein were conducted at the Iowa Institute of Hydraulic Research at Iowa City. The writer is indebted to John S. McNown and Hunter Rouse, Members, ASCE, and Mr. Yih for advice and criticism. He is also indebted to Mr. Keulegan for reading the manuscript.

APPENDIX. NOTATION

The following symbols, adopted for use in the paper and for the guidance of discussers, conform essentially with "American Standard Letter Symbols for Hydraulics" (ASA Z10.2—1942), prepared by a committee of the American Standards Association with Society representation and approved by the association in 1942:

a = wave amplitude;
a/L = wave steepness;
b = width of flume;
C = celerity of wave;
C_m, C_t = measured and theoretical celerities;
d = depth of flow;
d/L = ratio;

d/k = relative roughness;
$\mathsf{F} = \bar{U}/\sqrt{g\,d}$, Froude number;
g = gravitational acceleration;
k = height of roughness element;
L = wave length;
L/d = relative length of wave;
$m = 2\,\pi/L$;
T = wave period;
$\bar{U}$ = mean velocity of flow;
U_0, U_1 = surface and bottom velocities of primary flow;
V = velocity of wave;
V_m, V_t = measured and theoretical wave velocities;
w = width of roughness element;
α = a parameter;
β = chanel-shape factor;
$\zeta = \dfrac{V_t - V_m}{V_m}$, deviation;
λ = spacing of roughness elements;
λ/w = relative spacing of roughness elements; and
ν = kinematic viscosity of the fluid.

AMERICAN SOCIETY OF CIVIL ENGINEERS
Founded November 5, 1852
TRANSACTIONS

Paper No. 2874

PERMEABILITY, PORE PRESSURE, AND UPLIFT IN GRAVITY DAMS

By Roy. W. Carlson,[1] A. M. ASCE

With Discussion by Messrs. Bryant Mather, J. Laginha Serafim, Serge Leliavsky, and Roy W. Carlson

Synopsis

Findings are presented of studies concerning the intensity of pore pressure in concrete dams and the resulting uplift force. The low permeability of concrete, even with as little as 2 bags of cement per cu yd, indicates that equilibrium pore pressure should never develop in a service dam. The effect of air entrainment is to reduce the penetration of pore pressure into a dam to a fraction of the penetration without air. An approximate solution for the determination of the percentage area subject to uplift pressure is offered; the area is expressed in terms of known voids and of the ratio of the elastic modulus of the solid constituents of the concrete to that of the composite concrete. The effective area is deduced to be approximately 100% of the gross area in the lean concretes investigated. However, in view of the low permeability, high intensity of pore pressure need never develop in the interior of a gravity dam if reasonable precautions are taken. Also, expansive strains caused by saturation and pore pressure are reported. These strains tend to increase the compressive stress near the upstream face and further improve the safety of a dam. Current (1956) design practice may, therefore, be overly conservative.

Introduction

One of the most doubtful steps in the design of a gravity dam is the allowance to be made for uplift pressure. The actual uplifting force caused by water in the pores always has been an uncertain factor. There has been doubt not only about the intensity of pressure in the pores of the concrete but also about the effective area over which that pore pressure acts.

Note.—Published, essentially as printed here, in May, 1955, as *Proceedings-Separate No. 700*. Positions and titles given are those in effect when the paper or discussion was approved for publication in *Transactions*.

[1] Cons. Engr., Berkeley, Calif.

The intensity of pore pressure in a dam depends primarily on the permeability of the concrete and the length of time the reservoir remains filled; it also depends on such factors as drainage and location of joints or cracks. Even without drains or joints, it may take centuries of the reservoir being full for equilibrium to be established—that is, for there to be a linear distribution of pore pressure from heel to toe. Despite this fact, most designs are based on some sort of equilibrium condition. Thus, the intensity of pore pressure to be expected in a particular dam seems to be worthy of study.

Differences of opinion have been aired for many years as to the effective area over which pore pressure acts, and many conflicting statements have appeared.[2] At first thought, it would appear that simple tests or measurements could be made to determine the uplift force caused by water pressure in the pores of concrete. The problem is not so simple, however, because, as long as the concrete is not jointed and pore pressure varies linearly from heel to toe, the stress distribution is the same when uplift pressure is acting as when there is no pressure. For example, one can assume the existence of a dam which is loaded by filling the reservoir so quickly that there is no pore pressure and whose dimensions and weight are such that the downward pressures are 100 lb per sq in. at the heel and 400 lb per sq in. at the toe. Pore pressure of an intensity varying linearly from 200 lb per sq in. at the heel to zero at the toe can then be added; the net downward force is still 100 lb per sq in. at the heel and 400 lb per sq in. at the toe in order to maintain a force balance. After the pore pressure has been added, however, the solid framework of the concrete near the heel is subjected to a tension of about 100 lb per sq in. of gross area (assuming approximately 100% of effective area) while the compression force in the pores is 200 lb per sq in. Should the concrete have been unable to carry the tension of 100 lb per sq in., a crack would have formed and 100% of area would surely have been subjected to pore pressure in the region of the crack—the stress distribution must then have been altered. Stress measurements alone would have given no clue as to the effective area in any part of the dam before failure or in the uncracked part after failure. The safety of the dam depends on the effective area even though the stresses may be unaffected. Only by measurements of strains or by tests depending on ultimate strength does there seem to be any hope of determining the effective area on which pore pressure acts.

DESIGN ASSUMPTIONS

The various agencies which are building dams have disagreed rather widely as to the uplift assumptions to be used in designing a gravity dam. The Bureau of Reclamation, United States Department of the Interior (USBR), has sometimes specified that the effective area should be two-thirds of the total area and that the pore pressure should vary linearly from full-reservoir pressure at the upstream face to tailwater pressure at the downstream face. The various districts of the Corps of Engineers, United States Department of the Army, have differed among themselves in the past, but many have used the assumptions of 100% area and two-thirds (more or less) of full-reservoir pressure at the upstream face, diminishing linearly to tailwater pressure at the downstream face. Occasionally, designers take advantage of drainage and assume reduced pore pressure at the location of the drains—the pressure then varying linearly to reservoir pressure at the upstream face and linearly also (but at a more gradual slope) from the drains to the downstream face. It is doubtful if any assumptions as to intensity of pore pressure are very close to the conditions which exist in the dams. There is less doubt about the area over which pore pressure acts in concrete, but, nevertheless, disagreement exists here also. Therefore, a better understanding of permeability, pore pressure, and resulting uplift pressure might serve to revise design assumptions to a sounder, more consistent, and more economical basis.

---

[2] "The Significance of Pore Pressure in Hydraulic Structures," by L. F. Harza, *Transactions*, ASCE, Vol. 114, 1949, p. 193.

TEST PROGRAM

Late in 1948, conferences were held in the Office of the Chief of Engineers to consider what tests could be made to clarify the question of uplift in gravity dams. At the outset, two phases of the problem were recognized. The intensity of pore pressure, as controlled by permeability, dimensions, duration of full reservoir, and other factors, was considered to be the more important phase of the problem. The uplift force caused by the pore pressure and the attendant strains in the concrete were grouped together as the second, and more difficult, phase of the problem.

The permeability of mass concrete was believed to be especially important in view of the trend toward lower cement content and the use of air entrainment.

All indications were that uncracked, rich concretes are so impermeable that pore pressure cannot develop to anywhere near the equilibrium condition in the body of a dam unless the reservoir is full for centuries; even lean concretes may be impermeable enough to permit lower pore pressure to be assumed in design. Very little is known about the permeability of lean concretes such as are (1956) being used in gravity dams, especially at greater ages and with air entrainment. The effect of continued saturation also is highly speculative and yet it may be a large factor in reducing the percolation of water into a gravity dam. Consequently, a program of permeability tests was developed to solve the first phase of the problem.

The permeability tests were planned to investigate a variety of concretes with special emphasis on the effects of (*a*) cement contents as low as 2 bags per cu yd, (*b*) air entrainment, (*c*) ages up to several years, and (*d*) continued saturation. Many refinements were introduced to be sure that the results would reveal the actual permeability of corresponding concrete in a gravity dam. Specimens were cast in metal containers and turned on their sides before setting in order that the permeability be measured in a direction corresponding to the horizontal direction in a gravity dam. Temperatures were controlled to simulate those in an actual dam. Water was controlled as to air content to prevent abnormal release of air within a specimen, where the pressure drops sharply. The tests were made in the Engineering Materials Laboratory of the University of California, at Berkeley, under the direction of Raymond E. Davis,[3] M. ASCE.

---

[3] "Permeability and Triaxial Tests of Lean Mass Concretes," by Raymond E. Davis, Report to the Chief of Engrs., U. S. Dept. of the Army, 1950 (mimeographed).

In addition to the permeability tests, another program of tests was developed to determine the effective area over which pore pressure acts and the strains which are caused by pore pressure. Although most engineers seemed to be convinced that the effective area was certain to be either nearly 100% or exactly 100%, there was a need for experimental verification in the working-stress region. Previous tests had indicated approximately 100% of area in specimens at time of failure, but no tests had yet been made to determine the effective area at working stresses. Some compression tests, however, had been reported which appeared to show that the area was about 100% in specimens subjected to moderate hydrostatic pressure. Current (1956) investigations proved that the interpretation of these tests was faulty because the hydrostatic compressibility was not dependent on pore area but only on the elastic properties of the solid constituents of the concrete. Furthermore, it was highly desirable to know what volume changes were to be expected from saturation and pore pressure in order that any accurate predictions could be made of stress at the heel of a gravity dam.

Many types of tests for determining effective pore area were suggested before one finally was adopted. The early preference was for tests of models of gravity dams, but no ready solutions were found for the many difficulties of obtaining results which would truly be indicative of uplift force. Therefore, the specimen finally adopted was a long cylinder which would be subjected to hydrostatic pressure around the sides and to mechanical pressure at the ends. Thus, there would be full pore pressure in the central region of the cylinder, diminishing to zero near the ends. Simultaneously an axial load could be applied at the ends of the cylinder, corresponding to expected heel stress in the dam. Strains were measured at the center of the cylinder to indicate change in length whenever hydrostatic or mechanical loads were applied or removed. In order to interpret the data, strain meters were embedded in companion specimens of the permeability series, and these specimens would be saturated and subjected to full hydrostatic pressure.[3]

RESULTS OF PERMEABILITY TESTS AND THEIR IMPLICATIONS

Many interesting revelations were obtained from the permeability tests, but only a few will be cited. In the particular mass mixes used, the permeability of 2-bag-per-cu-yd concrete averaged less than three times that of 3-bag-per-cu-yd concrete at the age of 3 months. Thus, the average permeability of the 2-bag-per-cu-yd concretes was only 580×10^{-12} cu ft per sec per sq ft for a unit pressure gradient. The same specimens, left saturated and retested at an age of 1 yr, showed a reduction in permeability to a fraction of the 3-month value.

Specimens tested at ages of 3 months, 18 months, and 24 months showed a progressive decrease in permeabilities, the average for 2-bag-per-cu-yd concretes being only 135×10^{-12} cu ft per sec at the age of 2 yr. An interesting revelation was that the 3-month specimens when retested at 1 yr were as impermeable as companion specimens initially tested at 2 yr. Thus, the saturation and testing at 3 months apparently hastened the process of hydration and lowering of permeability.

In the very lean mixes, the sand fineness had a significant effect on the permeability—the finer the sand, the lower the permeability. For the 2-bag-per-cu-yd mix, sand with a fineness modulus of 2.25 and a water-cement ratio of 0.86 resulted in a 2-yr permeability average of 81×10^{-12} cu ft per sec whereas a fineness modulus of 2.50 and a water-cement ratio of 0.80 gave a permeability average of 190×10^{-12} cu ft per sec. The finer sand more than offset the effect of the higher water content in this case.

The effect of air entrainment on permeability was favorable. For mixes having the same cement content, aggregate grading, and consistency, the permeability was 439×10^{-12} cu ft per sec for an air content of 6.2% and 662×10^{-12} cu ft per sec for the corresponding mix with no air-entraining agent but with 1.4% of air. Thus, the air entrainment reduced the permeability in this particular case by 34%. The mix in this case was 2.25 bags of cement per cu yd, the only one in which the effect of air entrainment was investigated.

In addition to reducing the actual permeability, the air entrainment delays the penetration of water into a mass of concrete by a much larger additional factor due to the storage capacity for water provided by the voids. In a dam the size of Detroit (Oregon) or Pine Flat (California), about 20×10^6 gal of water would be required to fill the voids produced by 5% of entrained air. Therefore, it may be worth while to compute the probable rate of penetration of water into a gravity dam under the pressure of a full reservoir.

As the water front moves farther into the concrete, it may be assumed that the air voids are completely filled by water behind the water front. Because water is relatively incompressible, very little additional water is needed to accommodate the reduction in volume as the pressure increases behind the advancing water front. Therefore, it can be assumed that a linear pressure gradient will prevail from reservoir level at the upstream face to zero at the farthest depth of water penetration, provided that the reservoir level remains constant. Under these assumptions, the following equation expresses in feet the distance D penetrated by water in T days into a mass of concrete in which the voids are 5%, the water head is 400 ft, and the permeability is 200×10^{-12} cu ft per sec:

$$D^2 = 0.2767\, T \qquad (1)$$

The permeability of 200×10^{-12} cu ft per sec was chosen for this example because test results indicate it to be about the 1-yr value for concrete containing only 2 bags of cement per cu yd. Of course, the permeability would be greater at earlier ages, but the reservoir is not likely to be filled before at least 1 yr after the concrete near the foundation is placed, and the permeability may be much lower at the ages indicated for deep penetration of water into the dam. Furthermore, Eq. 1 applies only to the case in which there is no relief by internal drains or ungrouted joints.

Fig. 1 shows the penetration of water into a 400-ft dam for various durations of full reservoir as computed by Eq. 1. Fig. 1 applies only to the continuous concrete of the dam and would be modified greatly near the base of a dam whose foundation is permeable. It would be modified considerably also if there were no air entrainment. After 200 yr of full reservoir, the indicated penetration is less than half the thickness of the dam. Under the conditions of this example (no joints or drains, no reduction in permeability after the age of 1 yr, and no drying from the downstream face), the water should appear at the downstream face in somewhat more than 1,000 yr. Of course, this applies only to sound concrete and does not consider the foundation to be permeable. However, it does definitely indicate that, as far as the concrete itself is concerned, low internal pore pressures are likely to prevail either with or without drainage, and that only a slight drainage would be effective against so slow a percolation rate.

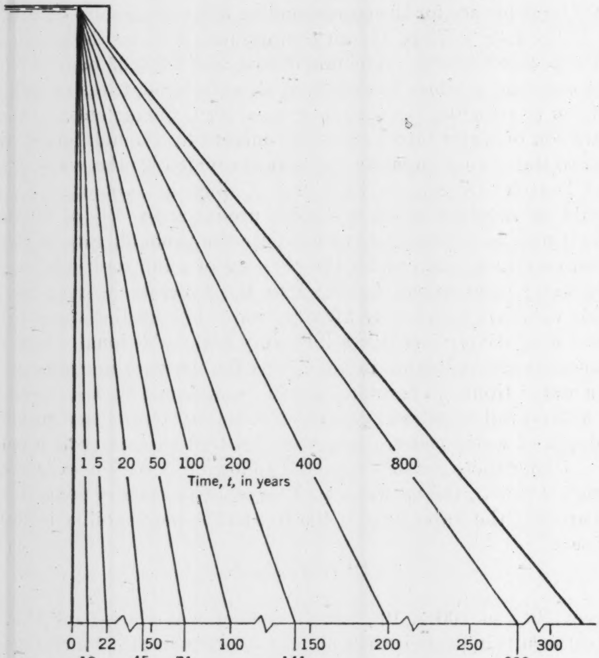

Fig. 1.—Penetration of Water into 400-Ft Dam for Various Durations of Full Reservoir

The foregoing considerations of permeability have neglected the effects of capillarity. An investigation of the computed and observed rates of penetration of water into the permeability specimens indicated that the rates were approximately as expected without any allowance for capillarity. However, it must be recognized that an abnormally large gradient existed in the specimens and that the effect of capillarity would, therefore, need to be very large to be evident. An investigation of the quantitative effect of capillarity is sorely needed.

Uplifting Force Produced by Pore Pressure

The problem of determining the area subject to pore pressure was hampered by erroneous beliefs of long standing and by the inherent complexity of a material like concrete. It was I. L. Tyler, M. ASCE, who disproved the long-published statement that the hydrostatic compressibility of concrete is related to the effective pore area. Douglas McHenry, M. ASCE, uncovered fallacies in several analyses which were developed by individuals and offered in review. Many others also helped in the slow progress toward a partial clarification of the problem of determining effective pore area.

When the test program was planned, it was believed that the only difference between a specimen subjected to full hydrostatic pressure and one with hydrostatic pressure around the sides only (ends open) would be the uplift forces caused by the pore pressure being zero at the ends in the latter case. Thus, it was specified that a simple subtraction of the strains in the two corresponding specimens would yield the strain caused by uplift. This strain was to be converted into uplift force by determining the axial load required to produce an equal strain. Later, it was proved that the difference was bound to yield 100% of "effective" area if the measurements were accurate. It became apparent that the step of going from a specimen loaded hydrostatically all around to a specimen loaded hydrostatically on the sides only amounted to removing the load both from the "effective" and from the "noneffective" area at the ends of the first specimen. Thus, the test program could not yield the effective area of the mass concretes in the simple manner which had been anticipated.

Using the observed strains as a guide, an approximate solution of the effective pore area of concrete was developed. The concrete was idealized to the extent of assuming most of the solids to be accumulated into cubes, regularly arranged, and connected by the remainder of the solids. At first thought this might seem to be an intolerable departure from actual concrete, but relative dimensions—instead of being chosen at random—were computed to make all pertinent properties identical with those of the concrete. Thus, the idealized concrete could be computed to have the correct void content, the correct modulus of elasticity of solid constituents (provided they are uniform), the correct modulus of elasticity of the concrete as a whole, the correct Poisson ratio for the solid constituents, and approximately the correct Poisson ratio for the concrete as a whole. It can be shown that an idealized concrete made up of a porous solid of uniform elastic properties will have a Poisson ratio of from about one-half to two-thirds that of the solid material, purely by virtue of the geometry. Thus, this idealized concrete is an accurate "particular" case of concrete although it evidently is not a general case.

The mechanics of the uplifting force in concrete have been clarified somewhat by the simplified analysis presented in the Appendix. For example, it can be proved that the uplift force on any section depends only on the pore pressure and area at that section and not on the area at other sections. Of course, there may be other forces applied in a dam, such as those caused by temperature changes, water loads, and gravity. However, what one defines as uplift is simply a matter of pore pressure and area at that section. This is contrary to a common belief about forces in specimens such as those tested by Mr. Davis.[3] It has sometimes been declared that the uplift on a section in the central region where a uniform pore pressure exists not only is caused by the diminution in pore pressure near the ends, but is dependent on the effective pore area near the ends where the pore pressure diminishes. It can be proved that no matter what the pore area may be in the regions where pore pressure drops to zero, as long as that pressure does drop to zero, the uplift on a section at midlength is the same. Also, it no longer is considered sound to think of uplift as causing an over-all pull on the concrete. As an illustration, one might consider again the long cylinder specimens subjected to pore pressure only in the midlength region. This cylinder, for example, might have a solid lens across the specimen, this lens having substantially no pore area. Such a condition is approached by taking a section through a maximum area of aggregates and other solids. By treating the half cylinder from such a section to one end (where forces are zero) as a free body, it is seen that there is no force on this section; this proves that there is no over-all pull on the specimen, but suggests instead that the uplift is produced locally by the pore pressure acting as a jack within the pores. As a contrast to the assumed solid section, one might find a section with a full 100% of pore area, such as a joint. Here the uplift would act over the whole area, and this would be the worst section, quite independent of pore areas elsewhere.

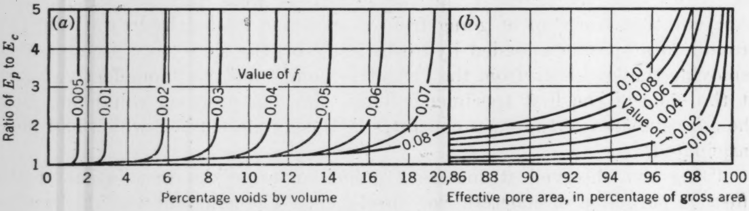

FIG. 2.—THE RELATIONSHIPS BETWEEN MODULI RATIO, VOID PERCENTAGE, AND PORE AREA FOR VARIOUS VALUES OF f

The actual areas disclosed by the tests and idealized analysis were not far from 100% for the lean concretes used. The sectional porosity, after hydration, was approximately 15% for all the concretes containing entrained air. The ordinary modulus of elasticity varied from approximately 4×10^6 lb per sq in. for the 2-bag-per-cu-yd concrete to 5.8×10^6 lb per sq in. for the 3-bag-per-cu-yd concrete. The modulus of elasticity of the solids was found to be approximately 17×10^6 lb per sq in. Thus, the ratios of moduli were 4.25 and 2.92, respectively. The corresponding areas can be found from the curves in Fig. 2; they range from 97% to 98%, the lower area being for the richer mix. These results are consistent with those tests to failure of Serge Leliavsky, M. ASCE, which are probably the most reliable to date.[4]

A surprising revelation came from applying the area equation to minerals. The physical properties of most aggregates indicate that they possess 100%

---

[4] "Experiments on Effective Uplift Area in Gravity Dams," by Serge Leliavsky, *Transactions*, ASCE, Vol. 112, 1947, p. 444.

of effective area. Very little published information is available to show the relative compressibility of minerals with and without impermeable cover to provide the values of E_c and E_p needed for the equation. However, W. A. Zizman[5] has listed these data for a dozen rocks. For all rocks, except obsidian, the compressibility due to fluid pressure when covered was much greater than when uncovered. Therefore, it is evident that the equation, developed in the Appendix, will yield a large fractional area, especially since the sectional porosity is small in most rocks.

For example, Quincy granite had a compressibility four times as great with an impermeable cover as it had without the cover. This means that the modulus of elasticity of the solid crystals was about four times that of the composite granite. Assuming the porosity to be 1% by volume, the value of f is seen to be about 0.004 from Fig. 2(*a*). Fig. 2(*b*) shows that the effective pore area would be more than 99% if the rock structure simulates the idealized porous solid envisioned for concrete.

Apparently, the pores in most minerals exist as poor contacts between crystals because, if the small volume of pores existed as well-distributed spherical cavities, for example, no such large differences in elastic moduli could be expected.

STRAINS DUE TO SATURATION AND PORE PRESSURE

An important contribution of the laboratory investigations, mentioned previously and conducted by Mr. Davis, is the revelation of actual strains or dimensional changes which accompany saturation and pore pressure. The results are such as to make the handling of strains quite simple due to the low compressibility of the solid constituents of the concrete and to a compensating expansion of the concrete caused by saturation. The measured expansion of the concrete in the long cylinders, from the saturated state without pore pressure to the addition of 200 lb per sq in. of pore pressure (free ends), was from 5×10^{-6} in. per in. to 10×10^{-6} in. per in. less than for an ordinary tensile stress of 200 lb per sq in. This is explained by the fact that, while the solid constituents are being compressed by the pore pressure and there is only a small average uplift force, most of the strain occurs in the filler material between the larger particles, and this is under a tensile stress of approximately 200 lb per sq in. The compensating factor regarding the strains is the effect of saturation. An average of results from strain measurements on permeability specimens, obtained prior to their regular testing, showed an expansion of 7×10^{-6} in. per in. due to saturating from a mass-cured condition. Adding this to the strain caused by pore pressure, one finds a total expansive strain which is almost exactly what one would expect if the uplift were a numerically equal mechanical tension. The designer can make good use of this result in computing the modification of stress due to restraint near the upstream face of a dam when the pore pressure penetrates only a moderate distance. Also, the engineer who analyzes measured strains in a structure should be gratified to learn that the strains due to pore pressure and saturation can be treated as mechanical strains. Only if the pore pressure differs greatly from the 200 lb per sq in. herein considered, or if the concrete were not of the lean mixes tested for this study, would a deviation from the simple treatment be necessary.

---

[5] "Compressibility and Anistropy of Rocks at and near the Earth's Surface," by W. A. Zizman, *Proceedings*, National Academy of Sciences, Vol. 19, 1933, p. 666.

RECOMMENDATIONS FOR FURTHER WORK

In the course of this investigation, the lack of information on many factors was noticed. Some of the subjects suggested for additional testing or investigation are as follows:

1. *Permeability at Greater Ages.*—It is highly speculative to compute the penetration of water into a concrete dam for decades when the permeability is known only up to the age of 1 yr. Provision should be made for tests up to at least 10 yr of age.

2. *Permeability of Concrete Continuously Saturated.*—The reduction in permeability of concrete is likely to be influenced greatly by continued hydration, and the continued hydration, in turn, may be expected to be affected by the availability of water in the pores.

3. *Permeability of Concretes Containing Pozzolans.*—Because some evidence indicates a many-folded reduction in permeability as a result of the inclusion of active siliceous materials in the concrete, this subject promises a large reduction in permeability and consequent pore pressure at low cost.

4. *Permeability of Concretes Containing Different Cements and Aggregates.*—Sweeping conclusions cannot be drawn from permeability tests on a single cement and aggregate. Different types of cements and aggregates should be "tied in" with the current investigations.

5. *Physical Properties of Aggregates.*—More information is needed on the hydrostatic compressibility of aggregates, both sealed and unsealed, and on the Poisson ratio of the minerals under the two conditions.

6. *Extraneous Deformations in Concrete Subjected to Hydrostatic Pressure.*—The hydrostatic compressibility of concrete is so small that any simultaneous deformation, such as might be due to gel expansion caused by squeezing water into unfilled pores, could introduce a serious error in the interpretation. A better understanding of the effect of water pressure on concrete is needed.

7. *Compressibility of Aggregates Due to Water Pressure.*—The reported tests on compressibility of minerals were made on very small specimens with kerosene as the fluid. Corresponding tests are needed on larger specimens subjected to water pressure.

8. *Effect of Capillarity on Percolation of Water.*—In view of the large theoretical effect of capillarity on the percolation of water through concrete, tests should be made to determine the rates of penetration of water into concrete specimens in which the pressure gradient is about the same as in a typical dam.

CONCLUSIONS

a. The permeability of well-designed mass concretes, even with mixes as lean as 2 bags of cement per cu yd, are so low as to indicate that equilibrium pore pressures are not likely to be achieved in a moderate number of decades, if ever.

b. The effect of entrained air is found not only to reduce the permeability of concrete but also to delay the penetration of water into a dam by a factor of several times, by virtue of the water capacity of the air voids.

c. The effective area over which pore pressure acts in concrete can be estimated from the relative compressibilities of sealed and unsealed specimens subjected to fluid pressure.

d. The maximum effective pore area to be expected in the lean concretes tested in the current program varies from 97% in the 3-bag-per-cu-yd mix to 98% in the 2-bag-per-cu-yd mix.

e. The effective pore area in most common aggregates appears to be more than 90%.

f. The expansion due to saturation and pore pressure is a large factor in reducing the likelihood of high tensile stress near the upstream face of a gravity dam, as long as the pore pressure is localized near the face.

ACKNOWLEDGMENTS

This report, although prepared by the writer, comprises the work of R. F. Blanks, M. ASCE, and Mr. McHenry of the USBR; T. C. Powers and Mr. Tyler of the Portland Cement Association; B. W. Steele, A.M. ASCE, F. B. Slichter, M. ASCE, J. R. Gilbert, A.M. ASCE, D. A. Buzzell, M. ASCE, and R. A. Barron, A.M. ASCE, of the Office of the Chief of Engineers; and Mr. Davis of the University of California.

APPENDIX. RELATIONSHIP BETWEEN STRAINS AND PORE AREA

Before 1956, the deformation (or strain) of concrete appeared to be the only measurable action which is closely related to uplift forces. Therefore, it is of importance to derive an equation for effective pore area in terms of measured strains.

Before becoming involved and possibly confused by the general treatment of uplift forces, one might first consider an "idealized" porous solid which has many of the characteristics of concrete. The idealized concrete can be likened to the section shown in Fig. 3, in which most of the solid particles have been collected into cubes and the remainder, together with the pores, comprise a filler material between cubes. The specimen in Fig. 3 is a large sphere, and the unit cell is exactly 1 cu in. Merely for convenience, the solid cube is assumed to be 0.9 in. on a side, leaving 0.05 in. all around for filler material. For further simplicity, the filler material is pictured as fibers or columns between cubes having a sectional area of exactly 0.1 sq in. per gross sq in. In this case the total pore space can be computed to be 24.4% of the volume, the void area on a section through the solid cube is 19% (chosen so as to miss the columns of filler material), and the void area on a section between cubes is 90%.

The expression for "percentage effective uplift area" can be determined in three steps:

1. An expression is first written for stress and consequent strain due to the application of a hydrostatic load on the spherical specimen of which the 1-in. cube is an interior, unit cell. For this first step, it is assumed that the specimen has its surface sealed against entrance of pressure into the pores, or else the specimen is large enough to prevent development of pore pressure in the interior. If the test actually is made by the application of water pressure to the surface of the sphere, some relief must then be provided for the pressure which will develop in the pores due to volume change because the equations will assume zero pore pressure for this step. Actually, it is simpler to make the test by applying an axial load to a cylindrical specimen and computing the corresponding strain for triaxial load (hydrostatic) by applying a double Poisson-ratio correction, one for load in each of the other two directions. The reference condition (zero strain) requires that the specimen be fully saturated but under no stress of any kind; this applies to the succeeding two steps as well.

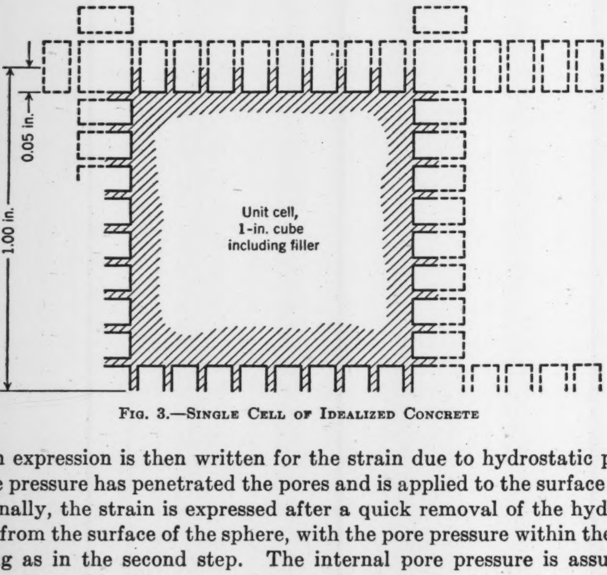

FIG. 3.—SINGLE CELL OF IDEALIZED CONCRETE

2. An expression is then written for the strain due to hydrostatic pressure when the pressure has penetrated the pores and is applied to the surface as well.

3. Finally, the strain is expressed after a quick removal of the hydrostatic pressure from the surface of the sphere, with the pore pressure within the sphere remaining as in the second step. The internal pore pressure is assumed to remain unchanged in this step, neglecting the effect of volume change, because it is desired to simulate the static condition in a dam.

It can now be shown that the change from Step 2 to Step 3 amounts to removing the pressure from 100% of the surface area, and because Step 1 amounts to applying the pressure to 100% of the area, a subtraction of the strain of Step 3 from that of Step 2 should equal the strain of Step 1, except for sign.

For the case in which the modulus of elasticity and the Poisson ratio of the solid material are known or assumed to be 8×10^6 lb per sq in. and 0.25, respectively, the solid columns in the filler material are assumed to have the same elastic properties. However, to make the case a little more general, it is assumed that this last fact was not known but that a measurement indicated the modulus of elasticity of the gross filler material to be 0.8×10^6 lb per sq in. This is merely the result of having one-tenth the sectional area. For further simplification, all expressions shall be determined for unit pressure, 1 lb per sq in., and the primary concern will be the vertical stresses in the unit cell.

Step 1.—The stress due to a surface pressure of 1 lb per sq in. is simply 1 lb per sq in. in all directions, with no pore pressure. The contribution to vertical strain by the filler material is equal to the stress times the length (0.05 in. above and 0.05 in. below, or 0.1 in.) and divided by E (0.8×10^6 lb per sq in.) and the area (1 sq in.). The Poisson-ratio effect is considered to be negligible in the filler material as far as this strain is concerned because pressure is not applied to the sides of the filler elements. The contribution to vertical strain by the solid cube is the stress times the length (0.9 in.) divided by E (8×10^6 lb per sq in.) and the area (0.81 sq in.). The Poisson-ratio effect reduces this strain by 25% for the stress in each lateral direction; the strain can simply be multiplied by 0.50 to take account of the Poisson ratio. Thus, for the total vertical strain in Step 1,

$$e_1 = -\frac{0.1}{0.8} - \frac{0.5 \times 0.9}{8 \times 0.81} = -0.1250 - 0.0693 = -0.1943 \times 10^{-6}.$$

Step 2.—Hydrostatic pressure in the pores, as well as at the surface, produces a compressive strain which is independent of the pore area. It is merely the stress divided by E(8×10^6 lb per sq in.), corrected for the Poisson ratio by subtracting 25% for each lateral direction. Thus, the strain in Step 2 is

$$e_2 = -\frac{0.5}{8} = -0.0625 \times 10^{-6}.$$

Step 3.—Quick removal of pressure from the surface of the sphere produces somewhat more complex stresses. If n is the fractional area subject to pore pressure in the filler material, the stress in the filler material is found by balancing the forces on a plane through the material and parallel to a face of the cube. The product of n and the pressure must equal the tensile force per gross square inch of filler as the external force is zero. Thus, the force in the filler is simply n pounds per square inch, based on the full area. The strain due to this force is n times the length (0.1 in.) divided by E(0.8 lb per sq in.). This must be corrected, however, for the additional expansion of the fibers due to water pressure around them, and this is the pressure (1 lb per sq in.) times the length (0.1 in.) times 0.50 (for the double Poisson ratio) and divided by E(8×10^6 lb per sq in. because of the solid fibers). In addition, there is a slight tension in the solid cube which can be found to be 0.19 lb by balancing the forces on a plane through the cube. The contribution to strain by this tension in the cube is 0.19 times the length (0.9 in.) times 0.50 to allow for the double Poisson-ratio correction and divided by E(8×10^6 lb per sq in.) and divided also by the area (0.81 sq in.). The terms for strain in Step 3 are then

$$e_3 = \frac{0.1\,n}{0.8} + \frac{0.1 \times 0.50}{8} + \frac{0.19 \times 0.5 \times 0.9}{8 \times 0.81} = 0.1250\,n + 0.0062 + 0.0132. \quad (2)$$

Inserting numerical values into

$$e_3 - e_2 = e_1 \qquad (3)$$

results in

$$0.1250\,n + 0.0062 + 0.0132 + 0.0625 = 0.1943 \qquad (4)$$

from which

$$n = \frac{0.1124}{0.1250} = 0.90.$$

Thus, it is seen that the effective pore area in the filler material (worst section) might have been found from an analysis of measured strains to be 90%, as it should be in this known case. This means that the specimen should fail when subjected to internal pore pressure (only) of an intensity about 10% above the tensile strength. However, it may be noted that the stress in the aggregate particles (cubes) is low.

It is of interest to examine the stress conditions on a practical scale before proceeding further. Suppose that the pore pressure were 200 lb per sq in. as at the base of a 460-ft dam, instead of 1 lb per sq in. The tensile stress in the fibers of the filler material of this idealized example must then be 200 × 10 or 2,000 lb per sq in. In any tensile loading of concrete, the stresses must be magnified similarly in those elements which support the stress applied to the gross section in porous regions.

Now the stress in the solid cube (simulating the aggregate) was found to be very low. In this example, in which the volume of voids was 24% (rather high for concrete), the tensile stress in the aggregate was found to be only 47 lb per sq in. (0.19 lb times 200 and divided by 0.81). Of course, this value cannot be applied directly to concrete because the volume percentage of voids has been deliberately made higher than that which would be deduced by taking a section through the aggregate. However, a fact, which is illustrated by the example, is that uplift force does not produce an over-all pull on the concrete nor is the tension anywhere near uniform from point to point. The tension is highest across sections where the void areas are greatest, which is not really surprising. Another fact illustrated by this example and consistent with strain studies on actual concrete is that the tensile strains due to the uplift force of pore pressure are almost as great as if there were actually an over-all pull on the concrete of the full amount of the "effective" uplift. This is merely a consequence of the relatively high modulus of elasticity of the solid constituents of the average concrete. The filler material (with its voids) is responsible for most of the deformation.

Development of Equation for Uplift Area

The nature of concrete is such that an exact mathematical expression for uplift cannot be developed from only those physical properties ordinarily known. For example, it is clear that any particle of aggregate which is unbonded over its entire surface should be considered to be part of the voids because it can take part in no structural action. Although aggregate particles are not likely to be unbonded over their entire areas, occasionally one may find particles to be unbonded over substantial parts of their areas and, in such cases, they would act partly as voids. Also, there are minor Poisson-ratio effects and property differences which are indefinite. Therefore, it appears inadvisable to strive for an exact mathematical expression for uplift area.

The area which must be determined is that of a section which passes through the largest possible number of voids without deviating too far from a plane section. This may be termed the "worst section" and one which yields the largest area. The requirement that it may not deviate too far from a plane section is used to avoid introducing shearing strength; this investigation is concerned only with the area of pore pressure which must be supported by tensile strength, or which produces tensile strain. It is fairly evident that an average plane section will have the same void area as the concrete as a whole, or about 15% for ordinary mass concrete with air entrainment. Thus, the worst section is a special one and highly localized. When dealing with a heterogeneous material like concrete, the worst section in one region may be somewhat different from that in another region. It should be realized that strain measured on a 10-in. gage length spans many worst sections, as well as many sections with low void areas. It appears to be expecting too much, therefore, for measured strains to reveal the one worst section. In the idealized analysis which follows, the intention is to reveal the worst plane section that might be expected with an arrangement of particles which maintains all the pertinent, known properties of the concrete.

It may be possible to obtain a fairly dependable solution of the effective-area problem by considering the concrete to be idealized as in the foregoing example. That is—assume most of the solid matter to be collected into cubes, with the remainder of the solids and the voids comprising the porous filler material between cubes. The exact quantity of filler material can be computed to satisfy the conditions, assuming that only that part of the solid matter which can be treated as columns between cubes shall be assigned to the filler. The volume of voids must be known, and the quantity of solids in the filler is then computed so as to account for the modulus of elasticity of the concrete being lower than that of the solids. Thus, Fig. 2(*a*) has been prepared to provide a method of determining effective thickness of filler material in terms of known ratio of elastic moduli and of known void content of a particular concrete. In this treatment, it is assumed that all solids have the same modulus of elasticity and the same Poisson ratio; this may be approximately true because voids are responsible for the large variations in elastic moduli among rocks. It may be seen from the development of the equation for uplift area that the Poisson ratio for composite concrete is not applicable. However, a computation will show that a reasonable ratio, considerably lower than that for the solids, is a natural consequence of the separate treatment of solids and paste (or filler).

The following is a short derivation of an equation for the effective uplift area, *n*. Because this derivation is exactly parallel with the example already given, little further explanation is necessary. The final result is independent of the Poisson ratio; because all the ingredients have the same inherent properties this is expected.

DEVELOPMENT OF MORE GENERAL EQUATION FOR EFFECTIVE UPLIFT AREA

If f is the linear amount of filler per inch (between cubes), F denotes the amount of solid per inch, P is the pore pressure, μ represents the Poisson ratio of all solid material, E_x is the modulus of elasticity of filler material (based on gross area), E_p equals the modulus of elasticity of solid material, E_c is the modulus of elasticity of concrete (composite filler and cubes), a denotes the void area $(1 - F^2)$, n is the fraction of area subject to uplift, and e represents strain—

$$e_1 = -\frac{P\,f}{E_x} - \frac{P\,F\,(1 - 2\,\mu)}{E_p\,F^2} \qquad (5)$$

for external load and no pore pressure,

$$e_2 = -\frac{P\,(1 - 2\,\mu)}{E_p} \qquad (6)$$

for hydrostatic load with pore pressure, and

$$e_3 = \frac{n\,f\,P}{E_x} + \frac{P\,f\,(2\,\mu)}{E_p} + \frac{a\,P\,F\,(1 - 2\,\mu)}{E_p\,F^2} \qquad (7)$$

for pore pressure and no external load.

The E_x-term can be eliminated by expressing it in terms of E_p and E_c. If 1 lb per sq in. is applied to layers of filler f inches thick and to a layer of solid F inches thick and F^2 in area, the sum of the deformations is that of 1 in. of the idealized concrete. Thus, the concrete strain for 1 lb per sq in. is

$$\frac{1}{E_c} = \frac{f}{E_x} + \frac{F}{F^2\,E_p} \qquad (8)$$

Solving for E_x and defining E_p/E_c as C, one finds

$$E_x = \frac{f\,F\,E_p}{F\,C - 1} \qquad (9)$$

Substituting this value for E_x wherever it appears, and further defining $(1 - 2\,\mu) = Q$, Eq. 3 leads to

$$\frac{n\,f\,(F\,C - 1)}{f\,F\,E_p} + \frac{f\,(1 - Q)}{E_p} + \frac{a\,Q}{E_p\,F} + \frac{Q}{E_p} = \frac{f\,(F\,C - 1)}{f\,F\,E_p} + \frac{Q}{F\,E_p} \qquad (10)$$

which can be simplified to

$$n = 1 - \frac{f\,F}{F\,C - 1} \qquad (11)$$

The effective area is thus expressed in terms of relative moduli of elasticity and of idealized cell dimensions. The idealized dimensions are in turn dependent on the relative moduli and the pore volume and they can be found most readily from Fig. 2(*b*).

DISCUSSION

Bryant Mather.[6]—Active consideration of the problems mentioned by Mr. Carlson is needed and, it is hoped, will be stimulated by this paper. This work by Mr. Carlson also appeared as an appendix to a report[7] published by the Waterways Experiment Station at Jackson, Miss.

The laboratory tests initiated by Mr. Davis for the Corps of Engineers have been continued by the Waterways Experiment Station. The work done at the University of California[3] and subsequent work up to 1951 by the Waterways Experiment Station have been reported on by Herbert K. Cook.[8] Results of these tests through an age of 2 yr are given in a report[7] and through an age of 5 yr in a revision thereof.[9] A summary of the average results is given in Table 1 and in this revision.[10]

TABLE 1.—Summary of Permeability Data from Tests on 14½-In. by 15-In. Concrete Cylinders at 200 Lb per Sq In.

Mix	Cement factor, in bags per cubic yard	Fineness modulus of fine aggregate	Water-cement ratio, by weight	Permeability Value,[a] K				
				3 months	1 yr[b]	1.5 yr	2 yr	5 yr
A	2.00	2.50	0.80	685	133	348	190	206
B	2.00	2.25	0.86	479	143	418	81	92
C	2.25	2.25	0.84	662	214	411	290	100
D	2.25	2.85	0.67	926	120	106	161	99
E	2.25	2.50	0.72	830	228	216	152	128
F	2.25	2.25	0.76	439	156	92	148	157
G	2.50	2.85	0.60	574	139	202	72	75
H	2.50	2.50	0.66	687	83	140	111	194
I	3.00	2.85	0.50	200	56	203	57	66
Average				609	141	237	140	124

[a] Value of K is given in cubic feet per second per square foot per foot of head per foot of length $\times 10^{12}$.
[b] The 3-month specimens were retested at an age of 1 yr. All other results are for initial testing.

J. Laginha Serafim,[11] M. ASCE.—This paper is of great interest to those who are concerned with uplift in dams because it deals with important items which have not been sufficiently considered in various publications on the subject.

The writer has had occasion to consider[12] the various aspects of uplift in masonry dams and to compare the different opinions expressed in the vast bibliography on this matter. One of the first conclusions resulting from this comparison is that there are actually three distinct problems, and not two, in the consideration of uplift:

---

[6] Civ. Engr. (Concrete Research), Concrete Div., Waterways Experiment Station, Corps of Engrs., U. S. Dept. of the Army, Jackson, Miss.

[7] "Permeability and Triaxial Tests of Lean Mass Concrete," by Bryant Mather, E. J. Callan, E. E. McCoy, and R. W. Carlson, *Technical Memorandum No. 6-380*, Waterways Experiment Station, U. S. Dept. of the Army, Vicksburg, Miss., March, 1954.

[8] "Permeability Tests of Lean Mass Concrete," by Herbert K. Cook, *Proceedings*, A.S.T.M., Vol. 51, 1951, pp. 1156–1165.

[9] "Revision A—Permeability of Concrete at Five Years Age," Supplement to *Technical Memorandum 6-380*, Waterways Experiment Station, U. S. Dept. of the Army, Vicksburg, Miss., July, 1955.

[10] *Ibid.*, p. 18 (revised), Table 3.

[11] Research Engr., Head, Dam Studies Section, National Civ. Eng. Lab., Lisbon, Portugal.

[12] "A Subpressão nas Barragens," by J. Laginha Serafim, *Publication No. 55*, Laboratório Nacional de Engenharia Civil, Lisbon, 1954.

1. What is the distribution of pressure of the water in the concrete pores?
2. What is the effective area over which that pore pressure acts?
3. What is the interpretation to be given to the stresses caused by these pressures?

As to the first problem Mr. Carlson gives some very useful information when presenting the implications of permeability tests. He shows, for example, that, as the time necessary for the complete saturation of a dam is considerable, only in very special cases will there be a linear pressure distribution across a dam. That is, the percolation of the water will not, as a rule, be steady. In an analysis[13] of unsteady flow of water through concrete it was concluded that this phenomenon is expressed by a differential equation of the type,

$$K\left(\frac{\partial^2 p}{\partial x^2}+\frac{\partial^2 p}{\partial y^2}+\frac{\partial^2 p}{\partial z^2}\right)=\left[C_1+C_2\frac{p_a}{(p+p_a)^2}\right]\frac{\partial p}{\partial t}+C_3\frac{\partial \theta}{\partial t}\ldots\ldots(12)$$

in which K is the coefficient of permeability; p represents the pore pressure; t is the time; p_a denotes the atmospheric pressure; C_1, C_2, and C_3 are constants which depend on the physical properties of the concrete and on the quantity of air trapped within the concrete pores during the filtration of the water; and θ is the sum of the three principal stresses,

$$\theta=\sigma_x+\sigma_y+\sigma_z\ldots\ldots\ldots\ldots\ldots\ldots\ldots(13)$$

which vary with p.

The similarity of Eq. 12 with Fourier's differential equation for heat conduction shows that the interpretation made by the Tennessee Valley Authority of the very interesting pore pressure observations in Hiwassee Dam (North Carolina) is justifiable.[14]

With regard to the remarks made about capillarity, the writer—by means of very simple equipment—determined capillary rises of approximately 50 ft for concrete.[15] This equipment was originally used for permeability tests with a view to verifying the validity of Darcy's law for the flow of water under low heads.

The problem of the effective area of porous bodies is closely related to the problem of the interpretation of the stresses set up by the pressures in the pores. Hence, it is convenient to discuss the latter first. In fact, it is believed that the lack of due consideration of this third problem is one of the reasons for the different opinions about the forces produced by pore pressure. Certain statements by Mr. Carlson, such as (in the "Introduction") "* * * the stress distribution is the same when uplift pressure is acting as when there is no pressure" or (under the heading, "Uplifting Force Produced by Pore Pressure") " * * * the uplift force on any section depends only on the pore pressure and area at that section * * * " or again (under the same heading) " * * * the uplift is produced locally by the pore pressure acting as a jack within the pores * * * " can be understood better if the third problem is discussed. That is, it is necessary to give acceptable interpretations to the terms "uplift" and "stress."

---

[13] "A Subpressão nas Barragens," by J. Laginha Serafim, *Publication No. 55*, Laboratório Nacional de Engenharia Civil, Lisbon, 1954, Chapter 4, p. 68.

[14] "Measurements of Structural Behaviour of Norris and Hiwassee Dams," *Technical Memorandum No. 67*, Tennessee Valley Authority, Knoxville, Tenn., 1950.

[15] "A Subpressão nas Barragens," by J. Laginha Serafim, *Publication No. 55*, Laboratório Nacional de Engenharia Civil, Lisbon, 1954, Chapter 5, p. 140.

Publications like those by J. H. Brahtz[16] clarify the meanings of these terms. On the one hand, when one speaks of stresses in concrete, mean stresses are considered—that is, their mean values in areas considerably greater than those of the pores or the size of the aggregates. When speaking of uplift stresses, the same meaning of the term stress has to be maintained, but, on the other hand, when dealing with forces produced by pore pressures, the scale of dimensions has to be reduced to the size of these pores and the size of solid bonds between grains.

If a porous body such as a concrete cylinder is submitted, externally and in the pores, to a uniform pressure, it will not break and the deformations produced in it will be negligible. The well-known breaking tests in tension[17] and in compression[18] on samples submitted to uniform pressures in the pores and on the outside show clearly (and it is doubtful whether they show more than this) that the strength of concrete, both tensile and compressive, is not altered by high pressures in the pores.

In view of the foregoing it can be stated that a body subjected to a uniform pressure produced by a fluid acting all around the entire surface of the solid material is not subjected to uplift forces; however, pressures are acting in its pores. In other words, it can be said that the "total stresses" in such a body are at all points equal to the pressures in its pores and that the "effective stresses" (those which rupture or deform) are nil. The expression "effective stress" for concrete can have a meaning analogous to that used in soil mechanics.

If the rupture of concrete in tension or compression appears to result from the rupture of the bonds between the solid particles,[19] in sections with a minimum area of solid, it is only of interest to consider the effective stresses in these sections. Such sections are simultaneously those of the greatest "effective area." Also, it is the deformations of the solid bonds which principally account for the deformations of the concrete when it is loaded externally. Therefore, the effective stress for soils is an indication of the forces between the grains and, for concrete, an indication of the forces transmitted by the solid bonds in the section of smallest bond area.

If a concrete pillar, 100 ft high, is embedded in impermeable rock at the bottom of a 200-ft-deep lake, the pores of the concrete at the base of the pillar would contain water at a pressure of 86 lb per sq in. and, at the same time, the uplift at the base of the pillar (taking the effective area as 100%) would only produce (effective) tensile stresses of 43 lb per sq in. Therefore, the value of the pore pressure does not give, by itself, the value of the stresses due to these pressures. It appears, therefore, more reasonable to admit that the uplift forces result from the gradients of pressures in the pores between the point under consideration and the surface of the body.

---

[16] "Pressures Due to Percolating Water," by J. H. Brahtz, *Transactions*, 2d Cong. on Large Dams, Vol. 5, Communication 18, Washington, D. C., 1938.

[17] "Versuche über die Zugfestigkeit bei allseitigen Wasserdruck," by P. Fillunger, Oesterreichische Wochenschrift für den Offentlichen Baudienst, *Heft 29*, 1915, p. 443.

[18] "The Effect of Uplift Pressure on the Shearing Strength of Concrete," by D. McHenry, *Transactions*, 3d Cong. on Large Dams, Vol. 1, Report 48, Stockholm, 1948.

[19] "Stress Conditions for the Failure of Concrete and Rock," by K. Terzaghi, *Proceedings*, A.S.T.M., Vol. 45, 1945, p. 777.

From the definition adopted previously for the effective stresses, it can easily be shown[20] that the forces caused by pore pressures are in the nature of body forces in which the components per unit volume are the derivatives of the pressure, p, times the effective area, n—$\partial(np)/\partial x$, $\partial(np)/\partial y$, $\partial(np)/\partial z$.

It should be noted that, if the effective area is not constant from one point to another, its variation is responsible for the presence of body forces. Hence, it can be concluded that the uplift at a point depends on and is produced by the presence of variations in the pore pressure or the effective area between one point and another. However, because the cement paste (which normally is the material having the greatest effective area) in concrete surrounds all the aggregate, n can be considered as constant in the computation of the stresses which interest the engineer (mean effective stresses).

From the consideration of the body forces referred to previously, it has been demonstrated[21] that a loading due to pore pressure (steady or unsteady flow) is analogous to the loading produced by temperature variations which is given by

$$T = \frac{1 - 2\mu}{\alpha E} n p \qquad (14)$$

in which E and μ are the elastic constants of the concrete and α is its coefficient of thermal expansion. It has also been demonstrated that, in simple cases (state of plane strain and pressures corresponding to a steady flow), the uplift stresses are given by the difference between the stresses which would act on the body if it were impermeable and the value of the product of the pressures in the pores by the effective area.

Karl Terzaghi, Hon. M. ASCE, has stated[22] that the effective area of permeable bodies could only be determined by tests. However, the deductions of Mr. Carlson are quite acceptable from the logical point of view and also do not contradict previous experimental results.

On the basis of various tests, the writer is of the opinion that the value of that area depends on the test conditions—that is, the effects of the pressures of a fluid in the concrete pores are different according to whether one is dealing with rupture tests or tests by measuring deformations and also according to the type of fluid used in the tests.

In the tests performed[4] by Mr. Leliavsky the samples were tested to rupture. Rupture was caused by tensile forces set up by the pressure variations in the pores, from the zone of failure to the external end of the samples. The values of the effective area found by Mr. Leliavsky (mean value 0.91) have therefore to be taken into consideration when the stability of construction in relation to rupture is to be verified.

---

[20] "A Subpressão nas Barragens," by J. Laginha Serafim, *Publication No. 55*, Laboratório Nacional de Engenharia Civil, Lisbon, 1954, Chapter 3, p. 46.

[21] *Ibid.*, Chapter 3, p. 54.

[22] "Simple Tests Determine Hydrostatic Uplift," by K. Terzaghi, *Engineering News-Record*, June 18, 1936, p. 872.

In tests performed by the writer (similar to those of Mr. Davis[4]) the object was to measure the forces and deformations produced by pore pressures. Ten series of mortar cylinders and two series of neat-cement-paste cylinders were tested. Using the equipment shown in Fig. 4 the tensile force set up by the longitudinal variation of pressure was obtained. To avoid rupture by tension the cylinders were maintained in constant axial compression during the test. The total longitudinal deformations, and also the strains, in the mean section were measured in percolation tests with nitrogen and with water. In the test in which strains were measured there was a compensating strain gage mounted on a small briquette (of the same material as the cylinder) placed in the chamber and, therefore, it was not necessary to subtract from the readings obtained the strains produced by the volumetric compression of the solid material. In fact, these were eliminated in the reading given by the strain indi-

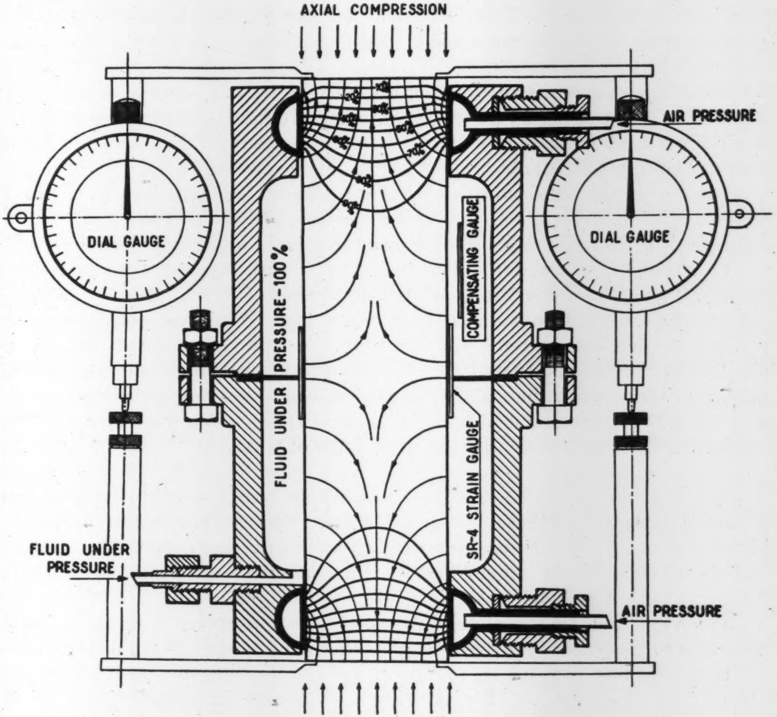

Fig. 4.—Test Equipment

cator. In the tests in which the total longitudinal deformations were measured by external dial gages, the longitudinal deformations due to the volumetric compressibility of the solid material were deducted from the values obtained.

The tensile forces caused by the percolation of the fluid were computed from the values of the deformation or strains produced by the longitudinal compression and from the values of the decrease of these deformations or strains caused by the pore pressure. These forces allowed the effective area of the samples to be estimated by taking into account the effect of creep.

The nitrogen tests on dry samples produced values of the effective area, *n*, varying from 0.8 to 1.0. The results showed that *n* increases slightly with the water-cement ratio, with the value of the pore pressures, and with the dryness of the samples. The tests in which water was used resulted in values between 0.40 for compact mortars and 0.80 for lean mixes. In one of the tests, water at a pressure of 560 lb per sq in. was maintained around the sample for 19 days, and there was no increase of *n* after 2 hr following the application of the water pressure around the sample.

The low values obtained by the water tests suggested the lack of mobility of the adsorbed water films. The nitrogen tests also showed that the area of solid bonds between particles is small when compared with the area of the voids.

The results of the writer's tests do not agree with the statement under the heading, "Uplifting Force Produced by Pore Pressure," "* * * the test program [of Mr. Davis] could not yield the effective area * * * in the simple manner which had been anticipated." If this were true, the values found now would always have been equal to unity. The writer feels very much more inclined to believe in tests rather than in the theoretical considerations even though they may have the interest and logical exactness of those which were presented by the author for[23] "experiment is the sole source of truth."

SERGE LELIAVSKY,[24] M. ASCE.—Essentially, this paper is a review of a set of investigations conducted in the United States on uplift in dams, beginning about 1948. It is, however, a significant point that Mr. Carlson disregards entirely the report[25] of the Subcommittee on Uplift in Masonry Dams, published in 1952.

The very fact that the conclusions of this report are thus disregarded indicates to the writer that the Subcommittee failed to settle the uplift problem.

In attempting to solve this problem, the author does not use the classical theory developed by Mr. Terzaghi but uses instead an artifice which he describes as "idealized concrete" (under the heading, "Uplifting Force Produced by Pore Pressure").

The number of oversimplified diagrams of this class which, it will be remembered, were first introduced into the theory of uplift by P. Fillunger[26] is legion. The danger of such oversimplifications is that an almost imperceptible alteration in the idealized model frequently reverses the result.

---

[23] "Readings in Philosophy of Science," by H. Poincaré, in "Science and Hypothesis," Dover Publications, New York,, N. Y., 1953, p. 31.

[24] Civ. and Hydr. Engr., Cairo, Egypt.

[25] "Uplift in Masonry Dams: Final Report of the Subcommittee on Uplift in Masonry Dams of the Committee on Masonry Dams of the Power Division, 1951," *Transactions*, ASCE, Vol. 117, 1952, p. 1218.

[26] "Neuere Grundlagen für die statische Berechnung der Talsperren," by P. Fillunger, *Zeitsch. d. Österr. Ing. u. Arch. Ver.*, 1914, p. 441.

How does the author apply the proposed method to the problem posed by Mr. Terzaghi in 1948?[27] Mr. Terzaghi asked what happens to the uplift pressure if all the imaginary solid particles of the "ideal pattern" are rearranged to form a number of vertical columns, and if all the voids are arranged to form vertical wells?

Idealized models of this description became obsolete when Mr. Terzaghi developed the differential equations by which the problem can be solved as definitely as the more general elastic problem was solved in the beginning of the nineteenth century. The point is that in addition to his experiments, which are frequently quoted, Mr. Terzaghi contributed a general theory of uplift which is essential in studying the problem. The failure to test conclusions against that theory[28] is a serious lack in Mr. Carlson's paper.

In any future effort to advance this branch of engineering science, the publications of Mr. Föppl,[29] Mr. Fillunger,[30] M. Rudeloff and Mr. Panzerbieter,[31] Oscar Hoffman,[32] and especially Mr. Terzaghi[28] must first be translated into English and thoroughly assimilated.

At a time when so much attention is focused on the concepts of "ultimate strength" or "limit" design, the methods and experiments described by the author are, in fact, a step backward. The method of testing which he describes is essentially the same as that used in 1940–1945 by the writer.[4] There is this difference however: Whereas the writer's conclusions were based on the "ultimate" or "limit" conditions, at which the test piece broke under the effect of uplift (that is, under the effect of the interstitial pressure of the water injected in the concrete), the author's results are derived from the deformation of unbroken specimens. The writer's method is the more correct and more advanced solution of the two.

If the author were required to verify the resistance of a bridge, would he base his conclusions on an average section of the girder or on its weakest section? The reply is obvious, and the same applies to the uplift problem because here, as in a bridge, failure occurs at the weakest section—that is, that section in which the effect of uplift is the greatest whereas the resistance is the lowest. This general principle defines the location and method of the surface of rupture. Therefore, any conclusions based on an average section of the specimen (as was the case in the author's experiments) are essentially valueless. Possibly they may have some value as additional information, throwing light on some secondary aspects of the problem but not as basic material for establishing design principles.

In this connection, an analogy with the main principles of reinforced concrete design might be enlightening. It is a matter of common knowledge that the sectional area controlling the deformation of a reinforced concrete beam is materially larger than that assumed in the calculation of resistance.

---

[27] *Proceedings*, 3d Cong. on Large Dams, Stockholm, 1948, Vol. I, Discussion on Question No. 8.

[28] "Die Wirksame Flächenporosität des Betons," by Karl von Terzaghi, *Zeitsch. d. Österr. Ing. u. Arch. Ver.*, 1934, Nos. 1–2, pp. 6–9.

[29] "Mitt. a. d. mech.-techn. Lab. d. k. Techn. Hochsch. München," 27 Heft, 1900, p. 16.

[30] "Neuere Grundlagen f. d. Statische Berechnung v. Talsperren," *Zeitschr. d. Österr. Ing. u. Arch. Ver.*, 1914, No. 23, p. 441.

[31] "Versuchen d. Porendruck d. Wassers im Mauerwerk," *Mitt. a. d. Königl. Materialsprüfungsamt*, Ergänzungsheft 1, 1912, Berlin.

[32] "Permeazioni d'aqua e loro effeti nei muri di ritenuta," Milan, 1928.

The former also includes some part of the extended concrete whereas the latter is confined to compressed area only. Deflection is an accumulated result of numberless infinitesimal deformations and depends, therefore, on average conditions throughout the entire length of the member. On the other hand, failure occurs in one point only—that is, in the weakest section, and it is this section, therefore, which must be (and is) included in the calculation of resistance. The same principle is also valid as regards the uplift experiments because here, as in a reinforced concrete beam, the observed deformation is symptomatic of average conditions (that is, an average uplift area) throughout the entire length of the specimen between the observation points. Conversely, failure occurs at the weakest point in which the percentage of the effective area is a maximum and the resistance a minimum, and the dam must be calculated accordingly—that is, depending on the results obtained with specimens tested to destruction rather than on the measured deformations of the unbroken test piece.

Experimental mathematics demonstrates that recorded figures based on one single section are more affected by accidental circumstances than are averages, and this explains the reason which prompted the writer to use the mathematical theory of probability in systematizing the results of his numerous tests on the failure of specimens. Experience of that nature is believed to be rather important for it allows a deeper insight into the physical circumstances of the failure, particularly when the latter is produced by interstitial pressure in combination with direct load. For instance, such phenomena as the "agony" period described by the writer[33,34] could not have been obtained otherwise.

Another fallacy incorporated in the author's argument is the implicit assumption that permeability and porosity, on the one hand, and the effective uplift area, on the other, are, of necessity, correlated.

Extensive practice with specimens tested to destruction tends to prove the existence of two different concepts—the microstructure and the microfailure. Since the author of the paper places so much faith on his idealized models, another idealized pattern may be suggested—just for once—although not as a proof but only as an explanation of what is meant by the two quoted concepts. In this connection attention is called to Fig. 1 which shows two schematized materials with obviously different porosities. In both cases, the effective uplift area is 100% if the failure surfaces between the pores are vertical and only 60% if these surfaces are inclined.

Thus, depending on the inclination of the surfaces of failure, any effective uplift area is consistent with any porosity. Consequently, the shape of the surface of failure is the all-important consideration for determining the uplift area, and it is obvious that in order to obtain experimental information on failure, the test piece must be made to fail.

---

[33] "Experiments on Effective Uplift Area in Gravity Dams," by Serge Leliavsky, *Transactions*, ASCE, Vol. 112, 1947, p. 483.

[34] *Ibid.*, p. 486.

As early as 1914, Mr. Fillunger showed that, had the surface of failure been plane, there would have been no uplift force because the additional weight of the water contained in the pores would have then balanced the additional interstitial pressure. The fact that uplift does exist and that it is, in fact, a significant parameter in designing dams was explained by Mr. Fillunger as the differences in the porosities of binding material and aggregate, respectively. Mr. Terzaghi propounded the much more convincing, and better established, principle that the surface of failure was not a plane and therefore the porosity of this surface was not the same as the average volumetric porosity of the material (and this, as a reasoned exception to Delesse's law). It follows that the effective uplift area cannot be determined from the deformations of specimens which depend on the average porosity.

This instance is believed to show that, before undertaking experiments which are intended as pioneer work, previous literature on the subject must be fully assimilated.

Another mirage the paper seems to be pursuing is revealed by the attempts to produce specimens of equal permeability. M. Mary[35] and the writer[33] have shown that no matter what results may be arrived at in the laboratory, in actual dam building wide differences may be expected even in samples taken from the same batch.

The 800-yr curve in Fig. 1 is certainly sensational but scarcely consistent with the fact that large quantities of percolating discharge develop frequently within a year after the dam is built. The logical chain—discharge, velocity, gradient, pressure—yields evidence that, at the very least, the diagram in question is misleading.

The paper contains some sweeping statements about discoveries made by numerous persons. The writer cannot agree with these "discoveries." For instance, the author is certainly wrong in stating (under the heading, "Uplifting Force Product by Pore Pressure") that it has been proved that there is no over-all pull in the specimen tested in the manner first used by the writer,[33,36] and later by Mr. Davies, and that "* * * the uplift is produced locally by the pore pressure acting as a jack within the pores."

The writer questions this statement. That interstitial pressure acts as a jack within the pores is correct, of course. However, because the infinitesimal solid between the pores is surrounded by the interstitial water on all its sides, one must imagine another jack being applied on the opposite side of the first jack, the net result being, therefore, an infinitesimal force equal to the difference between the forces of the two imaginary jacks—in reality, equal to the difference between the two interstitial water pressures, acting on either side of the infinitesimal solid.

It is the accumulated effect of these infinitesimal differences which causes the rupture of the specimen, or failure of the dam, as the case may be. This accumulated force can be transferred to the surface of rupture in no other way, except by what the author describes as the "over-all pull." This instance supplies a vivid demonstration of what was said earlier on "idealized" models—namely, the ease with which such a model (in this case, the jack) can be made to prove the extreme opposite of its original argument.

---

[35] "Un nouveau type de barrage en enrochements: Le batardeau de Marèges," by M. Mary, *Bulletin Periodique No. 7*, International Commission on Large Dams, December, 1938.

[36] "Pore versus Crack as Basis of Uplift Concept," by Serge Leliavsky, *Report 13*, 3d Cong. on Large Dams, Stockholm, 1948.

ROY W. CARLSON,[37] A. M. ASCE.—After studying the discussions by Messrs. Serafim and Leliavsky, the writer wishes to revise the conclusions regarding pore area subject to uplift. Conclusion 3 would then read as follows:

3. The maximum pore area in concrete subject to pore pressure cannot be determined from its effect on strains over customary gage lengths; strain measurements can, at best, yield only some sort of average area. The only known and defensible method for determining the one, maximum pore area which exists in a specific concrete is that of testing to failure, as was done[4] by Mr. Leliavsky. An approximate estimate can be made of the maximum area, however, by studying idealized models which have all the essential properties of concrete.

The discussion of Mr. Serafim shows a good understanding of the subject of uplift, but the writer cannot agree that the effective areas Mr. Serafim determined from strain measurements were the maximum areas of pores. The writer is convinced that strain measurements cannot reveal the "worst" area. Although it is true that strains in concrete subjected to pore pressure are affected most by regions of large pore area, they nevertheless represent a weighted average of all parts of the concrete within the gage length. There appears no logical reason why strains over a considerable gage length should reveal the one largest pore area in a specimen. The writer agrees with Mr. Leliavsky that the "weakest section" is the one which should govern.

Mr. Leliavsky points out the danger in oversimplification when considering an idealized model. However, much can be learned from such a model if it possesses all the essential, measurable properties of the concrete. Mr. Leliavsky (and Mr. Terzaghi) ask

> "*** what happens to the uplift pressure if all the imaginary solid particles of the 'ideal pattern' are rearranged to form a number of vertical columns, and if all the voids are arranged to form vertical wells?"

The answer to this is that one no longer has anything simulating concrete. Any idealized model must have all the essential properties of the concrete itself. If the model has vertical columns of solids, the modulus of elasticity will be too high because the modulus of elasticity of the solids is usually several times that of the concrete. Furthermore, the properties of the model will differ greatly in different directions. The model originally postulated, however, maintains all the essential, measurable properties of the concrete. Not only are the moduli of elasticity and Poisson's ratio of both solids and composite concrete preserved, but the porosity is correct also; the properties are the same in each of the three principal directions of measurement.

---

[37] Cons. Engr., Berkeley, Calif.

In support of the conclusion that concrete is relatively impermeable, it is maintained that the leakage which occurs through dams does not occur through sound concrete. After inspecting scores of dams in service, many of which leaked badly, the writer has yet to see evidence of water percolating through sound concrete. It is true that concrete varies greatly from point to point, but in a thick dam there are not likely to be any long percolation paths (still considering only the sound concrete), and the average permeability should be very nearly the governing one. Percolation of water through dams is a serious problem, but the percolation is likely to be through cracks and joints. This view is supported by the fact that trends toward lower cement contents in dams has led to lesser leakage rather than to greater.

Mr. Mather's contributions concerning other tests on lean concretes is greatly appreciated.

AMERICAN SOCIETY OF CIVIL ENGINEERS
Founded November 5, 1852
TRANSACTIONS

Paper No. 2875

EFFECT OF AIRPORT DISTANCE ON TRAFFIC GENERATION

By James C. Buckley[1]

Synopsis

Discussions of the landing-area requirements of jet-transport aircraft have a tendency to influence both engineers and laymen to think only in terms of developing new outlying airports rather than of redeveloping "close-in" airports. However, experience at the few locations for which usable data are available demonstrates clearly that airport distance of any magnitude has a decided depressive effect on air-traffic generation. In addition, the redevelopment of a close-in airport, as against the development of an outlying airport, saves the community the added costs which would result from longer ground travel; the value of the associated added ground time; the benefits of the airport payroll; and the loss of an important attraction of new industry. Consequently, before a choice is made between a distant location or a close-in location for a municipal airport, the effect of airport distance on air-traffic generation, and the resultant financial effects should be evaluated.

Introduction

During 1955 and 1956 several major airlines announced that they had placed orders for turbo-jet aircraft for use on domestic as well as overseas routes. On July 26, 1955, an airline inaugurated the first service with turbo-prop aircraft on United States domestic routes when it began operations on its Washington-Chicago and Washington-Norfolk flights. These two developments emphasize the problem of adjustment which must be accomplished between the requirements of turbo-prop aircraft and turbo-jet aircraft on the one hand and the facilities at major commercial airports on the other.

It is not the purpose of this paper to evaluate the problem posed by jet aircraft, with respect to either landing area and air-space requirements, or to the influence on surrounding areas of the noise nuisance which currently (1956) accompanies jet operation. Major penetration of domestic air trans-

---

Note.—Published, essentially as printed here, in May, 1956, as *Proceedings Paper 978.* Positions and titles given are those in effect when the paper was approved for publication in *Transactions.*

[1] Pres., James C. Buckley, Inc., Terminal and Transportation Consultants, New York, N. Y.

portation by turbo-jet aircraft will require production of aircraft with landing-area requirements reasonably within present recommended standards and with a noise level which can be tolerated at existing airports. Manufacturers can and will have to find the means to produce such aircraft.

The purpose of this paper, however, is to call attention to the fact that current discussions about jet aircraft are likely to strengthen a tendency among engineers and laymen to think only in terms of developing new outlying airports rather than redeveloping "close-in" airports. There are strong indications both from the standpoint of the community and from the standpoint of the maximum development of air transportation generally to indicate the importance of giving equal or greater consideration to the possibility of redeveloping and expanding close-in airport locations.

The effect of airport distance on a community's economy and the extent to which a community may be able to pay a premium price for a close-in airport will also be examined.

THE EFFECT OF AIRPORT DISTANCE ON AIR-TRAFFIC GENERATION

Unlike the policies adopted for marketing most goods and services, there is a feeling that the place of offering air services does not substantially affect the quantity of that service purchased by consumers. Thus, even businessmen who regard location as a vital factor in their own businesses may be led to disregard the same factor when thinking about airports.

To a considerable extent, the effect of airport distance on traffic generation has failed to be appreciated because there have been so few data available to illustrate and establish such effects. They can, of course, be measured on either of two general bases:

a. By examining changes in air-traffic generation at major air-transportation centers—where there has been a major change in the airport distance—on a "before and after" basis;

b. By examining air-traffic generation in relation to population in areas near and areas distant from a given airport or group of airports at a particular point in time.

Evaluations based on a "before-and-after approach" are limited because in the United States there are so few major air-traffic centers where there has been a significant change in airport distance to justify a conclusion. Evaluations based on air-traffic generation in relation to population at varying distances from a given airport or airports at a given point in time are even more difficult because so few data have ever been assembled on the local origins and destinations of air passengers. It has been possible, however, in the course of work on several airport and air-transportation projects to evaluate pertinent data on a group of situations covering both types of measurement, and the results and implications of these evaluations will be discussed here. They are important because they imply that a substantial volume of air traffic is lost because of airport distance. Data on the following have been assembled and evaluated:

1. The effect on a major segment of the Detroit (Mich.) air travel market by the removal of its airline airport from a location 6 miles from the city center to a location 31 miles from the city center;

2. The relationship between air-traffic generation and population at twenty-one California airports for the population less than 10 miles from each airport and for the population from 10 miles to 20 miles from each airport;

3. The relationship between air-traffic generation and population within the City of Dallas (Tex.) for areas close to the airline airport and for areas distant from the airline airport; and

4. The relationship between air-traffic generation and population for areas less than 15 miles from the Buffalo (N. Y.) airport and for areas 25 miles from that airport.

THE DETROIT EXPERIENCE

Early in 1947 scheduled airline operations at Detroit were moved from the Detroit Municipal Airport, 6 miles northeast of downtown Detroit, to the Willow Run Airport, 31 miles west of the city. The Willow Run Airport is 12 miles from Ann Arbor (Mich.), a city of 48,000, and only 3 miles from Ypsilanti (Mich.), a city of 18,000; both cities could be expected to contribute more traffic at Willow Run than at the old airport. A limited-access expressway connects Detroit with Willow Run Airport.

Sufficient time has elapsed to evaluate the effect of this airport move and to determine answers to the following questions: (*a*) Were any passengers lost to air transportation at Detroit as a result of the change in airport location? (*b*) If so, were these passengers ever regained?

A measurement of changes in passenger development at Detroit by itself would not be sufficiently refined because some changes would be expected even if the airport had not been changed. A better measurement would relate changes in passenger development at Detroit to the normal trend of the market as indicated by developments in another, or control, group of cities. The control group should not, of course, contain cities of too different a size in relation to Detroit nor should they be from sections of the country undergoing very different growth patterns since 1946.

A control group was established, therefore, consisting of all standard metropolitan areas of more than 500,000 population within 300 miles of Detroit. The cities constituting the control group were Buffalo, Chicago (Ill.), Cincinnati (Ohio), Cleveland (Ohio), Columbus (Ohio), Indianapolis (Ind.), Milwaukee (Wis.), Pittsburgh (Pa.), and Youngstown (Ohio). In September, 1946, before the airport move, Detroit's originating and terminating traffic with these cities was 53.2% of its total traffic, but in September, 1954, it was only 37.9%.

The universe of traffic pairs to be considered in the analysis consisted of 45 different traffic pairs. They are considered in two groups as follows:

1. The 9 traffic pairs consisting of Detroit paired with each of the 9 cities in the control group.
2. The 36 different traffic pairs consisting of each of the cities in the control group paired with each other such city.

The number of origin-destination passengers reported for each September for which Civil Aeronautics Board data are available was compiled for each such pair. The city totals for the control-group pairs (each such city paired with each other) and the grand total of control-group pairs are shown in Fig. 1 as solid curves. It will be noted that the trend of the sum of the pairs is representative of the trends for the individual cities.

The sum of the Detroit pairs and the sum of the non-Detroit pairs are shown in Fig. 1 as short and long dashed curves respectively. It is apparent that the trend of passenger development at the city which moved its airport (Detroit) is different from the trend for the control group. From these two curves it will be noted that: (*a*) From 1940 to 1946 traffic development for the Detroit pairs and the control-group pairs was parallel, or at almost the same rate of growth; (*b*) from 1949 to 1954 traffic development for the Detroit pairs and the control-group pairs was parallel, or at almost the same rate of growth; and (*c*) only between 1946 and 1949 was there a significant difference in the trend. (During this period the Detroit pairs declined, at first rapidly and then at a slower rate, whereas the control-group pairs had a generally upward trend.)

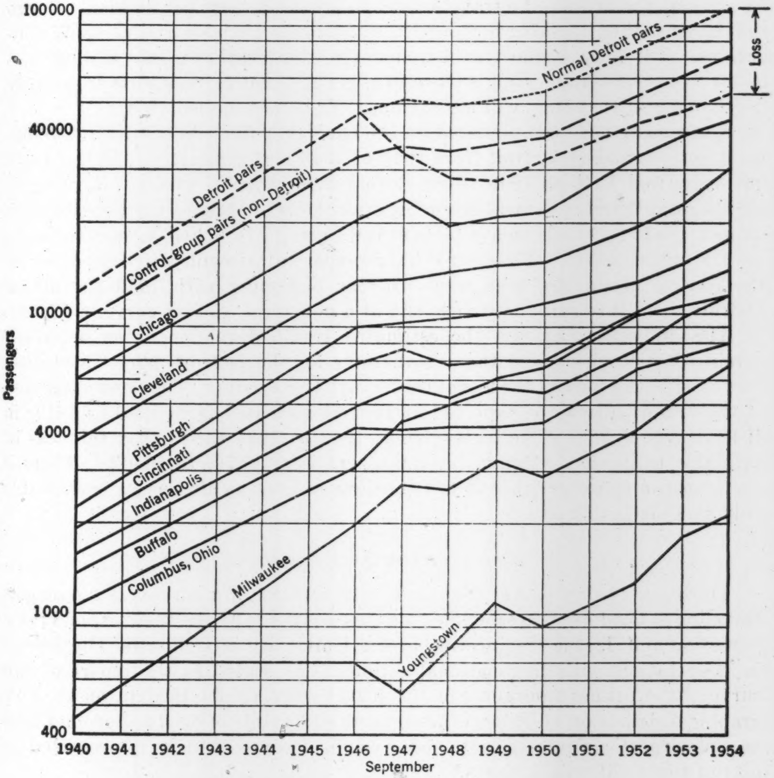

FIG. 1.—EFFECT OF AIRPORT DISTANCE AT DETROIT

From these observations it is concluded that the effect of moving the airport at Detroit took three years to manifest itself fully in reduced passenger traffic and that a normal rate of development resulted at the reduced level. The reasons for the effect's requiring three years to show itself fully can only be surmised. Apparently the manner in which air service is woven into the fabric of business and personal life in a modern metropolis is so complex that readjustments to changes in its place of offering can only be made gradually. As a group, the people who travel most by air cannot, perhaps, suddenly forego that habit without making it more difficult to meet business and personal obligations. For people who travel frequently, the location of the airport is a factor to consider in selecting a place to live, but a change in airports apparently does not mean that they will move from their homes immediately.

A summary has been prepared on the basis that the rate of traffic development was normal at Detroit from 1940 to 1946 and again from 1949 to 1953, but that from 1946 to 1949 traffic development was affected by the airport change, and that the control-group experience best indicates what would have happened had service been available at the Detroit Municipal Airport throughout the entire period. Thus, for the three-year adjustment period the trend of the control group has been used whereas beginning with 1949 the actual Detroit trend is reintroduced although at a new level (dotted curve in Fig. 1).

The difference between the estimated traffic development as described herein (dotted curve) and the actual traffic for the Detroit pairs (short-dash curve) is the measure of the loss of traffic with these pairs. The percentage loss of traffic normally to be expected at Detroit increased from 1946 to 1949; in 1949 it was 46.3%. The history from 1949 to 1954 shows that this loss of available traffic has continued in a range of from 39.7% to 49.0%. There is every reason to expect that it will continue as long as air service is available only at a distant airport.

The California Examples

During a 14-day period (September 10–23, 1950), a survey of passengers traveling in California on scheduled airlines was made by the Institute of Transportation and Traffic Engineering of the University of California (Berkeley), in cooperation with five national airlines. As stated in the report of this survey,[2] the primary purposes of the survey were to obtain data on the geographic distribution of homes of passengers and points of origin of ground trips to each airport. Summary data on the origin of ground trips were presented for all but two California airports.[3]

From the report it was possible to study the effect of airport distance on passenger-generation rates at a sufficiently large number of places. Obviously, the economic characteristics of cities using any one airport might be so different that their air passengers would not be true measures of the effect of distance on the generation of passengers. It has been possible, however, to study a large number of cases in which the larger cities are sometimes closer and sometimes farther away from the airports so that the chance characteristics of communities are eliminated in the final result. The procedures used were as follows:

---

[2] "Research Report 220. 10-1," Inst. of Transportation and Traffic Eng., Univ. of California, Berkeley, Calif., August, 1951.

[3] *Ibid.*, Table A-8.

1. Around each California airport were drawn two circles, one with a radius of 10 miles and the other with a radius of 20 miles. Any area which was within 20 miles of two or more separate airports was not considered.
2. For each airport all populated places reported in the United States Census of 1950 with 1,000 or more population were assembled into two groups—those within 10 miles of the airport and those more than 10 miles distant but within 20 miles of the airport.
3. The passengers reported on for each community were entered in the appropriate places.
4. The passenger-generating rates per 1,000 population were then computed for the cities in the 0–10 mile zone and also for those in the 10–20 mile zone.
5. The passenger-generating rate per 1,000 population in the 0–10 mile zone was taken as normal, assigned an index of 100.0, and, on this basis, the passenger-generating rate index of the 10–20 mile zone was computed.

TABLE 1.—EFFECT OF AIRPORT DISTANCE AT CALIFORNIA AIRPORTS

Airport	Loss in per-capita passenger generation of communities 10 to 20 miles from airport relative to communities 0 to 10 miles from same airport (%)
Burbank	7.8
San Luis Obispo County	11.3
Stockton Municipal	43.3
Palm Springs Municipal	48.0
Arcata-Humboldt County	56.9
Modcsto Municipal	58.4
Watsonville Municipal	67.6
Visalia Municipal	67.8
San Diego Municipal	68.2
Long Beach Municipal	70.8
Santa Barbara Municipal	71.3
Bakersfield—Kern No. 1	74.1
Ontario International	74.5
Napa County	75.6
Sacramento Municipal	75.9
El Centro	79.8
Merced Municipal	80.2
Redding Municipal	81.9
Santa Maria	88.5
Fresno Air Terminal	88.8
Oxnard-Ventura County	89.4
Arithmetic Average	65.7
Median	71.3
Modal Group	70–80

It was possible to make this comparison for a total of twenty-one airports in California. For the other airports, no comparison was possible either because there were no places reported in the U. S. Census with 1,000 or more inhabitants in one or the other of the two mileage bands, or because no passengers had been reported for such places, or because all points within 20 miles of the airport were also within 20 miles of another airport.

A summary of the percentage loss in per-capita passenger generation of communities in the 10–20 mile zone from the airport relative to communities in the 0–10 mile zone from the airport is given in Table 1.

From Table 1 it will be noted that at all but two of the twenty-one California airports more than a 40% reduction in per-capita passenger generation existed for communities 10–20 miles from their airports and that the typical loss of these communities was from 60% to 80% as compared with communities closer to their airports. These relationships are long-term relationships and reflect settled adjustment of communities to airport distances.

THE DALLAS EXAMPLE

In a general evaluation of its airport-development program, the City of Dallas in December, 1951, conducted a carefully controlled sample survey of passengers enplaning and deplaning at its airline airport to determine, among other things, the local origins and destinations of passengers originating from or terminating their journeys at Dallas. These data also included the length of air journey for each passenger interviewed. As a result, these data provide a basis for evaluating both the effect of airport distance on air-traffic generation and the extent to which the length of the air travel itself may minimize this effect. The analysis was conducted as follows:

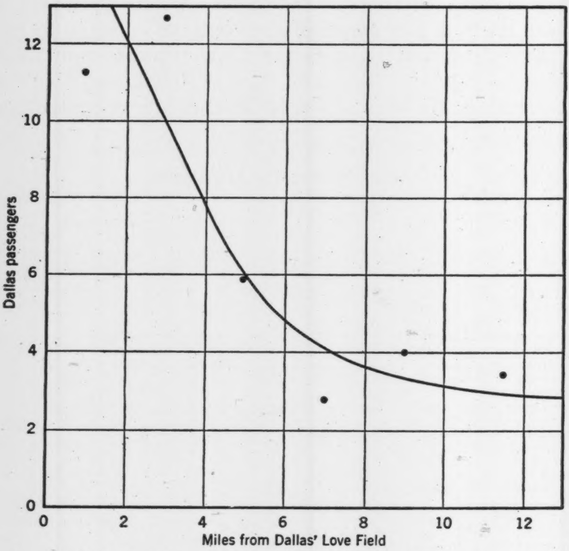

FIG. 2.—EFFECTS OF AIRPORT DISTANCE AT DALLAS

1. The local origins and destinations of Dallas' resident air passengers, as indicated by a sample survey at Love Field, were distributed by U. S. Census tracts within the city and by length of air trip.

2. The relative air-passenger potential of each Dallas census tract was computed by adjusting the family population in each tract for income. Higher-

income families were more heavily weighted than lower-income families on the basis of a survey of travel habits of various income groups.

3. The census tracts were divided into ground-distance bands from Love Field as nearly as possible into the following groups by miles: 0–2, 2–4, 4–8, 8–10, and 10–13.
4. The number of air passengers per thousand families (after adjustment for income) was computed for each ground-distance band and for each length of air trip.
5. The computations were interpreted in a series of graphs, each one showing the effect of ground distance on passenger generation for a different length of air trip. Curves were fitted to the points. The curve for all trips is shown in Fig. 2.

The graphs show that for very short-haul air trips the loss of air-passenger potential is only slightly greater than that for medium and long-haul trips and that severe losses in air-passenger potential occur with greater ground distance for all lengths of air trip. In Table 2 these losses for a ground haul of from 2 miles to 4 miles and for one of from 10 miles to 13 miles are compared.

TABLE 2.—PASSENGER LOSS

Length of air trip, in miles	Passengers per 1,000 Families (Adjusted for Family Income)		Percentage loss of air-passenger potential
	From 2 to 4 miles	From 10 to 13 miles	
0–99	0.12	0.00	100.0
100–149	0.20	0.00	100.0
150–199	1.91	0.30	84.3
200–249	1.79	0.30	83.2
250–299	1.35	0.89	34.1
300–499	2.07	0.44	78.7
500–999	1.91	0.74	61.3
More than 1,000	2.15	0.44	79.5

These data regarding the effect of airport distance on air traffic at Dallas certainly disprove the idea that airport distance is not a factor affecting long-haul air travel. They reinforce the views of those who believe that travel, regardless of distance, is only one facet of a complex of business and personal activity and that it can be encouraged and discouraged, not merely lost to another form of transport. This view is not inconsistent with the finding (as at Dallas) that for short-haul trips there is a greater loss of air-passenger potential than for the medium and long-haul trips.

THE BUFFALO EXAMPLE

Exhibits submitted by the City of Niagara Falls (N. Y.) in the Niagara Falls Airport Case[4] indicated a sound factual basis for determining the effect of distance on air-passenger generation in the Buffalo-Niagara Falls (New York) area. This was done by making a detailed analysis of 4,339 air-trip insurance policies written at the Buffalo Municipal Airport in March and September,

---

[4] **Niagara Falls Airport Case, *CAB Docket No. 6125*, May 26, 1954.**

1952, and September, 1953, in order to determine the incidence of air travel in relation to population for various distance zones around the Buffalo airport. The results were as follows:

Distance from the airport	Air passengers per 1,000 population
Less than 15 miles	393
15 to 25 miles	245
More than 25 miles	84

The data establish the fact that the area lying from 15 miles to 25 miles from the Buffalo airport generates 37.7% less air traffic in relation to population than the area within 15 miles of the airport.

CONCLUSIONS AS TO THE EFFECT OF AIRPORT DISTANCE ON AIR-TRAFFIC GENERATION

These examples covering experience in widely separated parts of the United States lead to the conclusions that (1) there is a demonstrable effect on air-traffic generation from airport distance; (2) the effect is substantial in terms of the difference between an airport from 5 miles to 7 miles away from major traffic concentrations and one 15 miles or more distant; and (3) the increment of passengers lost appears to be of the order of 40% or more. This lost traffic is probably far more valuable to the air carriers in terms of line-haul revenue and to the community in terms of time and money savings and added attractiveness to industry than any added expense which might be entailed in making a close-in airport suitable to accommodate needed scheduled airline services. To test this point, it will be worth while to consider the effect of airport distance on the economy of a community.

EFFECT OF AIRPORT DISTANCE ON THE COMMUNITY

Although almost no data are available as to the comparative impact on communities of close-in and distant airports, a carefully documented study of this problem was made by the City of Dallas and submitted to the Civil Aeronautics Board in the so-called Reopened Fayetteville Proceeding.[5]

The occasion was a hearing by the Civil Aeronautics Board on whether it should rescind an order which required a local service airline on one of its routes to serve Dallas through the Fort Worth (Tex.) International Airport, 18.3 miles from the Dallas city center, and prohibited service to Dallas on that route segment at the Dallas airline airport which is only 5½ miles from the city center.

Data were submitted which show that in Dallas the major concentrations of air passengers and air freight are immediately accessible to the Dallas airport and distant from the Fort Worth airport (Fig. 3).

Data were also submitted on the basis of extensive test runs between all sections of the city and each of the two airports to establish the added time and distance required between each section of the city and the more distant airport; the results are plotted as contours in Fig. 3. Indicative of the results of this investigation are the following data which indicate that more than 92% of

---

[5] Reopened Service to Fayetteville Case, *CAB Docket No. 5598 et al.*

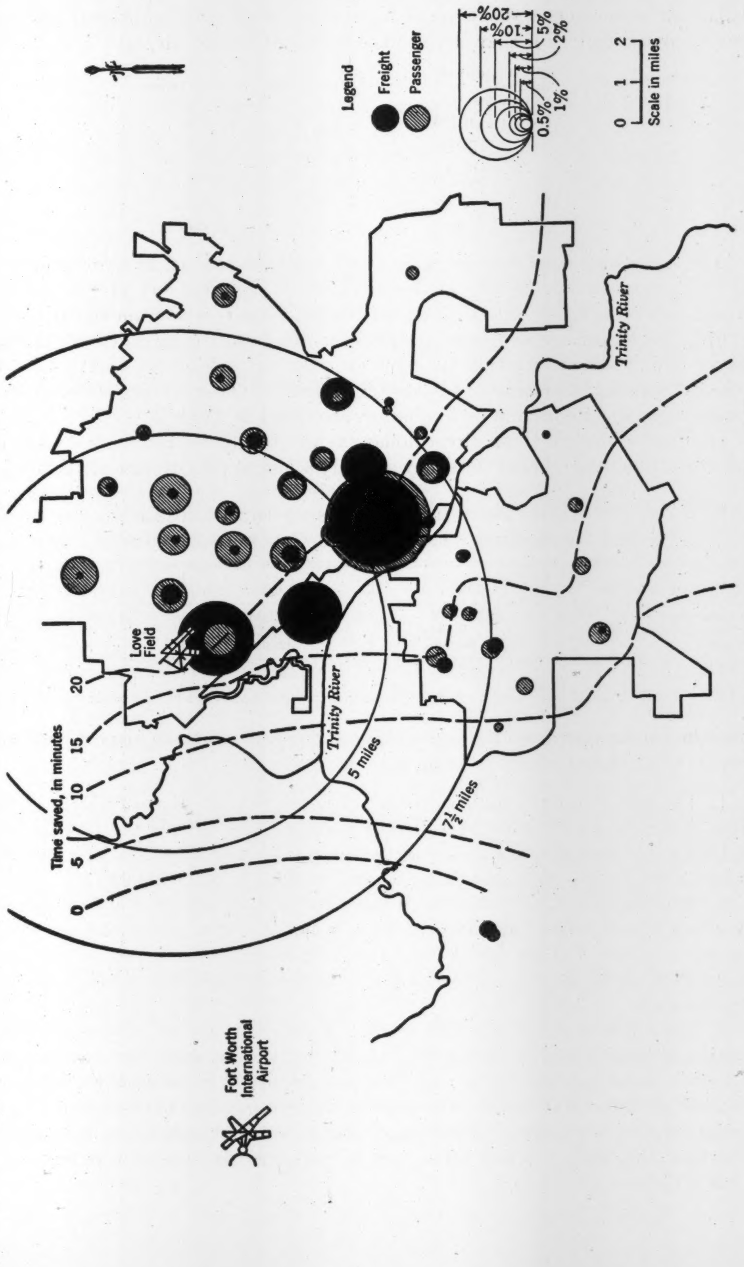
Time saved, in minutes
0
5
10
15
20
Love Field
Trinity River
5 miles
7½ miles
Trinity River
Fort Worth International Airport
Legend
Freight
Passenger
20%
10%
5%
2%
1%
0.5%
0 1 2
Scale in miles

FIG. 3.—EFFECT OF AIRPORT DISTANCE ON THE DALLAS ECONOMY

Dallas' air passengers would require more than 15 minutes additional ground time in each direction if they were to use the more distant airport:

Minimum ground time saved, in minutes	Percentage of Dallas' air passengers
More than 20	48.43
15–20	43.86
10–15	7.08
5–10	0.17
None	0.46

Also submitted were detailed data which established that, as a result of the use of its close-in airport, the Dallas economy is spending (*a*) 33.3% less on airport limousine fares; (*b*) 70% less on taxicab fares to and from the airport; (*c*) 67% less on private automobile expense to and from the airport; (*d*) 56.2% less on ground-transportation time for air passengers; and (*e*) 68.4% less of ground distance and associated costs for air freight. These savings, expressed in dollars as a lowest common denominator, are listed in Table 3.

Impressive though these direct dollar savings to the community's economy are, it must be remembered that they are only a minimum estimate of the benefit to the community from the availability and use of a close-in airport because they do not reflect indirect benefits such as:

TABLE 3.—ESTIMATED MINIUMUM SAVINGS TO THE DALLAS ECONOMY FROM THE AVAILABILITY AND USE OF A CLOSE–IN AIRPORT

Type of air traffic	1953	1955	1960
Air passengers	$1,566,018	$1,752,366	$2,380,132
Air freight	9,443	18,885	28,328
Air mail	20,000	20,000	20,000
Total	$1,595,461	$1,791,251	$2,428,460

1. The value to the community of the airport's payroll, most of which is lost when the airport is situated at a distant point usually outside the city limits. At Dallas, for instance, the airline airport currently provides jobs for approximately 3,000 people with an annual payroll of close to $20,000,000.

2. The value to the community of the airport as an attractor of new industry which is lost with a distant airport. At Dallas, for example, the principal executive of the Trinity Industrial District has stated that the convenient availability of the airport has been a major factor in attracting several of their large tenants.

3. The value to the community of the airport as an aid to the competitive position of local business enterprises. Again, at Dallas, some banks maintain an hourly messenger service to and from the airport to expedite the clearance of checks moving via air mail to and from their correspondent banks in small and medium-size communities. The bankers have said that they could not afford to perform this service, which helps their business greatly, if they were required to use a distant airport.

There is no reason to believe that conditions existing in Dallas differ from those which prevail at other major air-traffic centers throughout the United States. On the contrary, the factors benefiting the Dallas economy because of the availability and use of a close-in airport are factors common to most of the major metropolitan areas. In the light of these facts, it is hardly conceivable that either the engineer or the layman would wish any city to forego development or redevelopment of a close-in airport without a full evaluation of the benefits which would be lost from its abandonment as compared to the cost of its continuance. An example or two will illustrate the point even more clearly:

First, there is considerable concern currently about providing at each end of the principal runway of commercial airports the so-called Doolittle clear zone—that is, an area 1,000 ft wide and 2,640 ft long at each end of the runway. Because most airports have been providing from 1,000 ft to 1,200 ft of such clearance, a given airport might have to secure at both ends of its principal runway, land measuring 1,400 ft long and 1,000 ft wide—or about 35 acres. If this were miscellaneous improved real estate, such as that which might be found adjoining an airport from 5 miles to 7 miles from a city center, it might reasonably cost $250,000 an acre, or a total of $17,500,000 for the 70 acres. Although this appears to be a tremendous price to pay for 70 additional acres at an airport, it becomes almost a bargain in a community such as Dallas where this price is less than the ten years' saving that the community will realize from the use of its close-in airport; this expenditure saves the community the tremendous additional capital investment of acquiring land and developing a new airport at an outlying location.

Another example is one which many communities with close-in airports may face in the next ten years—the desirability of lengthening their principal runway by 1,000 ft or 2,000 ft for the better accommodation of jet aircraft. A 2,000-ft addition to an instrument runway with a parallel taxiway and warm-up path would require about 80 acres, which again might cost approximately $250,000 per acre for miscellaneous improved real estate, or $20,000,000 to acquire the needed land. Again, this apparently large expenditure for only 80 acres of land appears to be more of a sound business investment when it is remembered that the community will not have to develop a new airport which may cost from $25,000,000 to $50,000,000 and that annual benefits will continue. In a city like Dallas, annual benefits will total in eight years as much as the cost of the land required to keep the airport in use as a close-in facility.

CONCLUSIONS

The basic conclusion suggested from this study is that too little attention has been paid by engineers, planners, and laymen to the effect of airport distance on air-traffic generation, on the air carriers, and on the communities concerned. Although the available pertinent data are not as extensively developed as one would like, they are uniformly indicative of the fact that:

1. There is a very substantial loss in air traffic when a community must accept its air service through a distant airport.
2. This loss in air traffic has a direct and detrimental effect on the revenues of the air carriers.

3. The community concerned is burdened with a determinable expense because of the necessity of using a distant airport, an expense which appears substantially greater than the added costs of developing and extending close-in airports.

4. The community using a distant airport is at an additional disadvantage by not having substantial ancillary benefits, such as a stable working force within the city limits, a strong attraction to new and expanded industry, and a capacity to maintain and improve the competitive position of local industry.

From these facts it can be implied that it is the obligation of the engineer engaged on an airport location or relocation project to make certain that the community concerned evaluates well the benefits of a close-in airport in relation to any alleged disadvantages and compares these with the alleged benefits and demonstrable disadvantages of an outlying airport before finally abandoning the thought of developing or redeveloping close-in commercial airport facilities.

AMERICAN SOCIETY OF CIVIL ENGINEERS
Founded November 5, 1852
TRANSACTIONS

Paper No. 2876

STRESSES IN ELASTIC PLATES OVER FLEXIBLE SUBGRADES

By Eric Reissner[1]

Synopsis

Comparative studies are presented of the effect flexible surface layers have on the load-carrying capacity of the combined surface layer and subgrade. The analysis is based on the representation of the subgrade as a system of springs or, equivalently, as a heavy liquid.

Approximate formulas are obtained for the maximum tensile stress in the surface layer and the maximum deflection of the surface layer that are produced by loads distributed uniformly in circular areas. A limit is established for the range of applicability of these formulas and this bound also determines the range of usefulness of the surface layer.

In the range of usefulness, it is shown that reasonable nonuniformity of load distribution and built-in tensions of plausible magnitude are of secondary importance. Also, nonlinear effects caused by noninfinitesimal deflections are negligible if the deflections of the surface layer are no larger than approximately one-half the thickness of the surface layer.

Notation

The letter symbols adopted for use in this paper are defined where they first appear and are arranged alphabetically for convenience of reference in Appendix III.

Introduction

It is proposed to study herein various theoretical questions which arise when one considers the load-carrying capacity of a foundation consisting of a subgrade strengthened by a relatively thin surface layer that is stronger than the subgrade. The surface layer may be a mat, a concrete layer, or the subsoil itself which has been improved to a certain depth by the use of various additives.

Two basic questions confront the investigator at the outset of a study of this type. They are: (*a*) What should be assumed in regard to the behavior of

---

Note.—Published, essentially as printed here, in May, 1955, as *Proceedings-Separate No. 690*. Positions and titles given are those in effect when the paper was approved for publication in *Transactions*.

[1] Prof. of Mathematics, Massachusetts Inst. of Technology, Cambridge, Mass.

the subgrade, and (*b*) what should be assumed in regard to the behavior of the flexible surface layer?

It appears that in previous work of this type the subgrade has been considered as obeying Hooke's law of elasticity, or it has been assumed that the subgrade behaves like a system of parallel tension-compression springs. The latter assumption is equivalent to the consideration of the subgrade as a heavy liquid and is therefore often termed the liquid-subgrade assumption.

Either of the foregoing assumptions is, at best, an approximation of the actual behavior of the subgrade under load. Experience indicates, however, that the approximation is quite close for subsoils of normal consistencies carrying loads of such distribution as to permit the return to approximately original conditions upon removal of the loads. It is clearly one of the functions of the flexible surface layer to cause a distribution of load on the subsoil which would permit the existence of this condition for larger total loads than would be possible in the absence of the surface layer.

It is necessary to be more specific regarding the behavior of the flexible surface layer. The following types of action characterize a flexible surface: (1) Bending action, (2) tension-surface action, and (3) transverse-shear action. Action of types 1 and 3 are always present, although often one of them, usually type 3, is negligible compared to the other. Action of type 2 may or may not be present.

The manner in which the flexible surface may be represented for the purpose of analysis depends essentially on the ratio of the diameter of the load surface to the thickness of the surface layer. For values of this ratio beginning at approximately unity it is possible to consider the surface layer as a "thin plate," in a manner which will be explained subsequently, rather than as a three-dimensional continuum.

NATURE OF RESULTS OBTAINED

The quantities determined subsequently are primarily (*a*) the maximum value of the pressure on the subgrade at the interface of subgrade and surface layer and (*b*) the maximum value of the tensile stress in the surface layer.

These two quantities are determined by their dependence on what are believed to be the essential parameters that enter into the problem:

1. The elasticity of the surface layer;
2. The thickness of the surface layer;
3. The diameter of the load area;
4. The total load; and
5. The deformation characteristics of the subgrade.

In the course of the present analysis it was found that, subject to specific restrictions which are usually satisfied in practice, certain formulas that have been previously used can be justified on wider grounds than was heretofore possible. Although some of these restrictions may have been implicit in the earlier work, at least one of them, which is to be formulated herein, has previously been disregarded explicitly.

Because the object of this analysis is the comparative study of surface layers endowed with a variety of properties and because previous analyses have shown fairly close analogies between the "elastic" and the "liquid" subgrade behavior, it was considered justified to base the present work on only one assumption concerning subgrade behavior. For this one assumption it was natural to choose the simpler—that is, the assumption of a liquid subgrade characterized by a foundation constant, k.

The following four special problems pertaining to the various possible properties of the surface layer have been solved.

1. Infinite Elastic Plate: Uniform Load on a Finite Circular Area.—The plate is treated by conventional plate theory. The results for this case have been presented previously by G. Pickett and others,[2] and the present computations confirm the formulas of these authors. Added to these results is a requirement that these formulas not be used beyond a certain value of one of the basic parameters. For values of the parameter within the recommended range it is possible to simplify the formulas to emphasize more clearly the relative significance of thickness changes and elastic-modulus changes for the surface layers.

2. Infinite Elastic Plate: Load Distributed Parabolically over a Finite Circular Area.—Because the actual nature of the load-intensity distribution over the assumed circular area is not actually known, it seems appropriate to investigate the differences in plate stress and foundation pressure due to changes in load distribution for constant total load. The relevant computations are made for one family of significant load distributions. It is found that, up to a certain value of a basic parameter, the results for Problem 1 and Problem 2 are the same for all practical purposes. Significant discrepancies appear in Problem 2 at approximately the same values of the basic parameter which were found critical for Problem 1. This fact lends additional support to the restrictions advised in connection with the use of the analytical formulas for the plate with uniform load distribution. The formulas for Problem 2 have been specifically obtained for use herein, and it is possible that they have not been previously published anywhere.

3. Infinite Elastic Plate: Uniform Tension in Plane of Plate and Uniformly Distributed Lateral Load.—Because the installation of the flexible surface may build into it a state of pretension (for example, through shrinkage in a chemically treated surface), it seemed advisable to investigate the influence of built-in tension on foundation pressure and plate bending stresses. An explicit solution was obtained for this problem; it is believed that this solution is new. It is found that the tension possible in chemically treated surface layers is so small that its effect is minor. However, the analytical solution obtained should be of more value than just revealing this fact. The solution permits a numerical analysis of similar problems in a unified manner between the two extreme conditions of (*a*) the plate without built-in tension and (*b*) the case in which this tension is the dominating factor and the flexural resistance of the plate is negligible.

---

[2] "Deflections, Moments and Reactive Pressures for Concrete Pavements," by G. Pickett, M. E. Raville, W. C. Jones, and F. J. McCormick, *Bulletin No. 65*, Kansas State College, Manhattan, Kans. October, 1951.

4. Nonlinear Effects.—In most problems concerning transverse deflections of flat plates the relationships between loads and deflections are effectively linear as long as the deflections remain less than approximately one-half the plate thickness. Because plates on a flexible subgrade apparently have not heretofore been checked in regard to this property, such an analysis is presented herein. It is found that, for this condition also, nonlinearity becomes significant only for displacements of half the plate thickness or more. In many or most problems pertaining to flexible surfaces on flexible subgrades, this means that the ordinary linear, small-deflection theory is adequate. The present paper goes somewhat beyond establishing this result. It also includes a formulation of the nonlinear problem which is particularly convenient for the actual computation of nonlinear corrections to the linear theory, in the event that such computation might become desirable.

PROBLEM 1: UNIFORM LOAD

The differential equation for an infinite elastic plate carrying a load distributed uniformly over a finite circular area is

$$D \nabla^2 \nabla^2 w + k\, w = p \qquad (1)$$

in which w represents the plate deflection, in inches, and D is the plate-stiffness factor, equal to $E\, h^3/12\ (1 - \mu^2)$. For the present problem the load-intensity function, p, is

$$\left.\begin{array}{ll} p = p_0, & r \leq a \\ p = 0, & a < r \end{array}\right\} \qquad (2)$$

in which a is the radius of the circular load surface and r is the radial distance from the center of this surface.

To be determined are, in particular:

a. The foundation pressure distribution, σ_F, expressed by

$$\sigma_F = k\, w \qquad (3)$$

b. The bending stresses in the outermost fibers of the plate, in radial and circumferential directions. These are expressed as

$$\sigma_{rB} = \pm \frac{1}{2} \frac{E\, h}{1 - \mu^2} \left(\frac{d^2 w}{dr^2} + \frac{\mu}{r} \frac{dw}{dr} \right) \qquad (4a)$$

and

$$\sigma_{\theta B} = \pm \frac{1}{2} \frac{E\, h}{1 - \mu^2} \left(\frac{1}{r} \frac{dw}{dr} + \mu \frac{d^2 w}{dr^2} \right) \qquad (4b)$$

in which h is the plate thickness, E, the modulus of elasticity, and μ is the Poisson ratio. Eqs. 3 and 4 are independent of the form of the pressure-intensity function and will be used also in subsequent sections of this paper.

The solution of Eqs. 1 and 2 is of the following form:

$$\left.\begin{array}{ll} w = \dfrac{p_0}{k} \left\{ 1 + \dfrac{\pi}{2}\, Im\, [\nu\, H_1^{(1)}(\nu)\, J_0(\lambda\, r)] \right\}, & r \leq a \\ w = \dfrac{p_0}{k} \left\{ \dfrac{\pi}{2}\, Im\, [\nu\, J_1(\nu)\, H_0^{(1)}(\lambda\, r)] \right\}, & a < r \end{array}\right\} \qquad (5)$$

in which

$$\lambda = \sqrt{i}\sqrt[4]{\frac{k}{D}} = \frac{1+i}{\sqrt{2}}\sqrt[4]{\frac{k}{D}}$$

$$\nu = \lambda\, a$$

and in which J_1, $H_0^{(1)}$, and $H_1^{(1)}$ are Bessel and Hankel functions in the usual notation.

For the evaluation of Eq. 5 it is to be noted that $\sqrt{i} = e^{i\pi/4}$. Furthermore, if ρ equals $\sqrt[4]{k/D}$,

$$\lambda = \rho\, e^{i\pi/4}.$$

Then,[3]

$$J_{0,1}(\lambda\, r) = J_{0,1}(\rho\, r\, e^{i\pi/4}) = u_{0,1}\left(\rho\, r, \frac{\pi}{4}\right) + i\, v_{0,1}\left(\rho\, r, \frac{\pi}{4}\right)$$

$$Y_{0,1}(\lambda\, r) = Y_{0,1}(\rho\, r\, e^{i\pi/4}) = U_{0,1}\left(\rho\, r, \frac{\pi}{4}\right) + i\, V_{0,1}\left(\rho\, r, \frac{\pi}{4}\right)$$

and

$$H^{(1)} = J + i\, Y = (u - V) + i\,(v + U).$$

The symbol J represents Bessel functions of the first kind; Y, Bessel functions of the second kind; and u, v, U, *and* V, the real and imaginary parts of these Bessel functions.[3] Because all these functions, with subscripts zero and one, have been tabulated elsewhere[3,4] it is quite simple to plot the displacement profile, $w(r)$, as expressed by Eq. 5 in its dependence on r.

It is plausible and may be confirmed by computation that w is largest at the origin, $r = 0$. Therefore, the foundation pressure, σ_F, as expressed by Eq. 3 is also largest for $r = 0$. The value of the maximum foundation pressure, $\sigma_F(0)$, will be examined first. From Eqs. 3 and 5,

$$\sigma_F(0) = p_0\left\{1 + \frac{\pi}{2}\, Im\left[\nu\, H_1^{(1)}(\nu)\right]\right\} \ldots\ldots\ldots\ldots\ldots (6a)$$

The result of Eq. 6*a* is also given by Mr. Pickett and others.[5] It may be expressed in terms of a pressure coefficient, C, which is defined as the ratio $\sigma_F(0)/p_0$,

$$C = 1 + \frac{\pi}{2}\, Im\left[\nu\, H_1^{(1)}(\nu)\right] \ldots\ldots\ldots\ldots\ldots\ldots (6b)$$

The results expressed in Eqs. 6*a* and 6*b* may alternately be expressed in terms of the so-called Kelvin functions, which are real and imaginary parts of various types of Bessel functions with argument proportional to $\sqrt{i}$. In terms of these functions the pressure coefficient, C, is

$$C = 1 + \rho\, a\, \ker' \rho\, a \ldots\ldots\ldots\ldots\ldots\ldots\ldots (6c)$$

---

[3] "Table of the Bessel Functions $Y_0(z)$ and $Y_1(z)$ for Complex Arguments," Computation Lab., National Bureau of Standards, U. S. Dept. of Commerce, Columbia Univ. Press, New York, N. Y., 1950.

[4] "Table of the Bessel Functions $J_0(z)$ and $J_1(z)$ for Complex Arguments," Mathematical Tables Project, National Bureau of Standards, U. S. Dept. of Commerce, Columbia Univ. Press, New York, N. Y., 1947.

[5] "Deflections, Moments, and Reactive Pressures for Concrete Pavements," by G. Pickett, M. E. Raville, W. C. Jones, and F. J. McCormick, *Bulletin No. 65*, Kansas State College, Manhattan, Kans., October, 1951, Table 6.

Definitions and tables of the Kelvin functions, ber, bei, ker, kei, and their derivatives may be found conveniently in the tables of H. B. Dwight.[6]

At this point it is well to consider the actual behavior of the pressure coefficient, C, as a function of $\rho\, a = \sqrt[4]{k/D}\, a$. Table 1 supplies information on this point.

It would seem to be the object of the flexible surface layer to reduce appreciably the maximum value of the load pressure on the subsoil. Accordingly, for the flexible surface layer to be significant, pressure coefficients appreciably less than unity would be required. This requirement, according to Table 1, reduces the range of physically significant values of $\rho\, a = \sqrt[4]{k/D}\, a$ to values not greatly in excess of unity. Furthermore, redirecting attention to Eq. 5, it is only for as long as $\rho\, r \leq \rho\, a$ is not more than approximately unity that the deflection w inside the load area is substantially uniform, because only then is it true that $J_0(\lambda\, r)$ does not differ much from unity. The foregoing considerations suggest that technical application of flexible surface layers be restricted to values of $\rho\, a$ approximately equal to unity. Additional reasons for this restriction will become apparent subsequently.

Polynomial Approximation.—If $\rho\, a$ is not larger than approximately unity, it is possible to clarify the meaning of the pressure coefficient, C, as expressed by Eq. 6*a*, by introducing into Eq. 6*c* for $\mathrm{ker}'\rho\, a$ the first few terms of its series representation in the vicinity of the point, $\rho\, a = 0$. Mr. Dwight's tables[7] lead to the following approximate expression for C:

TABLE 1.—VALUES OF THE PRESSURE COEFFICIENT, C

$\rho\, a$	0	0.3	0.5	0.7	1.0	1.5	2.0	∞
C	0	0.034	0.090	0.166	0.305	0.55	0.787	1

$$C \approx \tfrac{1}{8}\,\pi\,(\rho\, a)^2 \ldots\ldots\ldots\ldots\ldots\ldots\ldots\ldots (6d)$$

Eq. 6*d* should not be used for values of $\rho\, a$ greater than unity. One may write Eq. 6*d*, with $\rho = \sqrt[4]{k/D} = \sqrt[4]{k\; 12\,(1 - \mu^2)/(E\, h^3)}$, in the following instructive, explicit form:

$$C \approx \frac{\pi}{4}\sqrt{3\,(1 - \mu^2)}\,\sqrt{\frac{k}{E}}\,\frac{a^2}{h^{3/2}} \ldots\ldots\ldots\ldots\ldots\ldots (6e)$$

In Eq. 6*e* the variables describing the surface layer are the modulus, E, and the thickness, h. It is seen that increasing the thickness, h, means reducing the pressure coefficient and, similarly, increasing the stiffness of the surface-layer material—that is, making E larger—reduces the value of the pressure coefficient. Use of the simple formula, Eq. 6*e*, requires that

$$\rho\, a = \sqrt[4]{12\,(1 - \mu^2)}\,\sqrt[4]{\frac{k}{E}}\,\frac{a}{h^{3/4}} \leq 1 \ldots\ldots\ldots\ldots\ldots\ldots (7)$$

---

[6] "Tables of Integrals and Other Mathematical Data," by H. B. Dwight, The Macmillan Co., New York, N. Y., 1947.

[7] *Ibid.*, p. 188, Formula 824.5.

but this requirement, as stated previously, should approximately cover the useful range of a flexible surface layer.

Bending Stresses.—Explicit values for bending stresses in accordance with Eqs. 4 will be given here only for the center, $r = 0$, where their values would be expected to be largest. Moreover, when $r = 0$, the values of radial and circumferential bending stress are the same. Introduction of w from Eqs. 5 into Eqs. 4 yields

$$\sigma_B(0) = \frac{E\,h}{1-\mu}\,\frac{i\,\pi\,\lambda^2}{16}\,\frac{p_0}{k}\left[\nu H_1^{(1)}(\nu) + \bar{\nu}\,H_1^{(2)}(\bar{\nu})\right] \quad \text{.........} \quad (8a)$$

in which $\sigma_B(0) = \sigma_{rB}(0) = \sigma_{\theta B}(0)$ and $\bar{\nu}$ is the complex conjugate of ν. Eq. 8 may also be expressed somewhat more conveniently in terms of the Kelvin functions. The result is

$$\sigma_B(0) = \frac{\sqrt{3}}{2}\sqrt{\frac{1+\mu}{1-\mu}}\,p_0\,\sqrt{\frac{E}{k\,h}}\,\rho\,a\,\mathrm{kei}'\,\rho\,a \quad \text{...........} \quad (8b)$$

Restricting attention again to the cases for which ρ a is less than approximately unity, one can use the first few terms of the series from Mr. Dwight's tables[7] for kei′ $\rho\, a$ and approximate for $\rho\, a$ kei′ $\rho\, a$ in Eq. 8*b* as follows,

$$\rho\,a\,\mathrm{kei}'\,\rho\,a \approx \tfrac{1}{2}\,(\rho\,a)^2 \log\left(\frac{2}{\rho\,a}\right).$$

Therewith,

$$\frac{\sigma_B(0)}{p_0} \approx \frac{3\,(1+\mu)}{2}\left(\frac{a}{h}\right)^2 \log\left[\sqrt[4]{\frac{4}{3\,(1-\mu^2)}}\,\sqrt[4]{\frac{E\,h^3}{k\,a^4}}\right] \quad \text{......} \quad (8c)$$

Use of Eq. 8*c* is allowed as long as the inequality (Eq. 7) is satisfied—that is, as long as

$$\sqrt[4]{\frac{E\,h^3}{k\,a^4}} \geq \sqrt[4]{12\,(1-\mu^2)} \approx 2.$$

Inspection of Eq. 8*c* reveals that, as the thickness, h, of the surface layer decreases, the bending stress increases. Furthermore, the bending stress increases as the modulus, E, of the surface layer increases.

Referring to Eqs. 6 and 8, it is seen that increasing h decreases both σ_F and σ_B whereas increasing E decreases σ_F but increases σ_B. This result is, as it should be, in agreement with data presented by J. H. Reynolds, Jr.,[8] J.M. ASCE. The only way in which the present results may at this point be considered an improvement on these earlier results is in the simple, explicit analytical expressions, Eq. 6*e*, Eq. 7, and Eq. 8*c*.

Eqs. 8 for $\sigma_B(0)$ are in agreement, for a suitably chosen value of the Poisson ratio, μ, with the test results mentioned previously.[9] The function F_3 of those results is related to Eqs. 8 as follows:

---

[8] "Design Criteria for Expediently Solidified Flexible Soil Surfaces," by J. H. Reynolds, Jr., *Memorandum*, Eng. Research and Development Labs., Fort Belvoir, Va., October, 1953, Figs. 1–4.

[9] "Deflections, Moments, and Reactive Pressures for Concrete Pavements," by G. Pickett, M. E. Raville, W. C. Jones, and F. J. McCormick, *Bulletin No. 65*, Kansas State College, Manhattan, Kans., October, 1951, Table 8.

$$F_3 = \frac{1+\mu}{16}\left[\nu\, H_1^{(1)}(\nu) + \bar{\nu}\, H_1^{(2)}(\bar{\nu})\right]$$

or

$$F_3 = \frac{1+\mu}{4\,\pi}\,\frac{a}{l}\,\mathrm{kei}'\,\frac{a}{l}.$$

It should finally be noted that expressions similar to Eqs. 6*d* and 8*c* have been obtained by H. M. Westergaard.[10]

Numerical Example.—It is assumed that $a = 9$ in., $h = 4.5$ in., $E = 10^5$ lb per sq in., and $k = 10^2$ lb per cu in. Hence,

$$\rho\, a = \sqrt[4]{\frac{10^2}{\frac{1}{12}\,10^5 \times 4.5^3}}\; 9 = \frac{4.82}{5} = 0.96.$$

From Table 1 (Eq. 6*c*), $C = \sigma_F(0)/p_0 \approx 0.3$. From Eq. 8*b*, for bending stress $\sigma_B(0)$, if μ is assumed to be $\frac{1}{4}$,

$$\frac{\sigma_B(0)}{p_0} = \sqrt{\frac{5}{4}}\,\sqrt{\frac{10^5}{10^2 \times 4.5}}\; 0.96 \times 0.35 \approx 5.5.$$

As $\rho\, a$ satisfies the restriction of Eq. 7, reasonable values of $\sigma_F(0)$ and of $\sigma_B(0)$ should follow from the approximate expressions, Eqs. 6*e* and 8*c*. From Eq. 6*e*, $C \approx 0.36$, and from Eq. 8*c*, $(\mu = 1/4)$, $\sigma_B(0)/p_0 \approx (3/2)(5/4)\ 4 \log 2.07 \approx 5.47$. Clearly, the numerical data following from the approximate formulas are adequate, even though one is close to the upper end of what was stated to be their usable range.

PROBLEM 2: PARABOLIC LOAD

Eq. 1 is also applicable to an elastic plate having the load distribution,

$$\left.\begin{array}{ll} p = p_0\left[\eta + 2\,(1-\eta)\left(\dfrac{r}{a}\right)^2\right], & r \le a \\ p = 0, & a < r \end{array}\right\} \qquad (9)$$

The parameter, η, may have any real value. The range between zero and 2 is of particular interest. When $\eta = 1$, the load distribution is uniform. When $\eta = 0$, the load intensity varies from zero at midpoint to maximum load at the outer rim of the load surface. When $\eta = 2$, the load intensity is greatest for $r = 0$ and decreases to zero at $r = a$. The total load—

$$\int_0^a 2\,\pi\, r\, p\, dr = \pi\, a^2\, p_0$$

—is independent of the value of η.

---

[10] "Analytical Tools for Judging Results of Structural Tests of Concrete Pavements," by H. M. Westergaard, *Public Roads*, Vol. 14, 1933, pp. 185–188.

The following expressions are obtained after many transformations:

$$\frac{\sigma_F(0)}{p_0} = 1 + \rho\, a \operatorname{ker}'\rho\, a + (1 - \eta)\left(-1 + \rho\, a \operatorname{ker}'\rho\, a + \frac{8 \operatorname{kei}'\rho\, a}{\rho\, a} - 4 \operatorname{ker}\rho\, a\right) \quad (10a)$$

$$\frac{\sigma_B(0)}{p_0} = \frac{\sqrt{3}}{2}\sqrt{\frac{1+\mu}{1-\mu}}\sqrt{\frac{E}{k\, h}}\left\{\rho\, a \operatorname{kei}'\rho\, a + (1 - \eta)\left[\rho\, a \operatorname{kei}'\rho\, a - 4 \operatorname{kei}\rho\, a - \frac{8 \operatorname{ker}'\rho\, a}{\rho\, a} - \frac{8}{(\rho\, a)^2}\right]\right\} \quad (10b)$$

When $\eta = 1$, Eq. 10*a* is reduced to Eq. 6*c* and Eq. 10*b* is reduced to Eq. 8*b*. One may write

$$\frac{\sigma_F(0)}{p_0} = C_F + (1 - \eta)\, C^*_F \quad (11a)$$

and

$$\frac{\sigma_B(0)}{p_0} = [C_B + (1 - \eta)\, C^*_B]\frac{\sqrt{3}}{2}\sqrt{\frac{1+\nu}{1-\nu}\frac{E}{k\, h}} \quad (11b)$$

In both Eq. 11*a* and Eq. 11*b* the second terms on the right describe the effect of nonuniformity of the load distribution. To be sure that the results for uniform load distribution are significant one should, it would appear, require that these second terms be negligible compared with the first terms; Table 2 is of use in this determination.

TABLE 2.—RELATIVE CONTRIBUTIONS TO σ_F AND σ_B

Pressure and bending stress coefficients	VALUE OF $\rho\, a$			
	0	0.5	1.0	2.0
C_F	0	0.090	0.31	0.79
C^*_F	0	−0.002	−0.02	−0.17
C_B	0	0.167	0.35	0.44
C^*_B	0	−0.030	−0.11	−0.32

Inspection of Table 2 reveals that, when $\rho\, a$ is appreciably larger than unity the effect of nonuniformity of the applied load can no longer be neglected. Because the actual distribution may not be uniform, computations based on uniformity of load distribution should be viewed with caution if $\rho\, a$ is greater than approximately unity.

PROBLEM 3: UNIFORM TENSION

In an infinite elastic plate subjected to a two-dimensional hydrostatic state of tension, σ, in the plane of the undeflected surface layer, the horizontal stress resultants are $h\, \sigma = N$. The effect of this state of tension on the resistance against lateral loads is expressed by modifying the differential equation for the deflection, w, as follows:

$$D\,\nabla^2\nabla^2 w - N\,\nabla^2 w + k\,w = p \quad \text{(12)}$$

Attention will be restricted to the case of a uniformly distributed lateral load, p, as expressed by Eqs. 2.

The solution, w, is found to be of the following form:

$$\left.\begin{aligned} w &= \frac{p_0}{k}\left[1 + C_1\,J_0(\lambda\,r) + \bar{C}_1\,J_0(\bar{\lambda}\,r)\right], & r &\leq a \\ w &= \frac{p_0}{k}\left[C_2\,H_0^{(1)}(\lambda\,r) + \bar{C}_2\,H_0^{(2)}(\bar{\lambda}\,r)\right], & a &< r \end{aligned}\right\} \quad \text{(13)}$$

in which

$$\lambda = \rho\,e^{i\phi}, \qquad \lambda = \rho\,e^{-i\phi} \quad \text{(14a)}$$

$$\rho = \sqrt[4]{\frac{k}{D}}, \qquad \cos 2\,\phi = -\,\frac{N}{2\,\sqrt{k\,D}} \quad \text{(14b)}$$

$$\nu = \lambda\,a = \rho\,a\,e^{i\phi} \quad \text{(14c)}$$

$$C_1 = \frac{\pi\,\nu}{4\,i}\,\frac{H_1^{(1)}(\nu)}{1 + \dfrac{N}{2\,D\,\lambda^2}} \quad \text{(15a)}$$

and

$$C_2 = \frac{\pi\,\nu}{4\,i}\,\frac{J_1(\nu)}{1 + \dfrac{N}{2\,D\,\bar{\lambda}^2}} \quad \text{(15b)}$$

For the numerical evaluation of the effect of the built-in tensile stress, $\sigma = N/h$, attention will be restricted to the values of the foundation pressure at the origin, $\sigma_F(0)$, and to the bending stress in the plate at the origin, $\sigma_B(0)$. The following expressions are obtained for these two quantities:

$$\frac{\sigma_F(0)}{p_0} = 1 + \frac{\pi\,\rho\,a}{4}\left(\frac{u_1 - V_1}{\sin\phi} + \frac{v_1 + U_1}{\cos\phi}\right) \quad \text{(16)}$$

and

$$\frac{\sigma_B(0)}{p_0} = \pm\sqrt{\frac{3\,(1+\mu)}{4\,(1-\mu)}}\sqrt{\frac{E}{k\,h}}\,\frac{\pi\,\rho\,a}{4}\left(\frac{u_1 - V_1}{\sin\phi} - \frac{v_1 + U_1}{\cos\phi}\right) \quad \text{(17)}$$

The quantities, u_1, v_1, U_1, and V_1, occurring in Eqs. 16 and 17 are tabulated functions[3] defined as follows:

$$\left.\begin{aligned} J_1(\nu) &= u_1\,(\rho\,a,\phi) + i\,v_1\,(\rho\,a,\phi) \\ Y_1(\nu) &= U_1\,(\rho\,a,\phi) + i\,V_1(\rho\,a,\phi) \\ H_1^{(1)}(\nu) &= (u_1 - V_1) + i\,(v_1 + U_1) \end{aligned}\right\} \quad \text{(18)}$$

In the absence of built-in tension—that is, for $N = 0$—Eq. 14b yields $\cos 2\,\phi = 0$ and $\phi = \pi/4$; the results are thus reduced to those of Problem 1. The solution presented in Eqs. 13, 14, and 15 is valid in the form stated so long as $|\cos 2\phi| < 1$—that is, so long as $N \leq 2\sqrt{k\,D}$. Subsequent numerical examples will show that this relationship is satisfied for practical values of N. However, to deduce from the results the limiting case of a "membrane" with $D = 0$, one would first have to write the results in a different form.

The use of Eqs. 16 and 17 and the influence of pretension on stresses will be illustrated by a numerical example.

Example.—It is assumed that $a = 9$ in., $h = 4.5$ in., $k = 10^2$ lb per cu in., and $E = 10^5$ lb per sq in. Hence, according to Eqs. 14,

$$\rho\, a = \sqrt[4]{\frac{10^2}{\frac{1}{12}\,10^5 \times 4.5^3}}\; 9 = 0.96$$

and

$$\cos 2\,\phi = \frac{-\,\sigma}{3{,}860}.$$

Attention will be restricted to cases in which σ is of the order of several hundreds of pounds per square inch. Then, $|\cos 2\,\phi| \ll 1$ or $2\,\phi \approx \pi/2$ and $\phi \approx \pi/4$. Taking the first value of ϕ in excess of $\pi/4$ for which the functions in the expressions for σ_F and σ_B are tabulated, $\phi = 5\,\pi/18 = 50°$ and $\cos 2\,\phi = \cos 100° = -\cos 80° = -\,0.1736$. Therefore, $\sigma = 3{,}860 \times 0.1736 = 670$ lb per sq in. Furthermore, $\sin 50° = 0.766$, $\cos 50° = 0.643$, and[11,12]

$$u_1(0.96, 50°) = +\,0.356, \qquad v_1(0.96, 50°) = +\,0.338,$$
$$U_1(0.96, 50°) = -\,0.785, \qquad V_1(0.96, 50°) = +\,0.579.$$

From Eq. 16, $\sigma_F(0)/p_0 = 0.26$, which indicates that the effect of a pretension of 670 lb per sq in. is to reduce the maximum foundation pressure by approximately 13% of its value in the absence of pretension.

Next, from Eq. 17 (setting $\mu = 1/4$), $\sigma_B(0)/p_0 = 5.25$, which indicates that the effect of pretension in this case reduces the maximum bending stress by approximately 5%.

Although further numerical examples can readily be solved in the same manner as the foregoing, it is apparent that pretension stresses of hundreds of pounds per square inch have only a relatively minor influence on foundation pressure and bending stress in a flexible surface layer, in the range of dimensions and rigidities that are under consideration.

PROBLEM 4: NONLINEAR EFFECTS

The analysis of nonlinear effects is based on the differential equations for finite deflections of elastic plates. These are, for the case of rotationally symmetric displacements,

$$D\,\nabla^2\,\nabla^2 w + k\,w = \frac{1}{r}\frac{d}{dr}\left(\frac{dF}{dr}\frac{dw}{dr}\right) + p \ldots\ldots\ldots\ldots (19a)$$

---

[11] "Table of the Bessel Functions $J_0(z)$ and $J_1(z)$ for Complex Arguments," Mathematical Tables Project, National Bureau of Standards, U. S. Dept. of Commerce, Columbia Univ. Press, New York, N. Y., 1947, p. 203.

[12] "Table of the Bessel Functions $Y_0(z)$ and $Y_1(z)$ for Complex Arguments," Computation Lab., National Bureau of Standards, U. S. Dept. of Commerce, Columbia Univ. Press, New York, N. Y., 1950, p. 203.

and

$$\nabla^2 \nabla^2 F = -\frac{E\,h}{2\,r}\frac{d}{dr}\left[\left(\frac{dw}{dr}\right)^2\right] \qquad \text{(19}b\text{)}$$

in which the load intensity function, p, is given by Eq. 2. The quantities D, ∇^2, w, k, p, and $E\,h$ are the same as those used in the linear small-deflection theory. The function, F, represents the stresses in the midplane of the plate which are negligible in the case of sufficiently small deformations. The foregoing equations correspond to those already considered[13] except that in the present treatment the horizontal subgrade reaction is considered negligible.

The following is a natural procedure for solving Eqs. 19:

a. The first of the two equations is solved for w as if the nonlinear term involving F were absent.

b. With the value of w so determined the second equation is entered and F is determined in terms of w.

c. Using these values of F and w, the nonlinear term in the first differential equation is computed. If this term, computed in this manner, is small compared with p, the nonlinear effect is negligible.

A systematic approach by means of the introduction of suitable dimensionless variables can furnish important qualitative information in this problem without performance of any numerical computations. It is assumed that a, the radius of the load surface, can be considered a "representative" length in the sense that significant changes are assumed to take place over distances of the order a. Then, in the linear theory, the bending term, $D\,\nabla^2\,\nabla^2 w$, is of importance, and the deflection is of the order of magnitude of $p\,a^4/D$ as though it were a plate of radius a supported along the edge instead of continuously by the subgrade. On the basis of these observations there is set

$$r = \xi\,a \qquad \text{(20}a\text{)}$$

and

$$w = \frac{p_0\,a^4}{D} f(\xi) \qquad \text{(20}b\text{)}$$

in which f is of the order of unity. Furthermore,

$$\nabla^2 w = \frac{p_0\,a^2}{D} \nabla^2_* f(\xi) \qquad \text{(20}c\text{)}$$

in which

$$\nabla^2_* = \frac{d^2}{d\xi^2} + \frac{1}{\xi}\frac{d}{d\xi} \qquad \text{(20}d\text{)}$$

Because of the assumption concerning a, the quantity, $\nabla^2_* f$, is also of the order of unity.

---

[13] "Deflections, Moments and Reactive Pressures for Concrete Pavements," by G. Pickett, M. E., Raville, W. C. Jones, and F. J. McCormick, *Bulletin No. 65*, Kansas State College, Manhattan, Kans. October, 1951, pp. 52–70.

Because it is desired to determine F in the first approximation from the second differential equation, one must make F nondimensional in such a manner that the terms containing F and w in this equation are of the same importance. This can be accomplished by setting

$$F = E\,h \left(\frac{p_0\,a^4}{D} \right)^2 g(\xi) \tag{20e}$$

The system of differential equations to be considered is now of the form:

$$\nabla^2_* \nabla^2_* f + \frac{k\,a^4}{D} f = \frac{E\,h}{D} \left(\frac{p_0\,a^4}{D} \right)^2 \frac{1}{\xi} \frac{d}{d\xi} \left(\frac{dg}{d\xi} \frac{df}{d\xi} \right) + \frac{p}{p_0} \tag{21a}$$

and

$$\nabla^2_* \nabla^2_* g = -\frac{1}{2} \frac{1}{\xi} \frac{d}{d\xi} \left[\left(\frac{df}{d\xi} \right)^2 \right] \tag{21b}$$

in which

$$\left. \begin{aligned} \frac{p}{p_0} &= 1, \qquad \xi \leq 1 \\ \frac{p}{p_0} &= 0, \qquad 1 < \xi \end{aligned} \right\} \tag{21c}$$

and

There are still two parameters in Eqs. 21, $k\,a^4/D$ and $(E\,h/D)(p_0\,a^4/D)^2$. The previous work concerning small deflections showed that $(k\,a^4/D)$ should be no more than unity. The remaining parameter, $(E\,h/D)(p_0\,a^4/D)^2$, indicates whether or not nonlinearity is important. If $(E\,h/D)(p_0\,a^4/D)^2$ is approximately unity, nonlinearity is important. However, if $(E\,h/D)(p_0\,a^4/D^2) \ll 1$, nonlinearity is not important. This condition may be expressed in terms of deflections. Setting $p_0\,a^4/D = \delta$, in which δ is the deflection according to the linear theory, and noting that $E\,h/D = 12\,(1 - \mu^2)/h^2$, the foregoing condition may be written in the form: $12\,(1 - \mu^2)\delta^2/h^2 \ll 1$. That is, nonlinear effects are negligible, as long as the deflection, δ, is small compared with the thickness, h, of the plate. This result, however, requires for its validity that $k\,a^4/D$ be not large compared with unity. If $k\,a^4/D$ is large compared with unity, a case not considered important here, a different procedure must be used for the analysis of the problem.

In the event that nonlinear corrections to the linear theory might be desired, an appropriate systematic procedure would be to develop f and g in powers of the parameter $(E\,h/D)(p_0\,a^4/D)^2$.

CONCLUSIONS

Comparative studies of flexible surface layers endowed with a variety of properties may be conducted most simply by representing the subgrade by a system of tension-compression springs. This type of subgrade has the same behavior as a heavy-liquid subgrade characterized by a foundation constant, k.

As long as the ratio of the diameter of load surface to the thickness of the surface layer, $2\,a/h$, is approximately unity or larger, it is permissible to consider the surface layer as a "thin plate." For values of $2\,a/h$ between approximately one and two, transverse-shear deformation in the plate is of quantitative significance. It is recommended that at some future date the work of the present paper be supplemented so as to coordinate the present results with results showing the correction effect of transverse-shear deformation.

It is suggested that the practical usefulness of a flexible surface layer requires satisfaction of the limit relationship,

$$\frac{2\,a}{h}\sqrt[4]{\frac{k\,h}{E}} \lesssim 1.5 \quad\text{(22a)}$$

So long as the foregoing limit relationship is satisfied, one has as simple formulas representing maximum foundation pressure, $\sigma_F(0)$, and maximum tensile (bending) stress in the surface layer, $\sigma_B(0)$, with only a small percentage of error,

$$\frac{\sigma_F(0)}{p_0} = \frac{\pi}{4}\sqrt{3\,(1-\mu^2)}\left(\frac{a}{h}\right)^2\sqrt{\frac{k\,h}{E}} \quad\text{(22b)}$$

and

$$\frac{\sigma_B(0)}{p_0} = \frac{3\,(1+\mu)}{8}\left(\frac{a}{h}\right)^2 \log\left[\frac{4}{3\,(1-\mu^2)}\,\frac{E}{k\,h}\left(\frac{h}{a}\right)^4\right] \quad\text{(22c)}$$

If the limit relationship of Eq. 22*a* is satisfied, one has the following assurances:

a. The loading stress on the subgrade is reduced more than half by the interposition of the flexible surface layer.

b. Nonuniformity of the loading-stress distribution is of secondary importance.

c. Built-in tensions of reasonable magnitude in the flexible surface layer are of negligible effect.

d. Nonlinear effects due to finite deformation are negligible so long as the transverse deflection due to load of the surface layer is smaller than half the thickness of the surface layer.

ACKNOWLEDGMENTS

This paper is based on a report prepared for the Engineer Research and Development Laboratories at Fort Belvoir, Va., under Contract DA-44-009 ENG-1863, the final report having been accepted in March, 1954.

The writer wishes to express his appreciation for helpful suggestions concerning the subject of this paper to Mr. Reynolds, who, at that time, was project engineer at Fort Belvoir, and to his colleagues, T. W. Lambe, M. ASCE, G. E. Murray, and the late D. W. Taylor of the Soil Mechanics group at the Massachusetts Institute of Technology at Cambridge.

APPENDIX I. INFINITE ELASTIC PLATE CARRYING A PARABOLICALLY DISTRIBUTED LOAD

Derivations.—The following derivations include the uniformly distributed load as a special case. The differential equation is

$$\left.\begin{array}{ll} D\nabla^2 \nabla^2 w + k\, w = p_0 \left[\eta + 2\,(1-\eta)\,\dfrac{r^2}{a^2}\right], & r \leq a \\ D\nabla^2 \nabla^2 w + k\, w = 0, & a < r \end{array}\right\} \ldots\ldots (23)$$

The total load is expressed as

$$2\,\pi \int_0^\infty p\, r\, dr = 2\,\pi\, p_0 \int_0^a \left[\eta + 2\,(1-\eta)\,\frac{r^2}{a^2}\right] r\, dr$$

$$= 2\,\pi\, p_0 \left[\eta\,\frac{a^2}{2} + 2\,(1-\eta)\,\frac{a^2}{4}\right] = \pi\, p_0\, a^2 \ldots\ldots (24)$$

and is independent of η. At the radius $r = a$, the solution w has to satisfy transition conditions which can be written in the form:

$$r = a;\ w,\ w',\ \nabla^2 w,\ \text{and}\ (\nabla^2 w)'\ \text{continuous} \ldots\ldots (25)$$

The general solution of the differential equation is

$$w = w_{hom} + w_{part} \ldots\ldots (26)$$

in which

$$w_{hom} = A_1\, J_0(\lambda\, r) + A_2\, Y_0(\lambda\, r) + A_3\, J_0(\bar{\lambda}\, r) + A_4\, Y_0(\bar{\lambda}\, r) \ldots\ldots (27)$$

and

$$\left.\begin{array}{ll} w_{part} = \dfrac{p_0}{k}\left[\eta + 2\,(1-\eta)\,\dfrac{r^2}{a^2}\right], & r \leq a \\ w_{part} = 0, & a < r \end{array}\right\} \ldots\ldots (28)$$

and in which

$$\left.\begin{array}{ll} & \lambda = \sqrt{i}\,\sqrt[4]{\dfrac{k}{D}} = \dfrac{1+i}{\sqrt{2}}\,\sqrt[4]{\dfrac{k}{D}} \\ \text{and} & \\ & \bar{\lambda} = \dfrac{1-i}{2}\,\sqrt[4]{\dfrac{k}{D}} \end{array}\right\} \ldots\ldots (29)$$

Suitable constants of integration are selected next. Because $Y_0(0) = \infty$- it is necessary to set A_2 and A_4 equal to zero in the region $r \leq a$. Further, more,[3,4] $J_0(\lambda\, r)$ and $J_0(\bar{\lambda}\, r)$ are conjugate complex, as follows:

$$\left.\begin{array}{l} J_0(\lambda\, r) = u_0\left(\rho\, r, \dfrac{\pi}{4}\right) + i\, v_0\left(\rho\, r, \dfrac{\pi}{4}\right) \\ J_0(\bar{\lambda}\, r) = u_0\left(\rho\, r, \dfrac{\pi}{4}\right) - i\, v_0\left(\rho\, r, \dfrac{\pi}{4}\right) \end{array}\right\} \ldots\ldots (30)$$

in which u_0 and v_0 are tabulated as functions of $\rho\, r$.

In order that w may be a real function one may write, for the region in which $r \leq a$,

$$w = \frac{p_0}{k}\left[C_1\, J_0(\lambda\, r) + \bar{C}_1\, J_0(\bar{\lambda}\, r) + \eta + 2\,(1 - \eta)\,\frac{r^2}{a^2}\right] \tag{31}$$

in which C_1 and $\bar{C}_1$ are conjugate complex.

In order to obtain the proper form for w in the region $a < r$, it is necessary to consider the behavior of the Bessel functions for large values of their arguments. In accordance with usage,

$$J_0 + i\, Y_0 = H_0^{(1)}$$

and

$$\left.\begin{aligned} J_0 + i\, Y_0 &= H_0^{(1)} \\ J_0 - i\, Y_0 &= H_0^{(2)} \end{aligned}\right\} \tag{32}$$

Because

$$\left.\begin{aligned} Y_0(\lambda\, r) &= U_0 + i\, V_0 \\ Y_0(\bar{\lambda}\, r) &= U_0 - i\, V_0 \end{aligned}\right\} \tag{33}$$

it is observed that

$$H_0^{(2)}(\bar{\lambda}\, r) = \overline{H_0^{(1)}(\lambda\, r)} \tag{34}$$

For large values of the argument,

$$\left.\begin{aligned} H_0^{(1)}(z) &\approx \frac{1}{\sqrt{z}}\, e^{iz} \\ H_0^{(2)}(z) &\approx \frac{1}{\sqrt{z}}\, e^{-iz} \end{aligned}\right\} \tag{35}$$

and consequently,

$$\left.\begin{aligned} H_0^{(1)}(\lambda\, r) &\approx \frac{1}{\sqrt{\lambda\, r}}\, e^{i(1+i)\rho r/\sqrt{2}} = \frac{1}{\sqrt{\lambda\, r}}\, e^{(-1+i)\rho r/\sqrt{2}} \\ H_0^{(2)}(\bar{\lambda}\, r) &\approx \frac{1}{\sqrt{\bar{\lambda}\, r}}\, e^{-i(1-i)\rho r/\sqrt{2}} = \frac{1}{\sqrt{\bar{\lambda}\, r}}\, e^{(-1-i)\rho r/\sqrt{2}} \end{aligned}\right\} \tag{36}$$

Both these functions decay exponentially for large values of $\rho\, r$, whereas $H_0^{(1)}(\bar{\lambda}\, r)$ and $H_0^{(2)}(\lambda\, r)$ increase exponentially. The latter functions must therefore be excluded from the solution of the present problem. Altogether, then, a real solution valid in $a < r$ is

$$w = \frac{p_0}{k}\left[C_2\, H_0^{(1)}(\lambda\, r) + \bar{C}_2\, H_0^{(2)}(\bar{\lambda}\, r)\right] \tag{37}$$

in which C_2 and $\bar{C}_2$ are conjugate complex.

For evaluation of transition conditions it is necessary to utilize the following Bessel-function differentiation formulas:

$$(J_0,\, Y_0)'(\lambda\, r) = -\,(J_1,\, Y_1)(\lambda\, r) \tag{38}$$

and

$$\nabla^2\,(J_0,\, Y_0)(\lambda\, r) = -\,\lambda^2\,(J_0,\, Y_0)(\lambda\, r) \tag{39}$$

To evaluate the transition conditions of Eq. 25, set

$$\lambda\, a = \nu, \qquad \bar{\lambda}\, a = \bar{\nu} \tag{40}$$

Combination of Eqs. 25, 31, and 37 gives

$$\left.\begin{array}{l} C_1\, J_0(\nu) + \bar{C}_1\, J_0(\bar{\nu}) + (2 - \eta) = C_2\, H_0^{(1)}(\nu) + \bar{C}_2\, H_0^{(2)}(\bar{\nu}) \\ C_1\, \nu\, J_1(\nu) + \bar{C}_1\, \bar{\nu}\, J_1(\bar{\nu}) - 4\,(1 - \eta) = C_2\, \nu\, H_1^{(1)}(\nu) + C_2\, \bar{\nu}\, H_1^{(2)}(\bar{\nu}) \\ C_1\, \nu^2\, J_0(\nu) + \bar{C}_1\, \bar{\nu}^2\, J_0\,(\bar{\nu}) - 8\,(1 - \eta) = C_2\, \nu^2\, H_0^{(1)}(\nu) + \bar{C}_2\, \bar{\nu}^2\, H_0^{(2)}(\bar{\nu}) \\ C_1\, \nu^3\, J_1(\nu) + \bar{C}_1\, \bar{\nu}^3\, J_1\,(\bar{\nu}) = C_2\, \nu^3\, H_1^{(1)}(\nu) + \bar{C}_2\, \bar{\nu}^3\, H_1^{(2)}(\bar{\nu}) \end{array}\right\} \tag{41}$$

From Eqs. 29 and 40, $\bar{\nu}^2 = -\nu^2$, which permits considerable simplification of Eqs. 41. Combining the first and third of Eqs. 41 by suitable addition,

$$2\, C_1\, J_0(\nu) + (2 - \eta) - \frac{8\,(1 - \eta)}{\nu^2} = 2\, C_2\, H_0^{(1)}(\nu) \tag{42a}$$

Combining the second and fourth equations by suitable addition,

$$2\, C_1\, \nu\, J_1(\nu) - 4\,(1 - \eta) = 2\, C_2\, \nu\, H_1^{(1)}(\nu) \tag{42b}$$

or

$$\left.\begin{array}{l} C_1\, J_0(\nu) - C_2\, H_0^{(1)}(\nu) = -\left(1 - \dfrac{\eta}{2}\right) + \dfrac{4}{\nu^2}\,(1 - \eta) \\ C_1\, J_1(\nu) - C_2\, H_1^{(1)}(\nu) = \dfrac{2}{\nu}\,(1 - \eta) \end{array}\right\} \tag{42c}$$

From Eq. 20*c*,

$$\Delta C_1 = \left[\left(1 - \frac{\eta}{2}\right) - \frac{4}{\nu^2}\,(1 - \eta)\right] H_1^{(1)}(\nu) + \frac{2}{\nu}\,(1 - \eta)\, H_0^{(1)}(\nu) \tag{43a}$$

$$\Delta C_2 = \frac{2}{\nu}\,(1 - \eta)\, J_0(\nu) + \left[\left(1 - \frac{\eta}{2}\right) - \frac{4}{\nu^2}\,(1 - \eta)\right] J_1(\nu) \tag{43b}$$

in which

$$\Delta = J_1(\nu)\, H_0^{(1)}(\nu) - J_0(\nu)\, H_1^{(1)}(\nu) \tag{43c}$$

The determinant, Δ, may be simplified by means of the identity,[14] $J_0(z)\, Y_1(z) - J_1(z)\, Y_0(z) = -2/\pi\, z$. Substituting Eqs. 32 into Eq. 43*c*, there follows $\Delta = J_1\,(J_0 + i\, Y_0) - J_0\,(J_1 + i\, Y_1) = i\,(J_1\, Y_0 - J_0\, Y_1)$ or

$$\Delta = \frac{2\, i}{\pi\, \nu} \tag{43d}$$

Hence,

$$C_1 = \frac{\pi}{2\, i}\left\{\left[\left(1 - \frac{\eta}{2}\right)\nu - \frac{4\,(1 - \eta)}{\nu}\right] H_1^{(1)}(\nu) + 2\,(1 - \eta)\, H_0^{(1)}(\nu)\right\} \tag{44a}$$

---

[14] "Table of the Bessel Functions $Y_0(z)$ and $Y_1(z)$ for Complex Arguments," Computation Lab., National Bureau of Standards, U. S. Dept. of Commerce, Columbia Univ. Press, New York, N. Y., 1950, pp. XXIII–XXIV.

and

$$C_2 = \frac{\pi}{2\,i}\left\{\left[\left(1-\frac{\eta}{2}\right)\nu - \frac{4\,(1-\eta)}{\nu}\right] J_1(\nu) + 2\,(1-\eta)\,J_0(\nu)\right\} \dots\dots (44b)$$

In the case of uniform load distribution for which $\eta = 1$, these expressions are simplified to

$$C_1 = \frac{1}{4}\,i\,\pi\,\nu\,H_1^{(1)}(\nu) \dots\dots (45a)$$

and

$$C_2 = \frac{1}{4}\,i\,\pi\,\nu\,J_1(\nu) \dots\dots (45b)$$

Introduction of Eqs. 45 into Eqs. 31 and 37 leads to Eqs. 5.

To obtain an expression for center deflections, Eqs. 44 are introduced into Eq. 31, giving

$$w(0) = \frac{p_0}{k}\,(\eta + C_1 + \bar{C}_1) \dots\dots (46)$$

The expression for foundation pressure, $\sigma_F(0)$, is

$$\frac{\sigma_F(0)}{p_0} = \eta + 2\,Re\,(C_1) \dots\dots (47)$$

in which, with $\sqrt[4]{k/D}\,a$ equal to κ,

$$C_1 = \frac{\pi}{2\,i}\left\{\left[\left(1-\frac{\eta}{2}\right)\frac{1+i}{\sqrt{2}}\,\kappa - \frac{4\,(1-\eta)}{\kappa}\,\frac{\sqrt{2}}{1+i}\right] H_1^{(1)}(\kappa\,e^{i\pi/4}) + 2\,(1-\eta)\,H_0^{(1)}(\kappa\,e^{i\pi/4})\right\} \dots (48)$$

From Eqs. 30, 32, and 33,

$$\begin{aligned} H_0^{(1)}(\kappa\,e^{i\pi/4}) &= J_0(\kappa\,e^{i\pi/4}) + i\,Y_0(\kappa\,e^{i\pi/4}) \\ &= u_0\left(\kappa,\frac{\pi}{4}\right) + i\,v_0\left(\kappa,\frac{\pi}{4}\right) + i\left[U_0\left(\kappa,\frac{\pi}{4}\right) + i\,V_0\left(\kappa,\frac{\pi}{4}\right)\right] \\ &= \left[u_0\left(\kappa,\frac{\pi}{4}\right) - V_0\left(\kappa,\frac{\pi}{4}\right)\right] + i\left[v_0\left(\kappa,\frac{\pi}{4}\right) + U_0\left(\kappa,\frac{\pi}{4}\right)\right] \end{aligned}$$

and[14]

$$H_0^{(1)}(\kappa\,e^{i\pi/4}) = -\frac{2}{\pi}\,\mathrm{kei}\,\kappa - \frac{2\,i}{\pi}\,\mathrm{ker}\,\kappa \dots\dots (49)$$

Analogously,

$$\begin{aligned} H_1^{(1)}(\kappa\,e^{i\pi/4}) &= u_1\left(\kappa,\frac{\pi}{4}\right) - V_1\left(\kappa,\frac{\pi}{4}\right) \\ &\quad + i\left[v_1\left(\kappa,\frac{\pi}{4}\right) + U_1\left(\kappa,\frac{\pi}{4}\right)\right] = \frac{2}{\pi}\left[\mathrm{kei}_1\,\kappa + i\,\mathrm{ker}_1\,\kappa\right] \dots (50) \end{aligned}$$

Therefore,

$$C_1 = \left[\left(1 - \frac{\eta}{2}\right)\frac{1+i}{\sqrt{2}}\,\kappa - \frac{4\,(1-\eta)}{\kappa}\,\frac{1-i}{\sqrt{2}}\right](\mathrm{ker}_1\,\kappa - i\,\mathrm{kei}_1\,\kappa)$$
$$- 2\,(1-\eta)(\mathrm{ker}\,\kappa - i\,\mathrm{kei}\,\kappa)$$

and

$$R\,e\,(C_1) = \left(1 - \frac{\eta}{2}\right)\frac{\kappa}{\sqrt{2}}\,(\mathrm{ker}_1\,\kappa + \mathrm{kei}_1\,\kappa)$$
$$+ \frac{4\,(1-\eta)}{\sqrt{2}\,\kappa}\,(-\,\mathrm{ker}_1\,\kappa + \mathrm{kei}_1\,\kappa) - 2\,(1-\eta)\,\mathrm{ker}\,\kappa.$$

Finally,[15] with

$$\mathrm{ker}_1\,\kappa = \frac{1}{\sqrt{2}}\,(\mathrm{ker}'\,\kappa - \mathrm{kei}'\,\kappa)$$

$$\mathrm{kei}_1\,\kappa = \frac{1}{\sqrt{2}}\,(\mathrm{ker}'\,\kappa + \mathrm{kei}'\,\kappa)$$

and

$$\mathrm{ker}_1\,\kappa + \mathrm{kei}_1\,\kappa = \sqrt{2}\,\mathrm{ker}'\,k$$
$$\mathrm{ker}_1\,\kappa - \mathrm{kei}_1\,\kappa = \sqrt{2}\,\mathrm{kei}'\,k,$$

there follows

$$R\,e\,(C_1) = \left(1 - \frac{\eta}{2}\right)\kappa\,\mathrm{ker}'\,\kappa + \frac{4\,(1-\eta)}{\kappa}\,\mathrm{kei}'\,\kappa - 2\,(1-\eta)\,\mathrm{ker}\,\kappa$$
$$= \frac{1}{2}\,\kappa\,\mathrm{ker}'\,\kappa + (1-\eta)\left(-\,2\,\mathrm{ker}\,\kappa + \frac{4}{\kappa}\,\mathrm{kei}'\,\kappa + \frac{\kappa}{2}\,\mathrm{ker}'\,\kappa\right)\ldots(51)$$

Introducing Eq. 51 into Eq. 47 finally results in the following expression for foundation pressure, $\sigma_F(0)$:

$$\frac{\sigma_F(0)}{p_0} = 1 + \rho\,a\,\mathrm{ker}'\,\rho\,a + (1-\eta)(-\,4\,\mathrm{ker}\,\rho\,a - 1$$
$$+ \frac{8}{\rho\,a}\,\mathrm{kei}'\,\rho\,a + \rho\,a\,\mathrm{ker}'\,\rho\,a)\ldots(52)$$

Eq. 52 is the same as Eq. 10*a*. If $\eta = 1$, Eq. 52 is reduced to Eq. 6*c*.

In accordance with Eqs. 4 for bending stresses,

$$\sigma_{rB} = \pm\,\frac{E\,h}{2\,(1-\mu^2)}\left(\nabla^2 w - \frac{1-\mu}{r}\,w'\right)\ldots\ldots\ldots\ldots(53a)$$

and

$$\sigma_{\theta B} = \pm\,\frac{E\,h}{2\,(1-\mu^2)}\left(\frac{1-\mu}{r}\,w' + \mu\,\nabla^2 w\right)\ldots\ldots\ldots\ldots(53b)$$

Eqs. 53 will be evaluated for $r = 0$. From Eqs. 9 and considering Eqs. 16

---

[15] "Tables of Integrals and Other Mathematical Data," by H. B. Dwight, The Macmillan Co., New York, N. Y., 1947, pp. 190–191.

and 17, so long as $r \leq a$,

$$w' = -\frac{p_0}{k}\left[C_1 \lambda\, J_1(\lambda\, r) + \bar{C}_1 \lambda\, J_1(\lambda\, r) - \frac{4\,(1-\eta)\, r}{a^2}\right] \ldots\ldots (54a)$$

and

$$\nabla^2 w = -\frac{p_0}{k}\left[C_1 \lambda^2\, J_0(\lambda\, r) + \bar{C}_1 \lambda^2\, J_0(\lambda\, r) - \frac{8\,(1-\eta)}{a^2}\right] \ldots\ldots (54b)$$

Because

$$\left.\begin{aligned} \lim_{r\to 0} \frac{J_1(r)}{r} &= \frac{1}{2} \\ \lim_{r\to 0} J_0(r) &= 1 \end{aligned}\right\} \ldots\ldots\ldots\ldots\ldots\ldots\ldots\ldots (55)$$

there follows from Eqs. 54:

$$\left[\frac{w'(r)}{r}\right]_0 = -\frac{p_0}{2\,k}\left[C_1 \lambda^2 + \bar{C}_1 \lambda^2 - \frac{8\,(1-\eta)}{a^2}\right] \ldots\ldots\ldots (56a)$$

$$(\nabla^2 w)_0 = -\frac{p_0}{k}\left[C_1 \lambda^2 + \bar{C}_1 \lambda^2 - \frac{8\,(1-\eta)}{a^2}\right] \ldots\ldots\ldots (56b)$$

With $\lambda\, a = \nu$ and $\lambda\, a = \bar{\nu}$, Eqs. 56 and 53 yield the following expressions:

$$\sigma_{rB}(0) = \mp \frac{E\,h}{1-\mu^2}\,\frac{p_0}{2\,a^2\,k}\left[\frac{1+\mu}{2}\,(\nu^2\, C_1 + \bar{\nu}^2\, \bar{C}_1) - 4\,(1+\mu)\,(1-\eta)\right] \ldots (57a)$$

$$\sigma_{\theta B}(0) = \mp \frac{E\,h}{1-\mu^2}\,\frac{p_0}{2\,a^2\,k}\left[\frac{1+\mu}{2}\,(\nu^2\, C_1 + \bar{\nu}^2\, \bar{C}_1) - 4\,(1+\mu)\,(1-\eta)\right] \ldots (57b)$$

Eqs. 57 may be written in the following form:

$$\begin{aligned} \frac{\sigma_B(0)}{p_0} = \frac{\sigma_{rB}(0)}{p_0} &= \frac{\sigma_{\theta B}(0)}{p_0} \\ &= \pm\,\frac{1+\mu}{4}\,\frac{E\,h}{(1-\mu^2)\,k\,a^2}\,[\nu^2\, C_1 + \bar{\nu}^2\, \bar{C}_1 - 8\,(1-\eta)] \ldots (58) \end{aligned}$$

With $\nu^2 = i\,\kappa^2$, from Eq. 44,

$$\begin{aligned} R\,e\,(\nu^2\, C_1) &= R\,e\left\{\frac{\pi\,\kappa^2}{2}\left[\left(1-\frac{\eta}{2}\right)\frac{1+i}{\sqrt{2}}\,\kappa - \frac{4\,(1-\eta)}{\kappa}\,\frac{1-i}{\sqrt{2}}\right] H_1^{(1)}(\nu)\right. \\ &\qquad\qquad \left. +\, \kappa^2\,\pi\,(1-\eta)\, H_0^{(1)}(\nu)\right\} \\ &= R\,e\left\{\frac{\pi\,\kappa^2}{2}\left[\left(1-\frac{\eta}{2}\right)\frac{1+i}{\sqrt{2}}\,\kappa - \frac{4\,(1-\eta)}{\kappa}\,\frac{1-i}{\sqrt{2}}\right]\frac{2}{\pi}\,(\mathrm{kei}_1\,\kappa + i\,\mathrm{ker}_1\,\kappa)\right. \\ &\qquad\qquad \left. +\, \pi\,\kappa^2\,(1-\eta)\left(-\frac{2}{\pi}\right)(\mathrm{kei}\,\kappa + i\,\mathrm{ker}\,\kappa)\right\} \\ &= \kappa^2\left[\left(1-\frac{\eta}{2}\right)\frac{\kappa}{\sqrt{2}}\,(\mathrm{kei}_1\,\kappa - \mathrm{ker}_1\,\kappa)\right. \\ &\qquad \left. -\, \frac{4\,(1-\eta)}{\sqrt{2}\,\kappa}\,(\mathrm{kei}_1\,\kappa + \mathrm{ker}_1\,\kappa) - 2\,(1-\eta)\,\mathrm{kei}\,\kappa\right] \\ &= \kappa^2\left[\left(1-\frac{\eta}{2}\right)\kappa\,\mathrm{kei}'\,\kappa - \frac{4\,(1-\eta)}{\kappa}\,\mathrm{ker}'\,\kappa - 2\,(1-\eta)\,\mathrm{kei}\,\kappa\right] \ldots\ldots\ldots (59) \end{aligned}$$

Introduction of Eq. 59 into Eq. 58 gives

$$\frac{\sigma_B(0)}{p_0} = \mp \frac{E\,h}{4\,(1-\mu)}\,\frac{1}{k\,a^2}\left\{\kappa^3 \operatorname{kei}'\kappa + (1-\eta)\left[\kappa^3 \operatorname{kei}'\kappa - 4\,\kappa^2 \operatorname{kei}\kappa - 8\,\kappa \operatorname{ker}'\kappa - 8\right]\right\} \quad (60)$$

Eq. 60 is modified by writing

$$\frac{E\,h}{4\,(1-\mu)}\,\frac{\kappa^2}{k\,a^2} = \frac{E\,h}{4\,(1-\mu)}\sqrt{\frac{k}{D}}\,\frac{a^2}{k\,a^2} = \frac{E\,h}{4\,(1-\mu)}\,\frac{1}{\sqrt{k\,D}}$$

$$= \frac{E\,h}{4\,(1-\mu)}\sqrt{\frac{12\,(1-\mu^2)}{E\,h^3\,k}} = \frac{\sqrt{12\,(1-\mu^2)}}{4\,(1-\mu)}\sqrt{\frac{E}{h\,k}}$$

$$= \sqrt{\frac{3}{4}\,\frac{1+\mu}{1-\mu}\,\frac{E}{k\,h}}.$$

Therewith,

$$\frac{\sigma_B(0)}{p_0} = \mp \sqrt{\frac{3\,(1+\mu)}{4\,(1-\mu)}}\sqrt{\frac{E}{k\,h}}\left[\rho\,a \operatorname{kei}'\rho\,a + (1-\eta)\left(\rho\,a \operatorname{kei}'\rho\,a - 4 \operatorname{kei}\rho\,a - \frac{8 \operatorname{ker}'\rho\,a}{\rho\,a} - \frac{8}{\rho^2\,a^2}\right)\right] \quad (61)$$

When $1 - \eta = 0$, Eq. 61 is reduced to Eq. 8*b*. Otherwise, it becomes Eq. 10*b* of the main text.

Series developments which are used are as follows:[16,17]

$$\operatorname{kei} x = \left(\log\frac{2}{x} - \gamma\right)\left(\frac{1}{4}x^2 - \frac{x^6}{2^6 \times 36} + \dots\right) - \frac{\pi}{4}\left(1 - \frac{x^4}{64} + \dots\right) + \frac{x^2}{4} - \left(1 + \frac{1}{2} + \frac{1}{3}\right)\frac{x^6}{2^6 \times 36} + \dots$$

$$\operatorname{ker} x = \left(\log\frac{2}{x} - \gamma\right)\left(1 - \frac{x^4}{64} + \dots\right) + \frac{\pi}{4}\left(\frac{x^2}{4} - \frac{x^6}{2^6 \times 36} + \dots\right) - \left(1 + \frac{1}{2}\right)\frac{x^4}{2^4 \times 4} + \dots$$

$$\operatorname{kei}' x = \left(\log\frac{2}{x} - \gamma\right)\left(\frac{x}{2} - \frac{x^5}{2^6 \times 6} + \dots\right) - \frac{1}{x}\left(\frac{x^2}{4} - \frac{x^6}{2^6 \times 36} + \dots\right) - \frac{\pi}{4}\left(-\frac{x^3}{16} + \frac{x^7}{2^7 \times 6 \times 24} - \dots\right) + \frac{x}{2} - \frac{11}{6}\,\frac{x^5}{2^5 \times 2 \times 6} + \dots$$

$$\operatorname{ker}' x = \left(\log\frac{2}{x} - \gamma\right)\left(-\frac{x^3}{16} + \dots\right) - \frac{1}{x}\left(1 - \frac{x^4}{64} + \dots\right) + \frac{\pi}{4}\left(\frac{x}{2} - \frac{x^5}{2^6 \times 6} + \dots\right) - \frac{3}{2}\,\frac{x^3}{2^4} + \dots$$

---

[16] "Tables of Integrals and Other Mathematical Data," by H. B. Dwight, The Macmillan Co., New York, N. Y., 1947, p. 184.

[17] *Ibid.*, pp. 187–188.

Hence,

$$1 + x \operatorname{ker}' x = \frac{\pi}{8} x^2 + \left[-\frac{1}{16}\left(\log \frac{2}{x} - \gamma\right) + \frac{1}{64} - \frac{3}{32} \right] x^4 + \ldots\ldots \quad (62)$$

$$\frac{2}{x} \operatorname{kei}' x - \operatorname{ker} x = \frac{1}{2} + \left(\frac{\pi}{32} - \frac{\pi}{16}\right) x^2 + \left[\left(-\frac{1}{2^5 \times 6} + \frac{1}{64} \right) \left(\log \frac{2}{x} - \gamma \right) \right.$$
$$\left. + \left(\frac{1}{2^5 \times 36} - \frac{11}{6}\frac{1}{2^5 \times 6} + \frac{3}{2}\frac{1}{2^4 \times 4} \right) \right] x^4 \ldots \quad (63)$$

$$\frac{8}{x} \operatorname{kei}' x - 4 \operatorname{ker} x + (x \operatorname{ker}' x + 1) - 2 = 2 - 2 + \left[4\left(\frac{\pi}{32} - \frac{\pi}{16}\right) + \frac{\pi}{8} \right] x^2$$
$$+ \left[4\left(\frac{1}{64} - \frac{1}{2^5 \times 6} \right) - \frac{1}{16} \right] \left(\log \frac{2}{x} - \gamma \right) x^4$$
$$+ \left(\frac{1}{2^5 \times 9} - \frac{11}{2^5 \times 9} + \frac{3}{2^5} + \frac{1}{64} - \frac{3}{32} \right) x^4 + \cdots$$
$$= -\frac{x^4}{48}\left(\log \frac{2}{x} - \gamma \right) - \frac{11\, x^4}{9 \times 64} + \ldots\ldots \quad (64)$$

Introduction of Eqs. 62, 63, and 64 into Eq. 52 yields the following expansion for the foundation pressure:

$$\frac{\sigma_F(0)}{p_0} = \frac{\pi}{8} (\rho\, a)^2 + (1 - \eta) \left[-\frac{(\rho\, a)^4}{48} \left(\log \frac{2}{\rho\, a} - \gamma + \frac{11}{12} \right) + \cdots \right] \ldots (65)$$

When $1 - \eta = 0$, Eq. 65 is reduced to Eq. 6*d*. Otherwise, Eq. 65 shows that, even for $1 - \eta \neq 0$, the foundation pressure is the same as if $1 - \eta = 0$, so long as $\rho\, a$ is small enough. This is in accordance with the appropriate statement made in the body of the paper.

It is finally noted that Eqs. 8*b* and 10*b* for $\sigma_B(0)/p_0$ may be developed in an entirely analogous manner, but the details are omitted.

APPENDIX II. INFINITE ELASTIC PLATE SUBJECTED TO UNIFORM TENSION AND CARRYING A UNIFORM LATERAL LOAD OVER A CIRCULAR AREA

Derivations.—The following derivations, in addition to giving important practical information, illustrate the usefulness of the numerical tables cited.[3,4]

For the differential equations,

$$D\nabla^2\nabla^2 w + N\,\nabla^2 w + k\, w = p_0, \qquad r \leq a$$

and

$$D\nabla^2\nabla^2 w + N\,\nabla^2 w + k\, w = 0, \qquad a < r \quad \Bigg\} \ldots\ldots\ldots\ldots (66)$$

the solutions are

and

$$\left.\begin{aligned} w &= w_h + \frac{p_0}{k}, & r &\leq a \\ w &= w_h + 0, & a &< r \end{aligned}\right\} \qquad (67)$$

in which w_h is the general solution for the homogeneous Eq. 66:

For brevity the subscript h will be omitted. The homogeneous Eq. 66 may be written in the form:

$$(\nabla^2 + \lambda^2)(\nabla^2 + \bar{\lambda}^2)\, w = 0 \qquad (68)$$

in which

$$\lambda^2 \bar{\lambda}^2 = \frac{k}{D}, \quad \text{and} \quad \lambda^2 + \bar{\lambda}^2 = -\frac{N}{D} \qquad (69)$$

Letting

$$\lambda^2 = \rho^2 e^{2i\phi}, \quad \text{and} \quad \lambda^2 = \rho^2 e^{-2i\phi} \qquad (70)$$

Eqs. 14*b* are applicable. The general solution of Eq. 68 is composed of the general solutions of the two equations: $(\nabla^2 + \lambda^2) f = 0$ and $(\nabla^2 + \bar{\lambda}^2) f = 0$. Accordingly, the real solution of Eq. 68 is

$$w = C_1 J_0(\lambda r) + \bar{C}_1 J_0(\bar{\lambda} r) + C_2 Y_0(\lambda r) + \bar{C}_2 Y_0(\bar{\lambda} r) \qquad (71)$$

According to references previously cited,[3,4]

$$J_0(\rho r e^{\pm i\phi}) = u_0(\rho r, \phi) \pm i\, v_0(\rho r, \phi) \qquad (72a)$$

and

$$Y_0(\rho r e^{\pm i\phi}) = U_0(\rho r, \phi) \pm i\, V_0(\rho r, \phi) \qquad (72b)$$

Knowledge of asymptotic behavior of the functions, J_0 and Y_0, is required in order to select the proper combination in the range, $r > a$. Setting

$$J_0(\lambda r) + i\, Y_0(\lambda r) = H_0^{(1)}(\lambda r) = H_0^{(1)}(\rho r e^{i\phi}) \qquad (73a)$$

and

$$J_0(\lambda r) - i\, Y_0(\lambda r) = H_0^{(2)}(\lambda r) = H_0^{(2)}(\rho r e^{i\phi}) \qquad (73b)$$

then,

$$H_0^{(1)}(\lambda r) \sim \frac{1}{\sqrt{\lambda r}} e^{i\lambda r} = \frac{1}{\sqrt{\lambda r}} e^{i\rho r(\cos\phi + i \sin\phi)} \qquad (73c)$$

and

$$H_0^{(2)}(\lambda r) \sim \frac{1}{\sqrt{\lambda r}} e^{-i\lambda r} = \frac{1}{\sqrt{\lambda r}} e^{-i\rho r(\cos\phi + i \sin\phi)} \qquad (73d)$$

Because $\sin\phi > 0$ it is true that $H_0^{(1)}(\lambda r)$ decays exponentially with increasing r-values if r is large and $H_0^{(2)}(\lambda r)$ increases exponentially with increasing r-values if r is large. The reverse is true for $H_0^{(1)}(\bar{\lambda} r)$ and $H_0^{(2)}(\bar{\lambda} r)$. Accordingly, in the range $r > a$, the proper combinations of Bessel functions which must be used are $H_0^{(1)}(\lambda r)$ and $H_0^{(2)}(\bar{\lambda} r)$.

When $r < a$ the singular behavior of the functions, Y_0, for the location, $r = 0$, excludes them from the solution of the problem.

In view of the foregoing considerations, the general solution of Eq. 66 is taken in the form,

$$w = \frac{p_0}{k}[1 + C_1 J_0(\lambda r) + \bar{C}_1 J_0(\bar{\lambda} r)], \qquad r \leq a \ldots\ldots\ldots (74a)$$

and

$$w = \frac{p_0}{k}[C_2 H_0^{(1)}(\lambda r) + \bar{C}_2 H_0^{(2)}(\bar{\lambda} r)], \qquad a < r \ldots\ldots\ldots (74b)$$

Eqs. 74 are the natural extensions of Eqs. 31 and 37, to which they reduce, for the case $\eta = 1$, when $N = 0$ and therefore, $\phi = \pi/4$.

The transition conditions are of the form of Eq. 25, and Eq. 40 is applicable. Making use of Eqs. 38 and 39, there are obtained the following transition equations:

$$1 + C_1 J_0(\nu) + \bar{C}_1 J_0(\bar{\nu}) = C_2 H_0^{(1)}(\nu) + \bar{C}_2 H_0^{(2)}(\bar{\nu}) \ldots\ldots\ldots (75a)$$

$$C_1 \lambda J_1(\nu) + \bar{C}_1 \bar{\lambda} J_1(\bar{\nu}) = C_2 \lambda H_1^{(1)}(\nu) + \bar{C}_2 \bar{\lambda} H_1^{(2)}(\bar{\nu}) \ldots\ldots (75b)$$

$$C_1 \lambda^2 J_0(\nu) + \bar{C}_1 \lambda^2 J_0(\bar{\nu}) = C_2 \lambda^2 H_0^{(1)}(\nu) + \bar{C}_2 \bar{\lambda}^2 H_0^{(2)}(\bar{\nu}) \ldots\ldots (75c)$$

$$C_1 \lambda^3 J_1(\nu) + \bar{C}_1 \bar{\lambda}^3 J_1(\bar{\nu}) = C_2 \lambda^3 H_1^{(1)}(\nu) + \bar{C}_2 \bar{\lambda}^3 H_1^{(2)}(\bar{\nu}) \ldots\ldots (75d)$$

In order to simplify Eqs. 75 one may use Eq. 69 and write

$$\bar{\lambda}^2 = -\lambda^2 - \frac{N}{D}, \quad \bar{\nu}^2 = -\nu^2 - \frac{a^2 N}{D} \ldots\ldots\ldots\ldots\ldots (76)$$

Eqs. 75 may be brought into the following alternate forms:

$$\left.\begin{aligned} &C_2 H_0^{(1)}(\nu) + \bar{C}_2 H_0^{(2)}(\bar{\nu}) - C_1 J_0(\nu) - \bar{C}_1 J_0(\bar{\nu}) = 1 \\ &C_2 H_0^{(1)}(\nu) - \bar{C}_2 H_0^{(2)}(\bar{\nu}) - C_1 J_0(\nu) + \bar{C}_1 J_0(\bar{\nu}) \\ &\qquad\qquad - \frac{a^2 N/D}{\nu^2}[\bar{C}_2 H_0^{(2)}(\nu) - \bar{C}_1 J_0(\bar{\nu})] = 0 \end{aligned}\right\} \ldots (77)$$

$$\left.\begin{aligned} &C_2 \nu H_1^{(1)}(\nu) + \bar{C}_2 \bar{\nu} H_1^{(2)}(\bar{\nu}) - C_1 \nu J_1(\nu) - \bar{C}_1 \bar{\nu} J_1(\bar{\nu}) = 0 \\ &C_2 \nu H_1^{(1)}(\nu) - \bar{C}_2 \bar{\nu} H_1^{(2)}(\bar{\nu}) - C_1 \nu J_1(\nu) + \bar{C}_1 \bar{\nu} J_1(\bar{\nu}) \\ &\qquad\qquad - \frac{a^2 N/D}{\nu^2}[\bar{C}_2 \bar{\nu} H_1^{(2)}(\bar{\nu}) - \bar{C}_1 \bar{\nu} J_1(\bar{\nu})] = 0 \end{aligned}\right\} \ldots (78)$$

From Eq. 77, by subtraction,

$$\bar{C}_2 \left(2 + \frac{a^2 N/D}{\nu^2}\right) H_0^{(2)}(\bar{\nu}) - \bar{C}_1 \left(2 + \frac{a^2 N/D}{\nu^2}\right) J_0(\bar{\nu}) = 1 \ldots\ldots (79)$$

From Eq. 78, by subtraction,

$$\bar{C}_2 \bar{\nu} \left(2 + \frac{a^2 N/D}{\nu^2}\right) H_1^{(2)}(\nu) - \bar{C}_1 \bar{\nu} \left(2 + \frac{a^2 N/D}{\nu^2}\right) J_1(\bar{\nu}) = 0 \ldots (80)$$

Eqs. 79 and 80 may be rewritten in simpler form. Taking conjugates of all constants and observing that $\overline{H_1^{(2)}(\bar{\nu})} = H_1^{(1)}(\nu)$,

$$\left.\begin{aligned} C_2\, H_0^{(1)}(\nu) - C_1\, J_0(\nu) &= \frac{1}{2 + a^2\,(N/D\,\bar{\nu}^2)} \\ C_2\, H_1^{(1)}(\nu) - C_1\, J_1(\nu) &= 0 \end{aligned}\right\} \qquad (81)$$

Hence,

$$C_1 = \frac{1}{2 + (N/D\,\bar{\lambda}^2)}\,\frac{-\,H_1^{(1)}(\nu)}{\Delta}$$

and

$$C_2 = \frac{1}{2 + (N/D\,\bar{\lambda}^2)}\,\frac{-\,J_1(\nu)}{\Delta} \qquad (82)$$

in which

$$\begin{aligned} \Delta &= -\,H_0^{(1)}(\nu)\,J_1(\nu) + H_1^{(1)}(\nu)\,J_0(\nu) \\ &= -\,(J_0 + i\,Y_0)\,J_1 + (J_1 + i\,Y_1)\,J_0 = i\,(Y_0\,J_1 - Y_1\,J_0) = \frac{-\,2\,i}{\pi\,\nu} \end{aligned} \qquad (83)$$

Further transformations are made as follows, using Eqs. 70 and 14*b*:

$$\begin{aligned} \frac{1}{2 + (N/D\,\bar{\lambda}^2)} &= \frac{1}{2 - 2\cos 2\phi\, e^{2i\phi}} = \frac{1}{2 - 2\cos^2 2\,\phi - 2\,i\cos 2\,\phi\sin 2\,\phi} \\ &= \frac{\sin 2\,\phi + i\cos 2\,\phi}{2\sin 2\,\phi} = \frac{1}{2}\,(1 + i\cot 2\,\phi) \end{aligned} \qquad (84)$$

Introducing Eqs. 83 and 84 into Eq. 82 yields

$$C_1 = \frac{\pi\,\nu}{4\,i}\,(1 + i\cot 2\,\phi)\,H_1^{(1)}(\nu)$$

and

$$C_2 = \frac{\pi\,\nu}{4\,i}\,(1 + i\cot 2\,\phi)\,J_1(\nu) \qquad (85)$$

Transforming C_1 further,

$$\begin{aligned} C_1 &= \frac{\pi\,\rho\,a}{4\,i}\,e^{i\phi}\,(1 + i\cot 2\,\phi)(J_1 + i\,Y_1) \\ &= \frac{1}{4}\,\pi\,\rho\,a\,(\sin\phi - i\cos\phi)\,(1 + i\cot 2\,\phi)(J_1 + i\,Y_1) \\ &= \frac{1}{4}\,\pi\,\rho\,a\,\frac{\cos\phi - i\sin\phi}{\sin 2\,\phi}\,[(u_1 - V_1) + i\,(v_1 + U_1)] \\ &= \frac{\pi\,\rho\,a}{4\sin 2\,\phi}\,\{(u_1 - V_1)\cos\phi + (v_1 + U_1)\sin\phi \\ &\qquad + i\,[(v_1 + U_1)\cos\phi - (u_1 - V_1)\sin\phi]\} \end{aligned} \qquad (86)$$

From Eq. 74*a*,

$$\frac{\sigma_F(0)}{p_0} = \frac{k\,w(0)}{p_0} = 1 + C_1 + \bar{C}_1 \qquad (87)$$

The combination of Eqs. 87 and 86 yields Eq. 16.

In expressing the bending stress at the center, the analogy between Eq. 74*a* and Eq. 31 indicates that the general expression, Eq. 58, with $\eta = 1$, remains applicable for the case of the plate under tension. Accordingly,

$$\frac{\sigma_B(0)}{p_0} = \mp \frac{1+\mu}{4} \frac{E\,h}{1-\mu^2} \frac{1}{k\,a^2} (\nu^2 C_1 + \bar{\nu}^2 \bar{C}_1) \ldots\ldots\ldots\ldots (88)$$

in which, from Eq. 85,

$$\begin{aligned}
\nu^2 C_1 &= \frac{\pi\,(\rho\,a)^3}{4\,i} e^{i3\phi} (1 + i \cot 2\phi)(J_1 + i\,Y_1) \\
&= \frac{\pi\,(\rho\,a)^3}{4\,i} [(\cos 3\phi - \sin 3\phi \cot 2\phi) \\
&\qquad + i\,(\sin 3\phi + \cos 3\phi \cot 2\phi)](J_1 + i\,Y_1) \\
&= \frac{\pi\,(\rho\,a)^3}{4\,i} \left(\frac{-\sin\phi + i\cos\phi}{\sin 2\phi} \right) (J_1 + i\,Y_1) \\
&= \frac{\pi\,(\rho\,a)^3}{8\,i} \left(\frac{i}{\sin\phi} - \frac{1}{\cos\phi} \right) (J_1 + i\,Y_1) \\
&= \frac{\pi\,(\rho\,a)^3}{8} \left[\frac{u_1 - V_1}{\sin\phi} - \frac{v_1 + U_1}{\cos\phi} + i \left(\frac{v_1 + U_1}{\sin\phi} - \frac{u_1 - V_1}{\cos\phi} \right) \right] \ldots\ldots (89)
\end{aligned}$$

Combining Eqs. 88 and 89 gives the following:

$$\frac{\sigma_B(0)}{p_0} = \mp \frac{E\,h}{1-\mu} \frac{(\rho\,a)^3\,\pi}{16\,k\,a^2} \left(\frac{u_1 - V_1}{\sin\phi} - \frac{v_1 + U_1}{\cos\phi} \right) \ldots\ldots\ldots (90)$$

Eq. 90 may be written in an alternate form, which is Eq. 17.

APPENDIX III. NOTATION

The following symbols, adopted for use in the paper and for the guidance of discussers, conform essentially with "American Standard Letter Symbols for Structural Analysis" (ASA Z10.8-1949), prepared by a committee of the American Standards Association with Society representation, and approved by the Association in 1949:

a = radius of a circular load surface, in inches;
C = pressure coefficient, $C = \sigma_F(0)/p_o = C_F + (1 - \eta)\,C^*_F$;
C_B = parameter defined by Eq. 11*b*;
D = plate stiffness factor, $D = E\,h^3/12\,(1 - \mu^2)$;
E = modulus of elasticity of the surface layer, in pounds per square inch;
F = a stress function occurring in nonlinear theory;
H = symbol for Hankel functions;
h = plate thickness, in inches;

Im = imaginary part of

J = symbol for Bessel functions of the first kind;

k = modulus of subgrade reaction, in pounds per cubic inch;

$N = \sigma h$, stress resultant;

p = load-intensity function, in pounds per square inch;

r = radial distance measured from the center of the load surface;

u, v, U, and V = symbols for the real and imaginary part of certain Bessel functions[3,4];

w = transverse plate deflection, in inches;

Y = symbol for Bessel functions of the second kind;

∇^2 = Laplace operator, $\nabla^2 f = (d^2f/dr^2) + r^{-1}\, df/dr$;

ξ = dimensionless coordinate, $\xi = r/a$;

η = parameter in parabolic load distribution;

$\lambda = \rho \sqrt{i}$;

μ = Poisson ratio of the surface-layer material;

$\nu = \lambda a$;

$\rho = \sqrt[4]{k/D}$;

σ = hydrostatic two-dimensional tensile stress:

σ_B = extreme fiber bending stresses in a plate; and

σ_F = foundation pressure.

AMERICAN SOCIETY OF CIVIL ENGINEERS
Founded November 5, 1852
TRANSACTIONS

Paper No. 2877

MISSOURI RIVER BASIN PLAN IN OPERATION

By WENDELL E. JOHNSON,[1] M. ASCE

SYNOPSIS

Progress has been made on the water-resource program which has been conducted in the Missouri River basin since World War II. Many projects are already in operation, and each year the benefits of flood control, power generation, irrigation, and navigation are being increasingly realized with each new feature of the program.

INTRODUCTION

During the ten years (1947 to 1956) that the Missouri River basin was under construction, the basin plan and the organizations which conducted it have been frequently discussed by engineers, politicians, educators, laymen, and individuals who have never visited the 530,000-sq-mile area.

The Corps of Engineers (United States Department of the Army) and the Bureau of Reclamation (United States Department of the Interior) have been constructing dams, levees, and channel works to harness the waters of the Missouri basin and to utilize them. Since 1949 the actual progress made by these and other agencies has begun to result in the benefits of flood prevention, irrigated acres, power revenues, and river traffic, instead of in percentages of completion.

BASIN DESCRIPTION

The Missouri basin is an area of 530,000 sq miles—one-sixth the area of the United States. The Missouri River begins in the Rocky Mountains in Montana; it runs through the semiarid plains of North and South Dakota, Nebraska, Kansas, and Missouri; and it empties into the Mississippi River near St. Louis (Mo.). Precipitation varies from less than 10 in. per yr in the western plains to more than 45 in. per yr in the eastern areas. The economy is predominantly agricultural; except for a few localities, industrial areas are located in the east and south. In the north and west, drought is the principal water-resource problem whereas, in the south and east, floods are the primary problem.

NOTE.—Published, essentially as printed here, in September, 1955, as *Proceedings Paper 800*. Positions and titles given are those in effect when the paper was approved for publication in *Transactions*.

[1] Chief, Eng. Div., Missouri River Div., Corps of Engrs., U. S. Dept. of the Army, Omaha, Nebr.

The 11-yr drought of the 1930's was followed by a series of wet years and disastrous floods. Near the end of this wet period, in 1951 there was a record-breaking flood in the lower basin, which resulted from torrential rains in Kansas. In 1952 there was a record-breaking flood in the upper and middle basins, which resulted from the rapid thaw of an abnormally high snow cover over ice-covered ground. These alternate periods of flood and drought caused a comprehensive water-development program to be developed to bring greater stability to the basin economy.

DESCRIPTION OF PLAN

The broad program for water-resource development planned in 1943 and 1944, which is being followed by the Corps and the Bureau, provides for storing flood waters in multiple-purpose reservoirs to reduce flood damages. It also provides for the subsequent regulated release of these waters to benefit irrigation, navigation, water supply, and pollution abatement, and to develop hydroelectric power.

Main-Stem Reservoir System.—The backbone of the basin development is the main-stem reservoir system in Montana and the Dakotas. Principal statistics regarding these reservoir projects are shown in Table 1.

TABLE 1

Project	Storage capacity, in acre-feet	Head, in feet	Power-plant capacity, in kilowatts	Status (as of 1955)
Fort Peck, Montana	19,400,000	213	165,000	In operation
Garrison, North Dakota	23,000,000	174	400,000	In partial operation
Oahe, South Dakota	23,600,000	208	595,000[a]	Under construction
Big Bend, South Dakota	1,570,000[a]	74[a]	217,000[a]	Authorized
Fort Randall, South Dakota	6,300,000	138	320,000	In operation
Gavins Point, Nebraska	540,000	51	100,000	In partial operation

[a] Tentative.

Fort Peck Reservoir (Montana) began to store water in 1938 and to generate power in 1943. Fort Randall Reservoir (South Dakota) began to store water in 1952 and to generate power in 1954. Storage in the reservoir at Garrison (N. Dak.) started in 1953, and power generation began in 1956.

The main-stem dams are all earth embankments with chute spillways in the abutments. At all the projects, except those at Big Bend and Gavins Point (Nebr.), tunnels are utilized for power releases and for general regulation. The embankments of three of the dams are among the largest earth fills in the world; Fort Peck Dam contains more than 100,000,000 cu yd placed hydraulically, and the Garrison and Oahe dams (South Dakota) each contain approximately 75,000,000 cu yd of rolled fill. Because of the size of the projects many unique construction techniques have been devised. For example, the moving of earth has been accomplished with very large equipment, such as 11-cu-yd shovels and 35-cu-yd trucks. The embankment at Fort Randall was closed by means of a dredge for pumping chalk, which had a maximum size of up to approximately 9 in. in diameter. The most recent development has been the use of a continuous mining machine in excavating the tunnels in the shale formation at the Oahe project near Pierre (S. Dak.). Fig. 1 shows some of this equipment at work on the earthwork embankment at Oahe Dam. Fig. 2 shows the mining machine outside one of the Oahe tunnels.

Bank Stabilization and Navigation.—Below this main-stem reservoir system the great flood plain of the Missouri River contains 2,000,000 acres of rich farm land. The width of the flood plain varies from a few miles to a maximum of 17 miles, and the river is in a meandering channel. Under natural conditions the river erodes an average of 10,000 acres every year. After many years of experimentation and intermittent isolated attempts to prevent erosion, in 1929 a comprehensive program of bank stabilization and contraction of the river was undertaken in a 760-mile reach extending from Sioux City (Iowa) to the mouth of the river. This will provide a 9-ft navigation channel and protect the bottom lands against erosion from the river. This program involves a system of pile dikes and rock revetments which uses the energy of the river to develop a single channel into a series of continuous, easy bends. The banks are then permanently stabilized, and a 9-ft channel is achieved through contraction. Although this part of the program was delayed because of a suspension of work in World War II, progress is now being made. Between Omaha (Nebr.) and the river mouth, the river has been controlled, and remaining operations are concentrated on improving alinements and on completing rock revetments. In the area extending from Kansas City (Mo.) to the mouth of the river, the present (1956) minimum depth is 7 ft; between Kansas City and Omaha the minimum depth is approxi-

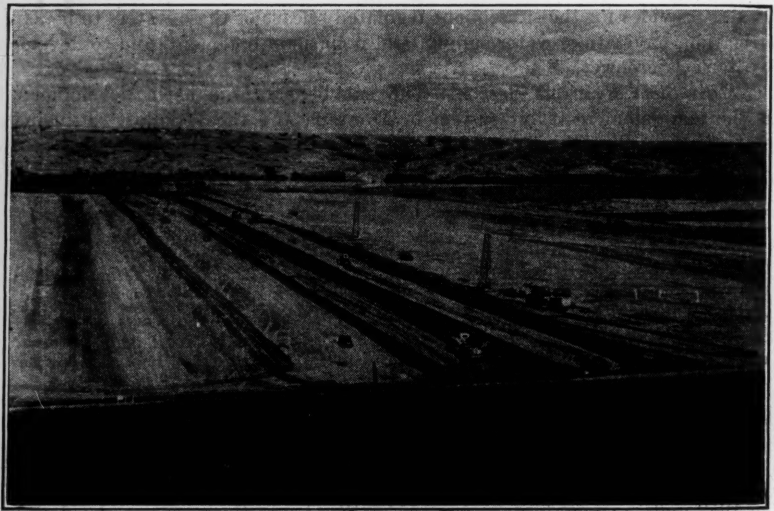

FIG. 1.—EMBANKMENT CONSTRUCTION, OAHE DAM

mately 6½ ft. Between Omaha and Sioux City the river is uncontrolled. However, in 1954, stabilization work was resumed, and it is expected that, from the point of view of construction, this reach will be the busiest part of the river during the next few years.

Local Protection Works.—In 1947 the work in the lower river was expanded by constructing the agricultural-levee system. Two hundred and twenty-five miles of levees protecting 195,500 acres of land have been constructed between Omaha and Kansas City. Since 1950 no new agricultural levees have been built, but present schedules show that this phase of the program may be resumed.

Municipal levees have been provided at Omaha, Council Bluffs (Iowa), Kansas City (Kans.), and Kansas City (Mo.), on the main stem, and at many places on the tributaries. At Omaha, Council Bluffs, and the Kansas Cities, the levees depend on upstream storage and primarily take care of the flows originating in the tributary areas below the reservoirs which are uncontrolled. In the case of the levees at Omaha and Council Bluffs, the required upstream storage is either in operation or under construction. However, at the Kansas Cities only a small part of the essential storage on the Kansas River has been provided.

FIG. 2.—MINING MACHINE, OAHE DAM

Lower Basin.—Kansas City is located at a point of the Missouri River which separates the Missouri basin from the progress that is being made on water-resource development. Above Kansas City a major part of the Corps, program and a large part of the Bureau's reservoir program have been completed or are being completed. However, at and below Kansas City, progress has not been satisfactory on the major tributaries of the Kansas River, the Grand River, and the Osage River which enter the Missouri River.

In the western and more arid part of the Kansas basin, relatively good progress has been made. Kanopolis Reservoir, constructed by the Corps, and Cedar Bluff Reservoir, constructed by the Bureau, effectively control the upper Smoky Hill River; Webster Reservoir and Kirwin Reservoir, under construction by the Bureau, will control the upper Solomon River; and Harlan County Reservoir, supplemented by smaller Bureau reservoirs upstream, controls the upper Republican River. In this western part of the basin only Wilson Reservoir on the Saline River, Glen Elder Reservoir on the lower Solomon River, Milford Reservoir on the lower Republican River, and several smaller reservoirs on the upper tributaries remain to complete an effective flood-control and water-conservation storage system. Some work has already been done on planning municipal levees. For example, because Kanopolis and Cedar Bluff are in operation, it will be possible to proceed with plans for a levee-and-channel project at Salina just downstream. A project at Abilene, which is independent of reservoir storage, is also scheduled to be constructed.

In the eastern part of the basin, the authorized plan includes Tuttle Creek Reservoir on the Blue River, Milford Reservoir on the lower Republican River, and Perry Creek Reservoir on the Delaware River. Other smaller reservoirs are being studied and appear promising. However, the residents in this part of the basin have different views on flood-control methods. Some prefer continuing with the approved reservoir-storage program, and others prefer relying on the upland-watershed and small-reservoir program of the United States Department of Agriculture, although that agency has stated that this program is designed for protecting upland areas and will not greatly affect major floods. Because there is divided opinion on flood-control methods, progress on the reservoir-storage system, the municipal protection in the lower Kansas basin, or on the agricultural levees below Kansas City has been delayed. In 1954 and 1955, however, a majority of the residents united behind the reservoir and levee program, and by 1956 construction on the Tuttle Creek Reservoir and planning of local protection projects were under way.

The controversy in the lower Kansas basin has affected two other major tributaries—the Osage River (Kansas), which is called the Marais des Cygnes, and the Grand River (Missouri)—and until recently no construction progress had yet been made on water-resource developments in these basins. In the Osage River area, however, a comprehensive plan has been formulated by the Corps and has been authorized by the United States Congress. By 1956 construction on the Pomme de Terre Reservoir had been initiated and detailed planning had been started on the Pomona Reservoir and Ottawa local protection project; a comprehensive plan for the Grand River basin is also being developed.

Tributary Reservoirs.—In the western and northern parts of the Missouri basin, a number of tributary reservoir projects has been initiated largely by the Bureau. Although most of these projects are concerned with irrigation, many projects also include flood-control storage. In accordance with the 1944 Flood Control Act,[2] the amount of flood-control storage and the regulations for operation of such storage are prescribed by the Corps. The Corps also operates irrigation storage in its multiple-purpose reservoirs, in accordance with Bureau recommendations; thus, coordination of operation is assured.

The tributary reservoirs of the Bureau are scheduled to have a total power-generating capacity of 1,200,000 kw. These power plants and the 1,500,000 kw on the main stem will generate an average of 15,000,000,000 kw-hr annually. The Bureau handles the marketing of all this power under the provisions of the 1944 Flood Control Act.

OPERATION

1951 Flood.—Although most of the interest shown in the basin program since 1946 has been connected with construction, in 1951 residents of the basin began to realize some of the benefits the basin development would provide. In July, 1951, intense storms in the Kansas River basin, which had been completely soaked by persistent rains since May, produced the greatest flood of record in the Kansas River; the peak flow was approximately 500,000 cu ft per sec at the mouth of the river at the Kansas Cities. The levees and the flood walls in the Kansas City area were not completed. The reservoir system upstream on the Kansas River did not exist except in some upper reaches, and the flood was substantially greater than the expected flood for which the works had been designed. Fig. 3 shows the areas affected. The Armourdale levee, the Argentine levee, and the Central Industrial District levee were overtopped. The levees on the Missouri River were not overtopped, although the Fairfax levee was inundated by a break in a sewer constructed by the Works Progress Administration, which had not been built to withstand heavy internal pressure. A contract for replacing this sewer with a fully pressurized sewer had already been made at the time of the flood, but work had not yet started. Although the damages resulting from this flood were catastrophic ($461,083,900 in Kansas City alone), the levees along the Missouri River prevented $264,640,000 in damages. If the levee system had been completed and if the sewer had been replaced, there would have been increased savings amounting to approximately $335,000,000.

In order to protect the levee system along the Kansas River from a similar flood, completing the authorized reservoirs is necessary in the Kansas basin—especially Tuttle Creek Reservoir, Milford Reservoir, Perry Reservoir, and several smaller reservoirs on tributaries near Topeka and Kansas City. Despite all the damage which resulted from the flood, the important fact is that the works which had been installed actually prevented substantial damages, and subsequent analyses have clearly demonstrated that complete protection against such a disaster is possible.

1952 Flood.—By March, 1952, the accumulated snowfall over the plains area in eastern Montana and in the Dakotas averaged 200% of normal. In general, this snowfall rested on a coating of ice over frozen ground. Then, late in March, a quick thaw caused the floods to begin. The peak of the flood

---

[2] *Public Law 534*, 78th Cong., approved December 22, 1944, Sections 7 and 9.

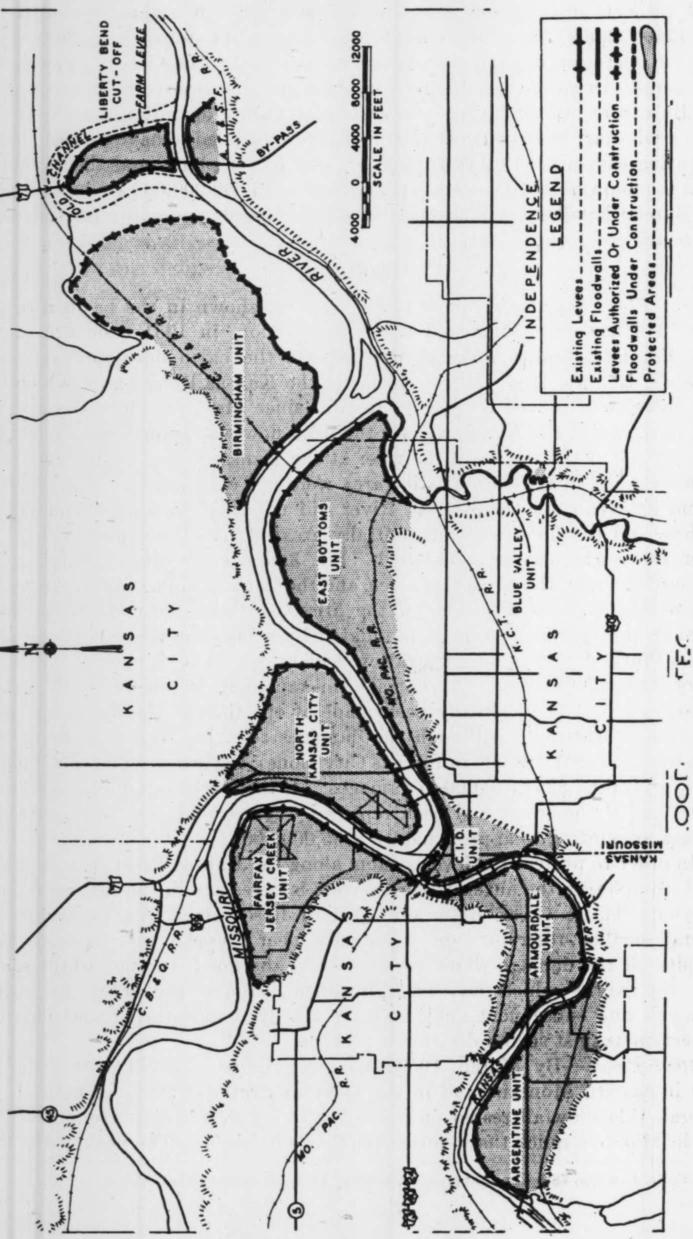
LIBERTY BEND CUT-OFF
FARM LEVEE
OLD CHANNEL
BY-PASS
A.T. & S.F. R.R.
RIVER
SCALE IN FEET
4000 0 4000 8000 12000
INDEPENDENCE
LEGEND
Existing Levees
Existing Floodwalls
Levees Authorized Or Under Construction
Floodwalls Under Construction
Protected Areas
BIRMINGHAM UNIT
C.R.I. & P. R.R.
EAST BOTTOMS UNIT
BLUE VALLEY UNIT
K.C.T. R.R.
KANSAS CITY
N
NORTH KANSAS CITY UNIT
MO. PAC. R.R.
C.I.D. UNIT
KANSAS
MISSOURI
FAIRFAX JERSEY CREEK UNIT
MISSOURI
C.B. & Q. R.R.
KANSAS CITY
ARMOURDALE UNIT
RIVER
KANSAS
ARGENTINE UNIT
MO. PAC. R.R.

FIG. 3.—AREA AFFECTED BY 1951 FLOOD

was accentuated by ice jams, which is a familiar phenomenon on the upper Missouri River.

Communities along the Missouri River, such as Bismarck (N. Dak.), Pierre, and Sioux City, which normally are high and dry even in flood years, experienced substantial damage. As the flood passed below Sioux City, it spread out over the broad valley, which has a maximum width of 17 miles near Blair (Nebr.). Many farming communities and hundreds of thousands of acres were inundated.

As the flood neared Omaha and Council Bluffs, where federal government levees had been constructed, the communities cooperated in a great effort to help control the flood. Army engineers, contractors, troops of the Fifth Army, and volunteer citizens worked to raise the levees, which had been designed for heavy floods, but which depended on the as yet incomplete upstream reservoir storage to take the peak off the flood. The levees had been designed for a flow of 250,000 cu ft per sec, but a flood peak of 400,000 cu ft per sec was reached on April 18, 1952; the levee with some emergency construction provided only just enough protection, with a few feet of freeboard. At this time only Fort Peck Reservoir in Montana and a few small tributary reservoirs were available for water storage, but they were able to reduce the peak stage a few feet so that with the emergency construction the levees passed the flood safely. This demonstrated forcibly the potentialities of the comprehensive plan. However, the most significant fact is that, if a similar flood were to occur at present (1957), Garrison Reservoir and Fort Randall Reservoir could essentially store the entire flood, and the flow at Omaha would be well below the banks. Fig. 4 shows the relationship of the levee height to the actual flood stage and also to stages modified by various conditions of reservoir operation. Surveys have shown that the damages which were prevented at

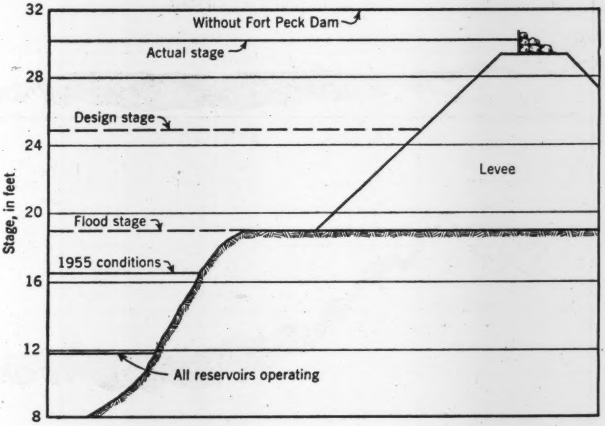

Fig. 4.—1952 Flood Stages at Omaha and Council Bluffs

Omaha and Council Bluffs amounted to more than $60,000,000, which is five times the cost of the levees.

Droughts.—In 1953 the cycle of floods was partly reversed, and droughts became a major problem, especially in Kansas and Missouri. In these areas the advantages of the reservoir system were demonstrated. In Kansas the completed reservoirs on the Smoky Hill River and on the upper Republican River helped maintain an adequate flow on the Kansas River. In the upper Missouri River, Fort Peck Reservoir collected approximately 2,000,000 acre-ft of water from a previous flood in Montana; this water was used to maintain adequate flows for water supply, public health, and navigation downstream. Fort Randall Reservoir, which was closed in July, 1952, assisted greatly in reducing the fluctuations of the Missouri River and produced a more uniform flow than the river had experienced in the past. During September and October of 1953, the stored water in the Missouri reservoirs was providing three-fourths of the total flow at Kansas City and approximately one-third of the flow at St. Louis. Without Fort Peck Reservoir, navigation on the Mississippi River to and beyond St. Louis would have been suspended in September. Fig. 5 shows the flows as they actually occurred and as they would have been without reservoir regulation.

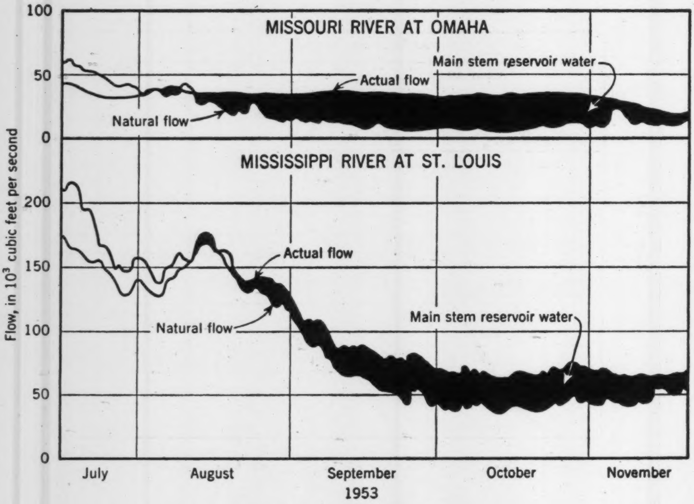

FIG. 5.—FLOWS DURING 1953 DROUGHT

Power Production.—Initial main-stem generation began in 1943 with the installation of the first 35,000-kw generator at Fort Peck; the third Fort Peck unit was installed in December, 1951. Two additional units in a second power plant are scheduled for installation in 1961. Initial power generation began at Fort Randall in March, 1954, with the first 40,000-kw generator. The eighth and last Fort Randall unit was placed in generation in January, 1956. Garrison units of 80,000 kw each were placed in operation in January, March, and August, 1956, respectively, with the remaining two units scheduled for installation in 1959 and 1960. The three Gavins Point power plant units of 33,300 kw each were placed in operation between September, 1956, and January, 1957. Power from these projects is integrated over a backbone grid transmission line and is being marketed by the Bureau in Montana, the Dakotas, Nebraska, Iowa, and Minnesota. By January, 1957, installed capacity amounted to 745,000 kw. Energy generation in the fiscal year of 1956 amounted to 1,724,000 kw-hr. Revenues in this year amounted to approximately $6,000,000. Fig. 6 shows additional data on power generation and revenues.

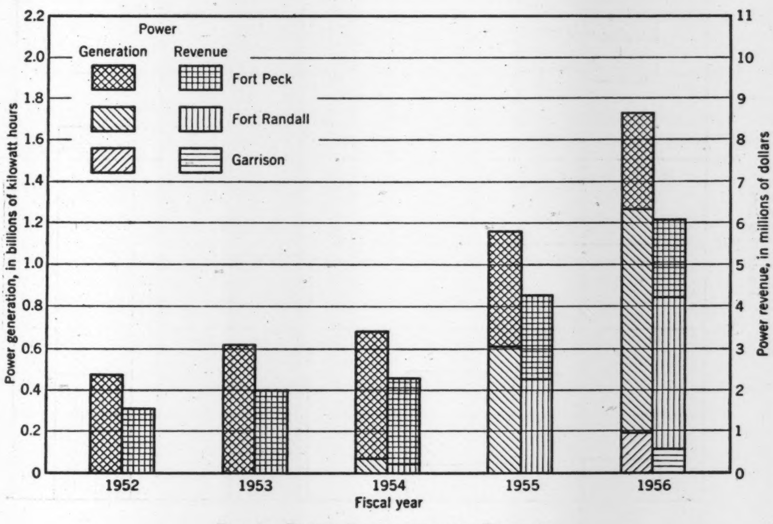

FIG. 6.—POWER GENERATION AND REVENUE

Navigation.—In 1954 substantial benefits began to be realized from another function of the water-development program. Navigation on the Missouri River has in the past been conducted on a pioneering basis, pending the final stabilization of the waterway and the development of a 9-ft channel. In 1954, however, two private towing companies started regular operations on the river and initiated plans for expanding their activities. One of these is utilizing a new 3,600-hp, 4-screw, 10-rudder towboat; the other has placed a 3,200-hp towboat in service, and other carriers are becoming increasingly concerned with traffic on the Missouri River.

Municipalities and private concerns are constructing dock facilities for handling cargo along the river. New facilities have been provided at Chamois (Mo.), Randolph (Mo.), St. Joseph (Mo.), Nebraska City (Nebr.), and

Brownville (Nebr.). Existing facilities at Omaha, the Kansas Cities, and other municipalities are being expanded and improved. Another benefit of navigation is the growing demand for river-front industrial sites that are accessible to both an assured water supply and a good navigable waterway. Commercial traffic, which reached a low point of 50,000 tons in 1952, increased to 150,000 tons in 1953, to 287,000 tons in 1954, and to 435,000 tons in 1955. The tonnage dropped to 312,000 tons in 1956 as a result of lowered rail rates on some of the principal commodities carried on the river. However, river traffic is expected to increase as the channel is improved. Most of the traffic upstream is of coal, steel, fuel, and molasses; downstream cargo is mainly of grain. A traffic study made in 1950 indicated that there should be 5,000,000 tons of traffic 20 yr after the project was completed, which appears to have been a conservative estimate. Fig. 7 shows traffic tonnage on the Missouri River from 1952 to 1955.

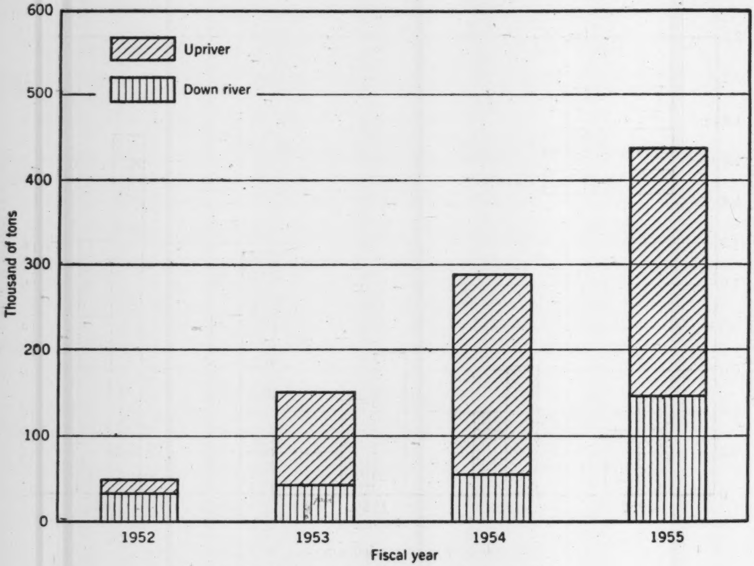

FIG. 7.—TRAFFIC TONNAGE ON THE MISSOURI RIVER

Basin Coordination.—The Missouri Basin Inter-Agency Committee coordinates the planning, construction, and operation of the development. This committee is composed of one representative from the United States Department of the Army, the United States Department of the Interior, the United States Department of Agriculture, the United States Department of Commerce, the United States Department of Health, Education and Welfare, the United States Department of Labor, and the Federal Power Commission; and is also composed of the governors of each state in the Missouri basin.

The committee meets once every two months and arranges to meet in each basin state about once a year. Working subcommittees meet more frequently, and some meet almost continually. This type of voluntary coordination has worked very well and has served not only to improve federal agency relationships but also to insure that the interests of the affected states and of the local citizens are adequately recognized and provided for.

A Reservoir Control Center located in Omaha operates the main-stem reservoirs. This group prepares a tentative annual operating plan based on water-supply forecasts and estimated demands which is submitted to a group of representatives of the federal agencies and the state engineers of the affected states. After all comments of this group have been received and discussed, a final plan is prepared and adopted. Execution of the plan is handled by the Reservoir Control Center, but close liaison is maintained with the other agencies and the states. This arrangement has been very effective in insuring a proper balance between all functions of the project.

The authorized program constitutes a basic framework of the larger and more important projects. The Corps, the Bureau, and the other agencies and states are constantly re-examining the program to determine whether modifications or additions are required. Additional projects have been recommended to Congress after studies have indicated their necessity and economic justification.

AMERICAN SOCIETY OF CIVIL ENGINEERS
Founded November 5, 1852

TRANSACTIONS

Paper No. 2878

SHEAR DEFLECTION OF WIDE-FLANGE STEEL BEAMS IN THE PLASTIC RANGE

BY WILLIAM J. HALL,[1] J. M. ASCE, AND NATHAN M. NEWMARK,[2] M. ASCE

SYNOPSIS

The following topics are included in this paper: (*a*) Results of tests of two continuous steel wide-flange beams, each having regions subjected to pure bending, bending combined with low shear, and bending combined with high shear; (*b*) a comparison of some of the test results with current design specifications; (*c*) data for estimating the component of deflection caused by shear when regions of the beam have undergone general shear yielding; and (*d*) theoretical examples illustrating the effects of general shear yielding of the web on the deformation characteristics of beams.

INTRODUCTION

The utilization of the reserve plastic strength of steel in structural design has merited considerable attention in recent years. The economy to be gained by so-called plastic-design methods lies in the fact that for redundant or complex structures the load corresponding to a specified deflection or to collapse may be considerably greater than that corresponding to the start of local inelastic action; occasionally deflection rather than load or stress may be the controlling factor in design.

Previous discussions of the deflection of structures loaded beyond the elastic limit have been restricted, for the most part, to the effect of bending alone. Although such restrictions are justifiable in many cases, it is important to be able to recognize when shear should be considered and to have concepts and data available which will make it possible to compute, or at least estimate, the shear deflection in both the plastic and the elastic ranges.

One objective of the beam tests and studies cited herein was to evaluate the importance of the effect of shearing stresses and deformations on the

---

NOTE.—Published, essentially as printed here, in October, 1955, as *Proceedings Paper 814*. Positions and titles given are those in effect when the paper was approved for publication in *Transactions*.

[1] Research Asst. Prof. of Civ. Eng., Univ. of Illinois, Urbana, Ill.

[2] Research Prof. of Structural Eng., Univ. of Illinois, Urbana, Ill.

behavior of beams, particularly with reference to load-carrying capacity. Information was sought for predicting the shear deflection of beam sections subjected to high shear forces. Also, additional data were obtained which are of interest in relation to current specifications for allowable shear stress in the webs of beams.

There is little theoretical or experimental information on the plastic deformation of structural beam sections subjected to high shear forces. In England the influence of shear forces on the behavior of I-sections has been investigated experimentally by J. F. Baker and J. W. Roderick,[3] and by A. W. Hendry[4]; a theoretical investigation has been made by M. R. Horne.[5] In the United States, B. G. Johnston, M. ASCE, C. H. Yang, and L. S. Beedle,[6] A.M. ASCE, have examined some of the implications of shear yielding of the web. A report by C.-F. A. Leth[7] treats the subject theoretically; this work is largely an extension of Mr. Horne's investigations.

These studies were mainly concerned with expected reduction in the so-called fully plastic moment. Several of the studies indicated that high shear forces caused a small or almost negligible reduction in the load-carrying capacity (except for extremely short sections); other studies indicated a marked reduction in the load-carrying capacity for some sections.

In the experimental part of the investigation cited herein two continuous-beam tests were made using one type of beam specimen. Each beam had sections subjected to pure bending, bending combined with low shear, and bending combined with high shear. The tests were carried far into the plastic range. In analyzing the data it was assumed that the bending and shear components of deflection could be separated and that their combined effect could be obtained by superposition. This approach resulted in data which can be used to estimate the shear deflection of other types of beam sections.

Obviously, two beam tests alone cannot provide a complete picture of the shear problem; they should be considered as exploratory tests which show what may be expected under certain conditions. Although the shear appeared to have little effect on the load-carrying capacity, it had considerable effect on the load-deflection response—a fact worth considering when assessing the applicability of standard specifications. It may be concluded from this study that the effect of high shear forces is not of great importance except for unusual loading conditions. Some of these conditions are described, and illustrations of the effects of high shear forces are presented.

BEAM SPECIMENS AND APPARATUS

Two continuous beams of section 8WF58 were tested in the as-rolled condition. This section was selected because it possessed (*a*) excellent rotation capacity—that is, ability to sustain the "hinge" moment through the required rotation without failure by local flange or web buckling; and (*b*) a relatively thick web which was desirable for sustaining large shear deformations.

---

[3] "Investigation into the Behavior of Welded Rigid Frame Structures. Second Interim Report," by J. F. Baker and J. W. Roderick, *Transactions*, Inst. of Welding, Vol. 3, 1940, pp. 83–92.

[4] "An Investigation of the Strength of Certain Welded Portal Frames in Relation to the Plastic Method of Design," by A. W. Hendry, *The Structural Engineer*, Vol. 28, 1950, pp. 311–326.

[5] "The Plastic Theory of Bending of Mild Steel Beams with Particular Reference to the Effect of Shear Forces," by M. R. Horne, *Proceedings*, Royal Soc. of London, Series A, Vol. 207, 1951, pp. 216–228.

[6] "An Evaluation of Plastic Analysis as Applied to Structural Design," by B. G. Johnston, C. H. Yang, and L. S. Beedle, *Research Supplement*, *The Welding Journal*, Vol. 32, 1953, pp. 224s–239s.

[7] "The Effect of Shear Stresses on the Carrying Capacity of I-Beams," by C.-F. A. Leth, *Technical Report A11-107*, ONR Contract N7onr-35801, Brown Univ., Providence, R. I., March, 1954, pp. 1–70.

The setup for the continuous-beam tests is shown in Fig. 1. The 9-ft central span was maintained in both tests, the central load points being symmetrically spaced at the one-third points for beam B1 ($a = b = 36$ in.), and at the one-sixth points for beam B2 ($a = 18$ in. and $b = 72$ in.). Symmetrical loading simplified analysis of the data; unsymmetrical loading would have made analysis difficult, as shown in examples presented in this paper.

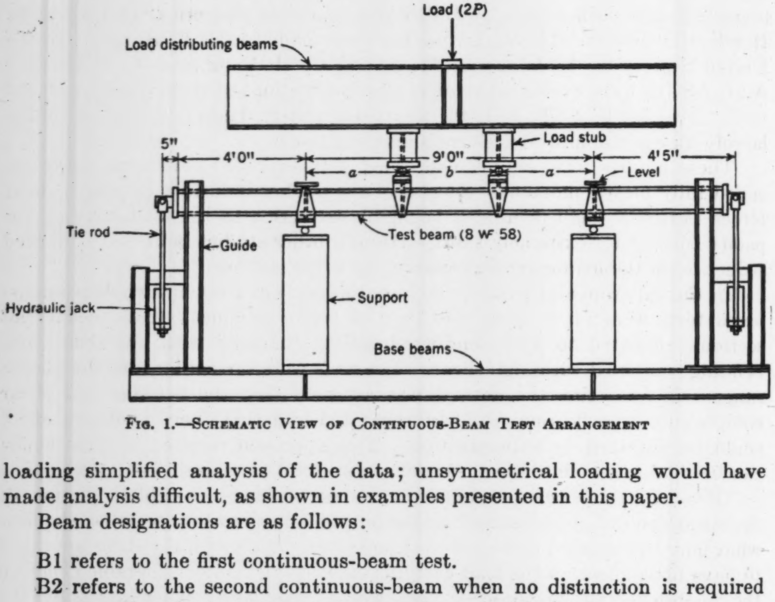

FIG. 1.—SCHEMATIC VIEW OF CONTINUOUS-BEAM TEST ARRANGEMENT

Beam designations are as follows:

B1 refers to the first continuous-beam test.
B2 refers to the second continuous-beam when no distinction is required regarding the two separate tests performed with this beam.
B2a refers to the first test of beam B2 in which shearing action was studied.
B2b refers to the subsequent pure-bending test of the central part of beam B2.

Each beam had sections under pure bending (the central section), bending combined with low shear (cantilever sections), and bending combined with high shear (the shear-moment (*V-M*) sections, which are the parts between the central load points and the reactions).

Both beams were tested to simulate fixed-end conditions by using the end cantilever sections to maintain zero rotation at the supports (beams B1 and B2a). After testing beam B2 as a continuous beam (B2a), the cantilevers were freed and the central part was tested in pure bending (B2b).

The load and reaction brackets were identical, the same type was used in both tests, and they were not designed to simulate any particular type of connection. To a certain extent they resembled splice plates, although not in the true sense, because the beam was not cut to insert the plates but was continuous throughout. The bracket plates were slotted to fit the wide-flange beam sections and were welded completely around the beam; they showed no signs of failure in either test.

Instrumentation for strain measurements included SR-4 wire-resistance gages (including post-yield gages) and mechanical gages. Deflection readings were made at selected points along the beam with reference to a line through the reactions. Whitewash was applied to more than half the beam in each test to indicate the yielding pattern and progression of yield zones. As an extension to the SR-4 rosette-gage readings in the web, shear detrusion on the shear-moment section was measured by direct-reading mechanical gages and gage holes on a 2-in.-square spacing. These gage holes were placed symmetrically about the longitudinal axis of the web and on both sides of the web. The level mounted on top of each reaction bracket was used to maintain the end fixity. Distribution of load between the load points was checked by two instrumented "load stubs" which were placed between the distribution beam and the rollers. The cantilever ends were loaded by means of jacks through instrumented tie rods.

TABLE 1.—SECTION PROPERTIES OF TEST BEAMS

Beam	Depth, in inches	Web thickness, in inches	Flange width, in inches	Flange thickness, in inches	Area, in square inches	I_x, in inches[4]	Z_x, in inches[3]
B1[a]	8.85	0.518	8.132	0.840	17.50	237	61.80
B2[a]	8.82	0.519	8.136	0.824	17.25	232	60.68
8W58[b]	8.75	0.510	8.222	0.808	17.06	227.3	...

[a] Average of measurements from two locations. [b] Standard values.

TABLE 2.—RESULTS OF TENSION-COUPON TESTS

Property	Unit	BEAM	
		B1	B2
Yield stress, σ_{yp}	kips per square inch	33.8	35.5
Modulus of elasticity, $E \times 10^{-3}$	kips per square inch	31.8	31.5
Strain corresponding to beginning of strain-hardening region, ϵ_{sh}	inches per inch	0.012	0.012
Maximum stress, σ_{max}	kips per square inch	60.8	62.8
Elongation of 8-in. gage length	percentage	33	32

Section properties of beams B1 and B2 are presented in Table 1, and the results of the tension-coupon tests are summarized in Table 2. These latter tests were based on nine coupons taken from one section, three from each flange, and three from the web. The test data are average weighted values, individual coupon results being weighted for the area represented and the distance from the neutral axis. Longitudinal, residual-strain measurements were made on a part of the piece from which beam B1 was cut. These measurements showed a maximum residual strain of 0.00045 in. per in. at the center of the web, or approximately 40% of the tensile yield-point strain.

The testing procedure consisted of loading with the 3,000,000-lb machine and of jacking down the ends of the cantilever to keep the level bubbles at the reaction points centered. When yielding occurs under constant load in the plastic range, it takes considerable time for the beam to come to rest. Under such conditions when the beams did not come to rest after 15 min to 20 min, the load was decreased slightly (from 1 kip to no more than 2 kips in a total load of from 200 kips to 400 kips) in order to stop the beam from deforming while readings were taken. In this manner it was possible to run each test in approximately 15 hr.

RESULTS AND INTERPRETATION OF TESTS

General Remarks.—Neither of the two continuous beams had reached its maximum load by the end of the test. The test of beam B1 was stopped at a load of 269 kips because of a jack failure. At that time the compression flanges inside each reaction—that is, in the shear-moment section—were just beginning to buckle. (This buckling was barely visible to the eye.) Beam test B2a was carried to a deflection which was considered sufficient to obtain the desired data, but the test was stopped while the central part was still in the elastic range in order to allow this part to be used in a subsequent pure-bending test.

The pure-bending test (B2b), consisting of freeing the cantilever ends and testing the central part as a simple beam, was made to obtain an experimental moment-curvature relationship to compare with that obtained from the tension-coupon test data. In addition, it was necessary to have reliable moment-curvature information to analyze the shear-moment data. The central section failed by gradual lateral buckling as the test was carried into the strain-hardening range.

Deflection computations were made by using the numerical integration procedure developed by one of the writers.[8] This and other procedures for computing flexural deflections of beams in the plastic range are summarized in a recent paper.[9] In making such computations it is customary to use assumptions as to the propagation of the plastic regions and the shape of the moment-curvature diagram. These assumptions tend to simplify the computations (which is preferable for many applications) but yield less accurate results. Where high accuracy is needed numerical integration is the most desirable.

The separate deformation concepts attributed to moment and shear are illustrated in Fig. 2. The basic hypothesis used in the reduction of the moment-shear data is that the bending and shear behaviors can be separated and treated independently in both the elastic and plastic ranges. That is, superposition is assumed to apply to the range of response under study. This appears to be the best method of handling the two effects. It is believed that, when these data are used to compute the shear deflection of other similar beams, the predicted deflections will be reasonably accurate. Data for making such an estimate of shear deflections when shear forces are high have not been available previously.

---

[8] "Numerical Procedure for Computing Deflections, Moments, and Buckling Loads," by N. M. Newmark, *Transactions*, ASCE, Vol. 108, 1943, pp. 1161–1234.

[9] "Plastic Strength and Deflections of Continuous Beams," by K. E. Knudson, C. H. Yang, B. G. Johnston, and L. S. Beedle, *Research Supplement*, *The Welding Journal*, Vol. 32, 1953, pp. 240s–256s.

In this paper, test results are presented in the order in which the analyses were made—pure-bending test, cantilever sections (bending combined with low shear), and V-M sections (bending combined with high shear). This is followed by an examination of certain phases of the test results in the light of current design specifications and by a presentation of data for predicting the shear deflection of beams after general shear yielding has occurred.

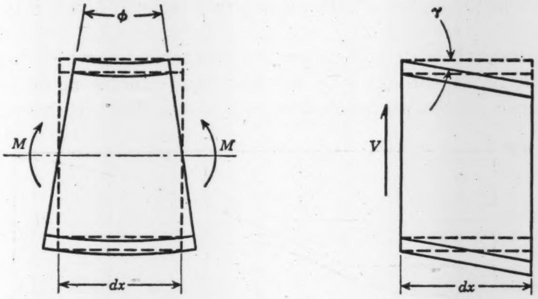

FIG. 2.—DEFORMATION OF A BEAM SECTION DUE TO BENDING MOMENT AND SHEAR

PURE BENDING

The simple plastic theory of pure bending of mild-steel beams assumes:

1. The flexural strain is distributed linearly over the cross section as in the elastic-bending theory.
2. The stress-strain relationship in a bent beam is the same as that determined from a static tension test of a coupon of the material.
3. The stress-strain relationship is the same in compression as it is in tension.

In the elastic range the moment, M, and the curvature, ϕ, of a bent beam, in terms of the modulus of elasticity, E, and of the moment of inertia, I, are $\phi = M/E\,I$.

In the plastic range the moment-curvature relationship is obtained by considering the stress-strain conditions. Computing the moment requires considering the stress block that is assumed to be acting on the section. Because the strain is distributed linearly, the stress block corresponding to a given strain distribution is actually the stress-strain curve (up to the maximum strain) with the strain axis adjusted to one-half the beam depth. For a given strain distribution and the corresponding stress block, the curvature and moment can be computed. Methods of computing the moment-curvature (M-ϕ) diagram are described elsewhere.[10,11]

Fig. 3 shows the M-ϕ diagram obtained from the pure-bending test of the center section (B2b). The experimental plot was obtained by a curve-

---

[10] "Shear Deflection of Wide Flange Steel Beams in the Plastic Range," by W. J. Hall, thesis presented to the University of Illinois, at Urbana, in 1954, in partial fulfilment of the requirements for the degree of Doctor of Philosophy.

[11] "Plastic Behavior of Wide Flange Beams," by W. W. Luxion and B. G. Johnston, *Research Supplement, The Welding Journal*, Vol. 27, 1948, pp. 538s–554s.

fitting process in which the curvatures were computed so as to make the derived deflections equal to the measured deflections. A check was obtained by computing the curvatures from the strain-gage readings. An independent check of the curve-fitting process was obtained by using the measured deflections and a second-order difference equation. All the latter values were so close to the original curve that they could not be distinguished with the scale used in Fig. 3. The initial slope of the curve corresponds to an $E\,I$-value of 69.3×10^5 kips per sq in. With I computed to be 232 in.^4, E is 29.9×10^3 kips per sq in.

The experimental curve falls below the theoretical curve (computed from tension-coupon data) through the flat part and climbs again toward the theoretical curve in the strain-hardening region. The decrease is approximately 9% of the theoretical value in the flat part and approximately $3\frac{1}{2}$% in the strain-hardening region. Observations of M-ϕ diagrams made in other publications[11,12] also showed decreases of the same order of magnitude. The experimental M-ϕ diagram obtained from beam test B2b was used in all computations for beam B2. An adjusted curve using the same 9% and $3\frac{1}{2}$% reduction values was used in the computations for beam B1.

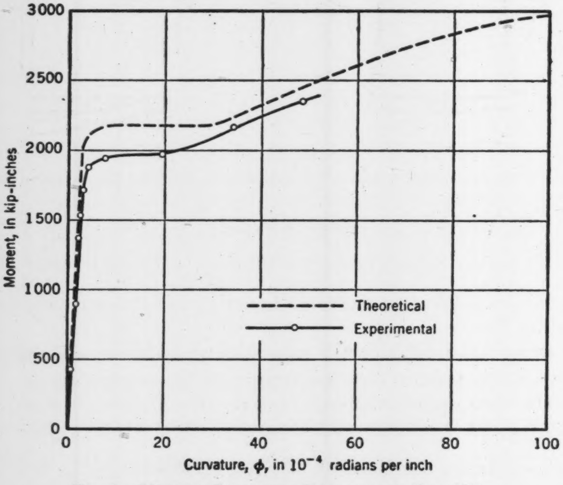

FIG. 3.—MOMENT-CURVATURE DIAGRAM FOR BEAM B2

In the moment-strain curve from beam B2b (Fig. 4) the strains are the average for the top and bottom of the section. The curve could be converted to a M-ϕ diagram by dividing the strain values by one-half the depth of the beam.

Fig. 5 shows the measured load versus the center-deflection curve for beam B2b and the load-deflection curve corresponding to the theoretical M-ϕ

---

[12] "Residual Stress and the Yield Strength of Steel Beams," by C. H. Yang, L. S. Beedle, and B. G. Johnston, *Research Supplement, The Welding Journal*, Vol. 31, 1952, pp. 205s–229s.

diagram of Fig. 3. A slight variation in the M-ϕ diagram for regions of pure bending can cause considerable differences in deflections; this is particularly true for long spans under pure bending.

COMBINED BENDING AND SHEAR SECTIONS

Because both continuous beams were loaded symmetrically, little or no shear was present in the central sections during the tests. The lengths of the cantilever sections, which were used to maintain the end fixity, were such that the shear in them was relatively low. Shear yielding did not occur in the web of the cantilever sections in either test. Between the reaction point and the central load point, the magnitude of the shear forces caused shear yielding of the web. The large shear deflections that resulted were of primary interest in this investigation.

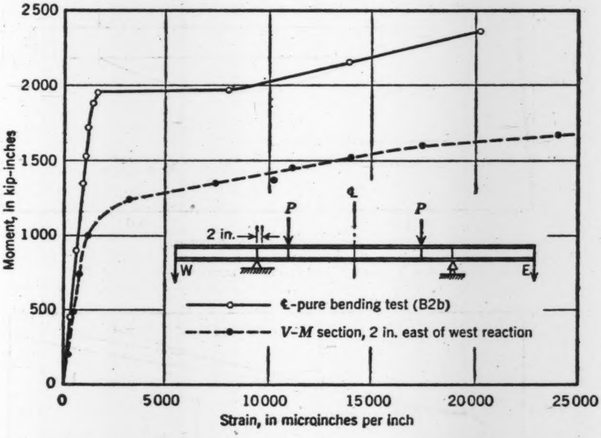

FIG. 4.—MOMENT VERSUS STRAIN FOR CENTER AND V-M SECTION OF BEAM B2

In Fig. 6 the fixed-end moments are plotted against end deflections for the cantilever sections of beam B1. The dotted curves, representing the deflections as they were computed from the adjusted M-ϕ diagram, include the component of deflection due to shear, which was elastic throughout and which constituted an almost negligible quantity.

In Fig. 7, in which the moment-strain curves for a cantilever section of beam B1 are shown, the strain values represent the average of the top and bottom strains at a section. These curves, which have the same shapes as moment-curvature diagrams, can be converted to such diagrams by dividing the strain values by half the depth of the beam—a procedure admissible only because the shear was low and did not greatly influence the linear-strain distribution.

The moment-load relationships for one-half the main span of beams B1 and B2a are shown in Figs. 8 and 9. The moment values corresponding to the theoretical start of yield, M_{YP}, and strain hardening, M_{SH} (from the adjusted M-ϕ diagrams) are indicated. The dotted curves represent the theoretical relationships resulting from considerations of flexure alone.

The method used to compute these theoretical relationships is of interest. In the elastic range the ratio between the end moment and the load-point moment was 2:1 for beam B1 and 5:1 for beam B2a. The latter ratio corre-

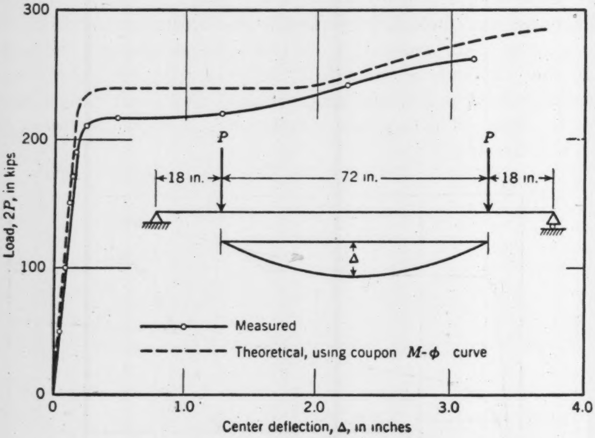

FIG. 5.—LOAD VERSUS CENTER DEFLECTION FOR BEAM B2b

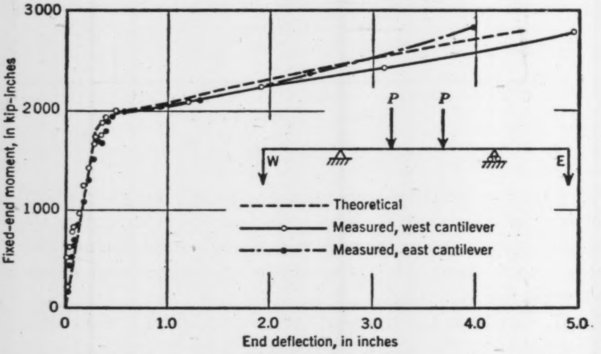

FIG. 6.—FIXED-END MOMENT VERSUS END DEFLECTION FOR CANTILEVER SECTIONS OF BEAM B1

sponds to an extremely steep moment gradient. In the elastic range, expressions for the moments can be obtained from any structural handbook; in the plastic range a trial-and-error method is needed. In the plastic range the method of analysis is not difficult because the beam is symmetrically loaded and, therefore, redundant to the first degree. (The slope at the ends and center must be zero because of symmetry.) The trial-and-error method consists of selecting the end moment and altering the load-point moment until the slope conditions are satisfied. Because shear deformation does not affect the moment-load relationship in symmetrically loaded beams, the agreement between the theoretical and experimental curves is generally good. A study of the moment-load relationship reveals that no appreciable reduction in the resisting moment exists which can be traced to shear.

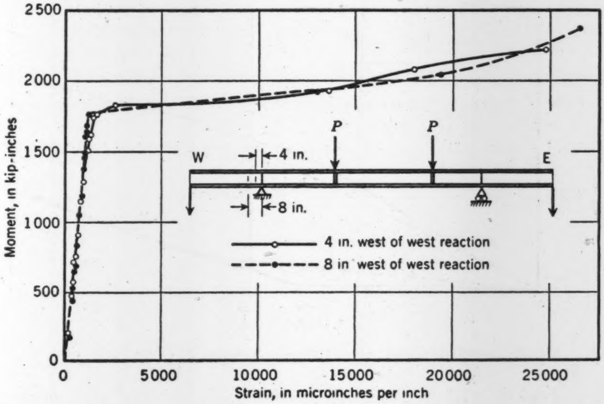

FIG. 7.—MOMENT VERSUS STRAIN FOR WEST CANTILEVER SECTION OF BEAM B1

A curve for the load versus center deflection, beam B2a (Fig. 10), illustrates the effect of the high shear force on the deflection of the main span. The dotted curve represents deflections for flexure alone. The additional deflection caused by the shearing action is noteworthy.

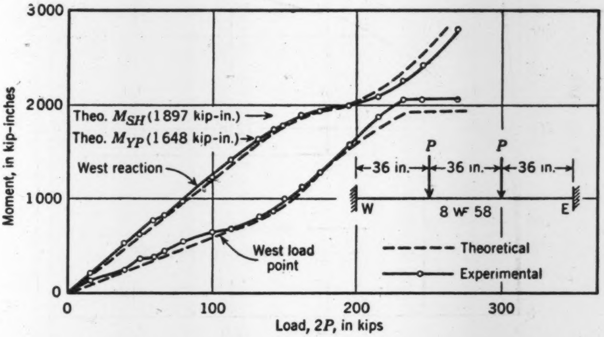

FIG. 8.—MOMENT-LOAD RELATIONSHIPS FOR BEAM B1; WEST END

Comparing the shapes of the load-deflection curves for the three conditions of loading encountered in each beam clearly indicates the expected trends. In the case of pure bending (Fig. 5) there is a relatively long, flat part before strain hardening commences and causes the load to increase. In the cantilever sections (Fig. 6), which have a moment gradient but low shear forces—that is, bending is still predominant—strain hardening commences quickly and causes the curve to rise almost immediately after yielding has occurred at the fixed end. For a region with a steep moment gradient and with corresponding high shear forces, general shear yielding of the web causes a break in the load-deflection curve (Fig. 10) which may be at a much lower load than would be expected from flexural yielding alone.

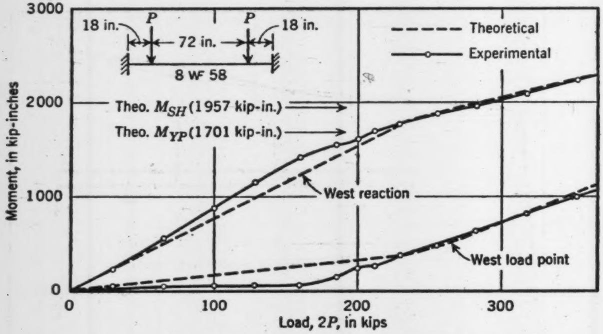

FIG. 9.—MOMENT-LOAD RELATIONSHIPS FOR BEAM B2a; WEST END

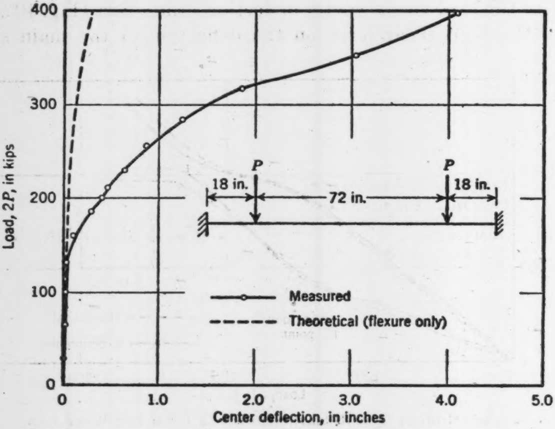

FIG. 10.—LOAD VERSUS CENTER DEFLECTION FOR BEAM B2a

The moment-strain curve for the *V-M* region of beam B2 (Fig. 4) is presented for comparison with one from a pure-bending section (Fig. 4) and one from a cantilever section (Fig. 7). General shear yielding of the web strongly influences the strains in the flanges. Therefore, such moment-strain curves have little significance. They should not be interpreted as an equivalent moment-curvature relationship for the shear-moment section because a study of other strain data taken in this region shows a differently shaped curve for each section. However, the load corresponding to the break-over in any moment-strain curve in the *V-M* section corresponds identically to the load at the sharp break in the load-deflection curve. The longitudinal strain distribution in the shear-moment sections is erratic, emphasizing the fact that the strain distribution is complicated in short sections. The boundary conditions and complex residual strain pattern influence the strain distribution.

The deformed shapes of the beams, as well as the test layout, are shown in Figs. 11 and 12. The central part of beam B2a (to the left in Fig. 12) is still in the elastic state and was later tested separately in pure bending (B2b). Views at close range of the cracked whitewash patterns in the shear-moment sections at two different loads are shown in Figs. 13 and 14. Flaking of the whitewash was initially observed at both the reaction and load ends of the *V-M* section in the web corners subjected to compressive flexural stress. This was to be expected because the residual strains in the web are compressive The yield patterns were almost identically symmetrical on either side of the web. Flaking started at loads of 50.5 kips in beam B1 (shear equals 24.2 kips) and 30 kips in beam B2a (shear equals 15.6 kips). These shears differ slightly from one-half the loads because there is a slight dissymmetry in the loading position and in the beam properties.

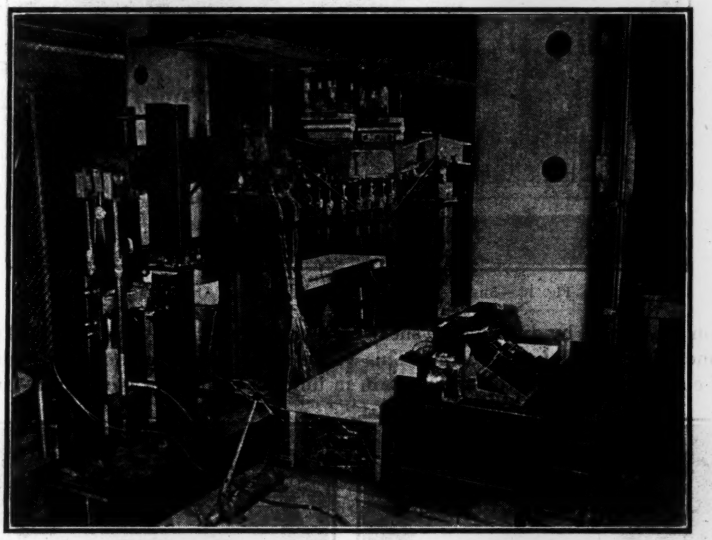

FIG. 11.—BEAM B1 AFTER TEST

Methods of estimating the elastic shear deflection of beams are well known. W. M. Fife and J. B. Wilbur,[13] summarizing data from some simple beam tests conclude that the nominal shear stress to be used in the shear-strain computation is obtained by dividing the shear by the gross web area—the web thickness times the depth of the beam. This value divided by the shearing modulus of elasticity, G, gives the shear strain in units of inches per inch which multiplied by the length will give the component of deflection due to shear. This conventional method of computing the elastic shear deflections of structural beams gives a reasonable solution. Many refinements can be made by con-

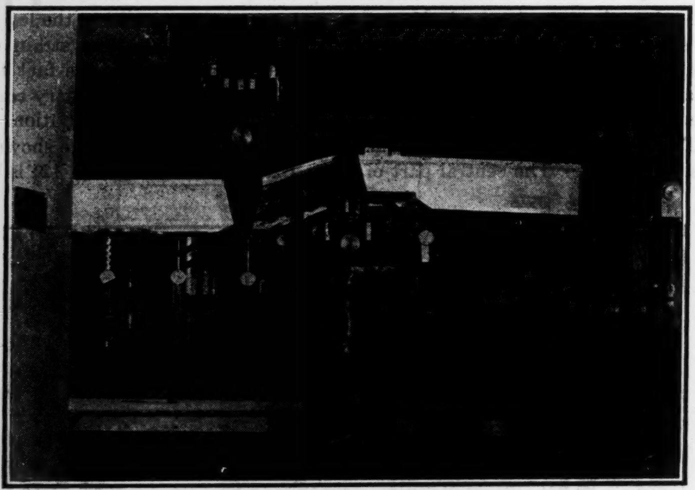

Fig. 12.—Shear Deformation of Beam B2a; After Test

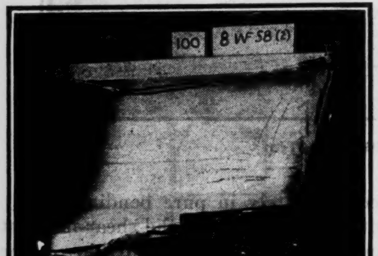

Fig. 13.—*V-M* Section of Beam B2a—Load = 100 Kips; Reaction on Right

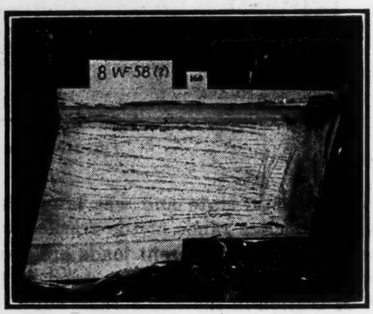

Fig. 14.—*V-M* Section of Beam B2a—Load = 160 Kips; Reaction on Right

sidering more accurate stress distributions; these are presented in many textbooks on strength of materials and theory of elasticity.

---

[13] "Theory of Statically Indeterminate Structures," by W. M. Fife and J. B. Wilbur, McGraw-Hill Book Co., Inc., New York, N. Y., 1937, p. 27.

One objective of this investigation was to obtain data for estimating shearing deflections for wide-flange beams loaded into the plastic range. Several methods were used to obtain the curve of shear versus shear strain for predicting shear deflections. One method consisted of (*a*) computing the deflections due to flexure alone, (*b*) subtracting these from the measured deflections, and (*c*) assuming the difference to be due to shear. These deflection differences were divided by the length between the deflection points to obtain a measure of the shear strain. Shear-strain values were also computed from a number of rosette gages which were mounted symmetrically on both sides of the web.

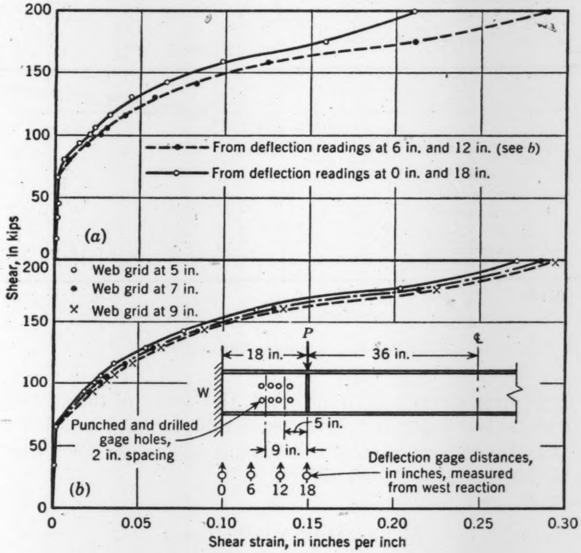

FIG. 15.—SHEAR VERSUS SHEAR STRAIN FOR WEST *V-M* SECTION OF BEAM B2a

For a given symmetrical pair of rosette gages the strain readings for corresponding arms were averaged and used in the rosette-strain analysis.

In order to extend the range of the shear-strain data obtained from the rosette gages, a series of gage holes was placed on both sides of the web. The angle changes in the grids were computed trigonometrically from measurements of the lengths of the sides and diagonals of the square gage grids at various loads. Because the grids were symmetrical about the midline of the web, the angle changes were the shear deformations.

Representative data obtained from the deflection procedure are presented in Fig. 15(*a*), the grid layout in Fig. 15(*b*), and the rosette gages in Fig. 16. The diagrams for shear versus shear strain obtained by the three methods show excellent agreement even when plotted to a larger scale.

The SR-4 strain-gage rosettes (Fig. 16) also provide information on the elastic shear-stress distribution. The rosette-gage shear-stress values, τ_{xy}, together with the values of $V\,Q/I\,b$ and V/A_w are listed in Table 3. The value of A_w is the web area taken from center to center of the flanges; V, the shear; Q, the static moment about the neutral axis of the area above the section at which the shearing stress is desired; and b, the width of the section at which the shearing stress is computed. The greatest discrepancy between the rosette values and the theoretical shear-stress values occurs for the rosettes which are closest to the reaction or load points.

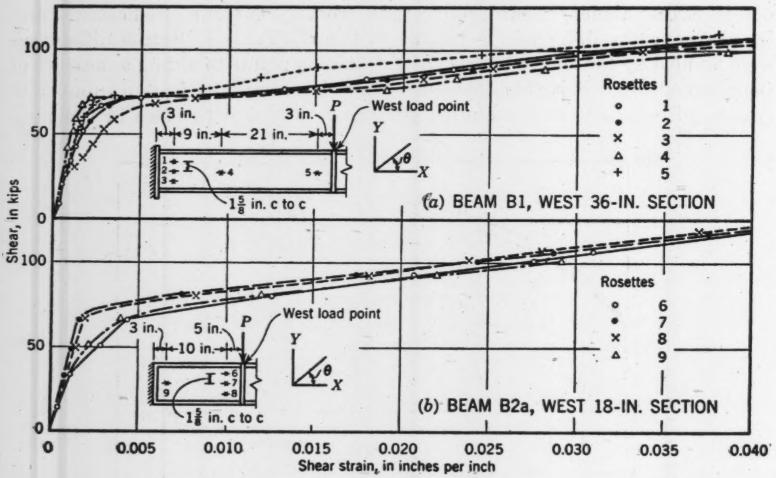

Fig. 16.—Shear Versus Shear-Strain

Application to Practice

The foregoing data are of some interest in relation to current design practice, and the more interesting aspects are cited subsequently. The first shear yielding of beam B1 was noted in the whitewashed part of the web at a load of 50.5 kips. As indicated in Table 3 the maximum shear stress for rosette gage set No. 3 at this load was computed to be 8,560 lb per sq in. and the nominal shear stress was 6,350 lb per sq in. The first shear yielding of beam B2a was noted at a load of 30 kips. The maximum shear stress for rosette gage set No. 6 at this load was computed to be 3,720 lb per sq in. and the nominal shear stress was 3,500 lb per sq in.

The appearance of yield lines at such low stresses does not mean that structural failure is imminent. The complex residual stress field in the web tends to initiate early yielding. The critical stage, from the deflection standpoint, is reached when general shear yielding of the web occurs and there is a corresponding sharp break in the load-deflection diagram (Fig. 10). This break-over corresponds to a shear of approximately 69 kips in both beams, which, based on the gross web area defined in the specifications, amounts to 15,000 lb per sq in. for the as-measured sections. With no corrections for the tension yield-point values, because they are only slightly more than 33,000 lb per sq in., a 15,000-lb-per-sq-in. shear stress provides a factor of safety against general shear yielding of only 1.15 based on the current specifications of the American Institute of Steel Construction (AISC) which calls for 13,000 lb per sq in. maximum on the gross web area. This low value is of interest and requires consideration.

In 1938 Mr. Johnston[14] indicated the implications of this sharp break-over in the load-deflection curve which results from general shear yielding. Actually, shear yielding may have a more direct bearing on the failure of a beam than flexural yielding under a concentrated load because, in the former case, a much greater part of the beam is affected.

TABLE 3.—COMPARISON OF SHEAR STRESS IN THE ELASTIC RANGE[a]

Load, in kips	Shear, in kips[b]	τ_{xy} from rosettes, in pounds per square inch			$(V Q)/(I b)$, in pounds per square inch	V/A_w, in pounds per square inch	τ_{xy} from rosettes, in pounds per square inch		$(V Q)/(I b)$, in pounds per square inch
		2	4	5			1	3	
				BEAM B1					
17.5	9.3	2,550	2,880	2,670	2,340	2,240	2,550	2,730	2,290
40	20.9	6,030	5,780	6,030	5,250	5,040	6,100	5,710	5,150
50.5	26.3	8,430	7,260	7,900	6,600	6,350	7,810	8,560	6,370
59.5	31.2	10,720	8,410	9,260	7,830	7,500	9,310	16,670	7,680
66.5	34.5	12,650	9,400	10,660	8,650	8,300	11,590	...	8,500
81.5	42.1	14,890	11,450	13,440	10,500	10,150	15,370	...	10,400
100	51.4	...	13,870	...	12,900	12,400	...	...	...
113	57.6	...	15,530	...	14,400	13,900	...	...	...
				BEAM B2a					
		7	9				6	8	
30	14.4	3,570	2,150		3,630	3,500	3,720	3,630	3,540
65.5	32.8	8,310	11,560		8,260	7,900	11,820	8,470	8,070
100	49.9	14,060	...		12,580	12,000	...	15,200	12,300
130	65.8	16,540	...		16,600	15,900	...	...	16,200

[a] Gage data in Fig. 16. [b] Shears are slightly different from one-half the load because of slight dissymmetry in the position of loading and in the beam properties.

Another item relating to current specifications which is of interest is the stress of 24,000 lb per sq in. allowed by AISC specifications on extreme fibers of beams which are continuous at interior supports. This is an approximate elastic equivalent of plastic design, but unlike the specifications of the American Railway Engineering Association (AREA) and the American Association of State Highway Officials (AASHO), there is no limit placed on the principal direct stress. These specifications limit the diagonal tension stress to 18,000 lb per sq in. in webs of girders and rolled beams at sections where maximum shear and bending occur simultaneously. In the case of beam B1, for a flexural stress of 24,000 lb per sq in. at the support, the moment is 1,287 kip-in. and the shear is 53.6 kips in the *V-M* section. For beam B2a the corresponding values are 1,263 kip-in. and 84.3 kips. In the former case, general shear yielding of the web had not occurred when the flexural stress was computed as 24,000 lb per sq in.; in the latter case, general shear yielding had occurred.

---

[14] "Shearing Stress in Steel Beams," by B. G. Johnston, *Civil Engineering*, Vol. 8, 1938, p. 273.

Thus, the position and type of loads must be considered when this specification is applied. It may be unwise to use the allowed stress value of 24,000 lb per sq in. unless the shear stress is adequately low. However, the AREA and AASHO specifications are more conservative. For a principal direct stress of 18,000 lb per sq in. at the support at the flange-web junction, the moment and corresponding shear are computed as 920 kip-in. and 38.3 kips for beam B1, and 740 kip-in. and 49.3 kips for beam B2. In the first case, a factor of safety against general shear yielding of 1.80 is provided; in the second case, the factor of safety is 1.40. The theoretical and measured moments and loads show close agreement for these tests (Figs. 8 and 9) so that the computed moments and shears cited approximate those actually measured.

Shear Stress-Strain Curve.—To use the shear-versus-strain data for predicting the shear deflections of other beam shapes, it is convenient to express the shear values in terms of the average shear stress in the web. The web area used in this conversion, $A_w = w\ (h - t)$, is considered a reasonable value that can be applied to shallow beams as well as to deep beams; w is the web thickness, h denotes the beam depth, and t is the flange thickness.

From the information gathered in both beam tests, a representative shear versus shear-strain curve was drawn. A study of this curve showed three rather definite regions: (*a*) The initial elastic part; (*b*) after the break-over, a gently sloping part extending to a shear-strain value of approximately 0.020 in. per in.; and (*c*) the remaining part, which resembled the strain-hardening part of a tension stress-strain curve. A curve-fitting scheme was used to obtain expressions for these parts in terms of the shear, V, and the shear strain, γ. The expressions were then divided by A_w for the 8W58 section to reduce the shear values to nominal shear stress in the web.

The mean shear value at the break-over in the V-γ curves is approximately 69 kips, which corresponds to a shear stress of 16,500 lb per sq in. for the 8W58 section. For a nominal yield point, σ_{yp}, of 32.3 kips per sq in. which corresponds to the experimental M-ϕ curve of beam test B2b, a shear stress of 16,500 lb per sq in. represents 0.51 σ_{yp}. These shear stresses are nominal values based on uniform distribution across the web. Nevertheless, they fall near the range of values reported by I. M. Lyse, M. ASCE, and H. J. Godfrey[15] who conducted torsion tests on specimens taken from the webs of structural beams and found that the ratio of yield strength in shear to that in tension varied from 0.505 to 0.634.

---

[15] "Shearing Properties and Poisson's Ratio of Structural and Alloy Steels," by I. Lyse and H. J. Godfrey, *Proceedings*, A. S. T. M., Vol. 33, 1933, pp. 274–292.

The curve-fitting process yielded the following expressions:

$$\gamma = \frac{\tau}{G} = 8.70 \frac{V}{A_w} 10^{-5} \begin{cases} 0 < \gamma < 0.00143 \text{ in. per in.} \\ 0 < \tau < 16.5 \text{ kips per sq in.} \end{cases}$$

$$\gamma = \frac{\tau - 16.06}{307} \qquad \begin{cases} 0.00143 < \gamma < 0.020 \\ 16.5 < \tau < 22.2 \end{cases}$$

$$\gamma = \left(\frac{\tau}{70}\right)^{3.40} \qquad \begin{cases} 0.020 < \gamma < 0.300 \\ 22.2 < \tau < 49.1 \end{cases}$$

The curve based on these expressions is presented in Fig. 17. It must be remembered that this diagram is based only on data obtained from the 8W58 section. However, unless other specific data are available from tests, this relationship may be used to estimate the shear deflections of other mild-steel wide-flange sections.

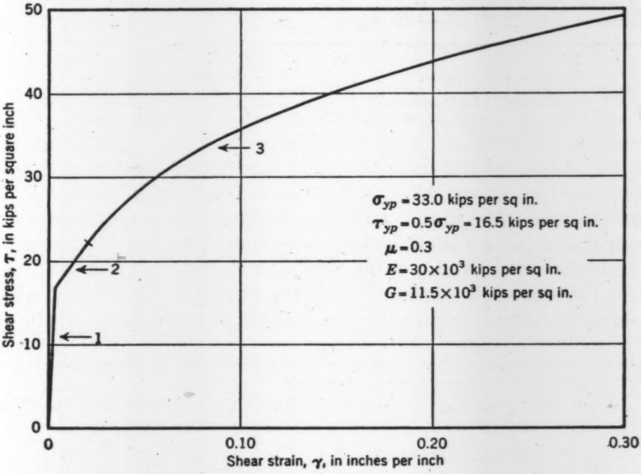

FIG. 17.—SHEAR STRESS-STRAIN DIAGRAM

To estimate the shear deflection of a beam it is first necessary to compute τ, which is equal to V/A_w; the curve should be entered with τ, and the shearing strain, γ, will be found. The shearing strain multiplied by the increment in length along the beam gives the component of deflection due to shear over that length. This procedure should be modified in special cases, as will be cited subsequently.

SHEAR DEFORMATION AND ITS EFFECT ON BEAM BEHAVIOR

Theoretical Examples.—Some of the effects of shear deformation on the behavior of a beam will be illustrated. For symmetrically loaded beams with symmetrical boundary conditions, shear causes no readjustment of moment and slope, even in the plastic range. However, for unsymmetrically loaded beams there is a readjustment of moment and slope. Some problems which can arise in the actual testing or analysis of an unsymmetrically loaded beam are illustrated as follows: A 12WF120 beam, having a span of 20 ft, and with the load 4 ft from one end, was selected and treated (*a*) as a simply supported beam (Fig. 18) and (*b*) as a beam with fixed supports (Fig. 19). In each case, bending alone and bending and shear combined are compared.

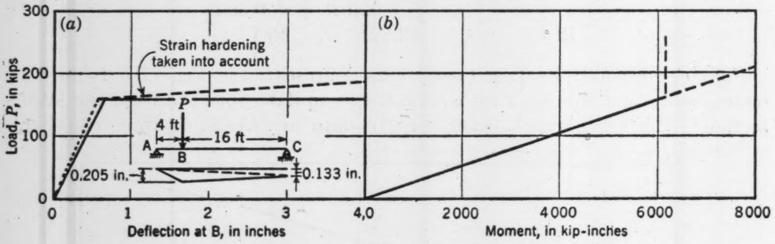

FIG. 18.—LOAD-DEFLECTION AND LOAD-MOMENT RELATIONSHIPS FOR AN UNSYMMETRICALLY LOADED SIMPLY SUPPORTED 12WF120 BEAM

Several assumptions were made in order to simplify the analyses. The M-ϕ curve used in the analyses assumes elastic behavior up to the fully plastic-moment value of 6,150 kip-in. and then becomes flat. In the first example, strain hardening is considered, and in the second example it is neglected. The inclusion of strain hardening would tend to reduce the deflections from those shown in the second example. Neglecting strain hardening also allows the plastic-hinge method of computing the deflections to be used,[5] which provides a further simplification in the computations. In the plastic-hinge method the beam has elastic regions and localized plastic hinges only.

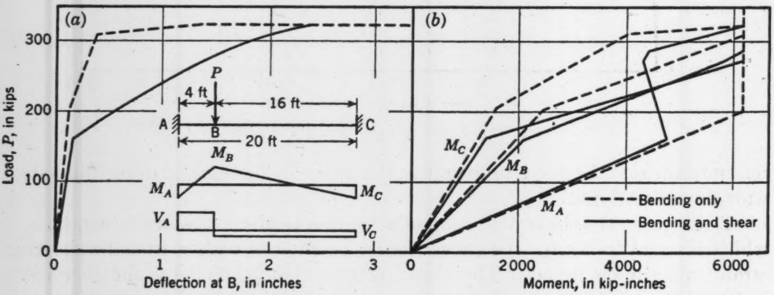

FIG. 19.—LOAD-DEFLECTION AND LOAD-MOMENT RELATIONSHIPS FOR AN UNSYMMETRICALLY LOADED 12WF120 BEAM WITH FIXED SUPPORTS

The shear stress-strain curve is taken from Fig. 17 with the exception that the second linear part is extended beyond 0.020 in. per in. to a shear strain of approximately 0.045 in. per in.; this approximation simplifies the computations. For the following examples the deflection at point B is computed.

Although it is not the maximum beam deflection, it approximates it in magnitude and illustrates the trend.

Simple Beam.—For the simple beam the moment increases linearly with the load. The beam remains elastic with regard to both bending and shear up to a load of 160 kips. The broken part of the graph represents the deflection due to bending alone whereas the solid line represents the combined deflection due to bending and shear. In accordance with the plastic-hinge concept, at a load of 160 kips the beam would become a mechanism with a hinge at point B and would deflect without any increase in load. This is represented by the solid horizontal line in the graph. However, to illustrate a point regarding shear deflection, strain hardening is considered; the deflection is represented by dashed lines. At a load of 185 kips the nominal shear stress in segment AB is 17.4 kips per sq in., which indicates that shear yielding has occurred. The flexural deflection at point B is 3.69 in. In Fig. 18(*a*) the shear deflection for segment AB is computed as 0.205 in. whereas that for segment BC is computed as 0.72 in., which indicates a lack of closure of 0.133 in. Because the shear angle-change at point B is fixed and the deflections must close out, the triangle is rotated to effect the closure which reduces the shear deflection at point B from 0.205 in. to 0.178 in. The total deflection at point B is the sum of 3.69 in. and 0.18 in., or a total of 3.87 in.

The physical significance of this lack of closure and necessary adjustment of the shear deflection is that the yielded segment AB should have deflected the full amount whereas the elastic segment could not and therefore restrained it to a certain extent. This action, in turn, caused a slight readjustment of the slopes at the ends of the beam, which can be computed. Obviously, the shear yielding of segment AB could have been induced while the flexural deflection was in the elastic range if the load had been closer to the end of the beam.

Beam Fixed at A and C.—The beam, fixed at points A and C, is twice indeterminate. In addition to the equilibrium equations, two relationships involving deformation must be utilized as follows: (*a*) The sum of the angle changes between points A and C must be zero and (*b*) the deflection of one end with respect to the tangent at the other must equal zero.

These conditions yield the following relationships for the elastic case:

$$M_A = \frac{P\,a\,b^2}{L^2} \quad \text{and} \quad M_C = \frac{P\,a^2\,b}{L^2}.$$

For bending alone (dotted lines in Fig. 19), the maximum moment initially occurs at point A and the first hinge forms at this point when the fully plastic-moment value of 6,150 kip-in. is reached at a load of 200 kips. As the load is increased the next hinge forms at point B at a load of 309 kips. The maximum load is 320 kips when the hinge moment is reached at point C. At this load the beam theoretically becomes a simple mechanism which deflects without any increase in load. It should be noted that the load-deflection curve and load-movment curve have two distinct breaks, characteristic of continuous beams when bending alone is considered.

For bending and shear the expressions for the moments become slightly more complicated. In this case the angle-change expression is not altered because the algebraic sum of the shear-angle changes will always be zero if statics are satisfied. However, there are added terms in the deflection relationship.

The two expressions are as follows:

$$\frac{1}{E\,I}\left(\frac{P\,a\,b}{2}-\frac{M_A\,L}{2}-\frac{M_C\,L}{2}\right)=0$$

and

$$\frac{1}{E\,I}\left[\frac{-P\,a\,b}{2}\left(\frac{L+b}{3}\right)+\frac{M_A\,L^2}{3}+\frac{M_C\,L^2}{6}\right]+\gamma_{AB}\,a-\gamma_{BC}\,b=0.$$

For the elastic case these reduce to

$$M_A=\frac{P\,a\,b}{L}-M_C \qquad \text{and} \qquad M_C=\frac{\dfrac{P\,a^2\,b}{6}+\dfrac{P\,a\,b}{K\,L}}{\dfrac{L^2}{6}+\dfrac{2}{K}}$$

in which

$$K=\frac{A_w\,G}{E\,I}.$$

As a check, if $a = b = L/2$ (the load is in the center of the beam), then $M_A = M_B = M_C = P\,L/8$, which is the same expression used for bending alone.

For bending combined with shear (solid lines in Fig. 19), just as for bending alone (dotted lines), the moment at point A is initially a maximum. The inclusion of the shear terms causes a slight readjustment of moment in the elastic range. At a load of 158 kips, before the hinge moment is attained at point A, general shear yielding occurs in segment AB which, in turn, continually transfers a larger proportion of the total load to segment BC. As the load is increased there is a marked readjustment of moment at all three points with a slight decrease in the moment at point A. The hinge moment is first reached at point C at a load of 271 kips; the next hinge forms at point B at a load of 284 kips; and the maximum load of 320 kips is attained when the last hinge forms at point A.

The equations given with the example are for the initial response only and should be altered as the hinges form or as the sections yield in shear. For many reasons the results of these analyses could not be expected to be exactly duplicated experimentally. For cases of unsymmetrical loading, high shear forces can change the values of moment and slope from those expected from flexure alone. This fact should be remembered when planning tests and performing analyses in which shear forces are high enough to be of importance.

General Observations.—There are many limitations to utilizing the reserve plastic strength, local flange and web buckling being two of the more serious of these limitations. Flange or web buckling may seriously impair the rotation capacity of the member. Thick flanges and webs tend to reduce the possibility of buckling; the use of such sections probably will be required wherever large rotation capacities are desirable. Thick flanges will provide greater moment capacity, especially as the strain-hardening capacity is utilized; larger moments may imply higher shear forces. Thus, the possibility of shear yielding in the web and its corresponding effect on the behavior of the structure must be considered in the study of desirable section properties. Also, strengthening beams by adding cover plates will often require that shear be considered.

In general, shear will be of primary importance only in unusual loading conditions, for example, in the case of a concentrated load near the end of a beam as in the use of offset columns in buildings. Because general shear yielding in the webs will cause excessive deflections, it is recommended that high shear be avoided whenever possible. However, when high shear forces are encountered, the data presented herein will permit estimates of the shear deflection.

Shear deflections in the elastic range are often quite important and it is a generally accepted rule that they should be considered when the span-depth ratio for simply supported beams is 8 or less. For a 12WF120 beam section, which is simply supported and has a span eight times its depth, the elastic shear deflection represents approximately 25% of the total deflection. The span-depth ratio, for which shear is important in plastic design, varies and depends on the boundary conditions and moment gradient. For a 12WF120 beam fixed at both ends and loaded at the center, general shear yielding in the web will occur at or before the yield moment is reached at the support or load point (both moments are equal) for a span-depth ratio of approximately 11. This emphasizes the fact that the span-depth ratio does not need to be extremely small for shear deformation to be important.

SUMMARY

The tests described represent the first large-scale tests of continuous beams loaded far into the plastic range with extremely high shear forces. On the basis of these tests it is concluded that there is no measurable reduction in the moment capacity for the section and span used.

Data are also provided which make it possible to predict the components of deflection due to shear when regions of the beam have experienced general shear yielding. When parts of the test results have been compared with current design specifications, they indicate that, wherever large shear forces are present, the factors of safety against general shear yielding may be somewhat low. This seems to be especially true of loadings of the type used in these tests, which are unusual, but not covered adequately by the specifications.

Theoretical examples are presented which show that, in unsymmetrically loaded beams when shear is considered, the moment and slope values differ from those computed on the basis of flexure alone; this could be of importance when general shear yielding of the web occurs.

ACKNOWLEDGMENTS

The experimental parts of the work were performed in the Structural Research Laboratory, Department of Civil Engineering, University of Illinois, at Urbana, as a part of the work of the Engineering Experiment Station of the university. This paper is based on a thesis by Mr. Hall[10] which was carried out under the direction of Mr. Newmark.

AMERICAN SOCIETY OF CIVIL ENGINEERS
Founded November 5, 1852
TRANSACTIONS

Paper No. 2879

RIVER-BED DEGRADATION BELOW LARGE-CAPACITY RESERVOIRS

BY M. GAMAL MOSTAFA,[1] A. M. ASCE

WITH DISCUSSION BY MESSRS. WHITNEY M. BORLAND AND CARL R. MILLER; MAURICE L ALBERTSON AND HSIN-KUAN LIU; SERGE LELIAVSKY; AND M. GAMAL MOSTAFA

SYNOPSIS

A simple method of predicting the condition of equilibrium attained by a river bed subject to degradation is presented herein; it is suggested that the rate of degradation be computed by a trial method. It is hoped that an examination of this subject will help clarify a problem of vital importance in dam design.

INTRODUCTION

The construction of a dam and of a storage reservoir on a stream causes a reduction in the transport ability of the stream upstream of the dam in relation to the actual sediment load; downstream of the dam, the actual sediment load, if any, is reduced below the transport ability of the stream. In both zones the regime of sediment transport is destroyed and the stream reacts accordingly. If the water released from the reservoir is relatively clear, the sediment transport immediately below the dam will be almost zero, although the sediment-transport ability of the flow remains high. Because the flow tends to establish equilibrium conditions, material from the bed and banks will accumulate and scour will occur. This tends to deepen and widen the channel and, at the same time, to flatten the slope. Finer fractions are removed from the bed by selective sorting, and the bed becomes progressively coarser because of scour. Finally, a regime is established with flow conditions incapable of scouring any more the bed surface, and the process of degradation is ended.

The writer will attempt to predict the extent of degradation below large-capacity reservoirs (due to the passage of clear water) and to predict the rate

---

NOTE.—Published, essentially as printed here, in September, 1955, as *Proceedings Paper 788*. Positions and titles given are those in effect when the paper or discussion was approved for publication in *Transactions*.

[1] Chf. Engr., Saad-el-Aali (High Dam) Dept., Cairo, Egypt.

of this degradation. The problem will be simplified by assuming that the discharge is constant between the dam and the first water-level-control works on the river downstream. A constant discharge is assumed between each pair of control works—that is, only where there is a water-level-control works does inflow reduce river discharge to some canals for irrigation or other purposes. The river is, therefore, divided into reaches as shown in Fig. 1. In the first reach there is a dam in its upstream end and a barrage-control works in its downstream end. Any other reach will have a barrage in its upstream end and another barrage in its downstream end. Each control works can maintain a certain water level in its immediate upstream stretch.

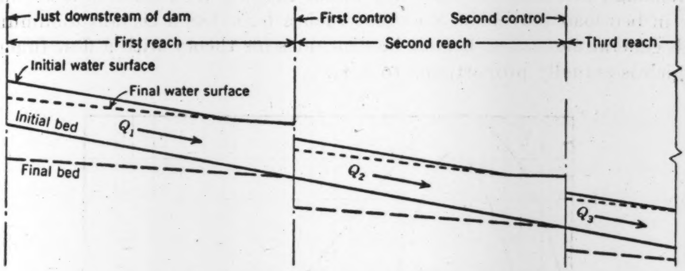

FIG. 1.—SIMPLIFIED CONDITIONS OF DEGRADATION

EQUILIBRIUM CONDITION AFTER COMPLETE DEGRADATION

The degradation process ceases when the river-bed material becomes coarse enough and the energy gradient becomes small enough so that the forces exerted by the flow on the bed material no longer cause general erosion. When such a condition is reached, the stream flow will be clear. In such a case one can apply the flow equation, given by G. H. Keulegan[2] and modified by Hans A. Einstein,[3] M. ASCE, to include smooth walls as well as rough walls:

$$u = u_* \, 5.75 \log_{10} \left(12.27 \frac{X R}{k_s} \right) \ldots\ldots\ldots\ldots\ldots\ldots (1)$$

in which u is the average flow velocity; u_* is the friction velocity equal to $\sqrt{\tau/\rho}$; R is the hydraulic radius; k_s is the representative grain diameter; τ is the shear stress exerted by the flow equal to γ_{RS}, in which S is the energy gradient; γ is the specific weight of fluid; X is the correction factor equal to a function of k_s/δ, in which δ is the thickness of laminar-boundary layer equal to $11.6 \, \nu/u_*$; and ν is the kinematic viscosity of the water.

Assuming that the minimum tractive force required to move bed material is the same as that reached when degradation is complete—that is, when the flow conditions at the end of erosion are similar to those at the start of bed-load movement—τ would be the so-called critical tractive force. During the past thirty years many laboratory experiments have been conducted to determine the value of the critical tractive force; these experiments resulted in an equation of the form,

---

[2] "Laws of Turbulent Flow in Open Channels," by G. H. Keulegan, *Journal of Research*, National Bureau of Standards, U. S. Dept. of Commerce, Washington, D. C., Vol. 21, 1938, pp. 701-741.

[3] "The Bed-load Function for Sediment Transportation in Open Channel Flows," by Hans A. Einstein, *Technical Bulletin No. 1026*, Soil Conservation Service, U. S. Dept. of Agriculture, Washington, D. C., 1950.

$$\frac{\tau_c}{(\gamma_s - \gamma)k_s} = K \qquad (2)$$

in which K was considered as being either a constant dependent on the uniformity of material or as a function of k_s/δ.

Although Mr. Einstein[4] does not accept the idea that traction is the major force in bed-load movement and that such a force has a certain minimum at which general movement begins, he concludes his theory with a flow function, ψ, which is actually proportional to τ/τ_c.

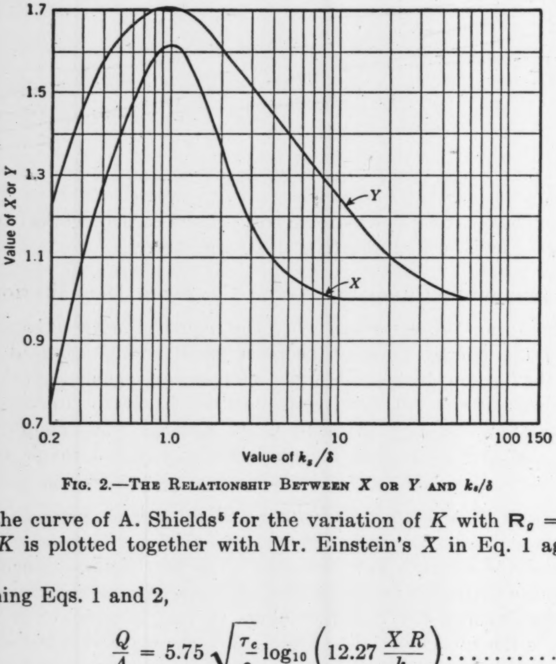

FIG. 2.—THE RELATIONSHIP BETWEEN X OR Y AND k_s/δ

Using the curve of A. Shields[5] for the variation of K with $\mathsf{R}_g = 11.6\, k_s/\delta$, $Y = 0.06/K$ is plotted together with Mr. Einstein's X in Eq. 1 against k_s/δ in Fig. 2.

Combining Eqs. 1 and 2,

$$\frac{Q}{A} = 5.75 \sqrt{\frac{\tau_c}{\rho}} \log_{10}\left(12.27\,\frac{X\,R}{k_s}\right) \qquad (3a)$$

and

$$\frac{Q}{A} = 5.75 \sqrt{\frac{0.06(\gamma_s - \gamma)k_s/Y}{\rho}} \log_{10}\left(12.27\,\frac{X\,R}{k_s}\right) \qquad (3b)$$

in which Q is the flow discharge and A, the cross-sectional area of flow.

---

[4] "Formulas for the Transportation of Bed Load," by Hans A. Einstein, *Transactions*, ASCE, Vol. 107, 1942, pp. 561–597.

[5] "Anwendung der Aehnlichkeitsmechanik und der Turbulenzforschung auf die Geschiebebewegung," by A. Shields, *Mitteilungen*, Preussischen Versuchsanst für Wasserbau und Schiffbau, Berlin, Vol. 26, 1936.

For every shape of cross section, A can be described in terms of R, as appears in Appendix I for cases of rectangular, triangular, and trapezoidal streams. Eqs. 3 become an expression for Q in terms of R, whereas $S = [(\gamma_s - \gamma)0.06\, k_s/Y]/\gamma\, R$ and is, therefore, inversely proportional to R. Thus, for every bed-material composition in a stream reach subject to degradation, the final hydraulic radius and slope for each discharge can be computed with accuracy if a proper value for k_s is used. Assuming that because the material left after degradation is composed of the coarsest bed material and is, therefore, more or less uniform and assuming that its characteristic size, k_s, can be chosen properly, the computation can be made by first assuming each value of X and Y as unity, the corresponding value of R to each discharge, and then by checking X and Y from Fig. 2. It would be necessary to repeat the computation if X or Y, or both, are not unity.

Choice of k_s.—Sample borings in the bed of a stream reach may result in the following: (*a*) Uniform-diameter sand through the bed; (*b*) a certain mixture of sand of different grain sizes; (*c*) mixtures of sand increasing in coarseness; (*d*) mixtures of sand decreasing in coarseness; and (*e*) layers with different grain sizes, the top layer being sand and the succeeding layers being gravel or rock.

In the first case, the diameter of sand would be used as k_s. In the second case, a diameter of from 90% to 98% finer is suggested for k_s, depending on whether the bed was subject to degradation (90%), stabilization (94%), or aggradation (98%) prior to the dam closure. Data of bed-material below Hoover Dam (Arizona-Nevada) at locations believed to have been subject to aggradation prior to the dam closure show that the mean size after erosion corresponds to as much as 98% finer of the surface bed material before erosion. Data of bed material from other cases would be of interest, especially in the case of a stream bed subject to degradation prior to dam closure. Data of sample analysis and depth of erosion at different locations in the Colorado River area show that degradation was still in process when Parker Dam and Imperial Dam were closed in 1939 and when Davis Dam was closed in 1950. These three dams are located in both Arizona and California. J. W. Stanley[6] has shown that there was a fast decrease in the rate of total volume of erosion in the first years after closing Hoover Dam. This is natural but does not mean that degradation had stopped before 1939. In fact, prior to any closure downstream of Hoover Dam, bed material in the Colorado River at a distance 83.5 miles downstream of the dam had a diameter of 0.17 mm at 35% finer and of 0.23 mm at 65% finer, whereas the tractive force exerted by the flow could move a material with a diameter of approximately 0.5 mm. Degradation started downstream of the dam and proceeded downstream as the material became coarser and more resistant to motion. The slope had not as yet been sufficiently flattened for equilibrium to have been reached. Table 1, taken from a report issued by the Bureau of Reclamation[7] (United States Department of the Interior) indicates the degradation that was taking place prior to closure downstream of Hoover Dam in 1938.

---

[6] "Effects of Dams on Channel Regimen," by J. W. Stanley, *Proceedings*, Federal Inter-Agency Sedimentation Conference, Washington, D. C., 1948.

[7] "River Control Work and Investigations, Lower Colorado River Basin," *Report*, Bureau of Reclamation, U. S. Dept. of the Interior, Washington, D. C., 1950-1951.

Data regarding the behavior of the stream bed prior to the passage of clear water because of dam closure are necessary to decide which diameter will be representative of the bed material at completion of erosion. Therefore, it is suggested that pending further investigation a diameter of 90% finer should be used for k_s, if the bed has been subject to some degradation; a diameter of 94% finer should be used for a bed that has been in equilibrium; and a diameter of 98% finer should be used for a bed that has been subject to aggradation.

TABLE 1.—DEGRADATION BELOW HOOVER DAM FROM 1935 TO 1938

Distance, in miles	Total scour, in feet	BED MATERIAL SIZE, IN MILLIMETERS		Change in slope
		35% finer	65% finer	
1	3	12	45	
5	10	0.4	0.7	
13	5.5	0.45	0.65	
43	4	0.22	0.28	Slope changed from 2 ft per mile to 1.7 ft per mile
83.5	0	0.17	0.23	

In the third case and in the fourth case one can assume a total scour depth, choose a corresponding value of k_s from samples in the vicinity of the assumed scour, compute a corresponding depth of scour from flow conditions and the Q-$R - k_s$ relationship, and then check the location of the sample. In the fifth case, the same procedure can be used unless the computed scour is deeper than the total depth of the sand layer. The exposed gravel would probably then be the limit of scour but can be treated in the same manner in exceptional cases.

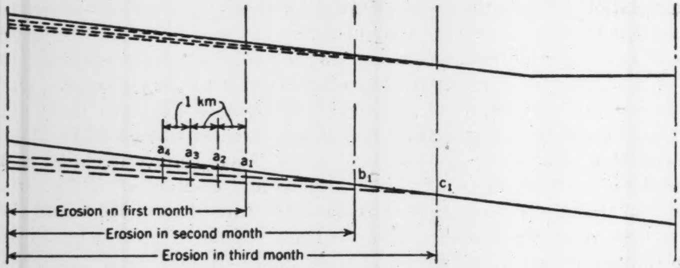

FIG. 3.—TRIAL METHOD FOR DEGRADATION

RATE OF DEGRADATION PROGRESS

Assuming a section, a_1 (Fig. 3), distance, L, from the dam which is assumed to be the range of scour during the first time interval of one month, the sediment-transport ability of the existing hydraulic condition can be computed. Assuming a certain amount of scour at a section, a_2, 1 km upstream of a_1, the volume of scour should be equal to the difference between the loads passing these two sections during the assumed time interval. Water-surface elevation at section a_2 can be computed by trial because the drop in water surface in a short reach is approximately equal to the mean of the energy slope at both sections multiplied by the reach length; the energy slope is a function of depth and geometric relations of the channel for a constant discharge. By using a suitable discharge equation and sediment-load equation, the conditions expected at the upstream end of the last kilometer can be determined; the conditions at another kilometer upstream can be similarly computed until one reaches the first kilometer immediately downstream of the dam where the sediment load should be zero. Otherwise, a different location for section a_1 should be chosen, and successive trials should be made. Starting with the bed and water profiles attained by the end of the first time interval, the scour trials can be repeated for the second time interval starting with a section, b_1, until final conditions are achieved.

DISCHARGE AND SEDIMENT LOAD EQUATIONS

The writer believes that the Manning equation for flow in open channels is inapplicable when there is sediment in transport. The value of Manning's *n* may vary from 0.016 to 0.06 in sediment-carrying flows and rivers and tends to increase with less sediment transport. Bed undulations and sediment movement, whether in suspension or as a bed load, affect friction,[8] and, hence, affect the relationship between different hydraulic conditions—that is, *R*, *S*, and *Q*. Until hydrosediment science is more widely accepted, it seems more practical to use empiricism for a river-discharge formula. For the Nile River, in Egypt, it has been found that, for almost all different discharges and sediment loads, the equation,

$$\frac{Q}{\text{unit width}} = M\,D^2\,S^{2/3} \qquad (4)$$

gives approximate results. In Eq. 4, *M* is a coefficient which, for the Nile River, is equal to 130 per sec.

The writer suggests that Eq. 4 may be used for different rivers as follows:

$$u = k\,R\,S^{2/3} \qquad (5)$$

in which *k* can be determined by a statistical study of river data.

Eq. 5 gives $S = (u/k\,R)^{3/2}$, which can be used in the successive-trial procedure for determining of degradation progress.

There have been so many investigations made of the sediment-transport ability of flow that it would be impracticable to cite them in this paper. Therefore, the writer wishes to refer to a previous summary made of these investigations.[9] Each equation that has been suggested shows good agreement with the collected data. It is suggested that an empirical equation be used, such as the one given by Lorenz G. Straub,[10] M. ASCE, simplifying the successive-trial computations. This equation is as follows:

---

[8] "Some Effects of Suspended Sediment on Flow Characteristics," by Vito A. Vanoni, *Bulletin No. 34*, *Proceedings*, 5th Hydraulics Conference, Univ. of Iowa Studies in Eng., Iowa City, Iowa, 1952.

[9] "Analytical and Experimental Study of the Effect of Flow Characteristics and Fluid Viscosity upon the Movement of Bed Load in Open Channels," by M. Gamal Mostafa, thesis presented to the University of Minnesota, at Minneapolis, in 1949, in partial fulfilment of the requirements for the degree of Doctor of Philosophy.

[10] "Detritus Transportation," by Lorenz G. Straub, *House Document 238*, 73d Cong., 2d Session, U.S. Govt. Printing Office, Washington, D. C., 1935, pp. 1124–1150.

$$G = N \frac{R\,S}{\gamma^2} (\tau - \tau_c) \quad\text{......}(6)$$

in which N is a sediment coefficient and G is the sediment load.

The sediment diameter which should be used in the choice of N and τ_c would be the mean size for the first time period and then would be gradually increased reaching from 90% to 98% finer for the last time period in which the degradation appears to approach asymptotically its maximum value for equilibrium. When such a condition is approached, the next reach of the river between the first and second control structures downstream of the dam will start to degrade when not enough load is being supplied by the first reach. Computations for this reach with its known discharge, Q_2, would be similar to those of the first reach except for the control-works section. In this section, G does not equal zero but is smaller than the flow-sediment capacity and also decreases in time; the same procedure can be followed for succeeding reaches.

With the exception of which water-flow formulas or which sediment-flow formulas are to be used, the degradation progress can be evaluated more accurately when the length and time intervals used in the successive-trial operations are smaller.

ACKNOWLEDGMENTS

The writer prepared this paper in 1954 when he was granted a United Nations Technical Assistance Fellowship in the United States to study sedimentation control. He wishes to thank Enos J. Carlson, M. ASCE, of the Hydraulic Laboratory, Bureau of Reclamation, for his kind cooperation in making available the Bureau's sedimentation reports and other published information.

APPENDIX I

The relation of hydraulic radius to area of flow is: (*a*) For a rectangular channel,

$$R = \frac{A}{B + 2\,A/B} \qquad B = \text{breadth}$$

(for a very wide channel, $R = A/B$); (*b*) for a triangular channel,

$$R = \tfrac{1}{2} \sqrt{\frac{\alpha}{1 + \alpha^2} A}$$

in which $\alpha/1$ = horizontal/vertical of side slopes; and (*c*) for a trapezoidal channel,

$$R = \frac{A/B}{1 + \sqrt{\frac{1 + \alpha^2}{\alpha^2}} \left(\sqrt{1 + \frac{4\,\alpha\,A}{B^2}} - 1 \right)}$$

in which B is the bottom width.

APPENDIX II. NOTATION

For the guidance of discussers, the following symbols used in this paper are described:

A = area of flow;
D = total depth of flow;
G = sediment load;
k_s = representative grain diameter of sediment;
n, k, K, N, and M = coefficients;
Q = discharge of water;
R = hydraulic radius of flow;
R_g = grain Reynolds number equals $11.6 \frac{k_s}{\delta} = \frac{k_s u_*}{\nu}$;
S = slope of the energy gradient;
u = average flow velocity;
u_* = friction velocity equals $\sqrt{\tau/\rho}$;
X and Y = correction factors;
α = side slope = $\frac{\text{horizontal}}{\text{vertical}}$;
γ = specific weight of water;
γ_s = specific weight of sediment;
δ = thickness of laminar boundary layer;
ν = kinematic viscosity;
ρ = water density;
τ = tractive force per unit area equals γ_{RS};
τ_c = critical tractive force per unit area; and
ψ = a function.

DISCUSSION

WHITNEY M. BORLAND[11] AND CARL R. MILLER,[12] ASSOCIATE MEMBERS, ASCE.—There is a continuing need in sediment engineering for developing procedures for predicting the stream-channel degradation that results from a change in the natural regime. The author's paper cites the condition in which clear water is released from a newly constructed storage dam. A similar problem results when a natural channel is used as a wasteway for irrigation-return flows.[13,14]

The author proposes a logical procedure for computing the degradation. Similar procedures have been used by engineers in the Bureau of Reclamation for predicting degradation that would result from constructing reclamation projects. Factors controlling the degradation are (*a*) size of the bed material as related to depth; (*b*) transport limit of the materials in the bed for the existing hydraulic conditions; (*c*) depth of the bed turnover and bed-armor development; (*d*) downstream controls; and (*e*) ability of the structure to retain the replenishing supply of bed material. In a completely homogeneous river channel—that is, a channel having no downstream-grade controls and no bed-material variation with depth, and having all transportable material—the degradation will be limited only by the reduction in slope. Eventually, a slope would be reached at which transport would cease. If bed material that cannot be transported is available, the degradation will be limited by the depth of turnover and by the creation of bed armor.

In the technical analysis of the problem the limitations of the basic data and modern bed-load formulas must be recognized. The author suggests the use of the Straub bed-load formula.[10] The writers have found that the various formulas are usually applicable only to the particular stream or set of conditions from which they were derived. None of the formulas, many of which are based solely on laboratory research, can be applied to a river or to a condition without first establishing its applicability. The Einstein bed-load function[3] and the modified Einstein procedure[15] have proved to be representative of conditions in varying types of alluvial streams in the United States. The Schoklitsch formula[16] has been consistently reliable for computations within the range of medium-sand to fine-gravel size (from 0.2 mm to 8.0 mm).

The author suggests that the 90%-to-98% size, which is determined from the size-distribution curve, is a measure of the stabilizing size. It is difficult to select bed-material samples that represent the average size within 5% accuracy. Fig. 4 shows some bed-material-size data for the middle Rio Grande area. The variation from day to day and from point to point at the same cross section should be noted. The 98%-finer size varies from 0.6 mm to 10.0 mm. Selection of the 98%-finer size to indicate the measure of stability does not appear justifiable in most cases. It might be more practical to select some relationship with the material, for example, the 75%-finer size in which the skew factor would not be so pronounced. In addition to the difficulty in selecting bed material to define the 90%-finer or 98%-finer size, the limitations of the laboratory analysis should be recognized. The magnitude of error increases with a decrease in quantity of material available in a particular size range.

---

[11] Head, Sedimentation Section, Hydrology Branch, Div. of Project Investigations, Bureau of Reclamation, U. S. Dept. of the Interior, Denver, Colo.

[12] Hydr. Engr., Hydrology Branch, Div. of Project Investigations, Bureau of Reclamation, U. S. Dept. of the Interior, Denver, Colo.

[13] "A Plan of Channel Erosion Control, Fivemile Creek, Riverton Project, Wyoming," *Report*, Hydrollogy Branch, Bureau of Reclamation, U. S. Dept. of the Interior, Washington, D. C., April, 1953.

[14] "A Study of Channel Erosion and Control, Muddy Creek, Riverton Project, Wyoming," *Report*, Hydrology Branch, Bureau of Reclamation, U. S. Dept. of the Interior, Washngton, D. C. June, 1954.

[15] "Computations of Total Sediment Discharge—Niobrara River near Cody, Nebraska," by B. R. Colby and C. H. Hembree, *Water Supply Paper 1357*, Geological Survey, U. S. Dept. of the Interior, Washington, D. C., 1955.

[16] "The Schoklitsch Bed-Load Formula," by S. Shulits, *Engineering*, London, June, 1935, p. 644.

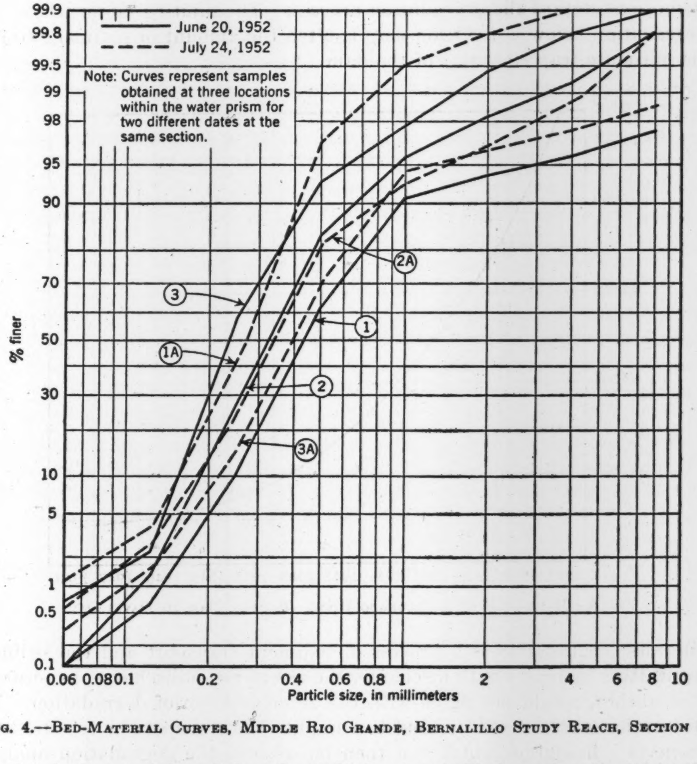

FIG. 4.—BED-MATERIAL CURVES, MIDDLE RIO GRANDE, BERNALILLO STUDY REACH, SECTION F

In order to develop procedures for predicting channel degradation, methods for deriving bed-material transport must be improved, representative bed-material samples and size distribution must be obtained, and factors that result in bed armor such as depth of turnover and necessary thickness of the armor layer must be determined. Without more complete definition of the foregoing factors, one can only approximate degradation based on bed-load formulas.

It is often necessary to predict the distance downstream that the degradation will extend, in addition to the depth of degradation. When two structures are involved the aggradation-degradation balance point is the limit and can usually be established within certain bounds. When no downstream control exists, the theoretical limit would be a bed grade which is parallel to the original bed grade. This never occurs because a completely homogeneous channel does not exist and because other factors, such as tributary sediment contributions, retard the degradation process. The limiting factor in the case of degradation below a diversion dam is often the amount of sediment storage or the ultimate trap efficiency of the dam.

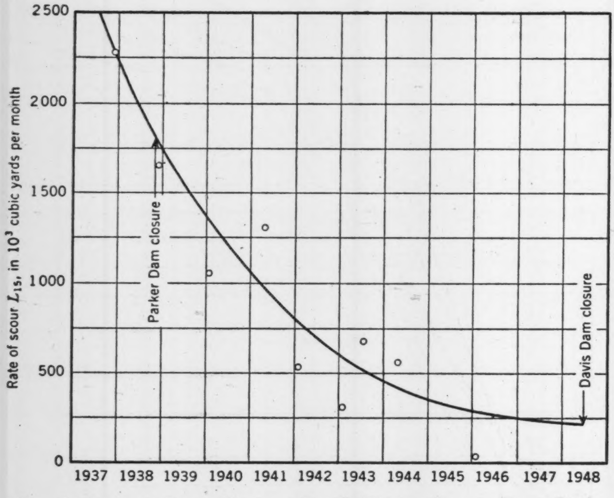

FIG. 5.—RATE OF SCOUR, COLORADO RIVER (HOOVER DAM TO DAVIS DAM)

Because degradation is a process of sediment transport and the sediment concentration increases with discharge, the use of mean discharge, as proposed by the author, would not agree with the determination of degradation. The flow-duration curve could be used to compute the transport or to establish a "dominant" discharge, which can then be used in the degradation analysis. The dominant discharge can be described as a discharge which has the most influence on the sediment transport and the channel shape. This discharge is readily established in a canal or in a completely controlled river, such as the lower Colorado River; it is difficult to establish in a river having a wide range in discharges, such as the Rio Grande.

The author, referring to a paper by Mr. Stanley,[6] states that the closing in 1938 of Imperial Dam and Parker Dam retarded degradation in the Colorado River below Hoover Dam. This implies that the relationship in Fig. 5, showing the degradation rate with respect to time, would have been different if Parker

Dam had not been built; in Fig. 5, L_{15} is the rate of scour (when Q is 15,000 cu ft per sec) computed from $L_Q\ (15{,}000)^2/Q^2$, in which L_Q is the measured rate of scour and Q is the actual average discharge. The writers do not agree with the author in this respect because it is believed that the backwater effect of Lake Havasu (Arizona-California) did not extend beyond the head of the Mojave Valley—that is, beyond the gaging station located just below Davis Dam. Fig. 5 indicates that the degradation rate was approximately 2,000,000 cu yd per month when Parker Dam was closed in 1938—approximately one-half the maximum rate after Hoover Dam was closed in 1935. The shape of the curve and the position of the points indicate that closing Parker Dam had no influence on the rate of degradation. Degradation below Hoover Dam was stopped by the closing of Davis Dam in 1948; the rate of degradation below Hoover Dam was influenced by factors other than the construction of Parker Dam. The author states that, in a purely homogeneous stream channel, the degradation below a storage reservoir would proceed far downstream and would, perhaps, be governed only by the ultimate base control, which is the ocean.[17] However, the fact is that natural stream channels are heterogeneous and not homogeneous. Wide valleys, such as the Mojave Valley near Needles (Calif.) above Topock Gorge, form areas for sediment deposition and prevent a generalized principle from being applicable to special cases.

MAURICE L ALBERTSON,[18] M. ASCE, AND HSIN-KUAN LIU,[19] A.M. ASCE.—River-bed degradation downstream from reservoirs is a subject of increasing concern to engineers throughout the world as more flow-regulating structures are being built. Therefore, the author should be thanked for presenting the results of his work on this subject.

Logic and observation in the field and in the laboratory have shown that scour and degradation will occur in any alluvial channel if the flow is not saturated with bed material. Therefore, for a given discharge and channel width, scour will occur until equilibrium is reached either by increasing the resistance of the bed to scour (increasing the size of the exposed bed material) or by decreasing the carrying capacity (decreasing the slope), or by a combination of both of these. In either case degradation occurs until a stable channel is reached.

In the first case the development of a stable channel is dependent on the availability of coarse material in the bed so that as selective sorting takes place the bed gradually becomes covered or plated with coarser material which can withstand the forces of scour. The necessary size of this material can be determined to some extent by using the stable-channel theories of Emory W. Lane,[20] M. ASCE, and Thomas Blench,[21] M. ASCE.

If the necessary size of coarse material is readily available in the bed, the amount of degradation will be small and equilibrium will be quickly reached.

---

[17] "The Importance of Fluvial Morphology in Hydraulic Engineering," by E. W. Lane, *Proceedings Paper 745*, ASCE, July, 1955.

[18] Prof. of Civ. Eng., Head of Fluid Mechanics Research, Colorado Agri. and Mech. College, Fort Collins, Colo.

[19] Asst. Prof. of Civ. Eng., Colorado Agri. and Mech. College, Fort Collins, Colo.

[20] "Design of Stable Channels," by Emory W. Lane, *Transactions*, ASCE, Vol. 120, 1955, pp. 1234–1279.

[21] "Regime Theory for Self-Formed Sediment-Bearing Channels," by Thomas Blench, *ibid.*, Vol. 117, 1952, pp. 383–408.

However, if the necessary size of coarse material is not available, degradation will continue until the slope is decreased to the point where the channel is stable for the coarser fractions of bed material. This ultimate slope also can be predicted by using the stable-channel theories. It is, therefore, possible that it would be helpful to apply the stable-channel theories to the problem of river-bed degradation.

The writers would like to show that, in a given alluvial channel having a steady, uniform flow, the various dependent variables are functions of certain independent variables, as follows:

$$\begin{array}{c}\text{Dependent}\\ \text{variables}\end{array} = \phi\left(\text{discharge,}\quad\text{slope,}\quad\begin{array}{c}\text{characteristics}\\ \text{of the water,}\end{array}\quad\begin{array}{c}\text{characteristics}\\ \text{of the bed and}\\ \text{bank materials}\end{array}\right) \ldots (7)$$

The dependent variables include the Chezy resistance coefficient, the concentration and distribution of the total load, and the suspended load of sediment, the shape of the channel cross section, and the depth of flow.

In most developments of Eq. 7 for turbulent flow by either analytical methods or dimensional analysis, or by a combination of both, the velocity of flow is found to vary with the square root of the slope; this is contrary to Eq. 5. Therefore, it is suggested that consideration be given to the following equation, which is derived from Eq. 7:

$$\frac{C}{\sqrt{g}} = \phi\left(\mathsf{R}, \frac{d}{R}\right) \ldots\ldots\ldots\ldots\ldots\ldots\ldots (8)$$

in which C is the Chezy resistance coefficient, $C/\sqrt{g} = u/\sqrt{g\,R\,S}$, R is the Reynolds number ($\mathsf{R} = u\,R/\nu$), d is the characteristic size of the bed material, u is the mean velocity, R is the hydraulic radius, and ν is the kinematic viscosity of the water. A significant correlation was found between Eq. 8 and data available from laboratory and field experiments. In addition, these data show clearly that beyond a certain value of R the roughness decreases and the concentration increases[22, 23] with increasing R, which agrees with the author's conclusion. However, the results of the writers show that for certain ranges of Reynolds numbers and relative roughness the opposite effect is also found.

Because degradation starts upstream at the toe of the dam and proceeds downstream, one can begin computing degradation by the successive increment method at the toe of the dam rather than at a distance downstream, such as that shown by a_1 in Fig. 3.

For a given discharge, slope of stream, size of sediment, and temperature of water, the stream has a certain capacity to carry sediment. If such a capacity is reached by eroding upstream reaches, the downstream bed will be unaffected at first. However, as soon as the bed within a reach is eroded (shown by section 0-1 in Fig. 6), the slope will decrease, the capacity of erosion will decrease, and the erosion process will shift downstream, accumulating

---

[22] "Some Aspects of Roughness of Alluvial Channels," by S. Ali, thesis presented to the Colorado Agricultural and Mechanical College at Fort Collins, in 1953, in partial fulfilment of the requirements for the degree of Doctor of Philosophy.

[23] "Roughness in Alluvial Channels," by Maurice L Albertson, *Research Report*, Colorado Agri. and Mech. College, Fort Collins, Colo., 1953.

more sediment in order to satisfy the capacity of the stream. The rate of erosion between sections 1 and 2 in the second time interval will not be as great as the first time interval between sections 0 and 1. However, the total sediment volume, Vol. 2, will be the same as Vol. 1, assuming no change has taken place in the composition of the sediment.

In order to estimate the rate of degradation more accurately, it is necessary to study the mechanics of degradation more thoroughly. Because degradation is a condition of nonequilibrium and of unsteady flow, knowledge of the mechanics of sediment transport is too limited to solve the problem accurately. The ideas presented by the author and in this discussion are oversimplified in so far as degradation in a natural stream is concerned. Nevertheless, by means of such simplification, a more exact and, perhaps a more complex, solution may eventually be found.

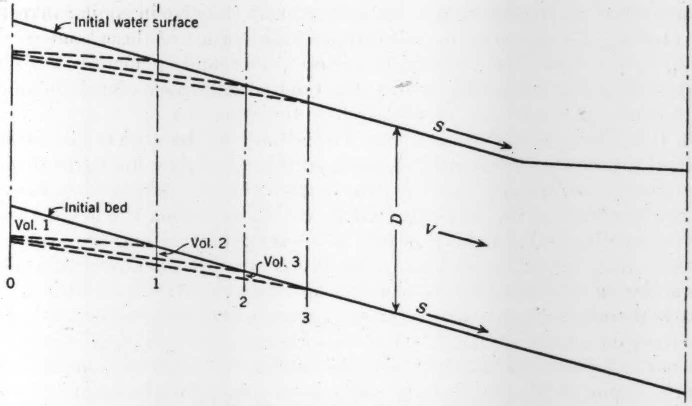

FIG. 6.—THE EROSION PROCESS

SERGE LELIAVSKY,[24] M. ASCE.—Credit is due Mr. Mostafa for having produced a particularly valuable and timely paper; it belongs to the group of analytical solutions that are based on parameters to be determined in the laboratory. From the more conservative standpoint, such a solution becomes an engineering fact only after it is applied to, and confirmed by, practical, actually executed designs.

The author's attention is directed to the fact that, with particular reference to the sediment-transportation problem, considerable research has been performed following the inverse route—that is, starting with the mathematical analysis of observations collected on natural rivers and ending with laboratory investigations.

Because Mr. Mostafa gives (under the heading, "Discharge and Sediment Load Equations") a number of formulas referring, in particular, to the Nile River, the writer ventures to present another formula for this river, which may well serve to illustrate the difference in the procedures described in the foregoing.

---

[24] Civ. and Hydr. Engr., Cairo, Egypt.

This formula was developed by the writer in 1922 while he was in charge of the mathematical analysis of a vast scheme of observations on silt, performed in Egypt, on irrigation canals and the Nile River.[25]

The principle embodied in this formula—namely,

$$v = [147 + 3.92\,(z - 10)^{0.383}]\, R^{0.85}\, S^{0.72} \qquad (9)$$

was not a preconceived postulate (as is frequently the case in similar investigations) but was a conclusion derived from an examination of these same records. In Eq. 9, v is the mean velocity, in meters per second; z denotes the silt in suspension, in grams per cubic meter; R is the hydraulic mean depth, in meters; S represents the slope; and 10 is the minimum value of z.

In fact, the principle contained in Eq. 9 was that, because of the presence of silt, the same channel is capable *ceteris paribus* of a larger discharge than the same channel containing entirely clear water. Eq. 9, usually known as the Beleida formula, is frequently quoted in the literature on the subject but is wrongly attributed to A. B. Buckley, in whose paper[26] it first appeared. At the time when it was first produced, Eq. 9 was possibly too advanced and met with a certain criticism because it was believed to be rather paradoxical.

It is therefore of particular interest to place on record the fact that recent laboratory data have confirmed what was originally derived from observations on a natural river. In point of fact, the well-known laboratory investigation by Vito Vanoni,[27] M. ASCE, fully confirms the principle which appeared to be a paradox when first produced.

It is tentatively suggested that the value of Mr. Mostafa's work may be enhanced, should its method be developed, by explicitly introducing therein the quantitative interdependence of C and z, as yielded by Eq. 9.

M. Gamal Mostafa,[28] A.M. ASCE.—The writer wishes to thank the engineers who have contributed discussions. The methods suggested by the writer for computing river-bed degradation were based on the assumption of ideal conditions which may, in some cases, be far from reality. However, as Messrs. Albertson and Liu have stated, "* * * by means of such simplification, a more exact and, perhaps, more complex, solution may eventually be found." Beginning with a simplified case and introducing the effect of natural conditions, a reasonable procedure may be reached by computing the rate and extent of degradation. Such a procedure may vary for different cases depending on the natural conditions and the existing man-made river structures. For example, it may be possible in some cases to assume that a river stretch between two control stations is straight and that its cross section is constant. In other cases the effect of every sharp turn may have to be studied separately.

---

[25] "Computation of the Beleida Formula," by Serge Leliavsky, *Minutes of Proceedings*, Inst. of C. E., London, Vol. CCXVI, Pt. II, 1922–1923, p. 207.

[26] "The Influence of Silt on the Velocity of Water Flowing in Open Channels," by A. B. Buckley, *ibid.*, p. 195.

[27] "Transportation of Suspended Sediment by Water," by Vito A. Vanoni, *Transactions*, ASCE, Vol. 111, 1946, p. 67.

[28] Chf. Engr., Sadd-el-Aali (High Dam) Dept., Cairo, Egypt.

Irregularity in the river section may decide the beginning and the length of the steps in the step-trial method of computation.

The use of a constant discharge for a river reach in the analysis did not represent mean discharge, as Messrs. Borland and Miller have stated. It is true that natural stream flow should be represented by a flow-duration curve. However, if, as is usual practice, a large-capacity reservoir is constructed so that the flow is regulated into its downstream, variation in discharge would probably be a seasonal occurrence rather than a daily natural phenomenon. Computations based on a constant discharge would, therefore, approximate actual conditions—for example, the Aswan "Sadd-el-Aali" High Dam (Egypt), which will be constructed on the Nile River with a reservoir capacity of 130,000,000,000 cu m for flood protection, generation of power, and development of agriculture. Because only water needed for irrigation and domestic use will be released from the reservoir, it is expected that the discharge variation will be seasonal, with a maximum of 240,000,000 cu m per day and a minimum of 100,000,000 cu m per day.

Assuming that a regime of natural equilibrium had been established in the Colorado River prior to closing Hoover Dam, valleys were areas where deposition and scour took place without a great change in levels from year to year. After Hoover Dam was closed, river-bed degradation started below the dam and progressed downstream. By 1938 the exposure of rock ledges, gravel, and coarse sands stopped the process in some near reaches; in some far reaches the bed surface was still composed of fine material. Therefore, degradation had been retarded but was still having some effect. Because the backwater effect of Lake Havasu did not extend beyond the head of the Mojave Valley does not mean that if Parker Dam and Davis Dam had not been built there would have been no degradation below the Mojave Valley.

The writer agrees with Messrs. Borland and Miller that natural stream channels are heterogeneous and that an assumption of a pure, homogeneous channel can never approximate reality. However, the ocean is the theoretical limit for degradation below a large reservoir whenever there is no dam or natural deposition trap downstream of that reservoir. In cases where there is a trap it is located only at the stream end as the stream approaches the ocean in the form of a delta.

The writer has recently conducted some laboratory tests at the Hydraulic Research Station, at Barrage, Egypt, to determine the characteristics of the bed armor after scour. Although these tests are still in progress, the following preliminary conclusions can be made: (1) Coarse material of approximately 5% bed composition can form an armor which can prevent excessive local scour by forces just less than the critical force necessary to cause its general movement, and (2) the limit of channel-bed degradation may not only be the formation of the armor but may lead to the determination of the minimum surface slope. The latter conclusion has not yet been described quantitatively. It is hoped that experiments which will soon be started in the 100-m-long and 1.5-m-wide experimental channel will help define the limiting slope. An additional preliminary conclusion is that taking the 75%-finer diameter as a relative index of stability needs further experimental verification. Mr. Lane[20] has recommended this size for stable-channel design.

Experiments to date (1955) have shown that 2% coarse material is not enough to form an armor at an early stage of degradation and that from 4% to 5% coarse material may be necessary.

During a degradation experiment, uniformly graded bed material was sorted so that the composition of the final top layer after equilibrium varied with the depth and location of the sample and had a maximum sample mean size corresponding to 85% finer of the original bed material.

Messrs. Albertson and Liu have recommended the application of an equation for the velocity of flow in the steady uniform condition which seems reasonable once ϕ is defined. In 1955 the writer was able to observe promising work done by Mr. Albertson in defining this function. Mr. Leliavsky suggests the use of Eq. 9 for velocity of flow in the Nile River; however, it is not possible to apply this formula to the computation of degradation because the value of Z should vary for every step and time interval.

The coefficient, k, in Eq. 5 of the paper is much more reliable than the Manning n; application of Eq. 5 to Nile River data has shown a maximum error of 35% whereas the Manning equation has shown errors of up to 200%.

The choice of Eq. 6 for the sediment load was justified because of its simplicity and applicability to bed loads of fine and medium sands which usually occur in degradation. The modified Einstein,[15] the Meyer-Peter,[29] and the Kalinske formulas[30] may all be applicable to a wider range of sediment size than the Straub formula. An interesting reference for different studies with respect to the formulas cited has been given by Ning Chien,[31] A.M. ASCE. Actually none of these formulas is a complete scientific solution because the field of hydrosediment science remains vast. The findings of Norman H. Brooks,[32] J.M. ASCE, at the California Institute of Technology at Pasadena may further complicate the choice of a sediment-transportation formula.

However, hydraulic characteristics of a stream flow should be interrelated with the sediment movement by the flow if this sediment is in total suspension on the stream bed or is distributed over the water section. The effect of sediment movement on the velocity of flow should be included in any equation describing the sediment load. At present, this is indicated in coefficients which may be given as functions of Reynolds number or of Froude number which represent flow conditions. A purely rational solution may be discovered that will describe accurately the flow of sediment in a stream by means of measurable factors. Engineers concerned with this problem are continually working toward this objective.

---

[29] "Formulas for Bed-Load Transport," by E. Meyer-Peter and R. Mullar, *Proceedings*, 3d Meeting of International Assn. for Hydr. Research, Stockholm, 1948.

[30] "Movement of Sediment as Bed Load in Rivers," by A. A. Kaliniske, *Transactions*, Am. Geophysical Union, Vol. 28, 1947, pp. 615–620.

[31] "The Present Status of Research of Sediment Transport," by Ning Chien, *Transactions*, ASCE, Vol. 121, 1956, p. 833.

[32] "Mechanics of Streams with Movable Beds of Fine Sand," by Norman H. Brooks, *Proceedings-Separate No. 668*, ASCE, April, 1955.

AMERICAN SOCIETY OF CIVIL ENGINEERS
Founded November 5, 1852
TRANSACTIONS

Paper No. 2880

STRUCTURAL VIBRATIONS PRODUCED BY GROUND MOTION

BY DONALD E. HUDSON[1] AND GEORGE W. HOUSNER,[2]
A. M. ASCE

SYNOPSIS

Simultaneous measurements of transient ground motion and of the resulting structural vibrations in a steel-frame building caused by a large quarry blast are described. Building accelerations computed from the measured ground accelerations are compared directly with measurements made in the building. The satisfactory agreement between the computed and measured building response indicates that the general method of replacing a complex structure by a simplified dynamic model yields results of engineering significance even for complicated transient loadings.

INTRODUCTION

The desire for continued improvement in the strength-weight efficiency of structures has led to an increased study of the effects of various dynamic loads on buildings. Among the loads which have been extensively investigated are those caused by earthquakes, by both air-borne and earth-borne explosive shocks, and by self-excited oscillations caused by wind. For a satisfactory analysis of such problems it must be possible to compute accurately the motions that would be caused by various loadings. Although considerable difficulty has been experienced in making theory and observation agree in this field, the work described in this paper shows that a satisfactory agreement can be obtained when all the factors are taken into consideration. The present investigation is concerned specifically with the transient loads caused by an explosive-generated ground shock; the methods of computation, however, are applicable to any kind of dynamic loading problem. A brief account of the methods used for such transient dynamic problems is first given, and test results illustrating the applicability of the theory are then presented.

NOTE.—Published, essentially as printed here, in October, 1955, as *Proceedings Paper 816*. Positions and titles given are those in effect when the paper was approved for publication in *Transactions*.

[1] Prof., Div. of Eng., California Inst. of Technology, Pasadena, Calif.

[2] Prof., Div. of Eng., California Inst. of Technology, Pasadena, Calif.

As a first step in computing the deflections or motion of any actual structure, it is necessary to make simplifying assumptions to reduce the complexity of the structure to the point where computations are practicable. For static problems many of the necessary simplifying assumptions have been so sanctioned by past experience that the designer hardly recalls that they are, in fact, assumptions. For dynamics problems, however, the additional complexity of the theory and the lack of sufficient experience and of test results have introduced an increased uncertainty as to which simplifying assumptions are really justified. Perhaps the most fundamental question to be answered in any theoretical design work is "How far can these simplifying assumptions be carried without losing some features of engineering significance?"

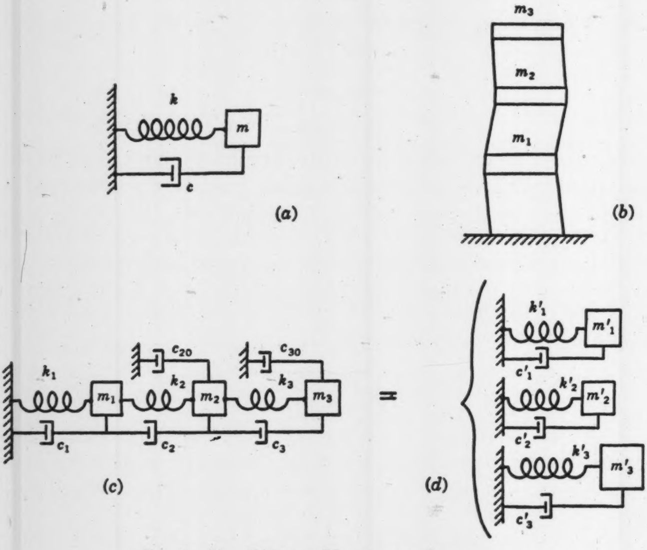

FIG. 1.—THE DYNAMIC MODEL OF A STRUCTURE

THE DYNAMIC MODEL OF A STRUCTURE

The three characteristics of a structure which determine its behavior under dynamic loads are (1) the masses of the various elements, (2) the stiffnesses of the members, and (3) the energy dissipations which arise from factors such as friction in joints, etc. The simplest dynamic model of a structure would be one in which each of these basic characteristics appeared in its simplest form. This simplest possible system (hereinafter referred to as the "simple system") is illustrated in Fig. 1(*a*). All the mass of the structure, *m*, is concentrated at one point; all the stiffness of the system is represented by one massless linear spring having a spring constant, *k*, and all the energy dissipating mechanisms in the structure are concentrated in one damping element described by a dissipation factor, *c*.

Actual structures will often have to be represented by more complicated dynamic models. If, for example, the horizontal motions of the three-story building shown in Fig. 1(*b*) were to be investigated, it would be possible to set up the dynamic model of Fig. 1(*c*) in which 3 masses, 3 springs, and 5 damping elements are used. A very important feature of these more complex models is that they can always be replaced by a number of simple systems. Thus, the behavior of the complex system of Fig. 1(*c*) can be computed by a superposition of the behavior of the three simple systems of Fig. 1(*d*).

Because of the great simplicity of the simple system compared to the actual structures of interest to the engineer, there has been a tendency for some engineers to doubt the value of work based on such a model. It should be emphasized, therefore, that the importance of the simple system of a dynamic model is based on two considerations:

1. In spite of its simplicity, the model does preserve the major features of many engineering structures so that it indicates their behaviors for many dynamic loads.
2. More complex structures can always be considered as equivalent to a series of simple systems, and the behavior of the complex structure can be obtained by adding the effects of the individual simple systems. The simple system can thus be considered as a "building block" for the more complex systems.

The Experimental Program

Because of the difficulty of generating large transient forces suitable for test purposes, there have been relatively few direct experiments on the effects of dynamic loads on actual structures. In connection with earthquake studies, there have been many steady-state vibration tests for finding the resonant periods of buildings. These tests have usually been made at very low stress levels because of the force limitations of the available mechanical oscillators and the danger of damage to the structure.

In the future, valuable data may be expected from the earthquake strong-motion accelerometer program of the Coast and Geodetic Survey (United States Department of Commerce). The data obtained under this program so far have been almost entirely in the form of ground acceleration records. There are at present (1957) several accelerometer installations in buildings, but as yet there has been no simultaneous measurement of both ground and building motions for earthquakes of a magnitude sufficient to cause significant structural loadings.

Quarry blasts are another possible source of test data. Most of these blasts, however, are small in size and are not located close enough to typical building structures to give usable results. In view of these difficulties, it was fortunate that a commercial quarry blast of a large magnitude was planned to occur sufficiently near a modern, well-designed and well-constructed building so that it would be subjected to a reasonably strong ground motion. This afforded the first opportunity to measure simultaneously relatively strong ground motion and the consequent motion of a typical building. It thus becomes possible to compare directly the measured building motion with the

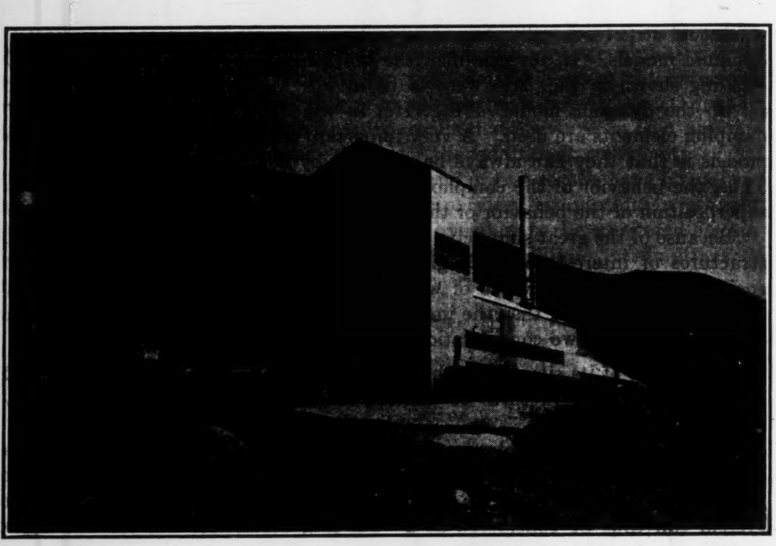

FIG. 2.—GENERAL VIEW OF TEST BUILDING

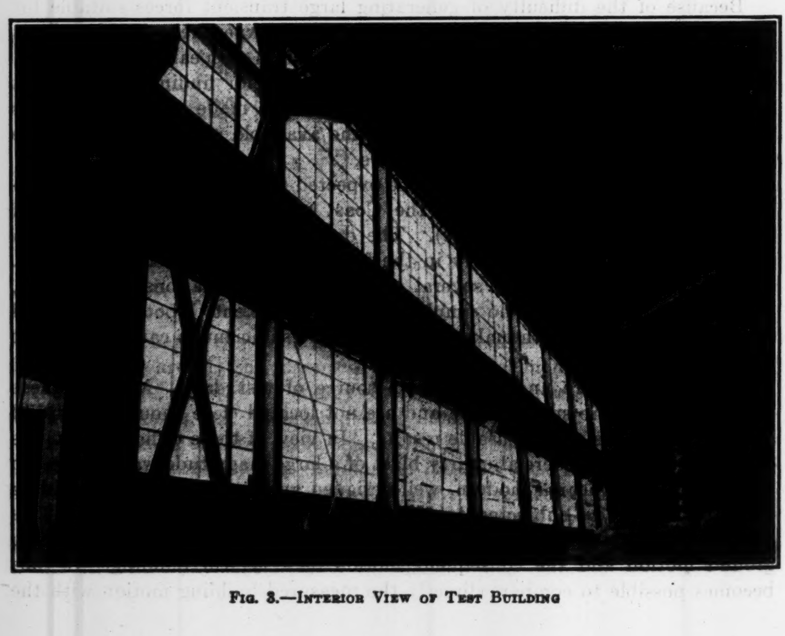

FIG. 3.—INTERIOR VIEW OF TEST BUILDING

motions that would be computed based on various simplified dynamic models, and hence to evaluate directly the practical value of the theoretical analysis.

Description of the Test Building.—In Figs. 2 and 3 are shown the general features of the steel-frame mill building in which the measurements were made. The building consists of two sections which in many respects act independently. The lower part of the building connects into the higher end at intermediate points in the vertical 10WF39 column members (points A and B in Fig. 4). Because of bending in these relatively long vertical members the connection between the two parts is not a very rigid one. The most important masses in the system are the 6-in.-thick concrete floor slab, located in the higher part of the building 45 ft 8 in. above the ground, which weighs about 180,000 lb, and the 1½-ft-thick concrete wall at the far end of the lower section, which weighs approximately 350,000 lb. The cross bracing in the end frames below the floor slab consists of 4H10 welded sections, and the other cross braces shown schematically in Fig. 4 are either 1-in.-diameter or 1½-in.-diameter round bars.[3]

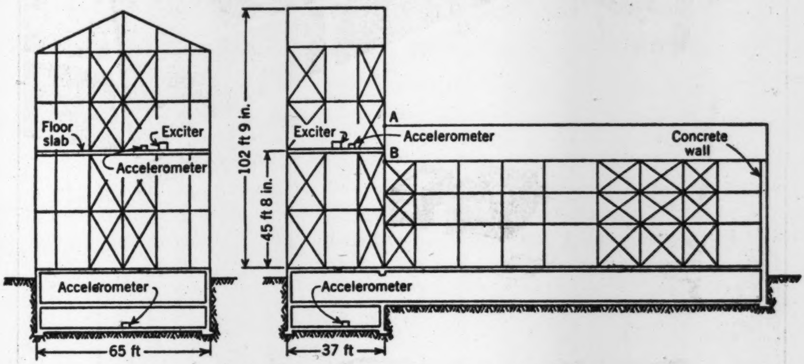

FIG. 4.—SCHEMATIC DRAWING OF TEST BUILDING

The Instruments.—The measuring instruments used for both the ground motion and the building motion were seismic type accelerometers. The particular instrument used had a variable-reluctance, balanced-armature type of seismic element, with a natural frequency of approximately 80 cycles per sec and fluid damping of about 60% of critical.[4] The accelerometer signal modulated the output of a 2,000-cycles-per-sec alternating current bridge. The output of the bridge circuit was then amplified, demodulated, and finally recorded on paper by a direct pen-writing oscillograph. The over-all frequency characteristics of the accelerometer-recorder system are essentially constant from zero to approximately 100 cycles per sec.

---

[3] "Measured Response of a Structure to an Explosive-Generated Ground Shock," by Donald E. Hudson, J. L. Alford, and George W. Housner, *Bulletin*, Seismological Soc. of America, Vol. 44, No. 3, July, 1954.

[4] "Ground Shock and Building Motions Produced by a Quarry Blast," by George W. Housner, Donald E. Hudson, and J. L. Alford, *Proceedings*, Soc. of Experimental Stress Analysis, Vol. XI, No. 2, 1954, p. 133.

In Fig. 5 the installation of this measuring and recording system at the upper floor slab position is shown. The recording oscillograph is at the right, and the larger instrument at its left contains the 2,000-cycle-per-sec oscillator, the amplifier, and the input bridge circuits. Connected to this amplifier unit at the left may be seen the small accelerometer, mounted on a right-angle bracket to record horizontal accelerations of the floor slab. The locations of the accelerometer and of the similar accelerometer and recording system in the subbasement are shown in Fig. 4. The accelerometers were oriented so that horizontal accelerations in the direction of the short side of the higher part of the building would be measured.

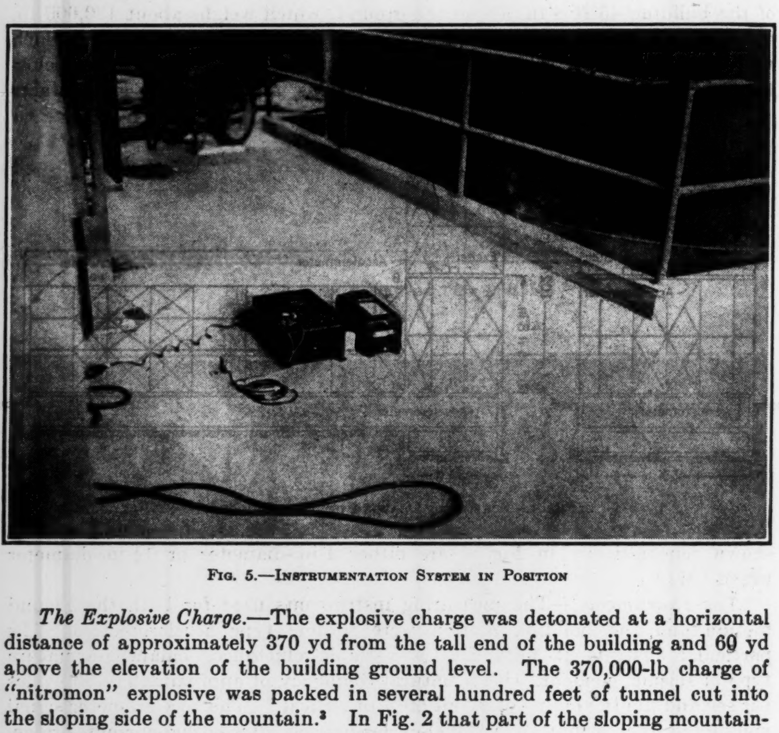

FIG. 5.—INSTRUMENTATION SYSTEM IN POSITION

The Explosive Charge.—The explosive charge was detonated at a horizontal distance of approximately 370 yd from the tall end of the building and 60 yd above the elevation of the building ground level. The 370,000-lb charge of "nitromon" explosive was packed in several hundred feet of tunnel cut into the sloping side of the mountain.[3] In Fig. 2 that part of the sloping mountainside behind the top of the tall telephone pole at the left of the building is the approximate location of the explosive charge.

THE RECORDED GROUND MOTION

In Fig. 6 is shown the measured ground motion as plotted from the oscillograph record. The acceleration shown is the horizontal component of the ground acceleration in a direction parallel to the short side of the tall part of the building. It is of interest to note that the magnitudes attained are equal to those of a moderately strong earthquake and that the general periods and wave form are similar to those for the initial part of a typical earthquake. The ground accelerations of some recorded strong earthquakes have been from two to three times as large as those shown in Fig. 6, and the motions have lasted from fifteen to twenty times as long.

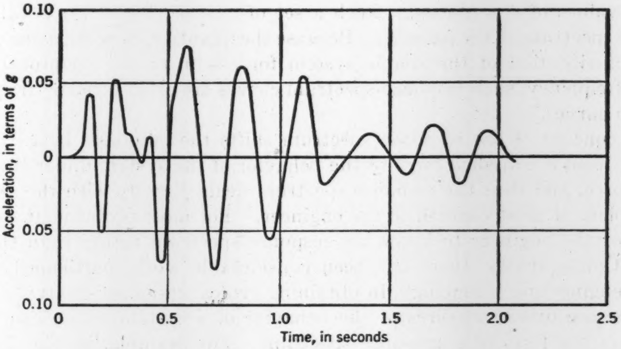

FIG. 6.—MEASURED GROUND MOTION

THE RESPONSE SPECTRUM OF THE GROUND MOTION

From the experimentally determined ground motion the forces acting on the building can be computed, and the anticipated behavior of the building can be determined. As stated in the "Introduction," the method will be to

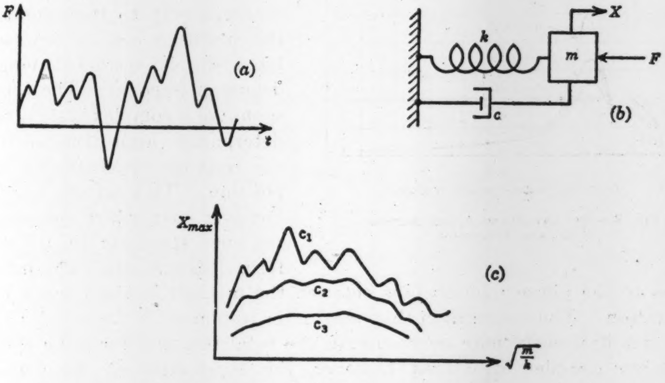

FIG. 7.—THE RESPONSE SPECTRUM OF A FORCE

replace the actual building structure by several equivalent simple systems. The first problem, therefore, will be to compute the behavior of a simple spring-mass system under the action of the recorded ground motion.

It has been found that a convenient way of describing the behavior of the simple system is by the so-called "response spectrum." Suppose that a force,

F, is given which varies with time in some known way (Fig. 7(a)). A quantity is then chosen to define the motion of the simple system, such as the displacement, X (Fig. 7(b)). In order to show in one set of curves the behavior of the system of Fig. 7(b) for all values of the basic characteristics, m, k, and c, the maximum value of the displacement, X_{max}, versus the quantity, $\sqrt{m/k}$, for various values of c is plotted. Such a set of curves (Fig. 7(c)) is called the response spectrum of the force, F. Because the quantity, $\sqrt{m/k}$, is the natural period of vibration of the simple system for $c = 0$, or the reciprocal of the natural frequency, such response-spectrum curves are often termed "frequency-response curves."

The concept of the response spectrum shifts the emphasis in a dynamics problem from the applied force to the behavior of the system under the action of the force, and thus the response spectrum deals directly with the aspect of the problem of most concern to the engineer. For most problems it would be better for the engineer to know the response spectrum rather than the force itself. Consequently, there has been considerable work, particularly in the field of engineering seismology, in obtaining typical response spectra.

There are other measures of the behavior of a system which can also be plotted in the form of a response spectrum. For example, in Fig. 7(b), the relative displacement between the mass and the support—that is, the total strain in the spring—or the relative or absolute velocities or accelerations of the mass, might be used as the response. The particular quantity selected will depend on the nature of the problem being studied. By using the more general term, "response," all these possibilities are included under one concept.

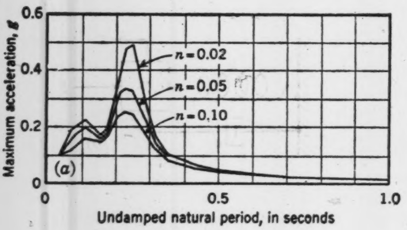

FIG. 8.—QUARRY-BLAST ACCELERATION RESPONSE SPECTRUM

The response spectrum will indicate directly the behavior of a structure only to the extent that the structure can be represented by a simple system having one degree of freedom. The total response of a complex system can be determined approximately from the response spectrum by superposition. This superposition is, however, not exact because the response spectrum in its simple form does not retain any information as to the phase relationships between the motions in the various modes of vibration. The assumption that maximum responses in the various modes occur simultaneously may overestimate the total response for some systems. For many complex structures, however, this summation of the maximum responses will give sufficiently accurate results so that even for complicated structures the response spectrum concept is of considerable utility.

For the problem under consideration the acceleration response spectrum will be used because acceleration is the quantity which is directly measured. The problem of determining the acceleration spectrum, given a complicated acceleration-time function as in the present problem, is difficult and is best solved by the use of high-speed computer techniques. In the present case, the spectrum was obtained by the use of the electric analog computer of the Analysis Laboratory at the California Institute of Technology at Pasadena.[5,6] The spectrum obtained for the quarry-blast ground acceleration is shown in Fig. 8. The damping factor, n, in Fig. 8 is the fraction of critical damping in the system, $n = \dfrac{c}{2\sqrt{k\,m}}$.

THE DYNAMIC MODEL OF THE BUILDING

From the response spectrum of Fig. 8 the behavior of the building can be predicted if the building can be replaced by a dynamic model consisting of several simple systems. In Fig. 4 it can be observed that the two main masses of the structure—the floor slab in the tall part and the vertical wall at the other end of the long section—are separated by a structure of considerable flexibility, and hence the two masses would not be expected to behave in the same way. The whole structure, therefore, cannot be represented by just one concentrated mass—that is, as one simple system; at least two masses and two springs must be retained in the model. As a tentative model for the structure the two-mass system shown in Fig. 9 is assumed. The mass, m_1, includes one-half of the mass of the concrete floor slab, plus a fraction of one-half of the mass of the roof and walls. The mass, m_2, includes part of the vertical concrete wall mass and a fraction of the roof and sidewall mass. The fractions of the roof and wall masses used were computed on the basis of tributary loads resisted by the wall frames. The cantilever spring, k_1, was the computed spring constant for one side frame which supports one-half of the concrete slab. This was determined by computing the static deflection caused by a given horizontal force applied at the floor slab. The cantilever spring, k_2, was similarly computed for the side framing supporting the roof and the vertical wall of the long part of the building. The coupling spring, k_3, was computed by considering the bending of the vertical members as at points A and B in Fig. 4. These com-

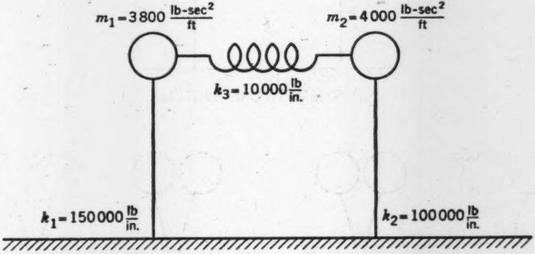
$m_1 = 3800 \frac{\text{lb-sec}^2}{\text{ft}}$
$m_2 = 4000 \frac{\text{lb-sec}^2}{\text{ft}}$
$k_3 = 10000 \frac{\text{lb}}{\text{in.}}$
$k_1 = 150000 \frac{\text{lb}}{\text{in.}}$
$k_2 = 100000 \frac{\text{lb}}{\text{in.}}$

FIG. 9.—DYNAMIC MODEL OF BUILDING

---

[5] "The Analysis of Strong-Motion Earthquake Records with the Electric Analog Computer," by George W. Housner and G. D. McCann, *Bulletin*, Seismological Soc. of America, Vol. 39, No. 1, January, 1949.

[6] "Spectrum Analysis of Strong-Motion Earthquakes," George W. Housner, R. R. Martel, and J. L. Alford, *ibid.*, Vol. 43, No. 2, April, 1953.

puted values of masses and spring constants are of course subject to some variation depending on the assumptions made as to mass distribution and joint rigidities, but it is believed that they should be within 10% of the correct values. From the later results it will be seen that this accuracy is sufficient for the present purpose.

Given the two-mass model of Fig. 9, the two natural periods can be computed.[7,8] The results for the numerical values of Fig. 9 are 0.278 sec for the shorter period and 0.347 sec for the longer period. The question arises as to which of these two periods would be excited by the ground motion. In Fig. 10, a still further simplification of the structure is introduced in that in this model the masses and the cantilever spring constants are equal. The two kinds of motion possible in Fig. 10(*a*) are shown in Figs. 10(*b*) and 10(*c*). In Fig. 10(*b*) the two masses move in the same direction whereas in Fig. 10(*c*) the masses always move in opposite directions. A very similar behavior would be expected from Fig. 9 because the masses and cantilever spring constants there are approximately equal.

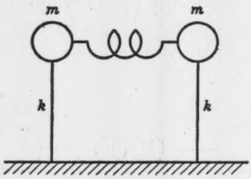

(*a*) SYMMETRICAL SYSTEM

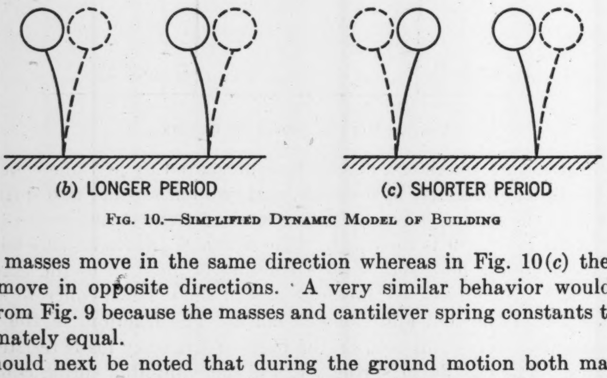

(*b*) LONGER PERIOD (*c*) SHORTER PERIOD

FIG. 10.—SIMPLIFIED DYNAMIC MODEL OF BUILDING

It should next be noted that during the ground motion both masses are acted on simultaneously by spring forces, and hence at the start of the motion both masses should move in the same direction. The ground motion would thus be expected to excite primarily the longer period. The magnitude of the acceleration which should correspond to this longer period could be determined from the spectrum curve of Fig. 8 provided the damping in the structure were known. It can be seen from Fig. 8, however, that, in the region of the 0.347-sec period, the response is not particularly sensitive to

---

[7] "Mechanical Vibrations," by J. P. Den Hartog, McGraw-Hill Book Co., Inc., New York, N. Y., 4th Ed., 1956, p. 79.

[8] "Vibration Problems in Engineering," by S. Timoshenko, D. Van Nostrand Co., Inc., New York, N. Y., 3rd Ed., 1955, p. 186.

damping; hence, a complete analysis of the damping in the structure is not necessary, and an approximate value based on past tests of building structures can be taken.[9] Using a damping value of $n = 0.05$, it is found from the spectrum curves of Fig. 8 corresponding to a period of 0.347 sec that the peak acceleration should be about 0.1 *g*. It is of interest to note that similar computations of the building response to several strong earthquakes that have been recorded show that the building motions caused by those earthquakes would have been much larger than 0.1 *g*.

Based on the analysis of the ground acceleration and the dynamics of the structure, the conclusion is that the floor slab should show a dominant period of approximately 0.347 sec and a peak acceleration of 0.1 *g*. This computation can now be compared directly with the test results.

THE TEST RESULTS

In Fig. 11 is shown the acceleration-time record obtained from the floor-slab accelerometer during the blast. It will be seen that although there is evidence of at least two periods, there is a dominant period and its magnitude checks satisfactorily with the computed one. The peak acceleration is also seen to be very close to the 0.1 *g* computed from the blast spectrum. It may thus be concluded from this satisfactory agreement between the computed and the measured motions that the main factors of engineering significance have been retained in the model even though many simplifications have been introduced.

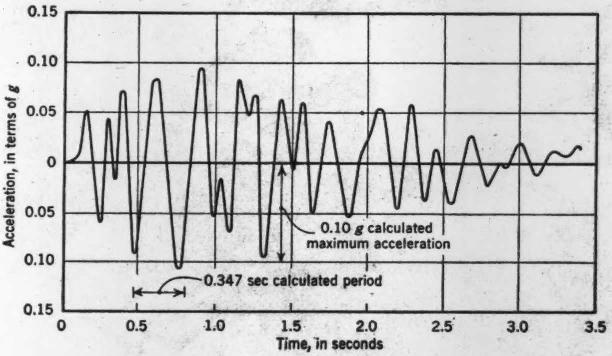

FIG. 11.—ACCELERATION-TIME RECORD OF FLOOR SLAB

VIBRATION TESTS OF THE BUILDING

Although for the building of the present tests the natural periods could be computed with reasonable accuracy, it would be expected that for some applications more accurate values of the periods than can readily be computed might be required. These more accurate values would probably best be obtained by a direct steady-state vibration test of the building. Such a vibration test would also give values of structural damping. Although the structural damping was not of critical importance in the present test, this was to a certain extent fortuitous; in general, damping would be expected to have an important effect on the response of a structure to dynamic loads. It was thus decided that, as an additional check and to provide a direct comparison of transient and steady-state response, vibration tests of the building should be made.

---

[9] "A Dynamic Test of a Four-Story Reinforced Concrete Building," by J. L. Alford and George W. Housner, *Bulletin*, Seismological Soc. of America, Vol. 43, No. 1, January, 1953.

The vibration exciter used as the source of an alternating sinusoidal force was a counter-rotating, unbalanced-mass machine borrowed from the Coast and Geodetic Survey. A photograph of this unit installed on the floor slab in the tall part of the building is shown in Fig. 12. The unit produces a total horizontal force, in pounds, given by the expression,

FIG. 12.—VIBRATION EXCITER UNIT IN POSITION

$$F = 12\,f^2 \quad \text{.........................} \quad (1)$$

in which f is the frequency in cycles per second corresponding to the rotational speed of the exciter. The unit was driven by a thyratron-controlled, variable speed, direct current motor which permitted a close adjustment of speed and a smooth variation of speed through the resonant periods. The exciter was adjacent to the upper floor slab accelerometer, as shown in Fig. 4, and was oriented so that the horizontal force was parallel to the short side of the tall part of the building.

It should be noted that there is a fundamental difference in the behavior of the building when acted on by the vibration exciter as compared with its response to the ground motion. Referring to Fig. 13(*a*) it will be seen that the ground motion (as previously stated) excites primarily the motion of the two masses in the same direction. The vibration exciter applies a force to just one mass of the system (Fig. 13(*b*)) and hence tends to excite the motion in which the two masses move in opposite directions. Thus, the resonant period excited by the shaking machine will be the shorter period whereas the period chiefly excited by the ground motion is the longer period. Because the coupling spring between the two masses is very soft as compared to the two cantilever springs, the second mass, which corresponds to the low part of the building, can be assumed to have no effect on the system for the opposite motion of the masses. Thus, for the vibration tests the tall part of the building can be considered as an independent structure.

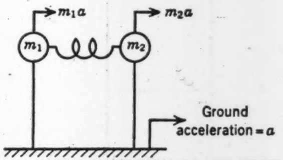

(*a*) GROUND-MOTION BLAST TEST

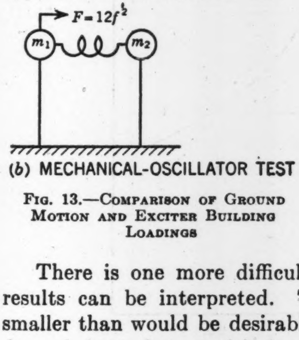

(*b*) MECHANICAL-OSCILLATOR TEST

FIG. 13.—COMPARISON OF GROUND MOTION AND EXCITER BUILDING LOADINGS

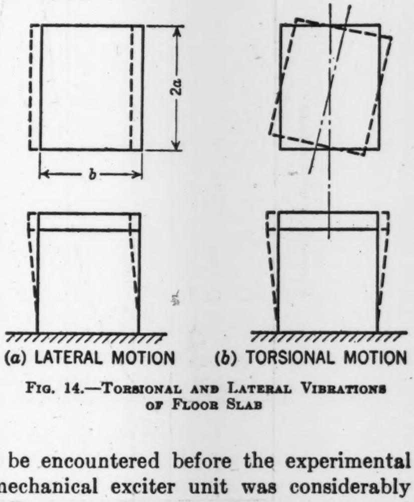

(*a*) LATERAL MOTION (*b*) TORSIONAL MOTION

FIG. 14.—TORSIONAL AND LATERAL VIBRATIONS OF FLOOR SLAB

There is one more difficulty to be encountered before the experimental results can be interpreted. The mechanical exciter unit was considerably smaller than would be desirable for the test, and, because the force generated depended on the rotational speed, for low speeds the force was insufficient to give a measurable motion to the building. This difficulty was avoided by noting that the torsional vibration of the floor slab had a period which corresponded to a sufficiently high exciter speed so that usable records could be obtained. Because there is a relatively simple relationship between the period of the torsional vibration and that of the desired lateral vibration, the lateral period could be easily computed.

In Fig. 14 are shown the motions corresponding to the torsional and the lateral vibrations. Considering the floor slab as a uniform rectangular slab of constant thickness, the relationship between these torsional and lateral periods is

$$\text{Lateral period} = (\text{torsional period}) \sqrt{\frac{12\,a^2}{4\,a^2 + b^2}} \quad \ldots\ldots\ldots\ldots (2)$$

(The symbols, *a* and *b*, are defined in Fig. 14.)

The same accelerometer and recording system that was used during the blast was used for the vibration test; the accelerometer was located in the same position. A second accelerometer was mounted at the edge of the floor slab about 25 ft from the first, and a simultaneous recording of the two accelerometers permitted a distinction between torsional and lateral vibrations. The vibration exciter was located a sufficient distance from the center of the slab so that torsional motions of the slab could be produced.

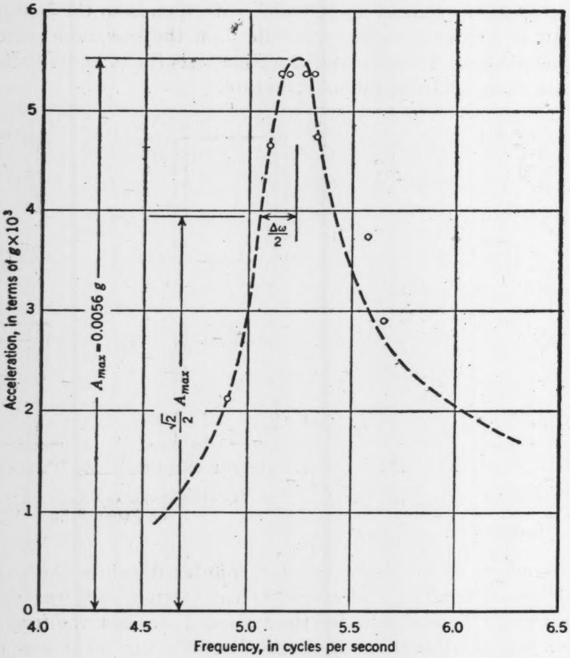

FIG. 15.—RESONANCE CURVE OF FLOOR SLAB TORSIONAL MOTION

In Fig. 15, the results of the vibration test may be seen in the form of a resonance curve, in which the amplitudes of the building accelerations are plotted versus the exciting frequency (the reciprocal of the period). It will be seen that the resonant period is 1/5.23 cycles per sec = 0.191 sec. This is the period of the torsional motion, and the desired lateral period can be computed from Eq. 2:

$$\text{Lateral period} = (0.191) \sqrt{\frac{(3)\ (65)^2}{(65)^2 + (37)^2}} = 0.289 \text{ sec} \ldots\ldots\ldots (3)$$

This value of 0.289 sec should be compared directly with the period of 0.278 sec previously computed for the system shown in Fig. 9. The difference of approximately 4% indicates the order of accuracy to be expected in work of this kind.

DETERMINATION OF DAMPING

The resonance curve of Fig. 15 is sufficiently well defined so that a value of the equivalent viscous damping can be determined by measuring its width. Because the lower frequencies can be more accurately measured from the record than the higher ones, the rising part of the resonance curve was used for this determination. If $\Delta\omega$ is the width of the resonance curve at an amplitude $\sqrt{2}/2$ times the resonant amplitude, it can be shown that, for small damping of the magnitude existing in the present test, the fraction of critical damping is approximately

$$n = 1/2\,\frac{\Delta\omega}{\omega} \qquad (4)$$

in which ω is the resonant frequency. For the resonance curve of Fig. 15, this gives a value of $n = 0.034$.

The dotted curve of Fig. 15 is a computed acceleration resonance curve for a simple spring-mass system. It is plotted from the equation,

$$\text{Acceleration} = \frac{K'\left(\frac{\omega}{\omega_n}\right)^4}{\sqrt{\left[1-\left(\frac{\omega}{\omega_n}\right)^2\right]^2+\left[2\,n\left(\frac{\omega}{\omega_n}\right)\right]^2}} \qquad (5)$$

in which the two unknown constants, K' and ω_n, are determined from the experimentally obtained damping and resonant frequency. It will be seen that the building does behave essentially like a simple system as far as this type of motion is concerned.

The value of equivalent viscous damping thus obtained is, of course, only an approximate one. The actual damping in the structure is not a viscous type dissipation, and, in addition, the resonance curve of Fig. 15 does not represent motion in a pure normal mode. It is believed, however, that the damping value obtained is useful for comparison with similar tests and as a basis for estimating the energy losses involved in such structural vibrations.

Referring to Fig. 14 it will be seen that the same structural members and the same structural deformations are involved in both the lateral and the torsional motions. The only difference is that in the lateral motion the two end frame structures move together whereas in the torsional motion they move in opposite directions. The same value of damping, experimentally determined for the torsional motion, would thus also apply to the lateral motions.

The low value of damping determined from the present tests (3.4%) shows that large dynamic amplification effects are possible in structures of this type. For this value of damping the maximum dynamic amplification factor at resonance is approximately 15. This value of 3.4% damping may be compared with a value of 7% obtained for a reinforced concrete building and also with values close to 3% which apply to typical aircraft structures.

COMPARISON OF TRANSIENT AND STEADY-STATE TESTS

In comparing the results of the blast and the vibration tests it is well to keep in mind that the amplitudes of the motions in the two tests were quite different and for some applications this might affect the comparison in a significant way. Although accelerations as high as 0.1 *g* occurred in the blast tests, the maximum accelerations during the vibration tests were of the order of 0.005 *g*. This difference in acceleration amplitude level could have two distinctly different effects on the results. In the first place the damping in the structure could be considerably greater at the higher amplitudes, and for some positions on the spectrum curve of Fig. 8 this could lead to different results. A second effect which might be caused by the large motions is the introduction of nonlinear effects. If the structure were loaded to the point where some plastic yielding or buckling of compression members were to occur, the nonlinear character of the restoring force would result in an effective lower natural period, which would alter the behavior of the building. With this thought in mind, computations were made of the forces acting in the structure and the stresses in the compression members. It was found that, even under the largest inertia forces of the ground shock motion, the axial compression forces did not approach the buckling values and that no significant structural members were stressed into the plastic region. It was fortunate that for this particular test neither of these amplitude effects operated to change conditions between the large and small amplitudes, and hence good agreement was obtained.

One other possible source of difficulty in comparing vibration tests in general with ground motion tests remains to be mentioned. The behavior of a structure under the action of ground motions may be quite different from that caused by a concentrated exciter force acting at one point. Because many vibration tests have been made on buildings with the idea of determining building response to earthquakes, it should be emphasized that the earthquake ground motion might excite motions and periods in a different way from a force applied at a single point in the structure. This has been a troublesome problem in similar vibration tests of aircraft structures in which it has been found that a number of vibration exciters located at various points throughout the structure, and operated simultaneously with the proper phase relationships, are necessary to excite properly the various wing and fuselage motions.[10]

CONCLUSIONS

The agreement between the computed and measured building responses is believed to be accurate enough for engineering application. It thus appears that it may often be possible to replace complex structures by simplified dynamic models that will retain the major features of engineering significance. The difficulty of computing the response of buildings to dynamic loads is a consequence of the complexity of most actual structures and of the exciting forces, rather than of any incompleteness or incorrectness of the dynamical theories applied. The theoretical computations follow directly from basic physical principles and do not require the inclusion of any empirical factors.

---

[10] "A System for the Excitation of Pure Natural Modes of Complex Structures," by R. C. Lewis and D. L. Wrisley, *Journal of the Aeronautical Sciences*, November, 1950, p. 705.

Although judgment must be exercised in selecting the best dynamic model to be used for the representation of a given complex structure, it is of importance to know that a rational method of analysis exists which can be applied to many structures and which leads to realistic results.

ACKNOWLEDGMENTS

Thanks are due the Minnesota Mining and Manufacturing Company, for permission to make the tests, and particularly R. E. Gundlach, regional manager, and G. J. LaVenture, production superintendent of the Corona quarry, for their very helpful cooperation. W. K. Cloud of the Coast and Geodetic Survey made arrangements for the use of the vibration exciter, and the Office of Naval Research cooperated in the financial support of the work.

AMERICAN SOCIETY OF CIVIL ENGINEERS
Founded November 5, 1852
TRANSACTIONS

Paper No. 2881

INELASTIC BUCKLING OF NONUNIFORM COLUMNS

By John E. Goldberg,[1] M. ASCE, John L. Bogdanoff,[2]
and Hsu Lo[3]

Synopsis

A numerical procedure is presented for computing the critical loads for nonuniform pin-ended columns in the elastic or inelastic range. The procedure is based on transformation of the differential equation to an integral equation which is solved numerically for trial values of the critical load.

Introduction

If an initially straight, pin-ended column is subjected to a slowly increasing axial load, the column will buckle when the load exceeds the value of P corresponding to the first eigenvalue[4] of the following differential equation[5] (together with appropriate boundary conditions):

$$E_t I \frac{d^2y}{dx^2} + P y = 0 \qquad (1a)$$

or

$$\frac{d^2y}{dx^2} = -\frac{P y}{E_t I} \qquad (1b)$$

in which $E_t = E_t(x, P)$ is the tangent modulus; $I = I(x)$ denotes the moment of inertia of the cross section; P represents the axial load; x denotes the longitudinal coordinate; and y is the lateral deflection.

Eq. 1 merely states that in some particular configuration, $y = y(x)$, which is arbitrarily small, the column is in a state of equilibrium when the applied load has been increased slowly to the critical load. Taking the internal bending

---

Note.—Published, essentially as printed here, in April, 1956, as *Proceedings Paper* 943. **Positions** and titles given are those in effect when the paper was approved for publication in *Transactions*.

[1] Prof. of Structural Eng., Purdue Univ., Lafayette, Ind.

[2] Prof. of Eng. Science, Purdue Univ., Lafayette, Ind.

[3] Prof. of Aeronautical Eng., Purdue Univ., Lafayette, Ind.

[4] "Advanced Calculus for Engineers," by F. B. Hildebrand, Prentice-Hall, New York, N. Y., 1949, pp. 200–202.

[5] "Buckling Strength of Metal Structures," by Friedrich Bleich, McGraw-Hill Book Co., New York, N. Y., 1952, pp. 15 and 62.

moment as

$$M = -E_t I \frac{d^2y}{dx^2} \qquad (2)$$

and equating this expression to the applied moment, $P\,y$, leads to Eq. 1.

For the case of a pin-ended column, the boundary conditions may be taken as

$$y(0) = 0 \qquad (3a)$$

and

$$y(L) = 0 \qquad (3b)$$

or, alternatively, because the bending moment vanishes at the ends of the column, as

$$\frac{d^2y(0)}{dx^2} = 0 \qquad (3c)$$

and

$$\frac{d^2y(L)}{dx^2} = 0 \qquad (3d)$$

in which L is the length of the column.

It is convenient to rewrite the foregoing equations in terms of a nondimensional independent variable,

$$s = \frac{x}{L} \qquad (4a)$$

and it is easily seen that

$$\frac{d^2y}{dx^2} = \frac{1}{L^2}\frac{d^2y}{ds^2} \qquad (4b)$$

Consequently, the substitution of Eqs. 4 in Eq. 1*b* results in

$$\frac{d^2y}{ds^2} = -\frac{P\,L^2}{E_t I}\,y \qquad (5a)$$

with the boundary conditions,

$$y(0) = 0 \qquad (5b)$$

and

$$y(1) = 0 \qquad (5c)$$

or, alternatively,

$$\frac{d^2y(0)}{ds^2} = 0 \qquad (5d)$$

and

$$\frac{d^2y(1)}{ds^2} = 0 \qquad (5e)$$

Eq. 5*a* is readily transformed to an integral equation by substituting a new dependent variable, $Y(s)$, for the second derivative of y, so that

$$\frac{d^2y}{ds^2} = Y(s) \qquad (6a)$$

$$\frac{dy}{ds} = \int_0^s Y(\zeta)\, d\zeta - C_1 \qquad (6b)$$

and, finally,

$$y = \int_0^s (s - \zeta)\, Y(\zeta)\, d\zeta - C_1 s - C_2 \qquad (6c)$$

in which C_1 and C_2 are constants of integration. It is observed that Eq. 6*c* and the boundary condition (Eq. 5*b*) at $s = 0$ require that

$$C_2 = 0.$$

The substitution of Eqs. 6*a* and 6*c* into Eq. 5*a* therefore yields the following Volterra integral equation of the second kind,

$$Y(s) = \frac{P\,L^2}{E_t\,I}\left[- s \int_0^s Y(\zeta)\, d\zeta + \int_0^s \zeta\, Y(\zeta)\, d\zeta + C_1 s\right] \qquad (7a)$$

while the boundary condition at $s = 1$ becomes

$$Y(1) = 0. \qquad (7b)$$

From Eq. 7*a* it is found that $Y(0) = 0$ which, of course, agrees with Eq. 5*d*.

A solution of Eq. 7*a*, linear in C_1, can be found by numerical methods described subsequently for any value of P. The values of P associated with solutions satisfying the boundary condition (Eq. 7*b*) represent estimates of critical loads corresponding to the various modes of buckling of the column. The lowest of these values of P which are greater than zero is the critical load of the column.

In terms of C_1 and for a given value of P, Eq. 7*a* represents an initial value problem for which an approximate solution may be found by the following method. The range of integration (0, 1) is divided in n equal segments with boundary and division points located at $s_0, s_1, s_2, \ldots, s_{n-1}$, and s_n. The points, s_0 and s_n, correspond to the ends of the column. The length of each segment is $b = 1/n$. At the jth division point, $Y(s)$ takes on the approximate value, Y_j. Between division points an interpolation of $Y(\zeta)$ is used, thus permitting evaluation of the sectionalized integrals of Eq. 7*a*. If the column is divided into a sufficient number of segments, the assumption that $Y(\zeta)$ varies linearly over each segment will give good results.

Assuming linear variation over each segment, the approximate form of $Y(\zeta)$ for integration in Eq. 7*a* takes on the polygonal character indicated in

Fig. 1. With this assumption, it is easily seen that

$$\int_0^{s_j} Y(\zeta)\, d\zeta = b\,\frac{Y_0}{2} + b\,Y_1 + \cdots + b\,Y_{j-1} + b\,\frac{Y_j}{2}$$

$$= b\left(\frac{Y_0}{2} + \sum_1^{j-1} Y_k + \frac{Y_j}{2}\right) \quad \text{..(8a)}$$

and

$$\int_0^{s_j} \zeta\, Y(\zeta)\, d\zeta = \frac{b}{3}\,\frac{Y_0\,b}{2} + b\,Y_1\,b + 2\,b\,Y_2\,b + \cdots$$

$$+ (j-1)\,b\,Y_{j-1}\,b + (j - \tfrac{1}{3})\,b\,\frac{Y_j\,b}{2}$$

$$= b^2\left[\frac{Y_0}{6} + \sum_1^{j-1} k\,Y_k + \left(\frac{j}{2} - \frac{1}{6}\right) Y_j\right] \quad \text{..(8b)}$$

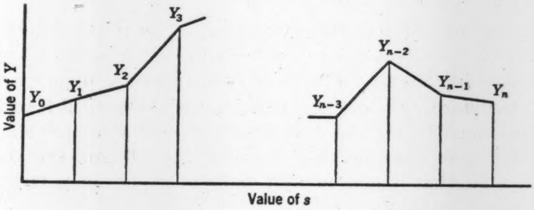

Fig. 1.—Polygonal Approximation for $Y(s)$

Substituting Eqs. 8 in Eq. 7*a*, collecting terms in Y_j, and making use of the fact that $Y_0 = 0$ leads to

$$Y_j\left(1 + \frac{P\,L^2\,b^2}{6\,E_t\,I}\right) = C_1\,j\,\frac{P\,L^2\,b}{E_t\,I} - \frac{P\,L^2\,b^2}{E_t\,I}\left(j\sum_1^{j-1} Y_k - \sum_1^{j-1} k\,Y_k\right) \quad \text{...(9a)}$$

which may be written as

$$Y_j\left(\frac{n^2\,E_t\,I}{P\,L^2} + \frac{1}{6}\right) = C_1\,j\,n - j\sum_1^{j-1} Y_k + \sum_1^{j-1} k\,Y_k \quad \text{.........(9b)}$$

If the summations in Eq. 9*b* are transposed to the left-hand side, it is seen that the solution must be linear in C_1. Consequently, for the present purposes, it suffices to select any convenient value, such as unity, for C_1.

Suggested Procedure

The following procedure, which is essentially a trial-and-error method, is suggested for the determination of the critical load of a nonuniform column:

1. Divide the column into *n* equal segments and tabulate area (*A*) and moment of inertia (*I*) at each division point and at the terminal point.
2. Select a trial value of the axial load (*P*).

3. Compute the average stress at each division point and at the terminal point, and determine the tangent modulus for each point at the applied stress. The tangent modulus may be determined from a tangent modulus curve or from a stress-strain curve, or it may be determined by means of an analytical expression for the stress-strain curve.

4. Using the following formula,

$$Y_j = \frac{j\,n - j\sum_{1}^{j-1} Y_k + \sum_{1}^{j-1} k\,Y_k}{\frac{n^2 E_t I}{P L^2} + \frac{1}{6}} \qquad (9c)$$

compute Y_j (at $j = 1, 2, \cdots, n$) either by desk computing methods or by a digital computer.

5. If Y_n is found to be zero and if Y_j has the same algebraic sign throughout, the trial load which has been used is a critical load corresponding to the lowest mode of buckling.

6. If Y_n is not zero or approximately zero, a new trial value of P should be selected and steps 2 to 5 repeated. If Y changes sign before the end point, n, is reached. This implies that a point of inflection or a hinge exists within the column and, therefore, the previous trial load is the critical load for a shorter column. Consequently, for the next trial, a lesser value of P should be used. Conversely, if Y does not change sign within the column, this corresponds to buckling of a somewhat longer column and, consequently, a larger value of P should be selected for the next trial.

It is, of course, unlikely that the boundary condition at s_n will be satisfied by the first trial. Because a second trial will be necessary it is desirable to use the results of the previous computation as a guide in selecting a new trial value of the axial load. By interpolation or extrapolation, the approximate point at which Y becomes zero may be found. If the point at which Y becomes zero is close to the end of the column, an estimate of the correction to the trial value of the critical load may be obtained by the following device. Let Δs be the distance of this inflection point from s_n, being positive if the inflection point lies beyond the end of the column and negative if it lies within the column. Then the correction, ΔP, to the previous trial value, P_1, may be taken as

$$\Delta P = 2\,P_1\,\Delta s \qquad (10)$$

and the value to be used as a second trial may be taken as

$$P_2 = P_1\,(1 + 2\,\Delta s) \qquad (11)$$

Eq. 10 is obtained by differentiating the Euler formula with respect to the length, assuming that the average tangent modulus does not change greatly. Thus,

$$P_1 = \frac{\pi^2 \bar{E}_t \bar{I}}{L^2} \qquad (12)$$

in which the bars over E_t and I indicate properties having the character of averages. Then,

$$\Delta P = -\frac{2\,\pi^2\,\bar{E}_t\,\bar{I}}{L^3}\,\Delta L \approx -\,2\,P_1\,\frac{\Delta L}{L} \qquad (13a)$$

or

$$\Delta P = 2\,P_1\,\Delta s \qquad (13b)$$

If the additional terms which enter into the total differential of Eq. 12 can be computed readily (that is, the terms involving the differentials of the tangent modulus and the moment of inertia), a more refined expression for the correction to the previous trial value may be obtained. However, it is doubtful whether under ordinary circumstances too much effort at this point is justified considering that the final result probably will be obtained by interpolation. Because Eq. 10 is generally not the total differential of Eq. 12, this equation should be used only as a means of estimating a correction. The final result is best obtained by interpolation or extrapolation from trial results which are reasonably well converged.

TABLE 1.—COMPUTATIONS FOR EXAMPLE 1

n	Y_{max}	Y_n	Y_{n-1}	Δs	Δp	p
			FIRST TRIAL ($p = 1.05$)			
20	0.16	−0.01193	0.01395	−0.0231	−0.0485	1.0015
10	0.16	−0.01031	0.04104	−0.0201	−0.0422	1.0078
5	0.16	−0.00401	0.09368	−0.0082	−0.0172	1.0328
			SECOND TRIAL ($p = 0.95$)			
20	0.15	0.01263	0.03576	0.0273	0.0573	1.0073
10	0.15	0.01403	0.05935	0.0309	0.0649	1.0144
5	0.15	0.01946	0.10358	0.0463	0.0972	1.0472

THIRD TRIAL (ALTERNATE INTERPOLATION PROCEDURE)

n	Y_n for p_1	Y_n for p_2	Interpolated p for $Y_n = 0$	Y_n for interpolated p
20	−0.01193	0.01263	1.00143	0.00016
10	−0.01031	0.01403	1.0076	0.00016
5	−0.00401	0.01946	1.033	0.00008

A variation of Eq. 9b is sometimes convenient for computation. Let the product, $E_t\,I$, at some station, such as s_0, be selected as a reference value and designated $(E_t\,I)_0$. Also, let

$$\frac{E_t\,I}{(E_t\,I)_0} = r(s, p) \qquad (14a)$$

and

$$\frac{\pi^2(E_t\,I)_0}{P\,L^2} = \frac{1}{p} \qquad (14b)$$

Eq. 14*b* represents that ratio of the Euler load of a uniform bar having the section properties of the reference station to the trial load. Then Eq. 9*b* may be written as

$$Y_j \left(\frac{n^2 r_j}{p \pi^2} + \frac{1}{6} \right) = C_1 j n - j \sum_1^{j-1} Y_k + \sum_1^{j-1} k Y_k \dots\dots\dots\dots (15)$$

Examples and Results

Example 1. Uniform Bar in the Elastic Range.—This example is included merely to establish the potentialities of the method with respect to accuracy. The problem was worked using five, ten, and twenty intervals. For a uniform bar, r_j in Eq. 15 is always equal to unity. As explained previously, C_1 is taken as unity.

In each case (Table 1), a first trial value was taken as 5% greater than the Euler load; hence, $p_1 = 1.05$. Second trials were made with $p_2 = 0.95$. In each case the correction formula of Eq. 13*b* was also applied to obtain a value which could be taken, if desired, for a subsequent trial. Linear interpolation or extrapolation was used to determine Δs, realizing, of course, that this is increasingly inaccurate as n decreases and that a second-order difference expansion should be used for better results. Starting with p_2 for n_5 and using extrapolation based on second differences to compute Δs gives a corrected value of p of 1.018 instead of 1.0472 as shown for linear extrapolation.

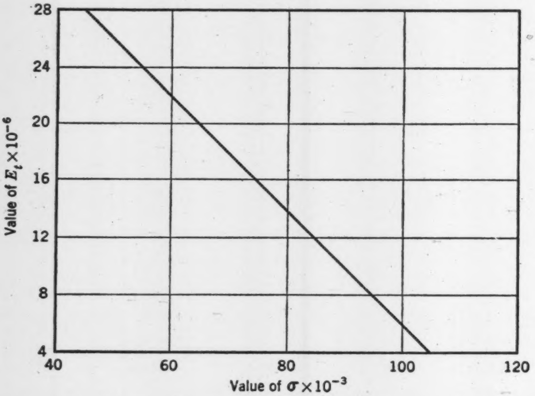

FIG. 2.—TANGENT MODULUS CURVE FOR EXAMPLE 2

An alternate procedure which consists merely of interpolating between p_1 and p_2 to find the value of p at which Y_n vanishes was also used. These interpolated values were taken as a third trial value, and the computations were repeated, leading to the results shown in the last part of Table 1.

Example 2. Column with Linearly Varying Thickness.—A 1-in.-wide, solid column having a thickness varying linearly from 1 in. to 0.5 in. and a length of

TABLE 2.—COMPUTATIONS FOR EXAMPLE 2

j (1)	$j\,n$ (2)	A (3)	I (4)	P/A (P/Col. 3) (5)	E_t (Fig. 2) (6)	$\frac{n^2 E_t I}{P L^2}$ (7)	Col. 7 + 1/6 (8)	$\sum_1^{j-1} Y_k$ (Col. 15 from previous row) (9)	$\sum_1^{j-1} k\,Y_k$ (Col. 16 from previous row) (10)	$j \sum_1^{j-1} Y_k$ (Col. 1 × Col. 9) (11)	Col. 2 + Col. 10 − Col. 11 (12)	Y_j $\left(\frac{\text{Col. 12}}{\text{Col. 8}}\right)$ (13)	$j\,Y_j$ (Col. 1 × Col. 13) (14)	$\sum_1^{j} Y_k$ (Col. 9 + Col. 13) (15)	$\sum_1^{j} k\,Y_k$ (Col. 10 + Col. 14) (16)
FIRST TRIAL (n = 10, P = 50,000 LB, AND $n^2/P L^2$ = 1/50,000)															
1	10	0.95	0.07145	52.6	25.0	35.70	35.87	0	0	0	10	0.279	0.279	0.279	0.279
2	20	0.90	0.06075	55.5	23.9	29.00	29.17	0.279	0.279	0.558	19.721	0.677	1.354	0.956	1.633
3	30	0.85	0.05118	58.8	22.5	23.10	23.27	0.956	1.633	2.868	28.765	1.235	3.705	2.191	5.338
4	40	0.80	0.04267	62.5	21.0	17.90	18.07	2.191	5.338	8.764	36.574	2.025	8.100	4.216	13.438
5	50	0.75	0.03516	66.7	19.3	13.58	13.75	4.216	13.438	21.080	42.358	3.080	15.400	7.296	28.838
6	60	0.70	0.02858	71.4	17.4	9.94	10.11	7.296	28.838	43.776	45.062	4.460	26.760	11.756	55.598
7	70	0.65	0.02289	76.9	15.2	6.96	7.13	11.756	55.598	82.292	43.306	6.074	42.518	17.830	98.116
8	80	0.60	0.01800	83.4	12.7	4.57	4.74	17.830	98.116	142.640	35.476	7.484	59.872	25.314	157.988
9	90	0.55	0.01386	90.9	9.6	2.66	2.83	25.314	157.988	227.826	20.162	7.124	64.116	32.438	222.104
10	100	0.50	0.01042	100.0	6.0	1.25	1.42	32.438	222.104	324.380	−2.276	−1.603			
SECOND TRIAL (n = 10, P = 49,000 LB, AND $n^2/P L^2$ = 1/49,000)															
1	10	0.95	0.07145	51.6	25.3	36.85	37.02	0	0	0	10	0.270	0.270	0.270	0.270
2	20	0.90	0.06075	54.4	24.2	30.04	30.21	0.270	0.270	0.540	19.730	0.653	1.306	0.923	1.576
3	30	0.85	0.05118	57.7	22.9	23.90	24.07	0.923	1.576	2.769	28.807	1.197	3.591	2.120	5.167
4	40	0.80	0.04267	61.3	21.5	18.75	18.92	2.120	5.167	8.480	36.687	1.939	7.756	4.059	12.923
5	50	0.75	0.03516	65.4	19.8	14.20	14.37	4.059	12.923	20.295	42.628	2.966	14.830	7.025	27.753
6	60	0.70	0.02858	70.0	18.0	10.49	10.66	7.025	27.753	42.150	45.603	4.278	25.668	11.303	53.421
7	70	0.65	0.02289	75.4	15.8	7.38	7.55	11.303	53.421	79.121	44.300	5.868	41.076	17.171	94.497
8	80	0.60	0.01800	81.7	13.3	4.89	5.06	17.171	94.497	137.368	37.129	7.338	58.704	24.509	153.201
9	90	0.55	0.01386	89.1	10.3	2.92	3.09	24.509	153.201	220.581	22.620	7.320	65.880	31.829	219.081
10	100	0.50	0.01042	98.0	6.8	1.45	1.62	31.829	219.081	318.290	0.791	0.488			

10 in. is considered. Values of the tangent modulus are taken from Fig. 2, in which σ denotes P/A. The computations are shown in Table 2 with $n = 10$.

A first trial was made using $P = 50{,}000$ lb and yielded $Y_n = -1.603$ as compared with a maximum value of Y equal to 7.48. This indicates that the trial value of P was too large. Using a rough curve of the values of Y_8, Y_9, and Y_n in lieu of an interpolation formula, the point of inflection was found to be approximately 0.1 of one segment above the bottom. Hence, Δs may be taken as -0.01, and by Eq. 13*b*, $\Delta P = 2(50{,}000)(-0.01) = -1{,}000$ lb. It is realized, however, that the apparent precision is misleading. Nevertheless, the indicated correction was applied and the process repeated with $P = 49{,}000$ lb.

It is seen that, for $P = 49{,}000$ lb, $Y_n = 0.488$. Interpolating between this result and the result for $P = 50{,}000$ lb gives a final critical load of 49,233 lb.

CONCLUSIONS

Numerous methods[6,7] exist for transforming Eq. 7*a* into a set of linear algebraic equations. In the foregoing, linear interpolation has been used with regard to each segment. This has led to a simple formula, Eq. 9*b*, for constructing a set of algebraic equations whose coefficients form a triangular matrix; hence, these equations are easily solved. It may be observed that if a greater number of stations are taken in order to improve accuracy—which may be justified particularly for irregular columns—the labor increases only proportionately and not as a higher power of the order of the matrix.

Rather than the linear interpolation which has been employed, it is clearly possible to use parabolic, cubic, or higher order interpolation formulas. This would require the simultaneous solution of the final equations by pairs in the case of the parabolic formula, by threes in the case of the cubic formula, and so on. An alternate procedure which retains the triangular nature of the system of equations and yet provides generally improved accuracy may be obtained by using single-step, forward-integration based on any desired degree of polynomial. Ultimately, one may construct an interpolating polynomial of the Lagrange type which covers all division points on the column. Such methods tend to lose the computational simplicity of Eq. 9*b*, and it is perhaps preferable to use the linear method with a larger number of stations if greater accuracy is desired.

The method which has been presented may be extended to the case of columns with one or more abrupt changes in section. Different arbitrary constants of integration will exist for each part, but relationships between them may be obtained from the continuity conditions at each step.

---

[6] "Application of Volterra Linear Integral Equations to the Numerical Solution of Beam Vibration Problems," by J. L. Bogdanoff, J. E. Goldberg, and Hsu Lo, *Proceedings* 1st Midwestern Conference on Solid Mechanics, Urbana, Ill., April, 1953, pp. 81–88.

[7] "Application of Volterra Linear Integral Equations to the Numerical Solution of Vibration Problems —II," by J. L. Bogdanoff, J. E. Goldberg, and Hsu Lo, *Journal of the Aeronautical Sciences*, Vol. 21, 1954, pp. 383–389.

AMERICAN SOCIETY OF CIVIL ENGINEERS
Founded November 5, 1852
TRANSACTIONS

Paper No. 2882

THE ACTION OF SOFT CLAY ALONG FRICTION PILES

BY H. BOLTON SEED[1] AND LYMON C. REESE,[2] ASSOCIATE MEMBERS, ASCE

WITH DISCUSSION BY MESSRS. LAWRENCE A. DUBOSE; YOSHICHIKA NISHIDA; JAMES D. PARSONS AND RALPH B. PECK; AND H. BOLTON SEED AND LYMON C. REESE

SYNOPSIS

Data are presented herein on the increase in supporting capacity of a pipe pile with the passage of time, the distribution of applied loads along the pile, and the pore-water pressures developed in the soil adjacent to the pile when driven into soft, saturated clay. Soil test data are interpreted to determine the effect of pile driving on the clay and the resistance of the clay to movement of the pile. A procedure is presented for using the results of vane shear tests to determine the relationship between load and settlement for a pile driven into clay.

INTRODUCTION

Many piles derive a major part of their supporting capacity from skin friction. Dynamic formulas have proved to be of limited value for determining the supporting capacity of such piles, whereas static formulas appear to hold the most promise for the development of rational design procedures. However, improvements in design methods are restricted by the limited available knowledge of the mechanics of the interaction between piles and soil. There is presented herein an investigation which attempts to further the understanding of the action of soil along the sides of friction piles.

Several 6-in.-diameter pipe piles from 20 ft to 22 ft long were driven approximately 15 ft into a stratum of soft, saturated clay. Electric strain gages were installed on one pile to measure the distribution of load and pressure along the pile. This pile was test-loaded soon after driving and a number of

---

NOTE.—Published, essentially as printed here, in December, 1955, as *Proceedings Paper 842*. Positions and titles given are those in effect when the paper or discussion was approved for publication in *Transactions*.

[1] Associate Prof. of Civ. Eng., Univ. of California, Berkeley, Calif.

[2] Asst. Prof. of Civ. Eng., Univ. of Texas, Austin, Tex.

times thereafter. Load-distribution curves were obtained for several loads, including the ultimate load, for each test loading. Total pressures and pore-water pressures, caused by the action of the soil against the pile wall, were measured at several points along the pile length during the pile driving and during the test period.

Several borings were made in the test area, and undisturbed soil samples were obtained. Soil tests were made to establish the relationships between strength and water content for (*a*) clay unaffected by pile driving, (*b*) clay next to a pile which had been in place 1 day, and (*c*) clay next to a pile which had been in place 30 days. The soil test results were interpreted to determine the effect of pile driving on the clay and the resistance of the clay to movement of the pile.

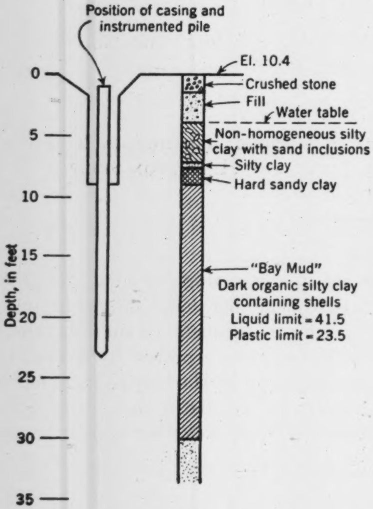
Position of casing and instrumented pile
El. 10.4
Crushed stone
Fill
Water table
Non-homogeneous silty clay with sand inclusions
Silty clay
Hard sandy clay
"Bay Mud"
Dark organic silty clay containing shells
Liquid limit = 41.5
Plastic limit = 23.5
Depth, in feet
0
5
10
15
20
25
30
35

Fig. 1.—Soil Profile

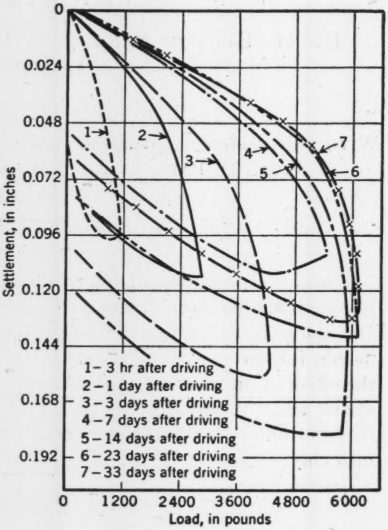

Fig. 2.—Load-Settlement Curves

In addition, a series of vane shear tests were made on the clay, and a procedure was developed for using the results of these tests to determine the load-settlement relationship for a pile driven into the clay. The load-settlement curve obtained in this way was compared with the results of load tests, and suggestions were made for the practical use of this procedure.

Location of Tests and Soil Conditions

The tests were conducted at a site adjacent to the San Francisco-Oakland Bay Bridge on the east side of San Francisco Bay in California. The soil conditions at this site (Fig. 1) consisted of 4 ft of fill, 5 ft of sandy clay, and a layer of organic silty clay containing shells (known locally as "bay mud"), which extended to at least 30 ft below the ground surface. The ground-water table was approximately 4 ft below the ground surface.

This site was chosen after extensive field tests had shown the soil conditions in the area to be relatively uniform.

DESCRIPTION OF PILES

The piles used in the investigation were made from 6-in.-diameter, spiral-welded steel pipe, No. 14 gage, and were fitted with conical driving points. One of the piles was cut lengthwise along a diameter so that the gages could be installed on the inside. The load-measuring system was made by cementing SR-4 gages directly to the pile wall; the pressure gages have been described elsewhere.[3]

In order to eliminate the effects of the upper 9 ft of nonhomogeneous soil on the supporting capacity of the pile, a 12-in.-diameter casing was installed to a depth of 9 ft, and the soil inside the casing was removed. The pile was then lowered to the surface of the clay at the bottom of the casing and driven into the clay using a 150-lb drop hammer; this arrangment of the casing is shown in Fig. 1. Several gages were damaged when the pile was driven, but a sufficient number of gages remained intact so that data on load distribution and pressures against the pile wall were successfully obtained.

After the pile was driven to position, large changes were found to be taking place in the pressures at the pile wall. These pressures were read as rapidly as possible, and at the same time the loading apparatus was being prepared for the first load test. It was assumed that pile loading would affect the pressure measurements, but it was hoped that this effect would be small if the pile settlement was kept to a minimum. Readings during the preliminary load test and during several subsequent load tests indicated that loading caused little, if any, permanent effect on the pressure-gage readings.

RESULTS OF LOAD TESTS

The first load test was begun 3 hr after driving was completed; the second load test was begun 21 hr after driving was completed; and subsequent tests were run on the same pile at times suggested by the results obtained. These times were approximately 3, 7, 14, 23, and 33 days after driving was completed.

The pile was loaded in increments of from 500 lb to 1,000 lb for the first few loads, and the increments were decreased as the ultimate supporting capacity of the pile was approached. All the load-measuring gages were read after the application of each load increment, except at loads near failure in several of the tests. The pressure gages were read usually after every second load increment was applied.

Pile settlement during loading was measured by two dial gages, each reading to 0.001 in. These dial gages were on opposite sides of the top of the pile, and their readings were averaged to obtain the settlement. Load-settlement curves were plotted as the test progressed, and loading was stopped when the settlement increased markedly with a small increase in load.

---

[3] "Pressure Distribution Along Friction Piles," by L. C. Reese and H. B. Seed, *Proceedings*, A.S.T.M., Vol. 55, 1955, pp. 1156–1182.

The load-settlement curves for the seven load tests are shown in Fig. 2. It was decided to consider the maximum load which the pile could support, without continuous deformation during a loading, as a measure of the bearing capacity of the pile at that time. Therefore, because it was desired to keep settlements to a minimum, care was required in the application of load increments as the ultimate load was approached. Most of the curves indicate that loading was stopped as soon as the ultimate load was reached.

For the first three loadings (Fig. 2) the settlement dials were read at zero load. In subsequent loadings, however, it was found more convenient to take the first settlement reading after a small seating load had been applied because of the difficulty in placing the settlement gages before the loading beam was positioned.

In practice, a load test is considered to be the best method of determining the supporting capacity of a friction pile, and the load-settlement curve is interpreted, in some way, to determine the safe load which can be carried by the pile. The load-settlement curves obtained from these tests and many others which have been obtained for friction piles have a characteristic shape: An initial part which is straight or slightly curved, a sharply curved transition part, and a final part which shows increasing settlement for no increase in load. The unloading curve is roughly parallel to the initial part of the loading curve. The safe load is usually taken as some proportion of the ultimate load, or as the load corresponding to some limiting value of the settlement.

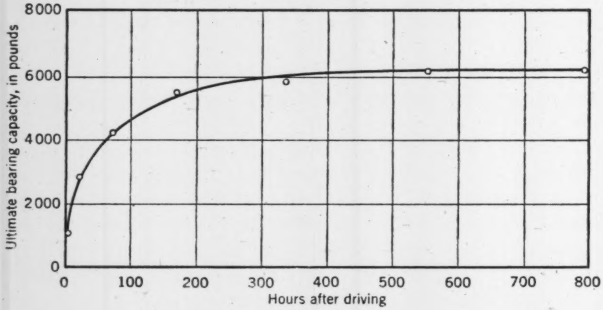

FIG. 3.—INCREASE IN ULTIMATE BEARING CAPACITY WITH TIME

The loading procedure used in this project differed from that recommended by most authorities in that the time between load increments was quite short. Therefore, it can be expected that the shape of the load-settlement curves will differ from those which are usually obtained for a friction pile. Using the recommended procedure there would have been a more gradual transition between the initial and final parts of the curve.

It was anticipated that there would be an increase in the supporting capacity of the pile with the passing of time, but the magnitude of the increase (Fig. 3) was surprising. The ultimate load for the final test was 5.4 times the initial ultimate load. The factor would have been greater had it been possible to determine the static bearing capacity of the pile immediately after driving, rather than 4 hr after driving. About 88% of the increase in the supporting capacity occurred in 8 days; the remaining 12% increase occurred during the next 25 days.

The change in strain-indicator readings for each load-measuring gage was multiplied by the appropriate calibration factor to obtain the load at each gage point. Measurements on opposite sides of the pile were averaged to obtain the load at each gage depth. A typical set of load-distribution curves, as measured during a test, is shown in Fig. 4(*a*). The dashed curve is an estimate of the load distribution which existed at the failure load. The load distribution could not be measured accurately at this stage because the pile was settling rapidly and there was not enough time to obtain the gage readings while maintaining the low values of pile settlement desired. Fig. 4(*b*) shows the load-distribution curves at the failure load for each of the load tests.

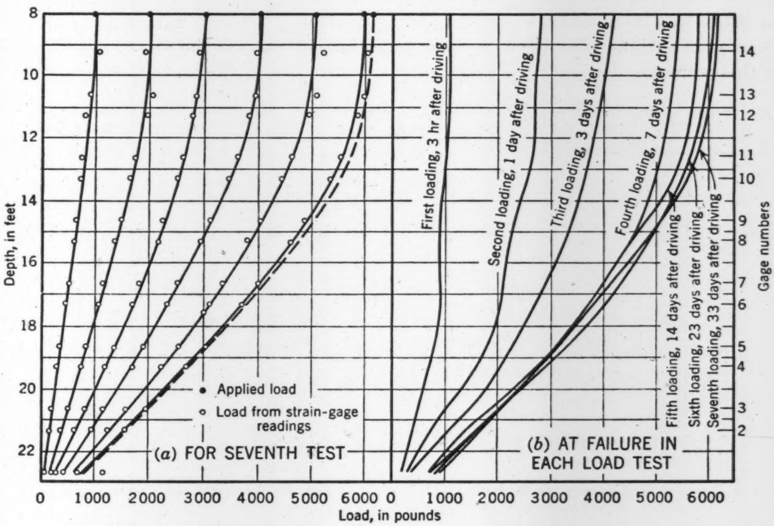

FIG. 4.—LOAD DISTRIBUTIONS ALONG PILE

The mechanics of the resistance of soil to the downward movement of a friction pile is illustrated in Fig. 5. If the pile were completely rigid, all points in the pile would move downward equally, and the soil deformation accompanying this downward movement would result in the development of shearing stresses in the soil. The shear stresses in the soil would cause the load in the pile to decrease with depth. However, because piles are not completely rigid, the observed settlement of the top of the pile exceeds the downward movement of the pile tip by a distance equal to the elastic compression of the pile, and, because the shear resistance of the soil around the pile—which depends on the magnitude of the shear deformation—causes the load in the pile to decrease with depth, the actual movements of points on the pile wall will increase with their distances from the pile tip.

It follows, therefore, that the distribution of load along a friction pile is associated with the relative stiffnesses of the pile and the surrounding soil. Because the soil will invariably deform more readily than the pile, it is difficult to imagine a practical case in which there would be no load transmitted to the pile tip. It will be seen (Fig. 4) that in these tests approximately 90% of the applied load was transferred to the soil by shaft resistance, and the remaining 10% was carried by the pile tip.

The load-distribution curves (Fig. 4) show that little load was removed by the top 3 ft of soil surrounding the pile. It is possible that this soil was displaced by the vibration of the pile during driving and that the overburden pressure was insufficient to cause bond to develop. Unfortunately not enough data were obtained from the pressure gages near the top of the pile to determine if this were so.

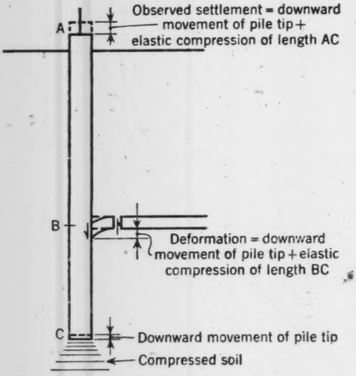
Observed settlement = downward movement of pile tip + elastic compression of length AC
A
B
Deformation = downward movement of pile tip + elastic compression of length BC
C
Downward movement of pile tip
Compressed soil

Fig. 5.—Soil Resistance to Downward Movement of a Friction Pile

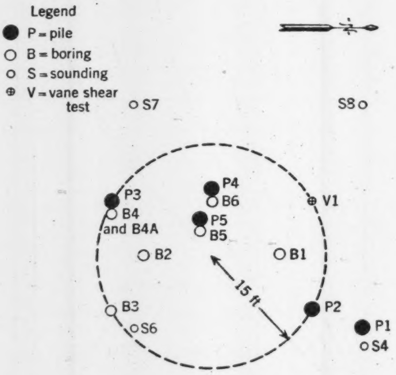
Legend
● P = pile
○ B = boring
○ S = sounding
⊕ V = vane shear test
S7
S8
P3
B4 and B4A
P4
B6
P5
B5
V1
B2
B1
15 ft
B3
S6
P2
P1
S4

Fig. 6.—Location of Field Tests

Knowing the distribution of an applied load along a friction pile and the corresponding downward movement of the top of the pile, the following information may be obtained:

1. The rate of load transfer from pile to soil or the shearing resistance of the soil around the pile. At any point along the pile this is equal to the slope of the load-distribution curve divided by the circumference of the pile.

2. The elastic compression of the pile from the top to any section along its length. This can be obtained by dividing the area under the load-distribution curve (to that section) by the area of the pile and the modulus of elasticity of the pile material. The elastic compression can then be subtracted from the observed pile settlement to obtain the movement of the pile at the section under consideration.

Thus, the shear resistance and the corresponding shear deformation of the soil around a pile at any point along the pile can be determined. The fact that such deformation can be obtained from load-distribution curves suggests the possibility that shear resistance-deformation curves obtained from soil shear tests might be used to determine load-distribution curves and load-settlement curves for friction piles; a procedure for determining such curves is presented subsequently.

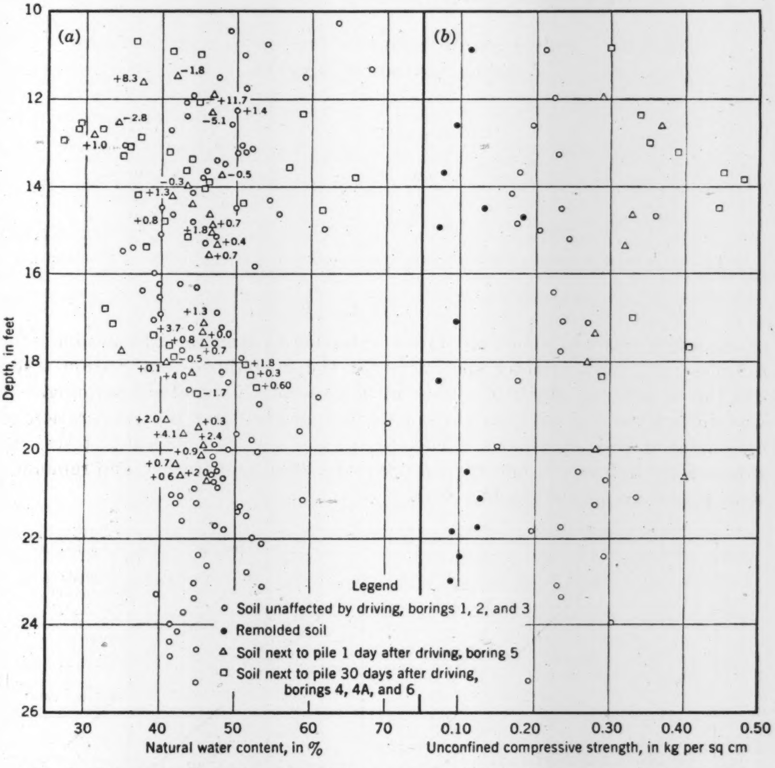

FIG. 7.—RESULTS OF SOIL TESTS (THE NUMBER TO THE SIDE OF SOME OF THE POINTS IS TO BE ADDED ALGEBRAICALLY TO OBTAIN WATER CONTENT OF PART OF SAMPLE FARTHEST FROM PILE)

RESULTS OF SOIL TESTS

Laboratory Tests.—The properties of the undisturbed soil were determined by a comprehensive series of tests on samples taken with a piston-type sampler in seamless steel tubes, 30 in. long and 2.87 in. in diameter. Three borings (Fig. 6) were made in the vicinity of the field work, and samples were taken as continuously as possible. Unconfined-compression tests were performed on 23 samples, and consolidation tests were performed on 5 samples. In addition, 13 unconfined-compression tests and 3 consolidation tests were performed on remolded samples of the soil.

The average of several determinations of the unit weight of the undisturbed silty clay was 112 lb per cu ft, and a liquid limit of 41.5 and a plastic limit of 23.5 were obtained as average values for the Atterberg limits. The results of the unconfined-compression tests on undisturbed and remolded samples are shown in Fig. 7. In these tests, most of the undisturbed samples failed suddenly upon reaching a strain of approximately 10% to 15%, and the sensitivity of the specimens was about 2. It was intended to trim the 2.87-in.-diameter samples to 1.4-in.-diameter specimens for the unconfined-compression tests, but the presence of shells in almost all the samples prevented trimming. It was difficult to find samples sufficiently free of shells for the preparation of consolidation-test specimens. The results of the consolidation tests are summarized in Table 1, and typical results for both undisturbed and remolded soil samples are plotted in Fig. 8(*a*).

TABLE 1.—SUMMARY OF RESULTS OF CONSOLIDATION TESTS ON UNDISTURBED SAMPLES

Test No.[a]	Compression index	Coefficient of permeability at a water content of 40%, in centimeters per second
2-184A	0.36	1.7×10^{-8}
2-184B	0.40	2.9×10^{-8}
3-253A	0.45	2.1×10^{-8}
3-253B	0.45	2.3×10^{-8}

[a] The first number represents the boring; the next three numbers represent the depth, in inches, to the sample.

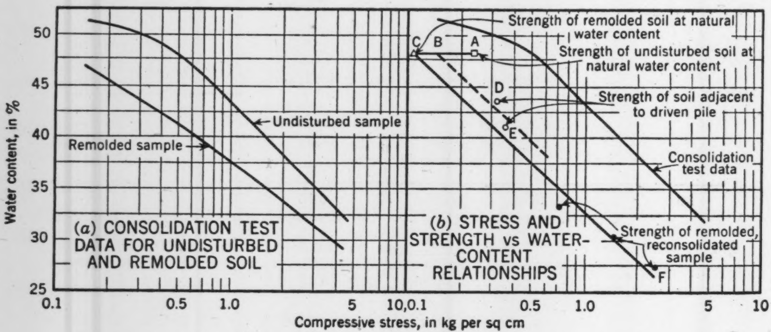

FIG. 8.—THE RELATIONSHIP BETWEEN WATER CONTENT AND COMPRESSIVE STRESS

In addition to these tests, three large samples of remolded soil were reconsolidated under pressures of 1 ton per sq ft, 2 tons per sq ft, and 4 tons per sq ft. Each of the reconsolidated samples provided four specimens, each 1.4 in. in diameter and 4 in. high, on which unconfined-compression tests and water-content determinations were made. The results of these tests are summarized in Table 2.

In order to determine the effects of pile driving on the soil adjacent to a driven pile, additional piles (numbers 3 and 4 in Fig. 6) were driven and samples were taken next to the piles. Boring 5 was made alongside a pile which had been in place for a period of 1 day; borings 4, 4A, and 6 were made alongside piles which had been in place for about 30 days. Unconfined-compression tests were performed on the samples obtained, and water-content determinations were made on specimens from the side of the samples nearest the pile wall and on specimens from the side of the samples farthest from the pile wall. The results of these tests are shown in Fig. 7, with the change in water content across the specimen designated in the figure.

TABLE 2.—SUMMARY OF RESULTS OF UNCONFINED-COMPRESSION TESTS ON RECONSOLIDATED SAMPLES

Test No.	CONSOLIDATION PRESSURE, IN TONS PER SQUARE FOOT					
	1		2		4	
	Unconfined-compression strength, in kilograms per square centimeter	Water content, in percentage	Unconfined-compression strength, in kilograms per square centimeter	Water content, in percentage	Unconfined-compression strength, in kilograms per square centimeter	Water content, in percentage
A	0.74	33.1	1.47	30.3	2.45	27.3
B	0.76	33.3	1.49	30.3	2.44	27.3
C	0.79	33.5	1.45	30.3	2.53	27.3
D	0.63	33.6	1.42	30.4	2.56	27.3
Average	0.73	33.4	1.46	30.3	2.49	27.3

The results of all the unconfined-compression tests are summarized in Table 3. Because at any particular time the unconfined-compression strength appeared to be approximately constant with depth, average values were used to determine the change in strength with time. It will be seen that the average unconfined-compression strength of the soil adjacent to a pile changed from an initial value of 0.24 kg per sq cm before driving to 0.32 kg per sq cm 1 day after driving, and finally to 0.36 kg per sq cm 30 days after driving. These increases in strength are accompanied by corresponding decreases in water content from an initial value of from 48.1% to 43.6% after 1 day and to 41.1% after 30 days.

TABLE 3.—AVERAGE VALUES OF UNCONFINED-COMPRESSION STRENGTH AND WATER CONTENT

Soil	Borings	Unconfined-compression strength, in kilograms per square centimeter	Water content, in percentage
Unaffected by driving	1, 2, 3	0.24	48.1
Next to pile, 1 day after driving	5	0.32	43.6
Next to pile, 30 days after driving	4, 4A, 6	0.36	41.1
Remolded soil	1, 2, 3	0.11	48.1

The percentage of shells, based on the dry weight of solids excluding shells in the unconfined-compression test specimens, ranged from 0% to 17%, the average being about 7%. Some of the shells were more than an inch wide. Approximately 14% of the moisture samples were entirely free of shells. Disturbance of the soil as a result of sampling was probably greater for those samples which contained shells than for those relatively free from shells. However, examination of the data failed to indicate a decrease in unconfined-compressive strength with an increase in shell content.

Field Tests.—In place shear tests were made on the silty clay prior to pile driving using a vane shear device. The vanes were each 1.5 in. wide and 4.5 in. high, and the rate of deformation was 10° per min. The results of these tests are shown in Fig. 9.

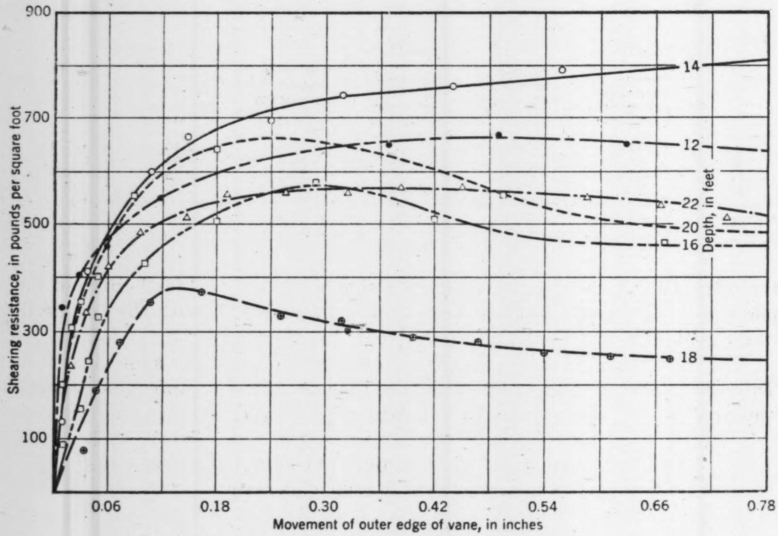

Fig. 9.—Results of Vane Shear Test

The shear strengths determined by the vane tests were considerably higher than those indicated by the unconfined-compression tests. This difference in strengths is probably caused by the presence of shells in the soil which appeared to have a marked effect on the vane shear strengths.

A 6-in.-diameter hand auger was used to advance a hole to within 2 ft of the depth at which the vane test was to be run. The vane device was then pushed or driven into position. In those instances where it could be pushed into position the shear strength was much lower than when the device had to be driven down. After the vane device had been withdrawn, the hand-auger cuttings showed that the difficulty in advancing the vane was due to the presence of shells in the soil. Two series of vane shear tests were made and the stress-deformation characteristics of the silty clay were determined at intervals of 2 ft of depth. The results shown in Fig. 8(*b*) are those exhibiting the lowest shear strength at any particular depth, and therefore are probably those least affected by the presence of shells.

EFFECT OF PILE DRIVING ON SOIL PROPERTIES

W. S. Housel and J. R. Burkey,[4] Members, ASCE, and A. E. Cummings, G. O. Kerkhoff, and R. B. Peck,[5] M. ASCE, have presented papers on the effect of pile driving on soil properties. Philip C. Rutledge,[6] M. ASCE, was able to show a reasonable quantitative interpretation of the data of Messrs. Cummings, Kerkhoff, and Peck based on the statement:

> "Previous work[7, 8] has shown that on a semilogarithmic plot of test data for saturated natural clay, the compressive strength-water content relation is a curve parallel to the virgin (or essentially straight-line) part of the consolidation test curve."

Such a plot is shown in Fig. 8(*b*). The consolidation-test data are those obtained from a test on an undisturbed sample, following the procedure suggested by Mr. Rutledge. Points A, C, D, and E were determined by soil tests as cited previously. Point A represents the average unconfined-compression strength of undisturbed samples, and point C shows the effect of remolding at no change in water content. Points D and E show results of unconfined-compression tests and water-content determinations on samples which had been taken next to piles installed 1 day and 1 month, respectively. Line C-F represents the compressive strength-water content relationship for reconsolidated remolded clay and was drawn from point C through an average of 3 points determined by experiment. It will be seen that line C-F is very nearly parallel to the virgin part of the consolidation-test curve.

The condition of the clay prior to pile driving is shown at point A. By drawing a dotted line parallel to line C-F, through an average of points D and E, point B was obtained. It would appear therefore that point B represents the condition of the clay next to a pile immediately after driving. The distance between points A and B shows the strength loss of the soil as a result of remolding caused by pile driving. Excess hydrostatic pressure was set up in the soil by the pile driving, and this pressure was related to consolidation of the soil next to the pile. The dotted line represents the change in soil properties because of consolidation, with points D and E showing the change occurring in 1 day and 1 month, respectively.

Other data which are pertinent are those showing the variation in water content across samples taken near a pile. Examination of the data in Fig. 7

---

[4] "Investigation to Determine the Driving Characteristics of Piles in Soft Clay," by W. S. Housel and J .R. Burkey, *Proceedings*, 2d International Conference on Soil Mechanics, Vol. 5, 1948, pp. 146–154.

[5] "Effect of Driving Piles into Soft Clay," by A. E. Cummings, G. O. Kerkhoff, and R. B. Peck, *Transactions*, ASCE, Vol. 115, 1950, p. 275.

[6] Discussion by Philip C. Rutledge of "Effect of Driving Piles into Soft Clay," by A. E. Cummings, G. O. Kerkhoff, and R. B. Peck, *ibid.*, p. 301.

[7] "Review of the Cooperative Triaxial Research Program," by Philip C. Rutledge, in "Triaxial Shear Research and Pressure Distribution Studies on Soils," Soil Mechanics Fact-Finding Survey, U. S. Waterways Experiment Station, Vicksburg, Miss., April, 1947, pp. 20-26 and pp. 79-100.

[8] "Strength of Natural Clays," by Philip C. Rutledge, paper presented at ASCE Meeting, Boston, Mass., October, 1948, *Civil Engineering*, November, 1948, p. 23 (abstract).

shows that for samples represented by point D the water content was an average of 1.31% higher for those parts of the samples farthest away from the pile; for samples represented by point E the water content was 1.33% higher for those parts of the samples farthest away from the pile.

From the information that has been presented, it can be argued that the water content of the soil next to the pile wall is progressively decreased with the passage of time after the pile has been placed, until some limit is reached, and that this decrease in water content is accompanied by an increase in the strength of the soil at the pile wall. The soil strength will be highest at the pile wall and it will decrease as the distance from the pile increases. Therefore, points D and E in Fig. 8(*b*) must represent an average value for soil properties near the pile because the samples were taken over a 3-in. distance. One could speculate on the value of the unconfined-compression strength at the pile wall on the basis of the differences in water content across the samples. However, when a friction pile is overloaded, failure usually occurs in the soil at some distance away from the pile wall; hence, some average value of the shearing strength of the clay near the pile wall will correctly define the effective strength. It is interesting to compare the rate of increase in soil strength with the passing of time as determined by soil testing with the rate of decrease in excess hydrostatic pressure with the passing of time as determined from pore-water pressure gages. Such a comparison is shown in Fig. 10, and there is excellent agreement between the rates.

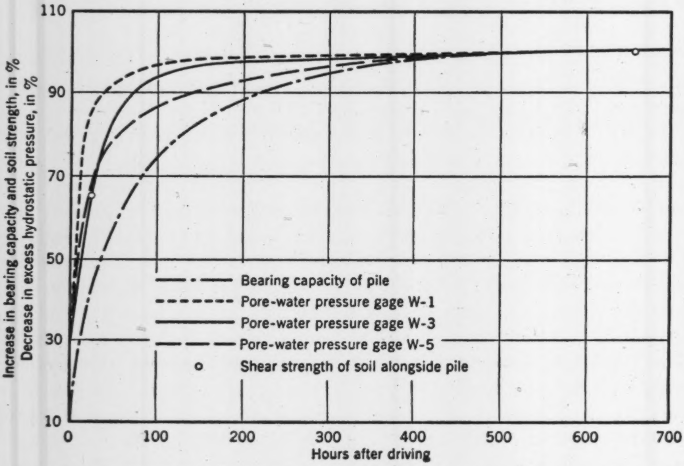

FIG. 10.—COMPARISON OF RATE OF CHANGE OF BEARING CAPACITY, SOIL STRENGTH, AND EXCESS HYDROSTATIC HEAD

RELATIONSHIP BETWEEN SOIL PROPERTIES AND LOAD-TEST DATA

From the results of a load test on a friction pile, a value for the average skin friction can be computed by dividing the maximum load which the pile can support by the embedded area of the pile. However, the variation in skin friction with depth can be seen by examining the distribution of the failure load along the pile. The slope of this load-distribution curve at any point is a measure of the rate of load transfer (skin friction) from the pile to the soil at that point. The rates of load transfer along the pile have been determined from the load-distribution curves for the failure load in each of the load tests, and the results are shown in Fig. 11. In general, the rate of load transfer at failure increases with increasing depth; it is about equal for depths of 20 ft and 22 ft, and it is very low for the shallow depths. The percentage increase in the rate of load transfer with the passing of time for all depths agrees, in a general way, with the percentage increase in bearing capacity of the pile.

In Fig. 11 the increase with the passing of time of the rate of load transfer from pile to soil (skin friction) at various depths in the soil, when the pile is supporting its maximum load, is compared with the increase in strength of the soil adjacent to the pile. The shear-strength values used in this comparison were those on the dotted line closest to points D and E in Fig. 8(*b*). For large values of time there is good agreement between the shear strength of the soil and the rate of load transfer, or skin friction, at the greatest depths; for small values of time the agreement is not so good, with the skin friction being appreciably less than the shear strength of the soil. The bearing capacity of the pile, computed on the assumption that the full shear strength of the soil is developed over the embedded area of the pile, would be greater than the measured value—with the largest error occurring at the smaller times. A similar lack of agreement between bearing capacity and strength data is shown in Fig. 10, in which it may be seen that in the early stages after driving

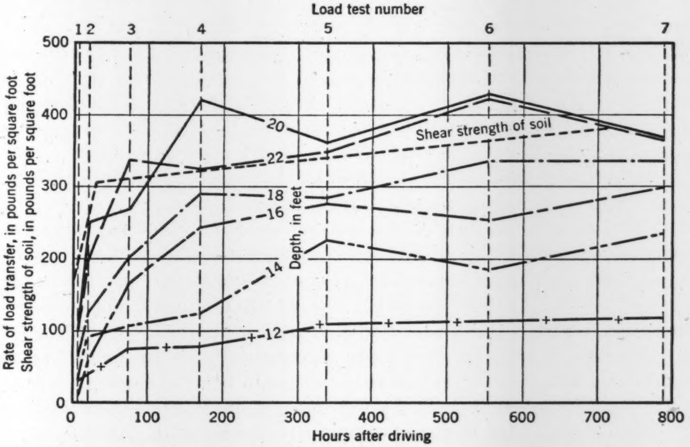

FIG. 11.—RATE OF LOAD TRANSFER FROM PILE TO SOIL COMPARED WITH INCREASE IN SHEAR STRENGTH OF SOIL NEXT TO PILE

the rate of increase in shear strength is considerably greater than the rate of increase in bearing capacity. In making these comparisons it is assumed that the shear strength of the soil is constant along the length of the pile because the test data in Fig. 7 show no definite trend in the relationship between shear strength and depth.

At the outset of this investigation it was assumed that the failure which occurs when a friction pile is overloaded occurs in the soil surrounding the pile and not at the interface between pile and soil. However, for the pile used in this investigation, the foregoing results indicate that this assumption should be modified as follows: For small values of time at all depths and for all values of time at shallow depths, the failure which occurred when the pile was overloaded did not occur in the soil but at the interface between the soil and the pile.

Arguments which favor this modified hypothesis are as follows:

1. The bearing capacity at time zero, as determined by extrapolating the bearing capacity-time curve (Fig. 3), was approximately 700 lb. The shear strength of the remolded clay, determined by taking one-half of the unconfined-compression strength of remolded samples, was 110 lb per sq ft; if this shear strength were effective over the entire embedded area, the bearing capacity of the pile at time zero would have been 2,360 lb. That the bearing capacity was less than one-third of the value indicated by the remolded shear strength probably indicates that failure occurred at the interface between the pile and the soil where a lower shearing resistance was developed.
2. The unconfined-compression tests showed no significant variation of the soil strength with depth, either before or after pile driving, but Fig. 11 shows significant changes in the rate of load transfer with depth. The changes in the rate of load transfer probably indicate that bond failed to develop at the interface between pile and soil at the shallow depths.
3. The data in Fig. 10 show good correlation between excess hydrostatic pressures and shear strength, but the increase in bearing capacity lags behind for small values of time. The lower rate of increase in bearing capacity probably indicates a lag in the development of bond at the interface.

It is recognized that the modified assumption is derived only from experiences with the piles used in this research; however, it seems probable that the modification will apply to other piles as well.

It is interesting to note that near the top of the pile the maximum skin friction was less than the shear strength of the undisturbed soil because failure occurred at the interface between pile and soil. Near the bottom of the pile, however, the maximum skin friction was greater than the shear strength of the undisturbed soil as a result of the increase in strength of the soil caused by disturbance and reconsolidation. It might be expected, therefore, that the average skin friction at failure, after sufficient time had elapsed to allow the soil around the pile to reconsolidate fully, would have a value approximately equal to the shear strength of the undisturbed soil. That this is in fact the case may readily be seen if the supporting capacity of the pile is computed on the assumption that the skin friction over the embedded area of the pile is equal to the shear strength of the undisturbed soil. The total skin friction based on this assumption is 5,400 lb. This value, together with a resistance of 200 lb at the pile tip, gives a total supporting capacity of 5,600 lb. This compares favorably with the maximum supporting capacity of 6,100 lb measured in the seventh load test. It appears that this method of computing the ultimate supporting capacity of the test pile gives good results because the length of the pile was such that the error caused by overestimating the skin friction at the upper end of the pile is approximately neutralized by the error caused by underestimating the skin friction at the lower end of the pile.

Load Distribution and Settlement for a Friction Pile from Shear Tests of Soil

In examining the load-distribution curves, the possibility of using data from shear tests of the soil to obtain load-distribution curves and load-settlement curves for a pile was cited. The accuracy of the results obtained will depend, of course, on the validity of the soil test data; if, however, reliable data on the shear characteristics of the soil adjacent to the pile can be determined, the behavior of the pile under load can be predicted by the method of analysis presented subsequently.

If a friction pile is driven through clay, the clay is remolded. Consequently, regardless of the properties of the undisturbed soil, the clay in the vicinity of the pile has nonbrittle stress-deformation characteristics. A loaded pile produces deformation in the surrounding soil, and the deformation varies from a maximum at the ground surface to a minimum at the pile tip. In usual cases, the pile is quite stiff in comparison to the soil so that at the ultimate pile load even the bottommost soil elements will develop their maximum shear resistance. Although the topmost soil elements will be deformed more because of the elastic compression in the pile, the additional deformation will not cause this shear resistance to be reduced below the maximum values. Thus, the load distribution at the ultimate pile load can be determined from a knowledge of the shear strength of the soil around the pile. It is possible that there will be failure at the interface between the pile and the soil; if so, some fraction of the shear strength of the soil might be used to account for the loss in strength resulting from the interface failure.

For a number of reasons it is useful to know the load distribution along a friction pile which is supporting a load less than the ultimate load. In this case, three problems exist: (1) Computing the resistance of the pile point; (2) relating the stress-deformation curves for the soil to pile movement; and (3) making the mathematical solution. At the present time (1956) the first two problems can be resolved approximately whereas the mathematical solution can be made by a method of successive approximations.

The point resistance of a pile in clay for a given downward movement of the pile point may be of minor importance if the pile support is supplied principally by shaft resistance; however, for a complete solution, the point resistance must be considered. Ultimately it is hoped that a method for determining point resistance, based on the stress-strain characteristics of the soil determined from triaxial compression tests, can be developed. However, as a temporary expedient, where the point resistance is very low, the resistance may be computed (as in the subsequent example) by considering the point to be replaced by an equivalent length of shaft. The shaft area to be added might be obtained by theoretical considerations or, as in the example, from the results of tests.

A more difficult problem is to relate the stress-deformation curves of the soil to the movement of the pile. If a point on the pile is assumed to move downward a certain distance, this downward movement must be related to the shear deformation in the soil at that point in order to determine a corresponding shear stress which will develop a resisting force along the pile. The methods of elasticity are of limited assistance in this problem because the soil is nonelastic. The stress-deformation curves used in this analysis should be those of the reconsolidated soil adjacent to the pile. However, such data cannot be determined readily, and therefore, as a trial, it is suggested that the stress-strain curves obtained from vane shear tests on the undisturbed soil be used. The vane imposes deformations similar to those imposed by a downward moving pile, and the radial movement of a point on the vane extremity is assumed to develop the same shear resistance as will an equal downward movement of a point on the pile. An attempt can be made to correct for the fact that failure may occur at the interface between the pile and the soil rather than in the soil by using only a certain part of the soil strength corresponding to a particular deformation.

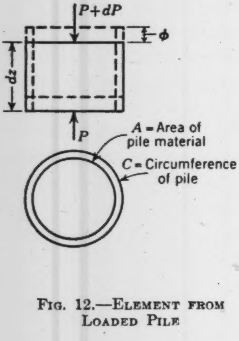

Fig. 12.—Element from Loaded Pile

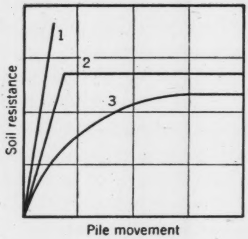

Fig. 13.—Pile Movement Versus Soil Resistance Curves

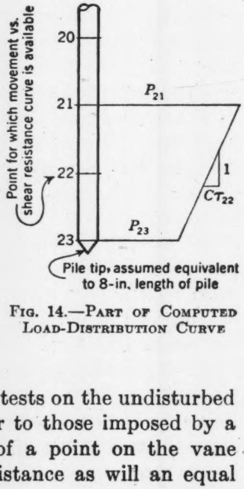
20
21
22
23
P_{21}
1
$C\tau_{22}$
P_{23}
Point for which movement vs. shear resistance curve is available
Pile tip, assumed equivalent to 8-in. length of pile

Fig. 14.—Part of Computed Load-Distribution Curve

The differential equation which defines the load distribution along the pile length can be approximated by considering an element cut perpendicular to the pile axis (Fig. 12). The movement of the pile wall at depth z differs from that at depth $z + dz$ by the elastic compression of the length, dz, of the pile. The unit strain of the pile at depth z is therefore

$$\frac{d\phi}{dz} = \frac{P}{E\,A} \qquad (1a)$$

in which E is the modulus of elasticity of the pile material; ϕ represents the movement of the pile at depth z; and P is the load on the pile at depth z. Then,

$$P = E\,A\,\frac{d\phi}{dz} \qquad (1b)$$

and

$$\frac{dP}{dz} = E\,A\,\frac{d^2\phi}{dz^2} \qquad (2)$$

If β is a function which defines the properties of the soil so that $\beta\phi$ is the shear resistance of the soil corresponding to a strain, ϕ,

$$dP = \beta\phi\,C\,dz \qquad (3)$$

and

$$\frac{dP}{dz} = \beta\phi\,C \qquad (4)$$

From Eqs. 2 and 4,

$$E\,A\,\frac{d^2\phi}{dz^2} = \beta\phi\,C \qquad (5)$$

and

$$\frac{d^2\phi}{dz^2} - \alpha\,\beta\phi = 0 \qquad (6)$$

in which

$$\alpha = \frac{C}{E\,A} \qquad (7)$$

This analysis ignores any deformation of a soil element next to the pile wall as a result of the nonuniform distribution of vertical load in the soil above this element and to this extent is approximate. The term, β, is a constant only if there is a linear relationship between soil resistance and pile movement, as expressed by a line such as line 1 in Fig. 13, for the full length of the pile. In that case and if α is also constant, a theoretical solution can be obtained readily for the differential equation. A theoretical solution can probably be obtained conveniently if the soil resistance and pile movement are related by a curve such as No. 2 in Fig. 13 for the full length of the pile. However, the usual case is that the soil resistance and the pile movement are related by a curve similar to No. 3 in Fig. 13 and that this relationship will vary with depth. In this case, a numerical procedure seems most suitable for the solution of Eq. 6. The procedure is analogous to the test loading of a pile, resulting in a series of load-distribution curves and in a load-settlement curve.

Computations Using Theory.—In order to illustrate the proposed method of analysis, computations have been made to determine the load-distribution curves and load-settlement relationship for the pile tested in the field. The stress-deformation relationships for the undisturbed soil as determined by vane shear tests (Fig. 9) were used in the analysis.

In order to correct for the fact that failure was found to occur at the interface between the pile and the soil rather than in the soil, only a certain proportion of the soil strength, corresponding to a particular deformation, was used. The proportions for the various depths were obtained from an examination of Fig. 11. A comparison of the shear strength of the soil with the rate of load transfer at the various depths enabled the following proportions to be obtained: 22 ft, 1.0; 20 ft, 1.0; 18 ft, 0.9; 16 ft, 0.7; 14 ft, 0.6; 12 ft, 0.3; and 10 ft, 0. It is recognized that such factors to be applied at various depths would not normally be known. However, experience with other piles and soils may ultimately be used to select appropriate factors.

A particular load-distribution curve is computed by assuming first a small downward movement of the pile tip. The stress-deformation curve for the soil at that depth is consulted (Fig. 9), and the rate of load transfer which is developed is obtained. The load on the pile tip is obtained by multiplying this rate of load transfer by the shaft area which is assumed to replace the pile tip. In this case it was found that the resistance of the pile tip could be approximated by the shaft resistance on an additional 8 in. of pile length.

TABLE 4.—COMPUTATION OF THE LOAD DISTRIBUTION ALONG A FRICTION PILE FOR AN ASSUMED POINT MOVEMENT OF 0.0012 IN.

Section depth, in feet	Assumed midpoint movement, in inches	Load transfer developed, in pounds per square feet	Surface area, in square feet	Load increment, in pounds	Total load, in pounds	Average load, in pounds	Compression of section, in inches	Total movement, in inches	Midpoint movement, in inches
Tip	0.1200	510	1.05	535	...	...	...	0.1200	...
23–21	0.1210	510	3.14	1,590	2,125	1,330	0.0008	0.1208	0.1204
	0.1204	510	3.14	1,590	2,125	1,330	0.0008	0.1208	0.1204
21–19	0.1217	600	3.14	1,880	4,005	3,065	0.0018	0.1226	0.1217
19–17	0.1239	340	3.14	1,070	5,075	4,540	0.0026	0.1252	0.1239
17–15	0.1268	328	3.14	1,030	6,105	5,590	0.0032	0.1284	0.1268
15–13	0.1303	380	3.14	1,190	7,295	6,700	0.0038	0.1322	0.1303
13–11	0.1343	170	3.14	535	7,830	7,565	0.0043	0.1365	0.1343
11–1	...	...	...	...	7,830	...	0.0224	0.1589	...

Next, a somewhat greater downward movement is assumed for a point on the pile a short distance higher and for which a corresponding stress-deformation curve for the soil is available. The rate of load transfer for the assumed movement is obtained, and the increase of load in the pile is computed. Then, using the area and modulus of elasticity of the pile material, the movement corresponding to this increase in load can be computed. If the computed movement does not agree with the assumed movement, a new computation is made, and the process is continued until agreement between movements is obtained. In this manner, a load-distribution curve can be computed for the entire pile length, corresponding to any assumed movement of the pile tip.

For the computation shown in Table 4, the downward movement of the pile tip at a depth of 23 ft was assumed to be 0.12 in. The stress-deformation curve for the soil at a depth of 22 ft was consulted, and a rate of load transfer of 510 lb per sq ft was obtained. The area of shaft for 8 in. of pile length was 1.05 sq ft; therefore, the load on the pile point was computed to be 535 lb.

The movement, ϕ, of the pile for a depth of 22 ft was assumed to be 0.1210 in. Then the rate of load transfer of 510 lb per sq ft was obtained from the appropriate stress-deformation curve (Fig. 9).

The load in the pile at a depth of 21 ft was computed as follows (Fig. 14):

$$P_{21} = P_{23} + \tau_{22}\, C\, L_{23-21} \ldots\ldots\ldots\ldots\ldots\ldots (8)$$

in which P_{21} is the load in the pile at a depth of 21 ft; P_{23} represents the load in the pile at a depth of 23 ft; τ_{22} is the rate of load transfer per unit area at a depth of 22 ft; C denotes the circumference of the pile; and L_{23-21} is the length of the pile from 23 ft to 21 ft. Thus,

$$P_{21} = 535 + (510)\,(1.57)\,(2) = 2{,}125 \text{ lb.}$$

To check the assumed movement of the pile, $\phi = 0.1210$ in., at a depth of 22 ft, the movement of the pile at a depth of 21 ft was computed from

$$\phi_{21} = \phi_{23} + \left(\frac{P_{23} + P_{21}}{2}\right)\left(\frac{L_{23-21}}{A\,E}\right) \ldots\ldots\ldots\ldots\ldots (9)$$

in which ϕ_{21} is the movement of the pile at a depth of 21 ft; A represents the cross-sectional area of the pile material (1.4 in.^{2}); and E is the modulus of elasticity of the pile material (30×10^6 lb per sq in.). Thus,

$$\phi_{21} = 0.1200 + \frac{535 + 2{,}125}{2} \times \frac{24}{(1.4)(30 \times 10^6)} = 0.1200 + 0.0008 = 0.1208.$$

The movement of the pile at a depth of 22 ft was assumed to be the average of the movements at 23 ft and 21 ft—that is, 0.1204 in. It is obvious that a more accurate computation could be made by using the area under the load-distribution curve from 23 ft to 22 ft, but the extra work involved does not appear to be justified. Thus, the computed movement, at a depth of 22 ft, of 0.1204 in. is not in agreement with the assumed movement of 0.1210 in. A new assumption was made and the computation was repeated (Table 4) until agreement was obtained between assumed and computed movements. Table 4 shows the entire computation for the full length of the pile.

By assuming various movements of the pile point, a series of load-distribution curves can be obtained. The series obtained for this pile is shown in Fig. 15. For each assumed point movement, corresponding values for movement and load at the top of the pile were determined. Reference to Table 4 shows that for the assumed point movement of 0.120 in., the movement of the top of the pile was 0.159 in. and the load at the top of the pile was 7,830 lb.

Movements and loads for the top of the pile were plotted to obtain a load-settlement curve (Fig. 16).

COMPARISON OF THEORETICAL AND TEST RESULTS

In Fig. 15, the load-distribution curves computed as described in the foregoing are compared with the actual load-distribution curve for the maximum load the pile was able to support (the ultimate load in the seventh load test). In Fig. 16, the computed load-settlement curve is compared with the load-settlement curve for the seventh load test; the results do not compare

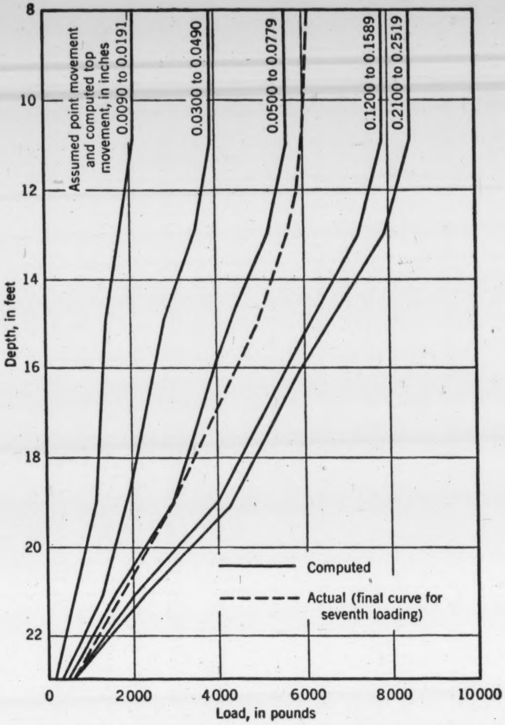

FIG. 15.—COMPARISON OF COMPUTED AND ACTUAL LOAD-DISTRIBUTION CURVES

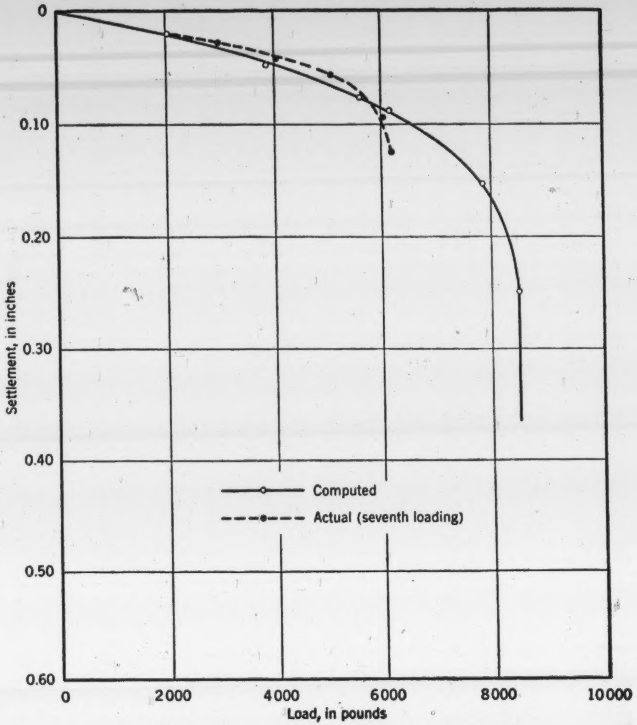

FIG. 16.—COMPARISON OF COMPUTED AND ACTUAL LOAD VERSUS SETTLEMENT CURVES

very favorably. However, the lack of agreement in this case is believed to be caused by errors associated with the use of the vane shear device for determining the properties of the particular soil used in this investigation. The presence of shells in the soil, cutting across the failure plane, undoubtedly, caused an increase in the resistance to movement of the vane with the result that the resistances computed from the dimensions of the vane were too high. This is evidenced by the fact that the shear strengths determined from the vane tests were higher than the maximum values of the rate of load transfer measured on the test pile. In a more uniform soil, for which a vane test would give more reliable results, the method of analysis would probably yield better agreement between computed and actual pile performance.

Even with a soil such as the one used for this investigation, however, the proposed method may have useful practical applications. If vane shear tests are performed at a site where a friction pile is being test-loaded, a pair of curves such as those shown in Fig. 16 could be obtained. From a practical standpoint, modifications could then be made in the vane-shear-test data so that the load-settlement curves would agree. The modified data from the vane shear test could then be used to determine load-distribution curves for other conditions of pile length and pile diameter.

The fact that the analysis does not take into account the deformation of the soil next to the pile wall caused by the nonuniform distribution of vertical load in the overlying soil would be expected to lead to computed settlements which are somewhat less than the actual settlements of the pile for any particular applied load. Further investigation may reveal a simple method of taking this factor into account. Furthermore, by using the data obtained by vane shear tests on the undisturbed soil, the effect of pile driving on soil properties is ignored. It is possible that research will reveal a more suitable way of determining the soil properties to be used in the analysis.

Characteristics of the Soil Adjacent to Driven Piles

In order to make a more accurate analysis of pile performance from soil tests, it would be necessary to determine the characteristics of the soil adjacent to a driven pile. For this purpose it would be necessary to determine the properties of the partly remolded soil corresponding to points B and E in Fig. 8(*b*) from the results of tests on soil samples obtained prior to pile driving. The properties of the undisturbed and completely remolded soil, corresponding to points A and C in Fig. 8(*b*), could be established as previously described, and the slope of a line corresponding to B-E could be correctly obtained, but the positions of B and E would be indeterminate.

How much disturbance will occur as a result of the pile driving? In this investigation the tests show that in going from point A to point B the soil lost 67% of the strength it would have lost in being completely remolded. This does not mean that some other clay would lose the same proportion of its strength as a result of pile driving, even if the same type of pile were used.

The conservative assumption could be made that full remolding would occur, but it would still be necessary to determine the increase in strength of the soil caused by reconsolidation. In these experiments the final strength of the soil next to the pile was approximately 60% more than the strength of the undisturbed soil, but there is no evidence to indicate that a different clay would show a similar increase in strength. Fully remolded soil attained a strength 60% higher than the strength of the undisturbed soil when reconsolidated in the laboratory under a pressure of approximately 1 ton per sq ft (about one-half the total pressure which developed during driving), but this relationship may not be true for other piles.

Therefore, at this time a complete procedure for predicting the performance of friction piles from soil properties cannot be formulated, and approximations must be made. It is believed, however, that the tests and analyses presented in the foregoing do indicate a procedure for obtaining a reasonably accurate determination of pile performance and that greater accuracy can be attained when basic work is performed to determine the mechanics of the consolidation process around a pile driven into clay so that peak pressures which are predicted can be translated into ultimate equilibrium pressures with accompanying consolidation and increase in shear strength of the clay.

SUMMARY

In the insensitive clay used in this investigation, the pile showed a marked increase in supporting capacity with the passage of time; the ultimate load for the final load test, about 30 days after driving, was 5.4 times as great as the ultimate load, measured several hours after driving. The increase in supporting capacity was attributed to an increase in the shear strength of the soil surrounding the pile.

The load-distribution curves for the pile showed that most of the load was removed from the pile by shaft resistance, with only approximately 10% of any particular load reaching the pile tip. The increase in supporting capacity was reflected by an increase in the rate of load transfer, as determined by the slope of the load-distribution curves; the increased rate of load transfer was exhibited by soil strata at all depths. The load-distribution curves for all loadings showed a general increase in rate of load transfer with depth, with no load being removed by the soil near the ground surface and a maximum rate of approximately 400 lb per sq ft being removed by soil at depths of 20 ft to 22 ft.

Relationships between strength and water content were established for undisturbed soil and for fully remolded soil. Tests of soil samples taken next to the pile wall showed that the strength loss caused by the disturbance when the pile was driven was approximately 60% to 70% of that which the soil would have lost as a result of complete remolding. The clay next to the pile wall subsequently gained strength, and at the end of the test period it had a strength 60% higher than the strength of the undisturbed soil. This increase in soil strength appeared to parallel the decrease in excess hydrostatic pressure, and the data indicated that these phenomena are directly related.

The supporting capacity of the pile was not so great as would have been obtained if a shear resistance equal to the strength of the reconsolidated soil had been developed over the embedded area of the pile. This fact and related data led to the conclusion that the failure of the overloaded pile occurred at the interface between the pile and the soil for shallow depths rather than in the soil.

A method was demonstrated for solving numerically the differential equation governing the distribution of load from a friction pile to the soil. From this procedure, the load-settlement relationship for a friction pile can be determined if the properties of the soil surrounding the pile are known. The method was applied to determine the performance of a test pile, using the stress-deformation characteristics of the undisturbed soil as determined by vane shear tests in the analysis. Results from the procedure were compared with experimental results, and fair agreement was obtained. It was suggested that better agreement would be obtained in a more homogeneous soil and if improved methods for determining soil properties could be developed. A procedure was also suggested for making the method useful in practice.

CONCLUSIONS

The following conclusions apply specifically to the investigation described herein—that is, to the study of a small-sized, displacement-type friction pile which was driven into a nonsensitive clay. The driving and testing procedures were, however, in many ways identical with engineering practice, and it is believed that most of the conclusions will apply to other displacement-type friction piles having similar surface characteristics.

1. Even in an insensitive clay, the increase in supporting capacity, with time, of a displacement-type friction pile may be large, and the final supporting capacity may be as much as five times the initial supporting capacity.
2. The loss of strength of the soil around the pile was the result of a disturbance caused by pile driving. As a result of this disturbance, the soil lost approximately 70% of the strength it would have lost because of complete remolding. The shear strength of the disturbed and reconsolidated soil was 60% higher than the undisturbed shear strength.
3. For small values of time for all depths, and for all values of time for shallow depths, the failure of the friction pile when overloaded did not occur in the soil but at the interface between the pile and the soil.
4. The supporting capacity determined for a single friction pile by multiplying the area of the embedded pile by the soil shear strength (obtained from unconfined-compression tests of undisturbed samples) must be considered an approximation although it is nearly equal to the true supporting capacity in some instances.
5. Load-settlement curves and load-distribution curves for a friction pile can be determined using a numerical procedure if the relationship between shear resistance and deformation for the soil surrounding the pile can be determined.
6. The proposed method for determining the performance of a friction pile from soil tests is useful even in heterogeneous soil, using the shear resistance-deformation characteristics of the undisturbed soil as determined by vane shear tests. Better results could be obtained if shear resistance-deformation curves for reconsolidated soil adjacent to a driven pile could be determined.

ACKNOWLEDGMENTS

The research reported on herein was performed in the Engineering Materials Laboratory of the University of California (Berkeley) and in the East Bay Yard of the San Francisco-Oakland Bay Bridge Railway. The permission of the chief engineer, San Francisco-Oakland Bay Bridge, California Division of Highways, to use the field test site is gratefully acknowledged. The writers also wish to thank the following members of the faculty and the research staff of the Division of Civil Engineering and the Institute of Transportation and Traffic Engineering, University of California, who gave valuable advice and assistance in developing the instrumentation and accomplishing other phases of the work: B. Bresler, A. M. ASCE, D. Pirtz, A. M. ASCE, R. Clough, A. M. ASCE, B. A. Vallerga, A. M. ASCE, C. L. Monismith, J. M. ASCE, F. N. Finn, A. M. ASCE, R. Brock, L. Trescony, E. L. Whittier, R. Lawrence, and G. Dierking.

DISCUSSION

Lawrence A. Dubose,[9] A.M. ASCE.—The interesting paper by Messrs. Seed and Reese can be used to illustrate an important deficiency in the field of soil mechanics and foundation engineering. This deficiency is the lack of rational and standard pile load-test procedures which associate the tolerable pile deformation during the load-testing program with stress and strain properties of the foundation medium. The influence of time should also be considered in designing the load-test procedures.

Despite the fact that the authors recognized that their load-test procedure differed (under the heading, "Results of Load Tests") "* * * from that recommended by most authorities in that the time between load increments was quite short," the influence of the short time interval on load-settlement relationships was not evaluated. Because an attempt was made by Messrs. Seed and Reese to correlate load-test results with computed values based on values of soil strength, the correctness of the load-test procedure used becomes of utmost importance.

The necessity of using a quick or short-term load-test procedure is recognized in evaluating the pile capacity 4 hr after the pile had been driven. However, the fact that pile driving remolds soft clay deposits and causes an initial low supporting capacity for the pile has been observed and reported numerous times.[10] Therefore, the load capacity of the pile immediately after driving appears to be primarily of academic interest. Of more practical value is the load-carrying capacity of the pile at some elapsed time interval related to actual construction loadings. Load tests conducted for this condition would permit the time factor to be considered. Although it is recognized that the method of placing the pile is important, it is felt that the time factor deserves consideration in performing load tests, whether the pile has been driven or drilled and cast in place.

The writer would like to present the results of load tests conducted on drilled and cast-in-place concrete piles for which the time factor was considered. Fig. 17(*a*) shows load-settlement curves for a long-term test and a short-term test conducted on a drilled and cast-in-place concrete pile. The pile diameter was 14 in., the effective length was 19 ft, and the total depth of the pile was 21 ft. The long-term test was continuous for a 194-hr period with four dial gages being read to the nearest 0.001 in. at 15-min intervals. (The first four tests reported by the authors were conducted within 168 hr after the pile had been driven. The actual testing time was probably only a small fraction of this time period.) For the long-term tests, the pile load was not increased until the settlement within a 4-hr period had not exceeded 0.010 in.; this was intended to represent a static equilibrium condition. The short-term test was conducted by increasing the pile load in 10-kip increments at 5-min intervals; the total time for this test was 50 min. One may note an increasing divergence of the two curves which begins at about 50 kips. Under a total load of 100 kips the pile had settled about 0.16 in. during the long-term test and only about 0.03 in. for the short-term test. Similar relationships were established for other piles subjected to both long-term tests and short-term tests. Tests were also conducted for which the pile loads were increased at intervals of 5 min, 15 min, and 30 min. There was little difference in load-settlement relationships for load tests conducted using these three time increments for increasing the pile load. However, the settlement occurring during the short-term load tests, as in the case of the data shown in Fig. 17(*a*), was much less than the settlement which occurred during the long-term load test.

---

[9] Associate Prof., Civ. Eng. Dept., Univ. of Alabama, University, Ala.

[10] "Soil Mechanics in Engineering Practice," by Karl Terzaghi and Ralph B. Peck, John Wiley & Sons, New York, N. Y., 1948, p. 461.

The soil at the test site for these piles is a stiff, desiccated clay with unconfined-compression strengths increasing from about 0.7 ton per sq ft at a depth of 2 ft to more than 2 tons per sq ft at a depth of 21 ft. Liquid-limit values ranged from 35% to 80%, and plastic-limit values were between 18% and 30%. The "in situ" water content was approximately equal to the plastic limit. The soils at the driven pile site (reported by the authors) had lower strengths and higher water contents and should have been much more compressible than the clay at College Station, Tex. It appears that time would have been of even greater importance in the load tests for the driven piles at the San Francisco Bay site.

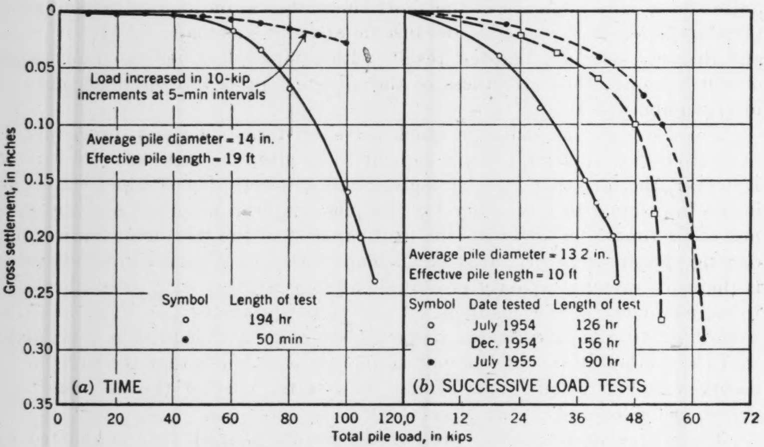

FIG. 17.—THE INFLUENCE OF TWO FACTORS ON THE RELATIONSHIP BETWEEN LOAD AND SETTLEMENT

Another important factor noted in conducting the tests on concrete piles was the increase in load capacity with successive tests. This is illustrated by the load-settlement curves in Fig. 17(*b*). Whereas the retests were conducted at intervals of approximately 6 months and 12 months after the initial test, the same general relationship was observed for retests conducted at shorter elapsed time periods. For the data shown in Fig. 17(*b*), the pile-load capacity increased from about 45 kips for the July, 1954, test to about 54 kips for the

December, 1954, test and to more than 60 kips for the July, 1955, test. The increase in pile capacity was associated with the retesting of the pile and not to an increase in soil strength resulting from changes in the in situ water content.

The writer feels that both of the foregoing factors must be evaluated before the validity of a load-test procedure can be established. Long-term load tests are time consuming and expensive, and many engineers would like to have a quick or short-term procedure for test-loading piles. However, the correctness of data should not be sacrificed for this reason. The engineer realizes that consolidation of a soft clay deposit under a loaded area will continue for weeks or even years. Therefore, it is not logical to assume that the correct relationship between load and settlement can be established by loading a pile for a few hours without first comparing long-term load-test data and short-term load-test data.

YOSHICHIKA NISHIDA.[11]—The authors have made many facts clear (quantitatively) concerning the remolding effect and time effect of pile driving on soil properties. They performed the load test and showed the load distribution along a pile. Although several engineers have performed similar tests, these last data seem to be more useful for the study of piles. Messrs. Seed and Reese also explained how to compute the supporting capacity and the load distribution of a pile from the measured data.

It is felt from the practical point of view in the field that the deformation in the surrounding soil produced by a loaded pile is zero and is not maximum at the ground surface because there is no shear resistance (shear stress and friction) at that point. The deformation will be larger at some point along a pile because the friction stress (load transfer) along a pile shaft seems to be larger at that section, as is seen from Fig. 4(*a*). The writer also obtained the same result after a theoretical computation[12] under some assumptions.

Referring to Eq. 6, there seems to be no direct relationship between it and the author's numerical example. The writer wishes to know the significance of Eq. 6 as it cannot be solved unless the rigorous knowledge of β is given, which is variable with depth as a function of ϕ itself.

The writer thinks that the methods of elasticity are useful for this problem although they are of limited assistance if applied to the state just before failure and if the soil is assumed to be elastic when compared with the pile. The writer obtained[13] and solved the following equation, under those boundary conditions and yields on soil which govern the soil deformation surrounding a pile:

$$\left(\frac{\partial^2}{\partial r^2} + \frac{1}{r}\frac{\partial}{\partial r} - \frac{1}{r^2} + \frac{\partial^2}{\partial z^2}\right)^2 \frac{\partial w}{\partial r} = 0 \ldots\ldots\ldots\ldots\ldots (10)$$

in which w is the vertical deformation of surrounding soil and r is the horizontal distance from the pile axis.

---

[11] Instructor of Civ. Eng., Univ. of Kanazawa, Ueno-hon-machi, Kanazawa-shi, Japan.

[12] "Theoretical Considerations on the Lateral Friction of Foundation Piles," by Yoshichika Nishida, *Transactions*, Brasilian Assn. of Soil Mechanics, Vol. 3, 1953, p. 17.

[13] "A Computation of the Skin Friction of a Foundation Pile Driven into the Cohesive Soil," by Yoshichika Nishida, *ibid*, Vol. 4, 1954.

The shear strengths determined from the vane shear tests are higher than the maximum values of the rate of load transfer measured on the test pile because of the presence of shells. At the same time, however, one should take note of the fact that the pile-to-soil shear strength must differ from the soil-to-soil shear strength if the failure takes place at the interface between the pile and the soil (as the authors found), and that only part of the length of the pile shaft (not the full length) develops the maximum resistance of the soil.

James D. Parsons[14] and Ralph B. Peck,[15] Members, ASCE.—Valuable data have been added to the store of information concerning the behavior of soft clay into which piles have been driven. It is noted that the average water content decreased from the original value of 48.1% to 43.6% adjacent to the pile within 1 day after pile driving and to 41.1% within 1 month after pile driving. Although the scattering of the values of water content is appreciable, the general decrease in the neighborhood of the pile appears well substantiated, particularly in view of the corresponding increase in unconfined-compressive strength.

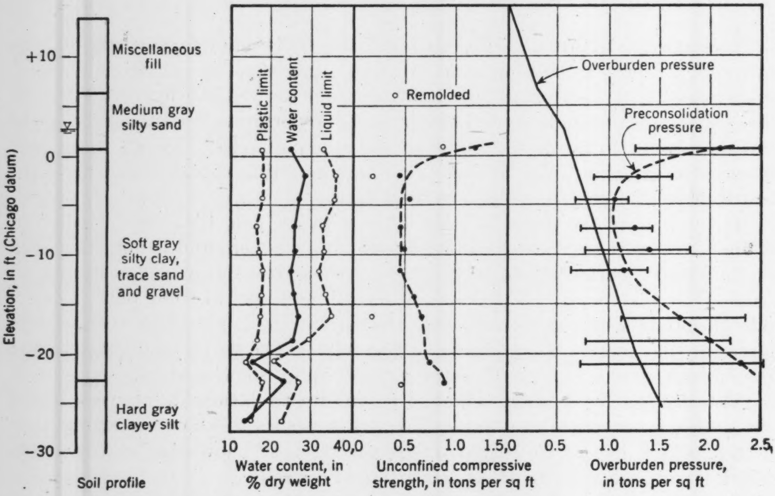

Fig. 18.—Properties of Undisturbed Soil

The data obtained by Messrs. Seed and Reese indicate substantial remolding adjacent to the pile, despite the relatively small diameter of each pile and the small number of piles in the group. The scattering of the values of water content, however, leaves considerable room for interpretation regarding the position of point B in Fig. 8(*b*) which established, quantitatively, the degree of remolding.

---

[14] Associate Partner, Moran, Proctor, Muesser and Rutledge, New York, N. Y.

[15] Research Prof., Soil Mechanics, Univ. of Illinois, Urbana, Ill.

The writers have made similar studies of the degree of remolding associated with the driving of displacement piles to end bearing through soft deposits of clay at a site in the Chicago (Ill.) area. The soil profile is shown in Fig. 18, together with values of the natural water content, liquid limit, plastic limit, and unconfined-compressive strength of undisturbed samples taken in a 3-in.-diameter, thin-walled piston sampler under carefully supervised field conditions. Between El. 0 and El. −15 the clay is quite homogeneous. The homogeneous layer is slightly overconsolidated except at its upper surface where it has been rather highly preconsolidated by desiccation.

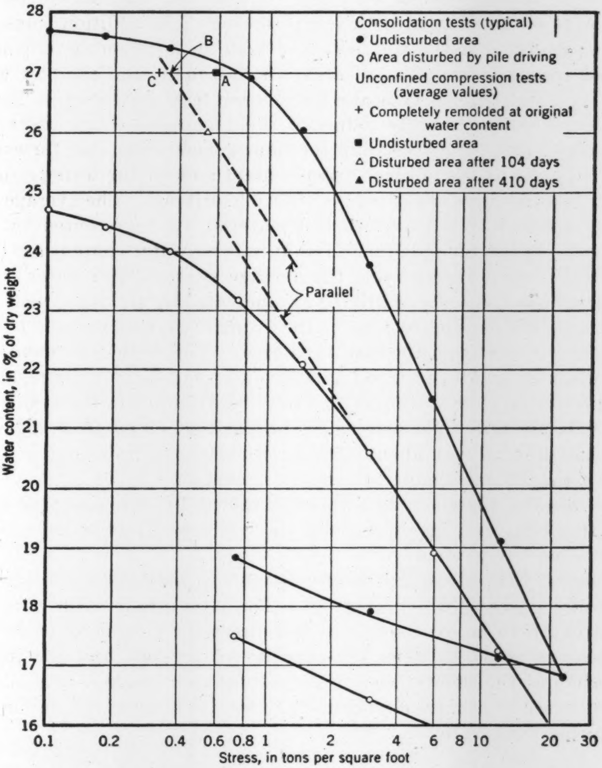

FIG. 19.—STRESS AND STRENGTH VERSUS WATER CONTENT RELATIONSHIPS

Piles were used to support a large, heavily loaded structure at the site. For the most part they were driven from the surface of an area excavated to El. 7 or to El. 0. The upper part of each pile consisted of a 12-in.-diameter, corrugated metal shell; the shell was generally about 35 ft long. The lower part of the pile, about 15 ft long, consisted of a closed-end, 10-in.-diameter, steel pipe pile. The entire pile was eventually filled with concrete.

In much of the area the pile clusters were spaced 14 ft by 17 ft and consisted of from nine piles to sixteen piles each, spaced on about 3-ft centers. Thus, the density and volumetric displacement of the piles were relatively great. Subsequent to pile driving, 2-in. Shelby tube samples were taken in the area of disturbance approximately 104 days after pile driving had been completed in the vicinity. At a time approximately 410 days after pile driving, two additional borings in the disturbed area were made, from which 3-in. piston samples were taken. Values of water content and unconfined-compressive strength were obtained from both sets of borings. In addition, consolidation tests were performed on the samples taken from the 3-in. boring for comparison with those from the undisturbed area where 3-in. piston samples were also recovered. The results of typical consolidation tests are shown in Fig. 19.

Fig. 19 also shows average values of the unconfined-compressive strength for the undisturbed samples within the homogeneous soft clay for completely remolded samples at the original water content and for the tests performed on samples taken 104 days and 410 days after pile driving. The average strength and water content of the undisturbed material are represented by point A whereas those of the remolded material at natural water content are indicated by point C. Points representing the average strength and water content of samples from the areas of pile driving are indicated by the triangular symbols; they define a line parallel to that of the straight part of the $e - \log p$ curve for a typical sample from the disturbed area. This is in agreement with the concept utilized by Messrs. Seed and Reese to represent their results. The upward projection of the strength line to point B indicates the strength of the soil immediately after pile driving. The position of point B suggests that the soil had lost all but about 15% of its strength immediately after pile driving, or that it was almost completely remolded.

These results, together with those obtained by the authors, appear to indicate that relatively insensitive soft clay soils are likely to be substantially or almost completely remolded by pile driving.

It is hoped that Messrs. Seed and Reese will indicate the location of the pore-pressure gages shown in Fig. 10. The large gradient in pore pressure and in strength to be expected in radial directions may account for some of the differences noted between the capacity of the pile and the progress of consolidation at the points where observations were made. It would also be of interest to see typical time-settlement curves for some of the load increments placed during the pile tests.

H. Bolton Seed[16] and Lymon C. Reese,[17] Associate Members, ASCE.—The contributions of Messrs. Dubose, Nishida, and Peck and Parsons in discussing this paper are greatly appreciated. As Mr. Dubose notes, the load-settlement relationship for a pile is certainly influenced by the rate of loading, and this factor should be considered in evaluating the supporting capacity of a pile for design purposes. However, the present investigation was concerned primarily with the mechanics of soil resistance to friction piles and the development of a better understanding of pile behavior. One of the objects of the investigation was to develop a relationship between the load-settlement curve of a pile and the stress-deformation characteristics of the soil. For this purpose it would seem desirable that the rate of loading of the soil in both the vane shear tests and in the pile loading tests should be approximately the same, and thus it is not necessary that the rate of loading be extremely slow. For this reason pile-load tests were performed as quickly as possible—the time being only long enough to make readings of the strain gages. The agreement between the predicted and the observed load-settlement relationships for the pile might have been improved if the rate of loading in the pile tests had been the same as that in the vane shear tests. The writers believe that once a satisfactory analysis of pile action has been developed the influence of rate of loading can be included in the analysis by using suitable soil test procedures.

---

[16] Associate Prof. of Civ. Eng., Univ. of California, Berkeley, Calif.

[17] Asst. Prof. of Civ. Eng., Univ. of Texas, Austin, Tex.

It is unfortunate that Mr. Dubose did not include the date of installing the pile in presenting the data in Fig. 17(*b*) which shows the increase in supporting capacity of the concrete pile under successive loadings. It would have been interesting to know the time which elapsed between placing the pile and the start of the first load test. In stiff clays such as those into which this pile was placed, over such long time periods, and for the drilled-pile method of construction, it is unlikely that there would be any appreciable change in water content as a result of radial flow, as is the case for soft clays during the first weeks after pile driving.

The writers would also have been interested in Mr. Dubose's reasons for associating the increase in supporting capacity with the retesting of the pile and in the data which showed that there were no in situ water-content changes. It would appear that the only effective method of determining water-content changes at the present time (1957) is by taking samples in a boring made immediately adjacent to the pile wall. Such a boring is likely to influence the subsequent behavior of the pile in further load tests. The data presented by Mr. Dubose in Fig. 17(*b*) are apparently for the same pile. It would, therefore, have been of interest to know the methods used to measure in situ water-content changes if borings were not made next to the pile wall.

In contrast to the data presented in Fig. 17(*b*), the writers would like to present the data in Fig. 20. Three load tests were performed in rapid succession on one of the piles used in the research program; this pile was of the same diameter and length as the pile on which the gages were installed. A study of Fig. 20 shows a reduction in supporting capacity of about 5% from Test 1 to Test 2 and no appreciable change in supporting capacity from Test 2 to Test 3. There was no apparent increase in supporting capacity associated with retesting of the pile in this case.

Possibly the results reported by Mr. Dubose might be influenced by thixotropic strength increases with time. However, for the soft clay tested by the writers, it appears that the water content and strength characteristics of the soil adjacent to a driven pile are associated with the excess pore-water pressure and vary with time after pile driving. To determine the behavior of a loaded pile, the skin friction resulting from these varying soil characteristics must be ascertained. The supporting capacity of a pile immediately after driving can-

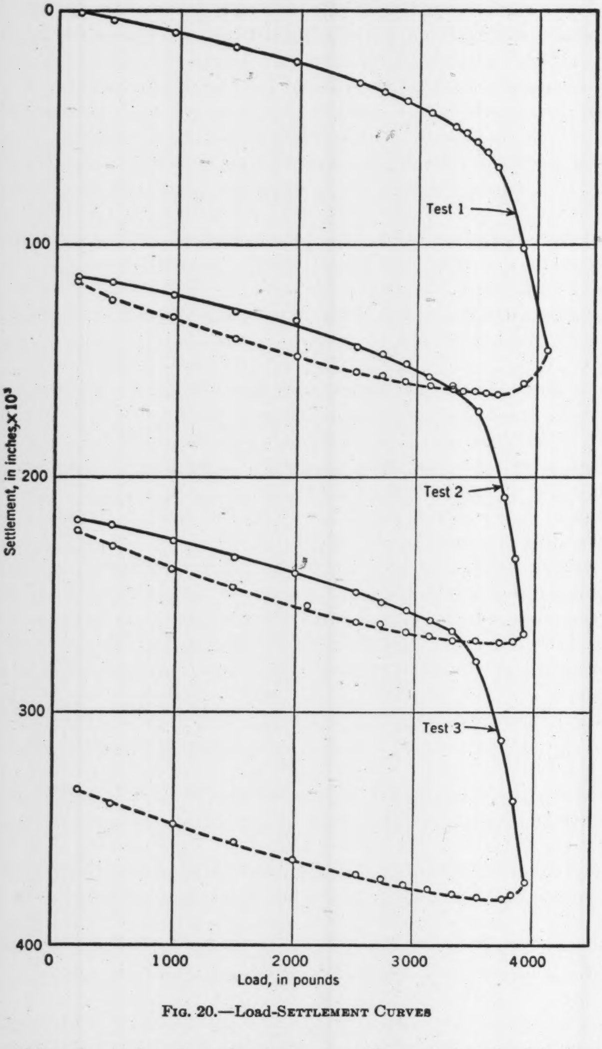

FIG. 20.—LOAD-SETTLEMENT CURVES

not be considered merely of academic interest if one is faced with the practical necessity of loading a pile soon after driving and is therefore interested in the rate of development of skin friction and its relationship to the properties of the soil adjacent to the pile.

The writers cannot agree with the implication of Mr. Dubose that long-time load tests are desirable in order to include the effects of consolidation in the measured pile settlement under load. Certainly in practice long-term load tests are desirable, but it should not be imagined that the results of such tests on individual piles will serve to indicate the probable settlement of a structure as a result of consolidation. A pile-load test is simply intended to evaluate the strength characteristics of a soil around a pile and does not necessarily bear any relationship whatsoever to the compressibility of the soil under the loads imposed by a structure.

The writers appreciate Mr. Nishida's comments. His observation that the deformation of the soil around a loaded pile is not a maximum at the ground surface is certainly substantiated by the results of this investigation. If a firm bond existed between the pile and the soil, the deformation of the soil would be a maximum at the ground surface. However, because the results indicate that failure occurred by slippage between pile and soil at shallow depths and that at a depth of 10 ft no skin friction was developed, the deformation of the soil at that depth must necessarily have been small. A similar condition would presumably exist near the ground surface if the pile were not driven through a 9-ft casing. This fact was considered in the analysis of pile performance by assuming the effective shear resistance to be zero in the upper 10 ft of soil.

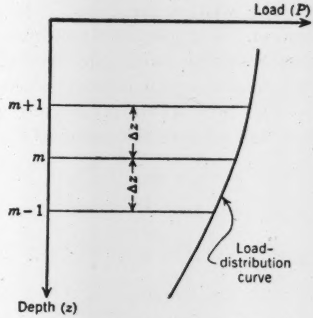

FIG. 21.—THEORETICAL LOAD-DISTRIBUTION CURVE

Mr. Nishida's equation (Eq. 10) for an elastic soil and a rigid pile will perhaps give an insight into certain phases of the problem. His inquiry concerning the relationship between the differential equation (Eq. 6) and the numerical computations can best be answered by rewriting Eq. 6 in the form of a difference equation as follows (Fig. 21):

$$\frac{\left(\frac{\Delta \phi}{\Delta z}\right)_{m+1} - \left(\frac{\Delta \phi}{\Delta z}\right)_{m-1}}{2\,\Delta z} = \alpha\,\beta\phi_m \quad \text{(11)}$$

From the expression for unit strain,

$$\left(\frac{\Delta \phi}{\Delta z}\right)_k = \frac{P_k}{E\,A} \quad \text{(12a)}$$

and

$$\alpha = \frac{C}{E\,A} \quad \text{(12b)}$$

Substituting these expressions into Eq. 11,

$$\frac{\frac{P_{m+1}}{E\,A} - \frac{P_{m-1}}{E\,A}}{2\,\Delta z} = \frac{C}{E\,A}\,\beta\phi_m \quad \text{(13)}$$

and

$$P_{m+1} - P_{m-1} = 2\,\Delta z\, C\, \beta\phi_m \qquad (14)$$

In the example in the original paper, $P_{m+1} = P_{21}$, $P_{m-1} = P_{23}$, $2\,\Delta z = L_{23-21}$, $C = C$, and $\tau_{22} = \beta\phi_m$. The other numerical expressions used therein proceed from elementary considerations.

The writers are grateful to Messrs. Parsons and Peck for the additional data on the degree of remolding of the relatively insensitive clay in the Chicago area resulting from pile driving. It was interesting to note that consolidation continued for many months after pile driving in this case.

The pore-water pressure gages mentioned in Fig. 10 were built into the pile wall and were located at the following depths:

Gage	Depth, in feet
W-1	22
W-3	18
W-5	14

The construction of the pore-water pressure gages and the results of pressure measurements on the wall of the pile have been described elsewhere.[3]

The pile-load tests for this research were performed rapidly compared with usual test procedures. Because the total time of each test was only about 2 hr, time-settlement curves were not plotted as in other load tests where the loading period might take several days.

AMERICAN SOCIETY OF CIVIL ENGINEERS
Founded November 5, 1852
TRANSACTIONS

Paper No. 2883

EDUCATION OF CIVIL ENGINEERS

A SYMPOSIUM

PAGE

FOREWORD

By Edwin H. Gaylord, Jr., M. ASCE 766

NEED FOR RECONSIDERATION

By L. E. Grinter, M. ASCE 767

WITH DISCUSSION BY MESSRS. Daniel C. Drucker, and L. E. Grinter. 776

TRAINING FOR CIVIL ENGINEERING

By Benjamin A. Whisler, M. ASCE 779

WITH DISCUSSION BY MESSRS. Alfred R. Golzé, and Benjamin A. Whisler 783

FOREWORD

By Edwin H. Gaylord, Jr., M. ASCE

Following a recommendation in 1951 of the Committee of Engineers' Council for Professional Development (ECPD) on Adequacy and Standards of Engineering Education, the American Society for Engineering Education (ASEE) appointed in May, 1952, a Committee on Evaluation of Engineering Education of which L. E. Grinter was chairman. The investigation was sponsored financially by the ASEE, the Engineering Foundation, the constituent societies of the ECPD, the General Electric Company, and the National Science Foundation.

This committee issued a preliminary report in October, 1953, an interim report in June, 1954, and a final report which was published in the *Journal of Engineering Education* for September, 1955.

In brief, the committee recommends increased emphasis on the basic sciences, the engineering sciences, and the humanistic and social studies, accompanied necessarily by a de-emphasis of engineering art and practice, and elimination of or reduction in time allotted to courses which have a high vocational or skill content. The papers in this symposium consider the implications of the final report from different points of view.

NEED FOR RECONSIDERATION

By L. E. Grinter,[1] M. ASCE

With Discussion by Messrs. Daniel C. Drucker, and L. E. Grinter

Synopsis

The American Society for Engineering Education (ASEE) Committee on Evaluation of Engineering Education was appointed in May, 1952, following discussion by Engineers' Council for Professional Development (ECPD) of the need for a thorough restudy of the objectives of engineering education. The committee was charged to determine what changes are needed in engineering education (1) for it to keep pace with the rapid advances that are occurring in science and (2) to provide the next generation with engineering leaders having the capacity to apply new scientific discoveries in a creative manner. The final report covers the committee's studies over a three-year period during which more than two hundred educational reports from institutional committees on engineering education, from engineering societies, from industrial organizations, and from individuals were studied. This resume is intended to give civil engineers a better insight into the problems of engineering education. It is hoped that many practicing engineers will read the full text of the report.

Objectives of Engineering Education

The objectives of engineering education are twofold and are related to the technical and social responsibilities of engineers. The technical goal is preparation for the performance of analysis and creative design or of construction, production, or operation in which a full knowledge of the analysis and design of the structure, machine, or process is called for. The Committee on Evaluation of Engineering Education of the American Society for Engineering Education (ASEE) concluded[2] that the greatest curricular deficiency in achieving the technical goal of engineering education lies in inadequate preparation of engineers in basic science (including mathematics), in engineering science, and in the planned use of this science background in engineering analysis, in the study of engineering systems, and in the preparation for creative design.

The second objective, the broad social goal of engineering education, includes the development of leadership, the inculcation of a deep sense of professional ethics, and the general education of the individual. In this area there is less unanimity of educational opinion, but there is a clear consensus of indus-

---

Note.—Published, essentially as printed here, in December, 1955, as *Proceedings Paper 858*. Positions and titles given are those in effect when the paper or discussion was approved for publication in *Transactions*.

[1] Dean of the Graduate School and Director of Research, Univ. of Florida, Gainesville, Fla.

[2] "Report on Evaluation of Engineering Education, 1952–1955," Am. Soc. for Eng. Education, Urbana, Ill., June, 1955.

trial and other employers who consider the young engineer to be unnecessarily handicapped by inability to convey ideas to others in a clear, logical, and interesting manner, using correct and concise oral or written language. There is wide agreement that technical competence alone is insufficient and that a reasonable fraction of the engineering curriculum must be directed toward achieving a liberal education for engineers.

Curricular Recommendations

The consideration of the curriculum takes an undue share of the original report and will take an even larger place in this brief summary. Actually, the report recognizes clearly that the competency of the faculty, its ideals, objectives, and methods, are far more significant than the curriculum because a truly distinguished faculty can mold any curriculum to its objectives. However, only a few faculties can exert such influence. The framework of the curriculum can maintain the reactionary influence of the past, not only into the present but far into the future. Since the great increase in students that is just "over the horizon" will soon make it necessary for engineering colleges to increase their faculties with many inexperienced teachers, the present seems a most appropriate time to consider whether curricula in civil engineering are designed in the best possible manner for producing the leaders that will be needed by the profession twenty-five years from now.

The great changes in physics and chemistry since the 1920's and the equally great advances in engineering practice do not seem to have produced an equivalent counterpart in a reorganization of engineering curricula. A group of industrial advisers to the committee has pointed out that the problems in production and manufacturing are demanding greater and greater scientific background for engineers. As one example, emphasis was placed upon automation as a current problem of the machine designer. The need for such instruction is critical in certain industries, and several of these offer such courses to their personnel. If this is generally true, engineering education may be a decade late in giving emphasis to electronics in the curriculum of mechanical engineering. Civil engineering is also beginning to feel the influence of automation. Greater adaptability to rapidly changing conditions seems clearly needed in engineering education.

Fortunately, however, some things do not change. A generation or a century ahead, reactions, stresses, and deflections will still occur and they will have to be calculated. Electrical currents and fields will follow unchanging laws. Energy transformation, thermodynamics, and heat flow will be as important to the next generation of engineers as to the present one. Solids, fluids, and gases will continue to be handled, and their dynamics and chemical behavior will have to be understood. The special properties of materials as dependent upon their internal structure will be even more important to engineers a generation hence than they are today. These studies encompass the solid unshifting foundation of engineering science upon which the engineering curriculum can be built with assurance and conviction.

Based upon such considerations, the committee recommends less specialization in terms of extensive intradepartmental offerings and greater dependence upon basic science, engineering science, humanities, and social studies. Departmental sequences serve their primary purposes as opportunities to apply fundamental scientific knowledge to analysis, design, and the study of engineering systems. The committee agrees with the basic concept expressed by industrial leaders that specific details of engineering practice change too fast to be of value for classroom study except as they may serve the high purpose of illuminating fundamental unchanging principles. If this criterion is applied rather forcefully by engineering faculties, it is felt that opportunity will be found within the usual time limits to increase basic studies in science and humanities as recommended in the report.

In particular, the committee sees the need for increased study of mathematics, physics, and chemistry. It sees mathematics through ordinary differential equations, an introduction to nuclear physics, and more attention to physical chemistry as normal requirements of modern curricula in engineering. Great emphasis is given to the importance of the instruction in engineering science and its proficient application to analysis and design in engineering. An engineering science by definition involves largely the study of basic scientific principles as related to and as interrelated through engineering problems and situations. The fields of engineering science are defined specifically in the report to include mechanics of solids (statics, dynamics, and strength of materials); fluid mechanics; thermodynamics; electrical theory (electrical circuits, fields, and electronics); transfer and rate mechanisms (heat, mass, and momentum transfer); and the nature and properties of engineering materials. Of course, these six titles of the engineering sciences should be regarded as generic and broadly definitive rather than as representative of courses now (1955) being offered. It is recognized that other engineering sciences may be expected to develop and that, alternately, there may be some curricula for which sciences other than those listed must be chosen—for example, an earth science or a life science.

It is recommended that about a quarter of the engineering curriculum be devoted to the study of the engineering sciences and about an equal fraction to their application in a departmental sequence in engineering analysis, design, and engineering systems. Hence, the organization of basic science, engineering science, and engineering analysis becomes an integrated sequential study of great importance.

Humanistic and Social Studies

Among the many comments from employers of engineers that have been received by the committee, none has come with greater frequency or stronger conviction than that urging the importance to engineers of the arts of communication and of social understanding. There is a nearly universal consensus among employers that engineers suffer unduly from lack of capacity for clear, concise, and interesting exposition and that they are limited in their ultimate development by an inadequate understanding of the humanities and the social studies. Although this viewpoint is accepted as true, there remains some question whether increase of fixed requirements of humanistic and social courses for all engineering students will eliminate this weakness.

In 1944, an ASEE Committee recommended[3] that about one-fifth of the curriculum be in humanistic and social studies but even this concession has not proved sufficient. Rather than establish an increased percentage of the curriculum beyond this widely accepted figure of 20%, the committee has concluded that a minimum of one course per semester for seven or eight semesters plus a broad opportunity for students to elect additional humanistic and social courses would be preferable. For students with cultural interests all electives might appropriately be chosen in the nontechnical field to produce about the same background as that of a liberal arts student who chooses "to major" outside of the humanities or social studies. The success of this approach will depend upon a genuine community of interest and more meaningful cooperation between teachers of engineering and those in the liberal arts. For true success in liberalizing engineering education, these two must respect and sustain each other.

The fields of the humanities and social sciences from which some courses must be selected include history, economics, and government wherein knowledge is essential to competence as a citizen, and literature, sociology, philosophy, and fine arts which afford means for broadening the engineer's intellectual outlook. In contrast, it is observed that many curricula list as humanistic or social courses such technical subjects as accounting, industrial psychology, investment economics, corporate organization, city management, or military training. The committee questions the value of such studies as a major contribution to liberal education and considers that they should be classified as nonengineering technical courses with appropriate additional time provided for humanistic and social studies.

AN EXPERIMENTAL CURRICULUM WITH SCIENTIFIC ORIENTATION

Emphasis is placed upon the fact that experimentation rather than standardization is needed in curriculum development. However, in order to demonstrate that its ideas are practical, the committee has found it necessary to offer an experimental time distribution for the scientifically oriented curriculum that it recommends for consideration:

Subject matter	Fraction of curriculum
Humanistic and social studies	about one-fifth
Mathematics and basic science	about one-quarter
Engineering science	about one-quarter
Major departmental sequence of analysis, design, and engineering systems including necessary technological background	about one-quarter
Choice of options or electives in (*a*) humanistic social, (*b*) basic science, (*c*) engineering science, (*d*) research or thesis, (*e*) engineering analysis and design, (*f*) management	about one-tenth

It will be noted that the fractions given do not total exactly 100%. Hence, it should be evident that the committee does not desire this suggested distribution of emphasis to be restrictive. There will be many reasons for variations among institutions and among departments of a single institution. Experimentation, however, is strongly encouraged.

---

[3] "Engineering Education: Progress Report of the Society's Professional Committee on Engineering Education for 1944," *Proceedings*, ASCE, March, 1946, p. 384.

The committee's interest in this curriculum outline is centered in: (1) The indication that the concept of a four-year scientifically-oriented curriculum is practical in many fields of engineering, although it takes no position that four years or any other length of curriculum represents the supreme desideratum; (2) the fact that considerably more than the "common freshman year" might be arranged, if desired, as one result of scientific orientation of curricula; (3) that even with an increased science background time may be provided for elective or option study to offer the student an opportunity to "try his wings" in one or two directions. Such elective study can contribute to a stronger humanistic-social background for some engineers and a stronger science background for others, with resultant over-all strengthening of the profession of engineering.

Interest of a Profession in Its Education

The fact that there may not be a broad base of interest concerning engineering education among practitioners of engineering leads to the question whether engineering is yet a profession, or whether possible organizational channelization within the profession produces this apparent, rather than real, lack of interest. An important characteristic of a profession is that it shall take a strong interest in its own education. Since this interest did not develop early in the history of engineering, it was necessary for a group of professors in 1896 to form the Society for the Promotion of Engineering Education which later became the American Society for Engineering Education. This society has been very active in the study of ways and means of improving engineering education, and civil engineers have been well represented; it is still unfortunate that very few practicing engineers have been involved personally. No real change can take place in this situation as long as the main engineering societies and ASEE are not associated more closely.

Coordination Through Engineers' Council for Professional Development

An association between professors and practicing engineers has been worked out through the Engineers' Council for Professional Development (ECPD), but one must report that this association is quite tenuous. The most effective work of ECPD by every measure has been the accrediting procedure for engineering curricula. However, the tradition behind this accreditation program is one of devoted service primarily of engineering educators. Accreditation was initiated by Karl T. Compton of the Massachusetts Institute of Technology (Cambridge), A. A. Potter of Purdue University (Lafayette, Ind.), and Harry S. Rogers, M. ASCE, of the Polytechnic Institute (Brooklyn, N. Y.). It has been carried on by S. C. Hollister, M. ASCE, Thorndike Saville, M. ASCE, and Harold L. Hazen with the aid of several hundred engineering educators and a few practicing engineers. Theoretically, the Society and the other engineering society members of ECPD appoint the lists of inspectors of engineering curricula. Practically, unless such appointments are pretested by a trial run where engineering educators are necessarily the judges, the whole accreditation structure could be destroyed in a few years. Experience has proved that very few practicing engineers either can give or will give the time and attention to accreditation inspections that engineering educators consider essential. Hence, the work of accreditation has fallen largely upon the shoulders of the educators themselves. Although the accreditation procedure of ECPD has been effective, it has not encouraged the entire engineering profession to develop the interest in engineering education that it should have.

Comparison with Medical Education

It is common procedure for writers on engineering education to attempt to idealize the procedure of medical education as an example to the engineering profession. Actually, the points of similarity are more evident by their absence than by their presence. If engineering education followed the medical pattern, probably about one-quarter as many engineers would graduate as at present because the requirements would be as follows: First, the pre-engineer would take a liberal arts course for four years with due emphasis upon the humanities and social sciences and special emphasis upon the physical sciences. At least one-half of those who started would drop out for the usual variety of reasons. Then the student engineer would begin a four-year program divided about equally between basic and engineering science on the one hand, as taught by research professors, and on the other hand some two years of practical engineering courses taught by practicing engineers. After his eighth year, he would graduate as an engineer and would start a two-year apprenticeship at a nominal wage where he would work for one of the top-flight industrial organizations or for a government laboratory. During this two-year period he would receive several hours a day of direct contact with a master engineer whose methods he would study. At the end of the two-year apprenticeship when he had reached the age of 28 or 30, he would be expected to be able to accept responsible charge of any engineering job within his field of specialization.

Learning the Art of Engineering

The educational picture presented is so divorced from concepts of engineering education and practice today as to appear fantastic. Freshmen engineering students are quite anxious to study engineering immediately and are not likely to progress rapidly in humanistic or social science courses that precede science and engineering studies. Their appreciation and progress in nontechnical studies is better in the junior and senior years. Also, the art of engineering must be learned on the job. Practical engineering work cannot be experienced adequately in the classroom or laboratory. There is no opportunity for practical education in engineering within a college comparable to animal experimentation or cadaver dissection in medicine.

Medical schools fortunately are associated with hospitals where the most advanced medicine is practiced by the professors and observed by the students. The teaching of engineering art in college is synthetic and relatively unproductive except as it is used to illustrate and teach the principles of engineering science and design. Anyone may clarify this point by considering to what extent he himself applied engineering art learned in college during his first years of experience. Instead, each person will conclude that he applied day by day the engineering art that he had observed others to be using successfully in practice. By this procedure, one accumulates over the years a storehouse of techniques, methods, tools, devices, and concepts—in short, a storehouse of engineering art that is always available for use.

The Study of Engineering Science

Since engineering art cannot be taught with real effectiveness in college, the technological emphasis of the curriculum should be placed upon engineering science instead. This procedure has the merit that all knowledge of engineering science and the basic sciences upon which it depends is transferable from field to field. An understanding of dynamics, for example, is applicable to the determination of the wind stresses in tall buildings, towers, or suspension bridges; to atomic blast effects upon structures; to the analysis of machine vibrations; and to airplane frame design. It is unimportant whether an understanding of dynamics is obtained in physics, mechanics, mechanical engineering, or civil engineering, or by a combination of exposures. If one understands fully the basic principles and necessary assumptions, applications may be made in many fields; in addition, such knowledge does not become out of date. In contrast, a knowledge of the art of handling concrete from the mixer to the forms is useful only in the field of concrete construction, a small segment of civil engineering, and such knowledge of the art is also subject to rapid obsolescence as new techniques and devices are developed.

It can be observed that the engineering science of the mechanics of solid bodies is transferable knowledge of permanent value for study by all student civil engineers whereas the art of concrete placement is better learned on the job by the limited number of graduates who happen to accept employment in that field of specialization. A similar parallel may be drawn between the broad usefulness of the engineering science of fluid flow and the relatively limited application of practical techniques for stream flow measurement. Unless the entire approach to engineering education should be revised more nearly along the lines of medical education, there is so little time for the study of engineering art that it can appropriately serve only as a tool for illuminating the principles of engineering science and engineering design and not as a basic approach for the transfer of engineering knowledge.

Graduate Study As Professional Education

The preceding remarks have applied largely to the undergraduate curriculum. In four or more years of undergraduate study, the college attempts to lay a foundation for the future development of a real understanding of engineering problems by its graduates. It does not expect to achieve through the undergraduate curriculum an adequate understanding of engineering science for the professional engineer. To achieve the appropriate status of a professional engineer, the engineering graduate has the choice of graduate study or of further self-education. It appears to be the trend for most professions to require either the master's degree or its equivalent in formal study before professional recognition is awarded. In engineering, where only a fraction of the graduates appear to desire professional recognition since attractive employment outside the professional field is readily available, there would be an obvious advantage in retaining the bachelor's degree in engineering as a normal termination for those who do not seek professional recognition, while establishing the master's degree as the normal channel for those who intend to become professional engineers.

There is widespread belief in engineering education that this natural solution to the problem of professional recognition is already well advanced and that it will either attain informal acceptance or be formally adopted within the next generation. The requirement of the master's degree in engineering science or its equivalent in self-education for professional recognition would do much to produce a true profession of engineering knit together by a common understanding of engineering science at a level commensurate with the demands that industry and government will place upon the new generation of engineers passing through colleges of engineering in the United States.

The foregoing leads to the conclusion that the objective of a modern curriculum in civil engineering, mechanical engineering, electrical engineering, or any other field of engineering specialization is to teach engineering science and its application to design. Specialization at the undergraduate level, including many courses unique to civil engineering, is the "topping on the cake," tasty and attractive and useful psychologically as a means of "selling the main package." Specialization usually partakes rather heavily of engineering art and should therefore not be overdone since knowledge of engineering art is less transferable and much more subject to obsolescence than knowledge of basic science, engineering science, and engineering design which are called the "fundamentals" of engineering education. Equally "fundamental," however, are English communication and certain nontechnical studies.

THE NONTECHNICAL SIDE OF ENGINEERING

Finally, it is well to inquire whether any or all of the things discussed herein are the most important in the education of an engineer. In a long article on decision-making by administrators in industry, the writer noted an amazingly light emphasis given to scientific, technical, or economic knowledge even though some such factors are involved in decision-making in nearly every instance. Instead, psychological, social, and human factors including strong character and a developed sense of ethics seem to weigh very heavily in the make-up of the successful administrator or decision-maker; and, since a large percentage of engineers eventually enter the realm of administration, one cannot feel comfortable about the lack of emphasis upon the humanities and the social sciences that has been particularly characteristic of civil engineering curricula.

As a start, educators must drop the confused thinking that has accepted technical nonengineering courses such as accounting, business or city management, cost analysis, marketing, finance, engineering economics, or military training as adequate substitutes for humanistic and social courses. When engineering educators face the issue that humanistic and social courses may be of the same order of importance as engineering science in the curriculum of engineering and that engineering art is useful primarily for illustrating applications of engineering science, they will be able to improve engineering curricula and will graduate stronger potential engineers. Since engineering schools can no longer hope to meet the demand for numbers of graduates, it is toward quality of graduates that they should now strive. The engineer must live his entire life among men. Unless due attention has been given to the education of the entire man (which means much more then the development of an able technologist), the engineering educator may have failed both the engineer of the future and the world itself.

ACKNOWLEDGMENTS

The investigation which forms the basis of the ASEE Report on Evaluation of Engineering Education was sponsored financially by the American Society for Engineering Education, the Engineering Foundation, the constituent societies of the Engineers' Council for Professional Development, the General Electric Company, and the National Science Foundation. Committee appointments were made in 1952 by Mr. Hollister, then president of ASEE.

DISCUSSION

Daniel C. Drucker,[4] M. ASCE.—The report of the ASEE Committee on Evaluation of Engineering Education[2] is a most encouraging portent of future progress of the engineering profession. The author's summary of the report is a clear and logical call for radical changes in current practice of most of the engineering schools of the country.

It may be of interest to know of the experience at Brown University (Providence, R. I.) in the period from 1948 to 1956 with almost exactly the type of curriculum proposed by the committee; this curriculum is outlined in Table 1. This experience within the framework of a private university devoted primarily to the liberal arts is not necessarily directly applicable to all colleges because such an environment is particularly well-suited for this type of engineering program; each school must work out a suitable program for its students and staff.

TABLE 1.—Outline of Engineering Curriculum, Brown University, Providence, R. I.

Semester 1	Semester 2	Semester 3	Semester 4
Chemistry Calculus Introduction to engineering English composition or elective[a]	Chemistry Calculus Introduction to engineering English composition or elective	Vector dynamics Differential equations Radiation physics Elective	Fluid mechanics Strength of materials Electricity and magnetism Elective
Semester 5	Semester 8	Semester 7	Semester 8
Electric circuits Thermodynamics Theory of structures Elective	Electrical machinery Thermodynamics Metallurgy and physics of solids Elective	Engineering option Engineering option Free elective Free elective	Engineering option Engineering option Free elective Modern physics

[a] Courses entitled "Elective," as distinguished from "Free elective," must not be chosen from the physical-sciences group. A minimum of two must be selected in the humanities and two in the social-studies group.

The first three years are common for all engineering students: Civil, electrical, mechanical, and aeronautical. This places the desired emphasis on science, mathematics, and engineering science as cited by Mr. Grinter. This emphasis obviously permits "considerably more than the 'common freshman year'." There are no "service courses" in engineering, such as electrical engineering for civil engineers or structures for electrical engineers. Except in student-chapter organizations there is no separation of students in accordance with their probable choice for the senior year. All students therefore get the fundamentals of all fields. The same basic philosophy applies to the liberal arts courses taken by arts, science, or engineering students.

Humanities and social studies occupy a prominent place in the program and may compose 30% of the total with a minimum of 20%. Courses in accounting, engineering economy, and other fields which, as the author explains, are not liberal arts, may be taken as free electives only. A five-year combined Bachelor of Arts and Bachelor of Science program is also offered. The basic curriculum is very advanced, not only in scope, but also in content. Several examples may help to make this point clear. Vector algebra is studied in the freshman year to prepare the way for vector dynamics, fluid mechanics, and electricity and magnetism in the sophomore year. The course in theory of structures treats the fundamental theorems of energy and of virtual work in their general form. Indeterminate and determinate elastic and elastic-plastic structures are considered. In all options, details of engineering design are postponed to the senior year along with advanced courses in theory. Again, fundamentals are emphasized so that, for example, both civil and aeronautical engineers take the same advanced course in theory of structures. The design courses are separate and involve introduction to design principles and are not repeated practice in design. As the author states under the heading, "LEARNING THE ART OF ENGINEERING":

---

[4] Prof. and Chmn., Div. of Eng., Brown Univ., Providence, R. I.

> "The teaching of engineering art in college is synthetic and relatively unproductive except as it is used to illustrate and teach the principles of engineering science and design."

The writer agrees that there is a need for "experimentation rather than standardization." All courses at Brown University are re-examined continually and are changed each year as the need for improvements is recognized. Adjustments are made among the courses to develop a more effective teaching and learning sequence with necessary but not wasteful repetition. Most experimentation takes place in the course entitled "Introduction to Engineering" which is given in the freshman year; this is the most vital course in the engineering curriculum because it is the first. At present (1956) it includes elementary mechanics, college algebra, descriptive geometry, drawing, and vector algebra. It is designed to bring the entering group of students to a high level of college work as quickly as possible from a varied background—smoothed only slightly by a two-week, presemester, engineering-orientation program.

Experience with this curriculum has been gratifying but must be carefully interpreted. Any change in curriculum will initially create at least as many problems as it solves. Eight years is not long, and many questions are still unanswered. A large number of students entering as Bachelor of Science engineers leave with a Bachelor of Arts degree just as they did years ago. It is difficult for the student or the admissions officer to evaluate correctly both interest and ability in engineering at any level. Admissions problems are increased greatly by any appreciable change in program. Counseling of students requires considerably more time.

One of the major unresolved difficulties, and one in which guidance is earnestly sought, is the matter of student-chapter activities and allied motivation. Because specialization is avoided so completely for the first three years most students do not think of themselves as civil engineers or electrical engineers, for example. Although this attitude may serve well the cause of unity of the profession in later years, interest in student chapters is not as strong as it should be. Activities tend to be marginal and sparsely attended. Here, the smallness of the group is a handicap. A fraction of the juniors plus all of the seniors in any one option do not add up to a chapter of optimum size to provide the necessary continuity from year to year.

With a curriculum of this type, there is some tendency toward lack of drive on the part of a small but not negligible number of students. They will drift along through the first years and decide on their option on the basis of which is easiest for them rather than most interesting.

Certainly the performance of the students of each class still ranges from poor work to excellent work just as it does everywhere. The important difference is that students who are average or better operate on a much higher and yet on a more fundamental level than before. Their ability to handle the diverse and difficult problems faced by engineers in research, design, construction, and management appears to be greatly enhanced, but approximately ten years must elapse before a real evaluation is possible. Surprisingly, perhaps their ability to do the routine problems on which so little time is spent now is as good and often better than before. This point can be checked fairly well by test and classroom performance.

Much more remains to be done to develop curricula which meet the needs of the profession. More and more mathematics, science, and improved laboratory science and technique must be incorporated in the engineering curriculum. The tendency for specialization will become stronger as engineering becomes more complex and difficult. There is no conflict, however, between specialization in practice and fundamentals in education. Quite the contrary, high specialization will require an increasingly broader base of knowledge.

Engineering societies should encourage frequent evaluations of engineering education in the hope that the productive results of the ASEE committee can be developed and then extended to meet the needs and resources of each college and university.

L. E. Grinter,[5] M. ASCE.—The important problem of the future trends in engineering education has been discussed by Mr. Drucker. The curriculum which he describes for the Bachelor of Science degree in engineering, without designation as to the specific field of study, fulfils the definition of a scientific curriculum in engineering. Several institutions have adopted this program in recent years, and others have begun its adoption since the publication of the committee's report.

However, the committee did not feel it necessary to recommend such revolutionary changes in engineering education. Rather, it seems preferable for evolutionary changes to take place within the traditional framework of present departmental curricula leading toward a more scientific background for engineers. A more significant influence will be had on engineering education by the gradual substitution of courses in engineering science and creative design for present courses that emphasize engineering art. Particularly in civil engineering education, it is the evolutionary process of curriculum adjustment toward a more scientific viewpoint that is needed most. There is encouraging evidence that such readjustments are receiving serious and favorable consideration.

---

[5] Dean of the Graduate School and Director of Research, Univ. of Florida, Gainesville, Fla.

TRAINING FOR CIVIL ENGINEERING

BY BENJAMIN A. WHISLER,[1] M. ASCE

WITH DISCUSSION BY MESSRS. ALFRED R. GOLZÉ, AND BENJAMIN A. WHISLER

SYNOPSIS

The present trend of engineering education is toward more technical courses in the basic sciences narrowly pointed toward careers in research and development in the manufacturing industries. Because most civil engineering graduates still go to field or office positions closely associated with the construction industry, increased attention to basic sciences at the expense of engineering courses is inappropriate for undergraduates. Present curricula, kept up to date in course content, are still most appropriate for the training of prospective civil engineers.

For several decades the American Society for Engineering Education (ASEE) has been an important influence on the attitudes and policies of engineering educators, colleges, and curricula. It is a society of approximately eight thousand members drawn from most engineering schools in the United States, from all academic ranks, and from industry. The leadership in the ASEE is at this time (1956) primarily from those fields closely associated with the manufacturing industries and is influenced by the needs and interests of a few large industries which maintain programs of research and development. Conditions, however, are so different in the field of civil engineering that changes which may be reasonable in other fields of engineering should not be applied here.

Present trends in engineering education are toward the inclusion of more mathematics, physics (including atomic physics), theoretical mechanics, and similar courses. These courses are being expanded in order to prepare the graduate engineer for development and research activities, and this expansion is being conducted at the expense of those courses which emphasize the true engineering aspects of the curricula.

In order to determine whether or not such changes are appropriate in the training of civil engineers, some of the factors which distinguish the civil engineer from other engineers should be examined. The historical development of civil engineering has resulted in its being closely associated with public works. The report[2] of the ASCE Committee on Employment Conditions showed that approximately 37% of all civil engineers were employed

---

NOTE.—Published, essentially as printed here, in December, 1955, as *Proceedings Paper 849*. Positions and titles given are those in effect when the paper or discussion was approved for publication in *Transactions*.

[1] Head, Dept. of Civ. Eng., Pennsylvania State Univ., University Park, Pa.

[2] "Returns from Questionnaire on Employment Conditions, 1953, Summarized," *Civil Engineering*, November, 1953, pp. 75-76.

by municipal, state, and federal government agencies and an additional 28% were employed in private practice, which is closely associated with public works such as sewage-treatment plants, water-treatment plants, and super-highways. In no other field of engineering does the employment of engineers in positions in government agencies or associated with government projects so predominate.

In addition to being associated with government agencies or projects, civil engineers are employed by small organizations. Consequently, relatively few civil engineering graduates receive the formal training or orientation courses such as those provided by large corporations.

Employment of civil engineers in the field of heavy construction is an important factor. A survey[3] of the employment of graduates of a large eastern university showed that nearly one-half its graduates are employed in field positions in heavy construction or on construction projects. Another third are employed in operation and maintenance positions which usually involve construction. Therefore, educators in civil engineering must keep in mind the fact that, in general, students must be trained for positions in the office or the field which are closely allied with the construction of nonduplicated projects and not with the mass production of general industry.

The practice of engineering in any field is, even today, both an art and a science. Many problems cannot be solved by the straightforward application of mathematical and physical principles but by judgment based on experience. For many reasons, the civil engineer, more than engineers in other fields, must use such judgment. He works with extremely variable and incompletely understood materials such as soils. He is prevented from using the best engineering solutions because he must satisfy the desires of nonengineering public authorities such as municipal councils and elected officials, and he is restricted by antiquated legal building codes. Consequently, he is continually required to make decisions which represent compromises with the theoretically best solution to a problem. Educational institutions can do little to provide the experience necessary to make such decisions, but they should do everything they can to provide a basis for making judgments by showing the student the role judgment plays in engineering and by providing him with the opportunity to exercise judgment based on his limited experience and knowledge. Such training cannot be a part of basic courses in mathematics and physics but must be a part of advanced courses in which scientific principles are applied to specific, practical engineering problems.

Research is needed in all branches of civil engineering in order to develop more economical methods of producing the desired results. This research is being continually conducted, but in civil engineering this is rarely done by large private industrial organizations. Research in civil engineering is conducted by engineering colleges and is supplemented in a few fields by independent, industry-supported organizations and by government research. These organizations do not employ many new engineers each year, and most of the engineers who are newly employed by them are men with experience in the field who have become interested in research activities. Therefore, colleges of the country are not training civil engineers for research positions but for positions in the field of heavy construction. These men will perform designing, supervisory, or operational functions in this field, and some of them will progress to positions of responsibility in their organizations. They will become chief engineers or presidents of railroads, chief engineers of highway departments or of government bureaus, owners of consulting firms, and owners of construction companies.

---

[3] "How Should We Educate Civil Engineers," by B. A. Whisler, *Journal of Engineering Education*, Vol. 45, No. 2, October, 1954.

What kind of education should be given to the young men who will occupy responsible civil engineering positions at any level of advancement? Because the student rarely knows until the end of his college career what specific branch of civil engineering he will enter, his college education must be of sufficiently broad scope to enable him to fill adequately any starting position in any branch of the field. The college must prepare him for work in design, construction, operation, or in a combination of these three.

However, there exist certain specific educational requirements for the student entering the general field of civil engineering. He must be an engineer with all the basic training in mathematics, physics, and mechanics necessary for civil engineering. He must have a knowledge of the basic principles involved in all branches of civil engineering such as structures, sanitation, hydraulics, surveying, and transportation in order that he may later make use of this knowledge in his chosen work and that he may be generally informed in the whole field. Because the young engineer frequently must make written reports, he must be particularly well grounded in the use of the English language. Some breadth must be given his education so his curriculum should include appropriate courses in the humanities, the social sciences, and the fine arts.

Because the civil engineering student does not know exactly what he will do after graduation and because his employer will not provide any special training, his curriculum should be broad in nature, with courses that are well balanced between the science and the art of engineering. The courses should also be sufficiently technical to enable him to be useful to his employer; they should provide a thorough grounding in the use of the English language; and they should include appropriate courses in nonengineering subjects.

Since the Wickenden Report[4] was issued, engineering colleges have been changing their curricula to meet these requirements. There has been general agreement on a reasonable and effective compromise among these requirements within the framework of a four-year curriculum which is evidenced by similarity of curricula at most institutions. Under these circumstances, it would appear that the best possible curricula have been developed and that normal and gradual modifications would keep the curricula up to date.

Many leaders in engineering education, however, believe that this stability in curricula is evidence of stagnation and that new developments, particularly in atomic science and electronics, require a complete revision of the methods of training engineers and of the subject matter involved. Such developments can have only small and peripheral effects on the field of civil engineering.

---

[4] "Report of the Investigation of Engineering Education, 1923–1929," Am. Soc. for Eng. Education, Pittsburgh, Pa., 1930.

Civil engineering has made steady progress over the years but actually there has been no startlingly new concept since reinforced concrete was introduced and there promises to be none in the near future. This is only natural because civil engineering works have been built for thousands of years and may be expected to be in a more mature state of development than those in other fields. However, progress has been made in the better understanding of the principles underlying soils and hydrology, the more economical use of materials, the use of photogrammetric mapping, the reduction in the costs of earth moving, and similar developments which should be brought to the students' attention.

The changes proposed for all engineering curricula include the addition of more mathematics to the calculus, atomic physics, or atomic engineering beyond that which is necessary to keep the student informed concerning progress in the field, "solid-state" physics or mechanics, and advanced electronics. These changes would damage civil engineering curricula because, if they were included, they would force out work in the advanced civil engineering subjects. It is more important for the young graduate civil engineer to be able to participate intelligently in the economic study of a highway location problem or the organization of a construction program than to be able to compute the efficiency of an atomic reactor.

The civil engineer who has an unusual job or who becomes a research worker will need specialized knowledge along certain lines. When this need arises he can always obtain this knowledge as he has in the past: Through his own efforts in the library, through his technical magazines, or by taking formal graduate work in a university.

When considering engineering curricula, it must be noted that the field of civil engineering is very different from other fields of engineering. The civil engineer is apt to work for a public agency, in construction, or by himself, and he is apt to have a wide variety of problems in his day's work. Civil engineering education should not be patterned after the engineering education of the mass production industries where research and development have become predominant but should be designed specifically for civil engineers.

DISCUSSION

Alfred R. Golzé,[5] **M. ASCE.**—This paper should be read by all civil engineering faculty members and by all members of the profession interested in having college graduates enter the profession with an adequate educational background.

While it may be true that there is more stability in civil engineering education than in the allied engineering arts and sciences, the university authorities responsible for the curricula should not become complacent. Progress in civil engineering is being made continuously, and where a practice has developed that is part of the profession this practice should be reflected in the curricula. For example, on graduation, a student should know that the modern civil engineer has new tools, such as prestressing of concrete and welding of structures, to help him do a more effective job. He should know, too, that the same basic principles of civil engineering apply to the design of small dams as well as to the design of the largest dams. He needs to be exposed to the economics involved in modern superhighway locations and he should understand the importance of estimating construction costs as a basis for securing funds for the work. It should be emphasized that a thorough understanding of civil engineering cannot be fully acquired in the four years of college training leading to a bachelor's degree.

Whenever a student can devote an additional year for a master's degree it is to his advantage. If the fifth-year curriculum includes subjects designed to increase the breadth of the student's education, it will certainly make him a better employee after graduation and increase his opportunities for positions of leadership in the engineering profession and related administrative fields. A fifth year of study could offer those students with an aptitude for research development a chance to develop that aptitude; it could also help the potential graduate select the occupational field for which he is best suited. However, because of the attractive salaries now being offered a graduate, it may be difficult to interest him in a fifth year. The young man anxious to begin his career might not realize the long-range value of a broader education. Therefore, anything the faculty members can do to interest fourth-year students to study another year will be of great service to the engineering profession.

The author mentions the lack of training courses for civil engineers after graduation. The need for such training programs by employers should be recognized. In some fields, such as electronics, in-service training is offered and may replace one or more years of graduate college work. Training courses for graduate civil engineers could be established with university participation so that credits toward a master's degree could be given. The Bureau of Reclamation (United States Department of the Interior) has worked closely with the universities on occasion in advancing the education of its engineering personnel, and on-the-job training is part of its program to advance qualified employees. Other government agencies have similar programs.

---

[5] Chief, Program Coordination and Finance Div., Bureau of Reclamation, U. S. Dept. of the Interior, Washington, D. C.

Proper training of young people is essential to progress in any field, and the field of civil engineering is no exception. Continuous constructive analysis, as outlined in the author's paper, shows that the universities are alert to their responsibilities.

Benjamin A. Whisler,[6] M. ASCE.—As Mr. Golzé has indicated, it is possible that a four-year curriculum leading to a bachelor's degree is no longer adequate for the education of the civil engineer. Educational institutions are under pressure to increase the basic scientific content as well as the nontechnical content of the civil engineering curricula. These pressures, however, have been resisted by those colleges recognizing that there can be no such increases within the framework of the traditional four-year curriculum without sacrificing courses designed specifically for civil engineers to the extent that it would no longer be a curriculum in civil engineering. The addition of another year to the undergraduate requirements would undoubtedly help relieve these pressures and, at the same time, retain the identity of the civil engineering curriculum. A few institutions have recently made this change with apparent success and are satisfied with the results.

The civil engineering teacher has had increasing difficulty in convincing his better students that a year or more of graduate work would be worth while. Mr. Golzé's views concerning the value of an extra year of study are apparently held by many practicing engineers and will help the civil engineering educator when he is trying to encourage his better students to take graduate work.

---

[6] Head, Dept. of Civ. Eng., Pennsylvania State Univ., University Park, Pa.

AMERICAN SOCIETY OF CIVIL ENGINEERS
Founded November 5, 1852
TRANSACTIONS

Paper No. 2884

A CONCEPT OF THE REGIME THEORY

By Ning Chien,[1] A. M. ASCE

With Discussion by Messrs. Gerald Lacey; Emory W. Lane; Thomas Blench; Ning Chien; and Hans A. Einstein

Synopsis

The regime theory is analyzed on the basis of the bed-load function. It has been found that, within the limits of the observed flows on which the regime theory was derived, the "silt" factor, f_{VR}, depends on the sediment concentration of the channel flow whereas another factor, f_{RS}, is a function of the size of the bed material. By using these functional relationships between sediment characteristics and silt factors, the depth and slope of an alluvial channel in regime can be determined either by the bed-load function or by the regime theory with almost no difference between the two. The use of the regime theory for conditions other than those in India and Pakistan should be approached with great care because the silt factor depends also on the characteristics of the flow.

Introduction

In northern India and Pakistan the rainfall, except in monsoon seasons, is usually not sufficient for the growth of crops whereas large rivers, flowing from the Himalaya Mountains, spread over the plains and carry discharges comparable to those of the Mississippi River in the United States. The great demand of water for agricultural purposes combined with an ample supply of river water make this section of the Indian plains ideal for a high development of irrigation. The water flowing out of the mountains is often heavily charged with sediment, and the Indus River and the Ganges River flow through an alluvial plain deposited by these two rivers during recent geologic periods. Maintenance work on some of the irrigation projects was expensive because of the continuous silting up of the channels. Engineers realized that certain natural laws must exist that control the characteristics of channels capable

---

Note.—Published, essentially as printed here, in February, 1955, as *Proceedings-Separate No. 620.* Positions and titles given are those in effect when the paper or discussion was approved for publication in *Transactions.*

[1] Associate Prof. of Hydraulics, Tsing Hwa Univ., Peiping, China.

of carrying given discharges and sediment loads without excessive aggradation or degradation. Edward S. Lindley,[2] A. M. ASCE, for example, stated in 1919 that "* * * the dimensions, width, depth and gradient of a (regime) channel to carry a given supply loaded with a given silt charge were all fixed by nature."

Since the end of the nineteenth century, various efforts, for the most part directed by British civil engineers, have been made to understand these natural processes. The most successful of these efforts was made by Gerald Lacey[3, 4, 5] who developed a complete set of formulas for determining width, depth, and slope of the channels in regime. This theory has been used extensively in India and Pakistan for the design of irrigation canals. Attempts to improve the theory have been made,[6, 7, 8] but the basic equations proposed by Mr. Lacey remain essentially the same, although they may be expressed in different forms with different interpretations.

The development of the Lacey regime theory is based on a mass of data and experience. However, the theory does not give a clear description of the physical aspect of the problem and it does not define what actually governs the characteristics of an alluvial channel. Therefore, engineers hesitate to apply the theory to conditions different from those in India and Pakistan. Mr. Lacey's formulas also involve factors which are essentially based on experience, thus making the application of the theory difficult for those lacking this experience. It is the purpose of this paper to evaluate these factors quantitatively in terms of the physical conditions imposed on the channel and also to show the possible limitations of the theory.

THE REGIME THEORY

The Lacey regime theory can be expressed as

$$\frac{V^2}{R} = 1.325\, f_{VR} \qquad (1)$$

$$R^{1/3} S^{2/3} = 0.0052\, f_{RS} \qquad (2)$$

and

$$p = a\, Q^{1/2} = 2.67\, Q^{1/2} \qquad (3)$$

in which V is the average velocity of the flow; R, the hydraulic radius of the channel; S, the channel slope; p, the wetted perimeter of the channel; a, a constant; Q, the discharge; and f_{VR} and f_{RS}, the silt factors. The silt factors are introduced in the same way as originally given by Mr. Lacey but they have since been shown to have different values. Eqs. 1, 2, and 3 can be applied only to channels which contain a bed of loose sediment of the same type that is moved along the bed; these channels should also be essentially at equilibrium. From these basic equations many other correlative relationships can also be derived.

---

[2] "Regime Channels," by Edward S. Lindley, *Minutes of Proceedings*, Punjab Eng. Cong., Lahore, India, Vol. 7, 1919, pp. 63–74.

[3] "Stable Channels in Alluvium," by Gerald Lacey, *Minutes of Proceedings*, Inst. of C. E., London, Vol. 229, 1929–1930, pp. 259–292.

[4] "Regime Flow in Incoherent Alluvium," by Gerald Lacey, *Publication No. 20*, Central Board of Irrig., Simla, India, 1940, p. 65.

[5] "A General Theory of Flow in Alluvium," by Gerald Lacey, *Journal*, Inst. of C. E., London, Vol. 27, 1946, pp. 16–47.

[6] "The Behavior and Control of Rivers and Canals," by Sir C. C. Inglis, *Publication No. 13*, Central Waterway, Irrig. and Nav. Research Station, Poona, India, 1949.

[7] "Hydraulics of Sediment-Bearing Canals and Rivers," by T. Blench, Evans Industries, Vancouver, B. C., Canada, 1951.

[8] "Regime Theory for Self-Formed Sediment-Bearing Channels," by T. Blench, *Transactions*, ASCE, Vol. 117, 1952, pp. 383–408.

BASIC PREMISES

This paper is based on four premises, two concerning the behavior of alluvial channels in general and two concerning the Lacey theory in particular. These premises are:

1. The equilibrium state of an alluvial channel is attained by adjusting the dimensions of the cross section and the slope of the channel to the natural conditions imposed on the channel by the drainage basin. These conditions, which are independent of the channel itself, include the sediment inflow, the discharge, and the gradation and size of the material of which the channel bed and banks are composed. It has long been recognized[9] that the sediment inflow is a primary factor governing the stability of an alluvial channel.
2. The alluvial channel differs from the fixed-boundary channel because the boundary of the former is molded by the flow and may change with it. The frictional resistance of alluvial-channel flow cannot be described by one formula with universal constants, such as the Manning formula. It must be interpreted as a composite effect of the following: (*a*) Resistance of the sediment grains which compose the channel bed; (*b*) resistance of banks; and (*c*) resistance of sand bars and other irregularities. Each of these effects follows different and independent laws.
3. Eqs. 1, 2, and 3 are empirical relationships based on field observations only. They should not be visualized as fixed laws with universal application.
4. The regime theory is the result of sixty years of experience in India and Pakistan. At present (1956) it is a useful tool for designing irrigation canals in those areas.

METHOD OF APPROACH

The writer does not intend to rationalize Eqs. 1, 2, and 3 by scrutinizing the physical significance of each formula. A philosophical basis for the regime theory is offered instead, indicating why the sediment load is not included in the theory.

The omission of the sediment load as an explicit variable in Eqs. 1, 2, and 3 can be explained by either of the following possibilities:

1. The silt factors in Eqs. 1 and 2 implicitly include the sediment load with the bed-material size.
2. Although the dimensions and slope of an alluvial channel must depend on the sediment inflow, a certain combination of these variables may rarely depend on the sediment load.

In testing these hypotheses, the graphical solutions as given by the writer,[10] in relating the channel depth and slope to the unit discharge and sediment load, are taken as the basis for analysis. These graphical solutions are constructed according to the bed-load function,[11] the only available working tool giving a complete description of the alluvial channel flow and the sediment transport.

---

[9] "Stable Channels in Erodible Material," by E. W. Lane, *Transactions*, ASCE, Vol. 102, 1937, pp. 123–142.

[10] "Graphic Design of Alluvial Channels," by Ning Chien, *Transactions*, ASCE, Vol. 121, 1956, p. 1267.

CONDITIONS UNDER WHICH THE REGIME THEORY WAS DEVELOPED

The physiographical and climatic conditions in northern India and Pakistan have been described.[7] Table 1 shows the range of variables used by Mr. Lacey in his analysis, as determined by taking the central 90% of the cumulative-frequency curve of each variable.[12]

TABLE 1.—RANGE OF VARIABLES UNDER WHICH THE REGIME THEORY WAS DEVELOPED

Variable	Unit	Canal Data			River Data		
		Punjab	Sind	Total	Punjab	Misc.	Total
Velocity	feet per second	1.5–2.8	1.5–2.9	1.5–3.0	2.0–13.5	2.4–7.5	2.0–7.6
Hydraulic radius	feet	1.1–8.0	1.6–11.0	1.2–10.3	2.5–13.3	3.1–15.3	3.0–15.6
Slope	feet per 1,000 ft	0.05–0.33	0.05–0.14	0.05–0.35	0.10–0.57	0.13–1.72	0.10–1.55
Discharge	cubic feet per second	20–4,500	35–8,500	20–6,500	...	...	...
Grain size	millimeter	0.20–0.38	0.05–0.15	0.05–0.33	...	...	...
f_{VR}	...	0.6–1.5	0.4–0.8	0.4–1.5	0.5–3.5	0.4–6.0	0.5–6.0
f_{RS}	...	0.6–1.5	0.5–0.8	0.5–1.5	0.6–2.5	0.8–6.0	0.6–6.0

The main source of data used by Mr. Lacey and other engineers arises from field observations of existing irrigation canals which were in equilibrium. For this class of information the range of bed-material size is particularly limited.

RESULTS OF ANALYSIS

The analysis was conducted in different steps: (*a*) The bank friction was neglected and the conditions, as given in Table 1, were investigated and computed; (*b*) this type of analysis was then extended to include conditions different from those prevalent in India and Pakistan; and (*c*) the bank friction was introduced and its effect was studied.

First Step.—In the first step the bank friction was neglected, the bed-material size was 0.25 mm (which corresponds to the average size of bed material in northern India and Pakistan), the hydraulic radius ranged from 2 ft to 25 ft, and the slope was from 0.001 to 0.004. Fig. 1 illustrates the results of this step in the investigation by showing the relationship between the silt factors and the sediment concentration. The computed points can best be approximated by straight lines of the following forms:

$$f_{VR} = 0.061 \left(\frac{q_T}{q}\right)^{0.715} \quad \ldots\ldots\ldots\ldots\ldots\ldots\ldots\ldots (4)$$

---

[11] "The Bed-Load Function for Sediment Transportation in Open Channel Flows," by H. A. Einstein, *Technical Bulletin No. 1026*, U. S. Dept. of Agriculture, Washington, D. C., 1950.

[12] "The Sediment Problem in the Indian Rivers: The Indian Approach and Its Comparison with the American Theory," by P. C. Playoust, thesis presented to the University of California at Berkeley, in 1954, in partial fulfilment of the requirements for the degree of Master of Science.

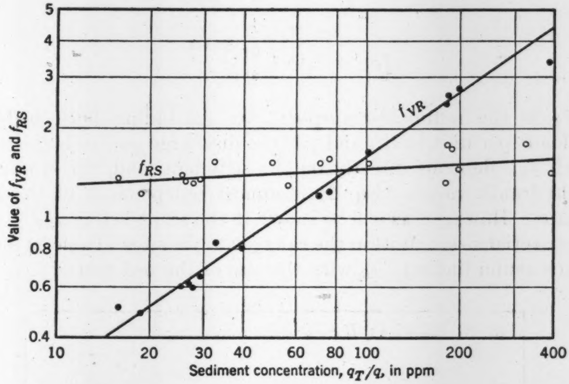

FIG. 1.—RELATIONSHIP BETWEEN SILT FACTORS AND SEDIMENT CONCENTRATION FOR NORTHERN INDIA AND PAKISTAN WITH $D = 0.25$ MM AND BANK FRICTION NEGLECTED (ACCORDING TO THE BED-LOAD FUNCTION)

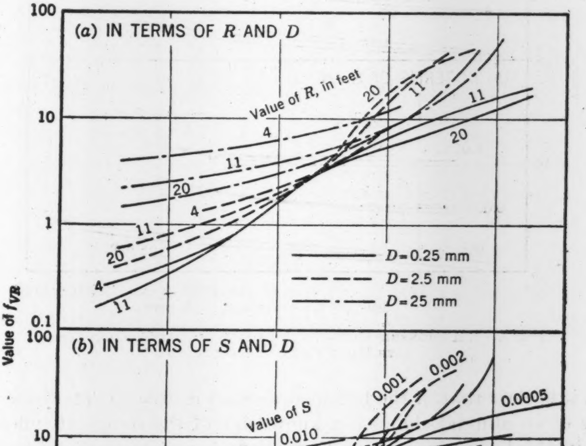

FIG. 2.—RELATIONSHIP BETWEEN f_{VR} AND SEDIMENT CONCENTRATION WITH BANK FRICTION NEGLECTED

and

$$f_{RS} = 1.18 \left(\frac{q_T}{q} \right)^{0.052} \qquad (5)$$

in which q_T is the sediment-transport rate (including both bed-load and suspended load) per unit width and q is the discharge per unit width.

Although f_{VR} depends directly on the sediment load, the combination of slope and hydraulic radius (Eq. 2) is almost independent of the sediment-transport rate. However, as will be shown in the second step, f_{RS} is a function of the bed-material size. Within the range of grain sizes (Table 1) no relationship has been found linking f_{VR} with the size of the bed material.

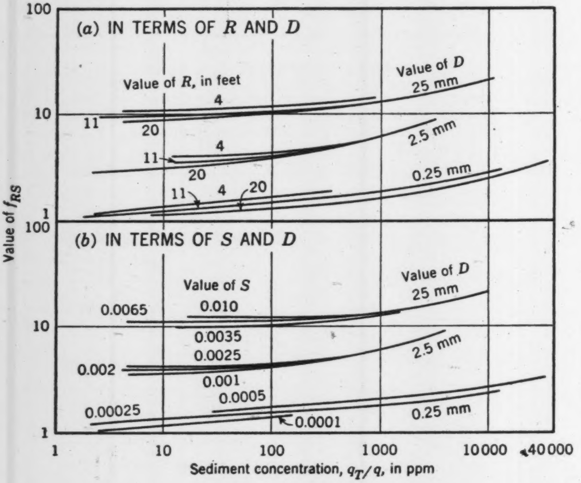

FIG. 3.—RELATIONSHIP BETWEEN f_{RS} AND SEDIMENT CONCENTRATION WITH BANK FRICTION NEGLECTED

Thus, it is clear that, if the bed-load method is used to determine the depth and slope of an alluvial channel, a knowledge of the sediment inflow and the material in the bed is required. Even though it is not simple to determine sediment inflow to irrigation canals,[10] this determination has physical significance. The use of the regime theory involves estimating silt factors which must represent functions of sediment load and size for existing conditions in India and Pakistan. Utilizing the regime theory in this manner and by using Fig. 1, the two methods give almost the same results.

Second Step.—In the second step bank friction was neglected; the bed-material size was 0.25 mm, 2.5 mm, and 25 mm; the hydraulic radius ranged from 2 ft to 30 ft; and the slope was from 0.001 to 0.005 for the 0.25-mm bed material, from 0.003 to 0.0025 for the 2.5-mm bed material, and from 0.001 to 0.01 for the 25-mm bed material. The relationships between the silt factors and the sediment concentration and size are given in Figs. 2 and 3. In Figs.

2(*a*) and 3(*a*), R is held constant and S varies; the reverse is true in Figs. 2(*b*) and 3(*b*).

In this wider range of variables, especially those of the sediment size, the trend of f_{RS} (Fig. 3) remains the same. With sediment size, D, as a variable and expressed in millimeters, Eq. 5 becomes

$$f_{RS} = 2.2\, D^{0.45} \left(\frac{q_T}{q}\right)^{0.052} \qquad (6)$$

for $q_T/q < 200$ ppm. The change of f_{VR} with sediment concentration (Fig. 2) not only follows a different pattern but is also quite erratic. For conditions different from those in India and Pakistan, f_{VR} depends also on the hydraulic characteristics of the channel, which makes general application of the regime theory extremely difficult. Lack of proper training or experience in estimating the values of the silt factors is not necessarily responsible for this difficulty, but experience in northern India and Pakistan may not be applicable to areas where the conditions are substantially different.

Third Step.—In the third step the bank friction was introduced with vertical side walls having an n-value of 0.02 (assuming growth of soft vegetation along the banks). The channel width in this step was given by Eq. 3; the bed-material size was 0.25 mm; the hydraulic radius was from 2 ft to 30 ft; and the slope ranged from 0.001 to 0.005.

The conclusions derived from the first two steps were obtained by ignoring the bank friction. It is important to ascertain whether the effect of bank friction will materially modify these conclusions in any way. This effect depends on the roughness of the banks and on the width-depth ratio of the channel. The selection of the Manning n of 0.02 for the bank roughness is arbitrary but representative. If the banks behave as if they were hydraulically smooth, as suggested by Thomas Blench,[7] M. ASCE, the net results of the analysis would fall somewhere between those indicated in Figs. 2(*a*) and 3(*a*) and those given in Fig. 4. The use of Eq. 3 in determining the channel width is justified as long as the range of variables is not significantly different from that listed in Table 1.

Comparing Figs. 2(*a*) and 3(*a*) with Fig. 4 clearly demonstrates that the bank friction has little effect on the over-all trends according to which silt factors vary with the sediment concentration. The inclusion of bank friction results in a slight shift of the relative position of both the f_{VR}- and f_{RS}-curves for small channels only.

The sediment load used in this study refers only to the bed-material load, which is the material that has been found to be abundant in the bed. The actual sediment concentration of the canal flow, including that of the wash load,[13] may be considerably higher than the values given in Figs. 1, 2, 3, and 4.

In using the bed-load function, the effect of bar resistance is determined from river measurements.[14] Some evidence indicates that, below a certain limit, the bar resistance is affected by the width of the channel. In a narrow channel the bars do not develop to full size because of the confinement of the banks. In effect, this will bring the values of f_{VR} and f_{RS} closer together at small sediment concentrations, but it will not materially change the conclusions derived from the present analysis.

---

[13] "The Laws of Sediment Transportation," by H. A. Einstein and J. W. Johnson, *Applied Sedimentation*, John Wiley & Sons, New York, N. Y., 1950, pp. 62–71.

[14] "River Channel Roughness," by H. A. Einstein and N. L. Barbarossa, *Transactions*, ASCE, Vol. 117, 1952, pp. 1121–1146.

CHANNEL WIDTH

The third Lacey relationship—linking the width of the channel to the discharge—cannot be appraised by comparing it with the bed-load function because it is beyond the scope of the latter. In a paper written by Luna B. Leopold, A. M. ASCE, and T. B. Maddock, Jr.,[15] in which a number of stream-channel characteristics in the Great Plains and southwest regions of the United States have been studied, it was found that a functional relationship between p and $Q^{\frac{1}{2}}$ exists among the various cross sections along the river length under the condition that discharge at all points is equal in frequency of occurrence. Messrs. Leopold and Maddock refer to the constant of proportionality, a (Eq. 3), which Mr. Lacey found to be 2.67, as follows:

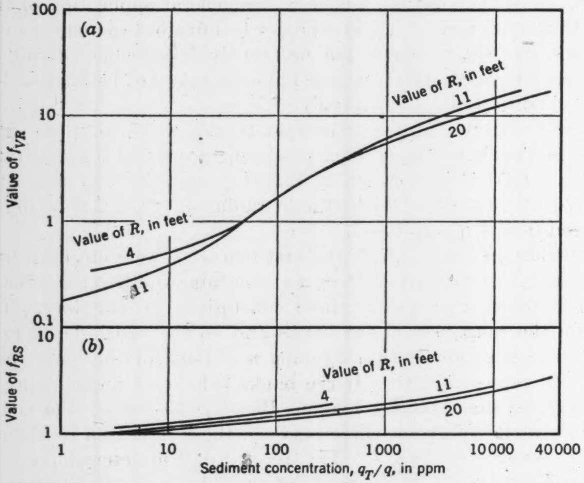

FIG. 4.—RELATIONSHIPS WITH BANK FRICTION INTRODUCED (n = 0.02) AND R HELD CONSTANT AS S VARIES WITH D = 0.25 MM

> "Lacey found so little variation of a in Indian regime canals that he considered it to be a constant for all streams. Inspection of the large differences in intercept of the lines * * * representing natural rivers indicates that the value of a is not a constant."

What determines a is not fully understood.

---

[15] "The Hydraulic Geometry of Stream Channels and Some Physiographic Implications," by Luna B. Leopold and T. B. Maddock, Jr., *Professional Paper No. 252*, Geological Survey, U. S. Dept. of the Interior, Washington, D. C., 1953, pp. 43-45.

CONCLUSIONS

The findings of this paper can be summarized as follows:

1. The silt factors in the regime theory have been correlated with the conditions imposed by the watershed on the channel according to the bed-load function.
2. In the case of the channels in the Indian-plains area, from which the regime theory was originally derived, f_{VR} depends on the sediment concentration of the flow whereas f_{RS} varies primarily with the bed-material size. Functional relationships between the silt factors and the sediment characteristics are given. Using these relationships, both the bed-load function and the regime theory give the same depth and slope of an alluvial channel in equilibrium.
3. The general application of the regime theory to conditions other than those in India and Pakistan is questionable because f_{VR} depends also on the flow characteristics, which makes the selection of the f-values difficult.

DISCUSSION

Gerald Lacey[16].—The author correctly states that the dimensions and slope of an alluvial channel having a given discharge, Q, must depend on the sediment load and on the bed-material size; his suggestion that a certain combination of the variables may depend only slightly on the sediment load is of value. It will be shown herein that in certain combinations the sediment load is entirely absent.

Sir Claude Inglis and Emory W. Lane,[6,9] Members, ASCE, were the first to stress the importance of the transported load as opposed to the size of the bed material. The precise manner in which both variables enter regime equations has yet to be determined. However, Mr. Chien's paper marks an advance in the solution of this problem.

The writer's basic equation for the silt factor, f, is

$$V = 1.155\, f^{1/2}\, R^{1/2} \qquad (7a)$$

or

$$f = 0.75\, \frac{V^2}{R} \qquad (7b)$$

If the mean depth, d, had been used rather than R, the silt factor would have been a function of the Froude number. One can reasonably conclude that the writer's relationship should preferably have taken this form.

The writer also proposed the formula:

$$f = 1.76\, m^{1/2} \qquad (8)$$

in which m is the size of the bed-material particle in millimeters. It became evident that the bed load should enter both of the writer's equations and that, as quoted, the equations could apply only to channels transporting an assumed constant, or regime, bed load.

The writer's flow equation, in terms of V, R, and S,

$$V = 16.0\, R^{2/3}\, S^{1/3} \qquad (9)$$

contained no silt factor or rugosity coefficient. Such variables were considered to be implicit in the actual depth and slope adopted by the channel in loose alluvium. Sir Claude proposed that, although the bed-material size might be implicit, the bed load could not be ignored in this relationship.

The writer's equation for the wetted perimeter (Eq. 3), which Messrs. Leopold and Maddock[15] have confirmed with respect to the power of 1/2 for natural channels, has the same defect. The precise grade of bed material does not appear to affect the constant but, as Messrs. Inglis and Lane have emphasized, the bed load is an important variable in determining width and should enter this question. With a regime bed load, the constant (except for the complication of stiff banks) would be approximately correct. In rivers the width varies greatly from point to point, and flow is seldom concentrated into one compact stable channel of minimum width. The writer now prefers to use the water-surface width, B, as a variable instead of the wetted perimeter, p. This procedure is consistent with modern practice.

---

[16] Consultant, Inst. of C. E., London, England.

Combining Eqs. 7 and 9, a number of silt factors can be obtained of which the following are examples:

$$f_{VR} = 0.75 \frac{V^2}{R} \qquad (10a)$$

$$f_{RS} = 192\, R^{1/3}\, S^{2/3} \qquad (10b)$$

and

$$f_{RS/V} = 3{,}072 \frac{R\, S}{V} \qquad (10c)$$

The author has used the first two silt factors and, from them, the third silt factor may be derived as follows:

$$f_{RS/V} = \frac{f^{3/2}{}_{RS}}{f^{1/2}{}_{VR}} \qquad (10d)$$

It is possible to determine the relationship between $f_{RS/V}$ and the sediment concentration. Referring to Fig. 4(a) and examining the general trend it will be noted that, for a sandy bed material with a mean diameter of 0.25 mm, these equations result in

$$f_{VR} = \text{const.} \left(\frac{q_T}{q}\right)^{1/2} \qquad (11a)$$

and

$$f_{RS} = \text{const.} \left(\frac{q_T}{q}\right)^{1/6} \qquad (11b)$$

Eq. 11a is the mean of the entire range, and Eq. 11b applies to sediment concentrations exceeding 1,000 ppm. Therefore, it can be concluded that the parameter, $R\, S/V$, is independent of the sediment concentration, q_T/q.

This combination of the variables is embodied in the flow equation,

$$V = 3{,}072 \frac{R\, S}{f} \qquad (12)$$

and on replacing f by the square root of the particle size, and inserting g, the gravitational acceleration,

$$V = \text{const.}\, g^{1/2} \frac{R\, S}{m^{1/2}} \qquad (13)$$

which is the Lacey-Malhotra equation.[17]

This dimensionally homogeneous equation (Eq. 13) has a physical significance because it implies a loose, moving bed of incoherent material and a linear-resistance law. Although it is preferable to express width and depth in terms of B and d, rather than in terms of p and R, the hydraulic mean depth should enter the linear-resistance-law flow equation because the slope, S, is involved. The value of R, the effective hydraulic mean depth, is obtained by dividing the cross-sectional area, $B\,d$, by the effective wetted perimeter, allowance being made for the different, and usually finer, texture of the banks; this point is of importance in all model work.

---

[17] "Regime Flow in Incoherent Alluvium," by Gerald Lacey, *Publication No. 20*, Central Board of Irrig., Simla, India.

Sir Claude[18] has added the sediment load as a variable to the regime equations. The variable, m, is retained but, in addition, the terminal velocity of the particle in water, V_s, is used, and $X = q_T/q$ is uniformly associated with the terminal velocity by means of the product, $X\,V_s$.

The following equations, or Inglis-Lacey[18] formulas, should be noted because they all involve the discharge and the sediment load—

$$V = \text{const. } m^{1/12}\,(X\,V_s)^{1/12}\,Q^{1/6} \qquad (14a)$$

$$D = \text{const. } m^{1/6}\,\frac{Q^{1/3}}{(X\,V_s)^{1/3}} \qquad (14b)$$

$$S = \text{const. } m^{5/12}\,\frac{(X\,V_s)^{5/12}}{Q^{1/6}} \qquad (14c)$$

and

$$W = \text{const. } \left(\frac{X\,V_s}{m}\right)^{1/4} Q^{1/2} \qquad (14d)$$

By using Eqs. 14, the grade, the terminal velocity, and the bed load can be eliminated which results in

$$V^4 = \text{const. } B\,d\,S \qquad (15)$$

Eliminating $X\,V_s$ from Eqs. 14a, 14b, and 14c,

$$\frac{V}{D\,S} = \frac{\text{const.}}{m^{1/2}} \qquad (16a)$$

which should be compared with Eq. 13. Also,

$$\frac{V^3}{W} = \frac{\text{const.}}{m^{1/2}} \qquad (16b)$$

Eqs. 16, which are independent of the sediment load, are of value and should stimulate research.

The comparable equation of Thomas Blench,[7]

$$\frac{V^2}{B} = s \qquad (17)$$

in which s is a "practical side factor" incorporating the smooth or coherent texture of banks does not apply to a channel which has been formed in loose, incoherent alluvium and whose banks consist of material transported by the channel and thrown down at the sides by secondary flow. Mr. Blench's side factor is applicable in nature because the banks may be composed of material different from the transported alluvium, but it does not apply to the basic regime problem of self-deposition.

---

[18] "The Effect of Variations of Charge and Grade on the Slopes and Shapes of Channels," by Sir C. Inglis, International Assn. for Hydraulic Structures Research, 1949.

The Inglis equation,

$$\frac{V^2}{g\,b} = \text{const.}\ (X\ V_s)^{1/2} \ldots\ldots\ldots\ldots\ldots\ldots\ldots (18)$$

in which the diameter of the particle does not enter, has yet (as of 1956) to be verified. However, when the bed material is formed of medium sand, Mr. Chien's data lend support to the power of 0.5. Eq. 6 also lends support to the power of 0.5 for the value of V_s which, in this instance, varies as the diameter. The problem is to verify that this equation is correct when applied to coarser material because it is possible that the final relationship that is derived may take a different form.

Mr. Chien has done a service to the profession in alining the work of Hans A. Einstein, M. ASCE, on the bed-load function with the regime theory. The valuable paper of Messrs. Leopold and Maddock[15] should be studied by those desiring to review the field of investigation. It is gratifying to note that the regime theory is of interest to research workers in the United States. It is hoped that formulas of physical significance may eventually be derived from the writer's early regime equations.

Emory W. Lane,[19] M. ASCE.—A valuable contribution has been made by Mr. Chien to the evaluation of the science of design of stable irrigation canals, which has been in progress since R. G. Kennedy proposed his equation in 1895.[20] Messrs. Kennedy and Lacey and other engineers developed a successful method of canal design in the plains region of India, which has been very helpful in solving many problems of stream control. However, the method has not proved to be generally applicable and, therefore, it has not been used widely in Egypt, the United States, or even exclusively in India.[21]

The writer believes that the principal weakness of Mr. Lacey's relationships is that they do not include the concentration of the sediment as a variable. Some engineers of India, including Sir Claude and Kanwar Sain, M. ASCE, believe that sediment concentration should also be considered. In comparing the results of the bed-load relationships, the author found the value of f_{VR} to be a function of the sediment concentration. However, the writer would urge a more limited application of the regime theory than that which Mr. Chien's third conclusion considers—restriction of the formula to India and Pakistan—because there are parts of India and Pakistan in which conditions differ from those in the plains sections. The writer would further limit the theory to the plains sections in which the relationships were developed or similar conditions. Even in these plains sections, conditions may change because of the introduction of water-storage reservoirs, which will materially change the sediment concentration in the canals supplied from the reservoirs. Therefore, calling attention to the limitation of the regime relationships is of particular importance.

---

[19] Hydr. Engr., Fort Collins, Colo.

[20] "The Prevention of Silting in Irrigation Canals," by R. G. Kennedy, *Minutes of Proceedings*, Inst. of C. E., London, Vol. 119, 1895, pp. 281-290.

[21] "The Canal System of the Hirakud Project," by E. P. Pilla and K. C. Thomas, *Indian Journal of Power and River Valley Development*, Calcutta, India, Vol. 4, No. 10, 1954, pp. 59-64.

As a result of the experience in the Imperial Valley (California), where the reduction of the sediment load in the water of the Colorado River by means of reservoirs and sediment-control works materially altered the regime of the canals, similar changes can be expected in canals in India and Pakistan. In the Imperial Valley, the slopes of the canals were reduced as much as two-thirds and depth was increased as much as 100%. Extensive protection of existing drops and the addition of numerous new drops were required. Although they may be less severe, similar changes will occur in India and Pakistan when reservoir water is introduced into the canals formerly carrying heavy sediment loads.

The author assumes that the bed-load function is reliable and that, when the results obtained by the use of regime relationships differ from those obtained by the use of the bed-load function, the regime relationships are in error. This is understandable because of the author's extensive experience with the bed-load function, but it may not be convincing to those who have had considerable favorable experience with the regime relationships and little or no experience with the bed-load function. The writer believes that perhaps the greatest need in the sediment-engineering field is extensive field measurements of the quantity of sediment transported in channels under a wide range of conditions, with which the relationships proposed by Mr. Einstein and others may be checked and the extent of their reliability determined. At the present time (1956) the engineering profession has as much knowledge of sediment transportation as it had of the flow of water in channels at the start of the twentieth century. Papers containing extensive data on sediment transport, comparable to those by E. Ganguillet and William Kutter,[22] Fred C. Scobey,[23] and Ivan E. Houk,[24] in the field of channel flow are needed to evaluate present formulas and to devise better ones if these formulas are not adequate. In order to solve sediment problems adequately it is necessary to learn to handle the flow of sediment quantitatively, as the flow of water is handled.

Mr. Chien has shown that, on the basis of the bed-load function, Mr. Lacey's value of f_{RS} is a function of $D^{0.45}$. The results, as shown in Fig. 3, are in approximate agreement with the Lacey relationship,

$$f = 8 \sqrt{D} \qquad (19a)$$

in which the bed grain diameter, D, was expressed in inches. This was later perfected to

$$f = 8.85 \sqrt{D} \qquad (19b)$$

---

[22] "A General Formula for the Uniform Flow of Water in Rivers and Other Channels," by E. Ganguillet and William Kutter, John Wiley & Sons, Inc., New York, N. Y., 1891.

[23] "Flow of Water in Irrigation and Similar Canals," by Fred C. Scobey, *Technical Bulletin No. 652*, U. S. Dept. of Agriculture, Washington, D. C., 1939.

[24] "Calculation of Flow in Open Channels," by Ivan E. Houk, in "Technical Reports," Pt. IV, Miami Conservancy Dist., Dayton, Ohio, 1918.

Mr. Lacey did not advocate the use of this relationship perhaps because it did not prove feasible when it was applied to the value of f_{VR}.

In selecting relationships for use in irrigation-canal design, engineers engaged in perfecting the science of canal design should keep the objective in mind—that is, the canal which will be the most economical from the standpoints of initial cost and maintenance. In order to minimize maintenance, the canal must not be subject to deposit and scour in large quantities. The regime theory of design was evolved because its aim was to provide freedom from both scour and deposit; it did not consider the element of first cost. As knowledge of sediment transportation increases, it may be possible to find channels of lower total cost (first cost plus maintenance) with characteristics somewhat different from those of channels that would be naturally formed by water flowing under equilibrium conditions. The regime relationships were developed because the maintenance problem, usually due to deposit, took precedence over the matter of first cost. The regime approach then offered the only means by which the problem of sediment deposit could be successfully handled.

However, in cases of clear water from reservoirs, the problem of deposit is eliminated because, if scour is prevented, there will be no sediment to be deposited. The analysis, therefore, must be to develop channels free of scour, and the relationships for these channels are likely to differ from those obtained by means of the usual regime methods. For clear water, disregarding bank sloughing, any combination of channel width and depth which will not scour will produce a stable canal. Such canals will allow more flexibility in the selection of sizes than canals carrying sediment. The lower slopes that can be used will, in some cases, make possible the command of wider areas for the same canal length and the production of greater hydroelectric power. It will thus change appreciably the analysis leading to the determination of the most economical development.

The science of canal design has not yet attained this degree of perfection. However, with additional study, it can probably be reached in the future. Mr. Chien's paper is a valuable contribution toward making this type of analysis possible.

THOMAS BLENCH,[25] M. ASCE.—Since the publication of the regime theory in 1929, the writer has had continuous experience in using, analyzing, and amending it slightly; he has also extended its application to rivers. Justice cannot be done to the theory without a knowledge of its prolonged investigation by the Irrigation Research Institutes and individual engineers of India, recorded in publications such as the Annual Reports of the Central Board of Irrigation and papers of the Institutes. Therefore, although the writer disagrees considerably with Mr. Chien, he can compliment him on a constructive and painstaking analysis of the matter at his disposal.

Mr. Lacey's regime theory cannot be expressed in terms of Eqs. 1, 2, and 3 because the theory was developed in terms of a single "silt factor," f, and the terms, f_{VR} and f_{RS}, were not used. The theory may be expressed by

---

[25] Cons. Engr. and Prof. of Civ. Eng., Univ. of Alberta, Edmonton, Alta., Canada.

$$\frac{V^2}{R} = 1.325\, f \qquad (20a)$$

$$V = 16\,(R^2\,S)^{1/3} \qquad (20b)$$

and

$$p = a\,Q^{1/2} = 2.67\,Q^{1/2} \qquad (20c)$$

Eqs. 20 are necessary and sufficient to fit the three degrees of self-adjustment of types of channels that are considered. For theoretical discussion the following equations, deduced algebraically from the basic equations, are useful:

$$\frac{p}{V\,R} = a^2 = 7.11 \qquad (21a)$$

and

$$V = \frac{1.35\,R^{3/4}\,S^{1/2}}{0.0225\,f^{1/4}} \qquad (21b)$$

For practical design the following algebraically deduced equations are also useful:

$$S = \frac{f^{5/3}}{1{,}788\,Q^{1/6}} \qquad (22a)$$

$$R = \frac{0.47\,Q^{1/3}}{f^{1/3}} \qquad (22b)$$

There are other possibilities, including Eq. 2.

Eqs. 20 and their derivatives proved to be acceptable to engineers and were recommended[26] by the central government (India). In 1932 the government of the United Provinces issued canal-design instructions in terms of the equations.[27] However, it was evident that some secondary corrections were needed. For example, although Lacey-designed channels would flow in regime, their widths could be altered and they would remain in the new regime. Therefore, although all Lacey channels were regime channels, not all regime channels were Lacey channels. Channels were designed as trapezoidal sections because they would retain approximately that shape; yet the design charts for trapezoidal channels[27] stopped at the lower limit of approximately 4 cu ft per sec because the equations gave unreal dimensions below that limit despite a number of normal channels flowing from 1 cu ft per sec to 2 cu ft per sec. When Mr. Lacey proposed that the "ideal" channel was probably of elliptic section, in order to solve the problem of limiting discharge, engineers observed that, for any one case, his equations enabled the choice of either a half ellipse with a horizontal major axis or half the same ellipse with a horizontal minor axis, which had never been observed in nature. Engineers in the province of

---

[26] "Constitution of the Research Committee of the Central Board of Irrigation with Resolutions up to July 1940," Central Board of Irrig., Simla, India, 1940.

[27] "Regime Diagrams for the Design of Canals and Distributaries," *Irrigation Branch Paper No. 1*, United Provinces Public Works Dept., Allahabad, India, 1932.

Sind (India) concluded, after exhaustive site analyses, that the power of 1/2 in Eq. 20*c* was correct but that the value of *a* was different from 2.67; the channels had relatively low values of *f*. Despite these objections, engineers used the equations with certain precautions—for example, in a definite sequence so that errors, if there were any, would only affect dimensions of little importance.

The Irrigation Research Institutes of the various provinces conducted extensive field investigations of the regime theory. In the Punjab men were posted at sites to make observations at intervals of a few days over periods of two or three years. Considerable time was spent in producing alternative formulas, particularly in terms of the sediment diameter rather than in terms of *f*, as discussed by Mr. Lacey.[3]

The Punjab Irrigation Research Institute attempted to verify the Lacey relationships by inserting field data into a variety of algebraically derived equations, such as Eqs. 22, and to check whether identical *f*-values resulted from each equation. The result was that the values of *f* from the separate equations were different but they were functionally related. This caused analysts to give suffixes to the differing values according to the equations from which they came. It would seem that the author may have incorrectly used such suffixes in Eqs. 1 and 2. Two interesting results were as follows: (*a*) The *f*-value from Eq. (22*a*) varied approximately as the square root of that from Eq. 20*a*; and (*b*) the *f*-value from Eq. 21*b* varied as an inverse power of that from Eq. 20*a*, showing that channels with large bed factors were actually smoother than those with small bed factors. This is a paradox arising from the peculiarities of dune formation.

The confusion about different *f*-values was caused by the fact that there are different phases of flow along the sides and the bed; therefore, the use of a single *f*-value for the entire perimeter is inadequate. Assuming a single *f*-value to be adequate and analyzing the systems of canals were equivalent to averaging out the "relative importance of side to bed." The resulting equations would refer to a physically possible set of channels but not to all channels. The writer found how to split the *f*-value into the side and bed factors,[28] and C. King[29] introduced the width-to-depth ratio into the slope relationship. The equations to replace the original Lacey equations are most conveniently expressed as

$$\frac{V^2}{d} = F_b \qquad (23)$$

$$\frac{V^3}{b} = F_s \qquad (24)$$

and

$$\frac{V^2}{g\,d\,S} = 3.63\left(\frac{V\,b}{\nu}\right)^{0.25} \qquad (25)$$

---

[28] "Effect of Dynamic Shape on Lacey Relations," by T. Blench, *Annual Report (Technical)*, Central Board of Irrig., Simla, India, 1941.

[29] "Practical Design Formulas for Stable Irrigation Channels," by C. King, *Annual Report (Technical)*, Central Board of Irrig., Simla, India, 1943.

in which b is breadth, F_b is bed factor, F_s is side factor, and ν is kinematic viscosity. Eq. 25 has been amended by the writer to

$$\frac{V^2}{g\,d\,S} = 3.63\left(\frac{V\,b}{\nu}\right)^{0.25}\left(1 + \frac{C}{233}\right) \quad (26)$$

in which C is the bed-load charge in thousandths of 1% by weight of the water flow and 233 is a provisional constant. The reasons for the introduction of charge and its limitations will be found in papers by the writer and by R. B. Erb.[30,31,32]

The bed and side factors, as defined by Eqs. 23 and 24, replace the Lacey value of f. When derived equations are compared with the Lacey regime equations, it is evident that the changes do not affect the indices of measurable variables in any of the Lacey regime equations. Also, the a-value of Eq. 20c appears as the ratio of the bed factor to the side factor, which explains the nontechnical term, "relative importance of sides to bed." Because the a-value appeared in the various derived regime equations to different powers, the functional relationship of the different f-values is explained. The values of p and R had to be replaced by values of b and d when the sides and beds were considered separately instead of the wetted perimeter as a whole. The physical significance of Eq. 25 was not apparent in the original regime theory. Therefore, the only alterations to the regime equations are in the splitting of the f-value and in the constants, but there are no alterations in the functional forms, as Mr. Chien has stated. The writer has attempted in his own publications to explain that, in the evolving of the regime theory, Mr. Lindley set forth the fundamentals and Mr. Lacey produced the dynamically satisfying formulas.

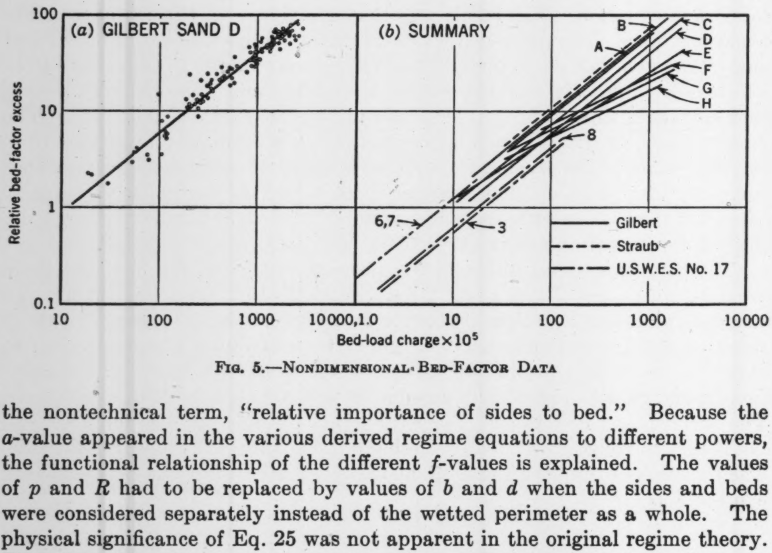

FIG. 5.—NONDIMENSIONAL BED-FACTOR DATA

---

[30] "Regime Behavior of Canals and Rivers," by T. Blench, Butterworths Scientific Publications, London, 1957.

[31] "Regime Formulas for Bed-Load Transport," by T. Blench, *Proceedings*, International Assn. for Hydr. Research, Delft, 1955.

[32] "Analysis of Bed-Load Data," by R. B. Erb, thesis presented to the University of Alberta, at Edmonton, Alta., Canada, in 1955, in partial fulfilment of the requirements for the degree of Master of Science.

The writer disagrees with the author's conclusions 2 and 3. The analyses by the writer and Mr. Erb[32] of the classic Gilbert data, on which the Meyer-Peter and Einstein formulas and curves depend, and of river-sand data in flumes show that:

1. The bed factor, which is practically the *f*-value free from side effect, is a definite function of sand size and of charge (ratio of weight of bed load per unit time to water weight per unit time), even in flumes with rigid sides.
2. Eq. 26 for regime slope is indicated when there are dunes.
3. When dunes vanish and flow becomes supercritical, the bed factor retains its significance. However, the relationship may suffer a discontinuity or, at least, a marked change; Eq. 26 ceases to apply.

Fig. 5 is presented[31,32] in support of items 1 and 3. In Fig. 5 the relative bed-factor excess is the ratio of the bed factor minus the bed factor at a vanishingly small charge to the latter quantity, whose value is exceedingly close to Mr. Lacey's empirical value of 1.9 times the square root of the mean particle size in millimeters. However, Eqs. 4, 5, and 6 would make this value zero instead of Mr. Lacey's empirical value—which is confirmed by flume experiments within fair limits. Presumably, Eqs. 4, 5, and 6 have been deduced from some theory concerning bed-load charges; they could not have been derived from Mr. Lacey's regime formula data as those data did not include charge.

Ning Chien,[33] A. M. ASCE.—The writer shares Mr. Lane's respect for Mr. Lacey who developed a set of empirical rules useful in designing stable channels in the plains of India at a time when little was known of basic fluid mechanics or sediment-transport mechanics. Even though this set of rules was successfully applied to the Indian plains region from which it originated, it has not been generally accepted by engineers in other areas because of the following weaknesses of the theory:

1. It omits the sediment supply as an independent variable, thus making difficult its physical comprehension.
2. It fails to apply empirical or analytical rules for determining the various constants or silt factors. Instead, selection of constants or silt factors is made on the basis of experience which, in itself, is a loose term with little meaning for engineers who have never worked in the Indian plains region.
3. It presents rules which have—as any other empirical rules—a limited application. These limitations have not been indicated in a clear and definite terms, and engineers do not know under what conditions these rules can or cannot be applied. According to Mr. Lane, this limitation of applicability is more serious than is generally known.

If these weaknesses had been properly corrected at the outset, the regime theory would be more widely used in the field of hydraulic engineering and on a larger scale in the areas where it can be applied. Unfortunately, some followers of the regime theory, because of successful experiences in the Indian plains region, have become dogmatic in the application of the theory. Instead of investigating the limitations of the rules, they assume that they are basic laws with universal applicability. Without taking advantage of the vast amount of available flume data on sediment transport in order to determine the effect of the sediment supply on these rules and their constants, these engineers discredited the usefulness of the flume data which, in many respects, covered a range of conditions much wider than that of the regime theory. Supporters of the regime theory believe that only this theory can be successfully applied to the solution of river problems, and that only engineers experienced in the application of this theory are qualified for this work. This attitude misleads beginners, confuses issues, and discredits the regime theory itself.

---

[33] Associate Prof. of Hydraulics, Tsing Hwa Univ., Peiping, China.

Mr. Lane has questioned the writer's justification for having evaluated the regime theory on the basis of another theory. The writer was convinced that a certain relationship existed between the silt factors and the characteristics of the sediment. After many trials, it was found that, in using the bed-load function and in expressing the sediment supply by the sediment concentration, a unique relationship between the silt factors and the size and concentration of the sediment was revealed for conditions in the Indian plains region. Because of the limited range of sediment size (from fine to medium sand) and the sediment supply in that area, the values of silt factors fell within a comparatively narrow range and could be accurately selected from experience. If this unique relationship had not been established by means of the bed-load method, thus demonstrating the usefulness of the regime theory in that area, this paper would not have been written.

On the other hand, the bed-load function also indicates that the relationship between silt factors and sediment characteristics becomes a function of the hydraulics when the conditions, especially the sediment size, are different from those existing in the Indian plains region. Regime theory is, after all, a set of empirical rules originating in the Indian plains region and cannot be assumed to apply outside that region. However, because the development of the bed-load function was based on the basic mechanics of fluid motion and sediment transport and because the constants involved were determined under a wide range of conditions (for example, particle size from fine sand to gravel), there is no reason why the bed-load function should be applied only to a river with a fine-to-medium sand bed and not to a river with a bed of coarse sand or gravel. The conclusions presented were based on these assumptions.

HANS A. EINSTEIN,[34] M. ASCE.—Before leaving the United States, the author authorized the writer to answer additional comments referring to his paper.

The discussions by Mr. Lane and Mr. Lacey were based on the understanding that the author attempted to find a bridge between the regime theory and the bed-load approach to problems of sediment transport. The discussion by Mr. Blench is that of one who is a sincere adherent to the regime theory.

The writer believes that both methods attempt to describe the same phenomena and, for that reason, they are comparable; their approach is different, however. The bed-load function attempts to use (*a*) concepts of general fluid dynamics and (*b*) empirical formulas only in cases where the physical effect of the solid particles necessitates their use, but these formulas are introduced only if they are physically explainable. Emphasis is placed on physical analysis and on a growing range of applicability. Mr. Blench has noted limits of applicability for some of his formulas and constants. The bed-load function is made complicated not only for discussion purposes but as a means of describing changes in formulas which become necessary as the range of conditions is enlarged. At present (1956), the range of applicability for the bed-load function is wide, but it needs further widening.

---

[34] Prof. of Hydr. Eng., Univ. of California, Berkeley, Calif.

The regime theory, on the other hand, is still a set of empirical equations, as stated by Mr. Inglis,[6] and becomes increasingly complicated. In contrast to the bed-load function, no attempt is made to use general fluid-dynamics equations. An effort has been made, however, to clarify the dimensional side of the equations, which become increasingly complicated and which will result in being identical to, or at least equal in content with, those of the bed-load function because they both describe the same phenomenon. The complication is, therefore, inherent in the problem.

One might question which is the better approach. The writer believes that such a general question is misleading and believes that both methods of approach must be developed simultaneously. According to their separate background, they should be used for different purposes. The more scientific and complicated method of the bed-load function would better provide a general description of the problem, which incorporates a variety of conditions nto a unified form. The empirical methods, however, should be as simple and as easily applicable as possible, even if the field of applicability for any set of constants and exponents becomes somewhat reduced. Such a set of equations has the advantage of being easily applied in any particular case.

The writer believes in having two such sets of equations available and in using them as follows: (*a*) The more general and more complicated method for finding the constants which must be inserted into the working equations in order to cover the range of conditions; and (*b*) the approximate, simpler equations for performing the practical computations, using the appropriate constants for the case in question.

AMERICAN SOCIETY OF CIVIL ENGINEERS
Founded November 5, 1852
TRANSACTIONS

Paper No. 2885

METHODS OF DETERMINING CONSUMPTIVE USE OF WATER IN IRRIGATION

By Ralph D. Goodrich,[1] M. ASCE

With Discussion by Messrs. Don M. Forester, and Ralph D. Goodrich

Synopsis

Attention is drawn herein to some of the early investigations of the "duty of water" in irrigation. As knowledge was acquired in this field of research, attention became focused on the "consumptive use of water" or "evapotranspiration." Standard methods of determination of rates of consumptive use are briefly described, and the utilization of the results thus obtained to measure farm use and valley use of water is examined.

Introduction

Investigations concerning the consumptive use of water by crops grown on irrigated farms have been conducted by state and federal agencies since before 1900. Because of the constantly increasing value of the water used and of the crops produced, such investigations should, and no doubt will, be continued indefinitely in order to increase irrigation efficiency with improved methods and procedures.

Early studies in this field of research concerned the "duty of water" on irrigated farms and projects. Among those making such investigations were Elwood Mead (1)[2] and John A. Widtsoe (2). In his early practice in irrigation engineering the writer made considerable use of reports by Don H. Bark (3) on cooperative investigations in Idaho.

Many other contributions to the knowledge of the duty of water and the consumptive use of water, such as descriptions of original research and experimentation, or explanations and examinations of the work of others, are found in standard textbooks and reference books (4) (5) (6) (7) (8). There are also

---

Note.—Published, essentially as printed here, in February, 1956, as *Proceedings Paper 884*. Positions and titles given are those in effect when the paper or discussion was approved for publication in *Transactions*.

[1] Eng. Consultant, Upper Colorado River Comm., Grand Junction, Colo.

[2] Numerals in parentheses—thus, (1)—refer to corresponding items in the Bibliography (see Appendix).

numerous papers and discussions published by the Society (9) (10) (11) (12) (13) (14) (15). All these sources and several others, including bulletins of the United States Department of Agriculture (16) (17) (18) (19) (20) (21), have been used extensively.

This paper, therefore, is a review and summary of work done by other investigators with whose books, reports, or papers the writer is most familiar and which were available for reference.

DEFINITIONS

The term, "duty of water," refers to the relationship of the area of land served by a given quantity of water. Sidney T. Harding, M. ASCE (5), drew attention to the fact that a high duty of water is associated with a small amount used whereas a low duty indicates a large use of water. Mr. Harding tried to avoid the confusion which often arises from such terminology by substituting the expression, "water requirement," which applies to the number of acre-feet of water necessary to maintain a given crop per acre of land irrigated. This expression is clear, but its use has been largely superseded by the term, "consumptive use of water," which was introduced by John E. Field (10).

Consumptive use of water may be defined (12) (16) (17) as:

> "The sum of the volumes of water used by the vegetative growth of a given area in transpiration and building of plant tissue and that evaporated from adjacent soil, snow, or intercepted precipitation on the area in any specified time, divided by the given area." (11)

It is usually expressed in units of acre-feet per acre per year (and sometimes per month) for the locality and crop, or vegetation or area considered. It is measured in various ways, such as by lysimeters or tanks, on experimental plots in selected fields, on a whole farm, on an irrigation project, or on the farms and projects in a river valley. The determination of the consumptive use of water for the entire drainage basin of a river system is often required—for example, the consumptive use of the Upper Colorado River Basin (which includes the Green River, the Colorado River, and the San Juan River in Colorado, New Mexico, Utah, and Wyoming), which is required by the terms of the Upper Colorado River Basin Compact of 1948.

It should be obvious that consumptive uses will vary for different crops. For any given crop the use will vary from year to year, and from one locality to another, with the length of the growing season, the average temperature, the precipitation, and the humidity. In addition to these climatic factors, there are many other factors which are also important, such as the character, condition, and treatment of the soil, and the practice of the irrigator applying the water. Because the foregoing definition includes water evaporated from the soil surrounding the plants which constitute the crop, or other vegetation, as well as the water used and transpired by the plants themselves, the term, "evapo-transpiration," is considered herein to be synonymous with the term, "consumptive use."

Several methods have been used to measure consumptive uses of water by crops and by native vegetation. Among the most useful of these methods are soil moisture, lysimeter, tank, and field-plot experiments (ground-water fluctuations, evaporation-pan records, the integration method, inflow-outflow measurements, effective heat, and the correlation of water use with climatological data). Some of these methods depend on the use of results obtained in previous work, and only a brief description of any method can be given within the limits of this review.

METHODS

Soil-Moisture Determinations.—The method of applying soil-moisture determinations to the measurement of evapo-transpiration is best adapted to experiments in which the total quantity of water made available to the plants or crops used in the investigation can be measured either as natural precipitation or as water artificially applied for irrigation. If there is a water table at a measurable distance below the surface, it should be at such a depth below the root zone that the plants cannot obtain water from the capillary fringe but will use only that water which is applied at the surface. Hence, if heavy rains occur so that deep seepage will result after a storm, or if an excessive amount of water is applied in irrigation, the amount of such seepage must be measured or estimated and proper corrections made. In localities where practically no precipitation occurs during the growing season, this method is well adapted to obtain reliable measurements of consumptive use. Soil samples are usually taken before and after each irrigation, and the moisture content is determined by standard laboratory procedure. Advantages of this method are that it can be used on experimental plots of any practical size and the plots can be selected so as to be surrounded by similar crops or vegetation. The experiments should then reflect the consumptive use of water under the most natural conditions for accurate results (6) (9) (11) (19) (21).

Tank or Lysimeter Experiments.—When lysimeters were first used in experiments to determine the consumptive use of water, the results obtained were qualitative rather than quantitative by present standards. Early experimenters did not always give full details of the conditions or procedures used, so that their results could not always be properly compared. Tanks of the largest practical size should be used and they should be placed so as to be surrounded by the natural conditions of local crops and vegetation, undisturbed soil, water table, and similar factors. Accurate observations and records should be secured of the effective precipitation, time, amount, frequency, and method of irrigation, water lost by deep seepage (if any), and the height and movement of ground water if the presence of such water is made a part of the experimental program. The most accurate means of determining evapo-transpiration when this method is used is by weighing (6) (11) (19). However, this is not always practical with the largest tanks. In experiments conducted by Ralph L. Parshall, A.M. ASCE (20), to determine the rates of evaporation from saturated soils and river sands, Mariotte tanks were successfully used to control water-table elevations.

Ground-Water Fluctuations.—When a considerable area of irrigated land is relatively flat and when there is an adequate water supply, it is sometimes possible to estimate the average consumptive use of water for the area by analyzing the fluctuations in the elevation of the ground-water table. After irrigation practice becomes well established, the ground-water table is usually somewhat higher than it was formerly. If there is a continuous inflow of underground water into the area and if capillary water is within reach of the root zone of the crops, recorders may be set at observation wells in order to obtain continuous records of the variations in the level of the water. By making the necessary allowances for irrigation water and precipitation and knowing the specific yield of the soil, it is possible to estimate the consumptive use for the area (6) (9). This method has been used with very satisfactory results in Arizona, California, and Utah (11).

Evaporation Pan Records.—Occasionally, one may need to estimate the losses of water from swamps or other low areas having vegetation that uses water heavily (phreatophytes). If evaporation pans are installed in such areas, it may be possible to utilize the evaporation data obtained to estimate the evapo-transpiration in that area. It is necessary with this method, as with all other methods, to take proper account of precipitation and irrigation water if either reaches the area; a factor depending on judgment or experience would also have to be applied to the observations. However, helpful information may be obtained for comparison with other data from similar areas (6).

Integration Method.—The determination of consumptive use for a variety of crops and native vegetation, made by the foregoing method or other methods, is required when the integration method is used to obtain the consumptive use of water on a farm or irrigation project. In certain cases this integration method has been used with satisfactory results to obtain project rates and even valley rates of consumptive uses.

To apply this method in a valley, having previously secured the rates of consumptive use for the various crops, one must obtain the acreage of each crop and of the pastures and incidental areas, together with the total area of each classification of the land use in the valley. Then, the sum of the products of the total area of each type of crop (or other class of land) and the average rate of consumptive use will give the total consumptive use or stream depletion in the valley. This total depletion quantity, divided by the total area, gives the weighted average rate of consumptive use (9) (10) (11) (18) (19). The foregoing description of the integration method may be an oversimplification of the procedure.

When applied by different individuals on different irrigation projects, the results may not always be properly compared. In a given valley there may be several irrigation projects, but annual records of the areas under cultivation may not be kept on exactly the same basis. The average in one case may be based on the acreage of the actual crops, excluding areas which include houses, barns, corrals, ditches, roads, and similar features, giving the evapo-transpiration rate for the net area cultivated. On another project the total amount of depletion computed may be divided by the total area of the project, thus giving a smaller rate of use.

Therefore, it is desirable to give the fullest explanation of all details in reports so that the results can be used to check and compare with data obtained by other methods or in other areas. For the purpose of comparison, results by the integration method have been of special value in connection with investigations in the Upper Colorado River Basin (17) (18).

Inflow-Outflow Method.—In theory, the inflow-outflow method, when applied to the determination of valley consumptive use, requires the actual measurement of all water entering the area. This water should include both surface and subsurface inflow and precipitation, especially that falling on the valley floor, and should also include quantitative data of any material changes in the amount of storage in the ground-water reservoir in the area. The difference between the inflow and the outflow (both surface and subsurface) plus the algebraic difference between ground storage at the beginning and at the end of the experimental period gives the consumptive use in a given area.

In mathematical terms this can be shown by

$$U = (I + R) + (G_s - G_e) - Q \ldots\ldots\ldots\ldots\ldots\ldots (1)$$

in which U is the consumptive use for the period selected (usually 12 months); I denotes the inflow; R represents the effective rainfall on the valley floor; Q is the quantity of outflow; and G_s and G_e are the volumes of water in ground storage at the beginning and end of the period, respectively.

All the quantities in Eq. 1 are given in acre-feet. Harry F. Blaney, M. ASCE (11) (19), has noted that any change in the amount of capillary water will be so small that it can be neglected.

The inflow-outflow method, or some modification of it, has been used by numerous engineers, such as Mr. Blaney, Wayne D. Criddle, John R. Erickson, Mr. Harding, Francis C. Hart, A. M. ASCE, Charles H. Lee, Robert L. Lowry, Arthur F. Johnson, A. M. ASCE, Karl V. Morin, Royce J. Tipton, M. ASCE, and Ralph I. Meeker, M. ASCE. In recent years this method has been adopted for use in connection with the negotiation and administration of several interstate river compacts, one of which was the Upper Colorado River Compact of 1948. Typical results obtained by this method are shown in Table 1, which has been copied from Table 5 of Mr. Blaney's paper (11*a*).

Correlation Methods.—The correlation of consumptive uses of water with certain climatological factors has been successfully developed by several investigators. Charles R. Hedke was one of the first to use the "effective heat" (or number of day-degrees) available to agricultural crops during the growing season or crop year. No attempt will be made herein to examine Mr. Hedke's method, but only to state that he used it as early as 1916 with gratifying results during investigations made in the Poudre River Valley and San Luis Valley (both in Colorado) and in the Rio Grande Valley in New Mexico (9).

The many years devoted by Mr. Blaney to constant research with a similar approach to this problem have resulted in a useful and reliable method which has many applications. Results obtained by his method have been checked by other methods in several instances with satisfactory agreement. The writer is more familiar with this method than with any other ever since the report made by Messrs. Blaney and Criddle for the Upper Colorado River Compact Commission in 1948. In this report, they state:

> "Briefly, the procedure is to correlate existing consumptive use data with mean monthly temperatures, percent of daytime hours and precipitation for the frost free period or irrigation season and for the entire year. The coefficients so developed for different crops are used to transfer consumptive use data from one section to other areas where only climatological data are available."

This method was more fully described by Messrs. Blaney and Criddle (17) in another report in which the procedure is described as follows:

> "Neglecting the unmeasured factors, consumptive use varies with the temperature and the daytime hours, and irrigation requirement is also dependent on precipitation. By multiplying the mean monthly temperature (t) by the monthly percent of daytime hours of the year (p), there is obtained a monthly consumptive use factor (f). It is then assumed that the consumptive use varies directly as this factor or, expressed mathematically, $U = K F$ where:
>
> U = Consumptive use of crop in inches for any period.
> F = Sum of the monthly consumptive use factors for the period (sum of the products of mean monthly temperature and monthly per cent of annual daylight hours ($t \times p$).
> K = An empirical coefficient.
> t = Mean monthly temperature in degrees Fahrenheit.
> p = Monthly per cent of daytime hours of the year.
> $f = t \times p$ = Monthly consumptive use factor.
>
> "By knowing the consumptive requirement of water by a particular crop in some locality an estimate of the use by the same crop in some other areas may be made by application of the formula. Table 1 gives a summary of the consumptive use of water (U) by alfalfa and cotton in various localities in the West as determined by investigators, together with the calculated

TABLE 1.—EXAMPLES OF VALLEY CONSUMPTIVE USE OF WATER DETERMINATIONS BY INFLOW-OUTFLOW METHOD[a]

Location	Year	Area, in acres	Annual Consumptive Use		Authority
			Total, in acre-feet	Average, in feet	
San Luis Valley, Colo.	1925 to 1935	400,000	664,900	1.66	Blaney-Rohwer[b]
San Luis Valley, Colo.	1936	400,000	685,423	1.71	Blaney-Rohwer[b]
San Luis Valley, Colo.	1930 to 1932	17,300	26,215	1.52	Tipton-Hart[b]
Isleta-Belen, N. Mex.	1936	17,500	38,700	2.28	Blaney-Morin[b]
Mesilla Valley, N. Mex.	1919 to 1935	109,000	297,756	2.73	Blaney-Israelsen[b]
Mesilla Valley, N. Mex.	1936	110,418	303,683	2.75	Blaney-Israelsen[b]
Carlsbad, N. Mex.	1921 to 1939	51,700	129,752	2.51	Blaney-Morin-Criddle[c]
Carlsbad, N. Mex.	1940	51,700	119,898	2.33	Blaney-Morin-Criddle[c]
New Fork, Wyo.	1939 to 1940	25,000	...	1.59	Lowry-Johnson[d]
Michigan-Illinois-Colorado	1938 to 1940	43,000	...	1.50	Lowry-Johnson[d]
Uncompahgre, Colo.	1938 to 1940	137,700	...	2.28	Lowry-Johnson[d]

[a] See Bibliography reference (11*a*). [b] "Water Utilization, Upper Rio Grande Basin," by Harry F. Blaney, Paul A. Ewing, O. W. Israelsen, Carl Rohwer, and F. C. Scobey, National Resources Committee, Washington, D. C., Part III, February, 1938. [c] "Consumptive Water Use and Requirements: Report of the Participating Agencies, Pecos River," by Harry F. Blaney, Paul A. Ewing, Karl V. Morin, and Wayne D. Criddle, Joint Investigation of the National Resources Planning Board, Washington, D. C., June, 1942. [d] "Consumptive Use of Water for Agriculture," by Robert L. Lowry, Jr., and Arthur F. Johnson, *Transactions*, ASCE, Vol. 107, 1942, p. 1243.

consumptive use factor (F) and the crop coefficients (K) in the areas studied. In planning to supply the irrigation requirements of any new project it then becomes necessary to estimate the acreage to be planted to each crop, determine the unit use of water by each crop based on known use in other areas and add the products for all the crops. This calculation will indicate the total consumptive use for the project (4). Allowance must, of course, be made for the use by native vegetation, water surface, evaporation and other minor uses.

TABLE 2.—EXAMPLES OF COEFFICIENTS, K, FOR IRRIGATED CROPS DEVELOPED FROM MEASUREMENTS OF CONSUMPTIVE USE AND CLIMATOLOGICAL DATA[a]

Location and crop	Year	Growing season or period	CONSUMPTIVE USE		
			Rate, U, in inches	Factor, F	Coefficient, K
ALFALFA					
Carlsbad, N. Mex.	1940	4/18 to 11/10	38.6	43.59	0.88
Fort Stockton, Tex.	1940	4/13 to 11/11	40.5	46.28	0.88
San Fernando, Calif.	1939	5/26 to 9/9	19.3	23.35	0.83
Ferron, Utah	1948	5/9 to 10/6	24.2	30.23	0.84
Mesa, Ariz.	1948	2/10 to 12/3	52.5	57.51	0.91
Ontario, Ore.	1941 to 1942	5/1 to 10/5	29.4	35.50	0.83
Gooding, Idaho		5/23 to 9/24	21.6	26.18	0.83
COTTON					
Mesa, Ariz.	1935	4/1 to 10/31	30.9	49.08	0.63
Bakersfield, Calif.	1927 to 1930	4/1 to 10/31	29.2	47.14	0.62
Carlsbad, N. Mex.	Normal	3/28 to 11/3	28.7	47.39	0.61
Fort Stockton, Tex.	1940	4/13 to 11/11	28.9	46.28	0.62
SMALL GRAINS					
Scottsbluff, Nebr.	1932 to 1935	4/20 to 7/25	14.72	20.02	0.74
Prosser, Wash.	1944	3/20 to 7/16	18.00	23.32	0.77
Ferron, Utah	1948	5/13 to 8/21	17.8	20.86	0.85
Davis, Calif.		3/1 to 6/7	12.0	17.73	0.68
ORCHARD — ORANGES					
Mesa, Ariz.	1931 to 1934	3/1 to 10/31	32.4	58.26	0.56
Azusa, Calif.	1929	4/1 to 10/31	21.8	43.19	0.50
San Fernando, Calif.	1940	4/1 to 10/31	22.1	43.73	0.51
ORCHARD — DECIDUOUS					
Ontario, Calif.	1928	4/1 to 9/30	28.4	37.73	0.75
Wenatchee, Wash.	1908	4/15 to 10/22	23.0	38.15	0.60
Albuquerque, N. Mex.	1936	5/1 to 9/31	19.5	33.94	0.58
PASTURE					
Vernal, Utah	1948	5/17 to 10/6	25.0	27.42	0.91
Murrietta, Calif.	1953	4/1 to 10/31	35.04	42.04	0.84
POTATOES					
Bonners Ferry, Idaho	1947	5/8 to 9/27	22.95	29.35	0.78
Utah County, Utah	1938	5/15 to 9/15	22.50	27.23	0.83
Prosser, Wash.	1945	4/20 to 8/4	16.65	22.81	0.73
Davis, Calif.		3/1 to 6/30	16.8	22.93	0.73
Logan, Utah	1902 to 1929	5/20 to 9/15	15.0	25.27	0.60
VEGETABLES					
Stockton, Calif.	1925 to 1928	5/1 to 9/30	21.4	33.91	0.63
Stockton, Calif.	1925 to 1928	4/1 to 10/31	24.6	44.18	0.56

[a] See Bibliography reference (19*a*).

"*Assumptions*: In order to apply the results of any study in one area to some other area, it is usually necessary to make certain minor assumptions. If sufficient basic information is available, some of the assumptions may be replaced by actual data, but rarely are all the data known in sufficient detail for reliable use. In other words, the more data available, the more accurate the estimates or assumptions, but some doubts still exist. For practical use the following assumptions must be made in applying the consumptive use formula between areas:

1—The fertility and producing power of the soils are similar.

2—Sufficient water is applied and at the proper time to maintain good growing conditions.

3—The length of growing season, to a large extent, determines the production and annual consumptive use of continuous growing crops such as alfalfa and pasture.

4—Consumptive use of water varies directly with the consumptive use factor."

The method devised by Messrs. Blaney and Criddle has certain advantages because the percentage of daylight hours in any month for various latitudes are given in published tables (11). With these quantities taken for the months and fractions during the growing season and with the mean monthly temperatures taken from reports of the United States Weather Bureau, consumptive-use factors can be computed for almost any crop in any western location because reliable records of experimental determinations of rates of consumptive use for many crops and vegetative types are also available. The necessary coefficient, *K*, can therefore be computed as the ratio of each observed value of consumptive use, *U*, by its corresponding factor, *F*. Typical rates of consumptive use for various crops are given in Tables 2 and 3. (Tables 2 and 3 are printed herein by permission of Mr. Blaney (19*a*).)

TABLE 3.—CONSUMPTIVE-USE COEFFICIENTS, *K*, FOR IRRIGATED CROPS IN WESTERN UNITED STATES[a]

Crop	Length of growing season or period	Consumptive-use coefficient, *K*
Alfalfa	Between frosts	0.80 to 0.85
Beans	3 months	0.60 to 0.70
Corn	4 months	0.75 to 0.85
Cotton	7 months	0.60 to 0.65
Flax	7 to 8 months	0.80
Grain, small	3 months	0.75 to 0.85
Grain sorghums	4 to 5 months	0.70
Orchard, citrus	7 months	0.50 to 0.65
Orchard, walnuts	Between frosts	0.70
Orchard, deciduous	Between frosts	0.60 to 0.70
Pasture, grass	Between frosts	0.75
Pasture, Ladino clover	Between frosts	0.80 to 0.85
Potatoes	3 1/2 months	0.65 to 0.75
Rice	3 to 5 months	1.00 to 1.20
Sugar beets	6 months	0.65 to 0.75
Tomatoes	4 months	0.70
Vegetables, small	3 months	0.60

[a] See Bibliography reference (19*a*).

It is assumed by Messrs. Blaney and Criddle, as stated in assumption 4, that consumptive-use rates vary directly with the consumptive-use factor. The data on alfalfa given in Table 2 were used to test the validity of this assumption by computing the mean, *M*, the standard variation, *S V*, and the coefficient of variation, *C V*, for each of the three quantities—the consumptive use, *U*, the consumptive-use factor, *F*, and the crop coefficient, *K*. The records shown in Table 2 are of experiments made in seven different states with consumptive uses varying from less than 20 acre-in. per acre in California to more than 40 acre-in. per acre for one year in Texas. However, the coefficients of variation, $C\ V$, of the consumptive uses, U, and of the consumptive-use factor, F, are 34.5% and 30.0%, respectively. That these two quantities are directly proportional for all practical purposes is also shown by the fact that the crop coefficient, K, has a variation indicated by its coefficient of 11.1%. This shows extremely high correlation between the consumptive use for this crop and the index of the heat available during the growing period. Once the coefficient, K, has been determined for any crop or type of vegetation, its use on other areas is certainly justified within reason. Table 3 gives values of K, as suggested by Mr. Blaney, for a number of the common crops grown by irrigation in the western United States. In using the consumptive-use coefficients given in Table 3, one should note that the lower values of K are for areas along the coast and the higher values are for more arid climates.

NATIVE VEGETATION AND MUNICIPAL AREAS

Some of the methods that have already been mentioned are available for determining evapo-transpiration rates from areas such as natural grassland and pasture and also for large plants or shrubs, orchards, and wooded areas. Consumptive-use rates for these areas are contained in several publications (17) (18) (19) (22). In addition, an excellent report is available by L. R. Rich (12).

Municipal areas are often considered as taking approximately the same evapo-transpiration rates per acre as the surrounding cultivated or native vegetation. Also available is a detailed and valuable report by George B. Gleason, A.M. ASCE (14), on the investigations conducted "* * * to determine a fair distribution of water rights in the Raymond Basin Area, of Pasadena, Calif." However, the limited scope of the writer's paper precludes examination of the foregoing papers, which should nevertheless be called to the attention of interested engineers.

UPPER COLORADO RIVER BASIN

The Upper Colorado River Commission was organized under the authority of the Upper Colorado River Basin Compact of 1948. There are five commissioners, one each from Colorado, New Mexico, Utah, and Wyoming; the chairman is appointed by the President of the United States. The commission is empowered to investigate each year the consumptive use or, more specifically, the man-made stream depletion in each of the aforementioned states and in the Upper Colorado River Basin as a whole, "by the inflow-outflow method." Hence, the engineering department of the commission has spent much time and effort in the study of methods for the determination of the consumptive use of water in irrigation and of how best to apply appropriate methods in determining man-made depletions of stream flow in the upper basin of the Colorado River (Colorado-Utah-Arizona).

The area of the upper basin is approximately 110,000 sq miles, or 70,400,000 acres. This area is 70,000,000 acres more than the area of the San Luis

Valley, which is the largest area reported by Mr. Blaney and Carl Rohwer, M. ASCE (19), as having determined valley consumptive uses by the inflow-outflow method. The irrigated area in this basin, however, is approximately 3% of the total area. It is divided into numerous subbasins, both large and small, which are separated by long, deep, and magnificent canyons on tributaries as well as on the main stem of the river. There are nearly 300 streams of varying size on which approximately 600 gaging stations have been operated by the United States Geological Survey (USGS) of the United States Department of the Interior for periods varying from two to three years to as many as fifty years. This does not include the large number of streams, from which many ditches take water but on which the USGS has never installed a gaging station. It has been estimated that there are from 15,000 to 20,000 canals and ditches diverting water for use on an equivalent area of 2,000,000 acres in the basin, which gives an indication of the magnitude of the task undertaken in these studies. Because there are only from two to three ground-water observation wells in the Upper Colorado River Basin, information on this source of inflow and storage is difficult to obtain. The records of annual discharge of the Colorado River at Lees Ferry (Ariz.), which is near the outflow point of the upper basin, have been good since 1922 when the recording gage was installed. However, with a limited number of rim stations, most of which have much shorter periods of continuous operation, it has been possible to use only indirect methods to obtain data which can be used in applying the inflow-outflow method in the valleys of this river system. The attack on this problem has therefore been to develop inflow indexes which are used with pertinent climatological factors in multiple-correlation relationships. These studies are not complete and, in fact, they may continue indefinitely as additional years of records become available and new facts are learned which tend to increase the accuracy of the inflow-outflow relationships that are being developed. Several problems must still be investigated, and as the investigation continues, questions will continue to arise which will require answers.

Because interest in this problem—which is among other problems considered by the Upper Colorado River Commission—seems to be rather widespread, the review of some of the methods of determining the consumptive uses of water in the west is presented, together with the special conditions governing the application of the inflow-outflow method to the measurement of man-made stream depletions on a basin-wide basis.

CONCLUSIONS

As of 1955, the Upper Colorado River Commission has not adopted any regulation or procedure by which to "make findings of fact" as to the amounts of man-made depletions either at Lees Ferry, located on the main stream of the Colorado River, 1 mile below the mouth of the Paria River (Arizona-Utah), or in each state. Progress reports are made from time to time (of which this paper is an example), which are reviewed by the committee on engineering advisers to the commission. When this committee makes recommendations to the commission which can be adopted for the application of the inflow-outflow method, it is hoped that the committee will also authorize a technical paper.

APPENDIX. BIBLIOGRAPHY

(1) **"The Use of Water in Irrigation,"** by Elwood Mead, together with **"Computations of Records,"** by C. T. Johnson, *Reprint Bulletin 86*, Annual Report of Irrigation and Drainage Investigation, U. S. Dept. of Agriculture, Washington, D. C., 1904.

(2) **"The Production of Dry Matter with Different Quantities of Irrigation Water,"** by John A. Widtsoe, *Bulletin 116*, Experiment Station, Utah State Agricultural College, Logan, Utah, 1912.

(3) **"Experiments on the Economical Use of Irrigation Water in Idaho,"** by Don H. Bark, *Bulletin 339*, U. S. Dept. of Agriculture, Washington, D. C., April, 1916.

(4) **"Duty of Water,"** Chapter X in "Irrigation Engineering," by Arthur P. Davis and Herbert M. Wilson, John Wiley & Sons, Inc., New York, N. Y., 1919, 7th Ed., pp. 147–151.

(5) **"Irrigation Practice and Engineering,"** by Bernard A. Etcheverry and Sidney T. Harding, McGraw-Hill Book Co., Inc., New York, N. Y., Vol. I, 2d Ed., 1933, pp. 64–119.

(6) **"Hydrology Handbook,"** *Manual of Engineering Practice No. 28, ASCE*, Chapter 4, Article 10, 1949, p. 136.

(7) **"Irrigation Principles and Practice,"** by O. W. Israelsen, John Wiley & Sons, Inc., New York, N. Y., 1st Ed., 1932, Chapter XIV.

(8) **"Hydrology,"** in "Physics of the Earth," edited by Oscar E. Meinzer, Chapter VIII by Charles H. Lee, 1st Ed., 1949.

(9) **"Consumptive Use of Water in Irrigation: "Progress Report of the Duty of Water Committee,"** *Transactions*, ASCE, Vol. 94, 1930, p. 1349.

(10) **"Consumptive Use of Water for Agriculture,"** by Robert L. Lowry and Arthur F. Johnson, *ibid.*, Vol. 107, 1942, p. 1243.

(11) **"Definitions, Methods, and Research Data,"** by Harry F. Blaney, in "Consumptive Use of Water: A Symposium," *ibid.*, Vol. 117, 1952, p. 949. (*a*) p. 963, Table 5.

(12) **"Forest and Range Vegetation,"** by L. R. Rich, in "Consumptive Use of Water: A Symposium," *ibid.*, p. 974.

(13) **"Irrigated Crops,"** by Wayne D. Criddle, in "Consumptive Use of Water: A Symposium," *ibid.*, p. 991.

(14) **"Municipal and Industrial Areas,"** by George B. Gleason, in "Consumptive Use of Water: A Symposium," *ibid.*, p. 1004.

(15) **"Special Case in Rio Grande Basin,"** by Robert L. Lowry, in "Consumptive Use of Water: A Symposium," *ibid.*, p. 1014.

(16) **"A Method of Estimating Water Requirements in Irrigated Areas from Climatological Data,"** by Harry F. Blaney and Wayne D. Criddle, Soil Conservation Service, U. S. Dept. of Agriculture, Washington, D. C., December, 1947 (mimeographed).

(17) **"Consumptive Use of Water Rates in the Upper Colorado River Basin,"** by Harry F. Blaney and Wayne D. Criddle, Soil Conservation Service, U. S. Dept. of Agriculture, Logan, Utah, April, 1949.

(18) **"Consumptive Water Use and Requirements in the Colorado River Area of Utah,"** by Willis C. Barrett and Cleve H. Milligan, *Special Report No. 8*, Experiment Station, Utah State Agricultural College, Logan, Utah.

(19) **"Evapo-Transpiration Measurements in Western United States,"** by Harry F. Blaney, paper given at the Tenth General Assembly of the International Union of Geodesy and Geophysics, Rome, September, 1954. (*a*) Tables 6 and 7 (mimeographed).

(20) **"Experiments to Determine Rate of Evaporation from Saturated Soils and Riverbed Sands,"** by Ralph L. Parshall, *Transactions*, ASCE, Vol. 94, 1930, p. 961.

(21) **"Irrigation Requirements of California Crops,"** *Bulletin No. 51*, Dept. of Public Works, Div. of Water Resources, California, November, 1945.

(22) **"Consumptive Use Requirements for Water,"** by Harry F. Blaney, *Agricultural Engineering*, Vol. 35, December, 1945, pp. 870–873, p. 880.

(23) **"Determining Water Needs for Crops from Climatic Data,"** by N. A. Halkias, F. J. Viehmeyer, and A. H. Hendrickson, *Hilgardia*, California Agri. Experiment Station, Davis, Calif., Vol. 24, No. 9.

DISCUSSION

Don M. Forester,[3] M. ASCE.—An excellent resume of many of the studies, of the so-called duty of water in irrigation is presented in Mr. Goodrich's paper. The many formulas and methods which have been developed emphasize the interest of the engineering profession in developing a theoretical means for the prior determination of the amount of water required for irrigation needs. The majority of the studies cited by the author are principally concerned with the water requirement of cultivated plants under various conditions of temperature, sunshine, rainfall, and other climatic factors. Perhaps it is possible to arrive at an empirical formula which, when properly applied, will give the correct answer for the previous irrigation season. There are many methods and formulas (11) which are thought to permit a fine determination of the consumptive use of water in irrigation; all give comparable results.

Engineers, who have the problem of designing an irrigation development, find in most instances that complete information on the water requirement is lacking. This is especially true for the semiarid regions of the western United States. Consumptive-use determinations are only a part of the problem in arriving at the amount of water necessary for a successful development. The total requirement includes—in addition to the consumptive use—evaporation, deep percolation loss, transmission losses, probable rainfall and degree of effectiveness, and irrigator efficiency and conservativeness.

The determination of present man-made depletions in the Upper Colorado River Basin is, without question, a vast and complex problem. To arrive at the ultimate man-made depletion, after partial or full development as presently envisioned by the commission, is even more complex. Depletion studies of consumptive use, based on various anticipated crops and native vegetation may or may not hold true for more than one, two, or three decades. Then, too, there will be many other influencing factors which must be evaluated and applied. All this serves to introduce the primary problem—that is, where is the stopping place for refinement of the "arithmetic" and "judgment" factors?

The Bureau of Reclamation, United States Department of the Interior (USBR), has adopted and used the method developed by Messrs. Lowry and Johnson (10) for determining consumptive use in planning irrigation developments or projects. This method, which is one of the inflow-outflow procedures mentioned by the author, has theoretical shortcomings, but the consumptive-use determination by this method compares favorably with that found by some of the more recently developed methods. In the design of an irrigation system the total and peak water requirements are of primary concern and the consumptive use is only one feature. Must the designer arithmetically refine his consumptive-use requirements to the nearest tenth of an inch or one-hundredth of a foot when he cannot determine his transmission and farm-waste loss much closer than from 5% to 20%, or more, of the diversion? Some methods of determining consumptive use place great emphasis on so-called "effective heat units" during an empirical growing season based on temperatures and the percentage of daylight hours. It is known that humidity directly affects the actual consumptive use of the plants. Also, the latitude and elevation in which the plants are grown have bearing on their consumptive use of water. It is generally recognized by designing engineers that the demand requirement in high-altitude developments is greater than that in areas of lower altitude, although the temperatures are the same (or higher in the lower areas). For refinement, this factor could possibly require studies of light intensities and of the relative effect on cultivated crops.

---

[3] General Engr., Bureau of Reclamation, U. S. Dept. of the Interior, Cody, Wyo.

Many empirical methods which have been developed for the determination of consumptive use entail long, laborious determinations, the results of which can be, at best, no more than approximations. Although the method developed by Messrs. Lowry and Johnson is somewhat less complicated than many other methods, it, too, approaches a degree of refinement in computation whose realistic practicability could be questioned. Some of the components of this method which can be questioned are:

a. The procedure outlined to determine the limits of the growing season. A more realistic approach would have been to use the running average of the consecutive daily minimum temperatures. The element of difference in the two methods of determination is insignificant.

b. The curve reflecting the relationship of consumptive use to effective heat has doubtless proved to be extremely helpful to the designer of irrigation projects although there are grounds for questioning the correctness of this curve. For example, the curve was determined on the basis of the average of determinations made for each of twenty locations. However, in several instances the basic data were arbitrarily corrected by Messrs. Lowry and Johnson. The curve does not correctly reflect the actual basic data; this curve can be expressed by

$$H = 6{,}500\ U - 5{,}600 \quad \text{(2)}$$

in which H is the effective heat in thousand day-degrees, and U denotes the consumptive use of water in feet of depth. By computation, using only the basic data and discarding the corrected adjustments, the relationship would be expressed by

$$H = 5{,}500\ U - 3{,}100 \quad \text{(3)}$$

The modified curve, as expressed by the computed formula, appears to overcome some of the criticism that has been made of the paper by Messrs. Johnson and Lowry.

In general, the distribution of the irrigation supply, based on the total diversion, ranges from 30% to 40% (or more) for canal waste and losses, and from 35% to 45% of loss for farm waste on unlined or partly lined gravity systems. Thus, it is evident that extreme arithmetical refinement in consumptive-use requirements is difficult to justify, in view of the necessary approximated values for wastes and losses of canals and farms. The foregoing observations, although made specifically in regard to the method developed by Messrs. Lowry and Johnson, are also generally applicable to almost all the methods outlined in the writer's paper. From the viewpoint of sound engineering judgment, the writer questions whether the extreme refinements used in determining approximate consumptive-use values are justified when designing a typical gravity irrigation system, large or small.

Ralph D. Goodrich,[4] **M. ASCE.**—It should be noted that the writer inadvertently omitted Mr. Meeker from the list of engineers who had made effective use of the inflow-outflow method for estimating the consumptive use of water in large areas. Further examination of the literature available has shown that Mr. Meeker has taken an active part in the study of problems of the consumptive use of water during his irrigation engineering practice in Colorado and Wyoming and that he has served on Society committees dealing with these problems. The writer very much regrets this unintentional oversight.

The pioneering work of Messrs. Lowry and Johnson will always be recognized in consumptive-use studies. The labor involved in the original determination of the factors necessary for applying their method in a new and different area is also recognized. When consumptive-use studies were conducted by the engineering advisory committee for the Upper Colorado River Basin Compact Commission, H. P. Dugan of the hydrology branch of the USBR in Denver, Colo., found that mean annual temperatures correlated very closely with the unit consumptive-use values found by Messrs. Lowry and Johnson at thirteen locations distributed in six western states; Fig. 1 shows the results of this study. An approximate formula expressing the relationship between the mean annual temperature in degrees Fahrenheit, T, and the average rate of consumptive use of water in acre-feet per acre is

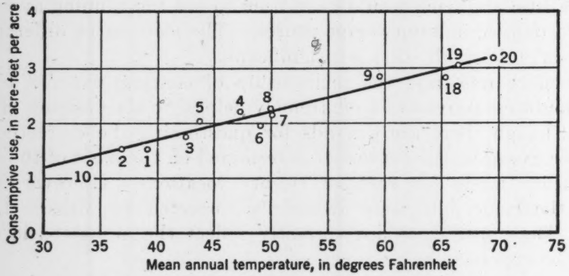

Fig. 1.—Curve of Temperature Versus Consumptive Use

$$U = 0.052\,T - 0.42 \quad \text{(4)}$$

The numbers shown in Fig. 1 refer to the projects given in Table 1 of Messrs. Lowry and Johnson (10). The distribution of these areas is as follows:

---

[4] Eng. Consultant, Upper Colorado River Comm., Grand Junction, Colo.

No.	Valley	State
1	New Fork	Wyoming
2	Michigan and Illinois	Colorado
3	Southwest area, San Luis	Colorado
4	West Tule Lake	California
5	Garland Division of Shoshone Project	Wyoming
6	North Platte	Wyoming and Nebraska
7	Mason Creek and Boise	Idaho
8	Uncompahgre	Colorado
9	Mesilla	New Mexico and Texas
10	Wagon Wheel Gap "A"	Colorado
18	East Fork of Trinity River	Texas
19	Cypress Creek	Texas
20	San Jacinto River	Texas

A report, which "* * * gives the results of studies on the correlation of some climatic measurements and the use of water by crops * * *," was published by the California Agricultural Experiment Station at Davis, Calif. (23). This report begins with an examination of the factors affecting transpiration and evaporation and states that the studies have been limited to the amount of water taken from the soil by plant transpiration and to the amount evaporated directly from the soil surface. In other words, soil-moisture determinations have been used to obtain the measurements of consumptive use in the investigations. The water that is used consumptively by various crops was correlated with the difference in evaporation as indicated by white-bulb and black-bulb atmometers; curves and tables are presented showing the results obtained. Table 3 of the report gives comparisons of the consumptive uses for seven different crops as measured by soil-moisture sampling with consumptive uses computed by four other methods. By using the first three methods, the computed results averaged approximately 20% higher than by soil-moisture sampling, whereas by using the atmometer method the results differed, on the average, by only 1.1% lower than by soil-moisture sampling.

Mr. Forester has drawn attention to the fact that, in the design of the canals and laterals of the distribution system of a large irrigation project, the amount of water actually used by the crops cultivated may be a small part of the total capacity for which the main canal and diversion structures must be designed. Although this fact is well known to irrigation engineers and is indicated indirectly in describing the use of correlation methods, it may be desirable to emphasize it more than the writer did in the paper.

Mr. Forester has also examined the method developed by Messrs. Lowry and Johnson of estimating the consumptive use of water by irrigated crops and presents his ideas concerning the practical application of this method. Therefore, any engineer contemplating the use of this method as an aid in applying integration in the inflow-outflow method should consider Mr. Forester's examination.

The writer does not intend to recommend one procedure in preference to other procedures for determining the consumptive use of water in irrigation, nor does he wish to limit the use of such determinations to the design of irrigation projects. Although the design of irrigation projects is a very important element in the future development of the Upper Colorado River Basin, such design is not a function of the Upper Colorado River Commission. A few of the engineering functions of the commission are described under the headings, "Upper Colorado River Basin" and "Conclusions."

An explanation should be made of the refinements used in determining approximate consumptive-use values in the engineering studies of the commission. As has already been shown, the determination of consumptive-use values was not made to design a typical gravity irrigation system, as Mr. Forester seems to have assumed; these values are to be used in connection with the administrative functions of the commission. With an approximate equivalent irrigated area of 2,000,000 acres in the basin and assuming an average unit consumptive-use rate of 1 acre-ft per acre, a difference of one-tenth of an acre-foot in the unit rate would indicate a difference of 200,000 acre-ft of water consumed. Whereas this may not seem important at present (1956) it may assume importance if future development attains an equivalent area of, say, 6,000,000 acres. Whether the resulting stream depletion is only 5,400,000 acre-ft or 6,600,000 acre-ft would be a matter of importance for the upper basin states.

Much useful information, which has not been mentioned heretofore, can be found in the bulletins of the experiment stations of agricultural colleges in the western United States.

The study of the material forming the basis for the writer's paper and discussions of it has led to the conclusion that research should be continued in the field of the consumptive uses of water and the consequent man-made depletion of streams.

AMERICAN SOCIETY OF CIVIL ENGINEERS

Founded November 5, 1852

TRANSACTIONS

Paper No. 2886

LATERAL BUCKLING OF ROLLED STEEL BEAMS

BY ROBERT A. HECHTMAN,[1] M. ASCE, JOHN S. HATTRUP,[2]
J. M. ASCE, EUGENE F. STYER,[3] AND
JOHN L. TIEDEMANN[4]

SYNOPSIS

In this experimental investigation of the lateral buckling of rolled steel beams under transverse loading, thirty-three beams with conditions of simple support in depths from 10 in. to 18 in. and twenty-one 10-in. beams with two types of bolted, semirigid end connections were tested. Close correlation between the experimental and theoretical values of the nominal bending strength was found for the more slender simply supported beams which buckled in the elastic range. The factor of safety, in terms of nominal bending strength of the test beams with respect to present and proposed design formulas, was determined.

NOTATION

The letter symbols adopted for use in this paper are defined where they first appear, in the illustrations or in the text, and are arranged alphabetically for convenience of reference in the Appendix.

INTRODUCTION

Prior to 1946, the design of rolled steel beams with laterally unsupported lengths was related to the slenderness ratio, L/b (in which L is the span and b is the width of the flange). Noting that this ratio neglected the influence of the torsional rigidity of the section and the restraint afforded by the tension flange, Karl de Vries,[5] M. ASCE, extended the work of S. Timoshenko[6] and

---

NOTE.—Published, essentially as printed here, in September, 1955, as *Proceedings Paper 797*. Positions and titles given are those in effect when the paper was approved for publication in *Transactions*.

[1] Prof. of Civ. Eng., Exec. Officer, The George Washington Univ., Washington, D. C.

[2] Civ. Engr., Light Div., City of Tacoma, Wash.

[3] Structural Engr., Boeing Airplane Co., Seattle, Wash.

[4] Bridge Designer, Glace & Glace, Harrisburg, Pa.

[5] "Strength of Beams As Determined by Lateral Buckling," by Karl de Vries, *Transactions*, ASCE, Vol. 112, 1947, p. 1245.

[6] "Theory of Elastic Stability," by S. Timoshenko, McGraw-Hill Book Co., Inc., New York, N. Y., 1936.

developed the parameter, $L\,h/b\,t$ (in which h is the depth of the section and t is the average thickness of the flange). This parameter resulted from equations which expressed the critical load and nominal bending stress for a simply supported, bisymmetrical, I-beam transversely loaded in the plane of its web in essentially the following forms:

$$P_{cr} = \frac{E\,I_y\,h}{L^3}\,16\,k \qquad (1)$$

and

$$s_{cr} = \frac{I_y}{I_x}\frac{h^2}{L^2}\,E\,k \qquad (2)$$

in which P_{cr} is the total critical load, E denotes the modulus of elasticity, I_y is the moment of inertia about the vertical axis, k denotes the torsional constant, s_{cr} is the critical stress, and I_x represents the moment of inertia about the horizontal axis. Eqs. 1 and 2 are applicable for the loading condition of two equal concentrated loads at the quarter-points of the span length.

The parameter, $L\,h/b\,t$, was deduced by Mr. de Vries from the elastic buckling strength of a large number of rolled beams under uniform top-flange load computed by equations of the general form of Eq. 2. He developed the formula,

$$s_{cr} = \frac{20{,}000{,}000}{\dfrac{L\,h}{b\,t}} \qquad (3)$$

as a reasonable basis for determining the buckling strengths for common types of transverse loading. G. Winter,[7] M. ASCE, showed that the buckling strength for such a beam under pure bending could be expressed by

$$s_{cr} = \frac{E\,\pi^2}{2\left(\dfrac{L}{h}\right)^2}\sqrt{\left(\frac{I_y}{2\,I_x}\right)^2 + \frac{k\,I_y}{2\,(1+\mu)\,I_x^2}\left(\frac{L}{\pi\,h}\right)^2} \qquad (4)$$

and that, with certain approximations which were slight for almost all rolled beams, the parameter, $L\,h/b\,t$, and Eq. 3 could be derived from this equation. In Eq. 4, μ is Poisson's ratio. The application of these same approximations to the quantity, $\dfrac{I_y\,h^2\,k}{I_x\,L^2}$, in Eq. 2 will also result in this form of the slenderness ratio and in Eq. 3.

For the design of slender beams, Mr. de Vries[5] incorporated a factor of safety of 1.67 in Eq. 3 and suggested

$$s = \frac{12{,}000{,}000}{\dfrac{L\,h}{b\,t}} \qquad (5)$$

Eq. 5 was adopted by the American Institute of Steel Construction (AISC)[8] for the design of structural carbon steel rolled sections, plate girders, and built-up members in bending with an $L\,h/b\,t$-ratio in excess of 600. For shorter beams an allowable unit bending stress of 20,000 lb per sq in. is used.

---

[7] Discussion by G. Winter of "Strength of Beams As Determined by Lateral Buckling," by Karl de Vries, *Transactions*, ASCE, Vol. 112, 1947, p. 1272.

[8] "Steel Construction Manual," A.I.S.C., 1946.

The L/b-parameter for beams with laterally unsupported lengths is in use in other steel specifications.[9,10] A formula based on it may be found subsequently in Eq. 7.

An expression for the critical buckling load of beams under two equal symmetrically placed transverse loads was developed by Mr. Winter and R. K. Schrader:[11]

$$P_{cr} = \frac{A\,E}{L^3}\left[-\frac{h\,I_y}{2} + \sqrt{\left(\frac{h\,I_y}{2}\right)^2 + B\left(\frac{h\,I_y}{2}\right)^2 + D\,C\,I_y\,L^2}\,\right] \ldots (6)$$

in which the factors A, B, and D depend on the same variables as the factor, k, in Eqs. 1 and 2, and C is the torsional moment required to produce an angle of twist per unit length of beam of one radian.

The present investigation had as its principal objectives:

1. The testing of rolled steel beams of the wide-flange type and standard I-beam type.
2. Correlation of the test results with theory where possible.
3. A critical examination of the $L\,h/b\,t$-parameter as a basis for predicting the buckling strength of standard rolled beams.
4. A preliminary exploration of the anticipated increase in strength that semirigid end connections would afford.
5. The determination of the factor of safety of rolled steel beams with respect to present and proposed design formulas.

Values of the factor, k, in Eq. 2 were available for two cases of interest in this investigation—simply supported beams with a midspan concentrated load or with uniform load over the entire span length.[5] There was the possibility of the existence of more severe loading conditions. Therefore, the methods by which Eqs. 1 and 2 were derived were used to compute the values of k for other loadings (Fig. 1). The most severe loading type was that of two equal loads at the quarter-points of the beam; this loading was used for all the tests.

It had been previously noted[12,13] that the parameter, $L\,h/b\,t$, would predict the value of the buckling strength less accurately for shorter beams than for longer beams because the shape of the cross section is more significant for the former. The desirability of choosing as test specimens three rolled sections with almost identical $h/b\,t$-ratios but with considerable difference in the shape of their cross sections led to the choice of the 10I25.4, 12WF27, 12WF27, and 18WF50 sections with $h/b\,t$-ratios of 4.37, 4.60, and 4.22, respectively. These

---

[9] "Specifications for Steel Railway Bridges," A.R.E.A., Vol. II, 1953.

[10] "Standard Specifications for Highway Bridges," A.A.S.H.O., 1953.

[11] Discussion by R. K. Schrader of "Lateral Stability of Unsymmetrical I-Beams and Trusses in Bending," by George Winter, *Transactions*, ASCE, Vol. 108, 1943, p. 247.

[12] Discussion by Neil Van Eenam of "Strength of Beams As Determined by Lateral Buckling," by Karl de Vries, *Transactions*, ASCE, Vol. 112, 1947, p. 1281.

[13] Discussion by Oliver G. Julian of "Strength of Beams As Determined by Lateral Buckling," by Karl de Vries, *ibid.*, p. 1303.

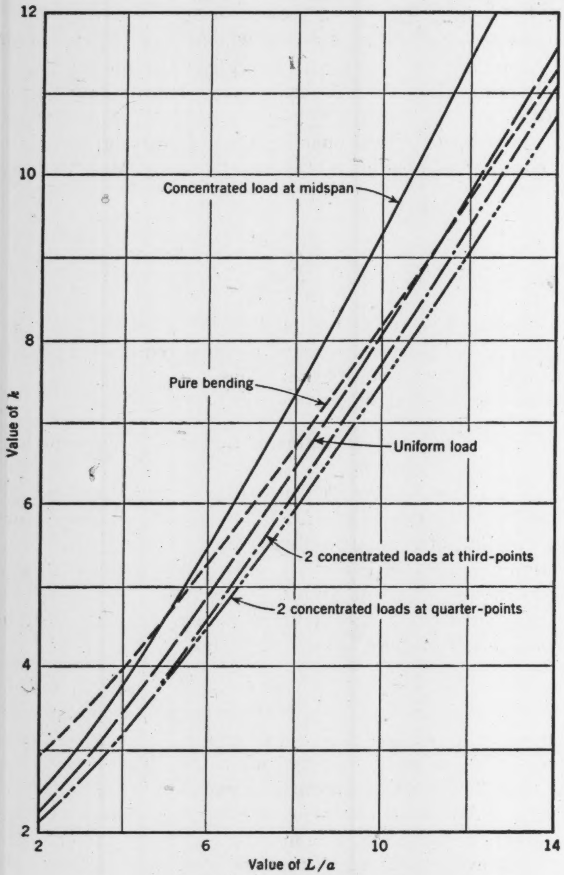

FIG. 1.—THEORETICAL k-VALUES FOR SIMPLY SUPPORTED BEAMS

three sections, the first with tapered flanges and the remaining two with almost parallel flanges, would be expected to develop almost equal buckling strengths for the same span, according to Eq. 3. The theoretical elastic buckling strengths of these sections and the 10B15 beams as predicted by Eqs. 2 and 3 are shown in Fig. 2.

Two types of end-support conditions were chosen for the test beams—first, simple support which would yield results that could be compared with the values predicted by the foregoing equations, and second, semirigid connections similar to those commonly found in steel structures.

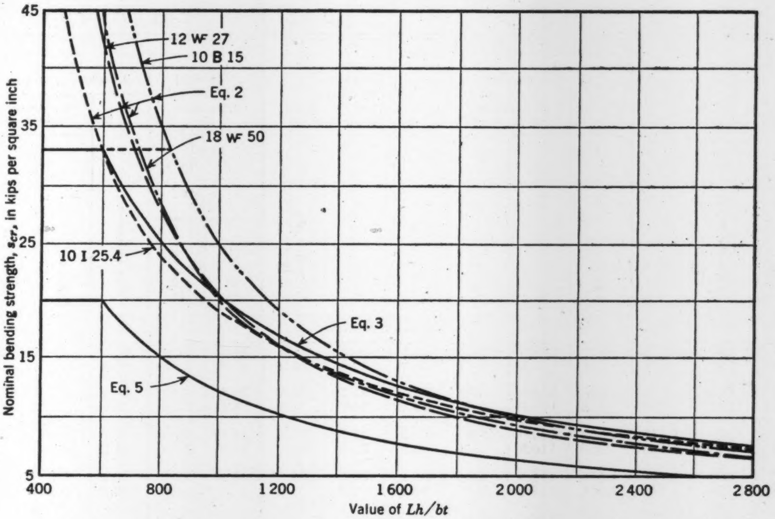

FIG. 2.—THEORETICAL s_{cr} OF SIMPLY SUPPORTED TEST SECTIONS FOR QUARTER-POINT LOADING

MECHANICAL PROPERTIES OF BEAM SECTIONS AND METHOD OF TESTING

All the beams tested in this investigation were rolled from the same heat of plain-carbon, semikilled structural steel meeting designation A 7-51 T of the American Society of Testing Materials (ASTM) or the type commonly termed "structural-carbon steel." Before each test the initial out-of-alinement and

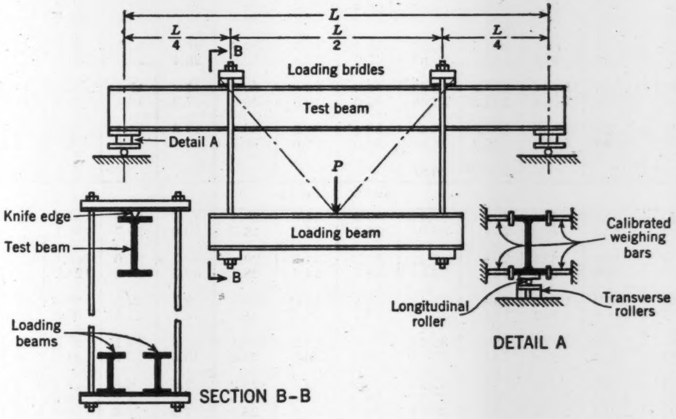
L
L/4
L/2
L/4
B
Loading bridles
Test beam
Detail A
P
Knife edge
Test beam
Loading beam
B
Calibrated weighing bars
Longitudinal roller
Transverse rollers
DETAIL A
Loading beams
SECTION B-B

FIG. 3.—END SUPPORTS AND LOADING OF SIMPLY SUPPORTED TEST BEAMS

TABLE 1.—SUMMARY OF RESULTS

(a) PROPERTIES OF TEST BEAMS											(b) SUMMARY				
Beam	Span, in inches	Slenderness Ratio, $L\,h/b\,t$		Actual Moment of Inertia,[a] in Inches^4		Average Compressive Properties,[b] in Kips per Square Inch			Nominal Bending Strength at Critical Load, in Kips per Square Inch		Critical Buckling		
		Actual[a]	Ideal	I_x	I_y	Yield point	Proportional limit	Modulus of elasticity × 10^{-3}	Eq. 3[e]	Test value	Test value[d]	Southwell's method	
												Donnell	Lundquist
10I25.4 SECTIONS													
1	120	576	526	119.9	6.37	35.5	30.2	31.6	33.0	27.0	44.1	. . .	54.0
2	120	574	526	115.8	6.36	35.6	30.5	29.2	33.0	25.3	41.4	. . .	. . .
3	150	696	658	125.0	6.83	33.5	31.7	31.6	28.8	22.9	29.9	. . .	40.0
4	150	700	658	116.5	6.54	34.5	30.0	31.1	28.6	21.8	28.5	. . .	32.0
5	240	1,115	1,052	125.0	6.83	33.5	31.7	31.6	18.0	16.0	13.1	13.5	13.1
6	240	1,120	1,052	116.5	6.54	34.5	30.0	31.1	17.9	17.4	14.2	14.3	14.2
7	360	1,720	1,576	114.5	6.36	35.6	30.5	29.2	11.6	12.6	6.8	6.8	6.6
8	360	1,731	1,576	118.5	6.37	35.5	30.2	31.6	11.6	11.6	6.3	6.9	6.6
				122.1	6.9[f]								
10B15 SECTIONS													
25	60	546	558	68.6	2.86	37.5	30.0	28.4	33.0	34.1	62.7	80.0	104.0
26	60	555	558	69.0	2.87	41.6	. . .	28.8	33.0	33.6	61.7	80.0	107.0
27	90	832	837	69.0	2.87	41.6	. . .	28 8	24.0	30.6	37.6	44.3	40.9
28	90	832	837	69.0	2.87	41.6	. . .	28.8	24.0	28.6	35.1	41.3	41.6
29	120	1,111	1,116	68.6	2.86	42.5	. . .	29.2	18.0	21.1	19.4	21.7	21.2
30	120	1,111	1,116	68.6	2.86	42.5	. . .	29.2	18.0	21.2	19.5	21.4	20.9
				68.8[f]	2.79[f]								
12W̅F27 SECTIONS													
9	120	575	552	207.2	17.35	38.5	31.2	30.4	33.0	29.5	66.9	. . .	114.0
10	120	576	552	200.3	16.40	38.5	31.2	30.4	33.0	28.4	64.3	. . .	70.0
11	150	723	690	203.2	16.98	36.5	30.3	30.3	27.7	25.7	46.9	. . .	. . .
12	150	705	690	203.9	16.83	37.9	33.8	30.3	28.4	20.3	36.9	. . .	. . .
13	240	1,130	1,104	206.2	16.83	37.9	33.8	30.3	17.7	17.4	19.6	19.8	19.8
14	240	1,155	1,104	203.2	16.98	36.5	30.3	30.3	17.3	16.4	18.5	19.3	20.7
15	360	1,725	1,656	203.8	16.40	38.5	31.2	30.4	11.6	11.1	8.4	8.5	8.8
16	360	1,680	1,656	200.7	16.66	39.5	31.6	30.7	11.9	11.5	8.7	8.8	9.0
				204.1[f]	16.6[f]								
18W̅F50 SECTIONS													
17	120	530	506	799	37.42	39.2	34.0	29.9	33.0	25.9	153.7	. . .	. . .
18	120	534	506	764	36.04	38.3	34.2	28.7	33.0	29.7	176.1	. . .	. . .
19	150	664	633	799	37.42	39.2	34.0	29.9	30.1	31.0	147.1	. . .	. . .
20	150	666	633	764	36.04	38.3	34.2	28.7	30.1	26.2	124.2	. . .	163.0
21	240	1,070	1,012	799	37.42	39.2	34.0	29.9	18.7	22.8	67.6	73.0	72.0
22	240	1,069	1,012	764	36.04	38.3	34.2	28.7	18.7	21.5	63.8	66.0	70.0
23	360	1,600	1,518	789	36.42	39.8	36.2	30.1	12.5	14.1	27.7	27.8	28.5
24	360	1,600	1,518	785	35.73	38.5	36.0	29.8	12.5	12.2	24.0	25.2	25.4
55a	600	2,660	2,530	799	37.42	39.2	34.0	29.9	7.5	6.8	8.2	8.4	8.4
55b	600	2,660	2,530	799	37.42	39.2	34.0	29.9	7.5	7.0	8.3	8.5	8.5
56	600	2,670	2,530	764	36.04	38.3	34.2	28.7	7.5	7.4	8.8	8.8	8.9
				800.6[f]	37.2[f]								

[a] Computed from measured dimensions of beams. [b] Averages of results (2-in. gage length) for two on beam. [e] Slenderness ratio greater than that permitted by code. [f] Ideal values.

FOR SIMPLY SUPPORTED BEAMS

OF TEST DATA					(c) FACTOR OF SAFETY					
Load, in Kips		Initial Out-of-Alinement of Flanges at Midspan[c]			Slenderness ratio, L/b	Factor of Safety				
Theoretical value						20 kips per sq in. base, AISC, Eq. 8	18-kips-per-sq-in. base			
									Proposed formula	
Eq. 2	Eq. 6	Top flange, in inches	Bottom flange, in inches	Angle of twist, in radians			AREA, Eq. 7	AASHO, Eq. 7	Parabolic cutoff, Eq. 9	Straight-line cutoff, Eq. 10
10I25.4 SECTIONS										
58.0	63.0	−0.03	−0.07	0.004	25.8	1.35	1.84	1.84	1.69	1.76
58.0	60.0	−0.04	−0.08	0.003	25.8	1.27	1.72	1.72	1.58	1.65
36.0	41.0	0.12	−0.02	0.014	32.2	1.32	1.78	•	1.53	1.59
36.4	39.0	0.08	0.02	0.005	32.2	1.26	1.69	•	1.45	1.57
13.8	15.7	0.10	0.03	0.007	51.6	1.48	•	•	1.48	1.45
13.8	14.8	−0.02	−0.09	0.007	51.6	1.62	•	•	1.62	1.58
6.2	6.4	0.11	0.08	0.003	77.3	1.81	•	•	1.81	1.81
6.3	6.7	0.19	0.13	0.006	77.3	1.67	•	•	1.67	1.67
10B15 SECTIONS										
111.0	122.0	0.01	−0.01	0.002	15.0	1.71	2.02	2.02	2.10	2.18
114.0	125.0	−0.02	−0.03	0.001	15.0	1.68	1.99	1.99	2.07	2.16
40.6	44.4	−0.01	0	−0.001	22.5	2.13	1.99	1.99	2.22	2.30
40.6	44.4	0.01	0.02	−0.001	22.5	1.98	1.86	1.86	2.07	2.15
18.9	21.1	0.04	−0.06	0.010	30.0	1.96	1.56	1.56	1.96	1.91
18.9	21.1	0.04	−0.03	0.007	30.0	1.96	1.57	1.57	1.96	1.92
12WF27 SECTIONS										
108.0	121.0	0.01	−0.04	0.004	18.4	1.48	1.81	1.81	1.84	1.92
108.0	116.0	0	0	0	18.4	1.42	1.74	1.74	1.78	1.85
63.0	67.0	−0.01	0.06	−0.006	23.1	1.55	1.68	1.68	1.72	1.82
60.0	64.0	0.02	0	0.002	23.1	1.19	1.33	1.33	1.35	1.42
18.9	20.6	0.04	0.10	−0.005	36.9	1.64	1.55	•	1.64	1.60
20.0	21.8	0.06	−0.11	0.014	36.9	1.58	1.46	•	1.58	1.52
8.4	8.8	0.09	0.07	0.002	55.3	1.60	•	•	1.60	1.60
8.3	9.0	0.12	0.12	0	55.3	1.61	•	•	1.61	1.61
18WF50 SECTIONS										
364.0	360.0	−0.03	−0.06	0.001	16.0	1.30	1.55	1.55	1.59	1.64
354.0	344.0	0	0	0	16.0	1.49	1.78	1.78	1.82	1.88
195.0	196.0	0.02	−0.06	0.004	20.0	1.71	1.94	1.94	2.03	2.11
195.0	190.0	0	−0.01	0.001	20.0	1.45	1.64	1.64	1.71	1.78
58.0	60.0	0.02	0.12	−0.006	32.0	2.03	1.78	•	2.03	2.00
60.0	60.0	0.02	0.01	0.001	32.0	1.92	1.68	•	1.92	1.89
24.0	25.4	−0.10	−0.37	0.015	48.0	1.88	•	•	1.88	1.88
23.6	24.8	0.10	0.07	0.002	48.0	1.63	•	•	1.63	1.63
7.7	8.0	0.08	0.01	0.004	80.0	1.53	•	•	1.53	1.53
7.7	8.0	−0.01	−0.08	0.004	80.0	1.56	•	•	1.56	1.56
8.6	8.4	−0.02	−0.08	0.003	80.0	1.66	•	•	1.66	1.66

specimens from each mill section, one for each beam flange. [c] With respect to span end points. [d] Total load.

TABLE 2.—SUMMARY OF RESULTS FOR

(a) PROPERTIES OF TEST BEAMS | (b) SUMMARY OF

Beam	Span, in inches	Slenderness Ratio, $L h/b t$		Actual Moment of Inertia,[a] in Inches^4		Average Compressive Properties,[b] in Kips per Square Inch			Nominal Bending Strength at Critical Load, in Kips per Square Inch		Critical Buckling		
		Actual[a]	Ideal	I_x	I_y	Upper yield point	Proportional limit	Modulus of elasticity $\times 10^{-3}$	Eq. 3[c]	Test value	Test value[d]	Southwell's method	
												Donnell	Lundquist
10B15 SECTIONS WITH TOP AND SEAT ANGLE CONNECTIONS													
37	90	822	837	70.5	2.96	43.8	39.5	29.8	24.3	35.6	43.7	54.0	53.5
38	90	822	837	70.5	2.96	43.8	39.5	29.8	24.3	38.1	46.7	50.5	54.1
39	120	1,111	1,116	67.6	2.79	43.3	40.5	27.9	18.0	35.5	32.7	...	33.6
40	120	1,111	1,116	67.6	2.79	43.3	40.5	27.9	18.0	29.7	27.3	30.8	31.0
41	180	1,679	1,674	68.4	2.82	38.3	37.0	27.7	11.9	21.8	13.4	14.1	14.4
42	180	1,679	1,674	68.4	2.82	38.3	37.0	27.7	11.9	23.8	14.7	15.0	14.9
43	240	2,207	2,232	68.8	2.90	40.5	35.5	28.6	9.0	19.8	9.1	...	9.5
44	240	2,215	2,232	68.5	2.87	40.2	36.0	28.7	9.0	20.5	9.4	...	...
57a	360	3,290	3,348	70.5	2.96	43.8	39.5	29.8	6.0	17.2	...	5.3	5.0
57b	360	3,290	3,348	70.5	2.96	43.8	39.5	29.8	6.0	15.9	...	4.9	4.7
58	360	3,350	3,348	67.6	2.79	43.3	40.5	27.9	5.9	15.0	...	4.6	4.5
				68.8[f]	2.79[f]								
10B15 SECTIONS WITH WEB-ANGLE CONNECTIONS													
47	90	826	837	68.1	2.82	42.6	40.2	27.8	24.2	34.8	42.7	45.5	45.2
48	90	826	837	68.1	2.82	42.6	40.2	27.8	24.2	33.2	40.7	44.5	44.7
49	120	1,108	1,116	68.1	2.82	41.5	33.0	26.6	18.1	25.5	23.5	25.2	24.8
50	120	1,108	1,116	68.1	2.82	41.5	33.0	26.6	18.1	27.2	25.0	25.2	25.1
51	180	1,649	1,674	68.5	2.86	41.7	31.0	28.3	12.1	17.9	11.0	11.4	11.3
52	180	1,649	1,674	68.5	2.86	41.7	31.0	28.3	12.1	18.1	11.2	11.6	11.5
53	240	2,268	2,232	67.9	2.90	40.3	35.7	29.7	8.8	13.6	6.2	6.2	6.2
54	240	2,183	2,232	68.6	2.86	37.5	30.0	28.4	9.1	14.0	6.4	6.5	6.4
59	360	3,302	3,348	68.1	2.82	42.6	40.2	27.8	6.0	12.4	3.8	3.8	3.7
60	360	3,320	3,348	68.8	2.82	41.5	33.0	26.6	6.0	11.7	3.6	3.6	3.7
				68.8[f]	2.79[f]								

[a] Computed from measured dimensions of beams. [b] Average of results (2-in. gage length) for two simple-beam-support conditions. Values at design load found by interpolation between nearest experimental

twist of the beam were measured as well as the dimensions of the cross section. From the latter were computed the actual slenderness ratios and moments of inertia recorded in Tables 1(*a*) and 2(*a*). The mechanical properties determined by compression tests of coupons cut from the beam flanges are listed in Tables 1(*a*) and 2(*a*).

The method of testing the simply supported beams is shown in Fig. 3. The span-end cross section of the beam was prevented from tipping by lateral

Beams with Semirigid End Connections

Test Data						(c) Factor of Safety					
Load, in Kips		Moment at Design Load,[c] in Kip-Feet		Moment at Critical Load, in Kip-Feet		Slenderness ratio, L/b	Factor of Safety				
Theoretical value							20-kips-per-sq-in. base, AISC, Eq. 8	18-kips-per-sq-in. base			
								AREA, Eq. 7	AASHO, Eq. 7	Proposed formula	
Eq. 2	Eq. 6	M_x	M_y	M_x	M_y					Parabolic cutoff, Eq. 9	Straight-line cutoff, Eq. 10
10B15 Sections with Top and Seat Angle Connections											
40.0	42.0	4.60	−0.07	10.70	−0.01	22.5	2.44	2.31	2.31	2.56	2.66
40.0	42.0	3.82	−0.06	10.08	...	22.5	2.61	2.47	2.47	2.74	2.84
18.7	20.0	3.12	−0.02	10.05	0.14	30.0	3.29	2.63	2.63	3.29	3.21
18.7	20.0	2.72	−0.12	8.60	0.00	30.0	2.75	2.20	2.20	2.75	2.68
7.6	7.9	2.26	0.00	7.59	0.35	45.0	3.05	[e]	[e]	3.05	3.05
7.6	7.9	1.90	0.00	7.59	0.21	45.0	3.33	[e]	[e]	3.33	3.33
4.5	4.7	1.66	0.03	7.56	0.30	60.0	3.67	[e]	[e]	3.67	3.67
4.5	4.7	1.67	−0.09	7.75	−0.15	60.0	3.80	[e]	[e]	3.80	3.80
2.0	2.0	0.44	0.00	10.54	0.69	90.0	4.72	[e]	[e]	4.72	4.72
2.0	2.0	0.62	0.01	9.50	0.68	90.0	4.37	[e]	[e]	4.37	4.37
1.9	2.1	0.61	0.02	9.05	0.73	90.0	4.19	[e]	[e]	4.19	4.19
10B15 Sections with Web-Angle Connections											
40.0	41.2	3.03	0.02	7.00	0.14	22.5	2.40	2.26	2.26	2.50	2.60
40.0	41.2	3.00	−0.04	6.96	−0.05	22.5	2.29	2.16	2.16	2.39	2.48
19.3	19.6	3.04	0.07	5.70	0.19	30.0	2.35	1.89	1.89	2.35	2.30
19.3	19.6	2.75	0.00	6.30	0.05	30.0	2.50	2.02	2.02	2.50	2.46
8.2	8.6	2.15	0.02	5.97	0.10	45.0	2.47	[e]	[e]	2.47	2.47
8.2	8.6	1.73	0.00	4.36	0.17	45.0	2.49	[e]	[e]	2.49	2.49
4.3	4.7	1.51	−0.01	5.53	0.67	60.0	2.57	[e]	[e]	2.57	2.57
4.5	4.7	1.47	0.01	3.58	0.37	60.0	2.55	[e]	[e]	2.55	2.55
2.0	2.0	0.54	0.02	5.41	0.53	90.0	3.41	[e]	[e]	3.41	3.41
2.0	2.0	0.57	0.00	5.02	0.45	90.0	3.24	[e]	[e]	3.24	3.24

specimens from each mill section, one for each beam flange. [c] Design load computed on assumption of values. [d] Total load on beam. [e] Slenderness ratio greater than that permitted by code. [f] Ideal values.

restraints on the toes of the flanges. A method of applying the loads was evolved which permitted manual adjustments of the loads in the lateral direction to keep their lines of action vertical.

The same method of loading was used for the beams with semirigid end connections. Rigid faces which remained parallel and free from rotation but which permitted axial translation were provided for the end connections in the manner shown in Fig. 4. Details of the end connections themselves appear in Fig. 5. The web-angle connection was scaled down from the standard beam connection[8] for a 14-in. depth in order to provide three bolts in line in the web. Bolts were of $\frac{5}{8}$-in.-diameter, high-tensile steel. All holes were $\frac{11}{16}$ in. in diameter, and carburized washers were placed under the heads and nuts of bolts.

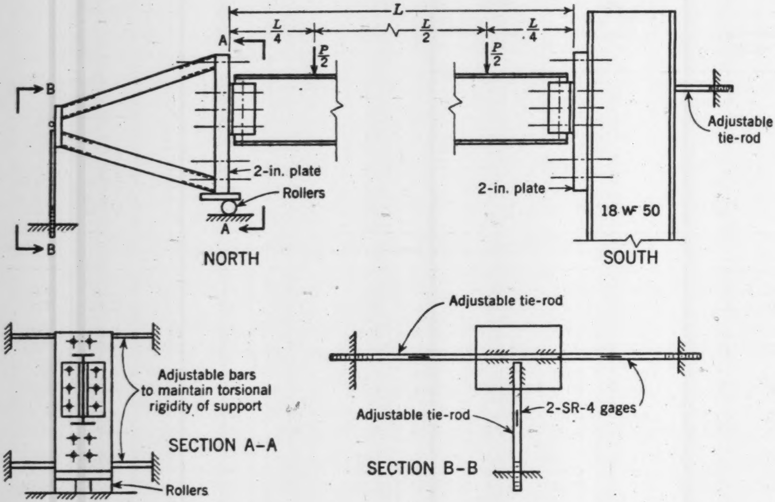
L
$\frac{L}{4}$
$\frac{L}{2}$
$\frac{L}{4}$
$\frac{P}{2}$
$\frac{P}{2}$
A
A
B
B
2-in. plate
Rollers
2-in. plate
18 WF 50
Adjustable tie-rod
NORTH
SOUTH
Adjustable bars to maintain torsional rigidity of support
SECTION A-A
Rollers
Adjustable tie-rod
2-SR-4 gages
Adjustable tie-rod
SECTION B-B

FIG. 4.—END SUPPORTS AND METHOD OF LOADING FOR BEAMS WITH SEMIRIGID END CONNECTIONS

In this program the quarter-point loads were first carefully located over the center plane of the web of the beam. Only in the case of the shorter beam (beam 25–30, beam 37–40, and beam 47–50) was the additional procedure of centering used.

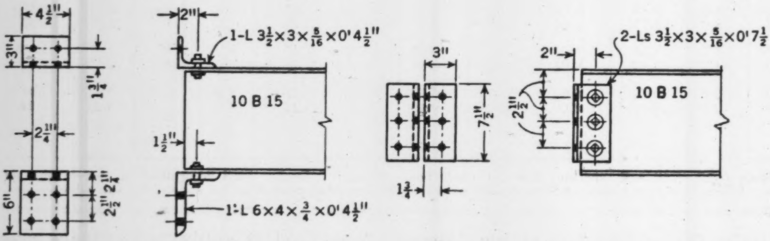
$4\frac{1}{2}''$
$3''$
$1\frac{3}{4}''$
$2\frac{1}{4}''$
$6''$
$2\frac{1}{2}''$
$2\frac{1}{4}''$
$2''$
1-L $3\frac{1}{2}\times3\times\frac{5}{16}\times0'4\frac{1}{2}''$
10 B 15
$1\frac{1}{2}''$
1-L $6\times4\times\frac{3}{4}\times0'4\frac{1}{2}''$
$3''$
$7\frac{1}{2}''$
$1\frac{3}{4}$
$2''$
2-Ls $3\frac{1}{2}\times3\times\frac{5}{16}\times0'7\frac{1}{2}$
$2\frac{1}{2}''$
10 B 15

TOP AND SEAT ANGLE CONNECTION WEB ANGLE CONNECTION

FIG. 5.—DETAILS OF SEMIRIGID END CONNECTIONS

In a beam under transverse loading no simple criterion of centering exists, as for an axially loaded symmetrical column. When the initially curved beam is loaded, it will twist as well as deflect laterally. The centering criterion could then be either of two possibilities—placement of the load so that no lateral deflection of the top flange of the beam at midspan occurred or placement of the load so that no rotation of the midspan cross section developed. The latter criterion was chosen after the earlier tests showed that the rotations of the beam cross sections were more sensitive to the positions of the loads and were more important in determining the buckling strength of the beam. Each load was independently adjusted laterally until the cross sections under the loads and at midspan showed very little or no rotation at a load estimated to be approximately 25% of the buckling load for the beam. After centering, the test was begun.

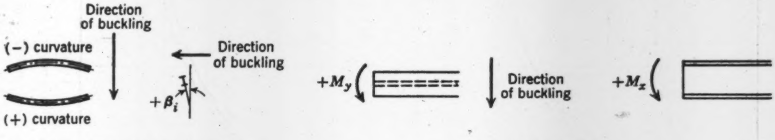

(a) MISALINEMENT AND TWIST (b) MOMENTS

FIG. 6.—SIGN CONVENTION

The lateral deflections of the top and bottom flanges, the vertical deflections of the beam, and the rotations of the cross sections were measured at the sixth-points of the span length at frequent load intervals up to buckling. The unit strains on the four toes of the beam flanges at midspan were determined by SR-4 strain gages. These data are not presented herewith. However, they served as a very useful means of observing the behavior of the beams and the imminence of failure.

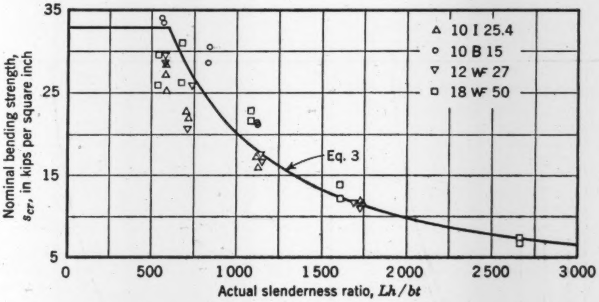

FIG. 7.—VALUE OF s_{cr} OF SIMPLY SUPPORTED TEST BEAMS

RESULTS OF TESTS

Summaries of the more important data of these tests appear in Tables 1(*b*) and 2(*b*).[14,15,16] In Fig. 6 the sign conventions used in this investigation for initial misalinement and twist are illustrated.

---

[14] "On the Analysis of Experimental Observations in Problems of Elastic Stability," by R. V. Southwell, *Proceedings*, Royal Soc. of London, Vol. 135A, 1932, p. 601.

[15] "On the Application of Southwell's Method for the Analysis of Buckling Tests," by L. H. Donnell, in "Contributions to the Mechanics of Solids: Dedicated to Stephen Timoshenko," The Macmillan Co., New York, N. Y., 1938.

[16] "Generalized Analysis of Experimental Observations in Problems of Elastic Stability," by E. E. Lundquist, *Technical Note No. 658*, National Advisory Committee on Aeronautics, Washington, D. C., 1938.

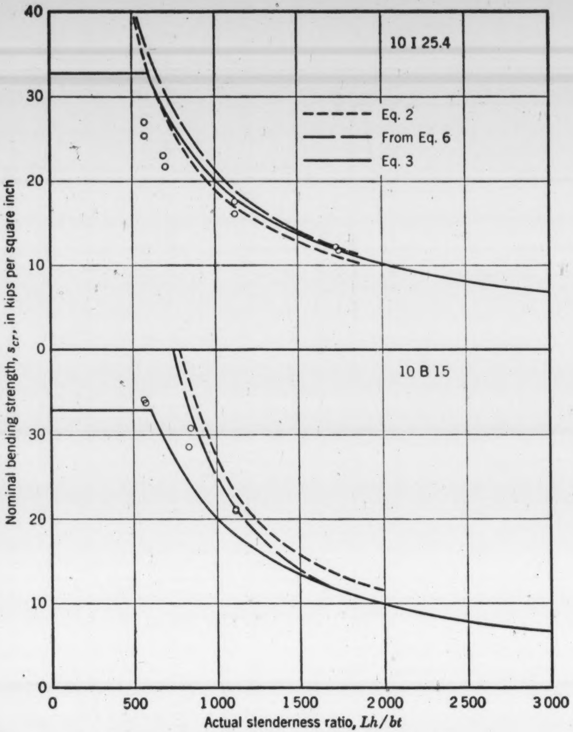

FIG. 8.—VALUE OF s_{cr} OF 10I25.4 AND 10B15 BEAMS

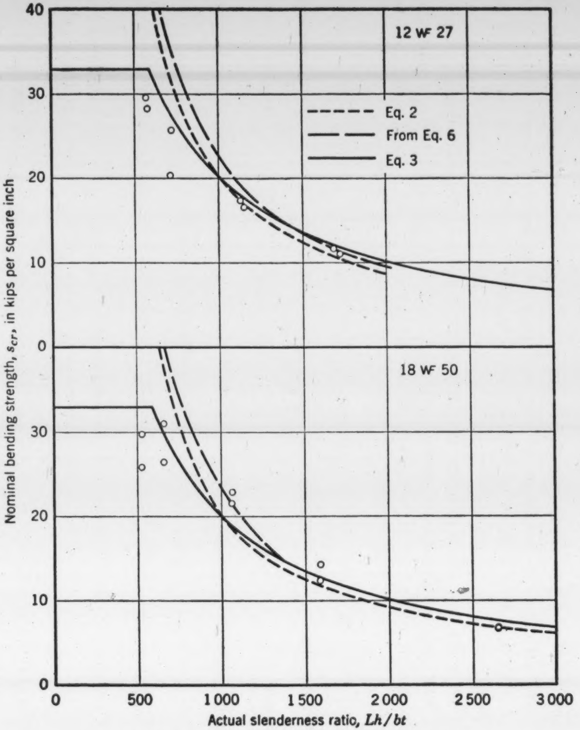

FIG. 9.—VALUE OF s_{cr} OF 12WF27 AND 18WF50 BEAMS

The plot in Fig. 7 shows the relationship between the nominal bending strength and the actual slenderness ratio, $L\,h/b\,t$, of the simply supported beams. This plot and the individual plots in Figs. 8 and 9 indicate that the buckling strengths of the shorter beams of the four section sizes were approximately of the same order as the theoretical strengths plotted in Fig. 2, the 10B15 section having the highest strength, the 10I25.4 section the lowest, and the 12WF27 and the 18WF50 sections falling in intermediate positions.

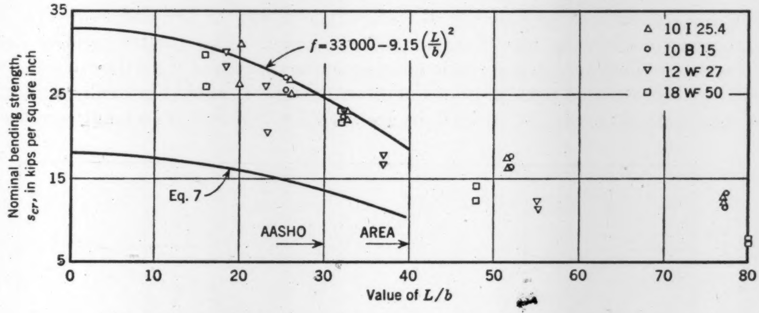

Fig. 10.—Comparison of s_{cr} and L/b for Simply Supported Beams

It seems reasonable to conclude that the $L\,h/b\,t$-parameter should be adequate for designing wide-flange and standard beams.[8] The greater accuracy of this parameter over L/b may be seen by examining the results of these tests when plotted against L/b (Fig. 10).

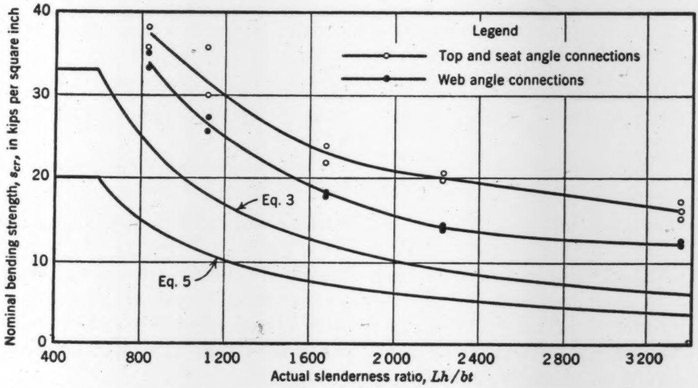

Fig. 11.—Comparison of s_{cr} and $L\,h/b\,t$ for 10B15 Beams with Bolted Semirigid End Connections

In Fig. 10 there is little tendency for the data to fall along a common curve. It can be shown that the transformation of the quantity, $\frac{I_y\,h^2}{I_x\,L^2}$, in Eq. 2 in terms of b, t, h, and L will result in the L/b-parameter. However, the important factor, k, is then omitted from the parameter whereas the parameter, $L\,h/b\,t$, contains the quantity, k.

The nominal bending strength developed by the beams with the top-and-seat-angle connection and the web-angle connection (Fig. 11) was computed on the assumption that they were simply supported. The actual nominal bending strength was related to the effective rigidity of the end connections and was considerably less than the values shown. The greater rigidity developed by the top-and-seat-angle connection as compared with the web-angle connection is in line with previous observations.[17] It should be realized that, when identical semirigid connections are used for different span lengths of the same beam section, the effective end restraint will increase as the span length increases.[17]

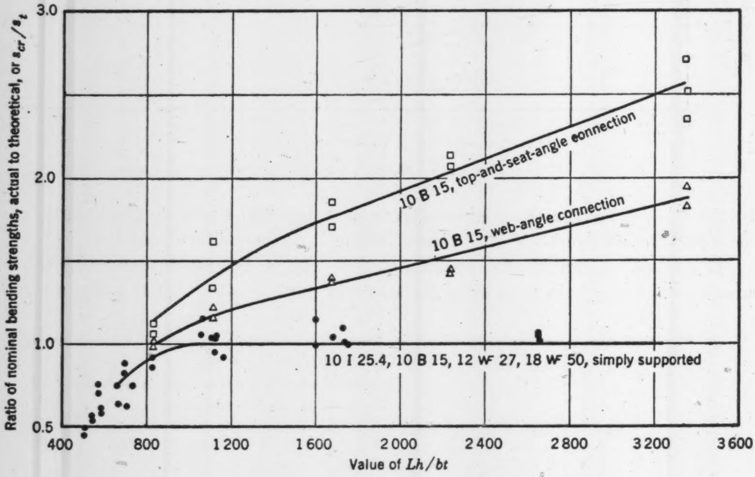

FIG. 12.—COMPARISON OF s_{cr} AND s_t FOR VARIOUS END-RESTRAINT CONDITIONS FOR SIMPLY SUPPORTED BEAMS

In Fig. 12 the experimental or actual nominal bending strength, s_{cr}, of all the beams is compared with s_t, the theoretical nominal bending strength, for the quarter-point loading. The points for $L\,h/b\,t$-ratios less than 600 were based on a theoretical critical stress which was greater than the yield point of the steel and must therefore be so interpreted.

From Fig. 12 it is possible to determine the $L\,h/b\,t$-ratio below which the beams buckled in the inelastic range by observing the value at which there was a downward turn in the curves. These values were approximately 1,100 for the simply supported beams and those with web-angle connections and approximately 1,300 for those with the top-and-seat-angle connections. Wherever the simply supported beams buckled in the elastic range fairly good correlation was found between the experimental results and the theoretical predictions. This correlation would suggest similar agreement if types of loading other than quarter-point loading had been used in these tests.

---

[17] "Riveted Semi-Rigid Beam-to-Column Building Connections," by R. A. Hechtman and B. G. Johnston, A.I.S.C., 1948.

The parameter, *L/a*, is used by Mr. Timoshenko[6] to describe the slenderness of a beam subject to lateral buckling; the term, *a*, is the torsion-bending constant. By use of Eq. 1 it was possible to compute the factor, *k*, developed by the beams. These values are compared with the actual *L/a*-value of the beams in Fig. 13. Where *L/a* was greater than approximately 3, the simply supported beams failed in the elastic range and the values of *k* fell near the theoretical curve. Because of the varying span-end rigidity of the beams with semirigid connections the experimental curves can best serve to give an approximate indication of the probable effectiveness of other similar connections.

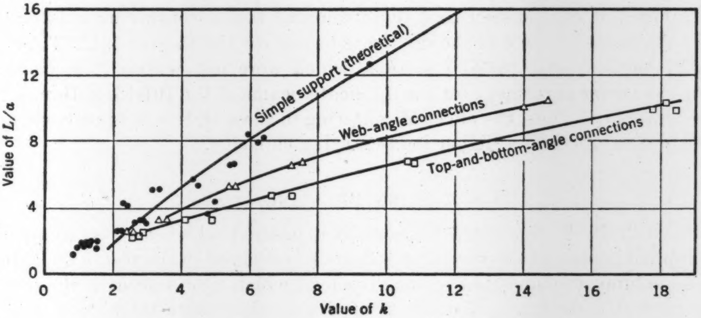

FIG. 13.—FACTOR *k* DEVELOPED BY TEST BEAMS

EFFECT OF INITIAL MISALINEMENT AND CENTERING ON THE BENDING STRENGTH

The initial misalinement of the test beams and its relation to the direction in which the beam finally buckled are given in Table 1(*b*). It was noted that:

1. The direction of buckling was always in the direction of the initial angle of twist of the web at midspan except in those cases in which both flanges were deformed in the direction of buckling with the greater curvature in the bottom flange.
2. The nature of the initial curvature and twist affected the buckling strength with the most adverse condition occurring when both the twist of the web and the curvature of the top flange were in the direction of buckling.
3. Strength was increased when the top flange was initially deformed in the direction opposite that in which the beam buckled.
4. The effect of misalinement on the buckling strength of the simply supported beams appeared to decrease as the value of $L\,h/b\,t$ increased.

Because the misalinement of the top flange determined the position of the load, and hence its eccentricity to the line joining the support points, these findings were quite logical. An exception to the pattern described in item 1 of the foregoing was beam 11 whose top flange was almost straight.

The purpose of centering is to move the load so as to counterbalance the adverse effect of the initial misalinement and twist of the beam. In items 1 and 2 of the foregoing the initial rotation of the cross sections of the beam would be in the direction of buckling. Centering increased the load-carrying capacity of these beams. The beams noted in item 3 tended to twist during the early stages of the test in a direction opposite to the final direction of buckling. It is important that the placement of the loads during centering be determined by the direction of the twist during the later stages of the test. Therefore, the load used in centering must be sufficiently large to develop the mode of deformation which is to prevail at failure.

In Fig. 7 it can be seen that there were, at times, considerable differences in the strengths of some of the duplicate beams for the shorter 10I25.4 section, 12WF27 section, and 18WF50 section, which were not centered; in contrast, there was better agreement for the duplicate beams of the 10B15 section, which were centered. Thus, the effect of centering in these tests was to produce more consistent results and a higher load-carrying capacity.

DETERMINING BUCKLING LOADS

In 1932, R. V. Southwell[14] described a method which used an analysis of the applied loads and the resulting deflections observed in the test of an initially curved column to compute the buckling load which would occur if the column were perfectly straight. Variations of this method were later developed by L. H. Donnell[15] and E. E. Lundquist,[16] M. ASCE; these latter methods were applied to the test data to yield the results shown in Tables 1(*b*) and 2(*b*). Where no value is shown the plot produced no conclusive evidence. These tests indicate that Mr. Lundquist's variation was more effective than that of Mr. Donnell in organizing the data into a consistent pattern, especially for the shorter beams.

A typical plot for both methods is shown in Fig. 14. Because the rotation β of the cross sections of a beam appears in the differential equation of equilibrium in a manner similar to that of the lateral deflection of a column, the angle of twist, β, was used in the Lundquist plots. This plot for the shorter beams consisted of three parts. At low values of the load the curve shown by the dashed line in Fig. 14 was obtained, and at greater loads a straight line, the inverse slope of which was used to compute the elastic buckling load. If the beam yielded, the upper part of the plot developed a curve with increasing slope; the inverse slope of the tangent to this last part of the curve at the point of buckling was the actual critical load for the beam. That Mr. Southwell's plot would give this shape of curve was mentioned by Mr. Donnell.[15]

The type of analysis first proposed by Mr. Southwell when used as an experimental tool could be said to have had three applications in these tests: (*a*) For those beams which failed by yielding, it both predicted the probable elastic buckling load and indicated the actual buckling load; (*b*) it could check the actual buckling load of the beams which failed in the elastic range; and (*c*) it enabled the experimental method of loading and the restraint of the end connections to be checked.

An example of the third point might be mentioned. The heel of the top connection angles of beams 57a, 57b, and 58 came into bearing at one end on the face of the supporting columns because of the large lateral deflections of the top flange upon approaching failure; these beams never actually buckled because of this increased restraint. The plot used by Mr. Lundquist for these beams near failure showed a decreasing slope corresponding to an apparent increase in buckling strength. By extrapolation of the straight-line part of the plot prior to this occurrence, the probable buckling load for the initial degree of restraint was determined. This value was used to compute the nominal bending strength of these three beams.

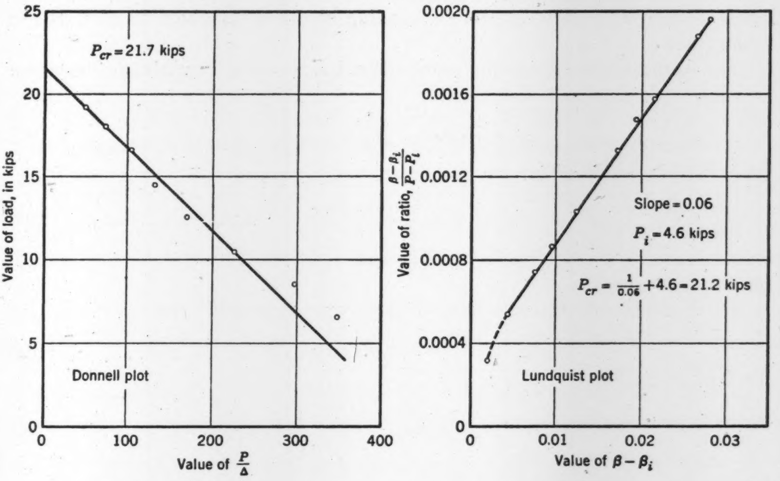

FIG. 14.—COMPARISON OF LUNDQUIST AND DONNELL PLOTS TO DETERMINE BUCKLING LOAD FOR BEAM NO. 29

FACTOR OF SAFETY WITH RESPECT TO DESIGN FORMULAS

The nominal bending strength developed by the test beams is compared in Tables 1(*c*) and 2(*c*) with the allowable unit bending stress permitted by the design formulas following in Eqs. 7, 8, 9, and 10 for structural carbon steel meeting ASTM Designation A 7-51 T. These formulas were derived on the assumption that the beam was simply supported.

The formula in the specifications of the American Railway Engineering Association (AREA)[9] and the American Association of State Highway Officials (AASHO)[10] is

$$s = 18{,}000 - 5\left(\frac{L}{b}\right)^2 \dots\dots\dots\dots\dots\dots\dots (7)$$

for $L/b \leqq 40$ (according to the AREA) and for $L/b \leqq 30$ (according to the AASHO).

The formulas in the specifications of the AISC[8] are

$$s = 20{,}000 \qquad (8a)$$

for $L\,h/b\,t \leqq 600$ and

$$s = \frac{12{,}000{,}000}{\dfrac{L\,h}{b\,t}} \qquad (8b)$$

for $L\,h/b\,t > 600$. The allowable bending stress, s, is given in pounds per square inch.

The formulas, incorporating parabolic cutoff, proposed by Mr. de Vries[5] are

$$s = 18{,}000 - 0.006\left(\frac{L\,h}{b\,t}\right)^2 \qquad (9a)$$

for $L\,h/b\,t \leq 1{,}000$, and

$$s = \frac{12{,}000{,}000}{\dfrac{L\,h}{b\,t}} \qquad (9b)$$

for $L\,h/b\,t > 1{,}000$.

Formulas incorporating a diagonal straight-line cutoff[18] are

$$s = 18{,}000 \qquad (10a)$$

for $L\,h/b\,t \leqq 250$,

$$s = 20{,}000 - 8\left(\frac{L\,h}{b\,t}\right) \qquad (10b)$$

for $250 < L\,h/b\,t \leqq 1{,}500$, and

$$s = \frac{12{,}000{,}000}{\dfrac{L\,h}{b\,t}} \qquad (10c)$$

for $L\,h/b\,t > 1{,}500$.

These formulas are plotted in Fig. 15. The allowable bending stress, s, permitted by the formulas was compared with the nominal bending strength at critical load developed by the test beams to give the factor of safety.

Comparison with the AREA and AASHO formula in Eq. 7 was possible in Fig. 10 only for the shorter beams permitted under these specifications. Because the L/b-parameter did not closely predict the nominal bending strength of the simply supported beams, the factors of safety with respect to this formula were subject to considerable variation, with the margin of safety, in general, being less for the more slender beams.

In the case of the simply supported beams the formulas based on the $L\,h/b\,t$-parameter gave a fairly uniform factor of safety for Eqs. 9 and 10, but for the AISC formula, Eqs. 8, only in the case of the more slender beams which buckled in the elastic range. For the shorter beams which buckled in the inelastic range the factor of safety was dependent on the yield point of the material and was as low as 1.19, as Table 1(*c*) shows. If these beams had had the minimum yield point of 33,000 lb per sq in. specified for structural carbon steel, their factor of safety with respect to the AISC specification (Eqs. 8) would have been even lower. The cutoff curves used by Eqs. 9 and 10 provided a much more adequate margin of safety for the shorter beams; with few exceptions, it was in excess of 1.50.

---

[18] "Report of Subcommittee," Research Committee E, Column Research Council, The Engineering Foundation, April 7, 1954 (unpublished).

The beams with the two types of flexible, semirigid connections all developed factors of safety in terms of simple-beam-bending strength much greater than that which is usually considered necessary in a member subject to possible buckling. For values of $L\,h/b\,t$ below 1,100 these types of connections would assure an entirely adequate margin of safety for beams designed by Eqs. 8. For larger slenderness ratios it would be desirable for design specifications to permit heavier loads than those now allowed in order to take advantage of the increased strength supplied by this type of connection, which is usually considered to have no moment-carrying capacity.

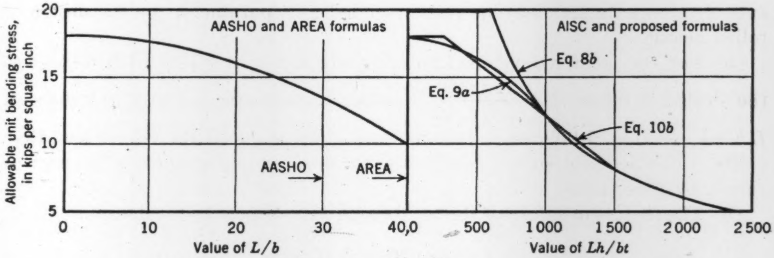

FIG. 15.—ALLOWABLE UNIT BENDING STRESSES BY PRESENT AND PROPOSED DESIGN FORMULAS

It might be well to note some of the uncertainties that exist in the design of beams with values of $L\,h/b\,t$ between 600 and 1,100. Factors which have a significant effect on the length of beams in this range of slenderness are: (*a*) The actual yield point of the material in the beam; (*b*) the initial misalinement of the beam; and (*c*) the adverse effect of failure to provide adequate lateral support of the span-end cross sections to secure them from rotating or tipping. Tests by N. C. Cyr and the senior writer[19] showed that short beams, having no lateral restraint at the span end but that given by the beam seat, might not even sustain the design load permitted by Eqs. 8 for a laterally unsupported simple beam.

CONCLUSIONS

The principal findings and conclusions of this investigation may be summarized as follows:

---

[19] "Lateral Buckling of Simply-Supported I-Beams," by N. C. Cyr and R. A. Hechtman, *Trend in Engineering*, Univ. of Washington, Seattle, July, 1950.

1. The test beams buckled in the elastic range when the value of $L\,h/b\,t$ was greater than approximately 1,100 for the simply supported beams and those with web-angle connections and greater than approximately 1,300 for beams with top-and-seat-angle connections. Below these slenderness ratios, the beams buckled in the inelastic range.

2. When the beams failed in the elastic range, correlation between the experimental and theoretical values of the buckling load and nominal bending strength was obtained. Either the formula developed by Mr. de Vries (Eq. 1) or that of Messrs. Winter and Schrader (Eq. 6) accurately predicted the critical buckling loads.

3. When the beams failed in the inelastic range and the yield point of the steel and the shape of the stress-strain curve became factors, the actual bending strength of the beams was less than the theoretical strength and could adequately be represented by a cutoff curve similar to that which has already been experimentally established for intermediate length columns.

4. Although the slenderness ratio, $L\,h/b\,t$, became less definitive in predicting the nominal bending strength of the test beams as its value decreased, it was entirely adequate and may be recommended as a parameter for the design of rolled beams.

5. The test beams developed an adequate factor of safety with respect to the design formula, $s = \dfrac{12{,}000{,}000}{L\,h/b\,t}$, when a parabolic cutoff for values of $L\,h/b\,t$ less than 1,000, or a diagonal straight-line cutoff for values less than 1,500. The need for such a cutoff in the case of simply supported beams was shown by these tests.

6. The factors of safety of the test beams with respect to the design formula,

$$s = 18{,}000 - 5\,(L/b)^2,$$

were subject to considerable variation and, in general, decreased as the value of L/b increased. The factors of safety for the sections tested were adequate, but it is possible that other sections would not have given such favorable results. Moreover, this design formula is not applicable to slender beams which showed good load-carrying capacity in these tests.

7. For beams with values of $L\,h/b\,t$ between 600 and 1,100, the two types of semirigid end connections provided an adequate factor of safety with respect to Eqs. 8, which assume simple beam support. For greater slenderness ratios it is desirable that design specifications take advantage of the increased strength supplied by this type of connection.

8. The buckling strength was found to be related to the initial misalinement and twist of the beams.

9. The Southwell method, as adapted by Mr. Lundquist,[16] was found to be a useful tool for analyzing the data of lateral buckling tests of beams.

ACKNOWLEDGMENTS

This research was performed as a cooperative project between the Column Research Council of The Engineering Foundation, of which Shortridge Hardesty was chairman, and the Engineering Experiment Station of the University of Washington (Seattle), of which F. B. Farquharson, M. ASCE, is director. Tests were made in the Structural Research Laboratory of the Department of Civil Engineering headed by R. B. Van Horn, M. ASCE. All work on the program was directed by the senior writer.

The writers are indebted to the members of Committee E of the Column Research Council for their interest and assistance as the advisory committee for this project; to B. G. Johnston and H. N. Hill, Members, ASCE, past chairmen of Committee E; to Mr. Hardesty who arranged the financial support for the program; to John J. Miles, A.M. ASCE, who assisted with the first tests; to K. T. Chang who extended available theoretical derivations to cover new loading conditions; and to H. E. Wessman, M. ASCE, Dean of the College of Engineering at the University of Washington, for his warm encouragement.

APPENDIX. NOTATION

The following symbols, adopted for use in the paper, conform essentially with "American Standard Letter Symbols for Structural Analysis" (ASA Z10.8–1949), prepared by a committee of the American Standards Association with Society representation, and approved by the Association in 1949:

a = torsion-bending constant of beam cross section, $\sqrt{E\,I_y\,d^2/4\,C}$;
b = width of beam flange;
C = torsional constant or stiffness of beam cross section, M_t/θ;
c = distance from neutral axis to extreme fiber;
E = modulus of elasticity;
G = modulus of elasticity in shear;
h = depth of beam;
I_x = moment of inertia of beam cross section about x-axis and the maximum moment of inertia;
I_y = moment of inertia of beam cross section about the y-axis and the minimum moment of inertia;
k = torsional constant of beam cross section, C/G;
L = span length or the laterally unsupported length of the compression flange of the beam;
M_s = simple beam moment of transverse loads on beam;
M_t = torsional moment about longitudinal axis of beam;
P = total load on beam;
P_{cr} = critical load;
s = allowable unit bending stress;
s_{cr} = nominal bending strength or critical stress, $M_s\,c/I$;
t = average thickness of beam flange;
β = rotation of cross section of beam with respect to vertical;
β_i = initial angle of twist at midspan;
θ = angle of twist per unit length of beam resulting from M_t; and
μ = Poisson's ratio.

AMERICAN SOCIETY OF CIVIL ENGINEERS
Founded November 5, 1852
TRANSACTIONS

Paper No. 2887

FIELD VANE SHEAR TESTS OF SENSITIVE COHESIVE SOILS

By Hamilton Gray,[1] M. ASCE

With Discussion by Messrs. Ebenezer Vey, Carl W. Fenske, Dale T. Harroun, and Hamilton Gray

Synopsis

The paper shows comparative test results which indicate that highly sensitive clays suffer a loss in strength not only during sampling but also in the preparation of test specimens. Uncertainty as to the magnitude of the effect of sample disturbance emphasizes the desirability of "in situ" tests in soils which change in mechanical properties as a result of distortion.

Introduction

During the past few years considerable effort has been expended in certain parts of Europe and, to a lesser extent, in the United States in appraising the significance of values of soil-shear strength based on test methods not requiring extraction of soil samples from the ground. The results of such methods have not been widely publicized, but it is believed that as the results become better known these new methods may, in many localities, because of reliability and economy, replace the ones conventionally used.

Despite successful efforts[2] to develop techniques for minimizing the "disturbance" to sensitive cohesive soils which results from sampling operations, there is available much evidence that the best "undisturbed" samples of many clays (also known as "practical undisturbed samples") do not reveal with desirable accuracy the actual mechanical properties of the various soil layers from which they are extracted. It is generally conceded that the stress changes associated with removal of soil examples from the ground must

---

Note.—Published, essentially as printed here, in July, 1955, as *Proceedings Paper 755.* Positions and titles given are those in effect when the paper or discussion was approved for publication in *Transactions.*

[1] Chairman, Dept. of Civ. Eng., Ohio State Univ., Columbus, Ohio.

[2] "Subsurface Exploration and Sampling of Soils for Civil Engineering Purposes," by M. J. Hvorslev, U. S. Waterways Experiment Station, Vicksburg, Miss., 1949, Chapters 4 and 6.

adversely affect the results of tests made on such samples and that distortions of the mineral skeleton will introduce relatively important changes in behavior under stress. Highly sensitive clays and the accompanying difficulty in preserving the soil structure have been encountered chiefly in alluvial, lacustrine, and marine deposits. On the other hand, in many regions mantled by residual soils, the sensitivity of the materials does not appear sufficient to warrant much concern with possible sample disturbances. The purpose of this paper is to relate experiences obtained in exploring deposits of glacial and marine clays in southern Maine. Whereas the results and conclusions are believed applicable to many similar deposits in the northern part of the United States they would not be equally significant for residual soils.

SENSITIVITY OF CLAYS

Certain sedimentary clays or silt clays possess extremely high "sensitivity." The sensitivity of a soil has been defined[3] in terms of the ratio of the unconfined compressive strength of an undisturbed sample of quality to the compressive strength of the same material after having been thoroughly remolded at unchanged water content. This sensitivity so defined is found to vary from values slightly greater than unity to as much as 30 or 40. In some cases where the natural water content exceeds the liquid limit a prism of remolded material will distort appreciably under its own weight. Therefore, the sensitivity can hardly be measured in the customary manner; it may even be said to approach infinity. Because partial remolding and, hence, some weakening of a soil may occur from sampling operations, such a definition of sensitivity is based on the natural consistency of available samples. If the sensitivity could be referred to the strength of the natural deposit, even greater values would frequently result.

Highly sensitive materials, fairly common in the northern half of the United States, can be detected by the obvious contrast between consistency in the undisturbed and remolded states, evident when the undisturbed soil is manipulated with the fingers. The sensitivity depends on the extent to which the natural moisture content differs from the liquid limit and on the magnitude of the preconsolidation load which strongly influences the undisturbed strength. Thus, the higher the moisture content relative to the liquid limit, the weaker the remolded material, and the higher the preconsolidation load, the stronger the undisturbed material. Consequently, if the natural water content of a highly preconsolidated soil is well above the liquid limit, the material will be excessively sensitive. If the natural moisture content approaches the plastic limit when the preconsolidation load is small, the sensitivity will be correspondingly small. Despite the fact that certain clays have been compressed under geologic loads exceeding 1 ton per sq ft, and, thus, have acquired strengths of the order of ¼ ton per sq ft to ½ ton per sq ft or more, the natural void ratios may be so high that the remolded materials exhibit an almost fluid consistency and, consequently, possess extreme sensitivity.

In engineering practice it is recognized that further compression of such soil involving a reduction in void ratio will increase the shearing strength.

---

[3] "Soil Mechanics in Engineering Practice," by K. Terzaghi and R. B. Peck, John Wiley & Sons, Inc., New York, N. Y., 1948, pp. 30–32.

Although such compression or decrease in void ratio may be produced through appropriate loading, it cannot materialize immediately on the application of a load because of the consolidation characteristics of the soil. That is, unless special provisions are made to allow for compression of the material, it is necessary to rely on only the strength which the material possesses prior to construction operations. This strength can be determined by applying shearing stresses in such a manner that the soil has no opportunity to compress, and consequently to acquire additional strength during the application of the shearing stresses. The type of test which reveals the existing strength of a clay soil is commonly referred to as "quick undrained," or merely "quick," because the speed of testing is assumed to preclude effective drainage.

Strength Determinations.—In the past it has been common practice to determine such strengths by unconfined compression tests because these tests can be made more rapidly and conveniently than the conventional direct shear test. Consequently, the compressive strength has been used both as a basis for measuring the effect of sample disturbance and for securing data for engineering studies of foundation conditions. Interest in the use of a method of determining the strength of soil in its natural bed was stimulated by the following observations and considerations.

It is generally believed that the soil adjacent to the wall of any type of sampling tube is weakened by frictional drag and by the consequent relatively severe distortion adjacent to the tube wall. In fact, data have been published showing that the compressive strength or consistency of miniature compression specimens located at varying distances from the wall of a sampling tube increases as the distance from the wall increases.[4] That is, the center of the sample is demonstrated to have been less damaged than the periphery by the sampling operation, thus confirming the visual evidence of excessive peripheral distortion which is often observed. Therefore, if a prism measuring, for example, 2 in. square in cross section is carefully trimmed from the innermost portion of a 3½-in.-diameter soil sample, it is logically assumed that the weakest material has been trimmed away and discarded leaving relatively undisturbed soil in the prism to furnish the basis for measuring soil strength. However, a comparison of the compressive strengths of certain undisturbed samples (secured in 3½-in. outside-diameter seamless tubing of No. 16-gage wall thickness) indicated that the strengths of compression specimens having a diameter equal to that of the inside of the tubing were not appreciably different from strengths of specimens which had been carefully trimmed with a wire saw from tube size to a cross section measuring 2 in. square. The test results thus indicated that the elimination of the peripheral material did not change the results of compression tests of many sensitive soils. It was necessary to conclude, therefore, that the trimming operation had seriously weakened the 2-in. by 2-in. prism. Consequently, the trimming operation appeared to be an unnecessary and time-wasting refinement.

The 2-in. by 2-in. prisms were trimmed carefully by hand with an ordinary wire saw guided by a miter box. It is possible that if such a saw were operated in conjunction with some high-frequency vibrator, less disturbance would occur during the trimming operation. However, the minimum required handling of the trimmed prism may in itself be just as damaging as the trimming operation. At any rate, if peripheral weakening occurs during sampling, as is generally conceded, some better means than trimming away peripheral material should be adopted if realistic strength values are to be consistently obtained for highly sensitive clays. The mere fact that much depends on the care exercised by the person trimming and otherwise preparing the prisms is sufficient cause to seek a means of eliminating this particular human factor.

---

[4] "A Method for Determining the Representative Character of Undisturbed Samples," by D. M. Burmister, *Proceedings*, 1st International Conference on Soil Mechanics and Foundation Eng., Harvard Univ., Cambridge, Mass., Vol. III, 1936, p. 26.

TEST RESULTS

Minimizing the Effect of Sensitivity on Test Results.—The logical way of eliminating the disturbance which accompanies the trimming and distortion of that part of a sample which is adjacent to the wall of the tube is to determine the strength of the central part of the sample in a manner which does not require that this part be either trimmed or removed from the tube. To accomplish this, a small four-bladed vane having a 1-in. diameter was constructed and placed in such a position that it could be inserted in the end of a tube sample and then rotated on bearings by means of a small torque wrench. Fig. 1 shows details of such a miniature vane and of its operation. When the results of such vane tests were compared with the results of unconfined compression tests performed on material taken from an adjacent part of the tube sample—either above or below the section which was subjected to the vane test—very con-

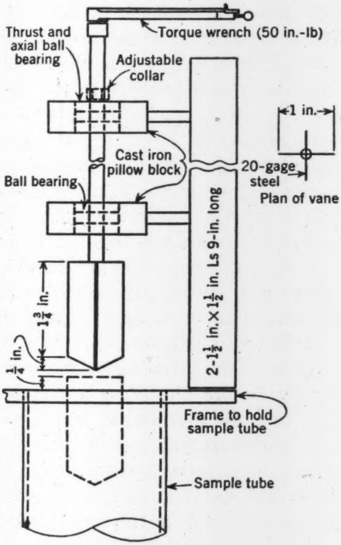
Thrust and axial ball bearing
Torque wrench (50 in.-lb)
Adjustable collar
1 in.
Cast iron pillow block
20-gage steel
Plan of vane
Ball bearing
2-1½ in.×1½ in. Ls 9-in. long
1¾ in.
¼ in.
Frame to hold sample tube
Sample tube

FIG. 1.—MINIATURE VANE SHEAR APPARATUS

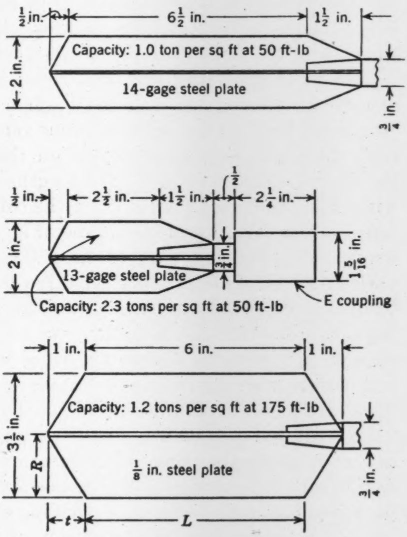
½ in.
6½ in.
1½ in.
Capacity: 1.0 ton per sq ft at 50 ft-lb
2 in.
14-gage steel plate
¾ in.
½ in.
2½ in.
1½ in.
½
2¼ in.
2 in.
¾ in.
1 5/16 in.
13-gage steel plate
Capacity: 2.3 tons per sq ft at 50 ft-lb
E coupling
1 in.
6 in.
1 in.
Capacity: 1.2 tons per sq ft at 175 ft-lb
3½ in.
R
⅛ in. steel plate
¾ in.
t
L

FIG. 2.—DETAILS OF VARIOUS FIELD VANES

sistent differences appeared. The vane strength is, with rare exceptions, usually attributable to heterogeneity of the sample, substantially greater than half the compressive strength. This confirmed the belief that the separation of the central part of a tube sample from the peripheral part, together with the other procedures involved in preparing this central prism for a compression test, introduced disturbances of sufficient magnitude to depress seriously the results.

It is obvious that this information, at best, could only imply that the miniature-vane test results more nearly approximated the true strength of the natural soil but that no indication has been obtained as to the accuracy of this approximation. That is, it still is necessary to extrapolate from the results of tests performed on samples in order to estimate the strength of the natural deposit. Any such extrapolation rests on no fully objective considerations and is therefore unsatisfactory.

There appeared to be no reason why the same testing principles should not be utilized, as has been suggested,[5] in measuring the soil strength in the field. Fig. 2 shows details of larger vanes which can be used to measure the soil strength at the bottom of bore holes 2½ in. or 4 in. in diameter. Such a vane (attached to the lower end of a string of drill rods) is inserted into the undisturbed material beneath the lower edge of the casing at the bottom of a cased drill hole. In order to prevent vertical movement of the vane during the test, the drill rods are supported on the top of the casing by a combination thrust and radial bearing. The lengths of vanes may be varied in accordance with the anticipated resistance of the soil so as to remain within the estimated safe loading capacity of each vane (Fig. 2). The vanes are rotated by torque wrenches applied at the top of the drill rods. The torque wrenches are likewise varied; for example, a more sensitive type of wrench is used where the total torque is expected to be small. The performance of each field vane test requires somewhat less time than is needed to take an undisturbed sample. It appears advisable to devote nearly as much care to the cleaning of the bore hole before making the vane test as is desirable before obtaining a sample. This care has a twofold purpose: (*a*) To insure that the material in which the vane is rotated is in no way disturbed and (*b*) to eliminate soil friction from the drill rods above the vane. The rotation of the vane requires less time than is usually allowed between driving and extraction of a sample tube. Once the vane test has been performed, a saving of time can result from the fact that no sealing, marking, and transportation of an undisturbed sample may be necessary; no unconfined compression test need be performed except to secure comparative data. On the other hand, the making of field vane tests does not necessarily eliminate the need for taking seamless tube samples inasmuch as consolidation data may be required. In any event, it is desirable to secure sufficient material from different elevations in the ground in order to reveal the variability of the subsurface formations by visual inspection and classification tests. Consequently, the real justification for such field vane tests is the seemingly greater reliability of the results.

---

[5] "Determination in Situ of the Shear Strength of Undisturbed Clay by Means of a Rotating Auger," by Lyman Carlson, *Proceedings*, 2d International Conference on Soil Mechanics, Rotterdam, Vol. I, 1948, p. 265.

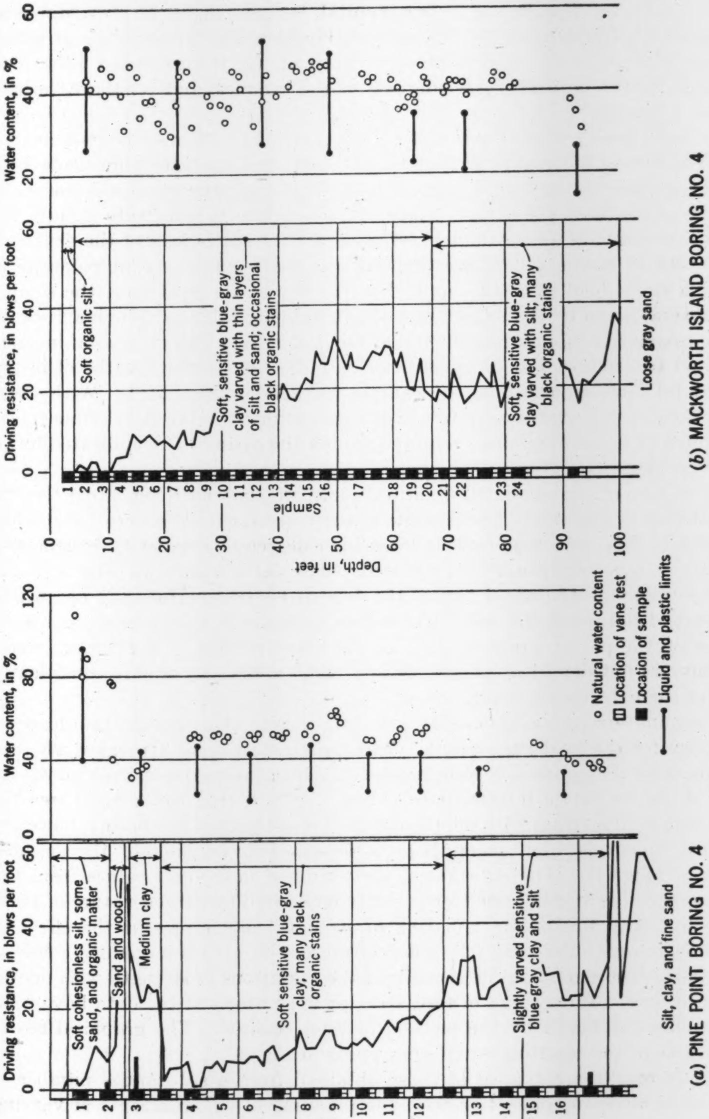

(a) PINE POINT BORING NO. 4

(b) MACKWORTH ISLAND BORING NO. 4

FIG. 3.—DRIVING RESISTANCE AND WATER CONTENT

Typical Test Results.—For two typical borings made on two different projects, Fig. 3 illustrates (*a*) the soil stratification, (*b*) the elevation at which soil samples and field vane tests were obtained, (*c*) the resistance offered to drilling, (*d*) the natural water contents of the samples, and (*e*) the Atterberg limits.

In both these borings the samples were secured in a 3½-in.-outside-diameter, seamless tubing of 16-gage wall thickness, and all vane tests were made with the large-diameter vane in Fig. 2. The bulk of the penetrated soil was sufficiently soft so that the sample tubes could be made to penetrate rapidly the necessary length of approximately 30 in. under the static load of the drill rods and a 300-lb hammer. Where the soil was too hard to permit penetration under a static load of 600 lb applied to the top of the drill rods, the sample tubes were driven by the impact of a 300-lb hammer falling through a distance of approximately 15 in. upon the top of the drill rods. The number of impacts required to produce 1 ft of penetration is indicated by the lengths of heavy horizontal bars adjacent to the sample markers in Fig. 3(*a*). With these exceptions it was unnecessary to use dynamic effort to drive the sample tubes. The number of hammer blows required to sink the casing 1 ft is indicated by an irregular line.

It will be observed that the natural moisture contents (Fig. 3(*a*)) tend to exceed the corresponding liquid limits in some instances by a very substantial amount. Thus, one requirement for a high degree of sensitivity is generally present in the soils penetrated by that particular boring. In Fig. 3(*b*) the water contents in the upper half of the deposit fluctuate erratically because of the varved nature of the soil. The water contents in this zone all appear to lie within the plastic range whereas in the lower portion of the boring, water contents do not depart as greatly from a mean value and remain consistently greater than the liquid limits.

Examination of the shear-strength data in Fig. 4 demonstrates clearly a tendency for the field vane test to yield the greatest shear strengths whereas the unconfined compression tests produce the least strengths and the miniature vane strengths attain intermediate values. In a boring the general trend is for strength to increase with depth; the uppermost part of the boring, however, exhibits relatively high strength as a result of desiccation of the surficial material (Fig. 4). The substantial scattering of individual values from the average trend is attributable to the thinly laminated or varved nature of these deposits. Any single determination of strength may represent the effect of more or less granular material which is present in a predominantly cohesive material. In order to aid in visualizing the variations in strength with depth, revealed by the three types of test, straight lines which fit the data have been determined for Fig. 4 by the method of least squares. The graphical representations of the resulting equations appear in Fig. 4.

These results are typical of those obtained from a substantial number of drill holes made in connection with the planning of embankments of varying heights. However, in these other borings less comprehensive data were usually secured in that less effort was made to determine the unconfined compressive strengths after vane tests had been made and the vertical intervals between vane tests were greater than in the two borings illustrated herein.

The less complete data substantiate those shown in Figs. 3 and 4. The primary consideration in each case was that the embankment not induce shearing displacements in the supporting ground. Settlements constituted a secondary consideration because, if a settlement of moderate magnitude was predicted on the basis of consolidation tests, it was generally felt that the displacement could be tolerated and even compensated either by appropriate temporary overloads which would accelerate compression during construction, or by future maintenance.

Significance of Results.—It is logical to believe that the differences observed between the results of field and laboratory vane tests are caused solely by sampling operations and that the differences between the laboratory vane and unconfined compression results are largely attributable to the preparation of the compression specimens. The first of these differences represents disturbance which occurs prior to any laboratory testing; the second type of difference indicates the extent to which laboratory preparation may further injure the structure of a sensitive soil.

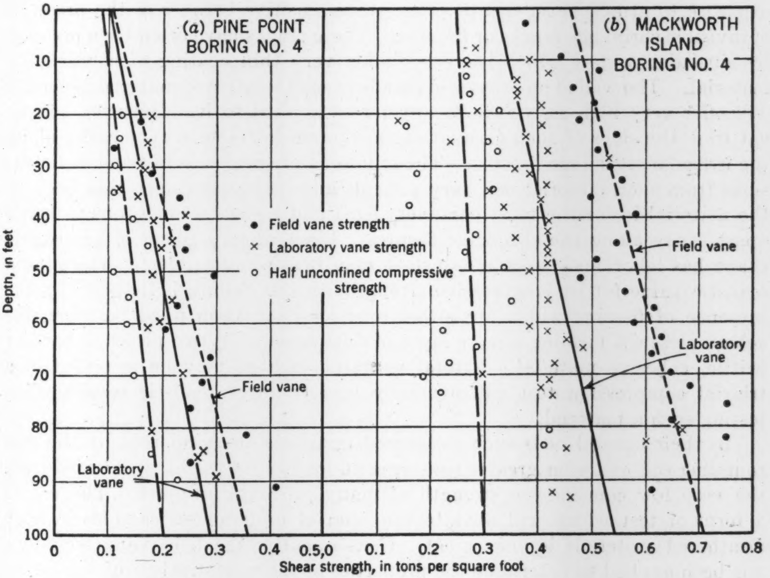

FIG. 4.—THE RELATIONSHIP OF DEPTH TO SHEAR STRENGTH

In comparative tests performed upon remolded soils, laboratory vane results tended to exceed somewhat the half-magnitudes of corresponding compressive strengths. The discrepancies were not serious and may be attributable to the fact that failure of compression specimens occurred by plastic deformation, whereas the vane resistances were associated with a surface of rupture. Inspection of Fig. 4 suggests that the greatest strength differences occur toward the bottoms of the drill holes where the natural strengths are higher, but where in many cases there does not appear to be a corresponding reduction in natural water content. In some instances the unconfined compressive strengths show very little tendency to increase with depth whereas in all cases field vane determinations do show such a tendency, and laboratory vane determinations have a similar though not as pronounced a tendency. One possible explanation of this behavior is found in the fact that in certain of these deposits the amount of varving or silt content appears to increase appreciably toward the bottom of the cohesive stratum. This tendency may be associated with a smaller unconfined compressive strength whereas the field vane strengths might well increase disproportionately because of the presence of this granular material.

Very stiff weathered materials derived from soft-clay deposits, as a result of exposure to atmospheric agents, often prove sensitive because of the presence of invisible shrinkage cracks or fissures. These cracks have often been invaded by silt-laden waters which leave behind a very thin coating of cohesionless material. The wall of an excavation made in such weathered material generally will offer very high resistance to any forces applied to it. However, prisms cut from the sides of such excavations are prone to fracture very easily along the irregular shrinkage fissures. The trimming of specimens of regular dimensions from such material is a very difficult and frustrating operation because the material is, for the most part, very hard and resistant but prone to break apart easily along the shrinkage fissures. Even when a prism of acceptable shape has laboriously been obtained it may prove impossible to determine a realistic value for its compressive strength because failure is induced by the presence of fissures which are either open or have been filled by very fine cohesionless silt forming a mere layer of dust separating two pieces of hard or brittle, cohesive material. Lateral restraint such as may be provided in a triaxial compression test will generally lead to more realistic results when testing such a material.

In their natural beds such weathered materials are supported by the surrounding soil and offer greater resistance to loads than might be inferred from the very low compressive strength of many prismatic samples. The use of a form of test which will obviate the need of undisturbed samples in such weathered materials is very great. Consequently, the field vane technique has been applied to determine the properties of these relatively stiff weathered materials. To this end the smallest vane is adapted (Fig. 2). Frequently, rather intense loading can be applied to such firm weathered soils which serve to distribute the pressure so that stresses in the softer underlying soils become moderate. Vane tests made at short vertical intervals provide more reliable and more comprehensive shear-strength data than can a more expensive procedure involving undisturbed sampling.

It appears doubtful that the true strength of sensitive soils can ever be directly measured by small-scale mechanical means other than the strength represented by a plate-bearing test. This is true because the insertion of a vane to some extent disturbs and weakens the adjacent soil. The results of vane tests made at the bottom of drill holes merely approach more closely the true strength values than do test results of even the best undisturbed samples.

In the case of the materials used as illustrations herein, predictions of behavior based wholly on the results of compression tests would be conservative to an unwarranted degree. In general, it would appear that the true strength of the soil may exceed the results computed from unconfined compression tests by as little as 30% or as much as 300% or 400%, depending on the type of soil. It is, of course, still impossible to state the true strength of such material other than to suggest it cannot be less than the values revealed by the field vane tests. In an analogous manner one may question the determination of the compression characteristics of undisturbed soil samples.

Implication for Other Soil Properties.—To date (1956) considerable thought has been directed toward the problem of estimating true preconsolidation loads through extrapolation of the results of laboratory tests.[6,7,8]

It is believed, probably with good reason, that if the results of a consolidation test yield a pressure-void ratio diagram with a sharp break or change in slope between the recompression and virgin branches of the diagram, the tested sample is reasonably representative of the natural deposit. However, there is considerable evidence that, although the absence of a sharp change in slope in a pressure-void ratio diagram appears a reliable indication of substantial disturbance of the material, the presence of such a sharp change does not guarantee that the sample is undisturbed. For example, in numerous cases where there was a pronounced difference between the results of field and of laboratory vane tests, consolidation samples gave results ordinarily classed as excellent on the basis of sharpness of curvature in the vicinity of the presumed preconsolidation load. It seems difficult to insist that when laboratory vane test results approximate—for example, only three-quarters of the corresponding field vane values—the consolidation test results should be considered highly reliable regardless of how little disturbance occurs during the preparation of consolidation samples. When the corresponding unconfined compressive strengths approximate only 50% of the field vane strengths, it is then evident that trimming a consolidation specimen is extremely likely to influence further the determination of the preconsolidation load. Furthermore, undisturbed samples from fairly uniform, deep deposits of sensitive soil often provide well-defined preconsolidation loads which do not vary regularly with depth.

The results of several consolidation tests made on samples taken from the boring of Figs. 3(*a*) and 4(*a*) indicated that the existing intergranular pressure (caused by overburden) in the layer of blue clay and the underlying varved silt and clay exceeds preconsolidation loads estimated from consolidation tests. The excess is rather small at depths less than 50 ft but is approximately half the overburden pressure at greater depths. This may be entirely due to erratic variation in the actual geological preconsolidation pressure. There are no data yet available to prove that the deposit is not still consolidating under its own weight. On the other hand, the information shown in Fig. 4(*a*) seems

---

[6] "Determination of the Preconsolidation Load and Its Practical Significance," by A. Casagrande, *Proceedings*, 1st International Conference on Soil Mechanics and Foundation Eng., Harvard Univ., Cambridge, Mass., Vol. III, 1936.

[7] "Relation of Undisturbed Sampling to Laboratory Testing," by P. C. Rutledge, *Transactions*, ASCE, Vol. 109, 1944, p. 1155.

[8] "The Undisturbed Consolidation Behavior of Clay," by John H. Schmertmann, *ibid.*, Vol. 120, 1955, p. 1201.

to warrant belief that the deposit may be naturally consolidated under the existing overburden because strengths increase regularly with depth. In certain instances, consolidation tests have yielded well-defined preconsolidation loads which were substantially less than the pressures exerted after completion of a structure. However, observations of these structures during and after construction revealed no significant settlement. This would seem to indicate the possibility that the true preconsolidation loads are actually considerably greater than those furnished by the test results even though such results appear to be of excellent quality.

Numerous consolidation tests were made on samples obtained from the boring detailed in Figs. 3(*b*) and 4(*b*). The estimated preconsolidation loads exceed the estimated overburden intergranular pressures from the ground surface to a depth of more than 60 ft beyond which depth preconsolidation pressures vary rather erratically. Above this 60-ft depth the estimated preconsolidation values all closely approximate 1½ tons per sq ft. The same is true at greater depths, except in the vicinity of the 80-ft mark where preconsolidation values of 2 and 3 tons per sq ft, respectively, were obtained from two tests. The estimated overburden pressure is 2 tons per sq ft at this depth. It is interesting to observe that the values of unconfined compressive strength in Fig. 4(*b*) generally are slightly less than 0.3 ton per sq ft but that at the 80-ft depth these values increase to more than 0.4 ton per sq ft; at the latter depth the laboratory vane results rather closely approximate the field vane results. The increase in the laboratory results at this depth is much greater than the increase of the field vane results. This appears to constitute strong evidence that the samples taken from this 80-ft depth were not as sensitive or at any rate were not damaged as much by sampling as the samples from somewhat smaller or greater depths. Unless the estimated magnitudes reflect sample disturbance, it is difficult to understand why the estimated preconsolidation load to a depth of nearly 70 ft would show no consistent tendency to vary with depth as contrasted with the variation exhibited by both types of vane shear test.

In consideration of the observed differences in shear-strength determinations shown herein, it is certainly questionable whether any extrapolation of the results of consolidation tests can be guaranteed to furnish reliable data. Relatively little is known about the susceptibility of the apparent preconsolidation load to sample disturbances, as compared with the susceptibility of shear strength to the influence of sample disturbance. Any extrapolation which is not based on the results of an analysis involving the variables pertinent to the phenomenon at hand is fraught with uncertainty. How can such a quantity as "degree of disturbance" be defined in objective terms—that is, numerical terms—without knowledge of the properties of a material possessing zero disturbance? Degree of disturbance perhaps could be related to the distortion or deformation of the soil skeleton, but the measurement of such distortion would certainly prove more difficult than measurement of the mechanical properties which it influences. It is suggested that consideration should be given the development of means for determining preconsolidation loads by testing the natural deposit rather than samples taken therefrom. It is apparent that such testing would in all probability be rather more difficult than the simple vane test described herein. Nevertheless, the development of such a test, even if it should prove to be of value only for research purposes, would at least provide an indication of the reliability of any procedure with respect to extrapolating the results of ordinary consolidation tests.

CONCLUSIONS

The primary purpose of the foregoing remarks is to stimulate interest in the possibilities which appear to reside in the use of simple and relatively inexpensive field tests. It is shown herein that, where shear strengths are determined by various techniques, those methods which entail the least amount of handling of material tend to give the largest values of strength. The various tests reported here were performed at comparable rates of deformation. In applying shear-strength data to practical problems many other details must be considered, among them:

a. The appropriate rate of shearing strain at which the determinations of strength should be made.

b. The possibility of progressive failure associated with the weakening which the soil experiences after subjection to large deformations.

c. The nonuniform distribution of shearing stresses within the soil mass.

All these previously mentioned factors should be considered of substantial importance in the determination of subsoil stability. Each appears to require extensive investigation before it would be possible to specify accurately the appropriate methods by which these factors should be taken into account in design work.

As long as determination of strength is subject to uncertainties of personal skill in preparing specimens as well as to the sensitivity of the particular soil in question, the most reliable procedure appears to be to utilize testing methods not requiring the removal of samples from the ground. The ease with which this can be accomplished is largely dependent on the nature of the test. It may very well be that the relative simplicity of the technique required to determine shear strength in the field cannot be approached for any other type of testing. Consequently, it may be that a correlation can be established involving laboratory consolidation and shear tests and field shear test results. As long as efforts are restricted to extrapolating laboratory results, there must be doubt as to the accuracy of such extrapolation. This doubt can be resolved only by the development of more realistic testing techniques.

APPENDIX. ANALYSIS OF LOADS ON VANES

The vanes are inserted in soil until the four vertical edges are completely embedded. Shearing resistance is assumed to develop on a cylindrical surface described by these vertical edges when the vane is rotated and also on a conical surface described by the bottom edges of the vane during rotation. It is assumed that the shearing stress has a constant magnitude over the surface of the cylinder and that upon the conical surface the resistance is either a constant and is equal in magnitude to that on the cylindrical surface, or else increases linearly from 0 at the axis to a maximum value at the radius of the cylinder—in other words is proportional to the radial distance. The resisting moment, M_c, developed on the cylindrical surface is given by

$$M_c = 2\,\pi\,R^2\,L\,\tau_{max} \tag{1}$$

in which R is the radius of the vane, L denotes the vane length, and τ_{max} is the shear stress. The resisting moment, M_r, developed on the conical surface when the shear stress on the surface is constant and is given by

$$M_r = M_c\,\frac{\sqrt{R^2 + t^2}}{3\,L} \tag{2}$$

whereas when the stress is proportional to the radial distance, the total resistance, M', on the conical surface is

$$M' = M_c\,\frac{\sqrt{R^2 + t^2}}{4\,L} \tag{3}$$

in which t is the dimension shown in Fig. 1. The total corresponding soil resistances for these two cases are therefore given by the following two expressions:

$$M = M_c\left(1 + \frac{\sqrt{R^2 + t^2}}{3\,L}\right) \tag{4a}$$

and

$$M = M_c\left(\frac{1 + \sqrt{R^2 + t^2}}{4\,L}\right) \tag{4b}$$

The difference between the two magnitudes given by Eqs. 4 is, for practical purposes, unimportant. For example, for the shortest vane illustrated in Fig. 2,

$$\frac{\sqrt{R^2 + t^2}}{L} = \frac{\sqrt{\frac{5}{4}}}{2\frac{1}{2}} = \frac{1}{\sqrt{5}}\,.$$

Thus,

$$\frac{1}{3\,\sqrt{5}} = 0.149$$

whereas

$$\frac{1}{4\,\sqrt{5}} = 0.112.$$

The difference between these results is therefore less than $3\frac{1}{2}\%$ of the magnitude of the total resistance given by either of Eqs. 4.

Similarly, for the longest vane in Fig. 2,

$$\frac{\sqrt{R^2 + t^2}}{L} = \frac{\sqrt{\frac{5}{4}}}{6\frac{1}{2}} = \frac{\sqrt{5}}{13};$$

thus,

$$\frac{\sqrt{5}}{3 \times 13} = 0.057$$

and

$$\frac{\sqrt{5}}{4 \times 13} = 0.043.$$

It follows from this that the difference between the values given by Eqs. 4 will be of the order of 1% of the total resistance.

It is considered, therefore, that the variation of shearing resistance over the conical surface generated by the lower edge of the vane during rotation is unimportant compared to natural variations in soil strength which would occur within short vertical distances.

DISCUSSION

Ebenezer Vey,[9] M. ASCE.—The tests described by Mr. Gray represent a valuable addition to information on the usefulness and reliability of the vane apparatus in determining the true shear strength of clay soils. The author is to be complimented for the painstaking care he exercised in preparing samples for laboratory tests and in performing the field tests.

In reference to the sample disturbance created by the insertion of thin-walled sampling tubes into the soil, it should be noted that a similar disturbance is produced by the insertion of the vane. In a series of laboratory tests which the writer and his associates performed on remolded soils, the friction between the vane blades and the soil was evidenced by a distinct depression produced in the soil surface by the insertion of the vane. This depression occurred in the three clays tested at all consistencies. It was greatest, however, when the moisture content of the clay was such as to cause the greatest stickiness. It was believed that this type of disturbance created stresses in the soil which were present when the vane shear test was made. At all events it seemed reasonable that the disturbance was likely to have some influence on the magnitude of the vane shear. To check this, two vanes of different lengths but of the same diameter were used in the same soil (Fig. 5) and the results compared (Table 1). In the large vane, such as Mr. Gray used in his field tests, the cylindrical surface on which shear occurred is farther from the central part of the vane than it is in the small vane. Because the disturbance caused by insertion is greatest near the center of the vane, the large vane values are probably less affected by this factor. It is believed that the thickness of the vane blades and the size of the vane shaft are not as important as the diameter of the vane itself.

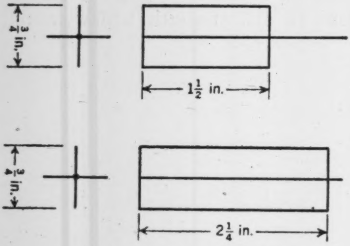

Fig. 5.—Two Field Vanes

The actual shear resistance as measured by the vane then depends on: (*a*) The diameter of the vane, (*b*) the length of the vane, (*c*) the stickiness of the soil, and (*d*) the shear strength of the soil. It is believed that vane shear values cannot be accepted as true unless all of these factors are properly evaluated.

The author states (under the heading "Test Results: Significance of Results"):

> "It is logical to believe that the differences observed between the results of field and laboratory vane tests are caused solely by sampling operations and that the differences between the laboratory vane and unconfined compression results are largely attributable to the preparation of the compression specimens."

---

[9] Prof. of Civ. Eng., Illinois Inst. of Technology, Chicago, Ill.

Because of these factors, vanes of the same size and shape would have to be used in the laboratory on samples of the same soil tested in the field to give a valid comparison.

There is an additional factor which would tend to give the lower values the author obtained using the small vane in the laboratory. The deposit tested was a varved clay consisting of alternate thin layers of clay, silt, and fine sand. The vane shear in the field measured not only the shear strength of the clay but also the shear strength of the silt and sand which would be a function of depth because of the increasing intergranular pressure with depth produced by the overburden. Because of the confined state of the laboratory sample, the cohesionless material would again be responsible for some, although much less, of the vane shear resistance. In the case of the unconfined compression test there is no confinement of the cohesionless layers. Because the shear strength obtained by this method would be almost entirely that of the clay, it would be expected to be much less than both the laboratory and the field vane strengths. Moreover, the unconfined compressive strength would be expected to remain fairly constant with depth, within the depth where the preconsolidation pressure was about the same. A more realistic measure of the strength for comparison with the vane data in this type of soil would be the triaxial shear. The data for the boring in Figs. 3(*b*) and 4(*b*) indicate that the increase in field vane shear over both the laboratory vane shear and the unconfined compression shear is more pronounced at the lower depths. It is also noted that the plasticity index values decrease with depth, which would indicate an increasing proportion of silt and sand. This increasing proportion would reduce the unconfined compressive strength even further, whereas the field vane shear would continue to increase with overburden pressure and the laboratory vane shear would show a smaller increase. There is considerable doubt that the vane results are reliable in highly silty or sandy soils.

TABLE 1

Test No.	Type of vane	Water content (%)	Moment (in. −lb)	$M_{II} - M_{I}$ (in. −lb)	Shear (lb per sq in.)
1	I	25.7	1.685		1.17
	II	25.7	2.260		1.07
				0.575	0.86
2	I	20.1	10.50		7.30
	II	20.6	13.86		6.55
				3.36	5.00

It is believed that the consolidation samples prepared and tested by Mr. Gray did give reliable preconsolidation loads and that the disturbance of sampling and trimming consolidation samples was really only of secondary importance. The fact that, as the author comments (under the heading, "Test Results: Implication for Other Soil Properties"): "***laboratory vane test results approximate—for example, only three-quarters of the corresponding field vane values***" is to be expected in this type of soil. However, although "***the corresponding unconfined compressive strengths approximate only 50%

of the field vane strengths***" this does not necessarily imply that the samples were dangerously disturbed and the consolidation data unreliable.

Mr. Gray mentions that at the 80-ft depth the unconfined compressive strength was more than 0.4 ton per sq ft compared with less than 0.3 ton per sq ft throughout the rest of the depth and that in the former region the laboratory vane results rather closely approximate the field vane results. He suggests that the soil at the 80-ft depth was not as sensitive or perhaps as damaged by sampling. The boring log description near this depth (Fig. 3(*b*)) shows "many black organic stains." This would indicate that this soil might have had a higher organic content than the soil above and below the 80-ft depth. Such soil content would provide a binder for the cohesionless material and thus give to the soil mass a high cohesive strength after having been consolidated under a pressure of 2 tons per sq ft. This mixture would accordingly derive its shear strength mainly from this cohesion; under the circumstances then, all three shear values would be expected to agree closely.

The writer believes that, in evaluating the discrepancies between shear strengths obtained by the three methods, Mr. Gray has overemphasized the effect of sample disturbance. It is believed that these differences were due principally to the varved nature of the clay rather than to the disturbance of sampling. Furthermore, the nature of the vane disturbance may also have been a factor in comparing the results obtained by the small vane on laboratory samples with those of the large vane in the field.

CARL W. FENSKE,[10] A.M. ASCE.—Commendations are due Mr. Gray for his paper which is intended to stimulate interest in the use of the field vane to secure in-place shear strengths of soils. This device has its definite place in the equipment that a soils engineer may use to obtain adequate and economical measurement of the shear strength of soils. The purpose of this discussion is to present additional information on the comparison of shear strengths as measured by the vane (both miniature and field) and by more conventional laboratory tests.

The writer has shear-strength data with which comparisons can be made between the results of miniature vane and unconfined compression tests. This information was obtained at a number of locations in the Gulf of Mexico off the coast of Louisiana. The soils are post-glacial deposits of the Mississippi River and, therefore, are of Recent Age. They are less sensitive than the soils studied by the author with the degree of sensitivity averaging approximately 2.5. The miniature vane tests were made by inserting a four-blade vane, 0.760 in. in diameter and 0.685 in. long, into the end of a Shelby tube sample as soon as the sample was recovered from the boring. The vane was rotated slowly, and the maximum torque required was observed. Rotation was continued and the minimum torque required to produce a continuous rotation was also observed. Maximum and minimum vane strengths were computed from these observed torque values. Unconfined compression tests were made at a constant rate of strain of about 2% per min. Good agreement was found between the maximum miniature vane strengths and the shear strengths from undisturbed unconfined compression tests for soils firm enough to be extruded from the sampling tube and prepared for testing without excessive disturbance. The only exceptions to this agreement have occurred when the tests were made on soils so soft that extrusion and preparation for the unconfined compression test could not be performed without noticeable disturbance. Similar good agreement has been found also between the minimum miniature vane strength and the shear strength from remolded unconfined compression tests.

---

[10] Senior Soils Engr., McClelland Engrs., Inc., Houston, Tex.

Investigations with a field vane, 3 in. in diameter and 6 in. high, were made at a few locations where miniature vane tests and tests on undisturbed samples were also performed. In these investigations, the agreement between the results of miniature vane and undisturbed unconfined compression tests cited previously was obtained, but significantly higher shear strengths were obtained by the field vane. However, the results of consolidated-undrained triaxial tests performed on undisturbed samples, with a lateral pressure equivalent to the computed effective overburden pressure at the depth from which the sample was obtained, were comparable with the field vane test results.

In the light of the foregoing information, the writer agrees with Mr. Gray's conclusion that the difference between the undisturbed unconfined compression and laboratory vane results for the sensitive soil studied is primarily caused by unavoidable disturbances in sample preparation. However, it is suggested that structural disturbance during sampling may not be the only factor causing the difference between the field vane and the laboratory vane strengths. There may be a more fundamental factor such as, possibly, the stress relief to which the sample is subjected in bringing it to the surface. This would mean that: (*a*) Even if tests were made on undisturbed samples that were perfect with respect to structural disturbance, there would still be an intrinsic difference between the results of field vane and unconfined compression tests; and (*b*) an agreement, especially at appreciable depths, between the results of these two tests should not be expected.

DALE T. HARROUN,[11] A. M. ASCE.—Any technique of performing soil tests in the field is highly desirable not only from the standpoint of minimizing sample disturbance but also in the saving of time and expense. Field soil tests, however, are subject to all the stresses and effects existing in a natural soil stratum without any screening or idealizing of conditions such as may occur, inadvertently or otherwise, in a laboratory.

A vane shear test is basically a direct-torsion shear test performed in a horizontal plane with a vertical axis of twist. In any direct shear test on typical soils having both cohesion and friction—

$$\text{Shear} = C + N \tan \phi.$$

In the case of the vane shear, the normal stress, N, is equal to the lateral soil pressure, which is in turn a function of the vertical soil pressure at that point. For a purely cohesive soil it also follows that the shear would be independent of the lateral soil pressure. However, a purely cohesive soil is an academic condition, most soils having at least a small angle of friction. The author mentions the silt content of the subject soil, for example.

---

[11] Prof. of Soil Mechanics, Univ. of Pennsylvania, Philadelphia, Pa.

Referring to the test data in Fig. 4(*b*), it is shown that the laboratory unconfined compression tests on the soil samples, free of any enclosing lateral stresses, display very little increase of strength with depth.

On the other hand, field vane shear results show an appreciable increase of strength in direct proportion to increase in lateral pressure. The laboratory vane shear tests conducted in the sample tubes display this direct increase of strength with depth to a lesser extent possibly because of the retention of some of the natural lateral soil pressure by the sample tube.

Because the vane shear test, like the unconfined compression test, measures only total shear, it is not possible to differentiate between the frictional and cohesive components. If conventional direct-shear test results were available, a more analytical study of the problem could be made.

The increase of field shear with lateral stress due to depth could also explain the author's observation (under the heading, "Test Results: Significance of Results") that the increase of shear value is attributed to a possible natural increase of soil strength with depth.

HAMILTON GRAY,[12] M. ASCE.—In commenting on the preceding thoughtful discussions the writer refers to a statement (under the heading, "Test Results: Significance of Results"):

> "It appears doubtful that the true strength of sensitive soils can ever be directly measured by small-scale mechanical means other than the strength represented by a plate-bearing test. This is true because the insertion of a vane to some extent disturbs and weakens the adjacent soil. The results of vane tests made at the bottom of drill holes merely approach more closely the true strength values than do test results of even the best undisturbed samples."

This statement recognizes the fact that the insertion of any object—be it a vane or a sampling device—into the soil produces some displacement and distortion so that the strength determinations which follow such insertion must reflect, to some extent, the effect of soil disturbance. The distortion and the effect thereof on measured strength vary not only with the magnitude and configuration of the displacement but also with the particular soil. That is, certain soils at appropriate consistency, when cut or indented, tend to undergo relatively large deformations remote from the area of applied stress whereas at softer or stiffer consistencies the separation or indentation causes a negligible deformation at remote points. The effect of distortion on strength also seems to vary with soil consistency and the ratio of natural water content to liquid limit.

The insertion of a large vane in a sample tube is obviously undesirable, but the use of a miniature vane in the field introduces different complications. Consequently, a comparison between field and laboratory vane tests wherein one and the same vane is used does not appear practicable except at very shallow depths.

---

[12] Chairman, Dept. of Civ. Eng., Ohio State Univ., Columbus, Ohio.

It is clear that the presence of granular varves introduces a complicating factor. Thickness of the individual varves is probably the most significant item because friction on the circular periphery of a very thin varve can hardly be important. Preliminary investigations have demonstrated that it is possible to rotate a vane in loose cohesionless soil. Sampling of such soils in a manner which will not greatly alter their density requires very elaborate procedures and is normally impracticable. Hence, some type of testing in situ is desirable, but whether vane testing of loose cohesionless deposits can yield valuable information remains to be seen. However, it is suggested that when a soil containing relatively thick varves of cohesionless material is sampled the density of the granular material may be altered so that when samples are tested in triaxial compression unduly high results are obtained. Furthermore, when a highly sensitive, purely cohesive soil is sampled and then subjected to consolidating pressures equal to the existing overburden or effective field pressure, the unavoidable sampling disturbance coupled with reconsolidating pressures will produce a void ratio which is smaller than the value in the original ground. Shearing the material at this reduced void ratio may result in a greater observed strength than that possessed by the natural deposit.

There is no comparison in the time required and cost involved in performing the field vane and triaxial tests, and hence if vane tests are reliable they are economically important. The writer is just as reluctant to accept the thesis that sampling and handling sensitive materials do not affect laboratory test results as others are to abandon it. Both attitudes are subjective, and one is not likely to change a subjective attitude unless it is challenged. The writer seriously doubts whether it can be proved that tests of samples of highly sensitive soils are more reliable than field tests and feels that up to the present time (1956) no semblance of such proof has been presented. Such proofs are not likely to result from a complacent attitude. Irrespective of the cause of the differences in field vane and laboratory test results, when such differences do occur it is likely that one value is more reliable than the other, and consequently a choice must be made as to which value is the appropriate one to use. The writer has not been persuaded that direct use of or extrapolation from laboratory test results is always as reliable as measurement of mechanical properties in the natural deposit in the field and therefore is inclined to favor the field tests.

In conclusion, the writer expresses his thanks to the various discussers and hopes that others will undertake to answer some of the uncertainties which are inherent in this aspect of soil mechanics.

AMERICAN SOCIETY OF CIVIL ENGINEERS
Founded November 5, 1852

TRANSACTIONS

Paper No. 2888

A PATTERN OF INTERSTATION AIR TRAVEL

By Daniel M. Belmont[1]

Synopsis

An analysis is made herein of airline travel between large- and medium-sized hubs of airway traffic. It is suggested that, for stations more than 800 miles apart, the number of trips between any two stations depends primarily on the total traffic at each of the stations and on the quality of service.

The forecasting of air traffic is an art greatly in need of reliable guiding principles. Long-range forecasting seems almost impossible; short-range forecasting is of course much easier and, in practice, much more important. Changes in airline service are usually based on effects expected in the next few months or years rather than in the next few decades. Short-range forecasting is by no means an exact science, and successful forecasts may owe more to good intuition than to scientific basis.

It is the purpose of this paper to call attention to a typical pattern of interstation airline travel and to suggest a simple underlying law in an attempt to provide a firmer ground for forecasting. (The data throughout the paper are domestic travel statistics reported by the Civil Aeronautics Board[2]).

When airline travel data are suitably organized, a rather remarkable pattern emerges, suggesting that, for stations more than approximately 800 miles apart, the number of trips between any two stations depends primarily on the total traffic at each of them and on the quality of service offered. It is independent of the distance between the stations.

To the extent that this law is valid, it should lead to an easy determination of the effect of important changes in quality of service. It will always be necessary to modify any such rule to accommodate local peculiarities, but the rule may at least provide a useful first approximation.

The foregoing pattern is exhibited in Fig. 1. Fig. 1(*f*) shows traffic involving Dallas, Tex. Each point represents one of the other sixty-one large

---

Note.—Published, essentially as printed here, in May, 1956, as *Proceedings Paper 987*. Positions and titles given are those in effect when the paper was approved for publication in *Transactions*.

[1] Associate Research Engr., Inst. of Traffic and Transportation Eng., Univ. of California, Berkeley, Calif.

[2] "Origin-Destination Airline Revenue Passenger Survey, September 17-30, 1954," Civil Aeronautics Board, Washington, D. C., 1954.

or medium hubs, showing the travel between the hub and Dallas in proportion to the former's total traffic. For example, the uppermost square is for travel between Dallas and New Orleans, La. (440 miles apart). During the survey period this amounted to 1,140 passengers, whereas the total traffic at New Orleans was 21,102 passengers. The ratio of 1,140 to 21,102 is 0.054, the value plotted.

It will be observed that the points decrease in height as distance increases to approximately 800 miles but that thereafter they lie in a substantially horizontal band. In particular, the squares, representing station-pairs having nonstop service, rather clearly exemplify this pattern.

Figs. 1(*a*) to 1(*h*) are strikingly similar. In each, for long-distance travel, the squares lie roughly on a horizontal line. On the average the solid circles (station-pairs having one-stop, through-plane service) also lie nearly horizontally, a little below the level of the squares. Lower still is a horizontal band of open circles, representing cities having less direct airline connection. Certain deviations from the pattern occur such as:

1. Traffic with Miami, Fla., Tampa, Fla., Minneapolis, Minn., and Fort Worth, Tex., is often too high.
2. The critical distance of 800 miles applies for most cities. For Denver, Colo., Los Angeles, Calif., San Francisco, Calif., and Seattle, Wash., however, a greater distance applies, perhaps 1,200 miles.

There is a venerable theory of transportation which holds that the traffic between two centers is proportional to the product of their populations, and inversely proportional to the square of the distance between them:

$$T_{AB} = k \frac{P_A P_B}{D^2_{AB}} \quad \ldots\ldots\ldots\ldots\ldots\ldots\ldots (1)$$

in which T_{AB} is the number of trips between centers A and B (in a given period); P_A and P_B are the respective populations of A and B; D_{AB} denotes the distance between them; and k is a constant independent of A and B. This law may have some applicability to short-distance airline travel. For long-distance travel, however, the horizontal tendency shown in Figs. 1 strongly suggests that the distance between stations has little or no effect on the airline travel between stations.

Suppose instead that long-distance travel between A and B is proportional simply to the product of their effective populations,

$$T_{AB} = k\, P_A\, P_B \quad \ldots\ldots\ldots\ldots\ldots\ldots\ldots (2)$$

The population served by an airport is not easily determined, and the effective population (in the sense required by the formula) is not necessarily determined by a census count. For the purposes of this paper, it is expedient to substitute the station's total airline traffic, T_A and T_B, for P_A and P_B. The total traffic of a station is a definite number and one which should reflect effective population closely enough.

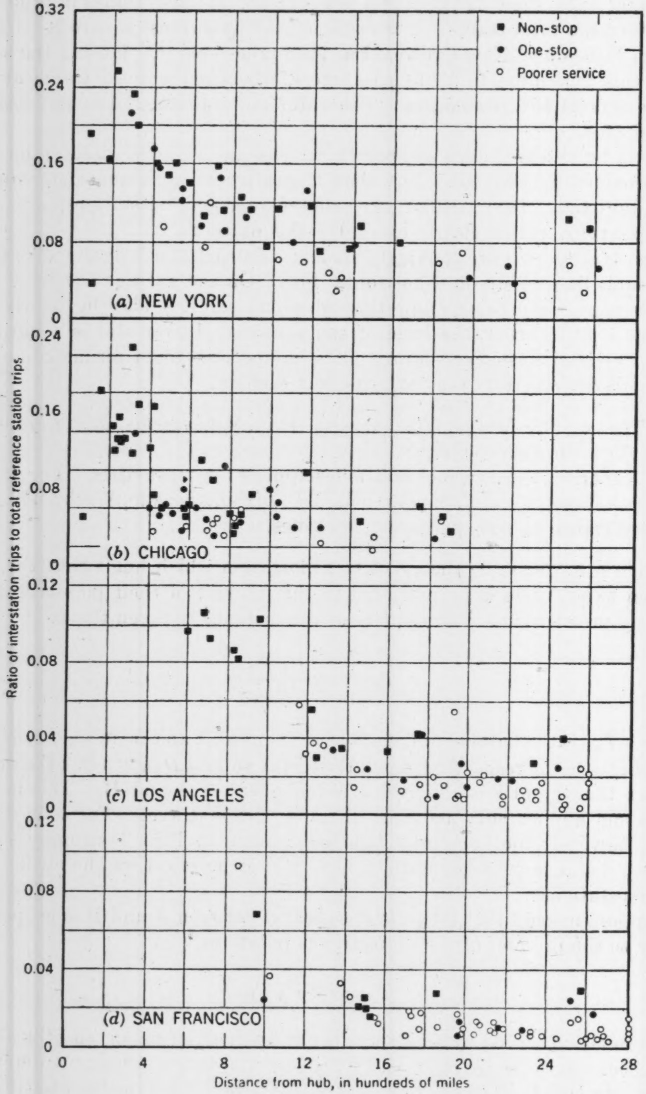

FIG. 1.—AIRLINE TRAVEL BETWEEN VARIOUS HUBS AND

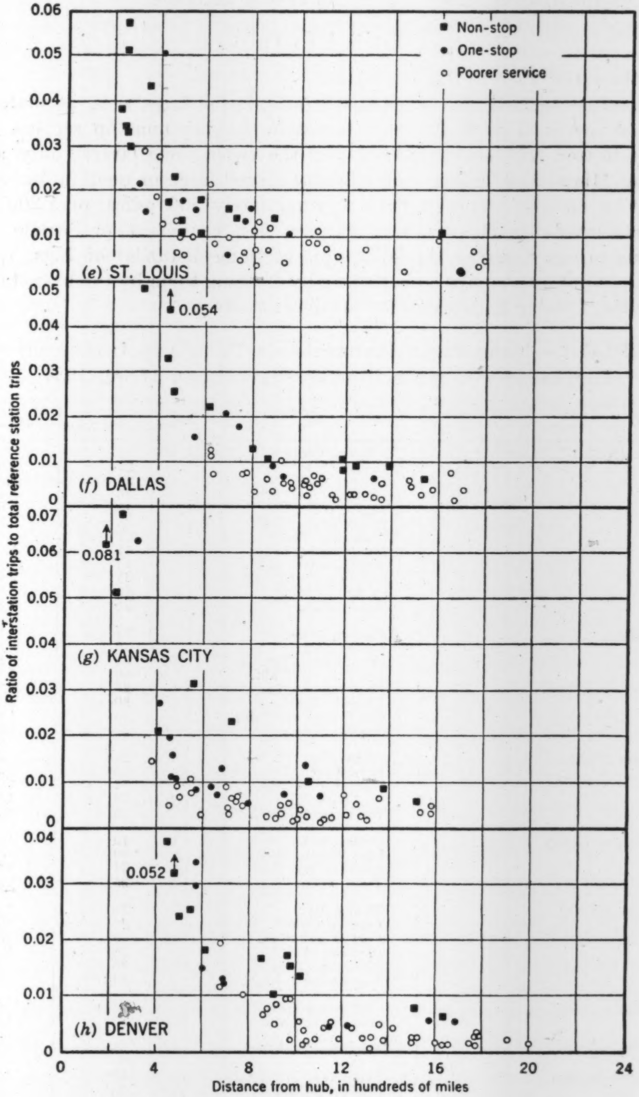

MAJOR REFERENCE STATIONS—SEPTEMBER 17–30, 1954.

It is assumed, then, that for A and B at long distance,

$$T_{\mathrm{AB}} = k\,T_{\mathrm{A}}\,T_{\mathrm{B}} \tag{3}$$

or that the ratio, $T_{\mathrm{AB}}/T_{\mathrm{A}}\,T_{\mathrm{B}}$, is constant.

This ratio—termed the "normalized interstation trips"—is, as multiplied by 10^8, shown in Fig. 2(*a*) for station-pairs having nonstop service. The points indicated represent trips between the twenty-one largest hubs and—excluding Miami and Tampa—all suitably served large or medium hubs with interstation distances greater than approximately 800 miles, or 1,200 miles for points involving Denver, Los Angeles, San Francisco, or Seattle. Fig. 2(*a*) thus brings together the solid squares (long distance) of Figs. 1, with their values put on a comparable footing by dividing them by the base station's total traffic. Table 1 identifies the stations involved.

TABLE 1.—NORMALIZED INTERSTATION TRIPS AND INTERSTATION DISTANCES—NONSTOP ROUTES—SEPTEMBER 17–30, 1954

From	To	Normalized trips	Distance
New York (N. Y.)	Atlanta, Ga.	41	760
	Dallas, Tex.	27	1,380
	Denver, Colo.	29	1,630
	Houston, Tex.	35	1,430
	Jacksonville, Fla.	46	840
	Los Angeles, Calif.	38	2,475
	Memphis, Tenn.	27	970
	Minneapolis, Minn.	41	1,020
	New Orleans, La.	43	1,190
	San Francisco, Calif.	34	2,580
	St. Louis, Mo.	41	890
	Tulsa, Okla.	25	1,230
Chicago (Ill.)	Boston, Mass.	34	860
	Dallas, Tex.	38	800
	Fort Worth, Tex.	23	815
	Los Angeles, Calif.	40	1,750
	New Orleans, La.	27	830
	Phoenix, Ariz.	30	1,450
	San Francisco, Calif.	33	1,860
	Seattle, Wash.	24	1,900
Los Angeles (Calif.)	Dallas, Tex.	28	1,245
	Fort Worth, Tex.	53[a]	1,220
	Kansas City, Mo.	34	1,370
	St. Louis, Mo.	32	1,600
	Washington, D. C.	26	2,230
San Francisco (Calif.)	Dallas, Tex.	19	1,530
	Fort Worth, Tex.	30	1,500
	Kansas City, Mo.	24	1,510
	Tulsa, Okla.	25	1,470
Washington (D. C.)	Dallas, Tex.	25	1,180
	Denver, Colo.	36	1,510
	Fort Worth, Tex.	58[a]	1,220
	Houston, Tex.	28	1,220
	Memphis, Tenn.	36	760
	New Orleans, La.	44	970
Dallas (Tex.)	Cincinnati, Ohio	33	860
	San Diego, Calif.	33	1,180
Seattle (Wash.)	Minneapolis, Minn.	55[a]	1,400
Minneapolis (Minn.)	Salt Lake City, Utah	67[a]	1,120
	Spokane, Wash.	56[a]	1,175
Kansas City (Mo.)	Phoenix, Ariz.	40	1,050

[a] Omitted in following statistics: Normalized Trips—mean 32.74; variance 44.13.

TABLE 2.—NORMALIZED INTERSTATION TRIPS AND INTERSTATION DISTANCES—ONE-STOP ROUTES—SEPTEMBER 17–30, 1954

From	To	Normalized trips	Distance
New York (N. Y.)	Birmingham, Ala.	38	870
	Fort Worth, Tex.	28	1,410
	Kansas City, Mo.	29	1,100
	Phoenix, Ariz.	20	2,170
	Salt Lake City, Utah	16	1,980
	Seattle, Wash.	19	2,620
	Spokane, Wash.	14	2,200
Chicago (Ill.)	Albuquerque, N. Mex.	25	1,130
	Houston, Tex.	33	1,040
	Jacksonville, Fla.	29	860
	Portland, Ore.	18	1,830
	Salt Lake City, Utah	25	1,260
	San Antonio, Tex.	42	1,045
	San Diego, Calif.	30	1,860
Los Angeles (Calif.)	Birmingham, Ala.	9	1,850
	Buffalo, N. Y.	17	2,220
	Cincinnati, Ohio	14	2,000
	Detroit, Mich.	26	1,970
	Minneapolis, Minn.	40[a]	1,770
	New Orleans, La.	17	1,680
	Omaha, Nebr.	32	1,330
	Philadelphia, Pa.	23	2,450
	Pittsburgh, Pa.	18	2,155
	San Antonio, Tex.	23	1,495
San Francisco (Calif.)	Cleveland, Ohio	13	2,160
	Hartford, Conn.	21	2,630
	Memphis, Tenn.	8	1,950
	New Orleans, La.	16	1.970
	Pittsburgh, Pa.	11	2,280
	Washington, D. C.	29	2,515
Washington (D. C.)	Kansas City, Mo.	30	950
	Omaha, Nebr.	37	1,020
	Tulsa, Okla.	27	1,050
Detroit (Mich.)	Denver, Colo.	21	1,130
	Spokane, Wash.	16	1,690
Boston (Mass.)	Atlanta, Ga.	18	950
Cleveland (Ohio)	Denver, Colo.	22	1,220
	Fort Worth, Tex.	30	1,065
Pittsburgh (Pa.)	Jacksonville, Fla.	39	830
	Phoenix, Ariz.	9	1,835
Philadelphia (Pa.)	Dallas, Tex.	18	1,300
	Denver, Colo.	26	1,580
	Kansas City, Mo.	53[a]	1,040
	Fort Worth, Tex.	52[a]	1,330
	Memphis, Tenn.	31	880
St. Louis (Mo.)	Albuquerque, N. Mex.	30	950
Dallas (Tex.)	Phoenix, Ariz.	27	880
Minneapolis (Minn.)	Portland, Ore.	31	1,450
Denver (Colo.)	Hartford, Conn.	24	1,685

[a] Omitted in following statistics: Normalized Trips—mean 23.46; variance 67.42.

Fig. 2(*b*) and Table 2 also show normalized interstation trips, but for station-pairs with one-stop, through-plane service as the most direct connection.

It will be seen that the points of Fig. 2(*a*) are in fair agreement with the foregoing assumption. The points lie rather uniformly in a horizontal band, supporting the theory that the distance between stations is irrelevant to traffic between them. There is of course considerable scatter among the points—they do not lie on a line. This is to be expected because of wide differences in quality of service, because of special community of interest, and other local factors. Perhaps some of the scatter is due to the use of the normalizing function; an improved normalizing function might pull the points together more effectively.

In Fig. 2(*b*) for one-stop routes, the points appear to decrease as distance increases. However, this variation from the horizontal is not very pronounced. To hold that the points are independent of distance is approximately as accurate as to hold that they are inversely proportional to distance. The standard deviation (excluding the points shown as open circles) is 8.2 for the assumption of independence of distance, and 6.8 for the inverse distance law.

A noteworthy difference between Figs. 2(*a*) and 2(*b*) is the average height of their points. Excluding the abnormally high points (open circles), the average for Fig. 2(*a*) is 32.7, whereas that for Fig. 2(*b*) is 23.5. This suggests that changing from one-stop service to nonstop service will, on the average, increase the interstation traffic by about 40%. Such a rule, if valid, would offer a very useful starting point for forecasting the effect of improvement in airline service. It would be especially useful if it could be refined to apply to several degrees of quality of service.

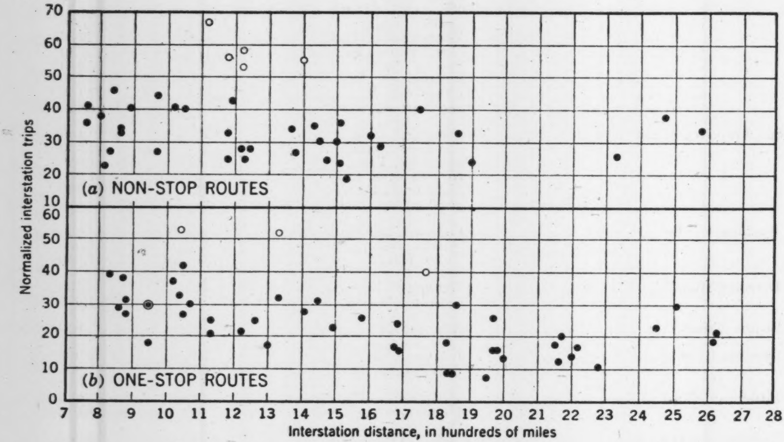

FIG. 2.—NORMALIZED INTERSTATION AIRLINE TRIPS VERSUS INTERSTATION DISTANCE.

The true significance of the patterns exhibited in this paper depends on the answer to a great many questions not yet investigated. Are the patterns the same for small hubs? Can the method be extended to shorter distances? Does the pattern change from year to year? Is September traffic typical (in the required respects) of the traffic existing throughout the year? How much of the scatter in Fig. 2(*a*) is due to differences in quality of service? Are differences between Figs. 2(*a*) and 2(*b*) due to differences in size among the cities represented? Why does distance have so little effect on airline travel?

Perhaps only the last question is easy to answer. The farther apart the stations are, the greater the advantage of air travel over competing forms of transportation. If total interstation travel by all modes were inversely proportional to distance, the airline portion would be greater for longer interstation distance and would tend not to decline with distance. A more important reason may be that the airlines have succeeded to a considerable degree in eliminating distance as a factor in travel. The difference in time between alternate destinations is relatively small, and one can cross the country for little more than it costs to go from San Francisco to Dallas. Whatever the future of air transport, it seems safe to predict that operations at the airline terminal will be of increasing importance both in airline costs and in passengers' total travel time. Interstation distance will matter very little.

AMERICAN SOCIETY OF CIVIL ENGINEERS
Founded November 5, 1852
TRANSACTIONS

Paper No. 2889

THE ANALYSIS OF WATER SAMPLES FOR CYCLICAL VARIATIONS

BY ALEX N. DIACHISHIN,[1] A. M. ASCE

SYNOPSIS

The more or less regular variation of the most probable number of coliform organisms, MPN, in the waters in the Metropolitan area of New York (N. Y.) with the tidal current has been noted. This paper presents an attempt to characterize the tidal variation of MPN-values by a quantitative, systematic method. After subjecting the data to this systematic method of appraisal, a further analysis is made of the unexplained variations which still remain after subtracting the variation accounted for by the tidal currents. The magnitude of the remaining variations is compared with the magnitude of both the theoretical variations to be expected with an MPN-test and the actual variations obtained when analyzing a sample of 20 replicas. Although the variation removed by the tidal effect is large, the remaining variation is still greater than either the theoretical residual variation or the experimental residual variation. However, the variations explained by both the sinusoidal variation due to the tide and the theoretically expected experimental error constitute a considerable part of the total variation.

INTRODUCTION

Pollution-control agencies in the seaboard states are often confronted with many data from samples of tidal waters. The interpretation of these data[2] is of great importance in many instances because it may mean the closing of beaches and the consequent curtailment of recreational activities for many people. Although the quality of inland waters is in general subject to variations that are more or less regular—for example, the seasonal variation ostensibly due to temperature changes—coastal waters have an additional variation due to the influence of the tides.

NOTE.—Published, essentially as printed here, in April, 1956, as *Proceedings Paper 930.* Positions and titles given are those in effect when the paper was approved for publication in *Transactions.*

[1] Cons. Engr., Bergenfield, N. J.

[2] "The Health Department's Role in New York Harbor Pollution Control," by Harold Romer, *Sewage and Industrial Wastes*, Vol. 28, 1955, p. 1495.

The method outlined subsequently presents a procedure whereby tidal-water data can be analyzed. Specifically, the magnitude of the tidal influence and its phase relationship to the tidal current can be determined, and the residual variation, whose magnitude determines the amount of tidal mixing to some extent, can be analyzed.

Although the method for analyzing tidal variations is presented, any cyclical variations, or combination of cyclical variations, can be analyzed. The general method was developed for the simultaneous analysis of seasonal and tidal variations in the waters of upper New York Harbor in New York.

PROCEDURE

A sinusoidal type of curve was chosen to represent tidal variations in MPN-concentrations inasmuch as both the tide (height of water) and the tidal current (horizontal movement of water) exhibit sinusoidal characteristics in New York Harbor.

The curve is represented by

$$Y = K_1 + K_2 \sin \frac{t - t_0}{p} \quad \text{.................... (1)}$$

in which $Y = \log_{10}$ MPN; K_1, K_2, and t_0 are constants; and p is the period of tidal cycle in New York Harbor equal to approximately 12.38 hr.

The method of "least squares" was used to evaluate the constants, K_1, K_2, and t_0. In the form of Eq. 1, the constants cannot be readily determined. However, because

$$\sin \frac{t - t_0}{p} = \sin \frac{t}{p} \cos \frac{t_0}{p} - \cos \frac{t}{p} \sin \frac{t_0}{p} \quad \text{.............. (2)}$$

which is the familiar trigonometrical subtraction formula, one obtains by substitution

$$Y = K_1 + K_2 \sin \frac{t}{p} \cos \frac{t_0}{p} - \cos \frac{t}{p} \sin \frac{t_0}{p} \quad \text{............ (3)}$$

from which

$$Y = K_1 + K_3 \sin \frac{t}{p} + K_4 \cos \frac{t}{p} \quad \text{................ (4)}$$

is obtained if

$$K_3 = K_2 \cos \frac{t_0}{p} \quad \text{........................ (5a)}$$

and

$$K_4 = - K_2 \sin \frac{t_0}{p} \quad \text{...................... (5b)}$$

Eq. 4 can then be used with the observed data. By summing the observations and by obtaining the partial derivatives of the summed equations with respect to the constants, K_1, K_3, and K_4, one obtains the three normal equations,

$$K_1 N \quad + K_3 \Sigma \sin \frac{t}{p} \quad + K_4 \Sigma \cos \frac{t}{p} = \Sigma\, Y \quad \text{(6a)}$$

$$K_1 \Sigma \sin \frac{t}{p} + K_3 \Sigma \sin^2 \frac{t}{p} \quad + K_4 \Sigma \sin \frac{t}{p} \cos \frac{t}{p} = \Sigma\, Y \sin \frac{t}{p} \quad \text{(6b)}$$

and

$$K_1 \Sigma \cos \frac{t}{p} + K_3 \sin \frac{t}{p} \cos \frac{t}{p} + K_4 \Sigma \cos^2 \frac{t}{p} = \Sigma\, Y \cos \frac{t}{p} \quad \text{(6c)}$$

in which N is the number of observations.

These equations can be written in the matrix form as

$$\left\| \begin{matrix} N & \Sigma \sin \frac{t}{p} & \Sigma \cos \frac{t}{p} \\ \Sigma \sin \frac{t}{p} & \Sigma \sin^2 \frac{t}{p} & \Sigma \sin \frac{t}{p} \cos \frac{t}{p} \\ \Sigma \cos \frac{t}{p} & \Sigma \sin \frac{t}{p} \cos \frac{t}{p} & \Sigma \cos^2 \frac{t}{p} \end{matrix} \right\| \left\| \begin{matrix} K_1 \\ K_3 \\ K_4 \end{matrix} \right\| = \left\| \begin{matrix} \Sigma\, Y \\ \Sigma\, Y \sin \frac{t}{p} \\ \Sigma\, Y \cos \frac{t}{p} \end{matrix} \right\| \quad \text{(7)}$$

and if the matrix involving the sum of the dependent terms on the left side of the equation is set equal to $\| A_i \|$, a simple form is obtained as follows:

$$\| A_i \| \left\| \begin{matrix} K_1 \\ K_3 \\ K_4 \end{matrix} \right\| = \left\| \begin{matrix} \Sigma\, Y \\ \Sigma\, Y \sin \frac{t}{p} \\ \Sigma\, Y \cos \frac{t}{p} \end{matrix} \right\| \quad \text{(8)}$$

If the inverse of the matrix, $\| A_i \|^{-1}$, can be found by premultiplying Eq. 8 by the inverse of the matrix,

$$\| A_i \|^{-1} \| A_i \| \left\| \begin{matrix} K_1 \\ K_3 \\ K_4 \end{matrix} \right\| = \left\| \begin{matrix} K_1 \\ K_3 \\ K_4 \end{matrix} \right\| = \| A_i \|^{-1} \left\| \begin{matrix} \Sigma\, Y \\ \Sigma\, Y \sin \frac{t}{p} \\ \Sigma\, Y \cos \frac{t}{p} \end{matrix} \right\| \quad \text{(9)}$$

from which the solution of the constants is obtained.

In many instances, the matrix, $\| A_i \|$, closely approximates a diagonal matrix because the terms, $\Sigma \sin t/p$, $\Sigma \cos t/p$, and $\Sigma \sin t/p \cos t/p$, are usually relatively small with respect to N, $\Sigma \sin^2 t/p$, and $\Sigma \cos^2 t/p$. The inverse can be expressed simply as

$$\| A_i \|^{-1} = \left\| \begin{matrix} \frac{1}{N} & 0 & 0 \\ 0 & \frac{1}{\Sigma \sin^2 \frac{t}{p}} & 0 \\ 0 & 0 & \frac{1}{\Sigma \cos^2 \frac{t}{p}} \end{matrix} \right\| \tag{10}$$

and the solution of the constants is

$$K_1 = \frac{\Sigma Y}{N}$$

$$K_3 = \frac{\Sigma Y \sin \frac{t}{p}}{\Sigma \sin^2 \frac{t}{p}}$$

and

$$K_4 = \frac{\Sigma Y \cos \frac{t}{p}}{\Sigma \cos^2 \frac{t}{p}}.$$

If sampling is conducted for other than a complete cycle or, more frequently, if it is conducted during only one part of the cycle, the matrix is not diagonal and the solution of Eqs. 6 must be performed by other methods, such as determinants.

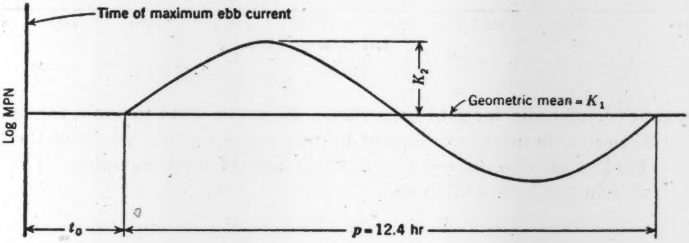

FIG. 1

As soon as the values of K_1, K_3, and K_4 have been determined, values for K_2 and t_0 can be computed, and the general prediction equation (Eq. 1) can be obtained. The constants, t_0 and K_2, can be determined from K_3 and K_4 by

$$K_3 = K_2 \cos \frac{t_0}{p} \tag{11a}$$

and

$$K_4 = -K_2 \sin \frac{t_0}{p} \tag{11b}$$

The physical concept of the various constants can be derived to some extent from Fig. 1. In Fig. 1, t is the elapsed time from an arbitrarily chosen starting point (the time at which the last maximum ebb current occurred); t_0 represents the time at which the sinusoidal code starts (or, in other words, the phase angle); and p is the period of the cycle, which, as previously stated, is equal to approximately 12.4 hr. The amplitude, which is the maximum displacement from the mean value, is equal to K_2.

ANALYSIS OF DATA

The observed values of MPN used for this analysis were obtained at a sampling point in New York Harbor. As is shown in Fig. 2, samples were collected every 20 min for a 14-hr period. However, data for only the first 12 hr and 35 min were used in order not to emphasize any one phase of the tidal cycle. Table 1 gives observed and derived data of these samples. The sum of various columns in the table are:

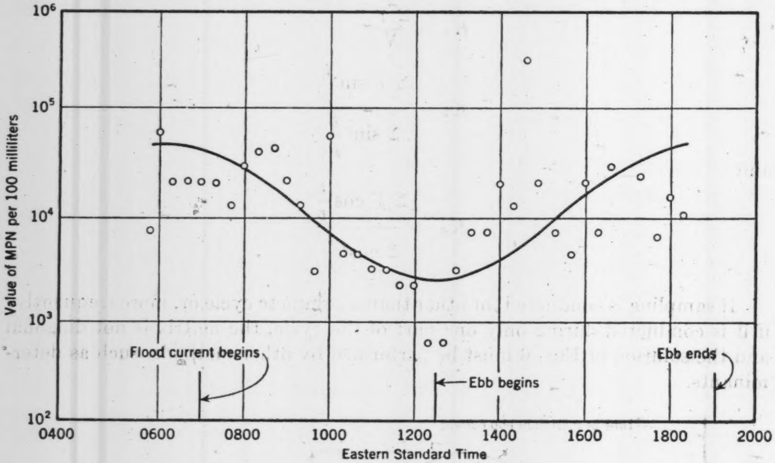

FIG. 2

$$\Sigma X_1 = +1.2407$$
$$\Sigma X^2_1 = +19.91224087$$
$$\Sigma X_2 = -0.5996$$
$$\Sigma X^2_2 = +18.07751444$$
$$\Sigma Y = +154.5207$$
$$\Sigma Y^2 = +639.62970095$$
$$\Sigma X_1 X_2 = +0.09358751$$
$$\Sigma X_1 Y = +12.84269021$$
$$\Sigma X_2 Y = +1.17102169$$

TABLE 1.—MPN DATA (JULY 22, 1951)

Time of observation[a] (1)	Elapsed time[b] (2)	Time interval[c] (3)	$\frac{\text{Col. 2}}{\text{Col. 3}} \times 360°$ (4)	MPN pre 100 ml = Y (5)	Sin Col. 4 (6)	Cos Col. 4 (7)	Log Col. 5 (8)	K_3×Col. 6 (9)	K_4×Col. 7 (10)	Predicted value of log MPN K_1+Col. 9 +Col. 10 (11)	Antilog Col. 11 (12)	Col. 11 −Col. 8 (13)
0545	2.3667	12.3500	69.0	7,900	0.9336	0.3584	3.8976	0.60213	0.02322	4.69168	49,170	0.7941
0600	2.6167	12.3500	76.3	70,000	0.9716	0.2368	4.8451	0.62664	0.01534	4.70831	51,090	−0.1368
0620	2.9500	12.3500	86.0	23,000	0.9976	0.0698	4.3617	0.64341	0.00452	4.71426	51,790	0.3526
0640	3.2833	12.3500	95.7	23,000	0.9951	−0.0993	4.3617	0.64180	−0.00643	4.70170	50,320	0.3400
0700	3.6167	12.3500	105.4	23,000	0.9641	−0.2656	4.3617	0.62181	−0.01721	4.67093	46,870	0.3092
0720	3.9500	12.3500	115.1	22,000	0.9056	−0.4242	4.3424	0.58408	−0.02748	4.62293	41,970	0.2805
0740	4.2833	12.3500	124.9	13,000	0.8202	−0.5622	4.1139	0.52900	−0.03642	4.55891	36,220	0.4450
0800	4.6167	12.3500	134.6	33,000	0.7120	−0.7022	4.5195	0.45921	−0.04549	4.48005	30,200	−0.0384
0820	4.9500	12.3500	144.3	46,000	0.5835	−0.8121	4.6628	0.37633	−0.05261	4.39005	24,550	−0.2727
0840	5.2833	12.3500	154.0	49,000	0.4384	−0.8988	4.6902	0.28275	−0.05822	4.29086	19,540	−0.3993
0900	5.6167	12.3500	163.7	23,000	0.2807	−0.9598	4.3617	0.18104	−0.06218	4.18519	15,320	−0.1765
0920	5.9500	12.3500	173.4	13,000	0.1149	−0.9934	4.1139	0.07411	−0.06435	4.07609	11,910	−0.0378
0940	6.2833	12.3500	183.2	3,300	−0.0558	−0.9984	3.5185	−0.03599	−0.06468	3.96566	9,240	0.4472
1000	6.6167	12.3500	192.9	64,000	−0.2233	−0.9748	4.8062	−0.14402	−0.06315	3.85916	7,230	−0.9470
1020	6.9500	12.3500	202.6	4,900	−0.3843	−0.9232	3.6902	−0.24786	−0.05981	3.75866	5,737	0.0685
1040	7.2833	12.3500	212.3	4,900	−0.5344	−0.8453	3.6902	−0.34467	−0.05476	3.66690	4,644	−0.0233
1100	7.6167	12.3500	222.0	3,300	−0.6691	−0.7431	3.5185	−0.43185	−0.04814	3.58665	3,861	0.0682
1120	7.9500	12.3500	231.7	3,300	−0.7848	−0.6198	3.5185	−0.50616	−0.04015	3.52002	3,311	0.0015
1140	8.2833	12.3500	241.5	2,300	−0.8788	−0.4772	3.3617	−0.56679	−0.03091	3.46863	2,942	0.1069
1200	8.6167	12.3500	251.2	2,300	−0.9467	−0.3223	3.3617	−0.61058	−0.02088	3.43487	2,722	0.0732
1220	8.9500	12.3500	260.9	680	−0.9874	−0.1582	2.8325	−0.63683	−0.01025	3.41925	2,626	0.5868
1240	9.2833	12.3500	270.6	680	−1.0000	0.0105	2.8325	−0.64496	0.00068	3.42205	2,643	0.5896
1300	9.6167	12.3500	280.3	3,300	−0.9839	0.1788	3.5185	−0.63458	0.01158	3.44333	2,775	−0.0752
1320	9.9500	12.3500	290.0	7,900	−0.9397	0.3420	3.8976	−0.60607	0.02216	3.48242	3,037	−0.4152
1340	10.2833	12.3500	299.8	7,900	−0.8678	0.4970	3.8976	−0.55970	0.03220	3.53883	3,458	−0.3588
1400	10 6167	12.3500	309.5	22,000	−0.7716	0.6361	4.3424	−0.49765	0.04121	3.60989	4,073	−0.7325
1420	10.9500	12.3500	319.2	13,000	−0.6534	0.7570	4.1139	−0.42142	0.04904	3.69395	4,943	−0.4199
1440	11.2833	12.3500	328.9	350,000	−0.5165	0.8563	5.5441	−0.33312	0.05547	3.78868	6,147	−1.7554
1500	11.6167	12.3500	338.6	23,000	−0.3649	0.9311	4.3617	−0.23535	0.06032	3.89130	7,786	−0.4704
1520	11.9500	12.3500	348.3	7,900	−0.2028	0.9792	3.8976	−0.12080	0.06343	3.99896	9,976	0.1014
1540	12.2833	12.3500	358.1	4.900	−0.0332	0.9995	3.6902	−0.02141	0.06475	4.10967	12,870	0.4195
1600	0.2667	12.4167	7.7	23,000	0.1340	0.9910	4.3617	0.08642	0.06420	4.21695	16,480	−0.1447
1620	0.6000	12.4167	17.4	7,900	0.2990	0.9542	3.8976	0.19284	0.06181	4.32098	20,940	0.4234
1640	0.9333	12.4167	27.1	33,000	0.4555	0.8902	4.5185	0.29378	0.05767	4.41778	26,170	−0.1007
1720	1.6000	12.4167	46.4	28,000	0.7242	0.6896	4.4472	0.46708	0.04467	4.57808	37,850	0.1309
1740	1.9333	12.4167	56.1	7,000	0.8300	0.5578	3.8451	0.53532	0.03613	4.63778	43,430	0.7927
1800	2.2667	12.4167	65.7	17,000	0.9114	0.4115	4.2304	0.58782	0.02666	4.68081	47,950	0.4504
1820	2.6000	12.4167	75.4	13,000	0.9677	0.2521	4.1139	0.62413	0.01633	4.70679	50,910	0.5929

[a] Eastern Daylight Time—24-hr clock. [b] Time from previous time of maximum ebb current, in hours. [c] Between maximum ebb currents.

and

$$N = 38$$

in which $X_1 = \sin t/p$ and $X_2 = \cos t/p$.

The fact that $\Sigma \sin^2 t/p + \Sigma \cos^2 t/p$ should be equal to N can be used to check the computations. The problem is then to find the inverse of the matrix,

$$\begin{Vmatrix} 38.0 & 1.2407 & -0.5996 \\ 1.2407 & 19.91224087 & 0.09358751 \\ -0.5996 & 0.09358751 & 18.07751444 \end{Vmatrix}$$

It is evident that the values are small, except for those in the principal diagonal. Hence, the approximation stated herein can be used to determine the values of K_1, K_3, and K_4, which are

$$K_1 = 154.5207/38 = 4.06633,$$

$$K_3 = 12.8426902/19.91224087 = 0.64496,$$

and

$$K_4 = 1.17102169/18.07751444 = 0.06478.$$

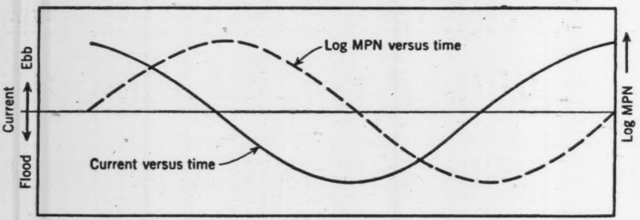

FIG. 3

A prediction equation such as Eq. 4, or an equation similar to Eq. 1, can be used. To obtain the values of K_2 and t_0 for use in Eq. 1, the procedure described in the foregoing can be used as shown by

$$K_2 \cos X = +0.64496$$

$$K_2 \sin X = -0.06478.$$

Therefore,

$$\cot X = -9.06478$$

from which

$$X = -5.7° = 354.3°$$

$$t_0 = 12.18 \text{ hr or } -0.20 \text{ hr}$$

$$\left.\begin{aligned} K_2 &= \frac{0.64496}{0.99506} = 0.648 \\ K_2 &= \frac{-0.06478}{-0.09932} = +0.652 \end{aligned}\right\}\text{use } 0.65.$$

TABLE 2.—ANALYSIS OF RESIDUAL ERRORS

Class range: log MPN (predicted) to log MPN (observed) (1)	Midpoint of class range (2)	Number of observations (3)	Deviation of class limit from mean (4)	Col. 4 ÷ σ (5)	Percentage area between class limit and mean (6)	Percentage area class interval (7)	Theoretical frequency (8)	χ^2 $\left(\frac{\text{observed-expected}}{\text{expected}}\right)^2$ (9)
−1.99 to −1.70	−1.85	1	−2.01	−4.02	49.997	0.028	0.01	98.01
−1.69 to −1.40	−1.55	0	−1.71	−3.42	49.969	0.029	0.08	0.08
−1.39 to −1.10	−1.25	1	−1.41	−2.82	49.760	1.081	0.41	0.85
−1.09 to −0.80	−0.95	1	−1.11	−2.22	48.679	3.941	1.50	0.17
−0.79 to −0.50	−0.65	2	−0.81	−1.62	44.738	10.124	3.85	0.89
−0.49 to −0.20	−0.35	5	−0.51	−1.02	34.614	18.338	6.97	0.56
			{−0.21	−0.42	16.276			
−0.19 to 0.10	−0.05	11	0.08	0.16	6.356	22.632	8.60	0.67
0.11 to 0.40	0.25	7	0.38	0.76	27.637	21.281	8.09	0.15
0.41 to 0.70	0.55	8	0.68	1.36	41.309	13.672	5.20	1.51
0.71 to 1.00	0.85	2	0.98	1.96	47.500	6.191	2.35	0.05
1.01 to 1.30	1.15	0	1.28	2.56	49.477	1.977	0.75	0.75
1.31 to 1.60	1.45	0	1.58	3.16	49.921	0.444	0.17	0.17
Total		38				99.918	37.98	103.86

NOTE.—Mean = 0.02289; σ^2 = 0.2498; and, therefore, σ = 0.4998.

TABLE 3.—VALUES OF MPN PER MILLILITER FOR TWENTY REPLICAS OF ONE SAMPLE

1. 790,000	6. 1,300,000	11. 230,000	16. 330,000
2. 1,300,000	7. 490,000	12. 460,000	17. 490,000
3. 330,000	8. 1,110,000	13. 790,000	18. 1,700,000
4. 2,220,000	9. 460,000	14. 1,300,000	19. 1,700,000
5. 330,000	10. 790,000	15. 490,000	20. 230,000

The fact that the value of t_0 is comparatively small (-0.20 hr) as compared to the length of the current period (12.38 hr) indicates that the current curve is approximately 90° out of phase with the MPN-curve, as shown in Fig. 3. This indicates that the values of MPN reach their maximum at the end of the ebb current (ebb-current slack). At the onset of the flood current, the values of MPN continue to drop until the end of the flood-current period, at which time the minimum values of MPN are reached. When the ebb current begins, values continue to rise again to their maximum at the end of the ebb current. It appears that high values of MPN are associated with the ebb currents.

For computational purposes (in order to draw a curve), Eq. 1 or Eq. 3 can be used. Eq. 3 has been used for this analysis.

The differences between the values predicted by Eq. 3 (sinusoidal) and the actual observed values were analyzed to determine whether these differences could be considered as normal experimental errors.

Table 2 presents the details of the analysis of the residual error. As this table shows, the residual errors do not form a normal distribution. This can be readily ascertained from the value of $\chi^2 = 103.86$. The values of χ^2 would be obtained theoretically less than 1% of the time if the distribution of residual errors were normal. However, the high value of χ^2 is almost entirely due to the observation of MPN-values at 1440 hr which were 350,000 per 100 miles. If the value of χ^2 is not considered, the remaining values of the residual errors are grouped normally. Inasmuch as the relatively high value of 350,000 may be due to "streaky" pollution, the remaining analysis is conducted after this maximum value has been deleted.

After the value of 350,000 has been deleted, the recomputed values for the variance and standard deviation are $\sigma^2_o = 0.167$ and $\sigma_o = 0.408$.

If this observed value of the variance compared favorably with the combined experimental and theoretical variance of the MPN-test, there would be a complete explanation of all observed values. W. G. Cochran[3] presents theoretical values for the variance and for the standard deviation as $\sigma^2_t = 0.067081$ and $\sigma_t = 0.259$. The observed variance is approximately $2\frac{1}{2}$ times that of the theoretically expected variance. However, the theoretical variance does not include the so-called "human" error. Any series of observations would, of course, include both the theoretical error and the experimental or human error.

A set of twenty replicas of a sample (Table 3) were used in order to estimate the total experimental and theoretical errors. An analysis of these replicas indicates that the variance and standard deviation of the sample were $\sigma^2_e = 0.0909$ and $\sigma_e = 0.3015$. Although the value of variance (0.0909) for this combined experimental and theoretical error is smaller than that obtained for the observed residual variance (0.167), the major part of observed residual variance can be accounted for by the combined experimental and theoretical error.

A quantitative method to determine whether a sinusoidal curve is a reasonable representation of the original data is outlined in Table 4. For the example used, there is a significant reduction in the total variation by the use of a sine curve. The residual mean square value obtained in Table 4 (0.253608) should check the value of the variance obtained in Table 2. The method of Table 4 for obtaining an estimate of the residual error is preferable to that of Table 2 because it involves considerably less labor; in Table 4, P is the probability of random occurrence and F is Fisher's ratio of the mean squares.

---

[3] "Estimation of Bacterial Densities by Means of the Most Probable Number," by W. G. Cochran, *Biometrics*, Vol. 6, 1950, p. 105.

The sinusoidal variation which accounted for much of the total variation in the values of MPN in the example analyzed can be thought to represent varying mixtures of two "reservoirs" of water, each with different concentrations of coliform organisms. The reservoir with high coliform concentrations contributes most of the water at the end of the ebb period. Values of MPN begin to lower as the high-MPN reservoir waters are diluted by the low-MPN reservoir waters until the lowest MPN occurs when the low-MPN reservoir waters are in their most concentrated form.

TABLE 4.—ANALYSIS OF VARIANCE

Source of variance	Sum of squares	Degrees of freedom	Mean squares
Total explained by curve[a]	2.167000	2	1.083500
Residual (by difference)	9.129896	36	0.253608
Total[b]	11.296896	38	...

$$F = \frac{1.083500}{0.253608} = 4.27 \quad \text{and} \quad 0.01 < P < 0.05$$

---

[a] Equal to $K_3 \; \Sigma \; Y \sin \frac{t}{p} + K_4 \; \Sigma \; Y \cos \frac{t}{p} - 2K_1 \left(K_3 \; \Sigma \sin \frac{t}{p} + K_4 \; \Sigma \cos \frac{t}{p} \right) -2 \; K_3K_4 \; \sin \frac{t}{p} \cos \frac{t}{p}$.

[b] Total $= \Sigma \; Y^2 - \frac{(\Sigma \; Y)^2}{N}$.

If the reservoir waters were completely mixed and if no other sources of variation other than the tide and the residual variance were present, then σ^2_o would be equal to approximately 0.10 and would represent the combined experimental and theoretical variations. The difference, $\sigma^2_o - \sigma^2_e$, is the amount of variation due to incomplete mixing. As can be seen in the χ^2-analysis of Table 2, the amount of mixing observed is rather uniform except for the sample obtained at 1440 hr and characterized as streaky.

It is obvious that applying the method to other factors of stream pollution—such as biochemical oxygen demand, dissolved oxygen, water temperature, and similar factors—is possible for cycles of various periods. Other cyclical variables encountered in the sanitary engineering field, such as the chlorine dosage required for a given chlorine residual, may well be applicable to similar analyses; the dosage can then be administered accordingly.

CONCLUSIONS

The relationship of the quality of tidal waters to tidal currents, the mean value of water quality over a tidal cycle, and the magnitude of the variation from the mean value can be determined by the statistical methods presented. Data for New York Harbor waters are susceptible to these methods, and the residual variation in the example data (after the variation due to the tides is subtracted) is consistent with the experimental data. By application of cylical statistical methods, tidal-water data can be conveniently summarized, interpreted, and utilized in the establishment of rational tidal-water-sampling programs.

AMERICAN SOCIETY OF CIVIL ENGINEERS
Founded November 5, 1852
TRANSACTIONS

Paper No. 2890

TRAFFIC DIVERSION TO TOLL ROADS

By John T. Lynch,[1] A. M. ASCE

Synopsis

This paper presents some of the results of traffic studies pertaining to the Maine and Pennsylvania Turnpikes made by the Bureau of Public Roads (United States Department of Commerce) in cooperation with state highway departments under a joint highway-planning program. State agencies regularly supply the federal bureau with detailed information on traffic over various turnpikes and with monthly traffic counts on other roads. For several of the turnpikes, comprehensive studies were made in which the origins and destinations of trips were determined. Analyses of the volume counts and trip origins and destinations are attempted herein in order to provide information on the diversion, generation, and growth of traffic.

Introduction

When a high-type facility such as a toll road is constructed, there is a large diversion of traffic to it from roads immediately parallel to it and a lesser diversion from more distant roads. In addition, there is an increase in traffic throughout the area known as "traffic generation." Some of this "generated" traffic is really diverted from public carriers, but a considerable part of it is composed of new travel which would not have been made if the high-type facility had not been available. This generation appears as a greater-than-normal growth of traffic over the first few years of the operation of the facility.

Annual Percentage Distribution of Traffic

Maine Turnpike.—The Maine Turnpike offers a good opportunity to study traffic generation and growth because (*a*) there is only one road through the area which runs closely parallel to the turnpike and (*b*) very little of the turnpike traffic could have been diverted to it from other more distant roads.

Note.—Published, essentially as printed here, in June, 1955, as *Proceedings-Separate No. 702.* Positions and titles given are those in effect when the paper was approved for publication in *Transactions.*

[1] Chief, Highway Planning Surveys Sect., Bureau of Public Roads, U. S. Dept. of Commerce, Washington, D. C.

In Fig. 1, the trend in traffic on U. S. 1 and on the Maine Turnpike from 1947 (the year preceding the opening of the turnpike) through 1953 is compared to the trend on other important roads throughout Maine. These traffic counts on U. S. 1 were taken near the middle of the turnpike area where the volume is lowest. This was done in order to eliminate local traffic from the count as much as possible because the turnpike could not be conveniently used for local travel. If the count had been made near Portland, Me., at the north end of the turnpike where there is generally a large amount of local travel, the comparison would have been less significant.

In Fig. 1, the 1947 traffic is taken as 100%. The line sloping upward represents the trend of traffic for other important roads throughout the state; it might be presumed that U. S. 1 traffic would have increased at a similar rate if the turnpike had not been built. After December, 1947, when the turnpike was opened, the traffic through the "corridor"—that is, on both the turnpike and U. S. 1—continued to increase more rapidly than traffic on other important roads in the state; therefore, it appears that there was continuing generation throughout this period.

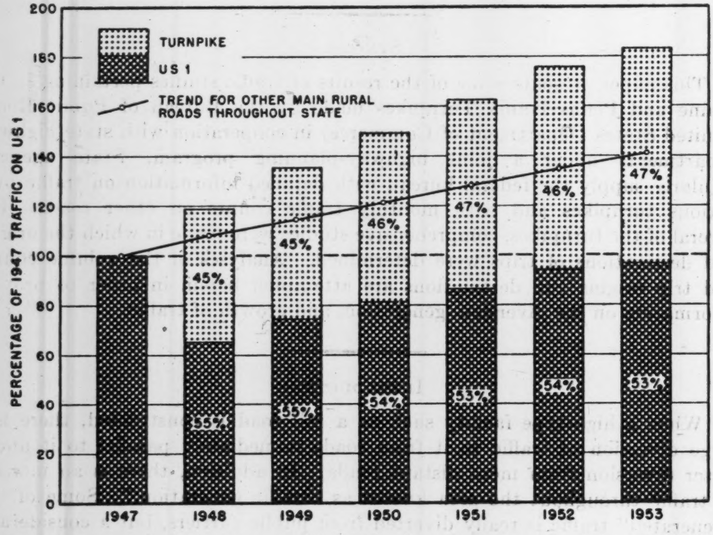

FIG. 1.—RELATIONSHIP OF TRAFFIC ON MAINE TURNPIKE TO THAT ON U. S. 1 AT MILE 29

The percentages within the bars indicate the distribution of corridor traffic between the turnpike and U. S. 1. In 1948, 45% of corridor traffic was on the turnpike (as shown in the upper part of the bar) and 55% was on U. S. 1 (as shown in the lower part). This relative distribution remained reasonably constant between 1947 and 1953. In 1953, 47% of the traffic was on the turnpike and 53% on U. S. 1. This slight expansion of proportionate turnpike usage occurred despite the fact that passenger-car toll rates were increased in May, 1949, from $0.50 to $0.60 for full-length trips of about 45 miles and again in May, 1952, from $0.60 to $0.75. In 1953, traffic on U. S. 1 was only 3% lower than the year before the turnpike was opened. It is apparent from this that U. S. 1 will soon become as congested as it was in 1947. When this occurs, a higher percentage of traffic will probably be diverted to the turnpike, varying, of course, with the steps taken to improve U. S. 1.

In determining the traffic expected on a proposed toll road, a common procedure is to:

a. Estimate the existing traffic on routes paralleling the toll-road location which would be diverted to the new facility;

b. Increase this by a generation factor to account for the new travel expected after this superior, high-speed route becomes available; and

c. Extrapolate this traffic on the basis of the trend forecasted for traffic on principal roads throughout the area.

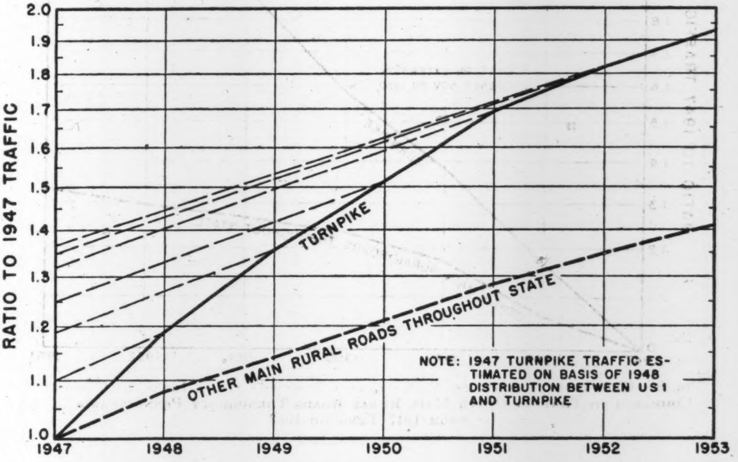

NOTE: 1947 TURNPIKE TRAFFIC ESTIMATED ON BASIS OF 1948 DISTRIBUTION BETWEEN US 1 AND TURNPIKE

FIG. 2.—GROWTH OF TRAFFIC ON MAINE TURNPIKE COMPARED TO THAT ON PRINCIPAL RURAL ROADS THROUGHOUT MAINE

Fig. 2 is so arranged as to test the reliability of this procedure and to facilitate determination of the generation factor that should have been used in forecasting traffic for the Maine Turnpike. This chart is plotted on semilog paper which has the characteristic of presenting equal growth rates as parallel lines regardless of the elevation of lines on the chart. The lower curve shows the trend in traffic (1947 to 1953) on the principal roads throughout Maine, exclusive of the turnpike. The upper solid curve shows the trend on the turnpike throughout this period. In both cases, the 1947 traffic is assigned a value of 1.0 on the chart.

The turnpike was not open in 1947, and its traffic for that year was estimated on the assumption that the distribution between the turnpike and U. S. 1 would have been the same as it was in 1948—that is, 45% on the turnpike and 55% on U. S. 1.

The sloping, broken lines above the turnpike curve in Fig. 2 are drawn from points on that curve for each year back to the vertical axis through 1947, parallel with imaginary lines from points for corresponding years on the curve for other main roads to the 1947 point on that curve (ordinate 1.0). These lines, therefore, show the part of turnpike-traffic increases attributable to normal growth as measured by the trend on other important roads throughout the state. The ordinate of the point of intersection of each line with the vertical axis through 1947 is the generation factor which, if used in the computations, would have resulted in a correct forecast of the turnpike traffic for each year, assuming that the normal growth trend had been accurately forecasted.

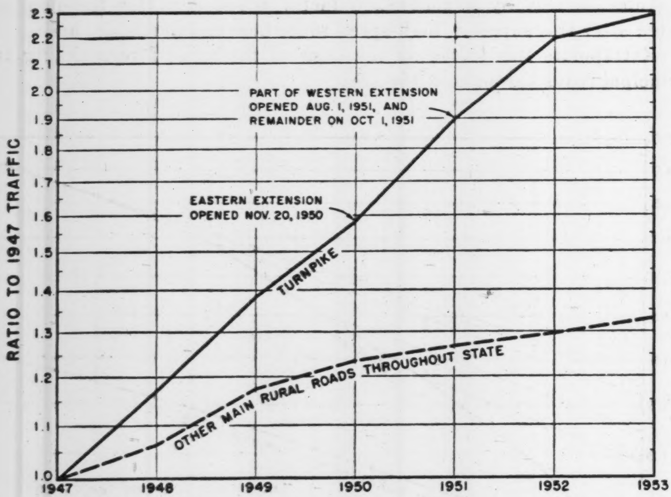

Fig. 3.—Growth of Traffic on Pennsylvania Turnpike (from Irwin to Carlisle) Compared to That on Other Main Rural Roads Throughout Pennsylvania from 1947 Through 1953

The relatively wider spread between these sloping lines toward the bottom of the chart indicates that traffic generation is largely accomplished in the earlier years. However, the space between the third and fourth lines is somewhat greater than that between the second and third lines, and this may be due to the generating effect of the opening of the New Hampshire Turnpike in June, 1950.

The value of the ordinate at the ordinate axis of the top line (1953) is 1.37. However, to say that this means a 37% generation for the period would not be entirely accurate because Fig. 1 showed a somewhat higher diversion from

U. S. 1 in 1953 than in 1948. Considering the entire traffic for the corridor, the 1953 generation factor computed in the same manner is 1.30. The difference between the 1.37-factor and the 1.30-factor is attributable to increased diversion to the turnpike from U. S. 1.

Pennsylvania Turnpike.—Fig. 3 compares the growth of traffic (1947 to 1953) on the original section of the Pennsylvania Turnpike (between Irwin, Pa., and Carlisle, Pa.) and on other rural roads in Pennsylvania. Between 1947 and 1952 the turnpike curve is steeper than the curve for the other roads; this indicates relatively faster traffic growth on the turnpike. Because the turnpike had been operating for seven years in 1947, this turnpike-traffic increase does not represent generation occurring soon after the opening of a new facility. There is no way of knowing whether this increase resulted from continuing generation or rather from increasing diversion. The fact that the rate of growth of traffic on the other main rural roads throughout the state is materially lower than that on comparable roads in nearby states suggests that increasing diversion may at least have been an important factor in this growth. The two curves are very nearly parallel between 1952 and 1953. The very steep slope of the turnpike curve (1950 to 1952) undoubtedly shows the effect of the opening of the eastern and western extensions of the turnpike. The former was opened in November, 1950, and the latter partly in August, 1951, and partly in October, 1951. This is a good illustration of the effect of turnpike extensions and connections on the traffic of the old section. However, it must be remembered that as the turnpike network is extended, com-

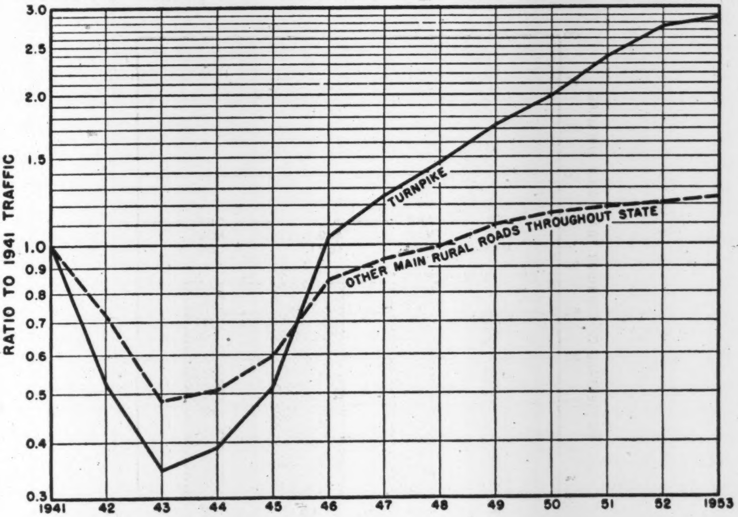

FIG. 4.—GROWTH OF TRAFFIC ON PENNSYLVANIA TURNPIKE (FROM IRWIN TO CARLISLE) COMPARED TO THAT ON OTHER MAIN RURAL ROADS THROUGHOUT PENNSYLVANIA FROM 1941 THROUGH 1953

petition between parallel routes also would result—even between routes quite far apart—which would have the effect of depleting the volume of traffic on a particular turnpike.

Fig. 4 shows the growth of traffic on the old section of the Pennsylvania Turnpike compared to that on other important rural roads in Pennsylvania for a longer period (1941 to 1953). During World War II, traffic on the turnpike decreased much more rapidly than that on other roads. After 1943, it increased so that in 1953 turnpike traffic was 187% higher than in 1941, whereas traffic on other principal roads in Pennsylvania was only 24% higher in 1953 than in 1941. Of course, the traffic increase on the other roads would have been greater if it had not been for diversion to the turnpike, but it would still have been less than the turnpike increase. The phenomenal growth of traffic on the Pennsylvania Turnpike is probably due to unique features of this particular project; it would be unwise to assume a corresponding growth for other projects.

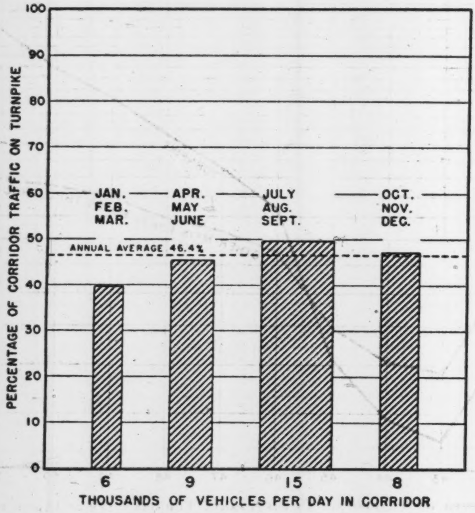

FIG. 5.—SIX-YEAR AVERAGE PERCENTAGE OF CORRIDOR TRAFFIC USING MAINE TURNPIKE AT MILE 29 IN EACH SEASON (1948–1953)

SEASONAL VARIATIONS IN TRAFFIC DISTRIBUTION

Fig. 1 shows that the annual percentage distribution of traffic between the Maine Turnpike and U. S. 1 has remained fairly constant since the first year of the opening of the turnpike. The question arises as to whether it is constant throughout the year or varies with the season.

Fig. 5 shows the variation in the percentage of the corridor traffic on the Maine Turnpike in the different seasons as an average of the six years of turnpike operation. The widths of the bars are proportional to the volumes of corridor traffic during the different seasons. In the winter season, when traffic is light, the turnpike is relatively less traveled than at other times of the year, such as during July, August, and September when there is very heavy traffic. This is of special interest because most studies of turnpike usage are made in the summer months, and it is important to estimate the extent to which conditions prevailing at that time are representative of conditions throughout the year. The horizontal broken line on the chart shows the annual average percentage of corridor traffic on the turnpike. It will be noted that this is only about 3% less than the percentage for the July, August, and September group. The lower percentage of the January, February, and March group does not greatly affect the average annual percentage because of the low volumes during that period. A similar relationship between the proportionate turnpike usage in the different seasons was found for the eastern extension of the Pennsylvania Turnpike, although the seasonal variations in traffic volume in Pennsylvania were somewhat less than in Maine.

Significant Factors in Growth and Distribution

In order to study how the relationships thus far described, which were based on simple traffic counts, would vary in different areas according to the composition and characteristics of traffic, intensive studies of trip origins and destinations and trip purposes were made on several turnpikes, among them the Maine Turnpike and the eastern extension of the Pennsylvania Turnpike. The field surveys were handled by the two state highway departments concerned and the analyses by the Bureau of Public Roads (United States Department of Commerce). Because detailed accounts of these origin and destination studies are available elsewhere[2, 3] it is sufficient to note merely that drivers were interviewed at selected points on roads parallel to the turnpikes on weekdays, Saturdays, and Sundays, mostly during the summer months, both before and after the turnpikes were opened, and at all turnpike toll stations after the turnpikes were opened. In the case of Maine, interviews were made during August and October, 1947, before the turnpike was opened, in August and October, 1948, after it was opened, and again in August, 1950, after the traffic had become more stabilized. The Pennsylvania interviews were conducted during the summers of 1950 and 1952, prior to and following that turnpike's opening.

Trip Length in the Maine Studies.—Fig. 6 gives the location of the Maine Turnpike and of U. S. 1 which parallels it. The turnpike is 44.9 miles long and U. S. 1 is 44.2 miles long between turnpike termini. The relatively greater length of the turnpike results from the right-angle turn near the northern end. This turn reduces traffic on the turnpike between Portland and points along the shore, as will be seen in the subsequent analysis. For purposes of studying the behavior of trips of different lengths through the turnpike area, the area

---

[2] "Proportionate Use of Maine Turnpike by Traffic Through Portsmouth-Portland Corridor," by J. C. Carpenter, *Proceedings*, Highway Research Board, National Research Council, Washington, D. C., Vol. 32, 1953, pp. 452–463.

[3] "Pennsylvania Turnpike Traffic Analysis," by Daniel O'Flaherty, *Public Roads*, Vol. 28, 1955, pp. 203–223.

is divided into three sections, A, B, and C, each containing an interview station on U. S. 1. Sections begin and end at turnpike toll stations. Unlike the other sections, there are two additional toll stations within section B, one at Kennebunk and one at Biddeford. With the exception of a few short trips to and from these two towns, all the travel which would be conveniently served by the turnpike would involve crossing one or more of the three sections.

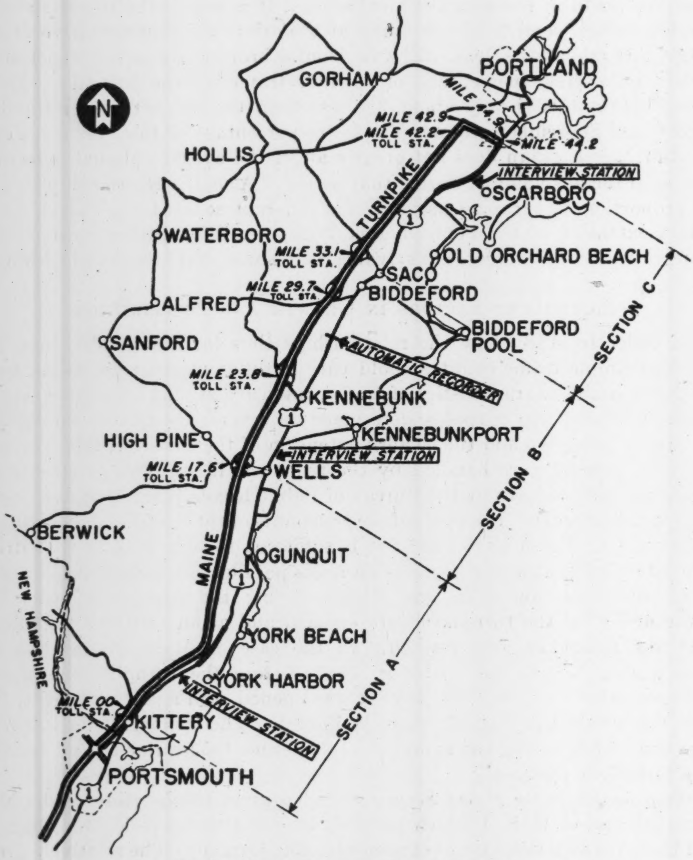
N
GORHAM
PORTLAND
MILE 44.9
MILE 42.9
MILE 42.2
TOLL STA.
MILE 44.2
INTERVIEW STATION
SCARBORO
HOLLIS
TURNPIKE
1
WATERBORO
MILE 33.1
TOLL STA.
OLD ORCHARD BEACH
SACO
MILE 29.7
TOLL STA.
BIDDEFORD
ALFRED
SANFORD
BIDDEFORD POOL
AUTOMATIC RECORDER
SECTION C
MILE 23.8
TOLL STA.
KENNEBUNK
1
KENNEBUNKPORT
HIGH PINE
INTERVIEW STATION
MILE 17.6
TOLL STA.
WELLS
SECTION B
BERWICK
OGUNQUIT
MAINE
1
NEW HAMPSHIRE
YORK BEACH
YORK HARBOR
MILE 0.0
TOLL STA.
KITTERY
INTERVIEW STATION
SECTION A
PORTSMOUTH
1

FIG. 6.—MAINE TURNPIKE TRAFFIC SURVEY

Fig. 7 shows, for August, 1950, the average daily number and the percentage of passenger-car trips distributed between the turnpike and U. S. 1 along the different lengths of the turnpike corridor, as shown by sections A, B, and C. The widths of the bands shown are proportional to the number of trips;

the figures in parentheses indicate the percentage distribution between the turnpike and U. S. 1. Trips by way of the turnpike appear above the center of the chart and those by way of U. S. 1 appear below the center of the chart. The first band above the center shows the through trips on the turnpike—that is, trips with one terminal south of the south end of the turnpike, and the other terminal north of the north end of the turnpike.

The first band below the center shows trips of corresponding length made through the area on U. S. 1. The distribution of this through traffic is 75% on the turnpike and 25% on U. S. 1.

The second band above the center shows the turnpike trips with one terminal south of the south end of the turnpike and the other terminal in section C, passing through sections A and B. The corresponding band below the center shows the number of corresponding trips using U. S. 1. Of the trips in this category, 55% were made on the turnpike. The third bands above and below the center indicate corresponding trips with one terminal north of the north end of the turnpike and the other in section A, passing through sections B and C. The percentage of turnpike use here is only 44%, the lower usage being due in part to the right-angle turn near the northern end of the turnpike.

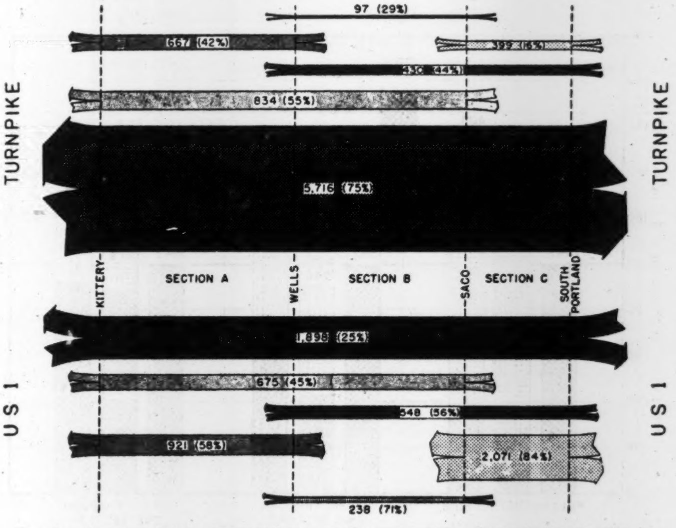

FIG. 7.—AVERAGE DAILY DISTRIBUTION OF PASSENGER-CAR TRIPS BETWEEN MAINE TURNPIKE AND U. S. 1 IN AUGUST, 1950

The next two pairs of bands, one pair above and the other below the center, show the trips with one terminal in the middle section and the other terminal beyond one end of the turnpike passing through end section A or section C. Of the trips between section B and Kittery and points south, 42% occurred on the turnpike, compared to only 16% for trips between section B and South Portland and points north. This shows the extent to which unfavorable turnpike alinement reduces use of the turnpike for comparatively short trips in and out of Portland.

The outermost bands above and below the center line represent trips with both origin and destination within the turnpike area, passing only through section B. Of these trips 29% were made on the turnpike.

It is seen that the length of a trip, or that part of it which extends onto the turnpike area, has an important bearing on choice of route. The turnpike usage by passenger cars traveling the entire 45 miles was 75%; by those traversing two of the three sections, from 44% to 55%; and by those driven only through one section, from 16% to 42%. Not shown in Fig. 7 were a large number of short trips on U. S. 1 which did not involve travel through an entire section and could not advantageously have been made on the turnpike.

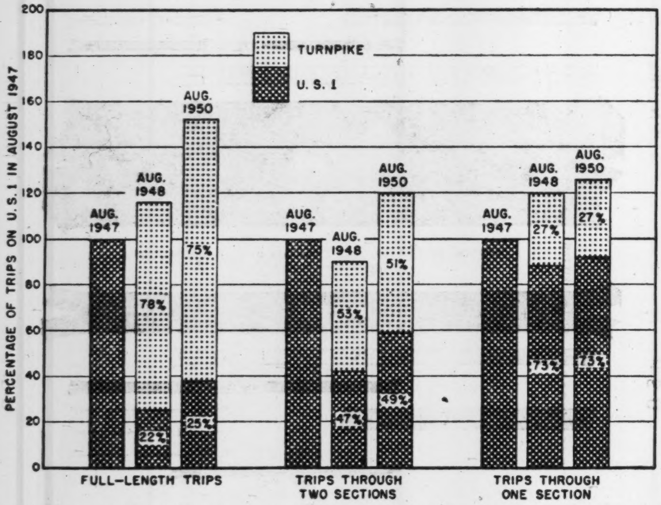

Fig. 8.—Growth in Average Daily Number of Passenger Cars Making Full Length Trips, Trips Through Two Sections, and Trips Through One Section, from August, 1947, to August, 1948, and to August, 1950, and Percentage Distribution Between Maine Turnpike and U. S. 1

Fig. 8 shows the growth (including generation) of passenger-car trips which extended through the entire turnpike area, through two sections, and through one section, for the three summers in which origin and destination studies were made. The number of trips on U. S. 1 in August, 1947, is taken as 100% for each trip class. The number of trips through the corridor in August, 1948, and in August, 1950, are shown by the heights of the bars as percentages of the number of trips in 1947; the distribution of trips between the turnpike and U. S. 1 in 1948 and 1950 are shown by the figures within the bars. From 1948 to 1950 the percentage distribution between the turnpike and U. S. 1 remained reasonably constant for trips of the three indicated lengths. For this period, the through trips increased by a considerably higher percentage than trips made part way through the area.

The effect of the total length of the trip, including that part of it which is beyond the turnpike area, on the percentage of turnpike usage is indicated in Fig. 9. This figure shows, for August, 1950, the percentage use of the turnpike for through passenger-car trips in different ranges of total length. The widths of the bars are proportional to the number of trips within the length range. The thin bar at the left (trips from 50 miles to 99 miles) designates trips mainly between Portsmouth and Portland. Only 53% of these trips were on the turnpike. The widest bar (lengths from 100 miles to 199 miles) includes the trips between Boston (Mass.) and Portland. Of the trips in this length range, 75% were on the turnpike. The third bar (trips from 200 miles to 299 miles) includes the trips between Boston and Bar Harbor, and Boston and Bangor. Of the trips in this group, 80% were made via the turnpike.

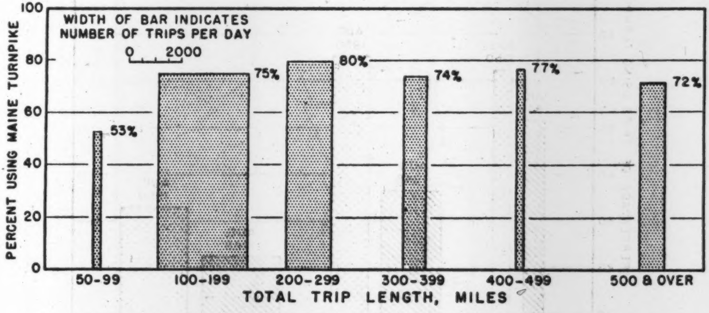

FIG. 9.—DISTRIBUTION OF AVERAGE DAILY PASSENGER-CAR THROUGH TRIPS IN THE CORRIDOR BY PERCENTAGE USE OF MAINE TURNPIKE AND BY TRIP LENGTH IN AUGUST, 1950

For longer trips the turnpike usage was approximately the same as for trips in the 100-mile-to-199-mile group. It might be concluded from this that the total length of a trip—up to a length of approximately 200 miles—affects the turnpike usage. Additional trip length appears to have little or no effect on turnpike usage. However, the location of Boston in relation to the turnpike may have some bearing on this case.

Variations in Turnpike Usage According to Vehicle Type.—For trips extending only part way through the turnpike area, the percentage use of the turnpike by trucks was about the same as by passenger cars. However, the number of these short truck trips was small. In August, 1948, the usage of the turnpike by trucks (particularly heavy trucks) driven through the entire area was much lower proportionately than the usage by passenger cars. Between August, 1948, and August, 1950, however, there was a large increase in the percentage of through truck trips diverted to the turnpike. Fig. 10 shows the distribution between the turnpike and U. S. 1 of the through trips by very light panels and pickups, other single-unit trucks, and combinations used principally by the large commercial haulers. The widths of the bars are proportional to the total number of trucks of each type driven through the corridor; the heights of the bars indicate the percentages of trips on the turnpike. There was a decline in the total number of trucks of all categories passing through the corridor, as indicated by the fact that the 1950 bar is narrower than the 1948 bar in each case. However, for all three classes, there was a much higher percentage of trips on the turnpike in August, 1950, than in August, 1948; there was, in fact, an actual increase in the number of trucks on the turnpike. The proportionate usage for the light panels and pickups and for other single-unit trucks passing through the corridor in August, 1950, was not so far below the passenger-car usage. However, the usage by the combinations was considerably lower, being only 33% of the total number passing through the corridor in August, 1950, compared to 75% for through passenger-car trips.

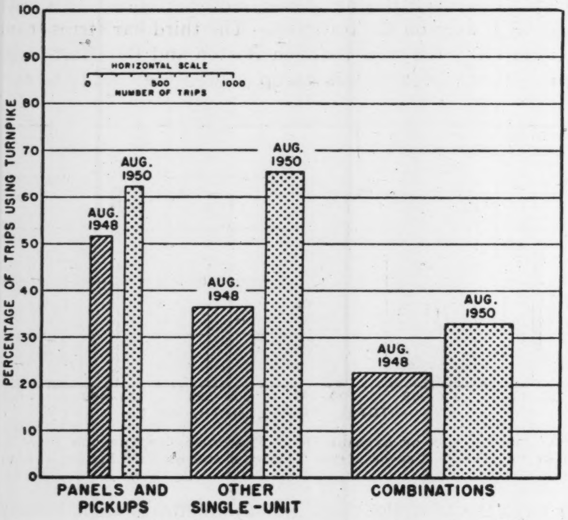

FIG. 10.—PERCENTAGE OF AVERAGE WEEKDAY THROUGH TRIPS BY TRUCKS OF DIFFERENT CLASSES USING MAINE TURNPIKE

The situation with respect to the eastern extension of the Pennsylvania Turnpike is quite different from that of the Maine Turnpike. As the mileage log at the bottom of Fig. 11 indicates, this 100-mile extension, from Carlisle to Valley Forge (Pa.) is not only longer than the Maine Turnpike but also it connects with the old section and forms a continuous turnpike of 327 miles which, including the western extension opened in 1951, extends from near Philadelphia, Pa., to Ohio.

The eastern extension was opened in November, 1950. It was along this extension that the interviews were taken before and after the extension was completed. Fig. 11 shows the location of the interview and automatic-recorder

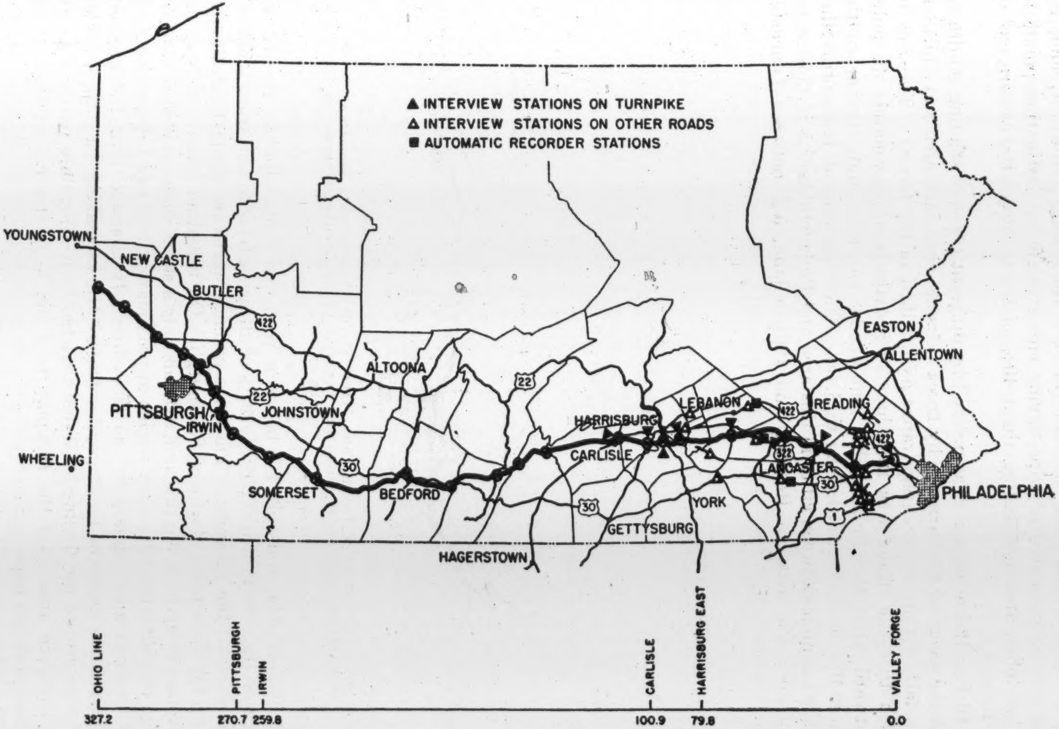
▲ INTERVIEW STATIONS ON TURNPIKE
△ INTERVIEW STATIONS ON OTHER ROADS
■ AUTOMATIC RECORDER STATIONS
YOUNGSTOWN
NEW CASTLE
BUTLER
422
ALTOONA
22
PITTSBURGH
IRWIN
JOHNSTOWN
WHEELING
SOMERSET
30
BEDFORD
HAGERSTOWN
HARRISBURG
CARLISLE
GETTYSBURG
LEBANON
YORK
LANCASTER
322
READING
EASTON
ALLENTOWN
PHILADELPHIA
1
OHIO LINE
PITTSBURGH
IRWIN
CARLISLE
HARRISBURG EAST
VALLEY FORGE
327.2
270.7
259.8
100.9
79.8
0.0

FIG. 11.—ZONES AND INTERVIEW STATIONS FOR PENNSYLVANIA TURNPIKE TRAFFIC STUDY IN SUMMER OF 1952

stations and the outlines of the zones used for grouping origins and destinations. The analysis of this study has not yet been completed. However, some results can be presented of trips having either origin or destination points in Philadelphia, and constituting about 40% of the traffic at the eastern end of the turnpike.

In Fig. 12 are shown areas marked by different types of shading, so drawn that the usage of the turnpike by truck trips between each area and Philadelphia falls within a percentage range as specified in the legend. The area in which turnpike usage was less than 20% extends approximately 40 miles westward from the Philadelphia end of the turnpike and, further south, almost 100 miles westward along U. S. 30. The percentage of trucks traveling on the turnpike between cities in this area and Philadelphia was in most cases very low—5% between Reading and Philadelphia, 5% between Lancaster and Philadelphia, and only 1% between York and Philadelphia. Harrisburg is within the area in which 20% to 40% of all truck trips to and from Philadelphia were on the turnpike. This area extends westward along U. S. 22 and U. S. 422 to a point north of Pittsburgh. On the other hand, south of the turnpike, along U. S. 30, this area extends only a short distance west of Gettysburg; the 80%-to-100% area begins approximately halfway between Carlisle and Bedford and extends to the Ohio line. It is noted that the greatest proportionate usage of the turnpike was by trucks making long trips. This is the reverse of the finding in Maine that trucks passing only partly through the turnpike area used the turnpike to a much greater extent than those making through trips.

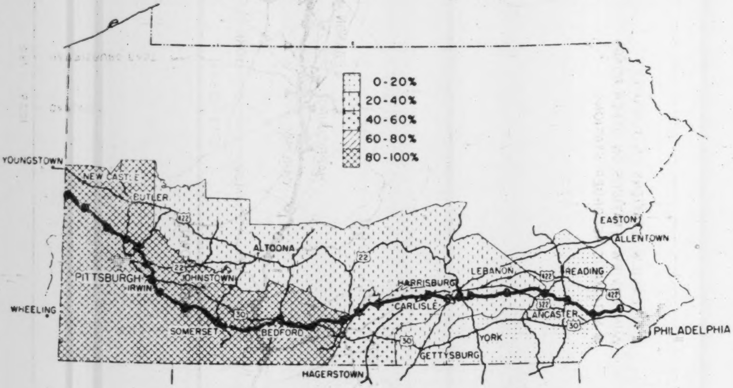
0-20%
20-40%
40-60%
60-80%
80-100%
YOUNGSTOWN
NEW CASTLE
BUTLER
422
ALTOONA
22
PITTSBURGH
IRWIN
JOHNSTOWN
WHEELING
SOMERSET
30
BEDFORD
HARRISBURG
CARLISLE
LEBANON
422
READING
EASTON
ALLENTOWN
322
LANCASTER
30
YORK
GETTYSBURG
HAGERSTOWN
PHILADELPHIA

FIG. 12.—PERCENTAGE OF TRUCK TRIPS MADE VIA THE PENNSYLVANIA TURNPIKE BETWEEN PHILADELPHIA AND AREAS ALONG THE TURNPIKE ON AN AVERAGE WEEKDAY IN THE SUMMER OF 1952

The high usage of the Pennsylvania Turnpike by trucks is unique in turnpike experience and is due principally to the very steep grades and sharp curves on U. S. 30. For example, the total rise and fall on U. S. 30 for 150 miles westward from Carlisle is 26,257 ft compared to 11,327 ft on the turnpike. The average time saved by trucks using the turnpike between Pittsburgh and Philadelphia is almost 3 hr. These advantages are not likely to be duplicated on many other toll roads.

The relative turnpike usage for passenger-car trips in and out of Philadelphia is given in Fig. 13 in the same manner as the information for truck trips is given in Fig. 12. As in the case of trucks, more than 80% of the passenger-car trips with origin and destination points in the area west of a point midway between Carlisle and Bedford were made on the turnpike. However, the 80%–100% area in Fig. 13 extends farther north (across U. S. 422 from just west of Johnstown) than the same percentage area in Fig. 12. In addition, this area contains a small section around Carlisle. Of the passenger-car trips between Pittsburgh and Philadelphia, 89% were on the turnpike; this compares with 72% of the passenger-car trips between Boston and Portland and 84% of those between Boston and Bar Harbor on the Maine Turnpike in August, 1950.

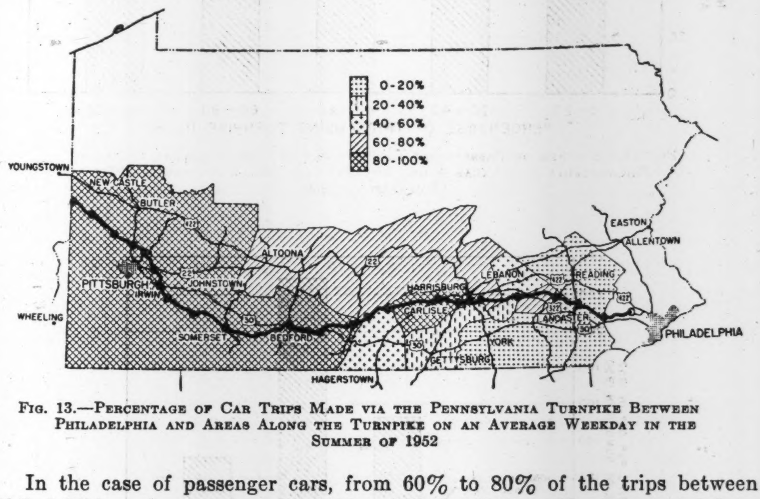
0-20%
20-40%
40-60%
60-80%
80-100%
YOUNGSTOWN
NEW CASTLE
BUTLER
422
ALTOONA
22
PITTSBURGH
IRWIN
JOHNSTOWN
22
30
WHEELING
SOMERSET
BEDFORD
HARRISBURG
CARLISLE
30
GETTYSBURG
YORK
LEBANON
322
READING
422
EASTON
ALLENTOWN
LANCASTER
322
30
PHILADELPHIA
HAGERSTOWN

FIG. 13.—PERCENTAGE OF CAR TRIPS MADE VIA THE PENNSYLVANIA TURNPIKE BETWEEN PHILADELPHIA AND AREAS ALONG THE TURNPIKE ON AN AVERAGE WEEKDAY IN THE SUMMER OF 1952

In the case of passenger cars, from 60% to 80% of the trips between Philadelphia and areas along U. S. 22 and U. S. 422 from Harrisburg to Johnstown were on the turnpike as contrasted with the 20%-to-40% usage by trucks. Between Harrisburg and Philadelphia, 76% of the passenger cars used the turnpike as compared with 36% for trucks. There was little usage of the turnpike by either passenger cars or trucks where less than approximately 40 miles of it could be used. This distance is almost equal to the length of the Maine Turnpike, where there is a 75% usage for through passenger-car trips.

Fig. 14 shows the growth in the number of passenger-car trips on all routes between Philadelphia and the different areas shown in Fig. 13 from 1950 (before the turnpike was opened) to 1952 (after it was opened). This is for summer weekday trips whereas the trips shown in the Maine charts were for average daily summer trips including Saturdays and Sundays. The 100%

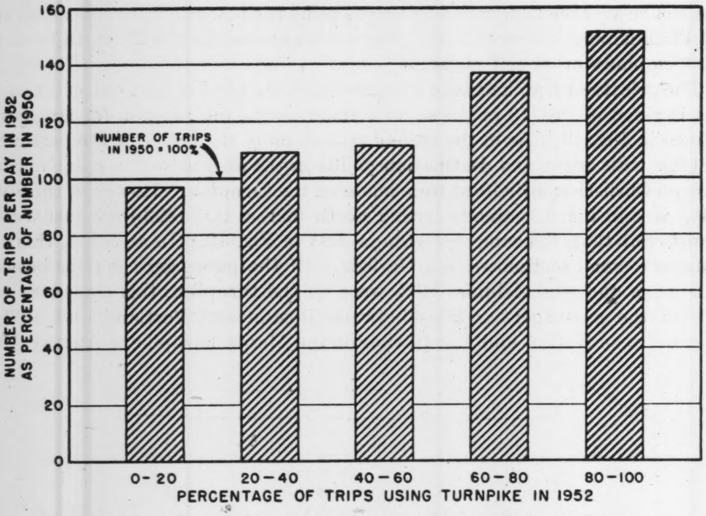

FIG. 14.—NUMBER OF PASSENGER-CAR TRIPS PER SUMMER WEEKDAY BETWEEN PHILADELPHIA AND AREAS ALONG THE PENNSYLVANIA TURNPIKE IN 1952 COMPARED TO 1950

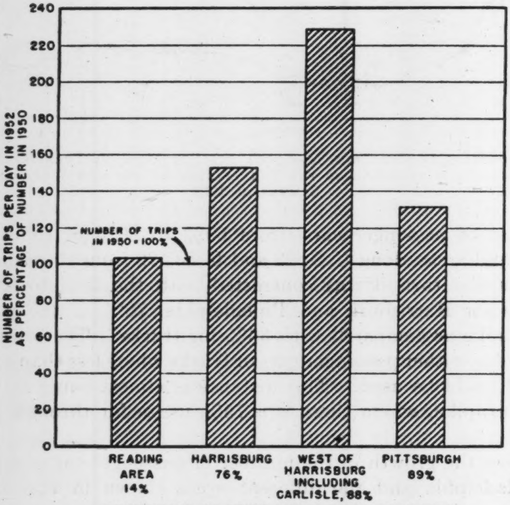

FIG. 15.—NUMBER OF PASSENGER-CAR TRIPS PER SUMMER WEEKDAY BETWEEN PHILADELPHIA AND CITIES ALONG THE PENNSYLVANIA TURNPIKE IN 1952 AS COMPARED WITH 1950

line in Fig. 14 represents the number of trips between the different areas and Philadelphia the summer before the turnpike was opened. For the area of less-than-20% turnpike usage, there was a 3% decline in the number of trips from 1950 to 1952. For the area of 20%-to-40% turnpike usage, there was a 9% increase; for the 40%-to-60% area, an 11% increase; for the 60%-to-80% area, a 37% increase; and for the 80%-to-100% area, a 55% increase. Thus, the higher the percentage use of the turnpike for trips to and from Philadelphia, the greater was the growth in the number of these trips on all routes after the turnpike was opened. This indicates definitely that the increase was caused by the existence of the turnpike.

Fig. 15 shows the percentage increase in the number of trips between Philadelphia and certain cities along the turnpike route after the turnpike was opened. For Reading, where the percentage use of the turnpike was 14% (indicated by the figure below the bar), there was only a 2% increase in the number of Philadelphia trips as indicated by the height of the bar; for Harrisburg, there was a 53% increase in the number of trips to and from Philadelphia. For Carlisle and the area west of Harrisburg, the increase in the number of Philadelphia trips was 129%. This area is at the western end of the eastern extension of the Pennsylvania Turnpike and travel between it and Philadelphia would benefit most from the construction of this section. For many years it has been convenient to travel between Philadelphia and Pittsburgh on the original section of the Pennsylvania Turnpike (from Irwin to Carlisle); the opening of the eastern extension was not so important, relatively, for this travel as it was for the travel between Carlisle and Philadelphia.

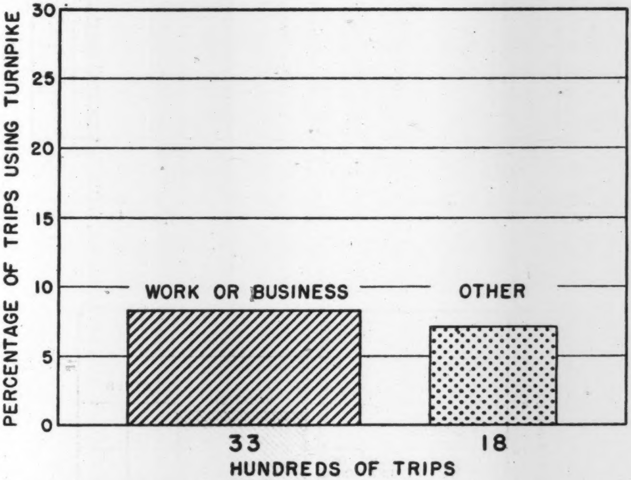

Fig. 16.—Percentage of Trips (by Trip Purpose) Between Philadelphia and 0%-to-20% Pennsylvania Turnpike Usage Area on the Turnpike on a Summer Weekday in 1952

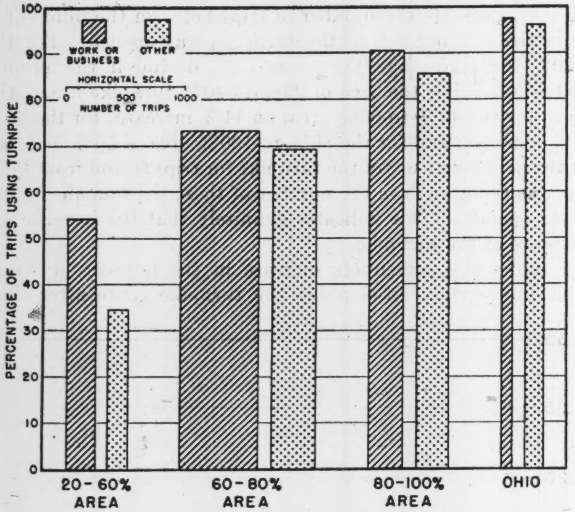

FIG. 17.—PERCENTAGE OF TRIPS (BY TRIP PURPOSE) BETWEEN PHILADELPHIA AND OTHER AREAS ON PENNSYLVANIA TURNPIKE FOR A SUMMER WEEKDAY IN 1952

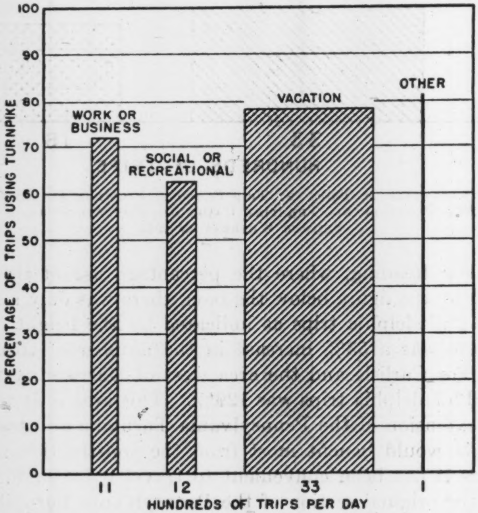

FIG. 18.—PERCENTAGE OF AVERAGE DAILY THROUGH PASSENGER-CAR TRIPS (BY TRIP PURPOSE) ON THE MAINE TURNPIKE, IN AUGUST, 1950

Thus, the percentage increase in trips from Pittsburgh to Philadelphia after the opening of the turnpike's eastern extension was only 31%.

Effect of Trip Purpose on Turnpike Usage.—Fig. 16 shows the percentage of work or business trips and other trips made on the turnpike between Philadelphia and the 0%-to-20% usage area shown in Fig. 13. The widths of the bars are proportional to the number of trips in each category. For this area, which is relatively close to Philadelphia, 8% of the work or business trips and 7% of the trips made for other purposes were on the turnpike.

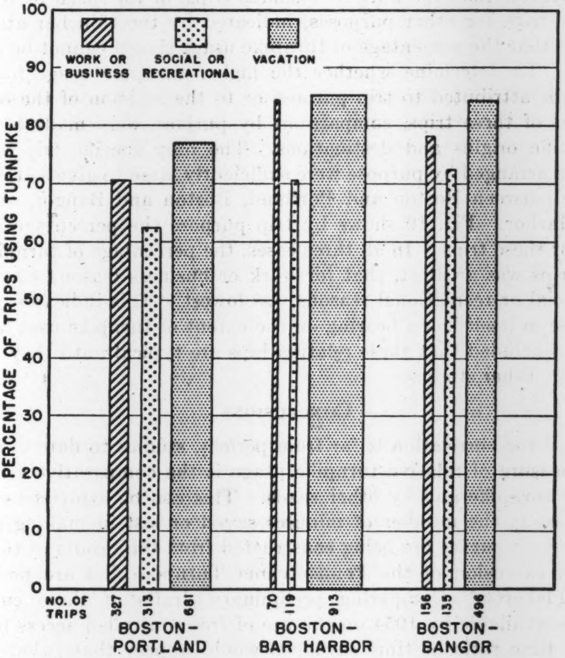

FIG. 19.—PERCENTAGE OF AVERAGE DAILY PASSENGER-CAR TRIPS (BY TRIP PURPOSE) BETWEEN BOSTON, MASS., AND POINTS NORTH OF MAINE TURNPIKE ON THE TURNPIKE, IN AUGUST, 1950

Fig. 17 shows, similarly, the relative usage of the turnpike by work or business trips and trips for other purposes between Philadelphia and other areas. The area percentage designations are those shown in Fig. 13 except that, because of the smallness of the sample when arranged according to trip purpose, it was necessary to combine the 20%-to-40% and the 40%-to-60% areas. These percentages indicate the extent to which trips between the zones in each of the areas and Philadelphia are made via the turnpike. Trips between Philadelphia and points in Ohio are also shown. In every case the percentage turnpike usage by work or business trips exceeded the usage by trips for other purposes. Most trips other than those for work or business (with origin or destination in Philadelphia) were of a social and recreational nature; very few were vacation trips. This is in contrast to Maine where, in August, most of the trips through the turnpike corridor were vacation trips.

In Fig. 18, pertaining to the Maine Turnpike study, the widths of the bars are proportional to the number of through trips for the different purposes. This figure pertains to through trips on an average day in August, 1950. The heights of the bars show that the proportionate turnpike usage for vacation trips was greater than for work or business trips, or for social or recreational trips. The trips for other purposes, indicated by the thin bar at the right, were so few that the percentage of turnpike usage shown cannot be considered significant. To determine whether the higher turnpike usage for vacation trips is to be attributed to trip purpose or to the location of the origins and destinations of these trips, comparisons by purpose were made for trips between specific origins and destinations. The only specific trip movements which when arranged by purpose were sufficiently large to give a stable sample were those between Boston and Portland, Boston and Bangor, and Boston and Bar Harbor. Fig. 19 shows by trip purpose the percentage use of the turnpike for these trips. In all three cases, the percentage of turnpike use for vacation trips was greatest, that for work or business reasons was next, and that for social or recreational reasons was lowest. This indicates, then, that trip purpose in itself has a bearing on the extent of turnpike use; however, it cannot be concluded that these relationships are typical until they have been confirmed by other studies.

Conclusions

Although the correlation is far from perfect, studies to date indicate that the best measure of relative turnpike usage is the comparative trip time by way of the turnpike and by other roads. This can be expressed either as a time ratio or as the number of minutes saved or lost in making use of the turnpike. Such curves are being constructed from the results of the study of the eastern extension of the Pennsylvania Turnpike and are presented by Daniel O'Flaherty.[3] Comparing preliminary drafts of these curves with information available by 1954 on the use of free controlled access facilities in relation to time ratio or time saved, it would appear that, where the time saving is large, the proportion of trips on the high-type facility would be approximately as high for a toll facility as for a free facility. Where the time saving is small the proportionate usage of a toll road would be much lower than that of a free road of comparable characteristics.

This conclusion is only tentative. Curves relating percentage usage with time saving, which are drawn solely from the data developed in the study of the eastern extension of the Pennsylvania Turnpike, would have to be confirmed by data developed for different situations before they could be accepted as generally applicable.

AMERICAN SOCIETY OF CIVIL ENGINEERS
Founded November 5, 1852

TRANSACTIONS

Paper No. 2891

MODEL TESTS, ANALYSIS, AND OBSERVATION OF AN ARCH DAM

By Manuel Rocha,[1] M. ASCE, J. Laginha Serafim,[2] M. ASCE, António F. da Silveira,[3] and José M. Ressurreição Neto[4]

With Discussion by Messrs. Merlin D. Copen; A. Warren Simonds; Joe T. Richardson; A. Carvalho Xerez; and Manuel Rocha, J. Laginha Serafim, António F. da Silveira, and José M. Ressurreição Neto

Synopsis

Studies made on the upstream cofferdam of Castelo do Bode Dam (on the Zêzere River in Portugal) are described. This dam is 34 m(111.55 ft) high. Stresses and displacements were measured on two models (plaster-diatomite and "alkathene") and the stresses and displacements in the structure were measured during the filling of the reservoir. Computations using the "abridged trial-load method" are presented and it is shown that the values from the model tests agreed closely with those observed in the structure.

1. Summary

The Zêzere River hydroelectric project in Portugal was begun in 1947 by the Hidro-Eléctrica do Zêzere with the erection of a dam at Castelo do Dode.[5] The project included an upstream concrete-arch cofferdam (Figs. 1 and 2) founded on crystalline shale. The dam is a slightly unsymmetrical structure 34 m high (1 m = 3.28 ft) and approximately 140 m long at the crown; the

---

Note.—Published, essentially as printed here, in May, 1955, as *Proceedings-Separate No. 696*. Positions and titles given are those in effect when the paper or discussion was approved for publication in Transactions.

[1] Director, National Civ. Eng. Lab., Lisbon, Portugal.

[2] Head, Dams Studies Section, National Civ. Eng. Lab., Lisbon, Portugal.

[3] Asst. Research Engr., National Civ. Eng. Lab., Lisbon, Portugal.

[4] Asst. Research Engr., National Civ. Eng. Lab., Lisbon, Portugal.

[5] "Le Barrage et l'usine hydroélectrique de Castelo do Bode (Portugal)," by A. C. Xerez, *La Technique des Travaux*, July and August, 1951.

ratio between length and height is therefore 4:1. The upstream face is a vertical, cylindrical surface with a radius of 65 m and the downstream face is concentric and conical.

Construction and study of the arch cofferdam were under the direction of the Laboratório Nacional de Engenharia Civil of Portugal (hereinafter referred to as the Laboratório). Castelo do Bode Dam was designed by André Coyne, Hon. M. ASCE. The Laboratório in collaboration with the Direcção Geral dos Serviços Hidráulicos (Board of Hydraulic Works) and the Hidro-Eléctrica do Zêzere outlined a program of extensive investigations of the arched cofferdam, including model tests, trial-load analysis, computation by the independent-arch theory, and observation of the dam during the filling and emptying of the reservoir. These studies would provide information on the structural behavior of arch dams and would help to evaluate the usefulness of the analytical and experimental methods used in predicting this behavior. The investigations were begun in 1947, and their experimental part was completed in 1951.

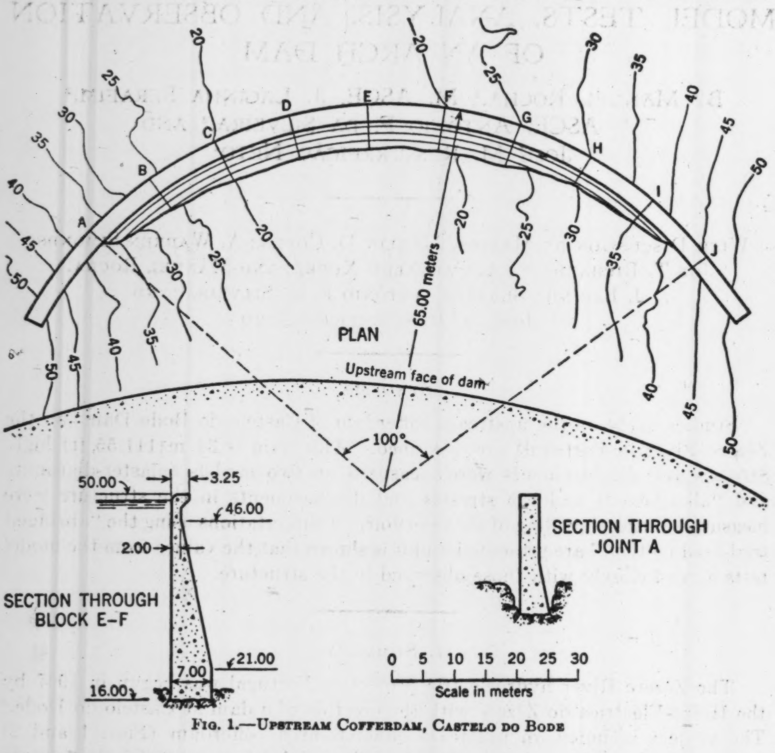
A
B
C
D
E
F
G
H
I
J
20
25
30
35
40
45
50
PLAN
65.00 meters
Upstream face of dam
100°
50.00
3.25
46.00
2.00
SECTION THROUGH BLOCK E–F
7.00
21.00
16.00
SECTION THROUGH JOINT A
0 5 10 15 20 25 30
Scale in meters

FIG. 1.—UPSTREAM COFFERDAM, CASTELO DO BODE

Tests were first conducted on a plaster-diatomite model. In this model a crack was induced by load at the base of the upstream face, and later observation of the prototype showed that an analogous crack had actually developed in the dam.

To ascertain the effect of this crack on the stress, use was made of a plastic ("alkathene") model. The plaster model, moreover, permitted analyzing the effect of some horizontal cracks (Fig. 2) developed at the downstream face of the prototype (a little below the crown) upon filling of the reservoir. The upstream and downstream stresses, as well as the radial deflections of the downstream face, were measured on both models. The tangential and vertical displacements were also measured on the plaster model (Fig. 3).

Stress analysis by the trial-load method included radial adjustments only, but the lack of symmetry of the structure was taken into consideration. The first approach having led to fairly high tensile stresses at the base of the cantilevers, a more accurate analysis was made on the assumption that the cantilevers cracked at the base.

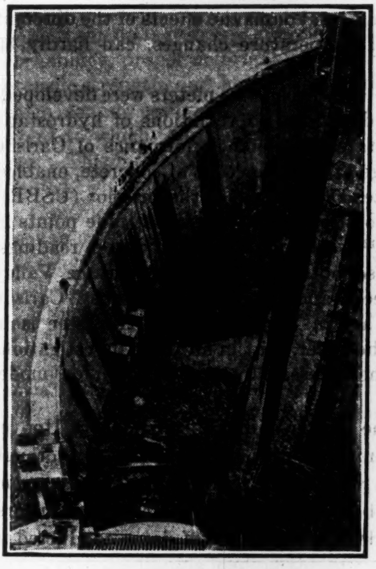

FIG. 2.—LEAKAGE AREAS IN COFFERDAM DURING FILLING OF RESERVOIR

FIG. 3.—PLASTER MODEL WITH THE ELECTRICAL STRAIN GAGES

It was possible to perform the test loading of the prototype when the temperatures of concrete, air, and water were about the same and when the loading-unloading cycle could be made quickly. Consequently, temperature changes were eliminated, and this afforded a simpler interpretation of the results.

The observation of the prototype included measurements of: Strains at interior points by vibrating-wire meters which also measured temperatures;

deflections of the downstream face and of the crown by geodetic and slide-target methods; joint openings; and angular displacements by clinometers. These were made after completion of much of the model tests and analytical computations. The cracks detected in the prototype entailed additional investigations which could not be pursued as far as desired without too much work. Consequently, this paper does not correspond to the initially outlined program. However, it was considered worth while to publish the results because there have been so few opportunities to compare the actual and predicted behavior of arch dams.

The observation of an actual structure to check the stresses and deflections given by computations or model tests was attempted for the first time in the test of the Stevenson Creek Dam,[6] in California, in 1922.

Construction and proper testing of trial dams entail considerable difficulties and expenditure. On the other hand, on actual dams the effects of the different loadings, especially water pressure and temperature changes, can hardly be separated.

In Europe, especially in Fance,[7,8,9,10,11] vibrating-wire meters were developed, and measurements of stresses in arch dams due to variations of hydrostatic pressure were made. In the United States the good performance of Carlson meters, together with a better knowledge of the properties of concrete, enabled the Bureau of Reclamation, United States Department of the Interior (USBR), to develop them further. The time evolution of the stresses at nine points in the base of Shasta Dam in California[12] was computed from meter readings. Reliable stress measurements were also obtained by the Tennessee Valley Authority (TVA) at Norris, Hiwassee,[13] and Fontana[14] Dams by Carlson meters. (Norris and Fontana Dams are in Tennessee, and Hiwassee is in North Carolina.) It should be noted, however, that in all those investigations no attempt was made to analyze the stresses by computation or model testing.

The remarkable investigations of the plaster and rubber models of Hoover Dam[15] in Arizona and Nevada were compared with the results from thorough trial-load analysis. Nevertheless, the results of stress and the displacement measurements for this dam have not been available thus far to the writers. Again, the results of the extensive model investigations of dams conducted in

---

[6] "Report of the Committee of Engineering Foundation on Arch Dam Investigation," *Proceedings*, ASCE, Pt. 3, May, 1928.

[7] "Mesures extensométriques du Barrage du Pas du Riot," by J. Bellier and D. Migny, *Report No. 33*, *Transactions*, Vol. II, 3d Cong. on Large Dams, Stockholm, 1948.

[8] "Mesures de déformations effectvées sur quelques barrages français," by A. Nizery, *Report No. 34*, *ibid.*

[9] "Rupture d'une voûte d'essai," by R. Bourriot, *Report No. 40*, *ibid.*

[10] "Mesures extensométriques effectuées sur le Barrage de Fabrèges lors de sa mise en eau," by Hamon, *Report No. 42*, *ibid.*

[11] "Auscultation du Barrage du Gour Noir," by J. Bellier and P. Blanchet, *Report No. 65*, *ibid.*

[12] "The Development of Stresses in Shasta Dam," by J. M. Raphael, *Transactions*, ASCE, Vol. 118, 1953, pp. 289–321.

[13] "Measurements of the Structural Behavior of Norris and Hiwassee Dams," *Technical Memorandum No. 67*, Tennessee Valley Authority, Knoxville, Tenn., February and August, 1950.

[14] "Measurements of the Structural Behavior of Fontana Dam," *Technical Memorandum No. 69*, Tennessee Valley Authority, Knoxville, Tenn., February and June, 1953.

[15] "Model Tests of Boulder Dam, Boulder Canyon Project, Final Reports," *Bulletin 3*, Bureau of Reclamation, U. S. Dept. of the Interior, Denver, Colo., 1939.

Italy and other European countries[16,17,18,19,20] have not been compared yet with those of prototype observations.

The results presented in this paper are those obtained from measurements. No corrections such as those for symmetry, continuity, or knowledge of the stress distribution have been made.

2. Model Investigations

Only the essential features of the investigations are presented here. A later detailed report is planned to cover all the model tests conducted at the Laboratório during the past eight years. The methods used so far have already been published.[21,22]

a. Plaster Model.—Based on experience from the model investigation of dams it was concluded that a mix of plaster and diatomite is the best material of those used.[15,21]

Certain characteristics command this material: Mechanical similarity, good workability, proper deformability, and low cost. However, it exhibits too low a tensile strength, and herein lies a serious drawback because cracks may occur which connot easily be detected. A further source of difficulty is the large extent to which the mechanical properties are affected by environmental moisture. This influence can be considerably reduced if the outer surface is waterproofed.

Considering the sensitivity and size of the gages used in earlier tests and the mechanical properties of the plaster-diatomite mix, the scale factor, $1/n = 1/75$, was selected for this model (Fig. 3). In casting the model, an accurate wooden mold was used in order to give directly every detail of its final shape.

The section of the foundation ground reproduced was 30 cm thick (1 cm = 0.3937 in.)—that is, approximately three times the maximum thickness of the dam model proper. The concrete tray used earlier for the model of Santa Luzia Dam[23] in Portugal was used again as the rigid base.

The model was made of a mixture of plaster and diatomite in the propertion of 2 to 1 by weight and water to produce a water-plaster ratio of 1.5 by weight. This water content gives a flowing mixture. The model was allowed to dry until moisture equilibrium with the environment was reached.

Application of hydrostatic pressure on the model was made by a properly shaped rubber bag filled with mercury. Thus, the ratio between the specific gravity of the liquids loading the model and the prototype is $G = 13.6$.

---

[16] "Ricereche sperimentali sul comportamento statico delle dighe," by G. Oberti, *L'Elettrotecnica*, Vol. XXXVI, No. 3, 1949.

[17] "Diga del Lumiei. Criteri di progetto e studi sperimentali," by G. Oberti, *L'Energia Elettrica*, September, 1948.

[18] "Modern Trends in Arch Dam Investigation and Design," by C. Jaeger, ***Civil Engineering and Public Works Review***, Vol. 45, No. 541, 1950, p. 572.

[19] "Statische Modellversuche zu Gewölbestaumauern," by E. Tschech and F. Jaburek, ***Schweizeriche Bauzeitung***, No. 16, 1951, p. 215.

[20] "L'etude sur modèle réduit des contraintes dans les barrages," by A. Nizery, G. Remenieras, and N. Beaujoint, ***Annales des Ponts et Chaussées***, July-October, 1953.

[21] "Dimensionnement experimental des constructions," by M. Rocha, ***Annales de l'Institut Technique du Bâtiment et des Travaux Publics***, No. 235, February, 1952.

[22] "General Review of the Present Status of the Experimental Method of Structural Design," by M. Rocha, ***Proceedings***, Cong .of the International Assn. for Bridge and Structural Eng., 1952.

[23] "Model Tests of Santa Luzia Dam," by M. Rocha and J. L. Serafim, ***Communication No. 5, Transactions***, 3d Cong. on Large Dams, Stockholm, 1948.

The mechanical properties of the model material were determined by compression-creep tests on prisms cut from the model. The prisms were subjected to stresses, σ (in kilograms per square centimeter) of 2, 4, 6, 8, and 10 (1 kg per sq cm = 14.2 lb per sq in.). The strains, ϵ, were measured after 0, 2, 5, 10, and 20 min (Fig. 4). The results show that the modulus of elasticity changes with time for stresses under 6 kg per sq cm, reaching the values indicated. The material may therefore be assumed to be perfectly elastic for each loading time. A modulus of elasticity of 15,400 kg per sq cm was adopted in evaluating model stresses; strains and deflections were read after a 10-min loading, each reading taking no longer than 1½ min. Poisson's ratio as given by tests was 0.20, no effect of creep having been measured.

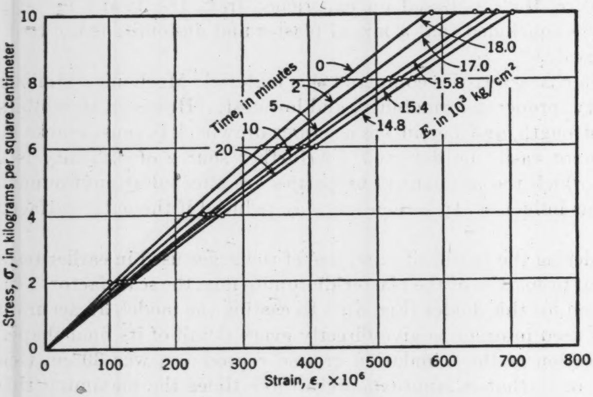

FIG. 4.—MODULUS OF ELASTICITY OF PLASTER FOR DIFFERENT DURATIONS OF LOADING

The following similarity relationships[23] exist between deflections, δ_p, δ_m, and stresses, σ_p, σ_m, respectively, in the prototype and model:

$$\delta_p = \frac{E_m}{E_p} \frac{n^2}{G} \delta_m$$

and

$$\sigma_p = \frac{n}{G} \sigma_m$$

in which E_p and E_m are the moduli of elasticity of the prototype and the model, respectively.

As will be shown subsequently in Sect. 6, a modulus of elasticity, E_p = 260,000 kg per sq cm, was assumed for the concrete. Thus, the similarity relationships are

$$\delta_p = 24.5\, \delta_m$$

and

$$\sigma_p = 5.50\, \sigma_m.$$

Despite the crack caused by the tensile stresses at the upstream face of the model near the boundary line between the dam and the ground, it was decided to continue the tests. At a later stage, horizontal cracks were cut at the upper part of the downstream face to simulate the prototype more closely.

b. Alkathene Model.—In order to learn the influence of the upstream crack at the base of the plaster model (which is very likely to develop in the prototype), it was decided to construct another model which could be tested before and after cracking. Since another plaster model cloud not be relied on, a commercial synthetic resin was sought having a fairly good tensile strength and conforming to the following requirements: Ability to be cast without pressure or special molds; good workability; constant mecahnical properties; and low modulus of elasticity so that small models could be used. This led to the adoption of alkathene, an English polyethylene resin. This material has the drawback of possessing a Poisson ratio higher than that for concrete, which could impair the similarity conditions. Construction is more complicated than it is for plaster because it requires metallic molds; furthermore, a pouring temperature of 130°C and very slow cooling are necessary.

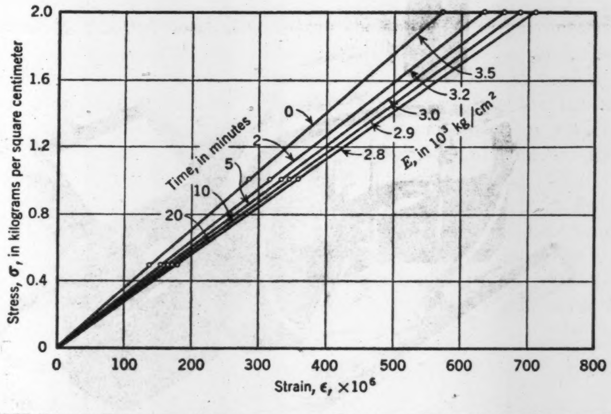

FIG. 5.—MODULUS OF ELASTICITY OF ALKATHENE FOR DIFFERENT DURATIONS OF LOADING (at 22°C)

The marked visco-elasticity of alkathene requires that considerable care be taken with regard to the time of loading the models. The high value of the coefficient of thermal expansion, about 0.0002 per degree Centigrade, together with the conspicuous influence of temperature on the mechanical properties, makes it absolutely necessary for the tests to be conducted in a temperature-controlled room. If these precautions are taken, alkathene appears to be a valuable material for model construction because of its high tensile strength, toughness and nonfriability (whereby the handling becomes easier), and its absolute homogeneity.

The mechanical properties of alkathene were also determined by subjecting prisms to compressive-creep tests, maintaining temperatures at 22°C. The results (Fig. 5) show that the modulus of elasticity changes with time. It was realized that the modulus of elasticity, *E*, corresponding to any duration of loading, changes with the temperatures, $\theta 1$ and $\theta 2$, in degrees Centigrade according to the equation:

$$E_{\theta 1} = E_{\theta 2}[1 - K(\theta 1 - \theta 2)]$$

in which the constant $K = 0.012$. Alkathene can therefore be used for model studies as if it were a perfectly elastic material, provided that sufficient time intervenes between tests so that the influence from the previous loading is avoided.

Readings of strains and deflections were taken 5 min after loading; thus, the value of 3,000 kg per sq cm was adopted for the modulus of elasticity.

Owing to this low value and to the possibility of using short-base strain gages, the scale factor, $1/n = 1/200$, was chosen for the alkathene model (Fig. 6). Poisson's ratio as determined by creep tests was found to be 0.44. No change in this value with time was detected. The model was subjected to a mercury load applied by a device similar to that used for the plaster model.

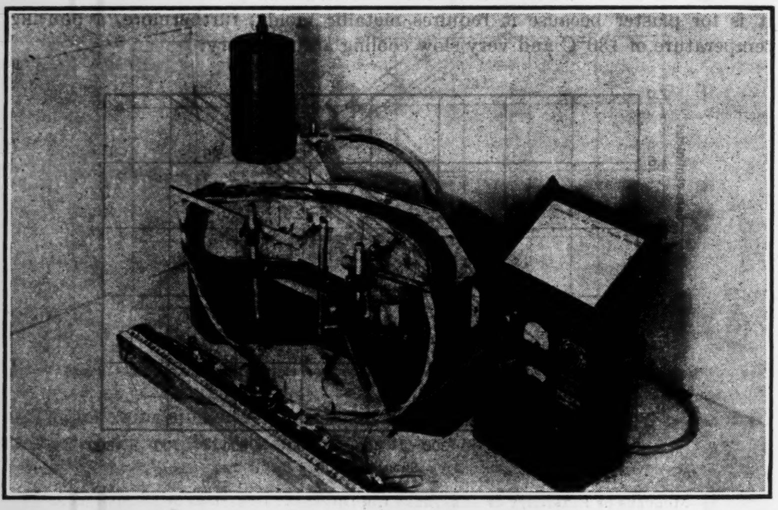

FIG. 6.—ALKATHENE MODEL WITH LOADING DEVICE, READING INSTRUMENT, DEFLECTOMETERS, AND STRAIN GAGES

The similarity relationships which apply for the deflections and the stresses are, respectively,

$$\delta_p = 33.9\, \delta_m$$

and

$$\sigma_p = 14.7\, \sigma_m.$$

3. MEASURING INSTRUMENTS

a. Strain Measurements.—At first vibrating-wire extensometers were to be used as in testing the model of Santa Luzia Dam;[23] however, after electrical strain gages proved to be so advantageous, efficient techniques of affixing these gages onto the surface of plaster models were attempted.

A shellac coating applied to the model surface and dried by infrared rays for approximately 30 min was found to be a proper base for fixing the Baldwin strain gages. At the downstream face some additional strain measurements were made by Huggenberger extensometers and these were found to be in complete agreement with those of the electrical strain gages. The latter have the advantage that they can be fixed quickly and used on the upstream face, where it is impossible to use mechanical extensometers if the pressure is applied by a liquid. It was found by tests that the direct influence of hydrostatic pressure on the extensometers can be neglected even for the highest applied pressure.

At first 4-gage rosettes were used and the four strains were always found to be in full agreement with one another, even when the rosette had not been properly fixed. Such agreement was inevitable because the 4 gages were mounted on the same paper base. It was therefore decided to use, instead of rosettes, single extensometers located successively at each point—one horizontal, one vertical, and one at 45° angles to the others. The gages had a 2-cm base. Readings were taken by a Baldwin "scanning recorder," enabling an observation of 48 gages in 1.5 min.

Because it was not possible to fasten the available extensometers on alkathene surfaces, the tests of that model required that special gages be designed and made at the Laboratório. These gages which had a 1-cm base consisted of electrical wire wound on a thin piece of cork, and were fixed to the model surface by melting the alkathene. The gages were calibrated by attaching them to test prisms whose strains were also measured by mechanical and optical extensometers.

b. Deflection Measurements.—Deflections were measured in both models only at the downstream face and by means of mechanical deflectometers (Fig. 6). On the plaster model, radial, tangential, and vertical displacements were measured. However, on the alkathene model, because of its small dimensions, only radial deflections were measured as it was too difficult to observe the others.

4. Results of the Model Tests

a. Plaster-Diatomite Model.—The plaster model was tested under mercury levels at elevations representing 40 m, 50 m, and 55 m. Water El. 55 lies 5 m above the crest of the prototype and corresponds to a flood over the dam. Of the results obtained, only those relating to El. 50 will be considered because the prototype was not loaded above that elevation.

In Fig. 7 are shown details of the model, position of cracks reproducing those developed in the prototype, location of gages, and calculated principal stresses both before and after providing the cracks.

The model was loaded successively as required for 8 readings for each extensometer. The magnitude and direction of the strains were then determined from the average values by means of the corresponding Mohr circles. The principal stresses were computed by Hooke's law and were applied to the prototype according to the similarity relationships. The pressure exerted by the mercury on the upstream face had to be considered in computing the stresses at that face. Considering the test conditions, the value of 2 kg per sq cm was assigned as the upper limit of error in the stress values.

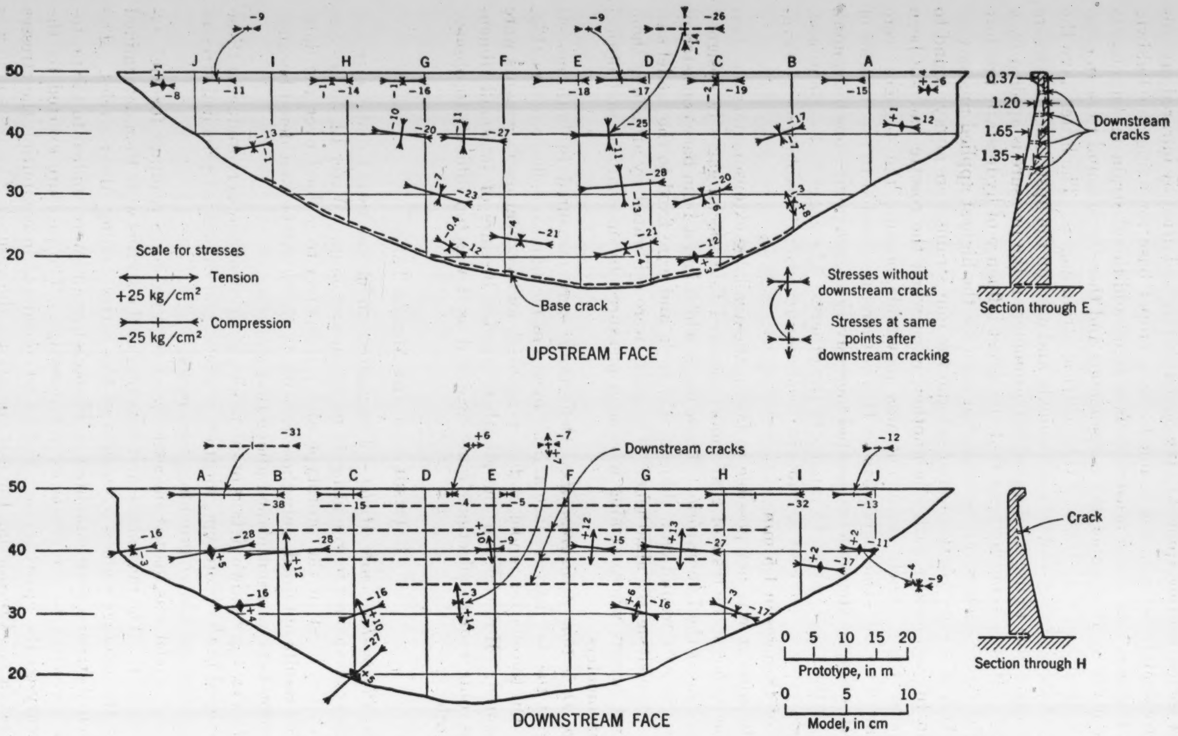
50
40
30
20
J
I
H
G
F
E
D
C
B
A
-9
-9
-26
-14
+1
-8
-11
-14
-16
-18
-17
-2
-19
-15
+4
-6
-13
-1
-10
-20
-11
-27
-25
-11
-17
-1
+1
-12
-28
-13
-20
-6
-3
+8
-7
-23
-0.4
-12
-4
-21
-21
-4
-12
+3
Scale for stresses
Tension
+25 kg/cm²
Compression
-25 kg/cm²
Base crack
UPSTREAM FACE
Stresses without downstream cracks
Stresses at same points after downstream cracking
0.37
1.20
1.65
1.35
Downstream cracks
Section through E
-31
+6
-7
+7
-12
Downstream cracks
-38
-15
-4
-5
-32
-13
-16
-3
-28
+5
-28
+12
+10
-9
+12
-15
+13
-27
+2
-17
+2
-11
4
-9
-16
+4
-16
+10
-27
+5
-3
+14
+6
-16
-3
-17
DOWNSTREAM FACE
0 5 10 15 20
Prototype, in m
0 5 10
Model, in cm
Crack
Section through H

FIG. 7.—STRESSES IN THE PROTOTYPE AS GIVEN BY THE PLASTER MODEL

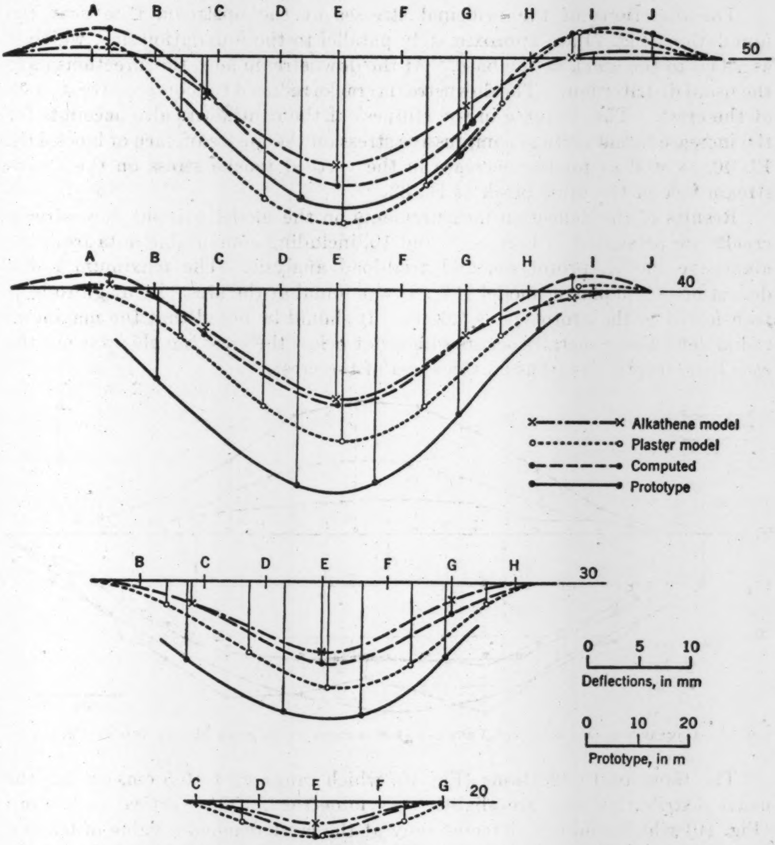

FIG. 8.—COMPARISON OF PROTOTYPE RADIAL DEFLECTIONS BY MODELS, ANALYTICAL CALCULATIONS, AND PROTOTYPE OBSERVATIONS

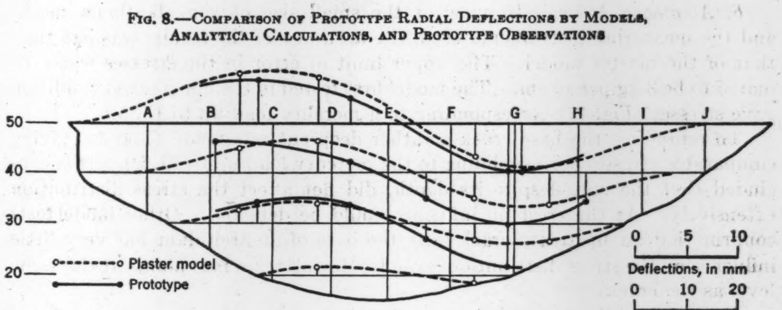

FIG. 9.—COMPARISON OF TANGENTIAL DEFLECTIONS BY PLASTER MODEL AND PROTOTYPE

The directions of the principal stresses at the upstream face near the foundation (Fig. 7) are approximately parallel to the foundation line, which is ascribed to the crack at the base. At the downstream face, the directions have the usual distribution. The downstream cracks reduced the compressive stresses at the crest. The decrease in the stiffness of the cantilevers also accounts for the increase in the vertical compressive stress on the upstream face of block DE, El. 40, as well as for the decrease in the vertical tensile stress on the downstream face of the same block at El. 32.

Results of the deflection measurements on the model without downstream cracks are presented in Figs. 8. 9, and 10, including comparable data from the alkathene model, prototype, and trial-load analysis. The maximum radial deflection of the plaster model (Fig. 8) was found at the crest; its magnitude as transferred to the prototype is 1.6 cm. It should be noted that the maximum radial deflection generally occurs somewhat below the crest but this was not the case here despite the unusual thickness of the crest.

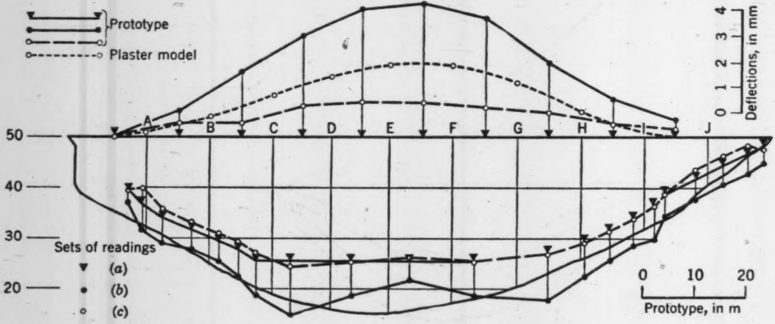

Fig. 10.—Comparison of Prototype Vertical Deflections by Plaster Model and by Prototype

The tangential deflections (Fig. 9), which range up to 0.5 cm, exhibit the usual distribution and are slightly unsymmetrical. The vertical deflections (Fig. 10) which could be detected only at the crest reached a value of 0.3 cm.

b. Alkathene Model.—In view of the small size of the alkathene model and the measuring instruments used, the accuracy of the results was less than that of the plaster model. The upper limit of error in the stresses was estimated to be 3 kg per sq cm. The model first tested in the noncracked condition gave stresses (Fig. 11) corresponding to a mercury load up to El. 50.

To reproduce the base crack a rather deep cut was made (Fig. 12) giving comparable stresses corresponding to the mercury load up to El. 50. It is concluded that the cut, despite its depth, did not affect the stress distribution extensively. At the crest no influence could be detected. Other model tests confirm that an upstream crack near the base of an arch dam has very little influence on the stress distribution, even for downstream face points at the same level as the crack.

As a result of the cut, an increase in both vertical and horizontal compressive stresses was found at the upstream face between El. 30 and El. 40—that is, at the middle part. The maximum compressive stress increased from 24 kg per sq cm to 29 kg per sq cm. At the lower part of the downstream face there is also some stress increase, with a maximum at El. 20 near the foundation. There the maximum compressive stresses increased by not more than 6 kg per sq cm, despite the nearby cut. At the base of the downstream face the cut was found to cause a slight decrease in both compressive stresses. Such a decrease does not appear possible; hence, by attributing it to some lack of accuracy in these tests, it can be concluded that there is practically no change in the stresses. The increase in the vertical stresses at both faces of the crown (DE block) at the middle part should be noted; it results from restraint lessened at the base of the cantilevers.

At its lower upstream part the crackless model exhibits rather high tensile stresses up to 25 kg per sq cm. The compressive stresses due to the dead weight of the prototype, as will be shown in the analytical studies, are only 10 kg per sq cm. The prototype would therefore be subjected to a tensile stress of 15 kg per sq cm which could cause an upstream crack at the base.

As a rule, comparison of the stresses as determined by the plaster model and the alkathene model leads to fairly good agreement except for downstream points near the right abutment. Such deviations are ascribed to a faulty bond at the abutment of the plaster model which had been molded in two steps to simplify the construction.

Recognizing the degree of accuracy of the measurements, such agreement shows that Poisson's ratio can be regarded as not having significant influences. The alkathene model generally exhibited higher values of the second principal stresses near the foundation, especially at its lower part; these stresses were compressive on the downstream face and tensile on the upstream (model in noncracked condition). Such deviations are probably due to the high Poisson ratio of alkathene, whose effect becomes more important at the foundation.

The radial deflections were measured on the model before and after making the upstream cut at the base. The results corresponding to the latter are presented in Fig. 8. The crest deflections are not much affected by the cut at the base, which confirms the similar results concerning the stresses. As anticipated, the cut caused an increase in the deflections below the crest.

5. Analytical Computations

To determine the stresses and displacements analytically both trial-load and independent-arch theories were used. In the trial-load analysis only the radial displacements were considered, and the modulus of elasticity of the foundation was assumed to be the same as that of the dam. Only the hydrostatic pressure was considered because no other type of load was applied to the model nor to the prototype during observation.

The trial-load analysis was computed according to the USBR procedure.[24] Four arches and six cantilevers were considered (Fig. 13). As the arch at El. 50 was assumed to have the thickness of the crest—that is, 3.25 m (Fig. 1)—no allowance for the changing thicknesses of the arches was made in the computations. Likewise, the cantilever, C_1, disregards the thickness of the right abutment ("A" joint, Fig. 1); on the other hand, only the thickness of the left

---

[24] "The Trial-load Method of Analyzing Arch Dams," Boulder Canyon Project. Final Reports, *Bulletin 1*, Bureau of Reclamation, U. S. Dept. of the Interior, Denver, Colo.

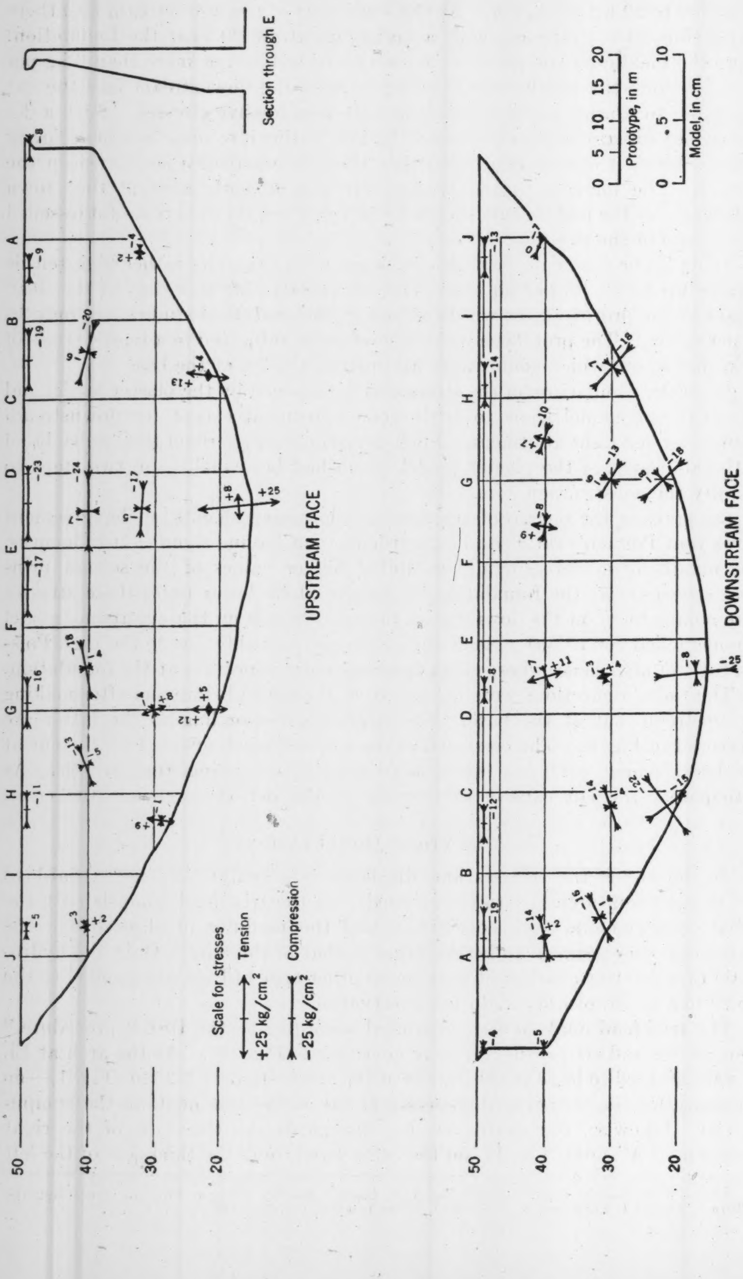
Section through E
UPSTREAM FACE
DOWNSTREAM FACE
A
B
C
D
E
F
G
H
I
J
50
40
30
20
Scale for stresses
+25 kg/cm²
Tension
−25 kg/cm²
Compression
Prototype, in m
0 5 10 15 20
Model, in cm
0 .5 10
−8
−9
−4
+2
−19
−20
−9
+13
+4
−23
−24
−17
−5
−7
+8
+25
−17
−18
−4
−16
−4
+8
+5
+12
−13
−5
−11
−1
+6
−5
−3
+2
−13
−7
−18
−14
−10
−13
−18
−8
+6
−8
−7
+11
−3
+4
−8
−25
−14
−12
−15
−16
−19
−14
+2
−4
−5

FIG. 11.—PROTOTYPE STRESSES FROM THE ALKATHENE MODEL BEFORE CRACKING

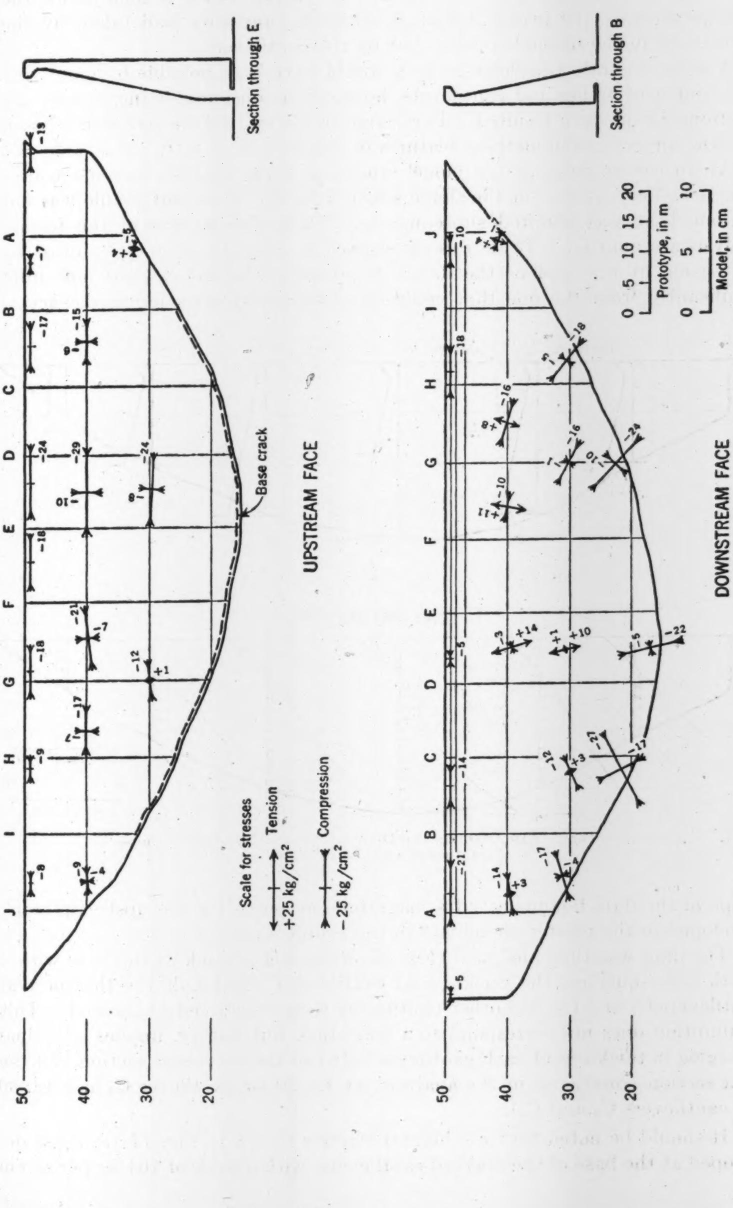
UPSTREAM FACE
DOWNSTREAM FACE
Section through E
Section through B
Base crack
Scale for stresses
+25 kg/cm2
Tension
−25 kg/cm2
Compression
Prototype, in m
0 5 10 15 20
Model, in cm
0 5 10
A B C D E F G H I J
50 40 30 20

FIG. 12.—PROTOTYPE STRESSES FROM THE ALKATHENE MODEL AFTER CRACKING AT BASE

abutment is considered in the cantilever, C_6. In Fig. 13 the shaded part of the total pressure in the load-distribution diagram represents load taken by the arches, and in the unshaded part, that by the cantilevers.

A more accurate trial-load analysis would have been possible by increasing the number of arches and cantilevers, however, a considerable increase in calculations would have resulted. Particular arches and cantilevers were chosen to allow for the unsymmetrical features of the dam.

At an earlier stage of the model studies a stress analysis was made in a noncracked condition, but the shape selected for the abutment profile was not the one that was adopted subsequently. Thus, the records of the former analysis are omitted. These records showed a vertical tensile stress of 38 kg per sq cm at the heel of the dam. Supposedly this stress does not differ significantly from the one that could be obtained by considering the actual shape of the dam boundary. Its magnitude accounts for the upstream crack developed in the plaster model and in the prototype.

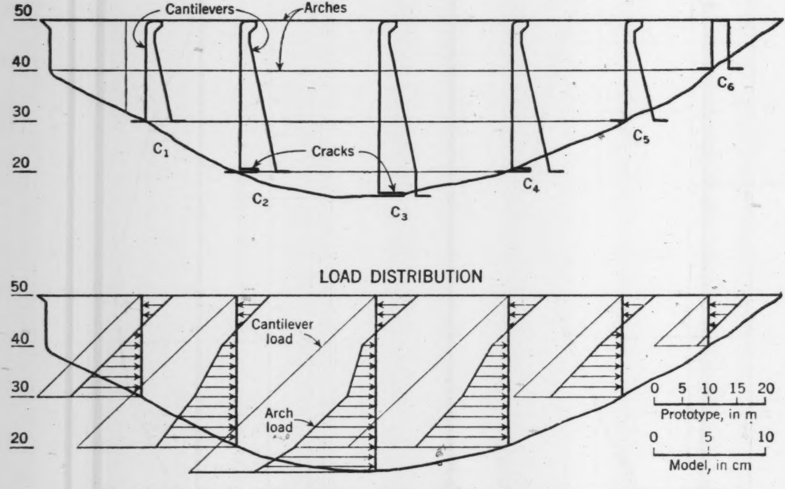

FIG. 13.—TRIAL-LOAD ANALYSIS AND DISTRIBUTION OF HYDROSTATIC PRESSURE ON ARCHES AND CANTILEVERS

The dam was then analyzed (Fig. 13) assuming a crack at the base with a depth three-quarters the thickness at cantilever C_3 and half the thickness at cantilevers C_2 and C_4; the other cantilevers were considered uncracked. This assumption does not correspond to a true crack but, rather, implies a gradual changing in thickness of each cantilever between the decreased section and the next section considered in the analysis (at El. 20 for cantilever C_3 and El. 30 for cantilevers C_2 and C_4).

It should be noted that the highest stresses shown in Fig. 14 are those developed at the base of the cracked cantilevers, with a peak of 104 kg per sq cm

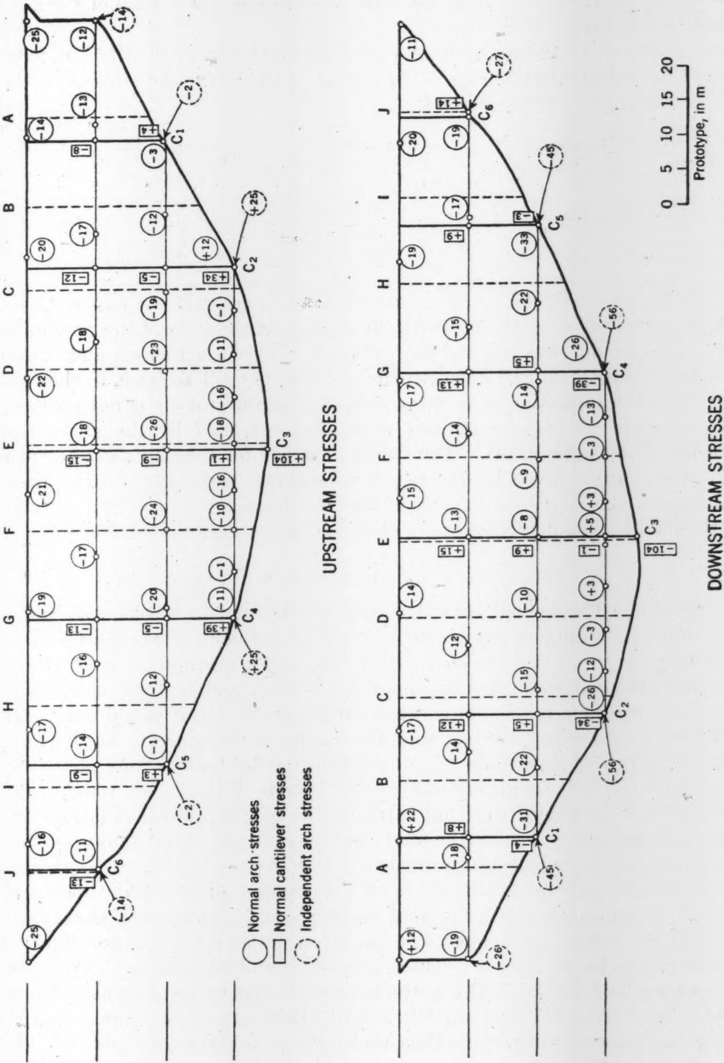
UPSTREAM STRESSES
DOWNSTREAM STRESSES
A
B
C
D
E
F
G
H
I
J
C1
C2
C3
C4
C5
C6
50
40
30
20
Normal arch stresses
Normal cantilever stresses
Independent arch stresses
0
5
10
15
20
Prototype, in m
+104
-104

FIG. 14.—PROTOTYPE STRESSES FROM TRIAL-LOAD ANALYSIS, IN KILOGRAMS PER SQUARE CENTIMETER

at the crown cantilever. The stresses are much lower at the base of the noncracked cantilevers.

The dead-weight stresses were computed as usual by assuming the dam to be divided into independent blocks. The values obtained for the stresses at the crown cantilever, C_3, are as follows:

Elevation (m)	Upstream face (kg per sq cm)	Downstream face (kg per sq cm)
40	3	1
30	6	1
20	8	1
15	10	2

If the crown cantilever, C_3, is assumed to have a crack at the base of three-quarters of its thickness, the dead-weight stresses at the ends of the remaining plain section would have reached the values of −308 kg per sq cm and + 260 kg per sq cm upstream and downstream, respectively. This leads to the conclusion that the formation of so deep a crack in the prototype is not possible.

To compare results, the stresses were also computed by the method of independent arches (Fig. 14). The values obtained for the abutment sections are far above those given by the trial-load analysis, especially on the downstream face. Radial displacements, which have been determined by assuming that the dam has an upstream crack (Fig. 8), have a normal distribution.

6. OBSERVATION OF THE ACTUAL STRUCTURE

a. General.—The arched cofferdam was constructed in blocks with joints A to J (Fig. 1). Concrete was placed in layers 1.5 m thick. Its cement content was 300 kg per cu m, and the coarse aggregate had a maximum size of 10 cm.

Because the cofferdam was an appurtenant work and in view of the difficulties in its erection, it was not constructed as carefully as it would have been had it been permanent. For example, the quality of the concrete was far from uniform; the rate of concreting was rather irregular (some lifts were poured on others approximately one year old); the concrete surfaces on which fresh concrete was to be placed were not carefully cleaned; and the foundation rock was not grouted. In particular, the joints were cement-grouted without pressure because no joint seals had been provided.

A period of high inflow provided an opportunity of filling the reservoir, impounding about 25×10^6 cu m of water in two days. On February 9, 1950, at 2 p.m. (stage *a*), the gates at the diversion tunnel inlet were shut and water started to be impounded. On February 11, at 2 p.m. (stage *b*), the water level had reached El. 50. The gates were then opened on February 12, at 10 a.m., the reservoir being completely emptied February 13, at 5 p.m. (stage *c*).

The loading-unloading cycle thus took only four days. In addition, the mean air temperature happened to be practically unchanged and to be the same as the water and concrete during that period—an extremely favorable circumstance.

The instruments for measuring relative and absolute deflections, strains, joint opening, and temperatures (Fig. 15) were placed during and after construction. During the loading and unloading operations and for four more days, readings were taken at every measuring instrument. Air and water temperatures were also recorded.

Properties of the concrete were found by testing prismatic specimens, 20 cm by 20 cm by 60 cm, cast during the construction; concrete cores, 32 cm in diameter; and prisms, 45 cm by 45 cm by 90 cm taken from the dam. The average instantaneous modulus of elasticity, E, as determined from the 20-cm prisms and the concrete cores, was found to be 280,000 kg per sq cm. The prisms were subjected to creep tests, giving E as 260,000 kg per sq cm corresponding to the time during which the prototype had been loaded. The latter value was used in interpreting the data. The average value of Poisson's ratio, found by testing the prismatic specimens, was 0.20.

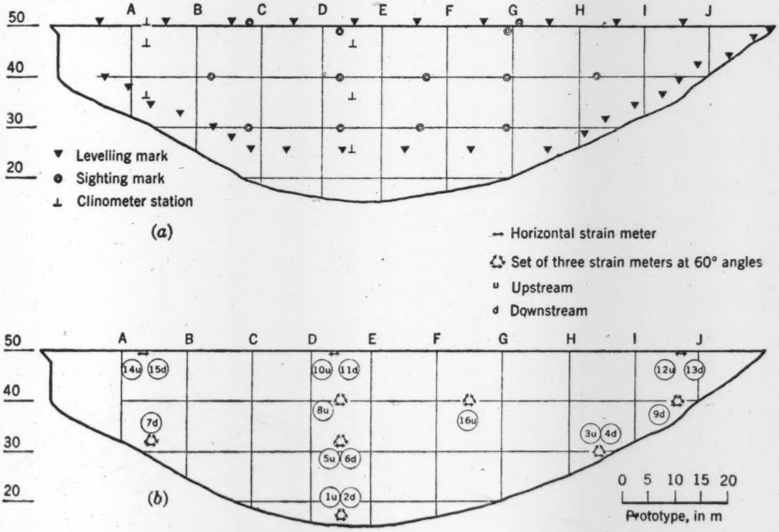
50
40
30
20
A
B
C
D
E
F
G
H
I
J
▼ Levelling mark
● Sighting mark
⊥ Clinometer station
(a)
→ Horizontal strain meter
Set of three strain meters at 60° angles
u Upstream
d Downstream
14u
15d
10u
11d
12u
13d
8u
16u
9d
7d
3u
4d
5u
6d
1u
2d
(b)
0 5 10 15 20
Prototype, in m

FIG. 15.—LOCATION OF (a) THE POINTS OF THE PROTOTYPE OBSERVED BY THE GEODETIC METHOD, PRECISION LEVELING, AND CLINOMETERS AND (b) STRAIN METERS

b. Absolute Deflections.—Absolute deflections were measured by the geodetic method[25] (Fig. 16) using a geodetic theodolite provided with a special centering device and following a plan to measure displacements likely to occur at stations I, II, and III between the abutments, from which the points on the downstream face (Fig. 15) were sighted. On the crest of the dam two stations, IV and V, were erected from which it was possible to sight both the fixed points on the banks and stations I, II, and III below.

The absolute displacements produced at stages *b* and *c* as determined by the geodetic method are given in Fig. 17. The error of the displacements was kept lower than 0.2 mm. This high standard of accuracy was achieved by refinement in the techniques used. The results show that the dam did not recover its initial shape after unloading.

---

[25] "Mesures des deplacements de deux barrages portugais par la méthode trigonométrique," by O. Rodrigues, *Report 64, Transactions*, 3d Cong. on Large Dams, Stockholm, 1948.

To measure promptly some absolute displacements during the loading-unloading cycle, station VI was erected on the right bank (Fig. 16), from which the components of the displacements at right angles to the lines of sight to stations IV and V were measured. The magnitudes of those components were plotted (Fig. 18) as a function of the water elevation, showing close agreement between the points and a nonreversible behavior of the dam. The displacement of both IV and V is 9 mm whereas the comparable displacements by the geodetic method are 7 mm and 10 mm, respectively, which is a good agreement.

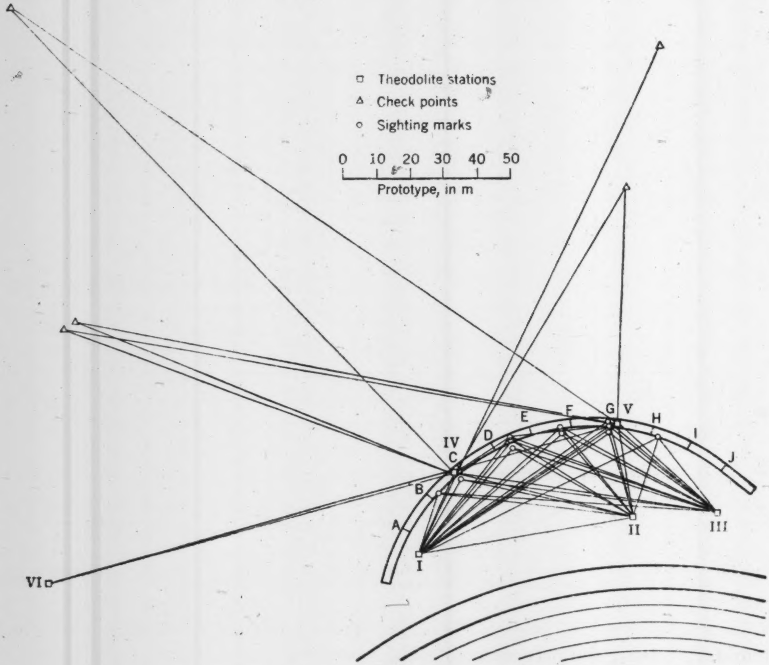

Fig. 16.—Prototype Observations by Geodetic and Slide-Target Methods

From Fig. 17 the diagrams for radial and tangential displacements (Figs. 8 and 9) were drawn. These will be compared (Sect. 8) with those predicted from model tests and analytical computations.

High precision leveling was performed for the points of the dam crest and for the downstream foundation line (Fig. 15), using invar sighting rods. The results appear in Fig. 10, together with the vertical crest deflections as given by the tests on the plaster model. The upward vertical deflections of the crest, which reached 0.5 cm, are not reversible. After unloading, the crest elevation remained higher than before.

Points near the foundation exhibit downward displacements during loading. After unloading they go back to their initial locations with very small deviations

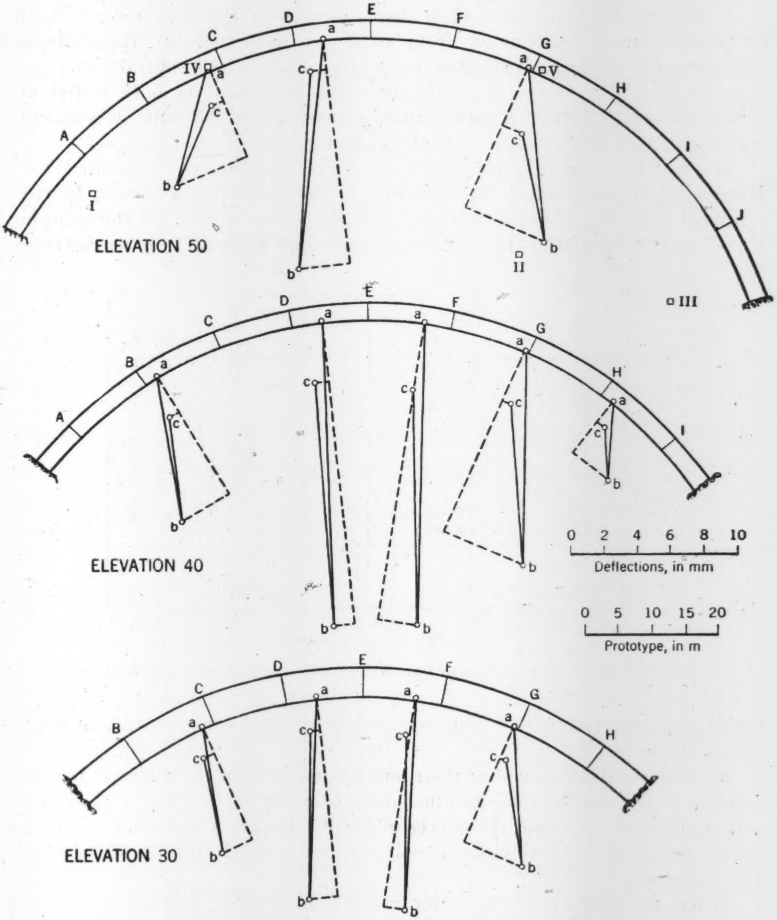
ELEVATION 50
A
B
C
D
E
F
G
H
I
J
IV
V
I
II
III
a
b
c
ELEVATION 40
ELEVATION 30
0 2 4 6 8 10
Deflections, in mm
0 5 10 15 20
Prototype, in m

FIG. 17.—DEFLECTION TRAJECTORIES OF THE POINTS OF THE PROTOTYPE BY THE GEODETIC METHOD

(Fig. 10). These displacements, about 0.2 cm, are probably due to the deflection undergone by the ground under the load of the impounded water. If the value of 200,000 kg per sq cm is assigned as the modulus of elasticity of the foundation, as based on the nature of the strata, it is easily shown by regarding the foundation as a semi-infinite body that the maximum settlement is about 0.2 cm. The fact that the foundation remains free from residual deflections shows that the residual top deflection is probably due to the cracking of the horizontal construction joints and to the uplift pressure exerted by water which percolated into the cracks.

c. Relative Displacements.—The displacements of the dam relative to its foundations were determined from rotations measured by Huggenberger clinometers at the points indicated in Fig. 15, which lie on a central section and on a section near the right abutment. The rotations on both radial and tangential vertical planes were measured at each point. Results were in good agreement with those obtained by the geodetic method.

d. Joint Opening.—The variation in joint opening was measured by a Huggenberger joint meter at the crest and the downstream face at fourteen locations (Fig. 19). Water levels and air-temperature curves are shown in Fig. 19. Minus values (showing that the joint edges approach each other) were found at all the joints, and displacements of about 1 mm occurred at several points of the crest.

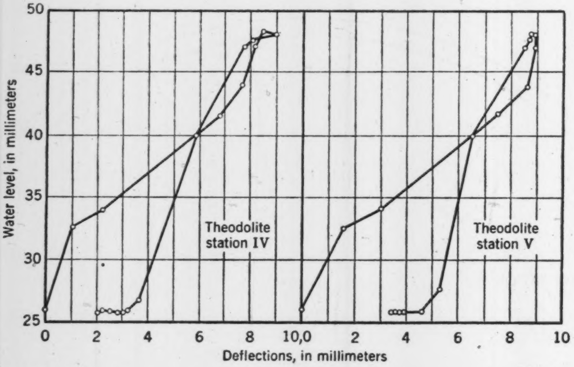

FIG. 18.—DISPLACEMENT UNDERGONE BY CROWN MARKS IV AND V BY THE TARGET METHOD

Some joints did not recover their initial opening after the reservoir had been emptied which explains the residual deflections observed (Fig. 17). For the period of empty reservoir, the curves of Fig. 19 disclose a clear-cut influence of the air temperature on the joint opening; a temperature rise causes a decrease, and conversely.

When the prototype was under water load, leakage was found to occur through vertical joints and through joints between concrete lifts at the middle of the dam. The leakage through the vertical joints is easily understood by reason of the grouting conditions. Leakage through the horizontal joints was found to occur at points where model tests had detected tensile stresses up to 15 kg per sq cm; these stresses were not balanced by the dead weight which produces compressive stresses up to 1 kg per sq cm only.

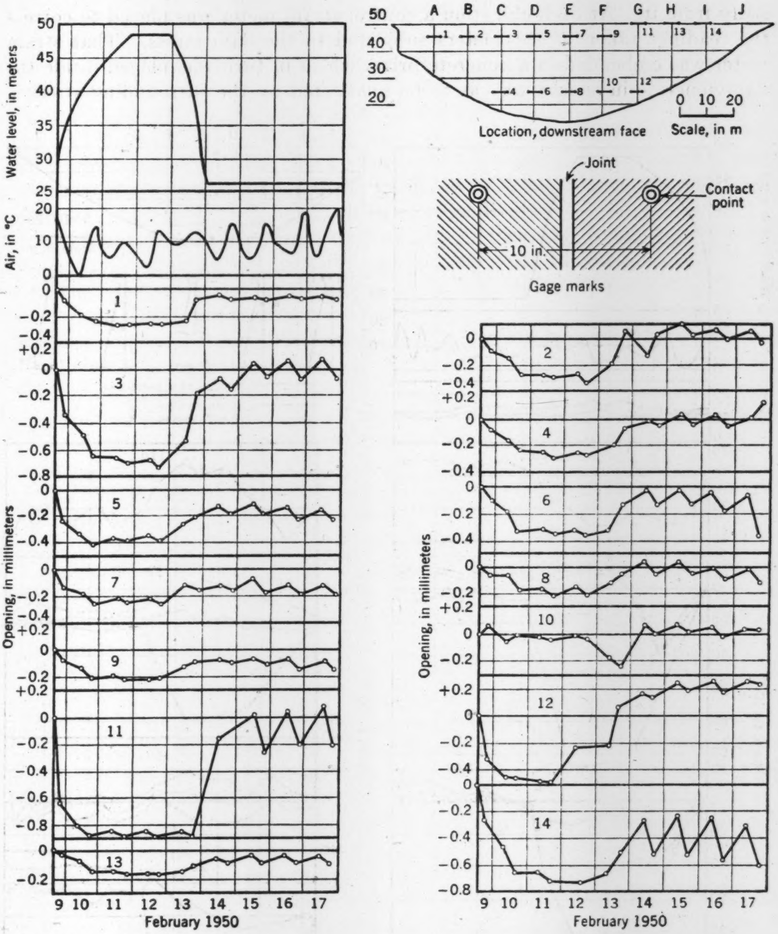

Fig. 19.—Joint-Opening Diagram of the Prototype

e. Strain Data and Stress Computation.—For measuring strains, use was made of the Coyne vibrating-wire strain meters[26,27,28] located at the 16 points shown in Fig. 15. At each point three strain meters were placed in the form of an equilateral triangle in a plane parallel to the face of the dam and 50 cm

---

[26] "Quelques résultats d'auscultation sonore," by A. Coyne, *Annales de l'Institut Technique du Bâtiment et des Travaux Publics*, July–August, 1948.

[27] "Vibrating-Wire Strain Gauge for Use in Long-Term Tests on Structures," by R. J. Mainstone, *Engineering* (London), 1953, No. 4566, pp. 154–156.

[28] "La Mesure de la déformation des solides," by R. L'Hermite, *Circulaires de l'Institut Technique du Bâtiment et des Travaux Publics*, Series F, No. 37.

away from it. At each elevation a control strain meter was placed to correct the readings taken at the meters subjected to the dam stress. That strain meter was embedded in a concrete prism which in turn was placed inside the dam concrete in such a way as to be unaffected by the surrounding stresses.

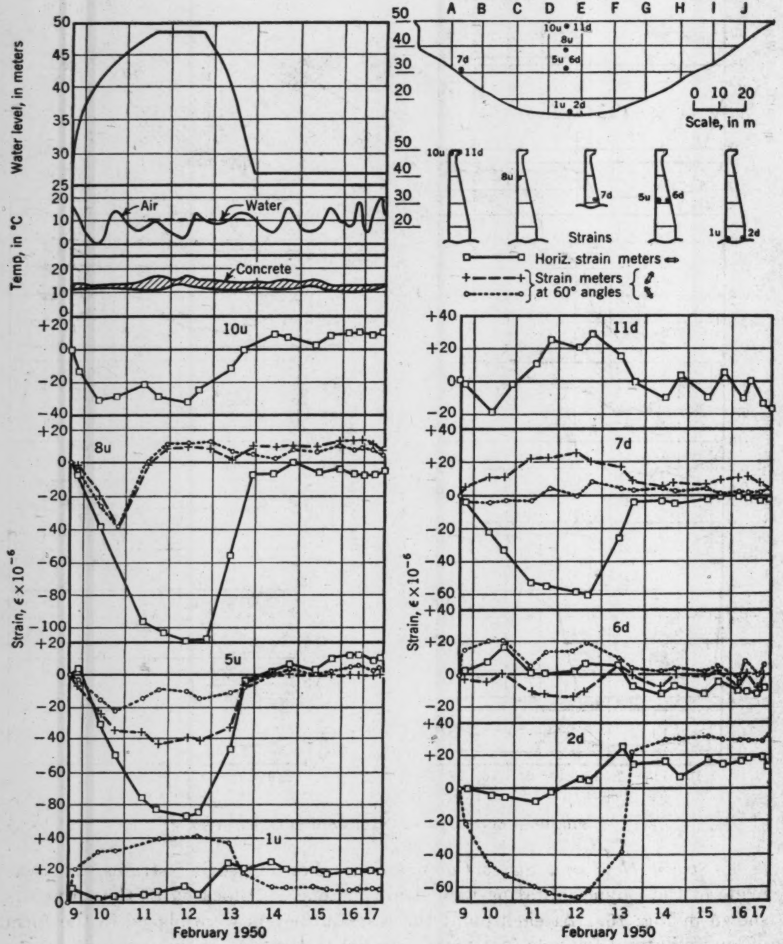

Fig. 20.—Diagram of Strains Measured in the Prototype

The control strain meters can detect the length changes undergone by concrete under changing temperature and moisture content. During the course of the tests, however, those meters detected only very small deviations, showing that the volume changes of the concrete had been due to stresses alone.

At the points of the crest, single horizontal strain meters were used instead of triangular sets. At some points on the downstream face, strain measurements were made by a Huggenberger joint meter, but the results were of no significance because of the large extent to which the strains in concrete near the face are affected by changes in air temperature.

In Fig. 20 the strain diagrams correspond to some of the more representative strain-meter groups. For the concrete temperature a zone is shown whose boundaries correspond to the highest and lowest temperatures recorded at the different strain meters during each stage of loading.

The analysis of the strain diagrams is interesting. Some vary like the water levels whereas others exhibit abnormalities due to cracking.

The crest strain meters, 10u and 11d, at first indicated compression, as expected, but strong disturbances were noticed in both meters after the water surface reached El. 42. From then on, the former indicated fairly constant strain whereas the latter detected tensile stresses even before the water reached its highest elevation.

Such behavior is understood if the results of the plaster model test (Fig. 7) are considered. As long as the downstream region of the model remains uncracked, compressive stress is induced there; as soon as cracks develop, a stress rearrangement takes place which produces a relief in upstream compression and gives rise to downstream tension. The behavior of meter 10u shows that, as expected, the cracks developed gradually as the water rose.

The strain meters of group 8u placed at 60° angles to the horizontal also disclosed a clear-cut influence of the downstream cracks which became noticeable as the water reached El. 44. The horizontal meter exhibited a normal behavior; this is also in full agreement with the observation of the plaster model which had shown that the horizontal stress is not noticeably affected by the cracks (Fig. 7). The regularity exhibited by the meters of group 7d evidences their not having been affected by the crack opening because of their location.

Groups 5u, 6d, and 8u show disturbances as the water reaches El. 44. Likewise, the upstream horizontal meter exhibits a regular behavior, but the downstream one is affected by the cracks. As a rule the disturbances are not so strong as they are in group 8u. This probably means that the cracks were not so deep at El. 30 as at El. 40 where the highest stresses tend to develop, as disclosed by both model tests and analytical computations.

In group 1u the 60° sloping meter, which detects tension, exhibits some disturbance as soon as the water surface reaches El. 32 and, contrary to expectations, shows no important length changes from El. 42 upward. This may be due to the development of a tension crack in the base of the dam. In group 2d the sloping meter exhibits a regular behavior which means that the upstream crack is probably not very deep.

After the dam was unloaded, all the strain meters of groups 1u and 2d disclosed noticeable tensile stresses which were probably due to uneven foundation deformations. Only 2 of the 36 strain meters embedded in the dam (also belonging to groups 1u and 2d) were damaged.

The magnitudes and directions of the principal strains were then determined from the strains measured during stage *b*. The values used for that purpose in meter groups 1u and 2d were the average strains of loading and unloading. The principal stresses induced by a rise of the water up to El. 50 were computed (Fig. 21) assuming the concrete (Sect. 6) to have a modulus of elasticity, $E_p = 260{,}000$ kg per sq cm, and a Poisson ratio, $\mu = 0.2$.

Taking account of the way the experiments were performed, the value of 5×10^{-6} can be assigned as the upper limit of error in the strains, which are obtained as the differences between two readings of the instruments. It is concluded that the upper limit of error affecting the principal stresses is about 3 kg per sq cm. As the modulus of elasticity of the concrete may very often differ by 10% from the average used in the computations, it is estimated that the stresses will be affected by a further error of 10%. The errors to be expected are therefore approximately 3 + 3 = 6 kg per sq cm for prototype stresses of the order of 30 kg per sq cm, 3 + 2 = 5 kg per sq cm for stresses of the order of 20 kg per sq cm, and so on.

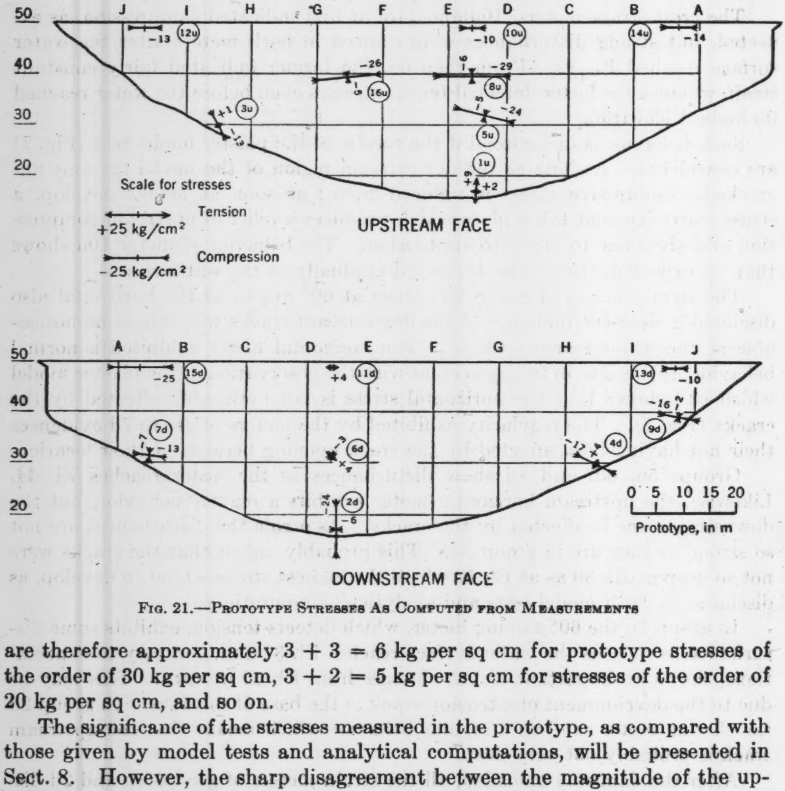
50
40
30
20
J
I
H
G
F
E
D
C
B
A
-13
12u
-10
10u
14u
-14
-26
16u
-29
8u
+1
3u
-13
-24
5u
1u
+2
Scale for stresses
Tension
+25 kg/cm²
Compression
-25 kg/cm²
UPSTREAM FACE
-25
15d
+4
11d
13d
-10
-16
7d
-13
6d
4d
9d
2d
-24
-6
0 5 10 15 20
Prototype, in m
DOWNSTREAM FACE

FIG. 21.—PROTOTYPE STRESSES AS COMPUTED FROM MEASUREMENTS

The significance of the stresses measured in the prototype, as compared with those given by model tests and analytical computations, will be presented in Sect. 8. However, the sharp disagreement between the magnitude of the upstream tensile stress observed at the base of the dam (9 kg per sq cm) and the value derived from the tests of the alkathene model (that is, 25 kg per sq cm) should first be noted. By considering the run of the strain diagram for that region (group 1u, Fig. 20) and the compressive stress of 9 kg per sq cm induced by dead weight at the point under observation, it is concluded that the hydrostatic pressure produced a crack which annulled the dead-weight compression. It cannot, however, be concluded that the concrete did not withstand tensile stresses because, in spite of these not having been detected by the strain diagram (Fig. 20), they might have developed between two consecutive readings.

The agreement between the downstream vertical compressive stresses at the base of the prototype and the homologous ones derived from the alkathene model leads, on the other hand, to the conclusion that the crack is probably not very deep; otherwise, the considerable tension induced by the dead weight at that region of the prototype (Sect. 5) would have caused a strong decrease in the compressive stress.

TABLE 1.—COMPARISON OF STRESSES

Point	Stresses (Kg per Sq Cm)						Deviations from the Prototype Values (Kg per Sq Cm)			
	Prototype	Model Tests			Analytical Computations		Model Tests		Analytical Computations	
		Plaster	Plaster cracked	Alkathene	Trial-load	Independent arches	Plaster cracked	Alkathene	Trial-load	Independent arches
1u	+9	....	....	+22[a]	+38[a]	....	....	....	....	....
	+2	....	....	+7[a]	....	....	....	....	....	....
2d	−6	....	....	−5	....	....	....	−1	....	....
	−24	....	....	−22	....	....	....	−2	....	....
3u	+1	....	....	+8	+3	....	....	−7	−2	....
	−13	....	....	−2	−6	−9	....	−11	−7	−4
4d	+4	−3	....	−4	−3	....	+7[b]	+8	+7	....
	−17	−17	....	−16	−28	−38	0[b]	−1	+11	+21
5u	−5	−11	....	−5	−7	....	+6[b]	0	+2	....
	−24	−25	....	−19	−23	−32	+1[b]	−5	−1	+8
6d	+4	+11	+7	+6	+7	....	−3	−2	−3	....
	−3	−5	−7	−3	−11	−15	+4	0	+8	+12
7d	−7	+5	....	−3	−2	....	−12[b]	−4	−5	....
	−13	−15	....	−15	−26	−38	+2[b]	+2	+13	+25
8u	−6	−8	−14	−6	−10	....	+8	0	+4	....
	−29	−23	−26	−24	−16	−22	−3	−5	−13	−7
9d	−2	+2	−4	+1	+9	....	+2	−3	−11	....
	−16	−11	−9	−7	−18	−24	−7	−9	+2	+8
10u	−10	−15	−7	−23	−21	....	−3	+13[c]	+11[c]	....
11d	+4	−6	−4	−7	−15	....	0	+11[c]	+19[c]	....
12u	−13	−11	−10	−7	−17	....	−3	−6	+4	....
13d	−10	−13	−11	−11	−19	....	+1	+1	+9	....
14u	−14	−18	....	−8	−16	....	+4[b]	−6	+2	....
15d	−25	−34	−28	−20	−21	....	+3	−5	−4	....
16u	−5	−7	....	−3	−13	....	+2[b]	−2	+8	....
	−26	−25	....	−18	−16	−22	−1[b]	−8	−10	−4

[a] Values obtained without a crack at the heel. [b] Values relative to the model without downstream cracks. [c] Values greatly influenced by downstream cracks.

7. STRUCTURAL BEHAVIOR OF THE DAM

Observation of the structure provided a judgment of the behavior of thin arch dams in wide valleys, which was found to be satisfactory except for leakage through both horizontal and vertical joints. Thin dams are bound to leak. In this case, however, such leakage could have been less had the construction been as careful as is usually the case with actual dams.

It is believed that an entirely satisfactory behavior can be achieved for thin arch dams, provided that their shapes are designed so as to avoid high tensile stresses.

8. Comparison of Results

a. Comparative Analysis of Stresses.—Only the stresses for those points observed in the prototype are herein compared. Because these points were 0.50 m from the dam faces, it was necessary to correct the values obtained from both model tests and analytical computations. Interpolation was also necessary for a few points to obtain the values at the observed points of the prototype. The results thus reached are shown in Table 1; the points are marked as in Figs. 15 and 21. Those from the plaster model with downstream cracks are also included.

In the alkathene model the magnitudes considered for evaluation were the average between the values obtained before and after upstream cracking. The reason was that the depth of the prototype crack was unknown and that this crack has little influence at the points whose stresses are compared, except for point 1u.

In Table 1 the values corresponding to the trial-load analysis are those of the arch and cantilever stresses without correction for those points at which the principal directions were not horizontal or vertical. The same applies to the values obtained from the independent arches.

In considering the comparison presented later it is necessary to bear in mind errors that affect the various determinations. The differences between the corresponding prototype and model values are as high as 9 kg per sq cm solely because of the degree of accuracy of the measurements; the differences between prototype and analytical values may, similarly, be up to 6 kg per sq cm.

A short analysis of the stresses at the points mentioned in Table 1 follows:

Point 1u.—The vertical tensile stress of 9 kg per sq cm has already been ascribed to the development of an upstream crack at the base of the dam; that crack released the compressive stress due to the dead weight (Sect. 6).

Point 2d.—There is close agreement between the two principal stresses as measured on the prototype and on the alkathene model (Sect. 6).

Point 3u.—For the highest stress there is a considerable difference between the values measured on the prototype and on the alkathene model. In so far as the observations of both models are concerned, this is the only difference not accounted for by the margin of error in the measurements or by the influence of cracks. The abnormal magnitude and direction of the principal stresses measured on the prototype, together with the agreement between the results of model and trial-load analysis, led to the conclusion that some error developed at this point of the prototype. As it is a point near the foundation, it may be assumed that any disturbance was due to nonuniform rock deformation.

Point 4d.—There is close agreement between prototype and both models in so far as the highest stress is concerned. On the other hand, analytical stress analysis, mainly by independent arches, lead to values lying far above those given by other methods.

Point 5u.—There is a fairly good agreement of all the values of the maximum compressive stress. Only the independent-arch theory leads to a considerably higher value.

Point 6d.—The extent to which the downstream cracking of the plaster model improved the agreement between the values of the tensile stresses—as was to be expected—should be emphasized. Similarly, the agreement between the lower compressive stresses at point 5u would also have been improved by observing the model after cracks had developed.

Points 7d and 8u.—There is again a close agreement between the values of the higher stresses as measured on the prototype and models. The values determined analytically are considerably larger.

Point 9d.—The differences in the maximum stress values, as found in both models, are slightly in excess of the probable errors of the measurements. Particularly noteworthy is the effect of the downstream cracks as observed on the plaster model, which justifies the second stress being a compressive one.

Points 10u and 11d.—A remarkably close agreement is obtained by considering the influence of the downstream cracks. This accounts for the great differences as compared with the alkathene model and trial-load analysis.

Points 12u and 13d.—There is agreement of the values determined by model tests and prototype observation, analytical methods having led to a rather higher value for point 13d.

Points 14u and 15d.—All the values are found to agree fairly closely.

Point 16u.—There is a fairly good agreement between prototype and model stresses whereas the trial-load analysis gives a lower value for the highest stress.

From the foregoing some general conclusions can be drawn. Considering first the absolute values of the maximum principal stresses at each point, the differences between the prototype and both models can be accounted for (except for point 3u) by the margin of error; in other words, the structural behavior as predicted by model testing closely agrees with the actual behavior of the prototype. It should be particularly noted that point 3u as well as point 9d, for which the differences encountered were a little too high, is located near the foundation where disturbances are likely to occur.

The situation is quite different for the maximum stresses by the trial-load analysis. There are a number of points (4d, 6d, 7d, 8u, 13d, and 16u) at which considerably greater differences were found than are accounted for by the observation error. For point 8u, at which the highest prototype compressive stress (namely, 29 kg per sq cm) was measured, the trial-load analysis gives slightly more than half—that is, 16 kg per sq cm—whereas it yields approximately double the stress for point 7d. Similar comparisons have not, as a rule, disclosed such marked inequalities. In this case the exceptional rigidity of the crown and the dissymmetry of the dam must have contributed to these discrepancies.

Consideration of a larger number of arches and cantilevers, as well as of the tangential and twist adjustments, would have given better results. However, the amount of work entailed would have been unfeasible because of the cost and time involved.

Among the values given by the trial-load analysis, reference should be made to the ones at the base of the cantilevers which were assumed to be cracked (Fig. 14). In fact, they are higher than those given by the alkathene model, especially for the crown cantilever (Fig. 12). Other model tests have shown that such a gradual change in the thickness, as considered in the trial-load analysis with cracked cantilevers, entails a significant rearrangement of the stresses in the dam. However, the actual stresses in the downstream part of the cracked sections are not so high as those computed analytically.

The method of independent arches leads to much higher values, sometimes more than twice those observed in the prototype at most points. An exception is the point of maximum compression, 8u, for which a lower stress is obtained by that method.

In so far as the minimum principal stresses, in absolute value, at each point are concerned, the model tests are found to yield rather important discrepancies, especially if account is taken of the small magnitude of those stresses. As in the case of the maximum stresses, the greatest discrepancies are observed at points in the vicinity of the foundation (4d and 7d). It is easily understood that the main effect of the irregular cracking of the rock may be a disturbance of the minimum principal stress because its direction is roughly parallel to the foundation surface. The trial-load analysis also leads to unsatisfactory values of the minimum stresses.

Among the minimum principal stresses, the tensile ones are worthy of note. It was seen, however, that the errors affecting the measurements do not enable any conclusion to be drawn as to the extent to which models or analytical computations are dependable for that purpose.

b. Comparison of Deflections.—The radial deflections observed at the prototype and in the model tests are presented in Fig. 8, together with those computed by trial-load analysis.

At El. 30 and El. 40 the deflections observed at the prototype are larger than those given by both model tests and trial-load analysis. The condition is quite different at the crest because the prototype deflections here are even smaller than those given by the plaster model. The large deflections at El. 30 and El. 40 are due to downstream horizontal cracks and to tightening of vertical joints (Sect. 6). The horizontal cracks, which entail a decrease in cantilever effect, contributed to the decrease of the crest deflection.

The deflections given by the alkathene model were found to be smaller at every elevation. Moreover, the deflection diagrams exhibit a different appearance near the abutments at El. 40 and El. 50. The tangential deflections measured at the prototype and at the plaster model (Fig. 9) are in reasonable agreement in their general appearance. The prototype gave higher values which were surely due to the tightening of the vertical joints. The vertical deflections at the prototype crest are larger than those obtained from the measurements on the plaster model (Fig. 10); the reasons have been explained previously.

9. CONCLUSIONS

The most remarkable result achieved in these investigations is the evidence of close agreement between the values of the maximum principal stresses at each point as observed on the prototype and on both models (Sect. 8). On the other hand, the trial-load analysis led to stresses differing considerably from those developed in the prototype, and the analytical method of independent arches gave results that are not to be accepted at all.

In view of the agreement between prototype and models, it may be concluded that the dam as a whole behaved as a continuous solid body, despite extensive cracking and percolation of water through the cracks. This conclusion is regarded as very significant because the observation of some similar structures could wrongly lead to the assumption that a dam behaves as a heap of concrete blocks rather than a continuous solid. Although the stress distribution may become irregular near the joints, such a lack of uniformity did not affect the stresses in the central part of the blocks, in which the strain meters were located. No failure was observed near the joints, which would have occurred had there been important stress concentrations.

The strong influence exerted by the horizontal downstream cracks on the state of stress at the crest must be emphasized. It was not until such cracks had been cut in one of the models that an agreement with the prototype could be achieved.

The tests performed on one of the models, together with those on models of other dams, indicate that, contrary to the general assumption, an upstream crack in the base of the dam does not change the state of stress even though it affects an important part of the dam thickness. This conclusion should be considered when judging the tensile stresses computed in most cases at the upstream part of the base of arch dams, even if compression due to dead weight is considered.

In so far as the minimum principal stresses are concerned, no conclusion could be drawn on the suitability of model tests or analytical methods because the accuracy of the measurements was not sufficient in view of the smallness of those stresses. With regard to the maximum as well as the minimum principal stresses, the more significant differences between prototype and model results were observed near the foundation, which discloses the influence of nonuniform deformation and cracking of the rock. Those disturbances are more significant for thin arch structures.

The agreement between the prototype and model deflections was found to be less close than that between the stresses. The deflections are evidently more affected by vertical joint opening, cracking, and foundation conditions.

The more important problems in the technique of model testing are the selection of materials and the measurement of deformations. As far as the materials are concerned, the experience gained in the attempts to improve the procedures leads to the conclusion that plaster-diatomite mixes are most suitable (Sect. 2). They have, however, the drawback of too low a tensile strength, which makes them less suitable when high tensile stresses are expected to develop. Alkathene, as well as other plastics used for model construction, does not have that drawback, but the influence of its high Poisson ratio, which changes from one case to another, has not yet been studied.

Electrical strain gages are best suited to measuring model strains. The observation of the prototype provided evidence of the high standard achieved in measuring strains and deflections. This is clearly seen from the diagrams for the strains as a function of the height of the reservoir (Fig. 20) and for the deflections along the dam (Fig. 17).

The behavior of the dam under load was satisfactory, except for leakage, which would not have occurred had the structure been carefully built and the shape designed to avoid considerable tension. The cracks reveal that it would have been possible to save concrete.

In view of the high standard of accuracy, the rapidity, and the economy achieved in model testing, it is believed that model studies should be made for all except minor projects. The trial-load analysis can be used in principle with any shape and foundation conditions. However, the necessity for reducing costs and time requires simplifications in the number of arches and cantilevers and in adjustments. This leads to results of unknown accuracy, especially with dams exhibiting dissymmetry, irregular foundation lines, heterogeneous foundations, and shape singularities such as cracks, bulky abutments, and spillway openings.

The only way of securing dependable information on the practical use of the analytical methods will be by systematically comparing their results with observations of models and prototypes.

DISCUSSION

Merlin D. Copen[29].—In the paper is reported one of the few available comparisons of model and prototype studies of deformations and stresses in a concrete arch dam. The authors are to be complimented for their lengthy study and for preparing the material.

In view of the obviously careful and detailed efforts expended in obtaining the reported material from the model and prototype, the question arises as to why these results were then compared with an admittedly incomplete and approximate trial-load stress analysis as noted by the statement (Sect. 5): "In the trial-load analysis only the radial displacements were considered * * *." The effects of tangential shear and twist cannot be disregarded if an unbiased comparison of model and analytical methods is to be made. This is illustrated (Fig. 22) by comparing the radial displacement of an arch element (in the proposed Yellowtail Dam in Montana) considering only radial-deflection agreement and the radial displacement including also the effects of tangential shear and twist. In Table 2 is a comparison of arch stresses at the crowns and abutments of horizontal elements in this same dam, showing the effects of tangential shear and twist. Similar effects on stresses in the crown cantilever are illustrated in Table 3. Because principal stresses are not normally computed on the basis of radial displacements only, the effects of tangential shear and twist on them are not available.

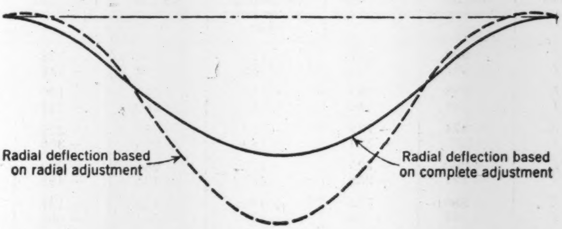
Radial deflection based on radial adjustment
Radial deflection based on complete adjustment

Fig. 22.—Effect of Tangential Shear and Twist on Radial Arch Displacement

The authors further state (Sect. 1):

> "The first approach having led to fairly high tensile stresses at the base of the cantilevers, a more accurate analysis was made on the assumption that the cantilevers cracked at the base."

It would be interesting to know how the extent of cracking was determined because a rather definite knowledge of the tensile stress necessary to produce failure in the concrete is required. Furthermore, the effects of tangential shear and twist often show such a reduction in tensile stress that an assumption of cracking would not be necessary (Table 3).

The authors refer to studies by the USBR on Shasta Dam and by the TVA at Norris, Hiwassee, and Fontana dams. They state (in Sect. 1):

---

[29] Engr., Bureau of Reclamation, U. S. Dept. of the Interior, Denver, Colo.

> "It should be noted, however, that in all those investigations no attempt was made to analyze the stresses by computation or model testing."

The difficulties encountered by foreign engineers in obtaining all available published material in the United States are realized. It is somewhat surprising, however, that the authors were not acquainted with the extensive analytical stress studies made at Shasta Dam. Reference is made here to only one study, but several design studies, based on both the linear and nonlinear assumption, have been made.[30] The results of stress computation on Norris Dam[31] by the USBR and stress analysis by the TVA of Hiwassee Dam[32] may also be obtained.

TABLE 2.—EFFECT OF TANGENTIAL SHEAR AND TWIST ON ARCH STRESSES[a] AT CROWN AND ABUTMENT SECTIONS OF YELLOWTAIL DAM

El.	Face of arch[b]	CROWN OF ARCH			ABUTMENT OF ARCH		
		Radial adjustment	Complete adjustment	Effect of tangential shear and twist	Radial adjustment	Complete adjustment	Effect of tangential shear and twist
3660	*E*	− 622	− 497	+ 125	− 543	− 158	+ 385
	I	− 262	− 350	− 88	− 342	− 138	+ 204
3600	*E*	− 793	− 685	+ 108	− 443	− 139	+ 304
	I	− 192	− 340	− 148	− 250	− 317	− 67
3550	*E*	− 874	− 732	+ 142	− 386	− 225	+ 161
	I	−135	− 324	− 189	− 295	− 366	− 71
3500	*E*	− 900	− 725	+ 175	− 284	− 202	+ 82
	I	− 121	− 258	− 137	− 435	− 488	− 53
3450	*E*	− 886	− 705	+ 181	− 135	− 137	− 2
	I	− 61	− 198	− 137	− 551	− 566	− 15
3400	*E*	− 832	− 666	+ 166	+ 15	− 104	− 119
	I	− 58	− 101	− 43	− 675	− 691	− 16
3350	*E*	− 765	− 568	+ 197	+ 106	− 42	− 148
	I	+ 2	− 93	− 95	− 717	− 778	− 61
3300	*E*	− 650	− 521	+ 129	+ 114	+ 4	− 110
	I	+ 44	− 41	− 85	− 619	− 696	− 77
3250	*E*	− 511	− 416	+ 95	+ 97	− 21	− 118
	I	+ 49	− 5	− 54	− 504	− 520	− 16
3200	*E*	− 377	− 277	+ 100	+ 30	− 149	− 179
	I	− 18	− 17	+ 1	− 383	− 413	− 30

[a] All stresses are in pounds per square inch. [b] *E* and *I* are the extrados and the intrados of the arch.

The last two paragraphs in the paper express the limitations found for the trial-load method, including the necessity for reducing costs and time.

In view of the fact that the specific time and expenditure of funds required for the model tests are not reported in the paper, it is difficult to understand the first part of this conclusion. In the paper it is stated (Sect. 1): "The investigations were begun in 1947, and their experimental part was completed in 1951." It is further stated (Sect. 2): "A later detailed report is planned to cover all the model tests conducted at the Laboratório during the past eight years." These statements indicate a considerable lapse of time and great expenditure of funds. This makes the criticism of the trial-load method on the basis of time and cost seem a little unnecessary.

---

[30] "Trial-Load Analysis of Nonlinear Stress Changes in Shasta Dam Due to Earthquake Effects," by Fred A. Houck and Donald S. Rand, *Technical Memorandum No. 618*, Bureau of Reclamation, U. S. Dept. of the Interior, Denver, Colo., July 14, 1941.

[31] "Design of Cross Section, Gravity Analyses, and Twist Studies for Norris Dam," by Ivan E. Houk, *Technical Memorandum No. 354*, Bureau of Reclamation, U. S. Dept. of the Interior, Denver, Colo., November 11, 1933.

[32] "A Technical Review of the Hiwassee Project," *Technical Memorandum No. 51*, Tennessee Valley Authority, Knoxville, Tenn., October, 1940.

The USBR with its experience, knowledge, and trained personnel has not found the trial-load analysis to be too time consuming and expensive. On the contrary, the possibility of saving materials by using this analysis in design studies has made the cost become insignificant. From previous experience in numerous stress studies it is possible to base designs of dams on greatly simplified trial-load studies, such as a simple adjustment of radial displacements of the crowns of arches and a crown cantilever. When a design containing the most desirable features—from both structural and economical standpoints—has been determined, a detailed trial-load study is made and any changes found necessary from its results are incorporated in the final design of the dam.

TABLE 3.—EFFECT OF TANGENTIAL SHEAR AND TWIST ON CROWN CANTILVER STRESSES[a] IN YELLOWTAIL DAM

El.	Face of dam[b]	Radial adjustment	Complete adjustment	Effect of tangential shear and twist
3600	U	− 135	− 132	+ 3
	D	+ 29	+ 26	− 3
3550	U	− 199	− 209	− 10
	D	+ 20	+ 30	+ 10
3500	U	− 209	− 241	− 32
	D	− 37	− 2	+ 35
3450	U	− 185	− 250	− 65
	D	− 129	− 58	+ 71
3400	U	− 137	− 243	− 106
	D	− 251	− 130	+ 121
3350	U	− 73	− 225	− 152
	D	− 387	− 212	+ 175
3300	U	− 1	− 196	− 195
	D	− 534	− 309	+ 225
3250	U	+ 80	− 152	− 232
	D	− 693	− 423	+ 270
3200	U	+ 170	− 93	− 263
	D	− 865	− 557	+ 308
3140	U	+ 292	+ 7	− 285
	D	− 1,091	− 755	+ 336

[a] All stresses are in pounds per square inch. [b] U and D are the upstream and downstream faces of the cantilever.

It should be stressed that the greatest value derived from the trial-load method of analysis is not necessarily the final numerical displacements and stresses obtained, but rather the determination by comparative studies of the most economical structure under a given set of conditions. Where the necessary design data are available, the actual time required to make a complete trial-load study, including tangential shear and twist, varies from three to six months depending on the conditions encountered. Generally three men, trained and thoroughly familiar with trial-load analysis, are required.

With the use of modern construction methods and grouting procedures, the objection to "irregular foundation lines" and "heterogeneous foundations" may largely be eliminated by careful excavation and preparation of the abutment and foundation area. Even if adverse conditions are encountered, it is doubtful if the accuracy obtainable from small-scale models is greater than that possible by use of trial-load procedures. In studies completed in the past a large variety of foundation conditions have been met and successfully included in the analysis with very little additional time required. In fact, it is safe to say that any or all of the difficulties mentioned as adding too much time and cost to trial-load studies can and have been included in analyses with little additional effort involved. "Shape singularities such as cracks" may be easily avoided by careful design. In this regard the use of trial-load analysis has definite advantages because, through the use of simplified methods and the application of experience and judgment, areas of tension may be reduced or eliminated without detailed study.

It might also be stated in defense of the trial-load method that the application of dynamic loads, such as earthquake and temperature variations, are easily included whereas such loads are extremely difficult or impossible to handle with any degree of accuracy on models. The authors were fortunate in having an ideal condition where these loads did not create a problem.

The next to the last paragraph is extremely perplexing because the authors are acquainted with the "* * * remarkable investigations of the plaster and rubber models of Hoover Dam * * *."[15] These investigations proved the practical value of trial-load analysis, and from these results it would not appear that such comparisons would have any further value except for unusual and difficult problems.

Commenting on the trial-load method, Von K. Goriupp in an article on the Hierzmann Arch Dam[33] states (as translated):

> "* * * only the analysis for the radial deflections were made. These results when compared with those had by experiment can be considered good in agreement. The deflection and stress diagrams show in both cases the same tendency and their numerical values give for comparisons such as these very satisfactory correspondence."

In view of the very brief evidence presented in this discussion, the exhaustive model tests on Hoover Dam, and the actual measurements of dams in service by the USBR—the conclusions arrived at in the paper regarding the trial-load method of analysis seem to be unjustified. Perhaps a more complete study based on further experience with trial-load analysis would be of value.

A. Warren Simonds,[34] M. ASCE.—The Laboratório has been fortunate in having had the opportunity of collaborating with the Direcção Geral dos Serviços Hidráulicos and the Hidro-Eléctrica do Zêzere in the extensive investigation of an arch dam by model tests, analytical computation, and observation. The opportunity of having a model and prototype available for research is indeed rare, and the results obtained are enlightening. In extremely thin arch dams, cracking of the concrete develops frequently, which complicates the analytical computations and also increases the difficulties in similitude for model tests. The fact that cracks developed in the prototype and were reproduced in the models and the fact that successful strain measurements were made are indications that models may be used advantageously to provide information on the structural behavior of arch dams and the predicted behavior.

---

[33] "Die Berechnung der Gewolbemauer am Hierzmann nach dem Versuchslastverfahren" (Analysis of Hierzmann Arch Dam by the Trial-Load Method), by Von K. Goriupp, *Österreichische Bauzeitschrift* (Vienna), 1950.

[34] Structural Engr., Bureau of Reclamation, U. S. Dept. of the Interior, Denver, Colo.

The tests of both the cofferdam at Castelo do Bode and its model were made under almost ideal conditions. For the prototype, the loading-unloading cycle was made during a fairly short period of time. This minimized the possibility of having the structure affected by temperature changes, changes in the elastic properties, or creep in the concrete. For the model tests, the laboratory conditions could be held constant throughout the test period, thereby eliminating many of the uncertainties traceable to changes in temperature and humidity. By eliminating these changes, simpler interpretation of the test results could be made.

A review of the comparable program for Hoover Dam covering two models and their tests is instructive. It will throw further light on the newer studies detailed in the paper. Prior to the design and construction of Hoover Dam, the USBR undertook an investigation program of structural behavior of arch dams. The USBR contributed to the test program of the Arch Dam Committee of the Engineering Foundation for the Stevenson Creek Dam and subsequently built and tested a model of this dam. This was followed by tests of models of Gibson Dam (in Montana) and Hoover Dam. At the prototype of these two models, extensive programs of structural behavior were undertaken. It should be emphasized that, at the time these investigations were begun (in the late 1920's), the equipment for measuring strains, stresses, and deflections was still in the development stage, and the results obtained were crude as compared with those obtained by the Laboratório which used modern equipment.

As a part of the program of investigating the structural behavior of Hoover Dam, two structural models were built and tested. This program included measurement of deflection in radial and tangential directions, angular displacements, foundation deformation, and measurement of strain. After making these observations, models were analyzed for loading conditions in the laboratory.

Plaster and Celite Model.—The first model of Hoover Dam was a mixture of commercial building plaster and celite (infusorial earth) which was a highly elastic lightweight material. The principal items of structural data and the assumptions for the analysis were as follows:

1. Scale of model, 1 to 240, or 1 in. = 20 ft;
2. Loading fluid: Mercury having a density of 13.6;
3. Weight of plaster-celite material, 42 lb per cu ft;
4. Modulus of elasticity of the plaster and celite material in tension and compression, 90,000 lb per sq in.;

5. Modulus of elasticity of the plaster and celite in shear, 37,500 lb per sq in.;

6. Normal stresses vary as a straight line from the upstream face to the downstream face of the model;

7. Cantilever stresses at the faces of the model acting parallel to the slopes of the faces are equal to the computed vertical stresses multiplied by the squares of the secants of the angles between the faces and the vertical directions;

8. The foundation deformation was adjusted and made to conform to the model measurements; and

9. The concrete support around the plaster-celite base and the support at the downstream side were both assumed to be rigid.

The trial-load method was used in the analysis of this model. Strains, stresses, rotations, and deflections due to the mercury load on the upstream face were determined by the analysis, and because the actual strains and deflections had been measured on the model, the results yielded a comparison between the computed and measured deflections.

For this purpose of the analysis, the model dam was replaced by two systems of elements—a system of vertical cantilevers and a system of horizontal arches. The mercury load was divided between arches and cantilevers and also between equal and opposite tangential and twist loads applied to the two systems in order to establish geometrical continuity throughout the structure. The required loads were gradually determined by trial so that the deflections and rotations in each system would be equal at all conjugate points. Because this satisfied the conditions of geometric continuity, the strains and stresses due to the applied trial loads were computed for both systems of elements.

The mercury load produced movements in radial directions, movements in tangential directions, and rotations in horizontal planes. These movements and rotations were considered, respectively, in the radial, tangential, and twist adjustments. In the radial adjustment, loads necessary to produce radial continuity were applied by trial to the arches and cantilevers; in the tangential adjustment, loads needed to restore tangential continuity were introduced; and in the twist adjustment, loads required to produce the same rotations in the arches and cantilevers were used.

The results of the series of tests on the plaster-celite model indicated that the computed deflections agreed closely with the measured deflections. The results of the strain measurements were not in such close agreement, however, mainly because the available gages for measuring strain were very crude as compared with those available subsequently. The strain measurements were made only on the downstream face of the model because the load was applied by hydrostatic pressure of mercury in a rubber bag braced against the upstream face.

Rubber and Litharge Model.—The second model of Hoover Dam tested was made of a compound of rubber and litharge which had a unit weight of 150 lb per cu ft. Because of its low modulus of elasticity the material could deform readily under hydrostatic pressure of water. Thus, it was possible to have the specific gravities of the model and the prototype the same and also to use the same loading mediums.

The principal items of structural data and the assumptions that were made for the purpose of analysis of this model were as follows:

1. Scale of the model, 1 to 180, or 1 in. = 15 ft;
2. Weight per cubic foot of water, 62.5 lb;
3. Weight per cubic foot of rubber and litharge compound, 150 lb;
4. Average modulus of elasticity in the rubber compound for tension and compression in the cantilevers, 343 lb per sq in.;
5. Average modulus of elasticity of the compound for tension and compression in the arches, 389 lb per sq in.;
6. Average modulus of elasticity of the compound for shear in the cantilevers, 114.33 lb per sq in.;
7. Average modulus of elasticity of the compound for shear in the arches, 129.67 lb per sq in.;
8. Average value of Poisson's ratio, 0.5;
9. Normal arch and cantilever stresses varied as a straight line from the upstream face to the downstream face of the model;
10. The foundation movements were adjusted and made to conform with the model measurements;
11. The concrete testing pit supporting the model and its foundation was assumed to be rigid; and
12. It was assumed that the rubber remained in contact with the concrete of the testing pit at all points.

In the trial-load analysis of this model, it was necessary to assume that the rubber and litharge compound was a homogeneous and isotropic material. It was not an ideal material, however, because it had pronounced directional properties which, in addition to an abnormally large Poisson ratio and a proportionally high tensile strength, made its elastic behavior different from that of concrete. However, it did permit making observations for strains on the upstream face when the model was subjected to water load.

Comparison Studies.—A comparison of the measured and computed deflections for both models showed that the analysis of the models by the trial-load method gave deflections very close to the actual values found from measurements on the models. The computed stresses were in reasonably close agreement with those obtained from the strain measurements on the models. If the improved models of strain gages had been available at the time of these tests, the agreement would probably have been closer.

The concluding step of the investigation of stresses in Hoover Dam has not been completed. Provisions for measuring the deflection and an extensive installation of embedded instruments—strain meters, joint meters, and thermometers—have been made at Hoover Dam for the purpose of observing the structural behavior of the prototype. It is hoped that eventually a series of observations can be made under conditions which will resemble those under which the models were tested—at maximum reservoir level and under uniform temperature conditions. In the prototype the reservoir level has not reached the maximum, and the temperature of the concrete has increased above that which existed at the time the contraction joints in the dam were grouted.

In comparing the stresses obtained from strain measurements at the Castelo do Bode cofferdam with those computed by the trial-load method, the results are in reasonably good agreement considering how the analysis was made. The deflections, however, were not in so close an agreement (as the authors point out) probably because only radial displacements were considered, the arch elements were assumed to be of uniform thickness, and the modulus of elasticity of the foundation was assumed to be the same as that of the dam. It is expected that a closer agreement of stress results would have been obtained if the trial-load analysis had included the effects of the nonuniform thickness of the arch elements and the tangential and twist adjustments. It is also possible that, if the modulus of elasticity of the foundation rock had been different from that which was assumed, it would have affected the computed deflections.

JOE T. RICHARDSON,[35] A. M. ASCE.—The authors have made contributions to the slowly accumulating published results of stress studies of actual, in-service dam structures along with allied model tests. The paper is a splendid presentation of results from several independent measurement sources, and the data are comprehensive and well correlated.

Few persons will probably realize the amount of time represented in these studies. Endless man-hours of work and a large staff are needed to accumulate data from models and prototypes, correlate laboratory studies, compute results for each study, and prepare plotted data—not to mention the time required for the trial-load study and other analytical studies. The organizations represented by these authors are to be complimented for conducting such a program. This summary is one of the first for which measured stress results are shown for an arch dam; it serves to establish, along with analogous gravity dam results,[12] information on which the engineer can gage methods of design.

It is hardly surprising that model and prototype results and the results of trial-load and other analytical studies are not comparable. It must be realized that studies of stress by measurement and by analytical methods are each on a different basis; each reflects the assumptions and conditions for which the particular analysis is made, and thus they cannot be expected to show the same final results. Perhaps the authors should have omitted results from their trial-load and other analytical studies at this time. As no attempt was made to explain the differences existing between these results and those of the model and prototype studies, the comparison of stress as presented is somewhat misleading and is not fair to the trial-load method. The authors indicated that trial-load studies were made only on the basis of a radial adjustment and did not include the effects of tangential shear and twist, as well as varying arch thickness.

In contrast to the procedure in the paper, the USBR practice has been to make an initial study based on radial adjustment and then to complete the study by including the effects of tangential shear and twist. In all cases the varying thickness of the arch is considered. The comparison of an initial and complete trial-load study shows quite different results. The authors' comparison using trial-load results that disregard important factors needs explanation.

---

[35] Engr., Structural Behavior of Concrete Dams, Dams Branch, Commissioner's Office, Bureau of Reclamation, U. S. Dept. of the Interior, Denver, Colo.

Temperatures as affected by factors of progressing construction, as well as by the varying conditions of reservoir, are reflected in the results of instrumental studies. These temperature effects are not easily represented in the analytical studies, and are not represented to the same degree in the model studies. Oftentimes the analytical study represents only stress conditions during a normal or some other fixed operational status for the structure whereas in-service conditions may not ever be comparable because loading, as represented in the analytical study, may not occur on the prototype until it has been in use a number of years. Even then, stress conditions may be entirely different because of the wide divergence in temperature and deflection between actual conditions and those used in design.

The analytical study must assume values for factors such as allowable concrete strength, modulus of elasticity, temperature effect, and Poisson's ratio; oftentimes the study does not recognize the effects of other factors such as concrete growth or shrinkage due to drying, or creep of concrete under sustained load. Likewise, the effect on stress of triaxial loading is not included; on massive volumes of concrete, as confined in a dam, this effect is not too well understood and thus cannot be included in the analytical study. These quantities are more or less automatically introduced—or at least accounted for to some extent—in the measurement studies.

Rock modulus is an uncertain quantity. Although its values for use in analytical studies are determined in the laboratory to the best of the engineer's ability to follow accepted methods, the modulus may often be only relative when thought of from the view of abutment and foundation rock considering the enormous volume of material surrounding a dam and the varying effect the dam and reservoir may have on that foundation rock mass.

In view of all of these factors collectively, it can easily be understood that many designers lose sight of the complex system of variables with which they are dealing in an arch dam and oftentimes are reluctant to accept results of measurement methods of analysis when they are not in agreement with analytical results. Conversely, many research workers do not want to accept results obtained by analytical methods when such results do not check with model and other measurement studies. In general, when a comparison is made, results must be qualified to avoid misleading the reader who may not be familiar with the basis of the study or the method used.

Many designers and researchers believe stress variation on a section of a cantilever or arch is of a linear nature, as expressed by accepted theoretical and mathematical methods. They are unwilling to recognize that variation shown by measured strain is very much nonlinear in nature, not recognizing that stress as well as load is a function of varying temperature. Sometimes, temperature effect on a massive structure is of far greater influence on stress than is load.

Only through results such as these presented in the paper are these facts made known, and only by the continuing joint efforts of engineers engaged on both measurement and analytical programs can sufficient information be accumulated to narrow the gap between design and in-service conditions for a structure. Results of these joint efforts will assure that future as-built structures will operate stresswise as anticipated by the design.

In an analytical study, the resulting stresses are somewhat an average resulting from the combination of loads, moments, shears, and twists. Considering a structure as a series of vertical elements analogous to posts or piling, and computing stress at required horizontal sections will result in an entirely different stress pattern on the vertical plane from that normally used, particularly near the base of the structure. This effect was illustrated in a previous paper[36] and is further strengthened by other similar studies. The results of in-service and trial-load studies show large differences in some cases. This post or piling explanation may partly account for these differences between "observed" and computed stress or "average" stress.

The authors will be interested to learn of the usefulness and reliability of external measurements on an arch dam. In the study of stress from measured strain in Hoover Dam (USBR), the stress trend in both cantilever and arch sections from embedded strain-meter measurements is reflected in the record from the plumb lines located in the elevator shafts and from the precise survey measurements made over the top of the dam and on the downstream face of the dam.

From the program presented in the paper, it is apparent that model and prototype structural studies provide as authentic and useful a source of data for evaluating the behavior of a structure as that provided by analytical studies. Although the trial-load and the independent-arch methods of analysis furnish an excellent beginning, they still do not guarantee that the structure will behave in accord with results of the respective stress studies. Thus, the model and prototype results are valuable in evaluating the analysis and for use as criteria in future structures; in the end, an attempt should be made to tie together the results of all three methods.

The authors' statement regarding behavior measurements at some American dams infers that (in Sect. 1) "* * * in all those investigations no attempt was made to analyze the stresses by computation or model testing."

They are reminded that the USBR structures have been analyzed by one or more methods. In the large concrete-arch gravity dams, analytical studies by one of several methods are made as well as a study of stress by internal and external measurements. In the case of Hoover Dam, the elaborate program of model testing[15, 37] was conducted simultaneously with the trial-load and other analytical studies. It is planned that data on stress from measured strain correlated with measurements of deflections and displacements will be made available.

In the prototype example offered by the authors, the loading-unloading cycle required only 4 days, which is far from the conditions experienced in most service structures. No mention is made regarding the property of creep of concrete under sustained load and its treatment in relation to the prototype study. Thus, it must be assumed during this short loading cycle that, for the purpose of a simple solution, creep may be neglected and only a modulus of elasticity at time of full load be used, with the resulting assumption that stress will follow directly from strain through direct application of Hooke's law.

---

[36] "The Development of Stresses in Shasta Dam," by J. M. Raphael, *Transactions*, ASCE, Vol. 118, 1953, p. 308.

[37] "Model Tests of Arch and Cantilever Elements, Boulder Canyon Project. Final Reports," *Bulletin 6*, Bureau of Reclamation, U. S. Dept. of the Interior, Denver, Colo., 1939.

The ingenious orientation of strain meters in the prototype is noted. Although this orientation is excellent from the economic aspect, it does not afford a method of checking strain at the gage points—which would be the case if a duplicate meter installation were made. Thus, measured strain values must be considered absolute, and strain for directions other than those of the meters must be computed by resolution. Although the authors may have had implicit faith in the reliability of their equipment and the methods used for installation, had any one of a trio failed, the complete trio would have been useless; also, without duplicate meters in each gage direction, there always exists the shadow of doubt regarding readings.

In contrast, the USBR practice provides for duplicate strain meters to be installed in the three major orthogonal planes and for supplementary meters to be placed in several planes at 45° angles with the primary meters. The usual installation includes 12 meters for each group. Thus, the multi-directional system affords three major directional lines of stress from strain at the gage point and, by addition of extra meters in midangle positions, provides the greatest possibility and reliability for stress investigation. This setup assures better compatibility of strain between trios of strain meters having one mutually perpendicular meter and adds to the reliability of results. In the authors' installation no strain meters were placed centrally in the dam, and hence results for stress variation through the section are unknown.

These comments are not to be construed as a critical view of the system used; they are made to emphasize the care and forethought required in planning an installation for reliable results. This comparison further stresses the contrast in practice between methods used for obtaining data in the United States and abroad.

The authors' results should leave little doubt in the mind of the engineer that each of the methods illustrated will serve a definite purpose in relation to dam design. In combination, they will be the criteria by which reliable information can be obtained and in the end afford a means by which that information can be used with a high degree of certainty to ascertain the stress behavior of an arch dam structure.

A. Carvalho Xerez.[38]—The paper is valuable in promoting a better knowledge of the structural behavior of arch dams and of the analytical and experimental methods used for their design. As the authors believe, it was indeed worth while to publish these results. The writer must add that it would be desirable for all laboratories to do the same and thus provide an opportunity for comparing their methods of testing and observation.

Concerning the model investigations, the authors properly conclude in Sect. 2 "* * * that a mix of plaster and diatomite is the best material of those used" mainly because this material has the same Poisson ratio as concrete and therefore the similarity requirements are fulfilled. However, for this same reason, the writer is not in complete agreement with the statement (Sect. 4) that "* * * Poisson's ratio can be regarded as not having significant influences" because he feels that it is very difficult to discuss this influence.

---

[38] Technical Director, Hidro-Eléctrica do Zêzere, Lisbon, Portugal.

The comparison of results presented is interesting, yet it would seem that the authors went too far in their analysis in comparing the stresses at all the observed points of the prototype. To justify the differences between the corresponding prototype and model values, a low degree of accuracy of the measurements had to be accepted and, additionally, some reasons had to be found to explain those differences which exceeded the tolerance. In the writer's opinion, it was enough and more natural only to express "* * * the evidence of close agreement between the values of the maximum principal stresses * * *," as stated at the beginning of Sect. 9.

The comparison between the observed prototype stresses and the analytical results is not significant due to the fact that neither the trial-load analysis with radial adjustments only nor the independent arch method can give true results for this type of dam. The latter method has the great value of simplicity, giving the superior limits of the principal compressive stresses.

Finally, the conclusion that "* * * an upstream crack in the base of the dam does not change the state of stress even though it affects an important part of the dam thickness" is very important. In fact, this conclusion is very helpful for designers of dams.

Manuel Rocha,[39] M. ASCE, **J. Laginha Serafim,**[40] M. ASCE, **António F. da Silveira,**[41] and **José M. Ressurreição Neto.**[42]—The writers are indebted to the discussers for the attention given to their paper. The questions raised by some discussers require further elucidation of certain points which, because of limited space, were not perhaps fully treated in the paper. The need for condensing led to the omission of many aspects and results obtained in the investigations.

From their own experience with the trial-load method the writers know the effect the tangential displacements and rotations have on the reduction of stresses obtained by radial adjustments. The results presented by Mr. Copen in relation to Yellowtail Dam agree fully with what is to be expected from this effect; when the dam supports loads by tangential stresses, it undergoes less radial displacements and therefore the normal stresses in the arches and cantilevers are lower. However, considering only the effect of hydrostatic pressure, the reductions of the maximum normal stresses through the introduction of the tangential shear and twist do not, as a rule, go beyond 30% for either the maximum tensile stresses or the maximum compressive stresses. This fact, which is well established in various USBR technical memoranda, has also been checked from comparisons of results of model studies of Portuguese dams with their trial-load calculations.

In their studies the writers made three simplified trial-load analyses, the first one with uncracked cantilevers. Even though this calculation showed that the dam would crack at the heel, it was made only after the observation of the prototype. This observation led to the decision as to what depth of crack should be considered.

---

[39] Director, National Civ. Eng. Lab., Lisbon, Portugal.

[40] Head, Dams Studies Section, National Civ. Eng. Lab., Lisbon, Portugal.

[41] Asst. Research Engr., National Civ. Eng. Lab., Lisbon, Portugal.

[42] Asst. Research Engr., National Civ. Eng. Lab., Lisbon, Portugal.

Bearing in mind the foregoing, the writers were able to conclude that the stresses determined by a complete calculation of the cracked zones of the dam under study could never give values of the order of those given by the models or observed in the prototype once they differed much more than 30% (see zones at points 1u and 2d). In view of the fact that the trial-load calculation is based on formulas of the strength of materials, it cannot be adequately applied to singular situations which occur, for example, near a crack or a hole.

This is one of the reasons why the writers considered it unnecessary to proceed with a complete trial-load calculation which would undoubtedly be too costly and time consuming because of the cracked cantilevers. In fact, the writers, in an application of the complete trial-load method for another arch dam, took about four times as long with the complete calculation as they did with a calculation with only radial adjustments. At the end they did not consider that the information obtained compensated for the added time.

Mr. Copen states:

> "* * *the greatest value derived from the trial-load method of analysis is not necessarily the final numerical displacements and stresses obtained, but rather the determination by comparative studies of the most economical structure* * *."

This is also an advantage that the writers have found in models because various studies can be made on the same model very economically, such as knowing the influence of a crack or an opening, or studying a thinner dam simply by removing some of the material from the model. It is to be noted too that a model makes it possible to obtain quite easily the stresses for all levels of the reservoir; this is not so easy with the calculations.

The writers would also like to mention that, whereas the analytical calculation of a dam becomes extremely laborious when the arches are not circular and the dam has a double curvature (as is the case of very recent rational designs for cupola dams), model studies are no more difficult in this case than for a dam having a circular cylindrical face and uniform thickness. The cases of dams having four-centered circular arches, or having parabolic or elliptical arches, which have been studied in Portugal, well demonstrated how the trial-load calculation becomes more complicated for these cases.

It should be mentioned here that the dam studied (the Castelo do Bode cofferdam) had arches of constant thickness, and consequently there was no simplification in the calculation of these elements.

When referring to the probable cost of model tests conducted in the Laboratório, Mr. Copen assumes that the tests on the cofferdam lasted without interruption from 1947 to 1951 and also that the expectation (Sect. 2)—"a later detailed report is planned to cover all the model tests conducted at the Laboratório during the past eight years"—refers to the model study of only one dam. However, the tests were not performed continuously, and the eight years' experience refers to various series of studies made on a number of dams.[43]

---

[43] "Arch Dams: Design and Observation of Arch Dams in Portugal," by Manuel Rocha, J. Laginha Serafim, and A. F. da Silveira, *Proceedings Paper 997*, ASCE, June, 1956.

When considering the comparative costs of the complete trial-load analysis and those of model studies, the facilities, the equipment, and the tradition which form the background of the question have to be considered. The establishment of a laboratory such as the one in Portugal, as well as one of an organization like the USBR, is costly. Once the organizations exist it may be cheaper to make model tests than computations, or vice-versa. The only question remaining is that of the scope of either of the methods in resolving the given problems; the advantage of model tests is greater.

With regard to the statement—when there is asymmetry, irregular lines of insertion, heterogeneous foundations, irregularities in shape, cracks, artificial abutments, or spillway openings—the trial-load method becomes very laborious and expensive. Mr. Copen suggests that objections to heterogeneous foundations may largely be eliminated by special preparation of the foundation area and that shape singularities such as cracks may be easily avoided by careful design. The writers, however, are of the opinion that, in spite of the suitable techniques available for foundation treatment, such heterogeneity cannot be avoided and also that, as cracks sometimes occur, it is important to have methods for studying their effects.

It is true that in model tests only the effect of hydrostatic pressure is considered. A comparison of the results of observations with the results of model tests can be made when studies are available, separating the effect of different loadings on the structure. Such studies are possible and are being undertaken by the Laboratório. On the other hand, comparisons made between model results and observations of the structures in which the different effects were separated gave truly remarkable agreement,[43] proving that the disadvantage of the other loadings not being considered in the models is minor. In addition, it should not be forgotten that it is the hydrostatic pressure that stresses the whole mass of the concrete although the temperature in zones covering relatively small volumes can produce high stresses (very much higher than those considered in the classical trial load). This point will be treated subsequently.

Finally, when referring to the calculation methods for arch dams, attention should be drawn to the remarkable British contribution for the resolution of the problem by relaxation methods which is based directly on the theory of elasticity.[44]

Mr. Simonds called special attention to the important model studies of Hoover Dam which undoubtedly were a notable step toward greater knowledge of arch dams. His reminder is very timely even though at Hoover Dam reliable stress measurements on the upstream face were not made because of a lack of adequate equipment. These tests showed that the complete trial-load method is a suitable calculation method for arch gravity dams, but one cannot conclude that it is also valid for thin arch dams. The tests conducted by the Laboratório on Cabril, Salamonde, Caniçada, and Bouçã Dams (in Portugal), all thin arch structures with vertical curvature, showed that in a complete trial-load method the vertical displacements could not be omitted. In these dams the displacements are very important and were not considered in the trial-load method of the USBR.

---

[44] "The Experimental and Mathematical Analysis of Arch Dams, with Special Reference to Dokan," by D. N. Allen, L. Chitty, A. J. S. P. Pippard, and R. T. Severn, *Paper No. 6113*, Inst. C. E., London, January, 1956.

Mr. Richardson makes some very interesting remarks about the influence of certain factors, such as temperature, on the behavior of the dams. Recently it has also been possible to gather enlightening results on this problem from observations on structures in Portugal.[45] The reasons for the differences when comparing the calculations, models, and observations should be considered. It is to be hoped that it will soon be possible to make a useful revision of the design criteria of dams after current studies of measurements in the actual structures have been completed in various countries.

An incomplete statement in the paper led to the criticism of a sentence which did not express the writers' full thought. Of course, they could not forget that the large and important dams of the USBR and of the TVA were the object of careful and detailed calculations during their design. What they meant to say was that, as far as they know, in all those investigations no attempt was made "to compare the observed stresses with stresses obtained for the existing conditions (during the time of observation)" by computation or model testing. They had in mind that it is always necessary to analyze the results obtained by observation by the existing theories and this can only be done by using in the analysis conditions which existed at the time the observations were made. The worst conditions, which are usually those of the design, do not permit this comparison because as in practice they seldom occur.

With regard to mounting strain gages, there has been a great advance in Portugal over the first use of these instruments.[45] The modern technique, one developed by the USBR, is doubtless much better than the one that was used first.

The writers, by comparing results obtained on equal models built of materials having a different Poisson ratio, have not found the great difficulty mentioned by Mr. Xerez in discussing the influence of the ratio. These results supplement the ideas given in the paper because they have shown that the Poisson ratio has an appreciable influence in the stress field of the dam only near the foundations. There the principal maximum stresses increase a little and the minimum ones are absolutely changed.

The statement that the comparison of the values observed on the prototype with the analytical results is not significant because neither the trial-load method with only radial adjustments nor the independent-arch method gives "true results" for this type of dam must be discussed. The calculation methods are, like all theories, only approximate and never exact; theory is not, in itself, nature. The comparison made is considered advantageous because these methods are used for design and it is necessary to show how near the "truth" they may be. It should be noted that it is precisely to this type of dam, more than any other, that they are usually applied.

An analysis of the stresses at all points of the dam was made to see how far the differences could be explained by errors in reading. It was concluded that in many cases the errors were responsible for them.

---

[45] "Measurement of Strains in Portuguese Concrete Dams," by J. Laginha Serafim, Réunion Internationale des Laboratoires d'Essais et de Recherches sur les Matériaux et les Constructions (RILEM)—Symposium on the Observation of Structures, Laboratório Nacional de Engenharia Civil, Lisbon, 1955.

AMERICAN SOCIETY OF CIVIL ENGINEERS
TRANSACTIONS
Founded November 5, 1852

Paper No. 2892

A GENERAL METHOD OF ANALYSIS OF RIGID FRAMES

BY PANAGIOTIS D. MOLIOTIS,[1] M. ASCE

SYNOPSIS

This paper describes a method for analyzing rigid frames by successive approximations. In contrast to the classical method of computation in two steps, this method unifies the steps so that, by new factors of distribution and transmission, a quicker and simpler solution is obtained.

INTRODUCTION

Nomenclature.—The rigid frames that are to be analyzed have straight members with a constant moment of inertia. The members are numbered 1, 2, 3, $\cdots$, i, and the joints are lettered a, b, c, $\cdots$. The bending moments are designated by M; the normal forces by N; the shear forces by Q; and, at the end section of a member, i, adjoining a joint, k, the bending moments, normal forces, and shear forces are termed M_{ki}, N_{ki}, and Q_{ki}, respectively.

These moments, normal forces, and shear forces, when they are considered as exerted by the member, i, on the joint, k (the joint which is assumed to be fully restrained against rotation and displacement), are termed "on-the-joint" moments, normal forces, and shear forces and are indicated by the symbols $\bar{M}_{ki}$, $\bar{N}_{ki}$, and $\bar{Q}_{ki}$. Evidently, the on-the-joint moments are equal and opposite in sign to the fixed-end moments of the members. The sum of the moments and forces exerted on the joint, k, by all the members meeting at k is the "unbalanced moment," $\Sigma\bar{M}_{ki}$, or normal force, $\Sigma\bar{N}_{ki}$, or shear force, $\Sigma\bar{Q}_{ki}$.

It is known that loaded structures undergo elastic deformations, the main characteristics of which are the movements of the joints. These movements are either rotations or displacements. In rigid frames with straight members the deformations caused by normal forces and shear forces are negligible compared with the deformations caused by the bending moments and therefore are neglected. The deformations caused by the bending moments result in inter-

---

NOTE.—Published, essentially as printed here, in October, 1955, as *Proceedings Paper 811*. Positions and titles given are those in effect when the paper was approved for publication in *Transactions*.

[1] Asst. Prof. of Civ. Eng., National Technical Univ., Athens, Greece.

related displacements of the joints. Therefore, the displacement of each joint is not independent of the displacements of other joints.

With the aid of virtual-displacement diagrams, all joint displacements can be expressed as functions of the displacements of certain joints. The number of these fundamental joints gives the degrees of elastic freedom of the frame. If the joints are replaced by hinges, the rigid frame can be converted into a structure which, as a rule, has a certain number of degrees of geometric freedom which can be eliminated by adding some imaginary simple restraints in the form of rollers.

The number of degrees of geometric freedom of the pin-connected structure mentioned herein is the same as the number of degrees of elastic freedom of the original rigid frame. The number of roller restraints that should be added to the nonrigid, pin-connected structure in order to convert it into a rigid structure again gives the number of degrees of elastic freedom of the original rigid frame. Thus, by adding one or more imaginary roller restraints, the degrees of elastic freedom of the rigid frame can be reduced by equal numbers. The introduced imaginary roller restraints are numbered I, II, III, ⋯.

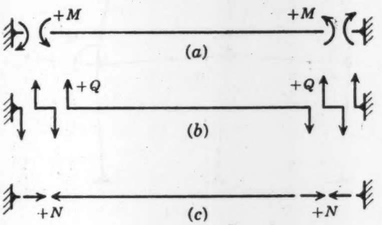

FIG. 1

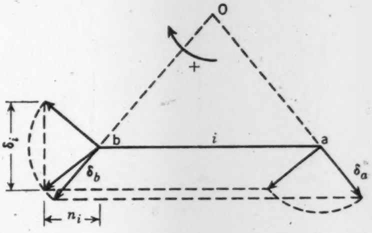

FIG. 2

The term, "group of condisplaced joints (members)," corresponding to a certain joint is taken as all the joints (members) of the frame which will be displaced if the roller restraint is removed. It is possible for joints and members of a frame to belong to two or more groups of condisplaced joints or members.

The following symbols will be used: $\delta_{m\mathrm{I}}$, the displacements of the frame joints; m, the joint; I, the group of condisplaced joints to which the joint, m, belongs; $\delta_{i\mathrm{I}}$, the displacements of the ends of a member, i, relative to each other and perpendicular to the direction of the axes of the member; i, the member; and $\eta_{i\mathrm{I}}$, the component of displacement of a member parallel to its axis, with suffixes, i and I, having the same meaning as heretofore mentioned.

Sign Convention.—A bending moment exerted by a member on a joint is positive when it is clockwise. Conversely, a bending moment at the end sections of a member is positive when counterclockwise (Fig. 1(*a*)). A shear force is positive when an infinite part of the member tends to turn clockwise under the action of the shear forces at its ends (Fig. 1(*b*)); a normal force is positive when it causes tension in the member (Fig. 1(*c*)); the angles of rotation of the joints are positive when clockwise; and the displacements, δ_i and η_i, are positive when they are caused by a clockwise rotation of a member, i, around the instantaneous center, O_i, of the member (Fig. 2).

Stress Analysis of the Frame.—In considering a frame (Fig. 3) loaded by external loads, P, the stress analysis of this frame can be accomplished in two steps by (1) computing the on-the-joint moments produced by the external loads on the members; and (2) computing the end bending moments and the normal and shear forces on the members produced by the unbalanced moments, $\bar{M}_d$, $\bar{M}_e$, $\cdots$, and the forces, $Z^0{}_{\text{I}}$, $Z^0{}_{\text{II}}$, $\cdots$ (Fig. 4).

The moments and forces developed in this step are represented by ϕ_0. The moments, $\bar{M}_d$, $\bar{M}_e$, $\cdots$, are given by

$$\bar{M}_k = \sum\nolimits_i \bar{M}_{ki} + M_k \ldots\ldots\ldots\ldots\ldots\ldots\ldots (1)$$

in which $\bar{M}_k$ is the unbalanced moment at the joint; M_k, an external moment applied to the joint, k (positive when clockwise); and $\sum_i$, the sum of the moments of all the members meeting at k.

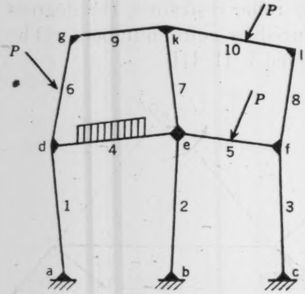

FIG. 3

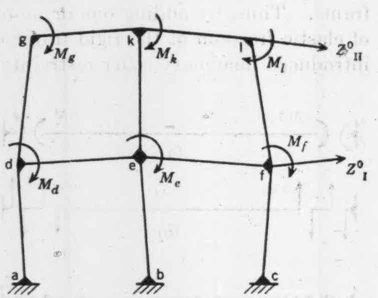

FIG. 4

The forces, $Z^0{}_{\text{I}}$, $Z^0{}_{\text{II}}$, $\cdots$, are equal and opposite to the reactions, $F^0{}_{\text{I}}$, $F^0{}_{\text{II}}$, $\cdots$, of the imaginary roller restraints, which are placed at certain joints of the frame to prevent their displacement. The forces, $Z^0{}_{\text{I}}$, $Z^0{}_{\text{II}}$, $\cdots$, are termed displacers of the frame. The forces, $F^0{}_{\text{I}}$, $F^0{}_{\text{II}}$, $\cdots$, are computed as reactions at the imaginary roller restraints of the corresponding statically determined pin-connected structure loaded by the unbalanced forces, $\bar{P}_d$, $\bar{P}_e$, $\cdots$.

The forces, $F^0{}_{\text{I}}$, $F^0{}_{\text{II}}$, $\cdots$, are termed fixing forces. The forces, $\bar{P}_d$, $\bar{P}_e$, $\cdots$, are the vector resultants of all the normal and shear forces and of any external forces applied to the joint; that is,

$$\bar{P}_k = \sum\nolimits_i \bar{Q}_{ki} + \sum\nolimits_i \bar{N}_{ki} + P_k \ldots\ldots\ldots\ldots\ldots\ldots (2)$$

in which $\bar{Q}_{ki}$ is the on-the-joint, k-shear force from the member, i; $\bar{N}_{ki}$, the on-the-joint, k-normal force from the member, i; and P_k, any external load applied on the joint, k. The summation of Eq. 2 is vectorial.

Solution of (ϕ^0) *by Successive Approximations.*—The solution of (ϕ^0) by successive approximations is performed in two stages: First, by unlocking each joint successively in so far as rotation is concerned (the rest of the joints remaining fixed against rotation and displacement); and, secondly, by setting free each joint (in turn) by removing successively each roller restraint to allow that joint to undergo linear displacement (the rest of the joints remaining fixed against rotation and displacement). When each joint is unlocked, the distribution factors, the carry-over factors, and the unbalanced moments can be used to compute the bending moments at the end sections of the members close to the joint and to those adjoining it.

Setting free each joint to rotate causes new fixing forces, F, on the imaginary roller restraints. These forces can be computed by multiplying the unbalanced moments by a factor. This factor corresponds to each imaginary roller restraint, the dimensions of which are 1/length. These factors are termed the restraining factors of the frame. The corresponding fixing forces are denoted by $F^a{}_{\mathrm{I}}$, $F^a{}_{\mathrm{II}}$, $\cdots$.

After the first unlocking of all the joints to free rotation, all the imaginary roller restraints are removed in turn. All the joints of the frame are then displaced under the action of the forces, Z_{I}, Z_{II}, $\cdots$. It is assumed that during these displacements the joints of the frame remain fixed against rotation.

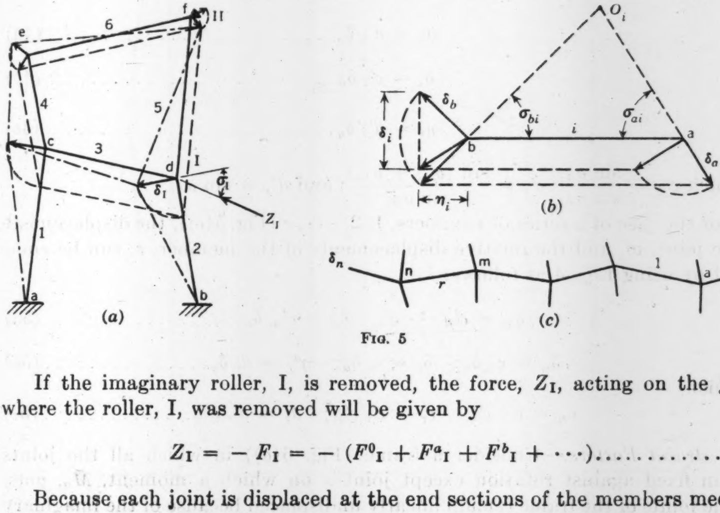

FIG. 5

If the imaginary roller, I, is removed, the force, Z_{I}, acting on the joint where the roller, I, was removed will be given by

$$Z_{\mathrm{I}} = -F_{\mathrm{I}} = -(F^0{}_{\mathrm{I}} + F^a{}_{\mathrm{I}} + F^b{}_{\mathrm{I}} + \cdots) \ldots\ldots\ldots\ldots (3)$$

Because each joint is displaced at the end sections of the members meeting at the considered joint, bending moments are developed which can be determined by multiplying the force, Z_{I}, by a factor corresponding to each member and having the dimension of length. These factors are termed distribution factors due to displacement.

On the remaining imaginary roller restraints, II, III, $\cdots$, because of the removal of the roller at I, new fixing forces, $F^{\mathrm{I}}{}_{\mathrm{II}}$, $F^{\mathrm{I}}{}_{\mathrm{III}}$, $\cdots$, are developed which can be determined by multiplying the force, Z_{I}, by numerical factors termed shear carry-over factors. In the same manner, all the imaginary rollers are removed in turn. The joints are successively unlocked against rotation and are set free against displacement repeatedly until unbalanced moments and forces, Z, are obtained which are negligible.

Diagram of Virtual Displacements.—The determination of the restraining factors, the distribution factors due to displacement, and the shear carry-over factors is given subsequently by the application of the principle of virtual work. Virtual deformations are adopted as finite displacements of the joints and bars produced by the successive removal of the imaginary roller restraints. These displacements are obtained by means of a diagram of virtual displacements (Fig. 5(*a*)).

The results of a displacement, δ_{I}, of the joint, d, from which the roller, I, was removed are used to draw the diagram of virtual displacements. The symbols, (n^{I}), (n^{II}), $\cdots$, will be used to denote diagrams of virtual displacements obtained by the successive removal of each roller restraint.

The displacements of the joints and the relative displacements of the ends of the members as functions of the displacements, δ_{I}, δ_{II}, $\cdots$, are determined with the aid of the instantaneous center of rotation (Fig. 5(*b*)) and with the angles, σ_{ai} and σ_{bi}. If the displacement, δ_a, of the end, *a*, is known, the remaining member displacements may be determined by

$$\delta_b = c'_b\,\delta_a \qquad (4a)$$

$$\delta_i = c'_i\,\delta_a \qquad (4b)$$

and

$$\eta_i = d'_i\,\delta_a \qquad (4c)$$

in which $c'_b = \dfrac{\sin\sigma_{ai}}{\sin\sigma_{bi}}$; $c'_i = \dfrac{\sin(\sigma_{ai} + \sigma_{bi})}{\sin\sigma_{bi}}$; and $d'_i = \sin\sigma_{ai}$.

For the case of a series of members, 1, 2, $\cdots$, *r* (Fig. 5(*c*)), the displacement of the joint, m, and the relative displacements of the member, *r*, can be computed by using Eqs. 4 as follows:

$$\delta_m = c'_b \cdots c'_m \quad \delta_a = \underline{c}'_m\,\delta_a \qquad (5a)$$

$$\delta_n = c_n\,\delta_a; \quad \delta_r = c_r\,\delta_a; \quad \eta^a{}_r = d_r\,\delta_a \qquad (5b)$$

in which

$$c_n = c'_n\,\underline{c}'_m; \quad c_r = c'_r\,\underline{c}'_m; \quad d_r = d'_r\,\underline{c}'_m \qquad (5c)$$

Restraint Factors.—Consider a frame (Fig. 6(*a*)) in which all the joints remain fixed against rotation except joint a on which a moment, $\bar{M}_a$, acts. All the joints of the frame remain linearly undisplaced because of the imaginary roller restraints, I, II, III, $\cdots$. The rotation of joint a causes fixing forces, $F^a{}_{\mathrm{I}}$, $F^a{}_{\mathrm{II}}$, $F^a{}_{\mathrm{III}}$, $\cdots$, at these imaginary rollers. Subsequently, the fixing force, $F^a{}_{\mathrm{I}}$, is determined. The determination of the remaining forces, $F^a{}_{\mathrm{II}}$, $F^a{}_{\mathrm{III}}$, $\cdots$, is performed in the same manner as for $F^a{}_{\mathrm{I}}$.

If the member, *i*, is isolated by two cuts near joints a and c and if the developed internal forces, *M*, *N*, and *Q*, are applied externally (Fig. 6(*b*)), the member, *i*, is in equilibrium under the action of these forces. The distributed moment, $M^a{}_{ai}$, and the carry-over moment, $M^a{}_{ci}$, are determined as functions of the applied moment as follows:

$$M^a{}_{ai} = -K_{ai}\,\bar{M}_a \qquad (6a)$$

and

$$M^a_{ci} = -\mu_i K_{ai} \bar{M}_a \dots\dots\dots\dots\dots\dots\dots (6b)$$

in which K_{ai} is the distribution factor of the member, i, and μ_i denotes the carry-over factor. It is known that the factor, μ_i, in a member with a constant moment of inertia, has the value of $\frac{1}{2}$ if the member, i, has its end fixed at c, but a value of 0 if this end is free to rotate.

The shear force is given by

$$Q^a_i = Q^a_{ai} = Q^a_{ci} = \frac{M^a_{ai} + M^a_{ci}}{l_i} \dots\dots\dots\dots\dots (7a)$$

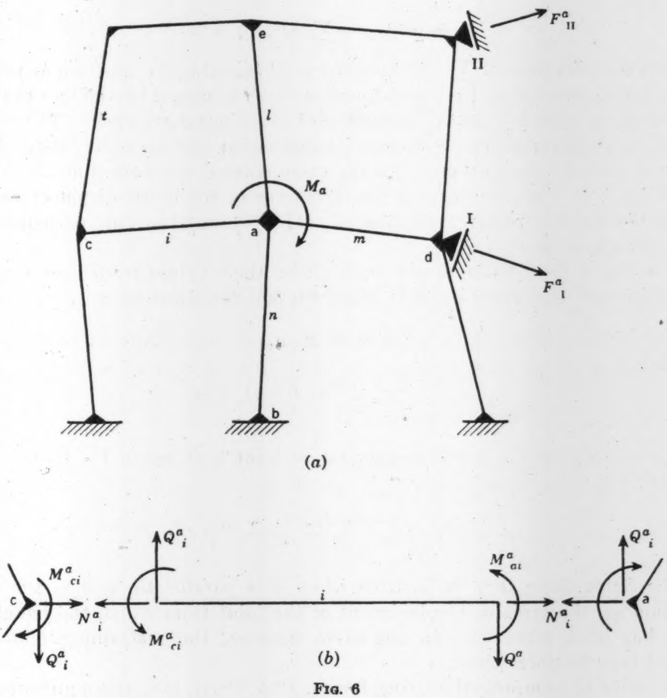

(a)

(b)

FIG. 6

and

$$Q^a_i = -\bar{M}_a \frac{K_{ai}\,(1 + \mu_i)}{l_i} \dots\dots\dots\dots\dots\dots (7b)$$

The normal forces, N^a_i, are not computed herein because they do not appear in the computation of the fixing forces, $F^a_I, \cdots$.

If any of the members, t, of the frame not meeting joint a are isolated (the joints which are met by the frame assumed not to rotate), this member is in equilibrium if it is acted on by the normal forces, $N^a{}_i$. The shear forces, $Q^a{}_i$, are zero.

If all members of the frame are isolated by cuts close to the joints and if the forces, N^a, Q^a, and F^a, are applied externally on the sections of the joints, each joint is in equilibrium under the action of these forces. So long as the systems of forces, N^a, Q^a, and F^a, on each joint are in equilibrium, then, evidently, they are in equilibrium if taken as a whole on all joints.

In order to determine the fixing force, $F^a{}_{\text{I}}$, the equilibrium of that total system of forces is expressed by applying the principle of virtual work for the virtual geometric displacements of the joints and members of the frame belonging to (n^{I}). The equilibrium of this total system of forces, Q^a, N^a, and F^a, is given by

$$F^a{}_{\text{I}}\,\delta_{\text{I}}\cos\sigma_{\text{I}} - \textstyle\sum_i Q^a{}_i\,\delta_{i\text{I}} = 0 \quad\ldots\ldots\ldots\ldots\ldots\ldots (8)$$

in which the summation, $\sum_i$, is extended to all members, i, meeting at joint a. The negative sign before the second part of Eq. 8 is caused by the fact that the positive shear with a positive displacement gives negative work. The forces, $N^a{}_i$, do not appear in Eq. 8 because, being equal and opposite, they cancel the work done by each other. For the same reason, the work done by forces, $F^a{}_{\text{II}}$, $F^a{}_{\text{III}}$, $\cdots$, are zero because the directions of the linear displacements of the joints where the imaginary rollers, II, III, $\cdots$, are placed are perpendicular to the directions of $F^a{}_{\text{II}}$, $F^a{}_{\text{III}}$, $\cdots$.

If in Eq. 8 the $Q^a{}_i$-forces are replaced by their values from Eqs. 7 and if $\delta_{i\text{I}}$ is expressed as a function of δ_{I}, then $F^a{}_{\text{I}}$ is determined from

$$F^a{}_{\text{I}} = -\bar{M}_a\,\sigma_{a\text{I}} \quad\ldots\ldots\ldots\ldots\ldots\ldots (9)$$

in which

$$\sigma_{a\text{I}} = \frac{1}{\cos\sigma_{\text{I}}}\sum_i \frac{c_{i\text{I}}\,K_{ai}\,(1+\mu_i)}{l_i} \quad\ldots\ldots\ldots\ldots\ldots\ldots (10)$$

The factor, $\sigma_{a\text{I}}$, is the restraining factor of joint a of group I. In the case, $\sigma_{\text{I}} = 0°$, Eq. 10 becomes

$$\sigma_{a\text{I}} = \sum_i \frac{c_{i\text{I}}\,K_{ai}\,(1+\mu_i)}{l_i} \quad\ldots\ldots\ldots\ldots\ldots\ldots (11)$$

The fixing force, $F^a{}_{\text{I}}$, is positive when it is parallel to, and in the same direction as, the positive displacement of the joint from which the imaginary roller has been removed. In the same manner, the restraining factors of group I may be determined.

In order to compute the fixing forces, $F^a{}_{\text{II}}$, $F^a{}_{\text{III}}$, $\cdots$, the equilibrium of the system of the forces is expressed, and the principle of the virtual work is applied for the virtual linear finite displacement of (n^{II}), (n^{III}), $\cdots$. Thus, the restraining factors, $\sigma_{a\text{II}}$, $\sigma_{a\text{III}}$, $\cdots$, of groups II, III, $\cdots$ can be computed.

Distribution Factors Due to Displacement.—The frame shown in Fig. 7(*a*) may be considered in which the imaginary roller, I, is removed and the joint, d, is acted on by the force, Z_{I}. In the deformation of the frame due to the action of Z_{I}, it is assumed that all the joints do not rotate. In this case the movements of the joints are linear displacements only.

Because of the relative displacements, δ_{iI}, of the members of the frame, the moments, $M_{ai}, \cdots$, are developed at the end sections of the members. The internal forces of any member, i, are determined by assuming that the member has its ends locked against rotation but that these ends can translate relative to each other in a direction which is perpendicular to the original axis of the member, an amount equal to δ_{iI}. Subsequently, the computation is given of the moments, M_{ai}, as functions of the force, Z_I.

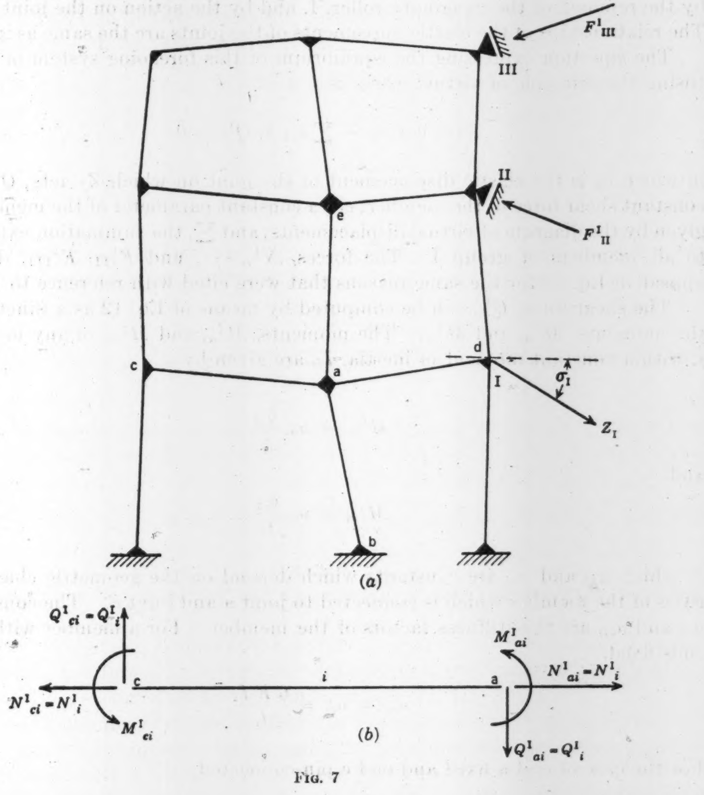

FIG. 7

The member may be isolated by two cuts at its ends and by the developed internal forces (Fig. 7(*b*)) which are applied there. The member, i, is in equilibrium under the action of these external forces. The shear forces, Q^I_{ai} and Q^I_{ci}, can be expressed as functions of the moments, M^I_{ai} and M^I_{ci}, by

$$Q^I_i = Q^I_{ai} = Q^I_{ci} = \frac{M^I_{ai} + M^I_{ci}}{l_i} \quad (12)$$

By cuts at their ends all the members may be isolated, and, on their end sections, may be applied Q^I_i, N^I_i, and Z_I and the fixing forces, F^I_{II}, F^I_{III}, $\cdots$, which are caused at the remaining imaginary roller restraints, II, III, · · ·, by Z_I. Forces Q, N, Z, and F, when acting on each joint, constitute systems of equilibrium and, consequently, when they are taken as a whole they are a system in equilibrium.

The equilibrium of the whole system of forces may be expressed by applying the principle of virtual work. This may be done by taking as the virtual displacements of the joints the actual displacements caused on the locked joints by the removal of the imaginary roller, I, and by the action on the joint of Z_I. The relationships of the elastic movements of the joints are the same as in (n^I).

The equation expressing the equilibrium of this foregoing system of forces (using the principle of virtual work) is

$$Z_\text{I}\, \delta_\text{I} \cos \sigma_\text{I} - \sum c_{i\text{I}}\, \delta_\text{I}\, Q^\text{I}{}_i = 0 \qquad (13)$$

in which δ_I is the elastic displacement of the joint on which Z_I acts; $Q^\text{I}{}_i$, the constant shear force of the member; $c_{i\text{I}}$, a constant parameter of the member, i, given by the diagram of virtual displacements; and $\sum$, the summation extended to all members of group I. The forces, $N^\text{I}{}_i$, · · ·, and $F^\text{I}{}_\text{II}$, $F^\text{I}{}_\text{III}$, do not appear in Eq. 13 for the same reasons that were cited with reference to Eq. 8.

The shear force, $Q^\text{I}{}_i$, can be computed by means of Eq. 12 as a function of the moments, $M^\text{I}{}_{ai}$ and $M^\text{I}{}_{ci}$. The moments, $M^\text{I}{}_{ai}$ and $M^\text{I}{}_{ci}$, of any member, i, with a constant moment of inertia, I_i, are given by

$$M^\text{I}{}_{ai} = u_{ai} \frac{\delta_{i\text{I}}}{l_i} \qquad (14a)$$

and

$$M^\text{I}{}_{ci} = u_{ci} \frac{\delta_{i\text{I}}}{l_i} \qquad (14b)$$

in which u_{ai} and u_{ci} are constants which depend on the geometric characteristics of the member which is connected to joint a and joint c. The constants, u_{ai} and u_{ci}, are the stiffness factors of the member. For a member with both ends fixed,

$$u_{ai} = u_{ci} = \frac{6\, E\, I_i}{l_i} \qquad (15)$$

For the case of end a fixed and end c pin-connected,

$$u_{ai} = \frac{3\, E\, I_i}{l_i}; \quad u_{ci} = 0 \qquad (16)$$

If, in Eq. 12, $M^\text{I}{}_{ai}$ and $M^\text{I}{}_{ci}$ are replaced by their values from Eqs. 14,

$$Q^\text{I}{}_i = \frac{\delta_\text{I}\, (u_{ai} + u_{ci})\, c_{i\text{I}}}{l_i} \qquad (17)$$

If, in Eq. 13, $Q^{\mathrm{I}}{}_i$ is replaced by its value from Eq. 17,

$$\delta_{\mathrm{I}} = Z_{\mathrm{I}} \frac{\cos \sigma_{\mathrm{I}}}{\sum_i \frac{c^2{}_{i\mathrm{I}}}{l^2{}_i} (u_{ai} + u_{ci})} \qquad (18)$$

in which the summation, $\sum_i$, applies to all members, i, of group I.

After the determination of the elastic displacement, δ_{I}, the moment, $M^{\mathrm{I}}{}_{kr}$, at the end section of any member, r, meeting joint k is computed by replacing δ_{I} in Eq. 14 with its value from Eq. 18. Then,

$$M^{\mathrm{I}}{}_{kr} = q^{\mathrm{I}}{}_{kr} Z_{\mathrm{I}} \qquad (19)$$

in which

$$q^{\mathrm{I}}{}_{kr} = \frac{\frac{c_{r\mathrm{I}}}{l_r} u_{kr}}{\sum_i \frac{c^2{}_{i\mathrm{I}}}{l^2{}_i} (u_{ai} + u_{ci})} \cos \sigma_{\mathrm{I}} \qquad (20)$$

The factors, $q^{\mathrm{I}}{}_{kr}$, are termed distribution factors due to displacement. For the case of $\sigma_{\mathrm{I}} = 0°$, Eq. 20 becomes

$$q^{\mathrm{I}}{}_{kr} = \frac{\frac{c_{r\mathrm{I}}}{l_r} u_{kr}}{\sum_i \frac{c^2{}_{i\mathrm{I}}}{l^2{}_i} (u_{ai} + u_{ci})} \qquad (21)$$

If the distribution factors due to displacement of all the members of group I are multiplied by the corresponding fractions, c_r/l_r, their sum is equal to unity; that is,

$$\sum_r q^{\mathrm{I}}{}_{kr} \frac{c_{r\mathrm{I}}}{l_r} = 1 \qquad (22)$$

in which the summation, $\sum_r$, extends to all members of group I. In the same way, one can determine the distribution factors due to displacement of groups II, III, $\cdots$.

Shear Carry-Over Factors.—When the imaginary roller restraint, I, is removed and the force, Z_{I}, is applied at that joint, the forces, $F^{\mathrm{I}}{}_{\mathrm{II}}$, $F^{\mathrm{I}}{}_{\mathrm{III}}$, $\cdots$ (Fig. 7(*a*)), are caused on the remaining rollers, II, III, $\cdots$.

For determining $F^{\mathrm{I}}{}_{\mathrm{II}}$, the equilibrium of the total system of the forces, Q^{I}, N^{I}, Z_{I}, and F^{I}, is expressed by applying the principle of virtual work in which the virtual geometric displacements of the joints and members of the frame are those of (n^{II}). The equation which expresses the equilibrium of the foregoing system of forces and which results from applying the principle of virtual work is

$$F^{\mathrm{I}}{}_{\mathrm{II}} \cos \sigma_{\mathrm{II}}\, \delta_{\mathrm{II}} - \sum_i \delta_{\mathrm{II}}\, c_{i\mathrm{II}}\, Q^{\mathrm{I}}{}_i = 0 \qquad (23)$$

in which δ_{II} is the virtual displacement of the joint at roller II; $c_{i\mathrm{II}}$ is a constant referring to the member, i, of group II; $Q^{\mathrm{I}}{}_i$ is the constant shear force in any member, i; and $\sum_i$ represents the summation extended to all members, i, of group II.

The solution of Eq. 23 results in

$$F^{\mathrm{I}}_{\mathrm{II}} = \frac{\sum_i c_{i\mathrm{II}}\, Q^{\mathrm{I}}_i}{\cos \sigma_{\mathrm{II}}} \quad \text{(24)}$$

The shear force, Q^{I}_i, as a function of the computed moment, is

$$Q^{\mathrm{I}}_i = (\cos \sigma_{\mathrm{I}})\, Z_{\mathrm{I}}\, \frac{q^{\mathrm{I}}_{ai} + q^{\mathrm{I}}_{ci}}{l_i} \quad \text{(25)}$$

If the value of Q^{I}_i in Eq. 25 is substituted into Eq. 24,

$$F^{\mathrm{I}}_{\mathrm{II}} = m^{\mathrm{I}}_{\mathrm{II}}\, Z_{\mathrm{I}} \quad \text{(26)}$$

in which

$$m^{\mathrm{I}}_{\mathrm{II}} = \frac{\cos \sigma_{\mathrm{I}}}{\cos \sigma_{\mathrm{II}}} \sum_i \frac{c_{\mathrm{I\,II}}}{l_i} (q^{\mathrm{I}}_{ai} + q^{\mathrm{I}}_{ci}) \quad \text{(27)}$$

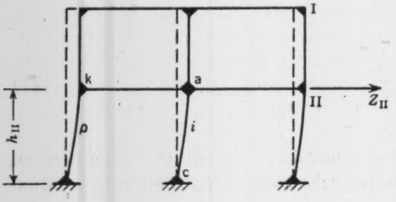

FIG. 8

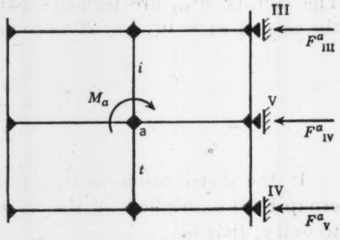

FIG. 9

For the case of angles, $\sigma_{\mathrm{I}} = 0°$ and $\sigma_{\mathrm{II}} = 0°$, Eq. 27 becomes

$$m^{\mathrm{I}}_{\mathrm{II}} = \sum_i \frac{c_{\mathrm{I\,II}}}{l_i} (q^{\mathrm{I}}_{ai} + q^{\mathrm{I}}_{ci}) \quad \text{(28)}$$

The factor, $m^{\mathrm{I}}_{\mathrm{II}}$, is termed the shear carry-over factor.

The forces, $F^{\mathrm{I}}_{\mathrm{III}}, \cdots$, are determined in the same manner by applying the principle of virtual work to virtual displacements of $(n^{\mathrm{III}}), \cdots$.

Rectangular Frames.—The foregoing restraining factors, distribution factors due to displacement, and shear carry-over factors have a simple form in the case of rectangular frames. In drawing the virtual-displacement diagram it is assumed that the section of the frame, above the imaginary roller which has been removed, moves without any elastic deformations (Fig. 8). For the case of a rectangular frame, the displacements, $\delta_{i\mathrm{I}}, \delta_{i\mathrm{II}}, \cdots$, are all equal in the columns and they are all equal to zero in the beams.

Applying the principle of virtual work, the following restraining factors (Fig. 9) are obtained:

$$F^{a}_{\mathrm{III}} = -\,(M_a)\, \sigma_{a\mathrm{III}} \quad \text{(29a)}$$

in which

$$\sigma_{a\mathrm{III}} = \frac{K_{ai}\,(1 + \mu_i)}{l_i} \ldots\ldots\ldots\ldots\ldots\ldots (29b)$$

In computing the forces, $F^a{}_{\mathrm{IV}}$, and in applying the principle of virtual work, it must be remembered that the computed force, $F^a{}_{\mathrm{III}}$, also performs work because of the displacement of the joint on which it acts. Therefore,

$$F^a{}_{\mathrm{IV}} + F^a{}_{\mathrm{III}} - (-M_a)\,\frac{K_{at}\,(1 + \mu_t)}{l_t} = 0 \ldots\ldots\ldots (30)$$

and

$$F^a{}_{\mathrm{IV}} = -\,(M_a)\,\sigma_{a\mathrm{IV}} \ldots\ldots\ldots\ldots\ldots\ldots (31)$$

in which

$$\sigma_{a\mathrm{IV}} = \frac{K_{at}\,(1 + \mu_t)}{l_t} - \frac{K_{ai}\,(1 + \mu_i)}{l_i} \ldots\ldots\ldots\ldots (32a)$$

$$F^a{}_{\mathrm{V}} = -\,(M_a)\,\sigma_{a\mathrm{V}} \ldots\ldots\ldots\ldots\ldots\ldots (32b)$$

and

$$\sigma_{a\mathrm{V}} = -\,\frac{K_{at}\,(1 + \mu_t)}{l_t} \ldots\ldots\ldots\ldots\ldots\ldots (32c)$$

The distribution factors due to displacement take the followimg simpler form (Fig. 8):

$$q^{\mathrm{II}}{}_{kp} = h_{\mathrm{II}}\,\frac{u_{kp}}{\sum\,(u_{ai} + u_{ci})} \ldots\ldots\ldots\ldots\ldots (33)$$

For the case of rectangular frames (Fig. 8), the shear carry-over factor for all stories is constant and equal to 1. Thus,

$$m^{\mathrm{I}}{}_{\mathrm{II}} = M^{\mathrm{II}}{}_{\mathrm{III}} = \cdots = -\,1 \ldots\ldots\ldots\ldots\ldots\ldots (34)$$

Arrangement of Computations.—The computations of the successive approximations can be arranged in tables as the writer has shown. These tables are arranged so that the distribution of the moments at each joint is effected.

Listed at the top of the tables to be cited subsequently are the joints, the members meeting at these joints, the distribution factors, the restraining factors, and the distribution factors due to displacement. The results of the moment distributions are placed in the corresponding columns for the joints.

Following the distribution of moments at each joint, the moments at the end section of each member are totaled; the moments resulting from the distribution are written in a rectangle in the corresponding column so that the distributions may be continuously checked.

The fixing forces, F_{I}, F_{II}, $\cdots$, are in the last columns to the right. After the moment, M, has been distributed at each joint, the moment, $-\,M$, is multiplied by the corresponding restraining factor, σ, for that joint. The results are then written in the columns to the right in which the fixing forces already appear.

Following the distribution at all joints, all the figures in the F_{I}-column are added to obtain the fixing force. This force (with a changed sign) is multiplied first by the factors, q^{I}_{ki}, and are noted in the column corresponding to each joint. Then, the force is multiplied by the factors, $m^{\mathrm{I}}_{\mathrm{II}}$, $m^{\mathrm{I}}_{\mathrm{III}}$, $\cdots$, to determine the fixing forces, $F^{\mathrm{I}}_{\mathrm{II}}$, $F^{\mathrm{I}}_{\mathrm{III}}$, $\cdots$. These products are noted in the corresponding columns for F_{II}, F_{III}, $\cdots$, and the same process is repeated in turn for the remaining fixing forces, F_{II}, F_{III}, $\cdots$.

After all the distributions have been completed, the final moments are obtained by adding the relative moments which are in the rectangles.

CONCLUSIONS

It is felt that the proposed method for computing frames by successive approximations has the following advantages:

1. In some cases the method may be quicker than the method developed by Hardy Cross,[2] Hon. M. ASCE.

2. Depending on the form of the structure and on the material to be used in construction (steel or reinforced concrete), it is possible to determine the number of successive approximations that are necessary so that the grade of accuracy in the computations does not affect the final section dimensions of the structural members.

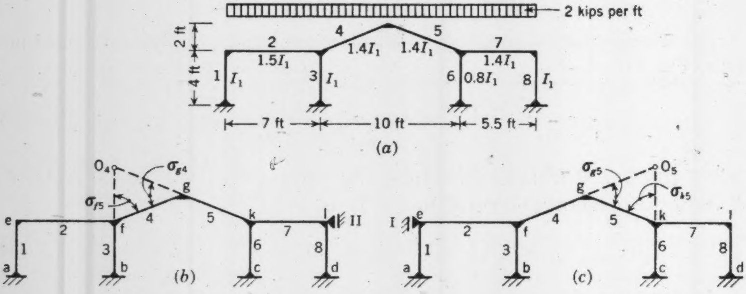

FIG. 10

In the examples cited herein the advantages of this method for solving rigid frames are clearly demonstrated.

Application.—The bending-moment diagram of the frame shown in Fig. 10(*a*) is required. The given conditions are $q = 2.0$ kips per ft; $I_2 = 1.5\, I_1$; $I_3 = I_1$; $I_4 = I_5 = 1.4\, I_1$; $I_6 = 0.8\, I_1$; $I_7 = 1.4\, I_1$; $I_8 = I_1$; $l_1 = l_3 = l_6 = l_8 = 4.00$ ft; $l_2 = 7.00$ ft; $l_4 = l_5 = 5.38$ ft; and $l_7 = 5.50$ ft.

***Diagrams of Virtual Displacements** (Figs. 10(b) and 10(c)).*—

---

[2] "Continuous Frames of Reinforced Concrete," by H. Cross and N. Morgan, John Wiley & Sons, Inc., New York, N. Y., 1949.

Displacement Constants—Group I.—

$$c_{1\text{I}} = 1; \quad c_{2\text{I}} = 0; \quad c_{3\text{I}} = 1;$$

$$c_{4\text{I}} = -\frac{\sin(\sigma_{f4} + \sigma_{c4})}{\sin(\sigma_{c4})} = -1.342; \quad c_{5\text{I}} = 1.342;$$

$$c_{6\text{I}} = c_{7\text{I}} = c_{8\text{I}} = 0.$$

Displacement Constants—Group II.—

$$c_{1\text{II}} = c_{2\text{II}} = c_{3\text{II}} = 0; \quad c_{4\text{II}} = +1.342;$$

$$c_{5\text{II}} = -1.342; \quad c_{6\text{II}} = 1.00; \quad c_{7\text{II}} = 0; \quad c_{8\text{II}} = 1.00.$$

Distribution Factors—Joint e.—

$$a_{e1} = \frac{4\,E\,I_1}{4.00} = 1.00\,E\,I_1; \quad k_{e1} = \frac{1.00}{1.857} = 0.538;$$

$$a_{e2} = \frac{4\,E\,1.5\,I_1}{7.00} = 0.857\,E\,I_1; \quad k_{e2} = \frac{0.857}{1.857} = 0.462.$$

Distribution Factors—Joint f.—

$$a_{f2} = \frac{4\,E\,1.5\,I_1}{7.00} = 0.857\,E\,I_1; \quad k_{f2} = \frac{0.857}{2.897} = 0.295;$$

$$a_{f3} = \frac{4\,E\,I_1}{4.00} = 1.00\,E\,I_1; \quad k_{f3} = \frac{1.000}{2.897} = 0.345;$$

$$a_{f4} = \frac{4\,E\,1.4\,I_1}{5.38} = 1.04\,E\,I_1; \quad k_{f4} = \frac{1.040}{2.897} = 0.360.$$

Distribution Factors—Joint g.—

$$k_{g4} = 0.500$$

$$k_{g6} = 0.500.$$

Distribution Factors—Joint k.—

$$a_{k5} = \frac{4\,E\,1.4\,I_1}{5.38} = 1.040\,E\,I_1; \quad k_{k5} = \frac{1.040}{2.860} = 0.364;$$

$$a_{k6} = \frac{4\,E\,0.8\,I_1}{4.00} = 0.800\,E\,I_1; \quad k_{k6} = \frac{0.800}{2.860} = 0.280;$$

$$a_{k7} = \frac{4\,E\,1.4\,I_1}{5.50} = 1.020\,E\,I_1; \quad k_{k7} = \frac{1.020}{2.860} = 0.356.$$

Distribution Factors—Joint l.—

$$a_{l7} = \frac{4\,E\,1.4\,I_1}{5.50} = 1.020\,E\,I_1; \quad k_{l7} = \frac{1.020}{2.020} = 0.505;$$

$$a_{l8} = \frac{4\,E\,I_1}{4.00} = 1.000\,E\,I_1; \quad k_{l8} = \frac{1.000}{2.020} = 0.495.$$

Restraint Factors—Group I.—

$$\sigma_{e\mathrm{I}} = \frac{(3)\ (0.538)}{(2)\ (4.00)} = +\ 0.202;$$

$$\sigma_{f\mathrm{I}} = \frac{(3)\ (0.345)}{(2)\ (4.00)} - \frac{(3)\ (1.342)\ (0.360)}{(2)\ (5.38)} = -\ 0.005;$$

$$\sigma_{g\mathrm{I}} = -\ \frac{(3)\ (1.342)\ (0.500)}{(2)\ (5.38)} + \frac{(3)\ (1.342)\ (0.50)}{(2)\ (5.38)} = 0;$$

$$\sigma_{k\mathrm{I}} = \frac{(3)\ (1.342)\ (0.364)}{(2)\ (5.38)} = 0.136;$$

$$\sigma_{l\mathrm{I}} = 0.$$

Restraint Factors—Group II.—

$$\sigma_{e\mathrm{II}} = 0;\quad \sigma_{f\mathrm{II}} = \frac{(3)\ (0.360)\ (1.342)}{(2)\ (5.38)} = +\ 0.135;$$

$$\sigma_{g\mathrm{II}} = 0;\quad \sigma_{k\mathrm{II}} = -\ \frac{(3)\ (0.364)\ (1.342)}{(2)\ (5.38)} + \frac{(3)\ (0.280)\ (1)}{(2)\ (4.00)} = -\ 0.031;$$

$$\sigma_{l\mathrm{II}} = \frac{(3)\ (0.495)}{2.400} = 0.186.$$

Stiffness Factors.—

$$u_{e1} = u_{a1} = \frac{6\ E\ I_1}{4} = 1.5\ E\ I_1;\quad u_{e2} = u_{f2} = \frac{6\ E\ 1.5\ I_1}{7.00} = 1.287\ E\ I_1;$$

$$u_{f3} = u_{b3} = \frac{6\ E\ I_1}{4} = 1.5\ E\ I_1;\quad u_{f4} = u_{g4} = \frac{6\ E\ 1.4\ I_1}{5.38} = 1.56\ E\ I_1;$$

$$u_{g5} = u_{k5} = 1.56\ E\ I_1;\quad u_{k7} = u_{l7} = \frac{6\ E\ 1.4\ I_1}{5.50} = 1.53\ E\ I_1;$$

$$u_{g6} = u_{k6} = \frac{6\ E\ 0.8\ I_1}{4.00} = 1.2\ E\ I_1;\quad u_{l8} = u_{d8} = \frac{6\ E\ I_1}{4.00} = 1.5\ E\ I_1.$$

Using Table 1 the following factors may be determined:

TABLE 1

Member	l_i	$c_{i\mathrm{I}}$	$c_{i\mathrm{II}}$	$\frac{c_{i\mathrm{I}}}{l_i}$	$\frac{c_{i\mathrm{II}}}{l_i}$	$\left(\frac{c_{i\mathrm{I}}}{l_i}\right)^2$	$\left(\frac{c_{i\mathrm{II}}}{l_i}\right)^2$
1	4.00	1.00	0.00	0.25	0.00	0.0625	0.000
2	7.00	0.00	0.00	0.00	0.00	0.000	0.000
3	4.00	1.00	0.00	0.25	0.00	0.0625	0.000
4	5.38	−1.342	+1.342	−0.25	+0.25	0.0625	0.0625
5	5.38	+1.342	−1.342	+0.25	−0.25	0.0625	0.0625
6	4.00	0.00	1.00	0.00	+0.25	0.000	0.0625
7	5.50	0.00	0.00	0.00	0.00	0.000	0.000
8	4.00	0.00	1.00	0.00	+0.25	0.000	0.0625

Distribution Factors Due to Displacements—Group I.—

$$\sum (\ ) = (0.0625)\ (2)\ (1.50 + 1.50 + 1.56 + 1.56)\ E\,I_1 = 0.765\ E\,I_1;$$

$$q^{\mathrm{I}}{}_{e1} = q^{\mathrm{I}}{}_{a1} = \frac{(0.250)\ (1.5)}{0.765} = 0.490; \quad q^{\mathrm{I}}{}_{e2} = 0; \quad q^{\mathrm{I}}{}_{f2} = 0;$$

$$q^{\mathrm{I}}{}_{f3} = q^{\mathrm{I}}{}_{b3} = \frac{(0.250)\ (1.5)}{0.765} = 0.490;$$

$$q^{\mathrm{I}}{}_{f4} = q^{\mathrm{I}}{}_{g4} = -\frac{(0.250)\ (1.56)}{0.765} = -0.510;$$

$$q^{\mathrm{I}}{}_{g5} = q^{\mathrm{I}}{}_{k5} = 0.510; \quad q^{\mathrm{I}}{}_{k6} = q^{\mathrm{I}}{}_{c6} = 0;$$

$$q^{\mathrm{I}}{}_{k7} = q^{\mathrm{I}}{}_{l7} = 0; \quad q^{\mathrm{I}}{}_{l8} = q^{\mathrm{I}}{}_{d8} = 0.$$

Distribution Factors Due to Displacements—Group II.—

$$\sum (\ ) = (0.0625)\ (2)\ (1.56 + 1.56 + 1.20 + 1.20)\ E\,I_1 = 0.727\ E\,I_1;$$

$$q^{\mathrm{II}}{}_{e1} = q^{\mathrm{II}}{}_{a1} = 0; \quad q^{\mathrm{II}}{}_{e2} = q^{\mathrm{II}}{}_{f2} = 0; \quad q^{\mathrm{II}}{}_{f3} = q^{\mathrm{II}}{}_{b3} = 0;$$

$$q^{\mathrm{II}}{}_{f4} = q^{\mathrm{II}}{}_{g4} = \frac{(0.250)\ (1.56)}{0.727} = 0.536; \quad q^{\mathrm{II}}{}_{g5} = q^{\mathrm{II}}{}_{k5} = -0.536;$$

$$q^{\mathrm{II}}{}_{k6} = q^{\mathrm{II}}{}_{c6} = \frac{(0.250)\ (1.20)}{0.727} = 0.413; \quad q^{\mathrm{II}}{}_{k7} = q^{\mathrm{II}}{}_{l7} = 0;$$

$$q^{\mathrm{II}}{}_{l8} = q^{\mathrm{II}}{}_{d8} = \frac{(0.250)\ (1.50)}{0.727} = 0.515.$$

Check:

$$\sum \frac{c_{i\mathrm{I}}}{l_i}\, q^{\mathrm{II}}{}_{ki} = (0.25)\ (2)\ (0.490 + 0.490 + 0.510 + 0.510) = 1$$

$$\sum \frac{c_{i\mathrm{II}}}{l_i}\, q^{\mathrm{II}}{}_{ki} = (0.25)\ (2)\ (0.536 + 0.536 + 0.413 + 0.515) = 1.$$

Shear Carry-Over Factors.—

$$m^{\mathrm{I}}{}_{\mathrm{II}} = (0.250)\ (-0.510 - 0.510) - (0.250)\ (0.510 + 0.510) = -0.510$$

$$m^{\mathrm{II}}{}_{\mathrm{I}} = (0.250)\ (0.536 + 0.536) + (0.250)\ (-0.536 - 0.536) = -0.536.$$

Active Moments.—

$$\bar{M}_{e2} = -\bar{M}_{f2} = \frac{(2)\ (7.00)^2}{12} = 8.16 \text{ kip-ft};$$

$$\bar{M}_{f4} = -\bar{M}_{g4} = \frac{(2)\ (5.00)^2}{12} = 4.16 \text{ kip-ft};$$

$$\bar{M}_{g5} = -\bar{M}_{k5} = \frac{(2)\ (5.00)^2}{12} = 4.16 \text{ kip-ft};$$

$$\bar{M}_{k7} = -\bar{M}_{l7} = \frac{(2)\ (5.50)^2}{12} = 5.04 \text{ kip-ft}.$$

TABLE 2

	a	b	e		f			g		k			l		c	d	fI	fII
	1	3	1	2	2	3	4	4	5	5	6	7	7	8	6	8	m^{I}_{I}	m^{I}_{II}
k_{ai}			0.538	0.462	0.295	0.345	0.360	0.500	0.500	0.364	0.280	0.356	0.505	0.495	...	...	...	−0.510
σ_{aI}			0.202		−0.005					0.136			...		...	...	m^{II}_{I}	m^{II}_{II}
σ_{aII}					0.135					−0.031			0.186				−0.536	
q^{I}_{ai}	0.490	0.490	0.490			0.490	−0.510	−0.510	0.510	0.510								
q^{II}_{ai}							0.536	0.536	−0.536	−0.536	0.413			0.515	0.413	0.515		
	−2.195		−4.390	8.160 −3.770	−8.160 −1.885		4.160	−4.160	4.160	−4.160		5.040	−5.040				12.500 −1.650	−12.500
		1.015	−4.390	4.390	1.735	2.030	2.120	1.060									−0.029	0.800
				0.868	−8.310	2.030	6.280	−0.530	−0.530	−0.265							...	...
							−0.265	−3.630	3.630	−0.224	−0.172	−0.219	−0.110		−0.086		−0.084	0.019
									−0.112	−4.649	−0.172	4.821	2.600	2.550		1.275	...	0.956
												1.300	−2.550	2.550				
	−5.270	−5.270	−5.270			−5.270	5.480	5.480	−5.480	−5.480							10.737	5.480
							2.810	2.810	−2.810	−2.810	2.160			2.700	2.160	2.700	−2.810	−5.245
	1.185		2.370	2.032	1.016												0.890	...
		−0.650	−2.900	2.900	−1.111	−1.300	−1.360	−0.680									0.019	−0.507
				−0.555	−0.095	−6.570	6.665	0.396	0.396	0.198							...	...
							0.198	8.006	−8.006	1.686	1.296	1.650	0.825		0.648		0.630	−0.140
									0.843	−6.406	3.456	2.950	−1.780	−1.745		−0.872	...	−0.655
	0.623	0.623	0.623			0.623	−0.648	−0.648	0.648	0.648		−0.890	−0.955	0.955			−1.271	−0.648
							1.045	1.045	−1.045	−1.045	0.805			1.000	0.805	1.000	−1.045	−1.950
	−0.018		−0.037	−0.031	−0.016												−0.014	...

		−0.208	0.586	−0.586	−0.355	−0.415	−0.432	−0.216									0.006	−0.163
				−0.178	−0.371	0.208	0.163	−0.313	−0.314	−0.157							. . .	. . .
							−0.157	−0.132	0.132	0.232	0.179	0.228	0.114		0.090		0.087	−0.020
									0.116	−0.322	0.984	−0.662	−0.563	−0.551		−0.275	. . .	−0.207
												−0.281	−0.449	0.449			−0.966	−0.493
	0.474	0.474	0.474			0.474	−0.493	−0.493	0.493	0.493							−0.474	−0.883
							0.474	0.474	−0.474	−0.474	0.363			0.455	0.363	0.455		
	−0.080		−0.159	−0.137	−0.069												−0.060	. . .
			0.315	−0.315	−0.068	−0.079	−0.082	−0.041									0.001	−0.031
		−0.039		−0.034	−0.137	0.395	−0.258	−0.038	−0.037	−0.019							. . .	. . .
							−0.019	−0.098	0.098	−0.030	−0.023	−0.029	−0.015		−0.012		−0.011	0.002
									−0.015	−0.030	0.340	−0.310	−0.222	−0.218		−0.109	. . .	−0.082
	0.267	0.267	0.267			0.267	−0.278	−0.278	0.278	0.278		−0.111	−0.237	0.237			−0.544	−0.278
	−0.062		−0.125	−0.108	−0.054		0.208	0.208	−0.208	−0.208	0.161			0.200	0.161	0.200	−0.208	−0.389
			0.142	−0.142	−0.037	−0.043	−0.044	−0.022									−0.047	. . .
		−0.021		−0.018	−0.091	0.224	−0.133	0.018	0.019	0.009							. . .	−0.017
							0.009	−0.074	0.074	−0.047	−0.036	−0.046	−0.023		−0.018		−0.018	0.004
									−0.024	0.032	0.125	−0.157	−0.089	−0.088		−0.044	. . .	−0.033
	0.134	0.134	0.134			0.134	−0.139	−0.139	0.139	0.139		−0.044	−0.112	0.112			−0.273	−0.140
	−0.032		−0.063	−0.053	−0.027		0.100	0.100	0.100	0.100	0.077			0.096	0.077	0.096	0.100	−0.186
			0.071	−0.071	−0.023	−0.026	−0.028	−0.014										
		−0.013			−0.050	0.108	−0.058	0.019	0.019	0.010								
								−0.034	0.034	−0.030	−0.023	−0.029	−0.014		−0.011	−0.020		
										0.019	0.054	−0.073	−0.042	−0.040				
													−0.056	0.056				
M_{el}	−4.974	−3.688	−6.176	6.176	−9.054	−3.605	12.659	4.038	−4.038	−11.356	4.787	−6.569	−4.356	4.356	4.177	4.409		

Fixing Forces.—

$$F^0{}_{\mathrm{I}} = 12.5 \text{ kips}$$
$$F^0{}_{\mathrm{II}} = -12.5 \text{ kips.}$$

The successive approximations and the arrangement of the operations are shown in Table 2.

The bending-moment diagram of the frame shown in Fig. 11 is required.

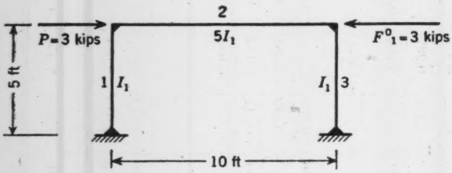
2
P=3 kips
$5I_1$
$F^0{}_1$=3 kips
5 ft
1
I_1
I_1
3
10 ft

FIG. 11

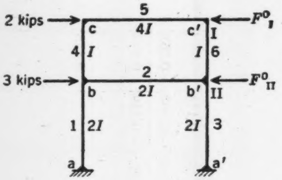
5
2 kips
c
4I
c'
I
$F^0{}_{\mathrm{I}}$
4
I
I
6
2
3 kips
b
2I
b'
II
$F^0{}_{\mathrm{II}}$
1
2I
2I
3
a
a'

FIG. 12

Distribution Factors—Joint c.—

$$a_{c1} = \frac{4\,E\,I_1}{5.00} = 0.800\,E\,I_1; \quad K_{c1} = \frac{0.8}{2.8} = 0.286;$$

$$a_{c2} = \frac{4\,E\,(5\,I_1)}{10.00} = 2.000\,E\,I_1; \quad K_{c2} = \frac{2.0}{2.8} = 0.714.$$

Distribution Factors—Joint d.—

$$K_{d2} = 0.714$$
$$K_{d3} = 0.286.$$

Restraining Factors.—

$$\sigma_c = \frac{(3)\,(0.286)}{(2)\,(50)} = 0.0858; \quad \sigma_d = 0.0858.$$

Stiffness Factors.—

$$u_{c1} = u_{a1} = u_{d3} = u_{b3} = \frac{6\,E\,I}{30} = 1.20\,E\,I.$$

Distribution Factors Due to Displacements.—

$$q_{a1} = q_{c1} = q_{b1} = q_{d1} = \frac{5.00 \quad 1.20}{(4)\,(1.20)} = 1.250.$$

Fixing Factors.—

$$F^0 = -3.00 \text{ kips.}$$

The successive approximations and the arrangement of the operations are tabulated in Table 3.

The bending-moment diagram of the frame shown in Fig. 12 is required.

TABLE 3

	a	c		d		b	f
	1	1	2	2	3	3	
k_{ai}	...	0.286	0.714	0.714	0.286	...	
σ_a	...	0.0858		0.0858		...	
ϕ_{ai}	1.250	1.250	...	...	1.250	1.250	
	3.750	3.750			3.750	3.750	−3.000
	−0.536	−1.072	−2.678	−1.339			−0.322
		2.678	−2.678	−1.720	−0.691	−0.345	−0.207
			+0.860	−3.059	3.059		−0.529
	0.661	0.661			0.661	0.661	
	0.029	0.057	0.142	0.071			0.017
		0.718	−0.718	−0.522	−0.210	−0.105	−0.063
			−0.261	−0.451	0.451		−0.046
	0.057	0.057			0.057	0.057	
	0.029	0.058	0.146	0.073			0.017
		0.115	−0.115	−0.093	−0.037	−0.019	−0.011
			−0.046	−0.020	0.020		0.006
	−0.008	−0.008			−0.008	−0.008	
	0.007	0.015	0.039	0.019			0.005
		0.007	−0.007	−0.008	−0.003	−0.002	−0.001
			−0.004	0.011	−0.011		0.004
	−0.005	−0.005			−0.005	−0.005	
	0.002	0.003	0.006	0.003			...
		−0.002	0.002	0.001	0.001		...
				0.004	−0.004		
M_{ki}	3.986	3.516	3.516	−3.515	3.515	3.984	

Distribution Factors—Joint c.—

$$a_{c4} = \frac{4\,E\,I}{4.00} = 1.00\,E\,I; \quad K_{c4} = \frac{1.00}{3.00} = 0.333;$$

$$a_{c5} = \frac{(4\,E)\,(4\,I)}{8.00}\,2.00\,E\,I; \quad K_{c5} = \frac{2.00}{3.00} = 0.667.$$

Distribution Factors—Joint c′.—

$$K_{c'3} = 0.667$$

$$K_{c'6} = 0.333.$$

TABLE 4

	c		c′		b			b′			a	a′	f_I	f_{II}
	4	5	5	6	4	2	1	6	2	3	1	3		
k_{ki}	0.333	0.667	0.667	0.333	0.300	0.300	0.400	0.300	0.300	0.400	. . .	. . .		m^I_{II}
σ_{kI}	0.125		0.125		0.1125			0.1125			. . .	. . .		−1.000
σ_{kII}	−0.125		−0.125		−0.0125			−0.0125			. . .	. . .		
q^I_{ki}	1.000			1.000	1.000			1.000						
q^{II}_{ki}							1.500			1.500	1.500	1.500		
	2.000			2.000	2.000			2.000					−2.000	−3.000
														−2.000
							7.500			7.500	7.500	7.500		−5.000
	−0.666	−1.334	−0.667		−0.333								−0.250	0.250
	1.334	−1.334	−0.889	−0.444				−0.222					−0.167	0.167
	−1.375	−0.445	−1.556	1.556	−2.750	−2.750	−3.667		−1.375		−1.834		−1.030	0.114
				−1.185	−1.083	−2.750	3.833	−2.370	−2.370	−3.161		−1.581	−0.890	0.099
						−1.185		−0.592	−3.745	4.337				
	2.337			2.337	2.337			2.337					−2.337	−2.337
							2.560			2.560	2.560	2.560		−1.707
	−0.172	−0.345	−0.172		−0.086								−0.065	0.065
	0.790	−0.790	−0.654	−0.326				−0.163					−0.123	0.123
	−0.544	−0.327	−0.826	0.826	−1.088	−1.088	−1.450		−0.544		−0.725		−0.408	0.045
				−0.628	1.163	−2.273	1.110	−1.257	−1.257	−1.676		−0.838	−0.471	0.052
						−0.628		0.917	−1.801	0.884				
	1.067			1.067	1.067			1.067					−1.067	−1.067
							1.170			1.170	1.170	1.170		−0.782
	−0.065	−0.131	−0.065		−0.032								−0.024	0.024

	0.458	−0.458	−0.249	−0.125				−0.062					−0.047	0.047
	−0.236	−0.124	−0.314	0.314	−0.473	−0.473	−0.631		−0.236		−0.315		−0.177	0.020
				−0.291	0.562	−1.101	0.539	−0.582	−0.582	−0.775		−0.387	−0.218	0.024
						−0.291		0.423	−0.818	0.395				
	0.466			0.466	0.466			0.466					−0.466	−0.466
							0.526			0.526	0.526	0.526		−0.351
	−0.035	−0.071	−0.035		−0.017								−0.013	0.013
	0.195	−0.195	−0.093	−0.047				−0.023					−0.017	0.017
	−0.102	−0.047	−0.128	0.128	−0.205	−0.205	−0.274		−0.102		−0.137		−0.077	0.008
				−0.130	0.244	−0.496	0.252	−0.260	−0.260	−0.347		−0.173	−0.098	0.011
						−0.130		0.183	−0.362	0.179				
	0.205			0.205	0.205			0.205					−0.205	−0.205
	−0.020	−0.036					0.234			0.234	0.234	0.234		−0.156
	−0.020	−0.036	−0.018		−0.010								−0.007	0.007
	0.084	−0.084	−0.038	−0.019				−0.010					−0.007	0.007
	−0.045	−0.019	−0.056	0.056	−0.090	−0.090	−0.119		−0.045		−0.060		−0.034	0.004
				−0.057	0.105	−0.220	0.115	−0.115	−0.115	−0.154		−0.077	−0.043	0.005
						−0.057		0.080	−0.160	0.080				
	0.091			0.091	0.091			0.091					−0.091	−0.091
							0.100			0.100	0.100	0.100		−0.067
	−0.009	−0.018	−0.009		−0.004								−0.003	0.003
	0.037	−0.037	−0.017	−0.008				−0.004					−0.003	0.003
			−0.026	0.026	−0.039	−0.039	−0.052		−0.020		−0.026		−0.015	0.002
					0.048	−0.096	0.048	−0.050	−0.050	−0.067		−0.033	−0.019	0.002
								0.037	−0.070	−0.033				
M_{kl}	2.898	−2.898	−2.906	2.906	1.039	−6.936	5.897	1.048	−6.956	5.908	8.993	9.001		

Distribution Factors—Joint b.—

$$a_{b4} = \frac{4\,E\,I}{4.00} = 1.00\,E\,I; \quad K_{b4} = \frac{1.000}{3.333} = 0.300;$$

$$a_{b2} = \frac{(4\,E)\,(2\,I)}{8.00} = 1.00\,E\,I; \quad K_{b2} = \frac{1.000}{3.333} = 0.300;$$

$$a_{b1} = \frac{(4\,E)\,(2\,I)}{6.00} = 1.333\,E\,I; \quad K_{b1} = \frac{1.333}{3.333} = 0.400.$$

Distribution Factors—Joint b′.—

$$K_{b'6} = 0.300$$
$$K_{b'2} = 0.300$$
$$K_{b'3} = 0.400.$$

Restraining Factors.—

$$\sigma_{c\mathrm{I}} = \left(\frac{3}{2}\right)\left(\frac{0.333}{4.00}\right) = 0.125; \quad \sigma_{c'\mathrm{I}} = 0.125;$$

$$\sigma_{b\mathrm{I}} = \left(\frac{3}{2}\right)\left(\frac{0.300}{4.00}\right) = 0.1125; \quad \sigma_{b'\mathrm{I}} = 0.1125;$$

$$\sigma_{c\mathrm{II}} = \left(-\frac{3}{2}\right)\left(\frac{0.333}{4.00}\right) = -\,0.125; \quad \sigma_{c'\mathrm{II}} = -\,0.125;$$

$$\sigma_{b\mathrm{II}} = \frac{3}{2}\left(\frac{0.400}{6.00} - \frac{0.300}{4.00}\right) = -\,0.0125; \quad \sigma_{b'\mathrm{II}} = -\,0.0125.$$

Stiffness Factors.—

$$u_{c4} = u_{b4} = u_{c'6} = u_{b'6} = \frac{6\,E\,I}{4.00} = 1.50\,E\,I$$

$$u_{b1} = u_{a1} = u_{b'3} = u_{a'3} = \frac{(6\,E)\,(2\,I)}{6} = 2.00\,E\,I.$$

Distribution Factors Due to Displacements.—

$$q^{\mathrm{I}}{}_{c4} = q^{\mathrm{I}}{}_{b4} = q^{\mathrm{I}}{}_{c'6} = q^{\mathrm{I}}{}_{b'6} = (4.00)\,\frac{1.50}{(4)\,(1.50)} = 1.00;$$

$$q^{\mathrm{II}}{}_{b1} = q^{\mathrm{II}}{}_{a1} = q^{\mathrm{II}}{}_{b'3} = q^{\mathrm{II}}{}_{a'3} = (6.00)\,\frac{2\,E\,I}{(4)\,(2\,E\,I)} = 1.50.$$

Fixing Forces.—

$$F^0{}_{\mathrm{I}} = -\,2.00 \text{ kips}$$
$$F^0{}_{\mathrm{II}} = -\,3.00 \text{ kips.}$$

The successive approximations and the arrangement of the operation are shown in Table 4.

AMERICAN SOCIETY OF CIVIL ENGINEERS
Founded November 5, 1852
TRANSACTIONS

Paper No. 2893

TRANSPORT HELICOPTER COST AND HELIPORT CONSIDERATIONS

BY F. DAVID SCHNEBLY[1]

SYNOPSIS

This paper considers the development—past, present, future—of the transport helicopter and the rapid incorporation of this machine in the existing air transport system. Examined here are the general problems of helicopter design and heliport facilities as related to operating cost.

INTRODUCTION

Since 1953, the transport helicopter has been the object of considerable commercial interest because of its possible use in scheduled short-haul air transport operations. One of the greatest growth potentials for the air transport industry lies in this so-called "mass short-haul air travel market." To date (1956), this market has been tapped only slightly by certified local-service airlines which, for the most part, operate DC-3 equipment over route segments. This is an operation for which the helicopter was not originally designed. Economic reasons force these aircraft to omit certain stops which might otherwise yield high passenger potential provided the time saving over surface travel were appreciable.

The development of the transport helicopter may be the solution to the short-haul air transport problem because of this aircraft's efficiency over the typical short-haul route segment and the fact that it wastes little time in taxiing, landing, and taking off—important time considerations in short-haul air-carrier operation. The development of helicopter air transportation is closely related to the availability of well-designed heliports both in the downtown metropolitan areas and in the rural communities which the machines will serve. The civil engineers responsible for the planning, design, and erection of future heliports and heliport facilities will indirectly, but quite decisively, determine the date when the transport helicopter will be in large-scale commercial service.

NOTE.—Published, essentially as printed here, in August, 1955, as *Proceedings Paper 778*. Positions and titles given are those in effect when the paper was approved for publication in *Transactions*.

[1] Mgr., Operations Research Dept., Hiller Helicopters, Palo Alto, Calif.

HELICOPTER TRANSPORTS—PRESENT AND FUTURE

Present.—At the present time, there are only three commercially certified heliocopters in production in the United States: The S-55, a 7-passenger or 8-passenger light transport (Fig. 1(*a*)); the model 12-B, a 2-passenger or 3-passenger general utility helicopter (Fig. 1(*b*)); and the model 47, a 2-place utility machine (Fig. 1(*c*)).

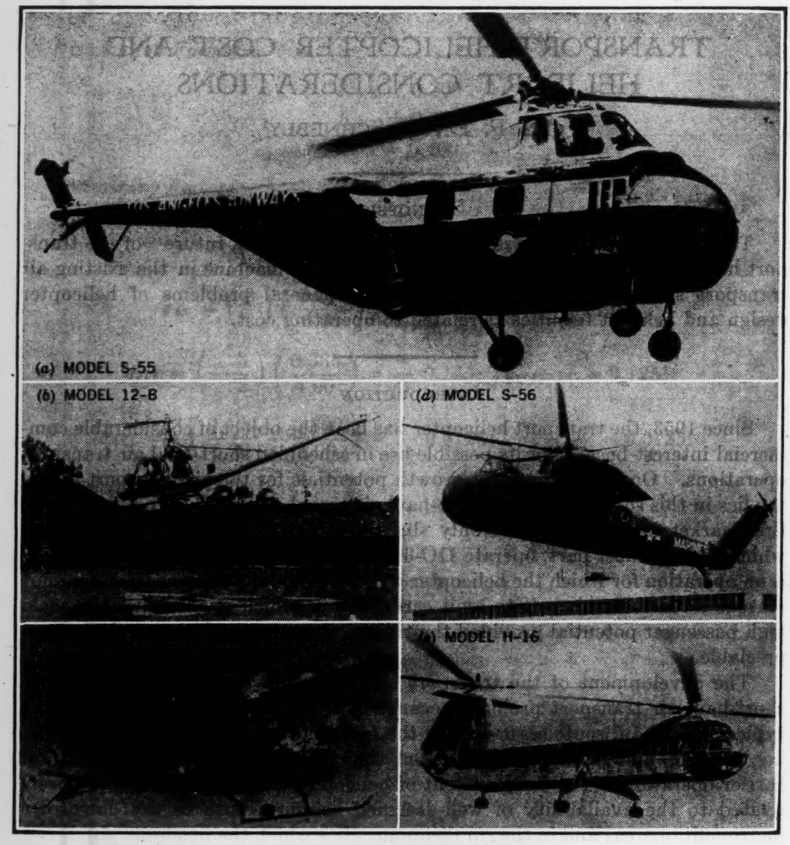

FIG. 1.—VARIOUS HELICOPTERS

The S-55 is the only transport type of helicopter in commercial service and is used by air carriers in Los Angeles (Calif.) and in New York (N. Y.). These companies have been certified for mail and passenger-hauling operations by the Civil Aeronautics Board, United States Department of Commerce (CAB), and do not engage in profit-making ventures but rather in government-subsidized learning operations for the purpose of developing the necessary operational techniques involved in helicopter transport operations. In addition to these carriers, a local-service airline in upstate New York and a well-known east coast trunk line carrier have purchased a S-55 helicopter for similar learning programs. However, these operations are without subsidy and were initiated by the carriers themselves in the belief that their particular air routes were especially suitable for helicopter operation.

The model 47 utility type of helicopter is used only by one CAB-certified air carrier operation in the United States; this company operates a fleet of six model 47 helicopters in an as yet experimental, inter-post-office-to-urban-area airmail operation. The model 47 helicopter also is used in other areas in general utility operations.

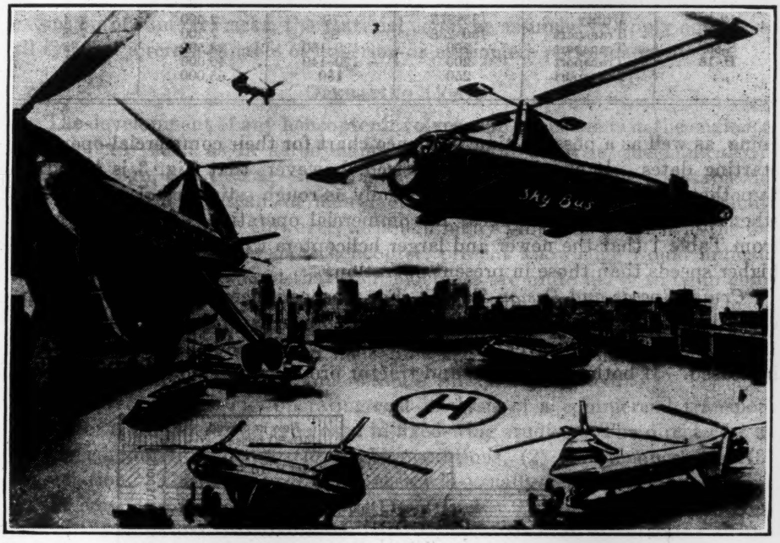

Fig. 2.—Future Transports at Heliport

The model 12-B utility type of helicopter is used in many countries in activities ranging from tree seeding, crop dusting, casualty rescue, and whale scouting to landing Santa Claus in downtown areas for the opening of the Christmas season. Four model 12-B helicopters are being used in charter passenger-carrying operations in Manila (Philippine Islands); others are being used in crop seeding and dusting operations in Asia and Europe.

Future.—Two large transport helicopters which might be developed for commercial operation are the 35-passenger S-56 (Fig. 1(*d*)) and the 45-passenger H-16 (Fig. 1(*e*)). The S-56 is going into military production, and the H-16 is in flight test (as of 1956). Both of these aircraft are twin-engined and may be the first large transport helicopters utilized for commercial service. Fig. 2 shows a design of a transport helicopter of the future (at right) as it hovers over a roof-top heliport.

Performance and Weight Data.—Table 1 and Fig. 3 list the range, cruise speed, gross weight, and payload of the particular models mentioned in the foregoing, as well as a possible time-sequence chart for their commercial-operation starting dates. It should be emphasized, however, that Fig. 3 is based on hypothetical data which are presented only as rough estimates of future dates when these aircraft may appear in commercial operation. It may be noted from Table 1 that the newer and larger helicopters will cruise at considerably higher speeds than those in present operation.

TABLE 1.—APPROXIMATE HELICOPTER WEIGHT AND PERFORMANCE DATA

Model	Type	Range, in miles	Cruise speed, in miles per hour	Gross weight, in pounds	Passenger capacity
47	Utility	170	70	2,400	2–3
12-B	Utility	135–275	70	2,500	2–3
S-55	Transport	150–235	85	7,200	7–8
S-56	Transport	200	120–150	28,500	35
H-16	Transport	200	120–140	40,000	45
..	Transport	250	150	65,000	50

Cruise Speeds and Design Types.—For reasons inherent in rotary-wing aircraft design, a "pure" helicopter is limited to speeds probably not exceeding 150 miles per hr. However, if a short "stub" wing is added, this speed can be increased. If both a stub wing and tractor propellers are added, the machine then becomes classed as a converti-plane and not as a pure helicopter, and the cruise speed increases even more. The vertical take-off type of airplane has cruise speeds as high as any transport airplane. All these types are being developed for use by the armed forces. However, it seems quite safe to assume that the first transport configuration to become operational will be a pure helicopter. A slightly modified stub-wing version of this type of helicopter

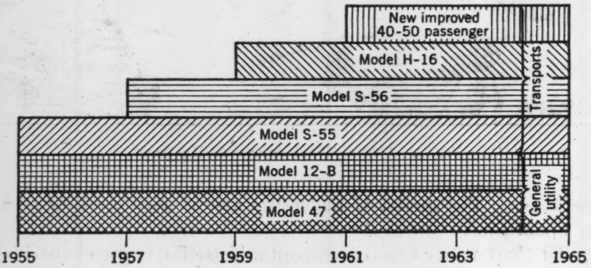

FIG. 3.—POSSIBLE COMMERCIAL OPERATION

will then be developed in a relatively short time at relatively small expense and will merely increase the allowable cruise speeds. The application of converti-plane and vertical take-off principles to configurations for large-scale commercial service is an undertaking for the future that will require a considerable period of initial experimentation. If and when such airplanes are developed and are put into commercial service, they will not necessarily cause the pure helicopter or the stub-wing configuration to become obsolete. The pure helicopter or stub-wing configuration in all probability will still offer the most efficient service on a certain part of the short-haul routes. The converti-plane aircraft will merely expand the possibilities for the air transport business in 200-mile to 700-mile long operations.

For purposes of this paper, therefore, the emphasis will be assumed to be on the pure helicopoter or the stub-wing version of it. However, by slight extension of some remarks, the material could be assumed to apply equally to all types of aircraft capable of hovering or motionless performance.

OPERATING COSTS

The development of any helicopter involves many specialists in the engineering sciences—such as in aerodynamics, structural analysis, mechanical dynamics, design, and testing—in the painstaking task of devising a suitable design. Then, another team of manufacturing specialists combines its talents to produce the design. However, although many problems do exist in the development of a large transport helicopter, present knowledge would indicate that they can be solved and that such machines are quite likely to be in commercial operation in the near future. For this reason, no attempt will be made herein to discuss any of the many design and development problems associated with the creation of a transport helicopter, and only those main points which will most directly affect its commercial use will be highlighted.

Cost Breakdown.—The operating-cost analysis of a commercial transport helicopter is similar to the type used in fixed-wing studies. The direct cost as usually computed involves: (1) Flight operations, (2) maintenance, and (3) depreciation. The flight-operations cost will usually reflect the funds spent for the crew, fuel and oil, training, and insurance. The maintenance cost consists of the total material and direct labor costs involved in maintaining all the system and mechanical components of the aircraft. The depreciation-cost breakdown merely allows for the write-off of the purchase price of the article.

The various trends in the direct operating cost as opposed to the range, work capacity, and utilization found from the results of a number of cost analyses on a number of different assumed designs are important to consider at this point.

Definition of Terms.—Before examining these trends, however, it might be well first to define two terms which are used most frequently: (1) Work capacity, which is the product of the payload times the block speed, and which represents the ton-miles per hour that the particular design is capable of moving; and (2) block speed, which represents the average speed from take-off to landing, and which is found by dividing the range or trip length by the sum of the time-to-cruise, the time-to-climb-and-descend, and the time-to-maneuver.

Block-Speed Variation.—Fig. 4(*a*) is a plot of block speed, V_B, versus trip length for two different cruise speeds, V_C. These trends merely indicate that, as the trip length increases, the block speed approaches asymptotically the cruise speed and that, as the trip length becomes very short, the climb-and-maneuver times become predominant and the block speed falls off rapidly. These same trends also appear in the case of fixed-wing aircraft, except that airplane maneuver time is obviously greater than that required by the helicopter.

Transport Helicopter Time-Saving Potential.—To compare transport airplane travel times with transport helicopter travel times, a specific type of mission must be stipulated and the time between city centers compared. If this is done and a limousine time from downtown to airport is assumed as 30 min each way for the airplane and 10 min for the helicopter, Fig. 4(*b*) may be drawn. Fig. 4(*b*) presents the ratio of helicopter over-all time to airplane over-all time for the DC-3 (cruising speed of 170 miles per hr) and the 150-mile-per-hr cruising helicopter. Fig. 4 indicates that for a 100-mile trip the helicopter would transport a passenger from one city center to another in one-half the time required by the airplane. Fig. 4 reveals that appreciable time saving is possible even for trip lengths of 200 miles. However, it must be noted that the travel time (10 min) between the city center and the heliport assumed a heliport in a close-in downtown location. The time saving made possible by close-in locations is one of the main reasons that the transport helicopter has much to offer the transportation industry.

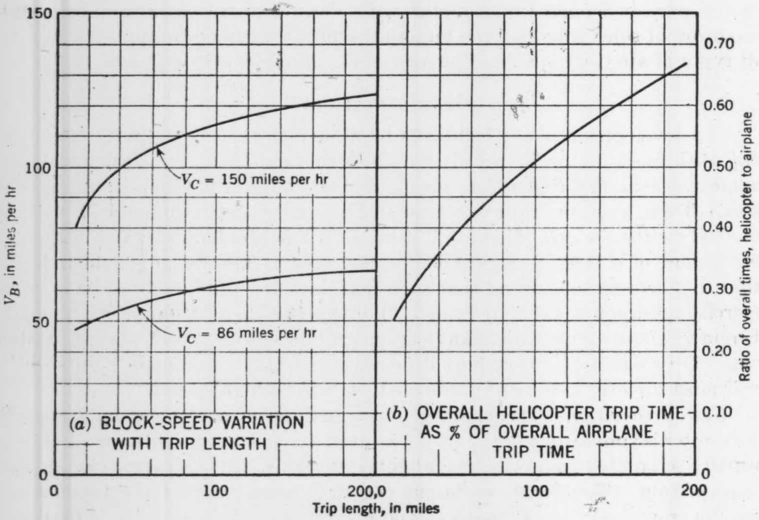

FIG. 4.—COMPARISON OF HELICOPTER AND CONVENTIONAL AIRPLANE

Effects of Work Capacity and Trip Length.—Fig. 5 is a presentation of direct operating cost versus work capacity, trip length, and utilization. Fig. 5(*a*) designates yearly utilizations of 1,000 hr per yr, 2,000 hr per yr, and 3,000 hr per yr. It may be seen that the direct operating cost reaches its minimum somewhere between 450 ton-miles per hr and 500 ton-miles per hr. For a 130-mile-per-hr cruise speed, this corresponds to a payload of from 35 passengers to 40 passengers. Obviously, the greater the yearly utilization, the lower the minimum point because the depreciation cost and portions of the insurance cost are on an annual basis.

In Fig. 5(*b*) direct operating cost is compared with trip length, and it may be seen that a minimum point occurs at about 200 miles for the 10-passenger, 20-passenger, and 35-passenger helicopters. This does not mean that all transport helicopters will operate most economically over a 200-mile length. This value merely indicates that the trip length for minimum operating cost occurs at the design range of the aircraft. Because the three helicopters considered in constructing Fig. 5(*b*) were all of 200-mile design range, their operating cost curves became minimized at that point. This, of course, assumes that the payload is limited by seating capacity and that on shorter trip lengths no additional payload can be carried because of reduced fuel weight. Cargo versions of these same helicopters might operate even more economically on a 75-mile trip, assuming operation always at design gross weight.

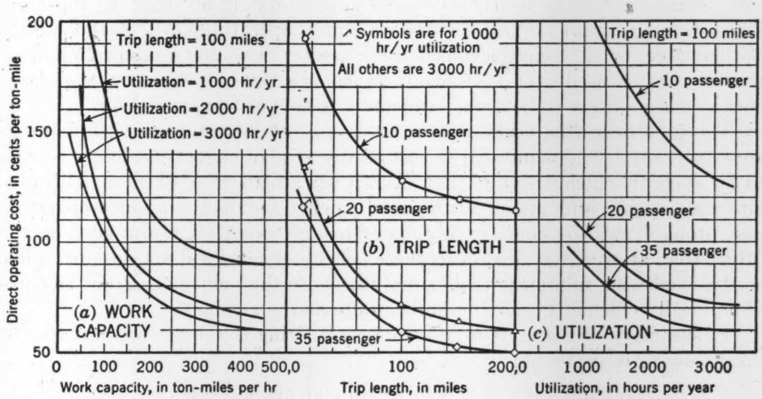

FIG. 5.—EFFECT OF VARIOUS FACTORS ON DIRECT OPERATING COSTS (LOAD FACTOR = 75%)

Design Range for Future Transports.—Because the transport helicopter offers a significant time saving over the airplane in trip lengths of up to approximately 250 miles, most of the transport helicopters which become commercially available will carry their design-point payload at from 200 miles to 250 miles and still maintain the proper fuel reserve.

Effect of Utilization.—Fig. 5(*c*) depicts direct operating cost versus yearly utilization for the 10-passenger, 20-passenger, and 35-passenger equipment. It can be seen that 3,000 hr per yr is a goal toward which every operator would strive—even those in the airplane industry. However, high utilizations of local-service operations—for instance, railroads and bus lines—have always been extremely difficult, if not impossible, to obtain.

In agreement with the fact that the transport helicopter will probably operate most efficiently over a 200-mile trip but will also be reasonably economical over much shorter distances, entire fleet studies on selected air carrier routes indicated yearly utilizations of from 2,500 hr per yr to 2,700 hr per yr. These figures are impressive to economists faced with the operation of aircraft having a break-even trip length of 400 miles over 75-mile to 100-mile lengths with a yearly utilization of less than 1,500 hr.

Operating-Cost Values and Comparison with Fixed-Wing Transport.—The minimum operating-cost data in Fig. 5 is based on past operational information and indicates minimum operating cost of approximately 50 cents per ton-mile. Fixed-wing transport aircraft display minimum operating costs of about 60% of this value for trip lengths considerably greater than 200 miles or 250 miles. However, when used over a 50-mile distance or a 100-mile distance, the transport airplane proves to be a very expensive means of transportation.

The high operating costs of helicopters are attributed mostly to maintenance expenses. The maintenance cost of any type of aircraft is closely related to the stage to which design of that aircraft has advanced. Because helicopter air-frame design and manufacture is advancing rapidly, minimum operating cost probably will be considerably closer to fixed-wing minimum costs in the future than at present. However, these helicopter costs will not become as low as the fixed-wing minimum costs simply because the helicopter is not as aerodynamically efficient in moving horizontally as the airplane.

In summary of the facts found from considering the operating-cost trends, the following is apparent:

1. The transport helicopter will provide significant time savings over the typical local service airplane operation to trip lengths of as much as 250 miles if heliports are provided in downtown centers.
2. These transports, to be most efficient, will have a passenger capacity of from 35 people to 40 people.
3. The transport helicopters in commercial operation will probably have design ranges of between 200 miles and 250 miles and will be able to operate economically over much shorter distances.
4. Due to their versatility, these transports will probably realize yearly utilizations much higher than those now found in local-service airplane operation.
5. The minimum operating cost per ton-mile for the transport helicopter will always be greater than the minimum cost for the transport airplane. However, the transport helicopter will be a formidable competitor of fixed-wing aircraft for the short-haul trips.

HELIPORT REQUIREMENTS

Transport Helicopter Performance Items.—Because the helicopter can hover motionless and rise vertically in take-off—and herein lies the predominant reason for its versatility and suggested use in air carrier operations—it requires only relatively small landing and take-off areas; in the United States these areas are termed "heliports" and in Great Britain, "rotor stations." However, the design of even such small landing areas must be such as to assure the safety of not only the passengers and cargo within the helicopter, but also the personnel and property near the heliport.

Helicopter Power Curves.—In order to understand the hovering and vertical performance characteristics of the helicopter, it is advisable to consider its power-required variation with forward flight speed. Fig. 6 represents a typical helicopter power-required curve showing the ratio of power required to total power available versus forward flight speed for two multiple-engine helicopters of advanced design. It is evident from this that the helicopter requires its greatest power while hovering. One machine, A, utilizes reciprocating-type power plants and is designed more in accordance with past design philosophy in that it exhibits a rather high power loading. The other machine, B, is designed around turbine power plants and has a relatively low-design power loading.

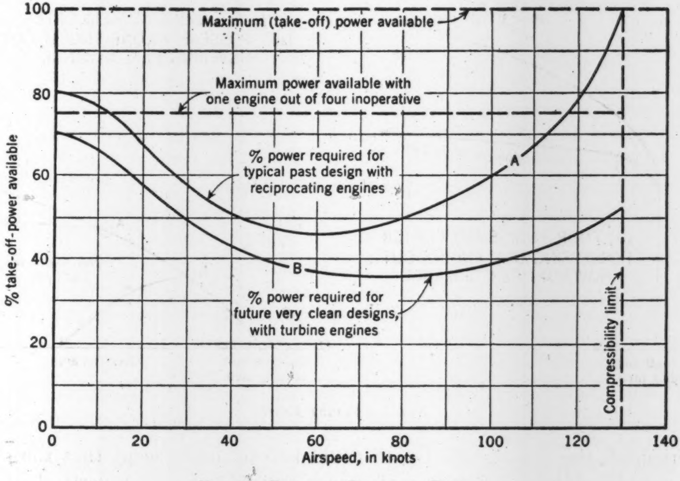

Fig. 6.—Chart of Required Power

It may be seen that helicopter A, the reciprocating type with high-power loading, cannot hover with only one of its four engines in working condition, but must attain a speed of approximately 12 miles per hr before safe level flight can be realized. Helicopter B, on the other hand, can hover with one engine inoperative. In Fig. 6 is emphasized the fact that future transport helicopters will probably display one-engine-out performance which will permit safe operation from smaller heliports.

Take-Off Path and Heliport Length Requirements.—Although it is far too early in the development of the transport helicopter for detailed predictions of future take-off patterns, it is permissable to generalize that, in the operation of a multiengined helicopter possessing one-engine-out hovering ability, an almost vertical take-off will not only be possible but should also be quite safe. If an engine failure were experienced, adequate power would still exist and no serious difficulty would be involved in bringing the aircraft safely back to the ground. Obviously, this would not be true for the machine displaying less than one-engine-out hovering performance. In the case of the latter, acceleration to the minimum one-engine-out flight speed would be required before any form of powered flight could continue after an engine failure. This naturally would require a larger heliport length to allow for a safe autorotational landing in the event that an engine failure occurred before the minimum one-engine-out flight speed had been attained.

Fig. 7 presents the estimated flight paths of the two performance types. It may be noted that the higher-performance machine can climb vertically and then accelerate to forward speed while in climb. Should an engine failure be experienced, the same general path could be executed except that the climb rate would be lower. Of course, the machine could execute a vertical landing after a single-engine failure, if so desired.

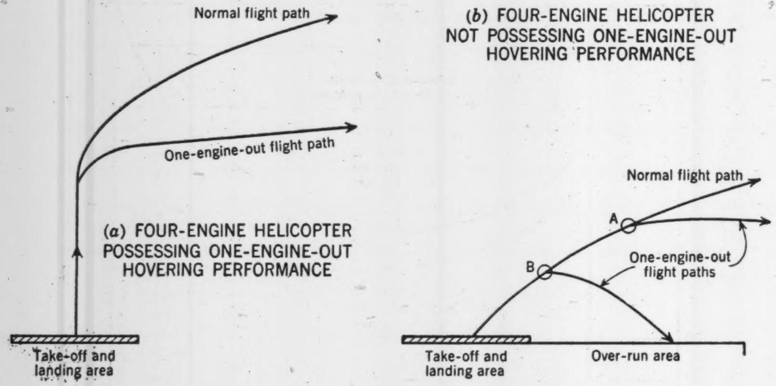
Normal flight path
One-engine-out flight path
(a) FOUR-ENGINE HELICOPTER POSSESSING ONE-ENGINE-OUT HOVERING PERFORMANCE
Take-off and landing area
(b) FOUR-ENGINE HELICOPTER NOT POSSESSING ONE-ENGINE-OUT HOVERING PERFORMANCE
Normal flight path
A
B
One-engine-out flight paths
Take-off and landing area
Over-run area

FIG. 7.—FLIGHT PATHS

The lower-performance helicopter, not being able to maintain hovering flight after an engine failure, must follow one of two courses in such a circumstance. If single-engine flight speed were obtained prior to the failure, the flight path shown from point A (Fig. 7 (*b*)) would be possible. If the failure were to occur before point A was reached, an autorotative landing on an overrun area adjacent to the heliport would be necessary.

The size of an overrun area depends strictly on the specific performance required of the helicopters using the particular heliport. However, a 400-ft area has been generally considered adequate. The minimum area required for the heliport landing and take-off might be 300-ft square. This would probably suffice for all twin-engined machines that might be used in commercial service. These dimensions are presented herein only as an aid for planning purposes because very few positive statements are possible without previous operational experience. The dimensions given should certainly be more than adequate for the helicopters now in operation, and because the future will probably bring equipment that will enable improved hovering performance the dimensions of heliport size ultimately will decrease. Even so, it is far better to plan for more than the required space than for too little space. This trend in heliport size, which in the future will probably vary inversely with helicopter weight and size, is opposite to the size ratio between vehicle and landing area experienced in the development of the fixed-wing transport.

Other Heliport Considerations.—Although heliport sites must be close-in to allow the aircraft to be most effective, the areas selected should be as free as possible from high obstructions in the approach area to provide for maximum flight safety and should be located where the noise levels will cause the least public annoyance. Access to surface transportation should also be considered in planning the heliport site.

Summary of Heliport Requirements.—From what has been outlined previously, the following points may be summarized:

1. The twin-engined helicopters that will be commercially operated will probably not possess single-engine hovering capabilities and will therefore require cleared, overrun areas adjacent to the heliport landings and take-off mats.
2. The heliport landing approach areas should be as free as possible from high obstructions and should be selected so as to create the least noise nuisance. The heliports themselves should be as close as possible to downtown areas and surface transportation.
3. Because of the incorporation of multiple and more suitable power plants and lower-design power loadings, the size requirement of heliport areas will probably decrease as larger and heavier machines become available, which will allow one-engine-out hovering performance.

Conclusions

Only the highlights of those items which will affect the large-scale use of the transport helicopter in commercial operations have been cited herein. Many other features will enter into the over-all development of this new transportation medium, but it is believed that operating cost and heliports are the most significant factors to be considered in the commercial acceptance of the vehicle.

The major facts and predictions of operating-cost trends and of heliport requirements for future transport helicopters have been presented in the hope that such data will aid in the long-range planning for what will probably be a major transportation medium of the not too distant future.

APPENDIX. BIBLIOGRAPHY

---

(1) **"Local Service Air Transportation and Metropolitan Helicopter Services,"** by Aviation Securities Committee of the Investment Bankers Assn. of America, New York, N. Y., 1953.

(2) **"Heliport Location and Design,"** by Dept. of Aviation, The Port of New York Authority, New York, N. Y., May, 1955.

(3) **"Planning for Urban Heliports,"** by Robert Horonjeff and Howard S. Lapin, Inst. of Transportation and Traffic Eng., Univ. of California, Berkeley, Calif., June, 1954.

(4) **"Preliminary Report on the Use of Helicopters in Scheduled Airline Operation,"** by The Committee on Helicopters, Air Transport Assn. of America, Washington, D. C., May, 1953.

(5) **"The Helicpoter—A Blueprint of Change in Airport Planning Standards,"** by L. Welch Pogue and Grahame H. Aldrich, Helicopter Council of the Aircraft Industries Assn. of America, Washington, D. C., 1954.

(6) **"Transportation by Helicopter—1955–1975,"** by Grahame H. Aldrich, Alex L. Hart, Joseph D. McGoldrick, and Lewis C. Sorrell, Dept. of Aviation, The Port of New York Authority, New York, N. Y., May, 1953.

AMERICAN SOCIETY OF CIVIL ENGINEERS
Founded November 5, 1852
TRANSACTIONS

Paper No. 2894

UNDERSEEPAGE, MISSISSIPPI RIVER LEVEES, ST. LOUIS DISTRICT

By Charles I. Mansur,[1] M. ASCE, and Robert I. Kaufman,[2] J. M. ASCE

Synopsis

Contained herein is a description of the underseepage problem along the Mississippi River levees between Alton (Ill.) and Gale (Ill.) and of the procedures used to design seepage-control measures. The paper includes: (1) A description of the investigations conducted; (2) the methods used to control the seepage; (3) examples of the design of the control measures; and (4) a description of the construction procedures used to install the control measures.

Introduction

Soil conditions in the alluvial valley of the Mississippi River are such that seepage beneath the levees along the river has always posed a serious problem during high waters. In fact, some crevasses in the levees along the Mississippi River have occurred as a result of sand boils and subsurface piping.

Prior to 1938, many of the levees along the Mississippi River in the St. Louis (Mo.) District, Corps of Engineers, United States Department of the Army, were below project-flood grade, and only relatively low heads could be developed against them. Although some underseepage had been experienced along these levees, only minor problems had occurred, mainly because of the low height of the levees. By authority of the Flood Control Acts of 1936 and 1938, the St. Louis District initiated a program to complete the levee systems and to raise the grade of existing levees so that they could withstand the project flood. Approximately 90% of this program was accomplished by 1955. A plan of the present levee systems along the Mississippi River from Alton (Ill.) to Gale (Ill.) is shown in Fig. 1. The increased height of the levees, however, has

---

NOTE.—Published, essentially as printed here, in January, 1956, as *Proceedings Paper 864*. Positions and titles given are those in effect when the paper was approved for publication in *Transactions*.

[1] Asst. Chief, Embankment and Foundation Branch, Soils Div., Waterways Experiment Station, Vicksburg, Miss.

[2] Chief, Design and Analytical Section, Embankment and Foundation Branch, Soils Div., Waterways Experiment Station, Vicksburg, Miss.

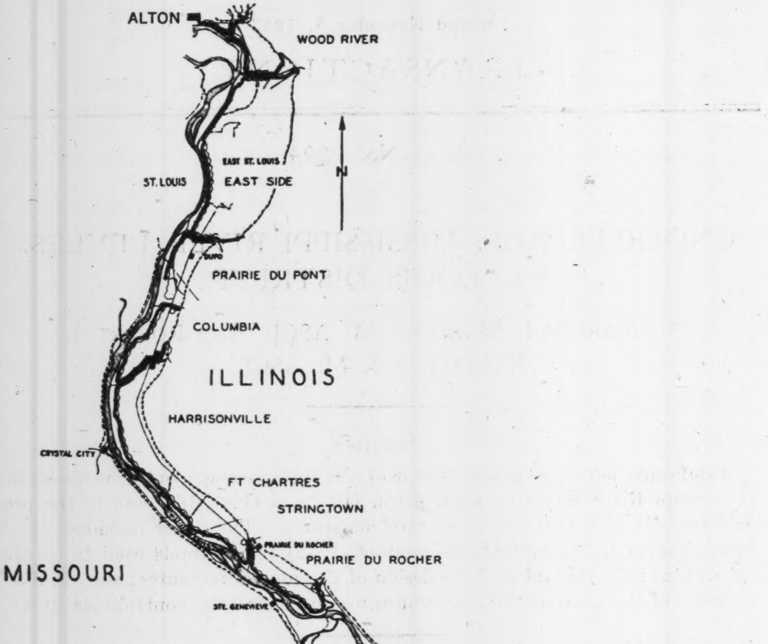
ALTON
WOOD RIVER
EAST ST. LOUIS
ST. LOUIS
EAST SIDE
N
DUPO
PRAIRIE DU PONT
COLUMBIA
ILLINOIS
HARRISONVILLE
CRYSTAL CITY
FT CHARTRES
STRINGTOWN
PRAIRIE DU ROCHER
PRAIRIE DU ROCHER
MISSOURI
STE. GENEVIEVE
CHESTER
PERRY COUNTY
DEGOGNIA
GORHAM
0 5 10 15
Scale in miles
GRAND TOWER
GRAND TOWER
PRESTON
MILLER POND
CLEAR CREEK
EAST CAPE GIRARDEAU
CAPE GIRARDEAU
NORTH ALEXANDER
GALE

FIG. 1.—PLAN OF LEVEES ALONG THE MISSISSIPPI RIVER—ALTON (ILL.) TO GALE (ILL.)

created a problem of underseepage which did not exist previously. Inasmuch as considerable head can now be developed against the levees, their safety against underseepage has become questionable.

Although it was realized that underseepage would be a problem along the new levee system, the control of underseepage was not specifically provided for in the design of the new levees. Following the 1951 and 1952 floods in the Omaha (Nebr.) and Kansas City (Mo.) Districts, the Office of the Chief of Engineers and the St. Louis District requested that the Waterways Experiment Station, Corps of Engineers, United States Department of the Army, make a comprehensive investigation of the seepage problem along the new levee system and design the necessary control measures. This investigation was initiated in October, 1952, and was essentially completed by June, 1955. Approximately 70% of the control measures indicated by these studies have been completed (as of 1955), and considerable additional work is under contract.

DEVELOPMENT OF UNDERSEEPAGE AND SAND BOILS

Whenever a levee is subjected to a differential hydrostatic head of water, as a result of river stages being higher than the adjacent land, seepage enters the pervious substratum beneath the levee through the bed of the river, and through riverside borrow pits and/or through the riverside top stratum. This seepage creates an artesian head and hydraulic gradient in the sand stratum under the levee. ,The gradient, in turn, causes a flow of seepage beneath and landward of the levee (Fig. 2). The seepage from the previous substratum which emerges at or landward of the levee toe is generally termed underseepage. Concentrated underseepage which carries sand up to the surface through an open channel in the top stratum is called a sand boil. Piping is the active erosion of sand or other soil from below the ground surface which occurs as a result of substratum pressure and the concentration of seepage in localized channels.

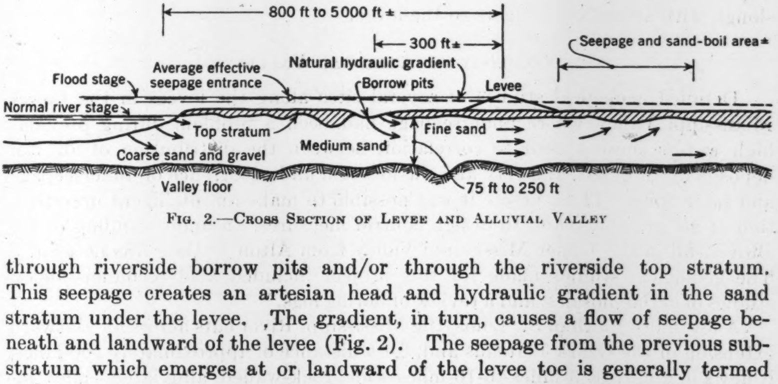

FIG. 2.—CROSS SECTION OF LEVEE AND ALLUVIAL VALLEY

If the hydrostatic pressure in the pervious substratum landward of a levee becomes greater than the submerged weight of the top stratum, the excess pressure will cause heaving of the top blanket, or will cause it to rupture at one or more weak spots with a resulting concentration of seepage flow in the form of sand boils. Where the foundation and top strata are heterogeneous in character, as is usually the case, seepage tends to appear at localized spots instead of causing the entire top stratum to heave or become "quick."

The hydraulic gradient required to cause heaving is called "the critical hydraulic gradient." This gradient is the ratio of the submerged unit weight of the soil to the unit weight of water and is usually approximately 0.85. Any tendency for the hydraulic gradient to increase above the critical gradient causes additional sand boils or increased percolation. In nature, high exit gradients and concentrations of seepage are usually found along the landside toe of the levee, at thin or weak spots in the top stratum, and adjacent to clay-filled swales or channels.

Where seepage is concentrated to the extent that it creates turbulent flow, the flow causes erosion in the top stratum and causes the development of a channel in the underlying silts and fine sands which frequently exist immediately below the base of the top stratum. As the channel increases in size or length, or in both, the concentration of flow into the channel becomes progressively greater, as does the tendency for erosion to occur beneath the levee. This is especially true if the top stratum is cohesive and the underlying soils are susceptible to erosion. Shrinkage cracks, root holes, and holes dug by man or by animals form channels in the top stratum susceptible to the development of localized flows and attendant piping. Not only is underseepage a hazard from the standpoint of underground erosion, but it also may saturate the landside slope of a levee and reduce its stability to such an extent that the slope may slough with attendant dangers to the levee.

Geology of Alluvial Valley

Detailed geological studies of several sites along the levees in the Lower Mississippi Valley where underseepage had been a problem during previous high waters show a definite correlation between the distribution of alluvial deposits of sand, silt, and clay and the location and occurrence of underseepage and sand boils. Thus, before it was possible to make an intelligent investigation of underseepage and to design control measures, an understanding of the alluvial fill in the Upper Mississippi Valley from Alton to Gale was necessary. The geological studies made for this project included field reconnaissances, studies of aerial mosaics, and a review of boring logs.

A few miles south of St. Louis, the Mississippi River cuts across an eastward extension of the Ozark Plateaus and, for a distance of approximately 100 miles, it flows in a narrow 3-miles-to-10-miles-wide, rock-walled, alluviated valley incised in ancient bedrock composed predominately of limestone. The river emerges from the plateaus through a narrow gorge called Thebes Gap into the broad Lower Mississippi Valley. The depth of the alluvial deposits in the St. Louis District is variable, ranging approximately from 75 ft to 200 ft with an average depth of approximately 125 ft.

In general, the river is adjacent to the bluffs on the Missouri side, with the floodplain east of the river in the State of Illinois. Tributary streams originate in the bluffs on the east, flow through the floodplain, and empty into the Mississippi River at frequent intervals between Alton and Gale. The levee system on the left bank in this area consists of levees which originate at the bluff, run parallel to the tributary streams toward the Mississippi River, and then along the Mississippi River to the next tributary stream (Fig. 1). Thus, the alluvial valley is subdivided into small areas, each with its own encircling levees.

Melting of the glaciers during late or postglacial times caused the entrenched valley to become filled with a series of sandy gravels, sands, silts, and clays, which can be grouped into two broad units: (1) A sand and gravel substratum and (2) a fine-grained top stratum.

The Pervious Substratum.—During the gradual rise of sea level which accompanied the final retreat of glacial ice, the Mississippi River became an overloaded, braided stream in which large quantities of gravel-bearing sands were deposited. As the sea level continued to rise and the deposits on the entrenched valley floor continued to thicken, stream slopes were progressively reduced and both the quantity and grain size of the material transported by the river decreased. The gravel-bearing sands were succeeded by coarse sands grading upward into progressively finer materials and terminating in deposits of very fine sand. This upward gradation from coarse to fine materials reflects the gradual adjustment between the transporting capacity of the river and the available load. Fine to very fine sands were not deposited until the sea level had essentially reached its present stand and the river had begun to change from a braided to a meandering stream. The substratum sands are quite pervious and have a high seepage-carrying capacity, as will be subsequently described.

The Top Stratum.—The predominantly fine-grained, top-stratum material was deposited by the Mississippi River as it meandered across the floodplain. Meander-belt deposits are characterized by marked lateral and vertical discontinuities and by wide variations in grain size and permeability. They are, therefore, of primary importance in the localization of underseepage and the design of control measures. Meander-belt deposits may be grouped as: (1) Point bar, (2) channel fill, (3) natural levee, and (4) backswamp. Such deposits can usually be identified in the field and on aerial mosaics.

Point-Bar Deposits.—As the radii of meander loops increase by erosion, deposition occurs on the inside bank where low sandy ridges are built up with intervening, elongated depressions which usually become filled with fine-grained deposits. Ridges and swales formed in this manner are known as point bars. Long sandy ridges, separated by clay-filled and silt-filled depressions which approximately parallel the margins of former river courses, are also characteristic of shifting river valleys and are especially common in the St. Louis District. These features appear to have been formed in migrating channels rather than on points and might well be referred to as channel bars and slough fillings. The upper part of these ridge and swale deposits is usually covered with clayey silts and silty clays which are deposited during gradual migration of the river channel from its former banks. Normally the slough fillings are approximately from 10 ft to 20 ft deep.

Channel-Fill Deposits.—When the river abandons its former course as a result of a cutoff, the central and lower parts of the old cutoff channel usually become filled with silts and clays which are relatively impermeable. Such deposits in the area studied may be from 40 ft to 80 ft deep.

Natural Levees.—When the river overflows its banks, the water spreads out, its velocity is reduced, and some of its sedimentary load is deposited. In this manner, long ridges known as natural levees are formed on the outside of meander loops and along both banks in straight reaches. Natural levee deposits found in the Upper Mississippi Valley appear to be predominantly sandy, approximately 5 ft high, and seldom more than 200 yd wide. Clearly distinct natural levees are relatively rare in the St. Louis District.

Backswamp Deposits.—Low-lying areas on the landside of natural levees are known as backswamps. These areas receive only quiet floodwaters and, as a result, the sediments deposited consist of fairly uniform silts and clays. Backswamp deposits create an almost impervious block to the emergence of subsurface seepage. There do not appear to be many, if any, true backswamp deposits in the St. Louis District; however, some thick clay top-stratum deposits resembling backswamp deposits were found adjacent to the valley walls.

Effects of Alluvial Deposits.—The emergence of seepage landward of a levee is influenced by: (1) Configuration of geological features, such as swale fillings and channel fillings, and their alinement relative to the levee; (2) characteristics and thickness of the top stratum; (3) cracks or fissures formed by drying and other natural causes; (4) borrow pits, post holes, seismic shot holes, ditches, and other works of man; and (5) decay of roots, uprooting of trees, animal burrows, crayfish holes, and other organic agencies. The severity of underseepage along a levee is frequently dependent on the configuration of geological features in that area. The greatest concentration of seepage always occurs along the edges of swales and the landside levee toe (Fig. 3).

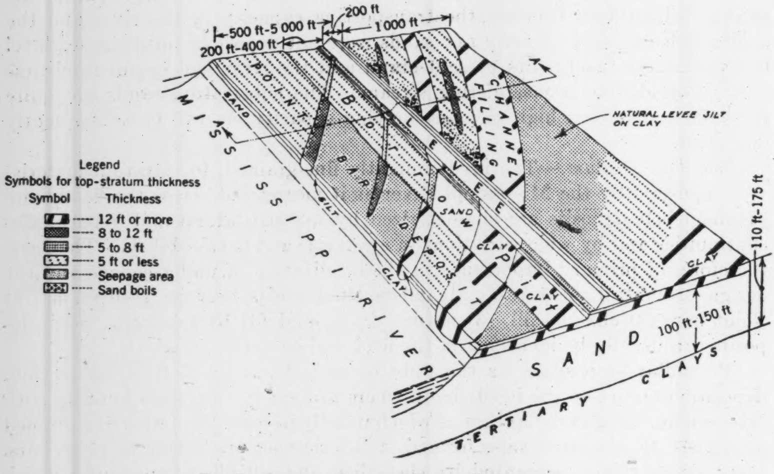
200 ft
500 ft-5 000 ft
1 000 ft
200 ft-400 ft
POINT BAR DEPOSIT
MISSISSIPPI RIVER
SAND
SILT
CLAY
BORROW PIT
LEVEE
CHANNEL FILLING
NATURAL LEVEE SILT ON CLAY
SAND
CLAY
CLAY
CLAY
A
A
SAND
100 ft-150 ft
110 ft-175 ft
TERTIARY CLAYS
Legend
Symbols for top-stratum thickness
Symbol Thickness
12 ft or more
8 to 12 ft
5 to 8 ft
5 ft or less
Seepage area
Sand boils

Fig. 3.—Seepage Through Point-Bar Deposits

Field Investigations

An extensive field investigation was made to ascertain the need for underseepage control measures and to obtain data on which to base their design. The field investigations consisted of a reconnaissance of all areas adjacent to the levees, the study of aerial mosaics, an intensive boring program, a geophysical investigation to determine the depth of the alluvial valley, and field pumping tests.

Field Reconnaissance.—Field reconnaissances were made along the levees for the purpose of noting features appearing on the ground surface that might affect the underseepage problem. The presence of geological features such as swales and sloughs and their orientation with respect to the levee were noted. The locations and extent of man-made features such as drainage ditches, stock ponds, and borrow pits were ascertained. The layout of new borings, made in the office on the basis of available soils data, levee heights, and a study of aerial mosaics, was checked in the field to insure adequate exploration of those features which would affect the underseepage problem and the design of control measures. The condition and depths of riverside borrow pits also were noted.

Aerial Mosaics and Maps.—Because there were no complete maps of the new levee system available to which the new borings, piezometers, and control measures could be referenced, a new folio of photomaps was prepared, showing all the Mississippi River levees and flood-control works in the area. These new maps will be used during flood-control operations and to record underseepage observations during future floods.

Boring Program.—At the beginning of the investigation the existing soils information was reviewed and a boring program planned to delineate soil conditions more precisely in potentially critical areas. Shallow borings to define the character and thickness of the top stratum along the landside toe of the levees were located on approximately 200-ft to 250-ft centers and at critical locations. Some shallow borings were also made farther landward of the levee in order to study pertinent geological features. A few borings were made in riverside borrow pits to determine the character and thickness of the remaining top stratum in these pits. In general, blanket borings were made with hand augers whenever water-table conditions would permit. Deeper borings (60 ft to 80 ft) were made on 1,000-ft to 1,500-ft centers to determine the characteristics of the subsurface sands for both the design and installation of relief wells in reaches where it was thought that control measures might be necessary. Some borings were extended to rock to determine the thickness of the pervious aquifer and to check geophysical determinations of the depth to rock.

Most of the deep borings were made using a 2-in., split-spoon sampler and using drilling mud to keep the hole open. Samples were generally taken at approximately 5-ft intervals and at points at which there were major changes in soil strata. A few undisturbed samples of the sand foundation were obtained with a 3-in. Shelby tube and drilling mud.[3] The reason for obtaining the undisturbed samples was to compare the grain size of the sands, as determined from such samples, with that of samples obtained with split-spoon and bailer samplers. Another reason for taking a few undisturbed sand samples was to study the stratification of the sand. A typical soil profile developed from field investigations is shown for a short reach of levee in the Harrisonville (Ill.) Levee District (Fig. 4).

---

[3] "Undisturbed Sand Sampling below the Water Table," *Bulletin No. 35*, Waterways Experiment tation, Vicksburg, Miss., June, 1950, pp. 1–19.

Geophysical Investigations.—Because of the difficulty and cost of ascertaining the depth to rock by means of borings, it was decided to obtain this information by means of geophysical explorations. At the beginning of the investigation the depths to rock were determined by the electrical resistivity method. In analyzing the data obtained, it became apparent that the depth to rock determined by the resistivity method was extremely sensitive to the method of interpretation and did not check very well the depths determined by borings. As a result, this method was abandoned in favor of the seismic method which involved making initial checks with a seismograph at locations where the depth to rock had been determined from deep borings and from excavation for the Chain of Rocks Canal Lock on the Mississippi River near St. Louis. Because good agreement was obtained, the seismic method was used for the remainder of the investigation.

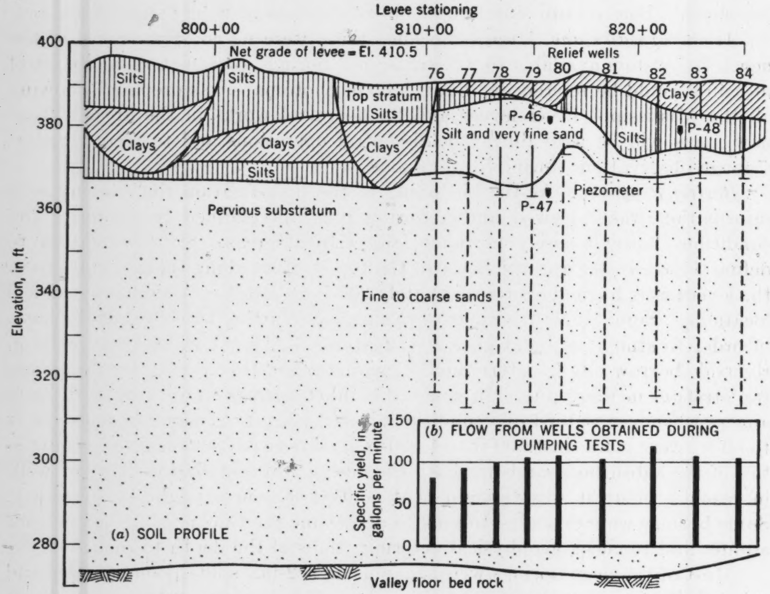

FIG. 4.—SOIL PROFILE, AND RELIEF-WELL AND PIEZOMETER-INSTALLATION DATA

Field Pumping Tests.—The design of relief wells along the levees in the St. Louis District was based on the assumption that the screens for the wells would penetrate the pervious aquifer underlying the levees to a depth which would result in the performance of a well system comparable to the performance obtained from a 50% penetration of a homogeneous, isotropic aquifer. Because the pervious strata underlying the levees along the Mississippi River generally become more pervious with depth, special pumping tests were performed on wells which fully penetrated the pervious aquifer. This was done for the purpose of determining the depth required for the well screens in order to achieve an effective penetration of 50%. The over-all permeability of the sand foundation at the sites of the test wells was also determined from these tests. The horizontal permeability of the various sand strata encountered at the test wells was determined by measuring the flow into the well screen from each sand stratum as previously delineated by a boring.

The field pumping tests consisted of pumping the wells at three different rates of flow, measuring the drawdown in the wells, and observing the drawdown in adjacent piezometers and wells. The flow in the well screen was measured at changes in strata by means of a calibrated, well-flow meter.[4] Head losses through the filter and the well screen and inside the well were measured by piezometers installed at the periphery of the gravel filter around the well screen. The over-all horizontal permeability, k_H, of the sand aquifer and of the individual sand strata was computed from the formula for artesian radial flow to a single well.

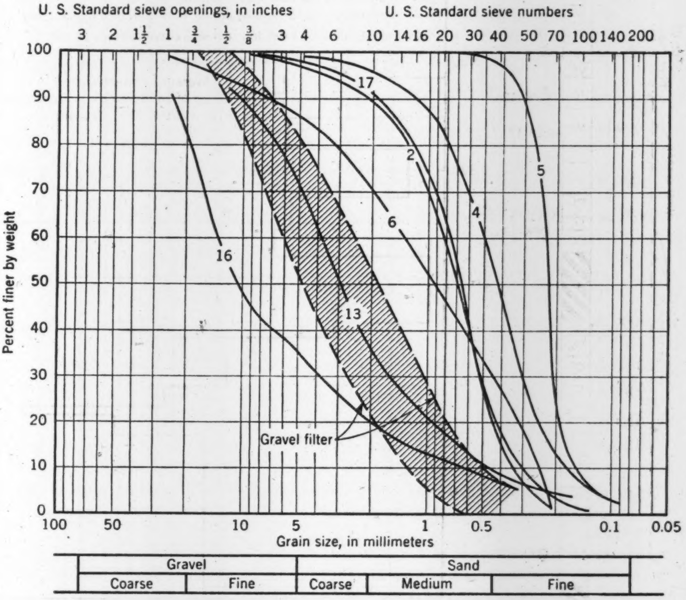

FIG. 5.—FOUNDATION SANDS AND FILTER GRAVEL–WELL FC-105

Grain-size curves of typical sands taken from a boring at one of the test wells (FC-105) together with the gradation of the filter gravel used around the well screen are shown in Fig.[5] 5. The permeabilities of the different sand strata encountered at well FC-105, as determined from laboratory tests and field pumping tests, are shown in Fig. 6.

---

[4] "Waterways Experiment Station Relief Well Flow Meter," *Miscellaneous Paper 5-83*, Waterways Experiment Station, Vicksburg, Miss., April, 1954.

The flow of the test wells was essentially artesian because of the existence of upper and lower impervious strata bounding the principal aquifer and because the water in the well was not drawn down below the top of the main sand stratum. As would be expected with artesian flow, drawdown in the test wells

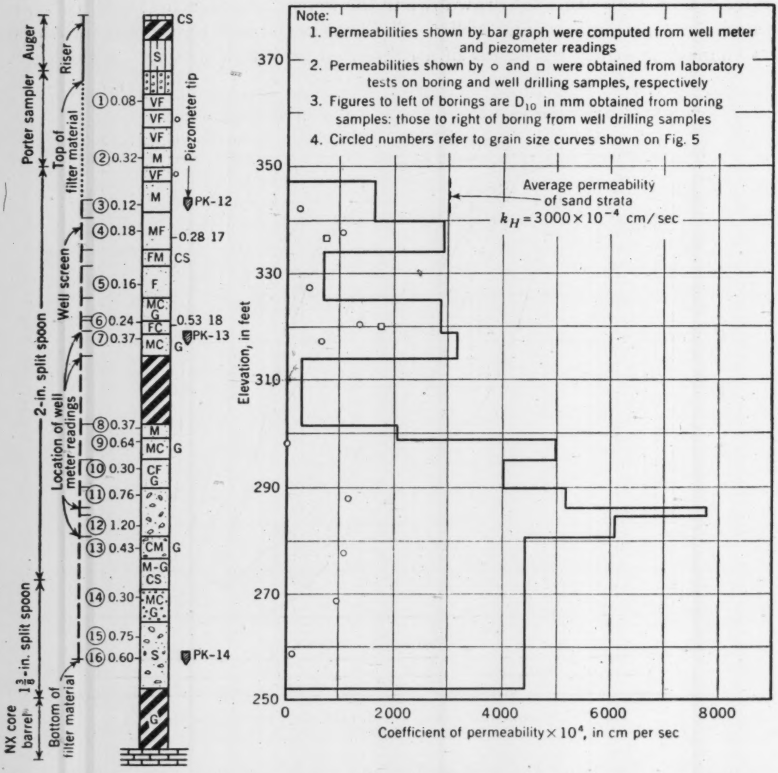

Note:
1. Permeabilities shown by bar graph were computed from well meter and piezometer readings
2. Permeabilities shown by ○ and □ were obtained from laboratory tests on boring and well drilling samples, respectively
3. Figures to left of borings are D_{10} in mm obtained from boring samples: those to right of boring from well drilling samples
4. Circled numbers refer to grain size curves shown on Fig. 5

FIG. 6.—COEFFICIENT OF PERMEABILITY AND EFFECTIVE GRAIN SIZE OF INDIVIDUAL SAND STRATA (WELL FC-105, LOCATED AT LEVEE STATION 301 + 25, FT. CHARTRES LEVEE DISTRICT, APPROXIMATELY 45 RIVER MILES SOUTH OF ST. LOUIS)

stabilized rapidly at a constant rate of pumping. Approximately 80% stabilization was achieved within 15 min to 30 min of pumping; full stabilization was achieved after 2 hr of pumping. Drawdown curves to the test wells, as plotted on semilog graph paper, resulted in straight lines, another indication of artesian flow to the test wells. The radius of influence of the different test wells ranged approximately from 500 ft to 1,000 ft. The specific yield from the test wells ranged approximately from 150 to 375 gal per min per ft of drawdown at the well. Head loss through the filter and wooden well screen was quite small, amounting to about 0.10 ft to 0.25 ft for a flow through the well screen of 10 gal per min per ft of screen. In analyzing the well test data, it was necessary to consider the hydraulic head losses in the well screen and riser pipe.

The results of the field pumping tests may be summarized as follows:

1. Little agreement was found between permeabilities determined in the laboratory on remolded samples and those obtained from the field pumping tests.

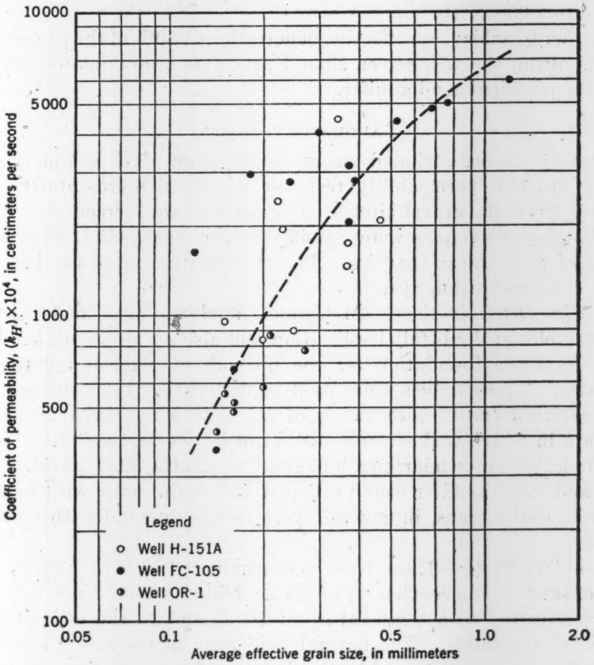

FIG. 7.—COEFFICIENT OF PERMEABILITY (k_H) VERSUS EFFECTIVE GRAIN SIZE (D_{10}) BASED ON FIELD PUMPING TESTS

There is no reason why the permeabilities should have agreed considering that the aquifer was stratified and that lenses of coarse sand and fine gravel existed. Generally, the field permeabilities for any given strata exceeded by from 2 to 4 times the permeability as normally determined in the laboratory.

2. A relationship between the effective grain size, D_{10}, and the coefficient of permeability, k_H, as determined from flow from individual sand strata is shown in Fig. 7. The scatter of points can probably be attributed to variation in uniformity of the grain-size curves and to the fact that the values of D_{10} used in the plot are based on the average of relatively few values of D_{10} for

each sand stratum tested. In the absence of pumping-test data, the curve shown in Fig. 7 may be of use to engineers concerned with seepage, water supply, or irrigation problems in the Mississippi River Valley.

3. The permeability of the principal seepage-carrying stratum at the test well sites ranged from 1,500 $\times 10^{-4}$ cm per sec to 3,000 $\times 10^{-4}$ cm per sec. The permeabilities of the individual sand strata varied from 200 $\times 10^{-4}$ cm per sec to 6,000 $\times 10^{-4}$ cm per sec. Pumping tests on relief wells subsequently installed throughout the St. Louis District indicated that the permeability of the principal seepage-carrying sand stratum generally ranges from 1,000 $\times 10^{-4}$ cm per sec to 2,000 $\times 10^{-4}$ cm per sec.

4. In order to achieve an effective penetration of 50% of the principal water-carrying stratum, the well screen should penetrate approximately 60% of the depth of the principal sand aquifer.

Laboratory Tests

Laboratory studies included visual classification of all samples, grain-size determinations and permeability tests on numerous representative samples, and filter tests on the gravel filter used around the well screens.

Classification.—Samples were classified both visually and, when in doubt, by means of mechanical analyses. The classification used was based on the Unified Soil Classification System.[5]

Grain-Size Determinations.—Mechanical analyses were made of any top-stratum samples of doubtful classification and also on numerous sand samples obtained from the foundation for the purpose of determining the D_{10}-size and D_{85}-size. These values were used in delineating the principal seepage-carrying stratum (sands with values of $D_{10} > 0.15$ mm) and in determining those strata in which well screens should not be set because of the possibility of the foundation sands migrating into and through the filter gravel. Although tests showed that the filter would satisfactorily drain sands with values of $D_{85} \geqq 0.15$ mm, well screens, in general, were not set in sand with values of $D_{85} < 0.25$ mm.

Permeability Tests.—These tests were conducted on a number of remolded samples of sand. The coefficients of permeability as determined in the laboratory were adjusted to a temperature of 20° C and to the estimated natural void ratio of the sands. The natural void ratio of the sands was estimated from the D_{50}-value of the sand.[6] Coefficients of permeability, as determined from laboratory tests on split-spoon samples of the alluvial sands, ranged from about 100 $\times 10^{-4}$ cm per sec to 2,000 $\times 10^{-4}$ cm per sec.

In connection with the permeability tests made on samples obtained with split-spoon samplers in mudded holes, it is emphasized that such samples are contaminated frequently by drilling mud. Therefore, it was necessary to wash all such samples thoroughly before performing any permeability tests. Some contamination of the samples taken with a Shelby tube in a mudded hole was also noted.

---

[5] "Unified Soil Classification System," *Technical Memorandum No. 3-357*, Waterways Experiment Station, Vicksburg, Miss., March, 1953.

[6] "Summary Report of Soil Studies," *Potamology Investigation Report 12-2*, Waterways Experiment Station, Vicksburg, Miss., October, 1952.

Filter Tests.—Several laboratory tests were also made to check the ability of the filter gravel specified for relief wells to protect foundation sands against piping into the well. The filter sample tested was on the coarse side of the gradation band specified. The thickness of filter tested was 6 in., the minimum required in the field.

Three relatively uniform sands, typical of the finer foundation sands encountered in the St. Louis District and having D_{85}-values of 0.20 mm, 0.15 mm, and 0.12 mm, respectively, were used in the tests. The tests proved that the filter would safely drain all the samples tested at gradients of less than 8. The maximum gradient existing at the interface between the sand foundation and filter during either pumping tests or flood periods when wells are in operation will probably not exceed 1. Therefore, it is concluded that if the filter material is satisfactorily placed and has a minimum thickness of 6 in. it should protect any sand with a D_{85}-value coarser than 0.15 mm.

METHODS OF UNDERSEEPAGE CONTROL

There are several methods which may be used for controlling seepage beneath levees. The choice depends on a number of factors, including the character of the foundation, cost, permanency, availability of right of way, maintenance, and disposal of seepage water. Devices that may be used to control underseepage are (1) landside berms, (2) relief wells, (3) impervious riverside blankets, (4) sublevees, (5) cutoffs, (6) drainage blankets, and (7) drainage trenches. Only the first two foregoing methods were considered practicable for the control of underseepage along the levees in the St. Louis District.

Landside Berms.—Landside berms have been used extensively for the control of underseepage. A berm serves to strengthen the top stratum, increase the base width of the levee, reinforce the landward slope of the levee against sloughing during high water, and move landward the emerging seepage or sand boils and piping from the levee proper. Landside berms were used along the levees in the St. Louis project wherever they were the most economical and where the top stratum landward of a levee was very thin or nonexistent and relief wells would have had to be installed excessively close together. Landside berms were also used where a levee was relatively low, but it appeared that certain precautions against underseepage and possible sloughing of the landside slope were desirable.

Relief Wells.—One method of controlling underseepage is to tap the underlying pervious strata with a series of relief wells. These wells will provide pressure relief and controlled seepage outlets which offer little resistance to flow and, at the same time, will prevent erosion of the foundation soils. This method has been used successfully by the Corps at a number of dams and along numerous levees underlain by a pervious foundation. Relief wells offer an advantage as compared to gravel toes, pervious blankets, and other surface measures where the foundation consists of stratified deposits of pervious materials in that they penetrate the more pervious strata in which pressure relief is necessary. With proper spacing and penetration, relief wells will reduce hydrostatic pressures landward of levees underlain by impervious foundations for a wide range of seepage entrances, foundation stratification, and landward top strata. In addition, seepage which formerly emerged landward of a levee in an uncontrolled manner without relief wells will be materially reduced, although the total of well flow plus seepage with wells will be increased.[7,8]

Impervious Riverside Blanket.—The natural top stratum riverside of levees frequently has been removed as a result of borrow operations in the construction of the levee, thereby exposing the pervious substratum and providing a ready source of seepage entry. In the St. Louis District no artificial, impervious blankets were placed riverward of the levees as a means of seepage control. However, where the river had scoured deep holes or channels in riverside borrow pits, these holes or channels were filled either by dredged or by hauled material, and abatis dikes were constructed to promote silting and the growth of willows in the pits.

Sublevees.—Areas known to be susceptible to dangerous underseepage may be encircled by one or more sublevees in which water can be impounded during high water to reduce the net effective head acting in this critical area. Construction of sublevees requires considerable right of way landward of a levee, skilful operation during high water to insure proper balancing of heads so as to prevent dangerous sand boils or blowouts, adequate spillways, and adequate section to insure that the sublevee itself will not fail during maximum flood stages because of a head of water in the sublevee basin. For these reasons, sublevees were not considered practicable as permanent underseepage control measures in the St. Louis District.

Cutoffs.—Where practicable, the most positive method of underseepage control is to cut off all pervious strata beneath a levee by means of an impervious barrier which will eliminate both excess substratum pressures and the problem of seepage water landward of a levee. However, completely cutting off pervious strata from 80 ft to 200 ft deep along extensive reaches of levees is not economically feasible. The installation of partly penetrating cutoffs will not reduce seepage and excess pressures significantly unless the cutoff penetrates 95% or more of the pervious aquifer. Because of this fact, which has been demonstrated by both mathematical and model studies,[9] no deep cutoffs were attempted along the levees in the St. Louis District. However, a few shallow cutoffs along the riverside toe of the levee were constructed to cut off relatively thin layers of either natural levee sands or crevasse sands which lie immediately under the base of the levee and which, in turn, are underlain by more impervious strata.

Drainage Blankets.—These blankets may be used for controlling underseepage where the levee is built on exposed sands and gravels of fairly homogeneous character. However, they are not effective for controlling seepage in deep substrata where the drain is underlain by impervious top strata or where stratified fine sands exist between the drain and the deeper, more pervious sand. No drainage blankets were used to control deep underseepage in the St. Louis District.

---

[7] "Relief Well Systems for Dams and Levees," by W. J. Turnbull and C. I. Mansur, *Transactions*, ASCE, Vol. 119, 1954, pp. 842–878.

[8] "Control of Underseepage by Relief Wells, Trotters, Miss.," *Technical Memorandum No. 3-341*, Waterways Experiment Station, Vicksburg, Miss., April, 1952, p. 61.

[9] "Efficacy of Partial Cutoffs for Controlling Underseepage Beneath Levees," *Technical Memorandum No. 3-267*, Waterways Experiment Station, Vicksburg, Miss., January, 1949, p. 63.

Drainage Trenches.—Drainage trenches may be used to control underseepage where the pervious foundation is of limited depth so that the trench substantially penetrates the formation. Where the pervious foundation is deep, a drainage trench of any practicable depth would attract only a small part of underseepage. The effect of this trench would be local, and detrimental underseepage would bypass the trench. Because of the depth of the pervious substratum along the Mississippi River levees, drainage trenches were not considered feasible for this project.

DESIGN OF SEEPAGE CONTROL MEASURES

Seepage control measures were considered necessary wherever the estimated head beneath the top stratum (at the landside toe of the levee or existing berm) at flood stages equal to the net grade of the levee would create an excessively high upward gradient through the top stratum. In agriculatural areas where it appeared that the upward gradient, i, would become equal to or exceed 0.85, seepage control measures were considered necessary. Where the gradient was between 0.67 and 0.85, piezometers were installed to measure the substratum pressure during future high-water periods; from these data, decisions will be made later as to the need for control measures. Where the gradient was less than 0.67, no control measures or piezometers were considered necessary. In industrial areas, control measures were considered necessary wherever i was expected to exceed 0.67 and were designed so that the gradient at the levee toe would not exceed 0.50.

The head, h_o, beneath the top stratum at the landside toe of existing levees was computed from the following:

$$h_o = \frac{H x_3}{s + x_3} \qquad (1)$$

in which H is the design net head on the levee; s denotes the distance from the landside toe of the levee to the effective seepage source; and x_3 is the distance from the landside toe to the effective seepage exit.

The design net head for riverfront levees was taken as the difference in elevation between the net grade of the levee and the average ground surface landward of the levee. Along the flank levees the design flood stage was taken as the elevation of the net grade of the river front levee at the intersection of the flank and riverfront levees. The distance to the effective source of seepage, s, was estimated from field reconnaissances of borrow pits, and the river, boring data, and piezometric data were obtained at similar sites along levees in the Lower Mississippi River Valley. For riverfront levees, values of s ranging from 600 ft to 1,000 ft were used for analytical and design purposes. Along flank levees where the seepage entrance is restricted to the bed of the tributary stream, values of s ranging from 800 ft to 1,500 ft were used. The distance from the landside-levee toe to the effective seepage exit, x_3 ,was computed from the following formula by Preston T. Bennett,[10] M. ASCE, which assumes that the top stratum is level and infinite in landward extent:

---

[10] "The Effect of Blankets on Seepage Through Pervious Foundations," by Preston T. Bennett, *Transactions*, ASCE, Vol. 111, 1946, pp. 215–252.

$$x_3 = \frac{1}{c} = \sqrt{\frac{k_f}{k_b} z\, d} \quad \ldots\ldots\ldots\ldots\ldots\ldots\ldots (2)$$

in which c denotes a constant; k_f/k_b is the ratio of horizontal permeability of the foundation to vertical permeability of the top stratum; z represents the top-stratum thickness in feet; and d equals the effective thickness of the aquifer in feet.

To simplify the preparation of design charts, it was assumed that $d = 80$ ft (variations in d between 50 ft and 120 ft do not greatly affect the values of h_o or x_3). Evaluation of the top-stratum thickness and of the permeability ratio was predicted largely on the thickness of the clayey part of the top stratum. The value of z was obtained by transforming the thickness of each layer of the top stratum into an equivalent thickness of material of constant vertical permeability. Where the top stratum was predominantly silty with less than 5 ft of clay, k_f/k_b was assumed equal to 400. When the top stratum consisted of 5 ft or more of fat clay, k_f/k_b was assumed equal to 1,000. The foregoing values of k_f/k_b were based on analyses of piezometric data from similar sites in the Lower Mississippi River Valley. By substituting x_3 (as given by Eq. 2) in Eq. 1, the head, h_o, can be expressed in terms of H and z for given values of s, k_f/k_b, and d. Design curves used for the computation of hydrostatic head at the landside toe of the levee without relief wells were developed from Eq. 1 and Eq. 2. A typical set of curves for $s = 800$ ft is shown in Fig. 8.

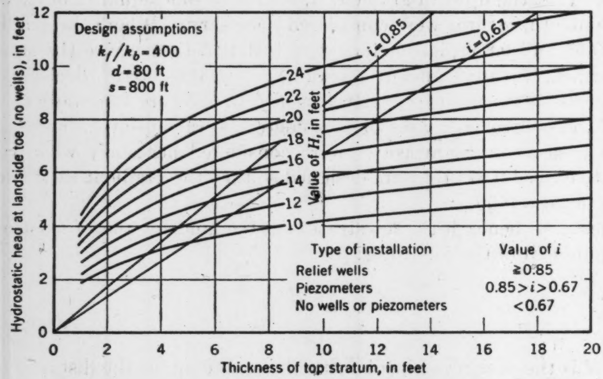

FIG. 8.—COMPUTED HYDROSTATIC HEADS AT LANDSIDE TOE OF LEVEES—NO RELIEF WELLS

Relief Wells.—Relief well systems were designed so that the gradient midway between wells would not exceed 0.67 in agricultural areas and 0.50 in industrial areas. The effective well radius, r_w, was taken as 0.9 ft, which is the distance to the periphery of the gravel filter. Design curves were developed from the equations of Reginald A. Barron,[11] A.M. ASCE, for an infinite line of fully penetrating wells with a semipervious top stratum. The curves were developed by computing the head midway between wells and then multiplying this head by the ratio of the head computed for 50% and for fully penetrating wells as obtained from formulas by T. A. Middlebrooks and William H. Jervis,[12] M. ASCE, and Morris Muskat,[13] respectively, for an impervious top stratum. Because the computed head midway between wells does not include hydraulic head losses in the well, these head losses were computed from the estimated flow from the well system and from hydraulic formulas, well-tank tests, and observations made on relief wells at Trotters (Miss.)[8] and added to the computed head midway between wells. The well spacing, a_c, was then adjusted so that the final head between wells, including hydraulic head losses, would not exceed the design values stated in the foregoing. Design curves were developed for $k_f/k_b = 400$ and for various distances to the source of seepage. Where $k_f/k_b = 1{,}000$, $a_c \cong 0.9\ a_c$ for $k_f/k_b = 400$. A typical set of design curves showing the relationship between the computed well spacing, a_c, adjusted for the head losses in the wells, and the top-stratum thickness for various heads on a levee is shown in Fig. 9. For the curves in Fig. 9 the penetration of the pervious aquifer by the well screen was 50%, and the head loss in the well was computed on the basis of a 25-ft riser and a 55-ft screen, assuming that $k_f = 1{,}000 \times 10^{-4}$ cm per sec and the top of the well at 0.33 ft above the ground surface.

---

[11] "The Effect of a Slightly Pervious Top Blanket on the Performance of Relief Wells," by Reginald A Barron, *Proceedings*, 2d International Conference on Soil Mechanics, Rotterdam, Vol. IV, 1948, p. 324.

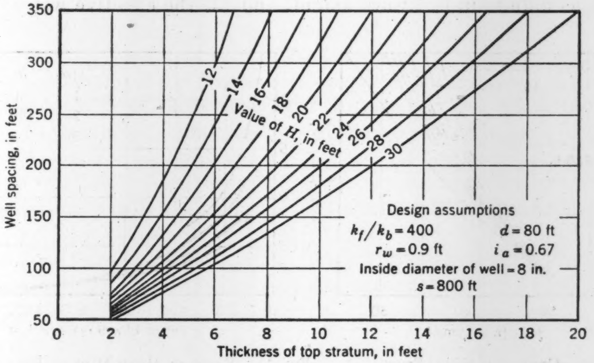

FIG. 9.—COMPUTED WELL SPACING ADJUSTED FOR HEAD LOSS IN WELL

The flow from relief well systems was obtained from Mr. Barron's formulas for fully penetrating wells, multiplied by the ratio of flow from 50% penetrating wells to that for 100% penetrating wells for an impervious top stratum as determined by Messrs. Middlebrooks and Jervis, and Mr. Muskat, respectively. The relationship between well flow, Q_w/H, for various top-stratum thicknesses and well spacings is shown in Fig. 10, in which the penetration of the pervious aquifer by the well screen is 50%. From the results of pumping tests conducted to date it now appears that the average k_f is approximately from 1,200 × 10^{-4} cm per sec to 1,500 × 10^{-4} cm per sec for the pervious substratum in the Upper Mississippi River Valley.

---

[12] "Relief Wells for Dams and Levees," by T. A. Middlebrooks and William H. Jervis, *Transactions*, ASCE, Vol. 112, 1947, p. 1321.

[13] "The Flow of Homogeneous Fluids Through Porous Media," by Morris Muskat, McGraw-Hill Book Co., Inc., New York, N. Y., 1937.

In a short, finite line of wells, the heads midway between the wells exceed those obtained for an infinite line of relief wells, both at the center and near the ends of the well system. Because numerous well systems were fairly short (less than 1,500 ft) it was necessary to reduce the computed well spacing for an infinite line of wells so that heads midway between wells in a short line of wells would not create an i-value in excess of the design value. The ratio of the head, midway between wells at the center of finite well systems, to the head between wells in an infinite line of wells is shown in Fig. 11 for various well spacings and exit lengths. In developing Fig. 10, it was assumed that (1) the penetration of the pervious aquifer by the well screen was 100%, (2) the semipervious top stratum was infinite in landward extent, and (3) the effective well radius was 1.0 ft. In Fig. 11, P_∞ is the head midway between wells in an infinite well line, computed from equations developed by Mr. Barron, and P_N denotes the head midway between wells at the center of a finite well line, computed from unpublished equations developed by W. E. Miner. Where a short line of wells was required, the spacing required was computed for an infinite line of wells, and this spacing then was divided by the ratio indicated in Fig. 11. In any finite line of wells of constant penetration and spacing, the head midway between wells near the ends of the system exceeds that at the center of the system. Thus, at the ends of both short and long well systems, the wells were generally made deeper to provide additional penetration of the pervious substratum so as to obtain the same head reduction as in the central part of the well line.

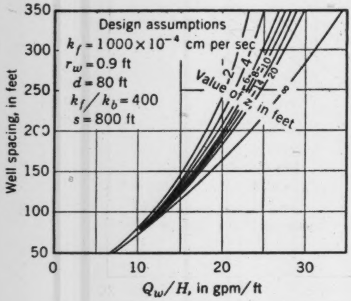

FIG. 10.—COMPUTED WELL FLOW

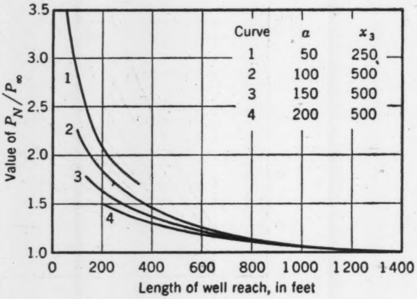

FIG. 11.—RATIO OF HEAD MIDWAY BETWEEN WELLS, AT CENTER OF A FINITE WELL SYSTEM, TO HEAD MIDWAY BETWEEN WELLS IN AN INFINITE LINE OF WELLS

The average well spacing for a given reach of levee was determined from design curves similar to those shown in Figs. 8 through 11 taking cognizance of the effect of geological features on seepage conditions. However, the location of each well was checked in the field and adjusted where necessary so that the wells would fit natural topographic features.

Seepage Berms.—These berms were designed by an empirical method developed by the Kansas City District that is based on electrical-analogy model studies in which it was assumed that the permeability of the berm would be the same as that of the top stratum. Adding a berm on the landside of a levee restricts the natural relief of pressure as a result of natural seepage through the top stratum and, thus, increases the hydrostatic head at the levee toe with respect to the original ground surface. This increase in head depends on the length, thickness, and permeability of the berm. The electrical-analogy model studies indicated that the effect of the berm on landside substratum pressures would be the same as if the impervious base width of the levee had been increased by 50% of the length of the berm. The nomenclature used in the design of seepage berms is shown in Fig. 12. The procedure used in designing seepage berms in the St. Louis District was as follows:

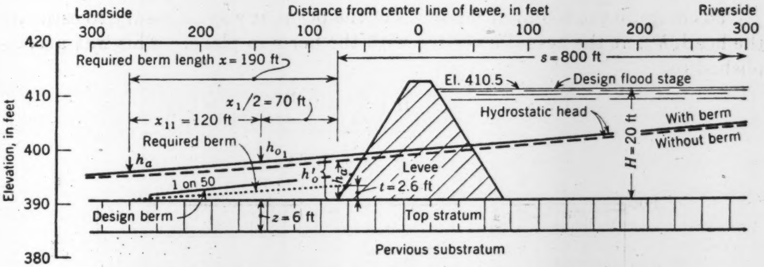
Landside
Distance from center line of levee, in feet
Riverside
300
200
100
0
100
200
300
420
410
400
390
380
Elevation, in feet
Required berm length $x = 190$ ft
$s = 800$ ft
El. 410.5
Design flood stage
$x_1/2 = 70$ ft
$x_{11} = 120$ ft
Hydrostatic head
With berm
Without berm
$H = 20$ ft
Required berm
h_{o_1}
h_a
h'_o
h_a
Levee
1 on 50
$t = 2.6$ ft
Design berm
$z = 6$ ft
Top stratum
Pervious substratum

FIG. 12.—NOMENCLATURE FOR DESIGN OF SEEPAGE BERMS

1. The head, h_o, at the landside toe of the levee without a berm was determined from Eq. 1. The allowable value of i_o with a berm was taken as 0.60 in agricultural levee districts and as 0.50 in industrial districts.

2. The allowable head at the berm toe, h_a, was taken as 0.85 z in agricultural levee districts and as 0.67 z in industrial districts.

3. The first trial length of berm x_1 was computed as that length of berm where the head, h_x, at the berm toe would be equal to h_a; this length was determined by means of Mr. Bennett's[10] blanket formulas.

4. The value of $x_1/2$ was then added to s, and the head, h_{o_1}, was computed from Eq. 1 at a point $x/2$ distant from the landside toe of the levee. The following equation results:

$$h_{o_1} = \frac{H\, x_3}{s + \frac{x_1}{2} + x_3} \qquad (3)$$

5. A new distance, x_{11}, from the assumed impermeable section ($x_1/2$ distant from the landside toe) was computed by means of the blanket formulas so that the head, h_x, at distance x_{11} would then be equal to the allowable head, h_a.

6. The required berm length, X, is then $x_1/2 + x_{11}$. To simplify the foregoing computations, it was found expedient to represent the blanket

formulas graphically as shown in Fig. 13, which shows the relationship between the ratio of head h_x (at a distance, x, landward of the levee) to the head, h_o, (at the toe) and the distance, x, divided by the exit length, x_3. By selecting h_a and substituting this value for h_x and knowing h_o and x_3, the distance, x, at which $h_x = h_a$ can readily be found.

To compute the required thickness of the berm, it was necessary to estimate the head, h^1_o, at the actual levee toe with the berm in place. This was accomplished by

$$h^1_o = \frac{H\left(\frac{x_1}{2} + x_3\right)}{s + \frac{x_1}{2} + x_3} \qquad (4)$$

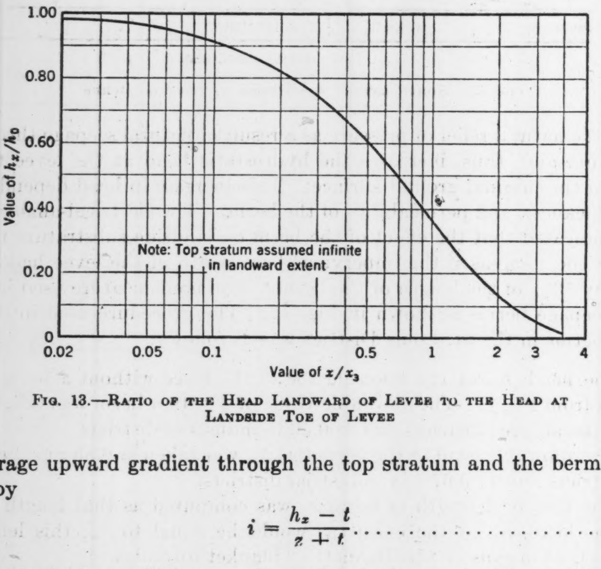

FIG. 13.—RATIO OF THE HEAD LANDWARD OF LEVEE TO THE HEAD AT LANDSIDE TOE OF LEVEE

The average upward gradient through the top stratum and the berm was expressed by

$$i = \frac{h_x - t}{z + t} \qquad (5)$$

in which t is the berm thickness. From Eq. 5, the required berm thickness, t at the levee toe can be found as

$$t = \frac{h^1_o - i_o\, z}{1 + i_o} \qquad (6)$$

in which i_o is the allowable upward gradient at the levee toe.

From Mr. Bennett's blanket formulas and from unpublished equations by Mr. Bennett for the design of seepage berms, an equation for determining the required length, X, of a berm was developed. This equation is as follows:

$$X = \frac{-A \pm \sqrt{A^2 - 24\,(2 + r)\left(1 + s\,c - \frac{H}{h_a}\right)}}{2\,c\,(2 + r)} \qquad (7)$$

in which A is equal to $6 + 3\,s\,c\,(r + 1)$; r denotes i_o/i_1; i_o is the allowable upward gradient at the landside toe of the levee; and i_1 is the allowable upward gradient at the landside toe of the berm. It should be noted that two values of X are obtained from Eq. 7. As a result of the sign convention adopted in developing the formula, the positive value of X gives the required berm length. The head, h^1_o, at the toe of the levee with the berm in place can be computed from the following:

$$h^1_o = h_a \left[1 + c\,X + \left(\frac{2 + r}{6}\right)(c\,X)^2\right] \ldots\ldots\ldots\ldots\ldots (8)$$

The required thickness of the berm at the levee toe is given by Eq. 6. The foregoing equations indicate the following required dimensions for the seepage berm illustrated in Fig. 12: $X = 175$ ft and $t = 2.5$ ft.

INSTALLATION AND CONSTRUCTION OF SEEPAGE CONTROL MEASURES

Relief Wells.—The relief wells along the levees in the St. Louis District have been and are being installed by the reverse-rotary method. This procedure for drilling holes for wells in sand is basically a suction-dredging method in which the material in the hole is removed by a suction pipe. The walls of the hole are supported by seepage forces acting against a thin film of fine-grained soil on the walls of the hole; the forces are created by maintaining a head of water in the hole several feet above the water table. A film of fine-grained soil is deposited on the walls of the hole by the drilling water as water and soil from the suction pipe are circulated through a sump pit. The sand settles out in the sump pit, and the water containing the fine-grained particles flows back from the pit into the hole. Successful drilling by the reverse-rotary method requires that the water table be approximately 7 ft or more below the ground surface and that there be an adequate supply of drilling water.

A typical reverse-rotary drilling unit is normally equipped with a large-capacity centrifugal pump and a 6-in.-diameter drill pipe, and is a bit similar in appearance to the cutterhead of a dredge. Where cobbles larger than approximately 3¾ in. are encountered, it is necessary to provide this type of equipment with a rock trap. Holes for relief wells also may be advanced by the reverse-rotary method using compressed air or a jet educator system, neither of which requires the use of rock traps.

A typical relief well consists of a screen section, riser pipe, gravel filter, sand backfill from the top of gravel filter to an elevation 10 ft below finished ground surface, and concrete backfill from the top of the sand backfill to ground surface. The riser and screen are of 8-in.-inside-diameter wood pipe. The screen is perforated with slots $\frac{3}{16}$ in. wide. The bottom of the well screen is closed with a wood plug. Tops of relief wells discharging on the ground surface are protected by metal well guards. (A schematic drawing of a typical relief well is shown in Fig. 14.)

As the boring for a relief well is advanced, samples of the foundation soil are obtained at 2-ft intervals by catching samples of the effluent from the drill rig in a bucket. The purpose of this sampling is to determine the depth at which the screen section of the well can be started and also to locate strata of silts, silty sands, and very fine sands through which unslotted sections of pipe are used instead of slotted screen. During or immediately after drilling operations, the well screen and riser pipe are assembled and guides are attached to the pipe to keep it centered in the hole as the filter gravel is placed. The hole for each well is overdrilled at by least 4 ft so as to provide a space at the bottom for filter gravel which may become segregated when the tremie pipe is first filled. The filter gravel is placed only after the screen and riser have been lowered to the correct depth and the top of the riser piper set about 4 in. above the natural ground surface. The filter gravel is placed by first lowering a perforated tremie to the bottom of the hole and filling it with filter gravel. The tremie then is slowly raised to allow the filter gravel to run out of the bottom as it is fed into the top. The tremie pipe is kept filled at all times with the filter gravel being

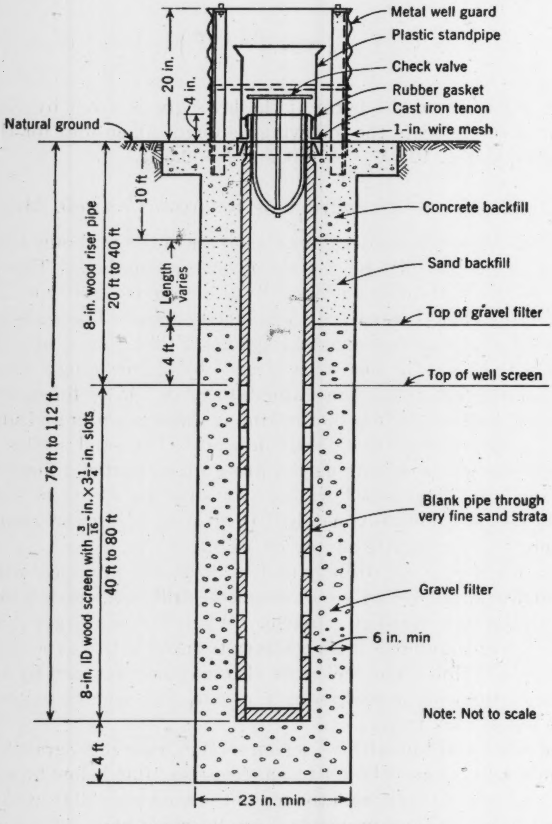
Metal well guard
Plastic standpipe
Check valve
Rubber gasket
Cast iron tenon
1-in. wire mesh
Natural ground
20 in.
4 in.
10 ft
Concrete backfill
Sand backfill
Length varies
20 ft to 40 ft
8-in. wood riser pipe
Top of gravel filter
4 ft
Top of well screen
76 ft to 112 ft
8-in. ID wood screen with 3/16-in.×3 1/4-in. slots
40 ft to 80 ft
Blank pipe through very fine sand strata
Gravel filter
6 in. min
Note: Not to scale
4 ft
23 in. min

FIG. 14.—RELIEF WELL AND APPURTENANCES

kept above the water surface so as to prevent any segregation of the gravel as it is placed. The filter gravel is placed to at least 4 ft above the top of the screen section so as to insure the existence of filter above the top of the screen after the well has been surged and developed.

After the filter is placed, material which has entered the well during the placing operations is removed, and the well is surged and pumped to remove drilling mud or other fines from the filter gravel. Surging and development pumping are started within 2 hr after the filter has been placed and are continued until the amount of material pulled through the screen between surging operations is less than 0.2 ft deep in the well. Surging is usually accomplished by lowering and raising a surge block made of a heavy rubber disk between two steel disks mounted on a steel rod. The rubber disk has a diameter of approximately 1 in. less than the inside diameter of the well, and the steel disks are 1 in. smaller than the rubber disk. The surge block is raised and lowered at a rate of travel of approximately 5 ft per sec.

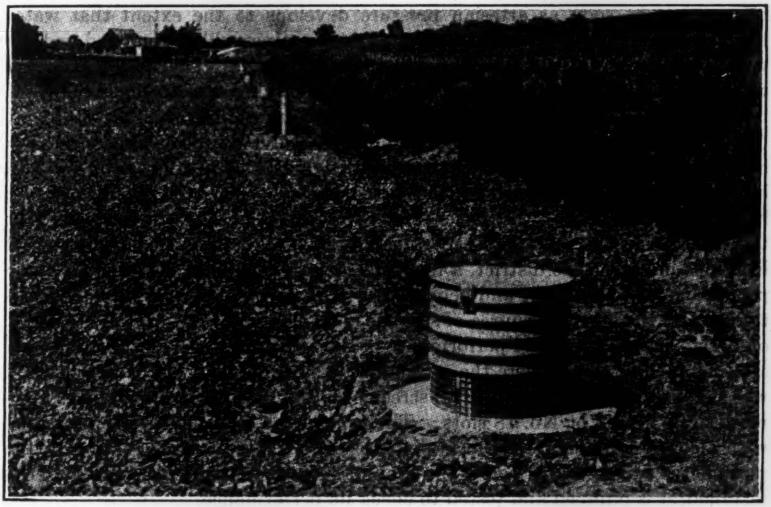

FIG. 15.—COMPLETED RELIEF-WELL SYSTEM

Each well is subjected to a pumping test after the completion of surging so as to achieve a drawdown of 5 ft in the well or a flow of at least 500 gal per min. The inflow of sand into a well during the pumping test is carefully checked for each well to prove its stability. This is accomplished by pumping the flow into a carefully baffled 1,000-gal sedimentation tank for 15 min. During this interval the sand in the tank is collected and measured, and the change in the amount of sand in the bottom of the well is determined. The pumping test is continued until the rate of inflow of sand into the well is less than 1 pt per hr. Fig. 4 illustrates a completed reach of a well system, showing the soil profile, spacing of wells, head on levee, and location of well screen and filter gravel; it also includes a bar graph of the specific yields of each well. A photograph of a completed well system is shown in Fig. 15.

The top of each well is protected against the backflow of muddy surface water by means of a specially designed rubber gasket and simple check valve as shown in Fig. 14. Accelerated full-scale laboratory tests have indicated this check valve to be very effective in preventing backflow of muddy water into a well under adverse conditions.

During periods of relatively low stages on the levees, relief wells will flow more than natural seepage. In agricultural areas each well is provided with a plastic sleeve which will raise the discharge elevation of the well to either 1 ft or 1.5 ft above the natural ground surface. These low sleeves or standpipes will prevent well flow at low river heads on the levee when no pressure relief is necessary. As soon as artesian pressure develops to the extent that water begins to spill over the top of the standpipes, the pipes will be removed and the well system allowed to operate as originally designed. The flow from relief wells in highly developed areas will be pumped over the levee during high water.

Piezometers.—Piezometers consisting of a 2-ft section of brass wellpoint (1¼ in. in diameter), plastic coupling, and 1¼-in. galvanized iron riser pipe have been installed in the pervious substratum immediately beneath the top stratum in almost all well reaches so as to check the efficacy of the well systems during high water. Generally these piezometers are installed between the wells near the end and in the middle of any sizeable reach of wells. At certain typical locations in each levee district, a few piezometers have been installed on a line perpendicular to the levee and beneath it. The purpose of these piezometers is to estimate the effective source of seepage entry at those locations and to check on design assumptions and performance of the well systems. Piezometers were also installed in areas where the estimated upward gradient at the design flood was between 0.67 and 0.85. The screens for the piezometers have either 40-mesh brass screen or No. 18 slots. The tops of the piezometers are protected with a column of concrete 6 in. in diameter which extends from just below the piezometer cap to 30 in. below the ground surface. After each piezometer is installed, it is pumped and tested to check its performance.

Seepage Berms.—These berms may be constructed by either hydraulic-fill methods or by hauling. Berms constructed of sand are preferable; however, the berms constructed to date (1955) in the St. Louis District have been generally built of random soil. In no event should a berm be constructed of soil that, when placed, is more impervious than the natural top stratum.

AMERICAN SOCIETY OF CIVIL ENGINEERS
Founded November 5, 1852

TRANSACTIONS

Paper No. 2895

A PRELIMINARY STUDY OF HIGH-RATE COMPOSTING

By John S. Wiley,[1] A. M. ASCE, and George W. Pearce[2]

With Discussion by Messrs. Pieter R. Krige; and John S. Wiley and George W. Pearce

Synopsis

Six 15-gal laboratory, mechanical composters (batch-type) for determining the criteria for the high-rate composting of organic wastes are described herein. Physical and chemical tests for indicating the degree of decomposition during composting are outlined, and typical results are presented. Optimum stirring and aeration rates, as well as the percentage of moisture in the initial charge, are presented for the laboratory units. The correlation of carbon dioxide and moisture production with the temperature of the compost is shown, together with the respiratory quotient for the decomposition.

Introduction

Garbage and refuse treatment and disposal in the United States are inadequate in most communities. The usual open dump is a public health hazard, an esthetic nuisance, a space consumer, and a waste of badly needed organic matter. Often, swine feed on raw garbage. This has devastating results, such as widespread outbreaks of vesicular exanthema and the less evident but important human disease, trichinosis. Burning more readily combustible material at a dump generally aggravates the nuisance without eliminating any other hazards. The second most popular method of refuse disposal, the sanitary landfill, eliminates the health and nuisance hazards, if properly operated, but this method still requires space and does not salvage organic matter for

---

Note.—Published, essentially as printed here, in December, 1955, as *Proceedings Paper 846*. Positions and titles given are those in effect when the paper or discussion was approved for publication in *Transactions*.

[1] Senior San. Engr., Dept. of Health, Education and Welfare, Public Health Service, Communicable Disease Center, Technical Development Labs., Savannah, Ga.

[2] Chief, Chemistry Section, Dept. of Health, Education and Welfare, Public Health Service, Communicable Disease Center, Technical Development Labs., Savannah, Ga.

return to the soil. Incinerators are expensive to build and operate and also destroy the organic matter. Although incinerators eliminate disease hazards associated with refuse disposal, they may increase the atmospheric pollution problem. If composting of garbage and refuse can be performed in mechanical units in a week or less than a week, health and nuisance hazards could be eliminated and a worthwhile by-product could be provided.

Composting of various organic wastes has been used for many years in Europe, Asia, and Africa. Generally, however, it is a slow process requiring from 6 months to 12 months under predominantly anaerobic conditions. Composting, as it was tried on a few occasions by cities in the United States, has largely failed. Recently, there has been considerable interest in aerobic, thermophilic composting in windrows or outdoor piles. The University of California,[3,4] at Berkeley, has conducted some outstanding studies on bin and windrow composting. These were the first basic studies to be made of the process in the United States. Additional studies on outdoor, aerobic composting have been conducted by the Communicable Disease Center, in Phoenix (Ariz.). There has also been considerable activity by several commercial groups and private individuals in aerobic, thermophilic composting in high-rate mechanical units.[5,6,7] Little research has been conducted to evaluate these processes or the basic factors of high-rate composting in mechanical units. However, Michigan State College, at East Lansing, has initiated such research,[8] and the field promises to produce a competitive method of treating refuse in a sanitary way.

STUDIES OF COMPOSTING

Studies being conducted at the Communicable Disease Center Laboratory at Savannah (Ga.) have as their objective the development of an economical method for converting organic wastes into usable by-products, while eliminating the health hazards created by disease vectors and pathogenic organisms. House flies in the form of eggs or larvae are often present in refuse reaching a dump and are attracted to and breed in exposed refuse. Rats and certain mosquito species, both of which may carry disease, are also problems in refuse disposal. Although pathogens may be or may not be an important public health problem in the disposal of community solid wastes, they constitute such a problem in sewage and sewage-sludge disposal.

Well-composted matter from the innumerable sources of organic wastes of a community may be of value to the farmer, the home gardener, and the nursery man. Such matter contains humus, which is badly needed in certain clay or sandy soils. Compost may also be beneficial to the soil in other ways: (*a*) By retaining moisture which would otherwise run off or percolate, (*b*) by checking excessive soil leaching, and (*c*) by improving the general texture and physical

---

[3] "Reclamation of Municipal Refuse by Composting," *Technical Bulletin No. 9*, San. Eng. Research Project, Univ. of California, Berkeley, Calif., June, 1953.

[4] "Stabilization of Municipal Refuse by Composting," by P. H. McGauhey and Harold B. Gotaas, *Transactions*, ASCE, Vol. 120, 1955, pp. 897–920.

[5] "A New Method of Garbage Disposal," by R. G. Kenyon, *Public Works*, June, 1952, p. 75.

[6] "Earp-Thomas Continuous Flow Digester," by G. H. Earp-Thomas, Earp Labs., Hampton, N. J.

[7] "Composting of Garbage and Sewage Sludge," by Eric Eweson, *Proceedings-Separate No. 312*, ASCE, October, 1953.

[8] "High-Rate Composting—A New Idea in Municipal Garbage Disposal," by John R. Snell, *Consulting Engineer*, August, 1954, pp. 49–53.

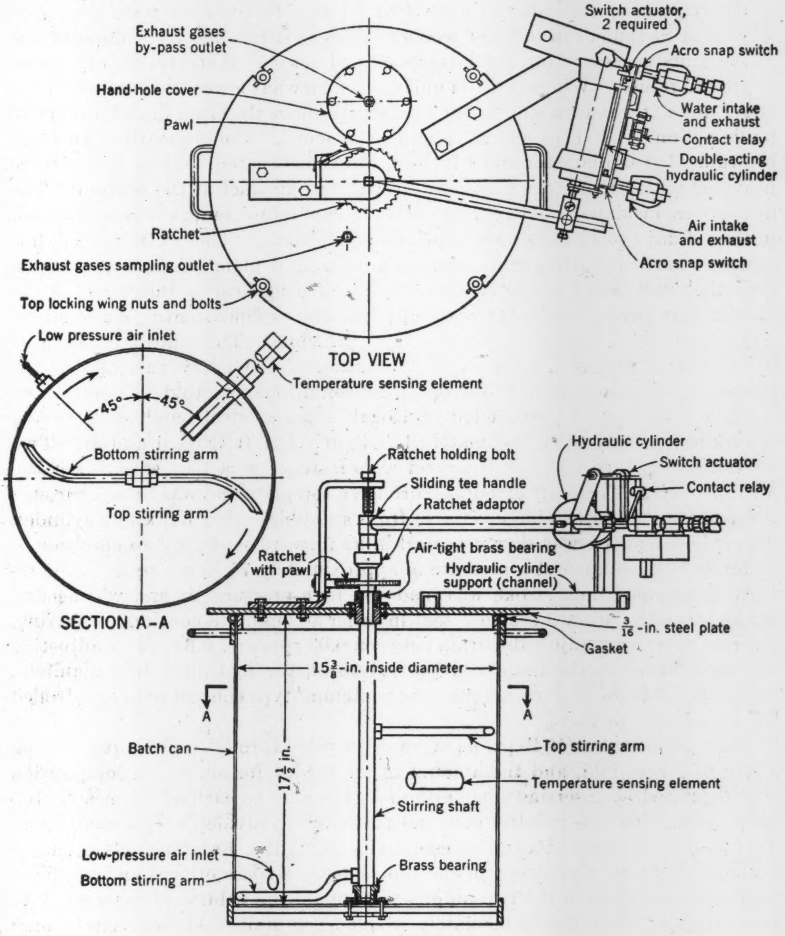
Switch actuator, 2 required
Acro snap switch
Exhaust gases by-pass outlet
Hand-hole cover
Water intake and exhaust
Pawl
Contact relay
Double-acting hydraulic cylinder
Ratchet
Air intake and exhaust
Exhaust gases sampling outlet
Acro snap switch
Top locking wing nuts and bolts
TOP VIEW
Low pressure air inlet
Temperature sensing element
45°
45°
Bottom stirring arm
Top stirring arm
SECTION A-A
Hydraulic cylinder
Ratchet holding bolt
Switch actuator
Sliding tee handle
Contact relay
Ratchet adaptor
Air-tight brass bearing
Ratchet with pawl
Hydraulic cylinder support (channel)
3/16-in. steel plate
Gasket
15 3/8-in. inside diameter
A
A
Batch can
17 1/2 in.
Top stirring arm
Temperature sensing element
Stirring shaft
Low-pressure air inlet
Brass bearing
Bottom stirring arm
CROSS SECTION FRONT VIEW

FIG. 1.—A COMPOSTING UNIT

condition of the soil.[9,10] Compost may be equal to or better than well-rotted stable manure when it is applied to the soil. The sale of such a by-product might reduce the cost of refuse disposal so that composting could compete economically with the less costly methods of disposal.

---

[9] "Wastes that Improve Soil," by Myron S. Anderson, in "Crops in Peace and War," *Yearbook of Agriculture*, U. S. Dept. of Agriculture, Washington, D. C., 1950–1951, pp. 877–882.

[10] "The Soil and the Microbe," by S. A. Waksman and R. L. Starkey, John Wiley & Sons, Inc., New York, N. Y., 1931.

Description of Laboratory Composting Units.—Preliminary tests were performed at Savannah in outdoor wooden boxes to determine the minimum size of the units necessary for the development of aerobic, thermophilic organisms in ground refuse. Whereas a 1-ft unit gave somewhat lower temperatures than larger units, it was apparent that temperatures above the lower limit for thermophilic action (113° F or 45° C) would be reached. Consequently, two units or drums, 1 ft in diameter and 1 ft deep, were constructed. These drums were provided with stirring mechanisms and with one air inlet at the bottom. The drums were insulated, held approximately 18 lb of refuse, and gave good compost in from 4 days to 11 days under optimum conditions. The central axis of one unit was vertical with stirring arms in a horizontal plane whereas the axis of the other unit was horizontal with vertical stirring arms. Inasmuch as the former unit gave slightly better results but did so consistently, six identical larger units were constructed on the same principle. The multiple units were developed to permit a more rapid evaluation of the many variables of the process in order to determine the optimum conditions for rapid decomposition.

These units were constructed of 15-gal, stainless-steel batch cans having a working capacity of approximately 11 gal, or 1.5 cu ft (Figs. 1 and 2). Two curved stirring arms ½ in. in diameter were fastened to a 1-in. square, vertical stirring shaft. The shaft extended through a top plate and was turned through a ratchet by an adjustable lever arm from a double-acting hydraulic cylinder. The cylinder piston was slowly pushed in its forward stroke by an emulsion of water and oil pumped at a pressure of approximately 75 lb per sq in. The return or nonoperating, stroke was made by high-pressure air and was accomplished rapidly (from 5 sec to 7 sec) in order to simulate continuous stirring. Stirring rates were adjustable from between 0.03 rpm and 0.6 rpm by adjusting the lever arms on the units and the valves on the hydraulic-fluid manifold. Three-way solenoid valves, actuated by a latching-type contact relay, controlled the liquid and air flows.

Low-pressure air (10 lb per sq in.) was provided through a pressure-reducing valve to a manifold, and the amount of air needed for aerobic decomposition was regulated by inserting small orifices in the lines to each unit. A steel top plate containing a 4-in. hand hole and plate, each provided with a gasket and thumb screws, made the units essentially airtight. Escaping gases passed through two hose nipples set in the top plates. Bypass orifices and sampling orifices were placed in the two nipples to regulate the volume of gases going to the samplers mounted immediately above each unit. Approximately one-twentieth of the air supplied to each drum was continuously passed through moisture and carbon-dioxide absorption tubes.

Temperature-sensing elements, connected to 3-pen, 24-hr recorders, were set 4 in. into the side of each drum at a height of 6½ in. above the bottom.

In most of the experiments the drums were covered with 2 in. of cotton duct insulation to reduce heat losses. Because all the operating mechanism is mounted above the top of the drums, the drums may be placed in water baths for temperature control if desired. The raw materials, which were ground, mixed, and sampled, were charged through the 4-in. hand hole into the drums. Subsequent samples of the solid materials were removed through the hand hole.

When a run was completed, the entire top and stirring mechanism was removed so that the drum could be emptied and cleaned.

Raw Materials and Method of Procedure.—After several unsuccessful attempts had been made to compost wet garbage from a hospital and a United States Air Force base, with and without adding dry materials such as paper, hay, and leaves, it was decided to use mixed garbage and refuse from the City of Savannah disposal area. Savannah has a combined collection system which includes mixed refuse and garbage with the exception of leaves, grass clippings, and tree limbs which are collected separately. Refuse collections are made three times a week from residential areas and are made on an average of from four to five times a week from business establishments. Present disposal (1955) is by sanitary landfill for both household refuse and yard refuse.

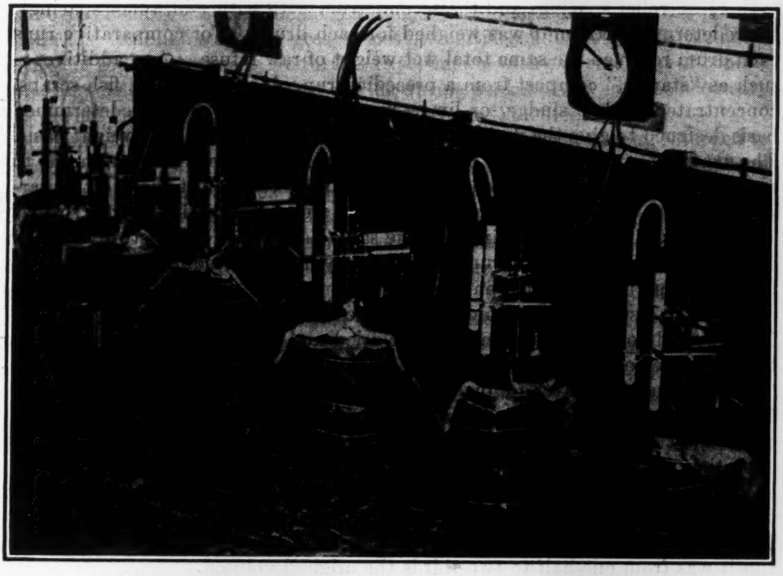

FIG. 2.—SIX LABORATORY COMPOSTERS IN OPERATION

Fresh material for experimental composting was collected by opening paper sacks of garbage recently dumped by collection trucks, throwing out most of the noncompostable items, and depositing the remainder in 30-gal cans. There was an excess of paper in the refuse, and the moisture content of the material to be composted was adjusted by the amount of paper included. It was estimated that residential refuse from Savannah had a moisture content of from about 30% to 35%, including paper of all kinds comprising more than 50% of the wet weight. From January 21, 1954, to April 12, 1955, average results from the analysis of 18 batches of raw refuse used in the experiments were:

Moisture (% of wet weight)	54.5
Volatile solids (% of dry weight)	91.5
Carbon (% of dry weight)	44.8
Nitrogen (% of dry weight)	1.21
Ratio of carbon to nitrogen	37.0
Protein (6.25N) (% of dry weight)	7.6
pH	5.5

Sufficient raw refuse was brought to the laboratory area where it was ground twice through a hammer mill provided with a roller screen. The first grind was with $1\frac{7}{8}$-in. roller spacings and the second grind with with $\frac{5}{8}$-in. roller spacings. A predetermined amount was weighed for each drum. For comparative runs each drum received the same total wet weight of raw refuse. Any additives—such as "starter," compost from a preceding run, chicken manure, fish scraps, concentrated sewage sludge, or lime—were also weighed on a predetermined basis designed to give the desired percentage of additive on a dry-weight basis. The exact moisture content of the initial mix was not known until from one to two days of the run had elapsed. When it was desired to test the effect of various additives, each unit received a computed amount of distilled water so that all units initially had approximately the same percentage of moisture.

Compost from preceding runs was generally used for seeding after some preliminary experiments had been made with runs having no additives and with runs having a starter (containing lime), lime by itself, and "finished" compost. The finished compost was generally air-dried and ground in the hammer mill through a perforated screen with $\frac{1}{4}$-in. holes.

Ingredients of a batch for one drum were thoroughly mixed and sampled before the drum was charged. Charging the six drums required from 1 hr to 2 hr of work by two men. At this time, stirring mechanisms and aeration were in operation. This period was needed to permit the charge to settle in the drum and to add more refuse. Quantities used per drum depended on moisture content, but they averaged approximately 36 lb (wet weight) and 16 lb (dry weight). The volume of the charge was reduced rapidly the first day. At the end of a run it was from one-half to two-thirds the original volume.

Several similar runs were made initially with all factors the same for each drum. Interruptions of stirring occurred frequently with an occasional interruption of air flow. These interruptions caused marked changes in the temperature of the compost, especially if they occurred on the second or third day when peak values were almost attained. Usually, stirring speeds, aeration rates, and sampling rates were held as constant as possible throughout a run. Some initial attempts at "tapered" aeration did not seem to produce the desired results.

At first, there were many mechanical difficulties. Some of these were failure of the hydraulic-fluid pump; inoperation or double operation of the relays, resulting in stoppage of the stirring; leaking of the O-rings in the cylinders (resulting in stoppage or diminished rates of stirring); bending or breaking of the stirring arms due to high torques; breaking of snap switches; power failure; and air-compressor failure. Gradual improvements in design and operation eliminated most of these difficulties.

Stirring rates were usually held from between 0.10 rpm and 0.16 rpm, with variations between drums in a single run being less than ±0.015 rpm. However, stirring rates are not critical, as will be shown subsequently. Aeration rates ranged from 0.24 to 0.27 cu ft per min per drum, or from 23 to 29 cu ft per day per lb of volatile solids in the initial charge.

Limited trials with and without the layer of insulating material around each drum indicated slightly higher temperatures, greater moisture evaporation and production, and slightly less carbon-dioxide production and volatile solids lost in the insulated drums. For the most part all drums have been insulated. In one trial, drums receiving air for aeration at average temperatures of 98° F and 67.5° F showed no significant differences in temperatures of the composting materials, although a slightly greater loss in volatile solids occurred in the drum receiving the warmer air. No further experiments with external heat or cooling were made, although it is felt that cooling during peak activity may be necessary to prevent the desired microorganisms from being killed.

The end of a run was indicated when all drums, or most of them, returned to approximately 10° F of room temperature. At that time, the entire top and stirring mechanism were removed, and the wet weight of the compost was obtained. Samples were analyzed so that the weights of the various components could be determined and compared with the initial values. Except in runs where the aeration rate or moisture of the initial mixture were varied, there was usually no drop in the percentage of moisture in the compost. The finished compost was adjusted to a suitable moisture content by partial air drying, or by adding water when necessary, rapidly mixed and aerated and placed in open cans for a reheating test. There should be little subsequent heating if the course of composting has been good. However, it has been determined that so-called finished compost will reheat sometimes more than once, when it is dried, reground to smaller sizes, and reconstituted with water. Reheating experiments were later conducted two or three times, including at least one drying and grinding operation.

Sampling and Testing Procedures.—Duplicate samples were collected for moisture determinations initially, every three days, and finally samples were collected in covered metal dishes having a capacity of approximately 250 ml. The moisture content was determined gravimetrically by drying in an oven at from 102° C to 105° C for about 48 hr. Drying periods of as short as 24 hr were found to be insufficient for the size of samples used (from 60 g to 150 g). Some of the more readily volatilized compounds, such as volatile acids, carbonates, and ammonia, may have been included as moisture in the oven-drying process. Moisture was reported as a percentage of wet weight. After drying, the duplicate samples were ground in a laboratory mill through a perforated screen with 1-mm holes, and the ground samples were stored in sealed jars.

A test for volatile solids[11] measured the amount of combustible matter or weight lost during the ashing of a sample. To determine volatile solids, duplicate samples of redried samples (from 3 g to 6 g) were ashed at from 650° C to 700° C for at least 2 hr in a muffle furnace. The percentage of volatile solids was computed on a dry-weight basis. The volatile solids represent primarily organic matter in the compost, but they may also include volatile minerals and carbon dioxide lost during ignition. Corrections for materials added to the refuse before or during composting have not been applied to the results reported. The addition of lime, starter, or compost from a previous run increased the ash content, thus decreasing the percentage of volatile solids.

---

[11] "Standard Methods for the Examination of Water, Sewage, and Industrial Wastes," Am. Public Health Assn., Inc., New York, N. Y., 10th Ed., 1955, p. 353.

The carbon content and nitrogen content of the oven-dried and ground samples after redrying at from 102° C to 105° C were also determined. The total carbon content was determined by a semimicro, wet combustion method[12]; approximately 15 mg of the sample were used. The carbon content, C, was reported as a percentage of dry weight.

The nitrogen content, N, excepting nitrites and nitrates, was determined by a micro-Kjeldahl procedure using from 10 mg to 15 mg of a ground, redried sample. The nitrogen content was reported as a percentage of dry weight. The protein content was estimated by multiplying the nitrogen content by the factor, 6.25. The carbon-nitrogen ratio was computed as C/N.

Samples of from 5 g to 10 g were collected daily for a pH-determination. They were diluted with distilled water free of CO_2, and determination was made by means of a glass-electrode pH-meter after vigorous stirring.

The temperature of the composting material was continuously recorded, and records were also maintained of the ambient (room) temperature. Temperatures of the inlet air admitted to the drums varied less than 2° F from the ambient temperature.

Special samples were removed from the drums whenever desired. Amounts removed because of all samplings, together with estimated losses or spills, were added to the final net weights of compost removed from the drums.

Carbon dioxide and moisture were the two major products of aerobic composting that were found in the outlet gases. The moisture collected from outlet gases was due to both the evaporation of free moisture in the composting mixture and to the biological oxidation of organic matter. In order to obtain a stoichiometric balance between the input and the output of each drum, measured portions of the outlet air were sampled continuously to determine their H_2O-contents and CO_2-contents. Moisture was sampled in 18-in. by $1\frac{1}{4}$-in.-diameter glass tubes containing Drierite (8-mesh anhydrous $CaSO_4$). These tubes contained from 300 g to 250 g of Drierite capable of absorbing approximately 75 g of moisture. The indicator color changed from blue to pink as the Drierite absorbed water. The moisture was determined gravimetrically for the measured quantity of air sampled. It was then converted by computation to the total quantity for the 24-hr flow for each drum and expressed in pounds per day per 100 lb of volatile solids (the initial charge in each unit). Tubes were changed once a day, the sampling periods varying from 1,000 min to 1,500 min. Drierite was regenerated by heating.

Carbon dioxide was similarly absorbed and determined gravimetrically following the removal of moisture by the Drierite tubes. Ascarite (sodium-hydroxide-impregnated asbestos, of from 8 mesh to 20 mesh) was used in 12-in. by $1\frac{1}{4}$-in.-diameter glass tubes. These tubes contained from 180 g to 205 g of

---

[12] "Rapid Methods for Assay of C-14 Labelled Compounds and Total Carbon in Organic Wastes," *Chemical Memorandum No. 3*, Communicable Disease Center, Technical Development Labs., Savannah, Ga., 1955.

Ascarite capable of absorbing approximately 60 g of carbon dioxide. The Ascarite changed color from light brown to white as it absorbed CO_2. The CO_2 was also reported as pounds per day per 100 lb of volatile solids. Air-sampling flows were measured with a wet test meter after the air had passed through the Drierite and Ascarite tubes. Total air flow to each drum was checked periodically with the wet test meter and was found to be essentially constant.

A few special or nonroutine tests were performed on raw refuse and compost. These tests included fly rearing; bacteriological plate counts of thermophilic bacteria, actinomycetes, and fungi; reducing sugars; and moisture determined by the method developed by Karl Fischer.[13] However, more work is necessary before these results can be reported.

Although other by-products, in addition to CO_2 and H_2O, were released atmospherically—such as volatile acids, occasional ammonia, and others—it was believed that the total of these products was small compared to the total mass being composted. As a result, everything with a significant total weight was measured except for the oxygen consumed in the oxidation process. The aerobic composting process might be represented by

$$\left[\begin{array}{ccc} & \text{Intake} & \\ C_pH_qO_rN_s + aH_2O + & & bO_2 \\ \text{(Raw garbage)} & & (O_2 \text{ used}) \end{array}\right] \rightarrow$$

$$\left[\begin{array}{cccc} \text{Output} & & & \\ C_tH_uO_vN_w + cH_2O + & dH_2O\uparrow \quad + & eH_2O\uparrow \quad + & fCO_2\uparrow \\ \text{(Finished compost)} & (H_2O\text{ evap-} & (H_2O\text{ pro-} & (CO_2\text{ pro-} \\ & \text{orated)} & \text{duced)} & \text{duced)} \end{array}\right] \quad ..(1)$$

The lower-case letters represent constants for given conditions. If only the organic matter that is destroyed is considered, Eq. 1 is simplified to

$$\underset{\text{(Volatile solids lost)}}{C_xH_yO_z} \quad + \quad \underset{(O_2\text{ used})}{b\,O_2} \rightarrow \quad \underset{(CO_2\text{ produced})}{x \quad CO_2\uparrow} \quad + \quad \underset{(H_2O\text{ produced})}{\frac{y}{2}\,H_2O\uparrow} \quad ..(2)$$

The weight of oxygen may be obtained by difference as all other constituents are known. The respiratory quotient (R.Q. = volume CO_2/volume O_2) may be computed and checked against other aerobic decomposition processes, such as the activated sludge process.[14]

Typical Composting Run.—A typical garbage-composting batch run is shown in Fig. 3, with curves for the temperature and the pH of the compost and for the H_2O and the CO_2 produced and evaporated in the outlet gases. The temperature of the composting mass increased rapidly to approximately 100° F in 24 hr. At this point, there was a reduction in the rate of temperature increase for approximately a day. Sometimes the curve showed a plateau or even a downward slope during this period. The temperature then increased rapidly into the thermophilic range, reaching a peak of from 140° F to 160° F, generally on the third or fourth day. The compost temperature then declined to within 10° of ambient, usually at the end of from 6 days to 9 days.

---

[13] "Aquametry," by John Mitchell, Jr., and Donald M. Smith, Interscience Publishers, Inc., New York, N. Y., 1948.

[14] "Biochemical Oxidation of Dairy Wastes. IV. Endogenous Respiration and Stability of Aerated Dairy Waste Sludge," by S. R. Hoover, Lenore Jasewicz, and Nandor Porges, ***Sewage and Industrial Wastes***, Vol. 24, 1952, pp. 1144–1149.

The initial phase of composting was acidic, the pH falling from an initial value of from 6.0 to approximately 4.5 in the first day or two. The second sharp rise in temperature usually coincided with a rapid increase in the pH, and peak temperatures were seldom reached until the pH was 7.0 or more. Most of the thermophilic action occurred under alkaline conditions, the pH reaching from 8.0 to 8.5 as temperatures reached their peak and started to decline. There was usually a slight drop in pH near the end of a run.

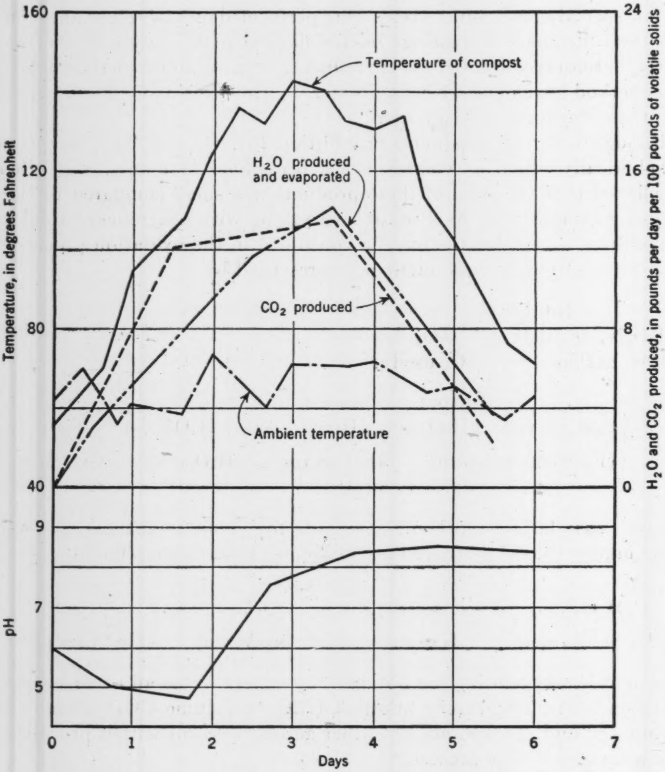

FIG. 3.—TYPICAL GARBAGE COMPOSTING RUN (RUN 25, DRUM 4—6.3% COMPOST ADDED, INITIAL MOISTURE, 65.7%)

Moisture and carbon dioxide in the outlet gases increased to a peak that was nearly simultaneous with the peak temperature and then decreased. Generally, the CO_2-output slightly exceeded the total H_2O-output during the first half of a run, and the reverse was true during the last half. Analyses for the same run shown in Fig. 3 are given in Table 1.

Percentage values of moisture, nitrogen, and protein increased. The carbon for all 6 drums in this run averaged 40.3% on the last day, indicating little or no change during the run, although results for drum No. 4 showed a slight increase. The C/N and volatile solids showed a decrease during the run.

TABLE 1

Day	Moisture content, in % of wet weight	Volatile solids, in % of dry weight	Carbon, C, in % of dry weight	Nitrogen, N, in % of dry weight	C/N
0	65.7	93.1	41.7	1.22	34
3	66.8	91.4	...	..	..
6	70.1	91.2	42.9	1.54	28

Whereas percentage values appeared to show little change during composting, the absolute weights showed a marked decrease, as indicated in Table 2 and Fig. 4. Losses in dry weight, especially the volatile-solids component, and total weight are considered important. Moisture loss by evaporation may be increased significantly by using more air, faster stirring, or better insulation of the units. The oxygen used and the CO_2 and H_2O produced are direct measurements of the activity of the microorganisms. The oxygen content was computed by subtracting the initial charge, 43.8 lb, from the total output, 49.8 lb. This value, 6.0 lb, can also be checked by means of the discharged materials and volatile solids that are lost.

TABLE 2

Component	Intake	Output	Loss	Loss, in %
Volatile solids	13.6	9.8	3.8	27.9
Ash	1.0	1.0	0.0	0.0
Total solids	14.6	10.8	3.8	26.0
Moisture	29.2	25.2	4.0	13.7
Total composting materials	43.8	36.0	7.8	17.8
Oxygen used	6.0	...	...	...
Water evaporated	...	4.0	...	...
Water produced	...	2.6	...	...
Carbon dioxide produced	...	7.2	...	...
Total	49.8	49.8	0.0	0.0

H_2O produced = 2.6 lb; H_2 = 0.29 lb; O_2 = 2.31 lb
CO_2 produced = 7.2 lb; C = 1.96 lb; O_2 = 5.24 lb
Total discharged: H_2 and C = 2.25 lb; O_2 = 7.55 lb
Total C, H_2, and O_2 recovered in outlet gases = 9.8 lb
Volatile solids lost = 3.8 lb
Difference, made up by the O_2 from air = 6.0 lb

Actually, 6.6 lb of moisture was recovered in the Drierite tubes during the run. The loss in moisture from the compost, 4.0 lb, was subtracted from the total moisture to give the net amount of H_2O produced by oxidation, which was 2.6 lb. Part of the O_2 needed for the oxidation, 1.55 lb, came from the organic constituents (primarily the carbohydrates, C H O), whereas the majority, 6.0 lb, was drawn from the air supplied. The respiratory quotient for this run is

$$\frac{\text{Volume CO}_2}{\text{Volume O}_2} = \frac{7.2/44}{6.0/32} = \frac{0.164}{0.188} = 0.87.$$

Average results for 25 runs with from 1 drum to 6 drums in operation are summarized in Tables 3 and 4, which give analyses and weight losses.

Weight balances were computed for 9 runs with from 1 drum to 6 drums, as shown in Table 5.

In general, losses in volatile solids varied from 17% to 53% with an average of 30% in 25 runs. This indicated that nearly one-third of the organic matter was decomposed to water and carbon dioxide. The moisture and carbon dioxide released weighed slightly more than 2.6 times the weight of volatile solids lost. This extra weight came from the oxygen used in the decomposition. The slight loss in ash content shown in Tables 4 and 5 is probably the result of sampling or of other errors. However, the fact that there was no appreciable gain in ash content indicates that little mineralization, if any, occurred.

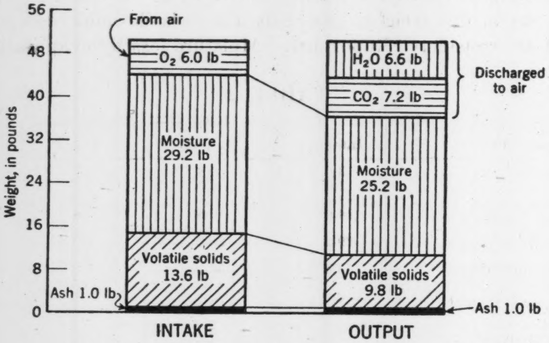

Fig. 4.—Stoichiometric Balance for Run 25, Drum 4

The composting periods averaged 7.3 days. However, in some cases runs were continued for from 1 day to 3 days longer than the time required for compost temperatures to reach within 10° F of ambient. Although compost temperatures, in most cases, fell to within 10° F of room temperature, the material at the end of a run still contained considerable organic matter subject to decomposition. The more readily oxidizable matter was decomposed, and the structure and character of the material was changed considerably. Paper, wood, cellophane, rags, bones, and similar materials showed little evidence of decomposition. However, most of the wet garbage was no longer recognizable.

Citrus peels and banana stalks could be distinguished, but they were shriveled to less than half their original size and were quite dark in color. The finished compost had an earthy or moldy odor like that of well-digested sewage sludge. It was dark brown when wet, light brown when dry, and was very fluffy after being air-dried and finely ground. It was thought that materials such as sugars, starches, pentosans, and similar compounds were completely destroyed whereas there was little or no destruction of cellulosic matter which probably comprised the bulk of the residual organic material. The average C/N was reduced from approximately 35 to 25 during composting. Soil humus has a C/N of approximately 10, despite the original source of the organic matter—that is, peat moss, manures, or compost.[15] It seems unlikely that garbage or municipal wastes can be produced with a C/N of this order by composting. However, garbage composts having C/N of from 25 to 30 could be expected to be readily converted to soil humus under most conditions. A suit-

TABLE 3

	Moisture content, in % of wet weight	Volatile solids, in % of dry weight	Carbon, in % of dry weight	Nitrogen, in % of dry weight	C/N	pH
Initial.....	56.4	89.4	42.1	1.21	35	5.74
Final......	53.3	85.3	41.9	1.67	25	7.99

TABLE 4

Component	Intake	Output	Loss	Loss, in %
Volatile solids................	11.3	7.9	3.4	30.1
Ash.........................	1.4	1.3	0.1	7.1
Total solids..............	12.7	9.2	3.5	27.6
Moisture......................	17.1	11.4	5.7	33.3
Total....................	29.8	20.6	9.2	30.9

TABLE 5

Component	Intake	Output	Loss	Loss, in %
Volatile solids...................	14.3	10.5	3.8	26.6
Ash..........................	1.5	1.4	0.1	6.7
Total solids.................	15.8	11.9	3.9	24.7
Moisture......................	22.3	14.6	7.7	34.5
Total composting materials...	38.1	26.5	11.6	30.5
Oxygen used..................	6.1	...	...	...
Water evaporated..............	...	7.7	...	...
Water produced.................	...	2.4	...	...
Carbon dioxide produced.........	...	7.6	...	...
Total......................	44.2	44.2	0.0	0.0

---

[15] "Artificial Manures," by Arthur B. Beaumont, Orange Judd Publishing Co., New York, N. Y., 1946.

able test for the desirable end point of composting has not been developed so far. Such a test should consider both the agricultural and health implications of the material, which may be distributed for use by the public.

The data available from 17 runs, in which initial and final nitrogen contents were determined, show that there was no loss of nitrogen for the average values:

	Initial	Final
Nitrogen, (% of dry weight)	1.21	1.67
Dry weight, in pounds	11.8	8.55
Nitrogen, in pounds	0.143	0.143

Some nitrogen loss was evident in a few runs because of an ammonia odor in the outlet gases. The presence of ammonia was variable, and the factors affecting its production have not been studied.

Physical Factors for Optimum Composting.—Although insulation and heating to speed up the composting process have been cited herein, neither appears necessary for large units (including those of commercial size). However, one or the other appears necessary for small laboratory units in which the area of surface exposure is large in proportion to the mass of material.

TABLE 6

	Run 23		Run 26	
Initial charge (same for each drum):				
Garbage and refuse, in pounds	28.0		34.0	
Compost, in pounds	2.0		2.0	
Total, in pounds	30.0		36.0	
Initial moisture, in % of wet weight	55.4		51.6	
Initial volatile solids, in % of dry weight	91.5		90.7	
Air supplied, in cubic feet per minute	0.26		0.25	
Speed	Drum	Stirring rates, in revolutions per minute	Drum	Stirring rates, in revolutions per minute
Low	6	0.035	1	0.05
	5	0.12	2	0.10
Medium	1	0.20	3	0.19
	4	0.27	4	0.35
High	3	0.52	6	0.55
	2	0.53	5	0.61

Duplicate runs were made with each of the six drums operating at a different stirring rate throughout the run and with all other variables held as constant as possible. Conditions for the two runs are shown in Table 6.

To determine the effect of stirring speed on the temperature of compost (Fig. 5), values were averaged for the two drums with the lowest speeds, the two drums with middle speeds, and the two drums with the highest speeds; there are four values in each group. Results indicated little difference within the speed ranges tested. This, of course, applied to the type of stirring in these particular units, in which only two curved stirring arms were attached to the shaft of each drum. This method of stirring was rather inefficient because the ½-in. stirring arms sometimes cut paths through the compost instead of mixing or moving the entire contents of the drums. A certain amount of caking of the material occurred on the bottom, on the stirring arms, and on the temperature-sensing element. Any slight advantage appeared to be in favor of the stirring rates in the range of from 0.19 rpm to 0.35 rpm because of the slightly higher peak temperature and quicker return to room temperature of the compost. Extremely slow speeds (0.035 rpm to 0.05 rpm) resulted in the lowest peak temperature, the slowest return to room temperature, and the smallest losses in the weight of volatile solids and moisture. Therefore, it was concluded that stirring rates of from 0.10 rpm to 0.61 rpm, and possibly faster rates, should be satisfactory for composting in the experimental units. If more efficient stirring is achieved or if the entire contents of a composter are tumbled or constantly mixed, different stirring or tumbling rates might be indicated. In addition, a high moisture content in the initial mix may require faster turning than a low moisture content. Better stirring may also reduce aeration requirements by providing more intimate contact between the organic particles and oxygen to be utilized and by better sweeping out of waste gases and vapors.

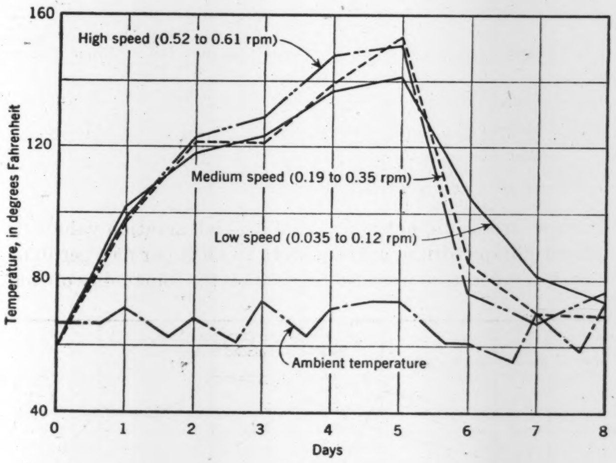

Fig. 5.—Effect of Stirring Speed on the Temperature of the Compost (Runs 23 and 26)

Variations in the aeration rate had a marked effect on the course of composting. In runs 24 and 27, the aeration rate was varied with all other factors held as constant as possible (Table 7).

Combining temperature values for both runs in the ranges of low, medium, and high aeration rates resulted in the curves shown in Fig. 6, in which the values contained in parentheses are the aeration rates in cubic feet per day per pound of volatile solids. Low aeration (from 0.035 to 0.055 cu ft per min per drum, or from 4.0 to 6.4 cu ft per day per lb of volatile solids in the initial charge) resulted in a late peak temperature (seventh day) and in incomplete compost by the ninth day. Medium aeration (from 0.10 to 0.26 cu ft per min per drum, or from 9 to 29 cu ft per day per lb of volatile solids) resulted in a peak temperature occurring on the fourth day with a slow decline until the ninth day when the composting was considered complete. Following the composting run, materials in these drums did not reheat. With high aeration values (from 0.35 to 0.67 cu ft per min per drum, or from 33 to 78 cu ft per day per lb of volatile solids) the peak temperature was also reached on the fourth day of composting. However, this peak temperature was followed by a rapid decline to room temperature by the sixth day. Nevertheless, even after composting had been continued for three additional days, the compost reheated to a temperature of more than 140° F after it was removed from the drum, mixed, aerated, and

TABLE 7

	Run 24		Run 27	
Initial charge (same for each drum):				
Garbage and refuse in pounds	30.0		34.0	
Compost, in pounds	2.5		2.0	
Total, in pounds	32.5		36.0	
Initial moisture, in % of wet weight	58.3		51.7	
Initial volatile solids, in % of dry weight	91.8		90.7	
Stirring rate, in revolutions per minute	0.08 to 0.10		0.10 to 0.11	
Aeration	Drum	Aeration rate, in cubic feet per minute	Drum	Aeration rate, in cubic feet per minute
Low	1	0.035	6	0.036
	2	0.055	5	0.055
Medium	3	0.11	4	0.10
	4	0.25	3	0.26
High	5	0.35	2	0.36
	6	0.67	1	0.65

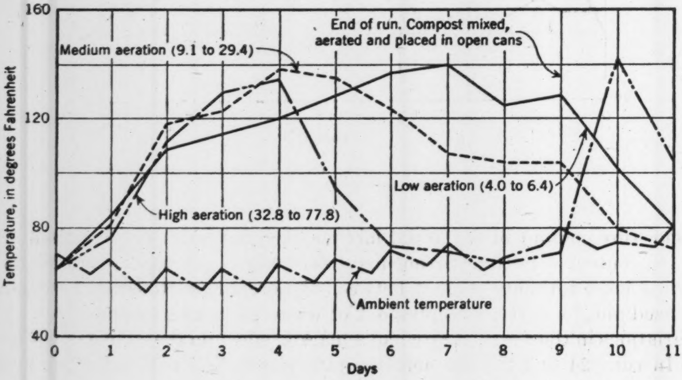

FIG. 6.—EFFECT OF AERATION ON THE TEMPERATURE OF THE COMPOST (RUNS 24 AND 27)

placed in open cans. This was a higher value than the value attained during the primary composting run. It could be concluded that low aeration provided either insufficient oxygen or insufficient sweeping out of waste gases. This resulted in a prolonged period of composting but with no reheating of the material after initial composting. Medium or adequate aeration values (from 10 to 30 cu ft per day per lb of volatile solids) resulted in a relatively rapid climb to the peak temperature, then in a slow decline to room temperature, followed by an inability of the compost to reheat. High aeration rates resulted in rapid cooling and dehydration of the compost, with apparent completion of the process in a short period but with reheating when subsequent wetting, mixing, and storage was accomplished. The latter result indicated that oxidation was incomplete and that the compost was not a finished product but a product which could become a nuisance or a health hazard unless it was treated further to reduce the oxidizable organic matter.

TABLE 8

	Run 25			Run 29		
Initial charge (same for each drum):						
Garbage and refuse, in pounds	25.0			22.9		
Compost, in pounds	1.25			1.25		
Total (excluding added moisture), in pounds	26.25			24.15		
Initial volatile solids, in % of dry weight	93.1			93.1		
Air supplied, in cubic feet per minute	0.25			0.25		
Stirring rate, in revolutions per minute	0.09 to 0.10			0.14 to 0.16		
Moisture	Drum	Moisture added, in pounds	Initial moisture, in % of wet weight	Drum	Moisture added, in pounds	Initial moisture, in % of wet weight
Low	1	..	44.6	1	..	40.2
	2	4.0	52.9	2	3.15	47.1
Medium	3	9.5	58.7	3	7.65	54.7
	4	17.5	65.7	4	13.75	61.9
				5	22.45	69.0
High	5	26.3	72.0	6	36.05	76.0
	6	36.8	76.6			

Moisture content also had a noticeable effect on the course of composting. In runs 25 and 29 the moisture content of the initial mix was varied and all other factors were maintained as constant as possible (Table 8).

In computing values for the temperature curves (Fig. 7), values from drums 1 and 2 of both runs were averaged, indicating low moisture (from 40% to 53%); values from drums 3 and 4 (run 25) and drums 3, 4, and 5 (run 29) were averaged, indicating medium moisture (from 55% to 69%); and the remaining three values, indicating high moisture (from 72% to 77%) were averaged. The curves for all ranges of moisture content showed a peak temperature on the third day. The average for the low moisture content came to a peak of 130° F, dropped to ambient temperature by the sixth day, and reheated to 101° F after adjusting the moisture, mixing, and aerating. The final moisture values were considerably lower than the initial values, and the loss of dry weight and volatile-solids weight was small. With a medium moisture content the peak temperature was 147° F and the compost was at room temperature on the sixth day with no subsequent reheating. Dry-solid and volatile-solid weight losses were favorable (from 17% to 31%), and the final moisture content was the same as or slightly higher than it was at first. The curve for the high-moisture drums had a peak temperature of only 109° F, and, by the sixth day, the temperature was still 20° above ambient (89° F). After the compost had been partly dried, mixed, and aerated, the temperature rose to approximately 97° F, indicating that the composting had not been completed. Under the conditions of these experiments it was concluded that optimum composting occurs when the moisture content of the refuse is started and maintained in the range of from 55% to 69%. Values below 50% are too low and values above 72% are too high. These values apply to garbage and refuse with a relatively high paper content because it was necessary to retain much of the paper found in the raw refuse in order to keep the initial moisture low in the basic materials for these experiments.

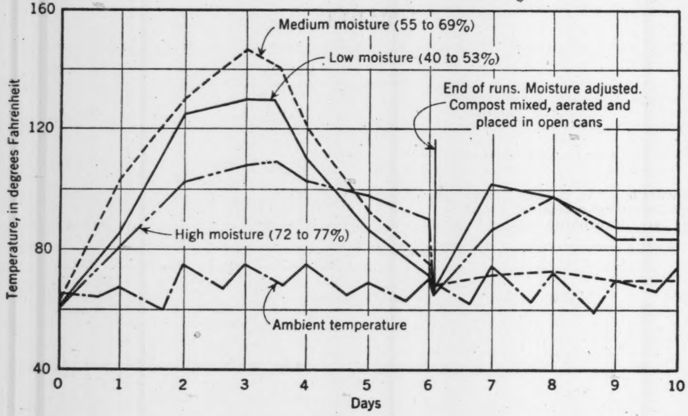

FIG. 7.—EFFECT OF MOISTURE ON THE TEMPERATURE OF THE COMPOST (RUNS 25 AND 29)

Correlation of CO_2 and H_2O with the Temperature of the Compost.—Because the production rates of CO_2 and H_2O during composting represent the rate at which decomposition is proceeding, they were compared with compost temperatures to determine any correlation between the two. Initial scatter diagrams on arithmetic paper showed good correlation, but the points seemed to lie on a concave curve. Plotting the points on semilog paper, with the CO_2 production rates and the H_2O production and evaporation rates on the log scale, gave better correlation and lines that were more nearly straight. This is understandable because the microorganisms experienced a logarithmic phase of growth under favorable conditions. Fig. 8 shows examples of the correlations obtained, together with the lines of best fit computed by the method of least squares.[16]

---

[16] "Statistical Methods," by George W. Snedecor, The Iowa State College Press, Ames, Iowa, 4th Ed., 1946.

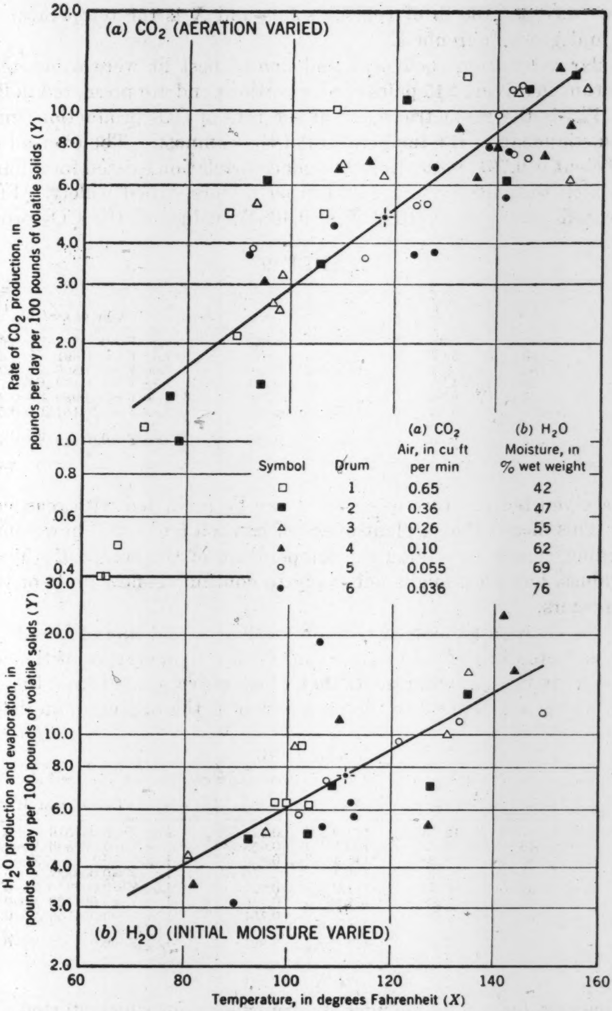

FIG. 8.—CORRELATION OF THE RATE OF CO_2 PRODUCTION (RUN 27) AND THE RATE OF H_2O PRODUCTION AND EVAPORATION (RUN 29) WITH THE TEMPERATURE OF THE COMPOST

Correlation between the CO_2 production rate and the temperature of the compost is shown for run 27 in which the aeration rates of the six drums differed widely. A correlation coefficient, r, of 0.844 was obtained with 54 pairs of observations, N, indicating excellent correlation. The line of best fit was $\log Y = 0.01177X - 0.7093$, in which Y is the rate of CO_2 production in pounds per day per 100 lb of volatile solids and X is the temperature of the compost in degrees Fahrenheit.

A similar correlation coefficient and line of best fit were computed for a total of 8 runs involving 245 pairs of observations and are presented in Table 9, in which Y_{mg} is the geometric mean of the rate of CO_2 production and X_m is the arithmetic mean of the temperature of the compost. The over-all correlation coefficient is 0.791, indicating that good correlation existed for a number of runs in which the initial charges and other factors varied widely. From the line of best fit ($\log Y = 0.01012\ X - 0.4084$), values of the CO_2 production rate for a given temperature of compost can be predicted with reasonable accuracy. This means that a plant operator can tell fairly well how composting is proceeding merely by taking the temperature of the compost. These particular values, however, might not apply to continuous-flow units or to plant-size composters.

TABLE 9

Runs	N	Y_{mg}	X_m	r	Line of best fit
14 to 16	47	7.30	124.9	0.653	$\text{Log } Y = 0.01225\ X - 0.6660$
25	36	5.07	100.4	0.871	$\text{Log } Y = 0.01091\ X - 0.3908$
26	54	5.31	111.2	0.832	$\text{Log } Y = 0.00896\ X - 0.2715$
27	54	4.79	118.0	0.844	$\text{Log } Y = 0.01177\ X - 0.7093$
28	24	8.02	127.9	0.784	$\text{Log } Y = 0.00989\ X - 0.3600$
29	30	5.65	111.3	0.712	$\text{Log } Y = 0.01181\ X - 0.5626$
Total	245	5.75	115.4	0.791	$\text{Log } Y = 0.01012\ X - 0.4084$

Fig. 8 (*b*) shows a similar correlation coefficient and line of best fit for the moisture collected in the outlet gases and for the temperature of the compost. The moisture in this case represents that which is evaporated from the compost and that which is produced by decomposition of the organic materials. The scatter diagram for run 29 includes six drums, each of which started with material having a different initial moisture content. The r-value of 0.751 with the N-value of 30 indicates good correlation. The formula for the line of best fit is $\log Y = 0.008565\ X - 0.0740$, in which Y is the H_2O produced and evaporated, in pounds per day per 100 lb of volatile solids, and X denotes the temperature of the compost in degrees Fahrenheit.

TABLE 10

Runs	N	Y_{mg}	X_m	r	Line of best fit
14 to 16	47	12.60	124.9	0.475	$\text{Log } Y = 0.007519\ X + 0.1614$
21	48	5.40	100.5	0.658	$\text{Log } Y = 0.008836\ X - 0.1590$
23	36	8.39	119.4	0.830	$\text{Log } Y = 0.1162\ X - 0.4687$
25	36	5.36	100.4	0.970	$\text{Log } Y = 0.008837\ X - 0.1582$
26	54	6.26	111.2	0.923	$\text{Log } Y = 0.007410\ X - 0.0274$
28	36	9.88	128.9	0.916	$\text{Log } Y = 0.009773\ X - 0.2646$
29	30	7.58	111.3	0.751	$\text{Log } Y = 0.008565\ X - 0.0740$
Total	287	7.52	113.6	0.827	$\text{Log } Y = 0.009142\ X - 0.1619$

The results of similar computations for a total of 9 runs with 287 pairs of observations are given in Table 10. The over-all coefficient of correlation is 0.827, and the formula for the line of best fit is $\log Y = 0.009142\ X - 0.1619$.

Runs 24 and 27 were omitted from these computations because they were the aeration experiments, and because widely different aeration rates greatly affect the moisture evaporated. Fig. 9 shows the effect of changing aeration rates on the relationship between the rate of moisture, which is produced and evaporated, and the temperature of the compost. High air flows evaporate much more moisture from the compost than low air flows, even though the temperature of the compost may be the same. There is no correlation between the H_2O which is produced and evaporated and the temperature under these conditions. The lines for each drum were drawn by eye. Under conditions in which aeration is in the optimum range, it is possible to predict the amount of moisture given off in the outlet gases from the temperature of the compost.

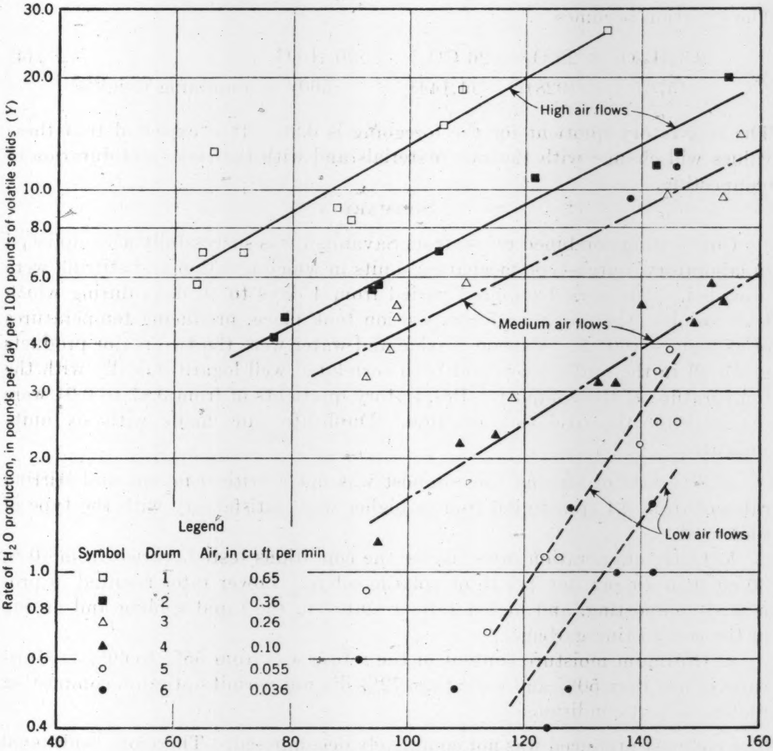

Fig. 9.—The Effect of Variation in Aeration on the Relationship of H_2O Production and Evaporation with the Temperature of the Compost

Continuous analyses of the discharge rates of H_2O and CO_2 were made for 9 runs. From these data, together with the loss in volatile solids and the oxygen utilized, it was possible to solve Eq. 2 for an empirical formula for the organic matter destroyed:

$$\begin{array}{ccccccc} C_xH_yO_z & + & bO_2 & \rightarrow & \times CO_2\uparrow & + & \frac{y}{2}H_2O\uparrow \ldots\ldots\ldots (3) \\ \text{(Volatile solids} & & \text{(}O_2\text{ used,} & & \text{(}CO_2\text{ pro-} & & \text{(}H_2O\text{ produced,} \\ \text{lost, 3.8 lb)} & & \text{6.1 lb)} & & \text{duced, 7.6} & & \text{2.4 lb)} \\ & & & & \text{lb)} & & \end{array}$$

The equation becomes

$$\begin{array}{ccccccc} 2C_{13}H_{20}O_7 & + & 29\ O_2 \rightarrow & 26\ CO_2\uparrow & + & 20\ H_2O\uparrow & \ldots\ldots\ldots\ldots\ldots\ldots\ldots (4) \\ (576) & & (928) & (1{,}144) & & (360) & \text{(combining weights)} \end{array}$$

The respiratory quotient for the foregoing is 0.90. It is expected that these values will change with the raw materials and with the stage and duration of composting.

SUMMARY

Composting combined refuse from Savannah was successfully accomplished in laboratory, batch-type mechanical units in which aeration and stirring were provided. The period required varied from 4 days to 10 days during which time aerobic, thermophilic decomposition took place, producing temperatures of as high as 160° F. Carbon dioxide and water were the two major products given off in the outlet gases and both correlated well logarithmically with the temperature of the compost. Respiratory quotients of from 0.87 to 0.91 were obtained for the oxidation reaction. Duplicate runs made with six units indicated:

a. The rate of stirring the compost was not a critical factor, and stirring rates of from 0.1 rpm to 0.6 rpm or higher were satisfactory with the type of unit used.

b. Optimum aeration rates, under the conditions tested, varied from 10 to 30 cu ft of air per day per lb of volatile solids. Lower rates resulted in prolonged composting, and higher rates resulted in the rapid cooling and drying of the composting garbage.

c. Optimum moisture content of the refuse was from 55% to 69%. Moistures of less than 50% and more than 72% did not permit optimum composting under the test conditions.

The compost produced was not completely decomposed. Therefore, additional experiments are needed to determine if this compost is suitable for use as a soil conditioner and humus, as determined by both public health criteria and agricultural criteria.

ACKNOWLEDGMENTS

The writers gratefully acknowledge the assistance of Lawrence B. Hall and Richard P. Lonergan in the design and construction of laboratory composting units. They also wish to thank Lewis W. Pyle for the determinations of carbon and nitrogen and Lawrence C. Gray, J.M. ASCE, for his assistance in conducting composting runs.

DISCUSSION

Pieter R. Krige[17].—A valuable contribution to the fundamental data on composting has been made by Messrs. Wiley and Pearce. The technical information offered will be most useful in certain phases of work in South Africa connected with the establishment of a semilarge-scale pilot plant to study more specifically the economics of producing compost from various forms of organic wastes.

Under the heading, "Studies of Composting: Raw Materials and Method of Procedure," the nature of the raw material used in the experiments was indicated, and mention was made of garbage, residential refuse, and raw refuse. When the writer visited the United States (November, 1954) the impression was gained that the terms, "garbage" and "refuse," were not synonymous. It is obvious, however, that the work conducted by the authors was confined to the use of garbage as the main ingredient.

In the preparation of raw materials for the laboratory experiments, "* * * throwing out most of the noncompostable items * * *" was accomplished. This procedure would be in order when laboratory studies are conducted to evaluate certain chemical and physical factors of composting, but it can become a major operation when it is tried in commercial installations.

Although it was mentioned that items such as manure and fish scraps were added to the garbage, it would have been interesting to see more data showing the effect of protein additions on the initial C/N-ratio and showing how lowering the ratio might result in higher temperatures but, perhaps, in a greater loss of ammonia.

The oven-drying method (105° C) for determining moisture leads to substantial errors because of the volatilization of ammonia which results in the adoption here of the toluene distillation of the Association of Official Agricultural Chemists. Have the authors considered allowing a bulk test sample to become air-dry, placing it in an airtight container, performing all the analyses on this air-dry sample, and correcting for the residual moisture which is determined by distillation?

In the section, "Typical Composting Run," the initial acidic phase is mentioned. This is no doubt due to a fermentation causing fatty acids. By the third day of the run, the acid-producing organisms were followed by the thermophilic groups, which were able to oxidize the organic acids as fast as they were produced and thereby correct the pH-factor to an alkaline condition.

With regard to the possible mineralization of the materials, the volatile-solids concentrations indicated that, when garbage contained from 90% to 93% of combustible material, mineralization during composting was insignificant. In conducting experiments with sewage sludge, grass, refuse, and other materials, the writer has found that volatile solids decreased from 42% to 25%. However, it would be interesting to see the volatile solids in the Savannah garbage compost at 6 months and at 12 months.

---

[17] National Chemical Research Lab., South African Council for Scientific and Industrial Research, Pretoria, South Africa.

The weight and stoichiometric balances were informative and well presented.

In the section, "Physical Factors for Optimum Composting," a thorough study of the effect of varying the important factors of the rate of stirring, aeration, and moisture were presented and the optimum values for these factors were developed. Such data are of great value in designing large-scale plants, but the writer feels that the authors should have varied the raw materials more to establish whether these data can be applied to different types of wastes and different C/N-ratios.

It was also shown that, in varying the rate of aeration, the two extremes should be avoided—that is, lack of oxygen and loss of heat due to overaeration. It is probable that air control could be simplified by installing an instrument continuously indicating CO_2 in the exhaust gases from the unit.

Much remains to be done to increase technical knowledge of the complex biological mechanisms of composting, and it is hoped that additional research will be made.

JOHN S. WILEY,[18] M. ASCE, AND GEORGE W. PEARCE.[19]—The interpretation of the Savannah data and their application to plant-scale conditions, in accordance with the South African experience reported by Mr. Krige, is very encouraging. Several countries, especially South Africa and New Zealand, are far in advance of the United States in applied research in the field of composting. The writers agree that there is a necessity for more basic and applied research before even a small pilot plant of the mechanical type can be built in the United States.

An attempt is made herein to clarify some of the questions raised by Mr. Krige concerning the work done in Savannah.

Refuse normally includes garbage. However, in the United States, separate collections are frequently provided—one for garbage and another one for other refuse. The raw material has been termed, "garbage and refuse," to show that it contains the all-inclusive domestic refuse. It contains probably only from one-third to one-fourth garbage and has a high paper content, which accounts for the high percentage of volatile matter. That part of the mixture which has been composted contains no grass, tree trimmings, street sweepings, or similar items. However, it does contain paper, trash, and garbage from the home, including small amounts of dust, floor sweepings, hair, and similar materials. The short, high-rate composting process scarcely alters paper and other cellulosic material. It primarily affects the garbage part of the mixture.

The sorting of noncompostable items would be a major operation in a full-scale plant and not all the undesirable materials may be economically removed. Salvage, of course, may reduce or cancel the cost of such sorting. However, all equipment must be constructed to withstand the toughest and hardest materials likely to occur in raw refuse, despite the degree of preliminary sorting. Some hard objects may be desirable in a type of mechanical composting unit such as a rotary drum because they may provide additional grinding or crushing during composting, provide a more open structure for air circulation, and prevent the sticking of wet material to the sides. A 110-gal rotary drum unit is now (1956) being tested at Savannah.

---

[18] Senior San. Engr., Dept. of Health, Education, and Welfare, Public Health Service, Communicable Disease Center, Technical Development Labs., Savannah, Ga.

[19] Chief, Chemistry Section, Dept. of Health, Education, and Welfare, Public Health Service, Communicable Disease Center, Technical Development Labs., Savannah, Ga.

Concerning C/N-ratios of raw materials, more experiments are planned in which the N-factor is increased in a variety of forms. There must be a sizable range in the C/N-ratio depending on the types of materials, in which aerobic composting may be accomplished without appreciable loss of ammonia. Some observations have indicated it may be desirable to keep maximum temperatures down, possibly to prevent desirable organisms from being destroyed.

It is assumed that by "* * * substantial errors because of the volatilization of ammonia" Mr. Krige means that these errors arise in the determination of either total or ammonia nitrogen rather than in the determination of moisture. Any error in moisture determination by the oven-drying method as a result of the volatilization of constituents other than water, is believed to be smaller (1.0% or less) than the sampling error (occasionally more than 2.0%). The volatilization of ammonia in drying may cause an appreciably low total nitrogen value. At Savannah no nitrogen determinations have been made on either fresh or air-dried samples; they have been made only on oven-dried samples.

TABLE 11.—Volatile Solids at Different Times

Run	Volatile Solids, in % of Dry Weight		
	Initial	End of run (from 6 days to 9 days)	After third reheat (from 26 days to 30 total days)
25	93.1	91.9	76.2
26	90.7	87.7	75.0
27	90.7	87.7	75.6
28	91.7	88.0	77.3
29	93.6	92.6	84.5
30	92.1	88.8	82.3
Average	92.0	89.45	78.5

A few ammonia determinations have been made on the liquid which condenses from the outlet gases because of the temperature drop from drum temperature to room temperature. The values ranged from 0 ppm to 600 ppm with average values for the run varying from 14 ppm to 260 ppm. However, these values should not be considered to be quantitative for either the outlet gases or for the composting material.

The hypothesis presented by Mr. Krige concerning the acidic phase of decomposition which occurs initially and below the normal thermophilic range in Savannah composting runs appears sound. A large amount of acid is produced because it was necessary to add 16% $Ca(OH)_2$ on a dry-weight basis to maintain alkaline conditions whereas 50% agricultural lime (dry basis) had little effect on the pH or the temperature of the compost. However, if there was sufficient alkaline buffer to prevent acid conditions, there was no temperature lag in the composting process.

The opposite effect also occurs. When the pH starts to rise and the temperature goes rapidly into the thermophilic range, it is difficult to reverse the reaction and maintain an acid condition in the compost. In one run five additions of glacial acetic acid, totaling 12.3% of the dry weight of the compost, resulted in fairly good control of the pH below 7.0. However, after the additions were stopped, the pH climbed to more than 8.0 on the ninth day.

With regard to mineralization, the writers have only determined volatile solids for a total composting time of from 26 days to 30 days. In the time subsequent to the run composting took place in open cans. Results of 6 runs, each run with 6 units operating, are shown in Table 11.

There is a considerably greater reduction in the percentage of volatile solids during approximately three weeks in open cans than in one week of composting in the mechanical units. Unfortunately, the actual dry weight or the volatile-solids losses occurring in the open-can composting were not determined.

It is agreed that the optimum physical factors for composting must be checked against variations in raw materials. However, this could mean a long study, especially if it involved many of the various types of solid organic wastes produced by various industries. It is hoped that some of the problems of municipal refuse composting may be answered first. Then those problems encountered in the composting of various other wastes should be dealt with. The consistency of analyses of the raw refuse from Savannah has been surprising. Enough experience should be gained with all types of municipal refuse before mechanical composting is universally recommended. With reference to the raw materials, the writers do not emphasize the C/N-ratio as has been done elsewhere.

Estimates of optimum aeration rates were admittedly based on indirect measures, such as speed of composting as indicated by temperature and pH, losses in weights, and moisture and carbon-dioxide production. Oxygen utilized during a run was determined by taking the difference between intake and output. Subsequently, it was learned that moisture-production figures have been low and that corrections will increase those values as well as the amounts of oxygen utilized. Direct oxygen readings during controlled runs should provide an additional check on the other determinations involving stoichiometric balance, as well as being a better criterion for judging optimum aeration rates. Although it is known that moisture measurements in the outlet gases are probably low, there are indications that there are some compensating errors in the opposite direction so that the material-balance estimates are not seriously inaccurate. The most reliable data on material balance are those data showing the gross loss in dry matter. It is believed that the carbon-dioxide estimates are reasonably accurate.

AMERICAN SOCIETY OF CIVIL ENGINEERS

Founded November 5, 1852

TRANSACTIONS

Paper No. 2896

THE EFFECT OF TRAFFIC ON THE CROSS SECTION OF A RUNWAY PAVEMENT

By Robert Horonjeff[1] and John Hugh Jones,[2]
Associate Members, ASCE

With Discussion by Messrs. Roger H. Williams; John F. Redus; and Robert Horonjeff and John Hugh Jones

Synopsis

This paper analyses the problem of whether or not it is necessary to construct runway pavements uniformly thick across their entire width. The fact is that traffic at many airports is concentrated at the center of the runway. An actual transverse traffic distribution compiled by observations made at several large commercial airports, together with an attempt to relate this distribution to the thickness of the runway pavement, is presented herein.

Introduction

During the past decade there have been great increases in airport traffic and in the size of aircraft which make up this traffic. These trends have led to larger investments in airport runways. The prospect of further airport expansions indicates the desirability of appraising runway design with a view to obtaining maximum load-handling capacity per dollar.

It is common practice to make the thickness of airport runway pavement uniform across the width of the runway. Observation of skid marks has indicated that traffic on the runway is fairly well centered. The traffic distribution for military airfields was observed in this manner by Hibbert Hill,[3] M. ASCE, in 1945. The present investigation was therefore undertaken to determine the actual transverse distribution of traffic at civil airports and to relate this dis-

---

Note.—Published, essentially as printed here, in June, 1955, as *Proceedings-Separate No. 720.* Positions and titles given are those in effect when the paper or discussion was approved for publication in *Transactions.*

[1] Prof. of Transportation Eng. and Research Engr., Inst. of Transportation and Traffic Eng., Univ. of California, Berkeley, Calif.

[2] Asst. Prof. of Civ. Eng., Inst. of Transportation and Traffic Eng., Univ. of California, Berkeley, Calif.

[3] Discussion by Hibbert Hill of "Military Airfields: A Symposium," *Transactions*, ASCE, Vol. 110, 1945, pp. 758-763.

tribution to pavement thickness; no attempt was made to determine the distribution of traffic in a longitudinal direction.

The Los Angeles, Oakland, and San Francisco airports (California) were selected for study. Traffic distribution was observed and compared for day and night operations under both visual and instrument flight conditions.

The transverse distributions were determined at three locations on the runway by means of electrical traffic detector tapes. These tapes, located at 600 ft, 1,000 ft, and 1,800 ft from the end of the runway, were capable of determining the transverse positions of a wheel within 10 ft. From the distribution of wheel loads an attempt was made to develop a design for runway pavement for varying thickness.

METHOD OF CONDUCTING TESTS

The tape locations were selected so as to detect significant variations in the transverse distributions along the runway.

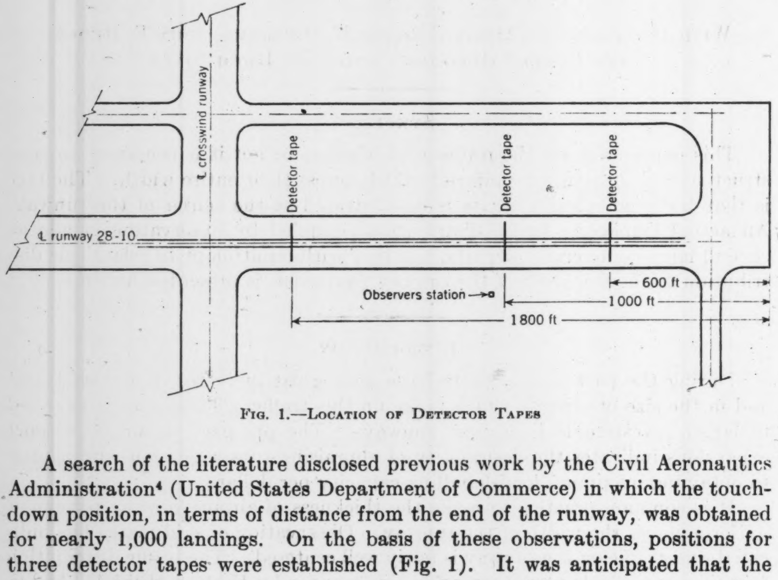

FIG. 1.—LOCATION OF DETECTOR TAPES

A search of the literature disclosed previous work by the Civil Aeronautics Administration[4] (United States Department of Commerce) in which the touchdown position, in terms of distance from the end of the runway, was obtained for nearly 1,000 landings. On the basis of these observations, positions for three detector tapes were established (Fig. 1). It was anticipated that the first tape, 600 ft from the runway end, would detect the transverse positions of 100% of all aircraft taking off and approximately 20% of all aircraft landing. The second tape, 1,000 ft from the runway end, would account for nearly all take-offs and 65% of the landings. The third tape, 1,800 ft from the runway end, would detect approximately 75% of all aircraft taking off and nearly all the aircraft landing.

---

[4] *Airport Engineering Bulletin No. 1*, Civil Aeronautics Administration, U. S. Dept. of Commerce, Washington, D. C., June 15, 1951.

The problem of determining the transverse positions of highway vehicles had been studied at the Institute of Transportation and Traffic Engineering, University of California (at Los Angeles), and a segmented electrical detector tape developed.[5] The tape, shown in Fig. 2, consists of two spring-steel elements which are normally held open by means of a gum-rubber spacer strip. The bottom contact extends throughout the length of the unit and serves as a common contact for all segments. The upper contact was made in 10-ft lengths.

Runway widths were 150 ft and 200 ft. For adequate coverage each tape was made 160 ft long and divided into 16 segments of 10 ft. Because many of the dual-wheel landing-gear assemblies are nearly 4 ft wide, it was felt that the accuracy gained by dividing the tapes into smaller segments was not warranted.

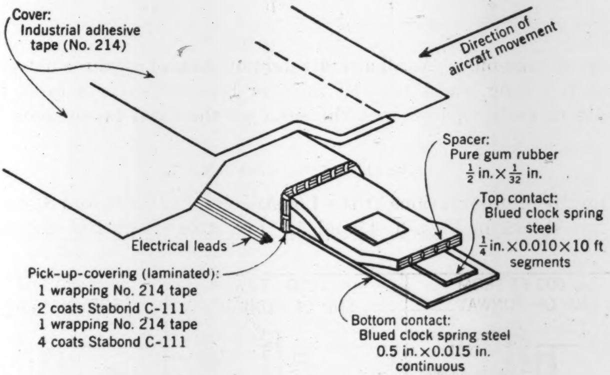
Cover:
Industrial adhesive tape (No. 214)
Direction of aircraft movement
Spacer:
Pure gum rubber
$\frac{1}{2}$ in. × $\frac{1}{32}$ in.
Top contact:
Blued clock spring steel
$\frac{1}{4}$ in. × 0.010 × 10 ft segments
Electrical leads
Pick-up-covering (laminated):
1 wrapping No. 214 tape
2 coats Stabond C-111
1 wrapping No. 214 tape
4 coats Stabond C-111
Bottom contact:
Blued clock spring steel
0.5 in. × 0.015 in.
continuous

Fig. 2.—Design Details of the Detector Tape

The tapes were attached to the runway with rubber cement and covered with two layers of industrial adhesive tape. The units proved remarkably resistant to abrasion, and only occasional patching with additional adhesive tape was necessary to provide satisfactory protection for the electrical units. A circuit was designed to indicate which segment was occupied by the left-hand wheel of moving aircraft. The indicator, which was stationed opposite the center detector tapes, consisted of 16 lighted neon tubes, each representing a 10-ft segment of tape. As the left wheel of the aircraft rolled across a particular 10-ft segment all tubes associated with segments to the left of the contacted tape remained lighted. It was necessary to reset the neon-tube indication after the aircraft had passed each tape in succession, but the time between crossings of the detector tapes was sufficient to obtain a reading and clear the circuit for the next tape.

Test Program

Observations were made during September and October, 1953. At each airport, night and day movements both under visual and instrument conditions were observed for all transport aircraft. The data recorded were time of landing or take-off, type of aircraft, whether movement was made under visual or instrument conditions, and the appropriate indication of transverse position as the aircraft crossed each of the three detector tapes. Wind velocity and direction were noted as these data were reported to pilots.

---

[5] "A Segmented Electrical Element for Detecting Vehicular Traffic," by J. H. Mathewson, R. Brenner, and R. J. Reiss, *Proceedings*, Highway Research Board, National Research Council, Washington, D. C., 1949, pp. 374–383.

The runways on which traffic tapes were placed at the three airports and their principal characteristics are listed in Table 1. Total movements refer to landings or take-offs. As all aircraft did not contact all three detector tapes due to landing long, short take-off runs, or bouncing over a tape, the total movements of each tape are not the same as the total movements listed in Table 1.

TABLE 1

Airport	Runway	Width (feet)	Length (feet)	Total movements
Los Angeles International	25R	150	8,500	263
Metropolitan Oakland International	27R	150	5,500	267
San Francisco International	28R	200	8,900	228

Analysis of Results

The results of observations at the Los Angeles, Oakland, and San Francisco airports are shown in Figs. 3, 4, and 5. Fig. 3(*a*) shows the distribution of wheel loads across the principal runway at each of the three airports at a point 600 ft from the end of the runway. Landings and take-offs during the day and night and during conditions of good and poor visibility are shown, and the number of observations at each airport is given in parentheses. The position of the left wheel of the main landing gear as it crossed the detector tape was observed in the field. The position of the right wheel was plotted 20 ft to the right. The actual distances between wheels varied from 18 ft to 28 ft. An analysis of the traffic at San Francisco International Airport indicates a weighted average of approximately 23 ft as the distance between the main

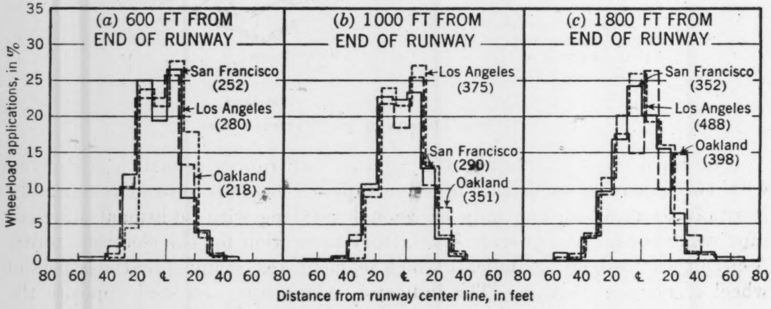

Fig. 3.—Distribution of Wheel-Load Applications

landing gears for transport aircraft. The adoption of 20 ft as the average distance does not seriously distort the results. It was felt that plotting the distance between main wheels for each type of aircraft was not warranted because the exact position of the left wheel was not known.

An examination of Fig. 3 reveals the following:

1. Traffic is concentrated within a 60-ft width of runway at the three tape locations. Less than 5% of the traffic occurs beyond these limits.

2. The maximum percentage of wheel-load applications in a 10-ft segment occurred at Los Angeles International Airport, 600 ft from the end of the runway, and amounted to 28% of the total number of wheel loads recorded at this location. At Metropolitan Oakland International Airport the corresponding figure is 26% and at the San Francisco airport, 27%.

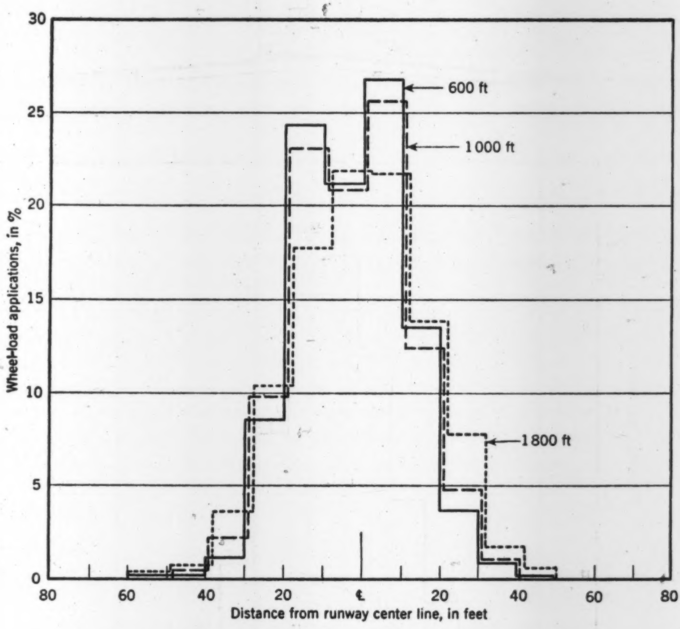

FIG. 4.—AVERAGE DISTRIBUTION OF WHEEL-LOAD APPLICATIONS

To indicate the variation along the runway of the transverse distribution of wheel loads, the average of the observations at the three airports was plotted for each detector tape position as shown in Fig. 4. It will be noted that the patterns are quite similar, indicating that the transverse distribution of wheel loads is approximately the same along the runway..

In order to use the data for the development of a design proposal an average distribution was made to represent all the observations at the three airports. This distribution is shown in Fig. 5. The standard curve of error which best fitted all the observations was computed, and the chart was drawn. This procedure was used in preference to an arithmetic mean because the latter would not have properly accounted for the different numbers of observations at each airport.

The data in Fig. 5 suggest that the pavement for the central 60-ft section of a runway could be designed for 25% of the total number of wheel-load applications which the runway would receive during its economic life. The remainder of the runway width would be designed for 3% of the wheel-load applications. It is recognized that 25% applied to the entire 60-ft section is conservative because only the 10-ft segment near the center line carries the 25%; however, a finer breakdown is not warranted at this time as only three airports have been investigated. Furthermore, the design criteria outlined

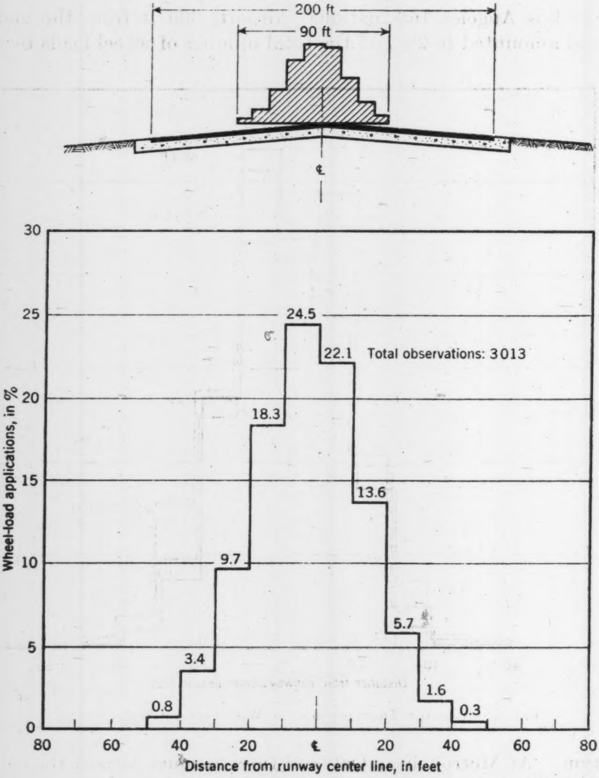

Fig. 5.—Composite Average Distribution of Wheel-Load Applications

are conservative in that traffic loading will be less at the upwind end of the runway than at the end at which most landings and take-offs occur.

At the beginning of the tests it was believed that visibility and cross winds might affect the pattern of wheel-load distribution on a runway; therefore, data on wind conditions and visibility were recorded in the field. An analysis of the observations indicates the following:

1. There was no significant difference in the pattern of wheel-load applications between night and day.
2. There was no significant difference in the pattern of wheel-load applications between a visual approach and an approach made under instrument conditions.
3. Within the range of cross-wind velocities encountered, up to 15 miles per hr, there was no observable effect on the pattern of wheel-load application. In several instances, however, incoming aircraft had to make several approaches in order to compensate for the wind before touching down on the runway. When they did touch down, their positions were not materially different from those observed at other times.

APPLICATION OF RESULTS TO PAVEMENT THICKNESS

In order to apply the data to the determination of pavement thickness it is necessary to use design procedures which include wheel-load repetitions as one of the variables.

For the purpose of this paper the procedure developed by F. N. Hveem and his associates in the California Division of Highways[6] was used to show the effect of wheel-load repetitions on pavement thickness.

Data from test tract studies made by the California Division of Highways and others have indicated that the destructive effect of wheel loads varies as the square root of the magnitude of the loads and that the necessary thickness of pavement varies as the logarithm of the wheel-load repetitions. The relationship between wheel loads and repetitions used by the California Division of Highways is

$$\sqrt{W_1} \log r_1 = \sqrt{W_2} \log r_2 \quad \text{.......} \quad (1)$$

in which W_1 and W_2 are the wheel loads and r_1 and r_2 designate the repetitions of wheel loads, W_1 and W_2. By applying this relationship all wheel loads can be converted to repetitions of a single arbitrarily selected wheel load. (For example, to learn the number of repetitions of a 50,000-lb load which would have the same destructive effect as 10,000 repetitions of a 20,000-lb load, the procedure would be as follows: $\sqrt{20{,}000} \log 10{,}000 = 10{,}000 = \sqrt{50{,}000} \log r_{50,000}$ from which $r_{50,000} = 338$.)

The equation for pavement thickness developed by the California Division of Highways, presented in nomograph form in Fig. 6, is

$$T = \frac{(K\,P\,\sqrt{a} \log r)\,\dfrac{90 - R}{100}}{\sqrt[5]{c}} \quad \text{.......} \quad (2)$$

---

[6] "The Factors Underlying the Rational Design of Pavements," by F. N. Hveem and R. M. Carmany, *Proceedings*, Highway Research Board, National Research Council, Washington, D. C., 1948, pp. 101–136.

in which T is the thickness of pavement, in inches; $K = 0.016$ for best correlation with test track data; P designates contact tire pressure, in pounds per square inch; a represents the contact tire area, in square inches; r is the number of load applications adjusted to an arbitrarily selected wheel load; R represents resistance value of the subgrade (scale 0 to 90); and c is the tensile strength of the pavement as measured by the cohesiometer.

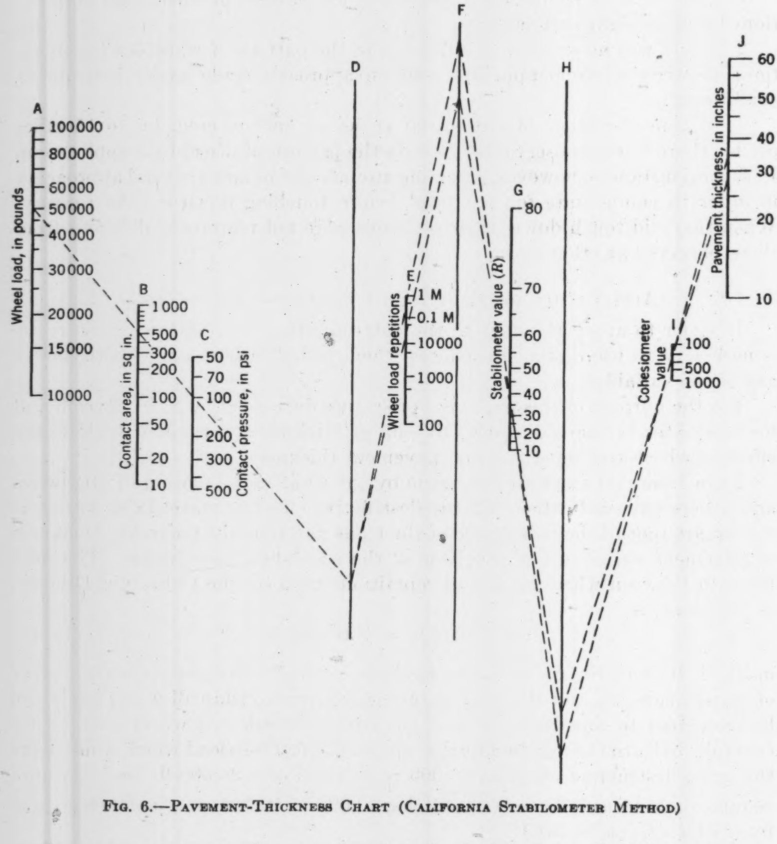

FIG. 6.—PAVEMENT-THICKNESS CHART (CALIFORNIA STABILOMETER METHOD)

Suppose, as an example, a runway is to be designed as a flexible-type pavement for 180,000 aircraft movements annually. Assume that the bearing capacity of the subgrade in terms of resistance value R is 35, which is approximately equivalent to a California Bearing Ratio of from 5% to 6%. The economic life of the pavement is assumed as ten years, making the total number of wheel-load applications on the runway 3,600,000. A record of landings and take-offs at the field indicates that the new runway will be used by aircraft having the following average weights.

Gross weight of aircraft (pounds)	Total traffic (%)
140,000	5
96,000	20
70,000	15
40,000	10
25,000	15
10,000	35

For the purpose of this problem it is assumed that the weight of the aircraft is distributed equally between the two main wheels and that the average tire contact pressure is 100 lb per sq in.

The central 60-ft section of the runway is to be designed on the basis of the wheel-load applications on the critical 10-ft central segment. This segment carries 25% (900,000) of the total applications. Similarly, the outer sections of the runway are to be designed on the basis of a 10-ft segment which is critical for those sections. This critical segment carries 3% (108,000) of the total load application.

TABLE 2

Wheel load (pounds)	Total loads (%)	Central Section		Outer Section	
		Wheel-load applications	Equivalent 50,000-lb applications	Wheel-load applications	Equivalent 50,000-lb applications
70,000	5	45,000	319,700	5,400	26,030
48,000	20	180,000	141,300	21,600	17,690
35,000	15	135,000	19,680	16,200	3,337
20,000	10	90,000	1,352	10,800	354
12,500	15	135,000	367	16,200	127
6,000	35	315,000	54	37,800	28
Total	100	900,000	482,453	108,000	45,566

A 50,000-lb load was chosen arbitrarily as the common denominator for the determination of wheel-load applications for use in the formula for pavement thickness. The result would have been the same regardless of the wheel load selected. The equivalent repetitions of a 50,000-lb load were computed as previously described, and the results are summarized in Table 2.

Using the nomograph (Fig. 6) a pavement thickness of 36 in. for 482,000 applications of a 50,000-lb wheel load, an *R*-value of 35, a cohesiometer value of 300, and a contact pressure of 100 lb per sq in. are obtained. Similarly, for 48,000 applications of the same wheel load, a pavement thickness of 30 in. is indicated.

The cohesiometer value will vary for each particular design depending on the thickness and character of the surfacing and the base; it can vary from a little more than 100 to as high as 1,000. For the purpose of this problem a value of 300 was selected to represent the combined tensile strength of the bituminous surfacing and the base course.

The pavement thickness derived by the procedure is conservative. Inasmuch as the landing-gear assemblies used on transport aircraft are not more than 4 ft wide and the detector tapes were in 10-ft segments, the wheel loads (as was assumed in the computations) are not applied to the same pavement area in a 10-ft segment with each aircraft movement.

A suggested pavement cross section based on the foregoing analysis is shown in Fig. 7. It consists of a 60-ft central section of 3 in. of bituminous plant mix, 9 in. of stabilized aggregate base course, and 24 in. of selected quarry-run material. The outer sections of the runway width consist of 2 in. of bituminous plant mix, 7 in. of stabilized aggregate base course, and 21 in. of selected quarry-run material.

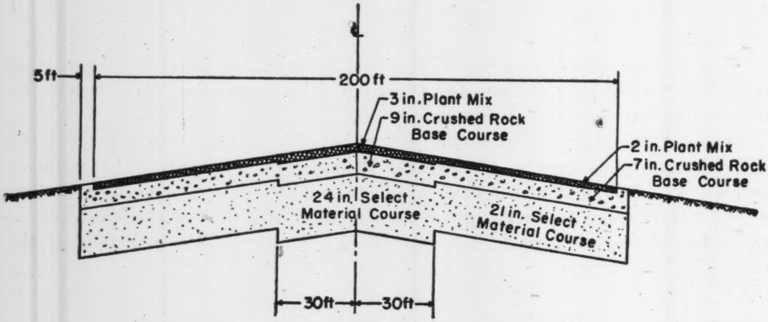
℄
5ft
200 ft
3 in. Plant Mix
9 in. Crushed Rock Base Course
2 in. Plant Mix
7 in. Crushed Rock Base Course
24 in. Select Material Course
21 in. Select Material Course
30ft
30ft

Fig. 7.—Suggested Runway Cross Section

Economic Considerations

In order to give an indication of the saving in cost which might be effected by a variable-thickness section as compared with a uniform section, costs were estimated for a runway 200 ft wide and 8,000 ft long with alternate pavements: (1) A uniform thickness of 36 in. and (2) a thickness of 36 in. in the central 60 ft and a thickness of 30 in. in the remaining 140 ft. These estimates are summarized as follows:

Uniform thickness pavement...........	$724,000
Variable thickness pavement...........	621,000
Saving in cost.....................	$103,000

In making these estimates, current prices in the San Francisco Bay area were used—namely, $6.50 per ton for bituminous plant mix, $2.60 per ton for stabilized aggregate base course, and $1.50 per ton for select material.

Summary

The foregoing analysis indicates some measure of the saving in cost that possibly could be made by taking into account the variation of load applications across the width of a runway. Such savings will naturally vary depending on the character of the native soil, the magnitude of the wheel loads, and the amount of traffic expected.

For the sake of simplicity the cost estimates do not provide for the fact that at taxiway connections to the runway it may be necessary to have the same thickness of pavement as the central 60-ft section.

The method of design adopted by the California Division of Highways was used for the example primarily because of the familiarity of the writers with this method. The basic data collected on wheel-load applications are applicable to any pavement design procedure which recognizes repetition of load as a variable.

The data presented in this paper were intended primarily for use in the design of civil airfields. On many military airfields, groups of two or three aircraft use the runway simultaneously. In such cases the pattern of load distribution would be different from those shown in this paper.

In Fig. 7 there is suggested a pavement section which abruptly changes from one thickness to another. In some cases a gradually tapering section might be more advantageous.

CONCLUSIONS

The pattern of wheel-load applications varies across the width of a runway and is concentrated in the central section. A runway for transport aircraft is of such width that substantial savings in cost may be effected by taking into account this variation in wheel-load applications in determining the thickness of the pavement.

ACKNOWLEDGMENTS

The writers express appreciation for the cooperation and assistance extended by Woodruff de Silva and Bert G. Lockwood (Los Angeles International Airport); Don W. Martin and F. McElwain (Metropolitan Oakland International Airport); George S. Dixon, Harold S. Messersmith, and F. Victor Philpot, M. ASCE (San Francisco International Airport); and Mr. Hveem, Ernest Zube, A.M. ASCE, and George Sherman, A.M. ASCE (California Division of Highways).

The writers are grateful for the assistance rendered by the following members of the staff of the Institute of Transportation and Traffic Engineering: Loren D. Fields, John R. Hall, and George B. Dierking.

DISCUSSION

Roger H. Williams,[7] M. ASCE.—The over-all pavement-thickness reduction in the example amounts to 16.7%, whereas the reduction of plant mix is 33.3%, the reduction of base course is 22.2%, and the reduction of select material course is 12.5%. Because the wearing surface is important in the durability of a properly designed and constructed pavement, the relatively large reduction of this course in relation to the reduction of the other courses and to the over-all reduction appears questionable.

The cost of excavating existing subgrade to place the thicker select material in the center section and the cost of common fill in the exterior sections, or both these costs, should also be included in the cost comparison as well as any increase in contractor bidding cost for placing the layers of varying thickness.

John F. Redus,[8] A. M. ASCE.—The authors are to be congratulated on a well-conducted study of a timely subject. The volume of current airfield construction requires the expenditure of large sums of money. Any means of reducing costs without impairing the ability of the pavement to function properly is certainly necessary.

Messrs. Horonjeff and Jones have mentioned that the traffic patterns on military fields might be different from those on civil fields. Traffic distribution on military fields will be examined herein.

The Waterways Experiment Station of the Corps of Engineers (United States Department of the Army) conducted a traffic-distribution study on military airfields (circa 1945) which was designed to determine the amount of traffic airfield pavements received so that proportional amounts could be applied to accelerated traffic test sections; this study has been summarized by C. R. Foster,[9] A. M. ASCE.

To determine the distribution of landings, tire marks were counted in 10-ft lanes across the width of the pavement at several places on each of the 28 fields that were studied. The runways were 150 ft wide, and the fields were classified in three groups according to the gross weights of the predominant planes as follows: (*a*) Less than 10,000 lb, (*b*) about 30,000 lb, and (*c*) about 60,000 lb. It was shown that the widths of the pavements in which 75% of the landings occurred were, for the three groups, 85 ft, 75 ft, and 50 ft, respectively. Seventy-five per cent of the traffic occurred in a width of approximately 40 ft (Fig. 5) at the fields observed by the authors. This is believed to compare favorably with the value shown for the planes in group (*c*) considering that these fields were training fields for the most part.

---

[7] Prin. Civ. Engr., Metcalf & Eddy, Cons. Engrs., Boston, Mass.

[8] Engr., General Investigation Section, Flexible Pavement Branch, Soils Div., Waterways Experiment Station, Corps of Engrs., U. S. Dept. of the Army, Vicksburg, Miss.

[9] "Development of CBR Flexible Pavement Design Method for Airfields: Design Curves for Single-Wheel Loads: A Symposium," by C. R. Foster, *Transactions*, ASCE, Vol. 115, 1950, p. 526.

Using the foregoing distribution and records from control towers of landings and take-offs, the number of coverages applied to the central section of a runway was computed by assuming uniform distribution over the central section. Although the distribution is not exactly uniform, it is approximate enough for this assumption to be made. These studies showed that, under intensive training conditions, the central section of the most used runway of a multi-runway field generally received approximately 5,000 coverages in a five-year period.

Runway traffic on take-offs is slightly different from runway traffic on landings. A single plane taking off alone tends to use the central section of the runway—the width used depends on the type and spacing of the main landing gear. However, take-offs are made on numerous fields with planes in a staggered pattern.

It can be seen, therefore, that traffic for military planes with a particular landing gear falls into a rather well-defined pattern. If it could be established that the planes using the field for the life of the pavement will be of a given type and that no widening of the pavements will be necessary, then a non-uniform cross section could be designed which would reflect considerable savings.

Since about 1952 guide lines have been painted on taxiways and apron taxilanes to aid pilots in keeping wheels on the pavement and to clear parked aircraft; this has resulted in "channelization" of traffic. However, insufficient data are available to examine channelized traffic in this paper.

ROBERT HORONJEFF[10] AND JOHN HUGH JONES,[11] ASSOCIATE MEMBERS, ASCE.—With regard to the reduction to 2 in. of asphalt surfacing, the writers feel that it is justifiable because the amount of traffic on the outer section of the runway is negliglble, as demonstrated by tests. At many airports throughout the United States the asphalt thickness is only 2 in. and has proved satisfactory. The Civil Aeronautics Administration has recommended the use of 2-in. surfacing for certain classes of airports. The writers feel that there is little need for placing a heavy thickness of asphalt in areas where there is only occasional traffic. Asphalt surfacing requires kneading action to prevent it from becoming brittle. It is considered that many cracks on the outer section of runways are due to lack of kneading action and are not due to traffic.

The cost of excavating the subgrade should be included in a comparison of costs for a specific project. It was felt, however, that this was not necessary for the generalized comparison. Furthermore, if the site requires both excavation and embankment, the profiles for the suggested design might be established so that the grading would not be more expensive than it would be for the uniform-thickness section.

The opinion of the writers is that the traffic pattern at large civil airports is fairly well established because it consists mostly of transport aircraft. Interviews conducted with several pilots have indicated that every effort is made to land on the central section of the runway. Pilots often execute a "missed-approach procedure" in order to avoid landing on the outer section of the runway. From the standpoint of safety there are many reasons for keeping the aircraft in the central section of a runway during take-offs and landings. A staggered pattern of take-offs is of course not permitted in civil operations. Consequently, as Mr. Redus has indicated, the patterns at civil and military fields could be quite different.

---

[10] Prof. of Transportation Eng. and Research Engr., Inst. of Transportation and Traffic Eng., Univ. of California, Berkeley, Calif.

[11] Prof. of Civ. Eng., Inst. of Transportation and Traffic Eng., Univ. of California, Berkeley, Calif.

AMERICAN SOCIETY OF CIVIL ENGINEERS
Founded November 5, 1852
TRANSACTIONS

Paper No. 2897

FAILURE OF PLAIN CONCRETE UNDER COMBINED STRESSES

BY BORIS BRESLER,[1] A. M. ASCE, AND KARL S. PISTER,[2] J. M. ASCE

WITH DISCUSSION BY MESSRS. FRANK A. BLAKEY AND F. DONALD BERESFORD; PAUL RICE; HENRY J. COWAN; AND BORIS BRESLER AND KARL S. PISTER

SYNOPSIS

The initial phase of an investigation of the failure of plain concrete under combined stresses is presented. Previous investigations of the failure of plain concrete revealed that the correlation of various criteria with test data has been either inadequate or inconclusive. To obtain further evidence on failure of plain concrete, hollow cylinders were tested under varying combinations of torsion and compression. Data obtained from these tests indicated a direct correlation between normal and shearing octahedral stresses at failure. Within the limits of available data, the octahedral-stress criterion was generalized to include the effect of the third stress invariant, and in this form the proposed criterion was shown to be in satisfactory agreement with the previously reported data.

INTRODUCTION

Knowledge of criteria of failure for concrete subjected to combined stress is of considerable practical importance. In considering the failure mechanism of reinforced concrete or prestressed concrete, it has often been stated that reinforcement or prestress alters the nature of the material and therefore changes the criteria of failure. Of course, bond between concrete and reinforcement and deformation in the reinforcement are important in the development of the failure mechanism. A reasonable assumption, however, is that the conditions producing local failure in concrete are essentially the same for both plain and re-

---

NOTE.—Published, essentially as printed here, in April, 1955, as *Proceedings-Separate No. 674*. Positions and titles given are those in effect when the paper or discussion was approved for publication in *Transactions*.

[1] Associate Prof. of Civ. Eng., Univ. of California, Berkeley, Calif.

[2] Asst. Prof. of Civ. Eng., Univ. of California, Berkeley, Calif.

inforced concrete. Therefore, knowledge of the conditions producing local failure in plain concrete should lead to a better understanding of the failure mechanism in reinforced or prestressed structural elements.

Formulation of failure criteria for concrete has received considerable attention. In engineering practice the most commonly proposed theories are those of maximum stress, internal friction, and maximum strain. However, the maximum-stress theory is unsatisfactory because it fails to agree with experimental data for biaxial and triaxial states of stress.[3,4,5,6]

Mohr's generalization of the internal-friction theory has been proposed for concrete.[6,7] Correlation of this theory with experimental data, however, is not entirely satisfactory, partly because of the approximation involved in the assumption that the failure criterion is independent of the intermediate principal stress. C. Torre[8] has demonstrated that for a given material there are as many Mohr envelopes as there are values of a parameter, α, defined as

$$\alpha = \frac{\sigma_2 - \sigma_1}{\sigma_1 - \sigma_3} \qquad (1)$$

in which σ_1, σ_2, and σ_3 are principal stresses. It follows that construction of a Mohr envelope from test data in which α is not constant cannot be justified.

The maximum-strain theory of failure is based on the premise that failure occurs when either maximum tensile strain or maximum compressive strain reaches a limiting value. For linearly elastic and isotropic materials this theory leads to a simple mathematical formula. In the cases of inelastic and anisotropic materials, such as concrete, this theory is not readily applicable. Approximate criteria of failure in terms of maximum concrete strain have been proposed for flexure in reinforced concrete members.[9] Comparison of these criteria with experimental data shows considerable scatter,[9] and the general use of these approximations cannot be justified.

Henry J. Cowan,[10] A.M. ASCE, has proposed criteria based on two distinct types of failure of plain concrete. According to one criterion, associated with a cleavage fracture, failure is governed by maximum tensile stress or strain. The other criterion, associated with crushing strength, states that failure is governed essentially by the Coulomb internal friction law. Mr. Cowan's experimental

---

[3] "The Inelastic Behavior and Failure of Concrete," by A. Freudenthal, *Proceedings*, 1st U. S. National Cong. of Applied Mechanics, Chicago, Ill., 1951, pp. 641–646.

[4] "Strength of Concrete Under Combined Compression and Shear," by E. Wollak, thesis presented to the University of California at Berkeley, in 1951, in partial fulfilment of the requirements for the degree of Master of Science.

[5] "A Study of the Failure of Concrete Under Combined Compressive Stresses," by F. Richart, A. Brandtzaeg, and R. L. Brown, *Bulletin No. 185*, Univ. of Illinois Eng. Experiment Station, Urbana, Ill., 1928.

[6] "Shearing Strength of Concrete under High Triaxial Stress—Computation of Mohr's Envelope as a Curve," by G. Balmer, Structural Research Lab. Report, *S. P. No. 23*, Bureau of Reclamation, U. S. Dept. of the Interior, Washington, D .C., 1949.

[7] "Über der Scherfestigkeit des Betons," by A. Leon, *Beton und Eisen*, Vol. 34, 1934–1935, pp. 130–135.

[8] "Einfluss der mittleren Hauptnormalspannung auf die Fliess und Bruchgrenze," by C. Torre, Österreichisches Ingenieur-Archiv, Wien, Vol. 1, 1947, pp. 316–342.

[9] "A Study of Combined Bending and Axial Load in Reinforced Concrete Members," by E. Hognestad, *Bulletin No. 399*, Univ. of Illinois Eng. Experiment Station, Urbana, Ill., 1951.

[10] "The Strength of Plain, Reinforced, and Prestressed Concrete Under the Action of Combined Stresses, with Particular Reference to the Combined Bending and Torsion of Rectangular Sections," by Henry J. Cowan, *Magazine of Concrete Research*, No. 14, December, 1953, pp. 75–86.

data[11] are limited to reinforced concrete elements subjected to bending and torsion and are insufficient for evaluating the validity of his hypothesis of failure for plain concrete.

In an effort to account for the heterogeneous nature of concrete, A. Brandtzaeg,[12] M. ASCE, has developed a theory based on an idealized (model) structure of the material. This theory is limited to cylindrical states of stress—that is, two of the three principal stresses are equal. The possibility of distinct shear or cleavage failure is considered. This theory defines a stress-strain relationship and a "critical" stress corresponding to the ultimate strength of the material. A series of biaxial and triaxial tests of concrete, conducted by F. Richart, A.M. ASCE, Mr. Brandtzaeg, and R. L. Brown, J.M. ASCE, indicated[5] reasonable agreement with Mr. Brandtzaeg's theoretical stress-strain relationship for stresses below the critical value, but showed significant discrepancies between the critical stress and the ultimate strength.

A. Freudenthal, M. ASCE, has examined[3] the problem of formulating failure criteria for concrete and has proposed a linear equation in terms of effective stress, σ_e, and mean stress, σ_m, as

$$\sigma_e = c_1 \sigma_m + c_2 \qquad (2)$$

in which

$$\sigma_e = \{\tfrac{1}{2}[(\sigma_1 - \sigma_2)^2 + (\sigma_2 - \sigma_3)^2 + (\sigma_3 - \sigma_1)^2]\}^{1/2} \qquad (3a)$$

$$\sigma_m = \tfrac{1}{3}(\sigma_1 + \sigma_2 + \sigma_3) \qquad (3b)$$

and c_1 and c_2 are constants of the material. To verify Eq. 2 for biaxial states of stress, Mr. Freudenthal performed a series of compression tests on notched cylinders. As noted by Mr. Freudenthal, it is doubtful that the notch stresses computed by elastic theory actually develop at failure; therefore, experimental evidence presented cannot be considered conclusive.

In addition to the theories discussed previously, various energy criteria for failure have been proposed for brittle materials.[13,14] A. Griffith has proposed a fracture theory which considers the effect on the total energy of the formation of macroscopic cracks within the material. For two cases of plane stress, assuming the cracks to be elliptic, Mr. Griffith obtained a theoretical tensile strength of fracture. It may be noted that for materials that exhibit nonlinear elasticity, Mr. Griffith's theory is not interpretable in terms of elastic-strain energy. Likewise, for materials subjected to three-dimensional states of stress, the solutions for plane stress become approximations. The philosophy expressed by Mr. Griffith's theory seems to have found utility in the studies of failure of cast iron by J. C. Fisher,[15] A.M. ASCE, and R. C. Grassi and I. Cornet.[16] A preliminary investigation by E. Wollak,[4] J.M. ASCE, revealed that for concrete the agreement of the available experimental evidence with Mr. Griffith's theory is not entirely satisfactory.

---

[11] "Reinforced Concrete in Combined Bending and Torsion," by Henry J. Cowan and S. Armstrong, *Preliminary Publication*, 4th Cong. of the International Assn. of Bridges and Structural Eng., Cambridge, 1952.

[12] "Failure of Material Composed of Non-isotropic Elements," by A. Brandtzaeg, Norske Videnskabers Selskabs Skrifter, No. 2, Trondhjem, I. Kommission Hos. F. Bruns Bokhandel, 1927.

[13] "The Phenomena of Rupture and Flow in Solids," by A. Griffith, *Philosophical Transactions*, Royal Soc. of London, Vol. 221, 1920–1921, pp. 163–198.

[14] "Der Spannungszustand an der Fliessgrenze (Plastizitätsbedingung)," by F. Schleicher, *Zeitschrift für Angewandte Mathematik und Mechanik*, Berlin, Vol. 6, 1926, pp. 199–216.

[15] "A Criterion for the Failure of Cast Iron," by J. C. Fisher, General Electric Research Lab. Report, Schenectady, N. Y., 1949.

[16] "Fracture of Gray Cast Iron Tubes under Biaxial Stresses," by R. C. Grassi and I. Cornet, *Transactions*, ASME, Vol. 71, 1949, pp. 178–182.

Existing (1955) failure criteria for plain concrete are neither adequately substantiated nor disproved. Most of the experimental data concerning the strength of plain concrete have been obtained for specimens subjected to (*a*) uniaxial, biaxial, or triaxial compression; (*b*) uniaxial tension; and (*c*) flexure. To the best of the writers' knowledge, data on failure of concrete subjected to shear-compression states of stress have not been obtained previously. To obtain experimental evidence for these states of stress, 24 hollow cylinders were tested under varying combinations of torsion and compression. The objectives of these tests were to obtain further verification of the various existing theories of failure, to correlate the new data with previously reported investigations, and to assist in formulating a more general criterion of failure. Data obtained from these tests indicated a linear relationship between normal and shearing octahedral stresses at failure. Previously reported data for biaxial states of stress agree reasonably well with the established linear relationship, but data for triaxial states of stress deviate from it. This deviation is shown to be related to the third invariant of the stress tensor,

$$I_3 = \sigma_1 \sigma_2 \sigma_3 \qquad (4)$$

A generalized form of failure criterion based on octahedral stresses and on the third stress invariant is proposed, and possible physical interpretations are examined.

TEST SPECIMENS AND PROCEDURE

Hollow concrete cylinders (9-in. outside diameter, 6-in. inside diameter, and 30 in. long) were made using mix proportions of 1:2.9:3.1 by weight and a ratio of water to cement of 0.6 by weight. The maximum aggregate size used was ½ in., and the slump averaged approximately 2 in. All specimens were cured at 100% humidity and 70°F and were tested at an age of 14 days.

Four 3-in. by 6-in. control cylinders were made for each specimen and tested in compression at an age of 14 days. The average compressive strength of these cylinders was taken as f'_c for the particular specimen.

Compression tests of hollow cylinders were made in a 200-kip hydraulic testing machine using a loading rate of 10 kips per min. Pure-torsion tests were made using special loading and anchor arms which were attached to the specimen by steel bands. The load was applied by use of an 8-in. screw jack, and the torque was computed as the product of the jack load and the lever arm (45 in.). The load on the jack was measured by use of a calibrated proving ring with SR-4 strain gages. Combined loads were obtained by using the torque apparatus and a screw-gear testing machine, as shown in Fig. 1.

In the combined-load tests, a predetermined compression was applied first, and then the torque was applied to produce failure; the compression load was kept sensibly constant during the test. The specimen was carefully centered in the testing machine, and the load was applied through a spherical bearing block. Special lubricated bearing plates were used to reduce friction between the top of the specimen and the head of the machine. These bearing plates permitted measurement of friction torque during the test and, although this never exceeded 4% of applied torque, the actual torque on the specimen was corrected for the friction.

TEST RESULTS

Typical failures obtained in this series of tests are shown in Fig. 2. The pure-torsion specimens exhibited approximately 45° helical fractures as a result of diagonal tension (Fig. 2). Under combined loadings, the specimens failed by helical cracks, the helix angle of which varied from 19° to 34° depending on the compression load. Pure-compression cylinders failed along irregular vertical, inclined, or circumferential cracks.

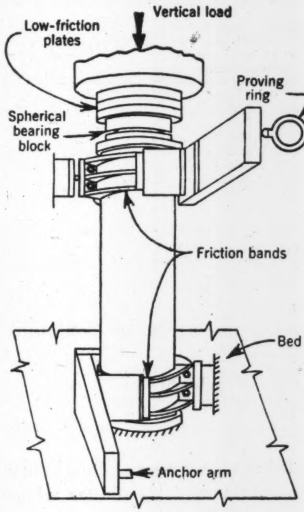
Vertical load
Low-friction plates
Spherical bearing block
Proving ring
Screw jack
Friction bands
Bed plate
Anchor arm

FIG. 1

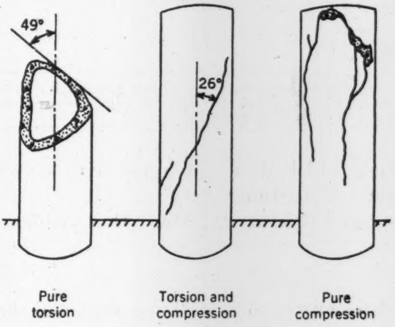
49°
26°
Pure torsion
Torsion and compression
Pure compression

FIG. 2

Stresses at failure were computed from the measured loads by use of

$$\sigma = \frac{P}{A} \qquad (5a)$$

and

$$\tau = \frac{T\,r}{J} \qquad (5b)$$

in which P is the compression load at failure, A is the area of test specimen, T is the corrected torque on the specimen at failure, r is the outside radius of hollow cylinder, and J is its polar moment of inertia. For groups of similar specimens, average values of the compressive, σ, and shearing, τ, stresses at failure, the nominal compressive strength, σ_c, and the helix angle of the major cracks are given in Table 1.

The compressive stress, σ, was computed by assuming that the load was perfectly axial and that the stress distribution was uniform over the entire cross section. The shearing stress, τ, was computed on the basis of elastic theory which, at failure, is only an approximation. If concrete were perfectly plastic, the shear stress at failure would be approximately 85% of the value given by elastic theory. However, the actual shear stress at failure is somewhere between these limits and it is approximated herein by elastic theory.

The principal stresses at failure, σ_1 and σ_2, and the dimensionless ratios, σ_1/σ_c and σ_2/σ_c, were computed for each individual specimen, and these dimensionless ratios are plotted in Fig. 3. With few exceptions, the data followed a pattern which does not agree with either the maximum stress or Coulomb's internal-friction theory.

TABLE 1

Group	Compressive stress, σ, in pounds per square inch	Shearing stress, τ, in pounds per square inch	Nominal compressive strength, σ_c, in pounds per square inch[a]	Helix angle, θ, in degrees
1	0	284	2,710	49
2	400	430	2,760	32
3	810	490	2,790	26
4	1,050	500	2,690	22
5	1,280	620	2,590	23
6	1,670	570	2,640	..
7	2,000	530	2,530	..
8	2,180	570	2,490	..
9	2,680	0	2,680	..

[a] Upon averaging results of test group 9, it was found that σ_c was equal to 86.6% of the value of f'_c determined from tests of 3-in. by 6-in. control cyclinders. Based on this relationship, σ_c-values were computed for all specimens.

It has been suggested[17] that yielding failure can be defined by

$$\tau_o = F(\sigma_o) \tag{6}$$

in which σ_o and τ_o are the normal and shearing octahedral stresses. Octahedral stresses occur on the sides of an octahedral element formed by planes whose normals make equal angles with the principal stress axes (Fig. 4) and are defined by

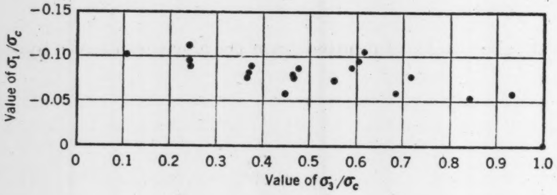

FIG. 3

$$\sigma_o = \tfrac{1}{3}(\sigma_1 + \sigma_2 + \sigma_3) \tag{7a}$$

and

$$\tau_o = \tfrac{1}{3}[(\sigma_1 - \sigma_2)^2 + (\sigma_2 - \sigma_3)^2 + (\sigma_3 - \sigma_1)^2]^{1/2} \tag{7b}$$

---

[17] "Theory of Flow and Fractures of Solids," by A. Nadai, McGraw-Hill Book Co., Inc., New York, N. Y., 1950, pp. 225–228.

A dimensionless plot of Eq. 6 for the test data is shown in Fig. 5. Fitting a straight line to the data by connecting the points obtained by averaging results of pure torsional tests and pure compressive tests yields

$$-\frac{\tau_o}{\sigma_c} = 1.16\,\frac{\sigma_o}{\sigma_c} + 0.086 \qquad (8)$$

To test further the validity of Eq. 8, results of a number of tests in which concrete was subjected to combined states of stress were considered. Of particular interest are biaxial tests[3] and triaxial tests.[5,6] The principal characteristics of the specimens and the test conditions are summarized in Table 2.

The data in Table 2 represent concretes of different ages, mixes, strengths, and moisture conditions at the time of test. The effect of these varying characteristics on the failure criteria cannot be readily defined. In this analysis the nominal compressive strength, σ_c, is used to account for the difference in the nature of the materials. As previously indicated, for hollow cylinders σ_c was determined as 86.6% of the strength of 3-in. by 6-in. control cylinders. For the specimens in Cols. 2 and 3 of Table 2, σ_c was taken as the compressive strength of corresponding control cylinders, and for Col. 4, σ_c was taken as the compressive strength of unnotched control cylinders.

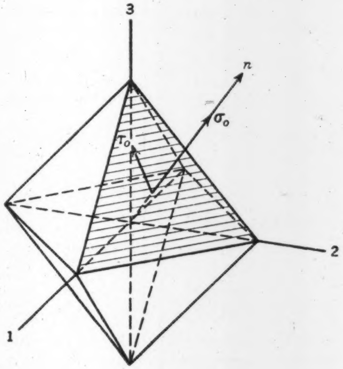

FIG. 4

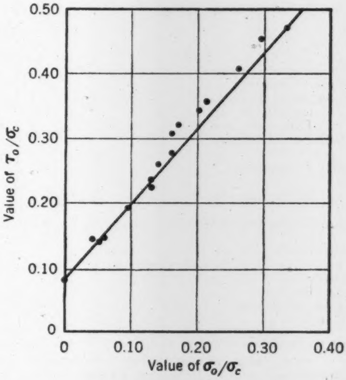

FIG. 5

Octahedral stresses, σ_o and τ_o, at failure and dimensionless ratios of σ_o/σ_c and τ_o/σ_c were computed for individual specimens, and average stresses and ratios were computed for groups of identical specimens. These dimensionless ratios are plotted in Fig. 6. Considering the heterogeneity of concrete and the variations in the type and in the conditions of tests, the scatter of the data is not significant. Furthermore, it appears that the data in the biaxial stress range can be adequately represented by a straight line, but those data corresponding to triaxial states of stress deviate appreciably from the assumed linear relationship. Because the third invariant, I_3, is identically zero for biaxial states of stress and is not zero for triaxial states of stress, it appears plausible that the deviation of triaxial data from the biaxial linear relationship may be related to the third stress invariant.

In a general case, any invariant symmetric function depending on state of stress—for example, a criterion of failure—is completely defined in terms of the three principal stress invariants. Therefore, a generalized failure criterion can be written as

$$F(I_1, I_2, I_3) = 0 \qquad (9)$$

in which

$$I_1 = \sigma_1 + \sigma_2 + \sigma_3 \qquad (10a)$$

and

$$I_2 = \sigma_1 \sigma_2 + \sigma_2 \sigma_3 + \sigma_3 \sigma_1 \qquad (10b)$$

TABLE 2

Description (1)	F. Richart, A. Brandtzaeg, and R. L. Brown[a] (2)	G. Balmer[b] (3)	A. Freudenthal[c] (4)
Type of loading	Triaxial[d]	Triaxial	Biaxial[e]
Specimen: Type	Cylinder	Cylinder	Notched cylinder
Length, in inches	8	12	10
Diameter, in inches	4	6	4
Number of tests	64	50	23
Mix Proportion	1:2.15:2.5 1:1:2 1:3:5	1:2.9:4.5	....
Maximum size of aggregate, in inches	3/4	$1\frac{1}{2}$	....
Water-cement ratio	0.88 0.64 1.25	0.58	....
Curing Conditions: Humidity, in %	Moist	100	100 and 70
Temperature, in °F	....	70	70
Duration of curing, in days	27	28	14
Age, in days	28	35 and 97	28
Test conditions	Air dry	Oven dry	....
Range of σ_c, in pounds per square inch	1,050 to 3,660	3,570 to 3,950	2,960 to 9,360

[a] "A Study of the Failure of Concrete Under Combined Compressive Stresses," by F. Richart, A. Brandtzaeg, and R. L. Brown, *Bulletin No. 185*, Univ. of Illinois Eng. Experiment Station, Urbana, Ill., 1928. [b] "Shearing Strength of Concrete Under High Triaxial Stress-Computation of Mohr's Envelope as a Curve," by G. Balmer, Structural Research Lab. Report, *S. P. No. 23*, Bureau of Reclamation, U. S. Dept. of the Interior, Washington, D. C., 1949. [c] "The Inelastic Behavior and Failure of Concrete," by A. Freudenthal, *Proceedings*, 1st U. S. National Cong. of Applied Mechanics, Chicago, Ill., 1951, pp. 641–646. [d] Series 2 and 3B omitted because of uncertain results caused by mechanical difficulties. [e] Tests with sustained load and fast loading rates are omitted.

This concept has been applied to the development of yield criteria for plastic materials by W. Prager, M. ASCE, and P. G. Hodge.[18] Octahedral stresses defined by Eq. 7 may also be expressed in terms of principal stress invariants, I_1 and I_2, as

$$\sigma_o = \tfrac{1}{3} I_1 \qquad (11a)$$

$$\tau_o = \tfrac{1}{3}[2(I^2_1 - 3 I_2)]^{1/2} \qquad (11b)$$

The failure criterion defined by Eq. 6 can be written as

$$F(I_1, I_2) = 0 \qquad (12)$$

---

[18] "Theory of Perfectly Plastic Solids," by W. Prager and P. G. Hodge, John Wiley and Sons, Inc., New York, N. Y., 1951, p. 22.

Therefore, a generalized form of the failure criterion given by Eq. 9 may be written in a form similar to Eq. 6 as

$$\tau_o = F'_1(\sigma_o) + F'_2(I_3) \quad \text{.....................} (13)$$

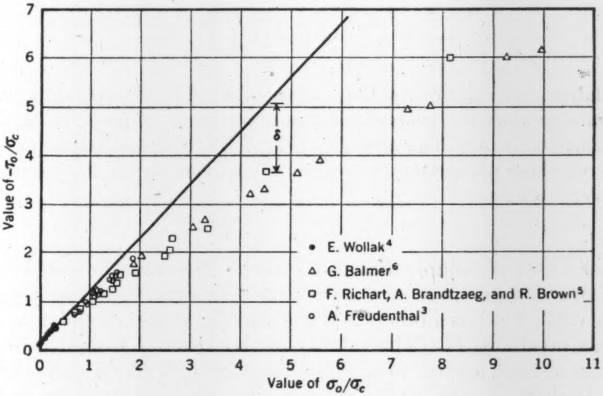

FIG. 6

in which F'_1 and F'_2 are functions characteristic of the material. Rewriting Eq. 13 into dimensionless form gives

$$\frac{\tau_o}{\sigma_c} = F_1\left(\frac{\sigma_o}{\sigma_c}\right) + F_2\left(\frac{I_3}{\sigma^3{}_c}\right) \quad \text{....................} (14)$$

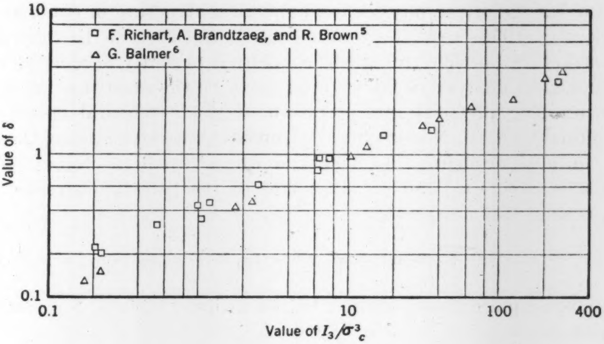

FIG. 7

For biaxial states of stress, $I_3 = 0$, and Eq. 14 yields

$$\frac{\tau_o}{\sigma_c} = F_1\left(\frac{\sigma_o}{\sigma_c}\right) + F_2(0) \quad \text{....................} (15)$$

It is seen from Fig. 6 that for states of stress for which I_3 is not zero the data deviate appreciably from the straight line defined by Eq. 8. This deviation, denoted by δ in Fig. 6, can be computed from test data. In terms of the proposed falure criterion, δ represents the difference between Eqs. 15 and 14:

$$\delta = F_2(0) - F_2\left(\frac{I_3}{\sigma^3{}_c}\right) \ldots\ldots\ldots\ldots\ldots\ldots (16)$$

Correlation between computed values of δ and corresponding values of $I_3/\sigma^3{}_c$ would support the generalized failure criterion proposed in Eqs. 12 and 13. A logarithmic plot of δ and $I_3/\sigma^3{}_c$ (Fig. 7) indicates a satisfactory correlation between these parameters, providing some evidence for the validity of the proposed hypotheses.

CONCLUSIONS

A general form of failure criterion for concrete has been proposed in Eq. 13. Eq. 13 indicates that failure occurs when the octahedral shear stress, τ_o, reaches a limiting value which is a function of the octahedral normal stress, σ_o, and the third stress invariant, I_3. The validity of this criterion is limited to the case in which (*a*) a single loading to failure is considered; (*b*) the duration of loading is relatively short; (*c*) the octahedral normal stress, σ_o, is compressive or zero; and (*d*) the stress distribution is approximately uniform. Evaluation of the effects of repeated cycles of loading, sustained loading, octahedral tensile stress, and nonuniform stress distribution requires additional experimental evidence.

There is no direct consideration of the effect of composition and structure of the material, rate and manner of loading, type and size of specimen, stress history, and volume changes depending on stress, humidity, and temperature. To obtain a criterion which would take into account these various factors requires knowledge of the physical and chemical structure of concrete beyond that presently (1955) available. Although basic research to determine the effect of structure on the strength of concrete is urgently needed, at this time phenomenological analysis of failure appears to be the most fruitful approach.

An interesting physical interpretation of the octahedral shearing stress has been noted by V. V. Novozhilov.[19] Consider, at a given point, the shearing stress, τ, on a plane defined by a normal whose direction cosines referred to principal axes are l, m, and n. In terms of the principal stresses and the direction cosines it is known that

$$\tau^2 = \sigma^2{}_1\, l^2 + \sigma^2{}_2\, m^2 + \sigma^2{}_3\, n^2 - (\sigma_1\, l^2 + \sigma_2\, m^2 + \sigma_3\, n^2)^2 \ldots\ldots (17)$$

The root-mean-square shearing stress, τ_a, on a closed surface, S, containing the point is defined as

$$\tau_a = \lim_{S\to 0}\left(\frac{1}{S}\int_S \tau^2\, dS\right)^{1/2} \ldots\ldots\ldots\ldots\ldots\ldots (18)$$

---

[19] "The Physical Meaning of the Stress Invariants of the Theory of Plasticity," by V. V. Novozhilov, Applied Mathematics and Mechanics, Academy of Science of U. S. S. R. Publication, Vol. 16, 1952, pp. 617–619.

In general, the value of τ_a will depend on the surface, S, over which the integration is performed. However, by choosing S to be the surface of a sphere of radius, r, all possible directions are weighted equally, and an "average" shearing stress at the point is obtained. Performing the integration of Eq. 18 leads to

$$\tau^2_a = \frac{1}{15}[(\sigma_1 - \sigma_2)^2 + (\sigma_2 - \sigma_3)^2 + (\sigma_3 - \sigma_1)^2] = \frac{9}{15}\tau^2_o \ldots\ldots (19)$$

Eq. 19 indicates that the "average" shearing stress, τ_a, differs from octahedral shearing stress, τ_o, only by a numerical constant. Using this formulation and noting that the octahedral normal stress, σ_o, is the average normal stress, the criterion of failure given by Eq. 8 can be written as

$$-\frac{\tau_a}{\sigma_c} = 0.897\frac{\sigma_o}{\sigma_c} + 0.066 \ldots\ldots\ldots\ldots\ldots\ldots\ldots (20)$$

For the biaxial states of stress considered, failure depends on the magnitude of the average shearing and normal stresses.

The failure criteria proposed herein are entirely phenomenological. However, some of the parameters used in these criteria may be associated with a physical interpretation of the failure mechanism. The types of possible failure that can be considered are (1) slip between grains, (2) slip within a grain, (3) cleavage between grains, and (4) cleavage within a grain. It seems plausible that such failures may be associated with the average shearing and normal stresses as defined by Eq. 20. In cases of triaxial compression, deviation of the experimental data from the simple relationship of Eq. 20 may be associated with the limited effectiveness of grain interlocking in increasing the resistance to intergranular slip.

Other interpretations of failure criteria based on considerations of strain or energy are possible. Verification of such formulations may provide some useful information regarding the mechanism of failure in concrete. It seems, however, that until the intragranular and intergranular behavior of concrete under load is better understood a phenomenological criterion of failure, such as proposed herein, is the most satisfactory.

DISCUSSION

Frank A. Blakey[20] **and F. Donald Beresford**[21].—Numerous tests have been performed by the writers on plain concrete beams, disks, and slabs arranged so that the failure under uniaxial tension, equal tensions at right angles, and equal compression and tension at right angles on concrete could be studied. The full details of these tests are available.[22, 23] As a result of these tests the formula governing the fracture of concrete was proposed in the form:

$$I^2_1 - 2\,I_2 + 2.4\,\sigma_b\,I_1 = 3.4\,\sigma^2_b \qquad (21)$$

in which σ_b is the failure stress of concrete in bending in beams.

Eq. 8, as formulated by Messrs. Bresler and Pister, may be placed in the form:

$$I^2_1 - 9.18\,I_2 + 9.18\,\sigma_b\,I_1 = 10.4\,\sigma^2_b \qquad (22)$$

if it is assumed that $\sigma_c = -10\,\sigma_b$. This assumption is supported by the results in Fig. 3, but any other assumed ratio for σ_c and σ_b would only alter the coefficients of the terms, $\sigma_b\,I_1$ and σ^2_b, in Eq. 22 but not change the agreement in the general form between the hypothesis of the authors and that of the writers.

This agreement in form can be demonstrated further if the physical interpretation of the stress invariants is considered.

If e is the volumetric strain or dilatation and U_s is the shear-strain energy (or energy of change of shape), it can be shown that

$$U_s = \frac{1+\mu}{3\,E}\,(I^2_1 - 3\,I_2) \qquad (23a)$$

and

$$e = \frac{1-2\,\mu}{E}\,I_1 \qquad (23b)$$

in which E is the modulus of elasticity and μ is Poisson's ratio. If these relationships are substituted in Eqs. 21 and 22, it will be found that

$$U_s\,\frac{3\,E}{1+\mu} + I_2 + 2.4\,\sigma_b\,\frac{E\,e}{1-2\,\mu} = 3.4\,\sigma^2_b \qquad (24a)$$

and

$$U_s\,\frac{3\,E}{1+\mu} - 6.18\,I_2 + 9.18\,\sigma_b\,\frac{E\,e}{1-2\,\mu} = 10.4\,\sigma^2_b \qquad (24b)$$

Thus, the fracture of concrete depends on the shear-strain energy, the volumetric strain, and an odd term associated with the second stress invariant. The effect of this latter form appears to be the most important difference between the two hypotheses.

---

[20] Senior Research Officer, Div. of Bldg. Research, Commonwealth Scientific and Industrial Research Organization, Melbourne, Australia.

[21] Technical Officer, Div. of Bldg. Research, Commonwealth Scientific and Industrial Research Organization, Melbourne, Australia.

[22] "Tensile Strains in Concrete," Pt. 1, *Report C2.2-1*, Div. of Bldg. Research, Commonwealth Scientific and Industrial Research Organization, Melbourne, Australia, 1953.

[23] "Tensile Strains in Concrete," Pt. 2, *Report C2.2-2*, Div. of Bldg. Research, Commonwealth Scientific and Industrial Research Organization, Melbourne, Australia, 1955.

Again, if the two hypotheses are plotted using as coordinate axes the dimensionless ratios, σ_1/σ_b and σ_2/σ_b, then Fig. 8 results; in Fig. 8 the results are plotted only for positive values of σ_1/σ_b because both equations are symmetrical about $\sigma_1/\sigma_b = \sigma_2/\sigma_b$. The differences in the first and adjacent parts of the second and fourth quadrants, although fairly large, are probably not practically significant and may well be within the margin of experimental error. The differences to the left of the line, $\sigma_1/\sigma_b = -\sigma_2/\sigma_b$, are much greater. However, it must be noted that the results of the authors fall entirely to the left of the line whereas those of the writers fall to the right of it (Fig. 8). In their report [21, 22] the writers emphasize that the choice of a circle as the curve to which the experimental points were fitted was based only on its simplicity. It was realized that further work might show other curves to be more suitable, but—as it was realized that any other second-degree curve should be capable of the same physical interpretation, as has been shown herein—there seemed to be little point in pursuing the matter further.

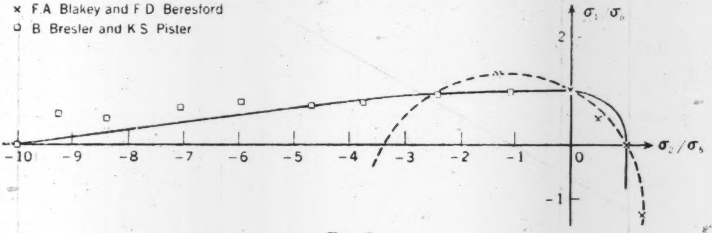

FIG. 8

There is, however, one important difference between the work of Messrs. Bresler and Pister and that of the writers. In the flexural specimens which they used it was found that microcracks developed—that is, the concrete material failed at loads well below that at which the specimens ultimately fell apart. It is with the stress conditions causing these cracks that the writers were concerned and to which their hypothesis applies. These microcracks were discovered through a detailed measurement of the strain distribution over the surfaces of the specimens used. It is rather disappointing that Messrs. Bresler and Pister omitted any reference to strain measurements. A complete study of the strain in the hollow cylinders would have been interesting. On the other hand, the writers have reason to believe that the extent to which these microcracks develop before final collapse of a specimen is a function of the mix proportions and the materials of the concrete. Perhaps the close qualitative agreement between the two hypotheses indicates that, although the microcracks developed at loads well below failure in the writers' tests, they developed at loads close to failure in the authors' tests.

PAUL RICE,[24] J.M. ASCE.—Data on the combination of tensile and compressive stresses have also been presented by G. M. Smith.[25] The purposes of this discussion are: (*a*) To correlate these additional experimental data and (*b*) to correlate data given by the authors with a suggested design equation given by Mr. Smith.

---

[24] Technical Director, Am. Concrete Inst., Detroit, Mich.

[25] "Failure of Concrete Under Combined Tensile and Compressive Stresses," by G. M. Smith, *Journal*, A. C. I., No. 50-8, October, 1953.

Mr. Smith's results agreed reasonably well with the simple design formula:

$$\left(\frac{\sigma_1}{M_R}\right)^2 + \left(\frac{-\sigma_3}{f'_c}\right)^2 = 1 \ldots\ldots\ldots\ldots\ldots\ldots (25)$$

in which M_R is the modulus of rupture and f'_c is the ultimate compressive strength of a 6-in. by 12-in. cylinder.

The results (scaled from the plotted data), when plotted as dimensionless ratios, $-\tau_o/f'_c$ and σ_o/f'_c, give close agreement with Eq. 8 for a criterion of failure. From Mr. Smith's data there is obtained the formula,

$$-\frac{\tau_o}{f'_c} = 1.15\frac{\sigma_o}{f'_c} - 0.115 \ldots\ldots\ldots\ldots\ldots\ldots (26)$$

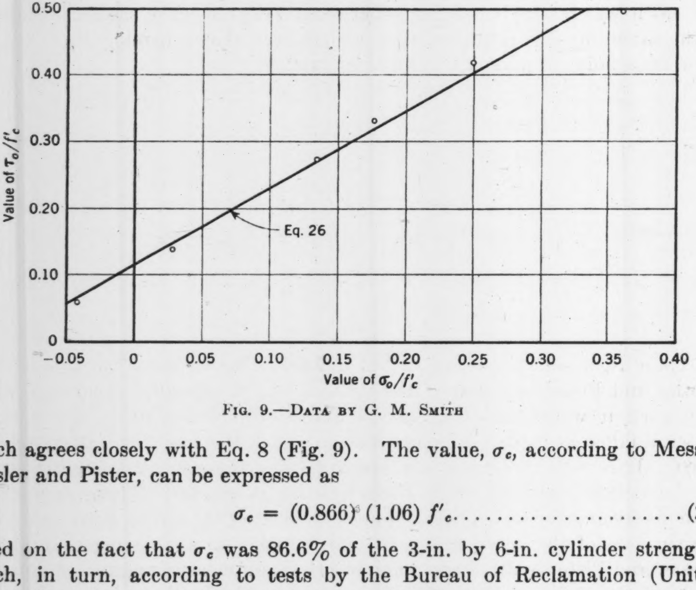

FIG. 9.—DATA BY G. M. SMITH

which agrees closely with Eq. 8 (Fig. 9). The value, σ_c, according to Messrs. Bresler and Pister, can be expressed as

$$\sigma_c = (0.866)\,(1.06)\,f'_c \ldots\ldots\ldots\ldots\ldots\ldots (27)$$

based on the fact that σ_c was 86.6% of the 3-in. by 6-in. cylinder strengths which, in turn, according to tests by the Bureau of Reclamation (United States Department of the Interior), are 106% of f'_c as determined from standard cylinders. With these conversion factors, Eq. 26 becomes

$$-\frac{\tau_o}{\sigma_c} = 1.15\frac{\sigma_o}{\sigma_c} - 0.125 \ldots\ldots\ldots\ldots\ldots\ldots (28)$$

A possible explanation for the difference in constants (in addition to errors in measurement) is that Mr. Smith's data are based on tension computed as $M\,c/I$ for beams in flexure. The value of the modulus of rupture when so determined usually differs from tensile strength as determined by direct tensile tests.

Using the average values for compressive and shearing stresses at failure as given in Table 1, principal stresses σ_1 and $-\sigma_3$ were determined. A comparison of these values with a curve for Mr. Smith's equation (Eq. 25), using the common approximation for ultimate tensile strength,

$$f'_t = 0.10\, f'_c \qquad (29)$$

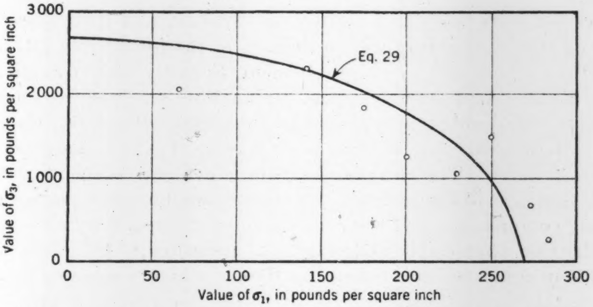

FIG. 10.—PRINCIPAL STRESSES (BRESLER-PISTER DATA FOR FIG. 3)

is shown in Fig. 10. The resulting design formula is

$$\left(\frac{\sigma_1}{0.10\, f'_c}\right)^2 + \left(\frac{-\,\sigma_3}{f'_c}\right)^2 = 1 \qquad (30)$$

It should be noted that Eq. 30 provides a rational pattern for the data shown in Fig. 3 and is presented in a form which is both convenient and familiar to structural engineers.

HENRY J. COWAN,[26] A.M. ASCE.—The authors are to be congratulated on having reduced the problem of the failure of concrete under combined stresses to a criterion similar to that which has been found to govern the failure of ductile materials. This is a significant advance in the theory of strength of materials. However, Messrs. Bresler and Pister dismiss too lightly some of the previous theories, notably Rankine's maximum-stress theory and Mohr's theory, of which Coulomb's internal-friction theory is a special case.

Although the mechanics of the failure of concrete are not fully known, the failure always appears to be initiated by the formation of very fine tension cracks, which, although invisible or barely visible, can be detected by careful measurement.[27,28,22,23] The ultimate failure of the concrete may, however, take the form of (*a*) a cleavage failure which results in a clean fracture and is associated with the existence of high tensile stresses; and (*b*) a crushing failure which is accompanied by an appreciable formation of debris and is associated with the existence of high compressive stresses. This ultimate failure is immediately obvious and leads to the collapse of a plain concrete specimen, either instantly or after a short period of time has been allowed for the completion of the process of failure. In a reinforced concrete specimen a cleavage failure can be prevented by inserting suitable tension or shear reinforcement; however, the strength of the specimen thereafter is dependent on the strength of the steel.

---

[26] Prof. of Architectural Science, Univ. of Sydney, Australia.

[27] "The Problem of Strength and Plasticity of Concrete," by O. Y. Berg, *Doklady Akademii Nauk S. S. R.*, Vol. 7, 1950, pp. 617–620 (translated from the Russian as *Road Research Library Communication No. 165*, Dept. of Scientific and Industrial Research of the United Kingdom, London, 1951).

[28] "A Method of Studying the Formation of Cracks in a Material Subjected to Stress," by R. Jones, *British Journal of Applied Physics*, Vol. 3, 1952, pp. 229–232.

It does not seem likely that a physical explanation of the process of failure in terms of atomic structure will be derived in the foreseeable future because the structure of concrete, or even of cement, is vastly more complicated than that of a metal. A phenomenological explanation is necessarily only approximate, and it is desirable that it should be associated with clearly observed phenomena. Because in concrete there are two types of failure, it seems reasonable to use two criteria. The cleavage fracture is evidently dependent largely on the tensile strength of the cement. The aggregate, however, plays a great part in resisting compression, and the cement does not apparently alter its angle of internal friction appreciably at low triaxial pressures;[5,6] therefore, the failure of concrete in compression is not unlike that of a highly cohesive granular soil. In offering this physical explanation, the writer is conscious that it is an over-simplification which will give way to a more precise interpretation when the structure of concrete is better understood.

The foregoing led the writer[29] to adopt the dual criterion of failure referred to by the authors. The maximum-stress theory has been used on numerous occasions to account for the cleavage (or tension) fracture of brittle materials, including concrete. Mohr's theory, using a curved envelope, has similarly accounted for the crushing failure of concrete. The first attempt at a unified criterion of failure appears to have been made by A. Leon,[7] using Mohr's theory with a continuous curved envelope, crossing the s-axis on the tension side. This criterion is represented by the curved line ABA in Fig. 11. Mr. Leon explained that a Mohr circle touching the envelope at B corresponds to a cleavage failure, and Mohr circles touching the envelope elsewhere correspond to compression failures. The curved envelope, however, is an unsatisfactory criterion for the concrete designer because it cannot be expressed in simple mathematical terms and it varies for different types of concrete. These difficulties are overcome by using a vertical limiting line DBD for the cleavage failure (Rankine's maximum-stress theory), and two limiting lines CC for the crushing failure. In the range of low triaxial stresses, straight limiting lines may be used with sufficient accuracy (Coulomb's internal-friction theory). Therefore, both the cleavage and the crushing failure can be expressed in terms of the principal stresses as a constant maximum tensile stress and a maximum compressive stress which varies linearly with the minor (tensile of compressive) principal stress. The dual criterion of failure can be readily applied to reinforced and prestressed concrete design. The linear relationship is sufficiently accurate for building construction; it does not apply to structures with high triaxial stresses such as large concrete dams.

The writer and S. Armstrong[30] have checked this criterion in an investigation on reinforced and prestressed concrete beams under combined bending and torsion and have suggested a procedure for structural design. The criterion has also been checked with the results of two earlier investigations on concrete and reinforced concrete in combined bending and torsion.[31,32] In both cases, generally, good agreement with the experimental data was found. The only significant difference between theory and experiment occurred at the transition from primary torsion (cleavage) to primary bending (crushing) failure because the dual criteria produced a sharp corner in the limiting line, whereas the experimental results followed a more gradual curve; however, this divergence is not of practical significance.

---

[29] "Strength of Reinforced Concrete under the Action of Combined Stresses, and the Representation of the Criterion of Failure by a Space Model," by Henry J. Cowan, *Nature*, Vol. 169, 1952, p. 663.

[30] "Experiments on the Strength of Reinforced and Prestressed Concrete Beams and of Concrete-Encased Steel Joists in Combined Bending and Torsion," by Henry J. Cowan and S. Armstrong, *Magazine of Concrete Research*, Vol. 7, 1955, pp. 3–20.

A three-dimensional representation,[33,29] in terms of the principal stresses, of the criteria used by Messrs. Bresler and Pister, Mr. Leon, and Mr. Armstrong and the writer shows that the difference between the criteria is caused primarily by the effect of the intermediate principal stress. That they are not as dissimilar as they appear to be when expressed in mathematical terms is revealed by a comparison with the experimental data. The intermediate principal stress does not play a significant part in the large range of combined-stress problems, notably those met in the design of reinforced and prestressed concrete structures. On the other hand, ease of application is of prime importance in these problems. The writer, therefore, feels that Messrs. Bresler and Pister have been a little harsh in their discussion of some of the previous theories. This comment is not intended, however, to detract from their important contribution to the theory of fracture of concrete.

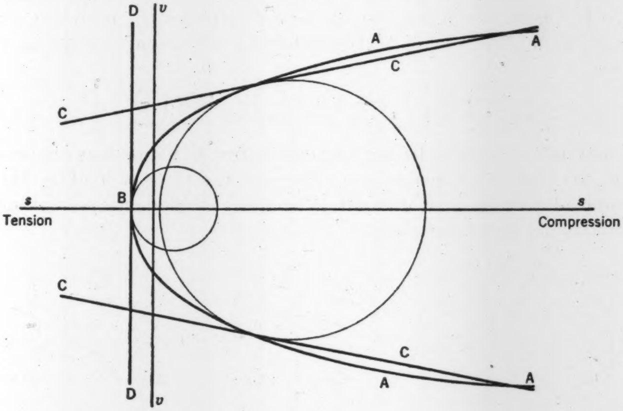

FIG. 11.—MOHR CIRCLE REPRESENTATION OF THE FAILURE CRITERIA OF A. LEON AND HENRY J. COWAN

---

[31] "Vridning och vridningsinspanning vid betongkonstruktioner," by H. Nylander, *Meddelanden No. 3*, Statens Kommitté för Byggnadsforskning, Stockholm, 1945.

[32] "The Strength of Concrete in Combined Bending and Torsion," by D. Fisher, thesis presented to the University of London, in 1950, in partial fulfilment of the requirements for the degree of Doctor of Philosophy.

[33] "New Graphical Method of Representing Strength Characteristics," by A. Meldhal, *Brown Boveri Review* (Switzerland), August, 1944, pp. 260–267.

Boris Bresler,[34] A.M. ASCE, and **Karl S. Pister,**[35] J.M. ASCE.—The comments of the discussers fall into two main categories: (1) Utility of the proposed failure criteria for design and (2) physical interpretation of failure criteria and mechanism of failure. Whether one form of failure criterion is superior to another depends largely on the use intended for it. The interaction formula proposed by Mr. Smith[25] is useful in design but is entirely empirical. Mr. Cowan proposes dual criteria which are somewhat more rational but are more difficult to apply. Neither criterion is applicable to triaxial states of stress. The writers' criterion, although not directly applicable to design, may be useful for correlating biaxial and triaxial tests and for furthering an understanding of the physical mechanism of failure. It was the writers' opinion that, once a valid criterion is established, simplifications suitable for design can be derived. For example, in the case of shearing stresses, τ, combined with compressive stress, σ, Eq. 8 leads to the following definition of shearing strength of concrete:

$$\frac{\tau}{f'_c} = 0.10 \left[0.89 + 8.9\left(\frac{\sigma}{f'_c}\right) - 10.8\left(\frac{\sigma}{f'_c}\right)^2\right]^{\frac{1}{2}} \dots\dots\dots\dots (31)$$

The writers are grateful to Mr. Rice for noting the agreement between their work and Mr. Smith's experiments. Because the type of loading Mr. Smith used produced a stress field difficult to analyze by elementary methods, such agreement seems rather fortuitous.

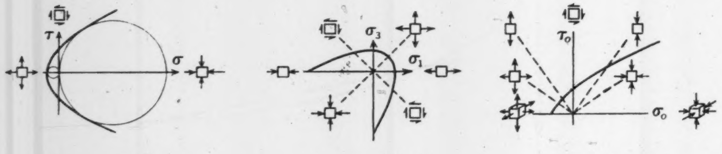

(a) $\tau = Fn(\sigma)$ (b) $\sigma_3 = Fn(\sigma_1)$ (c) $\tau_o = Fn(\sigma_o)$

Fig. 12

In formulating the failure law in terms of octahedral stress the writers were guided by several considerations:

1. The failure criterion in the form of Eq. 6 accounts for the effect of the intermediate principal stress, σ_2, and, thus, is a natural generalization of the Mohr theory of failure which neglects the effect of σ_2. Furthermore, use of octahedral stresses allows both biaxial and triaxial states of stress to be plotted in one plane. A comparison of three possible forms of representation of a failure criterion is shown in Fig. 12. In Fig. 12(*a*) is shown Mohr's failure theory in terms of normal and shearing stresses; in Fig. 12(*b*), a failure criterion for brittle materials in terms of principal stresses; and in Fig. 12(*c*), a similar criterion in terms of octahedral stresses. Radial lines define some of the possible states of stress, and only the octahedral form permits plotting triaxial states of stress in one plane.

---

[34] Associate Prof. of Civ. Eng., Univ. of California, Berkeley, Calif.

[35] Asst. Prof. of Civ. Eng., Univ. of California, Berkeley, Calif.

2. Octahedral stresses have physical interpretations which may lead to a better understanding of the mechanism of failure in concrete. The normal octahedral stress is the mean normal stress, and the shearing octahedral stress is proportional to the root mean shear stress at a point. Thus, it is possible from Eq. 6 to define the failure mechanism in terms of the mean shearing and normal stresses at a point. Another possible interpretation of octahedral stresses as noted by Messrs. Blakey and Beresford is related to the elastic strain energy and the volumetric strain. It seems doubtful that elastic-strain-energy concepts based on homogeneous materials with relatively constant values of elastic modulus and Poisson's ratio would be applicable to concrete. This view is supported by the presence of odd terms in the equations of Messrs. Blakey and Beresford, involving the second stress invariant, I_2, which apparently have no simple physical interpretations. A valid adaptation of strain-energy criteria to concrete must be based on a physical concept of the mechanism of deformation and failure.

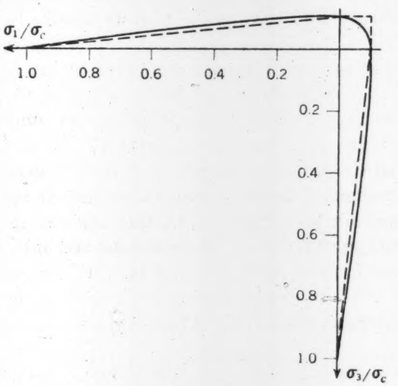

FIG. 13

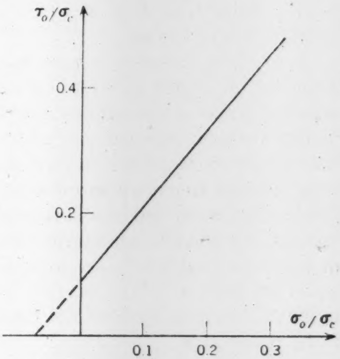

FIG. 14

3. Within the range of states of stress considered, the octahedral stress criterion has a further advantage in its simplicity of form, resulting in a simple linear equation—Eq. 8.

Mr. Cowan's linear criterion of failure, differentiating between cleavage and crushing failures, is shown in Fig. 13 by dashed lines. Whether the transition from a pure cleavage to a shear fracture in concrete is gradual or abrupt seems to be a matter that is still unsettled. The parabolic envelope assumed by Mr. Leon for brittle materials provides a gradual transition from cleavage to shear fracture. For a biaxial state of stress ($\sigma_2 = 0$) Eq. 8 may be rewritten in terms of principal stresses by substituting Eq. 7 into Eq. 8. This leads to a quadratic expression involving σ_1, σ_3, σ_c, and the experimental constants. The equation may be simplified by rotation of the σ_1 and σ_3 coordinate axes through a counterclockwise angle of 45°. If the new coordinate axes are denoted by

$\bar{\sigma}_1$ and $\bar{\sigma}_3$, there results

$$\frac{\left(\frac{\bar{\sigma}_1}{\sigma_c} + 0.257\right)^2}{0.0251} - \frac{\left(\frac{\bar{\sigma}_3}{\sigma_c}\right)^2}{0.0138} = 1.00 \qquad (32)$$

in which

$$\sigma_1 = \frac{1}{\sqrt{2}} (\bar{\sigma}_1 - \bar{\sigma}_3) \qquad (33a)$$

and

$$\sigma_3 = \frac{1}{\sqrt{2}} (\bar{\sigma}_1 + \bar{\sigma}_3) \qquad (33b)$$

Eq. 32 is the equation of a hyperbola in the principal stress plane, Fig. 13, and is similar to Fig. 8. It can be seen that, whereas Mr. Leon's theory[7] and the octahedral theory apply a single criterion to both cleavage and shear failures, Mr. Cowan proposes two distinct criteria with an abrupt transition between them. Aside from this, Mr. Cowan's theory and that of the writers appear to be in close agreement.

It must be understood that, as yet, the proposed linear octahedral theory is untested for states of stress in which the mean stress is tensile—that is, for states of stress to the left of the τ_o-axis in Fig. 12(*c*). It may well be that some modifications in the assumed linear curve may be necessary. In order to test the validity of Eq. 8 beyond the range of the writers' experimental data it may be of interest to extrapolate the straight line, as shown in Fig. 14, and evaluate the strengths for various states of stress on this basis. The uniaxial tensile strength based on this assumption is $0.10\,\sigma_c$ or $0.087\,f'_c$. The torsional strength, or biaxial, equal tension-compression strength, is $0.10\,\sigma_c$—that is, very nearly equal to tension. The biaxial, equal tension, tensile strength is $0.07\,\sigma_c$ or $0.061\,f'_c$—that is, 70% of the uniaxial tensile strength. These values appear to be reasonable.

Messrs. Blakey and Beresford define failure as the formation of microcracks at loads below the ultimate. The writers believe that the formation of microcracks is an important factor in the mechanism of failure but that the extent to which these cracks jeopardize the load-carrying capacity of concrete has not been definitely established. The work of the discussers indicates ratios of cracking to an ultimate load varying from 0.43 to 0.80. Until the mechanism of failure in concrete is better understood, the definition of failure shall remain arbitrary.

The writers agree with Messrs. Blakey and Beresford that a complete study of strain distribution in the hollow cylinders would have been of interest. This study was not included primarily because of the hazards involved in interpreting strain measurements in concrete. Only surface strains can be measured without disturbing the internal structure of the material. Thus, the interpretation that deviation from linearity of the load-strain curve is evidence of microcracking is strictly applicable only to the surface material. The fact that surface cracking occurs at small fractions of the ultimate load seems to indicate that propagation of surface cracking with increase in load is slow and that considerable load-resisting capacity is developed after initial cracking.

AMERICAN SOCIETY OF CIVIL ENGINEERS
Founded November 5, 1852
PAPERS

Paper No. 2898

THICK RECTANGULAR PLATES ON AN ELASTIC FOUNDATION

By DANIEL FREDERICK,[1] J. M. ASCE

WITH DISCUSSION BY MESSRS. HAROLD G. LORSCH,
AND DANIEL FREDERICK

SYNOPSIS

The governing equations and their solutions for the bending of thick rectangular plates resting on elastic foundations are presented using the theory of plates developed by Eric Reissner. An examination of various types of fixity of edges involving three boundary conditions is presented, and it is shown that the Levy and Navier solutions can be used.

INTRODUCTION

The thick-plate theory developed by Eric Reissner[2,3,4] in 1945 is significant because it includes the effects of shear deformation and normal pressure. In addition, the theory permits the specification of three boundary conditions on an edge and requires the evaluation of only two functions. A theory analogous to that of Mr. Reissner was developed by R. D. Mindlin,[5] in 1951, for the motions of plates. Since its development, Mr. Reissner's theory has been applied to the solution of several problems in the bending of plates. In 1952, Manfred Schäfer[6] presented an example of the bending of a rectangular plate under a

---

NOTE.—Published, essentially as printed here, in October, 1955, as *Proceedings Paper 818*. Positions and titles given are those in effect when the paper or discussion was approved for publication in *Transactions*.

[1] Associate Prof. of Applied Mechanics, Virginia Polytechnic Inst., Blacksburg, Va.

[2] "On the Theory of Bending of Elastic Plates," by Eric Reissner, *Journal of Mathematics and Physics*, Massachusetts Inst. of Technology, Cambridge, Mass., November, 1944, pp. 184–191.

[3] "The Effect of Transverse Shear Deformation on the Bending of Elastic Plates," by Eric Reissner, *Journal of Applied Mechanics*, Vol. 12, 1945, pp. 69–77.

[4] "On a Variational Theorem in Elasticity," by Eric Reissner, *Journal of Mathematics and Physics*, Massachusetts Inst. of Technology, Cambridge, Mass., July, 1950, pp. 90–95.

[5] "Influence of Rotatory Inertia and Shear on Flexural Motions of Isotropic, Elastic Plates," by R. D. Mindlin, *Journal of Applied Mechanics*, Vol. 18, 1951, pp. 31–38.

[6] "Über eine Verfeinerung der klassischen Theorie dünner schwach gebogener Platten," by Manfred Schäfer, *Zeitschrift für Angewandte Mathematik und Mechanik*, June, 1952, pp. 161–171.

sinusoidal loading. P. M. Naghdi and J. C. Rowley[7] extended the theory to include an elastic foundation that behaves according to the classical Winkler-Zimmerman assumption. A detailed history of the applications of Mr. Reissner's theory is contained in a paper by Mr. Naghdi.[8]

In the paper are discussed the thick-plate equations and their solutions for problems concerning the bending of rectangular plates resting on an elastic foundation. The basic equations are those obtained from Mr. Reissner's theory, modified to include an elastic foundation in the manner of Mr. Naghdi and Mr. Rowley; numerical examples are also presented.

THE FUNDAMENTAL EQUATIONS

Fig. 1 shows the coordinate system to be used and the stress resultants, M_x, M_y, M_{xy}, V_x, and V_y, in their positive directions. The displacements, u, v, and w, are positive when they act toward the positive ends of the x-axis, y-axis, and z-axis, respectively. They are assumed to be of the form, $u = z\alpha(x, y)$, $v = z\beta(x, y)$, and $w = \bar{w}(x, y)$; α and β are the rotations in the x-direction and y-direction, respectively, of a line element originally perpendicular to the neutral surface, and $\bar{w}$ is the vertical displacement of all points on this line element. They are defined as

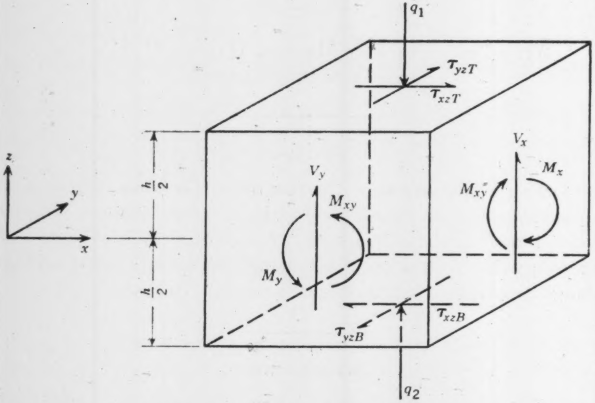

FIG. 1.—STRESS RESULTANTS FOR AN ELEMENT OF A PLATE FOR RECTANGULAR COORDINATES

$$\alpha = \frac{12}{h^3} \int_{-h/2}^{h/2} u\, z\, dz \qquad (1a)$$

$$\beta = \frac{12}{h^3} \int_{-h/2}^{h/2} v\, z\, dz \qquad (1b)$$

---

[7] "On the Bending of Axially Symmetric Plates on Elastic Foundations," by P. M. Naghdi and J. C. Rowley, *Proceedings*, 1st Midwestern Conference on Solid Mechanics, Univ. of Illinois, Urbana, Ill., 1953, pp. 119–123.

[8] "The Effect of Elliptic Holes on the Bending of Thick Plates," by P. M. Naghdi, *Journal of Applied Mechanics*, Vol. 77, 1955, pp. 89–94.

and

$$\bar{w} = \frac{3}{2\,h}\int_{-h/2}^{h/2} w\left(1 - \frac{4\,z^2}{h^2}\right) dz \ldots\ldots\ldots\ldots\ldots\ldots (1c)$$

Furthermore, it is assumed that the stresses, τ_{xz}, τ_{yz}, and σ_z, satisfy the equilibrium equations expressed in terms of the partial derivatives of the stress components. Therefore, these stresses are given by

$$\tau_{xz} = \frac{3\,V_x}{2\,h}\left(1 - \frac{4\,z^2}{h^2}\right) \ldots\ldots\ldots\ldots\ldots\ldots (2a)$$

$$\tau_{yz} = \frac{3\,V_y}{2\,h}\left(1 - \frac{4\,z^2}{h^2}\right) \ldots\ldots\ldots\ldots\ldots\ldots (2b)$$

and

$$\sigma_z = -\,\frac{q_1 + q_2}{2} + (q_2 - q_1)\left(\frac{3\,z}{2\,h} - \frac{2\,z^3}{h^3}\right) \ldots\ldots\ldots\ldots (2c)$$

in which q_1 is the pressure on the upper face and (assuming k as the foundation modulus) $q_2 = -\,k\,w$ is the pressure on the lower face of the plate. The stress resultants are defined as in the classical theory and are quantities per unit of length.

Basic Equations.—These equations are derived from the application of Mr. Reissner's variational principle,[4] considering the assumptions mentioned in the foregoing. They also include the shear stresses, τ_{xzT} and τ_{yzT}, on the top face of the plate and the shear stresses, τ_{xyB} and τ_{yzB}, on the bottom face of the plate. Eqs. 2*a*, 2*b*, and 2*c* now contain some additional terms involving these shear stresses on the top and bottom faces. After some rearranging, the basic equations may be written as

$$D\,\nabla^4\,\bar{w} - \left(\frac{h^2}{10}\right)\left(\frac{2-\nu}{1-\nu}\right)\nabla^2\,(q_1 + k\,\bar{w}) + (q_1 + k\,\bar{w}) + \left(\frac{h^3}{120}\right)\left(\frac{2-\nu}{1-\nu}\right)$$
$$\times\left(\frac{\partial \nabla^2 S^+{}_x}{\partial x} + \frac{\partial \nabla^2\, S^+{}_y}{\partial y}\right) - \frac{h}{2}\left(\frac{\partial S^+{}_x}{\partial x} + \frac{\partial S^+{}_y}{\partial y}\right) = 0 \,.\,.\, (3)$$

$$\frac{h^2}{10}\,\nabla^2\,V_x - V_x = D\,\frac{\partial \nabla^2\,\bar{w}}{\partial x} - \frac{h^2}{10\,(1-\nu)}\,\frac{\partial\,(q_1 + k\,\bar{w})}{\partial x} + \left(\frac{h^3}{120}\right)\left(\frac{2-\nu}{1-\nu}\right)$$
$$\times\left(\frac{\partial^2 S^+{}_x}{\partial x^2}\right) + \left(\frac{h^3}{120}\right)\left(\frac{\partial^2 S^+{}_x}{\partial y^2}\right) + \frac{h^3}{120\,(1-\nu)}\left(\frac{\partial^2 S^+{}_y}{\partial x\,\partial y}\right) - \frac{h}{2}\,S^+{}_x \,.\,.\, (4)$$

$$\frac{h^2}{10}\,\nabla^2\,V_y - V_y = D\,\frac{\partial \nabla^2\,\bar{w}}{\partial y} - \frac{h^2}{10\,(1-\nu)}\,\frac{\partial\,(q_1 + k\,\bar{w})}{\partial y} + \left(\frac{h^3}{120}\right)\left(\frac{2-\nu}{1-\nu}\right)$$
$$\times\left(\frac{\partial^2 S^+{}_y}{\partial y^2}\right) + \left(\frac{h^3}{120}\right)\left(\frac{\partial^2 S^+{}_y}{\partial x^2}\right) + \frac{h^3}{120\,(1-\nu)}\left(\frac{\partial^2 S^+{}_x}{\partial y\,\partial x}\right) - \frac{h}{2}\,S^+{}_y \,.\,.\, (5)$$

$$M_x = D\left[\frac{6\,(1-\nu)}{5\,G\,h}\left(\frac{\partial V_x}{\partial x}\right) - \left(\frac{\partial^2 \bar{w}}{\partial x^2} + \nu\,\frac{\partial^2 \bar{w}}{\partial y^2}\right) + \frac{3\,\nu}{5\,G\,h}\,(q_1 + k\,\bar{w})\right.$$
$$\left. - \left(\frac{2-\nu}{20\,G}\right)\left(\frac{\partial S^+{}_x}{\partial x}\right) - \left(\frac{\nu}{20\,G}\right)\left(\frac{\partial S^+{}_y}{\partial y}\right)\right] \,.\,.\, (6)$$

$$M_y = D\left[\frac{6\,(1-\nu)}{5\,G\,h}\left(\frac{\partial V_y}{\partial y}\right) - \left(\frac{\partial^2 \bar{w}}{\partial y^2} + \nu\,\frac{\partial^2 \bar{w}}{\partial x^2}\right) + \frac{3\,\nu}{5\,G\,h}\,(q_1 + k\,\bar{w}) - \left(\frac{2-\nu}{20\,G}\right)\left(\frac{\partial S^+_y}{\partial y}\right) - \left(\frac{\nu}{20\,G}\right)\left(\frac{\partial S^+_x}{\partial x}\right)\right] \quad (7)$$

$$M_{xy} = \frac{G\,h^3}{12}\left[\frac{6}{5\,G\,h}\left(\frac{\partial V_x}{\partial y} + \frac{\partial V_y}{\partial x}\right) - 2\,\frac{\partial^2 \bar{w}}{\partial x\,\partial y} - \frac{1}{10\,G}\left(\frac{\partial S^+_x}{\partial y} + \frac{\partial S^+_y}{\partial x}\right)\right] \quad (8)$$

$$\alpha + \frac{\partial \bar{w}}{\partial x} = \frac{6}{5\,G\,h}\,V_x - \frac{S^+_x}{10\,G} \quad (9)$$

and

$$\beta + \frac{\partial \bar{w}}{\partial y} = \frac{6}{5\,G\,h}\,V_y - \frac{S^+_y}{10\,G} \quad (10)$$

in which $S^+_x = \tau_{xzT} + \tau_{xzB}$ and $S^+_y = \tau_{yzT} + \tau_{yzB}$.

Eqs. 3 through 8 are the governing equations which contain six unknowns, $\bar{w}$, V_x, V_y, M_x, M_y, and M_{xy}.

Boundary Conditions.—In addition, boundary conditions also arise from the variational principle and are three in number for each edge of the plate, instead of two as in the classical theory. These conditions were described by Mr. Reissner;[2,3,4] several other authors have discussed applications of boundary conditions involving a particular edge.

Mr. Reissner[2,3] has discussed a free edge, Mr. Schäfer,[6] one type of simply supported edge, and R. A. Hirsch,[9] boundary conditions at the edge of a rigid circular inclusion.

Because three boundary conditions are to be satisfied, the usual definitions for the various types of fixity of an edge (simply supported, clamped, and others) must be extended. For the purpose of this investigation, a straight edge perpendicular to the x-axis will be used although the same statements would apply to an arbitrary curvilinear boundary. Mr. Reissner's boundary conditions are: (1) $M_x = M'_x$, or α prescribed; (2) $M_{xy} = M'_{xy}$, or β prescribed; and (3) $V_x = V'_x$, or $\bar{w}$ prescribed. Primed quantities are those prescribed on the boundary.

Simply Supported Edge.—In addition to the two usual conditions, $\bar{w} = 0$ and $M_x = 0$, a third condition for either β or M_{xy} must be specified. This may be either $\beta = 0$ or $M_{xy} = 0$. Because M_{xy} is not zero on a simply supported edge, according to the classical theory, the classical definition is perhaps more closely approximated by choosing $\beta = 0$. Physically, this condition may be achieved by using a knife-edge on the top and bottom of the plate if there is sufficient friction between the knife-edges and the plate to prevent rotation of the line elements in the y-direction. This scheme will prevent the uplift at the corners which in the classical theory is prevented by applying concentrated forces on the corners. The other possibility, $M_{xy} = 0$, would require an absence of friction between the knife-edges and the plate. The latter set of conditions was used by Mr. Schäfer[6] in his example of a rectangular plate under a sinusoidal loading.

---

[9] "The Effect of a Rigid Circular Inclusion on the Bending of a Thick Elastic Plate," by R. A. Hirsch, *Journal of Applied Mechanics*, Vol. 19, 1952, pp. 28–32.

Free Edge.—The free edge was used by Mr. Reissner[3] in an application concerning an infinite plate with a circular hole free of stress. Here, the two conditions of the classical theory, $M_x = 0$ and $V_x + \partial M_{xy}/\partial y = 0$, are replaced by $M_x = 0$, $M_{xy} = 0$, and $V_x = 0$. It is no longer necessary to transform the twisting moment into an equivalent vertical shear as in the classical theory. The vertical shear and the twisting moment must vanish separately.

Clamped Edge.—The usual conditions, $\bar{w} = 0$ and $\partial \bar{w}/\partial x = 0$, will be replaced by: (1) $\bar{w} = 0$, (2) $\alpha = 0$ or $\partial \bar{w}/\partial x = 0$, and (3) $\beta = 0$ or $M_{xy} = 0$. Although the clamped conditions may never be realized in an experiment, it appears that the condition, $\alpha = 0$, is closer to fulfilment than the condition, $\partial \bar{w}/\partial x = 0$. Also, since the statements made under the heading, "The Fundamental Equations: Simply Supported Edge," regarding the third condition, $\beta = 0$ or $M_{xy} = 0$, still apply, a clamped edge is perhaps best defined by $\bar{w} = 0$, $\alpha = 0$, and $\beta = 0$.

Elastically Restrained Edge.—If a thick elastic plate frames into a beam, for which the governing equations are the usual classical ones which do not include the effect of shear deformation, the boundary conditions for the plate can be written as

$$(M_x)_{plate} = C \frac{\partial}{\partial y} \left(\frac{\partial^2 \bar{w}}{\partial x \, \partial y} \right) \quad (11)$$

$$(M_{xy})_{plate} = B \frac{\partial^3 \bar{w}}{\partial y^3} \quad (12)$$

and

$$(V_x)_{plate} = B \left(\frac{\partial^4 \bar{w}}{\partial y^4} \right) \quad (13)$$

In these equations, B is the flexural rigidity of the beam and C denotes the torsional rigidity of the beam. These express the conditions that

a. The moment, M_x, in the plate must be associated with the twisting moment per unit length in the beam.
b. The twisting moment, M_{xy}, in the plate is equal to the bending moment per unit of length in the beam.
c. The vertical shear in the plate must be the load per unit of length on the beam.

If the theory governing the bending of the beam includes shear deformation, the beam terms would be modified accordingly. Other types of edges may be reconsidered in the same manner.

Solving the Basic Equations.—The basic equations (Eqs. 3 through 8) will be considered for the case in which $S^+_x = S^+_y = 0$. Solutions for this system of equations[10] can be found from the equations for $\bar{w}$, V_x, and V_y. The general solution for $\bar{w}$ will be written as the sum of a particular integral and a complementary function, as $\bar{w} = \bar{w}_H + \bar{w}_P$ in which

$$\nabla^4 \bar{w}_H - \left(\frac{c^2 k}{D} \right) (\nabla^2 \bar{w}_H) + \frac{k}{D} \bar{w}_H = 0 \quad (14)$$

---

[10] "On Some Problems in the Bending of Thick Plates," by Daniel Frederick, dissertation presented to the University of Michigan, at Ann Arbor, in 1955, in partial fulfilment of the requirements for the degree of Doctor of Philosophy.

and

$$\nabla^4 \bar{w}_P - \left(\frac{c^2 k}{D}\right)(\nabla^2 \bar{w}_P) + \frac{k}{D}\bar{w}_P = \left(\frac{c^2}{D}\right)(\nabla^2 q_1) - \frac{q_1}{D} \tag{15}$$

in which

$$c^2 = \left(\frac{h^2}{10}\right)\left(\frac{2-\nu}{1-\nu}\right) \tag{16}$$

Similarly, V_x and V_y can be written as the sum of a particular and complementary function: $V_x = V_{xH} + V_{xP}$ and $V_y = V_{yH} + V_{yP}$. If the function, $\psi(x, y)$, is introduced so that $V_{xH} = \partial\psi/\partial y$ and $V_{yH} = -\partial\psi/\partial x$, the governing equation for ψ is

$$\left(\frac{h^2}{10}\right)(\nabla^2\psi) - \psi = 0 \tag{17}$$

The particular solutions for V_x and V_y can be written as

$$V_{xP} = V^*_x + \frac{\partial(-D\,\nabla^2 \bar{w}_H + c^2 k\,\bar{w}_H)}{\partial x} \tag{18}$$

and

$$V_{yP} = V^*_y + \frac{\partial(-D\,\nabla^2 \bar{w}_H + c^2 k\,\bar{w}_H)}{\partial y} \tag{19}$$

in which V^*_x and V^*_y are functions which must satisfy the following equations by virtue of the governing equations of V_x and V_y:

$$\left(\frac{h^2}{10}\right)(\nabla^2 V^*_x) - V^*_x = D\,\frac{\partial\nabla^2 \bar{w}_P}{\partial x} - \frac{h^2}{10\,(1-\nu)}\,\frac{\partial(k\,\bar{w}_P + q_1)}{\partial x} \tag{20}$$

and

$$\left(\frac{h^2}{10}\right)(\nabla^2 V^*_y) - V^*_y = D\,\frac{\partial\nabla^2 \bar{w}_P}{\partial y} - \frac{h^2}{10\,(1-\nu)}\,\frac{\partial(k\,\bar{w}_P + q_1)}{\partial y} \tag{21}$$

Hence, for a rectangular plate, the complementary functions can be found from Eqs. 14 and 17, and the constants of integration associated with these can be evaluated from the twelve boundary conditions that can be developed from the four edges of the plate.

APPLICATIONS

In this section, two examples are presented, and the results are compared numerically with the predictions of the classical theory. In addition, some general solutions are cited.

Navier-Type Solution.—A rectangular plate of dimensions a and b (Fig. 2) has coordinate axes along two edges.[11] The plate is simply supported on each of the four edges in the following sense:

$$M_x(0, y) = M_x(a, y) = M_y(x, 0) = M_y(x, b) = 0 \tag{22}$$

$$\bar{w}(0, y) = \bar{w}(a, y) = \bar{w}(x, 0) = \bar{w}(x, b) = 0 \tag{23}$$

---

[11] "Theory of Plates and Shells," by S. Timoshenko, McGraw-Hill Book Co., Inc., New York, N. Y., 1940, pp. 117–134.

and

$$\beta\,(0, y) = \beta\,(a, y) = \alpha\,(x, 0) = \alpha\,(x, b) = 0 \qquad (24)$$

Furthermore, it is assumed that the top and bottom faces are free of shearing stress and that the loading function, $q_1\,(x, y)$, can be represented by a double Fourier sine series,

$$q_1\,(x, y) = \sum_{m=1}^{\infty} \sum_{n=1}^{\infty} a_{mn} \sin \frac{m\,\pi\,x}{a} \sin \frac{n\,\pi\,y}{b} \qquad (25)$$

The Fourier coefficients, a_{mn}, are determined by

$$a_{mn} = \frac{4}{a\,b} \int_0^a \int_0^b q_1\,(x, y) \sin \frac{m\,\pi\,x}{a} \sin \frac{n\,\pi\,y}{b}\, dx\, dy \qquad (26)$$

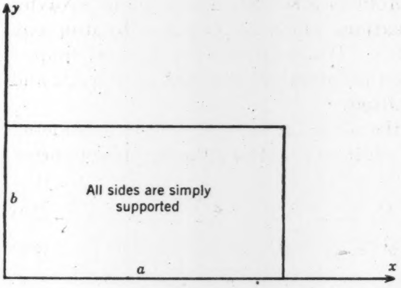

FIG. 2.—A RECTANGULAR PLATE WITH COORDINATE AXES

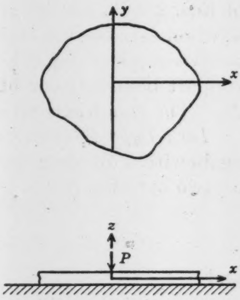

FIG. 3.—AN INFINITE PLATE WITH A LINE LOAD OF INTENSITY P

With the foregoing assumptions, $\bar{w}$, V_x, and V_y can be expressed in the Navier form, and the double Fourier coefficients can be found. The final expressions for $\bar{w}$, V_x, and V_y are

$$\bar{w} = \sum_{m=1}^{\infty} \sum_{n=1}^{\infty} w_{mn} \sin \frac{m\,\pi\,x}{a} \sin \frac{n\,\pi\,y}{b} \qquad (27)$$

in which

$$w_{mn} = -\frac{\left\{\frac{c^2}{D}\left[\left(\frac{m\,\pi}{a}\right)^2+\left(\frac{n\,\pi}{b}\right)^2\right]+\frac{1}{D}\right\} a_{mn}}{\left[\left(\frac{m\,\pi}{a}\right)^4+2\left(\frac{m\,\pi}{a}\right)^2\left(\frac{n\,\pi}{b}\right)^2+\left(\frac{n\,\pi}{b}\right)^4\right]+\frac{k\,c^2}{D}\left[\left(\frac{m\,\pi}{a}\right)^2+\left(\frac{n\,\pi}{b}\right)^2\right]+\frac{k}{D}} \qquad (28)$$

$$V_x = \sum_{m=1}^{\infty} \sum_{n=1}^{\infty} b_{mn} \cos \frac{m\,\pi\,x}{a} \sin \frac{n\,\pi\,y}{b} \qquad (29)$$

and

$$V_y = \sum_{m=1}^{\infty} \sum_{n=1}^{\infty} c_{mn} \sin \frac{m\,\pi\,x}{a} \cos \frac{n\,\pi\,y}{b} \qquad (30)$$

in which

$$b_{mn} = \frac{\frac{m\,\pi}{a}\left\{D\left[\left(\frac{m\,\pi}{a}\right)^2 + \left(\frac{n\,\pi}{b}\right)^2\right] w_{mn} + \frac{h^2}{10\,(1-\nu)}\,(k\,w_{mn} + a_{mn})\right\}}{\frac{h^2}{10}\left[\left(\frac{m\,\pi}{a}\right)^2 + \left(\frac{n\,\pi}{b}\right)^2\right] + 1} \qquad (31)$$

and

$$c_{mn} = \frac{\frac{n\,\pi}{b}\left\{D\left[\left(\frac{m\,\pi}{a}\right)^2 + \left(\frac{n\,\pi}{b}\right)^2\right] w_{mn} + \frac{h^2}{10\,(1-\nu)}\,(k\,w_{mn} + a_{mn})\right\}}{\frac{h^2}{10}\left[\left(\frac{m\,\pi}{a}\right)^2 + \left(\frac{n\,\pi}{b}\right)^2\right] + 1} \qquad (32)$$

The solutions given by Eqs. 27, 29, and 30 satisfy the boundary conditions of Eqs. 22, 23, and 24, and hence the problem is solved. The classical Navier solution satisfies the classical-plate equations which are obtained by dropping the terms containing h^2 in Eqs. 3 through 8. It also satisfies the classical, simple-support boundary conditions which are the conditions denoted by Eqs. 22 and 23. The conditions on α and β are omitted.

Levy-Type Solution.—The plate of the foregoing example will be considered again with a different set of boundary conditions.[11] It will be simply supported on two opposite edges, thus giving

$$M_x\,(0, y) = M_x\,(a, y) = 0 \qquad (33)$$

$$\bar{w}\,(0, y) = \bar{w}\,(a, y) = 0 \qquad (34)$$

and

$$\beta\,(0, y) = \beta\,(a, y) = 0 \qquad (35)$$

Furthermore, it may have any combination of boundary conditions on the other two edges consistent with the Reissner theory. In addition, it will be assumed that the function, q_1, is independent of y and can be represented by the Fourier sine series,

$$q_1\,(x) = \sum_{n=1}^{\infty} a_n \sin\frac{n\,\pi\,x}{a} \qquad (36)$$

Again, the Fourier coefficients can be evaluated and are

$$a_n = \frac{2}{a}\int_0^a q_1\,(x)\sin\frac{n\,\pi\,x}{a}\,dx \qquad (37)$$

Owing to the even derivatives occurring in Eq. 15, it is obvious that the particular solution, $\bar{w}_P$, can be written in the following form:

$$\bar{w}_P = \sum_{n=1}^{\infty} w_n \sin\frac{n\,\pi\,x}{a} \qquad (38)$$

Upon substituting Eq. 38 into Eq. 15, the coefficients, w_n, are found to be

$$w_n = -\frac{\left[1 + \left(\frac{n\,\pi}{a}\right)^2 (c^2)\right] a_n}{D\left(\frac{n\,\pi}{a}\right)^4 + c^2\,k\left(\frac{n\,\pi}{a}\right)^2 + k} \qquad (39)$$

Knowing $\bar{w}_P$, V^*_x can be determined from Eq. 20. This can be expressed in the same form because the left side of the governing equation contains the function and the even derivatives of the function:

$$V^*_x = \sum_{n=1}^{\infty} c_n \cos \frac{n \pi x}{a} \qquad (40)$$

in which

$$c_n = \frac{D\, w_n \left(\frac{n \pi}{a} \right)^3 + \frac{h^2}{10\,(1 - \nu)} (k\, w_n + a_n) \left(\frac{n \pi}{a} \right)}{1 + \frac{h^2}{10} \left(\frac{n \pi}{a} \right)^2} \qquad (41)$$

From Eq. 21, it can be seen that $V^*_y = 0$ because the right side contains derivatives with respect to y whereas $\bar{w}_P$ and q_1 are independent of y.

With the boundary conditions (Eqs. 33, 34, and 35) in mind, it is evident that for this problem, $\bar{w}_H$ can be taken in a Levy form,

$$\bar{w}_H = \sum_{n=1}^{\infty} Y_n\,(y) \sin \frac{n \pi x}{a} \qquad (42)$$

Upon substituting this value of $\bar{w}_H$ into Eq. 14, and solving the resulting differential equation for $Y_n\,(y)$, $\bar{w}_H$ becomes

$$\bar{w}_H = \sum_{n=1}^{\infty} [A_n \cosh\,(e_n\, y) \cos\,(f_n\, y) + B_n \cosh\,(e_n\, y) \sin\,(f_n\, y)$$
$$+ C_n \sinh\,(e_n\, y) \cos\,(f_n\, y) + D_n \sinh\,(e_n\, y) \sin\,(f_n\, y)] \sin \frac{n \pi x}{a} \qquad (43)$$

in which A_n, B_n, C_n, and D_n are independent constants of integration and in which

$$e_n = r^{\frac{1}{2}}_n \cos \frac{\theta_n}{2} \qquad (44a)$$

and

$$f_n = r^{\frac{1}{2}}_n \sin \frac{\theta_n}{2} \qquad (44b)$$

in which

$$r_n = \left[\left(\frac{n \pi}{a} \right)^4 + \frac{k\, c^2}{D} \left(\frac{n \pi}{a} \right)^2 + \frac{k}{D} \right]^{\frac{1}{2}} \qquad (45a)$$

and

$$\theta_n = \tan^{-1} \frac{\left(\frac{k}{D} - \frac{k^2\, c^4}{4\, D^2} \right)^{\frac{1}{2}}}{\left(\frac{n \pi}{a} \right)^2 + \frac{k\, c^2}{2\, D}} \qquad (45b)$$

Again, in view of the boundary conditions (Eqs. 33, 34, and 35), ψ will be taken as

$$\psi\,(x, y) = \sum_{n=0}^{\infty} \bar{Y}_n\,(y) \cos \frac{n \pi x}{a} \qquad (46)$$

After substituting this value of ψ in Eq. 17 and solving the resulting differential equation for $\bar{Y}_n\,(y)$, it is found that the final form for ψ can be written as

$$\psi\,(x, y) = \sum_{n=0}^{\infty} (G_n \cosh \beta_n\, y + H_n \sinh \beta_n\, y) \cos \frac{n\,\pi\,x}{a} \tag{47}$$

in which $\beta^2_n = (n\,\pi/a)^2 + 10/h^2$, and G_n and H_n are independent constants of integration.

With $\bar{w}_H$ and ψ given by Eqs. 43 and 47, respectively, the boundary conditions (Eqs. 33, 34, and 35) are automatically satisfied. There still remain six independent constants which can be determined by the six boundary conditions on the two remaining edges of the plate. In the classical theory, at the corresponding stage, the Levy solution has four constants which are determined by four boundary conditions on the two remaining edges of the plate.

The method also works for the case in which two opposite edges of the plate have the boundary conditions:

$$\alpha\,(0, y) = \alpha\,(a, y) = 0 \tag{48}$$

$$V_x\,(0, y) = V_x\,(a, y) = 0 \tag{49}$$

and

$$M_{xy}\,(0, y) = M_{xy}\,(a, y) = 0 \tag{50}$$

whereas the remaining edges have any combination of conditions. In this case, the solutions for $\bar{w}_H$ and ψ are taken as products of a function of y and cos $n\,\pi\,x/a$, and y and sin $n\,\pi\,x/a$, respectively. The boundary conditions (Eqs. 48, 49, and 50) apply to an infinite plate supported by equidistant columns; this case also has a counterpart in the classical theory.

Infinite Plate Resting on an Elastic Foundation.—A line load of intensity P (force per unit length) acts along the y-axis of an infinite plate (Fig. 3). Because the variable, y, does not enter into the solution, the governing equations are

$$\frac{d^4\bar{w}}{dx^4} - \left(\frac{k\,c^2}{D}\right)\left(\frac{d^2\bar{w}}{dx^2}\right) + \frac{k}{D}\,\bar{w} = \left(\frac{c^2}{D}\right)\left(\frac{d^2q_1}{dx^2}\right) - \frac{q_1}{D} \tag{51a}$$

$$\left(\frac{h^2}{10}\right)\left(\frac{d^2V_x}{dx^2}\right) - V_x = D\,\frac{d^3\bar{w}}{dx^3} - \frac{h^2}{10\,(1-\nu)}\,\frac{d(k\,\bar{w} + q_1)}{dx} \tag{51b}$$

$$\left(\frac{h^2}{10}\right)\left(\frac{d^2V_y}{dx^2}\right) - V_y = 0 \tag{51c}$$

$$M_x = \left(\frac{h^2}{5}\right)\left(\frac{dV_x}{dx}\right) - D\,\frac{d^2\bar{w}}{dx^2} + \frac{h^2\,\nu}{10\,(1-\nu)}\,(k\,\bar{w} + q_1) \tag{51d}$$

$$M_y = -\,\nu\,D\,\frac{d^2\bar{w}}{dx^2} + \frac{h^2\,\nu}{10\,(1-\nu)}\,(k\,\bar{w} + q_1) \tag{51e}$$

$$M_{xy} = \left(\frac{h^2}{10}\right)\left(\frac{dV_y}{dx}\right) \tag{51f}$$

$$\alpha + \frac{d\bar{w}}{dx} = \frac{6\,V_x}{5\,G\,h} \tag{51g}$$

and

$$\beta = \frac{6\,V_y}{5\,G\,h} \tag{51h}$$

Owing to the load, there is a uniform deflection along the y-axis. This deflection is denoted by w_o. Hence, the boundary conditions at the origin will be written as

$$\bar{w}\,(0) = -\,w_o \tag{52a}$$

$$\alpha\,(0) = 0 \tag{52b}$$

and

$$\beta\,(0) = 0 \tag{52c}$$

The general method of solution, in which a function, ψ, was introduced, will be used. For this particular example, because ψ is independent of y, the equation for ψ becomes

$$\left(\frac{h^2}{10}\right)\left(\frac{d^2\psi}{dx^2}\right) - \psi = 0 \tag{53}$$

Using the condition that $\bar{w}$, M_x, and V_x vanish as x approaches infinity, the solutions for ψ and $\bar{w}$ which are to be used take the following form:

$$w = (A\,e^{-e_o x})\,(\cos f_o\,x) + (B\,e^{-e_o x})\,(\sin f_o\,x) \tag{54a}$$

$$\psi = G\,e^{-\sqrt{10/h}\,x} \tag{54b}$$

in which

$$e_o = r^{\frac{1}{2}}{}_0 \cos\frac{\theta_0}{2} \tag{55a}$$

and

$$f_o = r^{\frac{1}{2}}{}_0 \sin\frac{\theta_0}{2} \tag{55b}$$

$$r_0 = \left(\frac{k}{D}\right)^{\frac{1}{2}} \tag{56a}$$

and

$$\theta_0 = \tan^{-1}\frac{\left(\dfrac{k}{D} - \dfrac{k^2\,c^4}{4\,D^2}\right)^{\frac{1}{2}}}{\dfrac{k\,c^2}{2\,D}} \tag{56b}$$

Upon application of the boundary conditions (Eqs. 52*a*, 52*b*, and 52*c*) the constants, G, A, and B, become

$$G = 0 \tag{57a}$$

$$A = -\,w_o \tag{57b}$$

and

$$B = -\,w_o\,\frac{e_o + \dfrac{6}{5\,G\,h}\,(D\,e^3{}_o - 3\,D\,e_o\,f^2{}_o - k\,c^2\,e_o)}{f_o - \dfrac{6}{5\,G\,h}\,(D\,f^3{}_o - 3\,D\,e^2{}_o\,f_o + k\,c^2\,f_o)} \tag{57c}$$

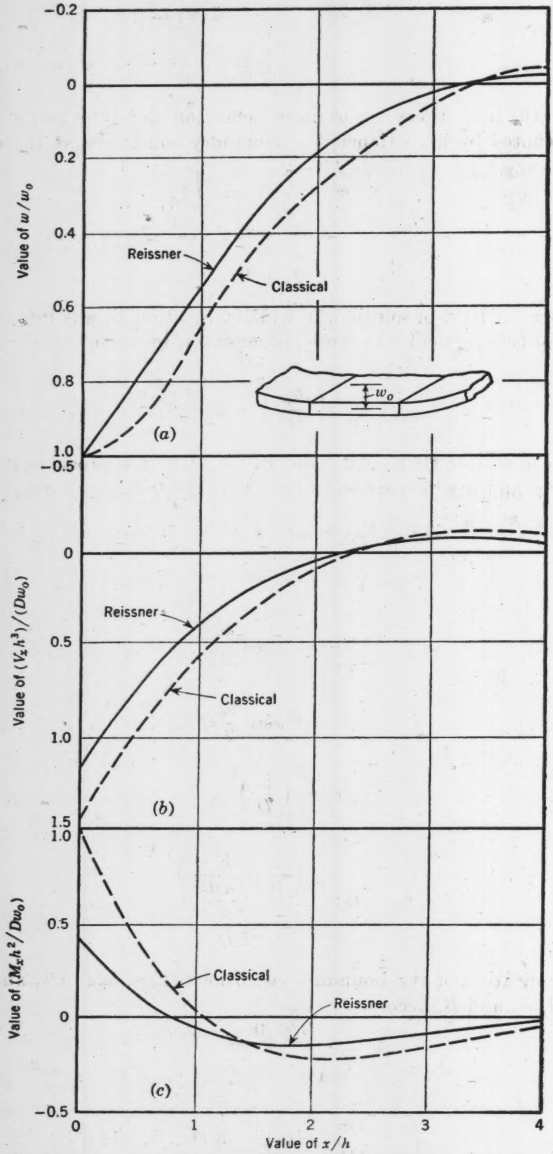

FIG. 4.—A COMPARISON OF THE DEFLECTIONS, MOMENTS, AND SHEARS IN TERMS OF w_o FOR THE LINE-LOAD PROBLEM WITH $\nu = \frac{1}{3}$

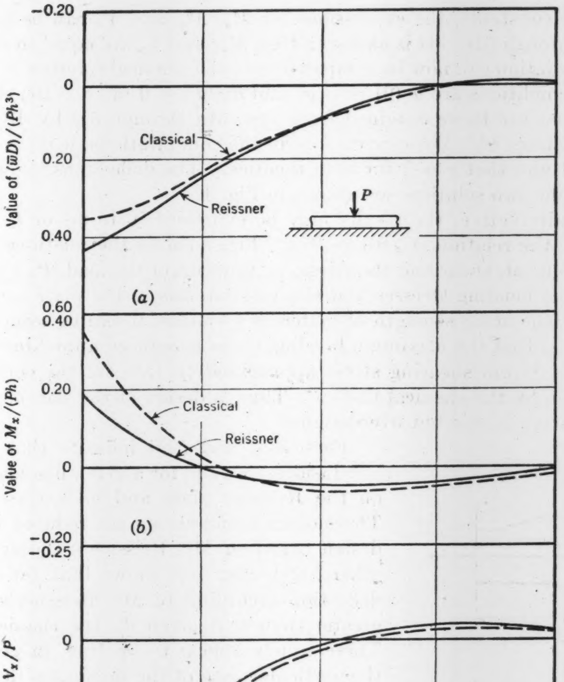

FIG. 5.—A COMPARISON OF THE DEFLECTIONS, MOMENTS, SHEARS, AND σ_z IN TERMS OF P FOR THE LINE-LOAD PROBLEM WITH $\nu = \frac{1}{4}$

With these constants, the expressions for M_x, M_y, and V_x can be found from Eqs. 51*b* through 51*e*. It is also seen that M_{xy} and V_y are equal to zero. The foregoing solution can now be compared with the classical solution in which the boundary conditions are $\bar{w}\ (0) = -\ w_o$ and $d\bar{w}/dx = 0$ (at $x = 0$); the governing equations are those obtained from Eqs. 51*a* through 51*f* by dropping the terms containing h^2. For convenience in the computations, it is assumed that $k\, h^4/D = 1$ and that $\nu = \frac{1}{3}$ for both theories. The deflections, moments, and shears for the two solutions are shown in Fig. 4.

As an alternative, the results may be expressed in terms of P instead of w_o through the relation, $V_x\ (0) = P/2$. Fig. 5 shows the relationship for deflection, moment, shear and the stress, σ_z, in terms of the load, P.

Since the bending stresses and shearing stresses in the plate are given by the usual elementary strength of materials formulas, it can be seen from Figs. 4(*b*) and 4(*c*) that the maximum bending stress is reduced approximately 55%, and the maximum shearing stress approximately 15%, of the corresponding values given by the classical theory. Thus, a design of the slab based on the classical theory is safe but overdesigned.

Figs. 5(*b*) and 5(*d*) indicate that the same conclusions are valid for a given line load pressing on the Reissner plate and on a classical plate. The moments and shears are reduced by using a design based on Mr. Reissner's theory. On the other hand, Fig. 5(*a*) shows that the maximum deflection according to Mr. Reissner's theory is greater than that given by the classical theory. These trends appear to be true, in general. In the particular case of the maximum deflection, it seems reasonable that a theory including the effects of shear deformation would give a deflection larger than that given by a theory which neglects it. Fig. 5(*d*) shows that the normal stress, σ_z, decreases as the distance from the load increases.

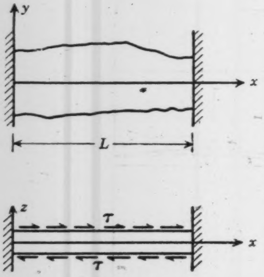

FIG. 6.—A PLATE WITH SHEAR STRESSES ON THE TOP AND BOTTOM FACES

Bending of a Plate Due to a Uniform Shear Stress.—To illustrate a boundary value problem involving shear stresses on the top and bottom faces, the plate shown in Fig. 6 is considered. In order to simplify the problem as much as possible, the plate has been assumed to be of infinite length in the y-direction, and the shear stress on the top and bottom faces has been taken as a constant. In addition, the foundation has been omitted because it would change only the form of the solution of $\bar{w}$. In practice, bending due to a shear stress might occur in a bin full of material in which there is friction at the wall of the bin due to packing of the material. This friction would produce both bending and extension of the plate; however, this example illustrates a method for handling the bending only.

Since all the quantities involved are independent of y, the governing equations are

$$S^+_y = 0 \tag{58a}$$

$$S^{+}_{x} = 2\,\tau \tag{58b}$$

$$\frac{d^4\bar{w}}{dx^4} = 0 \tag{58c}$$

$$\left(\frac{h^2}{10}\right)\left(\frac{d^2V_x}{dx^2}\right) - V_x = D\,\frac{d^3\bar{w}}{dx^3} - h\,\tau \tag{58d}$$

$$\left(\frac{h^2}{10}\right)\left(\frac{d^2V_y}{dx^2}\right) - V_y = 0 \tag{58e}$$

$$M_x = D\left[\frac{6\,(1-\nu)}{5\,G\,h}\,\frac{dV_x}{dx} - \frac{d^2\bar{w}}{dx^2}\right] \tag{58f}$$

$$M_y = -\,\nu\,D\,\frac{d^2\bar{w}}{dx^2} \tag{58g}$$

$$M_{xy} = \left(\frac{h^2}{10}\right)\left(\frac{dV_y}{dx}\right) \tag{58h}$$

$$\alpha + \frac{d\bar{w}}{dx} = \frac{6}{5\,G\,h}\,V_x \tag{58i}$$

and

$$\beta = \frac{6}{5\,G\,h}\,V_y \tag{58j}$$

For the edges which are clamped, the boundary conditions will be taken as

$$\bar{w}\,(0) = \bar{w}\,(L) = 0 \tag{59a}$$

$$\alpha\,(0) = \alpha\,(L) = 0 \tag{59b}$$

and

$$\beta\,(0) = \beta\,(L) = 0 \tag{59c}$$

Following a procedure similar to that used in the previous example, the solutions for $\bar{w}$ and ψ can be written as

$$\bar{w} = a_0 + a_1\,x + a_2\,x^2 + a_3\,x^3 \tag{60}$$

and

$$\psi = a_4 \sinh \sqrt{\frac{10}{h}}\,x + a_5 \cosh \sqrt{\frac{10}{h}}\,x \tag{61}$$

There are now six constants, a_0, a_1, a_2, a_3. a_4, and a_5, which are to be determined by the six boundary conditions (Eqs. 59*a*, 59*b*, and 59*c*). Omitting the detailed work, the final values of the constants are

$$a_0 = a_4 = a_5 = 0 \tag{62}$$

$$a_1 = \frac{3}{5}\,\frac{\tau\,L}{G\,d},\ a_2 = -\,\frac{9}{5}\,\frac{\tau}{G\,d},\ a_3 = \frac{6}{5}\,\frac{\tau}{G\,L\,d} \tag{63}$$

in which

$$d = \frac{L}{2}\left[1 + \frac{12\,h^2}{5\,(1 - \nu)\,L^2}\right] \qquad (64)$$

Hence. the expressions for $\bar{w}$, M_x, and V_x become

$$w = \frac{3}{5}\frac{\tau\,L^2}{G\,d}\left[\left(\frac{x}{L}\right) - 3\left(\frac{x}{L}\right)^2 + 2\left(\frac{x}{L}\right)^3\right] \qquad (65)$$

$$V_3 = \frac{\tau\,h\,L}{2\,d} \qquad (66)$$

$$M_x = \frac{9}{10}\frac{\tau\,h^3}{d}\left[1 - 2\left(\frac{x}{L}\right)\right] \qquad (67)$$

A plot of these equations for $\nu = \frac{1}{3}$ is shown in Fig. 7 for different values of h/L. This problem cannot be solved by the classical theory because the solu-

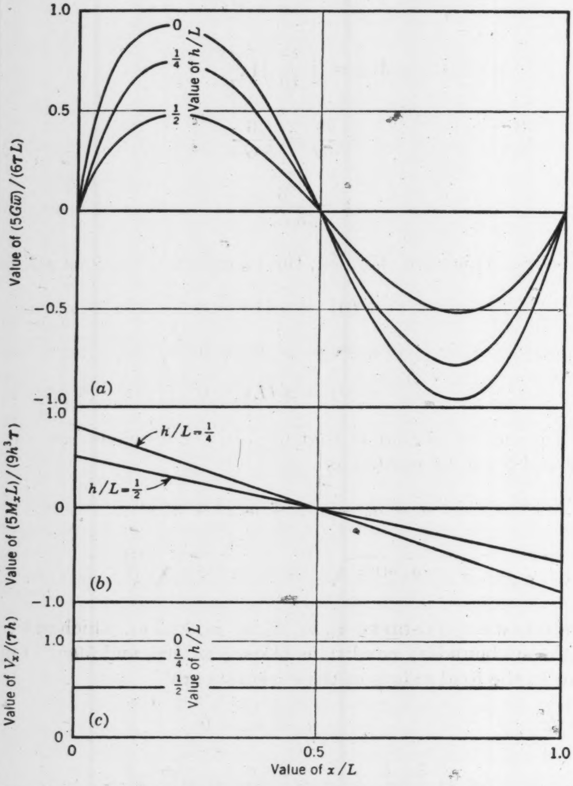

FIG. 7.—A COMPARISON OF THE DEFLECTIONS, MOMENTS, AND SHEARS FOR THE PLATE BENT BY SHEAR STRESSES

tion for $\bar{w}$ would be the same as the foregoing, but the boundary conditions, $\bar{w}(0) = \bar{w}(L) = d\bar{w}/dx$ (at $x = 0$) $= d\bar{w}/dx$ (at $x = L$) $= 0$, would require that all four constants of integration be zero. However, by letting $h/L \rightarrow 0$ with $\lim_{h \to 0} (\tau h)$ remaining finite, the solution for a plate of zero thickness subjected to a moment of magnitude, τh, at every point of the plate may be developed from the Reissner theory. These results are also shown in Fig. 7. The bending moment, M_x, for $h = 0$ is zero everywhere.

CONCLUSIONS

The thick-plate theory which was developed by Mr. Reissner, which includes the effects of shear deformation and normal pressure, can be used to solve certain problems in the bending of rectangular plates resting on an elastic foundation. In this paper, two examples were presented, and the results plotted graphically. The thickness-length parameter at which the effects of shear deformation and normal pressure become important can be determined from the graphical plots.

Finally, from the governing equations presented herein, solutions to other problems may be obtained. Furthermore, for certain types of boundary conditions the solution may be expressed in the Navier and Levy forms.

ACKNOWLEDGMENTS

The writer expresses appreciation for the assistance given by the Virginia Engineering Experiment Station, at Blacksburg, under the supervision of John W. Whittemore, and to Mrs. K. Greever for her patient efforts in typing the original manuscript.

DISCUSSION

Harold G. Lorsch,[12] A. M. ASCE.—An excellent presentation of an application of Mr. Reissner's theory of thick plates has been made by Mr. Frederick. The writer fears, however, that the graphs presented imply that a greater degree of discrepancy exists between results obtained by the classical theory and those obtained by the Reissner theory than might actually be the case.

Figs. 4 and 5 show the results for values of $k\,h^4/D = 1$, a ratio which the author states was chosen for convenience. Unfortunately, this value does not correspond to usual practical problems. For a lean concrete plate ($E = 2{,}000$ kips per sq in. and $\nu = 0.2$) and good soil ($k = 0.75$ kips per cu in.), the thickness of the plate corresponding to $k\,h^4/D = 1$ is almost 20 ft. It is reasonable to expect large shear effects in a plate of that thickness. For better concrete or for softer soil, or for both, the corresponding plate thickness would be even greater.

For a steel plate ($E = 30{,}000$ kips per sq in. and $\nu = 0.3$) on a thin concrete block ($E = 2{,}000$ kips per sq in. and $t = 1$ ft; thus, $k = 200$ kips per cu in.), the plate thickness for $k\,h^4/D = 1$ would be 13.75 in., a very unusual value.

The writer feels that the 55% reduction in bending stress should be viewed in the light of the foregoing numerical computations. Plates occurring in civil engineering have ($k\,h^4/D$)-ratios from 1/20 to 1/1,000. It would indeed be interesting if the author presented comparisons between the classical theory and Mr. Reissner's theory for this range. The writer expects the two methods to give nearly identical results for this range.

None of these remarks is designed to detract from the fundamental approach of Mr. Frederick but merely to reassure those engineers who might otherwise be inclined to disregard entirely the classical plate theory because of the large degree of error shown in this paper.

Daniel Frederick,[13] J. M. ASCE.—The writer wishes to express appreciation to Mr. Lorsch for his informative comments. For the example under discussion one notes that, for concrete or steel plates on soils where the usual values of $k\,h^4/D$ fall in the range of 1/20 to 1/1,000, bending stresses and other results obtained by Mr. Reissner's theory differ only slightly from those obrained by the classical theory. The value of $k\,h^4/D = 1$ will be significant for a concrete slab ($E = 2{,}000$ kips per sq in. and $\nu = 0.2$) on a rock foundation ($E = 3{,}000$ kips per sq in. and $t = 10$ in.; thus, $k = 300$ kips per cu in.), which gives a plate thickness of 0.581 in.

In writing the paper, the intentions were to show how Mr. Reissner's theory can be used in connection with plates on an elastic foundation and to present some solutions and methods of solving the governing equations. Therefore, no mention was made of any applications; it was also felt that corrections could be applied to particular problems where necessary. Values of $k\,h^4/D$ in the range 1/10 to 1/1,000 were used by the writer in preparing computations but were not presented in the final paper because of an effort to conserve space and a desire to have the corrections prominent in magnitude and direction.

---

[12] Asst. Prof. of Civ. Eng., The City College, New York, N. Y.

[13] Prof. of Applied Mechanics, Virginia Polytechnic Inst., Blacksburg, Va.

Because many believe that the Winkler-Zimmerman assumption does not yield a good approximation of the behavior of many soils, the engineer must use his discretion in deciding whether or not to use results based on the classical elastic foundation. On the other hand, there are many other practical problems for which $k\,h^4/D$ is approximately unity and for which the secondary effects are important. Some of these are, as follows:

1. Thick blocks of ice floating on large bodies of water;
2. A piston compressing a liquid in a cylinder;
3. Buckling and bending of thick layers of rock to explain certain phenomena in geophysics;
4. Plates of a low modulus of elasticity, which rest on a relatively stiff elastic foundation and which might be made of plastics, resins, rubber, wood, or metals at an elevated temperature where there has been a considerable decrease in the modulus of elasticity; and
5. Bending of finite thick plates.

It is important to emphasize that the infinite-plate example of the paper does not consider the ratio of the thickness of the plate to the length. As in the finite plate with no foundation, where the corrections to the classical theory are important for certain thickness-to-length ratios, it is expected that the corrections would be considerable for finite plates of certain configurations and loadings on a foundation, even when dealing with the range for $k\,h^4/D$ of 1/20 to 1/1,000.

AMERICAN SOCIETY OF CIVIL ENGINEERS

Founded November 5, 1852

TRANSACTIONS

Paper No. 2899

FLOW INTO A WELL BY ELECTRIC AND MEMBRANE ANALOGY

BY CHONG-HUNG ZEE,[1] DEAN F. PETERSON, JR.,[2] M. ASCE, AND ROBERT O. BOCK[3]

WITH DISCUSSION BY MESSRS. ROBERT E. GLOVER; VAUGHN E. HANSEN; JAMES N. LUTHIN; CHIA-SHUN YIH; AND CHONG-HUNG ZEE, DEAN F. PETERSON, AND ROBERT O. BOCK

SYNOPSIS

A study of radially symmetrical, unconfined flow to a well is presented herein. The discharge of such a system is related, using dimensional considerations, to the permeability of the aquifer and the geometric characteristics of the influence region. In order to study the problem, the electrical analogy for hydraulic flow is combined with the membrane analogy for a free surface. The experimental results obtained are combined with observations of other investigators to develop empirical relationships between the flow and the geometric variables.

NOTATION

The letter symbols adopted for use in this paper are defined where they first appear, and are arranged alphabetically, for convenience of reference, in the Appendix.

INTRODUCTION

Most drainage wells and many water-supply wells tap aquifers whose upper boundaries are not defined by impermeable strata. Solutions for the flow pattern under steady conditions, even for mathematically ideal wells of this class, are difficult because the location of the upper limiting boundary of the flow cross section is not known. Furthermore, the geometry of the flow system out-

---

NOTE.—Published, essentially as printed here, in October, 1955, as *Proceedings Paper 817*. Positions and titles given are those in effect when the paper or discussion was approved for publication in *Transactions*.

[1] Structural Designer, Ammann and Whitney, Cons. Engrs., New York, N. Y.

[2] Prof. and Head, Dept. of Civ. Eng., Colorado State Univ., Fort Collins, Colo.

[3] Senior Engr., Arma Corp., Garden City, N. Y.

side the well cannot be determined by knowing only the drawdown and the geometry of the well. Either both the well discharge and the permeability, or the elevation of the free water surface at a known radial distance from the well, must also be known. An additional complicating factor arises from hydrodynamic considerations, which require that the water surface stand at a higher elevation outside the well casing than inside it, even though hydraulic head losses through the casing are zero. Under certain conditions, this difference in elevation, termed the seepage face, may be considerable. The height of the seepage face is an important consideration where drainage wells are intended to produce a maximum lowering of the water table.

In 1863 a solution for a fully penetrating well in an unconfined aquifer was proposed by Jules Dupuit[4]:

$$h^2 - h^2_w = \frac{Q}{\pi K} \ln \frac{r}{r_w} \qquad (1)$$

in which h is the vertical distance from the bottom impermeable stratum to the free water surface at a radial distance, r, from the well axis; h_w denotes the depth of water in the well; r_w is the well radius; K represents the permeability of the aquifer; and Q is the discharge of the well. The solution proposed by Mr. Dupuit ignored the effect of curvilinear flow in a vertical plane. Investigations have shown that Eq. 1 can be used to predict the discharge correctly if r is chosen sufficiently far from the well. However, it cannot be used to describe the true position of the water surface near the well.

Most recent attempts to solve this flow problem have been by means of models and analogies. In 1932 R. D. Wyckoff, H. G. Botset, and M. Muskat[5] made an investigation using a sand model with a 15° sector. Because of capillarity, the position of the free surface near the well was not fully determined. In 1948 Harold E. Babbitt, M. ASCE, and David H. Caldwell,[6] M. ASCE, made similar studies using a sand wedge. An electrical analogy using a carbon wedge was also used by Messrs. Babbitt and Caldwell who suggested an empirical equation for the free surface. Vaughn E. Hansen,[7] J.M. ASCE, proposed that a depressed membrane under tension be used to simulate the free surface; Mr. Hansen also offered the functional expression,

$$\frac{Q}{K\, r^2_w} = f_1\left(\frac{h_s}{r_w}, \frac{h_w}{r_w}\right) \qquad (2)$$

which relates the depths of water outside the well and inside the well to the radius of the well, the discharge, and the permeability of the aquifer. Numerical analysis, using relaxation methods, was applied to six cases of unconfined radial flow by Shih-Te Yang[8] in 1949. Norman S. Boulton solved four additional cases[9] using relaxation techniques in 1951.

---

[4] "Études théoriques et pratiques sur le mouvement des eaux," by Jules Dupuit, Paris, 2d Ed., 1863.

[5] "Flow of Liquids Through Porous Media Under the Action of Gravity," by R. D. Wyckoff, H. G. Botset and M. Muskat, *Physics*, August, 1932, pp. 90–113.

[6] "The Free Surface Around, and Interference Between, Gravity Wells," by Harold E. Babbitt and David H. Caldwell, *Bulletin No. 374*, Eng. Experiment Station, Univ. of Illinois, Urbana, Ill., 1948.

[7] "Unconfined Ground-Water Flow to Multiple Wells," by Vaughn E. Hansen, *Transactions*, ASCE, Vol. 118, 1953, pp. 1098–1130.

During 1950 and 1951, the writers conducted experiments on this problem, in which the electrical analogy for flow was combined with the membrane analogy for a free surface. By using this method a relatively large number of cases were easily studied. Information from these experiments was combined with information from other sources[5,6,7,8,9] and from one field test in order to develop empirical curves showing the general relationships between geometric variables and flow variables expressed in dimensionless form.

THEORY

Seepage Flow in Cylindrical Coordinates.—Substituting the Darcy equation for flow in a saturated, isotropic, pervious medium into the differential equation of continuity for flow of an incompressible fluid leads to the Laplace equation for steady seepage flow. In cylindrical coordinates this is expressed by

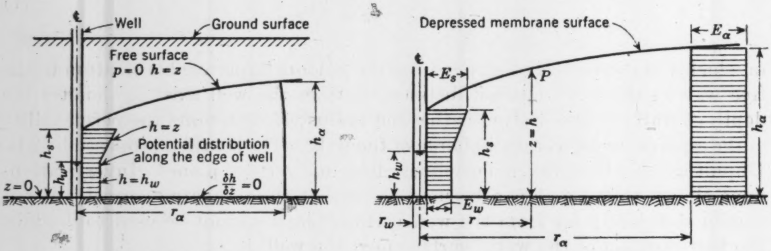

(*a*) IDEALIZED WELL (*b*) ELECTRICAL MODEL

FIG. 1.—BOUNDARY CONDITIONS

$$\frac{\partial^2 h}{\partial r^2} + \left(\frac{1}{r}\right)\left(\frac{\partial h}{\partial r}\right) + \left(\frac{1}{r^2}\right)\left(\frac{\partial^2 h}{\partial \theta^2}\right) + \left(\frac{\partial^2 h}{\partial z^2}\right) = 0 \ldots\ldots\ldots (3)$$

in which h is the piezometric head at a point having the coordinates (z, r) and θ. Boundary conditions for the idealized case of unconfined flow toward a central, fully penetrating well are shown in Fig. 1(*a*). The pervious medium, bounded by the impermeable stratum, is assumed to extend infinitely in a radial direction. At the well the outflow surface below the level of the drawdown is an isopotential surface on which the head is equal to the depth of water in the well, h_w. Above this elevation, along the seepage face and along the free water surface extending back from the well, the gage pressure is zero. The piezometric head along these boundaries must therefore be z.

An isopotential surface at some finite value of r may be chosen as the inflow boundary for a finite system. In order to correspond to the infinite system, this boundary should be slightly curved in a vertical plane, as shown in Fig. 1(*a*); the curvature decreases as r increases.

---

[8] "Seepage Toward a Well Analyzed by the Relaxation Method," by Shih-Te Yang, thesis presented to Harvard University, Cambridge, Mass., in 1949, in partial fulfilment of the requirements for the degree of Doctor of Philosophy.

[9] "The Flow Pattern near a Gravity Well in a Uniform Water Bearing Medium," by Norman Savage Boulton, *Journal*, Inst. of C. E., London, December 1951, pp. 534–550.

There are some interesting mathematical considerations in connection with the boundary conditions near the well—for example, the necessity that a real seepage face exists may be inferred, as will be shown subsequently.[10] Consideration of the properties of an interface between two fluids existing in media having different permeabilities leads to the conclusion that the free surface, or top streamline, must approach the well tangentially with a velocity of K. Below the elevation of the water surface in the well, the streamlines normally intersect the well boundary because this is an isopotential surface. If it is assumed that the top streamline intersects the water surface of the well, the resulting convergence of the streamlines near the elevation of the water in the well would imply infinite velocity rather than the velocity of K, as required. Also, if one assumes the depth h_w to be zero, nonexistence of the seepage face would result in a zero discharge area and infinite velocity through the well boundary. Actually, throughout the length of the seepage face, the direction of approach of the streamlines changes from being tantential at the top of the seepage face to being normal at the elevation of the water surface in the well. Theoretically, the exit velocity into the air along the seepage face is proportional to the cosecant of β, in which β is the angle of inclination of the streamline at the point of egress. This consideration again leads to the postulation of infinite velocity at the elevation of the water in the well. However, in this vicinity, the velocity probably exceeds the velocity for which the Darcy equation is valid and thus approaches some finite maximum. The function, $h(z)$, on the well boundary is not analytic at the elevation of the water surface in the well. Below this point, $h(z)$ equals h_w; above this point, $h(z)$ equals z.

Electrical Analogy.—The electrical analogy is based on the similarity between the Darcy equation and Ohm's law. In the analogy, the electromotive potential, E, corresponds to the head, h, and the current, I, corresponds to the hydraulic discharge, Q. The analog must be geometrically similar to the well and to the surrounding region. In addition, the voltage variation on any free surface must be linear in a vertical direction to correspond to the gravity head. This condition is expressed by

$$E_1 - E_2 = S\,(z_1 - z_2) \qquad (4)$$

in which E_1 and E_2 are voltages at points in the free surface or seepage face having the vertical coordinates, z_1 and z_2, respectively. The model constant, S, equals the electromotive potential gradient in a vertical direction on any free surface in the model and thus corresponds to the gradient of gravity in the prototype, which is unity. The constant, S, may best be introduced by considering the permeability, K, to be analogous to $S\,\sigma$, in which σ is the specific conductivity of the electrolyte.

Membrane Analogy.—The membrane analogy is based on the equation for the deflection of a membrane under uniform tension, which is clamped to a circular ring at the periphery and which is deflected by a small cylindrical rod at the center. The deflection, y, is approximated by

---

[10] "The Theory of Ground-Water Motion," by M. King Hubbert, *Journal of Geology*, Vol. 48, 1940, pp. 785–944.

$$\frac{d^2y}{dr^2} + \left(\frac{1}{r}\right)\left(\frac{dy}{dr}\right) + \frac{\gamma\, t}{T} = 0 \qquad (5)$$

in which T is the tension, t denotes the membrane thickness, and γ is the specific weight of the membrane.

For axially symmetrical flow, Eq. 3 reduces to

$$\frac{\partial^2 h}{\partial r^2} + \left(\frac{1}{r}\right)\left(\frac{\partial h}{\partial r}\right) + \frac{\partial^2 h}{\partial z^2} = 0 \qquad (6)$$

On the free surface, h is equal to y (except for a difference in the datum) and can be expected to satisfy Eq. 5 except for differences in the small, nonhomogeneous term. If this approximation is accepted, the membrane analogy may be used to study seepage flow.

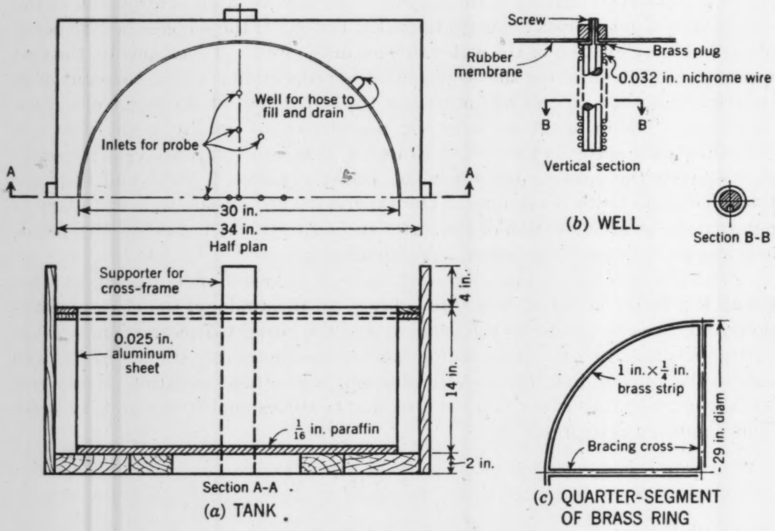
Well for hose to fill and drain
Inlets for probe
A
A
30 in.
34 in.
Half plan
Supporter for cross-frame
4 in.
0.025 in. aluminum sheet
14 in.
$\frac{1}{16}$ in. paraffin
2 in.
Section A-A
Screw
Rubber membrane
Brass plug
0.032 in. nichrome wire
B
B
Vertical section
Section B-B
1 in. × $\frac{1}{4}$ in. brass strip
Bracing cross
29 in. diam

(a) TANK

(b) WELL

(c) QUARTER-SEGMENT OF BRASS RING

FIG. 2.—EXPERIMENTAL APPARATUS

Dimensional Analysis.—Eq. 2 is a special case of a more general expression. The variables, Q, K, r_w, h_w, r, and h (in which h is the known depth of water at a radial distance, r), should be sufficient to define a particular system of flow. These variables may be arranged so that

$$\frac{Q}{K\, r_w^2} = f_2\left(\frac{h_w}{r_w}, \frac{h}{r_w}, \frac{r}{r_w}\right) \qquad (7)$$

By choosing $r = r_w$, h becomes h_s, and Eq. 2 is derived from Eq. 7. In addition, h_s might have been chosen instead of h_w as a pertinent variable to form

$$\frac{Q}{K\,r^2_w} = f_3\left(\frac{h_s}{r_w}, \frac{h}{r_w}, \frac{r}{r_w}\right) \quad (8)$$

Knowing the values of the water depth, h_1 and h_2, at two radial distances, r_1 and r_2, is sufficient to establish the corresponding free-surface profile for a well of a particular radius, r_w. Arranging this postulate into a dimensionless expression yields

$$f_4\left(\frac{h_1}{r_w}, \frac{h_2}{r_w}, \frac{r_1}{r_w}, \frac{r_2}{r_w}, \frac{h}{r_w}, \frac{r}{r_w}\right) = 0 \quad (9)$$

A single value of $Q/(K\,r^2_w)$ is associated with each dimensionless free-surface profile resulting from a particular solution of Eq. 9.

LABORATORY INVESTIGATIONS

Apparatus.—The basic apparatus used by the writers consisted of an open-topped, cylindrical tank; a rubber membrane assembly; and a simulated well. Because a cylindrical tank was used, the inflow boundary, as shown in Fig. 1 (*a*), could not be duplicated exactly. Actual boundary conditions that can be obtained with the model are shown in Fig. 1 (*b*). These conditions differ from those of Fig. 1 (*a*) only at the inflow boundary—a difference which becomes negligible for large values of r.

The model is shown in Fig. 2. The tank wall was made of sheet aluminum and the floor was made of plywood, which was waterproofed with paraffin. The membrane, which consisted of ordinary nursery-type rubber sheeting, was mounted on a ring made of brass strips. It was clamped to the ring with a tension band cushioned with strip rubber. The membrane assembly was supported by four threaded hangers from a cross frame mounted over the tank. The ring and membrane could thus be raised and lowered to provide different values of h_a, the depth of water at the inflow boundary. The thickness of the membrane was 0.12 in., and its specific gravity was 1.45. A tensile force of 70 g per cm produced a unit strain of 0.2 in the membrane material. In order to make sure that there was no difference in pressure between the two sides of the depressed membrane, the electrolyte was placed on both sides (Fig. 3). Along the circumference of the ring, the spare part of rubber sheet was raised so that current from the tank shell could not flow through the solution above the membrane. The surface profile of the depressed membrane was measured using a point-gage rule (Fig. 3).

The well was made of a plastic rod, $\frac{1}{4}$ in. in diameter, on which was wound a helix of nichrome wire 0.032 in. in diameter and with a resistance equaling 0.0193 ohms per cm. The wire was seated in $\frac{1}{4}$ in.-28 threads, thus giving a clearance of 0.0037 in. between adjacent turns of the wire. This arrangement made possible a uniform potential drop along the length of the rod. Prior to winding, a $\frac{3}{32}$-in. slot was milled lengthwise in the rod, and a $\frac{3}{32}$-in. brass tube was placed in the slot. This tube could slide in the slot to a height representing the water level in the well. Thus, by short-circuiting across the winding, the constant-potential section of the model well was provided.

The effective radius of the well model could not be determined by direct measurement because of the uncertainty regarding the electrical boundary of the wire helix. The subsequent indirect method was therefore used. The entire length of the well was maintained at a constant potential, and a radially symmetrical, polar, potential field was imposed in the surrounding electrolyte; such a field has radial, logarithmic distribution. By measuring the potential along a radius, this distribution was obtained, and the results were extrapolated to correspond to a radius having the same potential as the well. For the model well, the effective radius was found to be 0.314 cm.

The electrical circuits used are shown in Fig. 4. Alternating current was used to minimize polarization. Two power sources were necessary. One source provided the current, I_w, to maintain the required potential distribution along the well. (The value of I_w was used for all the tests and was maintained by adjusting the resistance, R_1.) The other source provided the current, I_T, which passed through the electrolyte and was analogous to the hydraulic discharge. The potential drop between any two points was measured using a potentiometer connected to an oscillograph through a preamplifier. Values of I_w and I_T were determined from measurements of potential drop across the resistances, R_2 and R_4, respectively. A water solution of 0.2% acetic acid was used for the electrolyte. After each run the conductivity of the electrolyte was measured using a cell especially constructed of plastic.

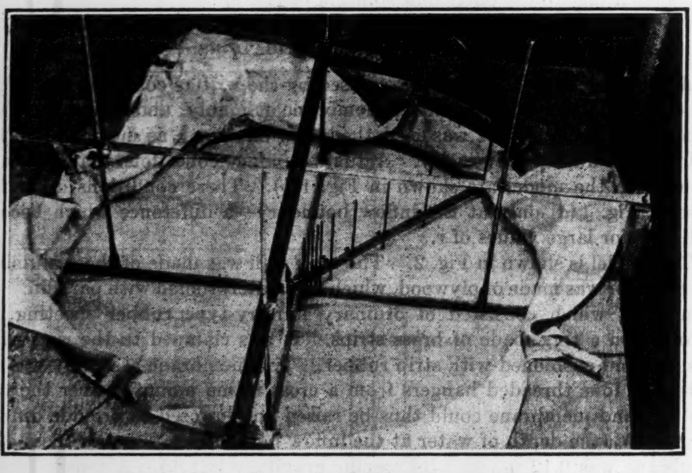

FIG. 3.—MODEL ELECTRICAL ASSEMBLY DURING THE TEST

The potential field in the electrolyte was surveyed using a probe inserted through holes in the bottom of the tank. This probe was constructed of straight glass tubing $\frac{3}{32}$-in. in diameter through which a 17-gage copper wire had been threaded. The probing end was sealed with paraffin, and eight holes for the probe were arranged radially and fitted with copper seal caps to prevent leakage.

Test Runs.—Eqs. 7 and 8 imply that single values of $Q/(K\,r^2_w)$ and h_w are associated with each particular set of values of h_α, r_α, h_s, and r_w. Selection of such a set for a single test run fixed the geometric configuration of the model. Also, selection of h_α and h_s determined the value of $(E_\alpha - E_s)$. The value of h_w and the value of E_w which is associated with it were found by trial as follows: The sliding tube in the analogous well was adjusted until Eq. 4 was satisfied by measured values of the potential along the membrane boundary and at the analogous water surface in the well.

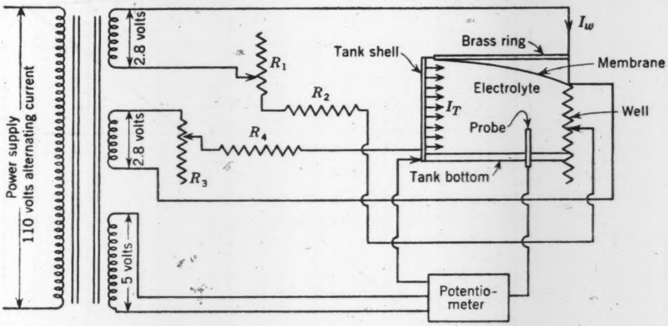

FIG. 4.—ELECTRICAL CIRCUITS FOR THE MODEL

The value of r_α was fixed by the size of the tank. Because the effective diameter of the well did not change, the value of r_α/r_w was 115 for all twenty-eight test runs.

MOSCA TEST WELL

During March, 1954, an experimental well located near Mosca, Colo., was tested by W. E. Code and Mr. Peterson, one of the writers of this paper. Natural conditions at this site correspond closely to the ideal conditions imposed on the laboratory experiments. The shallow topsoil is underlain by extensive water-bearing gravel and sand, there is no upper confining stratum, and the water table is practically level. The log for the well is:

Depth	Material
0 ft to 3 ft	Top soil
3 ft to 25 ft	Sand and gravel; clay lenses
25 ft to 45 ft	Brown sandy clay
45 ft to 57 ft	Blue clay

A hole, which was 24 in. in diameter, was drilled to a depth of 57 ft using cable tools. A 24-in. blank casing was placed to a depth of 35 ft, and the hole was backfilled with gravel to a depth of 29 ft below the ground surface. An 18-in. well casing was set and the blank casing was withdrawn. The ground elevation at the well as taken as +94.0 ft. Six observation wells were located on a radial line north of the pumped well at distances ranging from 6.0 ft to 600.0 ft. Other observation wells were located 112.0 ft west, 133.0 ft south, and 136.5 ft east of the test well.

Fig. 5 shows the initial elevation of the water in the observations wells, and the elevation after 64.6 hr of continuous pumping. After pumping, the water-surface elevation at the east, south, and west wells agreed closely with the drawdown curve for the north radius, indicating good radial symmetry.

After 64.6 hr of pumping, the discharge was 0.364 cu ft per sec. Application of the Dupuit equation (Eq. 1) gave $K = 2.23 \times 10^{-3}$ ft per sec. The Theis equation,[11] applied during the depletion period, gave $K = 2.28 \times 10^{-3}$ ft per sec. The initial depth of water in the well, h_α, was 22.0 ft; the depth, h_w, of water in the well after 64.6 hr of pumping was 10.0 ft. The usual method of extrapolating the logarithmic curve to the outside of the casing (Fig. 5) yields $h_s = 12.8$ ft. Subsequently a more accurate method of finding h_s will be shown. The effective radius, r_w, of the well was 0.72 ft.

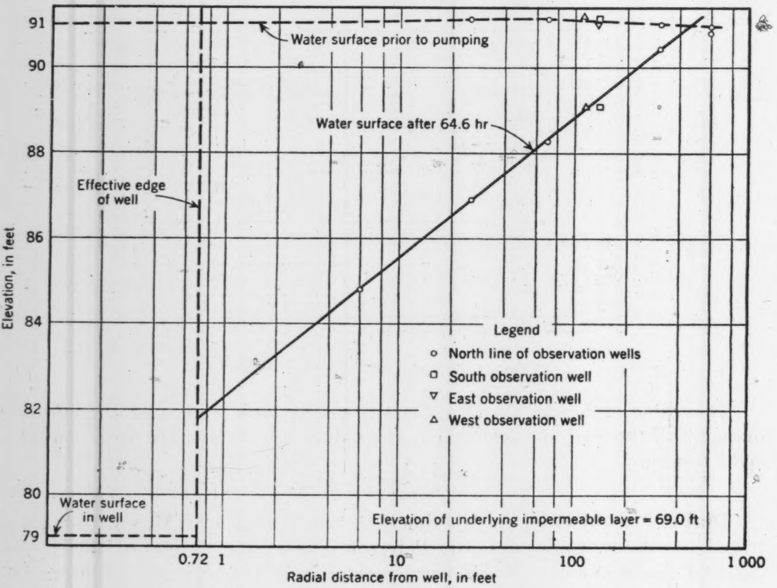

FIG. 5.—DRAWDOWN CURVE FOR THE MOSCA (COLO.) TEST WELL

RESULTS

Free-Surface Profiles.—In order to reduce the observed free-surface profiles to a single set of comparable curves, standard values of r_1 and r_2 need to be

---

[11] "Hydrology," by C. O. Wisler and E. F. Brater, John Wiley and Sons, New York, N. Y., 1949.

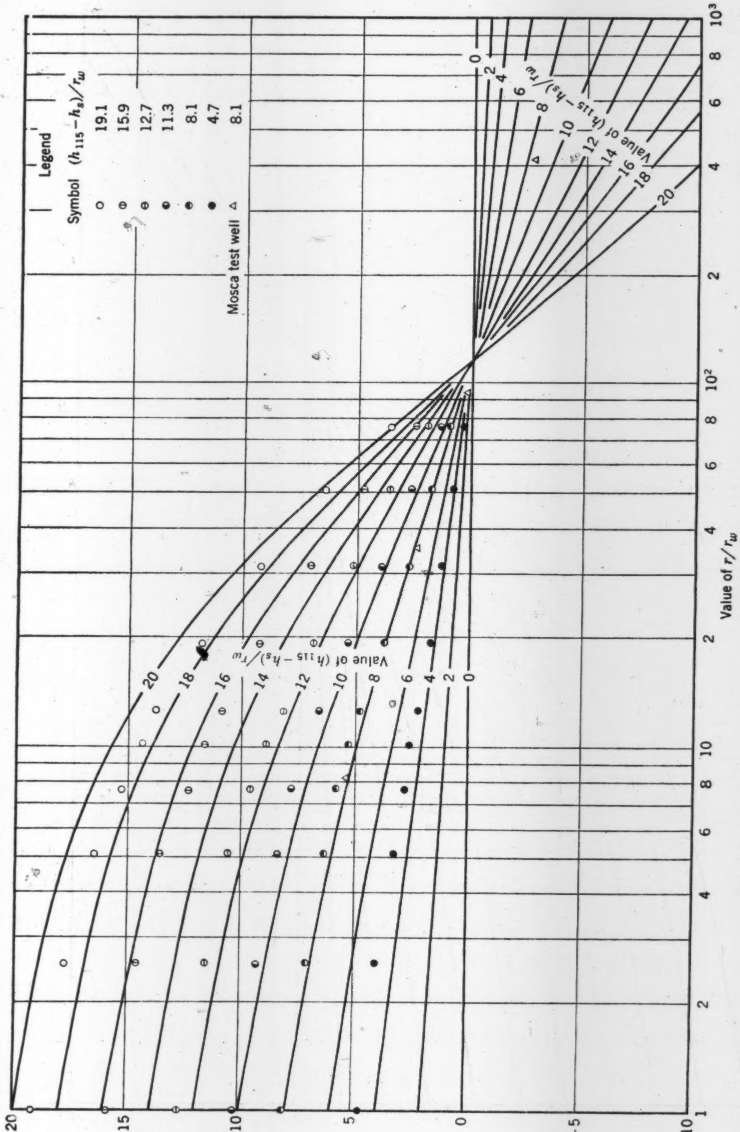

FIG. 6.—ANALOGY TEST RESULTS COMPARED WITH BEST FREE-SURFACE PROFILES

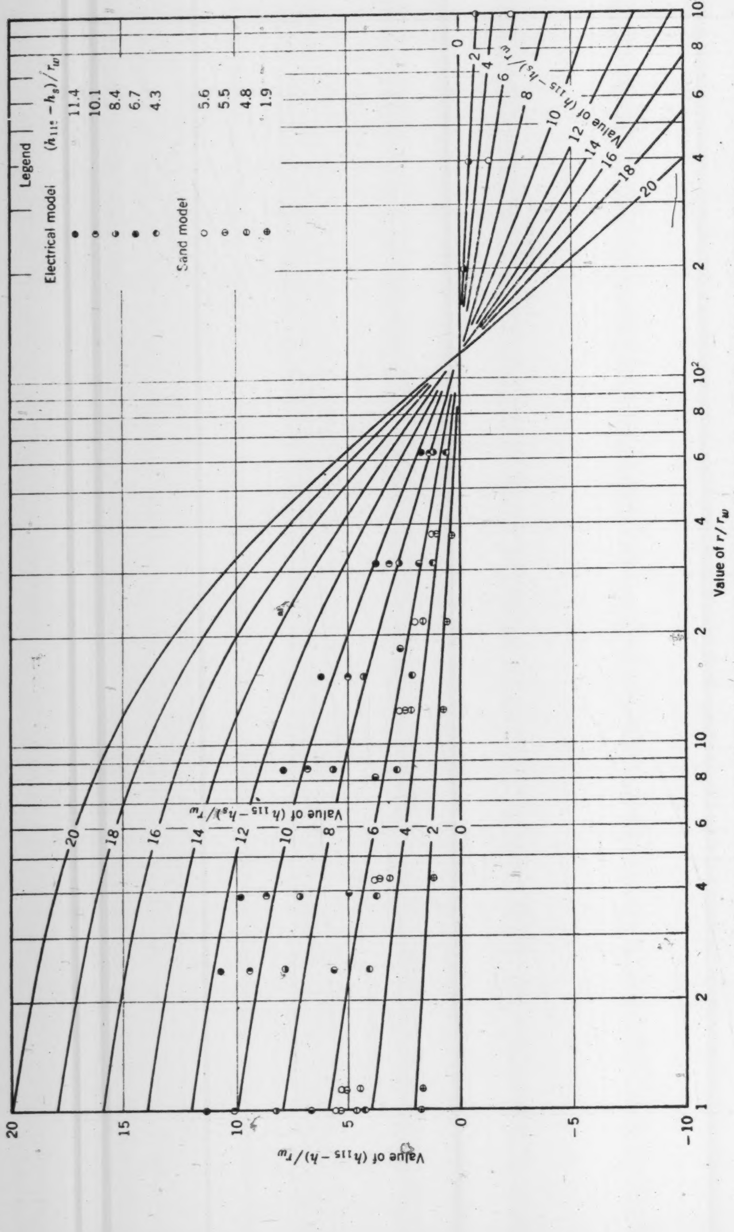

FIG. 7.—RESULTS OBTAINED BY MESSRS. BABBITT AND CALDWELL COMPARED WITH BEST FREE-SURFACE PROFILES

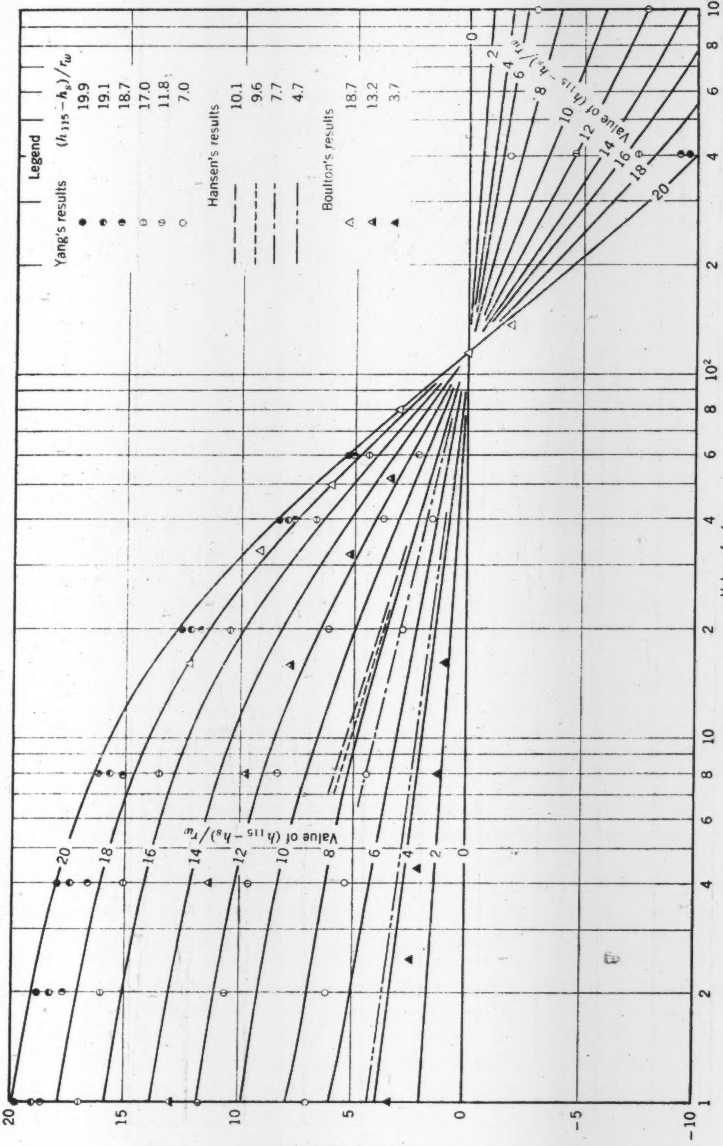

Fig. 8.—Results Obtained by Messrs. Yang and Hansen Compared with Best Free-Surface Profiles

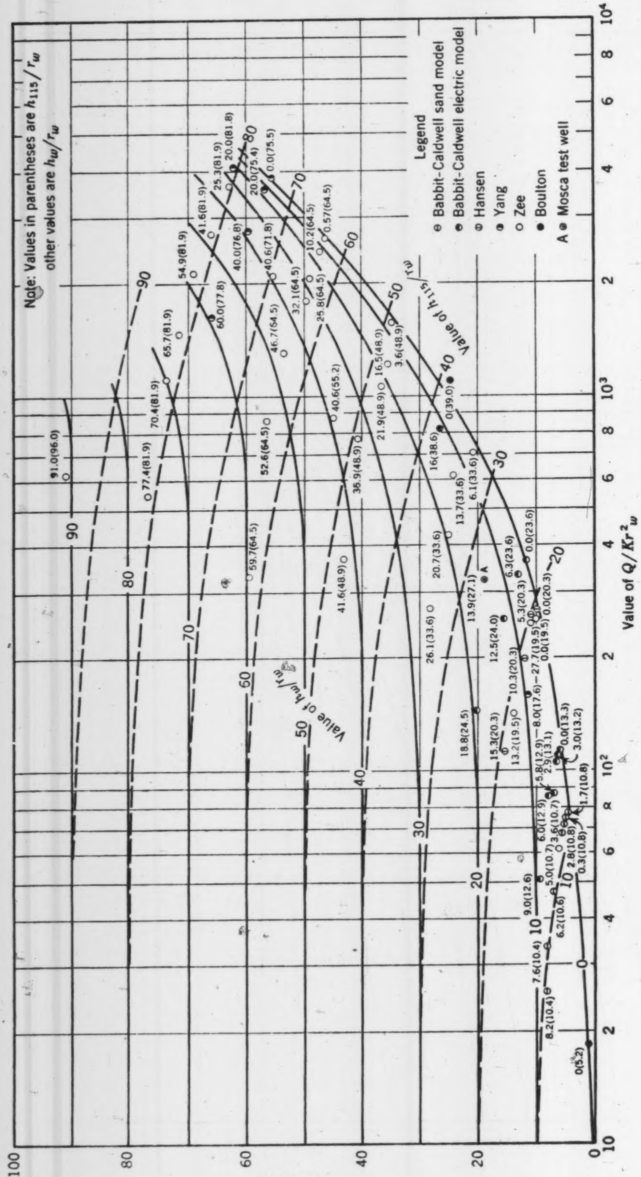

Fig. 9.—Relationship of Discharge and Geometric Parameters

chosen in Eq. 9. For this, r_1 was chosen as r_w, and r_2 was chosen as 115 r_w. The corresponding value of h_1 is h_s, and the value of h_2 is designated as h_{115}. The value of 115 r_w was arbitrarily chosen to correspond to the dimensions of the tank used. Choosing the elevation of h_{115} as the datum, Eq. 9 may be rewritten as

$$f_5\left(\frac{h_{115} - h_s}{r_w}, \frac{h_{115} - h}{r_w}, \frac{r}{r_w}\right) = 0 \ldots\ldots\ldots\ldots\ldots (10)$$

Available data from all sources were arranged in the form of Eq. 10 and were plotted. If data were adequate but did not extend to the radial distances of 115 r_w, they were extrapolated using the Dupuit equation. After careful consideration, curves having the best fit were drawn (Fig. 6). For simplicity only the data taken by the writers, including the data for the test well at Mosca, are shown in Fig. 6. The data of Messrs. Babbitt and Caldwell are shown in Fig. 7 and the data of Mr. Yang, Mr. Hansen, and Mr. Boulton, in Fig. 8. The plotted curves are the same for Figs. 6, 7, and 8.

Figs. 6, 7, and 8 show good correlation of the data from the various sources. The membrane profile agrees very well with profiles obtained elsewhere using models, analogs, or numerical solution of the differential equations, and with the field-test information. Whereas the membrane analogy is not theoretically exact because of the difference in the nonhomogeneous terms of Eqs. 5 and 6, the results indicate that the discrepancy introduced by this difference cannot be material for the range of variables covered. This establishes the practical validity of the membrane analogy. The data of Mr. Yang and Mr. Hansen indicate that the free-surface profile near a well is not a linear, logarithmic function of the radial distance in cases where the drawdown is large. This is important in the case of the Mosca well. Extrapolation of this free surface curve in Fig. 6 yields $h_s/r_w = 19$ or $h_s = 13.7$ ft instead of 12.8 ft found using the logarithmic extrapolation of Fig. 5.

The curves of Fig. 6 may be used to predict the free-surface profile for a well if the value of h_{115} and the depth at some other radius are known. By combining the use of these curves with those of Fig. 9, the free-surface profiles may also be predicted if discharge and permeability and either h_w, h_s, or h_{115} are known.

Discharge Data.—Discharge was first studied in its relationship to the geometric variables at the well—that is, in relation to r_w, h_w, and h_s, and to the permeability, K. For this purpose the variables were arranged in the form of Eq. 2; data from all sources were plotted as shown in Fig. 9; and curves were drawn (represented by solid lines) showing the variation of h_s/r_w and $Q/K\,r^2_w$ for various values of h_w/r_w.

Measurement of h_s is difficult both in the laboratory and in the field because of the rapidly changing water-surface elevation near the well and the effect of capillarity in sand models. The discharge information has more general use if it is defined in terms of a water depth measured at some distance from the well—an observation that can be made with confidence. For this purpose, h_w/r_w in Eq. 2 was replaced by h_{115}/r_w. The corresponding values of the latter variable are indicated in parentheses in Fig. 9 for each datum previously plotted. Curves showing the variation in h_s/r_w are drawn as dashed lines.

In general, the data from all sources correlate well in Fig. 9. Data obtained using the electric-membrane analogy agree closely with values obtained from other experiments, the numerical solutions of Eq. 6, and the field test. The advantages of the electric-membrane-analogy combination are: (1) Valuable information may be obtained rapidly and inexpensively; (2) capillary effects, which are often considerable in sand models, are eliminated; and (3) the water depth, h_s, immediately outside the well casing is directly and readily measured.

Knowledge of any two of the variables, $Q/K\,r^2_w$, h_s/r_w, h_w/r_w, or h_{115}/r_w, makes possible the prediction of the other two variables from Fig. 9. For instance, if the discharge parameter, $Q/K\,r^2_w$, and either h_w/r_w, h_s/r_w, or h_{115}/r_w are known, the other geometric variables may be predicted. With these variables, Fig. 6 may be used to predict the entire free-surface profile. Further uses of Fig. 9 include predicting discharge from drawdown and permeability information and predicting the height of the seepage face.

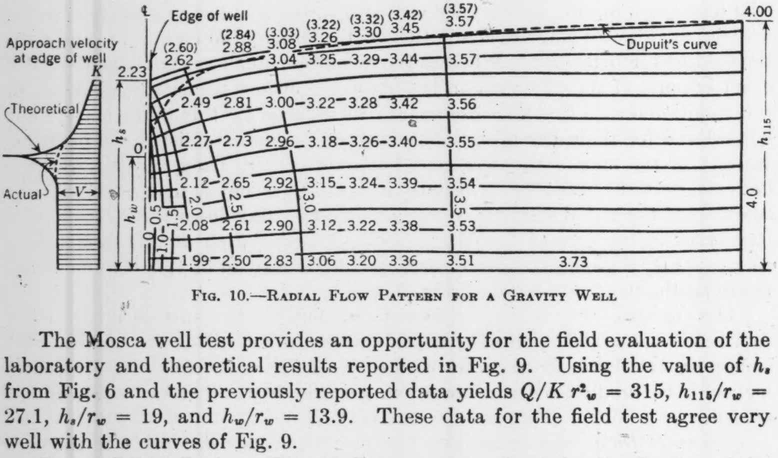

℄
Edge of well
Approach velocity at edge of well
K
Theoretical
Actual
V
2.23
h_s
0
h_w
0
0.5
1.0
1.5
2.0
2.5
3.0
3.5
(2.60)
2.62
(2.84)
2.88
(3.03)
3.08
(3.22)
3.26
(3.32)
3.30
(3.42)
3.45
(3.57)
3.57
4.00
Dupuit's curve
3.04
3.25
3.29
3.44
3.57
2.49
2.81
3.00
3.22
3.28
3.42
3.56
2.27
2.73
2.96
3.18
3.26
3.40
3.55
2.12
2.65
2.92
3.15
3.24
3.39
3.54
2.08
2.61
2.90
3.12
3.22
3.38
3.53
1.99
2.50
2.83
3.06
3.20
3.36
3.51
3.73
h_{115}
4.0

FIG. 10.—RADIAL FLOW PATTERN FOR A GRAVITY WELL

The Mosca well test provides an opportunity for the field evaluation of the laboratory and theoretical results reported in Fig. 9. Using the value of h_s from Fig. 6 and the previously reported data yields $Q/K\,r^2_w = 315$, $h_{115}/r_w = 27.1$, $h_s/r_w = 19$, and $h_w/r_w = 13.9$. These data for the field test agree very well with the curves of Fig. 9.

Potential Distribution.—Fig. 10 shows an example of the distribution of the potential in a radial plane determined for one of the test runs. The flow net was drawn from measurements of the potential made using the probe and the values are recorded in the figure.

The potential along a free surface must satisfy the gravity criterion expressed by Eq. 4. The numbers in parentheses in Fig. 10 were computed using observed values of z for the membrane. These values may be compared with the measured potential values to demonstrate the degree to which the depressed membrane actually satisfies the gravity criterion.

The velocity of the water approaching the seepage face was computed from the equation, $V = K \cos \beta$, using values of β obtained from the flow net. A curve showing the computed velocity distribution at the edge of the well is included in Fig. 10. This curve is based on the assumption that the well boundary below the elevation, h_w, remains an isopotential surface. Actually, the axial acceleration of the inflowing water along the length of the well screen modifies the uniform potential distribution along the length of the actual well[12]. Fig. 10, at least theoretically, shows how to place the well screen most economically in so far as best hydraulic performance is concerned.

Fig. 10 also shows the location of the free water surface computed with the Dupuit equation. Whereas deviations are large near the well, agreement is good at large distances. The Dupuit equation has been used for determining permeability by means of pumping tests. Fig. 10 may be used to indicate the distance from the well at which reasonably accurate results might be expected.

Effective Radius.—For a developed well or a well with a gravel envelope, the effective radius may be substantially different from the actual radius of the well screen. In 1947 C. E. Jacob[13] analyzed this problem and proposed methods for determining the effective radius of an artesian well. Fig. 9 may be used by trial and error to determine the effective radius of a steady-state well in an unconfined aquifer. If the values of Q, K (from a pump test), h_w, and h_{115} are known, a trial value of r_w is assumed, and $Q/K\, r^2_w$, h_{115}/r_w, and h_w/r_w are computed and plotted in Fig. 9. If r_w has been correctly assumed, this point will correspond with the curves of Fig. 9; if not, a new value of r_w can be assumed and the procedure can be repeated until substantial agreement is reached.

CONCLUSIONS

Even for the idealized case of a fully penetrating, steady-state well in an unconfined aquifer, exact mathematical expressions relating the geometric and flow variables have not been found. Much empirical information has been collected by many investigators, however. Some of this information has been obtained from field tests, but most systematic investigations have been made using sand models or electrical analogies using carbon wedges. The use of sand models is cumbersome and the capillary effects are large. When carbon wedges are used, the free surface must be carved to a radial profile located by trial and error. Numerical solution of the boundary-value problems by two different investigators for ten specific cases has also been accomplished, but this task is slow because of the radial convergence of flow.

To facilitate systematic interpretation of empirical information, dimensional considerations were used to arrange the variables in postulated functional expressions, which are stated as Eqs. 7, 8, 9, and 10. In order to obtain adequate data rapidly and with a minimum of effort, apparatus was used which combined the electrical analogy for flow with the membrane analogy for a free surface. Using this apparatus, data for a number of simulated cases were readily obtained. Data from one field test of a well under the rather idealized conditions of the problem were also collected. The validity of the membrane analogy is substantiated by the correspondence of results from numerical solutions, sand models, and an actual field test.

---

[12] "Effect of Well Screens on Flow into Wells," by Jack Sterling Petersen, thesis presented to Colorado State University, at Fort Collins, in 1951, in partial fulfilment of the requirements for the degree of Master of Science.

[13] "Drawdown Test to Determine Effective Radius of Artesian Wells," by C. E. Jacob, *Transactions*, Vol. 112, 1947, pp. 1047–1070.

The results are (1) geometric relationships of the dynamic system, (2) relationships between flow variables and geometric variables, and (3) potential-and flow-distribution patterns. Geometric relationships are presented in Fig. 6 as a single family of water-surface profile curves; the curves in this figure are based on data from all available sources. Fig. 6 also shows empirical data for comparison with these curves. Fig. 9 shows the relationship between the flow variables of discharge and permeability with the well radius, r_w, the depth of water in the well, h_w, the depth outside the casing, h_s, and the depth at a distance of 115 well radii, h_{115}. The curves of Figs. 6 and 9 may be used to predict values of the unknown variables if certain other variables are known. Of particular interest is the magnitude of the seepage face at the well boundary, which may be computed as the difference between h_s and h_w. Fig. 10 is a typical example of a radial flow net for a specific case which was investigated by the writers. Also shown in Fig. 10 is the velocity distribution at the boundary of the well for the specific case considered.

ACKNOWLEDGMENTS

The experimental work resulting in this paper was conducted by Mr. Zee in the physics laboratory of the Colorado State University at Fort Collins during 1950 and 1951 under the direction of Mr. Peterson and Mr. Bock. This work was accepted for a dissertation leading to a degree in irrigation engineering in 1952 at Utah State University in Logan. Mr. Hansen directed the writing of the dissertation, and Mr. Code and Mr. Peterson conducted the tests of the Mosca experimental well.

APPENDIX. NOTATION

The following symbols, adopted for use in the paper and for the guidance of discussers, conform essentially with "American Standard Letter Symbols for Hydraulics" (ASA Z10.2—1942) and "American Standard Letter Symbols for Electrical Quantities" (ASA Z10.5—1949) prepared by committees of the American Standards Association with Society representation, and were approved by the Association in 1942 and 1949, respectively:

E = electromotive potential or voltage;

E_a, E_s, E_w = electromotive potential at the tank boundary, at the outside of the well, and at the well, respectively;

f = functional relationship;

h = piezometric head at any point in the field; also the elevation of the free surface above the impermeable boundary;

h_a, h_s, h_w = piezometric head or elevation of the free surface at the tank boundary, outside the well, and at the well, respectively;

I = electrical discharge or current:

  I_T = electrical discharge through the electrolyte in the tank;

  I_w = electrical discharge through the well coil used to control the electrical potential at the simulated well;

K = the hydraulic permeability (sometimes designated as the hydraulic conductivity);
Q = total discharge of the hydraulic system;
R = electrical resistances;
r = radial coordinate measured from the well axis:
  r_w = radius of the well;
  r_α = radius of the tank;
S = model constant; electromotive-potential gradient in the direction, z, on a free surface;
T = unit tension in the membrane;
t = thickness of the membrane;
y = deflection of the membrane at a point;
z = a vertical coordinate measured from the impermeable stratum:
  z_1 = vertical coordinate of point 1;
β = angle of inclination of a streamline at the well boundary;
γ = unit weight;
θ = coordinate angle; and
σ = conductivity of an electrolyte.

DISCUSSION

Robert E. Glover,[14] M. ASCE.—The ingenious electrical analogy arrangement described by the authors facilitates investigation of flow conditions near a well in an aquifer having no upper confining bed. Such devices are often needed because the formulas usually used for engineering purposes are based on simplifications and approximations which exhibit their greatest shortcomings in this area.

A common idealization is based on the following simplifying assumptions: (1) The gradient of the free surface is conserved throughout the depth of the aquifer, and (2) the reduction of the area available for the flow of ground water, caused by the depression of the free surface as the well is approached, is neglected. These assumptions are equivalent to the requirement that the drawdown everywhere should be small compared to the original depth of water in the aquifer. The drawdowns in actual wells often exceed this limitation and thus induce a search for more elaborate solutions which will provide closer approximations. However, many actual cases involve transient phenomena, and the added mathematical difficulties introduced by the time factor provide powerful incentives for retaining the simple idealization previously described.

The best solution to these difficulties seems to be to use the simple idealization as long as the drawdowns retain tolerable values and to supplement these solutions with a special investigation in the zone of large drawdown near the well. The electrical analogy device should provide a means of making this investigation, and there is good reason for believing that, under certain identifiable conditions, this treatment will be adequate even though transient conditons must be considered.

If y represents the drawdown, or lowering, of the free water surface in an aquifer having an initial water depth, D, a permeability, K, and a ratio of drainable voids to total volume, v, the simple idealization described yields the following expression for the condition of continuity:

$$\frac{\partial y_1}{\partial t} = \frac{K\,D}{v}\left(\frac{\partial^2 y_1}{\partial r^2} + \frac{1}{r}\frac{\partial y_1}{\partial r}\right) \qquad (11)$$

For a steady state the right-hand member of Eq. 11 is zero, and a comparison with Eq. 5 shows that, if the weight of the membrane is neglected, the differential equations are of the same form. It follows that the membrane can take forms which closely represent the drawdowns obtained from this idealization. The steady-state solution of Eq. 11 which corresponds to Eq. 1 is

$$y_w - y = \frac{Q}{2\,\pi\,K\,D}\log_e\left(\frac{r}{r_w}\right) \qquad (12)$$

in which y_w represents the drawdown at the well.

---

[14] Research Engr., Bureau of Reclamation, U. S. Dept. of the Interior, Denver, Colo.

The transient-state solution for the case of a constant rate of withdrawal, Q, from a well of radius, r_w, is given by the exponential integral formula,[15]

$$y = \frac{Q}{4\,\pi\,K\,D} \int_{(v\,r2)/(4\,K\,D\,t)}^{\infty} \frac{e^{-u}}{u}\,du \qquad (13)$$

W. H. Taylor and E. D. Rainville[16] have noted that, if this integral is expressed in the usual series form in terms of powers of the quantity which appears as the lower limit of this integral with a logarithm term and a constant, the terms of the power series tend to vanish as time increases because the time appears in the denominators. The last term to disappear is the one which is raised to the first power. If this term is retained and two values of y are subtracted, an expression of the type of Eq. 12 is obtained, together with the difference of the two first power terms. It can then be seen that the transient case reverts to steady-state behavior between the radii, r_w and r_2, when

$$\frac{v\,(r^2{}_2 - r^2{}_w)}{4\,K\,D\,t} \ll 2 \log_e \frac{r_2}{r_w} \qquad (14)$$

It is inferred from these results of the approximate theory that, if r_2 represents a radius at which the drawdowns remain small compared to D, a steady state continuous with the solution to Eq. 13 at $r = r_2$ may be constructed in the interval, r_w to r_2, by electrical analogy or by other means to represent properly the true conditions between r_w and r_2 at that time.

What constitutes satisfaction of the requirement of Eq. 14 in any given case must be decided on the basis of the accuracy desired or attainable. The aquifers found in nature often depart materially from the homogeneity postulated in the idealization and, through these irregularities, often limit the accuracy which may be attained.

Vaughn E. Hansen,[17] M. ASCE.—The progress which is being made to solve the complex problem of the hydraulics of unconfined wells is encouraging. Significant advances have been made since the writer applied the membrane analogy to wells[18] and introduced the concepts of the discharge and well parameters.[7] The experimental data obtained recently by the authors have added considerably to the knowledge of unconfined wells. The design curves of Fig. 6 and Fig. 9 are useful and valuable summaries of these data.

In reviewing the dimensionless plottings of the free-surface profiles shown in Fig. 6, the writer believed that plots of this nature would become even more useful and meaningful if parameters could be selected which reflected a better picture of the actual free-surface profile. The disadvantage of basing the profile on an arbitrary radius 115 times the well radius could also be avoided by such a procedure.

---

[15] "The Relation Between the Lowering of the Piezometric Surface and the Rate and Duration of Discharge of a Well Using Ground Water Storage," by C. V. Theis, *Transactions*, Am. Geophysical Union, Sixteenth Annual Meeting, 1935.

[16] "Analysis of Pumping Test," by W. H. Taylor and E. D. Rainville, Bureau of Reclamation, U. S. Dept. of the Interior, Denver, Colo., February 2, 1937 (informal memorandum).

[17] Prof. of Irrig. and Drainage Eng., Utah State Univ., Logan, Utah.

[18] "Complicated Well Problems Solved by the Membrane Analogy," by Vaughn E. Hansen, *Transactions*, Am. Geophysical Union, Vol. 33, No. 6, December, 1952, p. 912.

In considering this need further it appeared reasonable that the following functional relationship of well variables would uniquely define the free-surface profile:

$$f_1(h, r, r_w, h_s, h_w) = 0 \quad \text{.....................} \quad (15)$$

The variables of Eq. 15 can be grouped in dimensionless form as

$$f_2\left(\frac{h}{r_w}, \frac{r}{r_w}, \frac{h_s}{r_w}, \frac{h_w}{r_w}\right) = 0 \quad \text{.....................} \quad (16)$$

Because four quantities are still too many to plot clearly on a two-dimensional graph, the following combination of the four parameters of Eq. 16 was considered in an attempt to find three parameters which would give the desired picture of the free surface and also provide a unique solution:

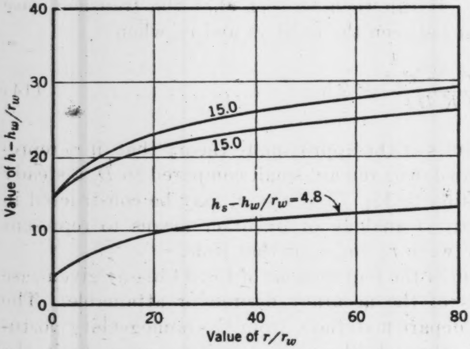

FIG. 11.—DIMENSIONLESS PLOTTING OF THE FREE-SURFACE PROFILE

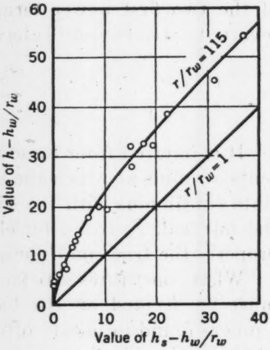

FIG. 12.—WELL PARAMETERS OF EQ. 17

$$\frac{h - h_w}{r_w} = f_3\left(\frac{r}{r_w}, \frac{h_s - h_w}{r_w}\right) \quad \text{...................} \quad (17)$$

The grouping of parameters shown in Eq. 17, when plotted with $(h - h_w)/r_w$ as the ordinate and r/r_w as the abscissa with a family of $[(h_s - h_w)/r_w]$-curves, would illustrate the free-surface drawdown as the water approached the well. It remained to ascertain if Eq. 17 would yield a unique solution.

To determine the uniqueness of Eq. 17, the values of the three dimensionless parameters were computed for three profiles previously shown by Mr. Zee.[19] The results of this computation are shown in Fig. 11. It is apparent that two free-surface profiles were obtained for the same value of $(h_s - h_w)/r_w = 15.0$. However, when other data were plotted for $r/r_w = 115$, as shown in Fig. 12, a distinct and unique relationship was observed which verifies (within the range of data available) the validity of Eq. 17. Unfortunately, the three profiles described by Mr. Zee contained, entirely by chance, two profiles with the same value of $(h_s - h_w)/r_w$ which deviated as widely as any data in his paper from the best-fit line. Because additional data are not available one cannot indicate the correct family of curves for Fig. 11. However, the proximity and random variation of the data from the best-fit curve of Fig. 12 does verify that a unique family of curves exists for Fig. 11 and Fig. 12. It is suggested that the family of curves be developed for Fig. 11 with the data used to develop Fig. 6. It is felt that Fig. 11 will be more useful than Fig. 6 because the resulting curves represent the free-surface profile and because the arbitrary radius of 115 well radii has been eliminated.

---

[19] "The Use of Combined Electrical and Membrane Analogies to Investigate Unconfined Flow into Wells," by Chong-Hung Zee, thesis presented to Utah State Agricultural College, at Logan, in 1952, in partial fulfilment of the requirements for the degree of Doctor of Philosophy.

JAMES N. LUTHIN.[20]—By combining the electric and membrane analogies the authors have been able to produce solutions to important practical problems of unconfined wells. The method used is simple, yields solutions of satisfactory accuracy, and is certainly an improvement over the laborious numerical methods and other techniques used previously.

With reference to two of the boundary conditions which are used by Messrs. Zee, Peterson, and Bock, the free water surface is an essential part of the solution and is provided by the membrane analogy. The free water surface is normally considered to be in equilibrium with the atmosphere (a surface at atmospheric pressure) and is usually assumed to be a limiting surface or boundary of the flow region. Mr. Muskat defines a free surface as a "streamline along which the pressure is uniform." If one accepts this definition (assuming atmospheric pressure along the free water surface), then the occurrence of a free water surface in ground-water flow is more or less fortuitous because streamlines do not necessarily coincide with equipressural surfaces. Also, the flow system is not limited by the free water surface because considerable flow can occur in the capillary zone lying above the water table. The water table simply represents an equipressural surface within the interior of the flow continuum and, in general, is not a stream surface.[21]

The importance of flow in the capillary zone is of course dependent on the relationship between the quantity of flow in the capillary zone and the flow in the ground-water zone or saturated zone lying below the water table. P. R. Day and the writer[22] have measured the lateral flow above a sloping water table. For the sand used in the experiment where the flow section below the water table was approximately 30 cm thick, about half the total flow was above the water table in the capillary zone. However, for a ground-water zone 50 ft thick the contribution of the capillary zone above it would be less than 2% of the total flow, indicating that the authors were correct in ignoring the capillary zone in their analysis.

The Laplace equation is not valid for flow in the capillary region, and any analysis of the total-flow continuum depends on a solution of

$$\operatorname{div}(K \nabla \phi) = 0 \quad \text{.......................} \quad (18)$$

---

[20] Associate Prof. of Irrig., Univ. of California, College of Agriculture, Davis, Calif.

[21] "The Flow of Homogeneous Fluids Through Porous Media," by M. Muskat, McGraw-Hill Book Co., Inc., New York, N. Y., 1937.

[22] "Lateral Flow Above a Sloping Water Table," by James N. Luthin and P. R. Day, *Proceedings*, Soil Science Soc. of America, Vol. 19, 1955, pp. 406–410.

in which K is a function of the soil-moisture tension. The relationship between K and the soil-moisture tension may be determined experimentally, although E. C. Childs and N. Colis-George[23] have proposed a method of computing this relationship from the soil-moisture characteristic (a plot of soil-moisture content versus tension).

Although the assumption of a free water surface may be justified in problems of well hydrology in which the flow region below the water table is very large compared to the capillary zone lying above the water table, it is doubtful if the concept can be applied with accuracy to certain problems of agricultural hydrology, highway drainage, and other flow problems involving thin-flow regions below the water table.

The existence of a seepage surface at the well boundary has been adequately investigated by the authors as well as by other engineers including Mr. Hansen.[7] However, as has been indicated, there is still an area of doubt as to the reason for the existence of a seepage surface. The reason usually given is that it must exist; because if it is assumed that there is a lack of a seepage surface, the impossible condition of intersecting streamlines with infinite velocities results. Having a seepage surface becomes apparently reasonable when the condition necessary for water to enter a well is considered. For water to pass as a liquid from a porous medium into the atmosphere the only requirement is that the pressure of the water in the porous media be equal to or greater than atmospheric.[24] Such a condition is encountered in the situation of ground-water flow toward a well.

In a homogeneous soil mass of uniform permeability the length of the seepage surface is independent of the soil permeability. Such uniform soil conditions are seldom encountered in practice, and usually the well penetrates a more permeable stratum. The greater the ratio of the permeability of the penetrated stratum to the permeability of the overburden, the smaller the seepage surface. This conclusion can be inferred from the results of experiments[25] in which the steady-state flow toward a well, penetrating an aquifer having a permeability 100 times that of the overburden, was analyzed. The distribution of hydraulic head indicates that the water moves vertically out of the overburden to the aquifer and then moves laterally to the well. One can infer that the seepage surface in this case would be rather small because water is passing from a layer of lower permeability to a layer of higher permeability.[26]

CHIA-SHUN YIH[27].—Congratulations are offered to the authors for their extensive contributions to well hydraulics. However, it should be emphasized that the membrane analogy really does not exist for unconfined wells in the exact sense. In Eq. 6 the second partial derivative of the piezometric head, h, with respect to the elevation, z, is not equal to zero for unconfined wells. It is true that on the free surface h is equal to z, but the equality of h and z is not maintained in the interior of the flow. The error therefore may not be small when the drawdown is not negligible compared to the asymptotic depth of the saturated layer. It is precisely because of this fact that the consistency of the data presented by Messrs. Zee, Peterson, and Bock with data obtained by previous investigations (particularly with those obtained by relaxation) is heartening. This consistency seems to indicate the general reliability of the results and establishes the fact that, in spite of the lack of a rigorous membrane analogy, an approximate membrane analogy nevertheless exists, the use of which has made extensive data possible.

---

[23] "The Permeability of Porous Materials," by E. C. Childs and N. Colis-George, *Proceedings*, Royal Soc. of London, Vol. 201, 1950, pp. 392–495.

[24] "Laws of Soil Moisture," by L. A. Richards, *Transactions*, Am. Geophysical Union, Vol. 31, 1950, pp. 750–756.

[25] "Numerical Analysis of Flow Through Aquifers Toward Wells," by James N. Luthin and V. H. Scott, *Agricultural Engineer*, Vol. 33, 1952, pp. 279–282.

[26] "Pressure Distribution in Layered Soils During Continuous Water Flow," by P. R. Day and James N. Luthin, *Proceedings*, Soil Science Soc. of America, Vol. 17, 1953, pp. 87–91.

[27] Associate Prof., Dept. of Eng. Mechanics, Univ of Michigan, Ann Arbor, Mich.

A great service would be rendered to the engineering profession if the task of finding the exact solutions were undertaken for a few cases in order to provide additional checks to the results obtained by Messrs. Zee, Peterson, and Bock, especially in the areas where only their own data exist. This would definitely establish the validity of the authors' results, which cover a wide range of practical interest.

CHONG-HUNG ZEE,[28] DEAN F. PETERSON, JR.,[29] M. ASCE, AND ROBERT O. BOCK[30].—The suggestions and comments of the discussers are most gratifying. Mr. Glover states that actual wells are almost invariably in a transient state. He correctly suggests that the transient-state equations are presently incapable of handling the complications introduced in the mathematical treatment of unconfined aquifers by wells or relatively large drawdown. Mr. Glover outlines the conditions under which a steady state may be postulated without material error. The use of methods of analysis suggested by the writers and their associates[7] makes possible the use of a substitute steady state in order to overcome these difficulties.

The writers agree that curves in the form of Eq. 17 would be better than those of Fig. 6. However, it is doubtful that the derivation of this equation made by Mr. Hansen has complete theoretical validity. Eq. 15 contains five variables all having the dimension of length. Because only one fundamental dimension is involved, dimensional analysis can reduce these variables to no less than four; therefore, Eq. 16 appears valid. Algebraic manipulation cannot reduce these variables to three as in Eq. 17. If Eq. 17 is valid, one of the variables of Eq. 15 would have to be redundant or insignificant. There can be an arbitrary choice for the fourth variable for Eq. 17; however, h_w/r_w appears logical. This would lead to

$$\frac{h - h_w}{r_w} = f_3\left(\frac{r}{r_w}, \frac{h_5\,h_w}{r_w}, \frac{h_w}{r_w}\right) \quad \ldots\ldots\ldots\ldots\ldots\ldots (19)$$

instead of to Eq. 17.

As a practical matter it is possible that h_w/r_w can be discarded, which is the same as discarding h_w in Eq. 1. The test for validity must be an experimental one, and an extension of the analysis presented by Mr. Hansen in his discussion is a logical approach. The writers regret that they have been unable to complete such an analysis; however, hydrodynamically, all five variables of Eq. 15 appear to be significant. The fact that the experimental data shown in Fig. 11 correlate fairly well at $r/r_w = 115$ may indicate that one of the variables becomes relatively unimportant at this distance. Eq. 10, on which Fig. 6 is based, follows from a consideration of the membrane only and is independent of hydrodynamics as such. The only relationship it has to the hydrodynamic case is through the validity of the membrane as an analogy.

---

[28] Structural Designer, Ammann and Whitney, Cons. Engrs., New York, N. Y.

[29] Prof. and Head, Dept. of Civ. Eng., Colorado State Univ., Fort Collins, Colo.

[30] Senior Engr., Arma Corp., Garden City, N. Y.

Mr. Luthin raises the question of capillary effects and describes the complicated phenomena involved when such effects are considered. The statement regarding the relative importance of such effects, in terms of specific field conditions, is useful in applying well hydraulics to practical problems. One obstacle to studying well hydraulics by utilizing simple scale models is the presence of capillary effects which cannot be scaled. The membrane analogy eliminates these effects and is valid if capillary effects in the field are negligible. This is a principal advantage of the method as compared to the sand-model method.

Mr. Yih states that the membrane analogy is not a rigorously correct one because the second derivative of h with respect to z is not zero. Although this is true, the differential equation for the membrane is not rigorously correct if the drawdown is appreciable because in deriving Eq. 5 it was assumed that the slope-length component, d_s, was equal to its horizontal projection. The writers do not know of a solution of the complete differential equations of elasticity for a circular membrane of finite unit weight and large central deflection. The similarity of Eq. 5 to Eq. 6 implies an approximate analogy which is borne out by the consistency of data obtained from its use with data from other sources, particularly with those from solutions using relaxation methods.

If $\partial^2 h/\partial z^2$ in Eq. 6 is equal to zero and if the weight of the membrane is ignored, for very small deflections the solutions to both Eq. 5 and Eq. 6 are of the form of Eq. 12—that is, linearly logarithmic in the radial direction. In this case both problems may be quite easily handled by the simple potential theory. The experimental data do not seem to substantiate a linear logarithmic distribution for either a well of large drawdown or a membrane of large deflection. It would not be surprising if, for correct boundary conditions, small deviations of the membrane from the true position of the free water surface made little difference in the discharge and seepage faces. However, the evidence substantiates that the membrane closely describes the true location of the free water surface. The membrane analogy, in combination with the electric analogy, therefore, constitutes a new and useful tool for the solution of problems of flow to a well.

AMERICAN SOCIETY OF CIVIL ENGINEERS
Founded November 5, 1852
TRANSACTIONS

Paper No. 2900

ANALYSIS FOR SHEET-PILE RETAINING WALLS

BY F. E. RICHART, JR.,[1] A. M. ASCE

WITH DISCUSSION BY MESSRS. PETER W. ROWE, AND F. E. RICHART, JR.

SYNOPSIS

A method for analyzing sheet-pile retaining walls is developed by considering the piling to be cut at the dredge line. The shear, moment, and backfill pressures, due to the material above the dredge line, are computed and then applied as loads to the embedded part of the pile. This embedded length is then treated as a beam on an elastic foundation in which the stiffness of the elastic foundation is assumed to increase linearly with the depth below the dredge line (zero at the dredge line). This type of foundation corresponds approximately to the behavior of sands. Curves have been prepared which show the variations in deflection and moment in this section of the pile, caused by a concentrated shear or moment at the dredge line or a uniform pressure along the embedded length. Using this information, a procedure for analyzing a chosen sheet-pile installation is presented, and the results for two examples are compared with those given by the "classical" procedures for such structures. The results of this study show the importance of the relative flexibilities of the pile section and foundation.

NOTATION

The letter symbols adopted for use in this paper are defined where they first appear, in the text or by illustration, and are arranged alphabetically, for convenience of reference, in the Appendix.

INTRODUCTION

The paper by Karl Terzaghi,[2] Hon. M. ASCE, emphasized the need for considering the wall flexibility in the design procedures for sheet-pile retaining

---

NOTE.—Published, essentially as printed here, in May, 1955, as *Proceedings-Separate No. 694*. Positions and titles given are those in effect when the paper or discussion was approved for publication in *Transactions*.

[1] Prof. of Civ. Eng., Univ. of Florida, Gainesville, Fla.

[2] "Anchored Bulkheads," by Karl Terzaghi, *Transactions*, ASCE, Vol. 119, 1954, p. 1243.

walls. Tests on models by P. W. Rowe[3] and by G. P. Tschebotarioff,[4] M. ASCE, have indicated a reduction of the maximum bending moment and the anchor load to values considerably below those computed from the classical "free-earth support" procedure, as a result of increasing the wall flexibility. In addition to considering wall flexibility, Mr. Rowe's tests also included an evaluation of the density of the material into which the model wall was embedded. Consequently, Mr. Terzaghi proposed that curves based on Mr. Rowe's tests could be utilized during the design of a particular sheet-pile wall. That is, the curves permit an estimate of the reduction below the free-earth-support values of bending moment and anchor pull caused by the wall flexibility and condition of the sand in the passive pressure zone.

However, Mr. Rowe's curves were based on laboratory tests of dry materials which had approximately the same density above and below the dredge line. The particular parameters investigated were: (1) The wall flexibility number, $\rho = (H')^4/E\,I$ ft^4 per lb in.^{2} per ft, in which H' is the total pile length, in feet; (2) the anchor-point location defined as the distance, $\beta\,H'$, from the top of the pile; (3) the length of pile embedded below the dredge line; (4) the surcharge; and (5) the type and density of material supported by the wall. Thus, considerable judgment is required to extrapolate this test information for use in actual pile design. However, such tests establish criteria for evaluating existing design procedures, and, until data from tests on prototype structures are reported, they are the most reliable available.

The reduction in bending moment and anchor pull found in the tests[3,4] was due to the partial fixity applied to the embedded length of the pile by sand pressures. Because the fixity depends on the relative stiffnesses of the sand and the wall in this region, the theory of subgrade reaction can be utilized to estimate the relative importance of each quantity under several types of loading conditions.

Previous analyses of this type have been made by Paul Baumann,[5] M. ASCE, I. Rifaat,[6] H. Blum,[7] and others to study the behavior of single piles and sheet-pile walls. This paper is an attempt to extend the previous analytical studies of sheet-pile walls. In order to make the results of rather tedious computation more usable, curves have been prepared for coefficients of deflection and coefficients of moment for each of three types of loading on the embedded part of a pile. Thus, the solution for any given pile problem can be obtained by superimposing these component solutions.

ASSUMPTIONS

The subgrade material is assumed to behave as a series of independent elastic springs. Furthermore, the rigidity of these springs is assumed to vary linearly with depth and to have a value of zero at the surface. This assumption appears valid within the range of depths which are normally encountered for sheet-pile walls embedded in sand. Loose sands have shown a linear relationship between the initial tangent modulus and the lateral confining pressure for pressures up to approximately 40,000 lb per sq ft. Dense sands exhibit a curved relationship between initial tangent modulus and confining pressure, but up to approximately 4,000 lb per sq ft of pressure the curve can be approximated by a straight line. Because an overburden height of 40 ft of dry sand or 60 ft of submerged sand is required to produce a pressure of 4,000 lb per sq ft, the usual embedded lengths of sheet piling (acting on sand) exhibit an approximately linear relationship between deformation and pressure for small deformations.

---

[3] "Anchored Sheet Pile Walls," by P. W. Rowe, *Proceedings*, Inst. of C. E., London, Vol. I, January, 1952, pp. 27–70.

[4] "Final Report, Large Scale Earth Pressure Tests with Model Flexible Bulkheads," by G. P. Tschebotarioff, Princeton Univ., Princeton, N. J., 1949.

[5] "Analysis of Sheet-Pile Bulkheads," by Paul Baumann, *Transactions*, ASCE, Vol. 100, 1935, pp. 707–797.

[6] "Die Spundwand als Erddruckproblem," by I. Rifaat, *Mitteilungen aus dem Institut für Baustatik*, Zurich, No. 5, 1935.

[7] "Beitrage zur Berechnung von Bohlwerken," by H. Blum, W. Ernst and Son, Berlin, 1951.

In analyzing a specific sheet-pile wall, the structure is cut at the dredge line, and the subgrade theory is used to analyze the behavior of the embedded length of pile due to the applied loads. These loads consist of a moment and a concentrated shear force, acting at the dredge line, as well as the horizontal pressure along the embedded length produced by the overburden pressure.

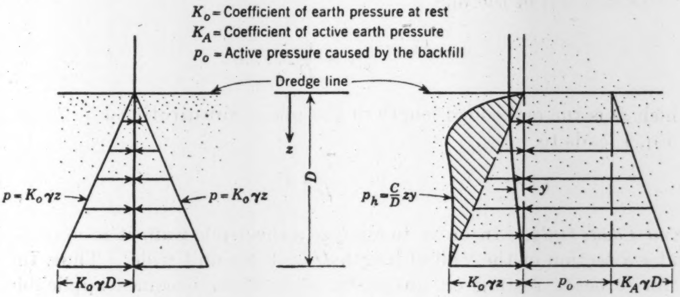
K_o = Coefficient of earth pressure at rest
K_A = Coefficient of active earth pressure
p_o = Active pressure caused by the backfill
Dredge line
z
D
$p = K_o \gamma z$
$p = K_o \gamma z$
$K_o \gamma D$
$p_h = \frac{C}{D} z y$
y
$K_o \gamma z$
p_o
$K_A \gamma D$

(*a*) NO BACKFILL (*b*) BACKFILLED

Fig. 1.—Pressures Acting on the Embedded Length of a Wall

This horizontal pressure is the active earth pressure generated by the weight of the backfill and the surcharge; it is assumed that this pressure is constant along the embedded length of the pile. Before backfilling or dredging, the embedded part of the pile is acted upon by the earth pressure at rest on both sides. As backfilling progresses the piling moves slightly outward. Thus, on the inside face the pressure consists of the active earth pressure exerted by the original embedment depth plus the active earth pressure exerted by the backfill depth.

On the outside face the original earth pressure at rest remains, but an increase in pressure due to the passive resistance of the soil is generated. Fig. 1 shows those conditions of pressure distribution. In this analysis, it is assumed that the active pressure on the inside face is equal to the earth pressure at rest on the outside face so that they cancel each other. This approximation contributes a conservative error to the analysis as it ignores the restraint offered to the pile by the difference between the earth pressure at rest and the active earth pressure. This leaves only the active earth pressure due to the backfill as a uniform load and the passive earth pressure as the reaction.

Analysis of Component Solutions

If the sand is considered to behave as an elastic medium, the relationship between the wall displacement and the horizontal reaction pressure it develops can be expressed as

$$p_h = k_h\, y \qquad (1)$$

in which k_h is the coefficient of horizontal subgrade reaction. For this study, k_h is assumed to vary linearly with depth, or

$$k_h = m_h\, z \qquad (2)$$

As a further designation, if C is the value of the coefficient of subgrade reaction at the bottom end of the pile,

$$m_h = \frac{C}{D} \qquad (3)$$

in which D is the embedded length of the pile. Substituting Eq. 2 and Eq. 3 into Eq. 1 leads to

$$p_h = \frac{C}{D}\, z\, y \qquad (4)$$

End Loads Only.—In order to analyze a sheet-pile wall, it is convenient to consider a section of the wall of length D and one unit wide. Thus, the solution for a beam resting on an elastic foundation becomes applicable. K. Hayashi[8] and later M. Hetényi[9] presented solutions for beams of uniform $E\,I$ resting on a foundation whose compressibility varies linearly along the length of the beam according to the expression,

$$k_x = k_A - b\, x \qquad (5)$$

in which k_A and b are constants and x is the distance along the beam from a fixed point, A. For the particular case of the subgrade coefficient equal to zero at the surface ($x = D$) and equal to C at the bottom of the pile ($x = 0$), Eq. 5 becomes

$$k_x = k_h = C - C\,\frac{x}{D} = C\,\frac{(D - x)}{D} = \frac{C\, z}{D} \qquad (6)$$

in which z is the distance from the top of pile. Using Eq. 6 in the differential equation of bending for a segment of a beam,

$$E\,I\,\frac{d^4 y}{dx^4} + \frac{D - x}{D}\, C\, y = 0 \qquad (7)$$

---

[8] "Theorie des Trägers auf elastischer Unterlag," by K. Hayashi, Julius Springer, Berlin, 1921.

[9] "Beams on Elastic Foundation," by M. Hetényi, University of Michigan Press, Ann Arbor, Mich., 1946.

By introducing a new variable,

$$\zeta = \frac{D - x}{D} = \frac{z}{D} \qquad (8)$$

there results

$$\frac{d^4y}{dx^4} = \frac{d^4y}{d\zeta^4}\left(\frac{d\zeta}{dx}\right)^4 = \frac{d^4y}{d\zeta^4}\frac{1}{D^4} \qquad (9)$$

and thus Eq. 7 takes the form,

$$\frac{d^4y}{d\zeta^4} + \alpha\,\zeta\,y = 0 \qquad (10)$$

in which

$$\alpha = \frac{C\,D^4}{E\,I} \qquad (11)$$

The term, α, is a dimensionless quantity which relates the stiffness of the soil (C) to the stiffness of the sheet-pile section ($E\,I/D^4$) and, consequently, it is designated the "flexibility coefficient" in this analysis.

The solution of Eq. 10 by means of the recursion formula gives y, in terms of four series, y_1, y_2, y_3, and y_4, as

$$y = c_1\,y_1 + c_2\,y_2 + c_3\,y_3 + c_4\,y_4 \qquad (12)$$

the component series involved in the general solutions are

$$y_1 = 1 - \frac{\alpha\,\zeta^5}{5!} + \frac{6\,\alpha^2}{10!}\zeta^{10} - \frac{6 \times 11\,\alpha^3}{15!}\zeta^{15} + \frac{6 \times 11 \times 16\,\alpha^4}{20!}\zeta^{20} - \cdots \qquad (13a)$$

$$y_2 = \zeta - \frac{2\,\alpha\,\zeta^6}{6!} + \frac{2 \times 7\,\alpha^2}{11!}\zeta^{11} - \frac{2 \times 7 \times 12\,\alpha^3}{16!}\zeta^{16} + \frac{2 \times 7 \times 12 \times 17\,\alpha^4}{21!}\zeta^{21} - \cdots \qquad (13b)$$

$$y_3 = \frac{\zeta^2}{2!} - \frac{3\,\alpha}{7!}\zeta^7 + \frac{3 \times 8\,\alpha^2}{12!}\zeta^{12} - \frac{3 \times 8 \times 13\,\alpha^3}{17!}\zeta^{17} + \frac{3 \times 8 \times 13 \times 18\,\alpha^4}{22!}\zeta^{22} - \cdots \qquad (13c)$$

and

$$y_4 = \frac{\zeta^3}{3!} - \frac{4\,\alpha}{8!}\zeta^8 + \frac{4 \times 9\,\alpha^2}{13!}\zeta^{13} - \frac{4 \times 9 \times 14\,\alpha^3}{18!}\zeta^{18} + \frac{4 \times 9 \times 14 \times 19\,\alpha^4}{23!}\zeta^{23} - \cdots \qquad (13d)$$

From the foregoing expressions for the deflection, the expressions for slope, moment, and shear at any point on the beam can be obtained by successive differentiations. That is,

$$\theta = \frac{dy}{dx} = \frac{dy}{d\zeta}\frac{d\zeta}{dx} = -\frac{1}{D}\frac{dy}{d\zeta} = -\frac{K_\theta}{D} \qquad (14a)$$

$$M = -E\,I\frac{d^2y}{dx^2} = -\frac{E\,I}{D^2}\frac{d^2y}{d\zeta^2} = -\frac{E\,I}{D^2}K_M \qquad (14b)$$

and

$$V = -EI\frac{d^3y}{dx^3} = \frac{EI}{D^3}\frac{d^3y}{d\zeta^3} = \frac{EI}{D^3}K_V \qquad (14c)$$

The boundary conditions at $\zeta = 0$ (dredge line) and at $\zeta = 1.0$ (bottom of pile) permit the evaluation of the constants in Eq. 12.

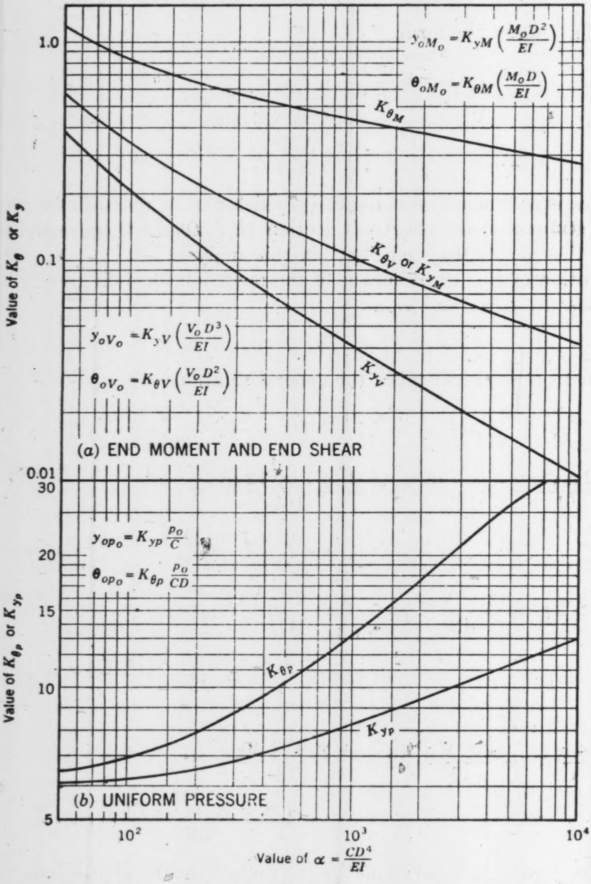

FIG. 2.—DEFLECTION AND SLOPE COEFFICIENTS AT THE DREDGE LINE

In Eq. 14 the various derivatives of y with respect to the dimensionless quantity, ζ, are represented as coefficients, K_θ, K_M, and K_V. These expressions for K have been evaluated for the range of ζ from 0 to 1.0 and for a range of α from 50 to 10,000 for end moment only and for end shear only (Figs. 2(a), 3, and 4).

Uniform Load Only.—When a uniformly distributed load is carried by a beam resting on the type of elastic foundation as described in the foregoing, Eq. 7 becomes

$$E\,I\,\frac{d^4y}{dx^4} + \frac{C\,(D - x)}{D}\,y = p_o \ldots\ldots\ldots\ldots\ldots\ldots (15)$$

By introducing the variable defined in Eq. 8 and rearranging, Eq. 15 becomes

$$\frac{d^4y}{d\zeta^4} + \alpha\,\zeta\,y = \frac{D^4}{E\,I}\,p_o = \frac{\alpha\,p_o}{C} = \text{constant} \ldots\ldots\ldots\ldots (16)$$

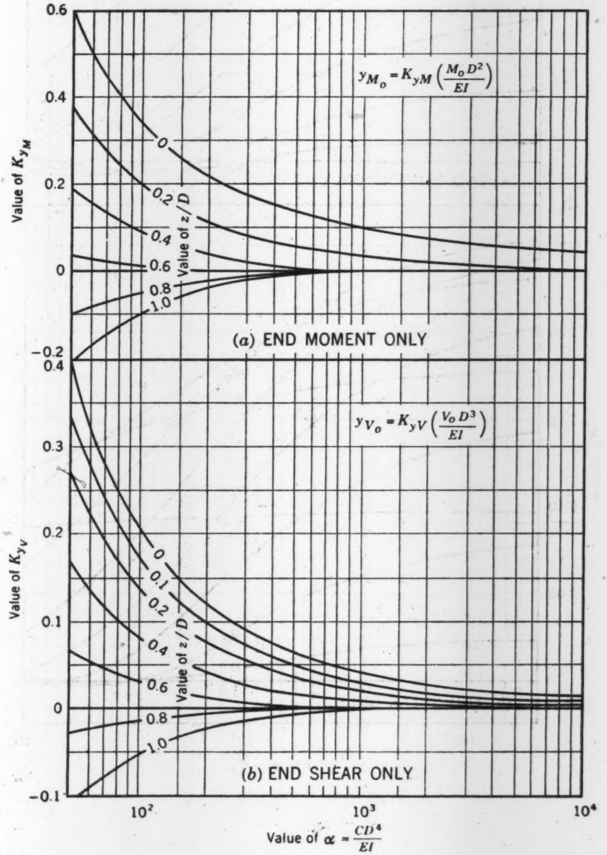

FIG. 3.—DEFLECTION COEFFICIENTS

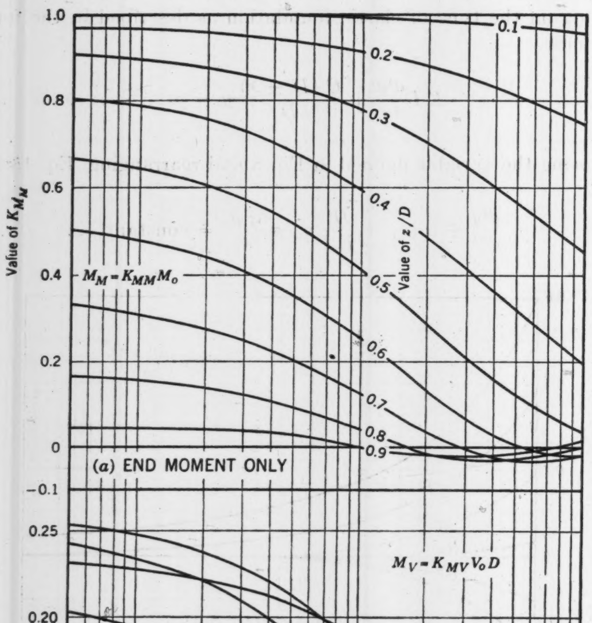

FIG. 4.—MOMENT COEFFICIENTS

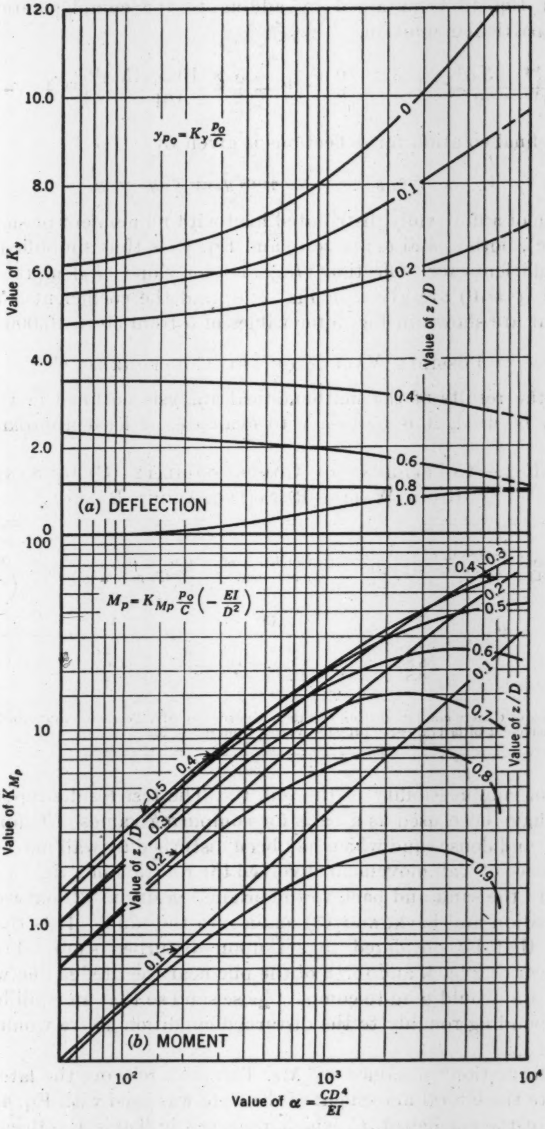

FIG. 5.—COEFFICIENTS FOR UNIFORM PRESSURE ONLY

Solution of Eq. 16 is obtained by adding to the complementary function (Eq. 12) a particular solution,

$$y_p = \frac{p_o}{C}\left(\frac{\alpha \zeta^4}{4!} - \frac{5\,\alpha^2}{9!}\zeta^9 + \frac{5 \times 10\,\alpha^3}{14!}\zeta^{14} - \frac{5 \times 10 \times 15\,\alpha^4}{19!}\zeta^{19} + - \cdots\right) \ldots (17)$$

so that the final solution for deflections is given by

$$y = c_1\,y_1 + c_2\,y_2 + c_3\,y_3 + c_4\,y_4 + y_p \ldots\ldots\ldots\ldots (18)$$

For the case of a uniformly distributed load with no moment or shear at $\zeta = 0$ (dredge line), both c_3 and c_4 are zero, and Eq. 18 is thus simplified.

The coefficients for deflection (K_y) and for slope (K_θ) of the pile at the dredge line ($\zeta = 0$) are given in Fig. 2(*b*), and the coefficients for deflection and moment are shown in Fig. 5 for values of α from 50 to 10,000.

POSSIBLE VALUES OF THE COEFFICIENT, *C*

Before the results of the mathematical analysis outlined in the foregoing section can be used, it is necessary to evaluate, at least approximately, the coefficient of compressibility of the soil, *C*. The test results reported by Mr. Terzaghi[10] have been used as a basis for computing values of *C* for loose sand, dense sand, and dense sand which had been disturbed by wall movement. The latter sequence of wall movement involved the rotation of a rigid wall about its base (1) into the sand and back to the original position, (2) outward from the original position and back, and (3) again into the sand. It is this third wall movement that is considered to act upon disturbed sand. For sheet-pile walls, the working back and forth of the pile near the dredge line would loosen dense sand and would tend to compact loose sand so that an equilibrium condition corresponding roughly to the disturbed condition above would eventually be reached.

TABLE 1.—COEFFICIENT OF COMPRESSIBILITY (*C*) OF SANDS FOR RIGID WALLS, ROTATING ABOUT BASE

Density of sand (lb per cu ft) (1)	Height of wall (D'), in contact with the sand (in.) (2)	Condition of the sand (3)	C (lb per cu in.)[a] (4)	C_{10} (lb per cu in.) $\left(C_{10} = \frac{120}{D'}C\right)$ (5)
90.1	62.4	Loose	12	23
100.0	58.8	Compacted	216	441
100.0	58.8	Disturbed	42	86

[a] The values of *C* were computed from test data reported by Mr. Terzaghi (footnote 10) for which the value of the coefficient of lateral earth pressure varied from 0.2 to 2.2.

Test information[10] obtained by Mr. Terzaghi, relating the lateral pressure coefficient to the lateral movement of the wall, was used with Eq. 4 to compute the values of the coefficient, *C*, which are given in Table 1. Because the embedded length of a sheet pile bends as well as rotates about some point near the tip, the distribution of passive pressures along this length is different from that along a rigid wall of comparable height. Consequently, it is assumed that for a preliminary analysis of a specific problem it will be satisfactory to determine the coefficient of subgrade reaction at the bottom of a given pile from the expression,

---

[10] "Large Retaining Wall Tests, I, Pressure of Dry Sands," by Karl Terzaghi, *Engineering News-Record*, Vol. 112, 1934, pp. 136–140.

$$C_n = \frac{D}{D'} C \qquad (19)$$

in which D' and C are given in Table 1, Cols. 2 and 4, respectively, and D is the embedded length of the particular pile. The subscript, n (corresponding to the number in feet), is used to denote the depth associated with a particular value of C.

GENERAL PROCEDURE FOR ANALYSIS

In order to use the coefficients given in Figs. 2, 3, 4, and 5, it is first necessary to determine the values of moment, shear, and overburden pressure which act at the dredge line. For cantilever piles, this is relatively easy as both moment and shear can be determined directly by statics. For anchored sheet-pile walls, however, the problem is statically indeterminate so that one or more of the boundary conditions must be incorporated into the problem. For a bulkhead with a single anchor point, it is convenient to consider the deflection of the anchor point to be zero as indicated by

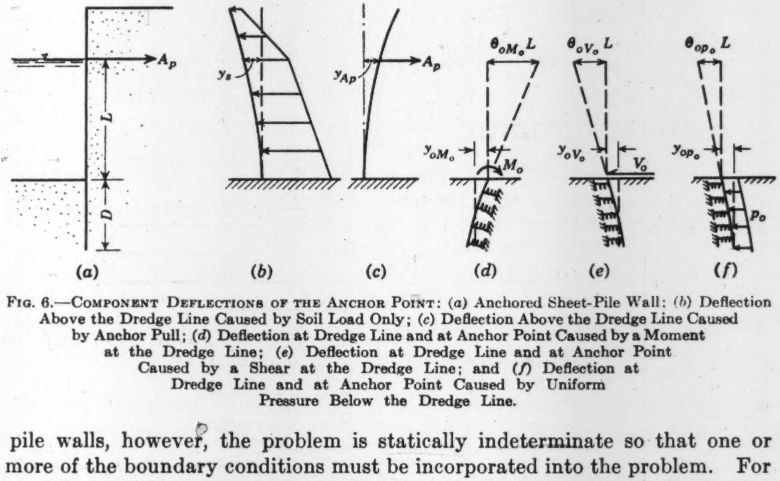

FIG. 6.—COMPONENT DEFLECTIONS OF THE ANCHOR POINT: (*a*) Anchored Sheet-Pile Wall; (*b*) Deflection Above the Dredge Line Caused by Soil Load Only; (*c*) Deflection Above the Dredge Line Caused by Anchor Pull; (*d*) Deflection at Dredge Line and at Anchor Point Caused by a Moment at the Dredge Line; (*e*) Deflection at Dredge Line and at Anchor Point Caused by a Shear at the Dredge Line; and (*f*) Deflection at Dredge Line and at Anchor Point Caused by Uniform Pressure Below the Dredge Line.

$$y_{anchor} = y_s - y_{A_p} + y_{oM_o} + y_{oV_o} + y_{op_o} + L\,(\theta_{oM_o} + \theta_{oV_o} + \theta_{op_o}) = 0 \qquad (20)$$

The subscript, o, in Eq. 20 designates the deflection at the dredge line due to moment, shear, or pressure.

These component deflections are shown in Fig. 6. In Fig. 6(*b*) the wall is considered to be a cantilever above the dredge line and to be loaded by the active pressure of the soil. The deflection at the anchor point produced by these soil loads is designated by y_s and is readily computed. The writer has found the procedure developed by Nathan M. Newmark,[11] M. ASCE, to be particularly useful for this type of computation as the shear, moment, and deflections are all obtained directly. Also, the computation of deflection is not complicated by an irregular load distribution or by a variation in moment of inertia of this part of the pile as would occur for a pile section reinforced by cover plates. Because the value of the anchor pull is unknown, the moment

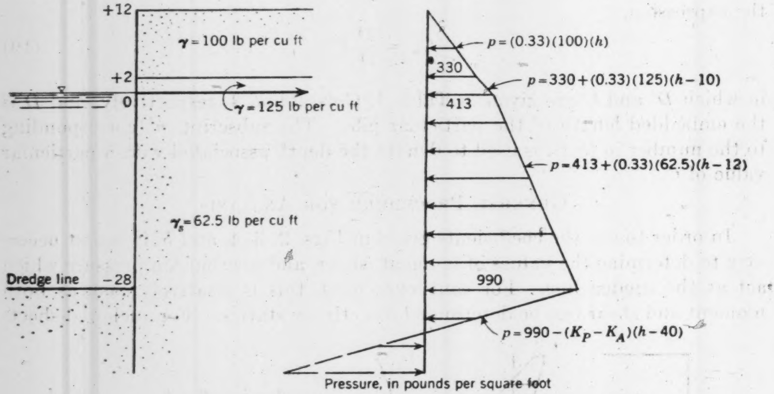
+12
γ = 100 lb per cu ft
+2
0
γ = 125 lb per cu ft
γs = 62.5 lb per cu ft
Dredge line
−28
p = (0.33)(100)(h)
330
p = 330 + (0.33)(125)(h − 10)
413
p = 413 + (0.33)(62.5)(h − 12)
990
p = 990 − (KP − KA)(h − 40)
Pressure, in pounds per square foot

(a) EXAMPLE A–SAND BACKFILL, $\phi = 30°$, NO SURCHARGE

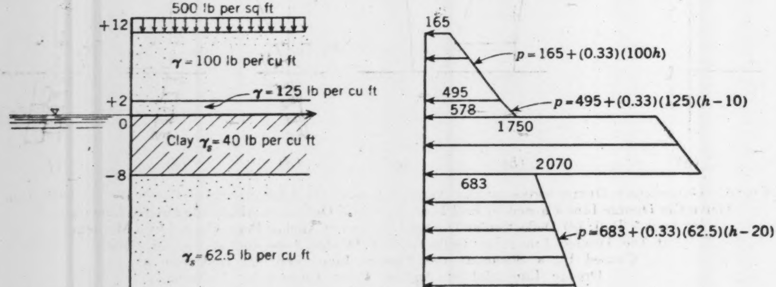
500 lb per sq ft
+12
γ = 100 lb per cu ft
γ = 125 lb per cu ft
+2
0
Clay γs = 40 lb per cu ft
−8
γs = 62.5 lb per cu ft
Dredge line
−28
165
p = 165 + (0.33)(100h)
495
578
p = 495 + (0.33)(125)(h − 10)
1750
2070
683
p = 683 + (0.33)(62.5)(h − 20)
1096
p = 1096 − (KP − KA)(γs)(h − 40)
Pressure, in pounds per square foot

(b) EXAMPLE B–SAND BACKFILL OVER CLAY LAYER, 500 LB PER SQ FT SURCHARGE

FIG. 7.—EXAMPLES OF ANCHORED SHEET-PILE WALLS

and shear at the dredge line may be written as

---

[11] "Numerical Procedure for Computing Deflections, Moments, and Buckling Loads," by N. M. Newmark, *Transactions*, ASCE, Vol. 108, 1943, pp. 1161–1188.

$$M_o = M_s - A_p\, L \qquad (21a)$$

and

$$V_o = V_s - A_p \qquad (21b)$$

in which M_s and V_s are the moment and shear, respectively, at the dredge line produced by the soil load above the dredge line.

Eq. 20 now contains two unknown quantities, α and A_p. Because α is a flexibility coefficient composed of the soil compressibility, C, the depth of embedment, D, and the E and I of the pile section, various arrangements of these quantities can yield the same value of α.

Two examples of anchored bulkheads were chosen to illustrate the use of the procedure. The dimensions and loading conditions of each are shown in Fig. 7. Example A represents a bulkhead driven into clean, cohesionless sand and backfilled with the same material. Example B is similar to Example A except that in Example B an 8-ft layer of soft clay is situated just below the anchor level and a 500-lb-per-sq-ft surcharge acts on the surface of the backfill. Example B represents an extreme case which would probably not occur in practice because the clay would be removed, at least in the vicinity of the bulkhead, and a sand dike would be used to reduce the lateral pressure on the bulkhead.

The maximum moment, indicated by the equivalent-beam procedure[12] was 92,000 ft-lb per ft for Example A and 118,000 ft-lb per ft for Example B. Using an allowable stress of 23,000 lb per sq in., the section moduli required are 48.0 cu in. per ft and 61.5 cu in. per ft, respectively. Thus, section MZ-38 (46.8 cu in. per ft) can be used for Example A, and MZ-38, reinforced with cover plates, $4\frac{3}{4}$ in. by $\frac{3}{8}$ in. (60.4 cu in. per ft), will be satisfactory for Example B. The reinforcement for Example B would not be carried below the dredge line so that the value of $E\,I$ for the embedded part of the pile will be the same for both examples.

Because C_n depends on the required length embedment, its value can be obtained by multiplying the value of C in Table 1 by the ratio D/D'. For the examples chosen, the sand was assumed to be in the disturbed condition.

Three embedment depths, 0.4 H (16 ft), 0.55 H (22 ft), and 0.70 H (28 ft), were used for the bulkheads of Examples A and B to give end restraints covering the range from free to fixed. Table 2 indicates the procedure for computing the anchor pull, and the moment and shear which act on the pile at the dredge line. Values of the deflection and slope coefficients at the dredge line are determined from Fig. 2 for each type of loading and for each particular value of the flexibility coefficient, α. The component deflections are then obtained by multiplying these coefficients by the structural constants and the values of the applied loads. Since these loads are given, as indicated in Eqs. 21, the final expression (Eq. 20) for the deflection at the anchor point involves only one unknown, A_p, which can then be evaluated directly. Once the value of the anchor pull is obtained, the moment and shear at the dredge line can be determined from Eq. 21. Then, by use of this shear and moment, and the uniform pressure acting along the embedded depth, D, the deflection curve for each case can be computed by use of the coefficients of Figs. 3 and 5(a), and, finally, the reaction pressures can be computed from Eq. 4. Figs. 8(a) and 8(b) show the variation in deflection and pressure which result from the three depths of embedment for Example A. In each case the value of C_n was determined by the relationship, 42 D/58.8, which denotes the same compressibility coefficient of the sand at each elevation for all three cases.

---

[12] "Theoretical Soil Mechanics," by K. Terzaghi, John Wiley & Sons, Inc., New York, N. Y., 1943, p. 225.

TABLE 2.—DETERMINATION OF SHEAR AND MOMENT AT THE DREDGE LINE (EXAMPLE A: $C = 86\ D/120$)

				Notes
Embedment depth, D (in.)	192	264	336	
(ft)	16	22	28	
$E\ I$ (lb-in.^{2} per in.)	6.880×10^8	6.880×10^8	6.880×10^8	
$D/E\ I$ (in.^{2} per lb-in.^{2})	$\frac{2.7910}{10^7}$	$\frac{3.8374}{10^7}$	$\frac{4.8840}{10^7}$	
$D^2/E\ I$ (in. per lb)	$\frac{5.3585}{10^5}$	$\frac{1.0131}{10^4}$	$\frac{1.6410}{10^4}$	
$D^3/E\ I$ (in.^{2} per lb)	$\frac{1.0228}{10^2}$	$\frac{2.6745}{10^2}$	$\frac{5.5138}{10^2}$	
$D^4/E\ I$ (in.^{3} per lb)	1.9754	7.0607	18.526	
C (lb per in.^{3})	140	190	240	
α	275	1,330	4,450	
K_{yM}	0.187	0.090	0.056	From Fig. 2(a)
K_{yV}	0.092	0.032	0.0157	From Fig. 2(a)
K_{yp}	6.85	8.60	11.0	From Fig. 2(b)
$K_{\theta M}$	0.595	0.415	0.327	From Fig. 2(a)
$K_{\theta V}$	0.187	0.090	0.056	From Fig. 2(a)
$K_{\theta p}$	8.60	14.8	24.4	From Fig. 2(b)
p_o (lb per in.^{2})	6.875	6.875	6.875	
p_o/C (in.)	0.0498	0.0364	0.0285	
y_s (in.)	13.585	13.585	13.585	Fig. 6(b)
y_{A_p} (in.)	$-0.01838\ A_p$	$-0.01838\ A_p$	$-0.01838\ A_p$	Fig. 6(c)
y_{oM_o} (in.)	$3.1474 - 0.003367\ A_p$	$2.8639 - 0.003064\ A_p$	$2.8855 - 0.003088\ A_p$	$y_{oM_o} = K_{yM}\left(\frac{M_o D^2}{E\ I}\right)$
y_{oV_o} (in.)	$1.7385 - 0.000947\ A_p$	$1.5719 - 0.000856\ A_p$	$1.5900 - 0.000866\ A_p$	$y_{oV_o} = K_{yV}\left(\frac{V_o D^3}{E\ I}\right)$
y_{op_o} (in.)	0.3413	0.3129	0.3138	$y_{op_o} = K_{yp}\frac{p_o}{C}$
$\theta_{oM_o} L$ (in.)	$17.5254 - 0.01875\ A_p$	$16.8071 - 0.01798\ A_p$	$16.8551 - 0.01803\ A_p$	$\theta_{oM_o} L = K_{\theta_M}\left(\frac{M_o D}{E\ I}\right) L$
$\theta_{oV_o} L$ (in.)	$6.1839 - 0.00337\ A_p$	$5.6269 - 0.00306\ A_p$	$5.6712 - 0.00309\ A_p$	$\theta_{oV_o} L = K_{\theta V}\left(\frac{V_o D^2}{E\ I}\right) L$
$\theta_{op_o} L$ (in.)	0.7498	0.6853	0.6961	$\theta_{op_o} L = K_{\theta p}\frac{p_o}{C\ D} L$
Total deflection (in.)	$43.2713 - 0.044814\ A_p$	$41.4530 - 0.04334\ A_p$	$41.5967 - 0.04345\ A_p$	
A_p (lb per ft)	11,600	11,500	11,500	
M_o (ft-lb per ft)	−10,700	−7,900	−7,900	
V_o (lb per ft)	10,450	10,560	10,560	

A further comparison was made by considering only the 28-ft depth of embedment, but by using C_{28} values of 15 lb per cu in., 72 lb per cu in., and 240 lb per cu in. The latter value corresponds to the disturbed condition and the smaller values are for loose sands. These particular values of C_{28} were chosen

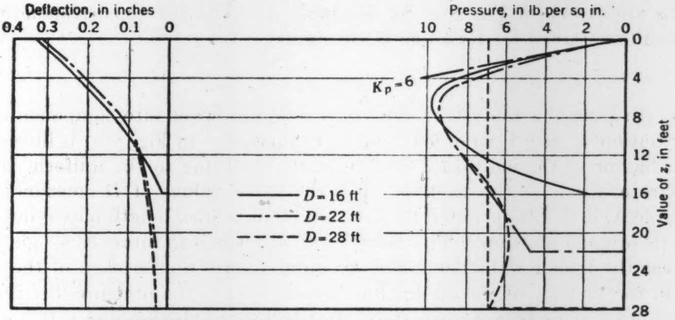

(a) DEFLECTIONS AND PRESSURES DUE TO UNIFORM LOAD

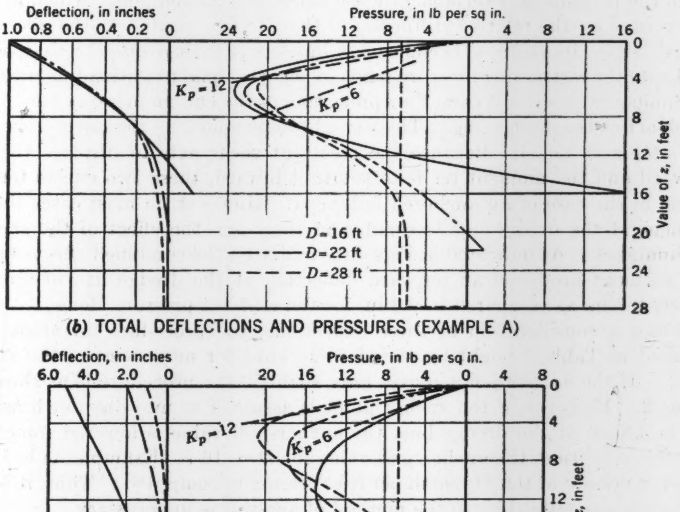

(b) TOTAL DEFLECTIONS AND PRESSURES (EXAMPLE A)

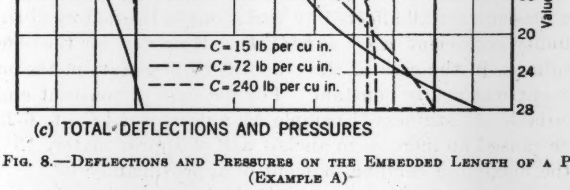

(c) TOTAL DEFLECTIONS AND PRESSURES

FIG. 8.—DEFLECTIONS AND PRESSURES ON THE EMBEDDED LENGTH OF A PILE (EXAMPLE A)

so as to give the same three values of α (275, 1,330, and 4,450) that were produced by the three different depths of embedment for $C_{28} = 240$ lb per cu in. The procedure for determining the anchor pull and bending moment is similar to that outlined in Table 2. The deflections and pressures for this set of conditions are shown in Fig. 8(*c*) for Example A. The curves corresponding to the results obtained for Example B are similar.

RESULTS

By dividing the analysis of sheet-pile retaining walls into components, the contribution of each type of load can be evaluated. In Fig. 8(*a*) is illustrated the behavior of the embedded section of the wall due to the uniform lateral pressure exerted by the backfill. For the three values of D considered for Example A, it should be noted that the entire embedded length moves outward from its original position. The shorter wall also tends to rotate as a rigid body whereas the longer walls bend so as to approximate the position of the short wall in the vicinity of the dredge line; consequently, the pressure-distribution curves are similar to approximately 14 ft below the dredge line. Below this depth the pressure is determined by the deflection at each point, which in turn is governed by the relative stiffnesses of the pile and sand. As the pile penetrates deeper, its stiffness becomes less important with respect to that of the sand, and the restraining pressure tends to become equal to the loading pressure.

Similar curves result from the application of the end moment and end shear which act at the dredge line. These can be determined by the use of Figs. 3(*a*) and 3(*b*) and Eq. 4. Because the resultant shear acts to displace the pile outward and the moment tends to rotate it inward, these two effects tend to cancel in the case of an anchored bulkhead. However, in most cases the net moment at the dredge line is small, and therefore, the effect of the shear is predominant. As indicated in Figs. 8(*a*) and 8(*b*), the combined effect of shear and moment produced an outward deflection at the dredge line of approximately 0.7 in. as compared to 0.3 in. for the uniform pressure alone.

From a consideration of these deflections, the procedure for analysis as outlined in Table 2 might be varied to account for movement of the anchor point. If the anchor point moves only slightly, the procedure is as shown in Table 2. However, if the anchor point is assumed to move as much as does the bulkhead at the dredge line, the anchor-pull value is lowered somewhat. For this condition, the anchor-pull value for $D = 16$ ft (Example A) is 11,300 lb per ft instead of the 11,600 lb per ft as originally computed. Thus, it is seen that such a modification in the method of analysis is unnecessary.

The design criteria of anchor pull, maximum bending moment, and maximum passive pressure are all affected by variations in the factors of the dimensionless flexibility coefficient, $\alpha \; (= C\,D^4/E\,I)$. However, for the condition of equal soil stiffness, in the case of three depths of penetration, the maximum bending moment was nearly constant. For the case of constant embedment depth and variable soil stiffness (Example A), a decrease of C_{28} to 6.25% of its original value caused an increase in anchor pull of approximately 15% and an increase in the maximum bending moment of approximately 40%. Values of anchor pull, maximum moment, depth of embedment, and maximum value of the coefficient of passive earth pressure are given in Table 3, as computed by the writer's method of analysis and by the conventional procedures.

The conventional procedures used for the analysis of the bulkheads were (1) the free-earth-support method, (2) the equivalent-beam method, and (3) the elastic-line method. In each method, values of 3.0 and 6.0 were used as the coefficient of passive earth pressure.

The values of anchor pull and bending moment computed by the subgrade theory were found to be approximately 10% and 20% lower, respectively, than those computed by the elastic-line method using $K_p = 6$. These reductions indicate the amount by which the flexibility of the pile affects the results in this particular case. However, these reductions of anchor pull and moment result from an elevation of the center of pressure of the passive pressure zone as indicated in Fig. 8. As this center of pressure moves upward, the pressure-distribution curve exhibits high pressure values near the dredge line. The dotted lines in Figs. 8(*a*), 8(*b*), and 8(*c*), which define the initial tangents of these curves, correspond to values of the coefficient of passive earth pressure. Computed values of K_p, ranging from 6 to 17, were obtained from analysis of the example problems, as indicated in Table 3 and Fig. 8.

TABLE 3.—COMPARISON OF ANALYTICAL RESULTS FOR THE BULKHEADS

Procedure		EXAMPLE A				EXAMPLE B			
		D (ft)	A_p (lb per ft)	M_{max} (ft lb per ft)	Max K_p	D (ft)	A_p (lb per ft)	M_{max} (ft lb per ft)	Max K_p
Sub-grade Theory	Disturbed sand	16	11,600	70,000	17	16	24,400	97,000	19
	Disturbed sand	22	11,500	69,000	17	22	24,300	96,000	19
	Disturbed sand	28	11,500	69,000	17	28	24,300	96,000	19
	$C = 15$ lb per cu in.	28	13,200	97,000	6	28	26,200	119,000	8
	$C = 72$ lb per cu in.	28	11,800	74,000	10	28	24,700	100,000	11
	$C = 240$ lb per cu in.	28	11,500	69,000	17	28	24,300	96,000	19
Free-earth support		17.3	15,450	140,000	3	18.1	29,600	182,000	3
		10.5	13,600	108,000	6	11.2	27,700	142,000	6
Equivalent-beam method		31.4	12,800	92,000	3	34.1	26,000	118,000	3
		17.8	12,700	90,000	6	19.4	25,900	117,000	6
Elastic-line method		29.4	14,200	116,000	3	34.0	28,500	165,000	3
		19.4	12,500	86,000	6	19.7	26,500	125,000	6

These high computed values of K_p are very likely unrealistic values because they exceed considerably the lower limiting values of K_p of 9.0 and 5.0 for dense and loose sands, respectively, which were suggested by Mr. Terzaghi.[2] However, in an actual situation, if the sand at the surface were overloaded, the necessary reaction would be developed at a slightly greater depth by an increase in pressure in this region. This, of course, results in a slight increase in both anchor pull and bending moment.

CONCLUSIONS

In the foregoing sections a method for analyzing sheet-pile installations has been devised which includes a numerical procedure for determining the shear, moment, and pressure at the dredge line, and uses the theory of subgrade reaction for the embedded pile length. This procedure permits computations of the anchor pull and the maximum bending moment in the pile which are comparable to those obtained by the conventional methods.

As illustrations of the procedure, two examples were studied. The computed values of the anchor pull and the maximum bending moment were slightly lower than those obtained from the conventional methods because of the high values of passive pressure developed near the dredge line. Because these high pressure values imply values of the coefficient of passive earth pressure which are unrealistic in some cases, caution is necessary in applying the analytical results obtained from this procedure.

Finally, the success of such a method of analysis depends on the reliability of the material constants involved. In this case it is the coefficient of compressibility, C, of the sand which is the critical quantity, although variations in C by a factor of three or four had little effect on the results of the examples studied. Several values of C have been estimated from the results of a few tests in which the passive resistance of sands was reported. In anticipation of more test results becoming available in the future, particularly those for full-size, sheet-pile walls, curves have been prepared for the deflection and moment coefficients caused by end shear or moment, or uniform pressure on the embedded pile length. Thus, values of C can be derived from bending-moment curves or deflection curves from such tests.

ACKNOWLEDGMENT

This study was sponsored by the Engineering and Industrial Experiment Station and the Department of Civil Engineering of the University of Florida, at Gainesville.

APPENDIX. NOTATION

The following symbols, adopted for use in this paper and for the guidance of discussers, conform essentially with the ASCE *Manual of Engineering Practice No. 22*, "Soil Mechanics Nomenclature," prepared by a committee of the Soil Mechanics and Foundations Division of ASCE, and were approved by the Society in 1941:

A_p = anchor pull;
b = constant;
C = coefficient of soil compressibility at the bottom of a pile:
  C_n = coefficient of soil compressibility at the bottom of a pile n ft long;
c_i = constants;
D = depth of sheet-pile penetration;
E = modulus of elasticity;
H = height of sheet pile above the dredge line;
H' = total length of sheet pile;
I = moment of inertia per unit width of the cross section of a sheet pile;
K_A = coefficient of active earth pressure:
  K_{MM}, K_{MV}, K_{Mp} = moment coefficients for the embedded part of the pile for the conditions of end moment only, end shear only, and uniform pressure, respectively;

K_o = pressure coefficient of earth at rest;

K_p = coefficient of passive earth pressure;

K_{yM}, K_{yV}, K_{yp} = deflection coefficients for the embedded part of the pile for the conditions of end moment only, end shear only, and uniform pressure, respectively;

$K_{\theta_M}, K_{\theta_V}, K_{\theta_p}$ = slope coefficients for the embedded part of the pile for the conditions of end moment only, end shear only, and uniform pressure, respectively;

k_A = constant;

k_h = coefficient of horizontal subgrade reaction at any depth;

k_x = elastic foundation reaction at a point, x;

L = distance between the dredge line and anchor point;

M = bending moment in the sheet pile at any location:

M_{M_o} = bending moment in the embedded length of sheet pile caused by M_o;

M_{V_o} = bending moment in the embedded length of sheet pile caused by V_o;

M_o = bending moment in the sheet pile at the dredge line ($M_o = M_s - A_p L$);

M_p = bending moment in the embedded length of sheet pile caused by the uniform pressure, p_o;

M_s = bending moment in the sheet pile at the dredge line, considering the pile fixed at the dredge line and supporting the soil loads as a cantilever beam;

m_h = rate of increase of k_h with depth;

p = horizontal pressure on the sheet pile:

p_h = horizontal reaction pressure due to passive earth resistance;

p_o = horizontal pressure on the sheet pile at the dredge line;

V = shear in the sheet pile at any location:

V_o = shear on the sheet pile at the dredge line ($V_o = V_s - A_p$);

V_s = shear on the sheet pile at the dredge line due to the soil loads only;

x = distance from the tip of the pile;

y = horizontal movement or deflection of the pile at any elevation:

y_{Ap} = deflection at the anchor point caused by the anchor pull acting on the pile which is considered to be a cantilever above the dredge line;

$y_{M_o}, y_{V_o}, y_{p_o}$ = deflection of the pile at any elevation caused by the moment or shear at the dredge line, or the uniform pressure;

y_i = component series;

y_p = component series for deflection due to p_o only;

y_s = deflection at the anchor point caused by the soil loads acting on the pile which is considered to be a cantilever above the dredge line;

z = distance below the dredge line;

α = flexibility coefficient $\left(\alpha = \frac{C D^4}{E I}\right)$;

β = ratio of the distance from the top of the pile to the anchor point to the total pile length;

γ = density of the sand;

θ = slope:

$\theta_{oM}, \theta_{oV}, \theta_{op}$ = slope at the dredge line of the embedded part of the pile loaded by M_o, V_o, or p_o, respectively;

ρ = Mr. Rowe's wall flexibility number $\left(\rho = \frac{(H')^4}{E I} \frac{\text{ft}^4}{\text{lb-in.}^2} \text{ per foot}\right)$; and

ζ = ratio of the distance below the dredge line to the total embedment depth $\left(\zeta = \frac{z}{D}\right)$.

DISCUSSION

PETER W. ROWE[13].—An interesting attempt has been made by Mr. Richart to develop an analytical design procedure for sheet-pile walls which takes into account the relative flexibility of the pile and the soil. His main additional objects have been (1) to provide for varying strata above the dredge level and (2) to present the design data in a form in which it can be used by a practicing civil engineer. The first objective was based on the belief that the writer's experimental tests[3] were made with sand at the same density above and below the dredge level. However, Figs. 16(*a*) and 16(*b*) of the report[3] show that tests were made with dense sand below the dredge level and loose sand above. In the "Correspondence"[14] following the report of those tests, further results were given for the case of water pressure above loose sand and dense sand. Both of these tests and mathematical analyses[15] of the problem show that it is only the stiffness of the subsoil below the dredge level that reduces the moment below that for an infinitely stiff wall. This latter value is computed by the free-earth-support analysis which takes into account, among others, the varying strata and differential water pressures. Thus, in Figs. 21 of the report[3] the ordinates of the operating curves vary from 17 to 4 for very poor to very good site conditions.

Mr. Richart then states in the "Introduction" that "* * * considerable judgment is required to extrapolate this test information for use in actual pile design." Considerable judgment is of course always necessary in civil engineering, but the writer would be grateful if Mr. Richart could explain this statement further.

The second objective has not been reached. First, the design has to proceed indirectly by trial and error. A section must be chosen and the stress checked. To choose the section in the first instance, the "equivalent beam" procedure is used. This means that two sets of computations are required. In addition, the process of checking involves extrapolation from eight curves and many tabulations.

In January, 1955, the writer published a theoretical and experimental study of sheet-pile walls, pinned[15] and encastré[16] at the anchorage, and Mr. Richart's basic differential equation is identical with the one which was developed from stress-strain considerations of sand. However, the analysis of 135 theoretical structures was completed, and the maximum bending moments were expressed as a ratio of the corresponding values for an infinitely stiff wall subject to the same strata conditions. As a result the writer found that, in agreement with previous experimental work,[3] the moment reduction depended mainly on the relative stiffness of pile and subsoil and, to a lesser degree, on the penetration depth. The amount of surcharge, position of tie rod, or varying densities above the dredge level had no influence on the percentage reduction. Consequently, previously published data were extended to the whole range of compressible cohesionless subsoils, whereas the simplicity of using a single reduction curve on the free-earth-support value for direct design was retained.

---

[13] Senior Lecturer, Eng. Dept., Univ. of Manchester, Manchester, England.

[14] Correspondence on "Anchored Sheet Pile Walls," by P. W. Rowe, *Proceedings*, Inst. C. E., London, Pt. I, September, 1952.

[15] "A Theoretical and Experimental Analysis of Sheet-Pile Walls," by P. W. Rowe, *ibid.*, January, 1955, p. 32.

[16] "Sheet Pile Walls Encastré at the Anchorage," by P. W. Rowe, *ibid.*, Pt. I, Vol. 4, January, 1955, p. 70.

Whereas the writer agrees with the form of Eq. 4 he cannot follow the reasons for the derivation of Eq. 3 and Eq. 19.

The coefficient, *C*, is identical with *m* in the writer's papers. The value of *m* decreases with soil strain. Consequently, the value of *m* increases from a low value at the dredge level to a maximum at the pile toe for a flexible piling. Analyses such as those of Mr. Richart and the writer assume that *m* is constant, and because very large variations in *m* are necessary to cause a significant variation in pile fixity, this procedure is admissible. However, it is not clear why it is satisfactory to use the value of C_n (Eq. 19) at the bottom of the pile.

The penetration depths of piling commonly range from 6 ft to 18 ft so that the mean overburden pressures at one-half the penetration depth in submerged sand on the passive side range from 200 lb per sq ft to 600 lb per sq ft. At these values the stress-strain curves for sand are steeper than at the pressures quoted. In addition, the important stiffness of the subsoil is close to the dredge level where the confining pressures are very small.

TABLE 4

Condition of the sand	log C	log C_{10}	log m
Loose	4.32	4.60	4.75
Disturbed	4.86	5.17	...
Dense	5.57	5.88	6.10

For these reasons the value of *C* may be higher than those given. In Table 4, the values of *C* from Table 1 are compared with the *m*-values previously published. For this purpose the units of *C* have been changed to pounds per cubic foot, and the logarithms are given.

Reasonable agreement is reached between log *m* and log C_{10}. However, it appears that C_{10} increases with an increase in the scale whereas *m* tends to decrease with an increase in the scale, as would be expected from the decrease in the slope of the ϕ-strain curve for sands with confining pressure.

The writer has designated *m* as the soil stiffness modulus. Because *m* or *C* increase in value with an increase in stiffness, the value of *C* does represent stiffness rather than compressibility. In addition, the word, coefficient, indicates a dimensionless number, and the term can be confused with the coefficient of compressibility used by Mr. Terzaghi in confined compression tests. Therefore, it is suggested that the term, soil stiffness modulus, is preferable.

F. E. Richart, Jr.,[17] A.M. ASCE.—The writer appreciates Mr. Rowe's comments and criticisms and is aware of the extensive studies he has made on the behavior of sheet piles. However, his excellent papers[15,16,18] appeared in print during the time interval between the submission of the paper (May, 1954) and its publication as ASCE *Proceedings-Separate No. 694* (May, 1955). Consequently, the writer did not have the benefit of Mr. Rowe's investigations prior to the time the paper was accepted.

Mr. Rowe's tests[3] on models of anchored, sheet-pile walls were made with sand of uniform density below the dredge line and with sand of uniform density (not necessarily the same as that below the dredge line) or water pressure above the dredge line. Unfortunately, the writer's statement did not make this completely clear, but it was intended to point out that in Mr. Rowe's tests the material above the dredge line was of uniform density. His mathematical analysis of the problem[14] also tied-in the loading above the dredge line to the analytical solution for the structural behavior of the wall.

By comparing the maximum bending moment and the tie-rod loads obtained from the mathematical analysis with those obtained from the free-earth-support procedure, Mr. Rowe was able to establish curves for use in design. These curves show the reductions below the free-earth-support values for maximum moment and tie-rod load which are associated with the soil stiffness modulus and the significant dimensions of the wall installation. Thus, his procedure is established as a correction to the values obtained by the free-earth-support, and by this consideration he provides for a layered backfill consisting of several different materials. However, as he has indicated, for conditions in which the sand is stiff with respect to the pile, Mr. Rowe's procedure for the moment reduction would tend toward low values, which would require that the design procedure include a check on the distribution of soil pressures to determine whether or not they conform to reality.

The procedure described in the original paper is based on a mathematical analysis which considers separately the load and structural behavior of the wall above the dredge line from that below the dredge line. By use of a numerical solution, the load and moment acting on the wall are determined in a continuous manner from the top of the wall to the dredge line. Table 5 illustrates this procedure as it applies to Example B (Fig. 7). Thus, the load, V_s, and the bending moment, M_s, due to the soil above the dredge line are obtained from Table 5 by evaluating the shear and moment at the dredge line as

$$V_s = 56{,}190\ (h/6) = 37{,}460 \text{ lb per ft} = 3{,}122 \text{ lb per in.}$$

and

$$M_s = 252{,}570\ (h^2/6) = 673{,}500 \text{ ft-lb per ft.}$$

The deflections of the anchor point when considering the pile as a cantilever above the dredge line are

$$y_s = \frac{114{,}220\ h^2\ 1{,}000}{12\ E\ I} = 30.33 \text{ in.}$$

---

[17] Prof. of Civ. Eng., Univ. of Florida, Gainesville, Fla.

[18] "A Stress-Strain Theory for Cohesionless Soil With Applications to Earth Pressure at Rest and Moving Walls," by P. W. Rowe, *Geotechnique*, Vol. 4, No. 2, June, 1954, p. 70.

due to the soil loads and

$$y_{A_p} = \frac{A_p L^3}{3 E I} = 0.01749 A_p \text{ in.}$$

due to the anchor pull. These values are used in the computation by the free-earth-support method and in Table 2.

By continuing the computations to a depth of 0.1 H below the dredge line, the moment and shear values lead directly to an analysis by the equivalent-beam method, whereas a continuation of the computations to a greater depth provides the basis for an analysis by the elastic-line method. When the computations are extended below the dredge line, it is necessary to include the passive pressure in computing the load on the wall at any depth. Thus, by arranging the computations in the form indicated in Table 5, one sheet-pile installation may be analyzed by several of the conventional procedures with only a small amount of work beyond that needed to determine the load due to the backfill and surcharge.

The symbol, C, was chosen to represent the value of the coefficient of subgrade reaction at the depth, D, to which the pile extends below the dredge line. This is a convenient point at which to identify the mechanical behavior of the soil close to a sheet-pile installation. It was not the intent of the paper to include rules or procedures for establishing numerical values for the soil stiffness quantities, but rather to investigate analytically the importance of variations in this parameter on the structural behavior of a sheet-pile wall.

In the "Conclusions" it was emphasized that, as more reliable values of the soil properties became available, they should be adopted. Mr. Terzaghi[19] has recently contributed an outstanding study of the coefficients of subgrade reaction and has established numerical values which may be used for design. He has designated l_h (tons per cubic feet) as the constant of horizontal subgrade reaction for sheet piles with free-earth support, depth of sheet-pile penetration D (value for $z/D = 1$). The term, l_h, may be substituted directly for m (soil stiffness modulus) in Mr. Rowe's analysis or for the C (coefficient of compressibility) in the paper. The writer agrees that the terminology used to define C could be confusing and that either of the other two terms is preferable.

The use of the procedure described by Eq. 19 implies that the soil behavior is not significantly affected by the movement of the wall. This is approximately true only if the soil is stiff with respect to the pile. In such cases, the degree of fixity at the dredge line (which permits the moment reduction) depends to a lesser degree on the depth of penetration than on the relative stiffnesses of pile and subsoil, as was noted by Mr. Rowe.

If the pile has a small depth of penetration and has a flexural rigidity which is great with respect to the stiffness of the subsoil, the depth of penetration has an important effect on the subsoil stiffness. For this case, the value of the constant, l_h, is equal to the soil stiffness at the tip of the pile. Thus, at a given depth below the dredge level the resistance offered by the soil, as a result of a unit horizontal displacement, varies inversely as the total depth of pile pene-

---

[19] "Evaluation of Coefficients of Subgrade Reaction," by K. Tergazhi, *ibid.*, Vol. V, No. 4, December, 1955, pp. 297–326.

TABLE 5.—NUMERICAL COMPUTATION FOR MOMENT, SHEAR, AND DEFLECTION

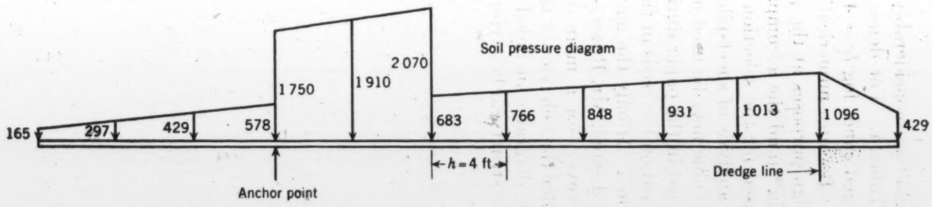

																									Common terms
Elevation (ft)	+12		+8		+4		0		−4		−8		−12		−16		−20		−24		−28		−32		
Pressure (lb per sq ft)	−165		−297		−429		−578 −1750		−1910		−2070 −683		−766		−848		−931		−1013		−1096		−429		
Equivalent concentrated force (lb per ft)	−627		−1782		−2591		−1585 −5410		−11,460		−6650 −2132		−4595		−5089		−5585		−6079		−3205 −2621		−1954		$\frac{h}{6}$
Shear (lb per ft)		−627		−2409		−5000		−11,995		−23,455		−31,637		−36,232		−41,321		−46,906		−52,985		(−56,190) −58.810		(−6076)	$\frac{h}{6}$
Moment (ft-lb per ft)	0		−627		−3036		−8036		−20,031		−43,486		−75,123		−111,355		−152,676		−199,582		−252,567		−311,377		$\frac{h^2}{6}$
Moment (in.-lb per in.)	0		−1.672		−8.096		−21.43		−53.42		−115.96		−200.33		−296.95		−407.14		−532.22		−673.51		−830.33		1,000
Angle change $\left(\frac{1}{\text{in.}}\right)$	0		1.672		8.096		21.43		53.42		115.96		200.33		296.95		407.14		532.22		673.51		830.33		$\frac{1,000}{E\,I}$
Concentrated angle change	0.768		24.82		104.06		275.02		671.59		1413.35		2416.21		3576.97		4900.57		6402.85		3750.4				$\frac{1,000\,h}{12\,E\,I}$
Slope		−23,536		−23,511		−23,407		−23,130		−22,460		−21,050		−18,630		−15,050		−10,150		−3750		(0)			$\frac{1,000\,h}{12\,E\,I}$
Deflection (in.)							114,220		91,090		68,630		47,580		28,950		13,900		3750		0				$\frac{1,000\,h^2}{12\,E\,I}$

tration. The use of this concept for conditions in which the pile is less than infinitely stiff with respect to the subsoil will lead to a conservative design; that is, computed bending moments will be larger than those which actually occur.

The numerical values of l_h given by Mr. Terzaghi[19] are considerably lower than the values of m indicated by Mr. Rowe in Table 4. For dense sands, $\log l_h = 4.60$ (dry or moist sand) and for submerged sand, $\log l_h = 4.41$ (as contrasted to $\log m = 6.10$ as shown in Table 4). Because numerical values for subsoil stiffnesses are being established for design purposes at the present time, it is suggested that the paper by Mr. Terzaghi[19] (and the accompanying discussions) as well as those of Mr. Rowe[15,18] be used for the selection of the appropriate soil stiffness modulus to be used in the analysis of sheet-pile walls.

After the soil constant has been established, its value may be used in place of the symbol, C, in the equations and curves included in the paper during the analysis of a sheet-pile installation which was designed on the basis of the free-earth-support method or the equivalent-beam method. If only the maximum bending moment in the wall and the tie-rod load are desired, Mr. Rowe's design curves would very likely involve less effort. However, for a more detailed analysis of a given installation, it is logical to consider the behavior of the wall above and below the dredge line separately. The diagrams included in the paper should be of appreciable value in studying the structural behavior of the embedded pile length.

AMERICAN SOCIETY OF CIVIL ENGINEERS
Founded November 5, 1852
TRANSACTIONS

Paper No. 2901

PLASTIC STRENGTH OF STEEL FRAMES

By Lynn S. Beedle,[1] A. M. ASCE

With Discussion by Messrs. Jack R. Benjamin; Zdeněk Sobotka; and Lynn S. Beedle

Synopsis

In order to demonstrate the applicability of plastic analysis to structural design in steel, the results of large-scale experiments are examined on the basis of theoretical predictions and correlated with current (1957) design specifications. The fundamentals of plastic analysis are described briefly. It is shown how the design of ordinary structural frames may be based on the maximum load the structure will support, as against the conventional methods which are based on the load at "first yield."

Although this paper does not purport to be a complete review of current investigations into the behavior of steel structures loaded beyond the elastic limit, sufficient evidence is presented to show that in many instances design may properly be based on maximum strength.

Introduction

Although the subject of design of steel frames on the basis of ultimate strength is not new, it is only in recent years (circa 1957) that sufficient tests of large-size structural members and frames have been performed and adequate analytical techniques developed to make the topic of practical use to engineers in the United States. Curiously enough, studies such as those under way at Lehigh University[2] (Bethlehem, Pa.) and at other institutions will enable the re-establishment of a technique that was accepted and used in Hungary in the 1920's in the design of apartment buildings[3]; therefore, historically, the topic is not new.

Note.—Published, essentially as printed here, in August, 1955, as *Proceedings Paper 764*. Positions and titles given are those in effect when the paper or discussion was approved for publication in *Transactions*.

[1] Chairman, Structural Metals Div., Fritz Eng. Lab., Civ. Eng. Dept., Lehigh Univ., Bethlehem, Pa.

[2] "An Evaluation of Plastic Analysis as Applied to Structural Design," by B. G. Johnston, C. H. Yang, and L. S. Beedle, *Welding Journal*, Vol. 32, 1953, p. 224-s.

[3] Discussion by N. J. Hoff of "An Evaluation of Plastic Analysis As Applied to Structural Design," by B. G. Johnston, C. H. Yang, and L. S. Beedle, *ibid.*, Vol. 33, 1954, p. 14-s.

Many investigators have contributed prominently to the application of plastic analysis in structural design. Foremost in stimulating progress in the period from 1942 has been J. F. Baker,[4] A. M. ASCE. Important contributions have also been made by J. W. Roderick,[4] M. R. Horne,[5] P. S. Symonds,[6] M. ASCE, and B. G. Neal.[6]

Purpose.—The purpose of this paper is to offer examples of structures (approaching full size) that have been tested beyond the elastic range and into the plastic range; to compare the maximum strength with the allowable load according to conventional elastic design; and to indicate how the reserve of strength beyond the elastic limit may be utilized in the design of ordinary structural frames.

Plastic Design.—It will first be necessary to give some thought to the criteria by which the usefulness of a structure is judged. The structural strength of a steel frame may be determined by a number of factors, any one of which may actually constitute a "limit of structural usefulness." These possible design criteria are: (1) First attainment of a hypothetical yield-point stress, (2) brittle fracture, (3) fatigue, (4) instability, (5) attainment of maximum plastic strength, and (6) large deflections.

A design based on any one of the six factors could be referred to strictly as a "limit design." "Plastic design" as an aspect of limit design and as applied to continuous beams and frames embraces primarily item 5—the attainment of maximum plastic strength.

Plastic design, then, is first a design on the basis of the maximum load the structure will carry (as determined from an analysis of strength in the plastic range). Secondly, it consists of consideration (by the use of rules or formulas) of certain "limitations" that might otherwise prevent the structure from attaining the computed maximum load. Many of these same limits may be present in conventional design (brittle fracture or fatigue). Others are inherently associated with only the plastic behavior of the structure. The unique feature of plastic design is that the ultimate load, rather than the yield stress, is regarded as the design criterion.

WHY PLASTIC DESIGN?

What is the justification for plastic design? One could reverse the question by asking, "Why use elastic design?" If the structure will support the load and otherwise meet its intended function, are the magnitudes of the stresses really important?

It is true that in simple structures the concept of the hypothetical yield point as a limit of usefulness is rational. This is because the ultimate load capacity of a simple beam is only from 10% to 15% greater than the hypothetical yield point, and deflections start increasing quite rapidly at such a load. Although it would seem logical to extend elastic stress analysis to indeterminate structures, such procedures have tended to overemphasize the importance of stress rather than strength as a guide in engineering design and have introduced a complexity that seems unnecessary for a large number of structures. Actually the idea of design on the basis of ultimate load rather than allowable stress is a return to the realistic point of view that had to be adopted by the engineering forefathers in a very crude way because they did not have the knowledge of mathematics and statics that would have allowed them to compute stresses.

---

[4] "Tests on Full-Scale Portal Frames," by J. F. Baker and J. W. Roderick, *Proceedings*, Inst. of C. E., London, January, 1952, p. 71.

[5] "New Methods in the Analysis and Design of Structures in the Plastic Range," by J. F. Baker and M. R. Horne, *British Welding Journal*, July, 1954, p. 307.

[6] "Recent Progress in the Plastic Methods of Structural Analysis," by P. S. Symonds and B. G. Neal, *Journal*, Franklin Inst., November, 1951, p. 383, and December, 1951, p. 469.

The introduction of welding, of course, has been a real stimulus to studies of the maximum strength of frames. By welding it is possible to achieve complete continuity at joints and connections—and to do it economically. The full strength of one member may thus be transmitted to another.

It has often been demonstrated that elastic stress analysis cannot be used to predict the real stress distribution in a building frame with anything comparable to the degree of accuracy that is assumed in the design. The work done in England by Mr. Baker and his associates as a forerunner to their maximum strength studies clearly indicates this fact.[7]

Examples of "imperfections" that cause severe irregularity in measured stresses are (*a*) differences in beam-column connection "fit-up" and flexibility, (*b*) spreading of supports, (*c*) sinking of supports, (*d*) residual stresses, (*e*) flexibility assumed where actually there is rigidity (and vice-versa), and (*f*) points of stress concentration. Such factors, however, usually do not influence the maximum plastic strength.

In summary, then, serious consideration is given to plastic design for the following reasons:

1. Simplicity.—Most of the tedious analysis of the equations necessary for the elastic solution of indeterminate frames is eliminated. Also, the imperfections usually can be disregarded.
2. Rationality.—By plastic analysis the engineer can determine the real maximum strength of the structure with an accuracy that far exceeds his presently available techniques. Thereby the factor of safety has more significance. It is not unusual for the factor of safety to vary from 1.65 to 3 or more for structures designed according to conventional elastic methods.
3. Economy.—Because the maximum strength can be determined quite accurately it is possible to utilize with assured safety the reserve of strength beyond the elastic limit.

Plastic design is not a technique that is intended to replace all design procedures. Structural design must preclude failure caused by such things as brittle fracture, fatigue, and buckling—factors that may themselves become the design criteria. In ordinary building construction, such limitations are usually the exception, however, and not the rule. Therefore, it can be expected that plastic design will find considerable application, particularly in continuous beams, industrial frames, and in tier buildings.

TESTS OF CONTINUOUS FRAMES

Fig. 1 (*a*) shows the third in a series of four frame tests performed at Lehigh University. The span of the girder was 30 ft, and the column height was

---

[7] "Shortcomings of Structural Analysis," by J. F. Baker, *Transactions*, North East Coast Inst. Eng. Ship, Vol. 68, 1951, p. 31.

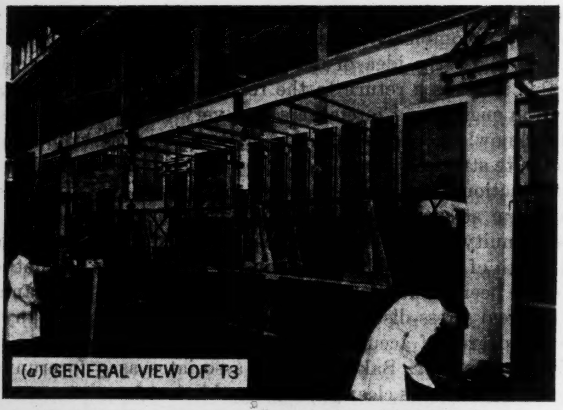

(a) GENERAL VIEW OF T3

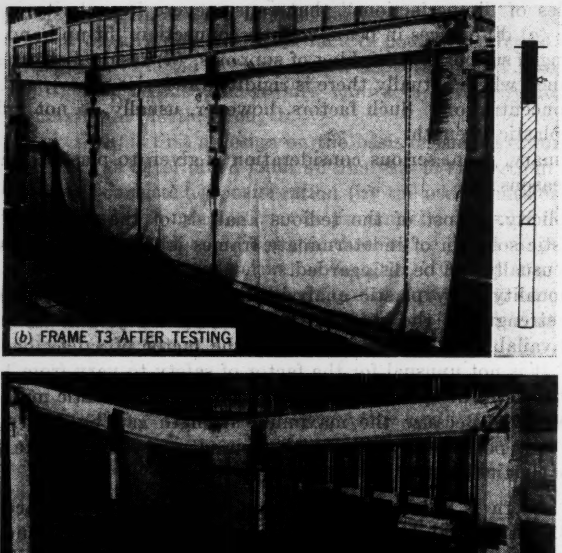

(b) FRAME T3 AFTER TESTING

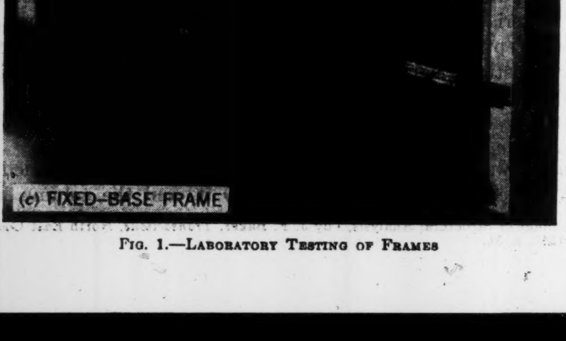

(c) FIXED-BASE FRAME

FIG. 1.—LABORATORY TESTING OF FRAMES

10 ft. The frame was pin-based and is shown in the early phase of the test in Fig. 1(*a*). The vertical load was applied with hydraulic jacks at the third points of the beam. Side load to simulate wind action was applied by the same technique. (The framing above the horizontal part of the test frame is part of the laboratory itself.)

In Fig. 1(*b*) the same frame is shown at the end of the test, as well as the arrangements for applying vertical and side load. With the solid line as a zero reference, the dotted line indicates the deflected shape when the frame first reached the predicted maximum load. The frame was deformed by jacking considerably beyond the maximum load to demonstrate the toughness of steel frames strained beyond the elastic limit.

The bar chart at the right of Fig. 1(*b*) indicates the considerable reserve of strength above the elastic limit that is not utilized (as of 1957) in conventional structural design. The allowable load, according to conventional elastic design, is at the top of the clear part of the chart. The predicted elastic limit is at the top of the cross-hatched part, and the top of the bar is the maximum reserve strength—a value that is above the predicted ultimate load shown by the short horizontal line. Even with the extensive jacking, when the test was stopped (at the arrow) the load was still above the maximum that could have been supported within the elastic limit.

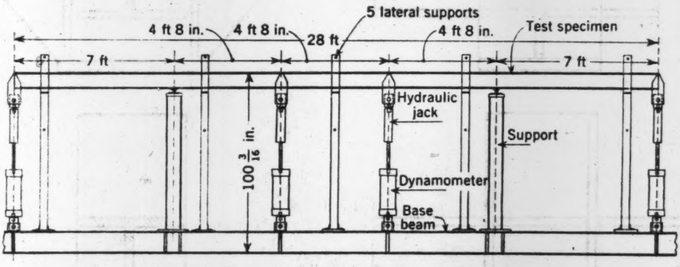

FIG. 2.—CONTINUOUS-BEAM TEST ARRANGEMENT

The fourth frame tested in this series of single-span frames is shown in Fig. 1(*c*). The column bases were fixed in this case, and this had the natural effect of decreasing the sidesway deflection. A second effect was to increase the capacity of the frame to carry side load; the ratio of side load supported by this frame and that of the frame in Figs. 1(*a*) and 1(*b*) was about 9 to 1.

A number of continuous beams also have been tested in the program. Fig. 2 shows a typical arrangement, designed in such a way that fixed-ended beams with intermediate degrees of end restraint might be simulated. The loading was applied at the third-points of a 14-ft span with end spans of 7 ft. A fixed-ended beam was simulated by maintaining the supports in a level position through proper adjustment of the end loads. Typical details of connections are shown in Fig. 3; an attempt was made to simulate practical structural details. In Fig. 4 there is shown a part of one of the continuous 8WF40 beams; one of the load points is at the left and a support is near the

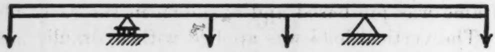

(a) TEST ARRANGEMENT

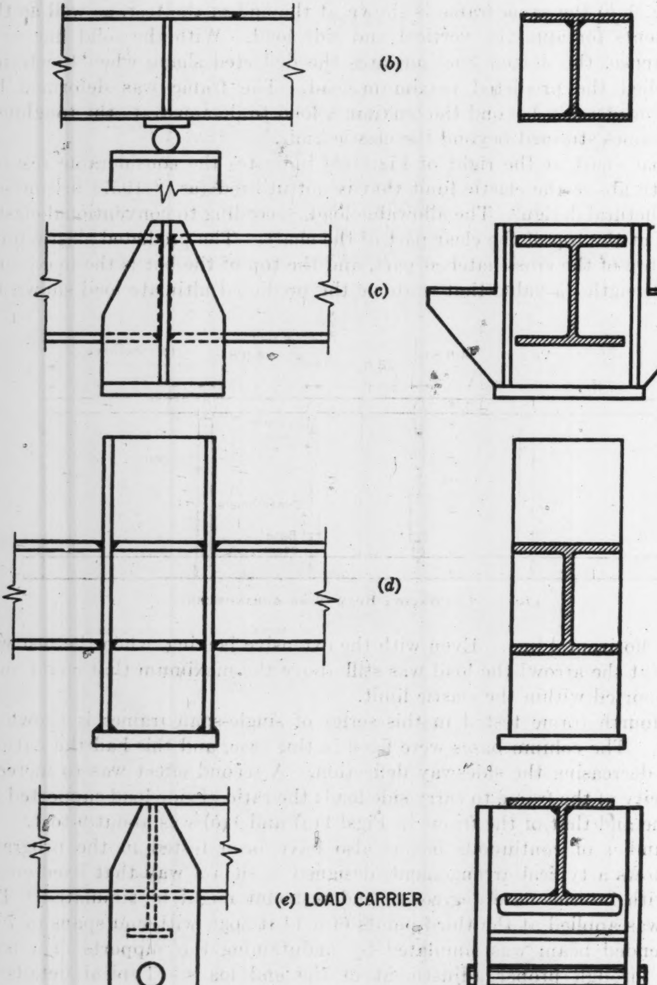
(b)
(c)
(d)
(e) LOAD CARRIER

FIG. 3.—CONNECTION DETAILS IN VARIOUS CONTINUOUS BEAMS

middle. To the side, the maximum observed strength (105%), the computed maximum strength (100%), and the computed elastic limit (67%) are shown with a bar graph. Also shown are the allowable loads on the beam for a stress of 20,000 lb per sq in. at the support (35%) and for the American Institute of Steel Construction (AISC) provision[8] of a maximum stress of 24,000 lb per sq in. at the support (42%). Such an increase of allowable stress at an interior support of a continuous beam is, of course, one method of utilizing some of the reserve of strength in design and was introduced into the AISC specifications in 1946.

It is seen from the foregoing illustrations that the reserve strength of steel is considerable and that it can be predicted with reasonable certainty. Now, there is the question, "How can use be made of this strength in structural design?"

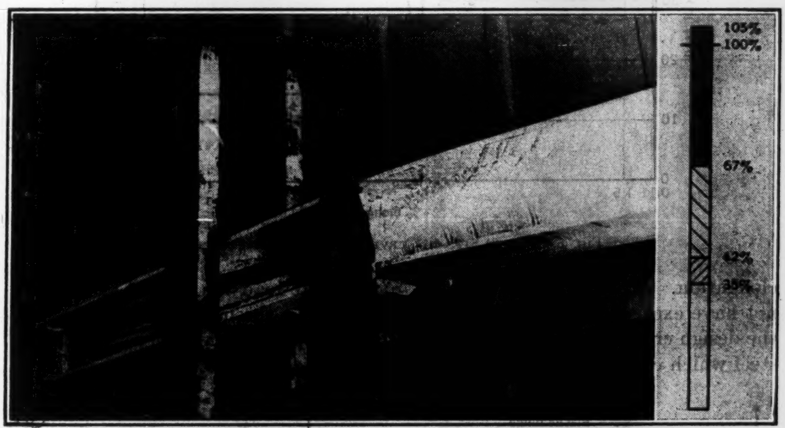

FIG. 4.—CONTINUOUS BEAM AT END OF TEST

The basis for computing this maximum plastic strength is the formation of "plastic hinges" at certain critical sections. The capacity of columns, connections, and beams to form these all-important hinges is the key to the development of high reserve strengths. Therefore, an examination will be made of the basis of hinge formation; this will be followed by a study of components that have developed plastic hinges.

DEVELOPMENT OF RESERVE STRENGTH

Plastic Hinges.—A typical example of the familiar stress-strain curve of ordinary structural steel is shown in Fig. 5. After the yield point is reached, a tensile specimen would stretch plastically without an increase in load for a distance that is from 10 to 15 times the extension at the elastic limit. This is followed by strain hardening, and at approximately 10% to 15% elongation the curve reaches the maximum point.

---

[8] "Steel Construction Manual," A.I.S.C., 1950.

Conventional elastic design makes use of only an insignificant part of the strain capacity of steel—up to the first light vertical line—or about 0.1% elongation. Even in plastic analysis, at ultimate load the critical strains will not have exceeded about 1.5% elongation. Thus, the use of ultimate load as the design criterion still leaves available a major part of the reserve ductility of steel which can be used as an additional margin of safety.

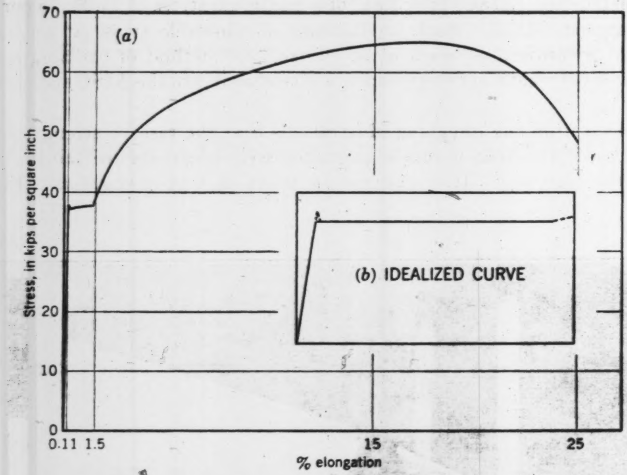

FIG. 5.—STRESS-STRAIN CURVE FOR STRUCTURAL STEEL

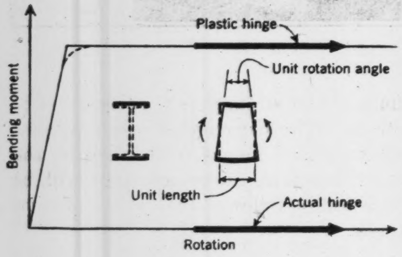
Plastic hinge
Unit rotation angle
Bending moment
Unit length
Actual hinge
Rotation

FIG. 6.—IDEALIZED MOMENT-ROTATION CURVE

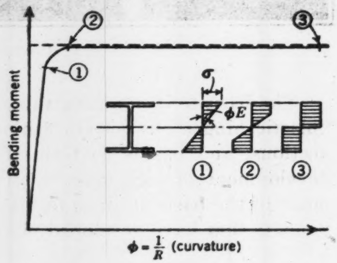
②
③
①
σ
φE
Bending moment
①
②
③
$\phi = \frac{1}{R}$ (curvature)

FIG. 7.—MOMENT-CURVATURE CURVE

Fig. 5(b) shows the first part of the stress-strain curve, drawn to larger scale. By keeping in mind this "idealized" curve, it is possible to follow the formation of plastic hinges.

In Fig. 6 bending moment is plotted against the rotation of a section bent by couples. This couple deforms the beam, introducing a certain unit rotation angle per unit length along the beam. If one imagines that all the material in the beam is concentrated in its flanges, the plot of moment versus curvature is the same as the stress-strain curve in Fig. 5; the compression flange acts as a compression specimen and the tension flange as a tension specimen. The analogy between an "actual hinge" and a "plastic hinge" is also shown in Fig. 6.

Fig. 7 shows a more realistic picture of the development of a plastic hinge and the successive change from elastic to plastic action. Point 1 is the elastic limit; at point 2 the member is partly plastic; and at point 3 it approaches the limiting "plastic-hinge moment," M_p. As is evident from the stress distribution, M_p may be computed from the yield stress and statical moment,

$$M_p = \sigma_y Z \qquad (1)$$

in which σ_y is the lower yield-point stress and Z denotes the plastic modulus, computed as twice the static moment of half the cross section. The term, Z, is analogous to S, the elastic section modulus.

One of the two sources of reserve strength beyond first yield is also shown in Fig. 7. The development of plastic yield of the full cross section results in an increase of bending strength beyond computed yield of approximately 14% for rolled wide-flange shapes. The term, "shape factor," denotes the ratio between the full strength (M_p) and first yield (M_y).

The Formation of Plastic Hinges in Structural Elements.—A large segment of the work at Lehigh University has involved testing of component parts of frames to see whether or not they actually develop the predicted plastic-moment strength.

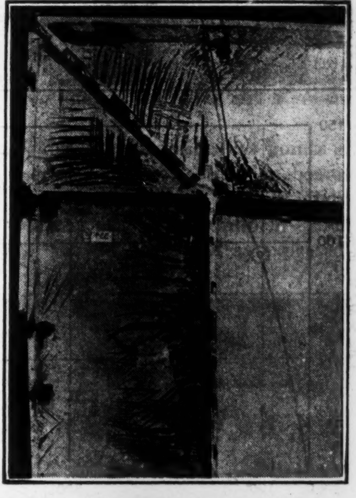

FIG. 8.—CORNER CONNECTING 12 WF36 WIDE-FLANGE SHAPES

In Fig. 8 there is shown a welded corner connection; a coating of whitewash was used to show the flaking of mill scale. In the corner of the connection it will be noted that the web has yielded rather extensively, transferring load to the diagonal stiffener that was inserted for the purpose of carrying that load. This connection joined two 12WF36 shapes, and the moments were such that the joint was being "closed" under the action of the forces. The lower part is the top of a column and it, too, participates to a considerable extent in the plastic action. The influence of direct stress is evident in the column as the inner flange (where bending and direct forces are additive) yielded more than on the tension side. The neutral axis is thus shifted to the left of center a small distance.

In Fig. 9 there is shown a connection of similar design but fabricated to join two 36WF230 beams; the behavior is similar to that of the smaller shapes. In Fig. 9(*d*) there is shown the nondimensional curve of moment versus deflection, the latter being measured between the two arms of the connection. Figs. 9(*a*), 9(*b*), and 9(*c*) are photographs of the knee taken at three different stages of the test and as indicated on the lower test curve. At computed yield (Fig. 9(*a*)) there is negligible deformation; as the maximum moment is approached (Fig. 9(*b*)) modest plastic yield zones have developed; only after the connection has been rotated beyond any practical overload does the deformation become severe (Fig. 9(*c*)). "Unloading" is caused by the combined effects of local and lateral buckling.

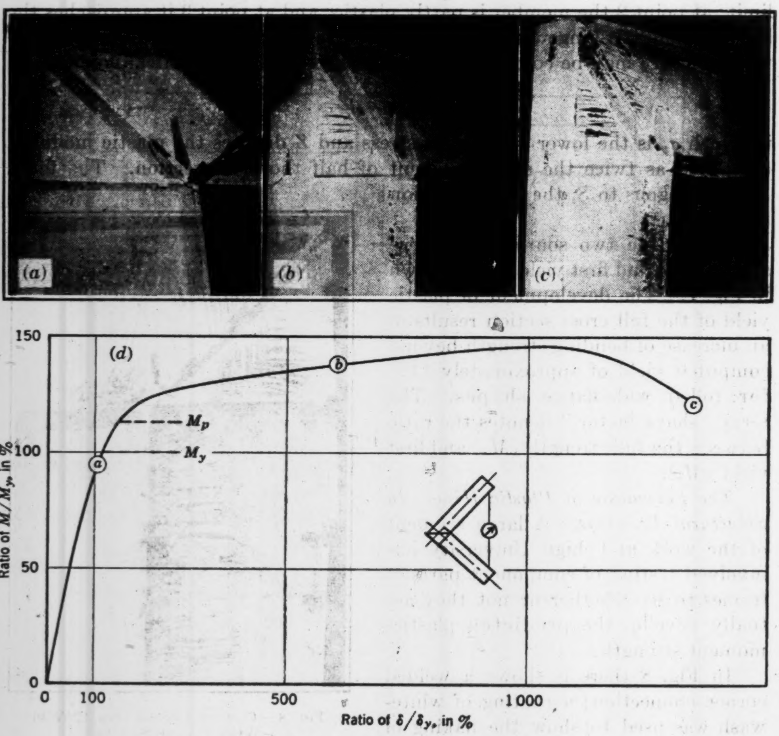

FIG. 9.—BEHAVIOR OF 36WF230 CORNER CONNECTION

Plastic hinges may form at load points or at supports in continuous beams. Examples are shown in Fig. 10. The general arrangement of the beam is shown at the top. Photograph (*a*) is a detail taken at the support as indicated in the sketch. Although somewhat obliterated by the auxiliary loading stiffener, the detail here is the same as that shown in Fig. 3(*b*). Photograph (*b*) shows the region between the two load points, the loading being such that the moment is uniform in this portion. The yield patterns differ, of course, depending on the magnitude of shear force that is present. However, studies of the influence of shear on the plastic moment have shown that it is not a severe limitation.

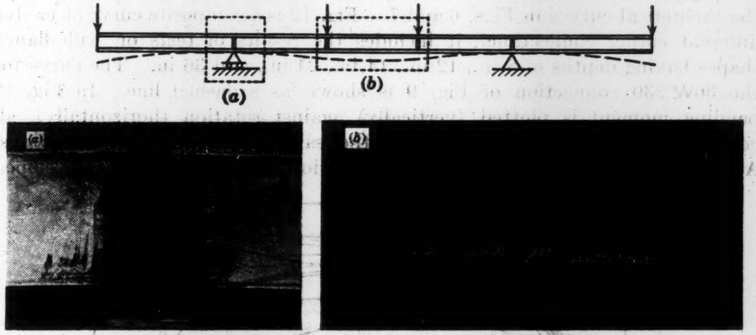

FIG. 10.—PLASTIC HINGES IN A CONTINUOUS BEAM

Plastic hinges may form in a continuous frame at connections, at points of concentrated load or reaction, and also at certain critical sections in beams where the bending moment is a maximum. Fig. 11 is typical of what might be expected for a beam in which the moment is practically uniform—such as at the center of a uniformly loaded span. Hinges form, and as expected, they extend over a somewhat longer length of the beam. Fig. 11 shows two views; in Fig. 11(*a*) the yield point has been passed and the moment is approaching M_p. In Fig. 11(*b*) there is shown a view of the beam after the curvature had far exceeded what would be required to satisfy the conditions of plastic

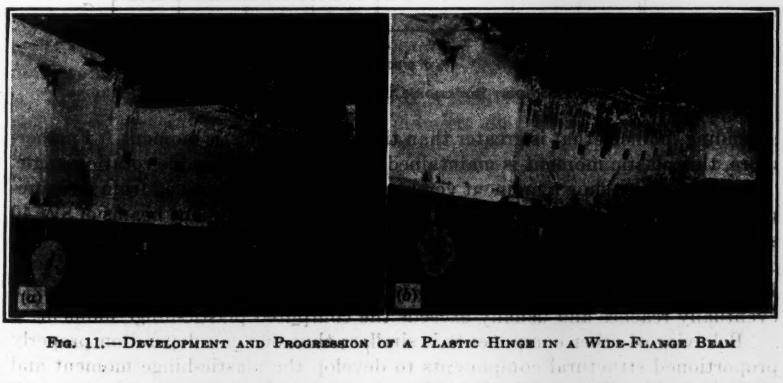

FIG. 11.—DEVELOPMENT AND PROGRESSION OF A PLASTIC HINGE IN A WIDE-FLANGE BEAM

analysis. The severe deformation seen in Fig. 11 is accomplished in order to obtain a complete load history. The deformation at maximum load is, of course, much less.

Moment versus rotation curves demonstrating the capacity of structural components to form hinges are shown in Figs. 12 and 13; they correspond with the theoretical curves in Figs. 6 and 7. Fig. 12 is a composite curve of twelve different corner connections; it includes the results of tests on wide-flange shapes having depths of 8 in., 12 in., 14 in., 24 in., and 36 in. The curve for the 36WF230 connection of Fig. 9 is shown as a dashed line. In Fig. 12 bending moment is plotted (vertically) against rotation (horizontally), all coordinates having been reduced to the same common percentage basis. Although there are some differences in behavior, all the connections developed a bending moment that is greater than the predicted plastic moment. Furthermore, this plastic moment is maintained through a considerable rotation angle.

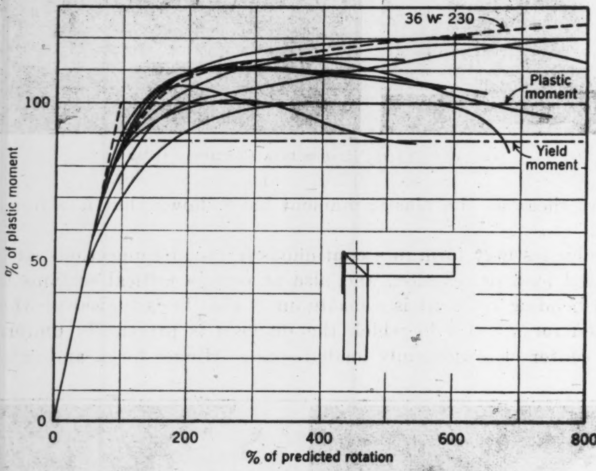

FIG. 12.—COMPOSITE MOMENT-ROTATION CURVES FOR VARIOUS CORNER CONNECTIONS

In Fig. 13 are shown moment versus rotation curves obtained from measurements made in the vicinity of the support of three continuous beams of 8WF40 shape. Sometimes the section develops a hinge moment that is a few percentages less than the predicted plastic moment in the early phase of the test. However, with adequate lateral support and continued straining, the strength eventually reaches and usually exceeds the computed plastic-hinge moment.

Behavior of other components is similar; thus one can depend on properly proportioned structural components to develop the plastic-hinge moment and to have an adequate reserve of curvature.

Redistribution of Moment.—Under the heading, "Development of Reserve Strength: Plastic Hinges," it was mentioned that one of the sources of reserve strength is the development of full plastic yield of the cross section (the shape factor). A second factor contributing to the reserve of strength—and usually to a much greater extent—is redistribution of moment due to the formation of these hinges (the "redistribution" factor). It is here that the importance of the flat part of the $(M\text{-}\phi)$-curve comes into action. When the plastic moment is reached at a critical section, this moment is maintained at approximately constant value as the section rotates, redistributing larger induced moments to other parts of the structure.

The fixed-ended, uniformly loaded beam of Fig. 14(*a*) will be used to illustrate how plastic hinges allow a structure to deform under load beyond the elastic limit and permit a redistribution of moment, thereby increasing the load capacity. The numbers, 1, 2, and 3, in Fig. 14 represent three phases of loading: (1) Attainment of first yield, (2) first attainment of computed ultimate load, and (3) an arbitrary deflection obtained by continued straining at the maximum load.

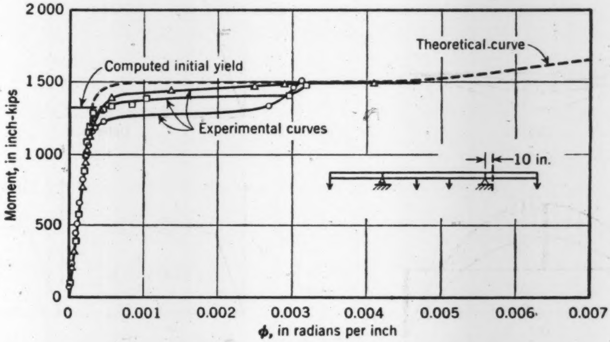

FIG. 13.—MOMENT-CURVATURE RELATIONSHIP OF CONTINUOUS 8WF40 BEAMS NEAR A SUPPORT

The idealized plastic hinge of Fig. 6 is assumed. In Fig. 14(*b*) are the deflection curves; in Fig. 14(*c*), the moment diagrams; in Fig. 14(*d*), the simplified load-deflection curve; and in Figs. 14(*e*) and 14(*f*), the $(M\text{-}\phi)$-action at the ends and at the center, respectively.

By an elastic analysis, the moment diagram of Fig. 14(*c*) could be determined when yielding commences (phase 1). The center moment is $p\,L^2/24$ and the end moment is $p\,L^2/12$, in which p is the distributed load per unit length and L is the span length. On the load-deflection curve of Fig. 14(*d*), the load has reached point 1. The moment capacity has been used up at the ends (Fig. 14(*e*)); however, from Fig. 14(*f*), because $M = \frac{1}{2} M_p$ at phase 1, moment capacity is still available at the center of the beam. Therefore, as load increases beyond phase 1, "hinge action" will start at the ends, and the beam behaves as if it were simply supported, except that the end moment remains constant at M_p. The deflection increases at a somewhat faster rate (the rate of increase being that of a simply supported beam of length L).

At phase 2 the beam reaches its maximum load as the moment capacity at the beam center is exhausted. Beyond phase 2, the beam will continue to deform under constant load (phase 3) in what has been termed a "mechanism."

The shaded part of Fig. 14(*c*) represents the simple-beam moment diagram that, due to redistribution of moment, is superimposed on the existing moment diagram (phase 1) and corresponds to the increase of load between phases 1 and 2 (Fig. 14(*d*)).

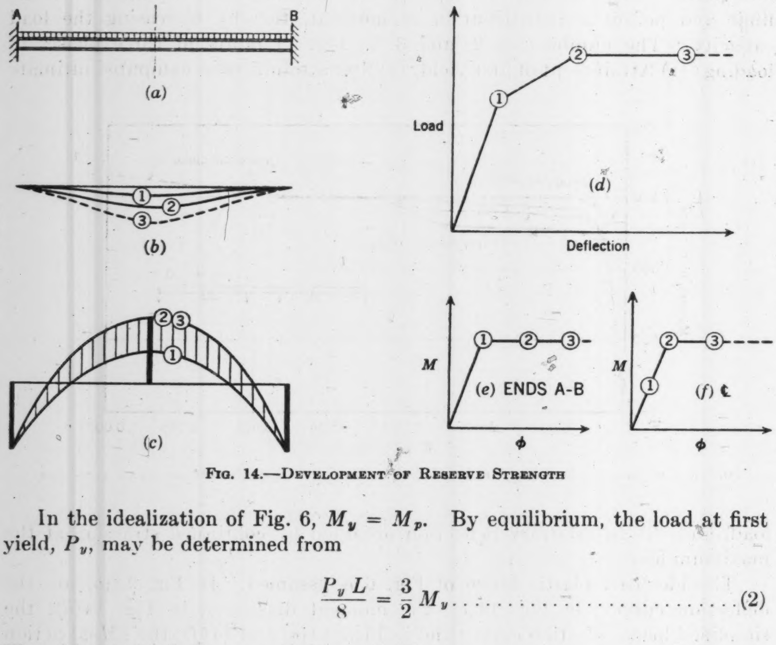

FIG. 14.—DEVELOPMENT OF RESERVE STRENGTH

In the idealization of Fig. 6, $M_y = M_p$. By equilibrium, the load at first yield, P_y, may be determined from

$$\frac{P_y L}{8} = \frac{3}{2} M_y \qquad (2)$$

The ultimate load, P_u, may be computed from

$$\frac{P_u L}{8} = 2 M_p \qquad (3)$$

The ratio between the ultimate load and the yield load is

$$\frac{P_u}{P_y} = \frac{2 M_p}{\frac{3}{2} M_y} = \frac{4}{3} \frac{M_p}{M_y} \qquad (4)$$

As has been noted, the ratio, M_p/M_y, is termed the "shape factor," with an average value for wide-flange shapes of 1.14. Therefore, using the more realistic (M-ϕ)-curve for rolled shapes (Fig. 7),

$$\frac{P_u}{P_y} = \frac{4}{3} \times 1.14 = 1.52$$

that is, the increase in load capacity of the beam beyond the load at initial yield is about 50%. The "shape factor" accounts for 14% and, in this example, the "redistribution factor" accounts for 33⅓% of the increase.

PLASTIC ANALYSIS

Eq. 3 is an equilibrium equation and constitutes the plastic analysis of a fix-ended beam that is uniformly loaded. Actually, the conditions were similar to those in elastic analysis except that the process was simpler. Messrs. Baker and Horne[5] have drawn a comparison between the basic conditions for each method.

In elastic analysis one must consider (*a*) continuity, in which the deflected shape is examined as the basis for continuity equations; (*b*) equilibrium because the load must be supported; and (*c*) limiting moment (or stress) because in elastic analysis the limiting moment is the yield moment. In plastic analysis three similar conditions (or modifications thereof) must be considered. With regard to continuity, the situation is just the reverse. Theoretically, plastic hinges interrupt continuity so that sufficient plastic hinges form to allow the structure (or part of it) to deform as a mechanism. This could be termed a mechanism condition. The equilibrium condition is the same—namely, the load must be supported. Instead of initial yield, the limit of usefulness is the attainment of plastic-hinge moments, not only at one cross section but at each of the critical sections; this is termed a plastic moment condition. The three conditions that must be considered in plastic analysis are therefore (1) mechanism condition, (2) equilibrium condition, and (3) plastic-moment condition.

To illustrate the foregoing by use of the example shown in Fig. 11, three plastic hinges are necessary before the structure will deform as a mechanism. The corresponding maximum load is determined from the equilibrium condition (Eq. 3). Because the maximum moment is nowhere greater than the plastic moment, M_p, the answer is the correct one.

These various conditions will next be considered in an analysis of the frame shown in Fig. 1(*c*). The frame with a 10-ft column height and a 30-ft span is shown in Fig. 15(*a*). The section (12WF36) is uniform throughout. The loading consists of vertical loads concentrated at the third points (to simulate uniformly distributed load); the side load, W, represents the action of wind on the side of the structure. Rather than distribute a total load of 2 W along the column height, the same action of the frame will be obtained in this problem if half the load is concentrated at the top of the column as load W. For the particular proportions of the frame, W was taken as 1/9 P. This fixed-base portal frame is redundant to the third degree.

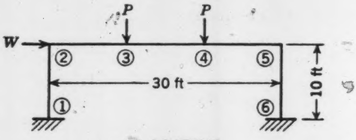

(a) LOADING

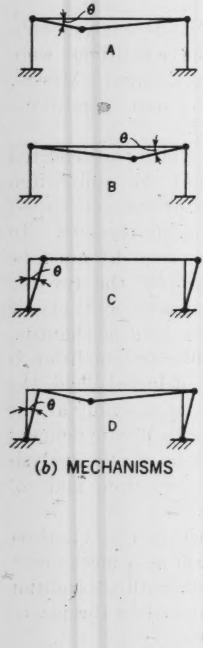

(b) MECHANISMS

$$P\frac{L}{3}\theta + \frac{1}{2}P\frac{L}{3}\theta = M_p\left(\theta + \frac{3}{2}\theta + \frac{1}{2}\theta\right)$$

$$P_u = \frac{6\,M_p}{L}$$

$$\frac{1}{2}P\frac{L}{3}\theta + P\frac{L}{3}\theta = M_p\left(\frac{1}{2}\theta + \frac{3}{2}\theta + \theta\right)$$

$$P_u = \frac{6\,M_p}{L}$$

$$\frac{1}{9}P\frac{L}{3}\theta = 4\,M_p\theta$$

$$P_u = 108\,\frac{M_p}{L}$$

$$\frac{1}{9}P\frac{L}{3}\theta + P\frac{L}{3}\theta + \frac{1}{2}P\frac{L}{3}\theta = M_p\left(\theta + \frac{3}{2}\theta + \frac{3}{2}\theta + \theta\right)$$

$$P_u = 9.3\,\frac{M_p}{L}$$

(c) VIRTUAL WORK EQUATIONS

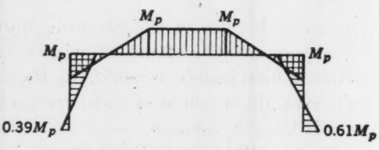

(d) EQUILIBRIUM MOMENT DIAGRAM

FIG. 15.—ILLUSTRATION OF PLASTIC ANALYSIS

The method of solution consists of examining the structure to see the different ways in which mechanisms can form by the development of plastic hinges (mechanism condition). An ultimate load corresponds to each possible mechanism and this may be quickly determined either by a semigraphical equilibrium method[9] by use of the principle of virtual displacements[6] or by other methods. The condition being satisfied is the equilibrium condition. It has been shown that the actual or correct mechanism for the problem is the one that gives the smallest value of the ultimate load.[10]

---

[9] "The Collapse Method of Structural Design," *Publication No. 5*, British Construction Steelwork Assn., London, 1952

Possible plastic mechanisms for the problem are shown in Fig. 15(*b*). These were not arrived at by guesswork, but their selection followed a systematic procedure that is equally effective for more complicated structures than the one shown.[6,11] Mechanisms A and B are beam mechanisms; conceivably "local failure" could occur in the girders by the formation of the indicated hinges. Mechanism C is a panel mechanism and involves failure of the frame by sway to the right. Mechanisms A, B, and C are termed elementary mechanisms whereas mechanism D results from a combination of mechanisms A and C. It will be noted that one of the hinges present in the two elementary mechanisms does not appear in the combined mechanism.

For each of the mechanisms, A through D, there exists a corresponding full plastic load, P_u. The principle of virtual displacements has been chosen to obtain this load. Using this principle, the external work done by the loads as the mechanism moves through a small displacement is equated to the internal work absorbed at each hinge as it rotates through a corresponding small angle. The resulting virtual-work equations are shown in Fig. 15(*c*).

As the structure deforms in mechanism A, for example, the load P at the left moves through a distance, δ, that is equal to the small angle, θ, times the distance, $L/3$; the load at the right moves through half the distance. Therefore, the external work is given by

$$W_e = \frac{P\,L\,\theta}{3} + \frac{\frac{1}{2}P\,L\,\theta}{3} \ldots\ldots\ldots\ldots\ldots\ldots\ldots (5)$$

During this motion, work is done at the hinges. At section 2 the internal work is equal to $M_p\,\theta$; at section 5 it is equal to one-half this value; at section 3 it is equal to $M_p\left(\theta + \frac{1}{2}\theta\right)$. Therefore, the total internal work during the mechanism motion is

$$W_i = M_p\left(\theta + \frac{3}{2}\theta + \frac{1}{2}\theta\right) \ldots\ldots\ldots\ldots\ldots\ldots (6)$$

Equating the two (for equilibrium) gives

$$P_u = 6\,\frac{M_p}{L} \ldots\ldots\ldots\ldots\ldots\ldots\ldots\ldots (7)$$

The lowest load is obtained in the case of mechanism A (or mechanism B which is identical). The ultimate load on the structure is therefore given by Eq. 7.

---

[10] "Limit Design of Beams and Frames," by H. J. Greenberg and W. Prager, *Transactions*, ASCE, Vol. 117, 1952, p. 447.

[11] "Analysis of Frames for Ultimate Strength," by B. T. Thurlimann, *Report No. 205.29*, Fritz Eng. Lab., Bethlehem, Pa., May, 1955.

As a check that the proper mechanism has been selected, the third (or plastic moment) condition is considered—at no point may the moment be greater than M_p. This check consists of computing by equilibrium the moments at each critical section in the frame and constructing the moment diagram. If at each point of the frame the moment is no greater than M_p, the answer is the correct one. The bending-moment diagram for the frame is shown in Fig. 15(*d*) for the case in which the side load, W, was equal to 1/9 of the concentrated vertical load, P.

Now, suppose the problem was to find how much side load the frame would stand while the full magnitude of the vertical load is maintained on the structure. (This situation might arise in a consideration of the blast resistance of frames.) There are two mechanisms by which the frame can fail under side load. These are mechanisms C and D and the procedure would be to try each. The virtual-work equation for mechanism D written in the terms of the unknown W is

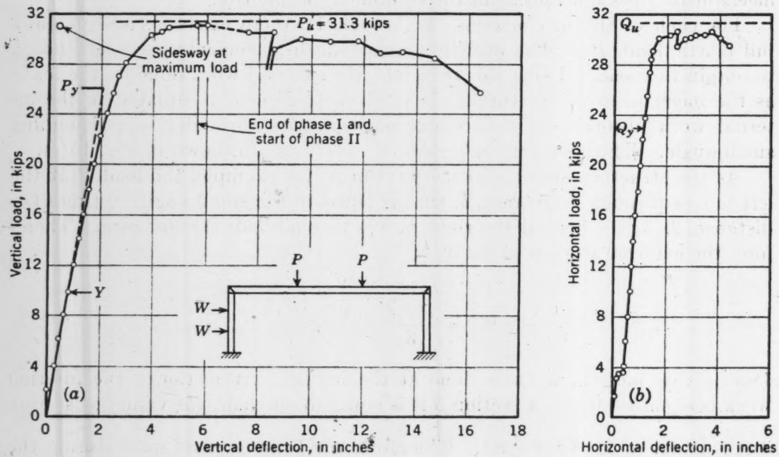

FIG. 16.—LOAD-DEFLECTION CURVES FOR TEST FRAME

$$\frac{W\,L}{3}\,\theta + \frac{P\,L\,\theta}{2} = 5\,M_p\,\theta \ldots\ldots\ldots\ldots\ldots\ldots (8)$$

Solving this for W (using a value of $P = 6\,M_p/L$), the allowable side load equals $6\,M_p/L$.

Now, for mechanism C the virtual-work equation in terms of the unknown W is given by

$$W\,\frac{L}{3}\,\theta = 4\,M_p\,\theta \ldots\ldots\ldots\ldots\ldots\ldots (9a)$$

or

$$W = 12\,\frac{M_p}{L} \qquad \text{(9b)}$$

Therefore, the correct maximum side load, W—which is the lowest value—is equal to 6 M_p/L or nine times the normal wind load.

How well does the test of a full-size frame bear out the theory? In Fig. 16 there are shown two load-deflection curves obtained from the test shown pictorially in Fig. 1(*c*). Fig. 16(*a*) is for the first test on the structure in which the side load was equal to 1/9 of the vertical load, representing the practical condition treated in Fig. 12. The frame carried the computed ultimate load. The test was then stopped and the second phase completed.

The resulting curve of horizontal load versus horizontal deflection as the side load was increased to a maximum value is shown in Fig. 16(*b*). The frame did not quite reach the value computed according to Eq. 11, but this is to be expected in view of the plastic deformations to which the frame had been subjected in the first test.

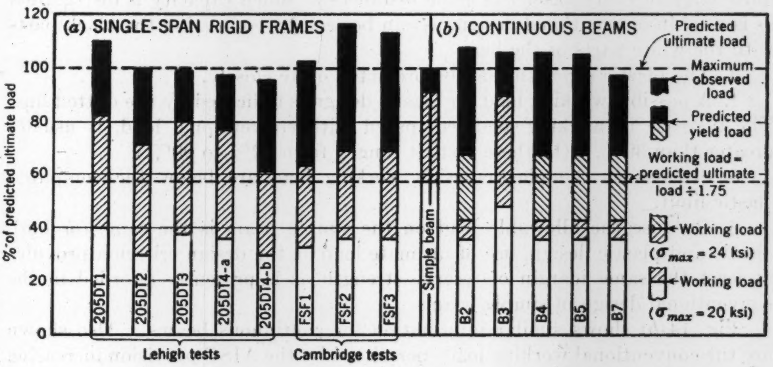

FIG. 17.—STRENGTH OF PORTAL FRAMES AND CONTINUOUS BEAMS

Fig. 16, therefore, shows that the predictions of plastic analysis are confirmed by actual tests.

RESERVE STRENGTH OF STEEL

Fig. 17(*a*) shows the maximum strength of single-span rigid frames. Each of the bar charts represents actual values from a series of frame tests made either at Lehigh University[12] or at the University of Cambridge in England under Mr. Baker's direction.[4]

---

[12] "Behavior of Welded Single-span Frames Under Combined Loading," by C. G. Schilling, F. W. Schutz, and L. S. Beedle, *Welding Journal*, May, 1956, p. 234–5.

The vertical scale is the percentage of the predicted ultimate load. Thus, a test that reached 100% on the vertical scale reached the load that is the basis of plastic analysis. The dotted line across Fig. 17 is a possible plastic-design working load.

The top of the open part of each bar represents the allowable conventional working load on a percentage-of-ultimate-load basis. The top of the cross-hatched part indicates the predicted yield load. The solid part up to the top of each bar represents the reserve of strength above the elastic limit and up to the maximum strength observed in the test. The predicted yield and ultimate loads are computed on the basis of measured material properties.

The case for plastic design is illustrated by the following observations in connection with Fig. 17(*a*):

1. The reserve in strength above present conventional working loads is considerable in continuous steel structures (from 150% to 200%).
2. The reserve of strength above the nominal theoretical yield point is quite large in every case. In some instances as much capacity is disregarded as is used in conventional design, as can be seen by comparing the black parts with the white parts of the bars.
3. The plastic strength may be predicted quite closely.
4. A possible working load for plastic design is indicated by the dotted line. The increase in working load, compared with conventional load, is usually greater than 30%. (In these tests it ranged from 42% to 90%.)
5. Stresses at the plastic-design working load are below the computed elastic limit.
6. Because the allowable load on the simple beam is the same for both elastic and plastic design, use of ultimate load as the design criterion provides at least the same margin of reserve strength as is presently afforded in the conventional design of simple beams.

Fig. 14(*b*) shows similar information for continuous beams. Also shown are the conventional working loads permitted by the AISC provision increasing the allowable stress to 24,000 lb per sq in. at the interior supports of continuous beams. It should be noted that these loads are substantially less than would be permitted using ultimate load design with a load factor of safety of 1.75. The general observations made concerning Fig. 17(*a*) are equally applicable to Fig. 17(*b*).

CONCLUSIONS

The aim of this paper has been to document the applicability of plastic analysis to structural design through an examination of test results correlated with applicable theory and in comparison with the provisions of present specifications. The following conclusions are presented in summary:

1. The unique feature of plastic design is that the ultimate load, rather than the yield stress, is regarded as the design criterion.
2. The justification for plastic design, in brief, is safety and economy resulting from balanced design. Substantial cost savings are indicated through

the more economical use of steel and a saving of time in the design office brought about by the use of the simpler plastic methods. At the same time, building frames are provided which are more logically designed for greater over-all strength.

3. Tests of continuous beams and portal frames in a size approaching full scale illustrate that the reserve strength of steel is considerable and that it can be predicted with reasonable certainty (Figs. 1 and 4).

4. Two factors account for the development of reserve strength in continuous structures. One is the "shape factor," representing the theoretical increase in moment strength of a section bent beyond the yield point; the ratio of full moment strength (M_p) to computed yield moment (M_y) averages about 1.14 (Fig. 7). The other factor is the "redistribution factor"; when the plastic moment, M_p, is reached at a critical section, the moment is maintained at approximately constant value while the section rotates, redistributing larger induced moments to other parts of the structure. (Fig. 14 has been used to describe this action.) Percentagewise, the latter factor is more important than the former.

5. Basic to the actual development of computed ultimate load is the proper formation of the "plastic hinges." Tests show that properly proportioned components (connections, columns, and beams) can be depended on to develop the plastic-hinge moment and to have adequate reserve of curvature (Fig. 12).

6. In the process of analyzing a structure to determine the maximum plastic strength, it is necessary to consider (*a*) a mechanism condition, (*b*) an equilibrium condition, and (*c*) a plastic-moment condition. These have direct parallels in elastic analysis. Based on these conditions, an indeterminate steel frame may be analyzed by a systematic procedure that is usually more rapid than the corresponding elastic analysis of the same structure.

7. The case for plastic design is illustrated by comparing the maximum strength of test frames with the computed ultimate load, with the computed first yield, and with the allowable load according to conventional design (Fig. 17). According to plastic design, the increase in working load, compared with allowable loads, is usually greater than 30%. At the same time, stresses at the "plastic design" working load are below the computed elastic limit. Furthermore, use of ultimate load as the design criterion provides at least the same margin of reserve strength as is presently afforded in the conventional design of simple beams.

ACKNOWLEDGMENTS

This report has been prepared as a result of research conducted at Lehigh University in the Fritz Engineering Laboratory. The work was done as part of a program on welded continuous frames and their components. It was supervised by the Lehigh Project Subcommittee of the Structural Steel Committee, Welding Research Council. Sponsors of the program are The American Institute of Steel Construction; the American Iron and Steel Institute; the Column Research Council (Advisory); the United States Department of the Navy (Contract 39303) Office of Naval Research, Bureau of Ships, and the

Bureau of Yards and Docks; and the Welding Research Council. Sincere appreciation is expressed to T. R. Higgins, M. ASCE, chairman of the committee, and to the members for their valuable advice.

This program was first started at Lehigh University by Bruce G. Johnston, M. ASCE. K. E. Knudsen, Bruno Thurlimann, A. M. ASCE, F. W. Schutz, J. M. ASCE, Robert L. Ketter, J. M. ASCE, and G. C. Driscoll, Jr., J. M. ASCE, were active in supervising various aspects of the study. The valuable contributions of these and of the numerous research assistants who have participated in the program are gratefully acknowledged.

DISCUSSION

JACK R. BENJAMIN,[13] A. M. ASCE.—The paper is extremely important and timely. It is unfortunate that it could not have included more information on joint details and how they should be designed. Much of this information could be applied to advantage with elastic-design procedures.

Unfortunately, Mr. Beedle has given the impression that the profession could safely adopt plastic procedures at the present time (1957). It is believed, however, that plastic procedures can only be applied to special small structures. The restrictions on plastic methods must be recognized by the proponents of the procedures.

The most important limitation on plastic procedures is that present knowledge is insufficient. Tapered sections or members in which a considerable length of the member is designed to pass through yielding at the same time have not been studied. Tier buildings cannot be analyzed until typical large-column sections have been tested under conditions of high axial stress. Unfortunately, the limited knowledge available on columns was not included by Mr. Beedle. Another difficulty with building frames is that the mode of failure of the entire structure at a particular floor must be known. Individual bent strengths may not be attained under conditions of over-all torsional failure.

Economy must be considered from two standpoints. Possible savings in a structure will depend entirely on the load factors of the local building code. An over-all factor of 2 will not produce enough saving over present procedures to warrant the adoption of plastic-design procedures. A load factor of less than 2 is questionable unless the loads are known and invariable. Furthermore, the economic problems of the design office must be considered. Plastic-design procedures are advocated as being faster and better than elastic procedures. Plastic designs will be better balanced with respect to a factor of safety, but the office-design costs will rise rather than decrease as engineers will have to be re-educated; this takes time and costs money. Furthermore, the procedures of plastic analysis assume one set of loads that increase gradually up to incipient collapse. In practice one deals with three classes of loads: (1) Dead loads that are fixed and that are subject to only minor variations; (2) vertical live loads that are generally known with a certain probability of change; and (3) unknown loads, such as wind, earthquake, and blast, that tend to be in the nature of allowances to assure a certain type of construction. How are these different quantities to be combined in an over-all design? The load factor should vary with the type of load under consideration. A complete re-examination of code provisions is therefore necessary. Certainly, the 33% overload provision with wind and earthquake should be discarded in favor of a more realistic loading pattern. Plastic-design procedures offer the only way to effect a major improvement in the design of steel structures. Adoption of these procedures should include a complete revision of codes if full advantage is to be obtained.

---

[13] Associate Prof. of Civ. Eng., Stanford Univ., Stanford, Calif.

Zdeněk Sobotka.[14]—The load-carrying capacity of structures in the plastic range may be computed with considerable simplification by a method which is based on the plastic equilibrium of the external loads and the internal forces which, in the case of pure bending, are represented by the plastic moments of the critical cross sections. This method may be termed the method of forces as opposed to the method of virtual work.

One may examine, for example, the plastic mechanism of a continuous beam with a variable cross section that is uniformly loaded. In any span three plastic hinges form at the ultimate load—namely, two at supports, A and B and the other one at an intermediate point, C (Fig. 18).

The middle plastic hinge, C, divides the span into two parts, AC, and CB. The plastic equilibrium condition of the left part, AC, may be written by equating the sum of the two plastic-hinge moments, M_{pA} and M_{pC}, to the static moment of the external ultimate uniform load p_u with respect to A:

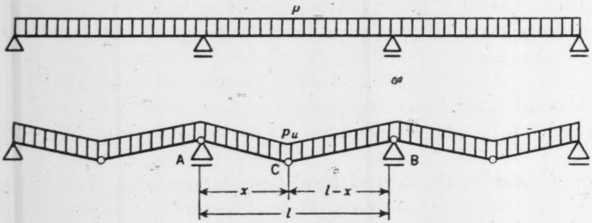

Fig. 18.—Continuous Beam with Variable Cross Section and Its Plastic Mechanism

$$\tfrac{1}{2}\,p_u\,x^2 = M_{pA} + M_{pC} \qquad \text{(10)}$$

Similarly, the plastic equilibrium of the other part, CB, is given by

$$\tfrac{1}{2}\,p_u\,(l - x)^2 = M_{pC} + M_{pB} \qquad \text{(11)}$$

Eqs. 10 and 11 express the plastic equilibrium of the two parts of the span of a uniformly loaded continuous beam with a variable cross section.

In the examples presented herein, the cross section will be assumed to be uniform in the middle part of the span where plastic hinge C forms; thus, there is a zero shear force at point C.

After dividing Eq. 11 by Eq. 10 and after taking the root, there results

$$\frac{l - x}{x} = \beta \qquad \text{(12)}$$

in which

$$\beta = \sqrt{\frac{M_{pC} + M_{pB}}{M_{pC} + M_{pA}}} \qquad \text{(13)}$$

---

[14] Docent of Strength of Materials and Theory of Elasticity, Technical Univ., Prague, Czechoslovakia.

From Eq. 12 the unknown distance of the middle plastic hinge, C, from the left support may be determined as

$$x = \frac{l}{1 + \beta} \qquad (14)$$

and then from Eq. 10 the value of the ultimate load, p_u, yields

$$p_u = \frac{2\,(M_{pC} + M_{pA})}{x^2} \qquad (15)$$

As another example of using the method of forces, the load-carrying capacity of a frame loaded by uniformly distributed load, p, and the side load, W (Fig. 19(*a*)) can be determined. The plastic mechanism is assumed as shown in Fig. 19(*b*).

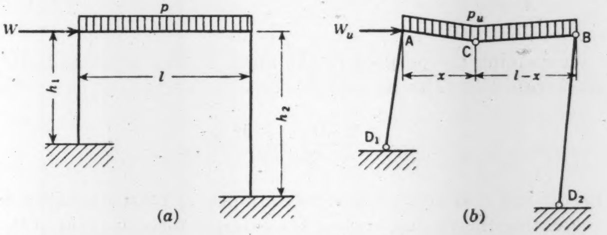

FIG. 19.—FRAME LOADED WITH UNIFORM VERTICAL LOAD AND HORIZONTAL LOAD AND ITS PLASTIC MECHANISM

The equilibrium of the three parts, D_1C, CB, and BD_2, of the plastic mechanism is given by

$$\Delta_1\, W_u\, h_1 + \tfrac{1}{2}\, p_u\, x^2 = M_{pD1} + M_{pC} \qquad (16)$$

$$\tfrac{1}{2}\, p_u\, (l - x)^2 = M_{pC} + M_{pB} \qquad (17)$$

and

$$\Delta_2\, W_u\, h_2 = M_{pB} + M_{pD2} \qquad (18)$$

in which $\Delta_1\, W_u$ and $\Delta_2\, W_u$ represent the two parts of the external side load supported by the columns, D_1A and D_2B.

After dividing Eqs. 16 and 18 by h_1 and h_2, respectively, adding them, and dividing the sum by Eq. 17,

$$\frac{w + \dfrac{x^2}{2\,h_1}}{\tfrac{1}{2}\,(l - x)^2} = \frac{\dfrac{M_{pD1} + M_{pC}}{h_1} + \dfrac{M_{pB} + M_{pD2}}{h_2}}{M_{pC} + M_{pB}} \qquad (19)$$

in which

$$w = \frac{W_u}{p_u} \qquad (20)$$

and is the given ratio between the ultimate values of the external horizontal force and the uniformly distributed load. From Eq. 19 an equation may be obtained for determining the unknown distance, x, of the hinge, C, from the left end of the frame:

$$\left(A - \frac{1}{h_1}\right) x^2 - 2\,A\,l\,x + A\,l^2 - 2\,w = 0 \qquad (21)$$

in which

$$A = \frac{\dfrac{M_{pD1} + M_{pC}}{h_1} + \dfrac{M_{pB} + M_{pD2}}{h_2}}{M_{pC} + M_{pB}} \qquad (22)$$

The solution of Eq. 22 is

$$x = \frac{A\,l}{A - \dfrac{1}{h_1}}\left[1 - \sqrt{1 - \frac{1}{A^2\,l^2}\,(A\,l^2 - 2\,w)\left(A - \frac{1}{h_1}\right)}\,\right] \qquad (23)$$

After determining the position of the hinge, C, the ultimate load, p_u, may be computed from Eq. 17 to be

$$p_u = \frac{2\,(M_{pC} + M_{pB})}{(l - x)^2} \qquad (24)$$

Mr. Beedle has also presented some examples of plastic analysis which are solved by equating the virtual work of the external forces to that of the plastic-hinge moments.

In the limiting state of a structure, so many plastic hinges form that the structure becomes a mechanism with one degree of freedom, as mechanism C and D in Fig. 15(*b*). In exceptional cases, particularly if there are only joint rotations and not joint displacements or if the joint displacements are small, the structure becomes a system with the possibility of virtual displacements as in system A and B in Fig. 15(*b*).

The structure may also become a system with more degrees of freedom—for example, when four plastic hinges develop at the corners and one in the girder in the portal frame. In this case, the frame has two degrees of freedom in the limiting state. This system results from the combination of mechanisms A and C in Fig. 15(*b*), and in this combined mechanism all plastic hinges present in the two elementary mechanisms appear—consequently, one more appears (at the left corner) than in mechanism D. However, the plastic hinges (in this case, two) which give the structure more degrees of freedom than one (or more than the virtual mobility) must develop simultaneously; or the structure must previously have lost itsst ability by becoming a mechanism with one degree of freedom.

Mr. Beedle has proposed a check of the selection of the proper mechanism and of the proper position of the plastic hinges considering the plastic-moment condition. This check may be accomplished by computing, by equilibrium, the moment at each critical section in the frame, by constructing the moment diagram, and by comparing the computed moments with the plastic moment, M_p, which cannot be exceeded.

From this an inverse method follows for computing the ultimate load of structures, starting from the possible equilibrium-moment diagram and from the ultimate equilibrium which the writer is presenting herein.

By comparing this procedure with that of the author, the plastic hinges with full plastic moments, M_p, at sections 2, 3, 4, and 5 (Fig. 15(*a*)), and the possible equilibrium-moment diagram on the girder (Fig. 15(*d*)) may be supposed. The ultimate equilibrium of the left part, 2–3, of the girder

$$\frac{p_u\,L}{3} = 2\,M_p \qquad (25)$$

gives directly

$$p_u = \frac{6\,M_p}{L} \qquad (26)$$

Taking, as does Mr. Beedle,

$$W_u = \tfrac{1}{9}\,p_u = \frac{2\,M_p}{3\,L} \qquad (27)$$

one gets, similarly, from the equilibrium of the columns, the moments at sections 1 and 6:

$$M_1 = 0.39\,M_p \text{ and } M_6 = 0.61\,M_p$$

as shown in Fig. 15(*d*).

Lynn S. Beedle,[15] A. M. ASCE.—A number of topics which are important but which were not covered in the paper have been mentioned by Mr. Benjamin. The purpose of the paper was primarily to document the applicability of plastic analysis to structural design. Concerning joint details, Mr. Benjamin correctly states that much of the information developed could be applied in elastic design; Figs. 6 and 7 are cases in point, and further information with regard to such details is available.[16, 17, 18]

The writer intended to leave the impression that the profession could safely adopt plastic design for certain steel structures. Of course, it will not replace all other design procedures; sometimes the design criterion will be fatigue, or buckling, or notch toughness. However, in ordinary building construction such limitations are the exception. In England, plastic design has been used on a considerable number of structures,[19] and one building was erected in Canada according to a design based on the plastic method.

Mr. Benjamin mentions the lack of information on members having a considerable length in the plastic region. On the contrary, most of the tests have been conducted on members in which one-third or more of the span was under pure bending or in a condition approaching it. This is true of the examples shown in Figs. 1(*b*), 1(*c*), and 8, all the "Lehigh tests" of Fig. 14(*a*), and all the tests of Fig. 14(*b*). Because this "pure bending" condition is not ordinarily found in practice, the typical behavior will usually be better than that evidenced by most of these tests.

---

[15] Chairman, Structural Metals Div., Fritz Eng. Lab., Civ. Eng. Dept., Lehigh Univ., Bethlehem, Pa.

[16] "Residual Stress and the Yield Strength of Steel Beams," by C. H. Yang, L. S. Beedle, and B. G. Johnston, *Welding Journal*, April, 1952, p. 205s.

[17] "Connections for Welded Continuous Portal Frames," by A. A. Tobrac, B. G. Johnston, and L. S. Beedle, *ibid.*, July, 1951, p. 359s; August, 1951, p. 397s; and November, 1952, p. 543s.

[18] "Plastic Design in Structural Steel," by L. S. Beedle, B. Thurlimann, and R. L. Ketter, lecture notes, A.I.S.C.-Lehigh Univ. publication, Bethlehem, Pa., September, 1955.

[19] "Some Steel Structural Frames Designed on Plastic Theory," by D. H. Little and A. Smith, *Proceedings*, Inst. C. E., London, May, 1955, Paper No. 44.

The other type of member mentioned is the tapered beam. It is true that studies of such beams have not been completed. (Tests of their lateral buckling characteristics are being conducted (1957) at Columbia University in New York, N. Y.). However, plastic design achieves its economy without the necessity for tapering the members. On the other hand, if there are instances where tapering might be desirable for other reasons, such a beam can be analyzed without difficulty by the plastic methods. This is illustrated by the subsequent example in which a comparison is made on the basis of a uniformly loaded, fixed-ended beam of a 40-ft span. Two possible solutions will be examined; the load may be supported (1) by a uniform member or (2) by one tapered from the ends to midspan. In the first instance, a 30WF108 beam ($S = 299.2$ in.^{3} and $Z = 340$ in.^{3}) on a 40-ft span will support a total distributed load of 375 kips according to Eq. 3. How will a tapered beam compare? In analyzing the tapered member, equilibrium of moment requires that

$$\frac{P_u L}{8} = M_{p1} + M_{p2} = 2 M_{p(\mathrm{WF})} \qquad (28)$$

in which M_{p1} and M_{p2} are plastic moments at the ends and center, respectively, and $M_{p(\mathrm{WF})}$ is the plastic modulus of the 30WF108 member. It is assumed that the member has a uniform taper, smaller at the center, and symmetrical about the center line. The ratio of M_{p1} and M_{p2} can be selected as any reasonable value—for example, $M_{p1} = 3M_{p2}$. Because the plastic modulus, Z, bears a linear relationship to M_p (from Eq. 1), then

$$Z_1 = 3Z_2 = \frac{3}{2} Z_{\mathrm{WF}} \qquad (29)$$

For a built-up member, the value of Z may be determined from

$$Z = 2 \int_0^{d/2} y \, dA \qquad (30)$$

from which

$$Z = bt\,(d - t) + \frac{w}{4}\,(d - 2t)^2 \qquad (31)$$

in which Z is the required plastic modulus; b, the flange width; t, the flange thickness; w, the web thickness; and d, the depth of the member. If the flange dimensions and the web thickness are selected to be about what would be found for such members ($b = 11.0$ in., $t = 0.75$ in., and $w = 0.625$ in.), then the only unknown in Eq. 31 is the depth, d, which may be obtained by solving

$$\frac{w}{4} d^2 + dt\,(b - w) - Z + t^2\,(b - w) = 0 \qquad (32)$$

For $Z_1 = \frac{3}{2} Z_{WF} = 510$ in.^{3} and $Z_2 = \frac{1}{2} Z_{WF} = 170$ in.^{3}, the required depth at the ends is 38 in. and that at the center is 16.8 in.

Comparing the weight of the two beams, the uniform member according to the plastic design weighs 4,320 lb. The weight of the plastically designed tapered beam is 4,440 lb. Thus, the two designs arrive at approximately the same weight with a slight advantage (3%) for the uniform member. Of course, there would have to be added to this the additional fabrication cost for the tapered member. Incidentally, conventional elastic design of the uniform beam would have required a section modulus of 429 in.^{3}. A 33WF141 section would have been used, the total weight being 5,640 lb, or an increase of 31% over the similar plastic design. In addition to showing the economy of material of plastic over elastic design, this example demonstrates that plastic design achieves economy without the necessity of tapering the members.

An examination of load factors was particularly avoided in the original paper. Although studies of the maximum strength of structures will be helpful in arriving at a rational load factor, many other factors also enter into the problem. Rather than confuse the presentation of plastic behavior of structures with a discussion of the factor of safety—a discussion, incidentally, which is equally applicable to conventional elastic design—the factor of safety was selected, under the heading, "Reserve Strength of Steel," on the basis of "* * * ultimate load as the design criterion provides at least the same margin of reserve strength as is presently afforded in the conventional design of simple beams." Depending on the shape factor selected, this value could vary from 1.75 to 2.03; the former was chosen for illustration.

Concerning "office-design costs," the techniques are relatively simple and are being learned by many practicing engineers. However, the task of instruction and education belongs with the colleges and universities, and many now include the subject in their curricula.

Code revisions are frequently mentioned. What form should a code or specification for plastic design take? A complete revision may not be necessary. In England and in Australia, specifications now permit use of the method, and this was done simply by adoption of an "enabling clause." A similar approach might be used in the United States. Of course, such a provision would be preceded by surveys and evaluations.[20, 2, 6, 18, 21] Two other documents eventually will be required, and work is being conducted on each: (1) Theoretical considerations, experimental verification, and guides for use in plastic design and (2) a manual of design examples.

The former will include a justification of provisions, a documentation by the inclusion of test results, and a summary of procedures. A first step in the completion of the task of formulating such "rules of practice" has been taken.[21] A joint task of the ASCE Committee on Plasticity Related to Design and the Welding Research Council's Structural Steel Committee, Lehigh Project Subcommittee, is being conducted to complete this report. Work on a manual of design examples is under way in the offices of the American Institute of

---

[20] "Rules of Practice in Plastic Design," by L. S. Beedle and B. G. Johnston, *Report No. 205.20*, Fritz Eng. Lab., Lehigh Univ., Bethlehem, Pa., August, 1954.

[21] "Plastic Design in Steel," *Proceedings*, National Engrs. Conference, A.I.S.C., April, 1956.

Steel Construction. Documents such as these should go far toward speeding the day when plastic design will be more frequently used by engineers.

Mr. Sobotka has discussed the case of a member of nonuniform cross section and has selected as a special case uniform members with cover plates or haunches at the supports. For this case, Eqs. 10, 11, 16, and 17 apply. In the general case of a tapered member, a vertical shear force is present at section C. Of course, if the member AB had been of uniform strength in the examples, then the shear force would truly have been zero at section C even if the moments at A and B were dissimilar. In the tapered-beam example cited earlier, the plastic hinge forms at the point of maximum moment (and zero shear) only because of the particular symmetrical arrangement chosen. Had the beam been tapered in the other direction (deeper at the center than at the ends), the hinge would not have formed at the center. Instead, two hinges would have formed simultaneously to the left and to the right of the center of those points where the moment capacity of the beam was just equal to the required statical moment of the member. The shear is of course not zero at those points. This simply underscores that the variation in moment capacity with distance along the beam must be considered in determining the location of plastic hinges therein.

Mr. Sobotka's "method of forces" is the same as the "semigraphical equilibrium method" noted by the writer and described in detail elsewhere[9] and used to solve the fixed-ended beam problem (Eq. 3).

In closing, the writer would like to thank Mr. Benjamin and Mr. Sobotka for the interesting points they have raised.

AMERICAN SOCIETY OF CIVIL ENGINEERS
Founded November 5, 1852
TRANSACTIONS

Paper No. 2902

WATER SUPPLY IN ARCTIC AREAS: DESIGN FEATURES

BY LLOYD K. CLARK[1] AND AMOS J. ALTER,[2] MEMBERS, ASCE

SYNOPSIS

Long, subzero winters and permanently frozen ground impose many restrictions on the design of water systems in the Arctic. The cost of construction is several times greater in the Arctic than it is in moderate climates, and operating conditions are more complicated. The results of a failure to recognize these factors are described herein, and design features are suggested for determining the source, treatment, distribution, and storage of a water supply.

INTRODUCTION

In 1932, Father Etienne Bazin, a Catholic missionary in the Iglulik Islands, located above the Arctic Circle in Canada, made the following entries in his diary (1)[3]:

> **"July 30—The mosquitoes are plentiful this year * * * something frightful; you can't put your nose out of the door. The ice is beginning to loosen; soon it will be gone * * ***
>
> **"August 25—Yesterday we had a white whale hunt and harpooned three * * ***
>
> **"August 27—There is already ice on the lake * * * the first snow fell today. As you see, summer is not very long."**

To those in a temperate climate, a 30-day summer season is unbelievably short. However, conditions in the Arctic include much that is unbelievable and paradoxical. In winter the sun barely rises over the horizon, if at all. However, many of the long nights are lighted by the shimmering colors of the aurora borealis. Each year in summer the Fairbanks, Alaska, baseball team traditionally starts a game at midnight without floodlights.

One may bask in 90° weather in July, but the frigid January winds will freeze exposed flesh in one minute. Although most of the underground soil is

---

NOTE.—Published, essentially as printed here, in April, 1956, as *Proceedings Paper 931*. Positions and titles given are those in effect when the paper was approved for publication in *Transactions*.

[1] Clark, Groff & Cave, Engrs., Salem, Ore.

[2] Chf. Engr., San Eng. Section, Alaska Dept. of Health, Juneau, Alaska.

[3] Numerals in parentheses, thus: (1), refer to corresponding items in the Bibliography (see Appendix).

permanently frozen (in some areas to depths of more than 1,000 ft), numerous hot springs exist. The Great Siberian Plain of Asia and the Great Central Lowland of North America, which comprise most of the Arctic land mass, are less than 1,000 ft in elevation. The Arctic seas are relatively shallow. On the other hand, most of Greenland, which is the largest land and ice mass to the north, is more than a mile in elevation.

Water supply is also paradoxical in the Arctic. The precipitation is usually less than 12 in. yearly, but most of the Arctic and sub-Arctic has an abundance of ponds and lakes. The design of a satisfactory community water system poses more than the usual complications.

This is not to say that the Arctic is impregnable, because men and machines have penetrated this area during the past decade (1945–1955) on a scale unequalled in the history of the Arctic. This penetration was caused by wartime demands and is being assisted by the discovery of the vast resources of the area and the ability to procure and use them. In the sub-Arctic the quest for precious and base metals—such as petroleum, iron and ferroalloys—is becoming increasingly rewarding. The harvest of the tremendous coniferous forests of the sub-Arctic region is at present (1956) just beginning.

To date, the climax of the penetration of the Arctic in the western hemisphere was reached in Operation Blue Jay at Thule, Greenland (2) (3), which is less than 900 miles from the North Pole. Here, in less than 100 days, a modern air base was built, complete with landing strip, hangars, and comfortable living accommodations for several thousand people. One of the principal problems to be overcome at this site is to obtain a suitable water supply.

The conquest of the Arctic appears to be well under way. Numerous water systems, both civilian and military, have been completed and are expanding. In Alaska approximately $20,000,000 have been spent for this purpose. The Distant Early Warning Stations that are being built across the top of the world by the armed forces must also be provided with water systems, although probably on a small scale.

Literature is gradually accumulating to relate the problems encountered and the means for solving them (4) (5) (6) (7) (8) (9) (10). The number of design engineers has increased, and these engineers are making rapid progress in learning and applying the disciplines imposed by Arctic conditions. Many designs and installations have been observed (11) so that an evaluation of their adequacy can at least be attempted.

Know the Arctic

It should be noted that this paper refers mainly to the inland Arctic areas and to those areas bounded by the Arctic seas or underlain with permanently frozen ground (permafrost) (12). Most of the communities in the north were first settled along the sea coasts of the northern Pacific Ocean and northern Atlantic Ocean. Currents from these oceans and trade winds are responsible for average annual temperatures of 30° F at locations above the Arctic Circle. Much of the coast of Greenland has these moderate temperatures whereas the Arctic area inland averages from 0°F to 10°F.

The lower limit of the sub-Arctic is generally considered to extend as far south as approximately the 50th parallel, which includes most of Canada on the North American continent; on the continent of Asia it extends from approximately the 60th parallel on the west to almost as far south as the 45th parallel in eastern Asia (13).

The principal effects of the prevailing low temperatures and the permafrost are shown by the retardation of biological and chemical reactions and by the changed physical properties of fluids, gases, and solids. Some of these effects are:

1. Ground water obtained from the permafrost area (14) through wells is subject to freezing in the withdrawal pipe when underpumped and to freezing in the aquifer when overpumped.
2. Frost heave (15) may damage well-pump installations; the freezing of pump bearings is an ever-present hazard.
3. Surface waters may freeze to the bottom whether in a flowing stream or a lake.
4. Creation of an impoundment by constructing a dam may alter the underground thermal regime to such an extent that the stability of the structure is endangered.
5. Intakes in surface sources are readily subject to clogging from frazil ice.
6. All chemical treatment processes are slowed down (16) to the extent that reaction chambers may become inadequate in capacity.
7. Subsidence of chemical floc and natural turbidities proceeds slowly.
8. Increased viscosity of water retards filtration.
9. Drainage devices, such as those provided for hydrants, are rendered inoperative.
10. Foundations of structures placed on permafrost are subject to complete failure.
11. Distribution of water through piping systems may be made difficult by frost penetration and subsequent freezing, which is also true for the storage of water (17) (18) (19) (20) (21).
12. Condensation and freezing on the exterior walls of buildings seriously deteriorate electrical and mechanical works mounted thereon.

In addition to the effects of low temperature and permafrost, there are conditions inherent in Arctic waters which must be taken into account (22). These are: (*a*) Surface waters possess fairly high pH-values and frequently contain considerable glacial silt in suspension, and (*b*) ground waters are, in general, highly mineralized—iron is usually present in objectionable quantities. From the conditions cited in the foregoing, it is apparent that to design properly for Arctic waters one must know Arctic conditions. It has been demonstrated too often that to ignore this fact is to invite disaster.

Operating Conditions.—The design of a water system must recognize the need for relative simplicity to insure operation during a period of extreme cold. Whenever an operator must work outdoors during this period, his major concern is keeping warm. Remote locations of intakes and storage facilities will, therefore, suffer from inadequate inspection; utilidors (large conduits) that cannot be easily entered complicate repair and replacement.

The operation of Arctic water systems in remote areas is complicated by the fact that trained personnel are scarce and are often incapable of maintaining numerous automatic and intricate electrical and mechanical equipment. Moreover, distances are great, and the weather is not always suitable for airplanes; thus, repair parts are difficult to obtain.

Economics and Design.—It is well known that construction costs in this region are extremely high. In the vicinity of Fairbanks these costs are approximately four times the costs in the United States. The Alaska Public Works office in Juneau, Alaska, reports that the bid price for 4-in. steel pipe in place at Palmer, Alaska, is $7.42 per ft. and that the bid price for 4-in. cast iron pipe is $10.90 per ft. The costs for water systems for the armed services in even more remote areas have not been revealed.

In view of such high costs, most Alaskan community utilities are assisted by funds from federal sources through the Alaska Public Works. Even with this assistance, a city's indebtedness to purchase a suitable water system may cost as much as $350 per capita. Apparently there is no federal relief to assist with operating costs, however, and the highly expensive plant is also costly to operate and maintain. It has been estimated that the maximum cost at Fairbanks for power alone would be $36,000 per yr. for a present population of 7,500. If one adds to this sum the cost of labor, chemicals, and general maintenance for a $5,000,000 installation plus the annual charges for interest and retirement of the city's share of the indebtedness for the first cost, the estimated annual total cost per capita is almost as much as the initial outlay, or approximately between $250 and $300. Thus, in spite of federal aid, water systems in the far north cost a great amount of money, which further restricts the designer.

DESIGN FEATURES

The following design features have been compiled from numerous sources. They are not all-inclusive, resulting largely from experience and from research by individuals and various agencies. Some of these features are in the form of suggestions for remedying deficiencies which have been observed in existing systems. They are presented with the sole intention of aiding those concerned with creating new systems or improving existing works.

Basic Factors.—The design should probably first consider the temperature and extent of ground frost in the soil for the area concerned (23) (24) (25). The factors which determine temperature and ground frost fall into two main categories as follows:

(1) Geographical position—latitude, altitude, proximity to bodies of water, terrain, and exposure to the sun; and

(2) Local conditions—ground cover, moisture content of soil, soil density, soil color, soluble salts in soil moisture, and thermal properties of soil.

Familiarity with these basic factors should automatically demonstrate the special conditions which will govern design in a given locality.

Selection of a Water-Supply Source—Surface Waters.—In comparatively rough terrain, such as that in Alaska, surface-water runoff is rapid in all areas except in the lowlands near rivers and river deltas. In permafrost areas, water sheds cannot normally be expected to retain precipitation similar to water sheds in temperate climates because percolation is restricted. Minimum stream flows exist during late winter and early spring.

Impoundment of surface waters must be preceded by a thorough study of underground conditions. The stored water may thaw permafrost which, depending on the nature of the soil in the permafrost, may in turn open underground channels for the release of the stored water. Thawing of permafrost under dam structures may render the foundations unstable, especially where soil particles are finely divided and possess a high moisture content and where no other precautions are taken.

Intakes should be placed in a suitable depth of water to allow the ice cover to protect against frazil ice. However, this is not necessarily the only solution to this problem. Controlling the velocity of flow may be indicated as well as supplying auxiliary heat.

Selection of a Water-Supply Source—Ground Waters.—In winter the ground waters are usually warmer than surface waters. This higher temperature means that less auxiliary heat is being added to the distribution system; the deeper ground waters are usually the warmest.

Water production from wells has been found to fluctuate, reaching a minimum in late winter and early spring. Some well supplies have become entirely depleted. Therefore, test pumping during this critical period is advisable to determine reliable yields prior to the final development of the well. D. J. Cederstrom (26) has prepared a comprehensive summary of ground-water development in Alaska.

The following features of natural topography indicate the possible availability of ground water:

a. Wide, shallow exposed channels, glacial streams, or alluvial fans;

b. Slopes at, or near, the foot of a mountain or hill where movement of ground water down the slope may be intercepted;

c. Locations immediately downgrade from poorly drained areas, such as muskeg swamps, which, due to retention by heavy vegetation, are apt to yield a continuing supply during winter; and

d. Any sudden reduction in natural channel gradient or channel width in such a way that the constriction would tend to accumulate water.

Where water sources are difficult to find on the ground, aerial studies have been helpful. Color photographs taken in the air during the late summer season may show up areas of dense green vegetation, which indicate the presence of ground water.

The sites selected for a water source should minimize the lengths of transmission lines because this saves heat and reduces inspection and maintenance. If possible, ground-water sources may be located near a source of waste heat as was done in Fairbanks near the city power plant. In an attempt to obtain a water supply in winter at more than freezing temperature, engineers in Anchorage, Alaska, have considered the underground storage of summer flows from a nearby river. (Recharging of ground-water supplies in Sweden has been practiced for many years.)

Well and Pumping Facilities.—In order to avoid damage from seasonal frost and from permafrost, the well and pumping-works design must incorporate some features in addition to the orthodox weatherproofing practice. Concrete slabs are poor insulators. They transmit the heat from water in well casings, intakes, and discharge lines to the outside cold sufficiently to cause the water to freeze. Concrete slabs may also occasionally thaw the underlying permafrost. When this moisture refreezes, heaving takes place which may damage pumping facilities and throw vertical well pumps and casings out of alinement.

The freezing of well casings in contact with permafrost is prevented by a judicious pumping program. Where pumping costs are excessive or pumping is not advisable for other reasons, different means must be provided to prevent freezing. Resistance-heating cables and hot water have been used with some success. In pumping wells care also should be taken not to exceed the recoverable yield of the aquifer because this may deplete the total quantity of water movement to the extent that freezing may occur from the encroachment of the surrounding permafrost. Wherever feasible, observation wells, in addition to the water well, are desirable in determining water yields and in charting the influence of various rates of pumping.

Permafrost temperatures should be determined for water wells and whenever permafrost is encountered in construction. These temperatures may vary from 15°F to 32°F. Permafrost having a temperature approaching 32°F may be removed with reasonable assurance that it will not return. Low-temperature permafrost will probably freeze back after a stratum has been disrupted.

Water Treatment.—Ground waters will usually require iron removal. A high iron content appears to be characteristic of most ground waters from Alaska to Greenland. The removal of hardness may also be desirable. The treatment required for surface waters varies considerably. In Alaskan areas, waters from melting glaciers carry large quantities of glacial silt, thus necessitating coagulation and filtration. Other Alaskan rivers and rivers in northern Canada are turbid and colored during spring and summer runoff, and treatment should be used. A fairly high pH-factor is common in these waters; this factor combined with low temperatures obviously retards disinfection by chlorination. Disinfection must be mandatory because in winter the ice on many streams is a dumping place for fecal and other wastes which are presumably carried away with spring break-up but much of which simply settle to the bottom (27).

The large lakes in northern Canada are usually suitable without treatment except for chlorination. Waters from muskeg areas are typically colored and soft and have low pH-values. The use of smaller lakes in the very cold regions should be approached with caution. In one instance when this was done the water was quite satisfactory during the first part of the winter. However, as the cold weather continued, the ice cover became thicker, and the water quantity lessened with the result that organic matter and minerals became highly concentrated. From January 15, 1949, to February 2, 1949, the total dissolved solids of this supply were doubled. Whereas from this system one could draw normal, relatively clear water in December the liquid emerging from the tap during the course of the winter literally resembled diluted sewage in appearance and odor. Treatment processes must taken into account (*a*) the increased viscosity of low-temperature water, permitting the carrying of greater silt loads and requiring settling chambers and a filter area nearly twice that of warmer waters; (*b*) the slowing-up of chemical reactions so that flocculation basins may have to be enlarged as much as three times the orthodox design; and (*c*) the increased solubility of oxygen, which may aggravate corrosion problems when the water is warmed.

The foregoing implications indicate the desirability of raising the temperature of the water prior to treatment. This has been done at the new treatment plant at Fairbanks where waste heat from the power plant is utilized. Even though waste heat may not be available, the designer should balance the costs of deliberately furnishing auxiliary heat against the increased costs of treating low-temperature water.

In addition, experimentation in chemical dosage, flocculation, and settling over the wide range of conditions encountered is doubly important. Laboratory facilities obviously should be included in any treatment-plant design.

Adequate insulation for the outside walls of treatment-plant construction and positive means for humidity control should be provided to prevent the condensation and freezing of moisture. Treatment-plant operation would probably be facilitated by the use of electrical control or air control of valves and by rate-of-flow controllers, as well as by indicating mechanisms, rather than by hydraulic methods.

Where seasonal turbidities are the only objectionable constituent in a small water supply, consideration should probably be given to the use of diatomaceous-earth filters. The initial cost of this system is only a fraction of the cost of the orthodox coagulation and filtration processes, and operation is greatly simplified. However, presettling should be used in this method when turbidities are high. (Aklavik, Canada, has used these filters with apparent success.)

Distribution.—The satisfactory distribution of water through piped systems is probably the most vexing problem facing the designer. Of the many different types of systems in use, most have involved difficulties of one kind or another.

Where heat is distributed from central heating plants (such as those at military bases), the prevention of freezing is somewhat simplified. The usual practice in this case is to construct utilidors, which contain both the heat and the water-transmission mains. Other utilities (including sewers) may also be placed in utilidors. This practice has serious disadvantages, however, because sewer lines jeopardize the safety of the water mains. Experience has shown that the large conduit may settle out of alinement causing water and sewer lines to become disjointed or broken. Water lines completely inundated with sewage have been observed.

Where water and sewage lines are placed in a single utilidor, the conduit should be of the walk-through type. If finances do not permit this costly construction, it is suggested that a smaller utilidor be sloped to drain throughout and that the sloped lines terminate in buildings or stations which require operating personnel to enter the utilidor at least daily and thus observe conditions. The roof of the utilidor, except perhaps for that of the walk-through type, should be so constructed that access to the interior is readily accomplished. Removable slabs with lifting hooks have been satisfactory for this purpose.

Distribution of water without using utilidors is commonly practiced, but auxiliary heat must usually be provided. This heat may be added at the source or at strategic points in the system. The source of heat is optional and probably depends on the local situation as to availability. Temperature-sensing instruments are essential for control, and, if desired, the present-day devices will insure almost automatic operation to keep the water above freezing. Heat is conserved by maintaining a temperature of only slightly more than 32°F.

The cost of insulating water pipe should be balanced against the cost of increased heating. Materials that are locally available—such as peat, moss, sands, and clay—have been used to economic advantage. Some insulation must surround water mains placed in permafrost to avoid excessive thawing and subsequent settling. However, this contingency can usually be provided for by backfilling with suitable materials such as sand and gravel, if available, to form a more substantial bedding for the pipe.

The recirculation of water through the system appears to be favored by many engineers. Although the two-pipe system with a smaller-sized return line has been used, the single-pipe system is probably preferable. This system assumes that service connections can be made without danger of freezing. Here, again, auxiliary heat may be used, although a recirculating service line is entirely feasible and is recommended.

To avoid seasonal frost, water mains should be laid below the average depths to which the frost penetrates. A 10-ft laying depth has been used in systems now operating, although where good insulation and heating are provided much shallower trenches have been used. One system places most of the water mains in insulated boxes on the ground surface. Another system provides a cover of from only 5 ft to 6 ft.

Storage.—Storage above ground has been used in part of the northern United States where riser pipes are well insulated and auxiliary heat is introduced at the base of the risers. Recirculation of water in the large-diameter risers may be sufficient, but temperature indicators should be provided in this case. In addition, the elevated tanks themselves should be enclosed with an insulated outside covering for the most economical operation. (The top section of the twelve-story city hall in Kemi, Finland, houses the city water-storage tank.)

Storage in surface and subsurface tanks and reservoirs should consider the underground conditions, the nature of any permafrost, and the soil contained in the permafrost. The relatively poor insulating qualities of concrete should be borne in mind, and supplemental insulation should be provided where transfer of heat must be retarded.

Structure Foundations.—Various attempts have been made to provide stable foundations for structures placed in or above permafrost as follows:

1. Removing finely divided soils with a high moisture content, and replacing with more stable material, such as gravel or crushed rock;
2. Jetting and driving piling into the permafrost and allowing the piling to freeze in place;
3. Inserting refrigerating coils into the underground soil to maintain continuous freezing;
4. Using plenum chambers below structures through which the outside air is circulated; and
5. Constructing completely above the surface of the ground so that the outside air may circulate freely.

Where plenum chambers are installed for circulating cold outside air during the winter, consideration might be given to the insertion of a refrigerating unit in the air-circulating ducts for summertime cooling. The use of refrigeration coils to keep the ground frozen should be approached with caution. If the thermal regime is such that the permafrost gradually thaws, the freezing coils may eventually become completely inadequate regardless of their capacity.

CONCLUSIONS

The design of water supplies for arctic conditions must take into account the rather severe restrictions imposed by the long, subzero winters and the permanently frozen ground. To overcome these restrictions the designer should (*a*) thoroughly study local conditions of temperature, permafrost, and the availability of insulating materials; (*b*) make allowance for the retardation of biological and chemical reactions; (*c*) consider the personnel who will operate the system; and (*d*) provide for ease of operation, inspection, and maintenance.

In addition, the extremely high costs of labor, materials, and equipment should be borne in mind so that the owner will be financially able to purchase the resulting utility and to operate it thereafter.

APPENDIX. BIBLIOGRAPHY

(1) **"Thawing Out the Eskimo,"** by A. G. Morice, The Society for the Propagation of the Faith, Boston, Mass., 1948.

(2) **"Arctic Engineering Know-How Gets Acid Test at Thule,"** by Samuel D. Sturgis, Jr., *Civil Engineering*, September, 1953, pp. 31–35.

(3) **"The Story of Blue Jay,"** by Lewis A. Pick, *The Military Engineer*, Washington, D. C., Vol. XLV, No. 306, July–August, 1953, p. 278.

(4) **"Winter Conditions and Controls at Bismarck, N. D.,"** *Water Works Engineering*, Vol. 98, No. 23, November 14, 1945, pp. 1306–1308.

(5) **"How to Prevent Pipeline Freezing,"** *Engineering News-Record*, November 9, 1950, pp. 38–41.

(6) **"Protecting Underground Utilities Located in Arctic Regions,"** by Carl Henry Billings, *Water and Sewage Works*, Vol. 100, 1953, p. 441.

(7) **"Calgary's (Alta.) Water Supply and Its Operating Problems,"** by W. E. Robinson, *Municipal Utilities*, Toronto, Canada, Vol. 83, October, 1950, p. 25.

(8) **"Cold Weather Operation of Distribution Systems,"** by E. J. Van Deusen, *Journal*, A.W.W.A., November, 1951, pp. 909–910.

(9) **"Two Water Systems in Northern Canada,"** by Stanley S. Copp, *Public Works*, September, 1953, p. 70.

(10) **"Review of Certain Properties and Problems of Frozen Ground, Including Permafrost,"** by Charles W. Lovell, Jr. and Moreland Herrin, *SIPRE Report 9*, Snow, Ice, and Permafrost Research Establishment, Corps. of Engrs., U. S. Dept. of the Army, Wilmette, Ill., March, 1953.

(11) **"Some Aspects of Sanitation and Water Supply in the Arctic,"** by Lloyd K. Clark, Report of the Symposium on Advanced Base Water Supply and Sanitation, U. S. Naval Civ. Eng. Research and Evaluation Lab., Port Hueneme, Calif., October 7–9, 1953.

(12) **"Permafrost—A Review,"** by Robert F. Black, *Bulletin,* Geological Soc. of America, Vol. 65, 1954, pp. 839–856.

(13) **Encyclopaedia Brittanica,** World Atlas, Plate 14.

(14) **"Arctic Sanitary Engineering,"** by Amos J. Alter, Federal Housing Administration, Washington, D. C., 1950.

(15) **"Frost Penetration in Montana Soils,"** *Journal,* A.W.W.A., November, 1951, pp. 904–908.

(16) **"Water Softening at Edmonton, Alta.,"** by E. L. Smith, *Water and Sanitation,* Canada, Vol. 88, March, 1950, p. 24.

(17) **"Freezing of Water in Exposed Pipe Lines,"** by Thomas M. Riddick, Norma L. Lindsay, and Antonio Tomassi, *TAPPI,* Technical Assn. of the Pulp & Paper Industry, New York, N. Y., Vol. 34, September, 1951, pp. 24a–40a.

(18) **"Spontaneous Freezing of Water,"** by N. Ernest Dorsey, *The Scientific Monthly,* Vol. LXXVIII, 1954, pp. 283–288.

(19) **"Arctic Water Supply: It Must Circulate or Freeze,"** *Engineering News-Record,* February 4, 1954, pp. 30–31.

(20) **"How a Water Supply Was Designed for a Permafrost Area,"** by John R. Wallace, Jr., *Public Works,* January, 1954, pp. 64–66 and pp. 133–134.

(21) **"Design of Water Distribution Systems for Service in Arctic Regions,"** by William B. Page, *Water and Sewage Works,* Vol. 101, 1954, p. 333.

(22) **"A Summary of Available Data on Quality of Arctic Waters,"** by Edward W. Moore, *Report,* National Research Council, Washington, D. C., 1949, 1950, and 1952.

(23) **"Arctic Sewer and Soil Temperatures,"** by William B. Page, *Water and Sewage Works,* Vol. 102, 1955, p. 304.

(24) **"Ground Temperature Conditions Governing the Design of Alaska Water Distribution Systems,"** by Amos J. Alter, *Proceedings,* 6th Alaska Science Conference, Fairbanks, June, 1955.

(25) **"Permafrost and Ground Water in Alaska,"** *Professional Paper 264-F,* Geological Survey, U. S. Dept. of the Interior, Washington, D. C., 1955.

(26) **"Summary of Ground-Water Development in Alaska, 1950,"** by D. J. Cederstrom, *Circular 169,* Geological Survey, U. S. Dept. of the Interior, Washington, D. C., 1952.

(27) **"Enteric Diseases in Alaska,"** by Frank P. Pauls, *Arctic,* The Journal of the Arctic Inst. of North America, October, 1953.

AMERICAN SOCIETY OF CIVIL ENGINEERS
Founded November 5, 1852
TRANSACTIONS

Paper No. 2903

INTERMITTENT DISCHARGE OF SPENT SULFITE LIQUOR

BY HERMAN R. AMBERG[1] AND ROBERT ELDER[2]

SYNOPSIS

Intermittent discharge of spent sulfite liquors into the Columbia River (Washington and Oregon) is proposed as a method of controlling slime growths. Laboratory studies showed that slime growths in a receiving stream could be controlled if the wastes were discharged intermittently into a river having sufficient volume and high velocity.

INTRODUCTION

A problem commonly associated with the discharge of organic wastes is excessive slime growth. The growth of slime in streams is a natural response to the increase in nutrients and, at times, the growth may become sufficiently great to cause serious pollution problems.

The filamentous bacteria, sphaerotilus natans, are usually found in streams receiving carbohydrate wastes, and growth of this particular organism may occur on extremely weak substrates. For example, under proper environmental conditions, from 0.5 ppm to 1.0 ppm of sugar is sufficient to produce considerable sphaerotilus growth. Excessive slime growth has been a problem on the lower Columbia River (Washington and Oregon) for a number of years, and this problem will undoubtedly increase with the industrial expansion of the area. During a period of low flow, slime growth reaches such levels that it interferes with the gill-net operations of the commercial fisheries.

The primary sources of pollution in the lower Columbia River are domestic sewage, spent sulfite liquor, and numerous industrial wastes. The spent sulfite liquor from the production of approximately 500 tons of pulp per day is discharged into the lower Columbia River (approximately 140 tons of wood sugar per operating day). Domestic sewage discharged in the critical area together

---

NOTE.—Published, essentially as printed here, in April, 1956, as *Proceedings Paper 929*. Positions and titles given are those in effect when the paper was approved for publication in *Transactions*.

[1] West Coast Res. Engr., National Council for Stream Improvement, Inc., Corvallis, Ore.

[2] Research Fellow, Eng. Experiment Station, Oregon State College, Corvallis, Ore.

with the carbohydrate load makes the problem worse by supplying enough organic nitrogen to stimulate excessive sphaerotilus growth.

Although the slime organism will develop on inorganic nitrogen, growth is stimulated by the addition of traces of organic nitrogen supplied by sewage. For example, C. C. Ruchhoft and J. F. Kachmer[3] found that sphaerotilus natans had difficulty using glucose in a medium containing only glucose and mineral salts. In one experiment in a medium containing glucose and mineral salts, only 41 ppm of the 1,000 ppm of glucose originally present were used in 120 hr by a culture of sphaerotilus natans. With settled sewage the organism was able to act on from 800 ppm to 900 ppm of glucose within from 24 hr to 48 hr after inoculation.

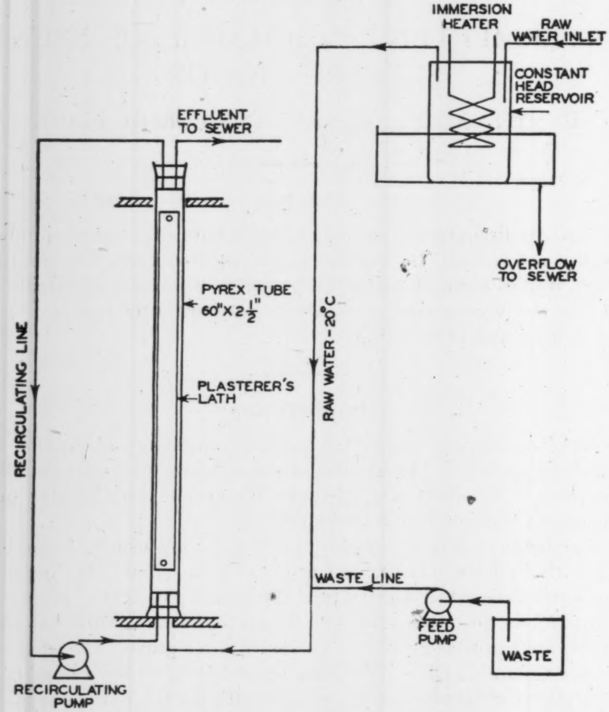
IMMERSION HEATER
RAW WATER INLET
CONSTANT HEAD RESERVOIR
EFFLUENT TO SEWER
OVERFLOW TO SEWER
PYREX TUBE 60"X2½"
PLASTERER'S LATH
RECIRCULATING LINE
RAW WATER - 20°C
WASTE LINE
FEED PUMP
WASTE
RECIRCULATING PUMP

FIG. 1.—CONTINUOUS-FLOW APPARATUS FOR SPHAEROTILUS GROWTH STUDIES

In 1955 experiments were started at the Engineering Experiment Station of Oregon State College, at Corvallis to find a method of discharge which would eliminate or reduce the slime problem. This paper is a summary of the initial phase of investigation conducted to determine the effect of intermittent feeding on the growth rate of sphaerotilus natans.

---

[3] "Studies of Sewage Purification. XIV. The Role of *Sphaerotilus natans* in Activated Sludge Bulking," by C. C. Ruchhoft and J. F. Kachmer, *Sewage Works Journal*, Vol. 13, 1941, pp. 3–36.

Because bacteria require a constant supply of nutrients for optimum growth and reproduction, elimination of nutrients during the major part of the logarithmic-growth phase should result in a substantial decrease in slime growth. Application of intermittent feeding by the sulfite mills on the Columbia River would require storage facilities sufficient to hold the waste for from 20 hr to 24 hr, with pumping facilities of sufficient capacity to discharge the spent sulfite liquor in from 2 hr to 4 hr per day.

In the studies reported, a continuous-flow apparatus was used to determine the effect of intermittent discharge of spent sulfite liquor on sphaerotilus growth.

APPARATUS

Fig. 1 shows a single unit of the study apparatus. A rack of twelve columns was used. Raw river water entered the constant-head reservoir, where it was heated to 20° C by an immersion heater controlled by a thermoregulator. Raw waste was injected into the water line by a multifeed, constant-displacement pump. The continuous water and waste flow entered the bottom of the column and was discharged at the top. Water flow was regulated by adjusting the height of the effluent line. A plasterers' lath was centered in the column to provide a surface for the attached slime growths, and a recirculation pump having a capacity of 2 liters per min was used to recirculate the water, thus ensuring sufficient velocity for slime growth.

Preliminary studies indicated that maximum growth was attained in seven days, and growth rapidly decreased after that period. At the end of seven days the columns were disconnected and drained. The growth was carefully scraped from the column walls and from the lath and was collected in a 2-liter graduated cylinder. The volume of growth was recorded after a 30-min settling period. The settled growth was dried, and determinations of total solids and volatile solids were made for each sample. Because of the voluminous nature of sphaerotilus growth, the volume determinations were more indicative of nuisance conditions than the dry weights. The solids determinations were affected by adsorption of silt and debris and gave poor indication of the slime growth.

TABLE 1.—ANALYSES OF SPENT SULFITE LIQUORS USED IN TESTS

	Ammonia base	Calcium base
Total solids (%)........	11.6	13.8
Volatile solids (%)......	89.1	...
B.O.D. (5-day at 20°C)..	30,000	39,000

The growths collected from each column were subjected to a careful microscopic examination to determine the type of growth. The fresh-water flow through the columns was maintained at 500 ml per min, and the water temperature ranged from 20° C to 22° C. Analyses of the ammonia-base and calcium-base liquors used in these studies are presented in Table 1.

Concentrations of the spent sulfite liquor are recorded herein as parts per million of bone-dry solids.

EXPERIMENTAL RESULTS

Ammonia-Base Liquor.—The initial experiment was designed to demonstrate the difference between intermittent and continuous feeding of ammonia-base liquor as measured by the slime growth at the end of the seven-day test period.

Extensive surveys of the Columbia River below the pulp-mill outfalls have shown that the maximum spent sulfite liquor a short distance below these outfalls is approximately 5 ppm. If the entire daily production of liquor were discharged during a 2-hr period, the maximum concentration in the receiving stream would be 60 ppm, and discharge over a 4-hr period would give a maximum concentration of 30 ppm. These concentrations would decrease further as the waste progressed downstream.

TABLE 2.—EFFECT OF INTERMITTENT FEEDING AND CONTINUOUS FEEDING ON SLIME GROWTH (21°C WATER TEMPERATURE AND 7-DAY RUN)

Spent-sulfite-liquor concentration, in parts per million of bone-dry solids	B.O.D. added, in parts per million	Feeding interval, in hours	Resting interval, in hours	Slime volume, in milliliters
(*a*) AMMONIA-BASE SPENT LIQUOR				
60	15.5	2	22	0
30	7.7	4	20	30
20	5.1	6	18	50
15	3.9	8	16	720
10	2.6	12	12	205
Control	0.5 to 1.0	...	...	50
5	1.3	24	...	800
10	2.6	24	...	1,240
60	15.5	24	...	1,950
(*b*) CALCIUM-BASE LIQUOR				
60	16.6	2	22	40
30	8.3	4	20	60
20	5.5	6	18	60
15	4.1	8	16	60
Control	0.5 to 1.0	24	...	40
5	1.4	24	...	550
10	2.8	24	...	840
15	4.1	24	...	730

The results of the initial experiment are presented in Table 2(*a*). Discharge of the spent sulfite liquor over periods of 2 hr, 4 hr, and 6 hr entirely eliminated sphaerotilus growth. Microscopic examination of the small amount of growth failed to show any signs of sphaerotilus natans. As the feeding period was increased to more than 6 hr, sphaerotilus growth was again noted.

The striking difference in growth can readily be seen by comparing the volume of growth under continuous-feeding conditions and intermittent-feeding conditions. For example, 60 ppm of sulfite solids fed over a 2-hr interval produced no visible growth whereas the same amount of solids fed continuously (5 ppm) produced 800 ml of growth at the end of seven days. Intermittent-feeding intervals of up to 6 hr produced growth comparable, on a volumetric basis, to the "control," which received no spent sulfite solids.

The elimination of slime growth at the 60-ppm concentration was not caused by any toxic effect because 60 ppm of spent sulfite solids fed continuously resulted in prolific growth (1,950 ml).

Calcium-Base Liquor.—In the second series of experiments, calcium-base liquor was substituted for the ammonia-base liquor. The results of this series are presented in Table 2(*b*).

No significant difference in slime growth could be detected in columns which were fed intermittently or in the control columns. Again, microscopic examination of the growth showed no sphaerotilus natans in any columns receiving intermittent doses of spent sulfite solids.

TABLE 3.—EFFECT OF AMMONIA-BASE FEEDING ON SLIME GROWTH

Spent-sulfite-liquor concentration, in parts per million of bone-dry solids		B.O.D. added, in parts per million		Feeding interval, in hours	Resting interval, in hours	Slime volume, in milliliters
Continuous	Intermittent	Continuous	Intermittent			
(*a*) AMMONIA-BASE RESIDUAL, INTERMITTENT FEEDING						
2	60	0.5	15.5	2	22	75
2	30	0.5	7.7	4	20	200
2	20	0.5	5.1	6	18	230
2	15	0.5	3.9	8	16	380
2	10	0.5	2.6	12	12	420
Control	...	0.5 to 1.0	...	...	...	50
2	...	0.5	...	24	...	110
(*b*) AMMONIA-BASE LIQUOR, TWO DAILY FEEDINGS						
2	60	0.5	15.5	2	...	300
0	60	0.0	15.5	2	...	50
2	40	0.5	10.2	3	...	590
0	40	0.0	10.2	3	...	130

Continuous feeding of equivalent amounts of calcium-base spent liquor produced considerable growth. Microscopic examination of the growth developed under continuous feeding showed that the growth was almost a pure culture of sphaerotilus natans.

Ammonia-Base Residual.—Because collection of spent liquor from the blow pits is not complete, it was thought practical to determine the effect of a continuous low concentration of spent sulfite solids on slime growth when an intermittent-feeding schedule was used. A background concentration of 2 ppm of spent sulfite solids was fed to the column on a continuous basis, and the intermittent-feeding schedule of the initial experiment was repeated.

Intermittent feeding on a 2-hr basis produced no significant difference in slime growth as compared to the control and the column receiving a continuous concentration of 2 ppm (Table 3(*a*)). Increasing the intermittent-feeding interval to from 4 hr to 6 hr resulted in some sphaerotilus growth, but this growth was considerably less than it was under a continuous-feeding schedule.

A careful microscopic examination of all samples of slime from the columns receiving 2 ppm of spent-sulfite-solids residual (continuous feed) showed sphaerotilus natans.

Two Intermittent Feedings per Day.—Two such feedings would have definite advantages over the single feeding because less storage capacity and smaller pumps would be required to handle the spent liquor.

In this experiment two daily feedings were used—one at 2-hr intervals twice a day and the other at 3-hr intervals twice a day. One series received a continuous discharge of 2 ppm of ammonia-base solids in addition to the intermittent discharges.

From Table 3(*b*) it can be seen that two intermittent feedings were very effective in eliminating slime growth, provided the water carried no continuous residual. In the presence of a continuous residual of 2 ppm, growth did develop, although it was much less than under a continuous-discharge schedule.

DISCUSSION OF RESULTS

All the laboratory results presented indicate that sphaerotilus growth can be eliminated or reduced by modification of the method of discharge at the mill. Results indicate that optimum growth occurs when spent sulfite liquor is discharged continuously at a constant concentration. Through the use of an intermittent-feeding schedule, the same amount of spent liquor can be discharged without subsequent increase in slime growth.

With an intermittent-feeding schedule, the organism is unable to adjust or become acclimated to any one condition. The intermittent schedule also eliminates a major part of the reproduction cycle during the phase of logarithmic growth. Although intermittent feeding to water containing a spent-sulfite-liquor residual resulted in some growth, the growth was substantially lower than if the same quantity of waste were discharged over a 24-hr period.

Table 2 and Table 3 clearly demonstrate the effectiveness of an intermittent-feeding schedule. Because there is always a possibility of some equalization upon discharge to a swift stream, it becomes advantageous to discharge over as short a period as possible. Intermittent discharge is effective in reducing slime growth, provided the growth is attached and does not grow in the flowing part of the stream and provided the velocity is sufficiently swift to prevent equalization of the intermittent discharges. The receiving stream must also have sufficient flow to absorb the intermittent discharges without depleting the oxygen supply and without creating a toxic problem.

The experimental data indicate that the period of discharge can be increased to as much as 6 hr without serious sliming, but, if equalization should increase the discharge period upon downstream translation in excess of 6 hr, a slime problem may develop. Flow in the Columbia River is swift, and it is doubtful whether merging of the intermittent discharges would ever occur.

The intermittent-discharge principle has considerable flexibility. For example, if there is a possibility of a certain amount of equalization of discharges, the resting period can be lengthened. By discharging the spent liquor from the production of 2 days over 4 hr, the possibility of developing a continuous-discharge pattern in the lower river would be eliminated.

The possibility of toxicity should also be considered. Voluminous survey data collected below the outfalls of the sulfite mills on the Columbia River have indicated that maximum spent-sulfite-liquor concentrations in the immediate vicinity of the underwater outfalls range from 3.0 ppm to 5.0 ppm of bone-dry solids when discharging over a 24-hr period. Discharge of the entire day's production over a 2-hr interval would result in a maximum concentration of 60 ppm below the outfall. Bioassays conducted indicated that these concentrations would not constitute a serious toxic problem. Although the fish may be exposed to concentrations of as much as 60 ppm, the time of exposure would be relatively short (from 2 hr to 4 hr), and this concentration would rapidly decrease upon passage downstream. For example, on the basis of available survey data, a discharge of 60 ppm at Camas (Wash.) would be reduced to less than 20 ppm at the Interstate Bridge at Vancouver (Wash.).

A report has been made[4] on the toxicity of spent sulfite liquor to salmon under experimental conditions. Twenty long-term experiments (thirty days) were conducted with Chinook, pink, and silver salmon of various age groups obtained from hatcheries. Table 4 shows the mortality "threshold indexes" (5% mortality) determined from seven long-term experiments.

With an intermittent-discharge schedule, the test specimens could undoubtedly tolerate much higher concentrations.

Engineering Implications.—The possible utilization of intermittent feeding of organic wastes as a method of waste disposal probably has a limited application. The stream utilized must have sufficient flow to handle the slug loadings in order to prevent toxicity and oxygen-depletion problems.

TABLE 4.—SPENT-SULFITE-LIQUOR CONCENTRATION TO RESULT IN A 5% MORTALITY OF SALMON

Type of Salmon	Age, in days	Parts per million of spent sulfite liquor
Chinook	38	117.5
	280	60.0
	305	56.0
Pink	102	155.0
	198	53.0
Silver	351	123.0
	412	101.5

However, the method may be successfully used in some locations to shift the critical dissolved-oxygen deficit or to lengthen the period of self-purification. It would be particularly applicable to streams where the major part of self-purification occurs through the action of slime growths on the river bottom. By eliminating the slime growths the rate parameter, k, would be reduced, and the waste may be shifted from a critical stream to a larger body of water where the purification capacity would be adequate to handle the waste.

The discharge of nitrogen-deficient wastes on an intermittent-feeding schedule would also be effective in reducing the rate of decomposition. For example, if one assumes a carbon-to-nitrogen ratio in a stream receiving an organic waste of 50 to 1, by discharging the waste over a 4-hr period the carbon-to-nitrogen ratio would be increased to 300 to 1, with a subsequent reduction in the rate of decomposition.

---

[4] "Toxic Effects of Sulfite Waste Liquor on Young Salmon," by R. W. Williams, E. M. Mains, W. E. Eldridge, and J. E. Lasater, *Research Bulletin No. 1*, State of Washington Dept. of Fisheries, Seattle, Wash., December, 1953.

Conclusions

From the experimental results presented herein the following conclusions can be made:

1. The most favorable feeding schedule for optimum growth of sphaerotilus natans is a continuous discharge of spent sulfite liquor.
2. The intermittent discharge of spent sulfite liquor to river water having a low-pollution residual produces no slime growth, provided the discharge interval is maintained below 6 hr.
3. The intermittent discharge of spent sulfite liquor to river water containing a background residual of 2 ppm of sulfite solids produces some slime growth, but the growth is much less compared with the continuous discharge of an equivalent pollution load.

AMERICAN SOCIETY OF CIVIL ENGINEERS
Founded November 5, 1852
TRANSACTIONS

Paper No. 2904

THE USE OF STATISTICS IN RESERVOIR OPERATIONS

BY VICTOR A. KOELZER,[1] A. M. ASCE

SYNOPSIS

Statistics can be very useful in reservoir operations as an assessment of the operational chances involved, particularly with respect to water supply. Operating plans must consider the probability of a variation in water supply from that considered to be most likely; in fact, the extreme variations frequently form the controls for a particular operation, rather than the most probable supply. The development of annual operating plans for reservoir systems deriving their primary water supply from snowmelt, as well as progressive, seasonal modifications to these plans, is demonstrated herein. Particular emphasis is given to the importance of probability analyses in determining limits for the development of the operational plans.

INTRODUCTION

The successful operation of any storage reservoir involves consideration and anticipation of a number of factors. Some of these factors are economic, such as power rates and water rental rates, which, for a given period of operation, are generally predictable within close limits. Others may be physical, such as reservoir, plant, and channel capacities, and are usually fixed. Legal and contractual obligations, generally also of a fixed nature, are frequently involved. Still other factors involve climatic conditions which are not usually predictable far in advance and are subject to relatively wide variations. These latter factors are of two types—water-use requirements and water supply.

Water-use requirements often involve both economic and climatic factors and, as a result, generally are not random occurrences. On the other hand, the occurrence of streamflow, if unregulated, is a natural phenomenon and, as such, is a random occurrence. Thus, a stream can be expected to follow the laws of probability, even though its probability curve will generally be skewed rather

---

NOTE.—Published, essentially as printed here, in June, 1956, as *Proceedings Paper 1008*. Positions and titles given are those in effect when the paper was approved for publication in *Transactions*.

[1] Hydr. Engr., Harza Eng. Co., Chicago, Ill.; formerly Hydr. Engr., Bureau of Reclamation, U. S. Dept. of the Interior, Washington, D. C.

than in accordance with the normal law. Therefore, it is in estimating water supply that the use of statistical procedures has the widest application.

Some engineers are reluctant to use statistical procedures because they consider them academic or too difficult to apply. It may seem preferable to use specifically observed figures, such as historical maximums or historical minimums. Hydrologists know, however, that this procedure can sometimes be very misleading, particularly if no consideration is given to whether the experienced extremes are out of proportion to the length of record.

Admittedly, the expression of water-supply potential in terms of probabilities may seem somewhat vague to the engineer who is accustomed to having a more solid foundation for his computations. However, because one is dealing with an element that is fundamentally unpredictable on a long-range basis, it should not be surprising if the best method of expression is somewhat less tangible than that used in most engineering practice. Most water-use projects will be in existence for many years, and the aim should be a successful operation during the life of the project. The probability approach does not guarantee protection against occasional mistakes, but it does offer the best assurance of a high-level performance over a long period of time. If such is the case, the approach is not academic—it is extremely practical.

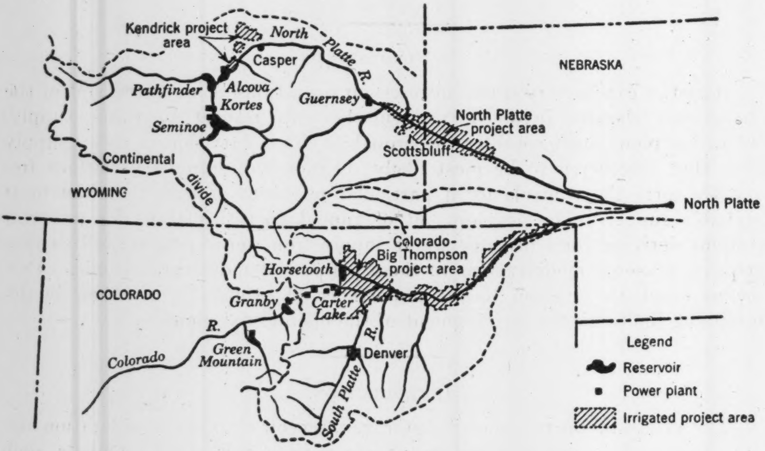
Kendrick project area
North Platte R.
Casper
Pathfinder
Alcova
Kortes
Guernsey
Seminoe
North Platte project area
Scottsbluff
NEBRASKA
Continental divide
WYOMING
North Platte
Colorado-Big Thompson project area
Horsetooth
COLORADO
Granby
Carter Lake
R.
Colorado
Green Mountain
Denver
South Platte R.
Legend
Reservoir
Power plant
Irrigated project area

Fig. 1.—Map of Operational Area

The emphasis placed on the proper evaluation of operational chances does not mean that common sense, good judgment, and observance of fixed operational requirements can be ignored. These must be basic in the determination of any reservoir-operations schedule. However, a so-called "feel of the river" is a valuable asset only if it refers to an intimate knowledge of the physical and hydraulic characteristics of a river, and is probably much overrated if it is intended to imply merely an intuitive knowledge of how a river will perform.

Concerning difficulty of use, only the simplest of statistical methods are needed. The time and effort spent in making the analyses represent only a minute part of the work involved in reservoir operations.

The intent of this paper is to demonstrate the use of statistical procedures, rather than to present arguments in favor of any specific type of analysis. Much information[2] is readily available on this subject, and it is considered outside the scope of the paper to justify any specific method of analysis.

TABLE 1.—DATA FOR RESERVOIRS, POWER PLANTS, AND PUMPING PLANTS

Name	RESERVOIRS		POWER PLANTS			PUMPING PLANTS		
	Type[a]	Total storage, in acre-feet	Installed capacity, in kilowatts	Hydraulic capacity, in cubic feet per second	Maximum gross head, in feet	Installed horsepower	Hydraulic capacity, in cubic feet per second	Maximum lift, in feet
Alcova	*R*	190,500	36,060	3,100	168			
Carter Lake	*S*	112,382						
Flatiron	*R*	760	63,000	960	1,118	13,000	440	297
			8,500[b]	440[b]	297[b]			
Granby	*S*	539,758				18,000	600	186
Grand Lake	*R*	511[c]						
Green Mountain	*S*	154,645	21,600	1,660	263			
Guernsey	*R*	44,800	4,800	920	90			
Horsetooth	*S*	151,752						
Kortes	*R*	4,744	36,000	2,700	205			
Lake Estes	*R*	3,068	45,000	1,300	568			
Lingle			1,400	230	106			
Mary's Lake	*R*	927	8,100	550	217			
Pathfinder	*S*	1,015,876						
Pole Hill			33,250	550	838			
Rattlesnake	*R*	2,181						
Seminoe	*S*	1,012,000	32,400	2,850	217			
Shadow Mountain	*R*	17,354						
Willow Creek	*R*	10,553				10,000	400	171

[a] *S* for storage, *R* for reregulating. [b] Pump unit which may be reversed for generation. [c] Active.

DESCRIPTION OF RESERVOIR SYSTEM

The probability approach has been used to estimate water supply in scheduling reservoir operations for one of the multiple-purpose systems designed by the Bureau of Reclamation, United States Department of the Interior (USBR). Physically, this system includes facilities of the Colorado-Big Thompson Project (Colorado), the North Platte Project (Wyoming), the Kendrick Project (Nebraska), and certain features of the Missouri River Basin Project in these same states. The major features of the system are shown in Fig. 1, and pertinent data are given in Table 1. Not shown is the extensive transmission grid which permits interconnected system operation of all power plants. The primary water supply for the system is derived from snowmelt from the Rocky Mountains. Early in the spring this water supply can be forecasted on the basis of the winter accumulation of snow and precipitation.

For maximum benefit, the reservoir operations of the entire interconnected system must be closely coordinated. Reservoir operations in the different river basins could be handled independently if only irrigation were involved. However, because the power plants in the two basins are interconnected, close coordination between the reservoir systems is essential. To effect the desired balance between reservoir systems and to arrive at the best integrated operation of all the features, a centralized operations office was established near Loveland (Colo.) in May, 1951. Its functions are primarily related to essential operational planning and coordination of multiple-purpose operations.

---

[2] "Review of Flood Frequency Methods," Final Report of the Subcommittee of the Joint Division Committee on Floods, *Transactions*, ASCE, Vol. 118, 1953, p. 220.

The Annual Operating Plan

Experience has indicated that the objective of optimum utilization of the water supply can be achieved only through careful budgeting of the anticipated water supply against water demands. This water budget is the basic element of what has become known as the "annual operating plan," which has been in use in the USBR system since the 1952 water year.

The annual operating plan is a defined course of future action. It includes operation studies, supporting charts, and an explanatory text, which together indicate how the facilities will be operated under various conditions. It must consider the possibility of extremes in water supply as well as in water demand. For this reason a complete operating plan includes provision for reasonable maximum and minimum conditions of water supply as well as for the most probable water-supply conditions. The plan must also allow for the revisions that will be made from time to time as the operational season unfolds and new information is obtained which indicates the desirability of change in operational direction.

It is in computing the reasonable maximum and minimum conditions to be provided for, both in the basic annual plan and in the subsequent within-season revisions, that the use of statistical analysis is most helpful. The existence of adequate streamflow records over a considerable period of time lends itself well to the use of statistical procedures for estimating probable variations in the annual water supply through the derivation of probability curves of annual flows. In a like manner, procedures for shorter-term forecasts of streamflow, such as for seasonal snowmelt runoff, generally include computation of the standard error of the forecast, which can be used in such cases in a manner similar to a probability curve.

An essential element of the operating plan is that it must have an initial firm schedule which is identical in some controlling feature under all assumed conditions of water supply. The controlling feature can be reservoir storage, reservoir release, power generation, or another feature. This feature should be identical for all operations until significant new information on possible inflow conditions is expected. The need for this initial firm schedule is obvious if the consequences are considered of developing a series of operating plans which immediately depart in different directions for any of the infinite number of possibilities of water supply. Such plans are unsuitable because no dependable course of action is established for any period of time. The course of the initial firm phase of operations can best be set by a month-by-month (or shorter period if necessary) operation study, which considers the possible future variations in water supply, water uses, and other controlling factors. The actual mechanics become somewhat of a trial-and-error process.

From the foregoing it can be seen that the operating plan has a firm schedule for the initial period only, and that after this initial period the operating plan is a series of plans to be applied under varying conditions rather than a single set plan. Also, the course of the initial, firm schedule is controlled by consideration of possible future extremes rather than of the most probable future occurrences. For example, under assumed, minimum inflow conditions, it will generally be desirable to fill a reservoir by the end of the snowmelt runoff season. At the same time, if maximum inflow conditions should occur, it will be desirable to pass all the water through the power plant. These two objectives, requiring consideration of opposite conditions, are the determining factors in establishing the operational position that will be gained during the initial period of the plan. Thus, the extremes, rather than the most probable occurrences, are the guide lines of operation, and it becomes essential to have reliable methods of computing the probability of the extremes.

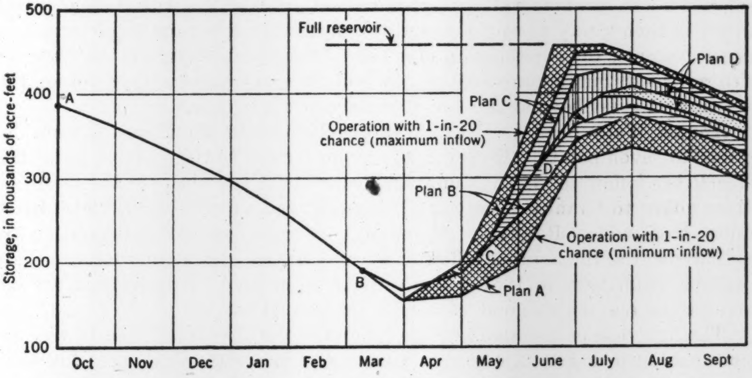

FIG. 2.—EXAMPLE OF REVISION OF OPERATION PLANS WITH PROGRESS OF RUNOFF SEASON

In actual operations, the firm schedule is followed until significant new information on water supply, water use, or other controlling elements are available. A new plan is then developed which extends the firm schedule beyond the one previously developed and considers various possibilities of the future. As the operations proceed, this process is continually repeated, using the same procedures. This process can best be demonstrated graphically (Fig. 2).

In Fig. 2, the element of the operating plan that remains constant for all conditions of inflow is reservoir storage. In such a case, the outflow must, of necessity, vary with different conditions of inflow during the initial period. At the beginning of the water year, at point A, operating plan A is developed; this plan has an initial firm schedule through March, and then has limits of storage necessary to accommodate the computed probable range of inflow. At point B, new inflow forecast information is available which indicates that a revision in plan is desirable. This plan, identified as plan B, has a set schedule extending into May, which then changes to limits of operation to accommodate the probable range of inflow. The probable range in plan B is the same as in plan A in terms of percentage change (1 in 20), but is smaller in terms of acre-feet because of increased forecast accuracy as the season progresses. The same process is repeated in plans C and D, until the critical operation time of peak storage is reached.

OPERATING PLANS BY PROBABILITY ANALYSES

General Considerations.—In the foregoing, the various factors to be considered in scheduling reservoir operations were examined with emphasis on their variability. The following examples were chosen for purposes of demonstrating the use of probability studies of water supply; therefore, they may not emphasize all the economic, legal, physical, and use-requirement considerations that would normally be involved. The somewhat simplified examples shown are not intended to detract from the consideration that must be given to such factors.

In certain cases probability curves may be useful for estimating water-use requirements. Although this possibility should not be overlooked, care should be taken not to combine water-use requirement probabilities with those of water supply in such a way as to compound the probabilities beyond those intended. As an example, the combination of a 1-in-20 maximum water-use requirement with a 1-in-20 minimum water supply will generally place a condition on the system that is far beyond the 1-in-20 chance of occurrence.

Annual Water Supply.—Natural streamflow enters the USBR system described at seven points. However, the major inflows to the system are (1) the Blue River inflow to Green Mountain Reservoir (Colorado), (2) the Colorado River inflow to Granby Reservoir (Colorado), and (3) the North Platte River inflow to Seminoe Reservoir (Wyoming). Streamflow estimates, either by measurement at the point of inflow or by correlations with nearby locations, are available from 1906 to 1957. The estimates obtained by correlation are believed to be reasonably good, especially the annual totals.

The five-year progressive average inflows to the three reservoirs in the system are shown in Fig. 3. For comparative purposes the flows are plotted as percentages of the historical average flow. These curves reveal definite high and low swings from which it might be feasible some day to determine a cyclic effect as further information is obtained on such potential climatic influences as sunspots. However, current knowledge is too limited to allow prediction on a cyclic basis of even general climatic conditions.

An inspection of the flows for individual years (not shown in Fig. 3) reveals that extreme high and low years have occurred, apparently at random, in any of the periods. Thus, any cyclic effect that might be determinable, although perhaps indicative of a general level of climatic conditions, would still be of questionable value in predicting the flow for any given year. In addition, trial correlations for these streams have revealed no significant influence on the runoff in one year on the runoff of the following year.

With these observations in mind, it was concluded that the probable range of occurrence of flows could best be estimated by considering the entire period of record and that probability procedures would be the best method of analysis. If future developments indicate that cyclic influences can be depended on to predict a general level of climatic conditions, it should still be possible to use probability methods to predict variations from the general level determinable from the cycle.

A reasonably reliable estimate of each year's flow, rather than a precisely accurate figure, is all that is required for a frequency analysis in that smooth curves are ultimately drawn through the plotted points. In lieu of a high degree of accuracy, it is probably more important to extend the period of record with reasonably reliable, estimated data in order to obtain the benefit of as long a hydrologic experience as possible. Although frequency curves can be misleading if stream flows are estimated for frequencies requiring extrapolation of the curve, the use of such curves is believed to be quite satisfactory if frequencies selected are well within the range of the curves. This is the case in the procedures described.

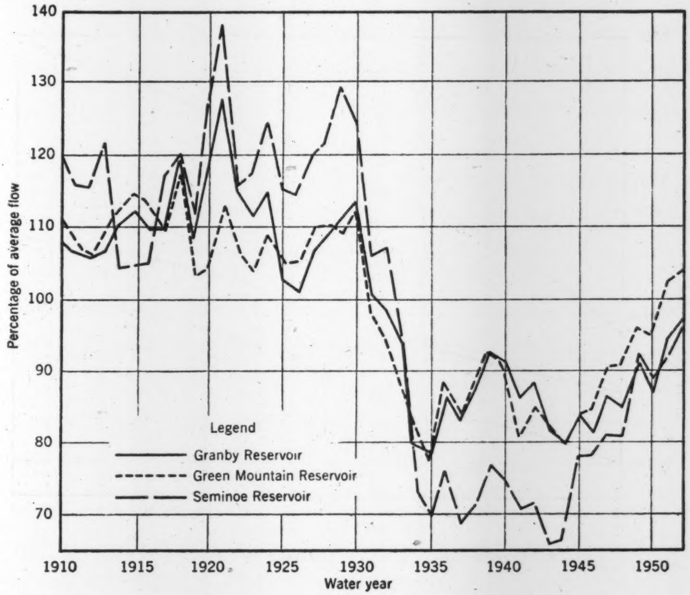

FIG. 3.—COMPARISON OF 5-YR RUNNING AVERAGE INFLOW EXPRESSED IN PERCENTAGES OF 1906–1952 AVERAGES

The procedure used consisted simply of arranging all annual flows in order of their magnitude, computing their plotting position, plotting on probability paper, and drawing a smooth curve. The location of the plotting position was determined by the formula,

$$p = 100 \left(\frac{2\,m - 1}{2\,n} \right) \dots\dots\dots\dots\dots\dots (1)$$

in which p is the percentage of the time that a given annual flow has been exceeded, m denotes the order number, and n is the years of record.

The resulting curves for the inflow to Seminoe Reservoir, Granby Reservoir, and Green Mountain Reservoir are shown in Fig. 4. They illustrate the percentage of time that given annual inflows at the three locations can be expected to be exceeded—that is, if the past is considered to be a reasonable representation of the future.

Short-Period Water Supply.—Short-period estimates of water supply are typified by the seasonal forecasts of water available from snowmelt. The development of such forecasts is a lengthy subject in itself and will not be described herein because considerable information on various procedures is available in engineering literature. Most procedures include a computation of the standard error of the estimate, from which various degrees of probability can readily be computed.[3] These probabilities are usable in the same manner as those selected from the curves in Fig. 4. As the snowmelt season progresses the probable error in the forecast decreases, and the range between given probabilities also decreases. For example, in 1953, the 9-in-10-chance range (between 5% chance and 95% chance) for inflows to Green Mountain Reservoir (April through July) varied from the 50% chance as follows:

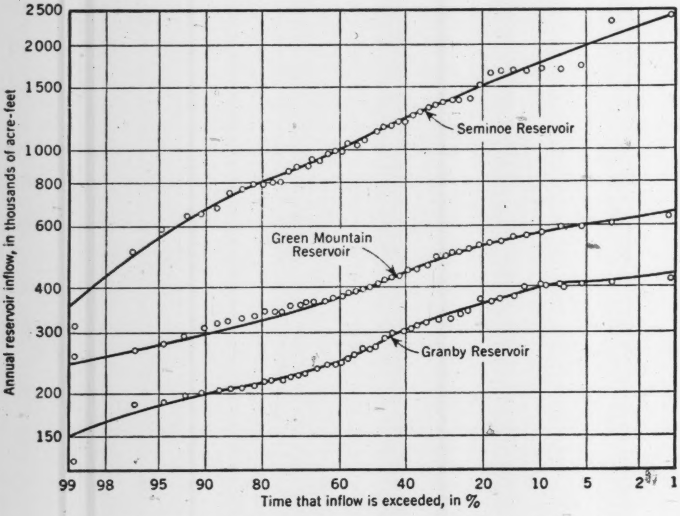

FIG. 4.—INFLOW FREQUENCY CURVES BASED ON 1906–1952 PERIOD

Date of forecast	9-in-10 chance range of inflow, in acre-feet
February 1	± 70,000
March 1	± 67,000
April 1	± 62,000
May 1	± 55,000

---

[3] "Multiple Correlation in Forecasting Seasonal Runoff," by Perry M. Ford, *Engineering Monograph No. 2*, Bureau of Reclamation, U. S. Dept. of the Interior, Denver, Colo., pp. 12–13 and p. 17.

Operating Plan for Green Mountain Reservoir.—The use of probability procedures can be demonstrated by the development of a simplified, annual operating plan for Green Mountain Reservoir. For purposes of simplicity it is assumed that all power can be sold at the same power rates. It is also assumed that certain minimum power generations must be maintained to fit system operations. The entire capacity of this reservoir is not needed for irrigation purposes. Therefore, although it is desirable to fill the reservoir, some chance that the reservoir will not be filled can be taken. A consideration of these factors indicates the desirability of taking equal chances of failing to fill and of spilling the reservoir.

TABLE 2.—ANNUAL-OPERATION PLAN FOR GREEN MOUNTAIN RESERVOIR

Month	UNDER REASONABLE MAXIMUM CONDITIONS (90% CHANCE)				UNDER MOST PROBABLE CONDITIONS (50% CHANCE)				UNDER REASONABLE MINIMUM CONDITIONS (10% CHANCE)			
	Inflow, in 10^3 acre-feet	Outflow, in 10^3 acre-feet	Storage, in 10^3 acre-feet	Generation, in 10^6 kilowatt-hours	Inflow	Outflow	Storage	Generation	Inflow	Outflow	Storage	Generation
September	...	...	111.9	...	...	...	111.9	...	...	...	111.9	...
October	19.0	21.9	109.0	4.2	13.8	16.7	109.0	3.2	10.2	13.1	109.0	2.5
November	13.4	19.4	103.0	3.6	9.7	15.7	103.0	3.0	7.2	13.2	103.0	2.5
December	11.2	18.8	95.4	3.5	8.1	15.7	95.4	2.9	6.0	13.6	95.4	2.5
January	10.1	18.7	86.8	3.3	7.3	15.9	86.8	2.8	5.4	14.0	86.8	2.5
February	9.0	18.7	77.1	3.2	6.5	16.2	77.1	2.8	4.8	14.5	77.1	2.5
March	11.2	26.7	61.6	4.4	8.1	23.6	61.6	3.8	6.0	21.5	61.6	3.5
April	25.2	36.8	50.0	5.6	18.2	29.8	50.0	4.5	13.5	25.1	50.0	3.8
May	105.8	110.5	45.3	16.9	76.5	30.0	96.5	5.0	56.7	32.0	74.7	5.0
June	186.5	92.3	139.5	18.0	134.9	81.4	150.0	17.3	99.9	25.6	149.0	5.0
July	96.3	81.2	154.6	18.6	69.7	65.1	154.6	15.0	51.6	45.0	154.6	9.0
August	46.5	51.1	150.0	11.4	33.6	38.2	150.0	8.5	24.9	39.0	140.0	8.7
September	25.8	25.8	150.0	5.5	18.6	23.6	145.0	5.0	13.8	31.8	122.0	6.6
Total	560.0	521.9	+38.1	98.2	405.0	371.9	+33.1	73.8	300.0	289.9	+10.1	54.1

Experience has indicated that approximately an 80%-chance range of annual inflows can be handled with equal chances of failing to fill and of spilling. Therefore, this range was selected for the first trial of the operating plan for the entire year. From Fig. 4, the following annual inflows were obtained for the 80%-chance range between 10% and 90%:

	Times flows were exceeded, in percentage	Inflow, in acre-feet
Reasonable maximum........	10	560,000
Most probable..............	50	405,000
Reasonable minimum........	90	300,000

The annual flows were distributed by months on the basis of the average historical distribution, and a month-by-month operation study was made, starting with conditions existing at the beginning of the operational year, October 1. The resulting annual operation plan for the reservoir is given in Table 2. The different phases of the plan were determined as follows:

1. To hold power head as high as possible, the minimum feasible drawdown is desirable during the low-flow winter period. Thus, the reservoir was operated during this period to meet minimum allowable power generations under minimum inflow conditions, as shown in the last four columns of Table 2. This procedure establishes a drawdown schedule that is used for the two other conditions of water supply, and is satisfactory even if the water supply should change during the winter to the reasonable minimum condition.

2. The duration for which the generation under minimum conditions is held to the minimum allowable is determined by operations during the snowmelt period to control the reasonable maximum inflows. Operation of the maximum condition in reverse (working backward at power-plant capacity from a full reservoir in July) will assure that no power water will be spilled under this condition. Thus, the point at which the two operations meet is the latest date at which generation can be held to the minimum under minimum conditions and still be able to pass all the water through the power plant in event of maximum conditions. This point is also the one at which the initial firm schedule, in terms of reservoir storage, begins to deviate to meet later inflow conditions.

3. After the reservoir is filled in July, operations are controlled by criteria for irrigation requirements, minimum generation, or drawdown to conserve rain floods.

The generation for July under minimum conditions is slightly higher than the 5,000,000 kw-hr that is required. This means that a lesser chance is being taken of failing to fill under minimum flows than there is of spilling under maximum conditions. A small adjustment in the flows selected, widening the range slightly from the 80%-chance range, and recomputation with the same procedure, will modify the operations as necessary to equalize fully the chances taken.

The foregoing operation shows the planned operation for the entire year as visualized on October 1. It contains the required ingredient of a firm schedule for all conditions for an initial period (an identical reservoir storage for all conditions until April 30). The plan can be firm, if necessary, until that date. If at any time prior to April 30 a forecast indicates that the operation in the original plan is not satisfactory, a new plan can be developed. For example, assuming that on April 1 the forecast for the April-to-July period, considering snow-water content, winter precipitation, and other factors, including the evaluation of the probabilities of occurrence as computed in the forecast equation, is as follows:

	Times flows were exceeded, in percentage	Inflow, in acre-feet
Reasonable maximum.......	5	± 328,000
Most probable..............	50	± 268,000
Reasonable minimum.......	95	± 208,000

Because such forecasts have narrower limits of error than the annual estimates, it is possible to operate with a greater assurance of either filling or avoiding spill. Therefore, the broader probability limits shown (from 5% to 95%) were selected for trial purposes.

The revised operating plan, based on the April 1 forecast, is given in Table 3. A firm schedule is chosen for the initial stages of the plan, again in terms of reservoir storage, which is identical for all types of inflow until May 20. A firm plan of operation is thus assured that can be followed through the development of the next inflow forecast, which will be prepared from snow survey and precipitation data observed as of May 1.

The operational schedules in this revision are developed in the same manner as in the original annual plan—that is, by working the minimum condition operation with minimum power requirements until it meets the maximum condition operation, worked in reverse from full reservoir at plant capacity. The process of revising the operating plans can be repeated as often as significant changes in forecasted conditions occur. Thus, a revised operating plan can be made after the May 1 and June 1 streamflow forecasts and as often during the rapidly changing heavy inflow period as changing conditions may require.

TABLE 3.—OPERATIONAL PLAN FOR GREEN MOUNTAIN RESERVOIR AFTER APRIL 1 FORECAST

Date		UNDER REASONABLE MAXIMUM CONDITIONS (95%)				UNDER MOST PROBABLE CONDITIONS (50%)				UNDER REASONABLE MINIMUM CONDITIONS (5%)			
		Inflow, in 10^3 acre-feet	Outflow, in 10^3 acre-feet	Storage, in 10^3 acre-feet	Generation, in 10^6 kilowatt-hours	Inflow	Outflow	Storage	Generation	Inflow	Outflow	Storage	Generation
March	31	...	...	61.6	...	...	...	61.6	...	...	...	61.6	...
April	10	4.0	9.5	56.1	1.4	3.2	8.7	56.1	1.3	2.5	8.0	56.1	1.2
	20	5.9	10.2	51.8	1.5	4.8	9.1	51.8	1.4	3.7	8.0	51.8	1.2
	30	10.5	12.3	50.0	1.8	8.6	10.4	50.0	1.5	6.9	8.7	50.0	1.3
May	10	17.4	17.4	50.0	2.6	14.2	14.2	50.0	2.1	11.0	11.0	50.0	1.7
	20	28.9	21.9	57.0	3.3	22.8	15.8	57.0	2.4	17.7	10.7	57.0	1.7
	31	40.8	26.1	71.7	4.4	33.2	18.5	71.7	3.1	25.8	11.1	71.7	1.8
June	10	57.6	31.1	98.2	5.8	47.1	20.6	98.2	3.8	36.6	10.1	98.2	1.8
	20	52.4	13.9	136.7	3.0	42.9	16.9	124.2	3.5	33.1	10.2	121.1	2.0
	30	41.3	26.1	151.9	6.0	33.8	16.2	141.8	3.5	26.2	9.6	137.7	2.0
July	10	28.2	25.5	154.6	6.0	23.9	15.7	150.0	3.5	18.5	9.1	147.1	2.0
	20	24.6	24.6	154.6	5.8	20.1	15.5	154.6	3.6	15.6	12.7	150.0	2.8
	31	16.4	21.0	150.0	4.8	13.4	18.0	150.0	4.1	10.4	10.4	150.0	2.3
August	31	37.8	37.8	150.0	8.7	30.8	30.8	150.0	7.1	24.0	40.0	134.0	8.9
September	30	20.9	22.2	148.7	5.0	17.1	28.0	139.1	6.4	13.2	35.0	112.2	7.0
Total		386.7	299.6	+87.1	60.1	315.9	238.4	+77.5	47.2	245.2	194.6	+50.6	37.7

The operations shown in Table 2 and Table 3 were controlled by the minimum and maximum conditions selected. These conditions form the guide lines that control the initial firm schedule, and the operation to meet such conditions is obviously satisfactory for the most probable conditions as well. This emphasizes the importance of the probability studies, which determine the minimum and maximum inflows in the operational scheduling.

Although the scheduling procedures described assure successful operations for the conditions cited, the limits chosen represent only a reasonable range and not the full range of possibilities. Occurrence of flows outside these limits are not only possible but should be expected to occur with the frequency indicated. Emergency operating plans should always be available to meet these conditions when they occur. The use of probability procedures will yield dividends over a long history of operations. However, they should not be "oversold" to the point of creating an impression that the flows will be positively within the limits selected for analysis.

North Platte Flood-Control Operation.—Another valuable application of the use of statistical methods in evaluating the chances involved occurred in 1952 on the North Platte River, when high flows of potential flood magnitude were considered a strong possibility. Instructions were received from appropriate administrative officials that the operational objective should be to prevent, if possible, uncontrolled damaging spills throughout the system and at the same time assure that all reservoirs would fill. These instructions were issued, of course, with the full knowledge that absolute guarantees could not be given of accomplishing both objectives. Such a guarantee was not possible because, in order to assure flood-control capability, advance releases to provide flood-control space would be required, which would cause some risk of failing to fill if the actual flow was substantially less than forecasted. Because there is no flood-control allocation in the system and, therefore, no formal flood-control regulations, it was understood that the operational chances to be taken should be consistent with the primary purposes of the reservoirs and with the benefits to be gained.

The situation was ideal for the use of statistical procedures. The basic streamflow forecasts were made in normal fashion, through multiple-correlation procedures, and included in their derivation a computation of the probable chances of missing the forecast by given amounts. Three basic types of operation studies were made, each using the operational scheduling procedure described previously. The three studies were:

1. A purely conservation operation, in which no reservoir releases in excess of power-plant capacity were allowed until the two reservoirs involved were filled. Such an operation indicated that damaging spills would very probably occur.
2. Operation to assure that reservoir outflows with 1-in-5 chance, maximum inflows would be held to acceptable limits.
3. Operations to assure that reservoir outflows with 1-in-20 chance, maximum inflows would be held to acceptable limits.

The latter operations involved taking some chance of failing to fill both reservoirs and consequently of wasting water for both irrigation and power.

Four factors were evaluated to determine the chances being taken of certain losses occurring because of operations under plans 1 and 2. These losses were (*a*) firm-energy loss. (*b*) dump-energy loss, (*c*) power-revenue loss, and (*d*) water lost to the system (the amount that the reservoirs fail to fill because of advance releases providing flood-control space).

An appraisal of the chances that would be taken of incurring various losses (in excess of the losses in a purely conservation operation), to assure control of the 1-in-5 chance and 1-in-20 chance, maximum inflows, is indicated graphically in Fig. 5. The chances are shown for two types of seasonal distribution of the forecasted inflows—that is, a normal distribution, and a critical or rapid concentration of the seasonal inflow.

The results, as presented in Fig. 5, were well suited to allow an administrative policy decision to be made on the chances that should be taken. The results indicated that substantial chances would be taken of losing water, energy, and power revenues if operations were initiated to assure control of the 1-in-20 chance, maximum inflows. Although these chances were less than 50-50, it was decided that the chances involved in controlling the 1-in-20 chance, maximum flood could not be taken because there is no flood-control allocation and because conservation of water has priority of use. On the other hand, it was noted that operation to assure control of the 1-in-5 chance flood could be initiated, and that the chances of any losses occurring would exceed 1 in 20 only if a critical distribution of inflow occurred. Other percentage chances could be analyzed in the same manner, but it appeared that operation to control the 1-in-5 chance flood involved about the maximum risk that could be taken of losing water. Therefore, based on these calculated risks, a decision was reached that operations should be geared to assuring control of the 1-in-5 chance flood to the desired flows.

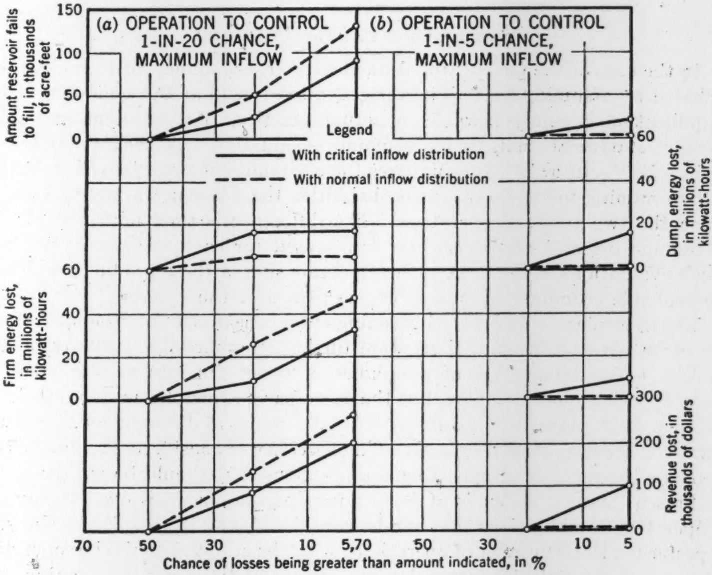

FIG. 5.—PROBABLE LOSSES RESULTING FROM GIVEN DEGREES OF FLOOD-CONTROL PROTECTION, NORTH PLATTE SYSTEM (USBR, 1952)

With this decision made, the job of scheduling reservoir operations was greatly simplified. As the flood season unfolded, successive forecasts of progressively increasing accuracy were made, which formed the basis on which operation studies could be performed. Using the general principles of scheduling discussed in the foregoing sections, operating plans were developed which, in each instance, were aimed at assuring control of the 1-in-5 flood, with maximum filling in event of low flows.

Actual operations were performed without mishap. Precipitation during the snowmelt season was about normal, which contributed toward a high degree of accuracy in the streamflow forecasts. All the reservoirs filled, and releases were controlled within the desired amounts.

System Operational Planning

In the case of the Green Mountain Reservoir, economic considerations were excluded by assuming that all power generated is sold at the same rate. This simplification is rarely possible in actual practice. An excellent method of utilizing statistical analysis for economic evaluation has been presented by Francis B. Blanchard.[4] He compares the economics of two types of operations by determining for various flow probabilities the difference in net revenue between the two types of operation. The difference is then multiplied by the percentage interval of probability represented for each probability limit for which evaluations were made. The algebraic sum of these products represents the probable economic advantage of one plan over the other.

The examples of operational planning cited considered only the operation of one or two reservoirs and, thus, were further simplified for purposes of illustrations. The integration of a number of reservoirs into system operation becomes much more complex, but the same basic principles may be used. In such a system, planning the number of combinations of different conditions that can occur becomes almost infinite. The necessity of considering economics also increases the number of operating combinations that should be weighed.

Present manual methods of performing operation studies limit the number of operating combinations that can be considered, and it is generally necessary to perform a small number of operations, with the adopted method of operations being selected partly by interpolation. The variety of possible combinations stresses the importance of developing economical, high-speed methods of performing integrated, system-operation studies. Such methods are not readily available. However, other USBR engineers and statisticians are working on procedures by which such studies may be processed on high-speed electronic computers, and some progress has been made. The methods under development, if successful, will allow quick processing of repeated operations with simple changes in operating criteria. This method of processing will satisfy an all-important need in operational planning by allowing a very large number of studies to be made rapidly at comparatively low cost. The development of such methods will allow the optimum potential of probability procedures to be realized in operational planning.

---

[4] "Operational Economy Through Applied Hydrology," by Francis B. Blanchard, *Proceedings*, 24th Annual Meeting of the Western Snow Conference, Portland, Ore., April, 1955.

Use of Statistics in Operation of Other Reservoirs.—Probability methods, inherent in forecasting procedures, form the basis for the development of operational plans for other USBR reservoirs, in addition to those described. For example, the operation of Hoover Dam and Lake Mead Reservoir (both in Arizona and Nevada) for flood control is based on protection against a maximum forecasted inflow of a given probability of occurrence.[5] The flood-control regulations currently in force provide that this maximum forecasted flow shall be that which (on the average) will not be exceeded 19 times out of 20.

Forecasting methods, based on multiple correlation and statistical procedures, are also the basis for tentative operating agreements for Arrowrock Reservoir and Anderson Ranch Reservoir (both in Idaho) and for Hungry Horse Reservoir (Montana). Similar use of such methods is under consideration for a number of other major USBR reservoirs in the west.

SUMMARY AND CONCLUSIONS

Statistical procedures can be very helpful in scheduling reservoir operations by furnishing an evaluation of the operational chances that are taken. The techniques are particularly applicable to the evaluation of water-supply probabilities.

Reservoir operating plans must consider all the potentialities for variation in water supply and must properly evaluate the probability of extremes occurring. The extremes of water supply frequently are the guides for a given operation, rather than the normal or most probable water supply. This emphasizes the need for proper evaluation of the probability of extremes occurring.

A complete operating plan must have an initial firm schedule which can be followed until significant new operating information can be anticipated. After the initial firm schedule, the plan should designate different courses of action for the various possibilities of water supply.

Adaptation of low-cost, high-speed, electronic computing methods for the processing of operational studies will be an invaluable aid to the development of fully coordinated operating plans and will allow the optimum potential of probability procedures to be realized.

ACKNOWLEDGMENTS

The work described was performed while the writer served with the USBR in Loveland. H. R. Brown was in immediate charge of the work performed, and Jesse L. Honnold had technical responsibility for the hydrologic phases of the work.

---

[5] "Use of Inflow Forecasts in Operation of Hoover Dam and Lake Mead for Flood Control," by Frantz R. Lupton, *Proceedings*, 18th Annual Meeting of the Western Snow Conference, April, 1950, pp. 35–47.

AMERICAN SOCIETY OF CIVIL ENGINEERS

Founded November 5, 1852

TRANSACTIONS

Paper No. 2905

AN APPROACH TO THE DESIGN OF TRICKLING FILTERS

By William T. Ingram,[1] M. ASCE

Synopsis

Trickling filters are accepted as an efficient means of secondary sewage treatment for wastes amenable to biological treatment. Among the reasons reducing their usefulness are (*a*) space requirements, (*b*) seasonal variations in efficiency, (*c*) clogging and pooling, (*d*) limitations on hydraulic and organic loading, and (*e*) limitations on the strength of applied sewage.

Many investigators have worked on improvements in filter design in an effort to overcome one or more of the objectionable characteristics of filters. The treatment field has profited from these investigations. Improvements have been made in media, circulation, hydraulic flow rates, and methods of applying sewage to the filter.

An entirely new approach to trickling filter design, which has been investigated in the laboratory for a year, will be presented herein. The results of these investigations show that it was possible, at laboratory scale and under controlled conditions, to treat settled domestic sewage efficiently at hydraulic rates as high as those used for rapid sand filtration of water.

The Basic Design Concept

When sewage is discharged into a shallow stream passing over and through gravel beds, the water soon emerges with few of the characteristics of sewage. Turbulence repeatedly exposes the water surface to aeration. The flow of sewage through slime-covered gravel and sand removes solids quickly. Depending, of course, on how well aerated the water is and how much filtration it receives, the water becomes clear and is capable of accepting additional sewage. Unless the water is so cold that biological growth is inhibited, the stream bed will reach a biological balance with sufficient organism growth capable of removing substantial organic loads.

Note.—Published, essentially as printed here, in June, 1956, as *Proceedings Paper 999*. Positions and titles given are those in effect when the paper was approved for publication in *Transactions*.

[1] Cons. Engr., Whitestone, N. Y.

The process of natural purification categorically described in the foregoing is the basis for the system of filtration proposed here, with the addition of controls making possible a design with predictable results. Sewage flow is kept continuous, and points of entry and quantities to be admitted to the filter are established. Filter space is provided with an adequate amount of oxygen to insure aerobic conditions, and enough filter depth is provided to carry conversion of organic materials to the degree of nitrification desired. The temperature of the filter water is maintained in the summer range of natural streams. Because oxygen is supplied at all depths of the filter, depth limitations become those of economics, convenience, and desired degree of treatment.

This process has been termed "controlled filtration," and the essential components include:

1. A trickling filter of sectional design;
2. Means for the introduction and distribution of controlled quantities of sewage to each section of the filter;
3. Means for the introduction of controlled quantities of air under each section of the filter;
4. Means for maintaining the influent, reaching and passing through the filter, at approximately the same temperature, preferably more than 15° C and less than 30° C;
5. A nonabsorbing filter media sized to some degree of uniformity in order to provide media surface and ample void space (for example, filter stone size of from 1½ in. to 3 in.); and
6. Means for removing the effluent from the filter section.

It is desirable to construct the filter so that the sectional effluent can be mixed with settled primary sewage or filter water as it passes through the filter.

CONTROLLED FILTRATION INVESTIGATIONS

Laboratory Filter Unit.—A diagram of the proposed filter is shown in Fig. 1. The laboratory unit was installed with metered control of settled domestic sewage taken from a sewer in the Bronx, New York (N. Y.), adjacent to the Lewis Van Carpenter Sanitary Engineering Laboratory of the College of Engineering at New York University (N. Y.). The total sewage flow was measured through a calibrated weir and pumped to the filter. Sectional feed through sections other than the top of the filter was metered through calibrated flow meters.

Air taken from the laboratory at room temperature was metered for total flow, and sectional feeds (to the bottom of each section) were metered to adjust the proportion of air flow to the several sections.

The filter, constructed as a special structure in the laboratory, was composed of six 3-ft sections of transite pipe with an inside diameter of 12 in. mounted separately on base plates, thus supporting each section separately. Each filter section was connected to the base plate with a transite collar drilled to provide inlet, outlet, and air connection on each collar. The collars were sealed to prevent escape of filter air. Each filter section was filled with from $1\frac{1}{2}$-in. to 3-in. filter stone. The bottom section was trapped with a water seal to prevent the escape of filter air, thus sealing the fiber except at the top.

Laboratory Studies.—During the initial ripening period, the hydraulic application rate to the top section was 40 million gal per acre per day (2.2 million gal per acre-ft per day). A series of six runs, each lasting from two weeks to one month, was conducted with top feeding only in an effort to determine the maximum hydraulic loading and the limiting organic loading with top feeding.

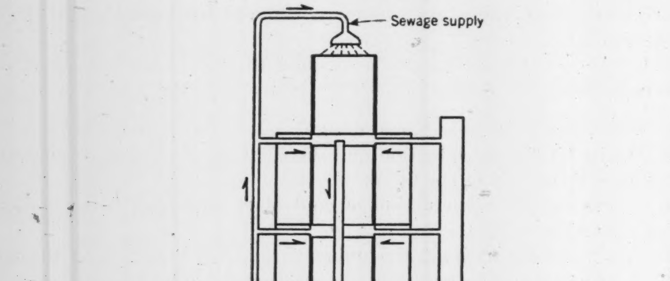

FIG. 1.—DIAGRAM OF THE LABORATORY FILTER UNIT

In this series, during which the hydraulic loading was carried up to 119.9 million gal per acre per day (6.6 million gal per acre-ft per day) and the organic loading was 4,150 lb per acre-ft per day (1.71 lb per sq ft per day), no measurable defection of the filter was noted. The sixth run at the highest rate gave the best effluent results, with a filter efficiency of 89.1% and an effluent containing 68 lb of biochemical oxygen demand (B.O.D.) per million gal or 8.1 parts per million (ppm).

Two runs of two weeks each were conducted with feeding on the top of the second section and into the beginning of the second section. The hydraulic loading was accelerated to 175.8 million gal per acre per day with an organic loading of 4,430 lb per acre-ft per day (1.72 lb per sq ft per day) in run 8. The average filter efficiency was 86.2% with 59 lb of B.O.D. per million gal in the effluent.

Runs 9 and 10 were conducted over a 28-day period with application to the first three sections. The hydraulic loading for run 10 was 199.8 million gal per acre per day with an organic loading of 6,900 lb per acre-ft per day (2.56 lb per sq ft per day). The filter efficiency was 80.8% with 107 lb of B.O.D. per million gal remaining in the filter effluent. It is noted here that the filter was deprived of flow for periods of from 1 hr to 3 hr during these runs. The deleterious effects of intermittent flow were easily observed. Filter sloughing always followed a resumption of flow. However, within an hour or so sloughing ceased and high-quality effluent was obtained.

One run was made in order to observe whether top feeding only, under the same general conditions, with interrupted flow and application rates of 199.7 million gal per acre per day, materially affected the filter efficiency. Run 11, at an organic loading of 6,830 lb per acre-ft per day (2.8 lb per sq ft per day) had an average efficiency of 75.9% with 10 days of feeding; 148 lb of B.O.D. per million gal remained in the effluent.

The strength of sewage was increased in runs 12 and 13. In run 12, which continued for 16 days, milk waste was added to the domestic sewage flow, and the flow was adjusted to bring the loading ratio (organic loading, in pounds per acre-foot per day, divided by the hydraulic flow rate, in million gallons per acre-foot per day) above 1,300 lb of B.O.D. per million gal. During the last 8 days of this run, the organic loading averaged 8,560 lb per acre-ft per day (3.03 lb per sq ft per day), and the flow was maintained at 95.88 million gal per acre per day. The filter efficiency was 84.1% with 219 lb of B.O.D. per million gal (26.2 ppm) remaining in the effluent. The over-all average efficiency for this run was 77.3% at a loading of 8,290 lb per acre-ft per day.

An effort was made to force a filter breakdown by increasing the hydraulic loading to 119.9 million gal per acre per day with an organic loading of 13,820 lb per acre-ft per day. After the third day, the filter began to recover from the shock, and on the sixth day the efficiency was 88.1% with a loading of 11,000 lb per acre-ft per day. On the second day, with a loading of 20,200 lb per acre-ft per day, the efficiency was 73.5%. On the third day, with a loading of 15,000 lb per acre-ft per day, the efficiency dropped to 57.8%, the lowest percentage recorded in the year of study. The average efficiency for this short run was 74.1% with 480 lb of B.O.D. per million gal remaining in the effluent. On the basis of comparisons of the filter behavior in the several runs, there was no reason to believe that the recovery did not represent filter biota adjustment with the same characteristically high efficiency of removal established in all the previous runs.

Table 1 summarizes the investigations, and Table 2 shows the maximum, minimum, and average results of B.O.D. application and removal for each run.

TABLE 1.—SUMMARY

Run	Applied section	Hydraulic Loading		Organic Loading (B.O.D.)			
		Million gallons per acre-foot per day	Million gallons per acre per day	Parts per million	Pounds per acre per day	Pounds per acre-foot per day	Pounds per square foot per day
1	1	2.2	40.0	108.5	36.15	2.01	.83
2	1	3.1	55.9	113.8	53.14	2.95	1.22
3	1	4.0	71.9	127.1	76.23	4.24	1.75
4	1	4.9	87.8	84.3	61.86	3.44	1.42
5	1	5.8	103.9	84.6	73.18	4.07	1.68
6	1	6.7	119.9	74.7	74.49	4.15	1.71
7	1,2	8.3	143.8	78.7	94.53	5.42	2.17
8	1,2	10.4	175.8	51.1	74.92	4.43	1.72
9	1,2,3	11.1	175.8	50.3	74.05	4.65	1.70
10	1,2,3	12.4	199.8	66.8	111.51	6.90	2.56
11	1	11.1	199.8	73.7	121.97	6.83	2.80
12	1,2,3	6.1	95.9	163.7	131.11	8.29	3.01
13	1,2,3	7.4	119.9	221.8	222.16	13.82	5.10

• Rates of air flow, in cubic feet per gallon of applied sewage: Runs 1 through 11 = 1,

Observations of the sectional efficiency of the filter were made periodically by extracting samples of liquid and of filter growth from each section. These profiles were of great value in assessing the behavior of the filter from top to bottom. Studies of the slime were limited to microscopic examination, but, nonetheless, the upward and downward adjustment of groups of organisms to meet changes in loading was noted in repeated observations. Comparison of sectional observations at the end of runs 6 and 12 (Table 3) demonstrated the organism response under top loading and 3-ft-section loading conditions.

TABLE 2.—RANGE OF APPLIED B.O.D.

Run	Applied B.O.D., in Parts per Million			Removal, in Percentage			Observation with removal of 80% or more, in percentage
	Maximum	Average	Minimum	Maximum	Average	Minimum	
1	155	109	50	96	82	70	59
2	162	114	85	95	79	56	56
3	209	127	72	94	84	73	82
4	125	84	30	97	88	80	100
5	125	85	60	98	88	75	85
6	130	75	40	99	89	82	100
7	153	79	45	99	92	85	100
8	85	51	25	91	86	79	85
9	80	50	36	92	86	78	86
10	173	67	35	95	81	66	50
11	100	74	50	87	76	58	20
12	258	164	78	88	77	55	63
13	325	222	175	88	74	58	40

Dissolved oxygen measurements on liquid taken sectionally showed quite conclusively the effectiveness of air admission to the sections. As was expected, the oxygen content was low at the top of the filter where the demand is greatest and increased progressively as the filter water flowed downward. The effluent contained oxygen (of from 3.2 ppm to 5.9 ppm) at all times. Table 4 summarizes the profile observations on oxygen content for the several runs.

OF INVESTIGATIONS[a]

Loading ratio, in pounds per million gallons	B.O.D. remaining, in pounds per million gallons	Filter efficiency, in percentage	Length of run, in days	TEMPERATURE, IN ° C		Run
				Maximum	Minimum	
914	169	82	31	24	21	1
952	200	79	31	24	21	2
1,063	173	84	14	25	21	3
705	85	88	19	25	22	4
705	88	88	14	22	18	5
623	68	89	14	21	18	6
656	52	92	14	21	18	7
426	59	86	14	19	18	8
420	61	86	7	20	18	9
557	107	81	21	19	18	10
615	148	76	10	19	17	11
1,366	219	77	18	20	17	12
1,851	479	74	6	19	18	13

run 12 = 2, and run 13 = 1.7. Runs 9 through 13 were made with interrupted feeding.

Profiles of B.O.D.-removal are demonstrated in Table 5, showing sectional efficiency under the several conditions of loading. The first section removed from 21% to 70% of the applied load. The significance of sectional removal characteristics will be examined more fully subsequently.

The pH-factor was checked on all profiles. When the applied sewage had a pH-factor of more than 7.0, there was only minor change through the filter to 7.2 or 7.3. When the applied waste was acid, the upward change was more pronounced—that is, + 0.5 or more. During these studies, the pH of the sewage normally remained between 6.9 and 7.2. With milk waste added, the lowest pH recorded was 6.0.

Nitrites and nitrates were checked at intervals. At 40 million gal per acre per day, nitrates of 4.8 ppm were measured. At higher rates, the nitrates were never more than 1.0 ppm and were usually present at a trace only. Nitrites were found in all samples analyzed and were approximately 0.5 ppm during run 6 and 0.05 ppm during run 10. There were too few nitrogen determinations to average.

Because over-all stability was of primary interest, routine tests of relative stability were made. In runs 2 through 8 the oxygen reserves from dissolved oxygen and nitrogen compound sources were ample to maintain relative stabilities of 60% or more, with the majority of all observations being more than 80%. Of 92 observations made over a span of 124 days, 45% showed a relative stability of 20 days or more (99^{+}%). It was noted that interrupted feeding and three-section feeding caused a sacrifice in stability. For example, during run 10 the relative stability ranged from 21% to 75% (from 1 day to 6 days).

Settleable solids in the filter effluent were measured routinely in an Imhoff cone. Although there were, of course, day-to-day variations, the solids disposition was reasonably uniform without pronounced sloughing. Averages for each run are shown in Table 6. For runs 1 through 8, the minimum observed was 0.3 ml, and the maximum was 13.6 ml. After the interruption

TABLE 3.—MICROSCOPIC EXAMINATION OF FILTER SLIME

Sample of slime taken from:	Run 6 Application to section 1 (119.9 million gal per acre per day)	Run 12 Application to sections 1, 2, and 3 (Total rate of 95.88 million gal per acre per day)
Top of section 1	Zooglea moderate Stalked ciliates moderate Rotifers numerous Flagellates few Filamentous bacteria few Branched filaments moderate Slime fairly active	Zooglea few Free swimming ciliates occasional Worms occasional Branched filaments moderate Much debris—dead sludge
Top of section 2	Zooglea moderate Stalked ciliates moderate Free swimming ciliates moderate Flagellates moderate Rotifers moderate Filamentous bacteria moderate Branched filaments moderate Worms rare Slime very active	Zooglea moderate Stalked ciliates few (small) Free swimming ciliates very few Flagellates few Branched filaments moderate Worms rare Organisms not very active
Top of section 3	Zooglea moderate Stalked ciliates very numerous Free swimming ciliates moderate Rotifers numerous Filamentous bacteria few Branched filaments numerous Slime very active	Zooglea very numerous Stalked ciliates few Branched filaments very numerous Slime not very active
Top of section 4	Zooglea moderate Stalked ciliates numerous Free swimming ciliates numerous Rotifers numerous Filamentous bacteria few Branched filaments few Worms few Slime very active	Zooglea numerous Stalked ciliates numerous Free swimming ciliates very few Rotifers very few Branched filaments numerous Organisms active
Top of section 5	Zooglea moderate Stalked ciliates very numerous Free swimming ciliates few Rotifers numerous Filamentous bacteria few Worms few Insects (8 legged) few Slime very active	Zooglea numerous Stalked ciliates very numerous Free swimming ciliates very few Branched filaments numerous Worms plentiful Organisms active
Top of section 6	Zooglea moderate Stalked ciliates very numerous Free swimming ciliates moderate Rotifers numerous Branched filaments numerous Worms few Slime very active	Zooglea numerous Stalked ciliates very numerous Free swimming ciliates few Rotifers few Branched filaments few Organisms active
Effluent sludge	Zooglea moderate Stalked ciliates numerous Free swimming ciliates numerous Rotifers moderate Organisms active	Zooglea moderate Stalked ciliates moderate Free swimming ciliates moderate Rotifers moderate Branched filaments moderate Worms moderate Organisms active

of filter flow during runs 9 through 12, the immediate slough measured as much as 40 ml, but the liquor cleared rapidly to a range of between 0.2 ml and 12.8 ml, as measured in routine sampling.

Present Filtration Practice and Results.—"The Tentative Standards for Sewage Works" established by the Upper Mississippi River Board of Public Health Engineers and the Great Lakes Board of Public Health Engineers have set limits on the loading for standard trickling filters of 15 lb per 1,000 cu ft (653.4 lb per acre-ft per day). At that loading, the Tentative Standards curves indicate a range of B.O.D.-removal of from 86% to 77% depending on the latitude. A general limitation is placed on hydraulic loading, so that the rate is less than 4 million gal per acre per day.

TABLE 4.—AVERAGE PROFILES OF OXYGEN CONTENT, IN PARTS PER MILLION

Section	Run											
	1	2	3	4	5	6	7	8	10	11	12	13
Influent	1.4	0.0	0.0	0.0	0.0	0.2	0.0	0.0	0.0	0.0	0.0	0.0
1	2.3	0.2	0.2	0.0	0.0	1.0	0.1	0.0	0.0	0.0	0.1	0.0
2	3.8	3.1	1.8	1.3	2.8	1.9	1.4	1.3	0.4	0.0	0.1	0.3
3	5.1	4.0	3.1	2.5	4.3	3.7	3.3	2.6	1.1	0.7	0.5	1.2
4	5.4	4.7	3.8	3.7	4.5	4.2	4.3	4.4	2.2	2.4	1.8	2.4
5	5.1	5.4	4.5	4.6	5.4	5.4	5.3	5.9	3.3	3.6	3.1	3.0
Effluent	5.5	5.4	5.2	4.7	5.4	5.3	5.5	5.9	3.2	4.0	3.5	3.4

TABLE 5.—AVERAGE SECTIONAL EFFICIENCY OF B.O.D. REMOVAL, IN PERCENTAGE

Section	Run											
	1	2	3	4	5	6	7	8	10	11	12	13
1	42.6	50.6	52.4	21.0	53.3	59.3	70.5	49.6	42.2	40.4	36.5	37.5
2	38.5	34.0	33.2	33.1	47.9	32.1	44.8	56.5	57.4	27.1	38.9	33.7
3	7.5	11.4	26.3	52.0	31.2	14.1	49.7	50.3	24.2	24.0	29.7	25.9
4	12.9	21.0	41.0	40.6	9.1	69.3	21.5	−18.9	7.7	5.1	29.3	5.2
5	21.1	5.3	0.0	29.8	37.0	−10.4	6.8	52.2	26.2	4.2	16.9	18.3
6	8.4	6.0	20.9	12.5	−18.2	37.5	29.4	7.0	1.6	16.1	14.1	8.2
1 through 6	79.5	79.7	89.1	90.8	88.3	94.9	94.1	92.2	80.3	74.8	80.4	70.6

TABLE 6.—SETTLED SOLIDS IN FILTER EFFLUENT

Run	AVERAGE SETTLEABLE SOLIDS, IN MILLILITERS, IN AN IMHOFF CONE (1,000 ML)		
	Maximum	Average	Minimum
2	5.3	2.7	0.5
3	5.2	1.5	0.3
4	13.6	2.3	0.3
5	5.2	2.6	0.5
6	3.8	1.7	0.3
7	4.2	1.6	0.3
8	1.6	1.1	0.4
9	4.6	2.0	1.2
10	5.2	2.1	0.2
11	12.0	3.4	1.5
12	12.8	5.3	2.6
13	4.4	3.8	2.8

When recirculation or high-rate filtration is practiced, the general limits are 30 lb per 1,000 cu ft (1,310 lb per acre-ft per day) and from 10 million to 30 million gal per acre per day. Up to 4,800 lb per acre-ft per day of applied load (including recirculation) is considered when a B.O.D. of 30 ppm or more is acceptable. Standard filter depths are suggested at from 5 ft to 7 ft above the underdrains.

The National Research Council (Washington, D. C.) conducted an exhaustive study of trickling filter performance and reported[2] a mathematical formula for computing the efficiency of filters with secondary and intermediate clarifiers.

C. J. Velz,[3] M. ASCE, presents a theory applicable to biologic beds which states:

> "* * * the rate of extration of organic material per interval of depth of a biological bed is proportional to the remaining concentration of organic matter measured in terms of its removability."

Mr. Velz further suggests that 1 lb of B.O.D. per sq ft per day at a temperature near 30° C is approximately the limit of loading, and additionally states that "* * * the removable fraction *L* can be expected to decrease as the rate of application of mgad increases."

Renville S. Rankin,[4] M. ASCE, in reviewing the work cited previously and applying the methods of evaluation to additional filter data, concludes that "* * * dosing rate, loading of the filter, or depth of filter have no significant effect within the range of values covered by the data." However, he indicates that the ratio of recirculation is important.

K. Imhoff,[5] M. ASCE, indicates that trickling filters can be highly loaded if dosed continually at loadings of 0.8 m per hr (2.62 ft per hr, or 20.5 million gal per acre per day). An example is cited of an experimental plant at Markleeberg (near Leipzig, Germany), in which surface loadings of 4.8 m per hr (15.7 ft per hr, or 122.8 million gal per acre per day) were achieved with a B.O.D.-removal of 90%. The depth of the filter was considered essential. The experimental plant was 8 m deep, and the hydraulic loading was approximately 4 times the loading of the usual high-rate filter.

One of the largest-scale operations with an enclosed aerated filter is the installation at a sewage plant in Glasgow (Scotland). A. Hunter and T. Cockburn,[6] and W. M. Cameron and A. R. Jamieson[7] describe in detail their experience with this filter, which is termed an "encased activated biological filter." It is 52 ft in diameter with 18 ft of filtering material. It was designed to handle hydraulically 388 gal per cu yd per day (14.37 imperial gal per cu ft, or 0.751 million gal per acre-ft per day.

During the years, 1938 to 1942, chemically precipitated sewage (approximately 137-ppm B.O.D.) was applied with removal ranging from 57% to 94% for the various test conditions. Maximum air supply was 5,000 cu ft per min introduced at the top of the filter. A comparison made with open filters indicated that the enclosed filter treated twice the volume of waste with an equal degree of purification.

---

[2] "Sewage Treatment at Military Installations: Report of Sub-committee on Sewage Treatment in Military Installations of the Committee on Sanitary Engineering, National Research Council," *Sewage Works Journal*, Vol. 18, 1946, p. 794.

[3] "A Basic Law for the Performance of Biological Beds," by C. J. Velz, *Sewage Works Journal*, Vol. 20, 1948, p. 607.

[4] "Evaluation of the Performance of Biofiltration Plants," by Renville S. Rankin, *Transactions*, ASCE, Vol. 120, 1955, p. 823.

[5] "How High Should a Trickling Filter Be," by K. Imhoff. *Gesundeits Ingenieur*, Vol. 74, 1953, p. 41.

[6] "Operation of an Enclosed Filter at Dalmarnock Sewage Works," by A. Hunter and T. Cockburn, *Journal and Proceedings*, Inst. of Sewage Purification, London, 1944, p. 12.

[7] "Further Operation of an Enclosed Filter at Dalmarnock Sewage Works," by W. M. Cameron and A. R. Jamieson, paper presented at a meeting of the Scottish Branch, Inst. of Sewage Purification, London, December, 1950.

The later studies[7] by Messrs. Cameron and Jamieson offer additional data on organic loading. Application ranged from 163 lb per acre-ft per day to 1,266 lb per acre-ft per day with removal of more than 80%. Hydraulic dosage was brought to 12.12 million imperial gal per acre per day (14.54 million gal per acre per day) during the last year of the records. The surface loading at that time was between 0.287 lb per sq ft per day and 0.531 per sq ft per day.

These two studies emphasize a number of important characteristics. Ponding was a problem at the flow rates cited in the preceding paragraph. The bottom half of the bed did not perform much biochemical work but did act as a refuge for scavengers. The retention of filter-water temperatures was an important influence. Recirculation was beneficial in controlling filter growth.

E. H. Arnold,[8] in studying the effects of low temperatures in trickling filters, compares open and enclosed filter performances at February and June temperatures. Winter temperatures of housed and open filter effluent were 43.6° F and 36.6° F; corresponding summer temperatures were 66.5° F and 67.1° F. It was observed that the efficiency of an open filter was only a little lessened under severe winter conditions and was higher during warm weather.

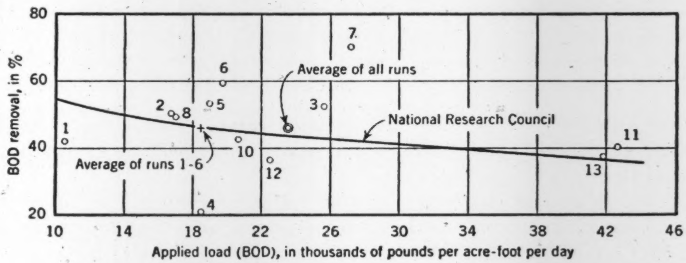

FIG. 2.—FILTER EFFICIENCIES FOR SEVERAL CONDITIONS OF LOADING

B. Gerber[9] shows that several variables of design and loading must be considered in combination. He suggests the use of a dimensionless product as a basis for design by plotting the ratio of the B.O.D. of the effluent to the applied B.O.D., (B.O.D.)$_D$/B.O.D., against the filter aerial loading, H, in feet per day, divided by the depth, D, times a constant, K_1, in units of 1/day, $H/(D K_1)$. A linear curve having a slope of 0.051 was derived for Baltimore (Md.) filter influent of from 120 ppm to 140 ppm of B.O.D. The value, $K_1 = 0.2$ at 20° C, was assumed for these computations. A variation in K_1 will change the intercept but does not affect the slope of the curve.

SIGNIFICANT CHARACTERISTICS OF CONTROLLED FILTRATION

The controlled filter is capable of handling extremely high hydraulic and organic loads by comparison with present practice. Assuming that the National Research Council efficiency curve applies at the organic loading rates used, an efficiency of 65% could be expected at a loading of 4,000 lb per acre-ft per day. It will be observed from Table 1 that in runs 5 and 6, efficiencies of 88% and 89% were obtained at a loading of approximately 4,000 lb per acre-ft per day. Fig. 2 shows filter efficiencies for the several conditions of loading, together with the National Research Council curve. Regardless of loading, the filter efficiencies obtained were well above the efficiency shown by the National Research Council curve.

---

[8] "Effects of Low Temperatures on Trickling Filter Operations," by E. H. Arnold, *Public Works*, October, 1946, p. 49.

[9] "A New Concept in Trickling Filter Design," by B. Gerber, *Sewage and Industrial Wastes*, Vol. 26, 1954, p. 136.

TABLE 7.—ANALYSIS OF FIRST-SECTION LOADING (3-FT SECTION)

Run	APPLIED B.O.D.			Sectional efficiency, in percentage	HYDRAULIC LOADING		Loading ratio, in pounds per million gallons	Filter efficiency, in percentage
	Thousand pounds per acre per day	Thousand pounds per acre-foot per day	Parts per million		Million gallons per acre per day	Million gallons per acre-foot per day		
1	31.68	10.56	95.0	42.6	40.0	13.36	792	79.5
2	50.13	16.71	107.4	50.6	55.9	18.63	896	79.7
3	76.83	25.61	128.0	52.4	71.9	23.96	1,068	89.1
4	55.62	18.54	75.8	21.0	87.8	29.30	632	90.8
5	56.97	18.99	65.7	53.3	103.9	34.63	548	88.3
6	59.04	19.68	59.0	59.3	119.9	40.0	492	94.9
7	81.33	27.11	81.3	70.5	119.9	40.0	678	94.1
8	51.03	17.01	51.0	49.6	119.9	40.0	426	92.1
10	62.04	20.68	62.0	42.2	119.9	40.0	517	80.3
11	127.89	42.63	76.7	40.4	199.8	66.59	640	74.8
12	67.38	22.46	155.4	36.5	51.94	17.31	1,297	80.4
13	125.76	41.92	209.5	37.5	71.91	23.97	1,748	70.6

Table 7 is an analysis of first-section loading. Performance of the first section is comparable to the performance expected, according to the National Research Council formula.[3] Average efficiency for the first six runs was 46.5% at an average loading of 18,350 lb per acre-ft per day for a 3-ft depth. The average removal for application to the first section for thirteen runs was 46.3%, with an average loading of 23,490 lb per acre-ft per day. The National Research Council efficiency at 18,000 lb per acre-ft per day would be 46.7%; at 24,000, the efficiency would be 43.2% (Fig. 3).

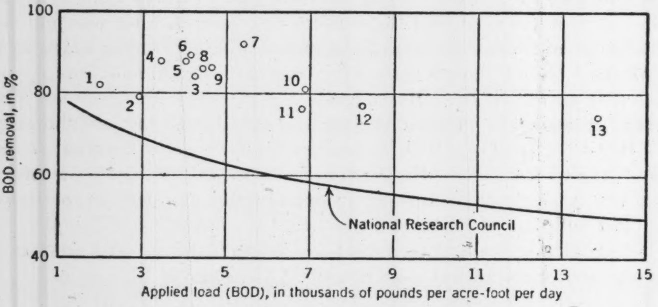

FIG. 3.—FILTER EFFICIENCIES FOR FIRST-SECTION LOADING

An attempt was made to reconcile the performance of the sectional filter with the theory advanced by Mr. Velz.[4] There were a number of considerations which made this almost impossible. As Table 5 illustrates, sectional extraction was not at a logarithmic rate. An approximate rate-of-removal line could be selected only by choosing straight lines connecting the removal values of B.O.D. at the beginning and at some depth.

The theoretical, total removable B.O.D., *L*, varied for the several runs, suggesting strongly that the ultimate amount of removable B.O.D. may be 95% or more. Removals were determined for each of runs 1 through 6, assuming that the B.O.D. of the effluent was entirely nonremovable. The value of *L*, therefore, varied from 0.794 to 0.949. Three reasonably straight lines were then plotted through the average points of the B.O.D. remaining (in percentage). The first break occurred at the bottom of section 3 and the second at the bottom of section 5, with the approximate *k*-value for the first three sections being 0.096 and for the first five sections, 0.111; the *k*-value is the logarithmic rate of B.O.D. extraction. It should be clear that each section actually had a different *k*-value.

Values of *k* were also computed on the assumption that 95% of the B.O.D. applied during all runs was removable (Fig. 4). The value of *k* approximated for each line connecting beginning and depth points varied from 0.044 in run 2 to 0.098 in run 6, with the average *k*-value for all runs equal to 0.065. If it could be assumed that all the B.O.D. was removable, the *k*-values for the first 6 runs would have ranged from 0.0382 to 0.0669.

The *k*-value computed by Mr. Velz for low-rate filters was 0.175 and for high-rate filters, 0.1505, with the assumption that *L*, the removable fraction, was 90.0% and 78.4%, respectively. The *k*-value for the first section during runs 2, 3, 5, and 6 closely approximated the *k*-value of Mr. Velz for high-rate filters. The value of *L*, therefore, without some fundamental difference in filter performance below the first section, should have been 0.784 for those runs. It is to be noted that the foregoing performance occurred at hydraulic loading rates of 55.9, 71.9, 103.9, and 119.9 million gal per acre per day, with corresponding organic loadings of 1.22, 1.75, 1.68, and 1.71 lb per sq ft per day. Filter liquor during three runs was approximately 23° C and during the fourth, approximately 20° C.

The performance of the first section is that which might be anticipated according to the theory proposed by Mr. Velz. However, organic loadings during these runs were well above the suggested upper limit of 1 lb per sq ft per day at 20° C, and hydraulic loadings were from 2.8 times to 6 times the rate of 20 million gal per acre per day used by Mr. Velz. Under these loading conditions, the removable fraction should have decreased whereas the reverse was apparently true because the total efficiency of filter removal increased for the runs, the values being 79.0%, 83.7%, 87.5%, and 89.1% for runs 2, 3, 5, and 6, respectively.

The controlled filter was operated for the first six runs as a single stage filter, with all waste being applied to the top of the filter. According to the Tentative Standards for single stage filters, maximum dosage should be less than 4 million gal per acre per day with less than 653.4 lb per acre-ft per day of B.O.D. Run 6 was dosed at 20 times this rate hydraulically and 6.4 times (average) organically at a temperature of ± 20° C. Run 11 was dosed hydraulically at more than 33 times the rate and was dosed organically at 10.4

times the rate. The average removal efficiency for all runs was, for practical purposes, within the limit allowed by curve C of the Tentative Standards which permits 23% of the B.O.D. to remain in the settled effluent. The efficiency of run 3 was better than curve B (18%), and removals during runs 4, 5, and 6 were better than curve A (14%).

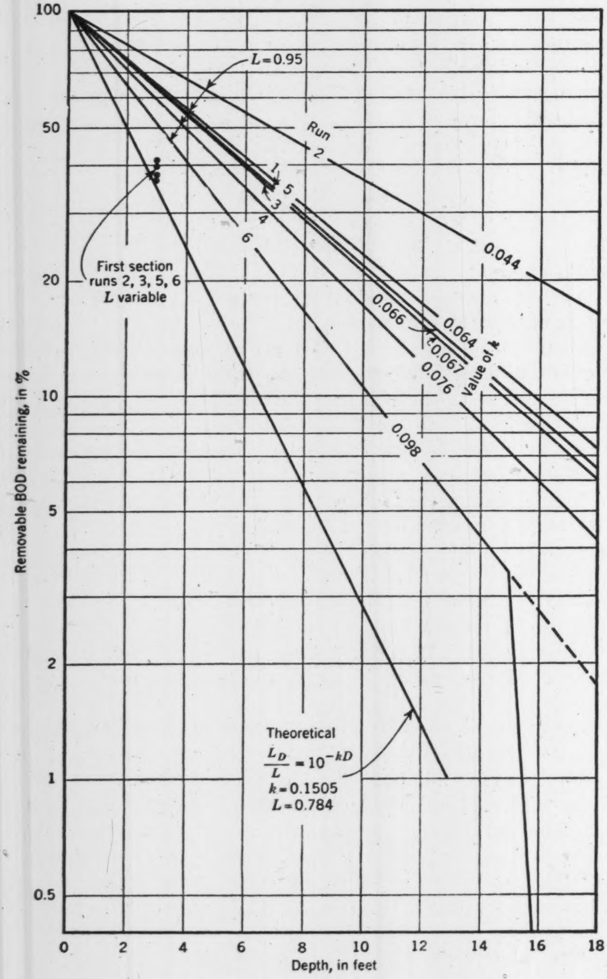

FIG. 4.—APPROXIMATE REMOVAL RATES BASED ON INFLUENT AND EFFLUENT OBSERVATIONS OF FILTER PROFILES

Sectional application to two sections (runs 7 and 8) had the effect of increasing both hydraulic and organic loading while maintaining efficiency of removal higher than curve B. Total surface loading averaged 39.5 times hydraulically and 8 times organically the loading of the standard filter during run 7, with an efficiency of B.O.D. removal of 92%. Loadings in run 8 averaged 43.9 times hydraulically and 6.8 times organically, with an efficiency of 86%.

Three-section application permitted still higher loadings without an excessive sacrifice of efficiency. Run 10, with a total averaged loading of 199.9 million gal per acre per day and 2.56 lb per sq ft per day (49.8 times and 10.6 times the standard filter loadings), maintained a removal efficiency of 81% which was better than curve C.

Stronger wastes were used during run 12. After allowing the filter time to adjust, the loadings averaged 95.9 million gal per acre per day and 3.03 lb per sq ft per day, or 24 times and 13.1 times the standard filter loading with a removal efficiency of 84%. The maximum organic loading was obtained during run 13 when an attempt was made to break the filter. This run was not as long as the others, but there was every indication that the filter was capable of readjustment to a loading averaging 5 lb per sq ft per day and reaching 7.5 lb per sq ft per day during the run. On the fifth day of the run, with a loading of 4.1 lb per sq ft per day (16.1 times the standard filter), the efficiency was 88.1%. Table 8 gives sectional information obtained from five profiles of the filter during run 12 (Fig. 5).

TABLE 8.—AVERAGE OF FIVE PROFILES

Filter section	B.O.D., in parts per million	Dissolved oxygen, in parts per million	Flow, in million gallons per acre per day	Organic loading, in pounds per acre per day	B.O.D. removed, in percentage
1 Top	155.4	0.0	51.94	67,380	36.5
1 Bottom	98.6	0.04	51.94	42,750	
Sewage added	155.4	0.0	28.76	37,320	
2 Top	118.8	...	80.70	80,070	38.9
2 Bottom	72.6	0.04	80.70	48,900	
Sewage added	155.4	0.0	15.18	19,680	
3 Top	85.7	...	95.88	68,580	29.7
3 Bottom	60.2	0.46	95.88	38,180	
4 Top	60.2	0.46	95.88	38,180	29.3
4 Bottom	42.6	1.82	95.88	34,080	
5 Top	42.6	1.82	95.88	34,080	16.9
5 Bottom	35.4	3.12	95.88	28,320	
6 Top	35.4	3.12	95.88	28,320	14.1
Effluent	30.4	3.54	95.88	24,330	

Note: Average efficiency = 80.4%

A brief comparison of controlled-filtration performance with the performance of high-rate filters illustrates that both hydraulic and organic loadings are higher on the controlled filter with a correspondingly higher B.O.D.-removal. From the Tentative Standards it may be assumed that 20 million gal per acre per day and 1,300 lb per acre-ft per day may be applied and that a B.O.D.-removal of 70% may be expected. All filter runs, regardless of loading condition, produced average effluents of higher quality. The minimum hydraulic loading was twice, and at maximum 10 times, that of the foregoing standard. Organic loadings began at 1.5 times the standard and reached 10.5 times the standard.

It is obvious that limitations now applied to the design of trickling filters need to be revised upward for application to controlled filtration. When the control principles given here are used, great flexibility in filter construction becomes possible. Depth can be increased by adding additional, independently supported sections. Loading can be controlled by sectional feeding.

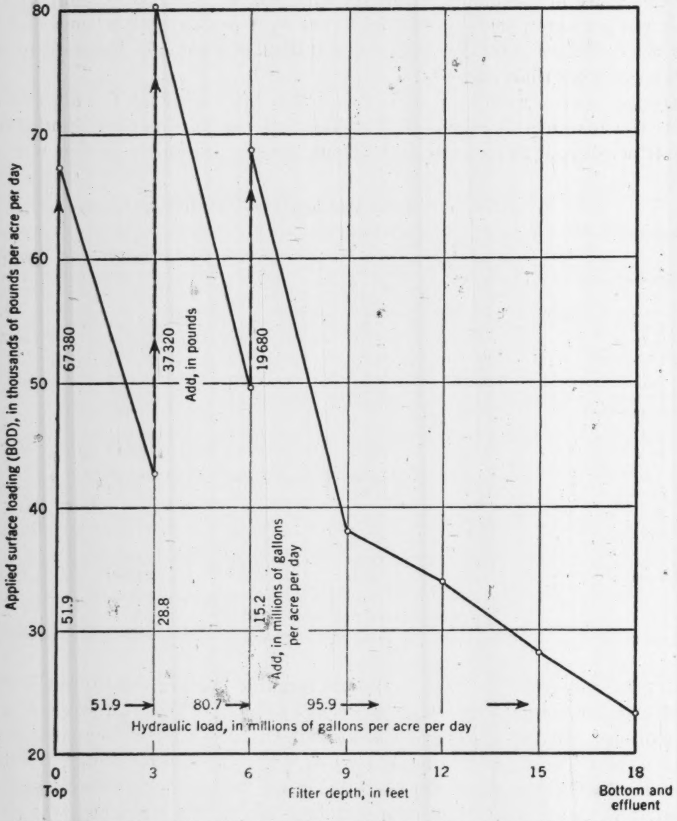

FIG. 5.—SECTIONAL APPLICATION OF SETTLED SEWAGE (AVERAGE OF FIVE PROFILES)

No indication of filter breakdown was experienced during the period of observations. Therefore, the upper limits for both hydraulic and organic loading have not been established by these studies. Filter sizing and area requirements can be reduced materially by using controlled filtration.

Stabilizing sections following feeding sections allow control of effluent stability. The data suggest that at least 9 ft of depth be provided for stabilization purposes.

Well-oxygenated effluent can be obtained with the method of air application without the development of excessive filter back pressure. At a high continuing flow there is no problem of filter pooling or clogging. The slime layer on filter media is thin and active and appears to adjust readily to the conditions of feed. When filter liquor temperatures are between 16° C and 25° C, organism growth appears prolific and seems to be more affected by loading conditions than by minor temperature changes. Future study should be given to well-organized investigations of organism functions in controlled filter purification. It appeared that the maintenance of reasonable warmth in the filter during the investigation secured a favorable temperature habitat for filter biota. Such temperatures can be maintained practicably by enclosure or by the injection of warm air into an insulated filter.

Short-circuiting in a filter of the depths used, or deeper, is a minor consideration. Downward liquid flow with counter-current air flow assures an intimate contact of oxygen-bearing air and filter water. Eventually, the aerated water will pass over filter media surfaces, and aerobic growth conditions are possible at all depths. Such conditions were established within 3 ft of the lowest sewage application point in all runs. By distributing approximately 50% of the total air flow to the bottom of the sections receiving sewage and by distributing the remainder to the bottoms of the remaining sections, a satisfactory dissolved-oxygen condition for the maintenance of aerobic growth in the filter was obtained. The actual proportioning of air to the sections was subject to analytical determination and plant adjustment to meet the demands of the sewage. The experimental work showed that a total air flow of approximately 1 cu ft per gal of sewage is adequate for treating settled domestic sewage containing as much as 200 ppm of B.O.D. It is possible that less air would suffice. It is important in controlled filtration that the filter air intake be positively controlled. A tight filter, trapped at the effluent point and open at the top, is also essential to the positive control of filter air.

FILTER FUNCTIONAL DESIGN

The experimental work described in the foregoing indicates that secondary treatment using controlled filtration could be accomplished with an average B.O.D.-removal of not less than 74% under the following conditions:

1. Maximum hydraulic flow rate (volumetric), L_H, of 12.4 million gal per acre-ft per day;
2. Maximum hydraulic flow rate (surface), H_s, of 200 million gal per acre per day;
3. Maximum organic loading rate (volumetric), L_B, of 13,800 lb per acre-ft per day;
4. Maximum organic loading rate (surface), B_s, of 222,000 lb per acre per day;
5. A maximum ratio, R_L, of organic to hydraulic loadings (volumetric) of 1,850 lb per million gal;

6. An air supply not exceeding 2 cu ft per gal of filter influent for extreme organic loadings, or approximately 1 cu ft per gal for influents containing from 50 ppm to 130 ppm of B.O.D.;

7. Temperature of the filter water between 17° C and 25° C;

8. Sectional application of settled sewage to one, two, or three sections as sewage strength increases; and

9. Sectional application of air.

Although the foregoing loading rates are not believed to be limiting, values not yet demonstrated should not be assumed for design purposes. Allowance should also be made for differences between laboratory and plant operating control. The following design ranges are suggested on the assumption that the principles of controlled filtration are to be used:

(*a*) L_H equal to from 4 to 12.4 million gal per acre-ft per day;

(*b*) H_s equal to from 72 to 200 million gal per acre per day;

(*c*) L_B equal to from 4,000 to 7,000 lb per acre-ft per day on the first section—12,000 lb per acre-ft per day total;

(*d*) B_s equal to from 43,000 to 120,000 lb per acre per day on the first section—200,000 lb per acre per day total;

(*e*) D (depth) equal to from 18 ft to 24 ft of filled section;

(*f*) R_L (filter loading ratio) equal to from 500 to 1,800 lb per million gal; and

(*g*) Sectional distribution, B_s, in percentage of total surface load, as follows:

	Section 1	Section 2	Section 3
One-section application	100	...	...
Two-section application	65–70	up to 35	...
Three-section application	55–60	up to 30	up to 15

Obviously, within the ranges stated there is great flexibility in design, useful in meeting the physical and topographical limitations of plant site and variations in plant daily flow and in sewage strength. For example, a part of the filter liquor may be returned to increase the flow and decrease the B.O.D. of the influent, or the flow may be maintained on the top section and variable flow added to the next section or next two sections during periods of peak flow.

Illustrative Example.—A sample design illustrates (*a*) a number of points of flexibility and (*b*) the use of the filter-loading ratio as a basic design tool. Assume that a controlled filter is to be designed for an average flow of 1 million gal per day; an average B.O.D. of sewage of 200 ppm; a primary-tank removal of 35% of the applied B.O.D.; an allowable effluent organic load of 250 lb per million gal; and a filter depth of 18 ft, required by topography and other considerations.

After a primary removal of 35%, the B.O.D. of the filter influent will be 130 ppm, or 1,085 lb per million gal. To reduce the B.O.D. to 250 lb per million gal requires a filter efficiency of 77%. Conservative loading rates for average flow should be chosen. The filter will be designed for application of average daily flow to the top of the filter. Peak flows (assumed as 180% of average) will be handled by sectional application as follows:

Section	Flow, in percentage	Flow, in million gallons per day
First	60	1.08
Second	30	0.54
Third	10	0.18
Total	100	1.80

The filter-loading ratio, R_L, is 1,085 lb per million gal and is equal to L_B/L_H. If L_B (on the first section) is assumed equal to 6,000 lb per acre-ft per day, $1{,}085 = 6{,}000/L_H$, giving $L_H = 5.53$ million gal per acre-ft per day or H_s (on the first section) = 99.54 million gal per acre per day. Therefore, the filter area required is 0.0108 acres, or 470 sq ft. A filter, 25 ft in diameter, yields 490.0 sq ft, or 0.0113 acres.

A filter, 25 ft in diameter and 8 ft deep, is tried. At maximum flow:

Section	H_s, in million gallons per acre per day
First	95.58
Second	47.79
Third	15.93
Total	159.3

and

Section	B_s, in percentage	B_s, in pounds per acre per day	L_B, in pounds per acre-foot per day
First	60	103,700	5,760
Second	30	51,850	3,460
Third	10	17,280	1,440
Total	100	172,830	10,660

To check the condition of minimum flow on the first section, assume a flow that is 70% of the average daily flow, or 0.7 million gal per day. For this flow, $H_s = 61.94$ million gal per acre per day, $B_s = 67{,}200$ lb per acre per day, and $L_B = 3{,}730$ lb per acre-ft per day. A check of the condition of average flow (1.0 million gal per day) on the first section yields $H_s = 88.5$ million gal per acre per day, $B_s = 96{,}400$ lb per acre per day, and $L_B = 5{,}350$ lb per acre-ft per day. Thus, the filter, the sizing, and the loading conditions are compatible with the suggested criteria, except at minimum flow. This deficiency is not serious enough to cause concern, and the design is adequate.

A standard filter, 6 ft deep, to meet approximately the same removal requirements of the foregoing example would require 24 times the area and 8 times the rock volume. A high-rate filter, 5 ft deep, would require approximately 14 times the area and 4 times the volume.

CONCLUSIONS

On the basis of the studies described, it may be presumed that the application of controlled-filtration principles makes possible the functional design of trickling filters, which are greatly reduced in filter area and volume. Such filters are capable of producing effluents of quality equal to or better than the quality required by present standards.

First-section performance of controlled filters is comparable with the performance of other high-rate filters. Thereafter, there are basic differences. No reliable limiting relationship of removal of the B.O.D. to either organic load or hydraulic load was found. The depth of the filter, the sectional construction, the sectional application of both sewage and air, and the filter-water temperature have a bearing on successful treatment at high rates and on the provision of a favorable habitat for sewage biota.

It is essential that continuous flow be maintained to obtain the higher rates of organic removal. Continuous and constant flow combined produce the best filter performance.

The filter-loading ratio, R_L, provides a simple basis for computing the filter size. It is the sewage strength expressed in terms involving depth of filter, area of filter, quantity of sewage, and weight of B.O.D.

ACKNOWLEDGMENTS

The investigation was performed as part of the research program of the Research Division of the College of Engineering at New York University. John Bevan monitored the equipment, and Gail P. Edwards examined the specimens of filter growth.

AMERICAN SOCIETY OF CIVIL ENGINEERS
Founded November 5, 1852
TRANSACTIONS

Paper No. 2906

TIME TO THINK

ADDRESS AT THE SUMMER CONVENTION BUFFALO, N. Y., JUNE 5, 1957

BY MASON G. LOCKWOOD,[1] PRESIDENT, ASCE

Speed has crowded reflective thought very nearly out of our lives. In this age, pure thinking is an almost complete casualty—as much so as walking or reading good literature. The newer influences tend to reject or to obviate or to depreciate contemplation. We have done little to resist the currents which have swept us along the path of diminishing individual thought.

At the request of President Dwight D. Eisenhower, the White House staff some time ago rearranged the Chief Executive's schedule to allow him to devote part of each day to thinking. The President had complained that the exigencies of his daily schedule allowed him no time to wrestle alone with the problems of his administration and to form conclusions and reach decisions before meeting with his advisers.

Few responsibilities undertaken by man impose demands so terribly crushing as those of the office of the President of the United States in these times; but, today, nearly everyone with business or professional responsibilities of any substantial significance finds himself faced with the necessity of getting along without adequate time for pure thinking.

This situation gets worse for the ordinary man year by year, just as it has for our presidents. Contrast President Eisenhower's problem now with circumstances prevailing before the turn of the century—or, for that matter, anytime prior to the last generation. A striking illustration of this is to be found in one of the "Executive Mansion Rules" brought to light by Walter Trehan from the 1893 Congressional Directory. It read:

> " 'Those having no business, but who desire to pay their respects, will be received by the President in the East Room at 1 o'clock P.M. on Mondays, Wednesdays and Saturdays.' "

According to *Newsweek*, Sarah Gibson Blanding, President of Vassar College, observed not long ago that when a college president

---

[1] Partner, Lockwood, Andrews & Newnam, Houston, Tex.

"* * * has accomplished each week's work, there is scarcely any time for academia or getting to know the students—presidential disciplines that were the indispensable prerequisites for the job a generation ago."

There would be adequate cause for individual concern if only highly placed personalities were troubled because they do not have enough time to think. Many of us may be affected by any impairment in their capacity to function best; but lack of thinking time is not merely an occupational disease of presidents. It strikes at all levels. In the world of engineering, circumstances no longer permit enough time for thinking. This is true of most designers, design draftsmen, construction engineers, specification writers, report writers, sales engineers, engineering educators, estimators, consulting engineers, supervisors, and engineering administrators. Generally, to be sure, the need for more thinking time increases with responsibility.

In all current communications media, the major emphasis is on appeal to mass emotion. Little is intended to stimulate individual thinking. We must conclude, therefore, that there is not enough of a mass demand for thinking stimuli to justify their cost. It is disquieting to consider how thoroughly our generation really has rejected thinking as a personal process, how quickly it has adjusted to spoon-feeding for all forms of intellectual nourishment, how impassively it reacts to unmaterial, intellectual challenges.

Man is, I believe, an unwilling victim of today's environment, caught up in a system which places an inordinate premium on speed, a system with little patience and less reward for a man known to be given to reflection. Present-day society has almost vanquished solitude. An active man with the inclination scarcely would dare arrange his life to allow himself time for thought. At best he risks being considered an antisocial plodder, at worst, a pathetic dreamer.

It is quite inconsistent to develop men intellectually, train them professionally, and then fail fully to utilize their potential. Knowledge cannot be fully applied without contemplation. While there was no intention to put this thought into good engineering language, it was indeed so phrased by Tryon Edwards when he said: "Contemplation is to knowledge what digestion is to food, the way to get life out of it."

Personal tension has become the badge of initiative; nervous restlessness, the emblem of successful drive. The hurried gait, the frantic manner, the harassed look—these are the unmistakable marks of achievement. An earlier grave is not the goal, but the successful man is obliged to behave as if it were. Pressure decisions clearly utilize nervous energy; but there is much evidence to indicate that calm reflective thought soothes and revitalizes. It is more likely that one may rely on a well-thought-out decision. Hence, it can soon be forgotten, whereas a hasty one may continue to consume nervous energy.

The influences which have so robbed us of time that little is left for creative thinking have perhaps struck hardest at the lives of business and professional men. The more creative the activity, the greater will be the damage. Thus, the engineering profession, for one, is especially hard hit.

More than ever before, industry and government understand that creativeness is essential to survival and that thinking is essential to creativeness.

Studied programs of wide scope are fostered solely to stimulate ideas and inventiveness. Opportunities for thinking in a relaxed atmosphere are deliberately provided, especially by industry; but most such programs are intended only for research people and business executives—and usually for group rather than individual application. The so-called "brain-storming" currently in vogue is a rather extreme example of the techniques being employed in the competitive effort to spark ideas. In this technique, the emphasis is on quantity production of ideas for application to a particular problem, with participants encouraged to say whatever the discussion may stimulate them to say, without fear of criticism, however wild the idea.

Some of the world's leading scientists have found it very worth while to participate in the Gordon Research Conferences of the American Association for the Advancement of Science. The primary purpose of these conferences is to provide an opportunity for free and unhurried discussion by small competent groups on scientific problems where current research is uncovering new fundamental information. There is neither the crowding nor the haste that marks most scientific and technical gatherings. Discussions proceed with small groups lounging in soft chairs. Nothing said is recorded, and no quotations are ever permitted.

Methods of this kind are being encouraged by industry and government for select groups; yet, in practice, almost everything possible is done to encourage speed-up. Executives are under great pressure and they in turn impose pressure on their subordinates. As one executive explained, what really happens is that, along the line, the man who is promoted is the one who takes his problems home with him.

These forced-draft working procedures are probably achieving maximum production of a sort at top levels. But, concurrently, fundamental professional thinking is being annihilated.

All this poses a grave professional problem. Relatively few engineers, however creatively disposed, are able any more to find the time to think. Such concentrated thinking as they are able to do will probably be done frantically in a pressurized atmosphere. We have been led to believe that this environment actually fires imagination and induces creativeness in some professions and vocations—journalism, for example, and in the creative aspects of the entertainment business. In engineering, it seems almost to have the opposite effect.

Competition is proudly acclaimed and justly identified as the underlying source of America's economic strength. Hence, it may correctly be concluded that competition is the fundamental source of our security, of our advanced scale of living, of our stability, and indeed of our nation's general welfare.

Competition, in one form or another, is also an underlying cause of the difficulties facing the engineering profession as a result of the ever-diminishing time for thinking. The income of active engineers, like the income of most other earners, is derived directly from individual effort. The ultimate source of this income, usually driven by competitive demands, generates pressures calculated to speed up everything in the interest of saving time. The urge to save time stems from the deeper desire to save money. Time saved usually means money saved—but not always, by any means. For example, more engineering applied at the expense of more time required, as well as some more engineering costs incurred, very frequently means more money saved for the ultimate supplier of the funds. Under the prevailing system, however, these relationships are seldom considered rationally. The wrong factors and influences control the time and the money expended on engineering—especially original or creative engineering—which is applied in particular undertakings. Seldom is there a particularized evaluation of the optimum proportion of engineering in the entire project. Hence, seldom is there a conscious balancing or a proper recognition of added benefits to be derived from such optimum engineering.

Factors and influences which most often control the extent of applied engineering are quite arbitrary. There may be little true relationship between these and optimum engineering in individual cases. Minimum engineering is the usual criterion under all competitive conditions. These minimums have their origin in customs in private, industrial, and public works practices. To a considerable degree, however, these origins are basically rooted in the schedules of median or minimum engineering fees which have been published from time to time by the engineering societies as general guides. These usually have been percentage related fees intended to provide generally appropriate compensation for services rendered by private practitioners. In practice, however, these minimum guides are often applied as a measure of the maximum allowable expenditure for engineering—whether it is to be done by engineers in the direct employ of the person or agency paying for the engineering or by outside firms engaged for the purpose.

It is not the intense competition in engineering arising from these practices which is harmful, but some of its evil effects. It tends to put too great a premium on engineering output, with inevitable sacrifice of quality. It tends to fix the time and thought required for applied engineering arbitrarily and without considering its far more significant relation to the over-all economy. A more rational determination would include the time-for-thinking element when justified—which is a nearly complete casualty under present conditions.

It is unprofessional for engineers to participate in competition for engineering services primarily on a price basis because that is neither in the public nor the professional interest. It is quite professional and highly desirable, however, for engineers to compete in all honorable ways because such competition is in both the public and the professional interest.

Despite these manifest truths, and the seeming paradox involved, thoroughly ethical engineers in both the employed and private practice categories these days are obliged indirectly to compete essentially on a price basis. In industry and in government, this competition is with budgets or appropriations, with other industry or other government agencies (civil and military) or with firms in the private practice of engineering. Firms in private practice are in competition with other such firms and with the engineering departments of industry and government. Even many engineering educators and their educational institutions are being affected increasingly by such competition. There is strong competition, for example, for industry- and government-financed, engineer-manned research. As underpaid educators have had to turn more and more to supplemental consulting service for economic survival, they are thrown into competition with each other and with full-time consultants.

To the extent that all these competitive pressures are responsible for reduced costs without impaired quality of engineering, the process is, of course, beneficial publicly and professionally. To the extent that these pressures are responsible for an end product which has had applied to it less than the optimum time for engineering thought, the system is wrong and harmful. This latter, quite frequently is the case.

Fundamentally, engineering is an applied science; but it is just as fundamentally a creative art. The art of engineering is not subject to mass production methods, although some engineering routines are. Nevertheless, excessive competition, combined with the current scarcity of engineers, is inspiring a variety of practices calculated to transform engineering art into routine mechanics.

Such efforts are not to be confused, however, with the very wholesome application of advanced techniques for the mass solution, presentation, or handling of laborious, time-consuming problems of engineering practice. Any such developments which save time and money without sacrifice of essential quality are indeed the very essence of the engineering art; but the sharp distinction between these engineering-related routines and original creative engineering is being obscured. Widespread evidence of this is to be found, and the degree of abuse usually increases with the number of engineers in a particular discipline. Industry perhaps is the chief offender, but government and private practice are hard at its heels. Engineering management seems not to recognize that almost all engineers—indeed almost all people—are creative to some degree. To suppress creativeness in engineers is to misuse engineers monstrously.

Business clearly recognizes the need for imaginative management. It knows the importance of creativity. Moreover business, industry, and government count heavily on scientific research, a pursuit for which they readily afford time for contemplation and independent thought. None of these seems consistently to recognize that engineers do much research, or that they might well do far more to good advantage had they the time and the essential climate.

Relatively few engineers are able any more to apply the uninterrupted thought necessary for the optimum solution. Time simply does not permit this. A harsh deadline must be met. Administrative details cannot be shelved. Personnel problems will not wait. Conference demands must be satisfied. Telephones are insistent and persistent. People must be met, courtesies extended. Meetings must be attended. Family demands cannot be ignored. Social amenities are essential, civic duties demanding.

In this atmosphere, thinking is spotty, uncoordinated, and appallingly inefficient. The best solutions are not achieved. Short cuts are contrived in desperation, usually based on methods copied from similar applications. Such hasty expedients do not necessarily lead to the best solution.

The shortened work week is another factor in the vanishing time for thinking. The professions, including engineering, have always lagged behind wage earners in adopting shorter hours. Self-employed people traditionally work longer, and this is true of self-employed engineers. In these days, however the vast majority of engineers are in the employee category. Nearly all of that group use the standard forty-hour work week, or in some instances an even shorter one. Large numbers, to be sure, work overtime, some quite regularly. For them, this means a work week in excess of forty hours, which can be ignored in this consideration. The very influences that have crowded out "thinking time" may be intensified by the conditions that bring about the overtime work.

Although self-employed and other engineers deriving their income wholly or in part from profits usually much exceed the standard work week, their working hours are influenced by the pattern of employed personnel. Also, the nature of the work they do in this excess time is usually quite different from that done during regular hours. Very likely the overtime hours are their most thoughtful and most productive.

We have less time for thinking, not only because we are at work fewer hours but also because we use more and more of these fewer hours for other things. Much of the lost thinking time can be accounted for. The theoretical eight-hour day in engineering offices actually averages no more than six and three-quarter hours. For many engineers it really averages much less. At least one and one-quarter hours per average day of nearly all engineers goes to vacation, sick leave, excused time off, recreation breaks, and other nonproductive time. In the higher grades perhaps another three-quarters of an hour per day may be lost from office work to meetings, technical conferences, and travel. For these, the office day is only six hours.

If engineers are to have more time to think as they once did—this time will need to be salvaged either from what is left of the working hours, or from nonworking hours, or both. This is an individual problem for all engineers. In the case of employed engineers, it is also a management problem.

Individually, the most promising efforts for improvement would seem to be elimination of all possible time-consuming, nonessential distractions. This means, first, improved personal efficiency. It means also release from all routine and administrative details that can be handled by subprofessional or clerical assistance.

In the case of supervisory or administrative engineers, it means delegation of more responsibilities. This must be done even though those to whom the responsibility is delegated are either thought or known to be less competent. Here many of us fail miserably. Almost invariably we underestimate the ability of others to assume responsibilities we have been handling. If we have perfectionist tendencies, the delegation problem is even more aggravated.

One notorious thief of time strikes at all engineering levels—on-the-job social visiting with associates and, to a lesser extent, with outsiders. The twice-daily recreational breaks, which have come to be an accepted and wholesome part of American business, industrial, and professional life, are proper times for such visiting; but abuses are reported everywhere. Probably the only effective remedy against excessive visiting is personal discipline. A thinking engineer who longs for more time for thought while at work might well examine and improve his personal habits in this regard.

Engineering entails much personal communication between design and supervisory personnel and between designers and sales representatives of manufacturers and suppliers. If they are to be successful, those interested in the sale of a product for use in an engineering undertaking must maintain personal contact with the engineers responsible for specifying materials, equipment, and nonengineering services. The frequency and duration of these interviews is some measure of the sales group's effectiveness. On the other hand, those who specify do lose time as a result of excessively long or frequent sales interviews.

The problem is a difficult one. Under our system of business practice, selling agents are entitled to a full hearing. Indeed they make a significant contribution to engineering. Nevertheless, it is both good judgment and acceptable professional etiquette to limit sales interviews to the length of time really required. The necessary discipline must be initiated by the engineer representing the ultimate owner or purchaser, not by the sales representative. Consistent insistence upon brevity usually leads to respect and mutual understanding, if ordinary business amenities are not breached in the process. It is quite unfair to selling agents to be inconsistent on this point, allowing moods and other factors of the moment to govern.

In administrative, executive, and supervisory capacities especially, the telephone is at once a tremendous time-saver and an astounding time-waster. Most telephone conversations during working hours are unnecessarily long. Usually they could be shortened materially without either reducing effectiveness or infringing courtesies.

Nearly all engineers of professional standing are obliged to participate in conferences of one kind or another. These conferences probably use, on the average, twice as many man-hours as necessary. Several factors are chiefly responsible for wasted conference time. The greatest, perhaps, is inadequate planning. Curiously, good planning is considered the special forte of the engineer. Another notable thief of time in conferences, also traceable to improper planning and direction, is the tendency to deal with matters affecting only a minority of those present.

Inadequate and incompetent stenographic and secretarial assistance, or inadequate dictating facilities, is a frequent and usually valid complaint of engineers, especially of those in situations requiring considerable use of such services or equipment. An organization that fails to provide its engineers with adequate services of this kind pays a very high price for its short-sightedness. This would be true even when engineers are plentiful; yet this is perhaps one of the most common time-thieves.

In his effort to recapture some time for thinking, the engineer might well examine the way in which he makes use of the dictating and stenographic facilities available to him. Sporadic dictation throughout the day, rather than more orderly, concentrated, uninterrupted periods of dictation, is wasteful. Another common and avoidable fault is the failure to make full use of stenographers' and secretaries' ability to compose, after only the briefest directions, the routine letters comprising a large part of an engineer's correspondence.

If collected, the minutes wasted throughout every work day would comprise a respectable total of perhaps one or two hours. This fact, coupled with the easily-overlooked responsibility of every engineer to make some use of his *own* time to his and his job's advantage, leaves us with less excuse for the current deplorable state of our workday schedule.

Granting the difficulties compared to those, say, of a century ago—or even of twenty years ago—it is still possible to supply oneself with time to think creatively. Only by finding a way to do so can an engineer, or any professional man, fulfil his ultimate responsibility. It is an effort—and not an easy one—which can originate only within the individual.

Only the very exceptional people are likely to be determined enough to persevere over these thought-inhibiting influences of our times. These will be able to base their important judgments on truly contemplative thought despite the adverse environment. Although the reason may not be generally recognized or appreciated by others, this is certain to distinguish them.

MEMOIRS OF DECEASED MEMBERS

ABSTRACTS

Past President

Edgar Morton Hastings 1231

Honorary Members

Charles Baker Burdick 1232
John Chatfield Page 1233

Other Members

Thomas Augustine Berrigan 1233
Frederick Louis Bixby 1234
James Churchill Boyd 1235
James Henry Brace 1235
Archibald Alexander Brown 1236
Richard Meyer Brown, Jr. 1237
Blair Irving Burnson 1237
Harry Cady Byrnes 1238
John Needels Chester 1238
John Belford Cleary 1239
Donald Omer Coe 1240
William Dewoody Dickinson 1240
DeMarcus D. Forgey 1241
Theodore Grahlman 1241
George Wellington Hamilton 1242
Charles Arthur Haskins 1243
Alfred Ronald Hiatt 1243
Walter Monroe Jarvis 1244
Hollister Johnson 1244
Frank Alvah Kittredge 1245
Oscar Henry Koch 1246
François Emile Matthes 1246
Gwynne Gravelle McCaustland 1247
Roy Gillespie McGlone 1248
Robert James Middleton 1248

John William Miller........ 1249
William Charles Mooney........ 1250
Thomas Clayton Mott........ 1250
Ray Messinger Murray........ 1251
Constantine Alexander Novie........ 1252
Sivert Edward Olsen........ 1252
Langdon Pearse........ 1253
John Carleton Phillips........ 1253
Herbert Spencer Ripley........ 1254
Arthur Winthrop Sargent........ 1255
Thomas Russel Simpson........ 1255
Alfred Kittoe Stillman........ 1256
Simon Weinberg Tarr........ 1256
Herman Franklin Tucker........ 1257
Charles Leopold Wartelle........ 1258
Walter Owen Washington........ 1258
Melvin Delano Williams........ 1259
Frank Wormald........ 1260
Arrigo Mazzucato Young........ 1260
Lloyd Otto Zapp........ 1261

EDGAR MORTON HASTINGS, PAST-PRESIDENT, ASCE[1]

DIED NOVEMBER 21, 1954

Edgar Morton Hastings, the son of Robert John and Ada (Heilig) Hastings, was born in Lutherville, Md., on May 5, 1883. He received his college education at the Baltimore Polytechnic Institute (Baltimore).

Mr. Hastings began his career with the Baltimore and Ohio Railroad Company and shortly thereafter, in 1903, joined the Richmond, Fredericksburg and Potomac Railroad Company in Richmond, Va. He progressed through subordinate positions until he became chief engineer in 1922. His administration was marked by the complete rehabilitation of the property in the post-World War I period, subsequent large-scale improvements, the replacement of station and bridge facilities at Fredericksburg, Va., the adoption of modern maintenance policies, and the use of heavy-section, continuous welded rail in main track.

He was selected by the Economic Cooperation Commission of the United States government in 1948 to inspect and report on the three principal railroads in China.

He also served the City of Richmond as a member of the City Planning Commission and as chairman of the Board of Zoning Appeals from 1935 to 1944.

In the course of his career, for more than forty-two years, he was very active in the American Railway Engineering Association. He served on its committees on Yards and Terminals, Cooperative Relations with Universities, and Standardization. He was director (1931-1934), vice-president (1937-1939), and president (1939-1940). In 1950 Mr. Hastings was made an honorary member of this organization.

He served the Society as President of the Virginia Section, as a member of several national committees, as Vice-President of Zone II in 1943-1944, and as President in 1947.

Other professional affiliations of Mr. Hastings included the American Society for Testing Materials, the National Society of Professional Engineers, the Engineers' Club of Hampton Roads, the Engineers' Club of Virginia Peninsula, and the Central Virginia Engineers' Club.

On February 27, 1908, he was married to Carmen Robertson. He is survived by his widow; two sons, Edgar M. and David C.; and three grandchildren.

Mr. Hastings was elected an Associate Member of the Society on June 30, 1910, and a Member on May 8, 1922. He became a Life Member in 1945.

NOTE.—Complete manuscripts have been filed in the Engineering Societies' Library, 29 West 39th Street, New York, N.Y., and are available for consultation. Many of these memoirs have been considerably abbreviated for printing in *Transactions*.

[1] Abstract of memoir prepared by P. A. Rice, A. M. ASCE.

CHARLES BAKER BURDICK, HON. M. ASCE[1]

Died February 17, 1955

Charles Baker Burdick, the son of William and Mary (Dewey) Burdick, was born in Chicago, Ill., on March 6, 1874. He was graduated from the University of Illinois (Urbana) in 1895.

Following graduation he was first employed by Alvord & Shields. This was followed by approximately five years with John A. Cole, consulting engineer, of Chicago. In 1902, Mr. Burdick formed a partnership with John W. Alvord which continued for forty years until Mr. Alvord's death. Until 1922, the partnership was known as Alvord & Burdick, and subsequently as Alvord, Burdick & Howson.

Mr. Burdick contributed markedly to the development of methods for both water and sewage treatment. He was also widely consulted on hydraulic problems related to stream flow, floods, and flood relief. In cooperation with Mr. Alvord he was author of a book on flood prevention and flood protection.[2] He early realized the economic possibilities in the use of super-heated steam in steam turbines and made some of the earliest installations of that type of equipment in waterworks service. In later years he converted many steam pumping stations to electric drive.

Mr. Burdick's advice was always widely sought throughout the United States. Some of his most outstanding developments are the Mokelumne River East Bay City project at San Francisco; the Deer Creek Water Development at Salt Lake City; the Moffat Filter Plant at Denver; and the extensive gallery system at Des Moines, which Mr. Burdick directed for more than forty years. He was consultant to the City of Chicago on the world's two largest filtration plants, on the Pioneer Mechanical Filtration plant at Niagara Falls with its phenomenal record of typhoid reduction, and to the Long Island Water Company in New York.

Mr. Burdick was active in Society affairs. He served as Director from 1935 to 1937 and as Vice-President in 1941-1942, and was chairman of many important committees.

He belonged to the American Institute of Consulting Engineers, the Illinois Society of Professional Engineers, the Western Society of Engineers, the American Water Works Association, and the Chicago Engineers' Club. He was an honorary member of the last four mentioned organizations.

In 1909 he was married to Mabel Taylor. She died in 1935. He is survived by two daughters, Mary (Mrs. R. C. Dallach) and Janet (Mrs. E. J. Hansman).

Mr. Burdick was elected an Associate Member of the Society on March 1, 1905; a Member on June 30, 1911; and an Honorary Member on October 14, 1946. He became a Life Member in 1940.

---

[1] Abstract of memoir prepared by L. R. Howson, M. ASCE.

[2] "Relief from Floods," by John W. Alvord and Charles B. Burdick, McGraw-Hill Book Co., Inc., New York, N. Y., 1918.

JOHN CHATFIELD PAGE, HON. M. ASCE[1]

DIED MARCH 23, 1955

John Chatfield Page, the son of Walter E. and Emma J. (Chatfield) Page, was born on October 12, 1887, in Syracuse, Nebr. In 1908 he received the degree of Bachelor of Science in civil engineering from the University of Nebraska (Lincoln). He also attended Cornell University (Ithaca, N. Y.).

Mr. Page's early experience in the field of reclamation, briefly interrupted by eighteen months of postgraduate study at Cornell, included conducting irrigation surveys in Idaho, Nebraska, and Colorado; a short term of service as assistant city engineer at Grand Junction, Colo.; and a few seasons of irrigation farming.

From 1911 to 1914 he was engaged in engineering and construction work on the Grand Valley Project of the United States Reclamation Service (later the Bureau of Reclamation) near Grand Junction. In 1915 when he returned to the project from Cornell, he became assistant to the project manager. In 1925 Mr. Page became superintendent of the Grand Valley Project and in 1930 he was selected office engineer of the Boulder Canyon Project (Hoover Dam) at Boulder City, Nev., and contributed to the successful completion of this project. In 1935 he was appointed assistant to Elwood Mead, the head of the United States Bureau of Reclamation in Washington, D. C.

On January 25, 1937, after a term of service as assistant commissioner of the bureau, he was promoted to commissioner. While serving as assistant commissioner and as a member of the national Great Plains Committee, Mr. Page made a thorough field study of the drought emergency of this region and supported investigations resulting in the initiation of the comprehensive Missouri River Basin Project.

In 1943, after unremitting devotion to his work, much of which was created by the demands of the war years, he resigned to become consulting engineer to the Bureau.

In 1914 he was married to Mildred R. Sloan in Oak Park, Ill. He is survived by his widow; two daughters, Jean (Mrs. Cecil L. Killgore) and Mildred (Mrs. Philip A. Danielson); and five grandchildren.

Mr. Page was elected a Member of the Society on July 6, 1936, and an Honorary Member on June 15, 1953.

THOMAS AUGUSTINE BERRIGAN, M. ASCE[2]

DIED MAY 11, 1956

Thomas Augustine Berrigan, the son of John F. and Mary E. (Dunn) Berrigan, was born at Boston, Mass., on May 29, 1895. He was graduated with the degree of Bachelor of Science from Massachusetts Institute of Technology (Cambridge) in 1916. He received the degrees of Bachelor of Laws from Northeastern University (Boston) in 1930 and Master of Science in Sanitary Engineering from Harvard University (Cambridge) in 1949.

---

[1] Abstract of memoir prepared by a committee of the Colorado Section consisting of Walker R. Young, Chairman, Frederick E. Schmitt, and Grant Bloodgood, Members, ASCE.

[2] Abstract of memoir prepared by Gordon M. Fair, M. ASCE.

Twice in his career Mr. Berrigan established himself in private practice, from 1921-1925, and upon his retirement from the Metropolitan District Commission of Boston in 1955. However, most of his professional life was spent in public service. He was a civil engineer with the Boston Transit Department (1925–1935) before he joined the Metropolitan District Commission as senior civil engineer, becoming director of the sewerage division and chief sewerage engineer in 1945.

Mr. Berrigan rendered outstanding public service also as chairman of the Joint Board consisting of the Merrimack River Valley Sewerage Board and the Massachusetts Department of Public Health, as a member of the National Pollution Control Board, United States Public Health Service (1949-1954), as director of the Boston Society of Civil Engineers, and as assistant district public works officer, First Naval District (July 1942–May 1945) for which he received a naval citation.

On September 13, 1937, at Boston, Mr. Berrigan was married to Helen L. Flynn. He is survived by his widow.

Mr. Berrigan was elected a Member of the Society on May 18, 1942.

FREDERICK LOUIS BIXBY, M. ASCE[1]

DIED NOVEMBER 13, 1955

Frederick Louis Bixby, the son of Russell and Annis (Smith) Bixby, was born in Moorehead, Minn., on July 1, 1880. He received the degree of Bachelor of Science in civil engineering in 1905 from the University of California (Berkeley) and the degree of Civil Engineer in 1918 from the University of Nevada (Reno).

After graduation Mr. Bixby was employed by the Oregon Short Line Railway on location and construction work in Idaho. In 1907 he made surveys and investigations for hydroelectric developments in the Salt Lake City area and in 1908 he joined the United States Department of Agriculture, later serving as office engineer in Washington, D. C.

In 1910 Mr. Bixby directed investigations on water resources and water uses in New Mexico and later continued in this capacity in Nevada. While in New Mexico, and during his early years in Nevada, he became a part-time member of the engineering faculty at the New Mexico College of Agriculture and Mechanic Arts, and also served in the same capacity in the Civil Engineering Department of the University of Nevada. He became a full-time member of the latter department in 1922, and chairman of the department in 1939. He retired in 1948.

---

[1] Abstract of memoir prepared by H. B. Blodgett, M. ASCE.

On December 31, 1907, in Berkeley he was married to Rhoda A. Orgren. He is survived by his daughter, Ruth Eleanor (Mrs. John M. Matley).

Mr. Bixby was elected an Associate Member of the Society on June 6, 1911, and a Member on March 11, 1919. He became a Life Member in 1946.

JAMES CHURCHILL BOYD, M. ASCE[1]

DIED JANUARY 18, 1954

James Churchill Boyd, the son of Samuel and Harriet E. (Churchill) Boyd, was born on August 19, 1871, in St. Louis, Mo. He was graduated from the Massachusetts Institute of Technology (Cambridge), in 1893.

After preliminary experience he joined (1897) the staff of the Boston Elevated Railway. Late in 1902 he joined Westinghouse, Church, Kerr & Company, Engineers and Constructors of New York, N. Y., and served that company until his retirement as construction engineer, chief engineer, vice-president, and first vice-president and acting president, successively.

Subsequent to his retirement (1920) he returned to Portland, Me., and to the practice of consulting engineering, except for a brief period with F. H. McGraw Company, New York.

In Portland, he was vice-president and director of The National Bank of Commerce; director of the The Boyd Corporation, Thomas Laughlin Company, and Felo Company; and vice-president and director of the State Loan Company.

On September 5, 1896, he was married to Ada Yerxa.

Mr. Boyd was elected a Junior of the Society on September 3, 1895; an Associate Member on May 1, 1901; and a Member on September 3, 1907. He became a Life Member in 1936.

JAMES HENRY BRACE, M. ASCE[2]

DIED APRIL 10, 1956

James Henry Brace, the son of James and Susan (Rork) Brace, was born in Sheridan Township, N. Y., on November 10, 1870. He was graduated a civil engineer from the University of Wisconsin (Madison) in 1892.

After preliminary experience, Mr. Brace became assistant consulting engineer (1903) on the construction of the East River Railway tunnels for the Pennsylvania Railroad. In 1908 he formed the construction firm of Fraser, Brace and Company, Limited. As general manager for thirty-seven years of this firm and of associated companies in Canada and the United States, Mr.

---

[1] Abstract of memoir prepared by George W. Burpee, Hon. M. ASCE.
[2] Abstract of memoir prepared by Gordon R. Stephen.

Brace directed construction of many industrial projects, including metallurgical refineries and smelters, chemical plants, pulp and paper mills, and hydroelectric developments.

In World War I, Mr. Brace served as a major in the Corps of Engineers, United States Army. During World War II, he was vice-president of the United Shipyards, Limited, which constructed cargo ships and auxiliary vessels.

Mr. Brace was a member of the St. James Club, the Engineers' Clubs of Montreal and New York, the Canadian Club, Forest and Streams Club, Royal Montreal Golf Club, and Copper Cliff Club in Ontario.

On September 6, 1897, in Chicago, Ill., he was married to Frances Gemmell. He is survived by two nephews.

Mr. Brace was elected an Associate Member of the Society on January 2, 1901 and a Member on September 6, 1904. He became a Life Member in 1936.

ARCHIBALD ALEXANDER BROWN, A.M. ASCE[1]

DIED NOVEMBER 26, 1955

Archibald Alexander Brown, the son of Archie and Mary (Ford) Brown, was born in DuBois, Pa., on June 19, 1884. He was graduated in 1906 as an engineer from the New Mexico College of Agriculture and Mechanical Arts (State College).

In 1908 Mr. Brown joined the office of the city engineer of San Francisco, Calif. He helped design a new sewer system, a fire protection system, and the Mission Street Viaduct. In 1911 Mr. Brown joined the Board of State Harbor Commissioners which administers the San Francisco water-front facilities, and later was chief draftsman for the 1915 Panama Pacific International Exposition. Late in 1915 he was employed by the California & Hawaiian Sugar Refining Corporation and for many years was retained by this company as a consultant. Subsequently, he was appointed assistant chief engineer for the Board of State Harbor Commissioners and was engaged in the construction of many structures for his own engineering office. He also served as engineering editor for *Architect and Engineer*.

Later he became vice-chairman of the San Francisco Bay Marine Piling Committee and was chairman of the subsoil committee of the San Francisco Section of the Society.

He belonged to the Berkeley Club, the Faculty Club of the University of California, the Presbyterian Church, and the Y.M.C.A.

On June 9, 1911, Mr. Brown was married to Sarah Josephine Work. He is survived by his widow and a son, Archibald.

Mr. Brown was elected an Associate Member of the Society on September 2, 1914. He became a Life Member in 1949.

---

[1] Abstract of memoir prepared by Arthur J. Grier, M. ASCE.

RICHARD MEYER BROWN, JR., J. M. ASCE[1]

Died April 8, 1954

Richard Meyer Brown, Jr., the son of Richard Meyer and Dorothy (Davies) Brown, was born on April 12, 1928, at Monroe, Wash. Mr. Brown was graduated from Garfield High School in Seattle in 1947 and from the University of Washington (Seattle) in August, 1951, with the degree of Bachelor of Science in civil engineering.

After graduation he was employed by the Boeing Airplane Company of Seattle in the engineering department. While on duty as ensign with Squadron VF 194, United States Naval Reserve, he was killed in dive-bombing practice maneuvers near Fallon, Nev.

He is survived by his father; his step mother, Lena Brown; two brothers; and one sister.

Mr. Brown was elected a Junior Member of the Society on December 10, 1951.

BLAIR IRVING BURNSON, M. ASCE[2]

Died October 26, 1955

Blair Irving Burnson, the son of G. Norman and Etla (Kelsey) Burnson, was born in Hettinger, N. Dak., on November 19, 1911. He was graduated with the degree of Bachelor of Science in civil engineering from the University of California (at Berkeley) in 1934.

While at the University of California, Mr. Burnson was president of Tau Beta Pi and Chi Epsilon, two honor societies.

After graduation Mr. Burnson was employed as a sanitary engineer by the East Bay Municipal Utility District, in Oakland, Calif. During his twenty-one years with the District, he advanced rapidly in the sanitary engineering field to increasingly responsible positions. During his last year with the District he became executive assistant to the general manager.

Mr. Burnson was very active in professional and civic groups, amongst which were the American Water Works Association, the American Public Health Association, and the Federation of Sewage and Industrial Wastes Association. He was a former director of the Oakland Junior Chamber of Commerce and was active in Rotary International.

At the time of his death Mr. Burnson was the vice-president of the San Francisco Section of the Society.

On September 6, 1940, at Oakland, Mr. Burnson was married to Evelyn Jorgenson. He is survived by his widow, mother, and two sisters.

Mr. Burnson was elected a Junior of the Society on October 29, 1934; an Associate Member on December 16, 1946; and a Member on September 29, 1954.

---

[1] Abstract of memoir prepared by Carl F. Ganong, M. ASCE.

[2] Abstract of memoir prepared by Donald G. Larkin, A. M. ASCE.

HARRY CADY BYRNES, M. ASCE[1]

Died November 7, 1955

Harry Cady Byrnes, the son of William and Addie (Miller) Byrnes, was born in Belle Plaine, Kans., on March 19, 1883. He studied civil engineering at the University of Kansas (Lawrence).

Mr. Byrnes served in the infantry during World War I. He maintained his officer standing as a reserve until 1943 when he resigned with the rank of lieutenant colonel of infantry.

Before setting up his own practice as a consulting engineer in Lamar, Colo., he was district construction engineer in the Colorado State Highway Department. In 1929 he became associated with the J. G. White Construction Company of New York, and represented them for two years in Panama as construction superintendent on a loading pier on the Pacific Coast and on the Panama Railroad. Later he represented the same company in Chile on construction of irrigation systems and a tunnel.

In 1933 Mr. Byrnes returned to the United States, joining the staff of the New England Division of the Corps of Engineers, United States Army. He retired in 1943 and moved to Whittier, Calif.

In 1909 he was married to Nelly Dillon. He is survived by his widow.

Mr. Byrnes was elected an Associate Member of the Society on October 11, 1920, and a Member on January 20, 1922.

JOHN NEEDELS CHESTER, M. ASCE[2]

Died November 1, 1955

John Needels Chester, the son of Hubert and Melvina (Needels) Chester, was born in Columbus, Ohio, on September 24, 1864. He was graduated from the University of Illinois (Urbana) in 1891 with the degree of Bachelor of Science in civil engineering and later received the degrees of Civil Engineer (1909) and Mechanical Engineer (1911).

After graduation, he entered the field of waterworks engineering. In 1894 he directed the installation of extensive waterworks equipment for a manufacturer of pumping machinery.

In 1899 Mr. Chester became chief engineer of the American Water Works & Guarantee Company which operated forty-two water plants. At this time he contributed greatly to the art of water filtration and to procedures for the installation of water-treatment plants.

Before organizing the firm of Chester & Fleming (1910), he was general manager of a pumping machinery company. For twenty-five years Mr. Chester was an active consultant in this partnership. He designed extensive improvements to waterworks plants and new construction and helped develop valuation and rate-making procedures, representing many communities and water companies.

---

[1] Abstract of memoir prepared by John M. Server, Jr., A. M. ASCE.
[2] Abstract of memoir prepared by D. E. Davis, M. ASCE.

Mr. Chester served as Director of the Society (1922-1924) and as Vice-President (1931-1932). He was a member of the Engineers' Society of Western Pennsylvania (past-president), the University of Illinois Association (director and president), and the University of Illinois Foundation (director).

He is survived by four sisters and one brother.

Mr. Chester was elected a Junior of the Society on December 6, 1892; an Associate Member on December 5, 1894; and a Member on March 6, 1901. He became a Life Member in 1929.

JOHN BELFORD CLEARY, M. ASCE[1]

DIED MAY 12, 1954

John Belford Cleary, the son of James and Katherine (Walker) Cleary, was born at Alma, Colo., on September 26, 1891. He was educated at the University of Wyoming (Laramie).

In 1920 he joined the Midwest Refining Company at Casper, Wyo., and for twelve years was in charge of all civil engineering activities. Concurrently, he undertook technical assignments for the City of Casper. He continued as district engineer for this company until 1935.

Through 1941, Mr. Cleary was engaged as United States mineral surveyor; superintendent of water distribution on the North Platte River; consultant and regional engineer to the Resettlement Administration, United States Department of Agriculture; and manager of the American Aggregate Company of Kansas City, Kans. He conducted research and wrote articles on the properties of Haydite concrete.

During World War II and until 1945, Mr. Cleary worked for the Pacific Car and Foundry Company in the construction of its Everett (Wash.) shipyards and engaged in other activities. He then established a private practice at Bothell, Wash., closing his career with varied projects in the Seattle area.

Mr. Cleary was a member of the Colorado Society of Engineers and the Wyoming Engineering Examining Board. He prepared the textbook for the International Correspondence Schools on United States land surveys.

On October 25, 1916 in Basin, Wyo., he was married to Farol Egbert. He is survived by his widow; two sons, James, and John; and a brother.

Mr. Cleary was elected a Junior of the Society on September 9, 1919; an Associate Member on June 6, 1921; and a Member on May 16, 1938.

---

[1] Abstract of memoir prepared by Sherman B. Green, M. ASCE.

DONALD OMER COE, M. ASCE[1]

DIED AUGUST 29, 1956

Donald Omer Coe, the son of Claude E. and Elizabeth (Thuma) Coe, was born at Crystal Lake, Iowa, on January 4, 1902. He received the degree of Bachelor of Science in civil engineering from Denison University (Granville, Ohio) in 1926. He did graduate work in civil engineering at the University of Wisconsin (Madison) and later studied naval architecture at Temple University (Philadelphia). Mr. Coe's professional experience had included employment in Boston, Mass., Ampere, N. J., and Philadelphia, Pa. While in Philadelphia, Mr. Coe was a structural designer and naval architect with the United States Department of the Navy. In 1941, Mr. Coe entered the employ of the Corps of Engineers, United States Army, Vicksburg, Miss. In the succeeding fifteen years of his career in the Corps, design work was his special concern until 1952 at which time he was promoted to the position of chief of the Safety Branch. He was serving in this capacity at the time of his death.

Mr. Coe was active in civic, fraternal, and church organizations.

On June 27, 1931, at Belmont, Mass., Mr. Coe was married to Katherine Kimball of Newburyport, Mass. He is survived by his widow, and two sons, Robert and Richard.

Mr. Coe was elected an Associate Member of the Society on June 10, 1942, and a Member on July 21, 1952.

WILLIAM DEWOODY DICKINSON, M. ASCE[2]

DIED JUNE 15, 1955

William Dewoody Dickinson, the son of George and Harriet (Brodie) Dickinson, was born in Arkansas City, Ark., on November 20, 1881. In 1903 he completed his engineering education at the University of Arkansas (Fayetteville). He was graduated from the Arkansas Law School in 1929.

His entire engineering career of more than fifty years was spent in his native state. After graduation he worked with the United States Geological Survey and then became assistant engineer on the construction of the Plum Bayou Levee—one of the first attempts by engineers to control the floodwaters of the Arkansas River and reclaim vast areas. Mr. Dickinson worked on this engineering problem throughout his professional life. Shortly after the levee system was completed he was promoted to the position of chief engineer for the Levee District, a position he held until his death.

---

[1] Abstract of memoir prepared by Norman R. Moore, M. ASCE.

[2] Abstract of memoir prepared by Leonard N. White and Abby W. Hardy, Members, ASCE.

In 1909 he formed the partnership of Dickinson and Watkins, Consulting Engineers, in Little Rock. During this long practice he designed and supervised the construction of many important works.

In 1905 Mr. Dickinson was married to Florence Watkins. He is survived by his widow and a son, William.

Mr. Dickinson was elected an Associate Member of the Society on May 3, 1910, and a Member on June 12, 1917. He became a Life Member in 1945.

DeMARCUS D. FORGEY, M. ASCE[1]

DIED APRIL 6, 1956

DeMarcus D. Forgey, the son of Elias and Amanda (Holman) Forgey was born in Anatone, Asotin County, Wash., on April 29, 1886. In 1909 he was graduated in civil engineering from Washington State College (Pullman). He was first employed in railway construction in Canada and later in hydroelectric development for the City of Seattle, Wash., on the Skagit River Project.

In 1925 Mr. Forgey joined the Washington State Highway Department and was located in Aberdeen, Wash., until 1935 at which time he was transferred to Seattle as a locating engineer. From 1945 to 1949 he served as construction engineer and afterwards as assistant engineer and district engineer in Wenatchee, Wash., and Vancouver, Wash., respectively. In 1951 he was appointed district engineer in Seattle and was serving in this capacity at the time of his death.

On December 31, 1941, in Sumas, Wash., Mr. Forgey was married to Ann Fitzgerald. He is survived by his widow; two daughters, Marie (Mrs. L. H. Scheibe) and Patricia (Mrs. J. W. McMahon); two foster children, Sister Charles Marie and Charles F. Courtman; a sister; and three grandchildren.

Mr. Forgey became a Member of the Society in 1954.

THEODORE GRAHLMAN, A. M. ASCE[2]

DIED JANUARY 23, 1956

Theodore Grahlman, the son of Frank and Loretta (Youngman) Grahlman, was born in Tacoma, Wash., on September 1, 1888.

Mr. Grahlman was educated in New York, N. Y. From 1909 through 1913 he held various positions with surveying organizations in the northwestern United States and Alaska. In 1913 he moved to New York and was a chief of party on highway location and construction in Palisades Interstate Park (New York and New Jersey until 1915. From that time until 1930 Mr. Grahlman performed various engineering duties for consultants and contractors in the New York area. From 1930 to 1940 he was assistant engineer for the Port of New York Authority and assisted in the construction of the Lincoln Tunnel for the New York City Tunnel Authority.

---

[1] Abstract of memoir prepared by Samuel DeMoss, M. ASCE.

[2] Abstract of memoir prepared by Carl F. Ganong, M. ASCE.

Because of poor health in recent years, Mr. Grahlman had not been able to carry on full employment but worked for the City of Seattle (Wash.) and the Pacific Testing Laboratories of Seattle.

On January 2, 1915 in Yonkers, N. Y., Mr. Grahlman was married to Mary Salvato. He is survived by his widow, a brother, and a sister.

Mr. Grahlman was elected an Associate Member of the Society on April 19, 1920. He became a Life Member in 1955.

GEORGE WELLINGTON HAMILTON, M. ASCE[1]

Died August 30, 1956

George Wellington Hamilton, the son of George and Almira Jane (Haas) Hamilton, was born on November 26, 1879, in Pottsville, Pa. Because of the death of his father he left school after completing two years (1898–1900) of the electrical course at Lehigh University (Bethlehem, Pa.).

Mr. Hamilton's extensive career of fifty-six years involved him in all major phases of electric utilities in the United States, Canada, and South America. After substantial experience, he was appointed vice-president of the Central Illinois Public Service Company in Mattoon, Ill. (1912-1919), and later vice-president in charge of hydraulic and electrical engineering of Middle West Utilities Company in Chicago, Ill. (1919–1931). Between 1931 and 1946 he engaged in private practice as a hydroelectric consulting engineer. After briefly serving as chief engineer for the U. S. Department of the Interior, Power Division, in Washington, D. C. (1946–1947), he returned to private practice as a consulting engineer.

Among the many important projects of Mr. Hamilton's career are three dams, which at the time they were developed under his supervision were the largest of their type, Dixon Dam in Illinois, Dix Dam in Kentucky, and Hamilton Dam, in Texas (which bears his name).

Mr. Hamilton was a fellow and charter member of the American Institute of Electrical Engineers and a member of the Western Society of Engineers.

On August 22, 1903, at Lancaster, Pa., he was married to Jane Follett Platt. She died in April, 1946. On December 21, 1946, at Evanston, Ill., he was married to Cinderella Hegg. He is survived by his widow and two sons, George and Harry.

Mr. Hamilton was elected a Member of the Society on July 14, 1930.

---

[1] Abstract of memoir prepared by Cinderella H. Hamilton.

CHARLES ARTHUR HASKINS, M. ASCE[1]

DIED DECEMBER 28, 1956

Charles Arthur Haskins, the son of Milton and Mary (Pierson) Haskins, was born on January 28, 1887, at Galva, Kans. He was graduated from the University of Kansas (Lawrence) with the degree of Bachelor of Science in 1910. He received the degree of Master of Science from Harvard University (Cambridge, Mass.) in 1914.

Mr. Haskins was formerly instructor and later professor of sanitary engineering at the University of Kansas (1913–1920). In this position he also held the title of assistant and later chief engineer of the State Board of Health. During this same period, by leave of absence, he served in the Army Sanitary Corps. He joined the staff of Black and Veatch, Consulting Engineers of Kansas City, Kans., in 1920, and in 1922, he headed his own engineering firm. From 1934 to 1939 Mr. Haskins served as chief engineer and architect for the Missouri State Building Commission.

Mr. Haskins was a member of Sigma Xi and Sigma Tau, and of numerous civic and technical groups. He was formerly president of the Kansas City Section of the Society (1929) and of the Kansas City Engineers' Club (1933).

On January 23, 1913, at Oskaloosa, Kans., Mr. Haskins was married to Tess Critchfield. He is survived by his widow; two daughters, Mary (Mrs. R. F. Barker) and Suzanne (Mrs. W. A. Tholen); two sisters; and one brother.

Mr. Haskins was elected an Associate Member of the Society on June 23, 1916, and a Member on June 6, 1921. He became a Life Member in 1951.

ALFRED RONALD HIATT, M. ASCE[2]

DIED MARCH 30, 1956

Alfred Ronald Hiatt, the son of Cassius and Cora (Fulghum) Hiatt, was born at Lynn, Ind., on January 25, 1898. At the termination of World War I and of his military service, and after having completed his sophomore year at Purdue University (Purdue, Ind.), Mr. Hiatt worked as an instrumentman for the City of Richmond, Ind. He also worked for the Pennsylvania Railroad, the Missouri Pacific Railroad, and the Baxter Engineering Company (Little Rock, Ark.) during the subsequent three years. Following this Mr. Hiatt taught mathematics for one year at Little Rock College (Little Rock). He then reentered Purdue University from which he received the degree of Bachelor of Science in civil engineering in 1925.

Subsequently Mr. Hiatt was employed as an engineer by the Baxter Engineering Company (1925-1928); the Arkansas State Highway Department (1929-1931 and 1935); and the Corps of Engineers, United States Army (1932-1934 and 1936-1955). From 1947 until his retirement in 1955, he was chief of the Planning and Reports Branch of the Vicksburg (Miss.) District Corps of Engineers, and was responsible for the planning on all flood control projects in the District.

---

[1] Abstract of memoir prepared by Mark C. Culbreath, M. ASCE.

[2] Abstract of memoir prepared by Ora G. Baxter, M. ASCE.

On June 19, 1947, at Jackson, Miss., he was married to Douglass Lord. He is survived by his widow, a sister, and a brother.

Mr. Hiatt was elected a Member of the Society on May 18, 1943.

WALTER MONROE JARVIS, M. ASCE[1]

DIED JULY 11, 1956

Walter Monroe Jarvis, the son of Thomas and Margaret (Hutton) Jarvis, was born in Barbourville, Ky., on September 10, 1895. He attended Union College (Barbourville) and the University of Kentucky (Lexington).

After working for the Kentucky State Department of Highways (1922-1932); engaging in private practice (1932–1934); being employed by the Federal Works Progress Administration, in eastern Kentucky (1935-1942); and, later, by Frazier-Brace, at Kingsport, Tenn.—Mr. Jarvis went to Oak Ridge, Tenn., to work on early road design programs for the Manhattan District and its successor, the Atomic Energy Commission. In succeeding years he was employed by private architect-engineer firms in similar work. At the time of his death, he was connected with the Oak Ridge National Laboratories.

Mr. Jarvis was a first lieutenant, United States Army, during World War I. He was a member of the Elks and of the A.F. & A.M.; he was one of the original trustees of the First Presbyterian Church in Oak Ridge.

On September 28, 1922, at Albany, Ind., Mr. Jarvis was married to Dorothy Eversole. He is survived by his widow; one son, Walter M.; and one daughter, Patricia (Mrs. Earle Good).

Mr. Jarvis was elected a Junior of the Society on August 31, 1925; an Associate Member on March 14, 1927; and a Member on July 13, 1936.

HOLLISTER JOHNSON, A. M. ASCE[2]

DIED NOVEMBER 1, 1955

Hollister Johnson, the son of Theron and Mary Elizabeth (Hollister) Johnson, was born at Willow Glen, N. Y., on December 19, 1890. He was graduated from Cornell University at Ithaca, N. Y., with the degree of Civil Engineer in 1912.

---

[1] Abstract of memoir prepared by Warren A. Niles, A. M. ASCE.
[2] Abstract of memoir prepared by Arthur W. Harrington, M. ASCE.

After preliminary experience with the New York State Highway Commission, the New York State Conservation Commission, and the Board of Black River Regulating District, Mr. Johnson joined the Water Resources Division, Surface Water Branch (Albany, N. Y.), United States Geological Survey, in 1934. He was assigned to the headquarters office (Washington, D. C.) in 1943 and, a few months prior to his retirement in 1952, to the Surface Water Branch at the Ithaca area office of the Albany District.

Mr. Johnson prepared or organized the preparation of reports on major floods throughout the United States as well as a flood specialist training program. He rendered outstanding contributions to the computations of peak flows by indirect methods.

Mr. Johnson was a member of the Royal Arch Masons of Dansville, N.Y., and had belonged to the Black River Valley Club of Watertown, N. Y., and the University Club of Albany.

On October 20, 1920, at Binghamton, N. Y., Mr. Johnson was married to Elizabeth L. Clark. He is survived by his widow; a son, Hollister; a daughter, Mary Anna; a brother; a sister; and two grandchildren.

Mr. Johnson was elected an Associate Member of the Society on May 15, 1917. He became a Life Member in 1951.

FRANK ALVAH KITTREDGE, M. ASCE[1]

Died December 11, 1954

Frank Alvah Kittredge, the son of Charles and Katherine (Forbes) Kittredge, was born at Glyndon, Minn., on March 29, 1883. He was graduated from the University of Washington (Pullman) with a degree in civil engineering in 1912. Later he received the degrees of Civil Engineer (1915) and Master of Science.

After serving as a road designer and planner with the United States Bureau of Public Roads (1917-1927) Mr. Kittredge began his career (1927-1952) in the National Park Service.

He became a high-ranking engineer and executive in the Service and was, successively, director of the regional office at San Francisco; superintendent of Grand Canyon National Park; and superintendent of Yosemite National Park.

For outstanding contributions to the development and protection of park resources Mr. Kittredge received the Pugsley silver medal of the American Scenic and Historic Preservation Society in 1951 and also the Department of the Interior's Distinguished Service Award.

On March 11, 1915, Mr. Kittredge was married to Catharine Mears. He is survived by his widow and one daughter, Catharine Jane (Mrs. Robert Andrews).

Mr. Kittredge was elected a Junior of the Society on March 1, 1910; an Associate Member on September 3, 1913; and a Member on October 12, 1921. He became a Life Member in 1948.

---

[1] Abstract of memoir prepared by Nathan A. Bowers, M. ASCE.

OSCAR HENRY KOCH, M. ASCE[1]

DIED AUGUST 7, 1955

Oscar Henry Koch, the son of John H. and Lena (Leffman) Koch, was born in Union, Mo., on March 27, 1890. In 1910 he received the degree of Bachelor of Science in civil engineering from Missouri State University (Columbia).

After graduation Mr. Koch was employed as a city planner by the Park Board Office at Kansas City. In 1913 he became an independent contractor in Dallas, Tex., and, in 1914, formed a partnership with James D. Fowler. During World Wars I and II, the company constructed camps and air bases.

Mr. Koch was a charter member, an honorary member, and president (1921-1922) of the Technical Club of Dallas, and represented the American Engineering Council. He was a member of the Water Policy Panel of the Engineers Joint Council (1950-1952) and, in 1949, was president of the Texas Society of Professional Engineers. In 1950 he was chairman of the National Society of Professional Engineers' Committee on International Relations.

He served the City of Dallas as a director of public works, director of the Chamber of Commerce, and in other capacities. He was a member of the Highland Park Presbyterian Church and the A.F. & A.M., and a Shriner. In 1950 he was elected to Tau Beta Pi.

Mr. Koch was a charter member of both the Texas Section and the Dallas Branch of the Society. In 1945 he was elected Director of District 15. He served as Vice-President (1928) and President (1931) of the Texas Section. He was a chairman of many Society Committees.

In 1911 he was married to Tena Sandker. He is survived by his widow; two daughters, Doris and Betty Sue; and five grandchildren.

Mr. Koch was elected an Associate Member of the Society on April 14, 1919, and a Member on November 21, 1921. He became a Life Member in 1954.

FRANCOIS EMILE MATTHES, A. M. ASCE[2]

DIED APRIL 18, 1948

François Emile Matthes, the son of Willem Ernst and Jonkvrouw Johanna Suzanna van der Does de Bije, was born on March 16, 1874, in Amsterdam, Holland. He was graduated from the Massachusetts Institute of Technology (Cambridge) with the degree of Bachelor of Science in civil engineering in 1895.

During fifty-one years with the Geological Survey, United States Department of the Interior, Mr. Matthes pioneered the surveying and mapping activities of many national parks and on the Bighorn Mountains, Wyo. (1898–1899); areas in Montana and Arizona (1900–1901 and the winter of 1902–1903); the section of the Grand Canyon of the Colorado River, Ariz., later known as the Grand Canyon National Park (1902–1904); and Yosemite Valley, Calif. (1905–1907), amongst others. From 1907–1913, Mr. Matthes served as an inspector of maps for the Survey, and between 1910–1911 he directed the mapping of Mount Rainier National Park, Wash. During the period between World War I and World War II, Mr. Matthes was primarily involved in the problems of geology of the Mississippi Valley (1928–1934) and of the Sierra Nevadas. Between World War II and his retirement in 1947 he worked on projects in connection with various scientific organizations and government agencies.

---

[1] Abstract of memoir prepared by Grayson Gill, M. ASCE.
[2] Abstract of memoir prepared by Fritiof Fryxell.

In addition to being a renowned mapper and surveyor, Mr. Matthes was a prolific writer and an eminent lecturer in the fields of geology and topography.

On June 7, 1911, at Georgetown, Md., he was married to Edith Lovell Coyle. He is survived by his widow and his twin brother, Gerard.

Mr. Matthes was elected an Associate Member of the Society on April 3, 1901. He became a Life Member in 1936.

GWYNNE GRAVELLE McCAUSTLAND, M. ASCE[1]

DIED JANUARY 18, 1957

Gwynne Gravelle McCaustland, the son of Elmer James and Annie (Gwynne) McCaustland, was born on May 23, 1894, at Salem, Ore. He was graduated from the College of Engineering of the University of Missouri (at Columbia) with the degree of Bachelor of Science in civil engineering, in 1916. He received the degree of Civil Engineer from that university in 1917.

After preliminary experience, Mr. McCaustland became (1930) engineer, and engineer-secretary for the City Plan Commission of Kansas City, Mo. In 1946 he was made principal planner and secretary to the Commission and Board of Zoning Adjustment. He was responsible for current planning, a study of the transit system, and for extensive revisions of the zoning ordinance. In 1951 he became zone and planning engineer and served in that capacity until his death.

Mr. McCaustland was a member of Tau Beta Pi, Psi Upsilon, the A. F. & A. M., the Presbyterian Church, and the American Institute of Planners, among others. He served in World War I as a captain, Coast Artillery Corps, United States Army, and in World War II as a colonel in this Corps.

On April 11, 1920, at Iola, Kans., Mr. McCaustland was married to Florence Hessler. He is survived by his widow and a son, Daniel.

Mr. McCaustland was elected an Associate Member of the Society on October 12, 1925, and a Member on July 14, 1930.

---

[1] **Abstract of memoir prepared by Edmund Wilkes, Jr., M. ASCE.**

ROY GILLESPIE McGLONE, M. ASCE[1]

DIED JULY 3, 1956

Roy Gillespie McGlone, the son of Rev. James A. and Emma (Brown) McGlone, was born in Mount Pleasant, Mich., on January 7, 1886. He was graduated with the degree of Bachelor of Science in mechanical engineering from Purdue University (Lafayette, Ind.) in 1907.

After preliminary experience with the Corps of Engineers, United States Department of the Army (1907–1908), and with private industry (1920–1922), Mr. McGlone became harbor engineer of the City of Long Beach, Calif. (1924–1931), and chief engineer and general manager of this port (1931–1935). He reentered the Corps (1935); served as chief of engineering of the Southwestern Division, at Dallas, Tex. (1941–1942; 1945–1950); and between March, 1950, and his retirement in 1956, as special assistant and supervisory consultant to the division engineer and head of the newly established Operations Division.

Mr. McGlone was a member of numerous professional and engineering societies and also of the Episcopal Church, the Dallas Athletic Club, and the A. F. & A. M. He served as a major during World War I and as a colonel during World War II. Among his many hobbies were his garden, a fine home workshop, and photography, in which he took an active interest.

On August 30, 1936, at Santa Ana, Calif., Mr. McGlone was married to Monta Trellis Reese. He is survived by his widow and one brother, Guy.

Mr. McGlone was elected a Member of the Society on November 10, 1930.

ROBERT JAMES MIDDLETON, A. M. ASCE[2]

DIED DECEMBER 21, 1954

Robert James Middleton, the son of Elisha and Nancy (Bennett) Middleton was born near Greenwood, Sebastian County, Ark., on September 29, 1881. In 1903 he was graduated from the University of Arkansas (Fayetteville) with the degree of Bachelor of Science in civil engineering.

After preliminary experience Mr. Middleton entered the employ of the Chicago, Milwaukee, St. Paul and Pacific Railroad. During the succeeding years he advanced to increasingly responsible positions within that organization. In 1918 he was made assistant chief engineer for the lines west of Mobridge, Wash.; in 1933, assistant chief engineer of the system, at Chicago, Ill.; in 1945, chief engineer, and in 1950, consulting engineer. He served in the latter capacity until his retirement in July, 1950.

---

[1] Abstract of memoir prepared by Grayson Gill, M. ASCE.
[2] Abstract of memoir prepared by Ernest B. Crane, M. ASCE.

Mr. Middleton held membership in the American Railway Engineering Association, the Engineers' Club of Seattle, and, prior to 1933, the City of Seattle Planning Commission. He was exceedingly active in affairs of the University Baptist Church in Seattle and was a member of Tau Beta Pi and Kappa Sigma.

On January 11, 1905, at Fayetteville, Mr. Middleton was married to Bertha Conner. He is survived by his widow; two daughters, Maurine (Mrs. L. Kelley) and Roberta (Mrs. C. L. Waterbury); one son, Robert; a half brother; six grandchildren; and two great-grandchildren.

Mr. Middleton was elected an Associate Member of the Society on December 4, 1907. He became a Life Member in 1942.

JOHN WILLIAM MILLER, A. M. ASCE[1]

Died February 26, 1953

John William Miller, the son of John H. and Ida (Nichols) Miller, was born in Springfield, Ill., on February 22, 1880. He was graduated from the University of Nebraska (Lincoln) in 1905 with the degrees of Bachelor of Science in civil and mechanical engineering and in 1928 received the degree of Civil Engineer.

Mr. Miller had a varied experience in railroad engineering. He worked for the Chicago and Northwestern and the Chicago, Burlington and Quincy lines.

Between 1909 and 1917, he was a member of the civil engineering faculty of the University of Washington (Seattle). He believed that summer student work should be a definite contribution to public works. Accordingly, in 1917, the engineering class surveyed 11,000 acres at Fort Lewis.

In 1917 and 1918, Mr. Miller was chief engineer of the Boeing Airplane Company. In 1919 he returned to the university as head of the aeronautics department but resigned shortly to re-enter the commercial aviation field.

Mr. Miller again returned to the university, serving from 1927 to 1937 as associate professor of aeronautical engineering. From 1937 until his retirement in 1947, he was a consultant, except for the last four years when he was a design engineer for the Lockheed Aircraft Corporation at Burbank, Calif.

On September 1, 1909, in Rapid City, S. Dak., Mr. Miller was married to Florence Lovetinsky. He is survived by his widow; one son, Charles; three daughters, Mercedes (Mrs. R. J. MacDonald), Vivian (Mrs. K. E. Pearson), Josephine (Mrs. E. S. Olason); and two brothers.

Mr. Miller was elected an Associate Member of the Society on September 3, 1913. He became a Life Member in 1946.

---

[1] Abstract of memoir prepared by Samuel DeMoss, M. ASCE.

WILLIAM CHARLES MOONEY, A. M. ASCE[1]

Died May 10, 1955

William Charles Mooney, the son of William A. and Elizabeth (Herman) Mooney, was born in Pittsburgh, Pa., on April 22, 1890. He attended the University of Michigan (Ann Arbor) for three years after which time he turned his attention to construction work.

In approximately 1922, he formed the William Mooney Construction Company in Detroit, Mich. In the early 1930's, he found employment as a field man with the Utley Construction Company of Detroit. He worked for that firm and for the Taylor-Gaskin Company (all in the Detroit area) until 1949 when health considerations prompted him to establish residence in Albuquerque, N. Mex.

For a number of years he did miscellaneous small construction work in that vicinity as owner of the Home Construction and Maintenance Service. In 1953 Mr. Mooney was instrumental in exposing the unethical activities surrounding the construction of a major city utility project in Albuquerque. He exemplified on this occasion and throughout his career a commendable sense of civic responsibility.

Mr. Mooney was a life member of the Bellevue Lodge of the A.F. & A.M., the first president of the Albuquerque chapter of the Sons of the American Revolution, and, for many years, a member of the Detroit Engineering Society.

In 1916 Mr. Mooney was married to Clarbelle Murchie. On December 23, 1946, he was married to Nina Coughlan. He is survived by his widow.

Mr. Mooney was elected an Associate Member of the Society on November 17, 1947.

THOMAS CLAYTON MOTT, M. ASCE[2]

Died May 2, 1955

Thomas Clayton Mott, the son of F. Edwin and Jennie (Richards) Mott, was born in Northumberland, N. Y., on August 3, 1886. He was graduated from Yale University (New Haven, Conn.) in 1908.

During the eighteen years preceding his employment in 1926 with Miller and Lux, Incorporated and Allied Corporations, Mr. Mott was engaged on a variety of important construction projects throughout the United States. As chief engineer and field manager of Miller and Lux (1926–1955) Mr. Mott was largely responsible for the successful negotiations reached on an issue basic to the Central Valley project (California), the exchange of San Joaquin River waters. He also prepared many engineering analyses of water rights and served as consulting engineer for the Central California Irrigation District (1951–1955).

---

[1] Abstract of memoir prepared by Nina C. Mooney.

[2] Abstract of memoir prepared by Harry Barnes and Howard Stoddard, Members, ASCE.

Mr. Mott exemplified civic leadership in his community of Los Banos, Calif., as one-time mayor, president of the Chamber of Commerce, trustee of Union High School District, chairman of the Red Cross, and trustee of the Methodist Church.

On August 31, 1906, in Troy, N. Y., he was married to Florence Elizabeth Mills. He is survived by his widow; a son, Thomas; two daughters, Marion (Mrs. T. C. Conwell) and Jeanne (Mrs. Walter G. Snyder); nine grandchildren; and one great-grandchild.

Mr. Mott was elected a Member of the Society on May 16, 1938.

RAY MESSINGER MURRAY, M. ASCE[1]

DIED OCTOBER 20, 1955

Ray Messinger Murray, the son of James and Mary (Haynes) Murray, was born on May 19, 1876, in Ada, Ohio. He earned the degree of Civil and Mechanical Engineer at Ohio Northern University (Ada) in 1897.

After a year of preliminary experience, he served on the faculty of his alma mater as instructor and dean of the College of Engineering. From 1902 to 1904 he was employed as a structural engineer for the American Steel and Wire Company and until 1910 as chief engineer of an interurban railway in Indiana.

Mr. Murray then moved to Billings, Mont., where he represented a bridge company and subsequently engaged in private practice until 1925. After a similar practice in Spokane, Wash., Mr. Murray became the chief engineer of the Union Bridge Company in Portland, Ore. He supervised the design and erection of the Twin Falls-Jerome Bridge over the Snake River and the Cascade Locks Bridge over the Columbia River.

In 1929 he moved to Seattle, Wash., where he resided until his death. During this period he was employed by the state and the City of Seattle on a number of major structures. From 1946 to 1950 he was consultant and designing engineer for the Alaska Street viaduct and the Battery Street subway in Seattle. The last few years of his life were spent in private practice.

On August 12, 1901, in Hartford, Ohio, he was married to Edith Mary Burnette. He is survived by his widow; two sons, Ray and Burnette; and two daughters, Vivien (Mrs. Schwarz) and Virginia (Mrs. Bone).

Mr. Murray was elected a Member of the Society on October 1, 1912. He became a Life Member in 1947.

---

[1] Abstract of memoir prepared by Samuel DeMoss, M. ASCE.

CONSTANTINE ALEXANDER NOVIE, A. M. ASCE[1]

Died October 2, 1956

Constantine Alexander Novie, the son of Alexander and Elizabeth (Menshikov) Novikov, was born on September 10, 1888, in Bargusin, Russia. Mr. Novie received the degree of Metallurgical Engineer in 1916 from the Institute of Technology (Tomsk, Russia).

Prior to the Bolshevik revolution, Mr. Novie worked as assistant director of the Bogoslovski mines in the Ural District. In 1919 he escaped from the Bolsheviks and worked briefly in a gold mine in Siberia, Russia, until the revolution overtook him. He then joined the White Russian Army and after its defeat went to Harbin, Manchuria, where he taught physics and mathematics in a boys' school until 1922. The following year he emigrated to the United States and became a citizen in 1929. Between 1923 and 1929 Mr. Novie worked at the Boeing Airplane Company, Seattle, Wash.

Mr. Novie joined the Corps of Engineers, United States Department of the Army, in 1936 as an inspector on river and harbor dredging. During his fifteen years in the Corps, he worked on construction of Mud Mountain Dam on the White River. He also assisted in the design of various civil works, and in foundation and materials research.

On November 2, 1912, at Tomsk, Mr. Novie was married to Anna Vozonzov. He is survived by his widow and two daughters, Lucy (Mrs. Donald R. Crow) and Gloria (Mrs. Bernard Burke).

Mr. Novie became an Associate Member of the Society on November 19, 1945.

SIVERT EDWARD OLSEN, A. M. ASCE[2]

Died March 25, 1956

Sivert Edward Olsen, the son of Frederick and Laura (Christiansen) Olsen, was born in Calumet, Mich., on November 30, 1904. He was educated at Michigan State University (East Lansing).

From 1930 to 1936 Mr. Olsen was employed by the Michigan State Highway Department, supervising road and bridge construction. In 1936 he joined the design section of the Tennessee Valley Authority in Knoxville, Tenn., as structural engineer. Because of world conditions in 1940, an accelerated construction program was authorized for the TVA, and Mr. Olsen was assigned to the field in charge of office engineering on construction of one of these large dams. By 1954 he had advanced to the position of assistant project manager on this project.

In January, 1955, Mr. Olsen became associated with Uhl, Hall & Rich, consulting engineers, on the St. Lawrence River power project near Massena, N. Y., for the Power Authority of the State of New York. He served as resident engineer on the construction of Long Sault Dam.

---

[1] Abstract of memoir prepared by A. S. Cary, A. M. ASCE.
[2] Abstract of memoir prepared by Sidney N. Smith, M. ASCE.

Mr. Olsen was a member and generous supporter of the United Lutheran Church. He was also active in Society affairs and a President of the Holston Branch of the Tennessee Valley Section (1952).

On May 26, 1936, Mr. Olsen was married to Gertrude Sattem of Escanaba, Mich. He is survived by his widow; and one son, Peter S.

Mr. Olsen was elected an Associate Member of the Society on April 12, 1948.

LANGDON PEARSE, M. ASCE[1]

DIED JULY 20, 1956

Langdon Pearse, the son of John Barnard and Mary Langdon (Williams) Pearse, was born in Boston, Mass., on November 12, 1877. He received the degree of Bachelor of Arts from Harvard College (Cambridge, Mass.) in 1899, and the degrees of Bachelor of Science in civil engineering (1901) and Master of Science (1902) from the Massachusetts Institute of Technology (Cambridge).

After early experience on water-supply projects, Mr. Pearse became an assistant engineer (1909) for the Sanitary District of Chicago (now The Metropolitan Sanitary District of Greater Chicago). His investigations and direction as assistant engineer, as division engineer, and—from 1921 to 1956—as sanitary engineer have served to increase substantially the amount of data available on large-scale sewage treatment.

Mr. Pearse was a member of the University Club, Indian Hill Club, Phi Beta Kappa, the American Academy of Arts and Sciences, and numerous engineering societies. For twenty years he was the chairman of the Committee on Sewage Treatment of the American Public Health Association, and helped to found the Federation of Sewage and Industrial Wastes Association. He was chairman for ten years of the Committee on Sewerage and Sewage Treatment of the Society, and was a prolific contributor to technical publications.

On June 1, 1910, Mr. Pearse was married to Eleanor Howard Dean. He is survived by his widow.

Mr. Pearse was elected a Junior of the Society on January 6, 1903; an Associate Member on October 7, 1908; and a Member on July 2, 1913. He became a Life Member in 1943.

JOHN CARLETON PHILLIPS, A. M. ASCE[2]

DIED OCTOBER 3, 1954

John Carleton Phillips, the son of Thomas and Hattie E. (Carleton) Phillips, was born in Port Townsend, Wash., on April 16, 1871. Mr. Phillips was selfeducated. He worked in a drugstore and later studied law and was admitted to the bar. He became interested in surveying and turned to land subdivision in 1890.

---

[1] Abstract of memoir prepared by Norval E. Anderson and H. P. Ramey, Members, ASCE.

[2] Abstract of memoir prepared by Samuel DeMoss, M. ASCE.

In 1899 he was employed by the Corps of Engineers, United States Army, and continued in this employment until his retirement in 1933. For part of this period he was engaged on the design of the concrete for the locks of the Lake Washington Ship Canal. The remainder of his work was on the construction of seacoast fortifications at Forts Worden, Casey, and Flagler. For a short time, Mr. Phillips worked on the Subic Bay fortifications in the Philippine Islands. During the last eleven years he was in active charge of maintenance of the fortification elements of the harbor defenses of Puget Sound.

Following his retirement, Mr. Phillips continued to live in the town in which he was born, quietly pursuing his hobbies of gardening and fishing.

On August 14, 1901, in Port Townsend, Wash., Mr. Phillips was married to Minnie Holmes Short. He is survived by his widow and a sister.

Mr. Phillips was elected an Associate Member of the Society on January 3, 1911. He became a Life Member in 1942.

HERBERT SPENCER RIPLEY, M. ASCE[1]

DIED MARCH 15, 1956

Herbert Spencer Ripley, the son of Henry Clay and Nellie (Arksey) Ripley, was born in Ann Arbor, Mich., on February 5, 1879. He was graduated from the University of Michigan (Ann Arbor) with the degree of Bachelor of Science in Civil Engineering in 1906.

During undergraduate years, Mr. Ripley worked with the United States Engineer Department (now the Corps of Engineers, United States Department of the Army) on various projects in the Great Lakes region and in Texas. Following graduation, he went to the Sanitary District of Chicago, Ill. Except for two years' leave, in 1907 and in 1908, respectively, during which time he prepared a special study concerning improvement of navigation on the Magdalena River in Colombia, South America, Mr. Ripley devoted his entire professional career to the complex problems of Chicago's sanitation. He retired as head of the District Engineering Department in 1949.

Mr. Ripley was a member of the Western Society of Engineers and the Illinois Society of Professional Engineers.

On August 31, 1905, in Galveston, Tex., Mr. Ripley was married to Caroline Kenison. He is survived by his widow; two sons, Herbert Spencer, Jr. and Henry Clay; a brother; and three grandchildren.

Mr. Ripley became a Member of the Society on November 28, 1916. He became a Life Member in 1950.

---

[1] Abstract of memoir prepared by Sherman B. Green, M. ASCE.

ARTHUR WINTHROP SARGENT, M. ASCE[1]

DIED JUNE 2, 1954

Arthur Winthrop Sargent, the son of Daniel and Charlotte (Thompson) Sargent, was born on June 19, 1871, at Barrington, Nova Scotia, Canada. In 1890 he went to Boston, Mass., where he worked for the city engineer and studied engineering.

He entered government service in 1896 at Peoria, Ill., working for the Corps of Engineers, United States Army, on river and harbor projects—largely lock and dam design and construction. He was transferred to the Seattle (Wash.) Office of the Corps of Engineers in 1905. He helped design Forts Casey and Flagler, two of the primary forts on Puget Sound, and later supervised construction of Fort Whitman.

In 1911 Mr. Sargent directed the construction of the Lake Washington Ship Canal and Locks in Seattle.[2] After the canal and locks were constructed, he became superintendent of the project. He held that position until his retirement in 1941.

On April 27, 1915, in Worcester, Mass., he was married to Nellie M. Watson. He is survived by his widow, two brothers, and a sister.

Mr. Sargent was elected an Associate Member of the Society on September 6, 1905, and a Member on March 13, 1917. He became a Life Member in 1940.

THOMAS RUSSEL SIMPSON, M. ASCE[3]

DIED APRIL 19, 1956

Thomas Russel Simpson, the son of Thomas and Eleanor (Perry) Simpson, was born on January 2, 1896, in Fresno, Calif. After serving as a lieutenant in World War I, he returned to the University of California (Berkeley) to receive the degree of Bachelor of Science in civil engineering in 1920.

From 1920 to 1950 Mr. Simpson was employed by the California State Division of Water Resources. He worked extensively in the adjudication of water rights, prepared special hydrological investigations of critical water-supply problems, and later directed inventories of water resources in the State of California. He also served as consultant to the joint Committee on Water Problems of the California legislature and to various state organizations.

In 1950 he left his position as principal hydraulic engineer with the water resources division to become professor of irrigation engineering at the University of California.

---

[1] Abstract of memoir prepared by Eugene I. Pease.

[2] "The Lake Washington Ship Canal, Washington," by W. J. Barden and A. W. Sargent, *Transactions*, ASCE, Vol. 92, 1928, p. 1001.

[3] Abstract of memoir prepared by H. B. Gotaas, M. ASCE.

Mr. Simpson was a member of the International Commission on Irrigation and Drainage and of the following societies: Tau Beta Pi, Sigma Xi, Chi Epsilon, and Sigma Iota Phi.

On May 1, 1928, he was married to Aileen Menzies. He is survived by his widow; a daughter, Barbara; a son, Thomas Russel; and a grandson.

Mr. Simpson was elected an Associate Member of the Society on July 6, 1925, and a Member on December 5, 1949.

ALFRED KITTOE STILLMAN, M. ASCE[1]

DIED NOVEMBER 30, 1954

Alfred Kittoe Stillman, the son of Frank P. and Eva M. (Kittoe) Stillman, was born on February 28, 1900, in Galena, Ill. He completed engineering courses at Washington State College (Pullman) and the University of Washington (Seattle).

For the next twenty years he practiced municipal, highway, and sanitary engineering in many of the western states. During World War II, he worked with the Corps of Engineers, United States Army, at Fort Lewis, Wash. In 1946 Mr. Stillman opened an office in Olympia, Wash., as a consulting engineer. In 1953 he formed a partnership in Seattle with DeWitt C. Griffin and in August, 1954, returned to Olympia and his own private practice.

Mr. Stillman also was a member of the National Society of Professional Engineers, the American Water Works Association, and the Federation of Sewage and Industrial Wastes Association.

On May 14, 1936, in Seattle, Mr. Stillman was married to Beulah Christensen. He is survived by his widow, a brother, and a sister.

Mr. Stillman was elected a Member of the Society on September 6, 1949.

SIMON WEINBERG TARR, M. ASCE[2]

DIED MAY 11, 1956

Simon Weinberg Tarr, the son of John and Regina (Weinberg) Tarr, was born in Moravia, Iowa, on June 27, 1873. He was graduated from Iowa State College (Ames) with a degree in civil engineering in 1898.

After some preliminary experience, Mr. Tarr embarked on a life-long career in the steel industry with the Oliver Iron Mining Company. In successive steps he became draftsman, structural engineer, assistant chief engineer (1922), and chief engineer (1928)—serving in the latter capacity until his retirement (1940). As chief engineer he was concerned with the process of "converting ore from the ground to the ore which is shipped to the blast furnaces." He advised the local municipalities necessarily affected by the company's extensive program as to their water, sewage disposal, and other problems.

---

[1] Abstract of memoir prepared by Sherman B. Green, M. ASCE.

[2] Abstract of memoir prepared by G. H. Butler, M. ASCE, and A. C. Giesecke, A. M. ASCE.

For many years Mr. Tarr was a member of the Board of Directors, St. Luke's Hospital, and chairman of its building committee. He was active in the Duluth Chamber of Commerce and the A. F. & A. M. He was a Past-President of the Duluth Section of the Society.

On August 28, 1901, he was married to Sarah Emma Argo. He is survived by two daughters, Margherita and Regina, and one son, Richard.

Mr. Tarr was elected a Member of the Society on May 31, 1916. He became a Life Member in 1944.

HERMAN FRANKLIN TUCKER, M. ASCE[1]

Died February 1, 1955

Herman Franklin Tucker, the son of William F. and Lauretta (Wheeler) Tucker, was born on January 8, 1878, in Weston, Mass. He was graduated with honors in civil engineering from Harvard University (Cambridge, Mass.) in 1901.

During his early practice in Boston, Mass., he assisted in designing the Harvard Stadium, one of the first reinforced concrete structures of its kind, and was later associated with a firm which planned the Boston elevated railroad and the Boston subway.

Mr. Tucker was a design engineer on the Panama Canal and participated in the design of the locks and valves.

He settled in Seattle, Wash., in about 1915 and for a time practiced as a consulting engineer. He was employed by the City of Seattle on the Skagit River hydroelectric development. Later he designed the large cranes used in the construction of Grand Coulee Dam as well as a number of bridges in King County, Washington.

Mr. Tucker was the author of a number of publications on engineering and design. He was a member of the Harvard Engineering Society and the Harvard Club of Seattle and was an associate member of the American Museum of Natural History.

On January 2, 1908, in Baltimore, Md., he was married to Wilhemina Meyers. He is survived by two sons, Bert A. and William F.; one daughter, Katherine; one brother; and three grandchildren.

Mr. Tucker was elected an Associate Member of the Society on December 7, 1904, and a member on November 13, 1939. He became a Life Member in 1939.

---

[1] Abstract of the memoir prepared by Carl F. Ganong, M. ASCE.

CHARLES LEOPOLD WARTELLE, M. ASCE[1]

DIED JUNE 1, 1954

Charles Leopold Wartelle, the son of Ferdinand and Valerie (LaStrappe) Wartelle, was born in Washington, La., on April 9, 1885. He was graduated a civil engineer from Louisiana State University (Baton Rouge) in 1907.

Mr. Wartelle joined the Seattle (Wash.) Engineering Department and rose from chief draftsman to district engineer, a position he held from 1924 to 1935. He was chief engineer for the State of Washington in the Public Works Administration until 1938 when he became city engineer of Seattle. He held this position until his retirement in 1948. Later he became associated with the Northgate development, the nation's largest suburban shopping center. He was consulting traffic engineer for the center at the time of his death.

During his long career in public office, he contributed greatly to Seattle's rapid physical development. He was in charge of hundreds of miles of sewer, water main, and paving projects. He instituted and implemented an extensive street rehabilitation program, a street lighting program, and modern arterial traffic plans, and designed many of the bridges spanning Seattle's numerous waterways.

On February 26, 1919, in Seattle, he was married to Zita Marie Curtis. He is survived by his widow; three sons, Robert, Edward, and William; one daughter; and three grandchildren.

Mr. Wartelle was elected a Member of the Society on January 10, 1944.

WALTER OWEN WASHINGTON, M. ASCE[2]

DIED JULY 4, 1954

Walter Owen Washington, the son of Thomas Pratt and Ella (Maxwell) Washington, was born on September 24, 1883, at Travis County, Texas. He was graduated from the University of Texas (Austin) with the degree of Bachelor of Science in civil engineering in 1904.

Mr. Washington rendered valuable services to the State of Texas both as an engineer and through active participation in civic, fraternal, technical, and other organizations. After preliminary experience, he became county engineer, Cameron County (1920-1939); he supervised the construction of a flood-control system in the Lower Rio Grande Valley (1920-1932). He was the construction engineer for an extensive irrigation program in Willacy County (1939-1940). As city engineer of Brownsville he supervised the building of war-time facilities (1941-1942). He directed the construction of synthetic rubber plants for the Defense Plant Corporation in Corpus Christi and in Ingleside (1943-1945). He was a senior partner of the firm, Washington and Ruff (1945-1950).

---

[1] Abstract of memoir prepared by Robert G. Wartelle, A. M. ASCE.

[2] Abstract of memoir prepared by John A. Focht, M. ASCE.

In addition to membership in numerous technical groups and his active support of the Methodist Church, Mr. Washington was also prominent in affairs of the Society. He helped organize the Lower Rio Grande Valley Branch, Texas Section, and served as President (1941) and Vice-President of the Texas Section (1945).

Mr. Washington was married to Bernice Haskell in 1910. He is survived by his widow; three sons, Walter, Wilber, and Thomas; three daughters, Elizabeth, Marjorie (Mrs. Randall Barker), and Mildred (Mrs. Lloyd Collier); a brother; a sister; and seven grandchildren.

Mr. Washington was elected an Associate Member of the Society on February 6, 1912, and a Member on September 9, 1919. He became a Life Member in 1947.

MELVIN DELANO WILLIAMS, M. ASCE[1]

Died September 28, 1955

Melvin Delano Williams, the son of John and Hanna (Webster) Williams, was born in Ogden, Iowa, on August 5, 1876. He was graduated in 1898 from the Colorado School of Mines (Golden) and soon after was working in the undeveloped areas of the west.

Mr. Williams participated in the topographical survey of the Colorado River including the Grand Canyon. For a time he had a private practice at Klamath Falls and Lakeview, in Oregon, and was later associated with the City of Los Angeles, Calif.

In 1919 Mr. Williams joined the Bureau of Public Roads and was in charge of forest highways for the Ogden, Utah, district. When the Public Roads office was established in Alaska, Mr. Williams became the first district engineer for the territory. At that time (1925) Alaskan road development was in its infancy. He pioneered in the solution of difficult location and construction problems peculiar to the north country and gained a host of friends throughout the territory.

Upon his retirement in 1945, Mr. Williams made his home at Edmonds, Wash. There, his lifetime love of flowers found full expression in one of the most beautiful gardens of the region.

On November 28, 1923, in Duchesne, Utah, he was married to Hortense Louise Lockhart. He is survived by his widow.

Mr. Williams was elected an Associate Member of the Society on January 17, 1921, and a Member on July 12, 1926. He became a Life Member in 1947.

---

[1] Abstract of memoir prepared by Harry Madison.

FRANK WORMALD, A. M. ASCE[1]

Died June 4, 1955

Frank Wormald, the son of George and Emily (Urianek) Wormald, was born on June 30, 1915, in New York, N. Y. He was graduated from the College of the City of New York in 1939 with the degree of Bachelor of Civil Engineering, and in 1949 was awarded the degree of Master of Science in Engineering from the University of California (Berkeley).

For a short time after graduation, Mr. Wormald taught engineering at the College of the City of New York. He then undertook two short assignments in New York State for the Geological Survey and the United States Engineers. From January, 1941, to March, 1946, he was a naval architect in the hull-design section at Mare Island Navy Yard, Vallejo (Calif.).

Except for a short interval of teaching and research at the University of California and a few weeks during which he was loaned to another structural engineering office in San Francisco, Calif., Mr. Wormald was employed by George Washington, civil and structural engineer, in San Francisco on structural design projects.

Mr. Wormald was a member of Tau Beta Pi and a licensed civil and structural engineer in California. He was a resident of Mountain View, Calif.

On December 9, 1945, he was married to Julia Armanini. He is survived by his widow; two daughters, Nancy and Lorraine; his father; and his brother.

Mr. Wormald was elected a Junior of the Society on April 4, 1940, and an Associate Member on March 27, 1950.

ARRIGO MAZZUCATO YOUNG, M. ASCE[2]

Died June 27, 1954

Arrigo Mazzucato Young, the son of Bicknell and Eliza (Mazzucato) Young, was born in London, England, on February 19, 1884. He was reared in Chicago, Ill., and attended Armour Institute (Chicago). He was graduated from the University of Michigan (Ann Arbor) in 1906.

Following graduation, he was associated with Pond and Pond, Architects, and later with the American Bridge Company. Mr. Young went to Seattle, Wash., in 1910 to organize the structural steel division of the Moran Company. In 1912 he established his own practice and in 1920 joined the firm of Schack, Young and Meyers, Architects. In 1940 he became the senior partner in the architectural firm of Young and Richardson, which subsequently became Young,

---

[1] Abstract of memoir prepared by Howard C. Wood, M. ASCE.
[2] Abstract of memoir prepared by Samuel DeMoss, M. ASCE.

Richardson, Carleton and Detlie. As an architect and engineer he planned many notable structures in the Pacific Northwest.

He was a member of the Seattle Building Code Commission in the 1920's and later of the City Planning Commission and the Seattle Housing Authority. He belonged to the American Institute of Architects and the Society of American Military Engineers.

Mr. Young was an accomplished musician. His maternal grandfather was director of La Scala Opera House in Milan.

On May 14, 1910, in Chicago, he was married to Edith Thackwell. He is survived by his widow; two sons, Thomas, and Richard; one daughter, Mrs. Jesse Haas; and eleven grandchildren.

Mr. Young was elected a Member of the Society on October 14, 1929.

LLOYD OTTO ZAPP, M. ASCE[1]

DIED OCTOBER 17, 1956

Lloyd Otto Zapp, the son of Hugo and Glendora (Otto) Zapp, was born on November 22, 1913, in Houston, Tex. He graduated from the Agricultural and Mechanical College of Texas (College Station) with the degree of Bachelor of Science in civil engineering in 1934.

Following graduation, he started a career of twenty-two years with the Humble Oil & Refining Company, a Texas corporation in which he rose to the position of senior supervising civil engineer (1948–1956). In this capacity he aided the assistant chief civil engineer (Houston office) in all construction work for the production department throughout the company's operations.

Mr. Zapp served as a major during World War II and in 1956 was promoted to the rank of lieutenant-colonel in the Houston marine corps reserve unit. Between June, 1951, and January, 1952, during the Korean Conflict, Mr. Zapp served with the Petroleum Administration for Defense, in Washington, D. C., as chief of the Construction Branch, Materials Division.

Mr. Zapp was an outstanding leader in civic and community affairs, as well as in company organizations. He was an active member of the Bethany Methodist Church of Houston; a member of the A. F. & A. M.; a president of the Humble Club, Houston (1950); and a director of the Humble Employees Federal Credit Union (1954–1955).

On February 21, 1935, at Houston, Mr. Zapp was married to Evelyn Baggett. He is survived by his widow; a son, Lloyd; a daughter, Shirley; his father; and one sister.

Mr. Zapp was elected a Junior of the Society on November 26, 1934; an Associate Member on October 20, 1947; and a Member on November 30, 1953.

---

[1] Abstract of memoir prepared by S. W. Oberg and H. N. Stamper, Members, ASCE; and W. A. Castille, A. M. ASCE.

TRANSACTIONS

OF THE

AMERICAN SOCIETY OF CIVIL ENGINEERS

INDEX

VOLUME 122

1957

Subject Index, Page 1264

Author Index, Page 1301

Titles of papers are in quotation marks when given with the author's name.

VOLUME 122

SUBJECT INDEX

ACCELERATION
See VELOCITY (cross references thereunder)

ACCIDENTS
See HIGHWAYS AND ROADS—Safety

ACCOUNTS AND ACCOUNTING
See COSTS ... ; *also* subheading Financing under relative subject

ADDRESSES
See AMERICAN SOCIETY OF CIVIL ENGINEERS—Addresses; *see also* under subject of address

AERATION
See also OXYGENATION
"A Preliminary Study of High-Rate Composting," John S. Wiley and George W. Pearce (with discussion), 1009.

AERIAL ...
See also AIR ...

AERIAL NAVIGATION
See AIR TRANSPORT

AGRICULTURE
See DRAINAGE; FERTILIZERS (cross reference thereunder); FLOOD ... ; IRRIGATION; RAINFALL (cross references thereunder); SOIL ... ; WATER, CONSUMPTIVE USE OF; WATER RIGHTS

AIRCRAFT
See also BUCKLING; WHEEL LOADS
Helicopter weight, performance data, speed (including comparison with airplane speed), and power requirements, 976, 978, 981.
Jet aircraft and their influence on airport developments, 614.
"Transport Helicopter Cost and Heliport Considerations," F. David Schnebly, 973.

Bibliography
Helicopter development in commercial transport, 983.

AIR ENTRAINMENT
See CONCRETE (General)

AIRFIELDS
See AIRPORT ...

AIRPLANES
See WHEEL LOADS

AIRPORT APPROACHES
"The Effect of Traffic on the Cross Section of a Runway Pavement," Robert Horonjeff and John H. Jones (with discussion), 1035.

AIRPORTS (structures and localities)
See also PAVEMENT AND PAVING ... ; TRAFFIC, AIRPORT
"A Pattern of Interstation Air Travel," Daniel M. Belmont, 864.
"Transport Helicopter Cost and Heliport Considerations," F. David Schnebly, 973.

Bibliography
Heliport facilities as related to helicopter operating costs, 983.

AIR SANITATION
See ODORS

AIR TERMINALS
See AIRPORTS

AIR TRANSPORT
See also COSTS, AIR TRANSPORT; TRANSPORTATION
Detroit Municipal Airport operations removal to Willow Run Airport and resulting operation changes, with 1940–1954 annual statistics, 615, 616
Normalized interstation trips between larger centers in United States, showing interstation distances (nonstop routes), September 17–30, 1954, 868.
"A Pattern of Interstation Air Travel," Daniel M. Belmont, 864.
"Transport Helicopter Cost and Heliport Considerations," F. David Schnebly, 973.

AIRWAYS
See AIR TRANSPORT

ALGAE
"Photosynthesis in Sewage Treatment," William J. Oswald and Harold B. Gotaas (with discussion), 73.

ALGEBRA, MATRIX
See STRUCTURES, THEORY OF

ALINEMENT CURVES
See CURVES (alinement curves)

ALLUVIATION
See SILT AND SILTING... ; VALLEYS

AMERICAN SOCIETY OF CIVIL ENGINEERS

Addresses
1957—Address at the Summer Convention, Buffalo, N. Y., June 5, 1957, Mason G. Lockwood, 1221.

Memoirs of Members. *See* name of member in Author Index. (*See also* p. 1229)

ANALOGS AND ANALOGIES
See under relative subject, e.g., WELLS; *see also* ELECTRIC ANALOGY (cross references thereunder)

ANALYSIS, DESIGN
See under relative subject, e.g., STRUCTURES, THEORY OF

ANALYSIS OF DATA
See EQUATIONS (cross reference thereunder); MATHEMATICS; PROBABILITY, THEORY OF; STRUCTURES, THEORY OF

ANALYSIS, STATISTICAL
See STATISTICAL ANALYSIS (cross reference thereunder)

ANALYSIS, STRUCTURAL
See STRESS AND STRAIN; STRUCTURES, THEORY OF

ANALYSIS, WATER
See WATER ANALYSIS

ANCHORAGES, COLUMN
See COLUMNS

ANCHORED BULKHEADS
See BULKHEADS (cross references thereunder)

APPARATUS
See under relative subject, e.g., CONCRETE; WAVES; *also* under general types of apparatus, e.g., VIBRATION RECORDING APPARATUS; *see also* INSTRUMENTS (cross references thereunder); TOOLS (cross references thereunder)

APPARATUS, DEFLECTION RECORDING
See DEFLECTION RECORDING APPARATUS

AQUIFERS
See WELLS

ARCH DAMS
See DAMS, ARCH (cross reference thereunder)

ARCHES
See DAMS, ARCH (cross reference thereunder); DOMES AND VAULTS; STRUCTURES, THEORY OF...

ARCHITECTS AND ARCHITECTURE
See under type of structure, e.g., BUILDINGS

ASPHALT PAVEMENT AND PAVING
See PAVEMENT AND PAVING, BITUMINOUS

ASSOCIATIONS
See SOCIETIES, TECHNICAL; *see also* AMERICAN SOCIETY OF CIVIL ENGINEERS

ATMOSPHERIC POLLUTION
See AIR SANITATION (cross reference thereunder)

AUTHORITIES
See RIVER VALLEY AUTHORITIES

AUTOMOBILE...
See TRAFFIC...

AUTOMOBILE ACCIDENTS
See HIGHWAYS AND ROADS—Safety

AUTOMOBILE TRUCKS
See MOTOR TRUCKS (cross reference thereunder)

AVIGATION
See AIRPORT APPROACHES

BACTERIA
"Intermittent Discharge of Spent Sulfite Liquor," Herman R. Amberg and Robert Elder, 1179.
"Photosynthesis in Sewage Treatment," William J. Oswald and Harold B. Gotaas (with discussion), 73.

BANKS AND BANK PROTECTION, RIVER
See RIVER BANKS AND BANK PROTECTION (cross references thereunder)

BANK STABILIZATION, RIVER
See RIVER BANKS AND BANK PROTECTION (cross references thereunder)

BASINS (depression in earth's surface)
See DRAINAGE; RIVER BASINS (cross references thereunder); RESERVOIRS... ; RIVER VALLEY AUTHORITIES; VALLEYS

BASINS, SPREADING
See SPREADING BASINS

BEACHES
See EROSION, BEACH; SHORES AND SHORE PROTECTION

BEAMS (General)
See BUCKLING; CONNECTORS AND CONNECTION; FLANGES (cross reference thereunder); STRUCTURES, THEORY OF—Beams and Girders (General); TORSION; *also* under name of material, e.g., STEEL; *also* under structure or structural part

BEAMS, CONTINUOUS
See STRESS AND STRAIN—Beams, Continuous; STRUCTURES, THEORY OF—Beams and Girders, Continuous; STRUCTURES, THEORY OF—Frames, Continuous

BEARING CAPACITY (foundations, rocks, soils)
For more general interpretation *see* cross references under LOAD
"The Action of Soft Clay Along Friction Piles," H. Bolton Seed and Lymon C. Reese (with discussion), 731.
"Field Vane Shear Tests of Sensitive Cohesive Soils," Hamilton Gray (with discussion), 844.
Soil resistance to downward movement of a friction pile, 735, 736.
"Stresses in Elastic Plates over Flexible Subgrades," Eric Reissner, 627.

BED LOAD
See RIVERS; SILT AND SILTING...; TURBULENCE; WATER, FLOW OF, IN OPEN CHANNELS

BED LOAD DISPOSAL
See SILT AND SILTING...

BENDING
See BUCKLING; MOMENTS; STRESS AND STRAIN; *also* under relative structure, structural part or material, e.g., PILES AND PILE DRIVING; TRUSSES...

BIBLIOGRAPHY
See subheading Bibliography under relative subject. (Comprehensive bibliographical footnotes existing in individual papers in which books and other material are cited)

BIOGRAPHIES OF DECEASED MEMBERS
See cross reference under MEMOIRS OF DECEASED MEMBERS. (*See also* p. 1229)

BITUMEN
See PAVEMENT AND PAVING, BITUMINOUS

BLASTING
"Structural Vibrations Produced by Ground Motion," Donald E. Hudson and George W. Housner, 705.

BOGS
See MARSHES

BOILER PLATE
See STEEL

BOLTED JOINTS
See JOINTS (General)

BOLTS
See ANCHORAGES, COLUMN (cross reference thereunder); JOINTS

BORINGS
See also DRILLS AND DRILLING
"Field Vane Shear Tests of Sensitive Cohesive Soils," Hamilton Gray (with discussion), 844.

BOUNDARY LAYER, THEORY OF (fluid flow)
See WATER, FLOW OF...

BREAKWATERS
See WATER PRESSURE; WAVES

BRIDGES (General)
See COLUMNS; PILES AND PILE DRIVING; VIBRATION

BUCKLING
"Inelastic Buckling of Nonuniform Columns," John E. Goldberg, John L. Bogdanoff and Hsu Lo, 722.
"Lateral Buckling of Elastically End-Restrained I-Beams," Walter J. Austin, Shahen Yegian and Tie P. Tung, 374.
"Lateral Buckling of Rolled Steel Beams," Robert A. Hechtman, John S. Hattrup, Eugene F. Styer and John L. Tiedemann, 823.
"Plastic Strength of Steel Frames," Lynn S. Beedle (with discussion), 1139.

BUILDING MATERIALS
See MATERIALS OF CONSTRUCTION (cross references thereunder)

BUILDINGS

See also COSTS...; FOUNDATIONS...; MATERIALS OF CONSTRUCTION; STRENGTH OF MATERIALS; STRESS AND STRAIN...; STRUCTURES...; VIBRATION; *also* under type of building

"Impulsive Motion of Elasto-Plastic Shear Buildings," Edward Cohen, Leon S. Levy and Leonard E. Smollen, 293.

Methods of determining moment-rotation characteristics for common types of column anchorages in light industrial buildings, 132.

BULKHEADS

See STRESS AND STRAIN—Bulkheads; WAVES

BULKHEAD WALLS

See RETAINING WALLS

BUOYANCY

See WATER PRESSURE

CANAL LININGS

"Measurement of Canal Seepage," August R. Robinson, Jr. and Carl Rohwer (with discussion), 347.

CANALS (General)

See IRRIGATION CANALS; LOCK-GATES; SEEPAGE; SILT AND SILTING, CHANNEL; WATER, FLOW OF, IN OPEN CHANNELS; WATERWAYS (cross references thereunder); WAVES

CANALS, IRRIGATION

See IRRIGATION CANALS

CARRIERS

See AIRCRAFT; MOTOR... (cross references thereunder); RAILROAD ... (cross references thereunder); TRANSPORTATION

CARS

See AUTOMOBILE... (cross references thereunder); TRAFFIC...

CHANNELS (waterways)

See EROSION, STREAM; RIVERS; SILT AND SILTING, CHANNEL; WATER DIVERSION (cross reference thereunder); WATER FLOW OF, IN OPEN CHANNELS; WATER POLLUTION

CHARTS

See under relative subject

CHEMISTRY

See under relative technical subject, e.g., OXYGENATION

CITIES

See also AIRPORTS; BUILDINGS; CITY PLANNING; COSTS...; DOCKS AND WHARVES; EXPRESSWAYS (cross reference thereunder); HEAT AND HEAT TRANSMISSION (cross references thereunder); HOUSING LAW; INDUSTRIAL...; MUNICIPAL... (cross references thereunder); ODORS; REFUSE DISPOSAL; SEWAGE DISPOSAL; STREETS; TRAFFIC ...; WATER FRONT (cross references thereunder); WATER SUPPLY; *also* geographical subheadings under relative subject, e.g., HARBORS—New York, N. Y.

New York City metropolitan area water cyclical variations, 872.

"Urban Renewal of American Cities," James W. Follin, 330.

CITY PLANNING (General)

See also HOUSING LAW; STREETS; TRAFFIC, STREET

"Observations on the Urban Transportation Problem," Harmer E. Davis, 286.

CIVIL ENGINEERS AND ENGINEERING

See AMERICAN SOCIETY OF CIVIL ENGINEERS; ENGINEERS AND ENGINEERING (and cross references thereunder)

CLAY

See also SHEAR; SOIL...; TILE (cross reference thereunder)

"Field Vane Shear Tests of Sensitive Cohesive Soils," Hamilton Gray (with discussion), 844.

COAST

See SEACOAST (cross references thereunder)

COFFERDAMS

"Model Tests, Analysis, and Observation of an Arch Dam," Manuel Rocha, J. Laginha Serafim, Antonio F. da Silveira and Jose M. Ressurreicao Neto (with discussion), 903.

COLLEGES AND SCHOOLS, ENGINEERING

See EDUCATION

COLUMNS

See also BUCKLING; CONNECTORS AND CONNECTIONS; FAILURES, COLUMN; STRUCTURES, THEORY OF—Columns; *also* under name of material, e.g., STEEL

COLUMNS (*Continued*)
"Moment-Rotation Characteristics of Column Anchorages," Charles G. Salmon, Leo Schenker, and Bruce G. Johnston, 132.

COMMERCE
See AIRPORTS; AIR TRANSPORT; CANALS (cross references thereunder); CHANNELS (cross references thereunder); CITIES; DOCKS AND WHARVES; HARBORS; LAKES; RIVERS; TRANSPORTATION and other relative subject headings; WATERWAYS (cross references thereunder)

COMPACTION
See BEARING CAPACITY; IMPACT

COMPOST AND COMPOSTING
See under type of waste, e.g., REFUSE DISPOSAL

COMPRESSION
See STRESS AND STRAIN

COMPRESSION MEMBERS
See COLUMNS

COMPRESSION TESTS, SOIL
See SOILS—Tests and Testing

CONCRETE (General)
See also FAILURES, CONCRETE; PAVEMENT AND PAVING, CONCRETE; SAND; SEEPAGE; STRESS AND STRAIN—Concrete (General); *also* under special structure or structural part, e.g., DAMS, MASONRY AND CONCRETE
Air entrainment effect on pore pressure penetration and permeability, 587, 590.

Construction
See under special structure

Cracks and Cracking
"Failure of Plain Concrete under Combined Stresses," Boris Bresler and Karl S. Pister (with discussion), 1049.

Design
Basic material in establishing design principles, 609, 610.

Mixes and Mixing
Lean mixes in their relation to permeability, pore pressure and air entrainment, 587, 591, 594, 596, 603.

Tests and Testing
Equipment for measuring forces and deformations produced by pore pressure, 607.
"Failure of Plain Concrete under Combined Stresses," Boris Bresler and Karl S. Pister (with discussion), 1049.

CONCRETE DAMS
See DAMS, MASONRY AND CONCRETE

CONCRETE—METAL
See cross reference under REINFORCED CONCRETE

CONCRETE PAVEMENT AND PAVING
See PAVEMENT AND PAVING, CONCRETE

CONCRETE, REINFORCED
See CONCRETE...

CONNECTORS AND CONNECTIONS
See also JOINTS...
"Lateral Buckling of Rolled Steel Beams," Robert A. Hechtman, John S. Hattrup, Eugene F. Styer and John L. Tiedemann, 823.

CONSERVATION
See FISH INDUSTRY (cross reference thereunder); GROUND WATER; SOILS—Conservation; WATER CONSERVATION

CONSOLIDATION TESTS, SOIL
See SOILS—Tests and Testing

CONSTRUCTION
See BUILDINGS; COSTS...; CURVES (alinement curves); FAILURES...; SPECIFICATIONS (cross reference thereunder); STRESS AND STRAIN...; STRUCTURES, THEORY OF...; *also* under type of construction

CONSTRUCTION CURVES
See CURVES (alinement curves)

CONSTRUCTION MATERIALS
See MATERIALS OF CONSTRUCTION (cross references thereunder)

CONSUMPTIVE USE (water)
See WATER, CONSUMPTIVE USE OF

CONTAMINATION, STREAM
See WATER POLLUTION

CONTINUOUS BEAMS
See BEAMS, CONTINUOUS (cross references thereunder)

CONTINUOUS FRAMES
See STRUCTURES, THEORY OF —Frames, Continuous; *see also* BEAMS (cross references thereunder); COLUMNS

CONTINUOUS GIRDERS
See GIRDERS, CONTINUOUS (cross reference thereunder)

CONVENTIONS (American Society of Civil Engineers)
See AMERICAN SOCIETY OF CIVIL ENGINEERS—Addresses

COSTS (General)
See also subheading Financing under relative subject

COSTS (of work)
See COSTS...

COSTS, AIR TRANSPORT
Nearby airport redevelopment compared with newly developed outlying airport with longer ground travel, 614.
"Transport Helicopter Cost and Heliport Considerations," F. David Schnebly, 973.

COSTS, CITY IMPROVEMENT AND SERVICE
Local and federal grants in relation to urban renewal programs, 335, 336.

COSTS, DRAINAGE
Earth fills with culverts versus bridges for cross drainage, 410.

COSTS, EROSION (FOUNDATION EROSION)
Flood erosion protection for highway fills, 532, 533, 541, 542, 543, 547, 553, 555.

COSTS, FRAME
Substantial savings in steel frame usage, 1158, 1161, 1167.

COSTS, IRRIGATION
"Pumping Ground Water for Irrigation and Drainage," Cleve H. Milligan, 228.

COSTS, JOINT
High strength bolted connections versus rivets, 20.

COSTS, LEVEE
Levee cost compared to damage prevented, 662.

COSTS, MODEL TESTING
Trial-load analysis computation and model studies compared, 947, 948.

COSTS, PAVEMENT AND PAVING
Runway pavement cost estimates compared for uniform and variable thickness, 1044, 1046, 1047.

COSTS, SEA WATER CONVERSION
Saline Water Conversion Program of United States Department of the Interior, and other techniques, 556.

COSTS, SEEPAGE
Ponding tests for measuring seepage rates in relation to costs, 349, 366.

COSTS, SEWAGE DISPOSAL
Algal cell separation cost as related to use of photosynthesis in sewage treatment, 93.
Plant cost estimating methods, 96, 98, 101, 105.

COSTS, TRANSPORTATION
Operating and usage costs in urban transportation, 289.

COSTS, WATER SUPPLY
Arctic water supply economic conditions in relation to high costs, 1172, 1177.

COURT DECISIONS
See under relative subject (under the subject LAW heading, e.g., GROUND WATER LAW)

CRACKS AND CRACKING
See under relative subject, e.g., CONCRETE—Cracks and Cracking; MODELS...

CREVASSES
See under relative subject, e.g., LEVEES

CULVERTS
See also FAILURES, CULVERT
"Rigid Culverts under High Overfills," R. Robinson Rowe, 410.

CURRENTS
See OCEAN CURRENTS; WAVES

CURVES (alinement curves)
"The Highway Spiral for Combining Curves of Different Radii," Paul Hartman, 389. *Discussion:* Thomas F. Hickerson, C. C. Wiley, Allen H. Brownfield, and Paul Hartman, 400.
Osculating circle "theory," 389, 402, 403, 409.
"Sight Distance at Undercrossings," Paul Hartman (with discussion), 64.

CURVES (construction curves)
See CURVES (alinement curves)

CURVES (design curves)
See relative subject of design, e.g., SHEAR

CURVES (transition curves)
See CURVES (alinement curves)

CURVES (vertical curves)
See CURVES (alinement curves)

CURVES, FREQUENCY
See PROBABILITY, THEORY OF; *see also* under topic

CYLINDRICAL SHELLS
See DOMES AND VAULTS

DAMPING
See STRUCTURES, THEORY OF

DAMS (General)
See also COFFERDAMS; GROUND WATER; MODELS, HYDRAULIC; RESERVOIRS . . . ; SPILLWAYS; WATER, FLOW OF, OVER DAMS AND WEIRS; WATER PRESSURE
"River-Bed Degradation Below Large-Capacity Reservoirs," M. Gamal Mostafa (with discussion), 688.

DAMS, ARCH
See STRESS AND STRAIN—Dams, Arch

DAMS, CONCRETE
See DAMS, MASONRY AND CONCRETE

DAMS, EARTH
See SEEPAGE

DAMS, GRAVITY
See DAMS, MASONRY AND CONCRETE

DAMS, MASONRY AND CONCRETE
See also DAMS, ARCH (cross reference thereunder); FAILURES, DAM; SEEPAGE; WATER PRESSURE
Hydrostatic uplift uncertainty and variances in design assumptions, 587, 588.
"Permeability, Pore Pressure, and Uplift in Gravity Dams," Roy W. Carlson, 587. *Discussion:* Bryant Mather, J. Laginha Serafim, Serge Leliavsky, and Roy W. Carlson, 603.

DEFINITIONS
See TERMINOLOGY

DEFLECTION RECORDING APPARATUS
Apparatus for measuring shear deflection of wide flange steel beams in the plastic range, 668.

DEFLECTIONS
See DEFORMATION (cross references thereunder); MOMENTS; SIDESWAY (cross reference thereunder); SLOPE DEFLECTION; STRESS AND STRAIN; STRUCTURES, THEORY OF; VIBRATION; *also* under relative structure or structural part, e.g., BEAMS . . . ; LOCK-GATES

DEFORMATION
See FAILURES . . . ; STRESS AND STRAIN; STRUCTURES THEORY OF; *also* under specific type of stress, e.g., BUCKLING; SHEAR; *also* under type of material, e.g., CONCRETE; SOILS; *also* under type of structure

DEMINERALIZATION OF WATER
See WATER TREATMENT

DESIGN
See under relative subject, e.g., CONCRETE; DOCKS AND WHARVES; *see also* DRAWINGS (cross reference thereunder); SPECIFICATIONS (cross reference thereunder); STRUCTURES, THEORY OF

DESIGN ANALYSIS
See under relative subject, e.g., STRUCTURES, THEORY OF

DESIGN CURVES
See CURVES (design curves) (cross reference thereunder)

DIAGRAMS
See under relative subject

DIKES
See RIVER BANKS AND BANK PROTECTION (cross references thereunder)

DISCHARGE
See GROUND WATER; PUMPS AND PUMPING; WATER, FLOW OF . . .

DISCHARGE COEFFICIENTS
See under relative subject, e.g., SPILLWAYS

DISEASE
See PUBLIC HEALTH (cross references thereunder)

DISTILLATION
"Recovery of Usable Water from Saline Water," David B. Smith and Charles E. Richheimer, 556.

DISTORSION
See STRESS AND STRAIN; TORSION

DIVERSION
See WATER DIVERSION (cross reference thereunder)

DIVERSION CANALS
See CANALS (cross references thereunder)

DOCKS AND WHARVES
See also HARBORS; PILES AND PILE DRIVING; STRESS AND STRAIN—Docks and Wharves
"The Design of Piers, Jetties, and Dolphins," David A. Hopkins, 22. *Discussion:* Zusse Levinton, and David A. Hopkins, 37.

DOMES AND VAULTS
See also STRUCTURES, THEORY OF—Domes and Vaults
"Moments in Domes Built into Cylinders," John V. Huddleston and Mario G. Salvadori, 235.

DRAINAGE
See also COSTS, DRAINAGE; CULVERTS; IRRIGATION; LAND RECLAMATION (cross references thereunder); PIPES AND PIPING; RUNOFF; VALLEYS; WELLS; *also* under type of drainage, e.g., HIGHWAYS AND ROADS—Drainage
Concise historic outline of land drainage in the United States, 118.
"Drainage in the Humid Areas of the United States," John G. Sutton, 115.
Historical outline of drainage in central and southern Florida, including the Everglades, 213.
"Pumping Ground Water for Irrigation and Drainage," Cleve H. Milligan, 228.
Research needed regarding drainage in humid areas of United States, 115.
Tile drainage failure problems and recommendations, 129.
"Water Control in Central and Southern Florida," Harold A. Scott, 211.

Financing
State wide program difficulties in Louisiana and North Dakota, 125.

DRAINAGE BASINS
See DRAINAGE

DRAIN WELLS
See WELLS

DRAWDOWN
See WELLS

DRAWINGS
See under relative subject, e.g., WELLS

DRILLS AND DRILLING
See also BORINGS
Reverse-rotary method of drilling holes for wells in sand, 1005.

DROP STRUCTURES
See DAMS

DUTY OF WATER
See WATER, DUTY OF

DYNAMICS OF FLUIDS
See HYDRODYNAMICS

DYNAMICS OF STRUCTURES
See STRUCTURAL DYNAMICS

EARTH...
See also GROUND...; LAND... (cross references thereunder); SOIL ...

EARTH DAMS
See DAMS, EARTH (cross reference thereunder)

EARTH MOVEMENTS
See EARTHQUAKES (cross reference thereunder)

EARTH PRESSURE
"Analysis for Sheet-Pile Retaining Walls," F. E. Richart, Jr. (with discussion), 1113.
"Stresses in Elastic Plates over Flexible Subgrades," Eric Reissner, 627.

EARTHQUAKES
See VIBRATION

EARTHS
See SOILS

EARTHWORK
See also DAMS, EARTH (cross reference thereunder); DRAINAGE; EMBANKMENTS; FOUNDATIONS...; LEVEES; SOILS
"Rigid Culverts under High Overfills," R. Robinson Rowe 410.

ECONOMICS
See also COSTS...; *also* under relative subject, subheading Financing
Airport distance and effect on economy of a specific community, 622.

EDUCATION
Curriculum outline in engineering education, 776.
"Education of Civil Engineers": A Symposium, Edwin H. Gaylord, Jr., L. E. Grinter, and Benjamin A. Whisler, 765. *Discussion:* Daniel C. Drucker, and L. E. Grinter, Alfred R. Golze, and Benjamin A. Whisler, 776, 783.

EFFLUENTS, SEWAGE
See SEWAGE DISPOSAL

ELASTICITY
See also PLASTICITY; STRESS AND STRAIN
"Impact on Pin-Jointed Trusses," Bruno A. Boley and Chi-Chang Chao, 39.
"Model Tests, Analysis, and Observation of an Arch Dam," Manuel Rocha, J. Laginha Serafim, Antonio F. da Silveira and Jose M. Ressurreicao Neto (with discussion), 903.
"Thick Rectangular Plates on an Elastic Foundation," Daniel Frederick (with discussion), 1069.

ELASTO-PLASTIC STRUCTURES
See STRUCTURES, THEORY OF—Elasto-Plastic Structures

ELECTRIC ANALOGY
See STRUCTURES, THEORY OF; WATER PRESSURE

EMBANKMENTS
See also DAMS, EARTH (cross reference thereunder); DIKES (cross reference thereunder); FOUNDATIONS, EMBANKMENT; LEVEES; SOILS
"Flood-Erosion Protection for Highway Fills," Chesley J. Posey (with discussion), 531.

EMPLOYEES AND EMPLOYMENT
Civil engineering education as related to future employment, 779.
Modern work procedures evaluated, 1221.

ENERGY
See HYDRODYNAMICS; INSOLATION; KINETIC ENERGY (cross references thereunder); STRUCTURAL DYNAMICS; STRUCTURES, THEORY OF; WATER, FLOW OF . . . ; WIND (cross reference thereunder)

ENERGY, KINETIC
See HYDRODYNAMICS; IMPACT

ENERGY, LOSS OF
See EVAPORATION (cross reference thereunder); FRICTION; WATER, FLOW OF . . .

ENGINEERING
See ENGINEERS AND ENGINEERING

ENGINEERING AND SOCIAL PROBLEMS
See cross references under SOCIAL PROBLEMS AND ENGINEERING

ENGINEERING BIBLIOGRAPHY
See BIBLIOGRAPHY (cross references thereunder)

ENGINEERING COLLEGES AND SCHOOLS
See EDUCATION

ENGINEERING EDUCATION
See EDUCATION

ENGINEERING GLOSSARIES
See TERMINOLOGY

ENGINEERING HISTORY
See AMERICAN SOCIETY OF CIVIL ENGINEERS; *also* under relative subject, e.g., DRAINAGE; JOINTS

ENGINEERING SOCIETIES
See SOCIETIES, TECHNICAL; *see also* AMERICAN SOCIETY OF CIVIL ENGINEERS

ENGINEERS AND ENGINEERING (General)
See also AMERICAN SOCIETY OF CIVIL ENGINEERS. (For memoirs of deceased members, *see* name of member in Author Index. (*See also* p. 1229); EDUCATION; EMPLOYEES AND EMPLOYMENT; RESEARCH; SOCIETIES, TECHNICAL; TERMINOLOGY
"Time to Think": Address at the Summer Convention, Buffalo, N. Y., June 5, 1957, Mason G. Lockwood, 1221.

ENTRAINMENT, AIR
See CONCRETE (General)

EQUATIONS
See under relative subject, e.g., TRUSSES . . .

ERECTION
See CONSTRUCTION (cross references thereunder)

EROSION, BEACH
"Beach Rehabilitation by Fill and Nourishment," Jay V. Hall, Jr. and George M. Watts, 155.

EROSION, FOUNDATION
See also COSTS, EROSION (FOUNDATION EROSION)
"Flood-Erosion Protection for Highway Fills," Chesley J. Posey (with discussion), 531.

EROSION, STREAM
"Missouri River Basin Plan in Operation," Wendell E. Johnson, 654.
"River-Bed Degradation Below Large-Capacity Reservoirs," M. Gamal Mostafa (with discussion), 688.

ESTIMATES
See COSTS

ESTUARIES
See RIVERS

EVAPORATION
See WATER, CONSUMPTIVE USE OF (in agriculture)

EXPERIMENTS AND EXPERIMENTATION
See MODELS . . . ; TESTS AND TESTING (cross references thereunder); *also* under material, structure or structural part tested; *also* under relative subject, e.g., BUCKLING

EXPLORATIONS
See BORINGS; FOUNDATIONS . . . ; PILES AND PILE DRIVING

EXPLOSION
See BLASTING

EXPRESSWAYS
See TRAFFIC, STREET

EXTENSOMETERS
See GAGES, STRAIN

FABRICATION
See under relative subject

FACT FINDING
See RESEARCH

FACTOR OF SAFETY
See under relative subject, e.g., BUCKLING

FAILURES (General)
See also ACCIDENTS (cross reference thereunder); BEARING CAPACITY; SAFETY (cross reference thereunder); STRENGTH OF MATERIALS; STRESS AND STRAIN; STRUCTURES, THEORY OF

FAILURES, COLUMN
Three ways a column anchorage fails, 133.

FAILURES, CONCRETE
"Failure of Plain Concrete under Combined Stresses," Boris Bresler and Karl S. Pister (with discussion), 1049.

FAILURES, CULVERT
Ground water and fill material problems, 419.

FAILURES, DAM
Principles involved in concrete dam failure theories, 610.

FAILURES, TILE
Drain failure causes and drain tile improvement recommendations, 130.

FASTENERS AND FASTENING
See BOLTS (cross references thereunder); CONNECTORS AND CONNECTIONS

FERTILIZERS
See COMPOST AND COMPOSTING (cross reference thereunder)

FIBER INDUSTRY
"Intermittent Discharge of Spent Sulfite Liquor," Herman R. Amberg and Robert Elder, 1179.

FILLING, HYDRAULIC
See HYDRAULIC FILLING

FILL, SETTLEMENT OF
See HYDRAULIC FILLING

FILTERS AND FILTRATION, SEWAGE
See also SEWAGE DISPOSAL
"An Approach to the Design of Trickling Filters," William T. Ingram, 1202.
Essentials and characteristics of controlled filtration, 1203, 1211.
Large scale aerated filter operations, 1210.

FINANCE
See COSTS . . . ; ECONOMICS; *also* subheading Financing under relative subject, e.g., DRAINAGE; WATER SUPPLY

FINITE DIFFERENCES, THEORY OF
See MATHEMATICS

FISH INDUSTRY
See under relative technical subject, e.g., WATER POLLUTION

FLANGES
See STRESS AND STRAIN—Flanges

FLEXURE
See STRESS AND STRAIN; STRUCTURES, THEORY OF

FLOOD CONTROL
See FLOOD ROUTING; RESERVOIRS, FLOOD CONTROL

FLOOD FORECASTING
See FLOODS

FLOOD ROUTING
"Water Control in Central and Southern Florida," Harold A. Scott, 211.

FLOODS (General)
See also DRAINAGE; LEVEES; MULTI-PURPOSE PROJECTS; RESERVOIRS, FLOOD CONTROL; RUNOFF; SPILLWAYS
"Flood-Erosion Protection for Highway Fills," Chesley J. Posey (with discussion), 531.
Forecasting methods based on multiple correlation and statistical procedures, 1201.

FLOODS (Geographical)
Missouri River
1951 and 1952 flood data and areas affected, 659.

FLOODWAYS
See FLOODS; SPILLWAYS

FLOOR BEAMS
See BEAMS... (cross references thereunder)

FLOW
See FLOODS; GROUND WATER; LIQUIDS, FLOW OF... ; RUNOFF; SEEPAGE; TURBULENCE; UNDERFLOW (cross references thereunder); WATER, FLOW OF...

FLOW, LAMINAR
See WATER, FLOW OF (General)

FLOW METERS
See METERS AND METERING

FLOW NETS
See HYDRAULIC FLOW NETS

FLOW OF FLUIDS
See LIQUIDS, FLOW OF; PIPES AND PIPING; WATER, FLOW OF...

FLOW OF LIQUIDS
See LIQUIDS, FLOW OF

FLOW OF OIL
See WELLS

FLOW OF SOLIDS
See SOLIDS, FLOW OF (cross references thereunder)

FLOW OF WATER
See WATER, FLOW OF...

FLUID FRICTION
See FRICTION

FLUID MECHANICS
See WATER, FLOW OF...

FLUIDS, DYNAMICS OF
See HYDRODYNAMICS

FLUIDS, FLOW OF
See LIQUIDS, FLOW OF; PIPES AND PIPING; WATER, FLOW OF...

FORMULAS
See under relative subject, e.g., RIVERS; WELLS

FOUNDATIONS (General)
See also BEARING CAPACITY; BORINGS; DRAINAGE; EROSION, FOUNDATION; STRUCTURES, THEORY OF—Foundations... ; WATER PRESSURE; *also* under special material, e.g., SOILS
Stable foundations for structures placed in or above permafrost, 1176.
"Thick Rectangular Plates on an Elastic Foundation," Daniel Frederick (with discussion), 1069.

FOUNDATIONS, BUILDING
See STRUCTURES, THEORY OF —Foundations, Building

FOUNDATIONS, EMBANKMENT
"Flood-Erosion Protection for Highway Fills," Chesley J. Posey (with discussion), 531.

FOUNDATIONS, HIGHWAY AND ROAD
See also HIGHWAYS AND ROADS —Roadbeds
"Flood-Erosion Protection for Highway Fills," Chesley J. Posey, 531. *Discussion:* Gerard H. Matthes; Emory W. Lane; Carl F. Izzard and Joseph N. Bradley; Carl E. Kindsvater; Parley R. Neeley; and Chesley J. Posey, 543.
Riprap protection against erosion during floods, 533.
"Stresses in Elastic Plates over Flexible Subgrades," Eric Reissner, 627.
Usage of "rock sausages" (or gabions), for protection of highway fills, 531.

FOUNDATIONS, LEVEE
"Underseepage, Mississippi River Levees, St. Louis District," Charles I. Mansur and Robert I. Kaufman, 985.

FOUNDATIONS, PILE
See PILES AND PILE DRIVING

FOUNDATIONS, UNDERWATER
See PILES AND PILE DRIVING

FRAMES (General)
See also COSTS, FRAME; STRESS AND STRAIN—Frames . . . ; STRUCTURES, THEORY OF—Frames . . . ; *see also* BEAMS . . . (cross references thereunder) ; COLUMNS
FRAMES, CONTINUOUS
See STRUCTURES, THEORY OF—Frames, Continuous; *see also* BEAMS (cross references thereunder) ; COLUMNS
FRAMES, RIGID
See STRESS AND STRAIN—Frames, Rigid
FRAMEWORKS
See STRUCTURES, THEORY OF
FRAZIL
See ICE
FREEZING
See also ICE; PERMAFROST (cross reference thereunder)
"Water Supply in Arctic Areas: Design Features," Lloyd K. Clark and Amos J. Alter, 1169.
Bibliography
Arctic permafrost effects, 1177.
FREQUENCY CURVES
See PROBABILITY, THEORY OF; *see also* under topic
FREQUENCY DISTRIBUTION
See under relative subject, e.g., VIBRATION
FRICTION
See also TURBULENCE
"The Action of Soft Clay Along Friction Piles," H. Bolton Seed and Lymon C. Reese (with discussion), 731.
"A Concept of the Regime Theory," Ning Chien (with discussion), 785.
FRICTION PILES
See PILES AND PILE DRIVING
FROST
See PERMAFROST (cross reference thereunder)
GABIONS (rock sausages)
See FOUNDATIONS, HIGHWAY AND ROAD
GAGES (General)
See also METERS AND METERING . . . ; INSTRUMENTS (cross references thereunder)
GAGES, PRESSURE
Piezometer type and usage in levee underseepage control work, 1008.
GAGES, STRAIN
Extensometer and other gage usage for stresses and displacements in arch dams, 905, 910, 921, 925, 933, 945.
GARBAGE DISPOSAL
See REFUSE DISPOSAL
GATES
See under type of gate, e.g., LOCK-GATES; WATER GATES . . .
GAUGES (measuring instruments)
See GAGES
GEOGRAPHY
See under relative technical subject
GEOLOGY
Studies of sites along alluvial valley of Mississippi River, 988.
GEOMETRY
See under relative subject, e.g., WELLS
GIRDERS (General)
See STRUCTURES, THEORY OF—Beams and Girders (General)
GIRDERS, CONTINUOUS
See STRUCTURES, THEORY OF—Beams and Girders, Continuous
GLOSSARIES
See TERMINOLOGY
GOVERNMENT
See AUTHORITIES (cross reference thereunder) ; LAW subject heading under related topic, e.g., GROUND WATER LAW
GRADES
See HIGHWAYS AND ROADS—Grades
GRADES, SUB-
See SUBGRADES (cross reference thereunder)
GRAPHICAL CHARTS
See under relative subject
GRAVITY DAMS
See DAMS, MASONRY AND CONCRETE
GRAVITY WAVES
See WAVES
GRAVITY WELLS
See WELLS
GROUND . . .
See also EARTH . . . ; LAND . . . (cross references thereunder) ; SOIL . . . ; UNDERGROUND . . . (cross references thereunder)

GROUND MOVEMENTS

See BLASTING; EARTHQUAKES (cross reference thereunder)

GROUND WATER

See also SEEPAGE; WATER SUPPLY

Apparatus for flow into drain wells and water supply wells, 1092, 1093, 1103.

Dupuit concept of Darcy's law of laminar flow through sands and gravels, 503, 512, 514, 517.

"Flow into a Well by Electric and Membrane Analogy," Chong-Hung Zee, Dean F. Peterson and Robert O. Bock (with discussion), 1088.

The Ghyben-Herzberg principle usage in problem of sea water intrusion in ground water basin, 466, 467, 474.

"Ground-Water Development": A Symposium, Robert O. Thomas, Harris R. McDonald, Paul Baumann, and Dean F. Peterson, Jr., 421. *Discussion:* Harold E. Thomas, Frank B. Clendenen, and Robert O. Thomas, Robert T. Knapp, Frederick L. Hotes, Norman H. Brooks, James A. Harder, Charles H. Lee, and Paul Bowmann, 434, 474.

Ground water utilization in history, 229.

"Pumping Ground Water for Irrigation and Drainage," Cleve H. Milligan, 228.

"Water Supply in Arctic Areas: Design Features," Lloyd K. Clark and Amos J. Alter, 1169.

GROUND WATER LAW

Legal status of ground water in California and the United States, 422, 455.

Problems of development and utilization, including influence of court decisions, 233.

GROUNDWORK

See EARTHWORK; FOUNDATIONS...

HARBOR POLLUTION

See WATER POLLUTION

HARBORS (General)

See also BREAKWATERS (cross references thereunder); BULKHEADS (cross references thereunder); CHANNELS (cross references thereunder); DOCKS AND WHARVES; JETTIES; PILES AND PILE DRIVING; RETAINING WALLS; SHORES AND SHORE PROTECTION; WATER POLLUTION; WAVES

HARBORS (Geographical)

New York, N. Y.

"The Analysis of Water Samples for Cyclical Variations," 872.

HEAD, LOSS OF

See AERATION; FRICTION; WATER, FLOW OF...

HEALTH, PUBLIC

See PUBLIC HEALTH (cross references thereunder)

HEAT AND HEAT TRANSMISSION

See DISTILLATION; EVAPORATION (cross reference thereunder); INSOLATION; TEMPERATURE

HEAT FLOW

See HEAT AND HEAT TRANSMISSION (cross references thereunder)

HELICOPTERS

See AIRCRAFT

HELIPORTS

See AIRPORTS

HIGHWAY BRIDGES

See BRIDGES (cross references thereunder)

HIGHWAY CURVES

See CURVES (alinement curves)

HIGHWAY GRADES

See HIGHWAYS AND ROADS—Grades

HIGHWAYS AND ROADS (General)

See also BRIDGES (cross references thereunder); CULVERTS; CURVES (alinement curves); EARTHWORK; FOUNDATIONS, HIGHWAY AND ROAD; PAVEMENT AND PAVING...; SOILS; STREETS; TRAFFIC...

Drainage

"Rigid Culverts under High Overfills," R. Robinson Rowe, 410.

Foundations. *See* FOUNDATIONS, HIGHWAY AND ROAD

Grades

"Sight Distance at Undercrossings," Paul Hartman, 64. *Discussion:* Thomas F. Hickerson, 72.

Location

Methods of improving valley crossings, 532.

HIGHWAYS AND ROADS (General) (*Continued*)

Roadbeds. *See also* FOUNDATIONS, HIGHWAY AND ROAD; SOILS

"Flood-Erosion Protection for Highway Fills," Chesley J. Posey (with discussion), 531.

Safety

"Sight Distance at Undercrossings," Paul Hartman (with discussion), 64.

Surfaces

"Stresses in Elastic Plates over Flexible Subgrades," Eric Reissner, 627.

Traffic. *See* TRAFFIC, HIGHWAY AND ROAD

HIGHWAYS AND ROADS (Geographical)

Maine

"Traffic Diversion to Toll Roads," John T. Lynch, 883.

Pennsylvania

"Traffic Diversion to Toll Roads," John T. Lynch, 883.

HIGHWAY TRAFFIC

See TRAFFIC, HIGHWAY AND ROAD

HINGED STRUCTURES

See JOINTS

HINGES

See JOINTS

HISTORY, ENGINEERING

See AMERICAN SOCIETY OF CIVIL ENGINEERS; *also* under relative subject, e.g., DRAINAGE; JOINTS

HOUSING LAW

Urban rehabilitation provisions of Federal Housing Act of 1954 as related to slum clearance and redevelopment provisions of Housing Act of 1949, 330.

HUMUS

See COMPOST AND COMPOSTING (cross reference thereunder)

HYDRAULIC FILLING

"Beach Rehabilitation by Fill and Nourishment," Jay V. Hall, Jr. and George M. Watts, 155.

HYDRAULIC FLOW NETS

Usage of flow nets for outflow from channel mounds, 464, 489, 491, 496.

HYDRAULIC MACHINERY

See under type of machinery, e.g., PUMPS AND PUMPING

HYDRAULIC MODELS

See MODELS, HYDRAULIC

HYDRAULICS

See AERATION; BREAKWATERS (cross references thereunder); BULKHEADS (cross references thereunder); CANALS (cross references thereunder); CHANNELS (cross references thereunder); COSTS . . . ; DAMS; DOCKS AND WHARVES; DRAINAGE; EROSION . . . ; FAILURES . . . ; FILTERS AND FILTRATION . . . ; FLOOD . . . ; FLOW . . . ; FLUID . . . ; FOUNDATIONS . . . ; FRICTION; GAGES . . . ; GROUND WATER; HARBORS; HYDRAULIC . . . ; HYDRO- . . . ; IRRIGATION; JETTIES; LAKES; LEVEES; LIQUIDS . . . ; LOCKGATES; METERS AND METERING; MODELS, HYDRAULIC; MULTI-PURPOSE PROJECTS; PILES AND PILE DRIVING; PIPES AND PIPING; POWER . . . ; PROBABILITY, THEORY OF; PUMPS AND PUMPING; RESERVOIRS . . . ; RETAINING WALLS; RIVER . . . ; RUNOFF; SEA . . . ; SEEPAGE; SEWAGE . . . ; SHORES AND SHORE PROTECTION; SILT AND SILTING, CHANNEL; SPILLWAYS; SPREADING BASINS; SPREADING, WATER; STRESS AND STRAIN . . . ; STRUCTURES, THEORY OF . . . ; TERMINOLOGY; TIDES (cross reference thereunder); TURBULENCE; VALLEY . . . ; WATER . . . ; WAVES; WELLS

HYDRAULIC STRUCTURES

See under type of structures, e.g., DAMS; SPILLWAYS

HYDRODYNAMICS

"Virtual Mass and Acceleration in Fluids," Thomas E. Stelson and Frederic T. Mavis (with discussion), 518.

HYDROLOGY

See DRAINAGE; FLOOD . . . ; GROUND WATER; INFILTRATION (cross references thereunder); LAKES; MARSHES; OCEAN . . . ; RIVER . . . ; RUNOFF; SEA WATER; SNOW; WATER . . .

HYDROSTATIC PRESSURE

See HYDROSTATIC UPLIFT (cross reference thereunder)

HYDROSTATIC UPLIFT

See WATER PRESSURE

ICE
See also PERMAFROST (cross reference thereunder)
"Water Supply in Arctic Areas: Design Features," Lloyd K. Clark and Amos J. Alter, 1169.

IMPACT
See also VIBRATION; WHEEL LOADS
"The Design of Piers, Jetties, and Dolphins," David A. Hopkins (with discussion), 22.
"Impact on Pin-Jointed Trusses," Bruno A. Boley and Chi-Chang Chao, 39.
Ship berthing impact in relation to structural flexibility and resilient ship fendering, 22.

IMPOUNDING, SEWAGE
See SEWAGE TREATMENT (cross reference thereunder)

IMPOUNDING, WATER
See RESERVOIRS, WATER STORAGE; WATER STORAGE

INDUSTRIAL PLANTS
See under specific type of plant, e.g., PAPER AND PULP MILLS; POWER PLANTS

INDUSTRIAL WASTE
See also ODORS; REFUSE DISPOSAL; SEWAGE DISPOSAL

Industrial Waste Pollution
"Intermittent Discharge of Spent Sulfite Liquor," Herman R. Amberg and Robert Elder, 1179.

INDUSTRIAL WATER SUPPLY
See IRRIGATION; RESERVOIRS . . . ; WATER SUPPLY

INDUSTRY
See under relative technical classification, e.g., LAND RECLAMATION (cross references thereunder); WATER, CONSUMPTIVE USE OF; *see also* EMPLOYEES AND EMPLOYMENT; *also* under type of industry or industrial plant e.g., FIBER INDUSTRY; POWER PLANTS

INFILTRATION
See FLOODS; GROUND WATER; LAND . . . (cross references thereunder); RUNOFF; SEEPAGE

INSOLATION
"Photosynthesis in Sewage Treatment," William J. Oswald and Harold B. Gotaas (with discussion), 73.

INSTRUMENTS
See GAGES . . . ; METERS AND METERING . . . ; *also* under general types of instruments, e.g., WATER INSTRUMENTS; *also* under specific type of instrument; *also* under usage, e.g., WATER, FLOW OF; *also* cross references under APPARATUS

IRRIGATION (General)
See also COSTS, IRRIGATION; LAND RECLAMATION (cross references thereunder); RESERVOIRS, IRRIGATION; WATER, CONSUMPTIVE USE OF; WATER, DUTY OF; WATER SUPPLY
"Pumping Ground Water for Irrigation and Drainage," Cleve H. Milligan, 228.

Bibliography
Consumptive use of water in agriculture, 816.

Power
"The Use of Statistics in Reservoir Operations," Victor A. Koelzer, 1187.

IRRIGATION (Geographical)

United States
"Drainage in the Humid Areas of the United States," John G. Sutton, 115.
"Ground-Water Development": A Symposium, Robert O. Thomas, Harris R. McDonald, Paul Baumann, and Dean F. Peterson, Jr. (with discussion), 421.
Historical development of ground water irrigation in United States, 443.

IRRIGATION CANALS
Evaluation of the science of design of stable irrigation canals, 797.
"Measurement of Canal Seepage," August R. Robinson, Jr. and Carl Rohwer (with discussion), 347.

JET AIRCRAFT
See AIRCRAFT

JETTIES
See also SHORES AND SHORE PROTECTION; WATER PRESSURE; WAVES
"The Design of Piers, Jetties, and Dolphins," David A. Hopkins (with discussion), 22.

JOINTS (General)
See also COSTS, JOINT; STRESS AND STRAIN—Joints; STRUCTURES, THEORY OF—Joints

JOINTS (General) (*Continued*)
"High-Strength Steel Bolts in Structural Practice," Mace H. Bell, 1. *Discussion:* William Hansen, and Mace H. Bell, 20.
High strength steel bolt specifications and their development in field assembly work, 1.
Pneumatic impact wrench usage, 1.

JOINTS, BOLTED
See JOINTS (General)

JOINTS, TRUSS
See TRUSSES

JOINTS, WELDED
Plastic hinge reserve strength, 1145, 1161.

KINETIC ENERGY
See HYDRODYNAMICS; IMPACT

LAKES (General)
See also HARBORS; SHORES AND SHORE PROTECTION; WATER . . . ; WAVES

LAKES (Geographical)
Florida
"Water Control in Central and Southern Florida," Harold A. Scott, 211.

LAMINAR FLOW
See WATER, FLOW OF (General)

LAND . . .
See also EARTH . . . ; GROUND . . . ; MARSHES; SOIL . . .

LAND RECLAMATION
See DRAINAGE; MARSHES; WATER RIGHTS

LATERAL FORCES
See EARTHQUAKES (cross reference thereunder); WIND (cross reference thereunder)

LATERAL PRESSURE
See EARTH PRESSURE; WATER PRESSURE

LAW
See LAW subject heading under related subject, e.g., GROUND WATER LAW; HOUSING LAW; *see also* GOVERNMENT (cross references thereunder)

LEGISLATION
See under relative subject (under the subject LAW heading, e.g., GROUND WATER LAW

LEVEES
See also COSTS, LEVEE; FOUNDATIONS, LEVEE
"Underseepage, Mississippi River Levees, St. Louis District," Charles I. Mansur and Robert I. Kaufman, 985.

LIFT GATES
See WATER GATES, MOVABLE

LIMIT DESIGN, THEORY OF
Plastic design as an aspect of limit design, 1140.

LININGS
See under relative type, e.g., CANAL LININGS; *also* under relative subject

LIQUIDS, FLOW OF (General)
See also WATER, FLOW OF . . .
"Virtual Mass and Acceleration in Fluids," Thomas E. Stelson and Frederic T. Mavis, 518. *Discussion:* Joseph M. Caldwell; Edward Silberman; and Thomas E. Stelson and Frederic T. Mavis, 526.

LITTORAL DRIFT
See SHORES AND SHORE PROTECTION

LOAD
See BEARING CAPACITY; BUCKLING; EARTH PRESSURE; FAILURES . . . ; IMPACT; STRESS AND STRAIN; STRUCTURES, THEORY OF; VIBRATION; WATER PRESSURE; WHEEL LOADS; *also* under structure, structural member or part, e.g., LOCK-GATES

LOAD, BED
See RIVERS; SILT AND SILTING . . . ; TURBULENCE; WATER, FLOW OF, IN OPEN CHANNELS

LOAD, SUSPENDED
See SEDIMENT AND SEDIMENTATION (cross references thereunder); SILT AND SILTING . . .

LOCK-GATES
See also STRUCTURES, THEORY OF—Lock-Gates
Gate leaf analysis as related to dead load shear and prestressing of diagonal members, 106, 114.
"Stiffening Lock Gates by Prestressing Diagonals," Carl L. Shermer, 106.

LOSS OF ENERGY
See EVAPORATION (cross reference thereunder); FRICTION; WATER, FLOW OF . . .

LOSS OF HEAD
See AERATION; FRICTION; WATER, FLOW OF . . .

LYSIMETERS

See WATER INSTRUMENTS

MACHINERY

See under types of machinery; *also* under usage; *see also* TOOLS (cross references thereunder)

MARINE...

See SEA...; WATER...

MARSHES

Work of Florida Everglades Engineering Commission and Everglades Engineering Board of Review, 214, 215.

MASS SUBMERGENCE (concrete solid matter)

See SOLIDS, FLOW OF (cross references thereunder)

MASS, VIRTUAL

See FLUIDS, FLOW OF (cross reference thereunder)

MATERIALS OF CONSTRUCTION

See CLAY; CONCRETE...; EARTHWORK; EROSION...; PERMEABILITY OF MATERIALS (cross references thereunder); QUARRIES AND QUARRYING (cross reference thereunder); SAND; SEEPAGE; SOILS; STEEL; STRENGTH OF MATERIALS; STRESS AND STRAIN...; STRUCTURES, THEORY OF; TILE (cross reference thereunder); *also* under types of materials, e.g., PLASTIC MATERIALS

MATERIALS, PERMEABILITY OF

See PERMEABILITY OF MATERIALS (cross references thereunder)

MATERIALS, STRENGTH OF

See STRENGTH OF MATERIALS

MATERIALS, TESTING OF

See TESTS AND TESTING (cross references thereunder)

MATERIALS, WASTE

See cross references under WASTE DISPOSAL

MATHEMATICS

See also EQUATIONS (cross reference thereunder); GRAPHICAL CHARTS (cross reference thereunder); PROBABILITY, THEORY OF; *also* under relative subject

"Impact on Pin-Jointed Trusses," Bruno A. Boley and Chi-Chang Chao, 39.

Theory of finite differences effectively used in solution of problems relating to impulsive motion of elasto-plastic shear buildings, 294.

MATRIX ALGEBRA

See STRUCTURES, THEORY OF

MEASURING INSTRUMENTS

See GAGES; METERS AND METERING; VIBRATION MEASURING INSTRUMENTS; WATER INSTRUMENTS

MECHANICS (General)

See also DYNAMICS,... (cross references thereunder); FLUID... (cross references thereunder); HYDRAULIC...; MATHEMATICS; STRENGTH OF MATERIALS; STRUCTURAL...; STRUCTURES, THEORY OF; TESTS AND TESTING (cross references thereunder)

MECHANICS, FLUID

See WATER, FLOW OF...

MECHANICS, SOIL

See SOILS

MEMBERS, COMPRESSION

See COLUMNS

MEMBERS, STRUCTURAL

See BEAMS... (cross references thereunder); COLUMNS; FRAMES... (cross references thereunder); GIRDERS (cross references thereunder); STRUCTURES (General) (cross references thereunder); STRUCTURES, THEORY OF; *also* under name of material, e.g., CONCRETE; STEEL; *also* under structure, e.g., BUILDINGS

MEMBRANE ANALOGY

See WELLS

MEMOIRS OF DECEASED MEMBERS

See name of member in Author Index. (*See also* p. 1229)

METALS

See MATERIALS OF CONSTRUCTION (cross references thereunder); REINFORCED CONCRETE (cross reference thereunder); STRENGTH OF MATERIALS; STRESS AND STRAIN...; STRUCTURES, THEORY OF...; *also* under specific metal or its alloy, e.g., STEEL

METERS AND METERING (General)

See also GAGES...; INSTRUMENTS (cross references thereunder)

METERS AND METERING (General) (*Continued*)
Merits of Weber Basin (Utah) storage meter when used for canal seepage studies, 366.
Well permeameter test results in forecasting canal seepage, 347, 351, 353, 372.

MILITARY ENGINEERS AND ENGINEERING
See under relative technical subject, e.g., AIRPORTS; WATER SUPPLY

MILLS
See under type of mill, e.g., PAPER AND PULP MILLS

MINERALOGY
See under relative technical subject, e.g., SOILS

MINERALS
See under relative technical subject, e.g. MATERIALS OF CONSTRUCTION (cross references thereunder); ROCK (cross reference thereunder); WATER, DEMINERALIZATION OF (cross reference thereunder)

MINES AND MINING
See BLASTING; BORINGS

MITER GATES
See LOCK-GATES

MODELS, HYDRAULIC
See also COSTS, MODEL TESTING
Cracking as it affects plaster-diatomite and alkathene models under stress, 905, 914, 918, 927, 930, 946.
"Discharge Coefficients for Spillways at TVA Dams," Kenneth W. Kirkpatrick, 190.
"Ground-Water Development": A Symposium, Robert O. Thomas, Harris R. McDonald, Paul Baumann, and Dean F. Peterson, Jr. (with discussion), 421.
"Model Tests, Analysis, and Observation of an Arch Dam," Manuel Rocha, J. Laginha Serafim, Antonio F. da Silveira and Jose M. Ressurreicao Neto (with discussion), 903.

MODELS, STRUCTURAL
Dynamic model of a structure, 706, 713, 714.
"Structural Vibrations Produced by Ground Motion," 705.

MOHR THEORY
See SHEAR; STRESS AND STRAIN

MOISTURE
See CLAY; REFUSE DISPOSAL; SEEPAGE; SOILS

MOMENT DISTRIBUTION
See STRUCTURES, THEORY OF

MOMENTS
See also STRESS AND STRAIN; STRUCTURES, THEORY OF; *also* under specific type of stress, e.g., BUCKLING; TORSION
"Analysis for Sheet-Pile Retaining Walls," F. E. Richart, Jr. (with discussion), 1113.
"Moment-Rotation Characteristics of Column Anchorages," Charles G. Salmon, Leo Schenker, and Bruce G. Johnston, 132.
"Moments in Domes Built into Cylinders," John V. Huddleston and Mario G. Salvadori, 235.
"Thick Rectangular Plates on an Elastic Foundation," Daniel Frederick (with discussion), 1069.

MOORINGS AND MOORAGES, SHIP
See DOCKS AND WHARVES

MOTOR TRUCKS
See TRAFFIC...

MOTOR VEHICLES
See TRAFFIC...

MOTOR VEHICLE ACCIDENTS
See HIGHWAYS AND ROADS—Safety

MOTORWAYS
See HIGHWAYS AND ROADS

MOVABLE WATER GATES
See WATER GATES, MOVABLE

MULTI-PURPOSE PROJECTS (RIVER PROJECTS)
See also RIVER VALLEY AUTHORITIES
"Missouri River Basin Plan in Operation," Wendell E. Johnson, 654.

MULTI-PURPOSE RESERVOIRS
See RESERVOIRS, MULTI-PURPOSE

MUNICIPAL ENGINEERS AND ENGINEERING
See AIRPORTS; BRIDGES (cross references thereunder); CITIES; CITY PLANNING; COSTS...; DRAINAGE; FILTERS AND FILTRATION...; HARBORS; PAVEMENT AND PAVING...; POWER...; REFUSE DIS-

MUNICIPAL ENGINEERS AND ENGINEERING (*Continued*)

POSAL; SANITATION (cross references thereunder); SEWAGE ...; SNOW; STREETS; TRAFFIC...; WATER...; and similar relative subjects

MUNICIPALITIES

See CITIES

NAVIGATION

See CANAL...; CHANNELS (cross references thereunder); DAMS...; FLOODS; HARBORS; LAKES; MULTI-PURPOSE PROJECTS; RIVERS; RIVER VALLEY AUTHORITIES; TIDES (cross reference thereunder); WATER RIGHTS; WATERWAYS (cross references thereunder)

NAVIGATION, AIR

See AIR TRANSPORT

NOMENCLATURE

See TERMINOLOGY

NONUNIFORM MEMBERS, STRUCTURAL

See MEMBERS, STRUCTURAL (cross references thereunder)

NUISANCES, ABATEMENT OF

See INDUSTRIAL WASTE; ODORS

OBITUARIES OF MEMBERS

See name of member in Author Index. (*See also* p. 1229)

OCEAN...

See also SEA...; WAVES

OCEAN BEACHES

See EROSION, BEACH; SHORES AND SHORE PROTECTION

OCEAN CURRENTS

See also EROSION, BEACH; WAVES

"The Analysis of Water Samples for Cyclical Variations," Alex N. Diachishin, 872.

OCEAN WAVES

See WAVES

ODORS

Sewage treatment plant odors (including odors of oxidation ponds) controlled by recirculation of pond effluents, 99.

OIL, FLOW OF

See WELLS

OPEN CHANNELS

See WATER, FLOW OF, IN OPEN CHANNELS

ORGANIZATIONS

See SOCIETIES, TECHNICAL; *see also* AMERICAN SOCIETY OF CIVIL ENGINEERS

OSCILLATION

See VIBRATION; WAVES

OSCILLOGRAPHS

See VIBRATION RECORDING APPARATUS

OXYGEN

See OXYGENATION

OXYGENATION

See also AERATION

"Photosynthesis in Sewage Treatment," William J. Oswald and Harold B. Gotaas (with discussion), 73.

PAPER AND PULP MILLS

See also FIBER INDUSTRY

"Intermittent Discharge of Spent Sulfite Liquor," Herman R. Amberg and Robert Elder, 1179.

PAVEMENT AND PAVING (General)

See also COSTS, PAVEMENT AND PAVING; SOILS; STRUCTURES, THEORY OF—Pavement and Paving; WHEEL LOADS

PAVEMENT AND PAVING, ASPHALT

See PAVEMENT AND PAVING, BITUMINOUS

PAVEMENT AND PAVING, BITUMINOUS

"The Effect of Traffic on the Cross Section of a Runway Pavement," Robert Horonjeff and John H. Jones, 1035. *Discussion:* Roger H. Williams; John F. Redus; and Robert Horonjeff and John H. Jones, 1046.

PAVEMENT AND PAVING, CONCRETE

"Stresses in Elastic Plates over Flexible Subgrades," Eric Reissner, 627.

PERCOLATION

See GROUND WATER; SEEPAGE

PERMAFROST

See SOILS

PERMEABILITY OF MATERIALS

See SEEPAGE; *also* under type of material, e.g., CONCRETE...; SAND; SOIL...

PERMEAMETERS

See METERS AND METERING (General)

PERSONNEL

See EMPLOYEES AND EMPLOYMENT

PHOTOSYNTHESIS
See OXYGENATION

PIERS (waterway structures)
See DOCKS AND WHARVES

PIEZOMETERS
See GAGES, PRESSURE

PILES AND PILE DRIVING
See also BEARING CAPACITY; GABIONS (cross reference thereunder); STRESS AND STRAIN—Piles; STRUCTURES, THEORY OF—Piles

"The Action of Soft Clay Along Friction Piles," H. Bolton Seed and Lymon C. Reese, 731. *Discussion:* Lawrence A. Dubose; Yoshichika Nishida; James D. Parsons and Ralph B. Peck; and H. Bolton Seed and Lymon C. Reese, 755.

"Analysis for Sheet-Pile Retaining Walls," F. E. Richart, Jr. (with discussion), 1113.

"The Design of Piers, Jetties, and Dolphins," David A. Hopkins (with discussion), 22.

PIN-CONNECTED TRUSSES
See TRUSSES, PIN-CONNECTED

PIPES AND PIPING (fluid conveyance)
See also CULVERTS

Arctic region piped system difficulties, and usage of utilidors, 1175.

PIPING (dam failure process)
See FAILURES, DAM; LEVEES

PLANNING
See under type of planning, e.g., CITY PLANNING; *also* under relative subject, e.g., STREETS—Planning and Design

PLANTS (industrial buildings and equipment)
See INDUSTRIAL PLANTS (cross references thereunder)

PLASTICITY
See also ELASTICITY; STRESS AND STRAIN

"Impulsive Motion of Elasto-Plastic Shear Buildings," Edward Cohen, Leon S. Levy and Leonard E. Smollen, 293.

Plastic design application, 1141.

"Plastic Strength of Steel Frames," Lynn S. Beedle, 1139. *Discussion:* Jack R. Benjamin; Zdenek Sobotka; and Lynn S. Beedle, 1161.

"Shear Deflection of Wide-Flange Steel Beams in the Plastic Range," William J. Hall and Nathan M. Newmark, 666.

"Soil Mechanics and Work-Hardening Theories of Plasticity," Daniel C. Drucker, Robert E. Gibson and David J. Henkel, 338.

PLASTIC MATERIALS
"Plastic Strength of Steel Frames," Lynn S. Beedle (with discussion), 1139.

PLASTIC STRUCTURES
See ELASTO-PLASTIC STRUCTURES (cross reference thereunder)

PLASTIC THEORY
See PLASTICITY

PLATES
See also STRESS AND STRAIN—Plates; STRUCTURES, THEORY OF—Plates

"Thick Rectangular Plates on an Elastic Foundation," Daniel Frederick, 1069. *Discussion:* Harold G. Lorsch, and Daniel Frederick, 1086.

POLLUTION, AIR
See AIR SANITATION (cross reference thereunder)

POLLUTION, STREAM
See WATER POLLUTION

PORE WATER PRESSURE
See WATER PRESSURE

POROSITY
See SEEPAGE

PORTS
See AIRPORTS; HARBORS

POWER (General)
See DAMS; DYNA-... (cross references thereunder); IRRIGATION—Power; PUMPS AND PUMPING; WATER POWER (cross references thereunder)

POWER PLANTS (General)
"The Use of Statistics in Reservoir Operations," Victor A. Koelzer, 1187.

PRECIPITATION
See RAINFALL (cross references thereunder); SNOW

PRESIDENTIAL ADDRESSES (American Society of Civil Engineers)
See AMERICAN SOCIETY OF CIVIL ENGINEERS—Addresses; *see also* under subject of address

PRESSURE
See BUOYANCY (cross reference thereunder); EARTH PRESSURE; IMPACT; LATERAL PRESSURE (cross references thereunder); PUMPS AND PUMPING; STRESS AND STRAIN; WATER PRESSURE

PRESSURE GAGES
See GAGES, PRESSURE

PRINCIPLE OF VIRTUAL WORK
See VIRTUAL WORK, PRINCIPLE OF

PROBABILITY, THEORY OF
"The Use of Statistics in Reservoir Operations," Victor A. Koelzer, 1187.

PROPERTY (landed property)
See LAND ... (cross references thereunder); STREETS—Planning and Design

PROTOTYPES AND MODELS
See MODELS

PUBLIC HEALTH
See SANITATION (cross references thereunder); WATER SUPPLY

PUBLIC SERVICES
See under type of service, e.g., REFUSE DISPOSAL; SEWAGE DISPOSAL

PUBLIC WORKS
See RIVER VALLEY AUTHORITIES; *see also* under type of structure or project

PULP MILLS
See PAPER AND PULP MILLS

PUMPING STATIONS
See DRAINAGE

PUMPS AND PUMPING (General)
"Ground-Water Development": A Symposium, Robert O. Thomas, Harris R. McDonald, Paul Baumann, and Dean F. Peterson, Jr. (with discussion), 421.
"The Use of Statistics in Reservoir Operations," Victor A. Koelzer, 1187.

PURIFICATION
See AIR SANITATION (cross reference thereunder); WATER TREATMENT

QUARRIES AND QUARRYING
See BLASTING

RADIANT HEAT
See HEAT AND HEAT TRANSMISSION (cross references thereunder)

RAILROAD CURVES
See CURVES (alinement curves)

RAILROADS (General)
See TRANSPORTATION

RAILROAD TRACKS
See CURVES (alinement curves); EARTHWORK

RAINFALL
See DRAINAGE; FLOODS; RUNOFF; SEEPAGE

RECLAMATION, LAND
See LAND RECLAMATION (cross references thereunder)

RECLAMATION, SEWAGE
See SEWAGE DISPOSAL

RECORDING APPARATUS
See under general types of apparatus, e.g., DEFLECTION RECORDING APPARATUS; VIBRATION RECORDING APPARATUS; *see also* under relative subject

REFUSE DISPOSAL
See also INDUSTRIAL WASTE; ODORS; SEWAGE DISPOSAL
Composting unit and operating procedure, 1011.
"A Preliminary Study of High-Rate Composting," John S. Wiley and George W. Pearce, 1009. *Discussion:* Pieter R. Krige; and John S. Wiley and George W. Pearce, 1031.

REGIME THEORY
See SILT AND SILTING...

REGIONAL PLANNING
See HIGHWAYS AND ROADS—Location

REINFORCED CONCRETE
See CONCRETE...

RELAXATION (numerical analysis)
See under relative subject, e.g., GROUND WATER; SEEPAGE

RELIEF WELLS
See WELLS

RESEARCH
See also MODELS ... ; PROBABILITY, THEORY OF; STRUCTURES, THEORY OF; SURVEYS (research data) (cross references thereunder); TESTS AND TESTING (cross references thereunder); *also* under relative subject, e.g., DRAINAGE
Bolted joint research in structural steel and changed concepts since 1947, 1.

RESERVOIRS (General)
See also DAMS; LAKES; SPILLWAYS: WATER STORAGE; WAVES
"The Use of Statistics in Reservoir Operations," Victor A. Koelzer, 1187.

RESERVOIRS, FLOOD CONTROL
"Missouri River Basin Plan in Operation," Wendell E. Johnson, 654.

RESERVOIRS, IRRIGATION
See also RESERVOIRS, WATER STORAGE
Ground water storage reservoirs in the United States, 443, 450.

RESERVOIRS, MULTI-PURPOSE
"Missouri River Basin Plan in Operation," Wendell E. Johnson, 654.

RESERVOIRS, WATER STORAGE
"Pumping Ground Water for Irrigation and Drainage," Cleve H. Milligan, 228.
"River-Bed Degradation Below Large-Capacity Reservoirs," M. Gamal Mostafa (with discussion), 688.

RESONANCE
See VIBRATION

RETAINING WALLS
See also BULKHEADS (cross references thereunder); EARTH PRESSURE; EARTHWORK
"Analysis for Sheet-Pile Retaining Walls," F. E. Richart, Jr., 1113. *Discussion:* Peter W. Rowe, and F. E. Richart, Jr., 1133.

RIGHTS, RIPARIAN
See RIPARIAN RIGHTS

RIGHTS, WATER
See WATER RIGHTS

RIGID FRAMES
See STRESS AND STRAIN—Frames, Rigid

RIPARIAN RIGHTS
American Rule of Reasonable Use as formulated by the New Hampshire State Supreme Court 1862, and partially adopted by the states, 456.

RIPRAP (stone protection layer)
See FOUNDATIONS, HIGHWAY AND ROAD

RIVER BANKS AND BANK PROTECTION
See EROSION, STREAM; FLOODS; LEVEES; RIPARIAN RIGHTS; SILT AND SILTING, CHANNEL

RIVER BASINS
See DRAINAGE; RAINFALL (cross references thereunder); RESERVOIRS...; RIVER VALLEY AUTHORITIES; VALLEYS

RIVER CHANNELS
See CHANNELS (cross references thereunder)

RIVER POLLUTION
See WATER POLLUTION

RIVER RECTIFICATION
See RIVER REGULATION (cross references thereunder)

RIVER REGULATION
See FLOOD ROUTING; RIVERS; RIVER VALLEY AUTHORITIES; WATER, FLOW OF, IN OPEN CHANNELS

RIVERS (General)
See also CHANNELS (cross references thereunder); DRAINAGE; EROSION, STREAM; FLOOD ROUTING; FLOODS; HARBORS; LEVEES; MODELS, HYDRAULIC; MULTI-PURPOSE PROJECTS; RAINFALL (cross references thereunder); RESERVOIRS...; RETAINING WALLS; RUNOFF; SILT AND SILTING, CHANNEL; VALLEYS; WATER...; WAVES
Oscillatory gravity waves as related to wave penetration in estuaries and scour in river beds, 565.

RIVERS (Geographical)
Colorado River
Rate of scour from Hoover Dam to Davis Dam, years 1937–1948, 698.
Columbia River
"Intermittent Discharge of Spent Sulfite Liquor," Herman R. Amberg and Robert Elder, 1179.
Florida
"Water Control in Central and Southern Florida," Harold A. Scott, 211.
India
"A Concept of the Regime Theory," Ning Chien (with discussion), 785.
Mississippi River
"Underseepage, Mississippi River Levees, St. Louis District," Charles I. Mansur and Robert I. Kaufman, 985.
Missouri River
"Missouri River Basin Plan in Operation," Wendell E. Johnson, 654.

RIVERS (Geographical) (*Continued*)
Nile River
Discharge and sediment load formulas (including Beleida formula), 693, 701, 702, 704.
Pakistan
"A Concept of the Regime Theory," Ning Chien (with discussion), 785.
Tennessee River
"Discharge Coefficients for Spillways at TVA Dams," Kenneth W. Kirkpatrick, 190.
Western States
"Methods of Determining Consumptive Use of Water in Irrigation," Ralph D. Goodrich (with discussion), 806.
RIVER VALLEY AUTHORITIES
See also RIVERS (under relative river); VALLEYS
"Missouri River Basin Plan in Operation," Wendell E. Johnson, 654.
RIVER VALLEYS
See VALLEYS
ROADBEDS
See CULVERTS; DRAINAGE; EARTHWORK; *see also* under specific type, e.g., HIGHWAYS AND ROADS—Roadbeds
ROADS
See HIGHWAYS AND ROADS
ROCK
See FOUNDATIONS...
ROCK SAUSAGES
See GABIONS (cross reference thereunder)
ROOFS AND ROOFING
See DOMES AND VAULTS
ROUGHNESS
See FRICTION
ROUTING, FLOOD
See FLOOD ROUTING
RUNOFF (General)
See also FLOODS; RAINFALL (cross references thereunder)
"The Use of Statistics in Reservoir Operations," Victor A. Koelzer, 1187.
RUNWAYS
See AIRPORT APPROACHES
SAFETY (General)
See HIGHWAYS AND ROADS—Safety
SAFETY FACTOR
See under relative subject, e.g., BUCKLING
SALT WATER
See SEA WATER
SALT WATER INVASION
See GROUND WATER
SAMPLING
See under relative material, e.g., SOIL ... ; *also* under relative subject, e.g., WATER ANALYSIS
SAND
See also PILES AND PILE DRIVING; SEEPAGE; SILT AND SILTING... ; SOILS; WATER, FLOW OF, THROUGH SAND (cross reference thereunder)
"Analysis for Sheet-Pile Retaining Walls," F. E. Richart, Jr. (with discussion), 1113.
Sand fineness as it affects concrete permeability, 591.
SANITATION
See AIR SANITATION (cross reference thereunder); COSTS... ; DRAINAGE; FILTERS AND FILTRATION... ; INDUSTRIAL WASTE; ODORS; PIPES AND PIPING; REFUSE DISPOSAL; SEWAGE DISPOSAL; WASTE DISPOSAL (cross references thereunder); WATER...
SAUSAGES, ROCK
See GABIONS (cross reference thereunder)
SCHOOLS AND COLLEGES, ENGINEERING
See EDUCATION
SCIENCE
See under specific science; e.g., EDUCATION; MATHEMATICS
SCIENTIFIC SOCIETIES
See AMERICAN SOCIETY OF CIVIL ENGINEERS; SOCIETIES, TECHNICAL; *see also* ENGINEERS AND ENGINEERING
SCOUR
See EROSION...
SEA...
See also OCEAN... ; WAVES
SEACOAST
See OCEAN CURRENTS; SHORES AND SHORE PROTECTION; WAVES
SEASHORE
See SHORES AND SHORE PROTECTION
SEA WALLS
See WATER PRESSURE

SEA WATER

See also COSTS, SEA WATER CONVERSION

"The Analysis of Water Samples for Cyclical Variations," Alex N. Diachishin, 872.

"Recovery of Usable Water from Saline Water," David B. Smith and Charles E. Richheimer, 556.

SEA WATER INTRUSION

See SALT WATER INVASION (cross reference thereunder)

SEAWAYS

See WATERWAYS (cross references thereunder)

SEDIMENT AND SEDIMENTATION

See SILT AND SILTING... ; TURBULENCE

SEEPAGE

See also COSTS, SEEPAGE; GROUND WATER

"Flow into a Well by Electric and Membrane Analogy," Chong-Hung Zee, Dean F. Peterson and Robert O. Bock (with discussion), 1088.

"Measurement of Canal Seepage," August R. Robinson, Jr. and Carl Rohwer, 347. *Discussion:* Raymond A. Hill; Dean C. Muckel; Calvin C. Warnick; N. Szalay; Cyril W. Lauritzen; and August R. Robinson, Jr. and Carl Rohwer, 364.

"Methods of Determining Consumptive Use of Water in Irrigation," Ralph D. Goodrich (with discussion), 806.

Methods of measuring canal seepage, 349.

Methods of underseepage control for levees, 997, 999, 1005.

Underseepage as related to sand boils, 987.

"Underseepage, Mississippi River Levees, St. Louis District," Charles I. Mansur and Robert I. Kaufman, 985.

SEISMOLOGY

See EARTHQUAKES (cross reference thereunder)

SETTLEMENT OF FILL

See HYDRAULIC FILLING

SETTLEMENT OF STRUCTURES

See BEARING CAPACITY; EARTH PRESSURE; FOUNDATIONS ...; SOIL...

SEWAGE DISPOSAL (General)

See also COSTS, SEWAGE DISPOSAL; FILTERS AND FILTRATION, SEWAGE; INDUSTRIAL WASTE; ODORS; WATER POLLUTION

"Photosynthesis in Sewage Treatment," William J. Oswald and Harold B. Gotaas, 73. *Discussion:* Isadore Nusbaum, and William J. Oswald and Harold B. Gotaas, 98.

Reclamation of nutrients, 95, 105.

SEWAGE DISPOSAL (Geographical)

New York, N. Y.

Controlled filtration investigations, with tabulated results (including effluent results), in Bronx area of New York, N. Y., 1203.

SEWAGE EFFLUENTS

See SEWAGE DISPOSAL

SEWAGE FILTERS AND FILTRATION

See FILTERS AND FILTRATION, SEWAGE

SEWAGE IMPOUNDING

See SEWAGE TREATMENT (cross reference thereunder)

SEWAGE RECLAMATION

See SEWAGE DISPOSAL

SEWAGE TREATMENT

See SEWAGE DISPOSAL

SEWAGE WORKS

See SEWAGE DISPOSAL

SHAFTS

Natural frequencies of torsional vibration of shafts, 250.

SHEAR

"The Action of Soft Clay Along Friction Piles," H. Bolton Seed and Lymon C. Reese (with discussion), 731.

"Analysis for Sheet-Pile Retaining Walls," F. E. Richart, Jr. (with discussion), 1113.

"Failure of Plain Concrete under Combined Stresses," Boris Bresler and Karl S. Pister (with discussion), 1049.

"Field Vane Shear Tests of Sensitive Cohesive Soils," Hamilton Gray (with discussion), 844.

"A General Method of Analysis of Rigid Frames," Panagiotis D. Moliotis, 950.

"Impulsive Motion of Elasto-Plastic Shear Buildings," Edward Cohen, Leon S. Levy and Leonard E. Smollen, 293.

SHEAR (*Continued*)
"Moment-Rotation Characteristics of Column Anchorages," Charles G. Salmon, Leo Schenker, and Bruce G. Johnston, 132.
"Moments in Domes Built into Cylinders," John V. Huddleston and Mario G. Salvadori, 235.
"Oscillatory Gravity Waves in Flowing Water," Turgut Sarpkaya, 564.
"Shear Deflection of Wide-Flange Steel Beams in the Plastic Range," William J. Hall and Nathan M. Newmark, 666.
"Soil Mechanics and Work-Hardening Theories of Plasticity," Daniel C. Drucker, Robert E. Gibson and David J. Henkel, 338.
Tangential shear and twist as they affect arch stresses, 935.
"Thick Rectangular Plates on an Elastic Foundation," Daniel Frederick (with discussion), 1069.

SHEARING STRESS
See SHEAR

SHEET PILING
See PILES AND PILE DRIVING

SHELL STRUCTURES
See DOMES AND VAULTS; PIPES AND PIPING

SHIP MOORINGS AND MOORAGES
See DOCKS AND WHARVES

SHOCK
See BLASTING; IMPACT; VIBRATION

SHORES AND SHORE PROTECTION (lands adjacent to lake, ocean or sea water)
See also BREAKWATERS (cross references thereunder); EROSION, BEACH; JETTIES; RETAINING WALLS; WAVES; *also* cross references under RIVER BANKS AND BANK PROTECTION
"Beach Rehabilitation by Fill and Nourishment," Jay V. Hall, Jr. and George M. Watts, 155.

SIDESWAY
See STRUCTURES, THEORY OF —Frames...

SIDEWALKS (General)
See CONCRETE; PAVEMENT AND PAVING...

SIGHT DISTANCE
See HIGHWAYS AND ROADS

SILT AND SILTING, CHANNEL
"A Concept of the Regime Theory," Ning Chien, 785. *Discussion:* Gerald Lacey, Emory W. Lane, Thomas Blench, Ning Chien, and Hans A. Einstein, 794.
Lacey regime theory and difficulty in applying theory under certain conditions, 786, 794, 797, 799, 803, 804.
Regime theory research studies conducted by Irrigation Research Institutes of various provinces of India, 801.
"River-Bed Degradation Below Large-Capacity Reservoirs," M. Gamal Mostafa, 688. *Discussion:* Whitney M. Borland and Carl R. Miller; Maurice L. Albertson and Hsin-Kuan Liu; Serge Leliavsky; and M. Gamal Mostafa, 696.
Traction as a force in bed load movement, 690.
"Underseepage, Mississippi River Levees, St. Louis District," Charles I. Mansur and Robert I. Kaufman, 985.

SKIN FRICTION
See FRICTION

SLIPS AND SLIPPAGE (movement of surfaces)
See JOINTS, BOLTED (cross reference thereunder)

SLOPE DEFLECTION
"Analysis for Sheet-Pile Retaining Walls," F. E. Richart, Jr. (with discussion), 1113.

SNOW
See also PERMAFROST (cross reference thereunder)
"Water Supply in Arctic Areas: Design Features," Lloyd K. Clark and Amos J. Alter, 1169.

SNOWFALL
See SNOW

SOCIAL PROBLEMS AND ENGINEERING
See under relative technical subject, e.g., CITIES; FLOODS; HOUSING...

SOCIETIES, TECHNICAL
See also AMERICAN SOCIETY OF CIVIL ENGINEERS; ENGINEERS AND ENGINEERING; *also* under relative subject
Resume of three year study on engineering education compiled by American Society for Engineering Education, 766, 767, 779.

SOIL...
See also EARTH...; GROUND...; LAND... (cross references thereunder)

SOIL MECHANICS
See SOILS

SOIL PRESSURE
See EARTH PRESSURE

SOILS (General)
See also BEARING CAPACITY; CLAY; DRAINAGE; EARTH PRESSURE; EROSION...; FOUNDATIONS...; FRICTION...; GROUND...; LAND... (cross references thereunder); PERMAFROST (cross reference thereunder); SAND; SEEPAGE; SILT AND SILTING...; STRESS AND STRAIN—Soils; *also* under name of soil structure, e.g., LEVEES
"Water Supply in Arctic Areas: Design Features," Lloyd K. Clark and Amos J. Alter, 1169.

Compaction. *See* BEARING CAPACITY

Conservation
United States Soil Conservation Service and assistance rendered in conservation districts, 115.

Tests and Testing
"The Action of Soft Clay Along Friction Piles," H. Bolton Seed and Lymon C. Reese (with discussion), 731.
Apparatus for vane shear testing, 847.
"Field Vane Shear Tests of Sensitive Cohesive Soils," Hamilton Gray, 844. *Discussion:* Ebenezer Vey, Carl W. Fenske, Dale T. Harroun, and Hamilton Gray, 858.
"Measurement of Canal Seepage," August R. Robinson, Jr. and Carl Rohwer (with discussion), 347.
"Soil Mechanics and Work-Hardening Theories of Plasticity," Daniel C. Drucker, Robert E. Gibson and David J. Henkel, 338.

SOIL TRANSPORTATION
See SILT AND SILTING...

SOLAR...
See SUN... (cross references thereunder)

SOLIDS, FLOW OF
See LIQUIDS, FLOW OF (General); SILT AND SILTING...; WATER, FLOW OF, IN OPEN CHANNELS

SPACE STRUCTURES
See under specific type of structure, e.g., DOMES AND VAULTS

SPACE TRUSSES
See STRUCTURES, THEORY OF—Trusses and Trussed Structures; TRUSSES

SPECIFICATIONS
See under relative subject, e.g., JOINTS

SPEED
See HIGHWAYS AND ROADS—Safety; VELOCITY (cross references thereunder)

SPILLWAYS (General)
See also DAMS; WATER, FLOW OF, OVER DAMS AND WEIRS

SPILLWAYS (Geographical)

Tennessee Valley Authority Dams
"Discharge Coefficients for Spillways at TVA Dams," Kenneth W. Kirkpatrick, 190.

SPIRALS
See CURVES (alinement curves)

SPREADING BASINS
Artificial recharge of ground water basins, and mound formations, 458.

SPREADING, WATER
"Measurement of Canal Seepage," August R. Robinson, Jr. and Carl Rohwer (with discussion), 347.

STABILITY
See BUCKLING; HYDRODYNAMICS; MECHANICS... (cross references thereunder); SOIL...

STATICALLY INDETERMINATE STRUCTURES
See STRUCTURES, THEORY OF

STATIONS
See under relative type of station; *see also* cross reference under TERMINALS

STATISTICAL ANALYSIS
See PROBABILITY, THEORY OF

STATISTICS
See under relative subject

STEEL (General)
See also REINFORCED CONCRETE (cross reference thereunder); STRENGTH OF MATERIALS; *also* under special structure or structural part, e.g., BEAMS (cross references thereunder)
"High-Strength Steel Bolts in Structural Practice," Mace H. Bell (with discussion), 1.

STEEL (General) (*Continued*)
"Plastic Strength of Steel Frames," Lynn S. Beedle (with discussion), 1139.
Reserve strength of steel, 1157.

STIFFNESS
"Analysis for Sheet-Pile Retaining Walls," F. E. Richart, Jr. (with discussion), 1113.
"A General Method of Analysis of Rigid Frames," Panagiotis D. Moliotis, 950.
"Natural Frequencies of Continuous Flexural Members," Anestis S. Veletsos and Nathan M. Newmark (with discussion), 249.

STORAGE
See RESERVOIRS . . . ; WATER STORAGE

STORM WATER
See DRAINAGE

STRAIN
See STRESS AND STRAIN

STRAIN GAGES
See GAGES, STRAIN

STREAM CONTAMINATION
See WATER POLLUTION

STREAM EROSION
See EROSION, STREAM

STREAM FLOW
See WATER, FLOW OF, IN OPEN CHANNELS

STREAMS
See RIVERS and cross references thereunder

STREETS (General)
See BRIDGES (cross references thereunder); CITY PLANNING; CURVES (alinement curves); FOUNDATIONS, HIGHWAY AND ROAD; FROST (cross reference thereunder); HIGHWAYS AND ROADS; PAVEMENT AND PAVING . . . ; PIPES AND PIPING; SIDEWALKS (cross references thereunder); TRAFFIC, STREET; WHEEL LOADS

Planning and Design
Atlanta, Georgia traffic expansion problems (1955) with estimated 1980 traffic capacity, 178.

STREET TRAFFIC
See TRAFFIC, STREET

STREET TRANSPORTATION
See TRANSPORTATION; WATER FRONT (cross references thereunder)

STRENGTH OF MATERIALS
See also FAILURES . . . ; STRESS AND STRAIN; *also* under specific material (*see* list of materials under MATERIALS OF CONSTRUCTION); *also* under fabricated structure or structural part, e.g., BEAMS (cross references thereunder); BOLTS (cross references thereunder)
Alkathene as a material of construction, 909, 911, 932.
"Lateral Buckling of Rolled Steel Beams," Robert A. Hechtman, John S. Hattrup, Eugene F. Styer and John L. Tiedemann, 823.
"Plastic Strength of Steel Frames," Lynn S. Beedle (with discussion), 1139.

STRESS AND STRAIN (General)
See also EARTH PRESSURE; ELASTICITY; FAILURES . . . ; GAGES, STRAIN; IMPACT; MOMENTS; STIFFNESS; STRENGTH OF MATERIALS; STRUCTURES, THEORY OF; VIBRATION; WATER PRESSURE; WHEEL LOADS; *also* under specific type of stress, e.g., BUCKLING; SHEAR; TORSION

Beams, Continuous
"Shear Deflection of Wide-Flange Steel Beams in the Plastic Range," William J. Hall and Nathan M. Newmark, 666.

Bulkheads
"Analysis for Sheet-Pile Retaining Walls," F. E. Richart, Jr. (with discussion), 1113.

Clay. *See* SHEAR

Concrete (General)
"Failure of Plain Concrete under Combined Stresses," Boris Bresler and Karl S. Pister, 1049. *Discussion:* Frank A. Blakey and F. Donald Beresford; Paul Rice; Henry J. Cowan; and Boris Bresler and Karl S. Pister, 1060.
Mohr's internal friction theory proposed for concrete, 1050, 1063, 1064, 1065.

Dams, Arch
"Model Tests, Analysis, and Observation of an Arch Dam," Manuel Rocha, J. Laginha Serafim, Antonio F. da Silveira, and Jose M. Ressurreicao Neto, 903. *Discussion:* Merlin D. Copen; A. Warren Simonds; Joe T. Richardson; A. Carvalho

STRESS AND STRAIN (*Continued*)
Xerez; and Manuel Rocha, J. Laginha Serafim, Antonio F. da Silveira and Jose M. Ressurreicao Neto, 935.

Dams, Masonry and Concrete
"Permeability, Pore Pressure, and Uplift in Gravity Dams," Roy W. Carlson (with discussion), 587.

Docks and Wharves
"The Design of Piers, Jetties, and Dolphins," David A. Hopkins (with discussion), 22.

Flanges
"Lateral Buckling of Elastically End-Restrained I-Beams," Walter J. Austin, Shahen Yegian and Tie P. Tung, 374.
"Lateral Buckling of Rolled Steel Beams," Robert A. Hechtman, John S. Hattrup, Eugene F. Styer and John L. Tiedemann, 823.

Frames, Rigid
"A General Method of Analysis of Rigid Frames," Panagiotis D. Moliotis, 950.
Method of analyzing rigid frames by successive approximations with advantages specified, 950, 962.

Joints
"High-Strength Steel Bolts in Structural Practice," Mace H. Bell (with discussion), 1.

Materials of Construction
Mineral compressibility with and without impermeable cover, 595.

Piles
"Analysis for Sheet-Pile Retaining Walls," F. E. Richart, Jr. (with discussion), 1113.

Plates
"Thick Rectangular Plates on an Elastic Foundation," Daniel Frederick (with discussion), 1069.

Soils
"Soil Mechanics and Work-Hardening Theories of Plasticity," Daniel C. Drucker, Robert E. Gibson and David J. Henkel, 338.

STRESS, SHEARING
See SHEAR

STRUCTURAL ANALYSIS
See STRESS AND STRAIN; STRUCTURES, THEORY OF

STRUCTURAL DYNAMICS
See also STRUCTURES, THEORY OF; VIBRATION
"Impact on Pin-Jointed Trusses," Bruno A. Boley and Chi-Chang Chao, 39.

STRUCTURAL JOINTS
See JOINTS

STRUCTURAL MATERIALS
See MATERIALS OF CONSTRUCTION (cross references thereunder)

STRUCTURAL MEMBERS
See MEMBERS, STRUCTURAL (cross references thereunder)

STRUCTURAL MODELS
See MODELS, STRUCTURAL

STRUCTURAL STEEL
See STEEL

STRUCTURES (General)
See BUILDINGS; CONSTRUCTION (cross references thereunder); FOUNDATIONS . . . ; MATERIALS OF CONSTRUCTION (cross references thereunder); MODELS, STRUCTURAL; STRENGTH OF MATERIALS; STRESS AND STRAIN; STRUCTURES, THEORY OF; VIBRATION; *also* under specific type of structure, e.g., DOCKS AND WHARVES; *also* under general types of structures

STRUCTURES, DROP
See DAMS

STRUCTURES, ELASTO-PLASTIC
See ELASTO-PLASTIC STRUCTURES (cross reference thereunder)

STRUCTURES, HINGED
See JOINTS

STRUCTURES, HYDRAULIC
See HYDRAULIC STRUCTURES (cross reference thereunder)

STRUCTURES, PLASTIC
See ELASTO-PLASTIC STRUCTURES (cross reference thereunder)

STRUCTURES, SETTLEMENT OF
See BEARING CAPACITY; EARTH PRESSURE; FOUNDATIONS . . . ; SOIL . . .

STRUCTURES, SHELL
See SHELL STRUCTURES (cross references thereunder)

STRUCTURES, SPACE

See SPACE STRUCTURES (cross reference thereunder)

STRUCTURES, STATICALLY INDETERMINATE

See STATICALLY INDETERMINATE STRUCTURES (cross reference thereunder)

STRUCTURES, SUB-

See SUBSTRUCTURES (cross references thereunder)

STRUCTURES, THEORY OF (General)

See also STRESS AND STRAIN; *also* under type of structure or structural part

Beams and Girders (General)

"Lateral Buckling of Rolled Steel Beams," Robert A. Hechtman, John S. Hattrup, Eugene F. Styer and John L. Tiedemann, 823.

Beams and Girders, Continuous

"Natural Frequencies of Continuous Flexural Members," Anestis S. Veletsos and Nathan M. Newmark (with discussion), 249.

"Shear Deflection of Wide-Flange Steel Beams in the Plastic Range," William J. Hall and Nathan M. Newmark, 666.

Buildings

Electric analog computer usage, showing damping factor, 713, 719.

Columns

"Inelastic Buckling of Nonuniform Columns," John E. Goldberg, John L. Bogdanoff, and Hsu Lo, 722.

"Moment-Rotation Characteristics of Column Anchorages," Charles G. Salmon, Leo Schenker, and Bruce G. Johnston, 132.

Domes and Vaults

Membrane theory used to eliminate discontinuities, 235.

"Moments in Domes Built into Cylinders," John V. Huddleston and Mario G. Salvadori, 235.

Elasto-Plastic Structures

"Impulsive Motion of Elasto-Plastic Shear Buildings," Edward Cohen, Leon S. Levy and Leonard E. Smollen, 293.

Foundations, Building

"Impulsive Motion of Elasto-Plastic Shear Buildings," Edward Cohen, Leon S. Levy and Leonard E. Smollen, 293.

Frames, Continuous

Continuous beam test arrangement, 1143.

Continuous frames without sidesway, 249, 263, 280.

"Natural Frequencies of Continuous Flexural Members," Anestis S. Veletsos and Nathan M. Newmark (with discussion), 249.

"Plastic Strength of Steel Frames," Lynn S. Beedle (with discussion), 1139.

Girders (General). *See* Beams and Girders (General) (hereunder)

Girders, Continuous. *See* Beams and Girders, Continuous (hereunder)

Joints

"Plastic Strength of Steel Frames," Lynn S. Beedle (with discussion), 1139.

Lock-Gates

"Stiffening Lock Gates by Prestressing Diagonals," Carl L. Shermer, 106.

Materials and Tests

"Plastic Strength of Steel Frames," Lynn S. Beedle (with discussion), 1139.

Pavement and Paving

"Stresses in Elastic Plates over Flexible Subgrades," Eric Reissner, 627.

Piles

"The Action of Soft Clay Along Friction Piles," H. Bolton Seed and Lymon C. Reese (with discussion), 731.

Plates

"Stresses in Elastic Plates over Flexible Subgrades," Eric Reissner, 627.

Trusses and Trussed Structures

"Impact on Pin-Jointed Trusses," Bruno A. Boley and Chi-Chang Chao, 39.

STRUCTURES, TRUSSED

See STRUCTURES, THEORY OF —Trusses and Trussed Structures

STRUCTURES, UNDERGROUND

See UNDERGROUND STRUCTURES (cross references thereunder)

SUB-...

See also UNDER-...

SUBGRADES

See PAVEMENT AND PAVING (cross references thereunder)

SUBMERGENCE, MASS (concrete solid matter)
See MASS SUBMERGENCE (cross reference thereunder)

SUBSTRUCTURES
See FOUNDATIONS... ; *also* under type of substructure

SULPHITE FIBER INDUSTRY
See FIBER INDUSTRY

SUN, EXPOSURE TO
See INSOLATION

SUN, RADIANT HEAT OF
See HEAT AND HEAT TRANSMISSION (cross references thereunder)

SURFACES, SLIPPAGE OF
See SLIPS AND SLIPPAGE (movement of surfaces) (cross reference thereunder)

SURFACING
See HIGHWAYS AND ROADS—Surfaces

SURVEYS (research data)
See under relative subject, e.g., SILT AND SILTING... ; TRAFFIC, HIGHWAY AND ROAD; *see also* RESEARCH

SUSPENDED LOAD
See SEDIMENT AND SEDIMENTATION (cross references thereunder); SILT AND SILTING...

SWAMPS
See MARSHES

SYMBOLS
See under relative subject

TAINTER GATES
See WATER GATES, MOVABLE

TECHNICAL SCHOOLS
See EDUCATION

TECHNICAL SOCIETIES
See AMERICAN SOCIETY OF CIVIL ENGINEERS; SOCIETIES, TECHNICAL

TEMPERATURE (General)
See also HEAT AND HEAT TRANSMISSION (cross references thereunder); ICE
Effect of temperature on seepage rates, 347, 358, 363.
Low temperature and permafrost effects on physical properties of fluids, gases and solids in Arctic regions, 1171.
"A Preliminary Study of High-Rate Composting," John S. Wiley and George W. Pearce (with discussion), 1009.

TENNESSEE VALLEY AUTHORITY
See RIVERS (Geographical)—Tennessee River

TENSILE STRESS
See STRESS AND STRAIN

TENSION
See STRESS AND STRAIN; STRUCTURES, THEORY OF

TERMINALS (structures and localities)
See AIR TERMINALS (cross reference thereunder)

TERMINOLOGY (Arranged hereunder by specific or comprehensive subject word when possible)

Aircraft. (Helicopter work capacity, block speed), 977.
Airports. (Heliport and rotor station usage differentiated), 981.
Boundary layer. (Transition point in its relation to laminar and turbulent flow), 317.
Buildings. (Shear type building properties), 293.
Concrete failure definition challenged in relation to microcracks, 1068.
Ground water basin recharge terms, mound wave, control, float, and basic parabola, 459, 462, 485.
Impact. ("Interference" as it relates to impact on trusses), 49, 57.
Photosynthesis as a process of biology, 75.
Rigid frame analysis terms, 950, 951.
Seepage rings usage as a term, 364.
Seepage. (Underseepage, sand boils, piping, and other terms), 987, 988, 990, 1003.
Sewage treatment. (Contaminants defined), 95.
Sewage treatment. (Controlled filtration defined), 1203.
Sewage treatment. (Sewage lagoons, industrial waste lagoons and oxidation ponds, as processing terms), 73.
Soil testing. (Clay soil test type usage), 846.
Traffic generation as a term, 883.
Vibration. (Natural frequencies defined), 284.

TERMINOLOGY (*Continued*)

Virtual mass in its relation to effective inertia, 518.

Water. (Duty of water, water requirement, consumptive use of water, and evapo-transpiration, as terms), 807.

Water pressure. (Free surface in ground water flow), 1109.

Water pressure. (Uplift and stress clarified as terms), 605.

Wells. (Effective radius when used in formulas for flow), 512.

TESTING MACHINES

See under use, material, structure or structural part tested

TESTS AND TESTING

See BUCKLING; ELASTICITY; FAILURES ... ; IMPACT; MODELS ... ; SHEAR; STRENGTH OF MATERIALS; STRESS AND STRAIN; STRUCTURES, THEORY OF—Materials and Tests; TORSION; WATER ANALYSIS; WATER, FLOW OF ... ; *also* under material, structure or structural part tested, e.g., JOINTS; SOILS —Tests and Testing

THEORIES

See cross references hereunder and under ANALYSIS OF DATA; *see also* STRUCTURES, THEORY OF; *see also* under relative subject or its relative science, e.g., MATHEMATICS

THEORY, MOHR

See SHEAR; STRESS AND STRAIN

THEORY OF BOUNDARY LAYER (fluid flow)

See BOUNDARY LAYER, THEORY OF (cross reference thereunder)

THEORY OF ELASTICITY

See ELASTICITY

THEORY OF FINITE DIFFERENCES

See MATHEMATICS

THEORY OF LIMIT DESIGN

See LIMIT DESIGN, THEORY OF

THEORY OF PLASTICITY

See PLASTICITY

THEORY OF PROBABILITY

See PROBABILITY, THEORY OF

THEORY OF STRUCTURES (General)

See STRUCTURES, THEORY OF

THEORY OF VIRTUAL WORK

See VIRTUAL WORK, PRINCIPLE OF

THEORY, PLASTIC

See PLASTICITY

THEORY, REGIME

See REGIME THEORY (cross reference thereunder)

TIDES

See OCEAN CURRENTS

TILE

See FAILURES, TILE

TOLL ROADS

See HIGHWAYS AND ROADS

TOOLS

See under types of tools or usage, e.g., JOINTS; *also* cross references under APPARATUS; INSTRUMENTS; MACHINERY

TOPOGRAPHY

Natural topography as related to availability of ground water in the Arctic regions, 1173.

TORSION

"Lateral Buckling of Rolled Steel Beams," Robert A. Hechtman, John S. Hattrup, Eugene F. Styer and John L. Tiedemann, 823.

"Stiffening Lock Gates by Prestressing Diagonals," Carl L. Shermer, 106.

TRACKS

See under type of track, e.g., RAILROAD TRACKS (cross references thereunder)

TRACTION

See SILT AND SILTING...

TRAFFIC (General)

See also HIGHWAYS AND ROADS —Safety; TRANSPORTATION; WHEEL LOADS

TRAFFIC ACCIDENTS

See HIGHWAYS AND ROADS—Safety

TRAFFIC, AIRPORT

"Effect of Airport Distance on Traffic Generation," James C. Buckley, 614.

"The Effect of Traffic on the Cross Section of a Runway Pavement," Robert Horonjeff and John H. Jones (with discussion), 1035.

"A Pattern of Interstation Air Travel," Daniel M. Belmont, 864.

TRAFFIC, BUS

See TRAFFIC, HIGHWAY AND ROAD; TRAFFIC, STREET

TRAFFIC, EXPRESSWAY
See TRAFFIC, STREET

TRAFFIC, HIGHWAY AND ROAD
See also HIGHWAYS AND ROADS —Location; HIGHWAYS AND ROADS—Safety

Maine Turnpike and Pennsylvania Turnpike traffic studies, with results indicated, 883.

Procedure for determining traffic expected on a proposed toll road, 885.

"Traffic Diversion to Toll Roads," John T. Lynch, 883.

TRAFFIC, STREET
"Integration of Streets with an Expressway System," Karl A. Bevins, 178.

TRAFFIC, VEHICULAR
See TRAFFIC, HIGHWAY AND ROAD and other relative traffic headings hereunder

TRANSITION CURVES
See CURVES (alinement curves)

TRANSPIRATION
See WATER, CONSUMPTIVE USE OF (in agriculture)

TRANSPORTATION
See also AIR TRANSPORT; COSTS, TRANSPORTATION; RIVERS; SOIL TRANSPORTATION (cross reference thereunder); TRAFFIC ...; WATER TRANSPORTATION (cross references thereunder)

Historical development of a typical American city over 125 year period, 286.

"Observations on the Urban Transportation Problem," Harmer E. Davis, 286.

TRIAXIAL SHEAR
See SHEAR

TRICKLING FILTERS AND FILTRATION
See FILTERS AND FILTRATION, SEWAGE

TRIGONOMETRY
See under relative subject

TRUCKS
See MOTOR TRUCKS (cross reference thereunder)

TRUSSED STRUCTURES
See STRUCTURES, THEORY OF —Trusses and Trussed Structures

TRUSSES, PIN-CONNECTED
"Impact on Pin-Jointed Trusses," Bruno A. Boley and Chi-Chang Chao, 39.

TRUSSES, SPACE
See STRUCTURES, THEORY OF —Trusses and Trussed Structures; TRUSSES

TUBES
See PIPES AND PIPING

TURBULENCE (water agitation)
See also FRICTION; WATER, FLOW OF...

Dependent variables for turbulent flow, with methods of computation, 700.

"An Experimental Study of Boundary-Layer Transition," Henry W. Bennett and Charles A. Lee, 307.

"Oscillatory Gravity Waves in Flowing Water," Turgut Sarpkaya, 564.

TURNPIKES
See HIGHWAYS AND ROADS

TWISTING
See TORSION; *also* under relative material, structure or structural part, e.g., LOCK-GATES

UNDER-...
See also SUB-...

UNDERFLOW
See SEEPAGE; WELLS

UNDERGROUND STRUCTURES
See under type of structure, e.g., CULVERTS; *see also* under related subject, e.g., SOILS

UNDERGROUND WATER
See GROUND WATER

UNDERGROUND WATER STORAGE
See WATER STORAGE

UNDERSEEPAGE
See SEEPAGE

UNDERWATER FOUNDATIONS
See PILES AND PILE DRIVING

UNIT COSTS
See COSTS...

UPLIFT, HYDROSTATIC
See WATER PRESSURE

URBAN...
See CITIES

VALLEY AUTHORITIES
See RIVER VALLEY AUTHORITIES

VALLEYS (General)

See also DRAINAGE; *also* under related subject, e.g., HIGHWAYS AND ROADS; WATER, CONSUMPTIVE USE OF (in agriculture)

VALLEYS (Geographical)

Colorado River Basin

Consumptive use of water determination for entire drainage basin, 807, 814, 815, 818, 820.

Mississippi River Valley

Geology of alluvial valley, 988.

VEHICULAR TRAFFIC

See TRAFFIC...

VELOCITY

See HYDRODYNAMICS; IMPACT; VIBRATION; WATER, FLOW OF...

VELOCITY DISTRIBUTION

See WATER, FLOW OF...

VERTICAL CURVES

See CURVES (alinement curves)

VESSELS

See SHIP... (cross reference thereunder)

VIBRATION

See also IMPACT

"Impulsive Motion of Elasto-Plastic Shear Buildings," Edward Cohen, Leon S. Levy and Leonard E. Smollen, 293.

"Natural Frequencies of Continuous Flexural Members," Anestis S. Veletsos and Nathan M. Newmark, 249. *Discussion:* Jacob Karol, and Anestis S. Veletsos and Nathan M. Newmark, 279.

"Oscillatory Gravity Waves in Flowing Water," Turgut Sarpkaya, 564.

"Structural Vibrations Produced by Ground Motion," Donald E. Hudson and George W. Housner, 705.

"Virtual Mass and Acceleration in Fluids," Thomas E. Stelson and Frederic T. Mavis (with discussion), 518.

VIBRATION MEASURING INSTRUMENTS

Seismic type accelerometer usage in ground and building vibration measurements, 709, 716, 718.

VIBRATION RECORDING APPARATUS

Oscillograph usage in quarry blast recording, 710, 711.

VIRTUAL MASS

See FLUIDS, FLOW OF (cross reference thereunder)

VIRTUAL WORK, PRINCIPLE OF

Application of principle in rigid frame analysis, 954, 958, 960, 961.

WALLS

See under relative structure or type of wall, e.g., RETAINING WALLS

WAR AND ENGINEERING

See cross references under MILITARY ENGINEERS AND ENGINEERING

WASTE DISPOSAL

See INDUSTRIAL WASTE—Industrial Waste Pollution; ODORS; REFUSE DISPOSAL; SEWAGE ...; WATER POLLUTION

WASTE MATERIALS

See WASTE DISPOSAL (cross references thereunder)

WASTE OF WATER

See WATER CONSERVATION; WATER, CONSUMPTIVE USE OF

WASTE WATER

See INDUSTRIAL WASTE; SEWAGE DISPOSAL; WATER POLLUTION

WATER...

See also COSTS...; DAMS; DRAINAGE; EROSION...; FILTERS AND FILTRATION...; FLOODS; FOUNDATIONS...; GOVERNMENT (cross references thereunder); GROUND WATER; HYDRAULIC...; HYDRO-...; ICE; IRRIGATION; MARSHES; METERS AND METERING...; MODELS, HYDRAULIC; OCEAN ...; OXYGENATION; PIPES AND PIPING; RESERVOIRS; RIVER...; RUNOFF; SALT WATER INVASION (cross reference thereunder); SANITATION (cross references thereunder); SEA WATER; SEEPAGE; SEWAGE DISPOSAL; SPILLWAYS; SPREADING BASINS; SPREADING, WATER; TERMINOLOGY; TURBULENCE; WAVES; WELLS

WATER ACCELERATION

See VELOCITY (cross references thereunder)

WATER ANALYSIS

See also BACTERIA; WATER TREATMENT

"The Analysis of Water Samples for Cyclical Variations," Alex N. Diachishin, 872.

WATER COLLECTION

See INFILTRATION (cross references thereunder); WELLS

WATER CONSERVATION

See also RESERVOIRS; RIVER VALLEY AUTHORITIES; WATER STORAGE

Artificial recharge of ground water basins as beneficial conservation measure, 458.

"Water Control in Central and Southern Florida," Harold A. Scott, 211.

WATER, CONSUMPTIVE USE OF (in agriculture)

"Methods of Determining Consumptive Use of Water in Irrigation," Ralph D. Goodrich, 806. *Discussion:* Don M. Forester, and Ralph D. Goodrich, 818.

Research needed in consumptive use of water, 822.

Valley consumptive use of water determination by inflow-outflow method and other methods, 809, 818, 820.

Bibliography

Consumptive use in agriculture, especially in western states, 816.

WATER, DEMINERALIZATION OF

See WATER TREATMENT

WATER DISTRIBUTION

See CANALS (cross references thereunder); IRRIGATION; PIPES AND PIPING

WATER DIVERSION

See FLOOD ROUTING

WATER, DUTY OF

Early research studies, 806.

"Methods of Determining Consumptive Use of Water in Irrigation," Ralph D. Goodrich (with discussion), 806.

WATER, FLOW OF (General)

See also FLOODS; FRICTION; GROUND WATER; HYDRAULICS (cross references thereunder); LIQUIDS, FLOW OF; MODELS, HYDRAULIC; SPILLWAYS; TURBULENCE; WATER GATES, MOVABLE; WELLS

Boundary layer transition apparatus, instruments and methods, 313, 315.

"An Experimental Study of Boundary-Layer Transition," Henry W. Bennett and Charles A. Lee, 307.

Laminar flow importance in boundary layer transition theory, 307.

"Water Supply in Arctic Areas: Design Features," Lloyd K. Clark and Amos J. Alter, 1169.

WATER, FLOW OF, IN OPEN CHANNELS

See also FLOODS; SILT AND SILTING, CHANNEL; WAVES

"A Concept of the Regime Theory," Ning Chien (with discussion), 785.

WATER, FLOW OF, IN OPEN CHANNELS

"Oscillatory Gravity Waves in Flowing Water," Turgut Sarpkaya, 564.

"River-Bed Degradation Below Large-Capacity Reservoirs," M. Gamal Mostafa (with discussion), 688.

WATER, FLOW OF, OVER DAMS AND WEIRS

"Discharge Coefficients for Spillways at TVA Dams," Kenneth W. Kirkpatrick, 190.

WATER, FLOW OF, THROUGH SAND

See GROUND WATER

WATER FRONT

See BREAKWATERS (cross references thereunder); BULKHEADS (cross references thereunder); DOCKS AND WHARVES; HARBORS; JETTIES; PILES AND PILE DRIVING

WATER GATES, MOVABLE

"Discharge Coefficients for Spillways at TVA Dams," Kenneth W. Kirkpatrick, 190.

WATER, GROUND

See GROUND WATER

WATER IMPOUNDING

See RESERVOIRS, WATER STORAGE; WATER STORAGE

WATER INSTRUMENTS

See also GAGES . . . ; METERS AND METERING

Lysimeter usage in determining consumptive use of water, 808.

WATER LAW

See RIPARIAN RIGHTS; WATER RIGHTS; *see also* other LAW subject headings, e.g., GROUND WATER LAW

WATER MAINS
See PIPES AND PIPING; WATER SUPPLY

WATER, OXYGEN SATURATION BY
See OXYGENATION

WATER PIPES AND PIPING
See PIPES AND PIPING

WATER POLLUTION
See also BACTERIA; INDUSTRIAL WASTE; OXYGENATION; SALT WATER INVASION (cross reference thereunder); SEWAGE DISPOSAL; WATER TREATMENT

"The Analysis of Water Samples for Cyclical Variations," Alex N. Diachishin, 872.

Fish industry gill net operations as affected by slime growths, 1179, 1185.

"Intermittent Discharge of Spent Sulfite Liquor," Herman R. Amberg and Robert Elder, 1179.

WATER POWER (General)
See DAMS...; MULTI-PURPOSE PROJECTS (RIVER PROJECTS); POWER (General) (cross references thereunder); POWER PLANTS; RIVER VALLEY AUTHORITIES

WATER PRESSURE
See also GAGES, PRESSURE; WAVES

"The Action of Soft Clay Along Friction Piles," H. Bolton Seed and Lymon C. Reese (with discussion), 731.

"Flow into a Well by Electric and Membrane Analogy," Chong-Hung Zee, Dean F. Peterson and Robert O. Bock (with discussion), 1088.

"Model Tests, Analysis, and Observation of an Arch Dam," Manuel Rocha, J. Laginha Serafim, Antonio F. da Silveira and Jose M. Ressurreicao Neto (with discussion), 903.

"Permeability, Pore Pressure, and Uplift in Gravity Dams," Roy W. Carlson (with discussion), 587.

"Soil Mechanics and Work-Hardening Theories of Plasticity," Daniel C. Drucker, Robert E. Gibson and David J. Henkel, 338.

"Underseepage, Mississippi River Levees, St. Louis District," Charles I. Mansur and Robert I. Kaufman, 985.

"Virtual Mass and Acceleration in Fluids," Thomas E. Stelson and Frederic T. Mavis (with discussion), 518.

WATER PURIFICATION
See WATER TREATMENT

WATER RESISTANCE
See FRICTION; HYDRODYNAMICS; SOLIDS, FLOW OF (cross references thereunder); TURBULENCE

WATER RIGHTS
See also RIPARIAN RIGHTS; *see also* WATER LAW (cross references thereunder)

Water rights difficulties in California and elsewhere and their causes, 435.

WATER, SEA
See SEA WATER

WATER SOFTENING
See WATER TREATMENT

WATER SPREADING
See SPREADING, WATER

WATER STORAGE
See also RESERVOIRS...; WATER CONSERVATION

"Ground-Water Development": A Symposium, Robert O. Thomas, Harris R. McDonald, Paul Baumann, and Dean F. Peterson, Jr. (with discussion), 421.

WATER, STORM
See DRAINAGE

WATER SUPPLY (General)
See also COSTS, WATER SUPPLY; DAMS...; FLOODS; GAGES ...; GROUND WATER; IRRIGATION; PIPES AND PIPING; PUMPS AND PUMPING; RAINFALL (cross references thereunder); RESERVOIRS; SILT AND SILTING...; SPREADING BASINS; WATER... (related subject headings thereunder); WELLS

Design features enumerated for Arctic regions, 1172, 1177.

Raw water constituents and United States Public Health Service standards (1946) compared for drinking water, 558.

Bibliography

Arctic water supply, 1177.

Financing

Future developments and their financing, 437, 442.

WATER SUPPLY (Geographical)

Arctic Regions

"Water Supply in Arctic Areas: Design Features," Lloyd K. Clark and Amos J. Alter, 1169.

California

"Ground-Water Development": A Symposium, Robert O. Thomas, Harris R. McDonald, Paul Baumann, and Dean F. Peterson, Jr. (with discussion), 421.

Florida

Historical outline of water supply in central and southern area, 213.

"Water Control in Central and Southern Florida," Harold A. Scott, 211.

United States

"Recovery of Usable Water from Saline Water," David B. Smith and Charles E. Richheimer, 556.

WATER TABLE

See WATER STORAGE

WATER TRANSPORTATION

See DOCKS AND WHARVES; LAKES; RIVERS

WATER TREATMENT

See also BACTERIA; WATER ANALYSIS; WATER POLLUTION

Apparatus for study of slime growths under continuous swift flow conditions, 1180.

Ground water treatment in Arctic regions, 1174.

"Recovery of Usable Water from Saline Water," David B. Smith and Charles E. Richheimer, 556.

WATER, UNDERGROUND

See GROUND WATER

WATER, WASTE

See INDUSTRIAL WASTE; SEWAGE DISPOSAL; WATER POLLUTION

WATER, WASTE OF

See WATER CONSERVATION; WATER, CONSUMPTIVE USE OF

WATER WAVES

See WAVES

WATERWAYS (General)

See CANAL... ; CHANNELS (cross references thereunder); COSTS ... ; DOCKS AND WHARVES; HARBORS; LAKES; OCEAN ... ; RIPARIAN RIGHTS; RIVERS; SEA... ; WATER DIVERSION (cross reference thereunder); WATER RIGHTS

WATERWAY TRANSPORTATION

See WATER TRANSPORTATION (cross references thereunder)

WATERWORKS (General)

See PIPES AND PIPING; RESERVOIRS; WATER SUPPLY (and cross references thereunder); WATER TREATMENT; WATER, WASTE OF (cross references thereunder); WELLS

WAVES

See also EROSION, BEACH; JETTIES; OCEAN CURRENTS; RETAINING WALLS; SHORES AND SHORE PROTECTION; WATER PRESSURE

"Oscillatory Gravity Waves in Flowing Water," Turgut Sarpkaya, 564.

Wave flume and wave generator apparatus, procedure and results, 572.

Wind generated oscillatory gravity waves in water, 565, 569.

WEATHER

See FLOODS; HYDROLOGY (cross references thereunder); RAINFALL (cross references thereunder); SNOW; TEMPERATURE; WIND (cross reference thereunder)

WEB BUCKLING

See BUCKLING

WELDS AND WELDING

See JOINTS, WELDED; METALS (cross references thereunder)

WELLS

See also GROUND WATER

Development of theoretical well hydraulics, 502.

Flow formulas for ground water into wells, 503.

"Flow into a Well by Electric and Membrane Analogy," Chong-Hung Zee, Dean F. Peterson and Robert O. Bock, 1088. *Discussion:* Robert E. Glover; Vaughn E. Hansen; James N. Luthin; Chia-Shun Yih; and Chong-Hung Zee, Dean F. Peterson and Robert O. Bock, 1106.

Gravity well radial flow pattern, 1102.

Pumping tests on relief wells in determining underseepage of Mississippi River levees, 992, 997, 1000, 1005.

WELLS (*Continued*)
  Research needed on hydrodynamic conditions near and through wells, 502.
  Schematic drawing of a typical relief well, 1005, 1006.
  "Water Supply in Arctic Areas: Design Features," Lloyd K. Clark and Amos J. Alter, 1169.
WHARVES
  See DOCKS AND WHARVES
WHEEL LOADS
  "The Effect of Traffic on the Cross Section of a Runway Pavement," Robert Horonjeff and John H. Jones (with discussion), 1035.
WIND
  See WAVES
WOOD
  See FIBER INDUSTRY; PAPER AND PULP MILLS; PILES AND PILE DRIVING
WORK, COST OF
  See COSTS
WORKS (industrial buildings and equipment)
  See under general types of works; *also* under specific types of works; *also* cross references under PLANTS
WORK, VIRTUAL
  See VIRTUAL WORK, PRINCIPLE OF
WRECKS
  See SAFETY (cross reference thereunder)

AUTHOR INDEX

(including Memoirs of deceased members)

Albertson, Maurice L.
River bed degradation, 699.

Alter, Amos J.
"Water Supply in Arctic Areas: Design Features," 1169.

Amberg, Herman R.
"Intermittent Discharge of Spent Sulfite Liquor," 1179.

Austin, Walter J.
"Lateral Buckling of Elastically End-Restrained I-Beams," 374.

Baumann, Paul
"Ground-Water Development (symposium): Basin Recharge," 458.

Beedle, Lynn S.
"Plastic Strength of Steel Frames," 1139.

Bell, Mace H.
"High-Strength Steel Bolts in Structural Practice," 1.

Belmont, Daniel M.
"A Pattern of Interstation Air Travel," 864.

Benjamin, Jack R.
Plastic strength, 1161.

Bennett, Henry W.
"An Experimental Study of Boundary-Layer Transition," 307.

Beresford, F. Donald
Concrete under combined stresses, 1060.

Berrigan, Thomas Augustine
Memoir of, 1233.

Bevins, Karl A.
"Integration of Streets with an Expressway System," 178.

Bixby, Frederick Louis
Memoir of, 1234.

Blakey, Frank A.
Concrete under combined stresses, 1060.

Blench, Thomas
Regime theory, 799.

Bock, Robert O.
"Flow into a Well by Electric and Membrane Analogy," 1088.

Bogdanoff, John L.
"Inelastic Buckling of Nonuniform Columns," 722.

Boley, Bruno A.
"Impact on Pin-Jointed Trusses," 39.

Borland, Whitney M.
River bed degradation, 696.

Boyd, James Churchill
Memoir of, 1235.

Brace, James Henry
Memoir of, 1235.

Bradley, Joseph N.
Erosion protection, 544.

Bresler, Boris
"Failure of Plain Concrete under Combined Stresses," 1049.

Brooks, Norman H.
Ground water, 483.

Brown, Archibald Alexander
Memoir of, 1236.

Brown, Richard Meyer, Jr.
Memoir of, 1237.

Brownfield, Allen H.
Highway spirals, 404.

Buckley, James C.
"Effect of Airport Distance on Traffic Generation," 614.

Burdick, Charles Baker
Memoir of, 1232.

Burnson, Blair Irving
Memoir of, 1237.

Byrnes, Henry Cady
Memoir of, 1238.

Caldwell, Joseph M.
Virtual mass, 526.

Carlson, Roy W.
"Permeability, Pore Pressure, and Uplift in Gravity Dams," 587.

Chao, Chi-Chang
"Impact on Pin-Jointed Trusses," 39.

Chester, John Needels
Memoir of, 1238.

Chien, Ning
"A Concept of the Regime Theory," 785.

Clark, Lloyd K.
"Water Supply in Arctic Areas: Design Features," 1169.

Cleary, John Belford
Memoir of, 1239.
Clendenen, Frank B.
Ground water, 437.
Coe, Donald Omer
Memoir of, 1240.
Cohen, Edward
"Impulsive Motion of Elasto-Plastic Shear Buildings," 293.
Copen, Merlin D.
Arch dams, 935.
Cowan, Henry J.
Concrete under combined stresses, 1063.
da Silveira, Antonio F.
"Model Tests, Analysis, and Observation of an Arch Dam," 903.
Davis, Harmer E.
"Observations on the Urban Transportation Problem," 286.
Diachishin, Alex N.
"The Analysis of Water Samples for Cyclical Variations," 872.
Dickinson, William Dewoody
Memoir of, 1240.
Drucker, Daniel C.
Engineering education, 776.
"Soil Mechanics and Work-Hardening Theories of Plasticity," 338.
Dubose, Lawrence A.
Friction piles, 755.
Einstein, Hans A.
Regime theory, 804.
Elder, Robert
"Intermittent Discharge of Spent Sulfite Liquor," 1179.
Fenske, Carl W.
Vane shear tests, 860.
Follin, James W.
"Urban Renewal of American Cities," 330.
Forester, Don M.
Consumptive use of water, 818.
Forgey, DeMarcus D.
Memoir of, 1241.
Frederick, Daniel
"Thick Rectangular Plates on an Elastic Foundation," 1069.
Gaylord, Edwin H., Jr.
"Education of Civil Engineers (symposium): Foreword," 766.
Gibson, Robert E.
"Soil Mechanics and Work-Hardening Theories of Plasticity," 338.
Glover, Robert E.
Well flow, 1106.
Goldberg, John E.
"Inelastic Buckling of Nonuniform Columns," 722.
Golze, Alfred R.
Engineering education, 783.
Goodrich, Ralph D.
"Methods of Determining Consumptive Use of Water in Irrigation," 806.
Gotaas, Harold B.
"Photosynthesis in Sewage Treatment," 73.
Grahlman, Theodore
Memoir of, 1241.
Gray, Hamilton
"Field Vane Shear Tests of Sensitive Cohesive Soils," 844.
Grinter, L. E.
"Education of Civil Engineers (symposium): Need for Reconsideration," 767.
Hall, Jay V., Jr.
"Beach Rehabilitation by Fill and Nourishment," 155.
Hall, William J.
"Shear Deflection of Wide-Flange Steel Beams in the Plastic Range," 666.
Hamilton, George Wellington
Memoir of, 1242.
Hansen, Vaughn E.
Well flow, 1107.
Hansen, William
High strength bolts, 20.
Harder, James A.
Ground water, 486.
Harroun, Dale T.
Vane shear tests, 861.
Hartman, Paul
"The Highway Spiral for Combining Curves of Different Radii," 389.
"Sight Distance at Undercrossings," 64.
Haskins, Charles Arthur
Memoir of, 1243.
Hastings, Edgar Morton
Memoir of, 1231.
Hattrup, John S.
"Lateral Buckling of Rolled Steel Beams," 823.
Hechtman, Robert A.
"Lateral Buckling of Rolled Steel Beams," 823.

Henkel, David J.
"Soil Mechanics and Work-Hardening Theories of Plasticity," 338.

Hiatt, Alfred Ronald
Memoir of, 1243.

Hickerson, Thomas E.
Highway spirals, 400.
Sight distance, 72.

Hill, Raymond A.
Canal seepage, 364.

Hopkins, David A.
"The Design of Piers, Jetties, and Dolphins," 22.

Horonjeff, Robert
"The Effect of Traffic on the Cross Section of a Runway Pavement," 1035.

Hotes, Frederick L.
Ground water, 475.

Housner, George W.
"Structural Vibrations Produced by Ground Motion," 705.

Huddleston, John V.
"Moments in Domes Built into Cylinders," 235.

Hudson, Donald E.
"Structural Vibrations Produced by Ground Motion," 705.

Ingram, William T.
"An Approach to the Design of Trickling Filters," 1202.

Izzard, Carl F.
Erosion protection, 544.

Jarvis, Walter Monroe
Memoir of, 1244.

Johnson, Hollister
Memoir of, 1244.

Johnson, Wendell E.
"Missouri River Basin Plan in Operation," 654.

Johnston, Bruce G.
"Moment-Rotation Characteristics of Column Anchorages," 132.

Jones, John H.
"The Effect of Traffic on the Cross Section of a Runway Pavement," 1035.

Karol, Jacob
Natural frequencies, 279.

Kaufman, Robert I.
"Underseepage, Mississippi River Levees, St. Louis District," 985.

Kindsvater, Carl E.
Erosion protection, 548.

Kirkpatrick, Kenneth W.
"Discharge Coefficients for Spillways at TVA Dams," 190.

Kittredge, Frank Alvah
Memoir of, 1245.

Knapp, Robert T.
Ground water, 474.

Koch, Oscar Henry
Memoir of, 1246.

Koelzer, Victor A.
"The Use of Statistics in Reservoir Operations," 1187.

Krige, Pieter R.
High rate composting, 1031.

Lacey, Gerald
Regime theory, 794.

Lane, Emory W.
Erosion protection, 544.
Regime theory, 797.

Lauritzen, Cyril W.
Canal seepage, 369.

Lee, Charles A.
"An Experimental Study of Boundary-Layer Transition," 307.

Lee, Charles H.
Ground water, 488.

Leliavsky, Serge
Gravity dams, 608.
River bed degradation, 701.

Levinton, Zusse
Piers, jetties and dolphins, 37.

Levy, Leon S.
"Impulsive Motion of Elasto-Plastic Shear Buildings," 293.

Liu, Hsin-Kuan
River bed degradation, 699.

Lo, Hsu
"Inelastic Buckling of Nonuniform Columns," 722.

Lockwood, Mason G.
"Time to Think": Address at the Summer Convention, Buffalo, N. Y., June 5, 1957, 1221.

Lorsch, Harold G.
Rectangular plates, 1086.

Luthin, James N.
Well flow, 1109.

Lynch, John T.
"Traffic Diversion to Toll Roads," 883.

Mansur, Charles I.
"Underseepage, Mississippi River Levees, St. Louis District," 985.
Mather, Bryant
Gravity dams, 603.
Matthes, Francois Emile
Memoir of, 1246.
Matthes, Gerard H.
Erosion protection, 543.
Mavis, Frederic T.
"Virtual Mass and Acceleration in Fluids," 518.
McCaustland, Gwynne Gravelle
Memoir of, 1247.
McDonald, Harris R.
"Ground-Water Development (symposium): Irrigation Aspects," 443.
McGlone, Roy Gillespie
Memoir of, 1248.
Middleton, Robert James
Memoir of, 1248.
Miller, Carl R.
River bed degradation, 696.
Miller, John William
Memoir of, 1249.
Milligan, Cleve H.
"Pumping Ground Water for Irrigation and Drainage," 228.
Moliotis, Panagiotis D.
"A General Method of Analysis of Rigid Frames," 950.
Mooney, William Charles
Memoir of, 1250.
Mostafa, M. Gamal
"River-Bed Degradation Below Large-Capacity Reservoirs," 688.
Mott, Thomas Clayton
Memoir of, 1250.
Muckel, Dean C.
Canal seepage, 364.
Murray, Ray Messinger
Memoir of, 1251.
Neeley, Parley R.
Erosion protection, 552.
Newmark, Nathan M.
"Natural Frequencies of Continuous Flexural Members," 249.
"Shear Deflection of Wide-Flange Steel Beams in the Plastic Range," 666.
Nishida, Yoshichika
Friction piles, 757.
Novie, Constantine Alexander
Memoir of, 1252.
Nusbaum, Isadore
Photosynthesis, 98.
Olsen, Sivert Edward
Memoir of, 1252.
Oswald, William J.
"Photosynthesis in Sewage Treatment," 73.
Page, John Chatfield
Memoir of, 1233.
Parsons, James D.
Friction piles, 758.
Pearce, George W.
"A Preliminary Study of High-Rate Composting," 1009.
Pearse, Langdon
Memoir of, 1253.
Peck, Ralph B.
Friction piles, 758.
Peterson, Dean F., Jr.
"Flow into a Well by Electric and Membrane Analogy," 1088.
"Ground-Water Development (symposium): Hydraulics of Wells," 502.
Phillips, John Carleton
Memoir of, 1253.
Pister, Karl S.
"Failure of Plain Concrete under Combined Stresses," 1049.
Posey, Chesley J.
"Flood-Erosion Protection for Highway Fills," 531.
Redus, John F.
Runway pavements, 1046.
Reese, Lymon C.
"The Action of Soft Clay Along Friction Piles," 731.
Reissner, Eric
"Stresses in Elastic Plates over Flexible Subgrades," 627.
Ressurreicao Neto, Jose M.
"Model Tests, Analysis, and Observation of An Arch Dam," 903.
Rice, Paul
Concrete under combined stresses, 1061.
Richardson, Joe T.
Arch dams, 942.
Richart, F. E., Jr.
"Analysis for Sheet-Pile Retaining Walls," 1113.
Richheimer, Charles E.
"Recovery of Usable Water from Saline Water," 556.

Ripley, Herbert Spencer
Memoir of, 1254.
Robinson, August R., Jr.
"Measurement of Canal Seepage," 347.
Rocha, Manuel
"Model Tests, Analysis, and Observation of an Arch Dam," 903.
Rohwer, Carl
"Measurement of Canal Seepage," 347.
Rowe, Peter W.
Sheet pile walls, 1133.
Rowe, R. Robinson
"Rigid Culverts under High Overfills," 410.
Salmon, Charles G.
"Moment-Rotation Characteristics of Column Anchorages," 132.
Salvadori, Mario G.
"Moments in Domes Built into Cylinders," 235.
Sargent, Arthur Winthrop
Memoir of, 1255.
Sarpkaya, Turgut
"Oscillatory Gravity Waves in Flowing Water," 564.
Schenker, Leo
"Moment-Rotation Characteristics of Column Anchorages," 132.
Schnebly, F. David
"Transport Helicopter Cost and Heliport Considerations," 973.
Scott, Harold A.
"Water Control in Central and Southern Florida," 211.
Seed, H. Bolton
"The Action of Soft Clay Along Friction Piles," 731.
Serafim, J. Laginha
Gravity dams, 603.
"Model Tests, Analysis, and Observation of an Arch Dam," 903.
Shermer, Carl L.
"Stiffening Lock Gates by Prestressing Diagonals," 106.
Silberman, Edward
Virtual mass, 527.
Simonds, A. Warren
Arch dams, 938.
Simpson, Thomas Russel
Memoir of, 1255.
Smith, David B.
"Recovery of Usable Water from Saline Water," 556.
Smollen, Leonard E.
"Impulsive Motion of Elasto-Plastic Shear Buildings," 293.
Sobotka, Zdenek
Plastic strength, 1162.
Stelson, Thomas E.
"Virtual Mass and Acceleration in Fluids," 518.
Stillman, Alfred Kittoe
Memoir of, 1256.
Styer, Eugene F.
"Lateral Buckling of Rolled Steel Beams," 823.
Sutton, John G.
"Drainage in the Humid Areas of the United States," 115.
Szalay, N.
Canal seepage, 368.
Tarr, Simon Weinberg
Memoir of, 1256.
Thomas, Harold E.
Ground water, 434.
Thomas, Robert O.
"Ground-Water Development (symposium): Planned Utilization," 422.
Tiedemann, John L.
"Lateral Buckling of Rolled Steel Beams," 823.
Tucker, Herman Franklin
Memoir of, 1257.
Tung, Tie P.
"Lateral Buckling of Elastically End-Restrained I-Beams," 374.
Veletsos, Anestis S.
"Natural Frequencies of Continuous Flexural Members," 249.
Vey, Ebenezer
Vane shear tests, 858.
Warnick, Calvin C.
Canal seepage, 366.
Wartelle, Charles Leopold
Memoir of, 1258.
Washington, Walter Owen
Memoir of, 1258.
Watts, George M.
"Beach Rehabilitation by Fill and Nourishment," 155.
Whisler, Benjamin A.
"Education of Civil Engineers (symposium): Training for Civil Engineering," 779.
Wiley, C. C.
Highway spirals, 402.

Wiley, John S.
"A Preliminary Study of High-Rate Composting," 1009.

Williams, Melvin Delano
Memoir of, 1259.

Williams, Roger H.
Runway pavements, 1046.

Wormald, Frank
Memoir of, 1260.

Xerez, A. Carvalho
Arch dams, 945.

Yegian, Shahen
"Lateral Buckling of Elastically End-Restrained I-Beams," 374.

Yih, Chia-Shun
Well flow, 1110.

Young, Arrigo Mazzucato
Memoir of, 1260.

Zapp, Lloyd Otto
Memoir of, 1261.

Zee, Chong-Hung
"Flow into a Well by Electric and Membrane Analogy," 1088.